F 1103

ACADÉMIE ROUMAINE

REVUE ROUMAINE DE CHIMIE

TOME 36

N°s 1—3

Janvier—Mars 1991

Rev. Poumanie Chim.

RRCHAH, 36, *1—3* 1—276 (1991), Bucarest

EDITURA ACADEMIEI ROMÂNE

ACADÉMIE ROUMAINE

CONSEIL DE DIRECTION

Rédacteur en chef :

I.G. MURGULESCU, membre de l'Académie Roumaine

Rédacteurs en chef adjoints :

A.T. BALABAN et V. EM. SAHINI, membres de l'Académie Roumaine

Collège de rédaction :

EM. BRATU, ECATERINA CIORĂNESCU NENITZESCU, P. SPACU CR. SIMIONESCU, GH. SUCIU, membres de l'Académie Roumaine ; M. ANDRUH, M. BANCIU , M.D. GHEORGHIU, I. HAIDUC, D.I. MARCHIDAN G. NIAC et D. SĂNDULESCU

La Revue Roumaine de Chimie paraît 10 fois par an. Toute commande de l'étranger sera adressée à ROMPRESFILATELIA — sectorul Export-Import Presă, P.O. Box 12—201, télex 10376, prsfir 78 104 Bucarest, Calea Griviței nr. 64—66, București, Roumanie

Les manuscrits, les livres et les revues proposés en échange, ainsi que toute correspondance seront envoyés à la rédaction :

REVUE ROUMAINE DE CHIMIE

125, Calea Victoriei, 79717 Bucarest, Roumanie, téléphone 50 76 80

EDITURA ACADEMIEI ROMÂNE

125, Calea Victoriei, 79717 Bucarest, Roumanie, téléphone 50 76 80

REVUE ROUMAINE
DE
CHIMIE

Tome 36, N°s 1–3 **Janvier–Mars, 1991**

P. SPACU, SILVIA PLOȘTINARU, LUMINIȚA PATRON, ADRIANA CONȚESCU, D. CRIȘAN and N. STĂNICĂ, Coordination compounds as raw materials for mixed oxides. VII. Mixed coordination compounds of lanthanides and Mn(II) as precursors of manganites 5–11

S. STERNBERG, T. VIȘAN, LIGIA MANOLIU, ADINA COTÂRȚĂ and I. LINGVAY, Polarization behaviour of the n-type and p-type silicon in hydroxide solutions 13–23

SOLOMON STERNBERG, MIHAELA UNGUREANU and SORIN ROȘCA, Electrochemical oxidation of carboxylic acids. II. Electrode processes in electrochemical oxidation of natrium monomethyl adipate on platinum 25–37

PAUL GH. ZUGRĂVESCU and JÁNOS FAZAKAS, The hollow cathode current as a factor affecting the influence of pressure on spectral line overlaps in electrothermal atomic absorption spectrometry 39–41

O. RADU and CONSTANȚA GHEORGHIU, As(III)–HCl–H_2O system. III. The liquid—liquid state 43–48

RADU MUTIHAC and ALEXANDRU OPREA, Thin films of Al_2O_3 and Ta_2O_5 obtained by magnetron reactive sputtering. 49–54

RADU VLĂDUȚESCU, Anionic layer optimization in a demineralization scheme using ion exchangers (in French) 55–64

ALEXANDRA SCHIOPESCU, ANCA ALBU and D. SĂNDULESCU, The ferrate (VI), $[FeO_4]^{2-}$, as oxidizing agent 65–69

F. SALINAS, J.J. BERZAS NEVADO and P. VALIENTE GONZÁLEZ, Iron determination by solvent extraction with salicylaldehyde guanylhydrazone and atomic absorption spectrophotometry. 71–75

A. MOLINA-DÍAZ, M.I. PASCUAL-REGUERA and L.F. CAPITÁN-VALLVEY, Study of the system iron(III)-3-nitrobenzohydroxamic acid-adogen 464 in toluene 77–83

LUCIA MUTIHAC and CONSTANTIN LUCA, Separation by extraction of amino acids with macrocyclic ligands 85–90

LUCIA MUTIHAC, CONSTANTIN LUCA, TITUS CONSTANTINESCU, MARIETA OPREA and MIHAI RADU, The influence of operational parameters upon the extraction of amino acids with macrocyclic ligands 91–99

MARIUS ANDRUH, Thermal behaviour of the complex cation-complex anion-type coordination compounds. III. Thermochromism in tris(phenanthroline)nickel(II)-tetrachloro-palladate complexes 101–107

Rev. Roumaine Chim. . . . . 36, *1–3*, 1–276 (1991), **Bucarest**

MARIUS ANDRUH, MICHAELA STĂNESCU, NICOLAE STĂNICĂ and MARILENA FERBINŢEANU, Mixed-ligands coordination compounds of cobalt(II) and nickel(II) with 9,10-dihydro-9,10-ethano-12-hydroxymethylene-anthracen-11-one and 2,2′-dipyridyl or 1,10-phenanthroline. 109—111

MARIUS ANDRUH, MICHAELA STĂNESCU, FLORIANA MUŞUROI and MARIA BREZEANU, Coordination compounds of cobalt(II), nickel(II) and copper(II) with 9,10-dihydro-9,10-ethano-12-hydroxymethylene anthracen-11-one . . . . 113—118

MICHAELA DINA STĂNESCU, MIRCEA D. BANCIU and FILIP CHIRALEU, Heterocycles with annelated dibenzocycloalkane skeletons. V. Pyrimidines with annelated dibenzobarrelene and dibenzohomobarrelene skeletons. . 119—125

IOANA ŞARAMET, MIRCEA D. BANCIU and CONSTANTIN DRĂGHICI, Synthesis and characterization of some 4,5-disubstituted-3-mercapto-1,2,4-triazoles . . . . 127—134

IOANA ŞARAMET, MIRCEA D. BANCIU and CONSTANTIN DRĂGHICI, Synthesis and characterization of some 5-substituted-3-mercapto-1,2,4-triazoles . . . . 135—143

A.T. BALABAN, J. BRUNVOLL and S.J. CYVIN, Chemical graphs. Part 54. Enumeration of unbranched catacondensed polyhexes with equidistant linearly condensed segments . . . . 145—155

FLORIN BADEA, ALEXANDRU T. BALABAN, ION COSTEA, FLORIN IORDACHE, AURELIA MEGHEA and DANIELA CARMEN ONICIU, Reaction of 3,5-di-*t*-butylnitrosobenzene with alkoxides and carbanions 157—169

H. SELIGER, M.B. BITAR, E. GÖLDNER, I. KITTEL and H.G. KILIAN, Preparation and properties of oligomers of defined chain length and structure as models for technical copolymers . . . . 171—185

M.A. El-SAFTY, S. El-BAHAEI, M.A. El-HASHASH, A. El-FARARGY and F. YASIN, Studies in the field of heterocyclic compounds. Synthesis and behaviour of 4-(4-chloro-3-methyl)phenyl-1-(2H)-phthalazinone towards some electrophiles and nucleophiles . . . . 187—195

S. YASSIN, I.I. ISMAIL, A.H. ABD El-ALEEM and A.A. ATTA, Some reactions of sultones . . . . 197—200

F.A. YASSIN, M.A. El-SAFTY, B.E. BAYOUMY and A.F. El FARARGY, Synthesis of 4,5,6,7-tetraphenyl-8(substituted)-3(2H)-phthalazinone derivatives with potential antihypertensive activity . . . . 201—208

S. El-BAHAIE and B.E. BAYOUMY, Synthesis of some new 1,2,3-selena- and 1,2,3-thiadiazolopyrimidines . . . . 209—213

ALEXANDRU C. RĂZUŞ, MIRCEA D. GHEORGHIU and EMERIC BARTHA, Dihydropyrans obtained in the reaction between 2-(acenaphthylen-1-yl)-ethanol and carbonylic derivatives . . . . 215—227

TEODOR-SILVIU BALABAN, MARIANA BOGAŢIAN, MARIETA PLĂVEŢI, VIRGIL M. BĂDESCU and GHEORGHE MIHAI, Diacylation of olefins. XXV. New pyrylium and pyridinium salts derived from hexahydropseudoionone. . . . . 229—234

A. ALKOURASHY and A.S. El-SHAHAWY, Electronic spectral analysis of benzo[b] pyrido[3,2-F] thiepin, 8-chlorobenzo[b] pyrido[3,2-F]thiepin and 8-chlorobenzo[b]pyrido[3,2-F] thiepin-6(5H)-one. . . . . 235—243

NADIA G. KANDILE, TAHIA M. ABDEL LATIF and WAFAA A. El SAYED, Synthesis and some reactions of 4-(N-acetyloxindolylidene)-2-aryl-5 (4H) oxazolones . . . . 245—250

CLAUDIU SUPURAN, GHEORGHE MANOLE, ANA SCHIKETANZ, MIRCEA D. GHEORGHIU and IOAN PUŞCAŞ, Carbonic anhydrase inhibitors. IV. Bifunctional derivatives of 5-amino-1,3,4-thiadiazole-2-sulfonamide 251–255
TEODOR COSEAC and EUGEN SEGAL, Basic program to generate the TG and DTG curves corresponding to thermal decompositions in solid—gas systems 257–262
MIRCEA V. DIUDEA and IOAN SILAGHI-DUMITRESCU, Molecular topology. 2. A computer program for multiple bond, cycle and radical approximations of D S index 263–269

BOOK REVIEW 271

IN MEMORIAM: GHEORGHE CLAUDIU SUCIU 273–275

Revue Roumaine de Chimie, **36**, *1–3*, 5–11 (1991)

COORDINATION COMPOUNDS AS RAW MATERIALS FOR MIXED OXIDES. VII[1]

MIXED COORDINATION COMPOUNDS OF LANTHANIDES AND Mn(II) AS PRECURSORS OF MANGANITES

P. SPACU, SILVIA PLOŞTINARU, LUMINIŢA PATRON, ADRIANA CONŢESCU,
D. CRIŞAN and N. STĂNICĂ

Center of Physical Chemistry, Bucharest, Splaiul Independenţei 202, Romania

Received June 4, 1989

A new class of mixed coordination complex compounds of Ln(III) and Mn(II) with gluconic acid was synthesized. These complex compounds were studied in order to obtain $LnMnO_3$ and $Ln_{1-x}Sr_xMnO_3$ oxides. All oxidic phases obtained by thermogravimetric decomposition were analysed by X-ray diffraction and were analysed by physico-chemical methods (electronic and IR spectra and magnetic measurements).

The references regarding the existence of mixed oxides of *3d* transition metals with lanthanides are relatively scarce in literature. The results we published so far referred to compounds of perovskite ($A^{3+}B^{3+}O_3$),[1,2] of K_2NiF_4 ($A_2^{3+} + B^{2+} + O_4$),[3] and garnet $Ln_3Fe_5O_{12}$(Ln^{3+} = Gd – Tm) type.[3]

The study of these oxides was initiated because they proved to be adequate catalysts in oxido-reduction, as well as hydrogenation reactions. From among perovskite – type oxides, cobaltite and manganites exhibit the highest catalytic activity.

Several oxide phases may be formed in Ln(III)–Mn(III)–O system depending on the possible states of valence of manganese: $LnMnO_3$, $LnMn_2O_5$, etc; the mixed perovskite oxide, $LnMnO_3$, with In(III) La–Tb, is the most common of them. In fact the most general form of these mixed oxides is $LnMn_x^{3+}Mn_{1-x}^{4+}O_{3+\delta}$. Formation of manganite with this composition is conditioned by the amount of oxygen absorbed from the atmosphere which, implicitly yields various amounts of Mn^{4+}, [4,5] ions.

The physico-chemical study of rare earth manganite has evidenced a good deal of magnetic and crystallographic properties, which originate in the presence of manganese ions whose valence is higher than three in manganites (following application of an adequate thermal treatment in oxygen atmosphere).

A similar increase of manganese valence was achieved through preparation of mixed crystals $In^{3+}Mn^{3+}O_3 - M^{2+}Mn^{4+}O_3$, ($M^{2+}$ = large divalent ions). Replacement of lanthanides with alkali-earth metals allows the obtention of Mn-mixed oxide containing Mn(IV) ions as well by calcination in usual atmosphere.[6,7]

This note deals with the synthesis and characterization of lanthanide manganites and lanthanide manganites substituted with Sr(II) from polynuclear complex compounds as precursors.

RESULTS AND DISCUSSION

The polynuclear complex compounds obtained from Ln(III)—Mn(II)-gluconic acid (Gluc) system were studied in order to obtain $LnMnO_3$ and $Ln_{1-x}Sr_xMnO_3$ oxides (Ln(III) = La-Tm).

The elemental chemical analysis and thermal decomposition have suggested the following general formulas:

$$[LnMn(Gluc)_4] \cdot nH_2O$$

where Ln(III) = La-Tm; n = 3—5
and

$$[Ln_{0,5}Sr_{0,5}Mn(Gluc)_4] \cdot nH_2O$$

where Ln(III) = La, Nd, Gd; n = 2,3.

The synthesized compounds were white or white-pink powders. All are water-soluble and hardly soluble in most of the usual organic solvents.

All these compounds were characterized from physico-chemical viewpoint (IR and electronic spectroscopy, magnetic and thermogravimetric determinations).

Electronic UV and visible spectra have supplied data regarding the structure of complex compounds. Fig. 1 shows the electronic spectrum of $[NdMn(Gluc)_4] \cdot 4H_2O$ complex compound. The UV spectrum of mixed complex is practically identical to that of the free ligand. Fig. 1 shows that in visible range the bands assigned to Mn(II) ion in O_h symmetry as well as those assigned to hyperfine *f-f* transitions of Nd(III) ion are present. The Mn(II) (d^5) ion exhibits in this configuration (like Fe(III), (d^5)) spin forbidden transitions from the ground level $^6A_{1g}$ to excited levels whose intensity is low (Fig. 1). To obtain a higher resolution of the spectrum the second derivative was drawn (Fig. 2 curve b).

The values of magnetic susceptibilities of the complex compounds:

$[GdMn(Gluc)_4] \cdot 3H_2O$

$[Gd_{0.5}Sr_{0.5}Mn(Gluc)_4] \cdot 3H_2O$

were determined at room temperature and the corresponding magnetic moments were calculated. The magnetic moment of the complex with Mn(II) and Gd(III) is 9.31 MB which confirms the existence of Mn(II) ion in an octahedral configuration of high spin. The value mentioned is lower than the sum of the magnetic momenta of the two ionic metals which points to the existence of some interaction between these ions.

The magnetic moment of the complex compound containing 50% Sr(II) is lower, i.e. 7.7 BM — which corresponds to a magnetic dilution caused by the divalent metal ion.

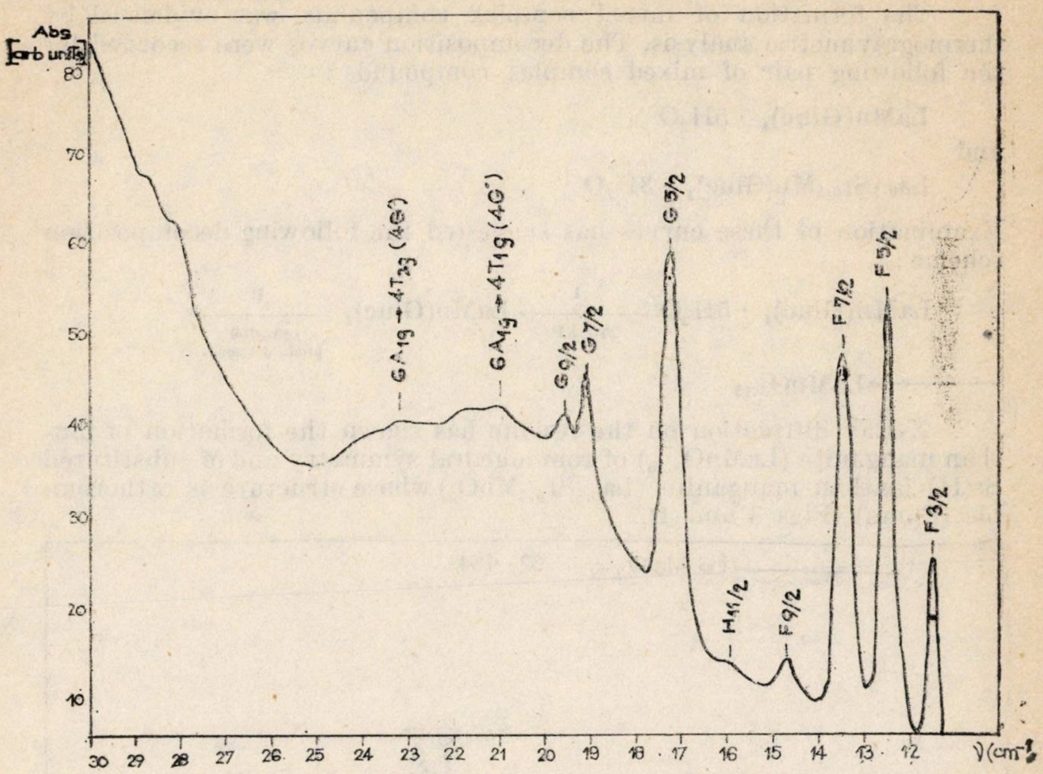

Fig. 1. — Electronic spectrum of NdMn(Gluc)$_4$ · 4H$_2$O.

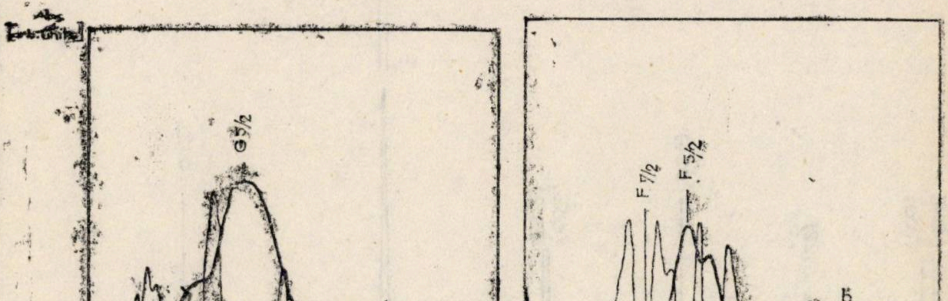

Fig. 2. — Electronic spectrum of [NdMn(Gluc)$_4$] · 4H$_2$O.

The formation of mixed complex compounds was evidenced by thermogravimetric analysis. The decomposition curves were recorded for the following pair of mixed complex compounds :

$LaMn(Gluc)_4 \cdot 5H_2O$

and

$La_{0.5}Sr_{0.5}Mn(Gluc)_4 \cdot 3H_2O$

Examination of these curves has suggested the following decomposition scheme :

$$LaMn(Gluc)_4 \cdot 5H_2O \xrightarrow[20-180^\circ]{\text{I}} LaMn(Gluc)_4 \xrightarrow[\substack{180-700^\circ \\ \text{prod. descomp.}}]{\text{II}}$$

$$\longrightarrow LaMnO_{3.15}$$

X-Ray diffraction on the residue has shown the formation of lanthan manganite ($LaMnO_{3.15}$) of rombohedral symmetry and of substituted Sr(II) lanthan manganite ($La_{0.5}Sr_{0.5}MnO_3$) whose structure is orthorombic (Pbnm) (Figs 3 and 4).

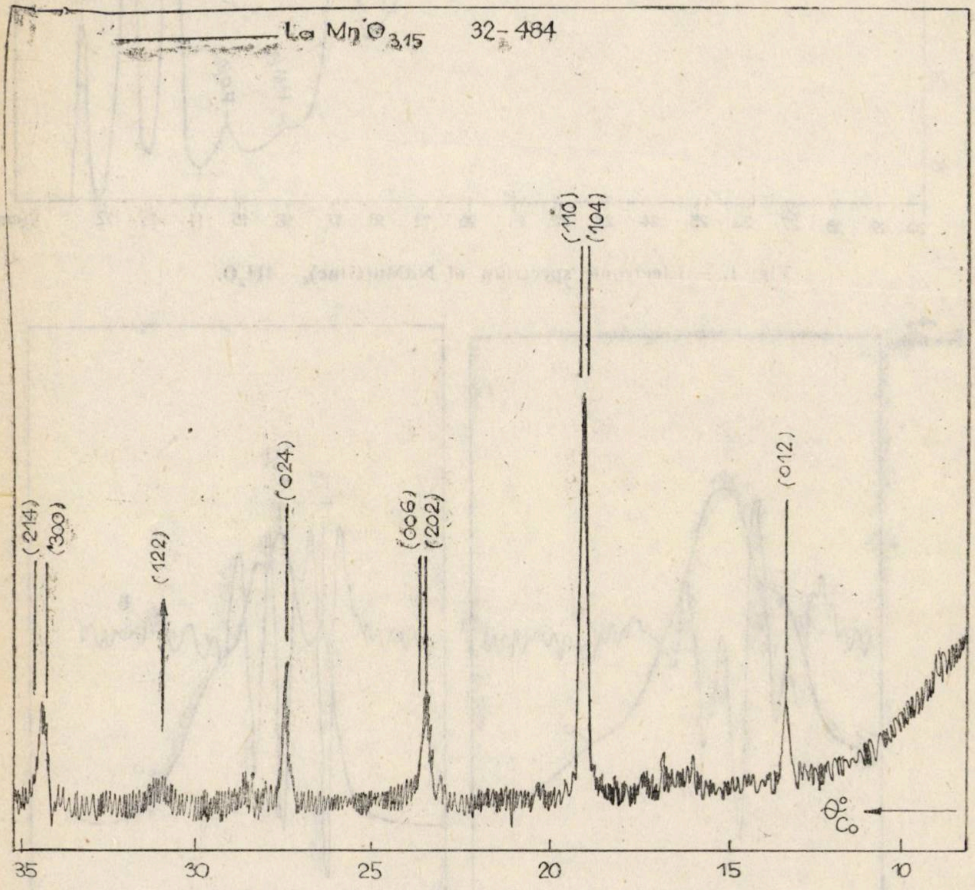

Fig. 3. — X-ray diffraction pattern of $LaMnO_{3.15}$.

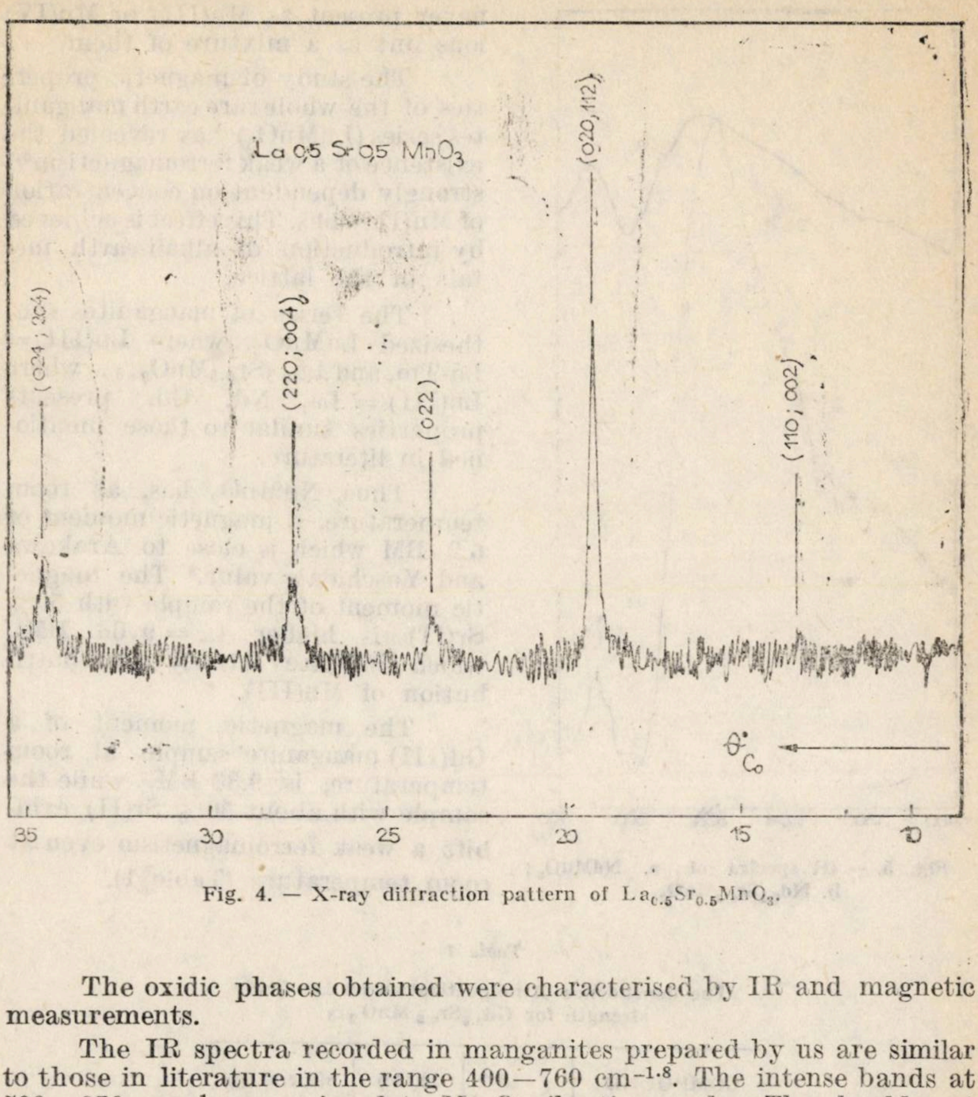

Fig. 4. — X-ray diffraction pattern of La$_{0.5}$Sr$_{0.5}$MnO$_3$.

The oxidic phases obtained were characterised by IR and magnetic measurements.

The IR spectra recorded in manganites prepared by us are similar to those in literature in the range 400—760 cm^{-1}[8]. The intense bands at 500—670 cm^{-1} are assigned to Mn-O vibration modes. The shoulder at 620 cm^{-1} in Mn$_2$O$_3$ is also present in the manganites of light lanthanides but is better resolved in the spectra of heavier manganites. The intense band at 608 cm^{-1} in Mn$_2$O$_3$ is present in all manganites at 590 cm^{-1}. Fig. 5 shows the IR spectra of NdMnO$_3$ and Nd$_{0.5}$Sr$_{0.5}$ MnO$_3$. The bands at 510, 545, 590 and 610 cm^{-1} mentioned in literature were also evidenced.

Discussions on the magnetic properties of mixed oxides assume that manganites are heteropolar compounds which, besides ions with rare gas configuration contain Mn(II) and Mn(IV) ions with $3d^4$ and $3d^3$ configuration. From theoretical viewpoint the manganites of rare earth are readily interpretable at first sight because the Ln(III) ions lie in the sites of a simple cubic lattice. However complications arise because manganese is never present as Mn(III) or Mn(IV) ions but as a mixture of them.

The study of magnetic properties of the whole rare earth manganites series ($LnMnO_3$) has revealed the existence of a weak ferromagnetism[6,9] strongly dependent on concentration of Mn(III) ions. This effect is achieved by introduction of alkali-earth metals in the lattice.

The series of manganites synthesized $LnMnO_3$, where Ln(III) = La-Tm, and $Ln_{0.5}Sr_{0.5}MnO_{3+\delta}$, where Ln(III) = La, Nd, Gd, presents properties similar to those mentioned in literature.

Thus, $NdMnO_3$ has, at room temperature, a magnetic moment of 6.2 BM which is close to Arakawa and Yoschida's value.[9] The magnetic moment of the sample with 50% Sr(II) is higher ($\mu = 9.06$ BM), which indicates clearly the contribution of Mn(III).

The magnetic moment of a Gd(III) manganite sample, at room temperature, is 9.33 BM, while the sample with about 50% Sr(II) exhibits a weak ferromagnetism even at room temperature (Table 1).

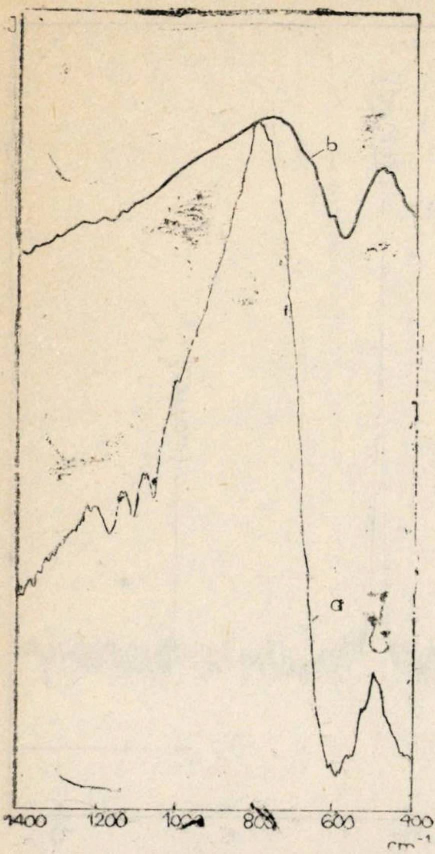

Fig. 5. — IR spectra of : a. $NdMnO_3$; b. $Nd_{0.5}Sr_{0.5}MnO_3$.

Table 1

The dependence of magnetization on the field strength for $Gd_{0.5}Sr_{0.5}MnO_{3+\delta}$

COMPOUND	$\chi \cdot 10^{-6}$	H(Oe)	σ(u.e.m./g)
$Gd_{0.5}Sr_{0.5}MnO_{3+\delta}$	161.40	1300	0.210
	141.03	1900	0.268
	137.13	2800	0.345
	119.70	3200	0.383

REFERENCES

[1] P. Spacu, Silvia Ploştinaru, Luminiţa Patron, Adriana Conţescu, D. Crişan and N. Stănică, *Rev. Roumaine Chim.*, **32**, 877 (1987).

[2] P. Spacu, Luminiţa Patron, Silvia Ploştinaru, Adriana Conţescu, D. Crişan and N. Stănică, *Rev. Roumaine Chim.*, **32**, 249 (1987).

[3] P. Spacu, Luminiţa Patron, Silvia Ploştinaru, Adriana Conţescu, D. Crişan and N. Stănică, *Rev. Roumaine Chim.*, **34**, 1275 (1989).

[4] H.L. Yakel, *Acta Cryst.*, **8**, 394 (1955).

[5] E.O. Wollan, *Phys. Rev.*, **100**, 545 (1955).

[6] G.H. Jonker and J.H. Van Banten, *Physica*, **16**, 337 (1950).

[7] D.W. Johnson, Jr., *Am. Ceram. Soc. Bull.*, 520 (1976).

[8] G.V. Subba and C.N.R. Rao, *J. Appl. Spectroscopy*, **24**, 436 (1970).

[9] T. Arakawa and A. Yoschida, *Mat. Res. Bull.*, **15**, 269 (1980).

[10] J.B. Goodenough, *Physica*, **100**, 564 (1955).

Revue Roumaine de Chimie, **36**, *1–3*, 13–23(1991)

POLARIZATION BEHAVIOUR OF THE n-TYPE AND p-TYPE SILICON IN HYDROXIDE SOLUTIONS

S. STERNBERG[a,*], T. VIŞAN[a], LIGIA MANOLIU[a], ADINA COTÂRŢĂ[b] and I. LINGVAY[c]

[a] Department of Applied Physical Chemistry and Electrochemistry, Polytechnic Institute of Bucharest, Romania

[b] Institute of Chemical and Biochemical Energetics, Bucharest, Romania

[c] Institute of Scientific Research and Designing for Electrotechnica Industry, Bucharesti, Romania

Received February 15, 1990

Potentiostatic polarization curves for n- and p-type silicon electrodes in alkali metal hydroxide solutions have been obtained in steady-state conditions. The anodic branch of curves showed an active region of silicon dissolution, silicon oxide film formation and dissolution ; its range is more extended in KOH and decreases in NAOH and LiOH solutions. The influence of semiconductor type and doping level has been demonstrated. The hydrogen evolution on cathodic polarization is also discussed.

INTRODUCTION

It is known that the surface processing of semiconductors is an important step in electronic devices technology. Thus, the study of electrode processes on silicon in different electrolytical media is related to the etching efficiency of the semiconductor device surfaces. Previous investigations on the behaviour of silicon electrodes in aqueous sulphuric acid [1,2] showed that at anodic polarization the surface covers gradually with an oxide film, which passivates the electrode. It has been also established that in HF-HNO_3 (HOAc) solutions the etching process is more efficient.[3] Another paper[4] showed that ammonium fluoride solutions are a moderate etching agent in comparison with hydrofluoric acid.

The present work studies the polarization behaviour of semiconductor silicon in different types of alkali metal hydroxides. We mention that there are only a few papers[5–7] which dealt with the study of silicon/alkaline solution interaction. The conditions of the etching of silicon in aqueous solutions of KOH-ethylic alcohol[8], KOH-n-propanol, KOH-isopropanol,[9] KOH$-NH_4Cl$[10] were also discussed. However, the reported results refer

---

[*] Deceased on 19 January, 1990

more to the influence of crystalline orientation and an adequate electrolyte composition for industrial applications, rather to the mechanism of the electrochemical process.

EXPERIMENTAL PART

Steady-state potentiostatic determinations were performed by the usual technique using a Princeton Applied Research potentiostat Model 173. The scheme of the device and the operating technique were described in a previous paper.[11]

The experiments were carried out in a three-electrode electrochemical cell. The working semiconductor electrodes were disks (plate wafers) with a surface area of 1 cm,^{2} made from monocrystaline silicon, sealed in Pyrex glass tubes. The counterelectrode was a bright platinum sheet, and the reference electrode was a saturated calomel electrode. The working electrode was polarized using potential steps of 50 mV ; for each potential step the current response was recorded. Chemical reagents of p.a. grade quality were used. The temperature during the experiments was kept at room temperature.

Construction and pretreatment of Si electrodes

The n- and p-type Si electrodes were cut as disks with 2 mm thickness from starting monocrystalline silicon (Wacker Chemie, Burghausen, Germany). Their resistivities and the free carriers densities at 27°C are listed in Table 1.

Table 1

Physical parameters of the silicon electrodes at 27°C

Electrode No.	Resistivity ($\Omega \cdot$ cm)	Charge carriers concentration (cm^{-3})
	n-type silicon	
1	0.01	5×10^{18}
2	1.6	1.7×10^{16}
3	20	1.5×10^{14}
4	70	7.5×10^{13}
	p-type silicon	
5	0.01	1.1×10^{19}
6	1	5×10^{16}
7	10	5×10^{14}
8	200	2.6×10^{13}

The n-type electrodes were doped with phosphorus from $POCl_3$ and the p-type electrodes were doped with boron from B_2O_3, using the technique described in the previous paper.[12] The doped silicon slices were metallized by chemical deposition of nickel and by gold electrodeposition in aqueous solution. The electric contact at polarization was made from a copper wire.

Prior to each experiment the surface renewal of silicon disk was accomplished. The electrode was etched in a mixture of HNO_3 (70%)—HF(50%) solution and rinsed in distilled water for 3 or 4 times. Then, the electrode was maintained for 10—15 minutes at a potential that ensures the complete surface cleaning by an intense evolution of hydrogen.

RESULTS AND DISCUSSION

The electrochemical behaviour of silicon in potassium hydroxide solution was investigated by us for two different concentrations : 2 M and 4 M KOH. By immersion in these hydroxide solutions, on the silicon electrode a steady-state potential was established, which is in fact a corrosion potential due to the silicon dissolution and the hydrogen discharge. In our case, this electrode potential ranges between −0.5 V and −1.4 V (vs. SCE) compared to the steadystate potential of about +0.2 V for determinations in H_2SO_4 solution.

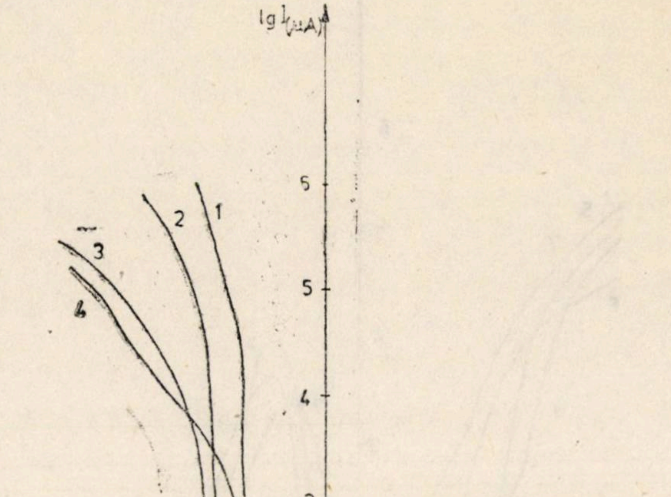

Fig. 1. — Steady-state i — E curves on n-Si electrodes in 2 M KOH (solid lines) and in 1 M H_2SO_4 (dotted line). For numbering of the electrodes see Table 1.

Figures 1–4 show the polarization curves (anodic and cathodic branches) for the two KOH concentrations. The polarization curves for Si/NaOH (Figures 5–6) and Si/LiOH (Figures 7–8) systems do not exhibit essential differences, but the currents are smaller, especially for the anodic ones.

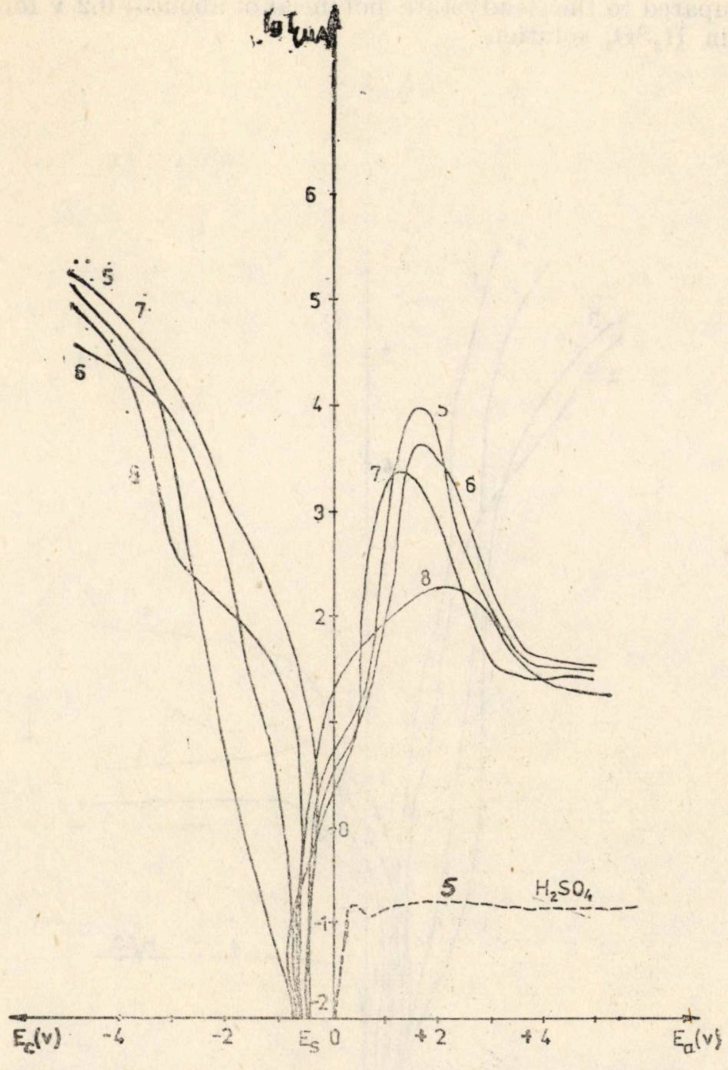

Fig. 2. — Steady-state i—E curves on p-Si electrodes in 2 M KOH (solid lines) and in 1 M H_2SO_4 (dotted line). For numbering of the electrodes see Table 1.

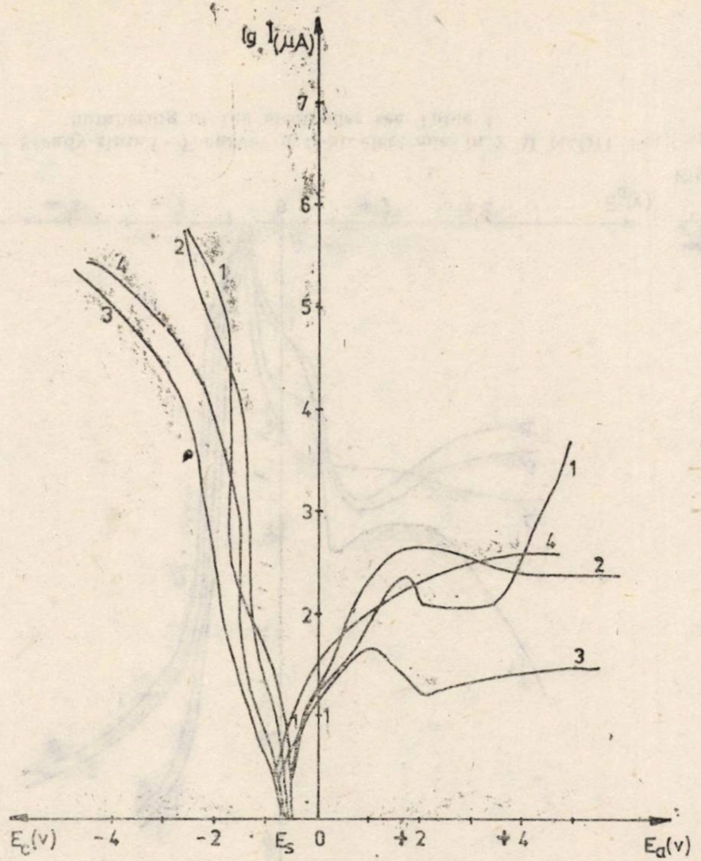

Fig. 3. — Steady-state i—E curves on n-Si electrodes in 4 M KOH. For numbering of the electrodes see Table 1.

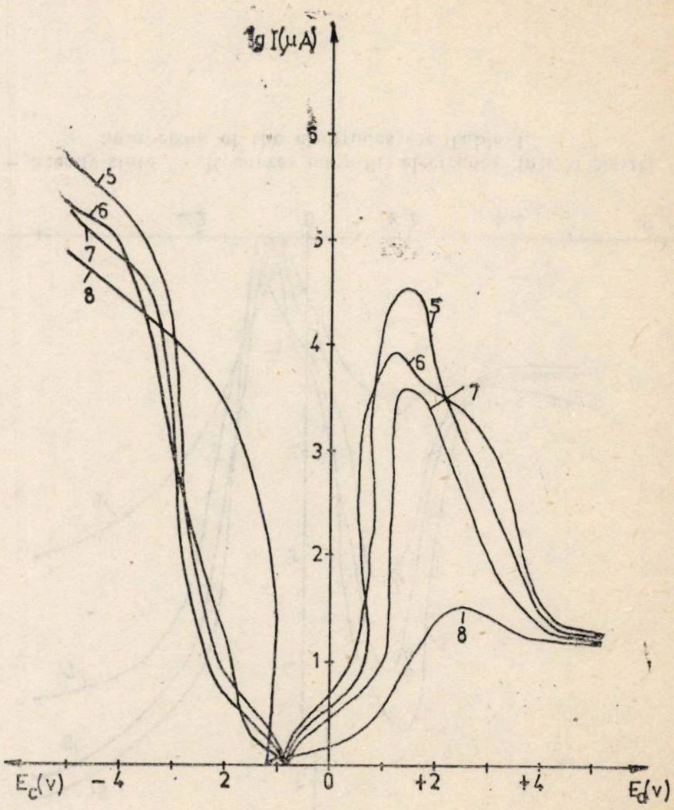

Fig. 4. — Steady-state i—E curves on p-Si electrodes in 4 M KOH. For numbering of the electrodes see Table 1.

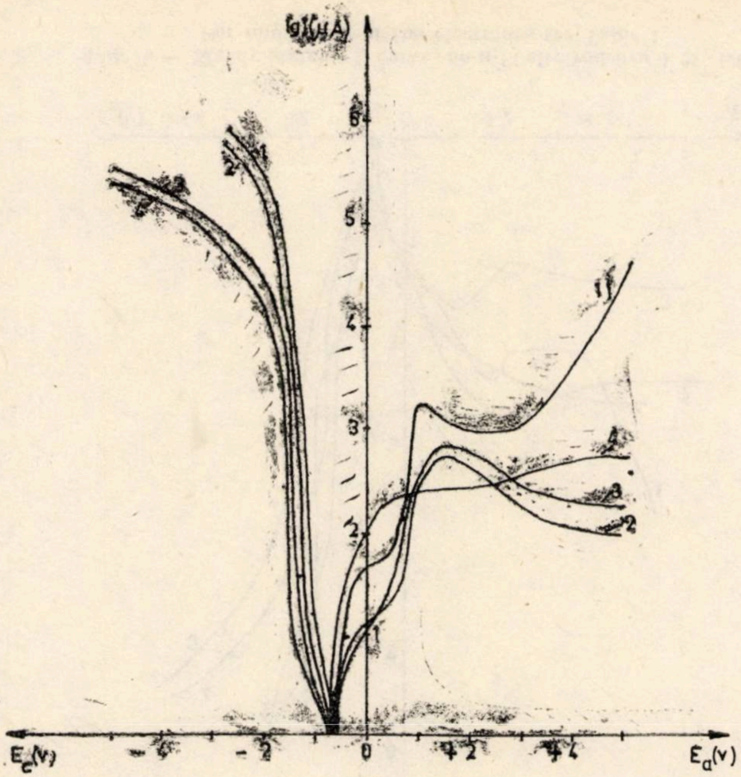

Fig. 5. — **Steady-state i—E curves on n-Si electrodes in 2 M NaOH. For numbering of the electrodes see Table 1.**

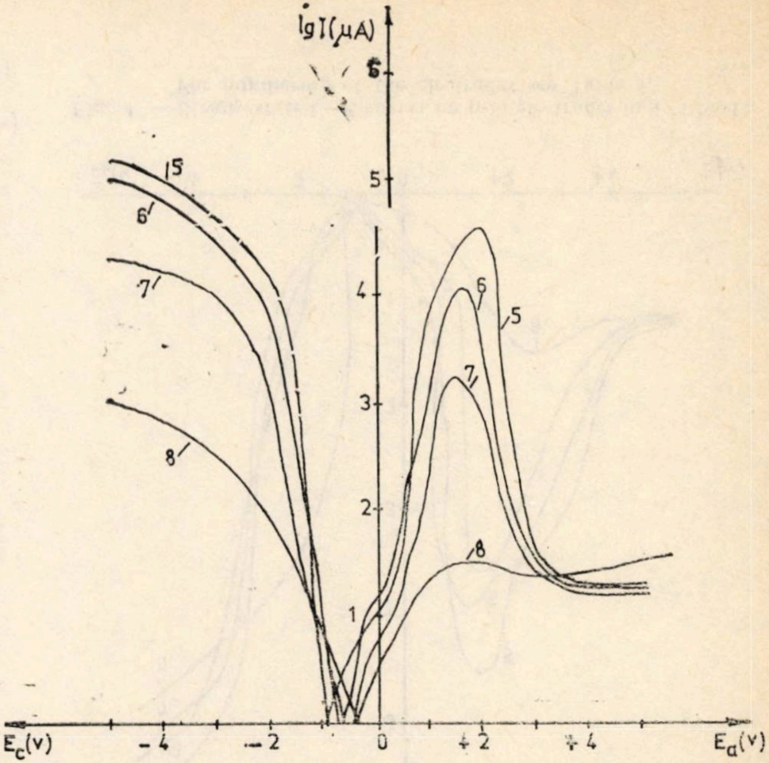

Fig. 6. — **Steady-state i —E curves on p-Si electrodes in 2 M NaOH. For numbering of the electrodes see Table 1.**

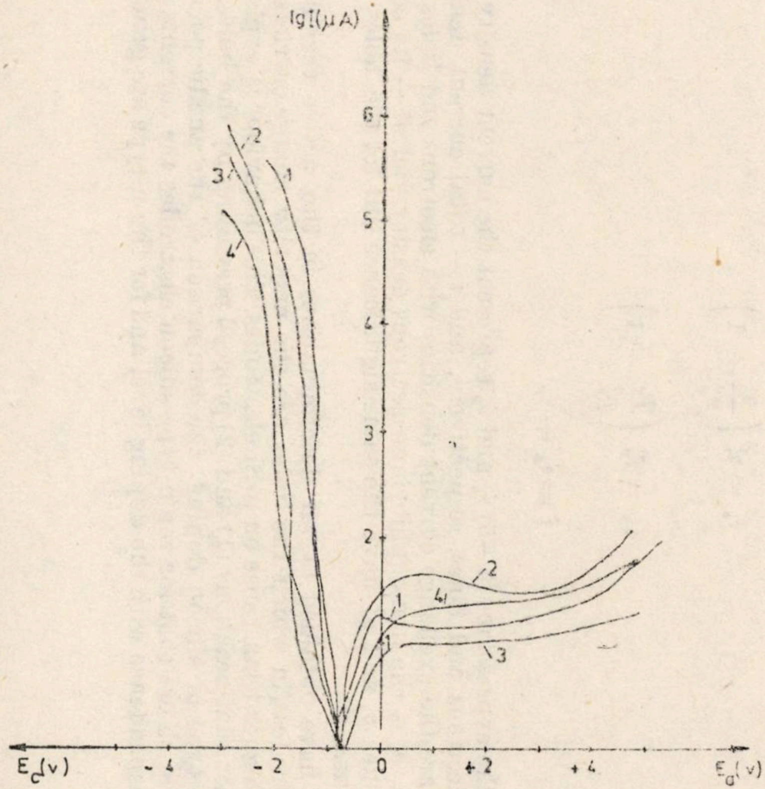

Fig. 7 — Steady-state i-E curves on n-Si electrodes in 2 M LiOH. For numbering of the electrodes see Table 1.

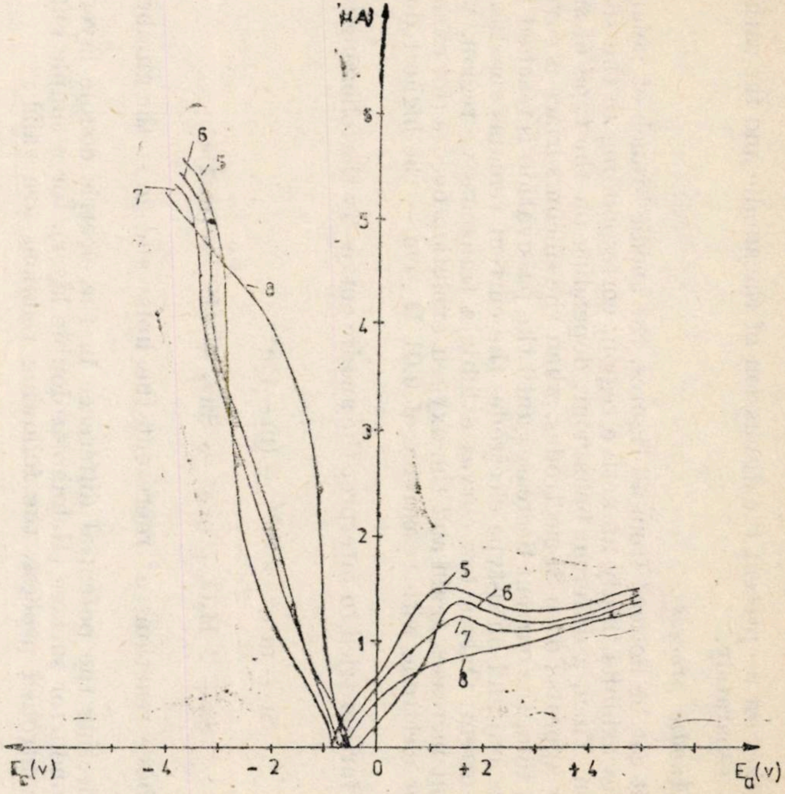

Fig. 8. — Steady-state i—E curves on p-Si electrodes in 2 M LiOH. For numbering of the electrodes see Table 1.

Further on we present the discussion of the anodic and the cathodic processes separately.

a) *Anodic process*

As it can be noticed from all figures, the anodic branch of polarization curves exhibits firstly an active region, corresponding to the silicon dissolution. Then, a different behaviour, depending on the type of semiconductor appears ; on p-Si electrodes, when the silicon surface is covered by a SiO_2 film, the current decreases until the passivation is reached (the passive region) and on n-type electrodes the current remains constant as limiting current. Only a few curves exhibit a transpassive region, when the current increases again and the oxygen evolution occurs (for example the n-type electrode with resistivity of 0.01 Ω . cm — the highest doped ones).

We further tried to interpret the anodic curves by the following reactions :

$$\mathrm{Si} + \mathrm{m\ e^+} \rightarrow \mathrm{Si^{4+}} + \mathrm{(m-4)e^+} \tag{1}$$

$$\mathrm{Si} + 2\ \mathrm{H_2O} + \mathrm{m\,e^+} \rightarrow \mathrm{SiO_2} + 4\mathrm{H^+} + \mathrm{(m\text{-}4)e^+} \tag{2}$$

In the above reactions e^+ represent the holes and m — the number of holes.

Neglecting the potential difference in the electric double layer on the semiconductor surface (Helmholtz double layer), for a simple charge transfer controlled process, the following relations are valid :

$$i_n = i_n^0 \left(\frac{n_s}{n_n^0} - 1 \right) \tag{3}$$

$$i_p = i_p^0 \left(\frac{p_s}{p_s^0} - 1 \right) \tag{4}$$

$$i = i_n + i_p \tag{5}$$

In the expressions (3—5) i_n and i_p represent the current density due to free electrons and holes, respectively, and i — total current density ; i_n^0 and i_p^0 are the exchange current densities with electrons and holes participation, n_s is the non-equilibrium electrons density and n_s^0 — its equilibrium value ; p_s and p_s^0 have the same significance but for the holes concentrations.

We have obtained in our determinations in the active region on p-Si electrodes (in which the holes are the majority charge carriers) the currents higher than those on p-Si electrodes. This behaviour is explained by the fact that reactions (1) and (2) proceed prevailing by the holes. For the same type of silicon doping, the comparison of the anodic polarization curves shows that for the p-type silicon electrodes the currents have a linear dependence with the doping level and for the n-type are generally in inverse proportion (in many cases the less doped electrodes exhibit the highest currents).

Referring to the passive region, we have noticed that the current is of approximately the same magnitude order for all p-type electrodes and that the passivation occurs faster for n-Si electrodes, reaching limiting currents. The descending of the passivation currents for the p-Si electrodes is due probably to the thickness and compactity of the insulating silicon oxide film. The existence of SiO_2 film was demonstrated by the current-time potentiostatic transients (an example is presented in Fig. 9) registered after an anodic polarization.

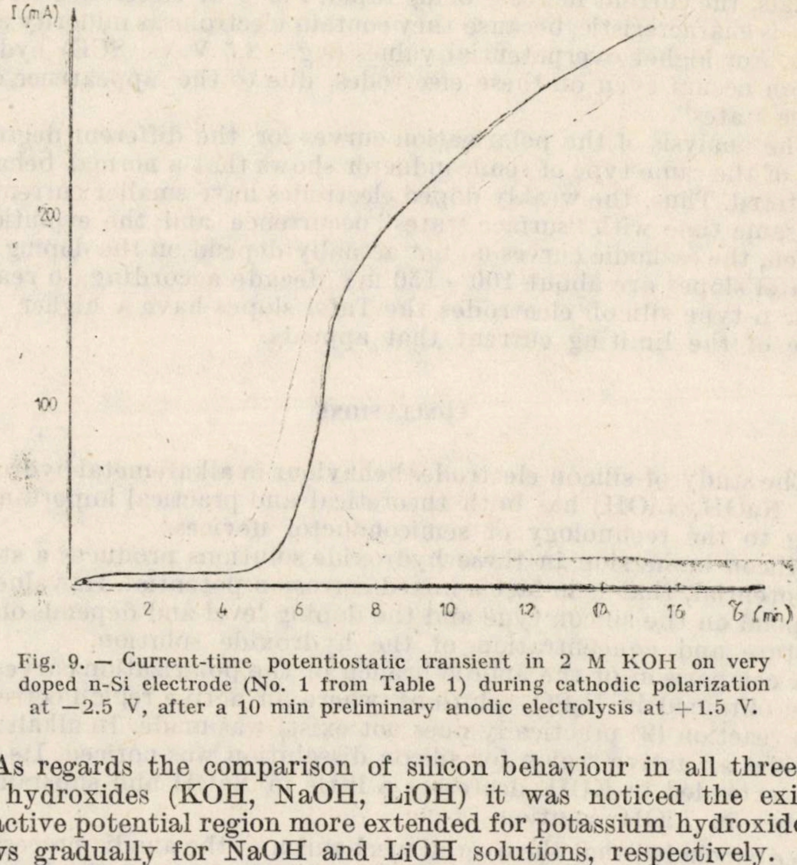

Fig. 9. — Current-time potentiostatic transient in 2 M KOH on very doped n-Si electrode (No. 1 from Table 1) during cathodic polarization at -2.5 V, after a 10 min preliminary anodic electrolysis at $+1.5$ V.

As regards the comparison of silicon behaviour in all three alkali metal hydroxides (KOH, NaOH, LiOH) it was noticed the existence of an active potential region more extended for potassium hydroxide, that narrows gradually for NaOH and LiOH solutions, respectively.

The etching effect of alkali metal hydroxides is represented by the reaction:

$$SiO_2 + 2HO^- + 2\ AlK^+ \rightarrow SiO_3^{2-} + H_2O + 2AlK^+ \qquad (6)$$

At anodic polarization of silicon in LiOH solution reaction (6) is very much diminished or does not occur at all; therefore, LiOH solution is a very weak etching agent.

b) *Cathodic process*

The cathodic branch of the polarization curves is more easily interpreted according to the hydrogen ion discharge:

$$H^+ + e^- \rightarrow \frac{1}{2} H_2 \qquad (7)$$

the reaction being thus favorized by the presence of free electrons.

In the case of n-type silicon electrodes, which have the electrons as majority charge carriers, the evolution of hydrogen occurs at small overpotentials, the current increase being rapid. For p-Si electrodes a current plateau is characteristic, because they contain electrons as minority charge carriers. For higher overpotential values (e.g. -2.5 V vs. SCE) hydrogen evolution occurs even on these electrodes, due to the appearence of the "surface states".

The analysis of the polarization curves for the different degrees of doping of the same type of semiconductor shows that a normal behaviour is registered. Thus, the weakly doped electrodes have smaller currents,but at the same time with "surface states" occurrence and the evolution of hydrogen, the cathodic curves do not actually depend on the doping level. The Tafel slopes are about 100–150 mV/decade according to reaction (7). For p-type silicon electrodes the Tafel slopes have a higher value because of the limiting current that appears.

CONCLUSIONS

The study of silicon electrodes behaviour in alkali metal hydroxides (KOH, NaOH, LiOH) has both theoretical and practical importance regarding to the technology of semiconductor devices.

Silicon immersion in these hydroxide solutions produces a steady-state potential, that is in fact a mixed corrosion potential. Its value does not depend on the silicon type and the doping level and depends only on the nature and concentration of the hydroxide solution.

A comparison of the anodic branch of the polarization curves with the one obtained in H_2SO_4 solutions (where an active region corresponding to reaction (2) practically does not exist) was made. In alkali metal hydroxides an active region for silicon dissolution was noticed. Its range is more extended in KOH, decreases a little in NaOH and substantially diminishes in LiOH solution.

We concluded that the overall mechanism of the anodic process contains two overlapped phenomena: silicon dissolution and the formation of SiO_2 film, that passivates the electrode. The silicon dissolution mechanism occurs mainly by means of holes (e^+) thus being intensified the dissolution of p-type electrodes, where the holes are the majority charge carriers. All n-type electrodes passivate more rapidly and their electrochemical properties do not depend anymore on doping level.

On cathodic branches, in all types of Si electrodes, the current increases even from the beginning, corresponding to the hydrogen evolution.

REFERENCES

[1] S. Sternberg, M. Ungureanu, V. Brânzoi and L. Apăteanu, *Rev. Roumaine Chim.*, **30**, 105 (1985).

[2] S. Sternberg, V. Brânzoi, L. Apăteanu and M. Ungureanu, *Rev. Roumaine Chim.*, **33**, 775 (1988).

[3] K.E. Bean, *I.E.E.E. Trans. Electron. Devices*, **ED-25**(10), 1185 (1978).

[4] S. Sternberg, M. Ungureanu and I. Lingvay, *Rev. Roumaine Chim.*, **31**, 3 (1986).

[5] Zhang Hongguang and Li Guozheng, *Sandong Daxue Xuebao, Ziran Kexueban*, **21** (2), **78** (1986).

[6] R.L. Smith and S.D. Collins, *Proc. Electrochem. Soc.* (Proc. Symp. Electrode Mater. Processes Energy Convers. Storage, 2-nd, 1987), **87—12**, 58(1987).

[7] E.D. Palik, O.J. Glembocki and I. Heard Jr., *J. Electrochem. Soc.*, **134**, 404 (1987).

[8] Hitachi Ltd., Jpn. Kokai Tokkyo Koho, JP-82, 145, 099 (1982).

[9] E.D. Palik, H.I. Gray and P.B. Klein, *J. Electrochem. Soc.*, **130**, 556 (1983).

[10] Yu. A. Kulagin, N.V. Rumak and V.P. Sergcev, USSR-524, 835 (1976).

[11] S. Sternberg, I. Lingvay and T. Vişan, *Electrochim. Acta*, **30**, 283 (1985).

[12] I. Lingvay, N. Iosif and A. Hluşcu, Rom-78, 126 (1979).

REFERENCES

[1] S. Steinberg, [illegible] and [illegible], Rev. [illegible] 36, 164 (1983).
[2] S. [illegible], [illegible] and M. [illegible], [illegible] 98, 776 (1983).
[3] [illegible] (1983).
[4] [illegible] and [illegible], Rev. [illegible] 2 [illegible]
[5] [illegible] (1983).
[6] [illegible] Smith and [illegible], Proc. [illegible] Symp. [illegible] Matter [illegible] (1983).
[7] [illegible] (1982).
[8] [illegible] 153, 145 (1982).
[9] [illegible] Gray and [illegible], J. [illegible] 130 (1982).
[10] [illegible] A. [illegible] and [illegible] (1976).
[11] S. [illegible] and T. [illegible] 34, 357 (1983).
[12] [illegible] (1979).

Revue Roumaine de Chimie, 36, *1–3*, 25–37 (1991)

ELECTROCHEMICAL OXIDATION OF CARBOXYLIC ACIDS. II[1]

ELECTRODE PROCESSES IN ELECTROCHEMICAL OXIDATION OF NATRIUM MONOMETHYL ADIPATE ON PLATINUM

SOLOMON STERNBERG[a,*], MIHAELA UNGUREANU[a] and SORIN ROȘCA[b]

[a] Laboratory of Applied Physical Chemistry, Faculty of Chemical Technology, Polytechnic Institute, 76206 Bucharest, Splaiul Independenței 313, Romania

[b] Department of Organic Chemistry, Polytechnic Institute, Bucharest, Romania

Received March 2, 1989

The electrode processes occurring in electrochemical oxidation of natrium monomethyl adipate in methanol with reduced water content (1 %) have been studied. Special attention has been given to the influence the anion concentration, the rate and the range of scanning as well as the free acid concentration have on the oxidation of platinum, on the oxidation of the solvent and on the carboxylate anion discharge.

INTRODUCTION

The electrochemical synthesis of the sebacic acid by anode condensation of monomethyl adipate is a process of great importance for industry. In order to explain the electrode processes, systematic studies[2,3,4] have been undertaken using generally stationary methods. For the study that makes the object of the present paper the cyclic voltammetry method has been used which provided additional information about the electrode processes occurring in the oxidation of monomethyl adipate.

EXPERIMENTAL

Potentiostatic measurements were performed in non-steady state conditions using a potentiostatic device, that was presented in a previous paper[1]. The working electrode was a platinum plate (area 0.28 cm^2). The platinum electrode was prepared before each measurement. [1] The reference electrode was an aqueous saturated calomel electrode. All potentials were referred to that of the normal hydrogen electrode. The electrolyte used for the experiment was a methanolic solution containing a small amount of water (1% in volumes), natrium monomethyl adipate (MNa) and free monomethyl adipate (MH) in various concentrations.

---

* Deceased on 19 January, 1990.

All the substances used for the experiment were analyticallly pure. The monomethyl adipate was synthesized by esterifying adipic acid with methanol and transesterifying the resulting dimethyl adipate with adipic acid. The monomethyl adipate resulted after the separation procedure contained 99.12% monomethyl adipate, 0.53% dimethyl adipate,0.34% light end-products and 0.01% methanol and water.

A mechanical stirring device driven by a synchronous motor with 1500 rpm was used to stir the electrolyte.

RESULTS AND DISCUSSION

Cyclovoltammograms on platinum electrode for various ranges of scanning resulted from the experiment. Figure 1 shows the successive cyclovoltammograms resulted for a MNa concentration (C_{MNa}) of 0.3M, a MH concentration (C_{MH}) of 0.5M on a range of scanning of about 4V.

The cyclovoltammograms shown in Figure 1 indicate three low rate overall (irreversible) oxidative processes. Considering, for example, cycle 1 one may notice that the first process (P I) starts at 0.9 V and reaches a maximum of about 0.6 mA at 1.2 V. The second process (P II) is superposed on the first, starting at about 1.4 V and reaching a maximum of about 1.4 mA at 1.9 V. Starting from about 2 V one may notice a third oxidation process (P III) involving currents that are exponentially increasing. At about 3.4 V the process begins to show a limitation. On the return path, the cyclovoltammograms exhibit a slight hysteresis in the P III region and a marked one in the P II and P I regions, which indicates that the processes I and II are irreversible to a greater extent than the process III.

Figure 1 also shows that the cyclovoltammograms for the first three successive cycles are not similar in the regions corresponding to the processes I and II while the cyclovoltammograms for the subsequent cycles are practically identical with the one for cycle 3.

Process I was attributed to the formation of a superficial layer of platinum oxides as a result of the anodic scanning. The subsequent oxidation processes develop on the surface of this oxides layer.

P II was accounted for by the oxidation of the solvent and P III by discharge of carboxylate ions. This attribution appears to be in agreement with the evanescence of the peak in P I in the subsequent cycles (Fig. 1) as the oxides layer is already formed. The solvent oxidation processes take place during the first cycle on a surface already partially covered with oxides, while both during and after the third cycle they take place on a relatively stable surface covered with oxides. The slowing down that may be noticed during the anion discharge process ($E > 2.8$ V) may be accounted for by the formation of a superficial film of products which had also been noticed in preparatory electrolysis.

As the cathodic limit of the range of scanning is shifted towards more electronegative potentials, P I does no longer disappear after the third cycle (Fig. 2). This is due to the decrease of the superficial layer of oxides when the potential reaches more electronegative values during the cathodic scanning. The superficial layer of oxides is formed again during

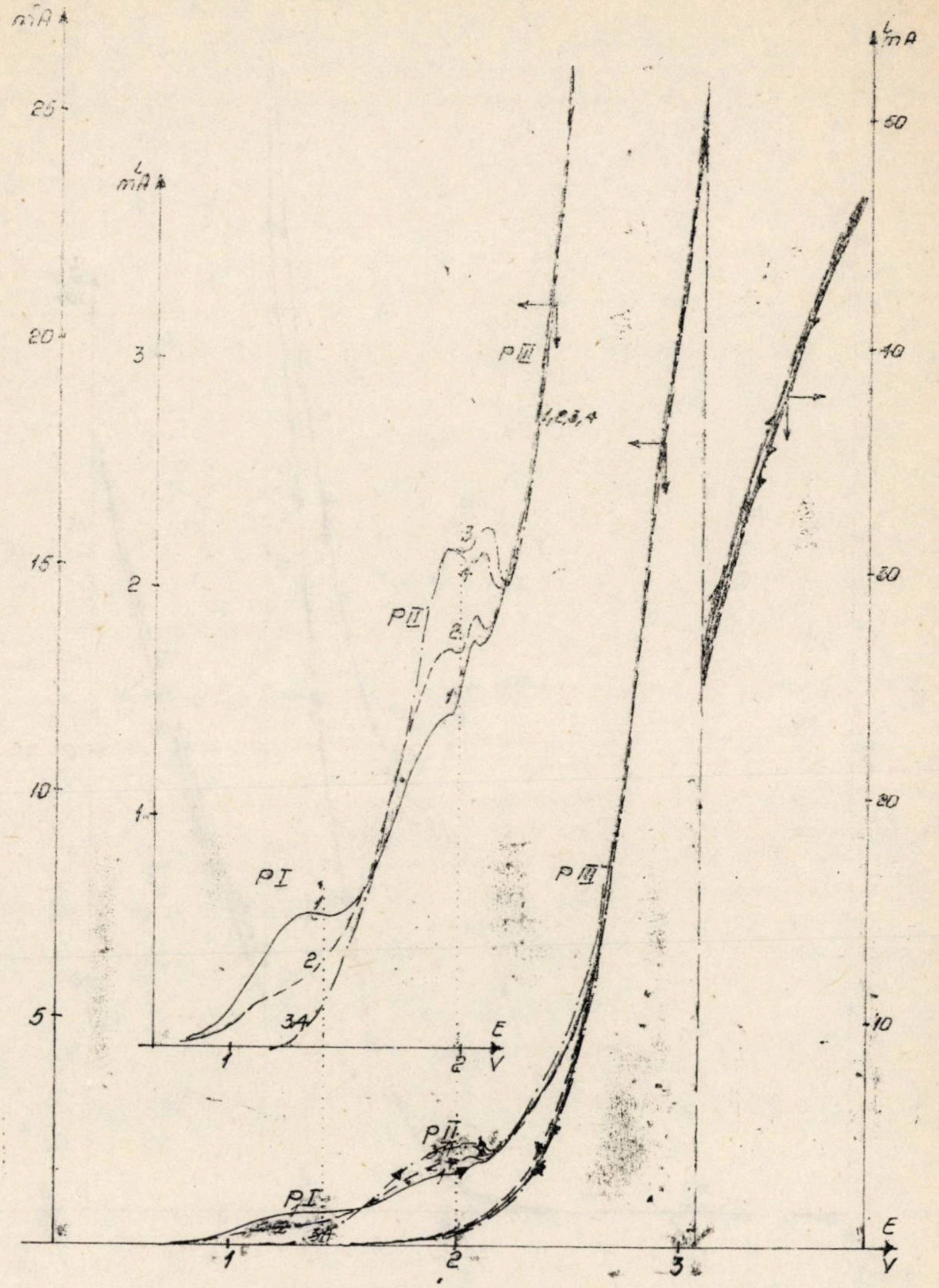

Fig. 1. — Successive cyclovoltammograms on platinum ($s = 0.8\ \mathrm{cm}^2$) ($v = 8$ mV/s; $c_{\mathrm{MNa}} = 0.3$ M; $c_{\mathrm{MH}} = 0.5$ M).

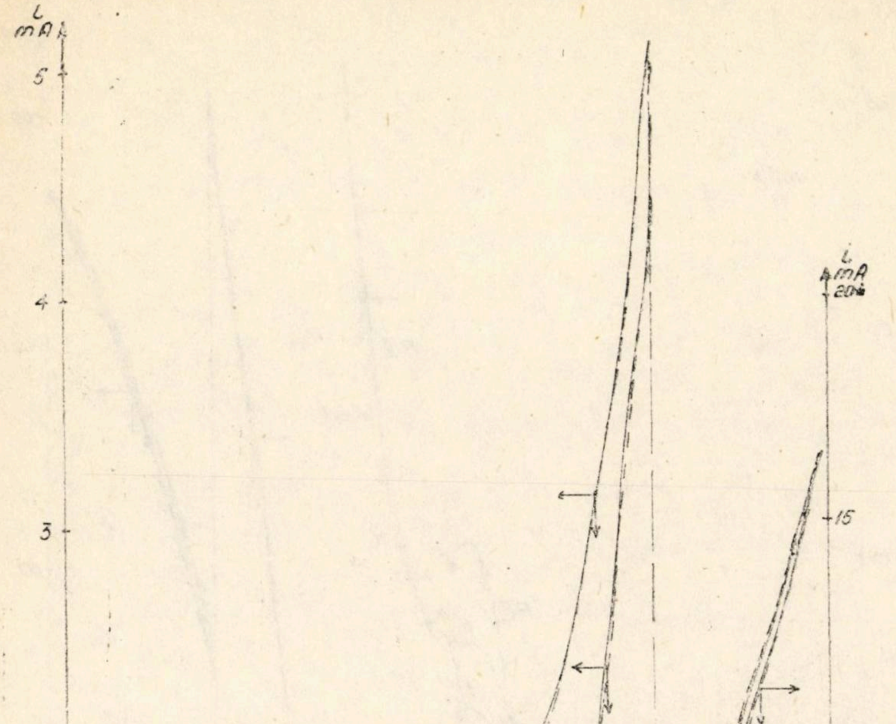

Fig. 2. — Successive cyclovoltammograms on platinum ($s = 0.8$ cm^2) with cathodic limit of -0.3 V ($v = 8$ mV/s ; $c_{MNa} = 0,3$ M ; $c_{MH} = 1$ M).

the anodic scanning. This hypothesis is confirmed by the cyclovoltammograms corresponding to narrower ranges of scanning (Fig. 3, Curves, 1, 2, 3). When the range of scanning is shifted towards even more electronegative values (Fig. 3, Curve 4), the reduction process of platinum oxides (P IV) becomes evident, followed by hydrogen discharge, which begins at about 0.2 V.

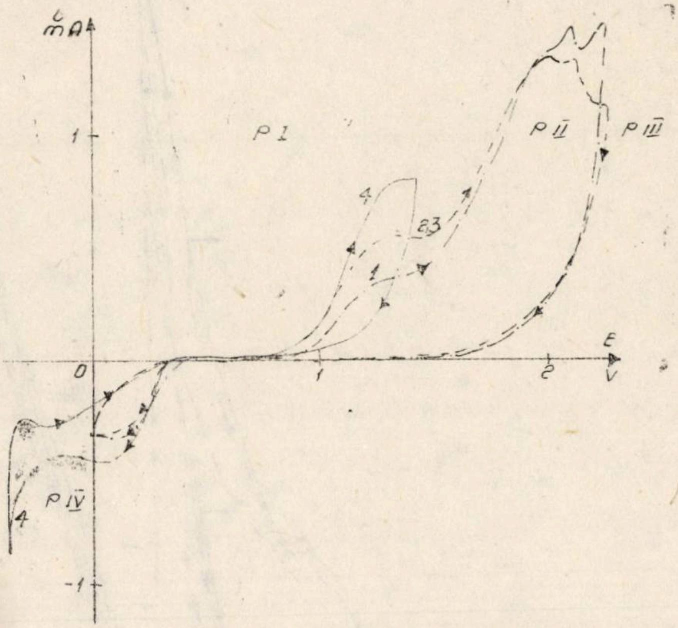

Fig. 3. — Cyclovoltammograms for narrow ranges of scanning: 2.5 V (the successive cycles 1(1), 2(2), 3(3) and 2 V (4): C_{MNa} — 0.3 M; $C_{MH} = 1$ M; $v = 5$ mV/s (1, 2, 3); $v = 6$ mV/s (4).

The cyclovoltammograms obtained using a platinum electrode in solutions that had been degassed by bubbling of argon are similar to those obtained without degassing.

The influence of the anion concentration on the shape of the cyclovoltammograms has been studied (Fig. 4). Cyclovoltammograms for C_{MNa} of 0.1M, 0.3M as well as 0.5M at constant concentration of acid $C_{MH} = 1M$ have been obtained. One may notice that the processes I and II are not infuenced by the concentration of the anion, while P III is strongly influenced, the value of the currents occurring during the anion discharge being higher at larger values of the anion concentration.

These facts are in agreement with the suggested explanations for processes I, II and III in the cyclovoltammograms. The currents involved in P I and P II do not depend on the anion concentration because the anion behaves as an indifferent electrolyte both in the process of surface oxides formation (P I) and in that of solvent oxidation (P II) in which the electrochemically active substances may be alcohol or water.

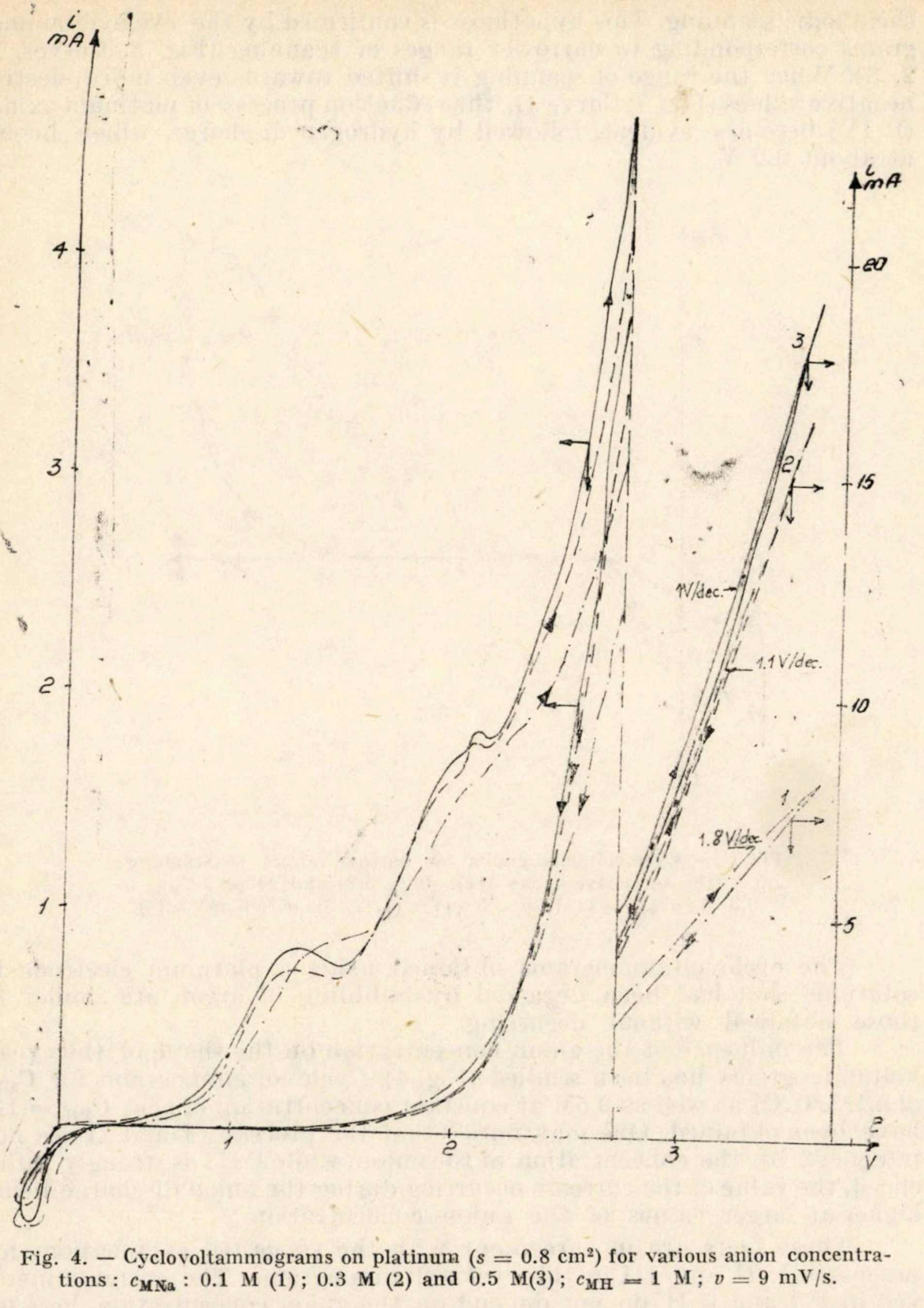

Fig. 4. — Cyclovoltammograms on platinum ($s = 0.8\ cm^2$) for various anion concentrations : c_{MNa} : 0.1 M (1) ; 0.3 M (2) and 0.5 M(3) ; $c_{MH} = 1$ M ; $v = 9$ mV/s.

The currents involved in P III increase strongly by increasing the anion concentration. For a wide range of values of the potential the partial order of reaction with respect to the anion is practically constant $n_{MNa} \sim 0.5$

(**Fig.** 5). The fact that the resulting order of reaction is less than unity is characteristic for a charge transfer process accompanied by adsorption.[5]

The influence of the rate of scanning on the cyclovoltammograms has also been studied. The results are given in Figure 6 and Table 1.

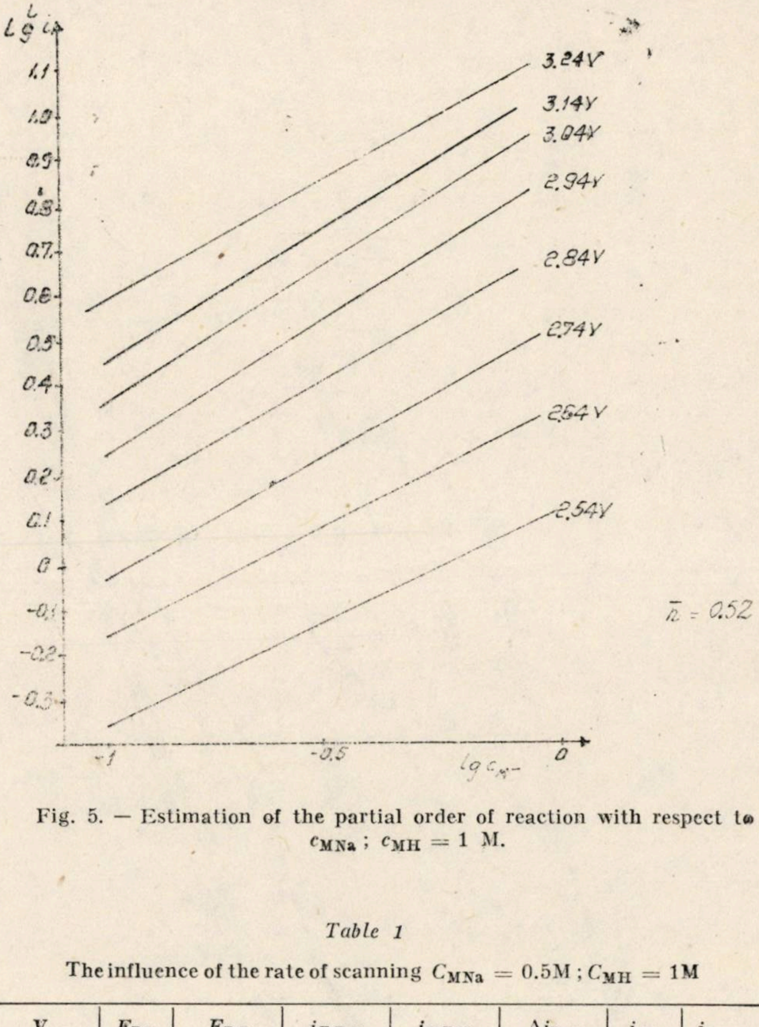

Fig. 5. — Estimation of the partial order of reaction with respect to c_{MNa} ; $c_{MH} = 1$ M.

Table 1

The influence of the rate of scanning $C_{MNa} = 0.5M$; $C_{MH} = 1M$

V (mV/s)	$E_{P\,I}$ (V)	$E_{P\,II}$ (V)	$i_{E,P\,I}$ (mA)	$i_{E,P\,II}$ (mA)	$\Delta i_{P\,II}$ (mA)	i_{3V} (mA)	$i_{P\,III,\,3V}$ (mA)
8	1.27	2.11	0.82	1.67	0.85	11.6	9.93
24	1.4	2.16	1.5	2.86	1.36	11.8	8.94
48	1.46	—	1.82	—	—	13.1	—
80	1.52	—	2.24	—	—	13.5	—

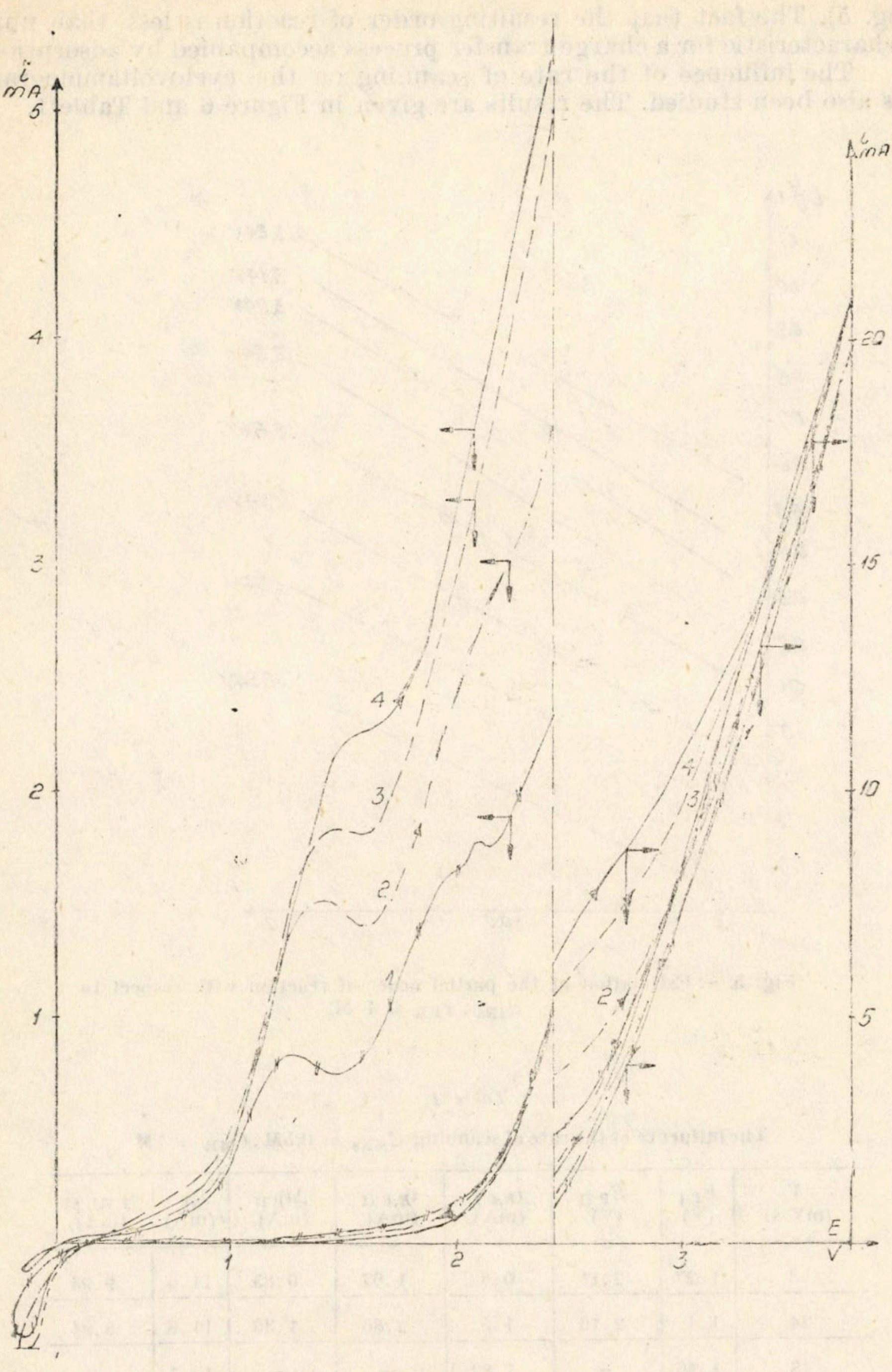

Fig. 6. — The influence of the scanning rate; v : 8 (1); 24 (2); 48 (3); 80 (4) mV/s; $c_{\mathrm{MNa}} = 0.5$ M; $c_{\mathrm{MH}} = 1$ M.

An increase of the currents in the processes I ($i_{E.P\,I}$) and III [$i_{E.P\,II}$ (total current) and $\Delta i_{E.PII}$ (partial current)] and simultaneously, a shift of the peaks corresponding to these processes (E_{PI}, E_{PII}) towards more electropositive potentials was noticed when the rate of scanning was increased.

In the region of III the current $i_{PIII,3V}$ [obtained by difference between the total current at 3V (i_{3v}) and the current at the foot of the curve for

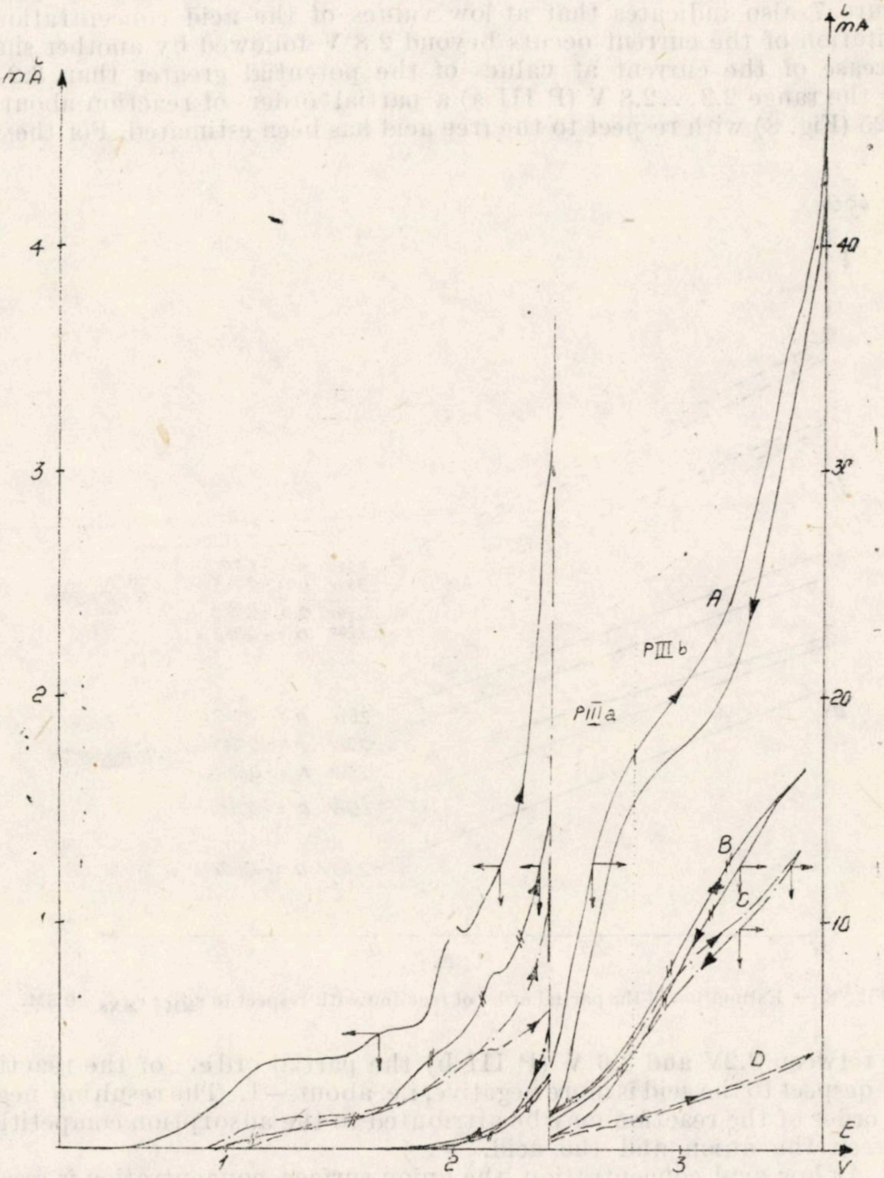

Fig. 7. — Cyclovoltammograms on platinum ($s = 0.24$ cm^2) for various acid concentrations: c_{MH} : 0.1 (A); 0.3 (B); 0.5 (C); 1(D); $c_{MNa} = 0.3$ M, $v = 8$ mV/s.

P III ($i_{E,PII}$)] does not practically depend on the rate of scanning, which proves that in the first approximation, at great concentrations of free acid, an ohmic control takes place even at high rates of scanning.

The influence of the acid concentration on the aforementioned oxidation processes was studied as well (Fig. 7). One may notice that the decrease of the acid concentration from 1M to 0.1M is accompanied by a sharp increase of the current in the region of P III. As one may notice, Figure 7 also indicates that at low values of the acid concentration a limitation of the current occurs beyond 2.8 V followed by another sharp increase of the current at values of the potential greater than 3.2 V. For the range 2.2...2.8 V (P III a) a partial order of reaction about —0.725 (Fig. 8) with respect to the free acid has been estimated. For the region retween 3.2V and 3.6 V (P III b) the partial order of the reaction with qespect to the acid is more negative, i.e. about —1. The resulting negative order of the reaction may be attributed to the adsorption competition between the anion and the acid.

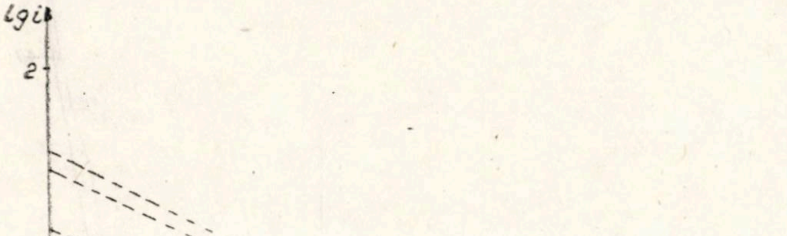

Fig. 8. — Estimation of the partial order of reaction with respect to c_{MH} ; c_{MNa}=0.3M.

At low acid concentration, the anion surface concentration is greater thus increasing the current of P III. That also determines a greater

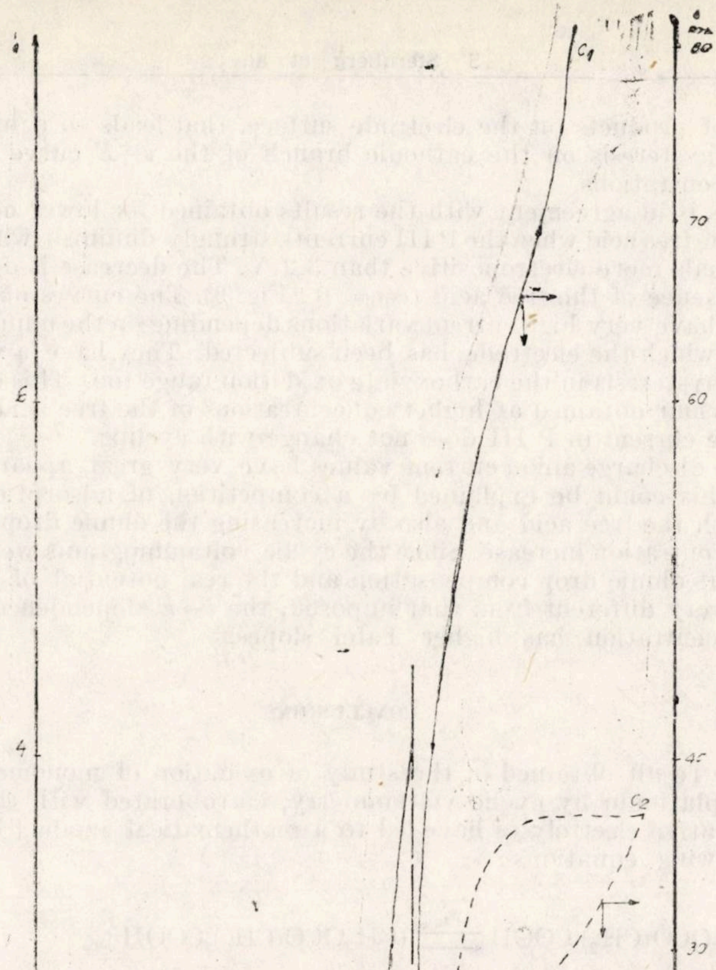

Fig. 9. — Successive cyclovoltammograms on platinum $s = 0.375$ cm²)
$c_{\mathrm{MH}} - 0$ M ; $c_{\mathrm{MNa}} - 0.3$ M ; $v - 8$ mV/s ; cycles 1 (1) ; 2(2) ; 3(3) ; 4(4).

amount of products on the electrode surface, that leads to a more pronounced hysteresis on the cathodic branch of the $i-E$ curve at lower acid concentrations.

This is in agreement with the results obtained for lower concentrations of the free acid when the P III currents strongly diminish with cycling at potentials more electropositive than 3.2 V. The decrease is dramatical in the absence of the free acid ($c_{MH} = 0$; Fig. 9). The curves obtained in this case have very high current variations depending on the number of the cycles to which the electrode has been subjected. They have a very pronounced hysteresis in the carboxylate oxidation range too. This differs by the behaviour obtained at higher concentrations of the free acid (Fig. 9), where the current in P III does not change with cycling.

The discharge anion current values have very great apparent Tafel slopes. This could be explained by a competition of adsorption of the anion with the free acid and also by increasing the ohmic drop with the acid concentration increase. Since the cyclic voltammograms were recorded without ohmic drop compensation and the real potential of the electrode is very different from that imposed, the $i-E$ dependence at great acid concentration has higher Tafel slopes.

CONCLUSIONS

The result obtained in the study of oxidation of monomethyl adipate on platinum by cyclic voltammetry, corroborated with the results of preparative electrolyses have led to a mathematical model,[5] based on the following equations:

$$CH_3OCO(CH_2)_4COOH \underset{k_{-1}}{\overset{k_1}{\rightleftharpoons}} (CH_3OCO(CH_2)_4COOH]_{ads} \qquad (1)$$

$$CH_3OCO(CH_2)_4COO^- \xrightarrow{k_2} [CH_3OCO(CH_2)_4^{\cdot}\cdot]_{ads} + CO_2 + e^- \qquad (2)$$

$$[CH_3OCO(CH_2)_4\cdot]_{ads} \xrightarrow{k_3} CH_3OCO(CH_2)_4\cdot_{sol} \qquad (3)$$

$$CH_3OCO(CH_2)^{\cdot}_{4sol} \xrightarrow{k_4} \begin{array}{l}\text{products}\\ [\text{mainly } CH_3OCO(CH_2)_8COOCH_3]\end{array} \qquad (4)$$

$$[CH_3OCO(CH_2)_4\cdot]_{ads} \xrightarrow{k_5} [CH_3OCO(CH_2)_4^+]_{ads} \qquad (5)$$

$$[CH_3OCO(CH_2)_4^+]_{ads} \xrightarrow{k_6} \begin{array}{l}\text{products (mainly ethers}\\ \text{and alcohols with normal}\\ \text{or isomerised chain)}\end{array} \qquad (6)$$

Equations (1) and (2) of the model show the adsorption competition between the carboxylic acid and the anion carboxylate. Equations (3) and (5) stand for the adsorption-desorption equilibrium of the radical formed in (2), the first stage of the electron transfer with decarboxylation. On platinum electrode $k_3 \gg k_5$, that means the radical is desorbed relatively easily leading mainly to products of radical origin (dimer and products of disproportionation and hydrogen atom extraction).

On graphite electrode, as will be shown in our next paper, $k_5 \gg k_3$ and the radical undergoes a second electron transfer, generating cationic products (esters and alcohols).

The different behaviour is explained by the existence of two kinds of adsorption centers on the electrode surface : I, adsorption centers with high energy and II, adsorption centers with low energy. On the I centers the radical is strongly adsorbed and undergoes the second electron transfer, leading to a carbocation. This is rapidly stabilised (partially isomerises) reacting with the solvent or other nucleophilic species in solution forming ethers, esters, alcohols.

On the II centers the radical is less adsorbed passing into solutions. In solution it undergoes characteristic stabilisation reactions of radicals (dimerisation, disproportion and hydrogen atom extraction) leading to monoelectronic oxidation products.

On the platinum electrode, the II adsorption centers prevail, the I adsorption centers being blocked by oxide formation. That is why the monoelectronic oxidation on platinum takes place at very high electropositive potentials in comparison with other anodic processes.

On the other hand, on graphite electrode the I adsorption centers prevail being favoured by the structure and metallic traces in graphite. The radical formed by electrodecarboxylation (2) remains adsorbed and undergoes the second electron transfer, leading to dielectronic oxidation products. This transfer takes place more easily at potentials of about 1 V more electronegative than the monoelectronic oxidation on platinum.

REFERENCES

[1] S. Sternberg, M. Ungureanu and S. Roşca, *Rev. Roum. Chim.* **34**, 337 (1989); **35**, 941(1990).

[2] E.P. Kovsman, G.N. Freidlin and G.A. Tarkhanov, "Electrochemical Synthesis of Monomers", Nauka, Moscow, 1980, p. 49

[3] Yu. B. Vassiliev, E.P. Kovsman and G.N. Freidlin, *Electrochim.* Acta, **27**, 953 (1982) ; **27**, 7 (1982).

[4] G. N. Freidlin, E. P. Kovsman and A. A. Adamov, "Elektrosintez monomerov", Moscow, 1981, p. 37.

[5] S. Sternberg, M. Ungureanu, *Rev. Roum. Chim.* in press.

[6] S. Torii, "Electroorganic syntheses. Part. I. Oxidations". Ed. Kondasha 1985, p.12.

Revue Roumaine de Chimie, 36, *1–3*, 39–41 (1991)

THE HOLLOW CATHODE CURRENT AS A FACTOR AFFECTING THE INFLUENCE OF PRESSURE ON SPECTRAL LINE OVERLAPS IN ELECTROTHERMAL ATOMIC ABSORPTION SPECTROMETRY

PAUL GH. ZUGRĂVESCU and JÁNOS FAZAKAS
Ministry of Chemical and Petrochemical Industry, Splaiul Independenței
R-70039 Bucharest, Romania

Received April 22, 1989

Increasing hollow cathode currents broaden the emission lines. Thus a better overlap becomes possible with the nearby absorption lines of other, interfering elements.

1. INTRODUCTION

Atomization under pressure[1-8] and its influence on spectral line overlaps[9,10] formed the subject of several previous investigations. The present paper continues our studies on fundamental and applied aspects of spectral line overlaps in electrothermal atomic absorption spectrometry (ET-AAS). In the following we shall discuss the influence of the hollow cathode current.

2. EXPERIMENTAL

Various details of the experimental system have been discussed in previous communications 1 – 10. We have used N_2 as purge gas. The choice was dictated by the fact that the red shift of the absorption lines is less important than in argon. In our case the investigated absorption line (Mn 403.307 nm) is already at longer wavelengths than our emission line (Ga 403.298). Thus the use of argon would increase the line separation. This would mean that in order to obtain meaningful signals one would have to use very high analyte concentrations. As a consequence we would depart very much from the conditions of a normal analytical situation.

3. RESULTS AND DISCUSSION

Fig. 1 shows the influence of atomization pressure on the Mn signal at various operating currents of the Ga hollow cathode lamp. As it is obvious from the figure, the signal strength of Mn increases considerably with increasing hollow cathode currents. The explanation is no doubt that the increasing current will cause a broadening of the source emission line due to a self-absorption effect. This implicitly means that there wil be a better overlap of the source emission line (Ga 403.298 nm) with the absorption line in the pressurized furnace (Mn 403.307 nm). It is interesting to note that probably the emission line broadening is very small. As evidenced in Fig. 1 the increase of the hollow cathode current by itself has no influence upon the degree of spectral line overlap at normal atomization pressure. Only the combination of the increasing current and the increasing atomization pressure has a visible influence upon spectral line overlaps.

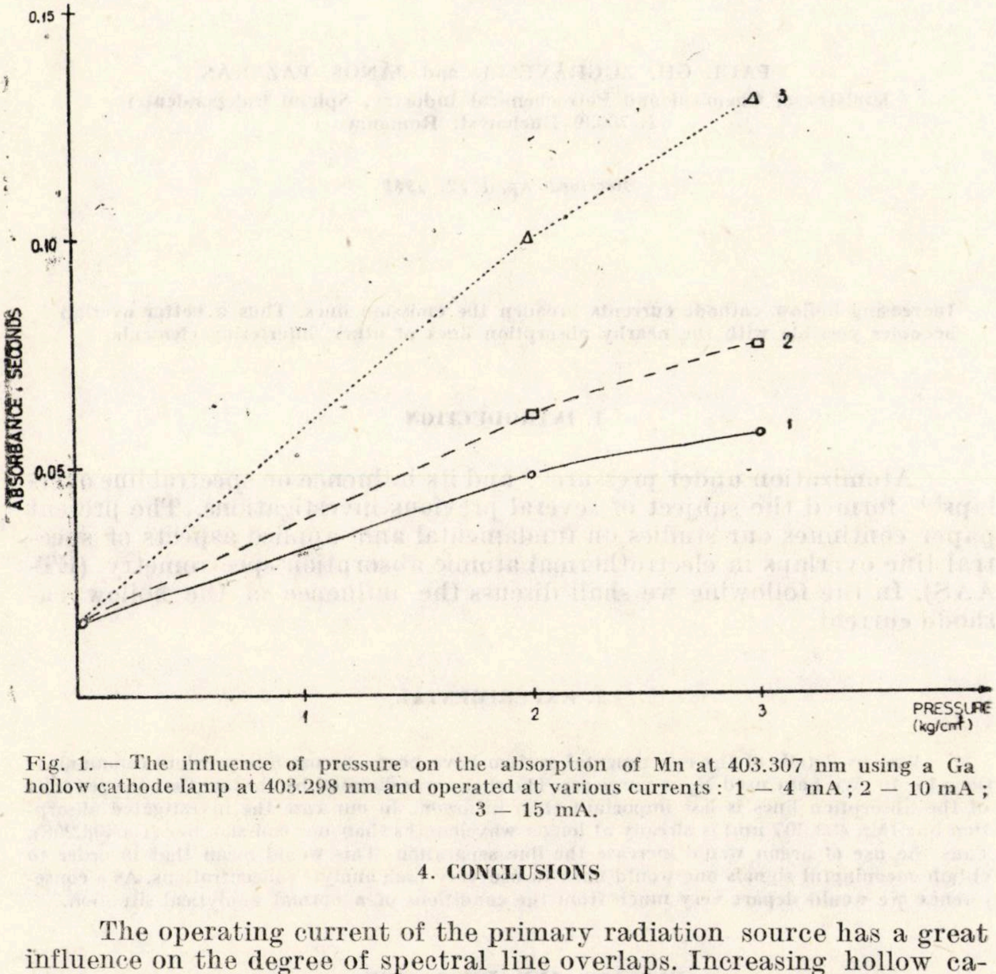

Fig. 1. — The influence of pressure on the absorption of Mn at 403.307 nm using a Ga hollow cathode lamp at 403.298 nm and operated at various currents : 1 — 4 mA ; 2 — 10 mA ; 3 — 15 mA.

4. CONCLUSIONS

The operating current of the primary radiation source has a great influence on the degree of spectral line overlaps. Increasing hollow cathode currents, while lowering analyte sensitivity improves the chances of an overlap with the nearby absorption lines of other elements. The broadening of the Ga 403.298 nm line is very small with increasing currents. Just by itself the broadening brought about by increasing currents is not manifest in an increase of the degree of spectral line overlap with the Mn 403.307 nm line. Only the combined effect of increased current and high atomization pressure have an observable influence on spectral line overlaps.

REFERENCES

[1] J. Fazakas, *Spectrochim. Acta*, **37B**, 921 (1982).

[2] J. Fazakas, *Mikrochim. Acta*, **I**, 249 (1982).

[3] J. Fazakas, *Rev. Roum. Chim.*, **27**, 685 (1982).

[4] J. Fazakas, *Analyt. Lett.*, **15**, 1523 (1982).

[5] J. Fazakas, *Mikrochim. Acta*, **II**, 217 (1983).

[6] J. Fazakas and M. Hoenig, *Talanta*, **35**, 403 (1988).

[7] J. Fazakas and P. Gh. Zugrăvescu, *J.A.A.S.*, submitted.

[8] J. Fazakas and P. Gh. Zugrăvescu, *Appl. Spectrosc.*, **42**, 521 (1988).

[9] J. Fazakas, *Spectrochim. Acta*, **38B**, 455 (1988).

[10] J. Fazakas and P. Gh. Zugrăvescu, *Spectrochim. Acta*. **43B**, 897 (1988).

Revue Roumaine de Chimie, **36**, *1–3*, 43–48 (1991)

$As(III)-HCl-H_2O$ SYSTEM. III[1,2]

THE LIQUID – LIQUID STATE

O. RADU[a] and CONSTANŢA GHEORGHIU[b,*]

[a] Institute for Research and Production of Semiconductors, Sos. Gării Căţelu No. 5, Sector 3, Bucharest, România
[b] Polytechnic Institute of Bucharest, Dept. of Chemical Technology, Bucharest, România

Received March 14, 1989

The liquid – liquid state of $As(III)-HCl-H_2O$ formed by dissolution of $AsCl_3$ in HCl solution was studied. Use has been made of the additivity of volumes (resulted from the interpretation of volume changes) and of the stability limit of homogeneous phase (introduced by the authors); the solubility curves determined by other authors were extrapolated. Characterization of the homogeneous state through the stability limit has affor ded the simultaneous drawing of inter-phase equilibrium diagram. Thus the characterization of any two-phase state without knowledge of the initial state becomes possible.

The method of study applied in this note was presented earlier;[1,2] it consists basically of establishing certain relationships between the initial state (known values of parameters which define the interactions of system forming) and the final state (the parameters of equilibrium state of the system formed), relations which assume that the inter-phase equilibria are chemically determined. The inter-phase liquid–liquid state has not been thoroughly studied except for some determinations of $AsCl_3$ solubility in HCl solution within 30–100° temperature range and at acid concentrations between 5 and 11 N[3].

1. THE CHARACTERIZATION OF INITIAL STATE

The liquid–liquid inter-phase equilibrium is considered to be determined by the following sequence of chemical equilibria:

$$\underbrace{As(OH)_3 \xrightleftharpoons[H_2O]{HCl} As(OH)_2Cl \xrightleftharpoons[H_2O]{HCl} As(OH)Cl_2}_{\text{liquid phase 1}} \xrightleftharpoons[H_2O]{HCl} \underbrace{AsCl_3}_{\text{liquid phase 2}}$$

---

* Deceased in 1983.

Thus, the initial state is defined by the $AsCl_3 + HCl + H_2O$ interaction which is univocally determined by parameters R', C'_{HCl}, V'_{HCl}, which are related by the equation :

$$\frac{R'}{C'_{HCl}} \frac{V'_{HCl}}{n_{AsCl_3}} \tag{III-1}$$

The homogeneous → liquid-liquid transition is determined by the limited solubility of $AsCl_3$ in HCl solution which decreases with the concentration of the acid and temperature. Solving of $AsCl_3$ is a sequence of two processes : a chemical one of hydrolysis and a physicalo ne of mixing two partially miscible liquids. The variation of solubility with temperature and acid concentration is determined by hydrolysis. Gradual addition of $AsCl_3$ to a given volume of acid causes that in the homogeneous system C_{Cl} increases and R' decreases. As the amount of $AsCl_3$ increases, the degree of hydrolysis decreases to zero through total re-conversion of arsenic to $AsCl_3$. The maintenance of homogeneous state at further $AsCl_3$ addition is ensured by the partial miscibility. The transition in liquid-liquid two-phase occurs when the diminution of R' reaches the stability limit of homogeneous phase R'_{lim} ; the homogeneous → liquid-liquid isothermal transition is characterized by pairs of $C'_{HCl} - R'_{lim}$ values.

According to the idea of volume variations[1] it is assumed that :

(i) the volume increase against V'_{HCl} originates in the non-hydrolysed $AsCl_3$ fraction whose volume is additive to V'_{HCl} ;

(ii) in saturated solutions and two-phase system the hydrolysis of $AsCl_3$ is zero so that the volumes of acid and trichloride are additives.

(iii) in both instances arsenic is present only as $AsCl_3$, the system in question being ternary ($AsCl_3 + HCl + H_2O$).

2. RELATIONSHIPS BETWEEN THE SATURATED HOMOGENEOUS STATE AND THE INITIAL STATE

By virtue of the additivity of volumes at saturation, one may establish reciprocal relationships between the saturated final state and the initial state in standard conditions.

2.1. The homogeneous saturated final state as a function of the initial state

The volume of saturated solution is given by the equation :

$$V_{sat} = V'_{HCl} + V_{AsCl_3} = V'_{HCl} + \overline{V}_{AsCl_3} \cdot n_{AsCl_3} \tag{III-2}$$

Because at equilibrium $R' = R'_{lim}$, taking account of eqn. (III-1) and substituting the molar volume of $AsCl_3$ it results :

$$V_{sat} = V'_{HCl} \left(1 + 0.0843 \frac{C'_{HCl}}{R'_{lim}}\right) \tag{III-3}$$

Since in the homogeneous system $n_{Cl} = n'_{Cl} + 3n_{AsCl_3}$, the total chlorine concentration is given by the equation:

$$C_{Cl} = \frac{C'_{HCl}\,(R'_{1lm} + 3)}{0.0843\ C'_{HCl} + R'_{1lm}} \tag{III-4}$$

The basic equation $R = C_{Cl}/C_{As}{}^1$ in which at saturation $C_{As} = C_{AsCl_3} = S_{AsCl_3}$ and $R = R'_{1lm} + 3$, together with eqn. (III-4) yield for the solubility of $AsCl_3$:

$$S_{AsCl_3} = \frac{C'_{HCl}}{0.0843C'_{HCl} + R'_{1lm}} \tag{III-5}$$

The concentration of free hydrochloric acid in saturated solution ($n_{HCl(l)} = n'_{Cl}$) is given by the equation:

$$C_{HCl(l)} = \frac{C'_{HCl}}{1 + 0.0843\,\dfrac{C'_{HCl}}{R'_{1lm}}} \tag{III-6}$$

It turns out that the final homogeneous state may be characterized by R'_{1lm} whose dependence on C'_{HCl} has to be established. To do this the solubility curves of $AsCl_3{}^3$ were extrapolated yielding $S_{AsCl_3} - C'_{HCl}$ pairs of values plotted in Fig. III-1. Eqn. (III-5) affords calculation of R'_{1lm} and thus the pairs of $R'_{1lm} - C_{HCl}$ values shown in Fig. III-2 result. The variation of S_{AsCl_3} and R'_{1lm} is linear in $C_{HCl} < 7.5$ and $C_{HCl} > 7.5$, respectively. Thus, depending on the parameter of initial state, two pairs of empirical equations

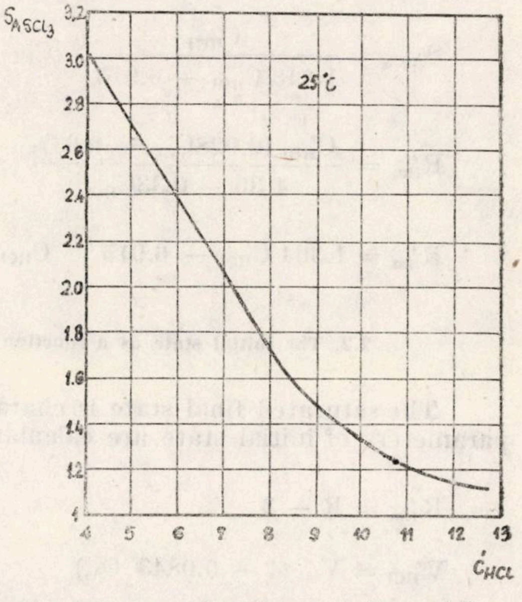

Fig. III—1. — The standard molar solubility of $AsCl_3$ versus the molar concentration of the acid.

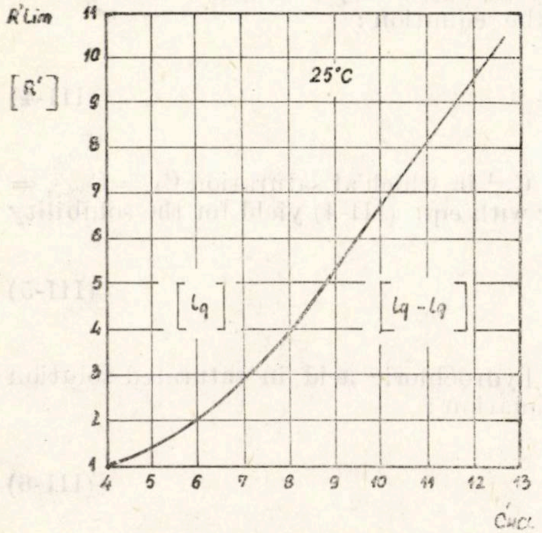

Fig. III–2. – The limit of stability of homogeneous phase versus the acid concentration. The standard liquid-liquid inter-phase equilibrium.

are obtained for S_{AsCl_3} and R'_{lim} which hold true provided that $R' = R'_{lim}$. The two pairs differ by linear and non-linear variation and cover all the concentration range:

$$S_{AsCl_3} = -0.33\ C'_{HCl} + 4.39 \qquad C_{HCl} \leqslant 7.5 \tag{III-7}$$

$$S_{AsCl_3} = \frac{C'_{HCl}}{1.448\ C'_{HCl} - 6.915} \qquad C_{HCl} \geqslant 7.5 \tag{III-8}$$

$$R'_{lim} = \frac{C'_{HCl}\ (0.028C'_{HCl} - 0.63)}{4.39 - 0.33C'_{HCl}} \qquad C_{HCl} \leqslant 7.5 \tag{III-9}$$

$$R'_{lim} = 1.364\ C'_{HCl} - 6.915 \qquad C_{HCl} \geqslant 7.5 \tag{III-10}$$

2.2. The initial state as a function of the saturated final state

The saturated final state is characterized by C_{Cl}, C_{As} and V_{sat}; the parameters of initial state are calculated by the equations:

$$R'_{lim} = R - 3 \tag{III-11}$$

$$V'_{HCl} = V_{sat}\ (1 - 0.0843\ C_{As}) \tag{III-12}$$

$$C'_{HCl} = \frac{C_{Cl}\ (R - 3)}{R - 0.0843\ C_{Cl}} \tag{III-13}$$

3. THE FINAL STANDARD LIQUID-LIQUID STATE

Introduction of the parameters "stability limit of homogeneous phase" grants the advantage that together with the determination of its standard values one also gets the conditions of inter-phase equilibrium. Therefore, the stability curve of homogeneous phase in Fig. III-2 is also the diagram of standard inter-phase equilibrium as a function of the initial state if only the symbols in parentheses are considered. This allows the characterization of two-phase liquid-liquid state.

3.1. The molecular composition of the final two-phase state

The study of As(III)$-$HCl$-$H$_2$O system requires often determination of molecular composition of some final two-phase states whose initial states are not known. For this most general case one usually resorts to the equations of saturated final state.

a. The composition of the final two-phase state is characterized in basic terms. First its volume (V_e) is determined, then deionized water is added in small portions under stirring until the transition to homogeneous state occurs. After cooling and thermal equilibration C_{Cl} and C_{As}[1] are determined and n_{Cl} and n_{As} calculated.

b. Then the parameters of the corresponding initial state are calculated by the equations:

$$R' = \frac{n_{Cl}}{n_{As}} - 3 \qquad \text{(III-14)}$$

$$V'_{HCl} = V_s - 0.0843\ n_{As} \qquad \text{(III-15)}$$

$$C'_{HCl} = \frac{n_{Cl} - 3n_{As}}{V_e - 0.0843\ n_{As}} \qquad \text{(III-16)}$$

c. Calculation of R'_{lim} by eqs. (III-9) or (III-10) follows.

d. All data obtained allow calculation of the composition saturated hydrochloric phase by eqs. (III-5) and (III-6).

e. The distribution of arsenic trichloride among phases (1 = hydrochloric phase, 2 = AsCl$_3$ phase) and the volumes of phases are given by the equations:

$$n_{AsCl_3(1)} = n_{As} \frac{R'}{R'_{lim}} \qquad \text{(III-17)}$$

$$n_{AsCl_3(2)} = n_{As} \left(1 - \frac{R'}{R'_{lim}}\right) \qquad \text{(III-18)}$$

$$V_1 = V_e - 0.0843\ n_{As} \left(1 - \frac{R'}{R'_{lim}}\right) \qquad \text{(III-19)}$$

$$V_2 = 0.0843\ n_{As}\left(1 - \frac{R'}{R'_{lim}}\right) \qquad \text{(III-20)}$$

The validity of calculations is proved by the good agreement of the experimental and calculated data.

DISCUSSION

The characterization of final liquid-liquid state has become possible through :

(i) the interpretation of volume increase[1] which establishes that in saturated solutions and liquid-liquid systems (in which arsenic is completely converted into $AsCl_3$) the volumes are additive ;

(ii) the defining of the stability limit of homogeneous phase which has allowed the simultaneous characterization of saturated homogeneous state and two-phase state ;

(iii) extrapolation to standard condition of solubility curves determined by other authors[3] which have afforded the development of empirical equations for the stability limit.

The very good agreement between the experimental and calculated values confirms the validity of volume variation assertion.

LYST OF SYMBOLS

C'_{HCl} = the concentration of hydrochloric acid employed in dissolution of $AsCl_3$(mole/litre)

V'_{HCl} = the volume of hydrochloric acid of concentration C'_{HCl} (litres)

n'_{Cl} = number of gram atoms of chloride from hydrochloric acid of concentration C'_{HCl}

n_{AsCl_3} = number of moles of $AsCl_3$

$R' = n'_{Cl}/n'_{AsCl_3} = R - 3$

V_{AsCl_3} = the volume of $AsCl_3$ (litres)

$\bar{V}_{AsCl_3}$ = the standard molar volume of $AsCl_3$ = 0.0843 litres

V_{sat} = the volume of saturated hydrochloric acid solution in $AsCl_3$ (litres)

R'_{lim} = the stability limit of homogeneous phase at liquid-liquid transition

V_e = the volume of two-phase liquid-liquid state (litres).

See also parts I and II of this paper.[1,2]

REFERENCES

[1] **O.** Radu, *Rev. Roumaine Chim.*, **33**, 585 (1988).

[2] **O.** Radu and C. Gheorghiu, *Rev. Roumaine Chim.*, **33**, 677 (1988).

[3] V. V. Krapuhin, I. A. Sokolov and M. N. Kostuicenko, *Isv. Vissh. Uceb. Zaved. Taved. Met.*, **10**, 95 (1967).

Revue Roumaine de Chimie, **36**, *1–3*, 49–54 (1991)

THIN FILMS OF Al_2O_3 AND Ta_2O_5 OBTAINED BY MAGNETRON REACTIVE SPUTTERING

RADU MUTIHAC[a] and ALEXANDRU OPREA[b]

[a] Faculty of Physics, University of Bucharest, Romania
[b] Institute of Physics and Technology of Materials Bucharest-Măgurele, P.O. Box MG-7, Romania

Received February 15, 1990

A magnetron with 75 cm^2 effective area for reactive sputtering in pure oxygen was realised by modifying AV 500 standard equipment. Dielectric Al_2O_3 and Ta_2O_5 thin films of 30 cm^2 area and thickness between 0.1–1 μm were obtained. Their amorphous structure and excellent visible transmission recommend them for electroluminescent devices production.[1–3]

1. ZnS ELECTROLUMINESCENT DEVICES

The development of electronic and computer techniques requests large display systems. Electroluminescent devices based on monocrystalline semiconductors are quite expensive because of the monocrystalline compounds involved (GaAs, GaP). There is an increasing interest in electroluminescent devices made of polycrystalline thin film semiconductors. The most promising results were obtained with devices of ZnS (Fig. 1).

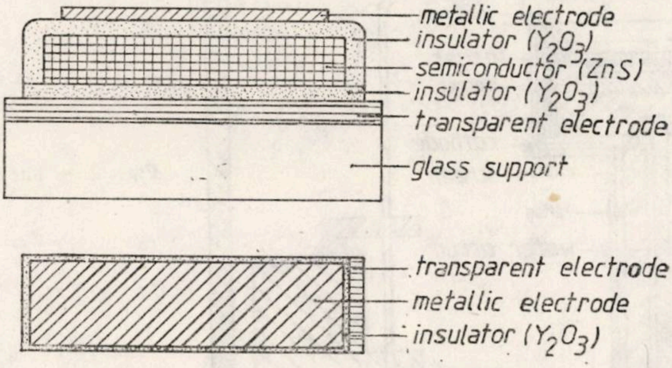
metallic electrode
insulator (Y_2O_3)
semiconductor (ZnS)
insulator (Y_2O_3)
transparent electrode
glass support
transparent electrode
metallic electrode
insulator (Y_2O_3)

Fig. 1. — ZnS electroluminescent device.

They consist of five layers : an active one of ZnS, two dielectric ones and other two conductive layers of which a transparent one at least (SnO_2 or ITO). For optimum results, uniform and stoechiometric layers are necessary. The semiconductor layer must be polycrystalline, homogeneously doped and grown perpendicularly relatively to its support.

The conductive layers have to exhibit as low as possible electrical resistance and the transparent one must also have very high transmission coefficient.[5]

The dielectric layers determine the behaviour of the device in the capacitive mode, limiting the dissipative component of the current. One of the dielectric-semiconductor interface releases electrons under the action of the electric field, which being accelerated determine the excitation of the electroluminescent centers. The other interface collects the electrons after crossing the semiconductor and then their functions are exchanged. Therefore there are necessary high dielectric constants for the dielectric layers, small dielectric losses and as high as possible transparence in the spectrum of interest (0.57 – 0.63 μm).

Two kinds of dielectrics are in use today :[6–10] oxide type (Al_2O_3, Ta_2O_5, Y_2O_3, HfO_2) and ferroelectric type ($BaTiO_3$, $PbTiO_3$). Practically they are quite equal from the price/performance point of view.

2. REACTIVE SPUTTERING

We realised and tested the oxide type dielectrics (Al_2O_3 and Ta_2O_5) using magnetron reactive sputtering in pure oxygen. A magnetron is a sputtering system of the dc diode type which has the cathode included in a magnetic system in order to increase the magnetic field around the target. Therefore the ionisation of plasma is increased and lower voltages (200 – 800 V) are necessary and higher sputtering rates are achieved (Fig.2).

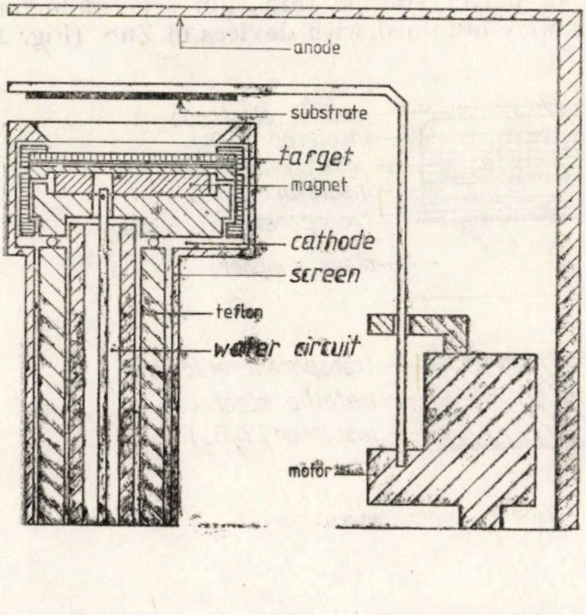

Fig. 2. – The magnetron.

Using dc magnetron reactive sputtering we obtained discharging currents higher then 1 A and firing voltages of 250 V and even lower. The powers involved (100 W and 250 W) determined growth rates of 0.5–1 μm/hour for Al_2O_3 and of 500–1000 Å/hour for Ta_2O_5. The experiments indicated the optimum pressure for pure oxygen to be 10^{-2} torr for Al_2O_3 and 0.5 torr for Ta_2O_5.

The shape of discharge during sputtering is shown in Fig. 3.

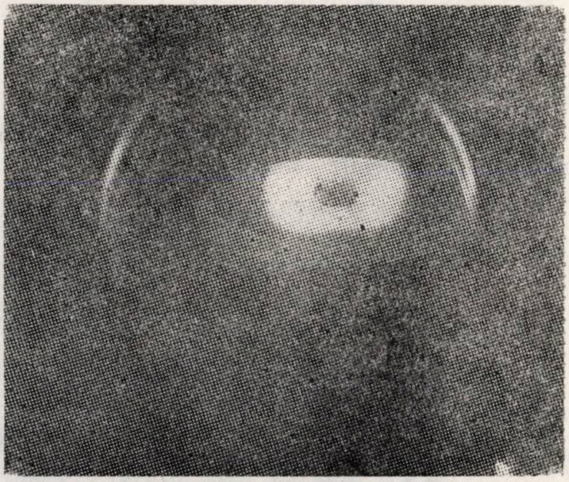

Fig. 3. — The shape of discharge.

3. CHARACTERISTICS OF Al_2O_3 AND Ta_2O_5 DIELECTRIC LAYERS

The layers deposited on good quality glass were 60 mm × 50 mm (Fig. 4).

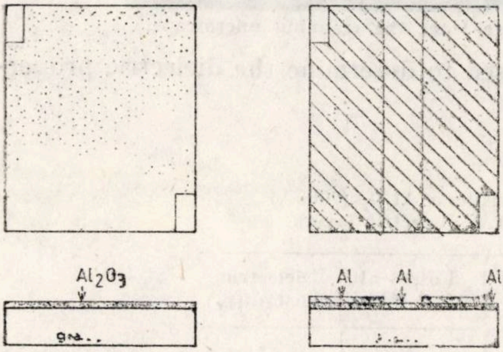

Fig. 4. — The geometry of the dielectric layers.

Their thickness was measured by reflexion with an Epival interferometric microscope after covering with a thin Al layer for contrast. Thickness measurements are concentrated in the distributions presented in Fig. 5.

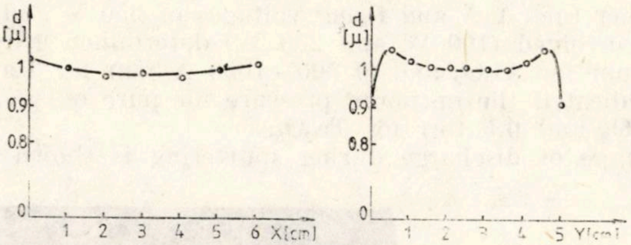

Fig. 5. — Thickness distributions along the dielectric layers.

Cross section investigations were performed by an electronic microscope at different enlargements and the results are shown in Fig. 6.

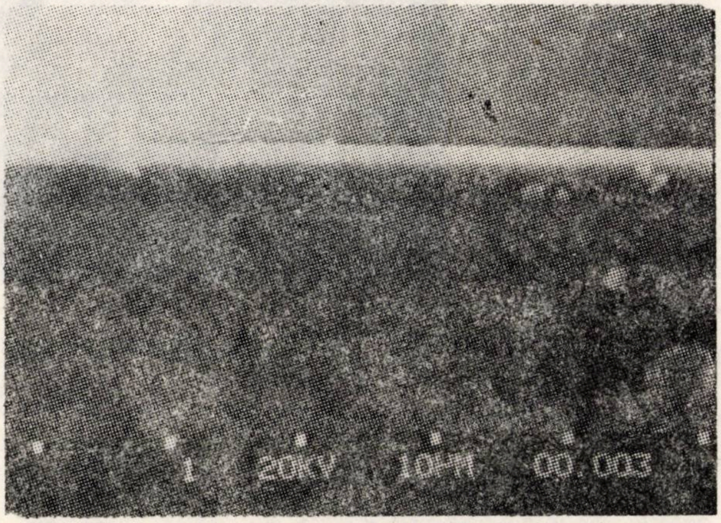

Fig. 6. — Cross section image from the scanning microscope.

Capacitive techniques were used to determine the dielectric properties of the samples (Table 1).

Table 1

Electrical characteristics of Al_2O_3 (7000Å) and Ta_2O_5 (1000 Å) dielectric layers

Sample	Specific capacity	Losses at 1.5 KHz	Dielectric constant(ε_r)
—	$\mu F \cdot cm^{-2}$	%	—
Al_2O_3	0.0106	1.86	8.55
Al_2O_3	0.0108	2.13	8.58
Al_2O_3	0.0109	1.59	8.64
Al_2O_3	0.0096	2.09	9.61
Ta_2O_5	0.2667	9.55	25.16
Ta_2O_5	0.3333	9.00	27.75

The amorphous structure of our layers was checked by X-ray difractometry which indicated no presence of crystals (Fig. 7).

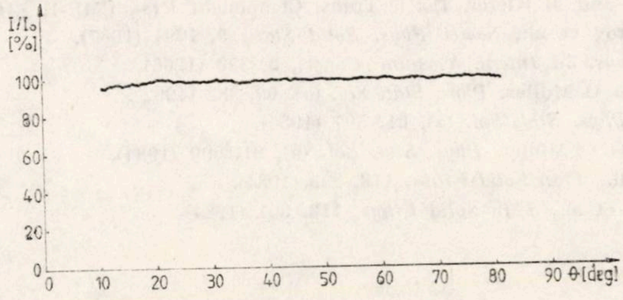

Fig. 7. — The optical transmission versus the directions.

The optical transmission was studied with UV-VIS Carl Zeiss and Carry spectrometers. The absorption spectra indicate a transmission better than 85% for both oxide species (Fig. 8).

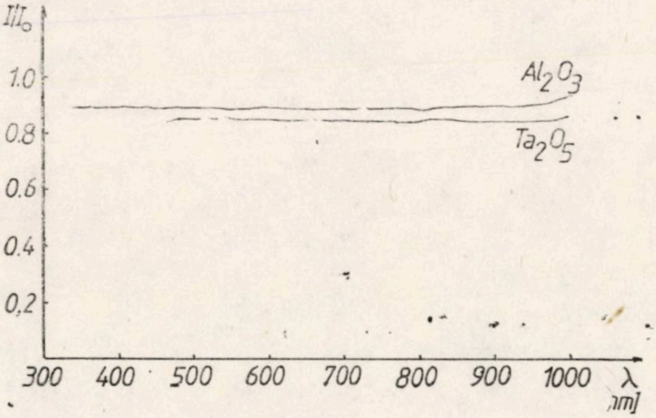

Fig. 8. — The absorbtion spectrum of the dielectric layers.

4. CONCLUSIONS

The whole set up was designed for reactive sputtering in pure oxygen There were realised Al_2O_3 and Ta_2O_5 dielectric thin layers with 90% average transparency in the visible range. Special masks were designed for electrodes and contacts deposition.

The results recommend Al_2O_3 and Ta_2O_5 dielectric layers for electroluminescent devices.

REFERENCES

[1] G. J. Tibol and W. R. Hull, *J. Electrochem Soc.*, **111**, 1368 (1964).

[2] C. D. Hodgman (ed), "Handbook of Chemistry and Physics", Ohio Rubber, 1968.

[3] B. H. Vromen and J. Klerer, IEEE Trans. Component Pts., PMP-1, S1(1965).

[4] Yu. A. Prokharov et al., *Soviet Phys. Solid State*, **9**, 1091 (1967).

[5] K. Taylor, *Trans.* 3d *Intern. Vacuum Congr.*, **2**, 329 (1966).

[6] R. Mach and G. O Müller, *Phys. Stat. Sol.* (a), **69**, 382 (1982).

[7] G. O. Müller, *Phys. Stat. Sol.* (a), **81**, 597 (1984).

[8] R. Mach and G. O. Müller, *Phys. Stat. Sol.* (a), **81**, 609 (1984).

[9] S. Schiller et al., *Thin Solid Films*, **118**, 255 (1984).

[10] D. K. Hohnke et al., *Thin Solid Films*, **118**, 301 (1984).

Revue Roumaine de Chimie, **36**, *1–3*, 55–64(1991)

OPTIMISATION DE L'ÉTAGE ANIONIQUE D'UN SCHÉMA DE DÉMINÉRALISATION À ÉCHANGEURS D'IONS

RADU VLĂDUŢESCU

IPROMED – Institut de Projets pour l'Environnement, Sos. Panduri 90–92,
Bucarest, Roumanie

Reçu le 25 mars 1990

Dans une installation de déminéralisation de l'eau, les échangeurs d'ions composant l'étage anionique imposent le dimensionnement global de la chaîne et les durées des cycles d'échange, donc la production d'eau traitée et le moment d'introduction en service des chaînes. L'optimisation de cet étage devient, par conséquent, le facteur le plus important qui conduit a l'accroissement de l'efficacité de l'installation.

In a demineralization plant, the steps of the anionic stage generally impose the dimensioning of the operating capacity (concerning the duration of both service and regeneration run), therefore the sequence of the filter lines starting. The optimizing of this stage becomes, for this reason, the most important agent of rise in plant efficiency.

INTRODUCTION

Le choix du schéma optimal de déminéralisation de l'eau comporte l'analyse des données de base suivantes : composition de l'eau brute, débit à traiter, qualité requise de l'eau traitée, chaînages présumés, types de résines échangeuses d'ions recommandés, durée du cycle d'échange, nature du régénérant, température de la soude pendant la régénération, opportunité de la neutralisation des éluats. On doit aussi tenir compte de la gamme d'équipements de traitement de l'eau qu'on a à sa disposition.

Dans un schéma de déminéralisation de l'eau à échangeurs d'ions, les résines cationiques ne posent pas de problèmes particuliers. En revanche, les résines anioniques sont très sensibles aux conditions de travail et surtout aux facteurs de pollution.

Au premier abord, le choix de la composition de l'étage anionique est fait parmi 8 variantes de base[1] : $[A]\downarrow$, $[A]\uparrow$, $D-[A]\downarrow$, $D-[A]\uparrow$, $(a)-[A]\downarrow$, $(a)-[A]\uparrow$, $(a)-D-[A]\downarrow$, $(a)-D-[A]\uparrow$, établies sur des critères techniques et économiques, en fonction de la salinité totale et de l'analyse de l'eau brute (teneur en bicarbonates).

En ajoutant les deux types (1 et 2) d'échangeurs d'anions forts, le nombre de combinaisons s'accroît à 16. En tenant compte des détails concernant les conditions de travail des résines (nécessité de rétention réversible des matières organiques, utilisation des résines polystyréniques – gel et macroporeuses – ou bien des celles polyacryliques, possibilité de réunion des deux résines anioniques dans la même colonne à lits superposés), le nombre des variantes possibles pour l'étage anionique devient à peu près 60 (dégazeur de CO_2 inclus).[2] La solution optimale sera établie à la suite d'un calcul technique et économique complexe. Certainement, la diversité des résines envisagées dépend de la gamme de produits de chaque fournisseur ; généralement on peut considérer quelque 3 à 4 types d'échangeurs d'anions faiblement basiques et 6 à 7 types fortement basiques, pour chacun d'eux existant des recommandations spécifiques aux conditions de travail.

Dans ce qui suit on présentera quelques aspects essentiels de la composition d'un étage anionique, en soulignant les avantages mais aussi les limites de chaque solution proposée.

ADOPTION DU TYPE 2 D'ÉCHANGEUR ANIONIQUE FORTEMENT BASIQUE

L'échangeur fortement basique type 1 est une résine polystyrénique ayant des groupements fonctionnels triméthylamine, chimiquement très stables. L'échangeur de type 2 a des groupements fonctionnels diméthyléthanolamine, dont la basicité est légèrement plus faible et la stabilité chimique moindre.

Le type 1 est utilisé afin d'obtenir une fuite en silice très basse. En revanche, lorsqu'on veut un rendement de régénération très bon (capacité utile d'échange élevée, obtenue avec une consommation de soude assez basse) et/ou un bon comportement à l'égard des matières organiques (fixation quasi totale et élution intégrale) on préfère le type 2.

Sur les figures 1 et 2 on a représenté la capacité utile de base, respectivement la régénérabilité, en fonction du taux de régénération des deux types de résines anioniques fortes polystyréniques.

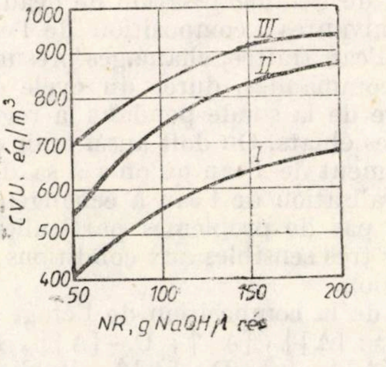

Fig. 1. — Capacité utile de base des échangeurs fortement basiques en fonction du niveau de régénération (cocourant) : I — résine polystyrénique type 1 (gel) ; II — résine polyacrylique ; III — résine polystyrénique type 2 (gel).

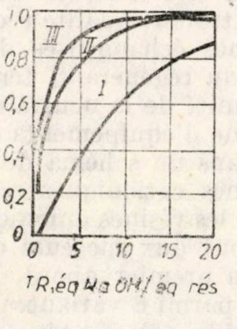

Fig. 2. — Régénérabilité des échangeurs fortement basiques en fonction de la quantité de soude (taux de régénération).

L'échangeur de type 2 a une résistance thermique faible. Le phénomène de dégradation des groupements forts mène souvent à la constitution de groupes faibles. La capacité fortement basique de la résine de type 2 diminuera, donc, dans une mesure beaucoup plus importante que sa capacité totale (voir figure 3). Le comportement de la résine à l'augmentation de la température de travail est différent, selon qu'il s'agit de la phase de saturation (épuisement) ou bien de celle de régénération.

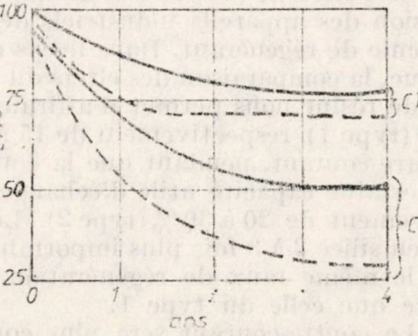

Fig. 3. — Dégradation de la capacité des échangeurs fortement basiques type 2 : CT — capacité totale ; CF — capacité forte ;
— épuisement à 40°C et régénération à 20°C ;
——épuisement à 20°C et régénération à 40°C.

Le taux d'oxygène dissout et d'oxydants présents dans l'eau à traiter exerce une influence importante sur le degré de décomposition de la résine. Par exemple, les courbes présentées sur les figures 1 et 2 se rapportent à une eau saturée en oxygène ; après 4 ans de service, la résine de type 2 perd environ 30 % de sa capacité totale et 50—70 % de sa capacité forte. En travaillant pendant 6 ans sur une eau sans oxygène (après dégazeur thérmique), la résine a perdu seulement 17 % de sa capacité totale, respectivement 40 % de celle fortement basique.[3]

Les acides forts sont fixés par l'ensemble des fonctions basiques. La capacité utile est liée surtout au total des fonctions faibles et fortes. La dégradation des groupements forts créant de nouveaux groupes faibles, son influence sur la capacité utile n'est pas importante dans le cas des eaux à haut pourcentage d'acides forts. La fixation par les groupements faibles est réalisée à un rendement de régénération meilleur, pendant que la fuite en silice devient excessive seulement après que 50 % de la capacité forte soit épuisée.

Dans le cas des eaux contenant de fortes quantités de CO_2 et de SiO_2 (relatives à la teneur en chlorures et sulphates) on préfère le type 1, placé en aval d'un échangeur faiblement basique.

La résine de type 2 présente toutefois un certain risque d'empoisonnement par la silice insuffisamment éluée à une température de régénération trop basse, phénomène amplifié par un taux de régénération près de la quantité stoéchiométrique (surtout dans le cas des eaux à fort pourcentage d'acides faibles).

L'échangeur de type 1 ne présente pas une dégradation notable à des températures au-dessous de 60°C ; quelquefois on obtient des résultats très satisfaisants même à 80—90°C. On connaît des cas où la capacité totale a diminué de 50 % après environ 500 jours d'utilisation à 80 C de la résine.

En ce qui concerne les matières organiques, le comportement du type 2 est nettement supérieur, surtout pour l'élution du régénérant alcalin.[4]

RÉGÉNÉRATION À CONTRE-COURANT DE L'ÉCHANGEUR ANIONIQUE FORTEMENT BASIQUE

Depuis plus de 15 ans les experts sont unanimement d'accord sur les avantages de la régénération à contre-courant : une qualité exceptionnelle de l'effluent (des fuites ioniques situées fréquemment à la limite de précision des appareils industriels de mesure), doublée d'une importante économie de régénérant. Dans le cas des échangeurs anioniques fortement basique, la comparaison des effets du système de régénération sur le même type de résine nous permet d'affirmer que la fuite en silice baisse de 5 à 7 fois (type 1), respectivement de 15 à 25 fois (type 2) par la régénération à contre-courant, pendant que la consommation de soude (pour obtenir une certaine capacité utile d'échange) baisse de 10 à 25% (type 1), respectivement de 20 à 30% (type 2). Le type 2 régénéré à cocourant a une fuite en silice 2 à 3 fois plus importante que celle du type 1. En échange, pour le même taux de régénération, la capacité utile est de 50% plus grande que celle du type 1.

Le contre-courant sera plus convenable pour le type 2, sur lequel on obtient, pratiquement, la même fuite en silice que dans le cas du type 1.

Dans les chaînages de déminéralisation modernes, la régénération à contre-courant des filtres fortement acides et basiques est devenue quasi-obligatoire, surtout lorsqu'on veut obtenir une eau traitée de haute qualité, dans des conditions de rendement élevé.

LITS SUPERPOSÉS ANIONIQUES

Les lits superposés (Duobed, Stratabed) représentent un cas particulier d'application de la régénération à contre-courant d'un échangeur fort en série avec un échangeur faible. Dans la même colonne on prévoit les deux résines du même signe : la résine faible, qui est plus légère que la résine forte se trouve à la partie supérieure du lit.

La régénération de bas en haut (contre-courant) fait que la soude rencontre d'abord l'échangeur fortement basique et puis celui faiblement basique. Le premier reçoit donc un excès de régénérant, ce chaînage en série améliorant encore le rendement par l'économie de soude réalisée. On utilise une résine anionique faible ayant une bonne cinétique d'échange et une importante capacité travaillée. Ceci, parce que le cycle actif (d'épuisement) sera prolongé au-delà du point de fuite en chlorure, jusqu'à l'épuisement de l'échangeur fort (l'apparition de la fuite en silice). Comme échangeur fortement basique on préfère un type 2 plutôt qu'un type 1 pour sa meilleure capacité utile et pour sa résistance à l'empoisonnement par les matières organiques, ce qui est très important puisque l'échangeur faible travaille au-delà de la fuite normale.

Le rapport volume de résine faible sur le volume total de résine anionique dépend de la durée du cycle actif, de la valeur absolue de l'acidité «-m» (SAF) et du rapport SAF/ST. La solution optimale correspond à une durée de cycle plus courte que celle habituelle et donc à un rapport volume résine faible sur volume total anionique situé dans les environs de 20 à 35%.[5]

Si on réussit à réaliser une très nette séparation à la limite des deux résines (donc des granulométries parfaitement mises au point) et si la teneur en silice de l'eau brute ne dépasse pas 20 % du total anions, la capacité utile du filtre anionique à lits superposés pourra atteindre 1000 eq/m^3 pour un rendement de régénération de 110 % seulement.

La granulométrie strictement contrôlée suppose la réduction à un minimum de la quantité de billes fines d'échangeur faiblement basique, dans le but de limiter l'expansion du lit de résine et pour éviter le colmatage du drainage de reprise des éluats, ainsi que la prohibition des billes trop grosses au fond du lit anionique fort, qui empêcheraient la séparation des résines pendant le soulèvement.

Une alternative très intéressante pour les lits superposés consiste à utiliser des composants acryliques. Les avantages en seront soulignés dans un chapitre suivant.

On a obtenu de très bons résultats aussi avec une résine faible polystyrénique et une résine forte polyacrylique, le facteur déterminant en étant la granulométrie.

Le calcul d'optimisation, dans les conditions spécifiques d'analyse de l'eau brute, de taux de régénération et de caractéristiques de travail des résines choisies peut conduire à un rapport volume échangeur faible sur volume anionique total de 40 jusqu'à 60 %.[6]

ÉCHANGEURS ANIONIQUES MACROPOREUX

Les résines type gel retiennent les matières organiques en fonction de leur poids moléculaire et proportionnellement au degré de porosité des billes de résine. L'élution pendant la régénération est incomplète, ce qui engendre une contamination irréversible de la résine, conduisant à une perte vertigineuse de la capacité d'échange anionique.

Les résines macroporeuses permettent la fixation des matières organiques dans les ramifications des canaux créés à dessein, et aussi leur élution quasi totale, même lorsqu'il s'agit de celles à haut poids moléculaire. En plus de cette adsorption, la résine accomplit aussi son devoir fondamental : l'échange ionique correspondant à ses groupements fonctionnels.

Les données géométriques optimales pour la fixation réversible des matières organiques sont bien établies[7] : de 40 à 80 m^2/g pour l'aire de la surface totale interne et de 300 à 500 Å pour le diamètre moyen des pores. Dans le cas des eaux à plusieurs types de matières organiques on recommande une gamme plus large de dimensions des pores.

L'exploitation d'un étage anionique composé d'un échangeur faible macroporeux et d'un échangeur fort semi-poreux fonctionnant jusqu'au point de fuite en silice a démontré que le pouvoir d'adsorption de la résine faible reste pratiquement constante, même après l'épuisement des groupes faiblement basiques.[8] Dans ce cas, l'échangeur fort agit en poste de finition pour les traces de matières organiques.

Certainement, le comportement de la résine à l'égard de ces matières est bien différent pour chaque fabricant, pour chaque produit même. Il existe des cas dans lesquels devient obligatoire un poste « barrière » (scavenger) précédant la chaîne de déminéralisation.

La limite au-dessous de laquelle on considère que les échangeurs d'anions tiennent tête sans protection (barrière) aux matières organiques est bien variable : dans certains cas on donne la valeur absolue du contenu exprimé en mg $KMnO_4$/l (par exemple, devant l'échangeur fort, lorsqu'il est précédé par un échangeur faible : 10 pour le type 1, respectivement 20 pour le type 2) ; d'autres fois on donne la quantité totale de matières organiques retenue par le volume d'échangeur, exprimée en g$KMnO_4$/l résine ; le plus souvent on donne la valeur-limite du facteur (chiffre) d'empoisonnement N (rapport entre la teneur en matières organiques, en mg/l et la salinité à fixer, en meq/l). Les valeurs recommandées pour les différents types d'échangeurs anioniques sont les suivantes [2] :

— polystyréniques gel type 1	2 mg/méq
— polystyréniques macroporeuses type 1	4
— polystyréniques gel type 2	6
— polystyréniques macroporeuses type 2	8
— polyacryliques fortement basiques	20
— polystyréniques faiblement basiques	20
— polyacryliques faiblement basiques	40

Lorsque le facteur N dépasse la valeur maximum admise pour le type respectif de résine on peut améliorer le comportement à l'égard des matières organiques en augmentant le volume de résine chargé dans la colonne. De cette façon, la quantité fixée par litre de résine sera réduite jusqu'au-dessous de la limite acceptée et la capacité opératoire sera inférieure à la capacité utile potentielle correspondant au même taux de régénération.

RÉSINES ANIONIQUES À STRUCTURE ACRYLYQUE

La structure acrylyque des résines anioniques leur confère une excellente stabilité physique et mécanique, une capacité utile d'échange élevée et une efficacité de fixation des matières organiques comparable à celle des résines polystyréniques macroporeuses (mais à laquelle vient s'ajouter une résistance à l'empoisonnement accrue, due à l'élution pratiquement complète pendant la régénération).

La résistance physique de cette résine, surtout en tenant compte de l'attrition permanente et des variations brusques de la pression osmotique auxquelles elle est soumise constitue un grand avantage, qui devient plus important dans le cas des installations dimensionnées pour des durées relativement réduites de la phase d'épuisement (par exemple, ayant plus de 250 cycles actifs par an).

En ce qui concerne la capacité utile d'échange, la résine fortement basique acrylique se comporte à peu près comme une résine polystyrénique macroréticulée de type 2 (voir la figure 1 pour le cocourant et la figure 4 pour le contre-courant), pendant que la fuite en silice est comparable à celle du type 1.[9]

Les résines polyacryliques faiblement basiques offrent des avantages plus évidents concernant la cinétique d'échange ionique : leur capacité utile dépasse de 20 à 30 % celle des résines polystyréniques macroporeuses et leur stabilité chimique est excellente, même pour le traitement des eaux « difficiles ». La régénérabilité des groupements actifs en fonction du taux de régénération peut être suivie sur la figure 2.

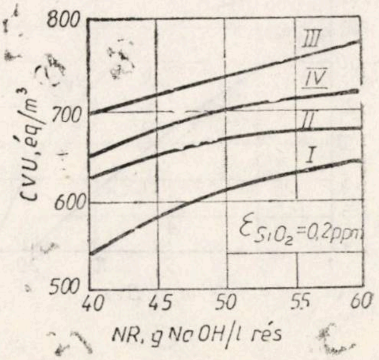

Fig. 4. — Capacité utile de base des échangeurs fortement basiques en fonction du niveau de régénération (contre-courant) ; IV — résine polystyrénique type 2 (macroporeuse).

Le comportement à l'égard des matières organiques représente le trait significatif essentiel des résines anioniques polyacryliques. En considérant les matières organiques comme un long radical organique hydrophobe sur lequel sont greffés des groupes carboxyliques hydrophiles on peut expliquer leur élution intégrale par le fait que le régénérant (NaOH) a la force nécessaire pour déplacer l'échange ionique qui a pris part à la fixation des groupements carboxyliques et aussi pour vaincre l'attraction assez faible entre la matrice hydrophyle de la résine et les radicaux hydrophobes des matières organiques. Ce phénomène ne se produit pas avec les résines polystyréniques, l'attraction entre leur squelette aromatique hydrophobe et le radical hydrophobe des matières organiques étant très forte. De cette manière, les matières organiques s'accumulent cycle après cycle, jusqu'à l'empoisonnement irréversible de la résine. Quelquefois dans de tels cas, même la décontamination à saumure alcaline n'est plus efficace.

Pour les échangeurs fortement basiques acryliques, une telle décontamination n'est pas nécessaire tant que la quantité de matières organiques retenue pendant le cycle actif ne dépasse pas 5 gKMnO$_4$/l de résine.[10]

Les résines faiblement basiques polyacryliques retiennent réversiblement des matières organiques jusqu'à une valeur du facteur N de 40 mgKMnO$_4$/méq.

En ce qui concerne la stabilité thermique, les échangeurs fortement basiques de type acrylique sont plus sensibles que les autres : il est recommandé de ne pas dépasser 35°C à l'épuisement, la régénération devant être effectuée, de préférence, à température ambiante. Exceptionnellement, afin d'améliorer le procès d'élution de la silice dans les conditions d'un taux de régénération baissé on peut chauffer la soude jusqu'à 35°C tout au plus.

Par même leur nature, les résines acryliques ont des caractéristiques de rinçage différentes des celles des résines polystyréniques correspondantes. Si pour les échangeurs fortement basiques la différence est assez peu significative, pour les faiblement basiques, en échange, celle-ci se manifeste d'une manière saisissante (fig. 5). Par exemple, afin d'obtenir une conductivité de 20 µS/cm dans l'éluat sont nécessaires de 12 à 14 volumes d'eau de rinçage (acryliques), contre 3 à 5 volumes seulement, dans le cas d'une résine polystyrénique macroréticulée. Cette caractéristique est extrêmement importante pour le traitement des eaux très salines, lorsque l'eau de rinçage consomme une bonne partie de la capacité d'échange de la résine.

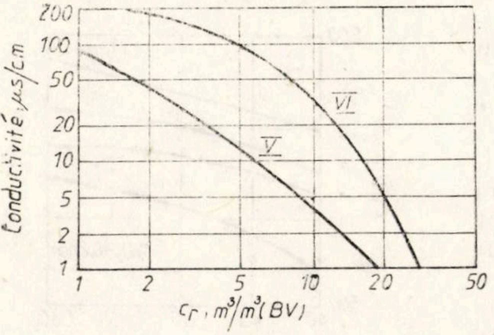

Fig. 5. — Caractéristiques de rinçage des échangeurs faiblement basiques : V — résine polystyrénique macroporeuse ; IV — résine polyacrylique.

EXEMPLE DE CALCUL

« On considère une eau qui, après passage par l'étage cationique et le dégazeur de CO_2, a l'analyse suivante : SAF = 2,0 méq/l; CO_2 = 0,3 még/l ; SiO_2 = 5 ppm ; matières organiques : 10—20 ppmKMnO$_4$.

On admet une fuite en sodium après l'échangeur cationique de 0,02 méq/l et une fuite en silice dans l'eau déminéralisée de 0,1 ppm, avec l'arrêt du cycle à une valeur maximale de 0,2 ppm.

L'eau déminéralisée doit avoir une conductivité maximum de 1,0 µS/cm. Le débit net produit est de 70 m³/h ».

Après une première étape d'analyse, pendant laquelle on élimine plusieurs variantes possibles pour l'étage anionique restent en compétition cinq chaînages, pour lesquels on fait des calculs détaillés, à base des courbes caractéristiques de chaque résine. Ces schémas sont les suivants :

1. Echangeur faible acrylique — échangeur fort type 1, régénéré à contre-courant.
2. Echangeur faible macroporeux — échangeur fort acrylique.
3. Echangeur fort acrylique, régénéré à contre-courant.
4. Echangeur fort type 2, régénéré à contre-courant.
5. Echangeur faible acrylique — échangeur fort acrylique, en lits superposés (Duobed).

Les conclusions des calculs sont présentées dans le tableau 1. On peut remarquer que la variante nº 5 est optimale du point de vue du comportement à l'égard des matières organiques, mais qu'elle a un coût élevé de l'investissement. On préfère, dans le stade actuel des technologies, la variante nº(1 valeur d'investissement de 16 % plus basse et consommation de soude de 4% moindre).

Quoique l'échangeur fortement basique de type 1 n'a pas une élution satisfaisante des matières organiques retenues, le couplage en amont d'un échangeur faiblement basique acrylique réalise une très bonne proection et — sur l'ensemble de l'étage anionique — le comportement à l'égard des matières organiques est bon, permettant la mise en valeur des avantages techniques et économiques de ce couplage.

Tableau 1.

Schéma de l'étage anionique (variante)	Valeur relative de l'investissement [%]	Régénérant [NaOH 100%]		Matières organiques [%]	
		Consommation spécifique [g/m³ eau démin.]	Taux de régénération [%]	retenues de l'eau	éluées de la résine
1	118,2	114,0	119	95	98
2	126,8	147,6	154	95	96
3	119,6	234,5	244	75	100
4	100,0	138,4	136	70	80
5	139 9	118 8	124	97	100

CONCLUSIONS

Le choix de la composition optimale de l'étage anionique d'un schéma de déminéralisation de l'eau nécessite une analyse complexe de toutes les possibilités techniques et économiques concernant la réalisation de ce chaînage.

En tenant compte tant des unités d'échange ionique possibles, du comportement des résines envers les caractéristiques de l'eau, des technologies de travail, des types de résines existants, que des marques spécialisées d'échangeurs anioniques, propres à chaque fournisseur et à chaque utilisation on peut affirmer que l'optimisation de l'étage anionique ne peut être faite correctement et complètement que sur la base d'un programme sur ordinateur, qui tienne compte de toutes les nouveautés du domaine de la production des échangeurs d'ions. Dans ce sens, les programmes de calcul existants [11, 12, 13], contenant — parmi d'autres — un élément de finesse remarquable (l'évolution dans le temps de l'usure chimique et mécanique des résines, avec toutes les implications qui en découlent sur le dimensionnement des installations de déminéralisation) peuvent être complétés avec les possibilités d'utiliser de nouvelles structures d'échangeurs d'ions (présentées dans le chaspitres précédents de cet ouvrage), tout comme des technologies modernes : lits superposés, lit flottant, système continu. Cette opération s'impose d'autant plus qu'on reconnaît le fait qu'un étage anionique optimisé représente la clef de voûte de la qualité de l'eau déminéralisée et le facteur de base de la réduction des frais de production.

NOTATION UTILISÉE

[A] ↓ = échangeur anionique fortement basique, régénéré à cocourant
[A] ↑ = idem, régénéré à contre-courant
D = dégazeur de CO_2
(a) = échangeur anionique faiblement (moyennement) basique

BIBLIOGRAPHIE

[1] C. Fodor, *Energetica*, **2**, 59 (1975).

[2] T. V. Arden et F. de Dardel, "Opérations chimiques unitaires. Echange d'ions", Rohm&Haas France SA, Inf. 8601F, J2861.

[3] * * * ,,Stabilité thermique des résines échangeuses d'ions fortement basiques et évolution de leurs performances en cours d'utilisation", Dia-Prosim, Inf. 76003F (1976).

* * * ,,Conditions optimales d'utilisation des résines anioniques", Dia-Prosim, Inf. 75003F (1975).

[5] J. J. Wolff, ,,L'eau et l'Industrie", **10**, 76 (1976).

[6] * * * "La technique et le calcul des lits superposés", Dia-Prosim, Inf. 80001F (1980).

[7] F. Martinola et A. Richter, "Makroporöse Ionenaustauscher und Adsorbentien zur Aufbereitung organisch belasteter Wässer", Bayer AG, OC/I1544 (1976).

[8] F. Martinola, "Ion Exchangers, indispensable aids for water treatment, power engineering and chemical technology", Bayer AG, OC/I20361 (1978).

[9] A.-D. Prunac, "Les échangeurs d'ions à structure acrylique utilisés dans la déminéralisation de l'eau", L'Eau, l'Industrie, les Nuisances, 72, 41 (1983).

[10] * * * "Les résines échangeuses d'ions acryliques en déminéralisation d'eau. Expérience industrielle", Dia-Prosim, Inf. 81001F (1981).

[11] C. Fodor, M. Damian et I. Stiger, *Energetica*, **4**, 178 (1986).

[12] C. Fodor, M. Damian et I. Stiger, *Energetica*, **6**, 271 (1986).

[13] C. Fodor, M. Damian et I. Stiger, *Energetica*, **7**, 327 (1986).

Revue Roumaine de Chimie, 36, 1–3, 65–69(1991)

THE FERRATE(VI), $[FeO_4]^{2-}$, AS OXIDIZING AGENT

ALEXANDRA SCHIOPESCU, ANCA ALBU and D. SĂNDULESCU
Department of Chemistry, Institute of Petroleum and Gas, Bd. Bucureşti 39, Ploieşti, Romania

Received July 25, 1990

Data are presented on the possibility of employing ferrate-(VI) ion as oxidizing agent; the results of kinetic studies regarding oxidation of some alcohols by potassium ferrate (VI) are reported.

INTRODUCTION

Oxidation of alcohols by metallic ions or oxyanions corresponding to metals in higher oxidation states was mentioned in literature.[1–3]

A kinetic study of reactions aiming at establishing the mechanism (especially the coordinated intermediate species that appear in reaction) and at evaluating the possibility of selective oxidation of alcohols in presence of mixed functions (double bonds, amines, etc.), is, beyond doubt, very interesting.

It is also important to ensure the controlled oxidation of the substrate to aldehyde or ketone, eliminating from the sequence the reactions of oxidation to acid. Ferrate (VI) ion belongs to the oxianion of transition metals in higher oxidation states.

Although the literature mentions the outstanding advantages of selective oxidation of alcohols by ferrates (VI), the data on this problem are scarce. [4]

In the previous articles Audette, Quail and Smith have reported some data on oxidation of alcohols by potassium ferrate (VI).[5]

In this contribution we continue some kinetic studies on oxidation of alcohols with potassium ferrate (VI).[5–6]

EXPERIMENTAL

To elucidate the mechanism of alcohol oxidation we studied the reaction kinetics by monitoring the fading of potassium ferrate (VI) colour at $\lambda = 500$ nm and 25°C. Samples were previously thermostated; the spectrophotometric measurements were also taken in a thermoset cell.

The determinations were carried out in ethylic, propylic, isopropylic, butylic and isobutylic alcohols in aqueous solutions within the $1 \cdot 10^{-4} - 4 \cdot 10^{-4}$ mol/ml of potassium ferrate (VI) and $2 \cdot 10^{-4} - 6 \cdot 10^{-4}$ mol/ml of the corresponding alcohol.

The absorbance of the solution was determined at certain time intervals.

The results were plotted as absorbance A versus time, $A = f(t)$.

RESULTS AND DISCUSSION

The curves of solutions absorbance versus time, which have their specific shape, evidence the possibility that some autocatalytic reactions occur which are caused by formation of $Fe_2O_3 \cdot nH_2O$ during the reaction. Thus, the oxidation of alcohols by ferrate (VI) appears as an autocatalytic reaction.

To determine the rate equation use has been made of the initial rate method which ensures elimination of secondary effects induced either by the presence of $Fe_2O_3 \cdot nH_2O$ precipitate or by the variations of pH during the advancement of reaction.[7-8]

This method of calculation has yielded the data listed in Tables 1 and 2 which specify the reaction orders as a function of the alcohols studied and ferrate (VI).

Table 1

The reaction order with respect to the alcohol (m)

Alcohol	m
Ethylic alcohol	0.7
Propylic alcohol	1
Isopropylic alcohol	1.5

Table 2

The reaction order with respect to ferrate (VI) (n)

Alcohol	n
Ethylic alcohol	0.5
Propylic alcohol	0.3
Isopropylic alcohol	1.5

The sequence of decreasing reaction order is: isopropylic alcohol〉propylic alcohol〉ethylic alcohol.

An analogy with decomposition of $KMnO_4$ in alkaline medium[9,10] may be employed in determination of potassium ferrate (VI) reaction mechanism.

The first attempts to determine the reaction mechanism in decomposition of $KMnO_4$ in alkaline medium have not given conclusive results.[11]

Symons study [12] reports the kinetic data and the mechanism of decomposition of $KMnO_4$ in alkaline medium. In this process OH^- radical appears as active oxidizing species.

This model adapted to the reaction mechanism of $(FeO_4)^{2-}$ may be conceived as follows:

$$1.\ FeO_4^{2-} + OH^- \underset{k_{-1}}{\overset{k_1}{\rightleftharpoons}} FeO_4^{3-} + \cdot HO$$

$$2.\ \cdot HO + OH^- \underset{k_{-2}}{\overset{k_2}{\rightleftharpoons}} \cdot O^- + H_2O$$

$$3.\ FeO_4^{2-} + OH^- + \cdot O^- \underset{k_{-3}}{\overset{k_3}{\rightleftharpoons}} FeO_4^{3-} + HO_2^-$$

4. $FeO_4^{2-} + HO_2^- \underset{k_{-4}}{\overset{k_4}{\rightleftarrows}} FeO_4^{3-} + HO_2$

5. $HO_2 + OH^- \underset{k_{-5}}{\overset{k_5}{\rightleftarrows}} O_2^- + H_2O$

6. $FeO_4^{2-} + O_2^- \underset{k_{-6}}{\overset{k_6}{\rightleftarrows}} FeO_4^{3-} + O_2$

The following equation is obtained under the assumption that the reactive species are quasistationary (Christiansen principle):

$$\frac{dt}{dx} = \frac{K_1}{(a-x)b} + \frac{K_2 x}{(a-x)b} + \frac{K_3 x}{(a-x)^2 b^3} + \frac{K_4 x^2}{(a-x)^3 b^3} + \frac{K_5 x^3}{(a-x)^3 b^4} +$$

$$+ \frac{K_6 x^3}{(a-x)^4 b^4}$$

where

$K_1 = \frac{1}{k_1}$; $K_2 = \frac{k_{-1}}{k_1 k_2}$; $K_3 = \frac{k_{-1} k_{-2}}{k_1 k_2 k_3}$ etc. (according to the scheme).

$(a - x)$ stand for the concentration of $(FeO_4)^{2-}$ at time t and x for the concentration that disappeared at time t.

Considering K_6 (which takes low values) integrating the rate equation and disregarding the sixth term in the first part of the equation one gets:

$$t = -x\left[\frac{k_2 a}{b^2} - \frac{k_5}{b^4}\right] - \ln\left(\frac{a}{a-x}\right)\left[\frac{k_1}{b} + \frac{k_2}{b^2} - \frac{k_3 k_4}{b^3} + \frac{3k_5 a}{b^4}\right] +$$

$$+ \left[\left(\frac{a}{a-x}\right) - 1\right]\left[\frac{k_3 2k_4}{b^3} - \frac{3k_5}{b^4}\right] + \left[\frac{a_2}{(a-x)^2} - 1\right]\left[\frac{k_4}{2b^3} + \frac{k_5 a}{2b^4}\right]$$

The integrated equation of reaction rate shows the difficulties implied by the experimental verification of the reaction mechanism advanced for difficulties encountered in utilization of a simplified form of this equation for all discussed alcohols. This is due to the fact that the terms of the equation contribute to a greater or less extent to the overall kinetic effect because of the distinct values the rate constants of elementary reactions take in the various alcohols.

The attempts to test the equation have shown that over certain conversion ranges the equation may be linearized in $1/A^2$ terms (as a function of time) or in $\ln A$ (as a function of time) for the reaction of potassium ferrate (VI) with the alcohols studied. This may be exemplified for the reaction of potassium ferrate (VI) with butylic alcohol.

The time variation of absorbance for the reaction above is shown in Figs 1 and 2.

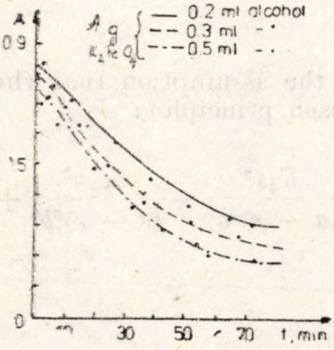

Fig. 1. — The time variation of absorbance for the reaction of potassium ferrate (VI) and butylic alcohol (constant amount of ferrate).

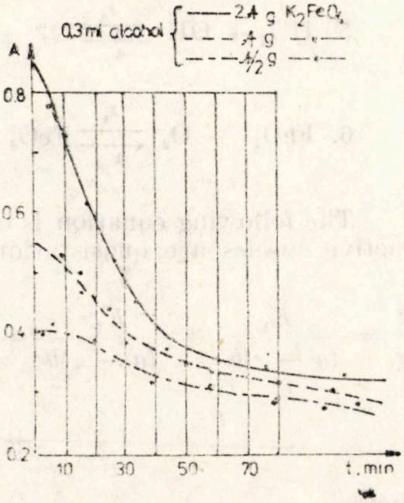

Fig. 2. — The time variation of absorbance for the reaction of potassium ferrate (VI) and butylic alcohol (constant amount of alcohol).

The verification of rate equation for the reaction of potassium ferrate (VI) with butylic alcohol is shown in Figs 3 and 4.

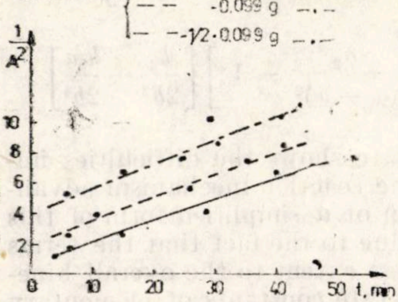

Fig. 3. — Verification of rate equation for the reaction of potassium ferrate (VI) with butylic alcohol ($1/A^2$ versus time).

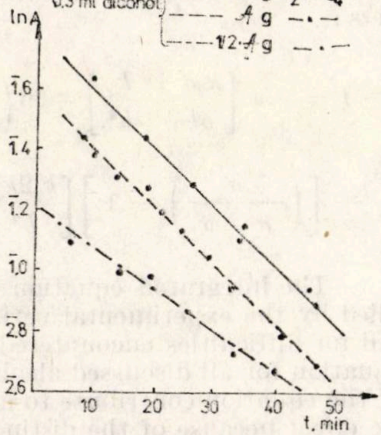

Fig. 4. — Verification of rate equation for the reaction of potassium ferrate (VI) with butylic alcohol (ln A versus time).

CONCLUSIONS

The combination of iron in higher oxidation state — Fe(VI) — was used as oxidizing agent of some alcohols in aqueous medium. The alcohols utilized were ethylic, propylic and butylic. The reaction orders with respect to the alcohols studied and ferrate (VI) were evaluated by the method of initial rate.

The attempts of verifying the rate equation have shown the possibility of linearizing it over certain conversion ranges; the data obtained so far do not allow the selection of a certain type of rate equation valid in all the alcohols studied.

REFERENCES

[1] W. Richardson, "Oxidation in Organic Chemistry", Academic Press, New-York, 1965.
[2] J. Holum, *J. Org. Chem.*, **26**, 4814 (1961).
[3] J. Baneyee and K. K. Sengupta, *Current Sci.*, **34**, 14 (1963).
[4] R. J. Audette and J. W. Quail, *Inorg. Chem.*, **11**, 1904 (1972).
[5] R. J. Audette and J. W. Quail, *Tetrahedron Letters*, **1971**, 279.
[6] J. M. Schreyer and L. T. Ockermann, *Analyt. Chem.*, **22**, 691, (1950).
[7] W. Wagner, J. Gump and E. Hart, *Analyt. Chem.*, **24**, 1997 (1952).
[8] M. Wronska, *Bull. Acad. Polon Sci. Chem.*, **7**, 137 (1959).
[9] A. Berka and J. Hapolo, *Coll. Czech. Chem. Commun.*, **31**, 222, (1966).
[10] A. Kharin, *Izv. Vyssh. Ucheb. Zaved. Khim. Khim. Tekhnol.*, **14**, 495, (1971).
[11] R. Stewart, "Oxidation Mechanisms", Benjamin, New York, 1964.
[12] Ferguson, Lerch and Day, *J. Amer. Chem. Soc.*, **53**, 126 (1931).

Revue Roumaine de Chimie, **36**, *1–3*, 71–75 (1991)

IRON DETERMINATION BY SOLVENT EXTRACTION WITH SALICYLALDEHYDE GUANYLHYDRAZONE AND ATOMIC ABSORPTION SPECTROPHOTOMETRY

F. SALINAS, J.J. BERZAS NEVADO and P. VALIENTE GONZÁLEZ
Department of Analytical Chemistry and Physical Chemistry, University of Extremadura,
06071 Badajoz, Spain

Received September 12, 1988

A simple method by solvent extraction and atomic absorption spectrophotometry for the determination of iron is described. The method is based on the extraction of the complex formed between iron and salicylaldehyde guanylhydrazone into methylisobutylketone. The method has been applied for determining iron in river water, Portland cement, magnesite and aluminium-bronze.

1. INTRODUCTION

Atomic absorption spectrophotometry (a.a.s.) is one of the instrumental techniques of analysis more used for its sensitivity, selectivity and quickness. However, the combination, of a.a.s. and liquid-liquid extraction is a recommendable method to increase the sensitivity, and reduce the interference from the matrix.[1]

Salicylaldehyde guanylhydrazone (SAG) reacts with iron (ferrous or ferric) giving always the same yellow complex in basic media and the same red complex in neutral and weak basic media. The yelow complex has been used for the spectrophotometric determination of trace amounts of iron in rare earths.[2] The red complex also was used for the extractive-spectrophotometric determination of iron in magnesite and Portland Cement.[3]

In this work a new method for iron determination by a.a.s. is proposed. The method is based on the formation of the red complex of iron and SAG which is extracted into methylisobutylketone (MIBK) in the presence of perchlorate. The new method is more sensitive and selective than the extractive-spectrophotometric method[3] and has been applied to waters and other samples.

2. EXPERIMENTAL

2.1. Reagents and apparatus

All solvents and chemical reagents used were of analytical grade.

SAG solutions in dimethylformamide (DMF)-water (1 : 20) were used at different concentrations. A standardized solution of Fe(III) was used. A buffer solution of pH = 7.3 of Tris-HCl 0.1 M and $NaClO_4$ 3.6 M was used.

A Perkin-Elmer 370 atomic absorption spectrophotometer equipped with standard burner of 10 cm flame path and the following optima instrumental conditions : Wavelength, 248.3 nm ; lamp current, 30 mA ; Slit width, 0.2 nm ; air flow rate, 16.5 $l.min^{-1}$; acetylene flow rate, 2 $l.min^{-1}$; height of lightpath above burner, 1.5 cm ; rate aspirate, 4 ml min^{-1} ; was used.

A Crison 501 digital pH-meter with a glass-AgCl electrode was used.

2.2. Recommended procedure for the determination of iron

In a separatory-funnel, take an aliquot of the sample solution containing to 40 µg of iron' add 5 ml of 0.2 % SAG solution and 7 ml of buffer solution (pH = 7.3 and 3.6 M $NaClO_4$)· Dilute to 50 ml with water. Mix well. Add 10 ml of MIBK. Shake for 2 min and allow the phases to separate. Transfer the organic layer into a dried glass tube and aspirate directly into the air-acetylene flame. Measure the atomic absorption at 248.3 nm using MIBK as a blank.

2.3. Determination of iron in Portland cement, magnesite and bronze

2.3.a. Portland cement. Take about 0.25 g of the sample and 0.5 g of ammonium chloride and add 5 ml of concentrated hydrochloric acid. Heat on a steam-bath for 30 min. Add 20 ml of hot water to the solution for complete dissolution of the soluble components of the cement sample. Filter and wash the precipitate with acidulated hot water. Cool the filtrate and dilute it to volume in a 100-ml standard-flask. In this solution, iron is determined following the recommended procedure.

2.3.b. Magnesite. Take about 0.5 g of the sample and dissolve it in a few ml of concentrated perchloric acid. Heat until dissolution is complete. Cool and dilute it to volume in a 100-ml standard flask. In this solution, iron is determined following the recommended procedure.

2.3.c. Bronze. Take about 0.25 g of the sample and dissolve it in 5 ml of concentrated nitric acid. Heat until dissolution is complete. Cool and dilute it to volume in a 100-ml standard flask. In this solution, iron is determined following the recommended procedure.

2.3.d. River water. The determination of iron in water was carried out without previous treatment of the sample and following the recommended procedure.

3. RESULTS AND DISCUSSION

3.1. Effect of pH

The effect of pH of the aqueous solution on the Fe(III)-SAG complex extraction into MIBK was studied using a fixed Fe(III), SAG and perchlorate concentrations and varying the pH of the aqueous solution with different buffer solutions (acetic acid/acetate ; Tris/hydrochloric acid and ammonia/ammonium chloride). The extraction yields have been calculated

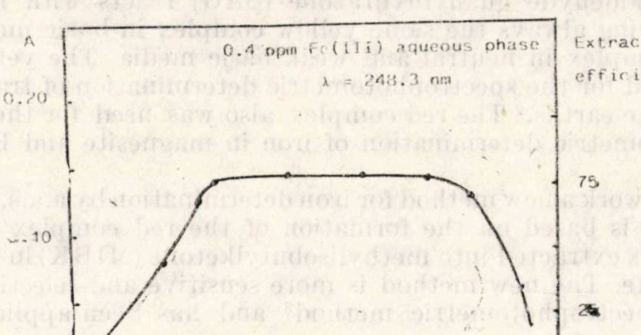

Fig. 1. Influence of pH on the Fe(III)-SAG complex extraction phase ratio 5:1 (aqueous phase:organic phase).

by determining iron from both aqueous and organic phases after extraction. Figure 1 shows that the greatest extraction occurred between 6–9 pH values with a yield higher than 80%. A buffer of pH = 7.3 and composition Tris/HCl was chosen.

3.2. Effect of SAG and perchlorate concentrations

The extraction was found to be maximal at $(ClO_4^-) > 0.25$ M and SAG must have a concentration of at least 0.01% in the aqueous layer. The effect of the perchlorate indicates the formation of an ion-association complex.

3.3. Effect of the other variables

The extraction was practically constant for aqueous/organic phase-volume ratios from 5 : 1 to 1 : 1. A shaking time of 30 sec. was sufficient, however a shaking time of 2 min is recommended for a best reproducibility. The stability of the samples in MIBK was studied and the absorbance remained constant for 2 hr. at least.

3.4. Characteristics of the analytical method

Using an aqueous phase of 50 ml and an organic phase of 10 ml, as previously described, was found that the calibration curve was linear up to 0.8 ppm Fe(III) in aqueous phase. The characteristic concentration was 0.012 ppm for 1% absorption (A = 0.0044). The coefficient of variation was 2.0% calculated from ten replicated analyses with 0.40 ppm in the aqueous phase. The detection limit was 0.003 ppm and the determination limit was 0.03 ppm.

3.5. Interferences

The interference of diverse ions was also studied in the determination of 0.40 ppm of iron. The tolerance limit was taken as the concentration of ion did not cause more than 5% change in the absorbance. The results are summarized in Table 1.

3.6. Applications

The method was applied satisfactorily to the determination of iron in Portland cement, magnesite, bronze and river water. The results are summarized in Tables 2 and 3.

Table 1

Effect of diverse ions in the determination of 0.40 ppm of iron

Maximum tolerable foreign ion/Fe ratio (w/w)	Ions
>250	Tartrate, oxalate, acetate, thiocyanate, Cl$^-$, F$^-$, K$^+$, NO$_3^-$
100	Mn(II), Cu(II), Hg(II), As(III), Pb(II) Ca, Ba, Mg, Cd(II), Zn(II), Mo(VI)
50	V(V), citrate.
25	Sn(II).
10	Co(II).
7.5	W(VI).
5	Al(III), Cr(III), Bi(III), As(III), Ni(II)
2.5	Ti(IV), Pd(II).
<1	EDTA, phosphate.

Table 2

Iron determination in standard samples

Sample	Composition %	Fe certified %	Fe found* %	% error
Portland Cement CS No. 372	SiO$_2$ (21.3) ; TiO$_2$ (0.33) Mn$_2$O$_3$ (0.06) ; CaO (65.8) Al$_2$O$_3$ (5.35) ; MgO (1.30) Na$_2$O (0.21) ; K$_2$O (0.62) SO$_3$(2.35); P$_2$O$_5$(0.19)	1.74	176	1.1
Bronze B.A.S. No. 32a	Cu (85.9) ; Zn(0.94) Mn (0.27) ;Ni(1.16) Al (8.8)	2.67	2.66	−0.4
Magnesite BCS No. 389	SiO$_2$ (0.89) ; TiO$_2$ (0.01) Al$_2$O$_3$(0.23) ; Fe$_2$O$_3$ (0.29) Cr$_2$O$_3$ (0.28) ; CaO (1.66) Na$_2$O (0.03) ;K$_2$O (0.01) MnO (0.008) ; B$_2$O$_3$ (0.029)	0.203	0.202	−0.5

* Mean of 3 determinations

Table 3

Iron determination in river waters

	Fe found (ppm)[a]	
Sample	Propo sed method	AAS with-out extractions[b]
Guadiana river	0.50	0.52
Ayuela river	0.62	0.63
Salor river	0.30	0.31

[a] Mean of 3 determinations.
[b] Samples with previous concentration.

REFERENCES

[1] M. S. Cresser, "Solvent Extraction in Flame Spectroscopic Analysis", **Butterworth and Co.** Ltd. London (1978).

[2] J. J. Berzas, A. Espinosa and P. Valiente, *Microchem. J.*, **30**, 380 (1984).

[3] F. Salinas, J. J. Berzas, A. Espinosa and P. Valiente, *An. Quim.*, **84 B**, 80 (1988)

Revue Roumaine de Chimie, **36**, *1–3*, 77–83 (1991)

STUDY OF THE SYSTEM IRON(III)-3-NITROBENZOHYDROXAMIC ACID-ADOGEN 464 IN TOLUENE

A. MOLINA-DÍAZ[2], M.I. PASCUAL-REGUERA[2] and L.F. CAPITÁN-VALLVEY*[1],
[1] Department of Analytical Chemistry, Faculty of Sciences, University of Granada,
18071 Granada. Spain.
[2] Department of Analytical Chemistry, University College of Jaén, University of Granada,
23071 Jaén. Spain

Received September 12, 1988

A new spectrophotometric method for determination of iron (III) based on the formation of Fe(III)-3-nitrobenzohydroxamic acid (NO_2BHA) complex at pH 3.3 and extraction into an Adogen 464-toluene solution is described. The orange extract has a maximum wavelength at 438 nm and the apparent molar absorbance of the 1 : 2 : 1 (Fe (III) : $3NO_2BHA$: Adogen 464) complex is $2.63 \times 10^4 L \cdot mol^{-1} \cdot cm^{-1}$ (Vaq/Vorg = 5). Properties of complex are compared with the Fe(III)-5-nitrosalicylhydroxamic acid (5-NO_2SHA). The system obeys Beer's law from 0.2 to 2.4 mg. L^{-1} of Fe(III) in aqueous phase using 3-NO_2BHA as reagent. The interference of foreign ions has also been determined and the mehod applied to the determination of iron in standard aluminium bronze samples.

INTRODUCTION

A large number of methods has been reported in the literature for the determination of iron (III) using hydroxamic acids as chelating agents in aqueous solution[1,2,3] as well as in extraction with organic solvents as hexanol,[4] methyl isobutyl ketone/tributyl phosphate[5] and so one.

However we only know a paper related with the extraction of charged iron complexes of hydroxamic acids in the presence of liquid ion exchangers. This system is iron : phenylacetohydroxamic acid : Adogen 464 in toluene.[6]

In the present paper, 3-nitrobenzohydroxamic acid is shown to be a selective and sensitive reagent for the determination of iron (III) at the microgram level. The orange complex formed at pH = 3.3 is extracted into toluene, only in the presence of Adogen 464 (ammonium quaternary resin). The composition of the extracted species and its aplication to the analysis of bauxites and aluminium bronzes are described. Properties of the complex are compared with Fe(III)-5-nitro-salicylhydroxamic acid at the same pH.

*** Author to whom any correspondence should be addressed.**

EXPERIMENTAL

Apparatus

A Bausch & Lomb Spectronic 2000 spectrophotometer with glass cells of 10 mm optical path length was used. All pH measurements were made with a Crison 501 Digit pH-meter fitted with a glass-calomel electrode assembly. A Selecta Vibromatic 384 mechanical shaker was used for the extraction process.

Reagents

All reagents and solvents were analytical-reagent grade chemicals.

Standard iron (III) solution 1.8×10^{-2} M, prepared from $Fe(NO_3)_3 \cdot 9H_2O$ in distilled water acidulated with HCl and standardized gravimetrically as oxide. Prepare working standards by suitable dilution as required.

3-Nitrobenzohydroxamic acid ($3\text{-}NO_2BHA$) and 5-nitrosalicylhydroxamic acid solutions of several concentrations. The reagents were synthesized by us[7], and the solutions prepared in water by addition of the stoichiometric amount of NaOH.

Buffer solution monohydrogen phthalate/HCl, pH = 2.7 $C_t = 0.05$ M and acetic acid acetate, pH = 3.3, Ct = 0.20 M.

Methyltrioctylammonium chloride solution (Adogen 464) 1.0×10^{-2} M in toluene.

Procedure

To an aliquot of the sample containing between 12.5 and 35 μg of iron, 0.75 mL of 1.0×10^{-2} M reagent, 10 mL of buffer solution acetic acid/acetate pH = 3.3 and 2.5 mL of 1 M solution of NaCl are added, leveling off finally to 25 mL with distilled water. Extract by shaking for 5 min. with 5 mL of. 1.0×10^{-2} M Adogen 464 solution using mechanical shaker and allow the phases to separate, filter the organic one by a paper to suppress the sligth turbidity in this layer. The absorbance is measured at 438 nm against a toluene solution of 1.0×10^{-2} M Adogen 464. The calibration graph over the range 0.2—2.0 mg $\cdot L^{-1}$ is prepared by using standard solutions of iron (III) treated identically.

Preparation of sample solutions

Aluminium bronze

A suitable weight of bronze, containing about 0.5 mg iron is dissolved in 10 mL of 1 : 1 HNO^3. Then, the solution is heated strongly until nitrous steam expulsion is completed, it is cooled and made up to 100 mL with distilled water. The iron content is determined on an aliquot following the recommended procedure.

Bauxites

A suitable weight of the samples is dissolved in a mixture of $HF-HCl-H_2SO_4$ (8) in a teflon crucible in the usual way and finally diluted to known volume. The iron is then determined according to the procedure.

RESULTS AND DISCUSSION

Absorption Spectra

The addition of an aqueous solution of $3NO_2BHA$ to another one of Fe(III) produces a violet complex in acid medium (maximum absorption at 520 nm), pink and pink-orangish colours at moderate pH and a strong yellow colour in basic medium (shoulder absorption at 520 nm). When these solutions are extracted with Adogen 464 in toluene, an orange colour is produced in all pH range, and their spectra show a maximum between 410 and 460 nm, being remarkable the increase of absorbance values with the extraction.

Optimum experimental conditions

Effect of pH. It was observed that the extraction of the orange species starts at pH 0.6 and resulted in maximum and constant absorbance of the organic phase over the pH range 1.9—5.0 (438 nm). At pH near 6 a hypsochromic effect is originated and the maximum wavelength displaced at 410 nm ; at higher pH values the extract turns brownish-orange in colour and this bathochromic effect moves the maximum wavelength at 460 nm. This suggests, at least, the extraction of two species at pH values smaller than 5 and higher than 9 respectively. pH 3.3 and 438 nm were chosen for further experiences.

Influence of buffer solution. A significant decrease in the absorbance of the extract was observed using hydrogenphthalate/HCl buffer solution. The acetic acid/acetate buffer solution between $C_t = 0.12-0.30$ M did not affect the absorbance of the extract, therefore, this one is used for further tests.

Influence of ionic strength. The presence of 0.1 M NaCl allows a quick and perfect phase separation after extraction.

Influence of 3-NO_2BHA and Adogen 464 concentrations. — A 11 and 7 fold molar excess of 3-NO_2BHA and Adogen 464 to Fe(III), respectively, was found to be suitable for the complete extraction of the complex.

Other experimental conditions. — A shaking time of 5 min was sufficient for equilibrium to be attained. The addition order is not critical and the absorbance of the extracts remains constant for at least 2 hours.

Nature of the extracted species

The stoichiometry of the Fe(III)-3-NO_2BHA binary complex was determined using the equilibrium-shift method.[9] The plot of the logarithm of the distribution ratio $A/(A_m-A)$ vs. the logarithm [3—NO_2BHA]at a fixed Fe(III) and Adogen 464 concentrations and pH 3,3 yields a straight line with slope 1.87 (r = 0.989) (Figure 1). This indicates a 3NO_2BHA to iron molar ratio of 2 : 1 in the extracted species. At the above mentioned pH the value of the global extraction constant, log K_e, was shown to be 7.20 (equilibrium-shift method).

The stoichiometric coefficient of Adogen in the ion association complex was established using the Yoe and Jones [10]and Asmus[11] methods modified to two phases and at fixed Fe(III) and 3NO_2BHA concentrations. The first method indicates a 1 : 1 stoichiometry. On the other hand the straight-line appears for the Asmus method for n = 1 (correlation coefficient, r = 0.9991 ; degrees of freedom, f = 3). Consistently we suppose that stoichiometry of the compound extracted is 1 : 2 : 1 (Fe : 3-NO_2BHA : Adogen) and the binary complex supports a negative charge.

Supposing that the equation $\log D = \log K_e + n\log[HA]aq + q\log[R_4N] + mpH$ holds, the plot of the logarithm of the distribution ratio (D) vs. pH for constant 3NO_2BHA and Adogen 464 concentrations, over the pH range 0.8—1.8 gave a straight line with a slope of 2.0 (Fig. 2), showing that two moles of hydrogen ions are released for each mole of metal complexed.

The distribution ratio values have been obtained as following : a known amount of Fe(III) is extracted at different pH values. When the equilibrium is reached, the iron in aqueous phase is determined according to the procedure and the extracted iron by substraction.

The extracted species could present the two possible formulas : $[FeA_2(OH)_2][R_4N]$ and $[FeA_2Cl_2][R_4N]$ in which the reagent (HA) acts in keto form as bidentate. This agrees with the loss of two protons per mole of extracted complex.

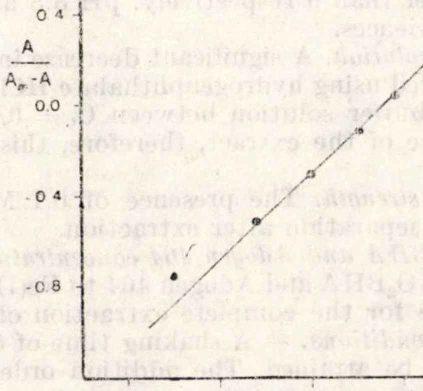

Fig. 1. — Equilibrium-shift method applied to the Fe(III)—$3NO_2BHA$—Adogen 464 system. $[Fe(III)] = 7.2 \times 10^{-5}$ M ; slope = 2 ; pH = 3.3 ; AcH/Ac^- buffer 0.19 M.

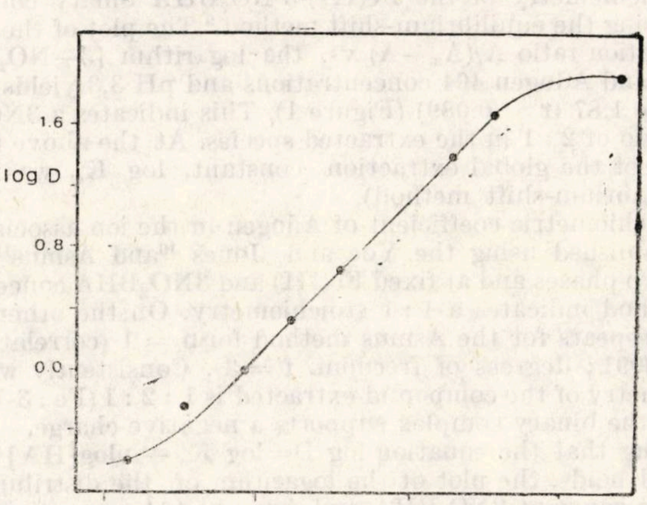

Fig. 2. — Variation of distribution coefficient of $3-NO_2BHA$ — Fe(III) complex between water and Adogen 464 — toluene with pH. $[3NO_2BHA] = 1.5 \times 10^{-5}$ M; $[Fe(III)] = 1.4 \times 10^{-4}$ M; $[Adogen] = 1.0 \times 10^{-2}$ M, wavelength 438 nm. $V_w/V_0 = 1$

However, the complex is extracted from solutions prepared in the same conditions but in the absence of Cl^- ion (NaCl is substitued by KNO_3 and the liquid anion exchanger is used in nitrate form, by shaking it successively with a saturated solution of $NaNO_3$ until the aqueous layer gave negative reaction for chloride). This suggests the first one as possible formula of the extracted species. Nevertheless its confirmation should be subject of later studies, because other methods applied for us (Yoe-Jones and Job[12]) suggest, however, a 4 :-1 $3NO_2BHA$: Fe(III) molar ratio.

The complex Fe(III)-3-NO_2BHA in aqueous solutions at pH 3.3. shows orange-red colour (480 nm) and we have observed, using the Yoe and Jones method a 2 :1 $3NO_2BHA$:-Fe(III) molar ratio. Similarly the complex Fe(III)-$3NO_2BHA$ has been extracted into isoamyl alcohol at pH 3.3 (450 nm) and Yoe and Jones method shows the 2 :-1 and 4 : 1 $3NO_2BHA$: Fe(III) molar ratios.

We also consider interesting the determination of the stoichiometry of the binary complex Fe(III)-5-nitrosalicylhydroxamic acid; a ligand in which steric effects could be, perhaps, remarkable in respect to the later 3-NO_2BHA.

The complex Fe(III)-$5NO_2SHA$ in aqueous solutions at pH 3.3 is orange-red (480 nm) and its stoichiometry established by the Yoe-Jones method is 2 : 1 ($5NO_2SHA$: Fe(III)). This complex extracted into Adogen 464-toluene from aqueous solutions at pH 3.3 possesses 2 : 1 ($5NO_2SHA$:Fe) stoichiometry established by Yoe-Jones, Harvey-Manning[13] and Job. The stoichiometric coefficient of Adogen 464 in the ion association complex was found to be (Adogen : complex) 1 : 1 (Yoe-Jones method).

From the above-obtained results we could think that the OH group of $5NO_2SHA$ does not introduce steric effect comparing to the $3NO_2BHA$. This complex could present the formula $[FeA_2(OH)_2][R_4N]$, the reagent acting as bidentate in keto form.

All these results agree with those given by other authors[14,15] for the same iron-hydroxamics acid complexes.

Extraction efficiency

Extraction efficiency was determined from the data of the influence of the pH on the distribution ratio. The extraction of Fe(III)-$3NO_2BHA$ complex begins at pH 0.5 (20% extracted) and it is achieved (99%) at pH 2.2.

Spectrophotometric characteristics

The volume ratio of the aqueous and organic phases can be varied between 1 : 1 and 5 : 1 without affecting the extraction efficiency and the absorbance being practically constant. The phase-volume ratio V_{aq}/V_{org} used in this work was 5 : 1.

Beer's law is obeyed over the range 0.2 and 2.4 $mg \cdot L^{-1}$ of iron in the aqueous phase with an optimal concentration range, evaluated by the Ringbom method[16] of 0.5—1.4 $mg \cdot L^{-1}$. The apparent molar absorptivity at 438 nm is 2.63×10^3 $L \cdot mol^{-1}cm^{-1}$. The Sandell index was 2.12×10^{-3} $\mu g \cdot cm^{-2}$.

The coefficient of variation obtained for eight replicate determinations of 1.6 mg $\cdot$ L^{-1} of iron was 1.4%. The IUPAC[17] detection limit was 11.6 μg $\cdot$ L^{-1} for a value of $K = 3$ and the determination limit ($K = 10$) 40.4 μg $\cdot$ L^{-1}.

Effect of foreign ions

The tolerance of the method to foreign ions was investigated using solutions containing 1.6 mg $\cdot$ L^{-1} of iron with various concentrations of foreign ions. The tolerance limit (Table 1) was taken as the concentration that did not cause an error greater than 5% in the recovery of Fe.

Table 1

Interference of foreign ions of the determination of 1,6 mg$\cdot$L^{-1} of Fe(III). [3NO$_2$BHA] = 3 $\cdot$ 10^{-4}M.

Ion tested	Tolerance (mg $\cdot$ L^{-1})
Cu(II)	400
Cl^-, Ac^-, BO_2^-, CO_3^{2-}, Ni(II), Al(III)	>100
NO_3^-	80
F^-	15
Bi(III), W(VI)	8
UO_2(II)	4
Ti(IV)	2
V(V), Mo(VI)	<1

Applications

The proposed method is applied to the determination of iron content in an aluminium bronze and two bauxites samples. The results given in table 2 are the mean value of five and seven determinations respectively. Accuracy and precision shown for the samples studied are satisfactory.

Table 2

Determination of iron in different samples

Certified sample	Fe %		t_{exp}	$t_{0.05}$
	Value	Found		
Aluminium bronze	0.21	0.208 ± 0.002	2.58	2.78 (n=4)
NBS 697 Bauxite (Dominican)	13.89	14.14 ± 0.21	1.88	2.45 (n=6)
NBS 69b Bauxite (Arkansas)	4.99	5.12 ± 0.13	2.36	2.45 (n=6)

Composition of the certified samples (%): Aluminium bronze = 91.34 Cu; 0.14 Pb; 8.19 Al; 0.09 Zn. Bauxite 697NBS 24.24 Al; 3.18 Si; 1.51 Ti; 0.048 Zr; 0.42 P; 0,035 V; 0,068 Cr; 0.32 Mn. Bauxite 69bNBS 24.82 Al; 6.27 Si; 1.139 Ti; 0.21 Zr; 0.051 P; 0.015 V; 0.0075 Cr; 0.085 Mn.

REFERENCES

[1] A. S. Bhaduri and N. H. Ghosh, *Z. Anorg. Chem.*, **303**, 117 (1960).

[2] Y. K. Agrawal, A. Mudaliar, A. L. Shashimohan, M. C. Chattopadhyaya and Rao Venkkatesh, *J. Indian Chem. Soc.* **53**, 617, (1976).

[3] F. Salinas and J. M. Estela, *An. Quim.*, **79**, B, 300 (1983).

[4] Fdez-Alba Rodriguez, A. PhD. Thesis. Univ. Granada. 1986.

[5] F. Capitán, D. Gázquez M. Sánchez and L. F. Capitán-Vallvey, *J. Anal. Atomic Spectrometry*, **1**, 457 (1986).

[6] M. A. Llompart, Licenciate Thesis. Univ. Palma de Mallorca, (1984).

[7] M^a. I. Pascual-Reguera, PhD. Thesis. Univ. Granada. 1987

[8] L. Shapiro and W. W. Brannock, "Rapid Analysis of Silicate Carbonate and Phosphate Rocks", U.S. Geological Survey Bulletin, 1–56 (1962).

[9] H. Diehl and F. Lidstrom, *Anal. Chem.*, **31**, 414 (1959).

[10] J. H. Yoe and A. L. Jones, *Ind. Eng. Chem. Anal. Ed.*, **16**, 111 (1944).

[11] H. Asmus, *Z. Anal. Chem.*, **178**, 104 (1960).

[12] P. Job, *An Chim.*, **9**, 114 (1927).

[13] A. E. Harvey and D. L. Manning, *J. Am. Chem. Soc.*, **72**, 4498 (1950).

[14] W. W. Brandt, *Record. Chem. Progress*, **21**, 159 (1960).

[15] A. K. Chakraburtty, Symposium of the Chemistry of Coordination Compounds. Agra (India). Part III, 235–248 (1959).

[16] A. Ringbom, *Z. Anal Chem.*, **115**, 332 (1938–9).

[17] *Spectrochim. Acta*, **33B**, 242 (1978).

Revue Roumaine de Chimie, 36, *1 3*, 85–90(1991)

SEPARATION BY EXTRACTION OF AMINO ACIDS WITH MACROCYCLIC LIGANDS

LUCIA MUTIHAC[a] and CONSTANTIN LUCA[b]

[a] Institute of Physical Chemistry, Roumanian Academy, Bucharest, Splaiul Independenţei, 202, 77 208, Bucharest, Roumania

[b] Polytechnical Institute Bucharest, Department of Analytical Chemistry

Received July 1, 1990

The possibility of separating amino acids from a mixture making use of macrocyclic ligands of crown ether type ([18]-crown-6) in a technique of simple extraction (acid aqueous phase — organic phase) or two step extraction (acid aqueous phase→organic phase ; organic phase→alkaline aqueous phase) was investigated. The two-step extraction was assisted by a pH gradient. The efficiency of extraction is ensured by the recycling of the macrocyclic ligand. The results obtained in model mixtures of amino acids were successfully aplied to mixtures of amino acids resulted from the acid hydrolysis of the proteins originating in Albumina Bovis and milk casein.

INTRODUCTION

The new class of chemical compounds — the macrocyclic ligands[1–10] which are able to specifically recognize through controlled interactions according to size, shape and structure various cations and then by their means, various anions — has allowed the study of amino acids whose amphion type molecule may appear either as cation in acid medium or as anion in basic medium.

The possibility of coupling two or more chemical species, according to a natural model by means of certain physico-chemical affinities without formation of covalent bonds is referred to as "recognition".[12]

In a previous contribution[13] the extraction constants of a series of amino acids with 1,4,7,10,13,16-hexaoxacyclooctadecane in water-1,2 dichloroethane by VIS absorption spectroscopy was reported.

The results of this study have suggested the possibility of classifying the amino acids as extractible and non-extractible from an acid aqueous phase into an organic phase under certain extraction conditions.

In the literature the solvent extraction of complexes with macrocyclic ligands was mentioned first by Pedersen[14] and Frensdorff[15]. M. Yoshio's and H. Noguchi's investigations on solvent extraction of some organic amines with macrocyclic ligands are worth mentioning.

This is a continuation of the study on separation of amino acids through a separation extraction technique.

EXPERIMENTAL

1. Equipment and reagents

pH determinations were carried out by digital MV-870 Pracitronic pH-meter with glass electrode and saturated calomel electrode, calibrated against standard potassium diphthalate (pH = 4.01) and solutions borax (pH = 9.18).

The amino acid concentrations in the two aqueous phases were determined by "Carlo Erba 3A28M" amino acid analyzer.

The macrocyclic ether [18]-crown-6 (Fluka) was of higher purity than 98%. All reagents were analytical grade.

The chromatographic determinations were carried out with a Carlo Erba — 6000 gas chromatograph equipped with capillary glass column (l = 40 m) and SE 30 stationary phase; the column temperature was 300°C, carrier gas hydrogen at a 315 ml/min flow rate, diffusion rate 1 : 20; the solvent 1,2 dichloroethane was distilled prior to utilization.

The volume of aqueous phases was 10 cm^3 while that of the organic phase 10 cm^3.

The aqueous phases were mechanically stirred to facilitate the operation. The experiments were carried out in a glass reactor and a group of two reactors of separation type.

2. Procedure

The following sequence of operation is suggested:

— extraction of protonated amino acids from aqueous phase I at acid pH (pH = 2) in an organic phase immiscible with the aqueous phase which contains the macrocyclic ligand, [18]-crown-6, (phase II) employing as pair anion the picrate anion introduced with the amino acids in aqueous phase (simple extraction);

— re-extraction of the amino acid and picrate anion from organic phase II in an alkaline aqueous phase, phase III, by decomposing the complex so that in phase III the amino acid appears as an anion ($-COO^-$) soluble in water while the macrocyclic ligand is free in the organic phase (two step extraction).

RESULTS AND DISCUSSION

The extraction of the amino acid from acid aqueous solution into an alkaline aqueous solution with [18]-crown-6 solution in 1,2 dichloroethane as intermediate has aimed at:

— reaching good extraction efficiency in two steps with the following sequence of operations: phase I → phase II; phase II → phase III.

— ensuring a handy and efficient procedure.

The results of this experiment are shown in table 1.

One can note that the extractible amino acids may be separated in an extraction cycle whose yield is highest in simple extraction (phase I→→phase II) ranging within 81—88%, depending on the amino-acid, and in two steps extraction (phase I→phase II; phase II→phase III).

L-cysteine is extracted at an efficiency of 50%. Mechanical stirring facilitates the separation.

Thus simple extraction results in a concentrate of non-extractible amino acids in the acid aqueous phase and a concentrate of extractible amino-acids in the organic phase; after processing by evaporation of the solvent, one can isolate the mixture of extractible amino-acids.

The concentration of amino-acids was determined chromatographically with an automatic amino-acids analyser.

Table 1

The efficiency of amino acid extraction

Amino acid	Initial concentration $M \cdot 10^{-4}$ (pH=2)	Concentration in phase II (simple extraction)		Concentration in phase(III two step extraction)	
		With stirring 1/2 h			
		$M \cdot 10^{-4}$	%	$M \cdot 10^{-4}$	%
L-Methionine	1.6	1.39	86.88	1.36	84.76
L-Isoleucine	1.6	1.39	86.88	1.30	81.25
L-Leucine	1.6	1.41	88.13	1.29	80.63
L-Phenylalanine	1.6	1.37	85.63	1.29	80.63
L-Valine	1.6	1.35	84.38	1.26	78.75
L-α-Alanine	1.6	1.30	81.25	1.20	75.00
L-Cysteine	1.6	0.88	55.00	0.80	50.00

The re-extraction of the amino acids and picrate from organic phase (1,2 dichloroethane) by decomposition of protonated amino acid-[18]-crown-6-picrate is carried out in alkaline aqueous phase.

In a previous study[18] it was shown that the optimum pH of aqueous phase III which affords the separation of the amino acids with high yield in this phase is 13 (achieved with LiOH because Li^+ ion of small diameter does not form a stable complex with the macrocyclic ligand [18]-crown-6[19]).

Recycling the macrocyclic ligand [18]-crown-6

The efficiency of extraction processes is partly determined by the possibility of recycling the organic phase II which contains the macrocyclic ligand in the two step extraction. This allows utilization of the organic phase in several extraction. There are two possibilities :

a) to change aqueous phases I and III for each extraction cycle;

b) to change only aqueous phase I which entails concentration of extractible compounds in aqueous phase III.

Case a. Four extraction cycles of extractible amino acids from a mixture were effected. The organic phase (1,2 dichloroethane) containing the macrocyclic ligand[18]-crown-6 extracts the (extractible) amino acid from acid aqueous phase I and passes it into organic phase as ion pairs. Then the organic phase is extracted with an alkali aqueous phase (pH = 13). The results are listed in table 2.

One can note losses of macrocyclic ligand [18]-crown-6 in case aqueous phases I and III were changed for each extraction cycle. Following 4 extraction cycles the amino acid extraction yield ranged within 26–41%, depending on the amino acid.

Case b. The experiment was carried out for 4 cycles in which the organic and aqueous alkaline phases were unchanged. The results are listed in table 3.

Smaller losses of macrocyclic ligand were noted. Besides separation of extractible and non extractible amino acids, there was a 2.5–2.7 times larger concentration of extractible amino acids in phase III.

Table 2

Concentration of extractible amino acids in the 4 extraction cycles with change of phases I and III for each extraction cycle

Amino acid	Initial concentration	No. of extraction cycles							
		1		2		3		4	
		$M \cdot 10^{-4}$	%	$M \cdot 10^{-4}$	%	$M \cdot 10^{-5}$	%	$M \cdot 10^{-5}$	%
L-Methionine	1.6	1.34	83.75	1.22	76.25	9.30	58.12	6.60	41.25
L-Isoleucine	1.6	1.34	83.75	1.22	76.25	8.90	55.63	6.10	38.13
L-Leucine	1.6	1.30	81.25	1.07	66.88	8.00	50.00	5.60	35.00
L-Phenylalanine	1.6	1.30	81.25	1.04	65.00	7.80	48.75	5.30	33.13
L-Valine	1.6	1.31	81.87	0.98	61.25	7.40	46.25	4.80	30.00
L-α-Alanine	1.6	1.19	74.38	0.93	58.13	6.70	41.88	4.10	25.63
L-Cysteine	1.6	1.77	48.12	0.45	28.12	2.50	15.62	—	—

$c_{[18]\text{-crown-6}} = 1 \cdot 10^{-2}$M

Table 3

The concentrations of extractible amino acids in the four extraction cycles; phase I was changed at each extraction cycle

Amino acid	Initial concentration $M \cdot 10^{-4}$	Concentration of amino acids in phase III $M \cdot 10^{-4}$			
		No. of extraction cycles			
		1	2	3	4
L-Methionine	1.6	1.36	2.16	3.04	3.84
L-Isoleucine	1.6	1.30	2.22	3.11	3.98
L-Leucine	1.6	1.29	2.25	3.14	3.99
L-Phenylalanine	1.6	1.29	2.19	3.15	3.95
L-Valine	1.6	1.26	2.17	3.03	3.75
L-α-Alanine	1.6	1.20	2.17	3.04	3.74
L-Cysteine	1.6	0.81	1.60	2.04	2.90

$c_{[18]\text{-crown-6}} = 1 \cdot 10^{-2}$M

In order that the loss of macrocyclic ligand that acted as complexing agent did not affect the extraction process, higher concentrations of complexing agent were employed which were established as a function of its partition coefficient[18] in water – solvent system.

The experimental results of a study on extraction of a series of amino acids from a mixture by the macrocyclic ligand [18]-crown-6 were applied to samples of acid hydrolysates originating in proteins from milk casein (Table 4) and Albumina Bovis (Table 5).

According to tables 4 and 5, the extraction yields i.e. 43–74% (depending on the amino acid) for casein and 51–72% for albumin are fairly high. Amino acid as aspartic acid (4.20% for casein and 5.25% for albumin) and lysine (15.58% for casein and 6.75% for albumin) were not extracted in the conditions mentioned from model mixtures.

The proteic hydrolysates as lysine and aspartic acid were extracted in this experiment with very low yield probably owing to a synergetic effect.

Table 4

Experimental results obtained in separation by two step extraction of the amino acid from the proteic hydrolysate of casein

Amino Acid	Initial amount µg/10 ml	Casein (1/2 h stirring)			
		Phase I(10 ml)[a]		Phase III (10 ml)[b]	
		µg	%	µg	%
Isoleucine	183.50	44.99	24.52	134.51	73.30
Leucine	225.50	63.25	28.05	158.28	70.19
Phenylalanine	132.30	48.85	36.92	79.49	60.08
Valine	180.00	100.24	55.68	77.76	43.20
Methionine	107.00	40.50	37.85	61.20	57.20
Alanine	107.05	56.23	52.53	45.82	42.82
Cysteine	28.00	11.20	40.00	15.40	55.00
Lysine	263.00	241.33	91.76	14.67	5.58
Histidine	84.00	84.38	100.45	—	—
Arginine	125.00	121.50	97.20	—	—
Aspartic acid	234.00	230.05	94.67	10.21	4.20
Treonine	140.00	144.86	103.47	—	—
Serine	180.00	179.72	99.84	—	—
Glutamic acid	643.00	617.60	96.05	—	—
Proline	233.00	221.34	94.99	—	—
Glycine	82.00	78.76	96.05	—	—
Tirosine	233.00	227.18	97.50	—	—

[a] Phase : I : amino acid ; [picric acid] = 1.6×10^{-3}M HCl 0.05 N (pH=2)
[b] Phase III : LiOH 0.1 N (pH=13)
Phase II : [[18]−crown−6] = 10^{-2} M/1,2 dichloroethane
Phase ratio 10 : 10 : 10 (v/v).

Table 5

Experimental results obtained in separation by two step extraction of the amino acids from the proteic hydrolisate of Albumina Bovis

Amino Acid	Initial amount µg (10 ml)	Albumina Bovis (1/2 h stirring)			
		Phase µg/10 ml)[a]		Phase III (10 ml)[b]	
		µg	%	µg	%
Isoleucine	87.25	20.01	22.93	62.21	71.34
Leucine	270.00	74.50	27.59	186.30	69.00
Phenylalanine	169.00	57.40	33.96	103.51	61.25
Valine	162.30	69.50	42.82	82.82	51.03
Alanine	202.00	85.50	43.33	111.91	55.40
Methionine	201.00	100.5	50.00	109.24	54.33
Cysteine	365.00	164.56	45.08	185.05	50.70
Lysine	358.00	330.84	92.41	24.16	6.75
Aspartic acid	250.00	233.50	93.40	13.12	5.25
Glycine	52.00	44.20	92.69	—	—
Histidine	114.00	109.52	96.07	—	—
Arginine	186.00	183.94	98.89	—	—
Treonine	183.00	172.38	94.19	—	—
Serine	133.00	127.02	95.50	—	—
Glutamic acid	469.00	462.90	98.70	—	—
Proline	133.00	128.60	96.69	—	—
Tirosine	172.00	169.25	98.40	—	—

[a] Phase I : amino acid ; [picric acid] = 1.6×10^{-3}M HCl 0.05N (pH = 2)
[b] Phase III : LiOH 0.1 N(pH=13)
Phase II : [[18]−crown−6] = 10^{-2}M/1,2 dichloroethane
Phase ratio 10 : 10 : 10 (v/v).

CONCLUSIONS

The experiments of amino acid extraction with macrocyclic ligands have confirmed the possibility of simple extraction and two step extraction. The two step extraction is assisted by pH gradient ; the higher this gradient the better the amino acid extraction by the macrocyclic ligand in the organic phase. The possibility of recycling the macrocyclic ligand raises the efficiency of the extraction process.

In simple extraction as well as in two step extraction the results have suggested the conclusion that the amino acids may be classified as extractible and non extractible according to the structural, characteristics imposed by the nature of the radical R which may be more hydrophobic or hydrophylic, respectively.[19]

The results were applied to model mixture of amino acids originating in proteic hydrolysates of Bovis Albumina and Casein. In this case the amino acids were separated by extraction with solvents, use has been made of the macrocyclic ligand and high extraction yields were obtained.

The results allow the concentration of certain amino acids whose analytical and preparative usefulness is obvious in synthesis of polypeptides, supramolecular chemistry, in medicine and biology.

REFERENCES

[1] C. J. Pedersen, *J. Inclusion Phenom.*, **6**(4), 337 (1988).

[2] C. J. Pedersen, *J. Am. Chem. Soc.*, **89**, 7017 (1967).

[3] D. J. Cram, *J. Inclusion Phenom.*, **6**(4), 397 (1988).

[4] T. J. Petsenko, S. N. Gaidarmaka and Yr. A. Serguchev, *Teor. Eksp. Khim.*, **24**(2), 191 (1988).

[5] T. Kakuchi, T. Takaoka and K. Iokota, *Makromol. Chem.*, **190**, 10 (1989).

[6] M. Ouchi, J. Inouc and K. Wada, *J. Org. Chem.*, **52**, 2420 (1987).

[7] F. Vogtle and E. Weber, "Host Guest Complex Chemistry Macrocycles ; Synthesis, Structures, Applications", Springer Verlag, Heidelberg, New York, Tokyo, 1985.

[8] C. J. Pedersen and H. K. Frensdorff, *Angew. Chem.*, **84**, 16(1972) ; *Angew. Chem. Int. Ed Engl.*, **11**, 16 (1972).

[9] E. Weber and F. Vogtle, *Inorg. Chim. Acta*, **45**, 165–167 (1980).

[10] F. Vogtle and P. Newmann, *Tetrahedron*, **26**, 5847 (1970).

[11] B. Dietrich, J. M. Lehn and J. P. Sauvage, *J. Chem. Soc. Chem. Commun.*, 1055 (1970).

[12] G. van Birst, "Design and Synthesis of Organic Molecules Based on Molecular Recognition" Springer Verlag-Berlin, Heidelberg, New York, (1986).

[13] C. Luca, L. Mutihac and T. Constantinescu, *Rev. Chim. (București)*, **39**, 12 (1988).

[14] C. J. Pedersen, *Fed. Proc. Fed. Am. Soc. Exp. Biol.*, **27**, 1305 (1968).

[15] H. K. Frensdorff, *J. Am. Chem. Soc.*, **93**, 4684 (1981).

[16] M. Yoshio, H. Nakamura and H. Noguchi, *Anal. Lett. Part A*, **13**(16), 1431 (1980).

[17] H. Noguchi, H. Nakamura and M. Yoshio, *Bull. Chem. Soc. Jpn*, **55**, 152 (1982).

[18] L. Mutihac, C. Luca, T. Constantinescu, M. Oprea and M. Radu, in press.

[19] C. Luca, L. Mutihac and T. Constantinescu, *Rev. Roumaine Chim.*, **35**, 467 (1990).

Revue Roumaine de Chimie, **36**, *1—3*, 91—99(1991)

THE INFLUENCE OF OPERATIONAL PARAMETERS UPON THE EXTRACTION OF AMINO ACIDS WITH MACROCYCLIC LIGANDS

LUCIA MUTIHAC[a], CONSTANTIN LUCA[b], TITUS CONSTANTINESCU[a], MARIETA OPREA[c] and MIHAI RADU[c]

[a] Institute of Physical Chemistry, Romanian Academy, Bucharest, Splaiul Independenţei 202, Bucharest, 77 208 Romania

[b] Department of Analytical Chemistry, Polytechnic Institute of Bucharest, 77 208 Bucharest, Romania

[c] Institute of Chemistry Research Bucharest, Splaiul Independenţei, 202, Bucharest, Romania

Received June 4, 1990

Partition processes occurring in two phases water-organic solvent (in solvent extraction of the complexes of amino acids with macrocyclic ligands of crown polyether type) in the system water (pH = 2) — organic solvent — water (pH = 13) and liquid membrane system were studied. The partition ratios of the amino acid in two phase system of macrocyclic ligand [18] — crown — 6 in two phase system (in case of extraction) and in case of liquid membrane were determined and the influence of pH upon these ratios was investigated. The results have afforded separation of groups of amino acids from a mixture by extraction and separation through liquid membrane making use of macrocyclic ligands [18]—crown-6.

The ability of macrocyclic ligands of complexing cationic species[1–10] has suggested a study[11] on complexing amino acids (DL-tryptophane, L-leucine, L-phenylalanine, L-methionine, L-valine, L-isoleucine, L-α-alanine and L-cystine) protonated at aminic group with [18]-crown-6 and various pair anions as complexing agents. Thus, the cationic complexes were extracted in 1,2 dichloroethane.

The results of this study, especially the values of extraction constants[11] offered the possibility of separating groups of amino acids by extraction and separation through liquid membranes [12–13]. This process has required a systematic study of partition processes occurring in a two phase system in various working conditions; this contribution presents the results of this study: the partition of the macrocyclic ligand between the phases of two phase systems, the partition ratio of the amino acid in the two phase system, the role of the compounds that may operate as pair anions and the influence of pH on partition.

EXPERIMENTAL

The chromatographic determinations were performed with a Carlo Erba 6000 apparatus; the concentrations of amino acids in the two phases were determined with a Carlo Erba 3A28M amino acid analyzer while pH was measured with a MV 870 Pracitronic digital pH-meter equipped with glass electrode and saturated calomel electrode calibrated against standard potassium disulphate (pH = 4.01) and borax (pH = 9.18) solutions.

The amino acids (Fluka) and the other reagents were analytical grade.

The macrocyclic ligand [18]-crown-6 was a 98% pure Merck-Schuchardt reagent.

The solvent 1,2 dichloroethane was distilled before use. The volumes of aqueous phases was 10 cm³ and of organic phase dichloroethane 10 cm³ as well.

RESULTS AND DISCUSSION

1. The amino acid partition ratio in water — organic solvent system

The influence of the composition and structure of amino acids upon the partition between phases has been studied. It is well known that α-amino acids $(\mathrm{R-\underset{\diagdown COOH^{2}}{CH}-NH_2})$ have the structure of amphions with one basic (-NH$_2$) and one acid (-COOH) group; the properties of these compounds are equally influenced by the whole structure of the molecule (R). The exponent of acidity is about 2 for (-COOH) group and about 10 for (-NH$_2$) group so that at certain pH both groups may be ionized, the amino acid appearing as an amphion $(\mathrm{R-\underset{\underset{COO^-}{|}}{CH}-NH_3^+})$.[14]

Whenever the aminic group ($-NH_3^+$) is protonated the partition ratio (D) of the amino acid between the two phases "s" and "w"of the system is defined as an experimental quantity as follows:

$$D = \frac{[\mathrm{R'NH_3LA}]_s}{[\mathrm{R'NH_2}]_w + [\mathrm{R'NH_3^+}]_w} \tag{1}$$

where:

R′ = R—CH—COOH
A = anion pair
L = macrocyclic ligand
The acidity constant K_{a2} of the couple $\mathrm{R'NH_3^+/R'NH_2}$:

$$K_{a2} = \frac{[\mathrm{R'-NH_2}][\mathrm{H_3O^+}]}{[\mathrm{R'-NH_3^+}]} \tag{2}$$

shows that for a pK_{a2} — 3 of aqueous phase 99.9% of the aminic group transforms into $-NH_3^+$ which suggests the conclusion that under such conditions:

$$D = \frac{[\mathrm{R'NH_3LA}]_s}{[\mathrm{R'NH_3^+}]_w} \tag{3}$$

In α-amino acids the acidity constant of $\mathrm{R'NH_3^+/R'NH_2}$ couple is $\approx 10^{-9.7}$ which shows that the $\mathrm{R'NH_3^+}$ cation is formed in a proportion of 99.9% at a pH ≈ 6. At a pH ≈ 6 the —COOH group of α - amino acids is practically dissociated because the value of the acidity constant (K_{a1}) of the —COOH/—COO⁻ couple is about $10^{-2.3}$.

The amphionic form $\mathrm{R-\underset{\underset{NH_3^+}{|}}{CH}-COO^-}$ is not extractible because of the two charges it carries and therefore the macrocyclic ligand [18]-crown-6 cannot ensure solubilization of this species in 1,2 dichloroethane through complexation of (NH_3^+) cation.

Lowering the pH value entails transformation of $(-COO^-)$ into $-COOH$ which makes the extraction possible. Therefore the extraction pH has to be so adjusted as to reach zero negative charge through formation of COOH.

Figure 1 shows the ranges of predetermined species derived from an amino acid as a function of pH ; the values were calculated by the Henderson equation.

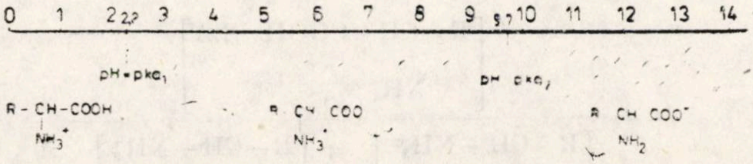

Fig. 1. — The ranges of predetermined species derived from an amino acid versus pH.

Likewise, Fig. 2 shows the fractions of formation of amino acids (in case of L-leucine) versus the pH ; they allow the calculation of the percent content of each of the three species in equilibrium as a function of pH.

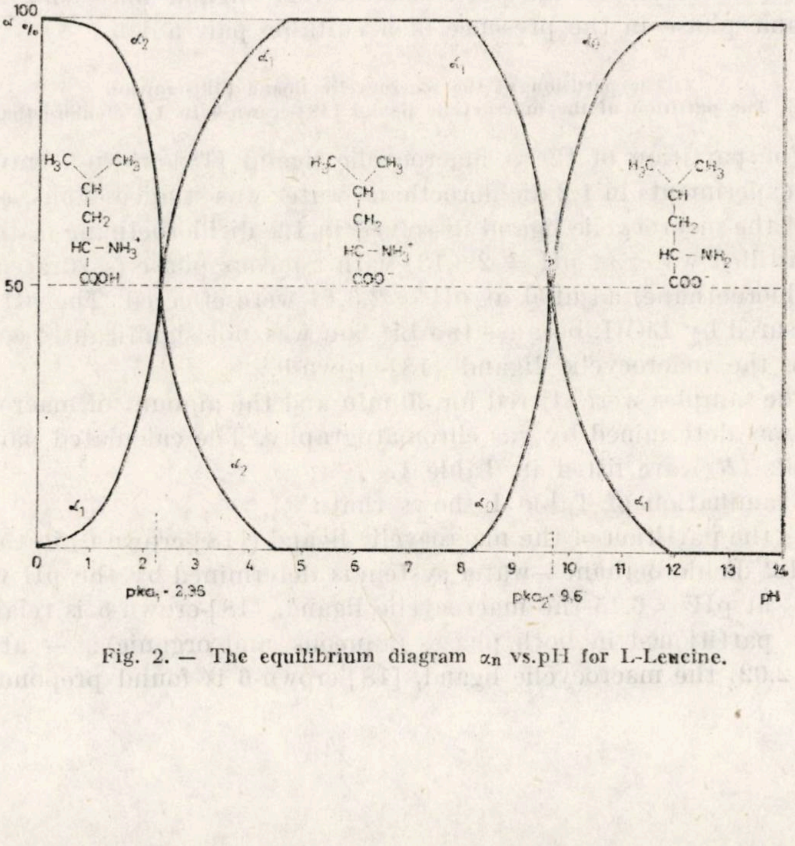

Fig. 2. — The equilibrium diagram α_n vs.pH for L-Leucine.

The $\alpha_n(\alpha_2, \alpha_1, \alpha_0)$ functions were calculated by the equations:

$$\alpha_2 = (1 + 10^{pH-pK}a1 + 10^{2pH-pK}a1^{-pK}a2)^{-1} \cdot 100$$

$$\alpha_1 = (1 + 10^{pK}a1^{-pH} + 10^{pH-pK}a2)^{-1} \cdot 100$$

$$\alpha_0 = (1 + 10^{pK}a2^{-pH} + 10^{pKa_1 + pK}a2 - 2pH)^{-1} \cdot 100$$

It results that the value of the partition ratio depends on pH at dH $\approx pK_{a1} \approx 2$ so that within this pH eqn. (1) becomes:

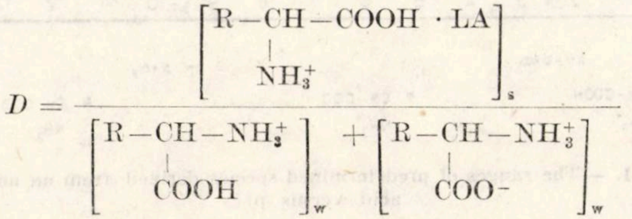

$$D = \frac{\left[\begin{array}{c}\text{R}-\text{CH}-\text{COOH}\cdot\text{LA}\\ |\\ \text{NH}_3^+\end{array}\right]_s}{\left[\begin{array}{c}\text{R}-\text{CH}-\text{NH}_3^+\\ |\\ \text{COOH}\end{array}\right]_w + \left[\begin{array}{c}\text{R}-\text{CH}-\text{NH}_3^+\\ |\\ \text{COO}^-\end{array}\right]_w} \qquad (4)$$

The partition ratio (D) is experimentally accessible because one can determine the concentration in organic phase of the extracted species $R'NH_3LA$.

In conclusion at pH $\approx$ 2 the amino acid is protonated in amine form ($-NH_3^+$), therefore an adequate macrocyclic ligand may solubilize it n organic phase in the presence of a suitable pair anion.

2. The partition of the macrocyclic ligand [18]-crown-6

2.1. The partition of the macrocyclic ligand [18]-crown-6 in 1,2 dichloroethane

The partition of the a macrocyclic ligand [18]-crown-6 employed in our experiments in 1,2 dichloroethane-water was studied. Thus, extractions of the macrocyclic ligand dissolved in 1,2 dichloroethane (saturated with distilled water at pH = 2,6,13) with aqueous phase (saturated with 1,2 dichloroethane) adjuted at pH = 2,6,13 were effected. The pH = 13 was ensured by LiOH, because the Li^+ ion was not significantly complexed by the macrocyclic ligand [18]-crown-6.[15]

The samples were stirred for 30 min and the amount of macrocyclic ligand was determined by gas chromatography. The calculated partition constants (R_L) are listed in Table 1.

Examination of Table 1 shows that:

— the partition of the macrocyclic ligand ([18]-crown-6) in the two phase 1,2 dichloroethane—water system is determined by the pH value;

— at pH = 6.45 the macrocyclic ligand, [18]-crown-6 is relatively equally partitioned in both phases (aqueous and organic); — at acid (pH = 2.02) the macrocyclic ligand, [18]-crown-6 is found preponderantly in water (probably owing to the formation of protonated chemical species "oxonium salt" which are well known in ether type compounds).

— at pH ⩾ 7 the macrocyclic ligand lies preferentially in the organic phase.

Table 1

The partition constant of the macrocyclic ligand ([18]—crown—6) in 1.2 dichloroethane-water system as a function of the pH of aqueous phase

pH	[18]—crown—6 Initial (g/100 ml)	[18]—crown—6 in organic phase (g/100ml)	R_L
2.02	0.0529	0.0228	0.760
6.45	0.0529	0.0269	1.035
13.05	0.0529	0.0289	1.204

2.2. The partition of the macrocyclic ligand [18]-crown-6 in membrane,water-solvent-water system

A system was studied consisting of the following components:

(a) acid aqueous phase (pH = 2) was the source phase in case of membrane system which was one of the subjects of study;

(b) organic phase which was the membrane as such was a carrier solution ([18]-crown-6, 10^{-2}M);

(c) acceptor phase consisted of a LiOH 0.1N solution (pH = 13.05).

The experiment was carried out in a tubular concentric[13] device. The phases were stirred at 180 turns/min. After 6 hour stirring 78.41% (determined by gas chromatography) of the initial amount of [18]-crown-6 was found in the organic phase.

In conclusion, in conditions of liquid membrane system, the loss of ligand in acid aqueous and alkaline phases is very low.

2.3. Selection of ion pair forming anion

The anion, the coupling partner in the forming of the ion pair with the amino acid macrocyclic ligand [18]-crown-6, plays an important part in the partition of the macrocyclic ligand in the two phases.

The selection of the organic anion was based on the following criteria: high molar absorption coefficient which affords spectral measurements (Table 2), its lipophilic character and the pH domain over which this anion and the cation of protonated amino acid coexist.

In conditions of the system mentioned at point 2.2, picric acid was added to the source phase (pH = 2.02). This experiment has evidenced the influence of picrate anion in three phase system (employed in membrane studies) with respect to the partition of the carrier between two phases of the system. In this case the amount of macrocyclic ligand found in the organic phase after a 6 hour stirring was 95.75% of the initial amount, i.e. 17% more than in the absence of the picrate anion

(Table 1). Under these circumstances the membrane operation is optimum with low loss of carrier which justifies utilization of picrate anion as forming anion of the ion pair with the complex cation of the amino acids ($R'NH_3^+L$).

Table 2

Molar absorption coefficients of the complexes of α-amino acids with [18] — crown — 6

AMINO ACID*	Molar absorption coefficients (ε) l mol⁻¹ .cm⁻¹	
	Diphenyl-aminoazo-benzene-p-sulphonic Acid** λ=418 nm	Picric Acid** λ=378 nm
DL-Tryptophane	27 .500	18 .030
L-Leucine	25 .450	17 .645
L-Phenylalanine	28 .000	16 .535
L-Methionine	31 .000	16 .750
L-Valine	23 .300	16 .000
L-Isoleucine	23 .300	17 .787
Glycine	22 .500	—
L-α-Alanine	—	15 .000
L-Cysteine	—	15 .200

$c_{[18]-crown-6} = 1\times10^{-2}M$; $c^* = 1\times10^{-2}M$; $c^{**} = 5\times10^{-5}M$

The picrate anion has fulfilled the conditions for its selection ; they up to the favourable partition data. The anion of diphenyl-amino-azobenzene-p-sulphonic acid which fulfills similar conditions was also employed for the same purpose.[11]

3. The influence of aqueous phase pH on extraction

3.1. The influence of aqueous phase pH on the extraction of amino acid complexes with [18]-crown-6 in the presence of the pair anion

The study of pH dependence of amino acid complexes extraction from an aqueous solution with [18]-crown-6 in 1,2 dichloroethane in the presence of picric acid has confirmed that the optimum extraction is achieved at pH = 2, where the protonated amino acid, the anionic form of coupling partner and the undissociated carboxylic group of the amino acid coexist. Figure 3 shows the influence of pH on the extraction of amino acid complexes with [18]-crown-6 as well as picrate and diphenyl-aminoazobenzene-p-sulphonic as associated anions.

Similar results were obtained in case diphenyl-aminoazobenzene-p-sulphonic acid was employed as pair anion.

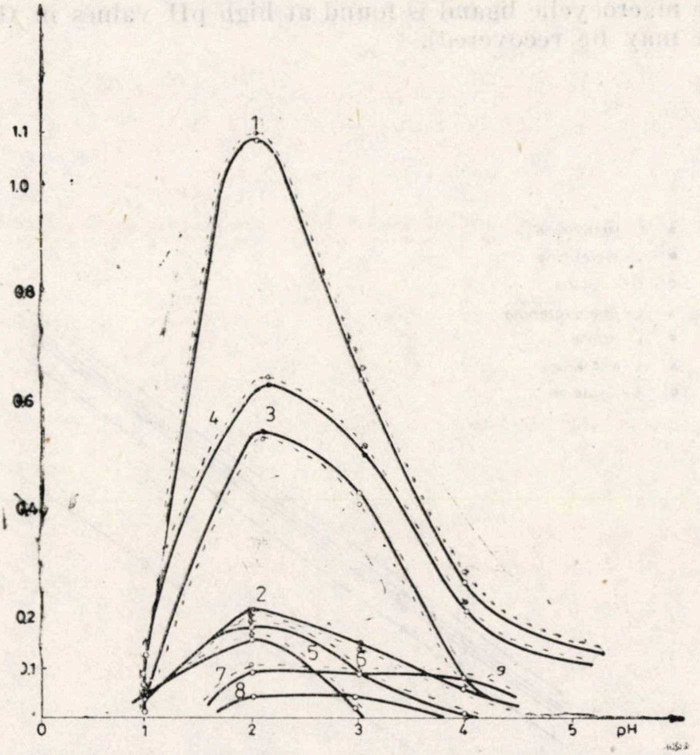

Fig. 3. — The dependence of extraction on the pH of aqueous phase (1) DL-tryptophan-[18]-crown-6-A ; (2) L-Leucine-[18]-crown-6-A ; (3)L-Phenylalanine-[18]-crown-6-A ; (4) L-Methionine-[18]-crown-6-A ;(5)L-Valine-[18]-crown-6-A ; (6) L-Isoleucine-[18]-crown-6-A; (7) L-α-Alanine-[18]-crown-6-A ; (8) L-Cysteine-[18]-crown-6-A ; (9) Glycine-[18]-crown-6A ; A = pair anion ; — picric acid ; — — — diphenylamino-azobenzene-p-sulphonic acid ; $c_{[18]-crown-6} = 1 \times 10^{-2}M$; $c_A = 8 \times 10^{-5}M$; $c_{amino\ acid} = 3 \times 10^{-4}M$.

3.2. The influence of aqueous phase pH on the extraction of amino acid from the complex protonated amino acid-[18]-crown-6-pair anion

The extraction of the amino acid and picrate from organic phase (1,2 dichloroethane) by breaking the protonated amino acid-[18]-crown-6-picrate ion pair is carried ont in an alkaline aqueous phase.

To determine the optimum pH, the extraction with aqueous phases was carried out at pH = 6 ; 11 and 13. The phases were stirred for 1/2 h. The extraction yields of the amino acids in aqueous phase are plotted versus the pH in Figure 4.

Examination of Fig. 4 shows that the yield is proportional to the pH of aqueous phase. The amino acid -[18]-crown-6-picrate ion pair which is present in the organic phase is relatively stable, breaking only at high pH values when the amino acid anion and picrate anion species are formed which are soluble in water. These species are also found in aqueous alkaline phase (the macrocyclic ligand is found at high pH values in the organic phase and may be recovered).

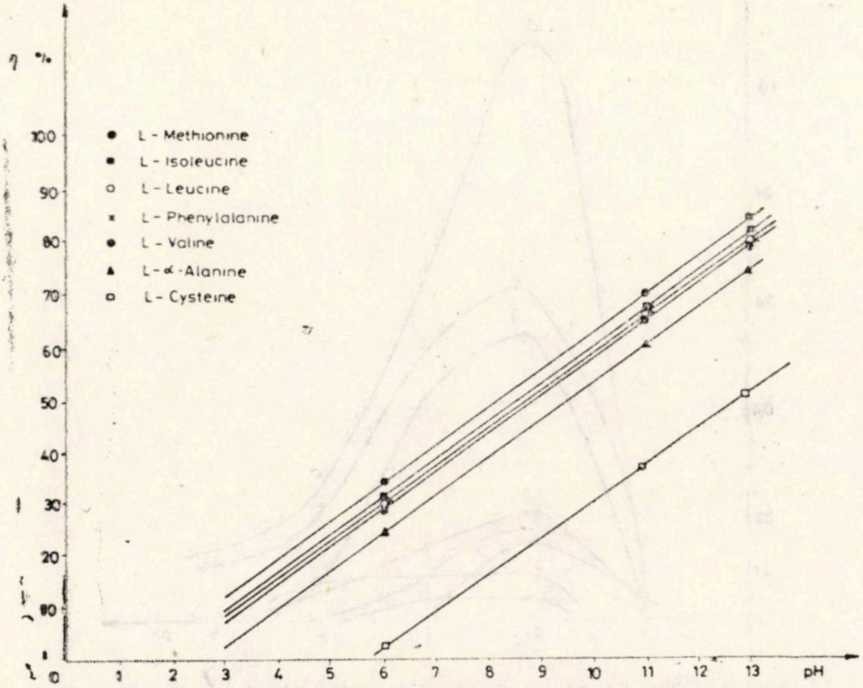

Fig. 4. — The amino acid extraction yield versus pH in aqueous phase.

The inverse transport of amino acids as anion in the presence of the picrate and macrocyclic ligand from alkaline aqueous phase to acid aqueous phase does not occur because LiOH was present to ensure the alkaline pH.

Thus, the optimum pH of alkaline phase is 13 because it ensures high yields of recovery of the amino acid from this phase.

CONCLUSIONS

This systematic study has shown that the parameter which undoubtedly influences the partition between the aqueous and organic phases in case of the complexes of amino acids with macrocyclic ligand and the pair anion is the pH. The extraction is optimum at pH equal to 2 which ensures the coexistence of the protonated amino acid, the coupling partner as aminic group and the undissociated carboxylic group of the amino acid.

The extraction of amino acids and associated anions from organic phase into aqueous phase by decomposition of protonated amino acid-[18]-crown-6 ion pair is optimum at pH = 13 ensured by LiOH; at this value there is no reverse transfer of amino acid into the organic phase (in anionic form) and the macrocyclic ligand is recovered from the organic phase.

All these findings have underlined the development of a procedure for separation of α-amino acids from a mixture consisting of a macrocyclic ligand of crown polyether type; use is made of separation by extraction and separation through liquid membranes.

REFERENCES

[1] H. K. Frensdorff, *J. Am. Chem. Soc.*, **93**, 4684 (1971).

[2] L. Sommer, "Analytical Absorption Spectrophotometry in the Visible and Ultraviolet", Akademiai Kiado, Budapest, 1989.

[3] E. Blasius and K. P. Ianssen, *Top Current Chem.*, **98**, 163 (1981).

[4] I. V. Piatnicki and A. Yu. Nazarenko, *Zh. Neorg. Khim.*, **25**, 1064 (1980).

[5] E. Pungor, "Ion Selective Electrodes" 5, Pergamon Press. Akademiai Kiado, 9—13 October, 1988, Hungary.

[6] H. Noguchi, H. Nakamura and M. Yoshio, *Bull. Chem. Soc. Jpn.*, **55**, 152 (1982).

[7] A. Yu. Nazarenko and Z. Z. Nizhnik, *Zh. Anal. Chim.*, **39**, 1308 (1984).

[8] J. D. Lamb, J. J. Christensen and S. R. Izatt, *J. Am. Chem. Soc.*, **102**, 3399 (1980).

[9] Ş. R. Izatt, R. T. Hawkins, J. J. Christensen and R. M. Izatt, *J. Am. Chem. Soc.*, **107**, 63 (1985).

[10] K. Maruyama, H. Tsukube and T. Araki, *J. Am. Chem. Soc.*, **104**, 5197 (1982).

[11] C. Luca, L. Mutihac and T. Constantinescu, *Rev. Chim. (Bucureşti)*, **39**, 12 (1988).

[12] C. Luca, L. Mutihac, T. Constantinescu and A. Csuma, *Rev. Roumaine Chim.*, **34**, 11—12 (1989).

[13] C. Luca, L. Mutihac and T. Constantinescu, *Rev. Roumaine Chim.*, **35**, 467 (1990).

[14] D. D. Perrin, "Dissociation Constants of Organic Bases in Aqueous Solutions", IUPAC, London, 1965.

[15] C. J. Pedersen, *Fed. Proc. Fed. Am. Soc. Exp. Biol.*, **27**, 1305 (1968).

Revue Roumaine de Chimie, 36, *1—3*, 101—107(1991)

THERMAL BEHAVIOUR OF THE COMPLEX CATION-COMPLEX ANION-TYPE COORDINATION COMPOUNDS. III*

THERMOCHROMISM IN TRIS(PHENANTHROLINE)NICKEL(II)-TETRACHLORO-PALLADATE COMPLEXES

MARIUS ANDRUH

Inorganic Chemistry Laboratory, Faculty of Chemistry, University of Bucharest, Str. Dumbrava Roșie 23, Bucharest Romania

Received June 12, 1990

The irreversible thermochromism of two coordination compounds of the type $[Ni(AA)_3][PdCl_4]\,nH_2O$, where AA = 11,0-phenanthroline (phen), and 4,7-diphenyl-1,10-phenanthroline (bathophen), is reported. The colour change is due to an unusual thermal behaviour of the complex cation-complex anion type coordination compounds, namely the migration of the organic ligand, in solid state, between the two coordination spheres of metal ions. The migration of the ligands is proved by means of TG and DSC studies, as well as by UV-VIS and IR spectral techniques. The first chromotropic phenomenon is accompanied by an exothermic effect.

INTRODUCTION

Known since a very long time, inorganic thermochromism has been extensively studied up to our days. The recent studies are mainly concerned with the causes of colour changes as well as of the chromotropic phenomena.[2] Generally speaking, the colour changes of transition metal compounds are usually correlated with phase transition, which may result from a change in the coordination geometry around the metal ion, namely a change in the coordination number, or a change in the coordinating ligands.

In preceding papers [1,3,4] we reported on the thermochromic behaviour of similar coordination compounds, containing $[ZnCl_4]^{2-}$ or $[SnCl_3]^-$ as anions:

$$[M(phen)_3][ZnCl_4] \rightarrow [M(phen)_2Cl_2] + [Zn(phen)Cl_2] \qquad (I)$$

M = Co :	yellow	red
M = Ni :	pink	green
M = Cu :	green	light green

---

* For Part II in this series, see Ref[1]

$$[Cu(dipy)_3][ZnCl_4] \rightarrow [Cu(dipy)_2Cl_2] + [Zn(dipy)Cl_2] \qquad (II)$$

blue green

$$[Co(dipy)_3][ZnCl_4] \rightarrow Co(dipy)_{1.5}Cl_2 + [Zn(dipy)Cl_2] + 0.5 \text{ dipy} \qquad (III)$$

yellow blue

$$[M(dipy)_3](SnCl_3)_2 \rightarrow [M(dipy)Cl_2] + 2[Sn(dipy)Cl_2] \qquad (IV)$$

M = Co : yellow blue

M = Ni : pink yellow

This is an irreversible thermochromism due to the migration in solid state of the organic ligand between the coordination spheres of two metal ions. Some information regarding the migration of the organic ligands in the solid state may be found in[5,6]. An early investigation on the thermal properties of $[M(en)_n][PtCl_4]$ complexes (where M = Ni, Zn, Cd, Cu) [5] emphasized the occurrence of reactions such as :

$$[Cu(en)_2][PtCl_4] \rightarrow [Pt(en_2)]Cl_2 + CuCl_2$$

In order to prove that this phenomenon exhibits a certain degree of generality and to emphasize the influence of both organic ligand and complex anion on thermal behaviour, the present work deals with two new systems, i.e. $[Ni(phen)_3][PdCl_4] \cdot 3H_2O$ and $[Ni(bathophen)_3][PdCl_4] \cdot 6H_2O$ (phen = 1,10-phenanthroline, bathophen =-4,7-diphenyl-1,10-phenanthroline).

EXPERIMENTAL

The $[Ni(AA)_3][PdCl_4] \cdot nH_2O$ complexes (AA = phen ; bathophen) precipitate from alcoholic solutions of $[Ni(AA)_3]Cl_2$ [7,8] while adding a $PdCl_2$ hydrochloric solution (HCl favoured the formation of $[PdCl_4]^{2-}$ anion). Both coordination compounds are pink and insoluble in ethanol. They have been filtered off, washed with ethanol and dried in vacuum over P_4O_{10}. The results of elemental chemical analyses are in agreement with proposed formulas. It is interesting to note that working with $PdCl_2$ hydrochloric solutions we get only nickel (II) complexes, whereas using $ZnCl_2$ solutions, both nickel (II) and cobalt (II) cation complex-anion complex type coordination compounds may be prepared [3] . For example, by treating a $[Co(phen)_3]Cl_2$ solution with $PdCl_2$ hydrochloric solution, a mixture containing only $[Co(phen)_2Cl_2]$ and $[Pd(phen)Cl_2]$ complexes is obtained. These differences might be explained by molecular orbital (or crystal field) stabilization energy considerations.

The electronic spectra were recorded by diffuse reflectance technique using MgO as a reference material. Infrared spectra were recorded in KBr pellets. The heating curves of the samples in air at atmospheric pressure have been recorded from the room temperature until 900°C, by help of a MOM Budapest Q-1500 type Paulik-Paulik-Erdey derivatograph. TG and DSC curves have been en registered by help of a DuPont 1090 thermal analyser.

RESULTS AND DISCUSSION

The TG curve of the compound $[Ni(phen)_3][PdCl_4] \cdot 3H_2O$ (Fig. 1) indicates a first decomposition step due to the loss of water molecules in the reaction:

$$[Ni(phen)_3][PdCl_4] \cdot 3H_2O(s) \rightarrow [Ni(phen)_3][PdCl_4](s) + 3H_2O(g) \qquad (V)$$

Between 106 and 371°C, the complex $[Ni(phen)_3][PdCl_4]$ seems to be stable, but the DSC curve (Fig. 2) indicates exothermic effects at 210.2, 221.8 and 258.8°C, without change of weight. One may note that on DSC curve the migration effect is shifted toward higher temperatures due to the particular working conditions (sealed pan): the derivatogram (DTA curve) exhibit exothermic effect at 210°C. At the same time, the colour of the sample changes from pink to green. These exothermic effects as well as the colour change (pink→green) are due to the migration of ligands, between two coordination spheres, according to the equation:

$$[Ni(phen)_3][PdCl_4](s) \rightarrow [Ni(phen)_2Cl_2](s) + [Pd(phen)Cl_2](s) \qquad (VI)$$

pink green yellow

The other complex, $[Ni(bathophen)_3][PdCl_4] \cdot 6H_2O$, exhibits the same type of reactions:

$$[Ni(bathophen)_3][PdCl_4] \cdot 6H_2O(s) \rightarrow [Ni(bathophen)_3][PdCl_4](s) + 6H_2O(g) \qquad (VII)$$

$$[Ni(bathophen)_3][PdCl_4](s) \rightarrow [Ni(bathophen)_2Cl_2](s) + [Pd(bathophen)Cl_2](s) \qquad (VIII)$$

pink green yellow

The migration of ligands, in reaction (VIII) is characterized also by an exothermic effect. It is interesting to observe that reaction (VIII) occurs at higher temperature (300°C on the derivato gram) than reaction (VI). This difference may be explained by the greater size of bathophenanthroline in comparison with unsubstituted phenanthroline. Consequently, the migration in solid state of the first mentioned ligand will be most difficult than that of the second one.

In order to prove that colour changes observed for both complex cation-complex anion type coordination compounds are due to migration of ligands, the electronic spectra of all complexes were recorded. Figs. 3b and 4b represent the diffuse reflectance spectra of the two green mixtures together with the electronic spectra of the parent complex cation-complex anion coordination compounds (Figs. 3a and 4a). The electronic spectra of $[Ni(AA)_3][PdCl_4] \cdot nH_2O$ complexes are similar, emphasizing the characteristic bands of both $[Ni(AA)_3]^{2+}$ [3, 7, 9] and $[PdCl_4]^{2-}$

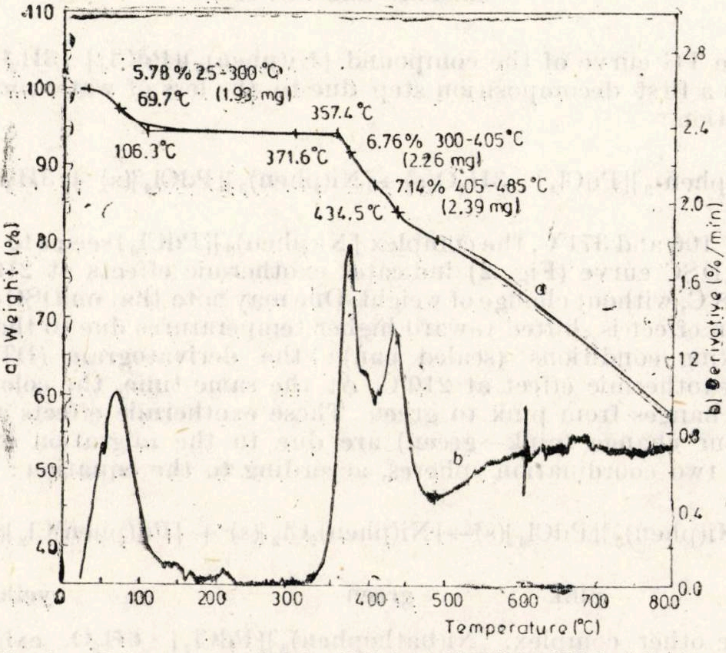

Fig. 1. — TG curve recorded for $[Ni(phen)_3][PdCl_4] \cdot 3H_2O$ at heating rate $\beta = 10\ K\ min^{-1}$ (weight of sample: 33.44 mg).

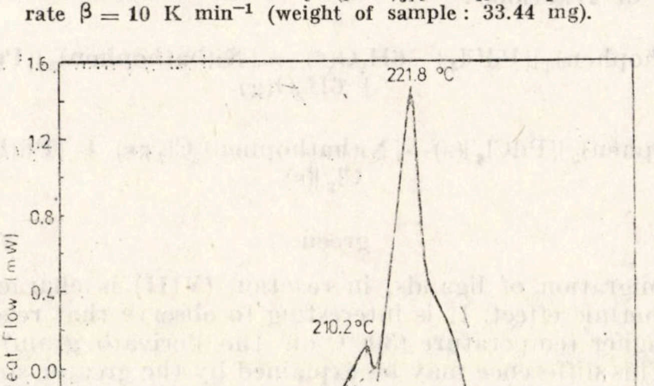

Fig. 2. — DSC curve recorded for $[Ni(phen)_3][PdCl_4]$ $\cdot 3H_2O$ at heating rate $\beta = 10\ K\ min^{-1}$.

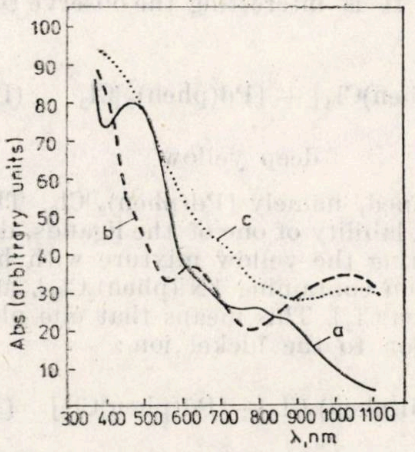

Fig. 3. — Diffuse reflectance spectra of a) $[Ni(phen)_3][PdCl_4]\cdot 3H_2O$ (—); b) $[Ni(phen)_2Cl_2]$ + $[Pd(phen)Cl_2]$(— — — — —); c) $[Ni(phen)Cl_2]$ + $[Pd(phen)_2]Cl_2$(. . . . . . .).

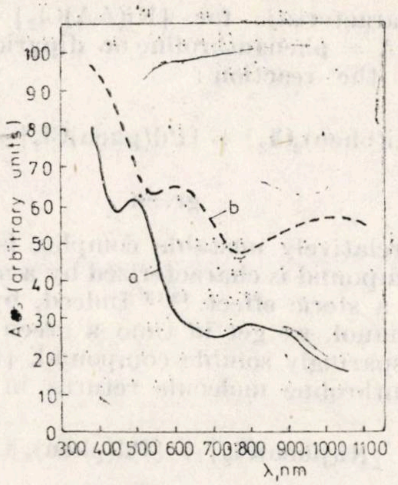

Fig 4. — Diffuse reflectance spectra of a) $[Ni(bathophen_3)][PdCl_4]\cdot 6H_2O$ (—); b) $[Ni(bathophen)_2Cl_2]$ + $[Pd(bathophen)Cl_2]$ [— — — — — — —).

ions.[10] On the other hand, the electronic spectra of the green samples exhibit the absorption bands due to the presence of $[Ni(AA)_2Cl_2]$ complexes[9]:

$$[Ni(phen)_2Cl_2]\ 16340\ cm^{-1}:\ {}^3T_{1g}(F)\leftarrow{}^3A_{2g}(\nu_2)$$

$$\sim 9520\ cm^{-1}:\ {}^3T_{2g}\leftarrow{}^3A_{2g}(\nu_1)$$

$$[Ni(bathophen)_2Cl_2]\ 16670\ cm^{-1};\ {}^3T_{1g}(F)\leftarrow{}^3A_{2g}(\nu_2)$$

$$\sim 9520\ cm^{-1}:\ {}^3T_{2g}\leftarrow{}^3A_{2g}(\nu_1)$$

By treating the green mixtures $[Ni(AA)_2Cl_2]$ + $[Pd(AA)Cl_2]$ with ethanol, we separated two complexes : nickel (II) compounds are soluble while palladium complexes are sparingly soluble in ethanol. From these alcoholic solutions, $[Ni(AA)_2Cl_2]$ complexes were crystallized by removing ethanol. The diffuse reflectance spectra for these nickel (II) complexes were also enregistered ; these spectra are identical with those reported in literature.[9]

By continuing the heating at 300°C, the green mixture $[Ni(phen)_2Cl_2]$ + $[Pd(phen)Cl_2]$ becomes deep yellow without change in weight. The electronic spectrum of this mixture (Fig. 3c) suggests the presence of two yellow compounds : $[Ni(phen)Cl_2]$and $[Pd(phen)_2]Cl_2$ the shoulders at ~700 nm and ~830 nm as well as the weak band at ~1050 nm are characteristic for $[Ni(AA)Cl_2]$ — polynuclear coordination compounds (AA = phenanthroline or dipyridyl)[11]. It is interesting the observe that in the reaction:

$$[Ni(phen)_2Cl_2] + [Pd(phen)Cl_2] \rightarrow [Ni(phen)Cl_2] + [Pd(phen)_2]Cl_2 \qquad (IX)$$

green deep yellow

a relatively unstable complex is obtained, namely $[Pd(phen)_2]Cl_2$. This compound is characterized by a marked lability of one of the ligands, due to a steric effect.[12,13] Indeed, by treating the yellow mixture with hot ethanol, we get in time a green solution containing $[Ni(phen)_2Cl_2]$, and a sparingly soluble compound, $[Pd(phen)Cl_2]$. This means that one phenanthroline molecule returns in solution to the nickel ion:

$$[Ni(phen)Cl_2] + [Pd(phen)_2]Cl_2 \rightarrow [Ni(phen)_2Cl_2] + [Pd(phen)Cl_2] \qquad (X)$$

Supplementary information regarding these chromotropic phenomena may be obtained also with the infrared spectra. The IR spectra recorded within the range 400—4000 cm^{-1} for $[Ni(phen)_3][PdCl_4] \cdot 3H_2O$ and $[Ni(phen)_2Cl_2]+[Pd(phen)Cl_2]$ samples emphasize some differences, respectively:

— the single band at 725 cm^{-1} in the spectrum of $[Ni(phen_3)][PdCl_4] \cdot 3H_2O$ is split into a doublet in the spectrum of the green sample (705 and 730 cm^{-1});

— the triplet centred around 1590 cm^{-1} is slightly modified going from $[Ni(phen)_3][PdCl_4] \cdot 3H_2O$ to $[Ni(phen)_2Cl_2] + [Pd(phen)Cl_2]$, namely: 1570, 1590 and 1610 cm^{-2} for the former and, respectively, 1560, 1595, 1625 cm^{-1} in the spectrum of the green mixture. At the same time, the relative intensities of these bands are also modified: the most intense peak in the spectrum of the unheated sample is located at 1610 cm^{-1}, whereas in the spectrum of the green sample the most intense peak is located at 1560 cm^{-1}.

The strong band located at 725 cm^{-1} is assigned to the in-phase, out-of-plane C—H bending mode, $\gamma(CH)$, of the hydrogen atoms on the carbocyclic ring.[14] The triplet near 1590 cm^{-1} is ascribed to C—C and C—N stretching vibrations on the heterocyclic ring system. These differences between the IR spectra may be accounted for by the inequivalency of the coordinated phenanthroline molecules in the green mixture. Indeed, as a consequence of different phenanthroline-nickel (II) and phenanthroline-palladium(II) interaction degrees, the three pairs of $\gamma(CH)$ on the heterocyclic rings as well as the C—N stretchings become inequivalent.[14]

Why are the chromotropic phenomena emphasized by tetrachloropalladate complexes exothermic, whereas those reported for similar tetrachlorozincate complexes[3] are endothermic? An explanation might be found taking into account crystal field (CFSE) or molecular orbital stabilization energies (MOSE).[15 16] For zinc (II) (d^{10}) complexes the MOSE is zero, whereas for palladium (II) (d^8 — low spin) complexes the contribution of MOSE is important :

$$[PdCl_4]^{2-} : MOSE = -6e'_{\sigma}(Cl)$$

$$cis\text{-}[Pd(phen)Cl_2] : MOSE = 3'_{\sigma}e(N) - 3e'_{\sigma}(Cl)$$

(e'_{σ} (X) are the Angular Overlap Model parameters).
The stabilization energies for the two nickel (II) complexes, in the frame of the Angular Overlap Model, are respectively :

$$[Ni(phen)_3]^{2+} : MOSE = -6e_{\sigma}(N)$$

$$cis\text{-}[Ni(phen)_2Cl_2] : MOSE = -4e_{\sigma}(N) - 2e_{\sigma}(Cl)$$

Accepting that $e_{\sigma}(N) > e_{\sigma}(Cl)$, $e'_{\sigma}(N) > e'_{\sigma}(Cl)$, $e'_{\sigma}(X) > e_{\sigma}(X)$ [16], one may predict that the migration processes

$$[Ni(phen)_3][ZnCl_4] \rightarrow [Ni(phen)_2Cl_2] + [Zn(phen)Cl_2]$$

$$[Ni(phen)_3][PdCl_4] \rightarrow [Ni(phen)_2Cl_2] + [Pd(phen)Cl_2]$$

are the former endothermic, the latter exothermic. However, this is only a qualitative explanation, the modification of lattice energy being neglected.

REFERENCES

[1] N. Dragoe, M. Andruh, A. Meghea and E. Segal, *Thermochim. Acta*, accepted for publication (1990).

[2] K. Sone and Y. Fukuda, "Inorganic Thermochromism", Springer, Berlin, Heidelberg, 1987.

[3] M. Andruh, M. Brezeanu, I. Paraschivoiu and E. Segal, *Thermochim. Acta*, accepted for publication (1990).

[4] M. Brezeanu, M. Andruh, L. Patron and V. T. Popa, *Rev. Roumaine Chim.*, **30**, 229 (1985).

[5] A. Grunberg and L. N. Pschenitzin, *Z. anorg. allgem. Chem.*, **157**, 173 (1926).

[6] W. W. Wendlandt and J. P. Smith, "Thermal Properties of Transition-Metal Ammine Complexes", Elsevier, Amsterdam, London, New York, 1967.

[7] R. D. Hancock and G. J. McDougall, *J. Chem. Soc. Dalton*, **1977**, 67.

[8] R. G. Inskeep, J. Inorg. Nucl. Chem., **24**, 763 (1962).

[9] C. M. Harris and E. D. McKenzie, *J. Inorg. Nucl. Chem.*, **29**, 1047 (1967).

[10] W. Roy Masson III and H. B. Gray, *J. Am. Chem. Soc.*, **90**, 5721 (1968).

[11] R. H. Lee, E. Griswold and J. Kleinberg, *Inorg. Chem.*, **3**, 1278 (1964).

[12] E. D. McKenzie, *Coord. Chem. Rev.*, **6**, 187 (1971).

[13] S. E. Livingstone and B. Wheelahan, *Aust. J. Chem.*, **17**, 219 (1964).

[14] E. König and K. Madeja, *Spectrochim. Acta*, **23A**, 45 (1967).

[15] J. K. Burdett, *Inorg. Chem.*, **15**, 212 (1976).

[16] D. W. Smith, *Struct. Bond.*, **35**, 88(1978).

Revue Roumaine de Chimie, 36, 1—3, 109—111 (1991)

MIXED-LIGANDS COORDINATION COMPOUNDS OF COBALT(II) AND NICKEL(II) WITH 9,10-DIHYDRO-9,10-ETHANO-12-HYDROXYMETHYLENE-ANTHRACEN-11-ONE AND 2,2′-DIPYRIDYL OR 1,10-PHENANTHROLINE

MARIUS ANDRUH[a], MICHAELA STĂNESCU[b], NICOLAE STĂNICĂ[c] and MARILENA FERBINŢEANU[a]

[a] Inorganic Chemistry Laboratory, Faculty of Chemistry, University of Bucharest, Str. Dumbrava Roşie 23, Bucharest, Romania

[b] Chair of Organic Chemistry, Faculty of Industrial Chemistry, Polytechnic Institute, Str. Polizu 1, Bucharest, Romania

[c] Institute of Physical Chemistry, Romanian Academy, Splaiul Independenţei 202, Bucharest, Romania

Received March 20, 1990

Mixed-ligands coordination compounds of cobalt (II) and nickel(II) of the type [ML$_2$(AA)] were synthesized (L = 9,10-dihydro-9,10-ethano-12-hydroxymethylene-anthracen-11-one ; AA = 2,2′-dipyridyl, 1,10-phenanthroline). They were characterized by means of elemental chemical analysis, electronic spectroscopy and magnetic measurements.

1. INTRODUCTION

Known since the latter half of the nineteenth century,[1] β-ketoenolate complexes have had considerable interest for both organic and inorganic chemists.[2,3] The number of β-ketoenolate complexes is increasing because many such potential ligands are prepared each year in the organic chemistry laboratories. The growing interest in inorganic derivatives of β-diketones is also due to the rich variety of coordinative interactions that occur between a metal ion and the ligand.[3]

Many β-ketoenolate complexes are able to bind additional ligands such as heterocyclic bases e.g. pyridine and its substituted derivatives, 4,4′-dipyridyl, pyrazine, quinoline or imidazole.[4,5]

In a previous paper [6] we reported the synthesis of cobalt (II), nickel (II) and copper(II) coordination compounds with a new β-dicarbonylic ligand, namely 9,10-dihydro-9,10-ethano-12-hydroxymethylene-anthracen-11-one, HL.

According to infrared and ^{1}H-NMR spectra,[7] only two tautomeric structures, **1** (ketoenol) and **2** (ketoaldehyde) are noticed to coexist in equilibrium (in $CHCl_3$ or $CDCl_3$ solutions).
In solid state, the equilibrium is displaced toward the enolic form, **1**. Intramolecular hydrogen bonding occurring in the enolic form, **1**, explains its higher stability with respect to the ketoaldehyde **2**.

Following our research, this paper deals with the synthesis and characterization of new mixed-ligands coordination compounds of the type [ML_2 (AA)], where (AA) stands for 2,2′-dipyridyl or 1,10-phenanthroline.

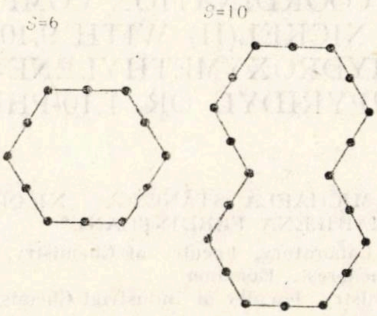

2. EXPERIMENTAL

The β-dicarbonylic ligand was synthesized according to[7]. The β-ketoenolate complexes were synthesized following the general scheme:

$$2HL + MCl_2 \cdot nH_2O \xrightarrow[\text{ethanol}]{CH_3COONa} [ML_2(H_2O)_2] \xrightarrow[\text{toluene}]{(AA)} [ML_2(AA)]$$

2.48 g HL (0.01 mols) were dissolved in 50 mL hot ethanol together with 1 g CH_3COONa (in order to facilitate the formation of the β-ketoenolate anion, L^-). To this solution, 0.005 mols of metal halides ($CoCl_2 \cdot 6H_2O$ or $NiCl_2 \cdot 6H_2O$) dissolved in 20 mL ethanol were added. The resulting mixture was warmed on a water bath for 15 min. On cooling these solutions, solid complexes precipitated: [$CoL_2(H_2O)_2$]-pink; [$NiL_2(H_2O)_2$]-light green. They were filtered off, washed with ethanol and dried in vacuum.

In order to obtain the mixed-ligands complexes with 2,2′-dipyridyl or 1,10-phenanthroline, the β-ketoenolate complexes, [$ML_2(H_2O)_2$], were dissolved in hot toluene and treated with toluenic solutions containing the stoichiometric amounts of 2,2′-dipyridyl or 1,10-phenanthroline. The four mixed-ligand complexes are sparingly soluble in toluene.

The results of elemental chemical analysis are in satisfactory agreement with the proposed formulas.

The electronic spectra were recorded by diffuse reflectance technique (within the range 380–1100 nm) using MgO as a reference material. Magnetic measurements were performed using Faraday's method, at room temperature with $HgCo(NCS)_4$ as a standard.

3. RESULTS AND DISCUSSION

According to infrared and ^1H-NMR spectra [6,7] we concluded that HL acts as an anionic ligand through ionization of hydroxymethylene group.

In order to establish the stereochemistry of the new complexes the electronic spectra were recorded. The shape of these spectra suggests an octahedral environment of the metal ions in all four complexes. Actually, taking into account the inequivalency of the ligands or of the donor atoms, these complexes are characterized by a pseudooctahedral configuration (C_{2v} microsymmetry). Consequently [$ML_2(AA)$] complexes are *cis*-octahedral, containing *cis*-[MO_4N_2] chromophores, but no obvious low symmetry splittings of the spectral bands are observed with the electronic spectra.

Table 1

Diffuse reflectance spectral data (kK)

Compound	Colour	ν_1	ν_2	ν_3
[CoL$_2$(2,2′-dipy)]	pink	9.52 $^4T_{1g}\rightarrow{}^4T_{2g}$	16.66 $^3T_{1g}\rightarrow{}^4A_{2g}$	21.05$^4T_{1g}\rightarrow{}^4T_{1g}$ (*P*)
[CoL$_2$(1,10-phen)]	pink	10.00 $^4T_{1g}\rightarrow{}^4T_{2g}$	16.34 $^4T_{1g}\rightarrow{}^4A_{2g}$	21.50$^4T_{1g}\rightarrow{}^4T_{1g}$ (*P*)
[NiL$_2$(2,2′-dipy)]	light-green	10.87 $^3A_{2g}\rightarrow{}^4T_{2g}$	18.18 $^3A_{2g}\rightarrow{}^3T_{1g}$	
[NiL$_2$(1,10-phen)]	light-green	9.76 $^3A_{2g}\rightarrow{}^3T_{2g}$	16.53 $^3A_{2g}\rightarrow{}^3T_{1g}$	

Table 1 lists the diffuse reflectance spectral bands together with their assignments. The shoulders appearing at ~12.5 kK (for both nickel complexes) are assigned to the spin-forbidden transition $^3A_{2g}\rightarrow{}^1E_g$.

The magnetic measurements for all complexes reported in this paper are also in agreement with an octahedral configuration of the metal ions (Table 2).

Table 2

Magnetic data for [ML$_2$(AA)]complexes

Compound	T, K	$\chi_M \cdot 10^6$, c.g.s.u.	μ_{ef}, MB
[CoL$_2$(2,2′-dipy)]	298	6925.9	4.21
[CoL$_2$(1,10-phen)]	298	8303.7	4.60
[NiL$_2$(2,2′-dipy)]	298	4381	3.42
[NiL$_2$(1,10-phen)]	298	4088.44	3.29

The values of the effective magnetic moments determined for both cobalt (II) complexes are greater than those predicted by the spin-only formula, these values including an orbital contribution (such an orbital contribution to the magnetic moment is expected for complexes having *T* ground states[8], e.g. octahedral complexes of cobalt (II)).

In conclusion, all the four complexes synthesized by us are characterized by a *cis*-octahedral configuration (C_{2v} microsymmetry).

REFERENCES

[1] A. Combes, *Comp. Rend.*, **105**, 871 (1887).
[2] J. P. Fackler, *Progr. Inorg. Chem.*, **7**, 361 (1967).
[3] D. W. Thompson, *Struct. Bond.*, **9**, 27 (1971).
[4] S. Ambe and F. Ambe, *J. Inorg. Nucl. Chem.*, **35**, 1109 (1973).
[5] A. W. Addison and D. P. Graddon, *Aust. J. Chem.*, **21**, 2003 (1968).
[6] M. Andruh, M. Stănescu, F. Mușuroi and M. Brezeanu, submitted for publication.
[7] M. Stănescu, M. Banciu and A. T. Balaban, *Rev. Roumaine Chim.*, **34**, 617 (1989).
[8] B. N. Figgis, "Introduction to Ligand Fields", Interscience, New York, 1966.

Revue Roumaine de Chimie, **36**, *1—3*, 113—118 (1991)

COORDINATION COMPOUNDS OF COBALT(II), NICKEL(II) AND COPPER(II) WITH 9,10-DIHYDRO-9,10-ETHANO-12-HYDROXYMETHYLENE ANTHRACEN-11-ONE

MARIUS ANDRUH[a], MICHAELA STANESCU[b], FLORIANA MUȘUROI[a] and MARIA BREZEANU[a]

[a] Inorganic Chemistry Laboratory, Faculty of Chemistry, University of Bucharest, Str. Dumbrava Roșie 23, Bucharest, Romania

[b] Organic Chemistry Laboratory, Faculty of Industrial Chemistry, Polytechnic Institute, Str. Polizu 1, Bucharest, Romania

Received June 12, 1990

Coordination compounds of Co(II), Ni(II) and Cu(II) with a new β-dicarbonylic ligand, 9,10-dihydro-9,10-ethano-12-hydroxy-methylene anthracen-11-one (HL), are synthesized. They have been characterized by means of elemental chemical analysis, infrared and UV-VIS spectroscopy as well as by magnetic measurements and EPR spectroscopy. They were also compared with the parent acetylacetonate complexes. Mixed-ligands coordination compounds containing L and heterocyclic bases (4-benzoyl-pyridine, 4,4′-dipyridyl) were also synthesized and characterized.

INTRODUCTION

Although known since a very long time,[1] the β-ketoenolate complexes are intensively studied up to our days, their structure and properties being of interest for both organic and inorganic chemists.[2,3] The number of β-ketoenolate complexes is increasing because many such potential ligands are prepared each year in the organic chemistry laboratories. The growing interest to inorganic derivatives of β-diketones is also due to the rich variety of coordinative interactions that occur between a metal ion and the ligand.[3]

This work deals with the synthesis and characterization of several coordination compounds with a new β-dicarbonylic ligand, 9,10-dihydro-9,10-ethano-12-hydroxymethylene anthracen-11-one, HL (**2**). The synthesis of the β-dicarbonylic ligand (**2**)starts from the ketone **1**.[4] According to infrared and ^{1}H-NMR spectra, only two tautomeric structures, **2a** (ketoenol) and **2b** (ketoaldehyde), are noticed to coexist in equilibrium[4] (in $CHCl_3$ or $CDCl_3$ solutions).

In solid state the equilibrium is displaced toward the enolic form **2a**.

The ketoaldehyde **2** seems to be a very interesting starting material for the syntheses of new organic and inorganic compounds.[4,5]

Many β-ketoenolate complexes are able to bind additional ligands such as heterocyclic bases, e.g. pyridine and its substituted derivatives, 4,4′-dipyridyl, pyrazine, quinoline ro imidazole.[6,7]

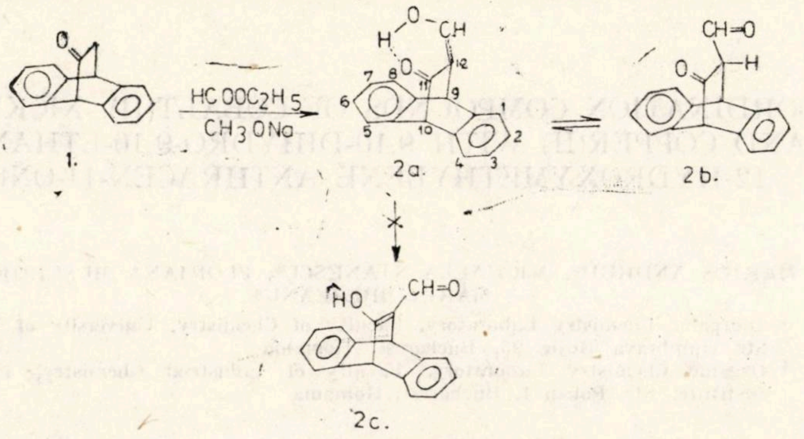

EXPERIMENTAL

The β-ketoenolate complexes were synthesized according to the following procedure: 2.48 g (HL) (0.01 mols) were dissolved in 50 mL hot ethanol together with 1 g CH_3COONa (in order to facilitate the formation of the β-ketoenolate anion, L^-). To this solution 0.005 mols of metal halide ($CoCl_2 \cdot 6H_2O$, $NiCl_2 \cdot 6H_2O$ or $CuCl_2 \cdot 2H_2O$) dissolved in 20 mL ethanol were added. The resulting mixture was warmed on a water bath for 15 min. On cooling these solutions, solid complexes were precipitated: $[CoL_2(H_2O)_2]$-pink; $[NiL_2(H_2O)_2]$-light-green; $[CuL_2]$-olive green. They were filtered off, washed with ethanol and dried in vacuum. In order to obtain their adducts with heterocyclic bases, the β-ketoenolate complexes were dissolved in hot toluene and then treated with toluenic solutions of 4-benzoyl-pyridine (4Bz-Py) or 4,4′-dipyridyl (4,4′-dipy):

$$2HL + MCl_2 \cdot nH_2O \xrightarrow[C_2H_5OH]{CH_3COONa} [ML_2(H_2O)_x] \xrightarrow[\text{toluene}]{2L'} [ML_2L'_y]$$

where M = Co, Ni; n = 6; L′ = 4Bz-Py, y = 2; L′ = 4,4′-dipy, y = 1; M = Cu, n = 2, x = 0, L′ = 4,4-dipy, y = 1. All these mixed ligand complexes are sparingly soluble in toluene.

The electronic spectra were recorded by diffuse reflectance technique (within the range 380–1100 nm) using MgO as a reference material.

Magnetic measurements were performed using Faraday's method, at room temperature, with $HgCo(NCS)_4$ as a standard. The EPR spectra of the copper(II)-complexes, in solid state, were recorded at room temperature, on a spectrograph operating in the X-band; DPPH was used as a standard in order to calculate *g* tensor values. Infrared spectra of the complexes were recorded as KBr pellets. ^1H-NMR spectra were recorded on a Varian EM-360L instrument, with TMS as internal standard.

The results of elemental chemical analysis are in satisfactory agreement with proposed formulas.

RESULTS AND DISCUSSION

Analysis of the ^1H-NMR spectrum of **2** indicates a keto/enol (**2b**/**2a**) ratio of 1/3 in $CDCl_3$. In DMSO only the enolic form **2a** was present. Intramolecular hydrogen bonding occurring in the enolic form **2a** explains its higher stability with respect to the ketoaldehyde **2b**. No trace of **2c** was noticed, probably due to the greater steric strain which would be present in such structure with a shorter $-\underset{|}{C}=\underset{|}{C}-$ bond in the bicyclic system than in **2a** and **2b**. Table 1 illustrates the spectral data for both tautomers[4]. According to these data, one may conclude that HL acts as an anionic ligand through ionization of hydroxymethylene group.

Table 1[4]

IR and ^{1}H-NMR spectral data of equilibrating ketoaldehyde **2b** and ketoenol **2a**

Compound	IR ($CHCl_3$, cm^{-1})	^{1}H-NMR ($CDCl_3$; δ^{ppm})					
		H^9	H^{10}	H^{12}	H^{13}	H_{arom}	OH
2b	1700 $_{C=O\ ket}$ 1725 $_{C=O\ ald}$ 2835 $_{C-H\ ald}$	4.95(d) J=2.5Hz	4.90(s)	3.20(d) J=2.5Hz	9.40(s)	7.0–7.6(m)	—
2a	1600 $_{C=C\ conj}$ 1672 $_{C=O\ conj}$ 3000–3300 large	5.00(s)[a]		—	7.0–7.6 (m)		9.7–10.3

[a] — accidental isochronism

In agreement with the electronic spectra, all complexes reported in this paper are characterized by a (pseudo)octahedral configuration of the metal ions, except the first copper(II) complex, $[CuL_2]$. In fact, these complexes are possible *trans*-octahedral (D_{4h} symmetry), but no obvious low symmetry spittings of the spectral bands are observed. Therefore, for some of the complexes reported in this paper only average values of the electronic parameters may be calculated. Table 2 lists the diffuse reflectance spectral bands together with their assignments (for cobalt(II) and nickel (II) complexes). In order to make a comparison between our complexes and the classical acetylacetonates, table 2 comprises also literature data for the similar metal-acetylacetonate complexes.[6–12]

It is obvious that $[ML_2(4,4'\text{-dipy})]$ complexes have polynuclear structures with 4,4′-dipyridyl bridges.

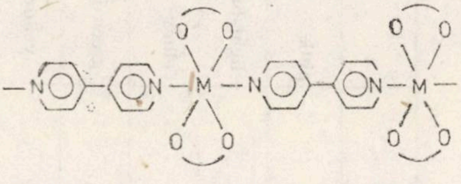

One may note that when methyl groups from acetylacetone are replaced by bulky groups, e.g. *t*-butyl, the stereochemistry of complexes is quite different from that of the corresponding acetylacetonates : nickel (II) and cobalt(II) acetylacetonates possess octahedral structures, while bis(dipivaloylmethanido) nickel(II), $[Ni(DPM)_2]$, is red, diamagnetic with square-planar stereochemistry of nickel(II), and $[Co(DPM)_2]$ has a tetrahedral configuration.[8] If our complexes, $[CoL_2(H_2O)_2]$ and $[NiL_2(H_2O)_2]$, have

Table 2

Diffuse reflectance spectral data (kK)

Compound	Colour	ν_1	ν_2	ν_3
$[CoL_2(H_2O)_2]$	pink	9.10 $^4T_{1g} \rightarrow {}^4T_{2g}$	16.13 $^4T_{1g} \rightarrow {}^4A_{2g}$	20.0 $^4T_{1g} \rightarrow {}^4T_{1g}$ (P)
$[Co(acac)_2(H_2O)_2]$		8.80	14.92	19.41
$[NiL_2(H_2O)_2]$	light-blue	9.10 $^3A_{2g} \rightarrow {}^3T_{2g}$	15.15 $^3A_{2g} \rightarrow {}^3T_{1g}$	—
$[Ni\ (acac)_2(H_2O)_2]$		9.22	15.87	—
$[CoL_2(4BIz\text{-}Py)_2]$	yellow	10.10 $^4T_{1g} \rightarrow {}^4T_{2g}$	19.60 $^4T_{1g} \rightarrow {}^4A_{2g}$	20.0 $^4T_{1g} \rightarrow {}^4T_{1g}$ (P)
$[Co(acac)_2(4Bz\text{-}Py)_2]$		10.20	(16.26)	19.42
$[NiL_2(4Bz\text{-}Py)_2]$	green-yellowish	10.53 $^3A_{2g} \rightarrow {}^3T_{2g}$	17.54 $^3A_{2g} \rightarrow {}^3T_{1g}$	—
$[Ni(acac)_2(4BIz\text{-}Py)_2]$		10.58	17.54	—
$[CoL_2(4,4'\text{-}dipy)]$	yellow	9.26 $^4T_{1g} \rightarrow {}^4T_{2g}$	(18.87) $^4T_{1g} \rightarrow {}^4A_{2g}$	—
$[Co(acac)_2(4,4'\text{-}dipy)]$		9.9	(19.23)	—
$[NiL_2(4,4'\text{-}dipy)]$	green-blueish	9.52 $^3A_{2g} \rightarrow {}^3T_{2g}$	16.13 $^3A_{2g} \rightarrow {}^3T_{1g}$	—
$[Ni(acac)_2(4,4'\text{-}dipy)]$		1.200	16.95	—

an octahedral configuration, one may conclude that the steric requirements of the anion L^- are not so important to hinder the achievement of a hexacoordination. In this case one may suppose that anhydrous ML_2-complexes (M = Ni, Co) may have $[M(acac)_2]_n$-like polynuclear structures.[5] Another conclusion derived from table 2 is that in nickel complexes our ligand exerts a weaker crystal field than acetylacetone (according to the values $\nu_1 = 10$ Dq).

The effective magnetic moment values, μ_{eff}, determined at room temperature (291 K) for $[CoL_2(H_2O)_2]$ ($\mu_{eff} = 4.86$ BM) and $[NiL_2(H_2O)_2]$ ($\mu_{eff} = 3.08$ BM) are also in agreement with a hexacoordination of both cobalt (II) and nickel (II) ions.

The analysis of the infrared spectra of $[CoL_2(H_2O)_2]$ and $[NiL_2(H_2O)_2]$ complexes emphasizes the shift to lower energies of the bands assigned to $_{(C=C)conj}$ and $\nu_{(C=O)conj}$ vibration modes as well as the occurrence of the $\nu_{(M-O)}$ vibration modes (Table 3).

Table 3

Selected IR data for some complexes (cm^{-1})

Compound	$\nu_{(C=C)_{conj}}$	$\nu_{(C=O)_{conj}}$	$\nu_{(M=O)}$
HL(**2a**)	1600	1672	—
$[CoL_2(H_2O)_2]$	1490	1620	440
$[NiL_2(H_2O)_2]$	1560	1650	420, 490

It is well known that lacking the X-Ray crystallographic data, the EPR spectra give the most useful information regarding the stereochemistry of copper(II) coordination compounds. Fig. 1 represents the EPR spectrum of $[CuL_2]$. The calculated g factor values are, respectively : $g_\perp = 2.073$; $g_\parallel = 2.278$. The EPR spectrum represented in fig. 1 is consistent with a square-planar or with an elongated-octahedral stereochemistry[13] (lowest $g > 2.04$). In the later case, one may suppose a semicoordination [4+2] of copper(II) ions, the axial fifth and sixth ligands being oxygen atoms from other $[CuL_2]$-units. On the other hand, the value of the parameter G,[13] defined by the ratio $(g_\parallel - 2)/(g_\perp - 2)$, namely $G < 4$, indicates that significant exchange coupling is present and the missalignment of "tetragonal" axes is appreciable. The mean value $g_0 =$

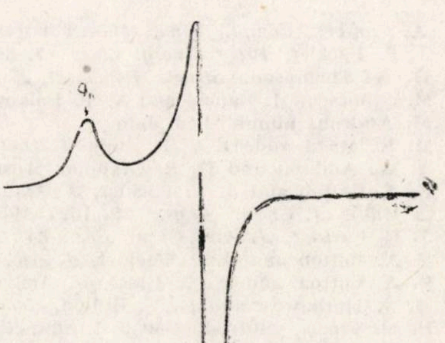

Fig. 1. — The EPR spectrum of the complex $[CuL_2]$.

$= \frac{1}{3}(2g_{\perp} + g_{\parallel}) = 2{,}141$ suggests an orbitally non-degenerate ground state.[14] The shape of the EPR spectrum recorded for [CuL_2(4,4′-dipy)] does not allow to calculateg accurate g values, but suggests an elongated octahedral symmetry. The changes in colour and stereochemistry going from [CuL_2] to [CuL_2(4,4′-dipy)] are reflected also by the electronic spectra (Fig. 2).

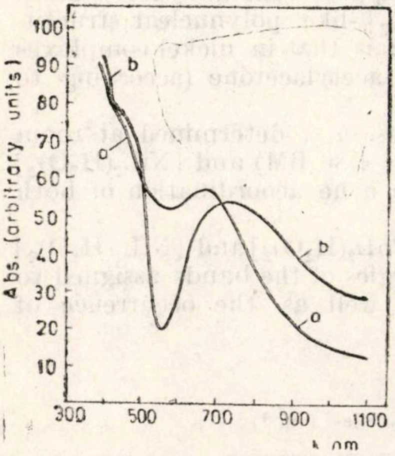

Fig.2. — The diffuse reflectance spectra of a) [CuL_2]; b) [CuL_2(4,4′-dipy)].

In conclusion, we have synthesized eight new complexes containing 9,10-dihydro-9,10-ethano-12-hydroxymethylene anthracen-11-one as a ligand. The ligand used by us seems to be sterically equivalent to acetylacetone, rather than to dipivaloylmethan, where the steric strains are very important.

REFERENCES

[1] A. Cambes, *Compt. Rend.*, **105**, 871 (1887).
[2] J. P. Fackler, *Progr. Inorg. Chem.*, **7**, 361 (1967).
[3] D. W. Thompson, *Struct. Bond.*, **9**, 27 (1971).
[4] M. Stănescu, M. Banciu and A. T. Balaban, *Rev. Roumaine Chim.*, **34**, 617 (1989).
[5] M. Andruh, unpublished data
[6] M. K. Misra and D. V. R. Rao, *J. Inorg. Nucl. Chem.*, **35**, 1109 (1973).
[7] A. W. Addison and D. P. Graddon, *Aust. J. Chem.*, **21**, 2003 (1968).
[8] F. A. Cotton and J. P. Fackler, *J. Am. Chem. Soc.*, **83**, 2818 (1961).
[9] C. Maki, *J. Chem. Phys.*, **29**, 162 (1959).
[10] J. P. Fackler, *J. Am. Chem. Soc.*, **84**, 24 (1962).
[11] F. A. Cotton and J. P. Fackler, *J. Am. Chem. Soc.*, **83**, 2818 (1961).
[12] F. A. Cotton and R. C. Elder, *J. Am. Chem. Soc.*, **86**, 2294 (1964).
[13] B. J. Hathaway and D. E. Billing, *Coord. Chem. Rev.*, **5**, 143 (1970).
[14] B. N. Figgis, "Introduction to Ligand Fields", Interscience, New York, 1966, p. 296.

Revue Roumaine de Chimie, **36**, *1–3*, 119–125(1991)

HETEROCYCLES WITH ANNELATED DIBENZO-CYCLOALKANE SKELETONS. V[1]

PYRIMIDINES WITH ANNELATED DIBENZOBARRELENE AND DIBENZOHOMOBARRELENE SKELETONS

MICHAELA DINA STĂNESCU,[a] MIRCEA D. BANCIU[a] and FILIP CHIRALEU[b]

[a] Organic Chemistry Department, Polytechnic Institute, TCH, Splaiul Independenței 313, 76206 Bucharest, Roumania

[b] Centre of Organic Chemistry, Roumanian Academy

Received April 11, 1990

Formyl derivatives **3** and **4** afford on treatment with urea, thiourea and guanidine the corresponding pyrimidines **5a-c** and **6a-c** with annelated dibenzobarrelene- and dibenzohomobarrelene skeletons respectively.

INTRODUCTION

In connection with our interest in the study of polycyclic heterocyclic compounds [2-4] we described recently[2] the synthesis of pyrazoles **1a–c** and **2a–c** which contain fused dibenzobarrelene and dibenzohomobarrelene skeletons respectively.

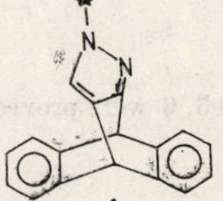

1

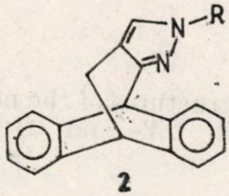

2

a; R = H
b; R = C_6H_5
c; R = $C_6H_3(NO_2)_2$

In this paper we describe the synthesis of some new pyrimidines including the same fused dibenzobicyclic moieties as **1** and **2**.

RESULTS AND DISCUSSION

Syntheses

The starting materials were the known formyl derivatives **3**[4] and **4**[5] existing mainly in their hydroxymethylenic tautomeric forms.

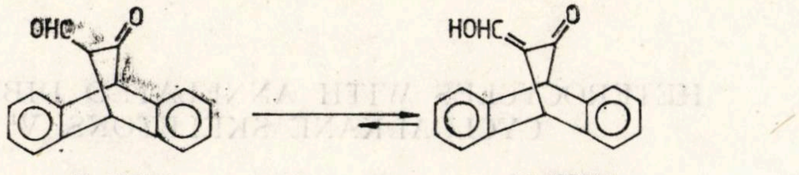

3a (25%) **3b** (75%)

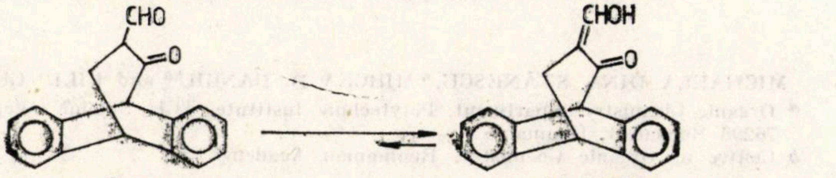

4a **4b** (100%)

Refluxing of **3** and **4** with urea, thiourea and guanidine in toluene/dimethylformamide in the presence of catalytic amounts of *p*-toluenesulphonic acid conducted to pyrimidines **5a-c** and **6a-c** with corresponding annelated bicyclic skeleton.

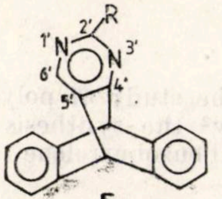

5

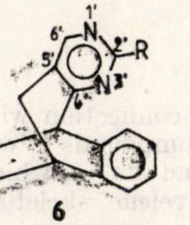

6

a; R = OH
b; R = SH
c; R = NH_2

The structures of the new pyrimidines **5**, **6** were proved on the basis of their IR- UV- and ^{1}H-NMR data.

IR spectra

The IR spectra (in KBr) are in agreement with the suggested structures. All investigated pyrimidines show characteristic absorptions of the hydrocarbon skeleton (see Experimental). Thus, compounds with the skeleton **5** present bands of γ_{CH} vibrations in *ortho*-disubstituted benzenes (between 735 – 770 cm^{-1}), ν_{CH} aryl vibrations (between 3020 and 3060 cm^{-1}) whereas the compounds **6** present additionally absorptions characteristic for $\nu^{sym}_{CH_2}$ and $\nu^{asym}_{CH_2}$ (at 2850 – 2860 cm^{-1} respectively 2920 – 2930 cm^{-1}). All the above-mentioned absorptions were found also in the pyrazoles **1**[2] and **2**[2] possessing the same polycyclic hydrocarbon skeletons.

On the other hand, the pyrimidines **5**, **6** show characteristic IR bands of functional groups. The hydroxy-derivatives **5a** and **6a** show large absorptions of ν^{assoc}_{OH} between 3100 and 3600 cm^{-1} as well as ν_{C-OH} absorptions at 1130 cm^{-1} and 1150 cm^{-1} respectively. The amino-derivatives **5c** and **6c** present ν_{NH_2} absorptions bands : whereas in **5c** these bands appear at 3390 cm^{-1} ($\nu_{NH_2}^{sym}$) and 3490 cm^{-1} ($\nu_{NH_2}^{asym}$) in compound **6c** two large $\nu_{NH_2}^{assoc}$ bands appear at 3100—3200 cm^{-1} and 3250—3400 cm^{-1} proving the association by hydrogen bonds. In the case of mercaptoderivatives **5b**, **6b** no ν_{SH} band is visible between 2550—2590 cm^{-1}, the usual domain of these vibrations. However it is known that ν_{SH} bands are very weak, often unobservable. Compound **5b** seems to present thiol⇌thione tautomerism **5bA⇌5bB :**

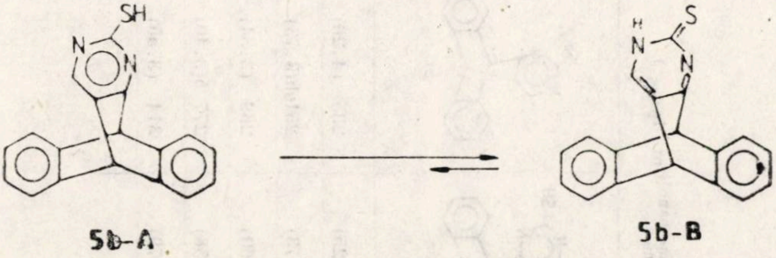

5b-A **5b-B**

Thus, in the IR spectrum of **5b** a strong absorption of $\nu_{C=S}$ appears at 1260 cm^{-1} along with two large absorptions of ν_{NH}^{assoc} at 3100—3200 cm^{-1} and 3200—3400 cm^{-1} proving the existence of thionic form **5b-B**. No ν_{NH} absorption is visible in the spectrum of **6b**.

Electronic spectra

The electronic spectral data of pyrimidines **5** and **6** are collected in Table 1. All compounds exhibit electronic spectra with the same general appearance including five similar absorption bands (1—5, table 1) except hydroxyderivatives **5a** and **6a** which present an additional band (6) at about 390 nm. From the first five absorptions those of about 265—269 nm (third band) and 273—277 nm (fourth band) are quite similar as wavelengths and extinction coefficients in all compounds **5** and **6**. The second bands, from 241—252 nm are generally shoulders of the previous strong absorptions of about 212—235 nm (first bands). The bands which indicate the largest shifts and the greatest ε-values variations are the fifth, which occur between 307.5 nm (in **6c**) and 353 nm (in **6b**). These absorptions could be associated with electronic transitions including differently substituted pyrimidine rings.

Very good similarities could be seen by comparison of the spectra corresponding to pyrimidines bearing the same substituent (**5a** with **6a**, **5b** with **6b** and **5c** with **6c** ; see Table 1). However, the fifth band indicates a hypsochromic shift on passing from system **5** to **6** both for hydroxy- and amino-substituted compounds, whereas for SH substituent a bathochromic shift is observed on passing from **5b** to **6b**. This behaviour could be ascribed to different hydrocarbon skeletons in **5** and **6** and, on the other hand to a possibly different thiol⇌thione tautomeric equilibrium in compounds **5b** and **6b**.

The existence (or preponderence) of thionic form **5b—B** (see also IR data) which is less conjugated than the fully aromatic **5b—A** could

Table 1

Electronic spectral data of pyrimidines **5a-c** and **6a-c** ($\lambda_{max}^{methanol}$nm ; $\lg\varepsilon_{max}$)

Absorption band	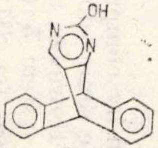 **5a**	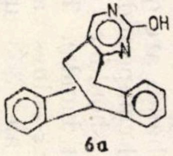 **6a**	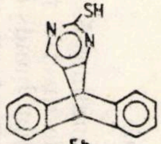 **5b**	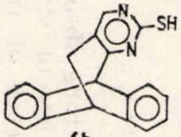 **6b**	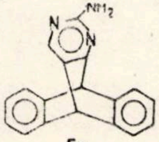 **5c**	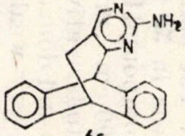 **6c**
1	216.5(4.24)	212.5(4.28)	212.5(4.30)	212.5(4.25)	235 (4.26)	220 (4.13)
2	251 (3.57)	252(3.66)	241sh(3.90)	250sh(3.73)	251sh(3.73)	245sh(3.80)
3	269 (3.54)	268(3.52)	267 (3.76)	268 (3.60)	269 (3.34)	265.5(3.30)
4	275 (3.58)	276 (3.63)	275 (3.79)	275 (3.58)	277.5(3.40)	273 (3.32)
5	339 (3.97)	312 (4.11)	332 (4.10)	353 (3.79)	314 (3.55)	307.5(3.41)
6	394.5(3.46)	389 (2.72)				

* sh = shoulder

explain the shorter wavelength of the absorption maximum ($\lambda_{max} = 332$nm) in **5b** in comparison with $\lambda_{max} = 353$ nm in the compound **6b** existing in aromatic thiolic form (see also IR data).

^{1}H-NMR spectra

The ^{1}H-NMR data for new pyrimidines **5a–c** and **6a–c** are collected in Table 2. The NMR spectra are in agreement with the proposed structures. As in the case of the previously investigated pyrazoles **1** and **2**[2] a good correlation could be seen between signals of similar protons from all compounds with annelated dibenzobarrelene skeleton on one hand and the compounds with annelated dibenzohomobarrelene skeleton on the other hand.

Table 2

^{1}H-NMR data for pyrimidines **5a-c** and **6a-c***

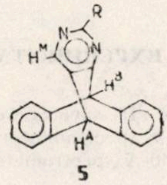

5

Compound	R	H^A	H^B	H_arom	H^M	Solvent
5a	OH	4.80(s)	5.05(s)	6.90–7.70(m)		d_6–DMSO
5b	SH	5.10(s)	5.35(s)	7.20–7.80(m)	8.10–8.25(m)	d_6-acetone
5c	NH_2	5.60(s)**		7.10–7.70(m)	8.10(s)	$F_3C-COOH$

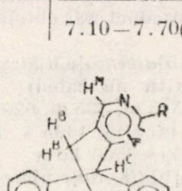

6

Compound	R	H^B	H^A	H^C	H_arom	H^M	Solvent
6a	OH	2.90(d)	4.30(t)	5.10(s)	7.20–7.80(m)		d_6-acetone+ $F_3C-COOH$
6b	SH	3.15(d)	4.50(t)	5.05(s)	7.20–7.80(m)	8.20(s)	$CDCl_3+d_6$– –DMSO
6c	NH_2	3.10(d)	4.30(t)	4.80(s)	7.30–7.80(m)	7.90(s)	$F_3C-COOH$

* s = singlet ; d = doublet ; t = triplet

** accidentally isochronous

The observed chemical shifts for protons of **5a-c** and **6a-c** (Table 2) corroborate well with those of the corresponding pyrazoles **1**[2] and **2**[2] as well as with those of triptycene[6], respectively homotriptycene.[7] The triptycene derivatives **5a-c** present singlets for bridgehead protons H^A and H^B whereas homotriptycene derivatives **6a-c** show a triplet/doublet/singlet pattern for $H^A/H^B/H^C$, confirming thus the proposed structures.

Unfortunately, the protons from functional groups of **5a—c** and **6a—c** could not be evidenced in the ^{1}H-NMR spectra. Due to the low solubility of all here investigated compounds, only d_6-DMSO, d_6-acetone and $F_3C—COOH$ could be used for registration of NMR spectra and in these solvents the OH, SH and NH_2 protons are included in solvent signals (respectively in that of water traces from these solvents).

In conclusion this work described the synthesis and physical characterization of six new pyrimidines with annelated dibenzobarrelene and dibenzohomobarrelene skeletons. These compounds are closely related with the pyrazoles, pyridines and pyrylium salts previously obtained in this laboratory.[2–4]

EXPERIMENTAL

Melting points are uncorrected. IR spectra were registered on a UR-20 apparatus and UV-VIS spectra on a Specord UV-VIS spectrophotometer both C. Zeiss Jena. ^{1}H-NMR spectra were performed on a Varian A 60-A spectrometer (TMS as internal standard).

General procedure for synthesis of pyrimidines 5 and 6

Hydroxymethylene ketone **3** (or **4**) (2 mmoles), urea (thiourea or guanidine carbonate), (3 mmoles), catalytic amounts of *p*-toluenesulphonic acid in 25 mL toluene and 5 mL dimethylformamide were refluxed for 12—15 hrs.

After cooling, the reaction mixture was washed with water, $NaHCO_3$ solution, again with water. If during this time a solid product appears it is solved in methylene chloride.

The organic layer was dried on anhyd. $MgSO_4$ then evaporated *in vacuo*. After scratching with petroleum ether a solid product was obtained (for the UV-VIS and ^{1}H-NMR spectra see text).

2′-Hydroxy-1′,3′-pyrimidino[b]*dibenzo*[e,h]*bicyclo*[2.2.2.]-*octa-2,5,7-triene* (**5a**); yield 63 %; m.p. 175—8°C (washed with methanol).

IR Spectrum (KBr; cm^{-1}): 515 m, 535 m, 620 w, 640 w, 700 w, 727 s, 745 m, 1070 m, 1130 s, 1145 m, 1205 m, 1350 m, 1455 m, 1495 s, 1610 s, 1680 s, 2870 w, 2920 w, 2950 w, 3015 w, 3040 w, 3065 w and 3100—3500 large.

2′-Mercapto-1′,3′-pyrimidino[b]*dibenzo*[e,h]*bicyclo*[2.2.2]-*octa-2,5,7-triene* (**5b**); yield 60.5 %; m.p. 232—3°C (ethanol).

IR Spectrum (KBr; cm^{-1}): 495 w, 580 m, 722 w, 758 s, 1040 s, 1140 s, 1260 s, 1360 s, 1510 m, 1605 s, 1660 s, 2380 w, 2970 w, 3060 w, 3075 w, 3100—3200 large and 3200—3400 large.

2′-Amino-1′,3′-pyrimidino[b]*dibenzo*[e,h]*bicyclo*[2.2.2]-*octa-2,5,7-triene* (**5c**); yield 70 %; m.p. 297—9°C (washed with methanol).

IR Spectrum (KBr; cm^{-1}): 465 w, 515 w, 595 w, 630 m, 780 m, 1165 m, 1195 w, 1422 s, 1450 s, 1560 m, 1590 s, 1602 s, 3040 w, 3070 w, 3175 w, 3390 m and 3490 m.

2′-Hydroxy-1′,3′-pyrimidino[b]*dibenzo*[f,i]*bicyclo*[3.2.2.]-*nona-2,6,8-triene*(**6a**); yield 60 %; m.p. 255°C (washed with cold methanol).

IR Spectrum (KBr; cm^{-1}): 615m, 635w, 680w, 753w, 1150s, 1230m, 1360m, 1430w, 1450w, 1470w, 1520w, 1570m, 1650m, 2850w, 2930w, 3010w, 3070w and 3200—3600 large.

2′-Mercapto-1′,3′-pyrimidino[b]*dibenzo*[f,i]*bicyclo*[3.2.2.]-*nona-2,6,8-triene*(**6b**); yield 58 %; m.p. 185—190°C (ethanol).

IR Spectrum (KBr; cm^{-1}): 640m, 700w, 735m, 750m, 770m, 1110m, 1165s, 1250s, 1325m, 1360m, 1400s, 1450m, 1475m, 1565s, 2340w, 2860w, 2920w, 3030w and 3070w.

2′-Amino-1′,3′-pyrimidino[b]*dibenzo*[f,i]*bicyclo*[3.2.2]-*nona-2,6,8-triene* (**6c**); yield 69 %; m.p. 168—170°C (washed with cold methanol).

IR Spectrum (KBr; cm^{-1}): 505w, 525w, 540w, 565w, 595w, 635m, 690m, 760m, 805 w, 1160w, 1192w, 1220w, 1408m, 1485s, 1550m, 1585s, 1660s, 1692m, 2860m, 2920w, 3040w, 3070w, 3100–3200 large and 3250–3400 large.

Note added in proofs. Compounds **1a** and **5c** had been synthesized–by other method–in the Doctoral Thesis of Axel Schmidt (1984, München, Germany); (personal communication of Dr. A.S.)

REFERENCES

[1] Note IV in this series: M. D. Banciu, F. Chiraleu, and A. Ciobanu *Rev. Roumaine Chim.*, **35**, 739 (1990).

[2] M. D. Banciu, M. D. Stănescu and F. Chiraleu, *Rev. Roumaine Chim.*, **34**, 1921 (1989).

[3] M. Banciu, A.T. Balaban, C. Drăghici and R. Vlad, *Rev. Roumaine Chim.*, **27**, 1037 (1982).

[4] M. Stănescu, M. Banciu and A. T. Balaban, *Rev. Roumaine Chim.*, **34**, 617 (1989).

[5] M. Banciu, *Rev. Roumaine Chim.*, **27**, 769 (1982).

[6] K. G. Kidd, G. Kotonycz and T. Schaefer, *Canad. J. Chem.*, **45**, 2155 (1967).

[7] S. J. Cristol and D.K.Pennelle, *J. Org. Chem.*, **35**, 2357 (1970).

Revue Roumaine de Chimie, **36**, *1–3*, 127–134(1991)

SYNTHESIS AND CHARACTERIZATION OF SOME 4,5-DISUBSTITUTED-3-MERCAPTO-1,2,4-TRIAZOLES

IOANA ŞARAMET[a], MIRCEA D. BANCIU[b] and CONSTANTIN DRĂGHICI[c]
[a] Organic Chemistry Department, Faculty of Pharmacy, Traian Vuia Street 6, Bucharest, Roumania
[b] Organic Chemistry Department, Polytechnic Institute, TCH, Splaiul Independenţei 313, Bucharest Roumania
[c] Centre of Organic Chemistry, Roumanian Academy

Received May 15, 1990

Some 4,5-disubstituted-3-mercapto-1,2,4-triazoles **1** with potential biologic activity were synthesized by cyclization of substituted mono- or bis-thiosemicarbazides **2**, respectively **3**, in alkaline medium. The structure of the new compounds **1a-f** was proved by elemental- and IR, UV, ^{1}H-NMR analysis.

INTRODUCTION

The utilizations of various substituted triazoles, especially of mercaptotriazoles as physiologically active compounds are well-known.[1-4] Introduction of an (arylsulphonyl)phenyl substituent in the triazolic ring seems to be interesting, keeping in mind the known pharmacologic activity of compounds possessing diarylsulphone moieties.[5] In this short note we describe the synthesis and physical characterization of some new 3-mercapto-1,2,4-triazoles **1** substituted with (arylsulphonyl)phenyl groups.

RESULTS AND DISCUSSION

The usual method applied for synthesis of 4,5-disubstituted-3-mercapto-1,2,4-triazoles seems to be the cyclization[6] accompanied by water elimination of 4-substituted-1-acylthiosemicarbazides, obtained on their turn by nucleophilic addition of hydrazides to isothiocyanates. The formation of 3-arylamino-1,2,4-triazoles as by-products in such reactions was mentioned and investigated.[7]

Synthesis of 4,5-disubstituted-3-mercapto-1,2,4-triazoles **1a–d** was performed by cyclization of substituted *para*-(arylsulphonyl) benzoylthiosemicarbazides **2a–d** on reflux with 1N-NaOH solution.

Synthesis of bis-mercaptotriazoles **1e, f** was realized similarly by alkaline (NaOH) double cyclization of bis-thiosemicarbazides **3a, b.**

Mono- and bis-thiosemicarbazides, **2** respectively **3**, were obtained[8a] on their turn by addition of the corresponding acid (mono- or bis-)hydrazides **4a–d**[8b] to ethyl – or benzyl – isothiocyanates.

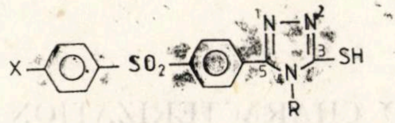

1

a; X = H; R = C_2H_5
b; X = Cl; R = C_2H_5
c; X = Br; R = C_2H_5
d; X = H; R = $C_6H_5CH_2$

e: X =

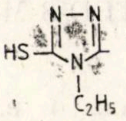

R = C_2H_5

f: X =

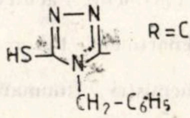

R = $C_6H_5-CH_2$

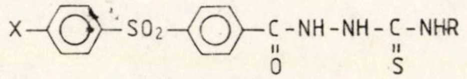

2

a; X = H; R = C_2H_5
b; X = Cl; R = C_2H_5
c; X = Br; R = C_2H_5
d; X = H; R = $C_6H_5CH_2$

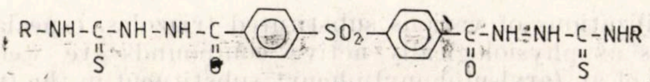

3

a; R = C_2H_5
b; R = $C_6H_5CH_2$

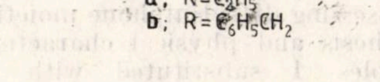

4

a; X = H
b; X = Cl
c; X = Br
d; X =

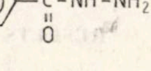

$\underset{\underset{O}{\|}}{C}-NH-NH_2$

The solid products **1a**−**f**, obtained in 70−80% yields, were characterized by elemental analysis (Table 1) as well as by their IR, UV and ^{1}H-NMR spectra (Table 2).

The IR spectra confirm the formation of mercaptotriazoles **1**. Thus, the amide I band ($\nu_{C=O}$) in the range of 1650−1690 cm^{-1} which is present in the spectra of the starting thiosemicarbazides **2**, **3**, disappears in the spectra of products **1** proving the cyclization. The ν_{SH} absorption though very weak is however visible in all mercaptotriazoles **1** at 2550 − 2570 cm^{-1}. No ν_{SH} absorption band is visible in the range of 3330−3500 cm^{-1} demonstrating the lack of thionic tautomers **5**.

Table 1

4,5-Disubstituted-3-mercapto-1,2,4-triazoles **1a f**

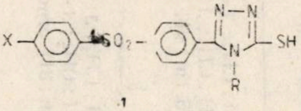

1

Comp.	X	R	m.p.(°C)*	Analysis (%) (Calc/Found)		
				C	H	N
1a	H	C_2H_5	218a)	55.65 55.70	4.35 4.28	12.17 12.18
1b	Cl	C_2H_5	254a)	50.59 50.38	3.69 3.90	11.06 11.02
1c	Br	C_2H_5	273b)	45.28 45.50	3.30 3.25	9.90 10.00
1d	H	$C_6H_5CH_2$	190c)	61.91 61.81	4.18 40.10	10.31 10.20
1e	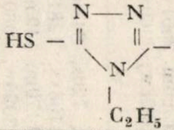	C_2H_5	293b)	50.85 51.22	4.24 4.30	17.79 17.80
1f	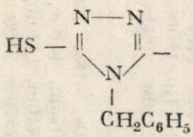	$C_5H_5CH_2$	187d)	60.40 60.10	4.03 4.10	14.09 14.00

* Recrystallization solvent: a) $CHCl_3$/petroleum ether; b) dioxane/petroleum ether; c) benzene; d) dioxane

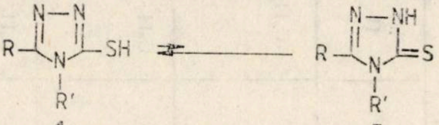

1 5

The attribution of the absorption band of 1269 — 1281 cm^{-1} to $\nu_{C=S}$ vibration in a presumable tautomeric form **5** could be denied in the present case due to the fact that a triazole related with **1d**, possessing S-benzyl group instead of SH one,[8a,9] presents the same absorption at 1280 cm^{-1}. Consequently, this band could be attributed to C-N vibrations in all compounds **1**. The characteristic absorptions of other structural moie-

Table 2

Spectral data of 4,5-disubstituted-3-mercapto-1,2,4-triazoles 1a-f

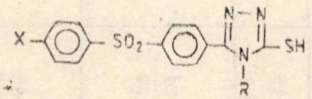

Comp.	X	R	IR (KBr)cm^{-1}	UV (MeOH) λ_{max};(lg ε_{max})	^{1}H–NMR(d_6-DMSO/$CDCl_3$) δppm ; J_{Hz}
1a	H	C_2H_5	550m, 590s, 620vs, 770vs, 850m, 1010m, 1070m, 1090m, 1165vs, 1280s, 1310s, 1440m, 1480m, 1545m ,1600m, 2550w, 2870m, 2927m, 2980m, 3035w, 3060w, 3090w	256.5 (4.42) 312 (3.74)	1.3 (t ; 3H ; CH_3 ; J=7.5) 4.18 (q ; 2H ; CH_2 ; J=7.5) 7.5 –8.25 (m ; 9H arom.)
1b	Cl	C_2H,	597s, 620s, 633s, 750m ,778s, 838s, 852s, 1010s, 1090s, 1105s, 1161vs,1275vs, 1321vs, 1470s, 1500m, 1562m, 1565m, 2559w, 2858m, 2915m, 2950m, 2985m, 3035m, 3085m	257 (4.46) 313.5 (3.70)	1.32 (t ; 3H ; CH_3 ; J=7) 4.22 (q ; 2H ; CH_2 ; J=7) 7.6–8.5 (m ; 8H arom.)
1e	Br	C_2H_5	575s, 620s, 731m, 762s, 830m, 848m, 1010s, 1075s, 1105s, 1159vs, 1281s, 1320vs, 1471m, 1500m, 1566m, 2561w, 2852w, 2920w, 2960w, 3028w, 3060w, 3080w	257 (4.56) 312.5 (3.76)	1.3 (t ; 3H ; CH_3 ; J=7) 4.2 (q ; 2H ; CH_2 ; J=7) 7.65–8.5 (m ; 8H arom.)
1d	H	$C_6H_5CH_2$	575s, 600s, 618s, 386s, 720s, 843m, 940m, 1075m, 1105s, 1158vs, 1281s, 1318s, 1410m, 1440m, 1470m, 1495m, 2370w, 2570w, 2920m, 3025w, 3060w 3095w	256 (4.51) 312 (3.77)	5.42 (s ; 2H ; CH_2) 7.0–8.3 (m ; 14H arom.)

Table 2 (continued)

Comp.	X	R	IR (KBr) cm^{-1}	UV (MeOH) λ_{max}; ($\lg\varepsilon_{max}$)	^1H-NMR ($d_6-DMSO/CDCl_3$) δ_{ppm}; J_{Hz}
1e	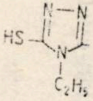	C_2H_5	575m, 595m, 625s, 640s, 775s, 833m, 847m, 960m, 1108s, 1160vs, 1269vs, 1323s, 1359s, 1420s, 1460s, 1471s, 2375m, 2560w, 2920m, 3020w, 3060w, 3090w	258 (4.73) 316 (4.21)	1.26 (t; 3H; CH_3; J=65). 4.18 (q; 2H; CH_2; J=6.5) 8.05 (d; 4H arom; J=8.5) 8.3 (d; 4H arom; J=8.5)
1f	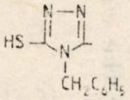	$C_6H_5CH_2$	580m, 625s, 635s, 700s, 731s, 768s, 845m, 940m, 1076m, 1107s, 1160vs, 1280s, 1325s, 1401m, 1420m, 1470m, 1492m, 2570w, 2920m, 3025w, 3060w, 3085w	260 (4.64) 317 (4.10)	5.44 (s; 4H; CH_2) 7.0–8.4 (m; 18H arom.)

ties from **1a**—**f** (e.g. SO_2 ; C-Halogen ; CH_3 ; CH_2 ; substituted aryl groups etc.) could be easily recognized in the IR spectra of the synthesized mercaptotriazoles (see Table 2).

All substituted triazoles **1a**—**f** present in the UV spectra (Table 2) two absorptions : the first at about 254—260 nm and the second at 309—317 nm. Whereas the former absorption bands, characterized by large lg ε values. (4.5—4.7) could be connected to electronic transitions in the benzenic rings, the latter absorptions, indicating smaller lg ε-values (3.7—3.8 in **1a**—**d** and 4.1—4.2 in bis-triazoles **1e**, **f**) seem to be characteristic to a conjugated moiety including the triazolic ring.

The ^{1}H-NMR spectra (Table 2) of mercaptotriazoles **1** are in agreement with their proposed structures. The protons from the benzenic ring adjacent to the triazolic one appear usually between 8—8.3 ppm. The thiolic proton signal overlaps in some spectra that of the H_{ortho} to SO_2 group.

The ethyl- and benzyl-protons from mercaptotriazoles **1** containing such groups appear normally as position and multiplicity (Table 2).

On the basis of the above data, it results that the thiosemicarbazides (**2** and **3**) could be easily cyclized to mercaptotriazoles. The mechanism of this cyclization could be rationalized as in the Scheme 1, the main intermediate being the tautomeric anion **7** which appears by cyclization of the initially formed anion **6** and is further converted by water elimination into the sodium salt **8** of **1**.

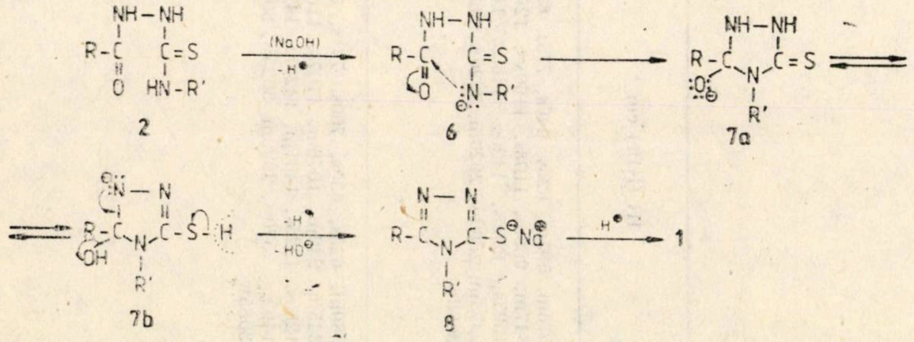

It should be also added here that the attempted synthesis of the same mercaptotriazoles **1** using the method of Pesson and co-workers,[10] namely the reaction of esters (e.g. **9a**) with thiosemicarbazides (e.g. **10**) in CH_3OH/CH_3ONa medium failed ; instead of triazole **1c** the methyl ester **9b** corresponding to **9a** was obtained. It seems that transesterification prevails over the condensation-cyclization sequence.

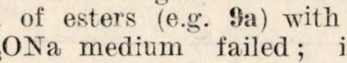

9

R = C_2H_5

R = CH_3

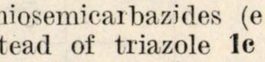

$H_2N\text{-}NH\text{-}\overset{\overset{\displaystyle S}{\|}}{C}\text{-}NH\text{-}C_2H_5$

10

In conclusion, in this paper some new — possibly biologically active — 3-mercapto-1,2,4-triazoles substituted in positions 4 and 5 with alkyl-(or arylalkyl-) and respectively arylsulphonyl)phenyl groups were synthesized and characterized.

EXPERIMENTAL

The melting points are uncorrected. The IR spectra were registered on a UR-20 C. Zeiss-Jena spectrophotometer, the UV spectra on a SPECORD UV-VIS C. Zeiss-Jena Spectrophotometer and the 1H-NMR spectra on a VARIAN A60-A spectrometer using TMS as internal standard.

para-**(Arylsulphonyl) benzoyl thiosemicarbazides 2a-d** were obtained [8a] by nucleophilic addition of *para*(arylsulphonyl) benzoic acid hydrazides **4a-e**[8b] to ethyl- or benzyl isothiocyanate (reflux of equimolar quantities in anhydrous ethanol).

Thiosemicarbazide **2a**, m.p. 220°; IR (KBr; cm^{-1}): 740, 775, 810, 1170, 1290, 1305, 1550, 1690, 2860, 2920, 2980, 3090, 3140, 3270.

Thiosemicarbazide **2b**, m.p. 232°; IR (KBr;cm^{-1}): 605, 740, 820, 1165, 1290, 1310, 1540, 1690, 2860, 2930, 2980, 3090, 3160, 3240, 3315.

Thiosemicarbazide **2c**, m.p. 221°; IR (KBr; cm^{-1}): 740, 820, 1160, 1290, 1310, 1550, 1680, 2850, 2915, 2960, 3090, 3145, 3290, 3340, 3420.

Thiosemicarbazide **2d**, m.p. 205°; IR (KBr;cm^{-1}): 700, 740, 815, 1160, 1290, 1305, 1550, 1680, 2850, 2920, 3075, 3140, 3300, 3380.

Bis-thiosemicarbazides of di(*para*-carboxyphenyl) sulphone, 3a,b, were prepared [8a] by addition of bis-acid hydrazide of di(*para*-carboxyphenyl) sulphone **4b**[8b] to ethyl - or benzyl isothiocyanate (reflux of equimolar quantities in anhydrous ethanol).

Thiosemicarbazide **3a**, m.p. 228°; IR (KBr; cm^{-1}: 850, 1160, 1290, 1325, 1550, 1685, 2850, 2915, 2970, 3080, 3170, 3270, 3300.

Thiosemicarbazide **3b**, m.p., 226°; IR (KBr; cm^{-1}): 720, 740, 1160, 1280, 1295, 1305, 1460, 1520, 1670, 2860, 2920, 3020, 3060, 3080, 3280, 3300.

General procedure for synthesis of 4,5-disubstituted-3-mercapto-1,2,4-triazoles 1a-f

The substituted thiosemicarbazides **2a-d** or **3a,b**(10mmoles) were refluxed with 50 ml N-NaOH solution for 45 minutes. The hot solutions were filtered then cooled. The solid sodium salts of mercapto-triazoles **1a-f** were filtered then converted into mercaptotriazoles by acidification with acetic acid. The crude products were recrystalized (Table 1) affording the following products (for spectra data see Table 2).

3-Mercapto-4-ethyl-5(phenylsulphonyl)phenyl-1,2,4-triazole (**1a**), m.p. 218°C; 70% yield.

3-Mercapto-4-ethyl-5(p-chlorophenylsulphonyl)phenyl-1,2,4-triazole (**1b**), m.p. 254°C; 83% yield.

3-Mercapto-4-ethyl-5(p-bromophenylsulphonyl)phenyl-1,2,4-triazole (**1c**), m.p. 273°C; 85% yield.

3-Mercapto-4-benzyl-5(phenylsulphonyl)phenyl-1,2,4-triazole (**1d**), m.p. 190°C; 70% yield.

Bis(para-*3-mercapto-4-ethyl-1,2,4-triazolyl)phenyl-sulphone* (**1e**), m.p. 293°C; 84% yield.

Bis(para-*3-mercapto-4-benzyl-1,2,4-triazolyl)phenyl-sulphone* (**1f**), m.p. 187°C; 80% yield.

REFERENCES

[1] E. G. Krysh, I. A. Mazur, N. N. Savenkova, V. R. Stets and A. A. Martynovski, *Khim. Farm. Zhur.*, **1983**, 798.

[2] S. P. Hiremath, J. S. Biradar and S. M. Kudari, *J. Indian Chem. Soc.*, **61**, 74 (1984).

[3] S. Evangelista, M. Ghelardoni, A. Meli, V. Pestelini, and G. Vitti, *Farmaco, Ed. Sci.*, **43**, 901 (1988).

[4] V. J. Ram, L. Mishra and D. S. Kushwaha, *Arch. Pharm.*, (Weinheim), **322**, 63 (1989).

[5] E. Cioränescu, ,,Medicamente de sinteză'', Ed. Tehnică, Bucharest, 1966, p. 35, 634.

[6] a) W. Marckwald and A. Bott, *Ber. dtsch. chem. Ges.*, **29**, 2914 (1986); b) E. Fromm, M.

Soffner and M. Frey, *Liebigs Annal. Chem.*, **434**, 285 (1923) ; c) E. Fromm and A Trnka, *Liebigs Annal. Chem.*, **442**, 150 (1925) ; d) E.F. Godefroi and E. L. Wittle- *J. Org. Chem.*, **21**, 1163 (1956) ; e) A. I. Mndzhoyan, V. G. Afrikyan and A. A. Dokhikyan, *Izv. Akad. Nauk Armyan SSR, Ser. Khim. Nauk*, **10**, 357 ; 363 (1957) — cf. *Chem. Abstr.*, **52**, 12851 (1958) ; f) S.G. Boots and C.C. Cheng, *J. Heterocyclic Chem.*, **4**, 272 (1967) ; g) I. Simiti and D. Ghiran, *Farmacia*, (*Bucharest*), **19**, 199 (1971) h) P. J. Kothari, V. Kishore, V. I. Stenberg and S. S. Parmar, *J. Heterocyclic Chem.*, **15**, 1101 (1978).

[7] I. Matei and E. Comaniţa, *Bull. Inst. Polytechn. Iassy*, **14**, 255 (1968).

[8] I. Saramet, *Ph. Dr. Thesis*, Polytechn. Inst. Bucharest, 1981 ; b) A. Mavrodin, V. Zotta, M. Stoenescu and D. Oţeleanu, *Pharm. Zentralhalle*, **95**, 353 (1956).

[9] These results will be reported in detail in a forthcoming paper.

[10] M. Pesson, S. Dupin and G. Polmans, *Bull. Soc. Chim. France*, **1961**, 1581.

Revue Roumaine de Chimie, 36, 1–3, 135–143(1991)

SYNTHESIS AND CHARACTERIZATION OF SOME 5-SUBSTITUTED-3-MERCAPTO-1,2,4-TRIAZOLES

IOANA ȘARAMET[a], MIRCEA D. BANCIU[b] and CONSTANTIN DRĂGHICI[c]
[a] Organic Chemistry Department, Faculty of Pharmacy, Traian Vuia Street 6, Bucharest, Roumania
[b] Organic Chemistry Department, Polytechnic Institute, TCH, Splaiul Independenței 313, Bucharest, Roumania
[c] Centre of Organic Chemistry, Roumanian Academy

Received July 25, 1990

Some new 5-substituted-3-mercapto-1,2,4-triazoles (2a-d) with potential biologic activity were synthesized by cyclization of acylthiosemicarbazides 4 or by reaction of acid hydrazides 3 with thiourea. The structures of triazoles 2a-d were proved by elemental analysis as well as by IR, UV and H-NMR spectra. Mercaptotriazoles 2 could be easily S-alkylated to thioethers 6a-e.

INTRODUCTION

In the previous note[1] we described the synthesis of some 4,5-disubstituted-3-mercapto-1,2,4-triazoles 1 with potential biologic activity. Continuing the researches in the same domain we present in this paper the synthesis and physico-chemical characterization of some related 5-substituted-3-mercapto-1,2,4-triazoles with the general formula 2. Due to the presence in the same molecular framework of the triazolic ring and of (arylsulphonyl)-phenyl substituent (R) the compounds 2 could be also regarded as potentially biologically active compounds.

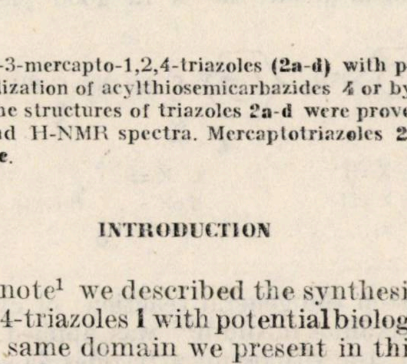

It could be also mentioned that some 5-substituted-3-mercapto-1,2,4-triazoles were used in the syntheses of interesting bicyclic thiazolotriazoles.[2]

RESULTS AND DISCUSSION

The 3-mercapto-1,2,4-triazoles **2** were synthesized by two different methods starting from the same key-intermediates, namely the known acid hydrazides **3a**—**d**.[3]

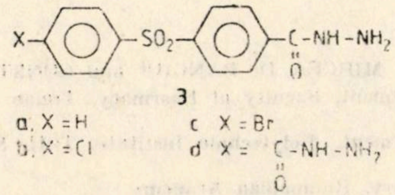

3

In the first procedure (method A) the hydrazides **3** treated (as hydrochlorides) with amonium or potassium thiocyanate afforded (arylsulphonyl)benzoyl-thiosemicarbazides **4a**—**d** in good yields (70—90%).[4]

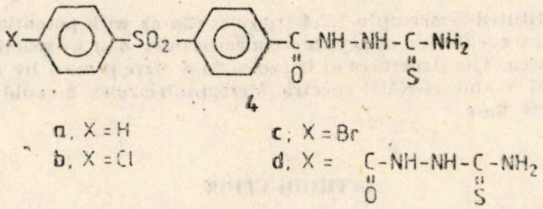

4

In the following step the general reaction of cyclization of 1-acylthiosemicarbazides in alkaline medium[5,6] was applied. Thus, heating of equimolar quantities of 1-acylthiosemicarbazides **4a**—**d** and sodium methoxide (in anhydrous methanol) conducted to mercaptotriazoles **2a**—**d** with 72—75% yields (Table 1).

The mechanism of the cyclization seems to be similar to that proposed[1] for 4,5-disubstituted-3-mercapto-1,2,4-triazoles (**1**) (Scheme 1).

In the second procedure (method B), the same mercaptotriazoles **2a**—**d** were obtained using the known general reaction between acid hydrazides and thiourea. Heating of hydrazides **3a**—**d**[3] with thiourea at 160—170°C afforded the triazoles **2a**—**2d** with 61—65% yields (Table 1).

Attempted synthesis of the triazole **2c** by reaction of the ester **5a** with thiosemicarbazide in methanol/sodium methoxide failed: the reaction product was the methyl ester **5b** formed by transesterification. The same preponderance of transesterification over condensation/cyclization sequence was observed in similar reactions of N-alkylthiosemicarbazides.

The structures of the new 3-mercapto-1,2,4-triazoles **2a**—**d** were proved by elemental analyses (Table 1) as well as by inspection of their IR, UV, and ^{1}H-NMR spectra (Table 2).

In the IR spectra of **2a**—**d** the characteristic $\nu_{C=O}$ band from the starting thiosemicarbazides **4a**—**d** (1685—1695 cm^{-1}) has disappeared proving the cyclization. The stretching vibration of the SH group appears

Table 1

5-Substituted-3-mercapto-1,2,4-triazoles 2

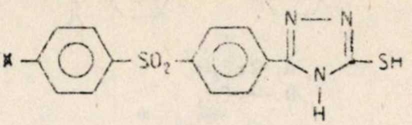
X
SO2
N
N
N
H
SH

2

Compound	X	m.p.(°C)recr. solvent*	yield(%) (method)**	Analysis % (calcd. found)		
				C	H	N
2a	H	282a)	72 (A) 63 (B)	52.99 53.29	3.47 3.70	13.25 13.20
2b	Cl	287a)	74 (A) 65 (B)	47.79 47.72	2.84 2.90	11.94 11.80
2c	Br	291a)	75 (A) 62 (B)	42.42 42.80	2.52 2.75	10.60 10.65
2d	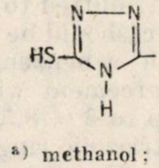	315b)	72 (A) 61 (B)	46.15 45.86	2.88 2.60	20.19 20.20

* a) methanol ; b) DMF/H_2O

** A — cyclization of acylthiosemicarbazides ; B—reaction of hydrazides with thiourea

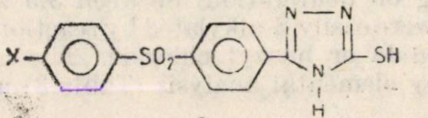
X
SO2
N
N
N
H
SH

2

a. X=H c X= Br

b X=Cl d. X =

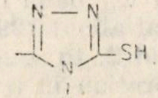

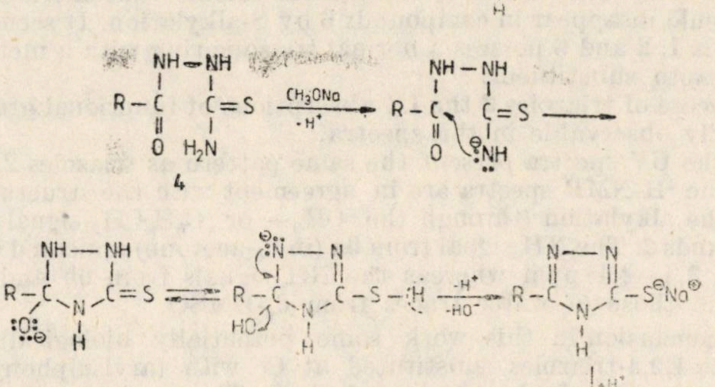
NH—NH
R—C
O
C=S
H2N
4
CH3ONa
-H+
NH—NH
R—C
O
C=S
NH
NH—NH
R—C
O
N
H
C=S
N
N
R—C
HO
N
H
C—S—H
-H+
-HO-
N
N
R—C
N
H
C—S⊖Na⊕
+H+

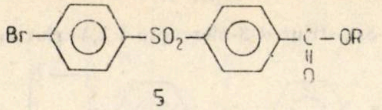

5
a; R = C_2H_5
b; R = CH_3

as a very weak band at 2540—2565 cm^{-}.^{1}All triazoles **2a**—**d** present specific SO_2 stretching bands at about 1160 cm^{-} ($\nu^{sym}_{SO_2}$) and at 1320 cm^{-1} $\nu^{asym.}_{SO_2}$). The characteristic absorptions of the remaining structural moieties from **2a**—**d** (e.g. C-Halogen; substituted phenyl groups, etc.) appear in the normal ranges. A strong absorption band occurring between 1280—1290 cm^{-1}in all triazoles **2a**—**d** could be attributted to ν_{C-N} vibrations and not to $\nu_{C=S}$ one (in a presumable thionic tautomeric form), on the basis of experimental evidence which will be discussed below.

The UV spectra of triazoles **2a**—**b** (Table 2) present three absorption bands: a) at 235—236 nm (lg ε = 4.09—4.24) b) at 251—258 nm (lg ε = 4.22—4.27) and c) a shoulder at 284—293 nm (lg ε = 3.96—4.08). Whereas the first two absorptions (a and b) could be attributted to transitions in substituted benzenic rings the latter absorption (c) should be ascribed to transitions in the triazolic ring conjugated with a benzenic one.

The ^{1}H-NMR spectra of **2a-d** (Table 2) are in agreement with the proposed structures. A relatively strong deshielding (up to δ = 8.5 ppm) of aromatic protons *ortho-* to SO_2 group and *ortho-* to triazolic ring could be easily seen. The NH and SH protons signals could be observed as large singlets (disappearing on deuteration) between 3.5 and 5.7 ppm.

The triazoles **2** were easily S-alkylated by reaction of their ammonium salts with methyl iodide or benzyl chloride. The new thioethers **6a-c** were characterized by elemental analysis (Table 3) and by spectral data (Table 4).

From the characteristic features of the spectra it could be mentioned:

a) the lack of ν_{SH} band from 2540—2565 cm^{-1} and the existence of the IR absorption at about 1290 cm^{-1}, attributed, as in the case of mercaptotriazoles **1**^{1} and **2**, to ν_{C-N} vibrations. If this band in **1** or **2** would be due to $\nu_{C=S}$ vibration in a presumable thionic tautomeric form (**2B**) then it would disappear in compounds **6** by S-alkylation. It seems that all compounds **1**, **2** and **6** possess a normal triazolic ring with a mercapto- or alkylmercapto substituent.
As in the case of triazoles **2** the IR absorptions of functional groups from **6** are easily observable in the spectra.

b) the UV spectra present the same pattern as triazoles **2**.

c) the ^{1}H-NMR spectra are in agreement with the structures **6** and confirm the alkylation (through the CH_3— or $C_6H_5CH_2$-signals lacking in compounds **2**. The NH signal from **6a** (in d_6-acetone) appeared as a large singlet at 3.4—4.1 ppm whereas the NH signals from **6b** and **6c** were included in those of water traces from d_6-DMSO.

In conclusion in this work some potentially biologically active 3-mercapto-1,2,4-triazoles substituted at C^5 with (arylsulphonyl)phenyl groups were synthesized and characterized. These compounds could be easily S-alkylated.

Table 2

Main spectral data of 5-substituted-3-mercapto-1,2,4-triazoles **2**

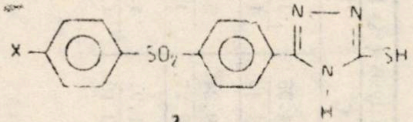

2

Comp.	X	IR* (KBr) cm	UV(CH_3OH) λ_{max}(lg ε_{max})	^1H-NMR**(TMS) δppm ;J_{Hz}(d_6-DMSO)
2a	H	691 s, 712 s, 759 s, 773 s, 853 s, 1160 vs$_{Hz}$ 1290 s, 1320 s, 1443 s, 1475 s, 1500 s, 1552 s, 1574 s, 2565 w, 3080 s, 3275 m	235 (4.09) 251 (4.22) 287 sh(3.96)	3.5–4.2 (large s ; 2H ; NH ; SH) 7.6–8.5 (m ; 9H$_{arom}$)
2b	Cl	695 w, 772 vs, 831 m, 842 m, 1160 vs, 1282 s, 1321 vs, 1381 m, 1471 s, 1554 m, 1575 vs, 2540 w, 3290 m	236 (4.24) 251 (4.26) 284 sh (4.06)	4.1–4.4 (large s ; 2H ; NH ; SH) 7.75 (d ; J=8.5 ; 2H ; H$_{ortho-Cl}$) ; 8–8.3 (m ; 6H$_{arom.}$)
2c	Br	605 m, 690 m, 770 s., 830 m, 852 m, 1160 vs, 1280 s, 1321 vs, 1390 m, 1470 s, 1567 m, 2560 w, 3080 w, 3265 m	236 (4.24) 255 (4.27) 287 sh(4.08)	3.9–4.4 (large s ; 2H ; NH ; SH) 7.9–8.2 (two large signals ; 8H$_{arom.}$)
2d	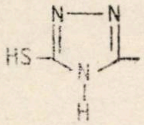	690 m, 766 m, 850 m, 1151 s, 1290 s, 1315 s, 1468 s, 1550 s, 1576 m, 2550 w, 3270 m	235 (4.22) 258 (4.24) 293 sh (4.01)	5.2–5.7 (large s, 4H ; NH ; SH) 8.17 (large s, 8 H$_{arom.}$)

*) w = weak ; m = medium ; s = strong ; vs = very strong
) s = singlet ; d = **doublet ; m = multiplet

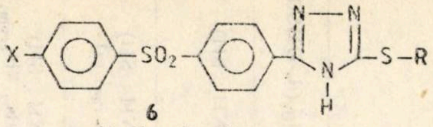

6

a. X = H ; R = CH_3
b. X = Cl; R = CH_3
c. X = H . R = $C_6H_5CH_2$

Table 3

5-Substituted-3-alkylmercapto-1,2,4-triazoles 6

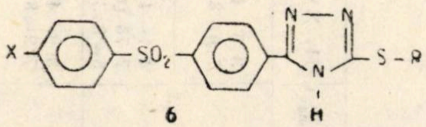

6

Compound	X	R	m.p.(°C) recr. solvent*	yield %	Analysis (%) (Calcd./Found)		
					C	H	N
6a	H	CH_3	208ᵃ⁾	80	54.38 54.42	3.92 4.20	12.68 12.70
b	Cl	CH_3	145ᵇ⁾	82	49.24 49.27	3.28 3.25	11.49 11.35
6c	H	$C_6H_5CH_2$	132ᵃ⁾	73	61.91 62.10	4.17 4.23	10.32 10.30

* a) benzene/petroleum ether ; b) methanol/water

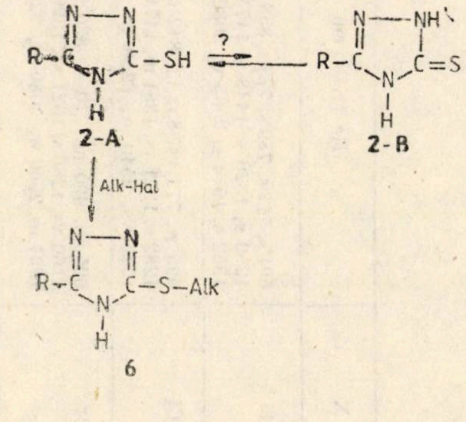

EXPERIMENTAL

The melting points are uncorrected. The IR spectra were registered on a UR-20. C. Zeiss-Jena spectrophotometer, the UV spectra on a SPECORD UV-VIS. C. Zeiss-Jena spectrophotometer and the ^{1}H-NMR spectra on a VARIAN A 60-A spectrometer using TMS as internal standard.

Table 4

Main spectral data of 5-substituted-3-alkylmercapto-1,2,4,-triazoles **6**

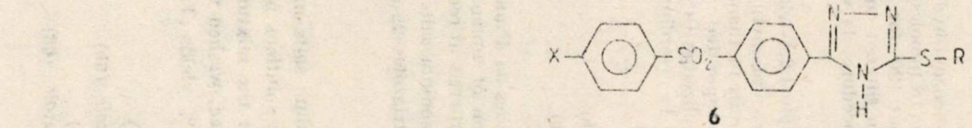

6

Compound	X	R	IR*(KBr)cm^{-1}	UV (CH_3OH) λ_{max}(lg ε_{max})	^1H-NMR** (TMS) δ ppm; JHz
6a	H	CH_3	685 m, 722 m, 760 m, 856 m, 1159 s, 1285 s, 1308 s, 1410 w, 1442 m, 1540 w, 1595 w, 3295 m	233 sh (4.12) 248 (4.19) 278 (4.10)	2.58 (s ; 3H ; CH_3) ; 3.4–4.1 (large s ; 1H ; NH) 7.4–7.75 (m ; 3H ; from C_6H_5) 7.8–8.4 (m ; 6H ; 2H from C_6H_5 and 4H from C_6H_4) (d_6-acetone-solvent)
6b	Cl	CH_3	710 m, 745 s, 770 s, 839 m, 1160 vs, 1290 vs, 1320 vs, 1390 m, 1420 m, 1449 m, 1461 m, 1510 m, 1571 m, 2920 w, 2988 w, 3090 m	234 (4.23) 251 (4.20) 280 (4.11)	2.7 (s ; 3H ; CH_3) 7.72 (d ; J = 8.5 ; 2H ; H_{ortho}–Cl) 8.0–8.35 (m ; $6H_{arom.}$) (d_6 -DMSO-solvent)
6c	H	$C_6H_5CH_2$	672 m, 719 m, 749 m, 851 w, 1158 s, 1290 s, 1308 vs, 1315 vs, 1410 m, 1441 m, 1490 m, 1595 w, 3258 s	223 (4.25) 253 (4.23) 273 (4.19)	4.48 (s ; 2H ; CH_2) 7.1–8.4 (m ; $14H_{arom.}$) (d_6-DMSO-solvent)

* w=weak; m=medium; s=strong; vs=very strong

** s=singlet; d=doublet; m=multiplet

para-(Arylsulphonyl)benzoyl-thiosemicarbazides 4a-d.[4]

Procedure 1: A solution of *p*-(arylsulphonyl)benzoylhydrazide **3a-d** (20 mmoles) in absolute ethanol (50 mL) was saturated at 0°C with anhydrous gaseous HCl. The solid hydrochlorides separated by filtration were dissolved in 50 mL absolute ethanol containing 28 mmoles ammonium thiocyanate. The solutions were refluxed for 12 hrs (the initial pink colour disappears). The solid products obtained after cooling were filtered, washed with water and recrystallized affording pure products **4a-d**. Good elemental analyses (C, H, N) were obtained for compounds **4a-d**.

Thiosemicarbazide **4a**, m.p. 165° (methanol); 89% yie'd; *IR spectrum* (KBr; cm^{-1}): 830w, 855w, 1165vs, 1260vs, 1305vs, 1450s, 1480s, 1540s, 1580s, 1640s, 1690vs, 3040m, 3090s, 3190s, 3280s, and 3370m; *UV spectrum* (Methanol) (λ_{max}; ε_{max}): 249 (26000); 351 (4500).

Thiosemicarbazide **4b**, m.p. (197° (methanol); 90% yield: *IR spectrum* (KBr; cm^{-1}): 780m, 825w, 850w, 1160vs, 1260vs., 1315vs, 1480s, 1530s, 1580s, 1605s, 1635s, 1690vs, 3090m, 3165m, 3320m, and 3410m.

Thiosemicarbazide **4c**, m.p. 208° (DMF-water: 70% yield): *IR spectrum* (KBr; cm^{-1}): 605vs, 755vs, 825w, 850w, 1160vs, 1260vs, 1315vs, 1480m, 1545m, 1575m, 1610m, 1635m, 1685vs, 3090s, 3160s, 3320s, and 3425m; *UV spectrum* (Methanol: λ_{max}^{nm}; ε_{max}): 253 (32170): 357 5800).

bis-Thiosemicarbazide **4d**, m.p. 282°; (DMF-water); 85% yield; *IR spectrum* (KBr, (cm^{-1}): 755s, 820w, 850w, 1160vs, 1260vs, 1310vs, 1450m, 1490m, 1535m, 1580s, 1635m, 1695vs, 3090m, 3180s, 3330s, and 3420m.

Procedure 2: Mixtures consisting from *p*-(arylsulphonyl)-benzoyl-hydrazide **3a-d** (13 mmoles), conc. hydrochloric acid (1.5 mL), potassium thiocyanate (18 mmoles) and anhydrous methanol (25 mL) were evaporated to dryness then heated at about 120° for 1 hr. The white solids obtained were heated gently with water (3 × 125 mL) then filtered and recrystallized. The thiosemicarbazides **4a-d** (identical to those prepared after procedure 1) were obtained in 70—76% yields.

General procedures for synthesis of 5-substituted-3-mercapto-1,2,4-triazoles 2a-d

Method A. Equimolar quantities (5 mmoles) of *para*-(arylsulphonyl)benzoyl-thiosemicarbazides **4a-d** and freshly prepared sodium methoxide in anhydrous methanol (15 mL) were heated at reflux on a water bath for 10 hours. The solvent was evaporated *in vacuo* and the remaining solid was treated with cold water (10 mL) then neutralized with acetic acid. The obtained crude products were filtered then recrystallized (Table 1) affording the pure compounds **2a-d** in 72—75% yields (for spectral data see Table 2):

3-Mercapto-5(phenylsulphonyl)phenyl-1,2,4,-triazole (**2a**)

3-Mercapto-5(p-chlorophenylsulphonyl)phenyl-1,2,4,-triazole(**2b**)

3-Mercapto-5(p-bromophenylsulphonyl)phenyl-1,2,4-triazole(**2c**)

Bis(para-3-mercapto-1,2,4-triazolyl)phenylsulphone (**2d**)

Method B. Equimolar quantities (10 mmoles) of acid hydrazides **3a-d**[3] and thiourea were heated (without solvent) at 160—170° for 8—10 hrs (the evolution of ammonia ceased). The crude reaction mixtures were dissolved in 5% NaOH solution and stirred at room temperature for 4 hrs. After filtration of some solid impurities the solutions of sodium salts of 3-mercapto-1,2,4-triazoles were cooled and acidified with acetic acid when the triazoles **2a-d** were obtained in 61—65% yields (Table 1).

5-Substituted-3-alkylmercapto-1,2,4-triazoles 6a-d

The triazoles **2** (3 mmoles) were converted into their ammonium salts on treatment with excess warm ammonium hydroxide solution (25 mL). Over these solutions methyl iodide or benzyl chloride (4 mmoles) was added at room temperature and the mixtures were stirred for 45 min.; the obtained yellowish-white precipitates were filtered, washed with water then recrystallized affording the following thioethers **6a-d** in 73—82% yields (Table 3; spectral data see Table 4):

3-Methylmercapto-5(phenylsulphonyl)phenyl-1,2,4-triazole (**6a**)

3-*Methylmercapto-5(p-chlorophenylsulphonyl)phenyl-1,2,4-triazole* (**6b**)

3-Benzylmercapto-5(phenylsulphonyl)phenyl-1,2,4-triazole (**6c**)

3-Benzylmercapto-5(p-bromophenylsulphonyl)phenyl-1,2,4-triazole (**6d**)

REFERENCES

[1] I. Şaramet, M. D. Banciu and C. Drăghici, *Rev. Roumaine Chim.*, **36**, 127 (1991).

[2] a) K. T. Pots and S. Husain, *J. Org. Chem.*, **36**, 10 (1971) ; b) A. I. Mohamed, A. B. Mostafa and A. Soliman, *J. prakt. Chem.*, **318**, 12 (1976) ; c) A. Singh, R. N. Handa and H. K. Pujari, *Indian J. Chem.*, **16 B**, 475 (1978).

[3] A. Mavrodin, V. Zotta, M. Vorel-Stoenescu and D. Oţeleanu, *Pharm. Zentralhalle*, **95**, 353 (1956).

[4] I. Şaramet, *Ph. Dr. Thesis*, Polytech. Inst. Bucharest, 1981.

[5] a) S. P. Dutta, A. K. Acharyya and U. P. Basu, *J. Indian Chem. Soc.*, **45**, 338 (1968); b) F. Russo and M. Ghelardoni, *Boll. Chim. Farm.*, **106**, 827 (1967).

[6] See also reference 1 and the literature cited therein.

Revue Roumaine de Chimie, 36, *1–3*, 145–155(1991)

CHEMICAL GRAPHS. PART 54.*

ENUMERATION OF UNBRANCHED CATACONDENSED POLYHEXES WITH EQUIDISTANT LINEARLY CONDENSED SEGMENTS

A.T. BALABAN,[a] J. BRUNVOLL[b] and S.J. CYVIN[b]

[a] Polytechnic Institute, Organic Chemistry Department, Spl. Independenţei 313, R–76206 Bucharest, Roumania

[b] Division of Physical Chemistry, The University of Trondheim, N–7034 Trondheim-NTH, Norway

Received July 15, 1990

Unbranched catacondensed benzenoids with equidistant linearly condensed segments of the lengths $s = 2$ and $s > 2$ were computer-generated and enumerated. These systems represent subclasses of fibonacenes and generalized fibonacenes, respectively. The abundancies of helicenic systems in these classes are discussed, as also is the case for the catafusenes in total. In this connection the numbers of catacondensed helicenes for h (the number of hexagons) $= 13$ and $h = 14$ are reported for the first time. Results from a computer-generation and enumeration of primitive coronoids with 2-segments only are reported.

1. INTRODUCTION

The enumeration of polyhexes is of constant interest to researchers in mathematical chemistry. This interest seems clearly to have increased after the appearance of a consolidated multi-author report[1] on this topic. We are using the term polyhex in a wide sense about the hexagonal systems so that they include both benzenoids (polyhexes without holes) and coronoids (polyhexes with holes).

In general, the enumeration problem for polyhexes is unsolved from the mathematical standpoint, but extensive computer-aided enumerations have been performed. Yet some partial solutions exist in exact mathematical terms. Firstly, one has the famous deduction of a generating function for the numbers of catafusenes by Harary and Read.[2] Here the term catafusene is used so as to include also catacondensed helicenes (or helicenic systems). Secondly, some explicit formulas have been derived for classes of polyhexes : (a) unbranched catafusenes ;[3,4] (b) L-transforms of a three-digit code[5] or *LA*-sequences,[6] which correspond to the objects called caterpillars in mathematics, and were enumerated by Harary and Schwenk;[7] (c) fibonacenes[8], a class of catafusenes to be defined below; (d) special annulenes,[9] a solution which has been adapted to "hollow hexagons", a subclass of primitive coronoids.[10,11]

---

* Part 53 is ref. 24. It should be noted that Part 51 is ref. 12, while Part 52 is ref. 25, erroneously indicated as Part 51.

We call s-segment a linearly condensed portion of a catafusene with s hexagons (benzenoid rings). At each kink the respective hexagon is counted twice for the two segments incident with this hexagon (see also below).

The recent analysis of fibonacenes (c)[8] is of special interest in the present work. A *fibonacene* is a special catafusene, which consists of 2-segments only (and therefore is "all-kinked"). The name is explained by the feature that it is a catafusene whose Kekulé structure count is a *Fibonacci* number. Very recently Balaban and Artemi[12] generalized the treatment of fibonacenes. They considered the numbers $N(h, s)$, which pertain to the unbranched catafusenes with h hexagons and having a longest segment of the length s.

In the present work the enumeration data on fibonacenes without helicenes are supplemented. Some reflections about the abundance of helicenic systems are offered.

Furthermore, a computer-aided enumeration of primitive coronoids with 2-segments only (all-kinked primitive coronoids) is reported for the first time.

Finally in this introduction we give the references to some monographs[13–15] with relevance to the subject of this work.

2. FIBONACENES

The class of polyhexes called fibonacenes was defined in the introduction above. As an alternative definition, a fibonacene is a single chain of hexagons with all of the hexagons angularly annelated apart from the two terminal ones (i.e. devoid of "anthracenic" subgraphs). It is emphasized that the fibonacenes include helicenic systems (helicenes).

Balaban[8] has derived explicit formulas for the number of fibonacenes and the fibonacenes of different symmetries. They can be written:

$$C(h) \begin{cases} 0\,; & h = 3,5,7,\ldots \\ 2^{(h-4)/2}\,; & h = 4,6,8,\ldots \end{cases} \qquad (1)$$

$$S(h) = 2^{[(h-3)/2]}\,; \qquad h = 3,4,5,6,\ldots \qquad (2)$$

$$U(h) = 2^{h-4} - 2^{[(h-5)/2]}\,; \quad h = 4,5,6,7,\ldots \qquad (3)$$

while $U(3) = 0$, and

$$T(h) = 2^{h-4} + 2^{[(h-5)/2]}\,; \quad h = 4,5,6,7,\ldots \qquad (4)$$

while $T(3) = 1$. Here C, S and U pertain to the centrosymmetrical (C_{2h}), mirror-symmetrical (C_{2v}) and unsymmetrical (C_s) systems, respectively, while T is used to designate the total. The number of hexagons is (as usual) denoted by h. The brackets (in the exponents) denote the floor function : $[x]$ is the largest integer smaller than or equal to x.

Here we use the term benzenoid for a planar (non-helicenic), simply connected polyhex. The term "planar" is used here in the geometrical rather than the graph-theoretical meaning ; helicenes are non-planar. It is clear that the class of unbranched catacondensed benzenoids with 2-segments only is a subclass of the fibonacenes ; the members are the planar fibonacenes. By an s-segment we mean a segment of the length s in terms of the number of hexagons ; a segment is the linear chain between two neighbouring angularly annelated hexagons (or a terminal and the nearest angularly annelated hexagon), the two end hexagons included.

We have enumerated, by computer aid, the planar fibonacenes up to $h = 21$, including the recognition of the different symmetries. The result is given in Table 1. The numbers agree with those of Balaban[8] or Balaban and Artemi,[12] who presented these numbers up to $h = 10$.

Table 1

Numbers of all planar fibonacenes (excluding helicenic systems) with $h = 3$ to 21

h	centrosym.	mirror-sym.	unsym.
3	0	1	0
4	1	1	0
5	0	2	1
6	2	1	2
7	0	3	5
8	4	2	9
9	0	6	19
10	7	4	35
11	0	11	69
12	13	7	125
13	0	18	238
14	24	12	430
15	0	33	800
16	44	22	1447
17	0	58	2662
18	81	36	4808
19	0	102	8779
20	147	68	15848
21	0	183	28813

3. GENERALIZED FIBONACENES

The class of unbranched catafusenes with S segments of s hexagons each has been considered by Balaban and Tomescu.[16] Fibonacenes clearly form a subclass of generalized fibonacenes, where $s = 2$.

The number of hexagons in a generalized fibonacene is

$$h = (s - 1)S + 1 \tag{5}$$

For fibonacenes in particular,

$$h = S + 1 (s = 2) \tag{6}$$

If h in Eqs. (1)–(4) is substituted by $S + 1$ according to Eq. (6), then the expressions are valid for any class of generalized fibonacenes where s is fixed (but arbitrary).

In the present work we have enumerated the planar generalized fibonacenes with $s = 3$ up to $S = 19$. Again the helicenic systems are excluded. The result given in Table 2, corresponds to the numbers of Table 1, which, however, are listed up to $S = 21$. It is inferred that the numbers of Table 2 are valid for any fixed s value is $s > 2$.

Table 2

Numbers of all planar generalized fibonacenes with $s > 2$ and $S = 2$ to 19

S	centrosym.	mirror-sym.	unsym.
2	0	1	0
3	1	1	0
4	0	2	1
5	2	2	2
6	0	3	6
7	4	3	11
8	0	6	25
9	8	6	47
10	0	11	96
11	15	11	181
12	0	20	358
13	29	21	674
14	0	36	1297
15	56	36	2445
16	0	68	4655
17	106	70	8762
18	0	123	16551
19	201	125	31129

4. ABUNDANCE OF HELICENES AMONG GENERALIZED FIBONACENES

The numbers of Tables 1 and 2 can be combined with the results from Eqs. (1)–(3) in order to give the numbers of helicenic systems for each entry. We have performed this analysis for the numbers of generalized fibonacenes in total. Table 3 shows the numbers of the planar and nonplanar systems separately; for the latter class the numbers are given in parentheses.

It is found that there are more helicenic fibonacenes ($s = 2$) than the helicenic generalized fibonacenes with $s > 2$ for the same number of segments ($S \geqslant 5$). This feature is not surprising. In this connection Fig. 1 is supposed to be elucidating.

Table 3

Numbers of planar generalized fibonacenes including fibonacenes ($s = 2$) in total, and the numbers of the corresponding nonplanar (helicenic) systems in parentheses

S	$s = 2$	$s > 2$
2	1 (0)	1(0)
3	2 (0)	2(0)
4	3 (0)	3 (0)
5	5 (1)	6 (0)
6	8 (2)	9 (1)
7	15 (5)	18 (2)
8	25 (11)	31 (5)
9	46 (26)	61 (11)
10	80 (56)	107 (29)
11	145 (127)	207 (65)
12	256 (272)	378 (150)
13	466 (590)	724 (332)
14	833 (1247)	1333 (747)
15	1513 (2647)	2537 (1623)
16	2720 (5536)	4723 (3533)
17	4925 (11587)	8938 (7574)
18	8881 (24015)	16674 (16222)
19	16063 (49729)	31455 (34337)

In general it is seen (Table 3) that the abundance of helicenic systems increases strikingly with increasing number of segments. This tendency is especially pronounced for the class of fibonacenes. Here it is found that the number of benzenoids is overbid by the number of helicenes for $S \geqslant 12$. For the generalized fibonacenes with $s > 2$ this feature occurs at $S \geqslant 19$.

5. CATAFUSENES

Here we give a note on the numbers of catafusenes as an apropos to the preceding section.

The catacondensed benzenoids (catafusenes without the helicenic systems) have been enumerated by several researchers. The numbers up to $h = 11$ are found in the consolidated report[1] mentioned in the present introduction, while the supplements thereof[17] contain the result for $h = 12$. Very recently the extension of these data to $h = 13$ and $h = 14$ has been reported.[18] All the numbers of catacondensed benzenoids up to $h = 14$ are collected in Table 4. We wish to compare them with the numbers of catacondensed helicenes. These numbers are obtained as differences if we know the numbers of catafusenes in total (benzenoids + helicenes) for the h values in question.

The numbers of catafusenes are the classical Harary-Read numbers. These authors[2] used their generating function to compute these numbers up to $h = 40$, but apart from the very number for $h = 40$ (a 24-digit in-

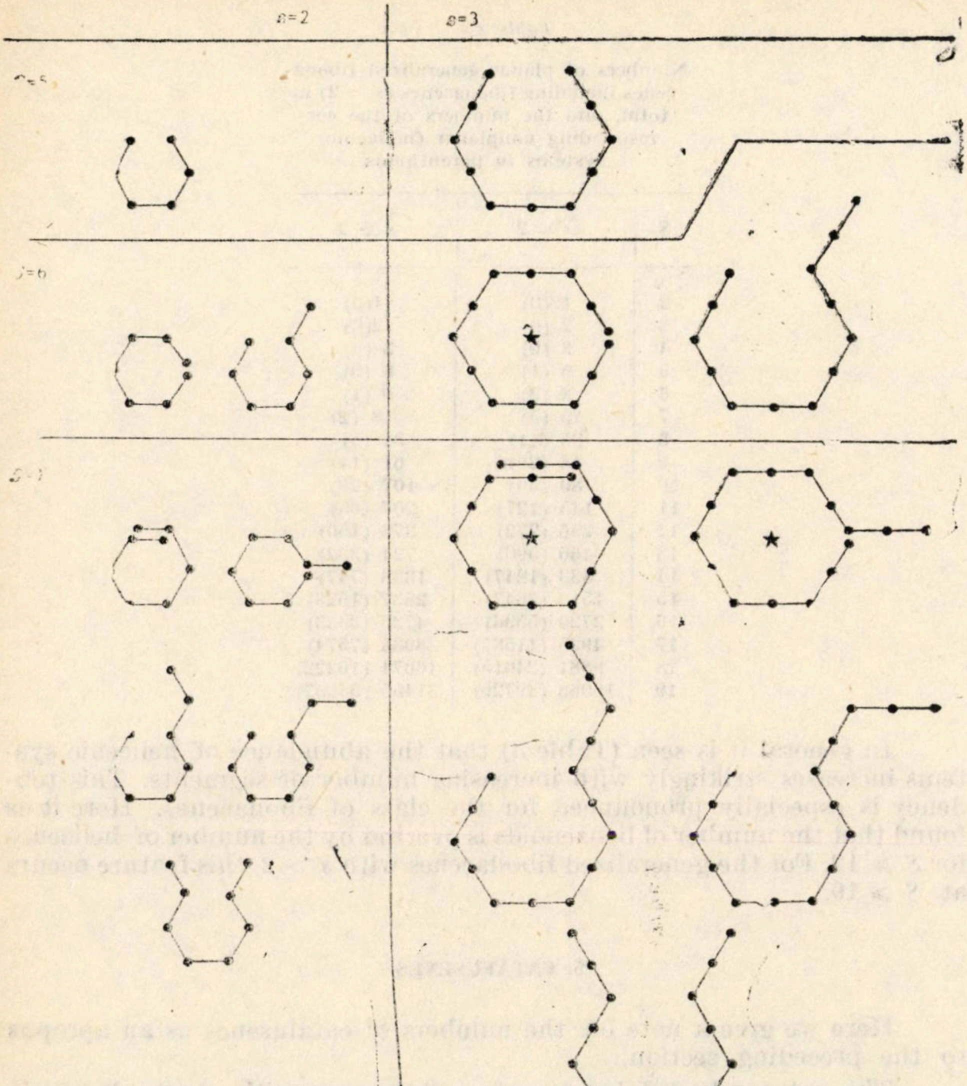

Fig. 1 — The eight smallest helicenic fibonacenes ($s=2$) and the corresponding generalized fibonacenes with $s=3$. Some members of the latter class indicated by asterisks, are helicenic; the others are not. Dualists are employed.

teger) they listed the numbers only up to $h = 12$. Now an extension of this list is acute. Based on the generating function of Harary and Read[2] we attained 467262 and 1981353 as the numbers of catafusenes with $h = 13$ and 14, respectively.

The numbers of catacondensed helicenes are now available up to $h = 14$. They are included in parentheses in Table 4.

Table 4

Numbers of the planar and nonplanar catafusenes : benzenoids and helicenes

h	Catacondensed	
	benzenoids	(helicenes)
1	1	(0)
2	1	(0)
3	2	(0)
4	5	(0)
5	12	(0)
6	36	(1)
7	118	(5)
8	411	(35)
9	1489	(200)
10	5572	(1121)
11	21115	(5919)
12	81121	(30509)
13	314075	(153187)
14	1224528	(756825)

It is seen from Table 4 that the relative abundance of helicenic systems among the catafusenes increases rapidly with increasing h values. It starts like a small contamination with 1 out of 37 systems (about 3 percent) at $h = 6$. Already at $h = 10$ the percentage of helicenes has increased to about 17. At $h = 14$ about 38 percent of the catafusenes are helicenic. For $h \leqslant 14$ there are still more benzenoids than helicenes among the catafusenes with the same h value. However, there is no reason to doubt that this situation becomes reversed at higher h values.

6. PRIMITIVE CORONOIDS WITH 2-SEGMENTS ONLY

A primitive coronoid is a single chain of hexagons in a macrocyclic arrangement achieved by corona-condensation; its dualist is simply a cycle.

In the present work we have produced the first computer-generated data for the title systems. These systems may be interpreted as the corona-condensed fibonacenes, but without helicenic systems. The correspond-

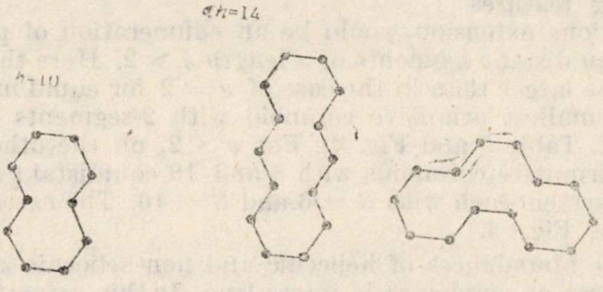

Fig. 2. — The smallest helicenic corona-condensed fibonacenes. Dualists are employed.

ing helicenic systems can also be defined, but their numbers are not obtainable by our computer algorithm. The smallest such systems are shown in Fig. 2.

No algebraic solution is known for the corona-condensed unbranched chains with equidistant segments, whether the helicenic systems are included or not.

The numbers of primitive coronoids with 2-segments only up to $h = 32$ are shown in Table 5, including the distribution into symmetry groups. The pertinent systems up to $h = 20$ are depicted as dualists in Fig. 3.

Table 5

Numbers of primitive coronoids with 2-segments only, classified according to symmetry

h	D_{6h}	D_{3h}	C_{3h}	D_{2h}	C_{2h}	C_{2v}	C_s	Total
12	0	1	0	0	0	0	0	1
14	0	0	0	1	0	0	0	1
16	0	0	0	0	0	1	0	1
18	1	1	0	1	1	1	0	5
20	0	0	0	0	0	3	2	5
22	0	0	0	4	2	4	5	15
24	0	2	1	0	0	6	20	29
26	0	0	0	5	9	19	48	81
28	0	0	0	0	0	22	159	181
30	2	4	3	9	29	48	422	517
32	0	0	0	0	0	59	1246	1305

It is observed that there is no system with C_{6h} symmetry of the class under consideration as far as the listing of Table 5 goes. Such systems do exist, however, the smallest of them presumably having 42 hexagons. This system is depicted in Fig. 4.

7. CONCLUSION

The present work is mainly a contribution to the enumeration of polyhexes (benzenoids and coronoids). It opens for possible future studies of interesting features.

An obvious extension would be an enumeration of primitive coronoids with equidistant segments of a length $s > 2$. Here the numbers are expected to be larger than in the case of $s = 2$ for equal numbers of segments. The smallest primitive coronoid with 2-segments only has $S = h = 12$ (cf. Table 5 and Fig. 3). For $s > 2$, on the other hand, there are already primitive coronoids with 6 and 10 equidistant segments, specifically one system each with $S = 6$ and $S = 10$. The cases for $s = 3$ are illustrated in Fig. 5.

Also the abundances of helicenic and non-helicenic systems among different classes of polyhexes is interesting. In this respect an extensive material for unbranched catafusenes is available.[19] The branched cata-

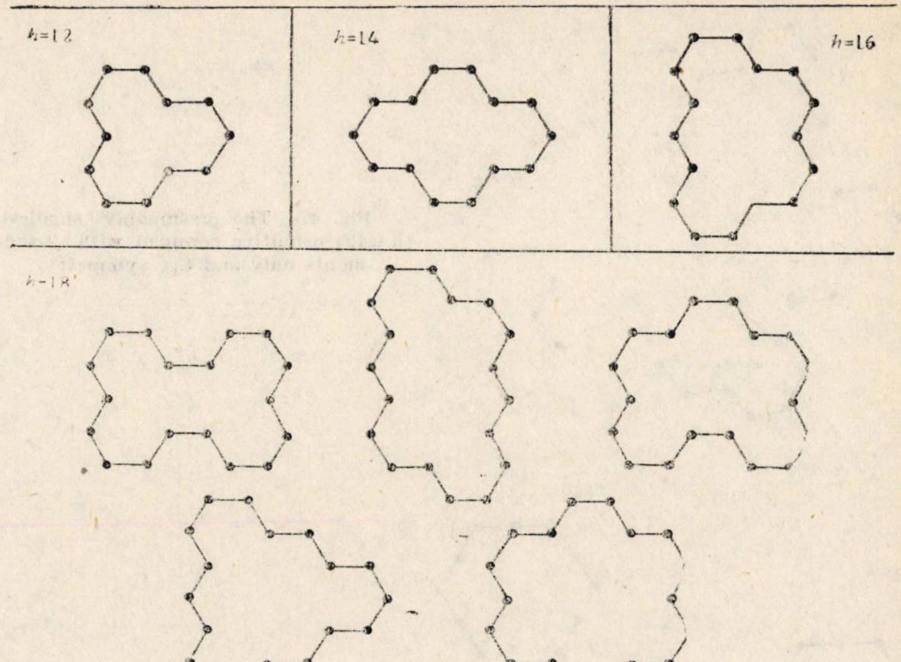

Fig. 3. — The thirteen smallest primitive coronoids with 2-segments only. Dualists are employed.

fusenes have also been treated under this scope.[20] Some reflections on this point for the catafusenes (unbranched and branched together) are offered in the present work (cf. especially Table 4).

Recently the regular trigonal $(D_{3h})^{21}$ and dihedral $(D_{2h})^{22}$ catacondensed benzenoids have been computer-generated and enumerated spe-

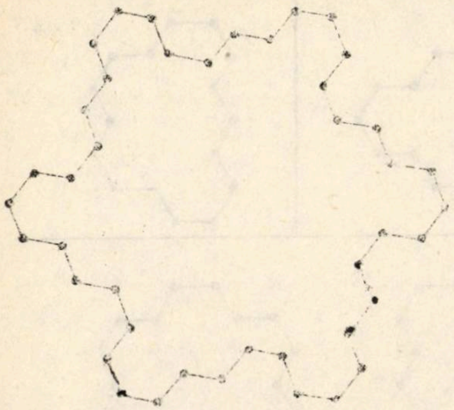

Fig. 4. — The presumably smallest ($h=42$) primitive coronoid with 2-segments only and C_{6h} symmetry.

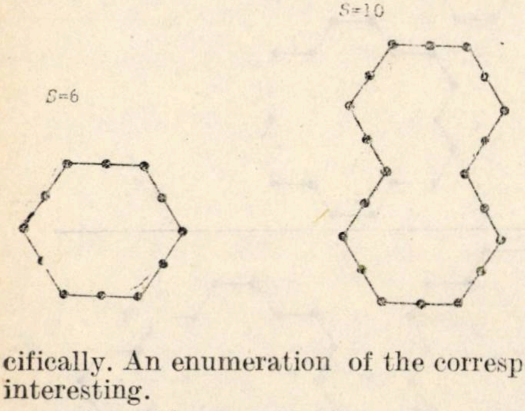

Fig. 5. — The two smallest primitive coronoids with 3-segments only.

cifically. An enumeration of the corresponding helicenic systems might be interesting.

An all-benzenoid (also called fully benzenoid[23]) is a benzenoid for which a Kekulé structure can be written so that all its double bonds belong to aromatic sextets. We have observed that the corona holes of the primitive coronoids with 2-segments only constantly are all-benzenoid systems. This is an interesting feature, which perhaps could be exploited in further enumerations.

REFERENCES

[1] A. T. Balaban, J. Brunvoll, J. Cioslowski, B. N. Cyvin, S. J. Cyvin, I. Gutman, W.C.He, W. J. He, J. V. Knop, M. Kovačević, W. R. Müller, K. Szymanski, R. Tošić and N. Trinajstić, *Z. Naturforsch.*, **42a**, 863 (1987).

[2] F. Harary and R. C. Read, *Proc. Edinburgh Math. Soc.*, **17** (Ser. II), 1(1970).

[3] A. T. Balaban and F. Harary, *Tetrahedron*, **24**, 2505 (1968).

[4] A. T. Balaban, *Tetrahedron*, **25**, 2949 (1969).

[5] A. T. Balaban, *Rev. Roumaine Chim.*, **22**, 45 (1977).

[6] I. Gutman, *Theor. Chim. Acta*, **45**, 309 (1977).

[7] F. Harary and A. J. Schwenk, *Discrete Mathematics*, **6**, 359 (1973).

[8] A. T. Balaban, *Math. Chem.*, **24**, 29 (1989).

[9] S. J. Cyvin, J. Brunvoll and I. Gutman, *Rev. Roumaine Chim.*, in press.

[10] S. J. Cyvin, J. Brunvoll and B. N. Cyvin, in "MATH/CHEM/COMP 1988, Proceedings of an International Conference on the Interfaces Between Mathematics, Chemistry and Computer Science, Dubrovnik, Yugoslavia, 20—25 June 1988" (Edited by A. Graovac), p. 127, Elsevier, Amsterdam, 1989.

[11] S. J. Cyvin, J. Brunvoll, B. N. Cyvin, J. L. Bergan and E. Brendsdal, *Struct. Chem.*, in press.

[12] A. T. Balaban and C. Artemi, *Polycyclic Aromatic Compounds*, **1**, 171 (1990).

[13] N. Trinajstić, "Chemical Graph Theory", volumes I, II, Boca Raton, Florida, 1983.

[14] S. J. Cyvin and I. Gutman, "*Kekulé Structures in Benzenoid Hydrocarbons*", Lecture Notes, in Chemistry No. 46, Springer, Berlin, 1988.

[15] I. Gutman and S. J. Cyvin, "*Introduction to the Theory of Benzenoid Hydrocarbons*", Springer, Berlin, 1989.

[16] A. T. Balaban and I. Tomescu, *Math. Chem.*, **17**, 91 (1985).

[17] W. J. He, W. C. He, Q. X. Wang, J. Brunvoll and S. J. Cyvin, *Z. Naturforsch.*, **43a**, 693 (1988).

[18] S. J. Cyvin and J. Brunvoll, *Chem. Phys. Letters*, in press.

[19] J. Brunvoll, R. Tošič, M. Kovačević, A. T. Balaban, I. Gutman and S. J. Cyvin, *Rev. Roumaine Chim.*, **35**, 85 (1990).

[20] A. T. Balaban, J. Brunvoll, B. N. Cyvin and S. J. Cyvin, *Tetrahedron*, **44**, 221 (1988).

[21] R. Tošić, Z. Budimac, J. Brunvoll and S. J. Cyvin, *J. Mol. Struct.* (*Theochem*), in press.

[22] R. Tošić, Z. Budimac, S. J. Cyvin and J. Brunvoll, *J. Mol. Struct.* (*Theochem*), in press.

[23] E. Clar, "The Aromatic Sextet", Wiley, London, 1972.

[24] C. Deleanu and A. T. Balaban, *Rev. Roumaine Chim.*, **35**, 349 (1990).

[25] A. T. Balaban, *Rev. Roumaine Chim.*, **34**, 1745 (1989).

S. J. Cyvin, J. Brunvoll and I. Gutman, Rev. Roumaine Chim., in press.

S. J. Cyvin, J. Brunvoll and B. N. Cyvin, in "MATH/CHEM/COMP 1988, Proceedings of an International Conference on the Interfaces Between Mathematics, Chemistry and Computer Science, Dubrovnik, Yugoslavia, 20–25 June 1988" (Edited by A. Graovac), p. 127, Elsevier, Amsterdam, 1989.

S. J. Cyvin, J. Brunvoll, B. N. Cyvin, J. L. Bergan and E. Brendsdal, Struct. Chem., in press.

A. T. Balaban and C. Artemi, Polycyclic Aromatic Compounds, 1, 171 (1990).

N. Trinajstić, "Chemical Graph Theory", Volumes I, II, CRC Press, Boca Raton, Florida, 1983.

S. J. Cyvin and I. Gutman, "Kekulé Structures in Benzenoid Hydrocarbons", Lecture Notes in Chemistry 46, Springer, Berlin, 1988.

I. Gutman and S. J. Cyvin, "Introduction to the Theory of Benzenoid Hydrocarbons", Springer, Berlin, 1989.

A. T. Balaban and J. Tomescu, Math. Chem., 17, 91 (1985).

W. C. He, W. J. He, Q. X. Wang, J. Brunvoll and S. J. Cyvin, Z. Naturforsch., 43a, 693 (1988).

S. J. Cyvin and J. Brunvoll, Chem. Phys. Letters, in press.

J. Brunvoll, R. Tošić, M. Kovačević, A. T. Balaban, I. Gutman and S. J. Cyvin, Rev. Roumaine Chim., 35, 85 (1990).

A. T. Balaban, J. Brunvoll, B. N. Cyvin and S. J. Cyvin, Tetrahedron, 44, 221 (1988).

R. Tošić, V. Bodroža, J. Brunvoll and S. J. Cyvin, J. Mol. Struct. (Theochem), in press.

R. Tošić, R. Doroslovački, S. J. Cyvin and J. Brunvoll, J. Mol. Struct. (Theochem), in press.

E. Clar, "The Aromatic Sextet", Wiley, London, 1972.

C. [illegible] and A. T. Balaban, Rev. Roumaine Chim., 35, 349 (1990).

A. T. Balaban, Rev. Roumaine Chim., 34, 1729 (1989).

Revue Roumaine de Chimie, 36, 1–3, 157–169 (1991)

REACTION OF 3,5-DI-*t*-BUTYLNITROSOBENZENE WITH ALKOXIDES AND CARBANIONS[1,2]

FLORIN BADEA, ALEXANDRU T. BALABAN, ION COSTEA, FLORIN IORDACHE, AURELIA MEGHEA and DANIELA CARMEN ONICIU

Department of Organic Chemistry, Polytechnic Institute, Bucharest, Romania

Received May 18, 1990

The reaction of 3,5-di-*t*-butylnitrosobenzene with alkoxides (MeOM,EtOM, *i*-PrOM and *t*-BuOM, where the metal M is either sodium or potassium) has been studied in different solvents (the corresponding alcohols, DMF, DMSO, N-methyl pyrrolidone, benzene and toluene), either in presence or in absence of camphor or a camphor derivative substituted in position 3 with a group RCO (R=H, OEt, COOEt). The reaction was followed by ESR-spectrometry, in order to detect the intermediate nitroxide radicals. The carbonyl compound is involved with certainty in the formation of the observed radicals in the case of 3-formylcamphor, **8**, and probably in the reaction performed in the presence of the unsubstituted camphor. In the absence of the carbonyl compounds, as well as in their presence, depending on the system base-solvent used in the reaction, a process similar to that described by Aurich et al.[3] was observed, leading to the anion radical of the nitrosoarene. The ESR spectra of the anion radical change in time, indicating the formation of another nitroxide radical. The results are discussed in relation with the reports of Aurich group and our own experience in this field.

In a previous investigation of our laboratory[1a,b] we generated free radicals by air oxidation of stable carbanions, derived either from substituted malonic esters[1a] or from the corresponding 1,2-diphenylpyrazolidine-3,5-diones[1b]. The resulted free radicals were spin-trapped with nitrosoarenes and the stable nitroxides were identified by ESR-spectrometry. Subsequent investigations by Schultz and coworkers confirmed and extended our results.[2]

In extending our work, we have observed that some carbanions prepared *in situ* from unsubstituted malonic ester, or from ketones with alkoxides, followed by air oxidation and addition of nitrosoarenes give rise to nitrogen free radicals, which do not seem to involve the carbanion precursor. We suspected that either the base used to generate the carbanion from the corresponding carbon acid, or the carbanion itself interact in some manner with nitrosoarenes forming the observed radicals.

Aurich, Dersch and Heinrich[3] have studied the reaction of nitrosobenzene with potassium *t*-butoxide and other bases in different solvents of decreasing ability for dissociating ion pairs (typically, *t*-butyl alcohol and benzene) and have admitted the reaction pathway given in Scheme 1:

Scheme 1

The reaction of nitrosobenzene with potassium *t*-butoxide in favouring dissociation solvents, according to Aurich and coworkers[3]

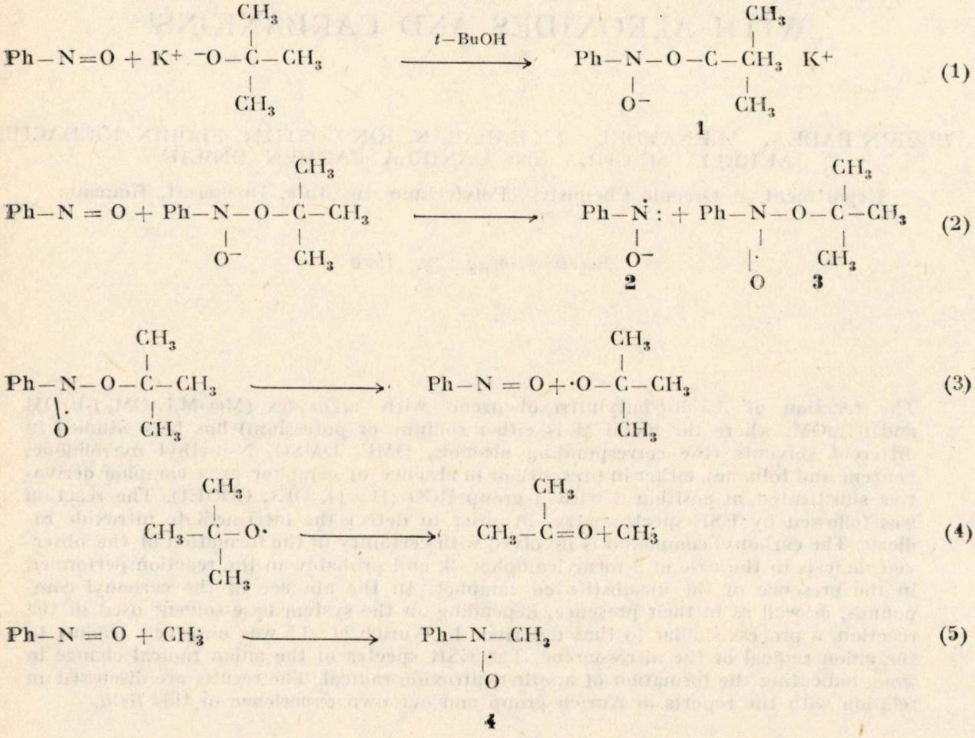

$$Ph-N{=}O + K^+\ {}^-O-C(CH_3)_3 \xrightarrow{t\text{-BuOH}} Ph-N(O^-)-O-C(CH_3)_3\ K^+ \quad \mathbf{1} \qquad (1)$$

$$Ph-N=O + Ph-N(O^-)-O-C(CH_3)_3 \longrightarrow Ph-\dot{N}(O^-) + Ph-N(\dot{O})-O-C(CH_3)_3 \quad \mathbf{2},\ \mathbf{3} \qquad (2)$$

$$Ph-N(\dot{O})-O-C(CH_3)_3 \longrightarrow Ph-N=O + \cdot O-C(CH_3)_3 \qquad (3)$$

$$(CH_3)_3C-O\cdot \longrightarrow (CH_3)_2C=O + \dot{C}H_3 \qquad (4)$$

$$Ph-N=O + \dot{C}H_3 \longrightarrow Ph-N(\dot{O})-CH_3 \quad \mathbf{4} \qquad (5)$$

In support to this scheme, they were able to identify by ESR-spectrometry the anion radical of nitrosobenzene **2** and methyl-phenyl-nitroxide **4**. It seemed possible that the radical species observed by us were the same as those identified by Aurich and coworkers.[3] However, our results differ in some respects from the published report, though they do not disagree. We consider that these differences, namely the pathway adopted by the reagents in the presence of a carbonyl compound able to generate a stable carbanion, are of interest and complete the electron-transfer mechanism to the nitrosoarenes.

RESULTS

1. Free radicals derived from camphor and camphor derivatives

Camphor (**5**) was treated with sodium ethoxide in benzene and the mixture was vigorously aerated for several hours. During 10 hours' aeration no radical species were detected by spin-trapping either with 3,5-di-*t*-butylnitrosobenzene **6** or with diphenylnitrone **7**. However, after 30 hours a radical was trapped with **7**, but not with **6**. The recorded ESR spectrum has the pattern of a nitroxide radical, three groups of 12 unresolved lines.

With alkoxides in the corresponding alcohols, either in presence of camphor or in its absence, by trapping with **6**, similar ESR-spectra were recorded (as seen further in this section).

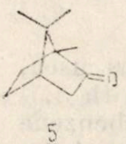

5

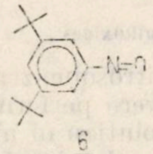

6

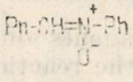

$Ph\text{-}CH{=}\overset{+}{N}\text{-}Ph$ with $\underset{|}{O^-}$ on N

7

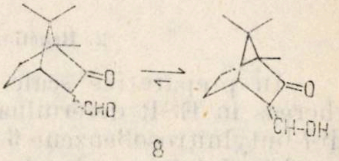

8

In contrast with unsubstituted camphor, 3-hydroxymethylenecamphor **8** (3-formylcamphor is a tautomer in small amount) in benzene with sodium ethoxide or methoxide give rise to a free radical, trapped both with **6** and **7**. The ESR spectrum obtained with 3,4-di-*t*-butylnitrosobenzene **6** consists of 27 well-resolved lines, a wide triplet split into twelve partly overlapping lines (Fig. 1.). The spectrum can be interpreted in terms of three hyperfine coupling constants: $a_N = 10.25$ G, $a_H = 3.85$ G for three (*ortho*/*para*) protons and $a_H = 2.75$ G for two protons (β to the nitrogen atom), namely the formyl and bridgehead protons.

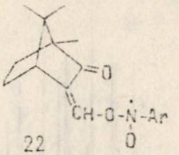

22

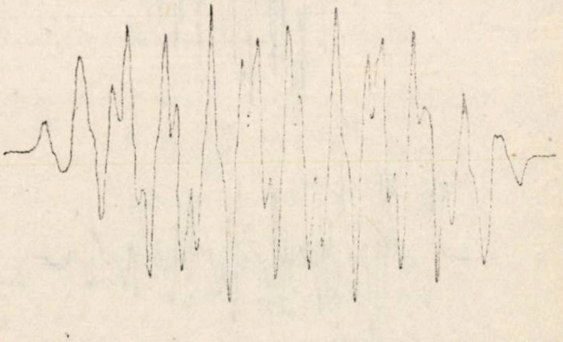

Fig. 1. — ESR spectrum of 3-formylcamphor in benzene, in the presence of sodium ethoxide and 3,5-di-*t*-butylnitrosobenzene.

Other camphor derivatives substituted in position 3 with groups able to stabilize the corresponding carbanion, such as **9** and **10**, failed to yield in a similar manner detectable free radicals.

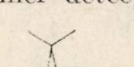

9

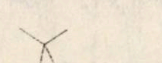

10

We have also checked the appearance of radicalic species during the Claisen condensation of camphor with formic and oxalic esters. A radical was generated and trapped in the condensation with methyl formate, but not in the reaction of dimethyl oxalate. The trapped radical gave rise to the same ESR spectrum as the spectrum shown in fig. 1.

2. Reaction of nitrosoarenes with alkoxides

In preparative scale experiments only nitrosobenzene was used, whereas in ESR determinations the reactions were performed with 3,5-di-*t*-butylnitrosobenzene **6**. On adding a green solution of nitrosobenzene in ethanol into a colourless solution of sodium ethoxide in ethanol, an

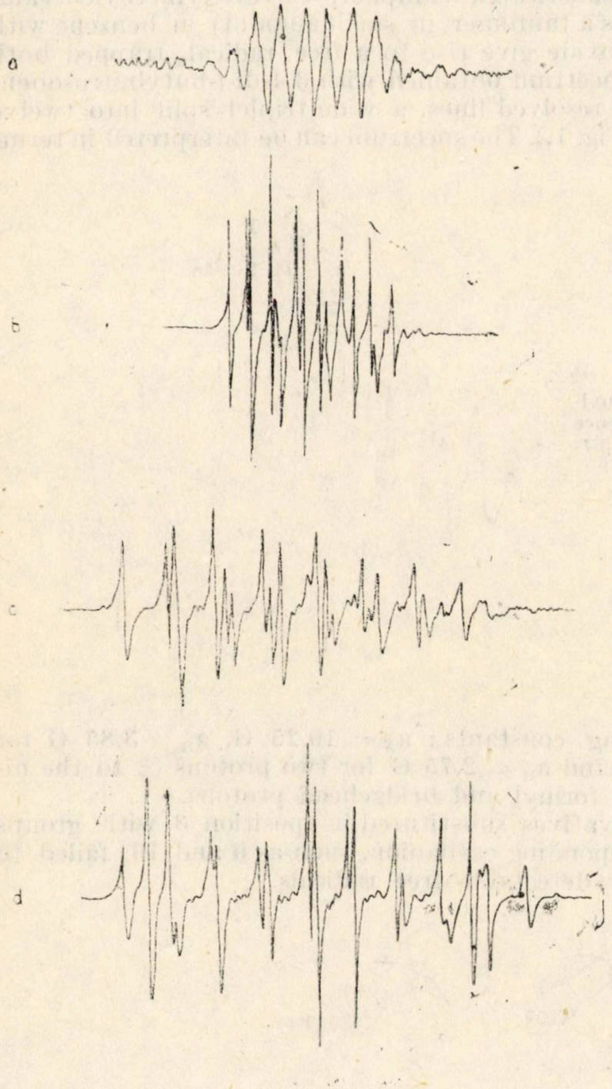

Fig. 2. — The variation in time of the ESR spectrum of potassium *t*-butoxide radical trapped with 3,5-di-*t*-butylnitrosobenzene in dimethylformamide; the spectra are recorded after: a — one minute; b — 3 minutes; c — half an hour; d — 24 hours (internal standard POD is marked with *).

intense orange colour was developed. After six hours' stirring at room temperature and neutralization of the solution, by working up the reaction mixture we were able to isolate only azoxybenzene. If the alcoholic ethoxide solution contained also one equivalent of camphor, the initially orange colour was reverted in a few days to the green colour of nitrosobenzene. If this solution was kept for several more days, the green colour turned to brown and impure azoxybenzene was again identified in the reaction mixture.

Di-*t*-butylperoxide was gas-chromatographically identified in the volatile products resulted in the reaction of nitrosobenzene with potassium *t*-butoxide. With all alkaline metal alkoxides ROM, where R : Me, Et, *i*-Pr, *t*-Bu ; M : Na or K, in the appropriate solvent (the corresponding alcohol or DMF) the ESR spectra were immediately recorded. In all cases nitrogen radicals were detected. The initially recorded spectra are stable a few hours in form and intensity, but change until the next day, due to the disappearance of the former radicals and the appearance of new radicals. In some cases, the coexistence of both radicals could be easily distinguished. In Fig. 2. an example is given of this variation of the spectra in time.

The reaction of potassium *t*-butoxide with 3,5-di-*t*-butylnitrosobenzene was followed by ESR-spectrometry also in other solvents, namely in aromatic hydrocarbons (benzene and toluene) and in aprotic dipolar solvents : dimethylsulfoxide (DMSO), and N-methylpyrrolidone (NMP). The recorded ESR spectra of the trapped radicals in DMSO and NMP were similar to those observed in DMF. In toluene, the nitroxide derived from benzyl radicals was the single identified species. The interpretation of the ESR spectra in terms of the calculated hyperfine coupling constants is given in Table 1.

Table 1

Hyperfine coupling constants of the nitroxide radicals formed in the reaction of 3,5-di-*t*-butylnitrosobenzene and alkali metal alkoxides (ROM) in different solvents

ROM	Solvent	Moment of recording the spectrum	Hyperfine coupling constants (Gauss)				g	Obs. [1]
			a_N	a_{2H}	a_{1H}			
MeONa	MeOH	—	10.5		4.3		2.0054	(1)
	DMF	—	8.4	4.0		3.2	2.0064	(2)
MeOK	MeOH	—	10.5		4.1		2.0055	(3)
EtONa	EtOH	—	10.5		3.9		2.0056	(4)
	DMF	initial	8.7		3.6		2.0057	(5)
		next day	11.2		3.6		2.0044	(6)
EtOK	EtOH	initial	10.0		3.9		2.0057	(7)
		next day	13.2		3.7		2.0045	(8)
t-BuOK	*t*-BuOH	initial	9.8		3.9		2.0057	(9)
	DMF	initial	8.0	3.9		3.2	2.0065	(10)
		next day	11.0	3.6		3.9	2.0047	(11)
	DMSO	initial	8.0	3.9		3.2	2.0065	(12)
	NMP	next day	11.5		3.6		2.0047	(13)
	toluene	next day	11.0		2.2		2.0057	(14)

[1] **Points corresponding to the diagram from Fig. 3 are indicated in brackets.**

DISCUSSION

1. Reaction of 3,5-di-t-butylnitrosobenzene with alkoxides

The data in Table 1 show that the hyperfine coupling constants a_N are associated in three different ways with the g factors, namely:

a. Low hiperfine coupling constants ($a_N = 8-8.4$ G) with high g factors (approx. 2.0065), observable in aprotic dipolar solvents (DMF, DMSO, NMP) with potassium *t*-butoxide and sodium methoxide, but not with sodium ethoxide.

b. Intermediate values of the a_N constants ($a_N = 9.8-10.5$ G) with moderate values of the g factor (2.0054−2.0057), observable in alcohols, where the smallest a_N constant is associated with the largest value and *vice-versa*.

c. Large hyperfine coupling constants ($a_N = 11.0-13.2$ G) and small g factors (2.0044−2.0047), observable either in protic or aprotic solvents, next day after mixing up the reagents.

All ESR spectra recorded present similar features (number and relative intensity of the lines), differing only in their width.

As far as we know, no published data report the g factors related to the hyperfine coupling constants for the paramagnetic intermediates resulted in the reduction of the nitrosoarenes. Therefore, we may inquire if the data in Table 1 indicate a single intermediate or several ones.

Three types of intermediates have been proposed for the reaction of nitrosobenzene with electron donors (nucleophiles):

i) Nitrosobenzene radical anion **2**, formed either by direct electron transfer between the donor and nitrosobenzene,[4–7] or by dissociation of other intermediates (see for example Scheme 1);

ii) Arylaminyloxides **11** observed in the reduction of nitrosobenzene with phenylhydroxylamine[4,6] in the presence of a base and even in acidic media:

$$\mathrm{Ph{-}N = O + Ph - NH - OH \longrightarrow 2Ph{-}NH\dot{-}O} \qquad (6)$$

11

iii) Nitroxide radicals, such as **3** or **4** (see Scheme 1), formed either from nitrosobenzene radical anion (7), or from nitrosobenzene with another radical species by spin trapping (8):

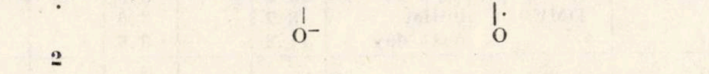

$$\mathrm{Ph{-}\underset{\cdot}{\ddot{N}}{-}O^- + R\cdot \longrightarrow PH{-}\underset{O^-}{\underset{|}{\ddot{N}}}{-}R \xrightarrow{-e^-} Ph{-}\underset{O}{\underset{|\cdot}{N}}{-}R} \qquad (7)$$

2

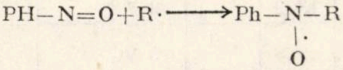

$$\mathrm{PH{-}N{=}O + R\cdot \longrightarrow Ph{-}\underset{O}{\underset{|\cdot}{N}}{-}R} \qquad (8)$$

It has been admitted by Russell and coworkers[6] that, in the reduction of nitrosobenzene with sodium dithionite, the radicalic species **12** is formed from the anion radical **2** and another molecule of nitrosobenzene.

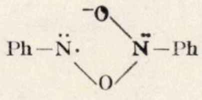

12

The hyperfine coupling constants of **2** and of related species **11** and **12** are resumed in Table 2, as they are cited in literature.

Table 2

Hyperfine coupling constants a_N (Gauss) of nitrobenzene radical anion **2** and of related species

Generation of the paramagnetic species		Hyperfine coupling constant a_N (G)	Type of radical	Ref.
Electron donor	Solvent			
Sodium p-chlorobezene thiolate	DMSO÷*t*-BuOH (2 : 1)	8.0	**2**	4
Sodium ethoxide	EtOH	10.10	**2**	6
Potassium *t*-butoxide	*t*-BuOH	9.30 9.60	**2**	6 3
Potassium *t*-butoxide	DMSO+*t*-BuOH (4 : 1)	7.90	**2**	6
K-Na Alloy	$MeOCH_2CH_2OMe$	8.60	**2**	6
Electrolysis	DMF	8.34	**2**	8
Sodium hydroxide-Phenylhydroxylamine	DMSO÷*t*-BuOH (4 : 1)	9.10	**11** $a_{NH}^{H} = 11.90$	5
Phenylhydroxylamine	benzene DMSO EtOH	9.02 8.89 8.80	**11**	6
Sodium dithionite	DMSO DMSO÷HOAc (2 : 1) DMSO÷H_2O (2 : 3) *t*-BuOH÷H_2O (3 : 2) EtOH	11.30 11.46 11.73 11.84 11.70	**12** **12** **12** **12** **12**	6 6 6 6 6

Large variations of the hyperfine coupling constants, a_N, were observed only for nitrosobenzene radical anion **2**, whereas for the other species (**11** and **12**) minor changes occur even when the solvents are largely varied (benzene-aprotic-unpolar ; ethanol-protic-polar ; DMSO — —aprotic—dipolar). It seemed thus that the hyperfine coupling constants initially observed correspond to the same species : the nitrosobenzene radical anion **2** ; however, the values determined next day would be associated with another species, probably **11** or **12**. In order to verify this assumption, the a_N values *versus* the g factors were plotted (Fig. 3). With one exception (sodium ethoxide in DMF), all the points of the initial ESR spectra recorded fall on a straight line, whereas the points corresponding to the values determined after 24 hours fall out from the correlation line.

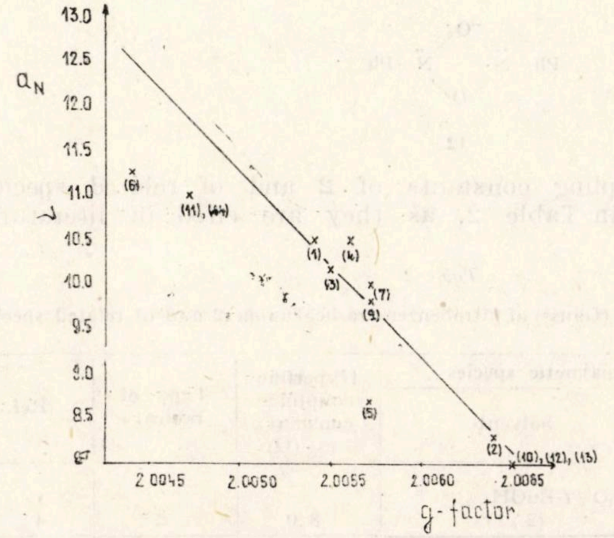

Fig. 3. — The correlation of hyperfine splitting constants a with the g-factors.

2. Direct electron transfer from the base to nitrosoarene, or indirect electron transfer from an adduct of the nitrosoarene with a nucleophile

Aurich and coworkers[3] assumed that nitrosobenzene radical anion **2** arises by an electron transfer from adduct **1** formed by addition of the alkoxide ion to the double bond of the nitroso group (Scheme 1, reaction (1)). Another possible interpretation is that the electron transfer occurs directly from the alkoxide ion to the nitroso group:

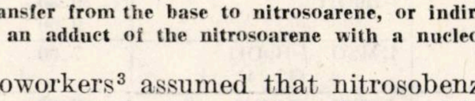

$$\mathrm{Ar{-}N{=}O + R{-}O^- \longrightarrow Ar{-}\underset{\underset{O^-}{|}}{\ddot{N}}\cdot + R{-}O\cdot}$$

2

If the first interpretation is correct, other strong nucleophiles would have a similar behaviour with that of the alkoxide ions. However, on treating 3,5-di-*t*-butylnitrosobenzene with potassium cyanide in DMF (favourable conditions for nucleophile reactions), no free radicals were detected by ESR spectrometry, although the nitroxide **14** is known to be stable[9], due to push-pull stabilization:

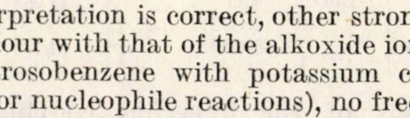

$$\mathrm{Ar{-}N{=}O + CN^- \underset{(DMF)}{\rightleftarrows} Ar{-}\underset{\underset{O^-}{|}}{N}{-}CN} \quad (10)$$

13

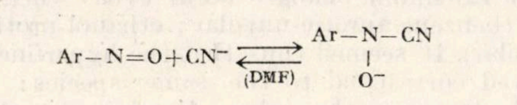

$$\mathrm{Ar{-}N{=}O + Ar{-}\underset{\underset{O^-}{|}}{N}{-}CN \longrightarrow Ar{-}\underset{\underset{O^-}{|}}{\ddot{N}}\cdot + Ar{-}\underset{\underset{O}{|}}{\dot{N}}{-}CN} \quad (11)$$

2 **14**

Reversible addition of the cyanide ion (10) cannot be ruled out by this experiment. Nevertheless, process (11) cannot occur.

Neither do carbanions, such as potassium camphor, generate the nitrosoarene radical anion, if alkoxide ion is not present in the reaction mixture. However, if a mixture of sodium ethoxide and camphor in benzene is stirred long enough (30 hours), a nitroxide radical is trapped with diphenylnitrone **7**, but not with 3,5-di-*t*-butylnitrosobenzene **6**. This result can be interpreted in terms of a very fast acid-base equilibrium (12). The much slower equilibrium (13) leads to the sterically hindered radical **15** which is unable to react with moderately reactive spin-trapping reagents (such as the sterically hindered **6**), but is able to be trapped by the more reactive species (such as nitrone **7**).

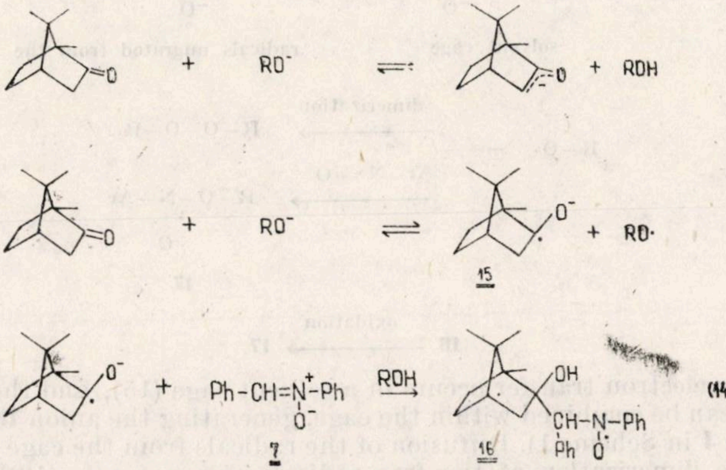

These experiments do not attest firmly the involvement of anionic species such as **1** (Scheme 1) in the generation of the nitrosoarene radical anions **2**, that is why more arguments are needed.

3. Transformation of radical ion 2 into another nitroxidic species

The most plausible explanation for the formation of another nitroxide radical was provided by Aurich and coworkers.[3] The alkoxy radicals split into carbonyl compounds and alkyl radicals, which are trapped by the excess of nitrosoarene (Scheme 1). However, we have not observed arylmethyl-nitroxides. Instead, we detected di-*t*-butylperoxide in the reaction of nitrosobenzene with potassium *t*-butoxide. The hyperfine coupling constants of the radical resulted from the initial radical ion **2** agree well with the values reported by Russell and coworkers[6] for radical **12**. However, we consider that the structure of the radical observed by us corresponds to an alkoxyphenyl-nitroxide **17**, similar to radical **3** proposed by Aurich and coworkers[3] as an intermediate in nitrosobenzene radical anion formation (Scheme 2).

Scheme 2

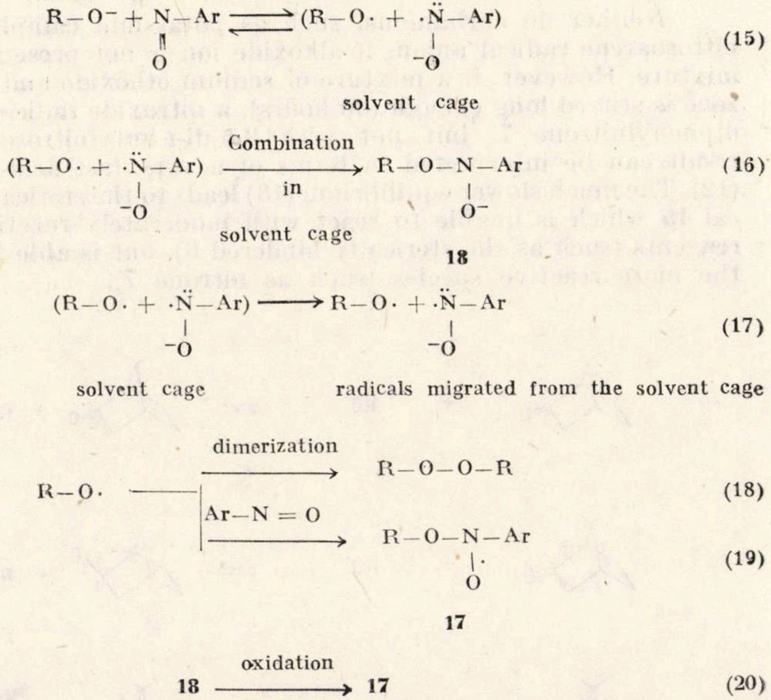
R–O⁻ + N–Ar ⇄ (R–O· + ·N̈–Ar)
O
⁻O
(15)
solvent cage
Combination
in
solvent cage
(R–O· + ·N̈–Ar) → R–O–N–Ar
⁻O
O⁻
(16)
18
(R–O· + ·N̈–Ar) → R–O· + ·N̈–Ar
⁻O
⁻O
(17)
solvent cage
radicals migrated from the solvent cage
dimerization
R–O·
R–O–O–R
(18)
Ar–N = O
R–O–N–Ar
O
(19)
17
oxidation
18 → 17
(20)

The electron transfer occurs in a solvent cage (15), and the resulted radicals can be combined within the cage, generating the anion **18** (equivalent with **1** in Scheme 1). Diffusion of the radicals from the cage (17) may allow the dimerization of the free radicals (for example (19)) or their trapping by nitrosobenzene (acting as a scavenger) to produce radical **17** (the reverse of reaction (3) in Scheme 1). The identification of di-*t*-butyl peroxide in the reaction of potassium *t*-butoxide with nitrosobenzene and the evidence of radical **17** (see further) is a support for this scheme. A different procedure of carrying out the experiments adopted by us has made possible another evolution of the reaction, leading to other conclusions than those of Aurich and coworkers.[3] In their work, dilute solutions of nitrosobenzene ($10^{-3}-10^{-4}$ molar) were treated either with a dilute solution of base deaerated previously or with a suspension of the base in the deaerated solvent, which did not make possible the combination of the radicals outside the solvent cage. Due to these conditions, the reverse of reaction (3) could not be observed and one observed only the radical transformation (4) and therefrom phenylmethyl-nitroxide **4**. If higher concentrations were used as in our procedure, the trapping of *t*-butoxy radical was possible.

Moreover, the deliberate presence of the air during the recording of the ESR spectra allowed the continuous generation (by air oxidation) of radical **17** from anion **18**. The spectra recorded in experiments performed with deaerated solvents showed that if oxygen was excluded, the radical **17** vanished rapidly from the reaction medium. The oxygen included seems to enable a longer lifetime (persistence) of the observed radical. As both *t*-butanol and DMF cannot be deaerated as easily as a hydrocarbon, we have also treated 3,5-di-*t*-butylnitrosobenzene with potassium *t*-butoxide in benzene, either aerated or deaerated and we have observed a similar behaviour, the detected radicals having a longer persistence in the nondeaerated experiments than in deaerated solutions.

4. The alkoxyaryl-nitroxides

The final stable radical obtained by us has the following characteristics :

i) It can be observed after the disappearance of the nitrosoarenes from the reaction medium. That means either that it is generated from the previously formed radical anion **2** or that it is more slowly generated from reagents and is more stable than the former.

ii) It must be very similar in structure with radical anion **2**, its ESR spectrum having the same shape as the nitrosoarene radical anion. No extra hyperfine splitting of the initial signal is observed.

iii) The hyperfine coupling constants and the *g* factor vary in a small degree with the condition of its generation (base and solvent), showing that it is a neutral species. The small *g* factor indicates that the spin is located in a larger extent to nitrogen than to oxygen.

iv) It has a larger persistence in the presence of oxygen than in its absence. That means either that it is continuously generated in the presence of oxygen, or that oxygen prevents its disappearance.

All these facts seem to indicate **17** as the detected radical :

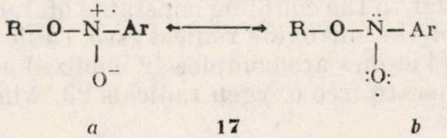

$$R-O-\overset{+\cdot}{\underset{\underset{O^-}{|}}{N}}-Ar \longleftrightarrow R-O-\overset{\cdot\cdot}{\underset{\underset{\underset{\cdot}{:O:}}{|}}{N}}-Ar$$

a **17** *b*

Indeed, the presence of the neighbouring alkoxy group would favour structure **17a** and disfavour structure **17b** (repulsion between the unpaired electrons; stabilization of the neighbouring positive change). The intercalation of the oxygen atom between nitrogen and alkyl group prevents the delocalization of the spin in the alkyl group. The fact that the initial spectrum is not changed with methoxide ion, neither in methanol nor in DMF (Table 1), agrees with the easy generation of formaldehyde from methoxy radical. The fact that the change of the spectrum is only incidentaly observed with alkoxides in the corresponding alcohols pleads in the same manner. Indeed, the continuous generation of **17** from **18** needs the cage combination of the nitrosoarene radical anion with the alkoxy radical ((16), Scheme 2). However, in alcohols, the radical anion **2** is rapidly solvated by the alcohol molecules and the concentration of **18** will fall down.

$$Ar-\underset{\cdot\cdot}{\dot{N}}-O^- + R-O-H \rightarrow Ar-\underset{=}{N}-\dot{O}^-\ldots H-O-R \qquad (21)$$

However, if RO⁻ is a very strong base, reaction (5) will have a high frequency and the high concentration of alkoxy radicals will ensure the formation of radical **17** (potassium ethoxide in ethanol, but not sodium ethoxide in ethanol, see Table 1).

The reported results agree well with Scheme 2.

5. Reaction of camphor derivatives 8 – 10

A different radical was observed in the reaction of 3-formylcamphor **8** in the presence of a base, by air oxidation. A relatively stable radical was generated which was afterwards trapped either with 3,5-di-*t*-butylnitrosobenzene **6** or with diphenylnitrone **7**. The structurally related compounds **9** and **10** behave differently, generating no detectable radicals even if the spin-trapping reagent was added initially in the reaction medium.

The spectrum given in Fig. 1 indicates that, beside the three hydrogen atoms from the arryl moiety, there must be other splittable hydrogen atoms in neighbourhood of the nitroxide group. The spectrum agrees well with nitroxide **22**.

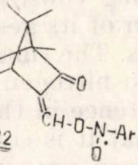

The values of the hyperfine coupling constants $a_N = 10.25$ G and $a_{3H} = 3.85$ G are similar to the coupling constants of radical **12**, suggesting a similar structure of the nitroxide radical (see Table 1). Moreover, it is known that α-formyl ketones are completely enolized and that the corresponding enolates generate free oxygen radicals **23**, which are more stable than alkoxy radicals:

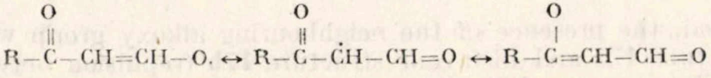

$$R-\overset{O}{\overset{\|}{C}}-CH=CH-O\cdot \leftrightarrow R-\overset{O}{\overset{\|}{C}}-\dot{C}H-CH=O \leftrightarrow R-\overset{\dot{O}}{\overset{|}{C}}=CH-CH=O$$

23

Such a radical will have the persistence to be trapped after its generation.

Lower stabilizations are expected for the enolate radicals derived from **9** and **10**. Moreover, the corresponding radicals will be less sterically accessible for spin-trapping than the enolate radical **24**.

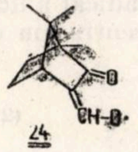

24

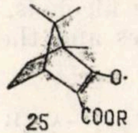

25

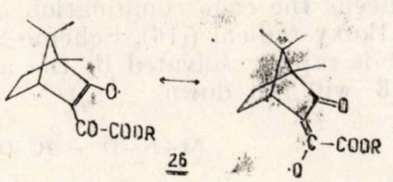

26

We consider that the formation of **22** is another proof for the interpretation given by us in Scheme 2.

REFERENCES

[1] a) F. Badea, A. T. Balaban, A. Dimitriu, F. Iordache, Aurelia Meghea and L. Stoenescu, *Rev. Roum. Chim.*, **31**, 903 (1986); b) F. Badea, F. Iordache, Aurelia Meghea, Roxana Marinescu, and Anne-Marie Ghivirigă, *Rev. Roum. Chim.*, **30**, 189 (1985).

[2] M. Schulz, L. Moegel, L. Omelka and A. Tkae, *J. Prakt. Chem.*, **328**, 222 (1986).

[3] H. G. Aurich, W. Dersch and J.M. Heinrich, *Liebigs Ann. Chem.*, 1271 (1981).

[4] F. J. Smentovski, *J. Amer. Chem. Soc.*, **87**, 122 (1965).

[5] G. A. Russel and E. J. Geels, *J. Amer. Chem. Soc.*, **87**, 122 (1965).

[6] G. A. Russel, E. J. Gells, F. J. Smentovski, K. J. Chany, J. Reynolds and G. Kaupp, *J. Amer. Chem. Soc.*, **89**, 3821 (1967).

[7] C. J. W. Gutch and W. A. Waters, *Proc. Chem. Soc.* (*London*), 203 (1964).

[8] P. B. Ayscough, F. P. Sargent and R. Wilson, *J. Chem. Soc. B.*, 903 (1966).

[9] D. Căproiu, Ph. D. Thesis, Polytechnic Institute, Bucharest, 1984.

Revue Roumaine de Chimie, 36, *1–3*, 171–185 (1991)

PREPARATION AND PROPERTIES OF OLIGOMERS OF DEFINED CHAIN LENGTH AND STRUCTURE AS MODELS FOR TECHNICAL COPOLYMERS

H. SELIGER, M.B. BITAR, E. GÖLDNER, I. KITTEL and H.G. KILIAN*
Universität Ulm, Sektion Polymere and
* Abteilung Experimentelle Physik, Oberer Eselsberg, D-7900 Ulm, Germany

Received July 1, 1990

Oligomeric segments of the macromolecules with defined structure have been prepared in an attempt to answer the question whether the thermal and mechanical properties of the elastomers (polyester) are mainly influenced by the segregation or by the structural heterogeneity. For the preparation of the oligoarylates the authors used monobenzylated bis-phenol A and terephthalic acid mono tert-butyl ester as starting compounds.

INTRODUCTION

Copolymers used as technical materials are in many respects heterogeneous. From their synthesis they are polydisperse. They are also heterogeneous with regard to their composition (sequence of constituents), their structure and other parameters. This multiple heterogeneity influences, or even determines, their properties in the solid and liquid state.

In many respects the properties of polymers are reflected in the behaviour of oligomeric segments of the macromolecules. Such oligomers can be synthesized as compounds of uniform size and structure and therefore be used as well-defined model compounds to evaluate the influence of chain length and structural parameters on physical properties of the polymers. Such studies have been initiated nearly three decades ago by Rothe and coworkers[1] as well as Zahn and his collaborators,[2] yet the interest in the preparation of such model systems has been limited for a long time and only recently revived. This is in contrast to the chemistry of biopolymers where the construction of oligomers of defined sequence and structure has been very well elaborated.

In our laboratory two types of macromolecules have been modelled by the construction of oligomers of uniform size and defined structure:

1. segmented block copolymers technically used as thermoplastic elastomers, and
2. main chain liquid crystalline copolymers applied e.g. in optoelectronics and as high tensile strength fibers.

The oligomers were prepared by stepwise synthesis in solution using a) protective groups to monofunctionalize the constituents, b) activating agents to effect condensation in good yields, and c) separation techniques, which allow to obtain the oligomers as individual compounds of high chemical purity. Parallel to our work such techniques have been elaborated independently for the preparation of segmented co-oligomers of defined structure by Wegner, Dröscher and coworkers.[3]

From mesogenic compounds the preparation of defined dimers or "twins" has been described in several papers,[4] but the only approach parallel to ours using a protection-activation scheme for the controlled elongation of liquid crystalline oligomers has been published by Keller.[5]

RESULTS AND DISCUSSION

Example 1 : Preparation and Investigation of Defined Oligomer Models for Segmented Block Copolymers

Segmented block copolymers used as thermoplastic elastomers are characterized by an alternation of "hard" (inflexible) and "soft" (flexible) structural elements within the polymer chain.[6] The elastomeric properties have been explained on the basis of a phase separation model involving an association of the hard and soft segments.[7] Hoping to contribute to a discussion of the question whether the thermal and mechanical properties of such elastomers are mainly influenced by the segregation as such or by the fact that, due to structural heterogeneity, soft segments must be included in the hard segment domain and vice versa, we have started a research program aiming at the preparation of oligomers composed of oligoarylate and oligomethylene units as models for "hard and soft" segments.[8] For the preparation of the oligoarylates we used monobenzylated bis-phenol-A- and terephthalic acid mono tert. -butyl ester as starting compounds. Chain elongation was done by 1. condensation of the phenolic and carboxylic component with dicyclohexylcarbodiimide as activating agent, 2. by deblocking of either the phenolic chain end through hydrogenation or of the carboxylic chain end by treatment with trifluoroacetic acid. The repetition of these steps resulted in the formation of a series of oligoarylates up to the penta(bisphenol-A-terephthalate) (Chart 1). Alternatively, oligoarylates containing terminal isophthalate or phthalate residues were prepared by the same reaction scheme. The further reaction of oligoarylates with commercial 1-bromodecan-10-ol resp. 1-bromo-icosan-20-ol (Chart 2) gave di- and tri-block oligomers containing terminal "soft" segments. Compounds containing an interior decane or icosane residue were obtained by reaction of oligoarylates with 1,10-decanediol resp. 1,20-icosanediol. The yields of these compounds are given in Table 1. Structural proof was obtained by elemental analysis, ^{1}H-NMR, UV- and IR spectroscopy.[8]

First studies on the physical properties of the defined oligomeric model compounds described above were focussed on their thermal behaviour.[9] Figure 1a shows a plot of the melting points (determined by DSC resp. on a heated plate) versus chain length for different series of protected and partially or completely unprotected oligoarylates. In all these series the melting points rise with increasing chain length, with a tendency to converge towards the T_m value of polybisphenol-A-terephthalate, which is at 350°C.[10,11] Also shown in Fig. 1a is the influence of a terminal unit that disfavours crystallization, i.e. isophthalate, phthalate, or decamethylene on the melting behaviour. Thus, the introduction of an isophthalate or phthalate unit leads to drastic depression of the melting point. This was to be expected from the practice of technical polyarylate production, where an isophthalate admixture has since long been used to improve the

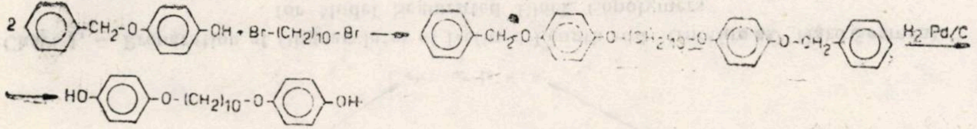

Synthesis of the [illegible]nol component

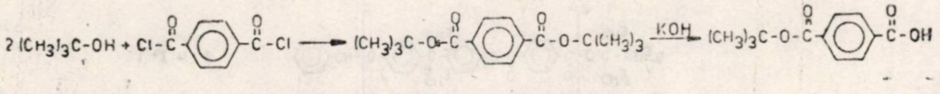

Synthesis of the monofunctional acid

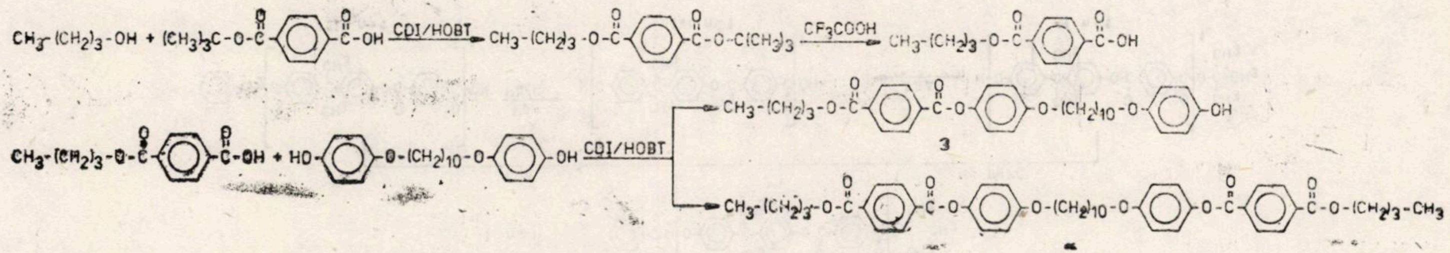

Synthesis of the 1-butyl esters

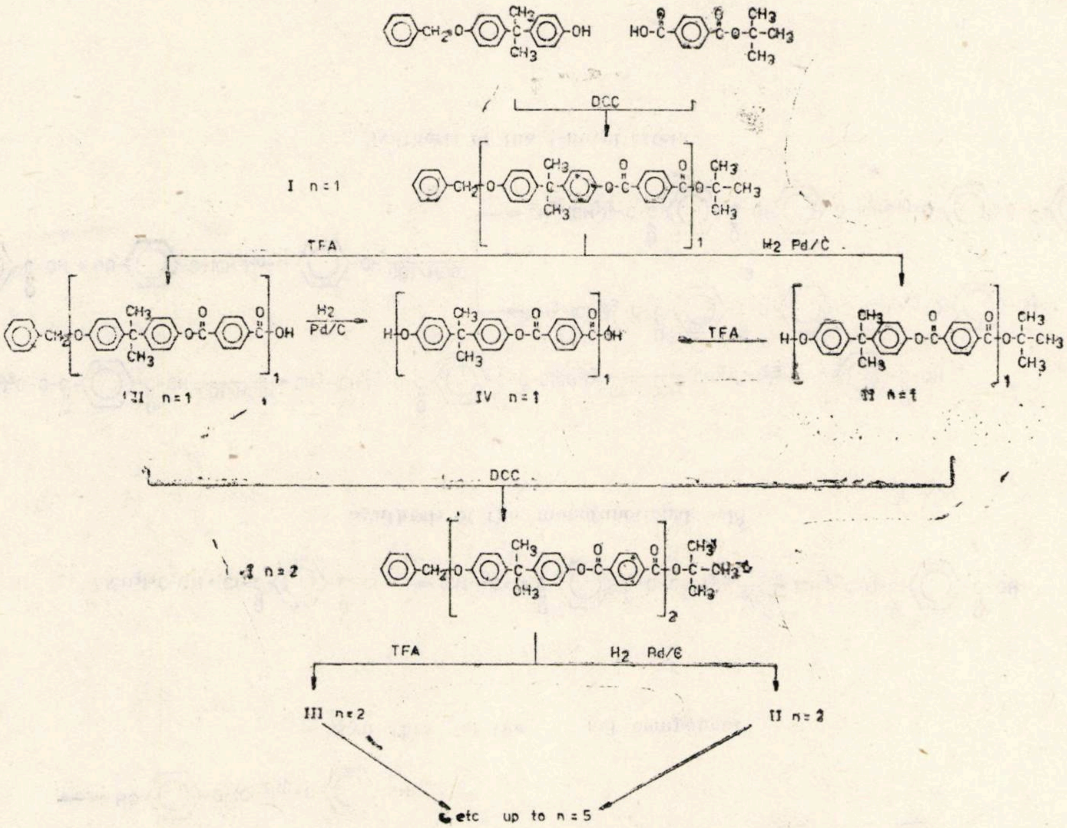
DCC
I n=1
TFA
H2 Pd/C
H2 Pd/C
TFA
III n=1
IV n=1
II n=1
DCC
I n=2
TFA
H2 Pd/C
III n=2
II n=2
etc up to n=5

Chart 1. — Preparation of Oligoarylates of Defined Length and Structure as "Hard Segments" for Model Segmented Block Copolymers

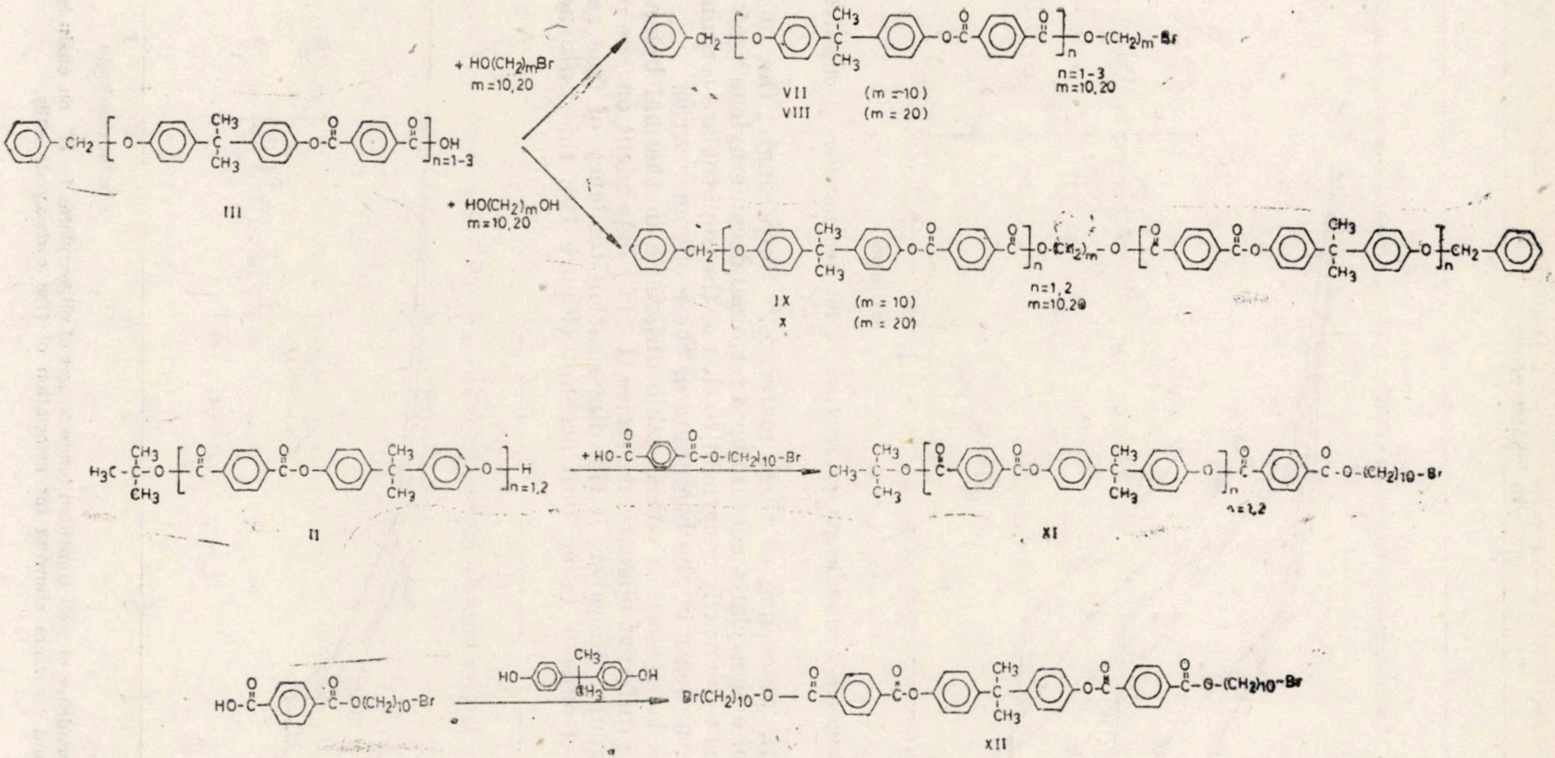
+ HO(CH2)mBr
m=10,20
+ HO(CH2)mOH
m=10,20
III
n=1-3
VII (m = 10)
VIII (m = 20)
n=1-3
m=10,20
IX (m = 10)
X (m = 20)
n=1,2
m=10,20
II
n=1,2
XI
n=1,2
XII

Chart 2. – Preparation of Oligomeric Models for Segmented Block Copolymers of Uniform Chain Length and Defined Structure

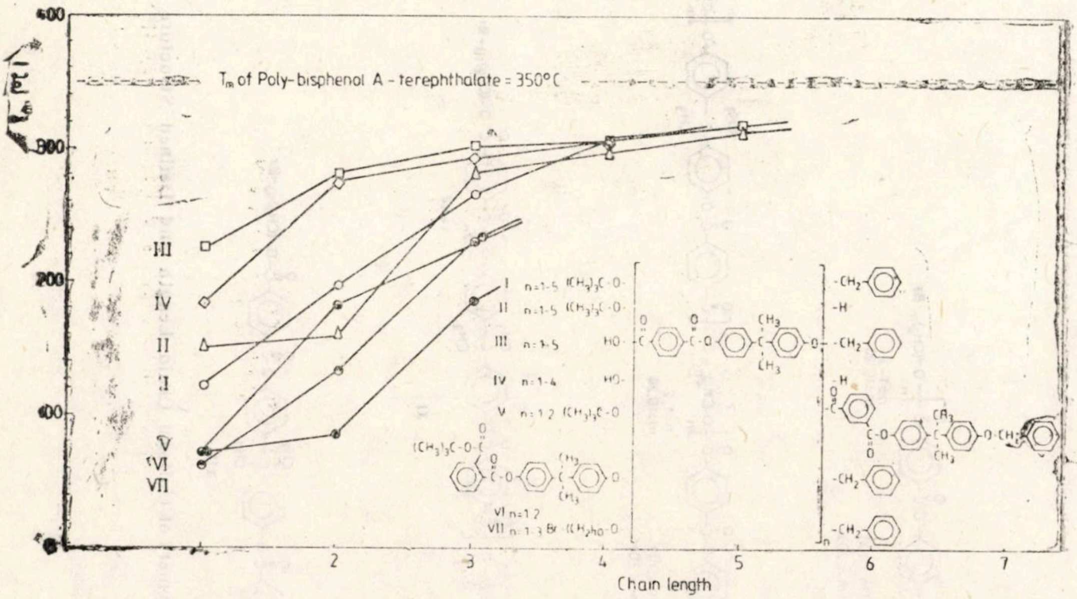

Fig. 1a. — Influence of chain length and structure on the melt transition of oligoarylates.

thermoplastic processing of these materials.[12] Surprisingly, the thermal behaviour of oligoarylates containing a terminal decamethylene "soft segment" seems to be nearly congruent to that of the isophthalate-terminated compounds, at least in the beginning of these oligomer series.

Figure la suggests a considerable difference in thermal behaviour between the different oligoarylate series (I—IV) dependent on the different end groups. However, if the dimerization tendency of free carboxylate end groups is taken into account (Figure 1b), this influence is

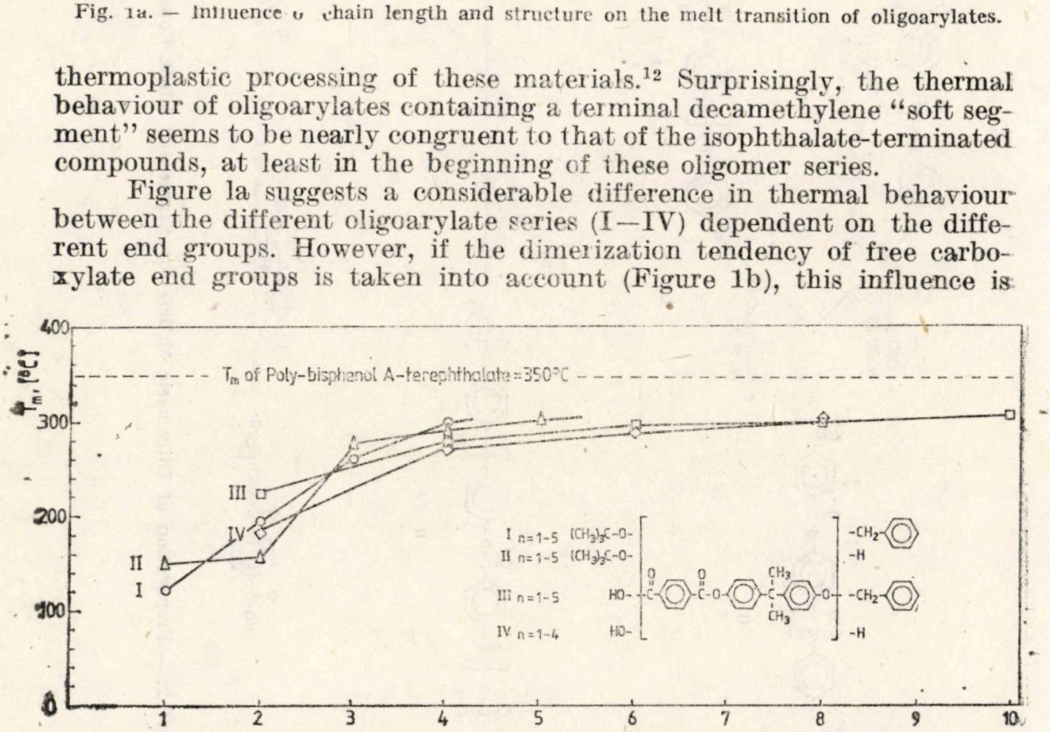

Fig. 1b. — Dependence of melt transition temperatures of oligoarylates I—IV on chain length and structure allowing for association of free carboxylate ends.

Table 1

Structures and yields of oligoarylates I–XII

Compound no.	Structures and End Groups			n	m	yield (%)
I,1 I,2 I,3 I,4 I,5	$(CH_3)_3CO-$		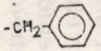	1 2 3 4 5	— — — — —	92 86 82 70 52
II,1 II,2 II,3 II,4 II,5	$(CH_3)_3CO-$		$-H$	1 2 3 4 5	— — — — —	95 80–92
III,1 III,2 III,3 III,4 III,5	$HO-$		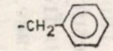 $-H$	1 2 3 4 5	— — — — —	90 80–90
IV,1 IV,2 IV,3 IV,4	$HO-$	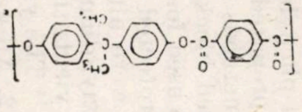	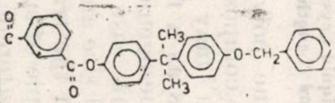	1 2 3 4	— — — —	80–90
V,1 V,2	$(CH_3)_3CO-$		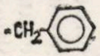	1 2	— —	76 68
VI,1 VI,2	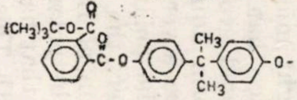		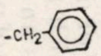	1 2	— —	70 58
VII,1 VII,2 VII,3	$Br-(CH_2)-O-$		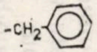	1 2 3	10 10 10	65–75
VIII,1 VIII,2 VIII,3	$Br-(CH_2)-O-$ 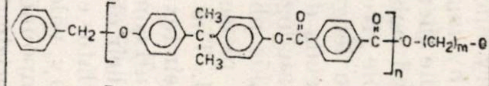		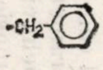	1 2 3	20 20 20	65–75
IX,1 IX,2			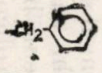	1 2	10 10	70 65
X,1	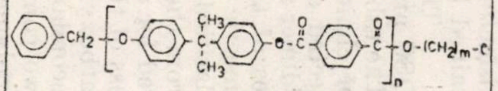		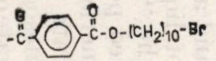	1	20	45
XI,1 XI,2	$(CH_3)_3CO$ |			1 2	— —	65 58
XII,1	$Br-(CH_3)_{10}-O-$		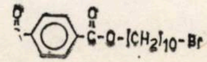	1	—	50

nearly eliminated, the melting points being very similar for different oligomers or pseudo-oligomers of the same chain length. These results, although preliminary, show different ways to a "tuning" of this segmented block copolymer system with respect to the thermoplastic behaviour. Further studies are in progress to investigate on the influence of structural alterations on the mechanical and elastomeric properties of such materials.

Example 2: Preparation of Main Chain Liquid Crystalline Oligomers of Defined Structure and Length

Main chain liquid crystalline polymers are usually prepared by polymerization of structural units composed of a low molecular mesogen and a spacer element. This "design" may lead to failure, if the formation of liquid crystalline phases occurs as a function of chain length, i.e. if the "monomer analogue" is not mesogenic, whereas the structurally related polymer is, or vice versa. In this case again, the preparation of oligomeric model compounds of defined size and structure may serve to elucidate the parameters which govern the transition from non-mesogenic to mesogenic behaviour. As an example of such a case, we chose to investigate on oligomeric models of polyoxy(terephthaloyloxy-)(1,4-phenyleneoxy-)(1,10-decamethyleneoxy-)1,4-phenylene.[13] Oligomers containing one or two mesogenic units were prepared by stepwise chain elongation using protection and activation methods similar to those described above for the preparation of segmented block cooligomers. Thus, benzyl and benzyloxycarbonyl groups were used for protection of phenolic ends, whereas carboxylate termini were protected as tertiary butyl ester residues. For comparison, 1-butyl esters were alternatively made. For activation we used a combination of carbonyl diimidazole with 1-hydroxybenzotriazole, which proved to give better yields than the dicyclohexylcarbodiimide employed previously (Chart 3).[14] The yields of the preparations of the compounds are shown in Table 2. All newly synthesized compounds gave satisfactory microanalytical analyses. Additional structural proof was obtained by mass spectrometry and ^{1}H-NMR and IR spectroscopy.[14]

The thermal and phase behaviour of these oligomers was studied by DSC and polarized light microscopy. The results are listed in Table 3. The table gives evidence that LC phases in the system occur as a function of chain length and end groups. The "monomer analogues" with protected ends do not form liquid crystalline phases at all. The protected "dimer analogue" shows a very narrow post-melting transition. The pictures of this phase in the polarizing light microscope resemble those of a smectic phase, however, the nature of this transition has to be further clarified. The formation of LC phases that can be classified as nematic from their texture in the polarizing light microscope, however, was observed for all compounds that have at least one free carboxlic end, regardless of their chain length. This is again explained by the association of the carboxylate end groups, which effect a "chain lengthening" through secondary valence forces. In line with this association phenomenon the two compounds **8** and **10** differing in chain length, but both capable of "polymerizing" through their free carboxylic termini are similar to each other and to the structurally related polymer in their transition temperatures and the temperature range of the nematic phases. Examples of some of the textures are shown in Figure 2a–d.

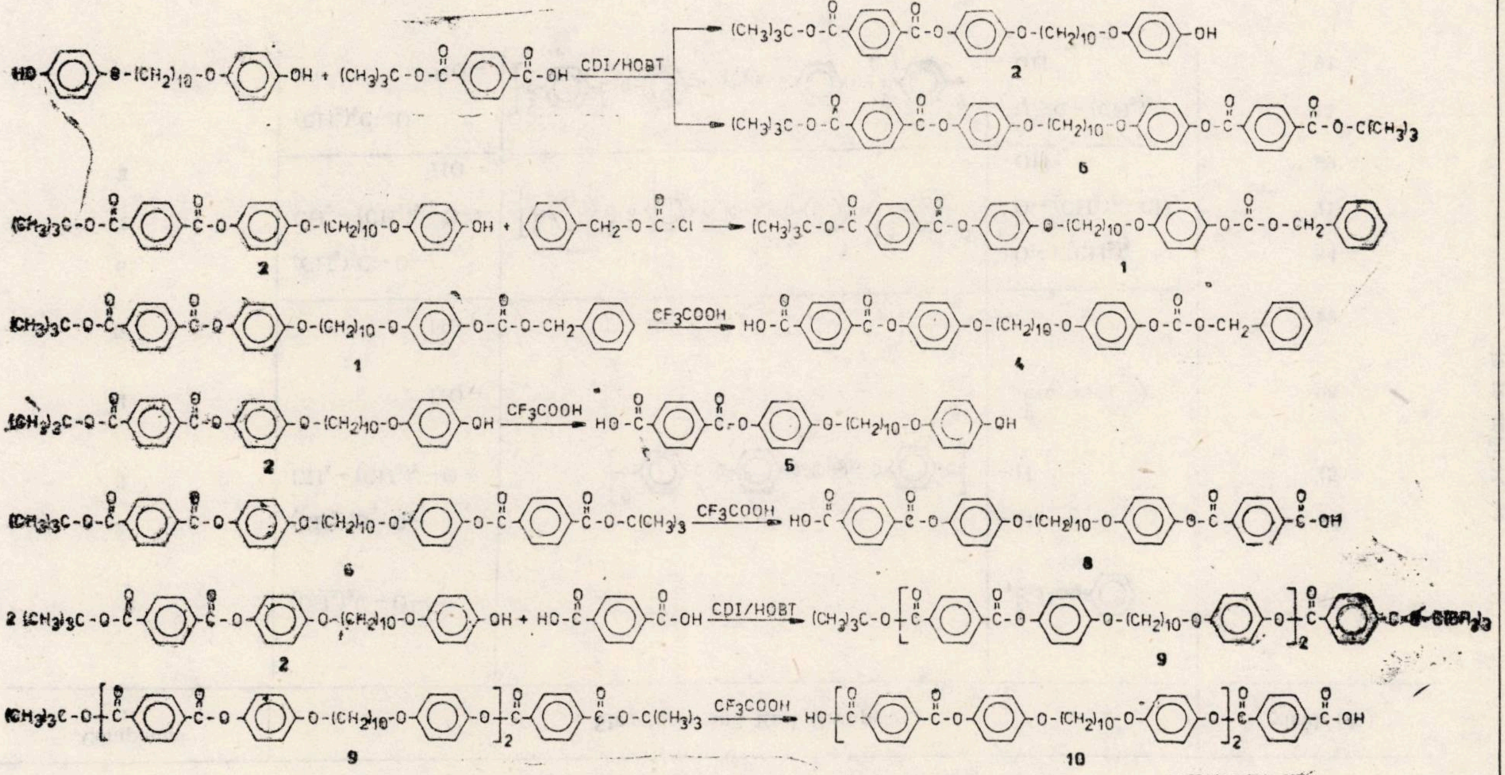
CDI/HOBT
2
6
1
CF$_3$COOH
4
5
8
9
10

Chart 3. – Preparation of Liquid Crystalline Oligomer-Models

Table 2

Structures and yields of liquid crystalline oligomer-models 1—10

Compound no.	Structures and End Groups			yield (%)
1	$(CH_3)_3C-O-$	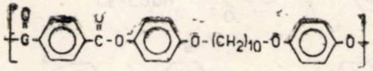	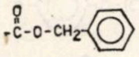	67
2	$(CH_3)_3C-O-$		$-H$	44
3	$CH_3-(CH_2)_3-O-$		$-H$	45
4	$HO-$		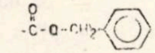	98
5	$HO-$		—	99
6	$(CH_3)_3C-O-$	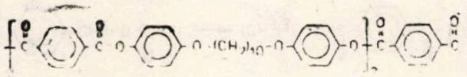	$-O-C(CH_3)_3$	84
7	$CH_3-(CH_2)_3-O-$		$-O-(CH_2)_3-CH_3$	21
8	$HO-$		$-OH$	99
	$(CH_3)_3C-O-$	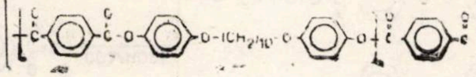	$-O-C-(CH_3)_3$	15
	$HO-$		$-OH$	91

Table 3

Thermal and phase behaviour of liquid crystalline oligomer-models 1—10 and polymer 11

Compound no.	Structures and End Groups			hase Transition Temperatures (°C)					Rangeof LC-Phase (°C) on		LC-Phase
				T_1	T_2	T_3	T_M	T_{cl}	Heating	Cooling	
1	$(CH_3)_3C-O-$	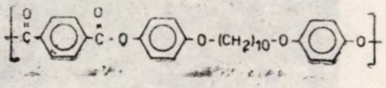	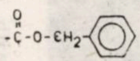	—	—	—	144	—	—	—	—
2	$(CH_3)_3C-O-$		$-H$	93	—	—	97	—	—	—	—
3	$CH_3-(CH_2)_3-O-$		$-H$	81 1) —	84 1) —	— —	90.5 1) 126	— —	— —	— —	— —
4	HO—		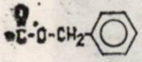	—	—	—	169	182	13	19	n ⇅
5	HO—		—H	— —	— —	— —	201 2) 179 2) 3)	— 191 2) 3)	— —	— 12 3)	n ↓
6	$(CH_3)_3C-O-$	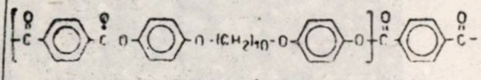	$-O-C(CH_3)_3$	—	—	—	134	—	—	—	—
7	$CH_3-(CH_2)_3-O-$		$-O-(CH_2)_3-CH_3$	—	—	—	132	—	—	—	—
8a	HO—		—OH	214	—	—	292	300	8	84 4)	n ⇅
8b	HO—		—OH**	234	—	—	285	293	8	38 .5	n ⇅
9	$(CH_3)_3C-O-$	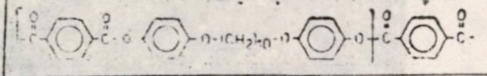	$-O-C(CH_3)_3$	147*)	—	—	172	177	5	2 2)	5) ⇅
10	HO—		—OH	257	—	—	265 2	293	28	81	n ⇅
11		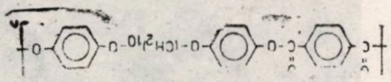		177	200*)	231	240	265	25	47	n ⇅

T_1, T_2, T_3 : Solid-Solid-Transitions ; T : Melt Transition ; T_{Cl} : Clearing Temp.
n = nematic ; *s* = smectic ; ⇅ : enantiotropic ; ↓ monotropic
* exothermic transition ** prepared by solid-phase method
[1] DSC determination on 2nd heating [2] observed from heating in polarizing microscope
[3] DSC determination on 1st cooling [4] DSC determination on 2nd cooling
[5] undetermined

Fig. 2a. — Nematic phase of **4** at 174°C during cooling (with λ-plate)

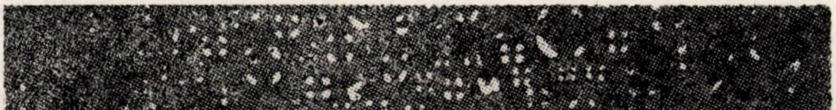

Fig. 2b. — Nematic droplets of 5 at 191°C (1st cooling) with pseudoisotropic phase

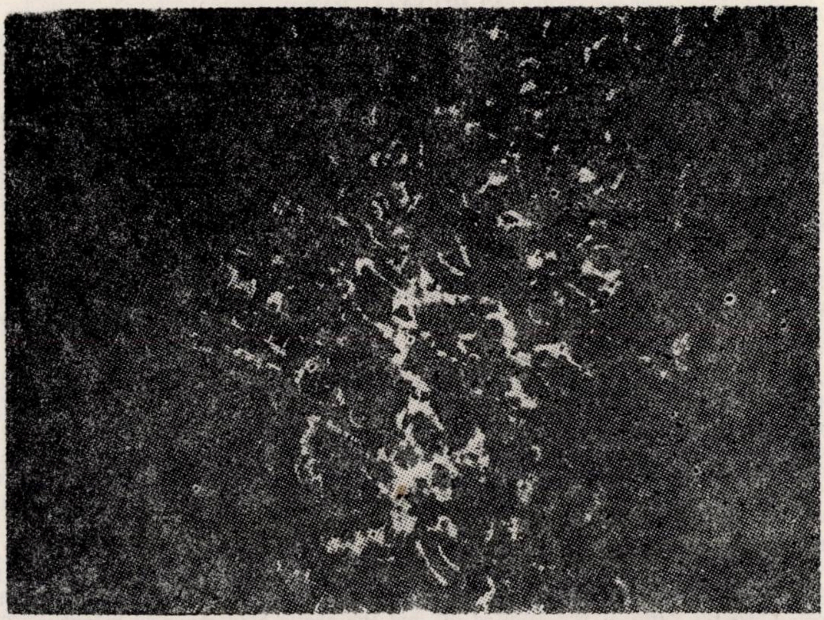

Fig. 2c. — Nematic schlieren-texture of 8a at 289°C (2nd heating)

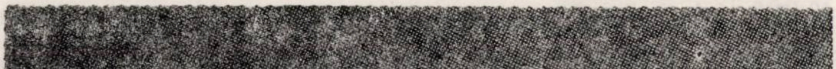

Fig. 2d. — Nematic schlieren-texture of 10 at 280°C (heating)

EXPERIMENTAL PART

Chemicals were purchased from Fluka, Buchs, Switzerland, and from E. Merck, Darmstadt, West-Germany. Materials for chromatography were: TLC-sheets coated with silicagel (from E. Merck), silicagel no. 7734 (E. Merck) and aluminium oxide ("Alox basisch") from Woelm, Eschwege, Germany.

UV-spectroscopy was done with a spectrophotometer PMQ III and a spectrograph DMR 21 (Carl Zeiss, Oberkochen, West Germany). IR-spectra were measured with a Perkin-Elmer 325, ^{1}H-NMR spectra with a Varian A 60A and a Perkin Elmer R 32 (90 MHz) and mass spectra with a Varian MAT 711.

4-[1-(4-Benzyloxyphenyl)-1-methylethyl] phenol (bisphenol A-monobenzylether) was prepared by modification of a procedure described by Newman and Cella.[15] tert. Butyl hydrogen terephthalate(-isophthalate, -phthalate) was prepared by modifying a procedure of Hässlin et al.[3b,8]

General procedure for the preparation of protected oligomers of the series I(I, n = 1—5): 0.04 ml of phenolic component were added with stirring to a solution of 0.04 mol of acidic component in 200 ml of abs. THF, containing a trace of 4-dimethylaminopyridine. After cooling to 0°C, 0.04 mol dicyclohexylcarbodiimid (DCC) were added. The mixture was first stirred 5 min. at 0°, then 3 hours at room temperature. Dicyclohexylurea was removed by filtration. The filtrate was concentrated in vacuo. The residue was taken up in a small volume of chloroform and the product crystallized from methanol or ethanol.

General procedure for the removal of the benzyl protecting group: 0.01 mol of oligomer I were dissolved in 300 ml of acetic acid. 2 g of a palladium/C (containing 10% Pd) were added and hydrogen was passed through the solution until the theoretical amount had been consumed. Then the catalyst was filtered off and the acetic acid removed in vacuo. The residue was crystallized from methanol.

General procedure for the removal of the tert.-butyl group: 0.01 mol of oligomer I were dissolved in 25 ml of chloroform and treated with 25 ml of trifluoroacetic acid. At room temperature the reaction was monitored by TLC until disappearance of the starting material. Chloroform and residual trifluoroacetic acid were evaporated and the precipitate crystallized from ethanol.

10-Bromo-1-decanol was prepared from commercial 1,10-decanediol by modification of procedures described by Schill[16] and Logemann.[17] 20-Bromo-1-icosanol was prepared from protected 10-bromo-1-decanol and 1,10-dibromodecane by modification of the procedure described by Schill and Merkel.[16]

Preparation of α-(Benzyl)-ω(benzyloxy)-(oxy-1,4-phenyleneoxy-1,10-decamethyleneoxy--1,4-phenylene): 37 g (185 mmol) of hydroquinonemonobenzylether were dissolved in 150 ml ethanol. 7.6 g (190 mmol) sodium hydroxide were added. The mixture was heated under reflux for 1 hour. Then a solution of 27 g (90 mmol) 1,10-dibromodecane in 70 ml ethanol was added dropwise at room temperature. The mixture was then refluxed for 3 hours, which led to a formation of a white precipitate, then stirred into 500 ml water. The precipitate was filtered with suction and washed with water, then dried in vacuo over phosphorus pentoxide. The product was recrystallized from dioxane.

The debenzylation of this compound was done as described above.

Procedure for the preparation of compounds *2* and *6*: 6.67 g (30 mmol) terephthalic acid mono- tert. butylester were dissolved in 200 ml abs. THF. 4.46 g (33 mmol) 1-hydroxybenzotriazole and 4.86 g (30 mmol) carbonyldiimidazole were added, and the clear solution was stirred until the evolution of carbon dioxide ended. The resulting mixture was added dropwise to 10.74 g (30 mmol) α-(hydrogen)-ω-(hydroxy)-(oxy-1,4-phenyleneoxy-1, 10-decamethyleneoxy-1,4-phenylene), dissolved in 400 ml abs. THF. The solution was stirred overnight, then the THF removed in vacuo, the residue dissolved in 500 ml chloroform and washed with water. The unreacted dihydroxy-component precipitated. The chloroform and water phases were filtered with suction. Then the organic layer was separated, dried and, after concentration to a small volume, chromatographed through a silicagel column (eluent methanol : methylene chloride = 1 : 99(v/v)). This compound was used for further duplication reactions.

If the similar reaction was done using only 15 mmol α-(hydrogen)-ω-(hydroxy)-(oxy-1,4--phenyleneoxy-1,10-decamethyleneoxy-1,4-phenylene), the main product was the disubstituted compound. The reactions could be similarly done with a mixture of dicyclohexylcarbodiimide and 1-hydroxybenzotriazole.

General procedure for the reaction of oligoarylate and oligomethylene derivatives: 0.04 mol tert. butyl hydrogenterephthalate and 0.04 mol 10-bromo-1-decanol in 100 ml abs. pyridine were reacted with 0.041 mol dicyclohexylcarbodiimide and 100 mg 4-dimethylaminopyridine at 0° for 3 hours. The dicyclohexylurea was removed by filtration, the solvent evaporated and the residue immediately deblocked by treatment with 50 ml trifluoroacetic acid. The resulting 10-bromodecyl hydrogenterephthalate was reacted with an equimolar amount of an oligoarylate with free phenolic end using 1 equivalent of dicyclohexylcarbodiimide and a trace of 4-dimethylaminopyridine in THF at 0° for 5 min., then at room temperature for 3 hours. After removal of the dicyclohexylurea by filtration the solvent was evaporated in vacuo and the residue purified by chromatography on a silicagel column (eluent chloroform).

The diesterification of 1,10-decanediol or 1,20-icosanediol with oligoarylates containing a free carboxylic end was done similarly at a ratio of arylate to diol = 2.2 : 1.

ACKNOWLEDGEMENTS

We are greatly indebted to A. Ruoff for IR measurements, to R. Kimmich and E. Neff for NMR measurements, and to G. Schmidtberg for mass spectroscopic measurements, as well as to V. Krivan for carrying out elemental analyses.

This project was financed by the Bundesministerium für Wirtschaft of the Federal Republic of Germany through the Arbeitsgemeinschaft Industrieller Forschungsvereinigungen (project no. 4686 and 6274). The content of this publication is solely in the responsibility of the authors. M.B. Bitar was recipient of a doctoral fellowship of the Deutsche Akademische Austauschdienst.

REFERENCES

[1] M. Rothe, *Makromol. Chem.*, **35**, 183 (1960) and literature cited there.

[2] H. Zahn, C. Borstlap and G. Valk, *Makromol. Chem.*, **64**, 18 (1963) and literature cited there.

[3] e.g. a) H.-W. Hässlin, M. Dröscher and G. Wegner, *Makromol. Chem.*, **179**, 1373 (1978); b) H.-W. Hässlin, M. Dröscher and G. Wegner, *Makromol. Chem.*, **181**, 301 (1980); c) R. Bill, M. Dröscher and G. Wegner, *Makromol. Chem.*, **182**, 1033 (1981); d) F.G. Schmidt and M. Dröscher, *Makromol. Chem.*, **184**, 2669 (1983).

[4] e.g. A.C. Griffin and T. R. Britt, *J. Amer. Chem. Soc.*, **103**, 4957 (1981); A. C. Griffin, N. W. Buckley, W. E. Hughes and D. L. Wertz, *Mol. Cryst. Liq Cryst.* (*Letters*), **64**, 139 (1981); R. B. Blumstein and E. M. Stickles, *Mol. Cryst. Liq Cryst.* (*Letters*), **82**, 151 (1982): A. C. Griffin and T. R. Britt, *Mol. Cryst. Liq. Cryst.* (*Letters*), **92**, 149 (1983); R. B. Blumstein, E. M. Stickles, M. M. Gauthier, A. Blumstein and F. Volino, *Macromolecules*, **17**, (1984), 177; J. A. Buglione, A. Roviello and A. Sirigu, *Mol. Cryst. Liq. Cryst.*, **106**, 169 (1984); R. Capasso, P. Iannelli, A. Roviello and A. Sirigu, *Macromolecules*, **18**, 2773 (1985): J.-I. Jin, E.-J. Choi, S.-C. Ryu and R. W. Lenz, *Polymer J.*, **18**, 63 (1986).

[5] P. Keller, *Mol. Cryst. Liq. Cryst.*, **123**, 247 (1985).

[6] H. Rinke, *Chimia*, **22**, 164 (1968).

[7] R. Bonart, *J. Macromol. Sci., Phys.*, **2**, 115 (1968).

[8] H. Seliger, M. B. Bitar, H. Nguyen-Trong, A. Marx, R. Roberts, J.-K. Krüger and H.-G. Unruh, *Makromol. Chem.*, **185**, 1335 (1984).

[9] J. K. Krüger, A. Marx, R. Roberts, H.-G. Unruh, M. B. Bitar, H. Nguyen-Trong and H. Seliger, *Makromol. Chem.*, **185**, 1469 (1984).

[10] M. Levine and S. C. Temin, *J. Polym. Sci.*, **28**, 179 (1958).

[11] W. M. Eareckson III, *J. Polym. Sci.*, **40**, 399 (1959).

[12] a) H. Schnell, *Angew. Chem.*, **68**, 633 (1956); b) G. Bier, *Polymer*, **15**, 527 (1974).

[13] J.-I. Jin, S. Antoun, C. Ober and R. W. Lenz, *Brit. Polym. J.*, **1980**, 132; S. Antoun, R. W. Lenz and J.-I. Jin, *J. Polym. Sci. Polym. Chem. Ed.*, **19**, 1901 (1981).

[14] a) E. Göldner, Dissertation, Univ. Ulm, **1987**, b) H. Seliger and E. Göldner, publication in preparation.

[15] M. Newman and J. Cella, *J. Org. Chem*, **39**, 214 (1974).

[16] G. Schill and C. Merkel, *Chem. Ber*; **111**, 1446 (1978).

[17] E. Logemann, Dissertation, Univ. Freiburg, **1976**.

Revue Roumaine de Chimie, **36**, *1–3*, 187–195**(1991)**

STUDIES IN THE FIELD OF HETEROCYCLIC COMPOUNDS. SYNTHESIS AND BEHAVIOUR OF 4-(4-CHLORO-3-METHYL)PHENYL-1-(2H)-PHTHALAZINONE TOWARDS SOME ELECTROPHILES AND NUCLEOPHILES

M.A. El-SAFTY[a], S. El-BAHAEI[a], M.A. El-HASHASH[b], A. El-FARARGY[a] and F. YASIN[a]

[a] Zagazig University, Faculty of Science, Zagazig, Egypt
[b] Ain Shams University, Faculty of Science, Abbassia, Cairo, Egypt

Received May 14, 1988

The phthalazinone derivatives 2a-f have been obtained *via* the interaction of *o*-(4-chloro-3-methyl)benzoyl benzoic acid with hydrazine derivatives. The behaviour of 2a towards carbon electrophiles and carbon nucleophiles has been investigated. The chlorophthalazine derivative 3S has been also synthesised from the action of $PCl_5/POCl_3$ on 2a. The behaviour of 3S towards nitrogen, and oxygen nucleophiles have been also described.

Recently,[1,2] 1(2H)-phthalazinones have been described as being useful as remedies for arteriosclerosis and thrombosis, and have also been found useful as developable light sensitive materials. This prompted us to synthesise some new phthalazinones *via* interaction of *o*-(4-chloro-3-methyl) benzoyl benzoic acid with hydrazine derivatives, and also in the hope of obtaining some pharmaceutical action.

The interaction of phthalic anhydride with *o*-chlorotoluene under Friedel-Crafts condition gives the *o*-(4-chloro-3-methyl) benzoyl benzoic acid (**1**), which reacts with hydrazines namely: hydrazine hydrate, phenylhydrazine, benzoylhydrazine, and salicyloylhydrazine in boiling butanol or with semicarbazide and thiosemicarbazide in boiling pyridine to give the corresponding phthalazinone derivatives **2a-f**.

The structure of compounds **2a-f** was confirmed from : (i) analytical data, (ii) IR spectrum of **2a** which shows bands at 1640, 1670, 3150, and 3400 attributable to $^{*\nu}C=O$, $^{\nu}C=N$, $^{\nu}NH$ and $^{\nu}OH$ respectively. This IR data illustrated that **2a** in solid state exists actually in lactam-lactim dynamic equilibrium. This is analogous with the results recently claimed by El-Hashash et al. [3] IR spectrum of **2e** exhibits bands corresponding to νmax of two carbonyl groups, $\nu C=N$ and νNH at 1680, 1665, 1640 and 3200 respectively. IR spectrum of **2f** shows bands at 1680, 1635, 1340 and 3200 attributable to $\nu C=O$, $\nu C=N$, $\nu C=S$ and νNH respectively.

The structure of compound **2c** was deduced *via* treatment of **2a** with benzoyl chloride in least amount of pyridine and comparison of m.p. and m.m.p. determination.

$^{*\nu}$ max expressed in cm^{-1} throughout the paper.

Recently,[4] it was reported that, in all solvents except petrol at high dilution, the 2- and 4-hydroxypyridines are extremely unfavoured in the equilibrium : polar solvation strongly favours the amide-like structures of the α- and γ- pyridones (lactam form).

The above results prompted us to study the behaviour of the 4-(4--chloro-3-methyl)phenyl-1-(2H)-phthalazinone (**2a**) towards some electrophiles and nucleophiles in different solvents. Thus the compound **2a** reacts with a variety of electrophiles namely, dimethyl sulphate, ethyl chloroacetate, and ethyl chloroformate in dry acetone, by using anhydrous K_2CO_3 as catalyst[5] to give 1-(methoxy, ethoxycarbonyl methoxy, or ethoxycarbonioxy)-phthalazine derivatives **3a-c** respectively. No N-alkyl derivative was obtained by this method, this may be due to the rapid interconversion of the lactam form to lactim form in the presence of acetone and K_2CO_3 which lead to the desired product.

Structure of compounds **3b** and **3c** was established from : (i) I.R. spectra which exhibit strong absorptions at 1635, 1740 attributable to νC=N and νC=O of ester ; ii) chemically, *via* the reaction of **3b** and **3c** with (a) aqueous sodium hydroxide to give the corresponding acids (**3d** and **3e**) respectively ; (b) hydrazine and phenylhydrazine in boiling butanol to give the corresponding hydrazides **3f-i**, (c) with primary amines namely aniline, ethylamine, benzylamine and *p*-anisidine in boiling butanol to give N-aryl or alkyl amide derivatives **3j-p**. The IR spectra of **3f-i** exhibit bands in the region 1660–1665 (νC=O carboxamide) and 3200–3300 νmax of two NH groups. Compounds **3j-p** show bands in the region of 1650–1665 and 3200–3300 attributable to νC=O and νNH respectively.

On the other hand, the ester **3b** reacts also with benzaldehyde in presence of potassium *tert*-butoxide at room temperature affording "Stobbe" product **3q** as major product and the "Claisen" product **3r** as minor product. This reaction is analogous with the previous work[6]. Compound **3r** was also converted to **3q** by hydrolysis with aqueous NaOH. I.R. spectrum of **3q** shows bands at 1620, 1635, and 1705 attributable to νC=C, νC=N and νC=O respectively.

Further proof for lactam-lactim equilibrium in phthalazinone **2a** has also been confirmed by converting the lactam form of phthalazinone **2a** to 1-chlorophthalazine **3S** which is the key starting material for numerous heterocyclic compounds. Thus treatment of **2a** with PCl_5 in presence of $POCl_3$ yielded **3S**. Structure of **3S** was deduced from : (i) Its IR spectrum which show no νC=O or νNH and (ii) chemically *via*, (a) reaction with oxygen nucleophiles e.g. sodium methoxide in methanol to give (3a) ; (b) treatment of **3S** with nitrogen nucleophiles e.g., hydrazine hydrate, phenylhydrazine, aniline and methylamine affording hydrazino, phenylhydrazino, anilino, and methylamino) phthalazine derivatives **3t-w**. Their IR spectra show bands in the region 1630–1625 and 3200–3300 attributable to νC=N and νNH respectively.

Recently,[7] it was reported that 6-substituted (phenyl)-1,2,4-triazolo--4,3-b pyridazines have pharmacological properties. Some of these derivatives also exhibited hypotensive activity when tested in spontaneously hypertensive rats (SHR). The present work also deals with the reaction

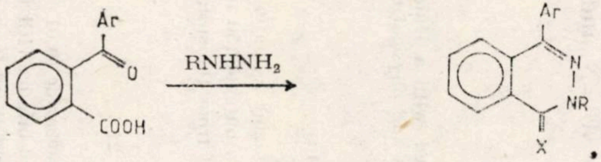
Ar
O
COOH
RNHNH₂
Ar
N
NR
X

(1) (2)

Ar = 4,3 − Cl, $CH_3C_6H_3$

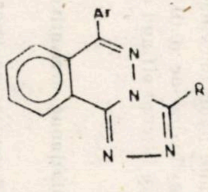

(4)

a, $R=C_6H_5$
b, $R=CH_2C_6H_5$
c, $R=C_6H_4-(OH)-(0)$

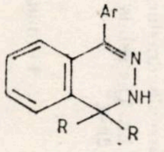

(7)

a, $R=CH_3$
b, $R=C_2H_5$

a, $R=H$
b, $R=C_6H_5$
c, $R=COC_6H_5$
d, $R=(C_6H_4CO)-OH-(0)$
e, $R=CONH_2$
f, $R=C(S)NH_2$
g, $R=H$
x = 0 except case of 2g $X=S$

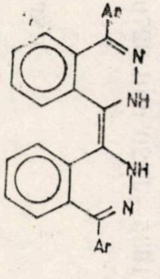
Ar
N
NH
NH
N
Ar

(6)

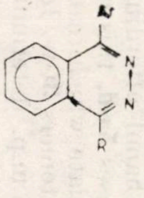

(3)

a, $R=OCH_3$
b, $R=OCH_2COOEt$
c, $R=OCOOEt$
d, $R=OCH_2COOH$
e, $R=OCOOH$
f, $R=OCH_2CONHNH_2$
g, $R=OCH_2CONHNHPh$
h, $R=OCONHNH_2$
i, $R=OCONHNHPh$
j, $R=OCH_2CONHPh$
k, $R=OCH_2CONHC_2H_5$
l, $R=OCH_2CONHCH_2Ph$
m, $R=OCONHPh$
n, $R=OCONHC_2H_5$
o, $R=OCONHCH_2Ph$
p, $R=OCONHC_6H_4-OCH_3(p)$
q, $R=O-C=CHPhCOOH$
r, $O-C=CHPhCOOEt$
s, $R=Cl$
t, $R=NHNH_2$
u, $R=NHNHPh$
v, $R=NHPh$
w, $R=NHCH_3$

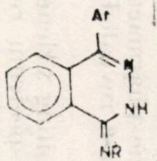

(5)

a, $R=NH_2$
b, $R=NHPh$
c, $R=C_6H_5$
d, $R=CH_3$

of the chlorphthalazine derivative **3s** with acylhydrazines namely, benzoylhydrazine, phenylacetylhydrazine, and salicyloylhydrazine in boiling butanol to give 6-(4-chloro-3-methyl)phenyl-1,2,4-triazolo-(4,3-b)-4,5-benzopyridazines (**4a-c**), in the hope of proving some pharmacological properties for these derivatives. The IR spectra for **4a-c** revealed bands at the region of 1640—1630 due to νC=N.

The reaction of phthalazinone **2a** with P_2S_5 in boiling xylene[3] gives the corresponding phthalazine thione **2g** whose IR spectrum revealed bands at 1340 and 3250 attributable to νC=S and νS—H or νNH.

It was reported,[9] that thiopyridazinones underwent condensation with nitrogen nucleophiles e.g. hydrazine or primary amines to give the corresponding hydrazones and Schiff-bases respectively. In the present work the authors try to compare the behaviour of the thione **2g** qualitatively (no data) towards the nitrogen nucleophiles with the thiopyridazinones. Thus, when **2g** was allowed to react with hydrazine hydrate, phenylhydrazine, aniline and methylamine in boiling ethanol affording **3t-w** and not the corresponding hydrazones or Schiff bases **5a-d**, this may be due to compounds **5** produced as fleeting intermediate which rearranges directly to the more thermodynamically stable tautomers **3t-w**. Identity of these products was deduced from m.p. and m.m.p. determinations.

Treatment of the thione **2g** with copper bronze in boiling xylene yielded the bis-compound **6**. Its IR spectrum exhibits bands at 1625 and 1618 attributable to νC=N and νC=C.

When **2a** was submitted to reaction with methyl magnesium iodide and ethylmagnesium iodide in dry ether-benzene mixture it affords 1-(4-chloro-3-methyl)phenyl-3,4-dihydro-4,4-dimethyl or diethylphthalazine (**7a** and **7b**) IR spectra of compounds **7** revealed absorption bands in the region 1635—1620 and 3270—3300 attributable to νC=N and νNH respectively.

EXPERIMENTAL

All melting points are uncorrected. IR spectra were determined with a Unicam SP 1200 spectrophotometer using KBr Wafer technique. Characterisations and physical data are llisted in Table 1.

Formation of phthalazinone derivatives (2a-d) :

A mixture of acid **1** (0.01 mole) and hydrazines namely, hydrazine hydrate, phenylhydrazine, benzoylhydrazine, and salicyloylhydrazine (0.01 mole) in *n*-butanol (50 mL) was refluxed for 3 hr. The solids separated were filtered off and crystallized from the suitable solvent to give **2a-d**.

Formation of phthalazinone derivatives 2e and 2f

A mixture of acid **1** (0.01 mole) and semicarbazide or thiosemicarbazide (0.01 mole) in pyridine (40 mL) was refluxed for 8 hr. The reaction mixture was poured into ice/HCl (100 gm ice and 20 ml conc. HCl). The solids obtained were filtered off and crystallized from the proper solvent.

Table 1

Characterisation and physical data for synthesised compounds

Compd	M.p. °C	Solvent (yield %)	Mol. formula	Analysis % Calcd.	Analysis % Found
2a	245	Toluene (50)	$C_{15}H_{11}ClN_2O$	C 66.54 H 4.06 N 10.35	66.50 4.00 10.00
2b	128	Benzene (65)	$C_{21}H_{15}ClN_2O$	C 72.72 H 4.32 N 8.08	72.62 4.21 8.00
2c	210	Benzene (63)	$C_{22}H_{15}ClN_2O_2$	C 70.49 H 4.01 N 7.47	70.01 4.00 7.25
2d	244	Ethanol (60)	$C_{22}H_{15}ClN_2O_3$	C 67.60 H 3.84 N 7.17	67.53 3.72 7.00
2e	258	Benzene (70)	$C_{16}H_{12}ClN_3O_2$	C 61.24 H 3.82 N 13.39	61.00 3.64 13.04
2f	260	Toluene (68)	$C_{16}H_{12}ClN_3OS$	C 58.27 H 3.67 N 12.74	58.20 3.57 12.60
3a	131	Benzene (65)	$C_{16}H_{13}ClN_2O$	C 67.48 H 4.56 N 9.84	67.25 4.32 9.75
3b	120	Light petrol 80–100° (65)	$C_{19}H_{17}ClN_2O_3$	C 63.95 H 4.76 N 7.85	64.23 5.09 7.56
3c	115	Light petrol 80–100°C (65)	$C_{18}H_{15}ClN_2O_3$	C 63.06 H 4.37 N 8.17	63.51 4.72 8.46
3d	240	Benzene (60)	$C_{17}H_{13}ClN_2O_3$	C 62.10 H 3.95 N 8.52	61.94 3.82 8.50
3e	245	Benzene (65)	$C_{16}H_{11}ClN_2O_3$	C 61.04 H 3.49 N 8.91	61.00 3.47 8.82
3f	241	Ethanol (55)	$C_{17}H_{15}ClN_4O_2$	C 59.56 H 4.36 N 16.35	59.22 4.30 16.00
3g	138	Ethanol (60)	$C_{23}H_{19}ClN_4O_2$	C 65.94 H 4.54 N 13.38	65.80 4.48 13.20
3h	240	Benzene (60)	$C_{16}H_{13}ClN_4O_2$	C 58.44 H 3.95 N 17.04	58.24 3.86 16.97

Table 1 (continued)

Compd	M.p. °C	Solvent (yield %)	Mol. formula	Analyse % Calcd.	Found
3i	217	Benzene (65)	$C_{22}H_{17}ClN_4O_2$	C 65.26 H 4.20 N 13.84	65.01 4.00 13.53
3j	131	Toluene (55)	$C_{23}H_{18}ClN_3O_2$	C 68.40 H 4.46 N 10.40	68.00 4.32 10.00
3k	130	Toluene (60)	$C_{19}H_{18}ClN_3O_2$	C 64.13 H 5.06 N 11.81	65.00 5.00 11.42
3l	220	Benzene (58)	$C_{24}H_{20}ClN_3O_2$	C 68.98 H 4.79 N 10.05	68.82 4.63 9.97
3m	206	Toluene (60)	$C_{22}H_{16}ClN_3O_2$	C 67.77 H 4.10 N 10.78	67.52 4.00 10.43
3n	238	Toluene (60)	$C_{18}H_{16}ClN_3O_2$	C 63.40 H 4.68 N 12.29	63.21 4.52 12.00
3o	230	Benzene (54)	$C_{23}H_{18}ClN_3O_2$	C 68.40 H 4.46 N 10.40	68.21 4.32 10.21
3p	205	Benzene (55)	$C_{23}H_{18}ClN_3O_2$	C 65.79 H 4.29 N 10.01	65.62 4.13 9.89
3q	85	Pet. ether 60–80° (45)	$C_{26}H_{21}ClN_2O_3$	C 70.19 H 4.72 N 6.29	70.00 4.56 6.01
3r	180	Toluene (55)	$C_{24}H_{17}ClN_2O_3$	C 69.14 H 4.08 N 6.72	69.02 4.00 6.52
3s	220	Toluene (60)	$C_{15}H_{10}Cl_2N_2$	C 62.22 H 3.46 N 9.68	62.03 3.40 9.57
3t	150	Benzene (55)	$C_{15}H_{13}ClN_4$	C 63.23 H 4.56 N 19.71	63.14 4.42 19.00
3u	144	Benzene (60)	$C_{21}H_{17}ClN_4$	C 69.90 H 4.71 N 15.53	69.75 4.62 15.01
3v	170	Toluene (63)	$C_{21}H_{16}ClN_3$	C 72.93 H 4.63 N 12.17	72.73 4.50 12.00
3w	142	Toluene (65)	$C_{16}H_{14}ClN_3$	C 67.72 H 4.93 N 14.81	67.40 4.82 14.50

Table 1 (continued)

Compd	M.p. °C	Solvent yield %	Mol. formula	Analysis %	
				Calcd.	Found
4a	233	Toluene	$C_{22}H_{15}ClN_4$	C 71.25	71.00
		(50)		H 4.04	3.94
				N 15.11	15.00
4b	214	Butanol	$C_{23}H_{17}ClN_4$	C 71.75	71.52
		(53)		H 4.42	4.40
				N 14.56	14.32
4c	222	Butanol	$C_{22}H_{15}ClN_4O$	C 68.30	68.40
		(60)		H 3.88	3.72
				N 14.48	14.25
2g	230	Xylene	$C_{15}H_{11}ClN_2S$	C 62.82	62.56
		(50)		H 3.83	3.74
				N 9.77	9.54
				S 11.16	10.09
6	251	Toluene	$C_{30}H_{23}Cl_2N_4$	C 70.86	70.73
		(60)		H 4.37	4.23
				N 11.02	10.97
7a	225	Toluene	$C_{17}H_{17}ClN_2$	C 71.70	71.53
				H 5.97	5.82
		(60)		N 9.84	9.73
7b	205	Toluene	$C_{19}H_{22}ClN_2$	C 72.72	71.93
		(65)		H 7.07	6.98
				N 8.93	8.82

Reaction of phthalazinone 2a with benzoyl chloride : Formation of 2c :

A mixture of **2a** (0.01 mole), benzoyl chloride (0.01 mole) and pyridine (1 ml) was refluxed for 3 hr. The cold reaction mixture was added gradually into ice-dilute HCl, the solid obtained was filtered off and crystallised from the proper solvent to give **2c**, which was identified by m.p. and m.m.p. determination.

Action of dimethylsulphate, ethyl chloroacetate and ethyl chloroformate on phthalazinone 2a : Formation of phthalazine derivatives 3a-c :

A mixture of **2a** (0.01 mole), alkylating agent namely, dimethyl sulphate, ethyl chloroacetate, and ethyl chloroformate (0.04 mole) ; and anhydrous potassium carbonate (0.04 mole) in dry acetone (50 mL) was refluxed for 20 hr. The excess of solvent was removed by distillation, then the reaction mixture was poured into water. The organic material was extracted by ether, evaporation of the dried ethereal solution gave the alkylating products **3a-c** respectively.

Alkaline hydrolysis of 3b and 3c : Formation of 3d and 3e.

A mixture of **3b** or **3c** (0.01 mole) and aqueous sodium hydroxide 10% (10 mL for each g of **3b** or **3c** was refluxed for 3 hr. The reaction mixture was cooled and extracted with ether to get rid of unsaponified material. The aqueous layer was acidified with very cold dilute hydrochloric acid, the solid obtained was filtered off and recrystallized from the proper solvent to give **3d** and **3e** respectively.

Action of hydrazines on 3b and 3c : Formation of hydrazides 3f-i :

A mixture of **3b** or **3c** (0.01 mole), hydrazine hydrate or phenylhydrazine (0.01 mole) was refluxed in *n*-butanol (50 mL)for 3 hr. The solid separated after concentrating and cooling was filtered off and recrystallized from the proper solvent.

Action of amines of 3b and 3c : Formation of amides 3j-p :

A mixture of **3b** or **3c** (0.01 mole), and primary amines, namely, aniline, ethylamine, benzylamine and *p*-anisidine (0.01 mole) was refluxed in *n*-butanol (50 mL) for 5 hr. The solid separated after concentrating and cooling was filtered off, and recrystallized from the proper solvent.

Action of benzaldehyde on 3b : Formation of cinnamic acid derivatives 3q and 3r :

A mixture of **3b** (0.01 mole) and benzaldehyde (0.01 mole) was added during 30 min. to a stirred solution of potassium *tert.* butoxide (in *tert.* butanol, 20 mL for each g of **3b**). The reaction mixture was left aside overnight at room temperature. The excess of alcohol was removed under reduced pressure. The residue was poured onto water and extracted with ether, then evaporation of the dried ethereal layer left an oily material, which solidified by trituration with light petrol (b.p. 40—60°). On recrystallization from the proper solvent **3r** was obtained. The aqueous layer upon acidification with very cold dilute hydrochloric acid gave a precipitate, which filtered off and recrystallized from the proper solvent and gave **3q**.

Action of $PCl_5/POCl_5$ on phthalazinone derivative 2a : Formation of chlorophthalazine derivatives 3s :

A mixture of phthalazinone **2a** (0.01 mole), PCl_5 (1 g) and $POCl_3$ (7 mL) was refluxed on a steam bath for 3 hr. The cold reaction mixture was poured slowly into crushed ice. The solid separated was filtered, dried and recrystallized from the proper solvent to give **3s**.

Action of hydrazines and amines on chlorophthalazine (3s) : Formation of 1-(hydrazino, phenylhydrazino, anilino and methylamino) phthalazine derivatives (3t-w) :

A mixture of chlorophthalazine (**3s**) (0.01 mole) and each of hydrazine hydrate, phenyhydrazine, aniline and/or methylamine (0.01 mole) was refluxed in benzene (40 mL) for 6 hr. The solids that separated on cooling were crystallized from the proper solvent.

Formation of 1-methoxyphthalazine 3a :

A mixture of chlorophthalazine (**3S**) (0.01 mole) and sodium methoxide (0.01 mole) in 30 mL methanol was refluxed for 3 hr. Excess of alcohol was removed by distillation, the reaction mixture was cooled and acidified with dilute hydrochloric acid, the solid that separated was filtered off and crystallized from the proper solvent to give (**3a**) which was identified by m.p and m.m.p. determination.

Action of acylhydrazines on chlorophthaleazine 3s : Formation of 1,2,4-triazolo-(4,3-b-4,5-benzopyridazines 4a-c :

A mixture of 1-chlorophthalazine (**3s**) (0.01 mole) and each of acylhydrazines, namely, benzoylhydrazine, phenylacetyl hydrazine and/or salicyloylhydrazine (0.01 mole) in *n*-butanol (40 mL) was refluxed for 48 hr. The solid that separated after concentrating and cooling was recrystallized from the proper solvent.

Action of P_2S_5 on phthalazinone derivative 2a : Formation of thione derivative 2g :

A mixture of (**2a**) (0.01 mole) and P_2S_5 (0.01 mole) in dry xylene (50 mL) was refluxed for 1 hr. The reaction mixture was filtered on hot. The solid obtained was recrystallized from the proper solvent.

Action of copper bronze on thione 2g : Formation of the bis compound 6 :

A mixture of the thione (**2g**) (0.01 mole) and copper bronze (1 g) in dry xylene (40 mL) was refluxed for 10 hr. The reaction mixture was filtered hot and the filtrate was concentrated. The solid separated was crystallized from the proper solvent.

Action of Grignard reagents on phthalazinone 2a :Formation of phthalazine derivatives 7a and 7b :

To an ethereal solution of methyl or ethylmagnesium iodide (0.02 mole) ,(0.01 mole) of phthalazione (2a) in dry ether (50 mL) was added with stirring. The reaction mixture was refluxed on a steam bath for 6 hr, left aside overnight at room temperature, then decomposed by saturated solution of aqeous ammonium chloride. The organic materials were extracted with ether. The ethereal layer was dried over anhydrous sodium sulphate. Slow evaporation of the ethereal solution left solids which were crystallized from the proper solvent.

REFERENCES

[1] M. Inou, M. Ishikawa, T.Tsuchiya and T. Shinamoto, Chem. Abstr., **83**, 136899, 179092 **(1975)**.

[2] S. Ikenoue, T. Masuda and S. Sakawaki, *Chem. Abstr.*, **94**, 9988 (1981).

[3] M. A. El-Hashash, G. H. Sayed and M. El-Kady, *Rev. Roumaine Chim.*, **25**, 839 (1980).

[4] J. Joule and G. Smith, "Heterocyclic Chemistry" ELBS edition Van Nostrand Reinhold Company LTD. (1982) p. 61.

[5] M. F. El-Nawaihy and M. A. El-Hashash, *J. Chem. Soc.* (*C*), **1971**, 2373.

[6] M. A. El-Hashash, M. M. Mohamed, F. A. Sayed and O. A. Abo-Baker, *Indian J. of Chem.*, **19B**, (1980).

[7] J. D. Albright, D. R. Morn, W. B. Wright, J. B. Collins, B. Beer, A. S. Lippa, E.N.J. Greenblat, *J. Med. Chem.*, **24**, 592 (1981).

[8] A. Essawy, M. A. El-Hashash, M. A. El-Gendy and M. M. Hamed, *Indian J. of Chem.*, **21B**, 593 (1982).

[9] G. H. Sayed, M. El-Kady and M. A. El-Hashash, *Rev. Roumaine Chim.*, in press.

Revue Roumaine de Chimie, **36**, *1–3*, 197–200 (1991)

SOME REACTIONS OF SULTONES

S. YASSIN, I.I. ISMAIL*, A.H. ABD El-ALEEM and A.A. ATTA
Mouneffia University Faculty of Science and National Research Centre Cairo*, Egypt

Received May 24, 1988

Condensation of 2,4-dimethyl-1,3-butadiene-1,4-sultone(**1**) with phenylenediamines gave the sultams 2a-e. The sultams **2** react with phenylisocyanate, *p*-anisylisocyanate or *p*-chlorophenylisocyanate to give the phenylurea derivatives **2d-l**. Sultam **2e** reacts with acetone, acetophenone, benzophenone, benzaldehyde or *p*-anisaldehyde to yield the Schiff bases **3a-e**. The reaction of **2d,e** with *p*-acetamidobenzenesulphonyl chloride afforded the sulphonamide derivatives, **4a-b**. Hydrolysis of **4b** yielded **5**. The compound **2e** reacts with acetyl chloride, benzoyl chloride, *p*-chlorobenzoyl chloride or benzyl chloride to yield **6a-d**.

INTRODUCTION

It is known that sultones react with amines to give either sulphonic acids or sultams.[1–4] This reaction has been applied to 2,4-dimethyl-1,3-butadiene-1,4-sultone **1**. Compound **1** condenses with *o*-, *m*- or *p*-phenylenediamine to give the sultams **2a-e**. The structure of **2** is based on correct analytical and spetroscopic data.

Phenylurea derivatives are known for their larvicidal activity and are found to be stable in soil and water.[5] The phenylurea derivatives **2d-l** are readily formed when **2a-e** is allowed to react with phenylisocyanate, *p*-anisylisocyanate or *p*-chlorophenylisocyanate. The structure of the products now reported rests on correct analytical data and on spectroscopic results.

Treatment of **2e** with acetone, acetophenone, benzophenone, benzaldehyde or *p*-anisaldehyde yielded the corresponding Schiff bases **3a-e**, respectively. The structure of **3a-e** is supported by analytical data and spectral results.

Sulphonamide derivatives are famous for their bacteriological activity and have been used widely under the name of sulpha-drugs as bacteriostatic agents.[6] Thus, when the sultams **2b** or **2e** were allowed to react with *p*-acetamidobenzenesulphonyl chloride they gave the sulphonamide derivatives **4a** or **4b**. Hydrolysis of **4b** with boiled alkali gave **5**. On the other hand, in the reaction of **2e** with acid chlorides such as acetyl chloride, benzoyl chloride or *p*-chlorobenzoyl chloride, HCl was evolved, with the formation of the amides **6a-e**. Treatment of **2e** with benzyl chloride yielded **6d**. The structure of **6a-d** is based besides the analytical data by the spectroscopic results.

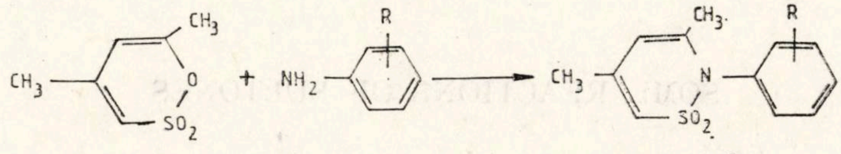
CH3
CH3
O
SO2
NH2
R
CH3
CH3
N
SO2
R

1 2

2a, R=$o-NM_2$

2b, R=$m-NH_2$

2c, R=$p-NH_2$

2d, R=$o-NH-CO-NH-C_6H_5$

2e, R=$o-NH-CO-NH-C_6H_4OCH_3(p)$

2f, R=$o-NH-CO-NH-C_6H_4Cl(p)$

2g, R==$m-NH-CO-NH-C_6H_5$

2h, R=$m-NH-CO-NH-C_6H_4OCH_3(p)$

2i, R=$m-NH-CO-NH-C_6H_4Cl(p)$

2j, R=$p-NH-CO-NH-C_6H_5$

2k, R=$p-NH-CO-NH-C_6H_4OCH_3(p)$

2l, R=$p-NH-CO-NH-C_6H_4Cl(p)$

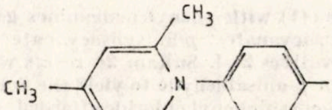
CH3
CH3
N
SO2
N = C
R
R'

3

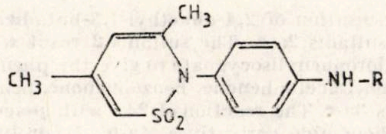
CH3
CH3
N
SO2
NH-R

6

3	R	R′
a	CH_3	$C\ H_8$
b	CH_3	C_6H_5
c	C_6H_5	C_6H_5
d	H	C_6H_5
e	H	$C_6H_4OCH_3(p)$

6a, R=$COCH_3$

6b, R=COC_6H_5

6c, R=$COC_6H_4Cl(p)$

6d, R=$CH_2-C_6H_5$

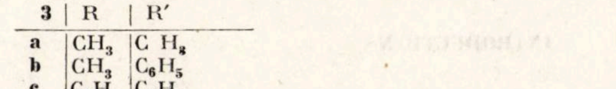
CH3
CH3
N
SO2
NH-SO2
NHCOCH3

4a, (m) 4b, (p)

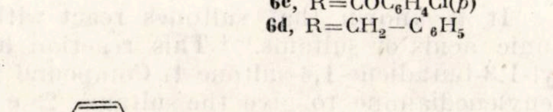
CH3
CH3
N
SO2
NHSO2
NH2

5

EXPERIMENTAL

Reaction of 2,4-dimethyl-1,3-butadiene-1,4-sultone with o-, m- or p-phenylenediamine. Equimolecular amounts of the sultone **1** and the amine, in a dry vessel, were heated in an oil bath. The reaction began at 130°C with evolution of water vapour. The temperature was kept at 130°C for an hour then, elevated to 150°C until the evolution of H_2O ceased. The reaction mixture was left to cool and a few drops of methanol were added. The separated solid was filtered off and crystallized from ethanol to give **2a-c**.

2,4-Dimethyl-N-(2-aminophenyl)-1,3-butadiene-1,4-sultam (**2a**) : M.p. 145°C ; yield 62 % — IR : 3470, 3370 cm^{-1} (NH_2), 1610, 1350 cm^{-1} (two conjugated double bonds), 1270 cm^{-1} (SO_2-N in sultam).

$C_{12}H_{14}N_2O_2S$ Calcd. C 57.55 H 5.63 N 11.20 Found C 57.65 H 5.81 N 11.11 %.

2,4-Dimethyl-N-(3-aminophenyl)-1,3-butadiene-1,4-sultam (**2b**) : M.p. 155°C ; yield 72 % – IR : 3475,3370 cm^{-1} (NH_2), 1610,1350 cm^{-1} (two conjugated double bonds), 1280 cm^{-1} (SO_2–N in sultam)-^{1}H NMR : $\delta = 7.2, 7.05$ (NH_2 protons), 6.4–6.8 (m 4H aromatic protons), 5.8,5.4 (s 1-H, 3-H sultam) 2.1,1.9 (s $2CH_3$).

$C_{12}H_{14}N_2O_2S$ Calcd. C 57.55 H 5.63 N 11.20 S 12.80 Found C 57.61 H 5.62 N 11.00 S 13.00 %.

2,4-Dimethyl-N-(4-aminophenyl)-1,3-butadiene-1,4-sultam (**2c**) : M.p. 164°C ; yield 80 %– IR : 3500, 3370 cm^{-1} (NH_2), 1600 – 1350 cm^{-1} (two conjugated double bonds), 1270 cm^{-1} (SO_2–N in sultam).

$C_{12}H_{14}N_2O_2S$ Calcd. C 57.55 H 5.63 N 11.20 Found C 57.50 H 5.61 N 11.61 %.

Reaction of the sultams **2a-c** *with isocyanates ; formation of* **2d-1**.

To a solution of the sultam 2(-2.5 g) in sodium – dried benzene (40 mL), 2mL of phenylisocyanate, *p*-anisylisocyanate or *p*-chlorophenylisocyanate and a few drops of triethylamine were added. The solution was refluxed for five hours. The product separated was filtered off, washed with benzene and crystallized from methanol to give **2d-l**.

N-Phenyl-Ń-[2-(2,4-dimethyl-1,3-butadiene-1,4-sultamyl-N)-phenyl]-urea (**2d**) : M.p. 203°C ; yield 75 %-IR : 1700 cm^{-1} (CO–N) 1270 cm^{-1} (SO_2–N sultam).

$C_{19}H_{19}N_3O_3S$ Calcd. C 61.77 H 5.18 Found C 61.50 H 5.51 %

N-4-Methoxyphenyl-Ň-[2-(2,4-dimethyl-1,3-butadiene-1,4-sultamul-N)-phenyl] - urea (**2e**) : M.p. 223°C ; yield 80 %-IR : 1700 cm^{-1} (CO–N), 1270 cm^{-1} (SO_2–N in sultam).

$C_{20}H_{21}N_3O_4S$ (399.47) Calcd. C 60.13 H 5.29 Found C 60.21 H 5.32 %.

N-4-Chlorophenyl-Ń-[2-(2,4-dimethyl-1,3-butadiene-1,4-sultamyl-N)-phenyl]-urea (**2f**) : M.p. 237°C ; yield 79 %-IR : 1700 cm (CO–N), 1290 cm^{-1} (SO_2–^{1} N sultam).

$C_{19}H_{18}N_3O_3SCl$ Calcd. C 56.50 H 4.46 Found C 56.81 H 4.23 %.

N-Phenyl-Ń-[3-(2,4-dimethyl3-1,-butadiene-1,4-sultamyl-N)-phenyl]-urea (**2g**) : M.p. 205°C ; yield 80 %-IR : 1700 cm^{-1} (CO–N), 1270 cm^{-1} (SO_2–N sultam).

$C_{19}H_{19}N_3O_3S$ 369.44) Calcd. C 61.77 H 5.18 N 11.37 S 8.67 Found C 61.51 H 5.01 N 11.20 S 8.55 %.

N-4-Methoxyphenyl-Ń-[3-(2,4-dimethyl-1,3-butadiene-1,4-sultamyl-N)-phenyl]-urea (**2h**) : M.p. 225°C ; yield 79 %-IR : 1700 cm^{-1} (CO–N), 1270 cm^{-1} (SO_2–N sultam).

$C_{20}H_{21}N_3O_4S$ (399.47) Calcd. C 60.13 H 5.29 Found C 60.50 H 5.50 %.

N-4-Chlorophenyl-Ń-[3-(2,4-dimethyl-1,3-butadiene-1,4-sultamyl-N)-phenyl]-urea (**2i**) : M.p. 230°C ; yield 84 % ; -IR. 1700 cm^{-1} (CO–N), 1270 cm^{-1} (SO_2–N sultam).

$C_{19}H_{18}N_3O_3SCl$ Calcd. C 56.50 H 4.46 N 10.40 Found. C 56.40 H 4.41 N 10.62 %.

N-Phenyl-N-[4-(2,4-dimethyl-1,3-butadiene-1,4-sultamyl-N-phenyl]-urea (**2j**) M.p. 200°C ; yield 84 %-IR : 1700 cm^{-1} (CO–N), 1280 cm^{-1} (SO_2–N sultam)-^{1}H NMR : $\delta = 8.8, 9$ (s two CONH), 7.75–7.2 (m 9H aromatic), 6.6, 5.8(s 1-H, 3-H sultam) 2.1, 1.9 ($2CH_3$).

$C_{19}H_{19}N_3O_3S$ Calcd. C 61.77 H 5.18 N 11.37 Found C 62.00 H 5.21 N 11.52 %.

N-4-Methoxyphenyl-Ň-[4-(2,4-dimethyl-1,3-butadiene-1,4-sultamyl-N-phenyl]-urea (**2k**) : M.p. 220°C ; yield 80 %-IR : 1700 cm^{-1}, (CONH), 1270 cm^{-1} (SO_2–N sultam).

$C_{26}H_{21}N_3O_4S$ (399.47) Calcd. C 60.13 H 5.29 Found C 60.29 H 5.48 %.

N-4-Chlorophenyl-Ń-[4-(2,4-dimethyl-1,3-butadiene-1,4-sultamyl-N-phenyl]-urea (**2l**) : M.p. 300, yield 80 %-IR : 1700 cm^{-1} (CO–N), 1280 cm^{-1} (SO_2–N)– ^{1}H NMR : $\delta = 9, 8.85$ (s two CONH), 7.65–7.25 (m 8H aromatic 6.6, 5.8 (1-H, 3-H sultam), 2.05, 1.85 (s $2CH_3$).

$C_{19}H_{18}N_3O_3SCl$ (403.88) calcd. C 56.50 H 4.46 Found C 56.60 H 4.50 %.

Reaction of **2c** *with carbonyl compounds : formation of* **3a-e**.

A solution of the sultam **2c** (0.01 mol) in 50 mL ethanol was treated with the appropriate carbonyl compound (acetone acetophenone, benzophenone, benzaldehyde or *p*-anisaldehyde (0.02 mol). A few drops of piperidine were added. The solution was refluxed for four hours. After concentration and cooling the solid product was crystallized from ethanol to give **3a-e**.

Reaction of **2c** *with acetone ; formation of* (**3a**) : M.p. 185°C ; yield 62 %-IR : 1620 cm^{-1} (C=N), whereas νCO and νNH_2 were absent.

$C_{15}H_{18}N_2O_2S$ Calcd. C 62.04 H 6.24 Found C 62.00 H 6.01 %.

Reaction of **2c** *with acetophenone ; formation of* (**3b**) : M.p. 175°C ; yield 60 %-IR : 1630 cm^{-1} (C=N)

$C_{20}H_{20}N_2O_2S$ Calcd. C 68.15 H 5.71 Found C 68.01 H 5.50 %.

Reaction of **2c** *with benzophenone ; formation of* (**3c**) : M.p. 180 C ; yield 67 %-IR : 1625 cm^{-1} (C=N)

$C_{25}H_{22}N_2O_2S$ Calcd. C 72.43 H 5.34 Found C 72.11 H 5.60 %.

Reaction of **2c** *with benzaldehyde ; formation of* (**3d**) : M.p. 170° C ; yield 82 %-IR : 1600 cm^{-1} (C=N), $^{-1}$H NMR : $\delta = 8.7$ (s N=CH), 7.96–8, 7.4–7.6 (m 9H aromatic), 6.6, 5.8 (1-H, 3-H sultam), 2.1, 1.85 (s 2CH$_3$).

$C_{19}H_{18}N_2O_2S$ Calcd. C 67.43 H 5.36 Found C 67.45 H 5.28 %.

Reaction of **2c** *with p-anisaldehyde ; formation of* (**3e**) : M.p. 120°C ; yield 62 %-IR : **1600** cm^{-1} (C=N).

$C_{20}H_{20}N_2O_3S$ Calcd : C 65.19 H 5.47 S 8.70 Found C 65.11 H 5.20 S 9.00 %.

Reaction of the sultam **2b** *or* **2c** *with acid chlorides or benzyl chloride ; formation of* **4a,b** *or* **6a-d**.

To a solution of the sultam (0.01 mol), in acetone (40 mL) and pyridine (1 mL), the appropriate acid chloride or benzyl chloride (0.015 mol) was added. The reaction mixture was refluxed for two hours. The solvent was driven off. The product was filtered off, washed with water, dried and crystallized from acetic acid to give **4a,b** or **6a-d**.

4-Acetamidobenzene-N-3- (2,4-dimethyl-1,3-butadiene-1,4-sultamyl-N) -phenyl-sulphonamide (**4a**) : M.p. 250°C ; yield 76 %-IR. 3350 cm^{-1} (NH), 1690 cm^{-1} (CO), 1290 cm^{-1} (SO$_2$-N), 1610–1350 cm^{-1} (two conjugated double bonds).

$C_{20}H_{21}N_3O_5S_2$ Calcd. C 53.69 H 4.73 Found C 53.31 H 4.80 %.

4-Acetamidobenzene-N-4- (2,4-dimethyl-1,3-butadiene-1,4-sultamyl-N) - phenyl-sulphonamide (**4b**) : M.p. 127°C ; yield 67 %.

$C_{20}H_{21}N_3O_5S_2$ Calcd. C 53.96 H 4.73 N 9.39 Found C 53.86 H 5 01 N 9.71 %.

N-(4-Acetamidophenyl)-2,4-dimethyl-1,3-butadiene-1,4-sultam (**6a**) : M.p. 220°C ; yield 75 %-IR : 3350 cm^{-1} (NH), 1690 cm^{-1} (CO), 1290 cm^{-1} (SO$_2$–N).

$C_{14}H_{16}N_2O_3S$ Calcd. C 57.51 H 5.51 N 9.58 Found C 57.10 H 5.80 N 9.70 %.

N-4-(benzoylamino)-phenyl-2,4-dimethyl-1,3-butadiene-1,4-sultam (**6b**) : M.p. 215°C ; yield 84 %-IR : 3350 cm^{-1} (NH), 1290 cm^{-1} (SO$_2$–N), 1960 cm^{-1} (CO)-^{1}H NMR = 8.7 (s NH), 8–7.4 (m 9H aromatic), 6.6, 5.8 (s 1-H, 3-H sultam), 2.1, 1.85 (s 2CH$_3$).

$C_{19}H_{17}N_2O_3S$ (Calcd. C 64.39 H 5.11 N 7.90 Found C 64.69 H 5.31 N 7.85 %.

2,4-Dimethyl-N-4-(4-chlorobenzoylamino)-phenyl-1,3-butadiene-1,4-sultam (**6c**) : M.p. 192°C ; yield 90 %-IR : 3350 cm^{-1} (NH) 1290 cm^{-1} (SO$_2$–N).

$C_{19}H_{17}N_2O_3SCl$ Calcd C 58.68 H 4.40 Found C 58.62 H 4.51 %.

2,4-Dimethyl-N-4-(benzylamino))-phenyl-1,3-butadiene-1,4-sultam (**6d**) : M.p. 190°C ; yield 73 %

$C_{19}H_{20}N_2O_2S$ Calcd. C 67.03 H 5.92 N 8.22 Found C 67.41 H 5.82 N 8.42 %.

Hydrolysis of **4b** ; *formation of* **5**

A solution of **4b** (4.4 g ; .01 mol) in 5 % NaOH solution (40 mL) was refluxed for five hours. After cooling, 2N HCl was added gradually with stirring till pH 6–7. The separated product was filtered off, washed, dried and crystallized from ethanol.

4-Aminobenzene-N-4-(2,4-dimethyl-1,3-butadiene-sultamyl-N)-phenyl-sulphonamide (**5**) : M.p. 240°C ; yield 56 %-IR : 3450, 3350 cm^{-1} (NH$_2$), whereas CO is absent.

$C_{18}H_{19}N_3O_4S_2$ Calcd. C 53.31 H 4.72 N 10.36 Found C 53.49 H 4.51 N 10 %.

REFERENCES

[1] B. Helferich and W. Klebert, *Liebigs Ann. Chem.*, **80**, 657 (1962).
[2] I. Zeid, I. Ismail and B. Helferich, *Liebigs Ann. Chem.*, **761**, 115 (1972).
[3] I. Zeid, I. Ismail and B. Helferich, *Liebigs Ann. Chem.*, **761**, 118 (1972).
[4] I. Zeid and I. Ismail, *J. Prakt. Chem.*, **317**, 369 (1972).
[5] K. Wellinga, R. Mulder and J. Doalen, *J. Agr. Food Chem.*, **21**, 993 (1973).
[6] A. Schonberg, N. Badran and N. Starkosky, *J. Amer. Soc.*, **75**, 4992 (1953).

Revue Roumaine de Chimie, 36, 1–3, 201–208 (1991)

SYNTHESIS OF 4,5,6,7-TETRAPHENYL-8(SUBSTITUTED-3(2H)-PHTHALAZINONE DERIVATIVES WITH POTENTIAL ANTIHYPERTENSIVE ACTIVITY

F.A. YASSIN, M.A. El-SAFTY, B.E. BAYOUMY and A.F. El FARARGY
Zagazig University, Faculty of Science, Department of Chemistry, Zagazig, Egypt

Received May 14, 1988

The interaction of tetraphenylphthalic anhydride with *o*-chlorotoluene under Friedel-Crafts conditions gives 2-(4-chloro-3-methyl)benzoyl-3,4,5,6 tetraphenyl benzoic acid (**1**) which on reaction with hydrazine derivatives gave phthalazinones **2a-d**. The behaviour of **2a** towards carbon electrophiles and carbon nucleophiles has been investigated. The chlorophthalazinones **3S** has been also synthesised through the action of $PCl_5/POCl_3$ on **2a**. The behaviour of **3S** towards nitrogen, and oxygen nucleophiles also has been described.

Recently[1,2] 3(2H)-phathalazinones have been described as being useful as remedies for arteriososclerosis and thrombosis, and have also been useful as antihypertensive materials. This prompted us to synthesize some new phthalazinones *via* interaction of 2-(4-chloro-3-methyl)benzoyl-3,4,5,6-tetraphenyl-benzoic acid (**1**), with hydrazine derivatives, also in hope of obtaining some pharmaceutical action.

The interaction of tetraphenylphthalic anhydride with *o*-chlorotoluene under Friedel-Crafts conditions gives 2-(4-chloro-3-methyl)benzoyl-3,4,5,6-tetraphenyl benzoic acid (**1**), which reacts with hydrazines namely, hydrazine hydrate, phenylhydrazine, benzoylhydrazine and salicyloylhydrazine in boiling butanol to give the corresponding phthalazinone derivatives **2a-d**. It reacts also with semicarbazide and thiosemicarbazide in pyridine to give **2e** and **2f**.

The structure of compounds **2a-f** was confirmed from : (i) analytical data (ii) IR spectrum of **2a** which shows bands at 1640, 1670, 3150 and 3400 attributable to *$\nu_{C=O}$, $\nu_{C=N}$, ν_{NH} and ν_{OH} respectively. This IR data illustrated that **2a** actually in solid state exist in lactam-lactim dynamic equilibrium.[3] The identity of the compound **2c** was deduced via treatment of **2a** with benzoyl chloride in least amount of pyridine and comparison of m.p. and m.m.p. determination.

The above results prompted us to study the behaviour of **2a** towards some electrophiles and nucleophiles in different solvents. Thus, the compound **2a** reacts with a variety of electrophiles namely, dimethyl sulphate, ethyl chloroacetate, and ethyl chloroformate in dry acetone, by using anhydrous K_2CO_3 as catalyst[4] to give 3-(methoxy, ethoxycarbonylmethoxy, and ethoxycarbonyloxy)-phthalazine derivatives (**3a-c**) respectively. No N-alkyl derivatives were obtained by this method, due to the rapid interconversion of the lactam form to lactim form in the presence of acetone and K_2CO_3 which lead to the desired product.

---

* ν_{max} expressed by cm^{-1} throughout the paper.

Structure of compounds **3b** and **3c** was established from : (i) IR spectra which exhibit strong absorptions at 1635, 1740 cm^{-1} attributable to $\nu_{C=N}$ and $\nu_{C=O}$ of ester. (ii) chemically, *via* the reaction of **3b** and **3c** with each of : a) aqueous sodium hydroxide to give the corresponding acids **3d** and **3e** respectively, b) hydrazine and phenylhydrazine in boiling butanol to give the corresponding hydrazides **3f-i**, (c) with primary amines namely, aniline, ethylamine, benzylamine and *p*-anisidine in boiling butanol to give the corresponding N-aryl and N-alkyl amide derivatives **3j-p**. The IR spectra of **3f-i** exhibit bands in the region 1660—1665($\nu_{C=O}$ carboxamide) and 3200—3300 ν_{NH} of two NH groups. Compounds **3j-p** show bands in the region of 1660—1665 and 3200—3300 attributable to $\nu_{C=O}$ and ν_{NH} respectively.

On the other hand, the ester **3b** reacts also with benzaldehyde in presence of potassium *tert*-butoxide at room temperature affording "Stabbe" product **3q** as major product and the "Claisen" product **3r** as minor product. This is analogous with the previous work.[5] The above ester was" converted to the corresponding acid **3q** by hydrolysis with aqueous NaOH. IR spectrum of **3q** shows bands at 1620, 1635 and 1705 attributable to $\nu_{C=C}$, $\nu_{C=N}$ and $\nu_{C=O}$ respectively.

Further proof for lactam-lactim equilibrium in phthalazinone **2a** has also been confirmed by converting the lactam form of **2a** to 1-chlorophthalazine **3S** which is the key starting material for diverse heterocyclic compounds. Thus, treatment of (**2a**) with PCl_5 in presence of $POCl_3$ gave 1-chlorophthalazinone **3S** whose structure was deduced from : (i) Its IR spectrum which shows the disappearance of $\nu_{C=O}$ and ν_{NH} ; (ii) chemically *via* its reaction with oxygen mucleophiles e.g. sodium methoxide in methanol to give 1-methoxy phthalazinone **3a**. Also via reaction of **3S** with nitrogen nucleophiles e.g. hydrazine hydrate, phenylhydrazine, aniline and methylamine, affording (hydrazino, phenylhydrazino, anilino and methylamino) phthalazine derivatives **3t-w**. Their IR spectra show bands in the region 1630—1625 and 3200—3300 attributable to $\nu_{C=N}$ and ν_{NH} respectively.

Recently,[6] it was reported that 6-substituted (phenyl), 1,2,4-triazolo-3,4-b pyridazines have pharmacological properties. Some of these derivatives also exhibited hypotensive activity when tested in spontaneously hypertensive rats (SHR). The present work also deals with the reaction of the chlorophthalazine derivatives **3S** with acylhydrazines, namely, benzoylhydrazine, phenylacetylhydrazine and salicyloylhydrazine in boiling butanol to give 1,2,4-triazolo-(4,3-b)-4,5-benzopyridazines **4a-c** in the hope of some pharmacological properties for these derivatives. The IR spectra of **4a-c** revealed bands at the region of 1640—1630 due to $\nu_{C=N}$.

The reaction of phthalazinone **2a** with P_2S_5 in boiling xylene[7] gives the corresponding phthalazine thione **2g** whose IR spectrum revealed bands at 1340 and 3250 attributable to $\nu_{C=S}$ and ν_{S-H} or ν_{NH}.

It was reported,[8] that thiopyridazinones underwent condensation with nitrogen nucleophiles e.g. hydrazines or primary amines to give the corresponding hydrazones and Schiff-bases respectively. In the present work the authors try to compare the behaviour of the thione **2g** towards the nitrogen nucleophiles with the thiopyridazinones. Thus, when **2g** was allowed to react with hydrazine hydrate, phenylhydrazine, aniline and methylamine in boiling ethanol, affording **3t-w** and not the corresponding hydrazones or Schiff-bases **5a-d**, this may be due to compounds **5** produced as fleeting intermediate which rearrange directly to the more thermodynamically stable tautomers **5**. Identity of these products was deduced from correct analytical data and from m.p. and m.m.p. determinations.

Treatment of the thione **2g** with copper bronze in boiling xylene yielded the bis-compound **6**. Its IR spectrum exhibits bands at 1625 and 1618 attributable to $\nu_{C=N}$ and $\nu_{C=C}$.

Action of Grignard reagents on **2a** : when **2a** was submitted to react with methyl magnesium iodide and ethyl magnesium iodide in dry ether-benzene mixture it affords **7a** and **7b** whose IR spectra show absorption bands in the region 1635—1620 and 3270—3300 attributable to $\nu_{C=N}$ and ν_{HN} respectively.

EXPERIMENTAL

All melting points are uncorrected. IR spectra were determined with a Unicam SP 1200 spectrophotometer using KBr Wafer technique. Characterisations and physical data are listed in table 1.

Formation of phthalazionne derivatives **2a-d** :

A mixture of acid **1** (0.01 mole) and hydrazines namely, hydrazine hydrate, phenylhydrazine, benzoylhydrazine, and salicyloylhydrazine (0.01 mole) in *n*-butanol (50 mL) was refluxed for 3 hrs. The solids separated were filtered off and crystallized from the suitable solvent to give **2a-d**.

Formation of phthalazinone derivatives **2e** *and* **2f** :

A mixture of acid **1** (0.01 mole) and semicarbazide or thiosemicarbazide (0.01 mole) in pyridine (40 mL) was refluxed for 8 hrs. The reaction mixture was poured into ice/HCl (100 gm ice and 20 ml conc. HCl). The solids obtained were filtered off and crystallized from the proper solvent.

Reaction of phthalazinone **2a** *with benzoyl chloride* : *Formation of* **2c** :

A mixture of **2a** (0.01 mole), benzoyl chloride (0.01 mole) and pyridine (1 mL) was refluxed for 3 hrs. The cold reaction mixture was added gradually into ice-dilute HCl; the solid obtained was filtered off and crystallised from the proper solvent to give **2c**, which was identified by m.p. and m.m.p. determination.

Action of dimethylsulphate, ethyl chloroacetate and ethyl chloroformate on phthalazinone **2a** : *Formation of phthalazine derivatives* **3a-c** :

A mixture of **2a** (0.01 mole), alkylating agent namely, dimethyl sulphate, ethyl chloroacetate, and ethyl chloroformate (0.04 mole); and anhydrous potassium carbonate (0.04 mole) in dry acetone (50 mL) was refluxed for 20 hrs. The excess of solvent was removed by distillation then the reaction mixture was poured into water. The organic material was extracted with ether; evaporation of the dried ethereal solution gave the alkylating products **3a-c** respectively.

Alkaline hydrolysis of **3b** *and* **3c** : *Formation of* **3d** and **3e** :

A mixture of **3b** or **3c** (0.01 mole) and aqueous sodium hydroxide 10% (10 mL) for each g of (**3b** or **3c**) was refluxed for 3 hrs. The reaction mixture was cooled and extracted with ether

Table 1

Characterisation and physical data for the synthesised compounds

Compd.	M.P. °C	Solvent (Yield %)	Mol. formula	Analysis		
					Calcd.	Found
2a	240	Toluene (65)	$C_{39}H_{27}ClN_2O$	C	81.32	81.02
				H	4.69	4.34
				N	4.86	4.71
2b	135	Benzene (63)	$C_{45}H_{31}ClN_2O$	C	83.01	82.71
				H	4.76	4.52
				N	4.30	4.00
2c	205	Benzene (60)	$C_{46}H_{31}ClN_2O_2$	C	81.35	81.00
				H	4.56	4.41
				N	4.12	4.01
2d	230	Ethanol (60)	$C_{46}H_{31}ClN_2O_3$	C	79.48	79.32
				H	4.46	4.35
				N	4.03	4.00
2e	260	Benzene (70)	$C_{40}H_{28}ClN_3O_2$	C	77.73	77.43
				H	4.53	4.42
				N	6.80	6.51
2f	258	Toluene (60)	$C_{40}H_{28}ClN_3OS$	C	75.76	75.54
				H	4.41	4.42
				N	6.62	6.33
2g	230	Xylene (63)	$C_{39}H_{27}ClN_2S$	C	79.25	79.00
				H	4.57	4.48
				N	4.74	4.65
3a	131	Benzene (55)	$C_{40}H_{29}ClN_2O$	C	81.56	81.46
				H	4.92	4.82
				N	4.75	4.65
3b	115	Light Petrol 80 – 100° (65)	$C_{43}H_{33}ClN_2O_3$	C	78.12	78.01
				H	4.99	4.87
				N	4.23	4.18
3c	110	Light Petrol. 80–100° (60)	$C_{42}H_{31}ClN_2O_3$	C	77.95	77.84
				H	4.79	4.62
				N	4.33	4.29
3d	240	Ethanol (50)	$C_{41}H_{22}ClN_2O_3$	C	77.78	77.68
				H	4.58	4.43
				N	4.42	4.40
3e	245	Ethanol (50)	$C_{40}H_{27}ClN_2O_3$	C	77.60	77.43
				H	4.36	4.23
				N	4.52	4.43
3f	235	Ethanol (55)	$C_{41}H_{37}ClN_4O_2$	C	76.01	75.98
				H	4.79	4.58
				N	8.66	8.53
3g	138	Ethanol (60)	$C_{47}H_{33}ClN_4O_2$	C	78.06	78.00
				H	4.84	4.73
				N	7.75	7.63

Table 1 (continued)

Compd.	M.P. °C	Solvent Yield %	Mol. formula	Analysis Calcd.	Analysis Found
3h	245	Benzene (65)	$C_{40}H_{29}ClN_4O_2$	C 75.88 H 4.58 N 8.85	75.64 4.48 8.73
3i	215	Benzene (65)	$C_{46}H_{33}ClN_3O_2$	C 84.08 H 5.02 N 6.39	84.00 4.93 6.21
3j	131	Toluene (60)	$C_{44}H_{34}ClN_3O_2$	C 79.71 H 6.08 N 4.80	79.69 6.00 4.72
3k	130	Toluene (65)	$C_{47}H_{34}ClN_3O_2$	C 78.24 H 6.52 N 6.36	78.13 6.48 6.23
3l	220	Benzene (55)	$C_{48}H_{36}ClN_3O_2$	C 79.83 H 4.98 N 5.82	79.77 4.89 5.73
3m	206	Toluene (60)	$C_{46}H_{32}ClN_3O_2$	C 79.59 H 4.61 N 6.05	79.49 4.52 6.00
3n	238	Benzene (60)	$C_{42}H_{28}ClN_3O_2$	C 78.56 H 4.48 N 6.54	78.46 4.43 6.49
3o	230	Benzene (55)	$C_{47}H_{30}ClN_3O_2$	C 80.17 H 4.26 N 5.97	80.00 4.19 5.88
3p	205	Benzene (55)	$C_{47}H_{30}ClN_3O_3$	C 78.38 H 4.16 N 5.83	78.21 4.13 5.79
3q	180	Toluene (55)	$C_{48}H_{33}ClN_2O_3$	C 79.94 H 4.58 N 3.88	79.94 4.49 3.79
3r	85	Petrol. ether 60—80° (45)	$C_{50}H_{37}ClN_2O_3$	C 80.16 H 4.94 N 3.74	80.00 4.91 3.69
3s	220	Toluene (60)	$C_{39}H_{26}Cl_2N_2$	C 79.05 H 4.39 N 4.72	78.93 4.28 4.69
3t	150	Benzene (55)	$C_{39}H_{29}ClN_4$	C 79.52 H 4.92 N 9.51	79.43 4.88 9.49
3u	144	Benzene (60)	$C_{45}H_{33}ClN_4$	C 81.26 H 4.96 N 8.42	81.25 4.95 8.36

Table 1 (continued)

Compd.	M.P. °C	Solvent Yield %	Mol. formula	Analysis		
					Calcd.	Found
3v	170	Toluene (63)	$C_{45}H_{32}ClN_3$	C H N	83.14 4.96 6.42	82.98 4.83 6.39
3w	142	Toluene (65)	$C_{40}H_{30}ClN_3$	C H N	81.70 5.10 7.14	81.65 5.00 7.01
4a	233	Toluene (50)	$C_{46}H_{31}ClN_4$	C H N	81.83 4.59 8.30	81.78 4.49 8.00
4b	214	Butanol (60)	$C_{47}H_{33}ClN_4$	C H N	81.91 4.79 8.13	81.83 4.73 8.12
4c	222	Butanol (60)	$C_{46}H_{31}ClN_4O$	C H N	79.94 4.48 8.10	79.90 4.46 7.94
6	251	Toluene (60)	$C_{78}H_{54}ClN_4$	C H N	90.65 5.23 5.42	90.00 5.18 5.32
7a	225	Toluene (60)	$C_{41}H_{33}ClN_2$	C H N	83.60 5.60 4.75	83.51 5.56 4.65
7b	205	Toluene (65)	$C_{43}H_{38}ClN_2$)	C H N	83.56 6.15 4.53	83.50 6.00 4.49

to get rid of unsaponified material. The aqueous layer was acidified with very cold dilute hydrochloric acid, the solid obtained was filtered off and recrystallized from the proper solvent to give **3d** and **3e**.

Action of hydrazines on **3b** *and* **3c** : *Formation of hydrazides* (**3f-i**) :

A mixture of **3b** or **3c** (0.01 mole), hydrazine hydrate or phenylhydrazine (0.01 mole) was refluxed in n-butanol (50 mL) for 3 hrs. The solid separated after concentrating and cooling, was filtered off and recrystallized from the proper solvent.

Action of amines on **3d** *and* **3c** : *Formation of amides* **3j-p** :

A mixture of **3b** or **3c** (0.01 mole), and primary amines, namely, aniline, ethylamine, benzylamine and *p*-anisidine (0.01 mole) was refluxed in *n*-butanol (50 mL) for 5 hrs. The solid separated after concentration and cooling was filtered off, and recrystallized from the proper solvent.

Action of benzaldehyde on **3b** : *Formation of cinnamic acid derivatives* **3q** *and* **3r** :

A mixture of **3b** (0.01 mole) and benzaldehyde (0.01 mole) was added during 30 min. to a stirred solution of potassium *tert.*-butoxide (in *tert.*-butanol), 20 mL for each g of **3b**). The reaction mixture was left aside overnight at room temperature. The excess of alcohol was removed under reduced pressure. The residue was poured onto water and extracted with ether then, evaporation of the dried ethereal layer left an oily material, which solidified by trituration with light petrol (b.p. 40—60°), and recrystallized from the proper solvent gave **3r**. The aqueous layer upon acidification with very cold dilute hydrochloric acid gave a precipitate, which filtered off and recrystallized from the proper solvent gave **3q**.

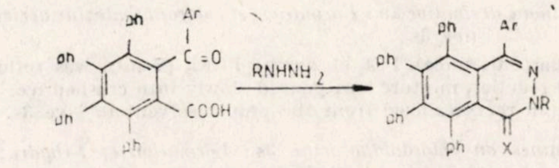
ph
Ar
C=O
COOH
RNHNH₂
N
NR
X

1.
2

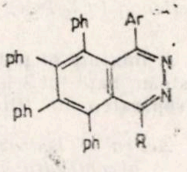

3.

$Ar = 4,3-Cl, CH_3C_6H_3$

a, $R = H$
b, $R = C_6H_5$
c, $R = COC_6H_5$
d, $R = (C_6H_4CO)-OH-(o)$
e, $R = CONH_2$
f, $R = C=SNH_2$
$X = O$
g, $R = H, X = S$

a, $R = OCH_3$
b, $R = OCH_2COOEt$
c, $R = OCOOEt$
d, $R = OCH_2COOH$
e, $R = OCOOH$
f, $R = OCH_2CONHNH_2$
g, $R = OCH_2CONHNHPh$
h, $R = OCONHNH_2$
i, $R = OCONHNHPh$
j, $R = OCH_2CONHPh$
k, $R = OCH_2CONHC_2H_5$
1, $R = OCH_2CONHCH_2Ph$
m, $R = OCONHPh$
n, $R = OCONHC_2H_5$
o, $R = OCONHCH_2Ph$
p, $R = OCONHC_6H_4 \cdot OCH$
q, $R = OCH=CHPhCOOH$
r, $R = OC=CHPhCOOEt$
s, $R = Cl$
t, $R = NHNH_2$
u, $R = NHNHPh$
v, $R = NHPh$
w, $R = NHCH_3$

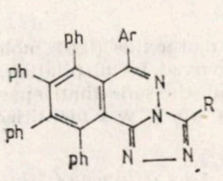

(4)

a, $R = C_6H_5$
b, $R = CH_2C_6H_5$
c, $R = C_6H_4(OH)-(o)$

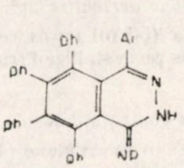

5

(5)

a, $R = NH_2$
b, $R = NHPh$
c, $R = C_6H_5$
d, $R = CH_3$

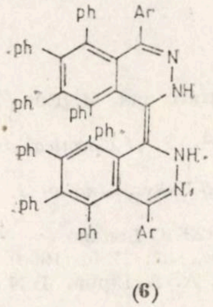
ph
Ar
N
NH
NH
N

(6)

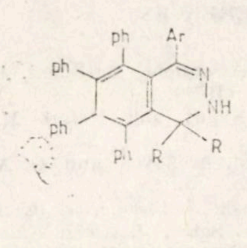

(7)

a, $R = CH_3$
b, $R = C_2H_5$

Action of $PCl_5/POCl_3$ on phthalazinone derivative **2a** : *Formation of chlorophthalazine derivative* **3s** :

A mixture of phthalazinone **2a** (0.01 mole), PCl_5 (1 g) and $POCl_3$ (7 mL) was refluxed on a steam bath for 3 hrs. The cold reaction mixture was poured slowly into crushed ice. The solid separated was filtered, dried and recrystallized from the proper solvent to give **3s**.

Action of hydrazines and amines on chlorophthalazine **3s** : *Formation of 1-(hydrazino, phenylhydrazino, anilino and methylamino) phthalazine derivatives* **3t-w** :

A mixture of chlorophthalazine **3s** (0.01 mole) and each of hydrazine hydrate, phenylhydrazine, aniline and/or methylamine (0.01 mole) was refluxed in benzene (40 mL) for 6 hrs. The solids that separated on cooling were crystallized from the proper solvent.

Formation of 1-methoxyphthalazine **3a** :

A mixture of chlorophthalazine **3s** (0.01 mole) and sodium methoxide (0.01 mole) in 30 mL methanol was refluxed for 3 hrs. Excess of alcohol was removed by distillation, the reaction mixture was cooled and acidified with dilute hydrochloric acid, the solid that separated was filtered off and crystallized from the proper solvent to give **3a** which was identified by m.p. and m.m.p. determination.

Action of acylhydrazines on chlorophthalazine **3s** : *Formation of 1,2,4,-triazole-(4,3-b)-4,-5-benzopyridazines* **4a-c** :

A mixture of 1-chlorophthalazine **3s** (0.01 mole) and each of acylhydrazines, namely, benzoylhydrazine, phenylacetyl hydrazine and/or salicyloylhydrazine (0.01 mole) in *n*-butanol (40 mL) was refluxed for 48 hrs. The solid that separated after concentrating and cooling was recrystallized from the proper solvent.

Action of P_2O_5 on phthalazinone derivative **2a** : *Formation of thione derivative* 2g :

A mixture of **2a** (0.01 mole) and P_2O_5 (0.01 mole) in dry xylene (50 mL) was refluxed for 1 hr. The reaction mixture was filtered on hot. The solid obtained was recrystallized from the proper solvent.

Action of copper bronze on thione **2g** : *Formation of the bis compound* **6** :

A mixture of the thione **2g** (0.01 mole) and copper bronze (1 g) in dry xylene (40 mL) was refluxed for 10 hrs. The reaction mixture was filtered upon hot, the filtrate was concentrated and the solid separated was crystallized from the proper solvent.

Action of Grignard reagents on phthalazinone **2a** : *Formation of phthalazine derivative* **7a** *and* **7b** :

To an ethereal solution of methyl or ethylmagnesium iodide (0.02 mole), (0.01 mole) of phthalazinone **2a** in dry ether (50 mL) was added with stirring. The reaction mixture was refluxed on a steam bath for 6 hrs, left aside overnight at room temperature, then decomposed by saturated solution of aqueous ammonium chloride. The organic materials were extracted with ether. The ethereal layer was dried over anhydrous sodium sulphate. Slow evaporation of ethereal solution left solids which were crystallized from the proper solvent.

REFERENCES

[1] G. Nannini, G. Biadoli, E. Perronk, A. Forgione, Butlinoni, A. Ferrari and M. Eur, *J. Med. Chem. Chim. Ther.*, **14**, 53 (1979).

[2] Maher. A. El-Hashash, Sayed, I. El-Nagdy and Refait M. Saleh, *J. of Chemical and Engineering Data*, **29**, 391 (1984).

[3] M. A. El-Hashash, M. M. Mohamed, M. A. Sayed and O. A. Abo-Baker, *Indian J. of Chem.*, **19B** (1980).

[4] M. F. El-Newaihy and M. N. El-Hashash, *J. Chem. Soc.* (*C*) **1971**, 2373, London.

[5] A. Mustafa, A. H. Hashash and A. A. Saleh, *J. Amer. Chem. Soc.*, **82**, 2735, (1960).

[6] J. D. Albright, D. B. Moran, W. B. Wright, J. B. Collins, B. Beer, A. S. Lippa, E.N.J. Greenblat, *J. Med. Chem.*, **24**, 592, (1981).

[7] M. M. Mohamed, M. A. El-Hashash, and M. El-Kady, J. *Revue Roumaine de Chimie*, **24**, 1381, (1979).

[8] G. H. Sayed, M. El-Kady and M. A. El-Hashash, *Revue Roumaine de Chimie*, **25**, 1375, (1980).

Revue Roumaine de Chimie, **36**, *1–3*, 209–213(1991)

SYNTHESIS OF SOME NEW 1,2,3-SELENA- AND 1,2,3-THIADIAZOLOPYRIMIDINES

S. El-BAHAIE and B.E. BAYOUMY
Department of Chemistry, Faculty of Science, Zagazig University, Zagazig, Egypt

Received May 14, 1988

5-Acetyl-2-aryl-4-mercaptoacetyl-chloride-6-methylpyrimidines **2** were allowed to react with isomeric amino acetophenone to give the corresponding anilides **3**. The latter compounds were reacted with semicarbazide and gave the corresponding semicarbazones **4**. Compounds **4** were subjected to oxidative cyclization either by selenium dioxide or thionyl chloride to give selena and thiadiazolopyrimidines respectively. The structure of the final compounds were deduced from elemental and spectral data.

INTRODUCTION

Recently, pyrimidine derivatives have exerted biological activities like cytostatic activity against tumour cells,[4] antithyroid activity[5] and exerted also diuretic action.[6] In addition both selena- and thiadiazoles are known through their antibacterial activities.[7–9] It was thought that incorporation of the pyrimidine moiety into selena and thiadiazoles might modify their biological activities.

EXPERIMENTAL

All melting points are uncorrected. IR (KBr disc) were carried out using a Pye unicame spectrometer model SP 200 G.

5-Acetyl-2-aryl-4-carboxymethylmercapto-6-methylpyrimidines **1a,b** *were prepared by the reported method.*[12]

Synthesis of 5-acetyl-2-aryl-4-mercaptoacetyl chloride-6-methylpyrimidines **2a,b** :

Compound **1a.b** (0.01 mole) was covered with 5 mL of thionyl chloride then heated under reflux on water bath for one hour. The excess of thionyl chloride was removed under vacuum. The precipitated product was filtered off, washed with sodium bicarbonate solution, dried and recrystallized from pet. ether 40–60/benzene mixture and gave buff crystals.

For compound **2a** m.p. 120–2°C ($C_{13}H_{11}N_2O_3SCl$) calculated : 50.24%C, 3.54% H, 9.01%N, found :50.20%C, 3.60% H, 9.10% N and for compound **2b** m.p. 92–3°C ($C_{16}H_{15}N_2O_3SCl$) calculated : 54.77% C, 4.27% H, 7.98% N, found : 54.80% C, 4.20% H, 7.80% N.

Synthesis of 4-mercaptoacetanilidopyrimidine derivatives **3a-d** :

A mixture of compound **2a,b** (0.01 mole) and 2, 3 or 4-aminoacetophenone (0.01 mole) in 30 mL of dry benzene was heated and stirred for 2 hours at 80°C. The reaction mixture was concentrated and cooled. The precipitated product was filtered off, washed with benzene, dried and recrystallized from ethanol giving yellowish brown crystals (Table 1).

Synthesis of semicarbazone of 4-mercaptoacetanilidopyrimidine derivatives **4a-d** :

Compounds **3a-** (0.001 mole) were dissolved in 30 mL of ethanol then added to a mixture of semicarbazide hydrochloride (0.01 mole) and anhydrous sodium acetate (0.02 mole), dissol-

Table 1

Comp.	Ar.	position of $-COCH_3$ group	m.p.°C	Yield %	Mol. Formula	Analysis		
						C	H	N
3a	2-Furyl	4—	183−4	33	$C_{21}H_{19}N_3O_4S$	Calcd. : 61 .61 Found : 61 .40	4 .64 4 .70	10 .26 10 .30
b	$p-OCH_3-C_6H_4$	4—	168-70	27	$C_{24}H_{23}N_3O_4S$	Calcd. : 64.14 Found : 64 .30	5 .12 5 .20	9 .35 9 .40
c	$p-OCH_3-C_6H_4$	3—	160−2	34	$C_{24}H_{23}N_3O_4S$	Calcd. : 64 .14 Found : 63 .90	5 .12 5 .30	9 .35 9 .30
	$_3-C_6H_4$	2—	174−5	38	$C_{24}H_{23}N_3O_4S$	Calcd. : 64 .14 Found : 64 .10	5 .12 5 20	9 .35 9 .60

ved in 10 mL of water. The reaction mixture was heated and stirred for 2 hours at 80°C, then cooled and diluted with water. The precipitated product was filtered off, dried and crystallized from ethanol/DMF mixture giving orange crystals (Table 2).

Table 2

Comp.	Ar.	Position of semicar-bazone	m.p°C	Yield %	Fol-Formula	Analysis		
						C	H	N
4a	2-Furyl	4—	214−6	42	$C_{22}H_{22}N_6O_4S$	Calcd. : 56 .65 Found : 56 .80	4 .72 4 .40	18 .02 18 .00
b	$p-OCH_3-C_6H_4$	4—	185−7	38	$C_{25}H_{26}N_6O_4S$	Calcd. : 59 .28 Found : 59 .30	5 .13 4 .90	16 .60 16 .40
c	$p-OCH_3-C_6H_4$	3—	173−4	27	$C_{25}H_{26}N_6O_4S$	Calcd. : 59 .28 Found : 59 .30	5 .13 5 .00	16 .60 16 .70
d	$p-OCH_3-H_6H$	2	190−2	32	$C_{25}H_{26}N_6O_4S$	Calcd. : 59 .29 Found 58 .90	5 .13 5 .30	16 .40 16 .40

Synthesis of 1,2,3-selenadiazolopyrimidine derivatives **5a-d** :

Powdered semicarbazones **4a-d** (0.01 mole) were dissolved in 30 mL of boiling glacial acetic acid. To the hot solution, finely powdered selenium dioxide (0.01 mole) was added portion wise, while stirring and heating on a water bath. After complete addition, heating and stirring was continued for one hour and the reaction mixture was filtered on ice-water. The precipitated product was extracted with chloroform and the organic layer was washed successively with 10% sodium bicarbonate solution and then with water. The chloroformic layer was dried over anhydrous sodium sulphate and evaported under vacuum. The residue was recrystallized from a proper solvent and gave yellowish brown crystals (Table 3).

Synthesis of 1,2,2,3 thiadiazolopyrimidine derivatives **6a-d** :

Powdered semicarbazones **4a-d** (0.01 mole) were added portion wise to 15 mL of thionyl chloride. The mixture was heated under reflux for one hour and the excess of thionyl chloride was removed under vacuum then added saturated solution of sodium carbonate and the reaction mixture was extracted for several times with chloroform. The chloroformic layer was dried over anhydrous sodium sulphate. The residue obtained after evaporation of the solvent and recrystallized from a proper solvent gave pale yellow crystals (Table 4).

Table 3

Comp.	Ar.	Position of thiadiazole	m.p°C	Yield %	Solvent of crystallization	Mol. Formula	Analysis C	H	N
5a	2-Furyl	4—	193—5	23	pet. ether 40—60	$C_{21}N_{17}N_5O_3SSe$	Calcd. : 50.60 Found : 51.00	3.41 3.60	14.05 13.90
b	p-$OCH_3 \cdot C_6H_4$	4—	145—6	30	Toluene	$C_{24}H_{21}N_5O_3SSe$	Calcd. : 55.40 Found : 53.40	3.70 3.70	13.01 13.20
c	p-$OCH_3 \cdot C_6H_4$	3—	130—1	22	ethan 1	$C_{24}H_{21}N_5O_3SSe$	Calcd. : 53.53 Found : 53.60	3.90 3.80	13.01 12.90
d	p-$OCH_3 \cdot C_6H_4$	2—	135—7	20	ethanol	$C_{24}H_{21}N_5O_3SSe$	Calcd. : 53.53 Found : 53.70	3.90 3.70	13.01 13.10

Table 4

Comp.	Ar.	Position of thiadiazolo	.p°C	Yield %	Solvent of crystaliization	Mol. Formula	Analysis C	H	N
6a	2-Furyl	4—	140—3	22	Toluene	$C_{21}H_{17}N_5O_3S_2$	Calcd. : 55.87 Found : 55.80	3.76 3.50	15.52 15.30
b	p-$OCH_3 \cdot C_6H_4$	4—	165—6	20	benzene pet.ether 40—60	$C_{24}H_{21}N_5O_3S_2$	Calcd. : 58.65 Found : 58.30	4.27 4.20	14.25 14.30
c	p-$OCH_3 \cdot C_6H_4$	3—	180—1	23	Toluene	$C_{24}H_{21}N_5O_3S_2$	Calcd. : 58.65 Found : 58.70	4.27 4.30	14.25 14.40
d	p-$OCH_3 \cdot C_6H_4$	2—	143—4	26	Toluene	$C_{24}H_{21}N_5O_3S_2$	Calcd. : 58.65 Found : 58.90	4.27 4.00	14.25 14.60

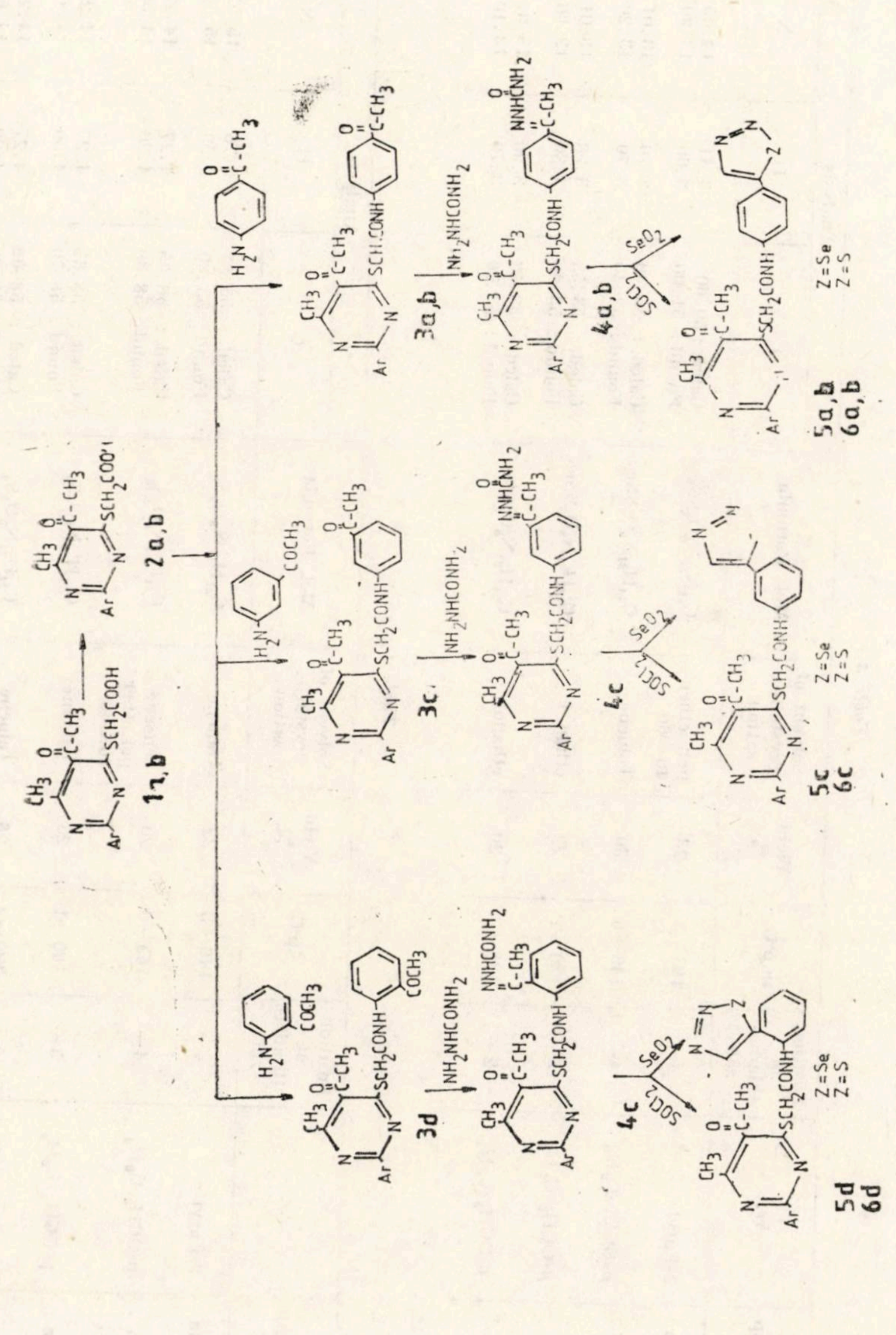
1a,b
2a,b
3a,b
3c
3d
4a,b
4c
5a,b
6a,b
5c
6c
5d
6d
$NH_2NHCONH_2$
SeO_2
$SOCl_2$
Z = Se
Z = S

RESULTS AND DISCUSSION

The synthesis of some new selena and thiadiazoles containing different heterocyclic moieties has been reported.[1-3]

Thus, the acid chlorides **2a,b** were allowed to react with 4-, 3- and 2-aminoacetophenone and gave the corresponding anilides **3a-d**.

The identification of compound **3b** was based on elemental analysis and IR spectra, which showed bands at 1680 cm^{-1} characteristic of $\nu C=O$ of secondary amide and at 3480 cm^{-1} characteristic of νNH of secondary amide.

Compounds **3a-d** were easily condensed with semicarbazide in ethanol[10] and aforded the corresponding semicarbazone **4a-d**.

The identification of compound **4b** was based on elemental analysis and IR spectral analysis, which showed absorption bands at 1630 cm^{-1} characteristic of $\nu C=N$ and at 3480 cm^{-1} characteristic of ν NH of secondary amide.

The purified semicarbazones **4a-d** were oxidized by selenium dioxide-glacial acetic acid to give 1,2,3-selenediazolopyrimidines **5a-d**.

The validity of the structure of compound **5b** was deduced from their correct elemental analysis and IR spectral data which showed band at 1320 cm^{-1}, characteristic of $\nu C-H$ in plane deformation and at 860 cm^{-1} characteristic of $\nu C-Se-N$.

On the other hand, the purified semicarbazones **4a-d** were allowed to react with thionyl chloride[13] giving 1,2,3-thiadiazolopyrimidines **6a-d**.

The structure of compound **6b** was confirmed by elemental analysis and IR spectral data, which showed bands at 1320 cm^{-1} characteristic of ν $C=N$, at 1740 cm^{-1} characteristic of $\nu C-H$ in plane deformation and at 770 cm^{-1} characteristic of $\nu C-S$.

REFERENCES

[1] H. S. El-Kashef, M. A. Abd-Alla, B. E. Bayoumy, and A. A. El-Timany, *J. Chem. Tech. Biotechnol.*, **33A**, 294 (1983).

[2] B. E. Bayoumy, A. Deeb, M. ElMobayed and M. A. Abd-Alla, *Egpt. J. Phaım. Sci.*, **27,** 17 (1986).

[3] B. E. Bayoumy, A. Hattaba and F. Zahran, *Oriental J.* (in press).

[4] F. Bayer and AKT Ges, *Ber.*, **25**, 810 (1959).

[5] M. Y. Kobak and A. Fridman, *Compt. Rend. Acad. Sci., USSR*, **51**, 733 (1946).

[6] S. L. Goodman, and A. Gilman, "The Pharmacological Basis of Therapeutics", The Mecmillan company, New York, London, Toronto, Third Eddition, 850 (1965).

[7] D. L. Pain and S. Slack, *J. Chem. Soc.* **1965,** 5166.

[8] W. Weuffen, W. Pyl Th. Gruebner and W. D. Juelich, *Pharmazie* **20**, 629, (1965).

[9] I. Lalezari, A. Shafiee and S. Yazdani, *J. Pharm. Sci.*, **63**, 628 (1974).

[10] B. Angla, *Chim. Appl.*, **22,** 10 (1940).

[11] I. Lalazari and A. Shafiee, *Tetrahedron Lett.* **1969,** 5105 .

[12] S. El-Bahaie, B. E. Bayoumy, and Sh. Youssif, *Egypt J. Pharm. Sci.* (in press).

[13] R. Roop and R. G. Micetich, *Canad. J. Chem.*, **46**, 1057, (1968).

Revue Roumaine de Chimie, **36**, *1–3*, 215–227(1991)

DIHYDROPYRANS OBTAINED IN THE REACTION BETWEEN 2-(ACENAPHTHYLEN-1-YL)ETHANOL AND CARBONYLIC DERIVATIVES

ALEXANDRU C. RĂZUŞ,[a] MIRCEA D. GHEORGHIU[b] and EMERIC BARTHA[a]
[a]Centre of Organic Chemistry, Spl. Independenţei 202 B 77208 Bucharest, Romania
[b]Department of Organic Chemistry, Polytechnic Institute, Bucharest, Romania

Received June 12, 1990

The reaction of 2-(acenaphthylen-1-yl)ethanol with a series of aldehydes or ketones, as well as with dimethylketals or vinylic ethers, was investigated. Structure proofs for the dihydropyrans obtained in this reaction are presented; possible mechanisms explaining the reaction course are proposed.

In the dehydratation of 2-methylpentane-2,4-diol, along with dienes and homoallylic alcohols, dihydropyrans are formed in small amount and it was supposed that dihydropyrans originate from the reaction between acetaldehyde and a homoallylic alcohol, both formed in secondary reactions.[1]

Later, it was established that the reaction between homoallylic alcohols and carbonylic compounds in acid catalysis is a general reaction, leading to mixtures of dihydropyrans **3**, **4** and **5** in which the dihydropyran **3** with an endocyclic double bond is the major component[2,3] (4-tetrahydropyranols in variable amounts were obtained in several cases[4]):

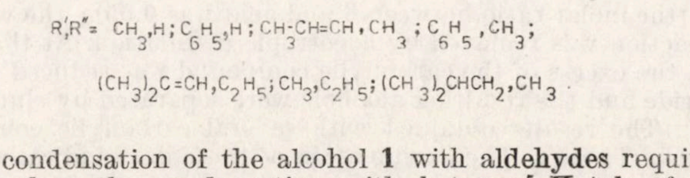

$R',R'' = CH_3,H; C_6H_5,H; CH_3\text{-}CH{=}CH,CH_3; C_6H_5,CH_3;$

$(CH_3)_2C{=}CH,C_2H_5; CH_3,C_2H_5; (CH_3)_2CHCH_2,CH_3.$

The condensation of the alcohol **1** with aldehydes requires milder conditions than the condensation with ketones.[5] Ketals of carbonylic compounds were also used as condensation reagent with the homoallylic alcohol **1**[6] and homollylic alcohols with more complicated skeleton were investigated.[7–10]

In previous papers[11,12] we reported that in the solvolysis in acid medium of several cyclopropylcarbinylic alcohols, dihydropyrans in variable amounts are formed, along with normal solvolytic products. The formation of dihydropyrans was explained by the reaction between one of the solvolytic products, namely a homoallylic alcohol, and acetaldehyde (or its ketal) present as impurity in the reaction medium (dioxane).[12] We decided to investigate the reaction between several homoallylic alcohols obtained in solvolytic reactions and carbonylic compounds or their derivatives.

The present paper describes only the behaviour of 2-(acenaphthylen-1-yl)ethanol **6**,* studying the dependence of the reaction course and reaction products ratio on the nature of the carbonylic compound or derivative. Several interesting structural features of the dihydropyrans obtained in this reaction will be specially emphasized.

RESULTS AND DISCUSSION

The first series of experiments involved the reaction between alcohol **6** and acetaldehyde, **7b**, in excess, with 0.5 M perchloric acid solution in aqueous dioxane (1 : 1 vol.), keeping the reaction mixture at 60°C until the disappearance of the alcohol (approx. three hours). The main reaction product was the dihydropyran **8b**:

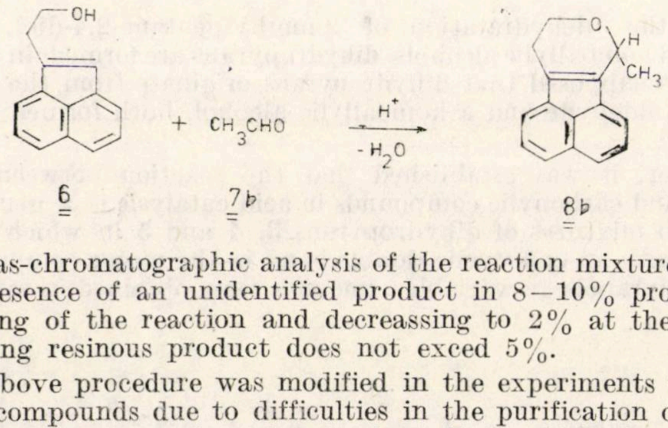

The gas-chromatographic analysis of the reaction mixture indicated also the presence of an unidentified product in 8–10% proportion at the beginning of the reaction and decreassing to 2% at the end. The accompanying resinous product does not exced 5%.

The above procedure was modified in the experiments with other carbonylic compounds due to difficulties in the purification of dioxane. Another procedure was adopted (procedure A) in which the mixture of the homoallylic alcohol **6** and the carbonylic compound **7** (molar ratio 1 : 2) was introduced into a 0.025 M solution of *p*-toluenesulfonic acid in benzene (the molar ratio between **6** and acid was 0.05); the water formed in the reaction was removed by azeotropic distillation. At the end of the reaction, the excess of the carbonylic compound was reduced with sodium borohydride and the resulting alcohols were separated by elution chromatography. The results obtained with several carbonylic compounds are presented in Table 1. The examination of these data indicates the formation of two isomeric dihydropyrans **8** and **9** in a ratio depending on the nature of the carbonylic compounds. In most cases, the isomer **8** separated spontaneously from mixture as crystals.

---

* The alcohol **6** was isolated from the reaction mixture in the acid solvolysis of spiro [acenaphthene-1,1′-cyclopropane]-2-ol.[12]

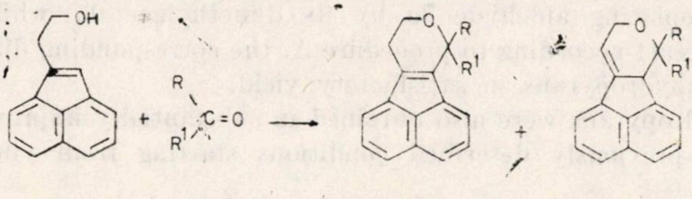

6 7a-g 8a-g 9a-g

Table 1

Isomeric dihydropyrans **8** and **9** obtained by condensation of alcohol **6** with carbonylic compounds **7a**–**g**, in benzene under TsOH catalysis

Carbonylic compounds			Yield$^{a)}$(%)	Ratio **8** : **9**
7	R	R¹		
a	H	H	70$^{b)}$	70 : 30
b	CH_3	H	90$^{b)}$	98 : 2
c	C_6H_5	H	40	70 : 30
d	$(CH_3)_2CH$	H	70	not determined
e	$o-CH_3OC_6H_4$	H	40	70 : 30
f	CH_3	CH_3	30$^{b)}$	95 : 5
g	CH_3	C_6H_5	30	90 : 10

a) Yield of dihydropyrans (mixture of isomers) related to alcohol **6**; b) Heating in sealed tube at 80°C for 2.5 hours.

The yield of the reaction decreases with increase of crowding at the carbonyl group, so that much smaller yields were obtained for ketones than for aldehydes. The pivalaldehyde, **7h**, gave the corresponding acetal **10**; under more severe conditions, only advanced resinification was observed.

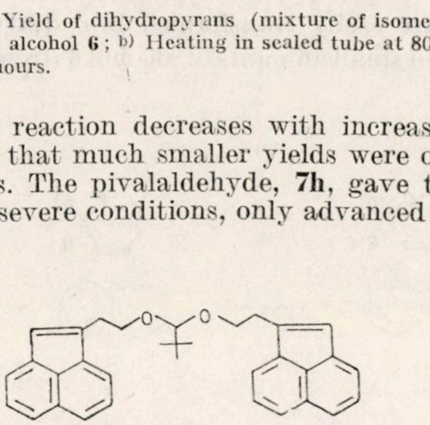

10

Benzophenone, **7i**, *t*-butylmethylketone, **7j**, pivalophenone, **7k**, or di-*t*-butylketone, **7l**, do not react under the conditions previously described.

However, starting from dimethylketals (procedure B) and using the same experimental conditions as in procedure A, several dihydropyrans either inaccessible or obtained in poor yields by procedure A, were obtained in good yields. For instance, an increase of the yield from 40 to 80% was obtained replacing aldehyde **7e** by its dimethylacetal; while ketone **7i** did not react according to procedure A, the corresponding dimethylketal gave dihydropyrans in satisfactory yield.

Dihydropyrans were also obtained in substantially improved yields under the previously described conditions starting from vinyl ethers (procedure C):

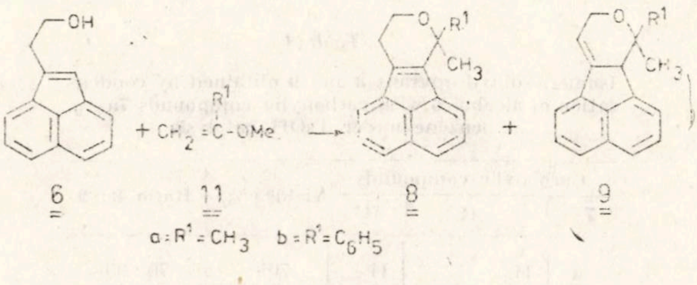

Starting from ether **11a**, a mixture of dihydropyrans **8f** and **9f** (in 93 : 7 ratio) was obtained in 90% yield; **11b** gave in 80% yield the mixture of **8g** and **9g** in 50 : 50 ratio.

It was experimentally proved that, under the reaction conditions, dihydropyrans **9** are easily transformed into dihydropyrans **8**, carbonylic compounds **7** and small amounts of alcohol **6** (from which dihydropyrans originate).

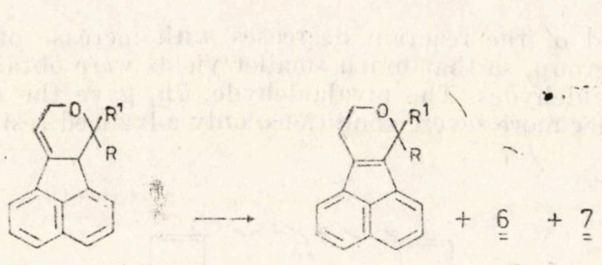

According to literature data,[2] the first step in the condensation of homoallylic alcohols with carbonylic compounds consists in a protonation with the formation of the carbocation **A**. The same cation is obtained starting from dimethylketals or vinyl ethers.

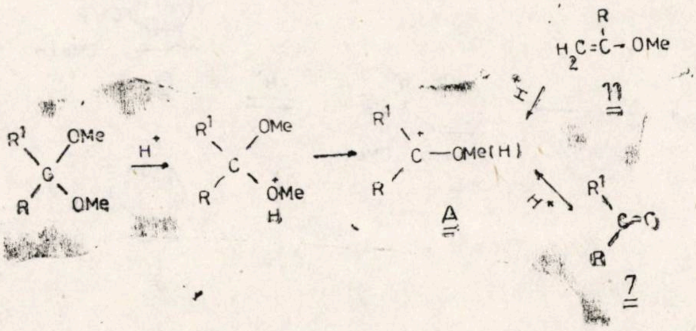
R¹
OMe
R
OMe
H⁺
R¹
OMe
R
OMe
H
R¹
C —OMe(H)
R
A
H⁺
R
H₂C=C—OMe
11
H⁺
R¹
C=O
R
7

Scheme 1 proposes the steps leading to dihydropyrans **8** and **9** from the homoallylic alcohol **6** and the carbocation **A** *via* the ketal **B** and the carbocations **D** and **E**. Deprotonation of the cation **E** gives the dihydropyrans **8** and **9**. Dihydropyran **8** prevails, being probably thermodynamically more stable (under thermodynamic control conditions, **9** passes into **8**).

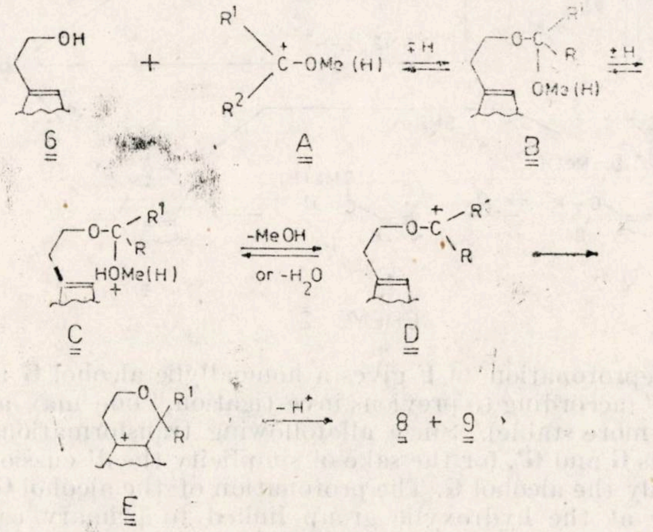
OH
6
+
R¹
C-OMe (H)
R²
A
± H
O-C
R¹
R
OMe (H)
B
± H
O-C
R¹
R
HOMe(H)
C
-MeOH
or -H₂O
O-C
R¹
R
D
O
R¹
R
E
- H⁺
8 + 9

SCHEME 1

In an alternate mechanism, similar to that for Prins condensation, an attack at the double bond generating the carbocation **F** may be infered (Scheme 2).

Williams and coworkers[2] consider the latter mechanism less probable because, on the one hand, Prins reaction is characteristic for aldehydes and, on the other hand, products specific for Prins reaction (like *m*-dioxanes) are lacking. However, an electrophilic attack on the double bond in the alcohol **6** investigated by us (scheme 2) is favored due to formation of benzylic ion **F** (a similar attack on the double bond in alcohol **6** was reported previously[10]).

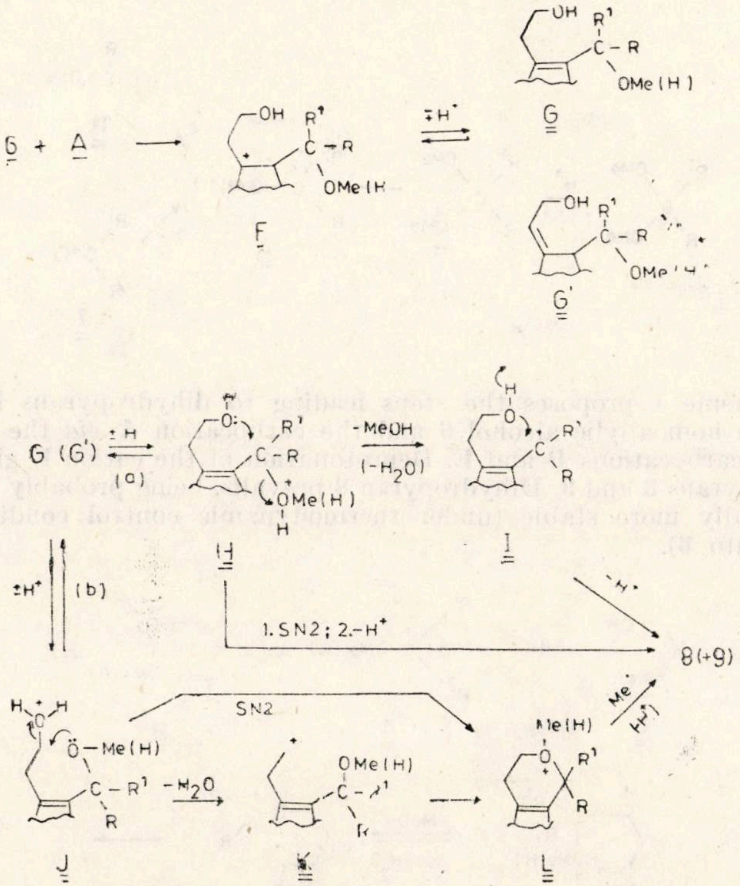

SCHEME 2

The deprotonation of **F** gives a homoallylic alcohol **G** and an allylic alcohol **G′** (according to previous investigation,[10] one may assume that alcohol **G** is more stable). Since all following transformations will imply both alcohols **G** and **G′**, for the sake of simplicity the discussion of scheme 2 regards only the alcohol **G**. The protonation of the alcohol **G** may take place either at the hydroxylic group linked to primary carbon atom, leading to ion **J** (route b) or at the other oxygen atom in the molecule, leading to the ion **H** (route a). The dihydropyranic ring closure in **H** may result from an SN2 attack of the hydroxylic group on the carbon atom in position 5, with elimination of water (or methanol) molecule and deprotonation, giving the dihydropyran **8** (similarly, **G′** gives **9**). Formation of dihydropyran **8** from **H** may follow an alternative route, through the carbocation **I.** The SN2 attack may be favoured by non-ionizing reaction medium (benzene).

Formation of dihydropyrans by route (b) may also have two alternatives : either an SN2 attack generating ion **L**, or water elimination giving ion **K**, following by ring closure leading to the same ion **L**. In the reaction starting from a carbonylic compound, dihydropyran **8** is formed from this ion by deprotonation. However, when the starting materials are methyl ketals or vinylic ethers, the last step implies the improbable elimination of a CH_3^+ fragment, consequently, path (b) can be excluded.

The literature data, as well as the results presented in this paper, are not sufficient to decide between these two mechanisms. There are experimental facts explainable by both mechanisms. For instance, regardless of mechanism, the higher stability of **A** when R and R^1 are phenyl groups compared to alkyls or hydrogen, determines a more difficult reaction course. Also, for both mechanisms, the protonation of the oxygen atom linked to a methyl group in **C** or in **G**, respectively, takes place, in principle, easier than the protonation of the hydrogen-bearing oxygen. Consequently, the reaction of the ketals and vinylic ethers is favoured in comparison with carbonylic compouns.

The mechanism depicted in scheme 2 route (a) via SN2 is supported by the argument that in non-ionizing medium, like that experimentally used, the SN2 mechanism is favored in comparison with the mechanism through carbocations.

Further informations are required to support one or the other of the mechanisms proposed.

STRUCTURE PROOF OF DIHYDROPYRANS

It was mentioned earlier that dihydropyrans **8** crystallized on standing from the mixture of isomeric dihydropyrans **8** and **9** and could be isolated and characterized by physical constants and spectral data. The dihydropyrans **9** could be obtained in pure state only in a few cases.

Dihydropyrans **8**. IR spectra of these compounds present the characteristic absorption bands of trisubstituted benzene, of C—O, C—H and =C—H bonds and some aromatic vibration bands. These data are presented for each compound in the experimental part. It is important to mention, as structure proof for dihydropyrans **8**, the absence of the absorption band around 1600 cm^{-1}, meaning that the double bond is tetra-substituted.

Table 2 displays the ^{1}H-NMR data for dihydropyrans **8**.

All these compounds present a $-CH_2-CH_2-$ characteristic fragment. The signals of these four protons do not present complicate multiplicity in compounds with R=R^1 (**8a**, **8f** and **8i**); for compounds in which R$\neq$R^1, the protons in each methylenic group are diastereotopic, due to the existence of a centre of chirality at C-7 and, consequently present different chemical shifts. Particular examples for each case will be discussed below.

Compound **8a** presents, besides the aromatic proton multiplet, three signals : a high-field multiplet for C-10 protons and two triplets at 3.96 and 4.86 ppm, assigned to the methylenic protons at C-9 and C-7, respectively. The multiplicity of the C-10 protons signal indicates, besides the coupling with C-9 protons, a long-range coupling (through the double bond) with the protons at C-7 and, consequently, the signal of the protons at C-7 appears as triplet. The coupling of the C-7 protons with the protons at C-10 through the double bond is preferred to the coupling with the C-9 protons, through the oxygen atom. The existence of such a coupling, as well as the unexpectedly high value (2.5 Hz) of the coupling constant, are not uncommon for dihydropyrans.[13]

Compound **8b** presents in the aliphatic protons region four signals whose area are in the ratio 1 : 2 : 2 : 3 (from downfield to upfield), belonging to the C-7 proton, methylenic protons at C-9 and C-10 and methyl

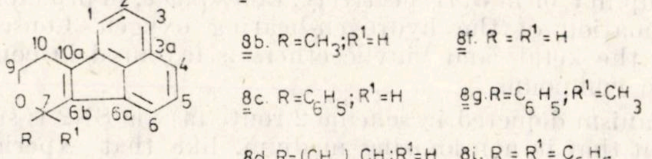

Table 2

^{1}H–NMR Spectra of 9,10-dihydro-7H-acenaphtho[1,2-c]pyrans (**8**) (δ, ppm, J, Hz)

Compound	Signal				
	H-10	H-9	R	R^1	aromatic protons[a]
8a	2.53–2.92, m, 2H	3.96, t, J=5.5, 2H	4.86, t, J=2.5, 2H(H-7)		7.15–7.92, m 6H
8b	2.53–2.90, m, 2H	3.60–4.33, m, 2H	1.58, d, J=7.5, 3H	4.63–5.18, m, 1H	7.27–7.80, m, 6H
8c	2.63–2.89, m, 2H	3.55–4.28, m, 2H	C_6H_5[a]	5.71, t, J=2.3, 1 H	6.78, dd, J=7; 1, 1H(H-6), 7.01–7.74, m, 10H
8d	2.03–2.92, m, 2H+1H[b]	3.50–4.53, m, 2H	0.80, d, J=7, 3H; 1.23, d, J=7, 3H	4.63–4.90, m, 1H	7.22–7.85, m, 6H
8e[c]	2.68–3.08, m, 2H	3.43–4.31, m, 2H	o-$CH_3OC_6H_4$	6.37, t, J=2.5, 1H	7.63–7.81, m, 10H
8f	2.72, t, J=7.5, 2H	3.97, t, J=7.5, 2H	1.63, s, 2×3H ($2\ CH_3$)		7.17–7.78, m, 6H
8g	2.68–3.11, m, 2H	3.30–4.22, m, 2H	C_6H_5[a]	2.02, s, 3H	7.17–7.87, m, 11H
8i	2.98, t, J=7.5, 2H	3.97, t, J=7.5, 2H	C_6H_5[a]	C_6H_5[a]	6.80, dd, J=6.5; 1 1H(H-6) 7.00–7.72, m, 15H

[a] The signals of the protons of the aryl substituents at C-7 are included; [b] one of the protons belongs to isopropyl group; [a] signal of the methoxy group: 3.87, s, 3H.

group at C-7, respectively. Irradiating the C-7 proton (signal consisting of nine lines), the doublet of the methyl group becomes singlet and the complex multiplet of the C-10 protons is simplified. Irradiating the C-10 protons, the signal due to the proton at C-7 becomes a quartet with a coupling constant equal to that of the doublet assigned to the methyl group at C-7.

The last observation concerning the ^{1}H-NMR spectra of dihydropyrans **8** is related to the signal of the C-6 proton in compounds possessing as substituents at C-7 at least one aromatic ring (**8c**, **8g** and **8i**). This proton is upfield shifted and detached from the aromatic protons multiplet.

^{13}C-NMR spectra of the dihydropyrans **8b** and **8f** are presented in the experimental part. Unambiguous assignments of the signals are based both on signals multiplicity and comparison with ^{13}C-NMR data for acenaphthylene[14] and acenaphthenone.[15]

The intensities of the molecular as well as isotopic peaks in the mass spectra are also structure proofs for dihydropyrans **8b** and **8f**.

Dihydropyrans **9**. Since dihydropyrans **9** are obtained in small amounts in the condensation reaction and their separation from isomeric compounds **8** is difficult, only four such dihydropyrans could be isolated and characterized, namely **9c**, **9f**, **9h** and **9i**.

The IR spectra of isomeric pairs of dihydropyrans **8** and **9** are similar, except for a weak band at approx. 1600 cm^{-1} appearing in the spectra of componds **9**, which can be assigned to tri-substituted double bond.

Although simple, the ^{1}H-NMR spectra of these dihydropyrans are not easy to be analyzed (Table 3).

All dihydropyrans **9** investigated possess at C-7 one or two aromatic substituents; consequently, the acenaphthenic proton at C-6, appearing as a doublet, is upfield shifted and detached from the other aromatic protons (similar with isomeric **8** with the same substituents).

The signal of the olefinic proton at C-10 appears at approx. 6 ppm. It has to be emphasized that in the skeleton, obtained by condensation of a homoallylic alcohol **6** with a carbonylic compound, the sole possible disposition of a double bond possessing a hydrogen atom is that in 6b,7-dihydro-9H-acenaphtho[1,2-c]pyrans, **9**. The signal of C-9 protons is a multiplet, but for $R=R^1=C_6H_5$ this multiplet appears as an AB quartet, further splitted by long-range coupling (difficult to be assigned). Normally, the signal of C-9 protons should be simplified for $R=R^1$ due to the disappearance of one of the centres of chirality in molecule. However, the sterical model indicates that the position of the two C-9 protons relative to the aromatic nucleus are quite different, leading to different chemical shifts for these protons.

The chemical shifts and multiplicities of the C-6b and C-7 protons, presented in table 3, are those expected for the structure proposed; in compound **9c** these two protons are overlapped, giving a multiplet, while in **9e** they appear at different field values.

EXPERIMENTAL PART

All melting and boiling points are uncorrected. IR spectra were recorded with a UR 10 Karl Zeiss Jena spectrometer. ^{1}H-NMR spectra were recorded with a Varian EM 360L, using TMS as internal standard. ^{13}C—NMR spectra were recorded with a Varian FT80 spectrometer,

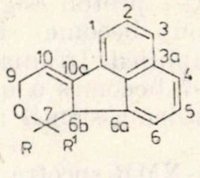

9c $R = C_6H_5$; $R^1 = H$

9e $R = o\,CH_3OC_6H_4$; $R^1 = H$

9g $R = C_6H_5$; $R^1 = CH_3$

9i $R = R^1 = C_6H_5$

Table 3

^{1}H-NMR Spectra of 6b,7-dihydro-9H-acenaphtho[1,2-c]pyran (**9**) (δ, ppm, J, Hz)

Signal	Compound			
	9c	**9e**[b]	**9g**[c]	**9i**
H-7	4.57–4.80, m, 2H	5.04, d, J=9, 1H	—	—
H-6b		4.20–4.58, m, 1H	4.20–4.30,m, 1H	3.90–4.97,m, m, 2H+1H
H-9	4.40, s, 2H	4.58–4.77, m, 2H	4.32–4.58, m, 2H	
H-6	6.14–6.48 m, 2H	6.38, dd, J=6.5 ; 1, 1H	6.50, dd, J=6.5 ; 1, 1H	6.54, dd, J=6.5 ;1, 1H
H-10		6.07–7.78, m, 1H	5.95–6.15, m, 1H	6.10, m, 1H
aromatic protons[a]	7.04–7.77, m, 10H	6.80–7.78, m, 9H	6.71–8.00, m, 11H	6.83–7.63, m, 15H

[a] The signals of the aryl substituents at C-7 are included ; [b] signal of the methoxy group : 3.65, s, 3H ; [c] signal of the methyl group at C-7 : 1.25, s, 3H

under the following conditions : Sw=400 Hz, Pw=18us, pulse delay=3s. Mass spectra were recorded with DP-102 GCMS (electronic ionisation, 250°C). Glc analyses were performed with a 18–3 Willy Giede apparatus, using flame ionisation detector and a separation column with the following characteristics : L=1 m, d=4 mm ; 5% neopentylglycolsuccinate on silanized Chromosorb w (60–80 mesh) ; carrier gas-hydrogen ; flowing rate 60 mL/min ; column temperature 200°C (isotherm) ; vaporisation temperature 250°C.

1. Starting materials

2-(Acenaphthen-1-yl)ethanol, **6**, was isolated from the solvolysis products in acidic medium of spiro[acenaphthene-1,1′-cyclopropane]-2-ol[12].

The carbonylic compounds are commercial reagents (p.a. grade), purified when necessary.

2,2-Dimethoxypropane and 2-methoxypropene are also commercial reagents.

Diphenyldimethoxymethane was obtained from dichlorodiphenylmethane[16] and sodium methoxide in methanol, in nearly quantitative yield, as white crystals, m.p.106°C (methanol, lit.,[17] 106–7°C, Et_2O).

1-Phenyl-1-methoxyethene was obtained according to literature data[18].

o-Methoxybenzaldehyde dimethylacetal was obtained from *o*-methoxybenzaldehyde and methanol in the presence of calcium chloride. The crude ketal was purified by reduction with sodium borohydride followed by chromatography on silicagel.

^{1}H–NMR ($CDCl_3$, δ, ppm) : 3.27 (s, 6H, OMe) ; 3.77 (s, 3H, OMe) ; 5.53 (s, 1H, CHO_2) ; 6.67–7.71 (m, 4H, CH-aromatic).

2. Synthesis of dihydropyrans

I. *Formation of dihydropyrans in aqueous medium under perchloric acid catalysis using alcohol* ***6*** *and acetaldehyde.*

In a glass ampoule (resistant to pressure) are introduced 1.96 g (10 mmoles) alcohol **6** dissolved in 100 mL dioxane and 80 mL water and 20 mL 5M aqueous perchloric acid and 3.9g (5 mL, approx. 90 mmoles) acetaldehyde are added to this solution. The sealed ampoule was heated for three hours in a thermostatic bath at 60°C. After cooling to room temperature, the ampoule was opened and its content was poured into 200 mL sodium bicarbonate solution. The mixture was extracted three times with 100 mL ethylic ether portions, the combined etheric solution was washed with water and dried over anhydrous magnesium sulfate. The ether was removed in vacuo, leaving an oily residue consisting mainly of dihydropyrans **8b** and **9b** along with small amounts of resins, separated through elution chromatography on silicagel (petroleum ether : ethylic ether 4 : 1). Similar results were obtained without dioxane using water-soluble carbonylic compounds (acetaldehyde, acetone) as solvent and reactant or using aqueous formaldehyde.

II. *Formation of dihydropyrans in benzene, under p-toluenesulfonic acid catalysis.*

Procedure A

1g (5 mmoles) alcohol **6** and 10 mmoles carbonylic compound are dissolved in 10 mL benzene. To this solution 10 mg (0.5 mmoles) *p*-toluenesulfonic acid are added. The mixture was boiled for 1—3 hours, with azeotropic distillation of water. After washing with saturated aqueous sodium bicarbonate solution and then with water, benzene was removed under reduced pressure leaving an oily residue. This residue was dissolved in aqueous methanol and treated with excess sodium borohydride for several hours. Working under general conditions, an oily product was obtained; the pure dihydropyranic fraction was separated from this oil by elution chromatography on silicagel (petroleum ether : ethylic ether 1 : 1).

The ratio between the isomeric dihydropyrans was determined either by gas-chromatography (for volatile compounds) or using the ^{1}H—NMR spectrum of the mixture. Usually, from this mixture crystallized as yellow crystals dihydropyrans **8**; in several cases, dihydropyrans **9** could be isolated as white crystals after a second chromatographic elution of the filtrate on a longer column. The yields and the ratio between isomeric dihydropyrans are presented in Table 1.

Procedure B

A solution of 1g (5 mmoles) alcohol **6** and 5 mmoles dimethylketal in 10 mL benzene was treated with 10 mg (0.5 mmoles) *p*-toluenesulfonic acid and then heated at 40—50°C on a water bath. The methanol formed in the reaction, along with a part of benzene was distilled under reduced pressure (50—60 Torr) during 2—3 hours. At the end of the reaction the remaining benzene was distilled under reduced pressure. The residue was dissolved in ethylic ether, washed with water for decomposition of ketal and then with saturated aqueous sodium bicarbonate solution. The worked-up is identical with that described in procedure A.

Procedure C

A solution of 1g (5 mmoles) alcohol **6** and 10 mmoles vinylic ether **11** in 10 mL solvent (benzene or ethylic ether) was treated with 10 mg (0.5 mmoles) *p*-toluenesulfonic acid and then left over night at room temperature. The worked-up of the reaction mixture was similar to those described above.

The following dihydropyrans were prepared according to the procedure indicated in brackets:

*7-methyl-9,10-dihydro-7*H*-acenaphtho[1,2-c]pyrane* **8b** (method I, 95%; method IIA) yellow crystals, m.p. 73—4°C (petroleum ether : ethylic ether 1 : 1).

IR (CS_2, CCl_4, cm^{-1}) : 784 vs, 822 vs, 857 w, 910 w, 961 w, 1037 w, 1051 w, 1069 m, 1089 s, 1113 s, 1141 w, 1283 w, 1326 w, 1363 m; 1428 m, 1477 m, 2715 w, 2829 m, 2853 m, 2917 m, 2976 m, 3041 m, 3065 m.

^{1}H—NMR (CD Cl_3, δ,ppm) : 1.58 (d, J=7.5 Hz, 3H, CH_3); 2.53—2.90 (m, 2H, H-10); 3.60—4.33 (m, 2H, H-9); 4.63—5.18 (m, 1H, H-7); 7.27—7.80 (m, 6H, aromatic protons).

^{13}C—NMR ($CDCl_3$, δ, ppm); 21.57 (q, CH_3) : 23.83 (t, C-10); 62.70 (t, C-9); 70.42 (d, C-7); 120.96 (d, C-1); 121.76 (d, C-6); 126.48 (d, C-2); 126.89 (d, C-5); 127.35 (d, C-3); 127.45 (d, C-4); 128.12 (s, C-3a); 128.67 (s, C-10c); 134.32; (s, C-10a); 137.54 (s, C-6b); 139.05 (s, C-10b); 139.12 (s, C-6a)..

MS (m/e, rel. intensity, %) 224 (M+2, 0.9) ; 223 (M+1, 10.8) ; 222 (M, 58.16) ; 207 (100) ; 194 (7.8) ; 192 (57.2) ; 191 (50.5) ; 189 (82.6); 178 (26.5) ; 165 (40.6) ; 152 (13.0) ; 150 (6.0) ; 94 (24.9).

9,10-dihydro-7H-acenaphtho[1,2-c]pyrane, **8a** (method I, **8a**+**9a**, 70% and method IIA) yellow oil.

IR (CS$_2$, CCl$_4$, cm^{-1}) : 772 vs, 782 sh, 816 s, 828 s, 882 m, 965 m, 978 s, 1012 w, 1035 w, 1072 s, 1095 m, 1112 s, 1138 m, 1189 w, 1221 w, 1285 w, 1340 w, 1387 w, 2825 m, 2852 s, 2915 s, 2959 s, 3044 m, 3060 m.

^{1}H–NMR (CDCl$_3$, δ, ppm) : 2.53–2.92 (m, 2H, H–10) ; 3.96 (t, J=5.5 Hz, 2H, H-9) ; 4.86 (t, J=2.5 Hz, 2H, H-7) ; 7.15–7.92 (m, 6H, aromatic protons).

7-phenyl-9,10-dihydro-7H-acenaphtho[1,2-c]pyrane, **8c** (method IIA) yellow crystals, m.p. 95–97°C.

IR (CCl$_4$, CS$_2$, cm^{-1}) : 702 s, 723 w, 788 s, 772 vs, 818 m, 830 m, 850 w, 903 w, 958 w 1032 w, 1068 m, 1088 m, 1103 m, 1140 m, 1272 w, 1360 w, 1430 m, 1450 w, 1477 w, 2828 m, 2850 m, 2912 m, 2958 m, 3035 m, 3058 m.

^{1}H–NMR (CDCl$_3$, δ, ppm): 2.63–2.98 (m, 2H, H-10) ; 3.55–4.28 (m, 2H, H-9) ; 5.71 (t, J=2.3 Hz, 1H, H-7) ; 6.78(dd, J$_0$=7 Hz, J$_m$ <1 Hz, 1H, H-6) ; 7.01–7.74 (m, 10H, aromatic protons).

7-phenyl-6b,7-dihydro-9H-acenaphtho[1,2-c]pyrane, **9c** (method IIA) white crystals, m.p. 74–5°C (hexane).

IR (CCl$_4$, CS$_2$, cm^{-1}) : 700 m, 710 w, 748 w, 761 w, 778 m, 801 s, 826 w, 837 w, 908 w, 968 w, 1018 w, 1112 s, 1368 m, 1600 w, 2822 w, 2878 w, 2922 w, 3035 w.

^{1}H–NMR (CDCl$_3$, δ, ppm) : 4.40 (broad singlet, 2H, H-9) ; 4.57–4.80 (m, 2H, H-6b and H-7) ; 6.22 (broad singlet, 1H, H-10) ; 6.29 (dd, J$_0$=7 Hz, J$_m$=1Hz, 1H, H-6) ; 7.04–7.77, (m, 10H, aromatic protons).

7-isopropyl-9,10-dihydro-7H-acenaphtho[1,2-c]pyrane, **8d** (method IIA) yellow oil.

^{1}H–NMR (CCl$_4$, δ, ppm) : 0.80 (d, J=7 Hz, 3H, CH$_3$) ; 1.23 (d, J=7 Hz, 3H, CH$_3$); 2.03–2.92 (m, max. 2.70, 3H, H-10 and H-2′) ; 3.50–4.53 (m, 2H, H-9) ; 4.63–4.87 (m, 1H, H-7) ; 7.22–7.85 (m, 6H, aromatic protons).

7-ortho-methoxyphenyl-9,10-dihydro-7H-acenaphtho[1,2-c] pyrane, **8e** (method IIA and method IIB, **8e**+**9e**, 80%) yellow crystals, m.p.=55–6°C (hexane).

^{1}H–NMR (CDCl$_3$, δ, ppm) : 2.68–3.08 (m, 2H, H-10) ; 3.43–4.31 (m, 2H, H-9) ; 3.87 (s, 3H, OCH$_3$) ; 6.37 (t, J=2.5 Hz, 1H, H–7) ; 6.63–7.81 (m, 10H, aromatic protons).

7-ortho-methoxyphenyl-6b,7-dihydro-9H-acenaphtho[1,2-c]pyrane, **9e** (method IIA and method IIB) white crystals, m.p. 43–7°C.

^{1}H–NMR (CDCl$_3$, δ, ppm) : 3.65 (s, 3H, OCH$_3$) ; 4.20–4.58 (m, 1H, H-6b) ; 4.58–4.77 (m, 2H, H-9) ; 5.04 (d, J=9 Hz, 1H, H-7) ; 6.07–6.27 (m, 1H, H-10) ; 6.38 (dd, J$_0$=6.5 Hz, J$_m$ =1 Hz, 1H, H-6) ; 6.80–7.78 (m, 9H, aromatic protons).

7,7-dimethyl-9,10-dihydro-7H-acenaphtho[1,2-c]pyrane, **8f** (method I, 70%, method IIA and method IIC, 90%) yellow crystals, m.p. 55–6°C.

^{1}H–NMR (CDCl$_3$, δ, ppm) : 1.63 (s, 6H, CH$_3$) ; 2.72 (t, 2H, H-10) ; 3.97 (t, 2H, H-9) ; 7.17–7.78 (m, 6H, aromatic protons).

^{13}C–NMR (CDCl$_3$, δ, ppm) : 23.91 (q, CH$_3$) ; 28.49 (t, C-10) ; 59.37 (t, C-9) ; 73.55 (s, C-7) ; 121.08 (d, C-1) ; 122.08 (d, C-6) ; 126.43 (s, C-2) ; 126.98 (d, C-5) ; 127.42 (d, C-3) ; 127.55 (d, C-4) ; 128.12 (s, C-3a) ; 128.75 (s, C-10c) ; 134.51 (s, C-10a) ; 137.54 (s, C-6b) ; 139 21 (s, C-10b) ; 139.31 (s, C-6a).

MS (m/e, rel. intensity, %) : 238 (M+2, 0.2) ; 237 (M+1, 2.9) ; 236 (M, 14.9) ; 221 (100) ; 206 (71.1) ; 205 (20.1) ; 191 (40.6) ; 190 (29.6) ; 189 (39.4) ; 178 (30.5) ; 165 (62.1) ; 152 (11.6) ; 118 (18) ; 110 (11.7) ; 95 (27.5).

7-phenyl-7-methyl-9,10-dihydro-7H-acenaphtho[1,2-c]pyrane, **8g** (method IIA and method IIC, **8g**+**9g**, 80%) yellow crystals, m.p. 115–6°C (hexene).

IR (CCl$_4$, CS$_2$, cm^{-1}) : 704 s, 748 w, 775 vs, 819 s, 841 w, 877 w, 923 w, 960 w, 985 w, 1030 w, 1047 w, 1080 s, 1110 w, 1224 w, 1361 w, 1427 m, 1474 w, 1548 w, 2828 w, 2862 w, 2929 w, 2960 w, 2983 w, 3061 w.

^{1}H–NMR (CDCl$_3$, δ, ppm) : 2.02 (s, 3H, CH$_3$) ; 2.68–3.11 (m, 2H, H-10) ; 3.30–4.22 (m, 2H, H-9) ; 7.17–7.87 (m, 11H, aromatic protons).

7-phenhyl-7-methyl-6b,7-dihydro-9H-acenaphtho[1,2-c]pyrane, **9g** (method IIA and method IIC).

^{1}H–NMR (CDCl$_3$, δ, ppm) : 1.25 (s, 3H, CH$_3$) ; 4.20–4.30 (m, 1H, H-6b) ; 4.32–4.58 (m, 2H, H-9) ; 5.95–6.15 (m, 1H, H-10) ; 6.50 (dd, J$_0$=6.5 Hz, J$_m$=1Hz, 1H, H–6) ; 6.71–8.00 (m, 11H, aromatic protons).

7,7-diphenyl-9,10-dihydro-7H-acenaphtho[1,2-c]pyrane, **8i** (method IIB, **8i**+**9i**, 80 %) yellow crystals, m.p. 213–4°C (benzene).

IR (CCl_4, CS_2, cm^{-1}): 706 vs, 740 m, 761s, 774 vs, 994 w, 1035 s, 1068 s, 1180w, 1222 w, 1426 w, 1442 w, 1477 w, 2830 w, 2868 w, 2920 w, 2963 w, 3035 w, 3059 w.

^1H–NMR ($CDCl_3$, δ, ppm): 2.98 (t, J=7.5 Hz, 2H, H-10); 3.97 (t, J=7.5 Hz, 2H, H-9); 6.80 (dd, J_0=6.5 Hz, J_m=small, 1H, H-6); 7.00–7.72 (m, 15H, aromatic protons).

7,7-diphenyl-6b,7-dihydro-9H-acenaphtho[1,2-c]pyrane, **9i** (method IIB), white crystals, m.p. 183–8°C (benzene).

IR (CCl_4, CS_2, cm^{-1}): 704 vs, 715 m, 732 m, 760 s, 777 m, 783 s, 800 vs, 833 w, 845 w, 913 w, 927 w, 950 w, 972 w, 1007 w, 1015 w, 1057 w, 1103 s, 1181 w, 1200 w, 1207 w, 1363 w, 1441 w, 1489 w, 1595 w, 2832 w, 2872 w, 2918 w, 3033 w, 3053 w, 3080 w.

^1H–NMR($CDCl_3$, δ, ppm): 3.90–4.97 (m, 3H, H-6b and H-9); 6.10 (m, 1H, H-10); 6.54 (dd, J_0=6.5 Hz, J_m=small, 1H, H-6); 6.83-7.63 (m, 15H, aromatic protons).

REFERENCES

[1] S. A. Ballard, R. T. Holm, and P. H. Williams, *J. Amer. Chem. Soc.* **72**, 5734 (1950).

[2] P. H. Williams, G. G. Ecke and S. A. Ballard, *J. Amer. Chem. Soc.* **72**, 5738 (1950).

[3] U. G. Hatullin, T. F. Petrushnina, Z. M. Nurtdinova, Yu. N. Popov and M. G. Safarov, *Khim. Geterotsikl. Soed.*, **1986**, 883.

[4] E. Hansche, *Chem. Ber.*, **88**, 1053 (1955).

[5] P. I. Kazarian, O. P. Avarian and A. A. Gevorkian, *Khim. Geterotsikl. Soed.*, **1985**, 1189.

[6] M. L. Melany, G. A. Lock and D. W. Thompson, *J. Org. Chem.*, **50**, 3925 (1985).

[7] I. Jirkovsky, L.G. Humber and Noureldin, *Eur. J. Med. Chem. Chim. Ther.*, **11**, 571 (1976).

[8] USA, Patent, 3, 904, 617, (9.09.1975); cf. CA **84**, 164794x.

[9] USA, Patent 3, 910, 954 (7.10.1975); cf. CA **84**, 43844e.

[10] USA Patent, 3, 995, 052 (15.01.1976); cf. CA **86**, 121162p.

[11] A. C. Răzuș, M. D. Gheorghiu and E. Bartha *Rev. Roumaine Chim.* **34**, 1263 (1989).

[12] A. C. Răzuș, M. D. Gheorghiu, Zs. Arvay, A. I. Iancu and E. Bartha, *Rev. Roumaine Chim.*, **34**, 1397 (1989).

[13] D. W. Cameron, D. G. I. Kingstone, N. Sheppard and L. Todd, *J. Chem. Soc.*, **1964**, 98.

[14] A. J. Jones, T. D. Algen, D. M. Grant and W. M. Litchman, *J. Amer. Chem. Soc.*, **92**, 2386 (1970).

[15] J. L. Marshall, L. G. Faehl and R. Kattner, *Org. Magn. Reson.*, **12**, 163 (1979).

[16] L. J. Andrews and W. W. Kaeding, *J. Amer. Chem. Soc.*, **73**, 1010 (1951).

[17] A. McKenzie, *J. Chem. Soc.*, **69**, 987 (1896); cf. I. Heilbron, "Dictionary of Organic Compounds", Ed. Moskow, 1949, vol. 1, p. 225.

[18] S. Winstein and L. L. Ingraham, *J. Amer. Chem. Soc.*, **77**, 1738 (1955).

Revue Roumaine de Chimie, **36**, *1–3*, 229–234 (1991)

DIACYLATION OF OLEFINS. XXV[1]

NEW PYRYLIUM AND PYRIDINIUM SALTS DERIVED FROM HEXAHYDROPSEUDOIONONE

TEODOR-SILVIU BALABAN,[a] MARIANA BOGAŢIAN,[a] MARIETA PLĂVEŢI,[a]
VIRGIL M. BĂDESCU[b] and GHEORGHE MIHAI[a]
[a] Centre of Organic Chemistry of the Romanian Academy, Splaiul Independenţei 202 B, 78100 Bucharest, Romania
[b] ICECHIM, Splaiul Independenţei 202, 78100 Bucharest, Romania

Received March 25, 1990

Hexahydropseudoionone **1** was converted into the crystalline pyrylium salt **4** (2,6-dimethyl-4-(4,8-dimethyl-1-nonyl)-pyrylium perchlorate) in which the 4-substituent is an isoprenoid alkyl group. This new pyrylium salt was transformed in high yields into the corresponding pyridine (**8**), N-methyl (**11**) N-phenyl-(**12**) and N-(4-*n*-butyl-phenyl)-pyridinium (**13**) salts. Beside pyrylium salt **4** (56%) two other isomeric pyrylium salts **5** (26%) and **6** (18%) are present in the diacylation mixture, as put into evidence by the GC-MS analyses of the corresponding mixture of pyridines (**8–10**).

INTRODUCTION

Pyrylium salts have become easily accessible by the diacylation of olefins and other methods, and have proven useful synthons for various heterocyclic and carbocyclic compounds.[2]

2,4,6-Trimethylpyrylium salts with various anions can be prepared by standard procedures.[3] On replacing one or more of the methyl groups with long alkyl groups one can derive new compounds which are summarized in Scheme 1. Pyrylium salts are easily converted into pyridinium salts by reaction with primary amines.[2] Scheme 1 presents also some pyridinium salts which can be derived from the corresponding pyrylium salts. Pyrylium salts are very reactive towards nucleophiles and are thus stable only at pH values less than 4. On the other hand, pyridinium salts are stable over a large pH range (1–14) and they are considerably less reactive.

One long alkyl side-chain (lipophilic) attached to the heterocyclic ring may confer interesting properties such as : (i) *tensioactive activity* ; (ii) *solubility* in less polar solvents, pyrylium and pyridinium salts without such long alkyl groups being usually soluble only in strongly polar solvents (protic or aprotic) ; (iii) *monolayer forming membranes.*

Two long alkyl side-chains may confer other properties depending on whether the polar group is excentric or not, and on the mutual orientation of the alkyl groups on the heterocyclic ring. Organization into bilayer-forming synthetic amphiphiles has been amply demonstrated [4] for related structures with single-chain,[5] double-chain,[6] and triple-chain[7] compounds. Scheme 1 summarizes all possibilities of pyrylium of pyridinium salts with up to four long alkyl side-chains having substituents only in the 2-, 6- (α); 4- (γ), or 1-positions.

All compounds from Scheme 1 can be synthesized by relative simple methods if a specific tailoring is desired. Starting materials are cheap and scaling up may be possible in certain instances.

In the present paper we describe the synthesis and some chemical and spectral properties of a crystalline pyrylium salt of type **A** (Scheme 1) with a long 4-alkyl side-chain of isoprenoid nature, as well as its conversion into the corresponding pyridine and pyridinium salts having N-methyl, N-phenyl, and N-(4-*n*-butylphenyl) groups.

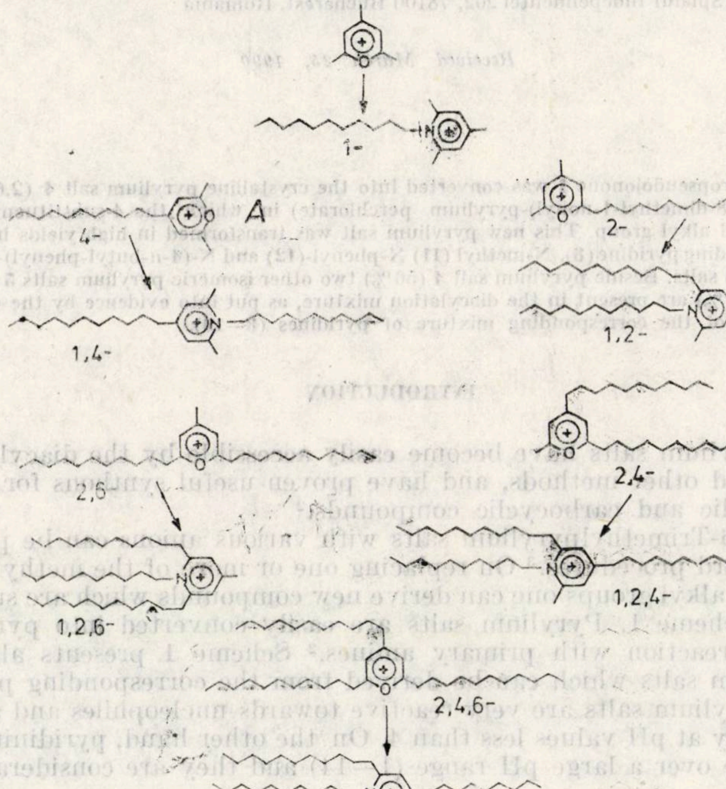

Scheme 1

RESULTS AND DISCUSSION

Scheme 2 presents the synthesis of 2,6-dimethyl-4-(4,8-dimethyl-1-nonyl) pyrylium perchlorate **4** starting from hexahydropseudoionone (6,11-dimeythylundecen-2-one, **1**) *via* the carbinol **2** and the mixture of alkenes **3a** and **3b**.

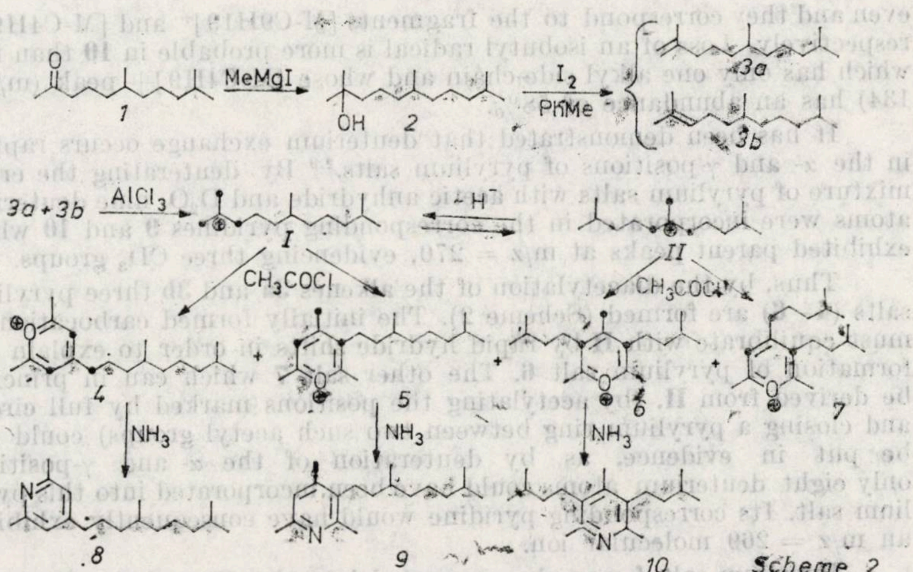

Scheme 2

Diacylation of the alkene mixture with acetyl chloride in carbon disulfide gave a mixture of pyrylium salts from which the salt **4** crystallized and could be separated in pure form. In order to analyse the diacylation of **3a** and **3b** the mixture of pyrylium salts was converted by reaction with aqueous amonia into the corresponding mixture of pyridines which was analysed by GC-MS. Rajoharisson and Roussel have shown that the composition of a mixture of pyrylium salts is reflected adequately by the composition of the corresponding pyridines, which can be easily analysed by GLC.[8]

The pure pyrylium salt **4** was converted into the pyridine **8** (83% yield) which was analysed by MS, IR, ^{1}H-NMR and UV spectra and by microanalysis as reported in the experimental section. With the structure of pyridine **8** firmly established (and consequently also that of the corresponding pyrylium salt **4**) we were able to interpretate the results of the GC-MS experiment on the mixture of pyridines.

Three isomeric pyridines (**8**—**10**) were present in this mixture, the pyridine **8** being the major (55.4%) component which was eluted as second on the capillary column (retention time 270 seconds). On the basis of their fragmentation patterns, and deuteration experiments (*vide infra*), we tentatively assign the structures **10** and **9** to the firstly eluted component (26.3%, RT = 297 s) and to the lastly eluted one (18.3%, RT = 209 s), respectively.

The parent peak of all pyridines is at m/z = 261 and has a relatively low abundance in pyridine **8** (22%) in comparison with **10** (30%) and especially **9** (48%)which have shorter alkyl side-chains and thus more stable molecular ions. The base peak is different in all pyridines **8**—**10**. While in the trisubstituted pyridine **8** the odd mass base peak at m/z = =121.2563 corresponds to loss of an alkene $C_{10}H_{20}$ from the isoprenoid side-chain, the base peaks of **9** (m/z = 134) and **10** (m/z = 204) are both even and they correspond to the fragments [M-C9H19]$^+$ and [M-C4H9]$^+$, respectively. Loss of an isobutyl radical is more probable in **10** than in **9** which has only one alkyl side-chain and whose [M-C4H9]+ peak (m/z= 134) has an abundance of 58%.

It has been demonstrated that deuterium exchange occurs rapidly in the α- and γ-positions of pyrylium salts.[2,9] By deuterating the crude mixture of pyrylium salts with acetic anhydride and D_2O, nine deuterium atoms were incorporated in the corresponding pyridines **9** and **10** which exhibited parent peaks at m/z = 270, evidencing three CD_3 groups.

Thus, by the diacetylation of the alkenes **3a** and **3b** three pyrylium salts (**4**—**6**) are formed (Scheme 2). The initially formed carbocation (**I**) must equilibrate with **II** by rapid hydride shifts in order to explain the formation of pyrylium salt **6**. The other salt **7** which can in principle be derived from **II**, (by acetylating the positions marked by full circles and closing a pyrylium ring between two such acetyl groups) could not be put in evidence, as by deuteration of the α- and γ-positions only eight deuterium atoms could have been incorporated into this pyrylium salt. Its corresponding pyridine would have consequently exhibited an m/z = 269 molecular ion.

Pyrylium salt **4** was also converted into the N-methyl-, N-phenyl and N-(4-*n* butylphenyl) pyridinium salts **11**, **12** and **13**, respectively (Scheme 3). We were unable to isolate the N-dodecyl-pyridinium salt from the reaction of **4** and dodecylamine-probably due to a greater solubility of this salt.

These pyridinium salts present relatively low melting points (51—52°C for **11** and 76—77 °C for **12**) but do not have nematic properties. Specific tailoring might produce a pyrylium or pyridinium salt with nematic properties over a desired temperature range.

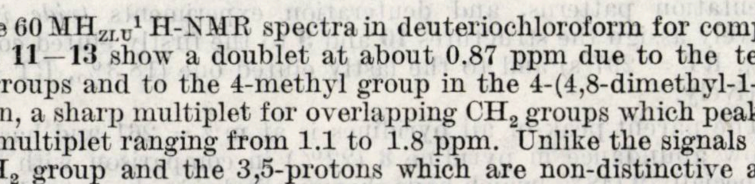

Scheme 3

The 60 MH$_{ZLU}$^{1} H-NMR spectra in deuteriochloroform for compounds **4**, **8** and **11**—**13** show a doublet at about 0.87 ppm due to the terminal methyl groups and to the 4-methyl group in the 4-(4,8-dimethyl-1-nonyl) side-chain, a sharp multiplet for overlapping CH_2 groups which peaks from a broad multiplet ranging from 1.1 to 1.8 ppm. Unlike the signals due to the 4-CH_2 group and the 3,5-protons which are non-distinctive as they appear in all compounds **4**, **8** and **11**—**13** the chemical shift of the signal due to the 2,6-dimethyl groups is characteristic for each of these compounds. Thus this signal is, as expected, more deshielded in the pyrylium salt **4** (2.94 ppm) and less in the N-methylpyridinium salt **11** (2.84 ppm) or pyridine **8** (2.44 ppm) since 0^+ is more electron-withdrawing than alkyl— N^+, which in turn, is more electron-withdrawing than N. The chemical shift for [illegible] methyl groups in pyridine **8** is consistent with the chemical shifts of other 2,6-dimethyl-polyalkyl substituted pyridines.[10]

In the N-phenylpyridinium salts **12** and **13** the phenyl ring shields the 2,6-dimethyl groups (2.41 ppm) explaining the lower chemical shift compared even with the pyridine **8**. This shielding property of N-aryl groups in 2,4,6-trimethyl-1-arylpyridinium salts has been used to assess the aromaticity of the aryl group from ^{1}H-,[11] and ^{13}C-NMR[12] spectra.

EXPERIMENTAL SECTION

^{1}H—NMR Spectra were recorded on a Varian A-60A spectrometer, IR spectra were run on Zeiss UR 20 apparatus and UV spectra were also run on a Zeiss instrument. Melting points were determined on a hot stage melting point apparatus equipped with a polariser and analyser for assessing nematic properties. GC-MS analyses were recorded on a 70-SE V.G. Analytical instrument. GLC analyses were run on a Carlo Erba Fractovap apparatus.

2,6-Dimethyl-4-(4,8-dimethyl-1-nonyl)pyrylium perchlorate **4**. Hexahydropseudoionone (198 g, 0.91 moles) 91% pure (by GLC with internal standard) was added dropwise into an ethereal solution of methylmagnesium iodide (1.1 moles). The reaction mixture after decompositon with a saturated aqueous solution of amonium chloride, ether extraction, and evaporation of the solvent, was dehydrated with iodine, the water being allowed to be collected by toluene in a Dean-Stark trap. Distillation in a Claisen flask gave a fraction (110 g, b.p.$_{1\cdot5\,\text{Torr}}$ 85—103 °C) which was redistilled over a short column (20 cm filled with Rashig rings of 2 mm diameter) affording 62 g **3a** and **3b** (35% yield relative to **1**). Diacylation of this fraction (36 g, 0.18 moles) was effected by adding it dropwise under efficient stirring and water cooling to a suspension of acetyl chloride (36 g, 0.46 moles) and aluminium chloride (25 g, 0.18 moles) in carbon disulfide (100 ml). The mixture after stirring (5 hrs.) at room temperature was left overnight, then subsequently heated to 40 °C until the evolution of hydrogen chloride subsided (about 5 hrs.). The reaction mixture was decomposed by pouring it over 200 g of crushed ice and concentrated aqueous hydrogen chloride (10 ml). The lower layer of carbon disulfide was separated and the aqueousupper layer was extracted four times with diethyl ether. The clear yellow solution was treated with perchloric acid which led to the separation of an upper oily layer. This oil was collected, washed with distilled water and was left to crystallise ; the crystalline pyrylium salt **4** (10.6 g, 16.2% yield based on the mixture of alkenes **3a** and **3b**) was separated from the residual oil (mixture of **4**, **5** and **6**). Recrystallization from water, acetic acid, ethanol, isopropanol or various mixtures of solvents met with difficulties. The initially separated crystals (m.p. 101—102 °C) were practically pure. Colourless needles (m.p. 95—101 °C) were obtained from acetic acid : water (1 : 1). Found : **C** : 59.59 ; **H** : 8.88 ; **Cl** : 9.96% ; $C_{18}H_{31}ClO_5$ requires **C** : 59.58 ; **H** : 8.61 ; **Cl** : 9.77%.

^{1}H—NMR ($CDCl_3$) : 0.87 (d, 9H, J=5.5 Hz, CH-*Me*), 1.21 (sharp m, about 6H CH_2CH_2CH), 1.2—1.7 (m, about 6H, CH_2CH_2CH), 2.73 (t, 2H, J=7 Hz, 4-CH_2 CH_2-) 2.94 (s, 6H, 2,6-Me_2), 7.82 (s, 2H, 3,5-H_2).

IR (KBr) : 625 s, 1100 s, 1460 mw, 1485 mw, 1540 m, 1640 m, 2870 mw, 2940 mw.
UV (ethanol) : $\lambda_{max}(\lg\varepsilon_{max})$: 244 (4.86).

2,6-Dimethyl-4-(4,8-dimethyl-1-nonyl)pyridine **8**. Pyrylium salt **4** (0.5 g, 1.38 mmoles) was treated with excess aqueous amonia, the pyridine was extracted into diethyl ether, the ethereal layer was dried and evaporated. Distillation gave 0.30 g of yellow oil (83% yield), b.p.$_{1\cdot\text{Torr}}$ 150 °C.Found **C** : 82.47 ; **H** : 11.88 ; **N** : 5.17% ; $C_{18}H_{31}N$ requires **C** : 82.69 ; **H** 11.95 ; **N** : 5.36%.

MS, m/z (%) : 263.50 (0.59), 262.47 (4.19), 261.4768 (21.6), 246 (12.9), 218 (6.2), 190 (7.7), 176 (5.9), 148 (10.2), 135 (18.0), 134 (58.7), 122 (8.96), 121 (100.0), 120 (13.0), 77 (7.1), 55 (5.9), 43 (13.6).

^{1}H—NMR ($CDCl_3$) : 0.87 (d, 9H, J=6 Hz, CH—*Me*), 1.23 (sharp m, about 6H, CH_2CH_2CH), 1.2—1.8 (m, about 6H, CH_2CH_2CH), 2.33 (t, 2H, J=7 Hz), 4-CH_2—CH_2-), 2.44 (s, 6H, 2,6-Me_2), 6.73 (s, 2H, 3,5-H_2).
IR (CC14) : 1218 m, 1470 m, 1600 mw, 2870 m, 2925 s, 2955 s.
UV (ethanol) : λ_{max} (lg ε_{max}) : 265 (4.22), 272 (4.21)

1,2,6-Trimethyl-4-(4,8-dimethyl-1-nonyl)pyridinium perchlorate **11**. Pyrylium salt **4** (0.5 g, 1.38 mmoles) was treated with excess of methylamine in ethanol and was heated for 30 minutes. Precipitation with hexane gave a crude slightly yellow oil. Recrystallization from isopropanol (cooling at −20 °C, overnight) gave colourless plates (0.40 g, 77% yield) with m.p. 51−52 °C. Found: **N**: 3.51%. $C_{19}H_{34}ClNO_4$ requires **N**: 3.73%.

^1H−NMR (CDC13): 0.88 (d, 9H, J=6 Hz, CH−*Me*), 1.24 (sharp m, about 6H, CH_2CH_2CH), 1.2−1.8 (m, about 6H, CH_2CH_2CH), 2.78 (t, 2H, J=7 Hz, 4-CH_2−CH_2−), 2.84 (s, 6H, 2,6-Me_2), 4.14 (s, 3H, N^+−Me), 7.52 (s, 2H, 3,5-H_2).

IR (CH_2Cl_2): 1100 vs, 1280 mw, 1450 mw, 1570 w, 1630 mw, 2865 w, 2930 mw, 2980 m, 3070 m.

2,6-Dimethyl-1-phenyl-4-(4,8-dimethyl-1-nonyl)pyridinium perchlorate **12**. Similarly, pyrylium salt **4** (84 mg, 0.19 mmoles) was heated in ethanol with excess of freshly distilled aniline. Precipitation with hexane gave a yellow oil which crystallized on cooling, (76 mg, 75% yield) m.p. 76−77°C. Found: **N**: 3.17% $C_{24}H_{36}ClNO_4$ requires **N**: 3.20%.

^1H−NMR ($CDCl_3$): 0.88 (d, 9H, J=6 Hz, CH−*Me*), 1.23 (sharp m) 1.1−1.6 (m, 12H, CH_2CH_2CH), 2.42(s,6H 2,6Me_2).2.87(m,2H,4-CH_2-CH_2-);7.37-7.68(rm,7H,3,5-H_2 and N-Ph).

IR (CH_2Cl_2): 1100 vs, 1380 mw, 1465 m, 1487 mw, 1557 mw, 1585 mw, 1629 m, 2870 mw, 2930 m, 2960 m, 3080 w.

UV (ethanol): λ_{max} (lg ε_{max}): 231 (4.98), 274 (4.76)

2,6-Dimethyl-4-(4,8-dimethyl-1-nonyl)-1-(4-butylphenyl)-pyridinium perchlorate **13**. Similarly, 0.5 g of **4** were treated in ethanol with freshly distilled 4-*n*butylaniline. Addition of hexane and cooling in the deep freeze led to the separation of an orange oil which was collected but could not be crystallized and satisfactorily purified. Found: **N**: 2.32% $C_{28}H_{44}ClNO_4$ requires **N**: 2.83%.

^1H−NMR ($CDCl_3$): 0.88−0.90 (d, 9H, J=6.5 Hz, CH−*Me* and t, 3H, CH_2-*Me*), 1.23 (sharp m), 1.15−2.0 (m, 16H, CH_2CH_2), 2.40 (s, 6H, 2,6-Me_2), 2.4−2.9 (m, 4H, 4-CH_2 and 4′-CH_2), 7.43 (unequal d, 2H, J=7 Hz, 3′, 5′-H_2), 7.53 (unequal d, 2H J=7 Hz, 2′, 6′-H_2) 7.68 (s, 2H, 3,5-H_2).

IR (CH2Cl2): 1100 vs, 1380 w, 1465 mw, 1503 w, 1560 w, 1628 m, 2880 m, 2930 s, 2955 s, 3075 w.

REFERENCES

[1] Previous part in this series, XXV: A. T. Balaban and T. S. Balaban, *Rev. Roumaine Chim.*, **34**, 41 (1989).

[2] A. T. Balaban, A. Dinculescu, G. N. Dorofeenko, G. W. Fisher, A. V. Koblik, V. V. Mezeheritskii and W. Schroth, "Pyrylium Salts. Syntheses, Reactions and Physical Properties", *Adv. Heterocyclic Chem.*, Suppl. Vol. **2**, A.R. Katritzky (editor), Academic press, New York 1982.

[3] A. T. Balaban and C. D. Nenitzescu, *Org. Synth.* Coll. **5**, 1106 (1973); K. Hafner and H. Kaiser, *ibid.*, 1088 (1973); A. T. Balaban and A. J. Boulton, *ibid.*, **1112**, 1114 (1973); A. Dinculescu and A. T. Balaban, *Org. Prep. Proc. Int.*, **14**, 39 (1982); A. Dinculescu, T. S. Balaban, C. Popescu, D. Teader and A. T. Balaban, *J. Belg. Chem. Soc.*, in press.

[4] T. Kunitake, *J. Macromol. Sci. Chem.*, **A1 3**, 587 (1979); T. Kunitake and S. Shinkai, *Adv. Phys. Org. Chem.*, **17**, 435 (1980); T. Kunitake in "Modern Trends of Colloid Science in Chemistry and Biology", Eicke (editor), Birkhaser Verlag, Basel, 1985.

[5] T. Kunitake, Y. Okahata, M. Shimomura, S. Yasunami and K. Takarabe, *J. Am. Chem. Soc.*, **103**, 5401 (1981).

[6] T. Kunitake and Y. Okahata, *J. Am. Chem. Soc.*, **99**, 3860 (1977).

[7] T. Kunitake, N. Kimizuka, N. Higashi and N. Nakashima, *J. Am. Chem. Soc.*, **106**, 1978 (1984); T. Kunitake and N. Higashi, *J. Am. Chem. Soc.*, **107**, 692 (1985).

[8] H. G. Rajoharisson and C. Roussel, *Nouv. J. Chim.*, **9**, 68 (1985).

[9] A. T. Balaban, E. Gard, A. Vasilescu and A. Barabas, *J. Labelled Comp.*, **1**, 166 (1965); E. Gard, I. I. Stanoiu, F. Chiraleu and A. T. Balaban, *Rev. Roumaine Chim.*, **13**, 257 (1973).

[10] T. S. Balaban, C. Uncuta, M. D. Gheorghiu and A. T. Balaban, *Tetrahedron Lett.*, **26**, 4669 (1985).

[11] A. T. Balaban, A. Dinculescu, H. N. Koutrakis and F. Chiraleu, *Tetrahedron Lett.*, 437 (1979); A. T. Balaban, A. Dinculescu, F. Iordache, F. Chiraleu and D. Patrascoiu, *Chem. Scripta*, **18**, 230 (1981).

[12] S. R. Salman, A. H. Hassan and M.A.R. Khayat, *Bull. Chem. Soc. Jpn.*, **61**, 2271 (1988).

Revue Roumaine de Chimie, **36**, *1–3*, 235–243 (1991)

ELECTRONIC SPECTRAL ANALYSIS OF BENZO[b] PYRIDO[3,2-F] THIEPIN, 8-CHLOROBENZO[b] PYRIDO [3,2-F]THIEPIN AND 8-CHLOROBENZO[b]PYRIDO[3,2-F] THIEPIN-6(5H)-ONE

A. ALKOURASHY and A.S. El-SHAHAWY*
Chemistry Department, Faculty of Education-Domiat, Mansoura, Univ., Domiat, Egypt
Chemistry Department, Faculty of Sciences, Assiut Univ., Assiut, Egypt

Received June 18, 1988

The electronic absorption spectra of thiepin compounds have been fully analyzed using the Gaussian line shape for energy scale. The resolution of UV spectra of these compounds to their individual components have a good coincidence with the calculated transition energies via SCF-CI calculations. Comparative electronic studies containing ionization potentials, electron affinities and charge densities have been done via SCF-method.

INTRODUCTION

The overlap of broad absorption bands prevents a simple and unique solution for the band parameter.[1,2] The resolution of the electronic absorption spectra has been performed by computer method using the Gaussian band shape function on the original data without previous indication of band parameters.

The electronic transition energies were calculated by the SCF-CI method.[4,4] The molecular orbital calculations progressed from simple HMO theory, then the SCF-MO method using the PPP approximations[5,6] together with that of Nishimoto and Forster.[7] Then, in a final step, configuration interaction calculations[7,8] were carried out between the ground configuration Φ_0 and the eight excited configuration $^1\Phi_1$, $^1\Phi_2$, $^1\Phi_3$, $^1\Phi_4$, $^3\Phi_5$, $^3\Phi_6$, $^3\Phi_6$ and $^3\Phi_8$. These configuration eigefunctions include the transitions between the highest two occupied molecular orbitals, ψ_{m-1} and ψ_m, and the lowest two vacant molecular orbitals, ψ_{m+1} and ψ_{m+2}.

EXPERIMENTAL

1. Chemicals

Benzo [b]pyrido[3,2-f] Thiepin, 8-chlorobenzo[b]pyrido[3,2-f]thiepin and 8-chlorobenzo[b]pyrido[3,2-f]thiepin-6 (5H)-one were prepared according to the methods cited in the literature.[10,11] Other chemicals used were of analytical grade.

---

* To whom all correspondences are directed: Dr. Anwar El-Shahawy, P.O. Box, 107 Assiut, Egypt.

2. Apparatus

A Varian 2300 spectrophotometer provided with coupled thermostat table accessory was used throughout this work. Stoppered far U.V. cells of path-lengths 0.5 and 1.00 cm were used. Corning pH-meter 1.9. All measurements were made at 23°C.

The Gaussian analysis of the electronic absorption spectra of thiepin compounds was carried out over a range of 10–430 nm. Such analysis was performed using the program UV-STRIP.[2]

RESULTS AND DISCUSSION

The purpose of spectral analysis

The spectra of such compounds, which are completely insoluble in the solvents recommended for work in UV-visible region, are complicated and highly overlapped. Then, the comparison of the theoretical results with the experimental data is not good enough since the ground of comparison is not clear for most cases. The resolution of a spectrum to its individual components might make the comparison easily and effective.

Computation of the spectral data

In order to extract the individual band parameters a curve analysis has been adopted due to the highly overlapped bands.[1'2] The absorption spectra of thiepin compounds are fully analyzed, using the Gaussian line shape, for energy scale.

The resolution of the experimental absorption spectrum into its compounds is used to determine the appropriate values for some spectroscopic parameter as indicated in tables 1, 2 and 3.

Through the analysis treatment the component bands were simply stripped from the experimental absorption spectrum. The stripping procedure was followed by both full refinement and least-squares fitting techniques to achieve the best possible fit of the analyzed Gaussian bands onto the experimental spectrum.

Electronic transition energies

It is obvious that these compounds have the Cs point gro up symmetry.

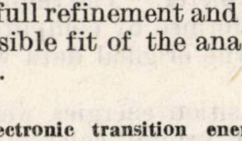

Benzo [b]pyrido [3,2-f]thiepin (compou nd

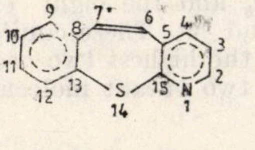

8-Chlorobenzo [b]pyrido [3,2-f]thiepin (compou nd II)

Table 1

Numerical values of some spectroscopic parameters of benzo[b]pyrido[3,2-f] thiepin in different solutions.
"The computation has been achieved for the transitions resulted by applying the full spectral anlaysis technique"

BAND	Medium	Without analysis		With full spectral analysis							
		Band maxima, nm	E_{max}, $(\times 10^{-3})$	Band position, cm^1 $(\times 10^{-3})$	E_{max}, $(\times 10^{-3})$	Area/10^6	Dipole strength, $(\times 10^{+17})$	Oscillator strength, f $(\times 10^{+2})$	Einstein's coefficients $(\times 10^{-8})$		Life time $(\times 10^{10})$
									B_{1j}	A_{1j}	
1	0.1 MHcl : Methanol (1 :1)	222 S	20.000	47.1982	24.8384	145.2112	12.2449	62.7063	17.7552	9.3220	10.7283
2		252	17.984	39.8316	17.3699	78.3383	7.8275	33.8285	11.3499	3.5814	27.9223
3		302	6.545	33.0873	6.4384	44.0784	5.3020	19.0340	7.6879	1.3905	71.9183
4		340 S	4.084	42.5480	4.5865	8.0543	0.7534	3.4779	1.0924	4.2013	238.0194
5				43.9147	4.3891	7.4432	0.6746	3.2142	0.9781	4.1361	241.7716
6				44.9765	2.4783	3.3603	0.2973	1.4509	0.4311	1.9586	510.5805
7				29.3484	1.5187	2.9932	0.4059	1.2925	0.58854	0.07428	1346.184
8				30.5870	0.2305	0.1779	0.02315	0.07682	0.03356	0.004796	20852.07
1	Phosphate buffer and methanol (1 :1) PH = 6.84	218 S	23.690	47.6900	25.0619	220.849	18.4312	95.3691	25.7252	14.4733	6.9093
2		228 S	15.573	38.2311	13.9789	37.926	3.9482	16.3775	5.7249	1.5973	62.6051
3		240 S	14.005	40.7773	10.3663	39.705	3.8753	17.1457	5.6192	1.9024	52.5650
4		260	17.801	33.9843	6.6008	32.169	3.7674	13.8915	5.4527	1.0706	93.4081
5		295	6.806	45.3983	2.3823	3.489	0.3059	1.5066	0.4435	0.2072	482.627
6		340 S	0.949								
1	0.1 NaOH : Methanol (1 : 1)	225 S	17.000	45.9249	19.3746	98.9366	8.5742	42.7237	12.433	6.013	16.6313
2		240 S	14.348	38.1024	12.8636	35.4622	3.7042	15.3136	5.371	1.484	67.4076
3		260	17.540	40.8738	13.1884	60.1782	5.8597	25.9867	8.497	2.897	34.5183
4		295	6.598	33.9560	6.6431	26.0015	3.0476	11.2282	4.419	0.864	115.757
5		340 S	0.947	29.8055	0.8882	3.6256	0.4841	1.5656	0.702	0.0928	1077.470

Table 2

Numerical values of some spectroscopic parameters of 8-Chlorobenzo (b) pyrido[3,2-f]thiepin in different solutions, computed after applying the full spectral analysis techniques

	Band	Medium	Without analysis		With full spectral analysis							
			Band maxima, nm	E_{max}, ($\times 10^{-3}$)	Band position, cm^{-1} ($\times 10^{-3}$)	E_{max}, ($\times 10^{-3}$)	Area/10^6	Dipole strength D($\times 10^{17}$)	Oscillator strength, f($\times 10^2$)	Einstein's coefficients ($\times 10^{-8}$) B_{ij}	Einstein's coefficients ($\times 10^{-8}$) A_{ij}	Life time ($\times 10^{10}$)
PH = z.84	1	0.1 MHCl :	218 S	27.757	47.042	30.065	212.513	17.980	91.769	26.070	13.551	7.3793
	2	methanol	240 S	19.626	44.509	0.638	0.813	0.0727	0.3511	0.1054	0.0464	2154.344
	3	(1 : 1)	253	22.617	41.888	4.316	10.982	1.0434	4.742	1.513	0.5552	180.104
	4		302.5	6.235	39.390	21.4096	102.618	10.369	44.313	15.034	4.588	21.7965
	5		337.5 S	3.289	33.2696	5.8688	26.155	3.129	11.295	4.537	0.8342	119.874
	6		355.0 S	1.251	30.012	2.4404	8.816	1.169	3.807	1.695	0.2288	437.040
	1	Phosphate	220 S	28.349	47.349	24.7713	169.815	14.1346	72.6138	20.4951	10.8629	9.2057
	2	buffer 8_c	261	22.118	45.064	8.9079	43.826	3.8706	18.9252	5.6124	2.5645	38.9935
	3	methanol	297	5.729	40.302	16.8397	69.697	6.8829	30.0771	9.9802	3.2620	30.6560
	4		340 S	0.629	37.850	15.3341	41.364	4.3495	17.8624	6.3068	1.7076	58.5625
	5				33.836	5.6930	24.941	2.9337	10.7704	4.2539	0.8228	121.5334
	1	0.1 Naoh(M)	227.8 S	19.231	45.2408	19.4809	64.7422	5.6956	27.9576	8.2586	3.8183	26.1897
	2	CH_3OH	261.0	22.119	39.4383	21.0367	168.4188	16.9963	72.7281	24.645	7.5483	13.2480
	3	(1 :1)	296.0	5.612	33.520	2.001	5.421	0.6437	2.341	0.9334	0.1755	569.726

Table 3

Numerical values of some spectroscopic parameters of 8-chlorobenzo[b]pyrido[-3,2-f]thiepin-6 (5H)-one, in different solutions. By applying the full spectral analysis technique

	Band	Medium	Without analysis		With full spectral analysis							
			Band maxima, nm	E_{max}, $(\times 10^{-3})$	Band position, cm^{-1} $(\times 10^{-3})$	E_{max}, $(\times 10^{-3})$	Area/10^6	Dipole strength, $(\times 10^{17})$	Oscillator strength, f $(\times 10^{+2})$	Einstein's coefficients $(\times 10^{-8})$		Life time, $(\times 10^{+8})$
										B_{ij}	A_{ij}	
PH = 6.94	1	0.1 Hcl :	236	21500	42.322	21.083	130.835	12.304	56.4984	17.841	6.753	0.148
	2	methanol			47.903	18.283	69.294	5.757	29.9231	8.348	4.582	0.218
	3	(1 : 1)	260 S	12545	38.031	6.303	19.100	1.999	8.2479	2.898	0.796	1.256
	4				29.979	4.460	17.330	2.301	7.4835	3.336	0.449	2.228
	5		285 S	6020	35.472	5.311	17.062	1.914	7.3678	2.776	0.619	1.617
	6				45.323	3.488	1.385	0.824	4.0527	1.195	0.556	1.800
	7		356	2975	32.704	2.177	5.679	0.691	2.4523	1.002	0.175	5.714
	8				28.403	0.872	1.826	0.256	0.7886	0.371	0.0425	23.556
		Phosphate	221 S	17850	41.307	19.969	70.324	6.776	30.368	9.825	3.458	0.289
		buffer and	241	22550	47.634	17.787	98.597	8.238	42.577	11.945	6.446	0.155
		Methanol	265 S	9825	38.490	6.583	17.036	1.762	7.357	2.554	0.727	1.375
		(1 : 1)	278 S	7450	43.871	8.242	30.554	2.772	13.194	4.019	1.695	0.590
			340	4295	36.095	7.105	28.781	3.174	12.429	4.602	1.081	0.926
					29.673	4.335	17.712	2.376	7.648	3.445	0.449	2.225
		0.1 M NaOH :	238	16180	47.498	18.624	345.969	28.900	148.938	41.906	22.421	0.0446
		meethyl	264	10250	28.721	8.347	42.433	5.885	18.338	8.533	1.009	0.9907
		al. (1 : 1)	287	10400	34.761	5.775	26.980	3.094	11.668	4.486	0.941	1.0629
			333 S	8250	41.423	2.754	5.336	0.512	2.301	0.742	0.264	3.7955
			345	9215								
			395 8	2600								

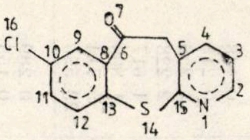

8-Chlorobenzo[b]pyrido[3,2-f]thiepin-6(5H)-one (compound III)

From the self consistent eigenvectors of these compounds, the charge densities are given below:

Table 4

Charge densities

Atom	Comp. I	Comp. II	Comp. III
1	−0.0571035	−0.0571037	−0.0573848
2	+0.0207087	+0.0207094	+0.0210904
3	−0.0042817	−0.0042823	−0.0045255
4	+0.0128818	+0.01288	+0.0136578
5	−0.0050237	−0.0050235	−0.0056737
6	−0.0003521	−0.0003507	+0.1576951
7	−0.0005462	−0.000547	−0.1847556
8	−0.003873	−0.003865	−0.011363
9	+0.0000052	−0.0001566	+0.0118848
10	−0.0029865	−0.00280089	−0.0034617
11	+0.0002905	+0.0001369	+0.0102648
12	−0.0044751	−0.0044663	−0.0050167
13	+0.0054265	+0.0053144	+0.0174228
14	+0.0124308	+0.0124292	+0.013989
15	+0.0269003	+0.0269005	+0.025938
16		+0.0002392	+0.0002386

From the previous data in table 4, with respect to compound I, it is clear that the charge densities on the pyridine nucleus are higher than those on the benzene nucleus, and this can be attributed to the presence of the fused nitrogen atom in the pyridine nucleus.

The introduction of the chlorine atom to the compound I affects the charge density on the carbon atom 9 from a positive charge to a negative charge. Hence, the carbon atom at position 9 is sensitive to the introduction of an electrophilic substituent in position 10.

The introduction of oxygen atom in compound II, to form a carbonyl group, increases the negative charge on the carbon atom at position 8 and the positive charge on the carbon atom at position 9 in the benzene nucleus.

From a general point of view, the carbon atom at position 3 in these compounds is sensitive to the electrophilic reactions and especially in compound III, since it has the largest negative charge with respect to the other compounds, I and II.

The sulfur atom in compound III has a higher positive charge, since it contributes highly in the π-cloud of compound III than its contribution in the other compounds, I and II.

Table 5

The SCF Eigenfunctions of the two HOMO's of compound I

Atom	ψ_7	ψ_8
1	−0.17609119	0.078381034
2	−0.0051934976	0.32537505
3	−0.18171304	0.15568722
4	−0.17284826	−0.21146834
5	0.012722672	−0.31467594
6	0.047426037	0.36547061
7	0.028944071	0.3642002
8	−0.049231798	0.31844676
9	−0.48836845	−0.22344548
10	−0.4301908	0.15052447
11	0.067859617	0.33403651
12	0.49793227	0.090243584
13	0.42010977	−0.26586249
14	−0.15592742	0.11477625
15	0.15323583	−0.27608703

The contribution of the fused nitrogen atom of pyridine nucleus in the two HOMO's is faint. The MOψ_7 is mainly spreaded over the benzene nucleus. But, the MOψ_8 is spreaded over the molecule, compound I, as a whole. The contribution of the sulfur atom in the MOψ_8 is higher than that in the MOψ_7.

Table 6

The SCF-Eigenfunctions of the two LUMO's of compound I

Atom	ψ_9	ψ_{10}
1	0.13948868	0.5212844
2	−0.35045769	−0.10294443
3	0.11631584	−0.4218208
4	0.26318298	0.51209346
5	−0.31509904	−0.0779292
6	−0.36452403	0.048044414
7	0.36694146	0.0049191589
8	0.30790817	−0.099023739
9	−0.24343015	−0.021019438
10	−0.12335887	0.11680592
11	0.3359966	−0.09334406
12	−0.12255135	−0.025287298
13	−0.24342876	0.11682878
14	0.0013675939	0.031215552
15	0.22729139	−0.47034032

These two LUMO's of compound I are mainly spreaded over the pyridine nucleus and the phenyl moiety, but the contribution of the sulfur atom in these two LUMO's is weaker than its contribution in the two

HOMO's. The contribution of the fused nitrogen atom in the MOψ_{10} is higher than its contribution in any molecular orbitals. The MOψ_{10} can be assumed that it is constructed mainly from the pyridine nucleus.

The ionization potentials, and the electron affinities have been calculated according to the following Pople equation.[12]

$$E_m = \sum_u \sum_v C_{mu} C_{mv} F_{uv}$$

Table 7

Ionization potentials and electron affinities.

Compound	E_m	E_{m+1}
I	9.118	2.019
II	9.118	2.018
III	10.071	1.857

From the previous data, it is clear that the introduction of a chlorine atom to the parent compound does not perturb the ionization potential and the electron affinity greatly. But the introduction of a carbonyl group to the compound II, increases the ionization potential and decreases the electron affinity of compound III.

The calculated transition energies of these compounds by SCF-CI method were compared with the transition energies via the Gaussian band shape as a function of the original data, as shown in tables 1, 2 and 3.

Compound I

Assignment	SCF—CI ΔE cm^{-1} (nm)	0.1 MHU + methanol Gaussian ΔE cm^{-1} (nm)
$\psi_8 \rightarrow \psi_9'$	31746.031 (315)	30587.0 (327)
$\psi_8 \rightarrow \psi_9^3$	35087.719 (285)	330878.0 Cm^{-1} (302)
$\psi_8 \rightarrow \psi_1'$	49019.607 (204)	47198.2 cm^{-1} (211)

N.B. : $\psi \rightarrow \psi'$ means singlet transition.
$\psi \rightarrow \psi^3$ means triplet transition.

Compound II

Assignment	SCF—CI ΔE cm^{-1} (nm)	(0.1 MHCl + Methanol) Gaussian ΔE cm^{-1} (nm)
$\psi_9 \rightarrow \psi_{10}'$	31259.6 (320)	30012 (333)
$\psi_9 \rightarrow \psi_{10}^3$	34647.3 (289)	33269.6 (300)
$\psi_8 \rightarrow \psi_{10}'$	43956.6 (228)	44509 (225)
$\psi_8 \rightarrow \psi_{10}^3$	46304.1 (216)	47042 (213)

Compound III		
Assignments	SCF—CI ΔE cm^{-1} (nm)	(0.1 MHCl+Methanol) 1 : 1 Gaussian ΔE cm^{-1} (nm)
$\psi_9 \rightarrow \psi'_{10}$	32185.2 (311)	32704 (305)
$\psi_9 \rightarrow \psi^3_{10}$	38156.3 (262)	38031 (263)
$\psi_9 \rightarrow \psi'_{11}$	43432.6 (231)	42322 (236)
$\psi_9 \rightarrow \psi^3_{11}$	43690.2 (229)	45323 (221)

From the previous transition energies data, we have good coincidence between the calculated transition energies by the SCF-CI method with the transition energies which have been obtained by the Gaussian analysis.

REFERENCES

Burny E. Barker and Malcom F. Fox, *Chem. Soc. Rev.*, **9**, 143 (1980).

Abdel-Ghany El-Kourashy and Roger Grinter, *J. Chem. Soc. Faraday Transactions II*, 1050 (1977).

[3] A. S. El-Shahawy, A. A. Harfoush and K. A. Idriss, *Spectrochim. Acta*, **41A**, 1463 (1985).

[4] A. S. El-Shahawy, M. M. Girgis and M. T. Ismail. *Spectrochim. Acta*, **43A**, 1371 (1987).

[5] R. Pariscar and R. C. Parr, *J Chem. Phys.*, **21**, 466, 767 (1953).

[6] J. A. Pople, *Trans. Faraday Soc.*, **49**, 1375 (1953).

[7] K. Nishimoto and L. S. Forster, *Bull. Chem. Soc. Japan*, **41**, 2254 (1968).

[8] Robert L. Flurry, Jr. "Molecuar Orbital Theories of Bonding in Organic Molecule", Marcel Dekker, Inc., New York, 1968.

[9] C. Sandorfy, "Electronic Spectra and Quantum Chemistry", Prentice Hall, Inc. Englwood Cliffs, New Jersey, 1964.

[10] M. Protiva, Z. Sedivy, J. Pomykacek, E. Svateko and J. Holubek, *Collect. Czech. Chem. Commun.*, **46**, 1199, 1981.

[11] V. Bartl, J. Metysova and M. Protiva, *Collect. Czech. Chem. Commun.*, **38**, 1693, 2778 (1973).

[12] J. A. Pople, *Trans. Faraday, Bull. Chem. Soc. Japan*, **41**, 2254 (1968).

Revue Roumaine de Chimie, **36**, *1–3*, **245**–250(1991)

SYNTHESIS AND SOME REACTIONS OF 4-(N-ACETYL-OXINDOLYLIDENE)-2-ARYL-5 (4H) OXAZOLONES

NADIA G. KANDILE, TAHIA M. ABDEL LATIF and WAFAA A. El SAYED

Chemistry and Chemistry & Nutrition Departments, University College for Women, Ain Shams University Heliopolis, Cairo, Egypt

Received June 13, 1988

Condensation of isatin with substituted glycine under Perkin conditions afforded the oxazolone derivatives **1**. The action of hydrazine hydrate, phenylhydrazine, aniline, ethylenediamine as well as alkaline hydrolysis on the oxazolone derivatives **1** were studied. The structures of all compounds were elucidated on the basis of chemical and spectroscopic data.

Glycine derivatives were known to condense with aldehydes and ketones under Perkin conditions to give the corresponding oxazolones[1,2,3].

As a continuation to our earliest work[4] on isatin, the present work aims to clarify the synthetic potentialities of oxazolones from isatin.

Condensation of isatin with acetylglycine and hippuric acid under Perkin conditions afforded 4-(acetyloxindolylidene)2-aryl-5(4H)oxazolones derivatives **1a, b** in fairly good yield. Elemental analysis coupled with the study of IR, UV and ^{1}H-NMR supported structure **1a,b** assigned to the product. Its IR spectra showed bands indicative of carbonyl group and $>C{=}N-$ linkage respectively. UV spectra of **1a,b** in ethanol showed strong absorption at λ_{max} 334–340 nm (Table 2). ^{1}H-NMR spectrum of **1a** in DMSO showed a 9-protons multiplet at τ2.5 (aromatic) and 3-protons singlet at τ7.7 ($CH_3{-}CO$). ^{1}H-NMR spectrum of **1b** in $CDCl_3$ showed a 4-protons multiplet at τ2.5 (aromatic), a 3-protons at τ 7.7(CH_3CO) and a 3-protons singlet at τ7.5 (CH_3).

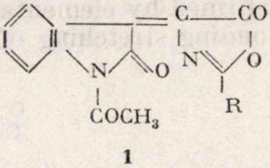

1

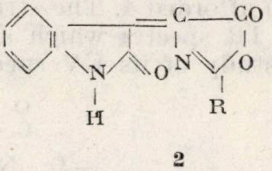

2

b: R = C_6H_5
a: R = CH_3

Hydrolysis of **1** using dilute hydrochloric acid (6N) afforded the corresponding oxindolylidene oxazolones **2**. The structure of **2** was inferred from elemental analysis and IR spectra which showed the corresponding stretching frequencies of ketones and amides. ^{1}H-NMR spectra of **2a,b** in DMSO showed a one proton singlet at τ 3.8 (NH) beside aromatic pro-

Table 1

List of newly synthesized compounds*

Product No.	Nt cry solvent	M.P. [°C]	Yield	Molecular Formula
1a	Acetic acid	235	70	$C_{19}H_{12}N_2O_4$
1b	Acetic acid	250	75	$C_{14}H_{10}N_2O_4$
2a	Methanol	259	80	$C_{17}JH_{10}N_2O_3$
2b	Methanol	170	75	$C_{12}H_8N_2O_3$
3a	Methanol	255	90	$C_{19}H_{14}N_4O_3$
3b	Methanol/H_2O	280	90	$C_{14}H_{12}N_4O_3$
4a	Ethanol-benzene	245	80	$C_{17}H_{12}N_4O_2$
4b	Ethanol/H_2O	270	85	$C_{12}H_{10}N_4O_2$
5a	Ethanol	250–1	90	$C_{25}H_{20}N_4O_4$
5b	Methanol	215–17	90	$C_{20}H_{18}N_4O_4$
5c	Toluene	240	85	$C_{26}H_{21}N_3O_4$
5d	Ethanol-benzene	208	90	$C_{21}N_{19}N_3O_4$
5e	Ethanol	250–1	95	$C_{25}H_{19}N_3O_4$
5f	Ethanol	>300	95	$C_{20}H_{17}N_3O_4$
6a	Ethanol	260	80	$C_{23}H_{16}N_4O_3$
6b	Ethanol	240	80	$C_{18}H_{16}N_4O_3$
6c	Methanol-benzene	253	85	$C_{24}N_{18}N_3O_3$
6d	Methanol	175	85	$C_{19}H_{17}N_3O_3$
6e	Methanol	280	80	$C_{23}H_{17}N_3O_3$
6f	Methanol	>300	80	$C_{18}H_{15}N_3O_3$
7a	Ethanol	179–80	90	$C_{21}H_{17}N_4O_3$
7b	Benzene	200	90	$C_{16}H_{14}N_4O_3$
8	Ethanol	260	80	$C_{19}H_{15}N_4O_2$
9a	Methanol	225–7	70	$C_{17}H_{12}N_2O_4$
9b	Methanol	215	75	$C_{12}H_{10}N_2O_4$

* All compounds gave satisfactory microanalytical data

tons of **2a,b** at τ (2.5 m) and aliphatic protons of CH_3 at τ (7.5 S) in case of **2b**.

Hydrazinolysis of **1a,b** with hydrazine hydrate at room temperature or under reflux gave the corresponding cyclic hydrazide **3a,b** *via* acyl oxygen cleavage of the oxazolone ring followed by cyclization. The structure of **3** was confirmed from elemental analysis and IR spectra which showed the corresponding stretching frequencies of arylketones, amides and lack NH (NH_2) Table 2. Also stability of its ring towards mineral acids and the nonformation of acylazide and benzaldehyde derivatives, excluded the open structure. Treatment of **3** with dilute hydrochloric acid (6N) afforded **4**. The structure of **4** was confirmed by elemental analysis and IR spectra which showed the corresponding stretching of NH and by study of its UV spectra (Table 2).

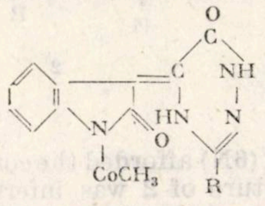

3

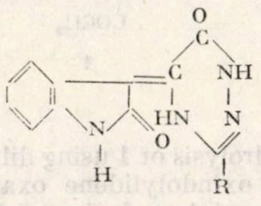

4

a ; R = C_6H_5
b ; R = CH_3

However treatment of **1a,b** with hot phenylhydrazine afforded the open adduct **5 a,b**.

Similarly aminolysis of **1a,b** with benzylamine and aniline in hot dry benzene gave N-(acetyloxindolidene)amide derivatives **5a-d**. The structure **5** was inferred other than elemental analysis, by its IR spectra which showed strong bands characteristic for the stretching frequencies of NH, C=O and C=C respectively (Table 2).

Lactimization of **5a-f** occurred on treatment with boiling (6N) hydrochloric acid to give **6a-f**.

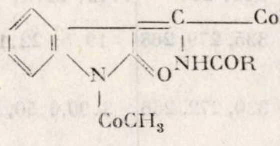

5

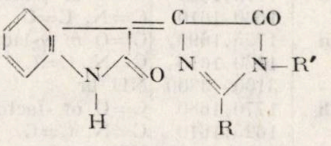

6

a ; $R = C_6H_5$, $R' = NH-C_6H_5$
b ; $R = CH_3$; $R' = NH-C_6H_5$
c ; $R = C_6H_5$, $R' = CH_2-C_6H_5$
d ; $R = CH_3$; $R' = CH_2-C_6H_5$
e ; $R = C_6H_5$, $R' = C_6H_5$
f ; $R = CH_3$, $R' = C_6H_5$

The structure of **6** was inferred from elemental analysis, and its IR spectra which showed the corresponding stretching frequencies of NH, C=O and C=C respectively (Table 2), also the change of its colour from yellow to orange-deep red.

As a point of interest, the interaction of **1a,b** with ethylene-diamine in ethanol and one drop of piperidene as catalyst yielded the product **7**.

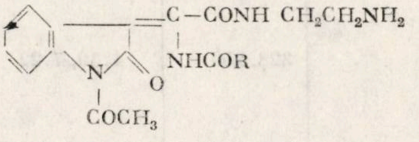

7

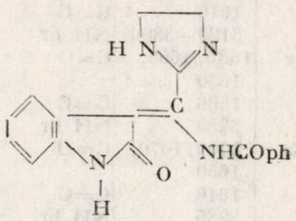

8

a, $R=C_6H_5$
b, $R=CH_3$

The structure of **7** was inferred from elemental analysis, its IR spectra which showed strong absorption bands characteristic of C=O, alicyclic CH_2 and NH (NH_2) respectively (Table 2). Also acid hydrolysis of **7** afforded **8**. The structure of the latter was confirmed by elemental analysis and its IR spectra which showed the expected bands of C=O, C=C and NH respectively (Table 12).

Finally alkaline hydrolysis of **1a,b** with sodium hydroxide afforded **9a,b** as expected.

Table 2

IR, and UV data

Compd No.	cm^{-1}	Attribution	λ_{max} nm	ε_{max} X10^{-3}
1a	1775,1690 1630,1610	C=O of -lactone and amide C=N, C=C	334, 275, 270	17.7,19.90, 20.05
1b	1770,1680 1630,1610	C=O of γ-lactone and amide C=N, C=C	340, 260	7.42, 11.81
2a	1775,1690 1630,1610 3100–3300	C=O of γ-lactone and amide C=N, C=C NH br.	335, 279, 268	19.5, 22.11, 22.47
2b	1770,1680 1625,1610 3100–3300	C=O of -lactone and amide C=N, C=C NH br.	330, 272, 266	3.90,6.50, 14.9
3a	1670 1630,1610 3180–3400	C=O C=C, C=N NHbr.	334, 273, 270	22.7, 26.69, 27.15
3b	1670 1630,1610 3100–3400	C=O C=N, C=C NH br.	350, 269, 246	5.85, 6.03, 6.03
4a	1670,1630 1610 3100–3350	C=O, C=N C=C NH br.	324, 310, 218	9.47, 10.42, 37.50
4b	1660,1630 1610 3100–3300	C=O, C=N C=C NH br.	325, 311, 220	8.77, 8.45, 34.45
5a	1730,1630, 1650 1610 3100–3500	C=O C=C NH br.	340, 270, 230	29.92, 35.64, 27.72
5b	1720, 1680, 1650 1610 3120–3300	C=O C=C NH br.	320	2.26
5c	1685, 1650, 1630 1600 3280	C=O C=C NH br.	334, 274, 270	22.5, 25.9, 27.44
5d	1700, 1670, 1650 1610 3285	C=O C=C NH br.	328, 250	4.39, 7.22
5e	1720, 1680, 1650 1610 3100–3300	C=O C=C NH br.	335, 272	40.37, 44.20
5f	1710, 1690, 1650 1610 3100–3280	C=O C=C NH br.		
6a	1680, 1630, 1610 3150–3400	C=O, C=N, C=C NH br.		
6b	1675, 1650, 1630 1610 3100–3400	C=O, C=N C=C NH br.		

Table 2 (continued)

Compd No.	cm^{-1}	Attribution	λ_{max} nm	ε_{max} X10^{-3}
6e	1680, 1650,	C=O, C=N	334, 274, 268	32.21, 36.95, 36.95
	1630 1610	C=C		
	3020–3320	NH br.		
6d	1690, 1650,	C=O, C=N		
	1630			
	1615	C=C		
	3000–3300	NH br.		
6e	1680, 1650,	C=O, C=N		
	1630 1610	C=C		
	3100–3300	NH br.		
6f	1685, 1650,	C=O C=N		
	1630			
	1610	C=C		
	3100–3300	NH br.		
7a	1670, 1650	C=O	340, 268, 232	1.9, 2.2, 1.7
	1600	C=C		
	3290, 3305	NH (NH_2)		
	2810, 2910	CH_2CH_2		
6b	1665, 1650	C=O		
	1600	C=C		
	3190, 3200	NH (NH_2)		
	2800, 2900	CH_2CH_2		
8	1660, 1650	C=O		
	1630, 1600	C=N, C=C		
	3100–3300	NH br.		
9a	1720, 1685	C=O		
	1610	C=C		
	3010–3320	OH, NH (br)		
9b	1720, 1680	C=O		
	1610	C=C		
	3005–3400	OH, NH (br.).		

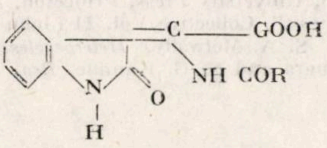

9

a; R=CH_3
b; R=C_6H_5

The structure of **9a,b** was inferred other than elemental analysis, by its IR spectra which showed the stretching frequencies of OH, NH and C=O respectively (Table 2).

EXPERIMENTAL

All melting points are uncorrected. The spectra were carried out using an EM 36 0 L Varian NMR spectrometer at 60 MHZ, the IR spectra were obtained with a Perkin-Elmer 398 spectrometer. UV spectra were carried out with a Perkin-Elmer 555 U.V.-Vis. spectrometer using ethanol as a solvent. Analyses were carried out in the Research Microanalytical Laboratory of Cairo University.

Condensation of glycine derivative with isatin : Formation of **1a,b** : A mixture of glycine derivative (0.01 mole), isatin (1.47 g ; 0.01 mole), freshly fused sodium acetate (0.82 g ; 0.01 mole) and 10 mL of acetic anhydride was heated on a hot plate until a solution was obtained. The reaction mixture was then transferred to a steam bath and heating was continued until crystals separated. The solid product was filtered off, washed with petroleum-ether (b.p. 40—60°) and finally crystallized from acetic acid.

Action of dilute hydrochloric acid on **1a,b**, **5a-d**, and **7** : The oxazolone (**1,a,b**) or **5a-d**, **7**, (lg) was dissolved in 30 mL acetic acid when a clear solution was obtained ; 10 mL of 6N hydrochloric acid were added and the reaction mixture was tefluxed for one hour. The solid product formed after cooling and filtration was crystallized from methanol-benzene to give **2a,b**, **6a-d** and **8**.

Action of hydrazine hydrate on **1a,b** :

Method A : a solution of **1** (0.01 mole) and hydrazine hydrate (0.05 mole), in 30 mL ethanol was left at room temperature for 24 hrs, then most of the solvent was evaporated and the solid separated was crystallized from methanol to give **3a,b**

Method B : The reaction was carried out as described in the above experiment, and the reaction mixture was refluxed for one hr ; after cooling and concentration, the solid product was rfiltered off and crystallized from methanol to give **3a,b**.

Aminolysis of **1a,b** : *Formation of* **5a-f**.

To a solution of **1**(0.01 mole) in 50 mL ethanol, phenylhydrazine, benzylamine, aniline or ethylenediamine (0.05 mole) was added ; the reaction mixture was refluxed for 2 hrs, then most of the solvent evaporated, the solid separated was crystallized from the suitable solvent.

Hydrolysis of **1a**, *with* 5% *sodium hydroxide* :

A mixture of the oxazolone (1g) and 20 mL of 5% sodium hydroxide was refluxed till clear solution. The solution after cooling was rendered acidic by dilute hydrochloric acid then made just alkaline with potassium hydroxide solution and finally acidic with acetic acid. The solid product was crystallized from methanol to give **ga,b**.

REFERENCES

[1] W. Thompson, R. R. Battain, H. M. Randall and R. S. Rasmussen in "The Chemistry of Penicillin", Princeton, University Press, Princeton, N.J., 1949, p. 387.

[2] A. H. Blatt, "Organic Synthesis", Collective Vol. II (John Wiley, New York), 1961, 55.

[3] A. Harb, S. E. Zayed and S. A. Metwally, *Heterocycles*, **24**, 1873, (1986).

[4] A. M. El-Abbady, M. A. Omara and N. G. Kandile, *Rev. Roumaine Chim.*, **19**, 79 (1974).

Revue Roumaine de Chimie, **36**, *1–3*, 251–255 (1991)

CARBONIC ANHYDRASE INHIBITORS. IV[1]

BIFUNCTIONAL DERIVATIVES OF 5-AMINO-1,3,4-THIADIAZOLE-2-SULFONAMIDE*

CLAUDIU SUPURAN[a],**, GHEORGHE MANOLE[b], ANA SCHIKETANZ[c], MIRCEA D. GHEORGHIU, and IOAN PUŞCAŞ[d]

[a] Department of Organic Chemistry, University of Bucharest, Bd. Republicii 13, Bucharest 1, Romania

[b] Builder's Clinical Hospital, Bucharest, Romania

[c] Department of Organic Chemistry, Polytechnic Institute – TCH, 77206 Bucharest 16, Romania

[d] Romanian Academy, Center for Research and Med. Assistance, Simleu Silvaniei

Received July 25, 1990

Bis-amides of type **5** were obtained by reaction of 5-amino-1,3,4-thiadiazole-2-sulfonamide (**4**) with acyl dichlorides. The nature of the group that spatiates the two thiadiazole rings was as follows: aliphatic, aromatic, heterocyclic and macrocyclic. The new compounds were characterized and tested for inhibitory action on purified enzyme. Inhibitory power was greater for compounds derived from heterocyclic/aromatic acids.

1. INTRODUCTION

Mono- and bicyclic aromatic/heterocyclic sulfonamides are strong carbonic anhydrase (CA) inhibitors.[2–4] The most important structural features that must be present in the molecule of such an inhibitor are: (i) the unsubstituted sulfonamido group(s), and (ii) an aromatic or heterocyclic moiety on which the SO_2NH_2 group is attached, which do not possess other bulky groups as substituents, in order to permit the easy access of the inhibitor within the active site of the enzyme.[5]

Bis-sulfonamides were tested as CA inhibitors from the very beginning of research in this class of substances. One of the first compounds to be tested was 1,3,4-thiadiazole-2,5-disulfonamide (**1a**)[3], which is a stronger inhibitor than the classical CA inhibitor in clinical use for the last 30 years, acetazolamide (5-acetylamino-1,3,4-thiadiazole-2-sulfonamide, **1b**) (Fig. 1).

Other compounds of this type include: thiophene-2,4-disulfonamide and some of its chloro- and methyl-substituted derivatives,[6,7] as well as bis-sulfonamides derived of diphenyl,[8] diphenyl ether,[8] diphenyl sul-

---

* Presented in part at the International Workshop-Carbonic Anhydrase, Spoleto, Italy, 4–7 March, 1990.

** Correspondence author.

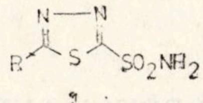

1

Fig. 1. — **1a** : R = SO_2NH_2
1b : R = CH_3CONH.

phide[8] and di-aryl/hetaryl-methane.[7,8] The structure of these compounds is presented in Fig. 2. An important observation for them was that the presence of two sulfonamido groups greatly reduces the toxicity of the drug.[7] Compounds of type **1**—**3** were prepared in different attempts to find effective diuretics.[5] On the other hand, dichlorophenamide (4,5-dichloro-1,3-benzene-disulfonamide), one of the first saluretics, is also known to possess a weak inhibitory action on CA[9] ; the thiazide diuretics are weak inhibitors just because the second structural feature presented above is not respected — the 1,3-disulfamoyl groups are too bulky when attached on the same cycle within the molecule. Even so, mention should be made that this line of sulfonamide research led to the design of two important classes of biologically active compounds : the thiazide saluretics and the high-ceiling diuretics.[5,9]

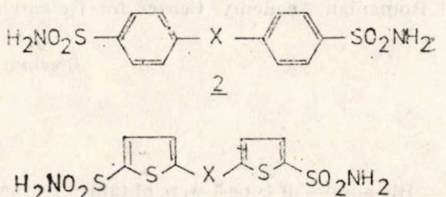

2

3

Fig. 2. — Aromatic and heterocyclic bissulfonamides :
2 : X = 0, S, CH_2 or lacking (diphenyl derivative) **3** : X = CH_2.

Recently, this class of compounds started to present an ever-increasing interest : it was proved that substituted benzene-disulfonamides possessing CA inhibitory action, are selective cerebrovasodilators and improve the function of the aging brain.[10]

The new compounds reported in this paper were designed in order to extend the study of CA inhibition by bis-sulfonamides. In this case, like for compounds **2** and **3**, two sulfonamide groups are attached on two heterocyclic rings, but these are spatiated by means of the fragment "A", whose nature may be aliphatic, aromatic, heterocyclic, as well as macrocyclic. These bis-amides were prepared by reaction of 5-amino-1,3,4-thiadiazole-2-sulfonamide (**4**) with acyl dichlorides, in the presence of pyridine, using well-known conditions for acylation of amines (Scheme 1). Mention must be made that in the case of the following acids : oxalic, malonic, succinic and fumaric, reaction of the corresponding acyl dichloride with amine **4** leads to the formation of a black or violet-black reaction-mixture, from which the desired bis-amide could not be isolated.

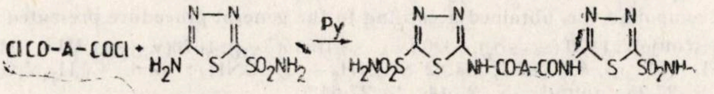

4

5

No. 5	A	Yield (%)
a	$-(CH_2)_4-$	71
b	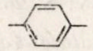	82
c	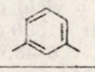	79
d	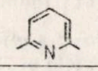	73
e	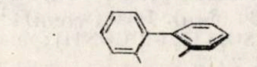	64
f	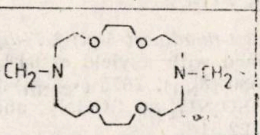	56

Scheme 1

The newly synthesized compounds were characterized by means of elemental chemical analysis, IR and ^{1}H-NMR spectroscopy, and were assayed for inhibitory action using purified bovine erythrocyte enzyme.

2. EXPERIMENTAL

The melting points were determined on a heating-plate microscope and are not corrected. IR spectra were taken in KBr pellets or in nujol suspension, with a Specord IR-71 spectrophotometer. ^{1}H—NMR spectra were recorded at 60 MHz on a Varian EM-360 L spectrometer. Chemical shifts are reported as parts per million relative to Me_4Si as internal standard. Because in many cases (compounds **5b-e**) the protons from the sulfonamido and amido groups appeared in the same region of the ^{1}H—NMR spectra as the other protons of the given compound, the first were assigned after deuteration with D_2O in the tube of the apparatus, when that region of the spectrum simplified. All compounds were analyzed and values obtained were $\pm 0.4\,\%$ of the theoretical value.

5-Amino-1,3,4-thiadiazole-2-sulfonamide was prepared from acetatolamide by literature procedures.[11] Carboxylic acids, pyridine, thionyl chloride and 1,10-diaza-18-crown-6 were from Merck. Diacyl chlorides were prepared from the corresponding acids and $SOCl_2$ · N,N′-Bis (carboxymethyl)diaza-18-crown-6 was prepared from 1,10-diaza-18-crown-6 by literature procedures.[12] Bovine erythrocyte CA was from Boehringer Mannheim.

General procedure for preparation of bis-amides **5**

3.60 g (20 mM) of amine **4** were suspended in 50 mL dry acetonitrile together with 20 mM of anhydrous pyridine. The acyl dichloride (10 mM) dissolved in 10 mL MeCN was dropped under good stirring, for a period of 30 min in the reaction mixture, maintaining the temperature under 35 C. Stirring was continued for 3—4 hours. The bis-amides **5** precipitated from the reaction mixture, were filtered off and purified as sodium salts, by recrystallization from acqueous methanol. The free sulfonamides **5** were reprecipitated thereafter by addition of acqueous hydrochloric acid to concentrated solutions of the sodium salts. Attempts to recrystallize directly the sulfonamides **5** were unsuccessful due to the poor solubility of these compounds in the usua. solvents. Yields were generally good (the table in Scheme 1).

N,N′-Bis(2-sulfonamido-1,3,4-thiadiazol-5-yl)adipamide **(5a)**

The compound was obtained according to the general procedure presented above (71%); mp284°C; IR(nujol); 1170 (ν_{s-SO_2}), 1300 (ν_{as-SO_2})1545(δ_{NH}), 1670(ν_{CONH}); ^{1}H–NMR(DMSO-d_6): 1.7 (m, 8H, $(CH_2)_4$), 8.1 (br s, 6H, 2 SO_2NH_2 + 2 CONH); anal. $C_{10}H_{14}N_8O_6S_4$ requires: N, 23.82; S, 27.25; found: N, 23.14; S, 27.64%.

N,N′-Bis(2-sulfonamido-1,3,4-thiadiazol-5yl)terephthalamide **(5b)**

The compound was obtained according to the general procedure. The yield was 82%; mp 297°C; IR (KBr); 800 (γ_{CH}), 1150 (ν_{s-SO_2}), 1300 (ν_{as-SO_2}), 1520 (δ_{NH}), 1660 (ν_{CONH}), 3070 (δ_{NH}): ^{1}H–NMR (DMSO-d_6): 8.0–8.6 (m, 4H, ArH), 8.4–8.6 (6H, 2 SO_2NH_2+2 CONH); anal; $C_{12}H_{10}N_8O_6S_4$ requires: N, 22.85; S, 26.14%; found: N, 22.07; S, 25.86%.

N,N′-Bis (2-sulfonamido-1,3,4,-thiadiazol-5-yl)isophthalamide **(5c)**

The compound was obtained with a yield of 79% according to the general procedure; mp 311°C; IR(nujol): 710 (γ_{CH}1170 (ν_{s-SO_2}), 1300 (ν_{as-SO_2}), 1540 (δ_{NH}), 1680 (ν_{CONH}); ^{1}H-NMR (DMSO-d_6): 7.5–8.7 (m, 4H, ArH), 8.6–8.9 (br s, 6H, 2 SO_2NH_2+2CONH); anal $C_{12}H_{10}N_8O_6S_4$ requires: N, 22.85; S, 26.14; found: N, 22.79; S, 26.74%.

N,N′-Bis(2-sulfonamido-1,3,4-thiadiazol-5-yl)-2,5-pyridine-dicarboxamide **(5d)**

The compound was obtained with a yield of 73%; mp 309°C; IR (nujol): 670, 750 (γ_{CH}), 1180 (ν_{s-SO_2}), 1300 (ν_{as-SO_2}), 1530 (δ_{NH}), 1690 (ν_{CONH}); ^{1}H–NMR (DMSO-d_6): 7.7–8.5 (m, 3H, ArH), 8.5–9.1 (br s, 6H, 2 SO_2NH_2+2 CONH); anal. $C_{11}H_9N_9O_6S_4$ requires: S, 26.09; N, 25.65%; found: S, 26.47; N, 25.87%.

N,N′-Bis(2-sulfonamido-1,3,4-thiadiazol-5-yl)-2,2′-diphenamide **(5e)**

The compound was obtained with a yield of 64%; mp 292°C; IR (nujol): 730 (γ_{CH}), 1180 (ν_{s-SO_2}), 1340 (ν_{as-SO_2}), 1530 (δ_{NH}), 1675 (ν_{CONH}); ^{1}H–NMR (DMSO-d_6): 7.5–8.7 (m, 8H,ArH), 8.6–9.1 (br s, 6H, 2 SO_2NH_2+2 COHN); anal. $C_{18}H_{14}N_8O_6S_6$ requirs: N, 19,78; S, 22.63; found: N, 20.11; S, 22.51%.

N,N,′-Bis(2-sulfonamido-1,3,4-thiadiazole-5-carboxamido-methyl)-1,10-diaza-4,7,13,16-tetraoxa-cyclooctadecan **(5f)**

The compound was obtained with a yield of 58%; mp276°C; IR (nujol): 1115 ($\nu_{AS-C-OC}$), 1160 (ν_{as-SO_2}), 1310 (ν_{s-SO_2}), 1560 (δ_{NH}) 1670 (ν_{CONH}); ^{1}H–NMR (DMSO-d_6): 2.45 (s, 4H, 2 CH_2CO), 2.80 (m, 8H, 4 N–CH_2), 3.60 (m, 16H, 8 O–CH_2), 8.3–8.5 (br s, 6H, 2SO_2NH_2+ 2 CONH); anal. $C_{20}H_{34}N_{10}O_{10}S_4$ requires: N, 19.93; S, 18,24; found: N, 20.05; S, 18.35%.

3. RESULTS AND DISCUSSION

CA inhibition with the new compounds was studied using the method of Maren et al. [13] The substrate – enzyme – inhibitor (SEI) technique was used and the assay was carried out at 4°C. I_{50} values for the new inhibitors were obtained from semilog plots of specific activity vs. concentration of inhibitor. These values represent the concentration of compound that inhibits 50% the CA catalyzed hydration of CO_2 and are presented in Table 1. All these compounds possess inhibitory activity; the most active are **5b-d**, which have I_{50} values comparable with acetazolamide ($2 \cdot 10^{-8}$ M, for the human enzyme, in the same conditions[14]).

Compounds **5e** and **f** are weaker inhibitors, probably due to the very bulky groups that are found in these molecules and which may cause a strong steric hindrance and the impossibility of access to the active site of the enzyme.

Qualitative structure-activity correlations for these and other related compounds are made elsewhere.[15]

Table 1

Compound	**5a**	**5b**	**5c**	**5d**	**5e**	**5f**	**1b**
$10^7 \cdot I_{50}$(M)	1.7	0.95	0.6	0.8	180	460	0.2

ACKNOWLEDGMENT. Thanks are addressed to dr. Iosif Schiketanz for providing some of the carboxylic acids used in this work, to Mr. Vasile Dinoiu for recording the IR spectra and to Ms. Olimpia Nagy for the help with the enzymatic determinations.

REFERENCES

[1] Part III of this series : I. Pușcaș, C. Supuran and G. Manole, *Rev. Roumaine Chim.*, **35**, 683 (1990).

[2] H. Davenport, *J. Biol. Chem.*, **158**, 567 (1945).

[3] R. O. Roblin and J. W. Clapp, *J. Amer. Chem. Soc.*, **72**, 4890 (1950).

[4] W. H. Miller, A. M. Dessert and R. O. Roblin, *J. Amer. Chem. Soc.*, **72**, 4893 (1950).

[5] T. H. Maren, *Ann. Rev. Pharm. Toxicol.*, **16**, 309 (1976).

[6] A. Buzas and J. Teste, *Bull. Soc. Chim.*, **1960**, 793.

[7] A. Buzas, J. Frossard and J. Teste, *Ann. Pharm. Fr.*, **19**, 449 (1961).

[8] Y. M. Beasley, B. G. Overell, V. Petrow and O. Stephenson, *J. Pharm. Pharmacol.*, **10**, 696 (1958).

[9] K. H. Baeyer and J. E. Baer, *Pharmacol. Rev.*, **13**, 517 (1961).

[10] P. E. Cross, B. Gadsby, G. F. Holland and W. M. McLamore, *J. Med. Chem.*, **21**, 9, 845 (1978).

[11] V. Petrow, *J. Chem. Soc.*, **1958**, 1508.

[12] H. Tsukuba, H. Adachi and S. Morosawa, *J. Chem. Soc. Perkin Trans.*, *I*, **1989**, 89.

[13] T. H. Maren, V. I. Ash and E. M. Bailey, *Bull. Johns Hopkins Hosp.*, **95**, 244 (1954).

[14] T. H. Maren, *Physiol. Rev.*, **47**, 595 (1967).

[15] C. Supuran, G. Manole, I. C. Pușcaș, A. T. Balaban, M.D. Gheorghiu, A. Schiketanz, M. Andruh and I. Pușcaș, "New Types of Carbonic Anhydrase Inhibitors" *in* "Carbonic Anhydrase — from Biochemistry and Genetics to Pharmacology and Clinical Medicine", R.E. Forster II and C. Botre Eds., VCH Verlag, 1991.

Revue Roumaine de Chimie, 36, *1–3*, 257–262 (1990)

BASIC PROGRAM TO GENERATE THE TG AND DTG CURVES CORRESPONDING TO THERMAL DECOMPOSITIONS IN SOLID–GAS SYSTEMS

TEODOR COSEAC and EUGEN SEGAL

Department of Physical Chemistry, Faculty of Chemistry, University of Bucharest,
Bulevardul Republicii 13, Bucharest, Romania

Received October 20, 1989

The authors present a program to generate the TG and DTG of the solid-gas decompositions using the determined values of the nonisothermal kinetic parameters according to the Coats-Redfern method.

One of the classical methods to evaluate the nonisothermal kineti parameters is based on the Coast-Redfern equation :

$$\ln \frac{F(\alpha)}{T^2} = \ln \frac{AR}{aE}\left(1 - \frac{2RT}{E}\right) - \frac{E}{RT} \qquad (1$$

where $F(\alpha)$ stands for the integral conversion function, T for the temperature, a for the heating rate, A for the preexponential factor, E for the activation energy and R for the gas constant. Using the "reaction order" model, according to the values of the reaction order, n, the integral conversion function is given by :

$$F(\alpha) = \frac{[1-(1-\alpha)^{1-n}]}{1-n} \qquad \text{for } n \neq 1 \qquad (2)$$

$$F(\alpha) = -\ln(1-\alpha) \qquad n = 1$$

According to equation (1) for the correct value of the reaction order, n, the plot $\ln F(\alpha) \cdot T^{-2}$ versus T^{-1} should be linear. The values of the preexponential factor A, and activation energies, E, can be obtained from the intercept and the slope of the straight line so obtained.

Usually, in equation (1) the term $\frac{2RT}{E}$ is neglected with respect to 1. To check if such an omission does not alter the values of the nonisothermal kinetic parameters as well as the accuracy of the Coats-Redfern nonisothermal kinetic parameters; it is useful to generate the TG and DTG curves with the determined values of n, and E. Thus one has to generate the (α, T) curves:

$$\left.\begin{aligned} &\alpha = 1 - e^{-\frac{AR}{aE}T^2e^{-\frac{E}{RT}}} && \text{for } n=1 \\ &\alpha = 1 - \left[1-(1-n)\frac{AR}{aE}T^2e^{-\frac{E}{RT}}\right]^{\frac{1}{1-n}} && \text{for } n \neq 1 \end{aligned}\right\}(3)$$

and the $\left(\frac{d\alpha}{dt}, T\right)$ curves

$$\left.\begin{aligned} &\frac{d\alpha}{dT} = \frac{AR}{aE}\left(2T + \frac{E}{R}\right)e^{-\left(\frac{AR}{aE}T^2e^{-\frac{E}{RT}} \quad \frac{E}{RT}\right)} && \text{for } n = 1 \\ &\frac{d\alpha}{dT} = \left[1-(1-n)\frac{AR}{aE}T^2e^{-\frac{E}{RT}}\right]^{\frac{n}{1-n}}\frac{AR}{aE}\left(2T+\frac{E}{R}\right)e^{-\frac{E}{RT}} \\ & && \text{for } n \neq 1 \end{aligned}\right\}(4)$$

In this paper we present a program written in BASIC language for the computers belonging to the SPECTRUM ZX family which allows to generate the TG and DTG curves using the values of the nonisothermal kinetic parameters determined by the Coast-Redfern method. The program uses both integral conversion functions given by (2). The TG and DTG curves are respectively generated in (α, T) and $\left[\frac{\left(\frac{d\alpha,}{dT}\right)_T}{\left(\frac{d\alpha}{dT}\right)_{T_{max}}}, T\right]$ coordinates, where T_{max} is the temperature corresponding to the maximum value of the reaction rate (the peak on the DTG curve).

The input data are introduced conversationally. If after the introduction of the data the listing of t(°C) and $d\alpha/dT$ values is interrupted by an error message the range of temperature values should be shortened. The maximum temperature values which should be used is the value at which the listing was interrupted or a value close to it. The temperature interval should be equally shortened even only if the TG curve is wanted

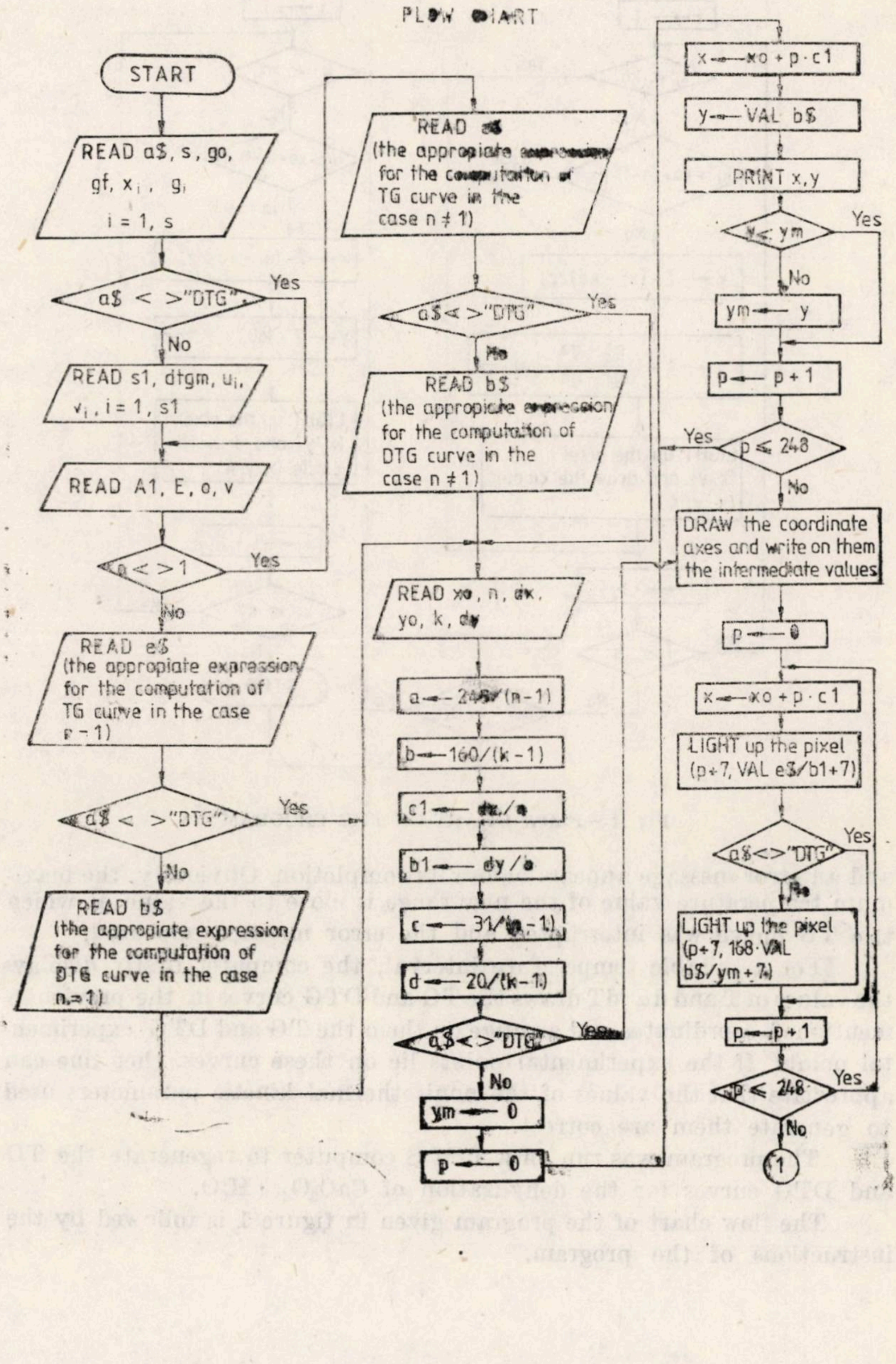
FLOW CHART
START
READ a$, s, go, gf, x_i, g_i i = 1, s
a$ < >"DTG"
Yes
No
READ s1, dtgm, u_i, v_i, i = 1, s1
READ A1, E, a, v
a < > 1
Yes
No
READ e$ (the appropiate expression for the computation of TG curve in the case n = 1)
a$ < >"DTG"
Yes
No
READ b$ (the appropiate expression for the computation of DTG curve in the case n = 1)
READ a$ (the appropiate expression for the computation of TG curve in the case n ≠ 1)
a$ < >"DTG"
Yes
No
READ b$ (the appropiate expression for the computation of DTG curve in the case n ≠ 1)
READ xo, n, dx, yo, k, dy
a ← 248/(n - 1)
b ← 160/(k - 1)
c1 ← dx/a
b1 ← dy/b
c ← 31/(n - 1)
d ← 20/(k - 1)
a$ < >"DTG"
Yes
No
ym ← 0
p ← 0
x ← xo + p · c1
y ← VAL b$
PRINT x, y
y ≤ ym
Yes
No
ym ← y
p ← p + 1
p ≤ 248
Yes
No
DRAW the coordinate axes and write on them the intermediate values
p ← 0
x ← xo + p · c1
LIGHT up the pixel (p+7, VAL e$/b1+7)
a$ < >"DTG"
Yes
No
LIGHT up the pixel (p+7, 168 · VAL b$/ym + 7)
p ← p + 1
p ≤ 248
Yes
No
1

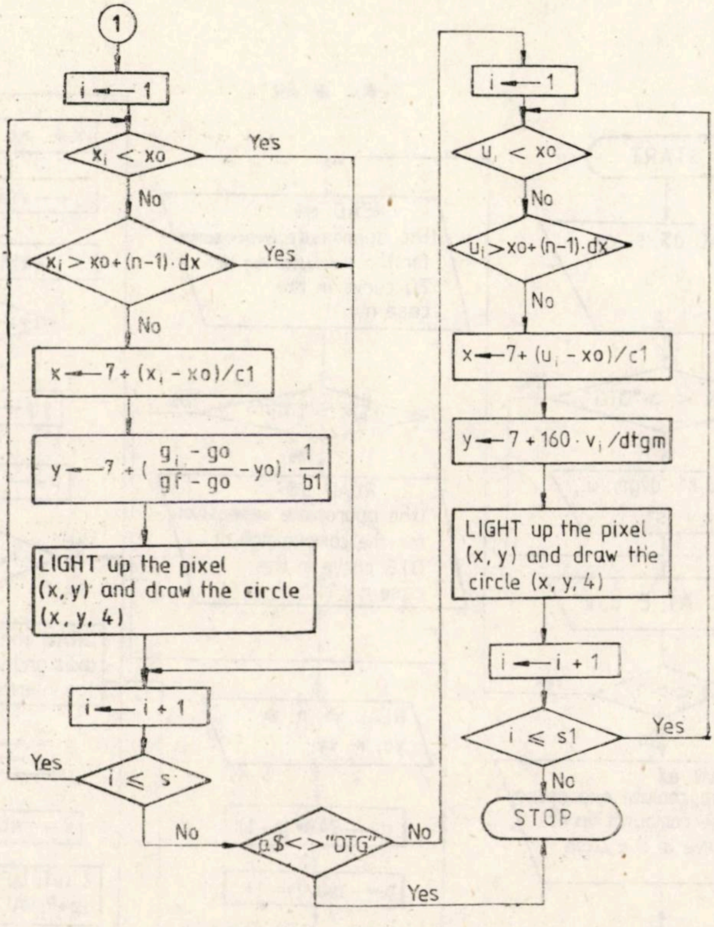

1
i ← 1
x_i < xo
Yes
No
x_i > xo + (n−1)·dx
Yes
No
x ← 7 + (x_i − xo)/c1
y ← 7 + ((g_i − go)/(gf − go) − yo)·1/b1
LIGHT up the pixel (x, y) and draw the circle (x, y, 4)
i ← i + 1
Yes
i ≤ s
No
p$<>"DTG"
No
Yes
i ← 1
u_i < xo
No
u_i > xo + (n−1)·dx
No
x ← 7 + (u_i − xo)/c1
y ← 7 + 160·v_i/dtgm
LIGHT up the pixel (x, y) and draw the circle (x, y, 4)
i ← i + 1
i ≤ s1
Yes
No
STOP

Fig. 1.—FLOW CHART OE THE PROGRAM

and an error message appears before its completion. Obviously, the maximum temperature value of the new range is close to the value at which the TG curve was interrupted and the error message appeared.

For a suitable temperature interval, the computer firstly displays the values of T and dα /dT draws the TG and DTG curves in the previously mentioned coordinates and arrange on them the TG and DTG experimental points. If the experimental points lie on these curves, then one can appreciate that the values of the nonisothermal kinetic parameters used to generate them are correct.

The program was run on a TIM S computer to regenerate the TG and DTG curves for the dehydration of $CaC_2O_4 \cdot H_2O$.

The flow chart of the program given in figure 1 is followed by the instructions of the program.

INSTRUCTIONS OF THE PROGRAM

```
  1 REM PROGRAM TO GENERATE TG AND DTG CURVES FROM COATS-REDFERN
 DETERMINED VALUES OF NONISOTHERMAL KINETIC PARAMETERS.
  10    INK 0
  20 INPUT "IF YOU WANT THE DTG CURVE THEN TAPE DTG,IF NOT PRESS
 ANY KEY",a$
  30 INPUT "NUMBER OF TG EXPERIMENTAL POINTS",s
  40 DIM x(s): DIM g(s): INPUT "INITIAL VALUE OF THE SAMPLE WEIG
HT OR A FIGURE PROPORTIONAL TO IT",g0: INPUT "FINAL VALUE OF THE
SAMPLEWEIGHT OR A FIGURE PROPORTIONAL TO IT ",gf
  50 PRINT  INK 7; PAPER 0;"TG EXPERIMENTAL POINTS(temperature C
,weight"
  60 FOR i=1  TO s: PRINT i: INPUT x(i),g(i): NEXT i
  70 IF a$<>"DTG" THEN  GO TO 120
  80 INPUT "NUMBER OF DTG EXPERIMENTAL POINTS",s1
  90 DIM u(s1): DIM v(s1): INPUT "MAXIMUM VALUE ON THE DTG CURVE
",dtgm
 100 PRINT  INK 7; PAPER 0;"DTG EXPERIMENTAL POINTS(temperature
C,DTG)"
 110 FOR i=1 TO s1: PRINT i: INPUT u(i),v(i): NEXT i
 120 INPUT "PREEXPONENTIAL FACTOR(1/s)",A1: INPUT "ACTIVATION EN
ERGY(cal/mol)",E: INPUT "REACTION ORDER",o: INPUT "HEATING RATE(
C/min)",v
 130 IF o<>1 THEN  GO TO 180
 140 RESTORE 150: READ e$
 150 DATA "1-EXP (-A1*1.986*(x+273)^2*60*EXP (-E/1.986/(x+273))/
v/E)"
 160 IF a$<>"DTG" THEN  GO TO 210
 170 RESTORE 175: READ b$
 175 DATA "A1*1.986*60*(2*(x+273)+E/1.986)/EXP (A1*1.986*60*(x+2
73)^2/EXP (E/1.986/(x+273))/v/E+E/1.986/(x+273))/v/E"
 176 GO TO 210
 180 RESTORE 185: READ e$
 185 DATA "1-(1-(1-o)*A1*1.986*60*(x+273)^2*EXP (-E/1.986/(x+273
))/v/E)^(1/(1-o))"
 190 IF a$<>"DTG" THEN  GO TO 210
 195 RESTORE 200: READ b$
 200 DATA "(1-(1-o)*A1*1.986*60*(x+273)^2/EXP (E/1.986/(x+273))/
v/E)^(o/(1-o))*A1*1.986*60/v/E*(2*(x+273)+E/1.986)/EXP (E/1.986/
x+273))"
 210 INPUT "INITIAL VALUE ON Y AXIS",Y0: INPUT "NUMBER OF VALUES
 ON Y AXIS",k: INPUT "DIFFERENCE BETWEEN TWO SUCCESIVE VALUES ON
 Y AXIS",dv
 220 INPUT "INITIAL VALUE ON X AXIS",x0: INPUT "NUMBER OF VALUES
 ON  X AXIS",n: INPUT "DIFFERENCE BETWEEN TWO SUCCESIVE VALUES O
 x AXIS",dx
 230 CLS : PRINT "IF AN ERROR MESSAGE APPEARS THEN TAPE GO TO 22
0 AND SHORTEN THE X INTERVAL"
 240 LET a=248/(n-1): LET b=160/(k-1): LET c1=dx/a: LET b1=dy/b:
 LET c=31/(n-1): LET d=20/(k-1)
 245 IF a$<>"DTG" THEN  GO TO 310
 250 LET vm=0: PRINT  PAPER 0; INK 7;"DTG COMPUTED VALUES"
 260 FOR p=0 TO 248
 270 LET x=x0+p*c1: LET v=VAL b$: PRINT x,y
 280 IF v<ym  THEN  GO TO 300
 290 LET vm=y
 300 NEXT p
 310 CLS : PLOT 7,7: DRAW 248,0: PLOT 7,7: DRAW 0,160
 320 FOR i=0 TO n-1: PLOT i*a+7,7: DRAW 0,3: NEXT i
 330 FOR i=0 TO k-1: PLOT 7,i*b+7: DRAW 3,0: NEXT i
 340 FOR i=0 TO n-1 STEP 2: PRINT AT 19,i*c;x0+i*dx: NEXT i
 350 FOR i=0 TO k-1: PRINT AT i*d,0;y0+(k-i-1)*dv: NEXT i
 360 FOR p=0 TO 248
 370 LET x=x0+p*c1: PLOT p+7,VAL e$/b1+7: IF a$<>"DTG" THEN  GO
TO 380
```

```
  375>PLOT p+7,160*VAL b$/ym+7
 380 NEXT p
 385 LET xf=x0+(n-1)*dx
 390 INK 2: FOR i=1 TO s
 400 IF x(i)<x0 OR x(i)>xf THEN  GO TO 430
 410 LET x=7+(x(i)-x0)/c1: LET y=7+((g(i)-g0)/(gf-g0)-y0)/b1 :PL
OT x,y: CIRCLE x,y,4
 430 NEXT i
 435 IF a$<>"DTG" THEN  GO TO 480
 440 FOR i=1 TO s1
 450 IF u(i)<x0 OR u(i)>xf THEN  GO TO 470
 460 INK 0: LET x=7+(u(i)-x0)/c1: LET y=7+160*v(i)/dtgm: PLOT x,
y: CIRCLE x,y,3
 470 NEXT i
 480 STOP
```

REFERENCE

A. W. Coats and J. P. Redfern, *Nature*, 20, 18 (1964).

Revue Roumaine de Chimie, **36**, *1–3*, 263–269 (1991)

MOLECULAR TOPOLOGY. 2

A COMPUTER PROGRAM FOR MULTIPLE BOND, CYCLE AND RADICAL APPROXIMATIONS OF D S INDEX[1]

MIRCEA V. DIUDEA* and IOAN SILAGHI-DUMITRESCU
University of Cluj-Napoca, Faculty of Chemical Technology, Arany Janos, 11, 3400–Cluj-Napoca, Romania

Received December 3, 1989

The D S index (DSI) is extended for multiple-bond-containing systems and aromatic compounds. A general formula and a computer program are given to compute it from the electronegativity degrees of vertices, over the whole molecule as well as for a radical portion, R; D S I was found to correlate well with log 1/c for inhibitors of *thymidine phosphorylase* as well as with molar refraction of olefins.

INTRODUCTION

In the previous paper of this series[1] we defined the valence (group) electronegativity for a vertex, and proposed, on this basis, a new Randić – type connectivity index DS, eq.1 :

$$\mathrm{DSI} = \sum_{\text{All edges}} (s_i s_j)^{-1/2} \tag{1}$$

where s_i, s_j are the degrees of electronegativity for two adjacent vertices.

The new index D S has found good correlation in the saturated, aliphatic series with molar refraction of amines and halogens and with polarizability and local anesthetic activity of alcohols.

MULTIPLE BOND APPROACH

Multiple bond approach in the Randić – type topological indices (TI's) was treated as a function of how the multiple bond and its endpoint valencies were counted.

Murray at al.[2] and Balaban[3–6] considered the conventional bond order b(1,2,3-for single, double and triple bond, respectively and 1.5 – for aromatic bond) for the endpoint degrees of multiple bond and counted it as a single edge when calculated *q* (number of edges in graph). In this approach the entries of multiple bond endpoints in the adjacency or distance matrices are multiplied by 1/b.

---

* Author to whom correspondence should be addressed

In the second approach, one counts each bond (considering e.g. a double bond as two edges) both in computing q and TI's.[5 7]

We adopted the second approach, by virtue of which the edge term $(s_i s_j)^{-1/2}$ is multiplied by b_{ij} = the conventional bond order for an edge having the i,j — atoms as endpoints, eq. 2 :

$$D\,S\,I = \sum_{\text{All edges}} b_{ij}(s_i s_j)^{-1/2} \qquad (2)$$

CYCLE APPROACH

Kier and Hall[7] treated the cyclic compounds by virtue of the spanning tree concept (eliminate one edge from different points of a cycle in order to equalize the cycle with its spanning trees — as number of edges). They addopted a mean value of 0.5 to diminish the initial $^1\chi$-value. The ring correction is applicable to any hexacyclic compound irrespective of its degree or type of substitution. When more than one $^1\chi$-term is used, this correction is not required.[7]

In agreement with the spanning tree concept, we propose a cycle approach which considers the edge mean value in a given cycle structure to be substracted from the initial D S I — value, eq.3 :

$$D\,S\,I = \left(1 - \frac{\mu}{q_{tot}}\right) \sum_{\text{All edges}} b_{ij}(s_i s_j)^{-1/2} \qquad \mathbf{(3)}$$

where q_{tot} is the total number of bonds in a connected graph, according to eq.4 :

$$q_{tot} = \sum_{ij} b_{ij} q_{ij} \qquad \mathbf{(4)}$$

with q_{ij} — the edge having i, j — atoms as endpoints.

In eq. 3, is the "cyclomatic number" (number of rings — see Baeyer, IUPAC and Chemical Abstracts nomenclature systems)[5,6] and is defined by eq. 5 :

$$\mu = q - n + 1 \qquad \mathbf{(5)}$$

where *n* is the number of vertices in graph and *q* refers only to sigma bonds.

Eq. 3 is applicable to any cyclic compounds irrespective of the type of cycle and its substituents.

Accurately, the cycle correction should be applied before counting the substituents. However, no large differences appear between the $^1\chi_D$-values corrected before and after counting the substituents. In a series of cyclohexanes with a $CH_3-(CH_2-CH_2)_m$-chain and $m = 1$ to 100 differences do not exceed 0.2% from the before-corrected D S I - values. Similar observation we could make about a series of monosubstituted decalines.

A quite special case is that of simple condensed aromatic hexacycles. Due to the conventional bond order $b_{ij} = 1.5$, in the calculation of q_{tot} by eq.4, there appears an "excess" of bonds. Of course, the exceeding bonds must be rejected off in the calculation of D S I. Thus, we propose a general eq.6, aplicable both for aliphatic and aromatic hexacycles, as well as for unsaturated structures :

$$D\,S\,I = \left(1 - \frac{\mu}{q_{tot}} + c\right) \sum_{\text{All edges}} b_{ij}(s_i s_j)^{-1/2} \qquad (6)$$

where *c* is the correction for condensed aromatic hexacycles, eq.7 :

$$c = \frac{A_G - \mu_{Ar}}{2q_{tot}} \qquad (7)$$

In eq.7, AG — is the number of aromatic groups in a molecule and μ_{Ar} represents the number of aromatic rings. It is obvious that *c* does not operate in the case of non-aromatic cycles ($AG = 0$; $\mu_{Ar} = 0$; $c = 0$), nor in the case of aromatic isolated cycles ($AG = \mu_{Ar}$; $c = 0$). Note that *c* is functional only for $\mu_{Ar} \geqslant 2$.

RADICAL APPROACH

It is known that many drug molecules, with similar biological properties, differ only by a radical, R, attached to a same skeleton. Moreover some properties could be a function of local structural or electronic features. Thus it would be useful to compute D S I only for R-portion of such molecules : D S I R.

This approach considers the atom directly attached to the skeleton as a *root vertex* and accounts for the broken bonds (in the "process" of R-forming) as follows :

$$v_{root} = v_i + n_{bb} \qquad (8)$$

where v_i and v_{root} — are the initial and actual connectivity (valence) of root vertex, respectively, and n_{bb} — stands for the number of broken bonds. Subsequently, the number of hydrogen atoms belonging to the root vertex, H_{root}, is calculated by :

$$H_{root} = (8 - G_{A,root}) - v_{root} \qquad (9)$$

with $G_{A,root}$ = the group in the periodic chart of the non-hydrogen atom of root vertex. Then, S_{root} = the valence (group) electronegativity and D S I R will be computed using the actual v_{root} and H_{root}—values (see[1]).

Our program for computing D S I accounts for the proposed radical approach (see also Table 1).

D S I – CORRELATING TESTS

We tested the ability of D S I (computed according to eq.6) to correlate with log 1/c (c – is here the inhibitory concentration) in a series of **thymidine phosphorylase** inhibitors[8] of a general structure I: Table 1 lists the D S I – values, computed over the whole molecule I as well as for the substituent R alone, along with the observed log 1/c. As comparison terms, we also introduced the $^1\chi_R$ (from. ref.[7]) and $^1\chi_v$ values (this work).

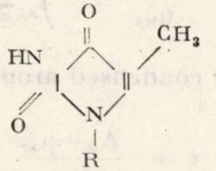

A first observation imposes: the correlation of T I's with the inhibitory activity of the listed thymidine derivatives is rather poor (see Table 1). This means that the topological feature of such compounds is not the sole determinant of their biological activity.

Second, no differences appear when are used the D S I R – values in regression instead of the D S I values computed over the whole molecule I (see also ref.[7], p. 189).

Third, D S I correlates by a parabolic function rather than by a linear one.

Table 1

Inhibitors of Thymidine Phosphotylase[8] (I-see text)

no.	R	DSI	DSIR	$^{a1}\chi_R$	$^b\ ^1\chi^v$	^{c}log 1/c	Statistics	
							R	s
1	Methyl	8.4647	0.6791	3.698	3.0729	$-2.30\,^1\chi_R$	0.9199	0.2125
2	Butyl	10.6329	2.8508	5.236	4.6490	$-1.35\ ^1\chi^v$	0.9220	0.2099
3	Isopentyl	11.3806	3.6009	5.592	5.0048	-1.30 DSI	0.8807	0.2568
4	Cyclopentyl	11.4948	3.7006	5.270	4.7003	-1.28 DSIR	0.8807	0.2568
5	Isohexyl	12.1035	4.3245	6.092	5.5048	$-1.17\,^1\chi^d$ DSI	0.9194	0.2262
6	Pentyl	11.3557	3.5744	5.736	5.1490	-1.15		
7	3-Phenyl-propyl	16.5554	8.7729	7.254	6.6614	-1.11		
8	2-Phenyl-ethyl	15.8321	8.0487	6.754	6.1614	-0.80		
9	Phenyl-methyl	15.1089	7.3244	6.254	5.6614	-0.76		
10	4-Phenyl-butyl	17.2787	9.4971	7.754	7.1614	-0.60		
11	5-Phenyl-pentyl	18.0020	10.2211	8.254	7.6614	-0.32		

[a] bond N–C(R) included; [b] from ref.; [c] this work (ring correction = −0.500;

[d] parabolic correlation – the following QSAR was found:

$$\log 1/c = 0.6226\ (\pm 0.2537)\ \mathrm{DSI} - 0.0177\ (\pm 0.0093)\ (\mathrm{DSI})^2 - 6.1194$$

$R = 11$; $R = 0.9194$; $s = 0.2262$; $F = 21.9$

DSI correlates with the molar refraction of olefins in a single variable function as well as χ^v does, in a three variable function (${}^0\chi^v$, ${}^1\chi^v$ and ${}^2\chi^v$; $r = 0.9985$; $s = 0.223$; $N = 39$).[7]

For the olefins file (Table 2) we found the following QSPR :

$$MR = 3.3395 + 6.1960 \text{ DSI} \tag{10}$$

$$N = 39 \text{ ; } r = 0.9980 \text{ ; } s = 0.2472$$

$$F = 4523.7 \text{ ; } T = 95.1 \text{ ; } EV = 0.9959$$

Table 2

Molar refraction

No.	Compound	DSI	Molar refraction[a]	
			Obs.	Calcd.
1	2-Methyl-2-butene	3.548	24.955	25.323
2	1-Pentene	3.446	24.858	24.691
3	3,3-Dimethyl-1-butene	4.228	29.598	29.536
4	2,3-Dimethyl-2-butene	4.323	29.590	30.125
5	2,3-Dimethyl-1-butene	4.244	30.063	29.635
6	4-Methyl-1-pentene	4.196	29.542	29.338
7	2-Methyl-1-pentene	4.216	29.398	29.462
8	2-Methyl-2-pentene	4.271	29.754	29.803
9	3-Methyl-1-pentene	4.198	29.485	29.350
10	2-Ethyl-1-butene	4.218	29.391	29.474
11	1-Hexene	4.169	29.208	29.170
12	2,3,3-Trimethyl-1-butene	5.001	33.980	34.326
13	4,4-Dimethyl-1-pentene	4.952	34.233	34.022
14	3,3-Dimethyl-1-pentene	4.955	34.011	34.041
15	2,3-Dimethyl-2-pentene	5.048	34.203	34.617
16	3,4-Dimethyl-1-pentene	4.949	33.919	34.003
17	3,4-Dimethyl-2-pentene	5.025	33.900	34.474
18	2-Ethyl-3-Methyl-1-butene	4.969	34.024	34.127
19	2,3-Dimethyl-1-pentene	4.969	34.005	34.127
20	5-Methyl-1-hexene	4.919	34.139	33.817
21	2-Methyl-2-hexene	4.995	34.395	34.288
22	2-Methyl-1-hexene	4.940	34.114	33.948
23	2-Methyl-3-hexene	4.972	34.223	34.146
24	4-Methyl-1-hexene	4.921	34.078	33.830
25	2-Ethyl-1-pentene	4.942	33.991	33.960
26	3-Ethyl-1-pentene	4.924	34.039	33.848
27	3-Ethyl-2-pentene	4.999	34.117	34.313
28	1-Heptene	4.893	34.136	33.657
29	2,4,4-Trimethyl-2-pentene	5.778	39.015	39.140
30	2,4,4-Trimethyl-1-pentene	5.723	38.769	38.799
31	2,3,4-Trimethyl-1-pentene	5.721	38.769	38.780
32	3,3,4-Trimethyl-1-pentene	5.707	38.499	38.700
33	2-Isopropyl-3-methyl-1-βutene	5.720	38.385	38.780
34	5,5-Dimethyl-1-hexene	5.676	38.785	38.500
35	4,4-Dimethyl-1-hexene	5.679	38.643	38.527
36	3,3-Dimethyl-1-hexene	5.679	38.548	38.527
37	2,5-Dimetyl-3-hexene	5.722	38.823	38.793
38	3,5-Dimethyl-1-hexene	5.671	38.764	38.477
39	3-Ethyl-4-methyl-1-pentene	5.675	38.591	38.502

COMPUTER PROGRAM

The computer program given below calculates the ¹D indices for both saturated or unsaturated organic derivatives, aromatic compounds or fragments of such molecules. Heteroatoms up to chlorine may be included. For other heteroatomic derivatives, the corresponding Saunderson electronegativities must be inserted as data statements at program lines 750—765.

The inputs are the same as for the previous version [1] completed with data necessary in the treatment of fragments or aromatic groups. For instance, the fragments may be treated when the following data are known: the number of break points, number of broken bonds and number of missing neighbours of each root vertex. The pertinent data of the fragment (   ) are the following.

```
Nr.   of break points = 4
VR    VB    VN
  1     1    11
  2     1     1
  5     1     1
  6     1     1
.....................
 ¹D        =6.5344
```

```
 90 REM DS INDEX Program VERSION 2
100 CURSOR 0,0
110 CLS#2 : CLS#0
120 RESTORE
130 DIM ga(100), Sa(100), h(50), d(100)
140 i=0
150 REPEAT READING
160 i=i+1 : READ ss
170 if ss = −999 then exit reading
180 sa(i) = ss
190 END REPEAT READING
200 INPUT "Molecule" ; t$
210 INPUT "Naton" ; na
220 INPUT "Is it a fragment" r$
230 IF r$ = "Y"  or r$ = "y" then
240 Input ,,Nr. or breaking points" ; bb : DIM vr(bb), vb(bb), vn(bb)
250 PRINT "Give no of root vertices"
260 PRINT "of broken bonds and missing"
270 PRINT "neighbours of each root vertex"
280 FOR ii = 1 to bb : INPUT vr(ii); vb(ii) ; vn(ii)
290 END IF
300 DIM a(na,na), s(na)
310 ainp :matip a, t$
320 PRINT "Input at.no. of elements"
330 FOR i=1 to na
340 PRINT i ; : PRINT "ga (" ;i ;") = " ; :INPUT ga(i
350 NEXT i
360 FOR i=1 to na
370 vi=0 :vj=0
380 FOR j=1 to na
390 if a(i,j) 〈 〉 0 then vi=vi+1 : vj=vj+a(i,j)
400 NEXT j
410 IF r$="Y" or r$ = "y" THEN
420 FOR ii = 1 to bb
430 IF vr(ii) = i then  vi=vi+vn(ii) : vj=vj+vb(ii)
```

```
440 NEXT ii
450 END IF
460 ng=ga(i)
470 ng=group(ng)
480 h(i) =8−ng−vj : ng = ga(i)
490 IF h(i) < 0 then h(i) = 0
500 a(i) = (sa(ng)×(sa(1)) ∧ h(i)) ∧ (1 + h(i)))
520 d(i) = (s(i)) ∧ (1/(1 + vi))
530 NEXT i
540 id=0 : q=0
550 FOR i=1 to na
560 FOR j=1 to na
570 IF a(i,j) 〈〉 0 THEN id=id+a (i,j)/sqrt(d(i) * d(j)) : q=q+1
580 NEXT j
590 NEXT i
600 PRINT “Do you wish to correct”
610 PRINT “for aromatic groups (y/n)?”; ar$
620 IF ar$=“Y” or ar$=“y” THEN
630 CLS : INPUT “No. of aromatic groups”; ag
640 INPUT “No of aromatic rings :” mar
650 INPUT “No of PI bonds”; npi
660 qt=q+npi : miu=q−na+1
670 cor=(1−miu/qt+(ag−mar)/(2*qt) : id=id*cor
680 END IF
690 PRINT : UNDER 1
700 PRINT t$ : UNIER 0
710 PRINT ”DS INDEX=”; id
720 INPUT “Other molecule (y/n)?”; r$
730 IF r$=“Y” or r$=“y” then RUN
740 STOP
750 DATA 2.592, 0, 0, 0
760 DATA 2.275, 2.746, 3.194, 3.654, 4.0, 0, 0, 0
765 DATA 2.138, 2.515, 2.957, 3.975, −999
770 DEFINE FUNCTION GROUP (ng)
780 gp=ng−2
790 if gp<0 then RETURN ng
800 gp=gp−8
810 IF gp<0 THEN RETURN gp+8
820 gp=gp−8
830 IF gp<O THEN RETURN gp+8
840 PRINT “This program does not work”
850 PRINT “with element no. ”; gp+8
860 END DEFINE
870 DEFINE PROCEDURE ainp
871 REM INSERT AINP FROM REFERENCE [1]
990 END DEFINE
1000 DEFINE PROCEDURE matip(a, t$)
1001 REM INSERT matip FROM REFERENCE [1]
1200 END DEFINE
```

REFERENCES

[1] M. V. Diudea and I. Silaghi-Dumitrescu, *Rev. Roumaine. Chim.*, **34**, 1175 (1989)

[2] W. I. Murray, L. B. Kier and L. H. Hall, *J. Pharm. Sci.*, **64**, 1978 (1975).

[3] A. T. Balaban, *Pure Appl. Chem.*, **55**, 199 (1983).

[4] A. T. Balaban, *Chem. Phys. Lett.*, **89**, 399 (1982).

[5] A. T. Balaban, I. Moţoc, D. Bonchev and O. Mekenyan, "Topological Indices for Structure-Activity Correlations", in "Topics in Current Chemistry", **114**, 21 (1983).

[6] A. T. Balaban and P. Filip, *Math. Chem.*, **16**, 163 (1984).

[7] L. B. Kier and L. H. Hall, "Molecular Connectivity in Chemistry and Drug Research", Acad. Press, 1976, New York.

[8] B. R. Baker and M. Kazawa, *J. Med. Chem.*, **10**, 302 (1967).

Revue Roumaine de Chimie, **36**, *1—3*,271 (1991)

BOOK REVIEW

"Advances in the Theory of Benzenoid Hydrocarbons" (Topics in Current Chemistry, No. 153) edited by I. Gutman and S.J. Cyvin. Springer Verlag, Berlin, 1990. Hard cover, 289 pp, 178 DM. ISBN 30-540-51505-4

In addition to the book "Introduction to the Theory of Benzenoid Hydrocarbons" by the above editors, published by Springer Verlag in 1989, volume 153 of *Topics Curr. Chem.* presents 14 more advanced chapters by active research chemists in this field.

The first chapter, by L.J. Allamandola, discusses benzenoid hydrocarbons in cosmos; IR emission bands give evidence that most interstellar carbon atoms may exist as such molecules. However, no mention is made of fullerene molecules.

All other chapters are theoretical. P.C. Hiberty stresses the distortive tendencies of delocalized pi-electronic systems, arguing that the D_{6h} regular geometry of benzene is due to the sigma-electronic framework, whereas in cyclobutadiene the pi-electron driving force prevails, leading to bond length alternation; heteroanalogues are also discussed.

D.L. Cooper, J. Gerratt and M. Raimondi present an interesting alternative approach to the MO and VB descriptions, namely via spin-coupled valence bond theory. In this chapter, azabenzenes are consistently misnamed as azobenzenes, and formulas of pyrrole and borazine contain misprints.

D.J. Klein's chapter (Semiempirical VB views for benzenoid hydrocarbons) is an overview blending graph-theoretic ideas with conventional quantum-chemical approaches; the Pauling-Wheland VB model, the Herndon-Simpson model, and the conjugated circuits of Randić are presented and discussed consistently and comparatively; VB theory is still very active and may eventually merge with MO theory

J. Cioslowski's chapter, "Scaling properties of topological invariants" refers to such topological invariants derived from the adjacency matrix of the hydrogen-depleted graph as eigenvalues, moments, numbers of Kekulé structures, and the HOMO-LUMO separation. Formulas correlating exactly or approximately such invariants with the numbers of vertices and edges in the graph are reviewed.

M. Zander reviews in his chapter reactivity indices for polynuclear aromatic hydrocarbons (PAH's) in such reactions as electrophilic substitution, Diels-Aldercy cloadditions, thermally-induced polymerization, and biochemical transformations.

In the chapter "A periodic table for benzenoid hydrocarbons", J.R. Dias continues to review applications of classifying benzenoid hydrocarbons according to two parameters: number of internal carbon atoms with degree three, and number of net tree disconnections.

P. John and H. Sachs review the literature of, and present algorithms for, the number of Kekulé structures, spanning trees, Pauling's bond orders, characteristic polynomials, and eigenvectors.

The next three chapters by Chinese authors present the theoretical and practical methods for finding out whether a given benzenoid system is, or is not, Kekuléan, i.e. whether it has at least a Kekulé structure. Systems with equal numbers of starred and unstarred vertices but devoid of Kekulé structures (di- or polyradicals, called concealed non-Kekuléans) can be constructed. The "peak-valley method" can be used for deciding whether a benzenoid or coronoid hydrocarbon is Kekuléan or non-Kekuléan. The Sachs and Sheng algorithms can also be used to that effect.

A group of five authors from China, Norway and Texas describe methods for enumerating Kekulé structures in certain peri-condensed benzenoids.

H.Hosoya discusses Clar's aromatic sextet and sextet polynomial in the light of graph-theoretical manipulations. The partial pi-electron density in benzenoids reflects strikingly Clar's ideas.

The last chapter, by S.El-Basil, presents correlations of physical and chemical properties of catafusenes by means of caterpillar trees in chemical graph theory according to Gutman.

In conclusion, this book is an important and up-to-date account of progress and development in the area of PAH's for all chemists involved in theoretical (both quantum-chemical and topological-computational) and practical (correlations with physico-chemical properties) investigations.

A. T. Balaban
Polytechnic **Institute** Bucharest

Revue Roumaine de Chimie, 36, 1-3, 273–275 (1991)

IN MEMORIAM

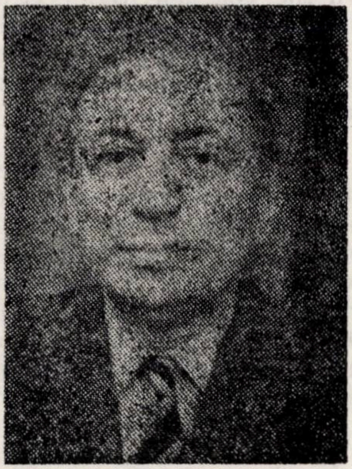

GHEORGHE CLAUDIU SUCIU

(1905–1990)

On December 11, 1990 the Roumanian chemistry and petrochemistry have lost one of their most remarkable representatives and the Roumanian Academy has lost one of its devoted members in the person of Prof. Dr. Doc. Gheorghe Claudiu Suciu.

G.C. Suciu was born on May 6, 1905 in Blaj, a town with a long resonance in Roumanian history. As a young boy, G.C. Suciu participated at the historical meeting at Alba-Iulia on the 1st December 1918, when Transylvania joined Roumania.

G.C. Suciu followed the primary and secondary schools in Blaj, Beiuș and Sibiu, proving his preference for the study of the natural sciences. After a one-year study in Rome with famous professors such as Nicola Paravanno and Enrico Fermi, G.C. Suciu returned to the University of Cluj where he obtained his B.S. in chemistry, with the mention "with distinction".

Based on six scientific papers elaborated under the guidance of Prof. Dr. Gheorghe Spacu during 1927–1929, the University of Rome granted G.C. Suciu the title of doctor in chemistry with the mention "110/110".

From 1930 to 1931 G.C. Suciu worked at the Bayway Refinery of the Standard Oil Company in New Jersey, USA, on two research assignments and took a full-time one year course in petroleum refining, consisting essentially in testing of processing units.

Between 1936—1939 he followed a Lubrication Engineering Course, given by correspondence by Standard Oil Company.

A great part of the scientific and technical activity of Dr. G.C. Suciu was linked with the Teleajen Refinery, a wholly owned subsidiary of Standard Oil Company, where he began to work from 1931 : one year in pilot plant design and operation, seven years as process engineer and seven years more as refinery assistant manager.

In 1948 he became technical manager of all the major oil refineries of Roumania.

From 1951 to 1964 G.C. Suciu was the project manager of the Onești Refinery and technical manager of the Roumanian Design Institute for Refining and Petrochemical Units.

Among the most prominent achievements one should mention his participation, between 1948—1950, in the design and commissioning of the first industrial installation for oil manufacturing entirely designed in Roumania and also his activity as project manager for the first refinery designed in Roumania, the Onești Refinery, where the work began by falling trees from the allotted plant site, in order to clear the ground.

He developed pipe ovens for the chemical and petrochemical industries, which were patented in France, England, India and Italy and were used at the refineries from Onești, Pancevo (Yugoslavia, 1978), Karachi (Pakistan, 1979).

Dr. G.C. Suciu never lost his interest in didactic activities begun in 1926 when he was assistant for chemistry at the Faculty of Sciences, the Cluj University, till 1929. From 1948 he was lecturer at the Institute of Petroleum, Gas and Geology (Bucharest), where he was appointed in 1951 as part-time professor and then, in 1964, as full-time professor of chemical engineering. He kept this position at the Institute of Petroleum and Gas — Ploiești till 1975 when he was appointed consulting professor.

His lectures treated mostly on momentum and heat transfer and on operations and equipment design for the hydrocarbon processing industry. He gave also UNIDO courses in English and French for chemical engineers from developing countries.

The research activity of Prof. G.C. Suciu had as object during 1926—1932 the inorganic and analytical chemistry and from 1930 onwards the chemical engineering applied to oil manufacture technology.

G.C. Suciu was author of three books ; editor, coeditor or coauthor of another six books ; author or coauthor of over 100 papers and communications at scientific or technical meetings. A great part of his activity, elaborated during 1930—1948, could not be published, being the private property of the enterprise where G.C. Suciu was employed.

G.C. Suciu was among the main authors of the "Chemical Engineer's Handbook" (1953—1954) and of the "Roumanian Technical Lexicon" (1956). Among his books one should mention "Elements of Chemical Engineering" (Cluj, 1946), "Thermal and Mechanical Separation Processes" (Bucharest, 1961, with a 2nd edition in 1962), "Engineering of Hydrocarbon Manufacturing. Petroleum — Petrochemistry" (2 volumes in 1973—1974 and a second edition in 3 volumes in 1983—1987), "Progresses in Hydrocarbon Manufacturing Processes" (Bucharest, 1977, 1984).

The remarkable scientific and technical achievements of Prof. Dr. Doc. G.C. Suciu were acknowledged by his election as a member of the Permanent Council of the World Petroleum Congresses (1967–1975), president of a Review Paper-Session of the World Petroleum Congress in 1971, president of an international UNIDO Meeting on "Transfer of know-how in the production and use of catalysts" (Bucharest, 1972) and by his inclusion in "Who's who in Petroleum".

In 1963 he was elected as a corresponding-member of the Roumanian Academy and in 1990 as a full member.

All those who have met Professor G.C. Suciu till his very last day will always remember his prodigious knowledge (of which that related to the hydrocarbon industry was only a part, truly his preferred one). But they also will remember the remarkable human qualities : kindness, earnestness and optimism, which were the tokens of a great man and scientist.

THE EDITORIAL BOARD
OF REVUE ROUMAINE DE CHIMIE

18th IUPAC INTERNATIONAL SYMPOSIUM ON THE CHEMISTRY OF NATURAL PRODUCTS

30 AUG. - 4 SEPT. 1992
STRASBOURG (FRANCE)

INVITATION TO ATTEND AND TO PRESENT A POSTER

The IUPAC Symposia on the Chemistry of Natural Products have been an occasion where major new results and trends in Organic Chemistry have been presented. The 1992 Symposium will endeavour to maintain this tradition. It will, for the first time, cover the chemistry of the molecules of Nature from the smallest to the largest, and from the oldest to the newest: Organic Cosmo- and Geochemistry, Prebiotic Chemistry, Organic aspects of Biotechnology, will find their place beside a large section devoted to Synthetic Chemistry and others devoted to major breakthroughs in Biosynthesis, in Chemical Interactions between living organisms, and in the Chemistry of Biologically or Biomedically active substances.

The programm will comprise **plenary lectures** (no parallel sessions!), **invited posters** and **proposed posters**. In the same premises, with a joint registration, will simultaneously be held the **3rd International Symposium on Iron Transport, Storage & Metabolism.**

The following distinguished scientists have already confirmed their participation as lecturers: P. Albrecht (Strasbourg), A. R. Battersby (Cambridge), D. Boger (West Lafayette), W. Boland (Karlsruhe), A. Brack (Orléans), D. P. Curran (Pittsburgh), P. Deslongchamps (Sherbrooke), Donglu Bai (Shanghai), A. Eschenmoser (Zürich), S. Hanessian (Montréal), G. Joyce (La Jolla), O. Kennard (Cambridge), H. Kunz (Mainz), S. Ley (London), Guo-qiang Lin (Shanghai), D. Lynn (Chicago), A. Marquet (Paris), K. Martinek (Praha), S. V. Moroz (Vladivostok), V. Naya (Osaka), K. C. Nicolaou (La Jolla), Oesterheld (Martinsried), F. Raulin (Créteil), J. Reisse (Bruxelles), M. Rohmer (Mulhouse), A. I. Scott (College Station), D. Tanner (Uppsala), P. F. Vlad (Kishinev), V. Vlassov (Novosibirsk), G. Wächtershäuser (Munich), M. J. Wyvratt (Rahway), J. S. Yadav (Hyderabad). This list is not final.

Beside hotels, cheap accomodation will be available in Student Residences, and a very limited number of bursaries will be offered to cover registration and local expenses for some doctoral students or young post-doctoral fellows, on a regional basis defined by the sponsors of this programme (e.g. Southern, Central and Eastern Europe, or developing countries; details will be available later).

Please register your interest in attending with the General Secretariat:
Ms. M. Cl. Dillenseger and A. M. Cheminat, Centre de Neurochimie, 5 rue
Blaise Pascal, F-67084-Strasbourg (France). (Fax + [33]88 60 76 20).

The Honorary President: J. M. Lehn

The Chairman: G. Ourisson

NOTE POUR LES AUTEURS

La Revue Roumaine de Chimie publie des articles en anglais, français, russe, allemand ou espagnol. Les auteurs sont pries d'envoyer des articles et des comptes rendus inédits.

Les manuscrits seront dactylographiés à double interligne. La bibliographie, les tableaux et la légende des figures seront placés après le texte.

Si l'article fait partie d'une série numérotée, la partie précédente sera donnée comme première reference.

Chaque article sera précédé d'un résumé comprenant quinze lignes au maximum.

Les rèfèrences bibliographiques dans le texte seront faites par des exposants sans parenthèses et paraitront à la fin de l'ouvrage.

Les publications périodiques montionnées dans la bibliographie seront présentées suivant les prescriptions internationales : le nom de auteur précédé de l'initiale du prénom, le titre du périodique abrégé conformément à «Chemical Abstract» et souligné par une ligne, le numéro du tome indiqué par des chiffres arabes et souligné par deux lignes, suivi de la première page de l'article : à la fin, l'année de la parution sera placée entre parenthèses. Le numéro de la revue ne sera pas indiqué si les pages du volume sont numérotées consécutivement.

Les textes des livres ou traités inclueront : le nom des auteurs, précédé de l'initiale du prénom, le titre du livre entre guillemets et sans être souligné, le numéro du tome précédé par l'abréviation «vol.»(ou «Bd»), le numéro de l'édition, les éditions (the publisher), la localité de la parution du livre, l'année de la parution et la page de la référence précédée(s) par l'abréviation «p»(ou «S»).

Les brevets seront indiqués comme suit : l'auteur ou la firme, le pays et le numéro du brevet, la date de la revue (*Chem. Abstr.*) Par ex. : M. Jones (to Union Carbide Co.) Brit. Pat. 610 238, 2 Sept. 1959: cf. *Chem. Abstr.*, 54, 12808 (1960).

Si la référence n'a pas été lue en original, on indiquera aussi la revue de références consultée.

Les diagrammes seront tracés à l'encre de Chine sur papier calque. Les tableaux et les figures (en nombre strictement nécessaire), ainsi que les courbes dans les figures seront numérotés par des chiffres arabes. Leur explication sera donnée dans la légende des figures. Prière de ne pas inscrire les mêmes données dans les tableaux et les figures. Chaque tableau aura un titre. On indiquera dans le texte la place approximative des tableaux et des figures. Les formules chimiques seront incluses dans le texte ; en outre, elle seront transcrites sur papier calque, à l'encre de Chine.

Les auteurs sont priés d'indiquer les caractères italiques (en soulignant les lettres au crayon), ainsi que tout autre caractère spécial : les préfixes *ortho*, *meta*, *para*, *cis*, *trans*, etc. seront soulignés pour indiquer leurs caractères italiques, et ne seront jamais écrits avec des majuscules.

Aucune correction à la main ne sera admise sur le manuscrit. Les corrections seront frappées à la machine. Les lettres grecques ou d'autres symboles spéciaux seront insérés à la main à l'encre clairement.

Le manuscrit sera signé par l'auteur.

Le titre courant aura 50 lettres au maximum.

L'entière responsabilité du contenu des articles appartient aux auteurs.

Sur demande on peut obtenir une note plus complète.

PRINTED IN ROMANIA

TRAVAUX PARUS AUX ÉDITIONS DE L'ACADÉMIE ROUMAINE

I. G. MURGULESCU, **Introducere in chimie fizică, vol. I. 1, Atomi, molecule, legătură chimică**, 1976, 560 p.

I. G. MURGULESCU, V. EM. SAHINI, **Introducere in chimia fizică, Vol. I, 2, Structura și proprietățile moleculelor**, 1979, 604 p.

I. G. MURGULESCU, E. SEGAL, **Introducere in chimia fizică, Vol. II. 1. Teoria molecular-cinetică a materiei**, 1979, 1036 p.

I. G. MURGULESCU, TATIANA ONCESCU, E. SEGAL, **Introducere în chimia fizică, Vol. II, 2. Cinetică chimică și cataliză**, 1981, 1024 p.

I. G. MURGULESCU, J. PĂUN, **Introducere în chimia fizică, Vol. I, 3. Nucleul atomic, reacții nucleare, particule elementare**, 1982, 606 p.

I. G. MURGULESCU, RODICA VÎLCU, **Introducere în chimia fizică. Vol. III. Termodinamica chimică**, 1982, 624 p.

I. G. MURGULESCU, O. M. RADOVICI, **Introducere în chimia fizică, Vol. IV, Electrochimia**, 1986, 416 p.

R. VÎLCU, M. LECA, **Polymer Thermodynamics by Gas Chromatography**, coédition avec Elsevier, 1990, 204 p.

F. CIUBAN, A. X. LUPEA, **Studiul structurii și sinteza peptidelor**, 1989, 282 p.

CRISTOFOR I. SIMIONESCU, VALERIA GORDUZA, **Implicații bioenergetice ale coloranților**, 1988, 208 p.

R. VÎLCU, M. LECA, **Termodinamica polimerilor prin cromatografie de gaze**, 1987, 238 p.

I. ZUGRĂVESCU, M. PETROVANU, **Cicloadiții 3+2 dipolare**, 1987, 446 p.

RAUL MIHAIL, ION GROZEANU, **Estimarea secvențială aplicată sistemelor chimice**, 1986, 406 p.

M. BREZEANU, I. PATRON, M. ANDRUH, **Combinații complexe polinucleare și aplicațiile lor**, 1986, 244 p.

A. T. BALABAN et al., **Labelled Compounds and Radiopharmaceuticals Applied in Nuclear Medicine**, coédition avec John Wiley and Sons, 1986, 742 p.

D. PURDELA, **Nomenclatura chimiei organice – IUPAC**, 1986, 451 p.

PETRU BUDRUGEAC, **Probleme de chimie**, 1986, 280p.

T. ONCESCU, S.G. IONESCU, **Conversie fotochimică și stocare de energie**, 1985, 272 p.

V. DRĂGUȚAN, A.T. BALABAN, M. DIMONIE, **Olefin Metathesis and Ring-Opening Polymerization of Cyclo-Olefins**, coédition avec John Wiley and Sons, 1985, 544 p.

C. LITEANU, I. RÎCĂ, **Optimizarea proceselor analitice**, 1985, 360 p.

N. PETRESCU, **Chimia extracției cu solvenți și aplicații**, 1985, 212 p.

V. EM. SAHINI, M. HILLEBRAND, **Chimie cuantică în exemple și aplicații**, 1985, 382 p.

1992 FEB 2 8

ISSN 0035–3930

S.C. UNIVERSUL c. 2280

43 426

Lei 120

F 1103

ACADÉMIE ROUMAINE

REVUE ROUMAINE DE CHIMIE

TOME 36

N°s 4–7

Avril–Juillet 1991

Rev. Roumaine Chim.

RRCHAX, 36, 4–7, p. 277–842(1991), Bucarest

EDITURA ACADEMIEI ROMÂNE

ACADÉMIE ROUMAINE

COMITÉ DE RÉDACTION

Rédacteur en chef:

I. G. MURGULESCU, membre de l'Académie Roumaine

Rédacteurs en chef adjoints :

A. T. BALABAN et V. EM. SAHINI, membres de l'Académie Roumaine

Collège de rédaction :

ECATERINA CIORĂNESCU-NENITZESCU, CR. SIMIONESCU, P. SPACU, membres de l'Académie Roumaine; M. BANCIU, I. HAIDUC, membres correspondants de l'Académie Roumaine; M. ANDRUH, M. D. GHEORGHIU, D. I. MARCHIDAN, G. NIAC et D. SĂNDULESCU

La Revue Roumaine de Chimie paraît 10 fois par an. Toute commande de l'étranger sera adressée à ROMPRESFILATELIA — sectorul Export-Import Presă, P. O. Box 12—201, télex 10376, prsfir 78 104 Bucarest, Calea Griviţei nr. 64—66, Bucureşti, Roumanie

Les manuscrits, les livres et les revues proposés en échange, ainsi que toute correspondance seront envoyés à la rédaction

REVUE ROUMAINE DE CHIMIE

125, Calea Victoriei, 79717 Bucarest, Roumanie, téléphone 50 76 80

EDITURA ACADEMIEI ROMÂNE

125, Calea Victoriei, 79717 Bucarest, Roumanie, téléphone 50 76 80

REVUE ROUMAINE DE CHIMIE

Tome 36, Nos 4–7 **Avril–Juillet 1991**

Professor A. T. Balaban's 60th anniversary 281–311

S. J. CYVIN, J. BRUNVOLL and B. N. CYVIN, Enumeration and classification of coronoid hydrocarbons. Part 12. Triple coronoids 313–332

E. B. GLUZ, M. E. KLETSKY and R. M. MINYAEV, Electronic and geometrical structure of 10π-electron systems : cyclooctatetraene dianion and its heteroatomic analogs 333–339

M. E. KLETSKY, E. B. GLUZ, V. YU. BIRYUKOV, R. M. MINYAEV and V. I. MINKIN, Electronic and geometrical structure of six-membered π-electron redundant systems 341–352

R. B. KING, Metal cluster topology. 12. Nickel carbonyl clusters 353–362

O. MEKENYAN, D. BONCHEV and D. N. DIMITROV, Information-theoretic approach to the aromaticity of chemical compounds based on superdelocalizability indices 363–377

IVAN GUTMAN, Topological properties of benzenoid systems. Merrifield-Simmons indices and independence polynomials of unbranched catafusenes . . 379–388

MILAN IVANUŠEVIĆ, SONJA NIKOLIĆ and NENAD TRINAJSTIĆ, A QSAR study of antidotal activity of H-oximes 389–398

IOAN MOȚOC and OSKAR E. POLANSKY, The effect of molecular topology on π-molecular orbital energies of pyridazine, pyrimidine, and pyrazine topomer triple 399–410

ILIE G. MURGULESCU and EUGENIA SĂLĂGEANU, The estimation of thermodynamic properties of fused silver halides 411–416

JOSETTE WEINBERG, ALEXANDRINA DONESCU, V. EM. SAHINI and M. COJOCARU, β-Lactam antibiotics. III. Electronic structure and physic-chemical properties of some antibiotic molecules and their intermediates 417–420

RODICA VÎLCU, I. GĂINAR, GH. ANIȚESCU and ȘT. PERIȘANU, A physical method for determining the solubility of gases in liquids at high pressures . 421–427

P. BUDRUGEAC and E. SEGAL, Derivatographic investigation of the compound *EVA* submitted to thermal accelerated ageing. Thermooxidative oxidation of the compound *EVA* 429–433

IULIA CONTINEANU, LUMINIȚA WAGNER, TATIANA ALEXANDRU and D. I. MARCHIDAN, The enthalpies of combustion and formation of 5-nitro-benzimidazol-2-one ; 5-amino-benzimidazol-2-one and 5-acetoacetylamino-benzimidazol-2-one 435–438

ALEXANDRU DUCA and DOINA BEJAN, Cyclic voltammetry of *p*-phenylendiamine 439–453

Rev. Roum. Chim. **36, 4–7, 277–842 (1991), Bucarest**

IRÉN E. KACSÓ, ANGELA BARAȘ-DIUDEA and MIRCEA V. DIUDEA, Molecular topology. 10. Fragmentation of molecular graphs within χ (Randić, [75Ran]) and Y [90Diu$_1$] topological indices . . . . 455—463

V. GOGONEA, D. CIUBOTARIU, E. DERETEY, M. POPESCU, I. IORGA and M. MEDELEANU, Surface area of organic molecules: a new method of computation . . . . 465—471

LUDOVIC KURUNCZI, RADU VÂLCEANU and ZENO SIMON, DEL RE calculations for dipole moments of phosphorus compounds. Parametrization and results . . . . 473—480

T. BRAUN and S. ZSINDELY, Trends and tendencies in instrumental analytical techniques with special emphasis on environmental analysis . . . . . . 481—506

WOLFGANG LINERT, VIKTOR GUTMANN, ALI TAHA and EL MARAGHY SALAH, Studies on chromotropic nickel(II)-complexes . . . . 507—517

P. SPACU, LUMINIȚA PATRON, SILVIA PLOȘTINARU and AL. BUTUCELEA, Complex compounds as raw materials for mixed oxides. VIII. Complex compounds of lanthanoids with Ba(II) and Cu(II) with malic acid . . . . 519—526

IONEL HAIDUC and IOAN SILAGHI-DUMITRESCU, The richness of structures available to P_2N_2 inorganic heterocycles. A topological and molecular orbital (EHMO) analysis . . . . 527—544

MARIA BREZEANU, LUMINIȚA PATRON, OANA CARP, MARIUS ANDRUH and NICOLAE STĂNICĂ, Coordination compounds as raw materials for spinelic oxides . . . . 545—550

LUCIA MUTIHAC, RADU MUTIHAC and CONSTANTIN LUCA, Mathematical modelling of ion pair carrier mediated transport through liquid membranes . . . . 551—561

MIECZYSŁAW MAKOSZA and ZBIGNIEW WROBEL, Vilsmeyer-Haack reaction of nitrobenzylic sulfones and nitriles . . . . 563—566

GEORGE A. OLAH, QI WANG, NORBERT KRASS and G. K. SURYA PRAKASH, Oxyfunctionalization of hydrocarbons. 16. Electrophilic hydroxylation and oxygenation of hydrocarbons with sodium percarbonate/trifluoromethanesulfonic acid . . . . 567—571

ALAN R. KATRITZKY, JACEK Z. BRZEZINSKI and JAMSHED N. LAM, 1-cyanobenzotriazole: a safe and convenient source of $^+$CN . . . . . 573—580

RENÉ BARONE, MICHEL ARBELOT, ANDRÉ BALDY, MICHEL CHANON and ROGER GALLO, RENE (REaction geNErator): a program to propose new reactions by construction of isomers and related reactive sets of simple functionalized compounds. Application to acids and esters . . . . . . 581—598

ERNST SCHMITZ and GISELA KOZAKIEWICZ, Formation of an α-lactone . 599—600

RICHARD NEIDLEIN, ZHIHUA SUI, WALTER KRAMER and ROLAND BOESE, Synthesis and structure analysis of 4-quinazolone derivatives from alkyl dicyanoacetates . . . . 601—611

CHRISTIAN ROUSSEL, HARIVELO G. RAJOHARISON and JACQUES METZGER, Acylation of alkenes using trifluoromethanesulphonic acid/acid halogenide acylation system (in French) . . . . 613—618

A. A. EL-BARBARY, M. FAHMY, M. EL-BADAWI, K. EL-BREMBALY and N. R. EL-BROLLOSI, Studies on 4-amino-5-aryl-1,2,4-triazole-3-thiones . 619—627

CARMEN ACERETE, MARÍA LUISA BAÑÓN, PILAR CABILDO, ROSA MARÍA CLARAMUNT, JOSÉ ELGUERO and JOSÉ LUIS LAVANDERA, Basicity-structure relationships in bisazolyl-methanes and -ethanes . . . 629—633

SHINJI NISHITANI and NICHOLAS BODOR, Polymer supported 1-benzyl-1,2-dihydroisonicotinamides as reducing agents . . . . 635—645

MARCUS E. BREWSTER, MING-JU HUANG, JAMES J. KAMINSKI, EMIL POP and NICHOLAS BODOR, Use of semiempirical molecular orbital parameters to probe dihydropyridine stability-implications to brain-targeting chemical delivery systems. 647—656

MARIA CAPROŞU, EUGENIA ŞTEFĂNESCU, MARGARETA UNGUREANU and MAGDA PETROVANU, New physiologically active pyridazines and phthalazines (in French) . . . . 657—663

SORIN MAGER, I. CRISTEA, LILIANA CRĂCIUN, F. IRIMIE and M. DIUDEA, New aminopyrimidinonic derivatives with potential biological activity . . . . 665—670

MIRCEA D. BANCIU, CĂTĂLINA HADA, MICHAELA DINA STĂNESCU, FILIP CHIRALEU and ECATERINA CIORĂNESCU, Heterocycles with annelated dibenzocycloalkane skeletons. VI. Six membered heterocycles with annelated 7H-dibenzo[a, c]cycloheptene skeletons . . . . 671—681

ANGELA POPESCU, LUMINITZA PÂRVULESCU, LAURENŢIU MEHEDINŢEANU, MARIETA PLĂVEŢI, MIRCEA D. GHEORGHIU, K. M. TURDIBEKOV and YU. T. STRUCHKOV, Synthesis of 1α, 2α-5,9-methano-5H-benzo[3,4]cyclobuta[1,2]cycloheptene derivatives. Molecular and crystal structure of 7-chloro-8-keto-1α, 2α-5,9-methano-5H-benzo[3,4]cyclobuta-[1,2]cycloheptene . . . . 683—691

SÎNZIANA ROŞCA, FILIP CHIRALEU and SORIN I. ROŞCA, Electrophilic aromatic substitution in arene-tricarbonyl-chromium complexes . . . . 693—705

ANGELA POPESCU, IRINA MATEI, MIRCEA D. GHEORGHIU, K. M. TURDIBEKOV and YU. T. STRUCHKOV, The synthesis of 8-substituted compounds of 7-H and 7-chloro-1β, 2β-5,9-methano-5H-benzo[3,4]cyclobuta[1,2]cycloheptenes. Molecular and crystal structure of 7,8α-dibromo-1β,2β-5,9-methano-5H-benzo[3,4]cyclobuta[1,2]cycloheptene . . . . . . 707—714

DAN STOICESCU and OVIDIU MAIOR, Phenoxatiin chemistry. Synthesis of pyrido[2,3-b]phenoxatiin . . . . 715—719

D. SCUTARU, I. MAZILU, M. VÂŢĂ, LUCIA TĂTARU, TATIANA LIXANDRU and V. BĂRBOIU, Functional derivatives of ferrocen-S-modifoed thioglycol acids (in German) . . . . 721—726

MARIUS ANDRUH, ELENA CRISTUREAN, RALUCA ŞTEFAN and CLAUDIU T. SUPURAN, Carbonic anhydrase inhibitors. 6. Novel coordination compounds of Pd(II), Pt(II) and Ni(II) with 6-ethoxy-benzothiazole-2-sulfonamide . . . . 727—732

GABRIELA STĂNCIUC, M. T. CĂPROIU, AGNETA CARAGHEORGHEOPOL and H. CĂLDĂRARU, Preparation and EPR spectra of capto-dative N-alkoxy-2,6-dinitro-α, α, α-trifluoro-p-tolyl-aminyls . . . . 733—739

MONICA POPESCU, REMUS ANDREESCU, SILVIA STĂNESCU, ŞTEFAN BRĂGĂREA and LUIZA JECU, An estimation of the possibilities for obtaining carotenoid- and chlorophyl-derived pigments from vegetal raw materials . . . . 741—748

SILVIA IOAN, MARIA BERCEA and BOGDAN C. SIMIONESCU, Flexibility parameter of high molecular weight polymers. 2. Polystyrene in solvent-nonsolvent mixtures . . . . 749—755

M. V. DIMONIE, N. N. MARINESCU and D. S. VASILESCU, Radical polymerization of acrylamide in homogeneous and heterogeneous systems. II. Emulsifier aggregates in organic media . . . . 757—760

MARCEL POPA and CLEOPATRA VASILIU OPREA, Mechanochemical reactions at the spinning from solution of the acrylonitrile — vinyl acetate — α-methyl styrene based ternary copolymer . . . . 761—770

RADU Z. TUDOSE, ECATERINA MERICĂ, ION MĂMĂLIGĂ and O. PETRUŞ, Study on mass transfer in thin film flow of suspensions . . . . 771—781

CAMELIA MIHĂILESCU, V. BULACOVSCHI and C. I. SIMIONESCU, Phase transfer free radical reactions. V. Copolymerization of methyl methacrylate with styrene under phase transfer conditions . . . . 783—788

GHEORGHIŢA JINESCU and VASILE LAVRIC, The multistage immobilised living yeast cells bioreactor . . . . 789—796

VALERIU V. JINESCU, The degradation of matter . . . . 797—808

N. I. IONESCU, M. S. CHIRCA and D. I. MARCHIDAN, The catalytic oxidation of methanol in oscillatory regime . . . . 809—818

ION BOLOCAN and FLAVIAN CUIBAN, Thermal decomposition of propylene . 819—828

MIHAI I. VASS and ION BALINT, Oxidative coupling of methane. The influence of reactant diffusion on the reaction . . . . 829—842

Revue Roumaine de Chimie, 36, 4–7, 281–311(1991)

PROFESSOR A. T. BALABAN'S 60th ANNIVERSARY

For Professor Alexandru T. Balaban's 60th anniversary, the Editorial Board of *Revue Roumaine de Chimie* expresses best wishes of good health and success in his career.

Alexandru T. Balaban was born in Timişoara on April 2, 1931. His father was an electromechanical engineer and the family lived in Reşiţa, Cluj, Bucharest, Petroşani, Baia Mare, and Bucharest again. Sandy Balaban studied in Bucharest (1937–1945) and Petroşani (1945–1949), and graduated in chemical engineering in 1953 after being a student at the Faculty of Industrial Chemistry in the Bucharest Polytechnic Institute. He was always classified first in his class. As a student, he appreciated much the lectures of Professors N. Racliş, P. Spacu, E. Bratu, and C. D. Nenitzescu.

In 1953 he took advantage of the just introduced possibility of Ph. D. fellowships for three years, starting to work in Prof. C. D. Nenitzescu's laboratory of organic chemistry, where he had already spent much time as a student. His Ph. D. thesis "Reactions Catalyzed by Aluminium Chloride" (1959) dealt with the mechanisms of the Scholl dehydrogenating condensation of aromatics, and of the reactions of alkanes and alkenes with carbon monoxide or with acid chlorides. In 1974, he obtained the title of Dr. Habil. (Docent, in Roumanian language).

In 1956, he became assistant at the Chair of Organic Chemistry of the Bucharest Polytechnic, and in parallel with the didactic tasks he again took advantage of a "once only" offer, one-year courses in nuclear physics and radiochemistry for the newly created Institute of Atomic Physics directed by Professor Horia Hulubei. He became a qualified radiochemist in 1957, and started to organize a Laboratory of Isotopically Labelled Organic Compounds, whose head he became in 1961. His small research group started to work with radioactive and stable isotopes; in addition, by interacting with physicists from the same Institute of Atomic Physics, this group embarked on chemical topics which could benefit from this interaction: stable free radicals for EPR spectroscopy, organoboron compounds for neutron capture therapy, and organic scintillators. Prof. Balaban remained associated with the Institute of Atomic Physics till 1974.

Professor Balaban's didactic career which had started at the Chair of Organic Chemistry continued, at the recommendation of Professor Nenitzescu, at the Chair of General Chemistry: lecturer (1962–1963), reader (1963–1966), and professor (1967). In 1970, he returned in the Chair of Organic Chemistry of the Bucharest Polytechnic as Professor, a position he holds also at present. He teaches not only Organic Chemistry for the 2nd and 3rd year students majoring in chemistry, but also optional courses on Homogeneous Catalysis, Strategy of Organic Syntheses, Homolytic Reactions. Since 1990 he has also taught General Chemistry in English for the Bucharest Polytechnic's Engineering Department.

For more than three years (1967–1970), Prof. Balaban interrupted his teaching (but not the contact with the research group in the Institute of Atomic Physics) for becoming Senior Research Officer at the Chemistry Section, Division of Research and Laboratories, International Atomic Energy Agency, Vienna, Austria; he was in charge with the organization of international standards for quality control of radiopharmaceuticals, and he organized several international meetings: Second Interamerican Conference on Radiochemistry in Mexico City, 1968; Latin-American Symposium on Radioisotope Production in Sao Paulo, Brazil, 1970; Symposium on Analytical Control of Radiopharmaceuticals, Vienna, 1970. He edited several books, and was the IAEA's liaison officer with the World Health Organization in Geneva on radiopharmaceuticals. In this quality, he was a consultant for the International Pharmacopeia, WHO, Geneva, 1971, and for several editions of Roumania's Pharmacopeia (1976).

Professor Balaban was elected a corresponding member of the Academy of Roumania in 1963, and a titular member in 1990. He became an annual active member of the New York Academy of Sciences in 1966, and in 1969 he was elected fellow of this Academy. In 1986 he was elected a fellow of the World Academy of Theoretical Organic Chemists (Paris). He is a member of the Royal Chemical Society, American Chemical Society, and Gesellschaft Deutscher Chemiker.

Since the foundation of *Revue Roumaine de Chimie*, Professor Balaban has been a member of the Editorial Board and is currently a

Deputy Head Editor. He was also a founding editor of the *Journal of Labelled Compounds* (and remained on the editorial board of this journal for 20 years) currently published by Wiley, and of *Mathematical Chemistry* (Mülheim an der Ruhr). He is a member of the Editorial Board for the following scientific journals: *Progresele Științei* (Bucharest), *Organic Preparations and Procedures International* (Boston), *Radioanalytical and Nuclear Chemistry* (Lausanne and Budapest), *Scientometrics* (Budapest), *Journal of Mathematical Chemistry* (Basel), *Polycyclic Aromatic Compounds* (London), *Advances in Heterocyclic Chemistry* (New York), *Journal of Computational Chemistry* (New York), *Journal of Chemical Information and Computer Sciences* (New York), *Bulletin des Sociétés Chimiques Belges* (Brussels).

In 1974, he was appointed UNESCO consultant for the CNRS—UNESCO Symposium on Current Trends in Coordination Chemistry held in Paris, but he was not allowed to attend the meeting, therefore he had to compile the secretary's report from transcripts and tape recordings.

At present, Professor Balaban is the chairman of three Commissions of the Roumanian Academy: for New Materials, for Scientics, and for Mathematical Chemistry. He was also vice-chairman of the Commission for the History and Philosophy of Science.

Professor Balaban is National Representative for IUPAC Commissions on Nomenclature of Organic Chemistry and on Physical Organic Chemistry. He is Editor of the series: "Roumanian adaptation of IUPAC chemical nomenclature" in which three volumes have already appeared (on inorganic, organic, and biochemical nomenclature).

For his scientific activity, Professor Balaban was awarded in 1962 the Chemistry Prize "N. Teclu" of the Roumanian Academy, and two Roumanian medals: Order or Labour (1963), and Order of Scientific Merit (1966).

At the age of 12—14 years, as a young "amateur chemist", he had published experiments in *Ziarul Științelor și Călătoriilor*, and obtained several prizes in competitions sponsored by this journal. Much later, his contact with the research school founded by C. D. Nenitzescu determined the style of Professor Balaban's research activity. Like Professor Nenitzescu, he invented new problems and went on to solving them. He grouped around him several young chemists tied only by their interest in research. About 20 coworkers obtained their Ph. D. degrees with him till now; some of them came from Egypt, Jordan, or Korea. For working with Professor Balaban, scientists have come from Britain, USA, USSR, Greece, and Turkey.

Having started to learn foreign languages in high school, professor Balaban speaks fluently English, French, and German, and has also lectured in Russian and Spanish. He attended many scientific meetings, and was invited to be plenary lecturer in several chemical congresses and symposia such as: Kekulé Symposium (Leipzig, 1966), Dozententagung (Halle, 1973), Quantum Chemistry Meeting (Czechoslovakia, 1969), Dynamic Stereochemistry Symposium (Brussels, 1972), Annual Chemistry Meeting (Ljubljana, 1972), Heterocyclic Chemistry Symposia (Kühlungsborn, 1976; Brussels, 1983), Aromaticity Symposium (Dubrovnik, 1979), Symposium on Labelled Compounds (Kansas City, 1982), European Symposia on Organic Chemistry (England, 1983; France, 1985), Theoretical Chemistry Symposia (Yugoslavia, 1982; Portugal, 1984), IUPAC Organic Synthesis Symposium (Moscow, 1986), NATO Symposium on Substituent Effects in Free Radical Chemistry (Louvain la Neuve, 1986), Correlational Analysis in Organic Chemistry (Poznan, 1988), International Conference on Nitroxide Radicals (Novosibirsk, 1989), 2nd World Conference of Theoretical Organic Chemists (Toronto, 1990).

In 1989 and 1990, he was appointed "Wilhelm Ostwald Professor for Theoretical Chemistry" at the Leipzig University.

Professor Balaban was invited to lecture at various universities abroad, and took part in lecture tours in India (1964), West Germany (1964, 1973, 1979, 1983), USA (1971, 1973, 1982, 1986, 1990), Israel (1969), England (1970, 1979), France (1980, 1985), Switzerland (1968), Belgium (1983), Denmark (1984), USSR (1975, 1986), and East Germany (1989). However, during the last twenty years, even more frequent were the cases when he was not allowed to attend scientific meetings to which he had been invited.

The research activity of Professor Balaban extends over three main areas: organic chemistry, labelled compounds, and theoretical chemistry. His publications include four edited books, eight authored books, more than 400 papers in scientific journals, 40 book chapters, and more than 20 Roumanian patents (most of which are in collaboration with Dr. A. Dinculescu on pyridinium salts with potential biological activity, and are not listed here).

(i) **Organic chemistry**

Organic reaction mechanisms. The theme of the Ph. D. thesis was the determination of reaction mechanisms for several reactions catalyzed by aluminium chloride; on replacing this catalyst by anhydrous benzenesulfonic acid, it was established that the Scholl reaction is an electrophilic substitution of an aromatic ring by the conjugate acid of another aromatic ring; the reaction of alkanes with carbon monoxide proceeds *via* nucleophilic attack of CO on carbocations. The reaction of phenylazide with anhydrous benzenesulfonic acid yields the benzenesulfonate ester of *para*-aminophenol *via* the same carbocationic intermediate as in the rearrangement of N-phenylhydroxylamine to *para*-aminophenol.

Pyrylium salts. A serendipitous discovery during the Ph. D. work was a new synthesis of pyrylium salts: from CO, tert-butyl chloride, and anhydrous aluminium chloride at high pressure, in addition to the products validating the abovereaction mechanism, a salt-like product was obtained in small yield, which proved to be 2,6-di-*t*-butyl-4-methylpyrylium chloroaluminate (without IR and NMR spectra!). This olefin diacylation was then transformed into a high-yield reaction by optimizing the reaction conditions. Independently, Praill in London discovered the same reaction, and this led to a life-long friendship. By systematic exploration of the scope and limitations of the diacylation of olefins, it was determined that this is the best synthesis of alkyl-substituted pyrylium salts with identical substituents in positions 2 and 6. The physical properties of pyrylium salts wereexplored systematically by Professor Balaban and his coworkers. The reactions of pyrylium salts with nucleophiles lead to a large variety of acyclic, carbocyclic and heterocyclic compounds (furan, pyrazoline, diazepine, indolizine and oxazoline derivatives were found by Professor Balaban; other reactions in this area were found by Dimroth in Marburg, by Schroth in Leipzig and Halle, and by Dorofeenko in Rostov/Don and again life-long collaborations were the result). In such reactions, the pyrylium cation behaves as an electrophilic conjugated carbonylic synthon of five carbon atoms vinylogous to acyl cations and β-halovinyl ketones. In cooperation with Professors Dorofeenko and Schroth and several younger coworkers, the first monograph on pyrylium salts was published as a supplementary volume in the series "Advances in Heterocyclic Chemistry" edited by A. R. Katritzky.

2-Acylfurans. Ring contraction of pyrylium salts under the attack by hydrogen peroxide leads in good yield to 2-acylfurans. In turn, these compounds serve as starting materials for the synthesis of other classes of compounds, and raise interesting conformational problems.

Oxazoles and thiazoles. 2,5-Diaryloxazoles are among the best organic scintillators for detecting nuclear radiations. A new synthesis of such compounds was devised starting from a recently-discovered acylaminoacylation of aromatic compounds under the catalytic influence of aluminium chloride, in cooperation with Professor Ecaterina Ciorănescu--Nenitzescu and L. Bîrlădeanu. In reviews on oxazole syntheses, this reaction is considered very promising. Recently, it was shown by Professor Balaban and coworkers that the reaction can be extended to other heterocycles such as thiazoles. The laser effect of 2,5-diaryloxazoles was investigated in collaboration with Dr. Rullière (Bordeaux).

Stable aminyl free radicals. Having prepared new analogs of N,N--diphenyl-N′-picryl-hydrazyl, Professor Balaban became curious to learn about the factors determining the stability of such free radicals. With his coworkers, a systematic exploration of steric and electronic factors was undertaken. It became apparent that in addition to steric shielding, the most important factor was the presence of an electron donor and an electron acceptor both attached to the same nitrogen atom. Thus, the first "push-pull" aminyls were prepared and studied by EPR spectroscopy; then, other donors such as alkoxy groups, and other acceptors such as cyano or arenesulfonyl groups were introduced. The latter acceptors are particularly interesting, as they lead to simple EPR spectra, and give rise to interesting magnetic non-equivalence owing to high rotation barriers. With acyl groups as acceptors, the rotation barriers were measured experimentally from variable-temperature EPR spectra.

Carbon-centered analogous free radicals were investigated by Katritzky who named them "mero-stabilized", and by Viehe, who coined the term "capto-dative" free radicals.

Organoboron compounds. In the search for boron compounds which might be stable towards hydrolysis for neutron capture therapy of tumors that are inaccessible to surgery, four-coordinated boron compounds were synthesized from diarylborinic acids or benzodioxaboroles and unsaturated hydroxy-ketones such as tropolones, 1,3-diketones, or 1,2-dibenzoyl-cyclopentadiene (in all cases a dipolar structure results, with the positive charge stabilized by electronic delocalization); the coordinative bond between boron and the carbonyl oxygen leads to the formation of

5-, 6-, and 7-membered chelate rings, respectively. The very large dipole moments confirm the structures. Spiranic systems give rise to chiral compounds when suitably substituted, as it was proved by NMR spectroscopy using diastereotopic isopropyl groups.

Rapidly fluctuating molecules. When in the above compounds boron was replaced by arsenic, the resulting compounds presented NMR spectra which seemed to indicate an equivalence of atoms as in the delocalized coordinated boron analogues. However, this was shown by X-ray crystallography to be due to rapidly fluctuating bonding; this class of molecules is among the most rapidly fluctuating structures as shown in a joint research with Professor V. I. Minkin from the University of Rostov/Don.

Stable free radicals with oxygen. Aroxyls with steric shielding around the oxygen atom, derived from 2,6-di-*t*-butylphenol, are important constituents of antioxidants and stabilizers. New derivatives of such systems were synthesized for investigations of spin density by means of EPR spectra. Another class of stable free radicals with many applications as spin labels, especially in biochemistry, is represented by nitroxides. New cationic nitroxides were synthesized with pyridinium residues; they were used in a joint research with Professors L. Packer and R. Mehlhorn from the University of California at Berkeley for studies of biomembranes. N-Aryl-N-nitroso-nitroxides were prepared for the first time by Professor Balaban and coworkers; their EPR spectra indicated by their spin densities a different conformation from that of the analogous N-acyl-N-aryl-nitroxides; this difference was rationalized theoretically in a joint paper with Professor P. von Ragué Schleyer (University of Erlangen-Nürnberg).

Charge-transfer salts of organic cations. It was observed that unlike salts with perchloric or fluoroboric acid, pyrylium iodides had a deeper colour. A systematic study was undertaken for this phenomenon, and it was found that pseudohalogens (thiocyanate, selenocyanate) gave still more pronounced charge transfer bands. Organic anions such as tetracyanopropenide and the 2-aza-analogue behaved likewise.

Pyridinium salts and intramolecular rotations barriers. Primary amines convert pyrylium salts into pyridinium salts. With aromatic amines, biphenyl analogues result; proton NMR spectra of 2,4,6,-trimethyl-derivatives can serve for measuring the ring current in the aromatic ring. Atropisomerism can give rise to chiral compounds or, when two *ortho*-tolyl substituents are attached to the pyridinium ring, to diastereoisomers. Rotation barriers were measured by dynamic NMR. With an N-9-fluorenyl residue, stable rotamers were prepared; they can interconvert thermally at elevated temperatures. With an N-1-indanyl group, the resulting chirality of the corresponding substituted pyridinium salt can be demonstrated by NMR *via* diastereotopic isopropyl groups. Also with N-alkyl groups it was possible to measure rotation barriers; they are among the highest yet determined for similar systems, probably because of the lower bond distance for ^+N-C bonds than for $C-C$ bonds.

Vinylogous pyrones. Propene derivatives can be diacylated to pyrylium salts, and it was shown that isobutene derivatives can be triacylated at all marginal carbons leading to vinylogous 4-pyrones. Doubly vinylogous pyrones were also prepared by Professor Balaban and coworkers.

A new naphthalene synthesis. 1,3-Diketones react with benzylmagnesium halides and the product can be dehydrated to a 1,3-disubstituted naphthalene. Independently, Professor Leitch (Canada) discovered the same reaction.

(ii) Isotopically labelled compounds

Deuterium-labelled compounds. On slight heating in heavy water, alkyl-substituted pyrylium salts exchange their hydrogens in benzylic positions attached to 2- and 4-standing alkyl groups on the pyrylium ring. This isotope exchange is regioselective, proceeding faster for 4-alkyls than for 2 (6) alkyls, and this allowed the preparation of selectively deuterated pyrylium salts and pyridines. With benzyl groups bearing various substituents, it was possible to influence the rate of this isotope exchange so that the reaction in 4-position became the slower one. Then the deuterated pyrylium salts can be converted into other compounds, which cannot be deuterated as easily as pyrylium salts.

Isotope effects. The rate of de-deuteration is lower than that of deuteration, and the process is again regioselective; this fact was put to use synthetically. It was observed that selectively deuterated pyridines present secondary isotope effects which depend both on steric factors of the substituents in 2 and 6 positions, and on the electronic effects of substituents in positions 2, 4, and 6; this was valid for quaternization with methyl iodide, as shown in a joint study with Proffessors C. Roussel and J. Metzger from the University of Marseille. In protonations, only the electronic effect operated (the proton is the smallest electrophile), while in lanthanide-induced shifts only the steric effect was manifest, because of the large volume of the lanthanide shift reagent.

Tritiations. Aluminium chloride catalyzes the tritiation of aromatic and aliphatic compounds by tritiated water *via* the formation of a superacid, as shown in several papers published in collaboration with the late Constantza Măntescu.

Catalytic automerization of polycyclic aromatics. On treatment with aluminium chloride, it was known that chrysene equilibrates with benzanthracene. This fact led to the supposition that naphthalene and phenanthrene might undergo degenerate rearrangements (for which Professor Balaban coined the term "automerizations"). An investigation with naphthalene labelled with carbon-14 in hot benzene solution seemed to indicate such a reaction, but on re-checking with carbon-13 it became apparent that the previous results had been erroneous (for reasons still unknown). Recent investigations with phenanthrene labelled with carbon-13 in various positions in a melt of $AlCl_3 \cdot NaCl$ around 200° gave evidence that the automerization does occur. Previously, it had been found by L. T. Scott that polycyclic aromatic hydrocarbons automerize at temperatures above 1000°.

Compounds labelled with carbon-14. The reversibility of the Friedel-Crafts aliphatic acylation was demonstrated by means of labelling. Labelled alkanes were also synthesized.

(iii) Theoretical chemistry

Aromaticity. One of the first theoretical studies of Professor Balaban was a systematic approach to predicting all possible monocyclic aromatic (carbocyclic and heterocyclic) compounds on the basis of Pauli's principle and Hückel's rule. The partition of atoms belonging to aromatic rings into three types was independently considered by Katritzky (hence the long friendly relationship), and has been adopetd in monographs on heterocyclic chemistry. On associating each atom type with an "aromaticity constant", a quantitative prediction of global electronegativity and stability of the aromatic system became possible.

Valence isomers of annulenes and cognate systems. By applying graph theoretical principles, it was possible for the first time to predict all possible valence isomers of benzene and other annulenes. Then valence isomers of benzoannulenes, heterocyclic aromatic systems, or homoannulenes were considered. On this basis, a comprehensive review was published in book form.

Chemical applications of graph theory. In addition to the above topics, graph theory can be useful to chemistry in many problems. Professor Balaban is a pioneer in the recent renaissance of graph-theoretical applications in chemistry. He used, in a long collaboration with professor F. Harary (University of Michigan at Ann Arbor), "dualist" graphs of polycyclic aromatic hydrocarbons (PAH's) for the complete enumeration, coding, and nomenclature of such systems. Based on dualist graphs, new definitions of cata-, peri-, and corona-condensed PAH's were proposed, and a corresponding nomenclature was devised; the carcinogenic PAH's with bay regions were enumerated. In another collaboration with Professor I. Tomescu (Faculty of Mathematics, Bucharest University), the enumeration of Kekulé structures for certain PAH's was achieved algebraically. In collaborations with Professor S. J. Cyvin (University of Trondheim, Norway) and with other chemical graph-theorists, a consensus on the naming of PAH's was published.

The first "reaction graphs" were introduced by Professor Balaban, and he edited the first book on chemical applications of graph theory. Two graphs are known in the literature as "Balaban graphs". New terms were introduced by him: *isoarithmic* PAH's have the same numbers of Kekulé structures e.g. *fibonacenes* (helicenes or zig-zag *catafusenes* with the same numbers of benzenoid rings).

Topological indices. For quantitative structure-activity or structure-property relationships, molecular structures can be associated with numbers, called "topological indices" (TI's). Professor Balaban devised many new TI's and used them for rationalizing octane numbers of alkanes and physico-chemical properties of organic compounds. The highly discriminating TI denoted by J is known in the literature as "the Balaban index".

Computer-aided chemical documentation. In a series of papers published with Professor D. Bonchev and Dr. O. Mekenyan (Burgas, Bulgaria), a system for input and retrieval of topological information on molecular structures was published making use of hierarchically ordered extended connectivities.

Cages. The reaction graphs are related to what is known by graph-theorists under the name of "cages", i.e. minimal highly symmetric regular graphs of degree three whose minimal circuit (girth) has a given number of points. In a mathematical excursion, Professor Balaban found the yet unknown cages with girth 10 and 11. He also noticed relationships among cages having homologous girths.

Carbon and its nets. In addition to the diamond and graphite lattice, other nets can be imagined for elemental carbon. The first to analyze theoretically such alternative nets was Professor Balaban ; these investigations were continued in joint papers with Professor Roald Hoffmann (Cornell University).

Aza-analogues of platonic hydrocarbons. Jointly with Professor J. Elguero (Madrid), energies and stabilities of aza-analogues of tetrahedrane, cubane, and dodecahedrane were investigated, in order to predict which of these compounds stand better chances to be synthesized.

Dications. Professor Balaban's prediction that the dication of dioxygen (which is isoelectronic with the dinitrogen molecule) should be stable was verified experimentally later. More recently, in a joint paper with Professors Schleyer and Pople, the ethane dication was calculated to have a carbenium-carbonium structure, rather than a structure analogous to the isoelectronic diborane.

Isoprenoid structures. For establishing whether a given chemical structure is decomposable into isoprenoid subgraphs, computer programs were devised in collaboration with Professor S. Marcus (Faculty of Mathematics of the Bucharest University).

Modelling of polymers. For stereoregular polymers and elastomers, as well as for regularly repeating sequences in copolymers, all possible higher-order systems were found.

★

In all the above research activity, Professor Balaban has been assisted by many younger coworkers, who are too numerous to be listed here, and whose names appear in the appended bibliography. They have learnt from him that, even under the unfavourable circumstances in which research was and is being carried out in Romania (by comparison with advanced countries), one can make significant contributions if one tries hard enough, and if one is dedicated to one's mission.

With this anniversary volume, the colleagues from Roumania and abroad, Professor Balaban's students, and his many friends, enclose good wishes for a long and productive life for many happy years to come.

A. ARTICLES IN SCIENTIFICAL PERIODICALS

1. C. D. Nenitzescu and A. T. Balaban, *Chem. Ber.*, 1958, **91**, 2109–2116 : Zum Chemismus der Hybrid-Übertragung bei der Schollschen Reaktion.
2. A. T. Balaban and P. T. Frangopol, *Studii şi cercetări chimice, Acad. R. P. România*, 1958, **6**, 427–432 : Prepararea 2,5-difeniloxazolului (PPO), scintilator organic în soluţie.
3. A. T. Balaban, *Studii şi cercetări chimice, Acad. R. P. România*, 1959, **7**, 257–295 : O încercare de sistematizare a compuşilor aromatici monociclici (Aromaticitate. I).

4. A. T. Balaban and C. D. Nenitzescu, *Studii şi cercetări chimice, Acad. R. P. România*, 1959, **7**, 521—529 : Despre decarbonilarea clorurii acidului 1,4-dihidronaftalin-1-carboxilic şi consecinţele asupra mecanismului reacţiilor Scholl şi Gattermann-Koch.
5. A. T. Balaban and C. D. Nenitzescu, *Liebigs Ann. Chem.*, 1959, **625**, 66—73 : Aluminiumchlorid-Katalysen. XXVI. Die Reaktion der Alkane mit Kohlenoxyd.
6. A. T. Balaban and C. D. Nenitzescu, *Liebigs Ann. Chem.*, 1959, **625**, 74—88 : Aluminiumchlorid-Katalysen. XXVII. Eine Synthese von Pyryliumsalzen aus Säurechloriden und Olefinen (Pyrylium Salts, I).
7. A. T. Balaban, *Tetrahedron Letters*, **1959**, No. 5, 14—15 : Possible formation of tetraphenylcyclobutadiene.
8. A. T. Balaban and C. D. Nenitzescu, *Tetrahedron*, 1960, **10**, 55—64 : Reactions Catalysed by Aluminium Chloride. XXVIII. The reaction of cycloalkanes with carbon monoxide.
9. A. T. Balaban and C. D. Nenitzescu, *Chem. Ber.*, 1960, **93**, 599—602 : Ringverengung von Pyryliumsalzen zu Furanderivaten.
10. A. T. Balaban, V. E. Sahini and E. Keplinger *Tetrahedron*, 1960, **9**, 163—174 : Electronic absorption spectra of alkyl- and phenyl-substituted pyrylium salts.
11. A. T. Balaban and C. D. Nenitzescu, *Izv. Akad. Nauk SSSR, Otdel. Khim. Nauk*, **1960**, 2064—2065 : Ultravioletovyi spektr pogloshchenia khlorata pirilia.
12. A. T. Balaban, *Izv. Akad. Nauk SSSR, Otdel. Khim. Nauk*, **1960**, 2260—2261 : K voprosu o sistematizatsii tipov troinoi sviazi.
13. N. Martalogu, D. Mumuianu, M. Magda and A. T. Balaban, *Studii şi cercetări chim., Acad. R. P. Romania*, 1960, **8**, 329—338 : Analiza pentametilbenzenului deuterat la nucleu prin spectrometrie de masă.
14. A. T. Balaban and C. D. Nenitzescu, *Tetrahedron Letters*, **1960**, No. 2, 7—10 : Preparation of pyrylium salts by olefin diacylation : The pyrylium salts formed in amylene diacetylation with various catalysts.
15. A. T. Balaban and C. D. Nenitzescu, *J. Chem. Soc.*, **1961**, 3553—3560 : Pyrylium salts obtained by diacylation of olefins. II. The two pyrylium salts formed in the diacetylation of 2-methyl-2-butene.
16. A. T. Balaban and C. D. Nenitzescu, *J. Chem. Soc.*, **1961**, 3561—3563 : Pyrylium salts obtained by diacylation of olefins. III. Diacylation of cyclic olefins and a novel synthesis of isoquinoline derivatives.
17. A. T. Balaban, C. D. Nenitzescu, M. Gavăt and G. Mateescu, *J. Chem. Soc.*, **1961**, 3564—3565 : Pyrylium salts obtained by diacylation of olefins. IV. Di- and triacetylation of allylbenzene.
18. A. T. Balaban and C. D. Nenitzescu, *J. Chem. Soc.*, **1961**, 3566—3572 : Reaction of pyrylium salts with alkali cyanides (Reaction of pyrylium salts with nucleophiles. I.).
19. A. T. Balaban, A. Ghenea and C. D. Nenitzescu, *Izv. Akad. Nauk SSSR, Otdel. Khim. Nauk*, **1961**, 1102—1107 : Pirilievyie soli poluchennyie bisatsilirovaniem olefinov. V. Bisatsilirovanie di- i triizobutilena.
20. A. T. Balaban, G. Mateescu and C. D. Nenitzescu, *Studii şi Cercetări Chim. Acad. R. P. Romania*, 1961, **9**, 211—218; *Rev. Chim. Acad. R. P. Romania*, 1961, **6**, 295—302 : Pyrylium salts obtained by diacylation of olefins. VI. Acetylation of benzylketones.
21. A. T. Balaban and C. D. Nenitzescu, *Studii şi cercetări chim., Acad. R. P. Romania*, 1961, **9**, 251—274; *Rev. Chim. Acad. R. P. Romania*, 1961, **6**, 269—294 : Investigations in the class of pyrylium salts.
22. A. T. Balaban, P. T. Frangopol, M. Mărculescu and I. Bally, *Tetrahedron*, 1961, **13**, 258—267 : Factors affecting stability and equilibria of free radicals. I. Steric factors in hydrazyls.
23. P. T. Frangopol, A. T. Balaban, L. Bârlădeanu and E. Cioränescu, *Tetrahedron*, 1961, **16**, 59—67 : Synthesis of 2,5-diaryloxazoles through Friedel-Crafts reaction of azlactones with aromatic hydrocarbons (Aminoketone synthesis. III).
24. A. T. Balaban, G. Mihai, R. Antonescu and P. T. Frangopol, *Tetrahedron*, 1961, **16**, 68—73 : Tropovinylene spiroborates, a novel class of dipolar boron heterocycles (Heterocyclic organoboron compounds. I).
25. A. T. Balaban, M. Mărculescu, I. Pascaru, M. Rotaru, A. Valeriu and M. Weiner, *Z. Phys. Chem. (Leipzig)*, 1962, **219**, 285—294 : ESR hyperfine structure in hydrazyl free radicals (Factors affectin g stability and equilibria of free radicals. II.).
26. A. T. Balaban and Z. Simon, *Tetrahedron*, 1962, **18**, 315—321 : Aromaticity constants (Aromaticity. II.).
27. A. T. Balaban, P. T. Frangopol, G. Mateescu and C. D. Nenitzescu, *Bull. Soc. Chim. France*, **1962**, 298—302 : Structure et réactions des pyranolhydrazides (Réactions des sels de pyrylium avec les nucléophiles. II).

28. E. Gârd and A. T. Balaban, *J. Electronal. Chem.*, 1962, **4**, 48—50 : Polarographic reduction of pyrylium salts.
29. A. T. Balaban, G. Mihai and C. D. Nenitzescu, *Tetrahedron*, 1962, **18**, 257—259 : Reduction of pyrylium salts with sodium borohydride. (Reactions of pyrylium salts with nucleophiles. III).
30. A. T. Balaban, D. Farcașiu and C. D. Nenitzescu, *Tetrahedron*, 1962, **18**, 1075—1078 : Pyrylium salts obtained by diacylation of olefins. VII. Diacylation of propene to 2,6-disubstituted pyrylium salts.
31. A. T. Balaban M. Gavăt and C. D. Nenitzescu, *Tetrahedron*, 1962, **18**, 1079—1081 : Pyrylium salts obtained by diacylation of olefins. VIII. Intramolecular diacylation.
32. A. T. Balaban, P. T. Frangopol, A. R. Katritzky and C. D. Nenitzescu, *J. Chem. Soc.*, **1962**, 3889—3895 : Pyrylium salts obtained by diacylation of olefins. IX. Formation of vinylogous pyrones by triacylation of isobutene.
33. A. T. Balaban, E. Barabaș and M. Fărcașiu, *Chem. and Ind.*, **1962**, 781—782, Pyrylium salts obtained by diacylation of olefins. X. Diacetylation of 2-methyl-2-butene catalysed by beryllium chloride.
34. A. T. Balaban, G. D. Mateescu and M. Elian, *Tetrahedron*, 1962, **18**, 1083—1094 : Infrared absorption spectra of pyrylium salts.
35. N. I. Shuikin, I. F. Belskii, A. T. Balaban and C. D. Nenitzescu, *Izv. Akad. Nauk SSSR, Otdel. Khim. Nauk*, **1962**, 491—493 : Kataliticheskoe prevrashchenie gomologov 2-atsetilfurana v trialkiltetragidropirany.
36. A. T. Balaban, M. Mărculescu-Frangopol and P. T. Frangopol, *Isotopentechnik*, 1962, **2**, 235—237 : Darstellung von Pyryliumsalzen durch Diacylierung von Alkenen. XI. ^{14}C-Kernmarkierte aromatische Verbindungen aus Pyryliumsalzen.
37. E. Ciorănescu, L. Bârlădeanu, A. T. Balaban and C. D. Nenitzescu, *Tetrahedron Letters*, **1962**, 359—361 : Influence of water in the $AlCl_3$-catalysed reaction of unsaturated azlactones with aromatics (Erratum, *ibid.*, p. 887).
38. Z. Simon and A. T. Balaban, *Rev. Chim. Acad. R. P. Romania*, 1962, **7**, 15—22 : Relative stability of isomeric aromatic monocyclic systems appreciated by M.O. methods. (Aromaticity. III.).
39. E. Ciorănescu, L. Bârlădeanu, A. T. Balaban and P. T. Frangopol, *Rev. Chim. Acad. R. P. Romania*, 1962, **7**, 755—762 : Aminoketone synthesis. IV. Preparation of 2-(1-naphthyl)-5-aryloxazoles.
40. A. T. Balaban, *Rev. Chim. Acad. R. P. Romania*, 1962, **7**, 675—682 : Contribution to a systematization of heterolytic reactions.
41. A. T. Balaban, P. T. Frangopol and M. Keplinger, *Spectrochim. Acta*, 1963, **19**, 367—368 : Steric hindrance evidenced by absorption spectra of 2-acyl-3,5-dialkylfurans and their polynitrophenylhydrazones.
42. Z. Simon and A. T. Balaban, *Studii și Cercetări Chim. Acad. R. P. Romania*, 1963, **11**, 53—60; *Rev. Chim. Acad. R. P. Romania*, 1963, **8**, 199—206 : Simple MO treatment of electronic spectra of five-membered aromatic heterocycles.
43. I. Necșoiu, A. T. Balaban, I. Pascaru, E. Sliam, M. Elian and C. D. Nenitzescu, *Tetrahedron*, 1963, **19**, 1133—1142 : The mechanism of the Etard reaction.
44. C. Măntescu and A. T. Balaban, *Canad. J. Chem.*, 1963, **41**, 2120—2121 : Tritiation of aromatics by HTO-promoted aluminium chloride. (Tritiations by HTO-promoted aluminium chloride. I.).
45. A. T. Balaban, I. Bally, P. T. Frangopol, M. Băcescu, E. Ciorănescu and L. Bîrlădeanu, *Tetrahedron*, 1963, **19**, 169—176 : Preparation of 2-(4-biphenylyl)-5-aryloxazoles by Friedel-Crafts reaction of azlactones with aromatics. Electronic absorption spectra of 2,5-diaryloxazoles (Aminoketone synthesis. V.).
46. A. T. Balaban, *Tetrahedron Letters*, **1963**, 91—94 : Pyrylium salts formed in olefin diacylation. XII. Diacylation of 2-methylpropenylbenzene.
47. A. T. Balaban, *Rev. Chimie (București)*, 1963, **14**, 158—160 : Numere magice de electroni și nucleoni.
48. A. T. Balaban and I. Stănoiu, *Rev. Chim. Acad. R. P. Romania*, 1963, **8**, 197—198 : Sulphur cell windows for infrared spectra of aqueous solutions.
49. A. T. Balaban, *Comptes rendus*, 1963, **256**, 4041—4043 : Préparation des halogénures de pyrylium.
50. A. T. Balaban, *Comptes rendus*, 1963, **256**, 4239—4242 : Sur le mécanisme de la formation des sels de pyrylium par deshydrogenation des 1,5-dicétones.
51. A. T. Balaban, L. Bîrlădeanu, I. Bally, P. T. Frangopol, M. Mocanu and Z. Simon, *Tetrahedron*, 1963, **19**, 2199—2201 : Preparation and spectra of para-substituted 2,5-diphenyloxazoles (Aminoketone synthesis VI.).

52. A. T. Balaban, E. Barabaş and G. Mateescu, *Rev. Chim. Acad. R. P. Romania*, 1963, **8**, 139—148 : A product obtained from benzoin and beryllium chloride.
53. A. T. Balaban, *Rev. Chimie (București)*, 1963, **14**, 603 : Prepararea fluorurii de bor.
54. A. T. Balaban, I. Pascaru and I. Stănoiu, *Ann. Phys.*, 1963, **8**, 513 : Spectres de résonance paramagnétique électronique des solutions d'acides organiques dans le chlorure de chromyle.
55. A. T. Balaban, M. Mocanu and Z. Simon, *Tetrahedron*, 1964, **20**, 119—130 : Charge transfer spectra of pyrylium iodides. (Molecular complexes with aromatic cations as electron-acceptors. I.).
56. A. T. Balaban, C. Bratu and C. Rențea, *Tetrahedron* 1964, **20**, 265—269 : One-electron reduction of pyrylium salts.
57. A. T. Balaban, I. Bally, R. J. Bishop, C. N. Rențea and L. E. Sutton, *J. Chem. Soc.* **1964**, 2382—2387 : Novel spiroborațes and a dipole moment study of tropophenylene spiroborates (Heterocyclic organoboron compounds. II).
58. A. T. Balaban, M. Gavăt, P. T. Frangopol, M. Mocanu and C. D. Nenitzescu, *Rev. Roum. Chim.*, 1964, **9**, 79—92 : Pyrylium salts obtained by olefin diacylation. XIII. Pyrylium salts with *para*-substituted phenyl groups. *Studii și Cercetări Chim. Acad. R. P. Romania*, 1964, **12**, 71—85.
59. D. Fărcașiu, M. Fărcașiu and A. T. Balaban, *Rev. Roum. Chim.*, 1964, **9**, 137—145 : Pyrylium salts obtained by diacylation of olefins. XIV. Diacylation of α,β-unsaturated ketones, β-chloroketones and β-hydroxyketones derived from 2-methyl-2-butene. *Studii și Cercetări Chim. Acad. R. P. Romania*, 1964, **12**, 131—138.
60. A. T. Balaban, G. R. Bedford and A. R. Katritzky, *J. Chem. Soc.*, **1964**, 1646—1649 : The nuclear magnetic resonance of heterocyclic systems. Part I. Pyrylium salts.
61. A. T. Balaban and C. D. Nenitzescu, *Org. Synth.*, 1964, **44**, 98—103 : 2,4,6-Trimethylpyrylium perchlorate. Reprinted in *Org. Synth. Coll. Vol. 5*, 1106—1108 (1973).
62. A. T. Balaban, E. Gârd and C. N. Rențea, *Abh. Dtsch. Akad. Wiss., Klasse Chem. Geol. u. Biol.*, **1964**, 659—663 : Isotopic exchange of methyl hydrogens in aqueous solutions of 2,4,6-trimethylpyrylium salts. (Isotopic exchange of active methyl hydrogens. I).
63. A. T. Balaban and Z. Simon, *Rev. Roum. Chim.*, 1964, **9**, 99—104 : Aromaticity. IV. On the aromaticity of boron- and nitrogen-containing five-membered heterocycles. *Studii și Cercetări Chim. Acad. R. P. Romania*, 1964, **12**, 93—98.
64. M. Frangopol, A. Ghenunche, P. T. Frangopol and A. T. Balaban, *Tetrahedron*, 1964, **20**, 1881—1888 : Pyrylium salts formed by diacylation of olefins. XV. ^{14}C-Tracer study of the acetylation of 4-chloro-3,4-dimethyl-2-pentanone.
65. D. Fărcașiu, A. T. Balaban and M. Gutman, *Rev. Roum. Chim.*, 1964, **9**, 727—741 : On the acetylation of 4-chloro-3,4-dimethylpentan-2-one with acetyl chloride-1-^{14}C.
66. Z. Simon and A. T. Balaban, *Rev. Roum. Chim.*, 1964, **9**, 339—349 : Energy levels of pyrylium salts with *para*-substituted phenyl groups. *Studii și Cercetări Chim. Acad. R. P. Romania*, 1964, **12**, 345—355.
67. A. T. Balaban, C. N. Rențea and M. Mocanu, *Tetrahedron Letters*, **1964**, 2049—2054 : Spiroborates ; symmetry and coordination of spiranic substituted 3-hydroxy-2-propen-1-one *o*-phenylene and *o*-vinylene borates.
68. A. T. Balaban, A. Barabaș and A. Arsene, *Tetrahedron Letters*, **1964**, 2721—2724 : 1,3,2-Dioxaborinium and 4,5-benzo-1,3,2-dioxaborinium cations, novel aromatic systems.
69. A. T. Balaban, A. Arsene, I. Bally, A. Barabaș, M. Paraschiv and E. Romas, *Tetrahedron Letters*, **1965**, 3917—3923 : 1,3,2-Dioxaborinium (Boroxaropyrylium) salts and their decomposition to bis-1,3-diketonatoboronium salts.
70. A. T. Balaban, C. N. Rențea, M. Mocanu-Paraschiv and E. Romaș, *Rev. Roum. Chim.*, 1965, **10**, 849—864 : Heterocyclic organoboron compounds. III. Symmetry and coordination of spiranic substituted 3-hydroxy-2-propen-1-one *o*-phenylene and *o*-vinylene borates.
71. A. T. Balaban, T. H. Crawford and R. H. Wiley, *J. Org. Chem.*, 1965, **30**, 879—882 : Configurations of substituted 5-cyanosorbic acids. An intramolecular Ritter reaction.
72. C. Măntescu, A. Ghenunche and A. T. Balaban, *J. Labelled Compds.*, 1965, **1**, 178—181 : Tritiation of pyrimidines by HTO in the presence of aluminium chloride (Tritiations by HTO-promoted aluminium chloride. II).
73. A. T. Balaban, C. N. Rențea and M. Băcescu-Roman, *Rev. Roum. Chim.*, 1965, **10**, 863—877 : Heterocyclic organoboron compounds. IV. Unichelated spiroborates prepared from 2-*n*-butoxy-1,3,2-benzodioxaborole and bidentate ligands.
74. A. T. Balaban, *Rev. Roum. Chim.*, 1965, **10**, 879—885 : Heterocyclic organoboron compounds V. Novel 1,3,2-dioxaboraazulene-2-spiro-2′-(1′,3′,2′-benzodioxaborole) (tropophenylene spiroborate) derivatives.

75. C. Bratu and A. T. Balaban, *Rev. Roum. Chim.*, 1965, **10**, 1001–1008 : Electrochemistry of carbonium ions. I. Electrooxidation of 1,5-diketones.
76. E. Gârd, I. Bally, A. Vasilescu, A. Arsene and A. T. Balaban, *J. Labelled Compds.*, 1965, **1**, 182–187 : Isotopic exchange of active methyl hydrogens. II. Deuteration of diphenylmethylpyrylium and methyltropylium salts.
77. A. T. Balaban, E. Gârd, A. Vasilescu and A. Barabaş, *J. Labelled Compds.* 1965, **1**, 266–274 : Isotopic exchange of active methyl hydrogens. III. Preparation of 2,4,6-tri-d$_3$-methylpyridine, 3,5-di-d$_3$-methylphenol, 3,5-di-d$_3$-methyl-2-acetylfuran and 4,6,8-tri-d$_3$-methyl-azulene from 2,4,6-tri-d$_3$-methylpyrylium perchlorate.
78. A.T. Balaban and Z. Simon, *Rev. Roum. Chim*,. 1965, **10**, 1059–1092 : Aromaticity. V. Stability of monocyclic aromatic compounds.
79. A Barabas, C. Mântescu, D. Duţă and A. T. Balaban, *Tetrahedron Letters*, **1965**, 3925–3928 : Thermal decomposition of tritiated 2,4,6-triphenyl-5-t-1,3,2-dioxaborinium perchlorate.
80. I. Bally, A. Arsene, M. Băcescu-Roman and A. T. Balaban, *Tetrahedron Letters*, **1965**, 3929–3931 : Reaction of beta-ketoenols with diphenylborinic esters.
81. A. T. Balaban, E. Romaş and C. C. Renţea, *Tetrahedron*, 1966, **22**, 1–5 : Pyrylium salts formed by diacylation of olefins. XVI. A low-melting hydrate of 2,6-di-n-propyl-4-methylpyrylium perchlorate.
82. A. T. Balaban and C. Toma, *Tetrahedron*, **1966**, Suppl. 7, 1–8; Reaction of pyrylium salts with nucleophiles. IV. Isolation of an intermediate in the conversion of 2,4,6-triphenylpyrylium perchlorate into 2.4,6-triphenylpyridine.
83. C. Toma and A. T. Balaban, *Tetrahedron*, **1966**, Suppl. 7, 9–25 : Reaction of pyrylium salts with nucleophiles. V. Reaction with primary amines.
84. C. Toma and A. T. Balaban, *Tetrahedron*, **1966**, Suppl. 7, 27–34 : Reaction of pyrylium salts with nucleophiles. VI. Reaction with aminoacids.
85. A. T. Balaban and N. S. Bărbulescu, *Rev. Roum. Chim.*, 1966, **11**, 109–112 : Conversion of dicyclic ketones into pyrylium salts.
86. A. T. Balaban, *Rev. Roum. Chim.*, 1966, **11**, 1097–1116 : Chemical graphs. I. Valence isomerism of cyclopolyenes. (Erratum, *ibid.* **12**, Nr. 1, 103 (1967)).
87. C. C. Renţia, A. T. Balaban and Z. Simon, *Rev. Roum. Chim.*, 1966, **11**, 1193–1203 : HMO-Calculations of the ground state of pyrylium salts and correlations with experimental data for their reactivity and NMR spectra.
88. A. T. Balaban, D. Fărcaşiu and R. Bănică, *Rev. Roum. Chim.*, 1966, **11**, 1205–1227 : Chemical graphs. II. Graphs of multiple 1,2-shifts in carbonium ions and related systems.
89. C. Mântescu, A. Genunche and A. T. Balaban, *J. Labelled Compounds*, 1966, **2**, 261–266 : Tritiations by HTO-promoted aluminium chloride. III. Uracil, adenine, glycine, di- and triglycine.
90. C. Măntescu. A. Genunche, D. Duţă-Cristu and A. T. Balaban, *J. Labelled Compounds* 1966, **2**, 267–271 : Tritiations by HTO-promoted aluminium chloride. IV. Cyclohexane and n-heptane.
91. I. Stănoiu, A. P. Mihăilă, P. T. Frangopol, A. T. Balaban, G. A. Popescu, I. Oprescu and V. T. Truşcă, *Rev. Roum. Phys.*, 1966, **11**, 937–949 : Étude de la radiolyse de quelques fractions pétrolières roumaines dans le réacteur nucléaire I.F.A.
92. I. Bally, A. Arsene, M. Paraschiv, E. Romas and A. T. Balaban, *Rev. Roum. Chim.* 1966, **11**, 1409–1418 : Heterocyclic organoboron compounds. VI. New boron-oxygen chelate compounds with equivalent oxygens.
93. A. Barabaş, E. Gârd, A. Vasilescu and A. T. Balaban, *J. Labelled Compound.*, 1966, **2**, 359–366 : Isotopic exchange of active methyl hydrogens. IV. Preparation of 1,3-di-d$_3$-methylnaphtalene, d$_3$-mesitylene and d$_3$-mesitylene derivatives from 2,4,6-trimethylpyridinium perchlorates.
94. E. Gârd, A. Vasilescu, G. D. Mateescu and A. T. Balaban, *J. Labelled Compds.*, 1967, **3**, 196–205 : Isotopic exchange of active methyl hydrogens. V. Reactivity of *alpha* and *gamma* methyl groups and of *beta* hydrogens in pyrylium salts.
95. A. Arsene, A. T. Balaban, I. Bally, A. Barabaş, M. Paraschiv and C. N. Renţea, *Spectrochimica Acta*, 1967, **23A**, 1373–1383 : Electronic absorption spectra of spiroborates and of 1,3,2-dioxaborinium salts.
96. M. Frangopol, A. Genunche, N. Negoiţă, P. T. Frangopol and A. T. Balaban, *Tetrahedron*, 1967, **23**, 841–844 : A study of the reversibility of the Friedel-Crafts C-acetylations by means of ^{14}C-labelling.
97. A. T. Balaban and A. Barabaş, *Chem. and Ind.*, **1967**, 404 : 1,3-Dimethylnaphthalene from acetylacetone and benzylmagnesium chloride.

98. A. T. Balaban, *Rev. Roum. Chim.*, 1967, **12**, 875–898 : Chemical graphs. III. Reactions with cyclic six-membered transition states. (Reprinted in "Recherches sur la Philosophie des Sciences", p. 207–230, Ed. Acad. Bucarest).
99. A. T. Balaban, P. T. Frangopol, M. Frangopol and N. Negoiţă, *Tetrahedron*, 1967, **23**, 4661–4676 : Stability and equilibria of free radicals. III. Preparation of stable, sterically shielded, diarylnitrogen radicals with donor and acceptor groups in the same molecule.
100. A. T. Balaban and D. Farcașiu, *J. Amer. Chem. Soc.*, 1967, **89**, 1958–1961 : Automerization of naphthalene in the presence of aluminium chloride.
101. A. T. Balaban, A. R. Katritzky and B. Semple, *Tetrahedron*, 1967, **23**, 4001–4008 : Some novel t-butylation reactions in the conversion of phenyl-substituted 1,5-diketones to pyrylium salts.
102. E. Gârd, A. Runge, A. Barabaș and A. T. Balaban, *J. Labelled Compounds*, 1967, **3**, 151–154 : Isotopenaustausch des Sauerstoffatoms in Pyryliumsalzen.
103. A. T. Balaban and F. Harary, *Rev. Roum. Chim.*, 1967, **12**, 1511–1515 : Chemical graphs. IV. (Aromaticity. VI.) Dihedral groups and monocyclic aromatic compounds.
104. D. Fărcașiu, C. Uncuţa and A. T. Balaban, *Rev. Roum. Chim.*, 1967, **12**, 899–903 : Pyrylium salts obtained by diacylation of olefins. XVII. Acylations with acid chlorides catalysed by perchloric acid.
105. A. T. Balaban and D. Farcașiu, *Tetrahedron Letters*, **1968**, 1273–1276 : Possible mechanisms for rearrangements involving sigma-complexes.
106. A. T. Balaban, D. Farcașiu, V. A. Koptyug, I. S. Isaev, M. I. Gorfinkel and A. T. Rezvukhin, *Tetrahedron Letters*, **1968**, 4757–4759 : Automerization of naphthalene — A correction.
107. A. T. Balaban and F. Harary, *Tetrahedron*, 1968, **24**, 2505–2516 : Chemical graphs. V. Enumeration and proposed nomenclature of benzenoid *cata*-condensed polycyclic aromatic hydrocarbons.
108. A. T. Balaban, C. C. Renţia and E. Ciupitu, *Rev. Roum. Chim.*, 1968, **13**, 231–247 : Chemical graphs. VI. Estimation of the relative stability of several planar and tridimensional lattices for elementary carbon (Erratum, *ibid.*, p. 1233).
109. A. Barabaș, E. Ișfan, M. Roman, M. Paraschiv, E. Romaș and A. T. Balaban, *Tetrahedron*, 1968, **24**, 1133–1144 : Heterocyclic organoboron compounds. VII. Chelated bis-(1,3-diketonato)boronium salts with acetylacetone, benzoylacetone and dibenzoylmethane.
110. A. Trestianu, H. Niculescu-Majewska, I. Bally, A. Barabaș and A. T. Balaban, *Tetrahedron*, 1968, **24**, 2499–2504 : Proton magnetic resonance spectra of chelated boronium and beryllium bis-(1,3-di-ketonates).
111. I. I. Stănoiu and A. T. Balaban, *Rev. Roum. Chim.*, 1968, **13**, 127–132 : Preparation. and infrared absorption spectrum of d_3-pyrylium perchlorate.
112. I. Bally, A. Arsene, M. Roman, M. Paraschiv, E. Romaș and A. T. Balaban, *Rev. Roum. Chim.*, 1968, **13**, 1225–1233 : Heterocyclic organoboron compounds. VIII. Chelate compounds formed by alkyl-substituted benzodioxaboroles or by diphenylborinic esters with tropolone or 1,3-diketones.
113. C. Bratu and A. T. Balaban, *Rev. Roum. Chim.*, 1968, **13**, 625–629 : Properties of electrolytically generated cetyltrimethylammonium amalgam, a metallic-covalent surface agent.
114. A. T. Balaban, *Tetrahedron*, 1968, **24**, 5059–5065 : Reaction of pyrylium salts with nucleophiles. VII. Conversion of 2,4,6-triphenylpyrylium into isoxazole or pyrazole derivatives by hydroxylamine or phenylhydrazine.
115. A. T. Balaban, P. J. Halls and A. R. Katritzky, *Chem. and. Ind.*, **1968**, 651 : Stable radicals from 1-hydroxybenzimidazole-3-oxides.
116. A. T. Balaban, *Tetrahedron Letters*, **1968**, 4643–4644 : Pyrylium salts formed by diacylation of olefins. XVIII. Diacetylation of cyclododecene.
117. I. Bally, A. Arsene, A. T. Balaban and G. V. Boyd, *Rev. Roum. Chim.*, 1968, **13**, 1391–1393 : Heterocyclic organoboron compounds. IX. Chelates of 2-aminotropone with 1,3,2-benzodioxaboroles or diphenylborinic esters.
118. I. Bally, E. Ciornei and A. T. Balaban, *Rev. Roum. Chim.*, 1968 **13**, 1507–1510 : Heterocyclic organoboron compounds. X. Chelate compounds of *p*-anisyl-phenyl-borinic acid with 1,3-diketones.
119. A. T. Balaban, *Tetrahedron*, 1969, **25**, 2949–2956 : Chemical graphs. VII. Proposed nomenclature of branched *cata*-condensed benzenoid hydrocarbons.
120. A. T. Balaban, *Organic Preparations and Procedures*, 1969, **1**, 63–66 : 2-Acetyl-3,5-dimethylfuran.
121. P. T. Frangopol, M. Frangopol, N. Negoiţă and A. T. Balaban, *Rev. Roum. Chim.*, 1969, **14**, 385–387 : Stability and equilibria of free radicals. IV. t-Butyl-1-cyano-nitroxide.

122. E. Gârd, I. I. Stănoiu, A. T. Balaban and F. Chiraleu, *Rev. Roum. Chim.*, 1969, **14**, 247–252 Isotopic exchange of active methyl hydrogens. VI. Deuterations of 2,4,6-triphenyl- 2,3,5,6-tetramethyl-, and 2,3,6-trimethyl-4-phenyl-pyrylium salts.
123. A. B. Susan and A. T. Balaban, *Rev. Roum. Chim.*, 1969, **14**, 111–120 : Reaction of pyrylium salts with nucleophiles. VIII. Triphenylpyrylium and methylamine. Thermal degradation of N-methyl-2,4,6-triphenylpyridinium halides to methyl halides and 2,4,6-triphenylpyridine.
124. I. Bally and A. T. Balaban, *Studii și Cercetări Chim. Acad. R. S. Romania*, 1969, **17**, 431–462 : Heterocicli organoborici nesaturați cu legături bor-oxigen.
125. A. T. Balaban, M. Frangopol, N. Negoiță, P. T. Frangopol and M. Paraschiv, *Rev. Roum. Chim.*, 1969, **14**, 941–945 : Factors affecting stability and equilibria of free radicals. V. Synthesis and spectra of polynitrophenyl-alkoxyamines.
126. A. T. Balaban, *Rev. Roum. Chim.*, 1969, **14**, 1331–1332 : Pyrylium salts formed by diacylation of olefins. XIX. Characterization of olefins by diacylation : acid dealkylation of 3,5-di-t-butyl-pyrocatechol.
127. A. T. Balaban, *Rev. Roum. Chim.*, 1969, **14**, 1323–1330 : Aromaticity. VII. Electronic absorption spectra of *o*-phenylene carbonate and its conjugate acid.
128. A. T. Balaban, *Rev. Roum. Chim.*, 1969, **14**, 1281–1284 : Oxidation of pyrocatechol derivatives to *o*-quinones by iodosobenzene diacetate.
129. G. V. Boyd and A. T. Balaban, *Rev. Roum. Chim.*, 1969, **14**, 1575–1577 : A correlation between chemical shifts of methyl protons and electron densities in substituted pyrylium salts.
130. A. Camerman, L. H. Jensen and A. T. Balaban, *Acta Cryst.*, 1969, **25B**, 2623–2630 : The molecular structure of N-phenyl-2,4,6-trimethylpyridinium perchlorate.
131. O. Buchardt, C. P. Pedersen, U. Svanholm, A. M. Duffield and A. T. Balaban, *Acta Chem. Scand.*, 1969, **23**, 3125–3138 : Seven-membered heterocyclic rings. I. Formation of 4-H-1,2-diazepines from pyrylium salts and hydrazine.
132. A. T. Balaban, R. O. Davies, F. Harary A. Hill and R. Westwick, *Austral. J. Math.*, 1970, **11**, 207–215 : Cubic identity graphs and planar graphs derived from trees.
133. A. T. Balaban, A. Arsene, I. Bally, A. Barabaș, M. Paraschiv, M. Roman and E. Romaș, *Rev. Roum. Chim.*, 1970, **15**, 635–653 : Heterocyclic organoboron compounds. XII. 1,3,2-Dioxaborinium salts.
134. A. T. Balaban, *Tetrahedron*, 1970, **26**, 739–742 : Reaction of pyrylium salts with nucleophiles. IX. Formation of 1,2-diazepine or 2-pyrazoline derivatives from 2,4,6-triphenylpyrylium salts and hydrazine.
135. A. T. Balaban and W. Silhan, *Tetrahedron*, 1970, **26**, 743–749 : NMR Spectra of 5-substituted 1,3,5-triphenyl-2,4-pentadien-1-ones and of 1,3,5-triphenyl-5-imino-penten-1-ones. Magnetic non-equivalence of phenacyl methylene protons in 3,5-diphenyl-5-phenacyl-2-pyrazolines.
136. A. T. Balaban, I. Zugrăvescu, S. Avramovici and W. Silhan, *Monatshefte Chem.*, 1970, **101**, 704–708 : NMR Spectren von *trans*-Chalcon-oxim, -semicarbazon und -thiosemicarbazon und ihrer cyclischen Isomeren (3,5-Diphenyl-2-isoxazolin und 1-substituierte 3,5-Diphenyl-2-parazoline).
137. A. Arsene, M. Parschiv and A. T. Balaban, *Rev. Roum. Chim.*, 1970, **15**, 247–252 : Reaction of *o*-phenylene arsenite with tropolone.
138. A. T. Balaban *Rev. Roum. Chim.*, 1970, **15**, 463–485 : Chemical graphs. VIII. Valence isomerism and general cubic graphs.
139. A. T. Balaban, D. Farcașiu and F. Harary, *J. Labelled Compounds*, 1970, **6**, 211–223 : Chemical graphs. IX. Isotope isomerism of multiply-labelled compounds.
140. A. T. Balaban, *Rev. Roum. Chim.*, 1970, **15**, 1243–1250 : Chemical graphs X. (Aromaticity. VIII). Resonance energies of *cata*-condensed benzenoid polycyclic hydrocarbons.
141. A. T. Balaban, *Rev. Roum. Chim.*, 1970, **15**, 1251–1262 : Chemical graphs. XI. (Aromaticity. IX). Isomerism and topology of non-branched *cata*-condensed polycyclic conjugated non-benzenoid hydrocarbons.
142. C. Uncuța and A. T. Balaban, *Studii și Cercetări Chim. Acad. R. S. Romania*, 1970, **18**, 161–188 : Metode de degradare chimică cu ruperea legăturilor pentru localizarea marcării cu carbon-14.
143. A. M. Duffield, C. Djerassi and A. T. Balaban, *Org. Mass Spectrometry*, 1971, **5**, 87–93 : Mass spectrometry in structural and stereochemical problems. 201. Study of the fragmentation processes of some pyrylium salts.
144. A. T. Balaban, N Negoiță and I. Pascaru, *Rev. Roum. Chim.*, 1971, **16**, 721–723 : N-Nitroso-phenyl-nitroxide.

145. A. T. Balaban and F. Harary, *J. Chem. Documentation*, 1971, **11**, 258—259 : The characteristic polynomial does not uniquely determine the topology of the molecule.
146. D. Fărcaşiu, A. Vasilescu and A. T. Balaban, *Tetrahedron*, 1971, **27**, 681—685 : Synthesis and reactivity of 2,6-dimethylpyrylium salts.
147. A. T. Balaban and A. M. Duffield, *Rev. Roum. Chim.*, 1971, **16**, 1095—1098 : Derivatives of 2-biphenylcarboxylic acid.
148. A. T. Balaban, *Rev. Roum. Chim.*, 1971, **16**, 725—737 : Stable nitrogen free radicals.
149. I. Bally and A. T. Balaban, *Rev. Roum. Chim.*, 1971, **16**, 739—742 : Heterocyclic organoboron compounds. XIV. Boron chelates with bis-(1,3-diketones).
150. A. T. Balaban, *Tetrahedron*, 1971, **27**, 6115—6131 : Chemical graphs. XII. Configurations of annulenes.
151. A. Barabaş and A. T. Balaban, *Tetrahedron*, 1971, **27**, 5495—5503 : Mono- and bis-addition products of benzylmagnesium chloride to acetylacetone. A synthesis of 1,3-dimethylnaphthalene.
152. I. I. Stănoiu, M. Paraschiv, M. Roman and A. T. Balaban, *Spectrochim. Acta*, 1972, **28A**, 1001—1005 : Vibrational spectra of pyrylium, pyrylium-2-d, pyrylium-3-d, and pyrylium-d$_3$ cations.
153. A. T. Balaban, *Rev. Roum. Math. Pure et Appl.*, 1972, **17**, 3—16 : Chemical graphs. XIII. Combinatorial paterns.
154. A. T. Balaban, I. Pascaru and F. Cuiban, *J. Magnetic Resonance*, 1972, **7**, 241—246 : Factors affecting stability and equilibria of free radicals. VI. Oxidation of cyclic hydroxamic acids to nitroxides.
155. A. T. Balaban and N. Negoiţă, *Rev. Roum. Chim.*, 1972, **17**, 1227—1234 : Factors affecting stability and equilibria of free radicals. VII. Arenesulphonyl-phenyl-nitroxides and 1-arenesulphonyl-2,2-diphenylhydrazyls.
156. A. T. Balaban, *J. Combinatorial Theory*, 1972, **12**, 1—5 : A trivalent graph of girth ten.
157. A. T. Balaban, *Rev. Roum. Chim.*, 1972, **17**, 9—24 : Determination of hyperfine coupling constants from ESR spectra of organic free radicals.
158. A. T. Balaban and A. Vasilescu, *Tetrahedron Letters*, **1972**, 571—574 : 1,2-Bis-benzenesuphonyl-1,2-diethoxyhydrazine and its temperature-dependent proton magnetic resonance spectrum.
159. A. T. Balaban, *Rev. Roum. Chim.*, 1972, **17**, 865—881 : Chemical graphs. XIV. Valence isomers of [12]annulene.
160. A. T. Balaban, *Rev. Roum. Chim.*, 1972, **17**, 883—896 : Chemical graphs. XV. Degenerate Cope rearrangements of valence isomers of annulenes.
161. A. T. Balaban, *Rev. Roum. Chim.*, 1972, **17**, 1531—1543 : Chemical graphs. XVII. (Aromaticity. X) cata-Condensed polycyclic hydrocarbons which fulfill Hückel's rule but lack closed electronic shells.
162. M. Safta, F. Chiraleu, A. T. Balaban and G. Ostrogovich, *Rev. Roum. Chim.* 1972, **17**, 2055—2065 : Quantitative study of active methyl groups in C-methyl-s-triazines. I. Hydrogen exchange kinetics of 6-methyl-5-triazin-2,4 (1H, 3H)-dione and its N-methyl-derivatives.
163. A. T. Balaban, N. Negoiţă and R. Baican, *J. Magnetic Reson.*, 1973, **9**, 1—7 : Aryl-nitroso-nitroxides.
164. A. T. Balaban, *Rev. Roum. Chim.*, 1973, **18**, 635—653 : Chemical graphs. XVIII. Graphs of degree four or less, isomers of annulenes, and nomenclature of bridged polycyclic structures.
165. A. T. Balaban, *Rev. Roum. Chim.*, 1973, **18**, 841—854 : Chemical graphs. XVI. Intramolecular isomerization of octahedral complexes with six different ligands.
166. A. T. Balaban, *Rev. Roum. Chim.*, 1973, **18**, 855—862 : Chemical graphs. XIX. Intramolecular isomerization of trigonal-bipyramidal structure with five different ligands.
167. A. T. Balaban, *Rev. Roum. Math. Pure Appl.*, 1973, **18**, 1033—1043 : Trivalent graphs of girth nine and eleven, and relationships between cages.
168. E. Gârd, I. Stănoiu, F. Chiraleu and A. T. Balaban, *Rev. Roum. Chim.*, 1973, **18**, 257—261 : Isotopic exchange of active methyl hydrogens. VII. Kinetic study of 2,4,6-trimethylpyrylium salts in deuterium oxide.
169. I. Bally, E. Ciornei, A. Vasilescu and A. T. Balaban, *Tetrahedron*, 1973, **29**, 3185—3187 : Heterocyclic organoboron compounds. XVI. Chelated compounds with α, β-unsaturated β-aminoketones.
170. R. Istrăţoiu, I. Pascaru and A. T. Balaban, *Z. Naturforsch.*, (**B**), 1973, **28b**, 543—544 : Push-pull nitrogen free radicals from benzenesulphonanilides or benzanilides with donor *para*-substituents.

171. N. Negoiţă, R. Baican and A. T. Balaban, *Tetrahedron Letters*, **1973**, 1877—1878 : N-(2,4,6-Tricarbomethoxyphenyl)-alkoxyaminyls, new push-pull stable nitrogen free radicals.
172. A. T. Balaban and R. Istrăţoiu, *Tetrahedron Letters*, **1973**, 1879—1880 : N-Arenesulphonyl-N-(2,2,6,6-tetramethylpiperidinyl-1)-aminyls, hydrazyls with no nitrogen-bonded aromatic groups.
173. C. Pomponiu and A. T. Balaban, *Rev. Roum. Chim.*, 1973, **18**, 1173—1209 : Computing program for interpreting ESR spectra of organic free radicals.
174. N. Negoiţă, R. Baican, F. Domşa and A. T. Balaban, *Rev. Roum. Chim.*, 1973, **18**, 995—1004 : Use of ESR spectrum simulator for determining precisely hyperfine coupling constants of stable nitrogen free radicals.
175. A. T. Balaban, *Rev. Roum. Chim.*, 1973, **18**, 1609—1612 : Reaction of pyrylium salts with nucleophiles. X. N(12)-substituted 11,13-di-methyl-[9] (3,6)-pyridophanium perchlorates.
176. A. T. Balaban and A. J. Boulton, *Org. Synth.*, Coll. Vol. 5, 1112—1113 (1973) : 2,4,6-Trimethylpyrylium tetrafluoroborate.
177. A. T. Balaban şi A. J. Boulton, *Org. Synth.*, Coll. Vol. 5, 1114—1116 (1973) : 2,4,6-Trimethylpyrylium trifluoromethanesulfonate.
178. N. Negoiţă, R. Baican and A. T. Balaban, *Tetrahedron*, 1974, **30**, 73—74 : Factors affecting stability and equilibria of free radicals. VIII. 1-Cyano-2,2-diphenylhydrazyl.
179. A. T. Balaban, H. G. Aurich, J. Trösken, E. Brugger, D. Döpp and K. H. Sailer, *Tetrahedron*, 1974, **30**, 739—744 : Aminyloxides from 1-hydroxy-2-indolinones.
180. A. T. Balaban and C. Pomponiu, *Rev. Roum. Chim.*, 1974, **19**, 581—630 : Computer program for determining all possible ESR spectra with equivalent lines.
181. A. T. Balaban and F. Kerek, *Rev. Roum. Chim.*, 1974, **19**, 631—647 : Chemical graphs. XX. Graphs of parallel and/or subsequent substitution reactions.
182. A. T. Balaban, *Rev. Roum. Chim.*, 1974, **19**, 1185—1196 : Chemical graphs. XXI. Valence isomers of benzoannulenes.
183. A. T. Balaban, N. Negoiţă and R. Baican, *Chem. Phys. Letters*, 1974, **24**, 30—32 : 2,2-Diphenyl-1-(trifluoromethanesulphonyl)-hydrazyl.
184. A. T. Balaban, *Rev. Roum. Chim.*, 1974, **19**, 1323—1342 : Chemical graphs. XXII. Valence isomers of heteroannulenes or of substituted annulenes. Coisomeric cubic multigraphs.
185. A. T. Balaban, M. T. Căproiu, N. Negoiţă and R. Baican, *Tetrahedron Letters*, **1974**, 4091—4094 : Non-equivalence of aryl groups in 1,1-diaryl-2-benzenesulphonyl-hydrazyls⊙
186. A. T. Balaban, *Rev. Roum. Chim.*, 1974, **19**, 1611—1619 : Chemical graphs. XXIII. General cubic graphs with one loop, and homovalenes or their derivatives. Erratum, *ibid.*, 1978, **23**, 311.
187. A. T. Balaban and M. Paraschiv, *Rev. Roum. Chim.*, 1974, **19**, 1731—1734 : Molecular complexes with aromatic cations as electron-acceptors. II. Charge-transfer spectrum of 2,4,6-triphenylpyrylium thiocyanate.
188. A. Barabaş and A. T. Balaban, *Rev. Roum. Chim.*, 1974, **19**, 1927—1940 : Chemical graphs XXIV. Isomerizations and isographic transformations.
189. A. T. Balaban, *Rev. Roum. Chim.*, 1975, **20**, 239—244 : Chemical graphs. XXV. Isomers of the porphyrins, an exercise using Polya's counting theorem.
190. I. Bally, E. Gârd, E. Ciornei, M. Blitz and A. T. Balaban, *J. Labelled Compounds*, 1975, **11**, 63—69; Synthesis of ^{14}C-labelled isotope-isomeric alkanes. I. n-Heptane-1-^{14}C and -2-^{14}C.
191. I. Bally and A. T. Balaban, *Rev. Roum. Chim.*, 1975, **20**, 1471—1472 : Synthesis of ^{14}C-labelled isotope-isomeric alkanes. II. Preparation of 2,2,4-trimethylpentane-$^{14}C_2$ labelled at both methyl groups of the isopropyl moiety.
192. A. T. Balaban and V. Wray, *Z. Naturforsch.*, 1975, **30b**, 654—655 : ^{13}C-Magnetic resonance spectra of alkyl-substituted pyrylium salts.
193. A. T. Balaban, *Math. Chem.*, 1975, **1**, 33—60 : Some chemical applications of graph theory.
194. A. T. Balaban, *Math. Chem.*, 1975, **1**, 123—124 : Methods for the enumeration of isomers.
195. R. Baican, N. Negoiţă and A. T. Balaban, *Rev. Roum. Phys.*, 1976, **21**, 213—215 : A new proposed standard stable free radical for ESR measurements : 1-cyano-2,2-diphenylhydrazyl (CDPH).
196. A. Bota, A. T. Balaban and F. Chiraleu, *Rev. Roum. Chim.*, 1976, **21**, 101—106 : Pyrylium salts formed by diacylation of olefins. XX. NMR Spectra of 2,4,6-trimethyl-3-phenylpyrylium and -pyridinium cations.
197. A. T. Balaban, *Rev. Roum. Chim.*, 1976, **21**, 241—249 : Mass spectrum of 3,7-di-t-butyl-5-methyl-4H-1,2-diazepine : Possible steric inhibition of dinitrogen expulsion.

198. C. Uncuţa and A. T. Balaban, *Rev. Roum. Chim.*, 1976, **21**, 251—255 : Reaction of pyrylium salts with nucleophiles. XI. Chemical shift non-equivalence of isopropyl in atropisomeric 1-aryl-2-isopropyl-4,6-dimethylpyridinium salts.
199. R. W. Robinson, F. Harary and A. T. Balaban, *Tetrahedron*, 1976, **32**, 355—361 : The number of chiral and achiral alkanes and mono-substituted alkanes.
200. S. Bădilescu and A.T.Balaban, *Spectrochim. Acta.*, 1976, **32A**, 1311—1318 : Molecular complexes with aromatic cations as electron-acceptors. III. Charge transfer spectra of substituted pyrylium thiocyanates, selenocyanates and iodides.
201. A. T. Balaban, *Rev. Roum. Chim.*, 1976, **21**, 1045—1047 : Chemical graphs. XXVI. Codes for configurations of conjugated polyenes.
202. A. T. Balaban, *Rev. Roum. Chim.*, 1976, **21**, 1049—1071 : Chemical graphs. XXVII. Enumeration and codification of staggered conformations of alkanes.
203. A. T. Balaban and I. I. Bădilescu, *Rev. Roum. Chim.*, 1976, **21**, 1339—1343 : Pyrylium-salts formed by diacylation of olefins. XXI. Diacetylation of cyclodecene to 9,11-dimethyl-[7] (2,6)-pyrylophanium perchlorate.
204. A. T. Balaban, A. Bota and I. I. Stănoiu, *Rev. Roum. Chim.*, 1976, **21**, 1183—1187 : Pyrylium salts formed by diacylation of olefins. XXII. Triacylation of 2,3-dimethyl-2-butene.
205. A. T. Balaban, *Math. Chem.*, 1976, **2**, 141—142 : Discussion on the paper by E. C. Hass and P. J. Plath entitled "Graphentheoretische Behandlung des beschränkten Selbstwechselwirkungsproblems, dargestellt an pericyclischen Sechszentrenreaktionen.
206. A. T. Balaban, *Math. Chem.*, 1976, **2**, 51—61 : Enumeration of catafusenes, diamondoid hydrocarbons and staggered alkane C-rotamers.
207. A. T. Balaban, I. I. Stănoiu and F. Chiraleu, *Chem. Commun.*, **1976**, 984—985 : Steric origin of isotope effects in NMR shifts induced by lanthanide shift reagents.
208. M. Gheorghiu and A. T. Balaban, *Rev. Roum. Chim.*, 1976, **21**, 1513—1525 : Ground and excited state PPP calculations for pyrylium salts.
209. I. I. Stănoiu, F. Chiraleu, E. Gârd and A. T. Balaban, *Rev. Roum. Chim.*, 1977, **22**, 117—126 : Isotopic exchange of active methyl hydrogens. VIII. Deuterium kinetic isotope effects for α- and δ-isopropyl-substituted pyrylium salts.
210. A. T. Balaban, *Rev. Roum. Chim.*, 1977, **22**, 45—47 : Chemical graphs. XXVIII. A new topological index for catafusenes : L-transform of their three-digit codes.
211. A. T. Balaban, E. M. Palmer and F. Harary, *Rev. Roum. Chim.*, 1977, **22**, 517—523 : Chemical graphs. XXIX. Numbers of isomers with naphthalene and adamantane skeletons.
212. A. T. Balaban and V. Wray, *Org. Magnetic Resonance*, 1977, **9**, 16—22 : ^{13}C-NMR Spectra of some pyrylium salts and related compounds.
213. A. T. Balaban, A. Bota, F. Chiraleu, E. Şliam, A. Haneş and C. Drăghici, *Rev. Roum. Chim.*, 1977, **22**, 1003—1015 : Pyrylium salts formed by diacylation of olefins. XXIII. Isomeric ethyl-trimethylpyridines from the diacetylation of hexenes and methylpentenes.
214. M. T. Căproiu, N. Negoiţă and A. T. Balaban, *Tetrahedron Letters*, **1977**, 1825—1826 : Aryl-nitroso-aminyloxide, aryl-tosylaminyloxide and diaryl-aminyloxide, where the aryl is 3,5-di-t-butylphenyl.
215. I. I. Stănoiu, M. Paraschiv, E. Gârd and A. T. Balaban, *Rev. Roum. Chim.*, 1977, **22**, 865—867 : Isotope effects in electronic absorption spectra of CH_3/CD_3-substituted six-membered heteroaromatics.
216. A. T. Balaban, *Rev. Roum. Chim.*, 1977, **22**, 243—255 : Chemical graphs. XXX. Reaction graphs for degenerate rearrangements of homovalenium cations.
217. A. T. Balaban, N. Negoiţă and R. Baican, *Org. Magnetic Reson.*, 1977, **9**, 553—554 : A new stable spiropyranic aminyloxide (nitroxide).
218. I. I. Stănoiu, E. Gârd, C. Uncuţa, F. Chiraleu and A. T. Balaban, *Rev. Roum. Chim.*, 1977, **22**, 1359—1361 : Isotopic xchange of active methyl hydrogens. IX. Intramolecular kinetic comparison between α-methyl and α-isopropyl groups in pyrylium salts.
219. A. T. Balaban, *Rev. Roum. Chim.*, 1977, **22**, 987—1001 : Chemical graphs. XXXI. Benzohomovalenes.
220. A. T. Balaban, I. I. Stănoiu and E. Gârd., *Rev. Roum. Chim.*, 1977, **22**, 1191—1193 : Deuterium isotopic effect on the basicity of 2,4,6-trimethylpyridine.
221. I. I. Stănoiu, A. T. Balaban and F. Chiraleu, *Rev. Roum. Chim.*, 1977, **22**, 1499—1504 : Isotopic exchange of active methyl hydrogens. X. Activation parameters for deuteration and de-deuteration of isopropylpyrylium salts.
222. A. T. Balaban, M. T. Căproiu, N. Negoiţă and E. Baican, *Tetrahedron*, 1977, **33**, 2249—2253 : Factors affecting stability and equilibria of free radicals. IX. Nonequivalence of aryl groups in 1,1-diaryl-2-benzenesulphonylhydrazyls and related compounds.

223. A. T. Balaban, *Org. Prep. Procedures Internat.*, 1977, **9**, 125—130 : Improved synthesis of 2,6-di-t-butyl-4-methylpyrylium chlorostannate and perchlorate and 2,6-di-t-butylpyridine.
224. A. T. Balaban, I. Bally, V. I. Minkin and A. I. Usachev, *Tetrahedron*, 1977, **33**, 3265—3267 : Dipole moments of boron chelates with tropolone and 1,2-diketone derivatives.
225. A. T. Balaban, I. I. Stănoiu and F. Chiraleu, *Rev. Roum. Chim.*, 1978, **23**, 187—196 : Isotope effects in lanthanide-induced shifts of ^{1}H-NMR spectra of selectively side-chain deuterated pyridines.
226. A. T. Balaban, *Noesis*, 1978, **4**, 15—22 : Mathematical principles in chemistry.
227. A. T. Balaban, *Croatica Chemica Acta*, 1978, **51**, 35—42 : Chemical graphs. XXXII. Constitutional and steric isomers of substituted cycloalkanes.
228. A. T. Balaban, A. Bota, G. N. Dorofeenko, V. D. Karpenko and Y. I. Ryabukhin, *Tetrahedron*, 1978, **34**, 2035—2037 : 2,5,5-Trimethyl-2-oxazolin-4-one, its perchlorate and α-acetoxy-isobutyronitrile by acetylation of acetone cyanohydrin.
229. A. T. Balaban and M. Gheorghiu, *Rev. Roum. Chim.*, 1978, **23**, 1065—1077 : Solvent and lanthanide-induced shifts in the ^{1}H-NMR spectra of 4-acetonylidene-2,6-dimethyl-4H-pyran and its tautomeric pyrylium cations.
230. A. T. Balaban, I. I. Stănoiu, F. Chiraleu and I. Moţoc, *Rev. Roum. Chim.*, 1978, **23**, 143—146 : Isotopic exchange of active methyl groups. XI. Kinetics of deuteration of 2,6-diaryl-4-methylpyrylium salts.
231. A. T. Balaban, *Tetrahedron Letters*, **1978**, 599—600 : Synthesis of pyrylotrimethinecyanines.
232. A. T. Balaban, *Rev. Roum. Chim.*, 1978, **23**, 723—746 : Chemical graphs. XXXIII. Graphs for intramolecular rearrangements of tetragonal-pyramidal complexes.
233. A. R. Katritzky, R. M. Claramunt-Elguero, F. S. Yates, A. Dinculescu, A. T. Balaban and F. Chiraleu, *J. Chem. Res. (S)*, **1978**, 395 : *J. Chem. Res. (M)*, **1978**, 4783—4797 : The reactions of pyrylium salts with aliphatic diamines and chloro- and hydroxy-amines. (Reactions of pyrylium salts with nucleophiles. XII).
234. A. T. Balaban and P. von R. Schleyer, *Tetrahedron*, 1978, **34**, 3599—3609 : Systematic classification and nomenclature of polymantanes.
235. C. Rullière, J. Joussot-Dubien, J. Bellocq and A. T. Balaban, *J. Chim. Phys.*, 1978, **75**, 961—968 : Étude des propriétes fluorescentes et de l'effet laser de quelques nouveaux dérives oxazoliques.
236. A. T. Balaban and V. Baciu, *Math. Chem.*, 1978, **4**, 131—159 : Chemical graphs. XXXV. Application of Polya's theorem to catamantanes.
237. A. T. Balaban, *Tetrahedron Letters*, **1978**, 5055—5056 : Lanthanide-induced shifts of pyridines, pyridinium and pyrylium salts.
238. I. I. Stănoiu, E. Gârd, C. Uncuţa, F. Chiraleu and A. T. Balaban, *Rev. Roum. Chim.*, 1979, **24**, 209—217 : Isotopic exchange of active methyl hydrogens. XII. Kinetics of deuteration and de-deuteration of α- and γ-ethyl groups, and relative rates for ethyl *versus* methyl side-chains, in pyrylium salts.
239. A. T. Balaban, M. Barasch and S. Marcus, *Match*, 1979, **5**, 239—261 : Computer program for the recognition of acyclic regular isoprenoid structures.
240. A. T. Balaban, *Theor. Chim. Acta*, 1979, **53**, 355—375 : Chemical graphs. XXXIV. Five new topological indices for the branching of tree-like graphs.
241. A. T. Balaban, A. Dinculescu, H. N. Koutrakis and F. Chiraleu, *Tetrahedron Letters*, **1979**, 437—440 : Methyl chemical shifts in NMR spectra of 1-R-2,4,6-trimethylpyridinium salts as simple probes for the existence and magnitude of ring current in group R.
242. A. T. Balaban and I. Moţoc, *Math. Chem.*, 1979, **5**, 197—218 : Chemical graphs. XXXVI. Correlations between octane numbers and topological indices of alkanes.
243. A. Dinculescu, H. N. Koutrakis and A. T. Balaban, *Rev. Roum. Chim.*, 1979, **24**, 439—442 : Reaction of pyrylium salts with nucleophiles. XIII. Pyridinium salts from primary aromatic and heterocyclic amines.
244. S. Bădilescu, L. Manu and A. T. Balaban, *Rev. Roum. Chim.*, 1979, **24**, 947—955 : Molecular complexes with aromatic cations as electron-acceptors. IV. Charge-transfer spectra of pyrylium 2-aza-1,2,3,3-tetracyanopropenides.
245. I. Bally, E. Gârd, N. Negoiţă and A. T. Balaban, *Rev. Roum. Chim.*, 1979, **24**, 601—604 : Synthesis of ^{14}C-labelled isotope-isomeric alkanes. III. n-Tetradecane-1-^{14}C, 2-^{14}C, and 7-^{14}C.
246. A. T. Balaban, A. Bota and A. Zlota, *Synthesis*, **1980**, 136—138 : 1,1-Bis-(2-furyl)-ethanes from 1-(2-furyl)-ethanols.
247. D. Bonchev, A. T. Balaban and O. Mekenyan, *J. Chem. Inf. Comput. Sci.*, 1980, **20**, 106—113 : Generalization of the graph centre concept and derived topological centric indices.

248. A. T. Balaban and D. H. Rouvray, *Tetrahedron*, 1980, **36**, 1851—1855 : Graph-theoretical analysis of the bonding topology in polyhedral organic cations.
249. K. Balasubramanian, J. J. Kaufman, W. S. Koski and A. T. Balaban, *J. Computational Chem.*, 1980, **1**, 149—157 : Graph theoretical characterization and computer generation of certain carcinogenic benzenoid hydrocarbons and identification of bay regions.
250. A. T. Balaban, *Math. Chem.*, 1980, **8**, 159—192 : Chemical graphs. XXXVIII. Synthon graphs.
251. A. T. Balaban, M. Barasch and S. Marcus, *Math. Chem.*, 1980, **8**, 215—268 : Computer program for the recognition of standard isoprenoid structures.
252. M. Hillebrand and A. T. Balaban, *Rev. Roum. Chim.*, 1980, **25**, 995—1006 : Unrestricted Hartree-Fock spin densities in aryl-nitroso-nitroxides and in acyl-aryl-nitroxides.
253. A. T. Balaban, M. Barasch and S. Marcus, *Math. Chem.*, 1980, **8**, 193—213 : Picture grammars in chemistry. Generation of acyclic isoprenoid structures.
254. A. T. Balaban, *Pure Appl. Chem.*, 1980, **52**, 1409—1429 : Is aromaticity outmoded?
255. A. T. Balaban, M. D. Gheorghiu and C. Drăghici, *Isr. J. Chem.*, 1980, **20**, 168—172 : ^{1}H-NMR Conformational study of 2-acyl-3,5-dialkylfurans using lanthanide shift reagents.
256. A. T. Balaban, M. T. Căproiu and N. Negoiţă, *Rev. Roum. Chim.*, 1980, **25**, 1327—1333 : Factors affecting stability and equilibria of free radicals. X. 1-Cyano-2,2-bis-3,5-di-t-butylphenyl-hydrazyl.
257. V. Baciu and A. T. Balaban, *Rev. Roum. Chim.*, 1980, **25**, 1213—1220 : Chemical graphs. XXXIX. Valence isomers of monodehydro[n]annulenes.
258. A. T. Balaban, C. Uncuţa, A. Dinculescu, M. Elian and F. Chiraleu, *Tetrahedron Letters*, 1980, **21**, 1553—1556 : Rotation barriers in N-substituted 2,4,6-trimethylpyridinium cations.
259. A. Dinculescu and A. T. Balaban, *Rev. Roum. Chim.*, 1980, **25**, 1505—1528 : Reaction of pyrylium salts with nucleophiles. XIV. New pyrylium salts with potential biological activity.
260. R. Hoffmann, O. Eisenstein and A. T. Balaban, *Proc. Nat. Acad. Sci. USA*, 1980, **77**, 5588—5592 : Hypothetical strain-free oligoradicals.
261. D. Bonchev, A. T. Balaban and M. Randić, *Internat. J. Quantum Chem.*, 1981, **19**, 61—82 : The graph center concept for polycyclic graphs. Erratum, *ibid.*, 1982, **22**, 441.
262. A. T. Balaban, *Rev. Roum. Chim.*, 1981, **26**, 407—413 : Chemical graphs. XXXVII. A simple rule for classifying *peri*-condensed benzenoid hydrocarbons as closed-shell or open-shell (polyradicalic) systems using dualist (characteristic) graphs.
263. I. Moţoc and A. T. Balaban, *Rev. Roum. Chim.*, 1981, **26**, 593—600 : Topological indices : intercorrelations, physical meaning, correlational ability.
264. V. I. Minkin, L. P. Oleknovich, V. P. Metlushenko, N. G. Furmanova, I. Bally and A. T. Balaban, *Tetrahedron*, 1981, **37**, Suppl., 1, 421—427 : Molecular structure and tautomerism of the 1,3,2-benzodioxaarsole ether of tropolone.
265. A. T. Balaban, A. Dinculescu, F. Iordache, F. Chiraleu and D. Pătrăşcoiu, *Chem. Scripta*, 1981, **18**, 230—323 : Ring current determination from ^{1}H-NMR spectra of N-aryl-2,4,6-trimethylpyridinium salts : scope and limitations.
266. A. T. Balaban, *J. Labelled Comp. Radiopharm.*, 1981, **18**, 1621—1632 : Preparation of selectively side-chain deuterated pyridines *via* pyrylium salts (Isotope exchange of active methyl hydrogens. XIII).
267. M. Barasch, S. Marcus and A. T. Balaban, *Math. Chem.*, 1981, **12**, 25—64 : Codification of acyclic isoprenoid structures using context-free grammars and pushdown automata.
268. D. Bonchev and A. T. Balaban, *J. Chem. Inf. Compt. Sci.*, 1981, **21**, 2—23 : Topological centric coding and nomenclature of polycyclic hydrocarbons. I. Condensed benzenoid systems (polyhexes, fusenes).
269. A. T. Balaban, *Bulet. Inst. Politehnic Bucureşti, Ser. Chim. Metal.*, 1981, **43**, Nr. 4, 65—69 : Radicali liberi ai azotului persistenţi capto-dativi.
270. A. T. Balaban, A. Bota, D. C. Oniciu, G. Klatte, C. Roussel and J. Metzger, *J. Chem. Res.*, **1982**, (S) 44—45 : (M) 559—583 : Deuterium kinetic isotope effects in the quaternization of polymethylpyridines (CH_3 or CD_3) with methyl iodide or methyl iodide-d_3.
271. J. Herdan, G. Iordache, N. Negoiţă, N. Grecu and A. T. Balaban, *Rev. Roum. Chim.*, 1982, **27**, 69—73 : New 2,4,6-trisubstituted phenols and their corresponding aroxyls. (Synthesis and ESR spectra of aroxyls. I).
272. A. Dinculescu and A. T. Balaban, *Org. Prep. Proc. Internat.*, 1982, **14**, 39—44 : 2,4,6-Trimethylpyrylium sulfoacetate.

273. A. T. Balaban and M. Paraschiv, *Rev. Roum. Chim.*, 1982, **27**, 813—821 : Molecular complexes with aromatic cations as electron acceptors. V. Inter- and intramolecular charge-transfer of amino-substituted pyridinium salts evidenced by electronic absorption spectra.
274. I. Drăguţan and A. T. Balaban, *Can. J. Chem.*, 1982, **60**, 1512—1513 : Synthesis of new radical-cations with 2,2,6,6-tetramethylpiperidine-N-oxyl and pyridinium moieties.
275. A. T. Balaban, *Pure Appl. Chem.*, 1982, **54**, 1075—1096 : Challenging problems involving benzenoid polycyclics and related systems.
276. I. Schiketanz, A. T. Balaban and E. Ciorănescu, *Rev. Roum. Chim.*, 1982, **27**, 1125—1129 : Aminoketone and oxazole synthesis. VII. Conversion of bis-azlactones into bis-oxazoles.
277. M. Banciu, A. T. Balaban, C. Drăghici and R. Vlad, *Rev. Roum. Chim.*, 1982, **27**, 1037—1046 : Synthesis of pyrylium salts with an annelated benzo(f, i)-bicyclo[3.2.2]nona-6,8-diene skeleton (oxoniahomotriptycenes) and their reactions with nucleophiles.
278. A. T. Balaban, *Chem. Phys. Lett.*, 1982, **80**, 399—404 : Highly discriminating distance-based topological index.
279. A. T. Balaban, C. Uncuţa and F. Chiraleu, *J. Labelled Comp. Radiopharm.*, 1982, **19**, 783—794 : Regioselective deuteration kinetics of 2-, 4- and 6-methyl groups in D_2O solutions of pyrylium and N-methyl-pyridinium perchlorates possessing also 3-methyl or 3-phenyl groups. (Isotopic exchange of active methyl(ene)hydrogens. XIV).
280. A. T. Balaban and A. Bota, *Org. Prep. Proc. Internat.*, 1982, **14**, 31—38 ; 2,3,4,6-Tetramethylpyrylium perchlorate and 2,3,4,6-tetramethylpyridine.
281. I. Moţoc and A. T. Balaban, *Rev. Roum. Chim.*, 1982, **27**, 735—739 : Geometrical significance of Taft-like steric parameters.
282. P. von R. Schleyer, A. J. Kon, J. A. Pople and A. T. Balaban, *J. Amer. Chem. Soc.*, 1982, **104**, 3771—3773 : Carbenium-carbonium structure $H_3C^+-CH_4^+$ for the ethane dication.
283. I. Moţoc, A. T. Balaban, O. Mekenyan and D. Bonchev, *Math. Chem.*, 1982, **13**, 369—404 : Topological indices : inter-relations and composition.
284. A. T. Balaban and I. Tomescu, *Math. Chem.*, 1983, **14**, 155—182 : Algebraic expressions for the number of Kekulé structures of isoarithmic *cata*-condensed benzenoid polycyclic hydrocarbons.
285. M. T. Căproiu, M. Elian, N. Grecu, N. Negoiţă and A. T. Balaban, *J. Chem. Soc. Perkin Trans. II*, **1983**, 591—594 : Factors affecting stability and equilibria of free radicals. XI. 1-Benzoyl-2,2-bis-(3,5-di-t-butyl-phenyl)-hydrazyl and its temperature-dependent ESR spectra.
286. A. T. Balaban, *Pure Appl. Chem.*, 1983, **55**, 199—206 : Topological indices based on topological distances in molecular graphs.
287. A. T. Balaban, M. D. Gheorghiu and T. S. Balaban, *Org. Mass Spectrometry*, 1983, **18**, 433—437 : Electron impact mass spectra of 3,5,7-triaryl- and -trialkyl-4H-1,2-diazepines.
288. J. Herdan, A. T. Balaban, N. Negoiţă and N. Grecu, *Rev. Roum. Chim.*, 1983, **28**, 129—137 : 4-Substituted 2,6-di-t-butylphenols and their corresponding aroxyls possessing 4-(1-methylenebenzimidazolyl) or 4-(1-sulfonyl-benzimidazolyl)groups. (Synthesis of aroxyls. II).
289. A. T. Balaban, M. Fahmy, M. D. Gheorghiu and V. Wray, *Liebigs Ann. Chem.*, **1983**, 1807—1817 : Doubly vinylogous 4H-pyrones from pyrylium salts and aryl β-chlorovinyl ketones.
290. A. T. Balaban, U. Bologa, M. T. Căproiu, N. Grecu, N. Negoiţă and R. I. Walter, *Bull. Soc. Chim. Belges*, 1983, **92**, 617 : Internal rotation in hydrazyls and in captodative aminyls using temperature-dependent ESR and ^{15}N-labelling.
291. M. Banciu and A. T. Balaban, *Chem. Scripta*, 1983, **22**, 188—194 : Schemes and transformations for benzo- and dibenzoderivatives of valence isomers of [10]annulene.
292. M. T. Căproiu, N. Negoiţă and A. T. Balaban, *Tetrahedron*, 1983, **39**, 3943—3945 : Factors affecting the stability and equilibria of free radicals. XII. Capto-dative diarylaminyls with polynitrophenyl and 3,5-di-t-butyl-phenyl groups.
293. A. T. Balaban and L. V. Quintas, *Math. Chem.*, 1983, **14**, 213—233 : The smallest graphs, trees and 4-trees with degenerate topological index J.
294. A. Dinculescu, M. Fahmy, F. Chiraleu and A. T. Balaban, *Rev. Roum. Chim.*, 1983; **28**, 699—705 : Reactions of pyrylium salts with nucleophiles. XVI. New N-substituted 2,4,6-trimethylpyridinium salts and their ^1H-NMR spectra.
295. C. Roussel, A. T. Balaban, U. Berg, M. Chanon, R. Gallo, G. Klatte, J. A. Memiaghe, J. Metzger, D. Oniciu and J. Pierrot-Sanders, *Tetrahedron*, 1983, **39**, 4209—4219 : Gear effect. X. Conformational aspects of the so-called positive or negative buttressing effects of groups : polymethylpyridines.

296. A. T. Balaban, M. D. Gheorghiu and T. S. Balaban, *J. Labelled Comp. Radiopharm.*, 1983, **20**, 1097–1104 : Isotopic exchange of active methyl(ene)hydrogens. XV. The aryl group controls the α/γ regioselectivity in deuterations of 2-(p-substituted benzyl)-4,6-dimethylpyrylium salts.
297. A. T. Balaban, T. S. Balaban, C. Uncuţa, M. D. Gheorghiu and F. Chiraleu, *J. Labelled Comp. Radiopharm.*, 1983, **20**, 1105–1112 : Isotopic exchange of active methyl(ene) hydrogens. XVI. Regioselective deuteration kinetics of 2,3,6-trimethyl-4-phenylpyrylium and 2,6-dimethyl-3,4-diphenylpyrylium salts.
298. E. Stepan and A. T. Balaban, *Rev. Roum. Chim.*, 1983, **28**, 707–714 : Reactions of pyrylium salts with nucleophiles. XVII. New 2,4,6-trisubstituted bis- and tris-pyridinium salts and their ^{1}H-NMR spectra.
299. C. Uncuţa, I. Bally, C. Drăghici, F. Chiraleu and A. T. Balaban, *Rev. Roum. Chim.*, 1984, **29**, 121–129 : Heterocyclic organoboron compounds. XVII. Axial chirality of boron chelates evidenced by ^{1}H-NMR spectroscopy in the presence of chiral additives.
300. A. T. Balaban and M. Banciu, *J. Chem. Educ.*, 1984, **61**, 766–770 : Schemes and transformations for valence isomers of $(CH)_8$ and $(CH)_{10}$ hydrocarbons.
301. A. T. Balaban, M. D. Gheorghiu and T. S. Balaban, *J. Mol. Struct.*, 1984, **114**, 363–366 : Isolable rotamers of N-(9-fluorenyl)-pyridinium salts owing to restricted rotation around the $C(sp^3)$-$N(sp^2)$ single bond.
302. A. T. Balaban and I. Tomescu, *Croatica Chem. Acta*, 1984, **54**, 391–404 : Chemical graphs. XL. Three relations between the Fibonacci sequence and the numbers of Kekulé structures for non-branched *cata*-condensed polycyclic aromatic hydrocarbons.
303. V. T. Ciorba, S. Bădilescu, A. Meghea, I. Schiketanz and A. T. Balaban, *Rev. Roum. Chim.*, 1984, **29**, 817–827 : Molecular complexes with aromatic cations as electron-acceptors. VI. A new method for preparing polyphenylpyrylium salts with 7,7,8,8-tetracyano-*para*-quinodimethane radical-anions.
304. A. T. Balaban and P. Filip, *Math. Chem.*, 1984, **16**, 163–190 : Computer program for topological index J.
305. G. Stănciuc and A. T. Balaban, *Org. Prep. Procedures Internat.*, 1984, **16**, 401–405 : 0-Alkyl-N-arylhydroxylamines : N-alkoxy-2,4,6-tri- and -2,6-dinitroanilines.
306. A. Dinculescu and A. T. Balaban, *Org. Prep. Procedures Internat.*, 1984, **16**, 407–410 : 2,4,6-Triphenylpyrylium hydrogen sulfate.
307. A. T. Balaban, *Sigsam Bull.*, 1984, **18**, (2), 29–30 : Numerical and non-numerical methods in chemistry : present and future.
308. M. Banciu, C. Popa and A. T. Balaban, *Chem. Scripta*, 1984, **24**, 28–37 : Schemes and transformations in the $(CH)_{2k}$ series. Valence isomers of [12]annulene.
309. A. T. Balaban, C. Uncuţa, M. Elian, F. Chiraleu and A. Dinculescu, *Tetrahedron*, 1984, **30**, 2547–2553 : Hindered rotation around the $N(sp^2)$–$C(sp^3)$ single bond in 2,4,6-trimethyl-N-alkylpyridinium cations : ^{1}H-DNMR analysis.
310. J. M. Risley, R. L. Van Etten, C. Uncuţa and A. T. Balaban, *J. Amer. Chem. Soc.*, 1984, **106**, 7836–7840 : ^{18}O-Isotope effect in ^{13}C nuclear magnetic resonance spectroscopy. VIII. Oxygen exchange in 2,4,6-trimethylpyrylium cation.
311. O. Mekenyan, A. T. Balaban and D. Bonchev, *Chem. Phys. Lett.*, 1984, **109**, 85–88 : Hierarchically ordered extended connectivities. Reflection in the ^{1}H-NMR chemical shifts of condensed benzenoid hydrocarbons (HOC-7).
312. O. Mekenyan, D. Bonchev and A. T. Balaban, *J. Comput. Chem.*, 1984, **5**, 629–639 : Unique description of chemical structures based on hierarchically ordered extended connectivities (HOC procedures). V. New topological indices, ordering of graphs, and recognition of graph similarity.
313. F. Badea, F. Iordache, A. Meghea, A. T. Balaban, R. Marinescu and A. M. Ghiviriga, *Rev. Roum. Chim.*, 1985, **30**, 189–198 : Carbanions and free radicals derived from 1,2-diphenylpyrazoline-3,5-diones. I. Trapping of the free radical formed in phenylbutazone oxidation.
314. A. T. Balaban and I. Tomescu, *Math. Chem.*, 1985, **17**, 91–120 : Chemical graphs. XLI. Numbers of conjugated circuits and Kekulé structures for zigzag catafusenes and (j, k)-hexes; generalized Fibonacci numbers.
315. A. T. Balaban, *J. Mol. Struct. (Theochem)*, 1985, **120**, 117–142 : Graph theory and theoretical chemistry.
316. A. T. Balaban, N. Ionescu-Pallas and T. S. Balaban, *Math. Chem.*, 1985, **17**, 121–146 : Asymptotic values of topological indices J and J′ (Average distance sum connectivities) for infinite acyclic and cyclic graphs.

317. A. T. Balaban and I. Gălăţeanu, *Physiologie (Physiology)*, 1985, **22**, 71—74 : Étude comparative des possibilités offertes aux investigations médicales par les isotopes stables et radioactifs.
318. C. Rullière, A. Declémy and A. T. Balaban, *Canad. J. Phys.*, 1985, **63**, 191—194 : Corrélation entre possibilité d'effet laser et force oscillatrice de la transition fluorescente.
319. A. T. Balaban, P. Filip and T. S. Balaban, *J. Comput. Chem.*, 1985, **6**, 316—329 : Computer program for finding all possible cycles in graphs.
320. A. T. Balaban, V. Wray, N. G. Furmanova, V. I. Minkin, L. S. Minkina, Yu. E. Czernysch and G. S. Borodkin, *Liebigs Ann. Chem.*, **1985**, 1587—1595 : Dipole moment, DNMR and molecular structure of vinylogous 4H-pyrones.
321. Z. Simon, A. T. Balaban, D. Ciubotariu and T. S. Balaban, *Rev. Roum. Chim.*, 1985, **30**, 985—1000 : QSAR for carcinogenic activity of polycyclic aromatic hydrocarbons versus delocalization energy, MTD and topological indices.
322. A. T. Balaban, D. Biermann and W. Schmidt, *Nouv. J. Chim.*, 1985, **9**, 443—449 : Chemical graphs. 42. Dualist graph approach for correlating Diels-Alder reactivities of polycyclic aromatic hydrocarbons.
323. A. T. Balaban, A. Dinculescu, J. Elguero and R. Faure, *Magn. Reson. Chem.*, 1985, **23**, 553—558 : Carbon-13 NMR studies of pairs of primary amines and 2,4,6-trimethylpyridinium salts with identical substituents on nitrogen.
324. A. T. Balaban, *J. Chem. Inf. Comput. Sci.*, 1985, **25**, 334—343 : Applications of graph theory in chemistry.
325. T. S. Balaban, M. D. Gheorghiu, C. Roussel and A. T. Balaban, *Z. Naturforsch.*, 1985, **40b**, 1555—1557 : Chiral rotamers of N-(1-indanyl)-pyridinium salts and their restricted rotation around the C(sp^3)—N(sp^2) single bond.
326. D. Bonchev, O. Mekenyan and A. T. Balaban, *Math. Chem.*, 1985, **18**, 83—99 : Unique description of chemical structures based on hierarchically ordered extended connectivities (HOC procedures). IV. Recognition of graph isomorphism and graph symmetries.
327. O. Mekenyan, A. T. Balaban and D. Bonchev, *J. Magn. Reson.*, 1985, **63**, 1—13 : Unique description of chemical structures based on hierarchically ordered extended connectivities (HOC procedures). VI. Condensed benzenoid hydrocarbons and their ^{1}H-NMR chemical shifts.
328. T. S. Balaban, C. Uncuţa, M. D. Gheorghiu and A. T. Balaban, *Tetrahedron Letters*, 1985, **26**, 4669—4672 : Factors affecting the interaction of lanthanide shift reagents with substituted pyridines.
329. C. Uncuţa, T. S. Balaban, M. D. Gheorghiu, L. Stănescu, A. Petride and A. T. Balaban, *Tetrahedron Letters*, 1985, **26**, 4673—4676 : Janus-type isopropyl groups revealed by ^{1}H-NMR spectra of alkylpyridines with lanthanide shift reagents (LSR).
330. I. Schiketanz, A. Schiketanz, M. D. Gheorghiu and A. T. Balaban, *Rev. Roum. Chim.* 1985, **30**, 977—984 : Aminoketone and oxazole synthesis. VIII. Acylaminoacylations using azolactones of fluorosubstituted hippuric acid, and 2,5-diaryloxazoles derived therefrom.
331. A. T. Balaban, I. Schiketanz, M. D. Gheorghiu and A. Schiketanz, *Rev. Roum. Chim.*, 1985, **30**, 977—984 : Aminoketone and oxazole synthesis. IX. 2,2-(*p*-Phenylene)-bis(5-aryloxazoles) and 2,2-(1,4-naphthalenedinyl)-bis(5-aryloxazoles) via acylaminoacylation of aromatic hydrocarbons.
332. A. T. Balaban, O. Mekenyan and D. Bonchev, *J. Comput. Chem.*, 1985, **6**, 538—551 : Unique description of chemical structures based on hierarchically ordered extended connectivities (HOC procedures). I. Algorithms for finding graph orbits and canonical numbering of atoms.
333. O. Mekenyan, D. Bonchev and A. T. Balaban, *J. Comput. Chem.*, 1985, **6**, 552—561 : Unique description of chemical structures based on hierarchically ordered extended connectivities (HOC procedures). II. Mathematical proofs for the HOC algorithm.
334. A. T. Balaban, O. Mekenyan and D. Bonchev, *J. Comput. Chem.*, 1985, **6**, 562—570 : Unique description of chemical structures based on hierarchically ordered extended connectivities (HOC procedures.) III. Topological, chemical and stereochemical coding of molecular structure.
335. A. T. Balaban, G. Marton and I. Schiketanz, *Rev. Roum. Chim.*, 1986, **31**, 37—47 : Reaction of pyrylium salts with nucleophiles. XVIII. Synthesis of 4-(p-n-butoxyphenyl)-2,6-dimethylpyridine and of 2,6-dimethyl-4-(p-n-pentylphenyl)-pyridine.
336. A. T. Balaban, *Rev. Roum. Chim.*, 1986, **31**, 679—694 : Chemical graphs. 44. Isomer enumeration for substituted saturated polyhedral valence isomers of annulenes.
337. A. T. Balaban, *Rev. Roum. Chim.*, 1986, **31**, 695—708 : Chemical graphs. 45. Edge-labelled graphs as unsaturated valence isomers of annulenes; applications of Polya's theorem.

338. A. T. Balaban, *Rev. Roum. Chim.*, 1986, **31**, 795–810 : Chemical graphs. 46. Enumeration of valence isomers of adamantane using Polya's theorem.
339. M. Bugeanu, V. E. Sahini, V. T. Ciorba and A. T. Balaban, *Rev. Roum. Chim.*, 1986, **31**, 1013–1018 : Molecular complexes with aromatic cations as electron acceptors. VII. Spectrometric, conductimetric and dipolar data of phenyl-substituted pyrylium salts with tetracyano-para-quinodimethane anions.
340. F. Badea, A. T. Balaban, A. Dimitriu, F. Iordache, A. Meghea and L. Stănescu, *Rev. Roum. Chim.*, 1986, **31**, 119–130 : Carbanions and free radicals derived from 1,3-diphenylpyrazolidine-3,5-diones. II. Trapping of the free radicals derived from diethyl fluoromalonate, n-butyl- and phenyl-malonate.
341. N. Ralev, S. Karabunarliev, O. Mekenyan, D. Bonchev and A. T. Balaban, *J. Comput. Chem.*, 1986, **6**, 587–591 : Unique description of chemical structures based on hierarchically ordered extended conectivities (HOC procedures). VIII. Implementation of the algorithm.
342. A. T. Balaban, R. Vancea, I. Moţoc and S. Holban, *J. Chem. Inf. Comput. Sci.*, 1986, **26**, 72–76 : Chemical graphs. 43. Fortran-IV program for computing the numbers of general cubic graphs on p vertices.
343. M. Giurginca, G. Ivan, A. Meghea and A. T. Balaban, *Rev. Chimie (Bucureşti)*, 1986, **37**, 860–864 : Comportarea termică a unor nitroderivaţi aromatici în matrice de elastomeri. Spectre în IR, UV-Viz şi RES.
344. A. T. Balaban, *Math. Chem.*, 1986, **21**, 115–122 : Chemical graphs. 48. Topological index J for heteroatom-containing molecules taking into account periodicities of element properties.
345. A. T. Balaban, *Computers and Maths. with Applic.*, 1986, **12B**, 999–1020 : Symmetry in chemical structures and reactions. Reprinted in : "Symmetry Unifying Human Understanding", ed. I. Hargittai, Pergamon Press, New York, 1986, p. 999–1020.
346. G. Stănciuc, M. T. Căproiu, A. Caragheorgheopol, H. Căldăraru, A. T. Balaban and R. I. Walter, *J. Magn. Reson.*, 1987, **75**, 63–72 : Factors affecting stability and equilibria of free radicals. XIII. N-Alkoxy- and N-aralkoxypicrylamines and ESR spectra of the corresponding capto-dative persistent aminyls.
347. A. T. Balaban, E. U. Würthwein and P. von R. Schleyer, *Tetrahedron*, 1987, **43**, 405–408 : Model MNDO calculations for rotamers of α-acylnitroxides and of N-nitrosonitroxides.
348. A. T. Balaban, I. Niculescu-Duvăz and Z. Simon, *Acta Pharm. Jugosl.*, 1987, **37**, 7–36 : Topological aspects in QSAR for biologically active molecules.
349. A. T. Balaban and E. Stepan, *Rev. Roum. Chim.*, 1987, **32**, 155–177 : Reactions of pyrylium salts with nucleophiles. XIX. Novel bis-pyridinium salts with potential biological activity.
350. A. T. Balaban and C. Deleanu, *Rev. Roum. Chim.*, 1987, **32**, 271–294 : Enumeration of valence isomers of [14] annulene (Chemical graphs, 47).
351. T. S. Balaban and A. T. Balaban, *Tetrahedron Letters*, 1987, **28**, 1341–1344 : Δ^3-Dihydropyrans and tetrahydropyrans by reduction of pyrylium salts with sodium borohydride in acetic acid.
352. P. A. Filip, T. S. Balaban and A. T. Balaban, *J. Math. Chem.*, 1987, **1**, 61–83 : A new approach for devising local graph invariants : derived topological indices with low degeneracy and good correlation ability.
353. A. T. Balaban and C. Artemi, *Math. Chem.*, 1987, **22**, 3–32 : Mathematical modeling of polymers. I. Enumeration of non-redundant (irreducible) repeating sequences in stereoregular polymers, elastomers or in binary copolymers.
354. C. Artemi and A. T. Balaban, *Math. Chem.*, 1987, **22**, 33–66 : Mathematical modeling of polymers. II. Irreducible sequences in n-ary copolymers.
355. A. T. Balaban, C. Artemi and I. Tomescu, *Math. Chem.*, 1987, **22**, 77–100 : Algebraic expressions for Kekulé structure counts in non-branched regularly cata-condensed benzenoid hydrocarbons.
356. A. T. Balaban, J. Brunvoll, J. Cioslowski, B. N. Cyvin, S. J. Cyvin, I. Gutman, He Wenchen, He Wenjie, J. V. Knop, M. Kovacević, W. R. Müller, K. Szymanski, R. Tosic and N. Trinajstić, *Z. Naturforsch.*, 1987, **42a**, 863–870 : Enumeration of benzenoid and coronoid hydrocarbons.
357. C. Uncuta, M. D. Gheorghiu and A. T. Balaban, *Tetrahedron Letters*, 1987, **28**, 3143–3144 : Formation of 6,6-dimethyl-2,6-cyclohexadienylidene-1-imines from primary amines and 2,6-diisopropylpyrylium salts.
358. A. Dinculescu, T. S. Balaban and A. T. Balaban, *Tetrahedron Letters*, 1987, **28**, 3145–3146 : Synthesis of indolizines starting from pyrylium salts.

359. A. T. Balaban, N. Negoiţă, S. M. Shein and A. D. Khmelinskaya, *Rev. Roum. Chim.*, 1987. **32**. 501–508 : Factors affecting and equilibria of free radicals. XVIII. Capto-dative (push-pull) diarylaminyls with 2,4,6-tri-(methanesulphonyl)-phenyl or 2,4,6-tri-(N,N-dimethyl-sulphonylamido)-phenyl groups.
360. A. T. Balaban, M. D. Gheorghiu, I. V. Shcherbakova, E. V. Kuznetsov and I. A. Yudilevich. *Tetrahedron*. 1987, **43**, 409–414 : 2-Benzopyrylium salts. XXXI. Analogs of Reissert compounds from 2-benzopyrylium salts and sodium cyanide.
361. I. V. Shcherbakova, E. V. Kuznetsov, L. Yu. Ukhin, M. D. Gheorghiu, A. Meghea, J. Herdan and A. T. Balaban, *Rev. Roum. Chim.*, 1987, **32**, 417–426 : 2-Benzopyrylium salts. XXXII. Synthesis and some chemical and spectral properties of 1- and/or 3-(3,5-di-t-butyl-4-hydroxyphenyl)-substituted 2-benzopyrylium salts.
362. A. T. Balaban, T. S. Balaban and G. V. Boyd, *Synthesis*, **1987**, 577–578 : A novel aromatic electrophilic substitution : acylation of aromatics with cyclic isoimidium salts to yield N,N-disubstituted-aroyl-carboxamides.
363. M. C. Balaban, I. Schiketanz, A. T. Balaban, A. Schiketanz and M. D. Gheorghiu, *Rev. Roum. Chim.*, 1987, **32**, 957–978 : Aminoketone and oxazole synthesis. X. Acylation and alkylation of arenes with the azlactone of cinnamoylglycine.
364. I. Schiketanz, A. Ştefănescu, M. C. Balaban, A. Schiketanz, M. D. Gheorghiu and A. T. Balaban, *Rev. Roum. Chim.*, 1987, **32**, 1175–1180 : Aminoketone and oxazole synthesis. XI. Extension to the synthesis of thiazoles from 2-aza-1,4-diketones or via electrophilic substitution of arenes with 2-thiazolin-5-ones (thioazlactones).
365. U. Bologa, A. T. Balaban, N. Grecu, N. Negoiţă, M. T. Căproiu and R. I. Walter, *J. Org. Chem.*, 1987, **52**, 4176–4179 : Factors affecting the stability and equilibria of free radicals. Part. XIV. Unexpected spin densities in 1-trifluoroacetyl-2,2-diarylhydrazyls revealed by ^{15}N-labelling.
366. K. M. Merz Jr., R. Hoffmann and A. T. Balaban, *J. Amer. Chem. Soc.*, 1987, **109**, 6742–6751 : 3,4-Connected carbon nets : through-space and through-bond interactions in the solid state.
367. M. Banciu, M. Stănescu, C. Florea, A. T. Balaban and E. Ciorănescu, *Rev. Roum. Chim.*, 1987, **32**, 1161–1170 : Ring contraction and additional annelation in the dibenzobullvalone system.
368. A. T. Balaban and Choi Il, *Rev. Roum. Chim.*, 1988, **33**, 377–383 : Reaction of pyrylium salts with nucleophiles. XX. Synthesis of 3-(N-pyridinium)-4′-dialkylaminoazobenzene and of 4-(4-dialkylaminophenylazo)-4′-(N-pyridinium)-biphenyl derivatives.
369. A. T. Balaban, *Rev. Roum. Chim.*, 1988, **33**, 359–362 : On a 3-connected carbon net (infinite tridimensional lattice of sp^2-hybridized carbon atoms) and congeneric systems.
370. A. T. Balaban and C. Artemi, *Makromol. Chem.*, 1988, **189**, 863–870 : Mathematical modelling of polymers. 3. Enumeration and generation of repeating irreducible sequences in linear bi-, ter-, quater- and quinquenary copolymers and in stereoregular homopolymers.
371. A. T. Balaban, J. Brunvoll, B. N. Cyvin and S. J. Cyvin, *Tetrahedron*, 1988, **44**, 221–228 : Enumeration of branched catacondensed benzenoid hydrocarbons and their numbers of Kekulé structures.
372. T. S. Balaban and A. T. Balaban, *Org. Prep. Proc. Internat.*, 1988, **20**, 231–236 : 4-Phenyl-Δ^3-dihydropyrans by reduction of pyrylium salts with sodium borohydride in acetic acid.
373. A. Dinculescu, T. S. Balaban and A. T. Balaban, *Org. Prep. Proc. Internat.*, 1988, **20**, 237–243 : Synthesis of alkylindolizines from pyrylium salts.
374. T. S. Balaban A. Dinculescu and A. T. Balaban, *Org. Prep. Proc. Internat.*, 1988, **20**, 289–292 : Preparation of 2,6-dimethyl-4-phenylpyrylium sulfoacetate.
375. A. T. Balaban, *J. Mol. Struct. (Theochem)*, 1988, **165**, 243–253 : Topological indices and their uses : a new approach for the coding of alkanes.
376. A. T. Balaban, *Rev. Roum.*, *Chim*. 1988, **33**, 699–707 : Chemical graphs. Part. 49. Open problems in the area of condensed polycyclic benzenoids : topological stereoisomers of coronoids and congeners.
377. C. Uncuţa, M. D. Gheorghiu, F. Chiraleu, M. Plăveţi, M. Elian and A. T. Balaban, *Rev. Roum. Chim.*, 1988, **33**, 719–727 : Reaction of pyrylium salts with nucleophiles. XXI. Unexpected formation of 6,6-dimethyl-5-isopropyl-2,4-cyclohexadienylidene-1-imines from primary amines and 2,6-diisopropylpyrylium salts.
378. A. T. Balaban, *Rev. Chimie (Bucureşti)*, 1988, **39**, 1026–1031 : Modelarea structurilor chimice prin grafuri şi a acestora prin indici topologici.

379. A. T. Balaban and I. Tomescu, *Discrete Appl. Math.*, 1988, **19**, 6—16: Alternating 6-cycles in perfect matchings of graphs representing condensed benzenoid hydrocarbons. Reprinted in "Applications of Graphs in Chemistry and Physics" (J. W. Kennedy and L. V. Quintas, editors), North-Holland, Amsterdam, 1988, p. 5—16.
380. O. Mekenyan, D. Bonchev and A. T. Balaban, *J. Math. Chem.*, 1988, **2**, 347—375: Topological indices for molecular fragments and new graph invariants.
381. I. V. Shcerbakova, E. V. Kuznetsov, I. A. Yudilevich, O. E. Kompan, A. T. Balaban, A. H. Abolin, A. V. Polyakov and Yu. T. Struchkov, *Tetrahedron*, 1988, **44**, 6217—6224: 2-Benzopyrylium salts. XXXVII. Oxygen analogs of Reissert compounds: molecular structure and reactions with sodium hydroxide.
382. A. T. Balaban, J. W. Kennedy and L. V. Quintas, *J. Chem. Educ.*, 1988, **65**, 304—313: The number of alkanes having *n* carbons and a longest chain of length *d*. An application of a theorem of Polya.
383. A. T. Balaban, U. Bologa, M. T. Căproiu, N. Grecu, N. Negoiță and R. I. Walter, *J. Chem. Res.*, (S) **1988**, 274—275: *J. Chem. Res.*, (M) **1988**, 2101—2126: Factors affecting stability and equilibria of free radicals. XV. Effects of the acceptor group on spin distribution and other properties.
384. I. Drăguțan, H. Căldăraru, A. T. Balaban and R. J. Mehlhorn, *Bull. Soc. Chim. Belg.*, 1988, **97**, 453—455: Stable nitroxides with delocalized positive charge.
385. A. T. Balaban și T. S. Balaban, *Rev. Roum. Chim.*, 1989, **34**, 41—50: Pyrylium salts formed by diacylation of olefins. Part. XXIV. Synthesis of *meta*-terphenyl derivatives and heterocyclic analogues *via* bis-pyrylium salts obtained by bis-diacylation of *meta*-diisopropenyl-benzene.
386. M. Stănescu, M. Banciu and A. T. Balaban, *Rev. Roum. Chim.*, 1989, **34**, 617—622: 1-Oxonia and 1-aza analogues of triptycene.
387. M. Ciureanu, J. Herdan and A. T. Balaban, *Rev. Roum. Chim.*, 1989, **34**, 739—748: Electrochemical oxidation of N-(nitro-substituted-phenyl)-4-amino-2,6-di-tert-butylphenols studied by cyclic voltammetry.
388. M. D. Gheorghiu, A. Schiketanz, A. Necula and A. T. Balaban, *Rev. Roum. Chim.*, 1989, **34**, 1005—1008: Carbon-13 nuclear magnetic resonance assignments of the saturated segment from 1,2,3,4-tetrahydrophenanthrene by means of ^{13}C and ^{2}H labelling.
389. U. Bologa, A. Schiketanz, C. Mușat, D. Vîlcică, C. Drăghici, M. D. Gheorghiu and A. T. Balaban, *Rev. Roum. Chim.*, 1989, **34**, 1131—1137: Synthesis and stereochemistry of 3,5-dialkyl-2-furyl p-substituted styryl ketones.
390. C. Uncuța, T. S. Balaban, A. Petride, F. Chiraleu and A. T. Balaban, *Rev. Roum. Chim.*, 1989, **34**, 1425—1437: Reactions of pyrylium salts with nucleophiles. XXII. Regioselectivity (formation of aniline derivatives from primary amines and non-symmetrically substituted pyrylium salts) and chemoselectivity (pyridinium vs. aniline formation).
391. J. Herdan, N. Grecu, N. Negoiță, M. D. Gheorghiu and A. T. Balaban, *Rev. Roum. Chim.*, 1989, **34**, 1515—1521: Synthesis and ESR spectra of persistent aroxyls. III. Dialkyl 3,5-di-t-butyl-4-hydroxy-benzylphosphonates and their corresponding aroxyls.
392. A. T. Balaban, G. R. De Maré and R. A. Poirier, *J. Molec. Struct. (Theochem)*, 1989, **183**, 103—119: Ab initio study of neutral O_2, SO, S_2, C_2H_2 and their mono- and dications.
393. A. T. Balaban, M. D. Gheorghiu, A. Schiketanz and A. Necula, *J. Amer. Chem. Soc.*, 1989, **111**, 734—735: Catalytic automerization of phenanthrene.
394. A. Schiketanz, I. Pogany, M. D. Gheorghiu, A. Necula and A. T. Balaban, *J. Labelled Comp. Radiopharm.*, 1989, **27**, 971—976: Use of solvent vapour pressure to evacuate the installation in carbonations of Grignard reagents.
395. G. Stănciuc, M. T. Căproiu, H. Căldăraru, A. Caragheorgheopol, T. Constantinescu and A. T. Balaban, *Rev. Roum. Chim.*, 1989, **34**, 1985—1905: Factors affecting stability and equilibria of free radicals. 16. Preparation and EPR spectra of capto-dative N-alkoxy-dinitrophenyl-aminyls.
396. G. Stănciuc, M. T. Căproiu, H. Căldăraru, A. Caragheorgheopol, T. Constantinescu and A. T. Balaban, *Z. Naturforsch.*, 1989, **44b**, 1459—1463: Factors affecting stability and equilibria of free radicals. 17. EPR Evidence for formation of N-alkoxypicramides on oxidation of N-alkoxy-dinitroanilines. Electronic structure of aminyl radicals.
397. A. T. Balaban, *Computers and Maths. with Applic.*, 1989, **17**, 397—416: Carbon and Its Nets. Reprinted in "Symmetry. II", edited by I. Hargittai, Pergamon Press, Oxford, 1989, p. 397—416.
398. I. Tomescu and A. T. Balaban, *Math. Chem.*, 1989, **24**, 289—309: Decomposition theorems for calculating the number of Kekulé structures in coronoids fused via perinaphthenyl units.

399. D. Bonchev, O. Mekenyan and A. T. Balaban, *J. Chem. Inf. Comput. Sci.*, 1989, **29**, 91–97 : Interative procedure for the generalized graph center in polycyclic graphs.
400. A. T. Balaban and J. Brocas, *J. Mol. Struct. (Theochem)* ; 1989, **185**, 139–153 :Modes of rearrangements and reaction graphs for XeF_6.
401. A. T. Balaban, *Math. Chem.*, 1989,**24**, 29–38 : Chemical graphs. Part 50. Symmetry and enumeration of fibonacenes (unbranched catacondensed benzenoids isoarithmic with helicenes and zigzag catafusenes).
402. A. T. Balaban and C. Artemi, *Polycyclic Aromatic Compounds*, 1990, **1**, 171–189 : Chemical graphs. Part. 51. Enumeration of nonbranched catafusenes according to the numbers of benzenoid rings in the catafusene and in its longest linearly condensed portion.
403. A. T. Balaban, *Rev. Roum. Chim.*, 1989, **34**, 1745–1752 : Chemical graphs. Part 52. Valence isomers of bis-homoannulenes.
404. I. Alkorta, J. Elguero, I. Rozas and A. T. Balaban, *J. Mol. Struct. (Theochem)*, 1990, **206**, 67–75 : Theoretical studies of azaanalogs of platonic hydrocarbons. I. Cubane and its azaderivatives.
405. J. Brunvoll, R. Tosic, M. Kovacevic, A. T. Balaban, I. Gutman and S. J. Cyvin, *Rev. Roum. Chim.*, 1990, **35**, 85–96 : Enumeration of catacondensed benzenoid hydrocarbons and their numbers of Kekulé structures.
406. C. Uncuța, F. Chiraleu, M. D. Gheorghiu and A. T. Balaban, *Rev. Roum. Chim.*, 1990, **35**, 323–338 : Reactions of pyrylium salts with nucleophiles. XV. Stereoisomers of polyarylpyridinium salts and their interconversation.
407. M. D. Gheorghiu, I. Schiketanz, A. Schiketanz and A. T. Balaban, *Rev. Roum. Chim.*, 1990, **35**, 339–343 : ^{13}C-NMR Spectral assignments for 2,5-diarylthiazoles.
408. I. Schiketanz, A. Ștefănescu, M. D. Gheorghiu, A. Schiketanz and A. T. Balaban, *Rev. Roum. Chim.*, 1990, **35**, 345–348 : Aminoketone, oxazole and thiazole syntheses. Part XII. 2,5-Diarythiazoles from thioazlactones and aromatic hydrocarbons.
409. C. Deleanu and A. T. Balaban, *Rev. Roum. Chim.*, 1990, **35**, 349–391 : Chemical graphs. Part. 53. Benzo- and polybenzo-derivatives of valence isomers of [12]annulene.
410. C. Supuran, A. T. Balaban. M. D. Gheorghiu, A. Schiketanz, A. Dinculescu and I. Pușcaș, *Rev. Roum. Chim.*, 1990, **35**, 399–405 : Carbonic anhydrase inhibitors. II. Membrane-impermeable derivatives of 1,3,4-thiadiazole-2-sulfonamide.
411. J. Herdan, V. Dinoiu, A. Meghea, M. D. Gheorghiu, A. Schiketanz, M. Giurginca and A. T. Balaban, *Rev. Roum. Chim.*, 1990, **35**, 407–414 : Synthesis and EPR spectra of persistent aroxyls. IV. *ortho*, *ortho'*-Disubstituted phenols possessing in the *para*-position a 2-bonded-1,3-dicarbonylic (or a functionally related) group.
412. A. Marton, U. Bologa, T. S. Balaban, M. D. Gheorghiu and A. T. Balaban, *Rev. Roum. Chim.*, 1990, **35**, 415–419 : ^{1}H-NMR assignments for 2,4-diaryl-pyrylium salts and -pyridines having fused 5- or 6-membered saturated rings bridging 5,6-positions.
413. D. C. Oniciu, N. Negoiță, M. Morjan, M. D. Gheorghiu and A. T. Balaban, *Rev. Roum. Chim.*, 1990, **35**, 421–426 : Synthesis of substituted benzoins and the corresponding bis-1,2-enedihiol complexes of nickel, platinum and palladium.
414. D. C. Oniciu, A. Marton, T. S. Balaban, S. Vlad and A. T. Balaban, *Rev. Roum. Chim.* 1990, **35**, 561–565 : Synthesis of 2,6-dimethyl-4-styrylpyrylium salts (from 2,4,6-trimethylpyrylium and donor-substituted benzaldehydes) and their conversion into pyridines.
415. A. T. Balaban și T. S. Balaban, *J. Math. Chem.* 1991, **8**, 383–397 : New vertex invariants and topological indices of chemical graphs based on information on distances.
416. A. T. Balaban, D. Ciubotariu and O. Ivanciuc, *Math. Chem.*, 1990, **25**, 41–70 : Design of topological indices. Part. 2. Distance measure connectivity indices.
417. M. V. Diudea, O. Minailiuc and A. T. Balaban, *J. Comput. Chem.* 1991. **12**, 527–535 : Molecular topology. IV. Regressive vertex degrees (new graph invariants) and derived topological indices.
418. I. Alkorta, J. Elguero, I. Rozas and A. T. Balaban, *J. Mol. Struct. (Theochem.)* 1990, **67**, 63–78 : Theoretical studies on azaanalogs of platonic hydrocarbons. II. Tetrahedrane and its azaderivatives.
419. I. Alkorta, J. Elguero, I. Rozas and A. T. Balaban, *J. Mol. Struct. (Theochem.)* 1991, **28**, 47–60: Theoretical studies on azaanalogs of platonic hydrocarbons. III. Dodecahedrane and its azaderivatives.
420. A. T. Balaban, J. Brunvoll and S. J. Cyvin, *Rev. Roum. Chim.*, 1991, **36**, 145–155 : Chemical graphs. Part. 54. Enumeration of unbranched catacondensed polyhexes with equidistant linearly condensed segments.

421. C. Uncuţa, I. Păun, A. Ghiţescu, C. Deleanu, T. S. Balaban, F. Chiraleu, M. D. Gheorghiu and A. T. Balaban, *Tetrahedron Letters*, 1990, **31**, 5645—6548 : Stereoisomers due to restricted rotation in N-substituted 2,6-di-*ortho*-tolylpyridinium cations. A molecular design enabling unambiguous indentification of isomers.
422. T. S. Balaban, A. T. Balaban, D. E. Daia, K. M. Turdybekov, S. V. Lindeman and Yu. T. Struchkov. *Structural Chemistry* (in press) : Crystal and molecular structure of 2-acetyl-5-methyl-3-phenyl-furan.
423. N. G. Furmanova, N. I. Sorokina, V. I. Andrianov, U. Bologa and A. T. Balaban, *Struct. Chem.* (in press) : Crystal and molecular structure of α-(3,5-dimethyl-2-furyl)-*p*-methylstyryl ketone.
424. T. S. Balaban, A. T. Balaban, N. G. Furmanova and N. I. Sorokina, *Struct. Chim.* (in press) : Crystal and molecular structure of *syn*-periplanar N-(9-fluorenyl)-2-isopropyl-4,6-dimethylpyridinium perclorate.
425. A. T. Balaban, C. Catană, M. Dawson and I. Niculescu-Duvăz, *Rev. Roum. Chim.*, 1990, **35**, 997—1003 : Applications of weighted topological index J for QSAR of carcinogenesis inhibitors (retinoic acid decivatives).
426. M. C. Balaban, T. S. Balaban, U. Bologa and A. T. Balaban, *Rev. Roum. Chim.*, 1990, **35**, 1005—1008 : Synthesis of novel furyl-substituted 3-cyano-2-pyridones.
427. J. M. Herdan, V. Dinoiu, A. Meghea, A. Schiketanz, M. D. Gheorghiu and A. T. Balaban, *Rev Roum. Chim.*, 1990, **35**, 1017—1024 : Synthesis and EPR spectra of persistent aroxyls. V. Aroxyls derived from chalcone and derivatives.
428. F. Badea, A. T. Balaban, I. Costea, F. Iordache, A. Meghea and D. C. Oniciu, *Rev. Roum. Chim.*, 1991, **36**, 157—169 : Reaction of 3,5-di-t-butylnitrosobenzene with alkoxides and carbanions.
429. T. Morikawa şi A. T. Balaban, *Math. Chem.*, (in press) : Topological formulas and upper/lower bounds in polygonal graphs, particularly in polyhexes (benzenoids).
430. A. T. Balaban, D. Ciubotariu and M. Medeleanu, *J. Chem. Inf.Comput. Sci.*, 1991, **31**, 517—523 : Topological indices and real vertex invariants based on eigenvalues or eigenvectors.
431. A. T. Balaban, U. Bologa, C. Muşat and J. Sieler, *Struct. Chem.* (in press) : Crystal and molecular structure of 3-(3,5-dimethylfuryl-2)-1-phenyl-5-*para*-tolyl-Δ^2-pyrazoline.
432. A. T. Balaban *Annals Discrete Maths.* (in press) : Solved and unsolved problems in chemical graph theory.
433. A. T. Balaban *J. Math. Chem.*, (in press) : Real numbers as vertex invariants.

B. BOOKS

1. A. T. Balaban (scientific editor) : "Analytical Control of Radiopharmaceuticals", International Atomic Energy Agency, Vienna, 1970 (223 pages), Proceedings of a Panel, 7—11 July 1969.
2. V. K. Iya, J. C. Maynard, A. T. Balaban and A. R. Palmer (editors) : "Radioisotope Production and Quality Control", Technical Reports Series No. 128, International Atomic Energy, Agency, Vienna, 1971 (968 pages).
3. A. T. Balaban (scientific editor) : "Radioisotope Production" (Proceedings of an IAEA Regional Meeting, Sao Paulo, October 1969), International Atomic Energy Agency, Vienna, 1970.
4. A. T. Balaban (editor) "Chemical Applications of Graph Theory" Academic Press, London, with chapters by the editor : A. T. Balaban and F. Harary : Early history of the interplay between graph theory and chemistry (p. 1—4) ; A. T. Balaban : Enumeration of cyclic graphs (p. 63—105). Total 389 pp.
5. A. T. Balaban, A. Chiriac, I. Motoc and Z. Simon, "Steric Fit in Quantitative Structure Activity Relations", Lecture Notes in Chemistry No. 15, Springer, Berlin, 1980, 178 pages.
6. A. T. Balaban, M. Banciu and I. Pogany, "Aplicaţii ale metodelor fizice în chimia organică", Ed. Ştiinţifică şi Enciclopedică, Bucureşti, 1983, 287 pages.
7. V. Drăguţan, A. T. Balaban and M. Dimonie, "Metateza olefinelor şi polimerizarea prin deschidere de inel a cicloolefinelor" Ed. Academiei, Bucureşti, 1981, 254 pages ; English version : "Olefin Metathesis and Ring-Opening Polymerization of Cyclo-Olefins", Wiley, Chichester, 1985, 545 pages.

8. A. T. Balaban, I. Gălăţeanu, G. Georgescu and L. Simionescu, "Compuşi marcaţi şi radiofarmaceutici cu aplicaţii în medicina nucleară", Ed. Academiei, Bucureşti, 1979, 495 pages: English version: "Labelled Compounds and Radiopharmaceuticals Applied in Nuclear Medicine", Wiley, Chichester 1986, 742 pages.
9. A. T. Balaban, A. Dinculescu, G. N. Dorofeenko, G. W. Fischer, A. V. Koblik, V. V. Mezheritskii and W. Schroth, "Pyrylium Salts. Synthesis, Reactions and Physical Properties", Adv. Heterocyclic Chem. Suppl. Vol. 2 (ed. A. R. Katritzky), Academic Press, New York, 1982, 454 pages.
10. A. T. Balaban, M. Banciu and V. Ciorba, "Annulenes, Benzo-, Hetero-, Homo Derivatives and Their Valence Isomers", CRC Press, Boca Raton, Florida, 1986, 3 volumes, 251 + + 231 + 206 pp. = 688 pp.
11. C. Andrei, I. Drăguţan and A. T. Balaban, "Fotostabilizarea polimerilor cu amine împiedicate steric", Editura Academiei Române, Bucureşti, 1990, 240 pp.
12. N. Voiculetz, A. T. Balaban, I. Niculescu-Duvăz and Z. Simon, "Modeling of Cancer Genesis and Prevention", CRC Press, Boca Raton, Florida, 1990, 251 pp.

C. BOOK CHAPTERS

1. C. D. Nenitzescu and A. T. Balaban: "O reacţie de diacilare a alchenelor ducînd la săruri de piriliu", in: "Aspecte din chimia hidrocarburilor", editura Inst. Romăno-Sovietic, p. 95–101, Bucureşti, 1960.
2. A. T. Balaban and C. D. Nenitzescu: "Dehydrogenating Condensations of Aromatics (Scholl and Related Reactions)", in "Friedel-Crafts and Related Reactions", editor G. A. Olah, Wiley-Interscience, New York, 1964, vol. 2, p. 979–1047.
3. C. D. Nenitzescu and A. T. Balaban: "Acylations of Aliphatics", in the same book, vol. 3, p. 1033–1152.
4. A. T. Balaban, C. Mântescu and O. Constantinescu: "Sinteza şi aplicaţiile compuşilor marcaţi", in "Tehnica nucleară în sprijinul producţiei (Unele realizări ale Institutului de Fizică Atomică al Acad. R.S. România)", Ed. Academiei R.S. România, Bucureşti, 1963, p. 73–83.
5. A. Valeriu and A. T. Balaban: "Două metode radiospectroscopice cu largi aplicaţii: rezonanţă magnetică nucleară (R.M.N.) şi rezonanţă paramagnetică electronică (R.P.E.)", in the same book, p. 131–144.
6. A. T. Balaban, M. Frangopol, P. T. Frangopol and E. Gârd, "Syntheses of Labelled Compounds Based on Pyrylium Salts", in "Preparation and Bio-Medical Application of Labelled Molecules", Euratom, Brussels, 1964, p. 45–53, ed. J. Sirchis.
7. A. T. Balaban, "Deacylation of Non-Conjugated Ketones and the Reversibility of C-Acylations" in "Omagiu pentru prof. Raluca Ripan", Ed. Academiei R.S. România, Bucureşti, 1966, p. 103–109.
8. A. T. Balaban, W. Schroth and G. Fischer, "Pyrylium Salts. I. Syntheses" in "Advances in Heterocyclic Chemistry" (editors A. R. Katritzky and A. J. Boulton), Academic Press, New York, 1969, vol. 10, p. 241–326.
9. E. Gârd, A. Vasilescu, A. T. Balaban and A. Barabas, "Préparation de composés aromatiques et hétérocycliques marqués au deuterium" in "Proceedings of the Second International Conference on Methods of Preparing and Storing Labelled Compounds", Brussels, November 28 – December 3, 1966, Euratom, Brussels, 1968, p. 649–654.
10. C. Mântescu, A. Genunche and A. T. Balaban, "Tritiation of aromatic, aliphatic and heterocyclic compounds by HTO in the presence of aluminium chloride" in the same book, p. 773–779.
11. A. T. Balaban and D. Farcaşiu, "Intramolecular isotopic isomerization of carbon atoms" in the same book, p. 611–630.
12. A. T. Balaban, "Composées coordinatifs du bore et systématique des composés coordinatifs", in "La nature et les propriétés des liaison de coordination", Colloque international du C.N.R.S. No. 191, Paris 27–31 octobre, pp. 233–240 C.N.R.S., Paris 1970.
13. A. T. Balaban, N. Negoiţă and I. Pascaru, Paramagnetic resonance of new stable nitrogen free radicals, in "Magnetic Resonance and Related Phenomena", Proceedings of the 16th Congress A.M.P.E.R.E., Bucharest 1–5 September 1970, Ed. I. Ursu, Ed. Academiei, Bucureşti, 1971, p. 1168–1171.
14. A. T. Balaban, Proc. 2nd Interamerican Conf. Radiochem., Mexico City, 22–25 April 1968: "Specifications of Radiopharmaceuticals. Possible International Aspects of Labelled Compounds Programs", Washington D.C., 1971, p. 10–15.

15. A. T. Balaban, "Aplicaţii ale teoriei grafurilor în chimie", in "Cercetările multidisciplinare şi interdisciplinare : originea, dezvoltarea şi perspectivele lor", p. 203—215, Ed. Academiei R.S. România, Bucureşti, 1972.
16. A. T. Balaban, "Final Report of the European Colloquium on Current Trends in Coordination Chemistry", UNESCO—CNRS, Paris, 2—4 Dec., 1974, p. 3—5 : Summary of the Round-Table Discussions. *Ibid.*, p. 1—2 : Final report (as consultant of UNESCO). *Ibid.*, p. 19—21 : Coordination compounds of 3rd and 5th main group elements.
17. R. Vasiliev, A. T. Balaban and I. Gălăţeanu, "Produsele radiofarmaceutice în Farmacopeea română şi suplimente", p. 21—24, in "Contribuţia ICSMCF la îmbunătăţirea medicamentului românesc", Ministerul Sănătăţii, Editura Medicală Bucureşti, 1977.
18. Monographs in "Farmacopeea Română IX" (1976) : Natrii radioiodati, Natrii radiophsphati, Natrii radiochromati, Radioactivitatea.
19. C. Simionescu and A. T. Balaban, in "Ştiinţa Contemporană" (ed. R. Taton) vol. IV, p. 443—451 : "Chimia românească", Ed. ştiinţifică, Bucureşti, 1976.
20. A. T. Balaban, "The pyrylium cation as a synthon in organic chemistry", in "New Trends in Heterocyclic Chemistry" (eds. R. B. Mitra, N. R. Ayyangar, V. N. Gogte, R. M. Acheson and N. Cromwell), Elsevier, Amsterdam, 1979, p. 79—111.
21. D. H. Rouvray and A. T. Balaban, "Chemical Applications of Graph Theory" in "Applications of Graph Theory", editors R. J. Wilson and L. W. Beineke, Academic Press, London, 1979, p. 177—221.
22. A. T. Balaban, "Steric versus electronic effects of deuterium", in "Synthesis and Applications of Isotopically Labelled Compounds" (eds. W. P. Duncan and A. B. Susan), Proc. Internat. Symp. Kansas City 1982, Elsevier, Amsterdam, 1983, p. 237—242.
23. A. T. Balaban, I. Moţoc, D. Bonchev and O. Mekenyan, "Topological indices for structure-activity correlations", in "Steric Effects in Drug Design" editors M. Charton şi I. Moţoc, Topics Curr. Chem., 1983, **114**, 21—55, Springer, Berlin.
24. A. T. Balaban, S. Bădilescu and I. I. Bădilescu, 'Infrared spectra of heterocyclic compounds", in "Physical Methods in Heterocyclic Chemistry" (ed. R. R. Gupta), Wiley-Interscience, New York, 1984, p. 1—139.
25. N. M. Grecu, N. Negoiţă, M. T. Căproiu, A. T. Balaban, U. Bologa and R. I. Walter, "ESR Evidence for rotation barriers in 1-benzoyl-2,2-diarylhydrazyls", in Proc. XXII Congres AMPERE on Magnetic Resonance and Related Phenomena, eds. K. A. Müller, R. Kind and J. Ross, Zürich, 1984, p. 455—6.
26. A. T. Balaban, "Topological indices : what they are and what they can do", in Proc. 2nd Balkan Chemistry Days, Varna.
27. A. T. Balaban, S. Bădilescu and I. I. Bădilescu, "Infrared absorbtion spectra of heterocyclic compounds", in "Physical Methods in Heterocyclic Chemistry" (ed. R. R. Gupta), Wiley, New York, 1984, p. 1—139.
28. R. J. Mehlhorn, L. Packer, R. Macey, A. T. Balaban and I. Drăguţan, "ESR Spin label probes of transmembrane proton movements", in "Water and Ions in Biological Systems", Proc. 3nd Internat. Conf. Bucharest, 1984, (eds. A. Pullman, V. Vasilescu and L. Packer), USSM Bucureşti, 1985, p. 167—174.
29. A. T. Balaban, "Steric versus electronic components of secondary deuterium isotope effects depend on the size of electrophilic probes", in "Water and Ions in Biological Systems", Proc. 2nd Internat. Conf. Bucharest, 1982 (eds. A. Pullman, V. Vasilescu and L. Packer), Plenum Press, New York, 1985, p. 655—663.
30. A. T. Balaban, "Vistas opened by Fourier-transform NMR in the area of compounds labelled with isotopes of hydrogen, carbon, nitrogen and oxygen", in "Synthesis and Applications of Isotopically Labeled Compounds 1985", ed. R. R. Muccino, Elsevier, Amsterdam, 1986, p. 505—510.
31. A. T. Balaban, "Symbolic computation and chemistry", in "EUROCAL-85", Lecture Notes in Computer Science, No. 203 (ed. B. Buchberger), Springer, Berlin, 1985, p. 68—79.
32. Z. Simon, D. Ciubotariu and A. T. Balaban, "Reactivity and stereochemical parameters in QSAR for carcinogenic polycyclic hydrocarbon derivatives", in "QSAR and Strategies in the Design in Bioactive Compounds", p. 370—373, VCH Verlagsgesellschaft, Weinheim, 1985 (Proc. 5th Eurcpean Symp. on QSAR, Bad Segeber), Ed. J. K. Seydel.
33. R. J. Mehlhorn, L. Packer, R. Macey, A. T. Balaban and I. Drăguţan, "Measurement of transmembrane proton movements with nitroxide spin probes", in "Methods in Enzymology", 1986, **127**, 738—745.
34. D. Bonchev, O. Mekenyan and A. T. Balaban, "Algorithms for coding chemical compounds", in "Mathematics and Computational Concepts in Chemistry", Ed. N. Trinajstic, Ellis Horwood Ltd., Wiley, Internat. Symp. Dubrovnik, Chichester, 1986, p. 34—47.

35. A. T. Balaban and I. Bally, "Isotopically labelled pyrimidines and purines", in "Isotopes in the Physical and Biomedical Sciences", Labelled Compounds (Part. A), editors E. Buncel and J. R. Jones, vol. 1, p. 288–329, Elsevier, Amsterdam, 1987.

36. A. T. Balaban, ''Numerical modelling of chemical structures : local graph invariants and topological indices", in "Graph Theory and Topology in Chemistry" (eds. R. B. King and D. H. Rouvray), Elsevier, Amsterdam, 1987, p. 159–176, (Studies in Physical and Theoretical Chemistry, No. 51, Proc. Internat. Conf., Univ. of Georgia, 1987).

37. M. Randic, D. J. Klein, V. Katovic, D. O. Oakland, W. A. Seitz and A. T. Balaban, in the same book, p. 266–284 : "Symmetry properties of chemical graphs. X. Rearrangement of axially distorted octahedra".

38. A. T. Balaban, "Pyrylium salts as useful synthons", in "Organic Synthesis : Modern Trends" (Proc. 6th Internat. Symp. on Organic Synthesis, Moscow), ed. O. Chizhov, Blackwell, Oxford, 1987, p. 263–274.

39. I. Niculescu-Duvăz, I. Baracu and A. T. Balaban, "Alkylating agents", in "Chemistry of Antitumour Agents", ed. D. E. V. Wilman, Blackie Publ., London (Chapman & Hall New York), 1990, p. 63–130.

40. E. V. Kuznetsov, I. V. Shcherbakova and A. T. Balaban, "Benzo[c]pyrylium salts : synthesis, reactions and physical properties" in "Advances in Heterocyclic Chemistry", ed. A. R. Katritzky, Academic Press, New York, 1990, 50, 157–254.

41. A. T. Balaban, "Enumeration of isomers", in "Chemical Graph Theory. Introduction and Fundamentals" (D. Bonchev and D. H. Rouvray, eds.), Abacus Press — Gordon and Breach, New York, 1991, pp. 177–234.

42. A. T. Balaban and O. Ivanciuc, FORTRAN-77 Computer program for calculating the topological index J for molecules containing heteroatoms, in MATH/CHEM/COMP 1988 (ed. A. Graovac), Studies in Physical and Theoretical Chemistry, No. 63, Elsevier, Amsterdam, 1989, p. 193–211.

Revue Roumaine de Chimie, **36**, *4*–*7*, 313–332 (1991)

Dedicated to Professor Dr. ALEXANDRU T. BALABAN
on his 60th anniversary

ENUMERATION AND CLASSIFICATION OF CORONOID HYDROCARBONS. PART 12.

TRIPLE CORONOIDS

S. J. CYVIN, J. BRUNVOLL and B. N. CYVIN
Division of Physical Chemistry, The University of Trondheim, N–7034 Trondheim–NTH, Norway

Received December 16, 1990

Triple coronoids (polyhexes with three holes each) are enumerated and classified. The gross totals were found to be 4, 71, 1214 and 15907 for *h* (the numbers of hexagons) = 18, 19, 20 and 21, respectively.

1. PREFACE

It is safe to say that the present work could not have been done without the pioneering studies of chemical graphs by Professor A. T. Balaban. The topic is an enumeration with computer aid of a class of coronoids. Here it is relevant to invoke Balaban's pioneering works for two reasons : (a) firstly for his contribution to the enumeration of polyhexes (to which coronoids belong) in general and (b) secondly for his fundamental treatments of coronoids in particular among other macrocyclic conjugated hydrocarbons (as the annulenes).

To take the first aspect (a), the paper on enumeration of certain classes of polyhexes by Balaban and Harary [1] in 1968 has become a classical reference in this area. It was followed by additional related works.[2,3] A part of this material is quoted in the important monograph of 1976, edited by Balaban.[4] An algebraic solution for the numbers of certain polyhexes (unbranched catafusenes), already found in the first citation,[1] was recently supplemented by similar solutions for other classes. [5,6] When the emphasis gradually shifted from algebraic to computerized solutions of the enumeration of polyhexes, Balaban was again a co-author of a pioneering work [7] of 1980, which inspired other researchers and initiated a new era within this topic. Later it has been advanced to an incredibly large extent. Also the present authors have contributed to these advances, and some of them in fruitful collaboration with Balaban.[8–12]

Within the frames of the second aspect (b), it must be recalled that probably the first graph-theoretical characterization of coronoids (under other names) is found already in the first two papers cited here.[1,2] The studies of coronoids is a natural continuation of the studies of annulenes,[4,13,14] on which Balaban is an undisputable capacity. In several articles, often with the character of reviews, Balaban [15-18] has mentioned coronoids and treated them as interesting systems.

2. INTRODUCTION

Coronoid (systems) are polyhexes with holes, referred to as corona holes. The systems correspond to conjugated (polycyclic) hydrocarbons in organic chemistry. A corona hole should have a size of at least two hexagons. When it is interpreted as a benzenoid (polyhex without hole) one speaks about the naphthalene hole, phenalene hole, pyrene hole, etc. Kekulene for instance, which has been synthesized,[19] corresponds to a coronoid with the coronene hole.

For general treatments of polyhexes we cite some monographs.[20-24] In one of them [24] a whole chapter is devoted to coronoids. It is implied that a coronoid by definition is a geometrically planar system. Hence the helicenic systems are excluded.

The coronoid systems studied most extensively so far, belong to single coronoids having exactly one hole each. Usually it has been tacitly assumed that the term "coronoid" refers to a single coronoid. A coronoid system with more than one hole is referred to as a multiple coronoid.[25]. In some recent theoretical works allowance was made for several holes.[26-28] Hall [27] referred to the number of holes as the genus (g) of the system. In the present terminology a coronoid of genus g would be a g-tuple coronoid.

The first Kekulé structure counts (K)[23] for multiple coronoids account for the numerical results of a few isolated double coronoids.[25-29] The example in the former work[25] belongs to a class (coronoids linked via phenylene units) of which the K numbers later were studied in general terms by Tomescu and Balaban.[30] Combinatorial K formulae for certain classes of multiple coronoids (perforated rectangles) have been reported. [31,32] Recently also a great number of machine-computed K values for double coronoids, and a few for triple coronoids, have been published in connection with the generation and enumeration of the systems. This is the main topic of the present work. References to previous works in this area are found in the next section.

3. WORKS ON GENERATION AND ENUMERATION OF MULTIPLE CORONOIDS

The first computer-aided generation and enumeration of multiple coronoids is due to Knop et al.,[33] who reported in a note the results for the smallest ($h = 13$ and 14) double coronoids. Here h is (as usual) the number of hexagons. In a "note to a note" the same authors together with Brunvoll et al.[34] extended the computations to $h = 15$. A detailed account on all nonisomorphic double coronoids with $h = 16$ is available,[35] (part 10 of the present article series) along with incomplete data for $h = 17$ and 18. In this report the first (rudimentary) numbers for triple coronoids are found; the four nonisomorphic systems with $h = 18$ are depicted therein. In a quite recent work [36] (part 11 of the present article series) it was succeeded to perform a complete generation and enumeration of the double coronoids for $h \leqslant 18$, in addition to the triple coronoids with $h \leqslant 19$. The total number of the nonisomorphic triple coronoids with $h = 19$ is 71,[36] still a relatively small number. Hence we were challenged to extend the computations, which is not at all a trivial matter. It is *not* only a prolonged computation by the same program.

In the present work the triple coronoids were generated and enumerated completely up to $h = 21$. Several classification schemes were taken into account.

As a special kind of classification of the triple coronoid systems, the numbers of chemical isomers were produced. The first such data for single coronoids are very rudimentary (and largely in error);[37] they are commented elsewhere.[35] The first substantial (but still modest) results for the chemical isomers of single coronoids were published only recently.[28] No such data have so far been available for multiple coronoids.

The present material for all triple coronoids with $h \leqslant 21$ was also classified with respect to the chemical isomers. This material is stored for a subsequent publication.

4. BASIC PRINCIPLES OF GENERATION AND ENUMERATION

Throughout this work, the number of hexagons, viz. h, is taken as the leading parameter.

Previously employed computer programs [29,38,39] were adapted to the generation and enumeration of multiple coronoids. Substantial revisions had to be made for this purpose, but started already with some of the previous enumerations.[34–36] Nevertheless, several special procedures had to be devised, especially for producing the extra systems mentioned in the next paragraph.

Firstly, nonisomorphic systems with $h + 1$ hexagons were produced by adding one hexagon at a time to all triple coronoids with h hexagons. Hexagons were added into all possible positions to the outer perimeter only, never into the corona holes. Secondly, the necessary extra systems, not obtained by the described additions of hexagons, were supplemented. These systems were also generated by computer aid, but followed and in part checked carefully by hand.

As a whole, the triple coronoid systems were produced by specific generation rather than recognition.[39] In other words, only triple coronoids were generated. After a first generation, however, the systems were automatically classified according to different principles. In particular, the different chemical isomers within a class of systems with a given h were obtained by recognition.

The generation of extra systems is a crucial part of the analysis inasmuch as they are not obtained just by running blindly a standard program.

5. CLASSIFICATION OF THE EXTRA SYSTEMS

The extra systems are called basic when they are of the first stratum.[26] The four triple coronoids with $h = 18$ are (naturally) all basic; they are shown in Fig. 1. By the first stratum ($str = 1$) it is meant, loosely speaking, that the corona holes are as close to each other as possible. More precisely, it should be possible to go from one hole to its neighbour by traversing not more than one hexagon. Two possibilities may occur: (a) two of the holes are not neighbours, or (b) all three holes are neighbours. In Fig. 1 the system I belongs to the former category (a), while the others, viz. II–IV, belong to the latter (b).

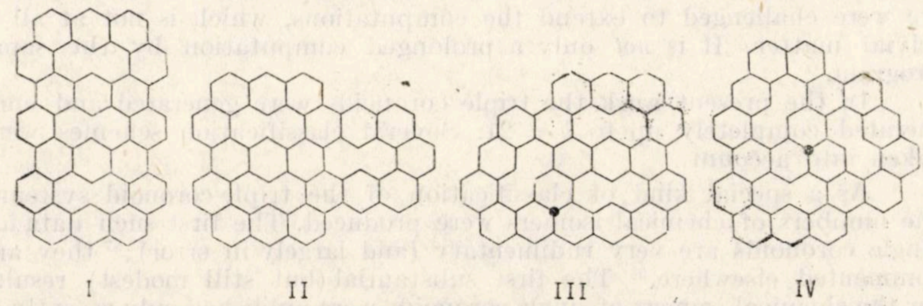

Fig. 1. — The four triple coronoids with $h = 18$; they are all basic. The black dots indicate internal vertices.

The concept of single primitive coronoids [29,40] is easily generalized to multiple coronoids as has been done at least for double coronoids.[35,36] (A) A primitive multiple coronoid is catacondensed, which means that it has no internal vertices. (B) It is obtained from single primitive coronoids where two and two neighbours share some hexagons. In Fig. 1, I and II are triple primitive coronoids. Such a system has always exactly four branching hexagons. The primitive (single or multiple) coronoids form a subclass of the basic systems. But it should be noticed that it is not sufficient to define a multiple primitive coronoid as being a catacondensed basic system. Fig. 2 shows an example of a catacondensed triple coronoid which is basic, but not primitive. Notice that it has five branching hexagons.

The non-primitive basic systems may be catacondensed as V (Fig. 2), but usually they are pericondensed, i.e. they possess one or more internal vertices. An internal vertex is defined as a vertex shared by three hexagons. The system V has $h = 22$ and is among the smallest triple coronoids of the category in question (non-primitive catacondensed basic). Therefore this type will not be encountered in our generations for $h \leqslant 21$. The systems III and IV (Fig. 1) are non-primitive basic and pericon-

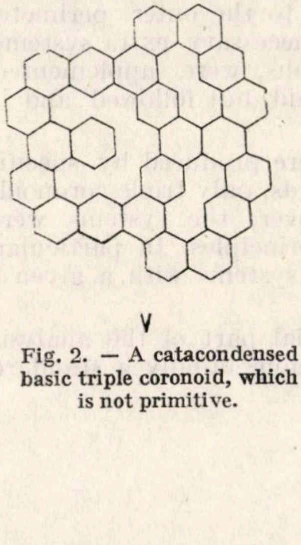

Fig. 2. — A catacondensed basic triple coronoid, which is not primitive.

densed. They have one internal vertex each. These systems are non-Kekuléan, i.e. they do not possess any Kekulé structure, as is characteristic for any polyhex with an odd number of internal vertices. Also Kekuléan systems (possessing Kekulé structures) are possible among the non-primitive basis systems. Polyhexes with an even number of internal vertices may be either Kekuléan or non-Kekuléan.

Finally one has, occurring for the first time at $h = 21$, some non-basic extra triple coronoids, which are of the second stratum.

6. SOME GENERAL CLASSIFICATION SCHEMES, AND RESULTS OF ENUMERATION

Table 1 gives the numbers of nonisomorphic triple coronoids for the four basic systems with $h = 18$ (see above and especially Fig. 1), and for the systems obtained by additions of hexagons to these basic systems. According to the present plan of the computations, the additions up to $h = 21$ are necessary.

Table 1

Triple coronoids derived from the 4 basic systems with $h = 18$

h	Type	Δ	D_{3h}	C_{3h}	D_{2h}	C_{2h}	C_{2v}	C_s	Total
18	*n*	0	0	0	1	0	1	0	2
	o	1	0	1	0	0	0	1	2
19	*n*	0	0	0	0	0	3	17	20
	o	1	0	0	0	0	0	21	21
	o	2	0	0	0	0	0	5	5
20	*n*	0	0	0	1	4	21	201	227
	e	0	0	0	0	1	1	0	2
	o	1	0	0	0	0	1	264	265
	o	2	0	0	0	0	1	69	70
	o	3	0	0	0	0	0	6	6
21	*n*	0	0	0	0	0	36	1897	1933
	e	0	0	0	0	0	2	47	49
	o	1	0	4	0	0	0	2537	2541
	o	2	0	2	0	0	1	719	722
	o	3	0	0	0	0	0	85	85
	o	4	0	1	0	0	0	2	3

The generated systems are divided into standard classes ;[8] see Table 1. Here Δ is the colour excess.[24] The "*neo*" classification implies the normal (*n*), essentially disconnected (*e*) and non-Kekuléan (*o*) systems. Precise definitions are found in the cited reference[8] and elsewhere.[23–25] Also the distribution into symmetry groups is indicated. Here it should be noted that only the six listed symmetry groups (cf. Table 1) are possible for triple coronoids. They can never have hexagonal symmetry.[35]

The system of listing was continued for $h = 19$ as the initial systems (Table 2) and $h = 20$ (Table 3). Finally, in Table 4, the data for the extra systems with $h = 21$ are collected. They imply the 767 basic systems ($str = 1$) and 20 non-basic extras with $str = 2$. A summary of Tables 1—4 is given as Table 5.

Table 2

Triple coronoids derived from the 25 basic systems with $h = 19$

h	Type	Δ	D_{3h}	C_{3h}	D_{2h}	C_{2h}	C_{2v}	C_s	Total
19	*n*	0	1	0	0	0	5	7	13
	o	1	0	0	0	0	0	10	10
	o	2	0	0	0	0	0	1	1
	o	3	0	1	0	0	0	0	1
20	*n*	0	0	0	0	0	8	180	188
	o	1	0	0	0	0	2	221	223
	o	2	0	0	0	0	0	58	58
	o	3	0	0	0	0	0	5	5
	o	4	0	0	0	0	0	1	1
21	*n*	0	0	0	0	0	65	2097	2162
	e	0	0	0	0	0	0	61	61
	o	1	0	0	0	0	2	2890	2892
	o	2	0	0	0	0	7	865	872
	o	3	0	0	0	0	0	127	127
	o	4	0	0	0	0	0	9	9
	o	5	0	0	0	0	0	1	1

Table 3

Triple coronoids derived from the 169 basic systems with $h = 20$

h	Type	Δ	D_{3h}	C_{3h}	D_{2h}	C_{2h}	C_{2v}	C_s	Total
20	*n*	0	0	0	1	9	12	57	79
	o	1	0	0	0	0	1	74	75
	o	2	0	0	0	0	2	12	14
	o	3	0	0	0	0	0	1	1
21	*n*	0	0	0	0	0	20	1271	1291
	e	0	0	0	0	0	0	54	54
	o	1	0	0	0	0	4	1760	1764
	o	2	0	0	0	0	0	491	491
	o	3	0	0	0	0	0	59	59
	o	4	0	0	0	0	0	4	4

Table 4

Extra 787 triple coronoids with $h = 21$

h	str	Type	Δ	D_{3h}	C_{3h}	D_{2h}	C_{2h}	C_{2v}	C_s	Total
21	1	*n*	0	0	0	0	0	21	291	312
		o	1	0	1	0	0	1	363	365
		o	2	0	1	0	0	7	77	85
		o	3	0	0	0	0	0	5	5
	2	*n*	0	0	0	0	0	1	17	18
		o	1	0	0	0	0	0	2	2

Table 5

Numbers of triple coronoids classified according to the *neo* classification and Δ values, including the distribution into symmetry groups

h	Type	Δ	D_{3h}	C_{3h}	D_{2h}	C_{2h}	C_{2v}	C_s	Total
18	*n*	0	0	0	1	0	1	0	2
	o	1	0	1	0	0	0	1	2
19	*n*	0	1	0	0	0	8	24	33
	o	1	0	0	0	0	0	31	31
	o	2	0	0	0	0	0	6	6
	o	3	0	1	0	0	0	0	1
20	*n*	0	0	0	2	13	41	438	494
	e	0	0	0	0	1	1	0	2
	o	1	0	0	0	0	4	559	563
	o	2	0	0	0	0	3	139	142
	o	3	0	0	0	0	0	12	12
	o	4	0	0	0	0	0	1	1
21	*n*	0	0	0	0	0	143	5573	5716
	e	0	0	0	0	0	2	162	164
	o	1	0	5	0	0	7	7552	7564
	o	2	0	3	0	0	15	2152	2170
	o	3	0	0	0	0	0	276	276
	o	4	0	1	0	0	0	15	16
	o	5	0	0	0	0	0	1	1

7. PRIMITIVE TRIPLE CORONOIDS

All the primitive triple coronoids for $h \leqslant 21$ were deduced by hand according to one of the previously described alternatives,[35] which was found to be the most useful one after its adaptation to triple coronoids. One starts with a primitive double coronoid. Let its number of hexagons be h'. Then a primitive single coronoid (with h'' hexagons, say) is combined with it so that the two systems share x hexagons and form a primitive triple coronoid. The resulting system then has

$$h = h' + h'' - x$$

which is used as a code (in parentheses). One needs the forms of primitive single and double coronoids, which have been published in sufficient amounts for our purpose, although they are scattered through several articles.[34-36,40]

In the start one combines the $h' = 13$ double coronoid with the $h'' = 8$ single coronoid by three common hexagons. The two possibilities, both with the code (13 + 8 − 3) are exactly I and II of Fig. 1, the two primitive triple coronoids with $h = 18$. This information is entered into Table 6. The rest of the table was produced in the same way by going systematically through all the possibilities. As a pleasing fact, the totals

Table 6

Numbers of primitive triple coronoids with different codes

h	Code	Number	h	Code	Number
18	(13+8−3)	2	20	(15+9−4)	2
				(16+8−4)	1
19	(13+8−2)	2		(13+10−2)	7
	(13+9−3)	1	21	(14+9−2)	6
	(14+8−3)	3		(15+8−2)	24
	(13+10−4)	1		(13+11−3)	4
	(14+10−5)	2		(14+10−3)	11
20	(13+9−2)	1		(15+9−3)	4
	(14+8−2)	9		(16+8−3)	15
	(13+10−3)	4		(13+12−4)	7
	(14+9−3)	2		(14+11−4)	2
	(15+8−3)	6		(15+10−4)	7
	(13+11−4)	2		(16+9−4)	4
	(14+10−4)	1		(17+8−4)	6

Table 7

Numbers of primitive, non-primitive catacondensed and pericondensed triple coronoids

h	Catacondensed		Pericondensed	Total
	primitive	non-primitive		
18	2	0	2	4
19	9	8	54	71
20	28	117	1069	1214
21	97	988	14822	15907

for each h value are consistent with the appropriate numbers of Table 7 They were derived by computer aid and in an entirely different manner using the number of hexagons in each of the three corona holes as the basis of a classification.

Figure 3 shows the forms (as black silhouettes on the background of a hexagonal lattice) of all nonisomorphic primitive triple coronoids with $h = 18$ through 21. In order to increase the amount of information the Kekulé structure counts (K) are given. They were computed by means of the determinant of the adjacency matrix[41] or, when necessary, by the Pfaffian of a skew-symmetric adjacency matrix.[42]

8. NON-PRIMITIVE KEKULÉAN TRIPLE COROIDS WITH NINETEEN HEXAGONS

The smallest non-primitive basic triple coronoids which are Kekuléan occur for $h = 19$. There are 4 such systems, which are depicted in Fig. 4. We have chosen, for the sake of brevity, not to reproduce the corresponding

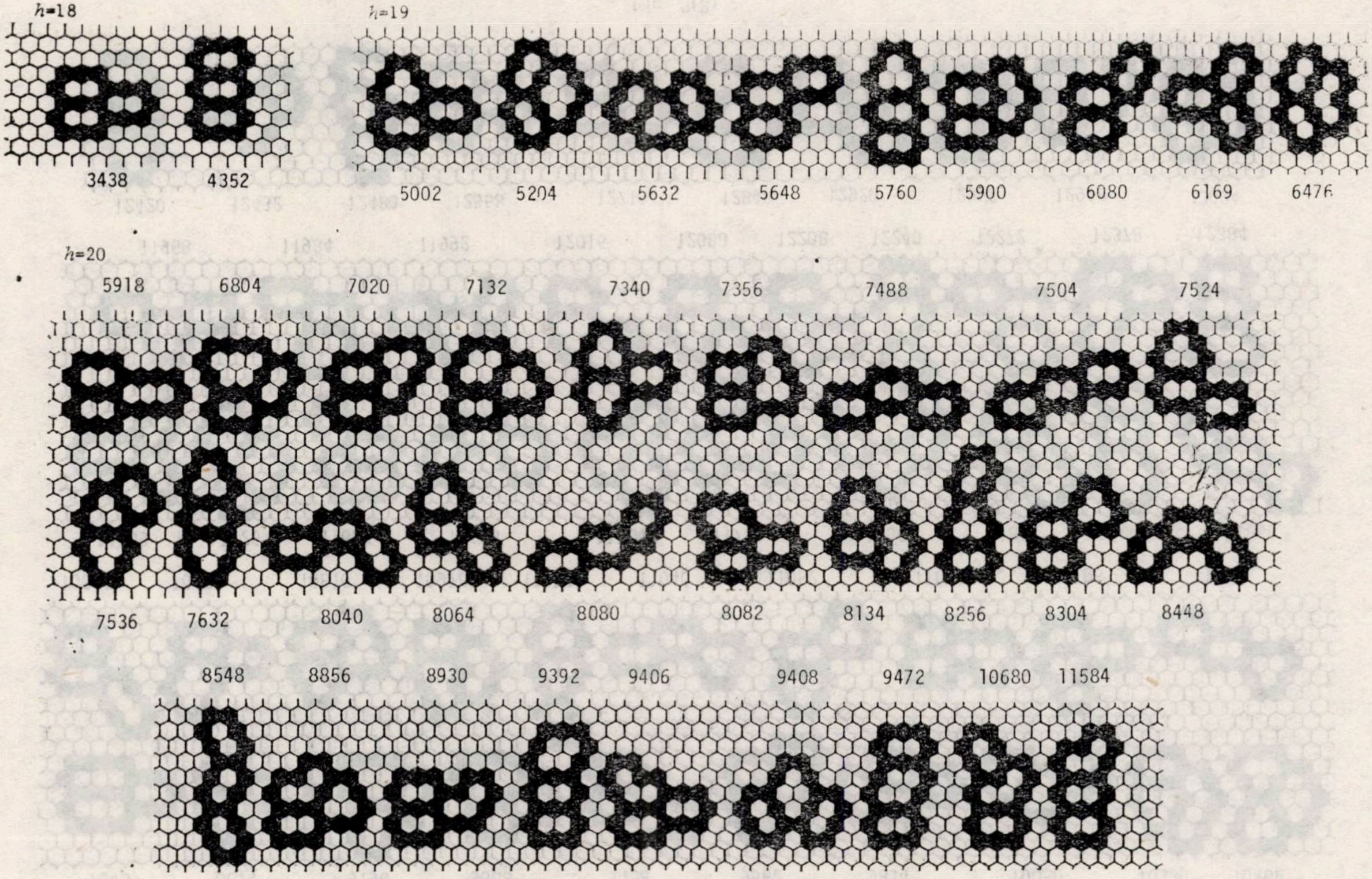

h=18
3438
4352
h=19
5002
5204
5632
5648
5760
5900
6080
6169
6476
h=20
5918
6804
7020
7132
7340
7356
7488
7504
7524
7536
7632
8040
8064
8080
8082
8134
8256
8304
8448
8548
8856
8930
9392
9406
9408
9472
10680
11584

Fig. 3(1). — All primitive triple coronoids with $h \leqslant 21$. K numbers are given.

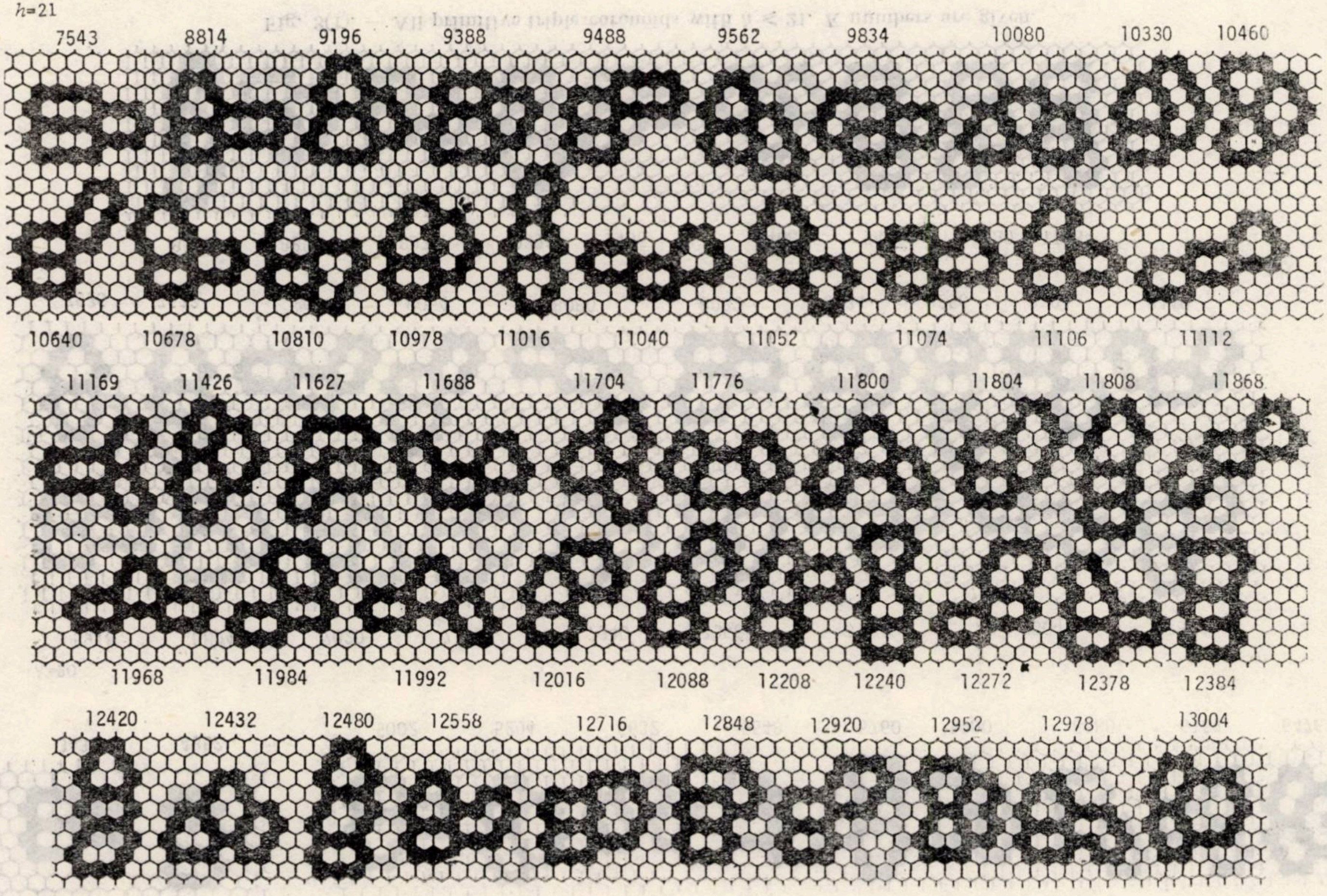
h=21
7543
8814
9196
9388
9488
9562
9834
10080
10330
10460
10640
10678
10810
10978
11016
11040
11052
11074
11106
11112
11169
11426
11627
11688
11704
11776
11800
11804
11808
11868
11968
11984
11992
12016
12088
12208
12240
12272
12378
12384
12420
12432
12480
12558
12716
12848
12920
12952
12978
13004

Fig. 3(2)

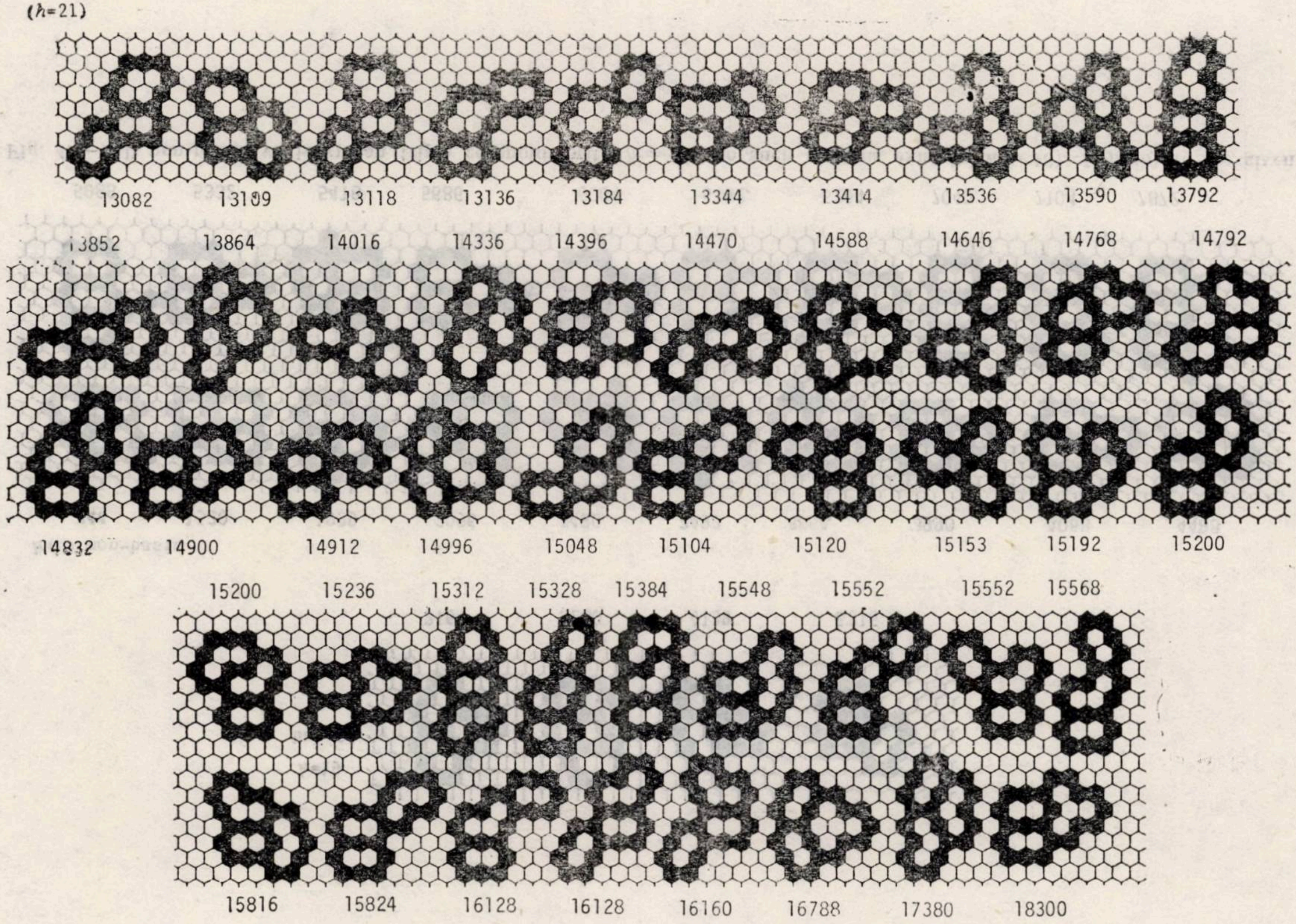
(h=21)
13082
13109
13118
13136
13184
13344
13414
13536
13590
13792
13852
13864
14016
14336
14396
14470
14588
14646
14768
14792
14832
14900
14912
14996
15048
15104
15120
15153
15192
15200
15200
15236
15312
15328
15384
15548
15552
15552
15568
15816
15824
16128
16128
16160
16788
17380
18300

Fig. 3(3)

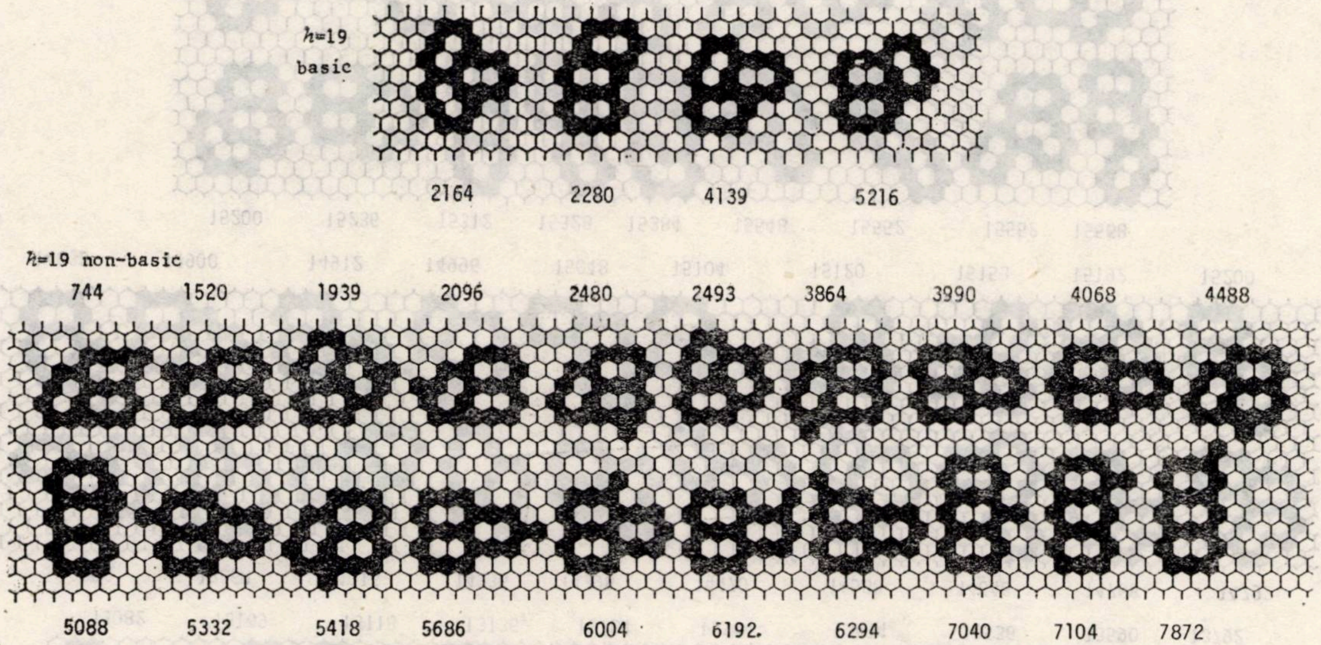
h=19
basic
2164
2280
4139
5216
h=19 non-basic
744
1520
1939
2096
2480
2493
3864
3990
4068
4488
5088
5332
5418
5686
6004
6192
6294
7040
7104
7872

Fig. 4. — All non-primitive Kekuléan triple coronoids with $h = 19$ (no such systems exist for $h = 18$). K numbers are given.

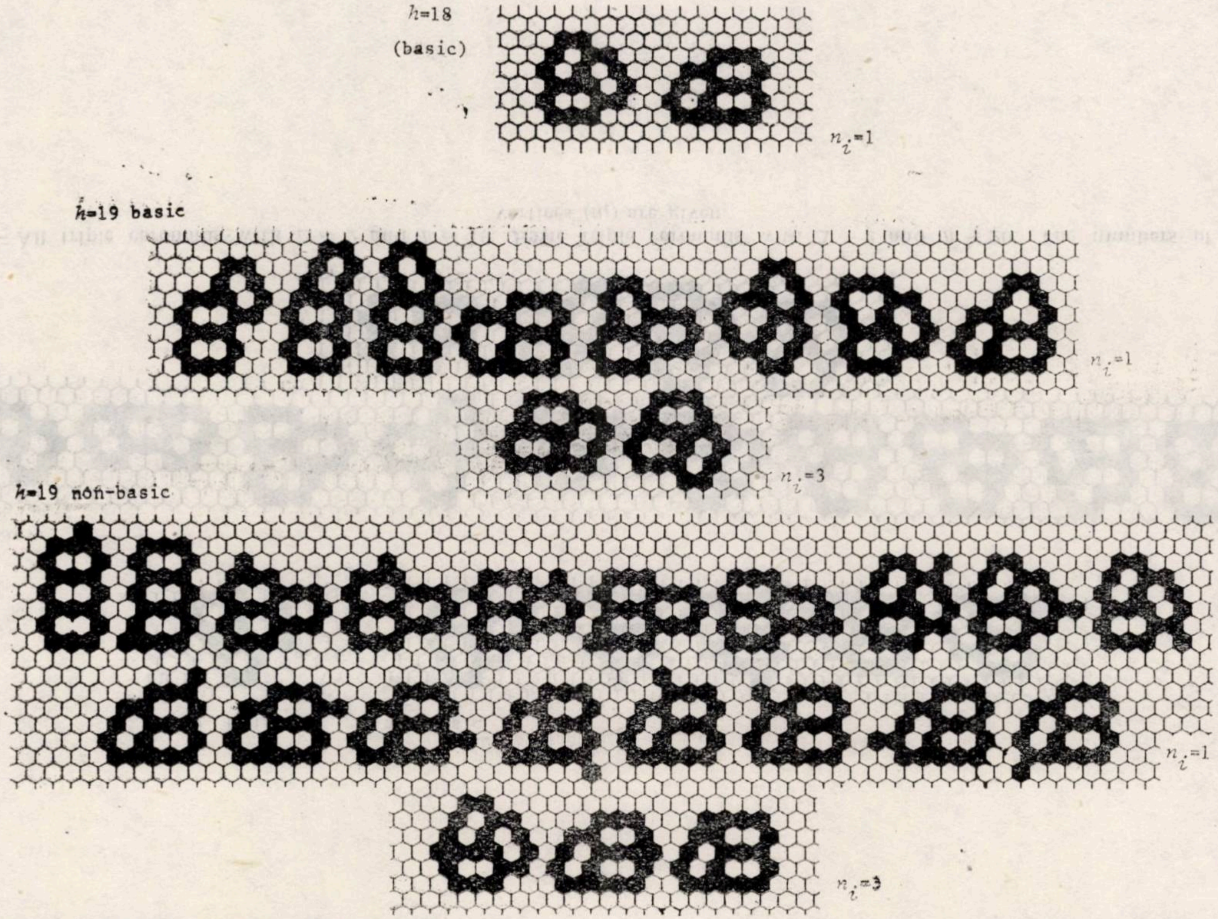
h=18
(basic)
n_i=1
h=19 basic
n_i=1
n_i=3
h=19 non-basic
n_i=1
n_i=3

Fig. 5. —All triple coronoids with $\Delta = 1$ and $h \leqslant 19$. They are non-Kekuléan. The numbers of internal vertices (n_i) are given.

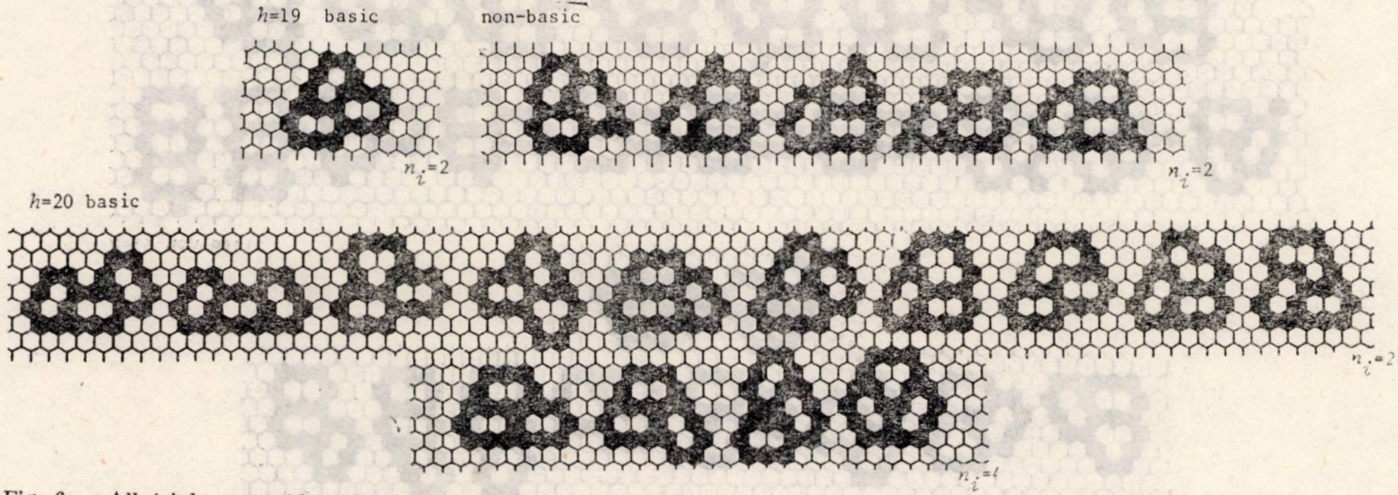
h=19 basic
non-basic
n_i=2
n_i=2
h=20 basic
n_i=2
n_i=4

Fig. 6. — All triple coronoids with $\Delta = 2$ and $h = 19$. Basic triple coronoids with $\Delta = 2$ and $h = 20$. The numbers of internal vertices (n_i) are given.

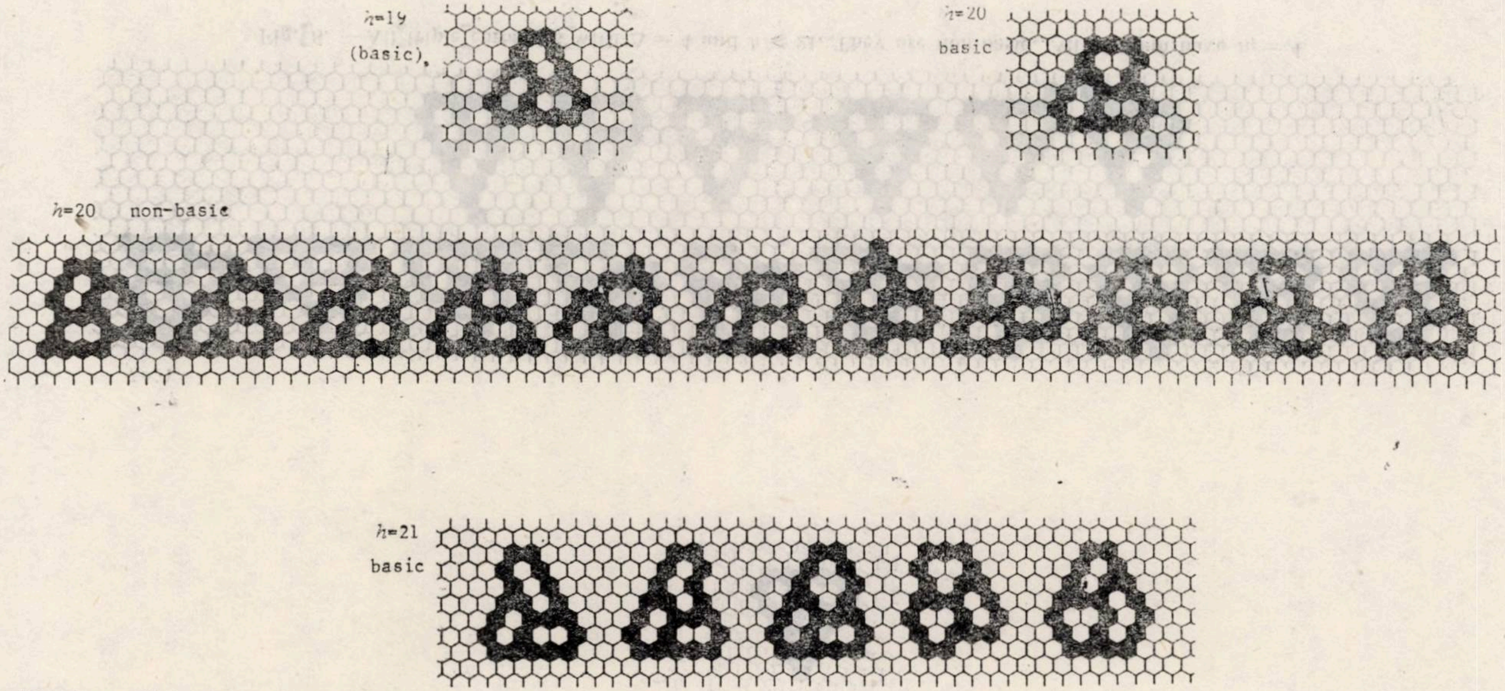
h=19
(basic),
h=20
basic
h=20 non-basic
h=21
basic

Fig. 7. — All triple coronoids with $\Delta = 3$ and $h \leqslant 20$. Basic triple coronoids with $\Delta = 3$ and $h = 21$. All these systems have $n_i = 3$.

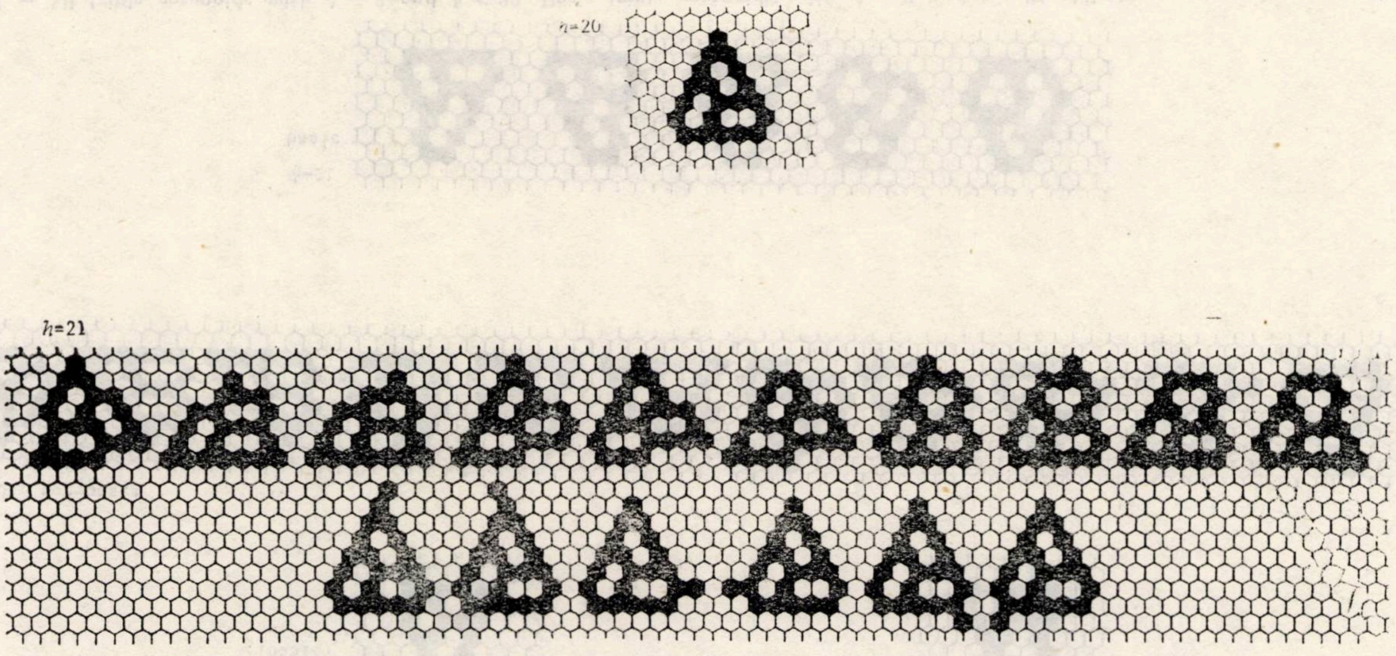

Fig. 8. — All triple coronoids with $\Delta = 4$ and $h \leqslant 21$. They are non-basic. All of them have $n_i = 4$.

systems with $h = 20$, of which there are 51. Instead we show in the same figure the 20 Kekuléan systems (8 catacondensed and 12 pericondensed) with $h = 19$, obtained by additions of hexagons to the $h = 18$ systems.

9. NON-KEKULÉAN TRIPLE CORONOIDS

The smallest non-Kekuléan triple coronoids are the 2 basic systems with $h = 18$ depicted in Fig. 5 (and Fig. 1). They have $\Delta = 1$. Figure 5 continues by displaying the $\Delta = 1$ triple coronoids with $h = 19$: 10 basic and 21 non-basic, the latter obtained by additions of hexagons to the $h = 18$ systems. For $h = 20$ and $h = 21$ the numbers of basic triple coronoids with $\Delta = 1$ are 75 and 365, respectively (cf Tables 3 and 4). They are too many to be depicted here, as also is the case for the non-basic systems with $\Delta = 1$ and $h > 19$.

Triple coronoids with $\Delta = 2$ start at $h = 19$. Figure 6 shows the unique basic and 5 non-basic systems of this category. Also included are the 14 basic systems with $h = 20$. The 85 corresponding systems with $h = 21$ (cf. Table 4) are not depicted.

Figure 7 shows the unique triple coronoid with $\Delta = 3$ and $h = 19$. It is basic. Also included are the 12 such systems with $h = 20$: 1 basic and 11 non-basic. Finally, Fig. 7 displays the 5 basic triple coronoids with $\Delta = 3$ and $h = 21$.

Triple coronoids with $\Delta = 4$ start with the unique non-basic $h = 20$ system; see Fig. 8. The figure includes the 16 systems with $\Delta = 4$ and $h = 21$, all of them non-basic.

It is found that there are unique extremal triple coronoids for $h = 19$ ($\Delta = 3$) and $h = 20$ ($\Delta = 4$); see Figs. 7 and 8, respectively. This regularity continues for $h = 21$ ($\Delta = 5$) and even for $h = 22$ ($\Delta = 6$), as can be inferred from the selection rules for Δ;[43] see Fig. 9.

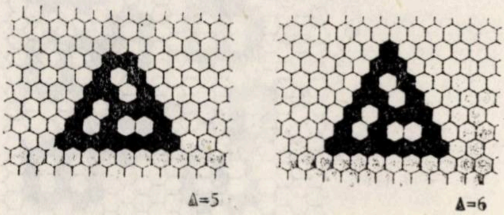

Fig. 9. — The unique extremal triple coronoids with $h = 21$ ($\Delta = 5$) and $h = 22$ ($\Delta = 6$).

10. TRIPLE CORONOIDS OF THE SECOND STRATUM WITH TWENTY-ONE HEXAGONS

There are 20 systems of the title category: 18 Kekuléan (6 catacondensed and 12 pericondensed) and 2 non-Kekuléan with $\Delta = 1$. All of them are additions to the smallest double coronoid, which has two naphthalene holes. The extra naphthalene hole is not as close as possible to any of the other holes. The systems are depicted in Fig. 10.

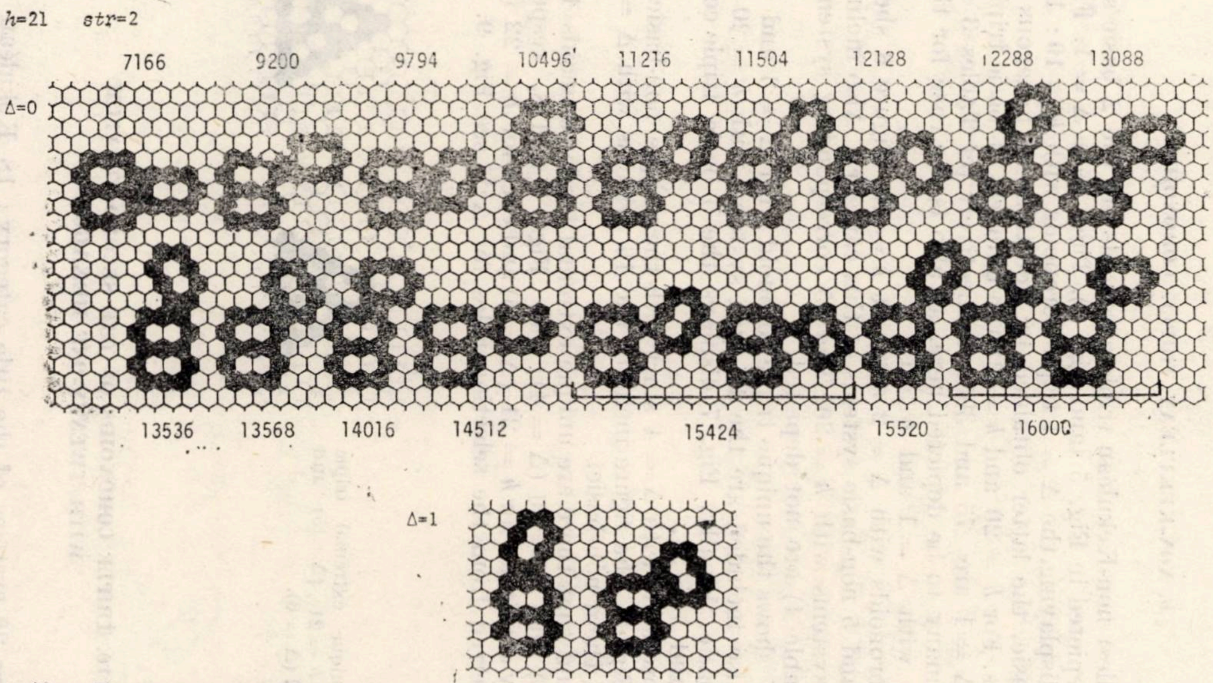
h=21
str=2
7166
9200
9794
10496
11216
11504
12128
12288
13088
Δ=0
13536
13568
14016
14512
15424
15520
16000
Δ=1

Fig. 10. — The triple coronoids with $str = 2$ and $h = 21$. K numbers for the Kekuléan systems are given. Bracketed systems are isoarithmic. The non-Kekuléan systems ($\Delta = 1$) have $n_i = 3$

11. CONCLUSION

It is useful to have the numbers of polyhexes according to coarse classification,[8] in addition to the finer details. Table 7 is such an example for triple coronoids. Some other coarse classifications of triple coronoids are presented in Table 8. All the numbers therein are obtainable by summations of the appropriate numbers in Table 5.

Table 8

Numbers of triple coronoids classified according to Δ, and their distribution into symmetry groups

h \ Δ	0	1	2	3	4	5
18	2	2				
19	33	31	6	1		
20	496	563	142	12	1	
21	5880	7564	2170	276	16	1

h	D_{3h}	C_{3h}	D_{2h}	C_{2h}	C_{2v}	C_s
18	0	1	1	0	1	1
19	1	1	0	0	8	61
20	0	0	2	14	49	1149
21	0	9	0	0	167	15731

The black silhouettes presented in Figs. 3–6 contain all triple coronoids with $h \leqslant 19$. In addition, members of selected classes for higher h values are depicted therein.

There is still much to be done in the area of multiple coronoids. With regard to the enumeration and classification of the systems, a study of the chemical isomers, which was mentioned above, seems to be of the greatest interest.

ACKNOWLEDGEMENT. Financial support to B. N. C. from the Norwegian Research Council for Science and the Humanities is gratefully acknowledged.

REFERENCES

[1] A. T. Balaban and F. Harary, *Tetrahedron*, **24**, 2505 (1968).
[2] A. T. Balaban, *Tetrahedron*, **25**, 2949 (1969).
[3] A. T. Balaban, *Math. Chem.*, **2**, 51 (1976).
[4] A. T. Balaban, in "Chemical Applications of Graph Theory" (Edited by A. T. Balaban), p. 63, Academic Press, London, 1976.
[5] A. T. Balaban, *Math. Chem.*, **24**, 29 (1990).
[6] A. T. Balaban and C. Artemi, *Polycyclic Aromatic Compounds*, **1**, 171 (1990).
[7] K. Balasubramanian, J. J. Kaufman, W. S. Koski and A. T. Balaban, *J. Comput. Chem.*, **1**, 149 (1980).

[8] A. T. Balaban, J. Brunvoll, J. Cioslowski, B. N. Cyvin, S. J. Cyvin, I. Gutman, W.C. He, W. J. He, J. V. Knop, M. Kovačević, W. R. Müller, K. Szymanski, R. Tošić and N. Trinajstić, *Z. Naturforsch.*, **42a**, 863 (1987).

[9] A. T. Balaban, J. Brunvoll, B. N. Cyvin and S. J. Cyvin, *Tetrahedron*, **44**, 221 (1988).

[10] J. Brunvoll, R. Tošić, M. Kovačević, A. T. Balaban, I. Gutman and S. J. Cyvin, *Rev. Roumaine Chim.*, **35**, 85 (1990).

[11] A. T. Balaban, J. Brunvoll and S. J. Cyvin, *Rev. Roumaine Chim.*, **35**, 985 (1990).

[12] S. J. Cyvin and A. T. Balaban, *Struct. Chem.*, in press.

[13] A. T. Balaban, *Tetrahedron*, **27**, 6115 (1971).

[14] A. T. Balaban, M. Banciu and V. Ciorba, "Annulenes, Benzo-, Hetero-, Homo- Derivatives and Their Valence Isomers", CRC Press, Boca Raton, Florida, 1987.

[15] A. T. Balaban, *Pure & Appl. Chem.*, **54**, 1075 (1982).

[16] A. T. Balaban, *J. Chem. Inf. Comput. Sci.*, **25**, 334 (1985).

[17] A. T. Balaban, *Rev. Roumaine Chim.*, **33**, 699 (1988).

[18] A. T. Balaban, in "Symmetry 2 Unifying Human Understanding" (Edited by I. Hargittai), *Computers Math. Applic.*, **17**, 397 (1989); Pergamon Press, Oxford, 1989.

[19] F. Diederich and H. A. Staab, *Angew. Chem. Int. Ed. Engl.*, **17**, 372 (1978).

[20] N. Trinajstić, "Chemical Graph Theory," Vols. I, II, CRC Press, Boca Raton, Florida, 1983.

[21] I. Gutman and O. E. Polansky, "Mathematical Concepts in Organic Chemistry," Springer—Verlag, Berlin, 1986.

[22] J. R. Dias, "Handbook of Polycyclic Hydrocarbons, Part A: Benzenoid Hydrocarbons," Elsevier, Amsterdam, 1987.

[23] S. J. Cyvin and I. Gutman, "Kekulé Structures in Benzenoid Hydrocarbons," *Lecture Notes in Chemistry*, **46**, Springer—Verlag, Berlin, 1988.

[24] I. Gutman and S. J. Cyvin, "Introduction to the Theory of Benzenoid Hydrocarbons," Springer—Verlag, Berlin, 1989.

[25] S. J. Cyvin, B. N. Cyvin and J. Brunvoll, *Chem. Phys. Letters*, **140**, 124 (1987).

[26] W. J. He and W. C. He, *Theor. Chim. Acta*, **70**, 43 (1986).

[27] G. G. Hall, *Theor. Chim. Acta*, **73**, 425 (1988).

[28] S. J. Cyvin and J. Brunvoll, *Chem. Phys. Letters*, **164**, 635 (1989).

[29] J. Brunvoll, B. N. Cyvin and S. J. Cyvin, *J. Chem. Inf. Comput. Sci.*, **27**, 14 (1987).

[30] I. Tomescu and A. T. Balaban, *Math. Chem.*, **24**, 289 (1989).

[31] S. J. Cyvin, B. N. Cyvin and J. Brunvoll, *Chem. Phys. Letters*, **156**, 595 (1989).

[32] R. S. Chen and S. J. Cyvin, *J. Mol. Struct. (Theochem)*, **200**, 251 (1989).

[33] J. V. Knop, W. R. Müller, K. Szymanski and N. Trinajstić, *J. Mol. Struct. (Theochem)*, **205**, 361 (1990).

[34] J. Brunvoll, B. N. Cyvin, S. J. Cyvin, J. V. Knop, W. R. Müller, K. Szymanski and N. Trinajstić, *J. Mol. Struct. (Theochem)*, **207**, 131 (1990).

[35] S. J. Cyvin, J. Brunvoll and B. N. Cyvin, *J. Chem. Inf. Comput. Sci.*, **30**, 210 (1990).

[36] J. Brunvoll, B. N. Cyvin and S. J. Cyvin, *Croat. Chem. Acta*, in press.

[37] J. R. Dias, *J. Chem. Inf. Comput. Sci.*, **22**, 15 (1982).

[38] J. Brunvoll, S. J. Cyvin and B. N. Cyvin, *J. Comput. Chem.*, **8**, 189 (1987).

[39] J. Brunvoll, B. N. Cyvin and S. J. Cyvin, *J. Chem. Inf. Comput. Sci.*, **27**, 171 (1987).

[40] J. Brunvoll, B. N. Cyvin, S. J. Cyvin, I. Gutman, R. Tošić and M. Kovačević, *J. Mol. Struct. (Theochem)*, **184**, 165 (1989).

[41] R. L. Brown, *J. Comput. Chem.*, **4**, 556 (1983).

[42] S. J. Cyvin, J. Brunvoll and B. N. Cyvin, *Struct. Chem.*, in press.

[43] J. Brunvoll, B. N. Cyvin, S. J. Cyvin and I. Gutman, *Z. Naturforsch.*, **43a**, 889 (1988).

Revue Roumaine de Chimie, **36**, *4*–7, 333–339(1991)

Dedicated to Prof. A. T. BALABAN
on the occasion of his 60th birthday

ELECTRONIC AND GEOMETRICAL STRUCTURE OF 10π-ELECTRON SYSTEMS : CYCLOOCTATETRAENE DIANION AND ITS HETEROATOMIC ANALOGS

E. B. GLUZ, M. E. KLETSKY and R. M. MINYAEV
Institute of Physical and Organic Chemistry, Rostov University,
Rostov-on-Don, 344711 USSR

Received January 7, 1991

Semiempirical AM1 quantum chemical calculations have been carried out for eight-membered 10π-electron cyclooctatetraene dianion and its nitrogen and oxygen heteroatomic analogs—diazocine and dioxocine molecules. The calculations predict that unlike the actually aromatic cyclooctatetraene dianion the 10π-electron neutral positional isomers of $X_2C_6H_6$ ($X=NH$, O) should be assigned to the class of antiaromatic compounds.

INTRODUCTION

The geometrical structure of cyclooctatetraene (COT) molecule, which is a nonaromatic annulene, demonstrates like the benzene structure a remarkable success of Hückel theory.

Neutral COT molecule, containing 8π-electrons and hence being antiaromatic in planar form, exhibits polyolefine features and therefore possesses a tub (boat-like) D_{2d}-conformation **1**.[1–3] According to calculations [4] the nonplanar chair-like structure **2** has the energy considerably higher than **1**. The D_{4h}-planar structure **3** and especially the antiaromatic D_{8h}-structure **4** are also thermodynamically destabilized in respect to structure **1**.[3–5] The flattening of the eight-membered ring may be achieved for example through annelation by small rings.[6] Eight-membered rings are flattened also in ions $C_8H_8^{2+}$ and $C_8H_8^{2-}$ which display aromatic features.[7,8]

However, as has been shown by experimental works of Schroth and coworkers,[9] some of the isoelectronic heterocycle analogs of COT^{2-}

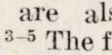
1, D_{2d}

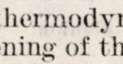
2

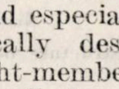
3, D_{4h}

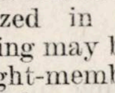
4, D_{8h}

containing 4n + 2 π-electrons, in contrast to prediction of Hückel theory are stable in nonplanar conformations and exhibit nonaromatic features. The Hückel MO calculations, carried out by Balaban and Simon in 1965 (see review [12]) also predicted the energy preference of nonplanar conformation for classical structures of dithio- and dioxocines. As has been shown by the same calculations, the nonclassical (mesoionic) structures possessed less bonding energy in comparison with classical structures and consequently are less aromatic (so-called pseudoaromatic systems). However, these pioneer calculations could not give the full understanding of structural and electronic properties of 10π-electron heterocyclic COT^{2-} analogs.

SINDO1 calculations,[12] also indicate that heteroatomic peripheral substitution in system **5** (X, Y=O, NH, NHAc, BH) influences critically the geometric properties (on the planarity) of 10π-electron eight-membered systems.

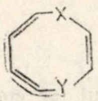

5

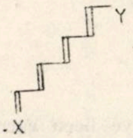

6

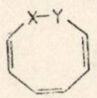

7

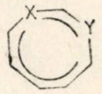

8

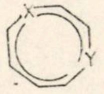

9

It should be emphasized that the Hückel calculations of system **5** have been done for the first time by Allinger and coworkers.[11]

In the present work we tackle the problem of electronic and geometric structure of COT dianion $C_8H_8^{2-}$ and its heterocyclic 10π-electron analogs with classical and nonclassical (mesoionic) structures **5**, **7**–**9** ($X=Y=CH^-$, O, NH) using semiempirical AM1 calculations.[13] Special attention will be devoted to the influence of heteroatomic positions in the cycle on the geometric structure and thermodynamic stability of the ring and finally on its aromaticity which can be characterized both by the ring planarization and π-electron delocalization.[14]

RESULTS

Structure of COT dianion

According to AM1 calculations in singlet electronic state the COT dianion is stable in planar configuration of D_{8h} symmetry in which C–C bond length equals 1.386 Å. As expected, this structure energetically is more stable by 57.2 kcal/mole than an open chain structure **6**, $X=Y=CH^-$. The D_{8h}-structure corresponds to the minimum ($\lambda = 0$) on the PES of $C_8H_8^{2-}$. Geometrical parameters of $C_8H_8^{2-}$ calculated by AM1 method are more consistent with *ab initio* (STO-3G) data ($l_{C-C} = 1.399$ Å),[8] than SINDO1 ($l_{C-C} = 1.432$ Å) results.[12]

It is interesting to notice that in triplet electronic state COT dianion, as predicted by AM1 calculations, thermodynamically is less stable than in singlet state ($\Delta H_f(S_0) = 133.4$, $\Delta H_f(T_1) = 179.2$ kcal/mol). The triplet state structure of $C_8H_8^{2-}$ has D_{4h} symmetry.

Quantum chemical calculations carried out in Hartree-Fock approximation show that the HOMO's energy of four-membered electron redundant dianion $C_4H_4^{2-}$ has a positive value (see, for example [15]). We have obtained the same results for $C_8H_8^{2-}$ ($\varepsilon_{HOMO} = 3.360$ eV). The decrease of HOMO energy should be expected in salts of type $M^{2+}C_8H_8^{2-}$, where M is alkali atom,[15] and in heteroatomic π-isoelectronic systems **5**, **7**—**9**. This is consistent with the stabilizing effect observed for cyclobutadiene dianion $C_4H_4^{2-}$.[16]

Molecular orbital analysis

The correlation MO diagram for systems $C_8H_8^{2-}$ and **5**, **7**—**9** (X=Y=O, NH) is presented in Fig. 1.

One can see that 1,k-disubstitution ($k = 2-5$) is reflected mainly in the change of HOMO and LUMO energies. The energy of another MOs negligibly depends on k. In all cases of disubstitution one can observe the removing of MO degeneration, but in 1,2-disubstituted isomer this effect is more slightly pronounced. 1,3-Disubstitution leads to destabilization of both frontier MOs but mainly of the HOMO. However, 1,4-disub-

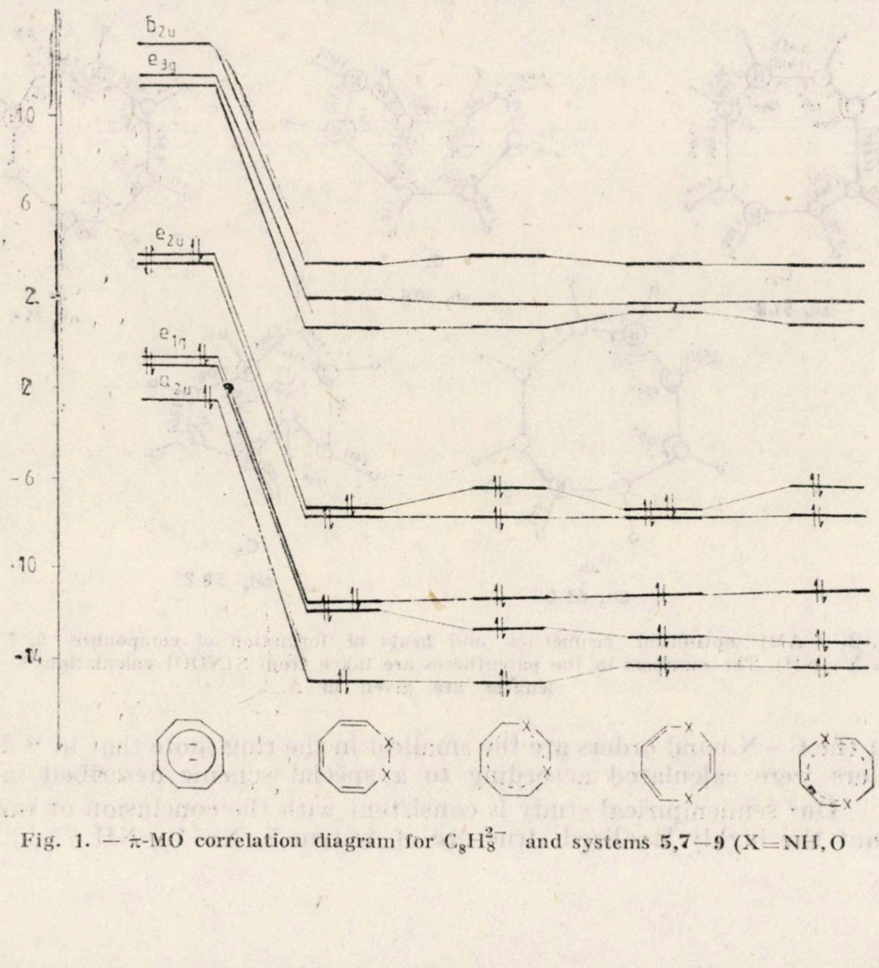

Fig. 1. — π-MO correlation diagram for $C_8H_8^{2-}$ and systems **5**,**7**—**9** (X=NH, O

stitution leads to the increase of the energy gap between frontier MOs especially at the expense of decreasing energy of HOMO in classical C_{2v} structures. The energies of frontier MOs for 1,5-disubstituted systems have the values close to those of 1,3-disubstituted systems (see Fig. 1).

Thus, the difference in type of substitution follows the difference in the thermodynamic stability of these isomers.

Diazocine and its positional isomers

According to AM1 calculations the classical structure **5** is the most stable among all diazocine positional isomers. On the singlet PES of $(CH)_6(NH)_2$ the planar structure **5** (C_{2v} symmetry) corresponds to a minimum ($\lambda = 0$). These results confirm well the spectroscopic (electronic and NMR) data.[17]

It is worth to note that although the alternation of bond length[8] obtained by SINDO1 method [12] is higher than that in AM1 calculations, (see Fig. 2) nevertheless both methods give similar orders of bond alternation.

For example, according to SINDO1 [12] and our calculations, two carbon atoms, located between nitrogen atoms, form the highest order bond, but the C—N bond orders are the smallest in the ring (note that in [12] bond orders were calculated according to a special scheme described in [18]).

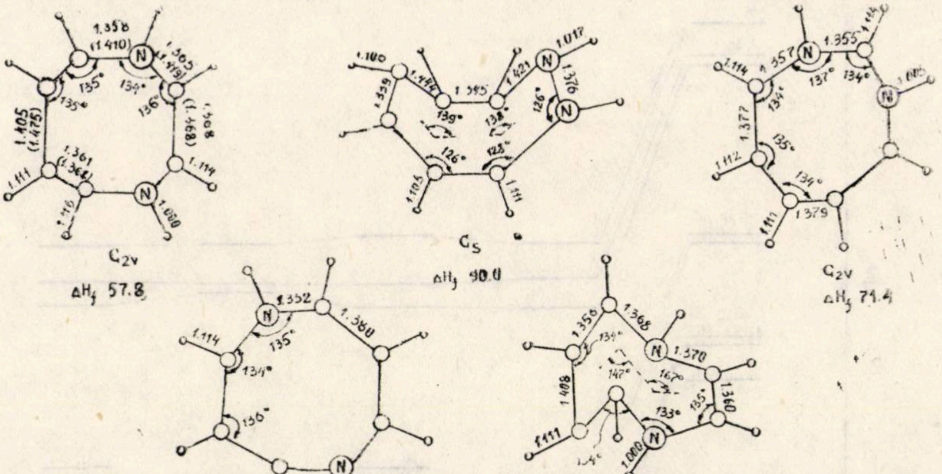

Fig. 2. — AM1 optimized geometries and heats of formation of compounds **5**, **7** — d (X=Y=NH). The numbers in the parentheses are taken from SINDO1 calculations[18]. Bon lengths are given in Å.

Our semiempirical study is consistent with the conclusion of work [17] about the highly localized structure of system **5**, X=Y=NH.

The structure corresponding to a minimum on the triplet PES energetically is less stable by 36 kcal/mol than that one on singlet PES. The singlet PES in the neighbourhood of minimum corresponding to the classical structure **5** is unusually flattenned. So according to our AM1 calculations the energy of this system changes negligibly when the puckering angle varies in a range from 147° to 180°. The structure with puckering angle equal to 147° is depicted in Fig. 2. This structure corresponds also to a minimum on the PES but its energy is nearly the same as the energy of the corresponding planar structure.

The next classical positional isomer — 1,2-diazocine **7** — in singlet electronic state corresponds to a saddle point of the first order ($\lambda = 1$) on the PES and has a nonplanar boat-like C_s-conformation. The analysis of the transition vector of this structure shows that it is a transition state for the ring opening reaction $\mathbf{5} \rightarrow \mathbf{6}$ (X=Y=NH). In addition, structure **7**, X=Y=NH has a very small N—N bond order (< 1.0). For comparison, the AM1 calculated N—N bond orders in pyridazine and hydrazine molecules amount to 1.47 and 1.02 respectively. According to the main ideas of refs.[12,18] such small values of cyclic bond orders mean a high degree of antiaromaticity in these systems (the idea of the relation between carbon-carbon bond orders and a degree of aromaticity was embodied in the aromatic stability index A [12,18]. In addition the structure **7** thermodynamically is less stable by 20.8 kcal/mol than structure **6**, X=Y=NH. Volpin was one of the first who pointed out the structural instability of system **7**.[19]

Unusual results were obtained for nonclassical (mesoionic) structures **8** and **9**, X=Y=NH. Both isomers correspond to minima on the singlet electronic state PES ($\lambda = 0$) and have lower energies than classical structure of system **7**. The systems **8** and **9** are stable in a C_{2v}-planar configuration and in the triplet electronic state ; thermodynamically ; they are less stable than in singlet electronic state by 23.3 and 26.4 kcal/mol respectively.

Moreover systems **8** and **9** are characterized in the ground singlet states by a less alternation of cycle bond orders than in planar classical isomer **5**. The estimation of this effect was carried out using the index A (for the evaluation of index A the calculated geometrical parameters were used). Thus the indices A were obtained to be equal to 0.965, 0.985 and 0.995 for systems **5**, **8** and **9** respectively (for comparison, in aromatic dianion $C_8H_8^{2-}$, $A = 1.0$).

Dioxocine and its positional isomers

According to AM1 calculations the 1,4-dioxocine corresponds to a minimum on the singlet PES in chair-like conformation with C_s-symmetry, which is consistent with the experimental data[9], see Fig. 3. In triplet electronic state the thermodynamically stable structure is less stable by 38 kcal/mol than in singlet one.

At the same time the 1,2-dioxocine is thermodynamically the least stable positional isomer among all 1,k-structures. Its heat of formation is about 62 kcal/mol higher than that for the ground state of isomer **5**. Similar to 1,2-diazocine the bond order between heteroatoms in system **7**

(X=Y=O) is less than 1.0. Furthermore this structure corresponds t the first order saddle point ($\lambda = 1$) on the singlet PES and is a transitio state for the ring opening reaction $5 \rightarrow 6$ (X=Y=O). Also the structure

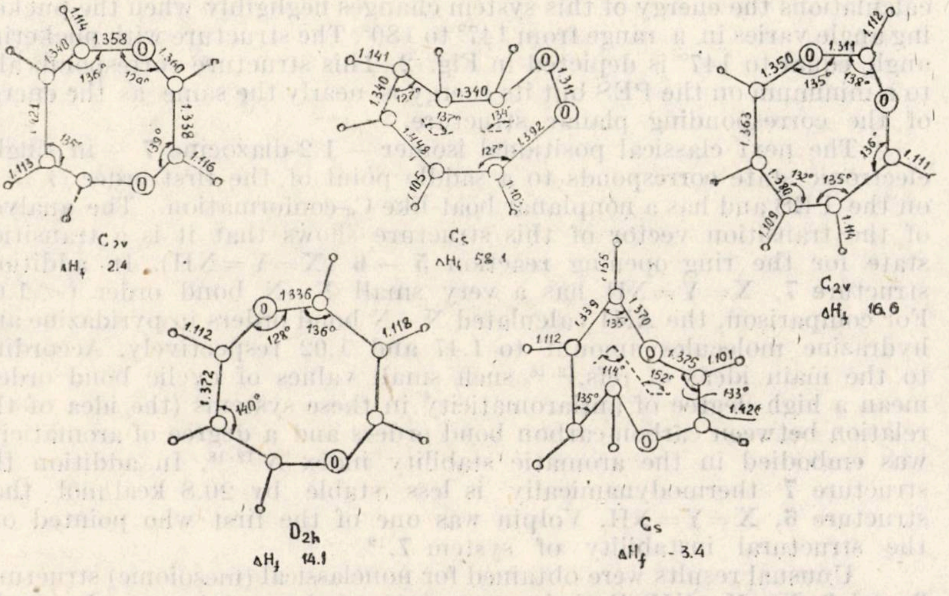

Fig. 3. — AM1 optimized geometries and heats of formation of compounds 5,7—9 (X=Y=O). Bond lengths are given in Å.

X=Y=O is thermodynamically less stable by 70.1 kcal/mol than open chain structure **6**, X=Y=O.

So 1,2-dioxocine like 1,2-diazocine is to be classified as antiaromatic system.

Mesoionic dioxocine isomers are thermodynamically less stable than classical 1,2-isomer (see Fig. 3). However among all positional 1,k-isomers only 1,5-dioxocine corresponds to a minimum ($\lambda = 0$) on the singlet PES.

1,3-Dioxocine (C_{2v} symmetry) corresponds to the first order saddle point ($\lambda = 1$). In triplet electronic state mesoionic structures **8** and **9**, X=Y=O are thermodynamically less stable by 12.1 and 13.0 kcal/mol respectively.

CONCLUSIONS

According to AM1 calculations the 10π-electron neutral systems **5**, **7**—**9** (X=Y=NH, O) are antiaromatic in contrast to an actually aromatic dianion $C_8H_8^{2-}$. In spite of that in planar configurations all these systems satisfy Hückel (4n + 2) rule ; nevertheless some of them do not correspond to a minima of the singlet PES. Even in the cases when the classical structures correspond to a minima, the calculated bond lengths indicate a structure with double and single bonds fixation which can be attributed to the antiaromatic features of these systems. It is interesting that the mesoionic positional isomers have less bond length alternation than classical structures ; however they also would be assigned to the class of antiaromatic compounds.

Method of calculation

In the present work we have used AMPAC program complex.[20]

REFERENCES

[1] L. A. Paquette, *Pure and Appl. Chem.*, **54**, 987 (1982).

[2] A. T. Balaban and M. Banciu, *J. Chem. Educ.*, **61**, 766 (1984).

[3] M. J. S. Dewar and K. M. Merz, *J. Phys. Chem.*, **89**, 4739 (1985).

[4] M. J. S. Dewar and K. M. Merz, *J. Chem. Soc. Chem. Commun.*, **1985**, 343.

[5] K. Hassenruck, H.-D. Martin and R. Walsh, *Chem. Rev.*, **89**, 1125 (1989).

[6] T. C. W. Mak and W.-K. Li, *J. Mol. Struct. (THEOCHEM)*, **89**, 281 (1982) ; H. N. C. Wong and W.-K. Li, *J. Chem. Res. (S)*, **1984**, 302 ; H. Durr, G. Klauck, K. Peters and H. v. G. Schnering, *Angew. Chem. Int. Ed. Engl.*, **22**, 332 (1983).

[7] P. J. Garratt in : J. F. Stoddart (ed.) "Comprehensive Organic Chemistry", D. Barton and W. D. Ollis (series eds.), 1979, v. 1, Pergamon Press, Elmsford.

[8] T. Wolfskill, *Int. J. Quant. Chem. Symp.*, **22**, 739 (1988).

[9] W. Schroth and J. Peschel, *Chimia*, **18**, 171 (1964) ; W. Schroth, W. Kiessling, J. Peschel and U. Schmidt, *Z. Chem.*, **4**, 302 (1964).

[10] A. T. Balaban and Z. Simon, *Rev. Roumaine Chim.*, **10**, 1059 (1965) ; A. T. Balaban, *Pure Appl. Chem.*, **52**, 1409 (1980), K. Jug., *J. Org. Chem.*, **49**, 4475 (1984).

[11] N. L. Allinger and G. A. Youngdale, *J. Org. Chem.*, **25**, 1509 (1960).

[12] K. Jug, *J. Org. Chem.*, **49**, 4475 (1984).

[13] M. J. S. Dewar, E. G. Zoebisch, E. F. Healy and J. J. P. Stewart, *J. Amer. Chem. Soc.*, **107**, 3902 (1985).

[14] V. I. Minkin, M. N. Glukhovtsev and B. Ya. Simkin "Aromaticity and Antiaromaticity", Springer Verlag, Berlin-Heidelberg-New York, 1991.

[15] B. A., Jr. Hess, C. S. Ewig and L. J. Schaad, *J. Org. Chem.*, **50**, 5869 (1985).

[16] G. Van Zandwijk, R. A. J. Janssen and H. M. Buck, *J. Amer Chem. Soc.*, **112**, 4155 (1990).

[17] M. Breuninger, B. Callenkamp, K.-H., Muller, H. Fritz, H. Prinzbach, J. J. Daly and P. Schonholzer, *Angw. Chem.*, **91**, 1030 (1979).

[18] K. Jug, *J. Org. Chem.*, **48**, 1344 (1983).

[19] M. E. Volpin, *Usp. Khim. (USSR)*, **29**, 298 (1960).

[20] "Quantum Chemistry Program Exchange (QCPE)," Program N506.

Revue Roumaine de Chimie, 36, 4–7, 341–352 (1991)

Dedicated to Prof. A. T. BALABAN
on the occasion of his 60th birthday

ELECTRONIC AND GEOMETRICAL STRUCTURE OF SIX-MEMBERED π-ELECTRON REDUNDANT SYSTEMS

M. E. KLETSKY, E. B. GLUZ, V. YU. BIRYUKOV, R. M. MINYAEV
and V. I. MINKIN
Institute of Physical and Organic Chemistry, Rostov University,
Rostov-on-Don, 344711, USSR

Received January 7, 1991

Semiempirical MNDO quantum chemical calculations have been carried out for six-membered π-electron redundant cyclic organic systems $[XY_2(CH)_3]^{\pm n}$, X, Y=NH, O, Hal, HalH ; n = 0, 1, 2. The calculations predict structural stability of nonclassical (mesoionic in the case of neutral systems) 8π-electron structures. These systems correspond to local minima on the potential energy surface (PES) of triplet electronic state. At the same time 10π-electron rings possessing two hypercoordinated halogen atoms do not correspond to minima on a singlet PES. The most stable isomers for these compounds are those containing five-membered rings.

INTRODUCTION

The concept of aromaticity is one of the key notions that constitute the rationale of theoretical organic chemistry. Some of the developments in this area which occurred during the last century have been reviewed elsewhere (see for example the well-known review of Balaban).[1]

At the same time the concept of aromaticity is still far from full understanding and final solving.[2,3]

A good deal of various criteria of aromaticity are known.[1-4] Usually aromaticity of a system is associated with π-electron delocalization and planarity of the ring. In contrast, antiaromaticity corresponds to π-electron localization and a trend to distortion from a planar conformation. On the basis of this simple connection between aromaticity (antiaromaticity) and conformation of the system, the conformational criterion of aromaticity (antiaromaticity) has been recently suggested and tested for 8π- and 10π-electron six-membered cycles **1**.[4]

In spite of its obvious attractiveness the conformational criterion does not seem to be convenient for neutral nonclassical (mesoionic) systems **2**[1],

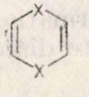

1

$X = CH^-, NH, N^-, O, \overset{+}{O}H, S$

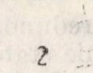

2

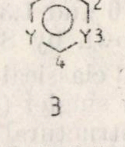

3

X, Y = NH, O, Hlg, HlgH;
n = 0, 1, 2

as well as for charged systems 3. In all these cases small energy gap between neighboring electronic surfaces (or inter crossing) of PESs for different electronic states, being typical for antiaromatic systems, is expected for π-electron redundant cycles.[3,5,6]

The π-electron redundant cyclic systems attract much attention not only from theoretical point of view concerned with different aspects of aromaticity but also because of their unusual physical and chemical properties. For example, these systems can serve as good potential acceptor components in charge-transfer complexes for purposes of design of new organic metals and semiconductors.[7] Likewise, heterocyclic mesoionic compounds have as a rule a wide spectra of biological activity like sydnones and munchnones.[8]

The parent six-membered π-electron redundant antiaromatic (or nonaromatic) hydrocarbon is benzene dianion 4 (R=H) which has not been observed experimentally up to now because of its high thermodynamic instability. This instability is a consequence of a high electron repulsion in the electron excessive cyclic system.[9] Estimation of the benzene and sodium interaction energy obtained by extrapolation of the experimental data for some aromatic polycyclic dianions, points out to a big endothermicity of the reaction

$$C_6H_6 + 2Na \rightarrow (Na^+)_2(C_6H_6)^{2-}, \quad \Delta\Delta H_f = 96.4 \text{ kcal/mol.} \qquad (1d)$$

However the substituted dianion 4, R=Ph, has been obtained through reduction of 1,3,5-triphenylbenzene by alkali metals.[10] Compounds 4, R=Ph and 8π-electronic dianion 2,4,6-triphenyl-symm-triazine 5, R=Ph, are stable in triplet ground state as it stems from their EPR spectra.[11,12]

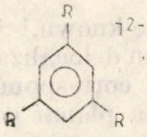

4, D_{3h}

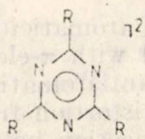

5, D_{3h}

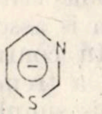

6

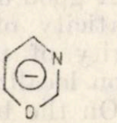

7

It was also found out by experimental study and quantum chemical calculations [12], that salts of dianion 4 have a triplet ground state irrespective of the nature of counterion, solvent and temperature. In contrast to this, for ions 5, R=Ph and R=CH_2Ph, the multiplicity of the ground state was proved to be strongly dependent on the above factors, see also.[13]

It is worth mentioning that a possibility of formation of reactive 1,3-thiazine 6 and 1,3-oxazine 7 anions isoelectronic to dianions 4 and 5 has been shown by Schmidt and coworkers.[14]

Neutral classical π-electron redundant systems 1, as shown in ref.[3,15], are stable in singlet (S_0) electronic state. However, for their nonclassical (mesoionic) structural isomers 2 and charged isoelectronic systems (see 3) the nature of their ground and lowest excited states is uncertain.

In this paper we tackled the problem of electronic structure and thermodynamic stability of π-electron redundant six-membered rings using semiempirical MNDO calculations.[16] The special attention was devoted to the six-membered structure **3** and to some of its position isomers. The scope and limitations of MNDO method have been analyzed in review papers.[17 18]

RESULTS

Molecular orbital analysis

The substitution of CH-groups in benzene molecule with heteroatomic fragments X in system **3** (D_{3h} symmetry) does not remove π-orbital degeneracy, the energy levels of all delocalized MO being decreased (see Fig. 1). In Fig. 1 shapes of the π-MOs and π-MO's correlation diagram for system **3** with D_{3h} symmetry are given.

Addition of two electrons to 6π-electronic benzene molecule, i.e. passing to 8π-electronic system **3** ($n = 1$; $X=Y=NH, O$; $n = 2, X=Hlg$) leads to occupation of double degenerate e''—MO by two electrons.

Filling $2e''$ π-MO with electrons converts system **3** ($X=Y$) in its singlet state to the Jahn-Teller type system which in D_{3h}-conformation must undergo geometrical distortion to remove the degeneracy of frontier MOs.

Transition to 10π-electron system, i.e. filling $2e''$ π-MO with four electrons, must cause enforcing geometric relaxation of the system in singlet state, similarly to the distortion of 8π-electron system in triplet state.

Further filling the upper antibonding π^*-MO, i.e. transition to 12π-electron systems is expected to lead to additional destabilization of the planar structure and its distortion towards a chair-like conformation. This distortion decreases antibonding and increases bonding interaction between p-AO's on neighboring centers (see Fig. 1).

Charged 8π-electron systems

According to the recent MNDO calculations [6] the ground electronic state of D_{6h} dianion **4** is triplet $^3A_{3g}$. Singlet $^1E_{2g}$ state undergoes expected first order Jahn-Teller distortion of which type is defined by E_{2g} vibration. This distortion reduces D_{6h} to D_{2h} symmetry for the structures **8** and **9**:

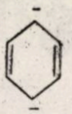

8, D_{2h}

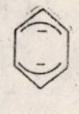

9, D_{2h}

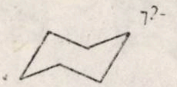

10, D_{3d}

Both structures **8** and **9** correspond to minima on the PES of $C_6H_6^{2-}$ ($\lambda = 0$). Nevertheless energy of these structures is higher than that for structure **4**, R=H with D_{6h} symmetry (electronic state $^3A_{2g}$). Energetic and electronic data for systems **4**, **8** and **9** are listed in table 1.

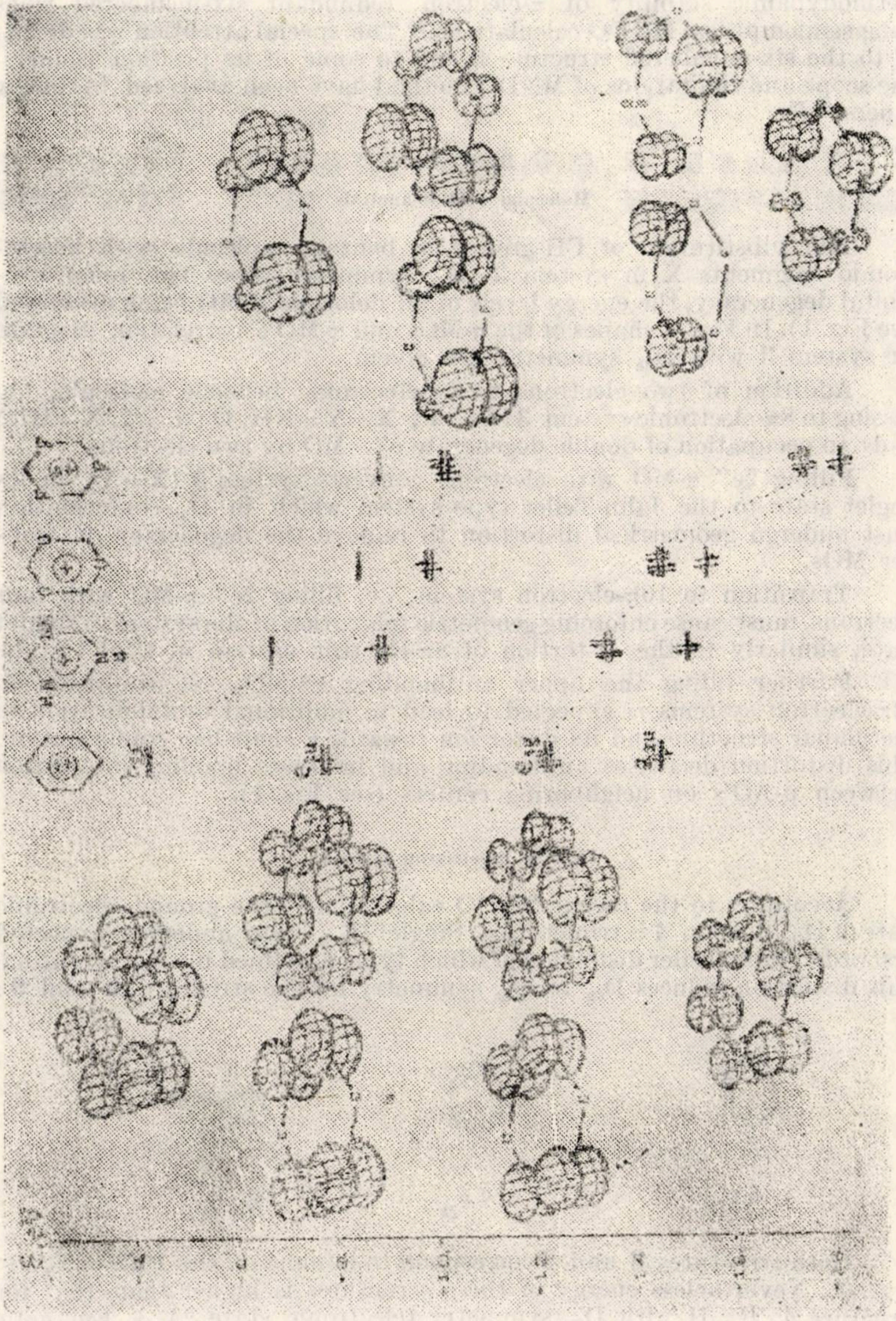

Fig. 1. —π-MO Correlation diagram and shapes of the π-MOs for systems 3.

Table 1

Heats of formations (ΔH_f, kcal/mol), relative energies (E_{erl}, kcal/mol), bond lengths (Å) for stable structures of benzene and $(CHNH)_3^{2-}$ dianions, and for cations $(CHO)_3^+$, and $(CHNH)_3^+$, calculated by MNDO method

Structure		ΔH_f	E_{rel}	l_{x1c2}*	l_{c2x3}	l_{x3c4}
4	$^3A_{2g}$	159.9	0	1.422	1.422	1.422
				(1.432)**	(1.432)	(1.432)
8		172.2	12.7	1.445	1.375	1.445
				(1.480)	(1.345)	(1.480)
9		171.0	11.5	1.393	1.481	1.393
				(1.378)	(1.541)	(1.387)
10		221.5	62.0	1.451	1.451	1.451
11	$^3A'_2$	11.7	0	1.344	1.344	1.344
13	X=O	138.7	27.0	1.412	1.310	1.407
14	X=O	138.4	26.7	1.306	1.406	1.312
15	X=O	206.8	95.1	1.399	1.399	1.399
12	$^3A'_2$	208.6	0	1.391	1.391	1.391
13	X=NH	228.5	19.9	1.426	1.335	1.390
14	X=NH	229.5	20.9	1.349	1.443	1.350
15	X=NH	317.9	109.3	1.399	1.399	1.399
16		228.6	20.0	1.389	1.338	1.425
5	$^3A'_2$	147.7	0	1.375	1.375	1.375
13	X=N	159.4	12.0	1.407	1.315	1.402
14	X=N	158.0	10.6	1.341	1.442	1.341

* Numeration of atoms is shown in structure 3.

** The numbers in parentheses are taken from *ab initio* calculations.[19]

The structure **9** occurs to be energetically a little more stable than the structure **8**. These results are in agreement with nonempirical calculations.[19]

The formation of the chair-like conformation **10** with D_{3d} symmetry and closed electronic shell through stabilization and filling b_1 MO (see Fig. 1) is another possible distortion of the D_{6h} dianion structure. However the calculations have shown that the energy of this structure in its singlet electronic state is considerably higher than that for triplet $^3A_{2g}$ electronic state. Furthermore the structure **10** corresponds to a saddle point of the second order ($\lambda = 2$) on the singlet PES (see Table 1).

Isoelectronic analogs of benzene dianion 4-3-symm-triazine dianion **5**, R=H cations of 1,3,5-(2,4,6-tridehydro)trioxanium **11** and 1,3,5-trihydrotriazinium **12** are more stable in triplet state (see also [12]).

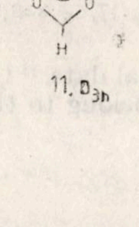

11, D_{3h}

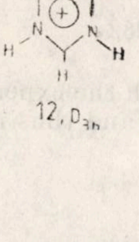

12, D_{3h}

As mentioned above D_{3d} structure **5** in singlet ($^1E'$) state is affected by first order Jahn-Teller distortion similar to that in $^1E_{2g}$ state of D_{6h} structure of benzene dianion. The D_{3h}-structure **5**, R=H corresponds to a saddle point on the PES ($\lambda > 2$). For E-terms the calculations of Hessian matrix must be performed according to special scheme[3,6]. Jahn-Teller isomers **13**, **14**, X=N, n = 2 are energy favorable compared to **5** (see Table 1). However these values are higher than for a triplet state of structure **11**.

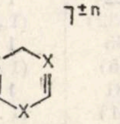

13, C_{2v}

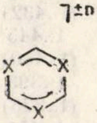

14, C_{2v}

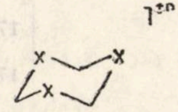

15, C_{3v}

X=O, NH; n=1 X=N; n=-2

The $D_{3h} \rightarrow C_{3v}$ distortion of **5** to structure **15** leads to a steady increase in energy. Moreover the structure **15** corresponds to the second order saddle point on the singlet electronic state PES ($\lambda = 2$).

Similar results were obtained for cations **11** [6] and **12**. Highly symmetric structures of these cations tend to distort to the less symmetric structures **13**, **14**, X=NH, O (n = 1), which energetically are least stable among all six-membered $C_3O_3H_3^+$ and $N_3C_3H_6^+$ isomers (see Table 1). In all these cases the triplet states are more stable and the corresponding structures pertain to minima on the PESs.

It has been shown earlier,[13,20,21] that the pyramidalization of carbon centers is one of the main geometrical features of some antiaromatic structures both in singlet ($^1A'$) and triplet ($^3A_2$) states. For the cation **12**, capable to nitrogen pyramidalization, one can expect that such a distortion leads to substantial electronic rearrangement and, consequently, to stabilization of the structure.

However according to MNDO calculations having been carried out, the isomeric cyclic structures **15**, X=NH, and **16** in their singlet electronic states are energetically less preferable than triplet state of D_{3h} structure **12** (the energy difference is 109.3 and 20.2 kcal/mol respectively). The only minimum on the PES of $(CHNH)_3^+$ is the C_s-structure **16**.

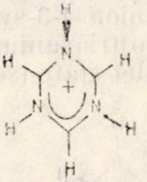

16, C_s

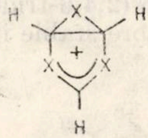

17, C_s; X=O, NH

In accordance with the experimental data [14] the bicyclic structure **17** may be formed from **3** and thus must belong to the critical point on the minimum energy path of decomposition reactions through heteroatom extrusion.

The C_s-cation **17** is stable in singlet electronic state.[22] Nevertheless bicyclic isomers **17** are energetically less stable than **11** and **12** only by 4.9 and 7.2 kcal/mol respectively. Noteworthy is that a photochemical recyclization of bicyclic structure **17** like the reaction (2) can serve as one of the ways of forming the structure **14**.[22]

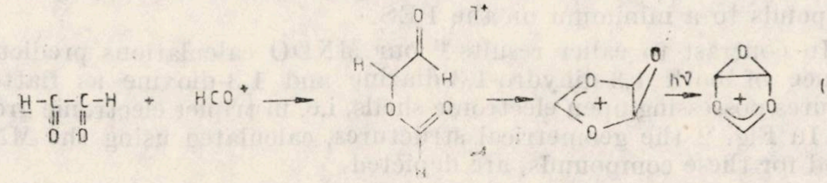

(2)

Neutral 8π-electronic systems

Electronic and geometric structure of π-electron redundant monocyclic systems are substantially determined by the intracyclic electronic repulsion. This effect is considerably higher in negatively charged systems : for example in benzene dianion $C_6H_6^{2-}$ the energy of electronic repulsion amounts to 7 eV.[12]

Both electronic repulsion and Jahn-Teller structural instability demand a lowering of the D_{3h}-symmetry in electron neutral systems. We chose different isomers of dihydrodiazine and dioxine molecules, which can be represented as classical **18**, **19** and nonclassical (mesoionic) structures **2**, X=O, NH, altogether with dioxazines **20**—**25** :

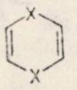

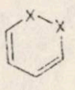

X = O, NH

18

19

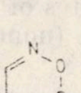

20

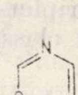

21

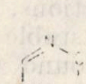

22

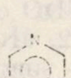

23

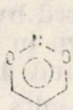

24

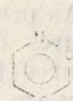

25

$\Delta H_f(S_0)$ 43.9 24.5 -14.2

The classical neutral 8π-electron systems were previously investigated.[4,15] Nevertheless there has not been any work (except [23]) in which the comparison of thermodynamic stability of classical and nonclassical (mesoionic) structures in different electronic states has been made (relative stability of some classical and mesoionic 6π- and 10π-electronic hetero-substituted cycles has been studied theoretically by Balaban et al.[1)].

Earlier a connection between mesoionic structures of 1,3-dihydro-diazine **2**, X=NH, 1,3-dioxine (X=O) and 1,3-dithiine (X=S) was investigated using the PPP method.[24] It has been shown that the structure of C_{2v} symmetry is characterized by a singlet instability of Hartree-Fock solutions. The MINDO/3 and *ab initio* (STO−3G) calculations have predicted that the structures of 1,3-dihydro-diazine with C_s symmetry corresponds to a minimum on the PES.

In contrast to ealier results [24] our MNDO calculations predict the existence of both 1,3-dihydro-1,3-diazine and 1,3-dioxine as flattened structures possessing open electronic shells, i.e. in triplet electronic ground state. In Fig. 2 the geometrical structures, calculated using the MNDO method for these compounds, are depicted.

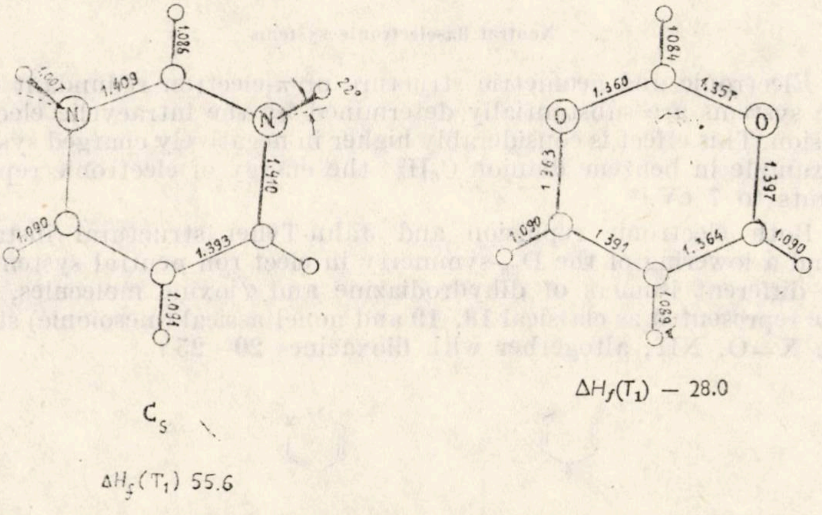

Fig. 2. – MNDO optimized geometries and heats of formation of compounds **2**. Bond lengths are given in Å.

As predicted by MNDO calculations, the triplet states of mesoionic structures shown in Fig. 2, are less stable than classical (nonmesoionic) structures **18** and **19** in singlet ground state.

Similar results have been obtained for the most symmetrical (C_{2v} symmetry) dioxazine isomers **23** and **24**, which are characterized by a singlet instability of Hartree-Fock solutions.

The heats of formation for classical and nonclassical isomers of dioxazine are close in value. Geometries and heats of formation for the stable structures of these compounds, calculated by MNDO method are represented in Fig. 3.

Noteworthy is that the mesoionic isomer **23** is the most stable among all other isomers (experimentally only five-membered mesoionic cyclic systems were observed [1,8]). However triplet electronic state for planar C_s structures of compounds **23**—**25** is more energetically favorable.

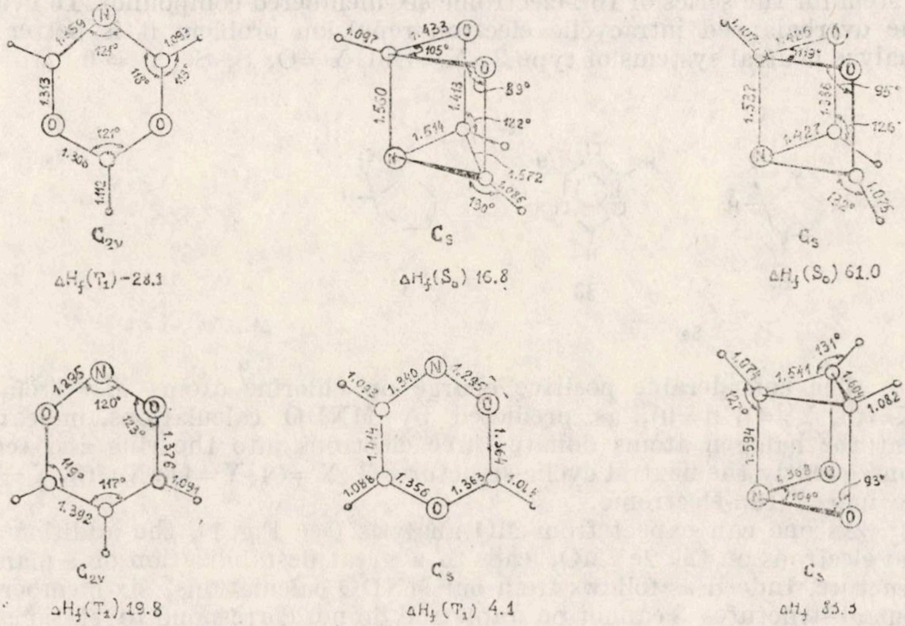
C2v
ΔHf(T1) -28.1
Cs
ΔHf(S0) 16.8
Cs
ΔHf(S0) 61.0
C2v
ΔHf(T1) 19.8
Cs
ΔHf(T1) 4.1
Cs
ΔHf 85.5

Fig. 3. — MNDO optimized geometries and heats of formation of compounds **23**, **26**, **27**, **24**, **25** and **28**. Bond lengths are given in Å.

As a rule for the systems with open electronic shells there exist low-energy intramolecular rearrangements which lead to more stable structures with closed electronic shells. Thus rearrangements of type (3) and (4) can be expected for the mesoionic compounds **23** and **24**:

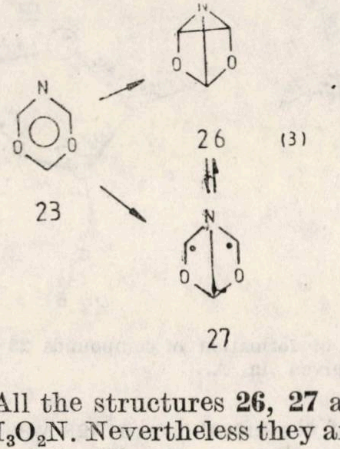

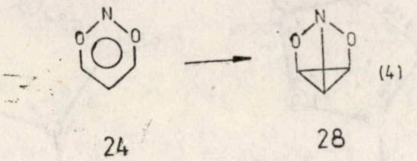

All the structures **26**, **27** and **28** correspond to minima on the PES of $C_3H_3O_2N$. Nevertheless they are less stable than the mesoionic structures presented in Fig. 3.

10π-and 12π-electronic systems

A hypothetical benzene tetraanion $C_6H_6^{-4}$ is the parent hydrocarbon system for the series of 10π-electronic six-membered compounds. To evade the overbalanced intracyclic electron repulsion problem it is better to analyze neutral systems of type **3**; X=Hal, Y=O, S, Se, n = 0.

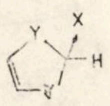

29

X = Hal ; Y = O, S, Se

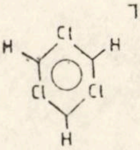
12+
Cl
H
H
Cl
Cl
H

30

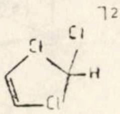

31

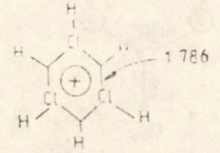
H
Cl
H
1.786
+
Cl
Cl
H
H
H

32

$\Delta H_f(T_1)$ 482.8

The considerable positive charge on chlorine atoms in system **3** (X=Cl, Y=O, n=0), as predicted by MNDO calculations, indicates that the halogen atoms donate three electrons into the ring π-system. Consequently the neutral cyclic structures **3** (X=Cl, Y=O; X=Cl, Y=S) are indeed 10π-electronic.

As one can expect from MO analysis (see Fig. 1), the addition of two electrons on the 2e″ MO, leads to a great destabilization of a planar structure. Indeed as follows from our MNDO calculations, six-membered neutral structures **3** cannot be stable and do not correspond to stationary points on the respective singlet PESs.

These six-membered compounds rearrange to five-membered cyclic structures **29**. In Fig. 4 calculated molecular geometries of compounds **29** (X=Cl, Y=O and X=Cl, Y=O) are represented.

The derivatives of 1,3-dithiolane and 1,3-dioxolane having five-membered rings are well known, see[25].

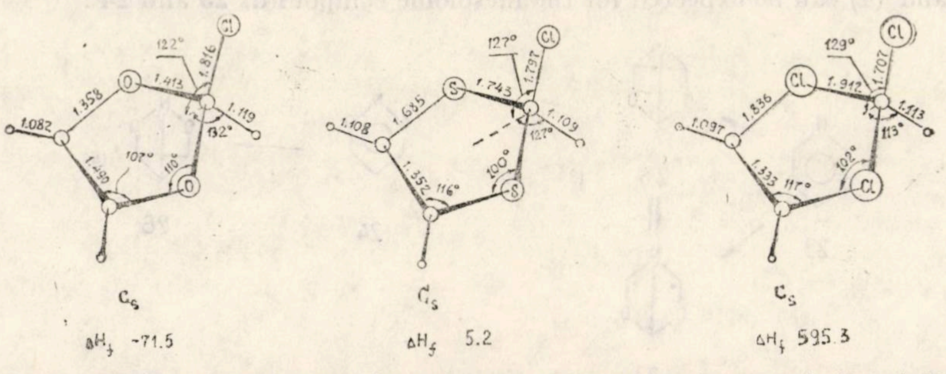
122°
Cl
1.816
1.413
O
1.358
1.082
1.119
132°
107°
116°
1.490
O
C_s
ΔH_f -71.5
127°
Cl
1.797
S
1.743
1.635
1.108
1.109
127°
100°
1.352
116°
S
C_s
ΔH_f 5.2
129°
Cl
1.707
Cl
1.912
1.336
1.097
1.113
113°
102°
1.333
111°
Cl
C_s
ΔH_f 595.3

Fig. 4. — MNDO optimized geometries and heats of formation of compounds **29** and **31**. Bond lengths are given in Å.

The same effect of destabilization of six-membered rings was discovered also for 10π-electron charged system **30** (D_{3h}).

According to our MNDO calculations system **30** like **3** (n = 0) does not correspond to any stationary point on a singlet PES. This structure is barrierlessly transformed into **31** with two hypercoordinated halogen atoms. The unusual structure **31** pertains to rather deep minimum on the singlet PES.

On the basis of MO analysis of system **3**, X=Y=Hal, (see Fig. 1) one can conclude that the planar six-membered cyclic systems are to be considered as 12π-electronic.

Our MNDO calculations have shown that the 12π-electron compound **32** $C_3Cl_3H_6^+$ with D_{3h} symmetry is thermodynamically stable (corresponds to a minimum on the PFS) only in triplet electronic state (see structure [32]).

CONCLUSIONS

Nonclassical (mesoionic in neutral cases) six-membered 8π-electronic systems irrespective of their symmetry and charge correspond to minima both on singlet and triplet PSSs, the triplet electronic state structures being thermodynamically more stable. At the same time 10π-electronic systems, containing two hypercoordinated halogen atoms, do not pertain to minima on the respective PESs and barrierlessly transform into isomeric five-membered structures on a singlet PES. Triplet PES for these compounds lies considerably higher in energy.

Method of calculation

The calculations have been carried out with program complex AMPAC.[26]

REFERENCES

[1] A. T. Balaban, *Pure and Appl. Chem.*, **52**, 1409 (1980).

[2] P. J. Garratt, "Aromaticity", Wiley, New York, 1986.

[3] V. I. Minkin, M. N. Glukhovtsev and B. Ya. Simkin, "Aromaticity and Antiaromaticity", Springer Verlag, Berlin—Heidelberg—New York, 1991.

[4] B. L. Podlogar, W. A. Glauser, W. R. Rodriguez and D. J. Raber, *J. Org. Chem.*, **53**, 2129 (1988).

[5] A. Minsky, Y. Cohen and M. Rabinovitz, *J. Amer. Chem. Soc.*, **107**, 1501 (1985).

[6] V. I. Minkin, R. M. Minayev, M. E. Kletsky and M. N. Glukhovtsev, *Zh. Org. Khim.* (1991) (in press).

[7] G. Boche, in : *Topics in Current Chem.*, **46**, 37 (1988) ; B. A. Kampar, *Usp. Khim. (USSR)*, **51**, 185 (1982) ; A. C. Wudl, *Acc. Chem. Res.*, **17**, 227 (1984) ; M. Aldissi, *Ed. Synth. Met.*, **1989**, 28.

[8] C. A. Ramsden, in : O. G. Sammes (ed.), "Comprehensive Organic Chemistry", D. Barton and W. D. Ollis (series eds.), 1979, v. 9, Pergamon Press, New York, p. 714.

[9] J. R. Stevenson, S. S. Zigler and R. C. Reiter, *J. Amer. Chem. Soc.*, **103**, 6057 (1981).

[10] R. E. Jesse, P. Biloen, R. Prins, J. D. W. Van Voorst and G. J. Hoijtink, *Mol. Phys.*, **6** 633 (1963).

[11] H. Van Willigen, J. A. M. Broekhoven and E. De Boer, *Mol. Phys.*, **12**, 533 (1967) ; J. L. Sommerdijk and E. De Boer, *J. Chem. Phys.*, **50**, 4771 (1969).

[12] J. A. M. Van Broekhoven, J. L. Sommerdijk and E. De Boer, *Mol. Phys.*, **20**, 993 (1971).

[13] G. Van Zandwijk, R. A. J. Janssen and H. M. Buck, *J. Amer. Chem. Soc.*, **112**, 4155 (1990).

[14] R. R. Schmidt and M. Dimmler, *Chem. Ber.*, **108**, 6 (1975).

[15] W. Kalm, *Angew. Chem. Intern. Ed. Eng.*, **22**, 171 (1983).

[16] M. J. S. Dewar and W. Thiel, *J. Amer. Chem. Soc.*, **99**, 4907 (1977).

[17] T. Clark, "A Haadbook of Computational Chemistry", Wiley Intersc. Publ., 1985, New York.

[18] A. A. Voytuk, *Zh. Struct. Khim. (USSR)*, **29**, 138 (1988).

[19] M. Nakayama, H. Ishikawa, T. Nakano and O. Kikuchi, *J. Mol. Struc. (THEOCHEM)*, **184**, 369 (1989).

[20] G. Winkelhofer, R. Janoschek, F. Fratev, G. W. Spitznagel, J. Chandrasekhar and P.v.R. Schleyer, *J. Amer. Chem. Soc.*, **107**, 332, 337 (1985).

[21] W.-K. Li, *J. Chem. Res.*, **1988**, 220.

[22] S. V. Borodaev, M. E. Kletstky, S. M. Luk'yanov and R. M. Minyaev, *Zh. Org. Khim. (USSR)*, 1991 (in press).

[23] K. Jug, *J. Org. Chem.*, **48**, 1344 (1983).

[24] M. N. Glukhovtsaev, B. Ya Simkin, V. I. Minkin and I. A. Yudilevich, *Zh. Struct. Khim. (USSR)*, **23**, 23 (1982).

[25] T. Okuyama and T. Fueno, *Bull. Chem. Soc. Jap.*, **59**, 327 (1986).

[26] *Quantum Chemistry Program Exchange (QCPE), program N506.*

Revue Roumaine de Chimie, **36**, 4–7, 353–362 (1991)

METAL CLUSTER TOPOLOGY. 12[1]*

NICKEL CARBONYL CLUSTERS

R. B. KING

Department of Chemistry, University of Georgia, Athens, Georgia 30602, U.S.A.

Received December 8, 1990

Graph-theory derived models of metal cluster bonding are now applied to the following types of nickel carbonyl clusters : (1) Nickel carbonyl clusters exhibiting three-fold symmetry including $Ni_6(CO)_{12}^{2-}$ with a globally delocalized octahedron, $Ni_9(CO)_{18}^{2-}$ consisting of a globally delocalized $Ni_3Ni_{3/2}$ octahedral cavity fused to an edge-localized trigonal $Ni_3Ni_{3/2}$ cavity by sharing a triangular face, and $Ni_{12}(CO)_{21}H_{4-n}^{n-}$ consisting of two fused globally delocalized $Ni_3Ni_{3/2}$ octahedra with external Ni atoms bridging each of the edges of the shared face ; (2) Nickel carbonyl clusters with five-fold symmetry including the globally delocalized icosahedra $Ni_9(AsPh)_3(CO)_{15}^{2-}$ and $Ni_{10}(AsMe)_2(CO)_{18}^{2-}$ with no central atom, $Ni_{12}E(CO)_{22}^{2-}$ with a central group 14 atom (E = Ge, Sn), $Ni_{10}[SbNi(CO)_3]_2(Ni)(CO)_{18}^{-4}$ with a central Ni atom with its 10 valence electrons in an H_g antibonding icosahedral orbital and therefore unavailable for skeletal bonding, and the arachno centered pentagonal antiprism $Ni_{10}Ge(CO)_{20}^{2-}$; (3) The nickel carbonyl carbides $Ni_{10}C(CO)_{18}^{2-}$, $Ni_{10}C_2(CO)_{16}^{2-}$, and $Ni_{16}(C_2)_2(CO)_{23}^{4-}$ with globally delocalized deltahedra or pseudodeltahedra as well as the nido capped square antiprism $Ni_9C(CO)_{17}^{2-}$ and the arachno square antiprism $Ni_8C(CO)_{16}^{2-}$.

1. INTRODUCTION

One of the areas of chemistry in which Prof. Balaban has been a pioneer involves chemical applications of graph theory. In my own work I have been interested in applications of graph theory to inorganic chemistry. This work has led to new approaches for the study of chemical bonding topology in polyhedral boranes, carboranes, metal clusters, and related compounds.[2,3,4] Compound types treated explicitly by these methods include post-transition element clusters[5,6,7] osmium carbonyl clusters,[8] gold clusters,[9,10] platinum carbonyl clusters,[9,11] rhodium carbonyl clusters consisting of fused polyhedra,[12,13] cobalt carbonyl clusters containing interstitial carbon atoms,[14] metal carbonyl clusters containing alkylphosphinidene vertices,[15] early transition metal halide clusters,[1,16,17] and gallium clusters.[18] These graph-theory derived methods have the following advantages :

---

* This paper is dedicated to Prof. ALEXANDRU T. BALABAN in recognition of his pioneering work in the applications of mathematics, particularly graph theory and topology, to the understanding of important chemical problems.

1. Minimal computation requirements to deduce important information about the electron counts and shapes of diverse metal clusters ;
2. The ability to generate electron-precise bonding models for metal clusters that appear intractable by methods not involving heavy computation ;
3. The ability to obtain information on the distribution of total cluster electron counts between skeletal bonding within the cluster polyhedral network and bonding to external groups ;
4. The ability to distinguish between localized and delocalized bonding in cluster polyhedra.

In addition, this graph-theory derived method has been compared with other approaches to metal cluster bonding such as the original Wade-Mingos skeletal electron pair method,[19–23] the extended Hückel calculations of Lauher,[24] the perturbed spherical shell theory of Stone,[25] and the topological electron counting method of Teo.[26–29] Furthermore, in the cases of the most symmetrical systems with the minimum number of orbitals, namely the octahedral and icosahedral boranes, the molecular orbital energy parameters found by various computational methods have been compared with those estimated by elementary application of graph-theory derived methods.[30–32]

This paper extends the application of these graph-theory derived methods to a study of various nickel carbonyl clusters arising from reactions of the octahedral nickel carbonyl cluster anion $Ni_6(CO)_{12}^{2-}$.[33] The reactions of $Ni_6(CO)_{12}^{2-}$ used to prepare most of these clusters are listed in Table 1. Such clusters include derivatives having both three-fold and five-fold symmetry as well as new types of metal cluster polyhedra containing interstitial carbon atoms.

2. BACKGROUND

The chemical bonding topology in metal clusters can be represented by a graph in which the vertices correspond to atoms or orbitals participating in the bonding and the edges correspond to bonding relationships. Previous papers [2,3,4,6,7,11,12] have shown that the energy parameter E_k for molecular orbital k is related to the eigenvalues x_k of the adjacency matrix A as follows :

$$E_k = \frac{\alpha + x_k\beta}{1 + x_k S} \tag{1}$$

Positive and negative eigenvalues, x, thus correspond to bonding and antibonding orbitals, respectively.

The valence orbitals of the atoms in metal clusters may be partitioned into internal and external orbitals. Internal orbitals participate in the internal metal cluster skeletal bonding whereas external orbitals participate in the bonding to atoms or groups external to the metal cluster. A normal vertex atom in a metal cluster such as a globally delocalized deltahedron uses three of its valence orbitals for internal orbitals. In the case of an interstitial atom located completely inside a metal cluster polyhedron, all of its valence orbitals are internal orbitals.

The two extreme types of skeletal bonding in metal clusters may be called edge-localized and globally delocalized.[2,3,4,11,12] An edge-localized metal cluster has two-electron two-center bonds along each edge of the cluster polyhedron and is favored when the numbers of internal orbitals of the vertex atoms match the number of edges meeting at the vertex in question (called the vertex degree). Since normal vertex atoms in metal clusters use three internal orbitals for skeletal bonding, cluster polyhedra exhibiting pure edge-localized bonding normally have only degree three vertices. A globally delocalized cluster has a multicenter core bond in the center of the cluster polyhedron and is favored when the numbers of internal orbitals at the vertex atoms do not match the vertex degrees.

The globally delocalized deltahedral clusters with n vertices have $2n + 2$ skeletal electrons with 2n of these electrons arising from the surface bonding and the remaining two electrons occupying the single bonding molecular orbital arising from the multicenter core bond.[2,3,4] Electron-rich polyhedra with n vertices and more than $2n + 2$ apparent skeletal electrons have one or more non-triangular faces which may be regarded topologically as holes in the otherwise closed surface.[2,3,4] The electron richness of such systems arises from splitting the n-center core bond in the $2n + 2$ skeletal electron globally delocalized system into a set of two or more bonds consisting of a multicenter core bond using fewer than n internal orbitals and one or more additional multicenter bonds located above the non-triangular faces. Thus electron-rich polyhedra with $2n + 4$ skeletal electrons have one non-triangular face and are called nido polyhedra particularly by boron hydride chemists. Similarly electron-rich polyhedra with $2n + 6$ skeletal electrons have two non-triangular faces or one large non-triangular face and are called arachno polyhedra.

A number of the metal clusters discussed in this paper contain interstitial atoms. Such interstitial atoms create certain volume requirements for the surrounding polyhedron.[34] The volume of a polyhedron containing an interstitial atom can be increased by decreasing the number of edges. In the case of a deltahedron this can be done by converting pairs of triangular faces sharing an edge into single quadrilateral faces by rupture of the edge shared by the two triangular faces similar to the "diamond-square" portition of the diamond-square-diamond process involved in polyhedral rearrangements.[35,36] An n-vertex non-deltahedron derived from an n-vertex deltahedron by volume expansion in this manner and containing an interstitial atom can still function as a globally delocalized $2n + 2$ skeletal electron system like the n-vertex deltahedron from which it is derived. Such non-deltahedra can be conveniently called pseudo-deltahedra; they have only triangular and quadrilateral faces with a limited number of the latter.

All of the valence orbitals of interstitial atoms in centered metal clusters are internal orbitals. For this reason all of the valence electrons of the interstitial atom are normally involved in the skeletal bonding. Exceptions to this rule can occur in highly symmetrical clusters containing an interstitial transition metal when some or all of the filled d orbitals of the interstitial atom correspond to irreducible representations found only in antibonding orbitals of the surrounding cluster polyhedron. In such cases these d electrons of the interstitial transition metal are unavailable for skeletal bonding and therefore cannot be included in the skeletal electron count. Such d electrons can be called latent d electrons. An example of a transition metal cluster with such latent d electrons is $CrZr_6I_{12}$ in which the four d electrons of the interstitial chromium atom in the e_g orbital cannot participate in the skeletal bonding because the e_g orbital corresponds to an antibonding rather than a bonding orbital of the surrounding Zr_6 octahedron.[1] Thus the interstitial chromium atom in $CrZr_6I_{12}$ is a donor of only $2(= 6 - 4)$ skeletal electrons rather than all of its six valence electrons. Another example of a symmetrical cluster with an interstitial transition metal with latent d electrons is $Ni_{12}Sb_2(CO)_{24}^{4-} = Ni_{10}[SbNi(CO)_3]_2'(Ni)(CO)_{18}^{4-}$ [37] in which the central nickel atom is a donor of zero skeletal electrons because all of its ten d electrons are in the antibonding H_g orbital of the $Ni_{10}Sb_2$ icosahedron.

3. NICKEL CARBONYL CLUSTERS WITH THREE-FOLD SYMMETRY

The nickel carbonyl clusters with three-fold symmetry of interest in the context of this paper are $Ni_6(CO)_{12}^{2-}$ containing a trigonal antiprism (topologically an octahedron) of nickel atoms, $Ni_9(CO)_{18}^{2-}$ containing a $Ni_3Ni_{3/2}$ trigonal antiprism fused to a $Ni_3Ni_{3/2}$ trigonal prism, and $Ni_{12}(CO)_{21}H_{4-n}^{n-}$ with a more complicated Ni_{12} configuration, which may be regarded as two fused $Ni_3Ni_{3/2}$ trigonal antiprisms (i.e., distorted octahedra) sharing a face with additional Ni atoms bridging each of the three edges of this shared face (Figure 1). The following electron-counting schemes pertain to these clusters:

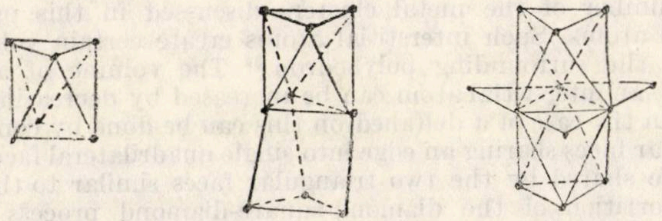

Fig. 1. — The arrangements of the nickel atoms in the nickel carbonyl clusters with three-fold symmetry.

A. $Ni_9(CO)_{12}^{2-}$ [33] : A total of $(6)(2) + 2 = 14$ skeletal electrons corresponding, respectively, to the six $Ni(CO)_2$ groups and the -2 charge. This skeletal electron count of $14 = 2n + 2$ for $n = 6$ is the correct skeletal electron count for a globally delocalized Ni_6 octahedron.

B. $Ni_9(CO)_{18}^{2-}$ [32] : The counting of skeletal electrons and orbitals for this cluster was presented in the previous paper of this series [1] and can be summarized as follows :

Sources of skeletal electrons and orbitals :

6 outer $Ni(CO)_2$ groups	12 electrons	18 orbitals
3 inner $Ni(CO)_2$ groups	12 electrons	12 orbitals
-2 charge	2 electrons	
Available for skeletal bonding	26 electrons	30 orbitals

Uses of skeletal electrons and orbitals :

Octahedral $Ni_3Ni_{3/2}$ cavity :		
6 Ni—Ni surface bonds	12 electrons	12 orbitals
1 6-center core bond	2 electrons	6 orbitals
Trigonal prismatic $Ni_3Ni_{3/2}$ cavity :		
6 Ni—Ni bonds along unshared edges	12 electrons	12 orbitals
Required for skeletal bonding	26 electrons	30 orbitals

In this model the six outer $Ni(CO)_2$ groups are considered to use the normal three internal orbitals whereas the three inner $Ni(CO)_2$ groups are considered to use four internal orbitals. The octahedral $Ni_3Ni_{3/2}$ cavity is globally delocalized and the trigonal prismatic $Ni_3Ni_{3/2}$ cavity is edge-localized.

C. $Ni_{12}(CO)_{21}H_{4-n}^{n-}$ [39] : The counting of skeletal electrons and orbitals for this type of Ni cluster is illustrated below for $Ni_{12}(CO)_{21}H_2^{2-} = Ni_9(CO)_{12}[Ni(CO)_3]_3H_2^{2-}$:

Source of skeletal electrons and orbitals :

6 $NiCO_3$ groups-3 internal orbitals	0 electrons	18 orbitals
3 $Ni(CO)_2$ groups-5 internal orbitals	18 electrons	15 orbitals
3 external $Ni(CO)_3$ groups :		
2 internal orbitals	6 electrons	
H_2	2 electrons	
-2 charge	2 electrons	
Available for skeletal bonding	28 electrons	33 orbitals

Use of skeletal electrons and orbitals :

9 Ni—Ni surface bonds	18 electrons	18 orbitals
2 6-center core bonds	4 electrons	12 orbitals
3 Ni—Ni two-center bonds around the central Ni_3 belt	6 electrons	6 orbitals
Required for skeletal bonding	28 electrons	36 orbitals

Note the following features of this model :

1. There are two globally delocalized $Ni_3Ni_{3/2}$ octahedral cavities sharing a common triangular face (Figure 1) which may be regarded as an Ni_3 "belt."

2. Nine atoms in these fused nickel octahedra are involved in the surface bonding of their global delocalization.

3. Additional Ni—Ni two-center bonds are located in each of the three edges of the Ni_3 belt.

4. The three edges of the Ni_3 belt are also each bridged by a $Ni(CO)_3$ group, which may be treated as a donor of two skeletal electrons.

5. The discrepancy between the 33 available skeletal orbitals and the 36 required skeletal orbitals can be rationalized by assuming four- and/or five-center rather than six-center core bonds in the two octahedral $Ni_3Ni_{3/2}$ cavities.

4. NICKEL CARBONYL CLUSTERS WITH FIVE-FOLD SYMMETRY

Reactions of $Ni_6(CO)_{12}^{2-}$ with halides of germanium, tin, arsenic, and antimony lead to nickel carbonyl clusters with five-fold symmetry based on the icosahedron (Table 1 and Figure 2). Such clusters include the uncentered icosahedra $Ni_9(AsPh)_3(CO)_{15}^{2-}$ and $Ni_{10}(AsMe)_2(CO)_{18}^{2-}$,[40] the centered icosahedra $Ni_{12}E(CO)_{22}^{2-}$ ($E = Ge, Sn$),[41] the arachno pentagonal antiprism $Ni_{10}Ge(CO)_{20}^{2-}$ derived from an icosahedron by removal of two antipodal vertices,[41] and the nickel-centered icosahedron $Ni_{13}Sb_2(CO)_{24}^{4-} = Ni_{10}[SbNi(CO)_3]_2(Ni)(CO)_{18}^{4-}$.[37] All of these clusters have the 26 skeletal electrons $= 2n + 2$ for $n = 12$ corresponding to a globally delocalized icosahedron. The skeletal electron counts for these clusters are obtained as follows:

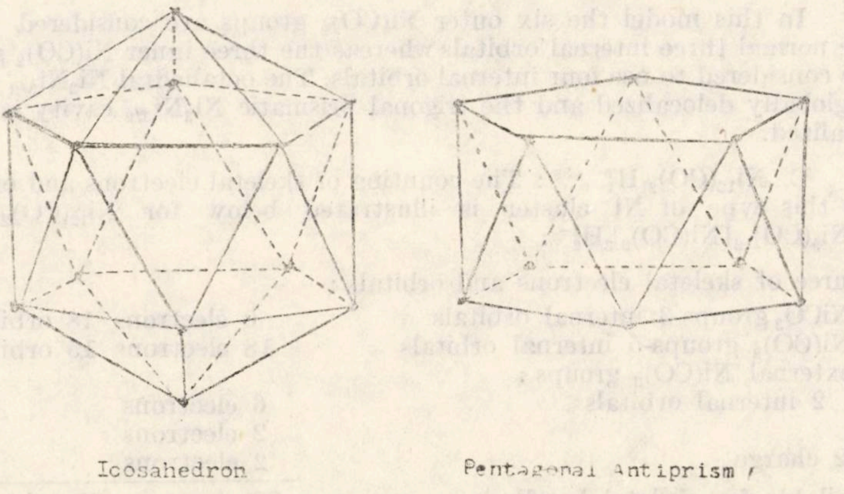

Fig. 2. — The icosahedron and pentagonal antiprism found in the nickel carbonyl clusters with five-fold symmetry.

A. $Ni_9(AsPh)_3(CO)_{15}^{2-}$: $18 - 6 + 12 + 2 = 26$ skeletal electrons arising from 9 $Ni(CO)_2$ vertices, a deficit of 3CO groups, the 3 AsPh vertices, and the -2 charge, respectively.

B. $Ni_{10}(AsMe)_2(CO)_{18}^{2-}$: $20 - 4 + 8 + 2 = 26$ skeletal electrons arising from 10 $Ni(CO)_2$ vertices, a deficit of 2CO groups, the 2 AsMe vertices, and the -2 charge, respectively.

Table 1

Nickel carbonyl clusters synthesized from $Ni_6(CO)_{12}^{2-}$

Reactant	Cluster Product	Yield, %	Literature
$Ni(CO)_4$	$Ni_9(CO)_{18}^{2-}$	~100	38
$NiCl_2$	$Ni_9(CO)_{18}^{2-}$	~100	38
$FeCl_3$	$Ni_9(CO)_{18}^{2-}$	80	38
H_2O(pH 6)	$Ni_{12}CO)_{21}H^{3-}$	50	39
$PhAsCl_2$	$Ni_9(AsPh)_3(CO)_{15}^{2-}$	40	40
$MeAsBr_2$	$Ni_{10}(AsMe)_2(CO)_{18}^{2-}$	40	40
$GeCl_4$	$Ni_{12}Ge(CO)_{22}^{2-}$	a	41
$SnCl_2 \cdot 2H_2O$	$Ni_{12}Sn(CO)_{22}^{2-}$	a	41
$SbCl_3$	$Ni_{13}Sb_2(CO)_{24}^{n-}$(n=2, 3, 4)	a	37
CCl_4(THF)	$N_9C(CO)_{17}^{2-}$	80	42
CCl_4 (MeCN)	$N_{10}C(CO)_{18}^{2-}$	3	42
C_2Cl_6 or C_2Cl_4	$Ni_{10}C_2(CO)_{16}^{2-}$	60	43

a The yield is not given.

C. $Ni_{12}E(CO)_{22}^{2-}$(E = Ge, Sn) : $24 - 4 + 4 + 2 = 26$ skeletal electrons arising from 12 $Ni(CO)_2$ vertices, a deficit of 2 CO groups, the interstitial Ge or Sn atom, and the − 2 charge, respectively.

D. $Ni_{10}Ge(CO)_{20}^{2-}$: $20 + 4 + 2 = 26$ skeletal electrons arising from 10 $Ni(CO)_2$ vertices, the interstitial Ge atom, and the − 2 charge- respectively. The 26 skeletal electrons correspond to $2n + 6$ for $n = 10$, i.e., the arachno 10-vertex pentagonal antiprism with its two pentagonal faces.

E. $Ni_{13}Sb_2(CO)_{24}^{4-} = Ni_{10}[SbNi(CO)_3]_2(Ni)(CO)_{18}^{4-}$: $20 - 4 + 6 + 0 + + 4 = 26$ skeletal electrons arising from 10 $Ni(CO)_2$ vertices, a deficit of 2 CO groups, the 2 $SbNi(CO)_3$ vertices, the interstitial Ni atom, and the − 4 charge. Note the following features of this model :

1. The two $SbNi(CO)_3$ vertices are donors of three skeletal electrons each since two of the five valence electrons of the antimony atom are coordinated to the external $Ni(CO)_3$ group leaving three electrons for the skeletal bonding.

2. The interstitial nickel atom is a donor of zero skeletal electrons. Table 2 shows the relationship of s, p, d, and f atomic orbitals to the non-degenerate bonding A_g level of eigenvalue $+5$, the triply degenerate bonding T_{1u} level of eigenvalue $+\sqrt{5}$, the quintuply degenerate antibonding H_g level of eigenvalue -1, and the triply degenerate antibonding T_{2u} level of $-\sqrt{5}$, respectively. Since the ten valence electrons of the interstitial nickel atom are d electrons, they must go into the H_g antibonding level where they cannot participate in skeletal bonding.

3. The reported[37] oxidation of $Ni_{13}Sb_2(CO)_{24}^{4-}$ to $Ni_{13}Sb_2(CO)_{24}^{3-}$ and $Ni_{13}Sb_2(CO)_{24}^{2-}$ can simply involve removal of one or two of the essentially non-bonding nickel d electrons which should affect very little the total energy of the cluster.

Table 2

The relationship of transition metal atomic orbitals to the molecular orbitals in an icosahedal cluster

Molecular orbital	Eigenvalue	Degeneracy	Atomic orbitals
a_g	$+5$	1	s
t_{1u}	$+\sqrt{5}$	3	p
h_g	-1	5	d
t_{2u}	$-\sqrt{5}$	3	f (3 of 7)

5. NICKEL CARBONYL CLUSTERS WITH INTERSTITIAL CARBON ATOMS

Reactions of $Ni_6(CO)_{12}^{2-}$ with chlorocarbons (Table 1) leads to the clusters $Ni_{10}C(CO)_{18}^{2-}$,[42] $Ni_9C(CO)_{17}^{2-}$,[42] and $Ni_{10}C_2(CO)_{16}^{2-}$.[43] The cluster $Ni_8C(CO)_{16}^{2-}$ is obtained by degradation of $Ni_9C(CO)_{17}^{2-}$ with carbon monoxide.[42] The largest nickel carbonyl carbide cluster $Ni_{16}(C_2)_2(CO)_{23}^{4-}$ is obtained by the degradation of $Ni_{10}C_2(CO)_{16}^{2-}$ with triphenylphosphine.[44] The capped square antiprism cluster $Ni_9C(CO)_{17}^{2-}$ and the square antiprism cluster $Ni_8C(CO)_{16}^{2-}$ are derived from the bicapped square antiprism cluster $Ni_{10}C(CO)_{18}^{2-}$ by removal of one and two antipodal vertices leading to nido and arachno structures, respectively (Figure 3). During the process of this successive vertex removal the skeletal electron count remains constant at 22 corresponding to $2n + 2$ for the Ni_{10} cluster, to $2n + 4$ for the nido

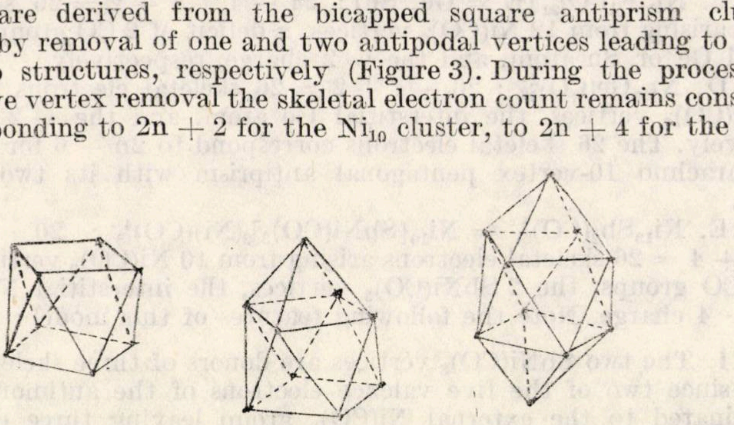

Fig. 3. — The nickel polyhedra in the nickel carbonyl carbide cluster.

Ni_9 cluster, and to $2n + 6$ for the arachno Ni_8 cluster. The larger nickel carbonyl carbide clusters $Ni_{10}C_2(CO)_{16}^{2-}$ and $Ni_{16}(C_2)_2(CO)_{23}^{4-}$ are based on larger Ni_{10} and Ni_{16} polyhedra necessary to contain the one or two interstitial C_2 units, respectively.

The details of the skeletal electron counting of these nickel carbonyl carbides are as follows :

A. $Ni_8C(CO)_{16}^{2-}$: $16 + 4 + 2 = 22$ skeletal electrons arising from 8 $Ni(CO)_2$ vertices, the interstitial carbon atom, and the -2 charge, respectively. This corresponds to the Ni_8 square antiprism (Figure 3) functioning as an arachno polyhedron with $2n + 6$ skeletal electrons for $n = 8$ in accord with the two square faces and in contrast to $Co_8C(CO)_{18}^{2-}$[14] where the Co_8 square antiprism functions as an eight-vertex pseudodeltahedron with only $2n + 2 = 18$ skeletal electrons.

B. $Ni_9C(CO)_{17}^{2-}$: $18 - 2 + 4 + 2 = 22$ skeletal electrons arising from 9 $Ni(CO)_2$ vertices, a deficiency of one CO group, the interstitial carbon atom, and the -2 charge, respectively. This corresponds to the nido $2n + 4$ skeletal electron capped square antiprism with one remaining square face.

C. $Ni_{10}C(CO)_{18}^{2-}$: $20 - 4 + 4 + 2 = 22$ skeletal electrons arising from 10 $Ni(CO)_2$ vertices, a deficiency of 2 CO groups, the interstitial carbon atom, and the -2 charge, respectively,corresponding to the $2n + 2$ skeletal electrons required for the observed closed deltahedron, namely the D_{4d} bicapped square antiprism.

D. $Ni_{10}C_2(CO)_{16}^{2-}$: $20 - 8 + 8 + 2 = 22$ skeletal electrons arising from the 10 $Ni(CO)_2$ vertices, the deficiency of 4 CO groups, the two interstitial carbon atoms, and the -2 charge, respectively, corresponding to the $2n + 2$ skeletal electrons required for a 10-vertex pseudodeltahedron.

E. $Ni_{16}(C_2)_2(CO)_{23}^{4-}$: $32 - 18 + 16 + 4 = 34$ skeletal electrons arising from the 16 $Ni(CO)_2$ vertices, the deficiency of 9 CO groups, the four interstitial carbon atoms, and the -4 charge, respectively, corresponding to the $2n + 2$ skeletal electrons required for a 16-vertex pseudodeltahedron.

Note that in the case of the nickel carbonyl carbides $Ni_{10}C_2(CO)_{16}^{2-}$ and $Ni_{16}(C_2)_2(CO)_{23}^{4-}$ each interstitial carbon atom is found to donate four skeletal electrons even though they are linked together in pairs to form C_2 groups. The interstitial carbon atoms in C_2 groups in all of the cobalt carbonyl carbide clusters except $Co_3Ni_7C_2(CO)_{15}^{3-}$ [14] each donate four skeletal electrons even when the C—C distance in the C_2 group indicates direct bonding. This suggests that in almost all cases the C—C bond in an interstitial C_2 group can overlap with the unique internal orbitals of the vertex atoms in the cluster polyhedron so that all of the interstitial carbon atoms (i.e., four electrons per carbon atom) can be used for the cluster skeletal bonding.

ACKNOWLEDGMENT : This manuscript was written in the Chemistry Department of Babeş-Bolyai University, Cluj-Napoca, Romania, during the course of a project development visit sponsored jointly by the Academies of Science of the U.S.A. and Romania. I am indebted to Prof. Ionel Haiduc and Dr. Ioan Silaghi-Dumitrescu for their kind hospitality during this visit.

REFERENCES

[1] For part 11 of this series see R. B. King, *Rep. Molec. Theor.* in press.

[2] R. B. King and D. H. Rouvray, *J. Amer. Chem. Soc.*, **99**, 7834 (1977).

[3] R. B. King in "Chemical Applications of Topology and Graph Theory", Elsevier, Amsterdam, 1983, p. 99–123.

[4] R. B. King in "Molecular Structure and Energetics"; Vol. 1, VCH Publishers, Deerfield Beach, Florida, 1986; p. 123–148.

[5] R. B. King, *Inorg. Chim. Acta.*, **57**, 79 (1982).

[6] R. B. King in "The Physics and Chemistry of Small Clusters," Plenum Press, New York, 1987; p. 79–82.

[7] R. B. King, *J. Phys. Chem.*, **92**, 4452 (1988).

[8] R. B. King, *Inorg. Chim. Acta*, **116**, 99 (1986).

[9] R. B. King in "Mathematics and Computational Concepts in Chemistry," Ellis Horwood, Ltd., Chichester, England, 1986; pp. 146–154.

[10] R. B. King, *Inorg. Chim. Acta*, **116**, 109 (1986).

[11] R. B. King, *Inorg. Chim. Acta*, **116**, 119 (1986).

[12] R. B. King, *Int. J. Quan. Chem. , Quant. Chem. Symp.*, **20**, 27 (1986).

[13] R. B. King, *Inorg. Chim. Acta*, **116**, 125 (1986).

[14] R. B. King, *New J. Chem.*, **12**, 493 (1988).

[15] R. B. King, *New J. Chem.*, **13**, 293 (1989).

[16] R. B. King in "Graph Theory and Topology in Chemistry," Elsevier, Amsterdam, 1987; pp. 325–343.

[17] R. B. King, *Inorg. Chim. Acta*, **129**, 91 1987).

[18] R. B. King, *Inorg. Chem.* **28**, 2796 (1989).

[19] D. M. P. Mingos, *Nature (London), Phys. Sci.*, **236**, 99 (1972).

[20] R. Mason, K. M. Thomas and D. M. P. Mingos, *J. Amer. Chem. Soc.*, **95**, 3802 (1973).

[21] K. Wade, *Adv. Inorg. Chem. Radiochem.* **18**, 1 (1976).

[22] D. M. P. Mingos, *Acc. Chem. Res.*, **17**, 311 (1984).

[23] D. M. P. Mingos, *Chem. Soc. Revs.*, **15**, 31 (1986).

[24] J. W. Lauher, *J. Amer. Chem. Soc.*, **100**, 5305 (1978).

[25] D. J. Wales and A. J. Stone, *Inorg. Chem.* **28**, 3120 (1989).

[26] B.K. Teo, *Inorg. Chem.*, **23**, 1251 (1984).

[27] B.K. Teo, G. Longoni, F. R. K. Chung, *Inorg. Chem.* **23**, 1257 (1984).

[28] B. K. Teo, *Inorg. Chem.*, **24**, 115 (1985).

[29] B. K. Teo, *Inorg. Chem.*, **24**, 4209 (1985).

[30] R. B. King, *J. Comput. Chem.*, **8**, 341 (1987).

[31] R. B. King‘ *Inorg. Chem.* **27**, 1941 (1988).

[2] R. B. King, B. M. Gimarc and B. Dai, *Inorg. Chim. Acta, in press.*

[33] J. C. Calabresse, L. F. Dahl, A. Cavalieri, P. Chini, G, Longoni and S.Martinengo, *J. Amer. Chem. Soc.*, **96**, 2616 (1974).

[34] G. Ciani, L. Garlaschelli, A. Sironi and S. Martinengo, *Chem. Commun.*, **1981** 563.

[35] W. N. Lipscomb, *Science*, **153**, 373 (1966).

[36] R. B. King, *Inorg. Chim. Acta*, **49**, 237 (1981).

[37] V. G. Albano, F. Demartin, M. C. Iapalucci, B. Longoni, A. Sironi and V. Zanotti, *Chem. Commun.* **1990** 547.

[38] D. A. Nagaki, L. D. Lower, G. Longoni, P. Chini, and L. F. Dahl, *Organometallics*, **5**, 1764 (1986).

[39] A. Ceriotti, P. Chini, R. Della Pergola and G. Longoni, *Inorg. Chem.*, **22**, 1595 (1983).

[40] D. F. Rieck, R. A. Montag, T. S. McKechnie and L· F. Dahl, *J. Amer. Chem. Soc.*, **108**, 1330 (1986).

[41] A. Ceriotti, F. Demartin, B. T. Heaton, P. Ingallina, G Longoni, M. Manassero, M. Marchionna and N. Masciocchi, *Chem. Commun.*, **1989** 786.

[42] A. Ceriott‘ G. Longoni, M. Manassero, M. Perego and M. Sansoni, *Inorg. Chem.*, **24**, 117 (1985).

[43] A. Ceriotti, G. Longoni, M. Manassero, N. Masciocchi, L. Resconi and M. Sansoni, *Chem. Commun.*‘ **1985** 181.

[44] A. Ceriotti, G. Longoni, M. Manassero, N. Masciocchi, G. Piro, L. Resconi and M. Sansoni, *Chem. Commun.*, **1985** 1402.

Revue Roumaine de Chimie, **36**, *4*–7, 363–377 (1991)

Dedicated to A. T. BALABAN, the pioneer
of mathematical chemistry, who prompted many
of us to join this fascinating field

INFORMATION-THEORETIC APPROACH TO THE AROMATICITY OF CHEMICAL COMPOUNDS BASED ON SUPERDELOCALIZABILITY INDICES*

O. MEKENYAN, D. BONCHEV and D. N. DIMITROV
Higher School of Chemical Technology, Burgas BU-8010, Bulgaria

Received January 18, 1990

A further development to the recent information-theoretic approach to aromaticity of Fratev et al. is presented on the basis of the degree of equalization of charges and bond orders in molecules. According to the novel approach, the closer the electron donor (or/and acceptor) capacities of atoms in a molecule the more aromatic the compound. Electron superdelocalizability indices as calculated by any of the MO-approximations can be used with this purpose. 54 conjugated compounds (alternant benzenoid and non-benzenoid, non-alternant, etc.) were examined by both PPP and HMO methods. The results allow the classification of compounds as aromatic, non-aromatic, and anti-aromatic, in good agreement with experiment and other theoretical aproaches, such as the Dewar & de Llano method, topological resonance energy, etc. The new measure reflects the change in aromaticity caused by topological factors like branching and cyclicity of molecular skeleton.

INTRODUCTION

Aromaticity of chemical compounds is one of the most challenging domains of contemporary experimental and theoretical chemistry.[1–15] Various new classes of aromatic compounds have been devised with structures often far from benzenoids, the standard for aromaticity. Remarkable progress has been achieved in predicting the aromatic character of unknown compounds. Theoretical chemistry thus guides the experimentalist by directing his efforts in the synthesis of aromatic compounds. Computed resonance energy, RE, is one of the main criteria used for such purposes either in the simplest Hueckel approximation [16–18] or by more sophisticated quantum-chemical [19–21] or topological [22–30] methods. This aromaticity criterion, however, is not free of pitfalls.[31] Thus, in order to provide a better prognostic accuracy one needs a large number of empirical parameters. RE is also calculated using a hypothetical standard structure which is sometimes difficult to construct, particularly for compounds in an excited state.

---

* **Reported at the 6th International Symposium on Novel Aromatic Compounds. Osaka, 20–25 August 1989.**

Resonance energy in its different versions (molecular orbital, valence bond or topological ones) is a measure for the additional stabilization an aromatic molecule gains, due to electron delocalization. Besides stability three other features characterize aromatic molecules. These are the ring currents, chemical reactivity, and specific geometry. More specifically, the latter implies an equalization of bond lengths or, otherwise, a decreased alternation of single and double bonds. As a consequence, the calculated bond orders of aromatic bonds are rather close to each other. The equalization of electron density along aromatic bonds is related to a decreased alternation (or equalization) of the atomic π-electron charges which intensify ring currents. A number of experimental and theoretical studies [32-36] evidence these manifestations of aromaticity which may be summarized as an equalization of electron distribution over the atoms and bonds in the molecule (or molecular fragment). Conversely, those molecules in which electron density is strongly localized on atoms and bonds display, as a rule, a high reactivity and should be classified as species of low aromaticity.

In information theory [37,38] the degree of unevenness in the distribution of matter or energy of a system is regarded as the most general definition of information,[39] i.e. information is a measure of the deviation of the system from its most probable uniform (or equalized) distribution. Therefore, one may assume that the molecular information content, calculated from a set of electronic distribution characteristics, might also be of use in evaluating the aromaticity of molecules or their fragments. Such an approach was applied by Fratev, Bonchev et al.[40,41] producing reasonably good aromaticity estimates for many chemical compounds in ground and excited states. It is the purpose of the present work to develop further this information-theoretic approach to aromaticity and to eliminate some of the drawbacks of the initial version.

BACKGROUND [40]

Electronic distribution in molecules may be described by means of the reduced density matrix. This quantum chemical matrix $A(A_{11}, A_{12}, \ldots \ldots, A_{mn}, \ldots)$ contains information on the distribution of electrons in the molecule.

Let

$$A = \sum_{mn} A_{mn} \, ; \quad p_i = A_{mn}/A \tag{1}$$

where

$$p_i \in \{p_i\} \qquad i \in <1, K>, \qquad \sum p_i = 1$$

The p_i quantities are regarded as relative characteristics of the electronic distribution normalized to unity. They have a probabilistic character since the matrix elements, i.e. the charged and bond orders, express the probability for electron distribution over orbitals and between them.

According to information theory,[37] each probability distribution $P(p_i, p_2, \ldots, p_i \ldots p_k)$ can be characterized by the mean entropy of the distribution $H(P)$:

$$H(P) = -\sum_{j=1}^{k} p_i \log_2 p_i \qquad (2)$$

This equation holds also for the "probabilistic" distribution described by eq. (1).

The uniform (or equalized) distribution $p_1 = p_2 = \ldots = p_i = \ldots \ldots = p_k$, after substituting in (1) and (2), results in an expression for the maximal entropy of distribution:

$$H_{max}(P) = \log_2 k \qquad (3)$$

The information content of a system is then specified as:

$$I(P) = H_{max} - H(P) \qquad (4)$$

i.e. I(p) is a measure for the system deviation from its most uniform (or equalized) electron density distribution which characterizes the most aromatic molecules. One should bear in mind that I(p) is not the *complete* information content of a molecule. Other distributions can be constructed to characterize molecular topology, symmetry, chemical composition, etc.[42–45]

By substituting (2) and (3) into (4), and taking also into account (1) one obtains:

$$I(\alpha) = \log_2\left(\frac{k}{A}\right) + \frac{1}{A}\sum_{mn} A_{mn}(\alpha)\log_2 A_{mn}(\alpha) \qquad (5)$$

The quantity $I(\alpha)$ is the molecular information content specified as a measure of the unevenness in the electron density (the matrix elements — charges and bond orders) according to the Shannon equation (5). Conversely, the evenness (or uniformity or equalization) of the distribution may be defined by a reciprocal index $\tilde{I}(\alpha)$, called the information index for aromaticity of a molecule in the ground ($\alpha = S_0$) or excited ($\alpha = = S_1, S_2, \ldots$) state:

$$\tilde{I}(\alpha) = I^B(0)/I^M(\alpha) \qquad (6)$$

where $I^B(0)$ is the information content of the benzene molecule (taken as a standard) in its ground state ($\alpha = S_0$), and $I^M(\alpha)$ is calculated by eq. (5) for the molecule M. All information indices are measured in bits and are specified within the following ranges:

$$I^M(\alpha) \geqslant I^B(0)$$

$$0 < \tilde{I}(\alpha) \leqslant 1$$

With the information index $\tilde{I}(\alpha)$ three ranges of ring aromaticity have been defined in a good agreement with other aromaticity estimates: high (1 to 0.666), moderate (0.666–0.333), and low (0.333–0).

As seen from the foregoing, $\tilde{I}(\alpha)$ is not based on particular chemical and physical assumptions but follows directly from most general information-theoretic considerations of equalized electron density distribution in aromatic molecules.

3. QUANTITATIVE AROMATICITY ESTIMATE BASED ON SUPERDELOCALIZABILITY INDICES

3.1. Some pitfalls of the first information-theoretic approach to aromaticity

(i) The information distribution function deals at the same time with two different electronic indices – the charges and bond orders. As known, the charges have a definite physical meaning (their sum equals the total number of electrons in the molecule) while the bond orders only formally are regarded proportional to the real electron density over the bonds.

(ii) The electronic charges basically characterize the capability of atoms to take part in electrostatic interactions (formation of ionic bonds). A quantitative measure of aromaticity should rather be associated with the charge-transfer from different reaction sites in the molecule (formation of covalent bonds).

3.2. Reactivity indices based on the Klopman and Hudson polyelectronic perturbation theory [46]

The capability of molecules to take a part in charge transfer interactions is usually characterized by the so-called superdelocalizability indices. Klopman and Hudson [42] developed a more general treatment of chemical reactivity which accounts for both charge and orbital interactions. This theory does not refer to π-conjugated molecules only. It is assumed that the interaction between the atoms r and s (from the reagents R and S, respectively) produces an energy change ΔE which depends on their nature, as well as on the distance d_{rs} between them:

$$\Delta E_{tot} = - q_r \cdot q_s \frac{M}{\varepsilon \cdot d_{rs}} + \Delta_{solv} + \sum_m \sum_n \frac{2(C_r^m)^2 \cdot (C_s^n)^2 \cdot \beta^2}{E_m - E_n} \qquad (7)$$

Here the first term describes the Coulomb electrostatic interaction where q_r and q_s are the total initial charges on atoms r and s, respectively, M is the Coulomb repulsion term between atoms r and s, and ε is the medium effective dielectric constant. This interaction results in an ionic type of bonding.

The second term in eq. (7) accounts for the same type of interaction with the solvent dipole molecules. The charge transfer effects are described by the third term. Originating from the direct interactions between the overlapping MO, these effects result in a covalent type of bonding.

Here c_r and c_s are the coefficients of the *r*th and *s*th AO in the occupied (m) and unoccupied (n) MO of the reagents R and S, respectively. E_m and E_n are the energies of these MO while β is the resonance integral.

When the difference $(E_m - E_n)/\beta$ in the energy of the occupied MO of the reagent R (the donor) and that of the unoccupied MO of the reagent S (acceptor) is large then the charge transfer is weak. In such cases the reaction is charge-controlled, what means a prevailing ionic type of bonding. In the opposite case, an orbitally controlled reaction occurs with covalent bond formation.

For congeneric compounds displaying the same interaction mechanism at a constant interaction medium, donor-acceptor superdelocalization capabilities are specified solely by the quantum chemical characteristics of the attacking reagent [47]:

$$\Delta E_{tot} = a \cdot q_{N_i} + b \sum_{m} \frac{2(C^m_{ri})^2}{E_m} + c \sum_{n} \frac{2(C^n_{si})^2}{E_n} \qquad (8)$$

Here q_{N_i} is the charge of the atom N in the *i*th molecule from the reacting class of compounds; C^m_{ri} and C^n_{si} are the AO coefficient in MO for positions r and s, respectively.

The second term in eq. (8) determines the reagent donor properties. The electron donor superdelocalizability index S^E_r is a measure of the reagent's ability to take part in electrophilic reactions, i.e. of its ability to form (partially) covalent bonds with a donation of charge from the atom r:

$$S^E_r = \sum_{\substack{m \\ \text{occ. MO}}} \frac{2(C^m_r)^2}{E_m} \qquad (9)$$

Analogously, the last term in eq. (8) characterizes the reagent acceptor properties. The S^N_r superdelocalizability index thus defined, quantifies the reagent's ability to take part in nucleophilic reactions with its atom r:

$$S^N_r = \sum_{\substack{n \\ \text{unocc.MO}}} \frac{2(C^n_r)^2}{E_n} \qquad (10)$$

Frontier orbital theory [48] makes use of the superdelocalization indices (9) and (10) by taking into account the coefficients and energies of the frontier occupied (HOMO) and unoccupied (LUMO) molecular orbitals only.

The superdelocalizability indices (9) and (10) along with their frontier orbital theory analogues and the atomic charges, calculated by various quantum chemical methods are widely applied in assessing the electronic factors influencing biological activity.[47,49–51] S^E and S^N mostly take into account the π-electron delocalization since it is the one to prevail in charge transfer effects.

3.3. Aromaticity Index Based on Superdelocalizability Indices

In this study, the donor and acceptor superdelocalizability indices specified above are used to determine a new variant of aromaticity indices. With this aim in mind they are substituted into eq. (1) :

$$A^E = \sum_r S_r^E \; ; \quad A^N = \sum_r S_r^N \tag{11a}$$

$$p_r^E = \frac{S_r^E}{A^E} \; ; \quad p_r^N = \frac{S_r^N}{A^N} \tag{11b}$$

Then, by inserting A^E and p_r^E into eqs. (2), (3), and (4) one obtains the information-theoretic aromaticity index I^D which accounts for the different capabilities of the atoms in the molecule to donate electron density. The less pronounced difference in (or equalization of) the atomic electron donor capabilities means less information content and high aromaticity. This global index reflects the molecule behaviour in electrophilic reactions. The analogous substitution of A^N and p_r^N into eqs. (2), (3), and (4) results in the aromaticity index I^A which accounts for the acceptor properties of atoms in molecules and characterizes the reactivity of molecules in nucleophilic reactions.

In this study we make use of a general aromaticity index which is an arithmetic mean of the donor and acceptor aromaticity indices introduced above :

$$I^{DA} = (I^D + I^A)/2 \tag{12}$$

Due to the MO symmetry the I^D and I^A indices in benzenoid hydrocarbons are equal. They differ, however, in non-alternant and heterocyclic molecules. In eq. (12) they are taken with an equal weight although the possibility for their different contribution to I^{DA} may also be taken into consideration.

4. RESULTS AND DISCUSSION

The test compounds (Fig. 1) have been selected to reflect the variety of organic π-electronic systems : alternant benzenoids with side-chains, alternant structures of mixed $(4n + 2,\ 4n)$ type, non-alternant compounds and acyclic alkenes. The choice was also aimed at covering the whole aromaticity scale. 55 compounds have been examined, the majority of them being alternant benzenoids and non-alternant hydrocarbons with 3, 5, and 7-membered rings. Due to the importance of the π-electronic structure for aromaticity, both the Pariser-Parr-Pople (PPP) and Hückel (HMO) quantum chemical methods have been used.

Within our information-theoretic approach the most aromatic compounds are characterized by the lowest values of the I^D and I^N indices, i.e., these are structures with the most equalized donor-acceptor properties

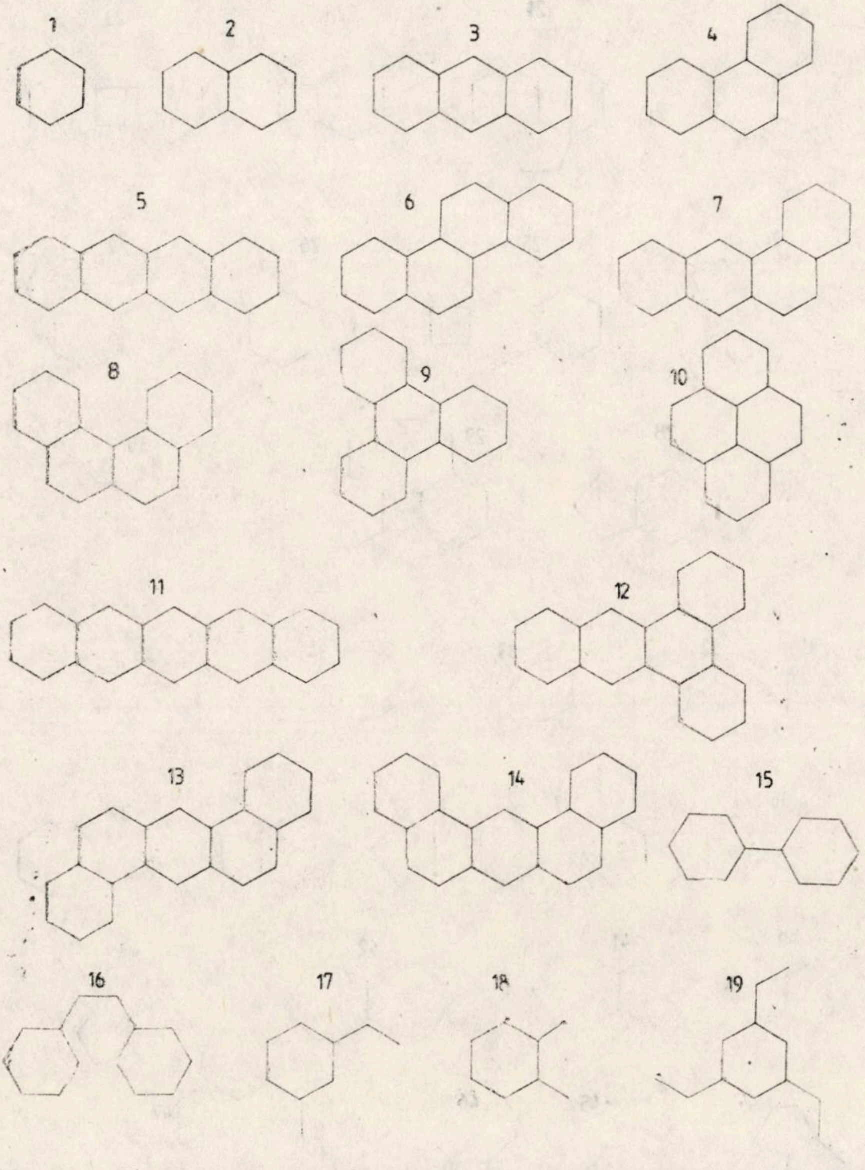

Fig. 1a. — 54 conjugated hydrocarbons whose aromaticity is examined in this work.

of their atoms. Otherwise, the lowest I^{DA} values correspond to high aromaticity and stability of compounds. The benzene molecule having the same donor-acceptor properties of all carbon atoms is thus regarded the most aromatic, its aromaticity index is minimal ($I^{DA} = 0$). This is in agreement with all aromaticity scales that take the benzene molecule as a standard for aromaticity.

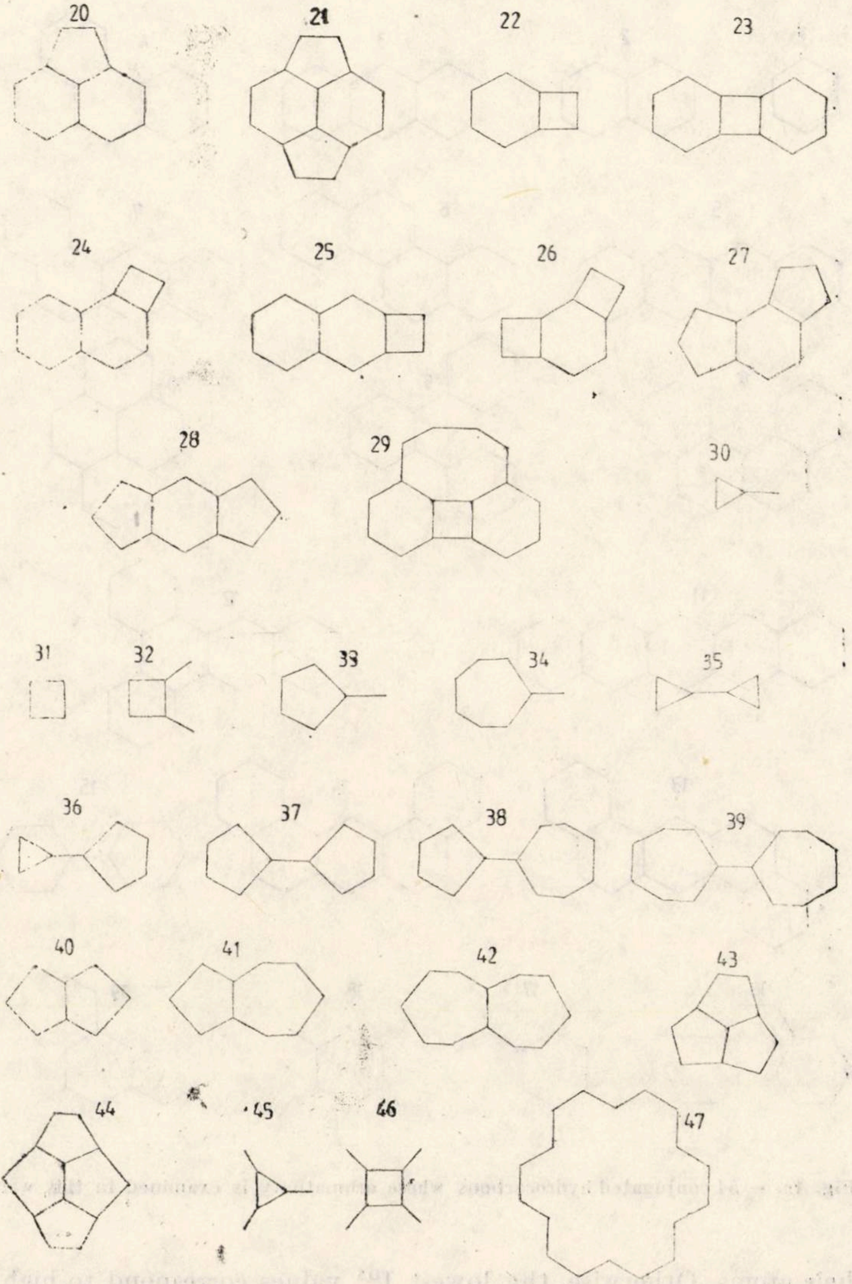
20
21
22
23
24
25
26
27
28
29
30
31
32
33
34
35
36
37
38
39
40
41
42
43
44
45
46
47

Fig. 1 b

The results of our calculations are summarized in Table 1 where the new information-theoretic indices I^{DA}_{HMO} and I^{DA}_{PPP} are given along with the initial version of this index,[40] $\tilde{I}$. They are compared there with

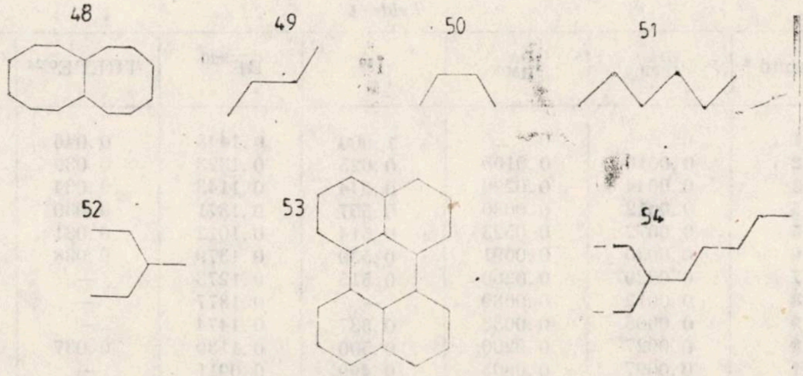

Fig. 1 c

three principally different aromaticity estimates. The first one is the Dewar and de Llano [20] resonance energy per atom ($\overline{RE}$, eV) regarded as the most rigorous aromaticity measure. It is defined as the difference between the heat of formation of given conjugated compound and that calculated for a corresponding classical structure with "localized" bonds. Both π-and σ-electronic energy contribute to the heat of formation. The topological resonance energy per electron (TREPE, in β units) introduced by Gutman, Milun and Trinajstić [24] was also taken as a representative of the wide class of topological aromaticity measures (see also [23–29]) which generally are in a good agreement with each other. This aromaticity measure does not require any empirical parameters; it is calculated by means of the difference in the roots of the characteristic polynominal and the acyclic polynominal of the respective molecular graph. Recently, Zhou, Parr and Garst [52] defined a new aromaticity index – the absolute hardness, η, which is approximated by the half of the HOMO-LUMO gap. They also introduced the concept of relative hardness [53] by relating the absolute hardness with that of an acyclic reference structure. Albeit the aromaticity range of values is not specified the results obtained are in parallel with some known aromaticity measures.

As seen from Table 1, the trends in aromaticity produced by the different approaches coincide for most classes of compounds. It is instructive to recall that according to the initial version of the information-theoretic approach (ITA-I) the test compounds have been grouped into three classes:

aromatic	($\tilde{I} = 1-0.45$),	compounds **1–7, 9–12, 15, 42**
non-aromatic	($\tilde{I} = 0.45-0.30$),	compounds **23, 34, 49, 51**
antiaromatic	($\tilde{I} = 0.30-0$),	compounds **22, 26, 31, 32**

Within the present variant of the approach (ITA-II) a different aromaticity scaling resulted for the I^{DA}_{PPP} index:

		compounds
aromatic :	$I^{DA}_{PPP} = 0-0.01$	**1–17, 19–26, 29, 32, 39, 46–48, 53**
non-aromatic :	$I^{DA}_{PPP} = 0.01-0.08$	**18, 27, 28, 30, 33–35, 37, 38, 41, 43–45**
antiaromatic :	$I^{DA}_{PPP} > 0.08$	**31, 36, 40, 42**

Table 1

Compound [a]	I_{PPP}^{DA}	I_{HMO}^{DA}	$\bar{I}^{40}$	$\overline{RE}^{b20}$	TREPE[c 24]	η^{c53}
1	0	0	1.000	0.1448	0.046	1.000
2	0.0016	0.0108	0.625	0.1323	0.039	0.618
3	0.0044	0.0296	0.544	0.1143	0.034	0.414
4	0.0012	0.0080	0.557	0.1371	0.039	0.605
5	0.0072	0.0523	0.514	0.1012	0.031	0.295
6	0.0030	0.0091	0.530	0.1379	0.038	0.520
7	0.0029	0.0200	0.515	0.1273	—	0.452
8	0.0012	0.0089	—	0.1377	—	0.468
9	0.0006	0.0033	0.537	0.1474	—	0.684
10	0.0027	0.0200	0.500	0.1139	0.037	0.445
11	0.0097	0.0803	0.499	0.0911	—	0.220
12	0.0017	0.0116	0.509	0.1390	—	0.499
13	0.0019	0.0137	0.501	0.1340	—	0.473
14	0.0020	0.0138	—	0.1340	—	0.492
15	0.0019	0.0026	0.646	0.1416	0.042	0.704
16	0.0011	0.0121	—	0.1230		0.504
17	0.0019	0.0161	—	0.1073	0.031	0.662
18	0.0140	0.1187	—	—	0.007	0.295
19	0.0042	0.0270	—	—	0.017	0.618
20	0.0069	0.0552	—	0.1112	0.030	0.461
21	0.0065	0.0281	—	—	0.009	0.207
22	0.0019	0.0481	0.232	—	−0.049	0.262
23	0.0030	0.0022	0.360	0.1122	0.010	0.445
24	0.0042	0.1425	—	—	−0.032	0.147
25	0.0022	0.0395	—	—	−0.010	0.339
26	0.0013	0.0166	0.191	—	−0.032	0.351
27	0.0196	0.0289	—	—	−0.025	0.033
28	0.0845	0.1616	—	—	0.005	0.309
29	0.0014	0.0337	—	—	−0.011	0.209
30	0.0571	0.2575	0.238	—	0.016	0.656
31	0.3532	0	0.070	—	−0.307	0.000
32	0.0047	0.0247	—	—	−0.027	0.555
33	0.0263	0.1933	0.294	0.0078	0.003	0.436
34	0.0142	0.1615	0.317	—	0.001	0.331
35	0.0390	0	—	—	−0.077	0.293
36	0.0886	0.1398	—	—	0.054	0.745
37	0.0150	0.0004	—	—	−0.030	0.182
38	0.0456	0.1101	—	—	0.023	0.508
39	0.0068	0.0006	—	—	−0.016	0.131
40	0.1370	0.0596	—	0.0008	−0.027	0.235
41	0.0297	0.0829	0.557	0.0169	0.015	0.439
42	0.0814	0.0447	—	0.0078	−0.012	0.156
43	0.0187	0.0149	—	—	−0.073	0.000
44	0.0118	0.0480	—	—	−0.045	0.064
45	0.0125	0.0734	—	—	0.002	0.516
46	0.0011	0.0628	—	—	−0.009	0.414
47	0.0019	0	—	0.0070	0.005	0.347
48	0.0006	0.0566	—	−0.0007	—	0.180 [d]
49	0.0042	0.0291	0.431	0.0008	—	0.620 [d]
50	0.0043	0.0290	—	0.0085	—	0.620 [d]
51	0.0044	0.2949	0.362	0	—	0.450 [d]
52	0.0074	0.0463	—	−0.0042	—	0.520 [d]
53	0.0028	0.0030	0.507	0.1310	—	0.347
54	0.0051	0.0523	—	−0.0010	—	0.300 [d]

[a] The compound numbers correspond to those in Fig. 1;
[b] In [eV]; [c] in β units; [d] calculated in this study

Inspection of Table 1 indicates that again compounds **1** to **15** and **17**, known as aromatic compounds are correctly classified having $I_{PPP}^{DA} < 0.01$. Two other structures, **53** and **16** (the latter being similar to biphenyl) are classified as aromatic in accordance with their high RE values (0.1455 and 0.1230, respectively). The hardness regarded as a measure of aromaticity in general also agrees with our results except higher polyacenes (**5** and **11**) for which very low numerical values are found.[18] Annulene also joins this class of compounds in agreement with the results of Haddon et al.[54] although in contradiction to the Dewar $\overline{\text{RE}}$ (0.007).

The I_{PPP}^{DA} index follows fairly well the aromaticity alteration in isomeric benzenoid hydrocarbons. The hardness index [53] also qualifies this compound as strongly aromatic. The increase in stability of these compounds with the increase in the branching of molecular skeleton has been attributed by Clar [3] to the increased number of "fully benzenoid" rings. As seen in Table 1, the I_{PPP}^{DA} index (which is an inverse proportional measure for aromaticity) decreases from 0.0044 to 0.0012 for the pair of isomers anthracene-phenanthrene (**3** and **4**), from 0.0072 to 0.0029 and then to 0.0006 in case of tetracene (**5**) — 1,2 — benzanthracene (**9**), respectively, and from 0.0097 for pentacene (**11**) to 0.0017 for 1—2, 3—4 dibenzanthracene (**12**). On the other hand, the increasing I_{PPP}^{DA} values for linear polyacenes with 1 to 5 benzene ring (0, 0.0016, 0.0044, 0.0072, and 0.0097, respectively) correlate well with the increasing reactivity and instability along this series of compounds.

The alteration in side-chain patterns is also correctly reproduced by the I_{PPP}^{DA} index as demonstrated by compounds **17** to **19** in agreement with hardness and TREPE estimates. The highest value (the lowest aromaticity) obtained for structure **18** corresponds to the lowest stability of this compound.

Our approach seems to fail in producing reliable results for alternant hydrocarbons containing $4n + 2$ and 4n-membered rings (**22**, **24**, **25**, **26**, **29**). The low I_{PPP}^{DA} values classify these compounds as typical aromatics, in accordance with their relatively high hardness values. However, this result disagrees with their instability, as well as with the TREPE antiaromaticity estimates [24] and the conjugated circuits concepts.[26] The trend toward overestimating the aromatic stability of $4n + 2$, 4n-compounds is also manifested although to a lesser extent in the case of biphenylene (**23**). The latter was found to have the same aromaticity index as the strongly aromatic compounds **6** and **7** in parallel with their hardness while both TREPE and $\overline{\text{RE}}$ estimates qualify biphenylene as borderline aromatic.

Better results were obtained for some non-alternant compounds. Thus, within the adopted aromaticity scale, compounds **20** and **39** are classified as weakly aromatic. The RE value 0.1112, TREPE = 0.030 and $\eta = 0.461$ support this finding for compound **20**, although the TREPE and hardness values for compound **39** (— 0.016 and 0.131, respectively) characterize it as a weak antiaromatic or antiaromatic. An aromatic character was also predicted for structure **21** which is similar to the aromatic compound **20**.

In the previous information-theoretic studies [40,41] the azulene molecule (**41**) was classified as aromatic in parallel with the hardness estimate ($\eta = 0.439$). The I_{PPP}^{DA} value of this molecule (0.0297), however, revises the previous results. The above-mentioned index value is close to those for structures **33** and **34** (0.0263 and 0.0142, respectively), the latter structure being often considered as a standard for non-aromaticity. The low TREPE (0.015) and, particularly, $\overline{RE}$ (0.0048) values may also be regarded in support of our finding.

Attempts to specify more precisely the bounds of the non-aromaticity region in our I_{PPP}^{DA} scale by investigating some acyclic compounds (**49**, **50**, **52**, **54**) were unsuccessful. The calculated hardness values also overestimate the aromatic character of these compounds. Actually, like ITA-I our approach provides a general measure for electron delocalization in molecules while aromaticity may be regarded as specific case of electron delocalization in cyclic structures.

In contrast, the low bound of the non-aromaticity region is well defined. The highest I_{PPP}^{DA} value (0.353) was obtained for the most typical antiaromatic compound, cyclobutadiene (**31**). The increase in stability of this compound when transformed into compounds **32** and **46** is reflected by the I_{PPP}^{DA} values (0.0047 and 0.0011, respectively), although the aromaticity thus predicted (as in the case of hardness assessments) seems high. On the other hand, the methylenecyclopropene (**30**) seems to be correctly predicted within the non-aromaticity region ($I_{PPP}^{DA} = 0.057$).

Two more compounds, pentalene (**40**) and heptalene (**42**) were also classified as antiaromatic by their high I_{PPP}^{DA} values (0.137 and 0.081, respectively). The ITA-I values placed these compounds at the non-aromaticity/antiaromaticity bound but the revised estimate seems more reliable in view of their low stability, low TREPE (− 0.027 and − 0.012), η (0.235 and 0.135) and $\overline{RE}$ (0.0008 and 0.0078) values.

The comparison of the I^{DA} index with other aromaticity measures reveals their close parallelism. Thus, after excluding compound **48** deviating strongly from the regularity found, the following regression was obtained for the Dewar and de Llano resonance energies [20]:

$$\overline{RE} = 0.1282 - 3.6036\, I_{PPP}^{DA} + 20.1365(I_{PPP}^{DA})^2 \qquad (13)$$

$$n = 25, \qquad r = 0.816, \qquad s = 0.010$$

The correlation is improved when dealing with benzenoid hydrocarbons only (**1**–**17**, **53**) and, particularly, when the HMO superdelocalizability indices are used:

$$\overline{RE} = 0.1453 - 1.3359\, I_{HMO}^{DA} + 8.3703(I_{HMO}^{DA})^2 \qquad (14)$$

$$n = 18, \qquad r = 0.899, \qquad s = 0.007$$

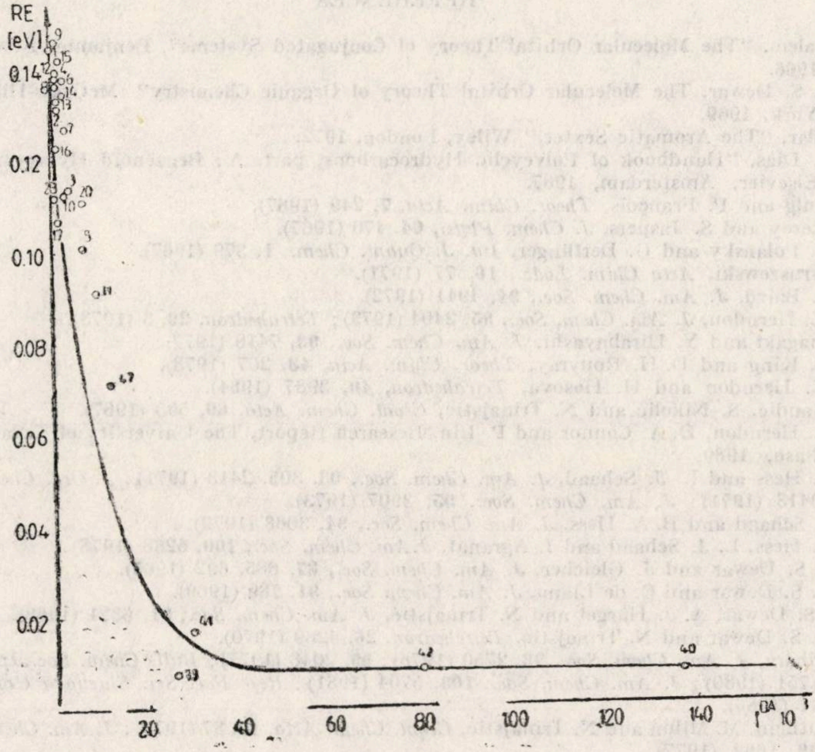

Fig. 2. — The Dewar-De Llano resonance energy [20] vs. the information aromaticity index calculated by the Pariser-Parr-Pople method.

On the other hand, the I^{DA}_{PPP} index was found to provide a higher correlation with the topological resonance energy (TREPE) [24] than I^{DA}_{HMO} :

$$\mathrm{TREPE} = -0.0007 + 0.3502\, I^{DA}_{PPP} - 3.4389 (I^{DA}_{PPP})^2 \qquad (15)$$

$$n = 39, \qquad r = 0.867, \qquad s = 0.032$$

The only other such correlation ($r = 0.78$) between the aromaticity indices from Table 1 was found to be that for TREPE and η.

Indeed, one should not expect our information-theoretic approach to produce exactly the same results as the resonance energy estimates, due to their different physical background. (In general, there is no hope that different aromaticity features will be reduced to a single one). Still, the reasonable parallelism found between them, along with the close connection of our information-theoretic index with electrophilic and nucleophilic substitution reactions, indicates the coherence in the different manifestations of the aromaticity phenomenon. The novel approach is applicable to the studying of excited states, radicals and ions.

ACKNOWLEDGMENTS. This study was supported by the National Committee for Science of Bulgaria (Grants nr. 233 and 385). The recommendations made by Prof. L. Shaad (Nashville) and Prof. T. Krygowski (Warszaw) are gratefully acknowledged.

REFERENCES

[1] L. Salem, "The Molecular Orbital Theory of Conjugated Systems", Benjamin, New York, 1966.

[2] M. J. S. Dewar, The Molecular Orbital Theory of Organic Chemistry" McGraw-Hill, New York, 1969.

[3] E. Clar, "The Aromatic Sextet," Wiley, London, 1972.

[4] J. R. Dias, "Handbook of Polycyclic Hydrocarbons, part. A : Benzenoid Hydrocarbons", Elsevier, Amsterdam, 1987.

[5] A. Julg and P. François, *Theor. Chim. Acta*, **7**, 249 (1967).

[6] G. Leroy and S. Jaspers, *J. Chem. Phys.*, **64**, 470 (1967).

[7] O. E. Polansky and G. Derflinger, *Int. J. Quant. Chem.*, **1**, 379 (1967).

[8] J. Kruszewski, *Acta Chim. Lodz.*, **16**, 77 (1971).

[9] N. C. Baird, *J. Am. Chem. Soc.*, **94**, 4941 (1972).

[10] W. C. Herndon, *J. Am. Chem. Soc.*, **95**, 2404 (1973) ; *Tetrahedron*, **29**, 3 (1973).

[11] S. Inagaki and Y. Hirabayashi, *J. Am. Chem. Soc.*, **99**, 7418 (1977).

[12] R. B. King and D. H. Rouvray, *Theor. Chim. Acta*, **48**, 207 (1978).

[13] W. C. Herndon and H. Hosoya, *Tetrahedron*, **40**, 3987 (1984).

[14] M. Randić, S. Nikolić and N. Trinajstić, *Croat. Chem. Acta*, **60**, 595 (1987).

[15] W. C. Herndon, D. A. Connor and P. Lin, Research Report, The University of Texas at El Paso, 1989.

[16] B. A. Hess and L. J. Schaad, *J. Am. Chem. Soc.*, **93**, 305, 2413 (1971) ; *J. Org. Chem.*, **36**, 3418 (1971) ; *J. Am. Chem. Soc.*, **95**, 3907 (1973).

[17] L. J. Schaad and B. A. Hess, *J. Am. Chem. Soc.*, **94**, 3068 (1972).

[18] B. A. Hess, L. J. Schaad and I. Agranat, *J.Am. Chem. Soc.*, **100**, 5268 (1978).

[19] M. J. S. Dewar and J. Gleicher, *J. Am. Chem. Soc.*, **87**, 685, 692 (1965).

[20] M. J. S. Dewar and C. de Llano, *J. Am. Chem. Soc.*, **91**, 789 (1969).

[21] M.J.S. Dewar, A. J. Harget and N. Trinajstić, *J. Am. Chem. Soc.*, **91**, 6321 (1969).

[22] M. J. S. Dewar and N. Trinajstić, *Tetrehedron*, **26**, 4269 (1970).

[23] J. Aihara, *J. Am. Chem. Soc.*, **98**, 2750 (1976) ; **99**, 2048 (1977) ; *Bull. Chem. Soc. Jpn.*, **53**, 1751 (1980) ; *J. Am. Chem. Soc.*, **103**, 5704 (1981) ; *Rep. Fac. Sci. Shizuoka Univ.*, **20**, 11 (1986).

[24] I. Gutman, M. Milun and N. Trinajstić, *Croat. Chem. Acta*, **48**, 87 (1976) ; *J. Am. Chem. Soc.*, **99**, 1692 (1977).

[25] W. C. Herndon, *Israel J. Chem.*, **20**, 270 (1980).

[26] M. Randić, *Chem. Phys. Lett.*, **38**, 68 (1976) ; *J. Am. Chem. Soc.*, **99**, 444 (1977).

[27] M. Randić and H. E. Zimmerman, *Int. J. Quantum Chem. Symp.*, **20**, 185 (1986).

[28] M. Randić and F. E. Nettleton, *Int. J. Quantum Chem. Symp.*, **20**, 203 (1986).

[29] M. Randić, D. Plavsić and N. Trinajstić, *Gazz. Chim. Ital.*, **118**, 441 (1988).

[30] N. Mizoguchi, *Chem. Phys. Lett.*, **158**, 383 (1989).

[31] N. D. Epiotis and R. L. Yates, *J Am. Chem. Soc.*, **98**, 461 (1976).

[32] F. Sondheimer, *Pure Appl. Chem.*, **27**, 4609 (1941).

[33] J. A. Elvidge and L. M. Jackman, *J. Chem. Soc.*, 859 (1961).

[34] J. F. Labarre and F. Crasnier, *J. Chem. Phys.*, **64**, 1664— (1967) ; J. F. Labarre, M. Graffeul, J. P. Faucher, M. Pasdeloup and J. P. Laurent, *Theor. Chim. Acta*, **11**, 423 (1968). J. P. Faucher, M. Pasdeloup and J. P. Laurent, *Theor. Chim. Acta*, **11**, 423 (1968).

[35] A. Julg. In : E. Bergmann, B. Pullman (eds) "The Jerusalem Symposia on Quantum Chemistry and Biochemistry", vol. III, The Israel Academy of Sciences and Humanities, Jerusalem, (1971), p. 383.

[36] J. Kruszewski and T. M. Krygowski, *Tetrahedron Lett.*, 3839 (1974) ; *Can. J. Chem.*, **53**, 945 (1974) ; M. Gdaniec, I. Turowska-Turk and T. M. Krygowski, *J. Chem. Soc. Perk. Trans.*, II 613 (1989).

[37] C. Shannon and W. Weaver, "Mathematical Theory of Communication", University of Illinois, Urbana, (1949).

[38] L. Brillouin, "Science and Information Theory", Academic Press, New York, (1956).

[39] V. Glushkov, in "Cybernetics, Thinking, Life", A. I. Berg, B. V. Biryukov, I. B. Novik, I. V. Kuznetzov and A. G. Spirkin (eds), Mist. Mosscow, (1964), p. 53 (in Russian).

[40] F. Fratev, D. Bonchev and V. Enchev, *Croat. Chem. Acta*, **53**, 545 (1980).

[41] F. Fratev, V. Enchev, O. E. Polansky and D. Bonchev, *J. Mol. Struct.*, **88**, 105 (1982).

[42] D. Bonchev, *MATCH*, **6**, 65 (1979).

[43] D. Bonchev and N. Trinajstić, *Int. J. Quant. Chem. Symp.*, **16**, 463 (1982).

[44] D. Bonchev, "Information Theoretic Indices for Characterization of Chemical Structures" Research Studies Press, Chichester, (1983).

[45] D. Bonchev, In : "Computational Chemical Graph Theory", D. H. Rouvray (ed), Nova Publications, New York, 1990.

[46] G. Klopman and R. E. Hudson, *Theor. Chim. Acta*, **8**, 165 (1967) ; G. Klopman, *J. Am. Chem. Soc.*, **90**, 223 (1968).

[47] F. Peradejordl, A. Martin and A. Cammarata, *J. Pharm. Sci.*, **60**, 576 (1971).

[48] K. Fukul, T. Yonezawa and C. Nagata, *Bull. Chem. Soc. Jpn.*, **27**, 423 (1954).

[49] O. Mekenyan, D. Peltchev, D. Bonchev and N. Trinajstić, *Arzneim. Forsch.*, **36**, 176 (1986).

[50] O. Mekenyan and D. Bonchev, *Acta Pharm. Jugosl.*, **36**, 225 (1986).

[51] O. Mekenyan, D. Bonchev and V. Enchev, *Quant. Struct-Act. Relat.*, **7**, 240 (1988).

[52] Z. Zhou, R. G. Parr and J. F. Garst, *Tetraedron Lett.*, 4843 (1988).

[53] Z. Zhou and R. G. Parr, *J. Am. Chem. Soc.*, **111**, 7371 (1989).

[54] R. S. Haddon, V. R. Haddon and L. M. Jackman, *Top. Curr. Chem.*, **16**, 103 (1971).

Revue Roumaine de Chimie, 36, 4–7, 379–388 (1991)

Dedicated to Professor ALEXANDRU T. BALABAN, a
pioneer in chemical graph theory, on the occasion
of his 60th birthday

TOPOLOGICAL PROPERTIES OF BENZENOID SYSTEMS. MERRIFIELD-SIMMONS INDICES AND INDEPENDENCE POLYNOMIALS OF UNBRANCHED CATAFUSENES

IVAN GUTMAN
Faculty of Science, University of Kragujevac, P.O. Box 60,
YU-34000 Kragujevac, Yugoslavia

Received December 8, 1990

A transfer-matrix technique is developed for the calculation of the independence polynomial and the Merrifield-Simmons index of an unbranched catafusene.

INTRODUCTION

The systematic examination of the topology of unbranched catafusenes began with the two seminal papers of Balaban [1,2] published in the late sixties. Since then a considerable amount of work has been done in this area, resulting in numerous discoveries and new theoretical concepts. A complete list of publications devoted to the topological properties of unbranched catafusenes would comprise several hundred titles. The interested reader should consult the books,[3,4] the reviews [5–8] and/or the research paper [9–33] as well as the references cited therein.

In this work we examine the independence polynomials and the Merrifield-Simmons indices of unbranched catafusenes and show that they can easily be calculated by means of a transfer-matrix technique.

Let G be a (molecular) graph. The number of ways in which k independent (i.e. mutually non-adjacent) vertices can be selected in G is denoted by n(G, k). By definition, n(G, 0) = 1 and n(G, 1) = n = number of vertices of G. Then the Merrifield-Simmons index of the graph G is given by :[34–39]

$$\sigma(G) = \sum_{k=0}^{n} n(G, k)$$

whereas the independence polynomial of G is defined as :[3,40–43]

$$\omega(G) = \omega(G, x) = \sum_{k=0}^{n} n(G, k)x^k.$$

It is immediately seen that $\omega(G, 1) = \sigma(G)$.

The quantity σ plays an important role in the Merrifield-Simmons' theory of molecular topology.[39] In particular, σ is the cardinality of the molecular topological space. Numerous chemical applications of σ can be found in the works [34–39] of Merrifield and Simmons.

The independence polynomial seems of be first examined by Motoyama and Hosoya [40] in 1977 and was named "king polynomial". They, however, defined it for (square) lattices rather than for graphs. The present author introduced the independence-polynomial concept within an algebraic approach to Clar's aromatic sextet theory.[3,41,43] The same author, together with F. Harary,[42] established the basic mathematical properties of $\omega(G)$. Unaware of all this, Balasubramanian and Ramaraj defined [44] the "color polynomial", which is precisely the same as $\omega(G)$. They [44] pointed at the relevance of ω in the theory of the magnetic properties of transition metal crystals as well as the kinetics of adsorption of diatomic molecules on metal surfaces.

In addition to the brute-force checking for independency of all the 2^n sets of vertices of the graph G, the only presently existing method for the calculation of $\sigma(G)$ and $\omega(G)$ is based on the recursion relations

$$\omega(G) = \omega(G - v) + x\omega(G - N_v) \tag{1}$$

$$\omega(G_1 \cup G_2) = \omega(G_1)\, \omega(G_2). \tag{2}$$

Here v denotes an arbitrary vertex of the graph G and N_v is the set containing v and all its first neighbors. By $G_1 \cup G_2$ we denote a graph composed of two disconnected components G_1 and G_2. By setting $x = 1$ in eqs. (1) and (2) we obtain the appropriate recursion relations for the Merrifield-Simmons indices.

Whereas in the case of molecular graphs with no or with few cycles the application of (1) and (2) enables a very efficient calculation of $\omega(G, x)$, difficulties arise if G is polycyclic. Then (1) and (2) have to be repeatedly applied many times, making thus the calculation very lengthy and error prone. Benzenoid hydrocarbons are typical molecules for which the application of (1) and (2) is difficult. As a consequence of this, σ-values were reported [37,39] only for benzene whereas $\omega(G, x)$ was reported [44] only for coronene and circumcoronene. In addition to this, the recurrence relation (11) for the Merrifield-Simmons index of linear polyacenes was established in a recent work.[45]

In this paper we design a transfer-matrix technique which makes possible a direct and easy calculation of both σ and ω of a class of benzenoid molecules, namely of unbranched catafusenes.

PRELIMINARIES

The molecular graph of an h-cyclic unbranched catafusene can be presented as follows:

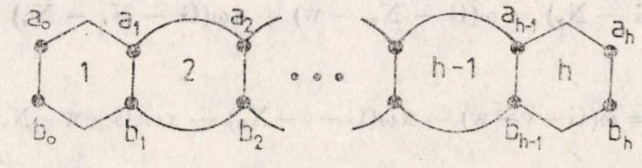

U_h

Denote by d(y, z) the (topological) distance between the vertices y and z. Then $d(a_i, a_{i+1}) + d(b_i, b_{i+1}) = 4$ for all $i = 0, 1, 2, \ldots, h-1$. Depending on the actual structure of U_h, $d(a_i, a_{i+1})$ is either equal to one or two or three. It is convenient to choose the vertices a_0 and a_h so that $d(a_0, a_1) = d(a_{h-1}, a_h) = 2$.

Now, according to Balaban [5-8] the structure of U_h is fully determined by an $(h - 2)$-tuple of symbols 0, 1 and/or 2, called the three-digit (3D) code. For the present considerations it is purposeful to augment this 3D-code by adding to both its ends a digit 0. Then, if C_i denotes the digit associated with the i-th hexagon, $i = 1, 2, \ldots, h$,

$$C_i = 0 \quad \text{when} \quad d(a_{i-1}, a_i) = 2$$

$$C_i = 1 \quad \text{when} \quad d(a_{i-1}, a_i) = 1$$

$$C_i = 2 \quad \text{when} \quad d(a_{i-1}, a_i) = 3.$$

For example, the augmented 3D-codes of the two catafusenes I and II are [0, 0, 1, 1, 2, 1, 0] and [0, 0, 1, 2, 2, 1, 0], respectively. Recall that the regular 3D-codes of these molecules are [0, 1, 1, 2, 1] and [0, 1, 2, 2, 1].

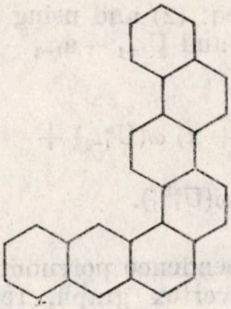
I

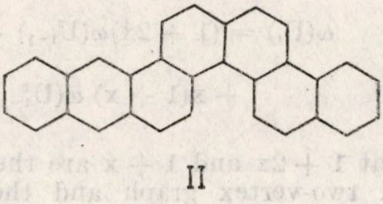
II

In what follows we shall need an immediate consequence of eq. (1). Let w be another vertex of the graph G. Then

$$\omega(G - v) = \omega(G - v - w) + x\,\omega(G - v - N_w)$$

$$\omega(G - N_v) = \omega(G - N_v - w) + x\omega(G - N_v - N_w)$$

resulting in

$$\omega(G) = \omega(G - v - w) + x\omega(G - v - N_w) + x\omega(G - w - N_v) + \\ + x^2 w(G - N_v - N_w). \tag{3}$$

One should note that if $d(v, w) = 1$ then $v \in N_w$ and $w \in N_v$ and eq. (3) reduces to

$$\omega(G) = \omega(G - v - w) + x\omega(G - N_v) + x\omega(G - N_w).$$

THE MAIN RESULTS

In order to deduce the required recurrence relation for $\omega(U_h)$ we onsider the i-cyclic catafusene U_i which is composed of the hexagons 1, 2, . . . , i of the previously described system U_h:

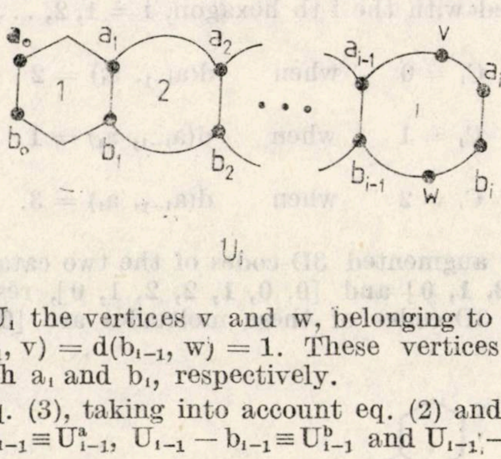

U_i

Choose in U_i the vertices v and w, belonging to the i-th hexagon, such that $d(a_{i-1}, v) = d(b_{i-1}, w) = 1$. These vertices may, but need not, coincide with a_i and b_i, respectively.

Applying eq. (3), taking into account eq. (2) and using the abbreviations $U_{i-1} - a_{i-1} \equiv U^a_{i-1}$, $U_{i-1} - b_{i-1} \equiv U^b_{i-1}$ and $U_{i-1} - a_{i-1} - b_{i-1} \equiv U^{ab}_{i-1}$ one obtains

$$\omega(U_i) = (1 + 2x)\omega(U_{i-1}) + x(1 + x)\,\omega(U^a_{i-1}) + \\ + x(1 + x)\,\omega(U^b_{i-1}) + x^2\omega(U^{ab}_{i-1}). \tag{4}$$

Recall that 1 + 2x and 1 + x are the independence polynomials of the connected two-vertex graph and the one-vertex graph, respectively.

We now have to separately consider the cases $C_i = 0$, $C_i = 1$ and $C_i = 2$.

If $C_i = 0$ then $v \neq a_i$, $w \neq b_i$ and in full analogy to eq. (4) we deduce

$$\omega(U_i^a) = (1 + x)\,\omega(U_{i-1}) + x(1 + x)\,\omega(U_{i-1}^a) + x\omega(U_{i-1}^b) + \\ + x^2\omega(U_{i-1}^{ab})$$

$$\omega(U_i^b) = (1 + x)\,\omega(U_{i-1}) + x\omega(U_{i-1}^a) + x(1 + x)\,\omega(U_{i-1}^b) + \\ + x^2\omega(U_{i-1}^{ab})$$

$$\omega(U_i^{ab}) = \omega(U_{i-1}) + x\omega(U_{i-1}^a) + x\omega(U_{i-1}^b) + x^2\omega(U_{i-1}^{ab}).$$

The above three relations together with eq. (4) furnish

$$\begin{bmatrix} \omega(U_i) \\ \omega(U_i^a) \\ \omega(U_i^b) \\ \omega(U_i^{ab}) \end{bmatrix} = \mathbf{T}_2 \begin{bmatrix} \omega(U_{i-1}) \\ \omega(U_{i-1}^a) \\ \omega(U_{i-1}^b) \\ \omega(U_{i-1}^{ab}) \end{bmatrix}$$

with

$$\mathbf{T}_0 = \begin{bmatrix} 1 + 2x & x(1 + x) & x(1 + x) & x^2 \\ 1 + x & x(1 + x) & x & x^2 \\ 1 + x & x & x(1 + x) & x^2 \\ 1 & x & x & x^2 \end{bmatrix}. \tag{5}$$

If $C_i = 1$ then $v = a_i$, $w \neq b_i$. Using (1) and (2) we immediately arrive at

$$\omega(U_i^a) = (1 + 2x)\,\omega(U_{i-1}) + x(1 + x)\,\omega(U_{i-1}^b)$$

$$\omega(U_i^{ab}) = (1 + x)\,\omega(U_{i-1}) + x\omega(U_{i-1}^b)$$

whereas (3) and (2) yield

$$\omega(U_i^b) = (1 + x)\,\omega(U_{i-1}) + x(1 + x)\,\omega(U_{i-1}^a) + x\omega(U_{i-1}^b) + \\ + x^2\omega(U_{i-1}^{ab}).$$

In matrix notation these relations read

$$\begin{bmatrix} \omega(U_i) \\ \omega(U_i^a) \\ \omega(U_i^b) \\ \omega(U_i^{ab}) \end{bmatrix} = \mathbf{T}_1 \begin{bmatrix} \omega(U_{i-1}) \\ \omega(U_{i-1}^a) \\ \omega(U_{i-1}^b) \\ \omega(U_{i-1}^{ab}) \end{bmatrix}$$

with

$$\mathbf{T}_1 = \begin{bmatrix} 1+2x & x(1+x) & x(1+x) & x^2 \\ 1+2x & 0 & x(1+x) & 0 \\ 1+x & x(1+x) & x & x^2 \\ 1+x & 0 & x & 0 \end{bmatrix}. \tag{6}$$

If $C_i = 2$ then a completely equivalent reasoning leads to

$$\begin{bmatrix} \omega(U_i) \\ \omega(U_i^a) \\ \omega(U_i^b) \\ \omega(U_i^{ab}) \end{bmatrix} = \mathbf{T}_2 \begin{bmatrix} \omega(U_{i-1}) \\ \omega(U_{i-1}^a) \\ \omega(U_{i-1}^b) \\ \omega(U_{i-1}^{ab}) \end{bmatrix}$$

with

$$\mathbf{T}_2 = \begin{bmatrix} 1+2x & x(1+x) & x(1+x) & x^2 \\ 1+x & x & x(1+x) & x^2 \\ 1+2x & x(1+x) & 0 & 0 \\ 1+x & x & 0 & 0 \end{bmatrix}. \tag{7}$$

We are now able to formulate our final results :

THEOREM 1. If the (augmented) 3D-code of an h-cyclic unbranched catafusene U_h is $[C_1, C_2, \ldots, C_{h-1}, C_h]$, $C_i \in \{0, 1, 2\}$, then

$$\begin{bmatrix} \omega(U_h) \\ \omega(U_h^a) \\ \omega(U_h^b) \\ \omega(U_h^{ab}) \end{bmatrix} = \mathbf{T} \begin{bmatrix} 1+2x \\ 1+x \\ 1+x \\ 1 \end{bmatrix}$$

where

$$\mathbf{T} = \mathbf{T}(U_h) = \mathbf{T}_{C_1}\mathbf{T}_{C_2} \ldots \mathbf{T}_{C_{h-1}}\mathbf{T}_{C_h}$$

and where the matrices $\mathbf{T}_0$, $\mathbf{T}_1$ and $\mathbf{T}_2$ are given by eqs. (5), (6) and (7).

Corollary 1.1.

$$\omega(U_h) = (1+2x)\,\mathbf{T}_{11} + (1+x)\,\mathbf{T}_{12} + (1+x)\,\mathbf{T}_{13} + \mathbf{T}_{14}.$$

THEOREM 2. For the catafusene U_h specified in Theorem 1,

$$\begin{bmatrix} \sigma(U_h) \\ \sigma(U_h^a) \\ \sigma(U_h^b) \\ \sigma(U_h^{ab}) \end{bmatrix} = \mathbf{t} \begin{bmatrix} 3 \\ 2 \\ 2 \\ 1 \end{bmatrix}$$

where

$$t = t(U_h) = t_{C_1} t_{C_2} \ldots t_{C_{h-1}} t_{C_h}$$

and where the matrices $\mathbf{t}_0$, $\mathbf{t}_1$ and $\mathbf{t}_2$ are given by eqs. (8)—(10):

$$\mathbf{t}_0 = \begin{bmatrix} 3 & 2 & 2 & 1 \\ 2 & 2 & 1 & 1 \\ 2 & 1 & 2 & 1 \\ 1 & 1 & 1 & 1 \end{bmatrix} \tag{8}$$

$$\mathbf{t}_1 = \begin{bmatrix} 3 & 2 & 2 & 1 \\ 3 & 0 & 2 & 0 \\ 2 & 2 & 1 & 1 \\ 2 & 0 & 1 & 0 \end{bmatrix} \tag{9}$$

$$\mathbf{t}_2 = \begin{bmatrix} 3 & 2 & 2 & 1 \\ 2 & 1 & 2 & 1 \\ 3 & 2 & 0 & 0 \\ 2 & 1 & 0 & 0 \end{bmatrix}. \tag{10}$$

Corollary 2.1.

$$\sigma(U_h) = 3t_{11} + 2t_{12} + 2t_{13} + t_{14}.$$

It is clear that Theorem 2 is obtained from Theorem 1 by setting $x = 1$. The matrices $\mathbf{T}_0$, $\mathbf{T}_1$ and $\mathbf{T}_2$, associated to particular hexagons of the unbranched catafusene in harmony with the 3D-code, are typical transfer matrices. Transfer-matrix techniques have already been proposed for the calculation of other topological characteristics of unbranched catafusenes, e.g. Wiener index,[31] number of Kekulè structures [20,25] and matching polynomials.[14,32] The method elaborated in this paper is based on ideas analogous to those used by Hosoya and coworkers.[14,31,32]

NUMERICAL WORK

In Table 1 are collected the σ-values of all possible unbranched catafusenes with $h \leqslant 7$. Note that the molecules whose 3D-codes are [1, 1, 1, 1], [0, 1, 1, 1, 1], [1, 1, 1, 1, 1] and [1, 1, 1, 1, 2] (and only these molecules) are nonplanar helicenic species. The molecules in Table 1 are ordered so that within groups of isomers (which have the same numbers of hexagons, h) the Merrifield-Simmons indices increase. We see that in all cases examined the unbranched catafusenes with the minimum and maximum value of σ are the zig-zag polyacene (A_h) and the linear polyacene (L_h), respectively. This turns out to be a general regularity. A rigorous mathematical proof of the bounds

$$\sigma(A_h) < \sigma(U_h) < \sigma(L_h)$$

will be reported elsewhere. In the above inequalities U_h stands for an arbitrary unbranched catafusene with h hexagons, different from A_h and L_h.

Many other regularities can be observed from Table 1. For instance, the larger is the number of digits 0 in the 3D-code, the larger is σ. In a few cases nonisomeric species have equal σ-values. The previously mentioned catafusenes I and II provide such an example (they both have $\sigma = 1137411$). Nevertheless, the isomer-distinguishing power of σ is found to be considerably higher than of some other topological indices.[46,47]

Table 1

Merrifield-Simmons indices (σ) of unbranched catafusenes with seven and less hexagons; the structure of the molecules is specified by Balaban's three-digit code; h = number of hexagons

h	3D code	σ index	3D code	σ index	3D code	σ index	3D code	σ index
1	—	18						
2	—	114						
3	1	717	0	726				
4	12	4509	11	4518	01	4563	00	4626
5	121	28353	122	28416	111	28452	102	28677
	101	28686	012	28695	011	28758	010	29037
	001	29073	000	29478				
6	1212	178284	1121	178689	1221	178725	1112	178941
	1122	179067	1111	179211	1021	180336	1012	180399
	0121	180435	1022	180741	1011	180777	0122	180840
	0112	180876	0111	181092	0102	182487	0101	182550
	0120	182613	1002	182712	1001	182721	0012	182829
	0110	183054	0011	183234	0010	185007	0001	185259
	0000	187842						
7	12121	1121049	12122	1123605	12112	1123884	11121	1125225
	12221	1125396	11211	1126134	11221	1126251	11112	1127115
	11122	1127646	11111	1128726	10212	1133955	12012	1134045
	10121	1134360	12012	1134486	01212	1134576	10211	1136511
	11021	1136601	10221	1136790	11012	1136853	10122	1136889
	10112	1137006	01211	1137159	01121	1137411	01221	1137411
	11102	1138131	10111	1138401	01222	1138779	01112	1138923
	11022	1139130	11011	1139274	01122	1139805	01111	1140669
	10201	1146861	10102	1147266	01021	1147572	10101	1147644
	01201	1147644	01012	1148013	01202	1148049	01210	1148265
	10021	1149003	10012	1149066	00121	1149633	01022	1150155
	01011	1150407	01102	1150479	01101	1150695	01120	1151100
	11002	1151559	10011	1151595	00122	1152216	00112	1152468
	01110	1152612	00111	1153836	01020	1161261	01010	1161702
	01002	1162692	00102	1162701	01001	1162755	00101	1163106
	00120	1163511	10002	1164285	10001	1164294	00012	1165023
	00110	1166346	00011	1167606	00100	1178757	00010	1178901
	00001	1180521	00000	1196982				

In Table 2 we present the first few σ-values for three distinguished homologous series of catafusenes — zig-zag and linear polyhexes as well as helicenes. Based on these data it is not difficult to recognize the

Table 2

Merrifield-Simmons indices (σ) of zig-zag polyhexes (A_h), helicenes (H_h) and linear polyacene (L_h) with h hexagons

h	$\sigma(A_h)$	$\sigma(H_h)$	$\sigma(L_h)$
1	18	18	18
2	114	114	114
3	717	717	726
4	4509	4518	4626
5	28353	28452	29478
6	178284	179211	187842
7	1121049	1128726	1196982
8	7049148	7109214	7627506
9	44324988	44776653	48604614
10	278715117	282021786	309722274
11	1752558843	1776287928	1973637462

recurrence relations

$$\sigma(L_{h+2}) = 7\sigma(L_{h+1}) - 4\sigma(L_h) \tag{11}$$

$$\sigma(A_{h+3}) = 7\sigma(A_{h+2}) - 4\sigma(A_{h+1}) - 3\sigma(A_h)$$

$$\sigma(H_{h+5}) = 7\sigma(H_{h+4}) - 4\sigma(H_{h+3}) - 15\sigma(H_{h+2}) + 75\sigma(H_{h+1}) + 18\sigma(H_h)$$

which hold for $h \geqslant 0$ and where $\sigma(L_0) = \sigma(A_0) = \sigma(H_0) = 3$.

A noteworthy correlation is found between the Merrifield-Simmons index (= number of sets of independent vertices) and the Hosoya index (= number of sets of independent edges).[14,32] These results will be reported elsewhere.

Note. This paper is part 76 of the series "Topological Properties of Benzenoip Systems". Part 75 is : I. Gutman, J. W. Kennedy and L. V. Quintas, *Chem. Phys. Letters*, **173**. 403 (1990). Parts 2, 9, 24, 47, 49, 50, 52, 60 and 70 are the present references 12, 41, 43, 17, 21, 26, 47, 28 and 45.

REFERENCES

[1] A. T. Balaban and F. Harary, *Tetrahedron*, **24**, 2505 (1968).

[2] A. T. Balaban, *Tetrahedron*, **25**, 2949 (1969).

[3] I. Gutman and S. J. Cyvin, "Introduction to the Theory of Benzenoid Hydrocarbons", Springer-Verlag, Berlin, 1989.

[4] I. Gutman and S. J. Cyvin (Eds.), "Advances in the Theory of Benzenoid Hydrocarbons" (Topics Curr. Chem., **153**), Springer-Verlag, Berlin, 1990.

[5] A. T. Balaban, *Pure Appl. Chem.*, **52**, 1409 (1980).

[6] A.T. Balaban, *Pure Appl. Chem* , **54**, 1075 (1982).

[7] A. T.Balaban, *J. Mol. Struct. (Theochem)*, **120**, 117 (1985).

[8] A. T. Balaban, *J. Chem. Inf. Comput. Sci.*, **25**, 334 (1985).

[9] A. T. Balaban, *Rev. Roumaine Chim.*, **15**, 1243 (1970).

[10] A. T. Balaban, *Rev. Roumaine Chim.*, **15**, 1251 (1970).

[11] A. T. Balaban, *Rev. Roumaine Chim.*, **22**, 45 (1977).

[12] I. Gutman, *Theor. Chim. Acta*, **45**, 309 (1977).

[13] A. T. Balaban and I. Tomescu, *Math. Chem.*, **14**, 155 (1983).

[14] H. Hosoya and N. Ohkami, *J. Comput. Chem.*, **4**, 585 (1983).

[15] S. El-Basil, *Theor. Chim. Acta*, **65**, 199 (1984).

[16] A. T. Balaban and I. Tomescu, *Math. Chem.*, **17**, 91 (1985).

[17] I. Gutman and O. E. Polansky, *Math. Chem.*, **20**, 115 (1986).

[18] S. El-Basil, *J. Chem. Soc. Faraday Trans. II*, **82**, 299 (1986).

[19] S. El-Basil, *J. Math. Chem.*, **1**, 153 (1987).

[20] D. J. Klein, T. Živković and N. Trinajstić, *J. Math. Chem.*, **1**, 309 (1987).

[21] I. Gutman, *Chem. Phys. Letters*, **136**, 134 (1987).

[22] A· T. Balaban, C. Artemi and I. Tomescu, *Math. Chem.*, **22**, 77 (1987).

[23] A. T. Balaban and I. Tomescu, *Discrete Appl. Math.*, **19**, 5 (1988).

[24] A. T. Balaban, J. Brunvoll, B. N. Cyvin and S. J. Cyvin, *Tetrahedron*, **44**, 221 (1988).

[25] D. J. Klein T. G. Schmalz, S. El-Basil, M. Randić and N. Trinajstić, *J. Mol. Struct. (Theochem)*, **179**, 99 (1988).

[26] I. Gutman and S. J. Cyvin, *Chem. Phys. Letters*, **147**, 121 (1988).

[27] S. El-Basil and M. Radnić, *J. Chem. Soc. Faraday Trans. II*, **84**, 1875 (1988).

[28] I. Gutman and S. J. Cyvin, *Bull. Chem. Soc. Japan*, **62**, 1250 (1989).

[29] J. Brunvoll, I. Gutman and S. J. Cyvin, *Z. Phys. Chem. (Leipzig)*, **270**, 982 (1989).

[30] D. Aboav and I. Gutman, *J. Serb. Chem. Soc.*, **54**, 249 (1989).

[31] O. E. Polansky, M. Radnić and H. Hosoya, *Math. Chem.*, **24**, 3 (1989).

[32] M. Randić, H. Hosoya and O. E. Polansky, *J. Comput. Chem.*, **10**, 683 (1989).

[33] J. Brunvol, R. Tošić, M. Kovačević, A. T. Balaban, I. Gutman and S. J. Cyvin, *Rev. Roumaine Chim.*, **35**, 85 (1990).

[34] H. E. Simmons and R. E. Merrifield, *Proc. Natl. Acad. Sci. USA*, **74**, 2616 (1977).

[35] R. E. Merrifield and H. E. Simmons, *Theor. Chim. Acta*, **55**, 55 (1980).

[36] R. E. Merrifield and H. E. Simmons, *Proc. Natl. Acad. Sci. USA*, **78**, 692 (1981).

[37] R. E. Merrifield and H. E. Simmons, *Proc. Natl. Acad. Sci. USA*, **78**, 1329 (1981).

[38] R. E. Merrifield and H. E. Simmons, *Proc. Natl. Acad. Sci. Usa*, **82**, 1 (1985).

[39] R. E. Merrifield and H. E. Simmons, "Topological Methods in Chemistry", Wiley, New York, 1989.

[40] A. Motoyama and H. Hosoya, *J. Math. Phys.*, **18**, 1485 (1977).

[41] I. Gutman, *Z. Naturforsch.*, **37a**, 69 (1982).

[42] I. Gutman and F. Harary, *Utilitas Math.*, **24**, 97 (1983).

[43] I. Gutman and S. El-Basić, *Z. Naturforsch.*, **39a**, 276 (1984).

[44] K. Balasubramanian and R. Ramaraj, *J. Comput. Chem.*, **6**, 446 (1985).

[45] I. Gutman and N. Kolaković, *Bull. Serb. Acad. Sci. Arts*, in press.

[46] D. H. Rouvray, *J. Comput. Chem.*, **8**, 470 (1987).

[47] I. Gutman, S. Marković, D. Luković, V. Radivojević and S. Rančić, *Coll. Sci. Papers Fac. Sci. Kragujevac*, **8**, 15 (1987).

Revue Roumaine de Chimie, 36, 4–7, 389–398 (1991)

Dedicated to Academician Professor Dr. ALEXANDRU T. BALABAN
on the occasion of his 60th birthday.
This is a fitting opportunity to thank him
for his kind help and encouragement
over the years.

A QSAR STUDY OF ANTIDOTAL ACTIVITY OF H-OXIMES

MILAN IVANUŠEVIĆ [a], SONJA NIKOLIĆ [b] and NENAD TRINAJSTIĆ [b]

[a] High Military Technical Schools, 41125 Zagreb, The Republic of Croatia, Yugoslavia

[b] The Rugjer Bošković Institute, 41001 Zagreb, The Republic of Croatia, Yugoslavia

> " 'Mr. Mayor,' says I, 'there is only one hope for you. Drugs will do you no good. But there is another power higher yet although drugs are high enough", says I.'
>
> " 'And what is that?' says he."
>
> " 'Scientific demonstrations,' says I...,
>
> O. Henry: "Jeff Peters as a Personal Magnet"[1]

Received January 4, 1991

Non-empirical QSAR models for antidotal activity of H-oximes are proposed. These models are based, respectively, on the zero $({}^0\chi^v)$, first-$({}^1\chi^v)$ and second-order $({}^2\chi^v)$ connectivity indices. All these three models exhibited excellent statistical characteristics. However, the model based on ${}^0\chi^v$ possesses slightly better characteristics than the other two models. Since ${}^0\chi^v$ linearly correlates with the number of atoms in a series of related molecules (which also represent a good measure of a molecular size), the corresponding model indicates that the size of H-oximes may be in the main responsible for their antisoman activities. Apparently, an optimum size of an H-oxime is needed to reactivate most efficiently the inhibited enzyme.

INTRODUCTION

Poisoning with organophosphorus compounds can be efficiently treated by means of mono- and bis-pyridinium oximes.[2] The therapeutic activity of these oximes is based on their ability to reactivate acetylcholinesterase inhibited by organophosphates.[3] A number of oximes, such as PAM-2 Cl (2-hydroxyiminomethyl-1-methylpyridinium chloride), TMB-4-(4-hydroxiiminomethyl-1-[3-(4-hydroxiiminomethyl(-1-pyridinio)propyl] dibromide) and toxogonin (4-hydroxiiminomethyl-1-[3-hydroxiiminomethyl

(-1-pyridinio)-2-oxapropyl]pyridinium dichloride), give a good protection against the action of anti-cholinesterase compounds because they can renew the activity of the inhibited enzyme by reactivation.[4] However, the very basic defect of these oximes is their slow or very weak action on CNS.[5] In addition, these oximes cannot efficiently reactivate enzymes inhibited by soman (1,1,2-trimethylpropylmethylphosphonofluoridate).[6]

In 1970 Oldiges and Schoene [7] discovered that some toxogonin-related compounds, used with atropine, protected mice against soman. Efforts to discover compounds with anti-soman activity led to preparation and antidotal testing of the class of compounds known in literature as H-oximes.[8]

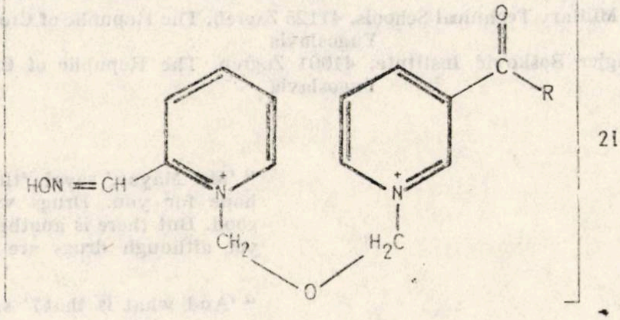

Fig. 1. — Diagram of studied H-oximes.

This work represents an attempt to establish a QSAR model of antidotal activity of H-oximes using topological (graph-theoretical) indices.[9–11]* Our strategy of building QSAR models with topological indices is detailed elsewhere.[18] We have considered 16 H-oximes whose basic structure is depicted in Fig. 1.

The codes and chemical names of these oximes are given in Table 1.

Experimental data on their antidotal activity (mean effective dose or ED_{50} value in $mol/kg \cdot 10^5$) against soman is taken from Gross.[8]

Mean effective dose or ED_{50} value is determined by the quantity of an antidote at which survives 50% of test animals poisoned with soman. The antidote is applied together with atropine (10 mg/kg) one minute after the poisoning of the test animal. Effective dose ED_{50} is based on the number of dead animals 24 hours after administering the antidote. In practice the antidote is more efficacious if the value of ED_{50} is smaller.

As the structural descriptors will be employed the valence—connectivity indices.[19–21]

This article is structured in the following way. In the next section we describe the valence—connectivity indices that will be used in this work. The third section contains results and discussion. We end the article with our concluding remarks.

---

* In this area of chemical applications of graph theory Academician Professor A. T. Balaban is one of the most creative and important contributors heretofore, e. g.[12–17]

Table 1

Codes and chemical names of studied H-oximes

No.	Code	Chemical Name
1	HGG 21	3-acetyl-1-[3-(2-hydroxyiminomethyl-1-pyridinio)-2-oxapropy] pyridinium diiodide
2	HGG 73	3-propionyl-1-[3-(2-hydroxyiminomethyl-1-pyridinio-2-oxapropyl] pyridinium diiodide
3	HGG 58	3-butyryl-1-[3-(2-hydroxyiminomethyl-1-pyridinio)-2-oxapropyl] pyridinium diiodide
4	HGG 101	3-isobutyryl-1-[3-(2-hydroxyiminomethyl-1-pyridinio)-2-oxapropyl] pyridinium diiodide
5	HGG 60	3-valeryl-1-[3-(2-hydroxyiminomethyl-1-pyridinio)-2-oxapropyl] pyridinium diiodide
6	HGG 52	3-isovarelyl-1-[3-(2-hydroxyiminomethyl-1-pyridinio)-2-oxapropyl] pyridinium diiodide
7	HGG 32	3-pivaloyl-1-[3-(2-hydroxyiminomethyl-1-pyridinio)-2-oxapropyl] pyridinium diiodide
8	HGG 69	3-hexanoyl-1-[3-(2-hydroxyiminomethyl-1-pyridinio)-2-oxapropyl] pyridinium diiodide
9	HGG 70	3-heptanoyl-1-[3-(2-hydroxyiminomethyl-1-pyridiniol)-2-oxapropyl] pyridinium diiodide
10	HGG 42	3-cyclohexylcarbonyl-1-[3-(2-hydroxyiminomethyl-1-pyridinio)-2-oxapropyl] pyridinium diiodide
11	HGG 93	3-octanoyl-1-[3-(2-hydroxyiminomethyl-1-pyridinio)-2-oxapropyl] pyridinium diiodide
12	HGG 82	3-nonanoyl-1-[3-(2-hydroxyiminomethyl-1-pyridinio)-2-oxapropyl] pyridinium diiodide
13	HGG 81	3-undecanoyl-1-[3-(2-hydroxyiminomethyl-1-pyridinio)-2-oxapropyl] pyridinium diiodide
14	HGG 77	3-isonitrosoacetyl-1-[3-(2-hydroxyiminomethyl-1-pyridinio)-2-oxapropyl] pyridinium diiodide
15	HGG 54	3-benzylcarbonyl-1-[3-(2-hydroxyiminomethyl-1-pyridinio)-2-oxapropyl] pyridinium diiodide
16	HGG 47	3-cinnamoyl-1-[3-(2-hydroxyiminomethyl-1-pyridinio)-2-oxapropyl] pyridinium diiodide

THE VALENCE-CONNECTIVITY INDICES

We will consider three valence—connectivity indices (χ^v) in this work. These are the zero-order, ($^0\chi^v$), the first-order ($^0\chi^v$) and the second-order ($^2\chi^v$) valence—connectivity indices. They are defined as follows.

(a) The zero-order valence — connectivity index

$$^0\chi^v = \sum_i (\delta_i^v)^{-0.5} \tag{1}$$

where δ_{ii}^v is the valence delta value of atom i and the summation is over all (weighted) non-hydrogen atoms in a molecule. The valence delta value of atom i δ_i^v is defined as

$$\delta_i^v = (Z_i^v - H)_i/(Z_i - Z_i^v - 1) \tag{2}$$

where Z is the atomic number, Z^v the number of valence electrons of atom i and H_i the number of hydrogen atoms attached to atom i.

(b) The first-order valence connectivity index

$$^1\chi^v = \sum (\delta_i^v \cdot \delta_j^v)^{-0.5} \tag{3}$$

where δ_i^v and δ_j^v are the valence delta values of atoms i and j making up the bond i — j. Therefore, the term $(\delta_i^v \cdot \delta_j^v)^{-0.5}$ represents the weight of the bond i — j. The summation in (3) is over all (weighted) bonds in a molecule.

(c) The second-order valence — connectivity index

$$^2\chi^v = \sum_{(i,j,k)} (\delta_i^v \cdot \delta_j^v \cdot \delta_k^v)^{-0.5} \tag{4}$$

where δ_i^v, δ_j^v and δ_k^v are the valence delta values of atoms i, j and k making up the path of length two i — j — k. The summation in (4) is over all (weighted) paths of length two in a molecule.

The studied H-oximes contain the following set of non-hydrogen atoms : C, N and O. Their valence delta values are given in Table 2.

Table 2

Valence delta values δ^v for carbon, nitrogen and oxygen in a given environment [a,b]

Atom	δ^v
$-CH_3$	1
CH_2	2
$=CH$	3
$=C<$	4
$=\overset{+}{N}=$	6
$=N-$	5
$-O-H$	5
$-O-$	6
$=O$	6

[a] L. B. Kier and L. H. Hall, *J. Pharm. Sci.*, **65**, 1806 (1976).

[b] L. B. Kier and L. H. Hall, "Molecular Connectivity in Structure Activity Analysis", Wiley, New York, 1986, p. 17.

In Table 3 we give as an illustrative example the calculations of $^{0}\chi^{v}$, $^{1}\chi^{v}$ and $^{2}\chi^{v}$ for HGG-58.

Table 3

The computations of $^{0}\chi^{v}$, $^{2}\chi^{v}$ and $^{2}\chi^{v}$ for HGG 58

(a) Skeleton of HGG 58 with valence delta values

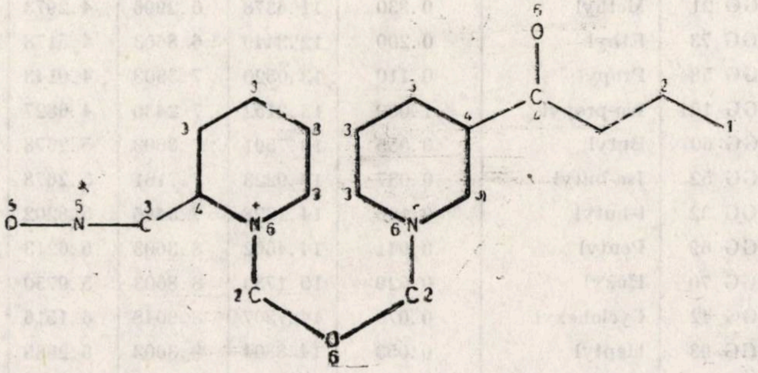

(b) Computation of $^{0}\chi^{v}$

$$^{0}\chi^{v} = 1 + 4\,(2)^{-0.5} + 9\,(3)^{-0.5} + 3\,(4)^{-0.5} + 2\,(5)^{-0.5} + 4\,(6)^{-0.5} = 13.0520$$

(c) Computation of $^{1}\chi^{v}$

$$^{0}\chi^{v} = (1 \cdot 2)^{-0.5} + (2 \cdot 2)^{-0.5} + (2 \cdot 4)^{-0.5} + 4\,(2 \cdot 6)^{-0.5} + 5\,(3 \cdot 4)^{-0.5} + 4\,(3 \cdot 4)^{-0.5} + (3 \cdot 5)^{-0.5} + 3\,(3 \cdot 6)^{-0.5} + (4 \cdot 4)^{-0.5} + 2\,(4 \cdot 6)^{-0.5} + (5 \cdot 5)^{-0.5} = 7.3603$$

(d) Computation of $^{2}\chi^{v}$

$$^{2}\chi^{v} = (1 \cdot 2 \cdot 2)^{-0.5} + (2 \cdot 2 \cdot 4)^{-0.5} + (2 \cdot 4 \cdot 4)^{-0.5} + (2 \cdot 4 \cdot 6)^{-0.5} + (2 \cdot 6 \cdot 2)^{-0.5} + 3\,(2 \cdot 6 \cdot 3)^{-0.5} + (2 \cdot 6 \cdot 4)^{-0.5} + 3\,(3 \cdot 3 \cdot 3) + 2\,(3 \cdot 3 \cdot 4) + 2\,(3 \cdot 3 \cdot 6)^{-0.5} + 2\,(3 \cdot 4 \cdot 3)^{-0.5} + 2\,(3 \cdot 4 \cdot 4)^{-0.5} + 2\,(3 \cdot 4 \cdot 6)^{-0.5} + (3 \cdot 5 \cdot 5)^{-0.5} + (3 \cdot 6 \cdot 3)^{-0.5} + (3 \cdot 6 \cdot 4)^{-0.5} + (4 \cdot 3 \cdot 5)^{-0.5} + (4 \cdot 3 \cdot 6)^{-0.5} + (4 \cdot 4 \cdot 6)^{-0.5} + 2\,(6 \cdot 2 \cdot 6)^{-0.5} = 4.9143$$

RESULTS AND DISCUSSION

In Table 4 are given the zero-order, first-order and second-order valence connectivity indices for 16 H-oximes and their experimental and calculated antisoman activities expressed as $(ED_{50})_{exp}$ and $(ED_{50})_{calc}$ respectively.

We have investigated several non-linear relationships betwen the three topological indices (TI = $^{0}\chi^{v}$, $^{1}\chi^{v}$, $^{2}\chi^{v}$) and the antisoman activities of H-oximes, such as exponential, logarithmic, quadratic, parabolic and higher-order polynomials. The best statistical characteristics were obtained

Table 4

Studied H-oximes with their experimental and calculated antisoman activities expressed as $(ED_{50})_{exp}$ and $(ED_{50})_{calc}$ and the zero-order, first-order and second-order valence connectivity indices

No.	H-oxime	R	$(ED_{50})_{exp}$	${}^0\chi^v$	${}^1\chi^v$	${}^2\chi^v$	$(ED_{50})_{calc}$[a]
1	HGG 21	Methyl	0.830	11.6378	6.2996	4.2973	0.839
2	HGG 73	Ethyl	0.200	12.3449	6.8603	4.5178	0.176
3	HGG 58	Propyl	0.110	13.0520	7.3603	4.9143	0.137
4	HGG 101	Iso-propyl	1.000	13.2152	7.2430	4.6827	1.079
5	HGG 60	Butyl	0.055	13.7591	7.8603	5.2678	0.103
6	HGG 52	Iso-butyl	0.037	13.9223	7.7161	5.2678	0.096
7	HGG 32	t-butyl	0.120	14.1378	7.5496	5.8202	0.087
8	HGG 69	Pentyl	0.041	14.4662	8.3603	5.6213	0.072
9	HGG 70	Hexyl	0.029	15.1733	8.8603	5.9750	0.044
10	HGG 42	Cyclohexyl	0.075	14.7507	8.9048	6.1516	0.061
11	HGG 93	Heptyl	0.053	14.8804	9.3603	6.2985	0.056
12	HGG 82	Octyl	1.500	16.5875	9.8603	6.6820	1.417
13	HGG 81	Decyl	1.500	18.0018	11.3603	7.2992	1.529
14	HGG 77	Hydroxyimino-methyl	0.062	14.7317	8.4174	5.6599	0.062
15	HGG 54	Benzyl	0.290	12.1096	6.5465	4.3500	0.192
16	HGG 47	Styryl	0.046	15.1793	8.6210	5.6827	0.046

[a] $(ED_{50})_{calc} = \pm\ [2p[{}^0\chi^v - 10.5)]^{0.5} + 0.4$
$(+)\ p = 0.085$ for $ED_{50} \geqslant 0.4$
$(-)\ p = 0.0135$ for $ED_{50} \leqslant 0.4$

for a parabolic-like model :

$$(ED_{50})_{calc} = \pm\ [2p(TI - X_0)]^{0.5} + Y_0 \qquad (1)$$

where the positive (negative) value of the parameter p is used when $ED_{50} \geqslant Y_0$ $(ED_{50}) \leqslant Y_0)$. Depending on the TI employed, the following three models have been established :

(i)
$$(ED_{50})_{calc} = \pm\ [2p({}^0\chi^v - 10.5)]^{0.5} + 0.4 \qquad (2)$$
$$(+)\ p = 0.085 \text{ for } (ED_{50} \geqslant 0.4$$
$$(-)\ p = 0.0135 \text{ for } ED_{50} \leqslant 0.4$$

(ii)
$$(ED_{50})_{calc} = \pm\ [2p({}^1\chi^v - 5.5)]^{0.5} + 0.35 \qquad (3)$$
$$(+)\ p = 0.0125 \text{ for } ED_{50} \geqslant 0.35$$
$$(-)\ p = 0.125 \text{ for } ED_{50} \leqslant 0.35$$

(iii) $$(ED_{50})_{calc} = \pm [2p(^1\chi^v - 4)]^{0.5} + 0.5 \qquad (4)$$

$$(+)\ p = 0.17 \quad \text{for } ED_{50} \geqslant 0.5$$

$$(-)\ p = 0.052 \quad \text{for } ED_{50} \leqslant 0.5$$

As an example we give in Fig. 2 a plot of $(ED_{50})_{exp}$ vs. $^0\chi^v$.

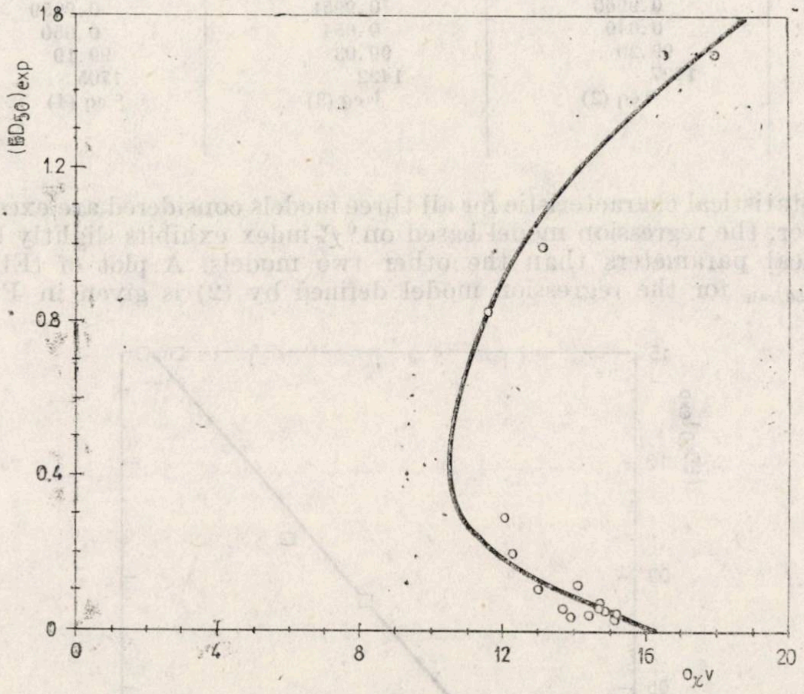

Fig. 2. — A plot of $(ED_{50})_{exp}$ vs. $^0\chi^v$ for studied H-oximes.

In this figure is clearly seen a parabolic-like relationship between the antisoman activities of H-oximes and the corresponding $^0\chi^v$ values. Since their parabolic relationship is asymmetric, the parameter p appears in the model with two different values depending on the part of a parabola considered. The threshold value of p in this model is equal to Y_0 when $TI = X_0$ (see eq. (1)).

A comparison between $(ED_{50})_{exp}$ and three sets of $(ED_{50})_{calc}$ via a linear regression :

$$(ED_{50})_{exp} = A(ED_{50})_{calc} + B \qquad (5)$$

is given in Table 5.

Table 5

A comparison between the $(ED_{50})_{exp}$ and $(ED_{50})_{calc}$ obtained by three models

	Model I[a]	Model II[b]	Model III[c]
n	16	16	16
A	1.0015 (±0.0241)	1.0037 (±0.0266)	1.0108 (±0.0245)
B	0.00326 (±0.0005)	0.00432 (±0.00007)	0.02027 (±0.00031)
r	0.9960	0.9951	0.9959
SD	0.049	0.054	0.050
EV	99.20	99.03	99.19
F	1727	1422	1705
	[a] eq (2)	[b] eq (3)	[c] eq (4)

Statistical characteristic for all three models considered are excellent. However, the regression model based on $^0\chi^v$-index exhibits slightly better statistical parameters than the other two models. A plot of $(ED_{50})_{exp}$ vs $(ED_{50})_{calc}$ for the regression model defined by (2) is given in Fig. 3.

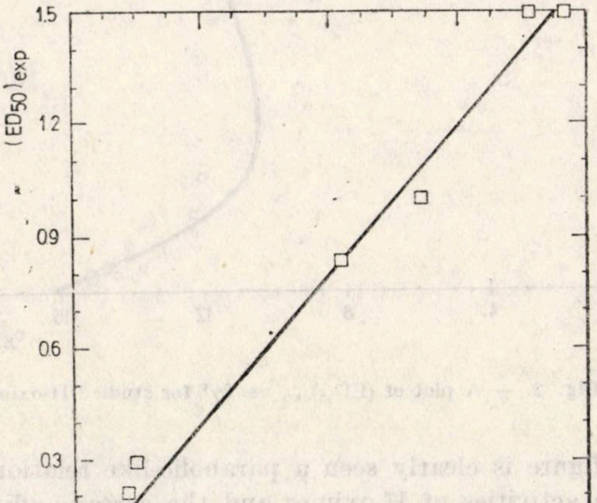

Fig. 3. — A plot of $(ED_{50})_{exp}$ vs $(ED_{50})_{calc}$ by means of the model based on $^0\chi^v$ index.

Since, all three models are close in their statistical characteristics the above results point to the fact that all three valence connectivity indices ($^0\chi^v$, $^1\chi^v$ and $^2\chi^v$) serve well as descriptors for the structures of H-oximes.

In the case of H-oximes the substituent R (see Fig. 1) has a considerable effect on the antidotal activity of a compound as well as on its toxicity. It should be noted that each antidote besides acting as a drug against a poison is also a toxic material.[7] It has been established [8] when **R** is an aliphatic chain, the increase of its length up to hexyl increases also the efficacity of antidotal activity of H-oximes. However, further increase in the length of the aliphatic chain decreases the antidotal activity which becomes undetectable when R = undecyl. This observation is probably related to the requiremend for the optimum structure of H-oximes in order to maximise the interaction with the receptor which might possess several active centres. In addition, the increase in the size of a molecule may hinder its transport in the biological system. This hindrance due to size, for example, affects the pharmacological action of a molecule because of its slow penetration through the blood-brain barrier.[22,23]

A weak point of a QSAR model formulated as (2) (as well as of models (3) and (4)) is that it predicts two values of ED_{50} for each new H-oxime considered. Thus ambiguity can, of course, be resolved only after testing the antidotal activity of a drug. However, the structural characteristics of a new compound may also help to decide which of the two predicted ED_{50} values is the "true " value. For example, the length of the side chain may help in this respect. Nevertheless, even if two ED_{50} values are predicted for each new compound, this information may still be valuable for the experimentator in a sense if neither of the two ED_{50} values are close to optimum ED_{50}, then the experimental work on such a compound should be discarded. On the other hand, if one of the two ED_{50} values is in a high range, then the preliminary experimental work (preparation and biotesting) must be done before discarding or further experimenting (to establish for example the toxic effects) with such a compound.

CONCLUDING REMARKS

A QSAR model of antidotal activity of H-oximes based on the zero-order valence connectivity index, is proposed. This model accounts for the structural changes in the side chain of the H-oximes and defines their structure — antidotal activity with high statistical characteristics. The proposed model may serve as a guide for the rational selection of different R-substituents (even containing heteroatoms) and preparation of novel compounds with enhanced antidotal activities. The work in this direction is in progress.

REFERENCES

1 "Complete Works by O. Henry", Doubleday, Gordon City, NY, 1953, p. 272.

2 R. I. Ellin and J. H. Wills, *J. Pharm. Sci.*, 53, 995 (1964).

3 L. P. A. de Jong and G. Z. Wolring, *Biochem. Chem.*, 29, 2379 (1980).

4 Z. Binenfeld, V. Deljac, M. Knežević, Lj. Pavlov, M. Maksimović, V. Markov, Lj. Radović and D. Rakin, *Acta Pharm. Jugosl.*, **31**, 5 (1981).

5 W. D. Erdman, in "Medical Protection Against Chemical Warfare Agents," SIPRI, Stockholm, 1976, p. 46.

[6] B. Bošković, *Fund. Appl. Toxicol.*, **1**, 203 (1981).

[7] H. Oldiges and K. Schoene, *Arch. Toxicol.*, **26**, 293 (1970).

[8] G. Gross, Entwicklugnen von Hochwirksamen gegenmitteln bei Vergiftungen mit toxischen Phosphonosaureestern, Ph. D. Thesis, Freiburg, 1980, p. 61.

[9] A. T. Balaban, A. Chiriac, I. Motoc and Z. Simon, "Steric Fit in QSAR", Lecture Notes in Chemistry, Vol. 15, Springer — Verlag, Berlin, 1980.

[10] A. Sabljić and N. Trinajstić, *Acta Pharm. Jugosl.*, **31**, 189 (1981).

[11] A. T. Balaban, I. Motoc, D. Bonchev and O. Mekenyan, *Topics. Curr. Chem.*, **114**, 21 (1983).

[12] A. T. Balaban, *Chem. Phys. Lett.*, **89**, 399 (1982).

[13] A. T. Balaban, *J. Mol. Struct. (Theochem)*, **120**, 117 (1985).

[14] A. T. Balaban, *J. Chem. Inf. Comput. Sci.*, **25**, 334 (1985).

[15] P. A. Filip, T.- S. Balaban and A. T. Balaban, *J. Math. Chem.*, **1**, 61 (1987).

[16] O. Mekenyan, D. Bonchev and A. T. Balaban, *J. Comput. Chem.*, **2**, 347 (1988).

[17] A. T. Balaban and O. Ivanciuc, in MATH/CHEM/COMP, 1988, A. Graovac, ed., Elsevier, Amsterdam, 1989, p. 193.

[18] N. Trinajstić, S. Nikolić and S. Carter, *Kem. Ind. (Zagreb)*, **38**, 469 (1989).

[19] M. Randić, *J. Amer. Chem. Soc.*, **97**, 6609 (1975).

[20] L. B. Kier and L. H. Hall, *J. Pharm. Sci.*, **65**, 1806 (1976).

[21] L. B. Kier and L. H. Hall, "Molecular Connectivity in Chemistry and Drug Research," Academic, New York, 1976.

[22] D. Pantelić and M. Maksimović, *Acta Pharm. Jugosl.*, **32**, 119 (1982).

[23] O. Wolthuis, R. A. P. Vanwersch and H. J. Van der Wiel, *Europ. J. Pharm.*, **70**, 355 (1981)

Revue Roumaine de Chimie, **36**, *4–7*, 399–410 (1991)

Dedicated to Professor A. T. BALABAN
on the occasion of his 60th birthday

THE EFFECT OF MOLECULAR TOPOLOGY ON π-MOLECULAR ORBITAL ENERGIES OF PYRIDAZINE, PYRIMIDINE, AND PYRAZINE TOPOMER TRIPLE

IOAN MOŢOC [a] and OSKAR E. POLANSKY [b]

[a] Bristol-Myers Squibb Co., Pharmaceutical Research Institute Princeton,
NJ 08543–4000, USA
[b] Max Planck Institute for Radiation Chemistry
D-4330 Muelheim a.d. Ruhr, FRG

Received February 1, 1991

Ab initio **molecular orbital calculations using various basis sets were performed for topologically related isomers (topomer triple) pyridazine (S_1), pyrimidine (S_2), and pyrazine (T). The SCFπ-MO eigenvalue patterns of S_2 and T are in complete agreement with the topological-effect-on-molecular-orbitals (TEMO) theorem, thus demonstrating the dominant influence of molecular topology on π-MO energies. A general perturbational procedure to relate computationally electronic and topological factors in SCF MO calculations was developed and used to trace the origin of the deviations from TEMO exhibited by the S_1 and T topomer pair.**

1. INTRODUCTION

The constitutional formula of a chemical compound indicates the types of constituent atoms and the pattern of chemical bonds existing among them. The topology of a molecule is delineated [1,2] by the constitutional formula and the latter is represented by simple molecular graphs. Thus, the molecular topology is rigorously defined [2,3] by the neighbourhood topology in the vertex set of the molecular graph. The vertex set together with its neighborhood topology constitutes a molecular topological space.

Two isomers with different constitutions are called topologically related if their respective topological spaces can be divided into two or more subspaces such that they are pairwise isomorphic.[4] Topological related isomers are called topomers.

The manner in which a pair of topomers can be constructed is called a topological model. Such a model is characterized by the number of subspaces used and the specifications by which these subspaces are connected among them.[5] In this paper two topological models are explicitely considered but properties of topomers pertaining to other topological models are used in discussing the *ab initio* results — for an in depth analysis of various topological models the reader is referred to refs. 5 and 8.

In the case of pyridazine and pyrazine, one uses two bivalent isomorphic topological spaces $A \simeq B =$ aza-allyl, with the topologically equivalent centers of residual valences a and b rendered inequivalent

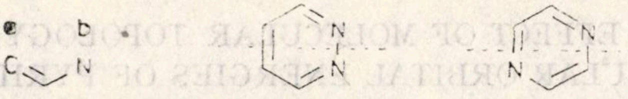

Fig. 1. — S_1 (pyridazine) and T (pyrazine) topomers.

by the distinct chemical nature of their corresponding atoms, i.e., N and C (Fig. 1). Pyridazine (S_1 topomer) is obtained by linking a with a, and b with b. Pyrazine (T topomer) is obtained by linking a with b, and b with a, respectively.

In the case of pyrimidine and pyrazine, three topological spaces are used : $A \simeq B =$ aza-ethenyl and $C =$ two disconnected CH groups

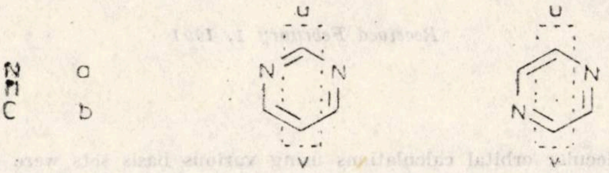

Fig. 2. — S_2 (pyrimidine) and T (pyrazine) topomers ; partial structure C is delineated by dotted lines.

(Fig. 2). Pyrimidine (S_2 topomer) contains the bond sequences a—u—a and b—v—b, while pyrazine (T topomer) corresponds to a—u—b and b—v—a sequences, respectively.

It was shown [6,7] that the zeros of the characteristic polynomials of an S and T pair ($x_j(A)$, $j = 1, 2, 3, \dots$ and $A = S$ or T) necessarily satisfy the interlacing rule (1),

$$\begin{gathered} x_1(S) \geqslant x_1(T) \geqslant x_2(T) \geqslant x_2(S) \geqslant \dots \geqslant x_{2j-1}(S) \geqslant \\ x_{2j-1}(T) \geqslant x_{2j}(T) \geqslant x_{2j}(S) \geqslant \dots \end{gathered} \tag{1}$$

For planar fully conjugated molecules, pattern (1) should be identified with the Hückel molecular orbital (HMO) energy levels (β units).

The interlacing (1) is obtained purely from topology and has been termed [4] topological effect on molecular orbitals (TEMO). It is noteworthy that by virtue of TEMO and the fact that S_1 and S_2 are related to the same T topomer, HMO patterns of this topomer triple should satisfy the interlacing rule (2),

$$\begin{gathered} \left.\begin{matrix} x_1(S_1) \\ x_1(S_2) \end{matrix}\right\} \geqslant x_1(T) \geqslant x_2(T) \geqslant \left\{\begin{matrix} x_2(S_1) \geqslant x_3(S_1) \\ x_2(S_2) \geqslant x_3(S_2) \end{matrix}\right\} \geqslant x_3(T) \geqslant x_4(T) \\ \geqslant \left\{\begin{matrix} x_4(S_1) \geqslant x_5(S_1) \\ x_4(S_2) \geqslant x_5(S_2) \end{matrix}\right\} \geqslant x_5(T) \geqslant x_6(T) \geqslant \left\{\begin{matrix} x_6(S_1) \\ x_6(S_2) \end{matrix}\right. \end{gathered} \tag{2}$$

The competition between topological and electronic factors in conditioning the eigenvalues patterns of pyridazine, pyrimidine and pyrazine can be investigated by *ab initio* SCF MO calculations. This approach is effective because the non-empirical SCF Hamiltonian matrix, in contrast to the topological one, considers all interactions among atoms without any restriction as to their equality. Further, as the three isomers are planar molecules, the eigenvectors of the σ- and π-MO's are decoupled, hence, one can rigorously treat the latter separately. Satisfaction of (2) argues for the dominance of topological factors, while deviations from TMO patterns may be traced to competing electronic factors.

2. DIAZINE TOPOMER TRIPLE : *AB INITIO* CALCULATIONS

Restricted Hartree-Fock calculations[9] using STO-3G, STO 4-31G, STO 6-31G, STO 6-13G*, and STO 6-31G** basis sets[10] were carried out for the three diazines retaining the electron diffraction geometries[11] of the three molecules. Tables 1—5 systematize the results.

Table 1

The π-MO eigenvalues (a.u.) of diazines : STO-3G basis

S_1	x^{I}_{i}	T	x^{I}_{i}	S_2
				−0.533779
		0.532547		
−0.531234				
	−0.505148			
		0.370204		
−0.347467				−0.362264
−0.339818				−0.335089
		0.322546		
	−0.261851			
0.214328				
		0.217117		
				0.220402
			0.227080	
		0.229832		
0.231243				0.231067
0.459924			0.339646	
		0.465042		
				0.468215
E_T-259.353775		−259.380090		−259.382749

Examination of Tables 1—5 indicates that most of the deviations from TEMO exhibited by the STO-3G π-MO spectra are due to insufficient flexibility of this basis set. Further, the eigenvalue spectra interlacing corresponding to S_2 and T pair is in complete agreement with TEMO, while S_1 and T pair exhibit only one persistent and stably located inversion of TEMO pattern (the inversion occurs in the region of virtual orbitals

Table 2

The π-MO eigenvalues (a.u.) of diazines: STO 4-31G basis

S_1	x^I_i	T	x^I_i	S_2
−0.586235				−0.588476
		−0.583771		
		−0.437990		
−0.407546				−0.427821
−0.395918				−0.387956
		−0.372412		
		0.094054		
0.095257				0.102502
0.117602				0.119920
		0.121434		
	0.189768			
0.331830				
		0.337088		
				0.338023
E_T-262.239435		−262.276478		−262.282931

Table 3

The π-MO eigenvalues (a.u.) of diazines: STO 6-31G

S_1	x^I_i	T	x^I_i	S_2
− 0.587025				0.589533
		0.584761		
		0.439143		
0.408286				−0.428926
0.397029				−0.389207
		0.373521		
		0.090465		
0.091518				0.098609
0.113674				0.115797
		0.117289		
	0.184658			
0.325701				
		0.330652		
				0.331078
E_T-262.519358		−262.555348		−262.561197

at an energy of about 0.19 hatrees; a discussion of TEMO inversions can be found in ref. 2). These results argue that the constraint imposed by molecular topology dominates in the case of S_2 and T, while the persistent TEMO inversion identified in the spectra of S_1 and T indicates that electronic factors compete with topology in determining the actual-interlacing of eigenvalues of this topomer pair.

Table 4

The π-MO eigenvalues (a.u.) of diazines : STO 6-31Gx

S_1	x^{I}_{i}	T	x^{I}_{i}	S_2
0.575670				0.577051
		0.573043		
		0.432294		
0.398675				0.421007
0.384990				0.376205
		0.358660		
		0.095639		
0.098022				0.106271
0.123472				0.126569
		0.128030		
	0.199821			
0.337427				
		0.342076		
				0.343283
E_T-262.644190		−262.681141		−262.690716

Table 5

The π-MO eigenvalues (a.u.) of diazines : STO 6-31Gx.x

S_1	x^{I}_{i}	T	S_2
−0.575462			0.576788
		−0.572777	
		−0.432052	
−0.398533			−0.420777
0.384856			−0.376064
		−0.358556	
0.097835			0.106009
0.122927			0.126117
		0.127417	
	0.199163		
0.335948		0.340648	
			0.342009
E_T-262.651277		−262.688170	−262.697659

3. EFFECTS OF PERTURBATIONS ON TEMO INTERLACING

Comparison of topological and non-empirical Hamiltonian matrices indicates that the actual anisotropy of the SCF tight binding and/or the SCF non-nearest neighbor interactions may represent, in the TEMO context, the relevant electronic factors which may compete with molecular topology in conditioning the actual interlacing of the *ab initio* π-MO energies.

The anisotropy of the tight binding interactions may cause violation of the isomorphism of the subspaces used to construct the topomers. The non-nearest neighbor interactions may picture these subspaces as multivalent. Consequently, the non-empirical matrices may mimic more complex topological models [2,5,8] for which TEMO interlacing is exibited in intervals bounded by successive inversion points.

To reconstitute the "history" of TEMO inversions, we found it advantageous to use a two-step perturbational procedure.[12,13] The zero-order Hamiltonian matrices represent effective one-electron tight-binding Hamiltonians operating on the π-electron functions of S and T, respectively. Their entries are obtained by suitably averaging [13] the appropriate elements of the topomers HF matrices. As this construction procedure maintains the isomorphism of the subspaces used to construct the topomers, TEMO assures that the eigenvalues corresponding to the zero-order matrices necessarily exhibit the interlacing (1).

In the first perturbational step one introduces the actual HF SCF tight-binding interactions, and the second perturbational step accounts for the HF SCF non-nearest neighbor interactions. Use of a modified version [13] of the generalized perturbational-variational Rayleigh-Ritz (PV-RR) procedure [14] permits accurate calculation of all MO eigenvalue perturbational corrections to arbitrarily high order, thus enabling one to monitor in a continuous manner the passage from molecular topology to physics.

As the largest number of TEMO inversions was obtained with the minimal basis set, we selected this case to illustrate our procedure.

For S_1 and T pair, the PV-RR-MO eigenvalue series obtained for the first perturbational step are collected in Table 6.

Table 6

Summation of π-MO PV-RR eigenvalue series (a.u.) through $n = 2$nd order of the first perturbational steps : S_1 and T isomers (STO-3G)

S_1	$n = 0$ T	S_1	$n = 1$ x^{I}_{i}	T	S_1	$n = 2$ x^{I}_{i}	T
0 .574826				−0 .574999			−0 .574991
	−0 .574325	−0 .571188			−0 .572222		
	−0 .324690		−0 .478372			−0 .472987	
−0 .318191				−0 .330091			−0 .330244
−0 .307824		−0 .311522			−0 .314153		
	−0 .301947	−0 .307856			−0 .308867		
	0 .197631			−0 .296605			−0 .296605
0 .202406			−0 .277956			−0 .255406	
0 .214376		0 .199901			0 .202761		
	0 .219731			0 .208706			0 .208706
	0 .469674			0 .209630			0 .209634
0 .470134		0 .212722			0 .214474		
		0 .464920			0 .464981		
				0 .470062			0 .470196

The PV-RR eigenvalue series for the second perturbational step are presented in Table 7.

Table 7

Summation of π-MO PV-RR eigenvalue series (a.u.) through n = 2nd order of the second perturbational steps : S_1 and T isomers (STO-3G)

S_1	n = 0 x^{I}_{i}	T	S_1	n = 1 x^{I}_{i}	T	S_1	n = 2 x^{I}_{i}	T
		-0 .574991			-0 .532523			-0 .532546
-0 .572232			-0 .530975			-0 .531167		
	-0 .472955			-0 .50194			-0 .503978	
		-0 .330243			-0 .370175			0 .370205
-0 .315066			-0 .344699			-0 .346645		
-0 .307935			-0 .342731			-0 .340712		
		-0 .296605			-0 .322546			0 .322546
	-0 .256532			-0 .259217			-0 .260589	
0 .202720			0 .214391			0 .214298		
		0 .208706			0 .216165			0 .217116
		0 .209633			0 .230760			0 .229833
0 .214507			0 .231100			0 .231280		
0 .464982			0 .459890			0 .459923		
		0 .470195			0 .465014			0 .465045

It is seen from Table 6 that the two inversion points of Table 1 appear in the first perturbational step and comparison of Tables 6 and 7 indicates that the second perturbational has no effect on the TEMO pattern established by the first perturbational step. It follows that the inversion points observed in the eigenvalue pattern of this topomer pair are due to the averaged effect of the anisotropy of the tight-binding interactions and, consequently, one concludes that STO-3G basis set pictures the aza-allyl moiety in S_1 and T, respectively, as non-isomorphic.

A similar analysis performed for S_2 and T pair provided the results presented in Tables 8 and 9.

Table 8

Summation of π-MO PV-RR eigenvalue series (a.u.) through n = 2nd order of the first perturbational steps : S_2 and T isomers

n = 0 S_2	T	S_2	n = 1 x^{I}_{i}	T	S_2	n = 2 x^{I}_{i}	T
-0.574445		-0.579370			-0.579995		
	-0.574325			-0.574999			-0.574991
	-0.324690			-0.330091			-0.330244
-0.319308		-0.323437			-0.323447		
-0.307449		-0.307150			-0.306879		
	-0.301347			-0.296605			-0.296605
	0.197631		0.208703			0.208695	
0.203453		0.208704			0.208698		
0.214029				0.208706			0.208706
	0.219731			0.209630			0.209634
	0.469674	0.212409			0.212459		
0.469794			0.299696			0.301823	
				0.470063			0.470196
		0.473405			0.473449		

Table 9

Summation of π-MO PV-RR eigenvalue series (a.u.) through n = 2nd order of the second perturbational steps : S_2 and T isomers

S_2	n = 0 x^I_i	T	S_2	n = 1 x^I_i	T	S_2	n = 2 x^I_i	T
−0.579721			−0.537212			−0.537750		−0.532546
		−0.574991			−0.532523			−0.370175
		−0.330243			−0.370175			
−0.323445			−0.362167			−0.362274		
−0.306887			−0.334751			−0.335114		
		−0.296605			−0.322546			−0.322546
	0.208685				0.217092			0.217115
0.208690			0.220286			0.220402		
				0.227618			0.227065	
		0.208706			0.229833			0.229833
		0.209633	0.230717					
				0.342313				
0.212467					0.465014	0.231079		
	0.302529		0.467680				0.339976	
		0.470195						0.465045
0.473449						0.468204		

The first perturbational step generates two inversion points, $x_1^I < x_2^I$, in the region of the virtual MO's. Comparison of Tables 8 and 9 indicates that only x_2^I is correctly and stably located by the first order perturbational corrections of the first perturbational step. It follows that x_2^I is due exclusively to the averaged effect of the anisotropy of the SCF tight-binding interactions. The origin of x_1^I is more complex and, by the same arguments as before, it may be traced to the averaged effects of the non-equality of the nearest-neighbor *and* the non-nearest neighbor interactions. Consequently, the STO-3G basis set pictures the topological spaces used to construct S_2 and T pair as non-isomorphic *and* multivalent.

As demonstrated above, the present procedure is able to identify electronic factors which may compete with molecular topology in conditioning the *ab initio* π-eigenvalue patterns. In order to analyze the behaviour of TEMO patterns in passing to the corresponding *ab initio* ones, we developed the computational procedure described in the next section.

4. BEHAVIOUR OF TEMO PATTERNS UNDER PERTURBATION

For any MO eigenvalue ε_q^R, q = 1, 2, . . ., R = S or T, one can calculate the corresponding power series (3) in the expansion parameter λ,

$$\varepsilon_q^R(\lambda) = \sum_j \varepsilon_{qj}^R \lambda^j \tag{3}$$

where the summation over j terminates when the desired numerical accuracy of $\varepsilon_q(\lambda)$ is achieved.

Table 10

The π-MO PV-RR eigenvalue series (u.a.) corresponding to the orbitals which cross in the first perturbation step

Topomer	ε_j	ε_{j_0}	ε_{j_1}	ε_{j_2}	ε_{j_3}	ε_{j_4}	ε_{j_5}
S_1	ε_1	−0.574826	0.363786 (−2)	−0.103335 (−2)	−0.988127 (−5)	−0.742157 (−6)	
	ε_4	0.202406	−0.250437 (−2)	0.286002 (−2)	−0.125974 (−4)	−0.298539 (−4)	0.127494 (−5)
	ε_5	0.214376	−0.165430 (−2)	0.175227 (−2)	0.246256 (−4)	0.834056 (−5)	
	ε_6	0.470134	−0.527375 (−2)	0.610735 (−4)	0.499658 (−6)		
T	ε_1	−0.574325	−0.662439 (−3)	−0.340792 (−5)			
	ε_4	0.197631	0.119989 (−1)	0.372517 (−5)			
	ε_5	0.219731	−0.110255 (−1)	0.225214 (−6)			
	ε_6	0.469674	0.388547 (−3)	0.134204 (−3)	−0.978380 (−6)		
S_2	ε_5	0.214029	−0.161988 (−2)	0.499689 (−4)	0.494800 (−5)	0.307219 (−5)	
	ε_4	0.203453	0.525090 (2)	−0.639989 (−5)	−0.476985 (−5)	−0.305842 (−5)	

Table 11

The π-MO PV-RR eigenvalue series (a.u.) corresponding to the orbitals which invert their order in the second perturbational step

Topomer	ε_j	ε_{j_0}	ε_{j_1}	ε_{j_2}	ε_{j_3}
S_2	ε_4	0.208690	0.115958 (−1)	0.107224 (−3)	0.897600 (−5)
T	ε_5	0.209633	0.745924 (−2)	0.234646 (−4)	0.104665 (−5)

Although only $\lambda = 1$ has physical significance, in what follows one will formally consider as a continuous variable and as a continuous function.

A TEMO inversion observed in the *ab initio* spectra implies that the q-th π-MO eigenvalues of S and T have crossed for $\lambda \in (0, 1]$. Such crossing implies that for some value of λ one has

$$\Delta\varepsilon_q(\lambda) = \varepsilon_q^T(\lambda) - \varepsilon_q^S(\lambda) = \sum_j (\varepsilon_{qj}^T - \varepsilon_{qj}^S)\lambda^j = 0 \tag{4}$$

$$\Delta\varepsilon_q(\lambda) = 0$$

The smallest positive root, λ_q^{crit}, of λ is called here the critical value of the expansion parameter. $\lambda_q^{crit} \geqslant 1$ indicates a tendency of the q orbitals to invert, but the inversion cannot be realized, while $0 < \lambda_q^{crit} \leqslant 1$ indicates an effective inversion in passing from topological to *ab initio* eigenvalues of the MO's in question.

Results reported previously [12,13] as well as in this paper indicate that the location of the TEMO inversions are correctly and stably located by the first-order perturbational corrections. Consequently, using (4) with the λ-expansion (3) truncated after the first order corrections should result in a sufficiently accurate approximation, $\lambda_{q,approx}^{crit}$, of the actual λ_q^{crit} values. Evidently,

$$\lambda_{q,approx}^{crit} = (\varepsilon_{q0}^T - \varepsilon_{q0}^S)/(\varepsilon_{q1}^S - \varepsilon_{q1}^T) = \frac{\rho_q}{\sigma_q} \tag{5}$$

Standard interpretation [15] of the first-order perturbation energy leads to the conclusion that λ_q^{crit} decomposes into two major factors : the resistance to distorsion of the unperturbed eigenvalues, $\rho_q = \varepsilon_{q0}^T - \varepsilon_{q0}^S$ and the relative strength of perturbation, σ_q, due to electronic factors "felt" by the topological pair of eigenvalues. Hence, the molecular system-dependent behaviour of TEMO patterns can be traced to the balance between different ρ vs σ values. Further, as changes in the ρ_q vs. σ_q, $q = 1, 2, \ldots$ tend to shift the actual λ_q^{crit} to values smaller or greater than one it is not surprizing that the *ab initio* π-MO eigenvalue patterns are sensitive to the choice of the basis set.

The PV-RR-MO eigenvalue series of the diazines orbitals which cross in the first perturbational step are collected in Table 10.

Table 11 displays the PV-RR series for the MO's which cross in the second perturbational step.

The critical values of the expansion parameters are systematized in Table 12.

Examination of Table 10 shows that the 4-th and 5-th eigenvalues of the T topomer invert their order in the first perturbational step at $\lambda = 0.959750$, i.e., *after* the TEMO pattern corresponding to this step has been established, and they invert again in the second perturbational step at $\lambda = 0.067832$, i.e., *before* the TEMO pattern corresponding to this step is established – hence, the indexing of the MO's in Table 12, second perturbational step.

Inspection of Table 12 indicates that represents a satisfactory estimate of and, therefore, the behaviour of the eigenvalue patterns under study can be attributed to the fact that the strength of perturbation overcomes the resistance to distorsion of the MO pairs listed in Table 12.

Table 12

The critical values of the expansion parameter, λ_q^{crit} and $\lambda_{q\ approx}^{crit}$

Perturbational step	Pair of MO's		λ_q^{crit}	$\lambda_{q\ approx}^{crit}$
Step 1	$\varepsilon_1^{S_1}$	ε_1^T	0.119954	0.1165
	$\varepsilon_4^{S_1}$	ε_4^T	0.353821	0.3292
	$\varepsilon_5^{S_1}$	ε_5^T	0.520370	0.5714
	$\varepsilon_6^{S_1}$	ε_6^T	0.082022	0.0821
	$\varepsilon_4^{S_2}$	ε_4^T	0.860962	0.8628
	$\varepsilon_5^{S_2}$	ε_5^T	0.604140	0.6062
Step 2	$\varepsilon_4^{S_2}$	ε_5^T	0.226902	0.2280

5. CONCLUSIONS

Ab initio calculations were performed for two pairs of topomers which share the same T isomer. The agreement between the results reported here and the TEMO theorem provides strong evidence for the dominant role of molecular topology on the eigenvalue spectra of these molecules.

Application of a two-step perturbational procedure allowed identification of electronic factors which compete with molecular topology in conditioning the actual interlacing of the *ab initio* eigenvalue spectra. The analysis gained in relevance by being applied simultaneously to three topologically related isomers.

An extension of the perturbational procedure (i.e., calculation of critical values) showed that the diverse behaviour of TEMO patterns in passing from topological eigenvalue spectra to the corresponding *ab initio* ones is due to the balance between the resistance to distorsion of the unperturbed system and the relative strength of perturbations.

REFERENCES

[1] V. Prelog, *J. Mol. Catalysis*, **1**, 159 (1975/76).

[2] I. Gutman and O. E. Polansky, "Mathematical Concepts in Organic Chemistry", Springer, Berlin, 1986.

[3] R. E. Merrifield and H. E. Simmons, *Theor. Chim. Acta (Berl.)*, **55**, 55 (1980).

[4] O. E. Polansky and M. Zander, *J. Mol. Struct.*, **84**, 361 (1982).

[5] O. E. Polansky, *J. Mol. Struct.*, **113**, 281 (1984).

[6] A. Graovac, I. Gutman and O. E. Polansky, *J. Chem. Soc. Faraday Trans. II*, **81**, 1543 (1985).

[7] I. Gutman, A. Graovoc and O. E. Polansky, *Chem. Phys. Lett.*, **116**, 206 (1985).

[8] O. E. Polansky, G. Mark and M. Zander, "Der Topologische Effekt on Moleculorbitalen. Grundlagen und Nachweise", Schriftenreihe des Max-Planck-Institut f. Strahlenchemie, no. 31, p. 1 – 403 (1987).

[9] A. Szabo and N. S. Ostlund, "Modern Quantum Chemistry", McGraw-Hill, New York, 1989.

[10] W. J. Hehre, L. Radom, P.v.R. Schleyer and J. A. Pople, "Ab Initio Molecular Orbital Theory", Wiley, New York, 1986.

[11] Cambridge Crystallographic Data Base, University Chemical Laboratory, Cambridge, England.

[12] I. Motoc, J. N. Silverman and O. E. Polansky, *Phys. Rev.*, **A28**, 3673 (1983); *Chem. Phys. Lett.*, **103**, 285 (1984).

[13] I. Motoc, J. N. Silverman, O. E. Polansky and G. Olbrich, *Ther. Chim. Acta (Berl.)*, **67**, 63 (1985).

[14] J. N. Silverman, *J. Phys.*, **A16**, 3471 (1983).

[15] D. S. Saxon, "Elementary Quantum Mechanics", Holden-Day, San Francisco, 1968.

Revue Roumaine de Chimie, 36, 4–7, 411–416 (1991)

Dedicated to Prof. ALEXANDRU T. BALABAN
on the occasion of his 60th anniversary

THE ESTIMATION OF THERMODYNAMIC PROPERTIES OF FUSED SILVER HALIDES

ILIE G. MURGULESCU and EUGENIA SĂLĂGEANU
Physical Chemistry Department, B-dul Republicii 13 Bucharest, Romania

Received February 8, 1991

The molten silver halides are assimilated to mixtures of ionic and covalent species. With this assumption expansion coefficients, compressibility coefficients and entropies of fused silver halides were calculated, using two rigid spheres equations of state.

The rigid spheres equations proved to predict quite well the thermodynamic properties of ionic liquids. However, the attempt to use such equations for molten silver halides reveals great discrepancies between experimental and estimated values, especially in isothermal compressibilities and entropies, discrepancies which seem to suggest a more complex structure for molten silver halides.

In order to improve the prediction, we have put the above-mentioned deviations on a marked covalent character of molten silver halides, considering them as mixtures of ionic and covalent liquids. The fraction of ionic character was roughly assimilated to the percentage of ionic bond as derived from Pauling [1] electronegativities.

We have checked this assumption by calculating thermal expansion coefficients, isothermal compressibility coefficients and entropies of molten silver halides with Buehler-Hirschfelder-Curtiss (B-H-C) (1) [2,3,4] and Thiele's [5] (2) equations of state:

$$PV = \nu RT \frac{1}{1 - \dfrac{\nu^{1/3}N^{1/3}\sigma}{\gamma^{1/3}V^{1/3}}} \tag{1}$$

$$pV = RT\frac{1 + x + x^2}{(1 - x)^3} \tag{2}$$

where

$$x = \frac{1}{6}\pi\sigma^3\nu\frac{N}{V} \tag{3}$$

In B-H-C equation, a face centered cubic lattice value was taken for the structure factor γ.

Both equations contain only two adjustable parameters, namely the mean particle diameter and the number of particles per molecular unit of molten salt.

As the procedure to set up P-V-T relationships for mixtures from the properties of pure components is not only cumbersome, but even inoperant in our case, because the individual properties of the components are not known, following Stillinger's [6] suggestion, we have considered the melt to be built up from identical particles, except for entropies calculations.

The mean radius was an average between ionic and covalent radii of the atoms :

$$\bar{r} = \frac{1}{3}\left(r_{Ag^+} + r_{X^-} + \sigma_{Ag-X}\right) = \frac{1}{3}\left(r_{Ag^+} + r_{X^-} + r_{Ag} + r_X\right) \qquad (4)$$

The number of particles per molecular formula weight was estimated through the ionisation degree, y, of the molten salt :

$$\nu = 1 + y \qquad (5)$$

THE THERMAL EXPANSION COEFFICIENTS

The two state equations quoted give the following expresions for the thermal coefficients :

$$\alpha = \frac{1}{V}\left(\frac{\partial V}{\partial T}\right)_p = \frac{1}{T}\,\frac{1 - \dfrac{\nu^{1/3}N^{1/3}\sigma^3}{\gamma^{1/4}V^{1/3}}}{1 - \dfrac{2}{3}\,\dfrac{\nu^{1/3}N^{1/3}\sigma}{\gamma^{1/3}V^{1/3}}} \qquad (6)$$

$$\alpha = \frac{1}{V}\left(\frac{\partial V}{\partial T}\right)_p = \frac{1}{T}\,\frac{1 - x^3}{(1 + 2x)^2} \qquad (7)$$

The radii for both ions and atoms are Pauling crystal radii. The estimated values are compared to the experimental ones, obtained from a linear dependence on temperature, of the density, with the Janz [7] data.

Table 1 contains besides the results for mixture, the values calculated for a completely ionised melt.

A it may be seen in table 1, the agreement is better for Thiele's equation under the mixture approximation. The differences between the values calculated for ionic melts and those for the mixture are too small to be a definite support for the mixture model.

Table 1

Thermal expansion coefficients for molten silver halides at their melting points

Salt	T_{m_1} K	V $\frac{cm^3}{mol}$	$\bar{r}$A°	r_iÅ		$\alpha \cdot 10^4 K^{-1}$								
						exp	eq 6	Δ%	eq 7	Δ%	eq 6*	Δ%	eq 7*	Δ%
AgCl	728	29.95	1.833	1.535	1.26	1.77	1.55	−12.4	1.86	5	2.30	29.9	2.16	22
AgBr	707	33.68	1.930	1.605	1.19	1.86	1.82	−2.0	2.00	10	2.19	17.7	2.15	15.6
AgI	829	42.09	2.063	1.710	1.09	1.81	2.54	36.5	2.12	17	2.16	19.3	1.96	8.3

* Values obtained for purely ionic melts

THE ISOTHERMAL COMPRESSIBILITY COEFFICIENTS

The isothermal compressibility coefficients derived from equations 1 and 2 are:

$$\beta_T = -\frac{1}{V}\left(\frac{\partial V}{\partial P}\right)_T = \frac{V}{\nu R}\left(1 - \frac{\nu^{1/3}N^{1/3}\sigma}{\gamma^{1/3}V^{1/3}}\right) \cdot \alpha \qquad (8)$$

$$\beta_T = -\frac{1}{V}\left(\frac{\partial V}{\partial P}\right)_T = \frac{V}{\nu R}\,\frac{(1-x)^4}{1-x^3} \cdot \alpha \qquad (9)$$

In the β_T calculation we have used compressibility radii which are shorter than Pauling radii. As we could not find the compressibility radii for silver ion and silver covalent halides, we have approximated them as follows:

— for the silver ion, we have interpolated the ratio of the compressibility to crystal radii of this ion, in a graph of similar ratios against crystal radii, dressed for alkaline ions; the value so obtained is 1.14 Å.

— the compressibility radii of silver covalent halides were appreciated under the assumption of a proportionality between crystal radii and compressibility crystal radii.

In the estimation of the isothermal compressibility coefficients, experimental values of the thermal expansion coefficients were used, so that the results are not rigorously the rigid spheres ones, but those for the real liquid, as Yosim claims out.[9]

The estimated results, compared to the experimental [10] values, as well as to those calculated for an entirely ionic melt are shown in table 2.

The compressibility coefficients obtained with the mixture acception of the melts are visibly improved. At the same time, we must emphasize that the use of the normal crystal radii of either ions or atoms, deepens sharply the disagreement between experimental and estimated values of the compressibility coefficients. May be the so-called compressibility radii of silver ion and silver covalent halides were rather roughly appre-

Table 2

Compressibility coefficients of molten silver halides at 873 K

Salt	$V \frac{cm^3}{mol}$	r_c, Å	r_{c_i} Å	ν	$\alpha \cdot 10^4$, K^{-1}	$\beta_T \cdot 10^{11}$ $m^2 N^{-1}$								
						exp	eq. 8	Δ%	eq. 9	Δ %	eq*8	Δ %	eq*9	Δ %
AgCl	30.19	1.56	1.307	1.26	1.79	10.3	9.6	−7.1	7.2	−30.6	6.6	−35.7	5.3	−48.5
AgBr	34.79	1.64	1.370	1.19	1.91	11.9	13.4	12.6	10.5	−11.8	8.2	−31.2	6.5	−48.4
AgI	42.43	1.76	1.472	1.09	1.82	17.0	18.7	10.0	15.6	−8.0	9.5	−43.8	7.3	−57.0

* Values estimated for a purely ionic melt

ciated, but we had not enough experimental data for a better estimation of them.

THE ENTROPIES OF MOLTEN SILVER HALIDES

In the calculation of liquid entropies, we have followed the way proposed by Yosim and Owens.[9] As the gas entropies of biatomic species differ markedly from that of a monoatomic one, on the account of rotationa and vibrational terms, the assumption of a liquid built up from identical mean particles cannot work in the estimation of the liquid entropies. Now we have to treat the melt as a mixture of mean monoatomic particles, averag ed onthe ionic species, and covalent biatomic molecules. The vaporisation entropy of the melt was derived on the following sequence of transformations :

1. $(Ag^+x^-)_{liq} \rightarrow (Ag^+x^-)_g = 2$ mean monoatomic particles
2. $(Ag - x)_{liq} \rightarrow (Ag - x)_g$
3. $y(Ag^+x^-)_{liq} + (1 - y)(Ag - x)_{liq} \rightarrow y(Ag^+x^-)_g + (1 - y)(Ag - x)_g$

The entropy of the liquid silver halide is given by the expression.

$$S_l = S_g - y\ S_1 - (1 - y)\ S_2 \tag{10}$$

The gas phase entropy, S_g, in the statistical value, averaged on the composition of the mixture made up from mono and biatomic species.

$$S_g = y(2S_{mono}) + (1 - y)\ S_{molecular} \tag{11}$$

In the estimation of the molecular silver halides gas entropies, Herzberg's [11,12] spectral data were used.

The vaporisation entropies of ionic and molecular liquids were derived with Yosim and Owens' relationship :

$$\Delta S^{vap} = \int_{V_1}^{V_g} \frac{P}{T} \cdot dv \tag{12}$$

B—H—C′ equation of state gives :

$$\Delta S_1 = 6R \ln \frac{V_g^{1/3} - \dfrac{2^{1/3}N^{1/3}\sigma_{ionic}}{\gamma^{1/3}}}{V_1^{1/3} - \dfrac{2^{1/3}N^{1/3}\cdot\sigma_{ionic}}{\gamma^{1/3}}} \tag{13}$$

$$\Delta S_2 = 3R \ln \frac{V_g^{1/3} - \dfrac{N^{1/3}\sigma_{cov}}{\gamma^{1/3}}}{V_1^{1/3} - \dfrac{N^{1/3}\sigma_{cov}}{\gamma^{1/3}}} \tag{14}$$

With Thiele's equation we get :

$$\Delta S_1 = 2R \left[\ln \frac{V_g}{V_1(1 - x_{ionic})} + \frac{3}{2} \frac{x_{ionic}(2 - x_{ionic})}{(1 - x_{ionic})^2} \right] \tag{15}$$

$$\Delta S_2 = R \left[\ln \frac{V_g}{V_1(1 - x_{cov})} + \frac{3}{2} \frac{x_{cov}(2 - x_{cov})}{(1 - x_{cov})^2} \right] \tag{16}$$

Throughout the calculation we have used the same value of V_1, for both ionic and covalent melts, as the assignment of specific values for the molar volumes of ionic liquid and covalent liquid, does not seem to affect sensibly the results.

The experimental values of liquid entropies were obtained by extrapolating the temperature dependence of the liquid entropies to the melting temperatures using the data of the Bureau of Mines Bulletin 605[13].

The result are presented in table 3. We have also tabulated the values calculated with an entirely ionic melt.

Table 3

Entropies of molten silver halides at their melting points

Salt	T (K)	r Å ionic	r Å cov.	S^1 cal mol^{-1} K^{-1}								
				exp	eq 1	Δ %	eq 2	Δ%	eq 1*	Δ %	eq 2*	Δ %
AgCl	728	1.535	1.215	39.9	39.1	−2.0	40.5	1.5	24.1	−39.7	19.29	−51.6
AgBr	707	1.605	1.290	41.8	42.8	2.4	44.6	6.7	25.0	−40.2	18.9	−54.6
AgI	829	1.710	1.385	47.1	48.6	3.2	51.4	9.1	30.1	−63.9	26.0	−44.7

* Values calculated for a purely ionic liquid

The values of entropies obtained under the mixture approximation agree very well with the experimental ones, while those calculated with a purely ionic liquid are far from being satisfactory. Thus, the assumption that the molten silver halides are mixtures of ionic and covalent species seems to be fully justified, at least for the entropies estimations.

REFERENCES

[1] L. Pauling, "Chimie Generală" Ed. Ştiinţifică, Bucharest, 1972 p. 185.

[2] J. O. Hirschfelder, C. F. Currtis and Byron Bird, "Molecular Theory of Gases and Liquids", John Wiley and Sons, New York, 1954.

[3] I. G. Murgulescu and E. Sălăgeanu, *Rev. Roumaine Chim.* **17**, 603 (1972).

[4] H. Reiss, H. L. Frisch and J. L. Lebowitz, *J. Chem. Phys.*, **31**, 369 (1959).

[5] E. Thiele, *J. Chem. Phys.*, **39**, 474 (1963).

[6] F. H. Stillinger jr. *J. Chem. Phys.*, **35**, 1681 (1961).

[7] G. Janz, "Molten Salts Handbook" New York Academic Press (1967).

[8] C. A. Carlson, "Valence", Oxford University Press, Oxford, 1959.

[9] S. J. Yosim and B. B. Owens, *J. Chem. Phys.*, **41**, 2032 (1964).

[10] S. Sternberg and V. Vasilescu, *Rev. Roumaine Chim.*, **21**, 1457 (1976).

[11] Herzberg "Molecular Spectra", N. Y., T. Van Nostrand Company Inc. (1957).

[12] "Tables of Interatomic Distances and Configuration of Molecules and Ions", Special Publication No. 11, the Chemical Society, Burlington House, W 1, London (1958).

[13] Buletin 605 of the Bureau of Mines, ed. C. Wick and F. E. Block, Washington 1963

Revue Roumaine de Chimie, **36**, *4*–7, 417–420 (1991)

Dedicated to Prof. ALEXANDRU T. BALABAN
on the occasion of his 60th anniversary

β-LACTAM ANTIBIOTICS. III *

ELECTRONIC STRUCTURE AND PHYSIC-CHEMICAL PROPERTIES OF SOME ANTIBIOTIC MOLECULES AND THEIR INTERMEDIATES

JOSETTE WEINBERG[a], ALEXANDRINA DONESCU[a], V. EM SAHINI[b] and M. COJOCARU[c]

[a] Centre of Physical Chemistry, Spl. Independenţei 202, Bucharest, Romania

[b] Bucharest University, Laboratory of Physical Chemistry, B-dul Republicii 13, Bucharest, Romania

[c] Antibiotic Plant, Valea Lupului 1, Jassy, Romania

Received May 23, 1990

LCAO-MO studies on a series of antibiotics pointed out that both the frontier electron density in a nucleophilic substitution at the carbon atom $C_{7(8)}$ belonging to the β-lactam cycle and in a electrophilic substitution at the nitrogen atom $N_{9(10)}$ belonging to the side chain of the same cycle, represent important reactivity parameters, accounting for the antimicrobian activity. In the same way the bond order may indicate a preferential route in the synthesis of such antibiotics.

In the present paper we report the results of an HMO computation of carbenicillin, ampicillin, oxacillin and seven cephalosporins electronic structure, some correction factors for β-lactam and thiazolidine (or dihydrothiazine) cycles nonplanarity, as well as for other π-conjugation, the discontinuity centers being applied.[1] Numbering of centers is according to Fig. 1. Table 1 presents the calculated reactivity indices.

As is well known, carbenicillin has been the first semisynthetical penicillin highly used in clinical practice due to its high activity against Gram-negative *Pseudomonas* and *Proteus* bacteria.[2] This activity is theoretically confirmed by Fukui density value $f^{N}_{C_7}$. Its instability in acid medium seems to be due both to the increased value of Fukui density of nitro-

---

* Part II: J. Weinberg, A. Donescu and V. Em. Sahini, *Rev. Roumaine Chim.*, **33**, 795 (1988).

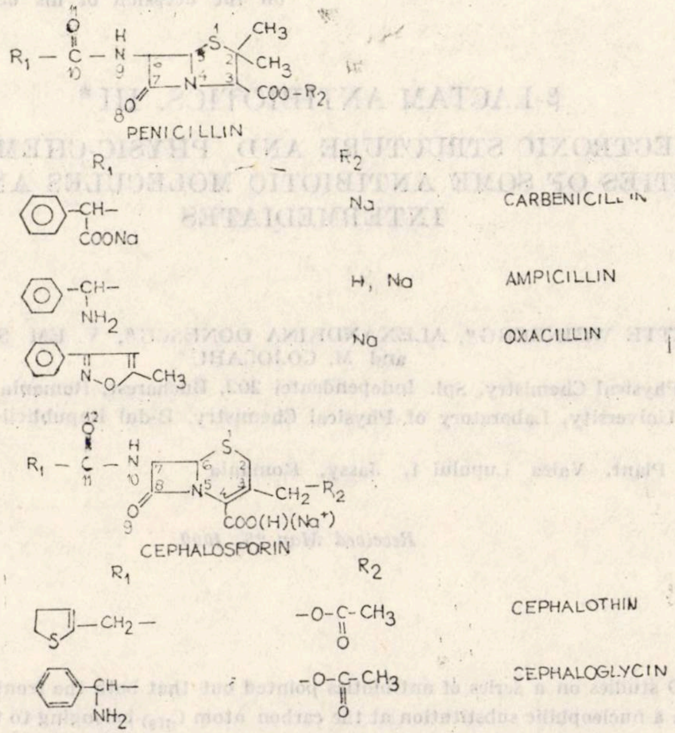
PENICILLIN
R1
R2
CARBENICILLIN
Na
AMPICILLIN
H, Na
OXACILLIN
Na
CEPHALOSPORIN
COO(H)(Na+)
R1
R2
CEPHALOTHIN
CEPHALOGLYCIN
CEFAZOLIN
CEPHACETRILE
CEPHRADINE
CEFADROXIL
CEFATRIZINE
CEFAMANDOLE

Fig. 1. — Structure of studied penicillins and cephalosporins.

Table 1

Frontier orbital densities f_r and bond orders P_{rs} *

Antibiotic	$f_{C_{7(8)}}$	$f_{N_{9(10)}}$	$P_{C_5-C_6(C_6-C_7)}$
Carbenicillin	2.23×10^{-3}	0.3240	0.45310
Ampicillin	2.32×10^{-3}	0.1656	0.45660
Oxacillin	0.6498	0.1657	0.80643
Cephalothin	9.81×10^{-3}	0.2402	0.68055
Cefazolin	1.41×10^{-2}	0.1704	0.63270
Cephacetrile	1.41×10^{-2}	0.1703	0.63278
Cefamandole	—	—	0.73036
Cephradine	2.65×10^{-3}	0.1483	0.61956
Cephaloglycin	5.21×10^{-4}	0.1202	0.86500
Cefadroxil	6.84×10^{-4}	0.2054	0.66380
Cefatrizine	—	—	0.54994

* Numbering according to penicilline (or cephalosporins)

gen atom $f^E_{N_9}$ and the low value of the bond order $P_{C_5-C_6}$ accounting for an energetically weak bond, easily to be destroyed, leading to a degradation of the antibiotic molecule. This particular lability of β-lactam cycle of carbenicillin makes it susceptible to a degradation process of the cycle.

As compared with carbenicillin and ampicillin, the oxacillin and the cephalosporins (especially cephaloglycin) appear to have a β-lactam cycle stabilized by delocalization. For this reason the carbenicillin is administered parenterally.[3]

In an electrophilic reaction (Table 1), the Fukui density $f^E_{N_9}$ has a remarkably low value in the case of oxacillin as compared with that in carbenicillin ; this density corresponds to those of orally administered cephalosporins, proving theoretically again the stability of the oxacillin in acid medium and explaining to some extent its oral administration.

The high reactivity of ampicillin, confirmed by Fukui index value in a nucleophilic reaction $f^N_{C_7}$ on one side and its stability in the acid medium as seen from the $f^E_{N_9}$ value (similar—table 1 — to that of oxacillin) on the other side, proves again theoretically the fact that this drug can be also orally administered.

II. An important stage in the process of obtaining carbenicillin is the ketenisation reaction. Due to the fact that its components are extremely reactive, this process is very sensitive to temperature — pressure — and light conditions.

The ketenisation takes places according to the following reaction[4] :

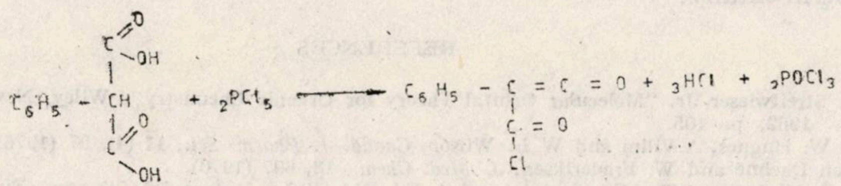

In addition to ketene chloride, the dichloride (Fig. 2) is also formed, which is transformed in ketene chloride by a thermolysis process.

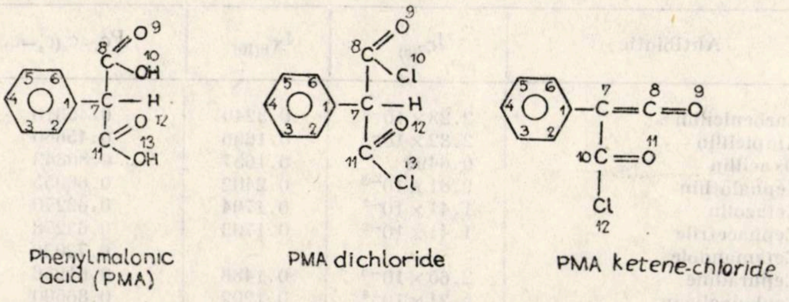

Fig. 2. — Numbering of atoms in PMA, PMA dichloride and PMA Ketene chloride.

An HMO study of electronic structure of participants to the ketenisation reaction and of the resulting products was performed. The results concerning the phenylmalonic acid (PMA), dichloride and ketene chloride are presented in table 2 and the atoms are numbered as shown in Fig. 2.

Table 2

Bond orders P_{rs} of PMA, dichloride of PMA and Ketene chloride of PMA

P_{rs}	PMA	Dichloride PMA	Ketene chloride PMA
P_{1-7}	0.3539	0.3394	0.3273
P_{7-8}	0.5328	0.5649	0.6362
P_{8-9}	0.6639	0.7064	0.6583
P_{8-10}	0.3594	0.1676	—
P_{7-10}	—		0.5287
P_{10-11}	—	—	0.7269
P_{10-12}	—		0.1722

Inspection of table 2 shows that by chlorination of PMA, the lability of the bonds 8—10 and 11—13 (expressed through the small value of the bond order $P = 0.3594$) indicates the preferential formation of the dichloride. This dichloride-through the small value of the bond order $P_{8-10} = 0.1676$-confirms theoretically the possibility of the direct coupling reaction of the dichloride with 6-aminopenicillanic acid as shown experimentally.

REFERENCES

[1] A. Streitwieser Jr. "Molecular Orbital Theory for Organic Chemistry", Wiley, New York, 1962, p. 105.

[2] D. W. Hugues, A.Vilim and W. L. Wilson, *Canad. J. Pharm. Sci.*, **11** (4), 97 (1976).

[3] Von Daehne and W. Frederiksen, *J. Med. Chem.*, **13**, 607 (1970).

[4] C. D. Nenițescu, "Chimie organică", vol. 1, Ed. Didactică și Pedagogică, 7th edn., Bucharest, 1973.

Revue Roumaine de Chimie, 36, 4–7, 421–427 (1991)

Dedicated to Prof. ALEXANDRU T. BALABAN on the occasion of his 60th anniversary

A PHYSICAL METHOD FOR DETERMINING THE SOLUBILITY OF GASES IN LIQUIDS AT HIGH PRESSURES

RODICA VÎLCU, I. GĂINAR, GH. ANIȚESCU and ȘT. PERIȘANU
Laboratory of Physical Chemistry, University of Bucharest, Bd. Republicii no. 13, Bucharest 70346, Romania

Received May 23, 1990

An apparatus for measuring the solubility of gases in liquids at high pressures is described. The solubility of CO_2 in N-methyl-pyrrolidone and glycerol-triacetate, at 25°C and pressures up to 50 atm is discussed. A comparison with previous high-pressure solubility data is made.

1. INTRODUCTION

The study of gas solubility in liquids has been the object of numerous papers.[1–7] The interest is due both to theoretical importance and potential practical applications. Solutions of gases in liquids having different structures and polarities allow the verification of various theoretical models describing the structure and properties of the liquids.[8] The aim of this paper is to describe a new equipment for measuring the solubility of gases in liquids at high pressures. The performances of the apparatus consist in the determination of Bunsen coefficients for the systems N-methyl-pyrrolidone + CO_2 and glycerol-triacetate + CO_2 at 25°C at pressures up to 50 atm and allow the comparison of our experimental data with those obtained by other authors.[9–10] A theoretical interpretation of the data is also made.

2. EXPERIMENTAL

Apparatus

The equipment, schematically presented in fig. 1, contains the following components :

- controlled supplying system for purified gas ;
- equilibrium gas-liquid cell provided with thermostating system ;
- sampling and analysis system to measure the amount of gas ;
- pressure measuring system.

The gas supplying system consists of a compressed gas bottle (1), a steel cylinder (2) for eliminating water traces using molecular sieves and an autoclave (3) as a manostate and a fine handling of gas supplying the equilibrium cell (7). The autoclave is made from stainless steel with an inner volume of about 100 mL hanged with two metal pillars on a plastic plate tightly fixed on a thermostat. The equilibrium cell, filled up with solvent, is basculated and stirred by means of an electromechanical device placed in the thermostat bath (Fig. 2). A better mixing of the two phases is thus achieved and phase equilibrium can therefore be attained in due time. Three capillary tubes made of stainless steel (0.2 mm inner diameter) passing through the equilibrium cell cover serve as follows : the first for direct gas supplying in the liquid phase, the second one for sampling of liquid saturated with the gas to be analyzed and the third one to eliminate the gas phase and to evacuate the equilibrium cell.

As thermostating liquid, ethyleneglycol-water mixture was used, allowing measurements for a wide range of temperatures.

The sampling and analysing system contains a refrigerator (8), a thermostated reservoir (9), an ampoule for samples (8′), a mercury manometer (10) and a precision cathetometer.

The role of the refrigerator is to condense the solvent vapours from the sample for very volatile solvents. The thermostated vessel (9) with an inner volume of 2000 mL is an expansion reservoir for the gas from the sample, under vacuum, serving for volumetric analysis together with the manometer (10) and cathetometer (precision : ± 0.01 mm).

The pressure measurement system works in two steps : the first one of gas supply controlled by a manometer with Bourdon tube (precision class 0.6) and the second one of equilibrium phase achievement using a pressure gauge (5) with rotative piston and weights (precision class 0.05). In order to avoid the condensation of solvent vapours in the pressure measuring system, a differential pressure manometer (4) was used.

Procedure

The equilibrium cell is first washed and then dried. It is filled up with about 50 mL of solvent, the cover is closed, attached to the stirrer and introduced into a Lauda Thermostat (model K4R) provided with an electronic system and Pt thermometer (accuracy of ± 0.02 K). Vacuum is made in the equilibrium cell and the thermostating is achieved at the desired temperature then the gas is slowly supplied up to a pressure value higher than that

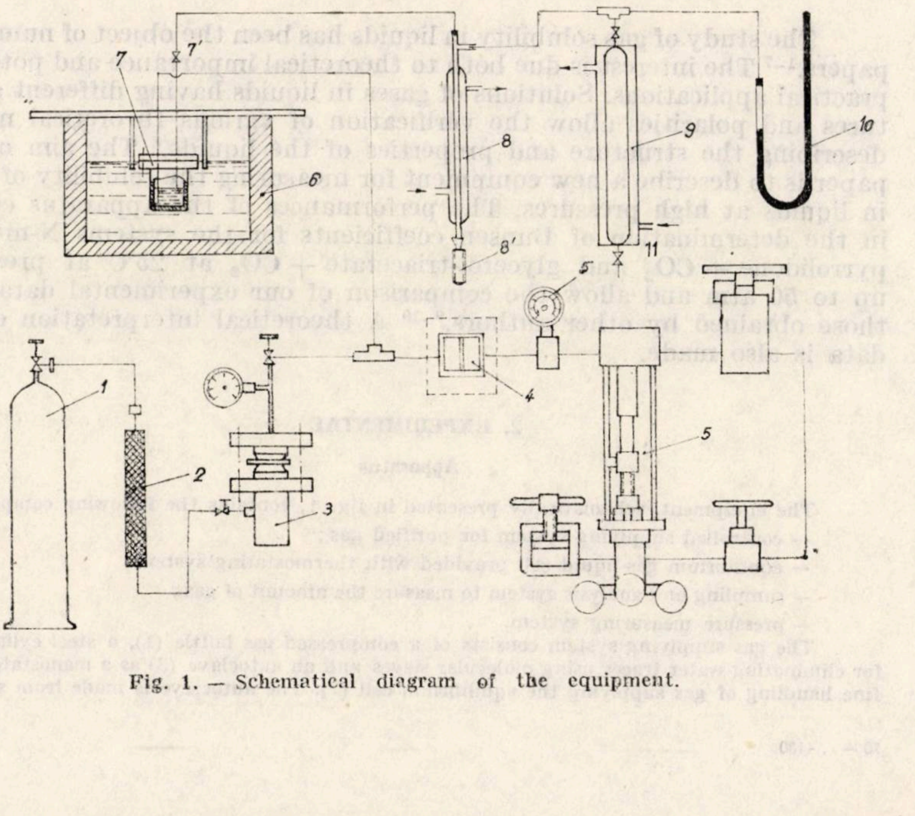

Fig. 1. — Schematical diagram of the equipment.

requested for the phase equilibrium. The equilibrium is attained under an energetic stirring in a few hours. The sampling system is then evacuated then the valve (7′) is carefully opened. A sample of about 1 mL of solvent is thus collected in the ampoule (8′). The solved gas is then desorbed and the pressure produced in this way is read by means of the cathetometer The volume, pressure, temperature and mole number of the desorbed gas can be correlated using a simple equation of state taking into account the low values of the pressure. We have used the virial equation of state containing only the second virial coefficient. After pressure reading the valve (11) is opened and air at the atmospheric pressure is then introduced. The ampoule (8′) is then detached and weighted. The volume of solvent is easily estimated knowing the solvent density and the mass of the ampoule.

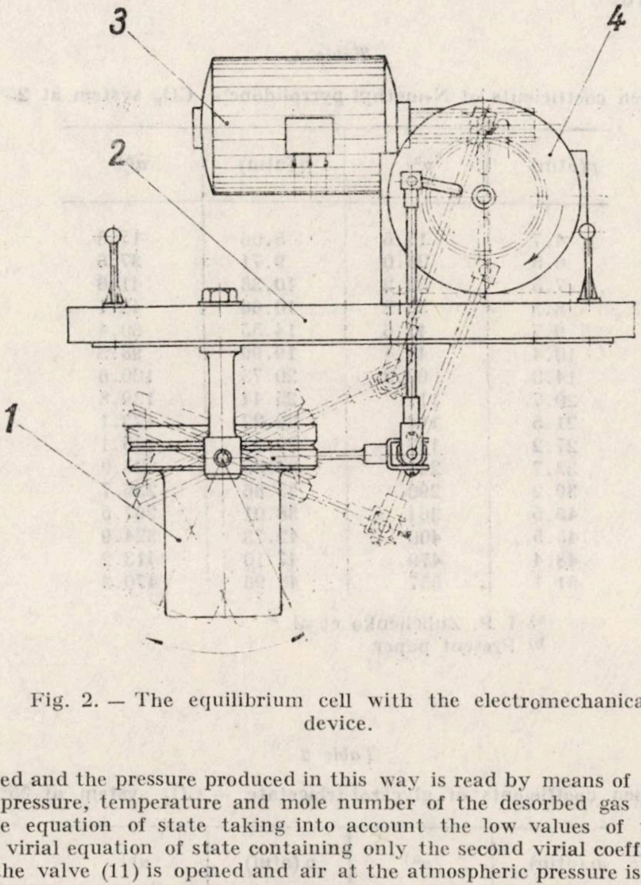

Fig. 2. — The equilibrium cell with the electromechanical device.

3. RESULTS AND DISCUSSION

From the experimental data discussed above, one may estimate the gas solubilities in liquids expressed in different ways (Bunsen or Ostwald absorption coefficients, mole fractions, etc.). We have preferred the Bunsen coefficient, α, calculated by the relationship :

$$\alpha = V_g T_0 / V_s T \tag{1}$$

where V_g is the desorbed gas volume calculated at 1 atm and the temperature of the thermostat bath, T, and V_s is the solvent volume in the sample.

At first, the binary systems have been studied, such as N-methyl-pyrrolidone + CO_2, glycerol-triacetate + CO_2 at 25°C, for which there are already published data for comparison. The experimental results obtained are presented in Tables 1 and 2, compared with those known from literature.

Table 1

Bunsen coefficients of N-methyl-pyrrolidone + CO_2 system at 25°C

p(atm)	$\alpha^{a)}$	p (atm)	$\alpha^{b)}$
4.7	17.6	5.06	17.8
6.5	26.0	9.71	37.6
7.5	30.2	10.38	41.6
8.3	30.2	10.66	42.1
9.7	42.6	14.55	60.4
10.4	41.4	19.99	98.5
14.0	63.3	20.73	100.6
20.7	111	25.44	139.8
21.5	114	29.22	173.1
27.2	158	29.32	175.1
33.7	241	34.35	227.0
39.2	290	35.66	236.7
45.5	364	38.01	267.5
45.5	400	42.73	324.9
48.4	479	47.10	413.2
51.1	557	48.96	470.3

a) I. P. Zubchenko et al. [9]
b) Present paper

Table 2

Bunsen coefficients of glycerol-triacetate + CO_2 system at 25°C

p (atm)	$\alpha^{a)}$	p (atm)	$\alpha^{b)}$
3.04	10.1	4.27	12.68
5.47	19.4	5.03	16.10
6.00	20.9	6.91	22.69
7.21	25.2	9.11	31.02
9.78	37.4	11.16	40.99
10.26	38.3	12.95	49.08
12.05	49.1	14.84	57.80
14.83	59.5	15.25	60.37

a) S. F. Shakova et al.[10]
b) Present paper

Fig. 3 and Fig. 4 show graphically our experimental values for the Bunsen coefficients compared with those from the literature. The agreement of data allows to ascertain that our experimental procedure can be favourably compared with the experimental techniques already reported. It must be mentioned that the precision with which α is calculated from experimental data proves to be better than that resulted from the reproducibility of the determinations (if they are made for many times under the same conditions). This fact suggests the conclusion that for the same P, V, T parameters, due to these fluctuations, an identical state is not always established.

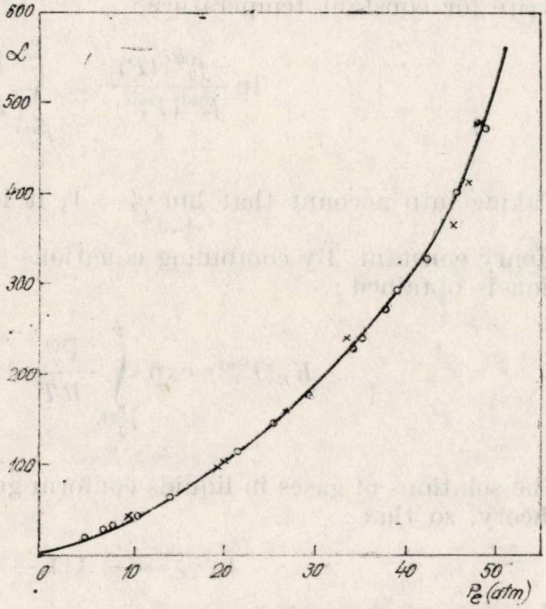

Fig. 3. — Comparative data about the dependence of the Bunsen coefficient with pressure (x — present paper ; ○ — I. P. Zubchenko et al.[9]) in N-metyl-pyrrolidone + CO_2 system at 25°C.

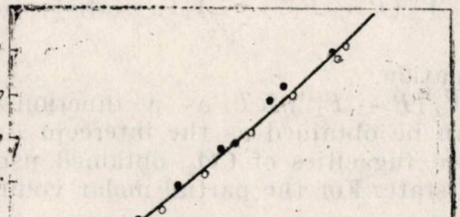

Fig. 4. — Comparative data about the dependence of the Bunsen coefficient with pressure (○ — present paper ; ● — S.F. Shakova et al.[10]) in glycerol-triacetate + CO_2 system at 25°C.

The quantitative treatment of data was made by means of the general liquid-vapour equilibrium equation :

$$f_2^{0*l} \cdot x_2^l \cdot \gamma_2^l = P \cdot x_2^g \cdot \gamma_2^g \qquad (2)$$

where f_2^{0xl} is the reference fugacity of the solute, γ_2^l is the activity coefficient of the solute in an unsymmetrical system, x_2^l and x_2^g are the mole fractions of the solute in the two phases and γ_2^g is the fugacity coefficient of gas in vapour phase.

The f_2^{0*l} is dependent on both temperature and pressure, so we can write for constant temperature :

$$\ln \frac{f_2^{0*l}(P)}{f_2^{0*l}(P_1^{\text{sat}})} = \int_{P_1^{\text{sat}}}^{P} \frac{\overline{V}_2^{0l}}{RT}\, \mathrm{d}P \tag{3}$$

Taking into account that $\lim\limits_{x_2^1 \to 0} \gamma_2^l = 1$, it is obvious that $f_2^{0*l} = K_H$, the Henry constant. By combining equations (2) and (3) the following equation is obtained :

$$K_H(P_1^{\text{sat}}) \cdot \exp \int_{P_1^{\text{sat}}}^{P} \frac{\overline{V}_2^{0l}}{RT} \mathrm{d}P\, \gamma_2^l x_2^l = f_2^g \tag{4}$$

The solutions of gases in liquids conform generally to the regular solution theory, so that :

$$\ln \gamma_2^L = -A[1 - (x_1^l)^2] \tag{5}$$

Equation (4) becomes :

$$RT \ln \frac{f_2^g}{x_2^1} = RT \ln K_H(P_1^{\text{sat}}) + \overline{V}_2^{0l}(P - P_1^{\text{sat}}) - A[1 - (x_1^l)^2] \tag{6}$$

khown as Krichewsky-Ilinskaya equation.

The variation of $\ln(f_2^g/x_2^l) - \overline{V}_2^{0l}(P - P_1^{\text{sat}})/RT$ as a function of $1 - (x_1^l)^2$ is linear, so that $\ln K_H$ can be obtained as the intercept and $-A/RT$ as the slope. We have used fugacities of CO_2 obtained using the Beattie-Bridgemann equation of state. For the partial molar volume at infinite dilution, we have taken the values of Zubchenko et al.[9] The parameters K_H and A obtained by the above-mentioned method and a regression program are listed in Table 3.

Table 3

Parameters K_H and A for N-methyl-pyrolidone + CO_2 (NMP + CO_2) and glycerol triacetate + CO_2 systems

Solvent	NMP	Glycerol triacetate
K_H(atm)	71.8	34.8
A (J/mole)	875	−855
Correl. coeff.	0.999	0.997

The reliability of our data was confirmed by the values of the correlation coefficient close to unit.

REFERENCES

[1] R. Battino and H. L. Clever, *Chem. Rev.*, **66**, 395 (1966).
[2] J. M. Prausnitz, "Molecular Thermodynamics of Fluid — Phase Equilibria", Prentice — Hall, New York, 1969.
[3] A. E. Markham and K. A. Kobe, *Chem. Rev.*, **28**, 519 (1941).
[4] R. Wiebe, V. L. Gaddy and C. Hein Jr., *Ind. Eng. Chem.*, **34**, 823 (1932).
[5] G. E. Gardiner and N. O. Smith, *J. Phys. Chem.*, **76**, 1195 (1972).
[6] T. D. O'Sullivan and N. O. Smith, *J. Phys. Chem.*, **74**, 1460 (1970).
[7] J. Jung, O. Knacke and D. Neuschutz, *Chem. Ing. Tech.*, **43**, 112 (1971).
[8] H. L. Clever and R. Battino, "The Solubility of Gases in Liquids", in *Techn. Chem.*, vol. 8, New York, 1975, p. 379.
[9] Yu. P. Zubchenko, S. F. Shakova and O. P. Ladyghina, *Khim. Prom.*, **9**, 535 (1985).
[10] S. F. Shakova, T. I. Bondareva and Y. P. Zubchenko, *Khim. Prom.*, **10**, 753 (1966).

Revue Roumaine de Chimie, **36**, *4–7*, 429–433 (1991)

Dedicated to Prof. ALEXANDRU T. BALABAN
on the occasion of his 60th anniversary

DERIVATOGRAPHIC INVESTIGATION OF THE COMPOUND *EVA* SUBMITTED TO THERMAL ACCELERATED AGEING. THERMOOXIDATIVE OXIDATION OF THE COMPOUND *EVA*

P. BUDRUGEAC[a] and E. SEGAL[b]

[a] Research Institute for Electrical Engineering, Bd. T. Vladimirescu 45–47, Bucharest 79623, Romania

[b] Department of Physical Chemistry, Faculty of Chemistry, Bd. Republicii 13, Bucharest, Romania

Received January 3, 1991

A derivatographic investigation has allowed us to demonstrate the changes undergone by the compound EVA (polyethylene + vinyl polyacetate) as a consequence of thermal ageing at 130°C and 145°C. The results obtained by thermal analysis have been correlated with the results concerning the relative elongation at break following accelerated thermal ageing.

INTRODUCTION

The use of solid polymeric electroinsulating materials needs knowledge on their behaviour at heating. With that end in view samples of electroinsulating materials are submitted to thermal accelerated ageing, and then the change of their mechanical properties (elongation at break, traction, compression resistance, etc) as well as of their electrical properties (dielectric strength, resistivity, etc) are followed. From the obtained results the thermal lifetime of the material at the temperature of its use [1] can be evaluated. Such measurements are usually associated with specific analyses, like thermal analyses which allow to determine the range of thermal stability of the material [2–8] as well as the changes undergone by the polymeric material as a consequence of thermally accelerated ageing.[3, 9, 10]

This paper presents the results obtained at a derivatographic investigation of some EVA compounds (polyethylene + vinyl polyacetate) samples submitted to thermal accelerated ageing in air at 130°C and 145°C. The results are correlated with those obtained at the change of the relative elongation at break after thermal accelerated ageing.

EXPERIMENTAL

The EVA compound used (polyethylene and 17% vinyl polyacetate with self-oxidants and fireproofing) was produced by ICECHIM — Brazi — Romania.

The heating curves of the powdered samples were recorded on a Q-1500 D, MOM, Budapest-type Paulik-Paulik-Erdey derivatograph in a static air atmosphere, in the temperature range 20—500°C at a heating rate of 3.1 K min^{-1}.

The accelerated thermal ageing of the test specimens took place in a WSU-200 oven with forced air circulation in which the temperature was kept constant with an accuracy of ± 2%.

The relative elongation at break of the initial test specimens as well as of those submitted to accelerated ageing was determined on a universal machine MONSANTO T-10/E with an accuracy of ± 1%.

The test specimens (dumb — bell test pieces) of EVA of 1 mm thickness were in agreement with ASTM-D-412 requirements.

RESULTS AND DISCUSSION

The thermal ageing of the compound EVA in the oven with forced air circulation was investigated under the following conditions:

(1) at 130°C with ageing times: 1000; 1500; 2525 and 3800 h;

(2) at 145°C with ageing times: 228; 467; 610; 949 and 1949 h.

Derivatograms (TG, DTG and DTA) were recorded for the initial test samples as well as for the aged ones. The elongation at break was determined for the same test samples.

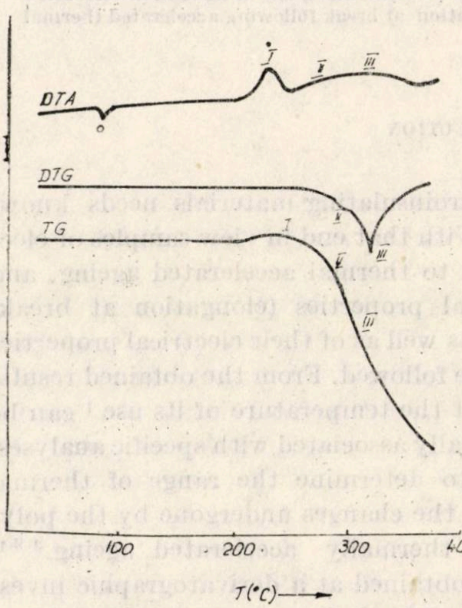

Fig. 1. — The derivatogram of the compound EVA thermally accelerated aged for 1000 h at 130°C

In figure 1 the derivatogram of the EVA compound thermally aged at 130°C for 1000 h is shown.

All the thermally aged samples give similar derivatograms. The nonaged samples give similar derivatograms, the only difference being a relatively small peak which preceds peak I at a close temperature on the DTA curve.

All the investigated samples exhibits a first order phase transition at 78–82°C (the peak 0) which correspounds to the soaking of the polymer material. As shown in figure 1, the compound EVA undergoes at heating the following thermooxidative degradation reactions :

— reaction I corresponding to the oxidation of polymer to solid products (the peak I on the DTA curve and a slight increase of weight on the TG curve) ;

— two exothermic reactions II and III, accompanied by the release of volatile compounds (the peaks II and III in the DTG curve).

Reaction I has been put in evidence at the thermooxidation of polyethylene,[11] polyacetylene [12] and of some elastomers.[13,14] In this oxidation step mainly hydroperoxides are formed, probably as a result of singlet oxygen ($^1O_2$, $^1\Delta_g$) attack on methylene groups of the monomeric units.[15] This process preceds the degradation of the polymer with release of volatile products. In the following we shall analyse the change of the thermal parameters corresponding to this process as a consequence of the thermal accelerated ageing of the polymer.

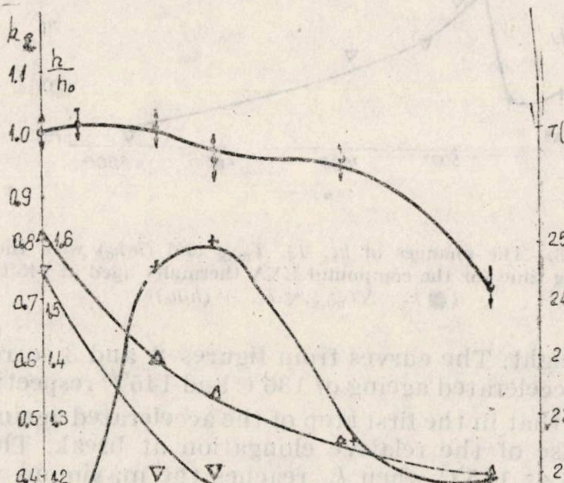

Fig. 2.—The changes of k_ε, T_i, $T_{\max}$ and (h/h_0) with the ageing time for the compound EVA thermally aged at 130°C (●k_ε ; $\Delta T_{\max}$; ∇T_i ; + (h/h_0))

In figures 2 and 3 the curves of change with the time of thermal accelerated ageing of the relative elongation at break (k_ε), the temperature at which the thermooxidation reaction I begins (T_i), the temperature of the DTA peak of reaction I (T_{max}) and the relative height of the peak I in the DTA curve ((h/h_0), h – corresponds to the aged sample, and h_0 to the nonaged one) are shown. The heights of the peak have been divided

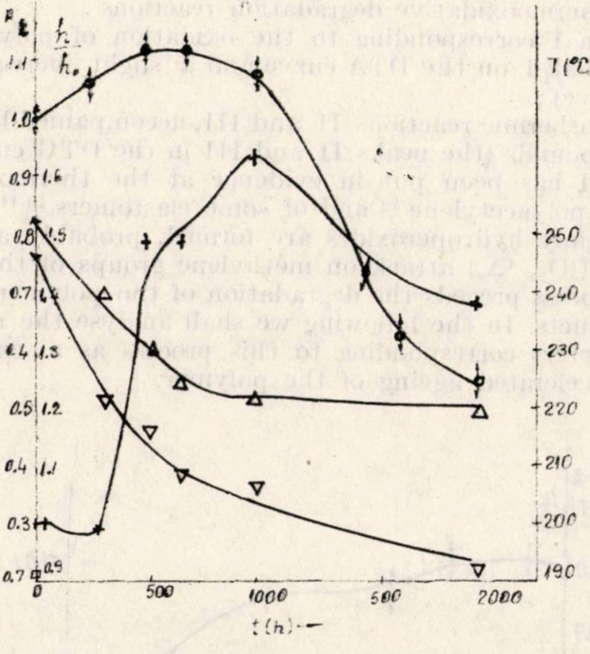

Fig. 3.—The changes of k_ε, T_i, T_{max} and (h/h_0) with the ageing time for the compound EVA thermally aged at 145°C (● k_ε; ΔT_{max}, ∇T_i, $+ (h/h_0)$)

by the sample weight. The curves from figures 2 and 3 correspond to the temperatures of accelerated ageing of 130°C and 145°C respectively.

One can see that in the first step of the accelerated ageing the samples exhibit an increase of the relative elongation at break. This increase is more pronounced at 145°C when k_ε reaches the maximum value of 1.12. Such results should be connected with the initial reticulation of the polymer which improves its mechanical properties. The change of the properties of the polymer through reticulation is reflected by the changes of (h/h_0), T_i and T_{max} with ageing time. The ratio (h/h_0) increases with reticulation and reaches a maximum value at ageing times which corresponds with the begining of k_ε decrease. The increase of (h/h_0) is due to the increase of the oxidability of the polymer leading to solid products. These oxidation reactions, as known, involve the tertiary carbon atoms.[11,16] Thus through reticulation of *EVA* compound the concentration of tertiary carbon atoms increases.

After the reticulation process, the polymer undergoes a thermo-oxidative degradation, the result of such a process being the decreases of the $\bar{k}_\varepsilon$ and (h/h_0) values.

From figures 2 and 3 one can notice that temperatures T_i and $T_{\max}$ decrease with the time of thermal ageing. This changes are more pronounced during reticulation. For higher ageing times these temperatures tend to constant values.

CONCLUSIONS

1) The samples of EVA compound nonaged and thermally accelerated aged at 130°C and 145°C, undergo three significant thermooxidative degradation reactions, one leading to solid products (I) and two with release of volatile products (II and III).

2) The thermal parameters of reaction I have been correlated with the results obtained at the investigation of the change of the relative elongation at break as a consequence of the thermal accelerated ageing.

3) The initial reticulation of the polymer is accompanied by an increase of the relative height of the oxidation peak in the DTA curve as well as by a decrease of the temperatures characteristic to it.

3) The reticulation is followed by the polymer degradation process which leads to the diminution of its thermooxidative capa city.

REFERENCES

[1] IEEE 383, Standard for Type Test of Class 1 E Electric Cables Field Splices and Connections for Nuclear Power Generating Stations, 1974.

[2] S. L. Madorsky, "Thermal Degradation of Organic Polymers", Interscience, New York, 1964.

[3] O. Vogl, I. Ivansung, H. C. Miller and H. W. Williams, *J. Macromol. Sci., A, Z,* **(1968)** 175.

[4] W V. Korshack, S. V. Viragradova, G. V. Danilov L. A. Beribze and S. N. Balazkin, *Vysokomol. Soedin.*, **12**, 129 (1970).

[5] A. A Berlin, B. G. Gherasimov and A. A. Ivanov, *J. Polym. Sci, C.*, **41** 183 (1973).

[6] T. J. Grademer, *J. Macromol. Sci, A*, **8**, 105 (1974).

[7] S. Ciutacu, D. Fătu and E. Segal, *Thermochim. Acta*, **131**, 279 (1988).

[8] D. Fătu, G. Geambaș, P. Budrugeac, S. Ciutacu and E. Segal, *Thermochim. Acta*, **149**, 181 (1989).

[9] E. Segal, P. Budrugeac, S. Ciutacu and G. Mareș, *Thermochim. Acta*, **164**, 161 (1990).

[10] E. Segal, P. Budrugeac and S. Ciutacu, *Thermochim. Acta*, **164**, 171 (1990).

[11] M. Iring, Z. H. Laszlo, T. Kelen and F. Tüdos in E. Buzagh (Ed), Proc. 4th International Conference on Thermal Analysis, Vol. 2, Budapest, 1975, Acad. Kiado, p. 127.

[12] F. G. Wil and D. W. McKee, *J. Polym. Sci, Polym. Chem. Ed.*, **21**, 3479 (1983).

[13] L. Slusarski, *J. Thermal Anal.*, **29**, 905 (1984).

[14] P. Budrugeac, E. Segal and S. Ciutacu, *J. Thermal Anal.* (in press).

[15] L. Slusarski and G. Ianowska, *J. Thermal Anal.*, **29**, 95 (1984).

[16] L. Reich and S. S. Stivala, "Autooxidation of Hydrocarbons and Polyolefins", M. Dekker, New York, 1969.

Revue Roumaine de Chimie, **36**, *4–7*, 435–438 (1991)

Dedicated to Prof. ALEXANDRU T. BALABAN
on the occasion of his 60th anniversary

THE ENTHALPIES OF COMBUSTION AND FORMATION OF 5-NITRO-BENZIMIDAZOL-2-ONE ; 5-AMINO-BENZIMIDAZOL-2-ONE AND 5-ACETOACETYL-AMINO-BENZIMIDAZOL-2-ONE

IULIA CONTINEANU[a], LUMINIŢA WAGNER[b], TATIANA ALEXANDRU[c] and D. I. MARCHIDAN[a]

[a] Institute of Physical Chemistry, Splaiul Independenţei 202, Bucharest 77208, Romania
[b] Research Center for Dyes, Splaiul Independenţei 202, Bucharest 77208, Romania
[c] Institute of Macromolecular Chemistry "Petru Poni", Aleea Gr. Ghica Vodă 41 A, Iassy 6600, Romania

Received September 18, 1990

The combustion enthalpies of 5-nitro-benzimidazol-2-one, 5-amino-benzimidazol-2-one and 5-acetoacetyl-amino-benzimidazol-2-one were determined in an oxygen static bomb calorimeter. The formation enthalpy was derived using data from the available literature. The results obtained are the following:

$C_7H_5N_3O_3(s) + 7.5\ O_2(g) = 7\ CO_2(g) + 2.5\ H_2O(1) + 1.5\ N_2(g)$

$\Delta cH°(298.15\ K) = -3045.5 \pm 0.25$ kJ/mol (-727.5 ± 0.06 kcal/mol)

$\Delta fH°(298.15\ K) = -424 \pm 0.25$ kJ/mol (-101.3 ± 0.06 kcal/mol)

$C_7H_7N_3O(s) + 8.25\ O_2(g) = 7\ CO_2(g) + 3.5\ H_2O(1) + 1.5\ N_2(g)$

$\Delta cH°(298.15\ K) = -3337 \pm 0.65$ kJ/mol (-797.2 ± 0.15 kcal/mol)

$\Delta fH°(298.15\ K) = -418 \pm 0.65$ kJ/mol (-100 ± 0.15 kcal/mol)

$C_{11}H_{11}N_3O_3(s) + 12.25\ O_2(g) = 11\ CO_2(g) + 5.5\ H_2O(1) + 1.5\ N_2(g)$

$\Delta cH°(298.15\ K) = -5590 \pm 0.56$ kJ/mol (-1335.5 ± 0.13 kcal/mol)

$\Delta fH°(298.15\ K) = -310.7 \pm 0.56$ kJ/mol (-74.2 ± 0.13 kcal/mol)

In order to determine the heat of formation of 5-nitro-benzimidazol-2-one, 5-amino-benzimidazol-2-one and 5-acetoacetyl-amino-benzimidazol-2-one, heats of combustion were measured. Use has been made of a calorimetric bomb and the procedure of processing data described elsewhere.[1] In this work the calorimeter constant was 10 243 J/K for the first substance and 10 465 J/K for the others. The pressure of oxygen employed in the bomb was 30 bar. The following values of heats of formation of carbon dioxide and water were utilized[2]:

$$\Delta fH°(298.15\ K) \qquad CO_2(g) = -393.51 \pm 0.13\ \text{kJ/mol}$$

$$-94.051 \pm 0.031\ \text{kcal/mol}$$

$$\Delta fH°(298.15\ K) \qquad H_2O(1) = -285.83 \pm 0.042\ \text{kJ/mol}$$

$$-68.315 \pm 0.01\ \text{kcal/mol}$$

These values were obtained by critical evaluation of the data in the literature[3] and are recommended as key values in scientific works. We adopted the following values: $\Delta fH^\circ(HNO_3) = 219.488$ cal/g, $\Delta fH^\circ(Fe_2O_3) = 1600$ cal/g and $\Delta cH^\circ(\text{cotton}) = 3885.15$ cal/g.

No data on heat of combustion of 5-nitro-benzimidazol-2-one are available in the literature. For molecular mass a value of 179 was used in calculations. The values obtained for the heat of combustion in solid state are listed in table 1. The heat of formation in standard conditions was calculated by the equation:

$$C_7H_5N_3O_3(s) + 7.5\ O_2(g) = 7\ CO_2(g) + 2 \cdot 5\ H_2O(l) + 1.5\ N_2(g)$$

and a value of -424 ± 0.25 kJ/mol was obtained.

Table 1

Heat of combustion of 5 nitro-benzimidazol-2-one ($C_7H_5N_3O_3$)

MW = 179

Substance (g)	K ΔT	Joules ($\Delta T \times$ calorim. const.)	ΔfH (Fe_2O_3)	ΔfH (HNO_3)	ΔcH (cotton)	J/g ΔU_B	kJ/mol ΔU_B
1.054	1.850	18950	56	72	902	17002	3043
1.1097	1.960	20076	54	58	1098	17001	3043
1.1372	1.987	20353	55	70	889	17005	3044
1.2549	2.200	22535	55	91	1057	17000	3043
1.792	3.073	31477	55	56	896	17003	3044

The calorimeter constant = 10243 J/K average value = 3043.4 kJ/mol

Standard deviation $\sigma = \sqrt{\Sigma\Delta^2/n(n-1)} = \pm 0.245$ kJ/mol

$$\text{Washburn's correction } \pi = \frac{0.3 \times 30 \times 7}{-3043}\left[-1 + 1.1\left(\frac{10-3}{28}\right) - \frac{2}{30}\right] = 0.02\%$$

$$\text{hence } \Delta cU^\circ(298.15\ K) = \frac{-3043.4 \times 99.98}{100} = -3043\ \text{kJ/mol}$$

For the reaction $C_7H_5N_3O_3(s) + 7.5\ O_2(g) = 7\ CO_2(g) + 2.5\ H_2O(l) + 1.5\ N_2(g)$ volume change is one unit so that $\Delta cH^\circ(298.15\ K) = -3043 - RT = -3043 - 2.479 =$
-3045.5 ± 0.25 kJ/mol $= -727.5 \pm 0.06$ kcal/mol

The values obtained for the heat of combustion of 5-amino-benzimidazol-2-one in solid state are listed in table 2. For molecular mass a value of 149 was used in calculations. The heat of formation in standard conditions was calculated by the equation:

$$C_7H_7N_3O(s) + 8.25\ O_2(g) = 7\ CO_2(g) + 3.5\ H_2O(l) + 1.5\ N_2(g)$$

and a value of -418 ± 0.65 kJ/mol was obtained.

Table 2

Heat of combustion of 5 amino-benzimidazol-2-one ($C_7H_7N_3O$)

MW = **149**

Substance (g)	K ΔT	Joules ($\Delta T \times$ calorim. const.)	ΔfH (Fe_2O_3)	ΔfH (NO_3H)	ΔcH (cotton)	J/g ΔU_B	kJ/mol ΔU_B
1.0152	2.185	22873	56	87	without	22730	3335
1.1624	2.501	26173	57	95	without	26022	3336
1.2348	2.656	27795	56	75	without	27670	3338
1.3028	2.802	29323	57	90	without	29176	3337

The calorimeter constant = 2500 cal/K = 10465 J/K average value = 3336.5 kJ/mol

Standard deviation $\sigma = \sqrt{\Sigma\Delta^2/n(n-1)} = 0.65$ kJ/mol

Washburn's correction $\pi = \dfrac{0.3 \times 30 \times 7}{-3336.5}\left[-1 + 1.1\left(\dfrac{14-1}{28}\right) - \dfrac{2}{30}\right] = 0.011\%$

hence $\Delta cU°(298.15\ K) = \dfrac{-3336.5 \times 99.99}{100} = -3336.2$ kJ/mol

For the reaction $C_7H_7N_3O(s) + 8.25\ O_2(g) = 7\ CO_2(g) + 3.5\ H_2O\ (l) + 1.5\ N_2(g)$ volume change is 0.25 so that $\Delta cH°(298.15\ K) = -3336.2 - 0.25\ RT = -3336.2 - 0.62 =$
$= -3337 \pm 0.65$ kJ/mol $= -797.2 \pm 0.15$ kcal/mol

For the heat of combustion of 5-aceto-acetyl-amino-benzimidazolo-2-one there are also no data in the literature. The molecular mass was taken as 233. The results obtained for the heat of combustion of solid 5-acetoacetyl-amino-benzimidazol-2-one are listed in table 3. The heat of formation in standard conditions was calculated by the equation:

$$C_{11}H_{11}N_3O_3(s) + 12.25\ O_2(g) = 11\ CO_2(g) + 5.5\ H_2O(l) + 1.5\ N_2(g)$$

which amounted to -310.7 ± 0.56 kJ/mol.

To bring the obtained values to standard state, calculations were more intricate, more complex the structure of the substance was. In the case of compounds with carbon, hydrogen and oxygen of the $C_mH_nO_q$ general formula the corrections of the procedure of reduction to standard state are summed by Washburn's equation: [4]

$$\pi = \frac{0.30 \times P \times m}{-U_B}\left[-1 + 1.1\left(\frac{2n-q}{4m}\right) - \frac{2}{P}\right]$$

where P stands for the initial oxygen pressure (in bar) and $-U_B$ for the heat of combustion; π is calculated in percents of experimental value. The above equation applies fairly well in the case of nitrogen compounds as well. The calculation of standard heat of combustion was effected after application of Washburn's corrections, by summation of the products RT

Table 3

Heat of combustion of 5 acetoacetyl-amino-benzimidazol-2-one ($C_{11}H_{11}O_3N_3$)

MW = 233

Substance (g)	K ΔT	Joules (ΔT × calorim. const.)	ΔfH (Fe_2O_3)	ΔfH (HNO_3)	J/g ΔU_B	kJ/mol ΔU_B
1.0335	2.383	24938	56.3	94	23984.23	5588
1.0802	2.491	26068.3	57	89	23997.7	5591
1.0922	2.517	26340.4	55.6	77.9	23994.6	5591
1.1182	2.575	26947.4	58	64.5	23898.4	5589
1.1407	2.629	27512.5	59	84.6	23993	5590
1.1626	2.675	27994	55.6	55.3	23983.4	5588

The calorimeter constant = 10465 J/K average value = 5589.5

Standard deviation $\sigma = \sqrt{\Sigma\Delta^2/n(n-1)} = 0.56$ kJ/mol

$$\text{Washburn's correction } \pi = \frac{0.3 \times 30 \times 11}{-5589.5}\left[-1 + 1.1\left(\frac{22-3}{4 \times 11}\right) - \frac{2}{30}\right] = 0.01\,\%$$

$$\text{hence } \Delta cU^\circ(298.15\text{ K}) = \frac{-5589.5 \times 99.99}{100} = -5589 \text{ kJ/mol}$$

For the reaction $C_{11}H_{11}O_3N_3(s) + 12.25\,O_2(g) = 11\,CO_2(g) + 5.5\,H_2O(l) + 1.5\,N_2(g)$ volume change is 0.25 so that $\Delta cH^\circ(298.15\text{ K}) = -5589 - 0.25\,RT = -5589 - 0.62 =$
$= -5590 \pm 0.56$ kJ/mol $= -1335.5 \pm 0.13$ kcal/mol

(equal to − 2.479 kJ/mol) times the number of volumes that entered and emerged from reaction. On combustion of organic compounds, which contain no nitrogen, nitric acid is formed by oxidation of nitrogen left as impurity in oxygen. On combustion of nitrogen containing compounds, much more nitric acid is formed. However most of the nitrogen contained in these compounds emerges from combustion reaction as gas and usually only 10% or less as nitric acid.

REFERENCES

[1] I. Contineanu and D. I. Marchidan, *Rev. Chim.* *(București)*, **30**, 1096 (1979).

[2] CODATA Bulletin no 28 (April 1978): "CODATA Recommended Key Values for Thermodynamics 1977".

[3] CODATA Task Group on Key Values for Thermodynamics. *J. Chem. Thermodynamics*, **4**, 331 (1972).

[4] E. W. Washburn, *J. Res. Nat. Bur. Standards*, **10**, 525 (1933).

Revue Roumaine de Chimie, **36**, *4–7*, 439–453 (1991)

Dedicated to Prof. ALEXANDRU T. BALABAN
on the occasion of his 60th anniversary

CYCLIC VOLTAMMETRY OF *p*-PHENYLENDIAMINE

ALEXANDRU DUCA and DOINA BEJAN
Faculty of Industrial Chemistry, Polytechnic Institute, Iassy, Splaiul Bahlui 71, Roumania

Received January 3, 1991

The electrochemical behaviour of *p*-phenylendiamine was studied by cyclic voltammetry on carbon paste electrode (C.P.E.) and on spectral carbon electrode (Sp.C.E.). The influence of electrode and support electrolyte nature, depolarizer concentration, scanning rate and sensitivity of the determination on the voltammogram shape and peak height and potential were investigated. The obtained data lead to the assumption that the electrode process has a mixed adsorption and diffusion, character, the proportion of these two components depending on several parameters.

Recently, the use of different carbon modifications as electrode materials has been much extended.[1–8]

The carbon electrodes, either as such or chemically modified, were used for the voltamperometric characterization of organic compounds,[9,10] namely some heterocyclic aminocompounds [10,11] and primary aromatic amines.[12–16]

In the present paper the electrochemical behaviour of *p*-phenylendiamine is studied. This aromatic aminocompound, used as raw material for some important dyes,[17] is able to be oxidized both chemically and electrochemically. The investigation was performed by cyclic voltammetry within the $-0.3 \rightleftharpoons +1.4$ V range with respect to the saturated calomel electrode (S.C.E.) by using two carbon electrodes : spectral carbon electrode (Sp.C.E.) and carbon paste electrode (C.P.E.).

The obtained data revealed the electrodic process to be a complex and mixed one, including diffusion and adsorption. Some observations on the residual current magnitude and on the reproducibility results, in connection with the surface phenomena characteristic to these electrodes, could also be made.

EXPERIMENTAL

Standard solution of *p*-phenylendiamine (*p*FDA), $5 \cdot 10^{-3}$ mol · L^{-1} was obtained by the dissolution of *p*FDA in twice-distilled water, at the room temperature obtained.

Supporting electrolyte solutions : 10^{-1} M HCl and 10^{-1} M Na_2SO_4, were prepared by the dissolution of p.a. reagents in twice-distilled water.

Spectral carbon electrode (Sp.C.E.) was obtained from a stick of spectrographic graphite by grinding on turning machine till the desired section (d = 3 mm), and then fixed in a polytetrafluoroethylene body. The electric contact was made by a threaded rod from stainless steel and a wire of stainless steel. The surface grinding was performed by means of an abrasive board with fine roughnesses (a layer of variable thickness was removed by cutting when required). The surface finish was made by rubbing on a quantitative filter paper with fine pores.

The C.P.E. (carbon paste electrode) was prepared as described in [4], from graphite powder and nujol; the mixture was homogenized in a mortar till the batter consistency and then introduced into a cavity of a polytetrafluor-ethylene body with a diameter, d = 3 mm. The electrode surface was finished by a slightly rubbing by a plane spattle on, a bright board and on a quantitative filter paper with fine pores.

The surface was renewed by removing a certain paste layer by turning around the metallic piston, which also ensures the electric contact. The electrode was also renewed by replacing the paste when required.

The polarographic cell, where the measurements of the cyclic voltammetry were made, was of the two-electrode type: C.P.E. or Sp.C.E. as working electrode and a S.C.E. as a reference electrode.

In order to record the cyclic voltammograms, the required amounts of the STOC solution of $5 \cdot 10^{-3}$ mol $\cdot$ L^{-1} *p*-FDA and the supporting electrolyte solution were introduced into the cell, till a final volume of 10 mL and pure nitrogen bubbled for 10 minutes for deaeration. Then the recording was performed on Polarograph OH-102-Radelkis.

RESULTS AND DISCUSSION

1. Influence of the supporting electrolyte

Taking into account the slightly basic character of *p*FDA ($Kb_1 = 1.1 \cdot 10^{-8}$; $Kb_2 = 3.5 \cdot 10^{-12}$) the pH of the medium might be assumed to influence somewhat its electrochemical behaviour in solution.

By using Sp.C.E. and basic solutions of different pH values (10^{-1} M HCl and 10^{-1} M Na_2SO_4) the potential of the anodic peak can be noticed to be placed within the more positive value range (+ 0.65 V) in the acid solution, as compared to the Na_2SO_4 solution (+ 0.40 V) (Table 1).

Table 1

Influence of supporting electrolyte on the characteristics of cyclic voltammogram (*p*FDA $5 \cdot 10^{-4}$ mol $\cdot$ L^{-1}; v = 50 mV/s; Sp.C.E.; potential range $-0.3 \rightleftarrows +1.4$ V versus S.C.E.; $S = 4 \cdot 10^{-7}$ A/div.)

Support electrolyte	Anodic peaks		Cathodic peaks		ΔE (V)	$\frac{ip_a}{ip_c}$	$b_{1/2}$ (V)		Symmetry *	
	Ep_a(V)	ip_a(μA)	Ep_c(V)	ip_c(μA)			anodic peak	cathodic peak	anodic peak	cathodic peak
10^{-1} M HCl	+0.65	4.8	+0.250	8.0	0.400	0.60	0.575	0.460	1 : 3	1 : 2
10^{-1} M Na_2SO_4	+0.40	10.0	+0.150	8.4	0.250	1.20	0.190	0.420	7 : 10	9 : 10

* Symmetry was estimated in V at the peak half-height

This fact confirms the stabilizing effect of the hydrogen chloride on the amino group, due to the forming of the corresponding hydrochloride ($ClH \, . \, NH_2-R$), which increases the resistance of *p*FDA toward oxidation.

With the same scanning rate (50 mV/s) and sensitivity (4. 10^{-7} A/div.) the anodic peak is much higher in the neutral solution (10 μA), than in the acidic one (4.8 μA). Instead, the cathodic peak heights are almost equal, which would indicate cathodic processes of the same mechanism and intensities in both media, the half-widths of these peaks being approximately equal, which supports the above assumption. The potentials characteristic to the cathodic peaks are less different than those of the anodic ones. The oxidative processes are more influenced by pH than the reduction ones. Thus, the anodic peak obtained in neutral solution is much better defined ($b_{1/2} = 0.190$ V), being a single peak (attraction of the redox centers), while in acid solution $b_{1/2} = 0.575$ V (repulsion). A careful examination of the voltammogram would lead to the identification of at least three superimposed peaks with $Ep_{a1} = +0.55$ V ; $ip_{a1} = 4.60$ μA ; $Ep_{a2} = +0.65$ V ; $ip_{a2} = 4.80$ μA ; $Ep_{a3} = +0.75$ V ; $ip_{a3} = 4.60$ μA.

This fact would support the assumption of an electrochemical oxidation proceeding in several stages in acidic medium.

The reversibility of the electrode process is partial in both cases, but higher in the 10^{-1} M Na_2SO_4 solution ($\Delta E = 0.250$ V and $ip_a/ip_c = 1.20$). In the 10^{-1} M HCl solution the reduction processes prevail ($ip_a/ip_c = 0.60$), while in the 10^{-1} M Na_2SO_4 solution the oxidation is more intense.

Anyway it is clear that the 10^{-1} M Na_2SO_4 solution is more suitable for following the anodic-cathodic process suffered by *p*FDA.

The high quality of the voltammograms obtained in 10^{-1} M Na_2SO_4 as background is also confirmed by the good symmetry of the anodic and cathodic peaks (7 : 10 and 9 : 11, respectively), expressed in volts and measured at the half-height of the voltammetric peak.

Consequently, the subsequent runs were carried out in 10^{-1} M Na_2SO_4 as a supporting electrolyte.

2. Influence of electrode nature

The recordings made with C.P.E. and Sp.C.E. under identical conditions (Na_2SO_4 10^{-1} M ; v = 50 mV/s ; *p*FDA $5 \cdot 10^{-4}$ mol · L^{-1} ; S = $= 4 \cdot 10^{-7}$ A/div.) revealed both different and similar behaviours of *p*FDA (Table 2).

The electrochemical process proceeding on the two electrodes is partially reversible ($\Delta E = 0.250$ V on Sp.C.E. and 0.210 V on C.P.E.,

Table 2

Influence of electrode nature on characteristics of the cyclic voltammograms

Electrode	Anodic peaks		Cathodic peaks		ΔE(V)	ip_a / ip_c	$b_{1/2}$ (V)		Symmetry	
	Ep_a(V)	ip_a(μA)	Ep_c(V)	ip_c(μA)			anodic peak	cathodic peak	anodic peak	cathodic peak
Sp.C.E.	+0.40	10.0	+0.150	8.40	0.250	1.20	0.190	0.420	7 : 10	9 : 10
	+0.100	0.60	−0.030	2.80	0.130	0.21	0.100	0.100	—	—
P.C.E.	+0.440	5.60	+0.230	4.20	0.210	1.33	0.275	0.210	4 : 7	1 : 2

hence much different from $\Delta E = 0.020$ V as a value admitted for the practical reversible processes).

The prevailing reaction is the oxidation ($ip_a/ip_c > 1.0$ in both cases), which confirms the tendency of the compound under study to this process. The peaks are not entirely symmetrical. It is worth mentioning that the symmetry value is closed to 1/2 on C.P.E. and 1/1 on Sp.C.E. for both anodic and cathodic peaks.

Under identical experimental conditions the reproducibility of the anodic-cathodic process is similar with the two electrodes. Only quantitative differences arise as regards the height of the principal peaks of the voltammograms, which are higher for Sp.C.E.

The potential of the anodic peaks are less different, while the cathodic peak obtained with Sp.C.E. is characterized by lower positive values. The anodic principal peak is very well defined for both electrodes, suggesting the prevailing of a single oxidative process, a secondary stage of a low intensity, being better evidenced on C.P.E. ($Ep_a = +0.100$ V ; $ip_a = 0.60$ μA) and only slightly noticed on Sp.C.E.

Instead, the range of the cathodic processes is quite differently expressed on the cyclic voltammograms drawn with the two electrodes. In the case of C.P.E., two successive reduction processes are clearly evidenced, the second being practically irreversible (Table 2). With Sp.C.E. the cathodic peak is wide ($b_{1/2} = 0.420$ V) defining a sum of reductive processes which are distinguished at scanning rates either higher or lower than 50 mV/s only.

Thus, at v = 8 mV/s two cathodic peaks are noticed and at v = 100 mV/s, three inflexions can be observed, which would suggest the existence of three processes strongly interfering.

3. Influence of potential scanning rate

The scanning rate of the potential is an important factor affecting the cyclic voltammogram, with both C.P.E. (Fig. 1, Table 3) and, mainly Sp.C.E., where the differences are significant, particularly in the range of the cathodic wave (Fig. 2, Table 4).

The maintenance of the potential value of the anodic peak with the modifying scanning rate is indicative of rapid anodic processes.

An intensification of the electrode processes with increasing scanning rate within both anodic and cathodic domains, can be noticed. The potentials of the anodic peaks are affected by the scanning rate to a lesser extent than the cathodic ones by Sp.C.E. and insignificantly by C.P.E. In comparison with the voltammograms obtained at v = 50 mV/s, new peaks are noticed to appear (Sp.C.E. at v = 100 mV/s) and others to disappear (C.P.E. at v = 8 mV/s).

By calculating the ip_a/ip_c ratio for the principal peaks, it can be noticed that it decreases with increasing scanning rate, becoming twice lower for v = 100 mV/s in comparison with the ratio value corresponding to the rate v = 8 mV/s.

This fact indicates the low rates to promote the oxidative processes and the high rates for the reductive ones. The intermediary rate of 50 mV/s ensures values of this ratio closed to unity, hence the quasireversibility

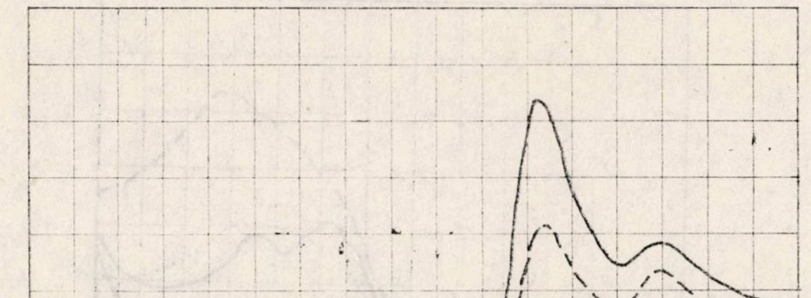

Fig. 1. — Influence of scanning rate on the characteristics of cyclic voltammograms (C.P.E ; pFDA $5 \cdot 10^{-4}$ mol · L^{-1} ; Na_2SO_4 10^{-1} M ; $-0.3 \rightleftharpoons +1.4$ V with respect to S.C.E. ; $S = 3.10^{-7}$ A/div.)

— · — · — v = 8 mV/s
— — — v = 50 mV/s
——— v = 100 mV/s.

Table 3

Influence of scanning rate on the characteristics of cyclic voltammograms (PCE, pFDA $5 \cdot 10^{-4}$ mol · L^{-1} ; Na_2SO_4 10^{-1} M ; potential range $-0.3 \rightleftharpoons +1.4$ V versus SCE ; $S = 3 \cdot 10^{-7}$ A/div.)

Scanning rate (mV/s)	Anodic peaks		Cathodic peaks		$\frac{ip_a}{ip_c}$ *
	Ep_a(V)	ip_a(μA)	Ep_c(V)	ip_c(μA)	
8	—	—	+0.030	0.75	2.18
	+0.370	3.60	+0.270	1.65	
50	+0.120	0.75	0.000	0.120	1.16
	+0.380	6.30	+0.260	5.40	
100	+0.120	0.30	0.000	0.30	1.07
	+0.410	9.30	+0.270	8.70	

* The ip_a/ip_c ratio was calculated for the main peaks

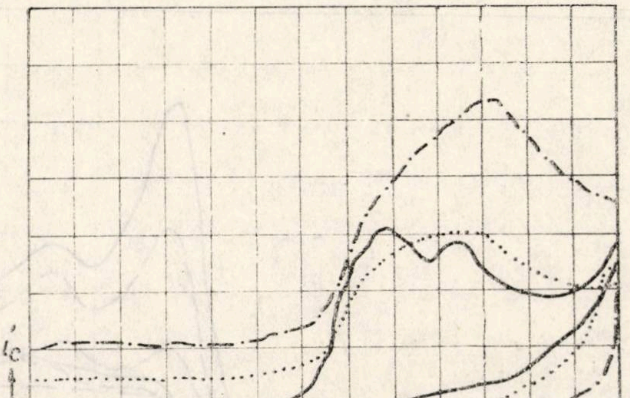

Fig. 2. — Influence of scanning rate on the characteristics of cyclic voltammograms (Sp.C.E. ; pFDA $5 \cdot 10^{-4}$ mol $\cdot$ L^{-1} ; Na_2SO_4 10^{-1}M ; $-0.3 \rightleftharpoons +1.4$ V with respect to S.C.E)

——— v = 8 mV/s ; S = $2 \cdot 10^{-7}$ A/div
— — — v = 50 mV/s ; S = $8 \cdot 10^{-7}$ A/div
—·—·— v = 100 mV/s ; S = $8 \cdot 10^{-7}$ A/div.

Table 4

Influence of scanning rate on the characteristics of cyclic voltammograms (Sp.C.E ; pFDA $5 \cdot 10^{-4}$ mol $\cdot$ L^{-1} ; Na_2SO_4 10^{-1}N ; potential range $-0.30 \rightleftharpoons +1.4$ V versus S.C.E)

Scanning rate (mV/s)	Anodic peaks		Cathodic peaks		$\frac{ip_a}{ip_c}$ *
	Ep_a(V)	ip_a(μA)	Ep_c(V)	ip_c(μA)	
8	+0.100 +0.380	0.20 4.20	+0.225 +0.060	3.00 2.60	1.40
50	+0.120 +0.425	0.80 9.20	+0.240 0.000	9.60 10.00	0.96
100	+0.130	1.20	+0.270	8.80	0.75
			+0.160	13.60	
	+0.425	13.20	−0.020	17.60	

* The ip_a/ip_c ratio was calculated for the main peaks

of the electrode processes. That is why this rate was considered the optimum for the following investigations.

The ip — v and ip — $\sqrt{v}$ plottings can give information on the nature of the predominant voltammetric current corresponding to anodic and cathodic processes, respectively.

With C.P.E. the intensity of the voltammetric current increases linearly with increasing scanning rate for the anodic process and partially linearly for the cathodic ones (Fig. 3).

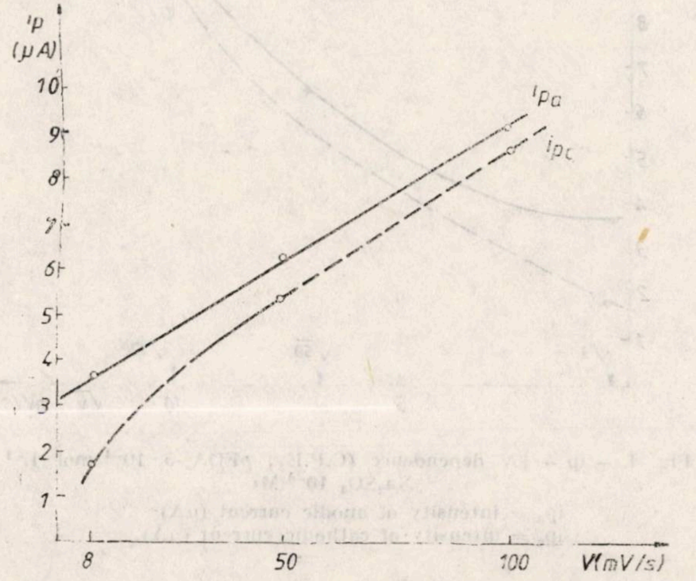

Fig. 3. — Influence of scanning rate on the intensity of voltammetric currents (C.P.E.; *p*FDA $5 \cdot 10^{-4}$ mol · L^{-1}; Na_2SO_4 10^{-1}M)
ip_a = height of anodic peak (µA)
ip_c = height of cathodic peak (µA).

Non-linearity is noticed with rates lower than 25 mV/s.

According by Murray [18] the proportionality $ip = k \cdot v$ between the intensity of the voltammetric current and the rate of potential recording is valid for a redox monolayer immobilized on the electrode surface if the electrode reaction is reversible.

The linear dependence ip — $\sqrt{v}$ is characteristic to the multimolecular layers participanting to a reversible process. The electrode might favour the formation of multi-molecular layers under certain conditions: for lower rates within the cathodic domain and for higher rates within the anodic domain (Fig. 4).

The loading of the electrode surface [18,19] $\left(\Gamma = \frac{Q}{nFA}\right)$ confirms the presence of multi-molecular layers ($\Gamma > 10^{-10}$ mol · cm^{-2}, a value accepted for a redox monolayer immobilized on the electrode surface). The electrode nature and scanning rate have a significant influence on the layer thickness (Table 5).

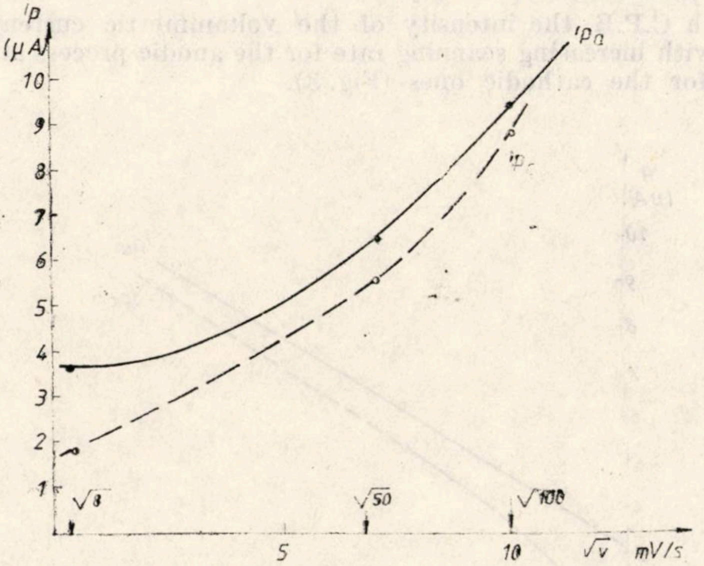

Fig. 4. — ip — $\sqrt{v}$ dependence (C.P.E.; pFDA $5 \cdot 10^{-4}$ mol · L^{-1}; Na_2SO_4 10^{-1} M)

ip_a = intensity of anodic current (µA)
ip_c = intensity of cathodic current (µA).

Table 5

Influence of electrode nature and scanning rate of the potential on the electrode surface loading

Scanning rate (mV/s)	Sp.C.E.		P.C.E.	
	Γp_a (mol · cm^{-2})	Γp_c (mol · cm^{-2})	Γp_a (mol · cm^{-2})	Γp_c (mol · cm^{-2})
8	$1.540 \cdot 10^{-8}$	$0.968 \cdot 10^{-8}$	$0.9088 \cdot 10^{-8}$	$0.3784 \cdot 10^{-8}$
50	$0.7045 \cdot 10^{-8}$	$0.920 \cdot 10^{-8}$	$0.2740 \cdot 10^{-8}$	$0.2575 \cdot 10^{-8}$
100	$0.4840 \cdot 10^{-8}$	$0.840 \cdot 10^{-8}$	$0.2045 \cdot 10^{-8}$	$0.2550 \cdot 10^{-8}$

The loading of the surface can be seen to be larger at lower scanning rates. The influence of the scanning rate is stronger in the case of the anodic processes. A rate of 50 mV/s ensures comparable surface loadings in both anodic and cathodic processes . C.P.E. favours the immobilization of a thinner layer of depolarizer in comparison with Sp.C.E.

The sensitivity of the run is known to be higher for thinner immobilized layers. This would explain the higher values obtained for ip_a and ip_c at $v = 100$ mV/s on both electrodes for the same concentration of *p*FDA and working conditions (Tables 3, 4).

The slopes of the $\lg ip_c - \lg v$ and $\lg ip_a - \lg v$ functions ($tg\ \alpha = 0.650$ and $tg\ \alpha = 0.433$, respectively) are indicative of the mixed character of the voltammetric currents on P.C.E., namely adsorption and diffusion for cathodic peak ($0.5 < tg\ \alpha < 1.0$) and diffusion for the anodic one ($tg\ \alpha \cong 0.5$) (Fig. 5)

On Sp.C.E. the reversible processes proceeding on monomolecular layer prevail (Fig. 6).

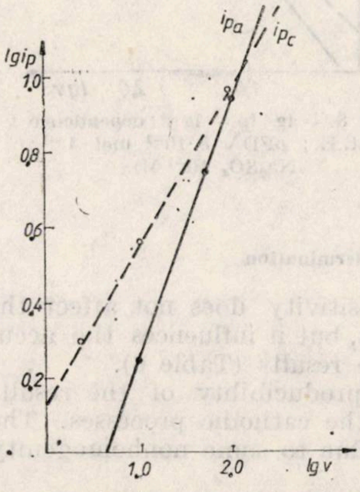

Fig. 5. — lg ip — lg v dependence (C.P.E.; *p*FDA $5 \cdot 10^{-4}$ mol · L^{-1}; Na_2SO_4 10^{-1} M)

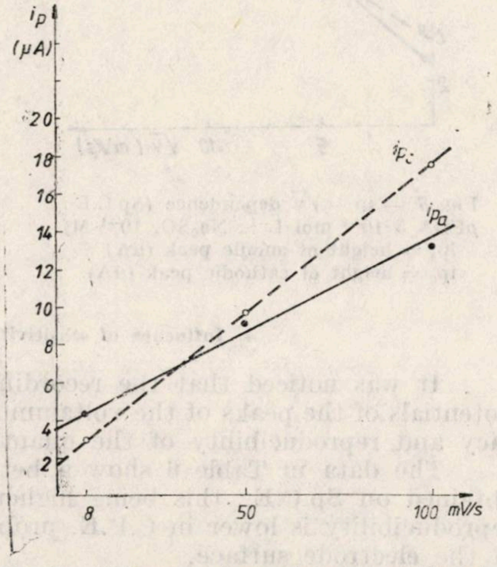

Fig. 6. — Influence of scanning rate on the intensity of voltammetric currents (Sp.C.E.; *p*FDA $5 \cdot 10^{-4}$ mol · L^{-1}; Na_2SO_4 10^{-1} M)
ip_a = height of anodic peak (μA)
ip_c = height of cathodic peak (μA).

Only within the domain of low scanning rates ($v < 50$ mV/s), the tendency of promoting the reversible processes in multi-molecular layers (Fig. 7) appears, both in the anodic range and in the cathodic one.

The anodic voltammetric current is controlled by diffusion ($tg\ \alpha = 0.44$, hence $\cong 0.50$), while the cathodic current has a mixed character of diffusion and adsorption ($tg\ \alpha = 0.60$ hence between 0.50 and 1.0) (Fig. 8).

With all scanning rates under consideration, the Sp.C.E. response in more intense than that of C.P.E., in both anodic and cathodic domain, for a certain concentration value. The Sp.C.E. may be considered as a more sensitive sensor.

The recording sensitivity is another parameter to be taken into account.

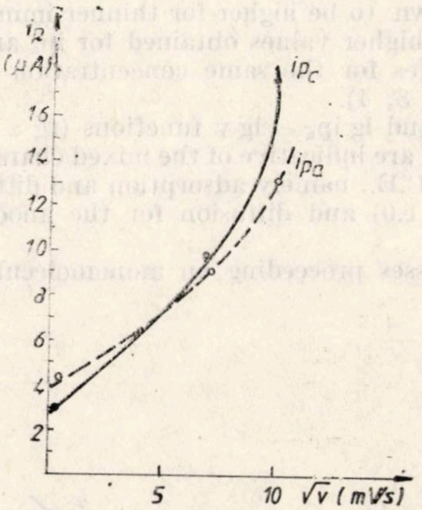

Fig. 7. — ip — $\sqrt{v}$ dependence (Sp.C.E ; *p*FDA $5 \cdot 10^{-4}$ mol $\cdot$ L^{-1} ; Na_2SO_4 10^{-1} M)
ip_a = height of anodic peak (μA)
ip_c = height of cathodic peak (μA).

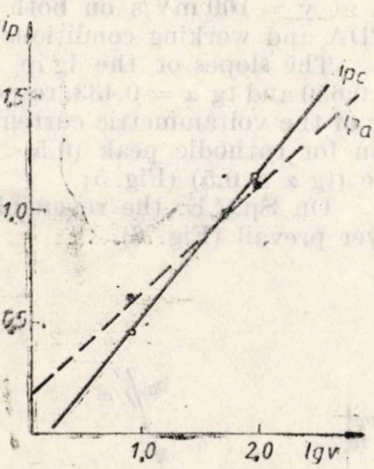

Fig. 8. — lg ip — lg v dependence (Sp.C.E. ; *p*FDA $5 \cdot 10^{-4}$ mol $\cdot$ L^{-1} ; Na_2SO_4 10^{-1} M).

4. Influence of sensitivity of determination

It was noticed that the recording sensitivity does not affect the potentials of the peaks of the voltammograms, but it influences the accuracy and reproducibility of the quantitative results (Table 6).

The data in Table 6 show a better reproducibility of the results obtained on Sp.C.E., this being higher for the cathodic processes. The reproducibility is lower in C.P.E. probably due to some nonhomogenity of the electrode surface.

However, both electrodes ensure a relatively reversible electrochemical process, which is confirmed by the ip_a/ip_c ratio value of about 1.0 ; from this point of view Sp.C.E. seems to be superior to C.P.E. The general shape of the cyclic voltammograms, hence the qualitative reflection of the electrode process, is practically independent of this parameter.

5. Influence of depolarizer concentration

The influence of the *p*FDA concentration on the cyclic voltammogram shapes recorder with C.P.E. and Sp.C.E. in 10^{-1} M Na_2SO_4 solution results in unsignificant variations of the peak potential and in proportional increase of their heights. The less intense peaks obtained at low concentrations become more pronounced at high concentrations.

These observations are also valid for the recordings resulting with Sp.C.E. in 10^{-1} M HCl solution.

The recording reproducibility is good, the intensity of the anodic and cathodic current becoming constant after three scanning cycles.

Table 6

Influence of sensitivity of determination on the characteristics of cyclic voltammogram (pFDA $5 \cdot 10^{-4}$ mol $\cdot$ L^{-1}; Na_2SO_4 10^{-1}M; v = 50 mV/s; potential range $-0.3 \rightleftharpoons +1.4$ V versus S.C.E.)

Electrode	Sensitivity A/div.	Anodic peaks		Cathodic peaks		$\frac{ip_a}{ip_c}$*
		Ep_a(V)	ip_a(μA)	Ep_c(V)	ipc_c(μA)	
Sp.C.E.	$8 \cdot 10^{-7}$	+0.100 +0.400	0.80 12.00	+0.250 +0.020	10.00 2.40	1.20
	$6 \cdot 10^{-7}$	+0.120 +0.410	0.90 11.10	+0.240 +0.020	10.20 2.40	1.10
	$4 \cdot 10^{-7}$	+0.120 +0.425	0.80 9.20	+0.240 +0.000	9.60 2.40	0.96
P.C.E.	$12 \cdot 10^{-8}$	+0.100 +0.360	0.30 4.20	+0.020 +0.260	0.36 3.60	1.16
	$2 \cdot 10^{-7}$	+0.100 +0.400	0.50 5.40	−0.030 +0.230	0.90 4.00	1.35
	$3 \cdot 10^{-7}$	+0.120 +0.380	0.75 6.30	0.000 +0.260	1.20 5.40	1.16
	$4 \cdot 10^{-7}$	+0.100 +0.440	0.60 5.60	−0.030 +0.230	0.40 4.20	1.33

* The ip_a/ip_c ratio was calculated for the principal peaks

Within the concentration range under investigation ($1-5 \cdot 10^{-4}$ mol $\cdot$ L^{-1} on C.P.E. and $2.5-7.5 \cdot 10^{-4}$ mol $\cdot$ L^{-1} on Sp.C.E.) in both support-electrolytes the intensity of the voltammetric currents for the principal peaks of the voltammograms, versus concentration, is linear (Figs. 9, 10, 11).

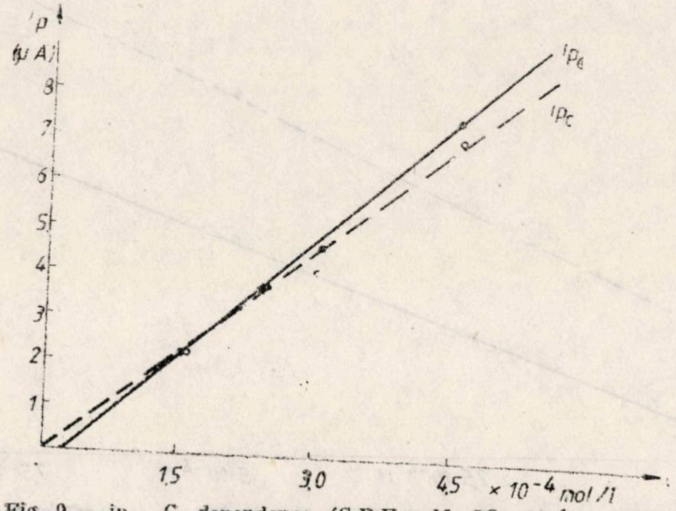

Fig. 9. — ip — C dependence (C.P.E.; Na_2SO_4 10^{-1} M; S = $4 \cdot 10^{-7}$ A/div.; v = 50 mV/s)
ip_a = height anodic peak (μA)
ip_c = height cathodic peak (μA)

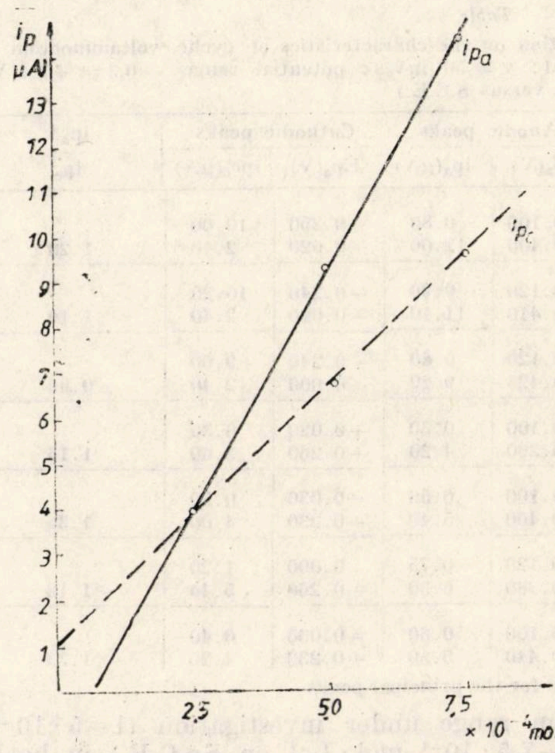

Fig. 10. — ip — C dependence (Sp.C.E.; Na_2SO_4 10^{-1}M; S = $= 4 \cdot 10^{-7}$ A/div.; v = 50 mV/s)
ip_a = height of anodic peak (μA)
ip_c = height of cathodic peak (μA)

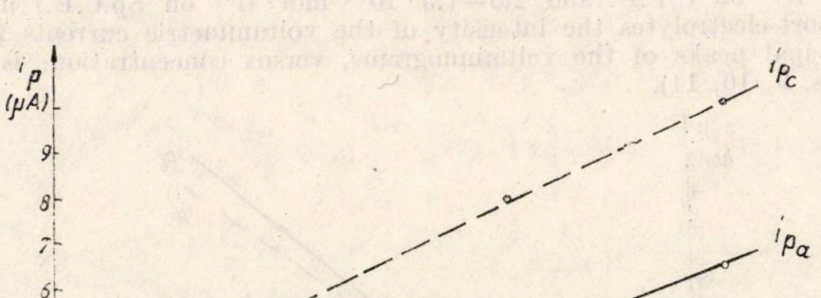

Fig. 11. — ip — C dependence (Sp.C.E.; HCl 10^{-1} M; v = 50 mV/s; S=$4 \cdot 10^{-7}$ A/div.)
ip_a = height of anodic peak (μA)
ip_c = height of cathodic peak (μA).

This fact confirms the diffusion to be the principal phenomenon of the electrode processes under the given conditions.

The high value of the residual current intensity in case of the recordings carried out on Sp.C.E. in 10^{-1} M HCl deserves mention.

Due to rather complex shape of the cyclic voltammograms, the overall voltammetric process was estimated by weighing the area of the cyclic voltammograms, in order to express more accurately the correlation between the electrode response and the concentration of the organic depolarizer.

The plottings of these dependences $(A(g) - C\ (\mathrm{mol} \cdot L^{-1}))$ drawn in Figs. 12, 13 and 14, confirm the linearity of the intensity of the overall electrode process versus concentration.

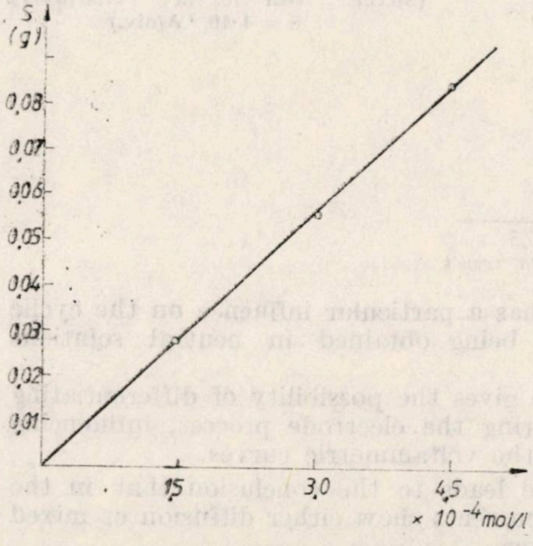

Fig. 12. — Area of the cyclic voltammogram versus pFDA concentration (C.P.E.; Na_2SO_4 10^{-1}M; v = 50 mV/s; S = 4 ·10^{-7} A/div.)

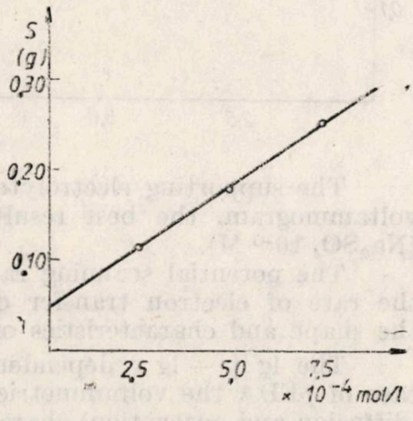

Fig. 13. — Area of the cyclic voltammogram (grams) versus pFDA concentration (Sp.C.E.; Na_2SO_4 10^{-1} M; v = 50 mV/s; S = 4 ·10^{-7} A/div.)

The areas of the voltammograms obtained in 10^{-1} M HCl solution on Sp.C.E. are noticed to be much larger than those in 10^{-1} M Na_2SO_4 solution.

If the intensity of the residual current is considered, the high qualities of the C.P.E. are clearly evidenced.

CONCLUSIONS

The pFDA can be characterized from the electrochemical point of view by cyclic voltammetry within the $-0.3\ V \rightleftharpoons +1.4\ V$ potential domain, with respect to S.C.E., by using Sp.C.E. and C.P.E. as working electrodes.

C.P.E. gives thin voltammograms of small areas and sharp peaks, but the sensitivity is lower. Sp.C.E. is more sensitive, but the residual current is of higher intensity.

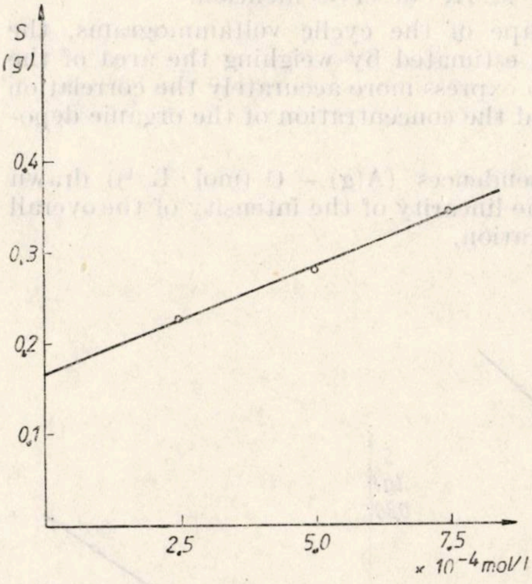

Fig. 14. — Area of the cyclic voltammogram (grams) versus *p*FDA concentration (Sp.C.E. ; HCl 10^{-1} M ; v=50 mV/s ; S = $4 \cdot 10^{-7}$ A/div.)

The supporting electrolyte has a particular influence on the cyclic voltammogram, the best results being obtained in neutral solutions (Na_2SO_4 10^{-1} M).

The potential scanning rate gives the possibility of differentiating the rate of electron transfer during the electrode process, influencing the shape and characteristics of the voltammetric curves.

The lg ip — lg v dependence leads to the conclusion that in the case of *p*FDA the voltammetric currents show either diffusion or mixed (diffusion and adsorption) character.

The heights of the main anodic and cathodic peaks of the cyclic voltammograms increase proportionally with increasing the concentration within the range under study ($1 \cdot 10^{-4} - 7.5 \cdot 10^{-4}$ mol · L^{-1}) which confirms the diffusion as the main phenomenon of the transport of the electroactive species toward the electrode surface.

The linear A(g) — C (mol · L^{-1}) dependence also confirms the overall electrode process to be controlled predominantly by diffusion.

It results that within the $-0.3 \rightleftharpoons +1.4$ V potential domain (with respect to S.C.E.) *p*FDA suffers a partially reversible oxidation — reduction process on both C.P.E. and Sp.C.E., the voltammetric current being controlled predominantly by diffusion within the anodic range and by diffusion and adsorption within the cathodic one.

Finally, by properly choosing the depolarizer concentration, potential scanning rate, recording sensitivity and suporting electrolyte, cyclic voltammograms particularly expressive for *p*FDA can be obtained with both electrodes.

REFERENCES

[1] R. N. Adams, "Electrochemistry at Solid Electrodes", Marcel Dekker, New York, 1969, p. 327 (*Bull. Soc. Chim. Fr.*, **5**, 791 (1987)).

[2] S. S. Lord, and L. B. Rogers, *Anal. chem*, **26**, 284 (1954).

[3] V. F. Gaylor, A. L. Conrad and J. H. Landere, *Anal. chem.*, **29**, 224 and 228 (1957).

[4] L. Kekedy, "Sensori electrochimici metalici și ionseselectivi", Ed. Academiei, 1987, p. 33.

[5] W. U. Malik, R. N. Goyal and Rajeshwari, *Bull. Soc. Chim. France*, **5**, 791 (1987).

[6] R. Lindquist, *J. Electroanal. chem.*, **52**, 37 (1976).

[7] R. P. Baldwin, J. K. Christensen and L. Kryger, *Anal. chem.*, **58**, 1790 (1986).

[8] S. V. Prabhu, R. P. Baldwin, and L. Kryger, *Anal. chem.*, **59**, 1074, (1987).

[9] Z. A. Gallai, N. M. Seina, N. V. Svedene and G. L. Oliferenko, *Zhur. Anal. Himii*, **41**, 1743 (1986) (*Ref. Zhur. Khim.* 18G285, 1986).

[10] G. N. Budnikov, *Zhur. Anal. Himii*, **41**, 1743 (1986) (*Ref. Zhur. Khim.* 3G 26, 1987).

[11] G. Caúquis, G. Fanvalot and J. Rigany, *Bull. Soc. Chim. France*, **12**, 4928 (1968).

[12] S. Wawzonek and T. W. McIntyre, *J. Electrochem. Soc.*, **114**, 1025 (1967).

[13] J. F. Price and R. P. Baldwin, *Anal. chem.*, **52**, 1940 (1980).

[14] J. Bacon and R. N. Adams, *J. Amer. Chem. Soc.*, **90**, 6597 (1968) (*Bull. Soc. Chim. France*, **5**, 794 (1987).

[15] A. R. Guadalupe, S. S. Jhaveri, K. E. Lin and H. D. Abruña, *Anal. chem.*, **59**, 2436 (1987).

[16] A. R. Guadalupe and H. D. Abruña, *Anal. Lett.*, **19**, 1613 (1986) (*Anal. chem.* **59**, 2436 (1987)).

[17] C. D. Nenitescu, "Chimie organică", vol. I, Ed. Tehnică, Bucharest, 1960, p. 521.

[18] R. G. Murray, "Electroanalytical Chemistry", vol. 13, Marcel Dekker, I.N.C., New York and Basel, 1984, p. 192.

[19] K. Ravichandran and R. P. Baldwin, *Anal. chem.*, **55**, 1586, (1983).

Revue Roumaine de Chimie, 36, 4–7, 455–463 (1991)

Dedicated to Prof. ALEXANDRU T. BALABAN
on the occasion of his 60th anniversary

MOLECULAR TOPOLOGY. 10*

FRAGMENTATION OF MOLECULAR GRAPHS WITHIN χ(RANDIĆ,[75Ran]) AND Y[90Diu$_1$] TOPOLOGICAL INDICES

IRÉN E. KACSÓ, ANGELA BARAŞ-DIUDEA and MIRCEA V. DIUDEA **
Department of Chemistry, "Babeş-Bolyai" University of Cluj
R-3400 Cluj, Romania

Received December 1, 1990

(Fragmental invariants within χ (Randić)[1] and Y[2] indices are derived in two variants: i) which preserves the degree of fragmentation vertices as in the whole graph and ii) with vertex degrees as in fragments. One point fragmental invariants on this ground are derived and the molecular branching within these indices is discussed.

1. INTRODUCTION

By cutting one or more edges in a molecular (hydrogen depleted) graph a univalent or a polyvalent molecular fragment is detached. The fragment, F, can be characterized by considering either its own atoms and edges (by the so-called "internal fragment indices/invariants", IFI [3]), or its interaction with the remainder of the molecule, G – F (by the "external fragment indices/invariants", EFI [3]). Mekenyan, Bonchev and Balaban [3] have made a detailed analysis of fragmentation of molecular graphs and the corresponding decomposition of several well-known graph invariants (topological indices).

The authors treated the IFI for fragments like the invariant I(G) for the whole molecule, whereas the EFI are specified as the difference in value between the global invariant and the internal fragment invariants for the two fragments, the detached and the remainder one:

$$\mathrm{EFI(F)} = \mathrm{I(G)} - [\mathrm{IFI(F)} + \sum_{c} \mathrm{IFI}(\mathrm{G} - \mathrm{F})_c] \qquad (1)$$

where c counts the components of the remainder graph (which can be a connected ($c = 1$) or a disconnected ($c > 1$) graph). In addition to the IFI/EFI, they used normalized invariants, NIFI/NEFI which were obtained by dividing by I(G).

---

* M.T.9. Composition rules for some topological indices, M. V. Diudea et al. MATCH (submitted).

** Author to whom correspondence should be addressed.

As the fragmental invariants must reflect the fragment topology in the same manner as the corresponding global invariants do,[3] the former ones were developed in connection with QSAR studies.[3,4–6] For details, see [3].

In this paper, we limit to discuss only two indices : χ (Randić's connectivity index,[1] and Y [2] vs. the molecular branching —as the main property they encode.

2. FRAGMENTAL INDICES

When the fragmentation of a molecular graph is made, the degree of the fragmentation points (the end points of cut edges) can be considered either like in the whole graph (the d_{Gi} — before cutting — variant) or as in the resulting fragments (the d_i — after cutting — variant). The two types of degrees are related by :

$$d_{Gi} = d_i + ce_i \qquad (2)$$

where ce_i stands for the cut edges incident in vertex i.
When $ce_i = 1$, the fragment is univalent whereas $ce_i > 1$ it is a polyvalent one.

2.1. Fragmental indices of connectivity, χ (Randić)[1]

$$\chi(G) = \sum_{(ij)\in G} (d_{Gi} \times d_{Gj})^{-1/2} \qquad (3)$$

i) d_{Gi} — variant

$$IF \cdot \chi(F) = \sum_{(ij)\in F} (d_{Gi} \times d_{Gj})^{-1/2}$$

$$IF \cdot \chi(G - F) = \sum_{c} \sum_{(ij)\in (G-F)_c} (d_{Gi} \times d_{Gj})^{-1/2}$$

$$EF \cdot \chi(F) = \chi(G) - \sum_{(ij)\in F} (d_{Gi} \times d_{Gj})^{-1/2} - \sum_{c} \sum_{(ij)\in (G-F)_c} (d_{Gi} \times d_{Gj})^{-1/2} =$$

$$= \sum_{(ij)\in fce} (d_{Gi} \times d_{Gj})^{-1/2} \qquad (4)$$

ii) d_i — variant[3]

$$IF \cdot \chi(F) = \sum_{(ij)\in F} (d_i \times d_j)^{-1/2}$$

$$IF \cdot \chi(G - F) = \sum_{c} \sum_{(ij)\in (G-F)_c} (d_i \times d_j)^{-1/2} \qquad (5)$$

$$\mathrm{EF}\cdot\chi(\mathrm{F}) = \chi(\mathrm{G}) - \sum_{(ij)\in(\mathrm{F})} (d_i \times d_j)^{-1/2} - \sum_{c}\sum_{(ij)\in(\mathrm{G-F})_c} (d_i \times d_j)^{-1/2} =$$

$$= \sum_{(ij)\in \mathrm{fce}} \{[(d_i + ce_i)(d_j + ce_j)]^{-1/2} +$$

$$+ \sum_{a,i\in \mathrm{F}} [[(d_i + ce_i) \times d_a]^{-1/2} - (d_i \times d_a)^{-1/2}] +$$

$$+ \sum_{c}\sum_{(a,j)\in(\mathrm{G-F})_c} [[(d_j + ce_j) \times d_a]^{-1/2} - (d_j \times d_a)^{-1/2}]\}$$

where *a* represents vertices adjacent to the fragmentation points and $\sum_i ce_i + \sum_j ce_j = 2N_{fce}$ (the number of fragment cut edges).

For $G_1 - G_3$ (see [3]) one obtains :

G	χ(G)	var.	IF · χ(G − F)	IF · χ(F)	EF · χ(F)
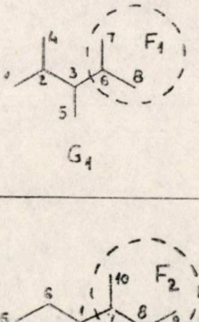	3.553418	d_{Gi} d_i	2.065384 2.270056	1.154701 1.414214	0.333333 −0.130851
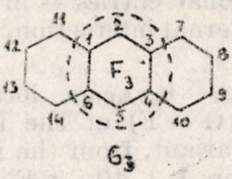	4.842535	d_{Gi} d_i	2.816497 3.000000	1.692705 1.914210	0.333333 −0.071680
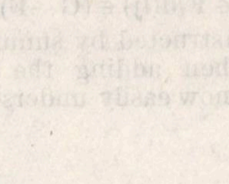 F₃ 1 2 3 4 5 6 7 8 9 10 11 12 13 14 G₃	6.932653	d_{Gi} d_i	3.000000 3.828430	2.299660 3.000000	1.632993 0.104220

2.2. Fragmental Y — indices

$$\mathrm{Y(G)} = \sum_{i,d(ij)\in \mathrm{G}} b_{\mathrm{G}i,d(ij)} \times 10^{-d(ij)} \tag{6}$$

where $b_{Gi,d(ij)} = \sum_{j:d(ij)=\text{const}} d_{Gj}$; with : $i, j \in G$; $d(ij) = \begin{cases} 0 ; & i = j \\ 0 < d(ij) \leqslant d_G ; & i \neq j \end{cases}$

$b_{Gi,d(ij)}$ — being the entries in the layer matrix of degree, B,

i) b_{Gi} — variant

$$\begin{aligned} IF \cdot Y(F) &= \sum_{i,d(ij) \in F} b_{Gi,d(ij)} \times 10^{-d(ij)} \\ IF \cdot Y(G - F) &= \sum_{c} \sum_{i,d(ij) \in (G-F)_c} b_{Gi,d(ij)} \times 10^{-d(ij)} \\ EF \cdot Y(F) &= Y(G) - \sum_{i,d(ij) \in F} b_{Gi,d(ij)} \times 10^{-d(ij)} - \\ &\quad - \sum_{c} \sum_{i,d(ij) \in (G-F)_c} b_{Gi,d(ij)} \times 10^{-d(ij)} \end{aligned} \tag{7}$$

ii) b_i — variant

$$\begin{aligned} IF \cdot Y(F) &= \sum_{i,d(ij) \in F} b_{i,d(ij)} \times 10^{-d(ij)} \\ IF \cdot Y(G - F) &= \sum_{c} \sum_{i,d(ij) \in (G-F)_c} b_{i,d(ij)} \times 10^{-d(ij)} \\ EF \cdot Y(F) &= Y(G) - \sum_{i,d(ij) \in F} b_{i,d(ij)} \times 10^{-d(ij)} - \\ &\quad - \sum_{c} \sum_{i,d(ij) \in (G-F)_c} b_{i,d(ij)} \times 10^{-d(ij)} \end{aligned} \tag{8}$$

Within the Y — index, which is built on the layer matrix, B, the interrelation between the fragments is less obvious. Since B can be derived from the DDG (distance — degree) matrix[2] we exemplify on the G_4 (Fig. 1).

The fragmental matrices, FB, are derived from the block — submatrices of the DDG matrix (with $d_{Gi} \setminus d_i$ — as diagonal entries — in the two proposed variants). From the matrices of the external interaction, EB, one obtains the following :

i) b_{Gi} — variant, from the rows $b_{Gk,d(kj) \in (G-F)} \setminus b_{G1,d(1j) \in F}$ located cf. the distance vectors $1 + d(kj) \in F \setminus 1 + d(lj) \in (G - F)$ of the fragmentation points, $k \in (G - F)/1 \in F$, and ii) b_i — variant, from the rows $b_{k,d(kj) \in (G-F)} \setminus b_{1,d(1j) \in F}$, located cf. the distance vectors $1 + d(kj) \in F \setminus 1 + d(lj) \in (G-F)$, added to the rows of the "ce-matrix" (the sequence (1,1) of the cut edge located cf. the vectors $d(kj) \in F/d(lj) \in (G-F)$.

The matrix B for the whole graph is thus constructed by summing FB and EB for F and (G—F) respectively and then adding the two above resulting matrices (as shown in Fig. 1). It is now easily understood

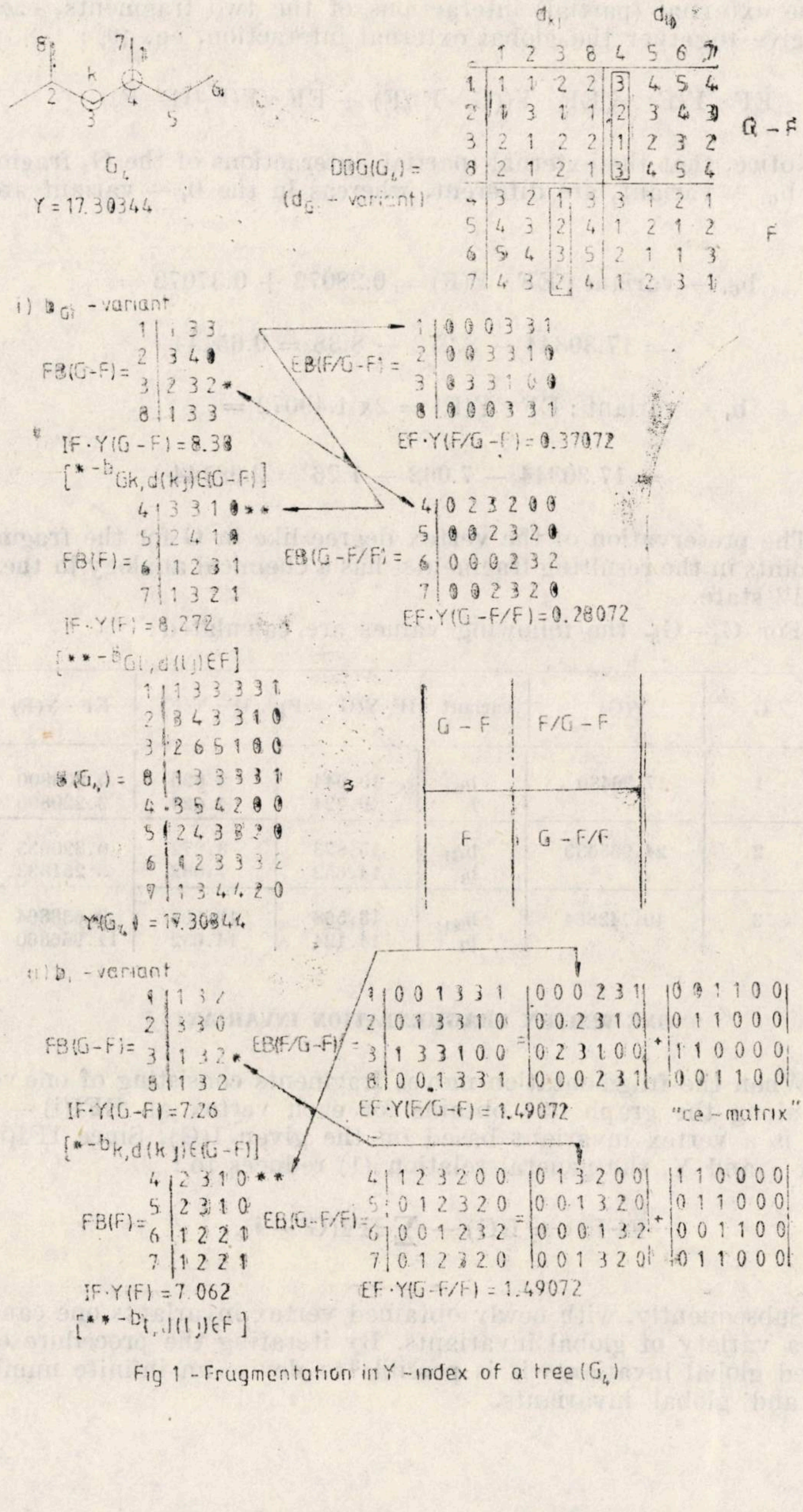
G_4
Y = 17.30344
DDG(G4) =
(d_G - variant)
d_{k1}
d_{l1}
G – F
F
i) b_{Gl} -variant
FB(G-F) =
IF·Y(G-F) = 8.38
EB(F/G-F) =
EF·Y(F/G-F) = 0.37072
[* - $b_{Gk,d(k)}$E(G-F)]
FB(F) =
IF·Y(F) = 8.272
EB(G-F/F) =
EF·Y(G-F/F) = 0.28072
[** - $b_{Gl,d(l)}$EF]
B(G4) =
Y(G4) = 17.30844
G – F
F/G – F
F
G – F/F
ii) b_l -variant
FB(G-F) =
IF·Y(G-F) = 7.26
EB(F/G-F) =
EF·Y(F/G-F) = 1.49072
"ce - matrix"
[* - $b_{k,d(k)}$E(G-F)]
FB(F) =
IF·Y(F) = 7.062
EB(G-F/F) =
EF·Y(G-F/F) = 1.49072
[** - $b_{l,d(l)}$EF]

Fig 1 - Fragmentation in Y-index of a tree (G_4)

that the external (partial) interactions of the two fragments, each on other, give together the global external interaction, eq. (9):

$$\mathrm{EF} \cdot Y(\mathrm{F}) = \mathrm{EF} \cdot Y((\mathrm{G}-\mathrm{F})/\mathrm{F}) + \mathrm{EF} \cdot Y(\mathrm{F}/(\mathrm{G}-\mathrm{F})) \tag{9}$$

Notice, that the external (partial)interactions of the G_4 fragments, in the b_{Gi} — variant, are different, whereas in the b_i — variant are the same.

$$b_{Gi} - \text{variant} : \mathrm{EF} \cdot Y(\mathrm{F}) = 0.28072 + 0.37072 =$$

$$= 17.30344 - 8.272 - 8.38 = 0.65144$$

$$b_i - \text{variant} : \mathrm{EF} \cdot Y(\mathrm{F}) = 2\mathrm{x}\, 1.49072 =$$

$$= 17.30344 - 7.062 - 7.26 = 2.98144$$

The preservation of the vertex degree like in G for the fragmentation points in the resulting fragments has a chemical analogy in the "free radical" state.

For $G_1 - G_3$, the following values are calculated:

G	Y(G)	variant	IF · Y(G − F)	IF · Y(F)	EF · Y(F)
1	17.56480	b_{Gi} b_i	10.944 9.724	5.820 4.620	0.800800 3.220800
2	24.965633	b_{Gi} b_i	15.873 14.652	8.272 7.062	0.820633 3.251633
3	40.742864	b_{Gi} b_i	18.568 14.124	19.536 14.652	2.638864 11.966860

3. ONE VERTEX FRAGMENTATION INVARIANTS[3]

When the fragmentation moves fragments consisting of one vertex/atom along the graph one obtains for each vertex an EFI(i) — value which is a vertex invariant based on the given I(G). Since IFI(i) = 0 within χ and Y, the general relation (1) reduces to:

$$\mathrm{EFI(i)} = \mathrm{I(G)} - \sum_{c} \mathrm{IFI(G - i)_c} \tag{10}$$

Subsequently, with newly obtained vertex invariants one can construct a variety of global invariants. By iterating the procedure on the resulted global invariants it is possible[3] to devise an infinite number of local and global invariants.

Table 1

The EFχ/EFY/Y indices in the graphs G_5-G_{14}

	G_5	G_6	G_7	G_8	G_9	G_{10}	G_{11}	G_{12}	G_{13}	G_{14}
1	0.5380 2.2664 —	0.5380 2.4664 —	0.5380 2.4664 —	0.5000 2.4466 —	0.5380 2.4686 —	0.5000 2.4445 1.2222	0.5607 2.4884 1.2442	0.5607 2.4884 1.2442	0.5607 2.4884 1.2442	0.5000 2.4488 1.2244
2	0.8938 5.1306 —	0.8938 5.1309 —	0.8938 5.1308 —	1.0380 4.9131 —	0.9107 5.1550 —	1.0000 4.8889 2.3222	0.8512 5.3730 2.5422	0.8513 5.3729 2.5422	0.8513 5.3729 2.5422	1.0607 4.9372 2.3442
3	0.8938 7.8168 —	0.8938 7.8195 —	0.8938 7.8197 —	0.3938 5.3775 —	0.8045 8.0856 —	0.5000 5.1333 2.4322	1.2071 10.7263 4.6322	1.2071 10.7261 4.6322	1.2071 10.7262 4.6322	0.3513 5.6217 2.6522
4	0.3938 5.3748 —	0.4796 5.3995 —	0.4796 5.4019 —	0.9796 7.8461 —	0.8903 8.1098 —	0.5858 5.1578 2.4432	0.4370 5.6467 2.6632	0.4371 5.6466 2.6632	0.4370 5.6664 2.6632	1.2929 10.7550 4.6432
5	1.0380 4.9128 —	0.5380 5.1575 —	0.6238 5.1819 —	0.4796 5.4019 —	0.4107 5.4016 —	0.5858 5.1603 2.4443	0.6464 5.2091 2.4663	0.6464 5.2090 2.4663	0.6464 5.2091 2.4663	0.4370 5.6491 2.6643
6	0.5000 2.4466 —	1.0000 4.8913 —	0.5000 5.1357 —	0.5380 5.1577 —	1.0380 4.9154 —	0.5858 5.1609 2.4446	0.5858 5.1653 2.4466	0.5858 5.1653 2.4466	0.5858 5.1653 2.4466	0.6464 5.2099 2.4666
7	0.3938 2.6862 —	0.5000 2.4447 —	1.0000 4.8891 —	1.0000 4.8913 —	0.5000 2.4468 —	0.5858 5.1654 2.4466	0.5858 5.1613 2.4448	0.5858 5.1610 2.4447	0.5858 5.1612 2.4448	0.5858 5.1703 2.4488
8	— — —	0.3938 2.6864 —	0.5000 2.4444 —	0.5000 2.4446 —	0.4107 2.7083 —	0.6464 5.2093 2.4664	0.5858 5.1630 2.4455	0.5858 5.1608 2.4446	0.5858 5.1632 2.4457	0.6464 5.2098 2.4666
9	— — —	— — —	0.3938 2.6864 —	0.3938 2.6886 —	0.4107 2.7103 —	0.4370 5.6494 2.6644	0.6238 5.1847 2.4553	0.5858 5.1631 2.4456	0.6238 5.1873 2.4565	0.4370 5.4695 2.6644
10						1.2929 10.7580 4.6443	0.4796 5.4022 2.5532	0.6238 5.1870 2.4564	0.4965 5.4291 2.5653	1.2929 10.7580 4.6443
11						0.4370 5.6467 2.6632	0.8938 7.8198 3.5322	0.4965 5.4266 2.5642	0.8903 8.1128 3.6532	0.4370 5.6466 2.6632
12						0.5607 5.2066 2.4542	0.8938 5.1309 2.4322	0.8523 8.0862 3.6442	0.8054 8.0860 3.6422	0.5607 5.1822 2.4542
13						1.0000 4.8938 2.3244	0.5380 2.4665 1.2332	1.2665 7.8172 3.5322	0.9107 5.1551 2.4432	1.0000 4.8937 2.3244
14						0.5000 2.6494 1.2224	0.3938 2.6865 1.3432	0.3727 2.6864 1.3432	0.5380 2.4686 1.2343	0.5000 2.4449 1.2224

	G_5	G_6	G_7	G_8	G_9	G_{10}	G_{11}	G_{12}	G_{13}	G_{14}
15						0.3133 2.9089 1.4544	0.3133 2.9065 1.4532	0.3727 2.6864 1.3432	0.4107 2.7084 1.3542	0.3133 2.9090 1.4544
16						0.3133 2.9089 1.4544	0.3133 2.9065 1.4532	0.4107 2.7084 1.3542	0.4107 2.7101 1.3553	0.3133 2.9090 1.4543
17								0.3133 2.9067 1.4532	0.3133 2.9064 1.4532	0.3133 2.9090 1.4543
18								0.3137 2.9064 1.4532	0.3133 2.9064 1.4532	0.3133 2.9087 1.4532
$EF\chi(G)$	8.8837	10.5196	12.2207	12.3708	11.7456	23.8770	23.2396	26.2430	26.1110	26.5542
$\overline{EF\chi(G)}$	1.4806	1.5028	1.5276	1.5464	1.4682	1.5918	1.5493	1.5437	1.5359	1.5620
$EFY(G)$	30.8342	35.9963	41.1563	41.1674	42.0014	78.9422	79.4366	90.5046	90.6228	90.9924
$\overline{EFY(G)}$	4.4049	4.4995	4.5792	4.5742	4.6668	4.9339	4.9648	5.0280	5.0346	5.0551
$Y(G)$						37.1039	37.3410	42.4718	42.4961	42.7012
$\overline{Y(G)}$						2.3189	2.3338	2.3597	2.3609	2.3723

We tested this idea, within χ and Y indices, on the graphs ($G_5 - G_{14}$) by constructing the EFI(G) like the original I(G). The results are collected in Table 1.

One can see that the EFI(i) – values reflect the type of vertex (its degree and location) and the global index EFI(G) follows in general the trend of the initial index I(G). Thus, the increased branching ordering of graphs, given by I(G) and EFI(G) is :

χ : $G_5 < G_6 < G_7 = G_8 < G_9 < G_{10} < G_{11} < G_{13} < G_{12} < G_{14}$

EF χ : $G_5 < G_6 < G_8 < G_7 < G_9 < G_{10} < G_{11} < G_{14} < G_{12} < G_{13}$

Y : $G_5 < G_6 < G_7 < G_8 < G_9 < G_{10} < G_{11} < G_{12} < G_{13} < G_{14}$

EFY : $G_5 < G_6 < G_7 < G_8 < G_9 < G_{10} < G_{11} < G_{12} < G_{13} < G_{14}$

The vertex invariants EFI(i) vary consistently towards the centers of complexity/branching (see [2]), with EFY(i) more sensitive to distance.

Notice that the ordering for EFχ we made in the spirit of χ whose values decrease as the branching of a graph increases. For other considerations on molecular branching consult [2,3,7]. Table 1 also includes the mean values $\overline{EFI(G)}$ as well as the invariants $\overline{Y(G)}$, Y(G) and Y(i) for the graphs (G10–G14).

Concluding, the fragmental parameters IFI and EFI, are useful tools in the topological investigation of molecular graphs as well as in the construction of interesting new invariants. The index Y is more sensitive to topological distance than the Randić index, χ, and its values better follow the intuitive concept of molecular branching (see [2,8]).

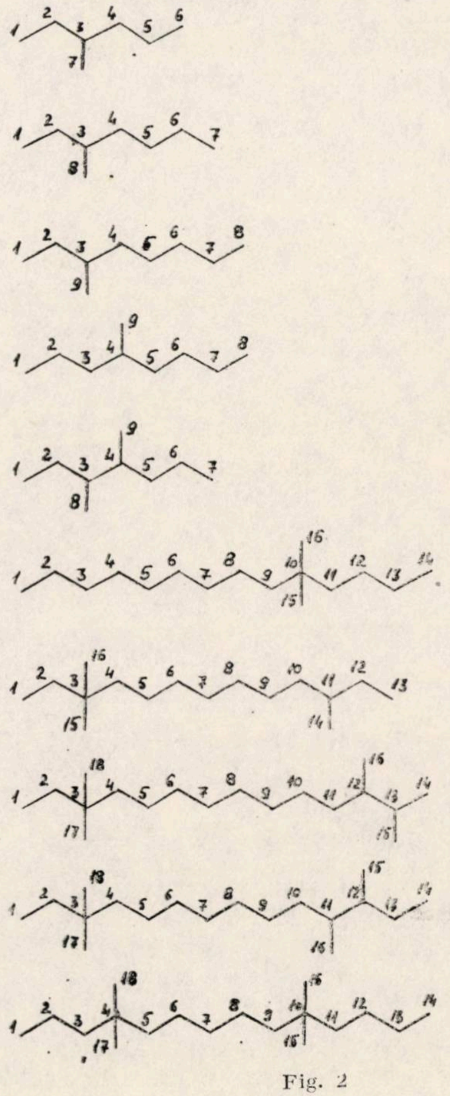
1 2 3 4 5 6 7
1 2 3 4 5 6 7 8
1 2 3 4 5 6 7 8 9
1 2 3 4 5 6 7 8 9
1 2 3 4 5 6 7 8 9
1 2 3 4 5 6 7 8 9 10 11 12 13 14 15 16
1 2 3 4 5 6 7 8 9 10 11 12 13 14 15 16
1 2 3 4 5 6 7 8 9 10 11 12 13 14 15 16 17 18
1 2 3 4 5 6 7 8 9 10 11 12 13 14 15 16 17 18
1 2 3 4 5 6 7 8 9 10 11 12 13 14 15 16 17 18

	χ	Y
G_5	3.30806	14.636827
G_6	3.80806	17.08148
G_7	4.30806	19.52595
G_8	4.30806	19.52813
G_9	4.21874	19.79180
G_{10}	7.62132	37.40393
G_{11}	7.51517	37.34108
G_{12}	8.38785	42.47183
G_{13}	8.42585	42.49611
G_{14}	8.32843	42.70124

Fig. 2

REFERENCES

[1] M. Randić, *J. Amer. Chem. Soc.*, **97**, 6609 (1975).

[2] M. V. Diudea, O. Minailiuc and A. T. Balaban, *J. Comput. Chem.*, **1—2**, 527 (1991).

[3] O. Mekenyan, D. Bonchev and A. T. Balaban, *J. Math. Chem.*, **2**, 347 (1988).

[4] L. B. Kier and L. H. Hall, "Molecular Connectivity in Chemistry and Drug Research", Academic Press, New York, 1976; L. B. Kier, W. J. Murray, M. Randić and L. H. Hall., *J. Pharm. Sci.*, **65**, 1226 (1976).

[5] A. T. Balaban and P. Filip, *MATCH*, **16**, 163 (1984).

[6] M. V. Diudea and B. Pârv, *MATCH*, **23**, 65 (1988).

[7] M. V. Diudea and I. Kacsó, *MATCH* (submitted).

[8] D. Bonchev and N. Trinajstić, *J. Chem. Phys.*, **67**, 4517 (1977).

Revue Roumaine de Chimie, 36, 4–7, 465–471 (1991)

Dedicated to Prof. ALEXANDRU T. BALABAN
on the occasion of his 60th anniversary

SURFACE AREA OF ORGANIC MOLECULES: A NEW METHOD OF COMPUTATION*

V. GOGONEA[a], D. CIUBOTARIU[b]*, E. DERETEY[b], M. POPESCU[c], I. IORGA[b] and M. MEDELEANU[b]

[a] ELOR Limited, Orăștie, Str. Plantelor No. 50, 2600 Orăștie, Romania
[b] Polytechnical Institute of Timișoara, Bd. 30 Decembrie No. 2, 1900 Timișoara, Romania
[c] Polytechnical Institute of Bucharest

Received December 29, 1990

A new nonanalytical procedure is proposed to calculate surface area of molecules. The concept of mesh uniformity used in the integrating procedure is accurately defined mathematically and further used to build up the algorithm. A critical view on a related method is given in the present paper. Comparative numerical results for several linear alkanes with respect to other computational methods are given, and an evaluation of the performances of the method according to the value of mesh grid is presented.

INTRODUCTION

The idea that molecular volumes and surfaces are of numerical significance is largely accepted now.[1] Confronting the geometrical attributes of simple molecules with the earlier established parameters of steric effects seems to be the current trend.[2,3] Ways to estimate surface areas have been developed [4,5,6] and the results have been evaluated.[7,8] Yet the main goals of published studies are the visualisation of surfaces and of the matching between forces of contiguous molecules to the similarity between related molecules.

Commonly, the molecule is treated as a solid in space which is defined by tracing spheres about the atomic nuclei. The dimensions of the molecular solid depend on the choice of the atomic radii. One option is to use van der Waals radii (r_w) as derived from crystallographic data, thus obtaining the van der Waals surface area (S_w). This practice is common in molecular graphics and in studies of molecules in liquid media. However, the van der Waals volume (V_w) enclosed by S_w does not fill the whole room that the molecule occupies in the liquid or even in a crystal. An alternative is to assign rather large radii to peripheral atoms (which are not part of the molecular backbone); these radii can be estimated by trial-and-error: one inflates the computed volume until it reaches the value derived from liquid density. The drawback is that the estimation of surface requires molecular volumes obtained from density in each particular case and calls for human decision during the computational process.

---

* To whom requests for reprints should be sent

THE CONCEPT OF MESH UNIFORMITY

The classical method of molecular volume and surface calculation,[9-11] and its variants [5,6,11] used a cuboid with minimal dimensions to enclose the molecule. A mesh intuitively defined as uniform is used for integrating procedure. The scan is conducted point-by-point, and with atom-by-atom checking whether the point is within distance r_a of any of the nuclei. If this is true, then it is taken to contribute an element g^3 (g stands for grid) to volume. If this is not true, then one checks whether it is within distance $r_a + g$, and if so, then it is taken to contribute an element g^2 to surface.

It is important to remark that the mesh uniformity feature is essential for the accuracy of the integrating method. In spite of the fact that this is considered to be true, it is not evident and mathematically proved. It is the isotropy of the Cartesian three-dimensional space which makes the right intuition. In a polar coordinate system, things are different. The idea of using polar coordinates to compute the molecular surface is not new, but we found it inadequately used.[5] Let us consider the facts : the mesh is generated with a stepwise variation in θ and φ angles, which are defined as in Fig. 1. Each atom i in the molecule is identified by a vector v_i containing the Cartesian coordinates of the atom centre and its van der Waals radius r_i. The atomic surface is sampled by a probe vector in the polar coordinates system with its origin in v_i and its radius $r = r_i$, touching each point of the surface by a stepwise variation in θ and φ angles. As already shown,[4] a non-uniform mesh is thus obtained which is inadequately used in the integrating procedure.

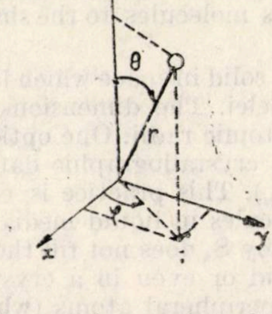

Fig. 1. — φ, θ and r coordinations definition.

Ways of improving the uniformity of this mesh were imagined and presented.[4] An attempt was made here to demonstrate that only certain coordinates could be chosen in order to obtain a uniform mesh by their stepwise variation. The condition to be fulfilled by these coordinates is : the first-order derivative of the surface function with respect to every coordinate must be a constant (see the appendix). In a two-dimensional Cartesian coordinate system, the area of a rectangle (with its sides parallel to the coordinate axes) as a function of the coordinates is shown in equation 1 :

$$S = f(x_1, x_2) = x_1 x_2 \tag{1}$$

$$\begin{aligned} \partial s/\partial x_1 &= x_2 \\ \partial s/\partial x_2 &= x_1 \end{aligned} \tag{2}$$

As it may be seen from equations 2, the first-order derivative of the surface function with respect to any of the two coordinates is a constant. This is why a uniform mesh in a cuboid may be obtained by stepwise variation of the Cartesian coordinates. In the case of polar coordinates the surface function has one of the following formulae :

$$S = f(\varphi) = 2r^2\varphi, \ 0 \leqslant \varphi \leqslant 2\pi$$

$$S = f(\theta) = 2\pi r^2(1 - \cos\theta), \ 0 \leqslant \theta \leqslant \pi$$

φ, θ and r are defined in Figure 1.

$$dS/d\varphi = 2r^2 \tag{3}$$

$$dS/d\theta = 2\pi r^2 \cdot \sin\theta \tag{4}$$

Eqs. 3 and 4 show that the φ coordinate is appropriate for mesh generation but for the θ coordinate is no longer.

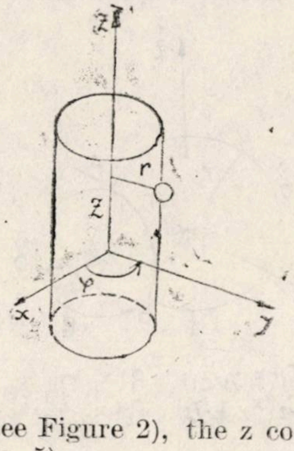

Fig. 2. — Cylindrical coordinations definition.

In the case of cylindric coordinates (see Figure 2), the z coordinate s adequate to be used in mesh building (eqs. 5) :

$$\begin{aligned} S &= 2\pi(z + r), \quad -r \leqslant z \leqslant +r \\ dS/dz &= 2\pi r = \text{constant} \end{aligned} \tag{5}$$

The second problem with respect to the concept of mesh uniformity is that the stepwise variation of the chosen coordinates must be replaced by a random selection of them, particularly in the case of a spherical surface. This must be done because the same number of points are placed on circles with nonequal radii, and a random selection does not arrange the points on circles. This justifies the use of the Monte Carlo method.

METHOD AND ALGORITHM

Although the idea to use the polar coordinate system to compute the molecular system is not new,[5] we consider our method as a new one. This is because the simple use of a stepwise variation of θ and φ angles in the integrating procedure is not appropriate, and no mention of another method was found.

The following formulae are used to transform the cylindrical coordinates into Cartesian coordinates :

$$\begin{aligned} c &= 1 - (z/r)^2 \\ x &= c^{1/2} \cdot \cos \varphi \\ y &= c^{1/2} \cdot \sin \theta \\ z &= z \end{aligned} \tag{6}$$

φ, θ and r are those from Figure 2.

Let us consider a solid made by two spheres intersecting as in Figure 3. The envelope of the solid is the sum of the two spherical fragments ABC and ABD. The ABC fragment consists of all P_1 points which fulfill the relationship :

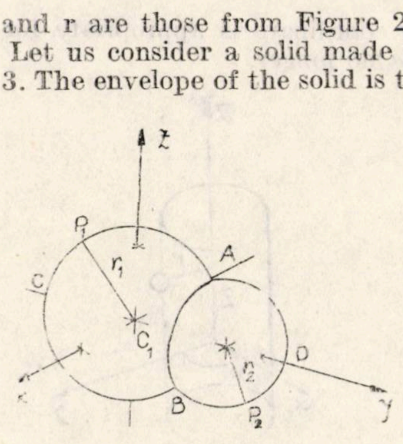

Fig. 3. — Principles of spheric envelope calculation.

$$(X_{P1} - X_2)^2 + (Y_{P1} - Y_2)^2 + (Z_{P1} - Z_2)^2 \geqslant (r_2)^2 \tag{7}$$

Similarly, the ABD fragment consists of all P_2 points which fulfill the following relationship :

$$(X_{P2} - X_1)^2 + (Y_{P2} - Y_1)^2 + (Z_{P2} - Z_1)^2 \geqslant (r_1)^2 \tag{8}$$

Extending the application of this method to a multi-spheres intersection, the relation which gives the solid envelope is

$$S_{env} = 4\pi \, \Sigma_i \, (P/P_T)^i \cdot r_i^2, \; i = 1, n \tag{9}$$

with the following restrictions for the P^i points :

$$(X_{P^i} - X_j)^2 + (Y_{P^i} - Y_j)^2 + (Z_{P^i} - Z_j)^2 \geqslant (r_j)^2, \; i \neq j, \; j = 1, \ldots$$

P_{T^i} is the total number of points on a certain sphere ; it depends on the radius and it is chosen to keep the same points density on the area unit.

The algorithm is as follows,

Step 1: Input data (Cartesian coordinates of atomic nuclei, van der Waals radii).

Step 2: Mesh generation on an atomic sphere.

Step 3: Each point of the mesh is tested to meet the restriction (9) ; if this is TRUE it is counted to contribute with an element g^2 at the molecular surface (g stands from mesh grid).

Step 4: Steps 2 and 3 repeat for each atom of the molecule.

RESULTS AND DISCUSSION

The computations are made on an IBM-PC XT computer. This method has been tested on a solid made of two spheres intersection. Our results have been compared with those obtained by means of the standard point by point scanning method. They are presented in Table 1.

Figures 4 and 5 are derived from Table 1.

Table 1

Computational results

grid[a]	time[b]	S[c]	time[b]	S[d]
0.0200	0.33	0.5168	2.13	0.5796
0.0100	1.40	0.5144	13.50	0.5566
0.0075	2.52	0.5100	28.23	0.5395
0.0050	5.62	0.5120	120.00	0.5120
0.0030	15.58	0.5109	—	—
0.0020	35.04	0.5101	—	—

[a] in nm ; [b] in minutes ; [c] computed with the Monte-Carlo method (in nm^2) ; [d] computed with standard point-by-point scanning method (in nm^2)

Both computing time and results accuracy are by far very good for Monte Carlo method. As could be seen in Table 1, while the surface of envelope computed by standard method equals 0.5210 nm² at a grid of 0.005 nm, the same quantity equals 0.5168 at a grid of no more than

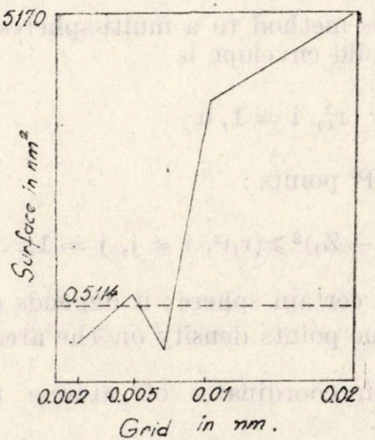

Fig. 4. — Precision of surface calculation as a function of grid.

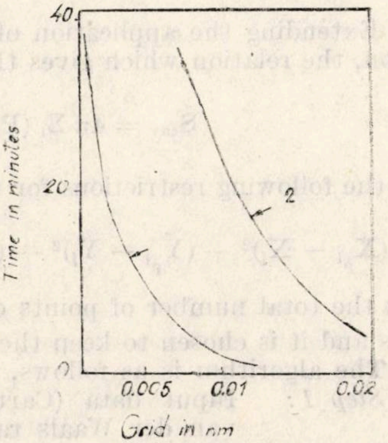

Fig. 5. — Calculation time as a function of grid.

0.02 nm for Monte Carlo method. Comparing computing time the discrepancy is huge. Figure 4 shows how the numerical values oscillate round the analytical value (0.5114 nm²). We used this method to compute the molecular van der Waals surface for some alkanes, both isomers and conformers. The results are presented in Table 2.

Table 2

Computed surfaces for some alkanes

Alkane	S[a]	S[b]	S[c]
methane	0.4758	0.4664	0.4730
ethane			
staggered	0.6801	0.6750	0.6810
eclipsed	0.6821	0.6779	—
propane	0.8863	—	0.8960
butane			
anti	1.0904	1.134[d]	—
gauche	1.0812	1.130[d]	—
eclipsed	1.0801	—	—
pentane	1.2881	1.2731	—
2-Me-butane	1.2686	1.2552	—
2,2-diMe-propane	1.2780	1.2474	—

All values are in nm².
[a] Computed with Monte Carlo program at g = 0.005 nm; [b] Reported in ref. 6; [c] Reported in ref. 5; [d] Reported in ref. 9.

CONCLUSIONS

As already recognised,[9] the standard point by point scanning method slowly converges and is less accurate. No doubt, the Monte Carlo method is better and it seems to be appropriate for computing atoms segments or parts of molecules. The calculated surfaces could be used as parameters in correlation analysis. At last, the computational effort is smaller than that of the corresponding standard method and this could be important for large molecules.

APPENDIX

DEFINITION OF THE MESH UNIFORMITY

Let E^n be the Euclidian n-dimensional space and $y = y(x_1,x_2,\ldots,x_n)$ be points in E^n. If y_i, y_j are points in E^n then $d(y_i, y_j) = \|y_i - y_j\|$ is called the distance between these points in the n-dimensional space.

Let M be a subset of E^n; M defines a mesh in E^n if and only if whatever $y_i, y_j \in M$ follows $d(y_i, y_j) > 0$.

Let D_M be the set of distances between points of M defined as follows

$$D_M = (d_{ij}\,;\, d_{ij} = d(y_i, y_j),\ y_i, y_j \in M)$$

and $d_{M'}$ be the minimal distance in D_M.

Axiom : The points y_i, y_j of M are adjacent, if and only if $d(y_i, y_j) = d_{M'}$.

Let N_i be the set of adjacent points of a certain point y_i and $n_i = \text{card}\ (N_i)$.

Theorem : The set M is a uniform network if and only if whatever be y_i, y_j of M follows $n_i = n_j$.

The above identity implies [2] that a uniform mesh can be built out of another one if the first order derivative of the transforming function is a constant.

ACKNOWLEDGEMENTS. We thank Professor Eiji Osawa, Hokkaido University for helpful correspondence and literature guidance . We also thank Professor A. T. Balaban for continuous support.

REFERENCES

[1] M. Charton and I. Motoc (eds.), "Steric Effects in Drug Design", *Top. Curr. Chem.*, vol. 114, 1983.
[2] D. Ciubotariu, V. Gogonea and E. Deretey, in preparation.
[3] A. Y. Meyer, *J. Chem. Soc. Perkin Trans. II*, **1986**, 1567.
[4] V. Gogonea, D. Ciubotariu and E. Deretey, Preprint, Univ. Timişoara, in press.
[5] A. Gavezzotti, *J. Amer. Chem. Soc.*, **107**, 962 (1989).
[6] A. Y. Meyer, *J. Comput. Chem.*, **7**, 144 (1986).
[7] G. L. Amidon, S. H. Yalkowski and S. Leung, *J. Pharm. Sci.*, **63**, 1858 (1974).
[8] S. C. Valvani, S. H. Yalkowski and G. L. Amidon, *J. Phys. Chem.*, **80**, 829 (1976).
[9] A. Y. Meyer, *J. Chem. Soc. Perkin Trans. II*, **1985**, 1161.
[10] D. Ciubotariu, PhD thesis, Polytechn. Inst. Bucharest, 1987.
[11] A. Y. Meyer, *Struct. Chem.*, **1**, 265 (1990).

Revue Roumaine de Chimie, 36, 4–7, 473–480 (1991)

Dedicated to Prof. ALEXANDRU T. BALABAN
on the occasion of his 60th anniversary

DEL RE CALCULATIONS FOR DIPOLE MOMENTS OF PHOSPHORUS COMPOUNDS. PARAMETRIZATION AND RESULTS

LUDOVIC KURUNCZI, RADU VÂLCEANU and ZENO SIMON *

Institute of Chemistry, B-dul Mihai Viteazu 24, 1900-Timișoara,
Romania

* Department of Biophysics, Univ. Medic. Pharm., P-ța Eftimie Murgu 2, 1900-Timișoara,
Romania

Received May 9, 1990

Based on experimental dipole moment values of fifteen molecules with known structural data, the PH, PC, PF, PP and PCl bond parameters were established for semiempirical Del Re molecular orbital calculations, and the following values were obtained : phosphorus electronegativity parameter 0.066 ; inductive (A–B/B–A bond respectively) and exchange parameters for phosphorus-hydrogen 0.362/0.744 and 0.747, –carbon 0.306/0.787 and 0.426, – fluorine 0.207/0.151 and 0.942, – phosphorus 0.279/0.279 and 0.837 and – chlorine 0.265/0.265 and 0.251, respectively. The above parameters allowed to calculate dipole moments for other trivalent phosphorus compounds with satisfactory accuracy and to draw some semiquantitative conclusions about the equilibrium of different conformations in compounds containing this type of bonds.

INTRODUCTION

In a previous note [1] dipole moments for trivalent phosphorus compunds calculated by the simple Del Re method and by advanced methods of quantum chemistry were compared with experimental dipole moments. The results of the Del Re method are generally in better agreement with the experiment than the results of advanced methods. This proves the utility of simple parametrized quantum chemical methods in limited areas, such as calculations of molecular charge distributions. Here we describe the parametrization method and a comprehensive view of our dipole moment calculations. As mentioned in note [1] we considered only molecules in which *sigma* character can be assumed for all bonds (*i.e.* simple PH, PC, PF, PP, PCl-bonds [2]).

CALIBRATION OF DEL RE PARAMETERS

Calibration of Del Re parameters is usually performed on the basis of dipole moment values.[3] Several sets of parameters were proposed for the *sigma* bonds of organic chemistry, but the bonds containing phosphorus were rather neglected from this point of view. A set of parameters for bonds of the P atom were proposed by Mihart *et al.*[4] based on general electronegativity considerations, but for pentavalent phosphorus.

For the bonds CH, CC, CO and CF which appear in our molecules we selected the parameters listed in table 1, based upon the best agreement between calculated and experimental dipole moment values.

Table 1

Del Re parameters used : literature values[a]

AB-Bond	ε_{AB}	γ_{AB}	γ_{BA}	δ°_{A}	δ°_{B}	Ref.
CH	1.00	−0.20	0.40	0.07	0.00	5
CC	1.00	0.10	0.10	0.07	0.07	3
CO	1.00	0.05	−0.50	0.07	0.40	6
CF	0.85	0.10	0.30	0.07	0.57	7

[a] ε — exchange parameter ;
γ — inductive parameters ;
δ° — electronegativity parameter ;
$\delta^{\circ}_{Cl} = 0.33$, [3]

The calibration of the parameters for P containing bonds was performed on the basis of a flexible simplex algorithm.[8,9] The basis system of the Del Re method is given by equations of type (1) :

$$\sum_{\substack{j=\text{neighbours}\\ \text{of } i}} \gamma_{ij}\delta_j - \delta_i = -\delta^{\circ}_i \tag{1}$$

from which the bond charges q_{ij} are calculated by equation (2).

$$q_{ij} = \frac{\delta_i - \delta_j}{2 \cdot \varepsilon_{ij}} \tag{2}$$

The molecular dipole moment is obtained hereafter by equation (3),

$$\mu = \frac{e}{2} \sqrt{\sum_{i,j} q^2_{ij}(\vec{r}_i - \vec{r}_j)^2} \tag{3}$$

where e is the electron charge, $\vec{r}_i$ and $\vec{r}_j$ the position vectors for atoms i and j, and the sum is performed only if there is a bond between the atoms i and j.

The values of some δ°, γ and ε's (those corresponding to the bonds with P atoms) are to be determined out of the experimental data. The calibration of these parameters corresponds to the search of the optimum of the following objective functions [10] :

$$\varphi[\mu(\delta^{\circ}, \gamma, \varepsilon)] = \sum_{\substack{\text{over all}\\ \text{molecules}}} (\mu_{\text{exp}} - \mu_{\text{calc}})^2 \overset{!}{=} \text{minimum} \tag{4}$$

The block scheme for the program of this search is given in figure 1.

A number of 15 molecules with known dipole moments (Table 2) were considered for the calibration. The literature quotations for the experimental dipole moments are listed in table 2. Unfortunately different methods were used for dipole moment determinations (microwave spectroscopy, gas phase and solution — Debye formula, corrected Higasi formula). The molecular geometry data are those given in the papers quoted in the same table (microwave spectroscopy, infrared spectroscopy, electron diffraction). The atomic position vectors from eq. (3) were calculated according to a program described in a previous paper.[34]

Table 2

Molecules selected for calibration of the Del Re parameters

Molecule	Dipole moments [a]		
	experimental	calcuated	Literature [b]
PH_3	0.574	0.650	[11], [12]
PF_3	1.025	1.062	[13], [14]
PCl_3	0.78	0.801	[15], [16]
PF_2H	1.32	1.184	[17], [17]
PF_2Cl	0.89	0.945	[18], [18]
$PH_2(CH_3)$	1.100	1.020	[19], [19]
$PH_2(CF_3)$	1.92	1.932	[20], [20]
$PF_2(CH_3)$	2.056	2.079	[21], [22]
$PCl_2(C_2H_5)$	2.18[c]	2.146	[23], [24]
$PH(CH_3)_2$	1.23	1.174	[25], [26]
$PCl(C_2H_5)_2$	2.44[c]	2.435	[23], [24]
$P(CH_3)_3$	1.192	1.274	[27], [28]
H_2PPH_2	0.92	0.921	[29], [29]
H_2PPF_2	1.71	1.711	[30], [30]
$P(CH_2O)_3CCH_3$	1.54	1.522	[31], [d]

[a] Dipole moments in Debye units (1 Debye = 3.336 $\cdot 10^{-30}$ cm).

[b] The first quotation refers to the source for the experimental dipole moment, the second to the source for molecular geometry data.

[c] Dipole moments corrected according to Jehlička.[32]

[d] Molecular geometry estimated by us, according to Verkade.[33]

The following limitations (see Fig. 1) were admitted : ε value interval from 0 to $+1$, γ values interval from -1 to $+1$. We considered $\gamma_{PCl} = \gamma_{ClP}$ according to Del Re.[3] Concerning the interval adopted for δ_P° : from geometrical data (bond angles and orthogonality of the P orbitals) we calculated [35] the mean s character for the bond orbitals of phosphorus using 44 compounds with known structure and containing PH, PC, PF, PP and PCl bonds. For the resulted value ($s = 0.1365$) the Hinze-Jaffé [36] orbital electronegativity was 2.55 (in Pauling units) and from the functional dependence [37] of known δ° values versus orbital electronegativities (straight line), the corresponding $\delta_P^0 = 0.069$ was obtained.

This was the middle of the interval of variation for δ_P^0 ($+0.014 - +0.124$). For the bond dipole moments of the PH and PC bonds the negative end was fixed at the P atom, while for PF and PCl — at the halogen atom.

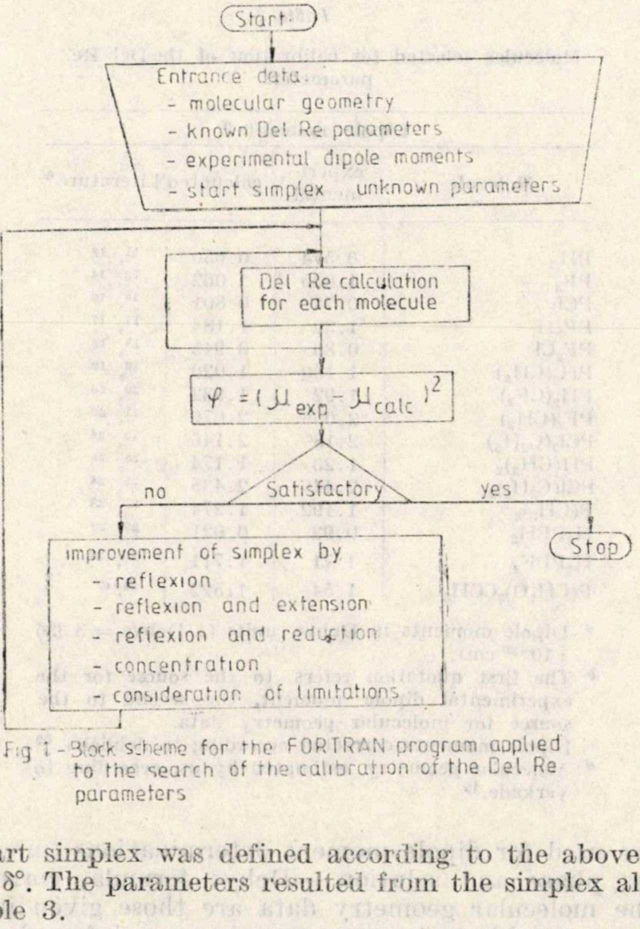
Start
Entrance data
- molecular geometry
- known Del Re parameters
- experimental dipole moments
- start simplex unknown parameters
Del Re calculation
for each molecule
$\varphi = (\mu_{exp} - \mu_{calc})^2$
Satisfactory
no
yes
improvement of simplex by
- reflexion
- reflexion and extension
- reflexion and reduction
- concentration
- consideration of limitations
Stop

Fig 1 - Block scheme for the FORTRAN program applied to the search of the calibration of the Del Re parameters

The start simplex was defined according to the above limitations for ε, γ and δ°. The parameters resulted from the simplex algorithm are listed in table 3.

The calculated dipole moments for the series of calibration compounds are in turn listed in table 2. The corresponding minimized value

Table 3

Calibrated Del Re parameters for bonds containing the P atom

Bond	$\overset{\circ}{\delta}_A$	$\overset{\circ}{\delta}_B$	γ_{AB}	γ_{BA}	ε_{AB}
PH	0.066	0.00	0.362	0.744	0.747
PC	0.066	0.07	0.306	0.787	0.426
PF	0.066	0.57	0.207	0.151	0.942
PP	0.066	0.066	0.279	0.279	0.837
PCl	0.066	0.35	0.265	0.265	0.251

of the objective function is 0.0474. The linear correlation coefficient between the experimental and calculated dipole moments afferent to this value is $r = 0.995$.

RESULTS

Excepting the test series molecules from table 2, dipole moment calculations were performed for other 25 compounds with known dipole moments. The results for a series of eight molecules with unique conformations were presented in table 2 of our previous note.[1] We mention here again these compounds, the experimental and the calculated dipole moments: PCl_2F, 0.86, 0.770; $PF_2(C_2H_5)$ – gauche, 2.168, 2.192; $PF_2(C_2H_5)$ – trans, 2.081, 1.896; $PH_2(C_2H_5)$ – gauche, 1.22, 1.12; $PH_2(C_2H_5)$ – trans, 1.226, 1.429; $PH_2(CH(CH_3)_2)$ – gauche, 1.23, 1.453; $PH_2(C(CH_3)_3)$, 1.17, 1.391 and $P(C(CH_3)_3)_3$, 1.59, 2.152 D. The experimental versus calculated values – correlation coefficient is $r = 0.937$ if the last compound is eliminated because of strong steric repulsion between the *t*-butyl groups.

Table 4 lists the results for molecules with two possible conformations, gauche and trans, with respect to the PC bond. Except for the first and the last compound, as well as for gauche-isopropylphosphine, no structural data were available, and we used standard bond lengths and angles. For the last molecule dipole moment calculations were performed with both standard and experimental structural data; the results are practically identical. The experimental dipole moments can correspond in principle to a mixture of the two conformations. Generally they fall indeed between those calculated for the two possible structures. For $H_2P(CH(CH_3)_2)$, in agreement with the experimental dipole moments as compared with the calculated ones, it is suggested that in the gas phase the gauche conformation has a greater concentration than in the liquid phase, where the trans is predominant.

Table 4[a]

Calculated and experimental dipole moments for compounds with two conformations (PC bond)

Compound	Calculated moment		Experimental moment		Conformation	
	g	t	G	L	G	L
H_2PEt	1.120[b]	1.429[b]	1.17; [38]	1.11, 1.15, [38]	t, g; [42,43]	
H_2PPr	1.125	1.369	1.09; [39]	1.09, 1.17; [39]		
H_2PBu	1.117	1.376		1.36; [40]		
H_2PHx	1.123	1.407		1.34; [40]		
$H_2P(i-Pr)$	1.453[b]	1.069	1.22; [39]	1.07, 1.13; [39]	g, t; [44]	t, g; [45]
$HPMe(Et)$	1.065, 1.255	1.547	1.28; [41]			
Me_2PEt	1.206 1.233[b]	1.632 1.655[b]	1.31; [41]		g, t; [46]	g, t; [47]

[a] Dipole moments in Debye units. Other notations: g – gauche; t – trans; G – gas phase; L – liquid phase; Me – methyl; Et – ethyl; Pr – propyl; Bu – butyl; Hx – hexyl

[b] Dipole moments calculated with experimentally determined structure[43,44,46]

Table 5 lists calculated and experimental dipole moment values for four compounds with two conformations, gauche and trans, with respect to the P—P bond. The first two compounds were used in the series of calibration. For tetramethyldiphosphine the experimental moment 1.75 D in liquid phase agrees with the conformational equilibrium data. For the last compound, supplementary conformations are possible due to the ethyl groups; the 1.728—3.138 D interval corresponds to the limits for the conformers without appreciable strain.

Table 5[a]

Calculated and experimental dipole moments for compounds with two conformations (PP bond)

Compound	Calculated moments[b]		Experimental moments		Conformation	
	g	t	G	L	G	L
H_2PPH_2	0.921	0	0.92; [29]		g; [29,48,49]	g; [50]
H_2PPF_2	0.833	1.711	1.71; [30]		t; [30]	
Me_2PPMe_2	2.107	0		1.75; [51]	t, g; [52,53]	g, t; [54,55]
Et_2PPEt_2	1.728—3.138	0		2.76; [51]		g; [55]

[a] Dipole moments in Debye units. Notations: g — gauche; t — trans; G — gas phase; L — liquid phase; Me — methyl; Et — ethyl.

Tables 6 and 7 discuss compounds with several conformations with respect to the two and respectively three PC bonds. Some sterically unlikely conformations were neglected. The experimental moments fall also between the limits of the calculated ones; they also indicate a displacement of the conformational equilibrium towards an increasing contribution of the trans position conformers with the increase of the substituent volumes, which is reasonable from a stereochemical point of view (repulsions due to the phosphorus lone pairs).[42,60]

Table 6[a]

Calculated and experimental dipole moments for secondary phosphines

Compound	Calculated values[b]					Experimental values	
	g—g	g—g′	t—g	t—g′	t—t	G	L
HPMe(Et)	1.255	1.065			1.547	1.28; [41]	
$HPEt_2$	1.101	0.981	1.603	1.621			1.36—1.40; [28,56]
$HPPr_2$	1.223	1.085	1.655	1.731			1.22—1.23 [39]
$MePEt_2$	1.155	1.230	1.706	1.645		1.58 [41]	
HP (i—Pr)$_2$	2.071	1.825	1.350	1.618	0.773		1.32—1.34 [39]

[a] Dipole moments in Debye units. The compounds are arranged in order of increasing substituent volume.
$MePEt_2$ was introduced for symmetry considerations.
For notations see table 4.

[b] With estimated structural parameters.

Table 7[a]

Calculated and experimental dipole moments for tertiary phosphines

Compound	Calculated values[b]						Exper. values
	g–g–g	g–g–g′	g–g–t	g–g–t	g–t–t	t–t–t	L
PEt_3	1.043	1.262	1.589	1.628	2.214	2.674	1.35–1.48; [38,56,58]
PPr_3	1.145	1.332	1.760	1.699	2.220		1.16–1.48; [39,57]
PBu_3	1.101	1.315	1.604	1.867	2.240		1.49–1.60; [57,59]
$P(i-Pr)_3$	2.784	2.715	1.700	1.687	0.958	0.121	1.32–1.36; [39]

[a] Dipole moments in Debye units. The compounds are arranged in order of increasing substituent volume.
For notations see table 4.

[b] With estimated structural parameters.

CONCLUSIONS

The dipole moments calculated in this note use the simple Del Re method calibrated especially on dipole moments. The number of compounds for a direct comparison with experimental data is relatively low, due to elimination of molecules with probable *pi* electronic contribution and of molecules with several conformations. For the limited number of compounds the agreement is satisfactory. For larger molecules with conformational equilibrium the experimental values generally fall between the limits of the calculated ones, and as a rule agree with the predominant conformations, where such data are available. For secondary and tertiary phosphines the comparison of the experimental and calculated dipole moments indicate an increasing contribution of trans type conformations simultaneously with increasing substituent volumes.

As a whole, our parametrization can be considered successful and recommendable for calculations of dipole moments and charge distributions also in other trivalent phosphorus compounds.

REFERENCES

[1] R. Vâlceanu, Z. Simon and L. Kurunczi, *Rev. Roum. Chim.*, **34**, 377 (1989).
[2] R. Vâlceanu, L. Kurunczi and Z. Simon, *Rev. Chim. (București)*, submitted.
[3] G. Del Re, *J. Chem. Soc.*, **1958**, 4031.
[4] C. Mihart, S. Ráduly and Z. Simon, *Rev. Roum. Chim.*, **28**, 857 (1983).
[5] J. Nagy and J. Réffi, *J. Organometal. Chem.*, **22**, 565 (1970).
[6] J. Nagy and L. Párkányi, *Acta Chim. Acad. Sci. Hung.*, **71**, 159 (1972).
[7] A. B. Sannigrahi and S. Noor Mohammad, *Indian J. Chem.*, **11**, 902 (1973).
[8] D. M. Himmelblau, "Process Analysis by Statistical Methods", Wiley, New York, 1970, p. 181.
[9] A. Woinaroschy and O. Smigelschi, "Ingineria sistemelor și optimizarea proceselor chimice", Ed. Didactică și Pedagogică, Bucharest, 1983, p. 80.
[10] L. Kurunczi and V. Eliu-Ceaușescu, *Analele Univ. Timișoara (Ser. St. fiz. chim.)*, **14**, 29 (1976).
[11] P. B. Davies, R. M. Neumann, S. C. Wofsey and W. Klemperer, *J. Chem. Phys.*, **55**, 3564 (1971).
[12] F. Y. Chu and T. Oka, *J. Chem. Phys.*, **60**, 4612 (1974).
[13] R. G. Shulman, B. P. Dailey and C. H. Townes, *Phys. Rev.*, **78**, 145 (1950).
[14] E. Hirota and Y. Morino, *J. Mol. Spectrosc.*, **33**, 460 (1970).

[15] U. Grassi, *Nuovo Cimento*, **10**, 3 (1933).
[16] G. Cazzoli, *J. Mol. Spectrosc.*, **53**, 37 (1974).
[17] R. L. Kuczkowski, *J. Am. Chem. Soc.*, **90**, 1705 (1968).
[18] A. H. Brittain, J. E. Smith and R. H. Schwendeman, *Inorg. Chem.*, **11**, 39 (1972).
[19] T. Kojima, E. L. Breig and C. C. Lin, *J. Chem. Phys.*, **35**, 2139 (1961).
[20] I. Y. M. Wang, C. O. Britt, A. H. Cowley and J. E. Boggs, *J. Chem. Phys.*, **48**, 812 (1968).
[21] E. G. Codding, R. A. Creswell and R. H. Schwendeman, *Inorg. Chem.*, **13**, 856 (1974).
[22] J. R. Durig, A. E. Stanley and Y. S. Li, *J. Mol. Struct.*, **78**, 247 (1982).
[23] J. P. Van Linthoudt, E. V. Van den Berghe and G. P. Van der Kelen, *J. Mol. Struct.*, **67**, 269 (1980).
[24] V. A. Naumov, L. L. Tuzova and N. M. Zaripov, *Zhur. Strukt. Khim.*, **18**, 67 (1977).
[25] R. Nelson, *J. Chem. Phys.*, **39**, 2382 (1963).
[26] J. R. Durig, S. D. Hudson, M. R. Jalilian and Y. S. Li, *J. Chem. Phys.*, **74**, 772 (1981).
[27] D. R. Lide and D. E. Mann, *J. Chem. Phys.*, **29**, 914 (1958).
[28] B. Beagley and A. R. Medwid, *J. Mol. Struct.*, **38**, 229 (1977).
[29] J. R. Durig, L. A. Carreira and J. D. Odom, *J. Am. Chem. Soc.*, **96**, 2688 (1974).
[30] R. L. Kuczkowski, H. W. Schiller and R. W. Rudolph, *Inorg. Chem.*, **10**, 2505 (1971).
[31] R. D. Bertrand, R. D. Compton and J. G. Verkade, *J. Am. Chem. Soc.*, **92**, 2702 (1970).
[32] V. Jehlička and I. Cibulka, *Collect. Czech. Chem. Commun.*, **40**, 3095 (1975).
[33] J. G. Verkade, *Coord. Chem. Reviews*, **9**, 1 (1972/73).
[34] L. Kurunczi and Z. Szabadai, *Analele Univ. Timișoara (Ser. St. fiz. chim.)*, **14**, 73 (1976).
[35] L. Kurunczi, unpublished data.
[36] J. Hinze and H. H. Jaffé, *J. Am. Chem. Soc.*, **84**, 540 (1962).
[37] H. Berthod and A. Pullman, *J. Chim. Phys.*, **62**, 942 (1965).
[38] G. Kodama, J. R. Weaver, J. La Rochelle and R. W. Parry, *Inorg. Chem*, **5**, 710 (1966).
[39] J. G. Morse and R. W. Parry, *J. Chem. Phys.*, **57**, 5367 (1972).
[40] H. Schindlbauer and G. Hajek, *Chem. Ber.*, **96**, 2601 (1963).
[41] J. G. Morse, *Inorg. Chim. Acta*, **41**, 161 (1980).
[42] J. R. Durig and A. W. Cox, jr., *J. Chem. Phys.*, **63**, 2303 (1975).
[43] J. R. Durig and A. W. Cox, jr., *J. Chem. Phys.*, **64**, 1930 (1976).
[44] J. R. Durig and Y. S. Li, *J. Mol. Spectrosc.*, **70**, 27 (1978).
[45] J. R. Durig and A. W. Cox, Jr., *J. Phys. Chem.*, **80**, 2493 (1976).
[43] J. R. Durig, J. F. Sullivan and S. Cradock, *J. Mol. Structure*, **145**, 127 (1986).
[47] J. R. Durig and T. J. Hizer, *J. Raman Spectrosc.*, **17**, 97 (1986).
[48] R. M. Lynden-Bell, *Trans. Faraday Soc.*, **57**, 888 (1961).
[49] S. Elbel, H. tomDieck and G. Becker, *Inorg. Chem.*, **15**, 1235 (1976).
[50] M. Baudler, M. Vogel-Raudschus and J. Dobbers, *Z. Anorg. allg. Chem.*, **347**, (1977).
[51] K. S. Mingaleva, G.-M. Bogolyubov, Yu. N. Shlyk and A. A. Petrov, *Zhur. Obshch. Khim.*, **39**, 2679 (1969).
[52] A. Mc. Adam, B. Beagley and T. G. Hewitt, *Trans. Faraday Soc.*, **66**, 2732 (1970).
[53] A. H. Cowley, M. J. S. Dewar, D. W. Goodman and M. C. Padolina, *J. Am. Chem. Soc.*, **96**, 2048 (1974).
[54] J. R. Durig and R. W. Mc Namee, *J. Mol. Structure*, **17**, 426 (1973).
[55] J. P. Albrand, A. Cogne and C. Taieb, *Org. Magn. Resonance*, **21**, 246 (1985).
[56] J. C. Bailar, jr., "The Chemistry of Coordination Compounds", Reinhold, New York, 1956. pg. 129.
[57] C. W. N. Cumper, A. A. Foxton, J. Read and A. J. Vogel, *J. Chem. Soc.*, **1964**, 430.
[58] J. P. Van Linthoudt, E. V. Van den Berghe and G. P. Van der Kelen, *J. Mol. Structure*, **67**, 269 (1980).
[59] J. P. Fayet, M. Pradayrol and P. Mauret, *C. R. Acad. Sci.*, **C**, **271**, 1033 (1970).
[60] P. Groner, J. S. Church, Y. S. Li and J. R. Durig, *J. Chem. Phys.*, **82**, 3894 (1985).

Revue Roumaine de Chimie, 36, 4–7, 481–506 (1991)

This paper is dedicated to Professor dr. ALEXANDRU T. BALABAN
on the occasion of his 60th birthday

TRENDS AND TENDENCIES IN INSTRUMENTAL ANALYTICAL TECHNIQUES WITH SPECIAL EMPHASIS ON ENVIRONMENTAL ANALYSIS

T. BRAUN[a] and S. ZSINDELY[b]

[a] Institute of Inorganic and Analytical Chemistry, L. Eötvös University, P.O. Box 123, 1443 Budapest, Hungary

[b] Information Science and Scientometrics Research Unit (ISSRU), Library of the Hungarian Academy of Sciences, Budapest, Hungary

Received December 24, 1990

An up-to-date review of trends and tendencies in instrumental analytical techniques is presented with special emphasis on environmental analysis.

Concern with the environment has become one of the most acute problems of the twentieth century. Since the 1970s, public opinion polls throughout Europe have shown that people worry more about the state of the environment than about inflation, poverty or unemployment.[1] Facing this situation recent studies [2] have highlighted the need to devise new ways of monitoring and reporting the state of the environment.

The success and widespread acceptance of economic and other indices in the post-war period inspired considerable interest in the late 1960s in ways of developing indices for the state of the environment. Early in the development of environmental indices there was some discussion about the difference between the terms index and indicator. Ott [3] calls a function based on one variable an indicator. A function based on two or more indicators is an index. An index is often used to reduce a large amount of unrelated data to a single measure of the quality of the whole or of a part of the environment. When dealing however with the above – mentioned problems it is always of paramount importance not to forget that the basis of building indices and indicators which could unobtrusively reflect the state of the environment is the analytical measurement. This measurement is done in the overwhelming majority of cases by instrumental analytical techniques.

Instrumental analysis basically deals with the quantitative characterization and measurement of the chemical species present in a sample. When it deals with the environment, samples mean implicitly environmental samples. Regardless of the measurements made, the actual experimental determination of a given chemical species in environmental samples is only one aspect of a much more comprehensive analytical procedure which takes into account:

1. Definition of the problem and the manner in which instrumental analysis will be relevant to its solution.
2. Identification of the appropriate chemical species to be measured.

3. Collection and preliminary treatment of the sample.
4. Selection of a suitable instrumental technique with respect to species concentration, accuracy, precision, cost and time.
5. Separation and/or preconcentration of the desired species if interfering components are present.
6. Measurement of the concentration of the species.
7. Evaluation of the data.

Just a simple look at each of these individual points, will provide an idea of the diversity and challenges involved in the problem solving aspect of instrumental analysis in environmental monitoring.

THE ENVIRONMENT

What is the environment which has to be characterized? About two decades ago toxicology defined it as the air, water, soil and food surrounding of man. Ecology has drawn specific attention to the dynamic equilibrium between the community of all living organisms (biozoen) with their non-living environment (biotope). Nowadays it is more common when speaking of the environment to mention the atmosphere, hydrosphere, lithosphere and biosphere. For characterizing the chemical element composition of the environment, Fig. 1 presents frequency distributions of mean element contents or concentrations of the abovementioned spheres. They are arranged according to the content of major, minor and trace element levels on the x-axis and the corresponding number of elements within one, increasing content range on the y-axis. In the figure the so-called toxic elements are labelled by a point in their box.

When comparing the distribution of toxic elements on the figures for the different environmental sample types it is worth mentioning that, as visible, there are quite many identical toxic elements in samples coming from very different environmental - spheres e.g. granite (lithosphere), river- or seawater (hydrosphere), plants of biomedical material (biosphere). It is very important to note that the toxicity of an element in the human organism always depends on its concentration. As such, a given element can be toxic, non-toxic or even essential according to its concentration in the respective-sphere, and there is no "ab ovo" toxicity of the elements. Morever, there is no reason to assume that "toxic" elements in e.g. granite powder (lithosphere) could be really toxic for the human organism (biosphere).

This leads to the very essential observation that monitoring the environment by element content alone is less than satisfactory. Of decisive importance in environmental research, monitoring, and more essentially in ecology, is the chemical (or molecular) form of the elements. The possible environmental concern of two different elements in the same chemical form is less evident than the difference of the same element in two different molecular forms.

The so-called "speciation" of the molecular form of an element can be determined by measuring the corresponding molecules, including ions, instead of elements alone.

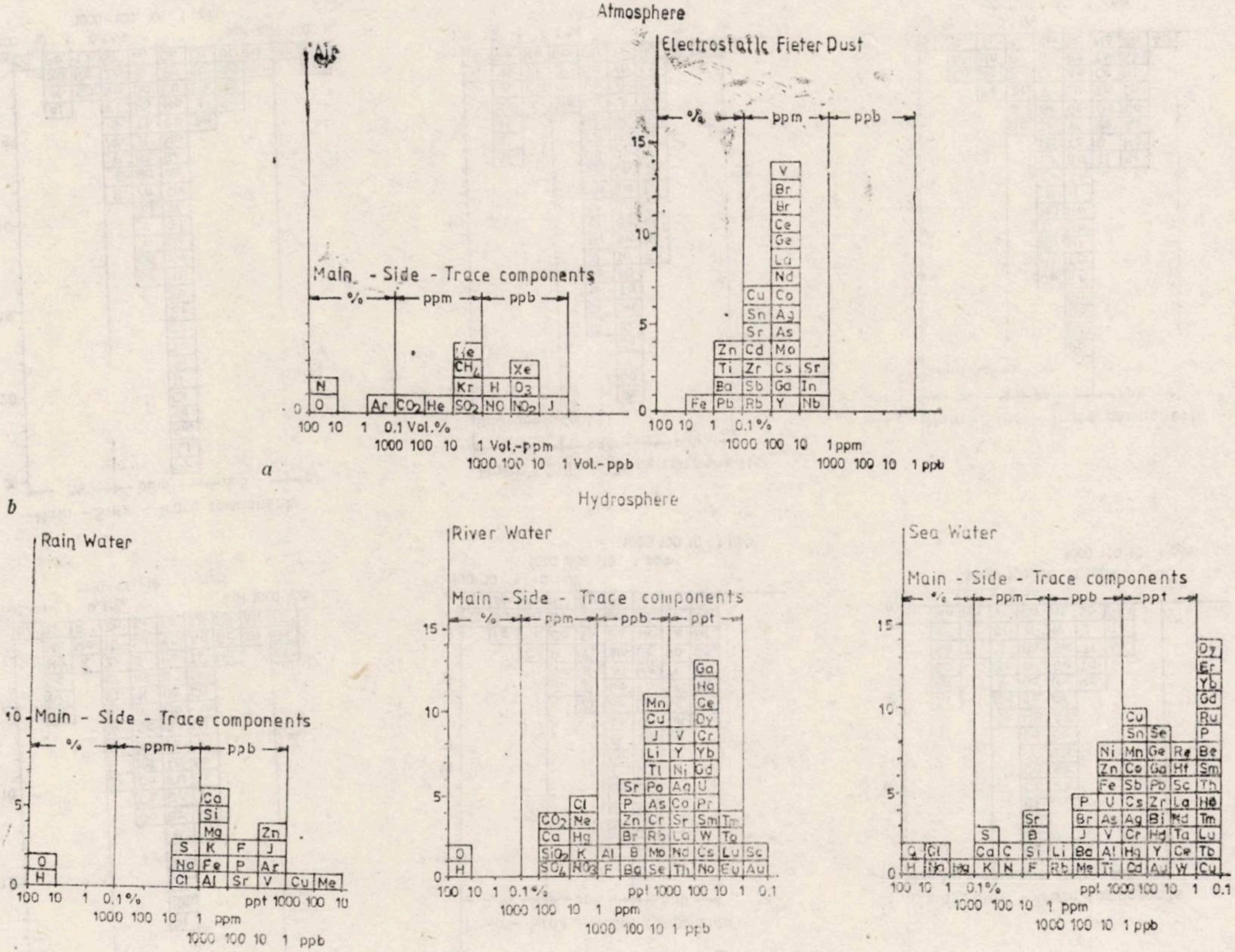
Atmosphere
Air
Main - Side - Trace components
% ppm ppb
N
O
Ar CO2 He
Ne CH4 Kr SO2
H NO
Xe O3 NO2 J
100 10 1 0.1 Vol.%
1000 100 10 1 Vol.-ppm
1000 100 10 1 Vol.-ppb
a
Electrostatic Fieter Dust
% ppm ppb
15
10
5
0
Fe Pb Rb Y Nb
Ba Sb Ga In
Ti Zr Cs Sr
Zn Cd Mo
Sr As
Sn Ag
Cu Co
Nd La Ge Ce Br Br V
100 10 1 0.1 %
1000 100 10 1 ppm
1000 100 10 1 ppb
b
Hydrosphere
Rain Water
Main - Side - Trace components
% ppm ppb
10
5
0
O
H
Cl Al Sr V
Na Fe P Ar
S K F J
Mg Si Ca
Zn
Cu Me
100 10 1 0.1 %
ppt 1000 100 10
1000 100 10 1 ppm
1000 100 10 1 ppb
River Water
Main - Side - Trace components
% ppm ppb ppt
15
10
5
0
O
H
SO4 Ca CO2
NO3 K Hg Ne Cl
F Al
Ba Se B Mo Rb Br Zn P Sr Tl Li J Cu Mn
Th Nd La Sr Co Ag Ni Y V
No Cs W Sm Pr U Gd Yb Cr Dy Ce Hg Ga
Eu Lu To Tm
Au Sc
100 10 1 0.1 %
ppt 1000 100 10 1 0.1
1000 100 10 1 ppm
1000 100 10 1 ppb
Sea Water
Main - Side - Trace components
% ppm ppb ppt
15
10
5
0
O H
Cl Na
Mg
Ca K S
C N
Si F B Sr
Li Rb
Ba Me J Br P
Ti Al V As U Fe Zn Ni
Cd Hg Cr Ag Cs Sb Co Mn Sn Cu
Au Y Hg Bi Zr Pb Ga Ge Se
W Ce Ta Nd La Sc Hf Re
Cu Tb Lu Tm Ho Th Sm Be P Ru Gd Yb Er Dy
100 10 1 0.1 %
ppt 1000 100 10 1 0.1
1000 100 10 1 ppm
1000 100 10 1 ppb

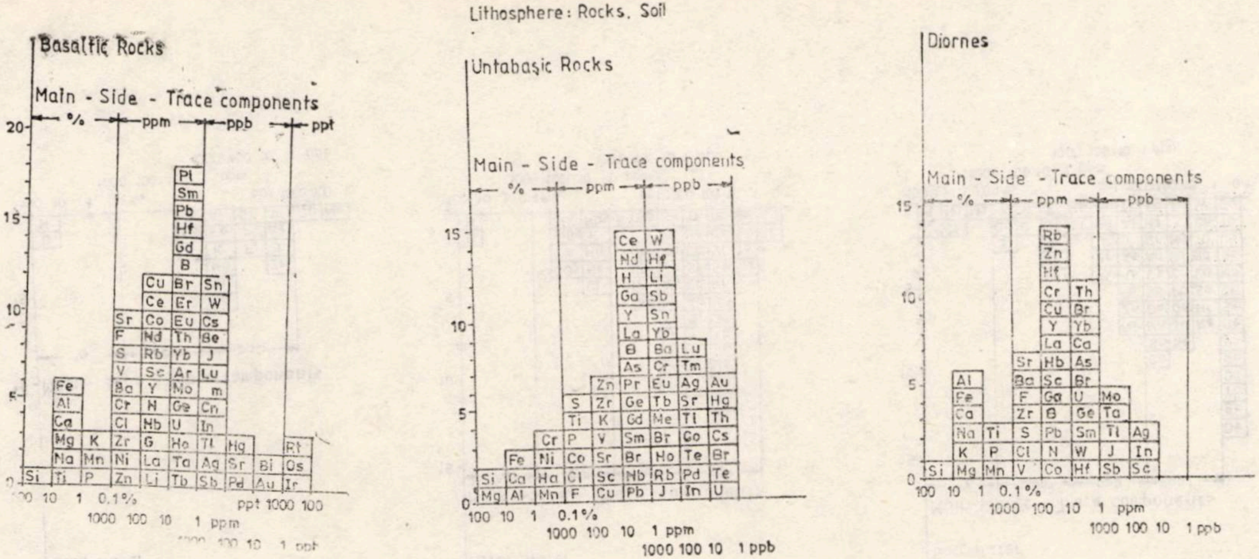
Lithosphere: Rocks, Soil
Basaltic Rocks
Main - Side - Trace components
% ppm ppb ppt
20 15 10 5 0
Pt Sm Pb Hf Gd B
Cu Br Sn
Ce Er W
Sr Co Eu Cs
F Nd Th Be
S Rb Yb J
V Sc Ar Lu
Fe Ba Y Mo m
Al Cr N Ge Cn
Ca Cl Nb U In
Mg K Zr G Ho Tl Hg Rt
Na Mn Ni La Ta Ag Sr Bi Os
Si Ti P Zn Li Tb Sb Pd Au Ir
100 10 1 0.1% ppt 1000 100
1000 100 10 1 ppm
1000 100 10 1 ppt
Untabasic Rocks
Main - Side - Trace components
% ppm ppb
15 10 5 0
Ce W
Nd Hf
H Li
Ga Sb
Y Sn
La Yb
B Ba Lu
As Cr Tm
Zn Pr Eu Ag Au
S Zr Ge Tb Sr Hg
Ti K Gd Me Tl Th
Cr P V Sm Br Co Cs
Fe Ni Co Sr Br Ho Te Br
Si Ca Ha Cl Sc Nb Rb Pd Te
Mg Al Mn F Cu Pb J In U
100 10 1 0.1%
1000 100 10 1 ppm
1000 100 10 1 ppb
Diornes
Main - Side - Trace components
% ppm ppb
15 10 5 0
Rb Zn Hf
Cr Th
Cu Br
Y Yb
La Ca
Sr Hb As
Al Ba Sc Br
Fe F Ga U Mo
Ca Zr B Ge Ta
Na Ti S Pb Sm Tl Ag
K P Cl N W J In
Si Mg Mn V Co Hf Sb Sc
100 10 1 0.1%
1000 100 10 1 ppm
1000 100 10 1 ppb

c

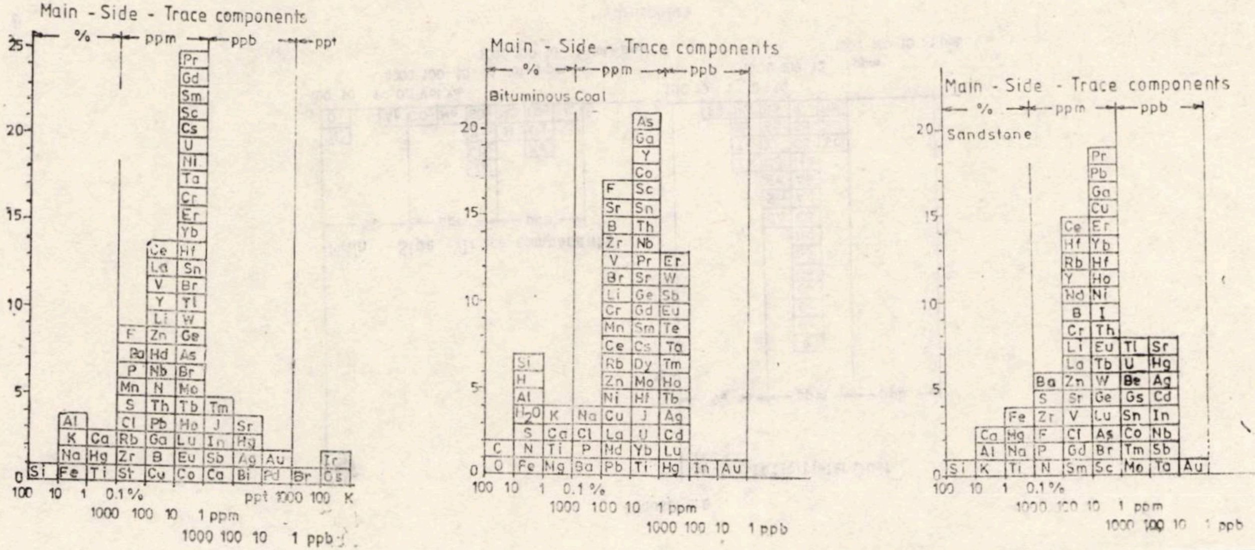
Main - Side - Trace components
% ppm ppb ppt
25 20 15 10 5 0
Pr Gd Sm Sc Cs U Ni Ta Cr Er Yb
Ce Hf
La Sn
V Br
Y Yl
Li W
F Zn Ge
Ba Hd As
P Nb Br
Mn N Mo
S Th Tb Tm
Al Cl Pb Ho J Sr
K Ca Rb Ga Lu In Hg
Na Hg Zr B Eu Sb Ag Au Ir
Si Fe Ti St Cu Co Ca Bi Pd Br Os
100 10 1 0.1% ppt 1000 100 K
1000 100 10 1 ppm
1000 100 10 1 ppb
Main - Side - Trace components
% ppm ppb
Bituminous Coal
20 15 10 5 0
As Ga Y Co
F Sc
Sr Sn
B Th
Zr Nb
V Pr Er
Br Sr W
Li Ge Sb
Cr Gd Eu
Mn Sm Te
Ce Cs Ta
Si Rb Dy Tm
H Zn Mo Ho
Al Ni Hf Tb
H₂O K Na Cu J Ag
S Ca Cl La U Cd
C N Ti P Nd Yb Lu
O Fe Mg Ba Pb Ti Hg In Au
100 10 1 0.1%
1000 100 10 1 ppm
1000 100 10 1 ppb
Main - Side - Trace components
% ppm ppb
Sandstone
20 15 10 5 0
Pr Pb Ga Cu
Ce Er
Hf Yb
Rb Hf
Y Ho
Nd Ni
B I
Cr Th
Li Eu Tl Sr
La Tb U Hg
Ba Zn W Be Ag
S Sr Ge Gs Cd
Fe Zr V Lu Sn In
Ca Hg F Cl As Co Nb
Al Na P Gd Br Tm Sb
Si K Ti N Sm Sc Mo Ta Au
100 10 1 0.1%
1000 100 10 1 ppm
1000 100 10 1 ppb

d

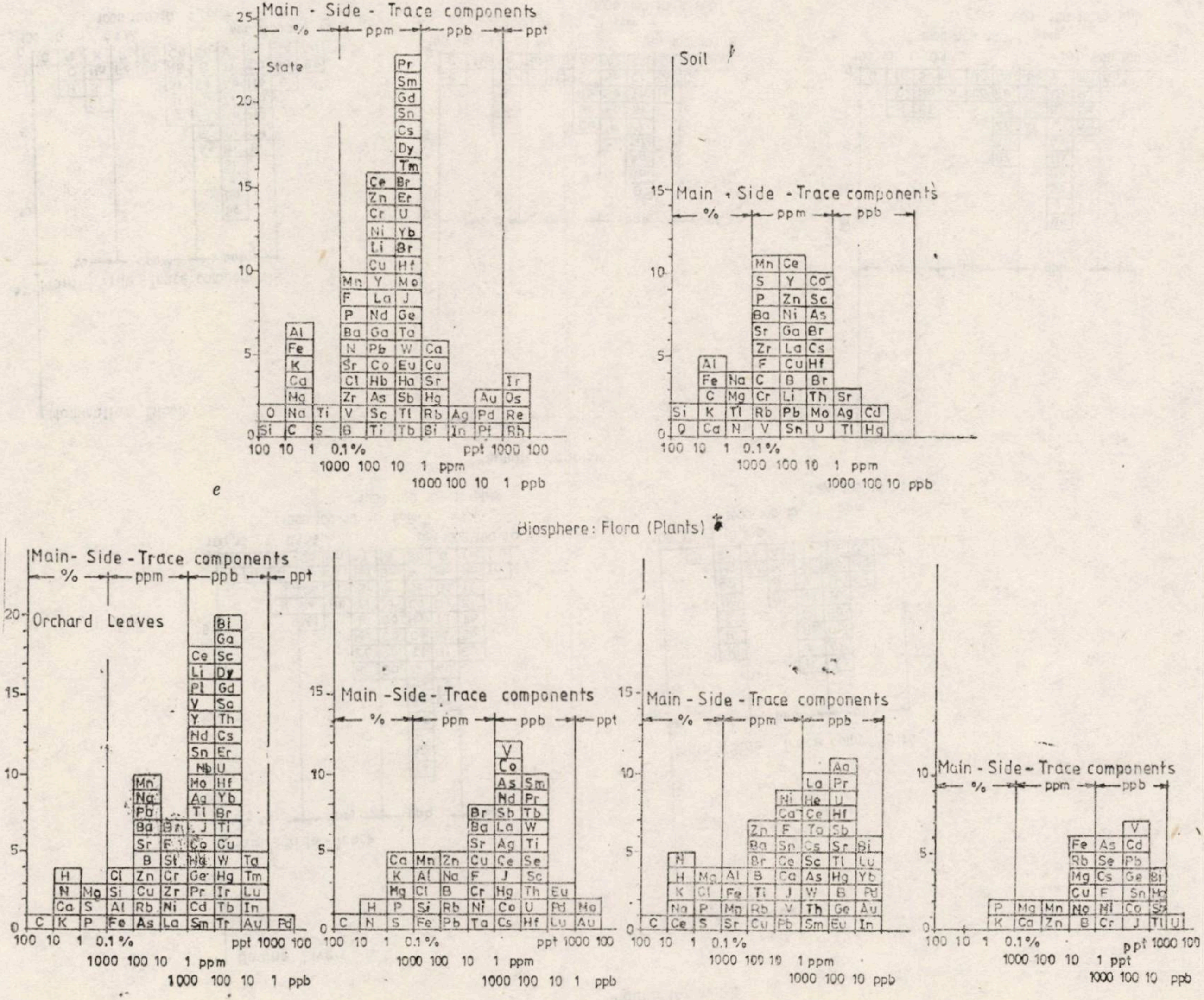
Main - Side - Trace components
% ppm ppb ppt
State
Soil
e
Biosphere: Flora (Plants)
Main- Side - Trace components
Orchard Leaves
f
100 10 1 0.1 %
1000 100 10 1 ppm
1000 100 10 1 ppb
ppt 1000 100

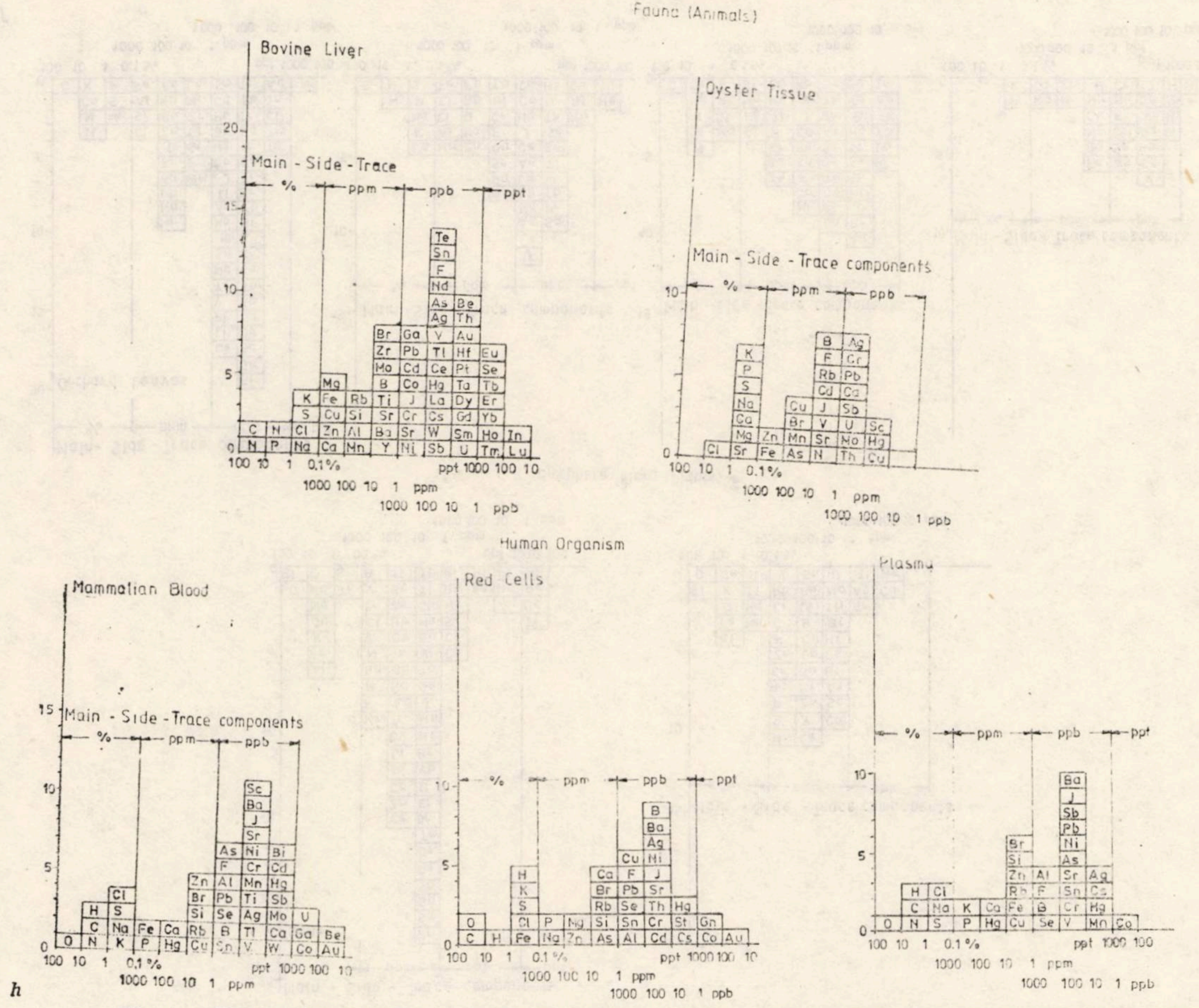

Fig. 1. — Elemental composition of environmental material (B. Sansoni, Pure & Appl. Chem.

The terms "species" and "speciation" have been borrowed by chemists from biology. In biology "species" refers to a population of organisms which possess hereditary traits and which interbreed, conserving these.

As mentioned, in chemistry "species" refers to the molecular form (configuration) of atoms of an element or cluster of atoms of different elements. In biology the term "speciation" denotes the processes by which species arise in the course of evolution. However, in chemistry the term "speciation" has been used in many different contexts, of which chemists are often not even aware. Chemical speciation has been used to describe :

1. The analysis of species leading to their identification and quantification in a defined area or in a volume (e.g. a sample) (species analysis).
2. The description of the abundance (or numerical distribution) of species of an element in a volume (species distribution or abundance).
3. The reactivity of a given species (species reactivity).
4. The transformation of one species into another (species transformation).

The species that actually exists in the environment is the "matrix species" or "functional species". This means that the term "chemical species" is actually an idealized concept. Analytical procedures generally convert the matrix species into a stable species (compound) that can be detected and quantified. The species which is detected is called the "analyte species". The different terms are illustrated for some mercury species in Fig. 2 and Table 1. The toxicities of organometallic species are determined by their structures and stabilities. Their toxic actions on organisms are encoded in the basic metal-carbon skeleted backbone. Mercury sulfide and methyl mercury compounds are celebrated, though

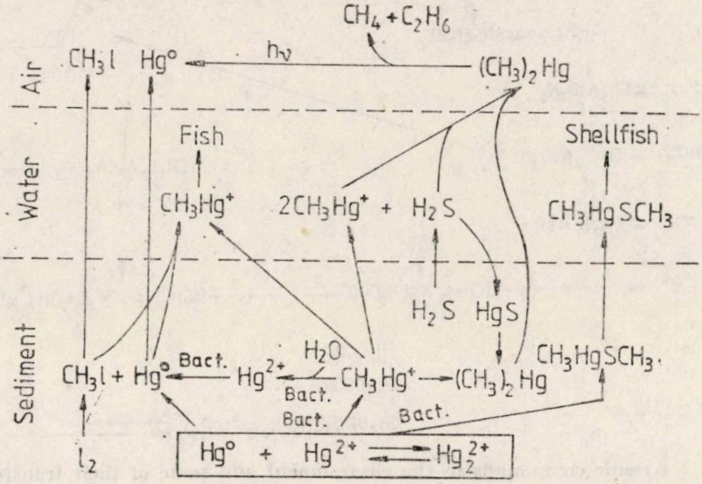

Fig. 2. — Schematic representation of mercury cycling in the environment.

Table 1

Parent species of methylmercury, some of its matrix species and the most common analyte species

Parent species	Matrix	Matrix species	Analyte species
CH_3Hg^+	Air	CH_3HgL (L = weakly bound ligand	Cl^- $\Rightarrow CH_3HgCl$
	Water	$CH_3Hg/OH)^+$	
	Biol. tissue	CH_3Hg — humic acid	
	Soil	CH_3Hg — humic acid	

infamous, examples of such relationships. Whereas the very insoluble mercury sulphide (HgS) is non-toxic because of its inertness, the lipid-soluble methylmercury derivatives are insidious and potent neurotoxins. Biota have unfortunately found a way for the methylation of mercury even in the form of its sulfides. Fig. 3 is an example showing that not all methylation reactions increase the toxicity of an element or compound. Arsenite which is rather toxic, is converted through methylation to methylarsonic acid and dimethylarsonic acid that are less toxic than arsenite. Although "total element" concentrations are rarely sufficient to describe environmental processes adequately, "total element" amounts are useful for the estimation of the quantitative importance of the species present.

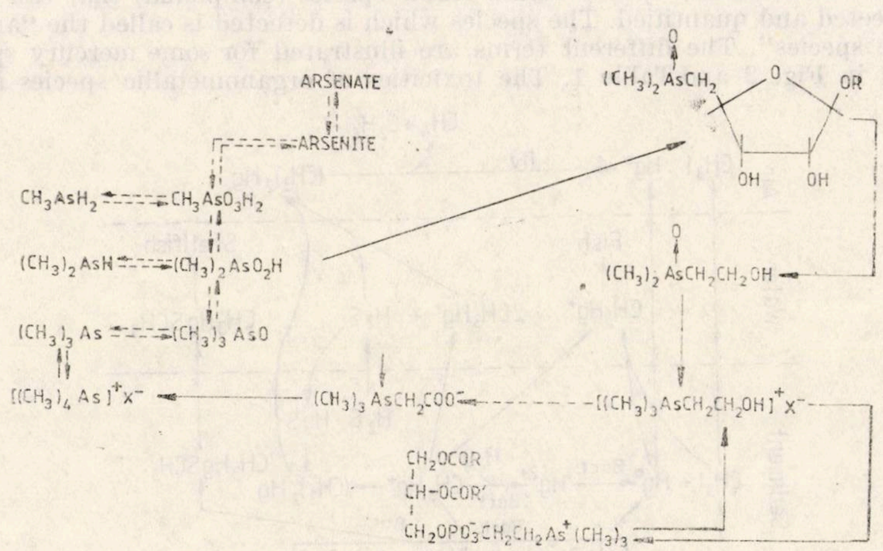
ARSENATE
ARSENITE
CH3AsH2
CH3AsO3H2
(CH3)2AsH
(CH3)2AsO2H
(CH3)3As
(CH3)3AsO
[(CH3)4As]+X−
(CH3)3AsCH2COO−
[(CH3)3AsCH2CH2OH]+X−
(CH3)2AsCH2
OR
OH
OH
(CH3)2AsCH2CH2OH
CH2OCOR
CH-OCOR′
CH2OPO3−CH2CH2As+(CH3)3

Fig. 3. — Arsenic compounds in the environment and some of their transformation (— — —methylation, — · — · —reduction, ...dimethylation, — · · — · · — · · —oxidation, ——— other reactions).

Just as an example for the utility of the determination of "total element" concentration for environmental purposes we mention the determination of mercury in wines of the same sort but of wintages of diffe-

Table 2

Mercury content of "Chateau d'Yquem" wines

Year	1784	1787	1869	1884	1921
Hg-content, $\mu g \cdot L^{-1}$	30	40	40	200	550

rent years. As visible in table 2, the increasing amount of total mercury in "Chateau d'Yquem" wines is a fairly good indicator of the influence of the increasing industrialization during the last centuries and of the accompanying increase of mercury emission on the mercury content of soils, plants and plant products.[4]

THE ANALYTICAL MEASUREMENT PROCESS

Major problems arise when attempts are made to determine trace and ultratrace concentrations of elements and species (Table 3). Today instrumental analysts are required to determine analytes at lower and lower concentrations; the lower limit for trace analysis has been decreased by a factor of 10^{11} (from $10^{-6} g \cdot g^{-1}$ to $10^{-17} g \cdot g^{-1}$) during the last decade or so.[5] Additionally, although trace and ultratrace concentrations of a chemical species may not cause a measurable effect directly, various organisms can concentrate specific chemical species by factors of $10^{-4}-10^{6}$ and concentrations that are toxic to the organism are reached. Compositional measurements on environmental samples are seldom made on an absolute basis. They are usually made on a comparative basis, relying heavily on the calibration/standardization of instruments and the use of environmental matrix-matched reference materials. Integrated into the process is the quality assurance program required to produce quality environmental monitoring data from a total instrumental analytical measurement system that is in statistical control. The basic objective of quality assurance is to estimate the uncertainty of measured or calculated values. Quality assurance has two components,[6] quality control and quality assessment. Quality control is the process used to control (reduce) errors. The elements of a quality control program include: good laboratory practices; good measurement practices; standard operating procedures; qualified personal with a "measurement" philosophy and atti-

Table 3

Typical concentration levels analyzed by instrumental analytical techniques

	$g_{analyte}/g_{sample}$	%
Major	$>10^{-2}$	>1
Minor	$10^{-3}-10^{-2}$	$0.1-1$
Trace	$10^{-7}-10^{-3}$	$0.00001-0.1$
Ultratrace	$<10^{-7}$	<0.00001

tude ; reliable, well-maintained, calibrated/standardized equipment ; reference materials to calibrate/standardize, and tests of the equipment and process. Quality assessment is the process used to see how effectively quality control is working.

ECONOMICAL ASPECTS OF ENVIRONMENTAL ANALYTICAL INFORMATION

One of the important goals of environmental analysis by using instrumental analytical techniques is to do that in a way which allows the value of the information present in the instrumental analytical result to be more worth than the cost of obtaining it. The economical value of an instrumental analytical result depends upon the amount of information the user actually receives, and upon whether the user indeed uses that information. The amount of the received information can be defined as the difference between the initial uncertainty (H_0) of the user before receiving the instrumental analytical result(s) and the remainder uncertainty (H_1) after having received the results. The net yield of information is thus $\Delta H = H_0 - H_1$. If we apply this definition to the case of environmental control, then H_0 is related to the variance of the controlled environment. When considering the cost-effectiveness of instrumental analytical effort, we should therefore, weigh the cost (C) of producing environmental analytical results by using instrumental techniques (H_1), against the return of profit (P), earned (in control) by applying the net amount of received information (ΔH) by the customer. Decision making in the instrumental analytical control of the environment is, therefore, focussed on maximizing the net profit ($P-C$). This obliges the manager of the instrumental analytical laboratory to keep evaluating the instrumental techniques and equipment in use, in relation to the changing demands for information and to the new technologies introduced on the market place. Today's instrumental analytical equipment is of an increasing sophistication, with capabilities to determine more analytes in a shorter time and with better precision and contains software to treat the complex data structures it generates.

INSTRUMENTATION

Figure 4 shows a set of S-curves (also known as learning curves or use curves) that are popular in many books describing innovation, or the lack thereof, in high technology business. S-curves are intended to show that a technology will eventually reach a plateau of performance and that prominent changes in performance most often come about through a departure from old technology and a jump to new technology, rather than from a single rising performance curve.

In figure 4, one possible labelling of these S-curves is shown for the changing character of instrumental analytical techniques. The increase of performance for all types of instruments is a result of a first conversion to internal control by modern analog and hybrid electronics, followed —

perhaps less serially than indicated — by a conversion to system control based on digital electronics approaches. The most recent change has been computerized equipment, which provides inherent operating intelligence a network of data flow, and autonomous analytical systems.

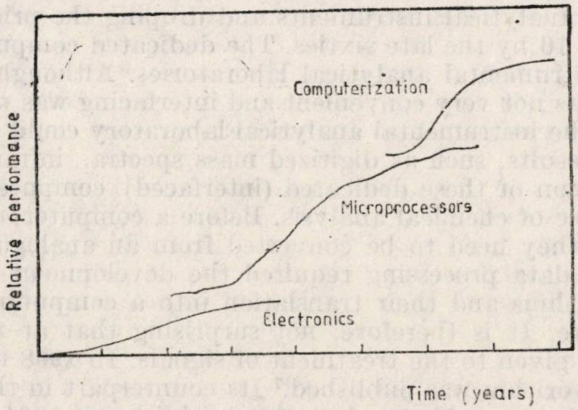

Fig. 4. — S—curves describing the impact of new technologies on performance improvement.

Table 4

Historical context of the generation of instrumental analytical information

	Barrier to instrumental analytical information	Solution	New problem
Pre 1960	Data generation	Electronic control	Kilometers of chart paper
1960's	Data acquisition	Digitizers	Masses of data and results
1970's	Data/result reduction	Mini/micro computers	Masses of information
1980's	Information management	Workstations, LIMS	Complexity of decisions
1990's	Intelligence	AI, expert systems	Fundamentals of analytical chemistry

The historical context of the generation of analytical (including environmental analytical) information by making use of the above-mentioned advances in instrumental analytical techniques is presented in table 4.

The pre-sixties was a period just before the second phase of the electronics revolution that took place in 1960. During and before the fifties, most of analytical equipment had to be controlled manually, making data collection slow and laborious. The measurement of a spectrum with a single beam spectrometer for instance, had to be carried out point by point, within between a manual adjustment of the monochromator and baseline. The principal barrier to the production of analytical information was, therefore, the data generation. It increased the demand of having recording istruments. The first spectrometers with automatic wavelength scanning and baseline correction became widespreadly available in the fifties. As a consequence, data generation became relatively easy and fast, causing however the production of kilometers of chart paper. The lack of the possibility to transform recorder traces into useful analytical information became the next barrier to the production of instrumental analytical information.

In the sixties, semiconductor devices were introduced, changing the design of analytical instruments and droping the price of computers by a factor of 10 by the late sixties. The dedicated computer appeared in the bigger instrumental analytical laboratories. Although access to such a computer was not very convenient and interfacing was not standardized and painful, the instrumental analytical laboratory could generate masses of data and results, such as digitized mass spectra, infrared spectra, etc. The introduction of these dedicated (interfaced) computers was going to change the face of chemical analysis. Before a computer can do anything with signals, they need to be converted from an analogue into a digital form. Digital data processing required the development of discrete, numerical algorithms and their translation into a computer readable code, called software. It is therefore, not surprising that at that time much attention was given to the treatment of signals. In 1968 the Fast Fourier Transform algorithm was published.[7] Its counterpart in the time domain, digital smoothing, was also developed[8] and published in 1964. The application of advanced algorithms on analytical signals became easier with the publication of complete program listings. The seventies were marked by tumultous developments. Computers evolved from an expensive tool for the few to a cheap, everywhere present tool, for everybody. In 1978 the first complete microcomputer system was introduced, first with relatively modest capabilities but later (80-ies) getting more calculating power than the obsolete mainframe of the sixties. Analogue meters were first replaced by digital BCD-displays. Later switches and buttons were replaced by a keyboard. Besides the process of further sophistication of existing measuring principles, new types of instrumental techniques for chemical analysis were introduced, for example, a chromatograph coupled to a mass spectrometer. This new type of equipment, by now called hyphenated instrumental technique, generates no longer one spectrum or one chromatogram, but is capable to measure several spectra at short time intervals. When operating such an instrument during 15 minutes, with one spectrum per second, digitized over 200 mass units, this data matrix contains 180.000 datapoints. If one point occupies 4 byte, 720 Kb information has been collected. The impact of these hyphenated systems in instrumental analytical chemistry can be read from figure 5, which shows the state of the art at the beginning of the 80-ties. As seen many different hyphenated instrumental techniques were available and lots of new ones were expected to appear in due course.

Many of these hyphenated instrumental techniques are a reality by now. This is one of the most remarkable achievements of the eighties. There are, of course, many other achievements worth to be mentioned. The ICP-AES technique e.q. has given birth to ICP-mass spectrometry (ICP-MS), and ICP-atomic fluorescence spectrometry (ICP-AFS).

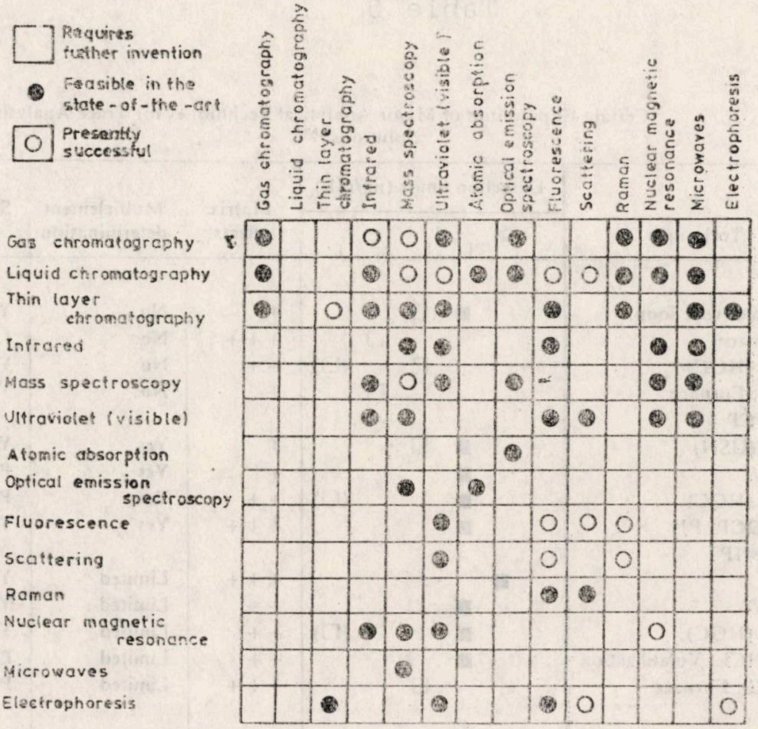

☐ Requires futher invention
● Feasible in the state-of-the-art
○ Presently successful

	Gas chromatography	Liquid chromatography	Thin layer chromatography	Infrared	Mass spectroscopy	Ultraviolet (visible)	Atomic absorption	Optical emission spectroscopy	Fluorescence	Scattering	Raman	Nuclear magnetic resonance	Microwaves	Electrophoresis
Gas chromatography	●			○	○	●		●			●	●	●	
Liquid chromatography	●			●	○	○	●	●	○	○	●	●	●	
Thin layer chromatography	●		○	●	●	●			●		●		●	●
Infrared					●	●			●			●	●	
Mass spectroscopy				●	○	●		●				●	●	
Ultraviolet (visible)				●	●				●	●		●	●	
Atomic absorption								●						
Optical emission spectroscopy					●		●							
Fluorescence						●			○	○	○			
Scattering						●			○		○			
Raman									●	●				
Nuclear magnetic resonance				●	●	●						○		
Microwaves					●									
Electrophoresis			●			●			●	○				○

Fig. 5. — The state of the art of the hyphenated instrumental techniques [7].

SENSITIVITY

A part per million was considered an impressive sensitivity a generation ago. Now a part per trillion ($1/10^{12}$) sensitivity is achieved for some routine analyses, while a special tandem-accelator mass spectrometer can detect three atoms of ^{14}C in the presence of 10^{16} atoms of ^{12}C[8]. Sensitivity depends on the efficiency of converting the analyte to a measurable species, and on the ability to measure this species. In addition, the actual detection limit (signal-to-noise ratio) is also affected by the response of interfering species present (that is, specificity). These measurable species include the photons whose absorption or emission is the basis of a variety of spectroscopic methods (X-ray, UV, IR, NMR, Raman, Mössbauer, and so on), and the charged species which are the bases of electron and mass spectrometry and of detectors (flame ionization, etc.) for chromatography. The efficiency of converting the analytes to photons (and even electrons and ions) has been dramatically improved with intense energy sources such as lasers, synchroton radiation, and plasmas. The capabilities of different instrumental analytical techniques is presented in tables 5—7.

Table 5

Certain Capabilities of Major Analytical Techniques for Trace Analysis of Solutions[a,b]

Technique	Detection limits (ng/mL)						Matrix effects	Multielement determination	Speciation analysis
		≥		1	≥				
AAS									
Flame (wire loop)			■	(□)			+	No	Yes (+)
Furnace					□		+ + +	No	Limited
HG (HGC)				□		(□)	+ +	No	Yes
ZAAS: Furnace					□		+	No	Yes
AES-ICP									
PN (USN)			■	□			+	Yes	Yes
ETV			■				+	Yes	Possible
HG (HGC)			■			(□)	+ +	Yes	Possible
AES-DCP: PN			■				+ + +	Yes	Yes
AES-MIP									
PN		■					+ + +	Limited	Yes (+)
ETV			■				+ +	Limited	Yes
HG (HGC)			■			(□)	+ +	Limited	Yes
AES-HCL: Volatilization			■				+ +	Limited	Possible
FANES: Furnace				□			+ + +	Limited	Possible
AFS									
Laser-ICP			■				+	Yes	Possible
ICP-ICP			■				+	Yes	Possible
HCL-ICP			■				+	Yes	Possible
Laser-furnace					□		+ + +	Yes	
CFS: Furnace			■				+ + +	Yes	Possible
OGS: Flame				□			+ + +	Limited	
XRS									
XRF	■						+ + +	Z > 6	Yes
PIXE		■					+ + +	Z > 14	No
TR				□			+	Z > 14	No
MS									
ID-ICP				□			+	Yes	Yes
ID-TI					□		+ +	Limited	No
ID-FD					□		+ +	Limited	
NAA									
INAA			■				(+)	Yes	Possible
RANAA						□	(+)	Limited	No
Voltammetry									
DPASV				□			+ + +	Limited	Yes
DPCSV				□			+ + +	Limited	Yes
Chelation									
GC-ECD					□		+ + +	Limited	Yes
HPLC-UVD			■				+ + +	Limited	Yes
Spectrophotometry		■					No	No	Yes
Fluorimetry				□			+ + + +	No	Yes

Table 6

Detection limits, in µg/g solid sample, for 17 elements in seven analytical techniques

Element	INAA	ED-XRF	PIXE	ICP-AES	ETA-AAS	LIF-ETA	ICP-MS
V	0.03	20	1.3	3.5	0.2	85	0.03
Cr	0.03	16	0.8	4	0.01		0.06
Mn	0.001	12	0.6	0.95	0.01	0.004	0.10
Fe	6	12	0.5	3	0.02	0.005	
Ni	3	5	0.4	6.5	0.2		0.10
Cu	0.03	6	0.3	3.5	0.02	0.003	0.32
Zn	0.3	5	0.3	1.2	0.001		0.21
As	0.03	4	0.4	35	0.2		0.04
Sc	0.03	2	0.4	50	0.5		0.79
Mo	0.3	5	1.9	5.5	0.02		0.04
Cd	0.6	6	10	1.7	0.003	0.001	0.06
In	0.0006		14	40		0.001	0.07
Sn	1	8	16	17	0.1		0.06
Sb	0.01	8	14	20	0.1		0.05
Hg	0.003	7	1.0	17	2		0.02
Tl			1.1	25	0.1	0.00004	
Pb		8	1.1	30	0.05	0.00003	0.05

Table 7

Summary of some characteristics of analytical techniques for bulk trace element analysis

Technique	Price of instr.[a]	Detec. limit[b] [µg/g] or [ng/ml]	Spectral interf.	Matrix effects	Multi-element	Preferred sample type
INAA	(++++)	0.001–1	low	low	yes	solid
XRF[c]	+/++	1–10	high-low	medium	yes	solid
TXRF	++	–0.2	high	medium	yes	liquid[d]
PIXE	(++++)	0.2–3	high	medium	yes	solid
ICP-AES	++	1–30	high	medium	yes	liquid
ETA-AAS	+	0.01–0.2	medium	high	no	liquid
LIF-ETA	+++	–0.001	low	high	no	liquid
ICP-MS	+++	0.03–0.1	high	high	yes	liquid

[a] Code for price of instrument: + indicates less than \$ 100 000, ++ from \$ 100 000 to \$ 250 000, +++ from \$ 250 000 to \$ 500 000, and ++++ more than \$ 500 000; (·) — the instrument cost is not a very relevant measure in PIXE and INAA.

[b] Detection limits are in µg/g for INAA, XRF and PIXE, and in ng/ml for the other techniques, including TXRF.

[c] The indications on this line before each slash apply to ED-XRF, those after each slash to WD-XRF.

[d] The dried residue of the liquid on a totally reflecting substrate is subjected to analysis.

COST OF EQUIPMENT FOR INSTRUMENTAL TECHNIQUES, PRICE PER SAMPLE ANALYSED AND SPEED OF ANALYSIS

The approximate capital cost of equipment for instrumental analytical techniques is shown in Table 8 and Fig. 6.

The world market for analytical instruments is considered to show a strength only dreamed about as little as 5–10 years ago. This is neatly reflected in figure 6. Chromatography is the fastest growing area, comprising 40%, or $ 1.5 billion, in 1987 world sales. The largest U.S. sales of individual instrument types, go for high-performance liquid chromatography (HPLC) and gas chromatography (GC) instruments. Gas chromatograph sales are growing at about the same rate as the total instrument market. Some of the newest innovations in GC technology are the production of more instruments with high-efficiency, high-resolution capillaries and supercritical fluid capability. Despite of having only a 3% share of the GC market, supercritical fluid chromatography (SFC) has attracted a great deal of attention since its introduction around 1985 and production of the first commercial instrument around 1986. SFC, which operates using a supercritical fluid as the mobile phase, bridges the gap between GC and HPLC. The use of these mobile phases allows for higher diffusion rates and lower viscosities than liquids, a greater solvating power than gases. Another area showing tremendous growth in sales is ion chromatography (IC).

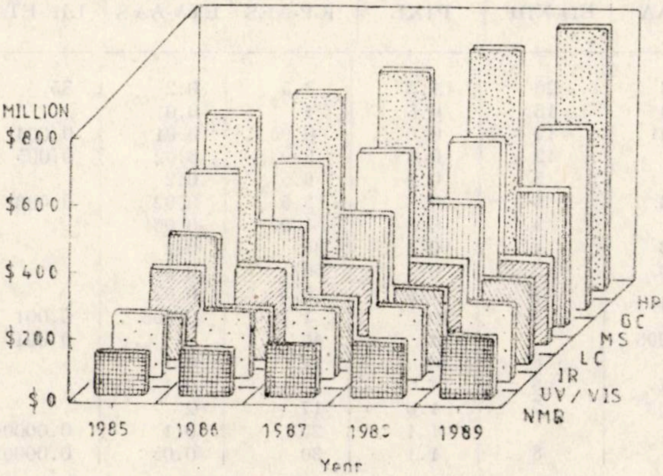

Fig. 6. — Sales of instrumental analytical equipment.

Table 8

Approximate capital cost of equipment

	(10^6 FF)	(10^3 DM)	(10^3 UK £)	(10^3 US $)
XRF	1.5	420	140	200
AAS	0.27	80	25	40
INAA *	0.20	60	20	30
ICP-AES	1.0	280	90	150
ICP-MS	1.8	520	170	270
EMP	3.0	1.000	300	470
IMA	6.0	2.000	600	1.000

* Excludes neutron source.

Mass spectrometry (MS) sales have been growing about 12% annually. Sales have always been high, especially since MS is the principal detection system in a number of hyphenated techniques as GC-MS, MS-MS and LC-MS. Innovation in interface technology such as inductively coupled plasma ICP-MS, SFC-MS and thermospray or particle beam interfaces for LC-MS had both advanced the technology and expanded the interest in applications. Increasing capability and importance have however contributed substantially to increasing cost of MS equipment (Fig. 7).

AAS instruments cost from $ 10.000 to $ 100.000 with flame AAS being cheaper than ETA-AAS. ICP-AES equipment costs from $40.000 to $ 200.000 and the price of an ICP-MS is in the order of $ 300.000. Prices for XRF instruments range from about $ 50.000 for simple ED-XRF machines to up to $ 200.000 or more for multichannel WD-XRF spectrometers. The price of INAA equipment, although having some indications in Table 6, is difficult to evaluate. The speed of analysis is high in most of the instrumental analytical techniques, with NAA being the major exception. The measuring time per sample is typically only a few minutes in ICP-MS, ICP-AES and AAS. However AAS suffers severely from the fact that it is a single-element technique. Measurement times in XRF can be as low as a few minutes, but may also extend to one hour or more (particularly in ED-XRF). In INAA, even much longer counting times are generally used (up to several hours). Moreover, each sample is measured 4 to 5 times over a period which may extend up to several

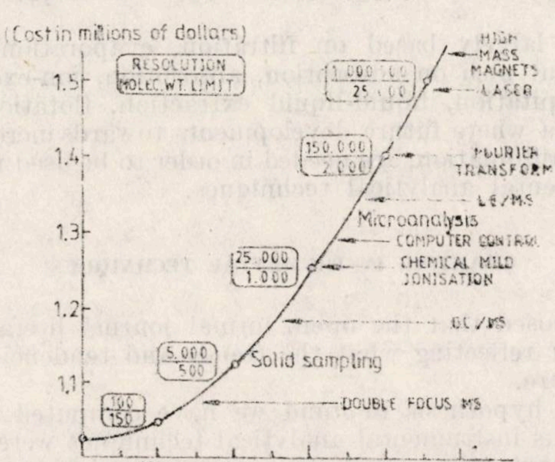

Fig. 7. — Increasing capability, increasing importance, increasing cost of MS equipment.

weeks. However, INAA and also XRF have the advantage over the other techniques that automated measurements of many samples can be done on a 24 hours/day, 7 days/week basis with virtually no human supervision.

PRECONCENTRATION

While the purely instrumental character of procedures for solid samples (INAA, XRF, etc.) not requiring a dissolution step is generally considered as the major advantage above other multi-elemental techniques such as ICP-AES, ICP-MS, Anodic Spripping Voltametry (ASV), this quality is lost when environmental aqueous samples are analysed. Therefore a large number of preconcentration techniques have been developed.

They are largely based on filtration, evaporation, freeze-drying (evaporation) but also on adsorption, absorption, ion-exchange precipitation, co-precipitation, liquid-liquid extraction, flotation, etc. This is certainly an area where future developments towards increased efficiency, selectivity and automation, are needed in order to be used with the sophisticated instrumental analytical techniques.

CHARTING INSTRUMENTAL TECHNIQUES

It is supposed that the open, formal journal literature is a quite adequate mirror reflecting what the trends and tendencies of the fields it deals with, are.

With this hypothesis in mind we have computed the number of times the various instrumental analytical techniques were used to determine different components in environmental matrices as reported in the *Analytical Abstracts* database.[9] The data were transferred into a computer file for further manipulations.

By classifying the various instrumental techniques according to the physical principles involved in the measurement process, there were, according to the indexing rules of *Analytical Abstracts*, approximately 150 different instrumental techniques. Some of these overlap considerably. They were merged into 7 groups (see Appendix). Conventional analytical methods were added for convenience.

Two aspects of this approach have to be emphasized.

— the different instrumental techniques taken into account were not selected, i.e. defined, by us but by the subject index classification system of the *Analytical Abstracts* database; the same is valid for the types of environmental matrices considered.

— our computing does not refer to the number of papers on instrumental analytical techniques but to the number of uses of these techniques, which is why, e.g., one paper can refer to the use of many instrumental techniques.

Tables 9—14 present the results. In all the tables percentages sum up horizontally. Although the tables are self-explanatory, a few comments are in order.

The upper part of table 9 shows e.g., that in analysing environmental air samples, of the total instrumental techniques used, 37.8% were optical, 10.4% nuclear, 5.4% electrical and so on. Viewed from the side of the instrumental technique used, the lower part of table 9 indicates e.g., that of the optical techniques used 27.7% were dedicated to the analysis of air, 65.5% to the analysis of water and so on.

Table 9

Instrumental techniques used for analyzing environmental matrix components, 1986–1989, % *

	OPT	NUCL	ELEC	CHROM	MISC	HYPH	CONV
AIR	37.8	10.4	5.4	37.4	0.9	7.1	1.0
WATER	40.2	7.5	12.6	22.2	3.8	12.6	1.1
EFFLUENT	30.5	6.6	10.9	25.4	4.7	19.8	2.1

	AIR	WATER	EFFLUENT
OPT	27.7	65.5	6.8
NUCL	35.6	57.5	6.9
ELEC	14.6	76.4	9.0
CHROM	39.5	52.3	8.2
MISC	8.4	78.3	13.3
HYPH	17.3	68.0	14.7
CONV	24.2	59.7	16.1

* Legend

OPT = optical ; NUCL = nuclear ; ELEC = electrical ; CHROM = chromatographic ; MISC = miscellaneous ; HYPH = hyphenated ; CONV = conventional.

Table 10

Instrumental techniques used for analyzing inorganic components in environmental matrices, 1986–1989, % *

	OPT	NUCL	ELEC	CHROM	MISC	HYPH	CONV
AIR	51.7	17.9	7.4	15.9	1.0	5.1	1.0
WATER	45.2	9.3	14.7	11.9	4.4	13.3	1.2
EFFLUENT	35.6	10.1	13.7	10.8	6.5	21.6	1.6

	AIR	WATER	EFFLUENT
OPT	25.4	68.5	6.1
NUCL	35.8	57.1	7.1
ELEC	12.9	78.8	8.3
CHROM	28.1	65.2	6.7
MISC	6.1	80.3	13.6
HYPH	9.6	76.3	14.1
CONV	18.8	70.8	10.4

* Legend

OPT = optical ; NUCL = nuclear ; ELEC = electrical ; CHROM = chromatographic ; MISC = miscellaneous ; HYPH = hyphenated ; CONV = conventional.

Table 11

Instrumental techniques used for analyzing organic compounds in environmental matrices, 1986–1989, % *

	OPT	NUCL	ELEC	CHROM	MISC	HYPH	CONV
AIR	19.2	0.6	2.9	66.2	0.3	10.2	0.6
WATER	23.7	1.1	5.4	57.1	1.7	10.7	0.3
EFFLUENT	17.8	0.0	5.0	55.7	2.9	15.7	2.9

	AIR	WATER	EFFLUENT
OPT	40.9	50.7	8.4
NUCL	36.4	63.6	0.0
ELEC	30.5	57.6	11.9
CHROM	48.7	42.2	9.1
MISC	11.8	64.7	23.5
HYPH	41.6	44.2	14.3
CONV	40.0	20.0	40.0

* Legend
OPT = optical; NUCL = nuclear; ELEC = electrical; CHROM = chromatographic; MISC = miscellaneous; HYPH = hyphenated CONV = conventional.

Table 12

Analyzing environmental matrix components by different instrumental techniques, 1986–1989, % *

	OPT	NUCL	ELEC	CHROM	MISC	HYPH	CONV
Ag	64.7	17.6	5.9	0.0	0.0	11.8	0.0
Al	53.6	8.7	8.7	4.3	2.9	21.7	0.0
As	54.7	18.8	9.4	6.3	0.0	10.9	0.0
Au	100.0	0.0	0.0	0.0	0.0	0.0	0.0
B	47.1	5.9	5.9	0.0	0.0	41.2	0.0
Ba	44.4	14.8	7.4	7.4	0.0	22.2	3.7
Be	60.9	20.0	4.3	13.0	0.0	21.7	0.0
Bi	58.3	4.2	20.8	4.2	0.0	12.5	0.0
Br	13.3	20.0	6.7	36.7	3.3	16.7	3.3
C	25.0	16.7	8.3	16.7	12.5	16.7	4.2
Ca	32.7	23.6	1.8	18.2	3.6	18.2	1.8
Cd	52.1	7.8	19.4	6.0	0.5	13.8	0.5
Ce	14.3	42.9	20.0	0.0	0.0	42.9	0.0
Cl	21.8	6.9	19.8	25.7	14.9	5.9	5.0
Co	44.5	10.9	15.5	15.5	1.8	11.8	0.0
Cr	45.0	18.3	12.5	6.7	2.5	15.0	0.0
Cs	28.6	57.1	0.0	14.3	0.0	0.0	0.0
Cu	50.4	6.9	20.2	6.9	2.8	12.5	0.4
F	23.9	2.2	28.3	32.6	8.7	2.2	2.2
Fe	45.2	21.0	7.3	5.6	4.0	16.1	0.8
Ga	80.0	20.0	0.0	0.0	0.0	0.0	0.0
Ge	75.0	0.0	0.0	12.5	0.0	12.5	0.0
Hg	56.0	13.0	14.0	10.0	2.0	5.0	0.0
I	21.1	13.2	18.4	18.4	7.9	21.1	0.0
In	60.0	20.0	0.0	0.0	0.0	20.0	0.0
K	35.1	24.3	8.1	16.2	2.7	13.5	0.0
Li	44.4	0.0	0.0	33.3	0.0	22.2	0.0
Mg	37.1	11.4	5.7	22.9	5.7	14.3	2.9

Table 12 (continued)

	OPT	NUCL	ELEC	CHROM	MISC	HYPH	CONV
Mn	56.0	10.3	10.3	4.3	3.4	14.7	0.9
Mo	37.5	12.5	16.1	3.6	3.6	26.8	0.0
N	47.6	4.8	0.0	14.3	19.0	4.8	9.5
Na	30.4	21.7	0.0	30.4	0.0	17.4	0.0
Ni	43.9	10.8	20.9	6.5	0.7	17.3	0.0
O	44.4	5.6	27.8	11.1	5.6	0.0	5.6
P	54.3	5.7	0.0	11.4	11.4	17.1	0.0
Pb	54.2	6.7	20.6	3.4	1.3	13.4	0.4
Pd	83.3	16.7	0.0	0.0	0.0	0.0	0.0
Pu	22.2	66.7	0.0	11.1	0.0	0.0	0.0
Rb	12.5	75.0	0.0	12.5	0.0	0.0	0.0
Ru	40.0	40.0	0.0	0.0	0.0	20.0	0.0
S	26.9	11.5	7.7	23.1	7.7	19.2	3.8
Sb	56.5	13.0	15.2	2.2	0.0	13.0	0.0
Se	54.4	19.3	10.5	5.3	1.8	8.8	0.0
Si	64.7	29.4	0.0	0.0	0.0	5.9	0.0
Sn	63.6	9.1	9.1	0.0	0.0	18.2	0.0
Sr	30.4	30.4	4.3	8.7	0.0	26.1	0.0
Te	83.3	16.7	0.0	0.0	0.0	0.0	0.0
Th	26.7	53.3	0.0	13.3	0.0	6.7	0.0
Ti	24.0	24.0	8.0	0.0	4.0	40.0	0.0
Tl	50.0	3.8	19.2	3.8	0.0	23.1	0.0
U	32.0	32.0	16.0	10.0	2.0	6.0	2.0
V	35.8	17.0	11.3	3.8	5.7	26.4	0.0
Y	14.3	28.6	0.0	0.0	0.0	57.1	0.0
Zn	45.8	11.4	17.5	6.6	0.6	18.1	0.0
Zr	27.3	36.4	0.0	0.0	0.0	36.4	0.0
ME	41.3	10.9	17.4	13.0	2.2	15.2	0.0
REE	28.6	28.6	14.3	0.0	0.0	28.6	0.0
MEL	32.4	27.1	6.4	13.8	3.2	16.0	1.1
aAs	88.9	0.0	0.0	11.1	0.0	0.0	0.0
aC	12.5	0.0	12.5	37.5	12.5	12.5	12.5
aCN	47.1	0.0	14.7	20.6	11.8	0.0	5.9
aCl	41.2	0.0	41.2	0.0	5.9	0.0	11.8
aCr	40.0	0.0	0.0	60.0	0.0	0.0	0.0
aN	43.1	0.0	5.4	36.2	12.3	2.3	0.8
aP	47.7	4.5	9.1	22.7	11.4	2.3	2.3
aS	30.4	2.2	13.0	34.8	8.0	4.3	7.2
aSCN	60.0	0.0	0.0	20.0	0.0	0.0	20.0
CH_4	83.3	0.0	0.0	16.7	0.0	0.0	0.0
CO	84.2	0.0	0.0	10.5	5.3	0.0	0.0
CO_2	62.5	0.0	29.2	8.3	0.0	0.0	0.0
COS	40.0	0.0	0.0	40.0	0.0	20.0	0.0
CS_2	55.6	0.0	11.1	33.3	0.0	0.0	0.0
H_2O	50.0	0.0	37.5	12.5	0.0	0.0	0.0
H_2O_2	72.0	0.0	8.0	12.0	8.0	0.0	0.0
H_2S	54.8	0.0	9.7	25.8	6.5	0.0	3.2
HCl	54.5	0.0	18.2	18.2	0.0	0.0	9.1
HF	50.0	0.0	33.3	16.7	0.0	0.0	0.0
NH_3	42.9	1.2	17.9	22.6	14.3	0.0	1.2
NO	80.0	6.7	6.7	6.7	0.0	0.0	0.0
NO_2	64.9	0.0	8.1	21.6	5.4	0.0	0.0
NOX	68.4	0.0	5.3	26.3	0.0	0.0	0.0
O_3	76.5	0.0	11.8	5.9	5.9	0.0	0.0
SO_2	58.7	0.0	11.1	20.6	1.6	1.6	6.3

Table 12 (continued)

	OPS	NUCL	ELEC	CHROM	MISC	HYPH	CONV
cCa	80.0	0.0	0.0	0.0	0.0	20.0	0.0
cN	58.1	0.0	0.0	41.9	0.0	0.0	0.0
cS	28.6	0.0	0.0	71.4	0.0	0.0	0.0
cSi	40.0	60.0	0.0	0.0	0.0	0.0	0.0
ORG	19.3	0.7	4.3	64.1	1.0	9.7	0.8
ORGHg	50.0	0.0	10.0	20.0	0.0	20.0	0.0
ORGPb	23.5	0.0	0.0	29.4	0.0	47.1	0.0
ORGSn	41.9	0.0	6.5	45.2	0.0	6.5	0.0
PAH	19.8	0.0	0.9	62.3	0.0	17.0	0.0
PCB	4.2	0.0	0.0	75.0	0.0	20.8	0.0
IND	26.3	1.4	3.8	54.5	3.3	8.1	2.4

* Legend

a... = anions of the element(s) indicated
c... = compounds of the element indicated but not mentioned individually
ME = metals
REE = rare earth elements
MEL = multi element analysis
ORG = organic compounds without organometallics, PAH, and PCB
ORG... = organometallic compounds of the metal indicated
PAH = polycyclic aromatic hydrocarbons
PCB = polychlorinated biphenyls
IND = industrial products and wastes (oils, detergents, fertilizers, polymers, exhaust gases, etc.)

No distinction has been made between metals and metal cations as well as between halogens and oxygen free halogen anions

Table 13

Analyzing matrix components in environmental samples, 1986–1989, % *

	Air	Water	Efluent
Ag	0.0	100.0	0.0
Al	15.9	78.3	5.8
As	14.1	78.1	7.8
Au	0.0	100.0	0.0
B	17.7	82.3	0.0
Ba	3.7	77.8	18.5
Be	13.0	78.3	8.7
Bi	8.3	81.7	0.0
Br	30.0	63.3	6.7
C	45.8	50.0	4.2
Ca	23.6	67.3	9.1
Cd	6.5	83.4	10.1
Ce	14.3	85.7	0.0
Cl	16.8	76.3	6.9
Co	8.2	87.3	4.5
Cr	19.2	59.2	21.6
Cs	0.0	100.0	0.0
Cu	6.0	85.5	8.5
F	26.1	69.6	4.3
Fe	15.3	77.4	7.3
Ga	0.0	60.0	40.0
Ge	0.0	100.0	0.0

Table 13 (continued)

	Air	Water	Effluent
Hg	20.0	63.0	17.0
I	18.4	79.0	2.6
In	20.0	80.0	0.0
K	27.0	62.2	10.8
Li	0.0	100.0	0.0
Mg	22.9	77.1	0.0
Mn	14.7	78.4	6.9
Mo	7.1	91.1	1.8
N	19.0	52.4	28.6
Na	21.7	78.3	0.0
Ni	10.8	77.0	12.2
O	22.2	77.8	0.0
P	5.7	65.7	28.6
Pb	13.5	78.1	8.4
Fd	0.0	100.0	0.0
Pu	11.1	88.9	0.0
Rb	25.0	75.0	0.0
Ru	60.0	40.0	0.0
S	50.0	38.5	11.5
Sb	15.2	80.4	4.4
Se	10.5	89.5	0.0
Si	41.2	58.8	0.0
Sn	21.2	75.8	3.0
Sr	17.4	78.3	4.3
Te	33.3	50.0	16.7
Th	13.3	80.0	6.7
Ti	12.0	64.0	24.0
Tl	7.7	80.8	11.5
U	12.0	84.0	4.0
V	17.0	77.4	5.6
Y	0.0	100.0	0.0
Zn	9.0	78.3	12.7
Zr	18.2	72.7	9.1
ME	13.0	76.1	10.9
REE	0.0	100.0	0.0
MEL	42.6	55.3	2.1
aAs	11.1	88.9	0.0
aC	0.0	100.0	0.0
aCN	17.7	50.0	32.3
aCl	11.8	82.3	5.9
aCr	0.0	80.0	20.0
aN	20.8	72.3	6.9
aP	6.8	86.4	6.8
aS	20.3	71.0	8.7
aSCN	0.0	60.0	40.0
CH_4	83.3	16.7	0.0
CO	94.7	5.3	0.0
CO_2	66.7	33.3	0.0
COS	100.0	0.0	0.0
CS_2	88.9	11.1	0.0
H_2O	87.5	12.5	0.0
H_2O_2	44.0	56.0	0.0
H_2S	83.9	12.9	3.2
HCl	100.0	0.0	0.0
HF	100.0	0.0	0.0
NH_3	46.4	42.9	10.7
NO	93.3	6.7	0.0

Table 13 (continued)

	Air	Water	Effluent
NO_2	97.3	2.7	0.0
NOX	100.0	0.0	0.0
O_3	70.6	29.4	0.0
SO_2	92.1	7.9	0.0
cCa	100.0	0.0	0.0
cN	83.9	12.9	3.2
cS	100.0	0.0	0.0
cSi	60.0	40.0	0.0
ORG	46.4	43.2	10.4
ORGHg	20.0	70.0	10.0
ORGPb	47.1	47.0	5.9
ORGSn	3.2	96.8	0.0
PAH	64.1	32.1	3.8
PCB	25.0	62.5	12.5
IND	19.6	64.6	15.8

* Legend

a... = anions of the element(s) indicated
c... = compounds of the element indicated but not mentioned individually
ME = metals
REE = rare earth elements
MEL = multi element analysis
ORG = organic compounds without organometallics, PAH, and PCB
ORG... = organometallic compounds of the metal indicated
PAH = polycyclic aromatic hydrocarbons
PCB = polychlorinated biphenyls
IND = industrial products and wastes (oils, detergents, fertilizers, polymers, exhaust gases, etc.)

No distinction has been made between metals and metal cations as well as between halogens and oxygen free halogen anions

Table 14

Instrumental techniques used for analyzing inorganic and organic matrix components, 1986–1989, % *

Compounds	OPT	NUCL	ELEC	CHROM	MISC	HGYPH	CONV
Inorganic	45.9	11.3	13.0	12.7	3.8	12.1	1.2
Organic	20.8	0.7	4.0	61.9	1.2	10.6	0.9

	Inorganic	Organic
OPT	84.6	15.4
NUCL	97.6	2.4
ELEC	89.1	10.9
CHROM	33.8	66.2
MISC	88.6	11.4
HYPH	74.0	26.0
CONV	77.4	22.6

* Legend

OPT = optical ; NUCL = nuclear ; ELEC = electrical ; CHROM = chromatographic ; MISC = miscellaneous ; HYPH = hyphenated ; CONV = conventional.

Table 9 also shows that optical methods and chromatographies ominate the instrumental analytical approach of environmental sam- les. What is however remarkable is the third position of hyphenated rocedures. The distribution of instrumental techniques used for analy- ing the three types of environmental matrices indicates that water has een the most frequently analyzed matrix.

When considering the determined analytes separately, table 10 ndicates that the use frequency ranking of instrumental techniques in ase of inorganic analytes shows a different picture. Optical procedures, nainly the different variants of atomic absorption spectrometry occupy ank 1, but in analyzing air samples, nuclear techniques climbed to the econd rank. Hyphenated procedures are also strongly used but chroma- ographies seem to be not yet established techniques in analyzing inor- anic analytes in environmental samples, although GC in case of air ana- ysis and ion chromatography in case of water and effluents are on the pward move.

The clear dominance of chromatographies is clearly revealed in heir use for determining organic analytes in environmental samples as hown in table 11. The quite negligible use of nuclear techniques for the ame purpose comes as no surprise. When considering individual analytes Table 12) it is visible that in the determination of traces of metals, optical ocedures are the most frequently used but there are some cases (Be, Ce, , Rb, Sr, Th, U, Y, Zr, REE) where nuclear techniques still occupy nk 1. In case of inorganic anions, chromatographies are competing ith spectroscopies mainly due to the progresses of the ion chromato- aphic techniques. The absolute dominance of chromatographies is best sible in case of analyzing organometallic analytes as well as some high xicity organics as PAH's and PCB's (see Table 12).

As concerns the frequency of analyzing different types of environ- ental matrices, table 13 shows that inorganic components are mainly etermined in water samples.

Finally table 14 shows rankings of instrumental techniques as well as their uses for analyzing environmental matrices.

For inorganic analyses the ranking is :
optical> electrical> chromatographic> hyphenated>
nuclear> miscellaneous> conventional techniques
For organic analytes however, the ranking changes to :
chromatographic> optical> hyphenated> electrical>
miscellaneous> conventional> nuclear.

ACKNOWLEDGEMENT. The generous assistance of Mrs. Lilian Vasvári in the computerized processing of our data is gratefully acknowledged.

APPENDIX

INSTRUMENTAL ANALYTICAL TECHNIQUES

Optical methods. Colorimetry, photometry, turbidimetry, fluorimetry, UV, visible and IR spectrometry, spectroscopy, polarimetry.

Nuclear methods. Neutron activation analysis, radiometry, gamma-spectrometry, X-ray fluorimetry and related methods.

Electrical methods. Potentiometry, coulometry, amperometry, conductometry, polar graphy, voltammetry, and related methods.

Chromatography. All kind of chromatographic methods (gas-liquid, gas-solid, soli gel, thin-layer, paper, capillary, ion-chromatography and other related methods, inclusi pyrolysis gas chromatography).

Miscellaneous. Mass spectrometry, nuclear magnetic resonance spectrometry, X-ra spectrometry, X-ray diffractometry, and related methods: thermal methods (thermometr thermogravimetry, enthalpymetry, calorimetry etc.), kinetic, enzymatic methods, as well methods which could not be ordered in any other group.

'Hyphenated methods'. Combined instrumental methods, *i.e.* gas chromatography—mas spectrometry, etc.

Conventional methods. 'Classical' analytical methods, *i.e.* gravimetry, titrimetry (en point indication with chemical indicators), extraction methods, pyrolysis (combustion m thods), gas-volumetry.

REFERENCES

[1] Commission of the European Communities, "The State of the Environment in the Europea Community 1986", Luxembourg, 1987.

[2] D. W. Pearce et al, "Blueprint for a Green Economy," Earthscan, London, 1989.

[3] W. Ott, "Environmental Indices: Theory and Practice", Ann Arbor, Michigan, 1978.

[4] H. Enschnauer, *Naturwissenschaften*, **73**, 281 (1986).

[5] L. A. Currie, *Pure Appl. Chem.*, **54**, 715 (1982).

[6] J. K. Taylor, *NBS Report NBSIR-84*, Gaithersburg, MD, USA.

[7] T. Hirschfeld, *Anal. Chem.*, **52**, 297A (1980).

[8] C. L. Bennett, *Am. Sci.*, **67**, 450 (1979).

[9] *Analytical Abstracts*, Royal Society of Chemistry, Cambridge, 1986—1989.

Revue Roumaine de Chimie, **36**, *4*–*7*, 507–517 (1991)

Dedicated to Professor ALEXANDRU T. BALABAN,
on the occasion of his 60th birthday

STUDIES ON CHROMOTROPIC NICKEL(II)-COMPLEXES

WOLFGANG LINERT,[a] VIKTOR GUTMANN,[a] ALI TAHA[b]
and EL MARAGHY SALAH[b]

Institute of Inorganic Chemistry, Technical University of Vienna, Getreidemarkt 9, A-1060 Vienna, Austria
Faculty of Education, Ain Schams University, Roxy, Cairo, Egypt

Received January 15, 1991

Thermodynamic and structural properties are reported on solvent- and substituent effects for square planar Ni(II) complexes with a diamine and a β-diketone as ligands. Solvent- and substituent effects point either in the same or in opposite directions. Both the Ni—O and Ni—N bonds are lengthened by donor solvents which form octahedral complexes *via* coordination. Electron withdrawing substituents at the β-diketone lead also to lengthening of the Ni—O bonds accompanied by increase in stability constant of the octahedral species, whereas electron releasing substituents at the β-diketone lead to shortening of these bonds and to decrease in stability constants.

INTRODUCTION

Square planar Ni(II)-complexes with a diamine and a β-diketone s ligands are known to show solvatochromism and thermochromism due o the equilibrium [1–8]

$$[\mathrm{Ni}(\beta\text{-dike})(\mathrm{diam})]^+ + 2\,\mathrm{D} \rightleftarrows [\mathrm{Ni}(\beta\text{-dike})(\mathrm{diam})\mathrm{D}_2]^+ \qquad (1)$$

square planar — octahedral
diamagnetic — paramagnetic
red — blue or green

n order to obtain more detailed information about the influence of the lonor solvents D and of different substituents on either of the ligands, he systems listed in Table 1 have been investigated.

EXPERIMENTAL

The Ni(II) complexes were prepared according to ref [1,2] and the solvents purified accord-ng to standard procedure.[9,10] The water content in the solvents was measured by Karl-Fischer itration and usually found less than 30 mg · dm^{-3}. The solvents used were : 1,2-dichloroethane DCE), acetonitrile (An), acetone (Ac), *n*-butanol (*n*-BuOH), formamide (Fa), N,N-dimethyl-ormamide (DMF), dimethylsulfoxide (DMSO) and pyridine (Py).

Visible spectra were obtained by means of a Tracor Northen TN-1170 spectrophoto-meter from Photo-Applied Physics Corporation and a Hitachi U-2000 Spectrophotometer

Table 1

Position of substituents at the ligands# in the investigated mixed Ni(II) complexes

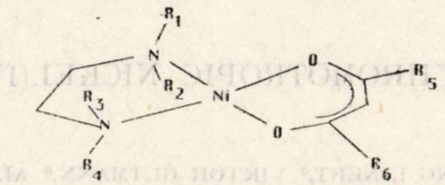

No.	Complex	R_1	R_2	R_3	R_4	R_5	R_6
1	$Ni(acac)(tmen)^+$	Me	Me	Me	Me	Me	Me
2	$Ni(bzac)(tmen)^+$	Me	Me	Me	Me	Me	Φ
3	$Ni(dbm)(tmen)^+$	Me	Me	Me	Me	Φ	Φ
4	$Ni(tfac)(tmen)^+$	Me	Me	Me	Me	Me	CF_3
5	$Ni(dipm)(tmen)^+$	Me	Me	Me	Me	t-Bu	t-Bu
6	$Ni(acac)(Me_3en)^+$	Me	Me	Me	H	Me	Me
7	$Ni(acac)(teen)^+$	Et	Et	Et	Et	Me	Me
8	$Ni(acac)(Et_3en)^+$	Et	Et	Et	H	Me	Me
9	$Ni(acac)(dipe)^+$	$(CH_2)_5$ [a]		$(CH_2)_5$ [a]		Me	Me
10	$Ni(acac)(medach)^+$	Me	$(CH_2)_2$ [a]		H	Me	Me

[a] bridging substituent

[#] Abbreviations for the used ligands are: acetylacetonate (acac), benzoylacetonate (bzac), dibenzoylmethane (dbm), dipiverylacetonate (dpm) and trifluoroacetonate (tfac); N, N, N′, N′-tetramethylethylendiamine (tmen), N, N, N′-trimethylethylendiamine (Me_3en), N, N, N′, N′-tetraethylethylendiamine (teen), N, N, N′-triethylethylendiamine (Et_3en) 1,2-dipiperidinomethane (dipe) and N-methyl-1,4-diacacycloheptane (medach).

using a cell with a path length of 3 cm, thermostated by means of a Haake F4-thermosta The temperature within the cell was measured before and after recording the spectra. Stoc solutions of the Ni-complexes in the solvents DCE were titrated with a donor-solvent, th recorded spectra stored in a multichannel memory unit and the spectral titration curves fitte by means of a combined Marquardt Newton method [11] to evaluate equilibrium constants and the extinctions ε_{NiL}.

Infrared spectra were recorded from nujol mulls using a Perkin Elmer 457 Gratin Spectrometer (5000–400 cm^{-1}). Far infrared spectra were measured with a Nicolet 20F FTIR spectrometer.

RESULTS AND DISCUSSION

The spectral features of the investigated systems are in line with those reported for the parent compound $Ni(acac)(tmen)^+$.[7] The positions of the UV-visible absorption bands vary with change in solvent and substitution (Fig. 1 and Fig. 2). The changes in the absorption bands of the octahedral species in the region between 570 and 670 nm are more pronounced by changes in substitution at the diamine ligand (lower part of Fig. 1 and Fig. 2) than by those at the β-diketonate (upper part in Fig. 1 and Fig. 2).

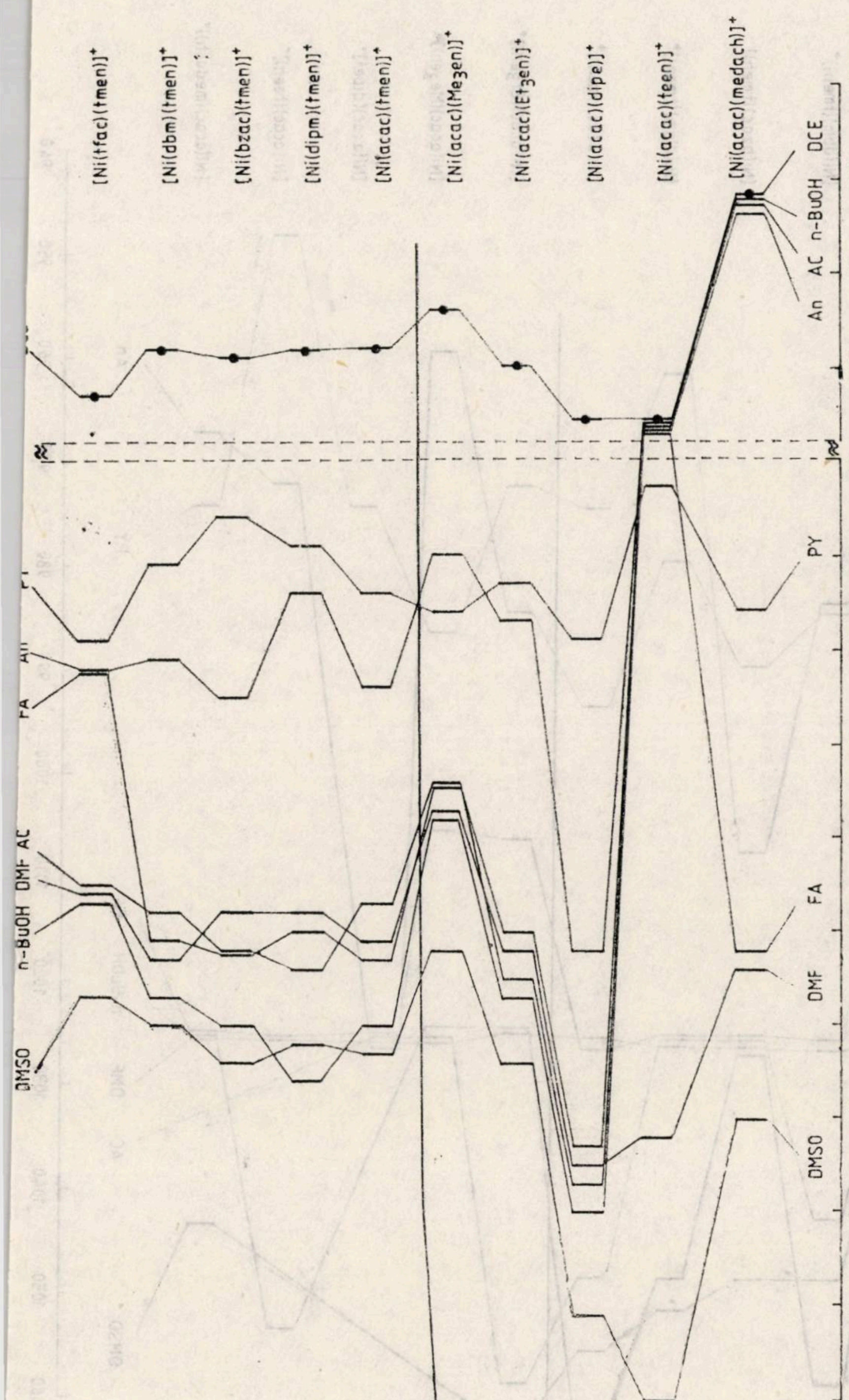

Fig. 1. — Positions of UV-visible absorption bands in dependence of the solvent and the ligand-substituents. (●: band of square planar complex).

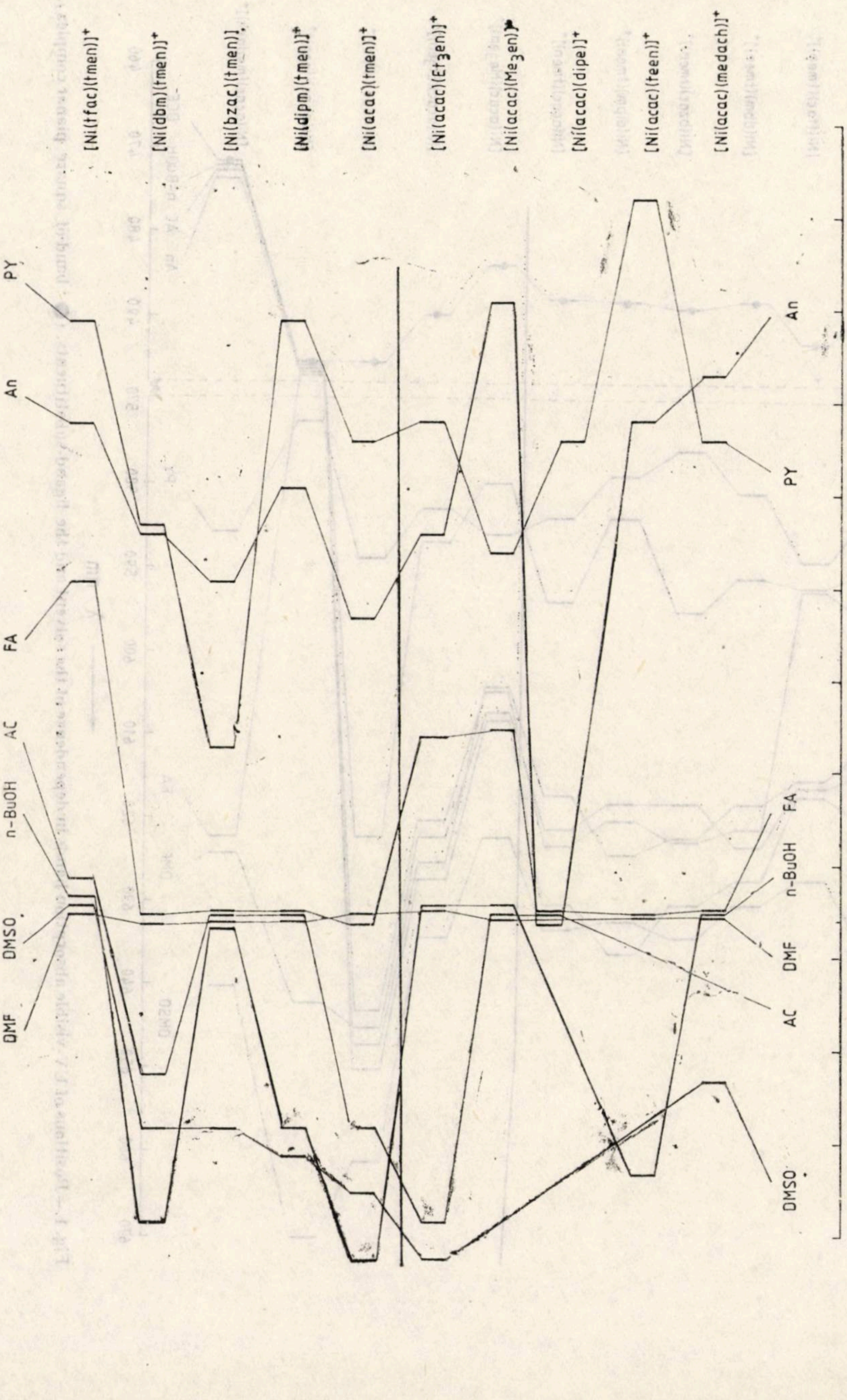
[Ni(tfac)(tmen)]⁺
[Ni(dbm)(tmen)]⁺
[Ni(bzac)(tmen)]⁺
[Ni(dipm)(tmen)]⁺
[Ni(acac)(tmen)]⁺
[Ni(acac)(Et3en)]⁺
[Ni(acac)(Me3en)]⁺
[Ni(acac)(dipe)]⁺
[Ni(acac)(teen)]⁺
[Ni(acac)(medach)]⁺
DMF
DMSO
n-BuOH
AC
FA
An
PY
DMSO
AC
DMF
n-BuOH
FA
PY
An
1060
1050
1040
1030
1020
1010
1000
990
980
970
960
950
940

The stability constants β as well as the reaction enthalpies and enopies are listed in Table 2.

Table 2

rium constants (at 298 K given in mol·L^{-1}), enthalpies (in kJ/mol) and entropies (in J/mol·K) changes of the reaction

$$\mathrm{Ni(\beta\text{-}dik)(diamine)^+ + 2L \rightleftarrows Ni(\beta\text{-}dik)(diamine)(L)_2^+}\ \text{in dichlorethane}$$

Complex		An	Ac	*n*-BuOH	FA	DMF	DMSO	Py
)(tmen)BΦ_4	β	2.24	0.157	0.976	5687	9141	2.84×10^4	1849
	ΔH	−54.21	−97.96	−69.71	−52.24	−54.67	−50.33	−71.1
	ΔS	−179	−348.1	−238.0	−105.8	−113.4	−84.7	−179
)(tmen)BΦ_4	β	7.33	0.265	1.66	2.43×10^4	3.25×10^4	1.4×10^5	1692
	ΔH	−52.77	−55.96	−77.0	−63.1	−55.76	−40.78	−94.78
	ΔS	−162.8	−201.6	−257.4	−129.4	−102.7	−40.1	−256.5
)(tmen)BΦ_4	β	11.69	0.31	1.68	2.26×10^4	5.96×10^4	2.0×10^5	1492
	ΔH	−44.1	−84.79	−54.07	−45.35	−61.7	−50.25	−52.46
	ΔS	−126.0	−295.3	−177.9	−65.63	−113.5	−64.8	−112.2
)(tmen)BΦ_4	β	5240	52,5	105.8	9.8×10^7	2.9×10^{10}	9.6×10^{10}	4×10^{10}
	ΔH	−96.44	−53.4	−130	—	—	—	—
	ΔS	−126.0	−150.3	−401.2	—	—	—	—
m)(tmen)BΦ_4	β	0.68	0.027	0.095	1036	6079	1.25×10^4	314.4
	ΔH	−9.19	−93.76	−63.25	−50.0	−39.2	−35.9	−58.5
	ΔS	−62.69	−348.5	−234.0	−112	−60.53	−43.38	−150.1
c)(Me$_3$en)BΦ_4	β	9.72	0.37	4.91	4.5×10^4	4.82×10^4	2.69×10^5	5.95×10^4
	ΔH	−23.05	−73.5	−116.5	−62.26	−46.5	−62.4	−68.6
	ΔS	−150.85	−262.6	−382.7	−121.2	−68.21	−108.5	−142
c)(teen)BΦ_4	β	—	—	—	1.65	31.20	51.74	1457
	ΔH	—	—	—	−112.7	−42.65	−38.36	−44.73
	ΔS	—	—	—	−383	−116.13	−97.53	−91.95
c)(Et$_3$en)BΦ_4	β	0.33	0.009	0.113	465.9	2159	8335	3320
	ΔH	−50.51	−78.76	−82.84	−87.22	−56.6	−33.97	−84.86
	ΔS	−180.8	−476.2	−299.2	−239	−127.9	−39.7	−128.7
c)(dipc)BΦ_4	β	1.08	0.023	0.033	4.26×10^4	1.96×10^5	3.91×10^6	1.52×10^4
	ΔH	−46.68	−46.92	−46.68	−54.2	−59.1	−131.8	−61.3
	ΔS	−186.97	−191.12	−186.97	−100.2	−100.5	−320.6	−128.7
c)(medach)BΦ_4	β	—	—	—	6.41	36.51	209.7	3264
	ΔH	—	—	—	−85.11	−51.93	−30.52	−50.51
	ΔS	—	—	—	−274	−144.46	−59.22	−105

The values of β are increased by increase in solvent donor number with the exceptions of An and Py as solvents :

$$\mathrm{Ac < BuOH < An < Fa < DMF < Py < DMSO}$$

For An the β-values are greater than expected from the consideration of its DN and this may be due to π-interactions between An and the coordination center, both of which may be classified as moderately soft. On the other hand, for Py as a solvent, the β-values are lower than expected and this may be due to the weaker donor properties of Py towards metal ions than towards $SbCl_5$.[12,13] The stability constants ar found to be related to the strengths of the Ni-D-bonds in the octahedra species. Substituents of the β-diketonate lead to increase in β-values i the following order:

$$\text{dpm} < \text{acac} < \text{bzac} \leqslant \text{dbm} \lll \text{tfac}$$

This is the sequence of increasing electron-attracting properties o the groups R_5 and R_6 (see Hammett plot, Fig. 3). The slope in the Hammett plots shows that with increasing electron withdrawing propertie of the substituents (paralleled by decreasing Lewis basicity of the diamine and diketonate ligands) the formation constants of the five-coordinated and the octahedral species is increased.[19] The additivity rule o the Hammett parameter σ for polysubstituted ligands appears to hold also for changes on both ligands.

The octahedral complex arrangement becomes less stable as the size of the diamine-group is increased. The substituents at the diamino-ligands are positioned out of plane of the square-planar configuration.[4] This is not reflected in the absorption bands in the near IR-region. In DMF the band near 1025 nm remains almost unaffected from the substituents. Change of substituents at the diamines leads to changes in

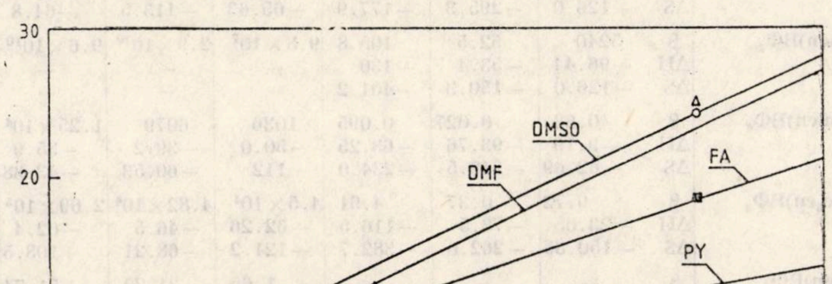

Fig. 3. — Hammett plot for overall equilibrium constant $\beta = K_1{*}K_2$ for different coordinating donor-solvent at 25°C.

the symmetry of the octahedral complexes. Substituents of the diamine ligands lead to decreasing in β-values in the following order :

$$\mathrm{Me_3en} > \mathrm{tmen} > \mathrm{dipe} > \mathrm{Et_3en} > \mathrm{medach} > \mathrm{teen}$$

This order is not in accordance with the increase of ligand field strength by variation of the substituents :

$$\mathrm{Me_3en} > \mathrm{medach} > \mathrm{teen} > \mathrm{Et_3en} > \mathrm{tmen} > \mathrm{dipe}$$

so that steric effects may be of importance.

The IR-absorption frequencies associated with the C=O vibration values ν(C=O) are influenced either by electron-releasing substituents and by electron-withdrawing substituents at the β-diketonate ligand (see Table 3) in the order :

$$\mathrm{dipm} < \mathrm{acac} < \mathrm{bzac} < \mathrm{dbm} < \mathrm{tfac}$$

Table 3

IR absorption frequencies (ν, cm^{-1}) of Ni(β-dik)(diam)BΦ_4 complexes

Complex	C=O	Ni—O	Ni—O	Ni—O	Ni—N
Ni(acac)(tmen)BΦ_4	1578	535	438	312	196
Ni(bzac)(tmen)BΦ_4	1585	531	441	307	203
Ni(dbm)(tmen)BΦ_4	1591	530	440	304	197
Ni(tfac)(tmen)BΦ_4	1606	515	446	296	216
Ni(dipm)(tmen)BΦ_4	1555	534	437	335	203
Ni(acac)(Me$_3$en)BΦ_4	1580	523	435	369	205
Ni(acac)(teen)BΦ_4	1578	512	436	375	198
Ni(acac)(Et$_3$en)BΦ_4	1569	522	437	363	203
Ni(acac)(dipe)BΦ_4	1580	515	432	337	185
Ni(acac)(medach)BΦ_4	1577	515	432	351	221

This is the same order as found for the values of the ligand field stabilisation energies Δ_0 (10Dq) in An and DMSO (Fig. 4).

The assignment of ν(Ni—O) in the IR spectra was made by comparison with the anhydrous [Ni(acac)$_2$] complex and its adduct with amines.[14] In this order ν(C=O) is shifted to higher frequencies whereas ν(Ni—O) is shifted to lower frequencies.

Correlations between ν(Ni—O), ν(C=O) and the electronic effects of the substituents (σ) show that increased donor capacity of β-diketonate ligands for the metal ion caused by electron releasing substituents leads to a decrease in C=O bond order and an increase in Ni—O bond order.

Electron-releasing substituents at the diamine have the same effect as electron-withdrawing substituent at the β-diketonate. The latter have a more decisive influence than the former. In other words, the decrease in electron density at the electron releasing substituent at one ligand leads to an increase in electron density at the electron-withdrawing substituent at the other ligand, whereas the electron density near the coordination center remains nearly invariant.[15,17] This is also concluded from the changes in UV/VIS spectra, which are more strongly influenced by variations of the substituents at the diamine.

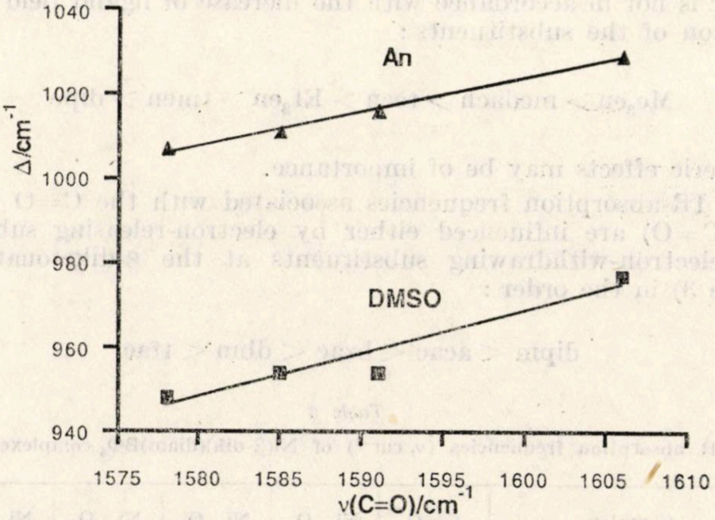

Fig. 4. — Relationship between the ligand field stabilisation energy Δo (10Dq) and νC=O for different mixed Ni(II) complexes.

Thus, electron-withdrawing properties of R_5 and R_6 positioned at the β-diketonate (see formula in Table 1) have the same effect as electron releasing properties of R_1; R_2; R_3 and R_4. These changes are as expected from the extended donor acceptor concept[8] and are shown in Fig. 5.

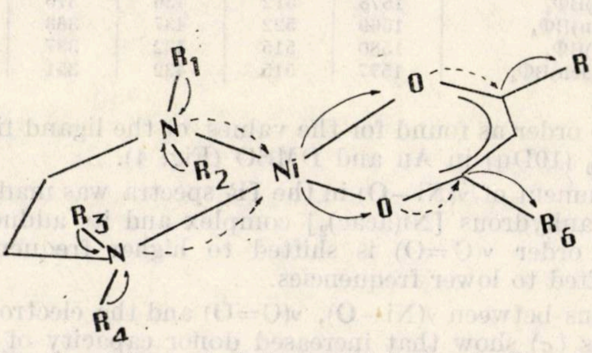

Fig. 5. — Scheme of electron redistribution in the square planar complexes induced by electron-releasing substituents at the diamine and by electron-withdrawing substituents at the β-diketonate.

→ charge transfer associated with decrease in bond length and increase in bond strength,

→ charge transfer associated with increase in bond length and decrease in bond strength.

Coordination of the donor solvent molecules D leads to lengthening of both the Ni—N and the Ni—O-bonds. With regard to the Ni—O-bonds, increase in DN of the solvent leads to an increase in bond length, just as increasing electron-withdrawing substituent groups at the β-diketonate and electron releasing at the diamine. With regard to the Ni—N-bonds, their increase by increase in DN is also induced by electron releasing substituents at the diamine and by electron-withdrawing substituents at the β-diketonate (see Fig. 6).

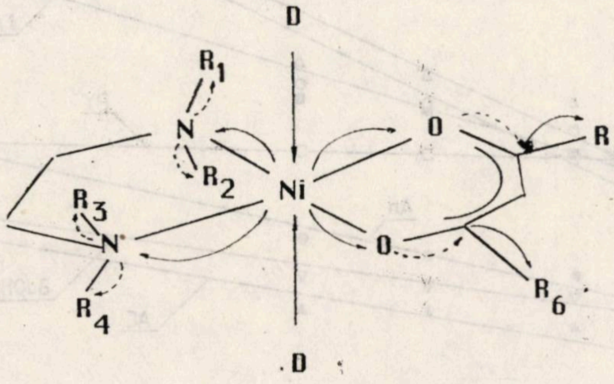

Fig. 6. — Scheme of electron redistribution in the octahedral planar complexes induced by the coordination of donor solvents.

Fig. 7 shows the relation between ν(C=O) and lnβ of the octahedrally coordinated complexes. All electronic changes lead to a redistribution of the electron density over the whole complex whereby the Ni-coordination center remains nearly invariant. Such features have been found for $[Fe(phen)_3]^{n+}$ complexes, in which the ligands with this π-electron systems are arranged symmetrically around the coordination center.[15] The latter conditions are not given for the systems with their π-ligand (β-dik) and one more rigid ligand (diamine). The results indicate that the more flexible ligand (β-dik) is of greater significance for the charge redistribution over the whole system and hence for the execution of the system organization [15–17] than the diamine.

The unique feature of these systems is that the electron density at the coordination center remains nearly constant irrespective of the properties of the substituents; the electronic changes are not located but distributed over the whole system so that the main changes are directed to the terminal positions of the unit.[16,17] This means that the coordination center appears to regulate the electronic changes in such ways that the molecular unit retains its main characteristics under different conditions.[8] Actually, the charge redistribution is not restricted to the solute but ex-

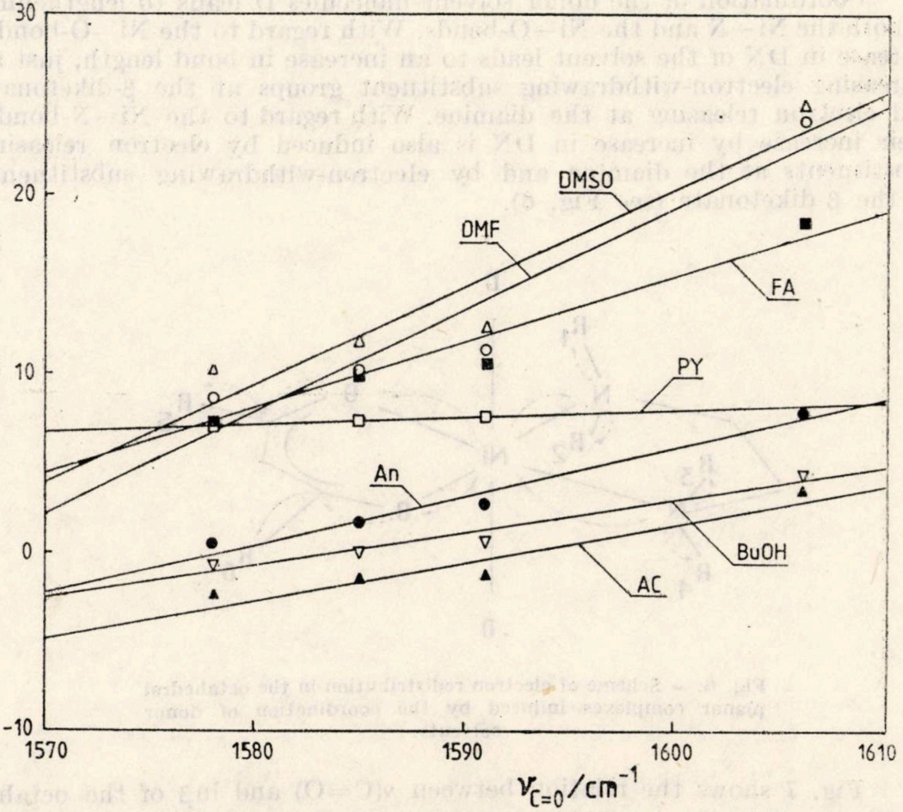

Fig. 7. — Overall equilibrium constant β versus νC=O IR-absorption frequencies of the complexes.

tends over the whole of the solution. This means that the information about the changes at the solutes is "smeared" over the whole solution.

ACKNOWLEDGEMENTS: The financial support of this investigation by the "Fonds zur Förderung der wissenschaftlichen Forschung in Österreich" (Projects 6907 and 7605) is gratefully acknowledged. Thanks are also due to the Ministry of Education of Egypt for its support of A.T. in Vienna and to our friend Professor Yutaka Fukuda, Tokyo, Japan for providing many of the complexes for this investigation.

REFERENCES

[1] Y. Fukuda and K. Sone, *Inorg. Nucl. Chem.*, **37**, 455 (1975).
[2] Y. Fukuda and K. Sone, *Bull. Chem. Soc. Jap.*, **43**, 2282 (1970).
[3] Y. Fukuda et al., *Bull. Chem. Soc. Jap.*, **49**, 1017 (1976).
[4] K. Sone and Y. Fukuda, "Inorganic Thermochromism" (Inorganic Chemistry Concept, Vol. 10), Springer, Heidelberg (1987).
[5] R. W. Soukup, *Chemie in unserer Zeit*, **17**, 163 (1983).

[6] H. Ogino et al., Abstracts of VI International Symposium on Solute—Solute-Solvent Interactions, Mino (Japan), No. 5P-30 (1982).

[7] W. Linert, R. Jedlicka, R. F. Jameson and V. Gutmann, *J. Coord. Chem.*, **17**, 347 (1988).

[8] V. Gutmann and G. Resch, *Monatsh. Chem.*, **119**, 1251 (1988).

[9] G. B. Porter and V. Hanten, *Inorg. Nucl. Chem.*, **18**, 2053 (1979).

[10] Organikum, 16th Edn., VEB Deutscher Verlag der Wissenschaften, Berlin (1986).

[1] D. W. Marquardt, *J. Soc. Ind. Appl. Math.*, **11**, 431 (1963).

[12] V. Gutmann, "The Donor-Acceptor Approach to Molecular Interactions", Plenum Press, New York, London (1978).

[3] K. Burger, "Solvation, Ionic and Complex Formation Reactions in Non-Aqueous Solvents", Akademiai Kiadó, Budapest, 1983.

[4] J. M. Haigh, N. P. Slabbert and D. A. Thornton, *J. Mol. Structure*, **7**, 199 (1971); **39**, 25 (1977).

[5] W. Linert, V. Gutmann, G. Wiesinger and P. G. Perkins, *Z. Phys. Chem.*, **142**, 221 (1984).

[6] V. Gutmann and G. Resch, *Monatsh. Chem.*, **116**, 1107 (1985).

[17] V. Gutmann and G. Resch, *Österr. Chem. Z.*, **89**, 143 (1988); **90**, 364 (1989).

Revue Roumaine de Chimie, **36**, *4–7*, 519–526 (1991)

Dedicated to Prof. ALEXANDRU T. BALABAN
on the occasion of his 60th anniversary

COMPLEX COMPOUNDS AS RAW MATERIALS FOR MIXED OXIDES. VIII.*

COMPLEX COMPOUNDS OF LANTHANOIDS WITH Ba(II) AND Cu(II) WITH MALIC ACID

P. SPACU, LUMINIȚA PATRON, SILVIA PLOȘTINARU and AL. BUTUCELEA
Center of Physical Chemistry, 202, Spl. Independenței, 77208 — Bucharest, Romania

Received February 12, 1990

The complex compounds of lanthanoids with Ba(II) and Cu(II) with malic acid were characterized by physico-chemical methods (IR spectra and thremogravimetric methods) in order to establish the nature of the species formed, the coordination of the ligand and the thermal behaviour.

Synthesis of some high critical temperature (T_c) superconductive materials has drawn the attention of the specialists ever since the discovery of the superconductivity phenomenon (1911), as an essential task, extremely important for science as well as for its multiple applications.

As a consequence of these efforts, Bednorz and Müller obtained in 1986 [1] superconductors with $T_c = 30$ K in the system La-Ba-Cu-O. In record time the studies were expanded to systems such as La-Sr-Cu-O and La-Cu-Cu-O, resulting in an about 10 K increase of T_c.[2] Later on, by studying the Y-Ba-Cu-O multiphase system, Chu and Whu [3] were able to separate and characterise the superconductive phase $YBa_2Cu_3O_{7-y}$, with $T_c = 90-92$ K. These oxidic materials with superconductive properties can be obtained relatively easy, in various forms — polycrystalline powders, single crystals, ceramic objects, fibres or films, etc.

The literature of the last 2—3 years offers a very large body of data relating to their preparation methods. Most of these studies have dealt with the preparation of oxidic phases by the ceramic method,[4–14] which is nevertheless inconvenient because it requires raw materials of advanced purity and thermal treatments at very high temperatures and for long periods (required by the solid-phase reaction). A relatively large number of studies have been concerned with the preparation of these materials by some unconventional techniques: thermal decomposition of oxalate [15–18] or carbonate [19] coprecipitates, pyrolysis of citrates [20–23] or acetates,[24] thermolysis of hyponitrites and alkoxides,[25] the sol-gel method.[26] These methods lead to very fine powders, with a very high degree of homogeneity.

---

* Part VII, *Rev. Roum. Chim.*, **36**, 5 (1991)

During the last few years, we have been concerned with preparing and characterising some mixed oxides of lanthanoids with transition metals using an unconventional method, starting from polynuclear complex compounds precursors.[27-33] Taking into account, on the one hand, the theoretical and practical importance of the Ln-Ba-Cu-O oxidic systems with superconductive properties and, on the other, our own experience in the synthesis of some types of oxides related structurally with the oxides mentioned above, we proposed ourselves to carry out a study on the possibility of obtaining $LnBa_2Cu_3O_{7-y}$, where Ln(III) = = Y, Tm, Gd.

In an earlier work [34] we have reported the first results on the Y-Ba-Cu-O and Tm-Ba-Cu-O systems, as well as the physico-chemical characterisation of the $YBa_2Cu_3O_{7-y}$ and $TmBa_2Cu_3O_{7-y}$ oxidic phases. In this paper, we will give the data obtained in what concerns the formation of an oxidic phase with superconductive properties by thermal decomposition of the coordinative compounds separated in the system :

Y(III) – Ba(II)–Cu(II) – Malic acid

The selection of the ligand was somewhat difficult, since very different coordination possibilities of the three elements had to be taken into account. Following several attempts, the best results were obtained by using as ligands the hydroxy-carboxilic acids (particularly gluconic and malic acids).

It is well known that insertion of hydroxy groups in the molecule of carboxylic acids used as ligands leads to an increase of the stability of the obtained complex compounds, due to the participation of these groups to the bonding, which leads to the formation of a chelatic ring. The literature offers a series of data concerning the synthesis of the complex compounds of transition metals with hydroxycarboxylic acids.[35,36]

In order to separate the mixed complex compounds, we chose, as a synthesis method, a variant of the method used by Melson and Pickering [37] and applied by these authors for synthesising the simple gluconates of transition metals. The separation of the mixed complex compound containing malic acid as ligand was carried out by extraction with ethanol from the reaction medium. The formula proposed for these complex compounds was arrived at based on elemental chemical analysis, in conjunction with various physico-chemical determinations (IR spectra, thermogravimetric analysis) :

$$YBa_2Cu_3(MA)_6 \cdot 8\,H_2O$$

where $MA = C_4H_4O_5^{2-}$.

All synthesised compounds appear as light-bluish powders, very soluble in water and hardly soluble in most common organic solvents.

By using this method of preparation, the simple compounds of malic acid with Y(III), Ba(II) and Cu(II) were obtained separately; the following chemical formulas were set up for these compounds:

$$CuMA \cdot nH_2O \qquad n = 2 - 3$$

$$BaMA \cdot H_2O$$

$$Y(MA)_3 \cdot 3\,H_2O$$

In order to obtain data on the way in which the ligand coordinates with the metal ions in the polynuclear complex compounds, the IR spectra were recorded in the 4000−200 cm^{-1} spectral range and these were compared to the IR spectra of the simple compounds with Y(III), Ba(II) and Cu(II), respectively, as well as to the IR spectrum of malic acid. Generally, the vibration spectra of the complex compounds are different from those of the free ligands, either due to the disappearance of some bands belonging to the ligand and the appearance of some new bands, or due to the shift and splitting of some bands.

As can be seen from the IR spectrum of the mixed complex compound $YBa_2Cu_3(MA)_6 \cdot 8\,H_2O$ and of the simple Ba(II) and Cu(II) malates, as a consequence of their formation the band located at 1730 cm^{-1}, which is present in the spectrum of the acid (being due to the uncoordinated carboxyl group), disappears, and the two bands of the carboxylate ion appear, $\nu_{sym\,COO^-}$ at 1400 cm^{-1} and $\nu_{asym\,COO^-}$ at 1600 cm^{-1}, due to the uncoordinated COO^- group (Table 1). Both the existence of the two bands typical to coordinated COO^- group and of a weaker band at 1700 cm^- can be noticed in the IR spectrum of $Y(MA)_3 \cdot 3\,H_2O$. Presence of the latter band can be associated with the existence of some uncoordinated carboxylic groups in the $Y(MA)_3 \cdot H_2O$ molecule (which is in agreement with the formulas established by chemical analysis).

In the case of polyhydroxycarboxylic ligands, coordination to the metal ion is also achieved by means of alcholic groups. The primary and secondary alcohol groups show absorption bands due to OH deformation, at 1250−1350 cm^{-1}, and to C−O(H) vibration, at 1000−1230 cm^{-1}. Comparison of the spectra recorded for the mixed complex compound and for the simple complex compound containing Y(III) with the spectrum of the free ligand shows a shift of the split CH−OH band at 1100−−1120 cm^- (for the free ligand) towards lower frequency values (1085 cm^- for Y(III) malate), which corresponds, according to literature data, to the cordination of one or more OH groups. In the case of Ba(II) malate, for which the interaction between the metal ion and the OH group of malic acid is minimal, the IR spectrum does not show any shift of this band. The same remark can be made for the case of $CuMa \cdot nH_2O$, which allowed us to draw the conclusion that the alcoholic group does not coordinate with the metal ion in this compound either.

The broad band occurring in the 3000−3600 cm^{-1} range (with a peak at 3400 cm^{-1}) in all recorded IR spectra can be assigned to the formation of hydrogen bonds in water and/or alcohols.

Table 1

IR spectra of malic acid, simple malates and of the coordination mixed complex compound

Acid malic	$YBa_2Cu_3(MA)_6 \cdot 8\,H_2O$	$CuMA \cdot 2\,H_2O$	$BaMa \cdot H_2O$	$Y(MA)_3 \cdot 3\,H_2O$	Assignment
1730 vs	—	—	—	1700 m	$\nu_{C=O}$
1650 sh	1610 vs	1605 vs	—	1600 vs	$\nu_{OCO\ asym.}$
				1460 sh,m	
1438 sh, m	—	—	—		$\nu_{CO} + \delta_{OH}$
1420 m	—	—	—		$\delta_{CH_2\ bond.}$
	1405 vs	1410 vs	1410 vs	1410 1400 } vs	$\nu_{OCO\ sym.}$
	1315 m	—	1315 m	1305 m	$\delta_{OH} + \nu_{CO}$
1295 m	—	—	—	1280 w	
1268 sh, w	—	1260 sh		1250 w	
1230 w					
1195 m	1195 m	1200 m	1200 w	1190 m	$\nu_{(CC)\ asym.}$
1120 s	—	1100 s	1095 s		ν_{C-OH}
1100	1090 s			1085 s	
	1040 m	1040 w	1040 w	1052 w	
				1040	
960 m	980 m	985 w	985 w	980 w	$\nu_{(CC)\ sym.}$
935 m, sh		940 w	960 m	975 w	
910	910		900 w	925 } w	
	890	895 m		905 } w	$\pi_{(OH)}$
	850 s		870 m	850 m	$\nu_{H_2O\ rock.}$
	845	840 w		840 w	
		825			
762 w	—	—	750 w		$\delta_{(COOH)}$
		700 m		700 sh	
		680 sh	680 sh		$\delta_{CH\ of\ CH_2}$
668 m	670 m	670 sh	672 m	665 sh	
				660 m	
642 m, sh					
	560 w	560 m	555 m	560 s	
542 w	540 w				

vs = very strong ; m = medium ; sh = shoulder ; w = weak

In order to ascertain to what extent the mixed complex compound $YBa_2Cu_3(MA)_6 \cdot 8\,H_2O$ may be used as a precursor for Y-Ba-Cu-O type mixed oxides, a thermogravimetric study was carried out and the obtained data were correlated with the analysis of the IR spectra recorded for the intermediates calcined at various temperatures.

Fig. 1 shows the decomposition curves obtained for the mixed complex compound $YBa_2Cu_3(MA)_6 \cdot 8H_2O$ and for a mechanical mixture of the three simple malates with Y, Ba and Cu, mixed in the molar ratio 1 : 2 : 3. The total loss is of 59.95% (at 930°) for the mixed complex compound and of 68.33% for the mechanical mixture, which corresponds to residues of 40.05% and 31.47%, respectively. This difference in the thermal behaviour can be taken as an argument for the formation of a mixed complex compound.

The weight loss obtained in the first temperature range (20–180°) corresponds to the loss of the 8 coordinated water molecules for the mixed complex compound (calc'd 9.67%, obs'd. 9.50%) and to the loss of 11

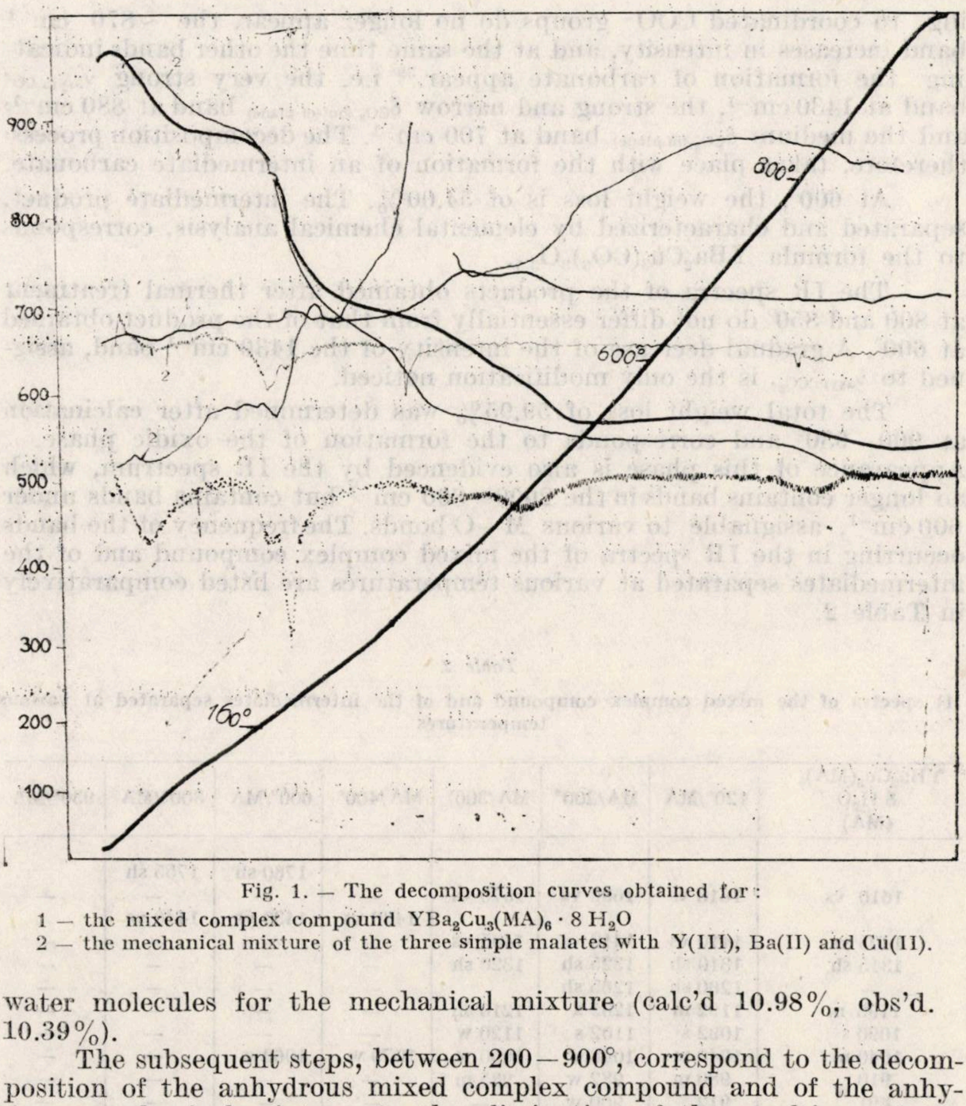

Fig. 1. — The decomposition curves obtained for:
1 — the mixed complex compound $YBa_2Cu_3(MA)_6 \cdot 8\,H_2O$
2 — the mechanical mixture of the three simple malates with Y(III), Ba(II) and Cu(II).

water molecules for the mechanical mixture (calc'd 10.98%, obs'd. 10.39%).

The subsequent steps, between 200—900°, correspond to the decomposition of the anhydrous mixed complex compound and of the anhydrous mechanical mixture, to the elimination of the resulting volatile products, and to the formation of the oxidic phases. The weight loss observed up to 300° is of 38.30% (for the mixed complex compound) which indicates an evolutive decomposition process. The IR spectrum recorded for the intermediate heated at this temperature shows, however, the two absorption bands at 1570 cm^{-1} and 1405 cm^{-1} assignable to the coordinated COO$^-$ groups. The 1090 cm^{-1} band, characteristic to the coordinated OH group, occurs only as a weak shoulder. These observations suggested that during decomposition up to this temperature, all coordinative M—OH bonds, but not all M—OOC bonds, are broken.

In the 400—440° range, the thermogram indicates a weight loss of 45%, whereas in the IR spectrum of this intermediate the bands belonging to coordinated COO^- groups do no longer appear, the ~870 cm^{-1} band increases in intensity, and at the same time the other bands indicating the formation of carbonate appear,[39] i.e. the very strong $\nu_{asym\,CO^3}$ band at 1430 cm^{-1}, the strong and narrow $\delta_{CO_3\,(out\text{-}of\text{-}plane)}$ band at 880 cm^{-1}, and the medium $\delta_{CO_3\,(in\ plane)}$ band at 700 cm^{-1}. The decomposition process, therefore, takes place with the formation of an intermediate carbonate.

At 600°, the weight loss is of 54.00%. The intermediate product, separated and characterized by elemental chemical analysis, corresponds to the formula $YBa_2Cu_3(CO_3)_3O_{3.5}$.

The IR spectra of the products obtained after thermal treatment at 800 and 850° do not differ essentially from that of the product obtained at 600°. A gradual decrease of the intensity of the 1430 cm^{-1} band, assigned to $\nu_{asym\,CO_3}$, is the only modification noticed.

The total weight loss of 59.95% was determined after calcination at 900–930° and corresponds to the formation of the oxidic phase. Appearance of this phase is also evidenced by the IR spectrum, which no longer contains bands in the 2000–800 cm^{-1} but contains bands under 600 cm^{-1}, assignable to various M–O bonds. The frequency of the bands occurring in the IR spectra of the mixed complex compound and of the intermediates separated at various temperatures are listed comparatively in Table 2.

Table 2

IR spectra of the mixed complex compound and of the intermediates separated at various temperatures

$YBa_2Cu_3(MA)_6 \cdot 8\,H_2O$ (MA)	120°/MA	MA/200°	MA/300°	MA/400°	600°/MA	800°/MA	930°/MA
					1760 sh	1755 sh	
1610 vs	1610 vs	1600 vs	1570 vs	—	—	—	—
				1430 vs	1430 vs	1440 vs	
1405 vs	1410 vs	1418 vs	1405 vs	—	—	—	—
1315 sh	1310 sh	1325 sh	1320 sh	—	—	—	—
—	1260 sh	1265 sh		—	—	—	—
1195 m	1192 m	1205 s	1210 sh	—	—	—	—
1090 s	1092 s	1102 s	1120 w	—	—	—	—
1040 m	1040 m	1048 w	1060 w	1070 w	1060 w	—	—
910	980 m	982 w	985 m	—	—	—	—
891 w	912	900 w	—	—	—	—	—
	890 w						
850 s	855 s	852 m	860 s	880 s	877 s	867 m	910 vw
			815 m				
670 w	678 m	700 s	680 s	695 s	700 s	700 w	—
608 w	610	612 w	623 w	—	—	—	—
	562 w						
560 sh		560 w	580 w	570 sh	570 sh	578 sh	570 sh
540 w	—	—	535	530	495	498	495
490 w	490 w	495 w	500	500	—	—	—
400 m	400 m	—	—	450 sh	455	440 sh	460
335 w	320 w	300	290 w	330 vw	350 w	342 m	335
310 w	290 w	—	—	—	315 w	312 m	275 m
225 w	260 w	—	—	—	—	—	240

vs = very strong; s = strong; m = medium; w = weak; vw = very weak; sh = shoulder

The obtained oxidic phase was subjected to a thermal treatment at 930° during 10 h. X-ray diffraction analysis has confirmed the formation of the mixed oxide $YBa_2Cu_3O_{7-y}$. This phase has also been characterised electrically and magnetically. The sample gave a value $T_c = 90K$ for the critical temperature, with a transition width $\Delta T = 2.3$ K. The measured value of the Seebeck coefficient was found to be $\alpha = 4.5$ uV/K, which suggests a pronounced metallic character at critical temperature. The regular decrease of the resistivity when the temperature is lowered down to $T_{onse}{}^{t}$ also indicates the metallic character of the sample.

EXPERIMENTAL

The complex compounds were synthesised and analysed by well-known methods.[28] The decomposition curves were recorded with a Paulik-Paulik Erdey-type MOM Derivatograph (Q-1500, Budapest), with heating rates between 2.4 – 10 K min^{-1}, in air.

The IR spectra were recorded with a M-80 Spectrometer (Carl Zeiss Jena – G.D.R.) operated under a flow of dried air, with a resolution of 2 cm^{-1} and an integration time of 3 s for each measured wavenumber point. The samples were prepared as pelets in KBr or CsI, using concentration of 1.00 – 3.00 mg sample/200 mg KBr or CsI.

REFERENCES

[1] J. G. Bednorz and K. A. Müller, *Z. Physik*, **B64**, 189 (1986).

[2] J. M. Tarascon et al., *Science*, **235**, 1373 (1987).

[3] C. W. Chu, P. H. Hor, R. L. Meng, L. Gao, Z. T. Huang and Y. Q. Wang, *Phys. Rev. Lett.*, **58**, 405 (1987).

[4] D. W. Murphy, D. W. Johnson, Jr., S. Jin and R. E. Howard, *Science*, **241**, 922 (1988).

[5] J. M. Tarascon, P. B. Barboux, B. G. Bagley, L. H. Green and G. W. Hull, *Mat. Sci. and Eng.*, Bl. 29 (1988).

[6] M. M. Garland, *Appl. Phys. Lett.*, **51**, 1030 (1987).

[7] A. Ono and Y. Ishizawa, *Japan J. Appl. Phys.*, **26**, L1043 (1987).

[8] Y. Maeno, M. Kato and T. Fujita, *Japan J. Appl. Phys.*, **26**, L329 (1987).

[9] A. J. Jacobson et al., "Chemistry of Oxide Superconductors", Blackwell Sci. Publ. IUPAC, 1988.

[10] Y. Khan, *J. Mat. Sci. Lett.*, **7**, 221 (1988).

[11] S. Kemmler-Sack et al., *J. Less Commun. Metals*, **138** L21 – L23 (1988).

[12] A. Ono and M. Tsutsumi, *Bull. Chem. Soc. Japan*, **60**, 3035 (1987).

[13] H. K. Lee, H. C. Kwon and J. C. Park, *J. Appl. Phys.*, **63**, 2 (1988).

[14] P. Murugaraj, J. Maier and A. Rabenau, *Solid State Commun.*, **66**, 736 (1988).

[15] A. Manthiram and J. B. Goodenough, *Nature*, **329**, 22 (1987).

[16] K. Kishio, J. Shimoyama and T. Hasegano, *Japan J. Appl. Phys.*, **26**, L 1228 (1987).

[17] T. Yamamoto et al., *J. Ceram. Soc. Japan. Ed.*, **96**, 375 (1988).

[18] F. Kloucec, W. E. Rhein and H. J. Bowen, *Physica C*, **153 – 155**, 789 (1988).

[19] Y. Saito et al., *Japan J. Appl. Phys.*, **26**, L 836 (1987).

[20] D. H. Blank, H. Kirnidhof and J. Flokstra, *J. Physica* D, 220 (1987).

[21] A. Junod et al., *Helv. Phys. Acta*, **61**, 460 (1988).

[22] D. H. A. Blank, J. Flokstra and G. J. Gerritsma, *Physica*, **145B**, 222 (1987).

[23] Z. Igbal, F. Reidinger and A. Bose, *Nature*, **331** (6154), 326 (1988).

[24] K. Bordia, H. S. Horowitz and M. A. Subramanian, *Mat. Res. Soc. Symp. Proc.*, **99**, 245 (1988).

[25] J. I. Rha and K. I. Yoon, *J. Amer. Ceram. Soc.*, **71**, C – 328 (1988).

[26] J. M. Tarascon et al., in press, *J. Appl. Phys.*

[27] P. Spacu, S. Ploștinaru, L. Patron, A. Conțescu and E. Segal, *Rev. Roum. Chim.*, **30**, 659 (1985).

[28] E. Eftimie, E. Segal, L. Patron, S. Ploştinaru and A. Conțescu, *Thermochim. Acta*, **91**, 369 (1985).

[29] P. Spacu, S. Ploştinaru, L. Patron, A. Conţescu, D. Crişan and N. Stănică, *Rev. Roum. Chim.*, **32**, 877 (1987).

[30] P. Spacu et al., *Rev. Roum.* Chim., **32**, 249 (1987).

[31] E. Eftimie, L. Patron, S. Ploştinaru, A. Conţescu and E. Segal, *Thermochim. Acta*, **98**, 379 (1986).

[32] P. G. Scullerus, S. Ploştinaru, A. Conţescu, L. Patron and E. Segal, *Thermochim. Acta*, **131**, 285 (1988).

[33] P. Spacu et al., *Rev. Roum. Chim.*, **34**, 1275 (1989).

[34] P. Osiceanu, L. Patron, S. Ploştinaru, A. Conţescu, L. Cristea and Gh. Aldica, *Rev. Roum. Chim.* **34**, 1541 (1989).

[35] S. P. Sinha, "Complexes of the Rare Earths", Pergamon Press, Ltd., (1966).

[36] U. V. Ustiak and Yu. J. Salinikov, *Koord. Himia*, **10**, 1636 (1984).

[37] G. A. Melson and W. F. Pickering, *Aust. J. Chem.*, **21**, 1205 (1968).

[38] N. S. Colthup, L. H. Daly and S. E. Wiberley, "Introduction to IR and Raman Spectroscopy", 2nd ed., Acad. Press. Inc., (1975).

Revue Roumaine de Chimie, 36, 4–7, 527–544 (1991)

THE RICHNESS OF STRUCTURES AVAILABLE TO P_2N_2 INORGANIC HETEROCYCLES. A TOPOLOGICAL AND MOLECULAR ORBITAL (EHMO) ANALYSIS *

IONEL HAIDUC and IOAN SILAGHI-DUMITRESCU
Chemistry Department, Babes-Bolyai University; RO-3400 Cluj-Napoca, Romania

Received January 29, 1991

A topological analysis of possible P_2N_2 ring derivatives, containing two-, three-, four-, five-, and six-coordinate phosphorus and two-, three- and four-coordinate nitrogen is performed and using Polya's theorem all isomers are enumerated. The extended Hückel calculation of molecular orbital energies gives information about the HOMO-LUMO separation and illustrates the most probable charges of the cyclic molecular ions formed.

INTRODUCTION

The title of this work was inspired by a paper of Roald Hoffmann *et al.*[1] which analysed the diversity of structures hidden behind the composition $C_5H_5MS_4MC_5H_5$. This is not a unique case, when structural variations of a basic unit lead to a great diversity of compounds.

As a part of our continuous interest in the chemistry of inorganic heterocycles [2,3] we have chosen the P_2N_2 small ring, which can give rise to a broad range of derivatives, containing tervalent and pentavalent, three-, four-, five- and six-coordinate phosphorus.[2,3] Nitrogen can also be di-, tri- or tetracoordinate. The association of these states leads to a broad diversity of monomeric units, which can be combined in various ways to give the four-membered P_2N_2 ring derivatives. The resulting monomeric units which can be combined to give the four-membered P_2N_2 ring derivatives are shown in Table 1.

The parent species for all compounds containing the four membered ring is a hypothetical diphosphorus dinitride, P_2N_2. This can be represented either as a molecule containing an alternation of single and double bonds **1** (like in cyclobutadiene):

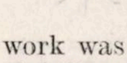

1

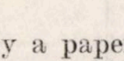

2

---

* This paper is dedicated to Prof. A. T. Balaban on his 60th birthday and is an attempt to extend the ideas and methods promoted by him to a new area of inorganic chemistry.

Table 1. — P–N fragments as monomeric units in P_2N_2 rings

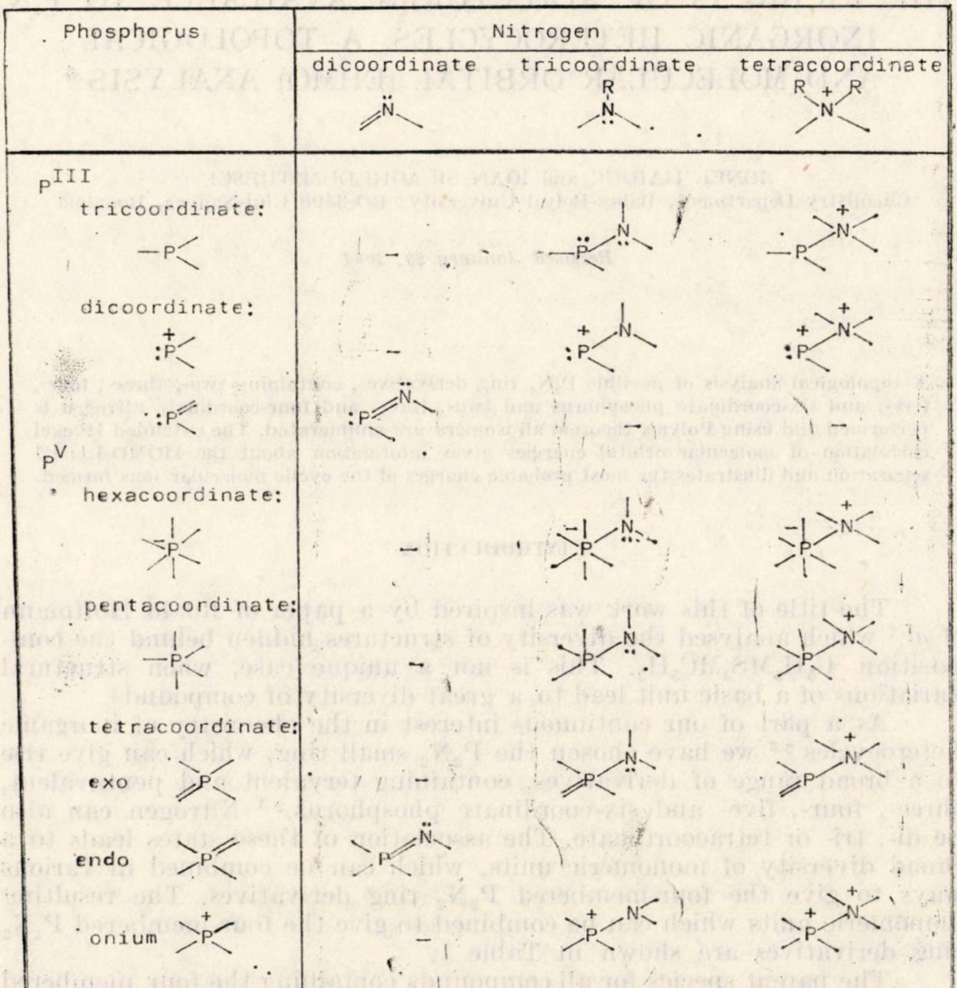
Phosphorus
Nitrogen
dicoordinate
tricoordinate
tetracoordinate
P^III
tricoordinate:
dicoordinate:
P^V
hexacoordinate:
pentacoordinate:
tetracoordinate:
exo
endo
onium
tricoordinate:
R
+
N
P

or as a polar species **2**, due to the equivalence between a formal double bond and a polar P—N bond :

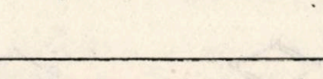

1 **2**

For this reason, throughout this paper, dicoordinate phosphorus will be represented as bearing a formal positive charge, while dicoordinate nitrogen as bearing a formal negative charge.

The attachement of additional substituents or groups to the parent P_2N_2 ring (**1** or **2**), with the increase of connectivity of phosphorus or nitrogen atoms to higher values, allowed by the "valence" of these two elements, produces all possible P_2N_2 ring derivatives. In order to calculate and to provide an enumeration of all possible species we performed a topological analysis based upon the graph theory[4] and analysed the electronic structure of some representative structures with the aid of the extended Hückel molecular orbital method.[5]

In this analysis we considered only P_2N_2 rings based upon heteroatom alternation of phosphorus and nitrogen. It is obvious that much more types of P_2N_2 ring derivatives can exist, based upon nonalternating rings, containing P—P and N—N bonds, e.g. **3**, or even cyclic isomers of smaller size, e.g. **4**.[6]

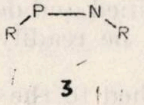

3

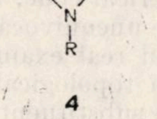

4

THE TOPOLOGICAL ANALYSIS

a) Rings containing two, three and four-coordinate phosphorus

Let's consider a planar P_2N_2 ring, as shown in **5**. This is a structure of D_{2h} symmetry, with eight possible substitution sites:

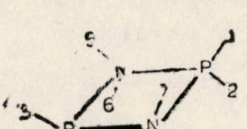

5

If only two-, three- and four-coordinate phosphorus and nitrogen atoms are considered at this stage, the occupancy of sites 1—8 will lead to all possible cyclic species, including *cis-trans* (geometrical) isomers. Their number can be calculated with the aid of Polya's theorem[4,7] using the algorithm suggested by Dolhane[8] in devising the computer program. The method takes into account the symmetry of the ring structure and constructs all the possible permutations of substituents, eliminating identical structures. More details are exemplified in the Appendix.

The output for substitutional isomers is given in Table 2.

Table 2

Substitutional isomers for P_2N_2 ring derivatives, containing two-, three- and four-coordinate phosphorus

number of substituents	number of structures
0	1 isomer
1	2 isomers
2	8 ,,
3	10 ,,
4	16 ,,
5	10 ,,
6	8 ,,
7	2 ,,
8	1 isomer

All the isomers are illustrated in Fig. 1A-C and each isomer is described by a numerical code, indicating the occupied sites. Thus every structure type can be unequivocally identified and described in an enumeration of isomers and real examples can be readily associated with the types predicted on a topological basis.

When only one substituent is attached to the ring it can be either at phosphorus or nitrogen and only two isomers are possible. With two (identical) substituents eight isomers are possible, including some geometrical (*cis-trans*) isomers. With three substituents the number of possible

1 SUBSTITUENT :

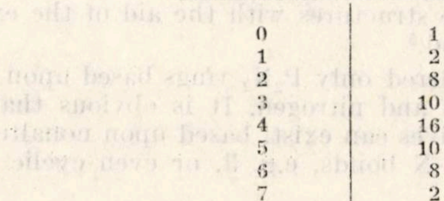

2 SUBSTITUENTS :

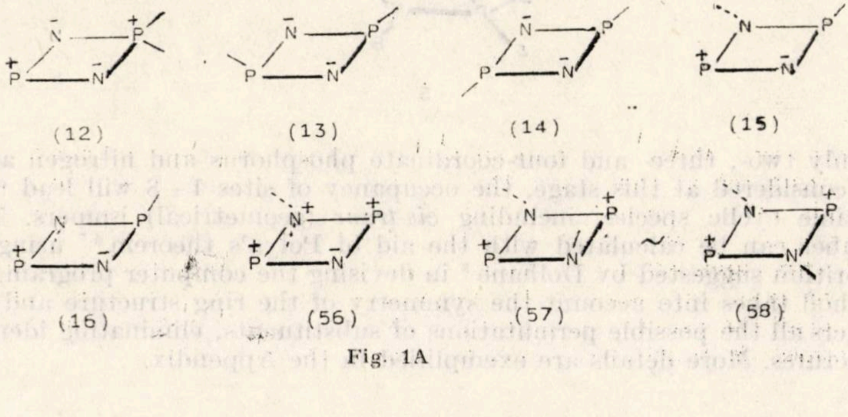

Fig. 1A

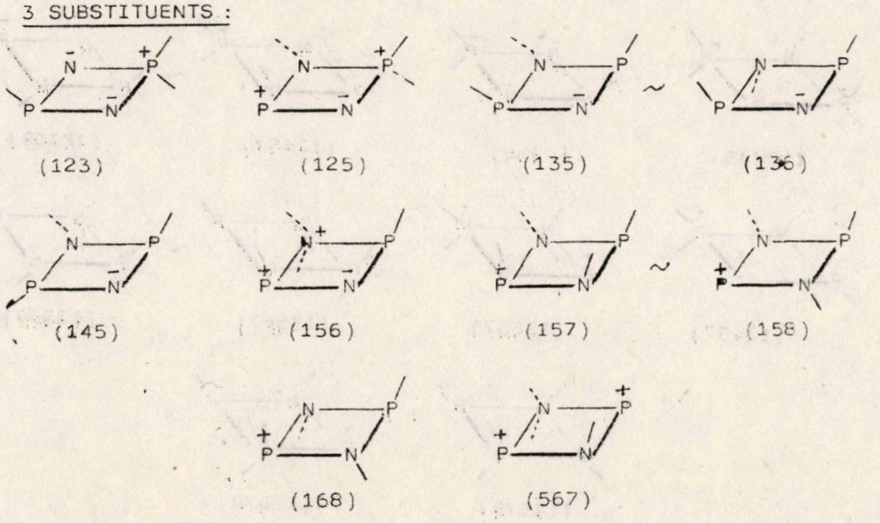
3 SUBSTITUENTS :
(123)
(125)
(135)
(136)
(145)
(156)
(157)
(158)
(168)
(567)

Fig. 1A

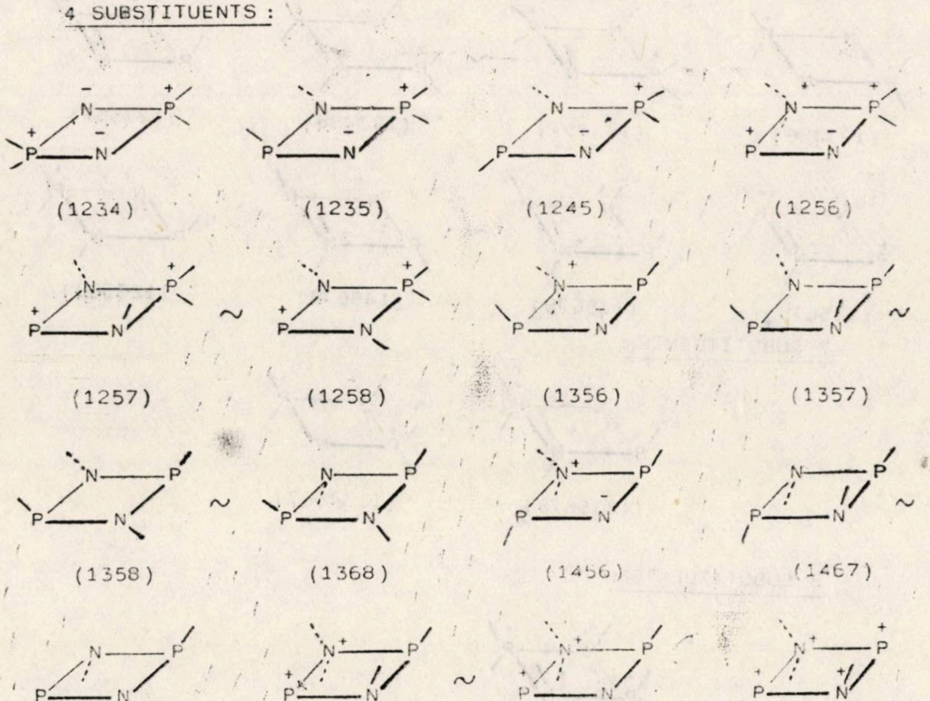
4 SUBSTITUENTS :
(1234)
(1235)
(1245)
(1256)
(1257)
(1258)
(1356)
(1357)
(1358)
(1368)
(1456)
(1467)
(1468)
(1567)
(1568)
(5678)

Fig. 1B

5 SUBSTITUENTS :

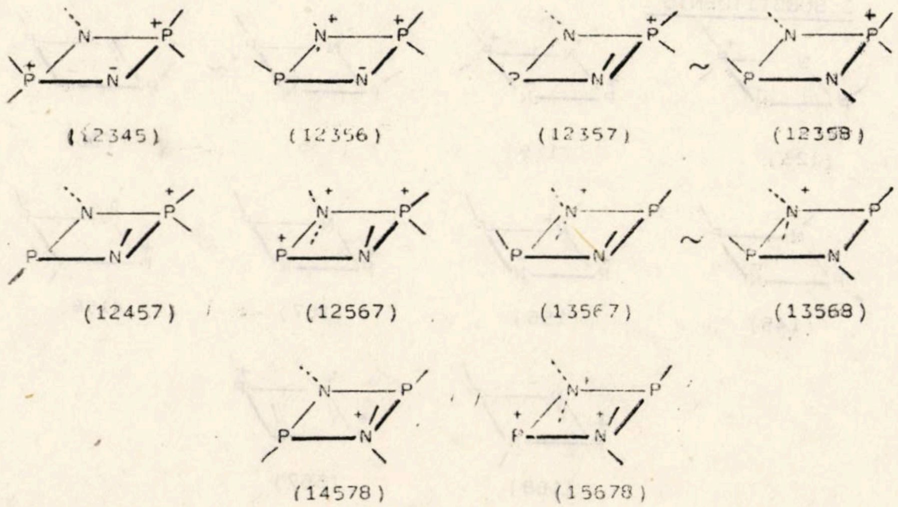

(12345) (12356) (12357) ~ (12358)

(12457) (12567) (13567) ~ (13568)

(14578) (15678)

Fig. 1B

6 SUBSTITUENTS .

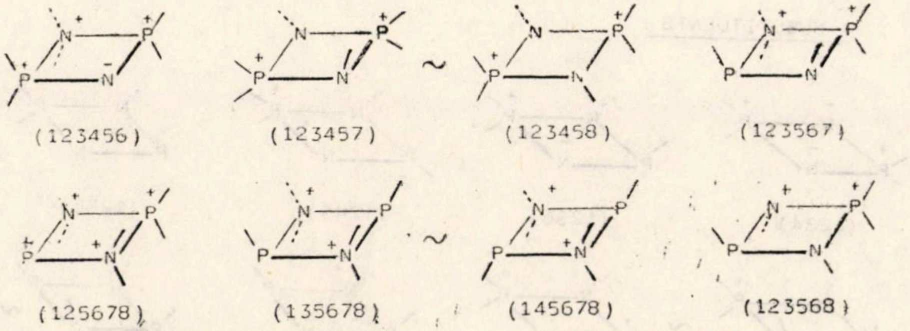

(123456) (123457) ~ (123458) (123567)

(125678) (135678) ~ (145678) (123568)

7 SUBSTITUENTS :

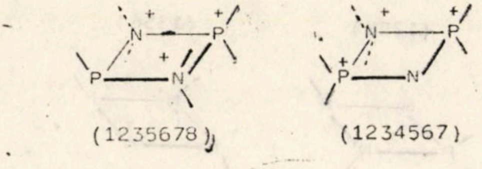

(1235678) (1234567)

8 SUBSTITUENTS :

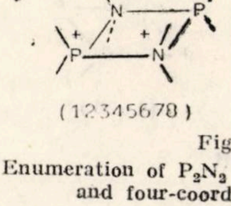

(12345678)

Fig. 1C

Fig. 1A, B, C. — Enumeration of P_2N_2 ring derivatives containing two-, three- and four-coordinate phosphorus.

isomers increases to ten, while the presence of four (identical) substituents leads to 16 isomers. The unsubstituted P_2N_2 species may be expected to occur in the vapor of phosphorus nitride *in vacuo*. So far no mono- or disubstituted species derived from a P_2N_2 ring has been reported, but a three-substituted ring species **6** has been cited in the literature.[9]

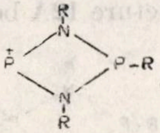

6

(157/8)

If the three bonds at nitrogen were pyramidal, two geometrical isomers, described by codes (157) and (158) in Fig. 1A would be possible. If the bonds at nitrogen are coplanar then the two structures (157) and (158) degenerate into a single one. Similar situations may occur in all other cases, when three-coordinate (monosubstituted) nitrogen is present in the ring. On the other side, three-coordinate (monosubstituted) phosphorus will always be considered as pyramidal.

Several isomers are known when four substituents are attached to the ring. These include the tricoordinate phosphorus(III) derivatives **7**,[10,11] the cyclodiphosphazene **8** ($R=NMe_2$) [12] and the unsymmetrical compound **9**.[13]

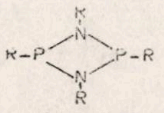

7

(1357/8)
(1368) cis
(1467/8) trans

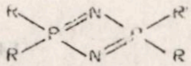

8

(1234)

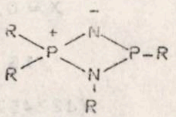

9

(1235/1245)

Cyclodiphosph(III)azanes **7** may occur as stereoisomers (the free positions are occupied by lone pairs of electrons) and both *cis* and *trans* isomers have been reported (e.g. refs.[14-16]) The number of possibilities seems to be reduced by the planarity or near-planarity of the three bonds at nitrogen. Thus the combinations (1356—1358) (P-*cis*) and (1467—1468) (P-*trans*) are degenerate. The cyclodiphosphazene **8** can be formulated either as shown, with alternating single and double bonds, or alternatively, with polar bonds, **10**. *Ab initio* theoretical calculations [17] seem to favor

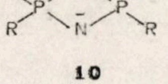

10

(1234)

the polar bond representation. Throughout this paper the polar representation will be used for P—N double bonds, but if preferred the corresponding formulae can be transcribed as Lewis formulae containing P=N double bonds.

Pentasubstituted derivatives are known as mixed P(III)-P(V) compounds **11** [6,18,19] and **12A-B**.[20-23] If the exocyclic PO double bond is represented as polar, then structure **12A** becomes **12B**.

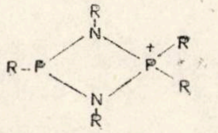

11

(12357/8)
(12457)

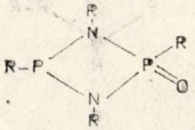

≡

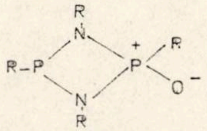

12A

12B

(12357/8)
(12457)

Some hexasubstituted P_2N_2 ring derivatives are also known. These include dioxo, dithio or diimino derivatives (*cis* and *trans* isomers) of type **13** [24,25] (neutral compounds) and **14** (dications).[26] If exocyclic P=X

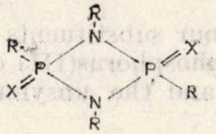

X = O, S, NR

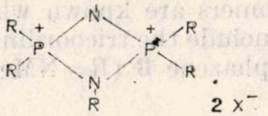

13

(123457)
(123458)

14

(123457)
(123458)

double bonds are conventionally represented as polar $P^+—X^-$ bonds, then these compounds are described by a degenerate pair of codes (123457/8) (the coordination at nitrogen is trigonal planar). It should be mentioned here that because of the different nature of the substituents at phosphorus (X and R) an additional geometrical isomerism occurs, which is not considered in our analysis.

b) Rings containing five-coordinate phosphorus

The prototype of rings containing five-coordinate phosphorus is structure **15**:

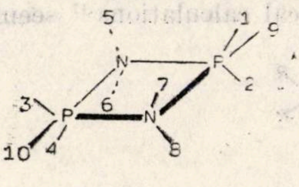

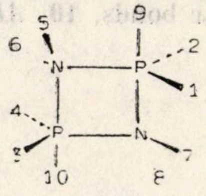

15A

15B

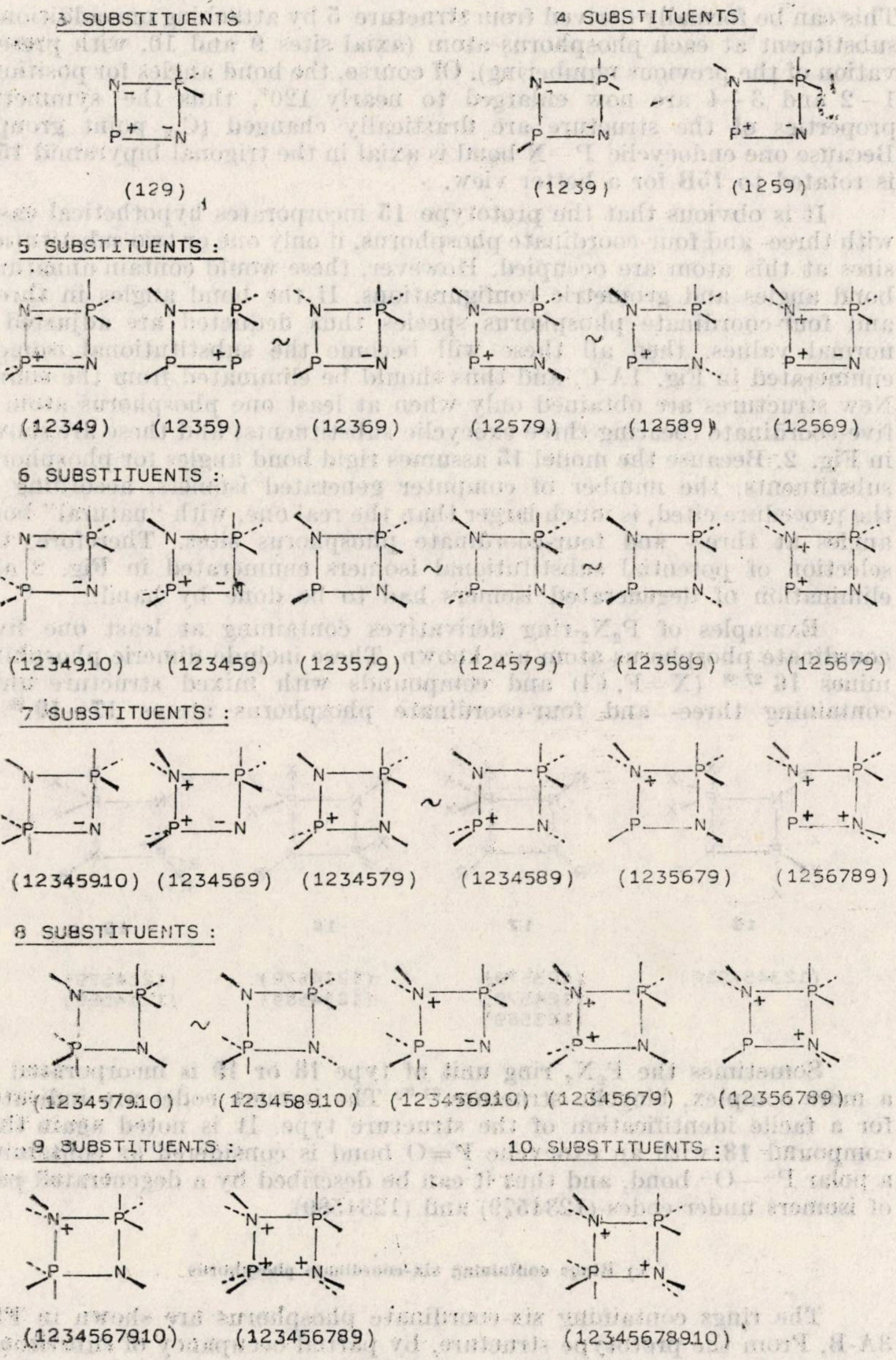
3 SUBSTITUENTS
(129)
4 SUBSTITUENTS
(1239)
(1259)
5 SUBSTITUENTS :
(12349)
(12359)
(12369)
(12579)
(12589)
(12569)
6 SUBSTITUENTS :
(1234910)
(123459)
(123579)
(124579)
(123589)
(125679)
7 SUBSTITUENTS :
(12345910)
(1234569)
(1234579)
(1234589)
(1235679)
(1256789)
8 SUBSTITUENTS :
(123457910)
(123458910)
(123456910)
(12345679)
(12356789)
9 SUBSTITUENTS :
(1234567910)
(123456789)
10 SUBSTITUENTS :
(12345678910)

Fig. 2. — Enumeration of P_2N_2 ring derivatives containing five-coordinate phosphorus.

This can be formally derived from structure **5** by attaching one additional substituent at each phosphorus atom (axial sites 9 and 10, with preservation of the previous numbering). Of course, the bond angles for positions 1—2 and 3—4 are now enlarged to nearly 120°, thus the symmetry properties of the structure are drastically changed (C_{2h} point group). Because one endocyclic P—N bond is axial in the trigonal bipyramid **15A** is rotated to **15B** for a better view.

It is obvious that the prototype **15** incorporates hypothetical cases with three- and four-coordinate phosphorus, if only one or two substitution sites at this atom are occupied. However, these would contain unnatural bond angles and geometric configurations. If the bond angles in three- and four-coordinate phosphorus species thus deducted are adjusted to normal values, then all these will become the substitutional isomers enumerated in Fig. 1A-C, and thus should be eliminated from the count. New structures are obtained only when at least one phosphorus atom is five-coordinate (bearing three exocyclic substituents) and these are shown in Fig. 2. Because the model **15** assumes rigid bond angles for phosphorus substituents, the number of computer generated isomers, according to the procedure cited, is much larger than the real one, with "natural" bond angles at three- and four-coordinate phosphorus sites. Therefore, the selection of potential substitutional isomers enumerated in Fig. 2 and elimination of degenerated isomers had to be done by hand.

Examples of P_2N_2-ring derivatives containing at least one five-coordinate phosphorus atom are known. These include dimeric phosphinimines **16** [27,28] (X=F, Cl) and compounds with mixed structure units containing three- and four-coordinate phosphorus atoms **17—19**.[29–31]

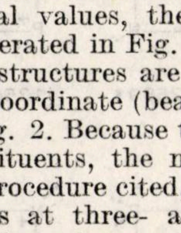

16

(123457910)

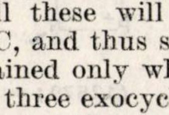

17

(123579)
(124579)
(123589)

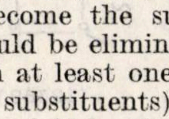

18

(1234579)
(1234589)

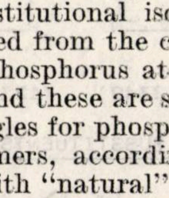

19

(1234579)
(1234589)

Sometimes the P_2N_2 ring unit of type **18** or **19** is incorporated in a more complex, bicyclic structure.[31,32] The isomers codes are indicated for a facile identification of the structure type. It is noted again that compound **18** with an exocyclic P=O bond is considered as containing a polar $P^+—O^-$ bond, and thus it can be described by a degenerated pair of isomers under codes (1234579) and (1234589).

c) Rings containing six-coordinate phosphorus

The rings containing six-coordinate phosphorus are shown in Fig. 3A-B. From the prototype structure, by partial occupancy of substituent sites, the previous three-, four- and five coordinate phosphorus substi-

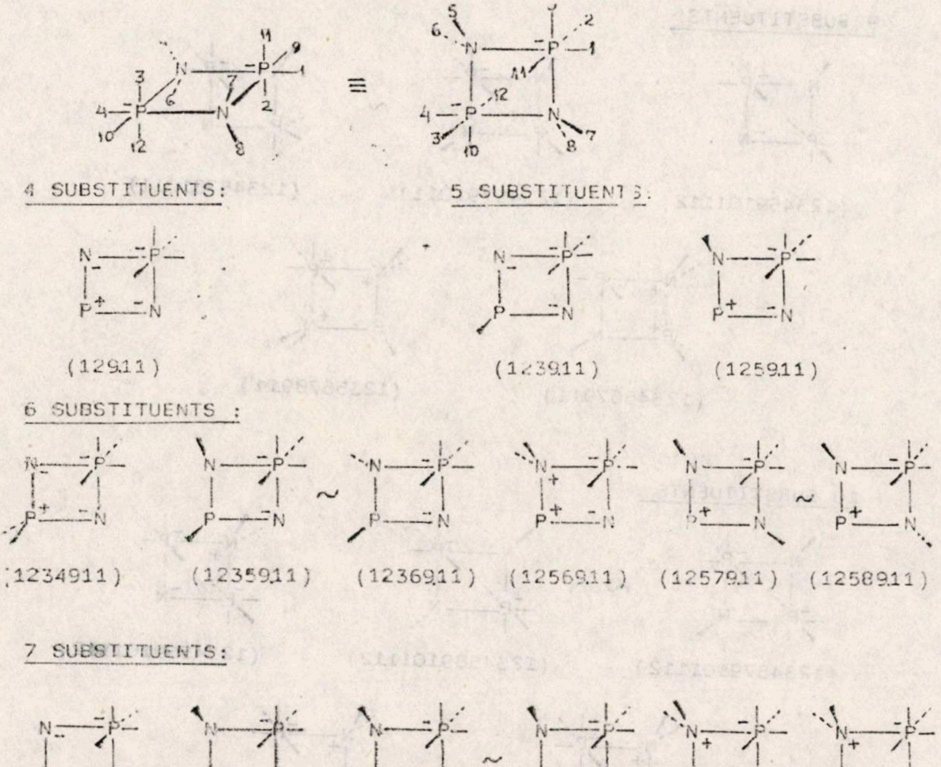
4 SUBSTITUENTS:
(12911)
5 SUBSTITUENTS:
(123911)
(125911)
6 SUBSTITUENTS :
(1234911)
(1235911)
(1236911)
(1256911)
(1257911)
(1258911)
7 SUBSTITUENTS:
(123491011)
(12345911)
(12357911)
(12358911)
(12356911)
(12567911
8 SUBSTITUENTS :
(12349101112)
(1234591011)
(1234791011)
(123457911)
(123458911)
(123456911)
(123567911)
(123568911)
(125678911)

Fig. 3A

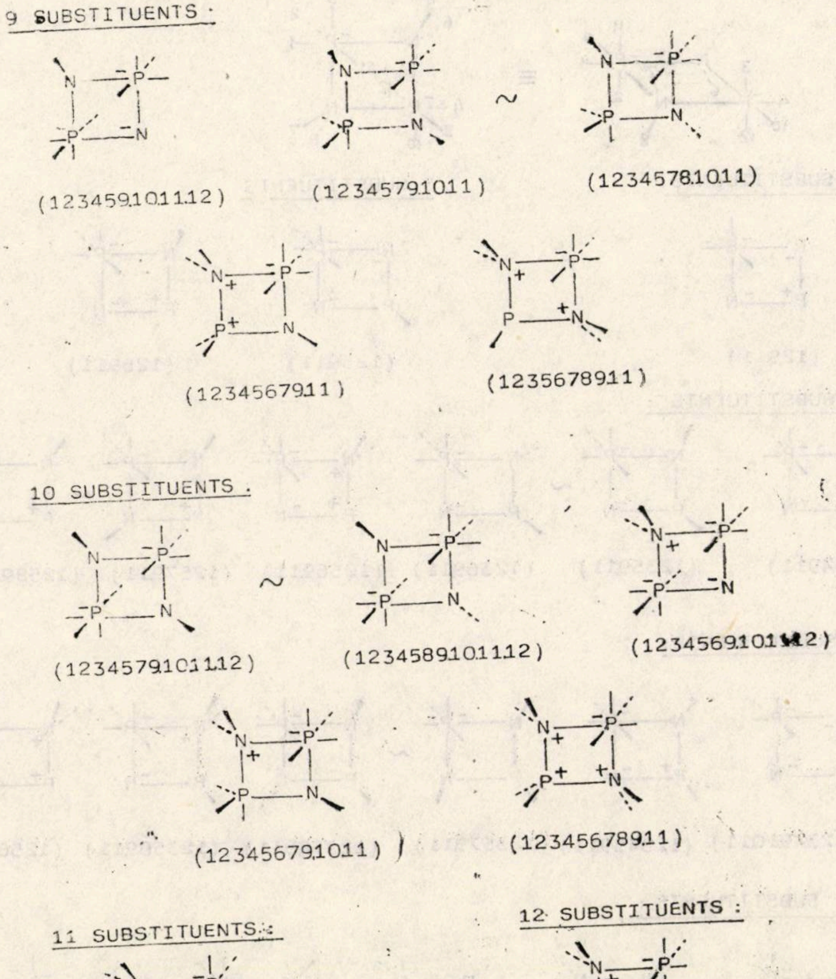
9 SUBSTITUENTS :
(12345910 11 12)
(123457910 11)
~
(123457810 11)
(1234567911)
(1235678911)
10 SUBSTITUENTS :
(1234579101112)
~
(12345891011 12)
(123456910 11 12)
(123456791011)
(12345678911)
11 SUBSTITUENTS :
(12345679101112)
(1234567891011)
12 SUBSTITUENTS :
(123456789101112)

Fig. 3 A, B. — Enumeration of P_2N_2 ring derivatives containing six-coordinate phosphorus.

tuents could be deduced, but the bond angles would be 90° (or 180°), therefore different from realistic values, close to tetrahedral, as depicted in Fig. 1. The number of computer generated isomers, by successive occupation of substituent sites, again would be too large and the elimination of the redundant structures had to be done by hand. New compounds occur only when at least four substituents are attached to the ring, all at a phosphorus site, as shown by code (129.11) in Fig. 3A. When five substituents are present, two isomers are possible, indicated by codes (1239.11) and (1259.11), depending on the attachment of the exocyclic group at phosphorus or nitrogen, respectively.

Examples of known P_2N_2 ring derivatives, containing six-coordinate phosphorus include compounds **20** (R=Bu^t,[33] **21** (R=Me)[34] and **22** (R=Me).[35-37]

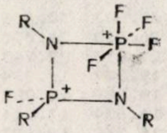

20

(1234579.11)

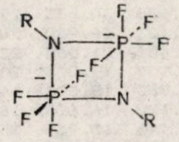

21

(1234579.10.11.12)
(123458 9.10.11.12)

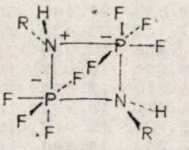

22

(123456789.10.11.12)

The enumeration introduced above covered all possible substituted P_2N_2 ring derivatives. Many of the structural types presented can be illustrated with real examples. Others would be rejected by the puritans as highly improbable, but it is very difficult to draw a line between possible and impossible compounds containing a P_2N_2 ring. However unlikely as some may be, they can teach us much about the structure of related compounds.

B. EXTENDED HÜCKEL MOLECULAR ORBITAL CALCULATIONS

In order to gain more insight into the structures of P_2N_2 ring compounds, we resorted to the extended Hückel molecular orbital method,[5] which allows a treatment of all cycles on a uniform level of accuracy. The orbital parameters were taken from refs.[38] and [39].

Some pertinent data obtained on hypothetic hydrogen-substituted cyclodiphosphazanes and cyclodiphosphazenes are shown in Table 3. The number of doubly occupied orbitals (DOO) and the charges on the rings (CH) are also included. The molecular orbital energy levels are given and the separation between HOMO and LUMO is indicated.

The unsubstituted P_2N_2 species (**1**) is formally isoelectronic with the P_4 tetrahedrane-like molecule. The planar form considered here has 12 low level molecular orbitals, but only ten of them are occupied in the neutral molecule **1** (or **2**) (see column A of Table 3). Thus, this species may not be able of existence as a stable entity. A two electron reduction would give the butterfly shape $P_2N_2^{2-}$ species **23**, **24** or monocyclic **25**, which reminds of the planar Se_4^{2+} (S_4^{2+}) isoelectronic cation and neutral S_2N_2 molecule. However, no one of **23**—**25** have been yet generated and characterized by some means. The LUMO of **23**—**24** could accomodate two more electrons, giving the four charged anion $P_2N_2^{4-}$, **26**. Its existence is quite probable in view of the fact that the homonuclear P_4^{4-} analog is known from the crystal structure of 9th and 10th group phosphides of MP_2 composition.[40,41]

Table 3

Molecular orbital energies of some cyclodiphosphazans and cyclodiphosphazene rings*

(-E(i), eV)

	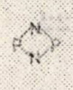	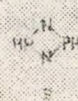	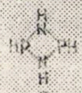	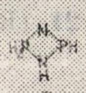	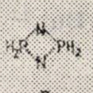	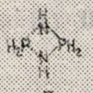	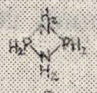	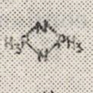	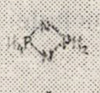	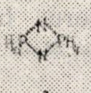	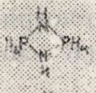	
	A	B	C	D	E	F	G	H	I	J	K	
1	30.804	30.605	30.663	27.141	30.605	30.663	30.635	29.837	30.607	30.608	30.655	
2	26.529	26.529	27.120	22.429	26.529	27.121	26.930	26.561	26.630	26.670	27.122	
3	19.290	20.410	20.450	20.768	21.481	21.481	21.065	22.182	21.817	22.243	22.243	
4	15.917	18.238	18.290	18.037	19.528	19.957	19.005	20.245	19.039	19.994	20.456	
5	15.811	15.917	16.710	17.496	17.172	17.363	18.373	16.879	18.089	18.089	18.089	
6	15.790	15.802	16.650	16.392	16.146	17.172	16.623	16.787	16.624	17.011	17.511	
7	14.498	14.787	15.920	15.917	15.917	16.146	15.936	15.949	16.570	16.623	17.011	
8	13.273	14.635	15.540	14.984	14.851	15.917	15.910	15.027	14.979	15.065	16.623	
9	13.090	13.273	13.470	13.622	14.558	15.536	15.527	14.602	13.888	14.587	15.927	
10	12.679	13.095	13.273	13.273	13.273	14.557	13.411	14.095	13.273	13.608	14.537	
11	11.475	12.535	13.130	13.143	13.094	13.273	13.384	13.325	13.236	13.273	13.273	
12	9.650	11.416	11.470	11.772	12.928	12.928	13.187	12.865	12.451	12.451	12.451	
13	2.168	2.168	2.168	6.064	2.168	2.168	8.112	12.504	11.806	12.151	12.264	
14	-3.602	0.133	-	2.168	-	-	8.088	11.873	11.233	11.487	11.487	
15	-	-	-	-	-	-	6.617	0.065	5.920	11.399	11.417	HOM
16	-	-	-	-	-	-	-	-	-	11.124	11.124	LUM
DOO	10	11	12	12	12	13	14	15	13	14	15	
CH	-4	-2	0	0	0	+2	+4	-4	-2	-4	-2	

* The continuous line indicates the HOMO-LUMO separation for the neutral molecular species. The dashed line indicates the HOMO-LUMO separation in stable charged species.

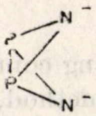

23

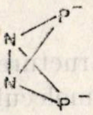

24

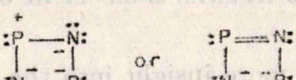

25

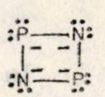

26

Now the total number of occupied molecular orbitals of $P_2N_2^{4-}$ is not changed if, formally, one to six protons are attached to phosphorus and/or nitrogen atoms. This way various mono-, di-. . .to hexa-substituted phosphazane or phosphazene rings are "constructed". The core of 12 favorable orbitals suggests that :

a) The species HPN_2PH (column B of Table 3), with only 22 electrons, should be doubly charged $[HPN_2PH]^{2-}$, with the negative charges localized at nitrogen sites **27.**

b) All C—E species have 24 electrons, the exact number required by 12 molecular orbitals, so they are expected to be neutral. The overall neutrality in E corresponding to codes (1234) is reached by alternating the charges at the phosphorus and nitrogen atoms.

c) In order to keep occupied only 12 mo's, $H_2P(NH)_2PH_2$ and $H_2P(NH_2)_2PH_2$ (F and G) lose two or four electrons, giving rise to doubly charged (on phosphorus) or quadruply positively charged species, corresponding to codes (123457/8) and (12345678) respectively.

The compounds containing one pentacoordinate phosphorus atom have 13 low lying molecular orbitals, while those with two five coordinate phosphorus have 14 such orbitals. If fully occupied, they need 26 or 28 electrons, respectively. Thus H_2PN_2PH has only 24 electrons, so two more will be necessary to fill 13 mo's, and a dianion of structure **28**,

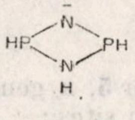

27

(13)

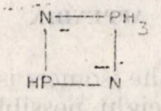

28

(1239)

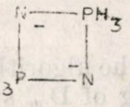

29

(12349.10)

as shown by code (1239) is expected to be favored over the neutral species. Phosphoranes with two pentacoordinate phosphorus require 28 electrons, so a hypothetical neutral $H_3PN_2PH_3$ (H) with only 26 electrons needs one more pair to give dianion **29** identified by code number (12349.10) in Fig. 2. One to five protons may be added to **28** (1239) and four to **29** (12349.10) without changing the number of low lying mo's. In this way the following mononegative, neutral, positive and dispositive species may be built up :

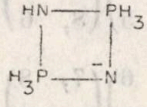

30

(123459.10)

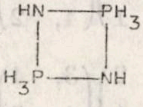

31

(1234579.10)

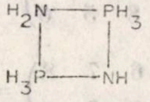

32

(1234579.10)

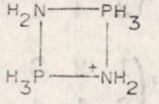

33

(123456789.10)

In species containing six- and five-, or two six-coordinate phosphorus atoms, 15 or 16 low lying mo's are found. The neutral $H_4PN_2PH_4$ has only 28 electrons, four less than necessary, so a basic structure with two six-coordinate phosphorus would have type **34**.

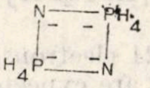

34

(12349.101112)

Again, up to four protons may be added without changing the number of lowest part of molecular orbital energies and 32 electrons (16 pairs) is still the right number which suits this system. No examples of structure **34** are known, but substituents (fluorine at phosphorus and hydrogen or methyl groups at nitrogen) gave the compounds **20**–**22** cited above.[33]

The extended Hückel method offers a remarkable illustration of the charges actually observed in highly substituted (hypervalent) derivatives of P_2N_2 rings reported in the literature.

APPENDIX

The algorithm of counting the isomers is illustrated for **5**, a generating ring of D_{2h} symmetry, with eight possible substitution sites :

1) act the symmetry operations (R) of the point group on **5** and get the length of cyclic permutations :

$$E\begin{pmatrix}1&2&3&4&5&6&7&8\\1&2&3&4&5&6&7&8\end{pmatrix}=\begin{pmatrix}1\\1\end{pmatrix}\begin{pmatrix}2\\2\end{pmatrix}\begin{pmatrix}3\\3\end{pmatrix}\begin{pmatrix}4\\4\end{pmatrix}\begin{pmatrix}5\\5\end{pmatrix}\begin{pmatrix}6\\6\end{pmatrix}\begin{pmatrix}7\\7\end{pmatrix}\begin{pmatrix}8\\8\end{pmatrix}$$

$$C_2^x\begin{pmatrix}1&2&3&4&5&6&7&8\\4&3&2&1&6&5&8&7\end{pmatrix}=\begin{pmatrix}1,&4\\4,&1\end{pmatrix}\begin{pmatrix}2,&3\\3,&2\end{pmatrix}\begin{pmatrix}5,&6\\6,&5\end{pmatrix}\begin{pmatrix}7,&8\\8,&7\end{pmatrix}$$

$$C_2^y\begin{pmatrix}1&2&3&4&5&6&7&8\\2&1&4&3&8&7&6&5\end{pmatrix}=\begin{pmatrix}1,&2\\2,&1\end{pmatrix}\begin{pmatrix}3,&4\\4,&3\end{pmatrix}\begin{pmatrix}5,&8\\8,&5\end{pmatrix}\begin{pmatrix}6,&7\\7,&6\end{pmatrix}$$

$$C_2^z\begin{pmatrix}1&2&3&4&5&6&7&8\\3&4&1&2&7&8&5&6\end{pmatrix}=\begin{pmatrix}1,&3\\3,&1\end{pmatrix}\begin{pmatrix}2,&4\\4,&2\end{pmatrix}\begin{pmatrix}5,&7\\7,&5\end{pmatrix}\begin{pmatrix}6,&8\\8,&6\end{pmatrix}$$

$$\sigma_h^{xy}\begin{pmatrix}1&2&3&4&5&6&7&8\\2&1&4&3&6&5&8&7\end{pmatrix}=\begin{pmatrix}1,&2\\2,&1\end{pmatrix}\begin{pmatrix}3,&4\\4,&3\end{pmatrix}\begin{pmatrix}5,&6\\6,&5\end{pmatrix}\begin{pmatrix}7,&8\\8,&7\end{pmatrix}$$

$$\sigma_h^{xz}\begin{pmatrix}1&2&3&4&5&6&7&8\\3&1&4&2&5&6&7&8\end{pmatrix}=\begin{pmatrix}1,&3\\3,&1\end{pmatrix}\begin{pmatrix}2,&4\\4,&2\end{pmatrix}\begin{pmatrix}5\\5\end{pmatrix}\begin{pmatrix}6\\6\end{pmatrix}\begin{pmatrix}7\\7\end{pmatrix}\begin{pmatrix}8\\8\end{pmatrix}$$

$$\sigma_h^{yz}\begin{pmatrix}1 & 2 & 3 & 4 & 5 & 6 & 7 & 8\\ 1 & 2 & 3 & 4 & 7 & 8 & 5 & 6\end{pmatrix}=\begin{pmatrix}1\\1\end{pmatrix}\begin{pmatrix}2\\2\end{pmatrix}\begin{pmatrix}3\\3\end{pmatrix}\begin{pmatrix}4\\4\end{pmatrix}\begin{pmatrix}5, & 7\\7, & 5\end{pmatrix}\begin{pmatrix}6, & 8\\8, & 6\end{pmatrix}$$

$$i\begin{pmatrix}1 & 2 & 3 & 4 & 5 & 6 & 7 & 8\\ 4 & 3 & 2 & 1 & 8 & 7 & 6 & 5\end{pmatrix}=\begin{pmatrix}1, & 4\\4, & 1\end{pmatrix}\begin{pmatrix}2, & 3\\3, & 2\end{pmatrix}\begin{pmatrix}5, & 8\\8, & 5\end{pmatrix}\begin{pmatrix}6, & 7\\7, & 6\end{pmatrix}$$

2) for each operation construct the polynomial

$$P(R, x) = (1 + x^{l_1})(1 + x^{l_2}) \ldots (1 + x^{l_n})$$

where l_k is the length of the k-th cycle in the permutation operator R
Thus : $P(E, x) = (1 + x)^8$

$$P(C_2^z) = (1 + x^2)^4 = P(C_2^y, x) = P(C_2^z, x) = P(h^{xy}, x) = P(i, x)$$

$$P(h^{yz}, x) = (1 + x)^4(1 + x^2)^2 = P(h^{xz})$$

3) Sum up $P(R, x)$ to get $Q(x)$:

$$Q(x) = 8 + 16x + 64x^2 + 80x^3 + 128x^4 + 80x^5 + 64x^6 + 16x^7 + 8x^8$$

4) Divide $Q(x)$ by $h = 8$, the order of D_{2h} group : the coefficient of x^m represents the number of m substituted isomers.

REFERENCES

[1] W. Tremel, R. Hoffmann and E. D. Jemmis, *Inorg. Chem.*, **28**, 1213 (1989).

[2] I. Haiduc, "The Chemistry of Inorganic Ring Systems", vols. 1–2, Wiley-Interscience, London, 1970.

[3] I. Haiduc and D. B. Sowerby, (editors) "The Chemistry of Inorganic Homo- and Heterocycles", vols. 1–2, Academic Press, London, 1987.

[4] A. T. Balaban, "Chemical Applications of Graph Theory", Academic Press, London, 1976.

[5] R. Hoffmann, *J. Chem. Phys.*, **39**, 1397 (1963).

[6] E. Niecke, D. Gudat and E. Symalla, *Angew. Chem.*, **98**, 817 (1986).

[7] O. E. Polansky, *MATCH*, **1975**, No. 1, p. 11.

[8] H. Dolhane, *Computers & Chemistry*, **5**, 41 (1981).

[9] A. H. Cowley, M. Lattman and J. C. Wilburn, *Inorg. Chem.*, **21**, 2916 (1981).

[10] R. Keat, in "The Chemistry of Inorganic Homo- and Heterocycles"; edited by I. Haiduc and D. B. Sowerby, Academic Press, London, 1987, vol. 2, p. 467.

[11] O. J. Scherer, *Nachr. Chem. Tech. Lab.*, **28**, 392 (1980).

[12] A. Baceiredo, G. Bertrand, J. P. Majoral, F. L. Anba, J. Jaud and J. Galy, *J. Amer. Chem. Soc.*, **106**, 6088 (1984).

[13] J. Boske, E. Niecke, M. Nieger, E. Ocando, J. P. Majoral and G. Bertrand, *Inorg. Chem.*, **28**, 499 (1989).

[14] K. W. Muir, *J. Chem. Soc. Dalton Trans.*, **1975**, 259.

[15] W. Schwarz, H. Hess and W. Zeiss, *Z. Naturforsch.*, **33B**, 723 (1978).

[16] S. Pohl, *Z. Naturforsch.*, **34B**, 256 (1979).

[17] G. Trinquier, *J. Amer. Chem. Soc.*, **108**, 568 (1986).

[18] C. Roques, M. R. Mazieres, J. P. Majoral and M. Sanchez, *Tetrahedron Letters*, **29**, 4547 (1988).

[19] I. S. Zaltsman, H. G. Koidan, A. P. Marchenko and A. M. Pinchuk, *Zh. Obshch. Khim.*, **59**, 2386 (1989).

[20] R. Appel, M. Halstemberg, *J. Organomet. Chem.*, **99**, C25 (1975).

[21] E. Niecke and W. Fluck, *J. Organomet. Chem.*, **105**, C23 (1976).

[22] R. Keat, D. S. Rycroft and D. G. Thompson, *J. Chem. Soc. Dalton Trans.*, **1979**, 1224.

[23] S. Kleemann and E. Fluck, *Z. Anorg. Allg. Chem.*, **526**, 133, 141 (1985).

[24] O. J. Scherer and G. Schnabl, *Chem. Ber.*, **109**, 2996 (1976) ; *Z. Naturforsch.*, **31B**, 142 (1976).

[25] R. Keat and D. G. Thompson, *J. Chem. Soc. Dalton Trans.*, **1980**, 928.

[26] A. P. Marchenko, V. V. Miroshnichenko, V. A. Kovenya, A. M. Pinchuk, A. N. Chernega, M. Yu. Antipin and Yu. T. Struchkov, *Zh. Obshch. Khim.*, **58**, 1758 (1988).

[27] A. Schmidpeter, in "The Chemistry of Inorganic Homo- and Heterocycles," edited by I. Haiduc and D. B. Sowerby, Academic Press, London, 1987, vol. 2, p. 617.

[28] M. Bermann, *Adv. Inorg. Chem. Radiochem.*, **14**, 1 (1972).

[29] G. V. Roschenthaler, K. Sauerbrey and R. Schmutzler, *Chem. Ber.*, **111**, 3105 (1978).

[30] M. Halstenberg and R. Appel, *Chem. Ber.*, **111**, 1815 (1978).

[31] A. Schmidpeter, M. Nayibi, P. Mayer and H. Tautz, *Chem. Ber.*, **116**, 1468 (1983).

[32] A. Schmidpeter and T. V. Criegern, *Z. Naturforsch.*, **33B**, 1330 (1978).

[33] H. Hahn, K. Utvary and W. Meindl, *Monatsh. Chem.*, **114**, 1167 (1983).

[34] W. Meindl and K. Utvary, *Monatsh. Chem.*, **110**, 129 (1977).

[35] K. Utvary and K. Kubjacek, *Monatsh. Chem.*, **117**, 287 (1986).

[36] H. Hahn, W. Meindl and K. Utvary, Monatsh. Chem., **115**, 899 (1984).

[37] H. Hahn, W. Meindl and K. Utvary, *Monatsh. Chem.*, **116**, 157, 279 (1985).

[38] A. G. Turner, "Methods in Molecular Orbital Theory," Prentice Hall Inc., New Jersey, 1974.

[39] A. Botrel and C. R. Guerillot, *J. Chim. Physique*, **71**, 1240 (1974).

[40] S. Rundquist, *Ark. Kemi*, **20**, 62 (1962).

[41] S. Rundquist and N. O. Ersson, *Ark. Kemi*, **30**, 103 (1969).

Revue Roumaine de Chimie, 36, 4–7, 545–550 (1991)

Dedicated to Prof. ALEXANDRU T. BALABAN
on the occasion of his 60th anniversary

COORDINATION COMPOUNDS AS RAW MATERIALS FOR SPINELIC OXIDES

MARIA BREZEANU[a], LUMINIȚA PATRON[b], OANA CARP[c], MARIUS ANDRUH[a]
and NICOLAE STĂNICĂ[b]

[a] Faculty of Chemistry, University, Bucharest
[b] Institute of Physical Chemistry of Roumanian Academy
[c] Institute of Chemical and Biological Energy, Bucharest

Received January 8, 1991

A new class of mixed coordination compounds of Fe(III) and Fe(II), Co(II) or Ni(II) with gluconic acid was synthesized. The complex compounds were characterized by elemental chemical analysis, electronic and IR spectra, magnetic measurements. Thermogravimetric decomposition of these compounds gives spinelic oxides $Fe_2(III)Fe(II)O_4$, $Fe_2(III)NiO_4$ and $Fe_2(III)CoO_4$.

Data on the obtention of mixed oxides with spinelic structure by thermal decomposition of polynuclear complex compounds are scarce in the literature.[1–3]

The present note deals with the possibility of employing such a method to obtain Fe_3O_4, Fe_2CoO_4 and Fe_2NiO_4.

The application of polynuclear complex thermolysis requires a thorough study of the synthesis conditions of these compounds containing Fe(III) and M(II), M(II)=Fe, Co, Ni, and, on the other hand, of the possibilities to decompose them in order to obtain the spinelic phase.

In order to be utilized as starting material, the complex compounds have to contain, as ligands, systems which are either volatile or decompose into volatile products. Selection of ligands is rather difficult because, besides the above-mentioned requirements, one has to take into account the relatively different coordination of the two transition metals.

In earlier publications we reported the results regarding the preparation of perovskite phase $LnMO_3$ (M(III)=Fe, Co, Ni, Cr, Mn) by the decomposition method of polynuclear complex compounds [4–6] using gluconic acid as ligand.

The gluconic acid – transition metal system was extensively studied,[7–12] because of the chelating ability of the acid, on the one hand, and of the distinct behaviour of each system, on the other hand; practically, there are not two gluconic acid – transition metal systems that behave in the same way.

Owing to their multiple applications, the following systems were studied :

$$M(III) - GH_4^- \quad M(III)=Al, Cr, Ln, Bi, Fe$$

respectively

$$M(II) - GH_4^- \quad M(II)=Fe, Co, Ni, Cu, Zn, Pb, Cd$$

The nature of the species found depends both on the pH of the reaction medium and on the nature of the transition metal ion involved. It is also worth specifying that the gluconic acid may act as ligand with one, two or even three negative charges.

Because in the literature there are no data on the possibility of coordination within the same species of two or more different transition metals, such a study may be regarded as interesting.

Therefore, the following systems were studied :

$$M(II) - Fe(III) - \text{Gluconic acid}$$

where $M(II)=Fe, Co, Ni$, for a ratio $M(II) : Fe(III) = 1 : 2$.

To isolate heteropolynuclear complex compounds, the synthesis was carried out according to Melson and Pickering's method.[13]

The elemental chemical analysis has evidenced the following series of heteropolynuclear complex compounds :

$$[Fe_2M(Gluc)_3] \cdot nH_2O$$

where $M(II)=Fe ; n = 6$

$M(II)=Ni ; n = 5$

and $[Fe_2Co(Gluc)_4] \cdot 8\,H_2O$

The same method was employed to prepare single gluconates of Fe(III), Fe(II), Co(II) and Ni(II) for which the following chemical formula was established :

$$[Fe(III)\,(Gluc)] \cdot 4\,H_2O$$

$$[Fe(II)\,(Gluc)_2] \cdot 2\,H_2O$$

$$[Co(II)\,(Gluc)_2] \cdot 3\,H_2O$$

$$[Ni(II)\,(Gluc)_2] \cdot 2H_2O$$

To determine the coordination of the ligand, IR spectra were recorded for heteropolynuclear complex compounds and single gluconates over the range 400—4000 cm^{-1}; these data were compared with those reported in the literature for IR spectra of glucono-δ-lactone and sodium gluconate, respectively.

The spectrum of glucono-δ-lactone shows a maximum at 1720 cm^{-1} assigned to $\nu_{C=O}$ vibration mode, which points to the existence of a free carbonyl group. After the formation of complex compound, this band vanishes and two bands of carboxylate ion appear : $\nu_{COO^- sym}$ at 1390 cm^{-1} and $\nu_{COO^- asym}$ at 1600 cm^{-1}, due to the coordinate COO^- group.

In the case of polyhydroxycarboxylic ligands, the coordination at metallic ions is achieved most often by alcoholic groups as well. The primary and secondary alcohol groups exhibit absorption bands attributed to the bending of OH at 1250—1350 cm^{-1} and to the C—O(H) frequency at 1000—1230 cm^{-1}.

Comparison of spectra recorded in heteropolynuclear complex compound and isolated simple complex compound with that of sodium gluconate (where in the interaction between the metal ion and alcohol group is electrostatic) shows a shift of the split band CH—OH from 1100—1090 cm^{-1} (in sodium gluconate) to lower values (according to the literature data). This shift is assigned to the coordination of one or several OH^- groups.

The broad band noted at 3000—3600 cm^{-1} (maximum at 3400 cm^{-1} in all IR spectra is assigned to the formation of hydrogen bonds in water and/or alcohols. As an example, figure 1 shows the IR spectra recorded for $FeCo(Gluc)_4 \cdot 8H_2O$ and $Co(Gluc)_2 \cdot 3H_2O$.

The electron spectra were recorded on all complex compound obtained and were compared with those of simple gluconates of transition metals.

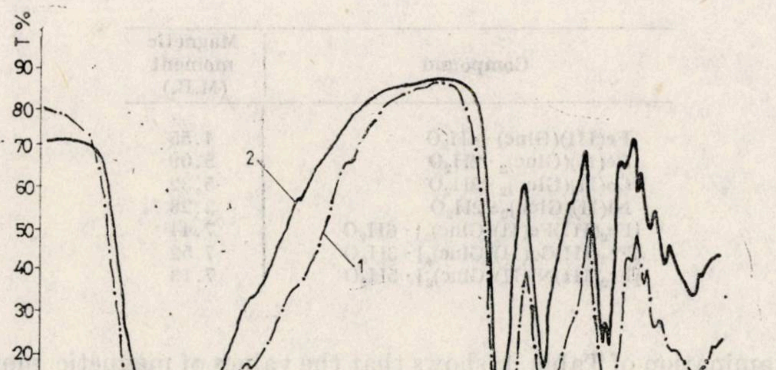

Fig. 1. — IR spectra of $FeCo(Gluc)_4 \cdot 8H_2O$ (1)
$Co(Gluc)_2 \cdot 3H_2O$ (2)

Examination of these spectra suggested the assignment of a high-spin octahedral configuration to Fe(III), (d^5), and also, to Fe(II), Co(II) and Ni(II). Figure 2 shows the spectrum of $Fe_2Ni(Gluc)_3 \cdot 5 H_2O$, heteropolynuclear complex compound. One can note the characteristic bands of Ni(II) ion in an octahedral high-spin configuration due to the transition from the ground state ${}^3A_{2g}(F)$ to the excited ones ${}^3A_{2g}(F) \rightarrow {}^3T_{2g}(F)(\nu_1)$ ($\sim$ 10 000 cm^{-1}) and ${}^3A_{2g} \rightarrow {}^3T_{1g}(P)(\nu_2)$ (13 500$-$14 000 cm^{-1}). The band assigned to the forbidden spin transition ${}^6A_{1g} \rightarrow {}^4T_{1g}(G)$ in a high-spin octahedral coordination of Fe(II) ion, also, appears as a shoulder.

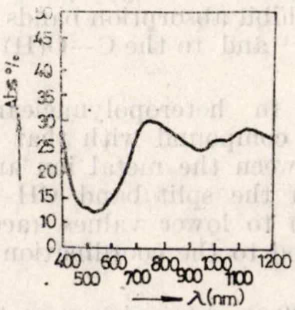

Fig. 2. — Electronic spectra of $Fe_2Ni(Gluc)_3 \cdot 5H_2O$

The values of magnetic susceptibilities (at room temperature) of heteropolynuclear complex compounds and of simple gluconates were determined and the corresponding magnetic moments were calculated (Table 1).

Table 1

Compound	Magnetic moment (M.B.)
$Fe(III)(Gluc) \cdot 4H_2O$	4.55
$Fe(II)(Gluc)_2 \cdot 2H_2O$	5.09
$Co(II)(Gluc)_2 \cdot 3H_2O$	5.32
$Ni(II)(Gluc)_2 \cdot 2H_2O$	3.28
$[Fe_2(III)Fe(II)(Gluc)_3] \cdot 6H_2O$	7.44
$[Fe_2(III)Co(II)(Gluc)_4] \cdot 3H_2O$	7.52
$[Fe_2(III)Ni(II)(Gluc)_3] \cdot 5H_2O$	7.13

Examination of Table 1 shows that the values of magnetic momenta of heteropolynuclear complex compounds are lower than those obtained by summing up the momenta of the three metallic ions. This finding points to the existence of some interactions between these ions.

Taking into account the aim of this study — the obtention of ferrites — the complex compounds synthesized were subjected to a thermogravimetric study to find out the steps of decomposition, the corresponding effects as a function of temperature and the optimal conditions for obtaining pure oxidic phase.

Our data and the similarity with those in literature, 14—16 on decomposition of Fe(III), Ln(III) and Cr(III), Ln(III) complex gluconates afford us to advance the following scheme of decomposition for the three heteropolynuclear complex compounds :

$$\text{I.}\qquad \mathrm{Fe_2(III)Fe(II)(Gluc)_3 \cdot 6H_2O} \xrightarrow[\substack{85-100^\circ \\ -6H_2O}]{\text{I}} \mathrm{Fe_2(III)Fe(II)\,(Gluc)_3} \longrightarrow$$

$$\xrightarrow[\substack{185^\circ \\ -CO_2 \\ -2H_2O}]{\text{II}} \mathrm{Fe_2(III)Fe(II)(C_4H_7O_5)_3} \xrightarrow[\substack{220^\circ \\ -H_2O}]{\text{III}} \mathrm{Fe_2(III)Fe(II)(CO_3)_4} \longrightarrow$$

$$\xrightarrow[\substack{350^\circ \\ -4CO_2}]{\text{IV}} \mathrm{Fe_2(III)Fe(II)O_3(CO_3)} \xrightarrow[\substack{400^\circ \\ -CO_2 \\ +1/2O_2}]{\text{V}} 3/2\ \mathrm{Fe_2O_3}$$

$$\text{II.}\qquad \mathrm{Fe_2(III)Co(II)(Gluc)_4 \cdot 3H_2O} \xrightarrow[67-70^\circ]{\text{I}} \mathrm{Fe_2(III)Co(II)(Gluc)_4} \longrightarrow$$

$$\xrightarrow[\substack{128-130^\circ \\ -CO_2 \\ -H_2O}]{\text{II}} \mathrm{Fe_2(III)Co(II)(CO_3)_4} \xrightarrow[\substack{298-300^\circ \\ -2CO_2 \\ -CO}]{\text{III}} \mathrm{Fe_2CoO_4}$$

$$\text{III.}\qquad \mathrm{Fe_2(III)Ni(Gluc)_3 \cdot 5H_2O} \xrightarrow[\substack{65^\circ \\ -5H_2O}]{\text{I}} \mathrm{Fe_2(III)Ni(II)(Gluc)_3} \longrightarrow$$

$$\xrightarrow[\substack{130^\circ \\ -H_2O \\ -CO_2}]{\text{II}} \mathrm{Fe_2Ni(II)(CO_3)_4} \xrightarrow[\substack{212-220^\circ \\ -2CO_2}]{\text{III}} \mathrm{Fe_2NiO_2(CO_3)_2} \xrightarrow[290-300^\circ]{\text{IV}} \mathrm{Fe_2NiO_4}.$$

The analysis of this decomposition scheme suggests the following conclusions :

- the decomposition of heteropolynuclear complex compounds with gluconate anion as ligand always occurs with formation of a mixed carbonate as intermediate ;
- the decomposition of the intermediate carbonate and the formation of oxidic phase takes place at very low temperature, below 300—400° ;
- passing from mixed carbonate to oxidic phase assumes the formation of an intermediate phase $\mathrm{Fe_2MO_3(CO_3)}$, where M=Fe(II) and Ni(II) ; this phase is not evidenced in the case of $\mathrm{Fe_2Co(Gluc)_4 \cdot 8\,H_2O}$ decomposition ;
- the decomposition of mixed carbonate $\mathrm{Fe_2(III)Fe(II)O_3(CO_3)}$ is accompanied by Fe(II) → Fe(III) oxidation :

$$2\,\mathrm{Fe_2O_3(CO_3)} \xrightarrow[+1/2O_2]{400^\circ} 3\mathrm{Fe_2O_3} + 2\mathrm{CO_2}$$

The products resulted from complex compounds decomposition were analysed by X-ray diffraction. The diagrams obtained have suggested the formation of $\mathrm{Fe_2O_3}$, $\mathrm{Fe_2NiO_4}$ and $\mathrm{Fe_2CoO_4}$.

The low temperatures at which these phases were obtained recommend the decomposition of heteropolynuclear complex compounds containing the gluconate anion as ligand as a possible alternative for obtaining Co(II) and Ni(II) ferrites.

REFERENCES

[1] J. Paris and R. Paris, *Bull. Soc. Chim. France*, **4**, 1138 (1965).

[2] L. Patron, A. Conțescu, G. Munteanu and M. Brezeanu, *Rev. Roum. Chim.*, **31**, 341 (1986).

[3] I. Ilie, M. Brezeanu, L. Patron, E. Segal and G. Filoti, *Rev. Roum. Chim.*, **32**, 1109 (1987).

[4] P. Spacu, L. Patron, A. Conțescu, N. Stănică and D. Crișan, *Rev. Roum. Chim.*, **34**, 1275 (1989).

[5] P. Spacu, L. Patron, S. Ploștinaru, D. Crișan, and N. Stănică, *Rev. Roum. Chim.*, **35**, 617(1990).

[6] P. Spacu, S. Ploștinaru, L. Patron, A. Conțescu, D. Crișan and N. Stănică, *Rev. Roum. Chim.*, **35**, 617 (1990).

[7] D. Askham and A. Wold, *J. Amer. Chem. Soc.*, **79**, 6365 (1990).

[8] A. Wold, *J. Amer. Chem. Soc.*, **76**, 1029 (1954).

[9] M. Crespin and W. K. Hall, *J. Catal.*, **69**, 358 (1981).

[10] Y. F. Yu. Yao, *J. Catal.*, **70**, 356 (1981).

[11] S. A. Nedil'ko, *Zh. Neorg. Khim.*, **24**, 1395 (1979).

[12] O. M. Parkash, *Mater. Res. Bull.*, **9**, 1173 (1974).

[13] G. A. Melson and W. F. Pickering, *Aust. J. Chem.*, **21**, 1205 (1968).

[14] P. Spacu, S. Ploștinaru, L. Patron and D. Crișan, *Rev. Roum. Chim.*, **34**, 323 (1989).

[15] P. G. Schullerus, L. Patron, S. Ploștinaru and E. Segal, *Thermoch. Acta*, **153**, 263 (1989).

[16] P. G. Schullerus, L. Patron, S. Ploștinaru, A. Conțescu and E. Segal, *Thermochim. Acta*, **133**, 285 (1988).

Revue Roumaine de Chimie, **36**, *4*–7, 551–561 (1991)

Dedicated to Prof. ALEXANDRU T. BALABAN
on the occasion of his 60th anniversary

MATHEMATICAL MODELLING OF ION PAIR CARRIER MEDIATED TRANSPORT THROUGH LIQUID MEMBRANES

LUCIA MUTIHAC[a], RADU MUTIHAC[b] and CONSTANTIN LUCA[c]

[a] Institute of Physical Chemistry, Romanian Academy, Splaiul Independenței, 202, Bucharest
[b] Faculty of Physics, University of Bucharest, Bucharest, Măgurele 76900, PO Box MG 11
[c] Polytechnical Institute, Department of Analytical Chemistry, Splaiul Independenței 202, Bucharest

Received December 17, 1990

The mechanisms of ion pair carrier mediated transport through unsupported liquid membranes in systems, proved to be rate limited by diffusion, were investigated both exprimentally and theoretically. The main purpose was to develop a simple mathematical model for computer simulation and then to optimize the rate of transport.

Carrier mediated transport through a liquid membrane offers a possible ground for separation techniques.[1] Three types of carrier mediated (or facilitated, transport are recognized [2]: (a) facilitated diffusion of single species, (b) facilitated diffusion of an ion-pair and (c) exchange diffusion of two species.

This paper is focused on modelling ion pair transport through liquid membranes mediated by crown ethers and assisted by pH gradient. The possibility of separating amino acids from a mixture making use of macrocyclic ligands of crown ether type (18-crown-6) in a technique of simple extraction (acid aqueous phase-organic phase) or two step extraction (acid aqueous phase – organic phase ; organic phase – alkaline aqueous phase) was previously investigated.[3] The macrocyclic ligands [4–6] which are able to specifically recognize through controlled interactions according to size, shape and structure various cations and then, by their means, various anions, have allowed the study of amino acids of which amphion type molecule may appear either as cation in acid medium or as anion in basic medium. The possibility of coupling two more chemical species, according to a natural model by means of certain physico-chemical affinities without formation of covalent bonds is referred to as "recognition".[7]

THE ION PAIR CARRIER MEDIATED TRANSPORT

The general model of ion pair carrier mediated transport through a liquid membrane is presented in Fig. 1.

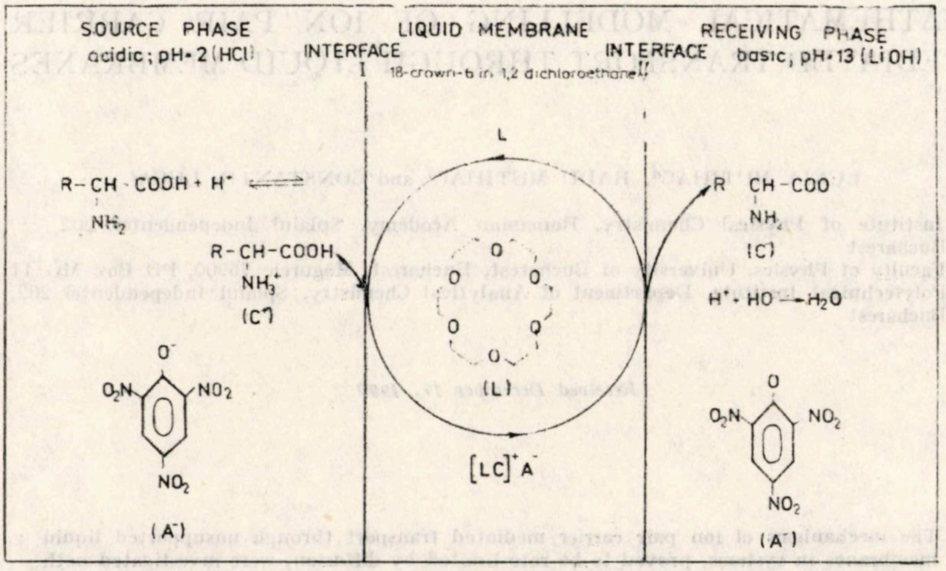
SOURCE PHASE
acidic; pH=2 (HCl)
INTERFACE
I
LIQUID MEMBRANE
18-crown-6 in 1,2 dichloroethane
INTERFACE
II
RECEIVING PHASE
basic, pH=13 (LiOH)
L
R-CH-COOH + H⁺
NH₂
R-CH-COOH
NH₃⁺
(C⁺)
O
(L)
[LC]⁺A⁻
R-CH-COO
NH₂
(C)
H⁺ + HO⁻ → H₂O
O⁻
O₂N
NO₂
NO₂
(A⁻)
O
O₂N
NO₂
NO₂
(A⁻)

Fig. 1. — Mechanism of carrier (L) mediated active transport of an ion pair (LC^+A^-) through bulk liquid membranes assisted by pH gradient.

This is the system most widely studied [8–12] especially in relation with the transport of bound monovalent cations (C^+) together with an external anion (A^-) by neutral ligands (L) like crown ethers and cryptands. Generally, some of the phases are stirred to provide convective transport. The overall process is complex, consisting of a mixture of diffusion and reaction steps at two independent, and possibly different, interfaces. Identification of the rate-limiting process is further complicated by the probable simultaneity of some steps and by other potential pathways involving complexation/decomplexation reactions in the bulk phases. Studies of the kinetics of substrate or ion-pair selective transport may reveal the importance of different steps.

In order to increase the efficiency of the process, an original design of the device [13] was used, as shown in Fig. 2. According to this system [14] in the source phase there is the protonated amino acid (C^+) to be transported and the picrate anion (A^-) in an aqueous solution at $pH = 2$ ensured by use of HCl. At the source phase/membrane interface, 18-crown-6 macrocyclic carrier complexes the amino acid through the protonated aminic group. The formed complex cation is extracted into 1,2 dichloroethane membrane by ion pairing with the picrate anion which diffuses through the membrane to the membrane/receiving phase interface. The receiving phase at $pH = 13$, transforms the protonated aminic group $-NH_3^+$ into

—NH_2 ; the amino acid is released from the complex and passes into receiving phase as a lithium salt. The empty carrier L diffuses back to the source phase/membrane interface where the whole cycle starts again and again until the equilibrium between the phases of the system is achieved. The basic pH of the receiving phase is ensured by using LiOH because

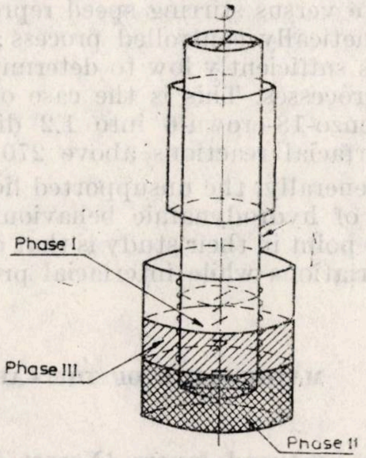

Fig. 2. — The device employed in separation of some amino acids through liquid membrane with macrocyclic carriers.

the Li^+ ion, being much smaller than the crown ether ring size, is not complexed by the macrocyclic carrier and so it does not determine any additional reactions which could influence the transport phenomenon.

Consequently, the acid medium of the source phase allows the formation of an ion pair complex (LC^+A^-) which diffuses through the membrane. The basic medium of the receiving phase facilitates the dissociation of the complex and thus the amino acid passes from the organic phase into the receiving phase. A coupled transport of amino acid and H^+ ions from source phase to receiving phase is accomplished this way. Therefore the transport occurs according to an active transport mechanism with pH gradient.

HYSICS OF THE CARRIER MEDIATED TRANSPORT

The overall process can be limited by the diffusion of the ion pair complex through the organic phase (LM) and/or by the rates of reactions occurring at the interfaces of the system. Theoretical approaches to the transport phenomena are mostly restricted to the case of fast interface reactions.[15] Therefore the membrane permeability is the limiting factor and it is treated as a diffusional process described by Fick's first diffusion law if the following assumptions are made : (i) steady state and (ii) linear concentration profiles through the membrane. The second assumption has already been proved theoretically [16] and checked experimentally [17] for countertransport as well as for the exchange diffusion process.[15] However, the predictions of a diffusion based model [18] fail to adequately explain all experimental results.[19] Consequently, alternative mechanism was proposed involving rate limiting adsorption/desorption reactions, consistent with the fast complexation/decomplexation kinetics [20] and high surfactant activity of the synthetic materials.

For cells of well defined hydrodynamic behaviour, extraction rate is a linear function of stirring rate at low speeds which reaches in some cases a limit value at higher speeds. The presence of a flat region in extraction rate versus stirring speed representation is taken as initial evidence of a kinetically controlled process; the thickness of the unstirred layer becomes sufficiently low to determine a faster diffusion than other interfacial processes. This is the case of the extraction of potassium picrate by dibenzo-18-crown-6 into 1,2 dichloroethane [21] which is rate-limited by interfacial reactions above 270 rpm stirring rate.

Generally, the unsupported liquid membranes do not permit a good control of hydrodynamic behaviour of cells involved. Nevertheless, the starting point in their study is that diffusional processes depend on stirring rate variations while interfacial processes do not.[12]

MATHEMATICS OF THE CARRIER MEDIATED TRANSPORT

As unstirred layers (Nernst layers) at the interfaces are known to play an important role in transport,[2,10] the interfacial turbulence caused by stirring makes it difficult to investigate the transport mechanism. However the simplest process of ion pair carrier mediated transport through bulk liquid membranes is considered under the following assumptions suggested by previously reported data [2,3]:

(1) Crown ether (L) exists more than 90% within the organic phase (LM);

(2) The protonated amino acid (C^+) is extracted into the membrane (LM) in the form of the ternary complex (LC^+A^-) with the crown ether (L) and a lipophilic anion (A^-);
and the following approximations, as well:

(3) If all phases are stirred, concentrations of all species may be considered constant throughout the bulk of each phase and concentration gradients are restricted to the unstirred boundaries (Nerst layers) at the interfaces;

(4) The diffusion constants of the free crown ethers and the ternary complex are equal;

(5) Steady state regime is accomplished at any stirring rate before interfacial turbulence occurs.

Our purpose is to derive a model of the transport mechanism, which should be understood as an equation in a differential or integrated form, describing the evolution of amino acid concentration in the receiving phase.

In a diffusion limited process, as the rates for complex formation and dissociation are fast compared to diffusion through membrane, the $[L]_0^{I,II}$ and $[LC^+A^-]_0^{I,II}$ concentrations at the membrane interfaces (indicated by the superscripts I and II, respectively) and the corresponding

$[A^-]_w^{I,II}$, $[C^+]_w^I$ and $[C^-]_w^{II}$ aqueous concentrations, obey the following equilibrium to form the ternary complex LC^+A^- :

$$K_{ext}^{I} = \frac{[LC^+A^-]_0^I}{[C^+]_w^I[A^-]_w^I[L]_0^I} \tag{1}$$

$$K_{ext}^{II} = \frac{[LC^+A^-]_0^{II}}{[C^-]_w^{II}[A^-]_w^{II}[L]_0^I} \tag{1'}$$

where $K_{ext}^{I,II}$ are the extraction constants at the membrane interfaces. The subscripts w and o are assigned to the species in the aqueous phase and in the organic phase, respectively.

Let us assume firstly that the concentrations at the interfaces are approximately equal to the concentrations in the bulk aqueous phases :

$$[C^+]_w^I \simeq [C^+]_w^{in} \text{ and } [A^-]_w^I \simeq [A^-]_w^{in} \tag{2}$$

$$[C^-]_w^{II} \simeq [C^-]_w^{out} \text{ and } [A^-]_w^{II} - [A^-]_w^{out} \tag{2'}$$

where superscripts in and out are assigned to the species in the bulk source phase and receiving phase, respectively. Therefore, the transport rate is limited by diffusion through the organic unstirred layers. At the initial steady state, the fluxes of amino acid $(J)^{I,II}$ are :

$$J^I = P^I([LC^+A^-]_0^I - [LC^+A^-]_0) \text{ and } J^{II} = P^{II}([LC^+A^-]_0 - [LC^+A^-]_0^{II}) \tag{3}$$

where $P^{I,II}$ is the permeation coefficient of the ternary complex and the free crown ether, both equal under the approximations considered. Consequently, the total concentration of the ligand is equal to the initial concentration $[L^0]$ throughout the organic phase :

$$[L^0] = [L]_0^I + [LC^+A^-]_0^I = [L]_0 + [LC^+A^-]_0 = [L]_0^{II} + [LC^+A^-]^{II} \tag{4}$$

and correspondingly the ligand and complex concentration profiles are symmetric with respect to $[L^0]/2$ (Fig. 3).
Hence, we have

$$J^I = P^I([L]_0 - [L]_0^I) \quad \text{and} \quad J^{II} = P^{II}([L]_0^{II} - [L]_0) \tag{5}$$

The continuity and steady state conditions lead to the following expression for the flux of amino acid (Appendix A) :

$$J = [L^0]\left(P^I K_{ext}^I \frac{[C^+]_w^I[A^-]_w^I}{1 + K_{ext}^I[C^+]_w^I[A^-]_w^I} - P''K''_{ext}\frac{[C^-]_w^{II}[A^-]_w^{II}}{1 + K_{ext}^{II}[C^-]_w^{II}[A^-]_w^{II}}\right) \tag{6}$$

It is a most common assumption, which is considered within this investigation, that the extraction constants K^{I}_{ext} and K^{II}_{ext} are the same $K^{I}_{ext} = K^{II}_{ext} = K_{ext}$ and constant for reactions at both interfaces during the transport process. Experimental arrangements could easily yield

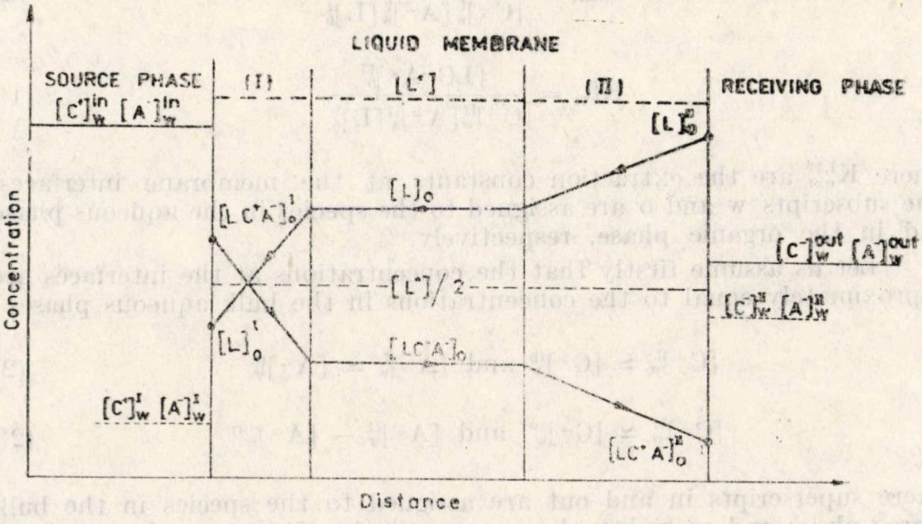
LIQUID MEMBRANE
SOURCE PHASE
$[C^+]^{in}_{w}\ [A^-]^{in}_{w}$
(I)
$[L^*]$
(II)
RECEIVING PHASE
$[L]^{II}_{o}$
$[L]_{o}$
$[LC^+A^-]^{I}_{o}$
$[C^-]^{out}_{w}\ [A^-]^{out}_{w}$
$[L^*]/2$
$[C^-]^{II}_{w}\ [A^-]^{II}_{w}$
$[L]^{I}_{o}$
$[LC^+A^-]_{o}$
$[C^+]^{I}_{w}\ [A^-]^{I}_{w}$
$[LC^+A^-]^{II}_{o}$
Concentration
Distance

Fig. 3. – Typical concentration profiles in the steady state at low saturation of the carrier ($[LC^+A^-]^{I,II}_{0}/[L]^{I,II}_{0}$) at both interfaces.

the same thickness (1) and area (σ) of both Nernst layers and according to Fick's first law under steady state conditions imposes all concentration gradients to be equal [2] (Fig. 3) and so $P^{I} = P^{II} = P$. Considering the approximations (2, 2′), we can rewrite the expression of the flux J:

$$J = PK_{ext}[L^0]\left(\frac{[C^+]^{in}_{w}[A^-]^{in}_{w}}{1 + K_{ext}[C^+]^{in}_{w}[A^-]^{in}_{w}} - \frac{[C^-]^{out}_{w}[A^-]^{out}_{w}}{1 + K_{ext}[C^-]^{out}_{w}[A^-]^{out}_{w}}\right) \quad (7)$$

or equivalent:

$$J = PK_{ext}[L^0]\frac{[C^+]^{in}_{w}[A^-]^{in}_{w} - [C^-]^{out}_{w}[A^-]^{out}_{w}}{(1 + K_{ext}[C^+]^{in}_{w}[A^-]^{in}_{w})(1 + K_{ext}[C^-]^{out}_{w}[A^-]^{out}_{w})} \quad (8)$$

This equation (8) is quite similar to the carrier mediated transport equation for biological membranes [2,22] where the concentration product [C][A] appears in place of the substrate concentration [S].

Depending on the experimental conditions, three regimes may be considered:

a) low saturation of the carrier at both interfaces, that is

$$[LC^+A^-]^{I}/[L]^{I}_{0} = K_{ext}[C^+]^{I}[A^-]^{I} \ll 1$$

and

$$[LC^+A^-]^{II}/[L]^{II}_{0} = K_{ext}[C^-]^{II}[A^-]^{II} \ll 1,$$

and consequently the flux is low:

$$J = PK_{ext}[L^0]([C^+]_w^{in}[A^-]_w^{in} - [C^-]_w^{out}[A^-]_w^{out}) \tag{9}$$

At the beginning of the process the flux expression may be considered to be:

$$J = PK_{ext}[L^0][C^+]_w^{in}[A^-]_w^{in} \tag{10}$$

which reflects a first order dependence of the concentration product.
b) high $[C^+]_w^I[A^-]_w^I$ concentrations product and/or high extraction constant K_{ext}, that is:

$$K_{ext}[C^+]_w^I[A^-]_w^I \gg 1$$

$$K_{ext}[C^-]_w^{II}[A^-]_w^{II} \ll 1$$

the amino acid flux increases as:

$$J = PK_{ext}[L^0]\frac{[C^+]_w^{in}[A^-]_w^{in} - [C^-]_w^{out}[A^-]_w^{out}}{1 + K_{ext}[C^+]_w^{in}[A^-]_w^{in}} \approx$$

$$\approx PK_{ext}[L^0]\frac{[C^+]_w^{in}[A^-]_w^{in}}{1 + K_{ext}[C^+]_w^{in}[A^-]_w^{in}} \tag{11}$$

The maximum value of the theoretically possible J is

$$J_{max} = P[L^0] \tag{12}$$

which is independent of K_{ext} and of the concentrations.
There are in the organic phase at this stage of saturation both free crown ether and ternary complex at the same concentration level:

$$[LC^+A^-]_o = [L]_o = [L^0]/2$$

providing the largest concentration gradients (the carrier is half-filled by the transported species):
c) high saturation at both interfaces, that is

$$K_{ext}[C^+]_w^I[A^-]_w^I \gg 1$$

$$K_{ext}[C^-]_w^{II}[A^-]_w^{II} \gg 1$$

the amino acid flux J decreases because of the complex formation at the receiving interface:

$$J \simeq PK_{ext}[L^0]\frac{[C^+]_w^I[A^-]_w^I - [C^-]_w^{II}[A^-]_w^{II}}{K_{ext}[C^+]_w^I[A^-]_w^I \cdot K_{ext}[C^-]_w^{II}[A^-]_w^{II}} \sim P[L^0]K_{ext}^{-1} \tag{13}$$

at this stage of saturation the carrier is filled by C^+A^- and there is no practical transport process.

CONCLUSIONS

As a general conclusion, the amino acid flux does not follow uniformly its relative affinity for the crown ether nor its concentration. According to the above results, in a diffusion limited process the highest rate of transport is obtained for a half-filled carrier.

When the complex formation at the receiving interface II can be neglected, rewriting equation (11) we have:

$$J = PK_{ext}[L^0]\frac{[C^+]_w^{in}[A^-]_w^{in}}{1 + K_{ext}[C^+]_w^{in}[A^-]_w^{in}} \qquad (14)$$

which indicates that J^{-1} and $([C^+]_w^{in}[A^-]_w^{in})^{-1}$ are in linear relationship described by:

$$J^{-1} = \frac{1}{PK_{ext}[L^0]}([C^+]_w^{in}[A^{-1}]_w^{in})^{-1} + \frac{1}{P[L^0]} \qquad (15)$$

Hence by plotting J^{-1} against $([C^+]_w^{in}[A^-]_w^{in})^{-1}$ one can determine the parameters P and K_{ext} which characterize the combination of ligand, amino acid, anion and the membrane.

The general expression of amino acid flux written here for convenience:

$$J = PK_{ext}[L^0]\frac{[C^+]_w^{in}[A^-]_w^{in} - [C^-]_w^{out}[A^-]_w^{out}}{(1 + K_{ext}[C^+]_w^{in}[A^-]_w^{in})(1 + K_{ext}[C^-]_w^{out}[A^-]_w^{out})} \qquad (16)$$

is valid as long as the approximations (2) are realistic. This is the case mostly at the beginning of the process. If the amounts of amino acid and anion are negligible in the organic phase, then it is relevant to express the concentrations in the aqueous phases as fractions of the initial concentration $[C^0]^{in}[A^0]^{in}$. Let us introduce the following simplifying notations:

$$[C^0]^{in}[A^0]^{in} = y_0$$

$$[C^-]_w^{out}[A^-]_w^{out} = fy_0$$

$$[C^+]_w^{in}[A^-]_w^{in} = (1 - f)y_0$$

where $0 < f < 0.5$, hence we have:

$$J/J_{max} = K_{ext}\frac{(1 - f)y_0 - fy_0}{(1 + K_{ext}(1 - f)y_0)(1 + K_{ext}fy_0)} \qquad (17)$$

which may be written also as :

$$J/J_{\max} = \frac{a_1 K_{ext}}{1 + b_1 K_{ext} + b_2 K_{ext}^2} \tag{18}$$

where $a_1 = (1 - 2f)y_0$, $b_1 = y_0$ and $b_2 = (1 - f)fy_0^2$

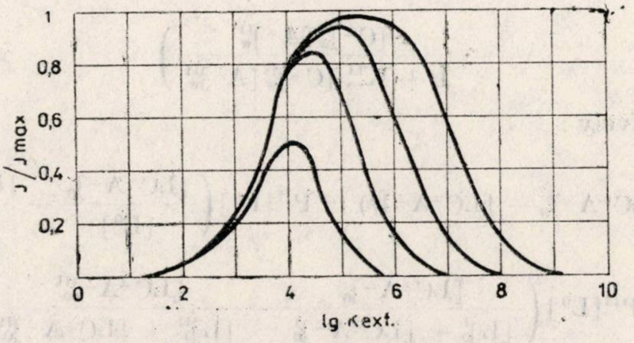

Fig. 4. — Graph of the normated amino acid flux $J/J_{\max}$ versus the thermodynamic extraction equilibrium constant K_{ext} at different stages of an experiment ($[C^0]^{in} = [A^0]^{in} = 1.6 \times 10^{-3}$ M, $f = 0.0001$, 0.001, 0.01 and 0.1 respectively and $[L^0] = 10^{-2}$M.

This last expression was computed and plotted as $J/J_{\max}$ versus $\lg K_{ext}$ for a given initial concentration y_0 at different stages f of an experiment (Fig. 4.)

The bell-shaped curves are superimposed for low K_{ext} and exhibit quite sharp maxima. Accordingly, there is an optimum value for $\lg K_{ext}$ where the transport is most efficient : $\lg K_{ext}^{\max} = 4 \ldots 6$ for a given f. As f increases, the maximum of $J/J_{\max}$ becomes lower, sharper and slightly moves towards lower K_{ext} values.

For a given experiment (y_0 and K_{ext} fixed, f variable) which is represented by a vertical section through the set of curves (Fig. 4), one may notice that the rate of transport is relatively constant only for $K_{ext} \ll K_{ext}^{\max}$. Our experiments are consistent with the model developed above.

APPENDIX A

The amino acid fluxes through the two interfaces may be written successively as :

$$J^{I} = P^{I}([LC^{+}A^{-}]_0^{I} - [LC^{+}A^{-}]_0) = P^{I}[L^0]\left(\frac{[LC^{+}A^{-}]_0^{I}}{[L^0]} - \frac{[LC^{+}A^{-}]_0}{[L^0]}\right) =$$

$$= P^{I}[L^0]\left(\frac{[LC^{+}A^{-}]_0^{I}}{[LC^{+}A^{-}]_0^{I} + [L]_0^{I}} - \frac{[LC^{+}A^{-}]_0}{[LC^{+}A^{-}]_0^{II} + [L]_0^{II}}\right) =$$

$$= P^{I}[L^{0}]\left(K^{I}_{ext}\,\frac{[C^{+}]^{I}_{w}[A^{-}]^{I}_{w}[L]^{I}_{0}}{[LC^{+}A^{-}]^{I}_{0}+[L]^{I}_{0}} - K^{II}_{ext}\,\frac{\dfrac{[LC^{+}A^{-}]_{0}}{[LC^{+}A^{-}]^{II}_{0}}\cdot[C^{-}]^{II}_{w}[A^{-}]^{II}_{w}[L]^{II}_{0}}{[LC^{+}A^{-}]^{II}_{0}+[L]^{II}_{0}}\right) =$$

$$= P^{I}[L^{0}]\left(K^{I}_{ext}\,\frac{[C^{+}]^{I}_{w}[A^{-}]^{I}_{w}}{1+K^{I}_{ext}[C^{+}]^{I}_{w}[A^{-}]^{I}_{w}} - K^{II}_{ext}\,\frac{[LC^{+}A^{-}]_{0}}{[LC^{+}A^{-}]^{II}_{w}}\cdot\right.$$

$$\left.\cdot\,\frac{[C^{-}]^{II}_{w}[A^{-}]^{II}_{w}}{1+K^{II}_{ext}[C^{-}]^{II}_{w}[A^{-}]^{II}_{w}}\right)$$

and respectively : (i)

$$J^{II} = P^{II}([LC^{+}A^{-}]_{0} - [LC^{+}A^{-}]^{II}_{0}) = P^{II}[L^{0}]\left(\frac{[LC^{+}A^{-}]_{0}}{[L^{0}]} - \frac{[LC^{+}A^{-}]^{II}_{0}}{[L^{0}]}\right) =$$

$$= P^{II}[L^{0}]\left(\frac{[LC^{+}A^{-}]_{0}}{[L]^{I}_{0}+[LC^{+}A^{-}]^{I}_{0}} - \frac{[LC^{+}A^{-}]^{II}_{0}}{[L]^{II}_{0}+[LC^{+}A^{-}]^{II}_{0}}\right) =$$

$$= P^{II}[L^{0}]\left(K^{I}_{ext}\,\frac{\dfrac{[LC^{+}A^{-}]_{0}}{[LC^{+}A^{-}]^{I}_{0}}\cdot[C^{+}]^{I}_{w}[A^{-}]^{I}_{w}[L]^{I}_{0}}{[LC^{+}A^{-}]^{I}_{0}+[L]^{I}_{0}}\quad K^{II}_{ext}\,\frac{[C^{-}]^{II}_{w}[A^{-}]^{II}_{w}}{1+K^{II}_{ext}[C^{-}]^{II}_{w}[A^{-}]^{II}_{w}}\right) =$$

$$= P^{II}[L^{0}]\left(K^{I}_{ext}\,\frac{[LC^{+}A^{-}]_{0}}{[LC^{+}A^{-}]^{I}_{0}}\cdot\frac{[C^{+}]^{I}_{w}[A^{-}]^{I}_{w}}{1+K^{I}_{ext}[C^{+}]^{I}_{w}[A^{-}]^{I}_{w}} - \right.$$

$$\left. - K^{II}_{ext}\,\frac{[C^{-}]^{II}_{w}[A^{-}]^{II}_{w}}{1+K^{II}_{ext}[C^{-}]^{II}_{w}[A^{-}]^{II}_{w}}\right) \qquad \text{(ii)}$$

The steady state conditions determine $J^{I} = J^{II} = J$. Expressions (i) and (ii) represent the same flux J, so identifying the coefficients of the two fractionary terms, we have :

$$P^{II}K^{I}_{ext}\cdot\frac{[LC^{+}A^{-}]_{0}}{[LC^{+}A^{-}]^{I}_{0}} = P^{I}K^{I}_{ext}$$

$$P^{I}K^{II}_{ext}\cdot\frac{[LC^{+}A^{-}]_{0}}{[LC^{+}A^{-}]^{II}_{0}} = P^{II}K^{II}_{ext}$$

So we may write the final expression for the amino acid flux through the membrane :

$$J = [L^{0}]\left(P^{I}K^{I}_{ext}\,\frac{[C^{+}]^{I}_{w}[A^{-}]^{I}_{w}}{1+K^{I}_{ext}[C^{+}]^{I}_{w}[A^{-}]^{I}_{w}} - P^{II}K^{II}_{ext}\,\frac{[C^{-}]^{II}_{w}[A^{-}]^{II}_{w}}{1+K^{II}_{ext}[C^{-}]^{II}_{w}[A^{-}]^{II}_{w}}\right)$$

REFERENCES

[1] J. M. Lehn, *Pure Appl. Chem.*, **51**, 978 (1979).

[2] J. P. Behr, M. Kirch and J. M. Lehn, *J. Am. Chem. Soc.*, **107**, 241 (1985).

[3] L. Mutihac, T. Constantinescu and C. Luca, *Rev. Roumaine Chim.*, **36**, 2 (1991).

[4] C. J. Pedersen, *J. Inclusion Phenom.*, **6** 337 (1988).

[5] D. J. Cram, *J. Inclusion Phenom.*, **6**, 397 (1988).

[6] T. Kakuchi, T. Takaoka and K. Iokota, *Makromol. Chem.*, **190**, 10, (1989).

[7] G. van Birst, "Design and Synthesis of Organic Molecule Based on Molecular Recognition", Springer, Berlin, 1985.

[8] C. F. Reusch and E. L. Cussler, *AIChE J.*, **19**, 736 (1973).

[9] K. H. Wong, K. Yagi and J. Smid, *J. Membr. Biol.* **18**, 379 (1974).

[10] J. D. Lamb, J. J. Christensen , J. L. Oscarson, B. L. Nielsen and B. W. Asay, *J. Am. Chem, Soc.*, **102**, 6820 (1980).

[11] M. Burgard, L. Jurdy, H. S. Park and R. Heimburger, *Nouv. J. Chim.*, **7**, 578 (1983).

[12] T. M. Fyles, *J. Membr. Sc.*, **24**, 229 (1985).

[13] C. Luca, L. Mutihac and T. Constantinescu, *Rev. Roumaine Chim.*, **35**, 467 (1990).

[14] C. Luca, L. Mutihac and T. Constantinescu, *Rev. Roumaine Chim.*, **34**, 2039 (1989).

[15] R. Wodzki, *Polish J. Chem.*, **63**, 557 (1989).

[16] J. P. Buck, *J. Phys. Chem.*, **91**, 2347 (1987).

[17] M. M. Kreevoy, "Trace Metal Removal from Aqueous Solution", Roy Soc. of Chem, London 1986, p. 103.

[18] E. M. Choy, D. F. Evans and E. L. Cussler, *J. Amer. Chem. Soc.*, **96**, 7085 (1974).

[19] T. M. Fyles, V. A. Malik-Diemer, D. M. Whitfield and C. A. Mc Gavin, *Can. J. Chem.*, **60**, 2259 (1982).

[20] B. G. Cox, J. Garcia Rosas and H. Schneider, *J. Amer. Chem. Soc.*, **103**, 1054 (1981).

[21] P. R. Danesi, R. Chiarizia, M. Pozzuchini and A. Saltelli, *J. Inorg. Nucl. Chem.*, **40**, 1119 (1978).

[22] M. H. Friedman, "Principles and Models of Biological Transport", Springer, Berlin, 1986, p. 70.

Revue Roumaine de Chimie, **36**, *4*–7, 563–566 (1991)

Dedicated to Prof. ALEXANDRU T. BALABAN
on the occasion of his 60th birthday

VILSMEYER-HAACK REACTION OF NITROBENZYLIC SULFONES AND NITRILES

MIECZYSŁAW MAKOSZA and ZBIGNIEW WROBEL
Institute of Organic Chemistry, Polish Academy of Sciences Kasprzaka Street 44,
01-224 Warszawa, Poland

Received February 18, 1991

The Vilsmeyer-Haack reagents produced from dialkylamides and phosphorus oxychloride react, with nitrobenzylic aryl sulfones and nitroarylacetonitriles to give substituted enamines.

The Vilsmeyer-Haack reagents **2** produced by treatment of dialkylamides **1** with phosphorus oxychloride are widely used for formylation of nucleophilic arenes [2] or introduction of dialkylaminomethylene groups into other nucleophiles.[3] There are, however only a few examples reporting the reactions of these and related reagents with carbanions. They are limited to such acidic carbanion precursors as acetylacetates, cyanoacetates and malonates — compounds which can be deprotonated by triethylamine, commonly used as a base in these reactions.[3,4]

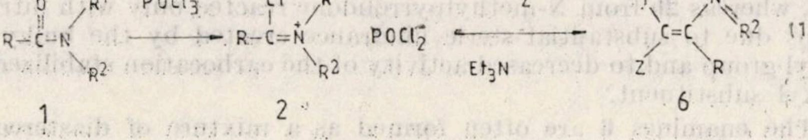

Y, Z = CN, COR, CO$_2$R, (3); O$_2$NAr, p-MeC$_6$H$_4$SO$_2$, (4); O$_2$NAr, CN, (5).

Taking into account the acidity criterion one could expect that nitro benzylic sulfones **4** and nitroarylacetonitriles **5** should also be able to react with **2** according to the same scheme. These compounds are readily available *via* vicarious nucleophilic substitution of hydrogen in nitroarenes in the reaction with carbanion of chloromethyl-tolyl-sulfone, chloroacetonitrile or aryloxyacetonitrile.[5] Because of high acidity of **4** and **5**, the corresponding carbanions are weak nucleophiles, nevertheless they do react with such electrophilic reagents as aldehydes and alkyl halides.[6]

They should therefore react also with such active electrophiles as the Vilsmeyer-Haack reagent **2**. Indeed, sulfone **4a** when treated in DMF-Et_3N solution with $POCl_3$ gave enamine **6a** in an excellent yield. Results of other reactions of **2** with sulfones **4** and nitriles **5** are given in table 1.

Table 1

Enamines **6** obtained from sulfones **4** and nitriles **5**

Entry	Substrate				Product (**6**)				Yield[a] [%]
	Nitroarene Z	Y		Amide		R	R^1	R^2	
1	5-chloro-2-nitrophenyl	Tos	**4a**	DMF	**6a**	Me	Me	H	72–91
2	5-methoxy-2-nitrophenyl	CN	**5a**	DMF	**6b**	Me	Me	H	87
3	5-methoxy-2-nitrophenyl	CN	**5a**	NMP[b]	**6c**	Me	$-(CH_2)_3$		
4	5-fluoro-2-nitrophenyl	CN	**5b**	DMF	**6d**	Me	Me	H	81
5	1-nitro-2-naphthyl	CN	**5c**	DMF	**6e**	Me	Me	H	61
6	1-nitro-2-naphthyl	Tos	**4b**	DMF	**6f**	Me	Me	H	62[c]
7	5-chloro-2-nitrophenyl	Tos	**4a**	NMP[b]	—	—	—	—	—
8	5-methoxy-2-nitrophenyl	Tos	**4c**	DMF	—	—	—	—	—

[a] isolated yields
[b] N-methyl pyrrolidone
[c] 30% of substrate **4b** recovered

For the reaction (eq. 1) to proceed, an excess of triethylamine was necessary. Without it, the enamines were not formed even upon heating of **4a** in DMF with $POCl_3$ up to 60°C.

So far we have found that the reaction is limited to rather highly acidic nitrobenzyl sulfones. For example **4c** containing electrodonating methoxy group in the aromatic ring, which undoubtedly decreases its acidity, does not react with **2** even when more basic tetramethylguanidine, diazabicycloundecane or potassium carbonate were used. Another factor limiting the reaction is connected with the structure of the Vilsmeyer-Haack reagent : that produced from dimethylformamide **2a** was the most active, whereas **2b** from N-methylpyrrolidone reacted only with nitriles **5**, perhaps due to substantial steric hindrance created by the bulky arylsulfonyl group and to decreased activity of the carbocation stabilized with an alkyl substituent.

The enamines **6** are often formed as a mixture of diastereomers. These isomers were not separated, composition of the mixtures was determined by the ^1H-NMR spectroscopy.

EXPERIMENTAL

Melting points are uncorrected, ^1H-NMR spectra were taken in $CDCl_3$ (chemical shifts are given in δ ppm referred to TMS) on Bruker AM–500 (500 MHz) spectrometer. In the cases when the mixtures of diastereomers are described, marks M and N refer to major and minor isomer respectively. Column chromatography was performed using Merck's silica gel 200–400 mesh and $CHCl_3$ or $CHCl_3-CCl_4$ mixtures as solvents.

5-Chloro-2-nitrophenyl 4-tolylsulfone[7](**4a**), 5-methoxy-2-nitrophenyl acetonitrile[8] (**5a**), 5-fluoro-2-nitrophenylacetonitrile[9](**5b**), 1-nitro-2-naphthyl acetonitrile[8](**5c**), (1-nitro-2-naphthyl) methyl 4-tolyl sulfone[10](**4b**), (5-methoxy-2-nitrophenyl)methyl 4-tolylsulfone[10](**4b**), (5-methoxy-2-nitrophenyl)methyl—4-tolyl sulfone[7](**4c**) were prepared according to the previously described procedures. Other reagents were commercial, dried and distilled before use.

General procedure

To a stirred solution of a nitroarene (1 mmol) in amide (4 mL) and triethylamine (1mL ca.10mmol), phosphorus oxychloride (0.25mL,ca.2.5mmol) was added dropwise at −20°C over 5 min. ; the resulted solution was allowed to warm to room temperature and stirred for 10 min. The mixture was poured into ice-cold 5% HCl (100 mL), extracted with methylene chloride(3 × 20 mL) the extracts were combined, dried and the solvent evaporated. The residue was purified *via* column chromatography followed by recrystallisation from ethanol. Ratio of the diastereoisomers was estimated on the basis of the ^{1}H-NMR spectra.

Dimethylaminomethylene (2-nitro-5-chlorophenyl)methyl-4-tolyl sulfone (**6a**) : yellow crystals, m.p. 151—154°C ; one isomer ; ^{1}H-NMR ; 2.38 (s, 3H ; CH_3—Tol) ; 2.80 (s, 6H ; N—CH_3) ; 7.13 (d, $J_{2-3} = 8.1$ Hz, 2H ; H—3 Tol.) ; 7.33 (d, $J_{2-3} = 8.1$ Hz, 2H ; H—2 Tol.) ; 7.38—7.40 (mult., 2H ; H—4 + H—6) ; 7.60 (s, 1H ; H-vinyl) ; 7.68 (d, $J_{3-4} = 8.54$ Hz, 1H ; H—3)
$C_{17}H_{18}N_2O_4SCl$ [381.90] found : C : 53.53 ; H : 4.38 ; N : 7.56 % ; calcd. : C : 53.62 ; H : 4.50 ; N : 7.36 %.

Dimethylaminomethylene(2-nitro-5-methoxyphenyl)acetonitrile (**6b**) orange crystals, 138—141°C ; two isomers : M/N = 5 :1 ; ^{1}H-NMR ; 2.74(N), 3.23(M) (s, s, 6H ; N—CH_3) ; M), 3.88(M), 3.90(N) (s, s, 3H ; OCH_3) ; 6.58 (M), 6.86 (N) (s, s, 1H ; H-vinyl) ; 6.78—6.81 (M), 6.87—6.92 (N) (mult., mult., 2H ; H—3 + H—5) ; 7.91 (M), 8.05 (N) (d, d, $J_{3-4} = 8.9$ Hz, 1H ; H—6)
$C_{12}H_{13}N_3O_3$ [247.28] ; found : C : 58.03 ; H : 5.41 ; N : 16.96 % ; calcd. ; C : 58.29 ; H : 5.30 ; N : 17.00 %.

(1-Methyl-2-pyrrolidylidene) (2-nitro-5-methoxyphenyl) acetonitrile (6c) ; red crystals, mp 89—92°C ; two isomers, M/N = 2 ; 1 ; ^{1}H-NMR : 1.82—1.88(N), 2.00—2.09 (M) (mult. mult., 2H ; N—CH_2CH_2) : 2.34(N), 3.06(M) (t, t, J = 7.7 Hz, 2H ; CH_2-allyl) ; 2.44(M), 3.99(N) (s, s, 3H ; N—CH_3) ; 3.44—3.65(mult.,2H,N—CH_2—) ; 3.88 (N), 3.89(M) (s, s, 3H ; OCH_3) ; 6.86—6.90(mult., 2H ; H—4 + H—6) ; 7.97(N), 8.02 (M) (d, d, $J_{3-4} = 9.0$ Hz, 1H ; H—3)
$C_{15}H_{15}N_3O_3$ [285.33] found : C : 61.59 ; H : 5.46 ; N : 15.22 % ; calcd. : C : 61.53 ; H : 5.53 ; N : 15.38 %.

Dimethylaminomethylene(2-nitro-5-fluorophenyl)acetonitrile (**6d**) : pale green crystals, mp 116—119°C ; two isomers : M/N = 9 : 1 ; ^{1}H-NMR : 2.77(N), 3.25(M) (s.s, 6H ; N—CH_3) ; 6.64(M), 6.90(N) (s.s, 1H ; H-vinyl) ; 6.97—7.01(mult., 1H ; H—6) ; 7.07—7.16 (mult., 1H ; H—4) ; 7.84—7.87(M), 8.02—8.04(N) (mult., mult, 1H ; H—3) $C_{11}H_{10}N_3O_2F$ [235.24] found : C :55.87 ; H : 4.22 ; N : 17.88 % ; calcd. : C : 56.17 ; H : 4.29 ; N : 17.86 %.

Dimethylaminomethylene(1-nitro-2-naphthyl)acetonitrile (**6e**) : orange crystals, mp 180—183°C ; two isomers : M/N = 12.5 : 1 ; ^{1}H-NMR : 2.73 (N), 3.23 (M) (s, s 6H ; N—CH_3) ; 6.73(M), 6.90 (N) (s, s, 1H ; H-vinyl) ; 7.53—7.67 (mult., 4H ; H—3 + H—5 + H—6 + H—7) ; 7.86 — 794 (mult., 2H ; H—4 + H—8)
$C_{15}H_{13}N_3O_2$ [267.31] found : C :67.41 ; H :4.73 ; N :15.68 % ; calcd. :C :67.41 ; H : 4.90 ; N : 15.72 %.

Dimethylaminomethylene(1-nitro-2-naphthyl)methyl 4-tolyl sulfone(**6f**) : pale yellow crystals, mp 188—192°C ; one isomer ; ^{1}H-NMR : 2.36 (s, 3H ; CH_3—Tol) ; 2.75 (broad s, 6H ; N—CH_3) ; 7.12(dq, $J_{2-3}=8.1$ Hz, $J_{3-5} = 1.6$ Hz, 2H ; H—3 Tol) ; 7.41 (dt ; $J_{2-3} = 8.1$ Hz, 2H ; H—2 Tol) ; 7.56—7.61 (mult., 4H ; H—3 + H—5 + H — 6 + H—7) ; 7.63 (s, 1H ; H-vinyl) ; 7.86—7.90 (mult., 2H ; H—4 + H—8)
$C_{21}H_{21}N_2O_4S$ [397.51] found : C : 63.61 ; H : 4.97 ; N : 7.08 % ; calcd. : C : 63.78 ; H : 4.84 ; N : 7.08 %.

REFERENCES

[1] "Reactions of Organic Anions", 179, Part 178 see ; M. Makosza, W. Lasek, *Tetrahedron* (in press).

[2] G. Simchen "Methoden der Organische Chemie" Houben-Weil, Band E3 : Aldehyde pp. 36—86, Georg Thieme Verlag, Stuttgart-New York, 1983.

[3] B. C. Challis and J. A. Challis, "Comprehensive Organic Chemistry", (Ed. by I. O. Sutherland) vol. 2, p. 1023, Pergamon Press, 1979.

[4] H. G. Viehe and Z. Janousek, *Angew. Chem.*, **85**, 837 (1973).

[6] M. Makosza and J. Winiarski, *Acc. Chem. Res.*, **20**, 282 (1987).

[7] M. Makosza and J. Baran, *J. Org. Chem.*, **49**, 1488 (1984).

[8] M. Makosza and J. Winiarski, *J. Org. Chem.* **49**, 1494 (1884).

[9] M. Makosza, M. Wenall, M. Golinski and A. Kinowski, *Bull. Pol. Acad. Sci.* **33**, 427 (1985).

[10] M. Makosza, W. Danikiewicz and K. Wojciechowski, *Liebigs Ann. Chem.*, **1987**, 711.

Revue Roumaine de Chimie, **36**, *4–7*, 567–571 (1991)

Dedicated to Professor ALEXANDRU T. BALABAN
on the occasion of his 60th birthday

OXYFUNCTIONALIZATION OF HYDROCARBONS. 16

ELECTROPHILIC HYDROXYLATION AND OXYGENATION OF HYDROCARBONS WITH SODIUM PERCARBONATE/TRIFLUOROMETHANESULFONIC ACID [1]

GEORGE A. OLAH,* QI WANG, NORBERT KRASS and G. K. SURYA PRAKASH *
Donald P. and Katherine E. Loker Hydrocarbon Research Institute and the Department of Chemistry, University of Southern California, Los Angeles, California 90089-1661, USA

Received January 23, 1991

Sodium percabonate in conjunction with trifluoromethanesulfonic acid has been used as a reagent for the electrophilic hydroxylation of benzene and toluene to their corresponding monohydroxylated compounds. The electrophilic oxygenation of adamantane gave excellent yield of 4-oxahomoadamantane. Related studies with substituted adamantanes as well as other alkanes are also reported.

INTRODUCTION

Acid promoted electrophilic hydroxylation is a convenient method for the preparation of hydroxyaromatics. Various reagent systems, such as peracids in the presence of boron trifluoride,[2] alkyl hydroperoxide-aluminum chloride [3] and diisopropyl peroxydicarbonate-aluminum chloride [4] have been used with electron rich aromatics and the corresponding hydroxy-derivatives were obtained in moderate yields. Hydrogen peroxide in the presence of aluminum trichloride,[5] boron trifluoride etherate,[6] concentrated sulfuric acid [7] and anhydrous HF[8] have also been used for the electrophilic hydroxylation of aromatics. These reactions can be generalized by the following scheme :

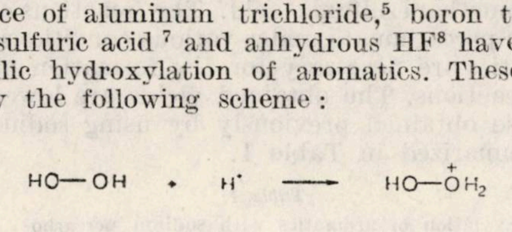

In the first step, an incipient hydroxyl cation (i.e. protonated or complexed hydrogen peroxide) is generated by reacting peroxides with protic or Lewis acids. It then reacts with aromatics to produce phenolic products. Secondary reactions of the hydroxylated products, however, frequently cause problems.

In 1978 Olah *et al.*[9] reported results of hydroxylation of aromatic compounds with 90% hydrogen peroxide in superacidic media, such as FSO_3H and $FSO_3H : SbF_5$. Phenols formed in these systems are protonated by the superacid and are thus deactivated against secondary reactions, resulting in preparatively acceptable yields of 50% or higher of monohydroxylated products. Two years later Olah [10] found that even 30% aqueous hydrogen peroxide was a suitable reagent for the hydroxylation of alkylbenzenes in pyridinium polyhydrogen fluoride solution. Subsequently, Olah and coworkers [11] found the use of aqueous hydrogen peroxide with hydrogen fluoride/boron trifluoride to be advantageous, because HF/BF_3 is inexpensive and recoverable. In search for an alternative of hydrogen peroxide, Olah and Ernst recently reported the use of bis-(trimethylsilyl)peroxide/trifluoromethanesulfonic acid as a convenient reagent for the laboratory electrophilic hydroxylation of aromatics[12a] as well as oxygenation of some polycyclic cage hydrocarbons.[12b] The yields of hydroxylation of aromatics with bis(trimethylsilyl)peroxide are generally good. However, the preparation of bis(trimethylsilyl)peroxide is tedious.[13] The 1,4-diazabicyclo[2.2.2]octane (DABCO) used to form adduct with hydrogen peroxide is relatively expensive. The purification of bis(trimethylsilyl)peroxide by distillation can also be potentially dangerous. It is desirable to find additional relatively inexpensive oxidants which are suitable for hydroxylation of aromatics. We recently reported results of the hydroxylation of aromatics with sodium perborate/trifluoromethanesulfonic acid.[14] In extension of these studies, we now report the use of sodium percarbonate/trifluoromethanesulfonic acid in the hydroxylation and oxygenation of hydrocarbons.

RESULTS AND DISCUSSION

Sodium percarbonate ($2Na_2CO_3 \cdot 3H_2O_2$) is an inexpensive industrial chemical. It has been widely used as bleaching agent in detergents. We considered it of interest to study whether sodium percarbonate ($2Na_2CO_3 \cdot 3\,H_2O_2$) can be used for hydroxylation of aromatics in the presence of superacidic trifluoromethanesulfonic acid. The reactions of toluene and benzene with sodium percarbonate under various conditions were investigated. Excess aromatics are necessary for the formation of hydroxylated products in those reactions. The obtained yields are lower (32%–38%) compared with those obtained previously by using sodium perborate.[14] The results are summarized in Table 1.

Table 1

Hydroxylation of aromatics with sodium percarbonate/trifluoromethanesulfonic acid

substrate	R×n temp (°C)	R×n time (h)	yield (%)
benzene	r.t.	8	12
benzene	0	8	32
benzene	−10	8	18
toluene	−10	8	36[a]

[a] isomer distribution was determined by GC. *ortho* : *meta* : *para* = 63 : 11 : 26

In connection with our studies, we also attempted to use sodium percarbonate to oxygenate alkanes. Electrophilic hydroxylation of alkanes was achieved previously by using various oxidants under superacidic conditions by Olah and his coworkers.[15] For example, even methane was converted to methanol in presence of H_2O_2 and superacids.[16] More recently, Olah *et al.*[12b] have oxidized the adamantane to 4-oxahomoadamantane **1** with bis(trimethylsilyl)peroxide/trifluoromethanesulfonic acid with major product being 4-oxahomoadamantane. The mechanism of 4-oxahomoadamantane formation was proposed to be the following: [12b]

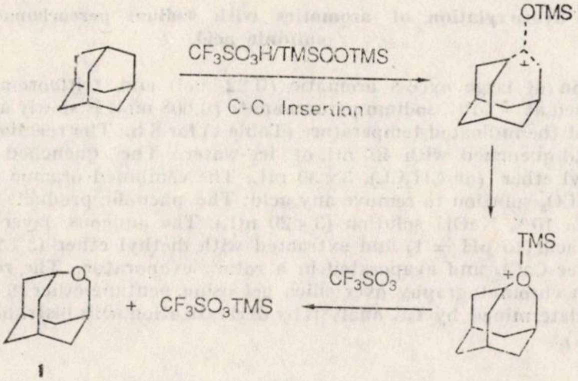

1

In our present study, the related reaction of adamantane with sodium percarbonate/trifluoromethanesulfonic acid was investigated. Sodium percarbonate was added in small portions to a mixture of trifluoromethanesulfonic acid and adamantane in methylene chloride solution. Upon workup, 4-oxahomoadamantane **1** was obtained in 84% isolated yield with no 1-adamantanol detected. When 1,3-dimethyladamantane was similarly reacted, two products were obtained in a total yield of 18%. The ratio between the two compounds is about 1 : 1. Based on the GC-MS and NMR studies, the mixture is indicated to be composed of isomeric dimethyloxahomoadamantanes **2** and **3**.

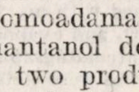

2

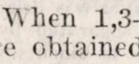

3

No reaction has been observed for 1,3,5-trimethyladamantane and the starting material was recovered unchanged. According to the proposed mechanism,[12b] the result seems reasonable as the methyl groups sterically hinder the insertion of oxygen into the carbon-carbon bonds.

The reaction of cyclohexane, methylcyclohexane and cyclododecane was also attempted under similar conditions, but no reaction was observed for these substrates. This is in accordance with the lower reactivity of the carbon-carbon bonds in these substrates.

EXPERIMENTAL SECTION

Adamantane, 1,3-dimethyladamantane, cyclohexane, methylcyclohexane, cyclododecane and the aromatic compounds were purchased from Aldrich. Trifluoromethanesulfonic acid was obtained from 3M company. Sodium percarbonate was bought from Burlington Chemical. 1,3,5-Trimethyladamantane was prepared from 1-bromo-3,5,7-trimethyladamantane (Aldrich) with a similar procedure used to prepare triphenylmethane from triphenylmethyl bromide.[17]

NMR spectra were obtained on a Varian Associates Model VXR-200 NMR spectrometer. Mass spectra were obtained in a Finnigan Incos-50 GC-MS instrument. Gas chromatographic analyses were performed on a Varian (model 3700) gas chromatograph using a quartz column coated with DB-1.

General method of hydroxylation of aromatics with sodium percarbonate/trifluoromethanesulfonic acid

To a solution of large excess aromatic (0.22 mol) and trifluoromethanesulfonic acid (0.11 mol) maintained at $-10°C$, sodium percarbonate (0.008 mol) is slowly added over a period of 2 h and stirred at the indicated temperature (Table 1) for 8 h. The reaction mixture was then cooled to $-78°C$ and quenched with 40 mL of ice-water. The quenched mixture was extracted with diethyl ether (or CH_2Cl_2), 3×30 mL. The combined organic extract was washed with aq. 10% $NaHCO_3$ solution to remove any acid. The phenolic products in the organic layer were extracted into 10% NaOH solution (3×20 mL). The aqueous layer was acidified with 30% hydrochloric acid (to pH = 1) and extracted with diethyl ether (3×20 mL). The ether layer was dried over $CaCl_2$ and evaporated in a rotary evaporator. The residue was further purified by column chromatography over silica gel using pentane/ether (9 : 1) as eluent. Isomeric ratios were determined by GC analysis by derivatization with bistrimethylsilyl trifluoroacetamide (BSTFA).

General procedure of oxygenation of alkanes with sodium percarbonate :

To a solution of alkane (8 mmol) and trifluoromethane-sulfonic acid (0.11 mol) in CH_2Cl_2 maintained at $-10°C$, sodium percarbonate (8 mmol) is added in portion over a period of 2 h and stirred at the same temperature for another 6 hours. The reaction mixture was then quenched with ice water. The quenched mixture was extracted with diethyl ether (or CH_2Cl_2), 3×30 mL. The combined organic extract was washed with aq. 10% $NaHCO_3$ solution to remove any acid. The ether layer was dried over $MgSO_4$ and evaporated in a rotary evaporator. The reaction mixture was separated by column chromatography over silica gel using pentane/ether (1 : 1) in sequence as eluents. Isomeric ratios were determined by GC.

4-Oxahomoadamantane :

MS : 152 (37.66) ; 134 (6.68) ; 122 (18.42) ; 107 (9.92) ; 93 (33.53) ; 79 (100).
$^{13}C(\delta)$: 74.2 ; 72.0 ; 37.6 ; 36.8 ; 35.2 ; 34.1 ; 26.5.

Isomeric Ethers obtained from 1,3-dimethyl-adamantane :

The mixture is a viscous liquid.

MS : 180 (36.56) ; 165 (13.15) ; 149 (15.17) ; 135 (7.50) ; 121 (28.76) ; 107 (100) ; 93 (81.80) ; 79 (48.14).

180 (15.74) ; 148 (21.61) ; 135 (4.47) ; 121 (4.41) ; 107 (100 ;) 93 (41.14) ; 79 (32.15).

$^{13}C(\delta)$: 79.4 ; 74.3 ; 72.0 ; 71.7 ; 52.0 ; 50.1 ; 44.4 ; 44.1 ; 43.8 ; 43.5 ; 42.6 ; 37.2 ; 36.1 ; 34.3 ; 31.8 ; 31.4 ; 30.7 ; 29.5 ; 29.3 ; 28.4.

ACKNOWLEDGEMENT : Support of our work by the National Science Foundation is gratefully acknowledged.

REFERENCES

[1] For Part 15, see : G. K. S. Prakash, N. Krass, Q. Wang and G. A. Olah, *Synlett.*, in press

[2] a) A. J. Davidson and R. O. C. Norman, *J. Chem. Soc.*, **1964**, 5404 ; b) H. Hart and C. A. Buehler, *J. Org. Chem.*, **19**, 2397 (1964).

[3] S. Hashimoto and W. Koike, *Bull. Chem. Soc. Jpn.*, **43**, 293 (1970).

[4] P. Kovacic and M. E. Kurz, *J. Amer. Chem. Soc.*, **87**, 4811 (1965).
[5] M. E. Kurz and G. J. Johnson, *J. Org. Chem.*, **36**, 3194 (1971).
[6] J. D. McClure and P. H. Williams, *J. Org. Chem.*, **27**, 627 (1962).
[7] D. H. Gerbyshire and W. A. Waters, *Nature*, **165**, 401 (1950).
[8] J. A. Vesely and L. Schmerling, *J. Org. Chem.*, **35**, 4028 (1970).
[9] G. A. Olah and R. Ohnishi, *J. Org. Chem.*, **43**, 865 (1978).
[10] G. A. Olah, T. Keumi and A. P. Fung, *Synthesis*, **1979**, 536.
[11] G. A. Olah, A. P. Fung and T. Keumi, *J. Org. Chem.*, **46**, 4305 (1981).
[12] a) G. A. Olah and T. D. Ernst, *J. Org. Chem.*, **54**, 1204 (1989) ; b) G. A. Olah, C. B. Rao and G. K. S. Prakash, *New J. Chem.*, **13**, 791 (1989).
[13] M. Taddei and A. Ricci, *Synthesis*, **1986**, 633.
[14] G. K. S. Prakash, N. Krass, Q. Wang and G. A. Olah, *Syntett.*, in press.
[15] Olah G. A., D. G. Parker and N. Yoneda, *Angew. Chem. Int. Ed. Engl.*, **17**, 909 (1978).
[16] G. A. Olah, D. G. Parker, N. Yoneda and F. Pelizza, *J. Amer. Chem., Soc.*, **98**, 2245 (1976).
[17] J. Y Corey and R. West, *J. Amer. Chem. Soc.*, **85**, 2430 (1963).

Revue Roumaine de Chimie, 36, 4–7, 573–580 (1991)

1-CYANOBENZOTRIAZOLE: A SAFE AND CONVENIENT SOURCE OF $^{+}$CN[a]

ALAN R. KATRITZKY, * JACEK Z. BRZEZINSKI[b] and JAMSHED N. LAM
Department of Chemistry, University of Florida,
Gainesville, FL 32611-2046. USA

Received January 17, 1991

Readily available 1-cyanobenzotriazole is a convenient reagent for the conversion of secondary amines into the corresponding cyanamides. Exploratory work with primary amines and with mercaptans is also reported.

INTRODUCTION

Most preparations of cyanamides have used cyanogen chloride (**2a**) (a toxic gas, m.p. – 6.5°C, b.p. 13°C,[1] and not readily available), or cyanogen bromide (**2b**) (a volatile toxic solid m.p. 52°C, b.p. 61.6°C[1]) in reactions with primary and secondary amines [2–5] (Scheme 1). The calcium and disodium salts of cyanamide **3** have been treated with alkyl, allyl and benzyl halides to afford the symmetrical N,N-disubstituted cyanamides **5** in moderate yields.[4,6,7] Cyanamides **5** have also been prepared from unsymmetrical N,N-disubstituted ureas or thioureas **4** *via* elimination of water or hydrogen sulfide.[4,8–10] Tertiary amines react with cyanogen bromide in the von Braun reaction to give disubstituted cyanamides, but side reactions often lead to complex mixtures.[11] Isothioureas **7** prepared from thiocyanates and secondary amines eliminate thiols in the presence of zinc, mercury and cadmium oxides [12] to give cyanamides in moderate yields. Monosubstituted cyanamides **5** (R^2=H) can be prepared by the elimination of methyl mercaptan (in the presence of potassium hydroxide) from isothioureas **7** (R=Me).[4,13]

---

[a] This paper is dedicated with admiration and affection to Academician A.T. (Sandy) BALABAN on his sixtieth birthday – for thirty years a friend and an example who's humanity and brilliance has overcome so many obstacles – A.R.K.

[b] Permanent address: Department of Organic Chemistry, Institute of Chemistry, University of Lodz, 90-136 Lodz, Poland.

orrespondence author.

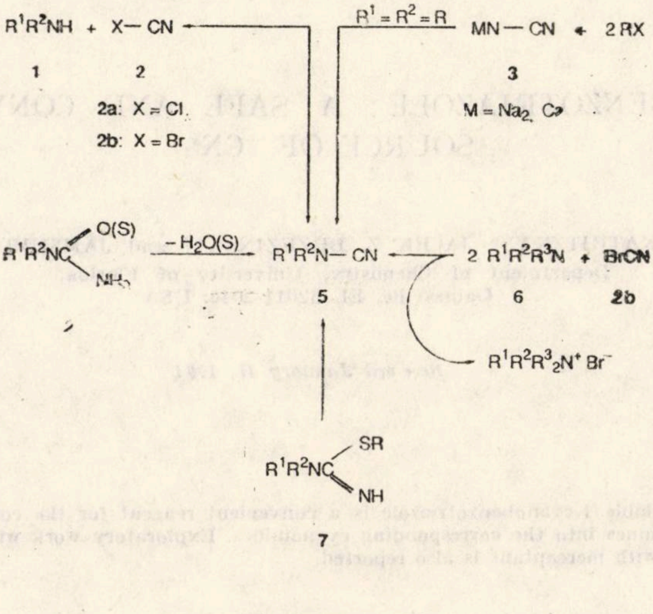
R¹R²NH + X— CN
1
2
2a: X = Cl
2b: X = Br
R¹ = R² = R
MN — CN + 2 RX
3
M = Na₂, Ca
R¹R²NC O(S) NH₂
– H₂O(S)
R¹R²N— CN
5
2 R¹R²R³N + BrCN
6
2b
R¹R²R³₂N⁺ Br⁻
R¹R²NC SR NH
7

Scheme 1

We now wish to report that 1-cyanobenzotriazole is a safe and stable source of "positive cyanogen", and can be used in place of the toxic cyanogen halides in several applications.

RESULTS

Preparation of 1-Cyanobenzotriazole

Two literature preparations[14,15] of 1-cyanobenzotriazole (**9**) both inconveniently used cyanogen chloride. Our attempted cyanation of benzotriazole with trichloroacetonitrile[16,17] failed. While a modified procedure of Whitten *et al.*,[18] gave 1-cyanobenzotriazole (**9**) in 76% yield from benzotriazole and 1-cyano-4-dimethylaminopyridinium bromide (**8**) (Scheme 2), considerably more convenient is our finding that cyanogen bromide and the sodium salt of benzotriazole under carefully controlled conditions (*vida infra*) affords **9** in over 90% yield : bis(bezotriazol-1-yl) methylimine (**10**) is formed as a minor byproduct in 3% yield. Cyanogen bromide usually behaves as a brominating agent[19–21] and only exceptionally as a cyanating agent.[11]

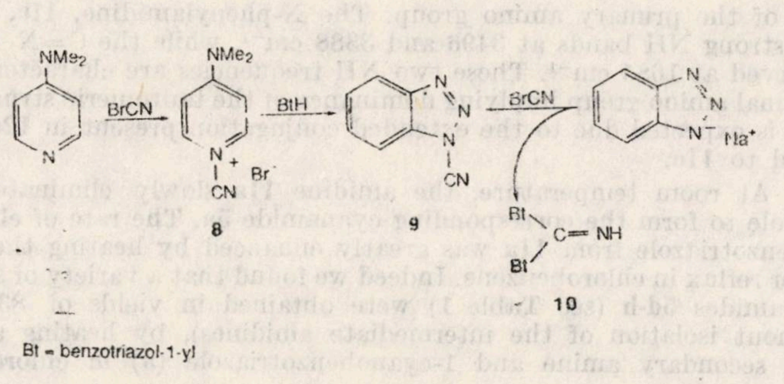
NMe₂
BrCN
NMe₂
Br⁻
CN
8
BtH
N
N
N
CN
9
BrCN
N
N
N⁻ Na⁺
Bt
C= NH
Bt
10
Bt = benzotriazol-1-yl

Scheme 2

Preparation of Cyanamides

Treatment of 1-cyanobenzotriazole (**9**) with amines in methylene chloride leads to additions across the triple bond, forming the amidines **11a-c** in high yields (Scheme 3). The dioctylamidine **11a** displayed the imino absorption at 1642 cm^{-1} and a single NH band at 3339 cm^{-1} in the IR spectrum. The literature [22] indicates that N-monosubstituted amidines exist (in chloroform and bromoform solutions) in two tautomeric forms **11** and **12** (Scheme 3). In agreement, the monooctylamidine **11b** displayed three signals for the N-H bond at 3462, 3407 and 3341 cm^{-1} and two bands for the C=N bond at 1690 and 1655 cm^{-1} in the IR spectrum. For N-alkylamidines the imino form **11** is known to be the predominant tautomer as evidenced by the weak asymmetric stretching vibra-

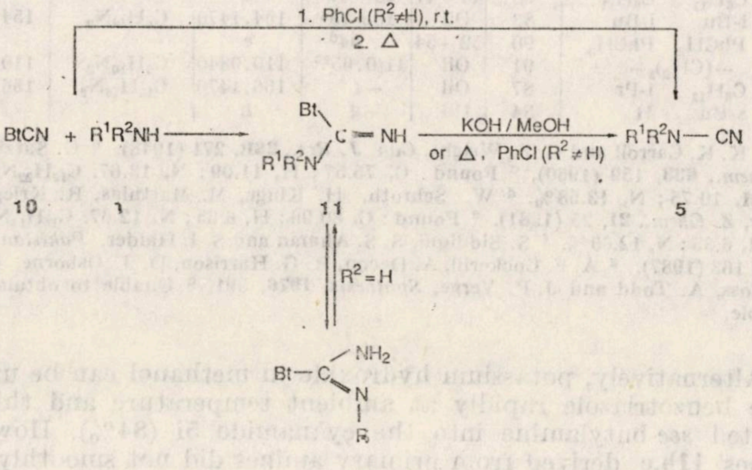
1. PhCl (R²≠H), r.t.
2. Δ
BtCN + R¹R²NH
Bt
C= NH
R¹R²N
KOH / MeOH
or Δ , PhCl (R² ≠ H)
R¹R²N— CN
10
1
11
5
R² = H
NH₂
Bt—C
N
R
12

Scheme 3

tion of the primary amino group. The N-phenylamidine, **11c**, displayed two strong NH bands at 3496 and 3388 cm^{-1}, while the C=N band was observed at 1685 cm^{-1}. These two NH frequencies are characteristic of a terminal amino group implying dominance of the tautomeric structure **12c**. This is expected due to the extended conjugation present in **12c** as compared to **11c**.

At room temperature, the amidine **11a** slowly eliminated benzotriazole to form the corresponding cyanamide **5a**. The rate of elimination of benzotriazole from **11a** was greatly enhanced by heating the amidine under reflux in chlorobenzene. Indeed we found that a variety of secondary cyanamides **5d-h** (see Table 1) were obtained in yields of 83 to 96% (without isolation of the intermediate amidines), by heating a mixture of a secondary amine and 1-cyanobenzotriazole (**9**) in chlorobenzene.

Table 1

Physical data of prepared Cyanamides R^1R^2NCN 5

Cpd. No.	Substituent		Yield (%)	MP(°C)/ BP(°C/mmHg)	Lit. MP(°C)/ BP(°C/mmHg)	HRMS			IR $\nu C\equiv N$ (cm^{-1})
	R^1	R^2				Calcd.	Mol. Formula	Found	
5a	C_8H_{17}	C_8H_{17}	96	Oil	162/0.5[a]	266.2722	$C_{17}H_{34}N_2$	266.2717	2207
5d	C_6H_{11}	C_6H_{11}	90	44−47	45−47[b]	c			2197
5e	i-Bu	i-Bu	83	Oil	109/15[d]	154.1470	$C_9H_{18}N_2$	154.1471	2207
5f	$PhCH_2$	$PhCH_2$	90	52−54	54[d]	e			2209
5g	$-(CH_2)_5-$		91	Oil	41/0.65[23]	110.0840	$C_6H_{10}N_2$	110.0770	2210
5h	C_6H_{11}	i-Pr	87	Oil	−f	166.1470	$C_{10}H_{18}N_2$	166.1482	2198
5i	s-Bu	H	84	Oil	−g	h			2215

[a] K. K. Carroll and G. F. Wright, *Can. J. Res.*, **26B**, 271 (1948). [b] G. Satzinger, *Liebigs Ann. Chem.*, **638**, 159 (1960), [c] Found: C, 75.57; H, 11.09; N, 13.67. $C_{13}H_{22}N_2$ requires C, 75.68; H, 10.75; N, 13.58%. [d] W. Schroth, H. Kluge, M. Matthias, R. Krieg and H.-D. Schadler, *Z. Chem.*, **21**, 25 (1981). [e] Found: C, 80.96; H, 6.35; N, 12.67. $C_{15}H_{14}N_2$ requires C, 81.05; H, 6.35; N, 12.60%. [f] S. Siddiqui, S. S. Ahman and S. I. Haider, *Pakistan J. Sci. Ind. Res.*, **30**, 163 (1987). [g] A. F. Cockerill, A. Decon, R. G. Harrison, D. J. Osborne, D. M. Prime, W. J. Ross, A. Todd and J. P. Verge, *Synthesis*, **1976**, 591. [h] Unable to obtain. Compound not stable.

Alternatively, potassium hydroxide in methanol can be used to eliminate benzotriazole rapidly at ambient temperature and this method converted *sec*-butylamine into the cyanamide **5i** (84%). However, the amidines **11b,c** derived from primary amines did not smoothly eliminate benzotriazole.

The only extensive spectroscopic data for cyanamides present in the literature deals with their IR spectra. Each of the cyanamides **5a**, and **5d-i** showed a sharp absorption band in the IR spectrum in the region between 2197 and 2215 cm^{-1} (Table 1). This is in contrast to 1-cyanobenzotriazole (8) which displayed the corresponding signal at 2254 cm^{-1}. The large shift is attributed to the electron withdrawing nature of benzotriazole.

With few exceptions.[23,24] there is no mention of any NMR study of cyanamides. Proton chemical shifts are recorded in Table 2. The nitrile group shifts the α-CH_2 groups downfield by 0.3−0.5 ppm compared to the parent amines.

Table 2

^{1}H-NMR Chemical Shifts (ppm) for cyanamides **5a**, **d-i** (in $CDCl_3$)

Cyanamides	R^1R^2N-		
	α-H	β-H	Others
5a	2.97(t, 4H, J 7.3 Hz)	1.56−1.71 (m, 4H)	1.19−1.43 (m, 20H) 0.88 (t, 6H, J 6.7 Hz)
5d	2.69−2.85 (m, 2H)	1.74−1.99 (m, 8H)	1.55−1.68 (m, 2H) 1.36−1.55 (m, 4H) 1.05−1.36 (m, 6H)
5e	2.80(d, 4H, J 7.4 Hz)	1.88−2.06 (m, 2H)	0.98 (d, 12H, J 6.7 Hz)
5f	4.08 (s, 4H)	—	7.32−7.42 (m, 6H) 7.24−7.32 (m, 4H)
5g	3.10−3.25 (m, 4H)	a	1.49−1.72 (m, 6H)
5h	3.23(sept, 1H, J 6.6Hz) 2.71−2.83 (m, 1H)	1.88−1.99(m, 2H) 1.76−1.88 (m, 2H) 1.26 (d,6H,J 6.6 Hz)	1.57−1.68 (m, 1H) 1.37−1.53 (m, 2H) 1.10−1.37 (m, 3H)
5i	3.16 (sext, 1H,J 6.5 Hz)	1.41−1.68 (m, 2H) 1.23 (d,3H,J 6.5Hz)	4.50 (brs, 1H) 0.96(t,3H,J 7.4 Hz)

[a] Obscured by other signals.

Table 3

^{13}C-NMR Chemical Shifts (ppm) for cyanamides **5a**,**d-i** (in $CDCl_3$).

Cyanamides	C≡N	R^1R^2N-				
		α-C	β-C	χ-C	Other	ω-C
5a	117.8	51.4	31.6	26.4	29.1, 29.0 27.6, 22.5	14.0
5d	115.4	57.9	31.7	25.1	—	25.0
5e	118.2	59.5	27.2	19.7	—	—
5f	118.1	54.1	134.2	128.5	128.7	128.4
5g	118.3	49.9	24.3	22.7	—	—
5h	114.9	57.9, 50.6	31.6, 21.2	25.0	—	24.9
5i	115.8	53.2	29.2, 19.8	9.9	—	—

Carbon chemical shifts are assigned in Table 3. For the cyanamides **5a**, and **5d-i**, the nitrile resonances were observed downfield between 114.9 and 118.3 ppm in the ^{13}C-NMR spectra as compared to 1-cyanobenzotriazole where the nitrile resonance appeared at 103.3 ppm. Similarly, the electron withdrawing ability of the nitrile group causes the N-C_α carbon to resonate 1−9 ppm downfield and the N−C_β carbon to resonate 1−6 ppm upfield as compared to the parent amine.

Reaction of 1-cyanobenzotriazole with mercaptans

Thiophenol reacts with 1-cyanobenzotriazole at 20°C to afford the imine **13** (Scheme 4). Treatment of **13** with *n*-butyllithium (in an attempt to eliminate benzotriazole) led to a nucleophilic displacement of the benzotriazole anion by the butyl anion to afford **14** in 85% yield.

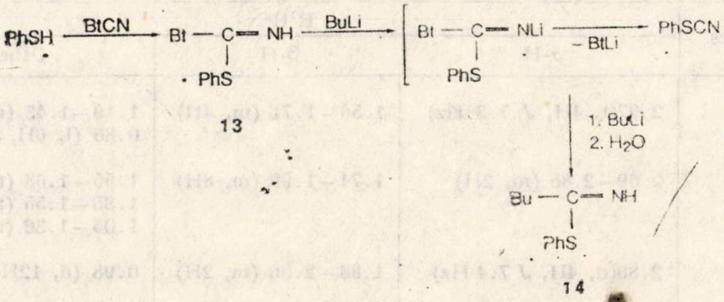

Scheme 4

This suggests that 1-cyanobenzotriazole could be used for the general synthesis of imino thioesters of type **14**.

EXPERIMENTAL

Melting points were determined on a bristoline hot-stage microscope and are uncorrected. ^{1}H-(300 MHz) NMR spectra were recorded on a Varian VXR-300 (FT mode) spectrometer with Me_4Si as internal standard. ^{13}C-NMR spectra were recorded at 75 MHz on the same instrument using solvent peaks ($CDCl_3$, δ 77.0 or DMSO-d_6, δ 39.5) as references. IR spectra were run on a Perkin-Elmer 1600 FTIR spectrometer. High Resolution Mass Spectromery was carried out on a Finnigan Mat 95. Elemental analyses (C,H,N) were carried out using a Carlo Erba 1106 elemental analyzer. Flash chromatography was run on EM Science silica gel 60 (230–400 mesh).

1-Cyanobenzotriazole (9). Method A : Cyanogen bromide (2.12 g, 20 mmol) was added to a solution of 4-dimethylaminopyridine (2.44 g, 20 mmol) in DMF (40 mL) at 10°C. The temperature of the reaction mixture increased to 20°C and a pale yellow precipitate (1-cyano-4-dimethylaminopyridinium bromide 8) was observed. The reaction was then cooled back to 10 °C, benzotriazole (1.19 g, 10 mmol) added and the mixture stirred at 35–40°C for 6 h. The DMF was removed under reduced pressure and the resulting solid triturated with benzene (30 mL). The insoluble material was filtered off and the solid washed with benzene. The benzene was evaporated off and the resulting solid sublimed (70–75°C/3 mm Hg) to afford 1.10 g (76%) of **9** as colorless needles, m.p. 73–76°C, lit.[14] m.p. 73–75°C.

^{1}H-NMR spectrum (*$CDCl_3$*, δ ppm) : 8.23 (dd, 1H, $J = 8.4$ and 0.9 Hz), 7.9–7.8 (m, 2H), 7.64. (ddd, 1H, $J = 8.3$, 6.4, and 1.9 Hz).

^{13}C-NMR spectrum (*$CDCl_3$*, δ ppm) : 143.3, 132.6, 131.6, 126.8, 121.4, 109.5, 103.7.

Method B : A solution of cyanogen bromide (**2b**) (2.22 g, 21 mmol) in tetrahydrofuran (10 mL) was added rapidly to a vigorously stirred solution (cooled to 10–12°C) of sodium benzotriazolate (2.82 g, 20 mmol) in dry tetrahydrofuran (50 mL). After addition was complete, the reaction mixture was allowed to reach ambient temperature and then stirred for an additional 1 h. The precipitate obtained was filtered off and washed with tetrahydrofuran. Evaporation of the tetrahydrofuran from the filtrate afforded a solid which was sublimed to afford 2.64 g (92%) of **9** as colorless crystals, m.p. 74–76°C identical in all respects to that prepared above. The residue from the sublimation was recrystallized from benzene to afford 0.15 g (3%) of bis (benzotriazol-1-yl)methylimine (**10**) as colorless needles, m.p. 167—170°C. Found: M^+ 263.0907; $C_{13}H_9N_7$ requires 263.0919.

^{1}*H-NMR spectrum* (*DMSO-d*$_6$, δ ppm): 11.79 (s, 1H), 8.45—8.3 (m, 3H), 7.88 (t, 1H, J = 7.6 Hz), 7.75—7.55 (m, 3H), 7.52 (d, 1H, J = 8.2 Hz).

^{13}*C-NMR spectrum*(*DMSO-d*$_6$, δ ppm): 145.87, 144.6, 140.7, 132.0, 131.7, 130,4, 129.6, 126.4, 125.6, 120.1, 119.8, 114.1, 111.9.

General Procedure for the Synthesis of 1-Amidinobenzotriazoles 11a-c. To a stirred solution of 1-cyanobenzotriazole (**9**) (0.29 g, 2 mmol) in methylene chloride (6 mL), the appropriate amine (2 mmol) was added. Stirring was continued for 0.5 h and the solvent was removed under reduced pressure at room temperature. The amidines **11a-c** were thus prepared:

1-(N^1, N^1-Dioctylamidino)benzotriazole (11a). The crude liquid was purified by column chromatography (methylene chloride/acetone, 97 : 3) to give 0.67 g (87%) of **11a** as a colorless liquid. Found: M^+ 385.3212; $C_{23}H_{39}N_5$ requires M^+ 385.3206.

^{1}*H-NMR spectrum* (*CDCl*$_3$, δ ppm): 8.11 (d, 1H, J = 8.4 Hz), 7.70 (d, 1H, J = 8.4 Hz), 7.6—7.5 (m, 1H), 7.5—7.4 (m, 1H), 6.60 (bs, 1H), 3.29 (t, 4H, J = 7.5 Hz), 1.75—1.5 (m, 4H), 1.4—1.0 (m, 20H), 0.86 (t, 6H, J = 6.7 Hz).

^{13}*C-NMR spectrum* (*CDCl*$_3$, δ ppm): 151.3, 145.4, 132.1, 128.8, 124.7, 120.1, 111.0, 48.9, 31.6, 29.1, 29.0, 27.6, 26.7, 22.5, 14.0.

1-(N^1-Octylamidino)benzotriazole (11b). The crude liquid was purified by column chromatography (methylene chloride/acetone, 97 : 3) to give 0.53 g (96%) of **11b** as a colorless oil which slowly solidified, m.p. 36—41°C. Found: M^+273.1936. $C_{15}H_{23}N_5$ requires M^+273.1953.

^{1}*H-NMR spectrum* (*CDCl*$_3$, δ ppm): 8.48 (d, 1H, J = 7.8 Hz), 8.0 (d, 1H, J = 8.3 Hz), 7.57 (t, 2H, J = 7.6 Hz), 7.42 (t, 2H, J = 7.7 Hz), 6.72 (br s, 0.67 H, N-*H*) 6.25, (br. s, 0.63H, *H*), 5.64 (br s, 0.7 H, *H*), 3.18 (m, 2H), 1.85—1.6 (m, 2H), 1.6—1.2 m, 10H), 0.88 (m, 3H).

^{13}*C-NMR spectrum* (*CDCl*$_3$, δ ppm): (Mixture of tautomers): 15.00, 146.5, 143.8, 131.3, 129.1, 124.8, 115.3, 46.9, 46.1, 41.1, 31.7, 29.1, 29.09, 29.0, 28.8,26.9, 22.5, 14.0.

1-(N^1-Phenylamidino)benzotriazole (11c). The crude solid was crystallized from methylene chloride/pentane to give 0.66 g (93%) of **11c** as colorless needles, m.p. 133.5—135.5°C. Found: C, 65.44; H, 4.60; N, 29.84. $C_{13}H_{11}N_5$ requires C, 65.81; H, 4.67; N, 29.52.

^{1}*H-NMR spectrum* (*CDCl*$_3$, δ ppm): 8.53 (d, 1H, J = 8.4 Hz), 8.09 (d, 1H, J = 8.4 Hz), 7.65—7.52 (m, 1H), 7.51—7.3 (m, 3H), 7.2—7.0 (m, 3H), 5.0 (bs, 2 H).

^{13}*C-NMR spectrum* (*CDCl*$_3$, δ ppm): 146.6, 146.58, 143.9, 131.2, 129.6, 129.3, 125.2, 123.8, 121.7, 119.7, 115.3.

General Procedure for the Direct Synthesis of Cyanamides 5 from 1-Cyanobenzotriazole. To a stirred solution of 1-cyanobenzotriazole (**9**) (0.72 g, 5 mmol) in dry chlorobenzene (15 mL) in a flask equipped with a calcium chloride drying tube, was added the appropriate amine (5 mmol). The mixture was stirred at ambient temperature for 0.5 h and then the reaction mixture was heated under reflux for 2 h. The chlorobenzene was removed under reduced pressure and the crude cyanamides purified by column chromatography. The cyanamides **3a,d-h** were prepared in this manner (Tables 1—3).

Dioctylcyanamide (5a) from the Amidine (11a). 1-(N^1,N^1-Dioctylamidino)benzotriazole (**11a**) (0.38 g, 1 mmol) in dry chlorobenzene (3 mL) was heated under reflux for 2 h. The crude mixture was worked up as above to afford 0.26 g (98%) of **5a** as an oil, identical in all respects to that prepared by the general method (Table 1).

1-Methylpropylcyanamide. (5i). To a stirred solution of 1-cyanobenzotriazole (1.01 g, 7 mmol) in methanol (20 mL), was added *sec*-butylamine (0.51 g, 7 mmol). Stirring was continued for 1 h and then potassium hydroxide (0.39 g, 7 mmol) was added and the whole stirred at ambient temperature for 5 h. The methanol was removed under reduced pressure (below 40°C), aqueous potassium hydroxide (2%; 7 mL) added, the mixture extracted with diethyl ether (5 × 3 mL) and the extracts dried over magnesium sulfate. The solvent was removed under reduced pressure and the crude cyanamide purified by column chromatography (chloroform/methanol, 19 : 1) to give 0.58 g (84%) of **5i** as a colorless oil (Tables 1—3).

Reaction of 1-Cyanobenzotriazole with Thiophenol. Thiophenol (0.77 g, 7 mmol) was added to a solution of 1-cyanobenzotriazole (1.01 g, 7 mmol) in tetrahydrofuran (20 mL). The reaction mixture was stirred at ambient temperature for 1 h and the solvent was removed *in vacuo* (below 35°C) to give an oily solid which upon crystallization from diisopropyl ether afforded 1.14 g (64%) of *1-(benzotriazol-1-yl)-1-phenylthiomethanamine* **13** as colorless needles, m.p. 113—121°C. Found: C, 61.20; H, 3.88; N, 22.39. $C_{13}H_{10}N_4S$ requires C, 61.40, H, 3.96; N, 22.03.

^{1}*H-NMR spectrum* (*CDCl*$_3$, δ ppm): 8.72 (s, 1H), 8.36 (dd, 1H, J = 8.3 and 0.8 Hz), 8.12 (d, 1H, J = 8.3 Hz), 7.7—7.65 (m, 2H), 7.6—7.5 (m, 4H), 7.5—7.4 (m, 1H).

^{13}*C-NMR spectrum* (*CDCl*$_3$, δ ppm): 158.4, 146.5, 136.8, 131.3, 131.2, 130.5, 129.5, 125.9, 125.5, 119.9, 114.7.

1-Phenylthiopentanimine (14). To a stirred solution of the imine **13** (0.64 g, 2.5 mmol) in tetrahydrofuran (7.5 mL) was added dropwise *n*-butyllithium (2.5 M in hexanes; 2 mL, 5 mmol) at 0°C. After addition was complete, the mixture was stirred at 0°C for 5 min and then at ambient temperature for 1 h. Water (2 mL) was added and the tetrahydrofuran was removed *in vacuo* (below 35°C). The aqueous mixture was washed with diethyl ether (5 × 3 mL) and the combined ethereal extracts dried over magnesium sulfate. The solvent was removed *in vacuo* and the residue purified by column chromatography (pentane) to afford 0.41 g (85%) of **14** as a colorless oil.

^{1}H-NMR spectrum ($CDCl_3$, δ ppm): 7.5 – 7.0 (m, 6H), 2.91 (t, 2H, $J = 7.2$ Hz), 1.75 – 1.3 (m, 4H), 0.91 (t, 3H, $J = 7.2$ Hz).

^{13}C-NMR spectrum ($CDCl_3$, δ ppm): 137.0, 128.8, 128.7, 127.5, 125.6, 33.2, 31.2, 21.9, 13.6.

REFERENCES

1 O. Glemser in "Handbook of Preparative Inorganic Chemistry" (G. Brauer, Editor), vol. 1, Academic Press, New York – London, 1963, p. 662 – 666.

2 W. P. Ericks and P. P. McClellan, *US Patent*, 2, 331, 670 ; cf. *Chem. Abstr.*, **38**, 1651 (1944).

3 W. L. Garbrecht and R. M. Herbst, *J. Org. Chem.*, **18**, 1003 (1953).

4 S. Petersen in "Methoden der Organischen Chemie (Houben-Weyl)", vol. 8, 1952, p. 172.

5 T. Mukaiyama, S. Ohishi and H. Takamura, *Bull. Chem. Soc. Jpn.*, **27**, 416 (1954).

6 W. Traube and A. Engelhardt, *Chem. Ber.*, **44**, 3149 (1911).

7 E. B. Vliet, *Org. Synth.*, **5**, 45 (1925).

8 F. Kurzer, *J. Chem. Soc.*, **1949**, 3033.

9 F. Kurzer, *J. Chem. Soc.*, **1950**, 3269.

10 W. Schroth, H. Kluge, R. Frach, W. Hodek and M. D. Schädler, *J. Prakt. Chem.*, **325**, 787 (1983).

11 H. A. Hageman, *Org. React. (N.Y.)*, **7**, 198 (1953).

12 A. G. Rybin, E. N. Zil'berman, V. I. Trachenko and A. M. Sotnik, *J. Gen. Chem. USSR (Engl. Transl.)*, **52**, 1606 (1982).

13 Société des usines chimiques Rhône-Poulonc, *Brit. Patent*, 649, 634 ; cf. *Chem. Abstr.*, **45**, 8040e (1951).

14 M. E. Hermes and F. D. Marsh, *J. Amer. Chem. Soc.*, **89**, 4760 (1967).

15 V. D. Sheludyakov, S. V. Sheludyakova, M. G. Kuznetsova, N. N. Silkina and V. F. Mironov, *J. Gen. Chem. USSR (Engl. Transl.)*, **50**, 705 (1980).

16 J. Houben and W. Fischer, *Chem. Ber.*, **63**, 2464 (1930).

17 L. A. Clizbe and L. E. Overman, *Org. Synth.*, **58**, 4 (1978).

18 J. P. Whitten, J. R. McCarthy and D. P. Matthews, *Synthesis*, **1988**, 470.

19 W. Langenbeck, *J. Prakt. Chem.*, **1928**, 77.

20 J. M. Cox and R. Ghosh, *Tetrahedron Letters*, **1969**, 3351.

21 H. Westmijze, J. Meijer and P. Vermeer, *Recl. Trav. Chim. Pays-Bas*, **96**, 168 (1977).

22 G. Häflinger in "The Chemistry of Amidines and Imidates", (S. Patai, Editor), John Wiley and Sons, London – New York – Sydney – Toronto, 1975, p. 53.

23 J. V. Pankstelis and M. Kim, *J. Org. Chem.*, **39**, 1494 (1974).

24 Y. L. Chow and K. E. Haque, *Can. J. Chem.*, **46**, 2901 (1968).

Revue Roumaine de Chimie, 36, 4–7, 581–598 (1991)

Dedicated to Prof. ALEXANDRU T. BALABAN
on the occasion of his 60th anniversary

RENE (REaction geNErator) : A PROGRAM TO PROPOSE NEW REACTIONS BY CONSTRUCTION OF ISOMERS AND RELATED REACTIVE SETS OF SIMPLE FUNCTIONALIZED COMPOUNDS. APPLICATION TO ACIDS AND ESTERS

RENÉ BARONE *,[a] MICHEL ARBELOT,[a] ANDRÉ BALDY,[a] MICHEL CHANON[a]
and ROGER GALLO[b]
[a] Faculté des Sciences de St Jérôme
Laboratoire AM3. Case 561. URA CNRS 1411
[b] ENSSPICAM. URA CNRS 1410
13397 Marseille cedex 13. France

We describe the program RENE (REaction geNErator). Its aim is to propose new challenges to invent reactions. The proposition of new reactions is made by the construction of the set of homotopomers and related reactive sets of a given substructure. The reactions are then written as transforms of one homotopomer into another one. The homotopomers are constructed by considering the array of bonds as a number written in base 4 and then limiting the number of possibilities by automatically discarding the generated propositions in disagreement with the basic rules of valency. RENE is written with QuickBasic and runs on IBM/PC microcomputer.

INTRODUCTION

Among the various directions in the field of Computer-Aided Organic Synthesis (CAOS) one seems particularly attractive : how to invent new reactions? As recalled in the recent review by Seebach the challenge of "finding a truly new reaction with the help of a computer program" is still open.[1]

Some CAOS programs are able to propose new reactions because they use a generalized description of reactions [2–4], but, to our knowledge, only two programs have been written specifically to invent new reaction schemes.[5,6] Otherwise general descriptions of reactions have been proposed.[7,8]

In EROS, precursors of a target are obtained by creating the "isomers" of the considered structure. These "isomers" are generated by means of reactions matrices which "mimic" the movement of electrons. The general description of a variety of reactions (elimination, nucleophilic substitution or addition, etc.) may be coded along those lines [2] (Scheme 1).

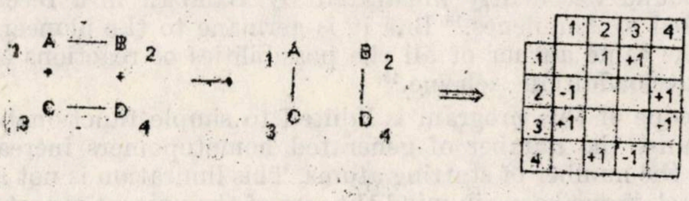

	1	2	3	4
1		-1	+1	
2	-1			+1
3	+1			-1
4		+1	-1	

R-Matrix

Scheme 1

In IGOR the generation of reactions is made by starting from a given reaction matrix and by constructing all the possible structural environments around this matrix.[6]

We describe here our attempts to develop an approach able to propose new reactions schemes by constructing the "isomers" of a given substructure. The main idea is similar to the one used in EROS, but instead of using reaction matrices which describe known reactions, we use a mathematical method to generate the isomers by means of a computer program.

The term of "isomer" was used outside of its usual meaning. We prefer the term of homotopomers because what is generated in this approach may be a set of molecules and atoms rather than a single compound (see scheme 2 : **2**—**6** are the homotopomers of **1**). Homotopomers convey the meaning that the topology of the overall considered set remains the same : the nature of the nodes being constant, but the number and the nature of the edges between the considered nodes varying.

Scheme 2 shows some homotopomers of substructure 1. Homotopomers **2**—**6** may be considered as potential precursors of **1**. This scheme shows how the program may be used : RENE generates naked ideas and the chemist has to "dress" them. The "solutions" given by RENE may be seen as a kind of chemical game in which the chemist has at his disposal the chemical knowledge in order to complete the substructures proposed. For example, homotopomer **6** looks like the oxidation of a saturated carbon. The chemist may add what he wants on the carbon atom, so solutions **6** may suggest synthesis such as **A**[9] or **B**[10] (scheme 2) and solution **5** may be seen as the schematic principle of the well known industrial Koch reaction **C**[11] or synthesis **D**[12] (scheme 2). These examples show that an interactive mode of use is absolutely needed for RENE. If some solutions are simple to "dress" such as **4** (oxidation of aldehyde for example) others, such as **5**, are less obvious.

The various substructures generated may represent intermediates such as carbenes, carbanions, carbocations, oxene, etc., as well as their precursors. The possibility that isolated atoms represent actual atoms is certainly open because heterogeneous catalysis of oxidation is certainly known to deliver O atoms, and metal vapor synthesis to create C atoms.[13,14] The first situation would correspond to a structural block M—O or O—O. The second simply to actual atoms of C. The substructures represent ground electronic states but the possibility of irradiating the reagents (IR or UV irradiation, sonochemistry) is not discarded.

With this definition of "homotopomer", our approach is therefore clearly different from the generation of all the structural isomers for a given compound excellently illustrated by Balaban in a recent monograph devoted to Annulenes.[15] But it is germane to the pioneering generation by the same author of all the possibilities of reactions associated with the cycloaddition scheme.[16]

The scope of this program is limited to simple functionalized compounds because the number of generated homotopomers increases drastically with the number of starting atoms. This limitation is not an important drawback if one keeps in mind the aim of the present raport : provide the chemist with new schemes of transformation. Indeed, in most of the

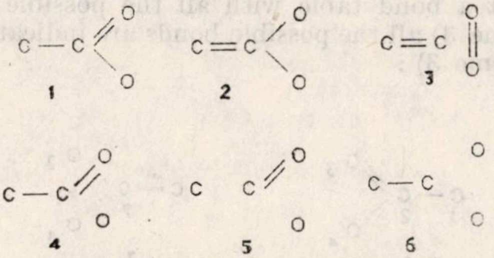

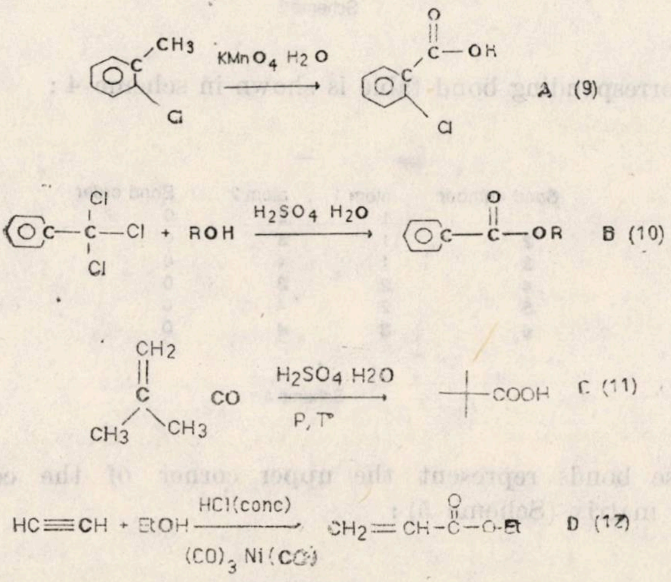
KMnO$_4$ H$_2$O
A (9)
H$_2$SO$_4$ H$_2$O
ROH
B (10)
H$_2$SO$_4$ H$_2$O
P, T°
C (11)
HCl(conc)
(CO)$_3$ Ni (CO)
D (12)

Scheme 2

already known chemical transformations the number of actually involved atoms of the structure seldom exceeds six. (For an exception to this statement see the concept of Holosynthon [17]).

PROGRAM

RENE generates the possible homotopomers by mathematical combination ; these homotopomers correspond to propositions of reactions schemes. The chemist has then to evaluate their interest and feasibility. Such an approach may suggest highly creative solutions because the mode of creation is independent from actual chemistry except from the point of view of basic valency rules.

The generation of homotopomers is done by the following principle : first, we construct a bond table with all the possible bonds. For the structure **1** (Scheme 3) all the possible bonds are indicated in dotted lines (Structure **7**, scheme 3) :

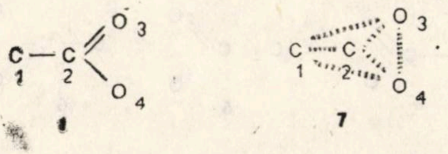

Scheme 3

and the corresponding bond table is shown in scheme 4 :

Bond number	atom 1	atom 2	Bond order
1	1	2	0
2	1	3	0
3	1	4	0
4	2	3	0
5	2	4	0
6	3	4	0

Scheme 4

These bonds represent the upper corner of the corresponding adjacency matrix (Scheme 5) :

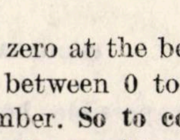

	1	2	3	4
1		▨	▨	▨
2			▨	▨
3				▨
4				

Scheme 5

The bond order is set to zero at the beginning of the program. The value of the bonds may vary between 0 to 3 and the bond order array may be seen as a base 4 number. **So to construct the isotopomers we have simply to construct all the possible numbers in base 4.** Binary numbers have been used by Hendrickson in the SYNGEN program to canonicalize and to code skeletons of structures.[18] Scheme 6 shows how the homotopomers are generated.

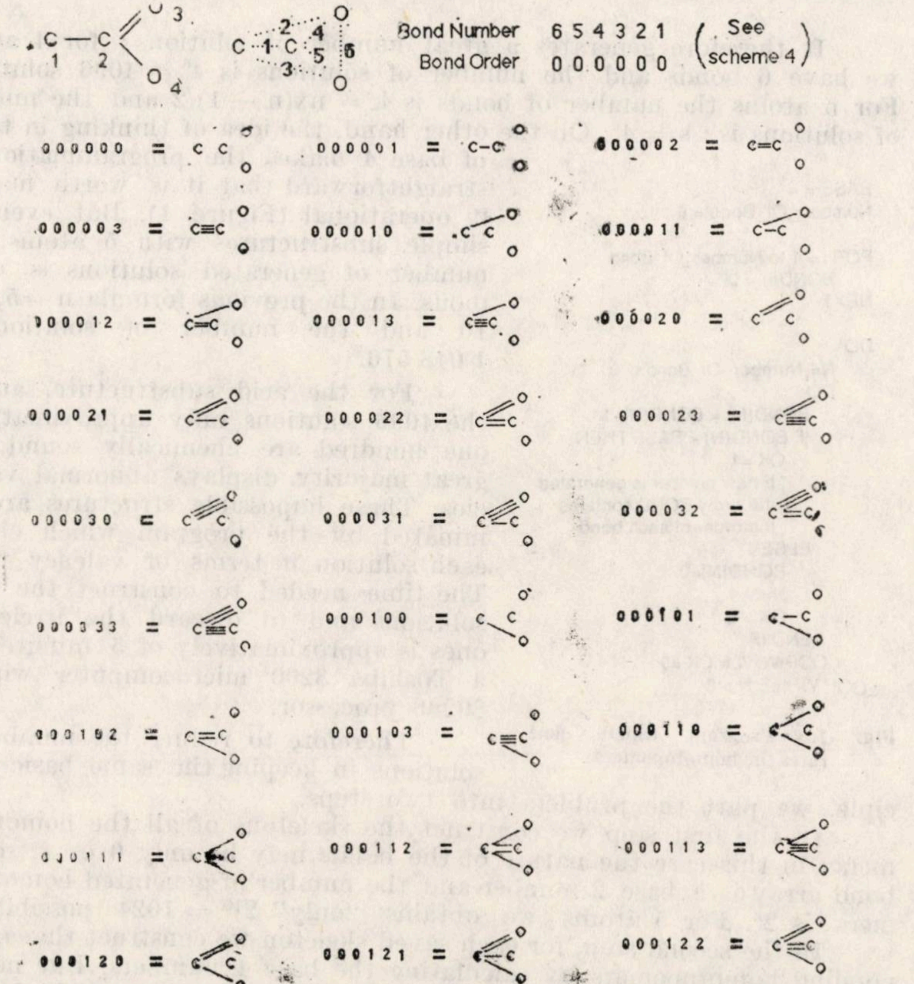
Bond Number 6 5 4 3 2 1
Bond Order 0 0 0 0 0 0
See scheme 4
000000 = C C
000001 = C–C
000002 = C=C
000003 = C≡C
000010
000011
000012
000013
000020
000021
000022
000023
000030
000031
000032
000033
000100
000101
000102
000103
000110
000111
000112
000113
000120
000121
000122
ETC.

Scheme 6

This approach has the disadvantage of generating, besides useful suggestions, totally unrealistic structures such as the ones presented in scheme 7 :

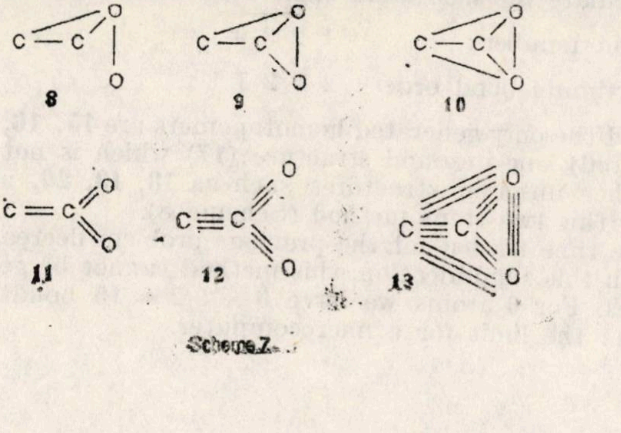
8
9
10
11
12
13

Scheme 7

It therefore generates a great number of solutions : for 4 atoms we have 6 bonds and the number of solutions is $4^6 = 4096$ solutions. For n atoms the number of bonds is $k = nx(n - 1)/2$ and the number of solutions is : $s = 4^k$. On the other hand, the idea of thinking in terms of base 4 makes the programmation so straightforward that it is worth making it operational (Figure 1). But even for simple substructures with 5 atoms, the number of generated solutions is enormous. In the previous formula $n = 5$, $k = 10$ and the number of solutions is 1 048 576.

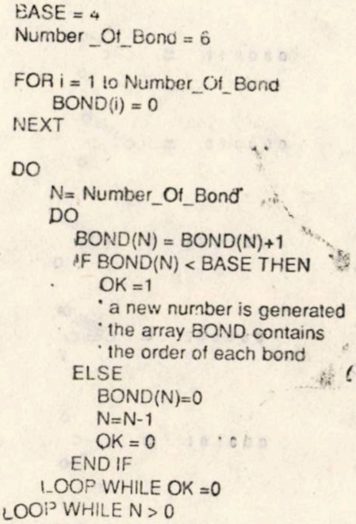

```
BASE = 4
Number_Of_Bond = 6

FOR i = 1 to Number_Of_Bond
    BOND(i) = 0
NEXT

DO
    N= Number_Of_Bond
    DO
       BOND(N) = BOND(N)+1
       IF BOND(N) < BASE THEN
          OK =1
          ' a new number is generated
          ' the array BOND contains
          ' the order of each bond
       ELSE
          BOND(N)=0
          N=N-1
          OK = 0
       END IF
    LOOP WHILE OK =0
LOOP WHILE N > 0
```

Fig. 1. — Program which generates the homotopomers.

For the acid substructure, among the 4096 solutions only approximatively one hundred are chemically sound, the great majority displays abnormal valencies. These impossible structures are eliminated by the program which checks each solution in terms of valency rules. The time needed to construct the 4096 solutions and to discard the irrelevant ones is approximatively of 5 minutes on a Toshiba 3200 microcomputer with a 80286 processor.

Therefore to reduce the number of solutions in keeping the same basic principle, we part the problem into two steps.

In the first step we construct the skeletons of all the homotopomers : in this case the nature of the bonds may be only 0 or 1, so the bond array is a base 2 number and the number of generated homotopomers is 2^k. For 5 atoms we obtains "only" $2^{10} = 1024$ possibilities.

In the second step, for each saved skeleton we construct the corresponding homotopomers by calculating the base 4 numbers. But not all the base 4 numbers are needed because in this case the skeleton is defined and we may calculate for each bond its maximum order. For the skeleton **14** (Scheme 8) generated during the first step, at the beginning the binary number describing the bond array of the substructures is 1 1 1 1. We may calculate the maximum order for each bond :

bond number :	1 2 3 4
maximum bond order :	2 1 2 1

And the only generated homotopomers are **15**, **16**, **17**, among which there is only one unsound structure (**17**) which is not displayed to the user. Other unsound structures such as **18**, **19**, **20**, are not generated by using this two steps method (Scheme 8).

The time needed for the previous problem decreases to 1′30″. But even with this simplification, this method cannot be generalized to large structures. For 6 atoms we have $6 \times 5/2 = 15$ bonds and $2^{15} = 32768$ skeletons : the limit for a microcomputer.

The homotopomers generated are the base for propositions of reactions. The chemist has then to evaluate their interest and feasibility as illustrated in the section results.

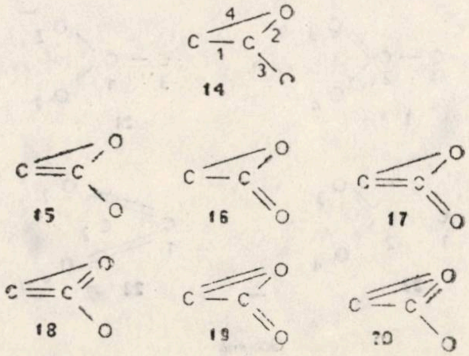

Scheme 8

The main steps of RENE operation are the following : The first step of RENE deals with the input of the substructure through the keyboard. This part of the program is similar to the one used in the SCORE program [19] and will not be discussed here.

The second step is the actual treatment of the involved substructure by RENE. For this treatment two options are available. The first one is to run the reaction generator itself and the second is used to display the solutions already recorded. The program may be used in an automatic or in an interactive mode.

To avoid the presentation of uninteresting solutions we have added one option :

— Some homotopomers contain atoms without bonds (see scheme 2). The user has the possibility to add as a constraint the maximum number of these isolated atoms tolerated in the homotopomers. For example if the constraint is : one isolated atom, the homotopomers **5**, **6** will not be displayed.

The program then explores the solutions. Every created solution is checked with the evaluation module which rejects those which contradict the demanded constraint. A test based upon the valence of atoms is also used in order to discard impossible skeletons such as **8** to **10** (scheme 7).

The program checks also if the homotopomers is a new one or has already been proposed. This comparison does not use directly the nature of the atoms but their equivalency classes obtained by canonicalization. We use the algorithm developed by Moreau.[20] For structure **1** (scheme 9) the program perceives the equivalence of atoms 3 and 4 and the canonicalized values for the atoms are those of structure **21** (scheme 9). Carbons 1 and 2 (structure **1**) are not identical and homotopomers **22** and **23** are considered as different and in fact if we think in terms of a chemical transform, the transformation of **22** to **1** is different from the one **23** to **1** (Scheme 9). In the first case there is only the formation of bond 1—2. In the second case there is the formation of bonds 1—2, 2—3, 2—4, and breaking of bonds 1—3 and 1—4.

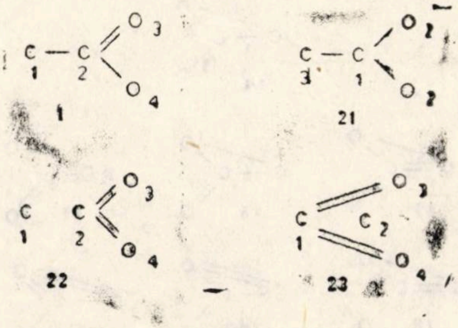

Scheme

In the interactive version the solutions are displayed on the screen for the user which decides to save them or not. In the automatic version all the solutions compatible with the rules of valency and starting constrains are directly saved.

When all the possibilities have been found the first part is achieved, then part 2 begins : for each skeleton saved the program generates the corresponding homotopomers by "colouring" the bonds as indicated previously. Again, a test is used to discard solutions in which atoms have abnormal valency. As in the first part, in the interactive version the solutions are displayed to the user which saves them or not and in the automatic version the solutions are directly saved. When this part is terminated the program returns to the main menu.

Figure 2 shows the screen when a solution is displayed to the user in the interactive version. It is possible to have a hardcopy of the screen, to move atoms in order to have a better graphical representation of the solution, to save the solution or to continue.

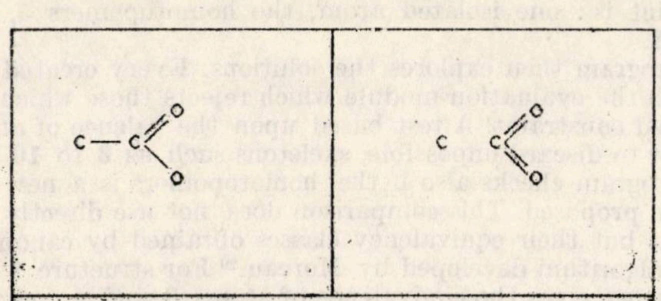

press any key to continue

Fig. 2. — View of the screen.

RESULTS

Tables 1 and 2 present the results obtained for the target substructure **1** (acid or ester). The constraint used was : two isolated atoms allowed.

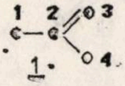

1

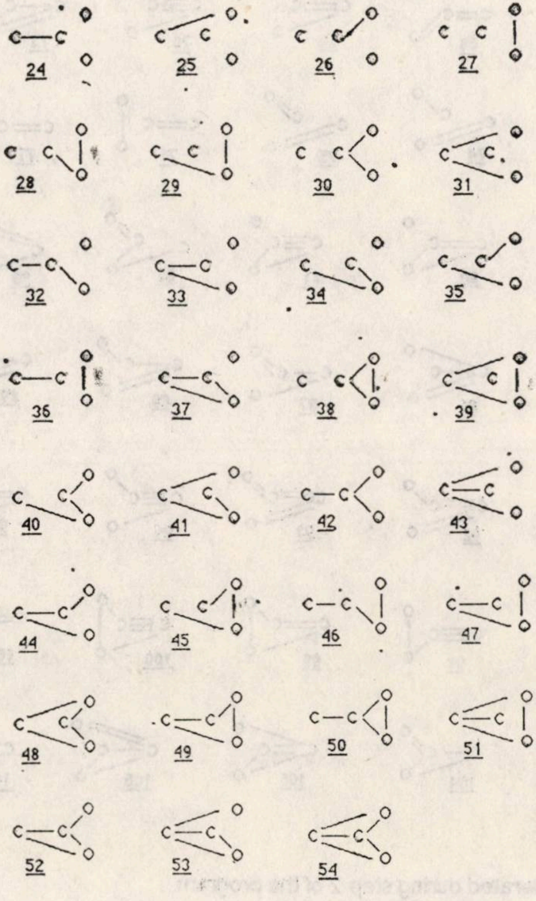
24
25
26
27
28
29
30
31
32
33
34
35
36
37
38
39
40
41
42
43
44
45
46
47
48
49
50
51
52
53
54

Table 1. Homotopomers generated during the first step of the program.

During the first part RENE generated 64 skeletons and among them 31 were compatible with the rules of valency and the starting constraint (homotopomers **24** to **54**, Table 1). In the second part 73 solutions were generated and 53 were sound (**55** to **107**, Table 2). The time necessary to create all these homotopomers is 1′30″ in the automatic mode.

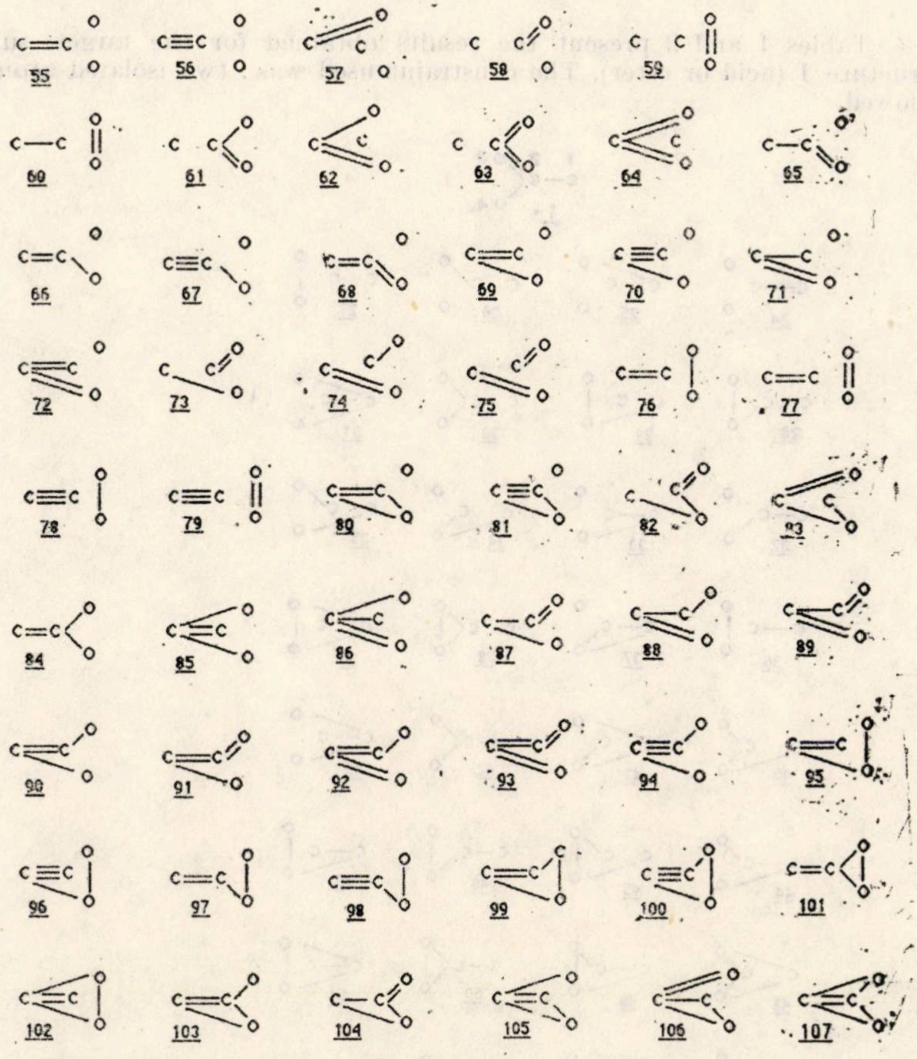
55
56
57
58
59
60
61
62
63
64
65
66
67
68
69
70
71
72
73
74
75
76
77
78
79
80
81
82
83
84
85
86
87
88
89
90
91
92
93
94
95
96
97
98
99
100
101
102
103
104
105
106
107

Table 2. Homotopomers generated during step 2 of the program.

These examples show the results provided and the part of interpretation left to the user : each homotopomer is a potential precursor (or product) of the starting structure. The chemist has to "imagine" the reaction "behind" the transform shown on the screen and the nature of the intermediates. For example homotopomer **28** shows C and C—O—O, the user has to interpret his "reaction" : formation of a bond between two carbon atoms, breaking of the O—O bond and formation of the C=O bond.

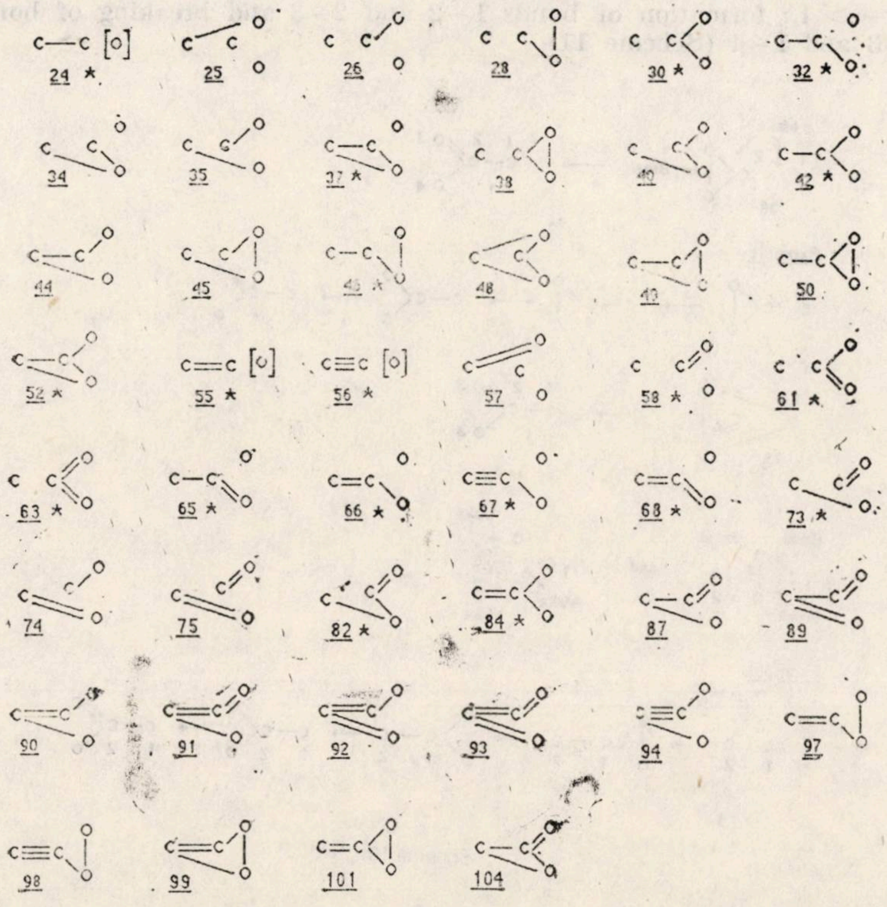
24 ★
25
26
28
30 ★
32 ★
34
35
37 ★
38
40
42 ★
44
45
46 ★
48
49
50
52 ★
55 ★
56 ★
57
58 ★
61 ★
63 ★
65 ★
66 ★
67 ★
68 ★
73 ★
74
75
82 ★
84 ★
87
89
90
91
92
93
94
97
98
99
101
104

Table 3.Homotopomers which seem interesting. * Indicates that an example is given in Table 4 or corresponds to well known synthesis.

The homotopomers of Tables 1–3 are drawn like the user see them on the screen : the atoms have the same position as in the starting structure in order to visualize the transform involved, the bonds to create and the bonds to break. That is why we draw homotopomer **39** with an internal C. This means that this C atom is atom 2 in **39** whereas in **38** the lone C is atom 1. So the transforms **38** – > **1** and **39** – > **1** are different. Case **38** – > **1** covers the following modifications : formation of bond 1–2, breaking of bond 3–4 and formation of a double bond between 2 and 3. For case **39** – > **1** the following modification occurs : formation of bonds 1–2, 2–3, 2–4 and breaking of bonds 1–3, 1–4, 3–4 (Scheme 10). In the same line one would have : case **82** – > **1** :

formation of bond between atoms 1—2 and breaking of bond 1—4. Case **83** — > **1** : formation of bonds 1—2 and 2—3 and breaking of bonds 1—3 and 1—4 (Scheme 11).

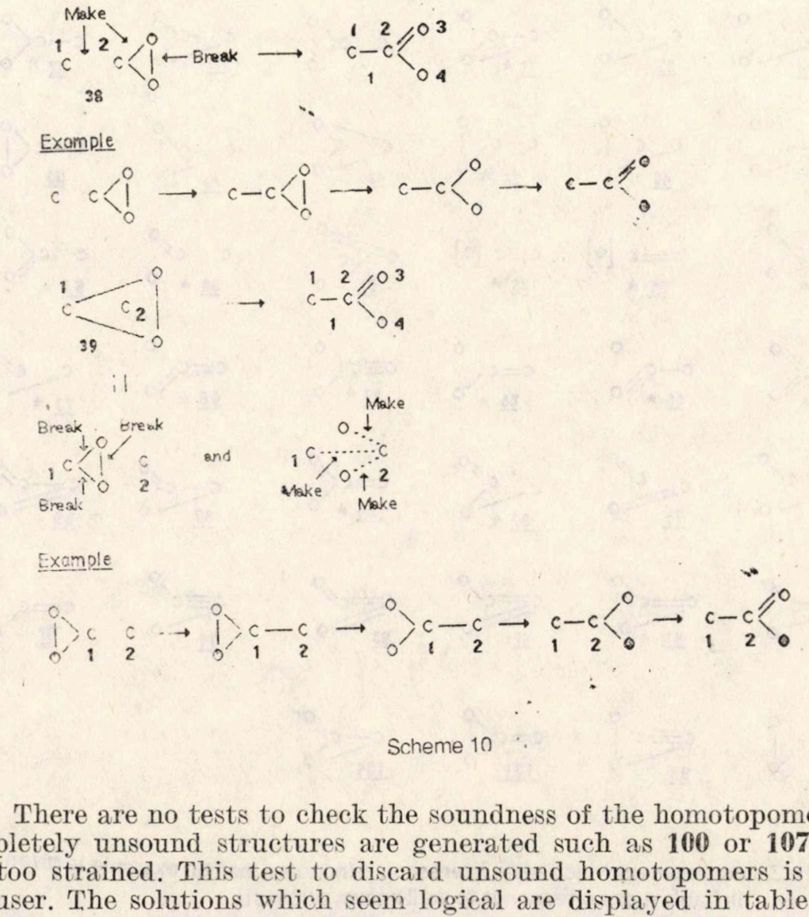

Scheme 10

There are no tests to check the soundness of the homotopomers and completely unsound structures are generated such as **100** or **107** which are too strained. This test to discard unsound homotopomers is left to the user. The solutions which seem logical are displayed in table 3. We delete several solutions in which one oxygen is bonded to atom 1 and involving a migration of O or breaking a C—O bond, adding one step in the "reaction" (see schemes 9 and 10). For example solution **29** is deleted because of solution **28** is simpler, also for **31** because of **30**, etc . . . One may notice that when we delete these solutions we seem to admit that atoms 1 and 2 are identical and **28** = **29**, **30** = **31**, **32** = **33**, etc. It is not the case : **73** and **74** seem identical but for **73** atom C 1 comes from alcohol and for **74** C 2 comes from C=O. In order to reduce the number of solutions in table 3, we summarize O O, O—O, O=O by the symbol [O].

With the 46 homotopomers left we can still formally imagine a great number of transformations. Formally they correspond to the p combinations of N homotopomers 2 by 2, i.e. : 1035. To keep this report in a reasonable size we have decided to explore only the transformations involving 1 using as a cheek test the reactions allowing the formation of acids or esters in the data bank REACCS.[21]

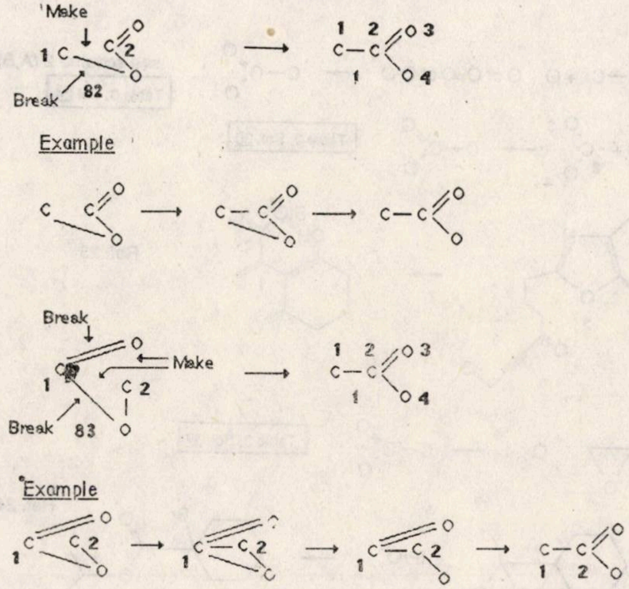

Scheme 11

At the start we found more than 4000 reactions of preparation but many of them correspond to the same homotopomeric principle. The interrogation of REACCS may be performed directly by using the homotopomers, for example : **37 — > 1**, **82 — > 1**, etc.

It is clearly beyond the scope of this paper to give all the references found in REACCS but for a clear chemical illustration of the use of RENE we illustrate in table 4 every homotopomer transformation by one or two actual example(s) from the literature, exception for well known synthesis such as oxidation of alcohol (**32**), aldehyde (**65**), ketene (**68**), or such as case **63** which suggests the reaction of a Grignard reagent on CO_2. Case **84** is the enolic form of the acid. All the known methods are not retrieved like hydrolysis of RCN because the starting substructure does not possess nitrogen. To find such solution it is necessary to introduce N with CCOO.

This work done, we are left with 28 principles of transformations which are propositions for new reactions. These cases are not marked by a star in table 3. Among them several involve not obvious intermediates such as **48**, **49**, **91**—**93**, **98**—**104**. Some substructures are very simple and seem to have not been used such as **44**, **75**, **87**.

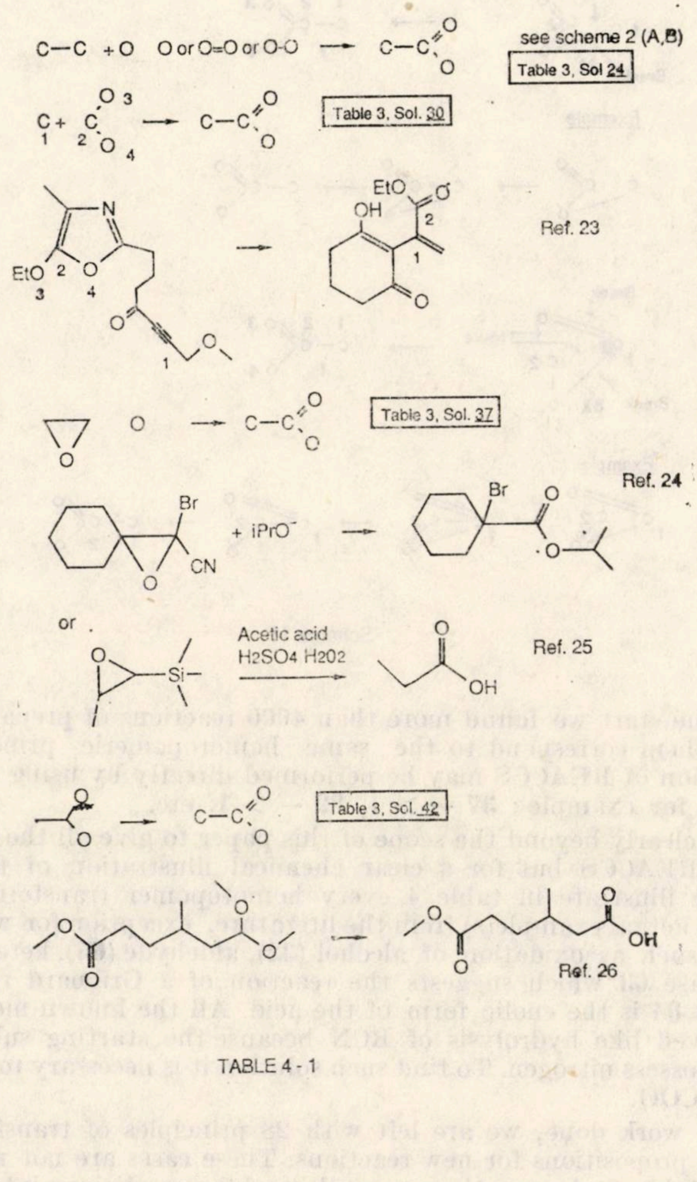
see scheme 2 (A,B)
Table 3, Sol 24
Table 3, Sol. 30
Ref. 23
Table 3, Sol. 37
Ref. 24
or
Acetic acid
H2SO4 H2O2
Ref. 25
Table 3, Sol. 42
Ref. 26

TABLE 4 - 1

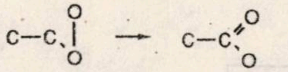

Table 3, Sol. 46

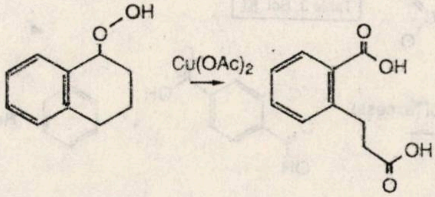

Ref. 27

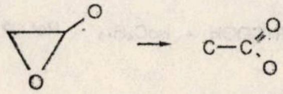

Table 3, Sol. 52

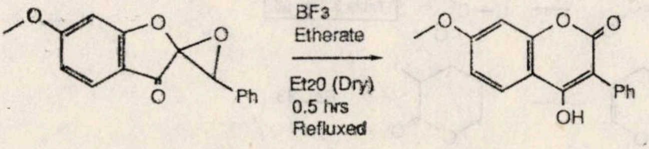
BF3
Etherate
Et20 (Dry)
0.5 hrs
Refluxed

Ref. 28

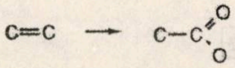

Table 3, Sol. 55

$tBuOH + CH_2{=}CCl_2 \xrightarrow{H_2SO_4\ H_2O} tBu\text{-}CH_2\text{-}COOH$ Ref. 29

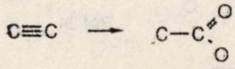

Table 3, Sol. 56

$$nC_6H_{11}C \equiv CH \xrightarrow[\text{3) H20, 4) HgSO4, H2SO4, AcOH}]{\text{1) nBuLi, THF, 2) PhSSPh}} nC_6H_{11}\,CH_2\,COOH$$ Ref.30

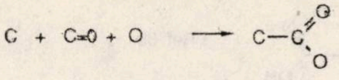

See Scheme 2 (C,D)

Table 3, Sol. 58

TABLE 4 - 2

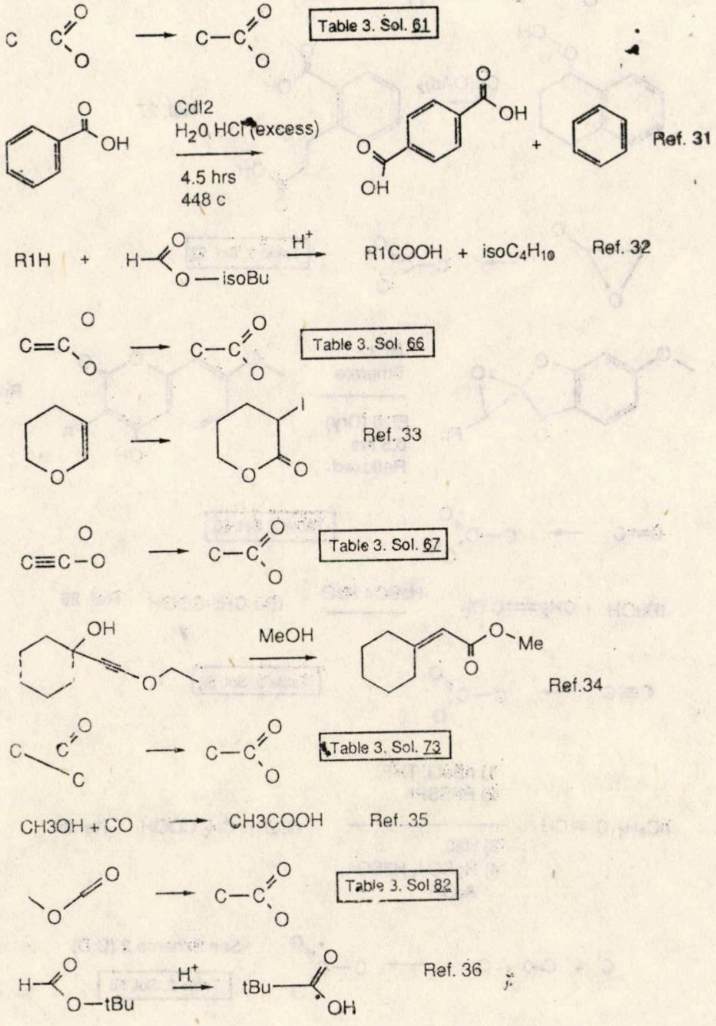
Table 3. Sol. 61
CdI2
H2O HCl (excess)
4.5 hrs
448 c
OH
Ref. 31
R1H + H–C(=O)–O–isoBu
H+
R1COOH + isoC4H10
Ref. 32
Table 3. Sol. 66
I
Ref. 33
Table 3. Sol. 67
OH
MeOH
O
Me
Ref.34
Table 3. Sol. 73
CH3OH + CO → CH3COOH
Ref. 35
Table 3. Sol 82
O–tBu
H+
tBu
Ref. 36

TABLE 4.3

The transformations suggested by these "naked ideas" are displayed in scheme 12 and the work of the chemist is to try to find the adequate substituents and the experimental conditions. Coupling of two carbonyl ligands (solution **75**) has been reported.[22]

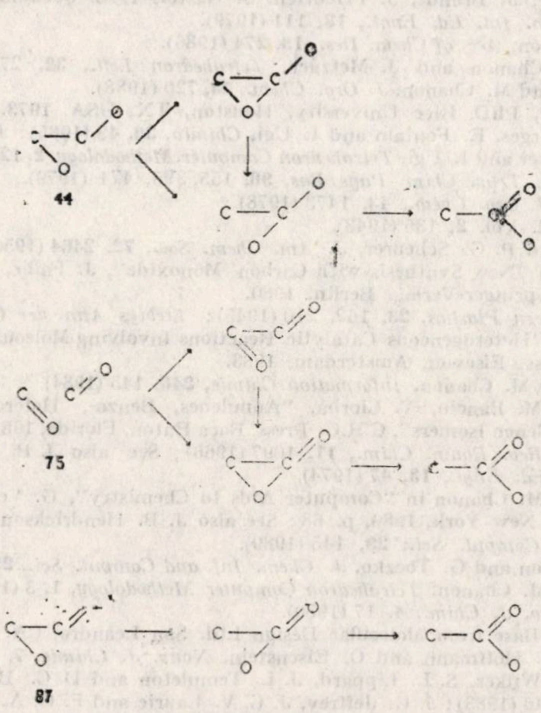

Scheme 12

CONCLUSION

By purely mathematical combinatory approach the program RENE is able to propose schemes of potentially new reactions. Propositions are provided to the chemist which has still to consider them in light of his own knowledge to determine if any could be worth to be tried experimentally. The core of the program which performs the combinations could also be used to enumerate isomers.[37] Also, it could be possible to use it in a computer-aided organic synthesis program in order to search solutions without chemical knowledge.

RENE is a new and simple approach in this new field of computer assisted generation of organic reaction. For the synthesis of acids and esters, and after this work the sentence of Seebach is still true and we are developing other approaches. But scheme 12 suggests that this simple approach may provide creative ideas.

RENE is written in Quick Basic and runs on IBM/PC and compatibles.

REFERENCES

[1] D. Seebach, *Angew. Chem. Int. Ed. Engl.*, **29**, 1338 (1990) : see also N. S. Zefirov and S. S. Tratch, *Analyt. Chim. Acta*, **235**, 115 (1990) and the references cited therein.

[2] I. Ugi, J. Bauer, J. Brandt, J. Friedrich, J. Gasteiger, C. Jochums, and W. Schubert, *Angew. Chem. Int. Ed Engl.*, **18**, 111 (1979).

[3] J. B. Hendrickson, *Acc. of Chem. Res.*, **19**, 274 (1986).

[4] R. Barone, M. Chanon and J. Metzger, *Tetrahedron Lett.*, **32**, 2761 (1974) ; P. Azario, R. Barone and M. Chanon, *J. Org. Chem.*, **53**, 720 (1988).

[5] T. Brownscombe, PhD, Rice University, Houston, TX, USA. 1973.

[6] J. Bauer, R. Herges, E. Fontain and I. Ugi, *Chimia*, **39**, 43 (1985) ; J. Bauer, E. Fontain, D. Forstmeyer and I. Ugi, *Tetrahedron Computer Methodology*, **2**, 129—132, (1988).

[7] J. F. Arens, *Rel. Trav. Chim. Pays Bas*, **98**, 155, 395, 471 (1979).

[8] D. C. Roberts, *J. Org. Chem.*, **43**, 1473 (1978).

[9] Org. Synth., coll. Vol. 2, 135 (1943).

[10] G. M. Lefave and P. G. Scheurer, *J. Am. Chem. Soc.*, **72**, 2464 (1950).

[11] H. Bahrmann, in "New Synthesis with Carbon Monoxide", J. Falbe, Ed., Chap. 5, "Koch Reaction", Springer-Verlag, Berlin, 1980.

[12] W. Reppe, *Modern Plastics*, **23**, 162, 210 (1945) ; *Liebigs Ann. der Chemie*, **582**, 1 (1953).

[13] G. I. Golodets, "Heterogeneous Catalytic Reactions Involving Molecular O^{2}", Engl. Trans. J. R. H. Ross, Elsevier, Amsterdam, 1983.

[14] J. C. Negrel and M. Chanon, *Information Chimie*, **246**, 145 (1984).

[15] A. T. Balaban, M. Banciu, V. Ciorba, "Annulenes, Benzo-, Hetero-, Homo-Derivatives and their Valence Isomers", C.R.C. Press, Boca Raton, Florida, 1987.

[16] A. T. Balaban, *Rev. Roum. Chim.*, **11**, 1097 (1966) ; See also J. B. Hendrickson, *Angew. Chem. Int. Ed. Engl.*, **13**, 47 (1974).

[17] R. Barone and M. Chanon in "Computer Aids to Chemistry", G. Vernin and M. Chanon. Ed., Wiley, New York, 1986, p. 68 : See also J. B. Hendrickson and Ping Huang, *J. Chem. Inf. Comput. Sci.*, **29**, 145 (1989).

[18] J. B. Hendrickson and G. Toczko, *J. Chem. Inf. and Comput. Sci.*, **23**, 171 (1983).

[19] R. Barone and M. Chanon, *Tetrahedron Computer Methodology*, **1**, 3 (1988).

[20] G. Moreau, *Nouv. J. Chim.*, **4**, 17 (1980).

[21] Reactions Data Base from Molecular Design Ltd, San Leandro, CA.

[22] C. N. Wilker, R. Hoffmann and O. Eisenstein, *Nouv. J. Chimie*, **7**, 535 (1983) ; R. Hoffman, C. N. Wilker, S. L. Lippard, J. L. Templeton and D. C. Brower, *J. Am. Chem. Soc.*, **105**, 146 (1983) ; J. C. Jeffrey, J. C. V. Laurie and F. G. A. Stone, *J. Organomet. Chem.*, **2**, 258 (1983) ; M. R. Churchill, H. J. Wassermans, S. J. Holmes and R. R. Schrock, *Organometallics*, **1**, 766 (1982).

[23] P. A. Jacobi, T. A. Craig, D. G. Walker, et al., *J. Amer. Chem. Soc.*, **106**, 5585 (1984).

[24] C. Legris, P. Coutrot and J. Villieras, *C. R. Acad. Sci. C.*, **278**, 77 (1974).

[25] G. Bufford, F. Cooke, P. Magnus, *Tetrahedron*, **39**, 867 (1983).

[26] V. R. Mamdapur, P. P. Pai, K. Chakravarti, U. G. Nayak and S. C. Bhattacharyya, *Tetrahedron*, **20**, 2601 (1964) ; R. O. Adlof, W. E. Neff, E. A. Emken and E. H. Pryde, *J. Amer. Oil Chem. Soc.*, **54**, 414 (1977).

[27] N. P. Emel'yanov and A. M. Shevchik, *Dokl. Akad. Nauk. SSSR*, **13**, 340 (1969) ; *Chem. Abstr.* **71**, 38537.

[28] M. Geoghegan, W. I. O'sullivan and E. M. Philbin, *Tetrahedron*, **22**, 309 (1966) ; C. Jain, V. K. Rohatgi and T. R. Seshadri, *Tetrahedron*, **23**, 2499 (1967).

[29] S. Randriamabeja, P. Deschamps and R. Gallo, *Synthesis*, **1985**, 493.

[30] S. R. Abrams, *Can. J. Chem.*, **61**, 2423 (1983).

[31] Y. Ogata, M. Tsuchida and A. Muramoto, *J. Amer. Chem. Soc.*, **79**, 6005 (1957) ; P. W. Sherwood, *Chem. Ind.*, **1960**, 1096.

[32] V. Lazzeri, R. Jalal and R. Gallo, French Pat., n° 89—05153 (April 04 1989).

[33] R. D. Evans and J. H. Schauble, *Synthesis*, **1986**, 727.

[34] E. A. Braude and O. H. Wheeler, *J. Chem. Soc.*, **1955**, 320 ; N. A. Milan and C. P. Priesing, *J. Am. Chem. Soc.*, **80**, 2189 (1958).

[35] K. Weissermel and H. Arpe, "Chimie Organique Industrielle", Masson, Paris, 1981.

[36] Swiss. Pat. 396 866 (26/07/1960).

[37] P. J. Hansen and P. C. Jurs, *J. Chem. Ed.*, **65**, 661 (1988).

Revue Roumaine de Chimie, **36**, 4–7, 599–600 (1991)

Dedicated to Prof. ALEXANDRU T. BALABAN
on the occasion of his 60th birthday

FORMATION OF AN α-LACTONE

ERNST SCHMITZ and GISELA KOZAKIEWICZ
Central Institute of Organic Chemistry, Rudower Chaussee 5, 0-1199 Berlin, Germany

Received January 30, 1991

On attempted preparation of α-lactone **2**, equivalent amounts of trimethylacetaldehyde **3** and carbon monoxide were obtained instead.

In contrast to the impressive development in synthesis of three-membered rings all attempts to obtain α-lactones have failed so far. Their existence was postulated as early as 1937.[1] The intermediacy of an α-lactone was concluded from the steric results of solvolysis of α-halocarboxylic acids. α-Lactones were also postulated as intermediates in radical decomposition of some peroxides and made plausible by formation of polyesters.[2] Proof of existence of α-lactones apparently has not made much progress since then.[3]

Several years ago we attempted to prepare α-lactone **2** by thermal decomposition of the sodium salt of α-bromo tert-butyl acetic acid **1**[4]; steric hindrance of the voluminous alkyl group was supposed to interfere with ring opening. A preliminary experiment yielded 8% of trimethylacetaldehyde **3** on thermal decomposition of dry salt **1**.

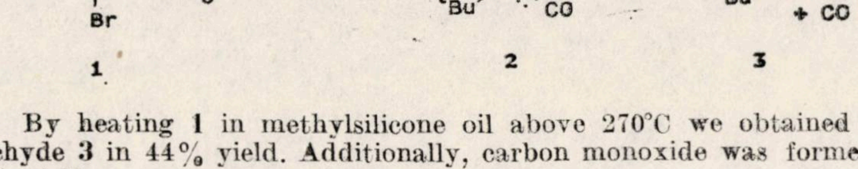

By heating **1** in methylsilicone oil above 270°C we obtained the aldehyde **3** in 44% yield. Additionally, carbon monoxide was formed in 57% yield.

α-Lactone **2** is believed to be an intermediate.

EXPERIMENTAL

Sodium α-bromo-tert-butyl acetate[5] (0.50 g, 2.3 mmol), suspended in 20 mL methylsilicone oil, was heated to 270°C. Volatile products were led through a solution of 2,4-dinitrophenylhydrazine in 2N-sulfuric acid by a stream of nitrogen. The reaction was completed by short heating to 450°C. Trimethylacetaldehyde-2,4-dinitrophenylhydrazone (0.27 g, 1.0 mmol) was obtained (44% yield), m.p. (ethanol) 210–212°C (Lit. [2]: 209°C); mixed m.p. without depression.

In an identical experiment carbon monoxide was recorded volumetrically and identified by gas chromatography (squalene on charcoal; 20°C).

REFERENCES

[1] W. A. Cowdrey, E. D. Hughes and C. K. Ingold, *J. Chem. Soc. (London)*, **1937**, 1208.

[2] P. D. Bartlett and L. B. Gertler, *J. Amer. Chem. Soc.*, **85**, 1864 (1963).

[3] A. R. Evans and G. A. Taylor, *J. Chem. Soc., Perkin I*, **1987**, 567.

[4] G. Kozakiewicz, *Ph. D. Thesis*, Berlin 1967.

[5] A. H. Homeyer, F. C. Whitmore and V. H. Wallingfeld, *J. Amer. Chem. Soc.*, **55**, 4209 (1933).

[6] R. L. Shriner and R. C. Fuson, ʻ The Systematic Identification of Organic Compounds", New York, London, 1948.

Revue Roumaine de Chimie, **36**, *4*–**7**, 601–611 (1991)

Dedicated in friendship to my dear colleague A. T. BALABAN,
with best wishes on the occasion of his 60th birthday

SYNTHESIS AND STRUCTURE ANALYSIS OF 4-QUINAZOLONE DERIVATIVES FROM ALKYL DICYANOACETATES

RICHARD NEIDLEIN *[a], ZHIHUA SUI**[a], WALTER KRAMER[a] and ROLAND BOESE[b]

[a] Pharmazeutisch-Chemisches Institut der Universität Heidelberg, Im Neuenheimer Feld 364, D-6900 Heidelberg, F.R.G.

[b] Institut für Anorganische Chemie der Universität Essen, Universitätstrasse 3–5, D-3500 Essen 1, F.R.G.

Received January 28, 1991

4-Quinazolones were obtained by nucleophilic attack of anthranilic acid (**2**) on one of the cyano groups in alkyl dicyanoacetate alkali salts **1**. ^{13}C-{^{1}H-selective} NOE spectroscopy and X-ray analysis was applied for structural assignments.

INTRODUCTION

Recently we have reported about a convenient method for the preparation of hitherto unknown 4-oxoimidazolines with ketene aminal structure [1] and related compounds with alkyl dicyanoacetates as starting materials.[2–5]

In this paper we will report on the synthesis and structural assignments of 4-quinazolones (Scheme 1) which are of interest for biological studies.[6–10]

RESULTS AND DISCUSSION

A mechanism to account for the formation of these derivatives is proposed in scheme 2. The reaction of anthranilic acid with potassium methyl dicyanoacetate [11] provides **3** when the reaction time was 20 h. However, if the reaction was interrupted after 8 h, the non-cyclized intermediate **13** could be isolated (Scheme 3). It can be assumed therefore, that the stereochemistry of the C(2)-C(9) double bond should be the same as in compound **3**.

---

* Correspondence author

** Part of the Ph. D. Thesis, University of Heidelberg, 1990

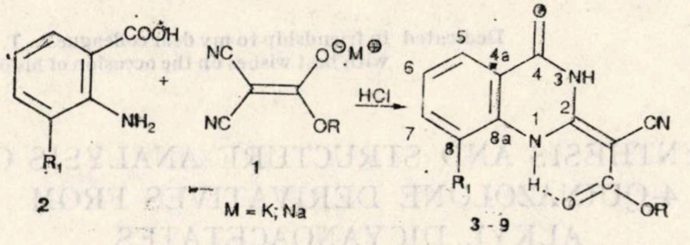
COOH
NH₂
R₁
2
+
NC
O⊖M⊕
NC
OR
1
M = K; Na
HCl
O
5
4a
4
3 NH
6
2
CN
7
8a
1
N
8
R₁
H
C
O
OR
3 - 9

	R	R₁		R	R₁
3	CH₃	H	7	CH₃	CH₃
4	C₂H₅	H	8	C₂H₅	CH₃
5	n-C₄H₉	H	9	CH₂C₆H₅	CH₃
6	CH₂C₆H₅	H			

Scheme 1

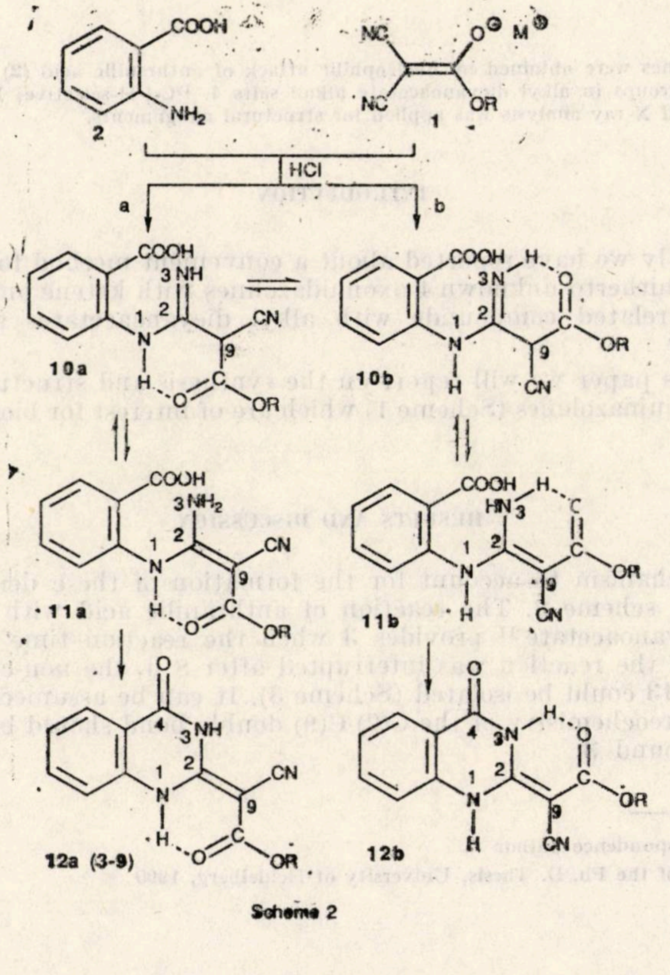
COOH
NH₂
2
NC
O⊖ M⊕
NC
OR
1
HCl
a
b
10a
10b
11a
11b
12a (3-9)
12b
COOH
3 NH
2
1
N
H
9
CN
C
O
OR
3 NH₂
HN 3
4
O

Scheme 2

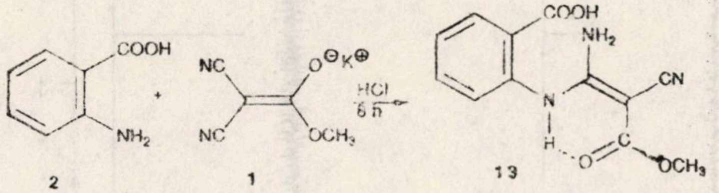

Scheme 3

Two stereoisomers can be formed of each of the compounds **3-9** and **17—18** but only one isomer could be isolated in each case. Since standard NMR techniques allowed to identify only the constitution, we tried to apply ^{13}C-{^{1}H-selective} NOE [12] for stereochemical studies. For representative structure elucidation we have selected compounds **4** and **13**.

In the ^{1}H- and ^{13}C-NMR spectra all signals were assigned on the basis of chemical shifts and NOEs by one- and two-dimensional methods starting with the identification of C(5)-H as the low field doublet and C(6)-H as the high field multiplet in the aromatic region of the ^{1}H-NMR spectrum.

Though C(7)-H and C(8)-H cannot be distinguished because of the accidental isochronism of their resonance frequencies, a two-dimensional ^{1}H-^{13}C chemical shift correlation spectrum (Figure 1) provides the complete assignment of all protonated carbon atoms.

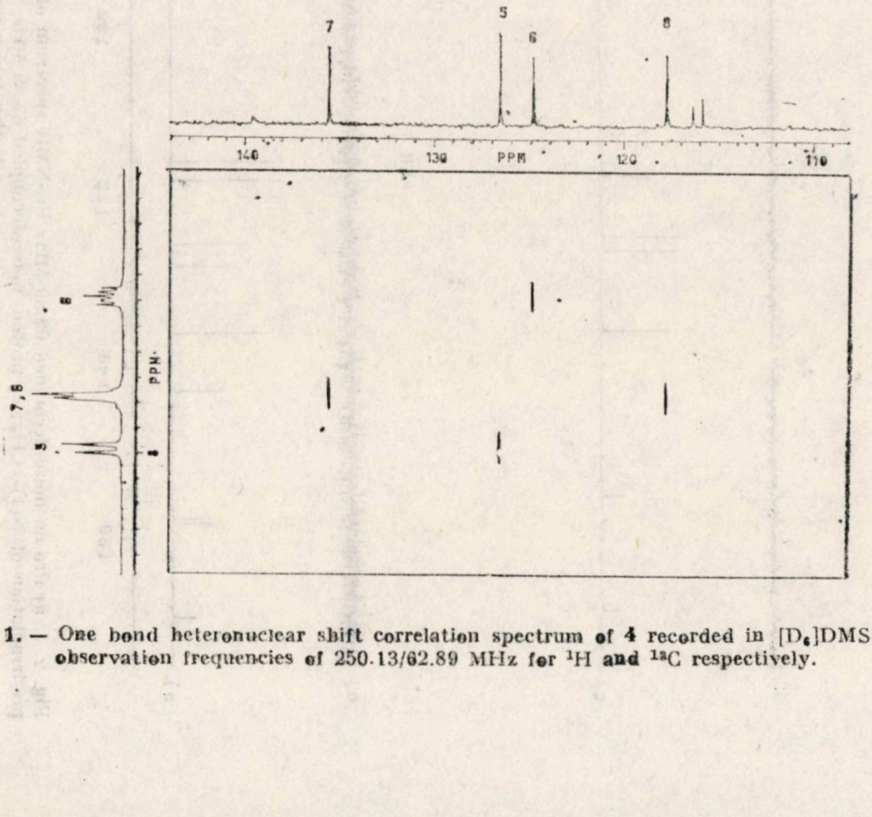

Fig. 1. — One bond heteronuclear shift correlation spectrum of **4** recorded in [D$_6$]DMSO at observation frequencies of 250.13/62.89 MHz for ^{1}H and ^{13}C respectively.

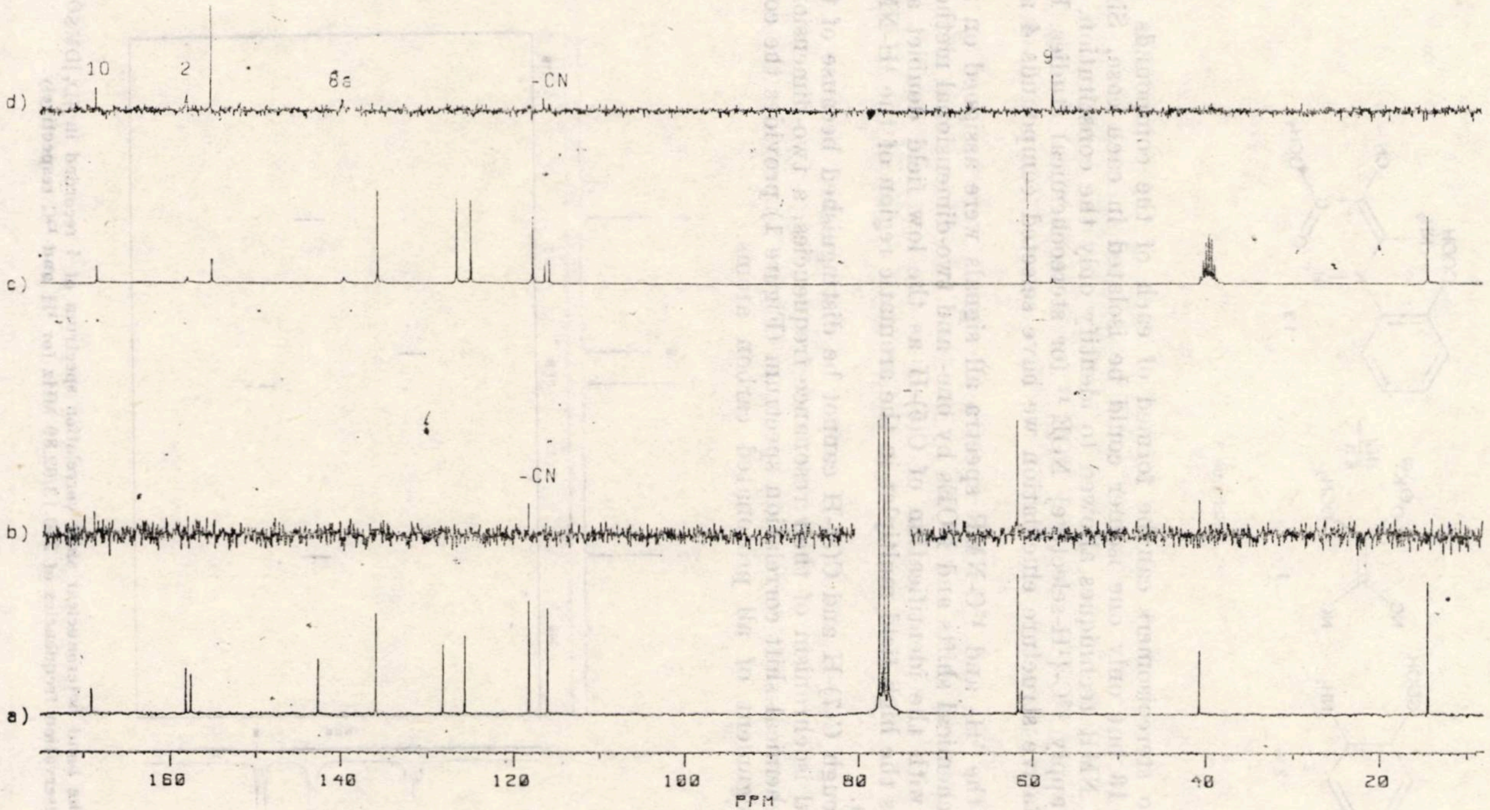

Fig. 2. — a) Proton noise-decoupled 62.89 MHz ^{13}C-NMR spectrum of **18** in CDCl$_3$; b) NOE difference spectrum obtained by selective low power pre-irradiation of N(1)−CH$_3$; c) proton noise-decoupled 62.89 MHz ^{13}C-NMR spectrum of **4** in [D$_6$]DMSO; d) NOE difference spectrum obtained by selective low power pre-irradiation of N(1)-Ph.

Unfortunately, both protons attached to the nitrogen atoms, i.e. N(1)-H and N(3)-H, undergo a slow chemical exchange which was detected by a homonuclear ^{1}H-NOE experiment. Therefore, it was impossible to irradiate selectively only one distinct N-H proton in a ^{13}C{^{1}H} nuclear Overhauser enhancement experiment. The obtained NOE difference spectra were the same either when the signal at 12.2 or 11.9 ppm was irradiated. Single-frequency ^{1}H pre-irradiation of one of these signals produces an NOE at both carbonyl groups, C(4) and C(10), so that the result was ambiguous. Further NOE enhancements of non-protonated carbon atoms occurred at the signals of C(2), C(8a), C(9) and the CN group (Figure 2) thus providing the unambiguous assignments of these carbon atoms, too.

The complication by tautomerism can be avoided by introduction of an alkyl group at either N(1) or N(3). The reaction of methyl N-methyl-anthranilate with potassium ethyl dicyanoacetate gives a derivative **18**, where the substituents at N(1) and N(3) cannot be interchanged by tautomerism. The position of the methyl group is determined by the educts and was in addition confirmed by a homonuclear NOE experiment.

Figure 2 shows the difference spectrum obtained from a heteronuclear NOE experiment. Pre-irradiation at the ^{1}H resonance frequency of N(1)-CH$_3$ only increased the intensity of the signal at 118.2 ppm by dipolar interaction of the N(1)-CH$_3$-protons with the CN carbon atom. This clearly demonstrates that the CN group but not the ester group is neighboured to N(1)-CH$_3$. Although the signal of the carbon atom to which the irradiated protons are directly bonded should not appear in the NOE difference spectrum because the protons of the ^{12}C, ^{1}H isotopomer are irradiated, overspill of the decoupler or signals of other protons nearby within a distance of about the half ^{13}C, ^{1}H coupling constant may result in NOEs at the corresponding carbon atoms by unavoidable irradiation of the ^{1}H signals of the ^{13}C, ^{1}H isotopomers. The signals at 62 ppm (-OCH$_2$CH$_3$) and 41 ppm (N(1)-CH$_3$) in the NOE difference spectrum of **18** shown in Figure 2 are artefacts in this sense.

For structure elucidation of compounds **3**–**9** an X-ray crystallography of compound **8** was performed. In this class of compounds the positions of CN and ester group at C(9) are reversed. Scheme 2 shows a series of equilibria preceding the cyclisation reaction. Because of the higher ability of N(1)-H in undergoing a hydrogen bond with the ester carbonyl group the conformation **10a** should be the preferred one. As a final result N(1) and COOR are Z to each other.

The lack of a proton at N(1) when anthranilic acid is replaced by methyl N-methylanthranilate and the steric hindrance of the N(1)-CH$_3$ group and the ester group in the intermediate product **15** seem to favour the E orientation of N(1)-CH$_3$ and COOR in compounds **17** and **18** (Scheme 4).

The bond lengths C(2)-C(9) (139.4 pm; standard double bond: 134 pm), C(11)-C(12) (145.2 pm) and C(11)-C(17) (143.2 pm) (standard single bond: 154 pm) reflect the push-pull character of the exocyclic double bond system. These values are in good agreement with those of similar systems.[13] Atom co-ordinates, equivalent isotropic displacement

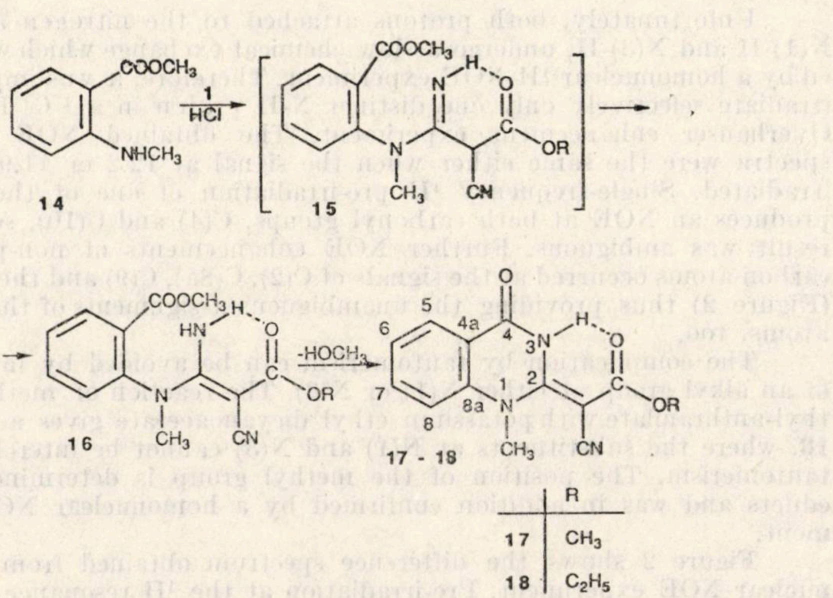
COOCH3
NHCH3
1
HCl
14
COOCH3
H
O
N
OR
N
CH3
CN
15
COOCH3
H
HN
O
-HOCH3
OR
N
CH3
CN
16
5
6
4a
4
3N
H
O
2
7
8a
1
N
OR
8
CH3
CN
17 - 18
R
17 CH3
18 C2H5

Scheme 4

factors, bond lengths and bond angles are presented in Tables 1—3; atom labelling and molecular conformation of compound 8 are illustrated in Figure 3 (the numbering in the text is referred to Scheme 1).

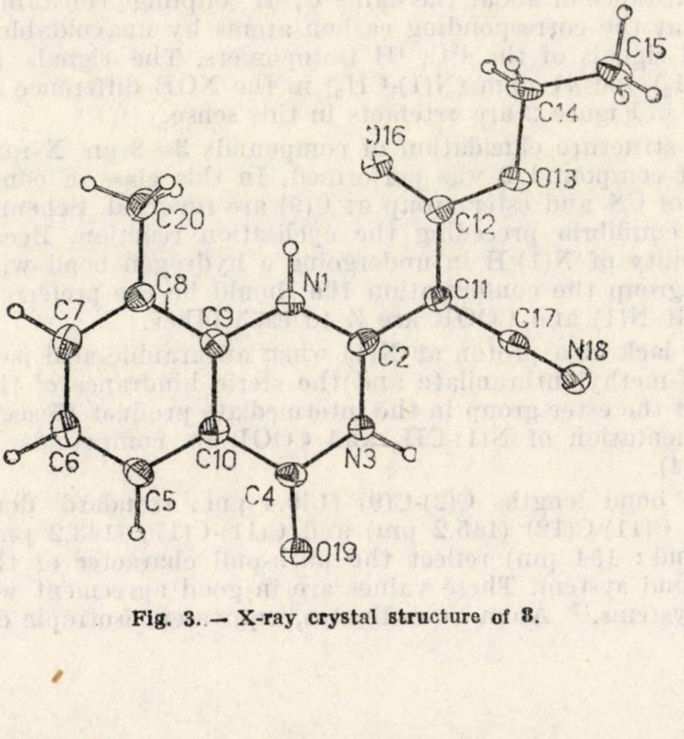
C15
C14
O16
O13
C20
C12
N1
C8
C11
C7
C9
C17
C2
N18
C6
C10
N3
C5
C4
O19

Fig. 3. — X-ray crystal structure of 8.

Table 1

Atomic coordinates ($\times 10^4$) and equivalent isotropic displacement factors ($Å^2 \times 10^3$)

	x	y	z	U_{eq}
N(1)	−1127(2)	3720(2)	1331(2)	22(1)*
C(2)	− 975(2)	4727(2)	1967(3)	21(1)*
N(3)	− 533(2)	4644(2)	3186(2)	21(1)*
C(4)	− 222(3)	3617(2)	3793(3)	22(1)*
C(5)	− 214(3)	1456(2)	3646(3)	25(1)*
C(6)	− 464(3)	462(3)	2957(3)	28(1)*
C(7)	− 923(3)	546(3)	1717(3)	27(1)*
C(8)	−1136(3)	1609(2)	1127(3)	24(1)*
C(9)	− 902(3)	2615(2)	1847(3)	21(1)*
C(10)	− 437(3)	2550(2)	3089(2)	22(1)*
C(11)	−1256(3)	5802(2)	1411(2)	20(1)*
C(12)	−1775(3)	5873(2)	139(3)	22(1)*
O(13)	−1999(2)	6981(2)	−212(2)	26(1)*
C(14)	−2607(3)	7151(3)	−1443(3)	27(1)*
C(15)	−2597(3)	8448(3)	−1681(3)	30(1)*
O(16)	−1995(2)	5035(2)	− 552(2)	30(1)*
C(17)	−1090(3)	6845(3)	2120(3)	22(1)*
N(18)	−945(2)	7682(2)	2700(2)	30(1)*
O(19)	212(2)	3641(2)	4879(2)	29(1)*
C(20)	−1609(3)	1700(3)	−213(3)	29(1)*

* Equivalent isotropic *U* defined as one third of the trace of the orthogonalized U_{ij} tensor.

Table 2

Bond lengths (Å)

N(1)—C(2)	1.345 (4)	N(1)—C(9)	1.397 (3)
C(2)—N(3)	1.373 (3)	C(2)—C(11)	1.394 (4)
N(3)—C(4)	1.378 (3)	C(4)—C(10)	1.449 (4)
C(4)—O(19)	1.235 (3)	C(5)—C(6)	1.376 (4)
C(5)—C(10)	1.403 (4)	C(6)—C(7)	1.398 (4)
C(7)—C(8)	1.387 (4)	C(8)—C(9)	1.402 (4)
C(8)—C(20)	1.504 (4)	C(9)—C(10)	1.402 (4)
C(11)—C(12)	1.452 (4)	C(11)—C(17)	1.422 (4)
C(12)—O(13)	1.341 (3)	C(12)—O(16))	1.228 (3)
O(13)—C(14)	1.460 (3)	C(14)—C(15)	1.506 (4)
C(17)—N(18)	1.148 (4)		

Table 3

Bond angles (°)

C(2)—N(1)—C(9)	124.2 (2)	N(1)—C(2)—N(3)	116.8 (2)
N(1)—C(2)—C(11)	121.4 (2)	N(3)—C(2)—C(11)	121.8 (2)
C(2)—N(3)—C(4)	125.1 (2)	N(3)—C(4)—C(10)	116.4 (2)
N(3)—C(4)—O(19)	120.0 (2)	C(10)—C(4)—O(19)	123.6 (2)
C(6)—C(5)—C(10)	119.0 (3)	C(5)—C(6)—C(7)	120.3 (3)
C(6)—C(7)—C(8)	122.5 (3)	C(7)—C(8)—C(9)	116.6 (2)
C(7)—C(8)—C(20)	122.5 (3)	C(9)—C(8)—C(20)	120.8 (2)
N(1)—C(9)—C(8)	120.2 (2)	N(1)—C(9)—C(10)	118.1 (2)
C(8)—C(9)—C(10)	121.7 (2)	C(4)—C(10)—C(5)	120.8 (2)
C(4)—C(10)—C(9)	119.4 (2)	C(5)—C(10)—C(9)	119.8 (2)
C(2)—C(11)—C(12)	121.2 (2)	C(2)—C(11)—C(17)	119.6 (2)
C(12)—C(11)—C(17)	119.1 (2)	C(11)—C(12)—O(13)	111.9 (2)
C(11)—C(12)—O(16)	125.2 (3)	O(13)—C(12)—O(16)	122.8 (2)
C(12)—O(13)—C(14)	116.6 (2)	O(13)—C(14)—C(15)	106.2 (2)
C(11)—C(17)—N(18)	179.2 (3)		

EXPERIMENTAL

Melting points were determined on a Reichert hot stage microscope and are uncorrected. Microanalyses were performed on a Heraeus automatical analyser. UV spectra were recorded on a Carl Zeiss DMR 10 spectrophotometer and IR spectra on a Perkin-Elmer 325 spectrophotometer. NMR spectra were recorded on a Bruker WM-250 spectrometer (for ^{1}H-NMR at 250.13 MHz, for ^{13}C-NMR at 62.89 MHz). Primary, secondary, tertiary and quaternary carbons were differentiated either by off-resonance decoupling, gated decoupling or J-modulated spin echo experiments (signal phase : $+ =$ C, CH_2 ; $- =$ CH, CH_3). Mass spectra were obtained on a Varian MAT 311 A instrument. For technique of heteronuclear NOE difference spectra see ref. 14.

Crystal Data for **8** : $C_{14}H_{13}N_3O_3$, M = 271.3, monoclinic, a = 1046.3(3), b = 1145.0(5), c = 1063.2(4) pm, $\alpha = 90$, $\beta = 90.89$ (3), $\gamma = 90°$, $V = 12.736(9) \times 10^8$ pm^3, space group $P2_1/n$, Z = 4, $d_{calc.} = 1.415$ gcm^{-3}. 1667 Independent reflections were measured on a Nicolet R3mV diffractometer with Mo-K radiation. Of these 1270 had $F_0 > 4\sigma(F)$ and were considered to be observed. The structure was solved by direct methods. The maximum residual electron density was 0.174 e/A^3.

Methyl (E)-2-cyano-2-[(1H,3H)quinazoline-4-one-2-ylidene]acetate (**3**) : A typical procedure for the preparation of **3** to **9**. A solution of 5.3 g (33 mmol) potassium methyl dicyanoacetate (**1**) and 4.1 g (30 mmol) anthranilic acid (**2**) in 2.7 mL conc. hydrochloric acid and 60 mL water was refluxed for 20 h. After cooling the precipitate was collected by filtration and then recrystallized from dioxane when 2.5 g (34%) of white crystals were obtained, mp : 287°C. — IR (KBr) : $\nu = 3220$ cm^{-1} (m, N—H), 3020 (w, aromatic), 2205 (s, CN), 1680 (s, C=O), 1670(s, C=O), 1635 (s, C = C), 1090 (s, C—O). — UV/VIS (acetonitrile) : $\lambda_{max}(\log\varepsilon) =$ = 214 nm (4.447), 296(4.602). — ^{1}H-NMR (250.13 MHz, [D_6]DMSO) : $\delta = 3.74$ (s, 3H, —OCH_3), 7.39 (mult, 1H, 6-H), 7.78 (d, 1H, 7-H and 8-H), 7.98 (d, 1H, 5-H), 11.95 (s, br., 1H, NH), 12.20 (s, br., 1H, NH). — ^{13}C-NMR (62.89 MHz, [D_6]DMSO) : $\delta = 51.7$ (q, OCH_3), 57.3 (s, = *C*(CN)($COOCH_3$)), 115.8 (s, C-4a), 116.4 (s, CN), 117.7 (d, C-7), 124.9 (d, C-5), 126.5 (d, C-6), 135.6 (d, C-8), 139.5 (s, C-8a), 155.0 (s, C-4), 157.9 (s, C-2), 168.7 (s, COO). — MS (80eV 178°C) : *m/z*(%) = 344(12) [$M^+ + 1$], 243(81) [M^+], 212(34) [$M^+ - OCH_3$], 211(100) [$M^+ - OCH_3$],

$C_{12}H_9N_3O_3$ (243.23) calcd. : 243.0644 found : 243.0644 (MS) ; calcd. : C 59.26 H 3.73 N 1708% ; found : C 59.28 H 3.86 N 17.06%.

Ethyl (E)-2-cyano-2-[(1H, 3H)quinazoline-4-one-2-ylidenel]acetate (**4**) : From 1.37 g. (10 mmol) anthranilic acid and 1.76 g (10 mmol) potassium ethyl dicyanoacetate in 0.9 mL conc. hydrochloric acid and 20 mL water 4 (0.91 g, 35%) was obtained, mp : 262—263°C. — IR (KBr) : $\nu = 3185$ cm^{-1} (w, NH), 3030 (w, CH-aromatic), 2980 (w, CH), 2210 (m, CN), 1700 (s, C=O), 1650(s), 1600 (s, aromatic), 1085 (m, C-O) — UV/VIS (acetonitrile) : $\lambda_{max}(\log\varepsilon)$ = 217 nm (4.333), 307 (4.449). — ^{1}H-NMR (250.13 MHz, [D_6]DMSO) : $\delta = 1.26$ (t, 3H, CH_2CH_3), 4.21 (q, 2H, OCH_2CH_3), 7.39 (mult, 1H, 6-H), 7.78 (d, 2H, 7-H and 8-H), 7.90 (d, 1H, 5-H), 11.94 (s, br., 1H, NH), 12.25 (s, br., 1H, NH). — ^{13}C-NMR (62.89 MHz, [D_6]DMSO) : $\delta = 14.3$ (q, CH_2CH_3), 57.4 (s, = *C*(CN)($COOCH_3$)), 60.4 (t, OCH_2CH_3), 115.8 (s, C-4a), 116.3 (s, CN), 117.7 (d, C-7), 124.9 (d, C-5), 126.5 (d, C-6), 135.6(d, C-8), 139.5 (s, C-8a), 155.0(s, C-4), 157.8 (s, C-2), 168.3 (s, COO). — MS (80eV, 140°C) : *m/z* (%) = 258(10) [$M^+ + 1$], 257(70) [M^+], 212(28) [M^+-OCH_2CH_3], 211(100) [M^+-$HOCH_2CH_3$], 186(11) [212-CN], 185(26) [211-CN]

$C_{13}H_{11}N_3O_2$ (257.26) ; calcd. : C 60.69 H 4.31 N 16.34% ; found : C 60.83 H 4.37 N 16.22%.

Butyl (E)-2-cyano-2-[(1H, 3H) quinazoline-4-one-2-ylidene]acetate (**5**) : From 1.37 g (10 mmol) anthranilic acid and 2.04 g (10 mmol) potassium butyl dicyanoacetate in 0.9 mL conc. hydrochloric acid and 40 mL water **5** (1.3 g, 46%) was obtained, mp : 227—228°C.— IR (KBr) : $\nu = 3180$ cm^{-1} (w, NH), 3030 (w, CH aromatic), 2980 (m, CH), 2940 (w), 2880 (w, CH), 2210 (m, CN), 1720 (s, C=O), 1675(s), 1640(s), 1090 (m, C-O). — UV/VIS (acetonitrile) : $\lambda_{max}(\log\varepsilon) = 216$ nm (4.347), 306(4.469). — ^{1}H-NMR (250.13 MHz, [D_6]DMSO) : $\delta = 0.91$ (t, 3H, CH_3), 1.38 (sext, 2H, CH_2CH_3), 1.61 (mult, 2H, $CH_2CH_2CH_3$), 4.19(t, 2H, OCH_2CH_2-), 7.31—7.45 (m, 1H, 6-H), 7.78 (d, 2H, 7-H and 8-H), 7.90 (d, 1H, 5-H), 11.89 (s, br., 1H, NH), 12.24 (s, br., 1H, NH). — ^{13}C-NMR (62.89 MHz, [D_6]DMSO) : $\delta = 13.5$ (q, CH_2CH_3), 18.6 (t, CH_2CH_3), 30.3 (t, $CH_2CH_2CH_3$), 57.4 (s, = *C*(CN)(COOR)), 64.0 (t, OCH_2CH_3), 115.8 (s, C-4a), 116.3 (s, CN), 117.7 (d, C-7), 124.9 (d, C-5), 126.5 (d, C-6), 135.6 (d, C-8), 139.5 (s, C-8a), 155.0 (s, C-4), 157.8 (s, C-2), 168.4 (s, COO). — MS (80 eV, 162°C) : *m/z* (%) = 286(9) [$M^+ + 1$], 285(51) [M^+], 230(9), 229(57) [M^+-C_4H_8,McLafferty-rearrangement], 213(5), 212(38) [M^+-OC_4H_9], 211(100) [M^+-HOC_4H_9], 186(9) [212-CN], 185(34) [211-CN], 157(23) [185-CO].

$C_{15}H_{15}N_3O_3$ (285.32); calcd.: C 63.15 H 5.30 H 5.30 N 14.73%; found: C 63.33 H 5.36 N 14.57%.

Benzyl (E)-2-cyano-2-[(1 H, 3H) quinazoline-4-one-2-ylidene]acetate (**6**): From 1.10 g (8 mmol) anthranilic acid and 2.14 g (9.6 mmol) sodium benzyl dicyanoacetate in 0.72 mL conc. hydrochloric acid and 40 mL water **6** (1.1 g, 43%) was obtained, mp: 273°C. — IR (KBr): $\nu = 3170\ cm^{-1}$ (w, NH), 3020 (w, CH aromatic), 2940 (w, CH), 2220 (m, CN), 1725 (s, C=O), 1675(s), 1650(s), 1600 (m, aromatic), 1085 (m, C-O), — UV/VIS (acetonitrile): $\lambda_{max}(\log\varepsilon) =$ = 223 nm (4.361), 309(4.513). — ^1H-NMR (250.13 MHz, $[D_6]$DMSO): $\delta = 5.25$ (s, 2H OCH_2-), 7.35—7.50 (m, 6H, 6-H/-C_6H_5), 7.78 (d, 2H, 7-H and 8-H), 7.90 (d, 1H, 5-H), 11.95 (s, br., 1H, NH), 12.15 (s, br., 1H, NH). — ^{13}C-NMR (62.89 MHz, $[D_6]$DMSO): $\delta = 57.4$ (s, = *C*(CN)(COOR)), 65.5 (t, O*C*H_2-), 115.9 (s, C-4a), 116.3 (s, CN), 117.8 (d, C-7), 125.0 (d, C-5), 126.6 (d, C-6), 127.7/128.0/128.4 (3d, C-2′-C-6′) 135.6 (d, C-8), 136.1 (s, C-1′), 139.4 (s, C-8a), 155.05 (s, C-4), 157.9 (s, C-2), 168.1 (s, COO). — MS (80 eV, 162°C): $m/z(\%) = 319(10)$ $[M^+]$, 275(2), 212(1) $[M^+\text{-}OCH_2C_6H_5]$, 185(1) [212-HCN], 157(3) [185-CO], 91(100) $[C_7H_7^+]$.

$C_{18}H_{13}N_3O_3$ (319.33); calcd.: C 67.77 H 4.10 N 13.16%; found: C 67.75 H 4.20 N 12.91%.

Methyl (E)-2-cyano-2-[8(1H, 3H)methylquinazoline-4-one-2-ylidene]acetate (**7**): From 1.51 g (10 mmol) 3-methylanthranilic acid and 1.7 g (9.6 mmol) potassium methyl dicyanoacetate in 0.9 mL conc. hydrochloric acid and 30 mL water **7** (0.98 g, 38%) was obtained, mp: 275°C. — IR (KBr): $\nu = 3175\ cm^{-1}$ (w, NH), 3155 (w, NH), 3090 (w, NH), 3005 (w, CH-aromatic), 2990 (w, CH), 2205 (m, CN), 1715 (s, C=O), 1665 (s, C=O), 1290 (s), 1150 (m), 1095 (m, C-O). — UV/VIS (acetonitrile): $\lambda_{max}(\log\varepsilon) = 219$ nm (4.365), 308(4.451). — ^1H-NMR (250.13 MHz, $[D_6]$DMSO): $\delta = 2.40$ (s, 3H, Ar-CH_3), 3.77 (s, 3H, OCH_3), 7.30 (t, 1H, 6-H), 7.69 (d, 1H, 7-H), 7.85 (d, 1H, 5-H), 12.05 (s, br., 1H, NH), 12.51 (s, br., 1H, NH). — ^{13}C--NMR (62.89 MHz, $[D_6]$DMSO): $\delta = 15.6$ (q, Ar-CH_3), 51.8 (q, OCH_3), 57.9 (s, = *C*(CN)($COOCH_3$)), 115.7 (s, CN), 115.9 (s, C-4a), 124.5 (d, C-6 and C-5), 124.6 (s, C-8), 136.3 (d, C-7), 136.7 (s, C-8a), 154.7 (s, C-4), 159.5 (s, C-2), 169.6 (s, COO). — MS (80 eV, 162°C): $m/z(\%) = 258(12)$ $[M^+ + 1]$, 257(82) $[M^+]$, 226(30) $[M^+\text{-}OCH_3]$, 225(100) $[M^+\text{-}HOCH_3]$, 198(4), 197(24) [225-CO]‘ 171(6) [197-CN].

$C_{13}H_{11}N_3O_3$ (257.26); calcd.: C 60.69 H 4.31 N 16.34%; found: C 60.97 H 4.35 N 16.45%.

Ethyl (E)-2-cyano-2-[8(1H, 3H)methylquinazoline-4-one-2-ylidene]acetate (**8**): From 1.51 g (10 mmol) 3-methylanthranilic acid and 1.76 g (9.6 mmol) potassium ethyl dicyanoacetate in 0.9 mL conc. hydrochloric acid and 40 mL water **8** (0.97 g, 36%) was obtained, mp: 259—260°C. — IR (KBr): $\nu = 3190\ cm^{-1}$ (w, NH), 3160 (w, NH). 3090 (w, NH), 2210 (s, CN), 1695 (s, C=O), 1660 (s, C=O), 1170 (s, C-O), 1095 (m, C-O). — UV/VIS (acetonitrile): $\lambda_{max}(\log\varepsilon) = 218$ nm (3.808), 311 (4.070). — ^1H-NMR (250.13 MHz, $[D_6]$DMSO): $\delta = 1.26$ (t, 3H, CH_2CH_3), 2.43 (s, 3H, Ar-CH_3), 4.25 (s, 2H, OCH_2), 7.23 (t, 1H, 6-H), 7.70 (d, 1H, 7-H), 7.86 (d, 1H, 5-H), 12.02 (s, br., 1H, NH), 12.56 (s, br., 1H, NH). — ^{13}C-NMR (62.89 MHz, $[D_6]$DMSO): $\delta = 14.3$ (q, CH_2CH_3), 15.6 (q, Ar-CH_3), 58.1 (s, =*C*(CN)($COOCH_3$)), 60.4 (t, OCH_2-), 115.7 (s, CN), 115.9 (s, C-4a), 124.5 (d, C-6 and C-5), 124.7 (s, C-8), 136.3 (d, C-7), 136.7 (s, C-8a), 154.7 (s, C-4), 159.5 (s, C-2), 169.2 (s, COO). — MS (80 eV, 162°C): $m/z(\%) =$ = 272(13) $[M^+ + 1]$, 271(70) $[M^+]$, 243 (4) $[M^+\text{-}CO]$, 227 (4), 226 (31) $[M^+\text{-}OCH_2CH_3]$, 225(100) $[M^+\text{-}HOCH_2\text{-}CH_3]$, 224(5), 200(12), 199(31) [225-CN].

$C_{14}H_{13}N_3O_3$ (271.29); calcd.: C 61.98 H 4.83 N 15.49%; found: C 62.16 H 4.88 N 15.53%.

Benzyl (E)-2-cyano-2-[8(1H,3H)methylquinazoline-4-one-2-ylidene]acetate (**9**): From 1.21 g (8 mmol) 3-methylanthranilic acid and 2.02 g (9.2 mmol) sodium benzyl dicyanoacetate in 0.72 mL conc. hydrochloric acid and 40 mL water **9** (0.61 g, 23%) was obtained, mp: 198—200°C. — IR (KBr): $\nu = 3170\ cm^{-1}$ (w, NH), 3100 (w, NH), 3070 (w, NH), 3040 (w, CH-aromatic), 2970 (w, CH), 2220 (m, CN), 1695 (s, C=O). — UV/VIS (acetonitrile): $\lambda_{max}(\log\varepsilon) = 215$ nm (4.251), 300 (4.317). — ^1H-NMR (250.13 MHz, $[D_6]$DMSO): $\delta = 2.37$ (s, 3H, Ar-CH_3), 5.28 (s, 2H, OCH_2-), 7.27 (t, 1H, 6-H), 7.31—7.43 (m, 5H, phenyl ring), 7.64 (d, $^3J = 8$ Hz, 1H, 7-H), 7.82 (d, $^3J = 8$ Hz, 1H, C-5), 12.01 (s, br., 1H, NH), 12.42 (s, br., 1H, NH). ^{13}C-NMR(62.89 MHz, $[D_6]$DMSO): $\delta = 15.6$(—, Ar—CH_3), 58.2(+, =*C*(CN)(COOR)), 65.5 (+, OCH_2-), 115.6 (+, CN), 116.0 (+, C-4a), 124.5/124.7 (—, C-6 and C-5), 124.8 (+, C-8), 127·6/128.0/128.5 (—, C-2′—C-6′), 136.1 (+, C-1′), 136.3 (—, C-7), 136.6 (+, C-8a), 154.7 +, C-4), 159.4 (+, C-2), 169.6 (+, COO). — MS (80 eV, 162°C): $m/z(\%) = 333(8)$ $[M^+]$, 9 (100) $[C_7H_7^+]$,.

$C_{19}H_{15}N_3O_3$ (333.36); calcd.: C 68.46 H 4.54 N 12.61%; found: C 68.05 H 4.82 N 12.03%

Methyl 3-Amino-3-(2-carboxy)phenylamino-2-cyanacrylate (**13**): A solution of 1.78 g (11 mmol) potassium methyl dicyanoacetate (**1**) and 1.37 g (10 mmol) anthranilic acid (**2**) in 0.9 mL conc. hydrochloric acid and 20 mL water was refluxed for 8 h. After cooling the precipitate was collected by filtration and then recrystallized from dioxane. mp: 273°C. — IR (KBr): $\nu = 3420\ cm^{-1}$ (m, NH), 3220 (m, NH), 3010 (w, CH-aromatic), 2960 (w, CH), 2200 (s, CN), 1670 (s, C=O), 1630 (s,), 1605 (s, C=C). — UV/VIS (acetonitrile): λ_{max}(log ε) = 211 nm (4.396), 240(4.023), 285(4.303). — ^{1}H-NMR (250.13 MHz, [D$_6$]DMSO): δ = 3.63 (s, 3H, OCH$_3$), 7.27 (t, ^{3}J = 7Hz, 1H, 5-H), 7.48 (d, ^{3}J = 7Hz, 1H, 3-H), 7.63 (t, 1H, 4-H), 7.96(dd, ^{3}J = 7Hz, 1H, 6-H), 10.08 (s, br., 1H, NH), 13.5 (s, br., 2H, NH$_2$). — ^{13}C-NMR (62.89 MHz, [D$_6$]DMSO): δ = 50.6 (q, OCH$_3$), 56.7 (s, =*C*(CN)(COOCH$_3$)), 118.6 (6, CN/C-1), 123.7 (d, C-3), 124.8 (d, C-5), 131.3 (d, C-6), 133.6 (d, C-4), 137.5 (s, C-2), 160.9 (s, COOH), 167.9 (s, > *C*=C(CN)(COOCH$_3$)), 168.5 (s, *C*OOCH$_3$). — MS (80eV, 162°C): *m/z*(%) = 262(4) [M$^+$+ 1], 261(28) [M$^+$], 244(10) [M$^+$-OH], 243(61) [M$^+$-H$_2$O], 212(39) [M$^+$-OCH$_3$], 211(100) [243-HOCH$_3$].

$C_{12}H_{11}N_3O_4$ (261.26) calcd.: 261.0754 found: 261.0750 (MS); calcd: C 55.17 H 4.24 N 16.09%; found: C 55.31 H 4.35 N 15.78%.

Methyl (E)-2-cyano-2-[1(1H, 3H)methylquinazoline-4-one-2-ylidene]acetate (**17**): A solution of 330 mg (2 mmol) methyl N-methylanthranilate and 324 mg (2 mmol) potassium methyl dicyanoacetate in 10 mL 2 mM hydrochloric acid was refluxed under nitrogen for 20 h. After cooling the precipitate was collected by filtration and then recrystallized from acetone, white crystals, 260 mg (51%), mp: 273°C. — IR (KBr): ν = 3090 cm^{-1} (w, NH), 2210(s, CN), 1710 (s, C=O), 1705(s, C=O), 1660(s), 1655(s, C=C), 1080 (m, C—O). — UV/VIS (acetonitrile): λ_{max}(log ε) = 210 nm (4.315), 305(4.486). — ^{1}H-NMR (250.13 MHz, [D$_6$]DMSO): δ = 3.76(s, 3H, OCH$_3$), 3.82(s, NCH$_3$), 7.39(t, 1H, 6-H), 7.68(d, 1H, 8-H), 7.91(dt, 1H, 7-H), 8.07(dd, 1H, 5-H), 12.64(s, br., 1H, NH). — ^{13}C-NMR (62.89 MHz, [D$_6$]DMSO): δ = 40.5(-, NCH$_3$), 520(—, OCH$_3$), 59.3(+, =*C*(CN)(COOCH$_3$)), 117.5(—, C-7), 117.7(+, CN), 117.9(+, C-4a), 125.5(—, C-5), 126.6(—, C-6), 135.8(—, C-8), 142.5(+, C-8a), 157.5(+, C-4), 157.6(+, C-2), 168.2(+, COO). — MS (80 eV, 162°C): *m/z*(%) = 258(15) [M$^+$+ 1], 257(100) [M$^+$], 226.(52) [M$^+$-OCH$_3$], 225(15) [M$^+$-HOCH$_3$], 200(11) [226-CN], 199(92) [226-HCN].

$C_{13}H_{11}N_3O_3$ (257.26) calcd.: 243.0644 found: 243.0644 (MS); calcd.: C 60.69 H 4.31 N 16.34%; found.: C 60.98 H 4.31 N 16.47%.

Ethyl (E)-2-cyano-2-[1(1H, 3H)methylquinazoline-4-one-2-ylidene]acetate (**18**): A solution of 570 mg (4.45 mmol) methyl N-methylanthranilate and 610 mg (3.45 mmol) potassium ethyl dicyanoacetate in 10 mL 3.45 mM hydrochloric acid was refluxed under nitrogen for 10 h. After cooling the precipitate was collected by filtration and then recrystallized from acetone. mp: 255—275°C. — IR (KBr): ν = 3100 cm^{-1} (w, NH), 2200(s, CN), 1715(s, C=O), 1705(s, C=O) 1645(s), 1640(s, C=C), 1635(s), 1615(s), 1085(m, C—O). — UV/VIS (acetonitrile): λ_{max}(log ε) = = 208 nm (4.294), 297(4.486). — ^{1}H-NMR (250.13 MHz, [D$_6$]DMSO): δ = 1.37(t, 3H, CH$_2$CH$_3$), 3.94(s, NCH$_3$), 4.32(q, 2H, OCH$_2$CH$_3$), 7.33(d, ^{3}J = 8, 1H, 8-H), 7.44(t, ^{3}J = 7, 1H, 6-H), 7.79(dt, ^{3}J = 7, ^{4}J = 2, 1H, 7-H), 8.22(dd, ^{3}J = 8, ^{4}J = 2, 1H, 5-H), 12.98(s, br., 1H, NH). — ^{13}C-NMR (62.89 MHz, [D$_6$]DMSO): δ = 14.4(—, CH$_2$CH$_3$), 40.7(—, NCH$_3$), 61.2(+, =*C*(CN)(COOC$_2$H$_5$)), 61.7(+, OCH$_2$CH$_3$), 116.1(—, C-7), 118.2(+, CN), 118.2(+, C-4a), 125.6(—, C-5), 128.1(—, C-6), 135.8(—, C-8), 142.6(+, C-8a), 157.5(+, C-4), 158.1(+, C-2), 169.1(+, COO). — MS (80 eV, 162°C): *m/z*(%) = 272(6) [M$^+$+ 1], 271(43) [M$^+$], 227(4), 226(24) [M$^+$-OC$_2$H$_5$], 225(3) [M$^+$-HOCH$_2$CH$_3$], 200(11) [226-CN], 199(100) [226-HCN].

$C_{14}H_{13}N_3O_3$ (271.29) calcd.: C 61.98 H 4.83 N 15.49%; found: C 61.95 H 4.85 N 15.37%.

ACKNOWLEDGEMENTS. Generous support of this work by *BASF AG*, *Verband der Chemischen Industrie-Fonds der Chemie-*, and *Deutsche Forschungsgemeinschaft* is gratefully acknowledged. We are indebted to *Mrs. G. Schormann* and *Mr. G. Beutel* for carrying out routine NMR spectra and elemental analyses, to *Mr. H. Rudy* and *Mr. P. Weyrich* for IR and mass spetra. Z. Sui thanks the *Konrad-Adenauer-Stiftung* for financial support; we also thank *Bayer AG* and *Hoechst AG* for general gifts of chemicals.

REFERENCES

[1] R. Neidlein and Z. Sui, *Chem. Ber.*, **123**, 2203 (1990).

[2] R. Neidlein and Z. Sui, *Synthesis*, **1990**, 959.

[3] R. Neidlein and Z. Sui, *Synthesis*, **1991** (submitted).

[4] R. Neidlein and D. Kikelj, *Chem. Ber.*, **121**, 1817 (1988).

[5] R. Neidlein and D. Kikelj, *Synthesis*, **1988**, 981.

[6] R. V. Coombs, R. P. Dama, M. Denzer, G. E. Hardtmann, B. Huegi, G. Koletar, J. Koletar, H. Ott, E. Jukmervicz, J. W. Perrine, E. I. Takesue and J. H. Trapold, *J. Med. Chem.*, **16**, 1237 (1973).

[7] H. Vinazzer, *Int. J. Clin. Pharmacol. Biopharm.*, **15**, 214 (1977).

[8] H. Yamamoto, C. Saito, H. Awata, M. Yamamoto, Y. Sakai and T. Komatsu, *Arzneimittel-Forsch.*, **23**, 1266 (1973).

[9] Y. Yanagi and T. Komatsu, *Biochem. Pharmacol.*, **25**, 937 (1976).

[10] Y. Yanagi, *Biochem. Pharmacol.*, **27**, 723 (1978).

[11] R. Neidlein, D. Kikelj, W. Kramer, Z. Sui, R. Boese, D. Bläser and D. Kocjan, *Chem. Ber.*, **122**, 1341 (1989).

[12] C. Cativiela and F. Sanchez-Ferrando, *Magn. Reson. Chem.*, **23**, 1073 (1985).

[13] Z.-T. Huang, W.-X. Gan and X.-J. Wang, *J. prakt. Chem.*, **330**, 724 (1988).

[14] R. Neidlein, W. Kramer and V. Ullrich, *Helv. Chim. Acta*, **69**, 896 (1986).

Revue Roumaine de Chimie, **36**, *4*–*7*, 613–618 (1991)

En hommage au Professeur A. T. BALABAN
pour son 60e anniversaire

ACYLATION D'ALCÈNES DANS LE SYSTÈME ACYLANT ACIDE TRIFLUOROMÉTHANESULFONIQUE-HALOGÉNURE D'ACIDE

CHRISTIAN ROUSSEL,* HARIVELO G. RAJOHARISON et JACQUES METZGER
ENSSPICAM, URA 1410, Université Aix-Marseille III, Avenue Escadrille Normandie Niemen,
13397 Marseille Cedex 13 France

Reçu le 15 janvier, 1991

The diacylation of 2-methyl-2-pentene and of related alcoholic precursors with trifluoromethanesulphonic acid/acetyl chloride was investigated. The initially formed pyrylium salts were converted directly into the corresponding pyridines. The influence of the reaction conditions (temperature ; molar ratios $AcCl/F_3CSO_3H$/alkene ; experimental procedure) was thoroughly examined permitting the observation of new aspects for the examined synthesis of pyrylium salts e.g. : a) formation of less substituted pyrylium salts **2** up to 94 % selectivity ; b) direct access to isomeric pyrylium salts **1** and **2** depending on the reaction conditions ; c) formation of triacylation products **3**, **4** which could be suppressed in favour of **2**. The described procedure presents also experimental advantages (no crackings ; easily tractable reaction mixtures).

INTRODUCTION

Le système acylant halogénure d'acide-acide protonique a été très peu utilisé dans la synthèse de sels de pyrylium par acylation d'alcènes.[1,2] Balaban et coll.[3] ont utilisé un mélange chlorure d'acétyle-acide perchlorique pour diacétyler l'isobutène (génére *in situ*) ou acétyler l'oxyde de mésityle en sel de 2,4,6-triméthyl pyrylium. A partir d'un alcène pouvant conduire à deux sels de pyrylium isomères les auteurs ont obtenu une réaction très régiosélective. Après traitement à l'ammoniaque, la 2,3,4,6-tetraméthylpyridine en mélange avec la 4-éthyl-2,6-diméthylpyridine a été obtenue avec une très grande sélectivité. Anderson et Stang[4] ont préparé le 2,6-ditertiobutyl-4-méthyl pyrylium par acylation de l'isobutène avec le chlorure de pivaloyle catalysée par CF_3SO_3H.

Nous avons montré que la réaction des chlorures d'acides benzoïques substituées avec les alcènes conduit en présence de CF_3SO_3H à des dérivés de chloroindènes inaccessibles dans les conditions classiques d'acylation catalysés par les acides de Lewis.[5,6]

Nous décrivons ici l'utilisation du système acylant CF_3SO_3H-halogénure d'acide dans la préparation des sels de pyrylium à partir d'isoalcènes ou de leurs précurseurs.

RÉSULTATS

Étude préliminaire

La réaction étudiée est celle de la diacétylation du 2-métyl-2-pentène. Catalysée par un acide protonique (CF_3SO_3H, CH_3SO_3H, $HClO_4$, acide carboxyméthanesulfonique, Nafion) et en présence d'anhydride acétique, cette réaction conduit à la formation de deux sels de pyrylium isomères **1** et **2** avec une sélectivité toujours en faveur du produit le plus substitué **1**.[7,8]

Tableau 1

Acétylation du 2-méthyl 2-pentène

Mode	Temp. (°C)	HX	Rapport[a]	Distribution des pyridines					Sélectivité	Rendement
				1	2	3	4	5	2/ 1 + 2	(%)
1 B2	50	CH_3SO_3H	12/3/1	66	34	—	—	—	34	48
2 B2	50	$HClO_4$	12/3/1	65	35	—	—	—	35	74
3 B2	50	CF_3SO_3H	12/3/1	26	65	1.5	1.4	5.4	71	90
4 A1	0	CF_3SO_3H	6/1/1	21	68			10.3	77	23
5 A2	0	CF_3SO_3H	6/1/1[b]	81	19	—	—	—	19	67
6 B1	50	CF_3SO_3H	6/1/1	7	63	6.1	7.1	16.4	89	32
7 B2	50	CF_3SO_3H	6/1/1	49	46	0.5	0.4	3.9	48	59
8 B2	50	CF_3SO_3H	12/1/1	52	48	—	—	—	48	60
9 B2	50	CF_3SO_3H	6/2/1	36	57	0.5	0.2	5.7	61	67
10 B2	50	CF_3SO_3H	6/3/1	28	64	—	—	7.5	69	92
11 B2	50	CF_3SO_3H	6/3/1[c]	30	70	—	—	—	70	55
12 B2	50	CF_3SO_3H	12/3/1[b]	20	73	2.1	2.0	2.6	79	87
13 B1	0	CF_3SO_3H	12/1/1	9.6	65	6.2	5.7	13.2	87	50
14 B1	0	CF_3SO_3H	12/2/1	7.5	63	6	6.1	14.3	89	35
15 B1	0	CF_3SO_3H	12/3/1	4	68	6.9	5.6	15.5	95	66
16 B1	0	CF_3SO_3H	12/4/1	3.7	60	10.8	16.2	9.7	94	70
17 B1	0	CF_3SO_3H	4/4/1	3	62	9.9	8.6	16.3	95	60

[a] Rapport CH_3COCl/ HX/ Alcène. [b] Précurseur : 2-méthyl 2-pentanol. c) Précurseur : 2-méthyl 1-pentène.

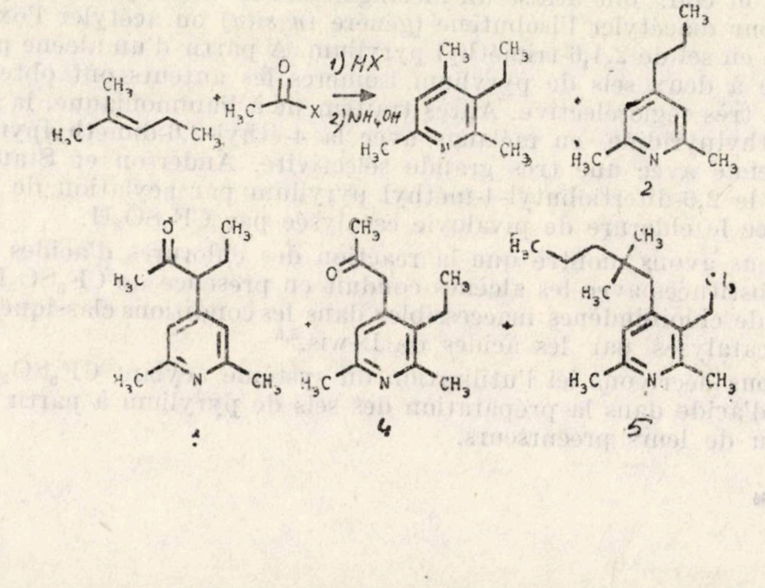

Nous rapportons dans le tableau 1 entrées 1,2,3, les résultats des essais conduits avec trois acides protoniques et le chlorure d'acétyle. Les résultats sont analysés à partir des pyridines obtenues par traitement à l'ammoniaque concentré (33%). Avec les acides méthanesulfonique et perchlorique, les deux pyridines attendues sont obtenues avec une sélectivité en faveur de la plus substituée inférieure à celle du mélange acylant anhydride d'acide — acide protonique. Avec le superacide CF_3SO_3H, *la pyridine la moins substituée* **2** *est obtenue preferentiellement*. Alors qu'une telle sélectivité est connue dans le cas des réactions catalysées par les acides de Lewis,[1,2,9] elle est observée ici pour la première fois dans un milieu acide protonique. Trois autres pyridines **3**, **4** et **5** correspondant aux réactions de triacylation du 2-méthyl 2-pentène et à la diacylation du dimère de l'alcène sont identifiées dans ce mode opératoire. Ce résultat nous a conduit à approfondir l'étude de la réaction en présence de CF_3SO_3H.

Quatre modes opératoires différents ont été testés en modifiant soit l'ordre d'addition des réactifs, soit la température des réactions. Nous avons choisi deux catégories de modes opératoires. a) Modes A : addition de CF_3SO_3H sur le mélange agité de CH_3COCl-alcène ; A_1 — addition et réaction à 0°C. A_2 — addition et réaction à reflux du chlorure d'acide. b) Modes B : addition de l'alcène sur le mélange agité de chlorure d'acétyle et de CF_3SO_3H ; B_1 — addition et réaction à 0°C. B_2 — addition et réaction à reflux du chlorure d'acide. Le rapport molaire CH_3COCl/CF_3SO_3H/alcène est fixé à 6/1/1, le temps de réaction est de 1 heure, les quantités de réactifs et le temps d'addition du troisième réactif ont été maintenus constants. Le mélange initial alcène/CF_3SO_3H n'a pas été envisagé pour éviter la polymérisation de l'alcène.[10] Dans tous les cas le traitement du milieu réactionnel est identique (traitement du brut réactionnel avec NH_4OH, extraction avec un hydrocarbure et traitements acide-base. Les résultats sont décrits dans le Tableau 1, entrées 4—7. La distribution des produits formés varie énormément avec les conditions opératoires. Le produit le moins substitué **2** est formé dans des proportions variant entre 19 et 89% par rapport à l'isomère **1**. Les produits de triacylation **3**, **4** peuvent constituer 0 à 13% du mélange et la pyridine **5** 0 à 16% du mélange. A basse température on favorise la formation du sel de pyrylium le moins substitué conduisant à **2** quel que soit l'ordre d'addition des réactifs. La dimérisation de l'alcène este favorisée dans ces conditions et la triacétylation si l'alcène est additionné en dernier. Lorsque l'acide est additionné à chaud sur le mélange alcène/CH_3COCl, le produit le plus substitué est obtenu. Lorsque l'alcène est additionné à chaud, les produits **1** et **2** sont obtenus en proportions équivalentes et les quantités de produits secondaires sont fortement réduites. Ce dernier mode B_2 sera retenu par la suite pour l'étude des variations des proportions de réactifs et de leur nature.

Le rapport CH_3COCl/CF_3SO_3H et la quantité de CF_3SO_3H par rapport à l'alcène ont une grande influence sur la distribution des produits (Tableau 1 entrées 3,7—10). L'augmentation de la quantité d'acide augmente la sélectivité en faveur de **2**. Les produits de triacylation restent sous la forme de traces alors que le produit de dimérisation augmente avec la quantité d'acide. Une augmentation de la quantité d'acide provoque en outre une augmentation nette des rendements globaux de la réaction. Un grand excès de CH_3COCl diminue la quantité de **5**.

Dans le tableau 1, entrées 3, 11, 12, nous rapportons les résultats obtenus suivant le mode opératoire B_2 pour différents précurseurs de l'alcène. Dans les trois cas la pyridine la moins substituée est obtenue en majorité. Le fait le plus marquant est l'absence des produits **3**, **4**, **5** à partir de l'alcool.

Les résultats d'expériences effectuées suivant le mode opératoire B_1 (température 0°C) (Tableau 1, entrées 13—17) montrent qu'on peut atteindre des sélectivités en isomère le moins substitué supérieure à 94%. La sélectivité est maximale lorsque le rapport CH_3COCl/CF_3SO_3H est inférieur à 4, en combinaison avec un excès d'acide par rapport à l'alcène. Les produits de triacylation peuvent atteindre 30% du mélange réactionnel.

Généralisation

La possibilité d'obtenir les pyridines (et donc les pyryliums) les moins substitués **2** dans des conditions évitant l'utilisation des catalyseurs de Lewis présente un intérêt certain en synthèse. En effet l'utilisation des acides de Lewis (chlorure ferrique ou chlorure d'aluminium) conduit à des modes opératoires souvent difficiles à mettre en œuvre à cause des milieux hétérogènes obtenus et de la présence de grandes quantités de sels metalliques qui ne sont pas facilement éliminés.[9] Dans le but de montrer l'intérêt synthétique de la nouvelle méthode que nous venons de décrire, nous avons réalisé une série d'expériences dans des conditions permettant de limiter la formation des produits de triacylation (température du reflux du chlorure d'acétyle et grand excès de celui-ci,utilisation d'un alcool comme précurseur de l'alcène).Les résultats sont rapportés dans le tableau 2 dans lequel nous avons ajouté pour comparaison, les résultats obtenus antérieurement dans le système acylant anhydride acétique/CH_3SO_3H.[7,8]

La différence de comportement est frappante : dans le milieu faiblement acylant $(CH_3CO)_2O/CH_3SO_3H$, le pyrylium le moins substitué est obtenu en minorité tandis que dans le milieu très acylant CH_3COCl/CF_3SO_3H, ce pyrylium est obtenu majoritairement. Les rendements de ces réactions n'ont pas été optimisés et par conséquent ils sont moins bons que ceux optimisés dans le mélange faiblement acylant.

Conclusion

Par l'utilisation du système acylant chlorure d'acide — acide trifluorométhanesulfonique, nous avons pu mettre en évidence de nouveaux aspects des réactions de polyacylation des alcènes ou de leurs précurseurs. L'utilisation de ce milieu acylant a permis de mettre en évidence pour la première fois dans une catalyse de Brönsted de la synthèse des sels de pyrylium :

— la possibilité d'obtention du sel de pyrylium le moins substitué à partir d'un isoalcène ou d'un précurseur,

Tableau 2.-Diacylation d'isoalcènes en présence d'acide protonique et de dérivés d'acide carboxylique.

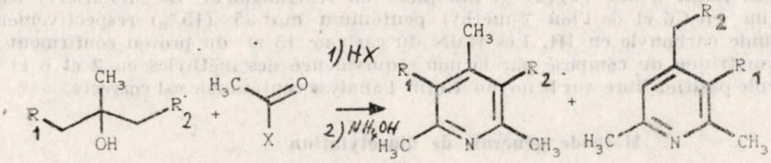

Précurseur	Sélectivité en pyridine la moins substituée (Rdt global)	
	$(CH_3CO)_2O$ / $CH_3SO_3H^a$	CH_3COCl / CF_3SO_3H
2-Méthyl-2-butanol (R_1=H, R_2=Me)	2 % (87%)	50% . (80%)
2-Méthyl-2-pentanol (R_1=H, R_2=Et)	5 % (81%)	70% (53%)
2-Méthyl-2-pentène (R_1=H, R_2=Et)	4 % (83%)	71% (90%)
3-Méthyl-3-pentanol (R_1=Me, R_2=Me)	13% (93%)	54% (72%)
2,4-Diméthyl-2-pentanol (R_1=H, R_2=iPr)	15 % (79%)	78% (44%)

a) Référence 7.

— la possibilité d'orienter suivant les conditions opératoires la réaction vers la formation préférentielle de l'un ou l'autre des sels de pyrylium,

— l'existence des réactions de triacylation en milieu protonique.

Par rapport aux réactions de polyacylation catalysées par les acides de Lewis, ce systéme acylant permet :

— de minimiser les réactions de triacylation tout en favorisant le sel de pyrylium le moins substitué,

— d'annuler les réactions de craquage et d'isomérisation de l'ion carbenium initial et de conduire ainsi a des mélanges réactionnels plus facilement utilisables[9].

PARTIE EXPÉRIMENTALE

Les différents produits obtenus au cours de cette étude ont déjà été caractérisés complètement par ailleurs et leurs caractéristiques comparées à des produits authenthiques. Seule la pyridine **5** est nouvelle. Son spectre de masse (70 eV) indique l'ion moléculaire à m/e 233 (8%) avec un pic de base à m/e 43. Une fragmentation importante à m/e 149 (48%) et une fragmentation plus faible à m/e 148 (21%) indiquent un réarrangment de McLafferty avec perte d'une oléfine en C6 et de l'ion 2-méthyl penténium m/e 85 (15%) respectivement. Il n'y pas de bande carbonyle en IR. Les RMN du carbone 13 et du proton confirment la structure non symétrique du composé par la non equivalence des méthyles en 2 et 6 et la présence d'une seule position libre sur le noyau. Enfin l'analyse centésimale est correcte.

Méthode générale de diacétylation

Dans un ballon tricol équipé d'un réfrigérant efficace (EtOH — 35°C), d'un thermomètre, d'une ampoule à brome et d'une agitation magnétique, on chauffe à reflux le mélange chlorure d'acétyle et CF_3SO_3H. puis on additionne goutte à goutte l'alcène ou son précurseur pendant environ 10 minutes. L'addition s'accompagne d'un grand dégagement d'acide chlorhydrique et d'une coloration rapide du milieu réactionnel en rouge brun. Après un temps de réaction défini (généralement une heure) à la température de reflux du chlorure d'acétyle (50°C), le mélange est refroidi à température ambiante puis versé goutte à goutte sur une solution agitée et refroidie (glace-eau) d'ammoniaque concentrée (34% NH_3).

Tous les produits organiques sont ensuite extraits par du pentane (ou hexane). Les pyridines formées sont récupérées par traitement acide base et extraction par du dichlorométhane. Le rendement de la réaction est établi par pesée après évaporation du solvent et la sélectivité est établie par analyses CPV et RMN du proton. L'identification des pyridines formées dans chaque réaction décrite ici a été faite par comparaison des caractéristiques CPV et CPV/SM du mélange pyridinique final avec celles des produits déjà préparés au laboratoire[7,8,9 et 11].

RÉFÉRENCES

[1] A. T. Balaban, A. Dinculescu, G. N. Dorofeenko, G. W. Fischer, A. V. Koblik, V. V. Mezheritzkii et W. Schroth, "*Advances in Heterocyclic Chemistry*", suppl. 2 (1982).

[2] A. T. Balaban, W. Schroth et G. Fischer, *Adv. Heterocyclic Chem.*, **10**, 241 (1969).

[3] D. Farcasiu, C. Uncuța et A. T. Balaban, *Rev. Roumaine de Chimie*, **12**, 899 (1967).

[4] A. G. Anderson et P. J. Stang, *J. Org. Chem.*, **41**, 3034 (1976).

[5] C. Roussel, H. G. Rajoharison, L. Bizzari et L. Shaimi, *J. Org. Chem.*, **53**, 683 (1988).

[6] C. Roussel, L. Shaimi et A. Chemlal, *Bull. Soc. Chim. France*, **1988**, 688.

[7] H. G. Rajoharison et C. Roussel, *Bull. Soc. Chim. France*, **1986**, 307.

[8] H. G. Rajoharison et C. Roussel, *Nouveau J. Chimie*, **9**, 681 (1985).

[9] A. Diallo, A. Hirchmüller, M. Arnaud et C. Roussel, *Nouveau J. Chimie*, **7**, 433 (1983).

[10] T. Masuda, M. Sawamoto et T. Higashimura, *Macromolek. Chem.*, **177**, 2981 (1976).

[11] M. Arnaud, A. Pedra, C. Roussel et J. Metzger, *J. Org. Chem.*, **44**, 2972 (1979).

Revue Roumaine de Chimie, 36, 4–7, 619–627 (1991)

Dedicated to Prof. ALEXANDRU T. BALABAN
on the occasion of his 60th anniversary

STUDIES ON 4-AMINO-5-ARYL-1,2,4-TRIAZOLE-3-THIONES

A. A. EL-BARBARY *[a], M. FAHMY [a], M. EL-BADAWI [a], K. EL-BREMBALY[b]
and N. R. EL-BROLLOSI [a]

[a] Chemistry Department, Faculty of Science, Tanta University,
[b] Chemistry Department, Faculty of Pharmacy, Tanta University, Tanta, Egypt

Received November 20, 1990

4-Amino-5-aryl-1,2,4-triazole-3-thiones **1** react with phenacylbromide at room temperature to give **2**, which could be converted to **3** on reflux. Treatment of **1** with chloroacetonitrile and potassium hydroxide in equimolar ratio and in excess yielded **4** and **6**, respectively. Acidic hydrolysis of **4** afforded **5**. Compound **7** which was obtained by reaction of **1** with ethylchloroformate at room temperature, could be converted to **9** on reflux. Reaction of **1** with isocyanates at room temperature afforded **9**, which on reflux gave **10**. Compound **1** reacted with some aliphatic acids and/or aliphatic aldehydes to give **11** and **12**, respectively.

INTRODUCTION

Our previous papers studied the chemistry of 1,2,4-triazoles due to their prominent utilizations as tuberculoslatic,[4] fungicidal,[5] bactericidal [6] and anti-inflammatory [7] compounds, as well as due to their use as photographic stabilizers [8] and agents which improve the heat resistance of polymers.[9] Accordingly, we decided to make further investigations of the chemistry of 5-aryl-1,2,4-triazole-3-thiones. Our results are reported in this paper.

RESULTS AND DISCUSSION

During the present investigation it was found that 4-amino-5-phenyl-1,2,4-triazole-3-thione (**1**) reacted with phenacylbromide in anhydrous pyridine at room temperature to give 4-amino-5-phenyl-3-(S-phe-

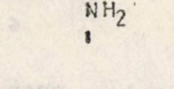
1

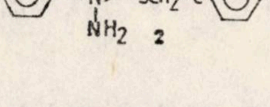
2

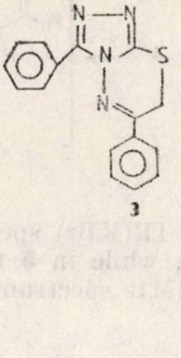
3

---

* Correspondence author

nacyl)mercapto-1,2,4-triazole (**2**),[10] which in turn could be converted to the cyclized form 7*H*-3,6-diphenyl-*s*-triazolo [3,4-*b*] [1,3,4] thiadiazine (**3**) by refluxing in anhydrous pyridine for 4 hr. Compound **3** is also obtained by refluxing compound **1** with phenacyl bromide in absolute ethanol for one hour.

The IR (KBr) spectrum of **2** showed bands at 1760 cm^{-1} and 3290 cm^{-1} due to C=O and NH_2, respectively. These bands were not observed in the spectrum of **3**.

The mass spectra of **2** and **3** showed the molecular ion peaks ($M^{+\cdot}$) at m/e = 310 and 231, respectively. Treatment of **1a,b** with an equimolecular amount of chloroacetonitrile[11] and potassium hydroxide in methanol at room temperature yielded 4-amino-5-aryl-3-cyanomethylthio-1,2,4-triazole (**4a,b**), respectively. Hydrolysis of **4a** with hydrochloric acid gave 4-amino-5-phenyl-3-carboxymethylthio-1,2,4-triazole (**5**). On the other hand, when **1a** reacted with chloroacetonitrile in ethanol at room temperature in the presence of an excess amount of potassium hydroxide it yielded 7H-6-amino-3-phenyl-*s*-triazolo [3, 4-*b*] [1,3,4] thiadiazine (**6**).

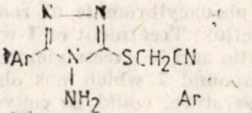

4

Ar
a. C_6H_5
b. p-ClC_6H_4

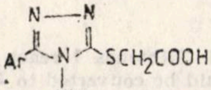

5

Ar= C_6H_5

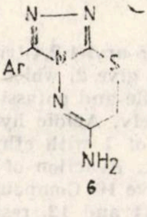

6

Ar= C_6H_5

Concerning the formation of **6**, the following mechanism is postulated :

A first nucleophilic attack of the chloroacetonitrile by **1a** yields **4a**, in which an internal nucleophilic attack takes place by the NH_2 on the C≡N affording the final product **6**.

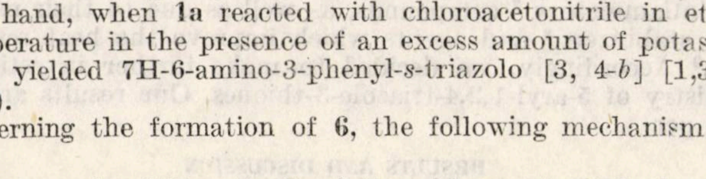

The IR(KBr) spectrum of **4** showed a band at 2260−2240 cm^{-1} for C≡N, while in **5** the C=O (COOH) band appeared at 1700 cm^{-1}. The ^{1}H-NMR spectrum of **4** showed a singlet at δ = 4.20 ppm, corresponding to 2H (S-CH_2—CN), a singlet at 6,20 ppm, corresponding to 2H (NH_2, exchangeable by D_2O) whereas that of **6** showed a singlet at $\delta = 3.40$ ppm, corresponding to 2H ($-CH_2-$), and a singlet at 3.80 ppm, corresponding to 2H $(NH)_2$. The mass spectrum of both **4a** and **6** showed the molecular ion peaks ($M^{+\cdot}$) at m/e = 231. The following scheme represents the fragmentation pattern of **6**.

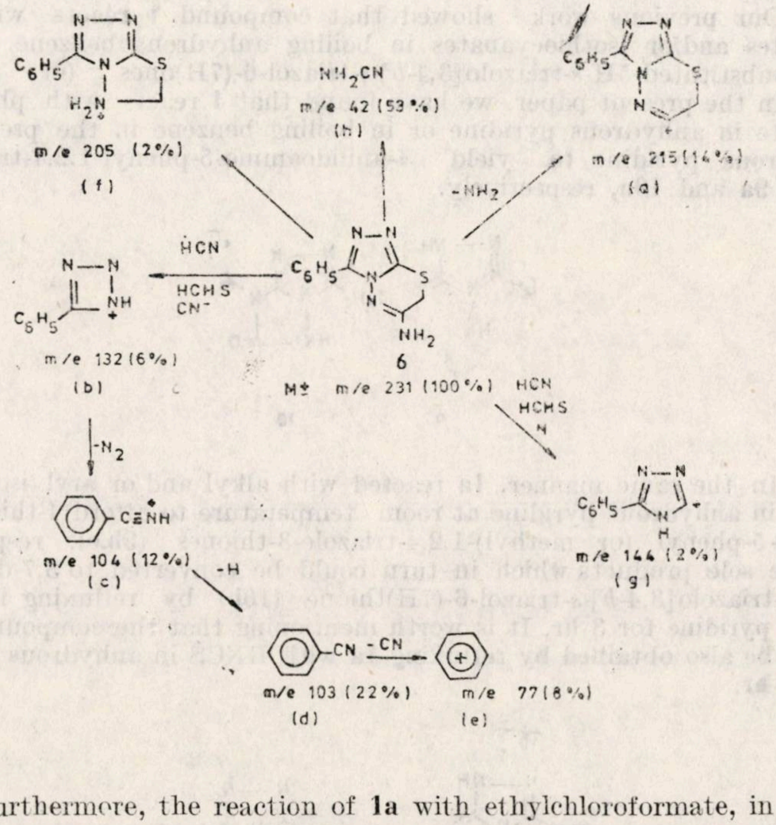
m/e 205 (2%)
(f)
NH2CN
m/e 42 (53%)
(h)
m/e 215 (14%)
(a)
-NH2
HCN
HCHS
CN⁻
m/e 132 (6%)
(b)
6
M⁺ m/e 231 (100%)
HCN
HCHS
N
-N2
m/e 104 (12%)
(c)
m/e 144 (2%)
(g)
-H
-CN
m/e 103 (22%)
(d)
m/e 77 (8%)
(e)

Furthermore, the reaction of **1a** with ethylchloroformate, in anhydrous pyridine at room temperature afforded 4-amino-5-phenyl-3-carboethoxythio-1,2,4-triazole (**7**), which on reflux in anhydrous pyridine for 4 hr gave 6-phenyl-3-oxo-1,2,4-triazolo[3,4-*b*]-4H[1, 3, 4] thiadiazole (**8**).[2,12] Compound **8** is also obtained through the elimination of one molecule of ethanol by refluxing **1a** with ethylchloroformate in absolute ethanol in the presence of fused sodium acetate.

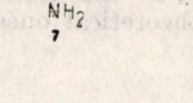
7

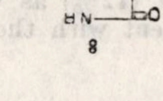
8

The IR(KBr) spectrum of **7** showed a band at 3290 cm^{-1} for NH_2 and a band at 1750 cm^{-1} for COOEt. The ^{1}H-NMR spectrum of **7** showed a triplet at $\delta = 1.40$ ppm, corresponding to $3H(CH_3-)$, a quartet at 4.50 ppm, corresponding to $2H(-CH_2-)$ and a singlet at 5.10 ppm, corresponding to $2H(NH_2)$. The ^{13}C-NMR spectrum of **7** showed signals at 13.845, 64.856 and 169.196 ppm, corresponding to CH_3, OCH_2 and $C{=}O$, respectively. The mass spectrum of **7** showed the molecular ion peak $(M^{+\cdot})$ at m/e = 264.

Our previous work [1] showed that compound **1** reacts with isocyanates and/or isothiocyanates in boiling anhydrous benzene to give 3,7-disubstituted-5H-*s*-triazolo[3,4-*b*]-*s*-triazol-6-(7H)ones (or thiones) (**10**). In the present paper, we have found that **1** reacts with phenylisocyanate in anhydrous pyridine or in boiling benzene in the presence of anhydrous pyridine to yield 4-anilidoamino-5-phenyl-1,2,4-triazole-3-tione **9a** and **10a**, respectively.

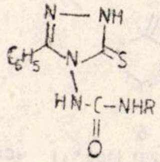

9

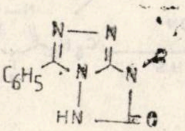

10

In the same manner, **1a** reacted with alkyl and/or aryl isothiocyanates in anhydrous pyridine at room temperature to afford 4-thioanilidoamino-5-phenyl (or methyl)-1,2,4-triazole-3-thiones (**9b,c**), respectively as the sole products which in turn could be converted to 3,7-diphenyl-*5H-s*-triazolo[3,4-*b*]-*s*-triazol-6-(7H)thione (**10b**) by refluxing in anhydrous pyridine for 3 hr. It is worth mentioning that the compounds **10b,c** could be also obtained by refluxing **1a** with RNCS in anhydrous pyridine for 3 hr.

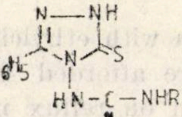

9b

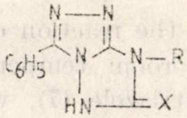

10

b, $R = C_6H_5$; X = S
c, $R = CH_3$; X = S

The IR (KBr) spectrum of **9a** showed a band at 1700 cm^{-1} for C=O, while a band at 1205—1200 cm^{-1} characteristic of C=S appeared in **9b** and **10b**. The mass spectrum of **10c** showed the molecular ion peak $(M^+)^{\cdot}$ at m/e = 231 (12%) as well as the isotopic peaks (M + 1) and (M + 2) in agreement with the theoretical ones.

It has been reported that 4-amino-5-aryl-1,2,4-triazole-3-thione, (1) reacted with some aromatic acids [1,13] in phosphorous oxychloride to yield 3,6-disubstituted-*s*-triazolo[3,4-*b*][1, 3, 4]thiadiazole. Similarly, when **1** was treated with formic acid and/or acetic acid in phosphorous oxychloride, 3-substituted-6*H*-*s*-triazolo[3,4-*b*][1, 3, 4]thiadiazole (**11a—d**), respectively, are obtained.

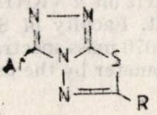

11a-d

	Ar	R
a,	C_6H_5	H
b,	C_6H_5	CH_3
c,	p-ClC_6H_4	H
d,	p-ClC_6H_4	CH_3

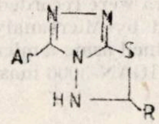

12a-c

	A	R
a.	C_6H_5	H
b.	p-ClC_6H_4	H
c,	p-ClC_6H_4	CH_3

The IR(KBr) spectrum of **11a—d** showed an absorption band in the region 1600—1590 cm^{-1} for C = N.

In our earlier invistigations,[14,15] compound **1** reacted with some aromatic aldehydes in boiling absolute ethanol to give *s*-triazolo derivatives. In an extension of this work, we have tried the reaction of **1** with some aliphatic aldehydes. Thus, on refluxing **1** with formaldehyde and/or acetaldehyde in absolute ethanol for 6 hr, 3-substituted-5,6-dihydro-6*H* (or methyl)-*s*-triazolo-[3,4-*b*][1, 3, 4]thiadiazole (**12a—c**), respectively, are obtained. The IR(KBr) spectrum of **12a—c** showed absorption bands in the region 3200—3120 cm^{-1} for (NH) and at 1600—1590 cm^{-1} for (C=N). The mass spectrum of **12c** showed the molecular ion peak ($M^{+\cdot}$) at m/e = 251 and the isotopic molecular ion peak ($M^{+\cdot}$+1) and ($M^{+\cdot}$ +2) with the ratio 3 : 2 : 1.

BIOLOGICAL ACTIVITY

The above compounds were screened against various types of bacteria using a modified Cup-test assay technique.[16,17] The data revealed that the majority of them showed activity against *Bacillus subtillis*, *Escherichia coli*, *Candida albicans* and *Sarcina lutea* (Table 1). Further investigations may be made to give more details.

Table 1

Biological activity of compounds 4, 5, 11, 12, and 13

Compound	Results on test organisms with m.m.		
	B. subtillis	*E. coli*	*S. lutea*
4a	10 m.m		
5			10 m.m.
11a	10 m.m	—	
11a	16 m.m		
12b	15 m.m	10 m.m	
13c	15 m.m		
13d	14 m.m	12 m.m	10 m.m.

EXPERIMENTAL

The melting points were recorded on a Gallenkamp apparatus and are uncorrected. The IR spectra were determined using UR 10 fully automatic double beam infra-red spectrophotometer Carl Zeiss Jena, and PYE UNICAM SP 200G and SP 100 spectrophotometers (using KBr). The ^{1}H-NMR spectra were recorded using a JEOL 90-MHZ spectrometer and a VARIAN-T 90-MHZ. $CDCl_3$ and d^6-DMSO were used as solvents and TMS as internal standard. The ^{13}C-NMR spectra were recorded at 20 MHz on a VARIAN-CFT-20 Spectrometer. Microanalyses were performed by Microanalyses Unit, Faculty of Science, Cairo University. The mass spectra were determined using a micromass 7070 mass spectrometer operating at 70 eV using direct inlet and a FINNIGAN-3000 mass spectrometer by the use of a direct inlet source and beam energy of 70 eV.

Reaction of compound 1 with phenacyl bromide. General procedure

A mixture of compound **1** (0.01 mole), phenacyl bromide (0.01 mole) and anhydrous pyridine (15 mL) was stirred at room temp. and/or under reflux for 1 — 3 hr. until the starting material was consumed (tlc). The reaction mixture was poured over ice-water mixture and the resulting solid was filtered off and crystallized from the suitable solvent.

a — 4-Amino-5-phenyl-3-(S-phenacyl)mercapto-1,2,4-triazole (2) :

The reaction proceeded at room temp. for one hour and the resulting solid was crystallized from aqueous ethanol to give compound **2**, m.p. 141°C (yield : 65 %) IR (KBr, cm^{-1}) : 1620 (C=N), 1670 (C=O), 3290 (NH_2), MS (rel. int. %), m/e = 292 (M$^+$, 100), 215(2), 192(45), 160(1), 144(1), 117(17), 103(89), 77(90), 51(29).

Anal. Calcd. for $C_{16}H_{14}N_4OS$: C, 61.9 ; H, 4.5 ; N, 18.1 ; S, 10.3 %. Found : C, 61.4 ; H, 4.9 ; N, 17.7 ; S, 10.0 %.

b — 7*H*-3-6-Diphenyl-s-triazolo(3,4-*b*)(1,3,4)thiadiazine (3)

The reaction mixture was refluxed for 3 hr and the resulting solid crystallized from ethanol to give compound **3**, m.p. 218°C (yield : 65 %).

This compound can also be obtained in good yield (82 %) by refluxing a mixture of compound **1** (0.01 mole) and phenacyl bromide (0.01 mole) in absolute ethanol (50 mL) for one hour until no more starting material could be detected (tlc). IR (KBr, cm^{-1}) : 3090(CH_2—), 1600(C=N).

^{1}H-NMR ($CDCl_3$, δ. ppm) : 3.30 (s ; 2H, $SC\mathit{H}_2$) and 7.60 8.20 (m ; 10H, aromatic protons).

MS (rel. int. %), m/e = 292 (M$^+$, 100), 215 (2), 189 (6), 131 (9), 103 (41), 77 (22).

Anal. Calcd. for $C_{16}H_{12}N_4S$: C, 65.7 ; H, 4.1 ; N, 19.2 ; S, 11.6 %. Found : C, 65.9 ; H, 4.3 ; N, 18.7 ; S, 11.0 %.

Reaction of compound 1 with chloroacetonitrile. Formation of 4-amino-5-aryl-3-cyanomethyl-thio-1,2,4-triazole (4)

A mixture of compound **1** (0.01 mole), chloroacetonitrile (0.01 mole), potassium hydroxide (0.01 mole) and methanol (20 mL) was stirred at room temp. for 12 hr until the starting material was consumed (tlc). The solvent was concentrated at room temp. to its half volume and the obtained solid was filtered off and crystallized from ethanol to give compound **4**, m.p. 161°C (yield : 90 %).

IR (KBr, cm^{-1}) : 3330 (NH_2), 3120 (CH_2), 2240 (C=N) and 1640 (C=N).

^{1}H-NMR ($CDCl_3$, δ, ppm) : 4.20(s ; 2H, $sC\mathit{H}_2CN$), 6.20 (s ; 2H, NH_2 ; exchangeable by D_2O) and 7.50 – 8.20 (m ; 5H, aromatic protons). MS (rel. int. %), m/e = 231 (M$^+$, 100), 220 (3), 192 (98), 104 (82), 103 (46), 77 (78), 29 (100).

Anal. Calcd. for $C_{10}H_9N_5S$: C, 51.9 ; H, 3.9 ; N, 30.3 %.

Found : C, 51.5 ; H, 4.2 ; N, 30.0 %.

6-Amino-7*H*-3-phenyl-s-triazolo(3,4-*b*)(1,3,4)thiadiazine (5)

The above method was used with an excess of potassium hydroxide and the resulting solid was filtered off and crystallized from methanol to give compound **5**, m.p. 192°C (yield: 65 %).

^{1}H-NMR ($CDCl_3$, δ, ppm): 3.40 (s; 2H, CH_2), 3.80 (s; 2H, NH_2), 7.20 (s; 2H, 2 NH due to the tautomeric forms) and 7.50–8.20 (m; 5H, aromatic protons).

MS (rel. int. %), m/e = 231 (M^+, 100), 215 (14), 132 (6), 104 (12), 103 (22) and 77 (8).

Anal. Calcd. for $C_{10}H_9N_5S$: C, 51.9; H, 3.9; N, 30.3; S, 13.9 %.

Found: C, 51.7; H, 4.0; N, 30.0; S, 13.6 %.

4-Amino-5-phenyl-3-carboxymethylthio-1,2,4-triazole (5)

A mixture of compound **4** (1 g) and 5 mL of 10 % HCl was refluxed for 4 hr until no more starting material could be detected (tlc). The reaction mixture was cooled and neutralized with NaOH. The resulting solid was filtered off and crystallized from ethanol to give **6**, m.p. 178°C (yield: 60 %).

IR (KBr, cm^{-1}): 3400 (OH), 3305 (NH_2), 3120 (CH_2), 1700 (C=O), 1630 (C=N).

Anal. Calcd. for $C_{10}H_{10}N_4O_2$: C, 48.0; H, 4.0; N, 22.4 %.

Found: C, 47.7; H, 4.3; N, 22.0 %.

4-Amino-5-phenyl-3-carboethoxythio-1,2,4-triazole (7)

A mixture of compound **1** (0.01 mole), ethylchloroformate (0.01 mole) and anhydrous pyridine (10 mL) was stirred at room temp. for 2 hr until no more starting **1** could be detected (tlc). The reaction mixture was poured onto ice-water mixture. The solid product was filtered off and crystallized from aqueous ethanol to give **7**, m.p. 120°C (yield: 88 %).

IR (KBr, cm^{-1}): 3290 (NH_2), 1750 (COOEt), 1620 (C=N).

^{1}H-NMR ($CDCl_3$, δ, ppm): 1.40 (t; 3H, CH_3), 4.50 (q; 2H, CH_2), 5.10 (s; 2H, NH_2, exchangeable by D_2O) and 7.80–8.20 (m; 5H, aromatic protons).

^{13}C-NMR. ($CDCl_3$, δ, ppm): 13.845 (CH_3), 64.856 (OCH_2), 123.846 (C_4), 128.281 (C_2), 128.521 (C_3), 131.305 (C_1), 148.204 (C_b), 149.684 (C_a) and 169.196 (C=O).

MS (rel. int. %), m/e = 264 (M^+, 46), 220 (3), 192 (98), 104 (82), 103 (46), 77 (78) and 29 (100).

Anal. Calcd. for $C_{11}H_{12}N_4O_2S$: C, 50.0; H, 4.6; N, 21.2; S, 12.1 %.

Found: 49.7; H, 4.2; N, 21.4; S, 11.8 %.

Cyclization of compound 7; Formation of compound 8

Compound **7** (1g) was heated under reflux in anhydrous pyridine (15 mL) for 5 hr until the starting material was consumed (tlc). The reaction mixture was cooled, poured onto ice-water mixture and filtered. The solid obtained was crystallized from aqueous ethanol to give **8**, m.p. 152°C (yield: 60 %). Its m.p. and mixed m.p. with an authentic sample of **8**[10] gave no depression.

Reaction of compound 1 with phenylisocyanate; Formation of 9 and 10

A mixture of compound **1** (0.01 mole), phenylisocyanate (0.01 mole) and anhydrous benzene (30 mL) was refluxed in the presence of anhydrous pyridine (3 mL) for 3 hr until the starting material was consumed (tlc). The reaction mixture was filtered off and the resulting solid was treated with a dilute solution of NaOH (20 mL) and filtered. The residual solid was crystallized from aqueous methanol to afford a solid which melted at 234°C (yield: 37 %). Its m.p. and mixed m.p. with an authentic sample of 3,7-diphenyl-5*H*-*s*-triazole[3,4-*b*]*s*-triazole-6-(7H)-one **10a**[8] gave no depression. The filtrate was acidified with HCl, the solid obtained was filtered off and crystallized from dioxane to give 4-anilidoamino-5-phenyl-1,2,4-triazole-3-thione **9a**, m.p. 239°C (yield: 43 %).

IR (KBr, cm^{-1}): 3210 (NH), 1700 (CONH) and 1600 (C=N).

Anal. Calcd. for $C_{15}H_{13}N_4OS$ (311.4): C, 57.9; H, 4.2; N, 22.5; S, 10.3 %.

Found: C, 57.5; H, 4.5; N, 22.0; S, 9.4 %.

Action of isothiocyanates on compound 1

i—a. On the cold. Formation of 4-thioanilidoamino-5-phenyl-1,2,4-triazole-3-thione 9b

Compound **1a** (0.01 mole) and phenylisothiocyanate (0.01 mole) were stirred in anhydrous pyridine (15 mL) at room temp. for 3 hr until no more starting material could be detected (tlc). The reaction mixture was poured onto ice-water mixture and filtered off. The solid obtained was crystallized from ethanol to give **9b**, m.p. 265°C (yield : 69 %).

IR. (KBr, cm^{-1}) : 3140 (NH), 1580 (C=N) and 1200 (CSNH).

Anal. Calcd. for $C_{15}H_{12}N_4S_2$: N, 21.4 ; S, 19.6 %.

Found : N, 21.00 ; S, 19.7 %.

b. On the hot. Formation of compounds 10b,c

Compound **9b** (1 g) was heated under reflux in anhydrous pyridine (15 mL), for 3 hr until the starting material was consumed (tlc). The reaction mixture was cooled, poured onto ice water mixture. The resulting solid was filtered off and crystallized from benzene to give a solid, m.p. 289°C (yield : 60 %). Its m.p. and mixed m.p. with an authentic sample of 3,7-diphenyl-5*H*-s-triazolo[3,4-*b*]-s-triazole-6(7H)thione **10b**[11] gives no depression.

ii. Route C

Compound **1a** (0.01 mole) and methylisothiocyanate (0.01 mole), were heated under reflux in anhydrous pyridine (20 mL) for 2 hr until the starting material was consumed (tlc). The reaction mixture was cooled, poured onto ice-water mixture, the resulting solid was filtered off and crystallized from ethanol to give 3-phenyl-7-methyl-5*H*-s-triazolo [3,4-*b*]-s-triazole-6(7H) thione **10c**, m.p. 194°C (yield : 75 %).

MS (rel. int. %), m/e = 231 (M$^+$, 12), 217 (32), 177 (14), 144 (100), 104 (7), 103 (5), 74 (44), 73 (14) and 30 (11).

Anal. Calcd. for $C_{10}H_9N_5S$: C, 51.5 ; H, 3.5 ; N, 30.0 ; S, 13.0 %.
Found : C, 51.9 ; H, 3.9 ; N, 30.3 ; S, 13.9 %.

Action of aliphatic acids on compound 1. Formation of 3,6-disubstituted-s-triazolo [3,4-b][1,3,4]thiadiazole 11. General method

A mixture of compound **1** (0.01 mole) and formic and/or acetic acid (0.015 mole) were refluxed in phosphorus oxychloride (15 mL) for one hour until no more starting material could be detected (tlc). The excess of phosphorus oxychloride was distilled off under reduced pressure and the residue was diluted with water ; the resulting solid was filtered off and crystallized from a suitable solvent.

Compound	Ar	R	M.P. (°C)	Yield (%)	Solvent* of cryst.	Formula	Analysis (%) Calc./Found. C	H	N	S	Cl
11a	C_6H_5—	H	99	61	A	$C_9H_6N_4S$	53.3 53.1	3.0 3.4	27.7 27.2	15.9 15.1	
11b	*p*-ClC_6H_4	H	237	63	A	$C_9H_5ClN_4S$	45.7 45.1	2.1 2.0	 —	13.5 13.1	15.0 15.3
11c	C_6H_5	CH_3	118	56	D	$C_{10}H_8N_4S$	55.5 55.0	3.7 4.1	— —	14.8 14.4	
11d	*p*-ClC_6H_4	CH_3	220	57	E	$C_{10}H_7ClN_4S$	47.9 47.3	2.8 2.6	22.3 22.1	12.8 12.4	 —

* A = Acetic acid, D = Dioxane ; E = Ethanol.

Action of aliphatic aldehydes on compound 1. Formation of 3,6-disubstituted-5H,6H-s-triazolo (3,4-b)(1,3,4) thiadiazole 12. General procedure

Compound 1 (0.01 mole), formaldehyde and/or acetaldehyde (0.01 mole) were refluxed in 30 mL absolute ethanol for 6 hr until no more starting material could be detected (tlc). The reaction mixture was concentrated to one third of its original volume and the resulting solid was filtered off and crystallized from the proper solvent to give 12

Compound	Ar	R	M.P. (°C)	Yield (%)	Solvent* of cryst.	Formula	Analyses (%) Calc./Found				
							C	H	N	S	Cl
12a	C_6H_5	H	235	70	A	$C_9H_8N_4S$	52.0 52.4	3.9 3.4	27.4 27.0	15.7 15.1	— —
12b	p-ClC_6H_4	H	272	65	A	$C_9H_7CLN_4S$	45.3 45.3	3.0 3.6	23.5 24.0	13.4 14.0	14.9 15.3
12c	p-ClC_6H_4	CH_3	155	61	E	$C_{10}H_9CLN_4S$	47.5 47.0	3.6 3.9	22.2 21.8	12.7 12.1	— —

* Acetic acid ; E = Ethanol.

REFERENCES

[1] A. A. El-Barbary, M. El-Borai and S. S. Guiguis, *Delta J. Sci.*, **10**, 607 (1986).

[2] A. A. El-Barbary, M. EL-Borai, M, Fahmy and H. H. E-Naggar, *Delta J. Sci.*, **12**, 102 (1988).

[3] M. El-Borai, A. A. El-Barbary, M. Fahmy and H. H. El-Naggar, *Delta J. Sci.*, **12**, 93 (1988).

[4] K. C. Joshi and K. Dubey, *Pharmazie*, **34**, 801 (1979) ; *Chem. Abstr.*, 92, 315372 (1980).

[5] B. A. Dreikorn and T. D. Thibault, *N.S. Patent*, 4, 8322 (1977) ; Chem. Abstr., **86**, 166387 (1977).

[6] A. K. Sengupta and A. A. Gupta, *Ind. J. Chem.*, **22(B)**, 263 (1983).

[7] M. Kadota and K. Honda, *Jap. Patent*, 7821, 197 (1978) ; Chem. Abstr., **89**, 43471 (1978).

[8] G. E. Hardtmann and F. G. Kathawala, *U.S. Patent*, 4,053, 600(1977) ; Chem. Abstr., **88**, 22970 (1978).

[9] D. Gerlach and E. Bader, *U.S. Patent*, 3, 585, 165 (1971) ; Chem. Abstr., **75**, 64907 (1971).

[10] T. George, R. Thilramani and D. A. Dobholkar, *Ind. J. Chem.*, **7**, 959 (1969).

[11] W. Rudnicka, Z. Osmialowska, *Acta Pol. Pharm.*, **36**, 411 (1979).

[12] A. A. El-Barbary, M. Anwar, A. A. Ghattas and A. F. Hashem, *Rev. Roumaine Chim.*, **26**, 449 (1981).

[13] H. Golgolab., I. Lalezari and L. H. Hosseini, *J. Heterocycl. Chem.*, **10**, 387 (1973).

[14] A. A. El-Barbary, I. Islam and A. M. Hashem, *J. Chem. & Eng. Data*, **29**, 477 (1984).

[15] M. Anwar, A. A. El-Barbary, A. A. Ghattas and A. M. Hashem, *Polish. J. Chem.*, **55**, **599** (1981).

[16] T. Yamagushi, T. Kashida, K. Netwa, I. Yajma, T. Miyagishima, Y. Ito and T. Okuda, *J. Antibiotics*, **23**, 373 (1970).

[17] A. A. Abouzeid, M. M. Abdel-Hamid and Y. M. Shehata, *Z. Allg. Microbiol.*, **16**, 337 (1976).

Revue Roumaine de Chimie, 36, 4–7, 629–633 (1991)

To Professor ALEXANDRU T. BALABAN
on the occasion of his 60th anniversary

BASICITY-STRUCTURE RELATIONSHIPS IN BISAZOLYL-METHANES AND -ETHANES

CARMEN ACERETE,[a] MARÍA LUISA BAÑÓN,[a] PILAR CABILDO, [b]
ROSA MARÍA CLARAMUNT,[b] JOSÉ ELGUERO[c] and JOSÉ LUIS LAVANDERA[b]
[a] Departamento de Química-Física Aplicada, Universidad Autónoma de Madrid, 28049 Cantoblanco, Spain
[b] Departamento de Química Organica, UNED, Ciudad Universitaria, 28040 Madrid, Spain
[c] Instituto de Química Médica, CSIC, Juan de la Cierva, 3, 28006 Madrid, Spain

Received November 20, 1990

The thermodynamic pK_a values of different bisazolyl-methanes and ethanes are reported. Considerations concerning basicity-structure relationships are also mentioned.

Although the basicity of simple azoles, like pyrazoles, imidazole and benzimidazoles has been thoroughly studied, [1] very few publication reported such studies in the case of molecules containing two of such rings A paper by Fruchier *et al.*[2] on some bispyrazolylmethanes and bisimidazolylmethanes where the azole rings are linked either by the carbon atoms (type a) or by a carbon and a nitrogen atom (type b) to the central CH_2, described the two successive pK_a's of such systems. Another work by Pozharskii *et al.*[3] reported the pK_a (in 1 : 1 water-alcohol) of *N,N'*-linked bisbenzimidazolylmethane and ethane (only the first ionization constant) (type c).

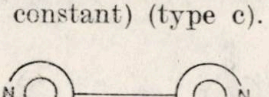
(a)

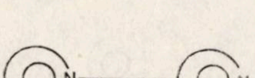
(b)

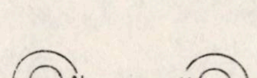
(c)

We report the thermodynamic values (water, 25°C) of both pK_a's of ten derivatives belonging to class (c). The azoles are pyrazoles, imidazoles and benzimidazole, and the central bridge, either CH_2 or CH_2–CH_2.

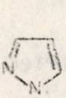
(pz)

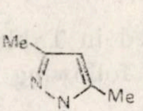
(dmpz)

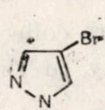
(brpz)

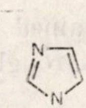
(im)

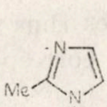
(mim)

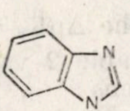
(bzim)

Table 1

Thermodynamic pK_a values of bisazolylalkanes and literature values of related *N*-methyl- and *N*-ethyl-azoles

Compound	pK_{a1}	pK_a	pK_{a2}
(1) pz-CH_2-pz	-2.12 ± 0.07		0.12 ± 0.02
(2) dmpz-CH_2-dmpz	0.37 ± 0.03		2.14 ± 0.09
(3) pz-CH_2-CH_2-pz	-0.24 ± 0.09		1.67 ± 0.04
(4) dmpz-CH_2-CH_2-dmpz	1.30 ± 0.04		3.39 ± 0.08
(5) brpz-CH_2-CH_2-brpz	-1.9 ± 0.2		0.0 ± 0.2
(6) im-CH_2-im	3.76		5.56
(7) mim-CH_2-mim	4.97		6.64
(8) im-CH_2-CH_2-im	4.87 [b]		6.41 [b]
(9) mim-CH_2-CH_2-mim	5.83		7.28
(10) bzim-CH_2-CH_2-bzim	3.71		4.61[a]
(11) pz-CH_3		2.06[1]	
(12) dmpz-CH_3		3.74[1]	
(13) brpz-CH_3		0.17[1]	
(14) pz-CH_2-CH_3		1.94[1]	
(15) im-CH_3		7.12[1]	
(16) mim-CH_3		8.00[1]	
(17) im-CH_2 CH_3		7.19[1]	
(18) bzim-CH_2-CH_3		5.62[1]	

[a] Lit.[3] gives 4.56 for water-alcohol 1 : 1. [b] for the error in potentiometric measurements, see experimental part (Sigma pH fit).

To discuss the pK_as of Table 1, some *N*-methyl and *N*-ethylazoles are also necessary. The idea is to consider both successive equilibria as reflecting the perturbation of the pK_a of a *N*-methylazole (-CH_2- series) or a *N*-ethylazole (-CH_2-CH_2- series) by an azole or an azolium protonated azole) substituent.

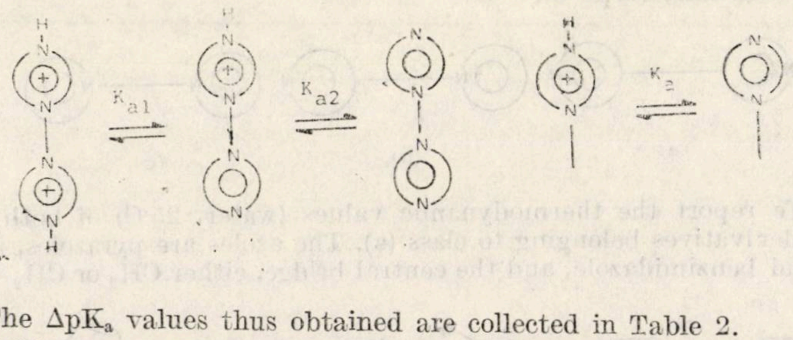

The ΔpK_a values thus obtained are collected in Table 2.

Table 2 values correspond roughly to the following expected observations :

i) Replacement of one hydrogen of the *N*-methyl or the *N*-ethyl substituent by an azolyl (neutral or charged) produces a base-weakening effect.

Table 2

Effect of an 1-azolyl and a 1-azolium substituent on the basicity of an azole through one (α effect) or two methylenes (β effect)

Pair of compounds	Substituent	ΔpK_a
(11) − **(1)**	pz (α)	−1.94
	pz^+ (α)	−4.18
(12) − **(2)**	dmpz (α)	−1.60
	$dmpz^+$ (α)	−3.37
(14) − **(3)**	pz (β)	−0.27
	pz^+ (β)	−2.18
1-ethyl-3,5-dimethylpyrazole[a] **(4)**	dmpz (β)	−0.23
	$dmpz^+$ (β)	−2.32
1-ethyl-4-bromo-pyrazole[b] **(5)**	brpz (β)	−0.05
	$brpz^+$ (β)	−1.95
(15) − **(6)**	im (α)	−1.56
	im^+ (α)	−3.36
(16) − **(7)**	mim (α)	−1.36
	mim^+ (α)	−3.03
(17) − **(8)**	im (β)	−0.78
	im^+ (β)	−2.32
1-ethyl-2-methylimidazole[c] − **(9)**	mim (β)	−0.79
	mim^+ (β)	−2.24
(18) − **(10)**	bzim (β)	−1.01
	$bzim^+$ (β)	−1.91

[a] Calculated $pK_a = 3.62$ [**(14)** + **(12)** − **(11)**]; [b] Calculated $pK_a = 0.05$ [**(14)** + **(13)** − **(11)**]; [c] Calculated $pK_a = 8.07$ [**(17)** + + **(16)** − **(15)**].

ii) The effect is larger in α than in β, i.e. through a methylene and two methylenes, respectively.

iii) The effect is larger for an azolium cation than for an azole.

A more detailed analysis of Table 2 reveals:

i) Through one methylene (α values), pyrazoles and pyrazolium ions are more base-weakening than imidazoles and imidazolium ions (averaged values: pyrazoles, −1.77, imidazoles, −1.46, pyrazoliums, −3.78, imidazoliums, −3.20) whereas the reverse is true for β values (averaged values: pyrazoles, −0.18, imidazoles, −0.78, pyrazoliums, −2.14, imidazoliums, −2.28). This surprising result is comparable, at least for neutral azoles, to the observation that the α methylene carbon in ^{13}C-NMR is more deshielded (35.1 ppm) by a pyrazole than by an imidazole (30.2 ppm) [4] whereas the β-methylene is more deshielded by imidazole (1.03 ppm) than by pyrazole (0.53 ppm).[5]

ii) There is no clear indication of stabilization of the monocation by chelation. This situation, possible only in the case of pyrazoles, would result in an increase of the difference between pK_{a1} and pK_{a2}. If the phenomenon is present in aqueous solution, the effect is rather insignificant.

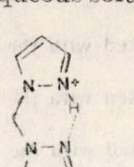

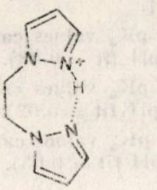

iii) The values for compound **5** are less precise. Values near -2.15 and -0.25 for pK_{a1} and pK_{a2}, respectively, would better fit with other compounds of Table 2 ($\Delta pK_a = -0.25$ and -2.20).

EXPERIMENTAL PART

Synthesis

Compounds (**1**),[6,7] (**2**),[6] (**3**),[5,8] (**5**),[5] (**6**),[6,9] (**7**),[10] (**8**),[5,8] and (**10**),[5] were previously described. Compounds (**4**) and (**9**) were prepared as follows: a suspension of the azole (29 mmoles), anhydrous potassium carbonate (29 mmoles), powdered potassium hydroxide (29 mmoles), tetrabutylammonium bromide (1.4 mmoles), and 1,2-dibromoethane (14.5 mmoles) in 50 mL of toluene or xylene were heated under reflux for 48 h. The hot reaction mixture was filtered and the solid residue was washed twice with 30 mL of anhydrous toluene or xylene. The solutions were dried over anhydrous sodium sulfate and the corresponding compounds purified by column chromatography on silica gel using petroleum ether/ethyl acetate (5 : 2) as eluent. The NMR spectra (δ, Hz) were recorded on a Bruker AC 200.

1,2-Bis(3,5-dimethylpyrazol-1-yl)ethane (**4**), yield: 75%, m.p. 126–7°C. Rf (Petroleum ether/ethyl acetate 5 : 2): 0.43; ^{1}H-NMR ($CDCl_3$): Me_3: 1.62 (s), H_4: 5.66 (s), Me_5: 2.20 (s), CH_2: 4.30 (s); ^{13}C-NMR ($CDCl_3$): Me_3: 13.4 ($^1J = 126.9$), Me_5: 9.5 ($^1J = 128.8$), C_3: 148.1 ($^2J = 6.1$), C_4: 104.8 ($^1J = 172.3$, $^3J = 3.8$), C_5: 140.4 ($^2J = 6.6$), CH_2: 48.7 ($^1J = 141.0$).

1,2-Bis(2-methylimidazol-1-yl)ethane (**9**), yield: 60%, m.p. 146–8°C, Rf ($CHCl_3$/EtOH 10 : 2): 0.20; ^{1}H-NMR ($CDCl_3$): Me_2: 2.05 (s), H_4: 6.90 (d), H_5: 6.58 (d), $J_{45} = 1.4$, CH_2: 4.12 (s); ^{13}C-NMR ($CDCl_3$): Me_2: 11.8 ($^1J = 128.5$), C_2: 144.6, C_4: 127.7 ($^1J = 189.3$, $^2J = 9.2$), C_5: 118.6 ($^1J = 188.0$, $^2J = 16.2$), CH_2: 46.5 ($^1J = 140.3$).

Basicity measurements

Spectrophotometry. For pyrazole derivatives (**1**)–(**5**), UV spectroscopy was selected as measurement technique, due to the expected low pK_a values. Compounds (**1**), (**2**), (**3**) and (**5**) were measured in concentrated sulfuric acid where the Hammett acidity function H_0 holds.[11,12] The experiments were carried out between $H_0 = -5.45$ and $H_0 = +3.00$. Compound (**4**), being more basic, was measured in hydrochloric acid solution between pH = 1.00 and pH = 5.00, using potassium chloride to adjust the ionic strength to 0.1.

For each compound, at least three series of measurements were performed using a Hewlett-Packard 841A diode array spectrophotometer. The temperature was maintained constant at 25.0 ± 0.1°C. For each series of measurements, the spectra of 20–25 samples of constant pyrazole concentration (3.10^{-3} M) and increasing acidity were recorded between 210 and 260 nm.

To determine the number of species present in solution, the TRIANG program were used.[13,14] In all cases, three species are present, corresponding to two pK_as. To calculate these pK_as, the SPECPK program [15] was used; it yields the values collected in Table 1.

Potentiometry. For much more basic imidazole and benzimidazole derivatives (**6**)–(**10**), potentiometry was chosen to determine their pK_a. Aqueous solutions about 10^{-3} M were prepared and their ionic strength adjusted to 0.1 [$I = 0.5$ for compound (**10**)] with potassium chloride.

The necessary quantity of HCl, plus a slight excess, to protonate both heterocycles were added. These solutions were titrated backwards with 0.1 M solution of KOH [0.5 M for compound (**10**)] at 25.00 ± 0.05°C under nitrogen atmosphere. A mixture glass-AgCl microelectrode and a Methrom E 536 potentiometer were used.

For each compound, at least three titrations were carried out. The corresponding pK_a values were calculated with the BEST program[16] and afterwards corrected to obtain the thermodynamic values of Table 1.

Compound (**6**): the pK_a values calculated with the program BEST were $pK_{a1} = 4.09$ and $pK_{a2} = 5.67$ (Sigma pH fit = 0.03).

Compound (**7**): the pK_a values calculated with the program BEST were $pK_{a1} = 5.30$ and $pK_{a2} = 6.75$ (Sigma pH fit = 0.02).

Compound (**8**): the pK_a values calculated with the program BEST were $pK_{a1} = 5.20$ and $pK_{a2} = 6.52$ (Sigma pH fit = 0.03).

Compound (**9**): the pK_a values calculated with the program BEST were $pK_{a1} = 6.16$ and $pK_{a2} = 7.39$ (Sigma pH fit = 0.02).

Compound (**10**): the pK_a values calculated with the program BEST were $pK_{a1} = 3.88$ and $pK_{a2} = 5.14$ (Sigma pH fit = 0.01).

The applied correction amounts to − 0.33 and − 0.11 for pK_{a1} and pK_{a2}, respectively, except for compound (**10**), where the corresponding corrections were − 0.17 and − 0.53.

REFERENCES

[1] J. Catalán, J. L. M. Abboud and J. Elguero, *Adv. Heterocycl. Chem.*, **41**, 187 (1987).
[2] E. M. Tjiou, A. Fruchier, V. Pellegrin and G. Tarrago, *J. Heterocycl. Chem.*, **26**, 893 (1989).
[3] M. M. Medvedeva, A. F. Pozharskii and A. M. Simonov, *Chem. Heterocycl. Comp.*, **1972**, 1280.
[4] J. Elguero, R. M. Claramunt, R. Garcerán, S. Juliá, L. Avila and J. M. del Mazo, *Magn. Reson. Chem.*, **25**, 260 (1987).
[5] J. Torres, J. L. Lavandera, P. Cabildo, R. M. Claramunt and J. Elguero, *J. Heterocycl. Chem.*, **25**, 771 (1988).
[6] S. Juliá, P. Sala, J. del Mazo, M. Sancho, C. Ochoa, J. Elguero, J. P. Fayet, and M. C. Vertut, *J. Heterocycl. Chem.*, **19**, 1141 (1982).
[7] R. M. Claramunt, H. Hernández, J. Elguero, and S. Juliá, *Bull. Soc. Chim. Fr.*, **1983**, II, 5.
[8] R. M. Claramount, P. Domiano, J. Elguero, and J. L. Lavandera, *Bull. Soc. Chim. Fr.*, **1989**, 472.
[9] R. M. Claramunt, J. Elguero, and T. Meco, *J. Heterocycl. Chem.*, **20**, 1245 (1983).
[10] R. M. Claramunt and J. Elguero, *An. Quím.*, **82**, 162 (1986).
[11] L. P. Hammett and A. J. Deyrup, *J. Am. Chem. Soc.*, **54**, 2721 (1932).
[12] K. M. Bascombe and R. P. Bell, *J. Chem. Soc.*, **1959**, 1096.
[13] A. Albert and E. P. Serjeant, "The Determination of Ionization Constants. A Laboratory Manual", Chapman and Hall. Third edition, 1984.
[14] R. M. Wallace and S. M. Katz, *J. Phys. Chem.*, **68**, 3890 (1964).
[15] L. P. Varga and F. C. Weatch, *Anal. Chem.*, **39**, 1101 (1967).
[16] R. J. Motekaitis and A. E. Martell, *Can. J. Chem.*, **60**, 2403 (1982).

Compound (9): the pK values calculated with the program BEST were $pK_{a1} = 5.49$ and $pK_{a2} = 7.9$ (Sigma pH fit = 0.02).

Compound (10): the pK_a values calculated with the program BEST were $pK_{a1} = 3.68$ and $pK_{a2} = 5.14$ (Sigma pH fit = 0.04).

The applied correction amounts to − 0.52 and − 0.41 for pK_{a1} and pK_{a2}, respectively, except for compound (10), where the corresponding corrections were − [illegible] and − 0.53.

REFERENCES

[1] P. Cabildo, J. L. M. Abboud and J. Elguero, J. Heterocycl. Chem., 41, 157 (1987).
[2] [illegible] Fruchier, V. Pellegrin and G. Tarrago, J. Heterocycl. Chem., 26, 503 (1989).
[3] M. M. Medvedeva, A. F. Pozharskii and V. M. Simonov, Chem. Heterocycl. Comp., 1975, 1530.
[4] J. Elguero, R. M. Claramunt, D. Carrera, S. Julià, L. Avila and J. M. del Mazo, [illegible] Chem., 28, 260 (1987).
[5] I. Torres, J. L. Lavandera, P. Cabildo, R. M. Claramunt and J. Elguero, J. Heterocycl. Chem., 25, 771 (1988).
[6] S. Julià, J. del Mazo, M. Sancho, C. Ochoa, J. Elguero, J. P. Fayet and M. C. Vertut, J. Heterocycl. Chem., 19, 1141 (1982).
[7] R. M. Claramunt, H. Hernández, J. Elguero and S. Julià, Bull. Soc. Chim. Fr., 1983, II-5.
[8] R. M. Claramunt, D. Domingo, J. Elguero and J. L. Lavandera, Bull. Soc. Chim. Fr., 1988, 472.
[9] R. M. Claramunt, J. Elguero and T. Meco, J. Heterocycl. Chem., 20, 1245 (1983).
[10] R. M. Claramunt and J. Elguero, An. Quím., 82, 102 (1986).
[11] L. P. Hammett and A. J. Deyrup, J. Am. Chem. Soc., 54, 2721 (1932).
[12] K. N. Bascombe and R. P. Bell, J. Chem. Soc., 1959, 1096.
[13] A. Albert and E. P. Serjeant, "The Determination of Ionization Constants. A Laboratory Manual", Chapman and Hall, Third edition, 1984.
[14] R. M. Wallace and S. M. Katz, J. Phys. Chem., 68, 3890 (1964).
[15] [illegible] and [illegible] Wentzell, Anal. Chem., 49, 1101 (1977).
[16] [illegible] and [illegible], Can. J. Chem., 60, 2203 (1982).

Revue Roumaine de Chimie, 36, 4–7, 635–645 (1991)

Dedicated to Professor ALEXANDRU T. BALABAN
on the occasion of his 60th birthday

POLYMER SUPPORTED 1-BENZYL-1,2-DIHYDROISONICOTINAMIDES AS REDUCING AGENTS

SHINJI NISHITANI * and NICHOLAS BODOR **

Center for Drug Discovery, College of Pharmacy, Box J-497 J. Hillis Miller Health Center, University of Florida, Gainesville, FL 32610

Received January 18, 1991

Polymer-supported dihydroisonicotinamides (2 and 3) capable of reducing pyridinium salts were prepared. Effects of reaction time, temperature and solvent were assessed in determining the most useful of these new reagents. It was found that the reagents may be recycled by regenerating the activated dihydropyridine moiety on the polymer. Reducing power of the regenerated reagents was studied.

INTRODUCTION

The use of polymer supported reagents in organic synthesis is widely accepted as a useful technique. These reagents are polymers that possess functional groups which participate in specific reactions such as hydrolyses, oxidations and reductions.[2] The method offers advantages over conventional synthetic methods; reaction work up is often greatly simplified as the spent reagent may be removed by simple filtration, and recycling of used reagent may be possible. In an industrial setting these features are particularly attractive, as they may allow for the establishment of flow systems in a synthetic procedure.

One of the most fruitful areas of polymer supported reagents is in the use of NAD$^+$ ↔ NADH models to effect stereospecific reduction of, for example, carbonyl functions.[3,4] Several groups have reported the use of these polymer supported 1,4-dihydronicotinamide systems.

We have developed a method for brain specific delivery of drugs using dihydropyridines as "carriers".[5,6] Preparation of the requisite dihydropyridines may in most cases be performed using the standard aqueous basic sodium dithionite method.[7] This method is generally applicable and useful for bench-scale reactions. The method is however unsatisfactory for the reduction of drug-carrier combinations that are base and/or water sensitive. In addition, work up of large scale preparations often requires tedious and awkward removal of inorganic salts from the reaction mixture, making it necessary to employ rather large volumes of volatile solvents to extract the product dihydropyridines. The need for production of large quantities of several of the dihydropyridine systems

---

* See reference No. 1.

** To whom all correspondence should be addressed.

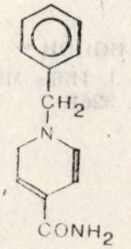

1

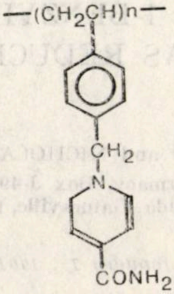

2

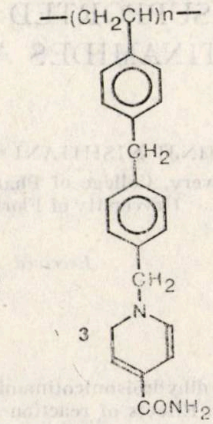

3

prompted us to devise a method for reduction of water and base labile systems, which would also be suitable for large scale use. Clearly, the NAD+ ↔ NADH reagents are not suitable for this reaction as the redox potentials of these reagents are too close to those of the substrates to allow the reaction to proceed to any useful extent. A method for the reduction of pyridinium, and quinolinium salts to the corresponding dihydro forms was recently described by Nuvole et al.[8] In this method, an "activated" dihydropyridine, 1-benzyl-1,2-dihydroisonicotinamide, (**1**), is mixed with a pyridinium or quinolinium salt, resulting in reduction of the salt to the corresponding dihydropyridine or isoquinoline. In many cases the by-product, a 1-benzyl-4-carbamoylpyridinium salt is easily removed by filtration. We recently applied this reduction method to a drug-carrier combination that is particularly sensitive to aqueous and basic media.[9] From a practical and scale-up standpoint, integration of the activated dihydropyridine reductant into a polymer supported reagent is extremely attractive. We now report the preparation of such reagents.

RESULTS AND DISCUSSION

Polymer bound 1-benzyl-1,2-dihydroisonicotinamides **2** and **3** were prepared as shown in Scheme I:

p-Chloromethylstyrene **4** was prepared by literature methods.[10] Homopolymerization of **4** was carried out by heating with benzoyl peroxide as radical initiator in toluene, giving the desired polymer **5** in 38% yield. Reaction of **5** with isonicotinamide in DMF for three days at

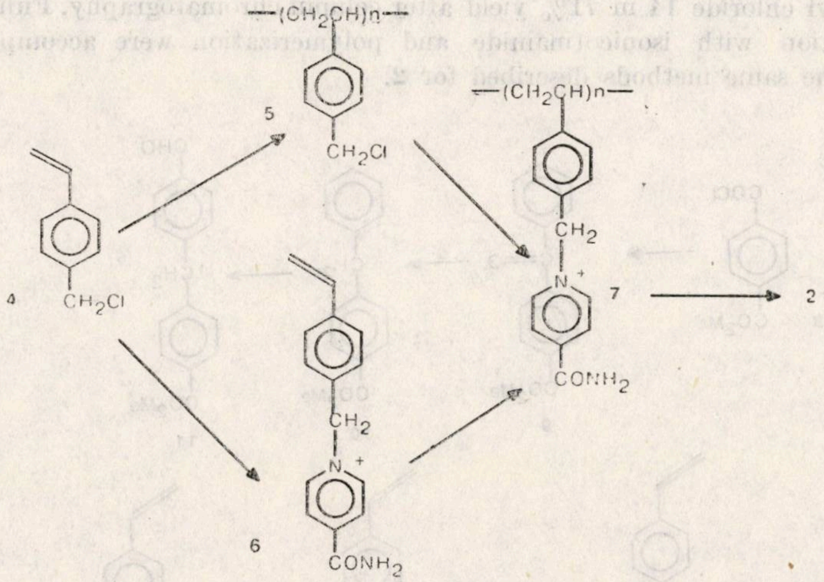

SCHEME I

70°C afforded the corresponding pyridinium salt **7** in 91% yield. Alternatively, **4** was converted to the pyridinium salt **6** in 71% yield on reaction with isonicotinamide. Reaction of **6** with potassium persulfate in water at 65°C for 17 hours gave the polymer **7** in 45% yield. Reduction of **7** with sodium borohydride in aqueous alkaline methanol at low temperature gave the desired polymer supported reducing agent **2** as an insoluble, yellowish solid in 97% yield. Structural determination of **2** was based on IR spectra, its ability to reduce pyridinium salts, and elemental analysis. No NMR spectra of **2** could be obtained due to the insolubility of the polymer in appropriate solvents.

A second polymer supported activated dihydropyridine, **3**, was also prepared. In **3** the dihydropyridine function is further away from the polymer backbone. It was considered possible that such a separation may influence the reactivity of the reagent. Polymer **3** was prepared as shown in Scheme II:

Friedel-Crafts acylation of benzene with the acid chloride **8**[11] gave the benzophenone derivative **9** in high (97%) yield. Reduction of **9** with triethylsilane and trifluoroacetic acid furnished the diarylmethane **10** in 96% yield.[12] Formylation of **10** was accomplished using titanium tetrachloride and α,α-dichloromethyl methyl ether in dichloromethane, giving 4-formyl-4'-methoxycarbonyl diphenylmethane **11** selectively in 63% yield. The formyl group was converted to a vinyl group by Wittig reaction in heterogeneous benzene-aqueous alkali media.[13] The resulting styrene was reduced with lithium aluminum hydride to give the alcohol **13** in 79% yield. Chlorination of **13** with thionyl chloride yielded the benzyl chloride **14** in 71% yield after column chromatography. Functionalization with isonicotinamide and polymerization were accomplished by the same methods described for **2**.

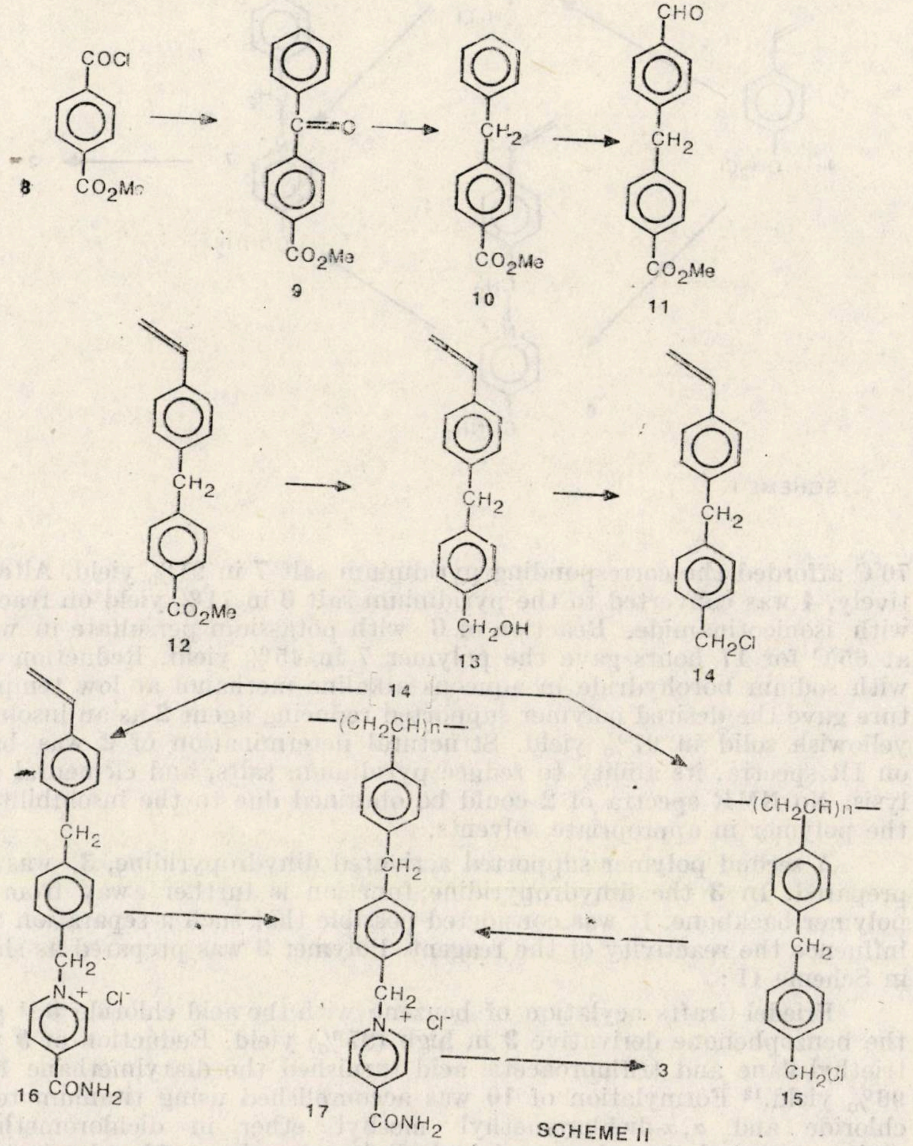
COCl
CO_2Me
8
C=O
CO_2Me
9
CH_2
CO_2Me
10
CHO
CH_2
CO_2Me
11
CH_2
CO_2Me
12
CH_2
CH_2OH
13
CH_2
CH_2Cl
14
14
$-(CH_2CH)_n-$
$-(CH_2CH)_n-$
CH_2
CH_2Cl
15
CH_2
CH_2
N^+ Cl^-
$CONH_2$
16
CH_2
CH_2
N^+ Cl^-
$CONH_2$
17
3

SCHEME II

In order to compare the reducing ability of **2** and **3** with that of the monomer **1**, a series of model reductions were carried out in which 1-benzyl-3-carbamoylpyridinium bromide **18** was reduced to give the relatively stable dihydropyridines **19** and **20**, as shown in Scheme III :

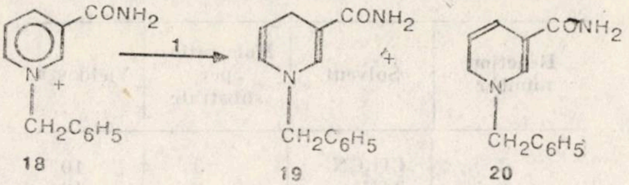

SCHEME III

The polymer (**2** or **3**) was mixed with **18** in dry methanol and the mixture was stirred for an appropriate time under a nitrogen atmosphere. After removal of the insoluble polymer by filtration, dihydropyridines **19** and **20** were collected as a mixture. Table 1 shows the yields of the reduction using **1**, **2** and **3**. It should be noted that the 1,4-(**19**) to 1,2-(**20**) isomer product distribution ratio is essentially the same as is obtained when the monomer **1** is used to effect the reduction.

Table 1

Reduction of **18** with polymer reagents **2** and **3**[a]

Reaction number	Polymer	Mole ratio per substrate	Yield %[b]
1	**2**	1	36
2	**2**	2	62
3	**2**	3	81
4	**3**	1	25
5	**3**	2	56
6	**3**	3	88

[a] Reaction conditions : solvent, methanol ; reaction time, 4 hrs ; temperature 25°C.

[b] Isolated as a mixture of 1,4 and 1,2 isomers-see text.

Table 1 shows that at least three equivalents of the polymer supported reducing agent are required to effect reaction in a reasonable time. The observation that reagents **2** and **3** behave almost identically suggests that the amount of contact between substrate molecule and polymer is the same for both species, even though one might expect that the more flexible system **3** might benefit from more intimate contact of the dihydropyridine moiety with the substrate **18** than does **2**. The effect of solvent on the reduction was examined and the results summarized in Table 2. It is evident from these data that the hydride transfer reaction is most successful in methanol. Time dependence of the reaction was also examined, and the results are shown in Table 3.

Table 2

Solvent effects on the reduction of **18** with polymer **3**[a]

Reaction number	Solvent	Mole ratio per substrate	Yield %[b]
7	CH_3CN	3	10
8	THF	3	12
9	CH_2Cl_2	3	10
10	MeOH	3	88

[a] Reaction conditions : reaction time, 4 hrs ; temperature 25°C.

[b] Isolated as a mixture of **19** and **20**.

Table 3

Time dependence of the reduction of **18** with **1**, **2**, and **3**[a]

Reaction number	Reagent	Mole ratio per substrate	Reaction time	Yield %[b]
11	**2**	3	30 min.	67
12	**2**	3	1 hr.	71
13	**2**	3	2 hr.	77
14	**2**	3	4 hr.	81
15	**2**	3	20 hr.	83
16	**3**	3	30 min.	59
17	**3**	3	1 hr.	70
18	**3**	3	2 hr.	82
19	**3**	3	4 hr.	88
20	**3**	3	20 hr.	90
21	**1**	1	5 min.	91[c]

[a] Reaction conditions : solvent, methanol ; temperature, 25°C.

[b] Isolated as a mixture of **19** and **20**.

[c] Our result ; literature [14] yield listed as 95 %.

The reaction is essentially over in four hours when three equivalents of the polymer reducing agent are used ; the yield approaches that obtained using the monomer **1**. These results imply that the reaction rate may increase if a greater excess of the polymer-bound reagent is used. Having established that the new polymers **2** and **3** will reduce the model system **18** the possibility of recycling the reagents was next considered. As shown in Scheme IV, spent polymer is expected to comprise the partially oxidized structure $\mathbf{2}_{ox}$. The oxidized pyridinium moiety must then be reduced in order to recycle and reactivate the reagent for further use. Both of the used polymers $\mathbf{2}_{ox}$ and $\mathbf{3}_{ox}$ were reduced with sodium borohydride in aqueous alkaline methanol. It is not clear whether or not the structures of the recycled polymers are identical to those of the freshly prepared reagents; however, no halogen was found in the recycled reagent, and the IR spectra of the fresh and recycled reagents were essentially identical.

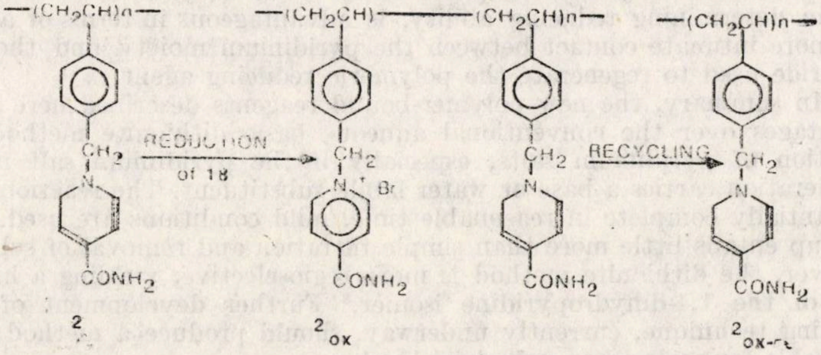

SCHEME IV

The reducing ability of the recovered and recycled reagents was next examined and the results summarized in Table 4.

Table 4

Reducing ability of the recycled polymers **2** and **3**

Reaction number	Polymer type [a]	Extent of reduction of the salt **18**[b] (%)
22	**2**	76
23	**2**(ox)	6
24	**2**(ox-re)	39[c]
25	**2**(ox-re)$_2$	40
26	**2**(ox-re)$_3$	31
27	**3**	77
28	**3**(ox)	26
29	**3**(ox-re)	73
30	**3**(ox-re)$_2$	65
31	**3**(ox-re)$_3$	54

[a] **2**, **3**, represent freshly prepared reagent (reactions 22 and 27). Reactions 23 and 28 were run using reagent that had been recovered from one reduction sequence, but was not recycled. The notation (ox-re)$_n$ refers to reagent that has been recycled n times.

[b] Reaction conditions: 3 equivalents of the reducing agent stirred with 1 equivalent of the salt **18** in dry methanol for 20 hr. at 25°C.

[c] Reaction time 66 hr.

Polymer **3** appeared to withstand recycling quite well, although reducing ability did decrease somewhat as the number of cycles was increased. Conversely, **2** did not fare nearly so well in the recycling study.

Reduction of the used polymers $2_{(ox)}$ and $3_{(ox)}$ does appear to be successful however, as demonstrated by the difference in % reduction of **18** observed on using the (**ox-re**) rather than the (**ox**) species. It is possible that the greater flexibility of **3** compared to **2**, shown to be of little consequence in determining reducing ability, is advantageous in terms of allowring more intimate contact between the pyridinium moiety and the borohydride used to regenerate the polymeric reducing agent.

In summary, the new polymer-bound reagents described here offer advantages over the conventional aqueous basic dithionite method for reduction of pyridinium salts, especially if the pyridinium salt under consideration carries a base or water labile substituent. The reactions are substantially complete in reasonable time, mild conditions are used, and work up entails little more than simple filtration and removal of solvent. However, the dithionite method is more regioselective, yielding a higher ratio of the 1,4-dihydropyridine isomer.[8] Further development of the recycling technique, currently underway, should produce a method that is suitable for scale-up to industrial levels.

EXPERIMENTAL

General

Microanalyses were performed by Atlantic Microlabs Inc., Atlanta GA. Melting points were determined on a Fisher-Johns melting point apparatus, and are uncorrected. ^{1}H-NMR spectra were recorded on a Varian EM360 (60 MHz) spectrometer with tetramethylsilane as internal standard. Infrared absorption spectra of solids dispersed in potassium bromide disks were recorded on a Beckman Infrared spectrophotometer. Low resolution mass spectra were obtained at 35 eV by electron impact (EI) on a Kratos MS80RFA instrument. Column chromatography was performed on silica gel (Merck, 70—230 mesh, 60).

1-Benzyl-1,2-dihydroisonicotinamide, **1**.

This material was prepared according to the method described by Paglietti[14]; mp 108—110°C. (Lit.[14] 112—115°C).

Poly(p-chloromethylstyrene) (**5**).

A solution of *p*-chloromethylstyrene (17.43 g) in 260 mL of toluene was washed successively with three times 45 mL portions of 5% aqueous sodium hydroxide and two times 30 mL portions of water, then dried over magnesium sulfate. After removing the drying agent, nitrogen gas was bubbled through the resulting solution for ten minutes and 430 mg of benzoyl peroxide was added. After heating at reflux for three hours, solvent was removed by evaporation and the residue was redissolved in 12 mL of chloroform. Methanol was added dropwise to the chloroform solution with vigorous stirring until a milky suspension was obtained. This suspension was in turn added to 750 mL of methanol and the mixture was stirred. The precipitate was collected by filtration, washed with methanol and air-dried, then the solid thus obtained was dissolved in 24 mL of chloroform. Reprecipitation of the polymer was performed once more by addition of methanol. Finally, the white precipitate was washed with saturated sodium bicarbonate, water and methanol. After drying under vacuum 6.46 g of a white polymer (38% yield) was obtained, mp 115—128°C. ^{1}H-NMR ($CDCl_3$) 1.2—2.0 (2H, bs), 6.4—6.9 (2H, bs), 6.9—7.4 (3H, bs). IR (KBr disk) 1250 cm^{-1}. Anal. calculated for $(C_9H_9Cl)n$: C, 70.83 ; H, 5.94; Cl, 23.23% ; Found : C, 70.72 ; H, 5.96 ; Cl, 23.29%.

N-(p-Vinylbenzyl)-4-carbamoylpyridinium chloride (**6**).

A mixture of *p*-chloromethylstyrene (2g, 13.10 mmol), isonicotinamide (1.44 g, 11.79 mmol) and 20 mL of ethanol was heated at reflux whilst stirring overnight, and then was allowed to stand at room temperature for one day. The resulting white precipitate was collected by filtration, washed with ethanol and dried under vacuum, yielding 2.19 g (68%) of **6**, mp 205—210°C (dec.). ^{1}H-NMR (DMSO-d_6) : 5.39 (1H, d, J = 18 Hz), 6.10 (2H, s), 6.85 (1H, dd, J = 10.5

and 18 Hz), 7.55—7.80 (4H, m), 8.35 (1H, bs), 8.66 (2H, d, J = 6.3 Hz), 9.06 (1H, bs), 9.60 (2H, d, J = 6.3 Hz). Anal. calculated for $C_{15}H_{15}N_2ClO \cdot 1/2\ H_2O$: C, 63.49 ; H, 5.68 ; N, 9.87 ; Cl, 12.49 % ; Found : C, 63.77 ; H, 5.64 ; N, 9.93 ; Cl, 12.60 %.

Poly(p-styrylmethylene-N-isonicotinamide chloride) (**7**).

(i) From **5** : To a solution of isonicotinamide (2.88 g, 23.6 mmol) in 36 mL of DMF was added poly(*p*-chloromethylstyrene) **5** (3 g, 19.7 mmol). The resulting mixture was heated at 80—90°C over a period of three days. The precipitate was collected by filtration and washed with toluene. The solid was redissolved in 32 mL of methanol and 8 mL of DMF ; ether was added to this solution dropwise with rapid stirring until a milky suspension was obtained. This suspension was in turn added to 600 mL of stirring ether. The resulting precipitate was removed by filtration and dried under vacuum at 80°C, yielding 5.26 g (97 %) of **7**. H-^{1}NMR ($DMSO-d_6 + CD_3OD$) 1.0—2.2 (2H, bs), 5.8—6.4 (2H, bs), 6.3—7.0 (2H, bs), 7.0—7.8 (3H, bs), 8.6 (2H, bs), 9.3—9.8 (2H, bs). IR (KBr disk) 3400, 3150 and 1660 cm^{-1}. Anal. calculated for $(C_{15}H_{15}N_2ClO \cdot 1/4\ H_2O)_n$: C, 64.51 ; H, 5.59 ; N, 10.03 ; Cl, 12.69 %. Found : C, 64.66 ; H, 5.71 ; N, 9.89 ; Cl, 12.72 %.

(ii) From **6** : To a solution of **6** (1 g) in 15 mL of water was added 30 mg of potassium persulfate as initiator. The resulting mixture was heated at 65°C and stirred for 17 hours. Acetone was added dropwise to the reaction mixture until a milky suspension resulted. This suspension was then added to 650 mL of stirring acetone. The resulting precipitate was collected by filtration and dried under vacuum to give 450 mg (45 %) of **7** as a pale yellow solid. Anal. calculated for $(C_5H_{15}N_2ClO \cdot [H_2O)_n$: C, 61.53 ; H, 5.85 ; N, 9.57 ; Cl, 12.10 % ; Found : C, 61.91 ; H, 5.81 ; N, 9.30 ; Cl, 11.69 %.

Poly(p-styrylmethylene-N-1,2-dihydroisonicotinamide), (**2**).

To a solution of the polymer **7** (4g, 14.6 mmol) in 24 mL of methanol and 8 mL of water was added 2M aqueous NaOH (10.9 mL) ; the temperature was maintained below — 10°C and nitrogen gas was bubbled through the mixture. Sodium borohydride (275 mg, 7.3 mmol) was added to the reaction vessel and the resulting mixture was stirred for 3 hrs. at — 10° to — 20°C. The resulting yellow precipitate was removed by filtration and washed with cold aqueous methanol under a nitrogen atmosphere. After drying in vacuo, 3.6 g (100 % yield) of a pale brown-yellow solid was obtained, mp > 150°C (dec.) IR (KBr disk) 3400, 3200 and 1650 cm^{-1}.

Methyl-4-benzoylbenzoate (**9**).

Compound **9** was prepared in 97 % yield following a literature method and was isolated as a white solid, mp 113—114°C. (Lit.[15] 106—107°C).

Methyl-4-benzylbenzoate (**10**).

Following a literature method **10** was prepared in 96 % yield and isolated as a colorles oil, bp 139—144°C/0.3 torr. (Lit.[16] 120—123°C/0.15 torr).

4-Formyl-4′-methoxycarbonyl diphenylmethane (**11**).

To an ice-cooled solution of **10** (84.6 g, 0.374 mol) in 850 mL of dry dichloromethane was added 164 mL (1.469 mol) of titanium chloride. To the resulting solution dichloromethyl-methyl ether (40 mL, 0.45 mol) was added slowly, maintaining cooling. The resulting mixture was stirred at 5°C for 3 hrs. and then at room temperature for 2 hrs. After this time, the reaction mixture was poured into ice-water and stirred to decompose the complex. The aqueous layer was extracted with dichloromethane (2 × 100 mL) and the combined organic layers were washed with water and dried over anhydrous magnesium sulfate. After evaporation of the solvent the residue was recrystallized twice from hexane-ethyl acetate yielding 59.4 g (63 %) of **11** as yellow needles, mp 75—77°C. ^{1}H-NMR ($CDCl_3$) 3.90 (3H, s), 4.10 (2H, s). 7.29 (2H, d, J = 8.7 Hz), 7.37 (2H, d, J = 8.7 Hz), 7.85 (2H, d, J = 8.7 Hz), 8.01 (2H, d, J = 8.7 Hz), 10.02 (1H, s). Anal. calculated for $C_{16}H_{14}O_3$: C, 75.57 ; H, 5.55 % ; Found : C, 75.55 ; H, 5.59 %.

4-Vinyl-4′-methoxycarbonyl diphenylmethane (**12**).

A mixture containing the aldehyde **11** (37.9 g, 0.149 mol), methyltriphenylphosphonium iodide (107.0 g, 0.265 mol), benzene (280 mL), and 5M aqueous NaOH (830 mL) was stirred for 40 hrs. at 40°C. The aqueous layer was then extracted with benzene (2 × 100 mL), the organic layers were combined, washed with water and brine. After drying over anhydrous magnesium sulfate, solvent was removed by evaporation at reduced pressure. The product was isolated after column chromatography (SiO_2, hexane : ethyl acetate, 8 : 1) giving 29.5 g of the styrene **12** as a pale yellow liquid. ^{1}H-NMR ($CDCl_3$) 3.90 (3H, s), 4.03 (2H, s), 5.25 (1H, d, J = 10.5 Hz), 5.75 (1H, d, J = 18 Hz), 6.76 (1H, dd, J = 10.5, 18 Hz), 7.2—7.5 (4H, m), 7.30 (2H, d, J = 8.7 Hz), 8.02 (2H, d, J = 8.7 Hz). Mass spectrum : (m/e) 252 (M^+).

4-Vinyl-4'-hydroxymethyl diphenylmethane (**13**).

To a suspension of lithium aluminium hydride (3.15 g 0.083 mol) in 200 mL of dry THF was added a solution of the styrene **12** (27.2 g 0.11 mol) in 80 mL of dry THF at 15——20°C for 15 min. under a stream of nitrogen. The resulting mixture was stirred at room temperature for 20 min. Following this time water (3.2 mL), 15 % aqueous sodium hydroxide (3.2 mL), and a further 9.6 mL of water were added successively with care. An insoluble gelatinous material resulted and was filtered, washed with brine and dried over anhydrous sodium sulfate. Solvent was removed by evaporation and the residue was recrystallized from pet. ether ethylacetate yielding 11.75 of colorless crystals. The filtrate was purified by column chromatography (SiO_2, CH_2Cl_2). Recrystallization of the major eluent from pet. ether-ethyl acetate gave a further 7.66 g of **13** for an overall yield of 79 % ; mp 70.5—71.5°C. ^{1}H-NMR ($CDCl_3$) 1.78 (1H, bs), 3.93 (2H, s), 4.63 (2H, bs), 5.20 (1H, d, J = 10.8 Hz), 5.70 (1H, d, J = 17.5 Hz), 6.71 (1H, dd, J=10.8, 17.5 Hz), 7.1—7.5 (8H, m). Anal. calculated for $C_{16}H_{16}O$: C, 85.68 ; H, 7.19 % ; Found : C, 85.74 ; H, 7.24 %.

4-Vinyl-4'-chloromethyl diphenylmethane (**14**).

To a stirred solution of the alcohol **13** (8.25 g, 36.8 mmol) in 90 mL of dichloromethane was added dropwise a mixture of thionyl chloride (5.69 g, 47.8 mmol), and pyridine (3.78 g, 47.8 mmol) in 25 mL of dichloromethane with ice-bath cooling. The resulting mixture was stirred at room temperature overnight, then washed with cold water and dried over anhydrous magnesium sulfate. After evaporation of solvent the residue was purified by column chromatography (SiO_2, hexane : benzene, 15 ; 1 to 12 : 1), giving 14.04 g (71 %) of **14**. A small amount of the liquid was purified further by vacuum distillation ; this sample was submitted for microanalysis ; bp > 100°C/0.1 torr. ^{1}H-NMR ($CDCl_3$) 3.91 (2H, s), 4.50 (2H, s), 5.16 (1H, d, J = 10.8 Hz), 5.66 (1H, d, J = 17.7 Hz), 6.71 (1H, dd, J = 10.8, 17.7 Hz), 7.0—7.4 (8H, m). Anal. calculated for $C_{16}H_{15}Cl$: C, 79.17 ; H, 6.23 ; Cl, 14.60 % ; Found : C, 78.97 ; H, 6.28 ; Cl, 14.53 %.

Poly[4-(4'-chloromethylphenyl)methyl styrene](**15**).

Compound **15** was prepared by the same method as described for **5**. Polymerization of the monomer **14** (10 g) gave the desired polymer (4.27 g, 43 %) as a white solid, mp 57—68°C. ^{1}H-NMR ($CDCl_3$) : 0.8—2.0 (2H, bs), 3.79 (2H, bs), 4.43 (2H, bs), 6.0—7.5 (9H, m). Anal. calculated for $(C_{16}H_{15}Cl)_n$: C, 79.17 ; H, 6.23 ; Cl, 14.62 % ; Found : C, 79.09 ; H, 6.25 ; Cl, 14.62 %.

N-[4-(4'-Vinylphenylmethyl)phenylmethyl]-4-carbamoylpyridinium chloride (**16**).

A mixture containing **14** (6 g, 24.7 mmol), isonicotinamide (2.72 g, 22.3 mmol), and 75 mL of 2-propanol was heated at reflux and stirred for 5 hrs. The white precipitate which resulted was collected by filtration and washed with 2-propanol. Recrystallization of the crude wet material from 120 mL of 2-propanol and 23 mL of water afforded 4.07 g (50 %) of **16** as a white, crystalline solid, mp 236—240°C (dec.). ^{1}H-NMR (DMSO-d_6 + D_2O) : 3.93 (2H, s), 5.20 (1H, d, J = 17.7 Hz), 5.85 (2H, s), 6.71 (1H, dd, J = 10.5, 17.7 Hz), (7.15—7.55(8H, m), 8.38 (2H, d, J = 6.3 Hz), 9.23 (2H, d ,J = 6.3 Hz). Anal. calculated for $C_{22}H_{21}N_2ClO \cdot 1/4H_2O$: C, 71.53 ; H, 5.87 ; N, 7.59 ; Cl, 9.60 % ; Found : C, 71.65 ; H 5.84 ; N, 7.56 ; Cl, 9.69 %

Poly{N-[4-(4'-vinylphenylmethyl)phenylmethyl]-4-carbamoylpyridinium chloride} (**17**).

(i) From **15** : Prepared as described for **7** (i) ; isolated in 80 % yield as a pale yellow solid, mp > 200°C (dec.). Anal. calculated for $(C_{22}H_{21}N_2ClO \cdot 1/2\,H_2O)_n$: C, 70.67 ; H, 5.93 ; N, 7.49 ; Cl, 9.48 % ; Found : C, 70.74 ; H, 5.93 ; N, 7.18 ; Cl, 9.17 %.

(ii) From **16** : Prepared as described for **7** (ii) ; precipitation of the crude product was effected by adding the milky suspension of the polymer in methanol and water to stirred ether. The resulting precipitate was collected by filtration giving a 78 % yield of a pale yellow powder, mp > 220°C (dec.). Anal. calculated for $(C_{22}H_{21}N_2ClO \cdot H_2O)_n$: C, 69.01 ; H, 6.06 ; N, 7.32 ; Cl, 9.26 % ; Found : C, 69.09 ; H, 6.03 ; N, 7.27 ; Cl, 9.17 %.

Poly[4-(4'-vinylphenylmethyl)phenylmethylene-N-1,2-dihydroisonicotinamide (**3**).

The same procedure as described for the preparation of **2** was used to prepare **3** ; isolated as a pale brown solid in 90 % yield, mp > 150°C (dec.). IR (KBr disk) 3400 and 1650 cm^{-1}. Anal. calculated for $(C_{22}H_{22}N_2O \cdot 1/4\,H_2O)_n$: C, 74.29 ; H, 7.03 ; N, 7.88 % ; Found : C, 74.31 ; H, 6.49 ; N, 7.40 %.

3-Carbamoyl-N-benzylpyridinium bromide (**18**).

Compound **18** was prepared as described in the literature[17]; mp 219–221°C. (Lit.[17] 210–211°C).

Reduction of the pyridinium salt **18** *with the polymeric reagent* **2** *or* **3**.

A typical procedure was as follows: To a solution of 100 mg (0.34 mmol) of the salt **18** in 5 mL of dry methanol was added the appropriate quantity of the polymer **2** or **3**. The mixture was stirred under a nitrogen atmosphere for the times indicated in Table 4. After insoluble materials were removed by filtration, solvent was removed at reduced pressure at room temperature. The residue was partitioned between dichloromethane and water, the phases were separated and the aqueous layer was extracted once more with dichloromethane. The combined organic layers were dried over anhydrous sodium sulfate and solvent was removed by low pressure evaporation at room temperature to give a mixture of the isomeric dihydropyridines **19** and **20** in essentially the same ratio as described in the literature[8] (4 : 1, **19** : **20**).

Recycling of the used polymers.

A typical procedure is described for recycling of the polymer $\mathbf{2}_{(ox)}$: To a suspension of the used polymer (300 mg) in 5 mL of methanol and 1 mL of water was added 0.3 mL of 2M aqueous sodium hydroxide, maintaining the reaction temperature at – 10 to – 20°C. Sodium borohydride (20 mg) was added to the stirred reaction mixture, kept under a nitrogen atmosphere at – 10 to – 20°C for 3 hrs. Isolation of the regenerated polymer was carried out by the same method as described for **2**; yield 258 mg, mp > 150°C (dec.). Anal. calculated for $(C_{15}H_{16}N_2O \cdot H_2O)_n$: C, 69.74; H, 7.02; N, 10.84%; Found: C, 69.00; H, 6.48; N, 9.42%. To ascertain that no quaternary species remained, bromine content was also determined and was found to be zero.

ACKNOWLEDGEMENTS. We would like to thank Dr. David Winwood for helpful discussions and assistance in preparing this manuscript.

REFERENCES

[1] On leave from Otsuka Pharmaceutical Company, 2nd Tokushima Factory, 463-10 Kagasuno Kawachi-cho, Tokushima, Japan.

[2] W. T. Ford in "Polymeric Reagents and Catalysts", American Chemical Society Symposium series, **308** (1985).

[3] G. Dupas, J. Bourgignon, C. Ruffin and G. Queguiner, *TetrahedronLett.*, **23**, 5141 (1982).

[4] A. Zicmanis and R. Nalivaiko, *Latvijas PSR Zinatnu Akademijas Vestis Kimijas Serija*, **3**, 360 (1982); *Chem. Abs.*, **93**, 187074n.

[5] N. Bodor, *Ann. New York Acad. Sci.*, **507**, 289 (1987).

[6] N. Bodor, H. Farag and M. E. Brewster, *Science*, **214**, 1370 (1981).

[7] L. J. Haynes and A. R. Todd, *J. Chem. Soc.*, **1950**, 303.

[8] A. Nuvole, G. Paglietti, P. Sanna and R. M. Acheson, *J. Chem. Res.* (s), **1984**, 356.

[9] K. S. Raghavan, E. Shek and N. Bodor, *Anti-Cancer Drug Design*, **2**, 25 (1987).

[10] S. Kondo, T. Ohtsuka, K. Ogura and K. Tsuda, *J. Macromol. Sci-Chem.*, **A 13**, 767 (1979).

[11] B. W. Hotten, *Ind. and Eng. Chemistry*, **49**, 1691 (1957).

[12] D. N. Kursanov, Z. N. Parnes and N. M. Loim, *Synthesis*, **1974**, 633.

[13] W. Takagi, I. Inoue, Y. Yano and T. Okonogi, *Tetrahedron Lett.*, **1974**, 2587.

[14] G. Paglietti, P. Sanna, A. Nuvole, F. Soccolini and R. M. Acheson, *J. Chem. Res.* (m), **1983**, 2326.

[15] M. G. Smith, *J. Amer. Chem. Soc.*, **43**, 1920 (1920).

[16] G. W. Gribble, W. J. Kelly and S. E. Emery, *Synthesis*, **1978**, 763.

[17] J. W. Bunting and S. Sindhuatmadja, *J. Org. Chem.*, **45**, 5411 (1980).

[18] J. V. Eys, *J. Biol. Chem.*, **233**, 1203 (1958).

3-Carbamoyl-N-benzylpyridinium bromide (18).

Compound 18 was prepared as described in the literature[illegible]; mp 219–221°C (lit.[illegible] 220–221°C).

Reduction of the pyridinium salt 18 with the polymeric reagent 2 or 3.

A typical procedure was as follows: to a solution of 100 mg (0.34 mmol) of the salt 18 in 5 mL of dry methanol was added the appropriate quantity of the polymer 2 or 3. The mixture was stirred under a nitrogen atmosphere for the times indicated in Table 1. After insoluble materials were removed by filtration, solvent was removed at reduced pressure at room temperature. The residue was partitioned between dichloromethane and water, the phases were separated and the aqueous layer was extracted once more with dichloromethane. The combined organic layers were dried over anhydrous sodium sulfate and solvent was removed by low pressure evaporation at room temperature to give a mixture of the isomeric dihydropyridines 19 and 20 in essentially the same ratio as described in the literature[5] (1 : 1, 19 : 20).

Recycling of the used polymers.

A typical procedure is described for recycling of the polymer 2ox. To a suspension of the used polymer (200 mg) in 3 mL of methanol and 1 mL of water was added 0.3 mL of 2M aqueous sodium hydroxide, maintaining the reaction temperature at − 10 to − 20°C. Sodium borohydride (20 mg) was added to the stirred reaction mixture, kept under a nitrogen atmosphere at − 10 to − 20°C for 3 hrs. Isolation of the regenerated polymer was carried out by the same method as described for 2; yield 288 mg; mp > 150°C (dec.). Anal. calculated for [illegible]: C, 69.74; H, 7.83; N, [illegible]. Found: C, [illegible]; H, [illegible]; N, [illegible]. To ascertain that no quaternary species remained, bromide content was also determined and was found to be zero.

ACKNOWLEDGEMENTS. We would like to thank Dr. David Wilkinson for helpful discussions and assistance in preparing this manuscript.

REFERENCES

[1] On leave from Otsuka Pharmaceutical Company, 2nd Tokushima Factory, 463-10 Kagasuno Kawauchi-cho, Tokushima, Japan.
[2] W. T. Ford in "Polymeric Reagents and Catalysts", American Chemical Society Symposium Series, 308 (1986).
[3] H. Dugas, [illegible], [illegible] and [illegible], *Tetrahedron*, [illegible] (1987).
[4] [illegible] and [illegible], [illegible]
[5] S. Shifrin, *Ann. New York Acad. Sci.*, [illegible] (1957).
[6] [illegible], *Science*, [illegible]
[7] [illegible] and A. H. [illegible], *J. Chem. Soc.*, 1958, 508.
[8] A. [illegible], [illegible] and R. M. Acheson, *J. Chem. Res.* (S), 1984, [illegible].
[9] K. S. [illegible], E. Steele and [illegible], *Anti-Cancer Drug Design*, 2, 25 (1987).
[10] S. Kondo, [illegible], *J. Macromol. Sci. Chem.*, A 13, 767 (1979).
[11] [illegible], 42, 1681 (1977).
[12] D. N. Kursanov, Z. N. Parnes and N. M. Loim, *Synthesis*, 1974, 633.
[13] W. [illegible], *Tetrahedron Lett.*, 1981, 2083.
[14] [illegible] and R. M. Acheson, *J. Chem. Res.* (M), 1983, 2838.
[15] [illegible] *J. Am. Chem. Soc.*, 42, [illegible] (1920).
[16] [illegible], W. J. Kelly and S. [illegible], *Synthesis*, 1978, 703.
[17] J. W. Bunting and S. Sindhuatmadja, *J. Org. Chem.*, 45, 5411 (1980).
[18] [illegible], *J. Biol. Chem.*, 243, [illegible] (1968).

Revue Roumaine de Chimie, **36,** 4–7, 647–656 (1991)

Dedicated to Prof. A. T. BALABAN
on the occasion of his 60th birthday

USE OF SEMIEMPIRICAL MOLECULAR ORBITAL PARAMETERS TO PROBE DIHYDROPYRIDINE STABILITY-IMPLICATIONS TO BRAIN-TARGETING CHEMICAL DELIVERY SYSTEMS

MARCUS E. BREWSTER,[a] MING-JU HUANG,[a] JAMES J. KAMINSKI,[b] EMIL POP[a]
and NICHOLAS BODOR *,[a]
[a] Center for Drug Discovery,
University of Florida, Gainesville, FL 32610,
Pharmatec, Inc., P.O. Box 730, Alachua, FL 32615
[b] Schering-Plough Corporation,
Bloomfield, NJ 07003

Received January 18, 1991

Semiempirical molecular orbital methods of the AM1 type were employed to examine the oxidative stability of 1-methyl-3-substituted-1,4-dihydropyridines. A highly significant correlation was obtained in the comparison of adiabatic ionization potentials and the log of the second order rate constants of ferricyanide-mediated oxidation. Attempts to use soft-hard acid-base theory to predict reactivity were unsuccessful.

INTRODUCTION

Dihydropyridines have emerged pharmaceutically as important drug substructures. Hantsch-ester dihydropyridines have potent calcium channel blocking activity and are used clinically as antihypertensives.[1,2] Another pharmacological use of dihydropyridines is as "drug targetors". Bodor has described a chemical delivery system (CDS) which utilizes reduced derivatives of nicotinic acid to achieve selective brain-deposition of drugs.[3–7] In this approach, a molecular targetor is covalently attached to the drug of interest. While a variety of carriers have been considered, best results are obtained for 1-methyl-1,4-dihydronicotinates (1,4-dihydrotrigonellinates). The attached moiety increases the lipophilicity of the drug and allows it to penetrate into many tissue compartments, such as the brain, which may be inaccessible to the parent compound. The targetor is, however, specially designed to undergo enzymatically mediated oxidation to the nicotinate (trigonellinate) salt. The now polar conjugate is readily lost from the systemic circulation due to its polarity but is retained in the central nervous system (CNS). This retention is in large part due to the blood-brain barrier (BBB) which prevents the rapid influx or reflux of polar molecules. The trapped drug-oxidized carrier conjugate can subsequently degrade to release the active agent. The design of this scheme provides for rapid peripheral elimination of the delivered agent and simultaneous central sequestration.

---

* To whom all correspondence should be addressed.

In the case of calcium channel blockers of the nifedipine/nisoldipine structural type, oxidation to the corresponding pyridine species is a major deactivating metabolic pathway.[1] By contrast, oxidation of the dihydronicotinate species in the CDS is necessary for CNS sequestration and optimal brain delivery. Given the importance of these oxidative processes, understanding the conversions and predicting the effects of substitutions and structural manipulations on dihydropyridine stability is highly desirable. To this end, a series of theoretical and experimental studies have been conducted to describe the mechanism of dihydropyridine oxidation as well as factors which impede or accelerate this conversion.[8-13] One important tool in these considerations is semiempirical molecular orbital approaches especially the AM1 approximation.[14,15] These all valence self-consistent field methods are computationally convenient and provide results within an acceptable error of experimentally derived data.

The AM1 approximation has been used to show that radically mediated oxidation such as that induced by the ferricyanide anion is dependent on dihydropyridine molecular ionization potentials.[11] Since the first and predominantly rate-determining step in ferricyanide-mediated oxidation is electron removal from the dihydropyridine to give the radical cation, the results confirm that the ease of electron loss is directly related to the energy of the molecular orbital containing the electron, i.e., the highest occupied molecular orbital (HOMO). In the present communication we expand these findings by examining a variety of substitution effects and attempt to correlate experimental data with the hard-soft acid-base theory.

METHODS SECTION

Energy calculations were performed using the AM1 all-valence electron self-consistent field molecular orbital approximation.[14,15] These computations were performed on either an IBM 3034 Model K dual processor computer (15 MIPS) or a Tektronix CAChe® system utilizing an Apple® platform. The CAChe® workstation consists of a MacIntosh® IIx 68030 processor with a 68882 floating point coprocessor. In addition, molecular orbital calculations are obtained on a 20 MHz Motorola 88000 RISC processor (17 MIPS). Molecular geometries and energies were obtained by minimizing the total energy of the system with respect to all structural variables using the Broyden-Fletcher-Goldfarb-Shanno optimization procedure. Vertical ionization potentials were calculated using Koopman's theorem while adiabatic ionization potentials were obtained as the difference between the radical cation and dihydropyridine heats of formation.

RESULTS AND DISCUSSION

Studies of ferricyanide-mediated oxidation of 1-(4-substituted phenyl)-1,4-dihydronicotinamides showed that the observed second order rate constants were fairly well correlated (r = 0.96) with AM1-derived vertical ionization potentials.[11] Interestingly, one compound, 1-(4-dimethylaminophenyl)-1,4-dihydronicotinamide, consistently deviated from the rate-energy relationships generated by the remaining derivatives. In reanalyzing the data, it was found that use of the adiabatic ionization potentials, which were derived from the heats of formation of the ground state and radical cations, provide for an increase correlation coefficient by linearizing the aberant dimethylamino value (Fig. 1). In evaluating this improvement, the adiabatic and vertical ionization potentials were studied. Figure 2 and Table 1 shows that with the exception of the 1-(4-dimethylaminophenyl)-1,4-dihydronicotinamide, vertical and adiabatic values are highly correlated. The slope of this relationship is 0.8 with adiabatic ionization potentials underestimating the vertical values by approximately

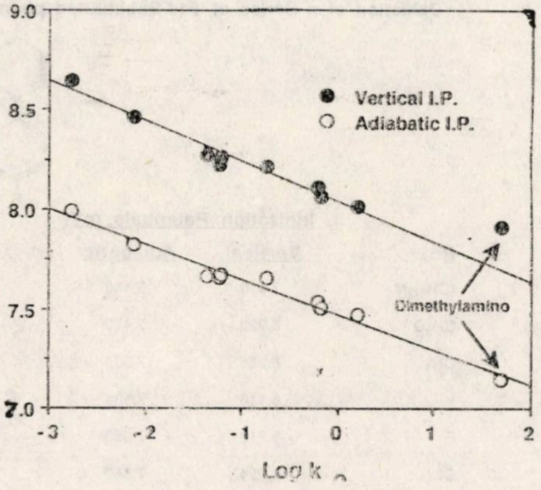

Fig. 1. — Correlation between the log of the second order rate constants for ferricyanide-mediated oxidation of a series of 1-(4-substituted phenyl)-1,4-dihydronicotinamides and AM1-derived adiabatic or vertical ionization potentials both expressed in electron volts (eV). The relationships differ in their correlation coefficients and the deviation of 1-(4-dimethylamino-phenyl)-1,4-dihydronicotinamide.

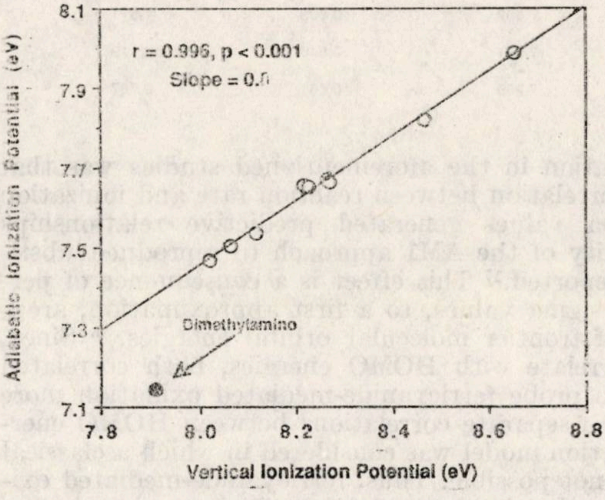

Fig. 2. Correlation between AM1-derived vertical and adiabatic ionization potentials for a series of 1-(4-substituted phenyl)-1,4-dihydronicotinamides. The relationship, excluding the dimethylamino derivative, was highly significant with a correlation coefficient of 0.996.

0.6 eV. The greater dependence of the rate on adiabatic ionization potential may be reflected in the mechanism of reaction. The adiabatic values incorporate radical cation relaxation in their magnitude suggesting that ferricyanide-mediated oxidation of dihydropyridines involves a rate-limiting electron transfer and that this process is sufficiently slow to allow for energetic molecular minimization prior to the subsequent step in the reaction, i.e., proton loss from the radical cation.[16]

Table 1. - Vertical and Adiabatic Ionization potentials, the Absolute Value of their Difference and the Log of the Second Order Rate Constants for Ferricyanide-mediated Oxidation of a Series of 1-(4-Substituted phenyl)-1,4-Dihydronicotinates

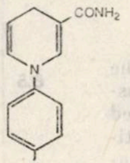

R	Ionization Potentials (eV) Vertical	Ionization Potentials (eV) Adiabatic	|Δ I.P. (eV)|	Log $k_2^{\ddagger}$
$(CH_3)_2N$	7.910	7.143	0.767	1.682
CH_3O	8.020	7.470	0.550	0.207
CH_3	8.065	7.506	0.559	-0.184
H	8.116	7.534	0.582	-0.211
F	8.216	7.658	0.558	0.745
Cl	8.224	7.652	0.572	-1.237
Br	8.264	7.671	0.593	-1.215
I	8.270	7.662	0.608	-1.371
CF_3	8.467	7.821	0.646	-2.119
NO_2	8.650	7.989	0.661	-2.767

An additional observation in the aforementioned studies was that in addition to significant correlation between reaction rate and ionization potentials, Hammett sigma values generated predictive relationships with kinetic data. The ability of the AM1 approach to reproduce substituent constants has been reported.[17] This effect is a consequence of perturbational theory in that sigma values, to a first approximation, are a measure of the variation of frontier molecular orbital energies. [18] Since, therefore, sigma values correlate with HOMO energies, both correlated with rate data. In order to probe ferricyanide-mediated oxidation more closely and in an attempt to separate correlations between HOMO energies and sigma value, a reaction model was considered in which a classical Hammett relationship was not possible. Thus, ferricyanide-mediated oxidation for a series of 1-methyl-3-substituted-1,4-dihydropyridines was completed and correlated with various semiempirical parameters. Table 2 provides rate information and ionization potentials for the compounds examined. Attempts to correlate vertical ionization potential with the log of the second order rate constants for oxidation were not fruitful as shown in Figure 3. By contrast a significant correlation ($r = 0.9$) was obtained when the corresponding adiabatic ionization potentials were employed. A comparison of vertical and adiabatic ionization potentials for this compound is shown in Figure 4. Unlike the relationship obtained

Table 2.-Vertical and Adiabatic Ionization potentials, the Absolute Value of their Difference and the Log of the Second Order Rate Constants for Ferricyanide-mediated Oxidation of a Series of 1-Methyl-3-substituted-1,4-dihydropyridines

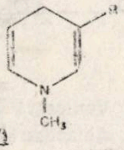

R	Ionization Potentials (eV) Vertical	Adiabatic	|Δ I.P. (eV)|	Log $k^{\ddagger}$
CHO	8.160	7.702	0.458	-1.301
CN	8.197	7.756	0.439	-0.678
$COCH_3$	8.095	7.614	0.481	0.072
$COOCH_3$	8.213	7.670	0.543	0.582
$COOC_2H_5$	8.195	7.637	0.558	0.635
$CONH_2$	8.196	7.565	0.631	1.776
$CON(C_2H_5)_2$	8.066	7.423	0.643	3.486
$CONHC_2H_5$	8.170	7.510	0.660	2.125
$CONHCH_2C_6H_5$	8.189	7.481	0.708	1.700
$CONH(CH_2)_2C_6H_5$	8.197	7.515	0.682	1.915
CO—N 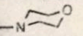	8.240	7.544	0.696	2.874

‡Ref. 10

for the substituted 1-phenyl-1,4-dihydronicotinamides, there was no correlation between ionization potentials. Molecular relaxation, therefore, acts to variably stabilize electron loss in the case of the 1-methyl-3-substituted-1,4-dihydropyridines (Table 2). In molecules where conformational possibilities are limited, differences in the two ionization potentials were minimal while greater entropic flexibility lend to produce greater energy minimization as a function of conformation space. 1-Methyl-3-cyano-1,4-dihydropyridine demonstrates a difference of 0.43 eV between vertical and adiabatic ionization potential while the 1-methyl-3-N'-benzyl-1,4-dihydronicotinamide shows a disparity of 0.71 eV. The ability of the latter to more easily find an energy well is associated with major conformation changes in going from the ground state to the radical cation. The N'-benzyl group, for example, rotates 46° in the radical in response to electronic oxidation while the 1-methyl substituent becomes more planar with the dihydropyridine moiety by 18°. Corresponding changes in the cyano derivative were minimal. The greater correlations of reaction rate with adiabatic relaxation processes are strongly suggestive that molecule minimization is a component of the reaction studied.

A second important theoretical treatment which can assess compound reactivity is the soft-hard acid-base theory as proposed by Pearson. In 1963, it was suggested that nucleophilic displacement reactions could be viewed as interactions of Lewis acids and bases and that the reaction was controlled by several factors including group polarizability and basicity.[19] These early studies gave rise to a series of classifications for soft and hard acids and bases. Briefly, soft bases are donor atoms of high polarizability, low electronegativity and easily oxidized while hard bases are difficult to polarize, highly electronegative and difficult to reduce. Soft acids are acceptor atoms of low positive charge, large in size and easily polarizable while hard acids have a high positive charge, small size and are poorly polarizable.[20]

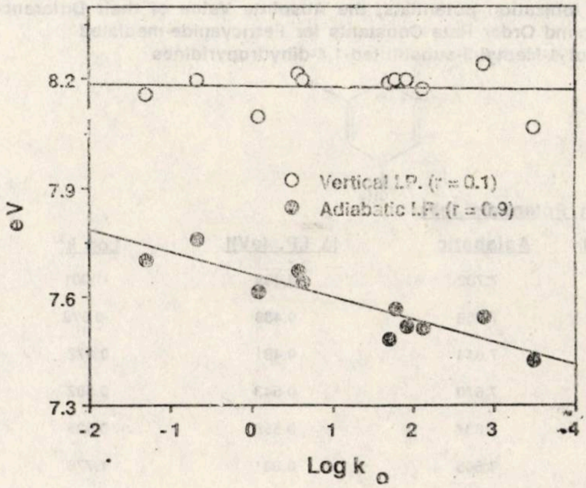

Fig. 3. — Correlation between the log of the second order rate constants for ferricyanide-mediated oxidation of a series of 1-methyl-3-substituted-1,4-dihydropyridines and AM1-derived adiabatic or vertical ionization potentials both expressed in electron volts (eV).

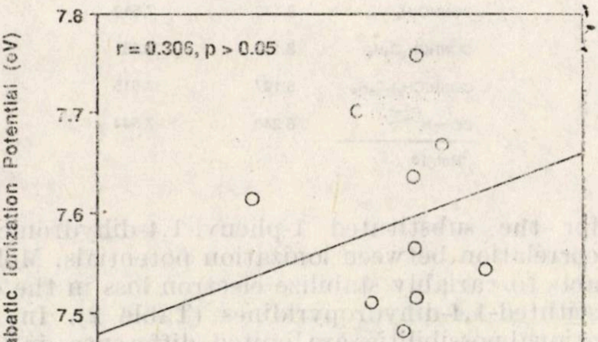

Fig. 4. — Correlation between AM1-derived vertical and adiabatic ionization potentials for a series of 1-methyl-3-substituted-1,4-dihydropyridines. The relationship was not significant at $p < 0.05$.

Several important parameters have been derived from the hard-soft acid-base theory. The tendency of a system to attract electrons is defined as electronegativity and in Pearson's nomenclature this absolute electronegativity (X) is defined as half the sum of the ionization potential and electron affinity [21]:

$$X_m = \frac{I + A}{2}$$

A complementary term is absolute hardness (η) which is defined as resistance to deformation.[21,22] This parameter is half the difference of a system's ionization potential and electron affinity.

$$\eta = \frac{I - A}{2}$$

These parameters have subsequently been incorporated into molecular orbital theory since according to Koopman's theorem, the negative of the HOMO energy is the ionization potential (I) and the negative of the lowest unoccupied molecular orbital (LUMO) is the electron affinity (A).[23] Thus, absolute electronegativity refers to the negative of the average HOMO and LUMO energies while the absolute hardness is half the HOMO-LUMO difference. According to these definitions, soft molecules which have a small HOMO-LUMO separation are polarizable since excitation energies are low.[20] In addition, a small energy gap should enhance chemical reactivity while a large HOMO-LUMO difference should decrease reactivity. Figure 5 and Table 3 gives a diagram correlating the log of the second order rate constants for ferricyanide-mediated oxidation for 1-methyl-3-substituted-1,4-dihydropyridines and the calculated absolute hardnesses. The data reveal a highly significant correlation between absolute

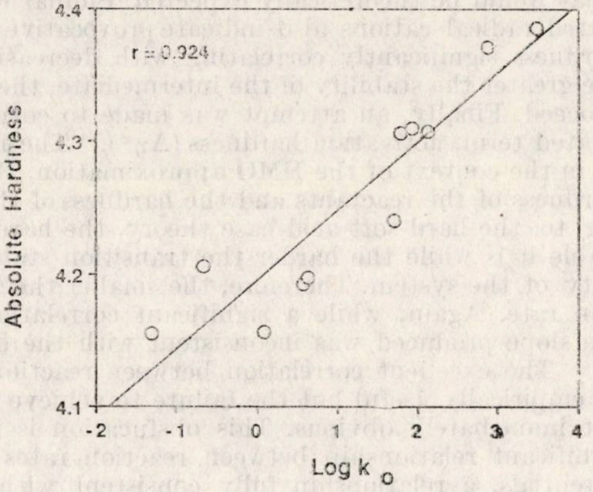

Fig. 5.—The relationship between the log of the second order rate constants for ferricyanide-mediated oxidation of a series of 1-methyl-3-substituted-1,4-dihydropyridines and the calculated absolute hardness.

Table 3.–Absolute Hardness of Various Dihydropyridines and their Corresponding Radical Cations and Activation Hardness Values for Ferricyanide-mediated Oxidation of a Series of 1-Methyl-3-substituted-1,4-dihydropyridines

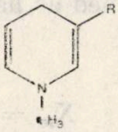

R	Absolute Hardness Dihydropyridine	 Radical Cation	Activation Hardness
CHO	4.155	1.150	3.005
CN	4.206	1.155	3.051
$COCH_3$	4.156	1.127	3.029
$COOCH_3$	4.192	1.085	3.107
$COOC_2H_5$	4.197	1.071	3.126
$CONH_2$	4.307	1.053	3.253
$CON(C_2H_5)_3$	4.386	1.023	3.363
$CONHC_2H_5$	4.307	1.018	3.289
$CONHCH_2C_6H_5$	4.241	0.981	3.259
$CONH(CH_2)_2C_6H_5$	4.310	0.992	3.318
CO— 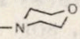	4.371	1.033	3.338

hardness and reaction rate. The obtained coefficient of correlation was r = 0.92. Interestingly, the relationship was characterized by a positive slope meaning that reaction rate increased with increasing hardness. Similarly, absolute electronegativity which correlated with log reaction rate showed a negative slope suggesting increasing reaction rate with decreasing electronegativity. The conclusions reached are opposite of what would be theoretically expected. Similar experiments with the associated radical cations also indicate provocative results with radical cation hardness significantly correlating with decreasing reaction rate. Clearly, the greater the stability of the intermediate, the faster the reaction should proceed. Finally, an attempt was made to correlate reaction rate with a related term, activation hardness ($\Delta\eta^{\neq}$).[24] The recently defined parameter is, in the context of the HMO approximation, the differences between the hardness of the reactants and the hardness of the transition state. According to the hard-soft acid-base theory, the harder the reactant, the more stable it is while the harder the transition state, the greater is the reactivity of the system. Therefore, the smaller the $\Delta\eta^{\neq}$, the faster is the reaction rate. Again, while a significant correlation was obtained (Fig. 6), the slope produced was inconsistent with the described theory.

The excellent correlation between reaction rate and hardness may be empirically useful but the failure to achieve theoretical convergence is not immediately obvious. This obsfucation is made more acute by the significant relationship between reaction rates and adiabatic ionization potentials, a relationship fully consistent with theoretical assumptions.

Several factors may contribute to the inability to apply soft-hard acid-base theory in this instance. First, the model used is a gas phase simulator. While such approaches have been found useful in examining enzymatic processes, they ignore the effect of solvation. In ferricyanide-mediated oxidation of dihydropyridines, radical cation formation is thought to be rate-determining or partially rate-determining. Thus, solvation energy which is expected to be significant for radical cation formation is excluded. Unfortunately, not considering transition state stabilization did not detract from rate versus adiabatic ionization potential correlations suggesting that this consideration is not necessarily crucial to obtaining theoretical convergence. Second, soft-hard acid-base theory has been extensively applied to hydrocarbon systems but not to the case presently examined. It is possible that for the tools used and the compounds evaluated, the approach is not appropriate.

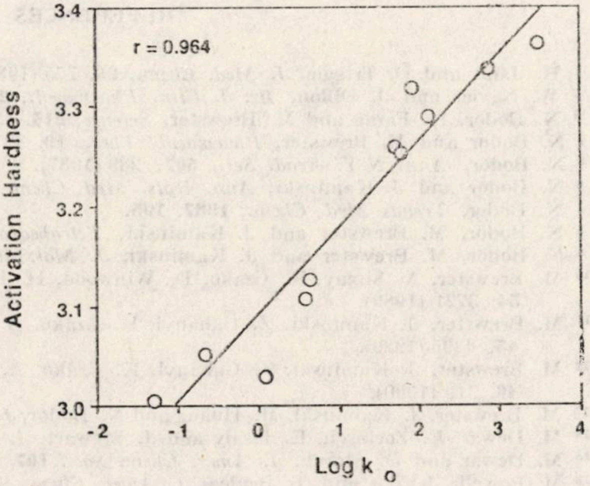

Fig. 6. — The relationship between the log of the second order rate constants for ferricyanide-mediated oxidation of a series of 1-methyl-3-substituted-1,4-dihydropyridines and the activation hardness.

These results figure singificantly in attempts to develop drug design methods which will allow prediction of biological activity. In the case of chemical delivery systems, an important component in their functioning is oxidative conversion of the administered transport form (dihydronicotinate) to the corresponding brain depot form (niocotinate salt). If this transmutation occurs too slowly, efficient brain trapping does not occur, whereas if oxidation is excessively rapid, conversion may occur prior to blood-brain barrier transit rendering the system useless. The described methods may allow for prediction of metabolic stability prior to chemical synthesis, thereby permitting a judicious choice of a variety of potential candidates.

In conclusion, semiempirical (AM1) molecular orbital methods were useful in describing the oxidative behavior of dihydropyridines. A highly significant relationship was observed between adiabatic ionization potentials and reaction rates. Unfortunately, a theoretically meaningful correlation could not be derived between reaction rate and hard-soft acid-base parameters such as absolute hardness or electronegativity. These findings may be useful in selecting candidates which may serve as brain-targeting chemical delivery systems.

ACKNOWLEDGEMENT. The authors are indebted to Anna Marie Martin for her expert editorial assistance.

REFERENCES

[1] R. Janis and D. Triggle, *J. Med. Chem.*, **26**, 775 (1983).
[2] W. Nayler and J. Dillon, *Br. J. Clin. Pharmacol.*, **21**, 975 (1986).
[3] N. Bodor, H. Farag and M. Brewster, *Science*, **214**, 1370 (1981).
[4] N. Bodor and M. Brewster, *Pharmacol. Ther.*, **19**, 337 (1983).
[5] N. Bodor, *Ann. N.Y. Acad. Sci.*, **507**, 289 (1987).
[6] N. Bodor and J. Kaminski, *Ann. Rpts. Med Chem.*, **22**, 303 (1987).
[7] N. Bodor, *Trends Med. Chem.*, **1987**, 195.
[8] N. Bodor, M. Brewster and J. Kaminski, *Tetrahedron*, **44**, 7601 (1988).
[9] N. Bodor, M. Brewster and J. Kaminski, *J. Mol. Struc.*, **206**, 315 (1990).
[10] M. Brewster, A. Simay, K. Czako, D. Winwood, H. Farag and N. Bodor, *J. Org. Chem.*, **54**, 3721 (1989).
[11] M. Brewster, J. Kaminski, Z. Gabanyi, K. Czako, A. Simay and N. Bodor, *Tetrahedron*, **45**, 4395 (1989).
[12] M. Brewster, J. Kaminski, Z. Gabanyi, K. Czako, A. Simay and N. Bodor, *Tetrahedron*, **46**, 319 (1990).
[13] M. Brewster, J. Kaminski, M. Huang and N. Bodor, *J. Org. Chem.*, **55**, 2361 (1990).
[14] M. Dewar, E. Zoebisch, E. Healy and J. Stewart, *J. Amer. Chem. Soc.*, **107**, 3902 (1985).
[15] M. Dewar and D. Storch, *J. Amer. Chem. Soc.*, **107**, 3898 (1985).
[16] M. Powell, J. Wu and T. Bruice, *J. Amer. Chem. Soc.*, **106**, 3550 (1984).
[17] T. Sotomatsu, Y. Murata and T. Fujita, *J. Comput. Chem.*, **10**, 94 (1989).
[18] O. Henri-Rousseau and F. Texier, *J. Chem. Educ.*, **55**, 437 (1978).
[19] R. Pearson, *J. Amer. Chem. Soc.*, **85**, 3533 (1963).
[20] R. Pearson, *J. Chem. Educ.*, **64**, 561 (1987).
[21] R. Pearson, *J. Amer. Chem. Soc.*, **107**, 6801 (1985).
[22] R. Parr and R. Pearson, *J. Amer. Chem. Soc.*, **105**, 7512 (1983).
[23] R. Pearson, *Proc. Natl. Acad. Sci. USA*, **83**, 8440 (1986).
[24] Z. Zhou and R. Parr, *J. Amer. Chem. Soc.*, **112**, 5720 (1990).

Revue Roumaine de Chimie, 36, 4–7, 657–663 (1991)

En hommage au Professeur A. T. BALABAN
pour son 60e anniversaire

NOUVEAUX DÉRIVÉS PYRIDAZINIQUES ET PHTALAZINIQUES DOUÉS D'ACTIVITÉ PHYSIOLOGIQUE

MARIA CAPROŞU[a], EUGENIA ŞTEFĂNESCU[b], MARGARETA UNGUREANU[b] et MAGDA PETROVANU[a]

[a] Université « Al. I. Cuza », Laboratoire de Chimie organique, Jassy, 11, rue M. Eminescu, Roumanie

[b] Université de Médecine et Pharmacie, Faculté de Pharmacie, Jassy, 16, rue Universităţii, Roumanie

Reçu le 16 février, 1991

Dans ce mémoire on présente onze nouveaux dérivés en série pyridazine et phtalazine. Les produits (5–11) ont été obtenus à partir de la 3-chloro-6-hydrazino-pyridazine par diverses réactions. Les produits **14–16** sont des dérivés de phtalazinium-ylures. Les tests biologiques effectués ont mis en évidence l'action antimicrobienne des produits **14**, **15** et **16**. Pour les autres produits synthétisés les tests biologiques sont en cours.

This paper reports eleven new pyridazines and phthalazines derivatives. Products **5–11** have been obtained starting from 3-chloro-6-hydrazino-pyridazine (**4**), by means of various reactions. Products **14–16** belong to the class of phthalazinium-ylids. The biological tests have shown the antimicrobial activity of products **14**, **15** and **16**. For the other products biological tests are still under way.

Gross, Druey et coll.[1] ont abouti à la suite de recherches laborieuses à un nouveau groupe de substances antihypertensives, dont les chefs de file sont l'hydralazine (hydrazino-phtalazine) **1** et la dihydralazine (dihydrazino-1,4-phtalazine) **2**.

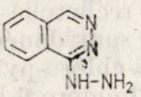

1

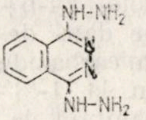

2

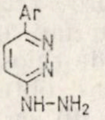

3

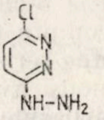

4

Abordant, dans des recherches antérieures [2,3,4] la classe des hydralazines, nous avons obtenu une série de produits 3-aryle-6-hydrazino-pyridaziniques **3**, certains d'entre eux manifestant des activités antihypertensives remarquables.

Dans le but de dépister de nouvelles structures actives et moins toxiques, nous avons envisagé de synthétiser de nouveaux dérivés pyridaziniques à partir de la 3-chloro-6-hydrazinopyridazine (**4**), produit qui manifeste une forte activité antihypertensive.[4]

Dans une première étape, on a synthétisé de nouvelles hydrazones du type **5** par condensation des acides α-cétoglutarique et pyruvique avec la 3-chloro-6-hydrazino-pyridazine selon le schéma réactionnel (A).

La sélection des produits carbonyliques est évidemment liée à leur participation au métabolisme.

Tenant compte du fait que certains dérivés du tétrazole sont utilisés dans la thérapie des maladies cardiovasculaires, nous avons envisagé de greffer un cycle tétrazolique sur le noyau pyridazinique.

Dans ce but, en utilisant quelques indications de la littérature,[5] nous avons synthétisé la 3-chloro-tétrazolo-[1,5-b]-pyridazine (**6**) en traitant la 3-chloro-6-hydrazino-pyridazine par l'acide nitreux. Nous supposons pour l'obtention de la tétrazolo-pyridazine le mécanisme réactionnel suivant : formation, en première étape, du cation de diazonium (a) qui se transforme en acide (b) par élimination de proton suivie de cyclisation intramoléculaire :

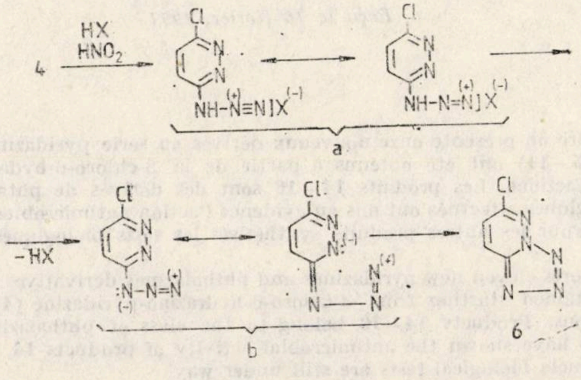

Il nous a paru intéressant de transformer la 3-chloro-tétrazolo-pyridazine (**6**) par attaque nucléophyle avec des amines aromatiques **7** en aryle-amino-tétrazolo-[1,5-b]-pyridazines **8** (schéma A).

Continuant nos recherches, nous nous sommes proposé d'introduire un noyau triazolique dans la molécule de diazine. Dans ce but, on a traité la 3-chloro-6-hydrazino-pyridazine avec de l'acide formique (80%). On a obtenu ainsi la 3-chloro-*s*-triazolo-[3,4-b]-pyridazine (**9**) (schéma A).

Tenant compte du fait que dans des recherches antérieures [2] on a constaté qu'une série de thiosémicarbazides sont douées d'activité antihypertensive nous avons obtenu la 1-(3'-*p*-chloro-pyridazinyle)-4-phényle-thiosémicarbazide (**10**) en traitant la 3-chloro-6-hydrazino-pyridazine avec l'isothiocyanate de phényle (schéma A).

Il nous a paru intéressant aussi de lier un cycle pyrazolonique à celui pyridazinique prenant en considération la large utilisation des pyrazolones dans la thérapie de certaines maladies.

Dans ce but on a condensé le produit 4 avec l'acétoacétate d'éthyle en obtenant la 1-(3'-chloro-pyridazinyle)-3-méthyle-5-pyrazolone (**11**) (schéma A).

Une autre voie de recherche que nous nous sommes proposé d'aborder dans le but d'obtenir de nouveaux dérivés 1,2-diaziniques doués d'activité physiologique est celle des phtalazinium-ylures et dérivés.

Schéma A

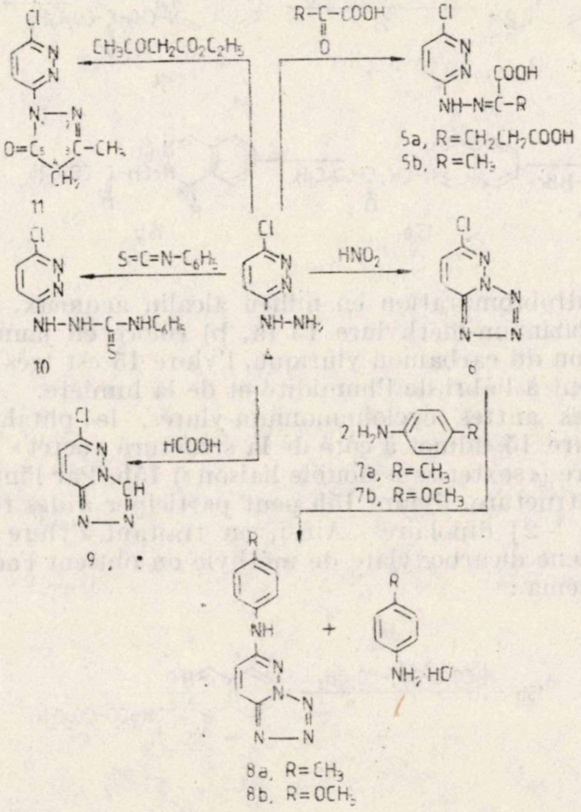
R–C–COOH
O
CH3COCH2CO2C2H5
5a, R=CH2CH2COOH
5b, R=CH3
11
S=C=N–C6H5
HNO2
10
4
6
HCOOH
? H2N–
7a, R=CH3
7b, R=OCH3
9
NH2·HCl
8a, R=CH3
8b, R=OCH3

Dans des recherches antérieures on avait constaté que certains sels de cycloimmonium – ylures et adduits cycliques en série pyridazinique et phtalazinique manifestent des activités biologiques intéressantes[6,7,8,9].

Poursuivant nos recherches dans la classe des phtalazinium-ylures nous avons étudié l'action du bromopyruvate d'éthyle **13** sur la phtalazine **12**.

A notre connaissance le bromopyruvate d'éthyle n'a pas encore été utilisé comme réactant α-halogénocarbonylique dans le but d'obtenir des sels de phtalazinium. En l'utilisant, nous avons tenté, d'une part, à introduire le reste d'acide pyruvique sur le noyau phtalazinique et, d'autre part, à obtenir des phtalazinium-ylures fortement stabilisés par le groupement $O=\underset{|}{C}-COOR$, qui exerce, évidemment, un effet accepteur d'électrons très puissant.

En traitant la phtalazine **12** avec le bromopyruvate d'éthyle **13** en milieu benzénique on obtient le bromure de N-éthyle-oxalyle-méthyl-phtalazinium **14** selon le schéma réactionnel :

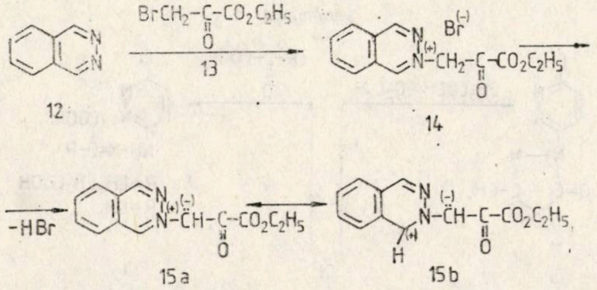

Par déhydrobromuration en milieu alcalin acqueux, le sel **14** conduit à la phtalazinium-méthylure **15** (a, b) coloré en jaune. Grâce à la forte stabilisation du carbanion ylurique, l'ylure **15** est très stable surtout si on le maintient à l'abri de l'humidité et de la lumière.

Comme les autres cycloimmonium-ylures, le phtalazinium-éthyloxalyle-méthylure **15** admet à côté de la structure « octet » **15a** une structure 1,3-dipolaire (« sextet sans double liaison ») **15b**. Par l'intermédiaire de cette dernière structure, l'ylure **15b** peut participer à des réactions de cycloadditions [3 + 2] dipolaires. Ainsi, en traitant l'ylure **15** « in situ » avec de l'acétylène dicarboxylate de méthyle on obtient l'adduit cyclique **16** selon le schéma :

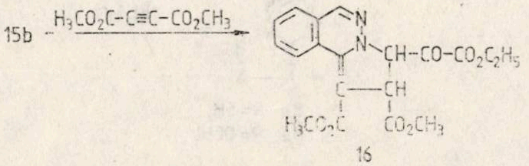

Les données des poids moléculaires, les points de fusion, les analyses élémentaires et spectrales des produits obtenus sont présentés dans le tableau 1.

TESTS BIOLOGIQUES PRÉLIMINAIRES

Nous présentons les résultats concernant l'activité biologique pour une partie des nouveaux produits synthétisés.

On a étudié l'activité antimicrobienne du sel **14**, de l'ylure **15** et de l'adduit cyclique **16**.

On a utilisé la méthode de diffusion. Les évaluations des activités ont été faites par rapport aux : *Staphylococus aureus Oxford*, *Escherichia coli* et la levure *Candida albicans*. Les produits testés ont été dissouts dans du DMFA, en concentration de 5 mg/ml.

D'après les données expérimentales biologiques, les produits **14**, **15** et **16** présentent une activité antimicrobienne. Le sel de cycloimmonium **14** est le plus actif envers le *Staphylococus aureus Oxford*. Envers

Tableau I

Caractéristiques physico-chimiques des produits **5**—**16**

Produits	Formule moléc.	p.f. °C	C %		H %		N %		Spectres I.R. cm^{-1}
			cal.	trouv.	cal.	trouv.	cal.	trouv.	
5a, R=CH_2CH_2COOH	$C_9H_9N_4O_4Cl$	191	39,6	39,8	3,3	3,8	23,4	23,9	νNH = 3330 ; νCO = 1755
5b, R=CH_3	$C_7H_7N_4Cl$	180	46,0	46,7	3,8	4,5	30,6	30,8	
6	$C_4H_2N_5Cl$	107	30,8	31,0	1,2	2,2	45,0	45,7	
8a, R=CH_3	$C_{11}H_{10}N_6$	235	58,4	58,8	4,4	5,2	37,1	37,0	νNH = 3310 ; νC—H ar. = 3100 νas. C—H(CH_3) = 1450
8b, R=OCH_3	$C_{11}H_{10}N_6O$	251	54,5	54,7	4,1	4,3	34,7	34,4	νNH = 3310 ; νC—H ar. = 3100 νas. C—H(CH_3) = 1441
9	$C_5H_3N_4Cl$	202	38,8	39,4	1,9	1,6	36,2	37,0	
10	$C_{11}H_{10}N_5ClS$	176	47,2	47,8	3,5	3,8	25,0	25,6	νNH = 3350 ;
11	$C_8H_7N_4ClO$	192	45,6	45,8	3,3	3,9	26,6	27,0	
14	$C_{13}H_{13}N_2O_3Br$	210					8,61	9,0	νCO = 1737 ; νC—O—C = 1210 νC = N = 1622, 1606, 1580, 1450
15	$C_{13}H_{12}N_2O_3$	284					11,4	11,0	νCO = 1737 νC = N = 1622, 1606, 1580
16	$C_{19}H_{18}N_2O_7$	184					7,2	7,8	νC=N = 1548, 1487 ν = 1280 νC=C = 1608, 1593 ; C—O—C

l'*Escherichia coli* les produits testés manifestent une activité presque égale. L'adduit cyclique **16** est doué d'une très prononcée activité antilévurique. Les tests biologiques pour les autres produits obtenus sont en cours.

PARTIE EXPÉRIMENTALE

Les points de fusion ne sont pas corrigés. Les spectres IR ont été enregistrés sur un spectromètre IR de type Specord 71.

Hydrazone de la 3-chloro-6-hydrazino-pyridazine avec l'acide α-cétoglutarique (5a)

On dissout à chaud 3 g de 3-chloro-6-hydrazino-pyridazine et 3 g d'acide α-céto-glutarique dans 25 ml d'éthanol chaque portion et on porte à reflux le mélange réactionnel pendant deux heures. La séparation de l'hydrazone commence après 4—5 minutes de chauffage. On obtient un produit crême, soluble dans l'acétone.

Hydrazone de la 3-chloro-6-hydrazino-pyridazine avec l'acide pyruvique (5b)

Même mode opératoire que précédemment.

3-Chloro-tétrazolo-(1,5-b)-pyridazine (6)

On dissout 5 g de 3-chloro-6-hydrazino-pyridazine dans 15 ml d'acide acétique 12% et on traite, en refroidissant avec une solution de 2,3 g d'azotite de soude dans 15 ml d'eau. Produit beige, recristallisé dans du benzène.

6-(4'-méthyle-phényle-amino)-tétrazolo-(1,5-b)-pyridazine (8a)

On porte à reflux un mélange de 3 g chloro-tétrazolo-pyridazine (0,02 moles) et 4,2 g *p*-toluidine (0,04 moles) dans 20 mL d'o-xylène pendant 3 heures. Après refroidissement on filtre les cristaux obtenus, on lave à l'eau chaude sur le filtre afin d'éliminer le chlorhydrate de la *p*-toluidine. Le produit est recristallisé dans du méthanol. Cristaux jaunes claires.

6-(4'-méthoxy-phényle-amino)-tétrazolo-(1,5-b)-pyridazine (8b)

Même mode opératoire que précédemment.

6-Chloro-s-triazolo-(3,4-b)-pyridazine (9)

On porte à reflux un mélange de 1,44 g (0,01 moles) (**4**) et de 10 ml acide formique 80% pendant 10 heures. Après évaporation d'une partie du solvant, on refroidit le reste de la solution. Il se forme un précipité blanc que l'on essore. Le produit est recristallisé dans du benzène.

1-(3'-p-chloropyridazinyle)-4-phényle-thiosémicarbazide (10)

On mélange une solution de 1,5 g (**4**) dans 10 ml éthanol avec une solution contenant 1,4 mL isothiocyanate de phényle en 10 mL éthanol et on porte à reflux le mélange réactionnel, pendant 10—20 minutes au bain-marie. On refroidit la solution. Il se forme un précipité blanc que l'on essore. Rdt. 35%.

1-(3'-chloro-pyridazinyl)-3-méthyl-5-pyrazolone (11)

On chauffe au bain-marie pendant 1—2 heures un mélange de 1,3 g (0,01 moles) acéto-acétate d'éthyle et 1,44 g (0,01 moles) de **4**. Après refroidissement on sépare une partie de la pyrazolone obtenue. On ajoute de l'éther éthylique pour précipitation complète. Le produit est recristallisé en alcool éthylique.

Bromure de N-éthyle-oxalyle-méthyl-phtalazinium (14)

On dissout 1,3 g phtalazine dans 40 mL benzène anhydre et on ajoute goutte à goutte 1,2 mL de bromopyruvate d'éthyle. Il se forme immédiatement le sel de cycloimmonium **14**, coloré en jaune, p.f. 210°C.

Phtalazinium-éthyle-oxalylo-méthylure (15)

On dissout 1,75 g sel 14 dans 30 ml d'eau et on ajoute, goutte à goutte, une solution de 0,7 g K_2CO_3 dissouts dans 10 mL d'eau. Il se sépare un produit jaune citron. On filtre et on lave avec de l'eau jusqu'à pH neutre. Après recristallisation dans du benzène —produit jaune à p.f. 84°C.

1,2-Dicarbométhoxy-3-éthyl-oxalyle-2,3-dihydro-pyrrolo-(2,1-a)-phtalazine (16)

On suspend 0,7 g de sel **14** dans 40 ml benzène, on ajoute 0,14 mL d'acétylène-dicarboxylate de méthyle et, goutte à goutte 0,3 mL de triéthylamine. On porte à reflux le mélange réactionnel pendant 4 heures. On filtre le solution bouillante afin d'éliminer le bromhydrate de la triéthylamine. On refroidit. Il se sépare un produit jaune foncé, à p.f. 184—185°C.

BIBLIOGRAPHIE

[1] F. Gross, J. Druey et R. Meier, *Experientia*, **6**, 29 (1950).

[2] M. Petrovanu, E. Gafiţanu, M. Caproşu et R. Dăneţ, *Archives de l'Union Médicale Balkanique*, **16**, 453 (1978).

[3] I. Zugrăvescu, M. Petrovanu, E. Rucinschi et M. Caproşu, *St. Cerc. Chim.*, **13**, 679 (1965).

[4] M. Ungureanu, E. Ştefănescu et M. Petrovanu, *An. şt. Univ. « Al. I. Cuza » Iaşi*, **15**, 47 (1969).

[5] N. Takahayashi, *J. Pharm. Soc. Japan.*, **75**, 776 (1955).

[6] V. Clipa, M. Petrovanu, M. Caproşu, E. Ştefănescu, E. Gafiţanu et E. Belousov, *Vol. Simpoz. Farmacie*, **1977**, 382.

[7] M. Petrovanu, E. Ştefănescu, *Arch. de l'Union Médicale Balkanique*, **16**, 456 (1978).

[8] M. Ungureanu, M. Dorneanu, E. Ştefănescu, M. Pavelescu, C. Radu et M. Petrovanu, *Rev. Med. Chir. Iaşi*, **4**, 709 (1984).

[9] M. Caproşu, E. Ştefănescu, M. Petrovanu et C. Radu, *Rev. Med. Chir. Iaşi*, **93**, 357 (1989).

Revue Roumaine de Chimie, **36**, *4*–*7*, 665–670 (1991)

Dedicated to Prof. ALEXANDRU T. BALABAN
on the occasion of his 60th anniversary

NEW AMINOPYRIMIDINONIC DERIVATIVES WITH POTENTIAL BIOLOGICAL ACTIVITY

SORIN MAGER, I. CRISTEA, LILIANA CRĂCIUN, F. IRIMIE and M. DIUDEA
Department of Organic Chemistry, "Babeş-Bolyai" University, 11 Arany Janos Str. 3400
Cluj-Napoca, Romania

Received March 10, 1991

In the industrial synthesis of fungicide, ethyrimol(I) (5-butyl-2-ethylamino-6-methyl-4-pyrimidinol), starting from ethylguanidine nitrate and butylacetoacetic ester, a by-product (15% of the main product) was also formed: the 2-amino-5-butyl-3-ethyl-4-pyrimidinone (II). In order to render valuable this by-product by means of some of its potentially biologic active derivatives, its 2-amino function was used. By acylation with phenoxyacetyl chlorides, tosyl chloride, *p*-acetylaminobenzenesulfonic chloride, the corresponding amides were obtained. The amino function was also replaced by the hydroxyl and chlorine groups. With phosgene the N,N-disubstituted urea was obtained. The new compounds were characterized by means of ^{1}H-NMR and IR spectra, some of them proving a biological activity.

Among the synthesis methods of the fungicide, ethyrimol (I) (5-butyl-2-ehtyl amino-6-methyl-4-pyrimidinol), the way chosen by us, starting from ethylguanidine (obtained from calcium cyanamide and ethylamine) and butylacetoacetic ester,[1] affords as a by-product (about 15% of main product) an isomer with a pyrimidinonic structure II.

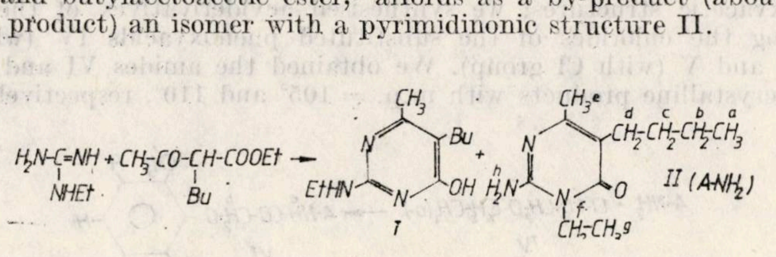

Scheme 1

The isomer II (2-amino-5-butyl-3-ethyl-6-methyl-4-pyrimidinone), separated from the main compound I by means of its insolubility in bases, was proved, in the laboratories of the Biological Research Center of Cluj-Napoca, to present a much higher toxicity ($LD_{50} = 182$ mg/Kgc) as compared to ethyrimol ($LD_{50} = 6902$ mg/Kgc). Because of its high amount (about 15%) formed in the industrial synthesis of ethyrimol, we tried to find some possibilities to render valuable the isomer II ($A\text{-}NH_2$) by means of some of its derivatives, mainly using its amino group. The isomer II was not characterized in the literature (m.p. = 189°).

Concerning the possible lactam-lactim tautomerism ($II_a \rightarrow II_b$) of the isomer II, the general problem has been well investigated in the chemical literature almost by means of the IR and UV spectroscopy of a large number of derivatives of pyrimidine. For 2-amino- and 4-hydroxypyrimidines the IR spectra clearly indicate the presence of the unchanged amino group and the ketonisation of the hydroxy group.[2] The same conclusion has been found by comparing the UV spectra of these compounds with their N-methylderivatives [3] and by examining the bathocromic shifts in the UV spectra of a number of substituted pyrimidines in aqueous buffer solutions.[4] Further evidence has shown that 2-aminopyrimidinones exist in the amino-oxo form[5,6]. For the isomer II the solid state, IR spectra and ^1H-NMR spectra, run by us, have offered further support for the structure II_a (see experimental part).

The amino function of the tautomeric form II_a was made obvious by acylation reactions, beginning with the most simple case of the reaction with benzoylchloride. Benzoylation of the isomer II_a (m.p. = 189°) gave the white crystalline product III (m.p. = 112°) whose ^1H-NMR spectrum shows clearly the appearance of the five aromatic protons in the molecule as compared to the spectrum of the isomer.

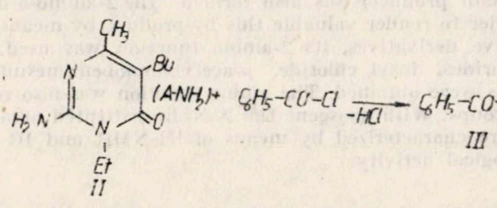

Scheme 2

In order to obtain potentially auxinomimetic compounds with phenoxyacetic structures, we synthesised acylderivatives of the isomer II using the chlorides of the substituted phenoxyacids IV (with CH_3 group) and V (with Cl group). We obtained the amides VI and VII as white crystalline products with m.p. = 105° and 110°, respectively.

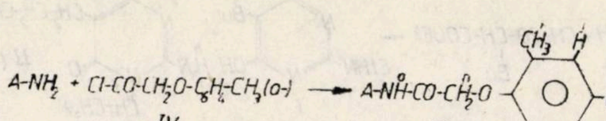

Scheme 3a

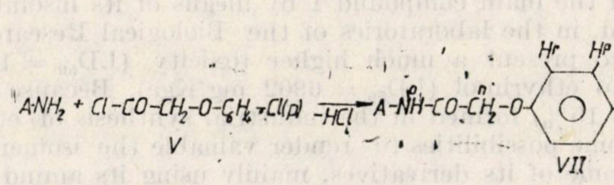

Scheme 3b

The ^{1}H-NMR spectra render obvious the formation of the amides showing the complex ABCD spin system for compound VI (protons H_{j-m}) and the AB pattern (for compound VII) of the aromatic protons H_p and H_r ($\Delta\delta/J = 4.8$).

The biological tests of compounds VI and VII show a significant auxinic activity, and very important, a lack of toxicity, as compared to the high toxicity of the starting isomer II.

The biological activity of the sulfonamides being known, we tried to obtain such compounds from the isomer II using the chlorides of some sulfonic acids. The tosyl chloride used for the beginning gave the sulfonamide VIII as white needle-shaped crystals (m.p. = 127°) showing in the ^{1}H-NMR spectrum the AB spin system ($\Delta\delta/J = 5$) of the aromatic protons H_p and H_r and the very deshielded signal ($\delta = 10.4$ ppm) of the sulfonamidic proton(s).

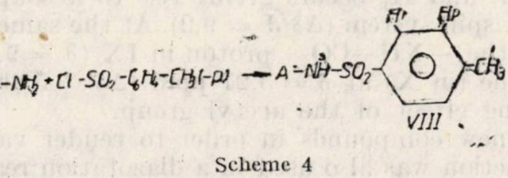

Scheme 4

Using the *p*-acetylaminobenzenesulfonyl chloride, the corresponding sulfonamide IX was obtained as a white crystalline product (m.p. = 148°).

The reaction was carried out in different solvents (1 : 1 molar ratio of reactants) using pyridine as base. From 50% in benzene and 70% in acetone, the yield increases to 57% in dichloromethane. The thin layer chromatography of the crude product (silicagel plates, 10 : 5 : 1 mixture of AcOEt, $CHCl_3$, MeOH as eluent and iodine vapours for developing), shows the existence of a more polar by-product, probably the bis-(acetylaminobenzenesulfonyl) derivative. The crystallization of the crude product from methanol leads to the pure compound IX (verification by TLC) with m.p. = 148°.

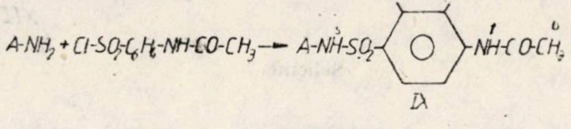

Scheme 5

Concerning its ^{1}H-NMR spectrum, it is interesting to mention that the opposite effect of the AcNH- and $-SO_2-NH-$ groups of the benzenic ring leads accidentally to the same value (a singlet with $\delta = 7.64$ ppm) for both kinds of protons (H_p and H_r); no splitting (AB pattern) can be observed.

In order to obtain the free amine of IX, its hydrolysis was performed with 10% NaOH solution. The pure *p*-aminosulfonamide X was obtained, after crystallization from methanol, as a white crystalline compound (m.p. = 152°).

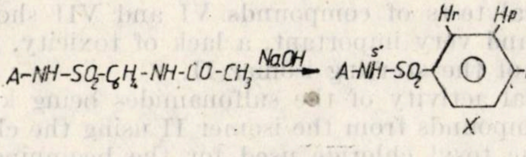

Scheme 6

A striking difference in the ^{1}H-NMR spectrum of X as compared with its acetylated compound IX, may be observed. Because of the strong shielding effect ($\Delta\delta = 0.75$ ppm) of the free amino group,[7] a big difference between H_r and H_p occurs giving rise to a coupling pattern close to that of an AX spin system ($\Delta\delta/J = 9.2$). At the same time the chemical shift ($CDCl_3$) of the —NH—CO— proton in IX ($\delta = 9.16$ ppm) is shifted for the free amine (in X) at $\delta = 3.27$ ppm ($\Delta\delta = 5.89$ppm) showing the strong deshielding effect of the acetyl group.

To obtain new compounds in order to render valuable the isomer II, its amino function was also used in a diazotation reaction followed by its transformation in the corresponding phenol XI (m.p. = 161—2°) and the chloroderivative XII (m.p. = 203—4°), which may be further used for other syntheses.

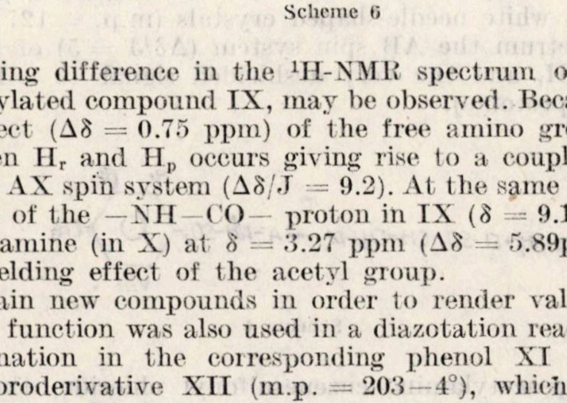

Scheme 7

The reaction of the isomer II with phosgene gave the new urea derivative XIII (m.p. = 219°) and the ammonium salt of the isomer, XIV (m.p. = 198°).

$$4\,A{-}NH_2 + COCl_2 \rightarrow \underset{XIIII}{A{-}NH{-}CO{-}NH{-}A} + \underset{XIV}{2A{-}NH_3]^{+}Cl^{-}}$$

All the new compounds III, VI—XIV were characterized by their physical constants and ^{1}H-NMR spectra.

EXPERIMENTAL

2-Amino-5-butyl-3-ethyl-6-methyl-4-pyrimidinone (II)

In a 250 mL round bottom flask, 22.5 g ethylguanidine nitrate, 8.5 g NaOH and 200 mL isobutanol were refluxed under stirring, for 1 hour. After this time 50 mL of the solvent were distilled in order to eliminate the water formed in the reaction. After cooling (40°) the suspension was filtered, obtaining the isobutanol solution of the free base of ethylguanidine. This solution was dropwise added under stirring and heating (at about 90°), for 3 hours, to 31 mL of butylacetoacetic ester. The mixture was then refluxed for 2 hours and finally 135 mL of the solvent (about 90 % of it) were distilled. About 220 mL water were then added and distilled in order to eliminate the solvent (remaining isobutanol) and the eventually unreacted buthylacetoacetic ester. The organic phase being removed, 6 g NaOH were added to the aqueous solution. After the dissolution of NaOH, 2 g of charcoal were added continuing the stirring until cooling at room temp. The suspension was then filtered and ethyrimol (I) was precipitated from its Na salt, at pH = 7 using HCl 1 : 1. The isomer II, insoluble in the alkaline solution, was then extracted under stirring, with hot HCl 1 : 1 from the above charcoal, filtered solution.

After cooling, the isomer II was precipitated by alkalinisation, as white crystals with m.p. = 189°. (If the hydrochloric solution is sufficiently concentrated, by cooling, the II-hydrochloride may be isolated. $C_{11}H_{20}N_3O$ Cl (245.8), m.p. = 198°). $C_{11}H_{19}N_3O$; N % calcd. 20.07, found 19.62 ; ^{1}H-NMR spectrum (δ ppm, $CDCl_3$) : $H_a = 0.79$ ppm, $H_{b,c} = 1.12-1.37$ ppm, $H_d = 2.28$ ppm, $H_e = 1.97$ ppm, $H_f = 3.89$ ppm, $H_g = 1.26$pp m. IR spectrum : $\nu_{NH_2} =$ = 3020, 3410 cm^{-1}, $\nu_{CO} = 1650$ cm^{-1}.

2-Benzoylamido-5-buthyl-3-ethyl-6-methyl-4-pyrimidinone (III)

Isomer II (5 g) was suspended in 25 mL dichloromethane then 10 mL of benzoyl chloride were dropped under stirring at room temperature. After one hour the pH was brought with NaOH to pH = 10, when white crystals were formed. The product was filtered, washed with water and crystallized from ethanol. 3.5 g (yield = 47 %) of pure compound (m.p. = 112°) were obtained. $C_{18}H_{23}N_3O_2$ (313.4 ; N % calcd. 13.4, found 12.95.

2-(o-Methylphenoxyacetamido)-5-butyl-3-ethyl-6-methyl-4-pyrimidinone (VI) and 2-(p-Chlorophenoxyacetamido)-5-butyl-3-ethyl-6-methyl-4-pyrimidinone (VII)

Phenoxyacetic acids IV (*o*-CH_3) or V (*p*-Cl), 0.2 mols in 1000 mL benzene were treated with 50 mL $SOCl_2$. The mixture was refluxed for 3 hours, then the solvents were evaporated and the residue was treated with 0.2 mols of II and 17 g $NaHCO_3$ in 1000 mL of benzene.

The mixture was refluxed for additional 1.5 hours. After the removal of benzene, the solid was crystallized from methanol. Compound VI was obtained as white crystals with m.p. = = 105° (yield = 35 %). $C_{20}H_{26}N_3O_3$ (356.4) C % calcd. 67.3, found 68.21 ; H % calcd. 7.85, found 7.11 ; ^{1}H-NMR spectrum (δppm., $CDCl_3$) : $H_n = 4.60$ ppm, $H_i = 2.17$ ppm, $H_{j-m} =$ = 6.50—712 ppm. Compound VII was obtained as white crystals with m.p. = 110 (yield = = 43 %). $C_{19}H_{24}N_3O_3Cl$ (377.9) C % calcd. 60.39, found 59.93 ; H % calcd. 6.40, found 6.12 ; ^{1}H-NMR spectrum (δppm ; $CDCl_3$) : $H_n = 4.56$ ppm, $H_p = 6.70$ ppm, $H_r = 7.02$ ppm.

5-Butyl-3-ethyl-6-methyl-2-tosylamido-4-pyrimidinone (VIII)

A mixture of 5 g isomer (II) and 10 g tosylchloride was suspended in 50 mL dichloromethane and 5 mL pyridine and boiled for 2 hours. The solvent was removed and 100 mL HCl 1 : 1 were then added. After cooling the precipitate was filtered and washed well with water. Crystallization from methanol gave white needle-shaped crystals with m.p. = 127°. $C_{18}H_{25}N_3O_3S$ (363.5) ; N % calcd. 11.56, found 11.2 ; ^{1}H-NMR spectrum (δppm ; $CDCl_3$) : $H_1 =$ = 2.25 ppm, $H_p = 7.10$ ppm, $H_r = 7.65$ ppm, $H_s = 10.4$ ppm.

2-(p-Acetylaminobenzenesulfonamido)-5-butyl-3-ethyl-6-methyl-4-pyrimidinone (IX)

4.2 g of II and 4.7 g of *p*-acetylaminobenzenesulfonyl chloride in 40 mL methylene chloride and 1 mL pyridine were boiled on a steam bath for 2 hours. The solvent was evaporated and the residue washed twice with HCl 1 : 1, then dissolved in 20 mL acetone and reprecipitated with water. The product was filtered and crystallized from methanol. Thus pure IX, white

crystalline product, was obtained. (5.4 g, 66%), m.p. = 148°. $C_{19}H_{26}N_4O_4S$ (406); N% calcd. 13.71, found 13.83; ^{1}H-NMR spectrum (δppm; $CDCl_3$): $H_p = H_r = 7.64$ ppm, $H_s = 10.4$ ppm, $H_t = 9.17$ ppm, $H_u = 2.13$ ppm.

2-(p-Aminobenzenesulfonamido)-5-butyl-3-ethyl-6-methyl-4-pyrimidinone (X)

4.1 g of IX in 30 mL 10% NaOH solution were boiled on a steam bath for 1.5 hours. The mixture was filtered, washed with water (20 mL) and the solution was neutralized with HCl 1 : 1 at pH = 7. The precipitate was filtered, washed with water and crystallized from methanol. A white crystalline product was obtained. (2.6 g, 72%), m.p. = 152°. $C_{17}H_{24}N_4O_3S$ (364); N% calcd. 15.38, found 15.49: ^{1}H-NMR spectrum (δppm; $CDCl_3$): $H_p = 6.55$ ppm, $H_r = 7.42$ ppm, $H_s = 10.38$ ppm, $H_v = 3.27$ ppm.

5-Butyl-3-ethyl-2-hydroxy-6-methyl-4-pyrimidinone (XI)

A solution of 0.7 g $NaNO_2$ in 5 mL water was added to a solution of 2 g isomer (II) in 5 mL 35% H_2SO_4 at −5–0°C.

The reaction mixture was then warmed at 60° for 2 hours. The solvent was distilled under vacuum and the formed solid was crystallized from benzene, giving 1.2 g (yield = 60%), white crystals with m.p. = 182°. $C_{11}H_{18}N_2O_2$ (210); N% calcd. 13.33, found 13.6.

5-Butyl-2-chloro-3-ethyl-6-methyl-4-pyrimidinone (XII)

A solution of 0.7 g $NaNO_2$ in 5 mL water was added to a solution of 2 g isomer (II) in 10 mL 6.2% HCl solution at −5°−0°C.

The reaction mixture was maintained at the same temperature for 30 min. The diazonium chloride of II was obtained as a water suspension of white crystalline product. Separately, a solution of CuCl in HCl conc was prepared from 4.3 g $CuSO_4$, 2.6 g KCl, 3.5 g Na_2SO_3, 15mL water and 12 mL conc HCl. The CuCl solution was added slowly under stirring to the diazonium salt at −5°−0°C. The mixture was maintained at the same temperature for 30 min. The precipitate was filtered and crystallized from $CHCl_3$, giving 1.2 g (yield = 53%), white crystals with m.p. = 203−204°. $C_{11}H_{17}N_2OCl$ (228.5); Cl% calcd. 15.53, found 15.73.

N,N-bis(5-butyl-3-ethyl-6-methyl-4-pyrimidinon-2-yl) urea (XIII)

A solution of 1.2 g phosgene in 4 mL tetrahydrofuran was added to a suspension of 5 g isomer (II) in 85 mL dichloroethane for 10 min. at 5−10°C. The reaction mixture was stirred for 2 hours at the same temperature, 50 mL water were then added to the suspension in order to destroy the unreacted phosgene and to dissolve the isomeric hydrochloride (XIV). The formed solid (XIII) was filtered and crystallized from dichloroethane, giving 1.4 g (yield = 56%), white crystals with m.p. = 218 − 220°. $C_{23}H_{36}N_6O_2$ (428); N% calcd. 19.62, found 19.23. ^{1}H-NMR spectrum (δppm; $CDCl_3$): $\delta_{NH} = 4.7$ ppm.

REFERENCES

[1] I. Panea, S. Mager, V. Fărcăşan, I. Hopârtean, F. Paiu and I. Cristea, Rom. Pat., 72028, 17 Dec. (1981).
[2] L. N. Short and H. W. Thompson, *J. Chem. Soc.*, **1952**, 268.
[3] D. J. Brown, E. Hoerger and S. F. Mason, *J. Chem. Soc.*, **1955**, 211.
[4] M. P. V. Boarland and J. F. W. McOmie, *J. Chem. Soc.*, **1952**, 3716.
[5] A. R. Katritzky and J. M. Lagowski, *Adv. Heterocycl. Chem.*, Supl. **1**, 339 (1976).
[6] J. S. Kwiatkowski and B. Pullman, *Adv. Heterocycl. Chem.*, **18**, 199 (1975).
[7] H. Spiesecke and W. G. Schneider, *J. Chem. Phys.*, **35**, 731 (1961).

Revue Roumaine de Chimie, 36, 4–7, 671–681 (1991)

Dedicated to Prof. ALEXANDRU T. BALABAN
on the occasion of his 60th anniversary

HETEROCYCLES WITH ANNELATED DIBENZOCYCLOALKANE SKELETONS. VI[1]

SIX MEMBERED HETEROCYCLES WITH ANNELATED 7H-DIBENZO[a,c]CYCLOHEPTENE SKELETONS

MIRCEA D. BANCIU,[a] CĂTĂLINA HADA,[a] MICHAELA DINA STĂNESCU,[a]
FILIP CHIRALEU[b] and ECATERINA CIORĂNESCU[a,b]

[a] Organic Chemistry Department, The Polytechnic, TCH, Spl. Independenţei 313, Bucharest 76206, Roumania
[b] Centre of Organic Chemistry, Roumanian Academy, Bucharest, Roumania

Received December 20, 1990

Reaction of formyl derivative 8b of 6H-5,7-dihydro-dibenzo[*a, c*]cyclohepten-6-one (7) with urea and thiourea affords the corresponding pyrimidines 9 and 10 with annelated dibenzo[*a, c*]cycloheptene skeleton. Heating of 8b in acetic acid/perchloric acid (in the absence as well as in the presence of a methyl(ene) ketonic component) gives rise to the same mixture of two isomeric pyrylium salts (11 + 12) containing two annelated dibenzo[*a, c*]cycloheptene skeletons. The doubly annelated pyrylium salts 15 and 17 were obtained from the dibenzobicyclic formylderivative 14b with ketones 7, respectively 13. Intramolecular charge-transfer interactions were observed for all these pyrylium salts. The pyrylium salts were converted into the corresponding pyridines by reaction with ammonia.

INTRODUCTION

In previous papers of this laboratory [2–5] the syntheses of different heterocycles with annelated dibenzobarrelene- (**1a-c**), dibenzohomobarrelene- (**2a-c**) and dibenzobullvalene- (**3a, b**) skeletons were described.

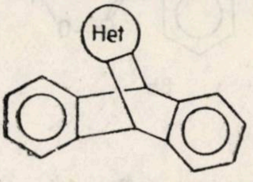

1

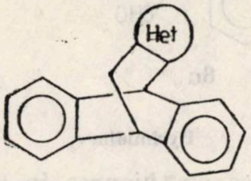

2

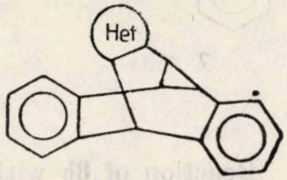

3

a , Het = pyrylium
b , Het = pyridinium
c , Het = pyrazole

More recently[6] we prepared pyrazoles with annelated 7H-dibenzo[*a*,*c*] cycloheptene skeleton **4a-c**.

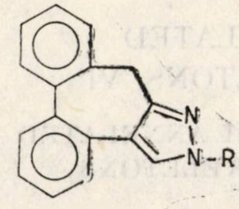

4

a, R = H
b, R = C_6H_5
c R = $C_6H_3(NO_2)_2$

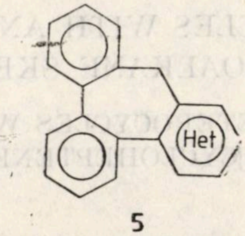

5

Het = pyrimidine

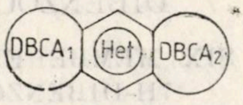

6

a: Het = pyrylium
b: Het = pyridine

In this paper we describe the synthesis of pyrimidines **5** possessing the same annelated skeleton as **4**, as well as the preparation of six-membered heterocycles **6** (pyrylium salts and pyridines) doubly annelated with identical or different dibenzocycloalkane (DBCA) moieties. The DBCA skeletons in **6** are of the 7H-dibenzo[*a*,*c*]cycloheptenic- and/or of the dibenzohomobarrelenic type.

RESULTS AND DISCUSSION

The key intermediate in the synthesis of heterocycles **5** and **6** was the formyl-derivative **8** of the known ketone **7**.[7] As we have shown previously[8] the formyl-derivative **8** is totally tautomerized into the hydroxymethyleneketonic form **8b**.

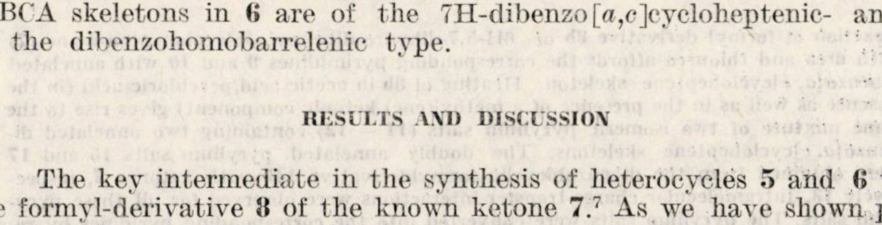

7 **8a** **8b**

Pyrimidines

Reaction of **8b** with urea or thiourea in toluene at reflux, in the presence of catalytic amounts of *p*-toluenesulphonic acid, conducted with good yields to the corresponding pyrimidines **9** (m.p. 298–299°) and **10** (m.p. 117–120°) of the type **5**. The much higher melting point of **9** as compared to **10** seems to be a result of associations through H-bonds occurring in **9**. A confirmation in this sense was brought by the large ν_{OH}^{assoc} absorption found between 3300 and 3600 cm^{-1} in the IR spectrum of **9**.

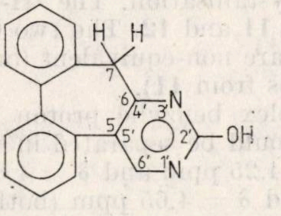

9

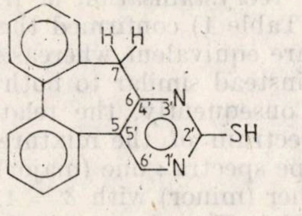

10

The spectral data of **9** and **10** (see Experimental) are in agreement with the proposed structures. Thus, in the IR spectra (in KBr), a strong absorption at 1620 cm^{-1} (in **9**) and at 1635 cm^{-1} (in **10**), characteristic to $\nu_{C=N}$ appears instead of the strong absorptions from 1600 cm^{-1} ($\nu_{C=C}$) and 1645 cm^{-1} ($\nu_{C=O}$) of hydroxymethyleneketone **8b**.[8] On the other hand, the ^{1}H-NMR singlet from $\delta = 8.05$ ppm due to the $=CH-O-$ proton in **8b**[8] disappeared also in cyclized products, the corresponding proton being included in the pyrimidinic + aromatic protons. The CH_2 protons from **9** and **10** appear as large singlets at about $\delta = 3.65$ ppm and $\delta = 3.8$ ppm respectively, suggesting a relatively slow conformational motion (by inversion of the middle ring).

Attempted similar synthesis of an aminopyrimidine **5** from **8b** and guanidine failed. Significant amounts of ketone **7** isolated from the products of this reaction suggest deformylation of **8b** (see also below).

Pyrylium salts

Synthesis of pyrylium salts with the skeleton **5** using the known[9] reaction of hydroxymethyleneketones with ketones having an α-methyl(ene) group also failed. Thus, reaction of **8b** with acetone, acetophenone or benzylphenyl ketone in the usual conditions (perchloric acid in acetic acid, 1.5 h at 110°) afforded no methyl- or phenyl-substituted pyrylium salts. Instead, in all the mentioned reactions, the same mixture of two doubly annelated pyrylium salts of the type **6**, namely **11** and **12**, was obtained.

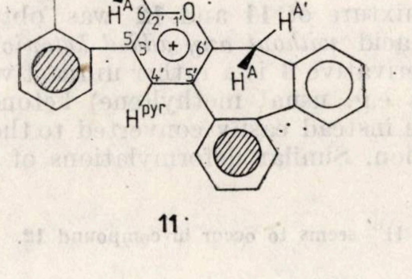

11

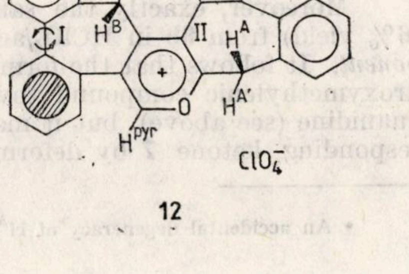

12

Formation of pyrylium perchlorates was proved by the 625 cm^{-1} and 1100 cm^{-1} IR bands characteristic of ClO_4^- as well as by the violent decomposition on heating. The mixture of **11** + **12** could not be separated by recrystallisation or fractional crystallisation. The ^{1}H-NMR spectrum (Table 1) confirmed the structures **11** and **12**. The two CH_2 groups in **11** are equivalent whereas in **12** they are non-equivalent (one of them, being instead similar to both CH_2 groups from **11**).

Consequently, the relatively complex benzylic proton signal from the spectrum of the mixture **11** + **12** could be separated in two simpler AB-type spectra : one (major) with $\delta = 4.25$ ppm and $\delta = 4.65$ ppm and the other (minor) with $\delta = 4.30$ ppm and $\delta = 4.65$ ppm (both with $J = 14$ Hz). The above signals were assigned to $H^AH^{A'}$ (from **11** and **12**) and to $H^BH^{B'}$ (from **12***), respectively. In both above cases the high-field signals ($\delta = 4.25$ and 4.30 ppm) are due to protons H^A and H^B respectively which are more shielded by the opposite phenyl rings (marked in formulas **11**, **12**) than their geminal protons $H^{A'}$ and $H^{B'}$. A ratio of about 3/2 between **11** and **12** was determined from the integral area of the signals corresponding to the pyrylium proton H^{pyr} in the above compounds ($\delta = 9.35$ ppm in **11** and 9.25 ppm in **12**).

Dreiding stereomodels reveal the symmetry of **11** (relative to the plane passing through O^+ and H^{pyr}, orthogonal to the pyrylium ring) as well as the absence of any steric hindrance. On the contrary, the model of **12** indicates some steric hindrance of $H^{B'}$ (in one conformation of dibenzocycloheptenic moiety I) or of H^B (in the second conformation of I resulted by twisting around the biphenylic bond in I) with the H^{ortho} of the sterically neighboring aromatic ring (see formula **12**). From the experimental results it seems that the above mentioned ketonic components do not enter into reaction with hydroxymethylene derivative **8b**. To further test this finding a similar reaction was performed using **8b** and a dibenzobicyclic ketone, namely **13** [10] when again the same mixture of **11** and **12** was obtained.

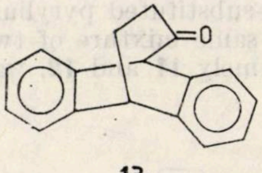

13

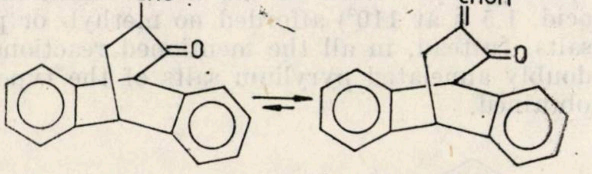

14a **14b**

Moreover, exactly the same mixture of **11** and **12** was obtained (6% yield) from **8b** in $HClO_4$/acetic acid *without any added ketonic component*. It follows that the formyl derivative **8** is a rather unreactive hydroxymethylenic compound towards e.g. usual methyl(ene) ketones or guanidine (see above), but it may be instead easily converted to the corresponding ketone **7** by deformylation. Similar deformylations of β-ketoaldehydes in acidic medium proceed sometimes with very good yields.[11] The further condensation of **8b** with **7** affords **11** and **12** by reaction of the aldehydic (hydroxymethylenic) — respectively of ketonic group from **8b**. Formation of **11** in higher ratio than **12** is in agreement with the higher reactivity of an aldehydic group as compared to a ketonic group.

---

* An accidental degeneracy of $H^{A'}$ and $H^{B'}$ seems to occur in compound **12**.

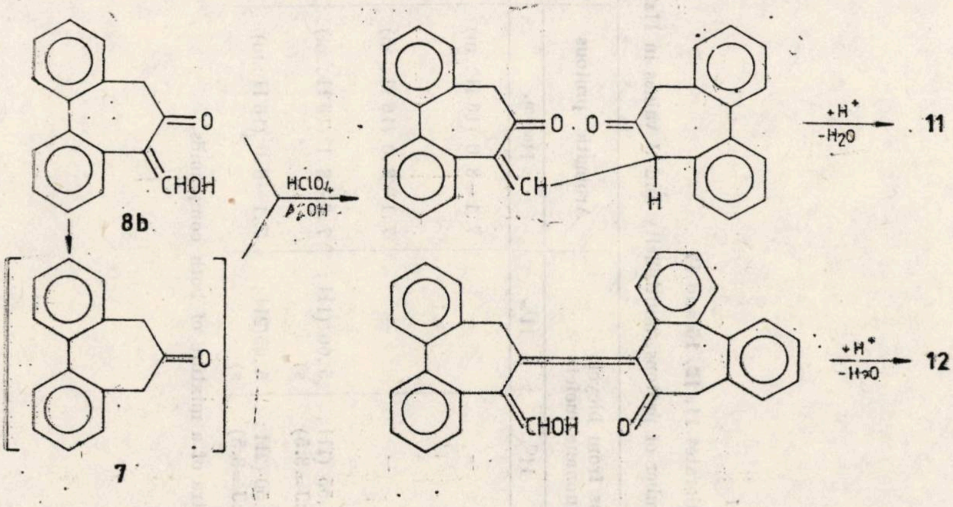
O
CHOH
8b
7
O
HClO₄
AcOH
O . O
CH
H
+H⁺
-H₂O
11
CHOH
O
+H⁺
-H₂O
12

On the other hand, condensation of the hydroxymethylene derivative **14b**[12] of ketone **13** with ketone **7** afforded as single product the pyrylium salt **15**, which could not be obtained from **8b** and **13**. This reaction confirms again the lower reactivity of the formyl-derivative **8b** as compared e.g. with **14b**, a compound known[2] to afford easily pyrylium salts with usual methylene ketones (acetophenone etc.).

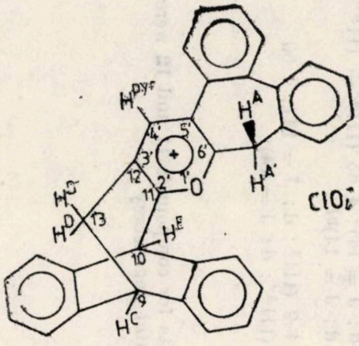
H^pyr
4'
5'
3'
6'
2'
1'
12
11
O
+
H^A
H^A'
H^D'
H^D
13
H^E
10
9
H^C
ClO₄⁻

15

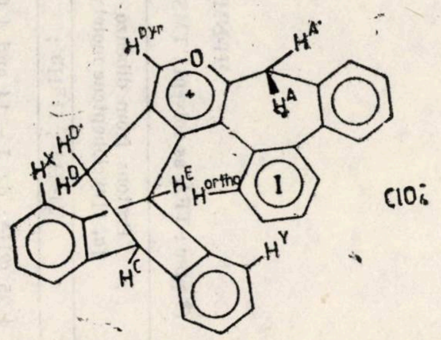
H^pyr
O
+
H^A'
H^A
H^X
H^D'
H^D
H^E
H^ortho
I
H^Y
H^C
ClO₄⁻

16

The structure **15** is confirmed by spectral data (see Experimental and Table 1). Thus, the ^{1}H-NMR spectrum shows the characteristic sequence: doublet, triplet, singlet for $H^{DD'}$, H^C and H^E, respectively

Table 1

^{1}H-NMR data for pyrylium perchlorates **11**, **12**, **15** and **17**

(δ ppm; TFA as solvent; TMS as internal standard; number of protons, multiplicity and J values in Hz)

Compound	Protons from dibenzo [*a*, *c*]cycloheptene moiety	Protons from bicyclo [3.2.2]nonane moiety			Aromatic protons	Pyrylium proton
	$H^AH^{A'}$; $H^BH^{B'}$;	$H^DH^{D'}$	H^C	H^E	$H^{arom.}$	$H^{pyr.}$
11 a)	4.25 ($2H^A$; d; J = 14 and 4.65 ($2H^{A'}$; d; J = 14)	—	—	—	7.1−8.0 (16 H; m)	9.35 (1H; s)
12 a)	4.25 ($1H^A$; d; J = 14); 4.30 ($1H^B$; d; J = 14); 4.65 ($1H^{A'} + 1H^{B'}$; d; J = 14)b)	—	—	—	7.1−8.0 (16 H; m)	9.25 (1H; s)
15	4.2 ($1H^A$; d; J = 14); 4.60 ($1H^{A'}$; d; J = 14)	3.6 (2H; d; J=3.5)	4.55 (1H; t; J=3.5)	5.60 (1H; s)	7.0−8.1 (16 H; m)	8.7 (1H; s)
17		3.30 (4H; d; J=3.5)	4.50 (2H; t; J=3.5)	5.65 (2H; s)	7.1−8.0 (16 H; m)	7.9 (1H; s)

a) The data for compounds **11** and **12** were extracted from the spectra of a mixture of both compounds.

b) accidental degeneracy

from the bicyclo[3.2.2] nonane moiety as well as the AB-type system of H^A, $H^{A'}$ from dibenzocycloheptenic part of the molecule. The difference of chemical shift between H^A and $H^{A'}$ is similar to that observed for **11** and **12** and has the same origin. The lack of isomeric pyrylium salt **16** as a product of reaction between **14b** and **7** could be explained after inspection of Dreiding stereomodels. In a presumable compound **16** the H^{ortho} (see formula **16**) should present serious hindrance with H^E and H^Y in one conformation of dibenzocycloheptenic moiety or with H^E and H^X in the other conformation of the same moiety. Moreover, the proton H^E in **16** should lie over the benzenic ring I only at about 1.6 Å ; such a position should bring a considerable shielding of this proton (shielding which is not visible in the ^{1}H-NMR spectrum of the reaction product, a normal value of $\delta_H E = 5.6$ ppm from **15** being instead observed as unique singlet). On the contrary, no steric hindrance is visible in the stereomodel of pyrylium salt **15**.

Another doubly annelated pyrylium salt **17** was obtained on condensation of hydroxymethylene-ketone **14b** with the ketone **13** possessing the same skeleton. In this case also a single product was obtained, namely that of the reaction of aldehydic group from **14b**. The ^{1}H-NMR spectrum (see Table 1) is in agreement with the highly symmetrical formula **17** and not with the isomeric formula **18**; in the latter compound two different H^E and $H^{E'}$ should appear, a situation which was not observed. The unicity of pyrylium proton H^{pyr} signal suggests that the reaction product is not a mixture of pyrylium salts. Moreover, the Dreiding models indicate strong overlaps between H^E and $H^{D''}$, $H^{D'''}$ in **18** whereas in **17** no steric hindrance is visible. The ^{1}H-NMR data are in perfect agreement with those of the pyrylium salt **15** and of the related monoannelated pyrylium salts **2a**.[2] The pyrylium proton in the compounds discussed above (see Table 1) shows very different chemical shifts which are however in agreement with the substitution pattern of pyrylium ring (phenyl substituents strongly deshielding and alkyl substituents shielding, the neighbouring proton). As concerns the DBCA skeletons in compounds **6**, the pyrylium salt **15** could be considered as a borderline compound between **11** and **12** on one hand and **17** on the other hand. The ^{1}H-NMR data (see Table 1) nicely reflect this situation.

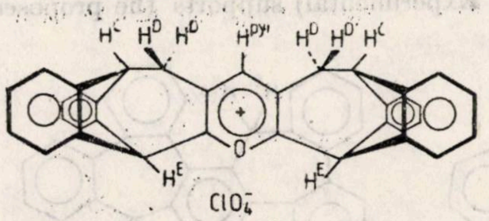

17

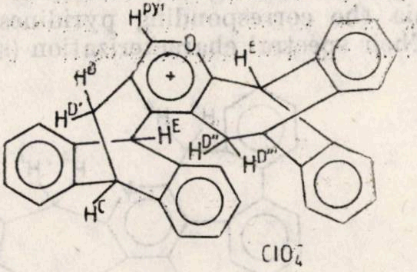

18

An interesting observation concerning the same pyrylium salts refers to the possibility of intramolecular charge transfer (CT) from aromatic rings towards the pyrylium one. Examination of the electronic spectra reveals the appearance of such charge transfer bands in the visible range. Whereas the mixture **11** + **12** presents (in CH_2Cl_2) three CT-bands at 486 ; 571 and 635 nm, the pyrylium salts **15** and **17** indicate a single CT band at 463 nm with different ε-values : 340 for **15** and 700 for **17**. On changing the solvent with acetonitrile the above band appears at 453 nm for **15** and at 454.5 nm for **17**. This blue shift observed on increasing the polarity of the solvent is in agreement with known data for CT bands.[13a,b] Similar CT-bands were observed by us previously [2–4] for mono-annelated pyrylium salts of the type **1**, **2** and **3**. In view of the recent interest of intramolecular CT-interactions [13] a more detailed analysis of such interactions in the here discussed systems will be described elsewhere.

Pyridines

The well-known reaction ot pyrylium salts with ammonia was used in order to obtain the doubly annelated pyridines of the type **6**. Upon performing the reaction of **11** + **12**, **15** and **17** with aqueous ammonia the corresponding pyridines : **19** + **20**, **21** and **22** were obtained. Their spectral characterization (see Experimental) supports the proposed

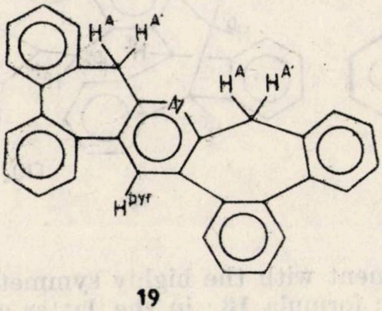

19

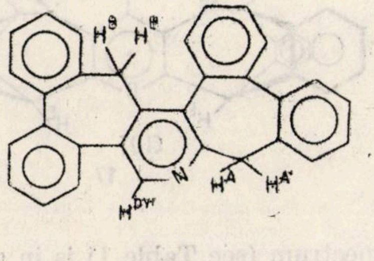

20

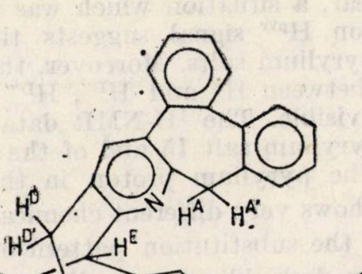

21

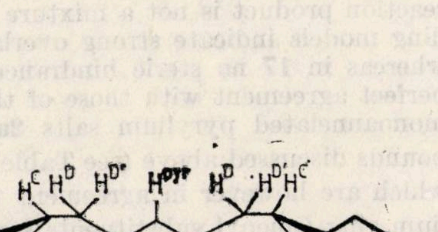

22

structures. The ^1H-NMR data corroborate well with those of the corresponding pyrylium salts (Table 1). A normal upfield shift of the signals in pyridines as compared to corresponding pyrylium salts (due to the disparition of positive charge) is easily visible. Unlike the pyrylium salts no CT-bands were observed in the visible spectra of the above pyridines.

In conclusion different new six-membered heterocycles : mono-annelated pyrimidines and doubly annelated pyrylium salts and pyridines including dibenzo[a,c]cycloheptene- and/or dibenzohomobarrelene skeletons were synthesized and characterized. The lack of reactivity of formyl-derivative **8b** towards usual methyl(ene) ketones as well as its easy deformylation which permitted the formation of doubly annelated pyrylium salts **11** and **12** starting only from **8b** was observed. Some conformational aspects as well as the appearance of intramolecular charge-transfer interactions within pyrylium salts were revealed.

EXPERIMENTAL

Melting points are uncorrected. IR spectra were registered on a UR-20 C. Zeiss Jena double beam spectrophotometer, electronic spectra on a SPECORD-UV-VIS C. Zeiss Jena double beam spectrophotometer, ^1H-NMR spectra on VARIAN A 60-A and VARIAN-Gemini 300 instruments.

2′-Hydroxypyrimidino-5,6(4′,5′)-7H-dibenzo[*a,c*]cycloheptene (9).

A mixture of hydroxymethyleneketone **8b**[8] (0.5 g ; 2 mmoles), urea (0.2 g ; 3 mmoles) and *p*-toluenesulphonic acid (catalytic amounts) in 50 mL toluene was refluxed for 24 h. The cooled reaction mixture was washed with water until pH 7, dried and evaporated *in vacuo*. The solid residue was recrystallized from toluene affording the pyrimidine **9** (0.25 g ; 43%), white crystals with 298–9°.

IR spectrum (KBr ; cm^{-1}) : 742m, 876m, 950w, 990m, 1080m, 1340s, 1395s, 1432s, 1460s, 1620s, 3020w, 3060w and 3300–3600 large.

UV spectrum ($CHCl_3$; λ_{max} nm ; $\log\varepsilon_{max}$) : 250(4.13) ; 311(3.62).

^1H-NMR spectrum (TFA ; δ ppm) : 3.5–3.8 (large s ; 2H ; CH_2) ; 7.2–8.1 (m ; 9H ; H_{arom}).

2′-Mercaptopyrimidino-5,6(4′,5′)-7H-dibenzo[*a,c*]cycloheptene (10).

The pyrimidine **10** was obtained (in 52% yield) from **8b** (2 mmoles) and thiourea (3 mmoles) similarly to hydroxypyrimidine **9** (see above). Mercapto-pyrimidine **10**, yellowish-white crystalls with m.p. 117–120° (ethanol).

IR spectrum (KBr ; cm^{-1}) : 739s, 750 m, 1255 m, 1295 m, 1380 m, 1440 m, 1470 m, 1635 s, 2870 w, 2900 w, 2950 w, 3020 w and 3060 w.

UV spectrum (methanol ; λ_{max} nm ; $\log\varepsilon_{max}$) : 240 (4.27) ; 333.5 (3.81) and 402.5 (shoulder ; 3.17).

^1H-NMR spectrum (TFA : δ ppm) : 3.7–3.95 (large s ; 2H ; CH_2) : 7.2–8.0 (m ; 9H ; H_{arom}).

[1′-Oxonia-5,6(2′,3′) ;(5′,6′]-benzo]-bis-7H-dibenzo[*a,c*]cycloheptene(11) and [1′-Oxonia-5,6(2′,3′) ; (4′,5′)-benzo) bis-7H-dibenzo[*a,c*]cycloheptene (12).

A solution of hydroxymethyleneketone **8b**[8] (1 g ; 4.23 mmoles) in 5 mL anhydrous acetic acid and 1 mL 70% perchloric acid was heated for 1.5 h at 105°, cooled and poured over 250 mL cold anhydrous diethylether. The obtained solid was filtered, washed with three portions of 30 mL anhydrous diethylether affording 125 mg (6% yield) of pyrylium salts **11** + **12**. After recrystallization from acetic acid a grey solid m.p. 284–290° was obtained. The ^1H-NMR spectrum (practically unchanged by recrystallization) indicated the presence of pyrylium salts **11** and **12** in 3/2 ratio. The same mixture of **11** and **12** was obtained always when hydroxymethyleneketone **8b** was treated in the above conditions with stoechiometric amounts of acetone, acetophenone, phenyl-benzyl ketone or bicyclic ketone **13**.

IR spectrum (**11** + **12**) (KBr ; cm^{-1}) : 625s, 735s, 750s, 760s, 1100vs, 1190w, 1420s, 1475s, 1590m, 2995w, 3060w.

Electronic spectrum (**11** + **12**) (CH_2Cl_2 ; λ_{max} nm) : 252 (strong) ; 263 sh ; 303 ; 372.5 ; 486 ; 571 and 635. The last three bands appear in CH_3CN at 480 ; 555.5 and 638 nm.

^1H-NMR spectrum (see Table 1).

[1′-Oxonia (11, 12) ; (2′, 3′)-benzo]-9,10-propeno-9,10-dihydroanthracene-(5, 6) ; (5′, 6′)-7H-dibenzo[*a,c*]cycloheptene (15).

Reaction of hydroxymethyleneketone **14b**[12] with ketone **7**[7] (1/1.1 molar ratio) and perchloric acid in acetic acid performed in the conditions described above for **11** + **12** afforded **15** as a green-yellow solid (26% yield) with m.p. 220–223°.

IR spectrum (KBr ; cm^{-1}) : 625s, 746s, 756s, 1095vs, 1425s, 1470s, 1585m, 3030w and 3060w.

Electronic spectrum (CH_2Cl_2 ; λ_{max} nm ; $\log\varepsilon_{max}$) : 249 (4.39) ; 275.5 (shoulder ; 4.13) ; 298.5 (3.95) ; 376(4.15) ; 463 (CT-band ; 2.53).

^{1}H-NMR spectrum (see Table 1)

[1′-Oxonia-11,12(2′,3′ and 5′,6′)-benzo]bis-9,10-propeno-9,10-dihydroanthracene (17).

Reaction of hydroxymethyleneketone **14b**[12] with ketone **13**[10] (1/1.1 molar ratio) and perchloric acid in acetic acid in the conditions described above for **11** + **12**, afforded the pyrylium salt **17** as a grey solid (9 % yield) with m.p. 234–6°. From the mother-liquids important quantities (0.50 g) of starting ketone **13** were obtained after evaporation of the solvent.

IR spectrum (KBr ; cm^{-1}) : 625s, 747s, 770m, 1100vs, 1410m, 1465s, 1580m, 2930w, 3030w and 3067w.

Electronic spectrum (CH_2Cl_2 ; λ_{max} nm ; $\log\varepsilon_{max}$) : 259.5 (3.73) ; 301 (3.76) ; 372.5 (4.11) ; 463 (CT-band ; 2.84).

^{1}H-NMR spectrum (see Table 1).

5,6[2′,3′ ; (5′, 6′)]Pyridino-bis-7H-dibenzo [*a, c*]cycloheptene (19) and **5,6[2′, 3′ ; (4′,5′)] Pyridino-bis-7H-dibenzo[*a, c*]cycloheptene (20).**

A warm filtered solution of pyrylium salts **11** + **12** (160 mg ; 0.31 mmoles) in 15 mL methanol was treated with excess aqueous ammonia (about 10 mL). The yellow precipitate was filtered, washed with water, dried then recrystallized from ethanol affording the mixture of pyridines **19** + **20** (75% yield) yellow solid, m.p. 190–213°. The mixture of pyridines **19** + **20** could not be separated into components by column chromatography on alumina or by fractional crystallization.

IR spectrum ($CHCl_3$; cm^{-1}) : 1080 s, 1105 m, 1140 m, 1158 s, 1198 m, 1410 s, 1430 s, 1442 s, 1480 s, 1585 m, 1645 m, 2830 w, 2930 w, 2970 w, 3025 w and 3060 m.

Electronic spectrum (Methanol ; λ_{max} nm) : 244 (strong) ; 307.5 and 459.

^{1}H-NMR spectrum ($CDCl_3$; δ ppm) : 2.8–4.1 (m ; 4H ; CH_2) ; 7.0–8.0 (m ; 17 H ; $H_{arom.}$).

[(11,12) ; (2′, 3′)-Pyridino]-9,10-propeno-9,10-dihydroanthracene-(5,6) ; (5′,6′)-7H-dibenzo [*a, c*]cycloheptene (21).

The pyridine **21** was obtained in 77% yield from pyrylium salt **15** and ammonia as described above for **19** + **20**. The yellow pyridine **21**, m.p. 174–176° (ethanol).

IR spectrum ($CHCl_3$; cm^{-1}) : 1120 m, 1412 s, 1450 s, 1475 s, 1600 w, 2928 m, 3028 m and 3065 m.

Electronic spectrum (Methanol ; λ_{max} nm ; $\log\varepsilon_{max}$) : 244 (4.31) ; 293 (3.91).

^{1}H-NMR spectrum ($CDCl_3$; δ ppm) : 3.26 (2H, $H^{D,D'}$; AB – system ; J = 18 Hz ; J = 3 Hz) ; 3.70 and 4.00 (2H ; $H^{A,A'}$; AB – system ; J = 13 Hz) ; 4.25 (1 H ; H^C ; t ; J = 3 Hz) ; 5.25 (1H ; H^E ; s) ; 7.0–7.7 (m, $H_{arom.}$).

[11, 12(2′, 3′ and 5′,6′)Pyridino]bis-9,10-propeno-9,10-dihydroanthracene (22).

The pyridine **22** was obtained from pyrylium salt **17** and ammonia as described above for **19** and **20** ; brown-yellow solid, m.p. 155–158° (73% yield).

IR spectrum (CCl_4 ; cm^{-1}) : 1160 m, 1416 m, 1438 m, 1450 m, 1473 m, 1590 w, 2920 m, 3028 m and 3070 m.

Electronic spectrum (Methanol ; λ_{max} nm ; $\log\varepsilon_{max}$) : 235 (3.98) ; 290 (4.17).

^{1}H-NMR spectrum ($CDCl_3$; δ ppm) : 3.00 (4H ; $H^{D,D'}$; d ; J=3.0 Hz) ; 4.15 (2H ; H^C ; t ; J = 3 Hz) ; 5.18 (2H ; H^E ; s) ; 7.0–7.7 (m ; $H_{arom.}$).

REFERENCES

1 Note V. M. D. Stănescu, M. D. Banciu and F. Chiraleu, *Rev. Roumaine Chim.*, **36**, 119 (1991).

2 M. Banciu, A. T. Balaban, C. Drăghici and R. Vlad, *Rev. Roumaine Chim.*, **27**, 1037 (1982).

3 M. Banciu, M. Stănescu, C. Florea, A. T. Balaban and E. Ciorănescu, *Rev. Roumaine Chim.*, **32**, 1161 (1987).

[4] M. Stănescu, M. Banciu and A. T. Balaban, *Rev. Roumaine Chim.*, **34**, 617 (1989).

[5] M. D. Banciu, M. D. Stănescu and F. Chiraleu, *Rev. Roumaine Chim.*, **34**, 1921 (1989).

[6] M. D. Banciu, F. Chiraleu and A. Ciobanu, *Rev. Roumaine Chim.*, **35**, 739 (1990).

[7] B. Eistert and H. Minas, *Chem. Ber.*, **97**, 2479 (1964).

[8] M. Banciu, Phan-Le-Thuy and L. Stănescu, *Rev. Roumaine Chim.*, **24**, 957 (1979).

[9] a) G. N. Dorofeenko and G. I. Junghietu, *Zhur. Obshchei Khim.*, **35**, 589 (1965) ; b) W. Schroth and G. Fischer, *Z. Chem.*, **3**, 147, 277 (1963).

[10] E. Ciorănescu, M. Banciu, R. Jelescu, M. Elian and C. D. Nenitzescu, *Tetrahedron Letters*, **1969**, 1871 ; *Rev. Roumaine Chim.*, **14**, 911 (1969).

[11] A. L. Wilds and C. Djerassi, *J. Amer. Chem. Soc.*, **68**, 1711 (1946).

[12] M. Banciu, *Rev. Roumaine Chim.*, **27**, 769 (1982).

[13] a) T. Nakazawa and I. Murata, *J. Amer. Chem. Soc.*, **99**, 1996 (1977) ; b) T. Nakazawa, N. Abe, K. Kubo and I. Murata, *Tetrahedron Letters*, **1979**, 4995 ; c)A. Tajiri, M. Hatano, T. Nakazawa and I. Murata, *Chem. Phys. Letters*, **76**, 490 (1980) ; d) H. Quast and H. L. Fuchsbauer, *Chem. Ber.*, **119**, 1016 (1986) ; e) N. Harada, H Uda, K. Nakasuji and I. Murata, *J. Chem. Soc. Perkin II*, **1989**, 1449.

[14] a) K. Dimroth and K. H. Wolf, "Newer Methods of Preparative Organic Chemistry", Academic Press, New York, 1964, vol. 3, p. 357 ; b) A. T. Balaban, A. Dinculescu, G. N. Dorofeenko, G. W. Fischer, A. V. Koblik, V. V. Mezheritskii and W. Schroth, "Pyrylium Salts : Syntheses, Reactions and Physical Properties", *Adv. Heterocyclic Chem.*, Suppl. 2, Academic Press, New York, 1982.

Revue Roumaine de Chimie, 36, 4–7, 683–691 (1991)

Dedicated to Prof. ALEXANDRU T. BALABAN
on the occasion of his 60th anniversary

SYNTHESIS OF 1α, 2α-5,9-METHANO-5H-BENZO[3,4]CYCLOBUTA[1,2]CYCLOHEPTENE DERIVATIVES. MOLECULAR AND CRYSTAL STRUCTURE OF 7-CHLORO-8-KETO-1α, 2α-5,9-METHANO-5H-BENZO[3,4]CYCLOBUTA[1,2]CYCLOHEPTENE[1]

ANGELA POPESCU,[a] LUMINITZA PÂRVULESCU,[a] LAURENŢIU MEHEDINŢEANU,[a] MARIETA PLĂVEŢI,[a] MIRCEA D. GHEORGHIU,*[,a] K. M. TURDIBEKOV [b] and YU. T. STRUCHKOV [b]

[a] Department of Organic Chemistry, Polytechnic Institute, 76206 Bucharest 16, Romania
[b] X-Ray Structural Centre, Section of General and Technical Chemistry, USSR Academy of Science, 28 Vavilov Str., 117813 Moscow, USSR

Received January 10, 1991

The substitution reactions carried out on the allylic fragment of the title compound made available compounds with acetoxy, hydroxy and keto group at C_8, while at C_7 were attached either a chlorine or a hydrogen atom. Ionic and radical reactions involved in the substitutions carried out on the allylic fragment have not promoted rearrangement of the bicyclo[3.2.1]octene skeleton. For the 7-chloro-8-keto-1α, 2α-5,9-methano-5H-benzo[3, 4]cyclobuta[1, 2]cycloheptene the molecular structure is discussed.

INTRODUCTION

The successful large scale synthesis of benzobarrelene was achieved by Jefford *et al.*[2], from benzobicyclo[3.2.1]oct-2-ene **1** by bromine addition and subsequent dehydrohalogenation. This precedence prompted us to examine whether a related rearrangement would be operational in the case of bromine addition to stereoisomeric bicyclo[3.2.1]oct-2-ene derivatives **4**[3a] and **5**[3a], respectively.

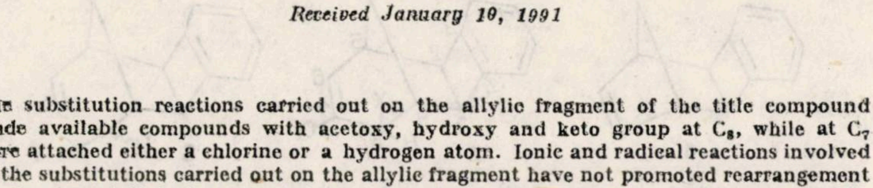

1 **2** **3**

---

* Correspondence author

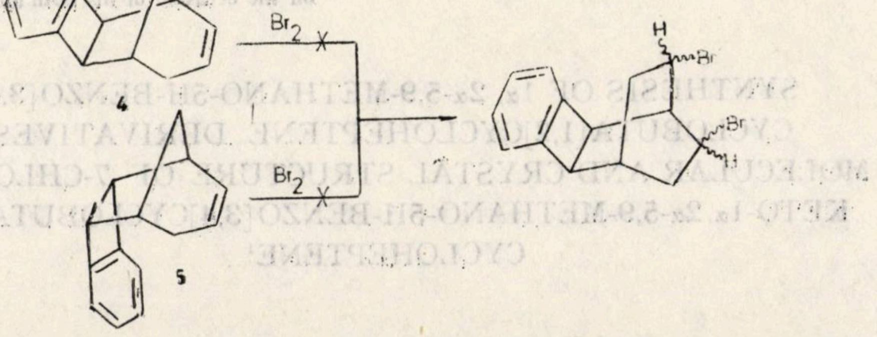

To our disappointment this was not the case. The four-membered ring is a rather poor anchimeric group; it does not assist a skeletal rearrangement which would end up in a dibromo precursor of the benzocyclobutabarrelene,[4] as it is depicted in scheme I.

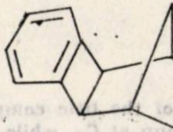

6

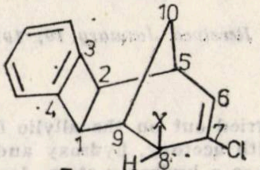

7

a) X : Cl
b) X : $OCOCH_3$
c) X : OH
d) X,H: O=
e) X: H

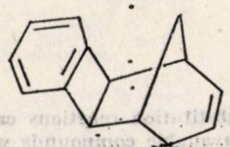

8

a) X : Br
b) X : $OCOCH_3$
c) X : OH
d) X,H: O=

However, we have explored some of the chemistry which turned out to be localized on the allylic fragment of derivatives of 4 and 5.

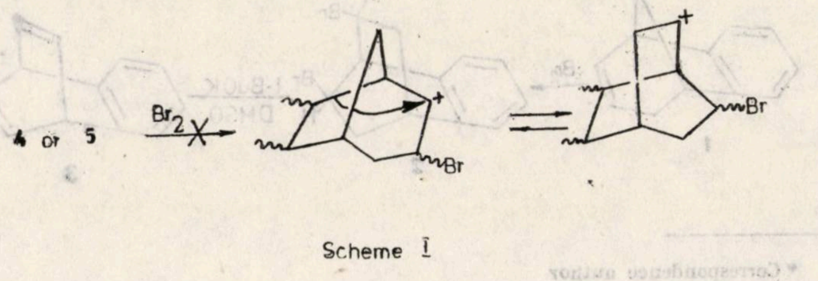

Scheme I

Thus, in the present paper we shall deal with reactions of the *exo*-benzocyclobutabicyclo[3.2.1]octene derivatives **7** and **8**, while for the *endo*-benzocyclobutabicyclo[3.2.1]octene derivatives the discussion will be presented in a forthcoming paper. The ^{1}H- and ^{13}C-NMR spectra of some derivatives of bicyclo[3.2.1]octene, mentioned in the present contribution, were already presented in our previous papers.[3b,3c]

DISCUSSION OF THE RESULTS

The dichlorocarbene cycloaddition to a norbornene skeleton resulted in the formation of dichlorobicyclo[3.2.1]oct-2-ene. A cyclopropane derivative was reported to be isolated only when the cyclopropanation was carried out on norbornene or norbornadiene.[6] But even in this case the cyclopropane rearranged thermally at quite low temperature (60°) to the corresponding bicyclo[3.2.1]oct-2-ene derivatives. Difluorocarbene cycloaddition to norbornene and norbornadiene, however, gave quite stable cyclopropanes.[7] In this latter case, thermally, the difluorocyclopropane is converted at 60°C from an *endo* configuration to *exo* configuration,[7,8] rather than experiencing ring enlargement.

In the case of *exo*-benzocyclobutanorbornene **6** the dichlorocarbene cycloaddition, irrespective of the generation of carbene, gave the bicyclo[3.2.1]octene dichloroderivative **7a**.[3,5] The stereochemistry of the compound **7a** was discussed in our previous contributions.[3,5] Thus the resulting dichloroderivative **7a** preserves the *exo* configuration of the benzocyclobutano fragment as it is in the original alkene **4**, and the chlorine at C_8 is in *exo* configuration as well. The allylic chlorine (bound to C_8) is relatively easily replaced with hydrogen by reduction of the dichloroderivative **7a** with $LiAlH_4$, in boiling ether, during 20 hrs. The chloroderivative **7e** resulted in 70% yield.

The reaction of the dichloroderivative **7a** with mercury(II) acetate in glacial acetic acid gave with 97% yield the 7-chloro-8α-acetoxy-benzocyclobutabicyclo[3.2.1]octene **7b**. The nucleophilic substitution should be unimolecular, since the stereochemistry of the acetoxy group is *exo*, as it results from the small magnitude (2.5 Hz) of H_8 coupling constant with the bridgehead H_9 proton.[6b,7b] In our forthcoming paper[9] we shall bring X-ray evidence that if the substituent at C_8 is indeed in *exo* configuration, the coupling constant $H_8 - H_9$ (bridgehead proton) has a rather small magnitude, less than 2 Hz.

By reduction of *exo* chloroacetoxy derivative **7b** with $LiAlH_4$ the alcohol **7c**, with the hydroxy group in the *exo* configuration, was obtained in 75% yield.

The oxidation of the alcohol **7c** gave the chloroketone **7d**, as crystalline compound, in 70% yield. The reaction was carried out with sodium dichromate and sulphuric acid at 0°C, during 15 minutes. The unsaturated ketone displays in the IR the characteristic streching frequency at 1680 cm^{-1}.

The parent hydrocarbon **4** reacts with N-bromosuccinimide (NBS) in CCl_4 in the presence of benzoyl peroxide to give a mixture of *exo*- and *endo*-8-bromo-benzocyclobutabicyclo[3.2.1]octenes **8a**. Presumably, this reaction occurs *via* the allylic radical, which reacts with bromine preferentially *exo*- facial, as it has resulted from the ^{1}H-NMR spectra of the crude reaction product.

The bromoderivatives **8a** were converted with mercury(II) acetate into the *exo*- and *endo*-8-acetoxy derivatives **8b**. The GC analysis has revealed only two isomers, in the ratio 85 : 15. The ^{1}H-NMR analysis (by integrating the two signals belonging to the CH_3 group from acetoxy) have revealed the same ratio of the isomers. Also, the same result was obtained from the integration of the ^{13}C signals assigned to C_8 atoms from the two isomers.

The reduction of the mixture of the acetoxy derivatives **8b** with $LiAlH_4$ and subsequent oxidation with $Na_2Cr_2O_7$ and sulphuric acid gave the α,β-unsaturated ketone **8d**.

Molecular structure of the 7-chloro-8-keto-1α,2α-5,9-methano-5H-benzo [3,4] cyclobuta[1,2]cycloheptene (7d)

The molecular structure of chloroketone **7d** is depicted in Fig. 1.

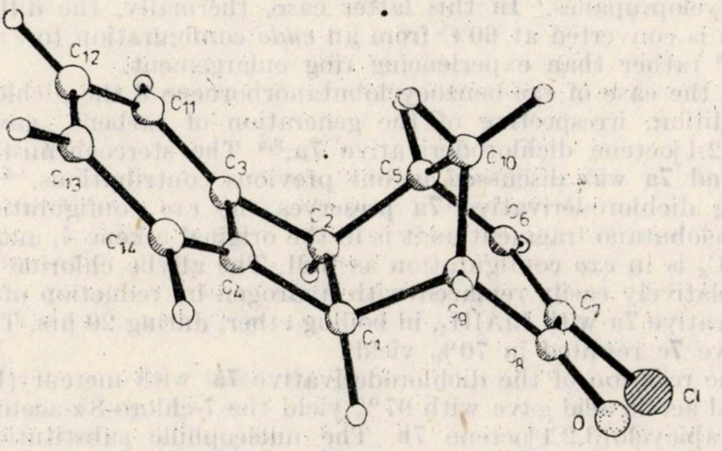

Fig. 1

The bond lengths are within the normal range expected for such structures.[10a] However, one should point out that the C_1-C_9 bond (1.592 Å) is longer. The bond angles around C_1 and C_2 are relatively altered, but such is the case for substituted four-membered rings.[10b]

The four-membered ring ($C_1-C_2-C_3-C_4$) is almost planar, the puckering along C_2-C_4 is 0.8°. The deviations of the chlorine (0.053 Å) and of the oxygen (0.070 Å) from the plane of atoms $C_6-C_7-C_8-C_9$ are so small that one should safely consider these atoms coplanar with the mentioned carbon atoms.

The dihedral angle among the four-membered ring $C_1-C_2-C_3-C_4$ and $C_5-C_2-C_1-C_9$ is 112.8°. The six-membered ring has a half-chair conformation as a result of the presence of the C_6-C_7 double bond. For saturated analogs of bicyclo[3.2.1]octane derivatives the same ring is in chair conformation.[10c]

Bond lengths and bond angles are presented in Table 1 and Table 2, respectively.

Table 1

Bond lengths d (Å) for compound **7d**

Bond	d	Bond	d
$Cl-C_7$	1.749(6)	C_1 C_4	1.527(9)
$O-C_8$	1.215(7)	C_4 C_{14}	1.379(9)
C_2-C_5	1.547(8)	C_1 C_9	1.592(8)
C_5-C_6	1.516(8)	C_8 C_9	1.519(8)
C_5-C_{10}	1.538(8)	C_9 C_{10}	1.539(7)
C_2-C_3	1.530(8)	C_7 C_8	1.484(8)
C_1-C_2	1.572(8)	C_6 C_7	1.338(8)
C_3-C_4	1.379(8)	C_{11} C_{12}	1.382(9)
C_3-C_{11}	1.394(8)	C_{12} C_{13}	1.402(9)
		C_{13} C_{14}	1.417(9)

Table 2

Bond angles ω (°) for compound **7d**

Bond angle	ω	Bond angle	ω
$C_2C_5C_6$	107.7(5)	$C_4C_1C_9$	111.0(5)
$C_2C_5C_{10}$	103.2(7)	$C_1C_9C_8$	107.0(5)
$C_6C_5C_{10}$	107.9(5)	$C_1C_9C_{10}$	103.0(4)
$C_5C_2C_3$	114.8(5)	$C_8C_9C_{10}$	108.1(5)
$C_1C_2C_5$	105.7(5)	$C_7C_8C_9$	114.4(5)
$C_1C_2C_3$	86.5(4)	$O C_8C_9$	122.3(5)
$C_2C_3C_4$	93.3(5)	$O C_8C_7$	123.3(5)
$C_2C_3C_{11}$	144.0(5)	$C_6C_7C_8$	123.4(5)
$C_4C_3C_{11}$	122.3(5)	ClC_7C_8	115.4(4)
$C_1C_4C_3$	93.9(5)	ClC_7C_6	121.2(4)
$C_3C_4C_{14}$	123.4(6)	$C_5C_6C_7$	118.5(5)
$C_1C_4C_{14}$	142.5(6)	$C_5C_{10}C_9$	102.3(4)
$C_2C_1C_4$	86.2(4)	$C_3C_{11}C_{12}$	116.1(6)
$C_2C_1C_9$	104.6(5)	$C_{11}C_{12}C_{13}$	121.4(6)
$C_4C_{14}C_{13}$	114.4(6)	$C_{12}C_{13}C_{14}$	122.4(6)

EXPERIMENTAL PART

The ^{1}H-NMR spectra were recorded on Varian EM-360L instrument, while the ^{13}C-NMR spectra were recorded on a Varian FT-80A instrument; occasionaly ^{1}H- and ^{13}C-NMR spectra were recorded with Brucker-400. All chemical shifts are quoted in ppm (parts per million) and are referred to internal tetramethylsilane. The multiplicity of signals is s(singlet), d(doublet), t(triplet), m(multiplet), coupling constants are expressed in Hz. The NMR solvents are reported for each compound. The IR spectra were recorded on a UR-20 Carl Zeiss Jena spectrometer. The intensity of absorption bands is s(strong), m(medium) and w(weak). Mass spectra were recorded on a DP-102 GCMS instrument; in parenthesis is quoted the intensity of the signal in % from the basic peak, considered 100%. The GC analyses were carried out on a Carlo Erba Model B GC instrument with flame ionization detector, using hydrogen as carrier gas. Melting points are uncorrected. In the case of X-ray measurements unit cell parameters and intensity data were collected on a Hilger-Watts automated four-circle diffractometer (λM_0K_α, graphite monochromator *via* a $\theta - 2\theta$ scan technique, $2\theta < 60°$). Crystals of **7e** were rhombic $a = 5.8088(7)$, $b = 9.6092(5)$, $c = 19.671(1)$ Å, $V = 1098.0(1)$ Å^3; $D_{calc} = 1.395$ g/cm^3; space group $P2_12_12_1$ with $Z = 4$ formula units/unit cell. The 759 reflections with $|F_0| > 2.0\sigma$ were considered in calculations. The structure was solved by direct methods and refined by full-matrix least square technique. Hydrogen atoms were not included. At convergence, $R = 0.052$ and $R_w = 0.043$. All calculations were carried out on Eclipse S/200 computer using the program INEXTL.[11] Atomic coordinates for chloroketone **7d** have been deposited with the Director of the Cambridge Crystallographic Data Center, University Chemical Lab., Lensfield Road, Cambridge CB2 1EW. *exo*-Benzocyclobutanorbornadiene **6** was obtained from anthranilic acid and norbornadiene, according to the reported literature procedure.[12] The synthesis of dichloroderivative **7a** was achieved according to our procedures.[3a-5]

7-Chloro-8α-acetoxy-1α,2α-5,9-methano-5H-benzo[3,4]cyclobuta[1,2]cycloheptene (7b)

A mixture of 5.6 g (22 mmoles) of dichloroderivative **7a** and 7g (22 mmoles) of mercury (II) acetate disolved in 100 mL of glacial acteic acid (freshly distilled) was refluxed 20 hours. After cooling to room temperature, the reaction mixture was poured on ice-water (*ca.* 250 mL) and was extracted with ethyl ether (5×50 mL). The etheral solution was washed with 5% $NaHCO_3$ solution to pH = 7. The organic layer was dried on anh. $MgSO_4$, then evaporated. The crude mixture was purified by column chromatography with CCl_4 as eluent resulting 5.93 g (97% yield) of the title compound as a viscous liquid.

IR(CS_2,CCl_4, cm^{-1}): 740 (m); 780 (m); 1227 (m); 1454 (s); 1600 (w); 1740 (s); 2854 (s); 2920 (s).

^1H-NMR(CCl_4): 1.35 (H_{10}^{anti}, d t, J = 12; 4; 4); 1.84 (H_{10}^{syn}, d, J = 12); 2.58 (H_9, m); 2.77 (H_5, m); 3.72 (H_2, d, J = 4); 3.8 (H_1, d, J = 4); 5.18 (H_8^{endo}, d, J = 2.5); 6.48 (H_6, d, J = 7); 7.25 (4H arom., m).

^{13}C-NMR($CDCl_3$): 21.04 (CH_3); 26.51 (C_{10}); 37.05 (C_5); 40.86 (C_9); 48.47 (C_1); 53.58 (C_2); 74.53 (C_8); 121.97 and 122.28 (2C-ortho); 127.95 and 128.01 (2C-meta); 128.60 (C_7); 135.86 (C_6); 144.67 (C_3); 144.91 (C_4); 170.13 (C=O).

MS: 274(4.3); 214(17.1); 197(18.7); 179(100); 178(31.2); 177(15.7); 175(29.5); 167(24.1); 165(16.1); 128(16.6); 102(18.5); 77(18.1).

Anal.: $C_{16}H_{15}ClO_2$ requires: C 69.98; H 5.46; Cl 12.9; Found C 69.57; H 5.8; Cl 13.4%.

7-Chloro-8α-hydroxy-1α,2α-5,9-methano-5H-benzo[3,4]cyclobuta[1,2]cycloheptene (7c)

A solution of 5.6 g (20 mmoles) of chloroacetate **7b** in 16 mL of anh. ethyl ether was added dropwise, under stirring, to a suspension of 0.65 g (17 mmoles) of $LiAlH_4$ in 20 mL anh. diethyl ether at a rate to maintain a gentle reflux. After additional 3 hours at reflux, the reaction mixture was cooled at 20°C and treated with 20 mL saturated aqueous solution of NH_4Cl until two layers are formed. The aqueous layer was separated and extracted with diethyl ether (3×25 mL). The etheral layers were then washed with saturated NaCl aqueous solution, dried over anh. Na_2SO_4, the solvent evaporated and the crude reaction product chromatographed on SiO_2 column, eluted with chloroform. The yield is 3.55 g (75%), m.p. 138—138.5°C.

IR (CS_2, $CHCl_3$, cm^{-1}): 692 (m); 740 (m); 1000 (s); 1027 (s); 1447 (m): 1627 (m); 2873 (w); 2940 (s); 3000 (w); 3060 (w); 3200—3550 (s); 3592 (m).

^1H-NMR($CDCl_3$): 1.23 (H_{10}^{anti}, d t, J = 11; 4; 4); 1.70 (H_{10}^{syn}, d, J = 11); 2.26 (OH, s); 2.53 (H_9, d, J = 2); 2.59 (H_5, d d, J = 6; 4); 3.72 (H_1, d, J = 4); 3.92 (H_8^{endo}, d, J = 2); 6.25 (H_6, d, J = 6); 7.08 (4H arom., m).

^{13}C-NMR($CDCL_3$): 26.12 (C_{10}); 37.21 (C_5); 42.68 (C_9); 48.89 (C_1); 53.53 (C_2); 74.23 (C_8); 122.01 and 122.14 (2C-ortho); 127.82 and 127.94 (2C-meta); 132.57 (C_7); 133.58 (C_6); 149.19 (C_3; C_4).

Anal.: $C_{14}H_{13}OCl$ requires C 72.29; H 5.58; Cl 15.24; found C 71.85; H 6.01; Cl 16.3%.

7-Chloro-8-keto-1α,2α-5,9-methano-5H-benzo[3,4]cyclobuta[1,2]cycloheptene (7d)

To a homogenous solution of 2 g (86 mmoles) of the chloroalcohol **7c** dissolved in 5 mL of ethyl ether and 2 mL of tetrahydrofuran, 9 mL of chromic acid [13] solution was added at 0°C during 2 minutes, (the chromic acid solution was obtained from 100 g (0.33 moles) of sodium dichromate, dissolved in 300 mL water and 136 g (1.34 moles) of sulphuric acid 96%, then completed with water to 500 mL), under mechanical stirring. The stirring was continued for additional 15 minutes at 0°C. The etheral layer was separated and aqueous layer was extracted with ethyl ether (3 × 25 mL). The combined etheral layers were washed with aqueous 5% $NaHCO_3$, water and then dried over anh. $MgSO_4$. After evaporation of the solvent was obtained a viscous yellow oil 1.1 g (70% yield); white crystals mp. 150 — 151°C (from ethanol).

IR($CHCl_3$, cm^{-1}) : 890 (s) ; 1050 (m) ; 1320 (m) ; 1450 (m) ; 1600 (w) ; 1680 (s) ; 2940 (s).
^1H-NMR($CDCl_3$) : 1.53 (H_{10}^{anti}, d t d, J = 12.1 ; 4 ; 1) ; 2.15 (H_{10}^{syn}, d, J = 12.1) ; 2.91 (H_5, d d, J = 8 ; 4) ; 3.09 (H_9, d, J = 4) ; 3.7 (H_2, d, J = 3.5) ; 3.86 (H_1, d, J = = 3.5) ; 7.0 (4H arom., m) ; 7.3 (H_6, d d, J = 8 ; 1).
^{13}C-NMR($CDCl_3$) : 34.99 (C_{10}) ; 39.14 (C_5) ; 47.66 (C_9) ; 51.44 (C_2) ; 52.30 (C_1) ; 122.03 and 122.64 (2C-ortho) ; 128.46 and 128.62 (2C-meta) ; 131.21 (C_7) ; 142.23 (C_3) ; 143.69 (C_4) ; 150.84 (C_6) ; 193.65 (C_8).
Anal. : $C_{14}H_{11}ClO$ requires : C 72.92 ; H 4.77 ; Cl 15.37 ; found C 72.41 ; H 4.95 ; Cl 16.02%.

7-Chloro-1α,2α-5,9-methano-5H-benzo[3,4]cyclobuta[1,2]cycloheptene (7e)

To a suspension of 1.3 g (34.3 mmoles) of $LiAlH_4$ in 30 mL of anh. diethyl ether was added dropwise, under stirring, a solution of 7.4 g (29.5 mmoles) of dichloroderivate **7a** dissolved in 60 mL of anh. diethyl ether. After 20 hours of reflux under stirring, to the reaction mixture was added 5 mL of water, then 5 mL of aqueous 15% NaOH. After filtration, the organic layer was separated, washed with saturated aqueous NaCl, dried over anh. $MgSO_4$ and the solvent was removed under reduced pressure. The residue was distilled and 4.5 g (70% yield) of the title compound was collected at 120°C/3 mmHg.

IR(CS_2, CCl_4, cm^{-1}) : 670 (s) ; 690 (s) ; 740 (s) ; 860 (s) ; 960 (s) ; 1020 (m) ; 1040 (s) ; 1460 (s) ; 1600 (w) ; 1640 (m) ; 2840 (m) ; 2940 (s) ; 3080 (s).
^1H-NMR(CCl_4) : 0.7 – 1.63 ($2H_{10}$, $2H_8$, m) ; 2.1 – 2.7 (H_5, H_9, m) ; 3.7(H_1, H_2, d, J = 4) ; 6.6 (H_6, d, J = 7) ; 6.8 – 7.2 (4 Harom, m).
^{13}C-NMR($CDCl_3$) : 29.99 (C_{10}) ; 31.91 (C_5) ; 32.74 (C_9) ; 41.58 (C_8) ; 53.93 (C_1) ; 56.86 (C_2) ; 121.84 (2C-ortho) ; 127.59 (C_7) ; 128.1 (2C-meta) ; 130.06(C_6) ; 144.42 (C_3 ; C_4).
Anal. : $C_{14}H_{13}Cl$ requires : C 77.63 ; H 6.00 ; Cl 16.36 ; found C 77.58 ; H 6.31 ; Cl 15.90%.

8α- and 8β-Bromo-1α,2α-5,9-methano-5H-benzo[3,4]cyclobuta[1,2]cycloheptenes (8a)

To a solution of **4** (2.5 g, 37 mmoles) in 30 mL of anh. CCl_4 was added 2.4 g (13.7 mmoles) of N-bromosuccinimide (NBS) and 0.05 g of benzoyl peroxide. The reaction mixture was subjected to a gentle reflux until all NBS was converted into succinimide (e.g. floating at the surface of the reaction mixture). After cooling, the succinimide was filtered, the solvent evaporated at 20 mmHg. 3.5 g (98% yield) of a viscous liquid of a mixture of two isomers **8a** resulted. The mixture of bromoderivatives **8a** was used as such for the synthesis of compounds **8b**.

8α- and 8β-Acetoxy-1α, 2α-5,9-methano-5H-benzo[3,4]cyclobuta[1,2]cycloheptenes (8b)

A mixture of 2.8 g (10 mmoles) of the bromoderivatives **8a** and 3.2 g (10 mmoles) of mercury (II) acetate was refluxed in 60 mL of the glacial acetic acid during 10 hours. After cooling, the reaction mixture was poured in ice-water and then was extracted with 3 × 25 mL of ethyl ether. The etheral layers were washed with aqueous 5% $NaHCO_3$, water and dried over anh. $MgSO_4$. The solvent removed and there was obtained 2.38 g (92% yield) of crude acetates **8b** as a viscous oil. The GC analysis (capillary column, 25 m, polyethylene glycol 20M, injection temperature 250°C, the column temperature was programmed with 12°/minute in the range 95–160°C, hydrogen flow rate 1.5 mL/minute) revealed 84.5% *exo* isomer and 15.5% of *endo* isomer of **8b**. The isomeric mixture has the following data :

IR(CS_2, CCl_4, cm^{-1}) : 917 (m) ; 952m ; 1013(s) ; 1234 (s) ; 1365 (m) ; 1450 (w) ; 1728 (s) ; 2920 (m) ; 3013 (w).

^1H-NMR(CCl_4) : 1.16(H_{10}^{ant}, d d t, J = 12 ; 7 ; 1.5) ; 1.65 (H_{10}^{syn}, d, J = 12) ; 2.06 (CH_3*exo*, s) ; 2.13 (CH_3*endo*, s) ; 2.45 (H_9, d d, J = 4 ; 3) ; 2.55 (H_5, d d, J = 7 ; 4) ; 3.47 (H_1, H_2, m) ; *ca.* 5 (H_8 *endo*, d d, J = 3 ; 4) ; 5.2 (H_8 *exo*, *m*) ; 5.42 (H_6, d d, J = 9 ; 4) ; 6.25 (H_7, d d d, J = 9 ; 7 ; 1.5) ; 6.75–7.3 (4H arom., m).

^{13}C-NMR($CDCl_3$) : 21.18 (CH_3) ; 26.83 (C_{10}*exo*) ; 32.51 (C_{10}*endo*) ; 36.07 (C_5 *endo*) ; 36.23 (C_5 *exo*) ; 40.01 (C_9) ; 46.69 (C_1 *endo*) ; 48.90 (C_1 *exo*) ; 53.92 (C_2 *exo*) ; 54.47 (C_2 *endo*) ; 71.40 (C_8 *exo*) ; 74.19 (C_8 *endo*) ; 121.82 and 122.09 (2C-ortho) ; 127.62 and 127.67 (2C-meta) ; 145.19 (C_3) ; 145.53 (C_4) ; 170.09 (C=O).

Anal. : $C_{16}H_{16}O_2$ requires : C 80.01 ; H 6.66 ; found C 79.63 ; H 6.49%.

8α- and 8β-Hydroxy-1α,2α-5,9-methano-5H-benzo[3,4]cyclobuta[1,2]cycloheptenes (8c)

The title compounds were obtained from acetoxy derivatives **8b** as colourless viscous oil, with 73% according to a similar procedure as it was described for **7c**. The isomeric mixture has the following data :

IR(CS_2, CCl_4, cm^{-1}) : 745 (s) ; 790 (m) ; 825 (m) ; 1026 (s) ; 1187 (m) ; 1395 (m) ; 1450 (m) ; 2859 (m) ; 2939 (s) ; 3034 (m) ; 3073 (m) ; 3340 (m).

^1H-NMR($CDCl_3$) : 1.16 (H_{10}^{anti}, d t, J = 12 ; 3.5 ; 3.5) ; 1.65 (H_{10}^{syn}, d, J = 12) ; 2.34 (H_9, m) ; 2.46 (H_5, m) ; 2.78 (OH, s) ; 3.30 – 3.71 (H_1, H_2, m) ; 3.89 (H_8, m) ; 5.50 (H_7, d d d, J = 9.5 ; 3.5 ; 1.5) : 6.83 (H_6, m) ; 6.75 – 7.3 (4H arom., m).

^{13}C-NMR($CDCl_3$) : tentative assignment :

exo-OH : 26.19 (C_{10}) ; 36.51 (C_5) ; 42.90 (C_9) ; 49.23 (C_1) ; 53.89 (C_2) ; 69.84 (C_8) ; 121.87 and 122.03 (2C-ortho) ; 126.48 (C_6) ; 127.48 and 127.55 (2C-meta) ; 137.06 (C_7) ; 145.83 (C_3) ; 145.91 (C_4).

endo-OH : 32.51 (C_{10}) ; 36.14 (C_5) ; 43.10 (C_9) ; 45.95 (C_1) ; 54.51 (C_2) ; 71.44 (C_8) ; 121.87 and 122.03 (2C-ortho) ; 127.48 and 127.55 (2C-meta) ; 127.98 (C_6) ; 135.26 (C_7) ; 145.83 (C_3) ; 145.91 (C_4).

Anal. : $C_{14}H_{14}O$ requires : C 84.86 ; H 7.11 ; found C 84.59 ; H 7.38%.

8-Keto-1α,2α-5,9-methano-5H-benzo [3,4]cyclobuta[1,2]cycloheptene (8d)

The title compound was prepared by a similar procedure as it was described for chloroketone **7d**, in 60% yield.

IR(CS_2, CCl_4, cm^{-1}) : 870 (m) ; 1030 (w) ; 1100 (m) ; 1200 (w) ; 1250 (m) ; 1305 (w) ; 1370 (w) ; 1450 (m) ; 1600 (w) ; 1680 (s) ; 2855 (m) ; 2870 (m) ; 2960 (s) ; 3030 (m) ; 3070 (m).

^1H-NMR(CCl_4) : 1.56 (H_{10}^{anti}, d t, J = 12 ; 4 ; 4) ; 2.04 (H_{10}^{syn}, d, J = 12) ; 2.90 (H_5, d d, J = 7 ; 4) ; 2.93 (H_9, dd, J = 4 ; 2) ; 3.7 (H_1, d, J = 3.5) ; 3.83 (H_2, d, J = 3.5) ; 5.83 (H_7, d d, J = 10 ; 2) ; 7.31 (H_8, d d, J = 10 ; 7) ; 7.15 (4H arom., m) ; 7.31 (H_6, d d, J = 10 ; 7).

^{13}C-NMR($CDCl_3$) : 34.92 (C_{10}) ; 37.99 (C_5) ; 48.0 (C_9) ; 51.72 (C_1) ; 52.67 (C_7) ; 122.17 and 122.48 (2C-ortho) ; 127.85 and 128.28 (2C-meta) ; 128.10 (C_7) ; 142.84 (C_3) ; 144.26 (C_4) ; 155.42 (C_6) ; 201.27 (C_8).

ACKNOWLEDGEMENT : We are indebted to Prof. A. T. Balaban for helpful discussions ; to chim. Ligia Stănescu for g.c. analysis and chim. V. Todan for IR spectra of a few compounds.

REFERENCES

[1] Taken in part from PhD Thesis of A.P. (Polytechnic Institute, Bucharest, 1989).

[2] R. P. Johnson, A. Exarchon, C. W. Jefford and R. C. Hahn, *J. Org. Chem.*, **42**, 3758 (1977) ; for the 3-bromoderivative of hydrocarbon **1** and rearrangement to benzobarrelene skeleton se : M. Balci, O. Cakmak and R. Harmandar, *Tetrahedron Letters*, **1985**, 5464.

[3] a) A. Popescu, L. Pârvulescu, L. Stănescu and M. D. Gheorghiu, *Rev. Roumaine Chim.*, **31**, 1025 (1986) ; b) for ^1H-NMR see : M. D. Gheorghiu, A. Popescu and Gh. Surpăţeanu, *Rev. Roumaine Chim.*, **34**, 481, (1989) ; c) for ^{13}C-NMR see : M. D. Gheorghiu and A. Popescu, *Rev. Roumaine Chim.*, **34**, 1779 (1989).

[4] For the synthesis of benzocyclobutabarrelene see : L. Enescu, I. Dinulescu and M. Avram, *Rev. Roumaine Chim.*, **24**, 995 (1979).

[5] L. Pârvulescu and M. D. Gheorghiu, *Rev. Roumaine Chim.*, **22**, 1059 (1977).

[6] a) W. v. Doering and A. K. Hoffman, *J. Amer. Chem. Soc.*, **76**, 6162 (1954) ; b) W. R. Moore, W. R. Moser and J. E. La Prade, *J. Org. Chem.*, **28**, 2200 (1963) ; c) R. C. De Selms and Ch. M. Combs, *J. Org. Chem.*, **28**, 2206 (1963) ; d) C. W. Jefford, *Proc. Chem. Soc.*, **1963**, 64 ; e) L. Ghosez and P. Laroche, *Proc. Chem. Soc.*, **1963**, 90 ; f) C. W. Jefford, S. Mahajan, J. Washyn and B. Waegell, *J. Amer. Chem. Soc.*, **87**, 2183 (1965) ; g) L. Ghosez, P. Laroche and G. Slinkx, *Tetrahedron Letters*, **1967**, 2767 ;

h) C. W. Jefford, S. N. Mahajan and J. Gunsher, *Tetrahedron*, **24**, 2971 ; i) C. W. Jefford and K. C. Ramey, *Tetrahedron*, **24**, 2927 (1968) ; j) C. W. Jefford, D. T. Hill, J. Gore and B. Waegell, *Helv. Chim. Acta*, **55**, 790 (1972) ; k) C. W. Jefford, A. Sweeney and F. Delay, *Helv. Chim. Acta*, **55**, 2214 (1972).

[7] a) P. R. Story and S. R. Fahrenholtz, *J. Org. Chem.*, **28**, 1716 (1963) ; b) C. W. Jefford, J. Mareda, J. C. E. Gehret, n Tanada Kabengele, W. D. Graham and U. Burger, *J. Amer. Chem. Soc.*, **98**, 2585 (1976) ; c) C. W. Jefford, J. C. E. Gehret and V. de los Heros, *Bull. Soc. Chim. Belg.*, **88**, 973 (1979).

[8] a) C. W. Jefford and R. Medary, *Tetrahedron*, **23**, 4123 (1967) ; b) idem, *Tetrahedron Letters*, **1960**, 2064 ; c) W. R. Dolbier, jr. and H. O. Enoch, *J. Amer. Chem. Soc.*, **99**, 4532 (1977).

[9] A. Popescu, I. Matei and M. D. Gheorghiu, *Rev. Roumaine Chim.*, **36**, 000 (1991).

[10] a) F. H. Allen, O. Kennard, D. G. Watson, L. Brammer, A. G. Orpen and R. Taylor, *J. Chem. Soc. Perkin Trans II*, **1987**, S1 ; b) F. H. Allen, *Acta Crystallogr.*, **B40**, 64 (1984) ; c) O. Buynkgenger, *Acta Crystallogr.*, **C40**, 75 (1989) ; d) O. Buynkgenger, M. Harmandar and M. Balci, *Acta Crystallogr.*, **C40**, 77 (1989).

[11] R. G. Gerr, A. I. Ianovsky and Yu. T. Struchkov, "Crystallography", 1983, vol. 28, pag. 1029 (in russian).

[12] M. N. Paddon-Row and R. Hartcher, *J. Amer. Chem. Soc.*, **102**, 662 (1980).

[13] H. C. Brown, C. P. Gary and Kwang-Ting Liu, *J. Org. Chem.*, **36**, 387 (1971).

Revue Roumaine de Chimie, 36, 4–7, 693–705 (1991)

Dedicated to Prof. ALEXANDRU T. BALABAN
on the occasion of his 60th anniversary

ELECTROPHILIC AROMATIC SUBSTITUTION IN ARENE-TRICARBONYL-CHROMIUM COMPLEXES

SÎNZIANA ROŞCA,[a] FILIP CHIRALEU[b] and SORIN I. ROŞCA[a] *
[a] Department of Organic Chemistry, The Polytechnic Institute, Bucharest, Romania
[b] Organic Chemistry Research Center, Bucharest, Roumania

Received March 3, 1991

The Friedel-Crafts acetylation and acid-promoted H-D exchange in tricarbonyl-chromium complexes of some diaryls, naphthalene and toluene were studied. For biphenyl and diphenylmethane complexes an assistance in electrophilic substitution by neighbouring Cr $(CO)_3$ was revealed. A reaction mechanism is proposed, comprising a preliminary formation of a relatively stable intermediate by the attack of electrophile on the chromium atom, followed by transfer into the key intermediate, in a rate determining step. The key intermediate is formed through an early transition state (resembling a π-complex) thus differing from free arenes where a late transition state (resembling a σ-complex) is operating. These features explain striking differences observed in orientation effects of complexes compared to "free" arenes.

INTRODUCTION

Arene-tricarbonyl-chromium complexes were reported to be readily prepared and to exhibit drastic changes in reactivity, when compared to their "free" arene counterparts. Due to enhanced reactivity and stereoselectivity of the complexes and to post-process mild release of the arenes, some reactions of the complexes became useful preparative tools.**

Despite the fact that the electrophilic aromatic substitution is the most typical reaction of aromatics, only sporadic investigations have been carried out regarding the electrophilic substitution in arene-tricarbonyl-chromium complexes. The Friedel-Crafts acylation of benzene,[3–5] alkylbenzenes,[6–9] indanes,[7,10] and diaryls complexes,[11] acid-promoted H-D exchange[12–15] and mercuration[16] of arene complexes have been so far, to some extent, studied. Both available experimental data and theoretical prediction[17] point to the suspicion that arene-tricarbonyl-chromium complexes do not undergo electrophilic aromatic substitution easily.

---

* To whom correspondence should be addresed

** See, for example, excellent reviews[1] as well as a recent survey[2] on the chemistry of arene-tricarbonyl-metal complexes and references therein.

However, as it was early shown[6,7] there is a striking difference in orientation effects in complexes as compared to corresponding uncomplexed arenes: *e.g.* acetylation of *t*-butylbenzene substrate, where the isomer ratios are $(o : m : p)$: 0 : 87 : 13 for complex, respectively 0 : 4.7 : 95.3 for uncomplexed arene.[7] This result points to an important difference in mechanistic path of the electrophilic substitution in complexes versus uncomplexed arenes, thus providing a convenient access to different regioisomers, starting from the same substrate.

In the present paper, we report some results regarding the Friedel-Crafts acetylation and acid-promoted H—D exchange that are thought to provide useful information concerning the mechanism of electrophilic substitution in arene-tricarbonyl-chromium complexes.

RESULTS AND DISCUSSION

Substrates and electrophilic reactions

The substrates chosen for this study were tricarbonyl-chromium complexes **1a** — **5a**.

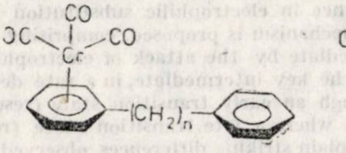

1a 2a 3a
n : 0 1 2

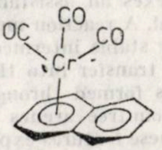

4a

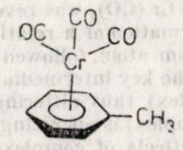

5a

These structures were selected for the following reasons: Mono-tricarbonyl-chromium complexes of diaryls (**1a** — **3a**) containing both complexed and non-complexed aromatic rings in the same molecule, are expected to afford reliable deductions concerning relative reactivities of complexed and non-complexed aromatic rings; moreover, various relative positions of complexed and non-complexed aromatic rings would, possibly, give rise to different mutual interactions noticeable by measuring the relative substitution ratios. Similar anticipations are applicable to the mono-tricarbonyl-chromium complex of a fused-ring system, **4a**; furthermore, in this case the primary formed acetylation product could easily undergo a subsequent haptotropic rearrangement.[18] The complex of toluene, **5a**, represents the simplest substrate suitable for observing orientation effects.

Two electrophilic substitution processes were studied, namely the Friedel-Crafts acetylation and acid-promoted D—H exchange. The Friedel-Crafts acetylation was selected since it may be conducted under mild conditions where ligand exchange is not important,[19] being normally highly selective and kinetically controled[20]; an acetylation of alkylbenzenes complexes showed[7] no alteration of regioisomer ratio by equilibration of products or by preferential decomposition of a particular complex.

The acid-promoted H-D exchange, although scarcely studied in the complex series,[12–14] was proved to be a typical electrophilic aromatic substitution process, also suitable for a kinetic study.[21]

Arene-tricarbonyl-chromium complexes **1a** – **5a** were prepared by the reaction between arene and chromium hexacarbonyl in refluxing diglyme or decaline, under nitrogen.[22]

The acetylations were performed following a described procedure,[7,23] in dichloromethane, at 25°, the electrophilic reagent being previously prepared (from acetyl chloride and aluminium chloride) and gradually added to arene-tricarbonyl-chromium complex containing solution, in order to assure a competition for electrophile of complexed and non-complexed aromatic rings.

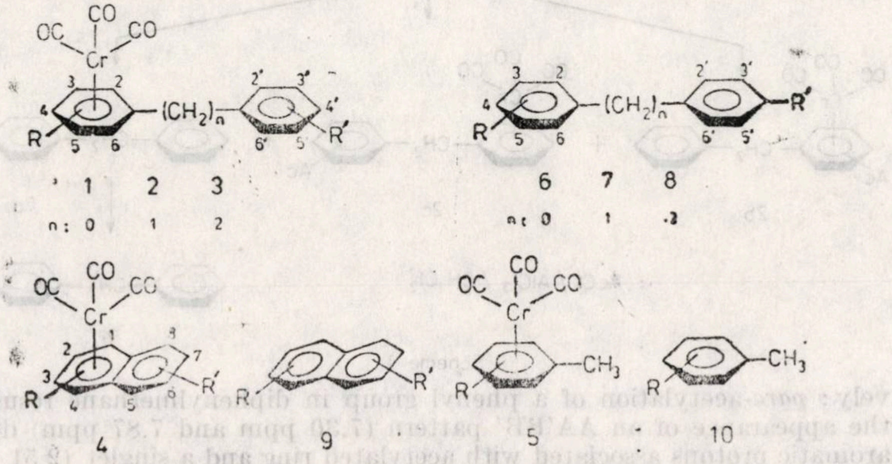

The composition of reaction product was determined by ^{1}H-NMR analysis. Preliminary experiments as well as previously reported data,[7,11] showed that the reaction mixture resulted from acetylation of mono-tricarbonyl-chromium complexes contains: unreacted starting complex (**1a** – **5a**); acetylated complex, with the acetyl group associated to the complexed ring (**1b** – **5b**); acetylated complex with the acetyl group associated to the non-complexed ring (**1c** – **4c**); "free" arene resulted by demetallation of the starting complex (**6a** – **10a**) and acetylated "free" arene resulted by subsequent *para*-acetylation of demetallated arene (**6c** – **10c** *vide, infra*). Consequently, of these possible components of the raw product, those unequivocally obtainable were prepared and their ^{1}H-NMR spectra were recorded.

In the case of diphenylmethane complex acetylation, for example, according to Scheme 1, the expected components present in the reaction mixture are the compounds **2a** – **2c**, **7a** and **7c**. Therefore, authentic samples of **2a**, **7a** and **7c** were prepared and their ^{1}H-NMR spectra were recorded. As shown by these spectra (see experimental section) complexation of a phenyl group by tricarbonyl-chromium moiety in diphenylmethane, cause an upfield shift in both aromatic (from 7.10 ppm to 5.05–5.35 ppm) and benzylic protons (from 3.93 ppm to 3.70 ppm) respecti-

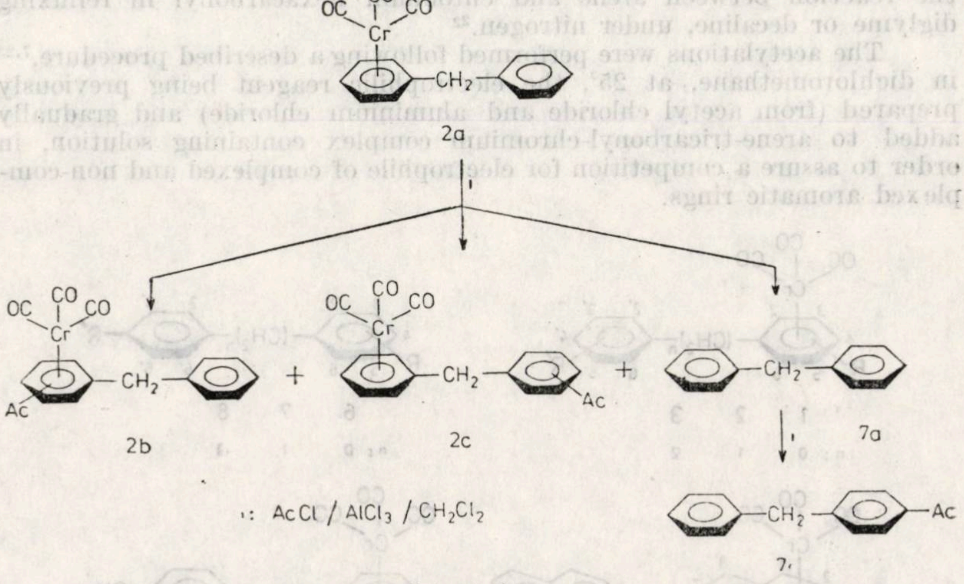

Scheme 1

vely; *para*-acetylation of a phenyl group in diphenylmethane results in the appearance of an AA′BB′ pattern (7.30 ppm and 7.87 ppm) due to aromatic protons associated with acetylated ring and a singlet (2.51 ppm) associated with COCH$_3$ group.

The raw product formed by acetylation of diphenylmethane complex **2a** was subjected to ^{1}H-NMR analysis. Taking into account the above

Table 1

Products distribution in the Friedel-Crafts acetylation of complexes **1a** — **5a**

Starting complex Products	**1a**	**2a**	**3a**	**4a**	**5a**
Acetylated in the complexed ring mol % (structure)	2 (**1b**)	14 (**2b**)	16 (**3b**)	0 (**4b**)	59 (**5b**)
Acetylated in the non-complexed ring mol % (structure)	22 (**1c**)	10 (**2c**)	9 (**3c**)	0 (**4c**)	—
"Free" arene[a] mol % (structure)	1 (**6a**)	2 (**7a**)	2 (**8a**)	95 (**9a**)	1 (**10a**)
"Free" arene, acetylated[b] mol % (structure)	19 (**6c**)	13 (**7c**)	13 (**8c**)	0 (**9b**)	10 (**10b**)
Unreacted complex mol % (structure)	56 (**1a**)	61 (**2a**)	60 (**3a**)	5 (**4a**)	30 (**5a**)

[a] Formed by demetallation of starting complex;

[b] Formed by demetallation of starting complex followed by rapid acetylation of formed "free" arene (see text).

a result of deactivation of the non-complexed one. Consequently, one could expect for complexes of diphenylmethane (**2a**) and biphenyl (**1a**) where the electron-withdrawing complexed ring becomes more closer, to exhibit a much lower reactivity of non-complexed ring. On the contrary, experimental data (this time in agreement with those already reported 11)) show a non-complexed ring acetylation of 42% for diphenylmethane complex and 92% for biphenyl complex. This clearly indicates that the electrophilic attack at the non-complexed ring is strongly assisted by neighbouring tricarbonyl-chromium, this latter effect prevailing on adverse inductive effect.

In the case of biphenyl complex, this electron-supplying effect (noticed also in solvolyses of 4-phenylcumyl-chlorides 30)) is most probably resonance phenomenon implying metal-arene bond ("vertical stabilization"[31] structure **16**).

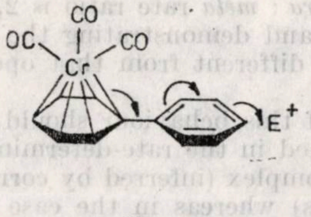

16

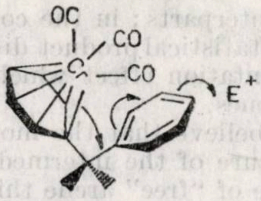

17

However, the electron-supply on electrophilic attack in the diphenylmethane complex is more obscure, although there are some precedents : Traylor and Goldberg[29] have recently showed that the anchimeric assistance in ligand exchange is greater for the diphenylmethane derivative, explicable in terms of a better proximity of the second phenyl group in this complex. Thus, the stabilization of the transition state leading to intermediate of electrophilic substitution in diphenylmethane complex could be depicted as a $\sigma - \pi$ homoconjugation (structure **17**).

Orientation effects in toluene-complex

In order to put into evidence orientation effects, acetylation and D-H acid promoted D-H exchange in the toluene complex were performed. For D-H exchange, rate constants were determined at 93° using specifically *o*, *m* and *p* deuterium labelled toluene-tricarbonyl-chromium complexes and 84% CF_3COOH. For acetylation, *o* : *m* : *p* ratios were evaluated by ^{1}H-NMR technique and are in good agreement with those reported elsewhere.[6]

The results are given in Table 3 and they point to a marked difference in behaviour of complexed and uncomplexed arenes. The relative rates of D-H exchange clearly reveal the following features : in the case of "free" arene, a typical *ortho*, *para* orientation is active ; the complex exhibits lower overall reactivity compared to "free" arene, although *meta* positions of the complex are more reactive than their "free"

Table 3

Acetylation and D-H exchange in methyl-substituted ring

Substrate	Isomer ratio in acetylation $AcCl/AlCl_3/CH_2Cl_2$;25°			Relative rates in D-H exchange ; 84 % CF_3COOH ; 93° value 1 taken for $k = 2 \cdot 1\ 10^{-6}\ s^{-1}$)		
	o(%)	*m*(%)	*p*(%)	*o*	*m*	*p*
5a[a]	37	15	48	1.9	1.5	3.0
10a[a]	5	2	93	45	1	71[b]

[a] For D-H exchange measurements, specifically, *o*- *m*- and *p*-deuterium labelled compounds [32] were used ;

[a] Compare to partial rate factors $f_o = 250$, $f_m = 4$ and $f_p = 420$ previously reported [33] in H-D exchange, at 70°, in CF_3COOH D_2O 62.9 : 12.5.

arene counterparts ; in the complex, *para* : *meta* rate ratio is 2, thus excluding a statistical product distribution and demonstrating the existance of an orientation effect which is much different from that operating in "free" arenes.

We believe that the motivation of this behaviour should be found in the nature of the intermediates formed in the rate-determining step : in the case of "free" arene this is a σ-complex (inferred by correlation of reactivity with stability of σ-complexes) whereas in the case of arene-tricarbonyl-chromium compounds, key-intermediate is a π-complex. In other words, in the rate determining step of the electrophilic substitution "free" arene will present a late transition state, similar in structure to a Wheland complex, whereas the complex will display an early transition state resembling a π-complex.

The following considerations demand that this π-complex should be oriented with respect to ring substituent :

The arene ligand (*e.g.*, benzene) is considered to be a η^6 bonding, six electrons system occupying three coordination sites of the metal (structure **18**). Due to its symmetry, all six positions of the complexed benzene ring are equivalent. However, in a benzene derivative (*e.g.*, toluene) the five positions are no more equivalent ; the electron density in chromium-carbon partial bonds should be larger for 2,4,6-positions as follows from most stable canonical structure **19**, drawn on the analogy of Wheland's type benzenium ions (the tricarbonyl-chromium moiety acts here as an "electrophile" for whose bond to arene a three-fold symmetry is conceivable). Electron densities in chromium-carbon partial bonds directed to 1,3,5-positions are somewhat lower, since corresponding electronic structures do not benefit by similar stabilization.

Consequently the electrophile, prefering electron rich possitions [34] will be directed to *para* and *meta* in a ratio proportional to specific weights of conformations **20a** and **20b**. In the case of toluene complex population of **20a** was estimated to be 67% [35] which is in excellent agreement with a *para* : *meta* ratio of 2, observed by us. Other evidence coming from electrophilic substitution of various substituted benzene complexes are now in preparation.

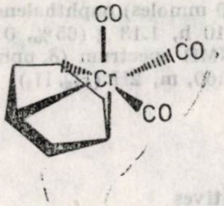

18

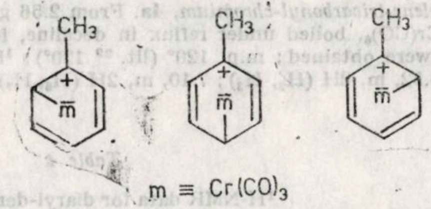

19

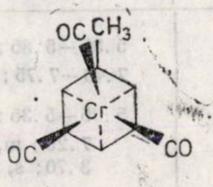

20a

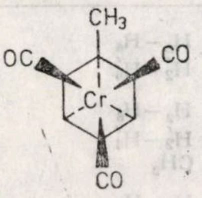

20b

Finally we should note that since the electron densities in metal-carbon partial bonds seem to be truly reflected by ^{1}H-NMR chemical shifts of corresponding ring protons, the latter can be used to estimate, orientatively, the reactivity in electrophilic substitution of a particular position.

EXPERIMENTAL

Melting points are uncorrected. ^{1}H-NMR spectra were recorded on a Varian A-60 spectrometer; approximately 8% solutions of the components in $CDCl_3$ and TMS as internal standard were used. Solvents were dried, freshly distilled and de-aerated by flushing with argon before use.

Arene-tricarbonyl-chromium complexes

Title compounds were prepared, according to Nichols and Whiting,[22] by heating the arene with chromium hexacarbonyl (molar ratio 2.7 : 1) in boiling diglyme or decalin, under nert, for 5—10 hours. After appropriate reaction time, the solvent and unreacted $Cr(CO)_6$ were removed by distillation under reduced pressure (unreacted chromium hexacarbonyl was ecovered). The residue was chromatographed on neutral alumina, products being eluted with petroleum-ether (b.p. 60 — 80°) and petroleum-ether : ether (4 : 1). Solvent evaporation of the latter fraction yielded raw complex, that was then recrystallized from *n*-heptane.

Biphenyl-tricarbonyl-chromium, **1a**. From 3.08 g (20 mmoles) biphenyl and 1.65 g (7.5 mmoles) $Cr(CO)_6$, boiled under reflux in diglyme, for 6 h, 0.82 g (54%, 0.5 g $Cr(CO)_6$ recovered) **1a** were obtained; m.p. 86° (lit. 87°[36]; 86°[11]); ^{1}H-NMR spectrum, see Table 4.

Diphenylmethane-tricarbonyl-chromium, **2a**. From 3.36 g (20 mmoles) diphenylmethane nd 1.65 g (7.5 mmoles) $Cr(CO)_6$, boiled under reflux in diglyme, for 5 h, 1.4 g (75%, 0.3 g $Cr(CO)_6$ recovered) **2a** were obtained; m.p. 97° (lit. 97°[37]; 98°[11]); ^{1}H-NMR spectrum, see Table 4.

1,2-Diphenylethane-tricarbonyl-chromium, **3a**. From 3.64 g (20 mmoles) 1,2-diphenylethane and 1.65 g (7.5 mmoles) $Cr(CO)_6$, boiled under reflux in diglyme, for 5 h, 1.4 g (72%,).4 g $Cr(CO)_6$ recovered) **3a** were obtained; m.p. 98° (lit. 98—100°[38]; 99°[11]; ^{1}H-NMR spectrum, ee Table 4.

Naphthalene-tricarbonyl-chromium, **4a**. From 2.56 g (20 mmoles) naphthalene and 1.65 g (7.5 mmoles) $Cr(CO)_6$, boiled under reflux in decaline, for 10 h, 1.13 g (65%, 0.2 g $Cr(CO)_6$ recovered) **4a** were obtained; m.p. 120° (lit.[39] 120°); ^{1}H-NMR spectrum (δ, ppm): 6.10, m, 2H (H_1, H_4); 5.52, m, 2H (H_2, H_3); 7.10, m, 2H (H_6, H_7); 7.60, m, 2H (H_5, H_8).

Table 4

^{1}H-NMR data for diaryl-derivatives

Entry	Structure	Position of protons	δ (ppm, TMS); Obs.
1	**1a**	H_2-H_6	5.35−5.85; m, 5H
		$H'_2-H'_6$	7.40−7.75; m, 5H
2	**2a**	H_3-H_6	5.05−5.35; m, 5H
3		$H'_2-H'_6$	7.25; m, 5H
4		CH_2	3.70; s, 2H
5	**3a**	H_2-H_6	4.90−5.40; m, 5H
6		$H'_2-H'_6$	7.10−7.30; m, 5H
7		$CH_3(\alpha)$	2.66; 2H A_2B_2
8		$CH_2(\beta)$	2.82; 2H
9	**6a**	H_2-H_6; $H'_2-H'_6$	7.30−7.70; m
10	**7a**	H_2-H_6; $H'_2-H'_6$	7.10; s, 10H
11		CH_2	3.93; s, 2H
12	**8a**	H_2-H_6; $H'_2-H'_6$	7.16; s, 10H
13		CH_2	2.80; s, 4H
14	**6c**	H_2-H_6	7.30−7.60; m, 5H
15		H'_2, H'_6	7.65; d, 2H AA′BB′
16		H'_3, H'_5	8.01; d, 2H
17		CH_3-CO	2.40; s, 3H
18	**7c**	H_2-H_6	7.10−7.25; m, 5H
19		H'_2, H'_6	7.30; d, 2H AA′BB′
20		H'_3, H'_5	7.87; d, 2H
21		CH_2	4.02; s, 2H
22		CH_3-CO	2.51; s, 3H
23	**8c**	H_2-H_6	7.20; m, 5H
24		$H_{2'}$, $H_{6'}$	7.22; d, 2H
25		H'_3, H'_5	7.86; d, 2H AA′BB′
26		CH_2 (α)	2.95; s, 2H
27		CH_2 (β)	2.95; s, 2H
28		CH_3-CO	2.52; s, 3H

Toluene-tricarbonyl-chromium, **5a**. From 2.8 g (30 mmoles) toluene and 3.3 g (15 mmoles) toluene and 3.3 g (15 mmoles) $Cr(CO)_6$ boiled under reflux for 6 h in a mixture of 20 ml diglyme and 5 ml *n*-heptane, 1.6 g (74%, 1.2 g $Cr(CO)_6$ recovered) **5a** were obtained; m.p. 82.5° (lit.[22] 82.5−83.5°); ^{1}H-NMR spectrum (δ, ppm): 5.05−5.50, m, 5H (H_2-H_6); 2.20, s, 3H (CH_3).

Arenes, **6a** − **10a**. Biphenyl, **6a**, naphthalene, **9a** and toluene **10a** were commercial products. Diphenylmethane[40] and 1,2-diphenylethane[41] were prepared following the procedures described in literature; ^{1}H-NMR spectra, see Table 4.

Acetylated arenes

The following procedure was applied to prepare acetylated arenes [7]: A solution of acetyl chloride (20 mmoles) in dry dichloromethane (20 ml) was added dropwise to a stirred suspension of freshly sublimated aluminium chloride (25 mmoles) in dichloromethane (20 ml). Thus obtained acetylating reagent was added dropwise to a stirred solution of arene (10 mmoles) in dichloromethane (20 ml). The mixture was stirred, at 0—20°, for 1 h under inert, then poured into ice (50 g) containing 3 ml concentrated hydrochloric acid. The organic layer was separated and the aqueous solution was twice extracted with dichloromethane. The combined extracts were washed with water, dried over $MgSO_4$, the solvent removed and the residue distilled under reduced pressure to yield acetylated arene. The following compounds were thus obtained :

4-Acetylbiphenyl, **6c**, was obtained, in 65 % yield, by acetylation of biphenyl ; m.p. 120° (lit.[42] 120.5°) ; b.p. 110°/10 mm ; ^1H-NMR spectrum, see Table 4.

4-Acetyldiphenylmethane, **7c**, was obtained, in 82 % yield, by acetylation of diphenylmethane ; m.p. 38° (lit.[43] 39°) ; b p. 127°/10 mm ; ^1H-NMR spectrum, see Table 4.

4-Acetylbibenzyl, **8c**, was obtained by acetylation of 1,2-diphenylethane, in 84 % yleid ; m.p. 82° ; b.p. 184°/10 mm ; ^1H-NMR spectrum, see Table 4.

1-Acetylnaphthalene, **9b**, was obtained by acetylation of naphthalene in CCl_4, in 55 % yield ; b.p. 165°/16 mm (lit. [44]170—170.5/20 mm).

4-Acetyltoluene, **10b**, was obtained by acetylation of toluene, in 82 % yield ; b.p. 85°/5 mm (lit [45] 93.5°/7 mm).

Acetylation of complexes

General procedure previously described [7] was used. A solution of acetyl chloride (0.424g, 5.4 mmoles) in dichloromethane (5 ml) was added, under inert, to a stirred suspension of powdered, freshly sublimated, aluminium chloride (0.8 g, 6 mmoles) in dichloromethane (20 ml) and stirred under ice cooling until most aluminium chloride had dissolved ; 5 ml of this acetylating reagent was added dropwise, with stirring under inert, to a solution of arene-tricarbonylchromium complex (1 mmole) in dichloromethane (3 ml). The reaction flask was protected from light and after 4 h, at 25°, the reaction mixture was poured into ice (5 g) and concentrated hydrochloric acid (0.5 ml). The organic layer was separated and aqueous layer was extracted with dichloromethane (5 ml). The combined organic layers were washed with water, then with 5 % Na_2CO_3 and again with water and dried over $MgSO_4$. The solvent was evaporated and the orange-yellow residue was analysed by ^1H-NMR spectrometry.

Composition of the raw acetylation product was determined using the following procedure (illustrated for the representative case of diphenylmethane complex, **2a**). Significant ^1H-NMR data for diarylsubstrates including mono-tricarbonyl-chromium complexes of diaryls (**1a** — **3a**) "free" diaryls (**6a** — **8a**) and *p*-acetylated diaryls (**6c** — **8c**) are displayed in Table 4.

When ^1H-NMR spectrum of raw product formed in acetylation of **2a** was inspected, the following peaks, well separated to obtain reliable integrals, were observed and attributed : two doublets (deshielded branches of AA′BB′ signals) at 7.84 — 7.87 ppm due to deshielded H'_3, H'_5 protons from 4′-acetylated **2b** and H'_3, H'_5 protons from **7c** (see Table 4, entry 20) ; a peak at 7.05 — 7.35 ppm including aromatic protons H'_2 — H'_6 from **2a** (entry 3), H'_2 H'_6 from **2b**, H'_2, H'_6 from **2c**, H_2 — H_6 and H'_2, H'_6 from **7a** (entry 10), H_2 — H_6 and H'_2, H'_6 from **7c** (entries 18, 19) ; a group of signals in the range 5.00 — 6.10 ppm including aromatic protons associated with complexed ring H_2 — H_6 from **2a** (entry 2), four protons from **2b** and H_2 — H_6 from **2c** ; two singlets at 3.95 — 4.03 ppm due to CH_2 groups in **7a** (entry 11) and **7c** (entry 21) ; a peak at 3.70 ppm due to CH_2 protons in **2a** (entry 4), **2b**, and **2c** ; a group of singlets in the range 2.38 — 2.53 ppm due to CH_3CO protons from **2b**, **2c** and **7c** (entry 22).

Taking as support the above assignments, balance equations were established for each ^1H-NMR peak and molar fractions of components in the product mixture were determined by multiple integrations of pertinent peaks.

Acid-promoted H-D exchange

H-D exchange in 1,2-diphenylethane-tricarbonyl-chromium, **3a**. Deutero-trifluoroacetic acid was prepared from trifluoroacetic anhydride (22.3 g, 0.106 moles) and deuterium oxide (2.13 g, 0.106 moles). Alkalimetric titration showed a concentration of 97 %. A solution of 1,2-diphenylethane-tricarbonyl-chromium (0.636 g, 2 mmoles) in the above obtained CF_3COOD (16 ml) was prepared. Aliquots of 3 ml were withdrawn and placed in vials, the air was thoroughly removed by flushing with argon, the vials were sealed and thermostated at 115°. After appropriate time, reaction was stopped by pouring the content of each vial into ice (10 g). The complex was extracted with ether, washed with water, dried ($MgSO_4$) and evaporated to afford 70 — 80 mg complex per each sample. From ^{1}H-NMR spectra of these samples of product, the values of signal integrals i_{CH_2} (methylene protons, $\delta = 2.50 - 3.10$ ppm) i_C (complexed aromatic-ring protons, $\delta = 4.90 - 5.40$ ppm) and i_N (non-complexed aromatic-ring protons, $\delta = 7.10 - 7.30$ ppm) were monitored. The first order rate constants were calculated as : $k_C = 1/t \ln (5i_{CH_2}/4i_C)$ and $k_N = 1/t \ln (5i_{CH_2}/4i_N)$ where indexes C and N stand for complexed and non-complexed rings, respectively.

H-D exchange in 1,2-diphenylethane, **8a**, was measured by monitoring of i_{CH_2} and i_A (aromatic ring protons) integrals at appropriate time intervals for a 0.1 molar solution of **8a** in 97% CF_3COOD, thermostated at 115°. The rate constant was calculated as : $k_A = 1/t \ln (10\ i_{CH_2}/4i_A)$.

D-H exchange in o-, m- and p-d-toluene and corresponding tricarbonyl-chromium complexes. *o*-, *m*- and *p*-d-Toluene were prepared by the reaction of corresponding organomagnesium compounds with deuterium oxide as previously described.[32] Tricarbonyl-chromium complexes were obtained as above described for compound **5a**. From chromium hexacarbonyl (1.1 g, 5 mmoles) and *o*-deuterotoluene (1.86 g, 20 mmoles) *o*-deuterotoluene-tricarbonyl-chromium (0.65 g, 70%, 0.2 g $Cr(CO)_6$ recovered) were obtained ; m.p. 81° (lit.[32] 80°) ; ^{1}H-NMR (δ, ppm) : 2.18, s, 3H (CH_3) ; 5.1—5.5, m, 4.05H (complexed ring protons). Analogously *m*-deuterotoluene-tricarbonyl-chromium, 68% yield ; m.p. 81° (lit.[32] 81°) ; ^{1}H-NMR (δ, ppm) : 2.20, s, 3H (CH_3) ; 5.1 — 5.5, m, 4.1 H (complexed ring protons) and *p*-deuterotoluene-tricarbonyl-chromium, 72% yield ; m.p. 82° (lit.[32] 83°) ; ^{1}H-NMR (δ, ppm) : 2.20, s, 3H (CH_3) ; 5.1 — 5.5, m, 4.1H (complexed ring protons) were obtained.

Kinetic measurements were carried out in sealed NMR tubes, at 93°, using approximately 0.1 molar concentrations of complexes or "free" arene respectively, in an aqueous 84% trifluoroacetic acid solution, thoroughly de-aerated before use. Rate constants were derived from conversions measured by multiple integrations of pertinent peaks at each time period.

REFERENCES

[1] R. P. A. Sneeden, "Organochromium Compounds", Academic Press, New York (1975) ; M. F. Semmelhack, *J. Organomet. Libr.*, **1**, 361 (1976) ; J. P. Collman and L. S. Hegedus, "Principles and Applications of Organotransition Metal Chemistry" University Science Books, Mill Valley, Ch. 14 (1980) ; W. E. Watts, "The Organic Chemistry of Metal-Coordinated Cyclopentadienyl and Arene Ligands" in : "Comprehensive Organometallic Chemistry", Ed. G. Wilkinson, F. G. A. Stone, E. W. Abel, Pergamon, Vol. 8, pp. 1013—72 (1982) ; G. Jaouen, *Pure Appl. Chem.*, **58**, 597 (1986) ; A. Solladie-Cavallo *Adv. Met. Org. Chem.*, **1**, 99 (1989).

[2] L. S. Hagedus, *J. Organomet. Chem.*, **380**, 169 (1990).

[3] R. Ercoli, F. Calderazzo and E. Mantica, *Chimica e Industria*, **41**, 404 (1959).

[4] R. Riemschneider, D. Becker and K. Franz, *Monatsh.*, 90, 571 (1959).

[5] D. A. Brown and F. J. Hughes, *Inorg. Chim. Acta*, **1**, 448 (1967).

[6] G. E. Herberich and E. O. Fischer, *Chem. Ber.*, **95**, 2803 (1962).

[7] W. R. Jackson and W. B. Jennings, *J. Chem. Soc. (B)*, **1969**, 1221.

[8] S. Jaouen and R. Dabard, *C.R. Acad. Sci. Paris*, **271**, *Serie C*, 1610 (1970).

[9] G. Jaouen, *Tetrahedron Letters*, **1973**, 1753.

[10] W. R. Jackson, *Aust. J. Chem.*, **39**, 303 (1986).

[11] J. L. von Rosenberg and R. Pinder, *J. Chem. Soc. Perkin Trans. I*, **1987**, 747.

[12] D. N. Kursanov, V. N. Setkina, N. K. Baranetskaya, V. I. Zdanovich and K. N. Anisimov, *Dokl. Akad. Nauk SSSR*, **190**, 1103 (1970).

[13] V. N. Setkina, V. I. Zdanovich, N. L. Baranetskaya, A. I. Jurtanov, K. N. Anisimov and D. N. Kursanov, *Zh. Obshch. Khim.*, **41**, 1338 (1971).

[14] D. N. Kursanov, V. N. Setkina, N. K. Baranetskaya, V. I. Zdanovich, A. I. Yurtanov and K. N. Anisimov, *Izv. Akad. Nauk SSSR, Ser. Khim.*, **1973**, 1359.

[15] W. S. Leong and N. J. Cooper, *J. Amer. Chem. Soc.*, **110**, 2644 (1988).

[16] G. K. I. Magomedov and V. G. Skyrin, *Zh. Obshch. Khim.*, **45**, 2533 (1975).

[17] D. A. Brown, *J. Chem. Soc.*, **1963**, 4389.
[18] T. A. Albright, P. Hofmann, R. Hoffmann, G. P. Lillya and P. A. Dobosh, *J. Amer. Chem. Soc.*, **105**, 3396 (1983).
[19] Yu. F. Oprunenko, I. A. Shaposhnikova, Yu. A. Ustynyuk, N. A. Ustynyuk and D. N. Kravtsov, *Izd. Akad. Nauk SSSR, Ser. Khim.*, **1987**, 703.
[20] G. A. Olah (editor), "Friedel-Crafts and Related Reactions", Vol. 3, "Acylation", Interscience, New York, (1964).
[21] S. I. Roşca, unpublished results.
[22] B. Nicholls and M. C. Whiting, *J. Chem. Soc.*, **1959**, 551.
[23] G. Perrier, *Chem. Ber.*, **33**, 815 (1900).
[24] G. A. Olah, G. D. Mateescu and Y. K. Mo, *J. Amer. Chem. Soc.*, **95**, 1865 (1973).
[25] A. Davison, W. Mc Farlane, L. Pratt and G. Wilkinson, *J. Chem. Soc.*, **1962**, 3653.
[26] D. N. Kursanov, V. N. Setkina, P. V. Petrovskii, V. I. Zdanovich, N. K. Baranetskaya and I. D. Rugin, *J. Organometal. Chem.*, **37**, 339 (1972).
[27] N. Cornelly and Z. Demidowicz, *J. Chem. Soc. Dalton Trans.*, **1975**, 2335.
[28] V. A. Piveni, I. S. Nekrasov, V. I. Dosilkina and D. V. Zagorevskii, *Izv. Akad. Nauk SSSR Ser. Khim.*, **1987**, 664.
[29] T. G. Traylor and M. J. Goldberg, *J. Amer. Chem. Soc.*, **109**, 3968 (1987).
[30] A. Z. Kreindlin, *Izv. Akad. Nauk SSSR, Ser. Khim.*, **1973**, 952.
[31] T. G. Traylor, W. Hanstein, H. J. Berwin, N. A. Clinton and R. S. Brown, *J. Amer. Chem. Soc.*, **93**, 5715 (1971).
[32] Sînziana Roşca, Renate Pătraşcu, F. Chiraleu and S. Roşca, *Rev. Roumaine Chim.*, **24**, 1069 (1970).
[33] W. M. Lauer, G. W. Matson and G. Stedman, *J. Amer. Chem. Soc.*, **80**, 6433 (1958).
[34] H. C. Brown and H. Junok, *J. Amer. Chem. Soc.*, **77**, 5579 (1955).
[35] F. van Meurs, J. M. van der Toorn and H. von Bekkum, *J. Organometal. Chem.*, **113**, 341 (1976).
[36] E. O. Fischer, N. Kriebitzsch and R. D. Fischer, *Chem. Ber.*, **92**, 3214 (1959).
[37] D. J. Cram and D. I. Wilkinson, *J. Amer. Chem. Soc.*, **82**, 5721 (1960).
[38] R. Ercoli, F. Calderazzo and A. Alberola, *Chim. Ind. (Milan)*, **41**, 975 (1959).
[39] E. O. Fischer and K. Öfele, *Z. Naturforsch.*, **13b**, 458 (1958).
[40] N. K. Moshchinskaya and R. L. Globus, *J. Applied Chem.*, **17**, 76 (1944).
[41] J. Buck and S. Jenkins, *J. Amer. Chem. Soc.*, **51**, 2166 (1929).
[42] K. Anwers and W. Jülicher, *Chem. Ber.*, **55**, 2183 (1922).
[43] H. Duval, *Bull. Soc. Chim. France*, **1910**, 791.
[44] F. Krollpfeiffer, *Liebigs Ann., Chem.*, **430**, 199 (1922).
[45] C. R. Noller and R. Adams, *J. Amer. Chem. Soc.*, **46**, 1813 (1924).

Revue Roumaine de Chimie, 36, 4–7, 707–714 (1991)

Dedicated to Prof. ALEXANDRU T. BALABAN
on the occasion of his 60th anniversary

THE SYNTHESIS OF 8-SUBSTITUTED COMPOUNDS OF 7-H AND 7-CHLORO-1β,2β-5,9-METHANO-5H-BENZO[3,4] CYCLOBUTA[1,2]CYCLOHEPTENES. MOLECULAR AND CRYSTAL STRUCTURE OF 7,8α-DIBROMO-1β,2β-5,9-METHANO-5H-BENZO[3,4]CYCLOBUTA[1,2]CYCLOHEPTENE [1]

ANGELA POPESCU,[a] IRINA MATEI[a], MIRCEA D. GHEORGHIU, [a]*
K. M. TURDIBEKOV[b] and YU. T. STRUCHKOV[b]
[a] Department of Organic Chemistry, Polytechnic Institute, 76206, Bucharest 16, Romania
[b] X-Ray Structural Centre, Section of General and Technical Chemistry, USSR Academy of Sciences, 28 Vavilov Str., 117813 Moscow, USSR

Received January 10, 1991

The allylic bromine or chlorine from either 7-H or 7-chloro derivatives of 1β, 2β-5,9-methano-5H-benzo[3,4]cyclobuta[1,2]cycloheptenes were replaced by acetoxy group, which then was converted into hydroxy and keto functionalities. The molecular and crystal structure of 7,8α-dibromo-1β,2β-5,9-methano-5H-benzo[3,4]cyclobuta[1,2]cycloheptene is discussed.

INTRODUCTION

In our previous contributions [2–6] we have described synthetic procedures for the preparation of *exo*- and *endo*-benzocyclobutabicyclo[3.2.1] octene,** allylic derivatives of the *exo*-benzocyclobutabicyclo[3.2.1]octene as well as of discussions of ^{1}H-NMR and ^{13}C-NMR of both *exo*- and *endo*-benzocyclobutabicyclo[3.2.1] derivatives. Here we would like to present the synthesis of the hitherto unknown *endo*-benzocyclobutabicyclo[3.2.1] octene allylic derivatives and the X-ray structure determination of the 7,8α-dibromo-*endo*-benzocyclobutabicyclo[3.2.1] octene.

SYNTHESIS

7,8α-Dichloro-*endo*-benzocyclobutabicyclo[3.2.1] octene **1a**[2,3] when treated with mercury(II) acetate in boiling acetic acid was converted in 98% yield in the acetoxy derivative **1b**. The configuration of the acetoxy group is *exo*, retaining the chlorine configuration in the dichloro precursor **1a**. An *exo* configuration at C_8 is definitely established by examining the magnitude of the H_8-H_9 coupling constant. When the configuration

---

* Correspondence author

** For convenience, throughout the present paper we shall use instead of the *Chem. Abstr.* nomenclature, as it is presented in the title, the simpler name : benzocyclobutabicyclo [3.2.1]octene. However, the *Chem. Abstr.* numbering of the carbon atoms is preserved.

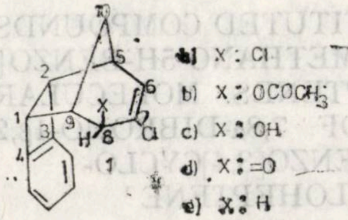

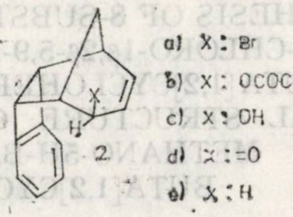

of a substituent at C_8 is *exo*, the coupling constant of allylic hydrogen atom with the bridgehead hydrogen is of *ca*. 2 Hz. For an *endo* configuration, the coupling constant is of *ca*. 4 Hz. As it will be discussed later in our paper, we shall present X-ray data for the 7,8α-dibromo-*endo*-benzocyclobutabicyclo[3.2.1]octene **4**, obtained from hydrocarbon **3** [7]

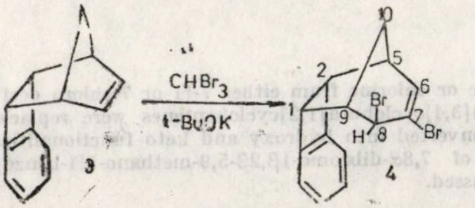

and dibromocarbene generated from bromoform and t-BuOK. The allylic bromine substituent has *exo* configuration. Indeed, for this compound, the allylic to bridgehead coupling constant is 2.191 Hz, the ^1H-NMR spectrum being recorded at 300 MHz.

By reduction of acetoxy derivative **1b** with $LiAlH_4$, the alcohol **1c** resulted in 75% yield. The hydroxy group has *exo* configuration on the basis of ^1H-NMR results, similar to that discussed above. Oxidation with sodium dichromate and sulphuric acid of the alcohol **1c** leads to the chloroketone **1d**, as white crystals.

The present hydrocarbon **2e**,[3] *endo*-benzocyclobutabicyclo[3.2.1]octene is easily converted with N-bromosuccinimide into the 8-bromoderivative **2a**. The configuration of the bromine at C_8 is *exo*. Unlike the *exo*-benzocyclobutabicyclo[3.2.1]octene, which by bromination with the same reagent gave a mixture of *exo*- and *endo*-isomers, the bromination of *endo*-benzocyclobutabicyclo[3.2.1]octene is stereospecific. Presumably, the *endo*-configuration of the benzocyclobutano fragment prevented an *endo* attack at the allylic C_8 atom. By reacting with mercury(II) acetate, the allylic halogen is easily replaced by an acetoxy group. The reaction was carried out at reflux in acetic acid, suggesting that the bromine is more reactive than chlorine. Lithium aluminium hydride reduction of the acetoxy group of **2b** gave in 70% yield the alcohol **2c** with *exo* configuration of the hydroxy group. Oxidation of the alcohol **2c** with sodium dichromate and sulphuric acid gave 70% yield the α,β-unsaturated ketone **2d**.

Molecular structure of the 7,8α-Dibromo-1β, 2β-5,9-methano-5H-benzo[3,4]cyclobuta[1,2]cycloheptene (4)

X-Ray measurements have confirmed the *endo* configuration ot the benzocyclobutano fragment and the *exo* configuration of the bromine atom at the allylic carbon atom, C_8.

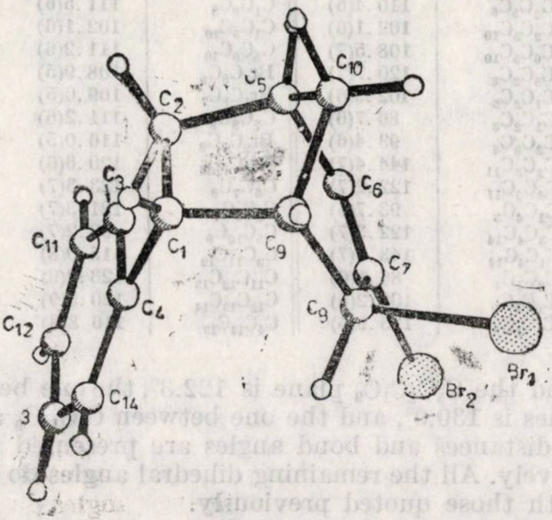

Fig. 1

The four-membered ring $C_1C_2C_3C_4$ in *endo* configuration is slightly folded, along $C_1—C_3$ the dihedral angle is 2.6°. Atom C_{10} is out of the $C_5C_2C_1C_9$ plane with 0.77 Å. The average plane among the atoms $C_5C_6C_7C_8C_9$

Table 1

Bond length d(Å) for compound 4

Bond	d	Bond	d
$Br_1—C_8$	2.004(7)	$C_1—C_4$	1.51(1)
$Br_2—C_7$	1.906(7)	$C_4—C_{14}$	1.37(1)
$C_2—C_5$	1.56(1)	$C_1—C_9$	1.54(1)
$C_5—C_6$	1.51(1)	$C_8—C_9$	1.524(9)
$C_5—C_{10}$	1.53(1)	$C_9—C_{10}$	1.55(1)
$C_2—C_3$	1.50(1)	$C_7—C_8$	1.482(8)
$C_1—C_2$	1.57(1)	$C_6—C_7$	1.31(1)
$C_3—C_4$	1.378(9)	$C_{11}—C_{12}$	1.40(1)
$C_3—C_{11}$	1.37(1)	$C_{12}—C_{13}$	1.36(1)
		$C_{13}—C_{14}$	1.39(1)

is rather poor (± 0.02 Å) and as a result, atoms Br_1 and C_{10} are placed at 1.73 Å and 0.87 Å, respectively, on one side, while Br_2 is situated at 0.21 Å on the other side. The dihedral angle between the four-membered ring $C_1C_2C_3C_4$ and the $C_5C_2C_1C_9$ plane is 122.3°, the one between $C_5C_2C_1C_9$ and $C_5C_{10}C_9$ planes is 130.0°, and the one between $C_5C_{10}C_9$ and $C_6C_7C_8C_9C_{10}$ is 119.4°. Bond distances and bond angles are presented in table 1 and table 2, respectively. All the remaining dihedral angles do not exceed 10°, as compared with those quoted previously.

Table 2

Bond angles ω (°) for compound 4

Bond angle	ω	Bond angle	ω
$C_2C_5C_6$	110.4(6)	$C_1C_9C_8$	111.5(6)
$C_2C_5C_{10}$	102.1(6)	$C_1C_9C_{10}$	102.1(6)
$C_6C_5C_{10}$	108.5(7)	$C_8C_9C_{10}$	111.2(6)
$C_5C_2C_3$	120.7(7)	$Br_1C_8C_9$	108.9(5)
$C_1C_2C_5$	102.9(6)	$Br_1C_8C_7$	109.0(5)
$C_1C_2C_3$	86.7(6)	$C_7C_8C_9$	111.2(6)
$C_2C_3C_4$	93.4(6)	$Br_2C_7C_8$	116.0(5)
$C_2C_3C_{11}$	144.4(7)	$Br_2C_7C_6$	120.6(6)
$C_4C_3C_{11}$	122.2(7)	$C_6C_7C_8$	123.3(7)
$C_1C_4C_3$	93.7(6)	$C_5C_6C_7$	121.3(7)
$C_3C_4C_{14}$	122.3(7)	$C_5C_{10}C_9$	99.2(7)
$C_1C_4C_{14}$	143.9(7)	$C_3C_{11}C_{12}$	115.0(8)
$C_2C_1C_4$	86.1(6)	$C_{11}C_{12}C_{13}$	123.2(9)
$C_2C_1C_9$	106.2(6)	$C_{12}C_{13}C_{14}$	120.5(9)
$C_4C_1C_9$	123.9(6)	$C_4C_{14}C_{13}$	116.8(8)

The six-membered ring has half-chair conformation as a result of the presence of the double bond at C_6-C_7 atoms. In the saturated isomers this ring has chair conformation.[8]

EXPERIMENTAL PART

The IR spectra were recorded on a UR-20 Carl Zeiss Jena IR spectrometer. In parenthesis is given the intensity of absorption bands: s(strong), m(medium), w(weak) quoted in cm^{-1}. The ^1H-NMR spectra were recorded with Varian EM 360L instrument and occasionally with Gemini 300 and Brucker 400. The ^{13}C-NMR spectra were recorded with Varian FT-80A instrument and occasionally with Gemini 300 and Brucker 400. All chemical shifts are quoted in ppm (parts par million) and are referenced to internal tetramethylsilane. The multiplicity of signals: s(singlet), d(doublet), t(triplet), m(multiplet) coupling constants are expressed in Hz. The solvents are reported for each compound. The MS were collected with DP-102 GCMS instrument; in parenthesis is quoted the intensity of the signal in % from the basic peak, considered 100%. GS analyses were run on a Carlo Erba Model 2450, equiped with a flame ionization detector and capillary column 25 m, coated with polyethyleneglycol 20M. Hydrogen was the carrier gas, 1.5 mL/minute, evaporation temperature 250°C, the column temperature was programmed with 12°/ minute, in the range 95°–160°C. Melting points are uncorrected. In the case of X-ray measurements the unit cell parameters and intensities data were collected with a Hilger-Watts automated four-circle diffractometer (λM_0K_α, graphite monochromator) *via* a $\theta - 2\theta$ scan technique, $2\theta < 60°$. Crystals of 7,8α-dibromo-1β,2β-5,9-methano-5H-benzo[3,4]cyclobuta[1,2]cycloheptene 4 were monoclinic, a = 12.999(2), b =

= 8.0511(7), c = 12.907(2) Å, β = 113.304(9)°, V = 1240.6(2) Å^3, M = 259.8, $D_{calc.}$ = = 1.824 g/cm^3, Z = 4, space group $P2_1/C$. Calculations were carried out with 1314 reflections with $|F_0| > 5\sigma$. The structure was solved by direct methods and refined by full-matrix least square technique. Hydrogen atoms were located from difference synthesis, refined with fixed isotropic thermal parameters. At convergence, R = 0.035 and R_w = 0.026. All calculations were done on Eclipse S/200 computer with aid of INEXTL program.[9] Atomic coordinates for dibromoderivative **4** have been deposited with the Director of the Cambridge Crystallographic Data Center, University Chemical Lab., Lensfield Road, Cambridge CB2 1EW. *endo*-Benzocyclobutanorbornadiene **3** was obtained according to the reported literature procedure,[7] 7,8α-dichloroderivative **1a** was obtained according to our published procedures,[2,3] the parent hydrocarbon **2e** was prepared according to reference 3.

7-Chloro-8α-acetoxy-1β,2β-5,9-methano-5H-benzo[3,4]cyclobuta[1,2]cycloheptene (1b)

A mixture of 3.2 g (12.7 mmoles) dichloroderivative **1a** and 4.1 g (12.7 mmoles) mercury (II) acetate dissolved in 60 mL of acetic acid (freshly distilled) was refluxed during 20 hours. After cooling, the reaction mixture was poured over 200 mL water and ice, and then was extracted with diethyl ether (3×50 mL). The combined organic layers were washed with aqueous 5% $NaHCO_3$ solution and water until pH = 7. The ethereal solution was dried over anh. $MgSO_4$, then the solvent was removed in vacuum; the residue was chromatographed on SiO_2 column, eluted with CCl_4, resulting 3.4 g (yield 98%) of title compound as a viscous oil.

IR(CS_2, CCL_4): 1220(s); 1370(s), 1445(m); 1620 (w); 1723 (s); 2865 (m); 2940 (s); 3000 (m); 3055 (m).

H -NMR(CCl_4): 1.71(H_{10}^{anti}, d t, J=11.5; 4.25; 4.25); 2.08 (H_{10}^{syn}, d, J=11.5); 2.5 (H_9, m); 2.8 (H_5, m); 3.83 (H_2, m); 3.97(H_1, m); 4.87 (H_8^{endo}, d, J=2.5); 5.65 (H_6,d, J = 7); 6.68 – 7.21 (4H arom., m).

^{13}C-NMR($CDCl_3$): 20.91 (CH_3); 35.30 (C_5); 36.09 (C_{10}); 37.60 (C_9); 47.68 (C_1); 52.17 (C_2); 72.68 (C_8); 122.60 and 123.34 (2C-ortho); 126.93 and 127.25 (2C-meta); 129.16 (C_6); 134.32 (C_7); 145.12 (C_3); 145.76 (C_4); 169.38 (C=O).

MS: 274(4.1); 234(3.2); 232(11); 214(19.9); 197(20.9); 180(16.5); 179(100); 178(35.8); 177(17.6); 175(33.7); 167(27.2); 165(18.4); 128(20.5); 115(18.2); 102(26.8); 89(8.5); 72(20.2).

Anal.: $C_{16}H_{15}ClO_2$ requires: C 69.98; H 5.46; Cl 12.90; found C 69.47; H 5 64; Cl 13.16%

7-Chloro-8α-hydroxy-1β,2β-5,9-methano-5H-benzo[3,4]cyclobuta[1,2]cycloheptene (1c)

A solution of 5.6 g (23.3 mmoles) of chloroacetoxy compound **1b** was added dropwise over a suspension of 0.7 g (18.4 mmoles) of $LiAlH_4$ in 40 mL anh. diethyl ether, sustaining a gentle reflux. The mixture was refluxed for additional 3 hours and then was added 20 mL of saturated aqueous NH_4Cl solution. After filtration, the organic layer was separated, while the aqueous layer was extracted with 3×50 mL of diethyl ether. The combined ethereal layers were washed with water, and then dried over anh. $MgSO_4$. After removal of the solvent, the crude product was chromatographed on SiO_2, $CHCl_3$ as eluent, resulting 3.2 g (72% yield) of the title compound, m.p. 89–90°C.

IR($CHCl_3$): 780 (m); 1020 (s); 1370 (m); 1445 (m); 1620 (s); 2875 (s); 2985 (m); 3000 (m); 3060 (w); 3200–3450 (m); 3585 (m).

^{1}H-NMR($CDCl_3$): 1.78 (H_{10}^{anti}, d t, J = 11; 4; 4); 2.18 (H_{10}^{syn}, d, J= 11); 2.4 – 3.1 (H_5, H_9 m); 3.76 (H_8^{endo}, d, J=2.5); 3.93 (H_1, H_2, m) 5.66 (H_6, d, J = 7.5); 6.8 – 7.3 (4H arom., m).

^{13}C-NMR($CDCl_3$): 35.83 (C_5); 35.93 (C_{10}); 39.49 (C_9); 48.15 (C_1); 52.44 (C_2); 72.25 (C_8); 122.99 and 123.46 (2C-ortho); 126.69 and 127.39 (2C-meta); 132.28 (C_6); 133.37 (C_7); 145.82 (C_3); 146.37(C_4).

MS: 234(2); 232(7.4); 198(10.4); 197(63.3); 196(20.4); 180(15.2); 179(79); 178(43 177(45.1); 176(25.5); 175(100); 169(19.8); 168(25.4): 167(69.6); 166(24.2); 165(45.7); 164(14.4); 163(12); 161(18.1); 155(14); 154(25.3); 153(30.2); 152(37.6); 151(12..5): 142(14.9); 141(63.3); 139(15.9); 129(31.8); 128(65.7); 116(19.4); 115(45 1); 104(209); 103(22.9); 102(26.7); 91(19.5); 89(15).

Anal.: $C_{14}H_{13}OCl$ requires: C 72.25; H 5.63; Cl 15.24; found C 71.86; H 5.89; Cl 16.17%.

7-Chloro-8-keto-1β,2β-5,9-methano-5H-benzo[3,4]cyclobuta[1,2]cycloheptene (1d)

To a cooled (to 0°C) solution of 1.8 g (7.65 mmoles) chlorohydroxy compound **1c**, dissolved in 10 mL of diethyl ether, was added during 5 minutes, dropwise, under mechanical stirring, 13 mL of chromic acid solution (made from 20 g $Na_2Cr_2O_7$ in 60 mL water, 14.8 mL (27.2 g) of sulphuric acid 98 % and then completed with water to 100 mL). The mixture is stirring for additional 15 minutes at 0°C. The organic layer was separated, while the aqueous layer was extracted with diethyl ether (3 × 30 mL). The combined organic layers were washed with 5 % aqueous $NaHCO_3$, then with water until pH = 7. After drying over anh. $MgSO_4$, the solvent was removed and the crude product was passed through neutral Al_2O_3, eluted with 1 : 1 (volumes) of petroleum ether (b.p 35°C) and diethyl ether resulting 1.1 g (61 % yield) of the title compound as a viscous oil.

IR($CHCl_3$) : 900 (m); 1067 (w); 1325 (w); 1450 (m); 1600 (w); 1680 (s); 2890 (w); 2960 (s); 3013 (m); 3065 (w).

^{1}H-NMR($CDCl_3$) : 2.14 (H_{10}^{anti}, d t, J = 12.5; 4.25; 4.25); 2.44 (H_{10}^{syn}, d, J = 12.5); 3.25 (H_9, H_5, m); 4.23 (H_1, H_2, m); 6.96 (H_6, d, J = 7); 7.16 (4H arom., m).

^{13}C-NMR($CDCl_3$) : 37.66 (C_{10}); 46.14 (C_5); 47.55 (C_9); 50.27 (C_2); 51.27 (C_1); 122.92 and 123.78 (2C-ortho); 127.89 and 128.23 (2C-meta); 133.53 (C_7); 145.14 (C_3, C_4); 149.03 (C_6); 192.81 (C_8).

MS : 232 (7.8); 230(22.5); 195(25.6); 188(16.7); 168(14.1); 167(100); 166(31.8); 165(56.4); 152(21.7); 103(15.3); 102(15.6); 82(17.9).

Anal. : $C_{14}H_{11}C10$ requires : C 72.92; H 4.77; Cl 15.37; found C 72.41; H 4.89; Cl 16.08 %

7-Chloro-1β,2β-5,9-methano-5H-benzo[3,4]cyclobuta[1,2]cycloheptene (1e)

A mixture of 0.5 g (2 mmoles) of dichloroderivative **1a** in 15 mL of anh. diethyl ether was added dropwise to a suspension of 0.08 g (2 mmoles) of $LiAlH_4$. The mixture was refluxed for 20 hours under mechanical stirring. After cooling, 5 mL of water and then 5 mL of 15 % aqueous solution of NaOH were added. The organic layer was separated, washed with water until pH = 7, and dried over anh. $MgSO_4$. Diethyl ether was removed under reduced pressure, the crude product was chromatographed on SiO_2 with petroleum ether (b.p 35°C) as eluent resulting the title compound as a viscous oil, 0.3 g (71 % yield).

IR(CCl_4) : 830 (m); 865 (s); 925 (s); 940 (m); 1025 (m); 1325 (s); 1575 (m); 1620 (m); 2835 (s).

^{1}H-NMR($CDCl_3$) : 1.46 – 2.2 (2H_{10}, 2H_8, m); 2.2 – 2.76 (H_5, H_9, m); 3.66 – 4.66(H_1, H_2, m); 5.46 (H_6, m); 6.6 – 7.6 (4H arom., m).

^{13}C-NMR($CDCl_3$) : 33.10 (C_5); 34.99 (C_9); 39.16 (C_8); 39.75 (C_{10}); 52.53 (C_1); 56.39 (C_2); 123.16 and 123.35 (2C-ortho); 126.32 and 126.9 (2C-meta); 131.24 (C_7); 132.15 (C_6); 146.36 (C_4); 147.30 (C_3).

8α-Acetoxy-1β, 2β-5,9-methano-5H-benzo[3,4]cyclobuta[1,2]cycloheptene (2b)

A mixture of 2.5 g (14 mmoles) of hydrocarbon **2e** [3], 2.5 g (14 mmoles) of N-bromosuccinimide (NBS), 0.1 g benzoyl peroxide in 25 mL of anh. CCl_4 was refluxed during 2 hours. When all NBS was converted in succinimide, it was removed by filtration and the solvent evaporated under reduced pressure. The crude bromoderivative **2a** was resulted in 95 % yield and was refluxed with 4.15 g (13 mmoles) of mercury (II) acetate dissolved in 75 mL of glacial acetic acid. After the work-up described for compound **1b**, the title compound was isolated as a viscous oil in 92 % yield. The ^{1}H-, ^{13}C-NMR and GC analysis are indicating a sole compound, *exo* acetoxy derivative **2b**.

IR(CCl_4) : 740(s); 1010(m); 1240 (s); 1362 (s); 1450 (m); 1600 (w); 1725 (s); 2860 (w); 2945 (s); 3040(w); 3062 (w).

^{1}H-NMR($CDCl_3$) : 1.69 (H_{10}^{anti}, d t, J = 11; 4.5; 4.5); 2.05 (H_{10}^{syn}, d, J = 11); 2.5 (H_9, m); 2.7 (H_5, m); 3.83 (H_2, m); 3.95 (H_1, m); 4.78 (H_8^{endo}, m); 5.1 (H_7, m); 5.66 (H_6, d d, J = 9.5; 7); 6.6 – 7.3 (4H arom., m).

^{13}C-NMR($CDCl_3$) : 20.72(CH_3) ; 33.93(C_5) ; 32.26(C_9) ; 47.95(C_2) ; 51.91(C_1) ; 69.83(C_8) ; 122.33(C_6) ; 123.05 and 123.95 (2C-ortho) ; 126.18 and 126.67 (2C-meta) ; 136.64 (C_7) ; 145.59(C_3) ; 146.14(C_4) ; 169.34 (C=O).

Anal. : $C_{16}H_{16}O_2$ requires : C 79.95 ; H 6.71 ; found C 79.85 ; H 6.32%

8α-Hydroxy-1β,2β-5,9-methano-5H-benzo[3,4]cyclobuta[1,2]cycloheptene (2c)

The title compound was obtained from acetoxy derivative **2b** as a viscous oil, with 70% yield according to a similar procedure as it was described for **1c**.

IR(CS_2, CCl_4) : 1213(m) ; 1600(w) ; 2840(s) ; 3100−3500 (m), 3626 (w, free OH).

^{1}H-NMR($CDCl_3$) : 1.61 (H_{10}^{anti}, d t, J=10.95 ; 4 ; 4) ; 2.05 (H_{10}^{syn}, d, J=10.95) ; 2.42 (H_9, m) ; 2.65 (H_5, m) ; 3.2 (OH, s) ; 3.67 (H_8^{endo}, m) ; 3.81 (H_1, H_2, m) ; 5.08 (H_7, m) ; 5.57 (H_6, m) ; 6.59−7.13 (4 H arom., m).

^{13}C-NMR($CDCl_3$) : 34.53 (C_5) ; 35.92 (C_{10}) ; 39.07 (C_9) ; 48.53 (C_1) ; 52.29 (C_2) ; 67.90 (C_8) ; 122.69 and 123.23 (2C-ortho) ; 126.21 and 126.81 (2C-meta) ; 128.06 (C_6) ; 134.81 (C_7) ; 146.48 (C_4) ; 146.89 (C_3).

Anal. : $C_{14}H_{14}O$ requires : C 84.86 ; H 7.06 ; found C 84.60 ; H 7.25%.

8-Keto-1β,2β-5,9-methano-5H-benzo[3,4]cyclobuta[1,2]cycloheptene (2d)

The title compound has resulted from the hydroxy derivative **2c**, as a viscous oil (70% yield), by a similar procedure as it was described for **1d**.

IR(CCl_4) : 700 (m) ; 748 (s) ; 820 (s) ; 848 (s) ; 1045 (m) ; 1113 (m) ; 1148 (m) ; 1190 (m) ; 1250 (m) ; 1291 (m) ; 1391 (s) ; 1455 (s) ; 1600 (w) ; 1680 (s) ; 2852 (m) ; 2930 (s) ; 3065 (m).

^{1}H-NMR (CCl_4 + $CDCl_3$) : 2.06 (H_{10}^{anti}, d t, J = 11 ; 4 ; 4) ; 2.38 (H_{10}^{syn}, d, J = 11) ; 2.7−3.2 (H_5, H_9, m) ; 3.92 (H_2, m) ; 4.28 (H_1, m) ; 5.4 (H_7, d, J = 10) ; 6.55 (H_6, m) ; 6.7−7.26 (4H arom., m).

^{13}C-NMR($CDCl_3$) : 36.05 (C_5) ; 46.07 (C_{10}) ; 47.49 (C_9) ; 50.03 (C_1) ; 51.13 (C_2) ; 122.25 and 123.28 (2C-ortho) ; 127.27 and 127.46 (2C-meta) ; 129.86 (C_7) ; 145.35 (C_4) ; 145,61 (C_3) ; 153.34 (C_6) ; 200.48 (C_8).

Anal. : $C_{14}H_{12}O$ requires : C 85.72 ; H 6.12 ; found C 85.54 ; H 5.76%.

7,8α-Dibromo-1β,2β-5,9-methano-5H-benzo[3,4]cyclobuta[1,2]cycloheptene (4)

To a mixture of 5 g (30 mmoles) of *endo*-benzocyclobutabicyclo[2.2.1]heptene **3**,[7] 6.8 g (60 mmoles) of potassium t-butoxyde and 25 mL of hexane, under mechanical stirring, was added dropwise a solution of 15.2 g (60 mmoles) bromoform in 10 mL of dry hexane, while the temperature was kept at 0−5°C. The stirring was continued for additional 1.5 hours. Then the reaction mixture was poured into water, the organic layer separated and the aqueous layer was extracted with diethyl ether (3×25 mL). The combined organic layers were washed to neutral pH with aqueous 5% HCl solution, then with water. After drying over anh. $MgSO_4$, the solvent was removed, the crude dibromoderivative **4** was purified on a SiO_2 column, with chloroform as eluent. The resulted title compound 7.3 g (yield 72%) has m.p. 93−94°C.

^{1}H-NMR($CDCl_3$) : 1.977 (H_{10}^{anti}, d t, J = 11.82 ; 4.5 ; 4.5) ; 2.540 (H_{10}^{syn}, d, J= 11.82) ; 2.918 (H_5, m) ; 2.977 (H_9, m) ; 3.978 (H_2 or H_1, m) ; 4.108 (H_1 or H_2, m) ; 4.531 (H_8, d, J = 2.191) ; 5.838 (H_6, d, J = 7.143) ; 6.9−7.3 (4H arom., m).

^{13}C-NMR($CDCl_3$) : 35.967 ; 36.874 ; 42.675 ; 50.040 ; 57.859 ; 122.286 ; 123.409 ; 123.440 ; 127.133 ; 127.844 ; 137.645 ; 144.863 ; 145.084.

X-Ray measurements see in the text (p. 3).

ACKNOWLEDGEMENTS : Authors are thankful to Prof. A. T. Balaban for helpful discussions, to chim. Ligia Stănescu for g.c. analysis and to C. Deleanu for recording the 300 MHz spectra of compound **4**.

REFERENCES

[1] Taken in part from the PhD Thesis of A.P. (Polytechnic Institute, Bucharest, 1989).

[2] L. Pârvulescu and M. D. Gheorghiu, *Rev. Roumaine Chim.*, **22**, 1089 (1977).

[3] A. Popescu, L. Pârvulescu, L. Stănescu and M. D. Gheorghiu, *Rev. Roumaine Chim.*, **31**, 1025 (1986).

[4] M. D. Gheorghiu, A. Popescu and Gh. Surpăţeanu, *Rev. Roumaine Chim.*, **34**, 481 (1989).

[5] M. D. Gheorghiu and A. Popescu, *Rev. Roumaine Chim.*, **34**, 1779 (1989).

[6] A. Popescu, L. Pârvulescu, L. Mehedinţeanu, M. Plăveţi, M. D. Gheorghiu, K. M. Turdibekov and Yu. T. Struchkov, *Rev. Roumaine Chim.*, **36**, 683 (1991).

[7] C. D. Nenitzescu, M. Avram and D. Dinu, *Chem. Ber.*, **90**, 2541 (1957).

[8] O. Buyukgenger, *Acta Crystallogr.*, **C40**, 75 (1989); O. Buyukgenger, M. Harmandar and M. Balci, *Acta Crystallogr.*, **C40**, 77 (1989).

[9] R. C. Gerr, A. I. Ianovsky and Yu. T. Struchkov, "Crystallography", 1983, vol. 28, p. 1029 (in Russian).

Revue Roumaine de Chimie, 36, 4–7, 715–719 (1991)

Dedicated to Prof. ALEXANDRU T. BALABAN
on the occasion of his 60th anniversary

PHENOXATIIN CHEMISTRY. SYNTHESIS OF PYRIDO[2,3-b] PHENOXATIIN

DAN STOICESCU[a] and OVIDIU MAIOR[b]
[a] Antitumor Drug Research Center, Bucharest
[b] University of Bucharest, Organic Chemistry Department,
Bd. Carol 13, Bucharest, Roumania

Received December 21, 1990

The nucleophilic addition of phenoxatiin amines to acetylenic esters is described ; mild acids or heat catalyzed cyclization of these enamines provides a facile route to pyrido[2,3-b]phenoxatiin derivatives. Chemical and spectral data supporting the structure of the products are presented.

INTRODUCTION

Since diverse biological properties are exhibited by several compounds with either phenoxatiin [1–8] or pyridine [9,10] nucleus, we have investigated the possibility of obtaining derivatives which would include both specified rings.

An attractive route to such derivatives is provided by the cyclization of 3-anilinoacrylates readily available from the reaction of aromatic amines and acetylenic esters.[11–14]

RESULTS AND DISCUSSION

We have used the following unsaturated esters and heteroaromatic amines :

$R-C\equiv C-COOR'$
$A: R=H,\ R'=CH_3$
$B: R=H,\ R'=C_2H_5$
$C: R=COOCH_3,\ R'=CH_3$

1: $X=S$
4: $X=SO_2$

The reactions of **1** were slightly exothermic and were completed at room temperature for 6 hours. Single recrystallization from methanol gave analytically pure materials, usually of mixed E and Z isomers. Compound **4** reacted very slowly at room temperature and even after heating at 68° for 12 hours, a minimal conversion to the corresponding acrylate was obtained. This might be rationalized in terms of electron withdrawing effect of the sulphonyl group present in **4**, similar to that of the nitro function in nitroanilines.[15] Reaction at higher temperature was precluded by the demonstrated instability of the adducts to prolonged heating.

The isomer ratios of such adducts were determined by ^{1}H-NMR spectroscopy (in DMSO-d_6). The proton alpha to the ester function could be clearly integrated in the E and Z acrylate as an indication of the isomer balance. For the Z acrylates the proton appeared at $\delta = 4.8$ ppm; for the E products at $\delta = 5.9$ ppm. These protons were typically AB doublets with $J = 8.5$ Hz for the Z and 13.5 Hz for the E isomers.[15,16]

According to these facts, the structure of **3**, as well as of **2** and **5**, was established as being mainly Z. It is admitted that E to Z conversion is spontaneous and does not require the presence of acids or heating; even in acid-free benzene, complete conversion occurred in a few days.

A tentative explanation rests on the assumption that the greater stability of the Z acrylates arises from the intramolecular NH...O=C hydrogen bonding.

The enamines were first cyclized by heating in diphenyl ether essentially as described by Price,[17] but the low yields (35–40%) and the tedious isolation of the products indicated the need of trying other methods. Among various reagents tried, the most efficient was polyphosphate ester (84–93% yields). It seems to be of general use in this respect since it gives good results in other instances too, e.g. for methyl 3-anilinoacrylate.

It was noticed that the E–Z isomer ratio in the acrylate does not affect the cyclization; it is likely that E to Z conversion must precede ring closure. Compound **5** failed to react even under forcing conditions because of the nucleus deactivation. Spectral analysis of **5** showed the existence of the lactam tautomeric form.

Further treatment of **6** with excess $POCl_3$, then with Zn in acetic acid led to the linear fused heterocycle pyrido[2,3-b]phenoxatiin **8** (Chart 1).

CHART 1

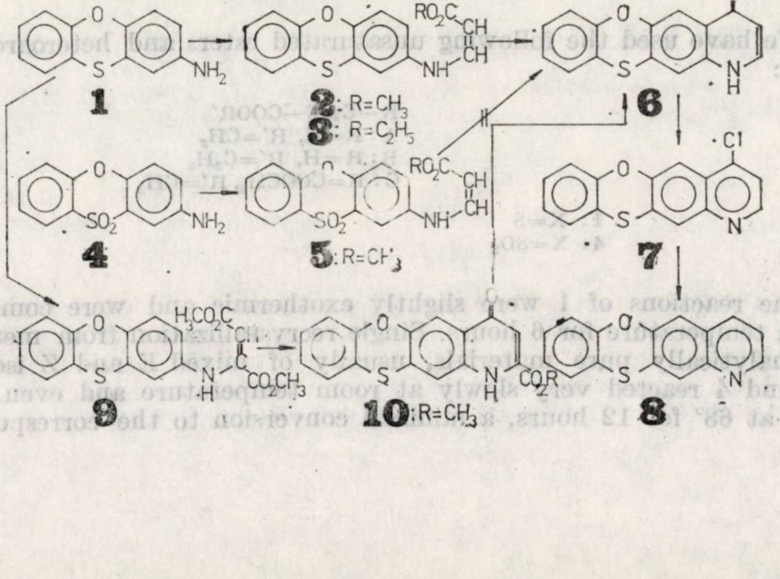

The proposed structure for **6** was also confirmed by another synthesis, using dimethyl acetylenedicarboxylate (Chart 1). The products prepared through these two different methods are listed in Table 1.

Table 1

Enamines and pyrido [2,3-b]phenoxatiin derivatives

Compound	Yield %	M.P.°C	Recrystallization solvent*
2	93	104–105	Methanol or *
3	91	108–110	Methanol
5	42	169–170	Isopropanol
6	89	244–245	Acetone-water or *
7	65	161–162	Acetic acid
8	60	122–123	Ethanol
9	67	215.5–216.5	Ethanol-diethyl ether
10	48	273–274	Chloroform
			(*or: chromatography on neutral Al_2O_3 with petroleum ether-diethyl ether 3 : 1 as eluent)

EXPERIMENTAL

Melting points were determined in open capillaries and are uncorrected. ^{1}H-NMR spectra were recorded on a Varian A-60 A spectrometer. IR spectra were taken on a C. Zeiss Jena UR 20 spectrophotometer. Ethyl propynoate is commercially available from Fluka AG.

Synthesis of ethyl 3-N-(2-phenoxatiinyl)-amino acrylate 3

To a solution of 2-aminophenoxatiin **1** (2.15 g, 0.01 mole) in 15 mL of methanol 0.98 g (0.01 mole) ethyl propynoate were added, then the mixture left at room temperature for 6 hours; after filtration and drying the precipitated solid, **3**, 2.84 g (91% yield) was obtained. Recrystallization from methanol or column chromatography (neutral alumina, dichloromethane as eluent) gave 2.4 g of colorless crystals with m.p. 108–110°. With concd. sulphuric acid an orange color results. IR : 1200 (C–O–C), 1640 (C=C), 1700 (C=O), 3280 (NH) cm^{-1}. ^{1}H-NMR : 1.2–1.4 (t–CH_3) 4–4.4 (q, –CH_2–), 4.75–4.95 (d, C=CH–$COOC_2H_5$) and 6.4–7.3 (aromatic protons) ppm.

Anal. Found : C, 65.59 ; H, 4.68 ; N, 4.45 ; S, 9.95% ; Calcd. for $C_{17}H_{15}NO_3S$: C, 65.14 ; H, 4.79 ; N, 4.47 ; S, 10.22%.

The same procedure was used for the preparation of **2** and **5** ; **5** needs 12 hours of heating at 68°.

Synthesis of pyrido[2-3,b]phenoxatiin-4-(1H)-one 6

Procedure A. A solution of **3**, 3.13 g (0.01 mole) in 80 mL of diphenyl ether is heated for 15 minutes at 250°. After cooling, the mixture is diluted with 250 mL of petroleum ether (b. p. 60–80°), the brown precipitate filtered, triturated with 2×100 mL petroleum ether and dried to give 1.08 g (40% yield) of **6**, with m.p. 236–240°. Analytically pure material, with m.p. 244–245° was obtained by chromatography over neutral alumina (petroleum ether-diethyl ether 3 : 1 as eluent) or by recrystallization from acetone-water ; a green fluorescence is obtained with concd. sulphuric acid. This procedure was applied for preparing **10**, with 48% yield.

Procedure B. A mixture of **3**,3.13 g (0.01 mole) and polyphosphate ester [18] (prepared from 10 g of phosphorus pentoxide 10 mL of diethyl ether and 20 mL of chloroform) is heated at reflux for one hour, then cooled, washed with 2×15 mL of 20% $NaHCO_3$ solution, 3×5 mL water and dried over anhyd. Na_2SO_4. The solvent was evaporated *in vacuo* and the residual yellow solid (2.4 g, 89%) crystallized from acetone-water and dried to give a light yellow mass of crystals weighting 2.18 g, m.p. 244–245°.

Procedure C. A mixture of **8**, 3.25 g (0. 01 mole) and 0.6 g NaOH in 15 mL ethylenglycole is stirred at reflux for 6 hours; after cooling, the solution is poured in 50 mL water and extracted with 2 × 40 mL diethyl ether. The ethereal extracts were washed with 10 mL water, 10 mL 10% HCl solution, 2 × 10 mL water, dried over anhyd. sodium sulphate and evaporated *in vacuo* to give 1.25 g (48%) of impure **6**, m.p. 237—241°; purification is made as described above. IR (KBr) : 868 (1,2,4,5-tetrasubstituted benzene ring), 1700(CO), 3290(NH) cm^{-1}; ^1H-NMR ($CDCl_3$, δ) : 4.8—4.7 (d, vinylic protons), 6.8—7.3 (aromatic protons).

Anal. Found : C, 67.60 ; H, 3.29 ; N, 5.55 ; S, 12.18% ; Calcd. for $C_{15}H_9NO_2S$: C, 67.41 ; H, 3.37 ; N, 5.24 ; S, 11.99%.

Synthesis of 4-chloro-pyrido[2,3-b]phenoxatiin 7

To a solution of **6**, 2.67 g (0.01 mole) in 12 mL of phosphorus oxychloride 0.5 mL of dimethylformamide were added and the mixture brought to reflux ; after one hour the clear solution was cooled and poured under stirring to 45 mL of 15% NH_4OH solution at 0—5°. The precipitated solid was filtered, washed with water, air-dried and recrystallized from acetic acid ; yield 1.85 g (65%) of product melting at 161—162° (violet-red color with concd. sulphuric acid). IR (KBr) : 690 (C—Cl), 870 cm^{-1} (tetrasubstituted benzene, 1, 2, 4, 5) ; no C=O band noticed.

Anal. Found : N, 5.03 ; S, 11.41% ; Calcd. for $C_{15}H_8NOCl$: N, 4.89 ; S, 11.20%.

Synthesis of pyrido[2,3-b]phenoxatiin 8

A mixture of **7**, 4.27 g (16.8 mmoles) and 1 g (0.0153 g atoms) of mossy zinc in 20 mL of glacial acetic acid is heated under efficient stirring at 90—95° for two hours, when another portion of zinc is added (0.5 g — 0.00765 g atoms) and the stirring and heating are continued for 2.5 hours. The reaction mixture was cooled, filtered and the filtrate diluted with 20 mL water under stirring and cooling (0—10°). The separated solid was collected by filtration, washed with water and air-dried giving 2.25 g of **8**. Recrystallization from ethanol afforded pure material with m.p. 122—123°. A light blue color was obtained with concd. sulphuric acid.

IR (KBr) : 756, 810, 868, 1370, 1450, 1470, 1580 (aromatic C—C and C—H) and 1200 (C—O—C) cm^{-1}.

^1H-NMR : 6.3—7.3 ppm (m, aromatic protons).

Anal. Found : C, 71.98 ; H, 3.91 ; N, 5.35 ; S, 12.48% ; Calcd. for $C_{15}H_9NOS$: C, 71.71 ; H, 3.58 ; N, 5.57 ; S, 12.74%.

Synthesis of dimethyl 2-N(2-phenoxatiinyl)-aminofumarate 9

A mixture of **1**, 4.30 g (0.02 mole) of and 1.2 g (0.02 mole) of dimethyl acetylenedicarboxylate in 90 mL methanol was heated at reflux temperature for 12—14 hours. Concentration *in vacuo* near dryness, below 45°, cooling, filtering and drying afforded 3.8 g (67% yield) of solid material ; recrystallization from ether-ethanol gave 3.2 g of white crystals of **9**, melting at 215.5—216.5° (deep blue color with concd. sulfuric acid). IR (KBr) : 1210 (C—O—C), 1630 (C=C) and 1690 (C=O) cm^{-1}.

Anal. Found : N, 4.13 ; S, 8.66% ; Calcd. for $C_{18}H_{15}NO_5S$: N, 3.90 ; S, 8.91%

REFERENCES

[1] D. S. Breslow and H. Skolnik, "Multi-sulphur and Sulphur and Oxygen Five and Six Membered Heterocycles", Interscience Publishers, New York, 1966.

[2] O. Maior, *Rev. Chim. (Bucureşti)*, **17**, 104 (1966).

[3] A. N. Grinev, *Khim. farm. Zhur.*, **7** (5), 5 (1973).

[4] G. N. Hamor, *J. Med. Chem.*, **15**, 215 (1972) and C. J. Paget and E. M. Dennis, *J. Med. Chem.*, **13**, 620 (1970).

[5] D. Sengupta, N. Anand, *Indian J. Chem.*, **25B**, 72 (1986).

[6] F. Martin, *J. Amer. Chem. Soc.*, **108**, 181 (1986).

[7] V. M. Anthony, J. M. Clough, J. M. Godfrey, P.L.C/*Eur. Patent* 270, 252 (1988) ; *Chem. Abstr.*, **110**, 39009 (1989).

[8] B. D. Palmer, M. Boyd, W. A. Denny, *J. Org. Chem.*, **55**, 438 (1990).

[9] J. Buchi, "Grundlagen der Arzneimittelforschung und der synthetischen Arzneimittel", Birkhauser Verlag, Basel, 1963.

[10] C. H. Sternbach, L. O. Randall and S. R. Gustavson, "Psychopharmacological Agents", M. Gordon Ed., Academic Press, New York, 1964.

[11] F. W. Gray, H. Mosher, F. C. Whitmore and T. S. Oakland, *J. Amer. Chem. Soc.*, **73**, 3577 (1951) and N. D. Heindel, T. A. Brodof and J. E. Kogelschatz, *J. Heterocyclic Chem.*, **3**, 22 (1967).

[12] E. Taylor and N. D. Heindel, *J. Org. Chem.*, **22**, 3339 (1967).

[13] N. D. Heindel, I. Bechara, P. Kennewell, J. Molnar, C. Ohnmacht, S. Lemke and T. Lemke, *J. Med. Chem.*, **17**, 685 (1974).

[14] A. W. Johnson, "The Chemistry of Acetylene Compounds", vol. 2, Longmans Green Ed., New York, 1950.

[15] N. D. Heindel, P. Kennewell and V. B. Fish, *J. Heterocyclic Chem.*, **6**, 77 (1969).

[16] R. Huisgen, K. Herbig, A. Siegel and H. Huber, *Chem. Ber.*, **99**, 2526 (1969) and J. E. Dolfini, *J. Org. Chem.*, **30**, 1298 (1965).

[17] R. C. Price, R. H. Reitsema and A. Leonard, *J. Amer. Chem. Soc.*, **68**, 1256 (1946).

[18] M. Fieser and L. E. Fieser, "Reagents for Organic Synthesis", vol. 1, Wiley Interscience New York, 1967, p. 892.

Revue Roumaine de Chimie, **36**, *4–7*, 721–726 (1991)

Herrn Professor Dr. A. T. BALABAN
zum 60. Geburtstag gewidmet

FUNKTIONSDERIVATE EINIGER MIT FERROCEN S-MODIFIZIERTEN THIOGLYKOLSAUREN

D. SCUTARU,[a] I. MAZILU,[a] M. VÂȚĂ,[a] LUCIA TĂTARU,[a] TATIANA LIXANDRU[a] und V. BĂRBOIU[b]

[a] Department of Organic Chemistry, Polytechnic Institute of Jassy, Bdul M. Eminescu Nr. 11, 6600 Jassy (Romania)

[b] Institut für Makromolekulare Chemie „P. Poni“, Jassy

Eingegangen am Januar 25. 1991

Es wurden 11 neue Methylester und 11 neue Hydrazide einiger mit Ferrocen S-modifizierten Thioglykolsäuren synthetisiert. Die erhaltenen Ester wurden durch IR Spektroskopie charakterisiert. Die Struktur der Hydrazide wurde mittels IR Spektralanalyse bestätigt sowie auch durch die Charakterisierung der Hydrazone, die durch die Reaktion mit Azeton erhalten wurden (Schmp., IR, ^{1}H-NMR).

Eleven new methyl esters and eleven new hydrazines of ferrocen-S-modified thioglycolacids were synthesized and characterized by IR spectroscopy. The structures of hydrazines were also confirmed by characterization of their corresponding hydrazones obtained through reaction with acetone (m.p.; IR; ^{1}H-NMR).

EINLEITUNG

In den letzten Jahren wurde der Herstellung einiger mit Ferrocen S-modifizierten Thioglykolsäuren eine besondere Aufmerksamkeit geschenkt, durch die Reaktion einiger Mono- und Di-α-hydroxylierten Ferrocen-Derivate mit der Thioglykolsäure in Anwesenheit von Trifluoressigsäure.[1,2] Die erhaltenen Verbindungen haben sich als sehr nützlich bewiesen zur Synthese einiger Ferrocenderivate,[3] für die Trennung einiger razemischen Gemische, zur Synthese einiger biologisch aktiven Verbindungen,[5] zum Studium der Mechanismen der nukleophilen Substitution,[4,6] usw.

ERGEBNISSE UND DISKUSSION

Die durchgeführten Untersuchungen haben die Synthese und Charakterisierung der Methylester und Hydrazide einiger mit Ferrocen S-modifizierten Thioglykolsäuren (I, II) verfolgt, zwecks Verwendung der erhaltenen Hydrazide zur Synthese von Riphamicinen mit Ferrocen.

Wegen den angetroffenen Schwierigkeiten bei der Verwendung der klassischen Synthesemethoden der Methylester wurde die Methylierung durch die Behandlung der Säuren I und II mit Diazomethan oder Methylchloroformiat realisiert.

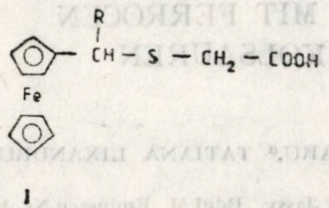
I

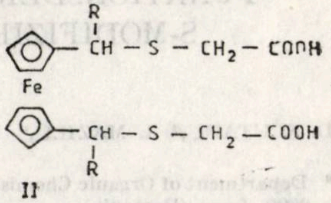
II

I. R = $-H$, $-CH_3$, $-C_2H_5$, $-C_3H_7$, $-CH(CH_3)_2$, $-C_6H_5$;
II. R = $-CH_3$, $-C_2H_5$, $-C_3H_7$, $-CH(CH_3)_2$, $-C_6H_5$.

Die Anwendung dieser Synthesevarianten hat sich als vorteilhaft erwiesen in Bezug auf die Ausbeute (über 80%), die Reinheit der Produkte (totale Umwandlung), die kurze Reaktionsdauer und die Einfachheit.

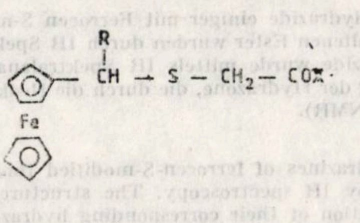
IIIa , IIIb , IIIc

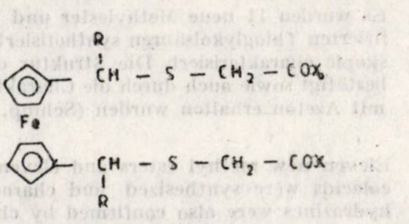
IVa , IVb , IVc

IIIa : $R = -H, -CH_3, -C_2H_5, -C_3H_7, -CH(CH_3)_2, -C_6H_5, X = -OCH_3$;
IVa : $R = -CH_5, -C_2H_5, -C_3H_7, -CH(CH_3)_2, -C_3H_5, X = -OCH_3$;
IIIb : $R = -H, -CH_3, -C_2H_5, -C_3H_7, -CH(CH_3)_2, -C_6H_5, X = -NH-NH_2$;
IVb : $R = -CH_3, -C_2H_5, -C_3H_7, -CH(CH_3)_2, -C_6H_5, X = -NH-NH_2$;
IIIc : $R = -H, -CH_3, -C_2H_5, -C_3H_7, -CH(CH_3)_2, -C_6H_5, X = -NH-N{=}C\Big\langle{}^{CH_3}_{CH_3}$
IVc : $R = -CH_3, -C_2H_5, -C_3H_7, -CH(CH_3)_2, -C_6H_5, X = -NH-N{=}C\Big\langle{}^{CH_3}_{CH_3}$

Die Umformung der Säuren I und II in die entsprechenden Methylester IIIa und IVa wurde durch Dünnschichtchromatographie (Benzol : Essigsäure 9 : 1 vol/vol) verfolgt.

Die erhaltenen Ester, mit Ausnahme der Fälle $R = -H$ und $-CH_3$, sind ölige Produkte. Ihre Charakterisierung wurde mittels der IR-Spektren realisiert. Tabelle 1 gibt die hauptsächlichen Charakteristiken der synthetisierten Ester wider.

Die den Strukturen vom Typ IIIb und IVb entsprechenden Hydraside sind von öliger Konsistenz und wurden gemäss der bekannten Synthesemethoden, [7] durch Hydrazinolyse der Methylester IIIa und IVa, hergestellt.

Wegen dem Vorhandensein der polaren Gruppe $-CO-NH-NH_2$ konnte die Reinigung durch Säulenchromatographie nicht befriedigend

Tabelle 1

Die hauptsächlichen Charakteristiken der Methylester der S-modifizierten Thioglykolsäuren

Lfd. Nr.	Radikal R	Ausbeute (%)		Charakteristiken (Schmp. °C, Aspekt)	IR Absorption (cm^{-1})		R_f-Werte	
		Methode A	Methode B		C=O	C—S—C	Säure	Ester
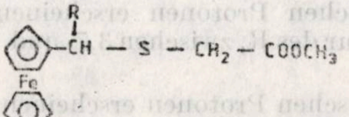								
1	—H	91	85	57—58	1735	700	0,39	0,52
2	$-CH_3$	87	86	53—55	1730	695	0,35	0,47
3	$-C_2H_5$	78	83	ölig	1740	685	0,38	0,53
4	$-C_3H_7$	85	89	ölig	1745	690	0,35	0,50
5	$-CH(CH_3)_2$	89	84	ölig	1740	690	0,37	0,46
6	$-C_6H_5$	90	87	ölig	1740	680	0,37	0,49
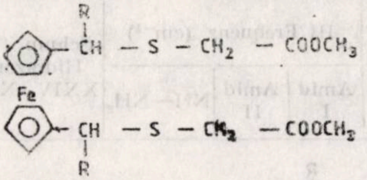								
7	$-CH_3$	91	89	ölig	1740	685	0,19	0,35
8	$-C_2H_5$	79	81	ölig	1740	690	0,24	0,39
9	$-C_3H_7$	85	85	ölig	1745	690	0,26	0,42
10	$-CH(CH_3)_2$	92	89	ölig	1735	695	0,28	0,38
11	$-C_6H_5$	85	83	ölig	1740	680	0,25	0,37

durchgeführt werden. Die Produkte wurden durch die Umwandlung der Hydrazide IIIb und IVb mittels Azeton in die entsprechenden Hydrazone IIIc und IVc gereinigt.

Die Hydrazone IIIc und IVc sind kristalline Substanzen mit eindeutigen Schmelzpunkten, leicht zu reinigen durch Rekristallisation aus Methanol oder mittels Säulenchromatographie (Al_2O_3/Azeton).

Die Hydrazide IIIb und IVb wurden durch die saure Hydrolyse der Hydrazone IIIc und IVc erhalten.

Die Bestätigung der Struktur der Hydrazide wurde mittels IR-Spektroskopie realisiert und durch die Charakterisierung der entsprechenden Hydrazone (Schmelzpunkte, Elementaranalyse, IR und ^{1}H-NMR).

Der Vergleich der IR-Spektren der Hydrazide und Hydrazone hat die differentiale Zuteilung der für νNH und νNH_2 charakteristischen Bänder erlaubt. Somit kann man in den IR-Spektren der Hydrazide IIIb und IVb zwei Bänder bei etwa 3300 cm^{-1} bzw. 3390 cm^{-1} hervorheben, während die Spektren der entsprechenden Hydrazone eine einzige Absorption bei etwa 3320 cm^{-1} aufweisen. Durch Vergleich wurde das Band mit niederer Frequenz der Valenzvibration νNH und jenes mit höherer Frequenz der Valenzvibration νNH_2 zugewiesen.

Die ^1H-NMR Spektren weisen eine Reihe von gemeinsamen Charakteristiken auf :

1. Die Protonen des Ferrocenyl- oder 1,1'-Ferrocenylen-Radikals erscheinen undifferenziert, als ein Singlet bei etwa 4,1 ppm.

2. Die methynischen Protonen erscheinen mit Vervielfachungen, abhängig von der Natur des R, zwischen 3,7 und 3,9 ppm (für $R = -C_6H_5$, $\delta = 5{,}08$ ppm).

3. Die methylenischen Protonen erscheinen als ein Singlet zwischen 3,26 und 3,5 ppm. Im allgemeinen, erscheinen sie bei δ-Werten, die um cca 0,15 ppm grösser sind als jene der entsprechenden Säuren,[2] als Folge einer von der Funktion $-CONH-N=C(CH_3)_2$ ausgeübten betonteren Entschirmung im Vergleich zu $-COOH$.

Tabelle 2

Charakteristiken der Hydrazide der S-modifizierten Thioglykolsäuren

Lfd. Nr.	Radikal		IR Frequenz (cm^{-1})			Schmp. (°C) Hidrazone XXIV, XXV	R_f-Werte		
	R	(%)	Amid I	Amid II	$NH-NH_2$		Ester	Hydrazid	Hydrazon
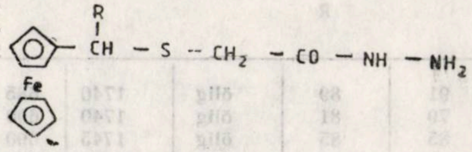									
1	$-H$	85,6	1645	1550	3225	103–105	0,95	0,86	0,91
2	$-CH_3$	80,4	1645	1530	3220	98–99	0,94	0,87	0,91
3	$-C_2H_5$	85,3	1670	1560	3250	119–121	0,92	0,86	0,93
4	$-C_3H_7$	82,7	1650	1525	3270	127–129	0,93	0,84	0,89
5	$-CH(CH_3)_2$	91,0	1660	1520	3300	123–124	0,95	0,87	0,90
6	$-C_6H_5$	79,4	1650	1550	3350	142–144	0,95	0,86	0,91
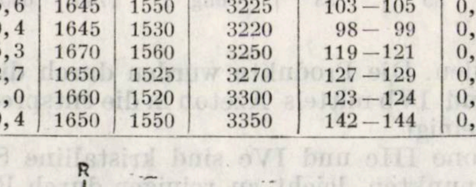									
7	$-CH_3$	72,4	1670	1535	3300	121–122	0,78	0,65	0,70
8	$-C_2H_5$	65,3	1650	1530	3270	117–118	0,77	0,68	0,71
9	$-C_3H_7$	81,4	1660	1530	3300	113–115	0,69	0,58	0,65
10	$-CH(CH_3)_2$	79,8	1650	1540	3250	108–109	0,81	0,66	0,74
11	$-C_6H_5$	60,0	1670	1550	3260	161–164	0,72	0,63	0,66

4. Die Methylgruppen des Isopropyliden-Radikals weisen jede ein Singlet auf als Folge der chemischen und magnetischen Unäquivalenz. In Analogie zu den chemischen Verschiebungen einiger verwandten Strukturen, wurde der kleinere δ-Wert der Gruppe $-CH_3$ „sin“ und der grösste der Gruppe $-CH_3$ „anti“ zugewiesen.

Die hauptsächlichen Charakteristiken der Hydrazide und Hydrazone sind in Tabelle 2 dargestellt.

EXPERIMENTELLER TEIL

Apparatur

Die ^{1}H-NMR Spektren wurden in DMSO bei 90°C mit einem Jeol 60 MHz Apparat aufgezeichnet; Die IR-Spektren wurden in $CHCl_3$ mit einem Spektrometer UR 20, Carl Zeiss Jena verzeichnet. Die Schmelzpunkte wurden mit einem Apparat Böetius bestimmt und sind nicht korrigiert. Der Reinheitsgrad der erhaltenen Verbindungen wurde durch Dünnschichtchromatographie auf Silikagel FG-254 geschätzt.

Reagenzien

Die Säuren vom Typ I und II wurden aus den entsprechenden Hydroxylverbindungen durch die Reaktion mit der Thioglykolsäure in Anwesenheit von Trifluoressigsäure [1,2] hergestellt

Synthesemethoden

1. Synthese der Methylester

1a mit Diazomethan

Zu einer Lösung, die 0,01 Mol saure Komponente I oder II in 100 mL wasserfreiem Äthyläther enthält, auf 0–5°C gekühlt, wird in Portionen (2—3 mL) eine ätherische Lösung von Diazomethan hinzugefügt bis chromatographisch (Benzol: Essigsäure 9 : 1) festgestellt wird, dass die Säure komplett umgewandelt ist. Die Reaktionsmasse wird bis zur Trockenheit konzentriert und der rohe Ester wird durch Säulenchromatographie (Al_2O_3/Benzol) gereinigt.

1b mit Methyl-Chloroformiat

Die saure Komponente I oder II (0,01 Mol) wird in 50 mL wasserfreiem CH_2Cl_2 gelöst; es werden 0,021 Mol Triäthylamin für jede Carboxylgruppe dazugegeben, es wird auf − 10°C gekühlt und dann werden 0,011 Mol Methylchloroformiat für jede Carboxylgruppe hinzugefügt. Die chromatographische Überwachung (Benzol: Essigsäure 9 : 1) gibt die totale Umformung der Säure nach 15 Minuten an.

Die Reaktionsmasse wird mit 3 × 15 mL Wasser ausgewaschen, auf $MgSO_4$ anhydrisiert und bis zur Trockenheit konzentriert. Die Reinigung wurde wie bei der Methode mit Diazomethan durchgeführt.

2. Die Synthese der Hydraside

Es werden 0,01 Mol Methylester IIIa oder IVa in 30 mL absolutem Methanol gelöst’ es werden 0,05 Mol Hydrazinhydrat für jede Estergruppe hinzugefügt und dann wird 2 Stunden mit Rückfluss gekocht. Die totale Umwandlung des Esters wird chromatographisch (Chloroform : Methanol 9 : 1) überwacht; Es werden 30 mL Wasser dazugegeben und es die ölige Komponente wird mit 3 × 20 mL CH_2Cl_2 extrahiert.

Die organische Phase wird mit 3 × 20 mL Wasser gewaschen, auf $MgSO_4$ anhydrisiert und bis zur Trockenheit konzentriert. Es werden die Hydrazide vom Typ IIIb und IVb als ölige Produkte erhalten.

Die erhaltenen Hydrazide werden in 20 mL wasserfreiem Azeton gelöst. Nach 30 min. wird die Lösung bis zur Trockenheit verdampft, die erhaltenen Hydrazone werden durch Säulenchromatographie (Al_2O_3/Azeton) gereinigt oder aus Methanol rekristallisiert. Die gereinigten Hydrazone wurden in 30 mL 80%-igem Methanol gelöst, es werden einige Tropfen Essigsäure dazugegeben und 60 min. auf 60°C erwärmt. Das Ende der Hydrolyse wird chromatographisch überwacht. Die Reaktionsmasse wird mit einer gesättigten Na_2CO_3 Lösung neutralisiert, mit 3×20 mL CH_2Cl_2 extrahiert. Die organische Phase wird mit 3×20 mL Wasser gewaschen, auf $MgSO_4$ anhydrisiert und bis zur Trockenheit konzentriert. Somit werden die Hydrazide IIIb und IVb in reinem Zustand erhalten.

LITERATURVERZEICHNIS

[1] A. Ratajczak, B. Czech und B. Misterkiewicz, *Bull. Acad. Polon. Sci., Sër. Chim.*, XXV, 541 (1977).

[2] D. Scutaru, I. Mazilu, L. Tătaru, T. Lixandru und Cr. Simionescu, *J. Organomet. Chem.*, **373**, 245 (1989).

[3] A. Ratajczak und B. Misterkiewicz, *J. Organomet. Chem.*, **91**, 73 (1975).

[4] A. Ratajczak und B. Misterkiewicz, *Chem. and Ind.*, **16**, 903 (1976).

[5] Unpublished results from this laboratory.

[6] D. Scutaru, L. Tătaru, I. Mazilu, B. Scutaru, T. Lixandru and Cr. Simionescu, *J. Organomet. Chem.*, **378**, 99 (1989).

[7] „Organicum", Ed. Ştiinţifică şi Enciclopedică, Bucharest, 1982, p. 447.

Revue Roumaine de Chimie, **36**, *4*–7, 727–732 (1991)

Dedicated to Prof. ALEXANDRU T. BALABAN
on the occasion of his 60th anniversary

CARBONIC ANHYDRASE INHIBITORS. 6[1]

NOVEL COORDINATION COMPOUNDS OF Pd(II), Pt(II) AND Ni(II) WITH 6-ETHOXY-BENZOTHIAZOLE-2-SULFONAMIDE

MARIUS ANDRUH,[a,*] ELENA CRISTUREAN,[a] RALUCA ŞTEFAN[a] and CLAUDIU T. SUPURAN[b,*]

University of Bucharest, Inorganic Chemistry Laboratory, Dumbrava Roşie 23, Bucharest, Romania

University of Bucharest, Department of Organic Chemistry, Bd. Republicii 13, Bucharest 1, Romania

Received December 23, 1990

Coordination compounds of Pd(II), Pt(II) and Ni(II) with 6-ethoxy-benzothiazole-2-sulfonamide (ethoxzolamide) were prepared and characterized by elemental chemical analysis, infrared and UV–VIS spectroscopy as well as magnetic measurements (for the Ni(II) complex). The three compounds proved to be strong inhibitors of red cell bovine carbonic anhydrase.

1. INTRODUCTION

In addition to classical carbonic anhydrase (CA) inhibitors, i.e., monovalent anions [2,3] and aromatic/heterocyclic sulfonamides,[4-6] we recently reported that Cu(II), Zn(II), Ag(I) and Ni(II) coordination compounds with heterocyclic sulfonamides as ligands act as powerful inhibitors of this enzyme.[7,8] Novel types of CA inhibitors are constantly designed and extensively studied, in the search for new drugs,[9] devoid of severe side-effects, and in order to elucidate the mechanism of CA catalysis and inhibition.[10-12] Such efforts have led to the recent discovery of topical CA inhibitors, successfully used in the management of glaucoma.[13-15] One such compound, MK-927 (**1**) [14a] was already evaluated in clinical trials,[16] and will be soon available as a new drug for the treatment of open-angle glaucoma (and eventually other CA-mediated disturbances), together with the now classical CA inhibitors, acetazolamide (5-acetamido-1,3,4-thiadiazole-2-sulfonamide, **2**) and ethoxzolamide (6-ethoxybenzothiazole-2-sulfonamide, **3**).

---

* To whom correspondence should be addressed.

In this paper we extend the previous studies of metal complexes as CA inhibitors, and report the preparation of coordination compounds of Ni(II), Pd(II) and Pt(II) with ethoxzolamide (**3**) as ligand. We focused our interest on this ligand, because it is one of the strongest CA inhibitors in clinical use;[6] on the other hand, we extended the range of complexating cations to Pd(II) and Pt(II), because of the well-known therapeutic use of some of their coordination compounds: cisplatin (*cis*-diamminodichloroplatinum(II)) was identified by Rosenberg et al.[17] as a powerful cytotoxic agent, being currently used in the treatment of certain neoplastic diseases.[18] Although a large number of Pt(II) coordination compounds were prepared thereafter, containing di- or tricarboxylic acids, diamines and aminoacids as ligands,[19] sulfonamides were not included in such studies, probably due to their known lower coordinating ability.[20] These facts, correlated with the recent finding of enhanced expression of CA activity in mixed tumours of skin (of eccrine gland origin) and major salivary glands (pleomorphic adenoma),[21] prompted us to prepare compounds possessing both inhibitory action on CA (due to sulfonamido ligands) and cytotoxic activity, due to the presence of heavy metal ions, such as Pt(II) or Pd(II). Such compounds might be useful candidates for studying different CA-mediated abnormal physiological conditions.

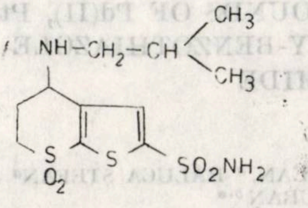
MK-927

1

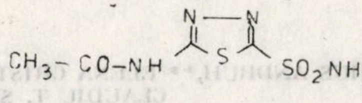
AAZ

2

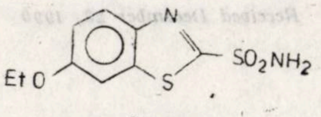
EZA

3

2. EXPERIMENTAL

The following complexes were synthesized and characterized: $[Ni(EZA)(H_2O)_2(OH)]_2 \cdot 6\,H_2O$ (green), $[Pd(EZA)Cl_2]$ (yellow) and $[Pt(EZA)Cl]_2$ (brown); in the above formulas, EZA means the corresponding anion of ethoxzolamide, excepting the palladium compound where ethoxzolamide acts as a neutral ligand. The nickel (II) complex has been synthesized according to the general procedure reported elsewhere.[7] Palladium (II) and platinum (II) complexes were prepared by treating aqueous solutions of $Na_2[PdCl_4]$ or $Na_2[PtCl_4]$ with a methanolic solution containing the ionized sulfonamide (in M^{2+} : EZA molar ratio of 1 : 1). The resulting mixtures were heated for 30 minutes on a water bath. The complexes precipitated from these solutions were filtered off, washed with water and methanol, and dried *in vacuo*. The results of elemental chemical analyses (metal, C, H, N, S) are in satisfactory agreement with the proposed formulas.

The electronic spectra were recorded by diffuse reflectance technique using MgO as reference material. Infrared spectra were recorded in KBr pellets, with a Specord IR-71 spectrophotometer. The magnetic measurements for the Ni(II) complex were performed according to Faraday's method at room temperature, using $Hg[Co(NCS)_4]$ as standard.

Ethoxzolamide was prepared by literature procedures.[22]

Inhibitors were tested at 4°C, using the micromethod of Maren and the substrate-enzyme-inhibitor technique,[23] as reported previously.[7,8] I_{50} values represent molar concentrations of inhibitor reducing the specific activity of enzyme with 50%, in the CO_2 hydration reaction. Stock solutions of inhibitor (10^{-3} M) were prepared in 50% (v/v) aqueous DMSO (Merck) and dilutions obtained thereafter with distilled deionized water. Bovine red cell CA was from Boehringer Mannheim.

Nickel (II) complex : IR(KBr) : 450, 530, 580, 650, 740, 840, 950, 1000, 1040, 1060, 1100, 1270, 1340, 1400, 1500, 1600, 2080, 3290, 3320 cm^{-1} ; analysis : found, Ni, 14.50, N, 6.76, S, 15.48%. $Ni_2C_{18}H_{40}N_4S_4O_{18}$ requires : Ni, 14.56, N, 6.91, S, 15.8%.

Palladium(II) complex : IR(KBr) : 420, 520, 560, 610, 750, 810, 890, 920, 1040, 1090, 1150, 1220, 1250, 1320, 1370, 1470, 1600, 2920, 2980 cm^{-1} ; analysis : found, Pd, 24.18, C, 25.20, H, 2.60, N, 6.40%. $PdC_9H_{10}N_2S_2Cl_2O_3$ requires : Pd, 24.43, C, 24.80, H, 2.29, N, 6.43%.

Platinum(II) complex : IR(KBr) : 420, 520, 610, 700, 750, 810, 920, 980, 1030, 1070, 1150, 1220, 1250, 1320, 1380, 1460, 1620, 2920, 2980 cm^{-1}; analysis : found, Pt, 39.21, C, 21.99, H, 2.43, N, 6.04%. $Pt_2C_{18}H_{18}N_4S_4Cl_2O_6$ requires : Pt, 39.94, C, 22.09, H, 1.84, N, 5.72%.

3. RESULTS AND DISCUSSION

According to the stoichiometry of the complex compounds synthesized, one may suppose that both ethoxzolamide and its anion act as bidentate ligands.

Generally speaking, nickel(II) complexes may have various stereochemistries : octahedral, square-planar and rarely, tetrahedral or other. The electronic spectrum of the complex $[Ni(EZA)(OH)(H_2O)_2]_2 \cdot 6\,H_2O$ clearly indicates a (pseudo)octahedral configuration of Ni(II) ions (Fig.1) ; the hexacoordination of nickel(II) is achieved most probably in a binuclear unit with two OH bridges.[24] It is interesting to note that the similar

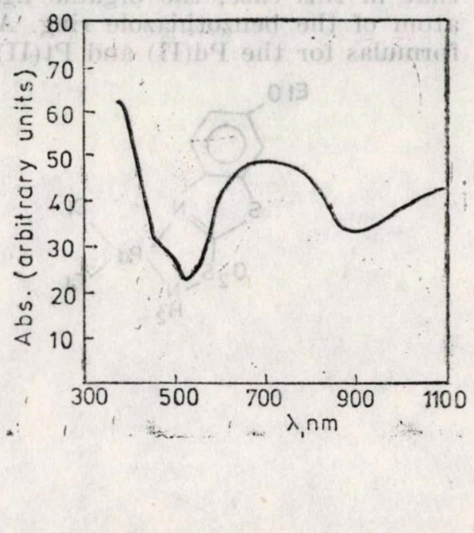

Fig. 1 — The diffuse reflectance electronic spectrum of compound $[Ni(EZA)(OH)(H_2O)_2]_2 \cdot 6H_2O$. The absorption bands are assigned to the following transitions : ${}^3A_{2g} \rightarrow {}^3T_{2g}$ (~1100 nm) and ${}^3A_{2g} \rightarrow {}^3T_{1g}$ (~700 nm).

compound, containing the anion of acetazolamide (2), AAZ,[7] [Ni(AAZ)(OH)$(H_2O)_2]_2 \cdot 6\,H_2O$, has the same stoichiometry and, probably, the same binuclear structure. We suppose also that the anion of ethoxzolamide interacts with nickel(II) ion through the nitrogen atom of the SO_2NH^- group, as well as with the neighbouring nitrogen atom, N-3, from the heterocyclic ring. This interaction with the metal ion has no special steric requirements. In this complex, two water molecules are also coordinated :

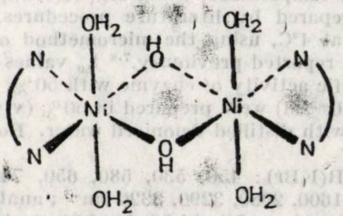

The hexacoordination of Ni(II) ions in such a structure is confirmed also by magnetic measurements : the value of the effective magnetic moment was found to be 3.33 MB at 20°C.

The other two complexes, $[Pd(EZA)Cl_2]$ and $[Pt(EZA)Cl]_2$, are most probably square-planar, in agreement with the well-known stereochemical preferences of Pd(II) and Pt(II) ions.

The IR spectra of the three coordination compounds display the characteristic frequencies of the organic molecule acting as ligand ; some of these are as follows :

	ν_{as-SO_2}	ν_{sym-SO_2}	(cm^{-1})
EZA	1370	1180	
$[Ni(EZA)(OH)(H_2O)_2]_2$	1280	1130	
$[Pd(EZA)Cl_2]$	1320	1150	
$[Pt(EZA)Cl]_2$	1320	1150	

The mentioned bands are slightly shifted at lower frequencies comparatively with the free organic ligand.

In the 650—750 cm⁻¹ region of the IR spectrum of the Pt(II) complex, the C—S bands of the benzothiazole ring are modified, as compared to the corresponding bands in the free ligand. This prompted us to conclude that in this case, the organic ligand coordinates through the sulphur atom of the benzothiazole ring. Accordingly, we propose the following formulas for the Pd(II) and Pt(II) complexes :

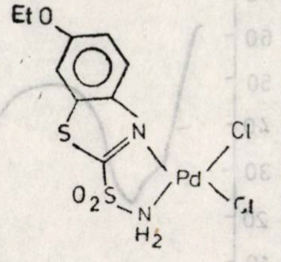

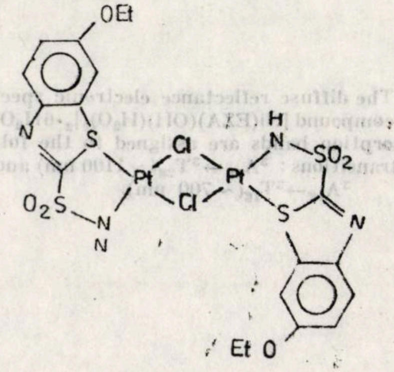

All the compounds reported in this paper proved to be strong CA inhibitors (Table 1), the most powerful being the palladium complex. Presently, they were not tested as cytotoxic agents, but work is in progress to establish whether they possess such properties.

Table 1

In vitro inhibition of CA by the new inhibitors and reference CA inhibitors

Compound	MK-927 (1)[a]	AAZ (2)[a]	EZA (3)[a]	Ni complex[b]	Pd complex[b]	Pt complex[b]
I_{50} (nM)	13	10	5	75	8	28

[a] Human CA II was used, and a pH-stat method (ref. 14c).

[b] Bovine red cell CA used, and the method of Maren[23] as described in the experimental part.

An important aspect in relation to these CA inhibitors is their mechanism of action, which is still unknown. We hypothesized earlier[8] that the strong inhibition observed with these compounds and the previously reported,[7] may arise as a result of the following processes: in dilute solution, in the assay system, the complex dissociates, forming sulfonamido anions and metal ions, which in turn, exert each one inhibitory action on the enzyme. As suggested by Lindskog,[25] the observed inhibition may be the sum of inhibition by free sulfonamide and free metal ions, but the possibility that more complicated processes occur, cannot be ruled out yet. Work is in progress to determine stability constants for these complexes, in conditions similar with those of the environment in the assay system.

ACKNOWLEDGMENTS. Thanks are addressed to professor Sven Lindskog (Univ. of Umeå) for helpful discussions, to dr. Michael F. Sugrue (Merck, Sharp and Dohme) for allowing us to use original data prior to their publication, and to Mr. Iuliu Ciupe for synthesizing the ethoxzolamide used in this work.

REFERENCES

[1] Part 5, C. T. Supuran, G. Manole, A. Dinculescu, A. Schiketanz, M. D. Gheorghiu, I. Pușcaș and A. T. Balaban, *J. Pharm. Sci.*, *in press.*

[2] T. H. Maren and C. E. Wiley, *J. Med. Chem.*, **11**, 228 (1968).

[3] T. H. Maren, C. S. Rayburn and N. E. Liddel, *Science*, **191**, 469 (1976).

[4] H. W. Davenport, *J. Biol. Chem.*, **158**, 567 (1945).

[5] H. A. Krebs, *Biochem. J.*, **43**, 525 (1948).

[6] T. H. Maren, *Physiol. Rev.*, **47**, 595 (1967).

[7] C. T. Supuran, M. Andruh and I. Pușcaș, *Rev. Roumaine Chim.*, **35**, 393 (1990).

[8] C. T. Supuran, G. Manole, I. C. Pușcaș, A. T. Balaban, M. D. Gheorghiu, A. Schiketanz, M. Andruh and I. Pușcaș, "New Types of Carbonic Anhydrase Inhibitors", *in* "Carbonic Anhydrase — From Biochemistry and Genetics to Physiology and Clinical Medicine", R. E. Forster and F. Botré Eds., Elsevier *(in press)*; Carbonic Anhydrase International Workshop, Spoleto, Italy, March 1990, Abstract Book pp. 128.

[9] S. Lindskog and P. J. Wistrand, "Inhibitors of Carbonic Anhydrase", *in* "Design of Enzyme Inhibitors as Drugs", M. Sandler Ed., Oxford Univ. Press, 1987.

[10] Y. Pocker and N. Janjič, *J. Amer. Chem. Soc.*, **111**, 731 (1989).

[11] R. G. Khalifah, *J. Biol. Chem.*, **246**, 2561 (1971).

[12] a) C. Tu, D. N. Silverman, C. Forsman, B. H. Jonsson and S Lindskog, *Biochem.*, **28**, 7913 (1989) ; b) G. Behravan, B. H. Jonsson and S. Lindskog, *Eur. J. Biochem.*, **190**, 351 (1990).

[13] a) T. H. Maren, L. Jankowska, G. Sanyal and H. F. Edelhauser, *Exp. Eye Res.*, **36**, 457 (1983) ; b) A. R. Katritzky, K. C. Kaster, T. H. Maren, C. W. Conroy and A. Bar-Ilan *J. Med. Chem.*, **30**, 2058 (1987).

[14] a) J. J. Baldwin, G. S. Ponticello, P. S. Anderson, M. E. Christy, M. A. Murcko, W. C. Randall, H. Schwam, M. F. Sugrue, J. P. Springer, P. Gautheron, J Grove, P. Mallorga, M.-P. Viader, B. M. McKeever and M. A. Navia, *J. Med. Chem.*, **32**, 2510 (1989) ; b) S. L. Graham, J. M. Hoffman, P. Gautheron, S. R. Michelson, T. H. Scholz, H. Schwam, K. L. Shepard, A. M. Smith, R. L. Smith, J. M. Sondey and M.F. Sugrue, *J. Med. Chem.*, **33**, 749 (1990) ; c) M. F. Sugrue, P. Gautheron, J. Grove, P. Mallorga, M.-P. Viader, H. Schwam, J. J. Baldwin, M. E. Christy and G. S. Ponticello, *J. Ocular Pharmacol.*, *in press*.

[15] R. F. Wang, J. B. Serle, S. M. Podos and M. F. Sugrue, *Arch. Ophthalmol.*, **108**, 511 (1990).

[16] T. H. Maren, A. Bar-Ilan, C. W. Conroy and W. F. Brechue, *Exp. Eye Res.*, **50**, 27 (1990).

[17] a) B. Rosenberg, L. VanCamp and T. Krigas, *Nature*, **205**, 698 (1960) ; b) B. Rosenberg, L. VanCamp, E. B. Grimley and A. J. Thomson, *J. Biol. Chem.*, **242**, 1347 (1967) ; c) B. Rosenberg, *Naturwissenschaften*, **60**, 349 (1973).

[18] P. Calabresi and R. E. Parks jr., "Antiproliferative Agents and Drugs Used for Immunosuppression" *in* "The Pharmacological Basis of Therapeutics", A. Goodman—Gilman et al. Eds., seventh edition, MacMillan Press, New York 1987, pp. 1247—1306.

[19] R. Böhm, *Pharmazie*, **42**, 793 (1987), and references cited therein.

[20] J. E. Coleman, *Ann. Rev. Pharmacol.*, **15**, 221 (1975).

[21] Y. Noda, Y. Takai, Y. Iwai, M. A. Meenaghan and M. Mori, *Virchows Arch. (Pathol. Anat.)*, **408**, 449 (1986).

[22] J. Korman, *J. Org. Chem.*, **23**, 1768 (1958).

[23] T. H. Maren, *J. Pharmacol. Exp. Ther.*, **130**, 26 (1960).

[24] We have not identified by elemental chemical analysis the presence of chloride ions.

[25] S. Lindskog, personal communication to C. T. Supuran.

Revue Roumaine de Chimie, 36, 4–7, 733–739 (1991)

Dedicated to Professor A. T. BALABAN
on the occasion of his 60th anniversary

PREPARATION AND EPR SPECTRA OF CAPTO-DATIVE N-ALKOXY-2,6-DINITRO-α,α,α-TRIFLUORO-p-TOLYL-AMINYLS

GABRIELA STĂNCIUC,[a] M. T. CĂPROIU,[a] AGNETA CARAGHEORGHEOPOL [b] and H. CĂLDĂRARU [b]

[a] Romanian Academy, Center of Organic Chemistry, Spl. Independenței 202B, 77208 Bucharest, Romania

[b] Romanian Academy, Institute of Physical Chemistry, Bucharest

Received February 15, 1991

N-Alkoxy-2,6-dinitro-α,α,α-trifluoro-p-tolyl aminyls (methoxy, ethoxy, isopropoxy and benzyloxy) were generated by oxidation of the corresponding secondary amines. Their well-resolved EPR spectra were interpreted by simulation and assigned. The results are in good agreement with those obtained for structurally related aminyl radicals.

INTRODUCTION

This paper reports the synthesis of N-alkoxy-2,6-dinitro-α,α,α-trifluoro-p-toluidines **2a**–**2d** which were converted by one-electron oxidation into the corresponding capto-dative aminyl radicals (Donor-$\dot{N}$-Acceptor), as single paramagnetic species:

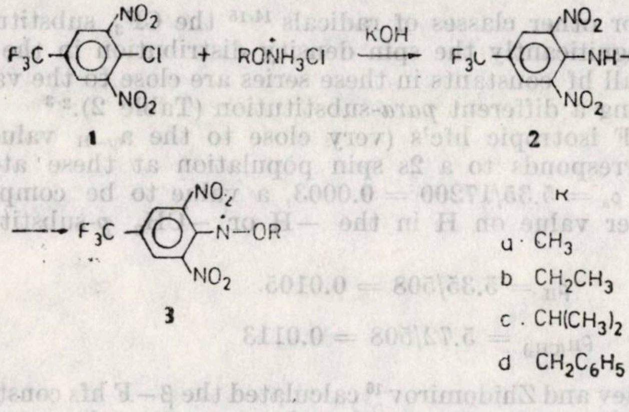

Scheme 1

The present work joins earlier investigations [1-3] to explore the effects of combining various donors (Don = $-NR_2$, $-OR$, donor-substituted aryl) with acceptors (Acc = $RCO-$, RSO_2-, $-CN$, acceptor-substituted aryl) on the properties of the aminyls Don-$\dot{N}$-Acc, started in 1967,[4] as part of efforts to obtain support for the concept of captodative stabilization.[5-13]

The present investigated Don-$\dot{N}$-Acc aminyls contain as strong acceptor a 2,6-dinitro-α,α,α-trifluoro-p-tolyl group, while the donor is an alkoxy (or benzyloxy) group.

The aminyls **3a**–**3d** were generated in toluene solution by oxidation of the corresponding toluidines **2a**–**2d** with partially decomposed lead tetraacetate. They could be detected in solution under static conditions, at room temperature by EPR spectroscopy.

EPR SPECTRA

The EPR spectra of aminyls **3a**–**3d** were completely interpreted by simulation and assigned on the basis of previous results.

The values of hyperfine splitting constants (hfc's) as well as their assignment are indicated in Table 1, and the experimental and simulated EPR spectra are presented in Figures 1–4.

Table 1

Hfc's (Gauss) of free radicals **3a**–**3d** obtained in toluene from **2a**–**2d** by oxidation with $Pb(OAc)_4$. In brackets the numbers of equivalent nuclei are shown.

Comp.	R	a_N	a_{NO_2}	a_F	$a_{(m-H)}$	$a_{\beta-H}$
3a	CH_3	9.57	0.77 (2)	5.35 (3)	1.65 (2)	3.47 (3)
3b	CH_2CH_3	9.44	0.81 (2)	5.40 (3)	1.54 (2)	3.17 (2)
3c	$CH(CH_3)_2$	9.96	0.87 (2)	5.35 (3)	1.66 (2)	2.48 (1)
3d	$CH_2C_6H_5$	9.58	0.85 (2)	5.36 (3)	1.62 (2)	2.97 (2)

As remarked for other classes of radicals [14,15] the CF_3 substitution does not influence signiticantly the spin density distribution in the rest of the radical; thus all hf constants in these series are close to the values of their analogs having a different *para*-substitution (Table 2).[2,3]

The observed F isotropic hfc's (very close to the a_{p-H} value in radicals **4** and **5**) corresponds to a 2s spin population at these atoms, which results to be $\rho_s = 5.35/17200 = 0.0003$, a value to be compared with the much higher value on H in the $-H$ or $-CH_3$ *p*-substituted radicals:

$$\rho_H = 5.35/508 = 0.0105$$

$$\rho_{H(CH_3)} = 5.72/508 = 0.0113$$

Schastnev, Balaev and Zhidomirov [16] calculated the β–F hfs constants in a series of CF_3-substituted radicals using the generalized hyperconju-

Table 2

Hfc's of free radicals 4—6 with general formula :

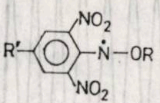

In brackets the numbers of equivalent nuclei are shown

Comp.	R′	R	a_N	a_{NO_2}	$a_{(p-H)}$	$a_{(m-H)}$	$a_{\beta-H}$
4a	H	Me	10.70	0.91 (2)	5.36 (1)	1.66 (2)	3.32 (3)
4b	H	Et	10.25	0.88 (2)	5.06 (1)	1.57 (2)	2.85 (2)
4c	H	iPr	10.25	0.84 (2)	6.00 (1)	1.50 (2)	2.50 (1)
4d	H	CH_2Ph	10.19	0.85 (2)	5.10 (1)	1.59 (2)	2.82 (2)
5a	Me	Me	10.10	0.87 (2)	5.72 (3)	1.53 (2)	2.92 (3)
5b	Me	Et	10.25	0.88 (2)	5.70 (3)	1.65 (2)	2.57 (2)
5c	Me	iPr	11.25	0.84 (2)	4.80 (3)	1.50 (2)	2.30 (1)
6a	tBu	Me	10.09	0.88 (2)	0.19 (9)	1.56 (2)	3.16 (3)
6b	tBu	Et	9.90	0.87 (2)	0.16 (9)	1.67 (2)	2.55 (2)
6c	tBu	iPr	9.98	0.82 (2)	0.16 (9)	1.43 (2)	2.19 (1)

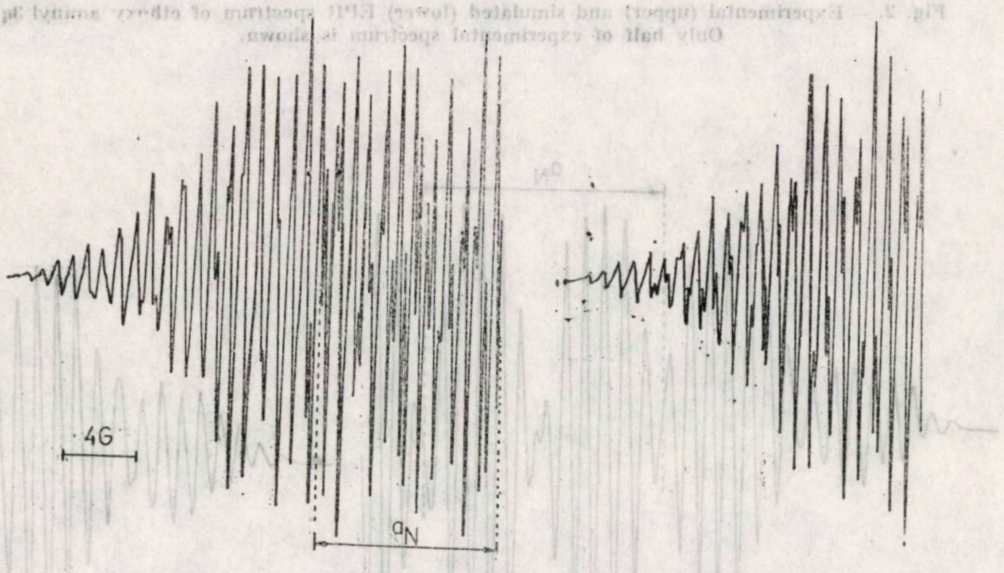

Fig. 1. — Experimental (left) and simulated (right) EPR spectrum of methoxy aminyl 3a. Only half of experimental spectrum is shown,

gation model. The results are in good agreement with the experimental hfc's and show that $Q_F^\beta = a_F/\rho_C$ is essentially different for different radicals, increasing with the increase of the odd electron energy level.

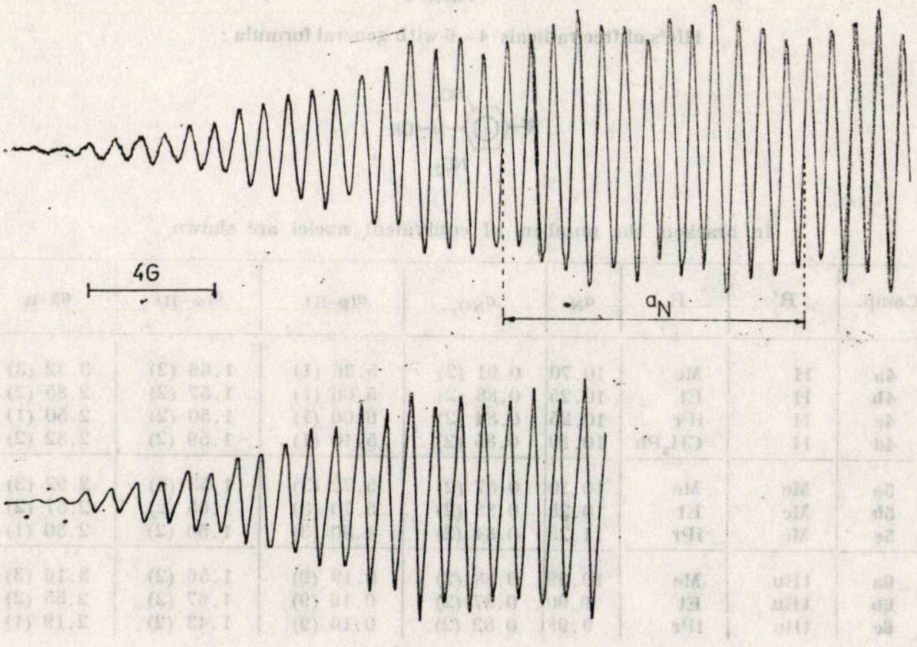

Fig. 2. — Experimental (upper) and simulated (lower) EPR spectrum of ethoxy aminyl 3q. Only half of experimental spectrum is shown.

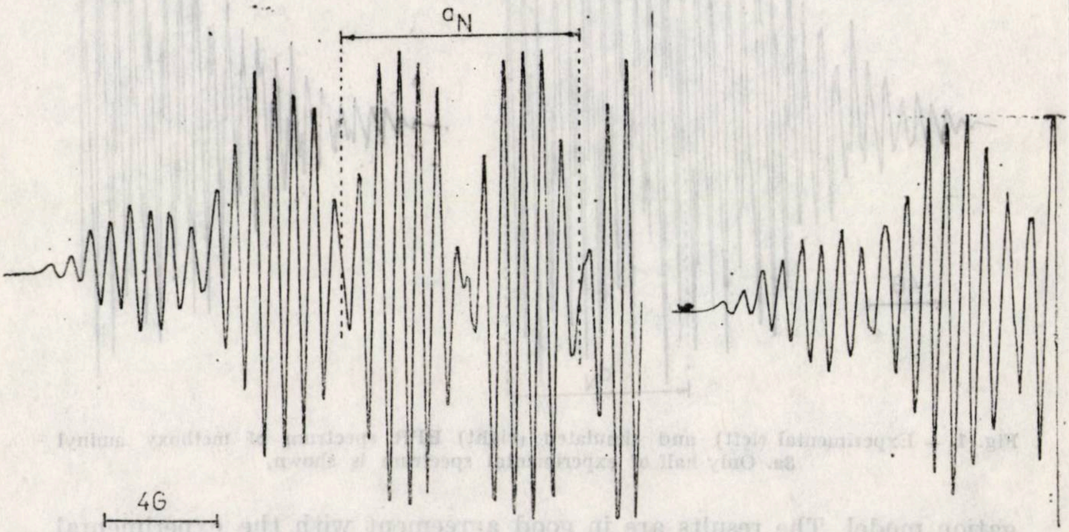

Fig. 3. — Experimental (left) and simulated (right) EPR spectrum of isopropoxy aminyl 3c. Only half of experimental spectrum is shown.

In our radicals, Q^{β}_{F} results to be very close to − 24 G.

The results also show that the aminyl radicals **3a**−**3d** similar to the previously studied series of radicals **4**, **5** and **6** also have a π-electronic structure.

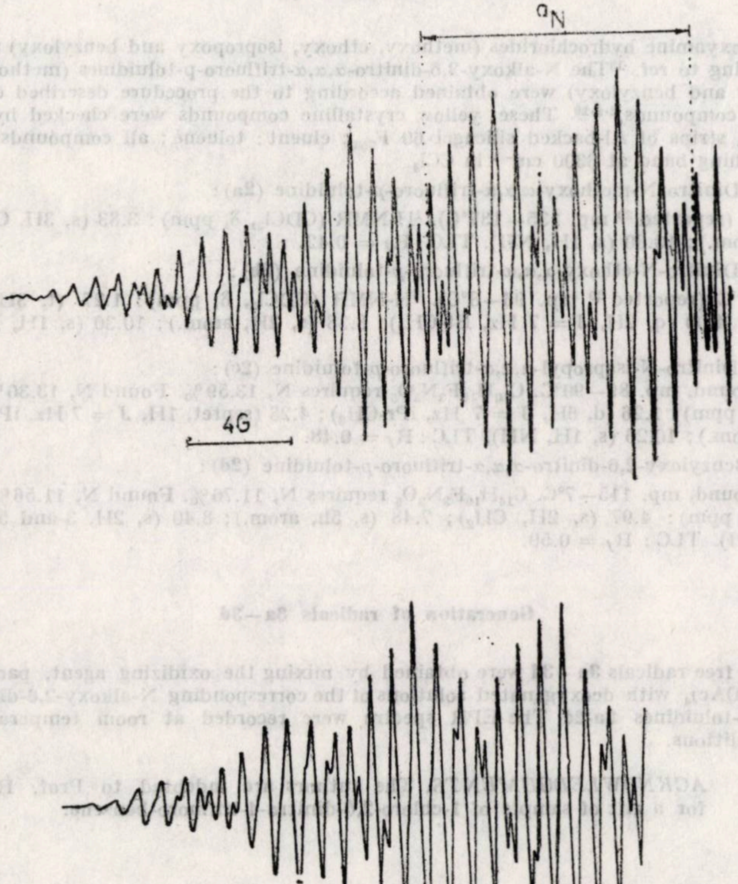

Fig. 4. — Experimental (upper) and simulated (lower) EPR spectrum of benzyloxy aminyl **3d**. Only half of experimental spectrum is shown.

EXPERIMENTAL

All melting points are uncorrected; IR spectra were recorded with a Jena UR-instrument; ^{1}H-NMR spectra were obtained at 60 MHz with a Varian EM-360 L instrument using $(CH_3)_4Si$ as internal standard; EPR spectra were recorded on a JES-3B (JEOL) spectrometer with 100 kHz modulation using X-band frequency. The hfc's was measured in comparison with potassium peroxylamine disulphonate ($a_N = 13.09 \pm 0.04$ G[17]). The simulated, spectra were computed and plotted with a Hewlett-Packard computer, using a Lorentzian-line shape.

Synthesis of aminyl precursors

Alkoxyamine hydrochlorides (methoxy, ethoxy, isopropoxy and benzyloxy) were prepared according to ref. [18]The N-alkoxy-2,6-dinitro-α,α,α-trifluoro-p-toluidines (methoxy, ethoxy, isopropoxy and benzyloxy) were obtained according to the procedure described elsewere for analogous compounds.[2,3,19] These yellow crystalline compounds were checked by analytical TLC using strips of Al-backed silicagel 60 F_{254}; eluent: toluene; all compounds exhibit an NH stretching band at 3300 cm^{-1} in CCl_4.

2,6-Dinitro N-methoxy-α,α,α-trifluoro-*p*-toluidine (**2a**):

mp. 138°C (reported [20] mp. 135—137°C). ^1H-NMR ($CDCl_3$, δ, ppm): 3.83 (s, 3H, OCH_3); 8.40 (s, 2H, arom.); 10.30 (s, 1H, NH). TLC: $R_f = 0.42$.

2,6-Dinitro-N-ethoxy-α,α,α-trifluoro-*p*-toluidine (**2b**):

mp. 94—5°C (reported [20] mp. 96—8°C). ^1H-NMR ($CDCl_3$, δ, ppm): 1.27 (t, 3H, J = 7Hz Et—CH_3); 4.00 (q, 2H, J = 7 Hz, Et-CH_2); 8.38 (s, 2H, arom.); 10.30 (s, 1H, NH). TLC: $R_f = 0.46$

2,6-Dinitro-N-isopropyl-α,α,α-trifluoro-*p*-toluidine (**2c**):

new compound, mp. 89—90°C. $C_{10}H_{10}F_3N_3O_5$ requires N, 13.59%. Found N, 13.30%. ^1H-NMR ($CDCl_3$, δ, ppm): 1.26 (d, 6H, J = 7 Hz, iPr-CH_3); 4.28 (septet, 1H, J = 7 Hz, iPr-CH); 8.32 (s, 2H, arom.); 10.26 (s, 1H, NH). TLC: $R_f = 0.48$.

N-Benzyloxy-2,6-dinitro-α,α,α-trifluoro-*p*-toluidine (**2d**):

new compound, mp. 115—7°C. $C_{14}H_{10}F_3N_3O_5$ requires N, 11.76%. Found N, 11.56%. ^1H-NMR ($CDCl_3$, δ, ppm): 4.97 (s, 2H, CH_2); 7.48 (s, 5h, arom.); 8.40 (s, 2H, 3-and 5-H); 10.23 (s, 1H, NH). TLC: $R_f = 0.50$.

Generation of radicals 3a—3d

The free radicals **3a—3d** were obtained by mixing the oxidizing agent, partly decomposed $Pb(OAc)_4$ with deoxygenated solutions of the corresponding N-alkoxy-2,6-dinitro-α,α,α-trifluoro-p-toluidines **2a-2d**. The EPR spectra were recorded at room temperature under static conditions.

ACKNOWLEDGEMENTS. The authors are indebted to Prof. R. Vîlceanu for a gift of sample of 1-chloro-2,6-dinitro-4-trifluoro-benzene.

REFERENCES

[1] G. Stănciuc, M. T. Căproiu, H. Căldăraru, A. Caragheorgheopol, A. T. Balaban and R. I. Walter, *J. Magn. Res.*, **75**, 63 (1987).

[2] G. Stănciuc, M. T. Căproiu, H. Căldăraru, A. Caragheorgheopol, T. Constantinescu and A. T. Balaban, *Z. Naturforsch.*, **44b**, 1459 (1989).

[3] G. Stănciuc, M. T. Căproiu, H. Căldăraru, A. Caragheorgheopol, T. Constantinescu and A. T Balaban, *Rev. Roum. Chim.*, **34**, 1895 (1989).

[4] A. T. Balaban, P. T. Frangopol, M. Frangopol and N. Negoiţă, *Tetrahedron*, **23**, 4661 (1967).

[5] A. T. Balaban, N. Negoiţă, S. M. Shein and A. D. Khmelinskaya, *Rev. Roum. Chim.*, **32**, 501 (1987).

[6] M. J. S. Dewar, *J. Am. Chem. Soc.*, **74**, 3353 (1952).

[7] D. Crans, T. Clark and P. von Schleyer, *Tetrahedron Lett.*, 3681 (1980).

[8] G. Leroy and D. Peeters, *TEOCHEM*, **2**, 133 (1981); G. Leroy, D. Peteers, C. Wilante and M. Khalil, *Nouv. J. Chim.*, **4**, 403 (1980).

[9] H. Wieland, *Justus Liebigs Ann. Chem.*, **381**, 200 (1911); H. Wieland and A. H. Lecher, Ber. Dtsch. Chem. Ges., **48**, 1078 (1915).

[10] R. I. Walter, *J. Am. Chem. Soc.*, **88** 1923 (1966).

[11] A. R. Katritzky and F. Soti, *J. Chem. Soc. Perkin Trans.*, **1**, 1427 (1974); A. R. Katritzky and F. Soti, *Heterocycles*, **1**, 67 (1973); R. W. Baldock, P. Hudson, A. R. Katritzky and F. Soti, *J. Chem. Soc. Perkin Trans.*, **1**, 1422 (1974).

[12] H.-G. Viehe, R. Merenyi, L. Stella and Z. Janousec, *Angew. Chem.*, **91**, 1028 (1979); Z. Janousek, F. Hays, L. Rene, M. Masqueller, L. Stella, R. Merenyi and H. G. Viehe, *Angew. Chem.*, **91**, 651 (1978); H. G. Viehe, Z. Janousek, R. Merenyi and L. Stella, *Acc. Chem. Res.*, **18**, 148 (1985).

[13] S. V. Park, S.-K. Chung and M. Newcomb, *J. Am. Chem. Soc.*, **108**, 240 (1986); J. B. Olson and T. H. Koch, *J. Am. Chem., Soc.*, **108**, 756 (1986).

[14] J. W. Rogers, W. H. Watson, *J. Phys. Chem.*, **72**, 68 (1968).

[15] L. M. Stock, J. Suzuki, *J. Am. Chem. Soc.*, **87**, 3909 (1965).

[16] P. V. Schastnev, A. V. Balaev, G. M. Zhidomirov, *Zh. Strukt. Khim.*, **12**, 719 (1971).

[17] R. J. Faber and G. K. Fraenkel, *J. Chem. Phys.*, **47**, 2462 (1967).

[18] A. Chimiak and T. Kolasa, *Bull. Acad. Pol., Ser. Chem.*, **22**, 195 (1974).

[19] G. Stănciuc and A. T. Balaban, *Org. Prep. Proced. Int.*, **16**, 401 (1984).

[20] J. C. Williams (Eli Lilly and Comp.), U. S. Pat. 4143073, March 1979.

Revue Roumaine de Chimie, 36, 4–7, 741–748 (1991)

Dedicated to Prof. ALEXANDRU T. BALABAN
on the occasion of his 60th anniversary

AN ESTIMATION OF THE POSSIBILITIES FOR OBTAINING CAROTENOID- AND CHLOROPHYL-DERIVED PIGMENTS FROM VEGETAL RAW MATERIALS

MONICA POPESCU, REMUS ANDREESCU, SILVIA STĂNESCU, ŞTEFAN BRĂGĂREA
and LUIZA JECU
Institute for Chemical and Biochemical Energetics, Splaiul Independenţei nr. 202, sector 6,
Bucharest, Romania

Received October 17, 1990

Taking into account the role of chlorophyls and carotenoids in the vegetal world, as well as their industrial applications, the paper reviews their main physico-chemical properties, followed by a presentation of the original methods and the results obtained using several vegetal raw materials (water plants, grassy plants, trees). The initial conditioning and characterizing method of the vegetal matter as well as the method of extraction and quantitative determination of the chlorophyls and carotens (determined as beta-carotens) are presented. The studies were done especially on alphalpha, a plant rich in carotenoids.

INTRODUCTION

The colours appearing in various animal- and vegetal tissues are determined by the presence of some complex organic combinations belonging to the following classes : anthocyans, chlorophyls, carotenoids, porphyrines, quinones.

Carotenoids are denominated as such owing to their abundance in carrot *(Daucus carrota)* roots. Various structures — aliphatic, aromatic or aliphatic-alicyclic — containing several (usually eight) isoprene residues, connected so that the two methyl groups situated closely to the center of the molecule are situated in the positions 1 and 6, all the other lateral methyl groups being situated in the positions 1 and 5 — belong to this class. The chromophore system is formed by the series of conjugated double bonds. Carotenoids are subclassified in two main groups : carotenes as such and oxy-carotenes. The first group includes carotenes containing hydrocarbon chains, whereas the second one comprises the hydroxylic, epoxy and furano derivatives of the first ones.[1]

Carotenoids are widespread in nature, annually regenerated amounts — through phytomass regeneration — being of the order of some hundred million tons.[1] They have the biochemical role of vitamin A precursor, proving a certain contribution in the absorption of radiant energy, in the transport of oxygen, in the colouring of animal and vegetal tissues from dark-yellow to dark-red or, after complexing with proteins, from green to blue. Natural extracts containing carotenoids are used as food dyes (bixine, crocine, capsantine, capsarubine). Beta-carotene was the first carotenoid commercially available through total chemical synthesis. Some companies are producing and selling beta-apo-8-carotenal and cantaxanthine.[1]

CHARACTERIZATION OF CAROTENES AND CHLOROPHYLS

The extractibility and properties of vegetal pigments are essentially influenced by the working conditions (pH, redox properties, the presence of hydrolytic enzymes, of some adsorbants and/or of received photonic energy) which determine the complexity of their quantitative determination in the vegetal raw material. Physical investigations are submitted to further interpretations, because in the chloroplasts and in the solid forms the absorption maxima are shifted to the red region of the visible spectrum as compared to the maxima registered in organic solvents. The absorption chromatography involves the prefractioning through distribution between two or more immiscible solvents, the saponification for the elimination of chlorophyls and a bidimensional chromatography or a chromatography in successive stages. The chromatography as such is hindered by the necessity of using alkaline beds (thus hindering the isomerization of carotenoids), by the work in inert gas atmosphere (thus minimising the decomposition of carotenes upon solvent evaporation), by the standardization of the extract concentrations and by the concentrations of the isocolour compounds.[2]

In the spectral determinations the carotenoids show three absorption maxima in the visible domain, owing to the presence of the conjugated double bonds (Table 1). Depending on the solvent used, the wavelengths of the absorption maxima are increasing from 449 nm in low-boiling gasoline (b.p. 30—60°C) to 453 nm in high-boiling gasoline (b.p. 88—99°C) and to 478 nm in carbon disulphide. The increase of the double bonds number in the molecule involves an increase with 20—22 nm of the absorp-

Table 1

Absorption maxima (nm) for certain carotenoids in several solvents

Pigment	Solvent			
	n-C_6H_{14}	CS_2	$CHCl_3$	C_6H_6
Alpha-carotene	420; 445; 475	477; 509	454; 485	—
Neo-beta-carotene	450; 481	478.5; 512.5	461; 493.5	461; 492
Beta-carotene	425; 451; 482	450; 485	466; 497	—
Neo-beta-carotene B	443.5; 475.5	520	—	—
5,6-epoxy-alpha-carotene	442; 471	471; 503	454; 483	455; 484

tion maximum (in carbon disulphide). When the double bond from the beta-iononic cycle is substituted by the 5,6-epoxy groups, the absorption maximum decreases with 6–9 nm.

The introduction of a ketonic group conjugated with the polyenic chain determines a red-shift of 3–5 nm whereas the introduction of the hydroxyl group has no influence upon the position of the maxima. The molar absorption coefficient $E^{1\%}_{1cm}$ also depends upon solvent interactions (Table 2).[3]

Table 2

Molar absorption coefficients ($E^{1\%}_{1cm}$) for certain carotenoids in several solvents

Pigment	$E^{1\%}_{1cm}$	Solvent
Alpha-carotene	2700–2730 2580–2710 2670	hexane 80% ethanol/20% diethyl ether isooctane
Neo-beta-carotene U	2520–2650 2490–2550	hexane 80% ethanol/20% diethyl ether
Beta-carotene	2450–2650 2490–2550 2510 1940	hexane 80% ethanol/20% diethyl ether isooctane carbon disulphide
Neo-beta-carotene B	1920	isooctane

The chlorophyls are determined in the acetonic extracts of the vegetal raw materials using the McKinney formula :

a-chlorophyl (mg/mL) $= 11.63\ E_{665} - 2.39\ E_{649}$

b-chlorophyl (mg/mL) $= 20.11\ E_{649} - 5.18\ E_{665}$

total chlorophyls (mg/mL) $= 6.45\ E_{665} + 17.72\ E_{649}$

For the characterization of the chlorophyllic pigment concentrates several elements have to be considered :

a) the absorption spectra of a- and b-chlorophylls in diethyl ether are characterized by two absorption maxima at 433 nm and 690 nm for a-chlorophyl and at 460 nm and 669 nm for b-chlorophyl ;

b) the absorption spectrum of the c-chlorophyl in diethyl ether has several maxima at $\lambda = 442$ nm, $\lambda = 580$ nm and 628 nm ;

c) the absorption spectrum of the d-chlorophyl in diethyl ether has several maxima at $\lambda = 395$ nm, $\lambda = 445$ nm and 686 nm.[4]

RESULTS AND DISCUSSION

1. Characterization of some phytomass species considering their pigment composition

In Table 3 the pigment concentrations for some water plants, grassy plants and trees are given. The grassy phytomass is the richest in pigments, the carrot roots contain the purest carotene, whereas the water species are drawn back by their high water content.

Table 3

Pigment concentrations in different phytomass species — referred to the dry matter content

Vegetal species	Dry matter (g/100 g)	Total chlorophyls (mg/100 g DM)	Carotenes (mg/100 g DM)
Water plants			
Sagittaria sagittifolia L	20	450	87.5
Lemna minor L	5	450	123
Salvinia natans	5	285	39
Nymphea alba L	10	950	315
Grassy plants			
Spinacia oleraceea	97	1470	356
Lactuca sativa	15	213.3	70.3
Daucus carota sativa (leaves)	25	171	22.5
Daucus carota sativa (roots)	20	0	170.2
Solanum lycopersicum (leaves)	15	296.6	46.9
Trees			
Populus marilandica	25	400	84.5
Salix babilonica	40	166.2	49.4
Quercus robur	35	157.1	52.4
Aesculus hypocastanus	35	697.1	99.6

2. The conditioning and storing of the vegetal raw materials

The conditioning and storing of the vegetal raw materials is significant owing to the rapid degradation of the pigments from these materials. The dynamics of the vegetal pigment concentrations was experimentally determined for different samples of ***Populus marilandica*** and ***Salix babylonica*** in different storage conditions (Table 4). The time degradation of the pigments is extremely rapid, that is why the selection of freshly harvested plants or of plants conditioned through drying in hot air flow at 40—50°C, followed by mechanical grinding as raw materials is preferred.

3. Preliminary experiments for carotenoid and chlorophyl pigments extraction from vegetal raw materials

The extraction experiments were accomplished with alphalpha from the first mowing, the raw vegetal material having the following characteristics :

— dry matter : 27.2 g/100 g

— aw protein : 22.16 g/100 g

— directly reducing sugars : 4.1 mg/100 g DM

Table 4

The degradation of the vegetal pigments from some phytomass species in different storing conditions

Vegetal species	Storage conditions	Dry matter (g/100 g)	Total chlorophyls (mg/100 g DM)	Total carotenes (mg/100 g DM)
Populus marilandica	— freshly harvested	25	400	84.5
	— stored for 24 hours in the refrigerator	50	189	48.4
	— stored for 24 hours at room temperature	35	275.7	77.8
	— stored for 48 hours at room temperature	35	240.5	63.0
Salix babylonica	— freshly harvested	40	168.7	49.4
	— stored for 24 hours in the refrigerator	50	166.2	35
	— stored for 24 hours at room temperature	40	102	44
	— stored for 48 hours at room temperature	40	69.5	37

— beta-carotene : 66.9 mg/100 g DM, a content which decreases upon drying to 47.2 mg/100 g DM, the yield of the preserving of useful compound being about 70%.

By extraction with a mixture of light gasoline/acetone 3/2 (v/v) one achieves an extraction dynamics presented in Fig. 1.

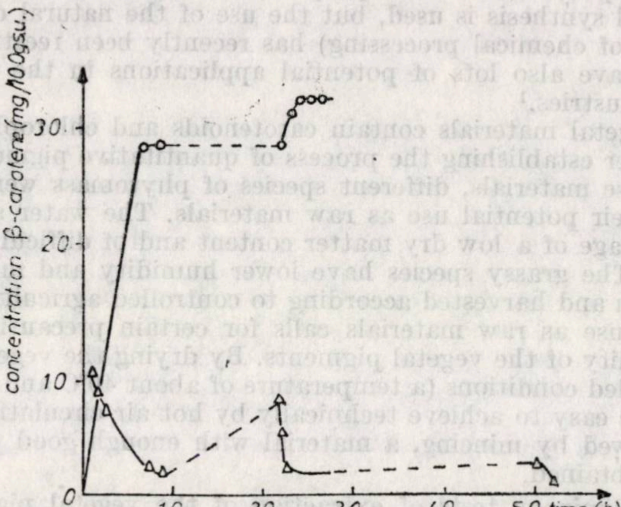

Fig. 1. — Extraction and concentration curve : — Δ — extraction from column, — O — concentration in blase ; the continuous line represents the dynamic extraction and the dotted line the static extraction.

The beta-carotene concentration in the raw extract is 32.4 mg/100 g DM and in the secondary extract, after saponification, 22.5 mg/100 g DM[2]. In a second experiment accomplished under identical conditions, the beta-carotene concentrations in the raw extract was 32.3 mg/100 g DM and in the final carotenoidic extract 26 mg/100 g DM.

Similar experiments were accomplished with alphalpha from the 2nd mowing, with a dry matter content of 20.35 g/100 g and initial beta-carotene of 78.2 mg/100 g DM. After drying at 40°C up to a dry matter contents of 89.9%, the beta-carotene content has decreased to 63.6 mg/100 g DM for a direct reducing sugars concentration of 4.01 mg/100 g DM and of raw protein of 27.2 g /100 g DM. The beta-carotene concentration in the raw extract was 38.6 mg/100 g DM and in the secondary extract, obtained after saponification, 30 mg/100 g DM.[2]

CONCLUSIONS

The biochemical role of carotenoids in the natural systems consists in : a) pigment help for energy transfer in the photosynthesis ; b) obtaining of photoresponses — for instance, the phototropism of certain forms of vegetal life ; c) photoprotection ; d) involvements in the metabolism of the oxygen ; e) physiological transformation of certain natural structures in vitamin A ; f) growth regulator for plants ; g) formation of compounds for the attraction of insects which pollinate the flowers. The carotenoids are used as provitaminic natural dyes in the food industry, either directly — by their mixing, for food products — or indirectly — by their addition to the food of birds, animals and fishes, followed by their absorption in tissues and depositing. For this purpose, the beta-carotene obtained by total chemical synthesis is used, but the use of the natural dyes (with a lower degree of chemical processing) has recently been reestimated. The chlorophyls have also lots of potential applications in the food and/or cosmetics industries.[1]

The vegetal materials contain carotenoids and chlorophyls in high amounts. After establishing the process of quantitative pigment determination in these materials, different species of phytomass were analyzed, estimating their potential use as raw materials. The water species have the disadvantage of a low dry matter content and of difficult harvesting possibilities. The grassy species have lower humidity and most of them may be grown and harvested according to controlled agricultural technologies ; their use as raw materials calls for certain precautions because of the instability of the vegetal pigments. By drying the vegetal material under controlled conditions (a temperature of about 40°C and the absence of light) quite easy to achieve technically by hot air circulation in closed areas — followed by mincing, a material with enough good preservation capacity is obtained.

The preliminary tests of extraction of the vegetal pigments with solvent mixtures, followed by saponification of raw extract with alcoholic KOH solution and by selective extraction of the carotenoids with petroleum ether, showed that carotenoidic and chlorophyllic solutions may be obtained and further used as intermediates.

EXPERIMENTAL PART

1. Chlorophyls and carotenes separation

A sample of 2 g of dried and minced vegetal raw material is thoroughly milled with 2 g $CaCO_3$ and 20 mL acetone for 3 — 5 minutes. The mixture is filtered on a G_4 crucible, the solid residue is washed away with 20 mL acetone and the filtrate is transferred to a 50 mL volumetric flask. The colour intensity is determined into 1 cm-cell at a wavelength of 663 nm for a-chlorophyl, and at 645 nm for b-chlorophyl.

A sample of 2 g of dried and minced vegetal raw materials is thoroughly milled with 2 mL methanol, the mixture is quantitatively transferred to a test tube with ground-glass stopper, the saponification being finished at 37°C in one hour. The whole mass is filtered on a G_4 crucible and the solid residue is washed again with 20 mL petroleum ether. The organic extract is washed with bidistilled water for alkalinity removal, dried on anhydrous Na_2SO_4 and transferred to a 50 mL volumetric flask with petroleum ether. The colour intensity is determined at a wavelength of 440 nm, with petroleum ether in 1 cm-cell, the pigments concentrations being calculated as follows:

— carotene (mg/L) $= 4.695\ E_{440}$
— a-chlorophyl (mg/L) $= 12.7\ E_{663} - 2.69\ E_{645}$
— b-chlorophyl (mg/L) $= 22.9\ E_{645} - 4.86\ E_{663}$
— total chlorophyls (mg/L) $= 8.02\ E_{663} - 20.2\ E_{645}$

the results being referred to the dry matter content, determined by drying at 105°C until a constant weight is obtained.[6]

2. Experimental laboratory equipment

The laboratory equipment used for pigments extraction from the vegetal raw materials is described in Fig. 2.

The dried vegetal material is loaded in the extraction column 1 filled with the extraction solvent mixture up to a constant level, corresponding to a useful capacity of 1350 mL. In the blase 2, 650 mL of the extraction solvent mixture are loaded. Upon the blase heating the solvent evaporates and condenses in the ascendent condenser 4, falls through the bed of vegetal material, is loaded with pigments and syphoned back to the blase. Through solvent evaporation the extract is concentrated; the continous feed of the installation may be achieved with fresh solvent mixture flow rates of 13 — 15 mL/min., thus achieving the complete recycling of the solvent in 2 hours. The analytical control of the process was achieved by sampling from both the extraction column and the blase.

The saponification is accomplished by reflux with 10% KOH ethanolic solution, in the same blase, aiming to transform the lipids, waxes and chlorophyls into hydrosoluble salts. The separation of the carotenoid pigments from these salts is achieved through extraction with petroleum ether and elimination of the residual alkalinity by washing with distilled water and drying on anhydrous sodium sulphate. The raw carotenoidic extract might be concentrated through evaporation of some solvent.

The conditioning of the vegetal raw material was accomplished through drying in air flow at temperatures of 40—45°C up to a dry matter content of 92%, followed by mechanical grinding.

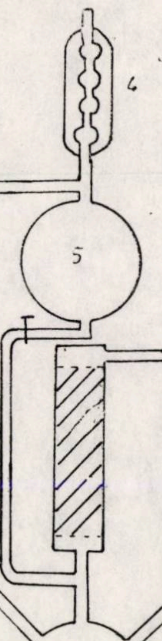

Fig. 2. — Laboratory installation for extracting and concentrating the pigments from vegetal raw materials: 1 — extraction column; 2 — concentration blase; 3 — ascending conduct; 4 — refrigerent; 5 — detention vase.

REFERENCES

[1] H. Kläui and J. C. Bauernfeind, "Carotenoids as Colorants and Vitamin A Precursors", Academic Press Inc., New York, 1981.

[2] Research Grant no. 535B, ICECHIM-IECB, 1982.

[3] J. Vernon and M. W. Seeley, "The Chlorophylls", Academic Press, New York, 1966.

[4] T. W. Goodwin, ed. "Chemistry and Biochemistry of Plant Pigments", Academic Press, London, New York, 1965.

[5] T. W. Goodwin, "Carotenoids" in "Modern Methods of Plant Analyses", Academic Press, New York, vol. III, 1955.

[6] Research Grant no. 535B, ICECHIM-IECB, 1981.

[7] Research Grant no. 535B, ICECHIM-IECB, 1983.

Revue Roumaine de Chimie, **36**, *4*–7, 749–755 (1991)

Dedicated to Prof. A. T. BALABAN
on the occasion of his 60th birthday

FLEXIBILITY PARAMETER OF HIGH MOLECULAR WEIGHT POLYMERS. 2*

POLYSTYRENE IN SOLVENT-NONSOLVENT MIXTURES

SILVIA IOAN,[a] MARIA BERCEA[a] and BOGDAN C. SIMIONESCU[b]

[a] "P. Poni" Institute of Macromolecular Chemistry, 6600 Iași, Romania
[b] Department of Macromolecules, Polytechnic Institute of Iași, 6600 Iași, Romania

Received January 2, 1991

The paper deals with the behaviour of high molecular weight polystyrene in benzene/ /n-hexane, benzene/methanol and benzene/isopropanol solvent/nonsolvent mixtures. The possibilities of determining the unperturbed dimensions of the polymer in theta conditions and using the Lenka extrapolation method are discussed. Long-range interaction parameters B were determined.

INTRODUCTION

In some previously published papers,[1,2] the conformational transitions of high molecular weight polystyrene in solvent/nonsolvent systems (benzene/n-hexane, benzene/methanol and benzene/isopropanol) were studied by viscometry as a function of composition and temperature. Polymer behaviour is affected by the preferential adsorption phenomena determining the appearance of two theta temperatures, one intramolecular ($B = 0$, $\alpha = 1$) and the other intermolecular ($A_2 = 0$). For very high molecular weight polystyrene, theta intramolecular strongly approaches theta intermolecular due to a decrease in selective adsorption, and in the vicinity of the theta condition the conformational transitions disappear.

Many studies are dealing with coil dimensions of polymers in mixed solvents.[3–5] Most of them involve liquid mixtures composed of a good and a poor solvent of the polymer. The action of mixed solvents has been reported to change coil dimensions, not only because excluded volume expansion but also because the interactions between the liquids modify the unperturbed dimensions of the coil.[6,7]

The present paper is concerned with the possibilities to determine the unperturbed dimensions, from viscosity measurements, for polystyrene in solvent/nonsolvent mixtures. The interaction of polymer with the mixed solvent is also analysed through the B parameter, and the thermodynamic properties of solvent/nonsolvent mixtures, described by the free (Gibbs) energy of mixing (the enthalpic and entropic parts), as a function of the nature of solvents, are estimated.

---

* Part 1 : see Ref. [1]

EXPERIMENTAL

Polystyrene (PS) was obtained by plasma-induced polymerization (for details on this synthesis technique, see, e.g.[8]). A PS sample with weight average molecular weight $\overline{M}_w = 3.065 \times 10^6$ was selected for this study. The solvents – benzene, n-hexane, methanol and isopropanol – were purified by standard procedures. The viscosities were measured with an Ubbelohde viscometer.

Huggins and Kraemer equations were used to analyse the data. Kinetic energy correction was found to be negligible.

RESULTS AND DISCUSSION

Unperturbed dimensions

Previously, it has been established that high molecular weight PS shows theta conditions (where theta-inter equals theta-intra) in benzene/n-hexane mixture at 20°C with $X_2 = 0.5359$, in benzene/methanol mixture at 25°C with $X_2 = 0.222$, and in benzene/isopropanol mixture at 25°C with $X_2 = 0.358$ (where X_2 is the volume fraction of nonsolvent – n-hexane, methanol or isopropanol).

A number of methods are available and currently used for the determination of unperturbed dimensions of polymer molecules, e.g., light scattering and/or viscosity measurements of polymer solutions at the theta temperature, and building-up suitable expressions relating the intrinsic viscosity (or other characteristic of the chain) to the molecular weight by following a mathematical extrapolation procedure. For high molecular weight polymers, the known extrapolation procedures yield much higher values of the unperturbed dimensions [9-11] due to curvatures of the linear dependences as given by the experimental points for high excluded volume.

In the present study, the relation proposed by Lenka et al.[12] was used for the determination of the cross-over point concentration (c_0) of the polymer in a number of solvents, in order to determine the unperturbed dimensions of the chain :

$$(\overline{r}_\theta^2)^{1/2} = 2.204 \times 10^{-8}(M/c_0)^{1/3} \quad (1)$$

where c_0 is the cross-over concentration in g/ml, and $(\overline{r}_\theta^2)^{1/2}$ is the unperturbed root-mean-square end-to-end distance. The condition for the cross-over point concentration is given by equation (2) (Heller's equation):

$$c/\eta_{sp} = (1/[\eta] - kc) \quad (2)$$

Figure 1 presents the dependence of $c/\eta_{sp} = f(c)$ for PS in benzene and benzene/methanol with $X_2 = 0.200$; 0.2069 ; 0.2143, with experimental values only in the diluted regime. From these dependences, expressed by the equations

$$c/\eta_{sp} = 0.23083 - 0.2667c \quad \text{(for benzene)} \tag{3}$$

$$c/\eta_{sp} = 0.4840 - 0.3763c \quad (\text{for } X_2 = 0.2143) \tag{4}$$

$$c/\eta_{sp} = 0.4510 - 0.3725c \quad (\text{for } X_2 = 0.2069) \tag{5}$$

$$c/\eta_{sp} = 0.4167 - 0.3303c \quad (\text{for } X_2 = 0.2000) \tag{6}$$

the cross-over point concentration was found to be $c_0 = 2.19503$ g/dl. From Figure 1, the obtained unperturbed dimension $(\overline{r}_\theta^2/M)^{1/2}$ is $0.654 \times \times 10^{-8}$ cm.

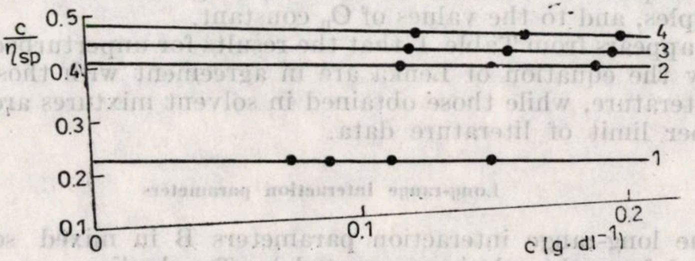

Fig. 1. — Reciprocal reduced viscosity c/η_{sp} as a function of concentration c for polystyrene in benzene (1) and benzene/methanol mixtures, at 25°C, with $X_2 = 0.200$ (2), 0.2069 (3) and 0.2143(4).

Table 1 presents the unperturbed dimensions obtained in solvent/nonsolvent mixtures at theta composition, as compared with the value issued from the equation of Lenka et al.[12]

Table 1

Intrinsic viscosities $[\eta]_\theta$, flexibility parameters K_θ and unperturbed dimensions $(\overline{r}^2/M)^{1/2}$ obtained for high molecular weight PS in theta conditions, in solvent/nonsolvent mixtures, and by the equation of Lenka et al.[12]

Solvent mixture (X_2)	$[\eta]_\theta$ (dl/g)	$K_\theta \times 10^3$ (ml/g)		$(\overline{r}_\theta^2/M)^{1/2} \times 10^8$ (cm)	
		$Ø_0 = 2.51 \times 10^{23}$	$Ø_0 = 2.87 \times 10^{23}$	$Ø_0 = 2.51 \times 10^{23}$	$Ø_0 = 2.87 \times 10^{23}$
benzene/n-hexane ($X_2 = 0.5359$, 20°C)	1.67	95.39^a		0.724^b	0.693^b
benzene/methanol ($X_2 = 0.222$, 25°C)	1.916	109.94^a		0.758^b	0.724^b
benzene/isopropanol ($X_2 = 0.358$, 25°C)	1.582	90.41^a		0.711^b	0.680^b
cf. Lenka et al.[12] (benzene/methanol mixtures, 25°C)		69.96^b	80.00^b	0.654	

[a] K_θ calculated from $[\eta]_\theta = K_\theta \times M^{0.5}$

[b] K_θ or $(\overline{r}_\theta^2/M)^{1/2}$ calculated from $(\overline{r}_\theta^2/M)^{3/2} = K_\theta/Ø_0$ with different values for $Ø_0$

With regard to the unperturbed dimensions expressed as K_θ, comparison with literature values is hampered by the disparity among the reported literature values.[13] Thus, for PS in cyclohexane, these range between 74×10^{-3} and 91×10^{-3} with an average of 82×10^{-3}. In mixed solvents, the values of K_θ are respectively lower, higher or equalize the values reported for single solvents. Also, for the unperturbed dimensions expressed as $(\bar{r}_\theta^2/M)^{1/2}$, directly measured in theta conditions, the range of variation presented in literature is from 0.651×10^{-8} [14] to 0.850×10^{-8}.[15] On the other hand, Yamakawa et al.[16] observed that the unperturbed dimensions in mixed solvents are significantly larger than in cyclohexane.

The relatively large scattering of the literature data can be attributed to the different methods used (in theta conditions or in good solvents), to the temperatures, nature of solvents, ranges of molecular weights of the samples, and to the values of Φ_0 constant.

It appears from Table 1 that the results for unperturbed dimensions given by the equation of Lenka are in agreement with those presented in the literature, while those obtained in solvent mixtures are situated at the upper limit of literature data.

Long-range interaction parameters

The long-range interaction parameters B in mixed solvents were calculated from the relation suggested by Tanaka[17]:

$$\alpha_\eta^5 = 1 + 1.90Z \tag{7}$$

with

$$Z = (1/4\pi)^{3/2}(B/A^{3/2})\, M^{1/2} \tag{8}$$

where $\alpha_\eta^3 = [\eta]/[\eta]_\theta$, $A = \langle S_\theta^2 \rangle/M$, Z is the excluded volume parameter, and $<S_\theta^2>$ is the unperturbed root-mean-square radius of gyration.

Figure 2 presents our previous data[1] for the variation of the intrinsic viscosity with mixed solvent composition X_2.

Generally, for solvent/precipitant mixtures, adding of precipitant decreases solvent quality. However, there are some particular mixtures, called "synergistic solvents", where the event of addition of precipitant causes an increase in the dissolving power of the mixture.[18-21] The phenomenon of synergism is associated with the sigmoidal form of the preferential adsorption.[21] This effect appears in the case of benzene/n-hexane mixture, although in the same study the decrease of preferential adsorption with increasing the molecular weight was mentioned. It was also observed that for high molecular weight PS, in benzene/methanol mixture, the intermolecular theta point strongly approaches the intramolecular theta point due to the decrease of selective adsorption.

The data in Figure 2 were used to calculate the viscometric expansion factors α_η, the excluded volume effect parameters Z, and the long-range interaction parameters B according to equations (7) and (8).

Figure 3 shows the plot of parameter B against inverse binary mixture composition $1/X_1$ for benzene/n-hexane system at 20°C and for benzene/methanol and benzene/isopropanol systems at 25°C. The diffe-

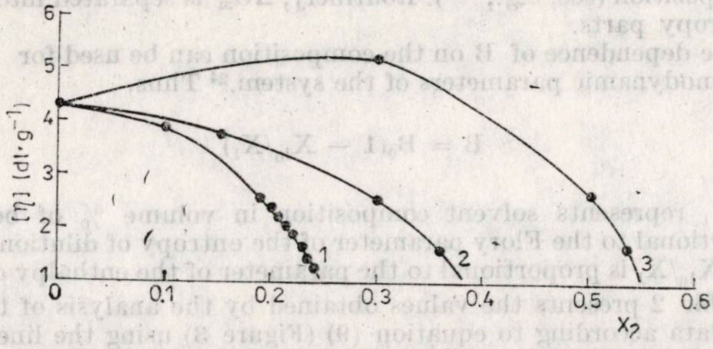

Fig. 2. — Plots of intrinsic viscosity [η] for polystyrene against binary mixture compositions X_2 : (1) benzene/methanol at 25°C, (2) benzene/isopropanol at 25°C, (3) benzene/n-hexane at 20°C.

rences observed for the values of B for $X_2 = 0$ ($1/X_1 = 0.01$) are yielded by the different values of $[\eta]_0$ in the three systems (Table 1).

The dimensions of a polymer coil in a mixed solvent medium are influenced largely by the thermodynamic properties of the binary liquid mixture. This effect has been characterized by the free (Gibbs) energy of mixing ΔG_m, which is known to be a function of pressure, temperature

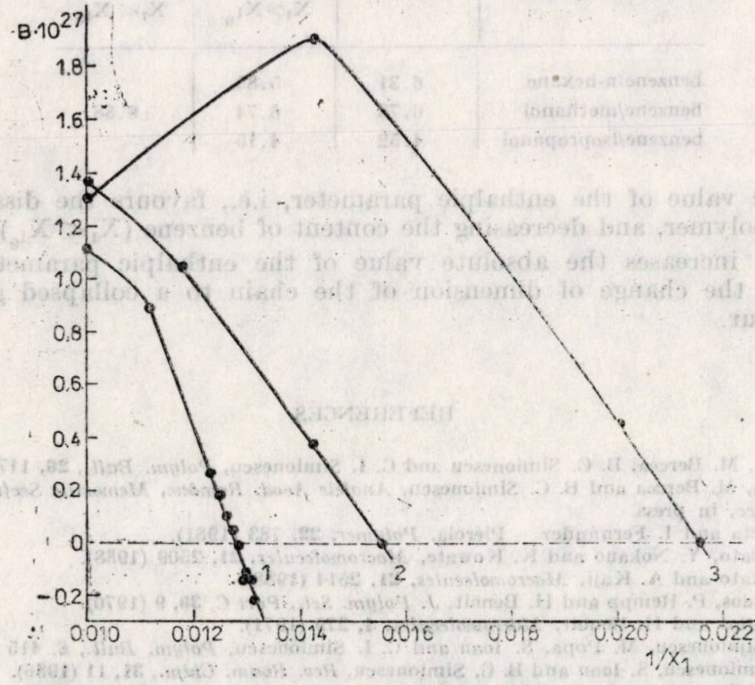

Fig. 3. — Dependence of interaction parameter B for polystyrene in benzene/methanol (1), benzene/isopropanol (2) and benzene/n-hexane (3) on reciprocal solvent composition $1/X_1$.

and composition (see, e.g.,[2,23]). Routinely, ΔG_m is separated into enthalpy and entropy parts.

The dependence of B on the composition can be used for estimating the thermodynamic parameters of the system.[24] Thus,

$$B = B_0(1 - X_{1\theta}/X_1) \tag{9}$$

where X_1 represents solvent composition in volume % of benzene, B_0 is proportional to the Flory parameter of the entropy of dilution, and similarly $B_0X_{1\theta}/X_1$ is proportional to the parameter of the enthalpy of dilution.

Table 2 presents the values obtained by the analysis of the experimental data according to equation (9) (Figure 3) using the linear part in the vicinity of the theta point.

Both parameters are positive, but the entropic exceeds the enthalpic one and this situation favours the dissolution of PS in the studied mixed solvents. Increasing the content of benzene in the mixture decreases the absolute value of the enthalpic parameter, i.e., favours the dissolution of the polymer, and decreasing the content of benzene ($X_1 < X_{1_\theta}$) in the mixture increases the absolute value of the enthalpic parameter, i.e., favours the change of dimension of the chain to a collapsed globular behaviour.

Table 2

B_0 and $B_0X_{1_\theta}/X_1$ parameters for PS in mixed solvent systems

Solvent system	$B_0 \times 10^{27}$	$(B_0X_{1_\theta}/X_1) \times 10^{27}$	
		$X_1 > X_{1_\theta}$	$X_1 < X_{1_\theta}$
benzene/n-hexane	6.31	5.85	
benzene/methanol	6.78	6.74	6.88
benzene/isopropanol	4.52	4.15	

REFERENCES

1 S. Ioan, M. Bercea, B. C. Simionescu and C. I. Simionescu, *Polym. Bull.*, **26**, 117 (1991).

2 S. Ioan, M. Bercea and B. C. Simionescu, *Analele Acad. Române, Memoriile Secţiilor Ştiinţifice*, in press.

3 H. Horta and I. Fernández — Piérola, *Polymer*, **22**, 783 (1981).

4 M. Nakato, Y. Nokano and K. Kowate, *Macromolecules*, **21**, 2509 (1988).

5 M. Nakato and A. Kaji, *Macromolecules*, **21**, 2514 (1988).

6 A. Dondos, P. Rempp and H. Benoit, *J. Polym. Sci., Part C*, **30**, 9 (1970).

7 A. Dondos and H. Benoit, *Macromolecules*, **4**, 279 (1971).

8 B. C. Simionescu, M. Popa, S. Ioan and C. I. Simionescu, *Polym. Bull.*, **6**, 415 (1982).

9 C. I. Simionescu, S. Ioan and B. C. Simionescu, *Rev. Roum. Chim.*, **31**, 11 (1986).

10 C. I. Simionescu, S. Ioan and B. C. Simionescu, *Eur. Polym. J.*, **23**, 69 (1987).

11 C. I. Simionescu, S. Ioan, A. Flondor and B. C. Simionescu, *Makromol. Chem.*, **189**, 2331 (1988).

[12] S. Lenka, P. L. Nayak and M. Dash, *J. Macromol. Sci., Chem.*, **A 19**, 321 (1983).
[13] A. Bozuaye and M. B. Huglin, *Polymer*, **20**, 44 (1979).
[14] B. A. Wolf, H. F. Bieringer and J. W. Breitenbach, *Polymer*, **17**, 605 (1976).
[15] A. Vrij, *J. Polym. Sci., Polym. Symposia*, **44**, 169 (1974).
[16] K. Takashina, K. Nakae, M. Shibada and H. Yamakawa, *Macromolecules*, **7**, 641 (1974).
[17] G. Tanaka, *Macromolecules*, **15**, 1028 (1982).
[18] H. Maillols, L. Bardet and S. Gromb, *Eur. Polym. J.*, **14**, 1015 (1978).
[19] D. Blanco, J. M. Teijòn and I. Katime, *Polym. Bull.*, **20**, 563 (1988).
[20] D. Blanco, J. M. Teijòn and I. Katime, *Eur. Polym. J.*, **26**, 249 (1990).
[21] I. Katime, D. Blanco and J. M. Teijòn, *British. Polym. J.*, **23**, 327 (1990).
[22] Y. Einaga, *Bull. Inst. Chem. Res. Kyoto Univ.*, **66**, 140 (1988).
[23] P. Munk, P. Hattan and Q. Du, *J. Appl. Polym. Sci., Appl. Polym. Symp.*, **43**, 373 (1989).
[24] T. Spychaj, D. Lath and D. Berek, *Polymer*, **20**, 437 (1979).

Revue Roumaine de Chimie, **36**, *4–7*, 757–760 (1991)

Dedicated to Prof. ALEXANDRU T. BALABAN
on the occasion of his 60th anniversary

RADICAL POLYMERIZATION OF ACRYLAMIDE IN HOMOGENEOUS AND HETEROGENEOUS SYSTEMS. II*

EMULSIFIER AGGREGATES IN ORGANIC MEDIA

M. V. DIMONIE, N. N. MARINESCU and D. S. VASILESCU
Laboratory of Macromolecular Chemistry, Polytechnic Institute, Calea Victoriei 149, Bucharest, Romania

Received May 16, 1990

Measurements of apparent molecular weights by vapour pressure osmometry indicate that the nonionic emulsifier, completely soluble in cyclohexane, tends to from associates; moreover, water molecules may be bound on the polyethyleneoxide chain of the emulsifier, even in organic media.

INTRODUCTION

Acrylamide polymerization in heterogeneous systems has been investigated by several workers.[1–3] The interest regarding this procedure is justified on the one hand by the high molecular weights of the polyacrylamide obtained and the lack of gel (crosslinked polymer); on the other hand, some topochemical peculiarities typical for such systems, unusual for other polymerization processes have been put in evidence.[4]

The systems studied by us, previously reported,[5] consist in an aqueous phase (a concentrated solution of polyacrylamide in water – 50% w/w) and an organic phase (cyclohexane); nonyl-phenol ethoxylated with four ethylene oxide molecules (NF4) has been used as a convenient emulsifier. A water-soluble redox system has provided the initiation.

Taking into account the complexity of the system, different parts of it have been investigated separately; for instance, we have shown the apparent molecular weight increase of acrylamide in water, as a result of association phenomena.[6] In the present work we report the investigation concerning the interactions between cyclohexane and NF4, as well as water bonding to emulsifier in the organic medium.

---

* Note 1; see *Rev. Roumaine Chim.*, **34**, 933 (1989).

EXPERIMENTAL

Cyclohexane, previously dried 24 hours on activated silicagel, was purified by distillation; its purity was checked by UV spectroscopy. Accurately measured amounts of NF4 were mixed with known volumes of pure cyclohexane. Preestablished volumes of water were introduced (using a chromatographic microsyringe) into these emulsifier-cyclohexane solutions. The mixture was subjected to an extensive shaking, in a sealed off phial; this procedure was followed by a period of several days, checking for any tendency towards phase separation. Only the mixtures that kept a homogeneous appearance were subjected to molecular weights measurements, using vapour pressure osmometry (VPO).

VPO was adopted as an appropriate method, taking into account the range of the molecular weights investigated. For this purpose, a Knauer-type VPO apparatus was used. The measurements took place with pure cyclohexane, at 25°: the average measuring time (in order to reach the thermodynamic equilibrium) was 30 minutes. The calibration was performed using cyclohexane solutions of benzyl or azobenzene, respectively, thus obtaining the number of equivalent divisions (for a standard amplification) corresponding to a concentration of 1 molal.

RESULTS AND DISCUSSION

In the first stage of this work, the effect of NF4 concentration (cyclohexane concentration) on the apparent molecular weight of NF4 has been studied: the main results are presented in table 1.

The molecular weight of NF4, according to its formula is 396; consequently, the first value presented in table 1 ($M = 418$) may be seen as a result of a certain polydispersity of the product, both in its hydrophilic part as well as in its hydrophobic part. Indeed, it is quite difficult to separe a "pure" NF4. However, the following values certainly indicate a monotonous tendency towards association; when the concentration reaches 12% (w/w), the apparent molecular weight becomes three times the initial value. We have not studied this dependence at higher concentrations, being out of range for practical applications: presenting the data from table 1 in a graphical form, one obtains a straight line.

Table 1

The influence of NF4 concentration on the apparent molecular weight of NF4 in cyclohexane

No.	NF4 concentration (% w/w)	Molar concentration (found)	Average numerical molecular weight
1	0.27	0.00647	418
2	1.32	0.02795	478
3	2.78	0.05542	517
4	3.21	0.05248	631
5	6.83	0.09196	797
6	11.48	0.11305	1148
7	12.40	0.11403	1242

Anyway, the values obtained clearly show the formation of simple associates and not of micelles, which should exhibit far higher molecular weights.

It has to be mentioned, that in studies concerning solubility phenomena for the heterogeneous system, we have noticed a remarkable increase for the volume of the organic phase (with regard to the initial one and, of course, after phase separation); the fact becomes more obvious as the acrylamide concentration in the aqueous phase decreases.[7]

At this behaviour is accompanied by a corresponding decrease in the volume of the aqueous phase, it may be attributed to a certain transfer of water towards the organic phase. One can reasonably suppose that water molecules may be bound on the polyethylene oxide chain, up to a certain limit.[8] For instance, we have noticed that as the water introduced in the cyclohexane solution of NF4 exceeds the molar ratio $H_2O/NF4 > 12$, then the system separates in two phases.

Table 2

Water bonds at the polyethoxylated chain of NF4 (NF4 concentration in cyclohexane – 2.78%)

No·	$H_2O/NF4$ (molar ratio)	Expected apparent molecular weight	Molecular weight experimentally found
3	0.0	—	517
8	1.27	540.2	552
9	2.53	565.5	576
10	5.02	607.0	619

In order to substantiate the above-described hypothesis, new tests (presented in table 2) have been carried out. These tests were performed under the previously mentioned conditions, when precisely measured water amounts were introduced in a cyclohexane solution of NF4 (2.78%).

The predicted (theoretical) values for the new apparent molecular weights were calculated taking into account a complete binding of water at the polyethoxylated chain. For instance (test no. 10), we have reckoned a theoretical molecular weight of $517 + 5.02 \times 18 = 607$. In our oppinion, there is an excellent concordance between the predicted and measured molecular weights; this fact is an important argument that favours the hypothesis of water bonds on emulsifier chain.

Repeating the same kind of experiments, this time for a higher NF4 concentration (5.91%), we have noticed significant differences between predicted and measured values for the molecular weight of "hydrated" emulsifier (see table 3).

The data listed in table 3 show that experimentally found values for M_n are sensibly higher than the predicted ones; this constitutes the experimental support for a model in which, besides ethylene oxide unit-water bonds, supplementary intermolecular hydrogen bonds become important. Nevertheless, the practical possibility that 10 moles of water may be bound to one mole of emulsifier has been experimentally proved, in agreement with literature data.[8] Unlike table 2, table 3 presents besides intensive values (concentrations, molar ratios etc.), extensive data as well,

Table 3

The effect of adding water in a solution containing cyclohexane — 70 ml (54.691 g) and NF4 — 3.4404 g (8.688 mmoles). on apparent molecular weight of NF4

No.	H_2O (g)	$\frac{H_2O}{NF4}$ (molar ratio)	Predicted M_n	Found	
				molal concentration	M_n
11	0.0	0.0	—	0.09349	672.8
12	0.4	2.5578	718.8	0.09122	768.7
13	0.7	4.4762	758.5	0.08828	857.6
14	1.12	7.1620	801.7	0.08730	950.5
15	1.33	8.5048	825.9	0.08607	1008.4
16	1.68	10.7429	866.1	0.08345	1115.8

suggesting the important water amount transferred in the organic phase, leading to the noticed volume increase.

REFERENCES

[1] J. W. Vanderhoff, F. V. DiStefano, M. S. ElAsser, R. O'Leary, O. M. Shaffer and D. L. Visiolü, *J. Disp. Sci. Technol.*, **5**, 323 (1984).

[2] W. Baade and K. H. Reichert, *Eur. Polymer J.*, **20**, 505 (1984).

[3] F. Candau, Z. Zekhuini and F. Heatley, *Macromolecules*, **19**, 1895 (1986).

[4] C. Holtzscherer, J. P. Durand and F. Candau, *Colloid and Polymer Sci.*, **265**, 1074 (1987).

[5] C. M. Boghină, C. D. Cincu, N. N. Marinescu, M. M. Marinescu, M. V. Dimonie, Minodora Lecca, Georgeta Popescu, C. G. Oprescu, Anca Roșanu and Magdalena Lungu, *J. Macromol. Sci.-Chem.*, **A 22**, 591 (1985).

[6] C. M. Boghină, C. D. Cincu, N. N. Marinescu, M. M. Marinescu, M. V. Dimonie and D. S. Vasilescu, *Rev. Roumaine Chim.*, **34**, 933 (1989).

[7] N. N. Marinescu, unpublished results.

[8] E. Cheever, F. D. Blum, K. R. Foster and R. A. MacKay, *J. Colloid Interface Sci.*, **104**, 121 (1985).

Revue Roumaine de Chimie, **36**, *4*–7, 761–770 (1991)

Dedicated to Prof. ALEXANDRU T. BALABAN with
the occasion of his 60th anniversary

MECHANOCHEMICAL REACTIONS AT THE SPINNING FROM SOLUTION OF THE ACRYLONITRILE – VINYL ACETATE – α-METHYL STYRENE BASED TERNARY COPOLYMER

MARCEL POPA and CLEOPATRA VASILIU OPREA

Polytechnic Institute of Jassy, Department of Macromolecules, 23 August Street, 11 A,
6600 Jassy, Roumania

Received January 3, 1991

The paper studies the mechanochemical degradation of the ternary copolymer acrylonitrile–vinyl acetate–α-methylstyrene in solution, in conditions simulating the spinning. The influence of some factors (geometrical characteristics of the capillaries, solution concentration, spinning pressure) on the efficiency of the mechanochemical destruction, on taking the variation of the intrinsic viscosity of the polymer as a criterion of molecular phenomena, was established. The tests accomplished on a micropilot installation prove the production of the mechanodestruction as well, in the conditions practically identical with those of industrial spinning. The undesirable and inevitable effects of mechanodegradation are used to obtain monofilaments with good tinctorial capacity which can be chemically dyed with acid colorants.

INTRODUCTION

The mechanical stressing of the polymers in solution has as effect the concentration of the mechanical energy directly and almost exclusively at the level of the macromolecules; thus we can consider that an authentic mechanochemical degradation is included here. Many studies have been dedicated to the destruction of the polymers in solution so that nowadays its laws, the mechanism and the influence factors of the reaction are very well known. Thus it has been emphasized that by ultrasonic treatment,[1–3] cryolize,[4,5] rapid stirring,[6–9] laminar [10] and turbulent flow [11,12] through thin tubes, the molecular weight is reduced, the efficiency of the mechanodegradation depending preponderantly on the parameters of the mechanical regime and on the concentration of the solution. But a few studies are still dealing with the mechanochemical degradation produced by shearing through capillary tubes, although the practical implications of this process are important especially in the case of the polymer spinning from solution.

Staudinger,[13] Frenkel,[14] Morris [15] and Grohn [16,17] broke new ground in this domain. On starting from this premise, we have approached the study of acrylonitrile-vinyl acetate-α-methyl styrene based ternary copolymer mechanodegradation under conditions simulating the industrial spinning. Our approach has been based, as well, on the experimental finding that the industrially-spun polymer undergoes a reduction up to 25% of the molecular weight, an argument for a mechanochemical process developed under these conditions. Therefore the purpose of this paper is the systematic research of this process so that the influence of some factors and the determination of the reaction mechanism peculiarities should be accomplished. The obtained results have allowed the elaboration of chemically dyeing procedure of the "Melana"-type monofilaments by using the inevitable effects of mechanodestruction.

EXPERIMENTAL PART

We have studied the mechanodegradation of a ternary polymer obtained by solution-suspension used for the manufacturing of the "Melana" — type synthetic fibres. The polymer has the following composition : 92.2% acrylonitrile (AN), 4.5% vinyl acetate (VA) and 3.3% α-methyl styrene (MS). The intrinsic viscosity in a dimethyl formamide (DMF) solution at 25°C is $[\eta] = 1.86$. The solutions subjected to shearing in capillaries have been obtained by dissolving the copolymer in DMF at $T = 60 \pm 5°C$, then by degasing (1 h, in vacuum). The experiments have been performed on a laboratory installation which allows the simulation of the industrial spinning process from solution.[18] The coagulation of the filaments has been done in water at $T = 20 \pm 2°C$. We have selected the intrinsic viscosity determined in DMF [19] as an evaluation criterion of the polymer mechanodegradation. The employed installation has permitted the study of the influence of some basic parameters on the mechanodegradation process, each of them being considered at five value levels (Table 1).

The results of some 96 experiments accomplished under different shearing conditions have been processed on a FELIX C 256 computer ; thus the regression equation which correlates $[\eta]$ with the parameters of the spinning process has been obtained.

Table 1

Parameters of the mechanodegradation process by spinning from solution and their value levels

Parameter	Value level				
— Length of the capillary (L, mm)	20	28	36	40	45
— Length/diameter ratio (L/D, mm/mm)	51.4	54	60	70	100
— Concentration of solution (C, %)	10	13	16	19	22
— Pressure (P, at)	5	7	9	11	15

To obtain information on the reaction mechanism, some experiments have been made under the condition of monofilaments coagulation in solutions containing radical acceptors (1% benzidine in methanol or 0.1% DPPH in methanol). The unreacted diamine amount has been determined by photocolorimetry.

The information obtained in laboratory has been used to accomplish the spinning of the ternary copolymer on a micropilot installation at the Central of Artificial Fibres — Brăila. Thus we have obtained monofilaments with free amino-groups, subsequently subjected to classic dyeing with "Modacryl" — type acid dyes.

RESULTS AND DISCUSSION

The obtained experimental results certify that the mechanodegradation is produced in all cases, being evaluated by the decrease of the polymer intrinsic viscosity. The intensity of the process depends on its variables. The regression equation which correlates with the considered parameters has the form

$$[\eta] = 1.427 + 7 \times 10^{-3}L + 2 \times 10^{-3}L/D + 2.1 \times 10^{-2}C + 5 \times 10^{-4}P + 10^{-4}L^2 - 10^{-3}(L/D)^2 - 5 \times 10^{-4}C^2 + 2.6 \times 10^{-4}P^2 - 10^{-4}L \times L/D + 2 \times 10^{-4}L \times C + 2 \times 10^{-4}L \times P - 2 \times 10^{-4}L/D \times C - 7 \times 10^{-4}L/D \times P + 7 \times 10^{-4}P \times C$$

The multiple correlation coefficient ($r = 0.8862$) and the "F" factor (21.2) indicate a good significance of the equation.

The variation of $[\eta]$, used as an evaluation criterion of the molecular phenomena which are taking place here with any parameters is shown in Figs. 1–4.

The length of the capillary is a first factor or influence whose action is illustrated in Fig. 1. The increase of the capillary length favours a longer action of the shearing stresses developed at its walls, responsible for the splitting of the chemical bonds, so that the efficiency of the mechanodegradation increases with this parameter.

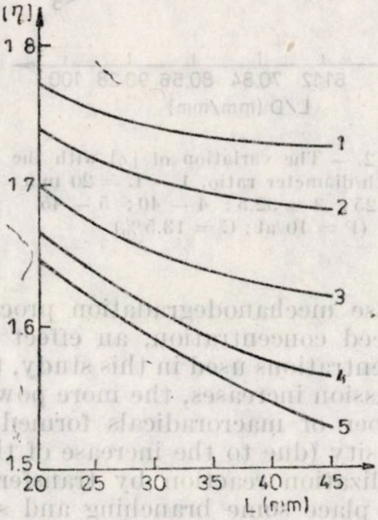

Fig. 1. — The variation of $[\eta]$ with the length of the capillary. 1 — L/D = = 51.4 ; 2 — 61 ; 3 — 75 ; 4 — 90 ; 5 — 100 (P = 10 at ; C = 13.5%).

The increase of the length/diameter ratio (another important variable of the process) has as effect the continuous decrease of $[\eta]$. The increase of this ratio value is due both to the increase of length and to the decrease of the capillary diameter. Generally speaking, capillary tubes with small diameter favour much more intense shearing stress at the wall, thus determining an advanced degradation. The same effect is obtained, as it has been previously shown, by the increase of the capillary length. Accordingly, $[\eta]$ suffers a much more decrease with the variable L/D than with the variable L, as resulting from Fig. 2.

Another important parameter of this mechanodegradation type is the concentration of the solution (Fig. 3). One can notice that the most intense mechanodegradation processes take place in the solutions with reduced concentration, an effect which is explained as follows: at the concentrations used in this study, the more the value of the variable under discussion increases, the more powerful the primary effects are. The great number of macroradicals formed under the condition of an increased viscosity (due to the increase of the solution concentration) favours their stabilization reaction by transfer to the polymer. Consequently, there take place some branching and some slight reticulations which lead to the increase $[\eta]$ of the polymer, emphasizing the effects of the mechanodegradation. Thus, it has been noted that the dissolving process of the monofilaments obtained by spinning the most concentrated solutions, is much slower (needing duration at least three times higher as compared

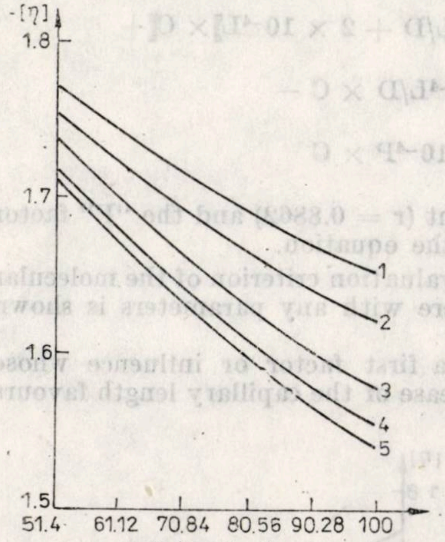

Fig. 2. — The variation of $[\eta]$ with the length/diameter ratio. 1 — L = 20 mm; 2 — 25; 3 — 32.5; 4 — 40; 5 — 45 (P = 10 at; C = 13.5%).

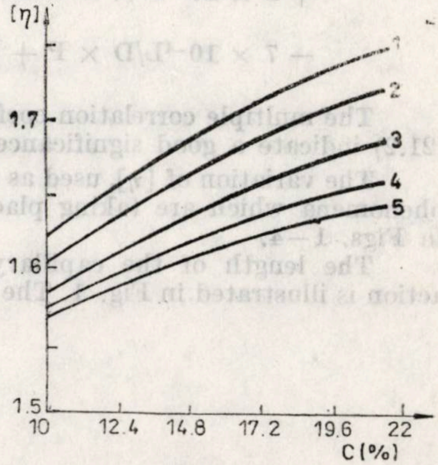

Fig. 3. — The variation of $[\eta]$ with the concentration of the solution. 1 — L = 20 mm; 2 — 25 mm; 3 — 32.5 mm; 4 — 40 mm; 5 — 45 mm (P = 10 at; L/D = 75.7).

to the other samples), an indirect proof of the slight reticulation of the structure.

An important variable of the process is the spinning pressure. The family of curves illustrating the influence of this parameter is shown in Fig. 4, presenting a minimum value of the intrinsic viscosity at P ≈ ≈ 10 atm. The downward branch of the curves (on the domain P = 5—10 atm) renders evident the diminishing of [η] with this parameter. The effect is evidently due to the intensification of the shearing effect at the capillary wall. Above the value P = 10 atm., the number of the molecular splitting increases, thus the concentration of the formed macroradicals increases as well. Beside their reciprocal stabilization by recombining and disproportionation, the chain transfer manifests more and more, being facilitated by the reduction of the "free volume" of the polymer due, in its turn, to the increase of pressure.[20,21] By the recombination of the secondary macroradicals thus formed, there are produced reticulation effects which are intensified with the increase of pressure, a fact which explains the increase of the value [η]. These data are in agreement with the decrease of the solubility of the monofilaments obtained by spinning at pressures above 10 atm.

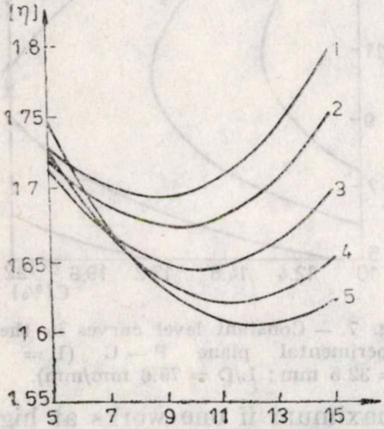

Fig. 4. — The variation of [η] with the spinning pressure. 1 — L = 20 mm; 2 — 25 mm; 3 — 32.5 mm; 4 — 40 mm; 5 — 45 mm (L/D = 75.7; C = 13.5%).

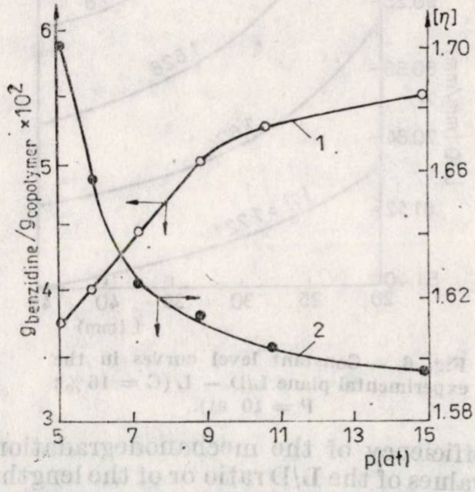

Fig. 5. — The variation of the amount of chemically reacted benzidine (1) and of the [η] with the spinning pressure (C = 10%; L/D = = 100; L = 20 mm).

By shearing at capillary tubes at pressures above 10 atm., in the presence of a radical acceptor (DPPH), dissolved in the copolymer solution, we have noticed the continuous decrease of [η], evidently due to the reaction of the macroradicals with DPPH and the prevention, in this manner, of the chain transfer reactions.

A supplementary argument in favour of the increasing number of primary macroradicals, at pressures above 10 atm., has been given by the experiment accomplished in the presence of benzidine as radical acceptor

(Fig. 5). On working on the domain P = 5—14 atm., we have noticed that at the same time with the increase of the pressure, greater and greater amounts of diamine are reacting, a result of a higher and higher concentration of free macroradicals with which the diamine reacts.

The effect is maintained as well at pressures higher than 9 atm. At the same time, the intrinsic viscosity of the copolymer decreases as the stabilization reactions of the macroradicals by chain transfer are prevented. Thus, it becomes clear that this increase of [η] renders evident at pressures above 9 atm; this is due to the slight reticulation of the polymer structure and not to the decreasing in the splitting numbers of the covalent bonds from the basic chain of the copolymer.

The analysis of the constant level curves presented in Figs. 6, 7 allows the establishing of the correlated influence of the mechanic regime parameters on the mechanodestruction. Thus, it can be noted that the efficiency of the mechanodegradation is maximum if one works at high values of the L/D ratio or of the length of the capillary, respectively (Fig. 6), or with small concentration solutions at pressures about 10 atm. (Fig. 7).

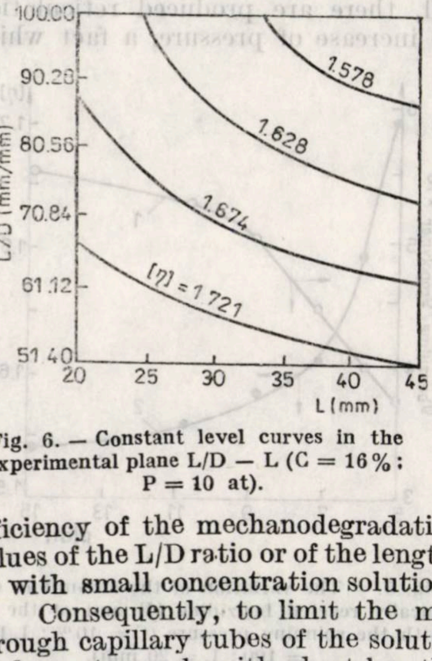

Fig. 6. — Constant level curves in the experimental plane L/D — L (C = 16%; P = 10 at).

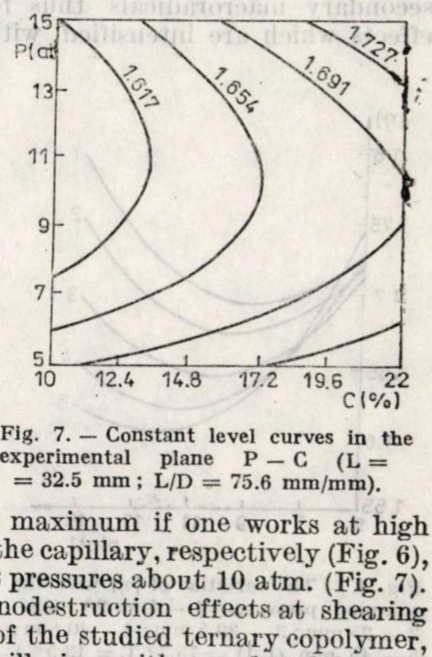

Fig. 7. — Constant level curves in the experimental plane P — C (L = = 32.5 mm; L/D = 75.6 mm/mm).

Consequently, to limit the mechanodestruction effects at shearing through capillary tubes of the solutions of the studied ternary copolymer, we have to work with short-length capillaries, with a reduced length/diameter ratio, at higher concentrations of the solutions (which are economical) and minimal pressures (also advantageous). In industry, these conditions are fulfilled by working with concentrated solutions and with 5 atm. pressure (in the case of manufacturing the "Melana" fibre).

The obtained experimental results render evident the fact that the polymer degradation takes place in any spinning regime. The reason for this reaction is the overstressing of the chemical bonds, especially of those placed in the vicinity of macromolecules centre, which undergoes an elongation in the direction of the flow due to the gradient of the flow speed from the centre of the capillary to the capillary walls. The effect increases in intensity with the square of the macromolecules length which splits homolytically when reaching the critical speed gradient.

To make evident the radical character of the mechanochemical destruction under conditions simulating the spinning from solution, we have introduced micromolecular compounds with a character of radical acceptor, in the coagulating bath. Thus, accomplishing the precipitation of the solution jet of the polymer in a DPPH solution, a violet coloured monofilament has been obtained. The intensity of the coloured monofilament has been obtained. The intensity of the colour has been maintained unchanged even after 48 hours of methanol extraction.

Knowing the radical acceptor character of aromatic diamines we have accomplished the coagulation of the polymer in a methanol solution of benzidine. Another working variant has been the introduction of a benzidine amount (0.03% as compared to the polymer) in the solution subsequently subjected to spinning. In all the cases, we have obtained filaments coloured according to the used diamines, while the witness samples accomplished by maintaining the uncoloured filaments in the diamine solution have not presented colour changes. The obtained colours proved to be stable, not being modified by extraction in methanol.

An indirect proof of the diamine chemical bonding is the possibility of accomplishing the diazotation and coupling reactions with components such as β-naphthol, resorcinol, "H" acid which led to the obtention of new colours for monofilaments.

On the basis of the gathered experimental data and discussed problems, we can formulate a chained radical mechanism of the mechanodegradation process of the studied polymer. In the initial stage, there appear primary macroradicals by splitting the bonds from the central zone of the macromolecule, especially those in which the quaternary carbon atom from the structural unity of α-MS is implied.[22]

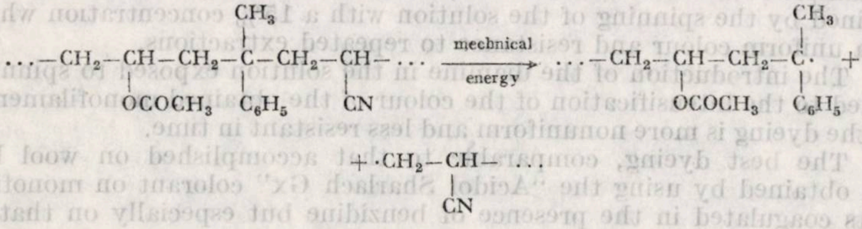

$$\ldots-CH_2-\underset{OCOCH_3}{CH}-CH_2-\overset{CH_3}{\underset{C_6H_5}{C}}-CH_2-\underset{CN}{CH}-\ldots \xrightarrow[\text{energy}]{\text{mechnical}} \ldots-CH_2-\underset{OCOCH_3}{CH}-CH_2-\overset{CH_3}{\underset{C_6H_5}{C}}\cdot + \cdot CH_2-\underset{CN}{CH}-\ldots$$

The formed macroradicals can react between them, stabilizing themselves either by disproportionation (a fact which explains the decrease of the intrinsic viscosity in the majority of the cases) or by chain transfer to the polymer followed by recombination (a fact explaining the slight increase of the intrinsic viscosity in some cases, by the formation of branched or reticulated structures).

In the presence of the micromolecular compound as radical acceptor (aromatic diamine), the stabilization of the macroradicals by transfer to diamine followed by recombination is being produced.

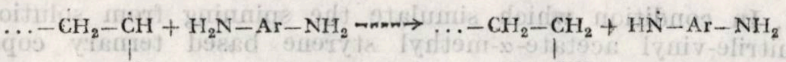

$$\ldots-CH_2-\underset{CN}{\dot{C}H} + H_2N-Ar-NH_2 \longrightarrow \ldots-CH_2-\underset{CN}{CH_2} + H\dot{N}-Ar-NH_2$$

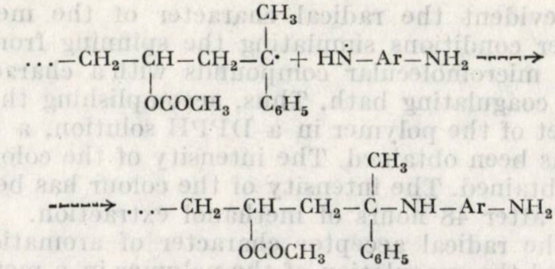

$$\ldots-CH_2-\underset{OCOCH_3}{\underset{|}{CH}}-CH_2-\underset{C_6H_5}{\underset{|}{\overset{CH_3}{\overset{|}{C}}}}\cdot + HN-Ar-NH_2 \dashrightarrow$$

$$\dashrightarrow \ldots-CH_2-\underset{OCOCH_3}{\underset{|}{CH}}-CH_2-\underset{C_6H_5}{\underset{|}{\overset{CH_3}{\overset{|}{C}}}}-NH-Ar-NH_2$$

Thus, there are obtained monofilaments having "grafted" on the surface aromatic aminic groups, ultimate or statistically disposed on the chain, in the case when the chain transfer reactions at the polymer have contributed as well as the stabilization of the primary macroradicals.

The experimental results on a laboratory level have led to the conclusion that the mechanodegradation process, although undesirable, is inevitable. The radical nature of its mechanism being proved, there appears the idea of using some specific reactions of the free radicals with the view of improving the tinctorial properties of the studied copolymer. Consequently, we have spun some solutions with various concentrations of the copolymer in DMF on a micropilot installation. We have worked out more variants, the obtained observations being selectively presented in Table 2.

One can notice that the used solutions present different spinning capacity, the best spinning capability being shown by that with a 15% concentration. The tinctorial properties, manifested by the dyeing of the monofilaments with "Modacryl" type acid colorants, vary as well from one sample to another. One can note, in this case as well, the monofilaments obtained by the spinning of the solution with a 15% concentration which has a uniform colour and resistance to repeated extractions.

The introduction of the diamine in the solution exposed to spinning has led to the intensification of the colour of the obtained monofilaments, but the dyeing is more nonuniform and less resistant in time.

The best dyeing, comparable to that accomplished on wool has been obtained by using the "Acidol Sharlach Gx" colorant on monofilaments coagulated in the presence of benzidine but especially on that of p-phenylene diamine.[23]

Therefore, the obtained results prove as well, the production of the mechanodegradation reactions in conditions similar to the industrial ones. However, we must check them out on the the industrial installation for producing the "Melana"-type monofilaments, to establish their behaviour on the entire technological flow, especially from the viewpoint of the physico-chemical and mechanical properties.

CONCLUSIONS

1. In condition which simulate the spinning from solution, the acrylonitrile-vinyl acetate-α-methyl styrene based ternary copolymer undergoes severe mechanodestructive processes.

Table 2

The behaviour of the "Melana" type filaments under spinning conditions on a micropilot installation, in the presence of radical acceptors

No.	Concentration of the solution (%)	Coagulation bath	Observations	
			on spinning	on dyeing with acid colorants
1	12	ethanol	— reduced spinning capability — reduced mechanical strength of the monofilaments	— reduced tinctorial capacity — the dyeing does not resist to repeated extractions
2	15	ethanol	— good spinning capability	
3	20	ethanol	— satisfactory spinning capability	
4	12	ethanolic solution of benzidine (1%)	— reduced mechanical strength of monofilaments — needs a small speed for spinning	— satisfactory dyeing, various shade ranges
5	12	ethanolic solution of p-phenylene diamine (0.3%)		— good dyeing
6	15	ethanolic solution of benzidine (1%)	— very good spinning capability — good mechanical strength of monofilaments — uniform thickness of monofilaments	— very good dyeing
7	15 (with 1.66% as compared to the copolymer)	ethanolic solution of benzidine (1%)	—idem—	— very good dyeing with a less loss of shade at repeated extractions
8	idem	ethanol	—idem—	— good dyeing, with a slight loss of shade at repeated extractions
9	20	ethanolic solution of benzidine (1%)	— small depth for dipping	— good but nonuniform dyeing
10	20	ethanolic solution of p-phenylene diamine (0.3%)	— quick clogging of the capillary	— weak and nonuniform dyeing

2. The intensity of the mechanodegradation under conditions simulating the spinning from solution of the ternary copolymer, depends on the geometrical characteristics of the capillaries, on the pressure and concentration of the solution.

3. Mechanodegradation is produced with maximum intensity at high values of the capillary length and of the length/diameter ratio, respectively, at small concentrations of the solution and medium values of the pressure.

4. The mechanodegradation mechanism is radicalic, the splitting of the macromolecular chains being done preferentially in the middle of chain.

5. The inevitable consequences of the mechanodestructive process which take places at spinning the ternary copolymer in solution, can be used to improve the tinctorial properties, allowing to obtain monofilaments which could be chemically dyed.

REFERENCES

[1] A. M. Basedow, and K. H. Ebert, *Makromol. Chem.*, **176**, 745 (1975).
[2] M. S. Doulah, *J. Appl. Polym. Sci.*, **22**, 1735 (1978).
[3] T. Amari and M. Nakamura, *J. Appl. Polym. Sci.*, **18**, 3329 (1974).
[4] M. M. Kuharcic and N. K. Baramboim, *Vysokomol. soedin.*, **A 14**, 843 (1972).
[5] S. Matsuzawa, K. Yamaura, Y. Umeda, Y. Inoue, H. Kitamura and S. Y. Pak, *Makromol. Chem.*, **180**, 2009 (1979).
[6] K. Yamaura, K. Nakada and S. Matsuzawa, *Makromol. Chem.*, **177**, 927 (1976).
[7] S. H. Agarwall and R. S. Porter, *J. Appl. Polym. Sci.*, **25**, 173 (1980).
[8] A. Nakano and Y. Minoura, *J. Appl. Polym. Sci.*, **19**, 2749 (1975).
[9] F. S. S. Yu, Y. L. Zakin and G. Patterson, *J. Appl. Polym. Sci.*, **23**, 851 (1978).
[10] G. Akay, Rheol. (Proc. Int. Cong. 8th), **8**, 351 (1980).
[11] H. G. Müller, *Angew. Makromol. Chem.*, **57**, 99 (1977).
[12] J. D. Culter, J. L. Zakin and G. Patterson, *J. Appl. Polym. Sci.*, **19**, 3235 (1975).
[13] H. Staudinger and V. Heurer, *Ber. Dstch. Chem. Ges.*, **67 B**, 1159 (1934).
[14] J. Frenkel, *Acta physicochim. URSS*, **19**, 51 (1944).
[15] J. W. Moris and R. Shurman, *Nature*, **1−0**, 674 (1967).
[16] H. Grohn and F. Krause, *Plaste und Kautschuk*, **11**, 2, 1964.
[17] F. Krause and H. Grohn, *Plaste und Kautschuk*, **11**, 6, 1964.
[18] Cl. Vasiliu Oprea and M. Popa, *Plaste und Kautschuk*, **32**, 337 (1985).
[19] * * * , "Polymer Handbook" (J. Brandrup and E. H. Immergut Eds.), J. Wiley and Sons, New York-London-Sidney-Toronto (1975).
[20] P. H. Goldblatt and R. S. Porter, *J. Appl. Polym. Sci.*, **20**, 1193 (1976).
[21] A. Casale, R. C. Peinwell and R. S. Porter, *Rheol. Acta*, **10**, 412, 1971.
[22] M. I. Chiparà, Cl. Vasiliu Oprea, L. Georgescu, M. Popa and F. Beuran, Proc. of ' Recent Advances in EPR Spectroscopy", University of Sheffield, England, 14—16 Sept. 1987.
[23] M. Popa, Ph. D. Thesis, Jassy (1989).

Revue Roumaine de Chimie, 36, 4–7, 771–781 (1991)

Dedicated to Prof. ALEXANDRU T. BALABAN
with the occasion of his 60th anniversary

STUDY ON MASS TRANSFER IN THIN FILM FLOW OF SUSPENSIONS*

RADU Z. TUDOSE,[a] ECATERINA MERICĂ,[a] ION MĂMĂLIGĂ[a] and O. PETRUŞ[b]

[a] Polytechnic Institute of Jassy
[b] "Al. I. Cuza" University – Jassy

Received December 8, 1990

In the present paper the manner in which the introduction of solid particles in a falling film of liquid influences the mass transfer is reported. Comparative studies were carried out for CO_2 absorption in thin liquid films of water and suspensions prepared with various solid materials, of various concentrations and particle sizes of the solids. The influence of Re number of the liquid phase, of the solid nature and concentration as well as of the particle size upon the mass transfer coefficient in liquid phase, k_L, has been followed and a general correlation between k_L and the process variables derived.

INTRODUCTION

The analysis of papers reported in the field of thin liquid film flow allows the selection of factors with potential influence on the mass transfer: interfacial area, inclination angle of the film flowing plane, liquid flowrate, column geometry, viscosity of the absorbant, presence of surfactants, temperature, rugosity and the presence of surface waves.[1-4]

Though the studies in the field of mass transfer are numerous, until 1986 no paper concerning the influence of solid phase presence on the mass transfer in flow of thin liquid film was reported. There is only a study on the hydrodynamics of a thin film of bentonite clay reported by Astarita,[5] but the obtained results have not been reproducible.

In a previous paper[6] a study on the mass transfer in flow of a thin film of suspensions of ABS copolymer (acrylonitrile-butadiene-styrene) of various concentrations and of two sizes of solid particles was reported. In the present paper the absorption of carbon dioxide in water and suspensions flowing in thin films is investigated and a comparison of all the

---

[*] Reported in part at the 9th International Congress of Chemical Engineering, Chemical equipment design and Automation, CHISA 87, Praha, CZECHOSLOVAKIA, August 30 – September 4, 1987

studied systems is made. The work has been structured in such a way as to allow the investigation of the following questions :

— how the presence of solid particles influences the mass transfer?

— which is the relationship between the Re number of the liquid phase and the liquid phase mass transfer coefficients, k_L?

— which is the dependence of the liquid phase mass transfer coefficient, k_L, on the solute diffusion coefficient?

— which of the features of the solid phase (nature, concentration and particle size) influences the transfer process and in what manner?

EXPERIMENTAL

The absorption of carbon dioxide in water and suspension, respectively, was investigated using the equipment depicted in Fig. 1. The absorption column (1—3) is formed of two concentric pipes.

The descending film flows on the external wall of the internal pipe (Ni-Cr alloy steel, length = 2 285 mm, external diameter 30 mm). In the annular space between the external pipe (plexiglass, internal diameter 60 mm) and the liquid film the carbon dioxide flows countercurrently.

At the top the column is provided with a distribution head which ensures the formation of a thin film on the internal pipe. The gap width is adjusted by the up and down displacement of the internal tube. The liquid is pumped from the supply tank to the level vessel 4 and enters the distribution head of the column. The two tanks work alternatively; while one receives the liquid, from the other the column is fed. Both tanks (V = 300 l) and the level vessel are provided with mixers for maintaining the particles in suspension.

The carbon dioxide is fed countercurrently from a gas tube and its flowrate was adjusted by means of two flowmeters, one for a coarse adjustement the other for a fine one.

To prevent the diffusion of water in gas the latter was saturated by bubbling it in water (vessel 13) prior to the admission in the column.

The liquid flowrate at the exit was measured by counting the time required for collecting a known volume of liquid.

MATERIALS AND WORKING PROCEDURES

As gas phase pure carbon dioxide has been used. All the runs have been performed using distilled water. As solid phase the materials listed in Table 1 have been used.

The solid materials have thus been chosen as to exhibit various chemical natures and densities; in case of polyvinylchloride prepared by two polymerization procedures — suspension and emulsion, respectively — the difference in behaviour and the influence of the emulgator presence have been followed.

The selection of the adequate particle size of the solids has been accomplished based on some technological considerations such as :

— the behaviour of the solid material in suspension ;

— the ratio between the size of the gap width of the distribution head, implicitly the film thickness and the particle size ;

— the availability of the desired fraction. In Table 1 the types of the investigated systems are listed.

The analysis of carbon dioxide in the liquid phase has been made by precipitating it as barium carbonate using a mixture of barium chloride and standard natrium hydroxide. The excess natrium hydroxide was then retitrated with hydrochloric acid to a phenolphthaleine end point.

Prior to each set of measurements a reference sample was taken, the initial content of carbon dioxide in water being thus determined. The liquid phase mass transfer coefficient based on mean logarithmic driving force has been calculated for the absorption of pure gas at a pressure of 1 atmosphere. In practical calculations the external surface of the internal pipe was assumed to be the mass transfer surface. Given the high purity of gas the resistance of gaseous phase has been neglected as well as the effect of water counterdiffusion, since the gas was previously saturated with liquid. The densities and viscosities of the suspensions have been determined experimentally

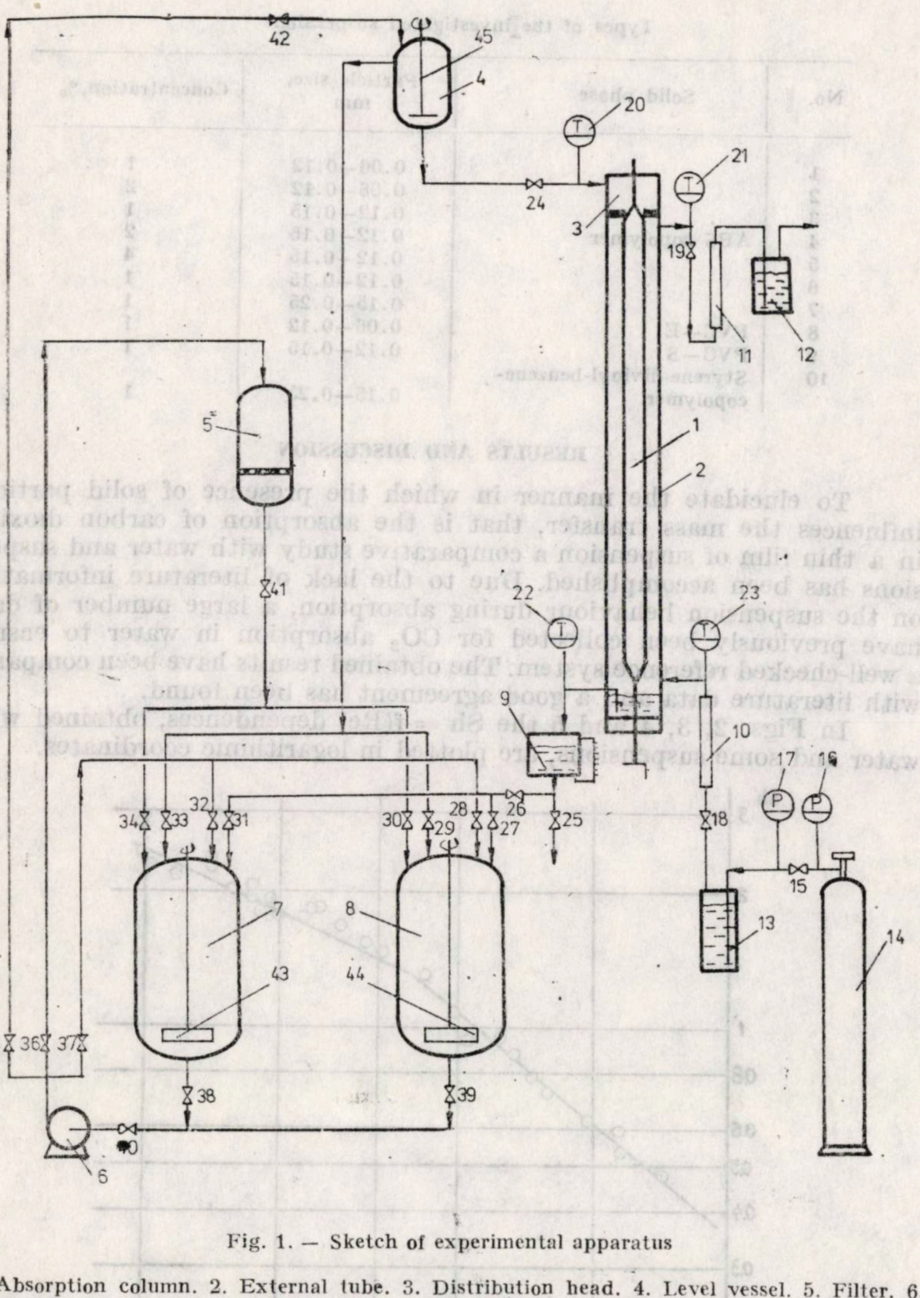
42
45
4
20
T
21
T
24
3
19
11
12
5
1
2
41
22
T
23
T
9
10
17
P
16
P
34
33
32
31
30
29
28
26
27
25
18
15
13
14
7
8
43
44
35
36
37
38
39
40
6

Fig. 1. — Sketch of experimental apparatus

1. Absorption column. 2. External tube. 3. Distribution head. 4. Level vessel. 5. Filter. 6. Pump. 7,8. Tanks. 9. Liquid flowrate measuring vessel. 10,11. Flowmeters. 12. Control vessel for CO_2 flow. 13. Vessel for CO_2 saturation with water vapours. 14. Gas tube. 15. Pressure reducing valve. 16,17. Manometers. 18,19. Valves. 20—23. Thermal resistances. 24—42. Valves. 43—45. Mixers.

Table 1

Types of the investigated suspensions

No.	Solid phase	Particle size, mm	Concentration, %
1	ABS copolymer	0.06—0.12	1
2		0.06—0.12	2
3		0.12—0.15	1
4		0.12—0.15	2
5		0.12—0.15	4
6		0.12—0.15	1
7		0.15—0.25	1
8	PVC—E	0.06—0.12	1
9	PVC—S	0.12—0.15	1
10	Styrene-divinyl-benzene-copolymer	0.15—0.25	1

RESULTS AND DISCUSSION

To elucidate the manner in which the presence of solid particles influences the mass transfer, that is the absorption of carbon dioxide, in a thin film of suspension a comparative study with water and suspensions has been accomplished. Due to the lack of literature information on the suspension behaviour during absorption, a large number of data have previously been collected for CO_2 absorption in water to ensure a well-checked reference system. The obtained results have been compared with literature data and a good agreement has been found.

In Figs. 2, 3, 4 and 5 the Sh = f(Re) dependences, obtained with water and some suspensions, are plotted in logarithmic coordinates.

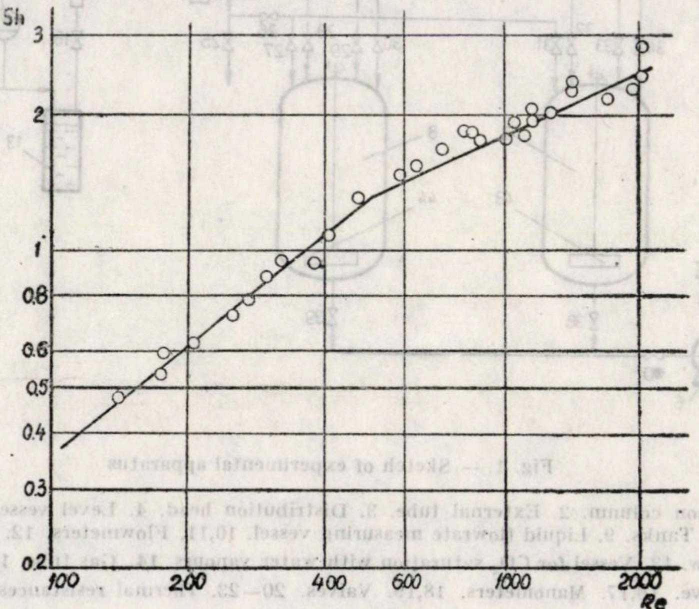

Fig. 2. — Sh vs. Re for the runs carried out with water.

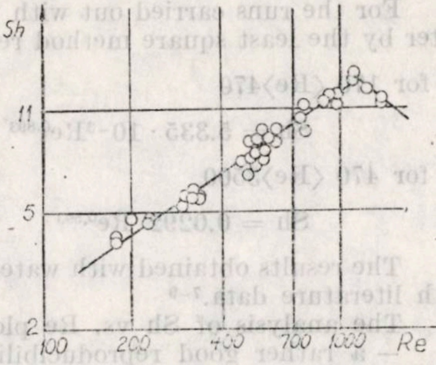

Fig. 3. — Sh vs. Re for the runs carried out with suspensions prepared with ABS copolymer (0.15—0.25 mm particle size).

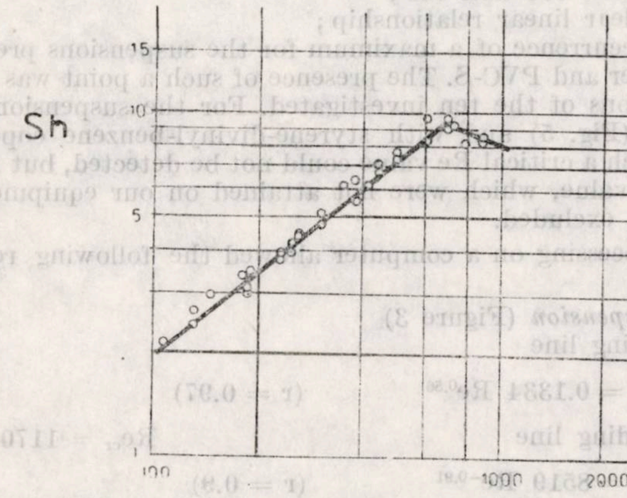

Fig. 4. — Sh vs. Re for the suspension prepared with PVC-S.

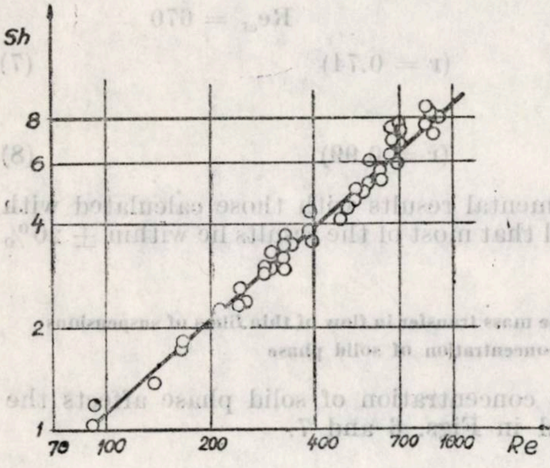

Fig. 5. — Sh vs. Re for the suspension prepared with PVC-E.

For the runs carried out with water, the data processing on a computer by the least square method resulted in the following relationships :

— for 170 ⟨Re⟩470

$$Sh = 5.335 \cdot 10^{-3} Re^{0.893} \qquad (r = 0.983) \qquad (2)$$

— for 470 ⟨Re⟩3500

$$Sh = 0.0292\ Re^{0.593} \qquad (r = 0.972) \qquad (3)$$

The results obtained with water were found to be in good agreement with literature data.[7-9]

The analysis of Sh vs. Re plots for suspensions shows :

— a rather good reproducibility of the results, especially for Re numbers between 100 and 500 ;

— the clear linear relationship ;

— the occurrence of a maximum for the suspensions prepared with ABS copolymer and PVC-S. The presence of such a point was noticed for eight suspensions of the ten investigated. For the suspensions prepared with PVC-E (Fig. 5) and with styrene-divinyl-benzene copolymer the presence of such a critical Re value could not be detected, but its presence at higher Re value, which were not attained on our equipment, cannot be completely excluded.

Data processing on a computer allowed the following relationships to be settled :

ABS suspension (Figure 3)

— the ascending line

$$Sh = 0.1334\ Re^{0.56} \qquad (r = 0.97) \qquad (4)$$

— the descending line $\qquad Re_{cr} = 1170$

$$Sh = 8519\ Re^{-0.91} \qquad (r = 0.9) \qquad (5)$$

PVC-S suspension

$$Sh = 0.0565\ Re^{0.796} \qquad (r = 0.98) \qquad (6)$$

$$Re_{cr} = 670$$

$$Sh = 120\ Re^{-0.39} \qquad (r = 0.74) \qquad (7)$$

— *PVC-E suspension*

$$Sh = 0.0198\ Re^{0.879} \qquad (r = 0.99) \qquad (8)$$

The comparison of experimental results with those calculated with the above relationships indicated that most of the results lie within ± 20% range.

Factors with potential influence on the mass transfer in flow of thin films of suspensions

Influence of concentration of solid phase

The manner in which the concentration of solid phase affects the mass transfer can be visualized in Figs. 6 and 7.

The fact that under the conditions of simultaneous variation of two parameters (concentration and Re) no clear differentiation occurs between the plots demonstrates the fact that the absorption mechanism is complex and indicates the close interaction between the process variables. The situation depicted in Fig. 7 is quite the opposite. It can be seen that for the same Re there is a clear relationship between k_L and solid concentration. Thus a concentration increase of the solid from 1 to 2% results in an increase of the liquid mass transfer coefficient but further increase of the solid concentration proves to be disadvantageous.

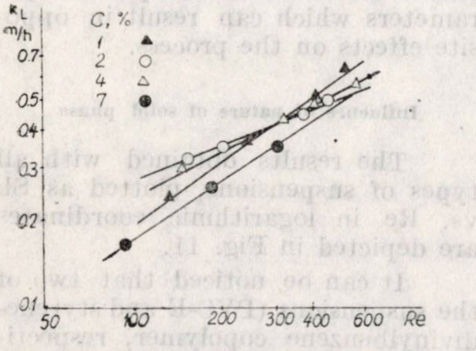

Fig. 6. — Variation of the mass transfer coefficient, k_L, with Re number for suspensions of ABS copolymer of various concentrations.

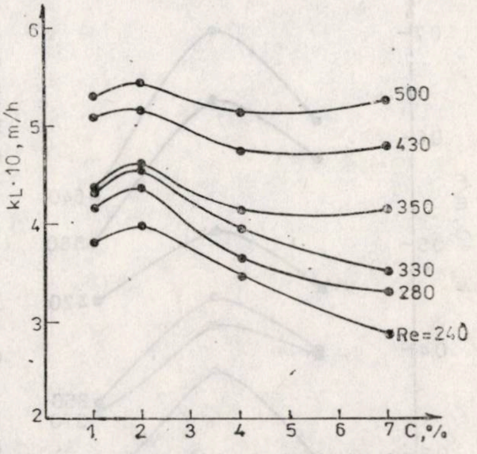

Fig. 7. — k_L vs. solid concentration for suspensions of ABS copolymer(0.12—0.15 mm particle size).

Influence of size of solid particles on the mass transfer coefficient

The effect of size of solid particles on the liquid mass transfer coefficient has been followed by carrying out experiments with the same material, at the same concentration of solid, but with solid particles of various sizes (Figs. 8, 9 and 10).

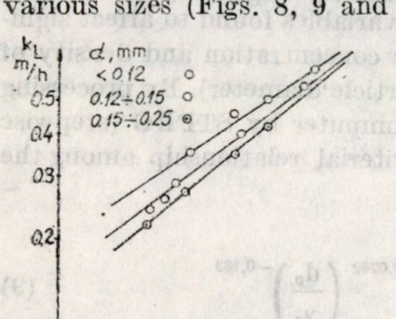

Fig. 8. — k_L vs. Re for suspensions of ABS of various particle sizes (concentration 1 %).

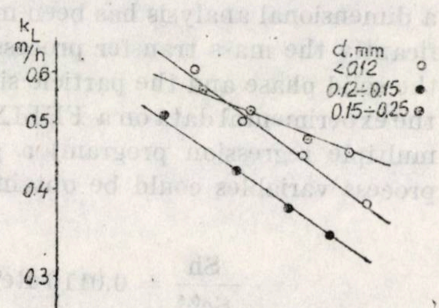

Fig. 9. — k_L vs. Re for suspensions of ABS of various particle sizes (concentration 1 %).

The best results are seen to be obtained with a medium particle size. But this effect is noticed only over a range of Re values up to the critical value (the ascending line). For Re values higher than the critical values the best results have been obtained with the largest particles while the lower k_L values were obtained with particles of medium size. These facts indicated the complex interaction between the process parameters which can result in opposite effects on the process.

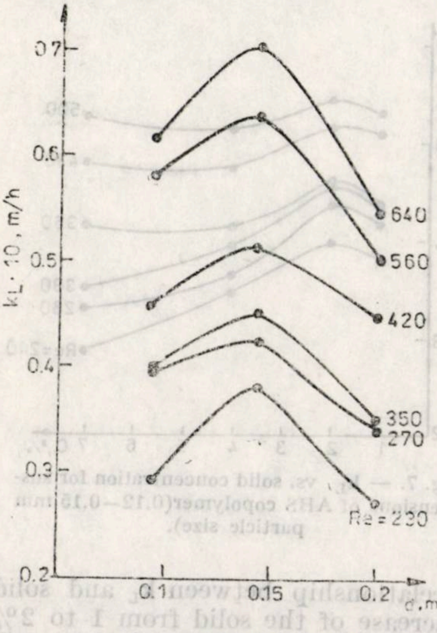

Fig. 10. — Influence of solid particle size on the coefficient of liquid phase mass transfer for suspensions of ABS copolymer (particle concentration 1%).

Influence of nature of solid phase

The results obtained with all types of suspensions, plotted as Sh vs. Re in logarithmic coordinates are depicted in Fig. 11.

It can be noticed that two of the suspensions (PVC-E and styrene-divinylbenzene copolymer, respectively) do not exhibit the same pattern of variation of the mass transfer coefficient with Re number. The analysis of plots evidences also that :

— the k_L values obtained with suspensions are several times higher than those obtained with water ;

— the intermediate position of the line for PVC-E suspension with respect to the water and the other suspensions which can be explained by the influence of the surfactant present in particles.

To find a correlation between the variables implied in the process a dimensional analysis has been made. The variables found to affect significantly the mass transfer process were the concentration and density of the solid phase and the particle size (the particle diameter). By processing the experimental data on a FELIX C-256 computer by STPRG (stepwise multiple regression program) a general criterial relationship among the process variables could be obtained :

$$\frac{\mathrm{Sh}}{\mathrm{Sc}^{0.5}} = 0.0116\ \mathrm{Re}^{0.385}\left(\frac{C}{\rho_p}\right)^{-0.0762}\left(\frac{d_p}{\nu_z}\right)^{-0.163} \tag{9}$$

where C, ρ_p, d_p and ν_z are the suspension concentration, the solid material density, the particle diameter and the characteristic (the equivalent)

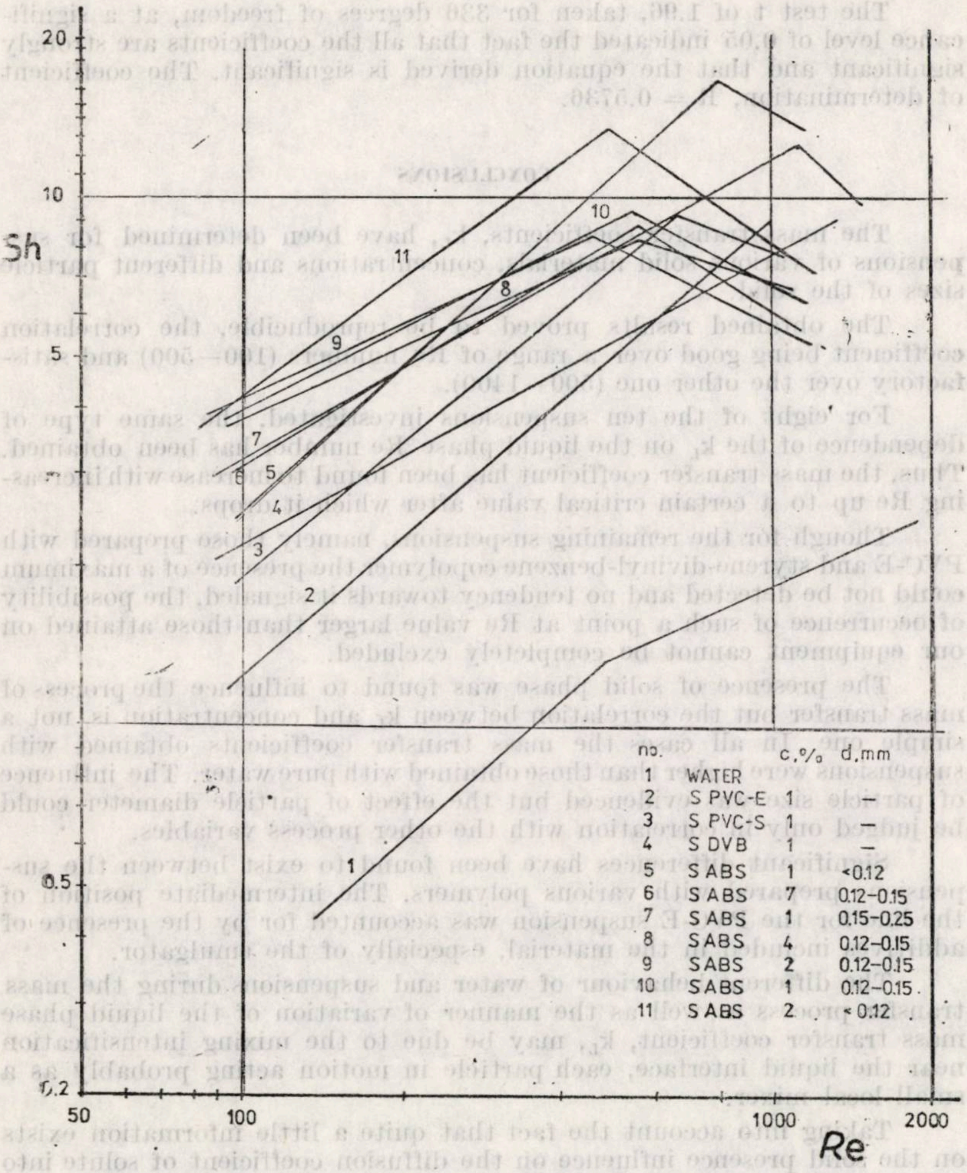

Fig. 11. — Sh vs. Re for all of the investigated systems. 1. water.

length, respectively. The latter has been calculated with the relationship:

$$v_s = \sqrt[3]{\frac{\eta^2}{\rho^2 g}} \tag{10}$$

where η, ρ and g are the suspension viscosity, the suspension density and the gravity acceleration, respectively.

The test t of 1.96, taken for 336 degrees of freedom, at a significance level of 0.05 indicated the fact that all the coefficients are strongly significant and that the equation derived is significant. The coefficient of determination, R = 0.5736.

CONCLUSIONS

The mass transfer coefficients, k_L, have been determined for suspensions of various solid materials, concentrations and different particle sizes of the solid.

The obtained results proved to be reproducible, the correlation coefficient being good over a range of Re numbers (100—500) and satisfactory over the other one (500—1400).

For eight of the ten suspensions investigated, the same type of dependence of the k_L on the liquid phase Re number has been obtained. Thus, the mass transfer coefficient has been found to increase with increasing Re up to a certain critical value after which it drops.

Though for the remaining suspensions, namely those prepared with PVC-E and styrene-divinyl-benzene copolymer the presence of a maximum could not be detected and no tendency towards it signaled, the possibility of occurrence of such a point at Re value larger than those attained on our equipment cannot be completely excluded.

The presence of solid phase was found to influence the process of mass transfer but the correlation between k_L and concentration is not a simple one. In all cases the mass transfer coefficients obtained with suspensions were higher than those obtained with pure water. The influence of particle size was evidenced but the effect of particle diameter could be judged only in correlation with the other process variables.

Significant differences have been found to exist between the suspensions prepared with various polymers. The intermediate position of the line for the PVC-E suspension was accounted for by the presence of additives included in the material, especially of the emulgator.

The different behaviour of water and suspensions during the mass transfer process as well as the manner of variation of the liquid phase mass transfer coefficient, k_L, may be due to the mixing intensification near the liquid interface, each particle in motion acting probably as a small local mixer.

Taking into account the fact that quite a little information exists on the solid presence influence on the diffusion coefficient of solute into a suspension and on the surface tension, an accurate explanation for the suspension behaviour is hardly to be advanced so more as the actual mechanism of mass transfer in a falling film of particle free liquid has not yet been entirely elucidated.

A general correlation between the liquid phase mass transfer coefficient for the investigated suspensions has been derived on the basis of a previous dimensional analysis. The data were processed by STPRG method on a FELIX-C-256 computer. A significant equation has been derived with a coefficient of determination R = 0.576.

REFERENCES

[1] Ch. Boyadjiev and V. Beschkov, "Mass Transfer in Liquid Film Flows", Publishing House of the Bulgarian Academy of Sciences, Sofia, 1984.
[2] G. Astarita, G. Marucci and G. Palumbo, *Ind. Eng. Chem. Fundls.*, **34**, 333 (1984).
[3] V. P. Metkin and V. N. Sokolov, *C.A.*, **104**, 7643 (1986).
[4] I. Ibănescu and R. Z. Tudose, *Rev. Chim.*, **23** (2), 114 (1972).
[5] K. Koziol, L. Broniarz and T. Nowicka, *Int. Chem. Eng.*, **20** (1), 136 (1980).
[6] R. Z. Tudose, Ec. Merică and St. Ungureanu, *Bul. Inst. Polit. Iași*, **XXXI(XXXV)**, fasc. supl., **1985**, 135.
[7] P. A. Lamourelle, C. Orwille and C. Sandall, *Chem. Eng. Sci.*, **27**, 1035 (1972).
[8] B. D. Prasher, A. L. Fricke, *Ind. Eng. Chem. Process Des. Develop.*, **13**, 336 (1974).
[9] K. Koziol, L. Broniarz and T. Nowicka, *Int. Chem. Eng.*, **20**, 143 (1980).

Revue Roumaine de Chimie, 36, 4–7, 783–788 (1991)

Dedicated to Prof. ALEXANDRU T. BALABAN
on the occasion of his 60th anniversary

PHASE TRANSFER FREE RADICAL REACTIONS. V.

COPOLYMERIZATION OF METHYL METHACRYLATE WITH STYRENE UNDER PHASE TRANSFER CONDITIONS

CAMELIA MIHĂILESCU, V. BULACOVSCHI and C. I. SIMIONESCU

Department of Macromolecular Chemistry, Polytechnic Institute of Jassy, 23 August 11A'
6600 Jassy, Romania

Received January 8, 1991

The phase transfer aided free-radical copolymerization of methyl methacrylate with styrene was studied. The reactivity ratios of the two monomers were calculated by the Fineman-Ross, Kelen-Tüdos and analytical methods. The triad sequence distributions were then determined.

INTRODUCTION

Free radical polymerization under phase transfer (PT) conditions has known great interest in recent years because of its efficiency in the synthesis of macromolecular compounds. One of the characteristics is the utilization of persulfate/PT catalyst complexes in nonaqueous free-radical polymerizations, as an unexpensive alternative for common organic soluble initiators.[1–5]

Whereas the persulfate/PT catalytic system has found extensive utilization in homopolymerization reactions, only few examples of phase transfer initiated free radical copolymerizations have been reported.[6,7]

In this study we have investigated the catalytic activity of persulfate/onium salts complexes in the copolymerization of methyl methacrylate with styrene and their influence upon the reactivity of monomers.

EXPERIMENTAL

Methyl methacrylate (MMA) and Styrene (S) were purified by usual methods before use.

Potassium persulfate and onium salts were purified by crystallization from the proper solvents. All other reagents were of chemical grade.

The copolymerization of inhibitor free monomers dissolved in the selected solvent, was conducted in glass vials previously charged with aqueous solution of the catalytic complex (persulfate/PTC). The whole system was sparged with nitrogen for five min, the vials sealed and placed in a constant temperature bath. The copolymer was recovered by precipitation in methanol, filtered off, washed and then dried.

Following the reaction, conversion of monomers to copolymer was determined by a simple gravimetric technique. The composition of copolymers was established from ^{1}H-NMR spectra registered on a JEOL 60 MHz apparatus in $CDCl_3$ solution.

RESULTS AND DISCUSSION

The copolymerization of MMA with S was carried out in a two phase system, water/ethyl acetate, starting from a monomer mixture of $X_{MMA} = X_S = 0.5$ (X denotes molar fraction). The concentrations of initiator and monomers, the ratio between water and the organic solvent (V_w/V_0) and the volume of the system were maintained constant (Table 1).

Table 1

Copolymerization of MMA with S under the phase transfer conditions (Org. Solvent — Ethyl Acetate ; T = 60° ; time = 3 h).

Catalyst	TMCA	PCABr	TPhMPBr	TPhBPCl	None
Polymer yield, %	21.8	19.04	3.30	5.59	Traces

Obs. TMCA — Trimethylcetylammoniumchloride ; PCABr — Pyridylcetyl-ammoniumbromide ; TPhMPBr — Triphenylmethylphosphoniumbromide ; TPhBPCl — Triphenylbenzylphosphoniumchloride.

$[MMA] + [S] = 5M$; $V_w/V_0 = 0.22$ (v/v) ; $K_2S_2O_8 = 5 \cdot 10^{-4}M$; $PTC/K_2S_2O_8 = 2:1$ (mol/mol) ;

Some features may be depicted from the obtained results. The ammonium salts are more active than the phosphonium ones whose reactivity depends on the dimension of onium ion. No significant influence of the halogen nature was observed.[8]

By changing the nature of the organic solvent, one may expect the copolymerization to be susceptible to medium polarity. Table 2 summarizes the data concerning this aspect, revealing that higher conversions are obtained when solvents with high dielectric constant are used. For similar polarities it seems that the miscibility of the two phases plays an important role. Thus, in dioxane — water system (homogeneous), the conversion is practically twice as compared to that obtained in benzene — water medium. It appears that the transfer of persulfate anion from aqueous to organic phase is easier in homogeneous media (Table 2).

Copolymer compositions were determined by using ^{1}H-NMR spectroscopy.[9] Then, reactivity ratios were determined by the Fineman-Ross, Kelen-Tüdos and analytical methods (Table 3).[10] Inspection of these data reveals that the obtained values are not far from those reported in the literature ($r_1 = 0.46$; $r_2 = 0.52$) (numbers 1 and 2 refer to MMA and S, respectively) for classical free radical copolymerization (initiator benzoyl peroxide).[11] This might be an evidence for a free radical mechanism in PT-assisted copolymerization of MMA with S. However, one may note a slight decrease, respectively an increase of MMA and S reactivities, which may find an explanation in the initiation particularities.

Table 2

The influence of the organic solvent nature on the copolymerization of MMA with S under the PT conditions
(Catalyst : PCABr ; time = 210 min)

Solvent	Polymer yield, %	
Dioxane	2.21	13.70
Benzene	2.28	6.39
Chloroform	4.80	11.58
Ethyl Acetate	6.02	10.32
Cyclohexanone	18.3	23.60

$[MMA] = [S] = 2.5$ M;
$K_2S_2O_8 = 0.01$ M ; $V_w/V_0 = 1.08$

Table 3

Reactivity rations for MMA and S copolymerized under the phase transfer conditions
(Catalyst : $K_2S_2O_8$/PCABr)

Method	r_1	r_2
Fineman — Ross	0.32	0.66
Kelen — Tüdos	0.39	0.67
Analytical	0.35±0.05	0.63±0.07
Literature data[a]	0.46	0.52

[a] Initiator benzoylperoxide.

The monomer reactivity ratios were used to calculate the MMA and S diads, also centered triad sequence distributions by using the relations :

$$P_{11} = \frac{r_1 y}{r_1 y + 1}; \quad P_{12} = 1 - P_{11}$$

$$P_{22} = \frac{r_2}{r_2 + y}; \quad P_{21} = 1 - P_{22}$$

and

$$P_{111} = P_{11}^2; \quad P_{212} = P_{12}^2; \quad P_{112} = 2P_{12} \cdot P_{11}$$

$$P_{222} = P_{22}^2; \quad P_{121} = P_{21}^2; \quad P_{221} = 2P_{21} \cdot P_{22}$$

where P_{11} and P_{1j} are the probabilities of formation of homogeneous and heterogeneous diads in the copolymerization process. P_{111}, P_{11j} and P_{1ij} are probabilities of triad formation.

$$y = [M_1]/[M_2].$$

Tables 4 and 5 contain the calculated values of diad and triad distributions for three compositions of the feed. The data were normalized to unity to provide a basis for comparison.

Table 4

Copolymerization of MMA with S under the PT conditions. Probabilities of diads formation

[MMA]/[S]	P_{11}	P_{12}	P_{21}	P_{22}
0.111	0.037	0.963	0.531	0.469
1.000	0.260	0.740	0.613	0.387
9.00	0.760	0.240	0.935	0.065

Obs. Catalyst: $K_2S_2O_8$/PCABr; solvent: ethyl acetate; $r_{MMA} = 0.39$; $r_S = 0.67$.

From the obtained data one may compute the probability α of a sequence of *n* MMA or S units in the copolymer:

$$\alpha_{n.MMA} = P_{11}^{n-1} \cdot P_{12} \quad \text{and} \quad \alpha_{n,S} = P_{22}^{n-1} \cdot P_{21}$$

It appears that the formation of a long homogeneous sequence has a little chance even at extreme composition of the feed (near 1% for a sequence of 12 units of MMA at $X_{MMA} = 0.9$ and 6 units of S at $X_{MMA} = 0.1$) but raises the probability of homogeneous triad population.

Table 5

Copolymerization of MMA with S under the PT conditions. Probabilities of triad formation

[MMA]/[S]	MMA centered triads			S centered triads		
	P_{111}	P_{212}	P_{112}	P_{222}	P_{121}	P_{221}
0.111	$1.42 \cdot 10^{-3}$	0.927	0.071	0.220	0.281	0.498
1.00	0.067	0.547	0.385	0.149	0.375	0.474
9.00	0.577	0.057	0.365	$4.305 \cdot 10^{-3}$	0.874	0.121

Obs. Catalyst: $K_2S_2O_8$/PCABr; Solvent: ethyl acetate; $r_{MMA} = 0.39$: $r_S = 0.67$

Figure 1 shows the normalized MMA and S centered triad populations vs. MMA (mol %) in the copolymers over the whole range of composition, with the triad concentrations determined from ^{1}H-NMR spectra. From these curves, it is evident that the concentration of P_{111} triads increases and that of P_{212} triads decreases as the concentration of MMA in the feed increases. P_{112} triad concentration is maximum when the feed contains 75% mol of MMA.

Similar behaviour is shown for the other triads but the maximum concentration for P_{221} triad is obtained when the feed contains 40 mol % of MMA.

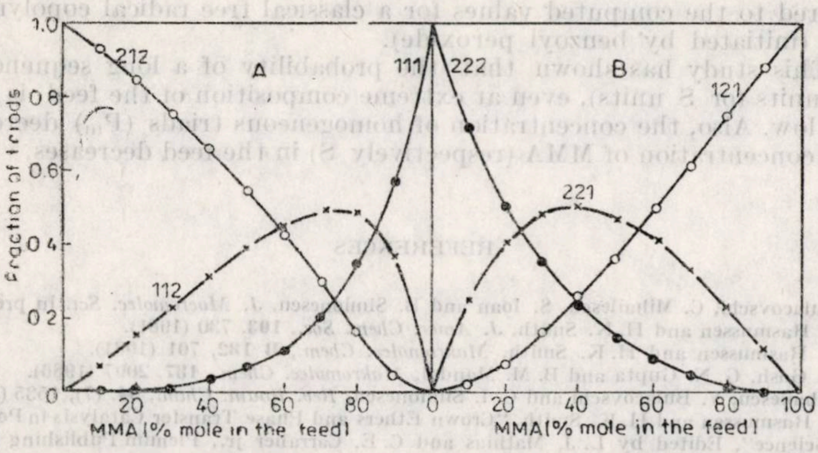

Fig. 1. — (A) Normalized methyl methacrylate (1) centered triad population vs. % methyl methacrylate in the feed of the system MMA + S. (B) Similar plots for styrene (2) centered triads.

The average product of the reactivity ratios is 0.228 indicating that the copolymerization is azeotropic. From the composition diagram (Fig. 2), it results that the azeotropic point is located at 40 mol % of MMA in the feed.

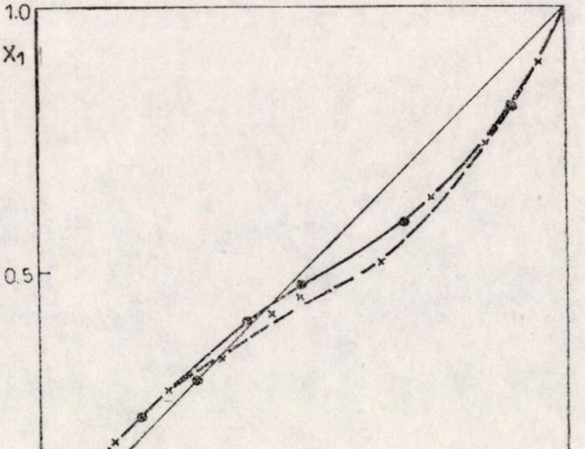

Fig. 2. — Composition diagram of the methyl methacrylate — styrene copolymer. (o) theoretical and (x) experimental data.

CONCLUSIONS

The copolymerization of MMA with S under the PT conditions proceeds by a free radical mechanism. Under these circumstances the reactivity ratios were found to be lower for MMA and higher for S as compared to the computed values for a classical free radical copolymerization (initiated by benzoyl peroxide).

This study has shown that the probability of a long sequence of MMA units (or S units), even at extreme composition of the feed, is relatively low. Also, the concentration of homogeneous triads (P_{111}) decreases as the concentration of MMA (respectively S) in the feed decreases.

REFERENCES

[1] V. Bulacovschi, C. Mihailescu, S. Ioan and B. Simionescu, *J. Macromolec. Sci.* in press.

[2] J. K. Rasmussen and H. K. Smith, *J. Amer. Chem. Soc.*, **103**, 730 (1981).

[3] J. K. Rasmussen and H. K. Smith, *Makromolec. Chem.*, **B 182**, 701 (1981).

[4] N. N. Gosh, G. N. Gupta and B. M. Mandal, *Makromolec. Chem.*, **187**, 2097 (1986).

[5] C. Mihailescu, V. Bulacovschi and C. I. Simionescu, *Rev. Roum. Chim.*, **34**, (7), 1535 (1989).

[6] J. K. Rasmussen and H. K. Smith, "Crown Ethers and Phase Transfer Catalysis in Polymer Science", Edited by L. J. Mathias and C. E. Carraher jr., Plenum Publishing Corp., N. Y., p. 105 (1984).

[7] R. Iu. Makushka, A. Iu. Usaitis, G. I. Baioras and M. Seno, *Vysokomol. Soed.*, **A31**, (7), 1419 (1989).

[8] C. I. Simionescu, C. Mihailescu and V. Bulacovschi, *Acta Polym.*, **38**, 502 (1987).

[9] A. S. Brar and A. K. Saini, *J. Appl. Polymer Sci.*, **32**, 4607 (1986).

[10] N. Cobianu and D. S. Vasilescu, "Copolimerizarea", Ed. Tehnică, Bucharest, p. 374, 1984.

[11] G. Odian, "Principles of Polymerization", Mc. Graw-Hill N. Y., p. 370, 1970.

Revue Roumaine de Chimie, **36**, 4–7, 789–796 (1991)

Dedicated to Prof. ALEXANDRU T. BALABAN
on the occasion of his 60th anniversary

THE MULTISTAGE IMMOBILISED LIVING YEAST CELLS BIOREACTOR

GHEORGHIŢA JINESCU and VASILE LAVRIC
Polytechnic Institute, Faculty of Industrial Chemistry; Chemical Engineering Department,
Polizu Street, 1, 78128 Bucharest, Roumania

Received December 20, 1990

In the present work a dimensionless mathematical model consisting from a system of ordinary differential equations, was developed for the monostage immobi lisedliving yeast cell bioreactor (MILYCB) for sugars bioconversion to ethanol. This model was used to simulate the multistage ILYCB (two and four stages, respectively) behaviour and, on this basis, to predict the enhancements implied by the total degasing of the liquid-phase between stages. It was emphasized that the productivity gain is considerable, especially for the low dilution rate cases. However, the number of stages and the corresponding working dilution rate for a given ILYCB are subject to a constrained optimization problem, involving both economic and engineering considerations.

INTRODUCTION

Many of the biological reactors functioning currently are discontinuous, with mechanical mixing. The concept of immobilised living yeast cells implies, however, continuous operation and the presence, in the biological medium, of such stress forces that could not permit the breaking down of the cells agregates. From the flow point of view, these bioreactors could be perfectly mixed or may have a plus flow.[1]

The perfectly mixed bioreactor has an extensive use because of the autocatalytic type of the biological reaction and, for such a reason, a critical value of the substrate concentration in the bioreactor medium exists and assures a maximum value for the biological reaction rate and, thus, an optimum dilution rate.[2] One of the major drawbacks of the perfectly mixed bioreactor is its incapacity to properly handle the bioreactions inhibited by the product. The reason is that, in every point of the biological medium, the cells are exposed at the highest product concentration level.[1]

In the plug flow type bioreactors, the substrate inhibition could be avoided feeding it in some axially distributed points. The product inhibition effect is diminished taking into account that ethanol is generated step by step, the maximum concentration being obtained at the bioreactor exit.[2]

The MILYCB is a familiar presence in the fermentation laboratories, many of them being vertically ordered, some attempts being made to perform the experiments in horizontal order.[3]

THEORETICAL CONSIDERATIONS

The physical model of the MILYCB

The MILYCB for sugars bioconversion to ethanol implies the presence, in its interior, of a triphasic system, consisting of a gas-liquid-solid medium.[4]

The gaseous phase, carbon dioxide, appears as a result of the fermentation and maintenance activities of yeast cells. The void fraction of this phase increases axially due to the fermentation process and the impossibility of local degasing of the fermentation medium.

The liquid phase is a solution of saccharides and ethanol. In the course of the fermentation process, the liquid phase density changes from input to output, because of the increase of ethanol and the decrease of substrate concentrations. As a consequence of the variable gas void fraction, the liquid velocity changes accordingly.

The solid phases is represented by the support (carragenan) and the immobilised living yeast cells. The solid support was chosen so that the thickness of the cells layer could be maintained stationary. The solid volume void fraction depends mainly on the support material, for the present study being close to 0.5.[4] The bioconversion process could be regarded as a result of a complex linkage of three main components [4]:

— the growing of the biological film on the solid support until cells maturity — afterwards, cells birth and death rates balance, the death cells being desorbed from the solid surface;

— the cells activity depends both on limiting substrate (monosaccharides) and on the product (which acts as an inhibitor) concentrations;

— the fermentation of monosaccharides to ethanol takes place only if the living yeats cells are into the liquid phase. All cells passed into the gas phase switch immediately to the maintenance activities.

The simplifying assumptions made on the basis of this physical model are detailed elsewhere,[4] together with the materials and methods used in the experimental approach.

The mathematical modelling

Consider a MILYCB vertically ordered, cross sectioned at the heights z and z + dz, cutting up this way an elementary volume with thickness dz and surface A (Fig. 1). For this elementary volume, one could express the mass balances for substrate and product, taking into account that the yield product is not constant and thus the substrate consumption and product formation have unrelated rates. The bioconversion kinetics is the one proposed by Luong [5] and the cell generation rate is that suggested by the binary fission mechanism.[6]

As was stated in a previous paper,[4] under steady state conditions, total and partial mass balances in the elementary volume are:

$$\frac{dg^*}{dz} = -\frac{v_{RS}A[1-(\varepsilon_G+\varepsilon_S)]}{D_{ma}} \quad (1)$$

$$\frac{de^*}{dz} = -\frac{v_{RP}A[1-(\varepsilon_G+\varepsilon_S)]}{D_{ma}} \quad (2)$$

$$\frac{dD_m}{dz} = v_{RP}\, f\, A[1 - (\varepsilon_G + \varepsilon_S)] \tag{3}$$

$$\frac{d\varepsilon_G}{dz} = \frac{\rho^0 g \varepsilon_G}{P} + \frac{v_{RP}\, f A[1 - (\varepsilon_G + \varepsilon_S)]}{\rho_G u_L} \tag{4}$$

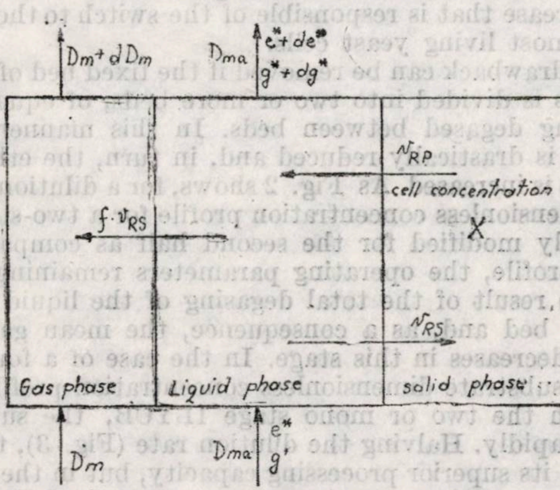

Fig. 1. — The elementary volume.

Taking into account the advantages of the nondimensional form of the ODEs model (1—4), the following dimensionless groups are utilized:

$$\eta = \frac{z}{H}\ ;\quad \Gamma = \frac{g^*}{g_0^*}\ ;\quad E = \frac{e^*}{\gamma g_0^*}\ ;\quad \Delta = \frac{D_m}{f\, D_{ma} g_0^*}\ ;\quad \pi = \frac{P}{P_0} \tag{5}$$

$$\Delta\pi = \frac{\rho^0 g H}{P_0}\ ;\quad \psi = \frac{D_{ma} g_0^*}{v_R(1 - \varepsilon_S)}\ ;\quad \Phi = \frac{\varepsilon_G}{1 - \varepsilon_G}$$

together with the dilution rate expression:

$$D = \frac{D_{ma}(1 + g_0^*)}{\rho v_R} \tag{6}$$

Substituting (5) and (6) in (1—4), after some mathematical manipulations, one obtains the dimensionless mathematical model of the MILYCB:

$$\frac{d\Gamma}{d\eta} = \frac{v_{RS}[1 - \Phi]}{\psi} \tag{7}$$

$$\frac{dE}{d\eta} = \frac{v_{RP}[1 - \Phi]}{\gamma\psi} \tag{8}$$

$$\frac{d\Phi}{d\eta} = \frac{\Delta\pi \cdot \Phi}{1 + (1 - \eta)\,\Delta\pi} + \frac{v_{RP}\, f\, H(1 - \Phi)^2}{\rho_G D} \tag{9}$$

RESULTS AND DISCUSSION

The detailed analysis of the algorithm used to solve the monostage ILYCB mathematical model is given in the cited paper.[4] The main conclusion was that the vertically ordered MILYCB suffers in its superior half a drastical drawback of its fermentation potential due to the gas phase void fraction increase that is responsible of the switch to the maintenance activities of all most living yeast cells.

This major drawback can be removed if the fixed bed of immobilised living yeast cells is divided into two or more beds, of equal height, the liquid phase being degased between beds. In this manner, the overall gas void fraction is drastically reduced and, in turn, the ethanol concentration derivative is increased. As Fig. 2 shows, for a dilution rate of 1 h^{-1}, the substrate dimensionless concentration profile for a two-stage fixed bed ILYCB is strongly modified for the second half as compared with the same MILYCB profile, the operating parameters remaining unmodified. This effect is the result of the total degasing of the liquid phase before the second fixed bed and, as a consequence, the mean gas phase void fraction sharply decreases in this stage. In the case of a four-stage fixed bed ILYCB, the substrate dimensionless concentration profile is different as compared with the two or mono stage ILYCB, the substrate being consumed more rapidly. Halving the dilution rate (Fig. 3), the four-stage ILYCB conserves its superior processing capacity, but in the fourth stage, the substrate concentration cancels at approximately half of the stage and, thus, the decaying S* profile. In this situation, the ultimate part of the bioreactor does not produce ethanol, because substrate is lacking and, for this reason, this part is not economically used.

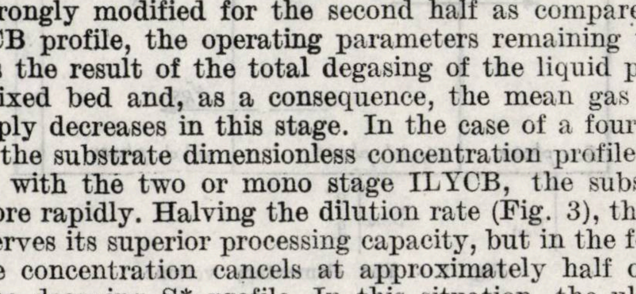

Fig. 2. — The profiles of the difference between dimensionless substrate concentrations along the monostage ILYCB, two-stage (— — — —) and four-stage (—×—) ILYCB, respectively; dilution rate equals 1.0 h^{-1}.

The same behaviour could be observed in Figs. 4 and 5, for the product dimensionless concentration in the two mentioned cases; as, in Figs. 6 and 7, for the nondimensional gas phase void fraction profiles. As could be observed from Fig. 4, there is a significant gain in the bioreactor productivity of the same volume of immobilised living yeast cells, divided in a two-stage fixed bed ILYCB.

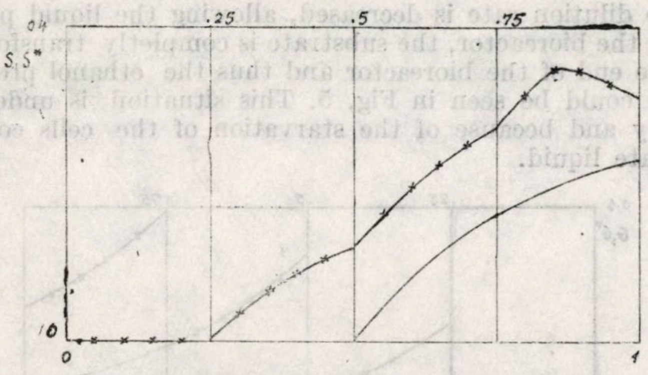

Fig. 3. — The profiles of the difference between dimensionless substrate concentrations along the monostage ILYCB, two-stage (————) and four-stage (— × —) iLYCB, respectively, for a dilution rate of 0.5 h^{-1}.

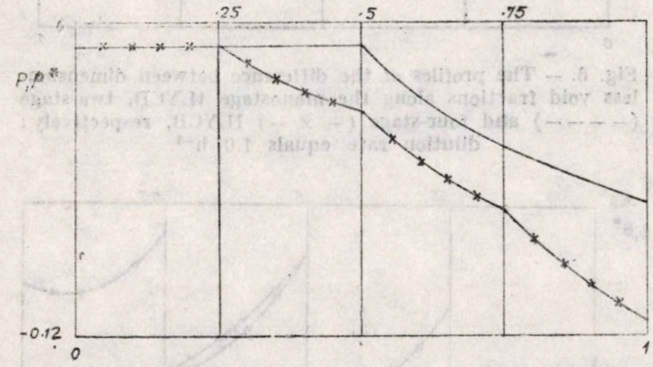

Fig. 4. — The profiles of the difference between dimensionless product concentrations along the monostage ILYCB, two-stage (————) and four-stage (— × —) ILYCB, respectively; dilution rate equals 1.0 h^{-1}.

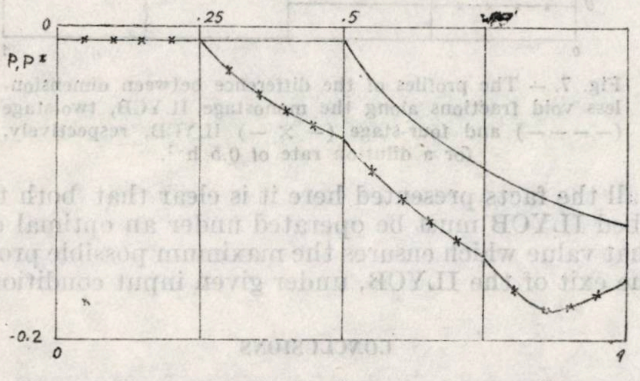

Fig. 5. — The profiles of the difference between dimensionless product concentrations along the monostage ILYBC, two-stage (————) and four-stage (— × —) ILYCB, respectively, for a dilution rate of 0.5 h^{-1}.

If the dilution rate is decreased, allowing the liquid phase to stay more inside the bioreactor, the substrate is completly transformed before reaching the end of the bioreactor and thus the ethanol production rate nullifies, as could be seen in Fig. 5. This situation is undesirable both economically and because of the starvation of the cells contacting the free substrate liquid.

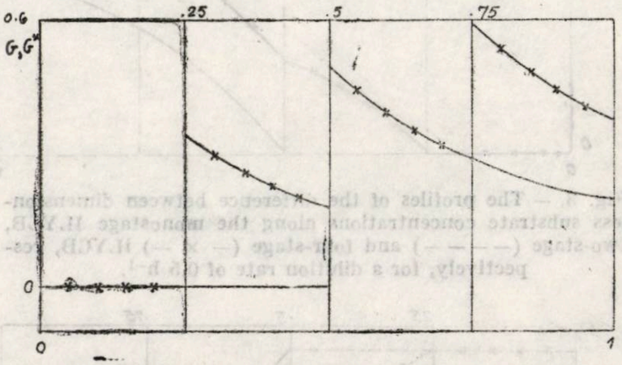

Fig. 6. — The profiles of the difference between dimensionless void fractions along the monostage ILYCB, two-stage (— — — —) and four-stage (— × —) ILYCB, respectively; dilution rate equals 1.0 h^{-1}.

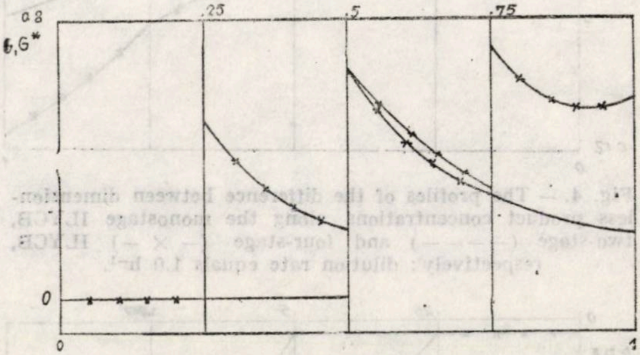

Fig. 7. — The profiles of the difference between dimensionless void fractions along the monostage ILYCB, two-stage (— — — —) and four-stage (— × —) ILYCB, respectively, for a dilution rate of 0.5 h^{-1}.

From all the facts presented here it is clear that both two and four-stage fixed bed ILYCB must be operated under an optimal dilution rate, defined as that value which ensures the maximum possible product concentration at the exit of the ILYCB, under given input conditions.

CONCLUSIONS

For the vertically ordered ILYCB, the equations of the mathematical model describing the steady state behaviour were deduced using phase circulation and biological processes simplifying hypotheses. The model, composed of a system of ODEs, enables the computation of the dimensionless concentrations and void fraction profiles for changing values of the operating variables. Based upon the closed correlation between experimental and computed data,[4] the model was used to predict the behaviour of a two or four-stage fixed bed ILYCBs, with total degasing of the liquid phase after each of the stages. Our assumption that using a multistage ILYCB, the bioreactor productivity will be increased was confirmed by our simulations, but in a greater amount than we expected for. It must be stressed that for a multi-stage fixed bed ILYCB an optimum dilution rate and a specific number of stages exist which ensure the economic utilization of such a bioreactor. To gain this optimum, one must use an objective function which is to be minimized in respect with the dilution rate and the number of stages, but this aspect is subject to a further paper.

NOTATIONS

A — reactor cross section [m^2]
D_m — mass flow rate of carbon dioxide [kg/s]
e^* — mass concentration of ethanol, with respect to water [$kg_{ethanol}/kg_{water}$]
E_d — difference between MILYCB and two-stage fixed bed ILYCB dimensionless void fractions
E_d^* — difference between MILYCB and two-stage fixed bed ILYCB dimensionless void fractions
f — conversion factor [$kg_{carbon\ dioxide}/kg_{ethanol}$]
g — gravity acceleration [m/s^2]
g^* — mass concentration of sugars, with respect to water [kg_{sugars}/kg_{water}]
H — total ILYCB height [m]
P — gas-phase pressure [Pa]
P_d — difference between MILYCB and two-stage fixed bed ILYCB dimensionless ethanol concentrations
P_d^* — difference between MILYCB and four-stage fixed bed ILYCB dimensionless ethanol concentrations
S_d — difference between MILYCB and two-stage fixed bed ILYCB dimensionless substrate concentrations
S_d^* — difference between MILYCB and four-stage fixed bed ILYCB dimensionless substrate concentrations
u_L — liquid-phase velocity [m/s]
v_R — total MILYCB volume [m^3]
v_{RP} — ethanol production rate [kg/m^3s]
v_{RS} — substrate consumption rate [kg/m^3s]
X — biomass concentration [kg/m^3]

Greek letters

ε_G — void fraction volume of the gas-phase
ε_S — void fraction volume of the solid-phase
ρ — entering liquid-phase density [kg/m^3]
ρ^0 — ILYCB mean liquid-phase density [km/m^3]

REFERENCES

[1] M. M. da Fonseca, G. M. Black and C. Webb, "Reactor Configuration for Immobilised Cells" in "Process Engineering Aspects of Immobilised Cell Systems.", C. Webb, G. M. Black and B. Atkinson (Eds.), The Inst. of Chem. Engs., Rugby, 1986.

[2] O. Levenspiel, "The Chemical Reactor Omnibook", OSU Bookstores, Corvallis, 1984.

[3] T. Shiotani and T. Yamane, *European J. Appl. Microbiol. Biotechnol.*, **13**, 96 (1981).

[4] G. Jinescu, V. Lavric, St. Brăgarea and M. Popescu, *Acta Biotechnol.*, **9**, 325 (1989).

[5] J. H. T. Luong, *Biotechnol. Bioengng.*, **27**, 280 (1985).

[6] C. L. Cooney, "Growth of Microorganisms", in "Biotechnology. Microbial Fundamentals." H.-J. Rehm and G. Reed (Eds.), Verlag-Chemie, Weinheim, 1981.

Revue Roumaine de Chimie, **36**, *4*–7, 797–808 (1991)

Dedicated to Prof. ALEXANDRU T. BALABAN
on the occasion of his 60th anniversary

THE DEGRADATION OF MATTER

VALERIU V. JINESCU

Polytechnic Institute of Bucharest,
Mechanical Engineering Faculty, Bucharest

Received December 9, 1990

The concept of matter degradation is defined on the basis of the principle of critical energy. Degradation can be reversible or irreversible and the relation expressing it depends both on the behaviour of matter and on the application rate of the exterior action on the material body. The calculation of reserve of degradation both for natural matter and for artificial, synthetic materials is also defined and discussed. In general, any natural and artificial process and phenomenon produces a certain irreversible degradation of matter. The concept presented herein can be applied both to the living matter and nonliving one.

By *degradation* or deterioration *of matter* it is generally understood the *diminution of its capacity* from a certain point of view. Any exterior action upon a material body brings about some changes of it. *The relative value of the change is called degradation and it is denoted by d.* Some actions are followed by the reduction of matter capacity ; others, on the contrary, oppose this reduction.

In its absolute value, the degradation, which is nondimensional, varies between 0 and 1. It means that $d \in [0 ; 1]$. In its relative value, $d \in [-1 ; 1]$.

How can the negative values of degradation be explained ? When an action opposes a process or phenomenon, then it contributes to the increase of matter capacity from the point of view taken into account. For instance, if actions A_1, A_2, A_3 produce the degradations d_1, d_2, and d_3 and the effect of A_2 is contrary to the effects of A_1 and A_3, then the total degradation is :

$$d = (d_1 + d_3) - d_2.$$

Whichever its forms (substance, field), the matter undergoes degradation. Degradation can occur slowly in time or instantly.

A consequence of the *slow degradation in time* is the change of matter behaviour. Such a degradation is, in general, *irreversible*. For instance : aging of materials, loading during creep, fatigue of materials, fatigue of light due to energy loss during interactions and others. *Instant degradation* is characterized by a sudden passing, in a $\Delta t \to 0$ period of time, from a degradation stage to another. This can be *reversible* or *irreversible*.

The quantitative evaluation of matter degradation must be done on the basis of the amount of energy involved in the process.

1. CONCEPT OF DEGRADATION

When applying an action upon a material body, a quantity of energy, E, is transferred to the body. This energy induces a (physical, chemical, biological...) process, P, into the body. Out of the E quantity of energy, only a part of it, E_p, is actually used for the process P. This is the main (dominant) process we are interested in. The remaining energy, $\Delta E_s = E - E_p$, is used for other *processes* which we consider as being *of less importance*.

During the development of the process P, irreversible or undesirable changes going further to the deterioration of the material can occur. These correspond to the moment when the so-called *critical state* (cracking or fracture, change of geometrical shape, carbonization, burning, death of material...) is reached.

The amount of energy acquired by the body for the process P, up to the moment when the critical state is reached, will be called *critical energy* and marked by E_{cr}.

On the basis of the *critical energy principle*[1], the concept of degradation of matter is defined by the relationship :

$$d = E_p/E_{cr} \qquad (1)$$

If $d < 1$, the critical state is not reached; when $d \geqslant 1$, the critical state is reached and even overpassed which brings about the deterioration or an undesirable, irreversible change.

The significance of the term "*degradation*" depends on the process to which matter is subjected, especially on the nature of the process (thermal, mechanical, electrical, magnetic, biological, etc.).

If a material body is subjected to some exterior actions and each of these induces one or more different processes in the body, then the total degradation, in the sense of any process P, results from summing up of the partial degradations :

$$d = \sum_j d_j \qquad (2)$$

where d_j is the partial degradation produced by the exterior action j which has transferred a certain quantity of energy to the body, out of which only the quantity $E_{p,j}$ contributes to the process P.

Because some of the actions oppose the process P, the general expression of partial degradation can be written as such :

$$d_j = \frac{E_{p,j}}{E_{cr,j}} \cdot \operatorname{sign}\left(\frac{E_{p,j}}{E_{p,r}}\right) \qquad (3)$$

where $E_{p,r}$ is the energy of the *reference* action, namely the energy which operates in the sense of developing the process P and

$$\operatorname{sign}\left(\frac{E_{p,j}}{E_{p,r}}\right)=\begin{cases}+1, & \text{if } E_{p,j} \text{ works in the sense of developing the process P;}\\ -1, & \text{if } E_{p,j} \text{ opposes the development of the process P.}\end{cases}$$

If $d < 1$, degradation does not occur.

But **degradation** can be also determined by *the loss of a certain quantity from the* **capable energy** of matter when it is in a certain state which decreases the intensity of energetic process as well as the reserve of degradation. The capable energy in this case is the critical energy of the analysed process; it is written at the denominator of d_j.

2. REVERSIBLE AND IRREVERSIBLE DEGRADATION

Reversible degradations disappear when the cause which has produced them is removed, while the *irreversible degradation* is a degradation which persists after the removal of the cause.

The reversible or irreversible type of degradation depends on the *behaviour of matter* towards an external action. The value of degradation under a given action is expected to depend on the rate of the external action.

Let us consider that the carrier of the external action is the generalized force Y, and that the effect of action is given by the physical dimension X.

The behaviour of matter versus the action Y is actually *nonlinear* and it can be expressed by a law of the type (Fig. 1):

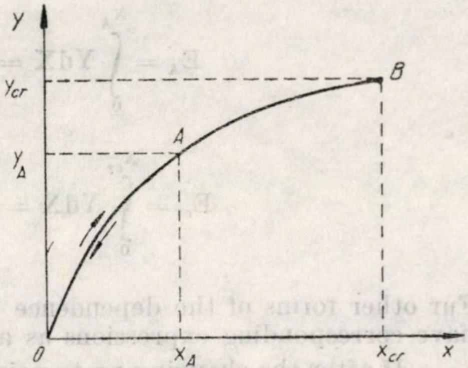

Fig. 1. — The $Y(X)$ dependence for a nonlinear reversible behaviour of matter.

$$Y = C \cdot X^n \tag{4}$$

where C and n are constants. Many theories assume the behaviour of matter as being linear ($n = 1$) to facilitate theoretical deductions.

By increase of Y, the characteristic curve goes along the section OA. If, in point A, a continuous decrease of Y starts, going down to zero, and if, in this case, the curve OA goes in the opposite sense, AO, then the process is reversible and the material body has a totally reversible behaviour. When the whole charge-discharge cycle is over, the final degradation is zero. The degradation corresponding to charging up to point A represents the ratio of the areas OAC and OBF (Fig. 2). These areas stand for the energy of charging up to point A and for the critical energy – E_{cr} – respectively.

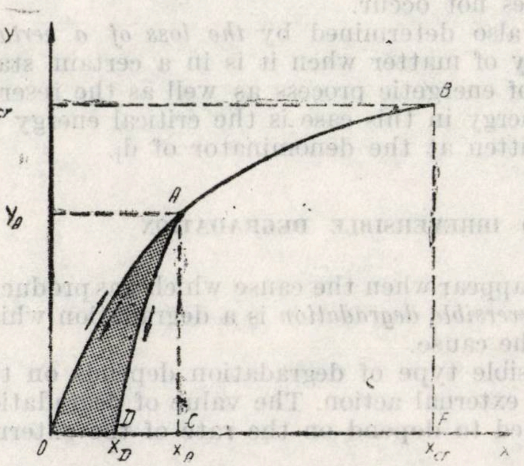

Fig. 2. – The $Y(X)$ dependence for a **nonlinear** *partly reversible* behaviour of matter.

For such a behaviour of matter the degradation is totally *reversible*; it is marked by d_r and is given by the expression:

$$d_r = E_A/E_{cr} \tag{5}$$

where

$$E_A = \int_0^{X_A} Y dX = C \cdot X_A^{n+1}/(n+1)$$

$$E_{cr} = \int_0^{X_{cr}} Y dX = C \cdot X_{cr}^{n+1}/(n+1). \tag{5.1}$$

Fur other forms of the dependence Y(X), the relationship (5.1) will also have corresponding expressions as a result of integration.

If after the changing up to point A (Fig. 2), the discharge is carried out following the curve AD, then the material body preserves (after the discharge) a remanent specific energy corresponding to the area OAD. The area ACD is the reversible energy by discharge. Such a material body is partly reversible – partly irreversible. The total degradation, d, in point A can be calculated using the relation (5). This has two components :

$$d = d'_r + d'_{ir},$$

where d'_r is the ratio of the areas DAC and OBF

$$d'_r = A_{DAC}/A_{OBF}$$

and the irreversible degradation is the ratio of the areas OAD and OBF

$$d'_{ir} = A_{OAD}/A_{OBF} \tag{6}$$

If AD is a straight line, then $A_{ADC} = 0.5 \cdot Y_A \cdot (X_A - X_D)$, so that (Fig. 2)

$$\left.\begin{aligned} d'_r &= 0.5\, Y_A(X_A - X_D)/E_{cr} \\ d'_{ir} &= (1/E_{cr}) \cdot \int_0^{X_A} Y dX - 0.5\, Y_A(X_A - X_D) \end{aligned}\right\} \tag{7}$$

where E_{cr} is given by the relationship (5.1).

If after the charging up to point A followed by a continuous decrease of Y, even falling to zero, X remains unchanged, $X = X_{cr}$, the vertical line AC is to be followed (Fig .3) the material body preserves the acquired energy which corresponds to the area OAC. In this case, the whole degradation brought about by charging up to point A, is irreversible :

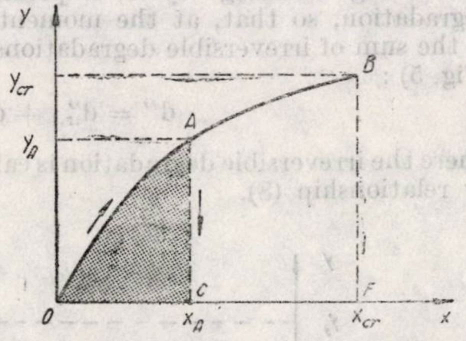

Fig. 3. — The $Y(X)$ dependence for a nonlinear *totally irreversible* behaviour of matter.

$$d''_{ir} = (1/E_{cr}) \int_0^{X_A} Y dX \tag{8}$$

3. THE EFFECT OF MATTER BEHAVIOUR UPON TOTAL DEGRADATION

Whether the behaviour of matter is reversible or irreversible is important in the case successive loads upon matter, separated by moments of charge falling to zero. When the charge falls to zero, reversible degradation does not occur, while irreversible degradation is preserved and added to the degradation of the next charging cycle.

For instance, a material body is subjected to successive charging Y_1, Y_2 and Y_3, with intervals of time among them (Fig. 4).

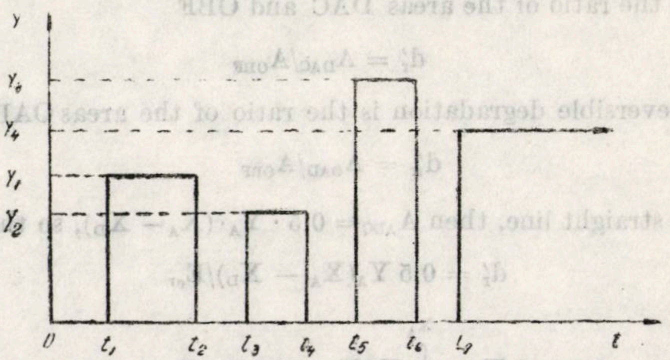

Fig. 4. — Successive charging (Y_1, Y_2, Y_3, Y_4) with intervals of time among them.

If the material body has a *totally reversible* behaviour, then the final degradation at the moment t_7 is zero, because, after each charge falling to zero, degradation also stops and $d = 0$.

If the material body has a *totally irreversible* behaviour, then after each charge-discharge cycle, it preserves the corresponding irreversible degradation, so that, at the moment t_7, the total degradation is equal to the sum of irreversible degradations corresponding to the three stresses (Fig. 5) :

$$d'' = d''_{ir,1} + d''_{ir,2} + d''_{ir,3} \tag{9}$$

where the irreversible degradation is calculated for each charge individually, by relationship (8).

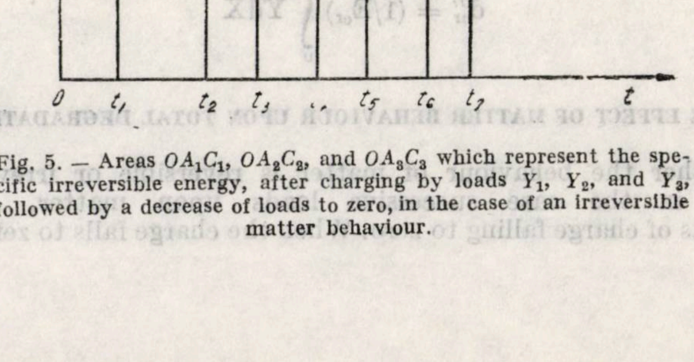

Fig. 5. — Areas OA_1C_1, OA_2C_2, and OA_3C_3 which represent the specific irreversible energy, after charging by loads Y_1, Y_2, and Y_3, followed by a decrease of loads to zero, in the case of an irreversible matter behaviour.

If the material body has a partially irreversible behaviour, then the total degradation at the moment t_7 is calculated by using the relationship (Fig. 6).

$$d' = d'_{ir,1} + d'_{ir,2} + d'_{ir,3} \tag{10}$$

where each partial irreversible degradation is calculated by relationship (6) or (7). Obviously, $d' < d''$.

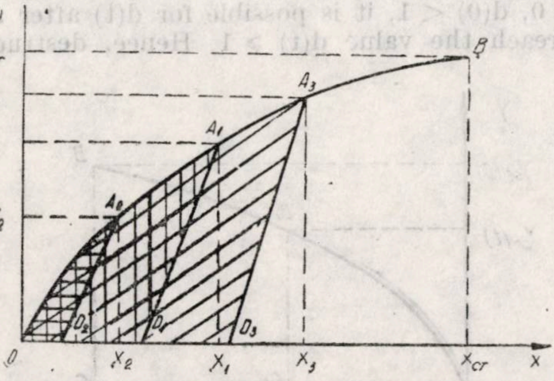

Fig. 6. — Areas OA_1D_1, OA_2D_2 and OA_3D_3 which represent the specific irreversible (partly) energy, after charging by loads Y_1, Y_2 and Y_3 followed by a decrease of loads to zero, in the case of a partly irreversible matter behaviour.

It results that the *value of matter degradation* at a certain moment depends on the behaviour of matter, the degree of its reversibility to external actions.

If, at the moment t_7, the three bodies are charged, for a long period of time, by Y_4, which produces the degradation d_4, then the total degradation during this interval of time depends on the behaviour of the body and it will have the following values :

— for the totally reversible material :

$$d_t = d + d_4 = d_4\,;$$

— for the partially irreversible material :

$$d'_t = d' + d_4\,;$$

— for the totally irreversible material :

$$d''_t = d'' + d_4.$$

From all data shown above, it obviously results that :

$$d''_t > d'_t > d_t = d_4.$$

The *irreversible behaviour* of matter is sometimes revealed by the *decrease in time of the critical parameters* Y_{cr} and X_{cr} (Fig. 7), which makes the critical energy depends on time, $E_{cr}(t)$, and decreasing in time. Consequently, for the same stress (hence for the same amount of energy, E_A) the degradation depends on time:

$$d(t) = E_A/E_{cr}(t) \tag{11}$$

Since $E_{cr}(t)$ decreases with time it results that $d(t)$ increases. This means that if for $t = 0$, $d(0) < 1$, it is possible for $d(t)$ after a certain period of time t, to reach the value $d(t) \geqslant 1$. Hence, destruction can occur.

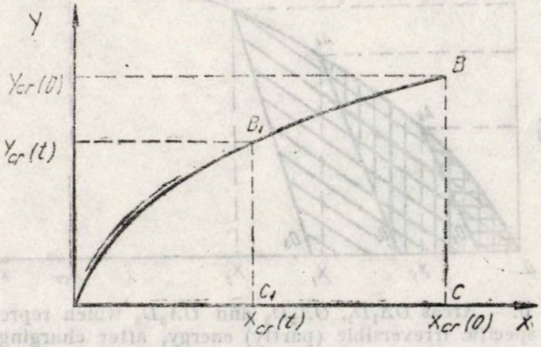

Fig. 7. — The decrease in time of the critical parameters from $Y(0)$; $X_{cr}(0)$ for $t = 0$ to $Y_{cr}(t)$; $X_{cr}(t)$ for the time $t = 0$.

In figure 7 one can notice that for $t = 0$, the dependence $Y(X)$ is given by the curve OB. After an interval of time t, the curve OB_1 is reached to which the following relation corresponds:

$$E_{cr}(t) < E_{cr}(0).$$

This is the case of material aging, of mild carbon steels exposed to the action of atomic hydrogen etc. In other cases (Fig. 8), after a certain period of time, t, instead of curve OB (from $t = 0$), the behaviour is given either by a curve as OB_2 or by another one as OB_3. In both cases $E_{cr}(t) < E_{cr}(0)$. This corresponds to the behaviour of some materials in case of fatigue (including fatigue of light) or creep.

4. THE EFFECT OF EXTERNAL LOAD APPLICATION RATE

From relationships (4), (5), it generally results that:

$$d = \left(\frac{Y}{Y_{cr}}\right)^{\frac{n+1}{n}} \tag{12}$$

The value of the exponent n depends on the behaviour of matter and this is influenced by the application rate of the external load.

Relationship (4) corresponds to a *slowly* applied load (*static load*).

If the load is applied instantly (impact, shock), Y increases from zero to its maximum value, before the occurrence of the effect X. In this case $1/n = 0$.

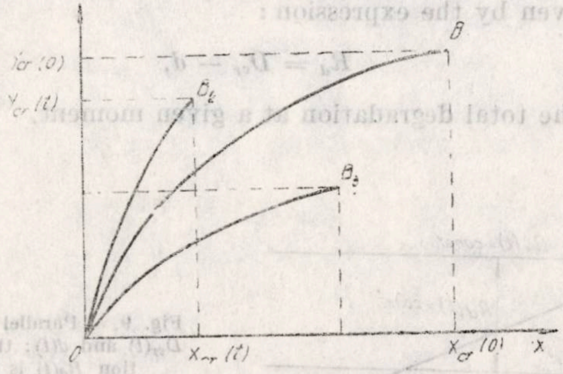

Fig. 8. — The change of matter behaviour after a period of time; Instead of the curve OB, for $t = 0$, the behaviour is given by the curve OB_2 or OB_3, for $t \neq 0$.

For an impact or *shock* load,

$$d = Y/Y_{cr} \tag{13}$$

For a rapid (fast) load whose rate is between that of the slow load and the rate of shock, it can be accepted — as a first approximation — that the exponent of d is the arithmetical mean of the exponents in relationships (12) and (13):

$$d = \left(\frac{Y}{Y_{cr}}\right)^{\frac{2n+1}{2n}} \tag{14}$$

5. RESERVE OF DEGRADATION

The value of degradation wherefrom the destruction of matter starts will be called *critical degradation* (D_{cr}).

For the *isotropic, homogeneous and natural matter* $D_{cr} = 1$.

For the *synthetic, artificial materials* and generally for materials whose behaviour is not completely similar from one sample to another, the critical characteristics Y_{cr} and X_{cr} are not unique; they form a dispersion characterized by a certain probability of return of a certain group of critical values (Y_{cr}, X_{cr}) and hence, the return of a certain value of the critical energy. We can write that for certain materials

$$E_{cr} \in [E_{cr,min}\, ;\, E_{cr,max}].$$

For such materials, this makes that :

$$D_{cr} \in [D_{cr,min} ; D_{cr,max}],$$

where $D_{cr,max} \leqslant 1$.

Whatever the nature of the material can be, the reserve of degradation (Fig. 9) is given by the expression :

$$R_d = D_{cr} - d, \tag{15}$$

where d is the total degradation at a given moment.

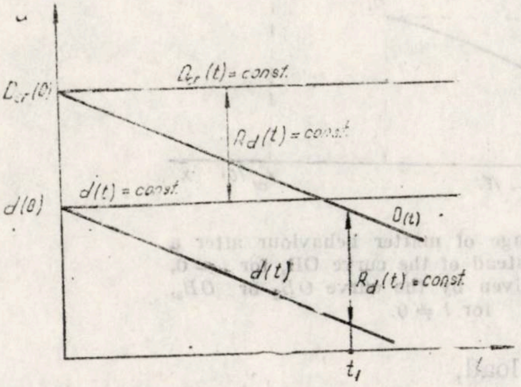

Fig. 9. — Parallel evolution vs. time of $D_{cr}(t)$ and $d(t)$; the reserve of degradation $R_d(t)$ is constant in time.

For a material with a *totally or partially irreversible behaviour, the degradation reserve, after the unloading of the exterior actions*, calculated by relation (15) is :

$$R'_d = D_{cr} - d_{ir}, \tag{16}$$

where d_{ir} is the corresponding irreversible degradation. For a recharging which determines the effective degradation d_1, the reserve of effective degradation is :

$$R_d = (D_{cr} - d_{ir}) - d_1 = R'_d - d_1 \tag{17}$$

This illustrates the negative influence of irreversible degradation.

The reserve of degradation is constant in time if both D_{cr} and d are constant (in time) and parallel (Fig. 9). The reserve of degradation $R(t)$ decreases in time if $D_{cr}(t)$ decreases (Fig. 10), if $d(t)$ increases in time (Fig. 11), or if $D_{cr}(t)$ decreases and $d(t)$ increases in time (Fig. 12). When the reserve of degradation depends on time, at a certain moment t_d, it falls to zero and $R(t_d) = 0$. At that moment the total destruction of material occurs.

6. CONCLUSIONS

Whichever its forms of existence may be, matter undergoes continuous more or less rapid changes. It deteriorates *reversibly* or — most of the time — *irreversibly*. Actually, by any process or natural phenomenon, a certain irreversible degradation occurs. In general, for relatively small values of action Y, as well as for proccesses or phenomena which develop very slowly in time, the irreversible component can be neglected, in comparison with the time of the possible experiment; it is only in these cases when we can speak about reversible degradation.

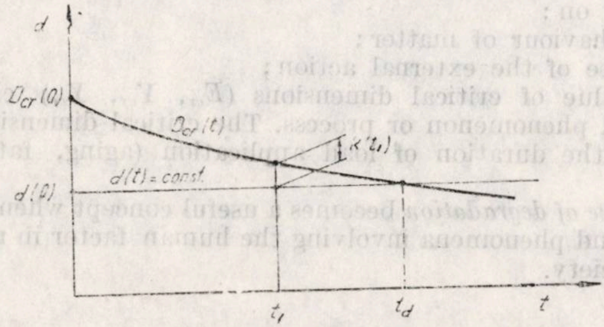
d
$D_{cr}(0)$
$D_{cr}(t)$
$R(t_1)$
$d(t) = const$
$d(0)$
t_1
t_d
t

Fig. 10. — Decrease in time of the reserve of degradation $R(t)$ due to $D_{cr}(t)$ decrease when $d(t)$ = constant.

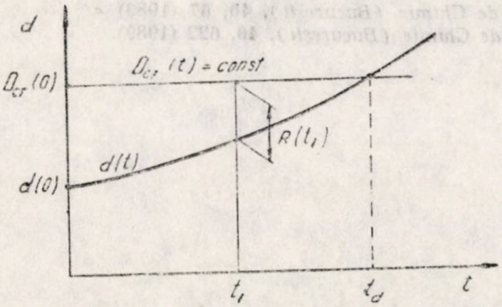
d
$D_{cr}(t) = const$
$D_{cr}(0)$
$R(t_1)$
$d(t)$
$d(0)$
t_1
t_d
t

Fig. 11. — Decrease in time of the reserve of degradation $R(t)$, due to $d(t)$ increase, when $D_{cr}(t)$ = constant.

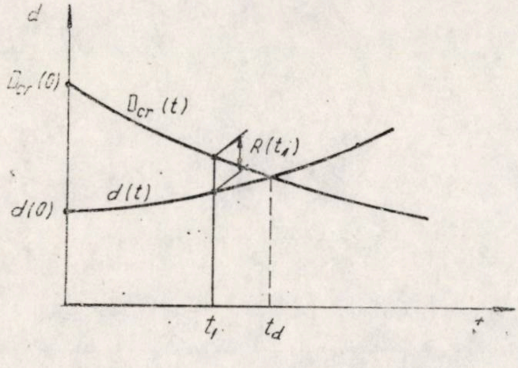
d
$D_{cr}(0)$
$D_{cr}(t)$
$R(t_1)$
$d(t)$
$d(0)$
t_1
t_d
t

Fig. 12. — Decrease in time of the reserve of degradation $R(t)$, due to $D_{cr}(t)$ decrease and $d(t)$ increase.

In the context of human experiments, the concept of reversible degradation can be accepted in numerous processes and phenomena. For instance, in case of a *perfectly elastic body*, as long as $d < 1$, its distorsion is reversible. But the distorsion of a *viscoelastic body* is only partly reversible while that of a *purely viscous body* is totally irreversible.

From this study it has also resulted that the value of matter degradation depends on :

— the behaviour of matter ;

— the rate of the external action ;

— the value of critical dimensions (E_{cr}, Y_{cr}, Y_{cr}) characteristic to the analysed phenomenon or process. The critical dimensions depend sometimes on the duration of load application (aging, fatigue, creep, and others).

The reserve of degradation becomes a useful concept when we consider the processes and phenomena involving the human factor in relation with nature and society.

REFERENCES

[1] V. V. Jinescu, *Revista de Chimie (București)*, **40**, 67 (1989).
[2] V. V. Jinescu, *Revista de Chimie (București)*, **40**, 622 (1989).

Revue Roumaine de Chimie, 36, 4–7, 809–818 (1991)

Dedicated to Prof. ALEXANDRU T. BALABAN
on the occasion of his 60th anniversary

THE CATALYTIC OXIDATION OF METHANOL IN OSCILLATORY REGIME

N. I. IONESCU, M. S. CHIRCA and D. I. MARCHIDAN
Institute of Physical Chemistry, Spl. Independenței 202, Bucharest 79611, Romania

Received January 15, 1991

Methanol oxidation on a palladium catalyst may proceed in oscillatory regime if an adequate correlation among various factors — reaction cell temperature, methanol content, oxygen flow rate, catalyst sample weight and its disposal on the metallic support — is realized. The influence of these factors upon the appearance and the characteristics of the thermal oscillations is presented. An attempt is made to propose a possible mechanism for the oscillatory behaviour, based on the reactivity of the intermediate Pd_xO phase.

INTRODUCTION

The study of the oscillatory reactions has grown up steadily in the last twenty years. These reactions challenge the researcher because the points of instability from the phase space, the multiplicity of steady states and the self-oscillations offer potential ways to discriminate among various kinetic models and also can bring new information concerning the catalytic act. At the same time, in some cases increased conversions of the reactants and better yields can be obtained by operating the chemical reactor in unsteady conditions.[1]

The oscillations which may appear in a reactor can also rise problems for the exploitation safety, because the transitions between the steady states and the unsteady ones are abrupt and till now the oscillatory reactions have not been adequately controlled.

In our previous papers [2–5] we have presented some of the experimental conditions in which the methanol oxidation on a palladium catalyst takes place in oscillatory regime. The present work enlarges the area for the variations of the parameters which determine the oscillatory behaviour and presents a possible mechanism for this process.

EXPERIMENTAL

The temperature difference between a catalyst sample and the ambient gaseous mixture was measured in a dynamic calorimeter realized by improving the models presented by Kral [6] and Jaeger.[7,8] A detailed scheme of the experimental installation was presented previously.[2]

The catalyst used was an industrial one, namely 0.5% $Pd/LiAl_5O_8$ (Bayer), with a granulation between 0.07 and 0.11 mm. The experimental conditions were varied within the following limits: weight of the catalyst sample 4 – 76 mg; temperature of the reaction cell 70 – 95°C; methanol content in the gaseous mixture of reactants 2.5 – 12.5%; oxygen flow rate 1.3 – 70.0 mL · min^{-1}. The analysis of the product was performed using a Carlo Erba gas-chromatograph.

RESULTS

The methanol oxidation on the palladium catalyst used in our experiments may proceed either in a stationary or in an oscillatory regime.[2–5]

The experimental borders in which the oscillatory regime can be detected are strictly determined by the weight of the catalyst sample, the temperature of the reaction cell, the methanol content in oxygen, the gaseous reactants flow rate and even by the catalyst sample disposal on the metallic support in the dynamic calorimeter.

The role played by each of the above-mentioned experimental parameters upon the appearance and the characteristics of the thermic oscillations will be further presented.

a) Weight of the catalyst sample

As previously shown [4,5] in the dynamic calorimeter used, the thermal oscillations could be detected only if the weight of the catalyst sample ranges between 15 and 55 mg, with an optimum value at 20 mg. An illustration of this assertion can be found in fig. 1, which presents the temperature of the catalyst during the catalytic oxidation of methanol, this value being measured on catalyst samples of various sizes and at different oxygen flow rates.

In the experimental range studied, the reaction can proceed in non-oscillatory or in oscillatory regime, the latter being illustrated by vertical arrows whose length is equal to the amplitude of the oscillations.

Fig. 1 shows that the highest amplitudes were obtained on 20 mg catalyst. For catalyst samples of 60 mg only oscillations which damped themselves in about 15 minutes were obtained.

The role played by the size of the catalyst sample is better evidenced in Fig. 2 which presents the temperature of the catalyst vs the weight of the catalyst sample, at various values for the reciprocal space velocity, defined as the ratio between the weight of the catalyst sample and the molar feed of methanol.

The experimental points which appear in Fig. 2 denote either the temperature of the catalyst in non-oscillatory regime, or the medium temperature when the reaction proceeds in oscillatory regime. As expected, for one size of the catalyst sample, the temperature of the catalyst is higher at lower values of the reciprocal space velocity, i.e. when a greater quantity of methanol reacts in the unity of time on the unity of mass of the catalyst.

The fact that the dependences presented in Fig. 2 are not linear proves that when bigger catalyst samples are used not the entire mass of catalyst is used in the catalytic reaction, because otherwise a linear dependence would be expected.

Fig. 1. — The variation of the catalyst temperature vs the oxygen flow rate on catalyst samples with various sizes (◐ — 20 mg ; ◑ — 46 mg ; ⊖ — 60 mg ; ⊖ — 76 mg). Temperature of the reaction cell : 80°C. Methanol content : 8.0 %.

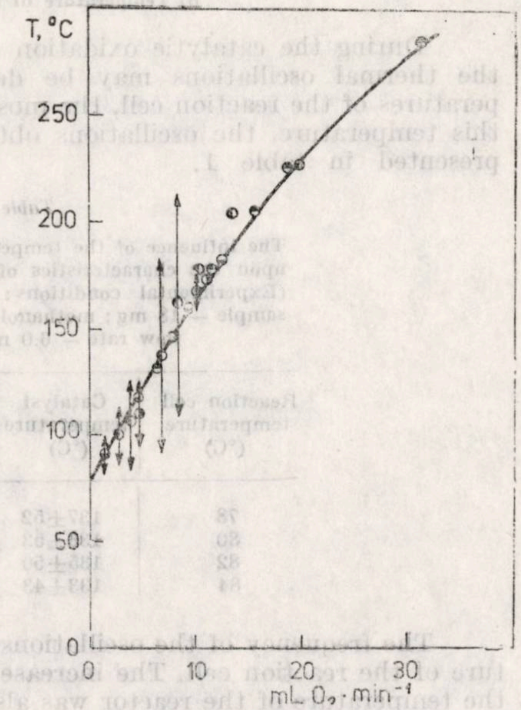

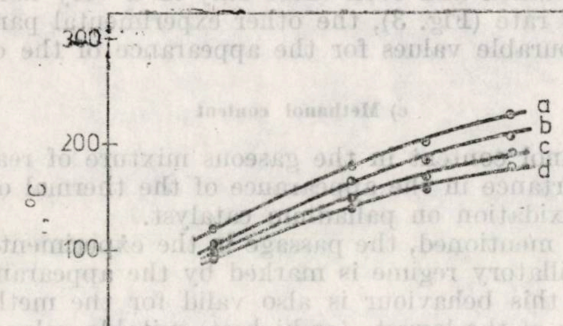

Fig. 2. — The variation of the catalyst temperature vs the weight of the catalyst sample at various values for the reciprocal space velocity, W/F (W — weight of the catalyst sample, g ; F — molar feed for methanol, mol · min^{-1}). Temperature of the reaction cell : 80°C. Values of the reciprocal space velocity W/F = 1 000 (a) ; 1200 (b) ; 1400 (c) and 1600 g · mol^{-1} · min.

b) Temperature of the reaction cell

During the catalytic oxidation of methanol on palladium catalyst the thermal oscillations may be detected in a narrow range of temperatures of the reaction cell, the most favourable being at 80°C. Around this temperature, the oscillations obtained have smaller amplitudes, as presented in table 1.

Table 1

The influence of the temperature of the reaction cell upon the characteristics of the thermal oscillations. (Experimental conditions: weight of the catalyst sample — 18 mg; methanol content — 5.0%; oxygen flow rate — 6.0 ml. · min^{-1})

Reaction cell temperature (°C)	Catalyst temperature (°C)	Oscillations amplitude (°C)	Oscillations frequency (h^{-1})
78	137±52	104	11
80	136±53	106	12
82	135±50	100	12
84	133±43	86	16

The frequency of the oscillations is also influenced by the temperature of the reaction cell. The increase of the frequency with the rise of the temperature of the reactor was also observed for the system CO/Pt.[9]

As for all the other experimental factors which influence the appearance of the thermal oscillations, the passage from oscillatory to non-oscillatory regime is not marked with a net border, but by the detection of damped oscillations. For example, at 90°C only damped oscillations can be obtained and even these only in a very narrow range for the oxygen flow rate (Fig. 3), the other experimental parameters being set at very favourable values for the appearance of the oscillations.

c) Methanol content

The methanol content in the gaseous mixture of reactants is also of decisive importance in the appearance of the thermal oscillations during methanol oxidation on palladium catalyst.

As already mentioned, the passage in the experimental area favourable to the oscillatory regime is marked by the appearance of damped oscillations and this behaviour is also valid for the methanol content. In the proximity of the lowest (or highest) suitable value, only damped oscillations were obtained, as presented in Fig. 4.

d) Oxygen flow rate

At a constant methanol content in the gaseous mixture, the rise of the oxygen flow rate causes evidently a rise of the temperature of the catalyst and in certain conditions thermal oscillations can be detected, as already presented in Fig. 1.

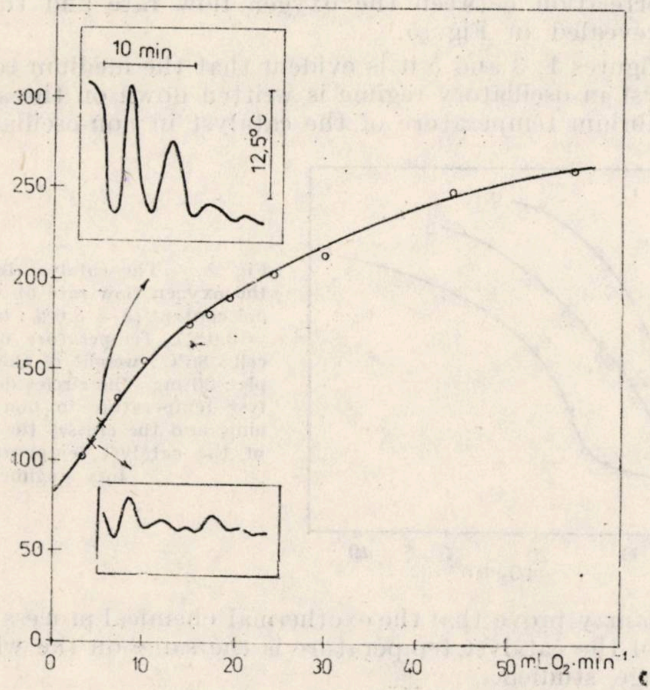

Fig. 3. — The variation of the catalyst temperature vs the oxygen flow rate when the temperature of the reaction cell was 90°C. Weight of the catalyst sample : 20 mg. Methanol content 5.0%. The circles denote the temperature of the catalyst in non-oscillatory regime.

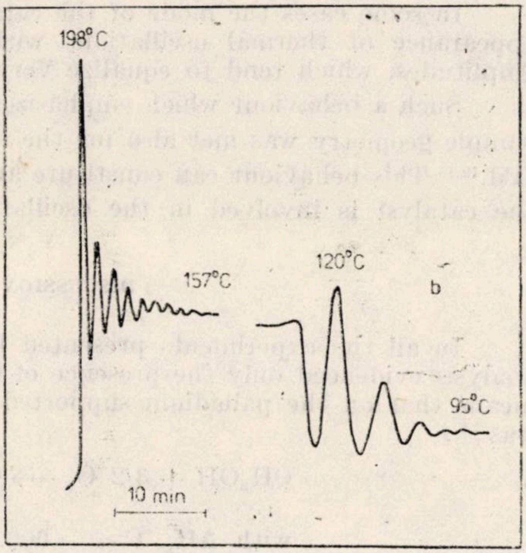

Fig. 4. — Damped oscillations during the catalytic oxidation of methanol. Experimental conditions : weight of the catalyst sample : 20 mg ; temperature of the reaction cell : 80°C ; methanol content 3.0% ; oxygen flow rate a — 22.0 mL · min^{-1} ; b — 16.2 mL · · min^{-1}.

The correlation between the oxygen flow rate and the methanol content is revealed in Fig. 5.

From figures 1, 3 and 5 it is evident that the medium temperatures of the catalyst in oscillatory regime is written down on the same curves as the equilibrium temperature of the catalyst in non-oscillatory regime and this fact may prove that the exothermal chemical process responsible for the rise of the catalyst temperature is the same on the whole experimental range studied.

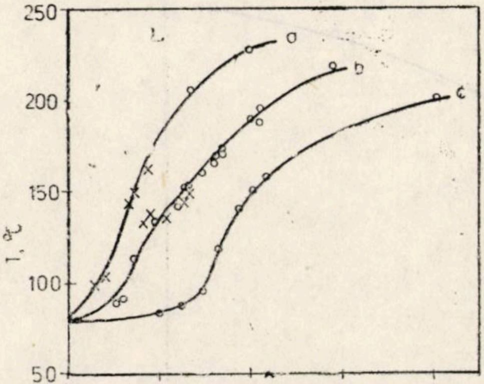

Fig. 5. — The catalyst temperature vs the oxygen flow rate at various methanol content (a — 8.0%; b — 5.0%; c — — 3.0%). Temperature of the reaction cell: 80°C; weight of the catalyst sample: 20 mg. The circles denote the catalyst temperature in non-oscillatory regime and the crosses the medium value of the catalyst temperature in oscillatory regime.

c) Geometry of the catalyst sample on the support

The catalyst sample disposal on the metallic support in the dynamic calorimeter also plays an important role in the characteristics of the oscillations, as presented in Fig. 6.

In some cases the mode of the catalyst disposal can determine the appearance of thermal oscillations with alternatively high and small amplitudes, which tend to equalize very slowly their values.

Such a behaviour which emphasizes the importance of the catalyst sample geometry was met also for the systems CO/Pt [10,11] and C_2H_5OH/ /Pd.[12,13] This behaviour can constitute another proof that only a part of the catalyst is involved in the oscillations appearance.

DISCUSSION

In all the experiments presented herein, the gas chromatographic analysis evidenced only the presence of CO_2 and H_2O as products. That means that on the palladium supported catalyst the oxidation reaction was [14]:

$$CH_3OH + 3/2\ O_2 \longrightarrow CO_2 + 2\ H_2O$$

$$\text{with } \Delta H_{80\,°C} = -606.3\ \text{kJ}\cdot\text{mol}^{-1}$$

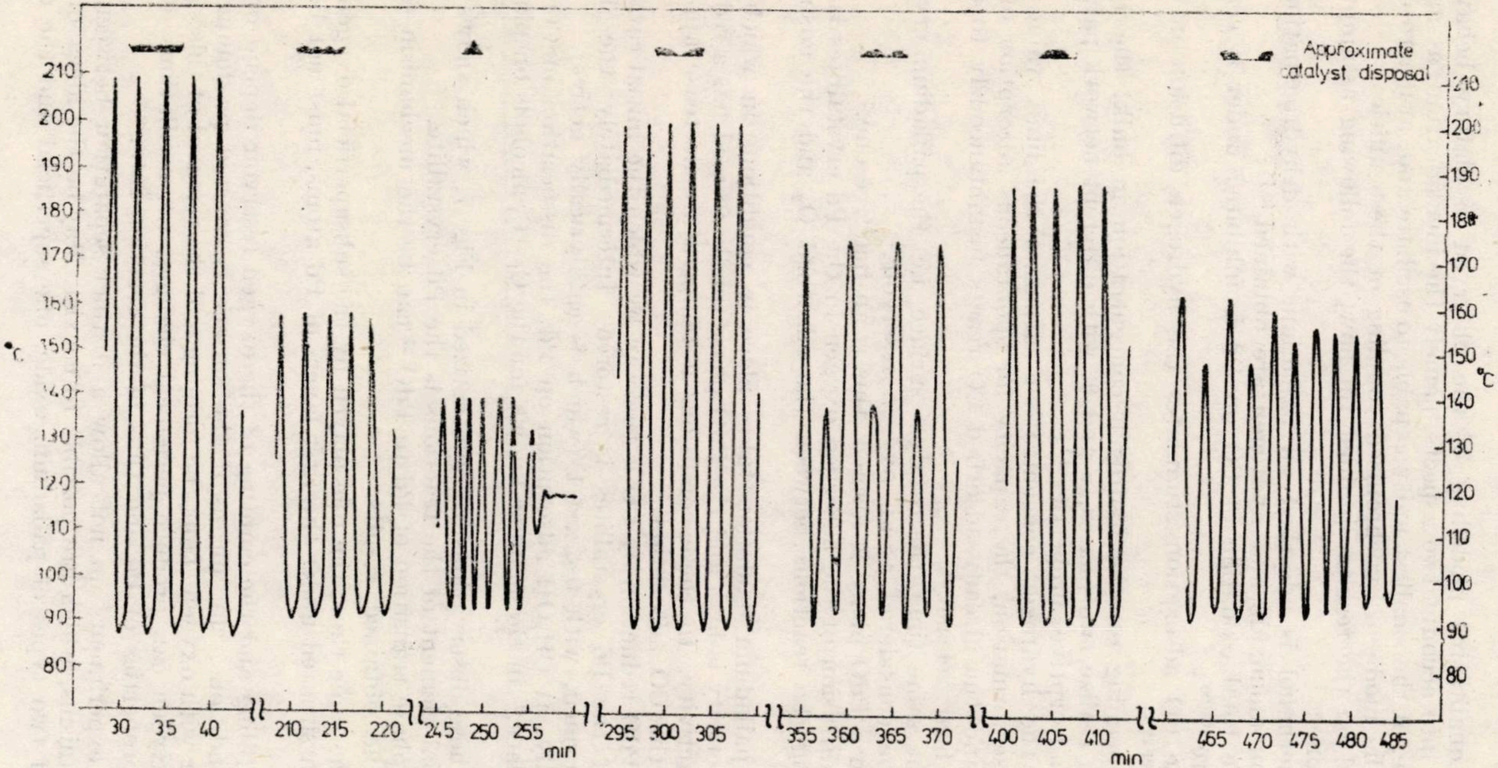

Fig. 6. — Different types of thermal oscillations obtained by only changing the disposal of the same catalyst sample on the metallic support in the reaction cell. Experimental conditions: weight of the catalyst sample: 18 mg; temperature of the reaction cell: 80°C; methanol content: 5.0%; oxygen flow rate: 5.0 mL · min^{-1}.

The qualitative modelling of the observed oscillatory behaviour must take into account two aspects, namely the identification, at microscopic scale, of the smallest unity capable to oscillate and, at macroscopic scale, of the mode of synchronised coupling of these unities.

Based on the results obtained till now, the following assumptions can be done:

— methanol is adsorbed on palladium with dehydrogenation so that carbon monoxide and hydrogen are obtained [12,15];

— the total oxidation of CO on Pd is inhibited under a certain temperature [16–20];

— the CO adsorption stimulates the hydrogen diffusion in bulk palladium [21,22];

— depending on the hydrogen concentration in bulk, the Pd-H system can realize two phases, α and β, with different network parameters and adsorptive properties [23];

— if the hydrogen concentration surpasses the limit values for the β phase formation, the capacity for spontaneous adsorption of CO decreases and the already adsorbed CO reacts instantaneously to form CO_2 with heat release.[24]

At the same time, the catalyst surface, i.e. the palladium crystallites can be considered as an oxygen reservoir.[25]

When a PdO phase is formed, this is an inactive one.[25–27]

The diffusion of the adsorbed oxygen in the Pd crystallites is realized during the reactions between the adsorbed O_2 and the adsorbed CO.

The palladium oxidation takes place in conditions in which the catalytic activity is high and the PdO phase finally formed has a reduced catalytic activity. In these conditions a temperature decrease appears, favouring the CO adsorption.

The PdO reduction by CO is the way by which the initial catalytic activity of the Pd crystallites is restored. Intermediately the Pd_xO phase is formed, with $0 < x < 1$ (which is catalytically active).

Finally, at CH_3OH adsorption on Pd, the dissociation in CO and H takes place,[25] in the manner known for the C_1-C_4 alcohols on platinic metals.[28]

All these observations are synthetized in Fig. 7, which shows that the essential element of the reactions is the Pd crystallite.

The phase transition of Pd to PdO [27] can be the mechanism which explains the obtained results.

At the same time, the role played by the subsuperficial oxygen, i.e. the oxygen situated under the first layers of Pd atoms, must not be neglected.[29]

The filling and the empting of the oxygen reservoir depend on the surface conditions, this means if the surface is covered predominantly with CO or with oxygen. Thus the forming and the removal of this subsuperficial oxygen can produce periodical changes, i.e. oscillations of the catalytic properties of Pd and thus of the reaction rate.[30]

Our experiments do not allow a distinct separation between the two mechanisms, which are possible to coexist. May be the ideea of coexistence of two types of palladium oxide, one superficial and the other in bulk, with various formation and reduction rates, could explain the role played by PdO and by the subsuperficial oxygen.

The mode in which the oscillating microunities couple themselves to give a thermal oscillation remains an open problem. Our experiments regarding the role played by the geometrical disposal of the catalyst on the metallic support in the reaction cell suggest that this coupling seems to be realised by heat transfer either by the metallic support which has a great thermal conductivity or by heat transfer among the catalyst portions and/or by convection. The coupling realized through the gaseous phase situated above the catalyst, in which both the initial and the final compounds are present, cannot also be neglected.

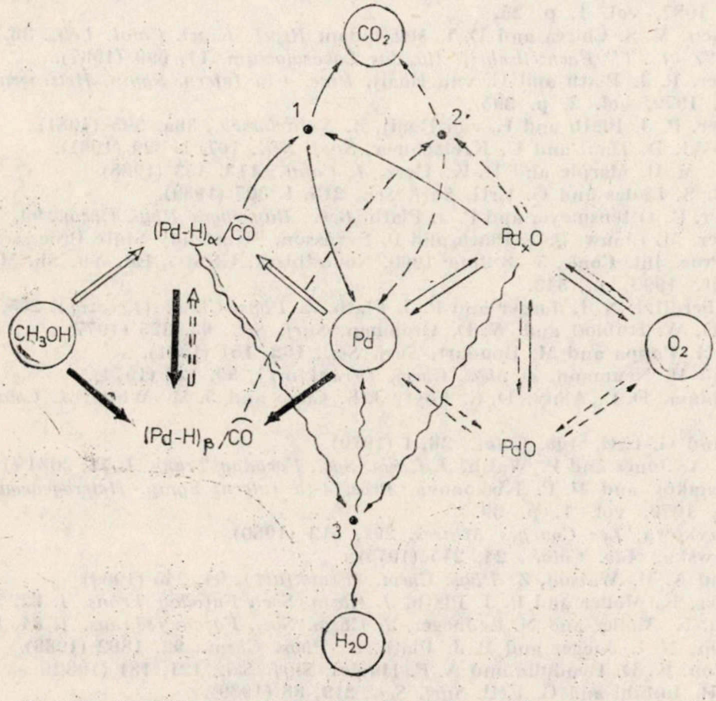

Fig. 7.—Possible ways for methanol total oxidation on the surface of a palladium catalyst.

═══ disociative adsorption of methanol as α phase

▬▬ methanol adsorption as β phase

—— oxygen adsorption as an active phase Pd_xO, with $0 < x < 1$

········ oxygen adsorption as an inactive phase PdO

1, 2, 3 junctions representing reactions of Langmuir-Hinshelwood type.

Further experiments may bring supplementary information in this problem.

As a conclusion, the determination of the experimental conditions in which the thermal oscillations can be obtained may be a valuable aid for a description of the mechanism that generates thermal oscillations during the catalytic oxidation of methanol.

REFERENCES

[1] L. A. Prazon and R. A. Schmitz, *Catal. Rev.-Sci. Eng.*, **28**, 89 (1986).

[2] N. I. Ionescu, M. S. Chirca and D. I. Marchidan, *Rev. Roumaine Chim.*, **31**, 671 (1986).

[3] N. I. Ionescu, M. S. Chirca and D. I. Marchidan, *React. Kinet. Catal. Let.*, **31**, 361 (1986).

[4] N. I. Ionescu, M. S. Chirca and D. I. Marchidan, *Proc. 6-th Intern.Symp. Heterogeneous Catal.*, Sofia, 1987, vol. 1, p. 25.

[5] N. I. Ionescu, M. S. Chirca and D. I. Marchidan, *React. Kinet. Catal. Lett.*, **38**, 249 (1989).

[6] H. Kral, "*G—I—T*" *Fachzeitschrift für das Laboratorium*, **11**, 699 (1967).

[7] N. I. Jaeger, P. J. Plath and E. van Raaij, *Proc. 4-th Intern. Symp. Heterogeneous Catal.*, Varna, 1979, vol. 2, p. 395.

[8] N. I. Jaeger, P. J. Plath and E. van Raaij, *Z. Naturforsch.*, **36a**, 395 (1981).

[9] D. Barkowski, R. Haul and U. Kretschmer, *Surf. Sci.*, **107**, L 329 (1981).

[10] P. K. Tsai, M. B. Marple and R. K. Herz, *J. Catal.*, **113**, 453 (1988).

[11] R. Imbihl, S. Ladas and G. Ertl, *Surf. Sci.*, **215**, L 307 (1989).

[12] N. I. Jaeger, R. Ottensmeyer and P. J. Plath, *Ber. Bunsenges Phys. Chem.*, **90**, 1075 (1986).

[13] N. I. Jaeger, M. Liauw, P. J. Plath and P. Svensson, "Unsteady State Processes in Catalysis" (Proc. Int. Conf., 5—8 June 1990, Novosibirsk, USSR), Ed. Yu. Sh. Matros, VSP, Utrecht, 1990, p. 343.

[14] A. Th. Haberditzl, N. I. Jaeger and P. J. Plath, *Z. Phys. Chem. (Leipzig)*, **265**, 449 (1984)

[15] H. Luth, G. W. Rubloff and W. D. Grobman, *Surf. Sci.*, **63**, 325 (1977).

[16] S. Ladas, H. Poppa and M. Boudart, *Surf. Sci.*, **102**, 151 (1981).

[17] G. Ertl and M. Neumann, *Z. phys. Chem. (Frankfurt)*, **90**, 127 (1974).

[18] T. Matsushima, D. C. Almy, D. C. Foyt, J. S. Close and J. M. White, *J. Catal.*, **39**, 277 (1975).

[19] T. Engel and G. Ertl, *Adv. Catal.*, **28**, 1 (1979).

[20] S. Gentry, A. Jones and P. Walsh, *J. Chem. Soc., Faraday Trans. I*, **76**, 2084 (1980).

[21] G. M. Bliznakov and M. P. Kiskonova, *Proc. 4-th Intern. Symp. Heterogeneous Catalysis*, Varna, 1979, vol. 1, p. 39.

[22] L. Ratajezykowa, *Les Couches Minces*, **201**, 513 (1980).

[23] W. Palczewska, *Adv. Catal.*, **24**, 245 (1975).

[24] P. Brill and A. M. Watson, *Z. Phys. Chem. (Frankfurt)*, **64**, 245 (1969).

[25] N. I. Jaeger, K. Möller and P. J. Plath, *J. Chem. Soc., Faraday Trans. I*, **82**, 3315 (1986).

[26] P. J. Plath, K. Möller and N. I. Jaeger, *J. Chem. Soc., Faraday Trans. I*, **84**, 1751 (1988).

[27] P. Svensson, N. I. Jaeger and P. J. Plath, *J. Phys. Chem.*, **92**, 1882 (1988).

[28] B. A. Sexton, K. D. Rendulic and A. F. Hugles, *Surf. Sci.*, **121**, 181 (1982).

[29] S. Ladas, R. Imbihl and G. Ertl, *Surf. Sci.*, **219**, 88 (1989).

[30] M. M. Slinko, N. I. Jaeger and P. Svensson, *J. Catalysis*. **118**, 349 (1989).

Revue Roumaine de Chimie, **36**, *4–7*, 819–828 (1991)

Dedicated to Prof. ALEXANDRU T. BALABAN
on the occasion of his 60th anniversary

THERMAL DECOMPOSITION OF PROPYLENE

ION BOLOCAN and FLAVIAN CUIBAN

Chemistry Department, Petroleum and Gas Institute, Blvd. București 39, 2000 Ploiești, Romania

Received January 10, 1991

Thermal decomposition of propylene at high temperatures (750 – 825°C) and conversions, in dynamic system is expressed by the relation : $k = 0.29 \cdot 10^{12} \cdot \exp(58500/RT)\mathrm{s}^{-1}$. Besides the principal products of reaction : methane, ethylene, hydrogen, butenes, butadiene, dependent on conversion significant amounts of ethane and propane are formed. No measurable quantity of allene was encountered. The "auto-in hibited" decomposition of propylene described in the literature occurs only at moderate temperature on account of oligomers formed in initial stages due to allyl type radicals. At these temperatures the initiation begins with bimolecular collisions giving propyl radicals and becomes ampler at increased temperature by dissociation into allyl and hydrogen radicals. At high conversion when the concentration of ethylene becomes significant, the initiation goes on by bimolecular collisions also with ethylene. The given ensemble of prevalent reactions and their succession is in accordance with the alteration of product distribution, dependent on conversion.

1. INTRODUCTION

Besides ethylene, propylene is one of the main useful products (up to 17%) obtained in any process of alkanes pyrolysis. They are formed through a chain of parallel and/or successive elementary reactions, whose contribution depends on the structure of pyrolysed alkanes and on the severity of process. Industrial pyrolysis is performed at high severities to obtain maximal yields of ethylene. In these severe conditions a part of propylene formed in primary stages undergoes a thermal decomposition. As a result, the yield of propylene varies with the conversion describing a convex curve, the maximal point moving to lower conversion with the increase of the pyrolysed alkane chain. In industrial practice, pyrolysis plants are frequently supplied with gaseous mixture impurified with propylene, its concentration sensibly exceeding the technological prescriptions (max. 3%).

The inhibitor role of propylene in radical processes is well-known for the reactions developed within moderate range of temperature due to the intervention of allyl type radical, more stable than alkyl radicals. Preserving of the inhibitor role of propylene in radical reactions at high temperature is little known and constitutes a controversial subject. In the literature a higher frequency of studies concerning the thermal decomposition of propylene in static system at low temperature (about 500°) is noticed while the pyrolysis of propylene at high temperature and short time of reaction has been less studied.[1,2] The data obtained in dynamic system reflect with more accuracy the actual process because the influence of reaction products — which are continuously eliminated out of the system — is considerably decreased. Only Kunugi [3] and Méllottée [4] have published systematic studies concerning thermal decomposition of propylene in dynamic conditions, but their results are somehow contradictory and difficult to compare. The difficulty of comparison appears since the conversions and kinetic parameters were related to the time of staying and not to the equivalent time of reaction, which includes the profile of temperature in the reactor. On the other hand, the times of reaction and the conversions are too low [3] or too high (up to 5 s.),[4] surpassing the time of staying of industrial importance. It was stated [4] that the order of reaction varies with the increase of temperature from 3/2 till 1 for high temperatures. In both studies, all possible radical reactions were taken into consideration, without specifying the contribution of prevalent reactions. Surprisingly and hard to accept is the generation of a significant quantity of allene [4] for those conditions of reaction. Although a radical chain reaction mechanism with an induction period, common both to static and dynamic systems is generally accepted, the mechanisms of reaction are considerably different. In the static systems, the initiation of radical chain is attributed to decomposition of oligomers resulted from initial stages of addition and combination with the participation of allyl radical. Under dynamic conditions it was stated that initiation takes place through butene-1, its decomposition generating reactive species H· and CH_3· which provoke proper initiation,[3] without taking into account the concentration of all products and reactive specia being present in the system at the moment.

Now, we have been studying quantitavively the thermal decomposition of propylene in dynamic system for a large conversion range near those employed industrially, in order to obtain experimental evidence concerning the main elementary reactions and their succession in straight decomposition of C_3H_6.

2. EXPERIMENTAL CONDITIONS AND COMPUTATION OF OBTAINED DATA

Propylene with a composition of 99.5% C_3H_6 and 0.5% C_3H_8 was used as raw material for pyrolysis. The experiments were carried out in a dynamic system, in a quartz tubular reactor 560 mm in length with an internal diameter of 14 mm. A quartz pipe 540 mm in length and 6 mm in external diameter was coaxially fixed inside the reactor. A thermoelement used for the determination of longitudinal profile of temperature was introduced inside that quartz pipe. The investigated range of temperature was 750—825°, at an equivalent reaction time between 0.1 and 2.8 seconds.

The analysis of the reaction products was made by gas chromatography : hydrocarbons C_2-C_4 in a column of activated alumina 4 m in length with an inside diameter of 4 mm, hydrogen and methane in a column of activated charcoal 2 m in length with an inside diameter of 4 mm. The conversion and the yields were determined by balancing the carbon atoms. The selectivity (S_i) was calculated with the relation :

$$S_i = \frac{\text{no. of mols } C_3H_6 \text{ transformed into ``i'' product}}{\text{total no. of mols } C_3H_6 \text{ transformed}} \times 100$$

To determine an order reaction according to a large range of conversion and time of reaction, a method described in [5] was used. For the computation of n value, when k remains constant for the studied range of conversion, 8 pairs of values (X_i, τ_i) from the graph $X = f(\tau)$ at the same temperature have been taken into consideration. These pairs have been introduced into the following relation :

$$k = \frac{1}{C_0^{n-1} \cdot \dfrac{V_e}{F}} \int_0^x \left(\frac{1 + (E - 1) \cdot X}{1 - X} \right)^n \cdot \mathrm{d}X$$

The system of equations obtained was solved for different values of n, bearing in mind that the order of reaction corresponds to the minimum deviation of the rate constant from its average value.

3. RESULTS

The values of propylene conversion are relatively low in comparison with those obtained at decomposition of alkanes in similar conditions (see Fig. 1). For a reaction time of one second, the conversion is 9% at 750°, respectively 42% at 825°. Higher conversions (approx. 70%) were obtained only at a longer time of reaction (about 2.8 seconds) and 825°. The influence of the reaction time on conversion is more important at high temperature. Thus, for an increase of time from 0.4 to 0.6 seconds, the conversion increases with 8% at 825° and with only 1.5% at 750°.

The principal products of decomposition are ethylene, methane, hydrogen, butene-1 and butadiene. The yield of ethylene is about 20% at 825° and $\tau = 1$ s. The distributions of the above-mentioned products as a function of reaction time are represented in figures 2 ÷ 6. It was stated that yields of ethylene, methane and hydrogen are monotonously increasing with time for all investigated temperatures, whereas the yields of C_4 components are monotonously increasing at 750° and describe a convex curve for $\tau = 1$ s at higher temperatures between 800 — 825°. The dependence of products selectivity on conversion is graphically presented in figure 7. For values of conversion lower than 40%, the selectivities of ethylene and methane increase parallel to conversion, the selec-

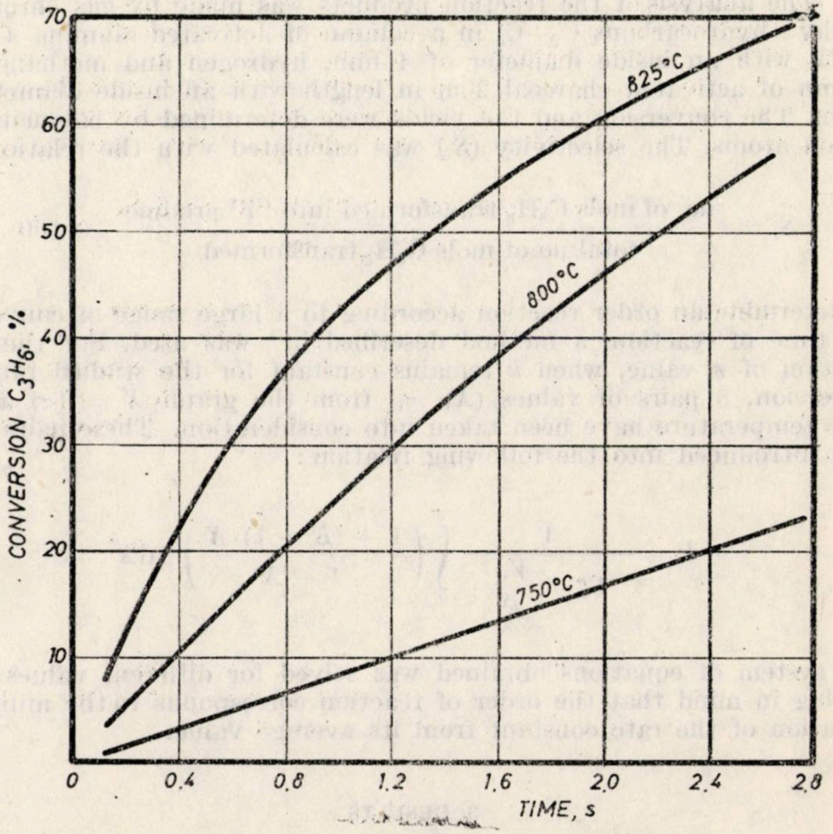

Fig. 1. — Conversion of propylene with reaction time.

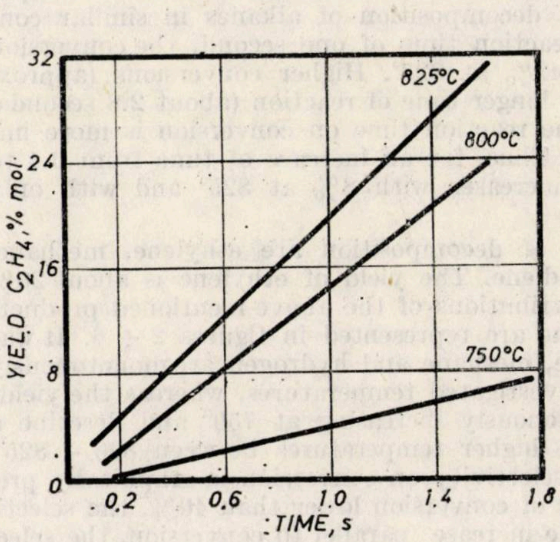

Fig. 2. — Yield of ethylene with reaction time.

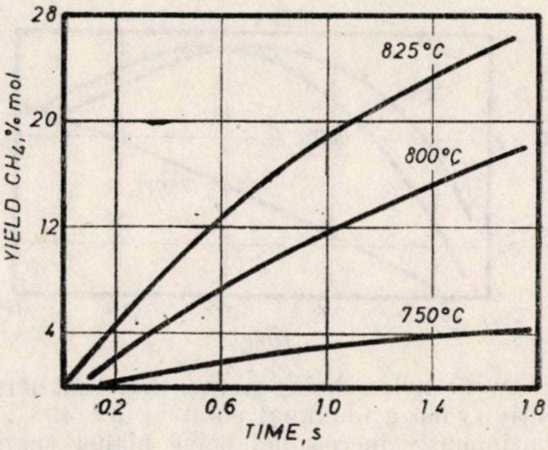

Fig. 3. — Yield of methane with reaction time.

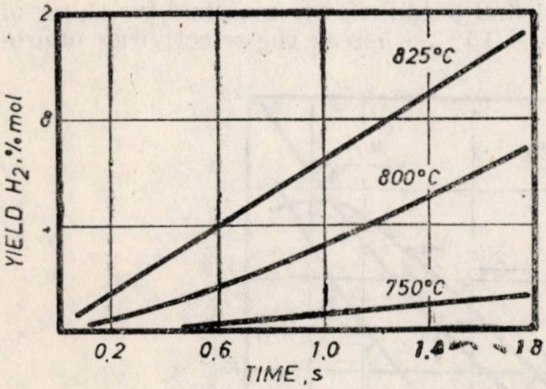

Fig. 4. — Yield of hydrogen with reaction time.

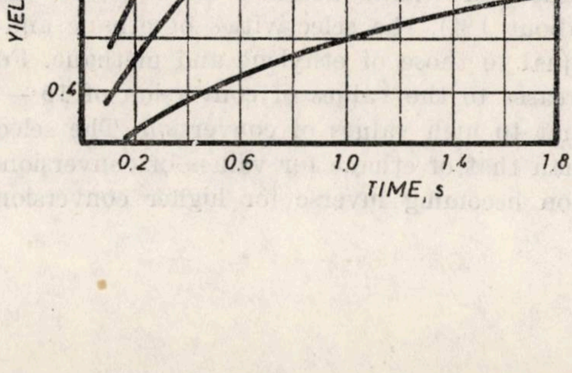

Fig. 5. — Yield of butadiene with reaction time.

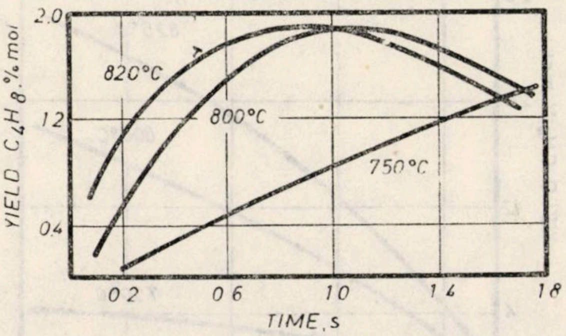

Fig. 6. — Yield of butenes with reaction time.

tivity of ethylene being greater than that of methane. The curve of C_2H_4 selectivity has a maximal point at $X=40\%$, whereas the CH_4 selectivity is continuously increasing, being higher than that of ethylene for conversions higher than 40%. The selectivity of hydrogen increases exponentially with conversion, being 3 or 4 times lower than the C_2H_4 selectivity. The selectivities of butene-1 and butadiene are maximal for values of conversion comprised between $5 \div 15\%$, whereas the selectivities of propane and ethane decrease with conversion. For very low conversions (about 1%), the selectivities of ethane and propane are approximately equal to those of ethylene and methane. For ethane the selectivity decreases to the values of conversion of $15-20\%$, increasing again after that to high values of conversion. The selectivity of propane is greater than that of ethane for values of conversion lower than 25%, the situation becoming inverse for higher conversions.

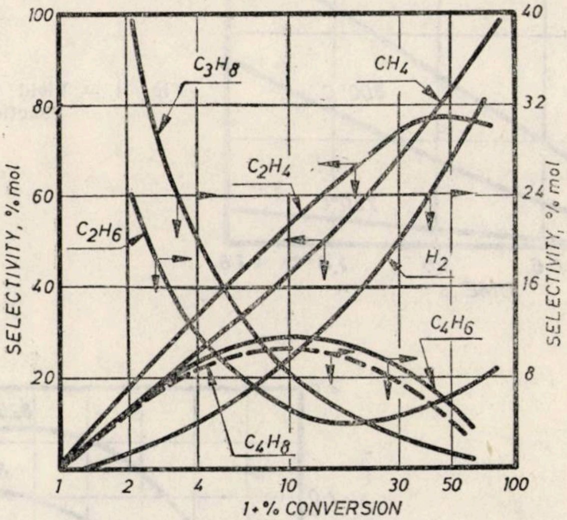

Fig. 7. — Selectivity of products as a function of log (1 + % conversion).

4. DISCUSSION

The lower values for conversion in thermal decomposition of propylene in comparison with those for propane are not unexpected because in conditions of pyrolysis, the olefines are thermodynamically more stable than the corresponding alkanes. Thus, the rate constant at 825° is only 0.65 s^{-1} for decomposition of propylene, 1.6 s^{-1} in the case of ethane and 4.7 s^{-1} for propane.[8] The order of reaction, calculated from experimental data is close to 1 for the range of temperature 750–825°. By determining A and E_a parameters, it becomes possible to express the rate constant for thermal decomposition of propylene with the relation :

$$k = 0.29 \cdot 10^{12} \cdot \exp(-58500/RT), \ (s^{-1}).$$

The value determined by us for energy of activation (58.5 kcal/mol) is greater than that obtained by Méllottée from a relation of first order (49.2 kcal/mol) but is less than Kunugi's value (63.2 kcal/mol), coming from an order of reaction equal to 3/2. These differences are due to the different methods used for the calculation of kinetic parameters. Using the methods of calculus exposed by the same authors,[3,4] our data are comparable and valid for the whole studied range of conversions, excluding any modification for the order of reaction. In opposition to previous studies,[3,4] in our experiments were not discovered significant quantities of allene.

The distribution of products and their variation with the conversion in different conditions of temperature allow us to assert, on experimental bases, the next succession of elementary reactions involved in propylene decomposition at high conversions, in dynamic conditions :

Initiating reactions	log A	E_a(kcal/mol)[3]
(1) $2\ C_3H_6 \rightarrow C_3H_5\cdot + C_3H_7.$	12.8	51
(2) $C_3H_6 + C_2H_4 \rightarrow C_3H_5\cdot + C_2H_5\cdot$	13.5	47
(3) $C_3H_6 \rightarrow C_3H_5\cdot + H\cdot$	15.0	88
Propagation reactions		
(4) $C_3H_7\cdot \rightleftharpoons C_2H_4 + CH_3\cdot$	13.9	31
(5) $C_2H_5\cdot \rightleftharpoons C_2H_4 + H\cdot$	14.0	40
(6) $H\cdot + C_3H_6 \rightleftharpoons C_3H_7\cdot$	13.0	3.6
(7) $H\cdot + C_3H_6 \rightleftharpoons C_3H_5\cdot + H_2$	12.4	1.1
(8) $C_3H_7\cdot + C_3H_6 \rightarrow C_3H_8 + C_3H_5\cdot$	11.0	8
(9) $CH_3\cdot + C_3H_6 \rightarrow CH_4 + C_3H_5\cdot$	10.3	7.2
(10) $CH_3\cdot + C_3H_6 \rightarrow$ sec-$C_4H_9\cdot$	11.5	7.4
(11) sec-$C_4H_9\cdot \rightleftharpoons H\cdot + C_4H_8\cdot$	14.8	47
(12) $H\cdot + C_4H_9 \rightarrow H_2 + C_4H_8\cdot$	14.0	3.6
(13) $C_4H_7\cdot \rightleftharpoons C_4H_6 + H\cdot$	13.7	47

Interrupting reactions

(14) $CH_3\cdot + C_3H_5\cdot \rightarrow 1\text{-}C_4H_8$
(15) $C_3H_5\cdot + C_3H_6 \rightarrow$ oligomers
(16) $2\ C_3H_5\cdot \rightarrow$ oligomers

Reactions (1), (2) and (3) have a decisive contribution to the initiating stage. The relatively high selectivity of propane at low conversions uphold the idea of formation in the initial stages of propyl radicals which may result from the molecular disproportion (1) or from addition of hydrogen atoms to propylene (6). The propyl radicals formed in these reactions explain the appearance of propane through a hydrogen atom extraction from propylene (reaction 8). Hydrogen results from the initiating reaction (3) followed by an atom transfer reaction (7) and (12). Actually at low conversions the selectivity of hydrogen is practically zero while the selectivity of propane is relatively high and these facts support an initiation under mild conditions through the generation of propyl radical from reaction of disproportion (1). In these conditions, at low severities, the contribution of hydrogen atoms at the initiation is practically zero. Having a higher energy of activation the initiating reaction (3) is facilitated by raising the temperature when an exponential increase of hydrogen selectivity with the conversion is observed, yet it lags behind the selectivities of ethylene and methane. These hydrocarbons are especially formed intermediary by means of propyl radicals resulted from (1) and (6), by β-cleavage (5) followed by an atom extraction (9).

Although the selectivities of ethylene and methane are different to a small extent, the lower values obtained for methane at conversions less than 40% might be explained by the participation of methyl radical in reactions of addition (10) — facilitated by low temperatures — and by interrupting through recombination with allyl radical (14). We noticed a real concordance between the selectivity of butene-1 and the difference between the lower selectivity of methane related to ethylene. We attributed this difference to the extent of methyl radical participation to addition and combination with allyl radical, in comparison with its share in reactions of atom transfer. For example, for a conversion of 10%, the selectivity of methane is 10% lower than that of ethylene, whereas the selectivity of butene-1 is about 10%. The increased selectivity of methane in comparison with that of ethylene — for conversions greater than 40% — is easily explained by its stability to pyrolysis.

For conversions greater than 40%, the selectivity of ethylene begins to decrease whereas in the same range of conversion the selectivity of ethane begins to increase. These facts support the contribution to the initiating stage of a new reaction of disproportion, with the participation of ethylene — presented in high concentration — and propylene (2). This reaction is geometrically facilitated in comparison with the reaction of disproportion (1) which supposes the participation of two molecules of propylene ($\log A_1 = 12.8$; $\log A_2 = 13.5$).[3] The period of induction mentioned — at low severities — by other researchers too [3,6,7] might be explained through the interruption of chain reaction caused by reactions of oligomerisation with the participation of propylene and allyl radicals (15,16). At high severities, the oligomers are broken generating supplementary reactive species which take part in the reactions of initiation and propagation. In these conditions, the increasing concentration of methyl radical at high temperature facilitates the interrupting reaction (14), implicitly the formation of butene-1.

5. CONCLUSIONS

— The kinetic parameters of propylene decomposition in dynamic system are given by the relation :

$$k = 0.29 \cdot 10^{12} \cdot \exp(-58500/RT),\ \mathrm{s}^{-1}$$

The relation is valid for a large range of conversion and explains the thermal stability of propylene comparatively to alkanes. The main products of decomposition are : methane, ethylene, hydrogen, butene and butadiene. No significant quantity of allene was encountered but measurable amounts of butene-1 were recorded.

— Besides the principal products of reaction, in initial stages, estimable quantities of propane – consumable at high conversions – and ethane are formed. The concentration of ethane, as a function of conversion, describes a curve with a minimum point.

— At moderate temperatures the initiation of propylene decomposition occurs prevalently by bimolecular collisions, having as result propyl radicals. At higher temperatures, the initiation becomes ampler through the contribution of propylene decomposition into allyl and hydrogen radicals. At high conversion, when the concentration of ethylene becomes significant, the initiation of propylene decomposition goes on by bimolecular collisions and also with ethylene. In this way the presence of propane and ethane might be explained in variable concentrations, dependent on conversion.

— The "autoinhibited" decomposition of propylene occurs only at moderate temperature on account of oligomers formed in initial stages, explaining the period of induction mentioned in the literature.

— The assembly of elementary reactions and their succession depict adequately the thermal decomposition of propylene for a large range of conversion suggesting the possibility of promoting its decomposition with the aim of ethylene forming.

6. NOMENCLATURE

X : conversion, %
S : selectivity, %
n : reaction order
k : rate constant, s^{-1}
E_a : energy of activation, kcal/mol
A : pre-exponential factor, s^{-1}
τ : equivalent time of reaction, s
T : temperature °C
E : expansion
C_0 : initial concentration, mol/l
F_0 : feeding flow, mol/s
V_e : equivalent volume of reaction, cm^3

REFERENCES

[1] V. Vântu, R. Mihail, V. Măcriş and Gh. Ivănuş, "Piroliza hidrocarburilor", Ed. Tehnică, Bucharest, 1980, p. 106.

[2] A. D. Stepuhovich and V. A. Ulitzkii, "Kinetika i termodinamika radical 'nih reaktzii krekinga", Ed. Himia, Moscow, 1975, p. 165.

[3] T. Kunugi, T. Sakai, K. Soun and Y. Sasaki, *Ind. Eng. Chem. Fuudam.*, **9** (3) 314 (1970).

[4] H. Méllottée, J. Tardieu de Maleissye and R. Delbourg, *Bull. Soc. Chim. de France*, **8** 2652 (1969).

[5] R. Dimitriu, A. Băsescu and Gh. Ivănuş, *Revista de Chimie*, **31** (6) 542 (1980).

[6] M. Simon and M. H. Back, *Can. J. Chem.*, **48** (2) 317 (1970).

[7] A. Amano and M. Uchiyama, *J. Phys. Chem.*, **68** (5) 1133 (1963).

[8] I. Bolocan, "Doctoral Dissertation", Petroleum and Gas Institute, Ploieşti, 1988, p. 79.

Revue Roumaine de Chimie, **36**, *4–7*, 829–842 (1991)

Dedicated to Prof. ALEXANDRU T. BALABAN
on the occasion of his 60th anniversary

OXIDATIVE COUPLING OF METHANE. THE INFLUENCE OF REACTANT DIFFUSION ON THE REACTION

MIHAI I. VASS and ION BALINT

Roumanian Academy, Institute of Physical Chemistry, Spl. Independenţei 202,
Bucharest 79611, Romania

Received January 8, 1991

The oxidative coupling of methane over lithium-promoted magnesium oxide was investigated in a fixed bed reactor at temperatures between 650°C – 850°C. Methane conversions, selectivities to C_2 compounds were determined as a function of the reaction parameters. Kinetic and diffusional domains were delimited for studied reaction.

1. INTRODUCTION

Methane, the major component of natural gas, is a relatively abundant and cheap raw material for chemical industry. Taking into account these advantages, many researchers have investigated the possibility of finding new ways of getting more valuable chemical compounds directly from methane. A turning point in this domain is Keller and Bhasin's work [1] published in 1982, which reports the possibility of obtaining C_2 compounds via oxidative coupling of methane, using basic metal oxides as catalysts. The study of methane oxidative coupling is also important from the theoretical point of view, the very stable C–H bond activation being a major challenge in the catalysis field.

Methane conversion to higher hydrocarbons via oxidative coupling has some advantages, especially concerning the transport and storage. The products of oxidative coupling may be transformed by oligomerization into liquid hydrocarbons. The fractions are important raw materials for polymer synthesis and for other valuable chemical compounds.

The applied technologies for methane utilization involve first, its conversion into carbon monoxide and hydrogen by steam reforming which requires a large energy input ($\Delta H^\circ = +206$ kJ/mol).

The temperatures at which the reaction takes place are high, 700–800°C. The second stage of methane transformation in to liquid hydrocarbons implies the reaction between carbon monoxide and hydrogen, which is exothermic ($\Delta H^\circ = -170$ kJ/mol). Another disadvantage of the Fischer-Tropsch method is the Schultz-Flory distribution of reaction products which cannot be avoided. In conclusion one can say that the

Fischer-Tropsch reactions for liquid hydrocarbon synthesis are energy intensive and capital intensive.

Reaction temperatures for the oxidative coupling of methane are also relatively high but the main reactions which take place are exothermic, therefore a part of energy for reactor heating is recovered from the heat released by the reactions :

$$\begin{array}{llrr}
 & & \Delta\, H_{25}\ ^{\circ}\mathrm{C(Kj/mol)} & \\
2\ CH_4 + 1/2\ O_2 = C_2H_6 + H_2O(g) & & -177 & (1) \\
C_2H_6 + 1/2\ O_2 = C_2H_4 + H_2O(g) & & -105 & (2) \\
C_2H_6 + 3/2\ O_2 = CO + 2H_2O(g) & & -520 & (3) \\
CH_4 + 2\ O_2 = CO_2 + 2H_2O(g) & & -803 & (4) \\
C_2H_6 = C_2H_4 + H_2 & & +137 & (5)
\end{array}$$

The secondary reactions (described by eq. 3,4) are favoured by the high temperatures at which oxidative coupling occurs.

Many papers in this field are devoted to the identification of the experimental conditions (temperature, reactants flow rate and concentrations, reactor design, catalysts) in order to ensure high conversions and selectivities to C_2 products and some of them to the understanding of reaction mechanism.

In this paper we report the results of preliminary investigations on the oxidative coupling of methane on 5% Li/MgO catalyst as well as on the identification of the kinetic conditions of the reaction.

2. SOME CHARACTERISTICS OF METHANE OXIDATIVE COUPLING CATALYSTS

The most used catalysts for methane oxidative coupling are the promoted basic metal oxides. Important increases of reaction selectivity have been reported when alkaline promoters are used. The role of alkaline promoters seems most clearly evidenced when the used catalysts are irreducible metal oxides.[2-7]

On reducible metal oxides (having two or more stable oxidation states), used as catalysts, a redox type mechanism has been advanced. In the first stage, the metal oxide is reduced by methane and then, in the second stage oxidized by the gas phase oxygen.[2,8,9] The redox type catalysts must be easily reducible, to activate CH_4, and taking into account the high reaction temperatures, they must have a good thermal stability.

Many authors consider that both the surface basicity [8,10] and the metal oxide bulk structure affect the oxygen mobility.[11]

The specific surface area of catalysts for oxidative coupling of methane is generally smaller than 10 m^2/g.[2]

Catalysts with one stable oxidation state are the doped or not doped oxides of earth-alkaline elements from II-A gr. The principal dopants used are the alkaline elements from I-A gr..

Another important group of irreducible catalysts are the oxides of elements from III-B gr. : Y_2O_3 and La_2O_3.

Frequently used reducible catalysts are the oxides from III-A, IV-A and V-A gr. High conversions and selectivities were obtained on Bi_2O_3[2] and PbO.[2,12] From the group of reducible transitional oxides which show high catalytic performances the manganese oxides [9] and cobalt oxides [13] could be mentioned.

Very active and selective catalysts for methane oxidative coupling are Sm_2O_3 (with or without alkaline dopants).[14] On the other side, only the promoted Ce, Pr, Tb oxides show good catalytic performances in methane oxidative coupling reaction.[15]

Promising results were reported when mixed oxides are used as catalysts : $Bi_2O_3-V_2O_5$, $Bi_2O_5-MoO_3-V_2O_5$.[16]

The great theoretical and practical interest of oxidative coupling of methane reaction is reflected by the diversity of compounds used as catalysts. Thus, not only the oxides show good catalytic performances. Different mixtures as $LiCl/CoO_3$, $Bi_2O_3-MoO_3-LiCl$ [16] have been reported to have good catalytic properties. Good catalytic performances show also pyrochlores with general formula $Ln_2Sn_2O_7$ (Ln = Y, La, Pr, Nd, Gd, Tb).[17]

A short review of the principal performances of the most used oxidative coupling catalysts seems useful.

The conversion obtained on Li/MgO catalyst is ranged from 3 to 43% whereas the reaction selectivity varies between 22 and 90%. [5,14,18,19] Methane conversion increases with temperature and oxygen pressure but the selectivity to C_2 compounds decreases under these circumstances. The high reactant pseudocontact time leads to low selectivity to C_2 compounds.

On the La_2O_3 catalysts the reported conversions were 5–20% at 59–80% selectivities.[20,21]

Sm_2O_3 is frequently quoted for its high catalytic performances. The reported conversions and selectivities ranged between 1–37% and 11–99% respectively[2,14]

Another relatively well studied catalyst is lead oxide, on which the conversion varies from 3 to 32% and the selectivity from 20 to 80%.[8,22,25] A major inconvenience of these catalysts are their high volatility at the reaction temperatures.

3. EXPERIMENTAL

The catalyst used in this study was prepared by mixing the lithium precursor (Li_2CO_3, Fluka AG r.g.) with magnesium carbonate (Merk, r.g.) and deionized water. The resulting slurry was homogenized and then heated until the excess water was evaporated. The mixture was then dried at 170°C for 8 h and crushed to a fine powder. The powder was pelletized and calcined in air at 850°C. In order to stabilize and activate the catalyst, it was treated for 2 hours at 850°C in oxygen with flow rate 1.5 cm^3/s.

The studies were performed in a fixed bed reactor in flow system. The reactor was made of fused quartz of 2 cm i.d.. The reaction mixture (CH_4,O_2 and N_2) was preheated in a quartz tube which is wound all around the reactor.

Oxygen, nitrogen and methane were dried by passing over a silica bed. Methane was also purified from traces of sulphur compounds on a special column packed with desulphuration catalysts. The mixture between CH_4, O_2 and N_2 was obtained by using a gas mixing pump (Wösthoff type 1 KM 100/a, 1 SA 27/3 a and 1 SA 18/3a).

The concentration of methane in the reaction mixture was maintained constant at 80% (vol). Different oxygen concentrations in the reactant feed, 4%, 12% and 20% (in volume) were used. The balance gas to 100% was nitrogen.

Reaction products were analyzed by a gas chromatograph (Pye Unicam type) with a thermal conductivity detector. The CO_2, C_2H_4 and C_2H_6 were separated on a Porapack Q column while CO, O_2 and N_2 with a Molecular Sieve 5Å column at 30°C. The used carrier gas was H_2 at 50 cm^3/min flow rate.

The catalyst surface area, measured by BET method was found to be very small, between 1 and 2.5 m^2/g.

The working temperatures domain was 650–850°C.

4. RESULTS AND DISCUSSION

Methane conversion is defined as the percentage of input methane converted to total products and the selectivity as the percentage of the amount of methane converted to particular products (C_2H_6,C_2H_4,CO_2,CO) to the total methane converted.

The pseudocontact time (W/F) is defined as the weight of catalyst divided by the feed gas flow rate at operating conditions.

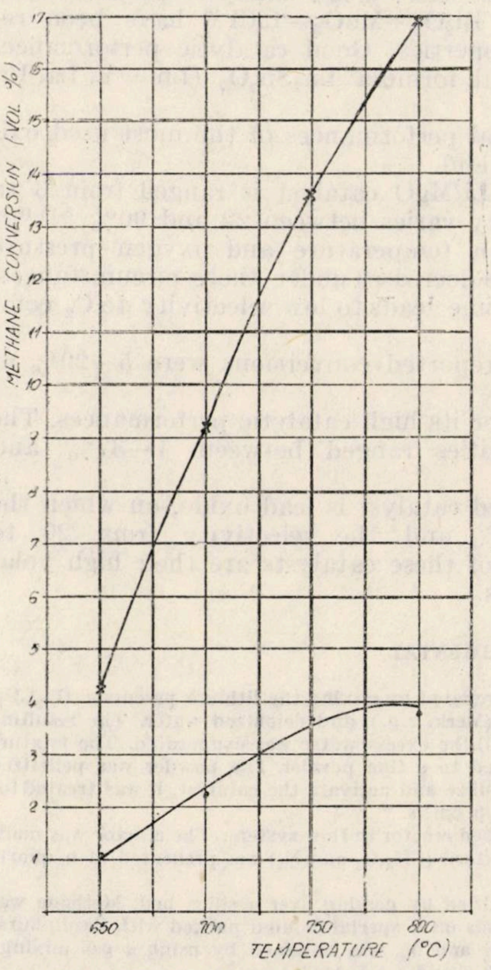

Fig. 1. – Effect of catalyst pretreatment on the methane conversion. Reaction conditions: $W/F = 3.4$ g · s/cm^3, 80% CH_4, 20% O_2.
× – catalyst treated, after calcination in air, in oxygen flow ($F = 1.5$ cm^3/s) 2 h at 850°C.
· – catalyst untreated in oxygen after calcination in air.

The 5% Li/MgO catalyst is particularly sensitive to the pretreatment condition. The effect of catalyst pretreatment on the methane conversion is represented in Fig. 1.

The influence of pseudocontact time (W/F) and temperature on the methane conversion, at different oxygen levels, is presented in Fig. 2. The methane concentration was maintained constant at 80% (vol).

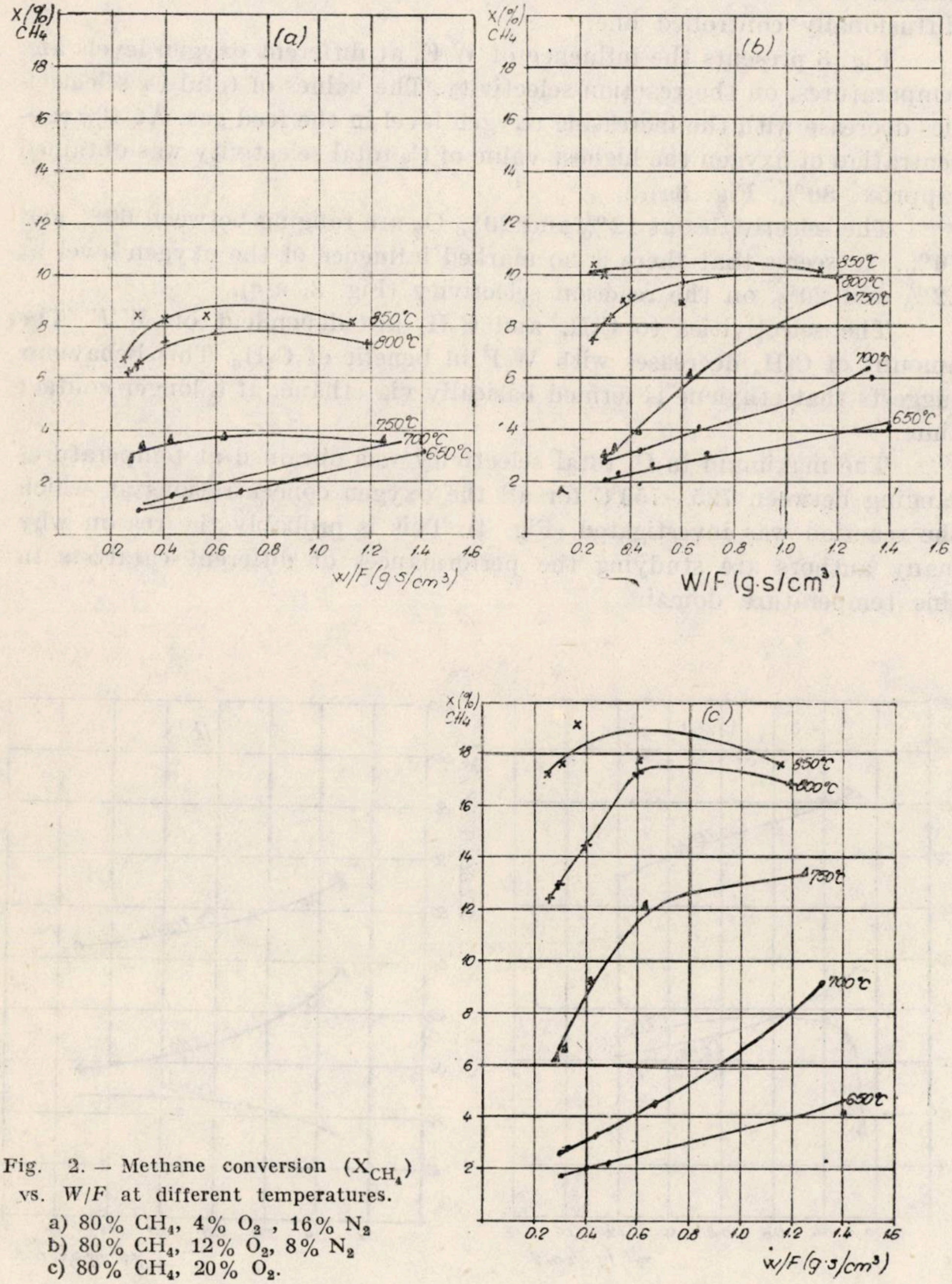

Fig. 2. — Methane conversion (X_{CH_4}) vs. W/F at different temperatures.

a) 80% CH_4, 4% O_2 , 16% N_2

b) 80% CH_4, 12% O_2, 8% N_2

c) 80% CH_4, 20% O_2.

By increasing the oxygen level and the temperature, the methane conversion increases. The curve of conversion vs. W/F shows a shape changing at temperatures higher than 700°C. The shape changing can be attributed to the transition from the kinetically controlled region to the diffusionally controlled one.

Fig. 3 presents the influence of W/F, at different oxygen levels and temperatures, on the reaction selectivity. The values of total C_2 selectivities decrease with the increasing oxygen level in the feed gas. At 4% concentration of oxygen the highest value of C_2 total selectivity was obtained (approx. 80%, Fig. 3a).

The selectivities at 12% and 20% O_2 are ranging between 60% and 70%. It seems that there is no marked influence of the oxygen level at 12% and 20% on the reaction selectivity (Fig. 3, a-e).

The selectivities to C_2H_6 and C_2H_4 are dependent on *W/F*. The amount of C_2H_4 decreases with W/F in benefit of C_2H_6. This behaviour suggests that ethylene is formed basically via ethane, at a longer contact time.

The maximum in C_2 total selectivity was obtained at temperatures ranging between 725–750°C for all the oxygen concentrations at which the reaction was investigated (Fig. 4). This is probably the reason why many authors are studying the performances of different catalysts in this temperature domain.

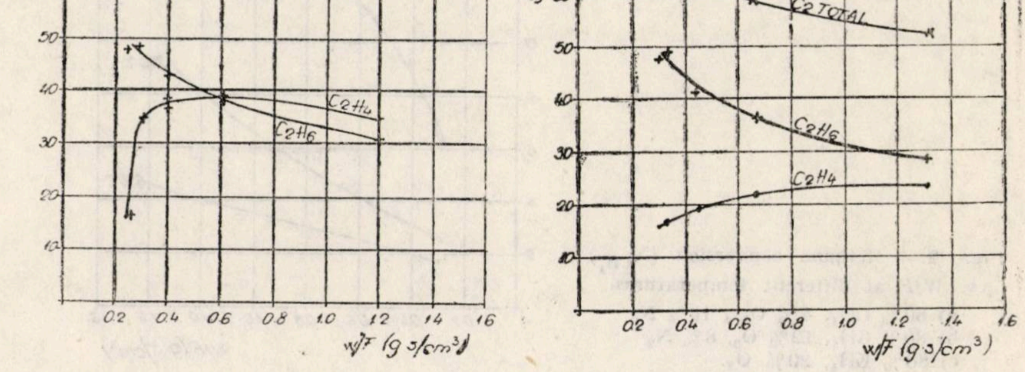

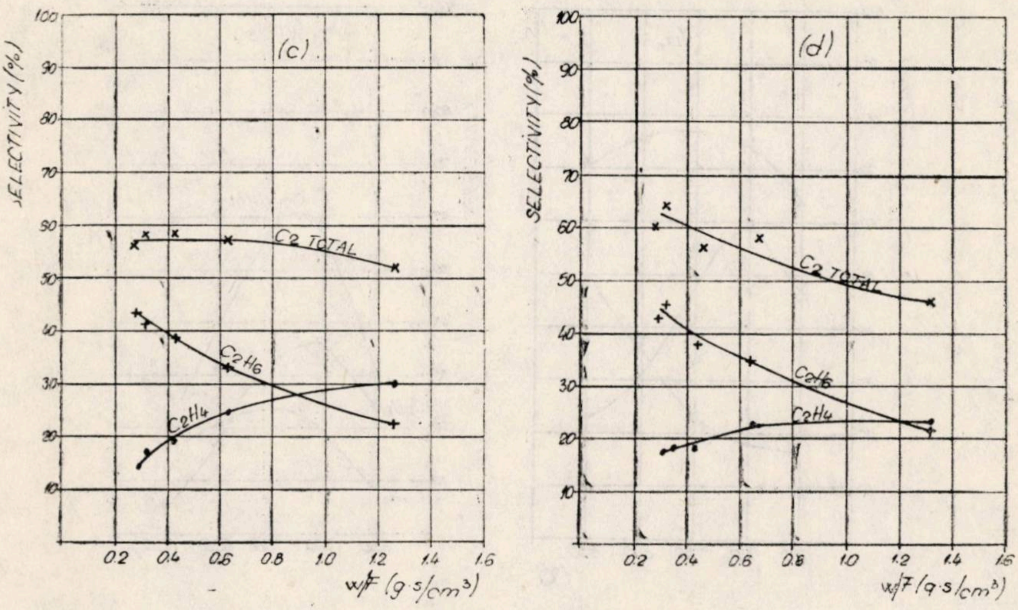

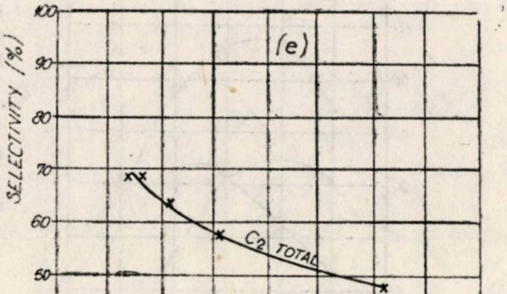

Fig. 3. — The influence of W/F on the reaction selectivity to C_2 compounds at different oxygen levels and temperatures.

a) 80% CH_4, 4% O_2, 16% N_2, 800 °C
b) 80% CH_4, 12% O_2, 8% N_2, 700 °C
c) 80% CH_4, 12% O_2, 8%N_2 750 °C
d) 80% CH_4, 20% O_2, 700 °C
e) 80% CH_4, 20% O_2, 750°C.

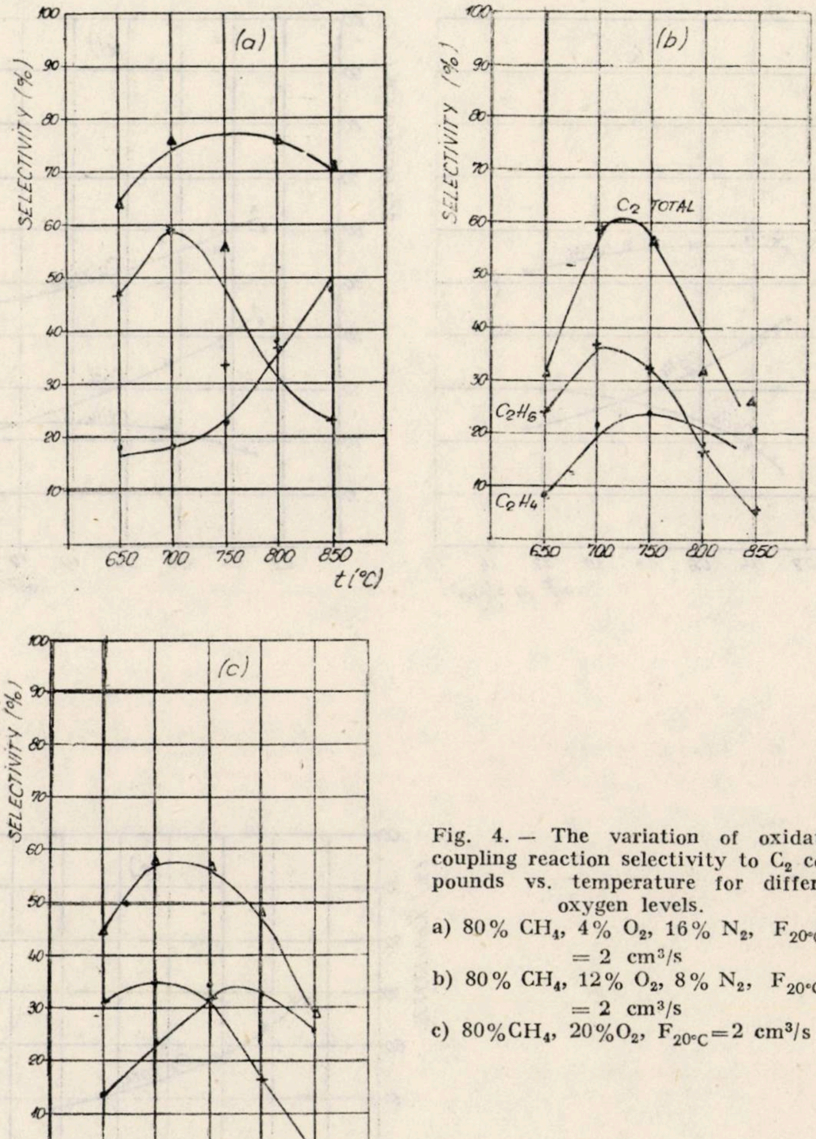

Fig. 4. — The variation of oxidative coupling reaction selectivity to C_2 compounds vs. temperature for different oxygen levels.
a) 80% CH_4, 4% O_2, 16% N_2, $F_{20°C}$ = = 2 cm^3/s
b) 80% CH_4, 12% O_2, 8% N_2, $F_{20°C}$ = = 2 cm^3/s
c) 80%CH_4, 20%O_2, $F_{20°C}$=2 cm^3/s

The reaction rate was determined at temperatures up to 850 °C. The results are represented in Fig. 5 (a, b and c). We can distinguish three regions :

1. Between 650 and 750°C the reaction rate increases slowly with temperature.

2. Between 750°C and 800°C the reaction rate increases dramatically.

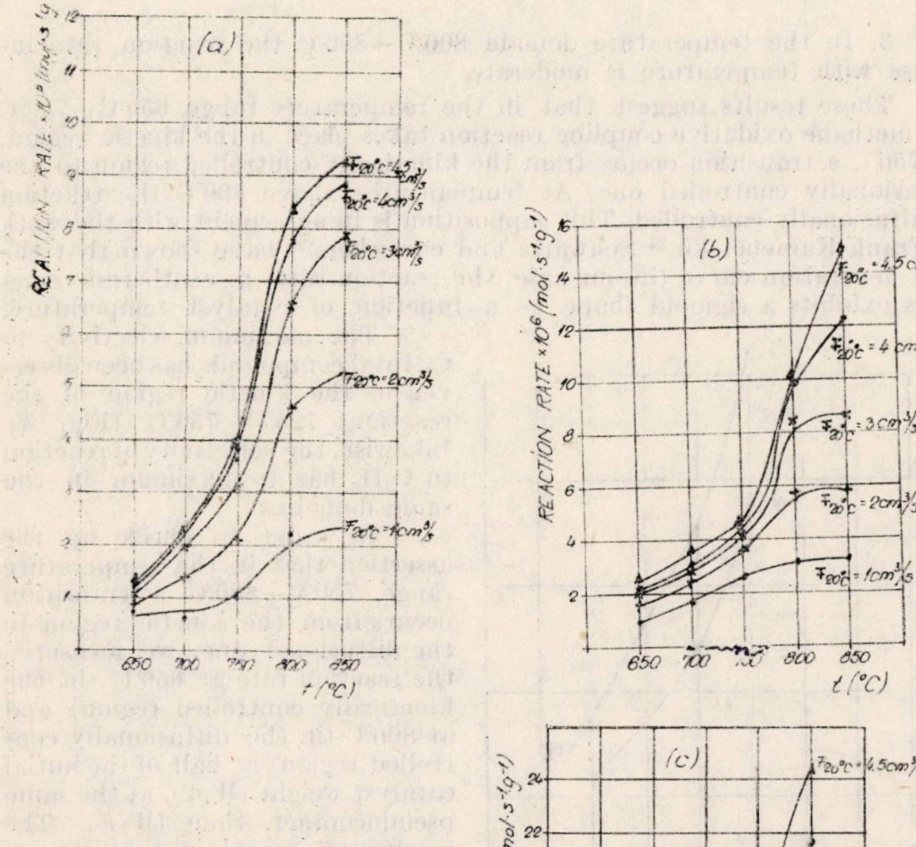

Fig. 5. — The variation of methane reaction rate vs. temperature for different reactants flow rates and oxygen levels.

a) 80% CH_4, 4% O_2, 16% N_2
b) 80% CH_4, 12% O_2, 8% N_2
c) 80% CH_4, 20% O_2

3. In the temperature domain 800°C – 850°C the reaction rate increase with temperature is moderate.

These results suggest that in the temperature range 650°C – 750°C the methane oxidative coupling reaction takes place in the kinetic region. At 750°C a transition occurs from the kinetically controlled region to the diffusionally controlled one. At temperatures above 800°C the reaction is diffusionally controlled. This supposition is in agreement with the work of Frank-Kamenetskii.[24] Schwartz and coworkers [25] have shown that the heat generation curve (in our case, the reaction rate) in exothermic reactions exhibits a sigmoid shape as a function of catalyst temperature.

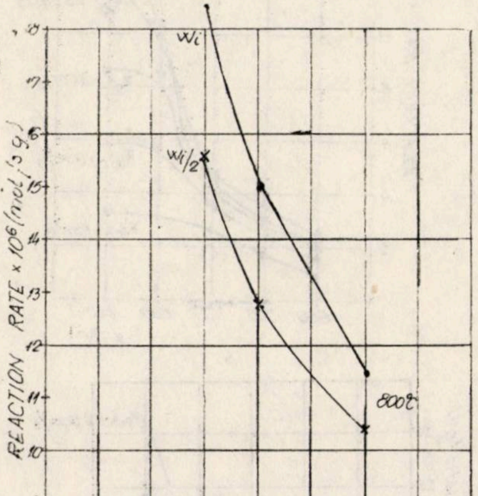

Fig. 6. – The influence of reactant diffusion on the reaction rate at 650°C and at 800°C.

The maximum selectivity to C_2 total compounds has been observed in the kinetic region of the reaction, 725°C – 750°C (Fig. 4). Likewise, the selectivity of reaction to C_2H_6 has a maximum in the same domain.

In order to check up the assertion that in the temperature range 750°C – 800°C a transition occurs from the kinetic region to the diffusional one, we measured the reaction rate at 650°C (in the kinetically controlled region) and at 800°C (in the diffusionally controlled region) at half of the initial catalyst weight ($W_i/2$), at the same pseudocontact time (W/F). The results are represented in Fig. 6.

At 650°C the differences between the reaction rates using W_i and $W_i/2$ g of catalyst are not significant. On the contrary, significant differences between the reaction rates have been obtained at 800°C. This behaviour suggests that at 800°C the diffusional effects on the reaction rate play an important role while at 600°C they are negligible. These conclusions are important because the estimation concerning the reaction mechanism can be made at temperatures below 750°C (in the kinetic region), where the diffusional effects are not important.

The dependences of the reactions rates for the principal reaction products vs. temperature and oxygen concentration are presented in Fig. 7 (a, b and c).

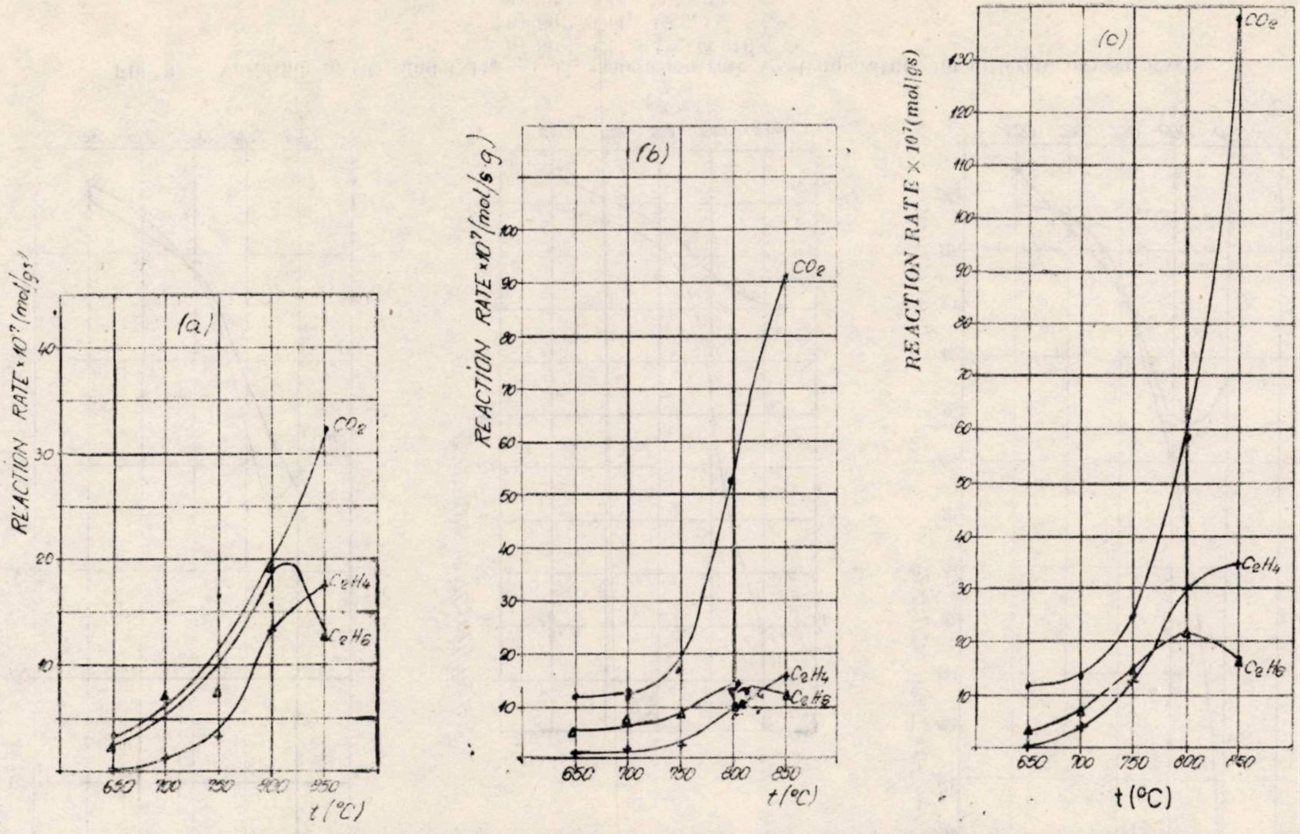

Fig. 7. — The dependence of the reaction rate vs. temperature for different oxygen concentrations.
a) 80% CH_4, 4% O_2, 16% N_2; $F_{20°C} = 4.5$ cm³/s
b) 80% CH_4, 12% O_2, 8% N_2; $F_{20°C} = 4.5$ cm³/s
c) 80% CH_4, 20% O_2; $F_{20°C} = 4.5$ cm³/s

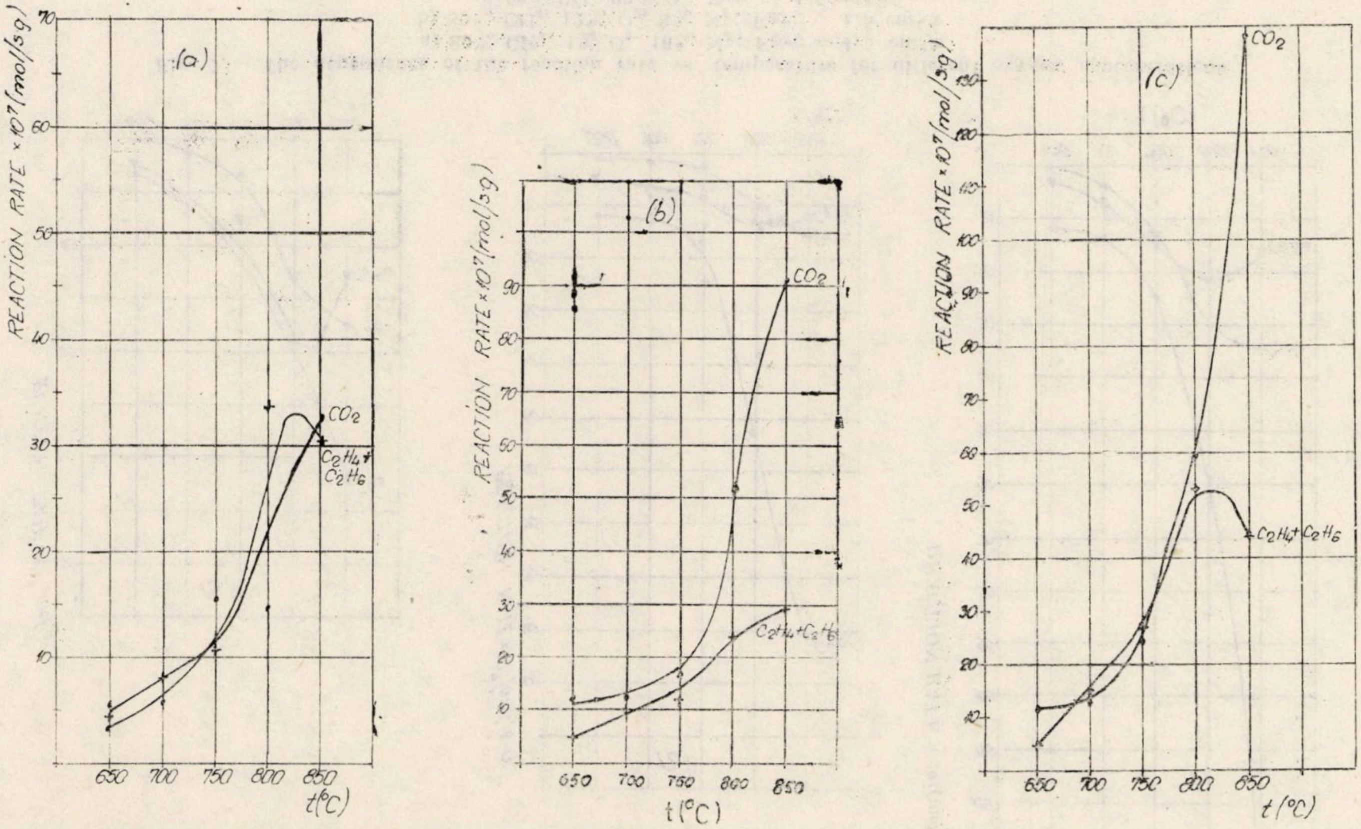

Fig. 8. — Variation of CO_2 and $C_2H_6 + C_2H_4$ generation rate vs. temperature for different oxygen levels.

a) 80% CH_4, 4% O_2 16% N_2
b) 80% CH_4, 12% O_2, 8% N_2
c) 80% CH_4, 20% O_2

At high oxygen concentrations (12%, 20%) the CO_2 production increases drastically at temperatures higher than 750°C, while the rate of C_2H_6 and C_2H_4 production decreases or remains constant (Fig. 7b and c). At low oxygen concentrations (4%) the reaction temperature did not significantly influence the ratio between CO_2 and C_2 products (Fig. 7a).

At high oxygen level in the feed mixture (12%, 20%) and temperatures above 800°C the increase of the rate of CO_2 production is faster than the increase of the rate of $C_2H_6 + C_2H_4$ generation. Likely, an important amount of CO_2 is generated by the combustion of CH_4 (Fig. 8b and c). At 20% O_2 it is clear that over 800°C even C_2H_4 and C_2H_6 are oxidized to CO_2 (Fig. 8c).

This research program is currently under way and is focused on the new catalysts and on the mechanism of oxidative coupling.

CONCLUSIONS

1. The treatment at 850°C in oxygen flow of Li/MgO catalyst enhances significantly its activity.

2. Our results regarding methane conversion, selectivity and reaction rate on 5% Li/MgO catalyst are in agreement with reported literature data.

3. Important diffusional effects have been evidenced in the reaction of methane oxidative coupling. At temperatures below 750°C the reaction is kinetically controlled. At temperatures between 750°C and 800°C a transition from the kinetic region to the diffusional region takes place. In this unstable region the reaction is diffusionally and kinetically controlled. The rate of reactant diffusion to the catalyst surface is balanced by the rate of surface reaction.

4. At high oxygen levels in the feed gas (12% and 20%) and temperatures above 800°C, C_2H_6 and C_2H_4 start to be totally oxidized. At the same time the combustion of CH_4 is enhanced.

5. The pseudocontact time (W/F) has an important effect on the reaction selectivity. A long pseudocontact time favours the appearance of C_2H_4 as main product while at short pseudocontact time the amount of C_2H_4 decreases in benefit of C_2H_6. This behaviour suggests that C_2H_4 is produced by the oxydehydrogenation of C_2H_6.

REFERENCES

[1] G. E. Keller and M. M. Bhasin, *J. Catal.*, **73**, 9 (1982).
[2] J. S. Lee and S. T. Oyama, *Catal. Rev.-Sci. Engn.*, **30**, (2), 249 (1988).
[3] N. W. Cant, C. A. Lukey, P. F. Nelson and R. J. Tyler, *Chem. Commun.*, 766 (1988).
[4] H. S. Zheng, J. X. Wang, D. J. Driscoll and J. H. Lunsford, *J. Catal.*, **112**, 366 (1983).
[5] S. J. Korf, J. A. Ross, N. A. DeBruijn, J. G. Van Ommen and J. R. H. Ross, *Appl. Catal.*, **58**, 131 (1990).
[6] X. D. Peng, D. A. Richards and P. C. Stair, *J. Catal.*, **121**, 99 (1990).
[7] J. A. Ross, S. J. Korf, R. H. J. Veehof, J. G. Van Ommen and J. R. H. Ross, *Appl.Catal.* **52**, 131 (1989).
[8] M. Baerns, "Successful Design of Catalysts", Elsevier Science Publishers, Amsterdam, 333 (1988).

[9] J. A. Sofranko, J. J. Leonard and C. A. Jones, *J. Catal.*, **103**, 302 (1987).
[10] J. A .S. P. Carreiro and M. Baerns, *J. Catal.*, **117**, 258 (1989).
[11] E. Iwamatsu, K. Aika, *J. Catal.*, **117**, 416 (1989).
[12] W. Hinsen and M. Baerns, *Chem. Ztg.*, **107**, 223 (1983).
[13] T. Komatsu, T. Amaya and K. Otsuka, *Catal. Lett.*, **3**, 317 (1989).
[14] G. J. Hutchings and J. R. Woodhouse, *J. Chem. Soc., Faraday Trans.* 1, **85**, 2507 (1989).
[15] A. M. Gaffney, C. A. Jones, J. J. Leonard and J. A. Sofranko, *J. Catal.*, **114**, 422 (1988).
[16] Y. Ohtsuka, M. Kuwabara and A. Tomita, *Appl. Catal.*, **47**, 307 (1989).
[17] A. T. Ashcroft, A. K. Cheetham, M. L. H. Green, C. P. Grey and P. D. F. Vernon, *Chem. Commun.*, 1667 (1989).
[18] R. J. Tyler and C. A. Lukey, ACS Div. A Fuel Meeting, New Orleans, **32**, 3, 249 (1989).
[19] G. J. Hutchings, M. S. Scurrel and J. R. Woodhouse, *Appl. Catal.*, **38**, 157 (1988).
[20] J. M. DeBoy and R. F. Hicks, *J. Catal.*, **113**, 517 (1988).
[21] J. M. DeBoy and R. F. Hicks, *Chem. Commun*, 982 (1988).
[22] G. Went, C. D. Meinecke and W. Schmitz, *Appl. Catal.*, **4**, 209 (1988).
[23] S. Ahmed and J. B. Moffat, *Appl. Catal.*, **54**, 241 (1989).
[24] F. Kamenetskii, D. A., "Diffusion and Heat Exchange in Chemical Kinetics", (N. Thorn, transl.) Princeton Univ. Press, Princeton, N. J., 1955.
[25] A. Schwartz, L. L. Holbrook and H. Wise, *J. Catal.*, **21**, 199 (1971).

NOTE POUR LES AUTEURS

La Revue Roumaine de Chimie publie des articles en anglais, français, russe, allemand ou espagnol. Les auteurs sont priés d'envoyer des articles et des comptes rendus inédits.

Les manuscrits seront dactylographiés à double interligne. La bibliographie, les tableaux et la légende des figures seront placés après le texte.

Si l'article fait partie d'une série numérotée, la partie précédente sera donnée comme première référence.

Chaque article sera précédé d'un résumé comprenant quinze lignes au maximum.

Les références bibliographiques dans le texte seront faites par des exposants sans parenthèses et paraîtront à la fin de l'ouvrage.

Les publications périodiques mentionnées dans la bibliographie seront présentées suivant les prescriptions internationales : le nom de l'auteur précédé de l'initiale du prénom, le titre du périodique abrégé conformément à « Chemical Abstracts » et souligné par une ligne, le numéro du tome indiqué par des chiffres arabes et souligné par deux lignes, suivi de la première page de l'article ; à la fin, l'année de la parution sera placée entre parenthèses. Le numéro de la revue ne sera pas indiqué si les pages du volume sont numérotées consécutivement.

Les textes des livres ou traités inclueront : le nom des auteurs, l'initiale du prénom, le titre du livre entre guillemets et sans être souligné, le numéro du tome précédé par l'abréviation « vol. » (ou « Bd. »), le numéro de l'édition, les éditions (the publisher), la localité de la parution du livre, l'année de la parution et la page de la référence précédée(s) par l'abréviation « p » (ou « S. »).

Les brevets seront indiqués comme suit : l'auteur ou la firme, le pays et le numéro du brevet, la date et la revue *(Chem. Abstr.)*. Par ex. : M. Jones (to Union Carbide Co), Brit. Pat. 601 238, 2 Sept. 1959 ; cf. *Chem. Abstr.*, 54, 12808 (1960).

Si la référence n'a pas été lue en original, on indiquera aussi la revue de références consultée.

Les diagrammes seront tracés à l'encre de Chine sur papier calque. Les tableaux et les figures (en nombre strictement nécessaire) ainsi que les courbes dans les figures seront numérotés par des chiffres arabes. Leur explication sera donnée dans la légende des figures. Prière de ne pas inscrire les mêmes données dans les tableaux et les figures. Chaque tableau aura un titre. On indiquera dans le texte la place approximative des tableaux et des figures. Les formules chimiques seront incluses dans le texte ; en outre, elles seront transcrites sur papier calque, à l'encre de Chine.

Les auteurs sont priés d'indiquer les caractères italiques (en soulignant les lettres au crayon), ainsi que tout autre caractère spécial ; les préfixes *ortho*, *meta*, *para*, *cis*, *trans*, etc. seront soulignés pour indiquer leurs caractères italiques et ne seront jamais écrits avec des majuscules.

Aucune correction à la main ne sera admise sur le manuscrit. Les corrections seront tapées à la machine. Les lettres grecques ou d'autres symboles spéciaux seront insérés à la main à l'encre clairement.

Le manuscrit sera signé par l'auteur.

Le titre-courant aura 50 lettres au maximum.

L'entière responsabilité du contenu des articles appartient aux auteurs.

Sur demande on peut obtenir une note plus complète.

PRINTED IN ROMANIA

1992 JUN 25

TRAVAUX PARUS AUX ÉDITIONS DE L'ACADÉMIE ROUMAINE

I. G. MURGULESCU, **Introducere în chimia fizică, Vol. 1. Atomi, molecule, legătură chimică,** 1976, 560 p.

I. G. MURGULESCU, V. EM. SAHINI, **Introducere în chimia fizică, Vol. I. 2. Structura şi proprietăţile moleculelor,** 1979, 604 p.

I. G. MURGULESCU, E. SEGAL, **Introducere în chimia fizică, Vol. II. 1. Teoria molecular-cinetică a materiei,** 1979, 1056 p.

I. G. MURGULESCU, TATIANA ONCESCU, E. SEGAL, **Introducere în chimia fizică, Vol. II. 2. Cinetică chimică şi cataliză,** 1981, 1024 p.

I. G. MURGULESCU, J. PĂUN, **Introducere în chimia fizică, Vol. I. 3. Nucleul atomic, reacţii nucleare, particule elementare,** 1982, 606 p.

I. G. MURGULESCU, RODICA VÎLCU, **Introducere în chimia fizică, Vol. III. Termodinamica chimică,** 1982, 624 p.

I. G. MURGULESCU, O. M. RADOVICI, **Introducere în chimia fizică, Vol. IV. Electrochimie,** 1986, 410 p.

O. IORDACHE, M. GHERGHE, S. CORBU, **Modelarea statistică şi estimarea parametrilor proceselor chimice,** 1991, 238 p.

C. ANDREI, I. DRĂGUŢAN, A. T. BALABAN, **Fotostabilizarea polimerilor cu amine împiedicate steric,** 1990, 240 p.

M. BREZEANU, E. CRISTUREANU, D. MARINESCU, A. ANTONIU, M. ANDRUH, **Chimia metalelor,** 1990, 244 p.

R. VÎLCU, M. LECA, **Polymer Thermodynamics by Gas Chromatography,** coédition avec Elsevier, 1990, 204 p.

FL. CUIBAN, ALFA-XENIA LUPEA, **Studiul structurii şi sinteza peptidelor,** 1989, 286 p.

CRISTOFOR I. SIMIONESCU, VALERIA GORDUZA, **Implicaţii bioenergetice ale coloranţilor,** 1988, 208 p.

R. VÎLCU, M. LECA, **Termodinamica polimerilor prin cromatografie de gaze,** 1987, 238 p.

I. ZUGRĂVESCU, M. PETROVANU, **Cicloadiţii 3+2 dipolare,** 1987, 446 p.

RAUL MIHAIL, ION GROZEANU, **Estimarea secvenţială aplicată sistemelor chimice,** 1986, 406 p.

M. BREZEANU, I. PATRON, M. ANDRUH, **Combinaţii complexe polinucleare şi aplicaţiile lor,** 1986, 244 p.

A. T. BALABAN et al., **Labelled Compounds and Radiopharmaceuticals Applied in Nuclear Medicine,** coédition avec John Wiley and Sons, 1986, 742 p.

D. PURDELA, **Nomenclatura chimiei organice — IUPAC,** 1986, 451 p.

PETRU BUDRUGEAC, **Probleme de chimie,** 1986, 280 p.

T. ONCESCU, S. G. IONESCU, **Conversie fotochimică şi stocare de energie,** 1985, 272 p.

V. DRĂGUŢAN, A. T. BALABAN, M. DIMONIE, **Olefin Metathesis and Ring-Opening Polymerization of Cyclo-Olefins,** coédition avec John Wiley and Sons, 1985, 544 p.

C. LITEANU, I. RÎCĂ, **Optimizarea proceselor analitice,** 1985, 360 p.

N. PERESCU, **Chimia extracţiei cu solvenţi şi aplicaţii,** 1985, 212 p.

ISSN 0035–3930

S.C. „UNIVERSUL" S.A. c. 3140

43 426

Lei 160

F 1103

ACADÉMIE ROUMAINE

REVUE ROUMAINE DE CHIMIE

TOME 36
Nº 8
Août 1991

Rev. Roumaine Chim.

RRCHAX, 36, 8, p. 843—988 (1991), Bucarest

EDITURA ACADEMIEI ROMÂNE

ACADÉMIE ROUMAINE

COMITÉ DE RÉDACTION

Rédacteurs en chef :

I. G. MURGULESCU, membre de l'Académie Roumaine

Rédacteurs en chef adjoints :

A. T. BALABAN et V. EM. SAHINI, membres de l'Académie Roumaine

Collège de rédaction :

ECATERINA CIORĂNESCU-NENITZESCU, CR. SIMIONESCU, P. SPACU, membres de l'Académie Roumaine ; M. BANCIU, membre correspondant de l'Académie Roumaine ; M. ANDRUH, M. D. GHEORGHIU, I. HAIDUC, D. I. MARCHIDAN, G. NIAC et D. SĂNDULESCU.

La Revue Roumaine de Chimie paraît 10 fois par an. Toute commande de l'étranger sera adressée à ROMPRESFILATELIA – sectorul Export-Import Presă, P. O. Box 12–21, télex 10376, prsfi r 78 104 Bucarest, Calea Griviței nr. 64–66, București, Roumanie

Les manuscrits, les livres et les revues proposés en échange, ainsi que toute correspondance seront envoyés à la rédaction

REVUE ROUMAINE DE CHIMIE

125, Calea Victoriei, 79717 Bucarest, Roumanie, téléphone 50 76 80

EDITURA ACADEMIEI ROMÂNE

125, Calea Victoriei, 79717 Bucarest, Roumanie, téléphone 50 76 80

ORSZÁGOS MŰSZAKI INFORMÁCIÓS KÖZPONT ÉS KÖNYVTÁR 1883

REVUE ROUMAINE DE CHIMIE

Tome 36, N° 8 **Août, 1991**

MAGDALENA MOMIRLAN and EUGEN PINCOVSCHI, Oxidation of the titanium alloy Ti 6Al 4V in air and oxygen 845–850

VALENTINA LĂZĂRESCU and M. VASS, Oxygen interaction with silver — gold alloy films 851–858

ALEXANDRA SCHIOPESCU and ANCA ALBU, Ferrate(VI) ion employed in preparation of some salts of the tetralutidinic complex combinations of nickel(II) and cobalt(II) 859–862

ALEXANDRU DUCA, MARIA GĂBURICI and DOINA BEJAN, Polarography of cysteine, cystine and thiourea with various electrodes (DME, ME, MFE) 863–876

I. COCÎRLĂ, LUCIA TĂTARU, M. VÂȚĂ, D. SCUTARU, I. MAZILU, LUMINIȚA WAGNER and CAMELIA PETRESCU, Absorption electronic spectra and reactivity of some As-naphthols 877–881

A. MATEESCU, C. D. MATEESCU, V. S. TEODORESCU and L. C. NISTOR, The influence of ClO_4^- ions upon the electrochemical system $Pb/H_2SO_4/PbO_2$ 883–899

S. A. ABBASI, Atomic absorption spectrometric determination of manganese in natural waters and industrial effluents after extractive separation of its ternary complex with n-phenyl-2-furohydroxamic acid and trioctylmethylammonium cation in MIBK 901–906

MIRCEA D. BANCIU, MIRCEA POP, AURICA PETRIDE and MICHAELA DINA STĂNESCU, Flow-vacuum pyrolysis of dibenzo[*c*, *g*]tricyclo-$[4.2.2.0^{2,5}]$-deca-3,7,9-triene (*syn*-dibenzo[*c*,*g*]Nenitzescu's hydrocarbon) and of tribenzo[*c*, *g*, *j*]tricyclo$[4.2.2.0^{2,5}]$deca-3,7,9-triene(tribenzo-Nenitzescu's hydrocarbon) 907–915

FLOREA DUMITRAȘCU, MARIETA PLĂVEȚI and DAN RĂILEANU, New convenient methods for the synthesis of 1,2-dihydro-3*H*-indazol-3-one and its 1-acyl derivatives 917–923

KERIMAN GÜNAYDIN, The synthesis of some 1-naphthylcycloalkanols and 1-naphthylcycloalkenes 925–929

MIHAI CONTINEANU, On intermediates involved in thermal decomposition of azibenzyl. Part I 931–936

CLAUDIU T. SUPURAN, ANTONIE DINCULESCU, GHEORGHE MANOLE, FLORINA SAVAN, IOAN PUSCAS and ALEXANDRU T. BALABAN, Carbonic anhydrase activators. Part 2. Amino acids and some of their derivatives may act as potent enzyme activators 937–946

Rev. Roumaine Chim. **36**, *8*, 843–988 (1991), Bucarest

SEVERIAN DUMITRIU and MARIA DUMITRIU, Bioactive polymers. 69. Cross-linked xanthan as drug-carrier matrices. 947–964

ZDENĚK SLANINA, FILIP UHLÍK and MICHAEL C. ZERNER, $C_5H_3^+$ isomeric structures : relative stabilities at high temperatures 965–974

MIRCEA V. DIUDEA and IOAN SILAGHI-DUMITRESCU, Molecular topology. 2. A computer program for multiple bond, cycle and radical approximations of DS index 975–982

IOANA JITARU, CORNELIA GURAN and MARIANA BICHER, Zinc chromite obtained from a residual chromium acetate solution 983–985

BOOK REVIEW 987

Revue Roumaine de Chimie, **36**, *8*, 845–850 (1991)

Dedicated to Professor PETRU SPACU on the occasion
of his 85th anniversary

OXIDATION OF THE TITANIUM ALLOY Ti 6Al 4V IN AIR AND OXYGEN

MAGDALENA MOMIRLAN[a] and EUGEN PINCOVSCHI[b]

[a] Institute of Physical Chemistry, Romanian Academy, Spl. Independenţei 202, Bucharest, Romania

[b] Polytechnic Institute, Bucharest, Romania

Received May 27, 1989

Titanium alloy Ti 6Al 4V is the most widely used of the titanium alloys in aerospace applications. A kinetic study of oxidation in air and oxygen of titanium alloy Ti 6Al 4V in the temperature range 400°C–600°C was carried out. During the oxidation of the samples, the partial pressure of oxygen was maintained at 50 and 150 mm Hg. The kinetic laws and the dependence of rate constant on oxygen pressure were determined. The resistance at oxidation in air of titanium alloy Ti 6Al 4V in comparison with other alloys was studied in direct connection with utilization in aerospace industry. The results of our experiments explain the limited domain of operation of the titanium alloy Ti 6Al 4V up to about 400°C.

Titanium is ductile in pure form but hardens considerably on alloying. Titanium alloys have excellent physical and chemical properties, being resistant to oxidation and corrosion in most dilute corrosive environments, including sea water, resulting in their widespread application in chemical plants, oil platforms, underwater engineering and medicine. Furthermore, with a low density of 4.5×10^3 kg/m^3 and strength well in excess of 1000 MPa, coupled with good crep resistance, certain titanium alloys have found extensive use in aerospace industry.

The physical metallurgy and alloying behaviour of titanium is however, rather complex due to its allotropy, involving a h.c.p. crystal structure (α) below 882.5°C and a b.b.c. crystal structure (β) above this temperature.

Titanium can be solubilized by almost all elements of periodic system. But the practical importance as alloying elements is attributed to aluminium and sometimes chromium, molybden, vanadium, manganese, tin, copper, nyobium, tantal, iron, wolfram and silicon.

Alloying elements may dissolve preferentially in α-titanium (α-stabilisers), in β-titanium (β-stabilisers) or in both (neutral), thereby increasing the stability range of these phases. They may also form compounds with titanium. Accordingly, titanium alloys are classed as α-alloys (predominantly α-phase), β-alloys and so on, each group having its own characteristic properties. Alpha and near alpha titanium alloys (containing additional small amounts of β-stabilisers) have very good creep resistance, high strength and good weldability. Beta titanium alloys have poor creep resistance, but good workability and formability. It is evident that a combination of useful properties can be achieved in an α + β-alloy.[1] Indeed one of the first aerospace alloys was an α + β-alloy, Ti 6Al 4V, also known in the United Kingdom as IMI 318 and in France as UTA 6V.

The present work on titanium-aluminium-vanadium system includes the effect of temperature and pressure on its oxidation in the temperature range 400°C—600°C and also the kinetic study of the oxidation of this alloy in comparison with the other titanium alloys.

EXPERIMENTAL PROCEDURE

The concentration of the alloying elements in titanium alloys used in our experiments are listed in table 1.

Table 1

The chemical composition of the titanium alloys

Trade mark of the titanium alloy	Chemical composition of the titanium alloy, atomic per cent
TA 6 V (UTA 6V — France; IMI 318 — United Kingdom)	Ti — 6Al — 4V (6 % Al — 4 % V — rest Ti)
Ti 685	Ti — 6Al — 5 Zr — 0,5 Mo — 0,25 Si (6 % Al — 5 % Zr — 0.5 % Mo — 0.25 % Si — rest Ti)
Ti 550	Ti — 4Al — 4 Mo — 2 Sn — 0,5 Si (4 % Al — 4 % Mo — 2 % Sn — 0.5 % Si — rest Ti)

The oxidation in air at 600°C of the titanium alloys samples was carried out for a long time (up to 60 hours) by the method of hanging the samples with a quartz thread in an electric vertical furnace. The temperature was maintained constant by means of a proportional thermoregulator. The Pt—Pt Rh thermocouple was piaced in the reaction zone at a distance of 0.5 cm from the sample. The variation of weight samples was measured from the difference between the initial weight of sample and the oxidized sample in air. The oxidized titanium alloys samples were examined by scanning microscopy and X-ray diffraction.[2,3,4,5]

The oxidation of the titanium alloys in oxygen was carried out at 400°C—550°C in a vacuum microbalance (Fig. 1).

At first, the microbalance was connected to vacuum equipment for cleaning the samples. The increase of weight of the samples during their oxidation was electronically determined when the oxygen was introduced in static regime.

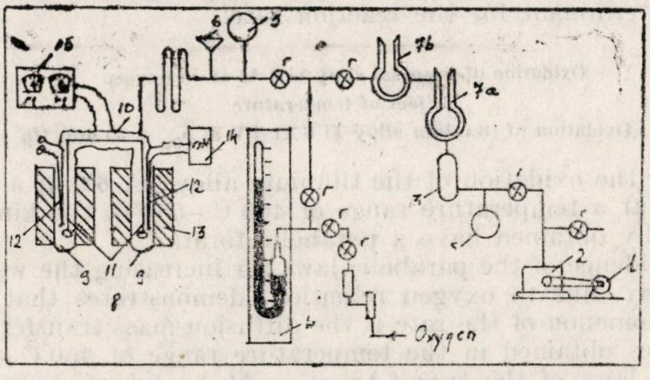

Fig. 1. — Sartorius type electronic microbalance connected to a vacuum line.

1, 2 — preliminary vacuum pump; 3 — diffusion pump; 4 — Hg manometer; 5 — preliminary vacuum flask; 6 — vacuum measuring lamp; 7a, 7b — nitrogen traps; 8 — microbalance; 9 — quartz tubes; 10 — lever; 11 — nacelle containing samples; 12 — thermocouple; 13 — furnaces; 14 — millivoltmeter; 15 — electronic registration of mass variation.

The diagrams of increasing the oxide weight formed on titanium alloy with the oxidation time were represented.

RESULTS AND DISCUSSION

A kinetic study of the oxidation in air of the three titanium alloys was done.

TA 6V was comparatively studied with other two titanium alloys: Ti 685 and Ti 550.

At 600°C, for all three alloys the dependence of increasing the weight on the oxidation time is given by a linear law. The kinetic law is of the type $\Delta m/q = k_1 t + k_2$ where $\Delta m/q$ represents the increase of weight on the surface unit and k_1, k_2 are the constants.

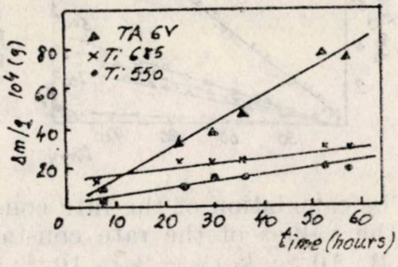

Fig. 2. — Kinetics of oxidation of some titanium alloys in air at 600° c.

Of all the titanium alloys oxidized, the TA 6V alloy has a greater oxidation rate (Fig. 2). This is due to the presence of vanadium, a phenomenon also reported in literature.[6, 7, 8]

The existence of the linear law of oxidation suggests that the diffusion and transport phenomena are rapid enough and the interfacial reactions are determinant for the reaction rate.

Oxidation of titanium alloy Ti 6 Al 4V in oxygen

Effect of temperature

Oxidation of titanium alloy Ti 6 Al 4 V at p_{O_2} = 50 mm Hg

During the oxidation of the titanium alloy TA 6V at a pressure of 50 mm Hg, at a temperature range of 400°C–550°C, the kinetic curves experimentally obtained have a parabolic form.

The evidence of the parabolic laws for increasing the weight of the titanium alloy, due to oxygen retention, demonstrates that the determinant phenomenon of the rate is the diffusion mass transfer. The three kinetic curves obtained in the temperature range of 450°C–550°C lead to parabolic laws of the type $(\Delta m/q)^2 = kt + c$ where $\Delta m/q$ represents the increase of the weight on the surface unit and k is the rate constant.

The rate constants were calculated by the method of the least squares.

At 550°C, a greater oxidation rate was calculated than that obtained at 500°C and 450°C.

The reports $k_{550°C}/k_{500°C} = 2.94$ and $k_{500°C}/k_{450°C} = 8.08$ indicate a limited practical domain of application of the TA 6V alloy and the impossibility of operation of this alloy at 550°C.

Our experiments are in a good concordance with recent studies which show that TA 6V is capable of operating up to about 350°C in aerospace applications.[1]

Oxidation of titanium alloy Ti 6Al 4V at p_{O_2} = 100 mm Hg

As is shown in Fig. 3 at the oxidation of TA 6V titanium alloy at an oxygen pressure of 100 mm Hg, at the temperature range 400°C–500°C, the oxidation laws are linear.

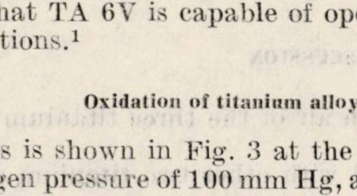

Fig. 3. — Titanium alloy Ti 6Al 4V. The variation of the weight on the surface unit, as a function of time in temperature range 400°C–500°C and at p_{O_2} = 100 mm Hg.

The calculation of the rate constants indicates that at 450°C, 475°C, 500°C the values of the rate constants are very close to one another: $k_{450°C} = 2\times10^{-4}$; $k_{475°C} = 2.7\times10^{-4}$; $k_{500°C} = 3.2\times10^{-4}$. At 550°C a rate constant of oxidation greater than at 500°C is obtained.

The $k_{550°C}/k_{500°C} = 8.37$ ratio indicates the impossibility of using the titanium alloy Ti 6Al 4V at temperature above 500°C.

The effect of oxygen pressure

For the elucidation of the influence of oxygen pressure on the character of the kinetic laws of the titanium alloy, the oxidation experiments were carried out at a temperature range 450°C—550°C at oxygen pressures varying between 50 mm Hg and 150 mm Hg. In the range of 450°C—550°C the difference between the reaction rates is higher when the temperature is lower.

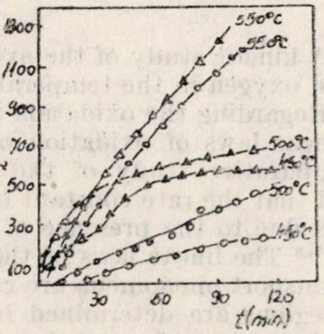

Fig. 4. — The effect of oxygen pressure at oxidation of titanium alloy Ti 6Al 4V in temperature range 450°C—550°C.

At 450°C and 550°C there is a more evident increase of the oxidation rate with the increase of the oxygen pressure, in comparison to what occurs at 550°C.

The results obtained by us are in a good agreement with the literature data, which mention a smaller dependence of the oxidation rate on pressure when the oxidation temperature is increased.[8] One observed that the oxygen pressure has an important influence on the rate constant values (Fig 5).

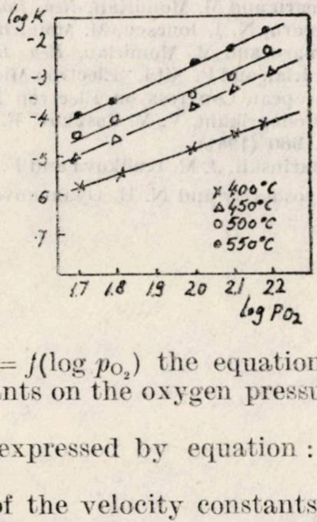

Fig. 5. — The variation $\log k = f(\log p_{O_2})$ in oxidation titanium alloy Ti 6 Al 4V in temperature range 400°C—550°C and at pressures 50—150 mm Hg.

Starting from the diagrams $\log k = f(\log p_{O_2})$ the equations establishing the dependence of the rate constants on the oxygen pressure were calculated.

The dependence $\log k = f(\log p_{O_2})$ is expressed by equation : $\log k = A + B \log p_{O_2}$.

The equations of the dependence of the velocity constants on the oxygen pressure were obtained by calculating A and B for each temperature.

The general form of the equations which represent the dependence of the rate constants on the oxygen pressure is : $k = ap_{O_2}^{b}$, where $a < 10^{-5}$ and $3.62 < b < 4.83$.

CONCLUSIONS

A kinetic study of the oxidation of the titanium alloy Ti 6Al 4 V in air and oxygen in the temperature range 400°C–600°C is presented.

Regarding the oxidation in air of titanium alloy Ti 6Al 4V at 600°C the linear laws of oxidation of type $\Delta m/q = k_1t + k_2$ were determined. A comparative study of the behaviour of three titanium alloys, concluded that the rate constant of titanium alloy Ti 6Al 4 V is the highest. This is due to the presence of vanadium in the alloy chemical composition.[6, 7, 8] The linear laws of the oxidation suggest that the diffusion and the transport phenomena are rapid enough and the reactions at the interface regions are determined by the reaction rate, the thickness of the oxide layer formed not being important for the oxidation rate of alloys.

At the oxidation of titanium alloy Ti 6Al 4V in oxygen at a temperature range of 400°C–550°C the parabolic and linear laws were determined.

Regarding the dependence on pressure of the rate constant in oxidation reaction of titanium alloy studied, we can conclude that, when the oxidation temperature is increased, the oxidation rate varies unsignificantly with the pressure.

REFERENCES

[1] A. Khatae, H. M. Flower and D. R. West, *Platinum Metals Rev.*, **33**, 106 (1989).

[2] D. Cismaru and M. Momirlan, *Rev. Roumaine Phys.*, **23**, 607 (1978).

[3] D. Cismaru, N. I. Ionescu, M. Momirlan and P. Niţă, *Rev. Roumaine Phys.*, **24**, 181 (1979).

[4] D. Cismaru and M. Momirlan, *Rev. Roumaine Chim.*, **23**, 1361 (1978).

[5] M. Momirlan and P. Niţă, "Electron Microscopy 1980", 1, Physics, Proceedings of the Seventh European Congress on Electron Microscopy, Haga, p. 222, 1980.

[6] M. N. Podoprikhin, V. V. Peshkov, F. S. Vorontsov and A. A. Borzunov, *Zhur. Fiz. Khim.*, **55**, 980 (1981).

[7] R. L. Barinskii, J. M. Kulikova and F. P. Shevoenko, *Izvist. Akad. Nauk SSSR*, **46**, 41 (1982).

[2] I. V. Lyosotskiy and N. B. Dyakonova, *Fiz. Metal Metaloved SSSR*, **53**, 681 (1982).

Revue Roumaine de Chimie, 36, 8, 851–858 (1991)

Dedicated to Professor PETRU SPACU on the occasion
of his 85th anniversary

OXYGEN INTERACTION WITH SILVER – GOLD ALLOY FILMS

VALENTINA LĂZĂRESCU and M. VASS

Institute of Physical Chemistry—Romanian Academy, Spl. Independenţei 202, Bucharest 79611, Romania

Received March 6, 1989

Cyclic voltammetry, an electrochemical technique that proved to be an efficient tool to evaluate the silver capacity to form a subsurface oxide, and work function change measurements, a sensitive method for observing the surface adsorption phenomena, have been associated to investigate the role of gold atoms in the oxygen interaction with Ag–Au alloy films. A pronounced increase in both the subsurface layer of Ag_2O and oxygen population of the surface have been observed to be promoted by the lower Au concentrations (5–10%). The results were considered as consequences of the inter-atomic charge transfers induced by alloying. Since gold is one of the materials reported to be promoters for ethylene epoxidation catalyzed by silver, a possible mechanism of the promotion action is also discussed.

INTRODUCTION

Silver distinguishes itself among all metals as the unique catalyst for ethylene epoxidation. Although the reaction mechanism is still under discussion and the identity of the active species, a matter for debate,[1, 2] there is general agreement that this remarkable property is due to its mode of interaction with oxygen.

Gold is one of the metals reported to be promoters for the selective ethylene oxidation. Flank and Beachell [3] and, recently, Toreis and Verykios [4] have found that silver alloys with low gold content show better catalytic performances than pure silver. As Backs et al.[5] reported that ethyleneoxide formation takes place only if both surface and subsurface oxygen are present, information concerning the influence of gold on the silver capacity to retain oxygen on its surface and in its bulk could be of importance for the discussion of promotion mechanism. It is the aim of this paper to investigate the role of gold in the oxygen interaction with Ag–Au alloys. Two sensitive experimental techniques have been, therefore, associated: work function change measurements for observing the surface adsorption phenomena and cyclic voltammetry for the investigations on the silver property to form a subsurface oxide.

EXPERIMENTAL

The measurements were performed on polycrystalline alloy films prepared by the simultaneous vacuum evaporation of the pure components and equilibrated by subsequent annealing at a sintering temperature (620 K) lying in between the Tammann temperatures of the two components, for 30 minutes.

The work function changes were monitored by the diode method in a working cell of the type described by Pritchard[6] — adapted[7] for alloy films — welded to an ultra-high-vacuum pumping line. The measurements have been performed at room temperature with an electrical circuit described previously.[8]

The electrochemical investigations were performed in 1M KOH solution in twice distilled water, in a three-compartment cell of conventional design. The alloy films, with thickness chosen to be greater than 3000 Å to avoid the substrate influence, were supported on optically polished glass surface, having two platinum wires embedded for electrical contacts. The other experimental details were described in a previous paper[9].

RESULTS

(a) Work function change measurements

The oxygen adsorption on silver surface brings about positive work function changes induced by the adsorbed species negatively charged. The work function variation was found to increase proportionally to oxygen exposures, for the films investigated, up to 10^6-10^7 L. This is an indication that, under the conditions of these experiments, the surface coverage remained at subunitary values.

The presence of gold has been observed to have important effects on the oxygen adsorption (Fig. 1). The small concentrations resulted in pronounced increases of the work function change, ΔΦ, at low as well as at high exposures. The higher gold content has been observed instead to inhibit rapidly the oxygen/silver interaction, whichever the exposure was. Our findings are in a good agreement with the results reported before by Fain and McDavid.[10]

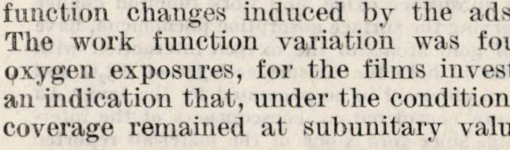

Fig. 1. — Change in the work function, ΔΦ, due to 600 L (×), respectively to 2×10^4 L(●) exposure to oxygen for Ag—Au alloys.

(b) Cyclic voltammetry investigations

The first stage of the anodic oxidation of silver in alkaline solutions was found to yield the formation of two layers of Ag(I) oxide, a subsurface one and a surface one, preceded by a minor process of the metal dissolution.[11] The second anodic oxidation step leads to a higher mixed oxide, formulated as $Ag(I)Ag(III)O_2$.

The same processes were shown to take place whatever the surface was of compact metal,[11,12] vacuum-deposited film [9] or alumina-supported catalyst.[13] However, the process of oxygen diffusion into the silver bulk has been observed to be greatly favoured by the more porous structure of the less sintered evaporated films.[9] Therefore, in order to follow the influence of gold on the silver capacity to retain oxygen in its bulk, we chose to work with films only partially annealed.

Typical cyclic voltammograms of 5, 10 and 15 at. % Au—Ag alloys are shown in Figs 2—4. The oxygen submergence into the silver lattice was found to be greatly enhanced by the small concentrations and hindered rapidly by the higher ones. 10 at. % Au gave rise to a maximum value of the coulombic charge involved in the subsurface oxide formation while 50 at. % Au resulted in a complete inhibition of the whole anodic oxidation of the silver (Fig. 5). The alloys with 50 at. % Au or more have been observed to exhibit a behaviour similar to that of pure gold electrode (Figs 6, 7).

The lower gold content was found to bring about also important changes in Ag(I) — oxygen bond strength. The cathodic reduction of Ag(I) oxide, taking place in one single step at pure Ag electrodes, was observed to occur in two steps at alloys containing 5 to 25 at % Au. The additional peak, appeared at more anodic potentials, shows that part of oxygen is more weakly bound to Ag atoms and hence, more easily to reduce.

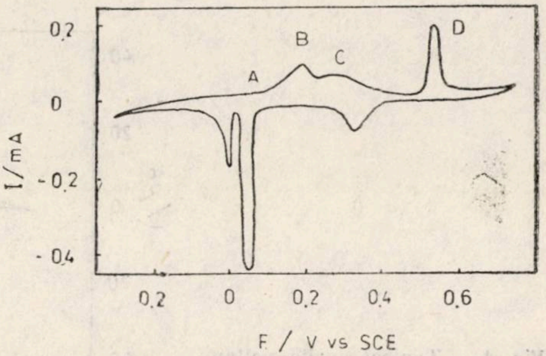

Fig. 2. — Typical cyclic voltammogram for 5 at. % Au—Ag alloy film in 1M KOH (A — metal dissolution, B — subsurface oxide formation, C — surface oxide formation, D — mixed higher oxide formation).

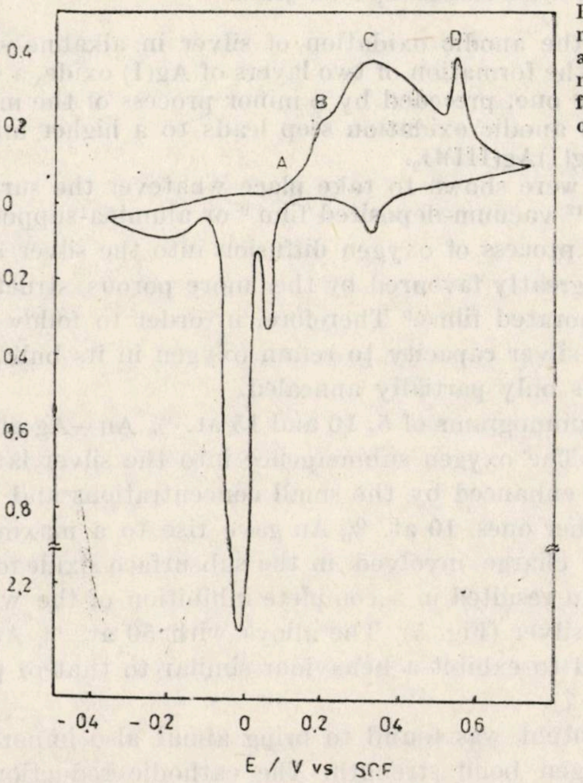

Fig. 3. — Typical cyclic voltammogram for 10 at. % Au—Ag alloy film in 1 M KOH (A — metal dissolution, B — subsurface oxide formation, C — surface oxide formation, D — mixed higher oxide formation).

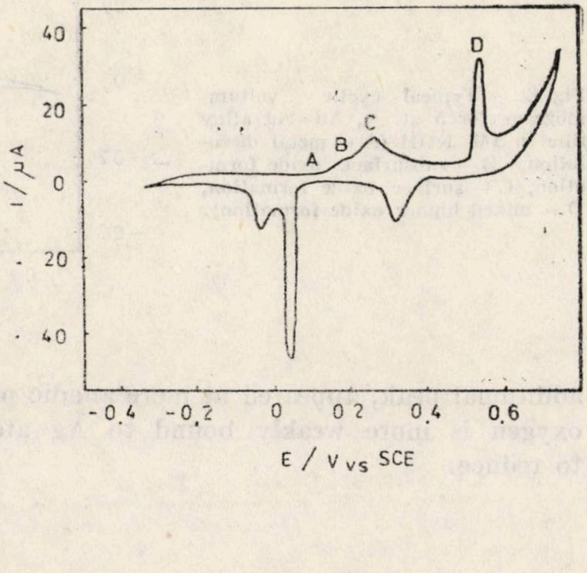

Fig. 4. — Typical cyclic voltammogram for 25 at. % Au—Ag alloy film in 1M KOH (A — metal dissolution, B — subsurface oxide formation, C—surface oxide formation, D — mixed higher oxide formation).

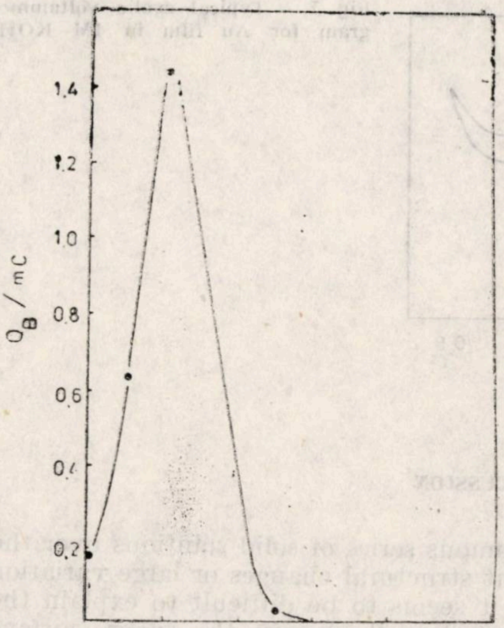

Fig. 5. — Effects of the gold content on the coulombic charge consumed in the subsurface oxide formation, Q_B.

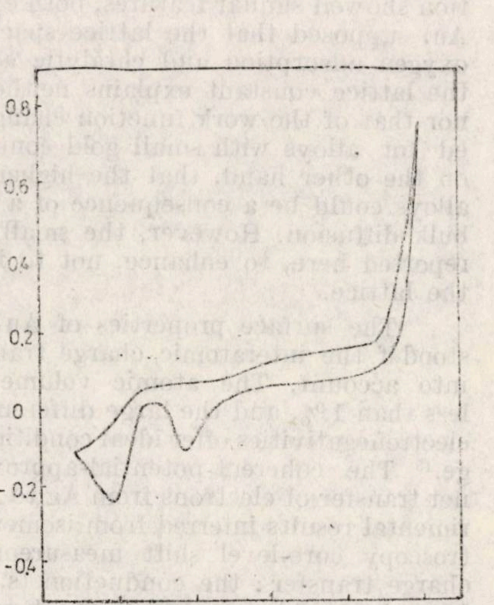

Fig. 6. — Typical cyclic voltammogram for. 50 at. % Au—Ag alloy film in 1M KOH.

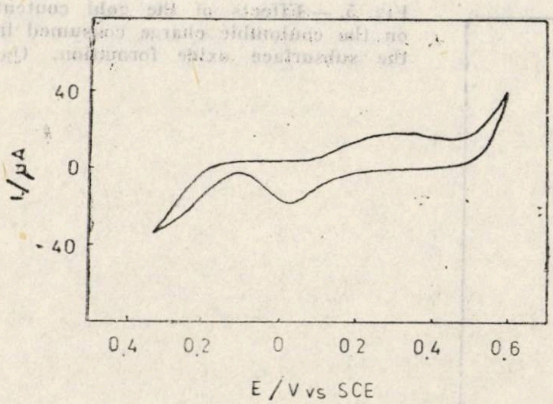

Fig. 7. — Typical cyclic voltammogram for Au film in 1M KOH.

DISCUSSION

Silver and gold form a continuous series of solid solutions over the entire compositional range, without structural changes or large variation in lattice parameter.[14] Therefore, it seems to be difficult to explain the pronounced changes brought about by alloying in the silver surface properties.

Flanck and Beachell,[3] who observed that the plot of the epoxidation rate constant and that of the lattice parameter versus the alloy composition showed similar features, both exhibiting a minimum around 60 at. % Au, supposed that the lattice spacing could play an important role in oxygen adsorption and catalytic activity. But the smooth decrease of the lattice constant explains neither the steep maximum of selectivity nor that of the work function change on oxygen adsorption, both observed for alloys with small gold content. Fain and McDavid [10] suggested, on the other hand, that the higher values of $\Delta\Phi$ exhibited by Ag-rich alloys could be a consequence of a presumable inhibition of the oxygen bulk diffusion. However, the small gold percent has been observed, as reported here, to enhance, not to inhibit the oxygen submergence into the lattice.

The surface properties of Au—Ag alloys could be better understood if the interatomic charge transfers induced by alloying are taken into account. The atomic volume difference of the two components, less than 1%, and the large difference (0.5) in the corresponding Pauling electronegativities offer ideal conditions for the interatomic charge exchange.[15] The coherent-potential-approximation calculations [15] indicated a net transfer of electrons from Ag to Au, in good agreement with the experimental results inferred from isomer shift and X-ray photoelectron spectroscopy core-level shift measurements.[16] Actually, there is a double charge transfer : the conduction (s, p) electrons are mainly transferred from Ag to Au to equalize the Fermi levels of the two metals but the valence d-electrons flow in the opposite direction, to compensate this effect.[15]

Since the electron deficit of the surface silver atoms increases with the gold content and the oxygen adsorption is an electron demanding process, a decrease in both the surface population of adsorbed species and silver-oxygen bond strength is expected. Except for the ΔΦ peak observed at Ag-rich alloys, that will be discussed farther, this is precisely what was observed in the work function measurements as well as in the cyclic voltammetry investigations.

The higher values of ΔΦ noted for alloys with 5—10 at. % Au may be the result of two different effects.

On the one hand, the silver sites, slightly depleted in electrons, may inhibit at first, the dissociative oxygen adsorption, allowing for (otherwise non-competitive) undissociative process to take place. A higher surface coverage and hence, a higher work function variation is expected to be observed, since the latter process requires only one adsorption site instead of the four adjacent sites, as the former does.

The small increase of the density of states in the Ag d-valence band, mentioned before, may increase, on the other hand, the charge ldonation into the π^* antibonding orbital of the oxygen molecule, favouring its dissociation. This might yield a higher surface population of atomic adsorbed species, unless the energy density of states resulted in the overall charge transfer inhibits it.

The experimental data reported by Fain and McDavid[10] have shown that up to 10—15 at. % Au, the alloy work function value is practically the same as for pure Ag. Although the equal work functions do not mean precisely equal Fermi levels, it may be appreciated that the changes in energy density of states are anyway small, in this case, and do not diminish the probability of electron transfers between the substrate and the adsorbate. Consequently, the higher values of ΔΦ might be also an indication of an increased surface population of atomic oxygen.

As long as the nature of the adsorbed oxygen species is still matter for debate,[17,18] it would be difficult to decide which explanation is more appropriate.

The small gold content has been observed to enhance not only the oxygen adsorption but also the oxygen diffusion into the silver bulk. This might be the consequence of the fact that the contracted size of the Ag sites, depleted in electrons, permits easier transport of oxygen atoms from surface to bulk. At higher gold concentrations, the shrinkage of the lattice parameter [3,4] associated with the decrease in the energy density of states — resulted in the overall charge exchange — inhibits step by step the process, till the complete ceasing.

CONCLUSIONS

The small gold percent, that has been reported to enhance the catalytic activity of silver in ethylene epoxidation, was observed to induce also important changes in the silver reactivity towards oxygen. The main effects were the increase in the surface population of the more weakly bound oxygen species — whichever is it, atomic or molecular — and the easier surface — bulk transport of chemisorbed oxygen.

It is interesting to note that, at least, the latter one, seems to be a sort of commun denominator for several elements known to act as promoters in ethylene epoxidation. Indeed, the lower K^+ ion concentrations added to alumina-supported silver,[19] the dissolved alkali in Ag bulk,[20] as well as the chlorine atoms [21] or ions [11] have been observed to enhance the oxygen diffusion beneath the surface. Since ethylene oxide is formed, as reported,[5] only if both surface and subsurface oxygen are present, the above observation leads to the tentative conclusion that the subsurface oxygen is the real selectivity promoter. The fact that the simple electrochemical oxygen pumping to or off the catalyst has been found to increase, respectively, to decrease the selectivity and ethyleneoxide yield [22] is a further reasoning to this assumption.

REFERENCES

[1] R. A. van Santen and C.P.M. de Groot, *J. Catal.*, **98**, 530 (1986).
[2] C. T. Campbell and B. E. Koel, *J. Catal.*, **92**, 272 (1985).
[3] W. H. Flank and H. C. Beachell, *J. Catal.*, **8**, 316 (1967).
[4] N. Toreis and X. E. Verykios, *J. Catal.*, **108**, 161 (1987).
[5] C. Backs, J. Moolhuysen, P. Geneen and R. A. van Santen, *J. Catal.*, **72**, 364 (1981).
[6] J. Pritchard, *Trans. Faraday Soc.*, **59**, 437 (1963).
[7] V. Lăzărescu, Thesis, Bucharest 1985.
[8] V. Lăzărescu, M. Vass, O. Radovici, E. Jugănaru, E. Corlăteanu and T. Bota, in "Proc. 2nd Symp. Appl. Electrochem., Timișoara 1985", Tome 1, p. 267.
[9] V. Lăzărescu, O. Radovici and M. Vass, *Rev. Roumaine Chim.*, **32**, 895 (1987).
[10] S. C. Fain and J. M. McDavid, *Phys. Rev. B*, **9**, 5099 (1974).
[11] V. Lăzărescu, O. Radovici and M. Vass, *Electrochim. Acta*, **30**, 1407 (1985).
[12] V. Lăzărescu, M. Vass and O. Radovici, *Rev. Roumaine Chim.*, **31**, 461 (1986).
[13] V. Lăzărescu, M. Vass, O. Radovici, C. Dașoveanu, M. Stanciu and M. Tolan, *Rev. Roumaine Chim.*, **30**, 933 (1985).
[14] W. B. Pearson, "Handbook of Lattice Spacings and Structures of Metals and Alloys" Pergamon Press, New York 1958.
[15] C. D. Gelatt, jr. and H. Ehrenreich, *Phys. Rev. B*, **10**, 398 (1974).
[16] R. E. Watson, J. Hudis and M. L. Periman, *Phys. Rev. B*, **4**, 2147 (1971).
[17] R. W. Joyner and M. W. Roberts, *Chem. Phys. Lett.*, **60**, 459 (1979).
[18] C. Backx, C. P. M. de Groot and P. Biloen, *Surf. Sci.*, **104**, 300 (1981).
[19] V. Lăzărescu, M. Vass, A. Popa, M. Stanciu and M. Tolan, in "Proc. 6th Int. Symp. Heterog. Catal." Sofia, 1987, Part I, p. 265.
[20] M. Kitson and R. M. Lambert, *Surf. Sci.*, **109**, 60 (1981).
[21] S. A. Tan, R. B. Grant and R. M. Lambert, *J. Catal.*, **100**, 383 (1986).
[22] M. Stoukides and C. G. Vayenas, *J. Catal.*, **70**, 137 (1981).

Revue Roumaine de Chimie, 36, 8, 859–862 (1991)

Dedicated to Professor PETRU SPACU on the occasion of his 85th anniversary

FERRATE(VI) ION EMPLOYED IN PREPARATION OF SOME SALTS OF THE TETRALUTIDINIC COMPLEX COMBINATIONS OF NICKEL(II) AND COBALT(II)

ALEXANDRA SCHIOPESCU and ANCA ALBU
Department of Chemistry, Institute of Petroleum and Gas, Bd. Bucureşti 39,
Ploieşti, Romania

Received June 9, 1990

Potassium ferrate(VI) was prepared in a basic medium with hypochlorite as oxidiser and was purified by reprecipitation from alkali KOH solutions of various concentrations. The following salts containing ferrate(VI) ion and complex combinations of nickel(II) and cobalt(II) were prepared

$[Ni\ (\alpha,\ \alpha' - Lut)_4](FeO_4)$ $[Co(\alpha,\ \alpha' - Lut_4)](FeO_4)$

$[Ni(\alpha,\ \gamma - Lut)_4](FeO_4)$ $[Co(\alpha,\ \gamma - Lut)_4](FeO_4)$

(Lut stands for lutidine). The infrared spectra of these compounds were recorded.

INTRODUCTION

The preparation of potassium ferrate (VI) is well known.[1–4]

We prepared the ferrate (VI) ion salts with complex cations. Infrared spectra have been obtained both in potassium ferrate (VI) and complex ammines.

The data obtained are correlated with the existing ones given by Griffith.[5] He studied the infrared spectra of the tetrahedral transition metal oxianions.

EXPERIMENTAL

In a first stage we prepared and purified potassium ferrate(VI) to obtain the purest product at a fairly good yield.

Certain changes in the procedure have allowed us to obtain potassium ferrate(VI) with an efficiency of 92%. The procedure is based on the following reaction :

$$3Fe(NO_3)_3 + 10\ NaOH + 3\ NaClO = 2\ Na_2FeO_4 + 3\ NaCl + 6\ NaNO_3 + 5\ H_2O$$

0.3 mol carbonate-free sodium hydroxide was added to 30 cm^3 distilled water. The resulting solution was cooled to 273 K with the help of a mixture of ice — sodium chloride.

By continuous stirring chlorine was slowly bubbled through this chilled solution. The chlorine was prepared in an auxiliary installation from $KMnO_4$ and concentrated HCl.

It is necessary to regulate the bubbling speed to a very small one, because an excess of chlorine would lead to a marked decomposition of the potassium ferrate(VI) obtained. It is also necessary to regulate the temperature; a sharp rise is not permitted. This is maintained in the range 275 K — 279 K. The operation of chloration lasts for about 40—45 min. The solution obtained was then made strongly basic by adding 0.9—1.0 mol of solid natrium hydroxide.

While the solution was constantly stirred, the temperature was allowed to rise up to 290 K when the hydroxide was added. The whole mixture was cooled in an ice-sodium chloride bath. After cooling, the precipitated alkali metal chloride was removed by filtration. The solution obtained was again introduced in the ice bath where it was kept for a period of 1/2 h.

After this, 13.5 mmol of pulverized nonahydrated ferric nitrate were added very slowly with continuous stirring. This operation must be performed very slowly, the necessary time was a period of 30—45 min. The temperature must be maintained at about 298 ± 2 K.

The mixture obtained is rapidly filtered through a filtre crucible (G_3 type) with the aid of a vacuum oil pump. In the resulting solutions, some solid potassium hydroxide was added by continuous stirring and maintaining the temperature below 300 K. The potassium ferrate(VI) was precipitated in the solution and recovered by rapid filtration through a filter crucible. The filtration was made with the aid of the same vacuum oil pump. The precipitated potassium ferrate(VI) was purified by dissolving and reprecipitating it in several solutions of potassium hydroxide. The dissolution took place in solutions of KOH 3M, and the reprecipitations in KOH 5M, KOH 6M solutions and saturated solution.

The precipitation that has remained was washed on the filter with three 10 cm^3 portions of dry benzene in order to remove the water in excess and then washed with four 15 cm^3 portions of anhydrous ether. The ferrate(VI) sample was stored in a vacuum dessiccator to prevent a slow decomposition due to the traces of water. The results of the analyses using the method of total iron[6] gave good yield of K_2FeO_4.

To obtain salts containing ferrate(VI) ion with complex combinations of nickel(II) and cobalt(II) the tetralutidinic complex combinations of nickel(II) and cobalt(II) were prepared.[7,8]

The following complex combinations have been prepared:

$$[Ni(\alpha,\ \alpha' - Lut)_4](FeO_4)\ ;\ [Ni(\alpha,\ \gamma - Lut)_4](FeO_4)\ ;$$

$$[Co(\alpha,\ \alpha' - Lut)_4](FeO_4)\ ;\ [Co(\alpha,\ \gamma - Lut)_4](FeO_4).$$

These compounds have been analysed: metal, hydrogen, nitrogen, iron, carbon, oxygen have been determined. The results obtained correspond to the calculated data. The results are shown in Table 1.

Table 1

Chemical analysis results

Compound		% Fe	% Ni	% Co	% C	% H	% N	% O	P.M.
$[Ni(\alpha, \alpha'-Lut)_4](FeO_4)$	calc.	9.23	9.68	—	55.38	5.93	9.23	10.55	606.7
	found	9.22	9.68	—	55.36	5.94	9.24	10.5	
$[Co(\alpha, \alpha'-Lut)_4](FeO_4)$	calc.	9.23	—	9.71	55.36	5.93	9.23	10.54	606.9
	found	9.23	—	9.70	55.33	5.94	9.24	10.56	
$[Ni(\alpha, \gamma-Lut)_4](FeO_4)$	calc.	9.23	9.68	—	55.38	5.93	9.23	10.55	606.7
	found	9.22	9.69	—	55.39	5.93	9.22	10.55	
$[Co(\alpha, \gamma-Lut)_4](FeO_4)$	calc.	9.23	—	9.71	55.36	5.93	9.23	10.54	606.9
	found	9.25	—	9.70	55.34	5.94	9.24	10.53	

The procedure to obtain salts of ferrate(VI) ion with Ni(II) and Co(II) tetralutidinic complex combinations is explained below.

The tests containing 0.02 freshly prepared K_2FeO_4 which was previously dissolved in 5 cm^3 distilled water have been put in contact with the tests containing 0.03 mol tetralutidinic compounds. The potassium ferrate(VI) solution was previously kept in an ice-sodium chloride bath.

The ferrate(VI) ion salts containing Ni(II) and Co(II) complex have been precipitated.

The infrared spectra of the ferrate(VI) ion salts with Ni(II) and Co(II) complex have been taken using a U.R. – 10 Zeiss-Jena spectrometer with the method of diluted samples in KBr disks.

RESULTS AND DISCUSSION

Infrared spectra were recorded in the salts of ferrate(VI) ion with complex combinations of Ni(II) and Co(II) and, for comparison in potassium ferrate(VI) and in tetralutidinic combinations of Ni(II) and Co(II) employed in the preparation of the corresponding salts. Regarding the free $(FeO_4)^{2-}$ ion one may claim that it belongs to a tetrahedral (T_d) symmetry. Of the four fundamental frequencies of T_d group only ν_3 and ν_4 are active in infrared ; the symmetric frequencies (ν_1 and ν_2) being inactive in infrared. If this ion is coordinated to a metal one may note besides a decrease of T_d symmetry, a splitting of degenerate vibrations into two or three components and the appearance of new infrared bands that correspond to active Raman bands of the free ion.

$(FeO_4)^{2-}$, like other oxianions of transition metals, exhibits a loss of symmetry, from T_d to $C_s \cdot \nu_3$ frequency shows up in infrared as a triplet ($2A' + A''$ type species) and ν_1 as a singlet (A' type).[9]

The frequency ν_2 was not observed.

However the frequency ν_3 appears in infrared not as a triplet but as a singlet at 810 cm^{-1} with a shoulder at 835 cm^{-1} while the frequency ν_1 is recorded at 790 cm^{-1}, which agrees with Audette's findings.[10]

These characteristic bands of $(FeO_4)^{2-}$ ion may also be found in the salts that contain it however shifted with respect to their normal position characteristic to the $(FeO_4)^{2-}$ ion.

The results are shown in Table 2 ; ν_1 is present as in singlet of average intensity.

Table 2

The frequencies ν_1 and ν_3 characteristic to $[FeO_4]^{2-}$ ion and the salts obtained

Compound	ν_1	ν_2
K_2FeO_4	790	810, 835 (shoulder)
$[Ni(\alpha, \alpha'-Lut)_4](FeO_4)$	780	870, 880 (shoulder)
$[Co(\alpha, \alpha'-Lut)_4](FeO_4)$	770	860, 875 (shoulder)
$[Ni(\alpha, \gamma-Lut)_4](FeO_4)$	780	865, 875 (shoulder)
$[Co(\alpha, \gamma-Lut)_4]FeO_4)$	770	870, 875 (shoulder)

A triplet corresponding to ν_3 could not be evidenced in any of the cases in question.

The contributions of complex tetralutidinic combinations of Ni(II) and Co(II) to the IR spectra are worth to be considered. One can note that in salts containing $(FeO_4)^{2-}$ ion combined with Ni(II) and Co(II) complex ions the bands characteristic to these latter are present in the spectrum.[11]

On the basis of the resulting data, in good agreement with the studies made by Allan [11] for the coordination compounds of pyridine, picoline, lutidine with transitional metals, it is concluded that the vibrational frequencies of substituted pyridine do not change significantly when these are coordinated with the metals. Due to the lattice effects or because of the departures from the ideal symmetry, some shifts are split in the complex combinations spectrum. The main region where there are registered these modifications is between 1400–1600 cm^{-1}.

Because the spectra of the compounds under study include the characteristic frequencies of ferrate(VI) ion we may assume that its T_d symmetry is, to a great extent, retained in these compounds. The presence of a maximum of average intensity assigned to ν_1 may be caused by a perturbation of the crystal field.

However the existence of a split of ν_3 into two components noted in some compounds supports the hypothesis of a distorted T_d symmetry which approaches a C_s symmetry.

The fact that in the spectrum of the salts containing $(FeO_4)^{2-}$ ion and tetralutidinic complex combinations of Ni(II) and Co(II) are present the frequencies characteristic to ferrate (VI) ion as well as to the complex combinations utilized, allows us to consider $[(FeO_4)^{2-} - M(L)_4]$ bond as predominantly ionic ($M = $ Ni(II); Co(II); $L = \alpha, \alpha'$ lutidine; α, γ lutidine).

CONCLUSIONS

Potassium ferrate(VI) was prepared; to continue a study on the chemistry of ferrates(VI), salts containing $(FeO_4)^{2-}$ ion with tetralutidinic complex combinations of Ni(II) and Co(II) were prepared by us for the first time. The IR spectra were recorded and discussed and the predominantly ionic character of $[(FeO_4)^{2-} - M(L)_4]$ bond was evidenced.

REFERENCES

[1] H. J. Hrostowski and A. B. Scott, *J. Chem. Phys.*, **18**, 105 (1950).
[2] F. R. Duke and T. W. Haas, *J. Chem. Phys.*, **65**, 304 (1961).
[3] R. Scholder and K. Kraus, *Z. anorg. Chem.*, **268**, 379 (1952).
[4] B. Helferich and V. Lang, *Z. anorg. Chem.*, **263**, 169 (1950).
[5] W. P. Griffith, *J. Chem. Soc.*, **1966**, 1467.
[6] J. M. Schreyer, G. W. Thompson and L. T. Ockerman, *Analyt. Chem.*, **22**, 691 (1950).
[7] A. Logan and V. Carle, *J. Amer. Chem. Soc.*, **74**, 5224 (1952).
[8] A. Sinha, *J. Indian Chem. Soc.*, **32**, 414 (1952).
[9] P. Tarte and G. Nizet, *Spectrochim. Acta*, **20**, 503 (1964).
[10] R. J. Audette and J. W. Quail, *Inorg. Chem.*, **11**, 1904 (1972).
[11] J. R. Allan, *J. Inorg. Nuclear Chem.*, **18**, 79 (1961).

Revue Roumaine de Chimie, 36, 8, 863–876 (1991)

Dedicated to Professor PETRU SPACU on the occasion of his 85th anniversary

POLAROGRAPHY OF CYSTEINE, CYSTINE AND THIOUREA WITH VARIOUS ELECTRODES (DME, ME, MFE) *

ALEXANDRU DUCA, MARIA GĂBURICI and DOINA BEJAN

Faculty of Chemical Technology, Polytechnical Institute of Iaşi, Splai Bahlui 71

Received April 18, 1988

The aim of the present study is to compare the main polarographic features (anodic and cathodic steps, $E_{1/2}$, h and reversibility) and the analytical ones (sensitivity, selectivity, reproductibility) as well as their application possibility for some systems characterization of technical and scientific interest, from the electrochemical point of view.**

1. INTRODUCTION

The cysteine, which is the precursor of other thiolic compounds in the organism (coenzyme A, phosphopantoteine), reacts reversibly with glutathione, releasing H_2S under the action of cystein-sulphydrase.

Besides cysteine, the cystine is of a major importance in the redox equilibra at the cellular level. In the organism it occurs as a result of cysteine enzymatic oxidation, the reaction being catalysed by cystine dehydrogenase (cystine-reductase).

The reversible oxido-reduction reaction between cysteine and cystine [1,2] can be represented like this :

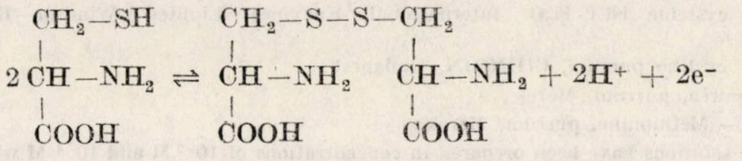

$$2\begin{matrix}CH_2-SH\\|\\CH-NH_2\\|\\COOH\end{matrix} \rightleftharpoons \begin{matrix}CH_2-S-S-CH_2\\| \qquad\qquad |\\CH-NH_2 \quad CH-NH_2\\| \qquad\qquad |\\COOH \qquad COOH\end{matrix} + 2H^+ + 2e^-$$

This reaction is particularly significant for the cellular oxido-reduction processes and breathing respectively, where cysteine plays the role of hydrogen carrier.

---

* DME — dropping mercury electrode
ME — stationary mercury electrode with large surface
MFE — mercury film electrode

** h — the height of polarographic wave

The polarography of cysteine and cystine has been investigated by a series of authors.[3-6]

Some authors [3] suppose that cysteine oxidation to cystine takes place through the formation of a Hg salt :

$$\mathrm{HOOC{-}CH(NH_2) - CH_2 - SH + Hg \rightleftharpoons}$$

$$\mathrm{\rightleftharpoons HOOC - CH(NH_2) - CH_2 - SHg + H^+ + e^-}$$

On the platinum electrode the cysteine oxidates reversibly to cystine.

The thiourea has been chosen as a model for H_2S or S^{2-} generating source, respectively (in acid or alkaline medium) and as component with strongly adsorptive features on various electrodes with applications in ASV (adsorptive stripping voltammetry).

The catalytic electrooxidation of compounds, having S with Co-phthalocyanine on carbon paste electrode has been recently examined.[7]

2. EXPERIMENTAL

In the runs a Radelkis OH-102 polarograph with various electrodes (DME, ME and MFE) and SCE (saturated calomel electrode) reference electrode with two cell types, with and without separation of the two compartments has been used.

The measurements have been performed with the following supporting electrolytes : hydrogen chloride, acetate, phosphate and ammonia (nitrate and ammonium chloride) buffer solutions and natrium hydroxide solution (Tables 1 and 2).

As the same time, the catalytic reaction has been followed with systems : ammonia buffer $+Co^{2+}$ and phosphate buffer $+Ni^{2+}$. The DME cappillary has the following characteristics :

$m = 2.65$ mg · s^{-1} ; $t = 3.125$ s determined at -1.02 V in ammonia buffer (Hg column height $H = 65$ cm).

The solution deaeration has been made by means of a nitrogen stream. The measurements have been carried out at 30 ± 0.5°C and within 20–30°C range.

Reagents

L – cysteine · HCl · H_2O. International Enzymes Limited Windsor–Berksshire–England ;

L – cystine purrum, CHINOIN, Budapest ;

Thiourea, purrum, Merck ;

DL – Methionine, purrum, Merck.

The solutions have been prepared in concentrations of 10^{-2} M and 10^{-4} M with distilled water and kept in the refrigerator.

3. RESULTS AND DISCUSSION

Some of the obtained results are listed in Tables 1 and 2.

In Fig. 1, the polarographic behaviour of cystine and cysteine on DME, in HCl 10^{-1} M is shown.

Table 1

Cysteine, cystine and thiourea polarographic behaviour in different supporting electrolytes :

DME — SCE ; $S = 2 \cdot 10^{-7}$ A/div. ; $H_{\mathrm{Hg}} = 60$ cm

Component	Supporting electrolyte	The characteristic of polarographic wave	$E_{1/2}$ (vs. S.C.E.)	Height of wave (μA)	Observations
Cysteine 10^{-3} M	HCl 0.1M	Anodic Cathodic	−0.14 −0.37	1.6 1.0	
Cystine 10^{-3} M	HCl 0.1M	Cathodic	−0.42	3.6	A good separation from cysteine wave
	HCl 0.1M + 0.04 ml gelatine 1 %	Cathodic	−0.92	3.6	
Thiourea 10^{-3}M	HCl 0.1M	Anodic	−0.11	0.8	
Cysteine 10^{-3}M	Phosphate buffer pH=6.6	Two anodic waves	−0.17 −0.55	2.4 2.4	
Cystine 10^{-3}M	—,,—	Cathodic	−0.81	5.0	Corresponds for low concentrations
Thiourea 10^{-3}M	—,,—	Anodic	−0.17	0.6	
Cysteine 10^{-3}M	Ammonia buffer ($NH_4NO_3 + NH_4OH$) pH=9.5	The anodic waves	−0.14 −0.58	2.0 2.6	Well defined waves
Cystine 10^{-3}M	—,,—	Cathodic	−0.92	4.2	
Thiourea 10^{-3} M	—,,—	Anodic	−0.14	4.6	
Cysteine 10^{-3}M	NaOH 0.1M	Anodic	−0.65	2.2	
Cystine 10^{-3}M	—,,—	Cathodic wave	−1.52	3.6	
Thiourea 10^{-3}M	—,,—	Anodic	−0.36	7.2	Corresponds for low concentrations

Table 2

Cystine, cysteine and thiourea polarographic behaviour on stationary mercury electrode with large surface ($s = 0.78$ cm^2); $S = 2 \cdot 10^{-7}$ A/div.

Component (10^{-3}M)	Supporting electrolyte	Characteristic of the wave	$E_{1/2}$ (V) (vs S.C.E.)	h μA	Observations
Cysteine	Ammonia buffer	Anodic	−0.11	6.4	Well defined
	($NH_4OH + NH_4NO_3$)	Anodic + cathodic	−0.57	6.6	
Cystine	—,,—	Cathodic	−1.25	9.6	
Thiourea	—,,—	Anodic–Cathodic	−0.145	7.6	
		Adsorptive wave	−1.0	17.6	
Cysteine	HCl 0.1M	Anodic–Cathodic rev.	$(E_{1/2})_a = -0.08$	2.4	On the free surface an adsorptive maximum is obtained ($E = -0.6$V)
			$(E_{1/2})_c = -0.12$	2.4	
Cystine	—,,—	—	—		
Thiourea	—,,—	Anodic–Cathodic rev.	−0.07	$h_a = 1.8$	
				$h_c = 1.2$	

As it can be seen in Fig. 1 the cysteine cannot be entirely separated from cystine (curve 3). There are two possibilities instead. According to the first one, taken into account the line $i = 0$, the cysteine curve is anodic, while that of cystine is cathodic.

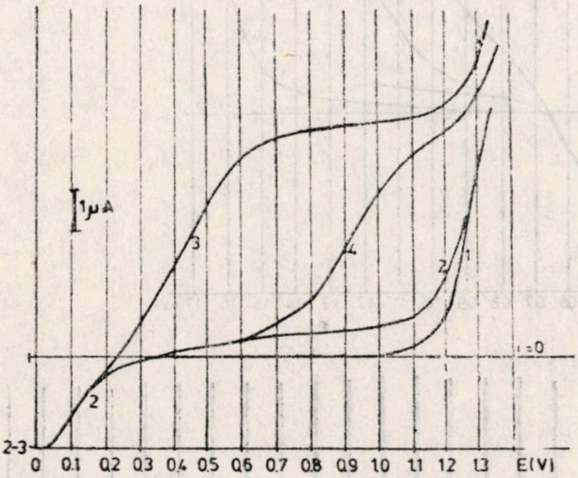

Fig. 1. — Cysteine, cystine and thiourea polarographic behaviour in HCl 0.1M on DME. $S = 2 \cdot 10^{-7}$ A/div., $H_{Hg} = 50$ cm, 400 mm/8 min :
1) 5 ml HCl 0.1M ; 2) 1 + 0.5 ml cysteine 10^{-2}M ; 3) 2 + 0.5 ml cystine 10^{-2}M ; 4) 3 + 0.04 ml gelatin 1 %.

The second possibility is connected to the fact that by adding gelatine 0.02—0.04 ml 1% solution), the cathodic wave of cysteine is shifted, towards more negative values, allowing a perfect difference of the two components.

The anodic wave of the thiourea has the same characteristic as cysteine but is approximately three times smaller.

In Fig. 2 the same measurements performed in 0.1 M ammonia buffer solution ($NH_4NO_3 - NH_4OH$) are plotted. Since the cystine exhibits two anodic waves and the thiourea only one (S^{2-} respectively), the possibility of their determination arises when they are together.

When adding a drop of 1% gelatine solution (0.02 ml), the cystine wave shifts towards more negative values, allowing the clear separation from that of cysteine.

The three components can be determined under these conditions. A good separation of the three components (10^{-3} M) is obtained in case of 0.1 M solution (without gelatine addition) — Fig. 3.

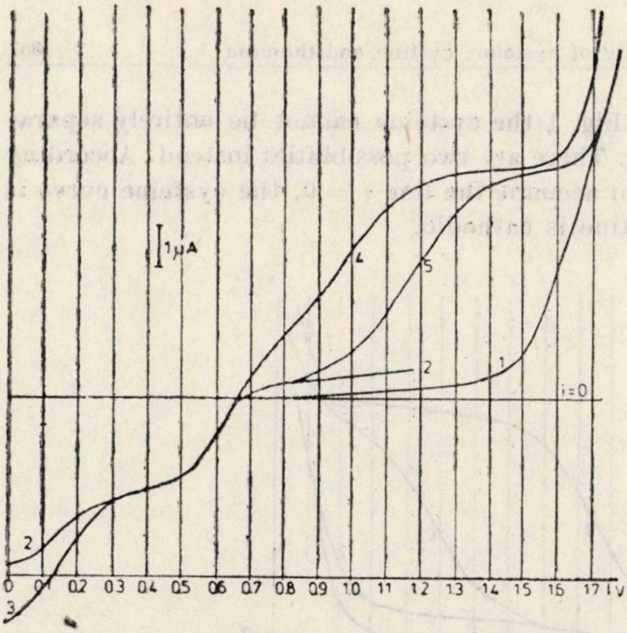

Fig. 2. — Cysteine and cystine polarographic behaviour in ammonia buffer (NH_4NO_3 — NH_4OH) on DME. $H = 50$ cm ; 50 mm/min.

1) 5 ml ammonia buffer 0.1 M ;
2) 1 + 0.5 ml cysteine 10^{-2} M ;
3) 2 + 0.5 ml thiourea 10^{-2} M ;
4) 3 + 0.5 ml cystine 10^{-2} M ;
5) 4 + 0.02 ml 1 % gelatin solutions.

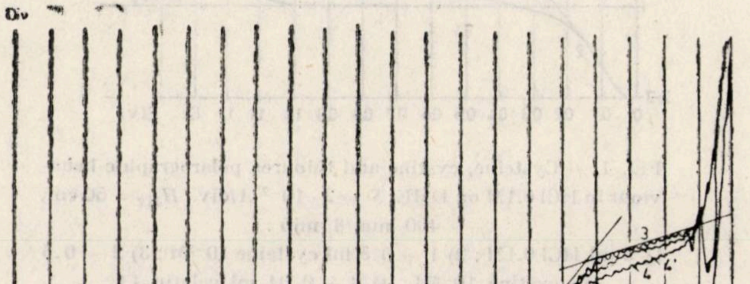

Fig. 3. — Cysteine, cystine and thiourea polarographic behaviour in 0.1M NaOH solution. System of electrodes : DME — SCE Ac. 4V ; $S = 2 \cdot 10^{-7}$ A/div. ; 50 mm/min.

1) 5 ml 0.1M NaOH solution ; 2) 1 + 0.5 ml cysteine 10^{-2}M ; 3) 2 + 0.5 ml cystine 10^{-2}M ; 4,4′) 3 + 0.2 ml thiourea 10^{-2}M.

In Fig. 4 the calibration curves for cysteine, cystine and thiourea, in HCl 0.1 M and ammonia buffer 0.1 M are depicted.

It can be noticed, by comparing the thiourea plots in concentration of 10^{-3}M in the two main solutions, that in HCl (H_2S) the anodic wave is nine times smaller than in buffer (S^{2-}).

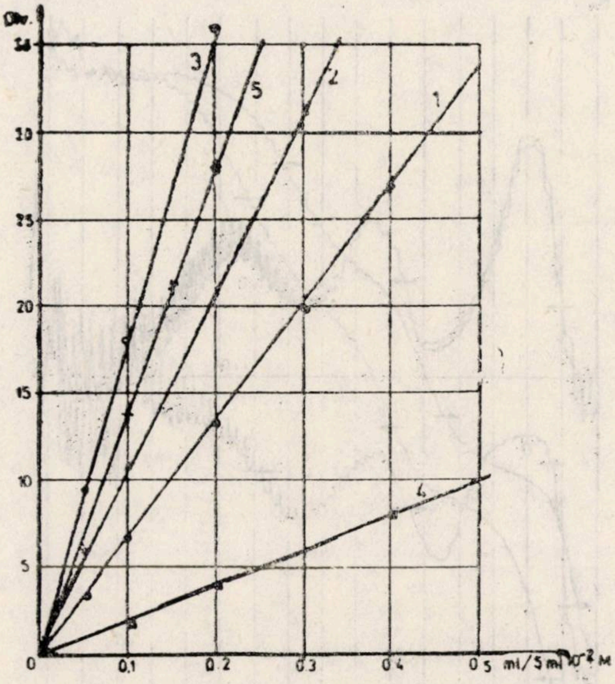

Fig. 4. — Calibration curves for cystine, cysteine and thiourea in 0.1M HCl solution and ammonia buffer. $S = 8 \cdot 10^{-3}$ A/div.

1) cysteine in 0.1M HCl solution ; 2) cystine in 0.1M ammonia buffer ; 3) thiourea in 0.1M ammonia buffer ; 4) thiourea in 0.1M HCl solution ; 5) cystine in 0.1M ammonia buffer solution.

In the case of cysteine the polarographic wave in HCl is 1.5 times smaller than ammonia buffer.

The cysteine wave (R—SH) in 0.1 M HCl solution is 3.4 times higher than that of thiourea.

These results point out the structural correlation with the polarographic behaviour and with ionic and molecular electroreactivity, respectively.

The practical limit of the test can be appreciated to be at about $5 \cdot 10^{-5}$ M for thiourea, cystine and cysteine in ammonia buffer.

From i versus $\sqrt{H}$ plots (H is the height of Hg column) for cysteine, cystine and thiourea in ammonia buffer the diffusion current percentage is higher than in HCl.

An interesting fact has been noticed in case of the measurements carried out in acetate buffer.

(a) Thus if the acetate buffer-cysteine is recorded, the cysteine wave (anodic-cathodic) is very small, and by adding thiourea, the anodic wave increases correspondingly (with 2.4 μA for instance).

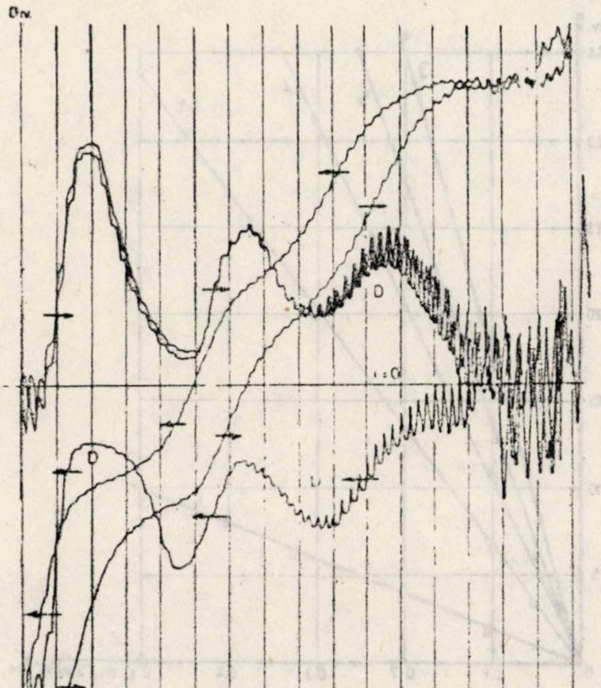

Fig. 5. — Polarographic curves ($S = 8 \cdot 10^{-8}$ A/div.), derived and cyclic voltammograms ($S = 2 \cdot 10^{-8}$ A/div) for cysteine and cystine 10^{-3}M in ammonia buffer 10^{-1}M.

(b) If the acetate buffer-thiourea is recorded, the thiourea wave (S^{2-} respectively) is very small and, by adding cysteine, the anodic step increases correspondingly. This behaviour is to be checked in the following.

Fig. 5 presents the normal polarographic plots ($S = 8 \cdot 10^{-8}$A/div.), the derived ones as well as the cyclic voltammetric curves ($S = 2 \cdot 10^{-8}$ A/div.) for 10^{-3}M cysteine and cystine in the 0.1M ammonia buffer solution (pH = 9–10).

The normal cyclic and derived curves exhibit three steps: the first one anodic, the second anodic-cathodic for cysteine and the third cathodic for cystine.

The separation between cystine and cysteine is clearer immediately after gelatine addition. The cyclic derived curve clearly separates the three stages. If one records from zero towards negative values, all the plots are found to lie above the line $i = 0$, respectively the cathodic one.

If one records in the opposite direction, from the negative values towards zero, all the steps lie under the line $i = 0$, respectively the anodic one. A comparison of the measurements in the two cells, with and without anodic and cathodic compartments separation with two and three electrodes DME — SCE — Pt can be seen in Fig. 6.

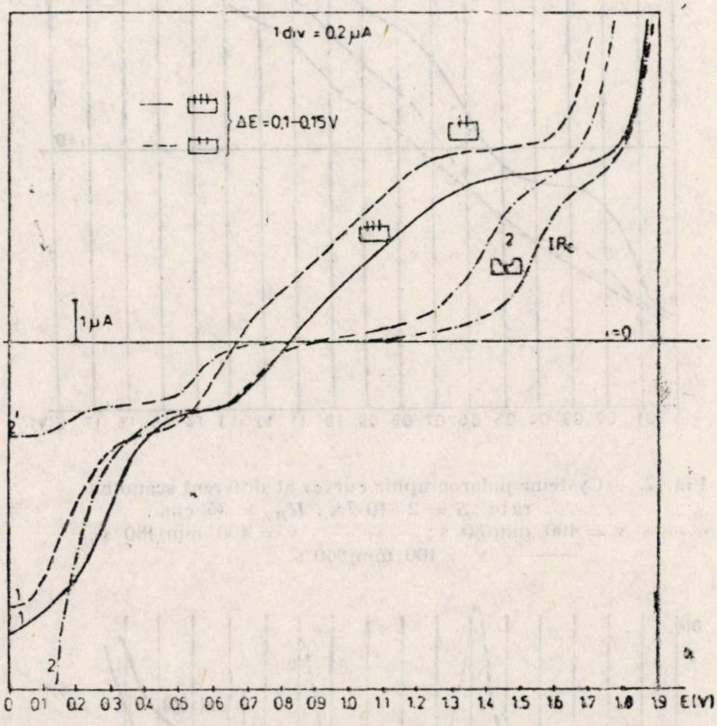

Fig. 6. — Cystine and cysteine polarographic behaviour ($S = 2 \cdot 10^{-7}$ A/div.).
1) 10 ml ammonia buffer (nitrate) + 1 ml cysteine 10^{-2}M ;
2) 1 + 1 ml cystine 10^{-2}M.

In both cases, when three electrodes are used, the polarographic waves are shifted towards more negative values by approximately 0.15 V.

In the cell with two separated compartments, cystine is very clearly separated from cysteine (without gelatine addition).

Gelatine behaviour is similar to that of glass foil separating the two compartments (anodic and cathodic ones). The recordings at various scanning rates : 400 mm in 80, 480 and 960 s respectively can be followed in Fig. 7.

The scanning rate of 400 mm/16 min. is noticed to be the most suitable but in practice, for analysis in series, the rate of 400 mm/8 min. can also be used.

The stationary mercury electrode (with large surface) behaviour can be followed in Fig. 8.

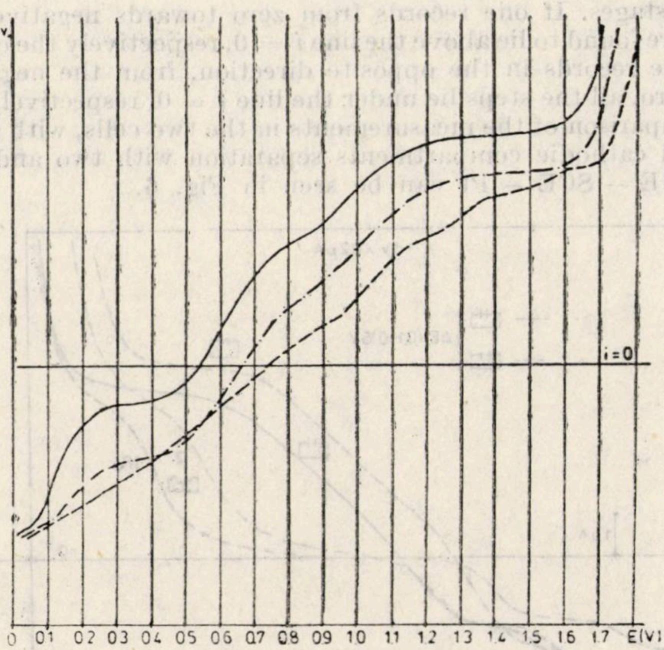

Fig. 7. — Cysteine polarographic curves at different scanning rate. $S = 2 \cdot 10^{-7}$A ; $H_{Hg} = 35$ cm.
.... v = 400 mm/80 s ; — · — · — · v = 400 mm/480 s ;
——— v = 400 mm/960 s.

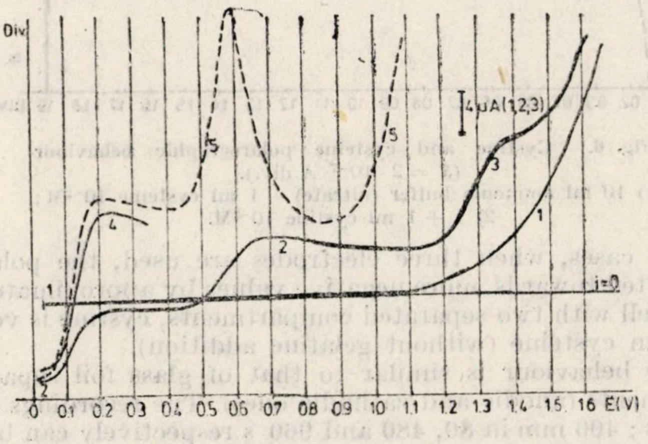

Fig. 8. — Cysteine and cystine polarographic curves on ME electrodes. $S = 8 \cdot 10^{-7}$ A/div. ; $v = 400$ mm/8 min.
1) 10 ml ammonia buffer 0.1M ($NH_4NO_3 + NH_4OH$) ; 2) 1 + 1 ml cysteine 10^{-2}M solution ; 3) 2 + 1 ml cystine 10^{-2}M solution ; 4) 10 ml HCl 0.1M + 1 ml thiourea 10^{-2}M ($S = 4 \cdot 10^{-7}$ A/div. ; 5) 10 ml HCl 0.1 M + 1 ml cysteine 10^{-2}M ($S = 2 \cdot 10^{-7}$ A/div).

This electrode is suitable for determining small cysteine and cystine concentrations ($10^{-4}M-10^{-5}M$). The polarographic curves are very well defined and the sensitivity is 2—3 times higher than with DME.

Cysteine anodic-cathodic step in 0.1M HCl is reversible.[8]

For cysteine and cystine concentrations, smaller than $10^{-4}M$, polarographic measurements can be successfully applied in ammonia buffer $+Co^{2+}$[9,10] or in phosphate buffer (pH = 6.6) $+Ni^{2+}$ [11].

As it has been already mentioned in literature, cysteine, cystine, glutathione, thiogluconic acid etc. compounds, containing sulphur and nitrogen, give catalytic steps in ammonia buffer solutions, in the presence of Co^{2+} [01]. Proteins, being more complicated products, exhibit characteristic double steps also in Co^{3+} solutions used in cancer diagnosis (the Brdička's reaction). The step height increases with increasing concentrations of the catalyst and the buffer solutions.[8]

Brdička assumed that between cobalt and —SH group a complex forms, due to the deformed —SH group dipole, so that the bond between $-S^-$ and H^+ is weakened; hydrogen catalytic discharge can take place at a more positive potential than in the cobalt absence.

The mechanism on the electrode processes involving catalytic prewave of hydrogen in the systems: Ni^{2+}-cysteine, Ni^{2+}-cystine and Ni^{2+}-glutathione in phosphate-acetate buffer (pH = 6.5) has been proposed.[12-15]

Unfortunately, these catalytic reactions have a high sensitivity but not a corresponding selectivity. By comparing the two catalytic reactions we found that the cystine and cysteine determinations are more sensitive in ammonia buffer $+Co^{2+}$ than in phosphate buffer $+Ni^{2+}$.

For this, the catalysis in ammonia buffer is maximum in the presence of Co^{2+} and smaller in the presence of Ni^{2+} (of the same concentration)

NO_3^- and NO_2^- in concentrations of 10^{-3} M lead to the annulation of the catalytic maximum of cysteine and cystine, but the shift of NH_4 wave remains the same.

The action of NO_3^- and NO_2^- ions in catalytic process is unclarified.

In ammonia buffer, in the presence of Cu^{2+}, Cd^{2+} and Z^{2+} catalytic steps are not obtained. The polarographic catalytic curves and the calibration curves can be followed in Figs 9 and 10.

The maximum of the catalytic curves for cysteine and cystine is found at —1.75 V and —1.80 V respectively.

It can be noticed that in buffer solutions of the same concentration (0.1M), the catalytic steps increase together with increasing Co^{2+} concentration (by about 1.5 times for a concentration twice as high).

In 0.05M buffer solution of the same Co^{2+} concentration, catalytic steps are higher than in 0.1M solution.

It is more convenient from the analytical point of view to use the following catalytic system: 0.1M ammonia buffer solution (chloride) $+10^{-3}MCo^{2+}$ for determining cysteine and cystine within $10^{-5}-10^{-6}$ M concentration range.

The practical limit of cysteine determination in the catalytic system is calculated to be $2 \cdot 10^{-7}M$.

The small thiourea concentrations can be determined on the mercury film electrode or stationary mercury electrode with large surface

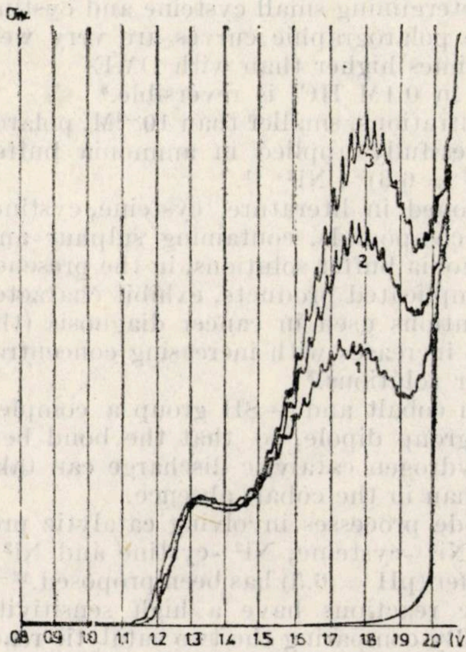

Fig. 9. — Catalytic curves for cystine and cystine in ammonia buffer 0.1M ($S = 4 \cdot 10^{-7} A$/div.) at DME — SCE. 1) $2 \cdot 10^{-6}$M ; 2) $4 \cdot 10^{-6}$M ; 3) $6 \cdot 10^{-6}$M

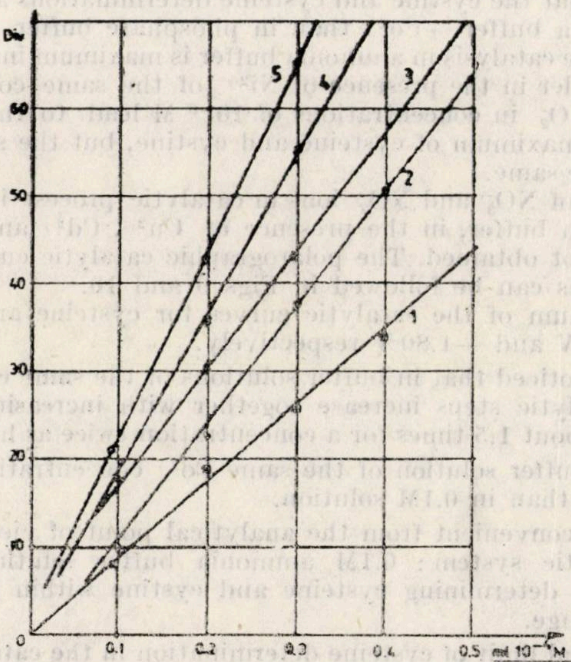

Fig. 10. — The calibration catalytic curves for cystine, cysteine, and thiourea in ammonia buffer 0.1M (1, 2, 3) and 0.05M (4 and 5) 1, 4 cysteine ; 2, 5 cystine ; 3 thiourea.

by ASV (adsorptive stripping voltammetry). For exemplification the plots for two concentrations of thiourea (10^{-5} and 10^{-7}M) are given in Fig. 11.

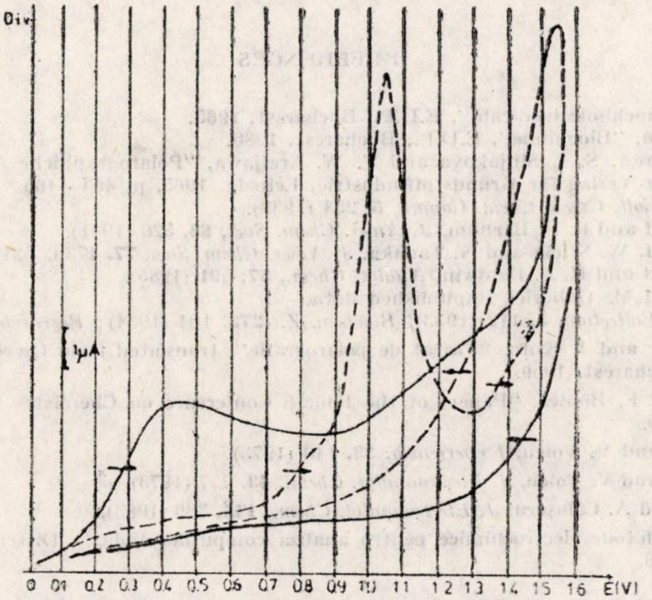

Fig. 11. — **Adsorptive stripping voltammetric curves for thiourea in ammonia buffer (M.E. — SCE)**

$t_{\text{accum}} = 5$ min. $E_{\text{ad}} = 0$V

------- 8 ml ammonia buffer 0.1M + 0.8 ml thiourea 10^{-4}M ;

——— 8 ml ammonia buffer 0.1 M+0.08 ml thiourea 10^{-4}M.

It can be noticed that both the shape and the size are different, as a function of concentration, respectively of the covering of electrode surface.

The ASV, a new variant of stripping voltammetry, enlarging the application range and the theoretical aspects, will be followed on various model substances in the next papers.

4. CONCLUSIONS

For determining cysteine, cystine and H_2S (respectively S^{2-}) in concentration $10^{-3}-10^{-4}$M, in various real systems, the polarography in ammonia-buffer (nitrate) with DME is recommended, while for smaller concentrations within $10^{-6}-10^{-7}$M range the catalytic reaction in ammonia buffer (chloride) + Co^{2+} with DME can be used. For concentrations of thiourea smaller than 10^{-5}M, the ASV is recommended.

Under our polarographical conditions the methionine could not be determined. The compounds with $R-S-CH_3$ bonds (methionine among them) may be determined by A.S.V.

Besides, methionine does not give catalytical wave because it cannot form a stable complex with Co^{2+}. Hence the Co—S bond is particularly important for the formation of catalytical complexes.

REFERENCES

[1] I. Manta, "Biochimie medicală", E.D.P., Bucharest, 1965.

[2] I. F. Dumitru, "Biochimie", E.D.P., Bucharest, 1980.

[3] T. A. Krjukowa, S. I. Sinjakova and T. W. Arefjawa, "Polarographiche Analyse", VEB Deutscher Verlag für Gründstoffindustrie, Leipzig, 1965, p. 464—465.

[4] R. Brdička, *Coll. Czech. Chem. Comm.*, **5**, 238 (1933).

[5] I. M. Kolthoff and C. P. Barnum, *J. Amer. Chem. Soc.*, **63**, 520 (1941).

[6] I. M. Kolthoff, W. Sticks and N. Tanaka, *J. Amer. Chem. Soc.*, **77**, 4739, 5211, 5215, (1955).

[7] M. K. Halbert and R. P. Baldwin, *Analyt. Chem.*, **57**, 591 (1985).

[8] Al. Duca and M. Găburici, unpublished data.

[9] R. Brdička, *Collection*, **5**, 112 (1933), *Biochem. Z.*, **272**, 104 (1934); *Research.*, **1**, 23 (1947).

[10] J. Heyrovsky and I. Kůta, "Tratat de polarografie", translated from Czech., Ed. Academiei, Bucharest, 1959.

[11] E. Diacu and F. Bănică, "Papers of the Fourth Conference on Chemistry", Buc., 17—18 Oct. 1985.

[12] A. Călușaru and V. Voicu, *Experientia*, **29**, 140 (1973).

[13] A. Călărușu and V. Voicu, *J. Electroanalyt. Chem.*, **43**, 257 (1973).

[14] F. Bănică and A. Călușaru, *J. Electroanalyt. Chem.*, **145**, 389 (1983).

[15] E. Diacu, "Metode electrochimice pentru analiza compușilor tiolici", Dissertation, Bucharest, 1986.

Revue Roumaine de Chimie, **36**, *8*, 877–881 (1991)

ABSORPTION ELECTRONIC SPECTRA AND REACTIVITY OF SOME AS-NAPHTHOLS

I. COCÎRLĂ, LUCIA TĂTARU, M. VÂȚĂ, D. SCUTARU, I. MAZILU,
LUMINIȚA WAGNER * and CAMELIA PETRESCU
Polytechnic Institute, Spl. Bahlui, 71,6600 Jassy, Romania
* ICECHIM, Research Center for Dyestuffs, Spl. Independenței 202, Bucharest
77208, Romania

Received December 14, 1987

Reactivity studies on three AS-naphthols based on electronic spectra and molecular diagrams have been undertaken. HMO calculations for the transitions between frontier orbitals evidenced a good agreement with experimental data.

INTRODUCTION

AS naphthols represent important coupling compounds for developing dyestuffs.

The present study deals with the characterization of anilide and toluidides (*o*-, *p*-) of the 2-naphthol-3-carboxylic acid, obtained by a non-conventional technique; they may be utilized in the obtainment of FGR permanent type pigments.

For correlating the electronic structures with their physical and chemical properties, the HMO method has been applied.

Electronic spectra of these compounds have been recorded with a UV–VIS spectrophotometer (Carl Zeiss Jena) in methanol solutions, at concentrations of $1 \cdot 10^{-5}$ M.

RESULTS AND DISCUSSION

For the theoretical interpretation of the reactivity of the compounds the following parameters have been used for heteroatoms[1,2].

$$h_{\dot{O}} = 0.7\,;\ h_{\ddot{O}} = 2\,;\ h_{\ddot{N}} = 1.4\,;\ k_{C-\ddot{N}} = 0.8\,;\ k_{C-\dot{O}} = 1.1\,;\ k_{C-\ddot{O}} = 0.6.$$

The value taken for the methyl group, in induction model, was $h_{C(CH_3)} = -0.2$.

Molecular diagrams (Fig. 1) show the same electronic distribution on the naphthol structure, regardless of the N amidic substitutes.

AS naphthols (I—III) are known as being coupled in position 1, by the electrophilic atack of the diazoic compound.[3]

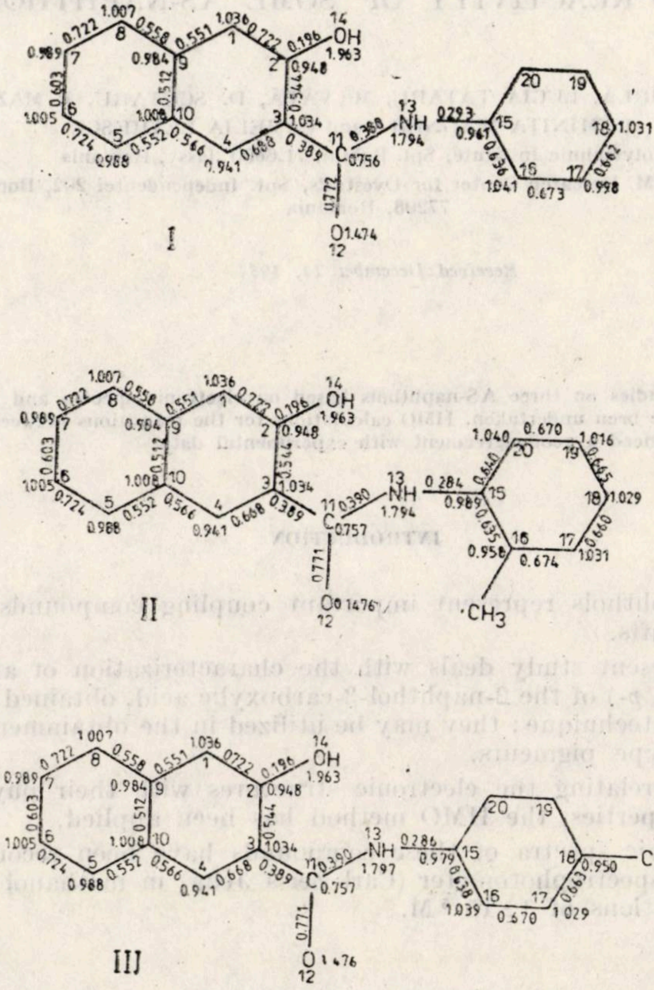
1.007
0.722
0.558
8
1.036
0.551
1
0.722
14
OH
0.196
1.963
0.989
7
0.984
9
2
0.948
0.603
0.512
0.544
1.005
6
1.008
10
3
1.034
13
NH
1.794
0.293
15
0.961
20
19
18
1.031
0.724
5
0.552
0.566
4
0.668
0.389
11
C
0.756
0.388
0.636
16
17
0.662
0.988
0.941
1.041
0.673
0.998
0.772
O
1.474
12
1.007
0.722
0.558
8
1.036
0.551
1
0.722
14
OH
0.196
1.963
0.989
7
0.984
9
2
0.948
0.670
1.040
20
19
1.016
0.603
0.512
0.544
0.640
0.665
1.005
6
1.008
10
3
1.034
13
NH
1.794
0.284
15
0.989
18
1.029
0.724
5
0.552
0.566
4
0.668
0.389
11
C
0.390
0.757
0.635
16
17
0.660
0.988
0.941
0.958
0.674
1.031
0.771
O
1.476
12
CH3
1.007
0.722
0.558
8
1.036
0.551
1
0.722
14
OH
0.196
1.963
0.989
7
0.984
9
2
0.948
20
19
0.603
0.512
0.544
1.005
6
1.008
10
3
1.034
13
NH
1.797
0.286
0.979
15
18
0.950
CH3
0.724
5
0.557
0.566
4
0.668
0.389
11
C
0.390
0.757
0.638
16
17
0.663
0.988
0.941
1.039
0.670
1.029
0.771
O
1.476
12

I

II

III

Fig. 1. — Molecular diagrams of the investigated compounds.

Molecular diagrams and the values of the electronic densities on the HOMO frontier orbital $f^E_{(r)}$, support — in conditions of electrophilic attack — (Table 1) this assertion. There is yet to be observed a higher reactivity of compounds II and III in this reaction, although the electronic density at atom 1 has the same value for all the three molecules. This may be explained only through the influence of the CH_3 group — modifying the frontier electronic densities. The introduction of methyl group

Table 1

Molecular characteristics of the investigated compounds

Molecule	$E_{\mathrm{HOMO}}(\beta)$	$E_{\mathrm{LUMO}}(\beta)$	$^*DE(\beta)$	$^*DE/n_\pi$	$^*f^E_{(r)}$
I	0.6011	0.4929	12.503	0.568	0.4048(1) 0.1391(6) 0.3541(8) 0.0005(16)
II	0.6011	0.4937	12.303	0.560	0.4499(1) 0.3539(8) 0.1608(6) 0.0013(18)
III	0.6011	0.4940	12.305	0.560	0.4497(1) 0.3536(8) 0.1607(6) 0.0012(16)

* DE — the delocalization energy

* n_π — the number of the π-electrons

* $f^E_{(r)}$ — the electron density at atom r for the HOMO (the electrophilic attack)

destabilizes molecule I (D E values) and, at the same time, lowers the interactions between molecules, leading to the decrease of the melting doints.[4]

Electronic spectra of molecules I—III show three absorption bands, ranging between 302—304, 237—240 and 204 nm respectively, representing the result of certain transitions $\pi \rightarrow \pi^*$ and $n \rightarrow \pi^*$. The correct assignment of the bands and the correlation of the results of HMO calculations with the experimental data may be performed by considering the electronic transitions between frontier orbitals as the most important ones (Fig. 2).

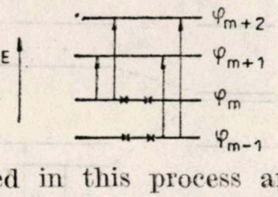

Fig. 2. — The transition between frontier orbitals.

The electronic configurations involved in this process are

$$\psi_0 = |\,\varphi_1\overline{\varphi}_1\varphi_2\overline{\varphi}_2 \,\cdots\, \varphi_m\overline{\varphi}_m\,| \tag{1}$$

for the fundamental states and

$$\psi_1 = \frac{1}{\sqrt{2}}\left\{|\,\varphi_1\overline{\varphi}_1\varphi_2\overline{\varphi}_2\cdots\varphi_m\overline{\varphi}_{m+1}\,| - |\,\varphi_1\overline{\varphi}_1\varphi_2\overline{\varphi}_2\cdots\overline{\varphi}_m\varphi_{m+1}\,|\right\} = (\varphi_m^{-1}\varphi_{m+1}) \tag{2}$$

for the $\varphi_m \rightarrow \varphi_{m+1}$ transition.

Further on, on applying the Dewar and Longuet-Higgins[5] notation, we get

$$\psi_2 = (\varphi_m^{-1}\varphi_{m+2}) \tag{3}$$

$$\psi_3 = (\varphi_{m-1}^{-1}\varphi_{m+1}) \tag{4}$$

$$\psi_4 = (\varphi_{m-1}^{-1}\varphi_{m+2}) \tag{5}$$

In these relations, φ_j represents the molecular orbitals of the LCAO form

$$\varphi_j = \sum_r c_{jr}\varkappa_r \tag{6}$$

where $\varkappa_r$ are the corresponding atomic orbitals, while the quantities among bars — the Slater determinants.[6]

The configurations resulting from the configurational interaction lead to the appearance of the absorption bands shown in Figure 3.

The band notation used was that proposed by Clar[7] for aromatic hydrocarbons. The β′ band has not been considered, as it does not appear in common UV.

For calculating the transition energies corresponding to the α, *p* and β bands, the configurational interaction has been approached empirically,[8] on taking molecule I as standard. Consequently, there results that

$$\Delta E_{\mathrm{exp}}(\alpha,\ p,\ \beta) = \Delta E_{\mathrm{theor}}(\alpha,\ p,\ \beta) \tag{7}$$

$$\Delta E_{\mathrm{theor}}(\alpha,\ p,\ \beta) = \Delta n\,\beta_{\alpha,p,\beta} \tag{8}$$

where Δn —coefficient variation of the coulombian parameter for OM, involved in the transition.

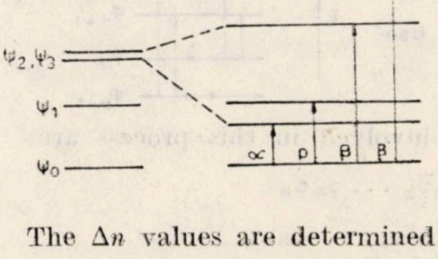

Fig. 3. — Configuration interactions and the absorption bands.

The Δn values are determined as

$$\Delta n(p) = n_{m+1} - n_m \tag{9}$$

$$\Delta n(\alpha;\ \beta) = 1/2[(n_{m+2} - n_m) + (n_{m+1} - n_{m-1})] \tag{10}$$

Experimental data referring to the position of the absorptions bands have been obtained from electronic spectra (Table 2).

Table 2

The calculated transition energies and their comparison with the experimental data

Investigated molecule	Electronic band	Δn	ΔE (eV)		$\Delta(\Delta E)$*
			Exper.	Theory	
I	α	1.3035	4.11	4.11	0
	p	1.0940	5.23	5.23	0
	β	1.3035	6.08	6.08	0
II	α	1.2913	4.11	4.06	0.05
	p	1.0948	5.23	5.23	0
	β	1.2913	6.08	6.01	0.07
III	α	1.2842	4.08	4.04	0.04
	p	1.0951	5.17	5.23	0.06
	β	1.2842	6.08	5.98	0.10

* $\Delta(\Delta E) = |\Delta E_{\text{exp}} - \Delta E_{\text{theor}}|$

Thus, the following calculation values are to be obtained for

$$\beta_\alpha = -3.15 \text{ eV}; \ \beta_p = -4.78 \text{ eV}; \ -\beta_\beta = 4.66 \text{ eV} \qquad (11)$$

The Δ (ΔE) differences between the calculated and the experimental values are presented in Table 2. As it can be observed, the theoretical data are in good agreement with the experimental ones.

REFERENCES

[1] A. Streitwieser, Jr., "Molecular Orbital Theory for Organic Chemistry", John Wiley & Sons, New York, 1961.

[2] W. P. Purcell and J. A. Singer, *J. Chem. Eng. Data,* **12**(2), Suppl. April (1967).

[3] H. Sanielevici and F. Urseanu, "Sinteze de coloranți azoici", vol. 1, p. 154, Ed. Tehnică, Bucharest, 1987.

[4] I. Heilbron and H. M. Bunbury, "Dictionary of Organic Compounds", vol. 2, London, 1946.

[5] M. J. S. Dewar and H. C. Longuet-Higgins, *Proc. Phys. Soc.*, **A67**, 795 (1954).

[6] M. Weisbluth, "Atoms and Molecules", Academic Press, New York, 1978, p. 240.

[7] E. Clar, "Aromatische Kohlenwasserstoffe", Springer Verlag, Berlin, 1952.

[8] I. Cocîrlă and C. I. Ghirvu, *Bul. Inst. Pol. Iași*, **T. XXIII** (XXVII), 69 (1977).

Revue Roumaine de Chimie, 36, 8, 883–899 (1991)

Dedicated to Professor PETRU SPACU on the occasion of his 85th anniversary

THE INFLUENCE OF ClO_4^- IONS UPON THE ELECTROCHEMICAL SYSTEM $Pb/H_2SO_4/PbO_2$

A. MATEESCU[a], C. D. MATEESCU[b], V. S. TEODORESCU[b] and L. C. NISTOR[b]
[a] "ACUMULATORUL" Enterprise, Bvd Biruinţei 102, Bucharest, Roumania
[b]Central Institute of Physics, I.F.T.M., C.P.MG–7 Măgurele, Bucharest, Roumania

Received August 31, 1990

The electroformation of the pasted positive plates in diluted sulphuric acid with perchloric acid and potassium perchlorate as additives was studied. It was established the optimum concentration of perchlorate ions for which the plate electroformation is possible and the mechanical and electrical properties of the active mass are improved. The ClO_4^- ions as additives have a considerable influence on the sulphatation process and on the electrochemical change of $PbSO_4$ to PbO_2, especially at the grid-active mass interface. The crystallographic structure of the formed active masses is considerably influenced by the presence of forming additives.

INTRODUCTION

The storage battery plates and especially those for lead-acid batteries are formed by changing their chemical composition, realized by applying a continuous current to the plates immersed in a dilute H_2SO_4 solution.

The chemical and electrochemical reactions following the formation process were described elsewhere.[1–4]

In up-to-date reports, the effects of different formation additives upon the mechanical properties of the active masses are presented.[5–11]

Relying on the experience accumulated on the utility of perchlorate ions in the electroformation of stationary plates, we studied the effects of perchloric acid and potassium perchlorate upon the formation of pasted plates.

EXPERIMENTAL PART

Both polarities electrodes were formed from pasted plates of 142 × 134 × 1.9 (1.5) mm, obtained by the classical technology.

For the plates formation, 1.75 M H_2SO_4 solutions were used.

The ammounts of $HClO_4$ (70%) added were between 5 and 35 mM/l and those of $KClO_4$ between 1 and 8 mM/l.

All the plates received the same quantity of electricity chosen so that no plate was completely formed, otherwise the possibility of comparison and observation being more difficult.

The experimental cells were composed of positive text plates placed between ordinary negative plates.

Periodically, the positive plates were analysed. They were first energetically washed in order to complete the elimination of perchlorate ions, then dried and analysed chemically and by X-ray diffraction.

The variation of the chemical compounds of the active mass during the electroformation process, for different amounts of forming additives was described by several equations. Their forms and coefficients were determined by mathematical regression analysis, using a Coral 4011 Computer.

The microprobes for scanning microscopy were covered by an aluminum layer of about 500 Å thickness, by evaporation in vacuum, in order to ensure a better electrical superficial conductivity of the sample.

RESULTS AND DISCUSSION

Electroformation in 1.75M H_2SO_4 with $HClO_4$ as additive

The complex electroformation process of the pasted positive electrode has been followed by Pavlov et al.,[1] through analysis of the phases present in the active material, during electroformation. No consideration was given to the role of additives.

In this paper, we report the studies upon the influence of perchloric acid as additive on the electroformation of pasted plates in comparison with the electroformation of the same kind of plates but formed in acid solutions without additives.

For the positive plates we observed a rising amount of PbO_2 in the formed active mass, subsequent to the increase of the amount of $HClO_4$ added to the formation electrolyte.

Maximum values for the PbO_2 content were obtained for $HClO_4$ amounts between 20—25 mM/l.

If the $HClO_4$ content is exceeded, the PbO_2 content begins to lower.

The chemical reactions assumed for the electroformation in H_2SO_4—$HClO_4$ mixed electrolyte, are the following :

$$Pb^{2+} + SO_4^{2-} \rightleftarrows PbSO_4 \qquad (1)$$

$$PbSO_4 + 2H_2O \rightleftarrows PbO_2 + HSO_4^- + 3H^+ + 2e \qquad (2)$$

$$PbSO_4 + 2H^+ + 2e \rightleftarrows Pb + 2H^+ + SO_4^{2-} \qquad (3)$$

$$PbO_2 + Pb + 4HClO_4 \rightleftarrows 2Pb(ClO_4)_2 + 2H_2O \qquad (4)$$

$$Pb(ClO_4)_2 + H_2SO_4 \rightleftarrows PbSO_4 + 2HClO_4 \qquad (5)$$

The first reaction is quick, while the second reaction, of oxidation, is slow, controlling the whole process. The reduction reaction (3) describes the active mass formation of the negative plate, finally consisting of metallic sponge lead.

Reaction (4) depends of the perchlorate ions concentration in the acid solution. For less than 25 mM/l ClO_4^- ions, reaction (4) is slow.

The perchlorate ions influence mainly the process of lead oxidation from the unformed active mass and from the interface layer between the grid and the active mass.

The conversion of the lead perchlorate formed in this area to $PbSO_4$ (reaction (5)) and then to PbO_2 (reaction (2)) eliminates the risk of an insulating irreversible layer of $PbSO_4$ between the active mass and the grid. This is a most important effect of the perchlorate ions.

$PbSO_4$ quantity (y) of the active positive mass, during the electroformation process, for different amounts of $HClO_4$ (x), varies according to equation (6) :

$$\ln y = a_0 + a_1 \ln x + a_2 \ln^2 x + a_3 \ln^3 x \qquad (6)$$

The perchlorate ion has also an influence on the crystallographic structure of the formed positive active mass.

The ratio of the crystallographic forms of lead dioxide ($\alpha PbO_2/\beta PbO_2$) and its variation during the electroformation process is given by equation (7):

$$\ln y = b_0 + b_1 \ln x + b_2 \ln^2 x + b_3 \ln^3 x \qquad (7)$$

The values for a_i and b_i coefficients are given in tables 1 and 2.

Table 1

Values of a_i coefficients from equation (6)

$HClO_4$ (mM/l)	a_0	a_1	a_2	a_3
0	2.909	0.717	−0.142	0.06
6.25	2.815	0.482	−0.120	0.06
12.50	2.999	0.448	−0.048	0.03
25.00	2.751	0.583	−0.144	0.007
30.00	2.947	0.504	−0.092	0.04

Small quantities of $HClO_4$ added to the forming electrolyte lead to a significant increase of the ratio C_α/C_β in comparison with a standard sample.

Table 2

Values of b_i coefficients from equation (7)

$HClO_4$ (mM/l)	b_0	b_1	b_2	b_3
0	−1.748	1.049	−1.175	0.007
6.25	−0.359	0.117	−0.042	0.002
12.50	−0.759	0.380	−0.092	0.004
25.00	−0.183	0.097	−0.020	0.001
30.00	−0.638	0.427	−0.085	0.003

The variation of PbO and PbO_2 amounts for 25 mM/l $HClO_4$ and 2 mM/l $KClO_4$ respectively, during the electroformation process is described by the following equations:

$$Y = \frac{1}{a + bx + cx^2} \qquad (8)$$

$$Y = \frac{m}{x} + nx + px^2 \qquad (9)$$

(The coefficient values are given in tables 3 and 4).

Electroformation in 1.75M H_2SO_4 with $KClO_4$ as additive

Similar to the perchloric acid, the potassium perchlorate influences the formation of the pasted plates. The results obtained (for PbO and PbO_2 are given by equations 8 and 9) proved the fact that $KClO_4$ is more active upon the electroformation process.

Table 3

Values of coefficients from equation (8)

Type of additives	without additives	$HClO_4$	$KClO_4$
quantity of additives (mM/l)	0	25	2
	a=−0.0141 b= 0.0277 c=−0.0007	a=0.0093 b=0.0039 c=0.00014	a=0.01 b=0.03 c=0.002

The final values of PbO_2 content are bigger when $HClO_4$ is used·

The best effects regarding the chemical and crystallographic composition of the formed active mass were obtained for 2mM/l $KClO_4$ added.

The increase of the $KClO_4$ amount above the mentioned quantity has not a significant influence on the formation process.

The negative plate of the lead-acid storage battery has received but little attention as compared to the positive one.

The equation for the negative plate may be written as :

$$Pb + SO_4^{2-} \underset{\text{Charge}}{\overset{\text{Discharge}}{\rightleftarrows}} PbSO_4 + 2e \tag{10}$$

The charge/discharge cycle at the negative plate involves a considerable redistribution of the active material during the dissolution, nucleation and growth of the solid phases.

We further present the microstructural changes during the electroformation process of the negative active masses, by conversion of the inferior lead oxides to metallic spongeous lead.

Table 4

Values of the coefficients from equation (9)

Type of additives	without additives	$HClO_4$	$KClO_4$
quantity of additives (mM/l)	0	25	2
	m=−18.228 n= 13.934 p=−0.525	m=18.232 n=13.192 p=−0.517	m=−28.27 n= 13.752 p=−0.537

The crystallographic structure of the active formed masses

The active mass microstructure was observed with an electronic microscope — TEMSCAN 200 CX. The scanning images show the negative and positive active masses formed in various situations.

Figure 1 presents the positive active mass formed in 1.75 M H_2SO_4 without additives. The active mass, consisting mostly of PbO_2 has a porous unfolded structure.

Two or several species of crystals can be observed in the positively formed active mass (Figs. 1a—1e). Some crystals have polyhedrical shapes with small but equal dimensions (2 or 3 μm), giving the general appearance of approximate spheres.

Among these crystals, larger crystals coexist (sometimes having the forms of thin rectangular plates), appearing on the surface of formed plates (Figs. 1d—1e).

The dimensions of these larger crystals is between 20 and 150 μm, being dependent on the paste composition before the formation process.

Crystals similar in form, dimensions and frequency of occurrence were observed also in the unformed regions of the same plate, pointing that these crystals were directly converted from sulphate to PbO_2 crystals, without a modification of the exterior shape.

According to the results published by other authors,[12-17] we assume that the small polyhedrical crystals are $\beta - PbO_2$ and those bigger are $\alpha - PbO_2$.

The individual PbO_2 crystals are 2 to 5 μm in thickness. The isolated $PbSO_4$ crystals have dimensions between 1 and 3 μm.

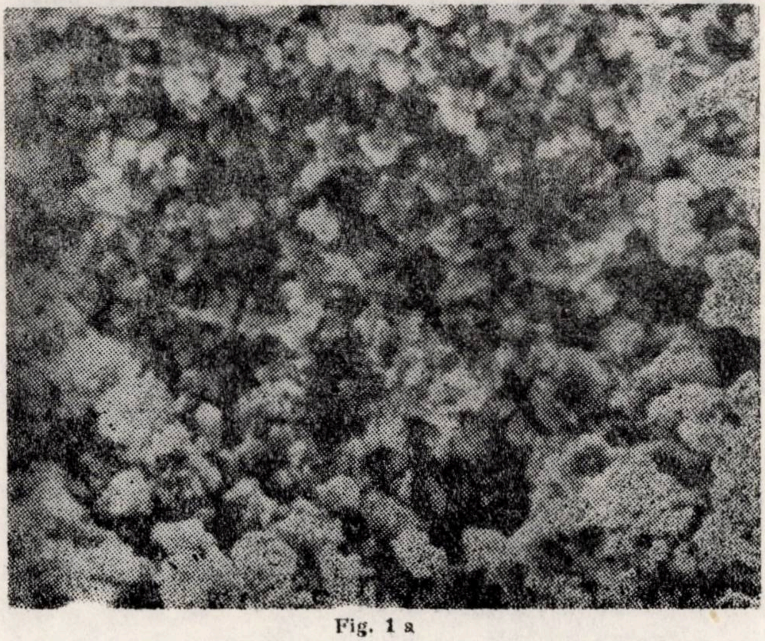

Fig. 1 a

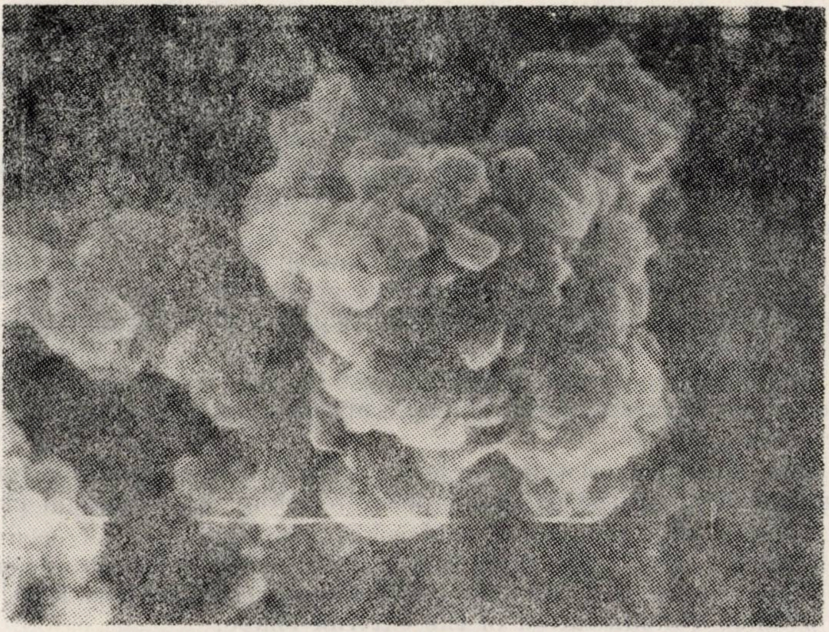

Fig. 1 b

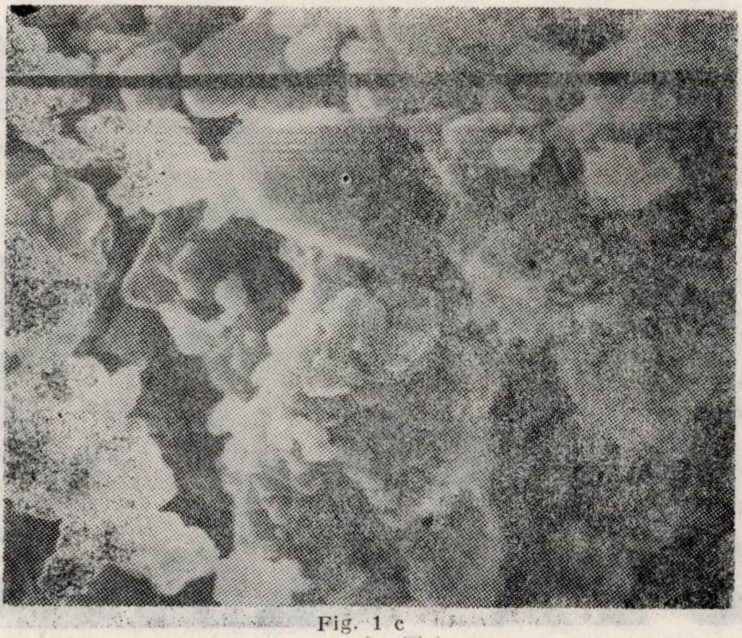

Fig. 1 c

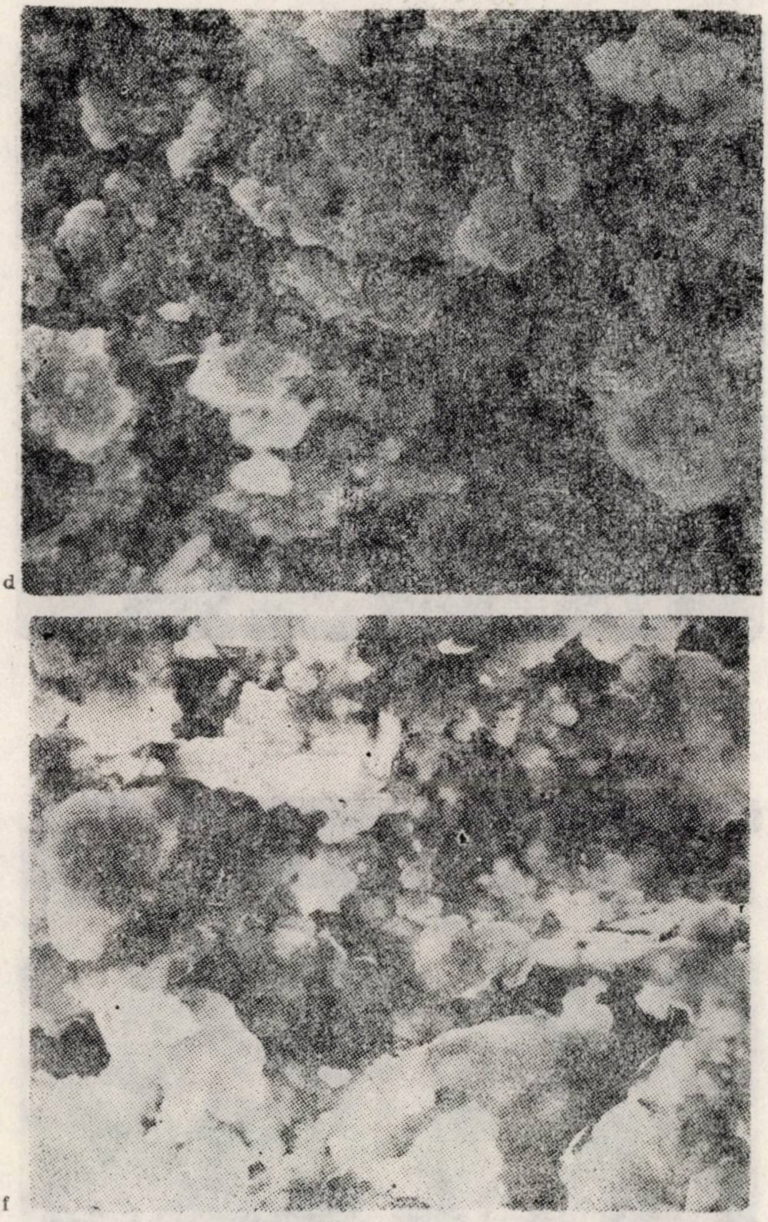

Fig. 1. — Scanning micrographs of the positive active mass formed in 1.75M H_2SO_4 without additives.

As can be seen in Figs. 1a and 1c, the $PbSO_4$ crystals may sometimes appear as conglomerates with coral structure.

The active mass of the formed negative plates, consisting mainly of metallic lead, is characterized by large spaces (sponge structure), an apparent lack of cohesion between the particles and by the presence of unchanged particles of lead sulphate (Fig. 2).

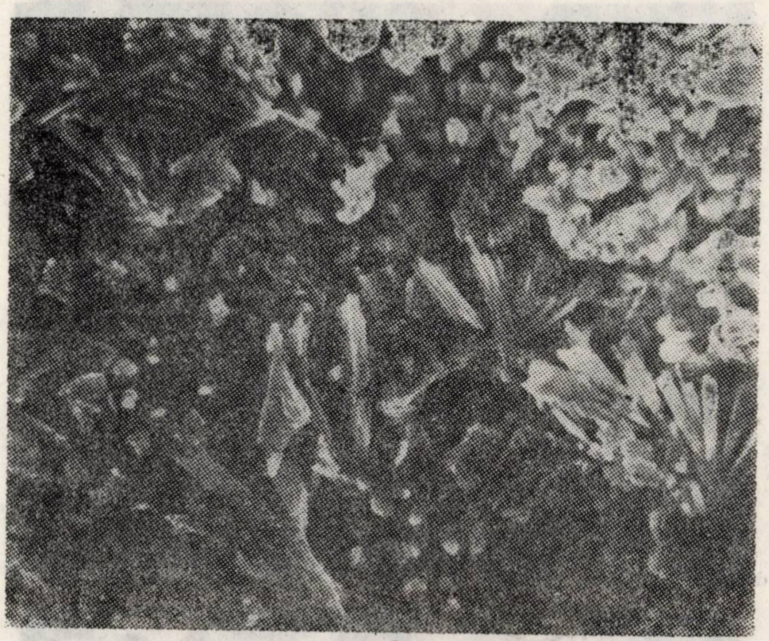

Fig. 2 a

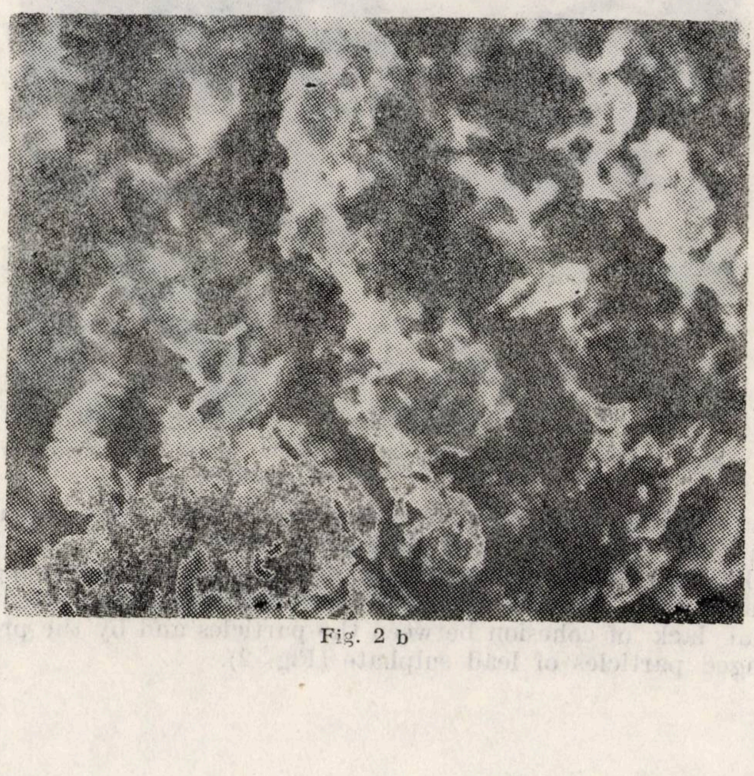

Fig. 2 b

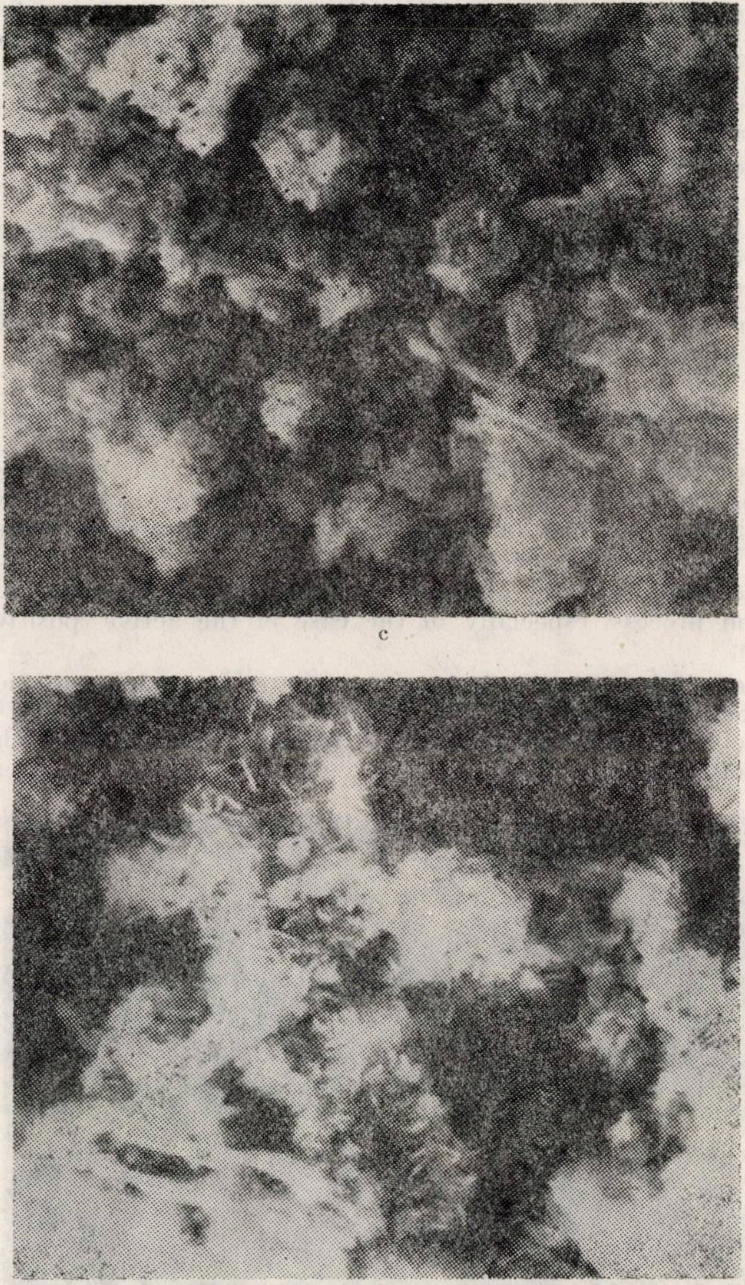

c

d

Fig. 2. — Scanning micrographs of the active negative mass formed in 1.75M H_2SO_4 without additives.

The active negative mass consists of a lattice of interrelated lead crystals (Figs. 2a and 2b) covered by smaller crystals with whiskers shape (Figs 2c and 2d).

The length and thickness of the individual whiskers correspond to a field range from 2—25 μm and respectively 2—6 μm.

The isolated crystals of lead sulphate of the active formed negative mass have from 1 μm to 3 μm dimensions.

It is interesting to notice that the studied additives present in the forming electrolyte have not a major influence on the active mass microstructure.

The microphotographs obtained for these cases do not differ essentially from those of fig. 2.

The influence of $HClO_4$ upon the structure of the formed positive plate

There are considerable differences between the scanning micrographs of the active positive mass formed in an electrolyte without additives and those obtained for the same active mass formed in an electrolyte with $HClO_4$ (30 mM/l) as additive.

The addition of perchlorate ions has a great influence upon the nucleation process, especially in the case of the active positive mass (Fig. 3a).

The cellular threedimensional structure, formed of a thick layer of whiskers (fig. 3b, 3c and 3d) extends in regions with higher density, this effect being determined by the previous localizations of the peaks of the polyhedrical crystals of $PbSO_4$, of unformed plate provenience.[11]

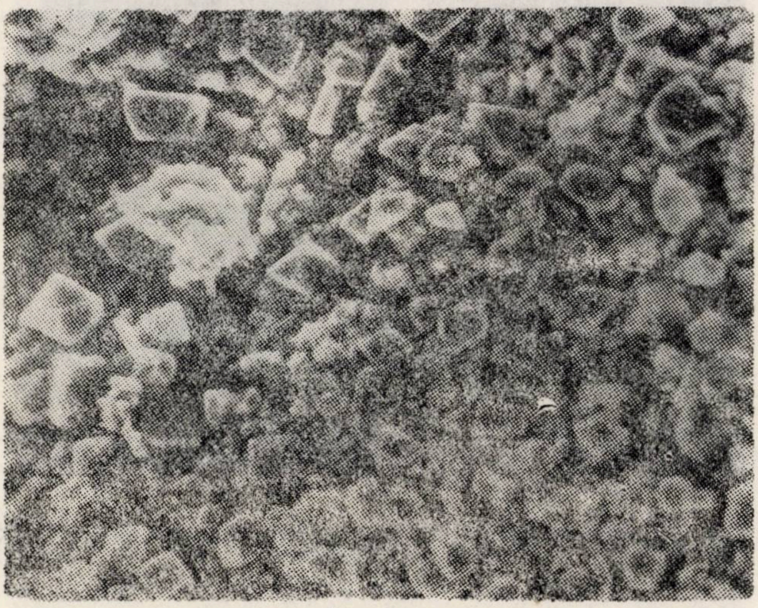

Fig. 3 a

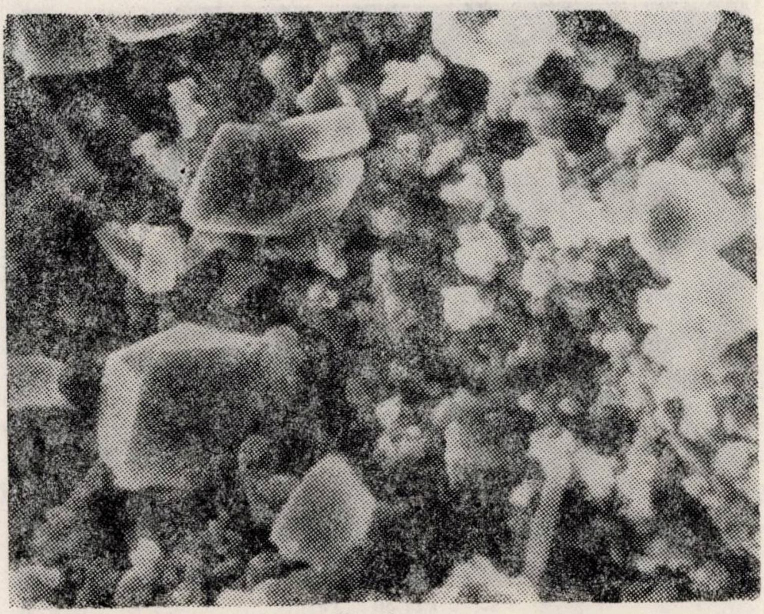

Fig.3b

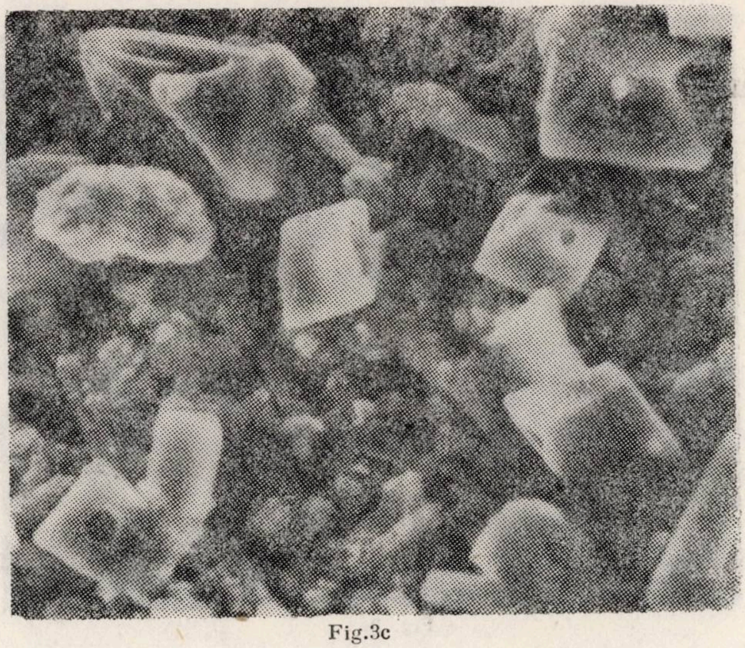

Fig.3c

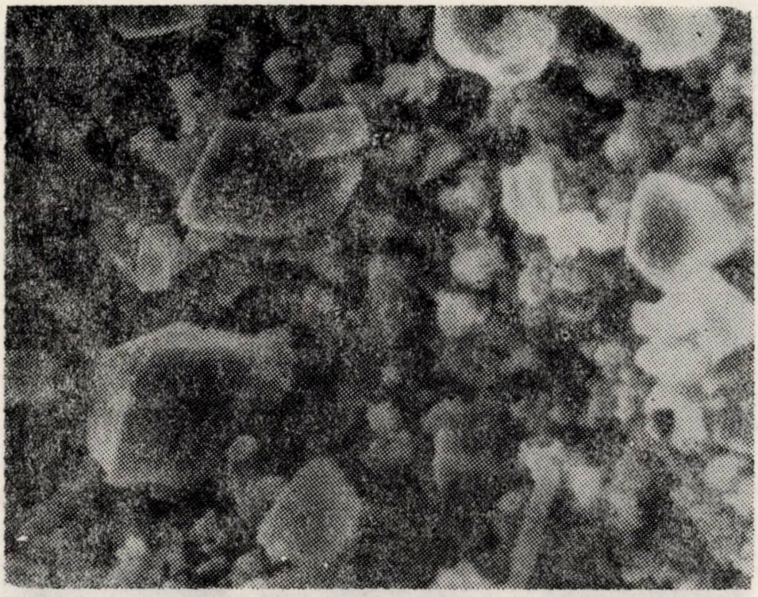

Fig.3d

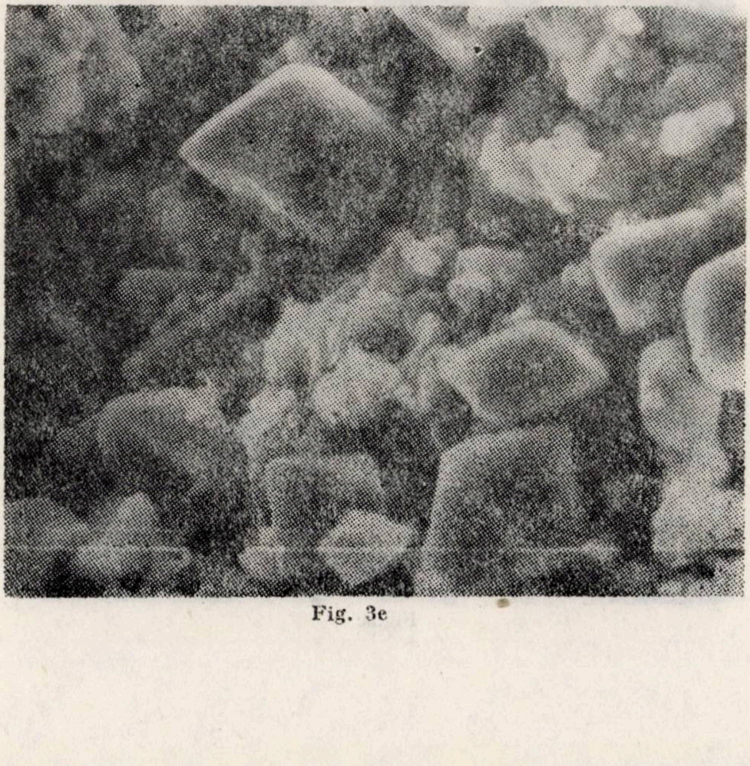

Fig. 3e

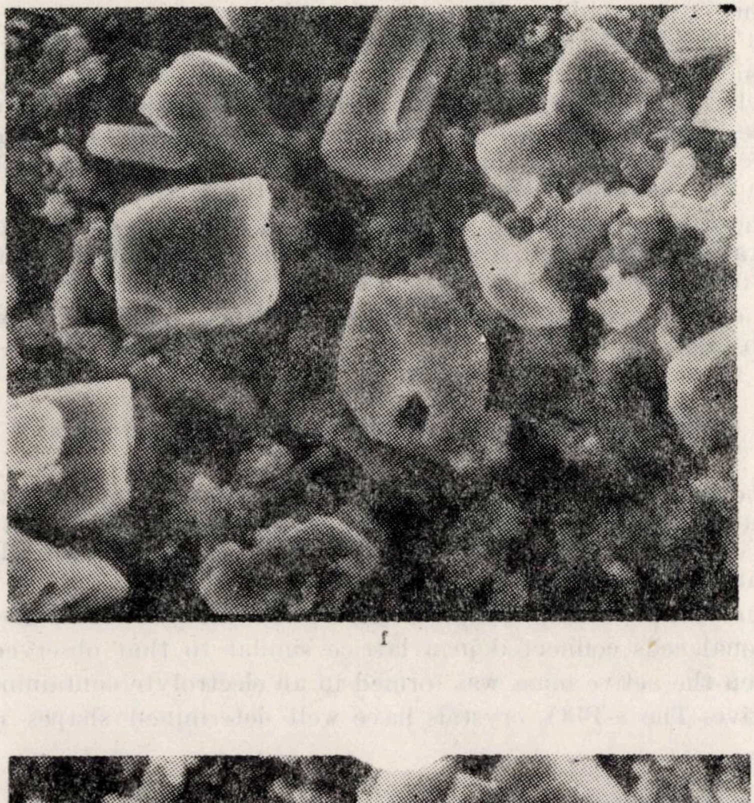
f

g

Fig. 3. — Scanning micrographs of the active positive mass formed in 1.75M H_2SO_4 with 30 mM/l $HClO_4$ as additive.

The correspondence between this slow solving of these crystals peaks ($PbSO_4$) and the shapes noticed in Figs 3d, 3e and 3f is obvious.

The mechanism of appearance of the substructural lattice is based on the change of $PbSO_4$ crystals to a preferential typical crystallographic sequence (Figs 3f and 3g) with the polyhedrical edges evolving slower than the plane areas, so that the crystal faces and the crystal bulk are first reacted, leaving behind a structure of the lattice edges.

The PbO_2 crystals are well determined, being characteristic for the perchlorate ions presence, a ratio between the two crystallographic forms closed to the optimum one (20% α PbO_2 and 80% β PbO_2).

The two crystallographic forms of PbO_2 are well determined (Figs 3b—3g).

The $KClO_4$ effect upon the formed positive plate microstructure

The insufficient formation of the positive active mass in an electrolyte containing $KClO_4$ (2 mM/l) as additive (Figs 4a—4c) leads to a peculiar pattern of PbO_2 evolving from the $PbSO_4$ structure (4c and 4d) of the active unformed mass.

The small β-PbO_2 crystals, agglomerated in bunches, give three-dimensional cells connected in a lattice similar to that observed in the case when the active mass was formed in an electrolyte containing $HClO_4$ as additive. The α-PbO_2 crystals have well determined shapes (Figs. 4c and 4e).

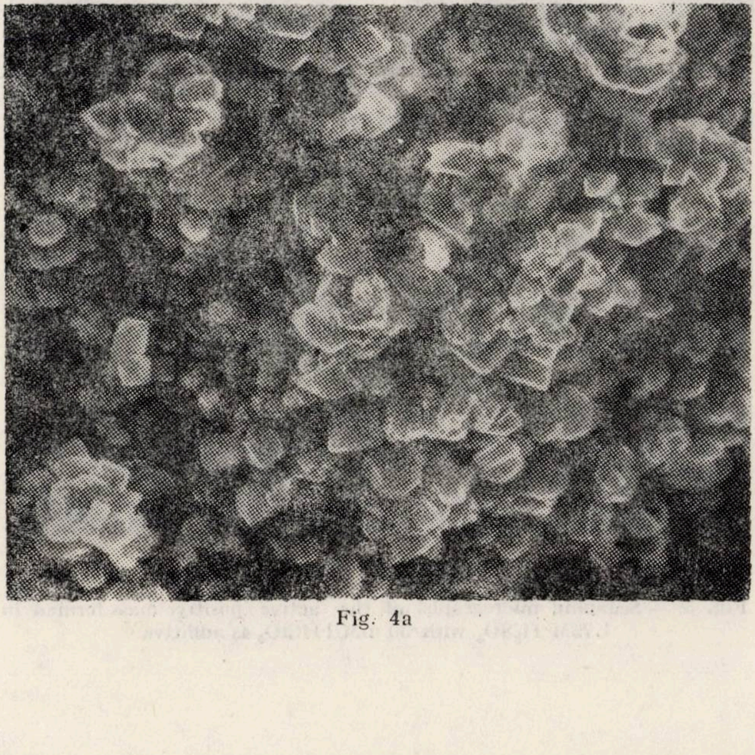

Fig. 4a

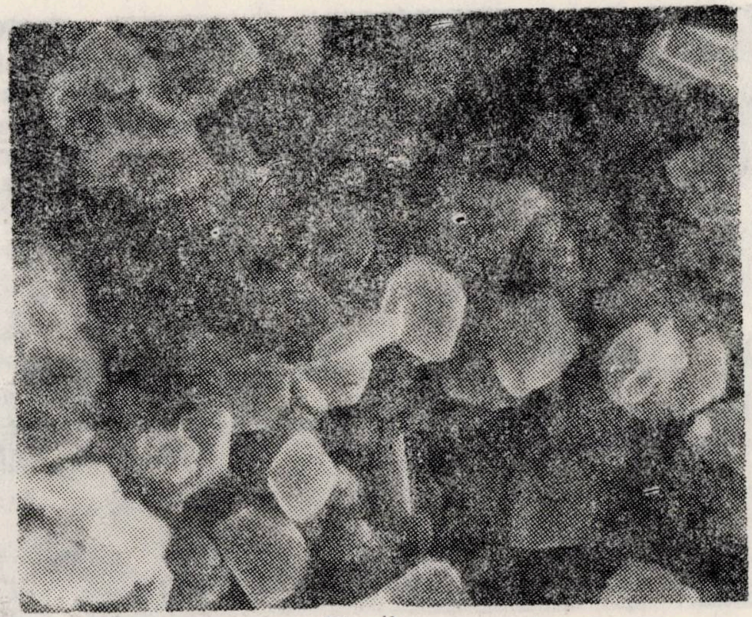

Fig. 4b

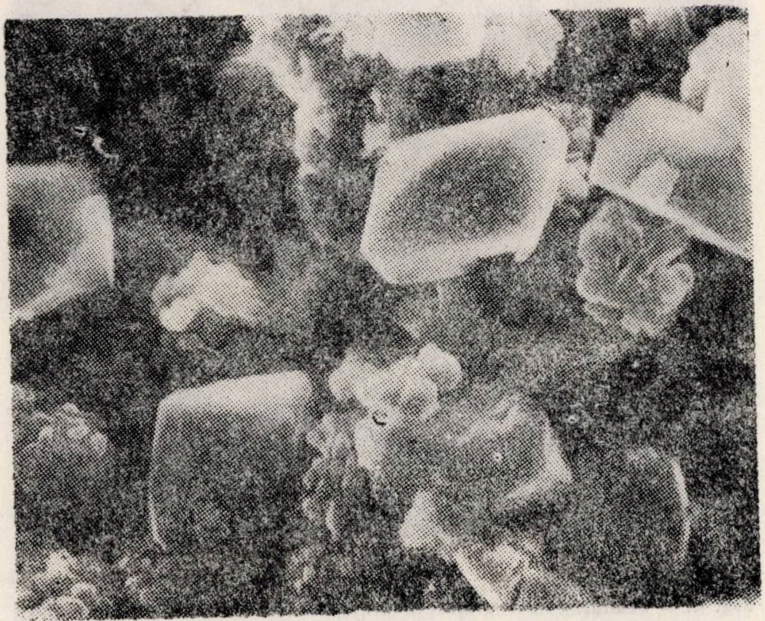

Fig. 4c

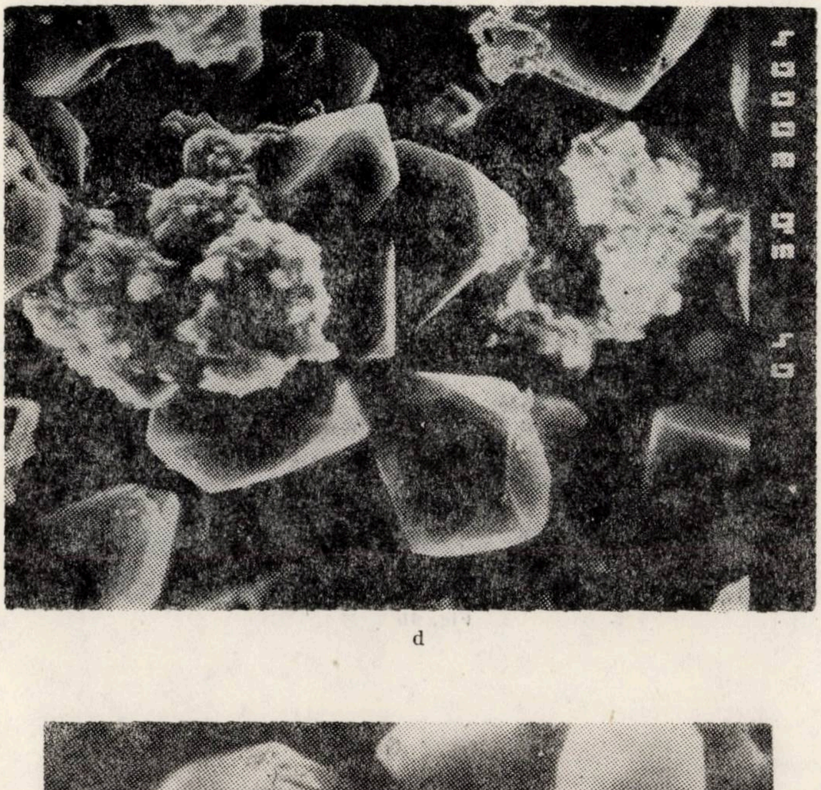

d

e

Fig. 4. — Scanning micrographs of the positive active mass formed in 1.75M H_2SO_4 with 2 mM/l $KClO_4$ as additive.

CONCLUSIONS

Perchlorate ions, present as additives in sulphuric acid solutions, used for the electroformation of the pasted plates in lead-acid batteries, have an influence upon both the chemical composition of the active masses thus obtained and on their microstructure.

It is presumed that the perchlorate ions influence especially the process of sulphates layers formation at the interface grid-active mass.

It is considered that there are ranges of perchlorate ions concentrations, when the mechanical and electrochemical properties of the active masses are improved in comparison with standard samples.

SYMBOLS LIST

mM = millimols
x = time of electroformation (hours)
y = percentage of the chemical compounds of the active positive formed mass
M = molar concentration
a_i, b_i, m, n, p = numerical constants

REFERENCES

[1] V. Pavlov, G. Papazov and V. Iliov, *J. Electrochem. Soc.*, **119**, (1), 8 (1972).
[2] C. F. Yarnell, *J. Electrochem. Soc.*, **119**, (1), 19 (1972).
[3] Burkett and Orsinoj J.U.S.Patent 2925505 – 1975.
[4] A. Mateescu, S. Sternberg, C. Dobos and E. Comănescu, *Rev. Chim.*, **34**, 732 (1983).
[5] N. Hampson and C. Lazarides, *J. Power Sources*, **23**, 181 (1981–1982).
[6] A. Mateescu, I. Toma, L. Şerbănescu and D. Mateescu, *Rev. Chim.* (under press).
[7] A. Mateescu, International Conference on Lead-Acid Batteries, LABAT-89, Abstracts, p. 38, Varna, Bulgaria, 1989.
[8] S. Sternberg, A. Mateescu, V. Brînzoi and L. Apăteanu, *Electrochimica Acta*, **32**, 349 (1987).
[9] S. Sternberg, A. Mateescu, V. Brînzoi and L. Apăteanu, 37th Meeting, International Society of Electrochemistry Vilnius, USSR, August, 1986, Extended Abstract, vol. IV, p. 249.
[0] J. Garche, H. Doring and K. Wiessener, 37th Meeting, International Society of Electrochemistry, Vilnius, USSR, August 1986, Extended Abstract, vol. IV, p. 191.
[11] A. Mateescu, Ph. D. Thesis, Polytechnic Institute, Bucharest, 1986.
[12] J. Perkins and M. T. Coyle, *J. Electrochem. Soc.*, **124**, 181 (1977).
[13] K. R. Bullock, *J. Electrochem. Soc.*, **126**, 360 (1979).
[14] I. K. Gibson and K. Peters, *J. Power Sources*, **8**, 143 (1982).
[15] D. Pavlov and V. Iliev, *J. Power Sources*, **7**, 153 (1981/1982).
[16] B. K. Mahato, *J. Electrochem. Soc.*, **124**, 365 (1977).
[17] W. J. Schlotter and C. W. Fleischmann, *J. Electrochem. Soc.*, **124**, 662 (1977).

CONCLUSIONS

Perchlorate ions, present as additives in sulphuric acid solutions, used for the electroformation of the pasted plates in lead-acid batteries, have an influence upon both the chemical composition of the active masses thus obtained and on their microstructure.

It is presumed that the perchlorate ions influence especially the process of sulphates layers formation at the interface grid-active mass.

It is considered that there are ranges of perchlorate ions concentrations, when the mechanical and electrochemical properties of the active masses are improved in comparison with standard samples.

SYMBOLS LIST

mM = millimols
x = time of electroformation (hours)
y = percentage of the chemical compounds of the active positive formed mass
M = molar concentration
a_0, b, m, n, β = numerical constants

REFERENCES

[1] V. Pavlov, G. Papazov and V. Iliev, J. Electrochem. Soc., 119, (1), 8 (1972).
[2] D. E. Yannell, J. Electrochem. Soc., 119, (1), 15 (1972).
[3] Hackett and Gutmann, U.S. Patent [illegible] (1972).
[4] A. Matescu, S. Sternberg, C. Dobos and E. Constantinescu, Rev. Chim., 34, 732 (1983).
[5] R. Hampson and C. Lazarides, J. Power Sources, 23, 181 (1981–1982).
[6] A. Matescu, I. Toma, L. Seremlescu and D. Stefanescu, Rev. Chim. (under press).
[7] A. Matescu, International Conference on Lead-Acid Batteries, LABAT-89, Abstracts, p. 85, Varna, Bulgaria, 1989.
[8] S. Sternberg, A. Matescu, V. Branzoi and L. Apateanu, Electrochimica Acta, 32, 349 (1987).
[9] S. Sternberg, A. Matescu, V. Branzoi and L. Apateanu, 37th Meeting, International Society of Electrochemistry, Vilnius, USSR, August, 1986, Extended Abstract, vol. IV, p. 295.
[10] I. Carcea, H. Doring and A. Matescu, 37th Meeting, International Society of Electrochemistry, Vilnius, USSR, August 1986, Extended Abstract, vol. IV, p. 194.
[11] A. Matescu, Ph. D. Thesis, Polytechnic Institute, Bucharest, 1989.
[12] J. Burbank and M. T. Coyle, J. Electrochem. Soc., 124, 481 (1977).
[13] K. R. Bullock, J. Electrochem. Soc., 126, 360 (1979).
[14] I. L. Gibson and K. Peters, J. Power Sources, 8, 143 (1982).
[15] D. Pavlov and N. Iordanov, J. Power Sources, 7, 153 (1981/1982).
[16] [illegible], J. Electrochem. Soc., 124, 805 (1977).
[17] W. A. Schultze and C. W. Fleischmann, J. Electrochem. Soc., 124, 932 (1977).

Revue Roumaine de Chimie, **36**, *8*, 901–906 (1991)

ATOMIC ABSORPTION SPECTROMETRIC DETERMINATION OF MANGANESE IN NATURAL WATERS AND INDUSTRIAL EFFLUENTS AFTER EXTRACTIVE SEPARATION OF ITS TERNARY COMPLEX WITH N-PHENYL-2-FUROHYDROXAMIC ACID AND TRIOCTYLMETHYLAMMONIUM CATION IN MIBK

S. A. ABBASI *

Water Quality & Environment Division,
Centre for Water Resources Development & Management,
Kunnamangalam P.O., Kozhikode 673 571
Kerala, India

Received September 5, 1988

A new, rapid and reliable method is presented for the atomic absorption spectrometric determination of manganese in waters after extractive separation from other ions as its ternary complex with N-phenyl-2-furylacrylohydroxamic acid and trioctylmethylammonium cation in methyl isobutyl ketone. The method enables determination of manganese at sub-ppb levels and was applied to the analysis of the metal in well water, lake water and industrial effluents.

INTRODUCTION

Manganese is an abundant element and though it does not occur naturally in the free state, it is a constituent of several minerals and is found at varying levels in airborne dust, natural waters, soils, plants and animals.[1,2] The average manganese concentration in the earth's crust has been estimated as 1000 ppm while sea water contains approximately 0.002 ppm of the metal. Vegetables, the germinal portions of grains, nuts, dried fruits, and tea are rich sources of manganese in food, whereas poultry, fish and shrimps are lean.[3] Manganese is an essential micronutrient for plants and animals and its deficiency in humans has been implicated with several disease states, including diabetes, nervous instability, convulsions, disorders of cartilaginous growth in infants and children, and rheumatoid arthritis.[1] Exposure to larger than trace concentration of

---

* Concurrently : Adjunct Professor, Sonoma State University, California, 94928, USA
Present Address : Professor, School of Ecology, Pondicherry Central University, No. 3, Viconte de Souillac Street, pondicherry-605 001.

manganese can be toxic ; the metal is respiratory irritant and a systematic poison when inhaled mainly as oxides in excessive amounts.[4] Processing of iron ores, in which manganese is present in significant concentrations, constitutes the major source of manganese pollution.[5] Numerous case studies on the hazards of occupational exposure to manganese have been reported.

Industrial toxicity through inhalation of manganese particulates is of two types ; the first results from acute short-term exposure and is known as manganese pneumonitis. Persons working in plants with high concentrations of manganese dust show an incidence of respiratory diseases 30 times greater than normal. The second and more serious disease results from chronic inhalation exposure to manganese dioxide, generally over a period of more than 2 years. In some cases the disease symptoms have appeared at much shorter exposure times.[6] The chronic manganese poisoning (manganism) leads to psychiatric disorders characterised by irritability, difficulty in walking, speech disturbances, and compulsive behaviour that may include running, fighting and singing. If the condition persists, a mask-like face, retropulsion or propulsion, and a Parkinson-like syndrome develop.[7] Victims of chronic manganese poisoning tend to recover slowly, even when removed from the excessive exposure.

The permissible concentration [4] of manganese in domestic water supplies is below 0.05 $mg\,l^{-1}$. The tolerance for manganese in irrigation water on a continuous use basis is 2.0 $mg\,l^{-1}$ and on a short-term use is 20 $mg\,l^{-1}$. The maximum allowable concentration of manganese in effluents discharged to a storm sewer or streams is 1.0 ppm. In a recent study on the water quality of seven borewells, monitored fortnightly for one year, Abbasi et al.[8] found manganese levels reaching a maximum of 0.17 ppm ; the metal levels in all wells were higher in summer than in the rest of the year.

It is desirable to have a rapid and accurate method for the determination of manganese in concentrations 0.05 ppm ($mg\ l^{-1}$) or lower so that the metal can be frequently monitored in drinking, industrial and irrigation waters for proper environmental management. Recently Salinas et al.[9] have proposed a method for the solvent extraction of manganese with isophthaidihydroxamic acid in toluenic Adogen 464 solution and spectrophotometric determination at 470 nm. However the method is not selective ; iron (II) and lead (II) interfer even when present in concentrations lower than manganese and a large number of anions and cations interfer when present in concentrations equal to or higher than that of manganese. The sensitivity is also low, ($>$ 100 ppb) precluding the application of the method in the environmental analysis of manganese.

In the present method manganese is rapidly and selectively determined by atomic absorption spectrometry at concentrations less than 1 ppb after extractive separation from aqueous solutions as its ternary complex with N-phenyl-2-furyl-acrylohydroxamic acid (PFHA) and tri-octylmethylammonium cation (TOMAC) in methyl isobutyl ketone (MIBK) at pH$>$ 9.5. We studied eight other hydroxamic acids, including *meta* or *para* methyl-, *meta* or *para* methoxy-, *para* chloro-, *para* bromo-, *para* iodo-, and *para* nitro- derivatives of PFHA. Of these the haloderivatives were unsuitable as they generated pungent combustion products in the AAS flame. The *methyl-*, *methoxy-* and *nitro-* derivatives were comparable to PFHA in their efficiency as extractants for manganese and in the sensitivity of the atomic absorption spectrometric determination involving their chelates, but PFHA was preferred over them as it can be prepared in significantly higher yields (~ 80%) than the other analogues.

MATERIALS AND METHODS

Reagent

PFHA and its analogues were synthesised by the general method of Tandon and Bhattacharya[10] and were purified and characterised as detailed elsewhere.[11] A standard manganese(II) solution (10^3 ppm) was prepared by dissolving 3.0764 g of $MnSO_4 \cdot H_2O$ in water containing 10 ml of hydrochloric acid and diluting to 1000 ml. This solution was standardised volumetrically.[12] All other reagents were analytical grade. Deionised double-distilled water was used throughout.

Apparatus

The atomic absorption spectrophotometric analysis was done on IL 951/551 instrument employing air-acetylene flame. The instrumental settings used are summarized in Table 1, Radiometer PHM 29 and Elico PE 132 pH meters were used for pH adjustments.

Table 1

Optimum instrumental conditions for the atomic absorption spectrometric determination of manganese

Characteristic	Setting recommended
Wavelength	279.3 nm
Lamp current	20 mA
Slit width	0.2 nm
Air flow rate	21.5 litre min^{-1}
Acetylene flow rate	2.6 litre min^{-1}
Height of light path above burner	2 cm
Rate of aspiration	5 ml min^{-1}

Procedure for the Extraction and Determination of Manganese (II)

An aliquot of sample containing 0.0015–0.015 ppm (1.5–15 ppb) of manganese was taken in a separatory funnel and the pH was adjusted to ~ 9.8 with ammonium hydroxide (8 M). To it 5 ml each of 0.05 M PFHA solution and 0.006 M TOMAC solutions, both in MIBK, were added and the contents were shaken vigorously for 10 minutes. The phases were allowed to separate and the organic layer was transferred into a glass-stoppered tube filtering by a paper moistened in ethyl acetate. The organic layer was aspirated directly into the air-acetylene flame. The atomic absorption was measured with the 279.3 nm resonance line using MIBK asa blank.

RESULTS AND DISCUSSION

Optimisation Studies on the Ion Pair Extraction of Manganese-PFHA-TOMAC ernary System

Effect of pH. The effect of pH on the extraction was investigated for a series of aqueous solutions buffered with NH_4Cl-NH_3 to various pH values. As shown in Fig. 1, Mn (II) is quantitatively extracted at pH values higher than 9.5. Extraction does not happen at pH values lower than 7.5. The extraction efficiency was calculated by application of the proposed method for manganese determination in the organic and aqueous phases after extraction.

A maximal and constant absorbance were obtained in the ammonium hydroxide concentration range from 0.05 to 0.4 M.

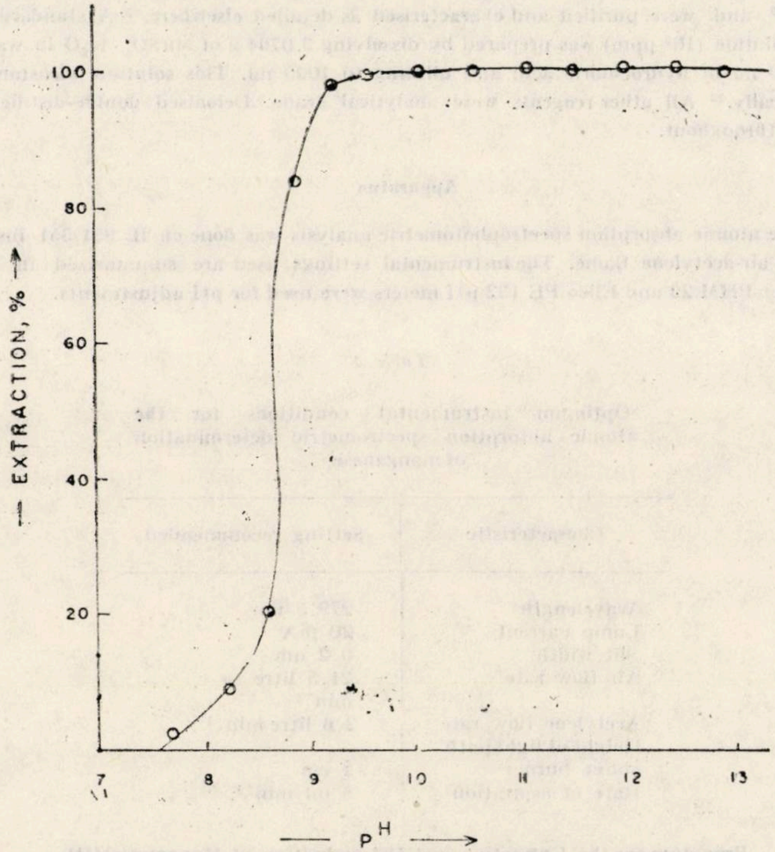

Fig. 1. — Effect of pH on the extraction of manganese by MFHA — TOMAC in methyl isobutyl ketone.

Effect of PGHA and TOMAC Concentrations. Molar excess of 50 in MFHA and 10 in TOMAC were adequate for the complete extraction of manganese. However, in the proposed method a higher molar excess is recommended because the reagents are also consumed by the interfering metal ions, and the presence of an excess of the reagents is recommended to ensure complete chelation and extraction of manganese.

Shaking time and stability. The extraction is complete after shaking for 2 minutes; however, when the extraction is carried out in the presence of high amounts of foreign ions, higher shaking times (~5 minutes) for the complete extraction of manganese are needed.

The atomic absorption of the extracted ternary manganese-MFHA—TOMAC system remains constant for at least 1 week if it is kept stoppered in a closed glass tube.

Calibration curve. Aliquots of standard solutions containing 0.20 μg of manganese (II) were diluted to 50 ml and extracted with 10 ml MFHA—TOMAC solution in MIBK as previously described. It was found that the calibration curve was linear in the range 1.5—15 ppb of manganese. The sensitivity was 0.1 ppb for 1% absorption. The coefficient of varition was 1.8% calculated from 12 replicate analyses with 6 ppb of Mn(II). The sensitivity is further enhanced by preconcentration of manganese from lean solutions through evaporation of water and manganese levels down to 0.1 ppb can be determined.

Effect of Diverse Ions

The tolerance limits of various anions and cations for the determination of 5 μg of manganese (II) within a relative error of ±1.5% are given in Table 2. The limits for iron (III), which is most frequently encountered with manganese in environment, can be further increased 1000-fold by prior extraction of the ion at pH 2 by PFHA (0.1 M) into MIBK.

DETERMINATION OF TRACE AMOUNTS OF MANGANESE IN INDUSTRIAL EFFLUENTS AND NATURAL WATERS

The present method was applied to the determination of manganese in industrial effluents and freshwaters. Manganese was determined with and without standard addition to test the reliability of the method against matrix interferences. The results (Table 2) indicate the accuracy and precision of the present method.

Table 2

Tolerance limits in the determination of 5 μg of manganese (II)

Diverse ions	Tolerance level, μg
Lithium, sodium, potassium, chloride, nitrate, sulphate, iron (III) *	>1000
Magnesium, calcium, barium, strontium, aluminium, acetate, fluoride	1000
copper (II) **, nickel (II) **, iron (II) **, cobalt (II), zinc (II), cadmium (II), mercury (II), vanadium (V) **, molybdenum (V) **, tungsten (VI), niobium (V), zirconium (VI) **, titanium (IV) **	500

* To be removed by prior extraction with MFHA at pH $\simeq 2$.

** Tolerance can be increased substantially by prior extraction at pH $\leqslant 2.5$.

Table

Analysis of manganese in natural waters and industrial effluents

Sample	Other major constituents (ppb)	Manganese added (ppb)	Manganese found (ppb)	Standard deviation
Well water	TDS (170×10^3), total hardness (65×10^3) iron (500), copper (7), zinc (4)	Nil	3.02	0.03
—do—	—do—	5.00	7.99	0.05
—do—	—do—	7.00	10.13	0.06
Lake water	TDS (65×10^3), total hardness (30×10^3), iron (350), copper (2), zinc (2)	Nil	2.95	0.04
—do—	—do—	5.00	8.01	0.05
—do—	—do—	10.00	13.02	0.07
Industrial effluent sample I *	Sodium (30×10^3), chloride (35×10^3) iron (1200), copper (900), zinc (900), cadmium (700)	Nil	150	3.1
—do—	—do—	25	176	3.7
Industrial effluent sample II *	Sodium (16×10^3), sulphate (9×10^3) chloride (5×10^3), iron (2500), nickel (2300), titanium (2300), vanadium (1900)	Nil	212	3.6
—do—	—do—	20	230	3.8

* Effluents from post-coagulation settling basins.

ACKNOWLEDGEMENTS. The author is grateful to Mr. P. P. Venkitachalam of M/s Techno Instruments for arranging to do the AAS analysis. Thanks are also due to the authorities of IIT Bombay, BITS Pilani and CWRDM Kozhikode for facilities.

REFERENCES

[1] E. Berman, "Toxic Metals and Their Analysis", Heyden, London, 1980, p. 221.

[2] R. J. Boila, T. J. Devlin, R. A. Drysdale and Lillie, *Canadian J. Anim. Sci.*, **65**, 861 (1985).

[3] E. J. Underwood, "Trace Elements in Human and Animal Nutrition", (3rd Ed), New York, Academic Press, 1978 ; p. 177.

[4] M. Sittig, "Toxic Metals : Pollution Control and Worker Protection", Noyes Data Corporation, New Jersey, 1976 ; p. 33.

[5] A. J. Goldberg, "A Survey of Emissions and Controls for Hazardous and other Pollutants", US Environmental Protection Agency, Washington, 1973.

[6] American Industrial Hygiene Association, "Manganese and its Inorganic Compounds", Hygienic Guide, American Industrial Hygiene Association, 1963.

[7] I. Mena, K. Horivchi, K. Burke and G. C. Lotzias, *Neurology*, **19**, 1000 (1969).

[8] S. A. Abbasi, R. Soni, K. Madhavan, V. Baji, K. Rehina, C. Radhakumari and K. V. M. Kunhi, Annual Review of Studies on Water Quality, Sediments and Aquatic Organisms in Kuttiadi Basin, Technical Report, CWRDM, Kozhikode ; 1987.

[9] F. Salinas, M. Jimenez-Arrabal and M. C. Mahedero, *Anal. Lett.*, **16**, 1449 (1983).

[10] S. G. Tandon and S. C. Bhattacharyya, *Anal. Chem.*, **33**, 1267 (1961).

[11] S. A. Abbasi, *Polish J. Chem.*, in press.

[12] A. I. Vogel, A Text Book of Quantitative Inorganic Analysis, (4th Ed), Longman, London and New York, 1978, p. 159.

Revue Roumaine de Chimie, **36**, *8*, 907–915 (1991)

Dedicated to Professor PETRU SPACU on the occasion of his 85th anniversary

FLOW-VACUUM PYROLYSIS OF DIBENZO[*c, g*] TRICYCLO[4.2.2.$0^{2,5}$]-DECA-3,7,9-TRIENE (*syn*-DIBENZO[*c, g*] NENITZESCU'S HYDROCARBON) AND OF TRIBENZO[*c, g, j*]TRICYCLO[4.2.2.$0^{2,5}$]DECA-3,7,9-TRIENE (TRIBENZO-NENITZESCU'S HYDROCARBON)

MIRCEA D. BANCIU[a], MIRCEA POP[b], AURICA PETRIDE[b] and MICHAELA DINA STĂNESCU[a]

[a] Organic Chemistry Department, Polytechnic Institute TCH, Splaiul Independentei 313, 76206 — Bucharest, Roumania

[b] Centre of Organic Chemistry, Roumanian Academy, Splaiul Independentei 202B, Bucharest, Roumania

Received February 15, 1991

Retro-diene reactions are the favoured pathways in the flow-vacuum pyrolysis of both title hydrocarbons 6 and 7. The main reactions products in the pyrolysis of 6 are : the angular dimer 17 of benzocyclobutene (Cava's dimer), naphthalene, dibenzo[*a, e*]cyclooctene and benzo[*a*]biphenylene. From the pyrolysis products of 7, anthracene, Cava's dimer 17 and dibenzo[*a, e*]cyclooctene were identified. The reaction mechanisms are discussed and a comparison with pyrolyses of related Nenitzescu's hydrocarbons is presented.

INTRODUCTION

Tricyclo[4.2.2.$0^{2,5}$]deca-3-7,9-triene (**1**) was synthesized in 1960 by Nenitzescu, Avram and Sliam.[1] This hydrocarbon, which was the first valence isomer of an annulene (corresponding to a non-separable graph) * was named — after Doering's proposal [2] — "Nenitzescu's hydrocarbon".

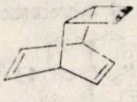

1

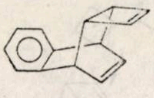

2

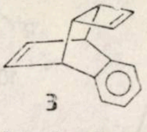

3

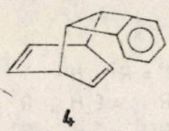

4

It is now well known [3] that this hydrocarbon played an important role in the development of the chemistry of valence isomers of annulenes and especially of $(CH)_{10}$ valence isomers. As in other related domains, the study of benzoannelated derivatives greatly contributed to the understanding of chemistry of the parent compounds. Thus, all the three possible benzo-Nenitzescu's hydrocarbons **2**,[4] **3**[5] and **4**[6] are now known. From the three possible dibenzo derivatives of **1** the isomers **5**[7] and **6**[8] were described by Nenitzescu and co-workers in 1966 and 1974 respectively. The unique tribenzo-Nenitzescu's hydrocarbon **7** was synthesized in 1963 by Cava.[9]

---

* Dihydroheptafulvalene or bitropyl, $(CH)_{14}$, the first valence-isomeric-annulenic hydrocarbon corresponding to a separable graph, was described in 1957 by Doering and Knox (*J. Amer. Chem. Soc.*, **79**, 352 (1957).

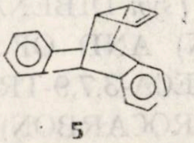
5

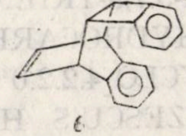
6

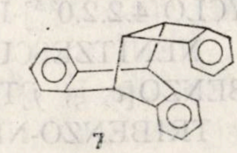
7

Pyrolysis of Nenitzescu's hydrocarbon **1** was first investigated[10] in the aim of obtaining cyclobutadiene. However, only traces of benzene (the product which should appear together with cyclobutadiene in a retrodiene reaction) were observed in the pyrolysis of **1** along with various other products. In spite of this discouraging result the pyrolyses of Nenitzescu's hydrocarbon **1** and of its benzo derivatives **2** and **3** as well as of the dibenzoderivative **5** were subsequently the object of numerous investigations, often accompanied by controversial mechanistic proposals. A review published in 1976[11] discussed all data available until then drawing the following essential conclusions :

— the mechanism for the pyrolysis of the parent compound **1** resulted as an extension of the mechanism proposed for *anti*-benzo-Nenitzescu's hydrocarbon **2** (with simpler product distribution) which could be easily rationalized.

— three different reaction pathways (Scheme 1) are generally available to the investigated hydrocarbons : (a) a Cope rearrangement,

Scheme 1

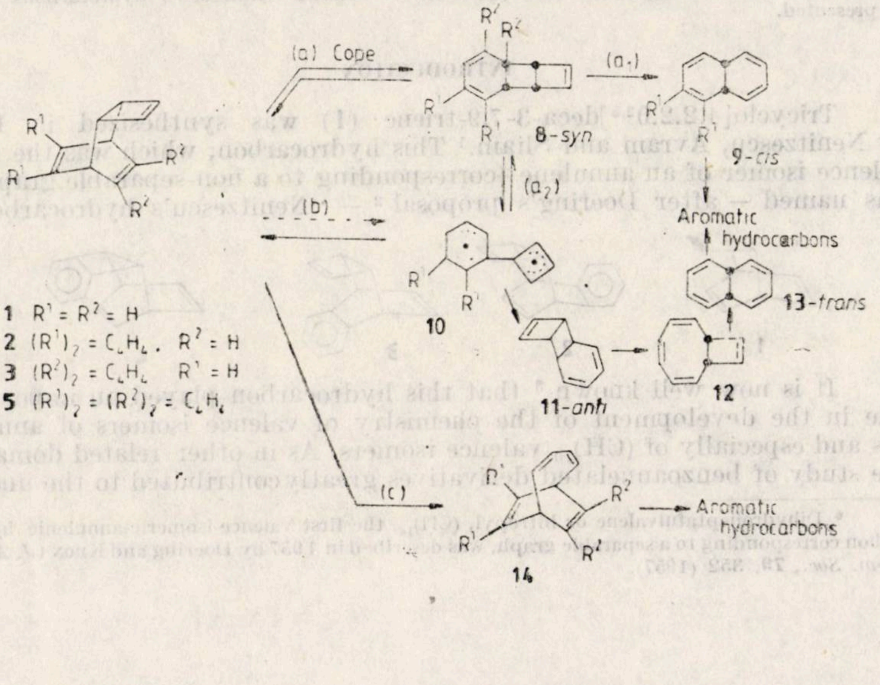

(b) a diradicalic mechanism and (c) a symmetry-forbidden cyclobutene ring opening. All these initial steps are usually followed by secondary reactions affording more stable compounds (dihydroaromatic or aromatic hydrocarbons).

— hydrocarbon **1** affords preferrentially the Cope product **8** (R^1, $R^2 = H$) which reacts further either by cyclobutene ring opening (a_1) to *cis*- dihydronaphthalene **9** ($R^1 = H$) or by a radicalic fission (a_2) conducting to **10** ($R^1 = H$); from **10** the *trans*-dihydronaphthalene **13** appears *via* **11** (*anti*) and **12**. Final stabilization of **9** and **13** gives rise to aromatic hydrocarbons (naphthalene, *cis*-phenylbutadiene, etc.).

— hydrocarbon **2** reacts also mainly *via* the Cope path (*a*) affording a product of the type **8** as precursor of dihydrophenanthrene **9**; $(R^1)_2 = C_4H_4$ and phenanthrene. A minor path (*c*) conducts from **2** to **14**, $(R^1)_2 = C_4H_4$; $R^2 = H$.

— diradicalic species of the type **10** are included in the observed minor thermal conversion of **2** into **3** (the actual steps being **2** → **8** → → **10** → **3**).

— the single available pathway for **3** and **5** seems to be the route (*c*) (Scheme 1) leading to butadiene-bridged hydrocarbons of the type **14**, which constitute in their turn, in these cases, the unique intermediates in the formation of aromatic hydrocarbons (phenanthrene and benzo[*a*]anthracene respectively). The temperatures needed by this reaction path are significantly higher than those of the Cope rearrangement. Thus at 380° the *syn*-benzo-hydrocarbon **3** was converted only 56% whereas at 370° *anti*-benzo hydrocarbon **2** was converted 98%; on the other hand the dibenzo-hydrocarbon **5** begins to react at about 450° and disappears at 600° among the reaction products.

— different reaction intermediates, e.g. **8** (R^1; $R^2 = H$) intuitively proposed by Nenitzescu,[10] before the enunciation of orbital symmetry selection rules, are now generally accepted.

On the other hand, pyrolysis of benzohydrocarbon **4**, described briefly in 1979[6] affords at 350°C benzene and the angular benzo-cyclobutene dimer **17** (Cava's dimer); benzo[*a*]biphenylene was also mentioned as a by-product.

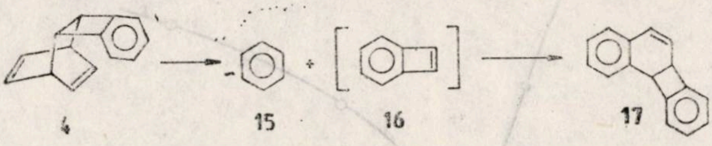

4 **15** **16** **17**

On the basis of these contrasting results obtained in the pyrolyses of **1** and **2**, of **3** and **5**, and of **4** respectively, it seemed interesting to study also the thermal behaviour of the yet uninvestigated dibenzo-Nenitzescu's hydrocarbon **6** and tribenzo-Nenitzescu's hydrocarbon **7**. The results obtained in pyrolyses of **6** and **7** are presented in this work.

RESULTS AND DISCUSSION

syn-Dibenzo[*c*, *g*] Nenitzescu's hydrocarbon (**6**) was obtained after the described procedure[8] starting from Nenitzescu's linear dimer **18** of benzocyclobutene, which reacts in its valence isomeric form **19** with fumaryl chloride to afford the adduct **20a** ; the corresponding acid **20c** is oxidatively decarboxylated to **6**.

Tribenzo-Nenitzescu's hydrocarbon **7** was prepared according to Cava [9] from anthracene and benzocyclobutene **16** (generated *in situ* from dibromobenzocyclobutane).

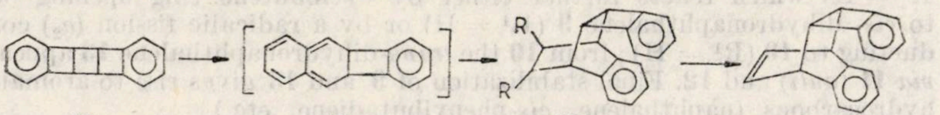

18 **19** **20** **6**

a : R = COCl
b : R = $COOCH_3$
c : R = COOH

The flow-vacuum pyrolyses of **6** were performed under an argon stream in an electrically heated quartz tube filled with quartz chips. The reaction temperature was varied between 350° and 650°C. The crude pyrbolysis mixtures were analyzed by v.p.c. The main products (identified by v.p.c. comparison with authentic samples on three different columns as well as from their ^{1}H-NMR signals) were : naphthalene **21**, the angular dimer **17** of benzocyclobutene (Cava's dimer), dibenzo[*a*, *e*] cyclooctene (**24**) and benzo[*a*]biphenylene (**30**). Small amounts of benzo[*a*]anthracene (**28**) and chrysene (**29**) were also identified in the pyrolysis mixture. The results obtained in pyrolyses of **6** performed at different temperatures are presented graphically in Fig. 1.

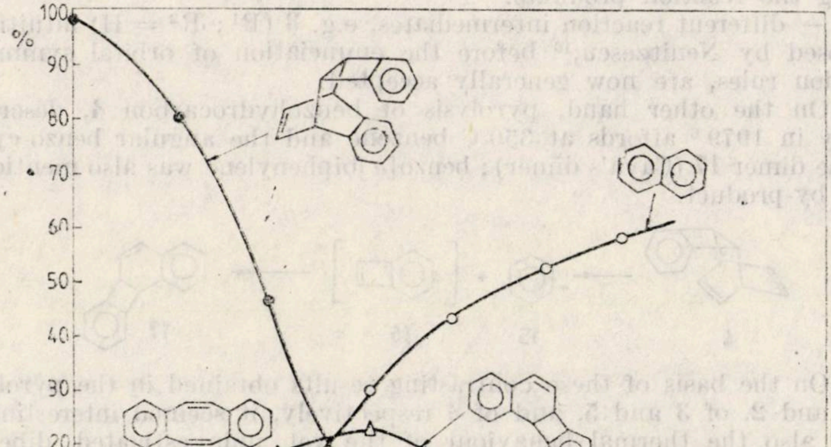

Fig. 1. — Product distribution in the flow-vacuum pyrolysis of dibenzo-Nenitzescu's hydrocarbon **6**.

The experimental results led to the following conclusions:

(a) two distinct domains may be delineated in Fig. 1, the former corresponding to temperatures between 350° and 500°C and the latter to temperatures above 500°C. The first domain is associated mainly to primary thermal reactions of **6** whereas the second domain corresponds to secondary reactions of the initially formed products (between 500° and 650°C, the starting hydrocarbon **6** practically disappears among the reaction products).

(b) the curves corresponding to Cava's dimer **17** and naphthalene (Fig. 1) run initially approximately parallel, the former being greatly surpassed by the latter at temperatures higher than 475°.

(c) dibenzo[*a*, *e*]cyclooctene indicates a plain curve (Fig. 1) situated always under 10% of the reaction mixtures.

(d) benzo[*a*]biphenylene (**30**) appears in crude pyrolysates of **6** above 500° and increases steadily towards higher temperatures.

(e) the amounts of benzo[*a*]anthracene and chrysene are low (0.5% at 400° and 6% at 650°); consequently these components were not included in fig. 1.

From the above data it results clearly that the preferred reaction path in the pyrolysis of **6** up to 475° (Scheme 2) is the retro-dienic fission (a thermally allowed cycloreversion), leading to benzocyclobutene **21** and naphthalene **22** (Scheme 2). Due to the known [3] instability of benzocyclobutene **21**, the corresponding isolable product is the well-known Cava's dimer **17**.[12] As it is now established,[12,13] the intermediate of this dimerization is the unstable polycyclic hydrocarbon **23** formed by a diene reaction; subsequent cyclobutene ring opening in **23** affords the stable dimer **17**.

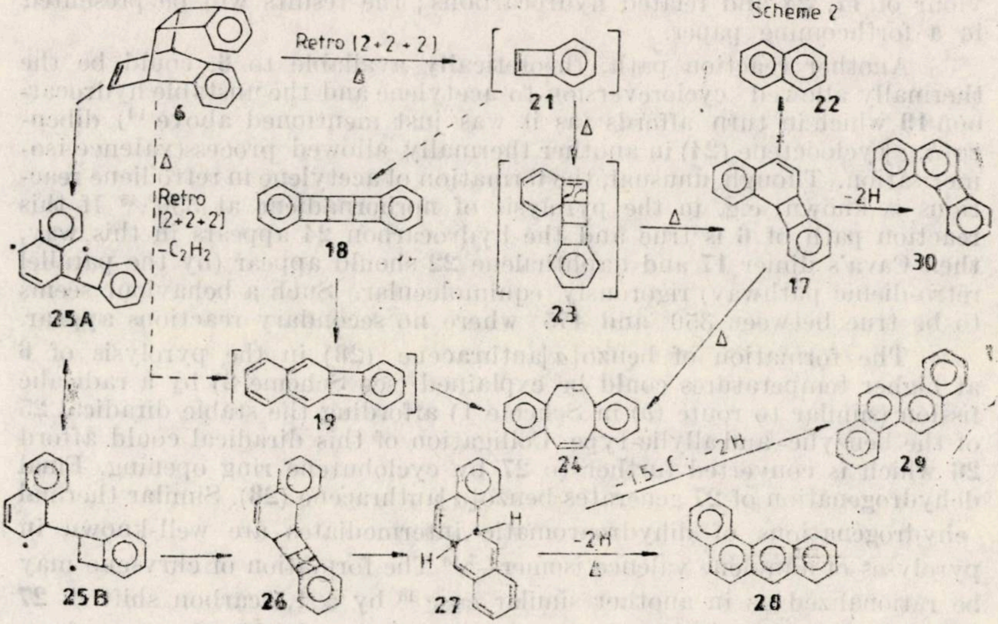
Scheme 2

In the above retro-diene reaction of **6** the products **21** and **22** should appear in equimolecular amounts. However, as the data from Fig. 1 show, above 475° the quantities of naphthalene are much greater than those of Cava's dimer of **21**. One explanation for the observed distribution of products could be a partial conversion of **17** into naphthalene occurring mainly at higher temperatures. This possibility was ruled out by control experiments in which samples of authentic Cava's dimer **17** were flow-pyrolysed at 600° and 650° in the same apparatus and conditions used for **6** and no naphthalene could be evidenced among the reaction products. Another explanation could be a partial conversion of benzocyclobutene **21**, or of its dimer **17**, into dibenzo[*a*, *e*]cyclooctene (**24**). An indication in this sense comes out from Fig. 1 where above 500° the decrease of **17** is accompanied by an increase of **24** (up to 570°). Only speculations may be made now concerning the conversion of the unstable **21** to **24**; an attractive intermediate could be the linear Nenitzescu's dimer **18** of benzocyclobutene which is known [9,14] to isomerize easily at its melting point (133°) into **24** *via* **19**. However, the formation of **18** from **21** could proceed thermally only by a non-concerted diradicalic mechanism but such a mechanism cannot be ruled out at temperatures above 450° used in this work.

On the other hand, the thermal conversion of **17** into **24** (Scheme 2) seems to be also an interesting transformation which was not described in the literature. A control experiment in which the pure **17** was flow-pyrolysed at 550° (in the conditions used for **6**) afforded important quantities of dibenzo[*a*, *e*]cyclooctene (about 28%). Due to the special interest of this observation in the context of the interconversions of dibenzo $(CH)_8$ hydrocarbons we undertook a more detailed study of the thermal behaviour of **17**, **24** and related hydrocarbons; the results will be presented in a forthcoming paper.

Another reaction path, theoretically available to **6**, could be the thermally allowed cycloreversion to acetylene and the unstable hydrocarbon **19** which in turn affords (as it was just mentioned above [14]) dibenzo[*a*, *e*]cyclooctene (**24**) in another thermally allowed process(valence isomerisation. Though unusual, the formation of acetylene in retrodiene reactions is known, e.g. in the pyrolysis of norbornadiene at 350°.[15] If this reaction path of **6** is true and the hydrocarbon **24** appears in this way, then Cava's dimer **17** and naphthalene **22** should appear (by the parallel retro-dienic pathway) rigorously equimolecular. Such a behaviour seems to be true between 350° and 475° where no secondary reactions appear.

The formation of benzo[*a*]anthracene (**28**) in the pyrolysis of **6** at higher temperatures could be explained (see Scheme 2) by a radicalic fission (similar to route (*b*) in Scheme 1) affording the stable diradical **25** of the benzylic- and allylic-type. Colligation of this diradical could afford **26** which is converted further to **27** by cyclobutene ring opening. Final dehydrogenation of **27** generates benzo[*a*]anthracene (**28**). Similar thermal ehydrogenations of dihydroaromatic intermediates are well-known in pyrolyses of annulene valence isomers.[3,16] The formation of chrysene may be rationalized as in another similar case [16] by a 1,5-carbon shift in **27** followed by aromatization. A thermal loss of two hydrogen atoms from

17 (a process which is favoured at higher temperatures) affords benzo[*a*]biphenylene (**30**).

The above data show that the thermal behaviour of **6** resembles well that of monobenzo-Nenitzescu's hydrocarbon **4** and strengthen the conclusion that Nenitzescu's hydrocarbons possessing a benzo-fused cyclobutenic ring afford mainly retro-dienic fission. A confirmation of this conclusion comes out from the flow-pyrolyses of tribenzo-Nenitzescu's hydrocarbon **7**. At 500° the conversion of **7** (in the conditions used for **6**) is 40%, at 550° is 70% and at 600° is 97%. The identified reaction products are : anthracene (**31**), Cava's dimer **17** and dibenzo[*a*, *e*]cyclooctene (**24**).

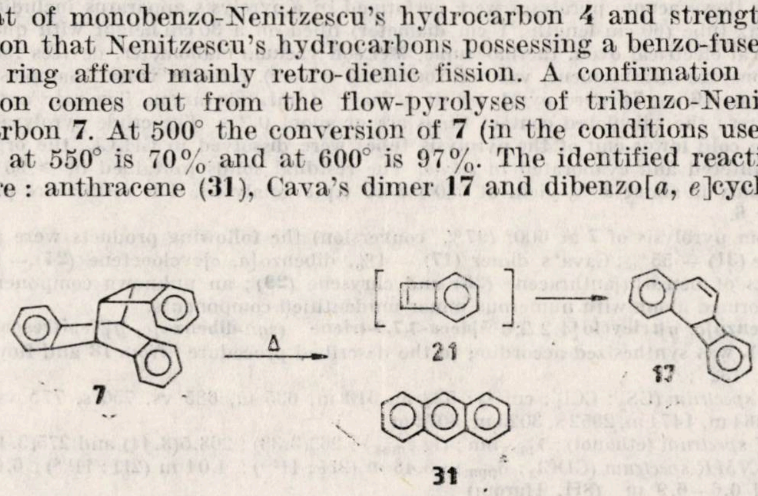

In conclusion, this work completes the mechanistic picture for pyrolyses of benzo-Nenitzescu's hydrocarbons allowing the assessment of the following three different behaviours : i) when a Cope rearrangement is possible (as for **1** and **2**) this is the preferred reaction path ; ii) when the Cope rearrangement is inoperative and the cyclobutene ring is not benzo-annelated (as in **3** and **5**) a symmetry-forbidden cyclobutene ring opening to butadiene-bridged compounds is preferred (at higher temperatures than Cope rearrangement) ; iii) when a Cope rearrangement is inoperative but the cyclobutene ring is benzoannelated (as in **4**, **6** and **7**) the retro-diene rearrangement appears (at temperatures higher than those for the Cope reaction but lower than those for the cyclobutene ring opening). Thus the retro-diene reaction searched by Nenitzescu [10] in the case of the parent hydrocarbon **1** seems to be rendered visible only in the cases when the cyclobutenic ring is benzoannelated (cyclobutadiene being much less stable than **21**).

EXPERIMENTAL

Melting points are uncorrected. IR spectra were registered with an UR-20 C. Zeiss-Jena double beam spectrophotometer, UV-VIS spectra with a SPECORD-UV/VIS spectrophotometer and ^{1}H-NMR spectra with a VARIAN-A60-A spectrometer using TMS as internal standard.

The v.p.c.-analyses were performed on a FRACTOVAP-2450 C. Erba apparatus using capillary glass columns and FID detector. For pyrolysates of dibenzo-Nenitzescu's hydrocarbon **6** the following three columns were used in order to corroborate the results : a) SE-30-methyl silicone polymer ; 25 m length ; 0.2 mm internal diameter ; temperature program from 100° to 280° with 10°/min heating rate ; carrier gas : hydrogen ; flow-rate 1 mL/min ; b) APIEZON L ; 30 m length ; 0.2 mm internal diameter ; temperature program from 100° to 270 ° with 10°/min heating rate ; carrier gas : hydrogen ; flow-rate 1 mL/min ; c) SP-1000-polyethyleneglycol ; 25 m length ; 0.2 mm internal diameter ; temperature program from 100° to 230° with 15°/min heating rate ; carrier gas : hydrogen ; flow-rate 1 mL/min. For pyrolysates of tribenzo-Nenitzescu's hydrocarbon **7** a SE 30 column with 25 m length and 0.2 mm internal diameter was used with temperature program from 100° to 160° with 7°/min and from 160° to 280° with 12°/min. heating rates ; carrier gas : hydrogen with 1 mL/min flow-rate.

The flow-vacuum pyrolyses were performed in a pyrolysis apparatus including : a vertical quartz tube (60 cm length ; 1 cm diameter) filled on a 30 cm height with quartz chips, a cylindrical electrical oven, thermocouple, McLeod vacuum manometer, devices for inert gas (argon) flow-rate measurement, vacuum source ($\leqslant$ 1 Torr), receiver vessel. Samples of 30 mg hydrocarbons (**6** or **7**) were pyrolysed at 1 Torr ; 4 mL/min argon flow-rate and different temperatures ; the calculated contact times are of about 0.2 s. The crude pyrolysates (solidified at the cold lower end of the pyrolysis tube) were dissolved in CH_2Cl_2, the organic solution was filtered and evaporated *in vacuo*. The residual solids (obtained in $\geqslant$ 95 % yield at 350° and only in about 80 % yield at 650°) were v.p.c.-analysed. The results are presented in Fig. 1 for **6**.

From pyrolysis of **7** at 600° (97 % conversion) the following products were identified : anthracene (**31**) — 55 % ; Cava's dimer (**17**) — 4 %, dibenzo[*a*, *e*]cyclooctene (**24**) — 2 %, along with traces of benzo[*a*]anthracene (**28**) and chrysene (**29**) ; an unknown component of 17 % was also formed along with numerous minor unidentified components.

Dibenzo[*c*, *g*]tricyclo[4.2.2.0^{2,5}]deca-3,7,9-triene (*syn*-**dibenzo[*c*, *g*]Nenitzescu's hydrocarbon) (6)**, was synthesized according to the described procedure [8] from **18** and fumaryl chloride ; m.p. 132° ;

IR spectrum (CS_2 ; CCl_4 ; cm^{-1}) : 522 m, 610 m, 635 m, 685 vs, 750 s, 775 vs, 1194 m, 1334 m, 1464 m, 1474 m, 2952 s, 3025 m, 3072 m

UV spectrum (ethanol) ; λ_{max}nm ; (lg ε_{max}) : 263(3.33) ; 268.5(3.44) and 275(3.41)

^{1}H-NMR spectrum ($CDCl_3$; δ_{ppm}) : 3.48 m (2H ; $H^{2,5}$) ; 4.04 m (2H ; $H^{1,6}$) ; 6.64 m (2H ; $H^{9,10}$) and 6.6—6.9 m (8H, Harom)

Tribenzo[*c*, *g*, *j*]tricyclo[4.2.2.0^{2,5}]deca-3,7,9-triene (tribenzo-Nenitzescu's hydrocarbon) (7) was prepared after Cava's procedure [9] from anthracene and benzocyclobutene (generated *in situ* from dibromobenzocyclobutane and zinc in dimethylformamide at reflux) m.p. 163°.

IR spectrum (CS_2 ; CCl_4 ; cm^{-1}) : 556 m, 575 m, 755 s, 785 m, 1461 m, 2937 m, 3022 w, 3070 w.

UV-spectrum (Methanol) : λ_{max} nm (lg ε_{max}) : 220 (4.03) ; 268(3.58) ; 275(3.61).

^{1}H-NMR spectrum ($CDCl_3$: δ_{ppm}) : 3.7 m (2H ; H^2, H^5) ; 4.55 m (2H ; H^1 ; H^6) and 6.75—7.5 m ($12H_{arom}$).

Dibenzo[*a*, *e*]cyclooctene (24) was obtained as previously described,[14] m.p. 108°C ; IR- and UV-spectra were identical to the described ones.[17]

^{1}H—NMR spectrum ($CDCl_3$; δ_{ppm}) : 6.75s(4Hvinylic) ; 7.0—7.2m($8H_{arom}$).

6a, 10b-Dihydro-benzo[*a*]biphenylene (**17**) was obtained after the procedure of Cava ;[12] m.p. 74° ;

IR spectrum (CS_2 ; CCl_4 ; cm^{-1}) : 595 m, 605 m, 705 m, 720 m, 735 s, 765 s, 775 m, 1454 m, 1494 w, 2904 m, 3030 m, 3070 m.

UV spectrum (ethanol) λ_{max} nm ; (lg ε_{max}) : 215 (4.50) ; 266 (3.96) and 273 (3.93).

^{1}H—NMR spectrum (CCl_4/d -acetone ; δ_{ppm}) : 4.2—4.5 m (1H ; H^{6a}) : 4.82d (1H ; H^{10b} ; J = 6 Hz) ; 6.12 m (1H ; H^6) ; 6.2 m (1H ; H^5) ; 6.9—7.5 m ($8H_{arom}$).

Benzo[*a*]biphenylene (30) was obtained from **17** similarly to Cava and Napier [12] but using dicyano-dichloro-*p*-benzoquinone (DDQ) as dehydrogenating agent (3 hrs reflux in benzene, followed by column chromatography on silica. The IR and UV-VIS spectra were identical to the described ones.[18]

ACKNOWLEDGEMENTS. This work was financially supported by the Ministery of Education and Science.

The ^{1}H-NMR spectra were performed by Dr. F. Chiraleu to whom our thanks are due.

REFERENCES

M. Avram, E. Sliam and C. D. Nenitzescu, *Liebigs Annal. Chem.*, **636**, 184 (1960).

[2] W. v. E. Doering and J. W. Rosenthal, *J. Amer. Chem. Soc.*, **88**, 2078 (1966).

[3] A. T. Balaban, M. Banciu and V. Ciorba, "Annulenes, -Benzo, -Hetero, -Homoderivatives and Their Valence Isomers", CRC-Press, Boca Raton, Fla., 1987, vol. II, p. 1.

[4] E. Vedejs and R. A. Shepherd, *Tetrahedron Letters*, **1970**, 1863.

[5] I. Murata, Y. Sugihara and N. Ueda, *Tetrahedron Letters*, **1973**, 1183.

[6] L. Enescu, I. Dinulescu and M. Avram, *Rev. Roumaine Chim.*, **24**, 995 (1979).

[7] M. Avram, I. G. Dinulescu and C. D. Nenitzescu, *Liebigs. Annal. Chem.*, **691**, 9 (1966).

[8] I. G. Dinulescu, M. Pop, F. Chiraleu, M. Avram and C. D. Nenitzescu, *Rev. Roumaine Chim.*, **19**, 1197 (1974).

[9] M. P. Cava and R. Pohlke, *J. Org. Chem.*, **28**, 1012 (1963).

[10] C. D. Nenitzescu, M. Avram, I. Pogany, G. Mateescu and M. Farcașiu, *Stud. Cerc. chim. Acad. R.P.R.*, **11**, 7 (1963).

[11] M. Banciu, *Rev. Roumaine Chim.*, **21**, 1083 (1976).

[12] M. P. Cava and D. R. Napier, *J. Amer. Chem. Soc.*, **79**, 1701 (1957).

[13] M. P. Cava and D. R. Napier, *J. Amer. Chem. Soc.*, **80**, 2255 (1958); M. P. Cava and J. F. Stucker, *J. Amer. Chem. Soc.*, **79**, 1706 (1957).

[14] M. Avram, D. Dinu and C. D. Nenitzescu, *Chem. Ind. (London)*, **1959**, 257; M. Avram, D. Dinu, G. Mateescu and C. D. Nenitzescu, *Chem. Ber.*, **93**, 1789 (1960); M. Avram, I. G. Dinulescu, D. Dinu, G. Mateescu and C. D. Nenitzescu, *Tetrahedron*, **19**, 309 (1963).

[15] J. H. Birey and J. P. Chesick, *J. Phys. Chem.*, **66**, 568 (1962).

[16] M. Elian, M. Banciu, L. Stănescu and E. Ciorănescu, *Rev. Roumaine Chim.*, **21**, 89 (1976).

[17] C. E. Griffin and J. A. Peters, *J. Org. Chem.*, **28**, 1715 (1963).

[18] M. P. Cava and J. F. Stucker, *J. Amer. Chem. Soc.*, **77**, 6022 (1955).

Revue Roumaine de Chimie, **36**, *8*, 917–923 (1991)

Dedicated to Professor PETRU SPACU on the occasion of his 85th anniversary

NEW CONVENIENT METHODS FOR THE SYNTHESIS OF 1,2-DIHYDRO-3*H*-INDAZOL-3-ONE AND ITS 1-ACYL DERIVATIVES

FLOREA DUMITRAŞCU, MARIETA PLĂVEŢI and DAN RĂILEANU
Organic Chemistry Center-ICECHIM, Spl. Independenţei 202 B. 78100 Bucharest,
Romania

Received June 7, 1989

The acid hydrolysis of the readily obtainable 3-(*o*-carboxyphenyl)sydnones (**6a**–**d**) afforded 3-indazolones (**3a**-**d**) in yields over 90%. By transacylation between 1-acyl-3-acyloxyindazoles (**11a**–**d**) and 3-indazolones (**3a**, **e**), the corresponding 1-acyl-3-indazolones **10a**–**d** resulted in pure state and yields also over 90%.

The historical synthesis of indazolone (**3a**) described by E. Fischer [1] and improved much later [2,3] is still most widely used in view of its good yields and easily available starting materials. It consists of the reduction of diazotized anthranilic acid (**1**) to *o*-hydrazinobenzoic acid (**2**) and cyclization of the latter (Chart 1). Nevertheless these methods seem somewhat laborious as large volumes of reaction mixtures are involved (about 19 L,[2] respectively 2.5 L,[3] per 100 g product) and one needs three days to obtain the final product from anthranilic acid.

We wish now to report a new convenient synthesis which appreciably reduces these disadvantages. The starting material is the readily obtainable phenylglycine-*o*-carboxylic acid (*4*).[4] Nitrosation and cyclization of the resulted nitroso acid 5a led to the 3-(*o*-carboxyphenyl)sydnone (**6a**), yields being over 70%. There is no need to isolate the intermediate N-(*o*-carboxyphenyl)-N-nitrosoglycine (**5**). The hydrolysis of sydnones **6a**–**d** was performed with 13–16% hydrochloric acid, the yields being over 90%. Volumes are reduced to 0.6 L per 100 g of product. The method is much less laborious than the classical one and an appreciably shorter period of time (one day instead of three) is necessary.

Besides indazolone **3a**, the 5-iodoindazolone **3b** could be easily obtained as well as two other halogenated derivatives (**3c**–**d**), mentioned in the literature and connected to physical measurements [5,6] or photographic materials,[7a] prepared in small yields. The 5-chloroindazolone which has been fully described [7b] could be obtained with yields of 43–44% from the corresponding anthranilic acid. The corresponding *o*-carboxyphenylglycines were easily prepared (yields 70–90%). *o*-Substituents to the amino group of *4* do not seem to interfere by steric hindrance, CHART 1

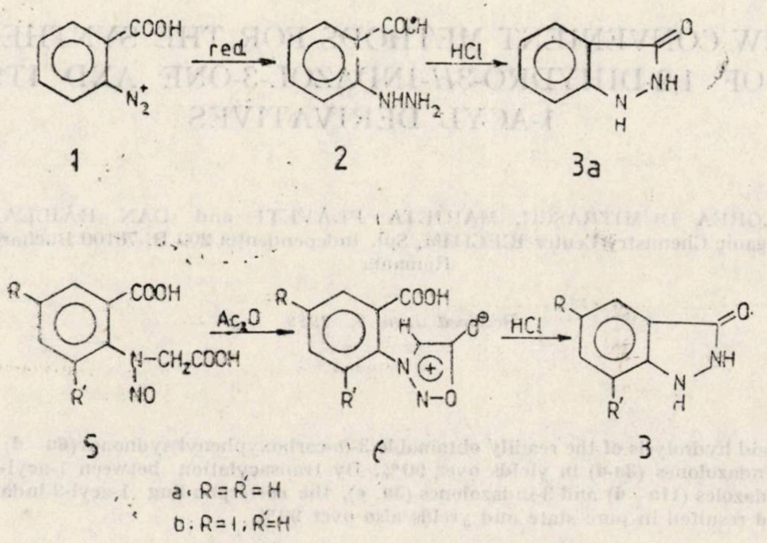
COOH
N$_2^+$
red.
COOH
NHNH$_2$
HCl
O
NH
N
H
1
2
3a
R
COOH
N–CH$_2$COOH
NO
R'
Ac$_2$O
R
COOH
H
O$^\ominus$
N
+
N–O
R'
HCl
R
O
NH
N
H
R'
5
6
3
a: R = R' = H
b: R = I; R' = H
c: R = Br; R' = H
d: R = R' = Cl

yields of the 3-(2-carboxy-4,6-dichlorophenyl)sydnone (**6d**) being only slightly lower than in the case of *o*-unsubstituted compounds.

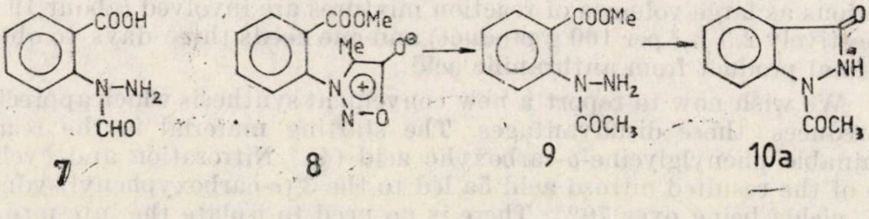
COOH
N–NH$_2$
CHO
7
COOMe
Me
O$^\ominus$
N
+
N–O
8
COOMe
N–NH$_2$
COCH$_3$
9
O
NH
N
COCH$_3$
10a

The hydrolysis mechanism of phenylsydnone is known.[8] In the presence of hydrochloric acid, the products are phenylhydrazine, formic acid and carbon dioxide. Isolation of 1-acyl-1-phenylhydrazines in strictly controlled conditions was considered as an evidence of their formation as transient intermediates during the course of the reaction.[9,10] When the acyl group was formyl its extreme lability rendered the operation extremely difficult and most of the times unreproducible.[8,9] Also in the case of the *o*-carboxyphenylsydnone **6a** we were not able to isolate the intermediate formylhydrazine **7**. However when the 3-(*o*-carbomethoxyphenyl)-4-methylsydnone (**8**) was submitted to strictly controlled acid hydrolysis the 1-acetyl-3-indazolone (**10a**) could be isolated. The methyl ester **8** was used for reasons of solubility. The ester group of the intermediate N-acylhydrazinobenzoic ester **9** brought about the cyclization to **10a**. Therefore the general mechanism does also operate in our case.

In the previous paper of this series [11] the rearrangement of 3-(*o*-carboxyphenyl)-4-alkylsydnones to 1-acyl-3-indazolones was described. Meanwhile the method recently described by Anderson [12] came to our attention. 1-Acyl-1,2-dihydro-3H-indazol-3-ones were obtained from stoichiometrical amounts of indazolone (**3a**) and acyl chlorides in pyridine either after two days at room temperature (yield 84% for acyl = Ac) or by reflux for two hours (yields 68–76%). In our hands the reaction mixtures monitored by ^{1}H-NMR only partly confirmed these results since mixtures of 1-acetyl- and 2-acetyl-3-indazolones were observed when acetyl chloride was used as acylating agent. In the first case the ratio between the 1-acetyl and 2-acetyl isomers was 20 : 80 while in the second one the percentages were reversed. The problem of the formation of 2-acyl-3-indazolones will be discussed separately in the next paper of this series.

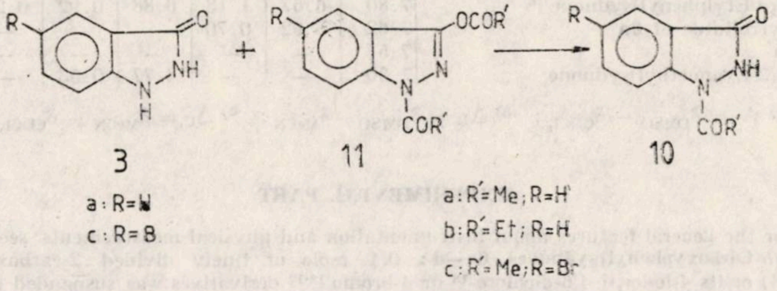

We have found now that a high purity of the 1-acyl-3-indazolones **10a**–**d** can be reached by intermolecular transacylation between 1-acyl-3-acyloxyindazoles (**11a**–**d**) and the corresponding indazolones **3a**, **c**. Two methods have been taken into consideration, both of them resulting in yields over 90% of 1-acyl-3-indazolones (**10a**–**d**) sufficiently pure for synthetic purposes. The first method involves the heating of an intimate mixture of the two compounds at its melting point followed by vacuum sublimation. Both the reaction and the purification take place in the sublimator. The second possibility which allows the preparation of larger amounts uses as a solvent pyridine at reflux. Monitoring by ^{1}H-NMR at the end of the reaction periods showed the exclusive presence of the 1-acyl isomer in both cases. The 1-acyl-3-acyloxyindazoles **11a**–**d** were obtained in practically quantitative yields from indazolones **3a**, **c** and the corresponding anhydride. The bromo derivatives were necessary for cross experiments in order to determine the nature of acyl migrations in indazolone derivatives. The results will be published in a separate paper as mentioned before.

^{1}H-NMR spectra. The 3-(*o*-carboxyphenyl)sydnones **6** are difficultly soluble in the majority of solvents so that d_6-DMSO was used for the ^{1}H-NMR spectral measurements. The chemical shifts of the 4-H proton appear as being unusually high as compared to those measured in other solvents for a wide range of sydnone derivatives.[13] Differences between d_6-DMSO and polar or nonpolar solvents could be registered in the case of the 3-(*o*-ethylphenyl)sydnone (Table 1). A plausible explanation is the

formation of hydrogen bonds between DMSO and the 4-CH group. This is supported by a ^{13}C-NMR study of sydnones[14] which confirms the tendency of the 4-CH group to form hydrogen bonds. This tendency is appreciably reduced when the 3-substituent is nonaromatic, for example the 3-(2-cyanoethyl)sydnone.

Table 1

Comparison of ^{1}H-NMR chemical shifts in d_6-DMSO and other solvents of the 4-H

	δ_{DMSO}	δ_{CDCl_3}	Δ_A^a	δ_{MeCN}	Δ_B^b	Δ_C^c
Ester **8**	7.83[15]	6.63	1.20	—	—	—
3-(*o*-Etylphenyl)sydnone[16]	7.80	6.67	1.13	6.88	0.92	0.21
Pyrrolidide of **6a**	7.62	6.92	0.70	—	—	—
6a	7.57	—	—	—	—	—
3-(2-Cyanoethyl)sydnone	7.30	—	—	6.77	0.53	—

[a] $A = \delta_{DMSO} - \delta_{CDCl_3}$; [b] $\Delta_B = \delta_{DMSO} - \delta_{MeCN}$; [c] $\Delta_C = \delta_{MeCN} - \delta_{CDCl_3}$.

EXPERIMENTAL PART

For the general features about instrumentation and physical measurements see Ref. 11.

3-(*o*-Carboxyphenyl)sydnones 6a—d: 0.1 mole of finely divided 2-carboxyphenylglycine (**4**) or its 4-iodo-,[17] 4,6-dichloro-[18] or 4-bromo[18,19] derivatives was suspended in 80 mL of water to which 20 mL of conc. HCl were added. Then with stirring and cooling to below 10° of the suspension, 7 g of sodium nitrite dissolved in 20 mL of water were gradually introduced. Stirring was stil continued for 20 min. The nitroso derivative **5a** dissolved in the reaction mixture the solution becoming clear while **5b—d** separated as oils. In all cases two extractions with 50 ml of ether each were applied. To the combined ethereal extracts 20 mL of benzene were added and thereafter the ether was removed in vacuo and also partly the benzene when crystallization of the nitroso acids **5a—d** occurred.

After the addition of 65 mL of acetic anhydride and 2 mL of pyridine to the crystalline residue impregnated with benzene dissolution occurred. The reaction mixture was evaporated straight away at 50—60 Torr on the water bath. The crystalline sydnones **6a—d** began to separate towards the end of the evaporation. After its completion a small amount of acetone was added and pure sydnones were obtained by filtration.

3-(o-Carboxyphenyl)sydnone (**6a**): yields of 70—75% based on **4** with mp 212° (dec.): lit.[20]: 205° (dec.).

UV: $\lambda_{max}^{EtOH}(\log \varepsilon) = 220\ (3.931)$, 300 nm (3.812). ^{1}H-NMR (d_6-DMSO): 7.57 (s, 1, 4-H), 7.97 (m, 4, 4′-, 5′-, 6′-H + COOH), 8.13 (q, 1, 3′-H).

6a, *Methyl ester*: with diazomethane as described before.[11] Yield 95% of a product with mp 102°: lit.[15]: 104—106° (from ethanol).

^{1}H-NMR ($CDCl_3$): 3.65 (s, 3, COOMe), 6.63 (s, 1, 4-H), 7.73 and 8.05 (multiplets, 4, arom. protons).

6a, *Pyrrolidide*. The solution of 3.1 g of the methyl ester of **6a** in 6 mL of pyrrolidine was left to stay over night after which the excess of pyrrolidine was removed *in vacuo*. The residue was treated with ether when crystallization occurred. After filtration, 3.2 g of the pyrrolidide of **6a** were obtained with mp 159—160° (from ethanol), yield 88%.

Found: C, 60.50; H, 5.30; N, 16.51. Calc. for $C_{13}H_{13}N_3O_3$: C, 60.23; H, 5.02; N, 16.21. ^{1}H-NMR ($CDCl_3$): 1.95 (broadened s, 4, CH_2), 3.43 (m. 4, N-CH_2), 6.92 (s, 1, 4-H), 7.80 (s, 4, *o*-phenylene); (d_6-DMSO): 7.62 (s, 1, 4-H).

3-(2-Carboxy-4-iodophenyl)sydnone (**6b**): yields 65—70%, mp 224—225° (dec.); from acetic acid.

Found: C, 32.29; H, 1.72; N, 8.54; J, 37.87. Calc. for $C_9H_5JN_2O_4$: C, 32.54; H, 1.51; N, 8.44; J, 38,23. IR (KBr): 1700 (sh.; COOH), 1740 (CO-sydnone), 3155 and 3165 cm^{-1} (4-H).

3-(4-Bromo-2-carboxyphenyl)sydnone (**6c**): yields 75—78%, mp 219—221° (dec.) from ethanol.

Found: C, 37.73; H, 1.89; N, 9.60; Br, 27.76. Calc. for $C_9H_8BrN_2O_4$: C, 37.90; H, 1.75; N, 9.83; Br, 28.04. IR (KBr): 1700 (sh.; COOH), 1730 (CO-sydnone), 3152 cm^{-1} (4-H). ^{1}H-NMR (d_6-DMSO): 5.82 (s, 1, COOH included in impurity of water), 7.58 (s, 1, 4-H), 7.87 (d, 1, 6'-H), 8.15 (dd, 1, 5'-H), 8.25 (d, 1, 3'-H).

-(*2-Carboxy-4,6-dichlorophenyl)sydnone* (**6d**): yields 70—72%, mp 234—235° (dec. from acetic acid.

Found: C, 39.24; H, 1.74; N, 9.89; Cl, 25.42. Calc. for $C_9H_4Cl_2N_2O_4$: C, 39.27; H, 1.45; N, 10.18; Cl, 25.82. UV; $\lambda_{max}^{EtOH} = 299$ nm. IR (KBr): 1690 (COOH), 1728 (CO-sydnone), 3171 cm^{-1} (4-H). ^{1}H-NMR (d_6-DMSO): 7.52 (s, 1, 4-H), 7.72 (s, 1, COOH), 8.12 (d, 1, 5'-H), 8.30 (d, 1, 3'-H).

1,2-Dihydro-3*H*-indazol-3-one (3a). A suspension of 10 g of **6a** in 20 mL of water to which 20 mL of conc. HCl were added, was refluxed until complete dissolution occurred, namely about 15 min. Refluxing was still continued for 15 min. The dil. HCl was removed *in vacuo* and the residue of the chlorohydrate dissolved in 30 mL of water and neutralized to pH 5—6 when the free indazolone separated. After filtration and drying 6.3 g of **3a** were obtained, yield of 97% with mp 243—245° (lit. [3]: 250°).

Halogenated 1,2-dihydro-3*H*-indazol-3-ones (3b—d): 6 g of sydnone (**6b—d**) were refluxed for 2—3 hrs in a mixture of 30 mL of ethanol, 20 mL of water and 30 mL of conc. HCl. The initial suspension became gradually homogeneous when a small amount of decolorizing carbon was added. The hot solution was filtered and left to crystallize. After filtration, washing with water and drying the halogenated indazolone was obtained.

*1,2-Dihydro-5-iodo-3*H*-indazol-3-one* (**3b**): yield of 96% with mp 250—252° (dec. with iodine liberation) from acetic acid.

Found: C, 32.63; H, 2.24; N, 11.03; I, 48.92. Calc. for $C_7H_5IN_2O$: C, 32.33; H, 1.94; N, 10.77; I, $^{40 \cdot 80}$.

*5-Bromo-1,2-dihydro-3*H*-indazol-3-one* (**3c**): [5,6] yield of 98% with mp 273—274° (dec.).

^{1}H-NMR (d_5-Py): 7.47 (dd, 1, 6-H), 7.65 (d, 1, 7-H), 8.37 (d, 1, 4-H), 11.37 (broad s, 2, NH).

*5,7-Dichloro-1,2-dihydro-3*H*-indazol-3-one* (**3d**): [5,7] yield of 98% with mp 238—240°. ^{1}H-NMR (d_5-Py): 7.55 (d, 1, 6-H), 8.07 (d, 1, 4-H), 9.32 (broad s, 2, NH).

Controlled hydrolysis of 3-(*o*-carbomethoxyphenyl)-4-methylsydnone (8): 2.2 g of the ester **8** were added to a mixture of 20 mL of dry benzene and 20 mL of dry ether which contains 0.365 g (10 mmole) HCl and 0.18 g (10 mmole) of water. A small amount of the ester **8** remained in suspension so that stirring was applied until dissolution occurred. The reaction mixture was kept at room temperature for 4 hrs starting from the beginning of the reaction. Most of the ether was removed when the 1-acetyl-3-indazolone (**10a**) began to crystallize and after filtration 1.4 g were obtained with mp 214°. A mixture with an authentic sample [11] showed no depression.

1-Acyl-3-acyloxyindazoles 11a—d. Indazolones **3a,c** were refluxed in 10 mL of acetic or propionic anhydride for 2—3 hrs. After evaporation *in vacuo* of the excess anhydride and working-up with a small amount of ethanol **11a—d** were obtained in yields of over 90%.

3-Acetoxy-1-acetylindazole (**11a**): 93% yield with mp 111° (lit.[21]: yield 58% aud mp 113°).

1-Propionyl-3-propionyloxyindazole (**11b**): yield of 95% with mp 79° (from methanol); lit. [12]: mp 76° and 84% yield.

3-Acetoxy-1-acetyl-5-bromoindazole (**11c**): yield 96% of a product with mp 119—120°. Found: C, 44.68; H, 3.25; N, 9.63; Br. 26.53. Calc. for $C_{11}H_9BrN_2O_3$: C, 44.44; H, 3.03; N, 9.43; Br, 26.93. IR (CCl_4): 1717 (N-$COCH_3$), 1780 cm^{-1} ($OCOCH_3$). ^{1}H-NMR ($CDCl_3$): 248 (s, 3, $OCOCH_3$), 2.73 (s, 3, (-$COCH_3$)' 7.72 (d, 1, 6-H), 7.77 (s, 1, 4-H), 8.37 (d, 1, 7-H).

5-Bromo-1-propionyl-3-propionyloxyindazole (**11d**): yield of 92% with mp 125—126° (from methanol).

Found: C, 48.30; H, 4.21; N, 8.82; Br, 25.01. Calc. for $C_{13}H_{13}BrN_2O_3$: C, 48.00; H, 4.00; N, 8.61; Br, 24.62. IR (CCl_4): 1718 (CO-amide), 1773 cm^{-1} (CO-ester). ^{1}H-NMR ($CDCl_3$): 1.33 and 1.37 (triplets, 6, CH_3), 2.80 (q, 2, $OCOCH_2$), 3.17 (q, 2, N-$COCH_2$), 7.75 (m, 2, 4- and 6-H), 8.43 (d, 1, 7-H); $J_{6,7} = 9$ Hz.

1-Acyl-1,2-dihydro-3*H*-indazol-3-ones 10a—d. A. Neatly. Equimolecular amounts of finely powdered indazolones **3a, c** and of their corresponding diacylated derivatives **11a—d** were intimately mixed and introduced into a sublimator. Heat was applied until melting of the reaction mixture took place when the temperature was further gradually raised up to 200°.

The reaction was completed in about 10 min when vacuum was applied (50—60 Torr) and the resulted 1-acylindazolones **10a—d** sublimed. The analysis samples were resublimed.

*1-Acetyl-1,2-dihydro-3*H*-indazol-3-one* (**10a**): yield of 94% with mp 212° (lit.[11] 214°).

*1,2-Dihydro-1-propiony-3*H*-indazol-3-one* (**10b**): yield of 93% with mp 190—191° (lit [11] 192°).

*1-Acetyl-5-bromo- 1,2-dihydro-3*H*-indazol-3-one* (**10c**): after resublimation mp 241—242° yield 93%.

Found: C, 42.59; H, 2.95; N, 11.23; Br, 31.72. Calc. for $C_9H_7BrN_2O_2$: C, 42.35; H, 2.74; N, 10.98; Br, 31.37.

*5-Bromo-1,2-dihydro-1-propionyl-3*H*-indazol-3-one* (**10d**): after resublimation mp 251—252°, yield 91%.

Found: C, 44.90; H, 3.60; N, 10.11; Br, 30.11. Calc. for $C_{10}H_9BrN_2O_2$: C, 44.61; H, 3.34; N, 10.40; Br, 29.74. ^{1}H-NMR (d_5-Py): 1.28 (t, 3, CH_3), 3.10 (q, 2, CH_2), 7.75 (dd, 1, 6-H), 8.18 (d, 1, 4-H), 8.58 (d, 1, 7-H); $J_{6,7} = 8.5$ Hz, $J_{4,6} = 2$ Hz.

B. In pyridine at reflux. In 100 mL of pyridine were introduced 13.4 g (0.1 mole) of 3-indazolone (**3a**) and 21.89 g (0.1 mole) of **11a** and the whole was refluxed for 3 hrs. After removal *in vacuo* of the pyridine a small amount of chloroform was added and after filtration 31.7 g of **10 a** with mp 212—213° were obtained (yield 90%). Similar results were registered in the cases of **10b—d**.

3-(2-Cyanoethl)sydnone: 12.8 g of N-(2-cyanoethyl)glycine [22] were dissolved in a mixture of water (15 mL) and conc. HCl (15 mL). After cooling with ice-water 7 g of sodium nitrite in 20 mL of water were dropped with stirring when a precipitate of the nitroso derivative separated. After cooling, filtration, washing with a small amount of water and drying in a vacuum desiccator, 14.5 of nitroso derivative were obtained with mp 116—118° (dec.), yield 91%. Lit.[23]: yield 38% with mp 117.5—118.5° (dec.) from ethyl acetate. The nitroso derivative (14.5 g) was dissolved in 60 mL of acetic anhydride and left at room temperature for three days and worked-up just as described by Stewart [23]: 11 g of sydnone were obtained with mp 79—81°, yield 87%. Lit.[23]: 60% yield with mp 81.5—82.5°.

^{1}H-NMR (d_6-DMSO): 3.37 (t, 2, CH_2CN), 4.82 (t, 2, CH_2-N^+), 7.30 (s, 1, 4-H).

REFERENCES

[1] E. Fischer, *Ber. dtsch. Chem. Ges.*, **13**, 681 (1880).

[2] E. Stephenson, *Org. Synth.*, coll. vol. 3, Wiley, 1955, p. 475.

[3] L. Baiocchi, G. Corsi and G. Palazzo, *Synthesis*, **1978**, 633.

[4] D. Răileanu, O. Constantinescu-Simon, E. Moșanu and C. D. Nenitzescu, *Rev. Roumaine Chim.*, **12**, 105 (1967); H. E. Fierz-David and L. Blangey, *Farbenchemie*, 6th ed., Springer, Vienna, 1946, p. 162; Ger. 127 178 (BASF; 1901/1900); *Forschr. Teerfarben-Fabrik* (ed. P. Friedländer), **6**, 538 (1900—1902).

[5] B. D. Chernokalski, A. T. Groisberg, N. F. Rakova and R. R. Shagidullin, *Khim. Geterotsikl. Soedin.*, **1966**, 96.

[6] P. Ballesteros, J. Elguero, R. Claramunt, R. Faure, M. De la Conception Foces-Foces, F. Hernandez Cano and A. Rousseau, *J. Chem. Soc., Perkin Trans.* 2, **1986**, 1677.

[7] (a) J. Jennen, U.S. 2 673 801 (Gevaerts; 1954); *Chem. Abstr.*, **48**, 9850 (1954); (b) J. S. Morley, *J. Chem. Soc.*, **1959**, 2280.

[8] S. Aziz, A. F. Cockerill and J. G. Tillett, *J. Chem. Soc.* (*B*), **1970**, 416 and references cited therein.

[9] S. A. Zotova and V. G. Yashunski, *Zhur. org. Khim.*, **3**, 942 (1967).

[10] B. V. Badami and G. S. Puranik, *Indian J. Chem.*, **12**, 671 (1974).

[11] F. Dumitrașcu and D. Răileanu, *Rev. Roumaine Chim.*, **34**, 1183 (1989).

[12] R. Anderson, *J. Chem. Res.* (*M*), **1985**, 3933—3959.

[13] M. Ohta and H. Kato, "Sydnones and Other Mesoionic Compounds", *Nonbenzenoid Aromatics*, vol. 1 (ed. J. Snyder), Academic Press, p. 138.

[14] Sum Ma, Hsien-Ju Tien and Suh Yun Fang, *Cheng Kung Ta Hsueh Hsueh Pao, Ko Chi, I Hsueh Pien*, **20**, 97 (1985) ; *Chem. Abstr.*, **107**, 133 782 (1987).

[15] P. Preston and K. Turnbull, *J. Chem. Soc., Perkin Trans.* 1, **1977**, 1229.

[16] D. L. Hammick and D. J. Voaden, *J. Chem. Soc.*, **1961**, 3303.

[17] W. Borsche, H. Weussmann and A. Fritzsche, *Ber. dtsch.* Chem. Ges., **57**, 1775 (1924).

[18] Germ. 148 615 (BASF ; 1903/1902) ; *Fortschr. Teerfarben-Fabrik* (ed. P. Friedländer), **7**, 289 (1902—1904).

[19] P. Friedländer, S. Bruckner and G. Deutsch, *Liebigs Ann. Chem.*, **388**, 34 (1911).

[20] R. A. Eade and J. C. Earl, *J. Chem. Soc.*, **1948**, 2307.

[21] I. J. Jennen and H. P. Eerdekens, U.S. 2 964 402 (Gevaert ; 1960) ; *Chem. Abstr.* **55**, 9129 (1961).

[22] L. L. McKinney, E. H. Uhing, E. A. Setzhorn and J. C. Cowan, *J. Am. Chem. Soc.*, **72**, 2599 (1950).

[23] F. H. C. Stewart, *J. Org. Chem.*, **27**, 687 (1962).

Revue Roumaine de Chimie, 36, 8, 925–929 (1991)

Dedicated to Professor PETRU SPACU on the occasion of his 85th anniversary

THE SYNTHESIS OF SOME 1-NAPHTHYLCYCLOALKANOLS AND 1-NAPHTHYLCYCLOALKENES

KERIMAN GÜNAYDIN
Istanbul Technical University, Department of Chemistry, Yeni Levent, Istanbul, Turkey

Received April 1, 1989

1-Naphthylcycloalkanols having 3, 4, 5, 6, 7, 12 and 15 ring carbons were synthesized from corresponding cyclic ketones and 1-naphthylbromide using Grignard reaction. The dehydration products of these naphthylcycloalkanolis were obtained. All the products were identified by means of IR- and ^{1}H-NMR spectra.

INTRODUCTION

In the previous works, cyclic alcohols obtained from the cyclic ketones having the 5, 6, 7 and 8 ring carbons were converted into corresponding alkenes by using different dehydration agents with rather poor yields.[1–3] In this work, the cyclic alcohols mentioned above were obtained with higher efficiency. Also four new 1-naphthylcycloalkanols having 3, 4, 12 and 15 ring carbons were prepared and spectroscopic and physical data of alcohols and their dehydration products are given.

For the synthesis of 1-naphthylcycloalkanols Grignard reagents and cycloalkanones were used whereas for the synthesis of 1-naphthyl cycloalkenes from 1-naphthylcycloalkanols H_3PO_4 in toluene was used as dehydration agent.[4]

For instance 1-napthylcyclopropanol (1) and 1-naphthylcyclopropene (1a) were prepared by the following reactions:

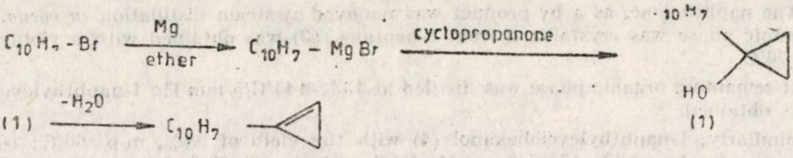

By this way 1-naphthylcyclobutanol (2) and 1-naphthylcyclobutene (2a); 1-naphthylcyclopentanol (3) and 1-naphthylcyclopentene (3a); 1-naphthylcyclohexanol (4) and 1-naphthylcyclohexene (4a); 1-naphthylcycloheptanol (5) and 1-naphthylcycloheptene (5a); 1-naphthylcyclooctanol (6) and 1-naphthylcyclooctene (6a); 1-naphtylcyclododecanol (7) and

1-naphtylcyclododecene (**7a**); 1-naphtylcyclopentadecanol (**8**) and 1-naphylcyclopentadecene (**8a**) were prepared.

EXPERIMENTAL

I — Spectroscopic and Chromatographic studies

The IR spectra were determined on a Schimadzu IR-400 spectrophotometer and the ^{1}H-NMR spectra were determined on a Varian T-60 instrument using TMS as internal standard. Gas chromatographic analyses were performed on a Schimadzu Model GC-5A instrument equipped with a flame ionization detector and $1/8 \times 12$ ft stainless steel columns packed with Silicone OV-17.3%. The chromatographic conditions were as follows: column temp.: 240°C, 200°C; detector and injector temp: 300°C, 240°C for carbinols having ring carbon number 6, 7, 8, 12, 15 and for carbinols having ring carbon number 3, 4, 5 respectively.

II — Preparation of 1-Naphthylcycloalkanols

a) 1-Naphthylmagnesiumbromide

Place 0.1 g-atome magnesium turnings into a dry 250 mL two necked flask equipped with a dropping funnel and a condenser with a calcium drying tube. 10 mL absolute ether and a small amount of iodine were added. A solution of 0.1 mole 1-naphthylbromide in absolute ether was added dropwise to Mg. Stirring was continued until Mg was almost completly consumed. The reaction vessel was gently warmed when required.

b) 1-Naphthylcyclopropanol (**1**)

To the above ethereal Grignard reagent 0.1 mole of cyclopropylketone in absolute ether was added. During the adding process the reaction vessel was cooled with dry ice. The reaction mixture was stirred for half an hour, then poured into a cold aqueous HCl solution (10%). The etheral phase was separated and washed successively with aqueous sodium bicarbonate solution and water. The neutral ethereal solution was dried over anhydrous sodium sulfate and the ether was evaporated. The crude product was distilled under vacuum: yield 91%. b.p: 178—184° C/7 mm Hg.

Similarly, 1-naphthylcyclobutene (**2**) was obtained and crystallized from CCl_4, yield 94%. m.p. = 98—99°C.

c) 1-Naphthylcyclopentanol (**3**)

As described in section (b), 0.1 g-atom Mg turnings and 10 mL absolute ether were placed into a dry 250 mL two necked flask. A mixture of 0.1 mole 1-naphthylbromide and 0.5 mole of cyclopentanone dissolved in absolute ether was added slowly on the magnesium turnings (*in situ*) at room temperature. After being stirred for three hours by warming, the etheral phase was shaken with aqueous sodium bicarbonate and water until it displayed no acid reaction to litmus. This ethereal solution was dried over anhydrous sodium sulfate. The ether was removed on a rotatory evaporator.

The naphthalene, as a by-product was removed by steam distillation *in vacuo*. Remaining organic phase was crystallized from *n*-heptane. (**3**) was obtained with a yield of 100%. m.p. = 76°C.

If remaining organic phase was distiled at 133—144°C/5 mm Hg 1-naphthylcyclopentene (**3a**) was obtained.

Similarly, 1-naphthylcyclohexanol (**4**) with the yield of 98%, m.p. 66°C; 1-naphthylcyclohexene (**4a**) bp: 168—170°C/8 mm Hg GLC analysis: 80/19.9 (*cis* + *trans*); 1-naphthylcyclopentanol (**5**) m.p. 77—78°C. Yield 70% and 1-naphtylcycloheptene (**5a**) b.p. = 154/0 mm Hg GLC analysis: 82.15/17.84 (*cis* + *traβs*: 1-naphthylcyclooktanol (**6**) m.p. = 83°C Yield 54%; 1-naphthylcyclooctene b.p. = 184—188°C/5 mm Hg GLC analysis: 70.33/29.6 (*cis* + *trans*) were obtained.

d) 1-Naphthylcyclododecanol (**7**)

As described in section (a) the Grignard reagent was prepared with 0.1 mole of 1 naphthylbromide, then a solution of 0.5 mole of cyclododecanone dissolved in absolute ether was added to the reagent. After the addition of ketone was completed the reaction mixture was heated for two hours and hydrolized in the usual manner. During the hydrolisation an ether-unsoluble part was precipitated. The solid phase was filtered and crystallized from THF at room temperature. 1-Naphthylcyclododecanol was obtained with a yield of 54%, m.p. = 179°C.

The filtrate was left overnight at 0°C and aldol of cyclododecanol was precipitated. m.p. = 154°C. The naphthalene remained in the ethereal phase.

e) 1-Naphthylcyclopentadecanol (8)

An ethereal solution of 0.1 mole cyclopentadecanone was added to the Grignard reagent prepared as described in section (a). The reaction mixture was hydrolized with an aqueous solution of HCl (10%). The alcohol obtained from the ethereal phase was crystallized with heptane. The yield was 100% m.p. = 131−132°C.
The IR and ^{1}H-NMR data of the alcohols were collected in Table 1.

Table 1

Spectral data of 1-naphthylcycloalkanols

Compounds	IR data (cm^{-1})	^{1}H-NMR data (δ ppm)
1	3570, 3400, 3500, 1600, 3000, 3100, 1500, 1020, 980, 900, 800, 760	7−8 ($C_{10}H_7$−, 7H) 1.95 (−H, 1H) 0.2−0.6 (−CH_2−, 4H)
2	3400, 3100, 3050, 3000, 2950, 1600, 1500, 1400, 1340, 1290, 1250, 1120, 1100, 1090, 1020, 1000, 960, 800	7−8 ($C_{10}H_7$−, 7H) 2.5−3 (−CH_2−, 4H) 2.1−2.4 (−CH_2−, 2H) 1.7 (OH, 1H)
3	3350, 3450, 3050, 2950, 2850, 1620 1600, 1500, 1440, 1380, 1100, 1000, 940, 770, 740	7−7.8 ($C_{10}H_7$−, 7H) 2.6 (OH, 1H) 2−22 (−CH_2−, 4H) 1.8 (−CH_2−, 2H)
4	3400, 3050, 2930, 2970, 2850, 1600, 1500, 1450, 1380, 1350, 1300, 1260, 1200, 1120, 1040, 960, 800, 780, 740	7−8 ($C_{10}H_7$−, 7H) 2−2.4 (−CH_2−, 4H) 1.9 (OH, 1H) 1.4−1.9 (−CH_2−, 6H)
5	3300, 3000, 3100, 2900, 2850, 1600 1500, 1460, 1440, 1240, 1170, 1020, 850, 910, 800	7.2−8 ($C_{10}H_7$, 7H) 2.3 (−CH_2−, 4H) 1.6−2 (−CH_2−, 8H) 4 (OH, 1H)
6	3450, 3050, 2920, 2850, 1600, 1500, 1440, 1380, 1260, 1200, 1150, 1000, 840, 770, 700	7−8($C_{10}H_7$−, 7H) 1.6 (−CH_2−4H) 2.2−2.9 (−CH_2−, 4H) 2.1 (−OH, 1H)
7	3300, 3000, 2800, 2950, 1600, 1500, 1450, 1390, 1065, 1020, 1075, 760, 720, 660	7.4−8 ($C_{10}H_7$−, 7H) 1.8−2.3 (−CH_2−, 4H) 1.3−1.6 (−CH_2−, 18H)
8	3300, 3100, 3050, 3000, 2920, 2850, 1600, 1500, 1480, 1390, 1380, 1340, 1280, 1180, 1120, 900, 850, 800, 780, 740	7.2−7.6 ($C_{10}H_7$−, 7H) 2.15 (OH, 1H) 1.3 (−CH_2−) 3 (OH, 1H)

III — Preparation of naphthylcycloalkenes

1-Naphthylcycloalkanol (0.02 mole) and 0.6 mL H_3PO_4 in toluene (45 mL) were refluxed for 8 hours. The organic phase was washed consecutively with water, 5% aqueous sodium bicarbonate and again with water and dried over anhydrous Na_2SO_4.

After distillation of toluene the olefin remains. From (1) 1-naphthylcyclopropene (1a m.p. = 46°C. GLC analysis: (decomposition) and from 1-naphthylcyclobutene (2a) b.p. =

$= 25°C/10$ mm Hg GLC analysis $= 100\%$ (*cis* isomer); from **(7)** 1-naphthylcyclododecene **(7a)** m.p. $= 54°C$ GLC analysis: 59.22%, 3831% (*cis* + *trans*); from **(8)** 1-naphthylcyclopenta decene **(8a)** b.p. $= 164°C/10$ mm Hg GLC analysis: 70.27%, 29% (*cis* + *trans*) were obtained. Compounds **3a, 4a, 5a,** and **6a** were prepared in the same manner from the corresponding alcohols.

RESULTS

In this work, eight 1-naphthylcycloalkanols and their dehydration products have been studied and their structure has been elucidated by IR, ^{1}H-NMR spectra and GLC analysis.

According to the reactivity of the ketones, Grignard reagent/ketone ratio has been chosen. For the reactive ketones for example cyclopropanone, cyclobutanone, and cyclopentadecanone, Grignard reagent/ketone ratio used was 1/1 and they gave high yields of alcohols. Because of the less reactivity of cyclopentanone, cyclohexanone and cyclooctanone, the application of usual method did not give good results, an excess of Grignard reagent was necessary. Although Grignard reagent/ketone ratio was 2/1 for cyclododecanone the result was not satisfactory because cyclododecanone gave an aldol product during the reaction.

After preparing the alcohols they were converted into the olefins by two ways: 1) using dehydration agent 2) thermally.

Because all of the alcohols were tertiary carbinols, they were readily converted to the olefins by the E_2 mechanism using H_3PO_4 in toluene as dehydration agent. But some of the alcohols could not be converted to alkenes thermally.

During the purification of the alcohols of cyclopentanone, cyclohexanone and cycloheptanone an interesting point was catched because IR- and ^{1}H-NMR data of the products obtained by distillation and crystallization were different. Crystallization process yielded an alcohol as expected whereas distillation of the crude reaction mixture produced an olefin. This result showed that during the distillation, alcohols changed into the olefins by E_1 mechanism in gas phase. So, similar spectral and physical properties were observed for the product obtained by using distillation or dehydration process (Table 2). Thus, it is possible to prepare olefins **3a**, **4a**, 5a, **6a**, by distillation of crude Grignard mixture without purification. But, if the goal of this reaction is to obtain pure alcohols, the mixture should be purified by crystallisation.

Alcohols prepared from cyclododecanone, cyclopentadecanone and cyclobutanone could not be converted into alkenes by distillation because of their failing to pass into the gas phase. On the other hand, these alcohols underwent a dehydration process within the GLC column, probably by the effects of heat and Silicone OV-17 %3.[4] This behaviour was further substantiated by the comparison of the chromatograms of the alcohols with that of the olefins obtained by dehydration agent.

Table 2

Spectral data of 1-naphthylcycloalkenes

Compounds	IR data (νcm^{-1})	^{1}H-NMR data (δppm)
1a	3000, 3050, 2950, 1600, 1500, 1460, 1420, 1380, 1250, 1000, 750	7–8 ($C_{10}H_7$, 7H) 3.65–4.35 (1H) 0.5 (–CH_2–12H)
2a	3020, 2960, 2950, 2900, 2850, 2820, 1680, 1590, 1570, 1500, 1440, 1390, 1370, 1160, 1250, 1150, 1060, 1010, 930, 900, 840, 820, 760	7–8 ($C_{10}H_7$–, 7H) 4.68–52 (1H) 3.2–3.7 (2H, –CH_2) 2–2.5 (2H, –CH_2)
3a	3030, 2930, 2825, 1630, 1590, 1500, 1430, 1380, 1300, 1250, 1360, 940, 840, 780, 760, 730	7.2–7.8 ($C_{10}H_7$–, 7H) 5.9 (1H) 2.6–3 (4H) 2.–2.3 (2H)
4a	3050, 2920, 2850, 2830, 1600, 1500, 1440, 1450, 1400, 1350, 1280, 1260, 1240, 1200, 1180, 1130, 1100, 1020, 920, 860, 840, 780, 740	7–7.8 ($C_{10}H_7$–, 7H) 6.1 (1H, *cis*) 5.6–5.8 (1H *trans*) 2–2.5 (4H) ; 1.4–1.8 (4H)
5a	3050, 2900, 2850, 1620, 1600, 1560 1500, 1440, 1200, 1010, 950, 870, 840, 780, 740	7–8 ($C_{10}H_7$–, 7H) 6–5.85 (1H, *cis*) 6.3–6 (1H, *trans*) 2.2–2.6 (4H) 1.3–1.8 (6H)
6a	3050, 2870, 2850, 1620, 1600, 1500, 1450, 1460, 1360, 1390, 1200, 1000, 890, 840, 810, 800	7–8 ($C_{10}H_7$–, 7H) 5.6–6 (1H, *cis*) 6–6.2 (1H, *trans*) 2–3 (4H) 1–2 (8H)
7a	3050, 2900, 2830, 1620, 1600, 1500, 1460, 1440, 1380, 1320, 1240, 1000, 940, 880, 760, 740, 720, 680	7.2–8 ($C_{10}H_7$–, 7H) 5.35–5.85 (1H) 2–2.8 (4H) 1.4 (16H)
8a	3050, 2950, 2850, 1920, 1800, 1640, 1600, 1580, 1500, 1460, 1400, 1350, 1300, 1240, 1200, 1140, 1020, 960, 860, 800, 780, 740	7.2–7.8 ($C_{10}H_7$–, 7H) 5.2–5.8 (1H) 2–2.7 (4H) 1.2 (22H)

REFERENCES

[1] B. Bergmann, *J. Amer. Chem. Soc.*, **59**, 1443 (1937).

[2] B. Kloetzel, *J. Amer. Chem. Soc.*, **60**, 2204 (1938).

[3] K. H. Lawrence, *J. Chem. Soc.*, **71**, 1431 (1936).

[4] K. Günaydin and Ü. Oyman, *Rev. Roumaine Chim.*, **31**, 497 (1986).

Revue Roumaine de Chimie, 36, 8, 931–936 (1991)

Dedicated to Professor PETRU SPACU on the occasion of his 85th anniversary

ON INTERMEDIATES INVOLVED IN THERMAL DECOMPOSITION OF AZIBENZYL. Part I

MIHAI CONTINEANU
Polytechnic Institute of Bucharest, Department of Physical Chemistry, Bdul. Republicii 13

Received June 15, 1989

The kinetics of formation and disappearance of radicals originated from diphenylketene produced in the process of azibenzyl thermolysis have been studied. Final reaction products in which diphenylketene is involved have been identified using electronic and IR spectra.

INTRODUCTION

Numerous studies have been issued on thermolysis of diazoketones most of them focusing on their decomposition in the presence of various reactants [1–4]; the reactivity of ketocarbenic radical towards these reactants was also investigated.

A paramagnetic intermediate was first mentioned by Singer,[5] who starting from analysis of hyperfine structure of EPR spectra and the hyperfine coupling constants has indicated the structure **1**:

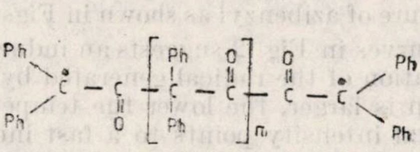

(1)

In two previous papers we studied the kinetics and the mechanism of azibenzyl thermal decomposition in benzene solution[4] and in the absence of the solvent[6]. The main product of thermal decomposition is diphenylketene, which is very reactive and decomposes in different sequences depending on the medium conditions.

In view of advancing a possible reaction mechanism using several experimental techniques and working conditions we evidenced the reaction products which imply the diphenylketene generated in the thermal decomposition of azibenzyl in the absence of the solvent.

EXPERIMENTAL

Azibenzyl was prepared by oxidising the corresponding hydrazone.[7] The main experimental technique employed was EPR using an ART 5 apparatus which operates in X band having high frequency modulation of 100 kHz. The spectroscopic splitting factor was determined with alkali peroxylamine-disulphonate as standard. To identify the final reaction products, the electronic and IR spectra were recorded by means of a Pye-Unicam SP 1800 spectrophotometer and a Zeiss-Jena UR10 apparatus, respectively.

RESULTS AND DISCUSSION

The azibenzyl samples heated to 60—200°C (melting point of azibenzyl being 80°C) and then EPR measured at room temperature show a singlet signal characterized by a factor $g = 2.00149$ and a peak to peak width $\Delta H = 7.49$ G. To study the hyperfine structure of this spectrum a 30% solution of azibenzyl in diphenyl was prepared and the EPR spectrum recorded under the same conditions indicated by Singer [5]; we obtained a similar spectrum, shown in Fig. 1.

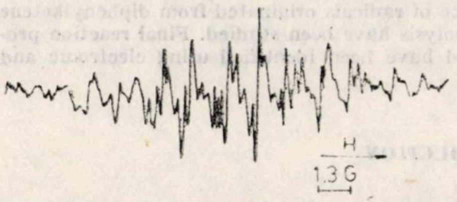

Fig. 1. — EPR spectrum of 30% azibenzyl in biphenyl solution recorded at 160°C.

The hyperfine structure originates in the interaction of an odd electron with two protons which results in a 2.8 G splitting, with four *ortho* protons resulting in a splitting of 2.7 G and four *meta* protons yielding a splitting of 1.71 G.

We studied the accumulation kinetics of the radicals at different constant temperatures in the range of 60—200°C, that is below and over the melting temperature of azibenzyl as shown in Figs 2 and 3, respectively.

The shape of curves in Fig. 2 suggests an induction time corresponding to the accumulation of the radical generated by diphenylketene. The duration of induction is larger, the lower the temperature. Then a linear variation of the signal intensity points to a fast increase of radical concentration. The slope of this linear portion allowed the calculation of the rate constant of radical formation which is temperature independent. One observes also that the intensity of the signal reaches faster a maximum, the higher is the temperature. These results suggest that before reaching this maximum value, the formed radical is immediately consumed in other processes characterized by a slower rate than the formation one. Then the curve declines slowly suggesting that the rate of radical depletion exceeds the formation rate. Each isotherm reaches a plateau and the concentration of the radicals which achieve this steady state is higher, the lower is the temperature. It is worth to note that the behaviour of the 60°C isotherm is in good agreement with our results obtained from absorbance measurements at different stages of the degased azibenzyl samples decomposed at 60°C and subsequently solved in benzene.[6] This variation was studied at two wavelengths corresponding to absorption of azibenzyl ($\lambda = 409$ nm) and diphenylketene ($\lambda = 320$ nm). As azibenzyl decomposes, diphenylketene is formed reaching its maximum concentration at 360 min., which is exactly the induction period of the radical accumulation (Fig. 2).

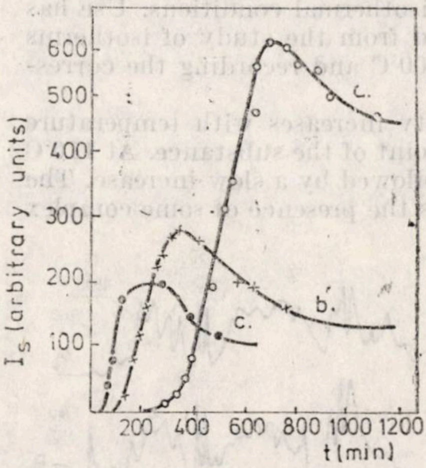

Fig. 2. — The dependence of EPR signal intensity on heating time: a) 60°C; b) 65°C; c) 70°C.

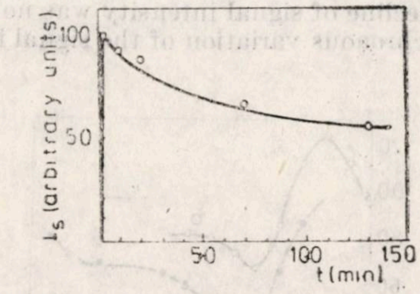

Fig. 3. — The EPR signal intensity versus heating time at 120°C.

To study the influence of O_2 upon the radical we carried out experiments with degased as well as with nondegased samples (Fig. 4).

Samples heated in air give smaller signals than those heated in vacuum and the influence of O_2 is more obvious if O_2 is bubbled. This is why at decomposition of degased benzenic solution, which gives an intense EPR signal, the introduction of air entails the vanishing of the signal. Moreover, our experiments have shown that O_2 addition to radical is

Fig. 4. — The variation of EPR signal intensity recorded at azibenzyl thermolysis at 80°C: a) vacuum; b) atmospheric pressure.

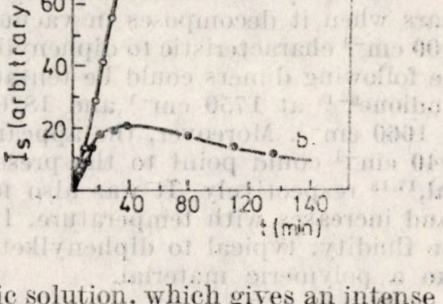

favored by low temperatures. Indeed, diphenylketene samples storred at -10°C exhibit an absorbance decrease 50% larger than those storred at room temperature.

Another series of experiments consisted of drawing the reaction isochrones i.e. the variation of signal in non-isothermal conditions. Use has been made of the degased samples resulted from the study of isotherms and heated 20 minutes every 10°C up to 200°C and recording the corresponding signal as shown in Fig. 5.

One observes that the signal intensity increases with temperature to reach a maximum at 80°C, the melting point of the substance. At 110°C a decline of signal intensity was noticed, followed by a slow increase. The isochronous variation of the signal indicates the presence of some complex processes of formation and recombination of radicals, with the appearance of some products whose stability depends on temperature.

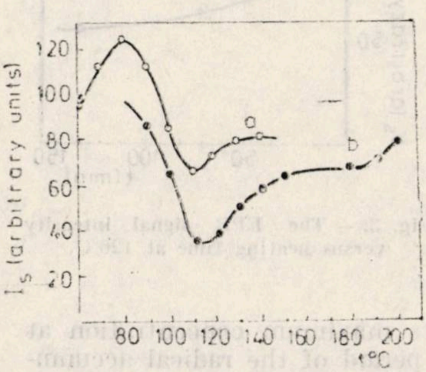

Fig. 5. — The isochronous variation of EPR signal in samples decomposed in vacuum : a) 60°C ; b) 80°C.

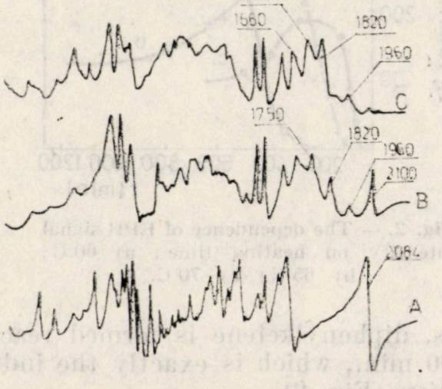

Fig. 6. — The infrared spectra of samples of : A — azibenzyl, B — azibenzyl decomposed in vacuum, C — azibenzyl decomposed in atmosphere.

The results regarding the thermal behaviour of these radicals correlate very well with the nature of products formed in system. They have been indentified especially by IR method, according to Fig . 6 .

Azibenzyl is characterized by the band at 2084 cm^{+1} which dissapears when it decomposes in vacuum being replaced by a new band at 2100 cm^{-1} characteristic to diphenylketene.[8] Among the reaction products, the following dimers could be tentatively identified : tetraphenylcyclobutandione[9–15] at 1750 cm^{-1} and 1820 cm^{-1} and tetraphenyl- -lactone [16,17] at 1660 cm^{-1}. Moreover, the appearance of the bands at 1720 cm^{-1} and 1940 cm^{-1} could point to the presence of a polymeric and alenic material,[17,18] respectively. It was also found that the intensity of the latest band increases with temperature. In fact the samples heated longer lose the fluidity, typical to diphenylketene, and turn into a breakable mass, like a polymeric material.

Figure 7 shows the electronic spectra (in hexane) of decomposed azibenzyl samples under different conditions in the absence of the solvent compared to those of pure diphenylketene and benzophenone. They supply an additional confirmation of the nature of the final products.

In these spectra recorded for azibenzyl samples decomposed in vacuum one could identify [19,20] tentatively the presence of diphenylketene by its maximum at 258 nm whereas in the presence at O_2 one notes a decrease of this maximum and the apperance of a new band at 250 nm characteristic to benzophenone.

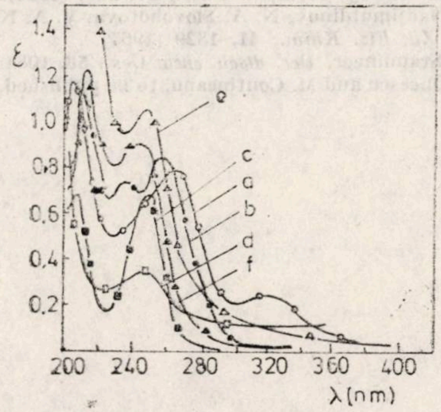

Fig. 7. — Electronic spectra recorded in samples of : a) undecomposed azibenzyl ; b) azibenzyl decomposed in vacuum ; c) pure benzophenone ; d) azibenzyl decomposed in oxygen atmosphere ; e) azibenzyl decomposed in atmosphere at 90°C ; f) diphenylketene bubbled with oxygen.

Among the final products of thermolysis of the nondegased azibenzyl samples we obtained a white powder also mentioned in the literature.[21] We could not establish its structure, but it can be a compound resulted from the reaction with O_2 of the radical generated by diphenylketene.

Our experimental results on the thermal decomposition of azibenzyl in the absence of the solvent offer the necessary information to establish a reaction mechanism, which will be published.[22]

REFERENCES

[1] R. Huisgen, *Angew. Chem.*, **67**, 439 (1955).

[2] V. Franzen, *Chem. Ztg.*, **81**, 359 (1957).

[3] L. Horner, E. Spietschka and A. Gross, *Liebigs Ann. Chem.*, **573**, 17 (1951).

[4] M. Contineanu, T. Oncescu and R. N. Schindler, *Rev. Roumaine Chim.*, **18**, 549 (1973).

[5] L. S. Singer and I. C. Lewis, *J. Amer. Chem. Soc.*, **90**, 4212 (1968).

[6] M. Contineanu, T. Oncescu and R. N. Schindler, *Rev. Roumaine Chim.*, **18**, 753 (1973).

[7] C. D. Nenițescu and E. Solomonica, *Organic Synthesis. Coll.* Vol. 2 Wiley, New York 1955, p. 496.

[8] A. Melzer and E. F. Jenny, *Tetrahedron Letters*, **43**, 4503 (1968).

[9] H. Staudinger, *Ber. dtsch. chem. Ges.*, **44**, 521 (1911).

[10] H. Staudinger, *Ber. dtsch. chem. Ges.*, **44**, 530 (1911).

W. Jügelt and D. Schmidt, *Tetrahedron*, **25**, 969 (1969).

[12] T. J. Clark and P. Yates, *J. Org. Chem.*, **27**, 286 (1962).

[13] R. Scarpati and D. Sica, *Gazz. chim. Ital.*, **92**, 1073 (1962).

[14] A. Abnöther, E. Jücker, E. Rissi, J. Rutschmann, E. Schreier, R. Steiner, R. Süess and A. Vogel, *Helv. Chim. Acta*, **42**, 927 (1959).

[15] B. Eistert, *Ber. dtsch. chem. Ges.*, **68**, 20 (1935).

[16] R. N. Hasek, K. D. Clark, E. U. Elan and J. C. Martin, *J. Org. Chem.*, **27**, 60 (1962).

[17] R. Anet, *Chem. and Ind.*, **33**, 1313 (1961).

[18] S. Nadjimutdinov, N. A. Slovohotova and V. A. Karaghin, *Zh. Fiz. Khim.*, **4**, 893 (1966).

[19] G. L. Hardy, *J. Chim. Phys.*, **21**, 281, (1924).

[20] S. Nadjimutdinov, N. A. Slovohotova, V. A. Karaghin, E. P. Cerneva and Iu. A. Cerbucov, *Zh. Fiz. Khim.*, **41**, 1829 (1967).

[21] H. Staudinger, *Ber. dtsch. chem Ges.*. **58**, 1084 (1925).

[22] T. Oncescu and M. Contineanu, to be published.

Revue Roumaine de Chimie, 36, *8*, 937–945 (1991)

Dedicated to Professor PETRU SPACU on the occasion of his 85th anniversary

CARBONIC ANHYDRASE ACTIVATORS. Part 2.[1]

AMINO ACIDS AND SOME OF THEIR DERIVATIVES MAY ACT AS POTENT ENZYME ACTIVATORS

CLAUDIU T. SUPURAN[a]*, ANTONIE DINCULESCU[b], GHEORGHE MANOLE[c],
FLORINA SAVAN[d], IOAN PUSCAS[d] and ALEXANDRU T. BALABAN[e]*

[a] University of Bucharest, Department of Organic Chemistry, Bd. Republicii 13, Bucharest 1, Roumania

[b] Chemical and Pharmaceutical Research Institute, Vitan 112, Bucharest, Roumania

[c] Builders' Clinical Hospital, Mandinesti str., 3–5, Bucharest, Roumania

[d] Roumanian Academy, Center for Research and Medical Assistance, Dunarii str., 37, 4775 Simleu Silvaniei, Roumania

[e] Polytechnic Institute, Department of Organic Chemistry, Polizu str., 1, Bucharest 12, Roumania

Received February 2, 1991

A number of 45 compounds, amino acids and derivatives, were tested as activators on isozymes I and II of carbonic anhydrase (CA). Some of these substances proved to be strong enzyme activators, while α-alanine is the only inhibitor in this series. The structural features leading to CA activation and the putative mechanism of action are discussed.

INTRODUCTION

Carbonic anhydrase (CA, EC 4.2.1.1), a highly efficient catalyst for the reversible interconversion of carbon dioxide and bicarbonate, plays an important role in the acid-base balance, in the transport of CO_2 between metabolizing tissues, in secretory processes such as gastric acid and ocular fluid secretions (in the case of vertebrates), as well as in photosynthesis (for the vegetal kingdom).[2] Inhibition of this enzyme by aromatic/heterocyclic sulfonamides [2,3] or monovalent inorganic anions [4] is extensively studied from the mechanistical point of view and in order to design novel drugs.[5,6]

In contrast to inhibition studies, activation of CA was a controversial issue for a long time. Van Goor [7] showed that activation of CA observed with some plasma proteins was in fact due to experimental artefacts, including denaturation of enzyme by violent shaking.[8] On the other hand, the report of Ho and Sturtevant [9] that EDTA is a strong CA activator was interpreted by Carter and Parsons[10] as a "shielding" of the enzyme from inhibitory heavy metals (possibly present in traces in solution, by chelation with the complexating agent), although the cited authors claimed that activation was induced by conformational alterations of CA produced by EDTA.[9] More recently, we [1,11,12] and others [13,14] proved that activation of CA is a phenomenon *per se*, and described some strong activators of this enzyme.

---

* To whom correspondence should be addressed.

In the present work we carried out an extensive study of CA activation with amino acids and derivatives, continuing our previous work [1] in determining the structural and electronic factors that must be present in the molecule of such a substance. As far as we know, this is the first comparative study of activation for the two most important isozymes of CA, namely CA I and CA II, and including the largest number of compounds tested.

EXPERIMENTAL

Enzymatic assays at 2°C were carried out by the micromethod of Maren,[15] as described elsewhere.[6b,c,12]. Concentrations of enzyme in the assay cell were approximately $3 \cdot 10^{-6}$M for CA I and approximately 10^{-8}M for CA II. Purified isozymes I and II of bovine origin were from Serva Feinbiochemica Heidelberg (batch No. 15882 for CA I and 15881 for isozyme CA II). The tested compounds had the following provenience : compounds **1**, **3**, **6**, **18**, **21**, **22**, **24**, **25**, **30**, **31**, **33**, **34**, **39**, **40**, **43**—**45** were from Serva ; compounds **2**, **4**, **7**, **19**, **20**, **23**, **27**, **35**, **38**, and **41** from Merck ; **32** and **37** from Fluka ; **13** from Reanal Budapest, **36** from Loba Feinchemie Vienna, and **42** from Nutritional Biochemicals. Compounds **5**,[16] **8**,[16] **9**—**12**,[17] **14**,[16] **15**—**17**,[17] and **26**—**29** [17] were prepared by literature procedures.

All compounds were tested in the concentration range 10^{-7}—10^{-3} mol/L. Stock solutions of the tested compound were prepared (10^{-2} M) in distilled deionized water, or water—DMSO (Merck) for the triaryl-pyridinium derivatives which have a poor water solubility. Successive dilutions were obtained in each case with distilled deionized water.

RESULTS AND DISCUSSION

As we have shown previously,[1,12] amines with the general formula I are CA activators, their potency depending primarily on the nature of the Ar group. Heterocyclic derivatives (Ar = 2-pyridyl, 4-imidazolyl, 5-amino-1,3,4-thiadiazol-2-yl, etc.) are stronger activators than aromatic compounds (Ar = phenyl, hydroxy-substituted phenyl, etc.).

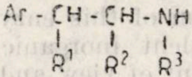

$\mathrm{Ar-\underset{R^1}{CH}-\underset{R^2}{CH}-\underset{R^3}{NH}}$

I

Fig. 1. — General Formula of CA Activators.

Ar = (substituted) aromatic/heterocyclic group.

R^1 = H, Me or OH.

$R^2 = R^3$ = H or Me.

On the other hand, Gargiulo et al.[14] showed recently, that dianionic species such as maleate, malonate, or hydrogen phosphate may act as CA activators for isozyme CA III. This is quite a surprising discovery, because it was reported previously that carboxylate anions act as CA inhibitors.[18] On the other hand, these authors showed that the dianionic activators do not compete for binding at the Zn(II) ion within the active site of CA III, but they have a different binding site, hypothesized to be Arg-67, a residue located 9 Å away from the Zn(II) ion.[14] They also hypothesized that the dianions acted as proton shuttle groups during the catalytic turnover, similarly with our hypothesis for compounds *I*, activators of isozyme CA *II*.[1,12]

Another recent and important finding is that of Parkes and Coleman [13] who showed that human erythrocyte or mouse hepatocyte membranes may efficiently activate human CA I and II. These authors also tested different compounds such as : membrane lipids, ion transport effectors (cAMP, caffeine, aldosterone, etc.), soluble proteins, and some amino acids for CA activation, and reported that only bovine serum albumine, myoglobin, lysine, polylysine, glycine and histidine are efficient CA activators (for human CA II). From the non-amino acid compounds tested, only imidazole proved to be activator for CA II, this compound being an inhibitor of CA I, as reported previously by Khalifah,[5b,19] and confirmed in this study of Parkes and Coleman.

All these recent findings prompted us to extend our study of CA activators to other compounds than amines *I*. Amino acids were considered good candidates for such a goal, especially taking into account the fact that some substances of this class have the general formula *I*, for $R^2 = COOH$ and $R^1 = R^3 = H$ (e.g. phenylalanine, tyrosine, histidine). As a consequence, a large series of substances were tested on the major isozymes, CA I and CA II, which possessed both free amino and carboxyl groups, but also derivatized compounds. The following groups of compounds were included in our study :

i) Natural and non-natural α-, β-, γ-, and ε-amino acids ;

ii) N-Alkyl- and N-acyl-amino acids (including phthalimido derivatives) as well as amino acid esters ;

iii) Trisubstituted pyridinium derivatives of amino acids, obtained by reaction of these amino acids with pyrylium salts, as reported by Balaban et al.[20]

iv) Dipeptides.

v) Aromatic aminoacids substituted with inductive electron withdrawing groups (OH, NH_2, F) at the aromatic moiety of the molecule.

In Table 1 we present activation data for the two CA isozymes with aliphatic aminoacids : glycine, β-alanine, γ-aminobutyric acid (GABA), ε-aminocaproic acid and some of their derivatives (II). In this group of compounds, the most active are Gly (**1**) and β-Ala (**7**). Alkylation/acylation of the amino group, as well as esterification of the carboxyl group, generally diminished the activation potency of the respective derivatives. An exception is hippuric acid (**2**) and its amino derivative (**3**), which preserve some of the activatory efficiency of glycine. On the other hand, more than three atoms between the two functional groups (II, $n \geq 3$), induced a loss of potency too. This is also true for all phthalimido derivatives III (Table 2), which possess a greatly diminished activity by comparison with the parent, underivatized amino acid. Generally, CA I was easier to activate than the high-activity isozyme, CA II.

Table 3 presents activation data with other types of amino acids, as well as their derivatives. Some surprising facts emerged during the study of these compounds. Thus, α-alanine (tested also by Parkes and Coleman [13] who reported it to be inactive against human isozyme CA II)

Table 1

CA activation with compounds of type II (CA I and II from bovine source; activator concentration in the assay cell : $5 \cdot 10^{-5}$ mol/L)

$$R^1NH-(CH_2)_n\ COOR^2$$

II

Compound No.	Name	R¹	R²	n	% Control CA activity [a] CA I	% Control CA activity [a] CA II
1	Glycine	H	H	1	150.2	151.2[b]
2	Hippuric acid	PhCO	H	1	131.6	119.3
3	4-Aminohippuric acid	$4-H_2NC_6H_4CO$	H	1	137.8	125.6
4	Ethyl sarcosinate	Me	Et	1	128.6	121.8
7	β-Alanine	H	H	2	152.8	139.7
13	GABA	H	H	3	112.0	115.0
27	ε-Aminocaproic acid	H	H	5	112.0	109.3
30	Methyl-ε-amino caproate	H	Me	5	100	100

[a] Control CA activity in the absence of activator is taken as 100%.

[b] For human CA II, Parkes and Coleman [13] found 177%, at $8 \cdot 10^{-4}$ M glycine.

Table 2

CA activation with phthalimido derivatives III (activator concentration $5 \cdot 10^{-5}$ mol/L)

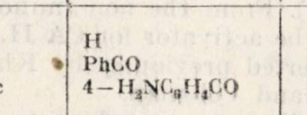

III

Compound No	n	% Control CA activity [a] CA I	% Control CA activity [a] CA II
5	1	109	100
8	2	113	100
14	3	106	100

[a] See Table 1.

was found by us to be inhibitor both for CA I and especially for CA II. Therefore, α-Ala is the only amino acid whose behaviour is similar with that of the carboxylic acids (more precisely, their sodium salts), from formic to hexanoic, which inhibit CA II.[18] The difference between α-Ala and its isomer, β-Ala, which is quite a potent activator, appears even more striking (see also Table 1). Then, the diamino monocarboxylic acids 19–22 and the hydroxy-amino acid 18 are also ineffective as CA activators, or possess only a weak activity. Again our data are somehow contradictory to those of Parkes and Coleman [13] who reported a stronger activation for lysine. The observed differences might be accounted for by the different source of enzyme and assay method in the two studies (the Wilbur—Anderson [21] method and human isozyme CA II, were used in their study, while we used bovine isozymes CA I and CA II and the method of Maren [15]). However our data are in good agreement with theirs for histidine (**41**), although the data from the mentioned study present a somehow greater activation (Table 3 and Fig. 2). Other compounds from this series such as cysteine, asparagine, glutamine, tryptophane, arginine and pyroglutamic acid show moderate activation at concentrations of $5 \cdot 10^{-5}$ M. Quite surprising is the fact that 0.001 M Arg produced a powerful activation (185%). But the most powerful activators in this

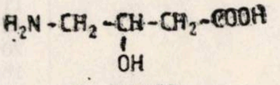

$H_2N-CH_2-\underset{OH}{CH}-CH_2-COOH$

18 : GABOB

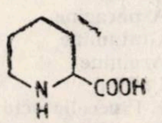

33 ; Pipecolic acid

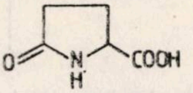

34: Pyroglutamic acid

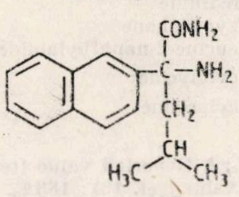

43

group were the following compounds : proline (**32**), pipecolic acid (homoproline, **33**), the leucine derivative **43**, as well as dipeptides **44** (glycylglycine) and **45** (glycylproline). These last two compounds are derivatives of two strong activators : glycine and proline, respectively. While the former is more efficient as activator than the parent aminoacid, the latter shows an intermediate potency, between Gly and Pro. This last amino acid is the strongest activator of CA which we have detected yet (Fig. 3).

In Table 4 we present activation data for derivatives obtained by reaction of amino acids with pyrylium salts.[17,20] These pyridinium derivatives preserve some potency as CA activators only in the case of trimethyl-substituted compounds derived from β-Ala, GABA, ε-aminocaproic acid and Asn, but their activity is diminished comparatively with the parent amino acid. The methyl-diphenyl- and triphenyl-substituted derivatives are completely devoid of such activity, a fact somehow similar with the situation of CA inhibitors possessing the same moiety and substitution.[22]

Finally Table 5 presents activation data of phenylalanine and some of its derivatives. All these compounds might be considered "classical CA activators", because formally they have formula I (with $R^2 = COOH$) of activators that we described earlier.[1] To our greatest surprise, these

Table 3

CA activation with natural/non-natural amino acids and their derivatives (activator concentration : $5 \cdot 10^{-5}$ mol/L)

Compound No.	Name	% Control CA activity[a]	
		CA I	CA II
6	D,L-Alanine	81.9	49.8[b]
18	D,L-GABOB	110.8	100
19	D,L-2,4-Diaminobutyric acid	100	100
20	L-Ornithine hydrochloride	100	100
21	L-Lysine hydrochloride	119.5	110.4[c]
22	N-α-Acetyl-L-lysine	110.3	100
23	L-Cysteine	121.7	114.3
24	L-Asparagine	131.6	112.7
25	L-Glutamine	118.6	100
31	L-Arginine	121.6	105.4[d]
32	L-Proline	207.5	203.9
33	D,L-Pipecolic acid (Homoproline)	168.9	163.7
34	L-Pyroglutamic acid	123.4	119.8
41	L-Histidine	138.7	152.3[e]
42	L-Tryptophane	124.8	118.0
43	L-Leucine-2-naphthylamide hydrochloride	140.1	127.4
44	Glycylglycine	163.9	162.8
45	Glycylproline	190.8	187.5

[a] See Table 1 ; [b] Reported value (ref. 13) : 100 %, for human CA II and 10^{-4} mol/L alanine ; [c] Reported value (ref. 13) : 183 %, for human CA II (the same concentration as for b) ; [d] At a concentration of 10^{-3} mol/L, Arg produced an activation of 185 % on bovine CA II ; [e] Reported value (ref. 13) : 170 %, on isozyme II, in a concentration of 10^{-5} mol/L His.

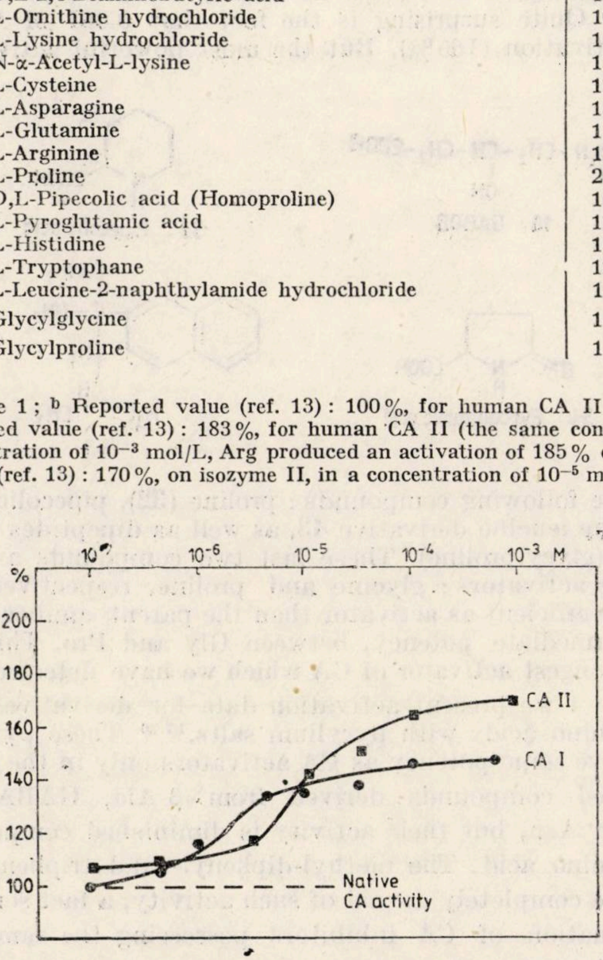

Fig. 2. — Activation of bovine CA I and II with histidine.

compounds are among the most active in the whole series of 45 substances tested by us (Fig. 4). Although the number and nature of substituents is quite diverse for this relatively small series of compounds, the activa-

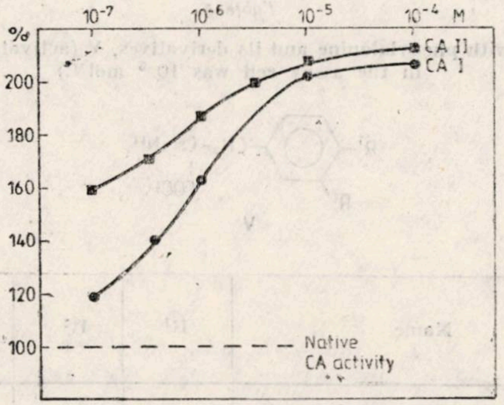

Fig. 3. — Activation of bovine CA I and II with proline.

Table 4

CA activation with pyridinium derivatives of amino acids, IV and **26** (activator concentration : $5 \cdot 10^{-5}$ mol/L)

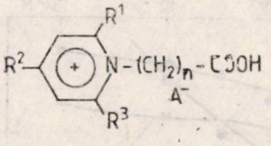

IV

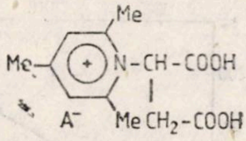

26

Compound No.	R¹	R²	R³	A	n	% Control CA activity[a]	
						CA I	CA II
9	Me	Me	Me	ClO_4	2	134.9	114.7
10	Me	Me	Me	BF_4	2	126.0	109.7
11	Me	Ph	Ph	ClO_4	2	100	100
12	Ph	Ph	Ph	ClO_4	2	100	100
15	Me	Me	Me	ClO_4	3	105	100
16	Me	Ph	Ph	ClO_4	3	100	100
17	Ph	Ph	Ph	ClO_4	3	100	100
26	see formula above			BF_4	—	121.8	112.6
28	Me	Me	Me	ClO_4	5	110.8	107.3
29	Me	Ph	Ph	ClO_4	5	100	100

[a] See Table 1.

tion efficiency does not vary too much, these compounds behaving in a similar manner. Another distinct feature is the fact that they activate to a greater extent isozyme CA II, in contrast to the other activators of this series which were more effective in activating isozyme I (the only other exceptions, together with Phe and its derivatives, are Gly and His).

Table 5

CA activation with phenylalanine and its derivatives, V (activator concentration in the assay cell was 10^{-5} mol/L)

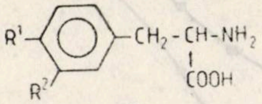

V

Compound No.	Name	R¹	R²	% Control CA activity[a]	
				CA I	CA II
35	L-Phenylalanine	H	H	178.3	186.7
36	L-Tyrosine	OH	H	165.9	189.1
37	L-3-Hydroxy-tyrosine	OH	OH	124.4	134.3
38	L-3-Amino-tyrosine	OH	NH_2	130.0	176.3
39	L-4-Fluorophenylalanine	F	H	132.5	167.7
40	D,L-4-Aminophenylalanine	NH_2	H	147.1	159.4

[a] See table 1.

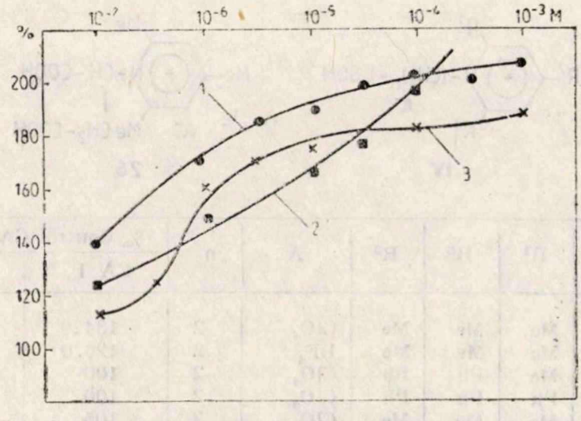

Fig. 4. — Activation data for CA isozymes I and II with phenylalanine and some derivatives;

1 : phenylalanine and CA II.
2 : tyrosine and CA I.
3 : 3-aminotyrosine and CA II.

CONCLUSIONS

The catalytic mechanism for the CA isozymes is well understood, especially after the emergence of such techniques as oligonucleotide-directed mutagenesis, which offered the possibility of obtaining variant enzymes with different properties.[23] As a consequence, it is actually known that the determinant step in the catalysis of CO_2 hydration is bicarbonate dissociation from the active site for CA I,[23] and a proton-transfer step for CA II.[3] In kinetic studies of Silverman's and Lindskog's groups, it was also discovered that the buffers may participate in such proton-transfer steps,[3b,c, 24] although it was claimed that the interaction between enzyme and buffer has little structural specificity.[3a]

Our results suggest that CA activation, which may be the result of proton shuttling, accomplished with the assistance of the activator, requires precise steric and electronic factors to be present in the molecule of such a compound. Discovery of activators of type I, as well as the strong activation observed with some amino acids, reported in the present study, brings some new insights in this field.

On the other hand, we observed that the most efficient amino acids as CA activators, such as Phe, Tyr, His, Trp, Asp, Gln, Cys, belong to the same group, of "semiconducting" side chained-amino acids, in the new classification of Sneddon et al.[25] based on the doublet acceptor energy levels (Pro, the most efficient activator, was not classified in this system). This classification suggests that some side chains (among which are also the "semiconducting" ones) propagate electronic coupling more effectively than others (like the "repulsive" or "insulating" side-chains, present in the molecules of amino acids which do not possess CA activating properties), and this fact might be important for CA catalysis.

In conclusion, our study demonstrated the efficiency of some amino acids and their derivatives as CA activators, and some relevant differences between the two isozymes CA I and CA II. In the following reports we will present the interaction of CA isozymes with other types of compounds that might affect the catalytic turnover.

ACKNOWLEDGMENTS. Special thanks are addressed to SERVA Feinbiochemica Heidelberg, and to Mr. Gert Hartmann, for the gift and fast delivery of enzymes and some reagents used in this work. We are extremely grateful to professor Brian W. Clare (Murdoch Univ., Western Australia) for his invaluable help.

REFERENCES

[1] First part in this series : I. Puscas and C. T. Supuran, "Carbonic Anhydrase Activators and Inhibitors — Structure Activity Relationship", *in* "Carbonic Anhydrase, From Biochemistry and Genetics, to Physiology and Clinical Medicine", R. E. Forster Ed., Elsevier, New York, 1991.

[2] T. H. Maren, *Physiol. Rev.*, **47**, 595 (1967).

[3] a) D. N. Silverman and S. Lindskog, *Acc. Chem. Res.*, **21**, 30 (1988) ;
b) B. H. Jonsson, H. Steiner and S. Lindskog, *FEBS Lett.*, **64**, 310 (1976) ;
c) D. N. Silverman and C. K. Tu, *J. Am. Chem. Soc.*, **97**, 2263 (1975).

[4] S. Lindskog, *Biochemistry*, **5**, 2641 (1966).

[5] a) Y. Pocker and N. Janjič, *J. Am. Chem. Soc.*, **111**, 731 (1989) ; b) R. G. Khalifah ,*Proc. Natl. Acad. Sci. USA*, **70**, 1986 (1973).

[6] a) S. L. Graham, J. M. Hofman, P. Gautheron, S. R. Michelson, T. H. Scholz, H. Schwam, K. L. Shepard, A. M. Smith, R. L. Smith, J. M. Sondey and M. F. Sugrue, *J. Med Chem.*, **33**, 749 (1990) ; b) C. T. Supuran, A. T. Balaban, M. D. Gheorghiu, A. Schi-

ketanz, A. Dinculescu and I. Puscas, *Rev. Roumaine Chim.*, **35**, 399 (1990) ; c) C. T. Supuran, G. Manole, A. Schiketanz, M. D. Gheorghiu and I. Puscas, *Rev. Roumaine Chim.*, **36**, 251 (1991)

[7] H. van Goor, *Enzymologia*, **13**, 73 (1948).

[8] A. M. Clark and D. D. Perrin, *Biochem. J.*, **48**, 495 (1951).

[9] C. Ho and J. M. Sturtevant, *Biochem. Biophys. Res. Commun.*, **3**, 20 (1960).

[10] M. J. Carter and D. S. Parsons, *J. Physiol.*, **215**, 71 (1971).

[11] I. Puscas, G. Buzas, P. Contrasiu and P. Suranyi, *Rev. Roumaine Biochim.*, **16**, 317 (1979).

[12] I. Puscas, C. T. Supuran and G. Manole, *Rev. Roumaine Chim.*, **35**, 683, (1990).

[13] J. L. Parkes and J. Coleman, *Arch. Biochem. Biophys.*, **275**, 459 (1989).

[14] N. J. Gargiulo, F. A. Santoll and R. S. Rowlett, Carbonic Anhydrase International Workshop, Spoleto, Italy, 1990, Abstract Book, pp. 38.

[15] T. H. Maren, *J. Pharmacol. Exptl. Ther.* **130**, 26 (1960).

[16] S. Gabriel, *Ber. dtsch. Chem. Ges.*, **41**, 242 (1908).

[17] a) A. Dinculescu and A. T. Balaban, *Rev. Roumaine Chim.*, **25**, 1505 (1980) ; b) A. Dinculescu, Ph. D. Thesis, Polytechnic Institute of Bucharest, 1979 ; c) A. T. Balaban, A. Dinculescu, G. N. Dorofeenko, G. W. Fischer, A. V. Koblik, V. V. Mezheritskii and W. Schroth, "Pyrylium Salts. Syntheses, Reactions and Physical Properties" *in* "Advances in Heterocyclic Chemistry", A. R. Katritzky Ed., Academic Press, 1982.

[18] Y. Pocker and T. L. Deits, *Ann. N. Y. Acad. Sci.*, **429**, 76 (1984).

[19] R. G. Khalifah, J. I. Rogers and J. Mukherjee, Carbonic Anhydrase International Workshop, Spoleto, Italy, 1990, Abstract Book, pp. 20.

[20] C. Toma and A. T. Balaban, *Tetrahedron*, Suppl. **7**, 27 (1966).

[21] K. M. Wilbur and N. G. Anderson, *J. Biol. Chem.*, **176**, 147 (1948).

[22] C. T. Supuran, G. Manole, A. Dinculescu, A. Schiketanz, M. D. Gheorghiu, I. Puscas and A. T. Balaban. *J. Pharm. Sci. (in press)*

[23] a) G. Behravan, B. H. Jonsson and S. Lindskog, *Eur. J. Biochem.*, **190**, 351 (1990) ; b) S. Lindskog, Carbonic Anhydrase International Workshop, Spoleto, Italy, 1990, Abstract Book pp. 8 ; c) D. N. Silverman, C. K. Tu and P. J. Laipis, *ibid.* pp. 10.

[24] R. S. Rowlett and D. N. Silverman, *J. Am. Chem. Soc.*, **104**, 6737 (1982).

[25] S. F. Sneddon, R. S. Morgan and C. L. Brooks III, *Biophys. J.*, **53**, 83 (1988).

Revue Roumaine de Chimie, **36**, *8*, 947–964 (1991)

Dedicated to Professor ALEXANDRU T. BALABAN on the occasion of his 60th anniversary

BIOACTIVE POLYMERS. 69 *

CROSS-LINKED XANTHAN AS DRUG-CARRIER MATRICES

SEVERIAN DUMITRIU and MARIA DUMITRIU

Polytechnic Institute of Jassy, Department of Macromolecular Chemistry
Bdul. Copou 11, R-6600, Jassy, Romania

Received January 15, 1991

Reticulation of xanthan with epichlorohydrin — as depending upon time and temperature — is studied. The reticulation degree of the polysaccharide is correlated with the sorption properties of water and of some organic compounds (alcohol, dioxan)/water mixtures. Depending on the synthesis conditions, xanthan gels with swelling degrees between 420 and 1000 % are obtained. Various drugs, such as isosorbite dinitrate, medroxyprogesteron have been introduced, through diffusion in the xanthan hydrogels, the following maximum values of inserted drug being obtained : isosorbite dinitrate = 150 mg/g ; medroxyprogesteron = 28 mg/g. All inserted drugs show a zero-order release kinetics. The neomycine — furazolidone — xanthan complex, in which neomycine is covalently linked to xanthan and furazolidone is inserted in the hydrogel formed by the reaction of neomycine with xanthan, is synthesized. The neomycine and furazolidone content in the complex depends on the ratio of the drugs present in the reaction medium. Thus, a zero-order kinetics is obtained for the release of both neomycine and furazolidone, in a basic medium. Consequently, the antimicrobial activity of the neomycine — furazolidone — xanthan complex is intensified.

INTRODUCTION

In recent years, extensive research has been directed towards the controlled release of pharmaceuticals. Polymeric materialas, especially the hydrogel, have been extensively studied because of their potential applications in this area.[1–5]

Advantages of hydrogels are the control of the release characteristics by an adjustable water-sorption and sorption rate and the often good compatibility with biological tissues and fluids.[6] Furthermore, matrix delivery systems based on hydrogel polymers have been developed, exhibiting zero-order release kinetics.[7–8]

Since Wichterle and Lim proposed the use of hydrogels for biomedical applications in 1960,[9] hydrogels have been extensively studied and used for a number of biomedical applications,[10,11] controlled drug release,[12-13] enzyme immobilization,[14,15] and other uses.[16-17] The efficacy of hydrogels as biomaterials results from the similarity of their hydrated structure to natural tissue. Nevertheless, hydrogels of extremely diverse chemical compositions have been prepared.[18-22]

Hydrogel is an acceptable material to insert from the standpoint of biocompatibility because it generally has a low stimulation to living tissue. Conventionally, the hydrogel is dipped in aqueous drug solution before insertion.[23,24] In these devices, the drug is first dissolved or dispersed within the polymeric matrix, which is usually in a glassy state. When these systems are placed into the dissolution medium (e.g. water), it penetrates the glassy region and the polymeric matrix begins to swell. In the presence of penetrant molecules (water), macromolecular chains in the polymeric network gain mobility. In this case, the swollen polymer is in a rubbery state and the rubbery region allows the drug to diffuse. These are known as swelling — controlled — release systems.[25-27] Depending on the relative magnitude of the rate of polymer swelling to the rate of drug diffusion, various release profiles may be possible. The situation where the polymer structural rearrangement has taken place rapidly in response to the swelling solvent as compared to drug diffusion generally leads to typical Fickian diffusion characteristics and the so-called first-order release behaviour. Various analyses and criteria have been reported in the literature [28-29] for predicting whether drug release from swelling-controlled polymer matrices will be first or zero-order (diffusion or relaxation controlled).

Soluble natural macromolecules have been suggested as carriers for different drugs. These include DNA, dextrans, plasma proteins notably albumin, antibodies and glycoproteins.[28-30] Nevertheless, these systems evidence some disadvantages, i.e. their increased solubility in water, which induces a too fast elimination after their oral administration.

Hydrogels based on modified (through reticulation or analogous polymer transformation) polysaccharides represent products with several applications in drug delivery systems.[31-35] Increasing attention is paid nowadays — on considering the production of controlled release systems — to xanthan, a polysaccharide obtained from the microbial synthesis of *Xanthomonas campestris* ; it is soluble in water, biocompatible, polyanionic. In this respect, special attention is paid to drug coupling through covalent bonding [36-38] or to formation of macromolecular complexes with polybasic antibiotics.[39-41] The transformation of xanthan into a water-insoluble hydrogel was performed through reticulation with epichlorohydrin or acetalization with glyoxal.[42-44]

The present study discusses the obtainment of a new type of semi-synthetic hydrogel, by the reticulation of xanthan with epichlorohydrin and its utilization in systems of controlled release with isosorbite dinitrate (ISDN), medroxyprogesteron (MP). By employing the reaction between xanthan and neomycine (Ne) — determining the formation of a hydrogel, furazolidone has been inserted, which resulted in a tricompound system of controlled release, of the Ne — furazolidone — xanthan type.

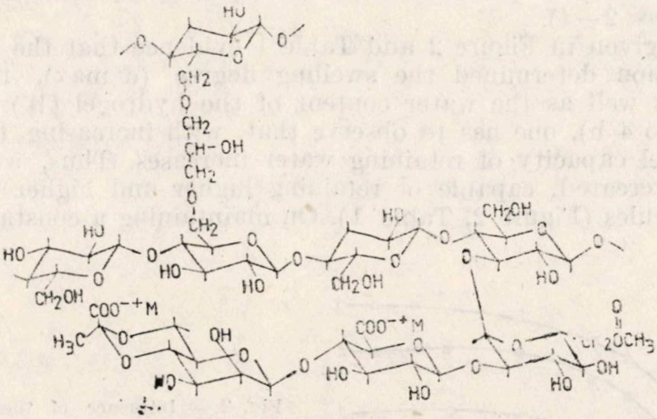

Fig. 1. — Structure of xanthan reticulated with epichlorohydrine.

ISDN AND XANTHAN DRUG – POLYMER CONJUGATE SYSTEMS

Reticulation of xanthan with epichlorohydrine has been performed by applying the method discussed in[45].

Study of the hydrogel swelling process has been performed on disks, 5 mm in diameter and 1.5 mm thick, cut up with a filmmade mould. The swelling degree (&) was determined by the static method through the introduction in water of samples of reticulated xanthan followed by keeping them for determined times, and weighing.

$$\& = \frac{\text{Swollen gel wt} - \text{Dry gel wt}}{\text{Dry gel wt}} \times 100 \qquad (1)$$

Graphical representation of the relation &-swelling time permits the determination of &max when & remains constant. The swelling rate, Q, and the water content of the hydrogel at the moment of the equilibrium installation, W, are obtained from relations 2 and 3 :

$$Q = \frac{\text{Weight of swollen gel}}{\text{Weight of dried gel}} \qquad (2)$$

$$W = \frac{\text{Swollen gel wt}^* - \text{Dry gel wt}}{\text{Swollen gel wt}^*} \times 100 \qquad (3)$$

where * — is the value obtained at the installation of the swelling degree is determined from &max.

By reticulation of xanthan with epichlorohydrin, a hydrogel with the structure given in Figure 1 — is obtained.

In order to appreciate the reticulation degree of the hydrogel, its swelling capacity has been determined in water or in various alcohol/water mixtures. Water is necessary for inducing a certain swelling degree for the hydrogel, which is required in the process of drug diffusion.

The reticulation process is influenced by temperature and the reaction time (Figures 2–4).

Data given in Figure 2 and Table 1 evidence that the temperature of reticulation determined the swelling degree (& max), the swelling rate (Q), as well as the water content of the hydrogel (W). With short times (up to 4 h), one has to observe that, with increasing temperature, the hydrogel capacity of retaining water increases. Thus, a reticulation network is created, capable of retaining higher and higher amounts of water molecules (Figure 2, Table 1). On maintaining a constant temperature of 40°C, on increasing the reaction time, the hydrogel sorption capacity decreases as a consequence of the formation of a compact reticulation network in which water molecules can no longer penetrate (Figure 3,

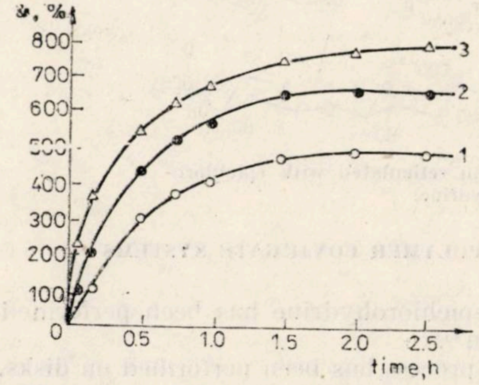

Fig. 2. — Influence of the reticulation temperature upon xanthan swelling degree. 1 = 40°C ; 2 = 60°C ; 3 = 80°C ; Time = 6 h.

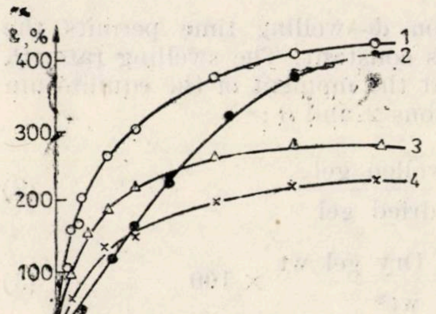

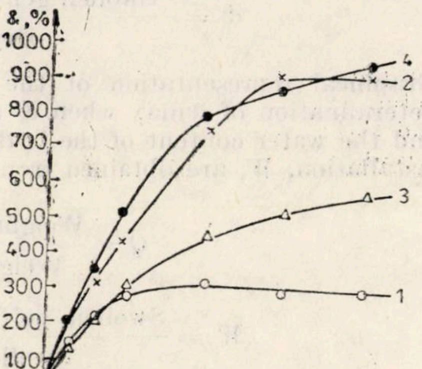

Fig. 3. — Influence of the reticulation time upon xanthan swelling degree. 1 = 3 h ; 2 = 4 h ; 3 = 6 h ; 4 = 9 h ; Temperature = 40°C.

Fig. 4. — Influence of temperature and reticulation time upon xanthan swelling degree. 1. Temperature = 50°C ; Time = 1.5 h ; 2. Temperature = 50°C, time = 17 h ; 3. Temperature = 60°C, time = 4 h ; 4. Temperature = 60°C, time = 9 h.

Table 1

Influence of xanthan reticulation temperature upon water sorption properties

Temperature (°C)	& max (%)	W (%)	Q
40	400	80.39	5.10
60	580	85.24	6.72
80	810	87.14	7.84

Time = 4 h

Table 2

Influence of temperature and time of xanthan reticulation degree upon water sorption properties

Temperature (°C)	Time (h)	& max (%)	W (%)	Q
40	3	440	80.85	5.22
40	4	400	80.39	5.10
40	6	260	73.85	3.82
40	9	240	70.29	3.36
50	1.5	300	75.63	4.10
50	17	900	90.19	10.19
60	4	560	85.24	9.77
60	9	950	90.54	10.57
80	4	800	87.14	7.48

Table 2). At temperatures over 40°C (50, 60, 80°C) reticulation occurs differently. Thus, the reaction time influences favourably the reticulation degree, and, implicitly, water's sorption capacity.

Such a phenomenon may be explained by the fact that — under conditions of medium alkalinity — epichlorohydrin is subjected to a rapid hydrolysis, thus an insufficient amount, even lower than when employing a 40°C temperature, remaining for the reaction. Consequently, quite a low number of reticulation bridges — expected to reduce, after a certain value, the swelling degree — are formed.

The process of swelling reticulated xanthan into the alcohol/water mixture was studied in order to establish the diffusional processes of ISDN in the hydrogel, the swelling curves being plotted in Figure 5. Figure 5 and Table 3 evidence that the alcohol/water ratio influences significantly the swelling parameters of the hydrogel. &max, W and Q values increase with increasing the amount of water in the alcohol/water mixture.

ISDN insertion was performed through their diffusion from various solutions of alcohol/water (5/1, 5/2, 5/3, v/v), having a drug concentration of 1.5 and 2.0 %. The alcohol is employed as solvent for ISDN, while water as swelling agent. The limit of ISDN precipitation from the alcohol (solutions up to 3 %) is met at an alcohol/water ratio of 5/4 (v/v). The diffusion was established by measuring the variation of the drug concentration into the solution.

ISDN diffusion into hydrogel depends on the alcohol/water ratio, and on the drug concentration into the diffusion medium (Figure 6). Alcohol/water ratios ranging between 5/1 and 5/3 (v/v) has been employed.

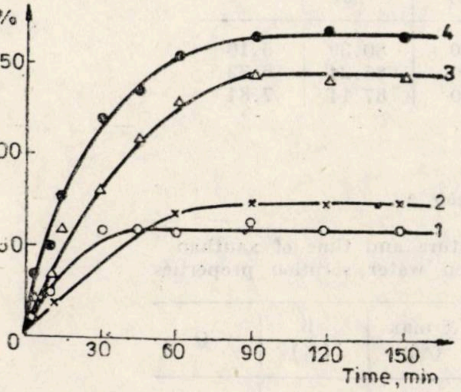

Fig. 5. — Influence of the alcohol/water ratio (v/v) upon the hydrogel based on reticulated xanthan 1. Aocohol/water ratio = 5/1 ; 2. 5/2 (v/v) ; 3. 5/3 (v/v) ; 4. 5/4 (v/v). Xanthan reticulated with & max = 678 %, $Q = 6.77$, $W =$ $= 85.24$ %.

Increasing the volume of water from the mixture employed and its concentration in ISDN leads to increase of the amount of diffused ISDN. Water plays the role of increasing the hydrogel swelling degree and, consequently, its permeability to ISDN. Increasing the concentration of the ISDN from the environment induces an increase of the gradient concentration, which permits increasing of the diffusion rate.

Table 3

Influence of the alcohol/water ratio upon the swelling process of reticulated xanthan

Alcohol/water ratio (v/v)	*W* (%)	*Q*
5/1	37.90	1.61
5/2	42.84	1.95
5/3	58.84	2.12
5/4	62.69	2.68

Reticulated xanthan with the following characteristics : & max = 678 %, $Q = 6.77$, $W = 85.24$ %.

On expressing the diffusional process by the diffusion rate (Figure 7), one may observe the presence of some maximum rates, their values depending on the concentration of water and of the ISDN from the system. Higher diffusion rates are to be obtained with increasing the water volume.

The peaks characterizing the diffusion rates (Figure 7) of ISDN in more concentrated solutions (2%) are wider. Such differences may be explained by the fact that, after the solvent — ISDN primary diffusion — when the hydrogel swelling occurs — in the case of more concentrated solutions, a higher concentration gradient is created, as compared with the one characterizing diluted solutions (1.5%).

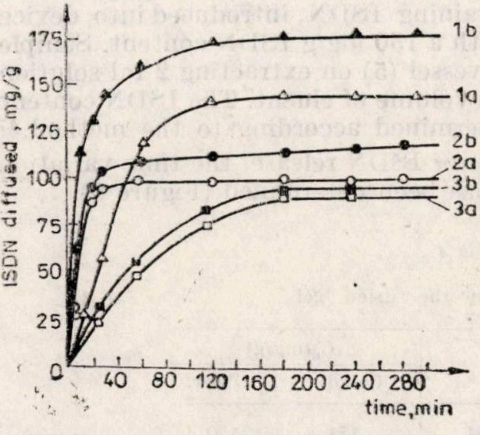

Fig. 6. — Time variation of the amount of ISDN inserted in the hydrogel as a function of ISDN concentration and alcohol/water ratio. 1a — alcohol/water ratio = 5/3 (v/v), ISDN concentration = 1.5%; 1b — alcohol/water ratio = 5/3 (v/v), ISDN concentration = 2.0%; 2a — alcohol/water ratio = 5/2 (v/v), ISDN concentration = 1.5%; 2b — aocohol/water ratio = 5/2 (v/v), ISDN concentration = 2.0%; 3a — alcohol/water ratio = 5/1 (v/v), ISDN concentration = 1.5%; 3b — alcohol/water ratio = 5/1 (v/v), ISDN concentration = 2.0%.

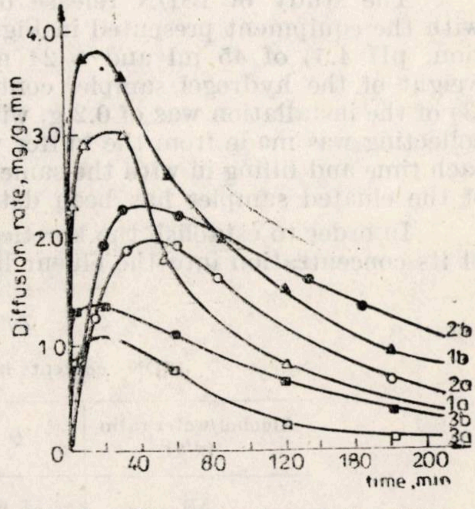

Fig. 7. — Time variation of the diffusion rate of ISDN into the hydrogel. 1a — Alcohol/water ratio = 5/3 (v/v), ISDN concentration = 1.5%; 1b — alcohol/water ratio = 5/3 (v/v), ISDN concentration = 2.0%; 2a — alcohol/water ratio = 5/2 (v/v), ISDN concentration = 1.5%; 2b — alcohol/water ratio = 5/2 (v/v), ISDN concentration = 2%; 3a — alcohol/water ratio = 5/1 (v/v), ISDN concentration = 1.5%; 3b — alcohol/water ratio = 5/1 (v/v), ISDN concentration = 2.0%.

The polar character of ISDN [45] contributes to the development of the diffusional process, since the support being known as a polyanion will interact electrostatically with the drug, thus permitting its insertion and fixation into the hydrogel.

The ISDN content in the dried hydrogel is determined by relation (4): [46]

$$C_{\mathrm{d}} = \frac{1000\,C\,(Q-1)/d}{[C(Q-1)/d] + 1000} \tag{4}$$

where C_d in the drug content of the dried gel (mg/g), C is the concentration of the drug in solution (mg/ml), and d (g/ml) is the density of the solvent. This equation is based on the assumption that both the solubility of the drug in the organic solvent, C, and the swelling ratio of the polymer, Q, are kept constant in the drug — solvent — polymer ternary system as in each binary system.

The values of C_d for the three alcohol/water ratios are given in Table 4. As shown in Table 4, the measured drug concentrations in the gel agree approximately with the values calculated by eq. (4).

The study of ISDN release of the hydrogel has been performed with the equipment presented in Figure 8. An eluent volume (buffer solution, pH 4.5) of 45 ml and a 24 ml/h flow have been employed. The weight of the hydrogel sample, containing ISDN, introduced into device (3) of the installation was of 0.2 g, with a 150 mg/g ISDN content. Sample collecting was made from the buffer vessel (5) on extracting 2 ml solution each time and filling in with the same volume of eluent. The ISDN content of the eluated samples has been determined according to the method.[47]

In order to establish the kinetics of ISDN release, the time variation of its concentration into the eluent has been determined (Figure 9).

Table 4

ISDN content in the dried gel

Alcohol/water ratio (v/v)	Q	C_d(mg/g)	
		Calcd.	Obser.
5/1	1.61	171	150
5/2	1.95	112	100
5/3	2.42	81	87

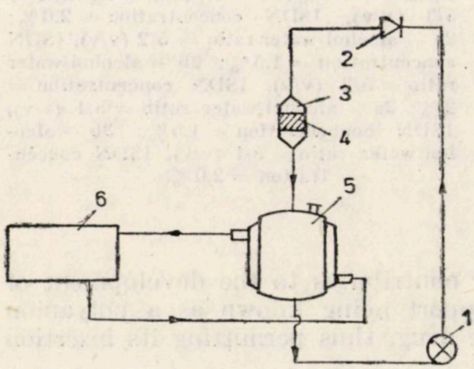

Fig. 8. — Apparatus for studying the kinetics of ISDN release 1 — Peristaltic pump; 2 — Flow regulator; 3 — Sample cell; 4 — Sample of controlled release ISDN; 5 — Effluent reservoir; 6 — Thermostate.

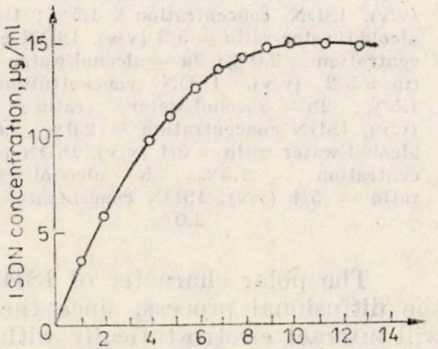

Fig. 9. — Time variation of the concentration of released ISDN. Eluent is buffer, pH 4.5; flow = 24 ml/h.

As seen from Figure 9, the concentration of ISDN into the eluent is constant after 10 h. The amount of ISDN released from the sample has been calculated according to the relation:

$$m_{\mathrm{ISDN}} = C_{\mathrm{ISDN}}\, V_{\mathrm{e}} + \sum_{i=0}^{n-1} C_i\, V_i \qquad (5)$$

where : m_{ISDN} — amount of ISDN released from the sample at a certain time (mg);
C_{ISDN} — concentration of ISDN in the extracted sample (mg/ml);
V_e — volume of eluent recirculated through the system (ml);
V_i — volume of the extracted sample, i, (ml);
C_i — concentration of ISDN in the extracted sample, i, (mg/ml).

Figure 10 plots graphically the dependence between the weight of released ISDN and time. Installation after 12 h, of a constant release domain is presented in Figure 9. The high value of the concentration in solution (Figure 9) and of the released ISDN weight (Figure 10), obtained in the first 11 h, is explained through the intense diffusion processes occurring between the retard ISDN and the eluent as determined by the

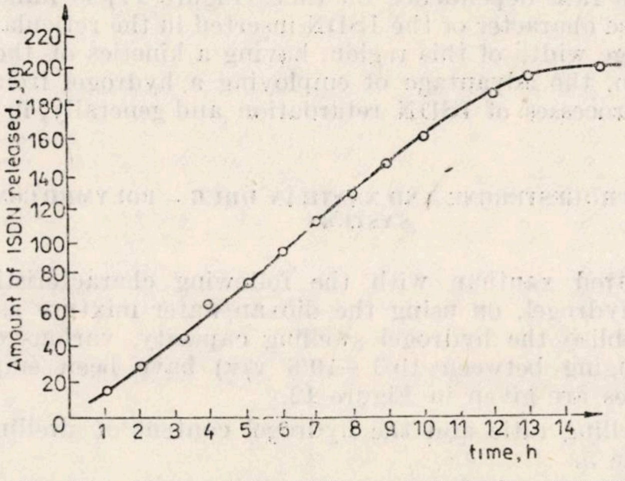

Fig. 10. — Time variation of the amount of released ISDN.

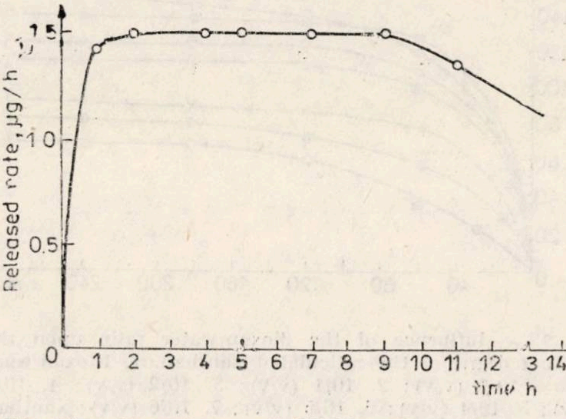

Fig. 11. — Dependence of ISDN, release rate on time.

high concentration gradient present within this time interval. As ISDN is accumulated in the eluent, the concentration gradient is reduced, the diffusion process being consequently reduced.

For the evaluation of the release rate the kinetic curve in Figure 10 has been employed, the amounts of ISDN released within an hour being thus established.

The release rate has been calculated according to the relation:

$$R = \frac{1}{m_{\mathrm{ISDN}}} \frac{\Delta m}{\Delta t} \tag{6}$$

where: m_{ISDN} — ISDN weight in the sample under study;
Δm — ISDN weight released over Δt.

The presence of constant rate domain in the graphical representation of the release rate dependence on time (Figure 11) is indicative of the delayed release character of the ISDN inserted in the reticulated xanthan. The quite large width of this region, having a kinetics of the zero order, evidences, too, the advantage of employing a hydrogel from reticulated xanthan in processes of ISDN retardation and generally, in drug retardation.

MEDROXYPROGESTERONE AND XANTHAN DRUG – POLYMER CONJUGATED SYSTEMS

Reticulated xanthan with the following characteristics MP was included in hydrogel, on using the dioxan/water mixture as solvent. In order to establish the hydrogel swelling capacity, various dioxan/water mixtures (ranging between 10/1–10/6 v/v) have been employed. The swelling curves are given in Figure 12.

The swelling ratio and the hydrogel content of swelling agent are given in Table 5.

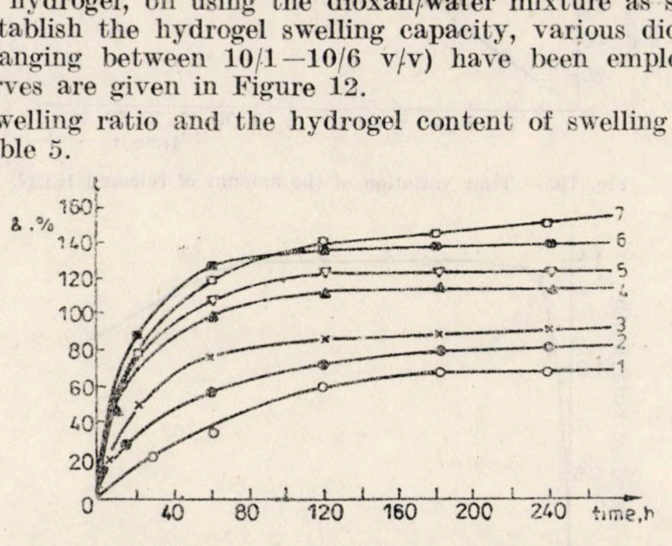

Fig. 12. — Influence of the dioxan/water ratio upon the swelling degree/of the reticulated xanthan. 1. Dioxan/waer ratio = 10/0 (v/v); 2. 10/1 (v/v); 3. 10/2 (v/v); 4. 10/3 (v/v); 5. 10/4 (v/v); 6. 10/5 (v/v); 7. 10/6 (v/v); xanthan reticulated with & max = 678, $Q = 6.77$, $W = 85.24\%$.

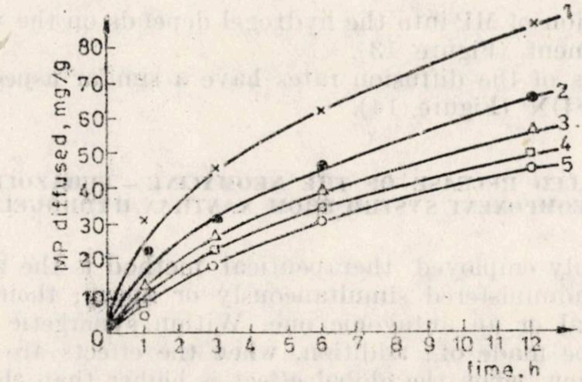

Fig. 13. — Time variation of the amount of MP diffused into hydrogel of reticulated xanthan. 1. Dioxan/water ratio = 5/2 (v/v); 2. 5/1.5 (v/v); 3. 5/1 (v/v); 4. 5/0.5 (v/v); 5. 5/0 (v/v). Xanthan reticulated with &max = 678 %, $Q = 6.77$, $W = 85.24$ %. Concentration MP = 1.5 %.

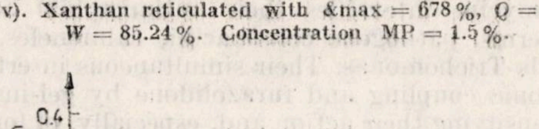

Fig. 14. — Time variation of the diffusion rate of MP into the hydrogel. 1. Dioxan water ratio = 5/0 (v/v); 2. 5/0.5 (v/v); 3. 5/1 (v/v); 4. 5/1.5 (v/v); 5. 5/2 (v/v). Xanthan reticulated with &max = 678 %, $Q = 6.77$, $W = 85.24$ %.

Table 5

Influence of the dioxan/water ratio upon the swelling process of reticulated xanthan

Dioxan/water ratio (v/v)	W (%)	Q
5/0	68.9	1.76
5/0.5	80.5	1.89
5/1	89.7	1.98
5/1.5	95.6	2.01
5/2	127.4	2.11
5/2.5	158.1	2.74
5/3	188.7	2.88

Reticulated xanthan with the following characteristics: & max = 678 %, $Q = 6.77$, $W = 85.24$ %.

The diffusion of MP into the hydrogel depends on the water content of the environment (Figure 13).

The curves of the diffusion rates have a similar aspect with those obtained for ISDN (Figure 14).

CONTROLLED RELEASE OF THE NEOMYCINE – FURAZOLIDONE BICOMPONENT SYSTEM FROM XANTHAN HYDROGEL

A commonly employed therapeutical method is the association of several drugs, administered simultaneously or apart; their action may be a synergetical or an antagonic one. Within synergetic interactions, mention must be made of: addition, when the effects are summed up, and intensification, when the global effect is higher than the sum of the partial effects.

Preliminary investigation [48] evidenced that association of furazolidone with neomycine intensifies their antimicrobial activity towards gram negative germs, pathogene colonbacilli, salmoneles, staphylococci, as well as towards Trichomonas. Their simultaneous insertion on xanthan (neomycine by ionic coupling and furazolidone by gel-insertion) has the advantage of intensifying their action and, especially, of forming a controlled release system with different rates, as a consequence of links specific to each drug.

Neomycine is coupled on xanthan through the formation of ionic bonds between the aminic groups of the drug and the carboxylic ones of xanthan. Furazolidone is inserted in the hydrogel formed by the reaction between neomycine (Ne) and xanthan.

For obtaining a delayed release, three solutions are prepared, from the Ne-Furazolidone-xanthan complex:

A. 0.2–1.0 g xanthan (Pharmaceutical grade) are dissolved in 100 ml water, under stirring;

B. 0.2–1.4 g Neomycine sulphate are dissolved in 100 ml water;

C. 0.2–0.8 g furazolidone (Fu) (Furoxane, Furoxone) are dissolved in 30 ml dimethylformamide, by careful heating up to 40–45°C, at dark.

Over solution A, solution C is added, in small amounts, under stirring. Further on, the formed mixture is treated with solution B, which leads to a precipitate representing the Ne-Fu-xanthan complex. Stirring goes on for other 15 minutes, then the obtained precipitate is filtered off and washed with 10 ml distilled water and finally with 100 ml ethanol. The reaction product is vacuum dried and jarred.

Dosing of Fu from the Ne-Fu-xanthan complex. 0.2 g of the reaction product – extracted quantitatively with 100 ml DMF – are weighed. The extracted Fu is dosed photocolorimetrically at 367 nm.

Dosing of Ne from the Ne-Fu-xanthan complex. The total nitrogen content of the Ne-Fu-xanthan complex – out of which the nitrogen ratio corresponding to the photocolorimetrically dosed Fu is subtracted – is determined. The Ne ratio is calculated from the value of the remaining nitrogen.

Kinetic study of the Ne and Fu release from the Ne-Fu-xanthan complex. The kinetic studies of Ne and Fu release were performed using the apparatus illustrated in Figure 8. The sample cell holds 1 ml and the eluent reservoir 50 ml. The peristaltic pump and the flow regulator circulating eluent at 1.4 ml/min. The measurement cell was maintained at 37°C. For every 1 ml sample taken from the eluent reservoir, 1 ml of eluent was added. The eluent used was a solution of NaOH with a pH value of 8.2 and 9.5, respectively. The Ne content of the sample taken was determined photocolorimetrically[50] at 570 nm while Fu at 367 nm.

Microbiological tests were performed on agar plates inoculated with *Staphylococcus aureus* 209 P and incubated for 24°h at 37°C.

Delayed release Ne is a complex of the carboxylic groups of xanthan and the aminic groups of Ne (Figure 15).

In the process of complexation, the supramolecular structure of xanthan is modified, passing from helicoidal[51] to a ball form, which is insoluble in water. In the precipitation phase, the hydrogel formed inserts the Fu present in the reaction medium.

The amounts of Ne and Fu in the complex with xanthan depend on their concentrations in solutions A, B and C (Table 6). The composition of the Ne-Fu-xanthan complex depends on the ratios established — in the reaction system — among the three compounds (Figures 16, 17).

Data given in Figure 16 evidence a linear dependence of the Fu

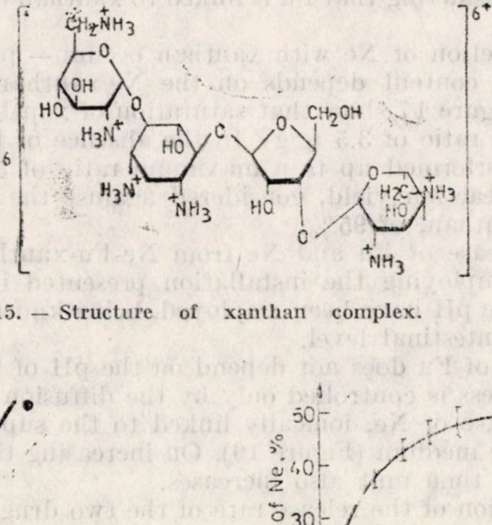

Fig. 15. — Structure of xanthan complex.

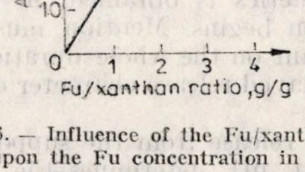

Fig. 16. — Influence of the Fu/xanthan ratio upon the Fu concentration in the Ne—Fu-xanthan complex. Ne concentration in solution $B = 0.2\%$.

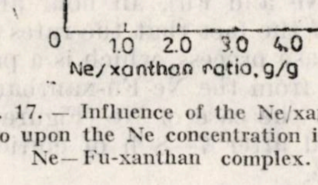

Fig. 17. — Influence of the Ne/xanthan ratio upon the Ne concentration in the Ne—Fu-xanthan complex.

Table 6

Composition of the Ne–Fu-xanthan complex as a function of the A, B and C solution

Concentration (%)			Ne (%)	Fu (%)
Xanthan in solution A	Ne in solution B	Fu in solution C		
0.2	0.2	0.2	38.58	20.09
0.2	0.2	0.4	38.14	33.24
0.2	0.2	0.6	31.43	50.11
0.2	0.2	0.8	27.52	60.04
0.4	0.2	0.6	36.12	40.13
0.6	0.2	0.6	37.06	42.13
1.0	0.2	0.6	26.98	40.98
0.4	0.4	0.6	38.52	31.73
0.4	0.6	0.6	41.36	26.48
0.4	0.8	0.6	44.50	34.16
0.4	1.0	0.6	47.90	27.03
0.4	1.4	0.6	48.50	25.45
0.4	0.4	—	56.33	—

content in the complex on the Fu/xanthan ratio. This linear correlation is normal, considering that Fu is linked to xanthan only through a process of insertion.

The reaction of Ne with xanthan occurs – practically – instantly, while the Ne content depends on the Ne/xanthan ratio in the system. Data from Figure 17 show that saturation of xanthan with Ne occurs, at a Ne/xanthan ratio of 3.5 (g/g). In the absence of Fu, coupling of Ne on xanthan is performed up to a maximum ratio of 58.76%, which corresponds to a reaction yield, considered against the content of carboxylic groups of xanthan, of 95%.

The release of Fu and Ne from Ne-Fu-xanthan complex was performed by employing the installation presented in Figure 8. Solutions having a basic pH have been employed, being known that Ne and Fu act only at the intestinal level.

Release of Fu does not depend on the pH of the eluent (Figure 18) once the process is controlled only by the diffusion of the absorbed drug. Yet, the release of Ne, ionically linked to the support, is influenced by the pH of the medium (Figure 19). On increasing the pH, the Ne weight released with time unit also increases.

Estimation of the release rate of the two drugs was made by means of the kinetic curves plotted in Figures 18 and 19.

The release rate-time dependence is graphically plotted in Figure 20 for Fu and Figure 21, respectively, for Ne.

Installation of a zero-order release kinetics is obtained, in both cases (Ne and Fu), an hour after the elution begins. Mention must be made of the fact that the rates remain constant on the whole duration of the release process, which is a proof of the delayed release character of Ne and Fu from the Ne-Fu-xanthan complex.

In the case of Ne (Figure 21), its total release from the support is observed after 7–8 h of elution. The eluent pH determines the release rate.

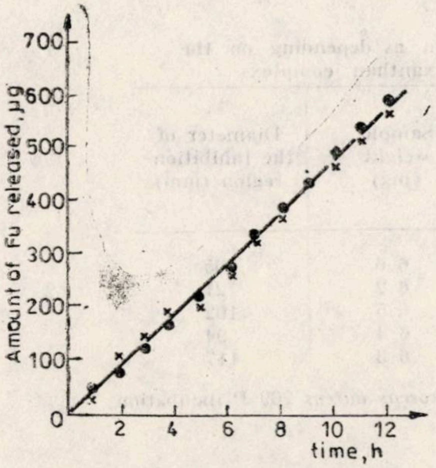

Fig. 18. — Variation of the amount of Fu released with time. Eluent flow 1.4 ml/min, m sample = 20.4 mg. ● — pH = 8.2 ; × — pH = 9.5 ; Ne—Fu-xanthan complex with composition : Ne = 38.50 %, Fu = 31.73 %.

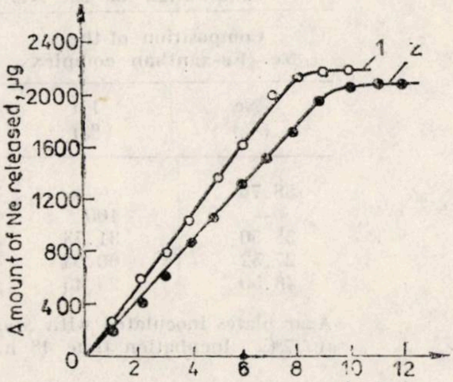

Fig. 19. — Variation of the amount of the Ne released with time and pH eluent. Eluent flow 1.4 ml/min ; 1 — pH = 9.5, m sample = 21.9 mg ; 2 — pH = 8.2, m sample = 21.0 mg. Ne—Fu-xanthan complex with composition : Ne = 38.5 % ; Fu = 31.73 %.

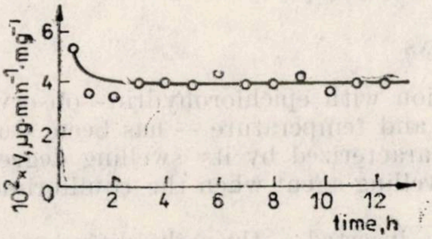

Fig. 20. — Time dependence of the release of Fu from the Ne—Fu-xanthan complex. Eluent flow = 1.4 ml/min ; pH = 9.5.

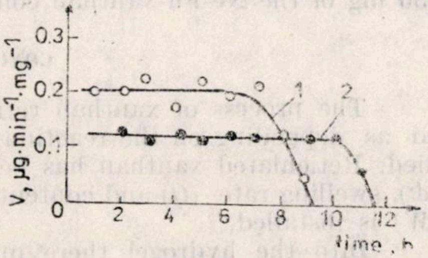

Fig. 21. — Time dependence of the release of Ne from the Ne—Fu-xanthan complex. Eluent flow = 1.4 ml/min, 1 — pH = 9.5 ; 2 — pH = 8.2.

As to the release of Fu, the rate of this process is lower with one order of magnitude, as compared to that corresponding to Ne ; such a behaviour may be explained by the much lower value of water solubility parameter of Fu, as compared to that of Ne (which is unlimitedly soluble in water).

Antimicrobial activity of the complex containing Ne and Fu with delayed release was determined by depositing exact weight amounts on plates inoculated with *Staphylococcus aureus* 209 P and measuring in time the diameter of the inhibition region, up to its stabilization (Table 7).

A significant increase of the antimicrobial activity — of about 50 % — is observed with the samples in which Ne and Fu have been inserted, as compared to those containing only Ne, which explains the intensi-

Table 7

Diameter of the inhibition region as depending on the composition of the NE—FU-xanthan complex

Composition of the Ne—Fu-xanthan complex		Sample weight (mg)	Diameter of the inhibition region (mm)
Ne (%)	Fu (%)		
58.76	—	6.6	65
—	100	6.2	21
38.50	31.73	6.5	102
27.52	60.04	6.4	94
48.50	25.45	6.3	117

Agar plates inoculated with *Staphylococcus aureus* 209 P incubation at 37°C. Incubation time 48 h.

fication action of Fu against Ne. At the same time, by their controlled release at an alkaline pH, a constant concentration of Ne and Fu in the intestinal region is thus ensured. The formed gel has a lower transit rate through the intestine, which is due to an increased adherence to the intestinal mucous membrane. [52]

The experiments performed on a batch of 50 patients suffering from salmonella evidenced their recovery after an administration of 2 doses of 250 mg of the Ne-Fu-xanthan complex, for 2 days.

CONCLUSIONS

The process of xanthan reticulation with epichlorohydrin—observed as depending on the reaction time and temperature — has been studied. Reticulated xanthan has been characterized by its swelling degree ($\mathfrak{C}$), swelling rate (Q) and content of swelling agent when the equilibrium (W) is installed.

Into the hydrogel there may be inserted — through diffusion — and retained, MP and ISDN. The hydrogel diffusion rate and retention capacity depend on the polarity of the drug's molecule.

The polar character of ISDN contributes to the development of the diffusional process because, the support being known as a polyanionic one will interact electrostatically with the drug thus permitting its insertion and fixation into the hydrogel.

The concomitant insertion of Ne and Fu into the xanthan led to the obtainment of a drug bicomponent system with controlled release.

Installation of a zero-order kinetics in the Ne and Fu elution demonstrates their character of retard drugs.

The effect of intensification, occurring concurrently with the controlled release, favours a constant drug concentration in the activity region and, at the same time, an increase of their action. The gel character of the system prolongs the duration of action into the intestinal tract.

The Ne-Fu-xanthan system is recommended in the treatment of intestinal infections, being active towards pathogene colon baccili, enterococci, staphylococci, salmonella.

REFERENCES

[1] S. Dumitriu, P. Vancea, D. Costin and M. Popa, *Clinical Materials*, **2**, 141 (1987).

[2] M. F. Saettone, B. Giannaccini, G. Leonardi, D. Monti, P. Chetoni, G. Galli and E. Chiellini, "Polymers in Medicine III", C. Migliaresi, L. Nicolais, P. Giusti and E. Chiellini ed. Elsevier, Amsterdam, pp. 209–224, 1988.

[3] S. Hosaka, H. Ozawa, H. Tanzawa, T. Kinimoto and R. L. Nichols, *Biomaterials*, **4**, 243 (1983).

[4] S. Dumitriu, M. Popa, P. Vancea, and D. Costin, *Journal of Bioactive & Compatible Polymers*, **3**, 370 (1988).

[5] P. Y. Wang and N. A. Samji, "Biomedical and Dental Applications of Polymers", C. G. Gebelein, F. F. Koblitz ed. Plenum Press, New York and London, pp. 29–37 (1981).

[7] J. G. Gilbert, J. Hadgraft, A. Bye and L. G. Brookes, International Journal of Pharmaceutics, **32**, 223 (1986).

[8] J. Hadgraft and J. R. Howard, *J. Pharm. and Pharmacol.*, **34**, 3P (1982).

[9] O. Wichterle and D. Lim, *Nature*, **85**, 117 (1960).

[10] K. Dorn, G. Hoerpel and H. Ringsdorf, "Bioactive Polymeric Systems", C. G. Gebelein and C. E. Carrahar, eds. New York : Plenum Press, pp. 531–585 (1985).

[11] J. G. Gilbert, J. L. Richardson, M. C. Davis and K. J. Palin, *J. Controlled Release*, **5**, 113 (1987).

[12] W. R. Good and K. F. Mueller, "Controlled Release of Bioactive Materials", R. Baker, ed. Academic Press., pp. 155–175 (1980).

[13] H. M. Creque, R. Langer and J. Folkman, *Diabetics*, **29**, 27 (1980).

[14] S. Dumitriu and V. Bulacovschi, *Rev. Roum. Chim.*, **25**, 989 (1980).

[15] Cr. Simionescu, S. Dumitriu, M. Popa, M. Dumitriu and D. Hritcu, *Colloid Polymer Science*, **262**, 705 (1984).

[16] H. B. Scher, "Controlled Release Pesticides", H. B. Scher, ed. ACS Symposium Series 53, American Chemical Society, Washington, D.C., pp. 127–135 (1977).

[17] F. W. Haris, "Proceedings of Controlled Release Pesticide Symposium", N. F. Cardarellin ed. Ohio : University of Akron, pp. 1–33 (1976).

[18] R. Langer, *Chem. Brit.*, **3**, *232* (1990).

[19] J. Kopecek, in IUPAC Macromolecules, H. Benoit and P. Rempp, ed. New York and Oxford : Pergamon Press, pp. 305–320 (1982).

[20] B. K. Davis, Proceedings of National Academy Science USA, **71**, 3120 (1974).

[21] S. W. Kim, *Phar. International*, **4**, 90 (1983).

[22] J. Heller, R. W. Baker, R. M. Gale and J. O. Rodin, *J. Appl. Polym. Sci.*, **22**, 1991 (1978).

[23] J. W. Shell and R. W. Baker, *Annales of Ophthalmology*, **6**, 1037–1045 (1974).

[24] G. J. Boer and Kruisbrink J., *Biomaterials*, **8**, 265 (1987).

[25] H. Benson, B. Harley and E. E. Schmitt, "Kirk-Othmer Encyclopedia of Chemical Technology", Vol. 17, New York : John Wiley & Sons, Inc., pp. 290–310 (1980).

[26] R. W. Baker and H. K. Lonsdale, "Controlled Release of Biologically Active Agents", A. C. Tanquary and R. E. Lacey eds. New York : Plenum Press, pp. 15–71 (1974).

[27] J. Kohn and R. Langer, *Biomaterials*, **7**, 176 (1986).

[28] M. F. Refojo, "Synthetic Biomedical Polymers Concepts and Applications", M. Szycher and J. W. Robinson, eds. Westport, Connecticut : Technomic Publishing, pp. 171–185 (1980).

[29] A. Marco, *Tumori*, **67**, 521 (1981).

[30] A. D. Trouet, Deprez-De Campeneere, and C. De Duve, *Nature New Biology*, **239**, 110 (1972).

[31] S. Dumitriu, M. Popa and M. Dumitriu, *Journal of Bioactive and Compatible Polymers*, **4**, 57, (1989).

[32] Cr. Simionescu, S. Dumitriu, M. I. Popa and L. Denisova, *Die Makromoleculare Chemie. Makromoleculare Chemie* Suppl., **9**, 179 (1985).

[33] S. Dumitriu, M. I. Popa and Cr. Simionescu, Bull. *Soc. Chim. Belges*, **95**, 283 (1986).

[34] P. Vancea, S. Dumitriu, M. Popa and M. Dumitriu, *Chimica Oggi*, **7–8**, 21 (1988).

[35] Schroder, U.n L. Gannholt, G. Nyberg and H. Eriksson, Proceeding of International Symposium of Controlled Release Bioactive Materials, **12**, 332 (1985).

[36] S. Dumitriu, M. I. Popa, I. Haulica, A. Cringu and A. Stratone, *Colloid Polymer Science*, **267**, 595 (1989).

[37] E. Schacht, F. Vandorne and J. Vermeersch, "Proceedings of International Symposium of Controled Release Bioactive Materials", **12**, 66 (1985).

[38] Cr. Simionescu, S. Dumitriu, M. Popa and M. Dumitriu, *Polymer Bulletin*, **16**, 319 (1986).

[39] C. Beldie, S. Dumitriu, N. Aelenei, M. Popa, M. I. Popa and D. Dumitriu, *Biomaterials*, **10**, 622 (1989).

[40] S. Dumitriu, C. Beldie, M. Popa and C. Dan, *Rom. Pat.* 127 892, 1987.

[41] S. E. Bloomfield, T. Miyata, M. W. Dunn, N. Bueser, K. H. Stenzelnand and A. L. Rubin, *Arch. Ophthalmology*, **96**, 885 (1978).

[42] P. Y. Wang, *Clinical Materials*, **2**, 91 (1987).

[43] P. Y. Wang and N. A. Samji, "Biomedical and Dental Applications of Polymers", C. G. Gebelein and F. F. Koblitz eds. New York and London : Plenum Press, pp. 29–37 (1981).

[44] S. Dumitriu, M. Dumitriu, *Biomaterials*, **1990**, in press.

[45] S. Dumitriu, M. Dumitriu and C. Matian, *Colloid & Polymer Science*, **1990** in press.

[46] Hosaka, S., H. Ozawa and H. Tanzawa, *J. Appl. Pol. Sci.*, **23**, 2089–2098 (1979).

[47] S. Dumitriu, M. Dumitriu and G. Teaca ,*Clinical Materials*, **6**, 265 (1990).

[48] M. Georgarakis, A. Panagopoulu, P. Hatzipantou, Th. Iliopoulos, M. Kondylis, and D. Grekas, Drug Development and Industrial Pharmacy, **16**, 315 (1990).

[49] S. Dumitriu, M. Popa and M. Dumitriu, *Journal of Bioactive and Compatible Polymers*, **5**, **89** (1990).

[50] D. T. Burns, G. H. Lloyd and J. W. Walker, *LABP*, **17**, 448 (1978).

[51] Kelco Company, "Xanthan Gum a Natural Biopolysaccharide for Scientific Water Control", Second Edition (1976).

[52] V. Maglietta, "Terapia Pediatrica Practica", Milano, Casa Editrice Ambrosiana, pp. 283–286 (1990).

Revue Roumaine de Chimie, **36**, *8*, 965–974 (1991)

Dedicated to Professor ALEXANDRU T. BALABAN
on the occasion of his 60th birthday

$C_5H_3^+$ ISOMERIC STRUCTURES: RELATIVE STABILITIES AT HIGH TEMPERATURES

ZDENĚK SLANINA,[a,*] FILIP UHLÍK[a,**] and MICHAEL C. ZERNER[b]

[a] Max-Planck-Institut für Chemie (Otto-Hahn-Institut), D-6500 Mainz, FRG
[b] Quantum Theory Project, University of Florida, Gainesville, Florida 32611, USA

Received January 17, 1991

Recent *an initio* calculations found the ethynylcyclopropenylium cation as the lowest energy structure among nine $C_5H_3^+$ isomers. These carbocations are abundant in fuel-rich flames and have been implicated in soot-formation mechanism. In this work the relative stabilities of the $C_5H_3^+$ isomers at high temperatures are evaluated, using a partition-function technique. The ethynylcyclopropenylium cation remains the most stable species even at very high temperatures. However, the relative populations of other isomers increase quite remarkably. At 2000, 3000, and 4000 K the ethynylcyclopropenylium cation forms 97.4, 85.3, and 69.5% respectively, of the isomeric equilibrium mixture. The isomeric interplay influences the (overall) values of thermodynamic characteristics of the system in a non-negligible way. The presence of isomers yields a temperature maximum in the heat capacity at constant pressure (at about 3900 K, the isomeric enhancement of heat capacity represents about 7% of its value).

INTRODUCTION

Isomer-enumeration studies have supplied[1–3] dozens of examples of a very rapid increase in the numbers of isomeric structures with increase of the number of atoms in a homological series. These enumerations have yielded useful suggestions as to the possible topologies of stationary points of the potential hypersurface for subsequent quantum-chemical studies. Although the number of local-energy minima on hypersurfaces can be lower[***] than the number of isomers from their enumeration, they can still be surprisingly large.[4] This was recently documented in an *ab initio* treatment [5] of $C_5H_3^+$ isomeric system, that uncovered nine low-lying local-energy minima. The system itself is important in one of the suggested mechanisms of soot formation [6–8] (via carbocations). Under the high-temperature con-

---

[*] The permanent and reprint-order address: The J. Heyrovský Institute of Physical Chemistry and Electrochemistry, Czechoslovak Academy of Sciences, Dolejškova 3, CS-18223 Prague 8-Kobylisy, Czech and Slovak Federal Republic.

[**] Undergraduate fellow. Faculty of Science, Charles University, Prague 2, Czech and Slovak Federal Republic.

[***] In principle, however, the number of hypersurface stationary points can also be larger than suggested by related graph-theoretical enumeration.

ditions of flames the importance of various isomers derived in a straightforward fashion from the potential energy might not be appropriate.[4,9,10] Thus, this report addresses the effects of temperature in the $C_5H_3^+$ isomeric system.

$C_5H_3^+$ is probably formed from condensation and condensation-elimination reactions such as :

$$C_3H_3^+ + C_2H_2 \rightarrow C_5H_5^+, \quad (A)$$

$$C_5H_5^+ \rightarrow C_5H_3^+ + H_2, \quad (B)$$

or :

$$C_3H_3^+ + C_4H_2 \rightarrow C_7H_5^+, \quad (C)$$

$$C_7H_5^+ \rightarrow C_5H_3^+ + C_2H_2. \quad (D)$$

These reactions in and by themselves may yield a specific isomer of $C_5H_3^+$. This report assumes that the barriers between isomers are sufficiently low that interconversion is easy and that steady-state thermodynamics among these isomers is appropriate. These are, admittedly, sizeable assumptions.

$C_5H_3^+$ ISOMERIC SYSTEM

Altogether nine minimum-energy structures were found in the quantum-chemical computational study[5] of the $C_5H_3^+$ system. Geometry optimisation was carried out[5] using the 6-31G* split valence plus polarization basis set. The vibrational analysis was performed in the 3-21G split valence basis set at the 3-21G equilibrium geometry. For each of the nine structures all 18 vibrational frequencies are real numbers ; i.e., genuine energy minima conditions are met. The relative energies were finally evaluated at the 6-31G* equilibrium geometries using second-order perturbation MP2/6-31G* treatment. Throughout this report we shall follow the numbering (Roman numbers) of structures introduced in Ref. 5 (cf. Table 1). At all levels of theory[5] the ethynylcyclopropenylium cation (I) represented the lowest potential-energy structure. Correction for zero-point vibrational energy does not change this ordering (Table 1). Only three of the structures possess some (non-trivial) rotational axis, viz. the structures I, V, and IX (C_{2v} point group of symmetry). One of them (IX) is triplet state (in fact, related to the structure V).

TEMPERATURE-INTERPLAY COMPUTATIONS

The ethynylcyclopropenylium cation (I) is lower in potential energy to all other isomers by at least about 88 kJ/mol. However, the high-temperatures observed in most flames might compensate the bias resulting from the potential terms. In addition, the important species for soot formation might even be a minority component of the isomeric mixture. An easiest way of considering temperature effects is represented [4] by simple Boltzmann factors :

$$w_i' = \frac{\exp[-\Delta E_i/(RT)]}{\sum_{j=1}^{n} \exp[-\Delta E_j/(RT)]}, \tag{1}$$

where ΔE_i stand for the potential energy terms of isomers in their n-membered set, related to a common reference energy level (here, to the energy of the ethynylcyclopropenylium cation (I) — see Table 1). However, the simple Boltzmann factors omit rotational-vibrational motions. The latter can be considered [11] through partition functions q_i of individual structures, yielding the weight factors :

$$w_i = \frac{q_i \exp[-\Delta H_{0,i}^o/(RT)]}{\sum_{j=1}^{n} q_j \exp[-\Delta H_{0,j}^o/(RT)]}, \tag{2}$$

where $\Delta H_{0,i}^o$ denote the relative ground-state energy terms (i.e., the ΔE_i terms corrected for the zero-point energy). A particular approximation of the partition functions is determined by computational demands, i.e. a rigid rotor and harmonic oscillator (RRHO) approximation [4] is assumed. The w_i' and w_i factors have a clear physical meaning, being mole fractions of the individual isomers in their equilibrium mixture. As interactions between the isomers are neglected the calculated partition functions correspond to an ideal gas. This assumption in high temperature flames is probably quite valid.

Assuming thermodynamic-equilibrium two kinds of thermodynamic terms can be distinguished ; viz.,[4] partial and overall terms. The standard partial terms ΔX_i^o belong to processes containing the individual isomers ; the overall terms ΔX^o to processes in which the equilibrium isomeric mixture acts as one pseudospecies (into the latter terms all the isomers contribute according to their weight factors w_i). Moreover, a third type quantity, the isomerism contribution, δX_1, has been introduced[12,13] :

$$\delta X_1 = \Delta X^o - \Delta X_1^o. \tag{3}$$

Table 1

Survey of the relative energetics (kJ/mol) in the $C_5H_3^+$ system*

Isomer	ΔE_i **	$\Delta H_{0,i}^o$ ***
I	0.0	0.0
II	97.1	102.1
III	87.9	89.8
IV	313.8	315.4
V	227.2	231.6
VI	444.3	441.9
VII	525.5	521.2
VIII	658.1	651.7
IX	354.4	347.8

* The MP2/6-31G* potential-energy data [5]; related to the ethynylcyclopropenylium cation (I).

** Potential-energy difference with respect to the ethynylcyclopropenylium cation (I).

*** Ground-state energy difference with respect to the ethynylcyclopropenylium cation (I) (i.e., ΔE_i corrected for zero-point vibrations).

Here X denotes standard enthalpy ($X = H$), entropy ($X = S$), or heat capacity at constant pressure ($X = C_p$). For example [12,13], for $X = C_p$:

$$\delta C_{p,1} = \delta C_{p,w,1} + \frac{1}{RT^2}\left[\sum_{i=1}^{n} w_i(\Delta H_i^\circ - \Delta H_1^\circ)^2 - (\delta H_1)^2\right], \tag{4}$$

where $\delta C_{p,w,1}$ stands for the so-called isofractional [12,13] isomerism contribution to the heat capacity:

$$\delta C_{p,w,1} = \sum_{i=1}^{n} w_i(\Delta C_{p,i}^\circ - \Delta C_{p,1}^\circ), \tag{5}$$

while the isomerism contribution to the enthalpy is given simply by [12,13]:

$$\delta H_1 = \sum_{i=1}^{n} w_i(\Delta H_i^\circ - \Delta H_1^\circ). \tag{6}$$

The $\delta C_{p,1}$ term from Eq. (4) is more general than the isofractional ones (5) as it includes the effects of changes in composition upon a temperature change. For this reason it has been called the relaxation isomerism contribution to the heat capacity.[12,13] In the isofractional contribution $\delta C_{p,w,1}$ the w_i terms are effectively considered to be temperature independent.

From the methodological standpoint it can be useful to consider not only the full nine-membered isomeric set, but also reduced sets created by omitting some isomers from the full set. This can be done in a systematic way [14] by recursively abandoning the isomer with highest identification number (Table 1) in each reduction step. If "9" denotes the full set, the reduced set "8" is created from it by omitting the isomer IX. In the next step, set "7" is created from "8" by removing the "VIII" structure, etc. The procedure is finished by creating set "2" composed of I and II isomers. This procedure represents a way of illustrating the role of individual isomers (though its convergency is clearly influenced by a particular isomer-labelling convention).

RESULTS AND DISCUSSION

Temperature evolution of the simple Boltzmann factors w_i' and the weight factors w_i are given in Fig. 1. Although the ethynylcyclopropenylium cation (I) is, throughout the very wide temperature interval considered, always the dominant species, other isomers clearly have importance at higher temperatures. As shown also in Table 2 structures III and II become significantly populated at high temperatures. It is clear from Fig. 1 that the simple Boltzmann factors represent only a rough approximation to the weight factors w_i. We note that although a scaling of calculated vibrational frequencies by a factor of 0.9 is suggested [5] in order to have better agreement with available experiment, it was shown [15] recently that

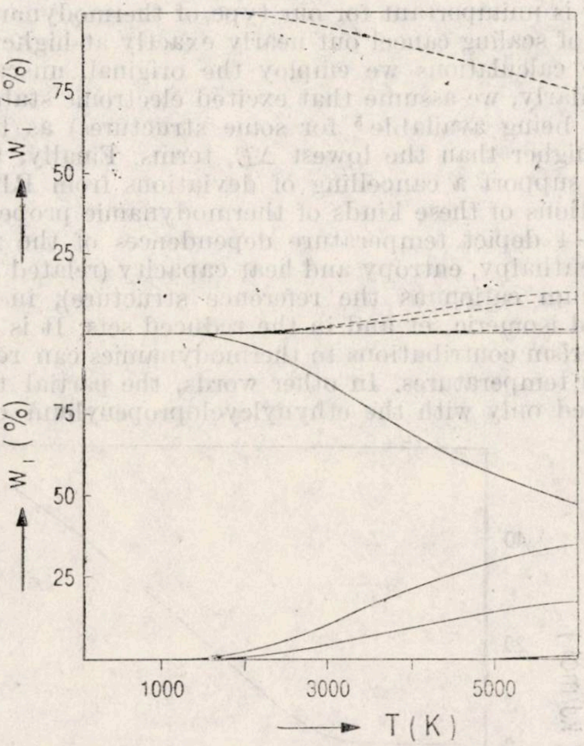

Fig. 1. — Temperature dependences of the simple Boltzmann factors w'_i (dashed lines, the upper part) and the weight factors, w_i (solid lines, the lower part) of isomers of $C_5H_3^+$. (Only some of the curves are apparent in the Figure with the scale used. For assigning the curves see Table 2).

Table 2

Relative populations of the individual $C_5H_3^+$ isomers in their equilibrium isomeric mixture

Isomer	w'* (%)			w_i(%)		
	2000 K	3000 K	4000 K	2000 K	3000 K	4000 K
I	99.2	95.2	88.8	97.4	85.3	69.5
II	0.3	1.9	4.8	0.7	4.3	9.6
III	0.5	2.8	6.3	1.9	10.4	20.9
IV	6×10^{-7}	3×10^{-4}	7×10^{-3}	2×10^{-6}	1×10^{-3}	2×10^{-2}
V	1×10^{-4}	1×10^{-2}	0.1	2×10^{-5}	1×10^{-3}	1×10^{-2}
VI	2×10^{-10}	2×10^{-6}	1×10^{-4}	3×10^{-9}	2×10^{-5}	1×10^{-3}
VII	2×10^{-12}	7×10^{-8}	1×10^{-5}	4×10^{-11}	1×10^{-6}	2×10^{-4}
VIII	6×10^{-16}	3×10^{-10}	2×10^{-7}	2×10^{-14}	8×10^{-9}	5×10^{-6}
IX	6×10^{-8}	6×10^{-5}	2×10^{-3}	1×10^{-6}	1×10^{-3}	4×10^{-2}

* Simple Boltzmann factors.

such a scaling is unimportant for our type of thermodynamic calculations as the effects of scaling cancel out nearly exactly at higher temperatures. Thus in these calculations we employ the original, unscaled set of frequencies. Similarly, we assume that excited electronic state are not populated (though being available[5] for some structures) as they mostly lie considerably higher than the lowest ΔE_i terms. Finally, there are arguments[11] that support a cancelling of deviations from RRHO behaviour in the calculations of these kinds of thermodynamic properties.

Figs. 2–4 depict temperature dependences of the isomerism contributions to enthalpy, entropy and heat capacity (related to the ethynylcyclopropenylium cation as the reference structure), in both the full, nine-membered isomeric set and in the reduced sets. It is clearly evident that the isomerism contributions to thermodynamics can reach quite large values at high temperatures. In other words, the partial thermodynamic terms associated only with the ethynylcyclopropenylium cation does not

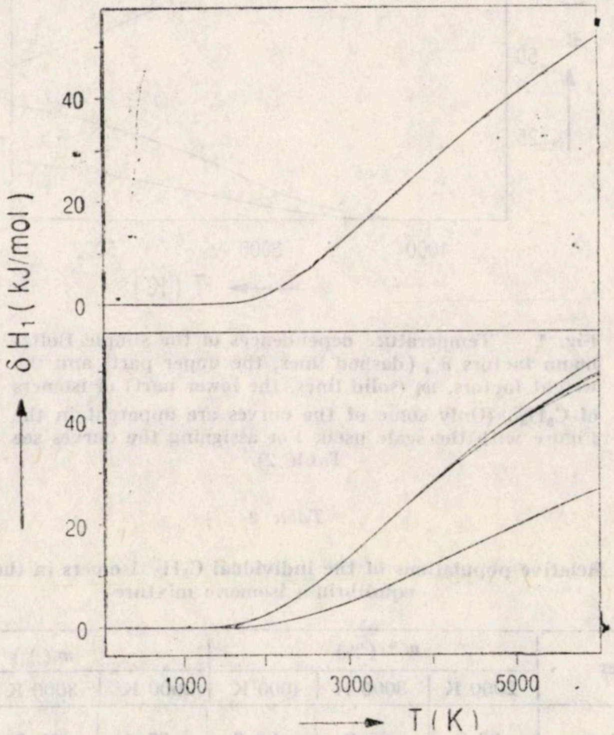

Fig. 2. — Temperature dependences of the isomerism contribution to enthalpy δH_1 for the $C_5H_3^+$ isomeric systems (the contributions are related to the ethynylcyclopropenylium cation (I) as the reference structure). The upper part belongs to the full, nine membered isomeric set; the lower part depicts dependences for the full and for reduced isomeric sets created recursively by abandoning the isomer with highest identification number (Table 1) in each step. (Only some of the curves are apparent with the scale used. For assigning the curves see Table 3.)

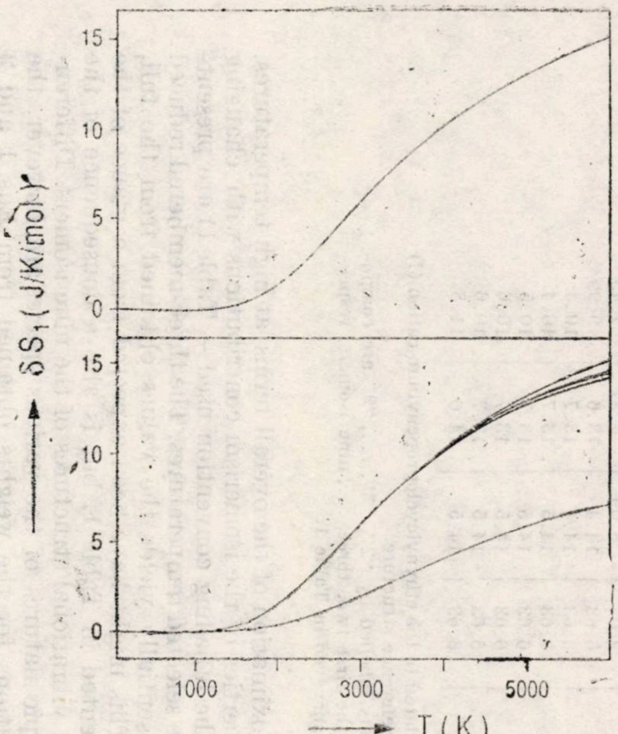

Fig. 3. — Temperature dependences of the isomerism contribution to entropy δS_1 for the $C_5H_3^+$ isomeric systems (the contributions are related to the ethynylcyclopropenylium cation (I) as the reference structure). The upper part belongs to the full, nine membered isomeric set ; the lower part depicts dependences for the full and for reduced isomeric sets created recursively by abandoning the isomer with identification number (Table 1) in each step. (Only some of the curves are apparent with the scale used. For assigning the curves see Table 3.)

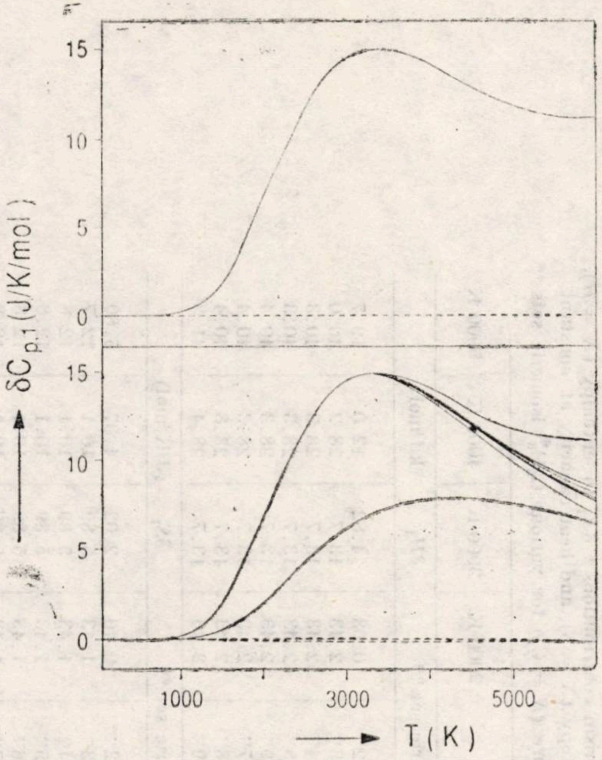

Fig. 4. — Temperature dependences of the isomerism contribution to heat capacity at constant pressure $\delta C_{p,1}$ (relaxation term) or $\delta C_{p,w,1}$ (isofractional term, dashed lines) for the $C_5H_3^+$ isomeric systems (the contributions are related to the ethynylcyclopropenylium cation (I) as the reference structure). The upper part belongs to the full, nine membered isomeric set ; the lower part depicts dependences for the full and for reduced isomeric sets created recursively by abandoning the isomer with highest identification number (Table 1) in each step. (Only some of the curves are apparent with the scale used. For assigning the curves see Table 3.)

Table 3

Isomerism contributions * δX_1 to enthalpy ($X = H$), entropy ($X = S$), and heat capacity at constant pressure ($X = C_p$) for various $C_5H_3^{\blacklozenge}$ isomeric sets **

	2000 K	3000 K	4000 K	5000 K
Isomeric set **		δH_1	(kJ/mol)	
"2"	0.68	4.82	12.0	19.7
"3"	2.43	13.7	28.2	40.0
"4"	2.43	13.7	28.3	40.3
"5"	2.43	13.7	28.3	40.3
"6"	2.43	13.7	28.3	40.4
"7"	2.43	13.7	28.3	40.4
"8"	2.43	13.7	28.3	40.4
"9"	2.43	13.7	28.4	41.3
Isomeric set **		δS_1	(J/K/mol)	
"2"	0.40	2.02	4.07	5.80
"3"	1.43	5.89	10.1	12.7
"4"	1.43	5.89	10.1	12.8
"5"	1.43	5.89	10.1	12.8
"6"	1.43	5.89	10.1	12.8
"7"	1.43	5.89	10.1	12.8
"8"	1.43	5.89	10.1	12.8
"9"	1.43	5.89	10.1	13.0
Isomeric set **		$\delta C_{p,1}$	(J/K/mol)	
"2"	2.04	6.09	7.81	7.45
"3"	6.63	14.4	13.6	9.99
"4"	6.63	14.4	13.7	10.4
"5"	6.63	14.5	13.7	10.4
"6"	6.63	14.5	13.7	10.5
"7"	6.63	14.5	13.7	10.6
"8"	6.63	14.5	13.7	10.6
"9"	6.63	14.5	14.0	11.8

* Related to the ethynylcyclopropenylium cation (I) at the reference structure.

** Sets labelled by "2", "3", ..., "9" are composed of the first two, three, ..., nine isomers, respectively, surveyed in Table 1.

represent a good approximation of the overall terms at high temperatures. The convergency properties of the isomerism contributions with changing dimension n (within the labelling convention used – Table 1) are presented in Table 3 for some selected temperatures. The three-membered reduced isomeric set ("3") essentially yields the values obtained from the full, nine-membered set. This might have been expected from a glance of the relative energies presented in Table 1, but is also a consequence of the similar rotational and vibrational structures of the nine isomers. Differences in the spectroscopic natures of the various species are, however, the reasons for the deviations for the weights obtained from Eqs. 1 and 2 and demonstrated in Figure 1.

The temperature dependence of the relaxation isomerism contribution to heat capacity deserves more attention as it exhibits a qualitative behaviour different from other terms presented in Figs. 2—4, i.e. it possesses a temperature maximum. The maximum is actually preserved even after transfer to the overall heat capacity at constant pressure of the (nine-membered) equilibrium isomeric mixture (i.e., to the pseudospecies $C_5H_3^+$). However, as can be seen in Fig. 5, the temperature maximum in the latter case is predicted to be very small. In addition to the maxima in the isomerism contribution to the heat capacity $\delta C_{p,1}$ and the overall standard heat capacity at constant pressure C_p^o, we report in Table 4 the maximum in the relative contribution of $\delta C_{p,1}$ into C_p^o (within the nine-membered $C_5H_3^+$ isomeric set). The highest isomeric enhancement to the overall heat capacity term (about 7.8%) represents a significant value with possible physical consequences.

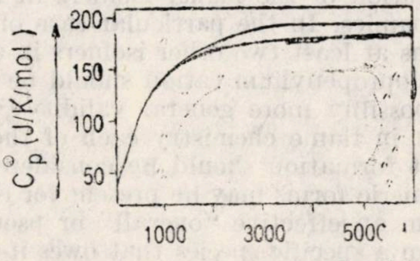

Fig. 5. — Temperature dependences of the standard molar heat capacity at constant pressure for the ethynylcyclopropenylium cation (I) ($C_{p,1}^0$, the dashed line) and for the equilibrium mixture of the nine $C_5H_3^+$ isomers (C_p^o, the solid line).

Table 4

Specification of temperature maxima in the isomerism contribution to heat capacity* δC_{p1}, the overall standard heat capacity at constant pressure C_p^o, and in the relative contribution of $\delta C_{p,1}$ into C_p^o for the nine-membered $C_5H_3^+$ isomeric set

Maximum	T (K)	w_1** (%)	$\delta C_{p,1}$ (J/K/mol)	$C_{p,1}^o$*** (J/K/mol)	$\delta C_{p,1}/C_p^o$ (%)	C_p^o (J/K/mol)
$\delta C_{p,1}$	3360	79.5	15.0	177	7.81	192
C_p^o	3903	70.9	14.3	178	7.40	193
$\delta C_{p,1}/C_p^o$	3317	80.2	15.0	177	7.81	192

* Related to the ethynylcyclopropenylium cation (I) as the reference structure.

** The mole fraction of the ethynylcyclopropenylium cation (I) in the nine-membered equilibrium mixture (cf. Table 2).

*** The partial standard heat capacity of 1 mole of the sole ethynylcyclopropenylium cation (I)

It should be mentioned for a completeness that an isomer enumeration in a parent system has already been carried out. Actually, graphs corresponding to the formula C_5H_4 have been enumerated by Balaban.[16]

They total 40, according to the following subtotals: seven $C_3(CH_2)_2$, six $C(CH)_4$, seven C_3CHCH_3, and twenty $C_2(CH)_2CH_2$. However, the number of corresponding cations $C_5H_3^+$ is considerably higher. Thus, an exhaustive search on the potential hypersurfaces[5] could still discover some other local energy minima.

In conclusion, it can be stated that an isomeric potential-energy separation even of about 100 kJ/mol need not necessarily prevent a manifestation of the higher isomers in high-temperature equilibrium thermodynamics. In the particular case of the $C_5H_3^+$ system under flame conditions at least two other isomers in addition to the energy-lowest ethynylcyclopropenylium cation should be considered (this being a conclusion of a possibly more general validity[17]). Considering the high temperatures met in flame chemistry each of the steps postulated to be important in soot formation should be considered from the point of view that many isomeric forms may be present for each species. Reactions then may occur from an effective "overall" or pseudo-species, or they might occur only from a specific species that owes its presence only through a temperature population.

ACKNOWLEDGEMENT. The study was in part carried out during a research stay of one of us (Z.S.) at the Max-Planck-Institut für Chemie (Otto-Hahn-Institut) supported by the Alexander von Humboldt-Stiftung. The support as well as the valuable discussions with Karl Heinzinger and the kind hospitality of him, of his group, and of the the Max-Planck-Institut für Chemie is gratefully acknowledged. We also acknowledge helpful discussions with Brian Weiner (Penn State University, Dubois) and last but not least constructive referee comments.

REFERENCES

[1] R. C. Read in A. T. Balaban, ed., "Chemical Applications of Graph Theory", Academic Press, London, 1976, pp. 25–61.

[2] A. T. Balaban in A. T. Balaban, ed., "Chemical Applications of Graph Theory", Academic Press, London, 1976, pp. 64–105.

[3] R. W. Robinson, F. Harary and A. T. Balaban, *Tetrahedron*, **32**, 355 (1976).

[4] Z. Slanina, "Contemporary Theory of Chemical Isomerism", Academia & D. Reidel, Prague & Dordrecht, 1986.

[5] B. Weiner, C. J. Williams, D. Heaney and M. C. Zerner, *J. Phys. Chem.*, **94**, 7001 (1990).

[6] A. G. Gaydon and H. G. Wolfhard, "Flames, Their Structure, Radiation and Temperature", Wiley, New York, 1979.

[7] D. B. Olson and H. F. Calcote in C. D. Siegla, G. W. Smith, eds., "Particulate Carbon: Formation during Combustion", Plenum Press, New York, 1981, p. 177.

[8] H. F. Calcote, *Combust. Flame*, **42**, 215 (1981).

[9] Z. Slanina, *Int. Rev. Phys. Chem.*, **6**, 251 (1987).

[10] Z. Slanina, *Thermochim. Acta*, **128**, 157 (1988).

[11] Z. Slanina, *Int. J. Quantum Chem.*, **16**, 79 (1979).

[12] Z. Slanina, *Thermochim. Acta*, **78**, 47 (1984).

[13] Z. Slanina, *J. Phys. Chem.*, **92**, 5836 (1988).

[14] Z. Slanina, *Comput. Chem.*, **13**, 305 (1989).

[15] Z. Slanina, *J. Phys. Chem.*, **95**, 1089 (1991).

[16] A. T. Balaban, *Rev. Roumaine Chim.*, **18**, 635 (1974); **19**, 338 (1975).

[17] A. Cameron, J. Leszczynski, M. C. Zerner and B. Weiner, *J. Phys. Chem.*, **93**, 139 (1989).

Revue Roumaine de Chimie **36**, *8*, 975–982 (1991)

Dedicated to Professor PETRU SPACU on the occasion of his 85th anniversary

MOLECULAR TOPOLOGY. 2

A COMPUTER PROGRAM FOR MULTIPLE BOND, CYCLE AND RADICAL APPROXIMATIONS OF DS INDEX [1]

MIRCEA V. DIUDEA * and IOAN SILAGHI-DUMITRESCU

"Babeş-Bolyai" University, Department of Chemistry, Arany Janos, 11,
3400 – Cluj, Romania

Received September 16, 1991

The DS index is extended for multiple bonds containing also aromatic compounds. A general formula and a computer program are given to compute it from the electronegativity degrees of vertices, over the whole molecule as well as for a radical portion, R. DS was found to correlate well with log 1/c for inhibitors of thymidine phosphorylase as well as with molar refraction of olefines.

INTRODUCTION

In the previous paper of this series [1] we defined the valence (group) electronegativity for a vertex, and proposed, on this basis, a new Randić-type connectivity index, DS – eq. 1 :

$$DS = \sum_{\text{all edges}} (S_i S_j)^{-1/2} \tag{1}$$

where S_i, S_j are the degrees of electronegativity for two adjacent vertices .

The new index DS has found good correlation in the saturated aliphatic series with molar refraction of amines and halogens and with polarizability and local anesthetic activity of alcohols.

MULTIPLE BOND APPROACH

Multiple bond approach in the Randić-type topological indices (TI's) was treated as a function of how the multiple bond and its endpoint valencies were counted.

Murray et al.[2] and Balaban [3–6] considered the conventional bond order b (1, 2, 3 – for single, double and triple bond, respectively and 1.5 – for aromatic bond) for the endpoint degrees of multiple bond and counted it as a single edge when calculated q (number of edges in graph). In this approach the entries of multiple bond endpoints in the adjacency or distance matrices are multiplied by 1/b.

---

* Author to whom correspondence should be addressed.

In the second approach, one counts each bond (considering e.g. a double bond as two edges) both in computing q and TI's.[5,7]

We adopted the second approach, by virtue of which the edge term $(S_iS_j)^{-1/2}$ is multiplied by b_{ij} — the conventional bond order for an edge having the i, j — atoms as endpoints, eq. 2 :

$$DS = \sum_{\text{all edges}} b_{ij}(S_iS_j)^{-1/2} \tag{2}$$

CYCLE APPROACH

Kier and Hall [7] treated the cyclic compounds by virtue of the spanning tree concept (eliminate one edge from different points of a cycle in order to equalize the cycle with its spanning trees — as number of edges. They adopted a mean value of 0.5 to diminish the initial $^1\chi$-value. The ring correction is applicable to any hexacyclic compound irrespective of its degree or type of substitution. When more than one $^1\chi$-term is used, this correction is not required.[7]

In agreement with the spanning tree concept, we propose a cycle approach which considers the edge mean value in a given cyclic structure to be substracted from the initial DS — value, eq. 3 :

$$DS = \left(1 - \frac{\mu}{q_{tot}}\right) \sum_{\text{all edges}} b_{ij}(S_iS_j)^{-1/2} \tag{3}$$

where q_{tot} is the total number of bonds in a connected graph, according to eq. 4 :

$$q_{tot} = \sum_{ij} b_{ij}q_{ij} \tag{4}$$

with q_{ij} — the edge having, i, j — atoms as endpoints.

In eq. 3, μ is the "cyclomatic number" (number of rings — see Baeyer, IUPAC and Chemical Abstracts nomenclature systems)[5,6] and is defined by eq. 5 :

$$\mu = q - n + 1 \tag{5}$$

where n is the number of vertices in graph and q refers only to sigma bonds.

Eq. 3 is applicable to any cyclic compounds irrespective of the type of cycle and its substituents.

Accurately, the cycle correction should be applied before counting the substituents. However, no large differences appear between the DS — values corrected before and after counting the substituents. In a series of cyclohexanes with a $CH_3-(CH_2-CH_2)_m$ — chain and m = 1 to 100, differences do not exceed 0.2% from the before-corrected DS-values. Similar observation we could made about a series of monosubstituted decalines.

A quite special case is that of simple condensed aromatic hexacycles. Due to the conventional bond order $b_{ij} = 1.5$, in the calculation of q_{tot} by eq. 4, there appears an "exces" of bonds. Of course, the exceeding bonds must be rejected off in the calculation of DS. Thus, we propose a general eq. 6, applicable both for aliphatic and aromatic hexacycles, as well as for unsaturated structures:

$$DS = \left(1 - \frac{\mu}{q_{tot}} + c\right) \sum_{\text{all edges}} b_{ij}(S_i S_j)^{-1/2} \tag{6}$$

where c is the correction for condensed aromatic hexacycles, eq. 7:

$$c = \frac{AG - \mu_{Ar}}{2q_{tot}} \tag{7}$$

In eq. 7, AG – is the number of aromatic groups in a molecule and μ_{Ar} represents the number of aromatic rings. It is obvious that c does not operate in the case of non-aromatic cycles ($AG = 0$; $\mu_{Ar} = 0$; $c = 0$), nor in the case of aromatic isolated cycles ($AG = \mu_{Ar}$; $c = 0$). Note that c is functional only for $\mu_{Ar} \geqslant 2$.

RADICAL APPROACH

It is known that many drug molecules, with similar biological properties, differ only by a radical, R, attached to a same skeleton. Moreover, some properties could be a function of a local structural or electronic features. Thus, it would be useful to compute DS only for R-portion of such molecules: DSR.

This approach considers the atom directly attached to the skeleton as a root vertex and accounts for the broken bonds (in the "process" of R-forming) as follows:

$$v_{root} = v_i + v_{bb} \tag{8}$$

where v_i and v_{root} – are the initial and actual connectivity (valence) of root vertex, respectively, and v_{bb} – stands for the number of broken bonds. Subsequently, the number of hydrogen atoms belonging to the root vertex, H_{root}, is calculated by:

$$H_{root} = (8 - G_{A,root}) - v_{root} \tag{9}$$

with $G_{A,root}$ – the group in the periodic chart of the non-hydrogen atom of root vertex. Then, S_{root} = the valence (group) electronegativity and DSR will be computed using the actual v_{root} and H_{root} – values (see[1]).

Our program for computing DS accounts for the proposed radical approach (see also Table 1).

Table 1

Inhibitors of Thymidine Phosphorylase[8] (I — see text)

No.	R	DS	DSR$^{a)}$	$^1\chi_R$$^{b)}$	$^1\chi^v$$^{c)}$	log 1/c	Statistics R	s
1	Methyl	8.4647	0.6791	3.698	3.0729	−2.30	$^1\chi^v$ 0.9199	0.2125
2	Butyl	10.6329	2.8508	5.236	4.6490	−1.35	$^1\chi_R$ 0.9220	0.2099
3	Isopentyl	11.3806	3.6009	5.592	5.0048	−1.30	DS 0.8807	0.2568
4	Cyclopentyl	11.4948	3.7006	5.270	4.7003	−1.28	DSR 0.8807	0.2568
5	Isohexyl	12.1035	4.3245	6.092	5.5048	−1.17	DS_d 0.9194	0.2262
6	Pentyl	11.3557	3.5744	5.736	5.1490	−1.15		
7	3-Phenyl-propyl	16.5554	8.7729	7.254	6.6614	−1.11		
8	2-Phenyl-ethyl	15.8321	8.0487	6.754	6.1614	−0.80		
9	Phenyl-methyl	15.1089	7.3244	6.254	5.6614	−0.76		
10	4-Phenyl-butyl	17.2787	9.4971	7.754	7.1614	−0.60		
11	5-Phenyl-pentyl	18.0020	10.2211	8.254	7.6614	−0.32		

a) bond N — C(R) included ; b) from ref. [7] ; c) this work (ring correction = −0.500) ; d) parabolic correlation — the following QSAR was found :

$$\log 1/c = 0.6226 \ (\pm 0.2537) \ DS - 0.0177 \ (\pm 0.0093 \ (DS)^2 - 6.1194 \quad N = 11 ;$$

$$R = 0.9194 ; \ s = 0.2262 ; \ F = 21.9$$

DS — CORRELATING TESTS

We tested the ability of DS (computed according to eq. 6) to correlate with log 1/c (c — is here the inhibitory concentration) in a series of thymidine phosphorilase inhibitors[8] of a general structure I :

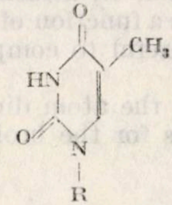

I

Table 1 lists the DS-values, computed over the whole molecule I as well as for the substituent R alone, along with the observed log 1/c. As comparison terms, we also introduced the $^1\chi_R$ (from ref.[7]) and $^1\chi^v$ values (this work).

A first observation one imposes : the correlation of TI's with the inhibitory activity of the listed thymidine derivatives is rather poor (see Table 1). This means that the topological feature of such compounds is not the sole determinant of their biological activity.

Second, no differences appear when using the DSR-values in regresrion instead of DS-values computed over the whole molecule I (se ealso sef.[7], pp. 189).

Table 2

Molar refraction of olefines

No.	Compound	DS	Molar refraction	
			Obs. [a]	Calcd
1	2-Methyl-2-butene	3.548	24.955	25.323
2	1-Pentene	3.446	24.858	24.691
3	3,3-Dimethyl-1-butene	4.228	29.598	29.536
4	2,3-Dimethyl-2-butene	4.323	29.590	30.125
5	2,3-Dimethyl-1-butene	4.244	30.063	29.635
6	4-Methyl-1-pentene	4.196	29.542	29.338
7	2-Methyl-1-pentene	4.216	29.398	29.462
8	2-Methyl-2-pentene	4.271	29.754	29.803
9	3-Methyl-1-pentene	4.198	29.485	29.350
10	2-Ethyl-1-butene	4.218	29.391	29.474
11	1-Hexene	4.169	29.208	29.170
12	2,3,3-Trimethyl-1-butene	5.001	33.980	34.326
13	4,4-Dimethyl-1-pentene	4.952	34.233	34.022
14	3,3-Dimethyl-1-pentene	4.955	34.011	34.041
15	2,3-Dimethyl-2-pentene	5.048	34.203	34.617
16	3,4-Dimethyl-1-pentene	4.949	33.919	34.003
17	3,4-Dimethyl-2-pentene	5.025	33.900	34.474
18	2-Ethyl-3-Methyl-1-butene	4.969	34.024	34.127
19	2,3-Dimethyl-1-pentene	4.969	34.005	34.127
20	5-Methyl-1-hexene	4.919	34.139	33.817
21	2-Methyl-2-hexene	4.995	34.395	34.288
22	2-Methyl-1-hexene	4.940	34.114	33.948
23	2-Methyl-3-hexene	4.972	34.223	34.146
24	4-Methyl-1-hexene	4.921	34.078	33.830
25	2-Ethyl-1-pentene	4.942	33.991	33.960
26	3-Ethyl-1-pentene	4.924	34.039	33.848
27	3-Ethyl-2-pentene	4.999	34.117	34.313
28	1-Heptene	4.893	34.136	33.657
29	2,4,4-Trimethyl-2-pentene	5.778	39.015	39.140
30	2,4,4-Trimethyl-1-pentene	5.723	38.769	38.799
31	2,3,4-Trimethyl-1-pentene	5.721	38.836	38.780
32	3,3,4-Trimethyl-1-pentene	5.707	38.499	38.700
33	2-Isopropyl-3-methyl-1-butene	5.720	38.385	38.780
34	5,5-Dimethyl-1-hexene	5.676	38.785	38.500
35	4,4-Dimethyl-1-hexene	5.679	38.643	38.527
36	3,3-Dimethyl-1-hexene	5.679	38.548	38.527
37	2,5-Dimethyl-3-hexene	5.722	38.823	38.793
38	3,5-Dimethyl-1-hexene	5.671	38.764	38.477
39	3-Ethyl-4-methyl-1-pentene	5.675	38.591	38.502

[a] from ref.[7]

Third, DS correlates by a parabolic function rather than by a linear one.

DS correlates with the molar refraction of olefines in a single variable function as good as χ^v does, in a three variable function

$$({}^0\chi^v,\ {}^1\chi^v \text{ and } {}^2\chi^v\,;\ r = 0.9985\,;\ s = 0.223\,;\ N = 39).^7$$

For the olefines file (Table 2) we found the following QSPR:

$$MR = 3.3395 + 6.1960\ DS \qquad (10)$$

$$N = 39 \,;\ r = 0.9980 \,;\ s = 0.2472$$

$$F = 4523.7 \,;\ T = 95.1 \,;\ EV = 0.9959$$

COMPUTER PROGRAM

The computer program given below calculates the DS indices for both saturated or unsaturated organic derivatives, aromatic compounds or fragments of such molecules. Heteroatoms up to chlorine may be included. For other heteroatomic derivatives, the corresponding Sanderson electronegativities must be inserted as data statements at program lines 750—765.

The inputs are the same as for the previous version (1) completed with data necessary in the treatment of fragments or aromatic groups. For instance, fragments may be treated if the following data are known: the number of break points, number of broken bonds and number of missing neighbours of each root vertex. The pertinent codes of the fragment (II) are as follows.

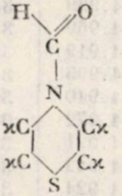

(II)

No. of break points = 4

VR	VB	VN
1	1	11
2	1	1
5	1	1
6	1	1

……………………

DS = 6.5344

```
 90 REM DS INDEX Program VERSION 2
100 CURSOR 0.0
110 CLS#2 : CLS#0
120 RESTORE
130 DIM ga(100), sa(100), h(50), d(100)
140 i=0
150 REPEAT READING
160 i=i+1 : READ as
170 if ss=-999 then exit reading
180 sa(i)=ss
190 END REPEAT READING
200 INPUT “Molecule.” ; t$
210 INPUT ”N atom :“ na
220 INPUT “Is it a fragment” ; r$
230 IF r$ = “Y” or r$ = “y” then
240 INPUT “Nr. of breaking points :” ; bb : DIM vr(bb)
    vb(bb), vn(bb)
250 PRINT “Give nr. of root vertices,”
260 PRINT “of broken bonds and missing”
270 PRINT “neighbours of each root vertex”
```

```
280 FOR ii = 1 to bb : INPUT vr(ii) ; vb(ii) ; vn(ii)
290 END IF
300 DIM a(na, na), s(na)
310 ainp : matip a, t$
320 PRINT “Input at. nr. of elements”
330 FOR i = 1 to na
340 PRINT i ; PRINT “ga(“ ; i ;”) = ” ; : INPUT ga(i)
350 NEXT i
360 FOR i = 1 to na
370 vi = 0 : vj = 0
380 FOR j = 1 to na
390 if a(i, j)⟨⟩0 then vi = vi + 1 : vj = vj + a(i, j)
400 NEXT j
410 IF rS = “Y” or r$ = “y” THEN
420 FOR ii = 1 to bb
430 IF vr(ii) = i then vi = vi + vn(ii) : vj = vj + vb(ii)
440 NEXT ii
450 END IF
460 ng = ga(i)
470 ng = group(ng)
480 h(i) = 8 − ng − vj : ng = ga(i)
490 IF h(i) < 0 then h(i) = 0
500 s(i) = (sa(ng)x(sa(1)) Λ h(i)) Λ (1/(1 + h(i)))
520 d(i) = (s(i)) Λ (1/(1 + vi))
530 NEXT i
540 id = 0 : q = 0
550 FOR i = 1 to na
560 FOR j = 1 to na
570 IF a(i, j)⟨⟩ 0 THEN Sd = id + a(i, j)/sqrt(d(i)xd(j)) : q = q + 1
580 NEXT j
590 NEXT i
600 PRINT “Do you whish to correct”
610 PRINT “for aromatic groups (y/n) ?” ; ar$
620 IF ar$ = “Y” or ar$ = “y” THEN
630 CLS : INPUT “Nr. of aromatic groups :” ; ag
640 INPUT “Nr. of aromatic rings :” ; mar
650 INPUT “Nr. of PI bonds :” ; npi
660 qt = q + npi : miu = q − na + 1
670 cor = (1 − miu/qt + (ag − mar)/(2xqt)) : id = idxcor
680 END IF
690 PRINT : UNDER 1
700 PRINT tS : UNDER 0
710 PRINT “DS INDEX=” ; id
720 INPUT “Other molecule (y/n) ?” ; rS
730 IF rS = “Y” or r$ = “y” then RUN
740 STOP
750 DATA 2.592, 0.0, 0
760 DATA 2.275, 2.746, 3.194, 3.654, 4.0, 0, 0, 0
765 DATA 2.138, 2.515, 2.957, 3.975, −999
770 DEFINE FUNCTION GROUP (ng)
```

```
780 gp = ng - 2
790 if gp < 0 then RETURN ng
800 gp = gp - 8
810 IF gp < 0 THEN RETURN gp + 8
820 gp = gp - 8
830 IF gp < 0 THEN RETURN gp + 8
840 PRINT "This program does not work"
850 PRINT "with element nr."; gp + 8
860 END DEFINE
870 DEFINE PROCEDURE ainp
871 REM INSERT AINP FROM REFERENCE (1)
990 END DEFINE
1000 DEFINE PROCEDURE matip(a, t$)
1001 REM INSERT MATIP FROM REFERENCE (1)
1200 END DEFINE
```

REFERENCES

[1] M. V. Diudea and I. Silaghi-Dumitrescu, "Molecular Topology 1. Valence Group Electronegativity as a Vertex Discriminator", *Rev. Roumaine Biochim.*, **34**, 1175 (1989).

[2] W. J. Murray L. B. Kier and L. H. Hall, *J. Pharm. Sci.*, **64**, 1978 (1975).

[3] A. T. Balaban, *Pure Appl. Chem.*, **55**, 199 (1983).

[4] A. T. Balaban, *Chem. Phys. Lett.*, **89**, 399 (1982).

[5] A. T. Balaban and P. Filip, *Math. Chem.*, **16**, 163 (1984).

[6] A. T. Balaban, I. Moţoc, D. Bonchev and O. Mekenyan, "Topological Indices for Structure — Activity Correlations" — in *Topics in Current Chemistry*, **114**, 21 (1983).

[7] L. B. Kier and L. H. Hall, "Molecular Connectivity in Chemistry and Drug Research", Acad. Press, 1976, New York.

[8] B. R. Baker and M. Kazawa, *J. Med. Chem.*, **10**, 302 (1967).

Revue Roumaine de Chimie, 36, 8, 983–985 (1991)

Dedicated to Professor PETRU SPACU on the occasion of his 85th anniversary

ZINC CHROMITE OBTAINED FROM A RESIDUAL CHROMIUM ACETATE SOLUTION

IOANA JITARU, CORNELIA GURAN and MARIANA BICHER
Inorganic Chemistry Department, Polytechnic Institute TCH, Splaiul Independenței 313,
76206-Bucharest, Roumania

Received June 10, 1991

Synthesis of a polynuclear complex compound, $[ZnCr_2(CH_3COO)_2(OH)_6(H_2O)_2]$ used as a precursor in zinc chromite preparation is presented. The precursor and zinc chromite are characterized by elemental analysis, electronic and vibrational spectra, X-rays spectra and differential thermal analysis.

INTRODUCTION

In our previous papers [1,2] we reported on chromium(III) salts (sulphate, acetate and alum) synthesis from residual acetic solutions. These solutions proceed from equipment of technical acetic acid purification (where chromium(VI) oxide is used as catalyst in oxidation of acetaldehyde to acetic acid).

In the present note we report on zinc chromite synthesis from these solutions.

Two classical methods for spinel zinc chromite synthesis are known : *a.* calcination above 1000° of zinc oxide and chromium(III) oxide mixture ; *b.* pyrolysis of zinc(II) and chromium(III) hydroxides or carbonates coprecipitates. A special method of zinc(II)chromite synthesis uses thermal treatment of some insoluble zinc(II) and chromium(III) polynuclear complex compounds.[3–5]

In this purpose, the zinc(II)chromite synthesis procedure indicated in the present note, includes : 1. residual solution processing (with excess of acetic acid elimination) ; 2. precursor synthesis from residual solution and zinc acetate (the precursor is a zinc(II) and chromium(III) polynuclear complex compound) ; 3. zinc chromite synthesis from precursor thermal treatment.

RESULTS AND DISCUSSION

The residual solution processing consists in free acetic acid distillation and the evaporation of dense solution. This compulsory stage is necessary since free acetic acid presence avoids the complete chromium(III) precipitation and requires a higher quantity of ammonium hydroxide (acetate anion and the other organic anions which can exist in residual solution block chromium(III) ion as some stable soluble complex compounds that cannot be destroyed by boiling or by hydrolysis).

In the second stage, precursor synthesis, our researches have established the optimum conditions of complete zinc(II) and chromium(III) ions "coprecipitation" by the following parameters modification : pH-precipitation ; precipitation temperature ; zinc to chromium atomic ratio ; heating time of "coprecipitates" in solution.

Our researches connected to some parameters optimization have established that, using 12.5% ammonium hydroxide solution as precipitation reactive, in pH = 7–8 range, at 80–90°C and zinc : chromium = = 1 : 2 atomic ratio it is possible to obtain a practically complete two ions "coprecipitation ; this "coprecipitate" is a dark green compound that was used as precursor in the following stage of zinc chromite synthesis.

Elemental chemical analysis and physico-chemical determinations (electronic, vibrational, X-rays spectra and thermal analysis) on isolated product established that it is probably a polynuclear coordination compound with molecular formulae, $[ZnCr_2(CH_3COO)_2(OH_6)(H_2O)_2]$. This product has its own structural characteristics.

Thermal analysis of the precursor shows that the total weight loss recorded on GT curve is $\sim 47\%$ (45.5% theoretically) and corresponds to zinc oxide -chromium(III) oxide mixture. The process of chromite formation ends at 550° ; this fact is observed from X-rays spectra also.

Vibrational spectra bring information referring to the nature of acetate and hydroxyl anions(monodentate ligands, bridging or ionic ligands). IR spectral data (in 650–4000 cm^{-1} range) for precursor and for certain compounds (zinc acetate or chromium acetates, known in literature [6]) support a structural formulae of precursor with bridging OH^+ and CH_3COO^- groups.

The electronic spectrum in visible range (400–1000 nm) of isolated precursor supports chromium(III) hexacoordination and the molecular electrical conductivity determination shows its nonelectrolyte nature.

In the third stage of the study we established optimum calcination time and temperature of the precursor. A blue-black compound was obtained by calcination of the precursor at 550°, for two hours. Its structure was determined by diffraction X rays analysis. The diffractogram of the obtained compound presents characteristic spinelic structure bands of zinc(II) chromite. Zinc oxide and chromium(III) oxide bands are not present.

The X-rays spectra determined on thermally treated products at different times show that the crystallinity degree of zinc chromite is reached after one hour of calcination. After three hours of calcination, crystallinity degree modifications do not appear.

In conclusion, this work proposes a zinc chromite synthesis method. This method has some economic advantages : recovery of the chromium(III), an expensive, critical element from a residual and polluant solution ; the obtained zinc chromite is a high purity product (free of zinc oxide or chromium(III) oxide).

EXPERIMENTAL

1. Residual Solution Processing. 100 mL residual solution was distilled into a simple distillation equipment. A volume of 31 mL product with d = 1.05 was distilled at 118°. The thick solution remained in distillation flask is dried on a sandbath. Dry product was the raw material in the following stage of precursor precipitation.

2. Precursor Synthesis. Samples of 5 g solid residue (1 g Cr) and 1.74 g $Zn(CH_3COO)_2 \cdot 2H_2O$ (0.6 g Zn) were dissolved in 150 mL distilled water. The obtained solution is heated up to 80—90° and a 12.5% ammonia solution is added up to pH = 7—8. The obtained precipitate (precursor) is filtered, washed with distilled water and dried in air.

3. Zinc Chromite Synthesis. The precursor previously isolated is calcinated at 550° for two hours.

4. Thermal Analysis was recorded in static air atmosphere between room temperature and 1000° using a MOM Budapest Q-1500 D derivatograph, Paulik-Paulik-Erdey type (heating speed-100 mg ; standard material-calcinated Al_2O_3).

5. Electronic Spectra have been recorded at room temperature on a VSU-2G spectrophotometer using, as a referring material, magnesium oxide. A large asymetrical band appears in the 450—550 nm range.

6. Vibrational Spectra — were recorded with a Perkin-Elmer spectrophotometer using a potassium bromide disk as reference. Bands in cm^{-1} : 3300 m, 1570 m, 1410 m, 675 m.

7. X-rays Diffraction Spectra were recorded on 63 nm powders, using a TUR-M-62, 40 kV, 18 mA diffractometer with Cu k_α radiation. (θ = 15.02 ; 18.0 ; 28.70 ; 31.50).

ACKNOWLEDGEMENTS. The X-ray spectra were performed by Dr. E. Andronescu to whom our thanks are due.

REFERENCES

[1] I. Jitaru, C. Guran, M. Bicher, M. Dinculescu and M. Micu, *Rev. Chim.*, **38**, 568 (1987).

[2] I. Jitaru, C. Guran, M. Bicher and M. Dinculescu, *Rev. Chim.*, **38**, 786 (1987).

[3] M. Kraus, Z. Zitny and A. Andreev, *Collect. Czech. Chem. Commun.*, **41**, 3586 (1976).

[4] N. E. Konyukhova, I. I. Kalinichenko and A. I. Purtov, *Izvest. Vyssh. Uchebn. Zaved., Khim. Khim. Tekhnol.*, **20**, 163 (1977).

[5] M. S. Erenburg, V. P. Fateeva and A. J. Minkov, *Isvest. Uchebn. Zaved., Khim. Khim Technol.*, **20**, 303 (1977).

[6] A. B. P. Lever, "Inorganic Electronic Spectroscopy", Elsevier, Amsterdam—London—New York, 1968, p. 265.

[7] K. Nakamoto, "Infrared Spectra of Inorganic and Coordination Compounds", Wiley Interscience, New York, London, Sydney, Toronto, 1970, p. 253.

Revue Roumaine de Chimie 36, 8, 987 (1991)

BOOK REVIEW

D. Klamann, Ed., *Methods of Organic Chemistry* (*Houben-Weyl*), 4th ed., Vol. E 12b, *Organotellurium Compounds*, by K. J. Irgolic, G. Thieme Verlag, Stuttgart, 1990 ; 1004 pages ;

This volume, edited by D. Klamann, continues the valuable series of "Houben-Weyl Methods of Organic Chemistry", which accustomed us with a complete and detailed description of preparative methods for a large range of organic and organometallic compounds.

The book provides a detailed presentation of the organotellurium chemistry, and is the result of a systematic study made by K. J. Irgolic (known for his interest in the field of tellurium organic compounds) on various groups of organotellurium compounds known until 1990 ; it offers a broad range of methods for preparing tellurium compounds and, at the same time, a rigorous classification of these compounds, related to either the oxidation states of the central element (Te) or to the ligands and bonds involved in their molecule.

The Introduction provides a brief history of organotellurium chemistry, as well as the classification and nomenclature used in the following ten Chapters of the book. Some safety precautions which must be taken into account are also mentioned.

In Chapter I (150 pages), methods for synthesis of tellurium compounds without a direct Te—C bond, but containing at least one carbon atom in their molecule, are presented.

The following nine Chapters are devoted to genuine organotellurium compounds, which contain one or more direct tellurium-carbon bonds. Thus, Chapter II (216 pages) describes the synthesis of di, tetra- and hexavalent organotellurium compounds with a single Te—C bond, Chapter III (308 pages) is devoted to compounds containing two single tellurium-carbon bonds or one tellurium-carbon double bond, while Chapter IV (33 pages) deals with triorganotellurium derivatives.

The synthesis of tetraorganotellurium, alkylidene diorganotellurium and hexaorganotellurium derivatives make up the subject of Chapter V (15 pages).

Chapter VI (5 pages) describes the synthesis of the few polymeric organic tellurium compounds known so far.

The last four Chapters are devoted to heterocyclic compounds containing at least one tellurium atom in the ring system. Thus, Chapter VII (2 pages) describes the synthesis of the few examples of tensioned three- and four-membered ring systems containing one or two Te atoms. The other three Chapters, *i.e.* VIII (83 pages), IX (67 pages) and X (1 page), are concerned with five-, six- and seven-membered heteroarenes, respectively.

The book contains a Bibliography listing the most important reviews and books on organic tellurium chemistry. The original references, including papers published up to 1990, are cited at the bottom of each page. A Subject and an Author Index conclude the book.

This book represents an exhaustive and, thus, a very useful guide on the methods of preparation of organic tellurium compounds. It is a must for every laboratory involved in the chemistry of organotellurium compounds. Being the most up-to-date and comprehensive monograph on organotellurium chemistry, this book has no competitor in the field and is highly recommended to all interested in this area.

Cristian Silvestru

Revue Roumaine de Chimie 36, 7, 867 (1991)

BOOK REVIEWS

D. Klamann, Ed., *Methods of Organic Chemistry (Houben-Weyl)*, 4th ed., Vol. E 12b, *Organotellurium Compounds*, by K. J. Irgolic, G. Thieme Verlag, Stuttgart, 1990; 1046 pages.

This volume, edited by D. Klamann, continues the valuable series of "Houben-Weyl Methods of Organic Chemistry", which accustomed us with a complete and detailed description of preparative methods for a large range of organic and organometallic compounds.

The book provides a detailed presentation of the organotellurium chemistry and is the result of a systematic study made by K. J. Irgolic (known for his interest in the field of tellurium organic compounds) on various groups of organotellurium compounds known until 1990. It offers a broad range of methods for preparing tellurium compounds and, at the same time, a rigorous classification of these compounds, related to either the oxidation states of the central element (Te) or to the ligands and bonds involved in their molecule.

The Introduction provides a brief history of organotellurium chemistry, as well as the classification and nomenclature used in the following ten Chapters of the book. Some safety precautions which must be taken into account are also mentioned.

In Chapter I (150 pages), methods for synthesis of tellurium compounds without a direct Te—C bond, but containing at least one carbon atom in their molecule, are presented.

The following four Chapters are devoted to acyclic organotellurium compounds, which contain one or more direct tellurium-carbon bonds. Thus, Chapter II (216 pages) describes the synthesis of di, tetra- and hexavalent organotellurium compounds with a single Te—C bond, Chapter III (308 pages) is devoted to compounds containing two single tellurium-carbon bonds or one tellurium-carbon double bond, while Chapter IV (82 pages) deals with triorganotellurium derivatives.

The synthesis of tetraorganotellurium, alkylidene diorganotellurium and hexaorganotellurium derivatives make up the subject of Chapter V (15 pages).

Chapter VI (6 pages) describes the synthesis of the few polymeric organic tellurium compounds known so far.

The last four Chapters are devoted to heterocyclic compounds containing at least one tellurium atom in the ring system. Thus, Chapter VII (2 pages) describes the synthesis of the few examples of tellurium-containing three- and four-membered ring systems containing one or two Te atoms. The other three Chapters, i.e. VIII (53 pages), IX (67 pages) and X (4 pages), are concerned with five-, six- and seven-membered heterocycles, respectively.

The book contains a bibliography listing the most important reviews and books on organic tellurium chemistry. The original references, including papers published up to 1990, are cited at the bottom of each page. A Subject and an Author Index conclude the book.

This book represents an exhaustive and, thus, a very useful guide on the methods of preparation of organic tellurium compounds. It is a must for every laboratory involved in the chemistry of organotellurium compounds. Being the most up-to-date and comprehensive monograph on organotellurium chemistry, this book has no competitor in the field and is highly recommended to all interested in this area.

Cristian Silvestru

NOTE POUR LES AUTEURS

La Revue Roumanie de Chimie publie des articles en anglais, français, russe, allemand. Les auteurs sont priés d'envoyer des articles et comptes rendus inédits.

Les manuscrits seront dactylographiés à double interligne. La bibliographie, les tableaux et la légende des figures seront placés après le texte.

Si l'article fait partie d'une série numérotée, la partie précédente sera donnée comme première référence.

Chaque article sera précédé d'un résumé comprenant quinze lignes au maximum.

Les références bibliographiques dans le texte seront faites par des exposants sans parenthèses et paraitront à la fin de l'ouvrage.

Les publications périodiques mentionnées dans la bibliographie seront présentées suivant les prescriptions internationales : le nom de l'auteur précédé de l'initiale du prénom, le titre du périodique abrégé conformément à « Chemical Abstracts » et souligné par une ligne, le numéro du tome indiqué par des chiffres arabes et souligné par deux lignes, suivi de la première page de l'article : à la fin, l'année de la parution sera placée entre parenthèses. Le numéro de la revue ne sera pas indiqué si les pages du volume sont numérotées consécutivement.

Les textes des livres ou traités incluront : le nom des auteurs, l'initiale du prénom, le titre du livre entre guillemets et sans être souligné, le numéro du tome précédé par l'abréviation « vol. » (ou « Bd »), le numéro de l'édition, les éditions (the publisher), la localité de la parution du livre, l'année de la parution et la page de la référence précédée(s) par l'abréviation « p » (ou « S. »).

Les brevets seront indiqué comme suit : l'auteur ou la firme, le pays et le numéro du brevet, la date et la revue *(Chem. Abstr.)* Par ex : M. Jones (to Union Carbide Co,) Brit. Pat. 601 238, 2 Sept. 1959 ; cf. *Chem. Abstr.*, **54**, 12808 (1960).

Si la référence n'a pas été lue en original, on indiquera aussi la revue de références consultée.

Les diagrammes seront tracés à l'encre de Chine sur papier calque. Les tableaux et les figures (en nombre strictement nécessaire) ainsi que les courbes dans les figures seront numérotés par des chiffres arabes. Leur explication sera donnée dans la légende des figures. Prière de ne pas inscrire les mêmes données dans les tableaux et les figures. Chaque tableau aura un titre. On indiquera dans le texte la place approximative des tableaux et des figures. Les formules chimiques seront incluses dans le texte ; en outre, elles seront transcrites sur papier calque, à l'encre de Chine.

Les auteurs sont priés d'indiquer les caractères italiques (en soulignant les lettres au crayon), ainsi que tout autre caractère spécial ; les préfixes *ortho,meta*, *para*, *cis*, *trans*, etc. seront soulignés pour indiquer leurs caractères italiques et ne seront jamais écrits avec des majuscules.

Aucune correction à la main ne sera admise sur le manuscrit. Les corrections seront tapées à la machine. Les lettres grecques ou d'autres symboles spéciaux seront insérés à la main à l'encre clairement.

Le manuscrit sera signé par l'auteur.

Le titre-courant aura 50 lettres au maximum.

L'entière responsabilité du contenu des articles appartient aux auteurs.

Sur demande on peut obtenir une note plus complète.

PRINTED IN ROMANIA

TRAVAUX PARUS AUX ÉDITIONS DE L'ACADÉMIE ROUMAINE

I. G. MURGULESCU, **Introducere în chimia fizică, Vol. 1. Atomi, molecule, legătură chimică**, 1976, 560 p.

I. G. MURGULESCU, V. EM. SAHINI, **Introducere în chimia fizică, Vol. 2. Structura şi proprietăţile moleculelor**, 1979, 604 p.

I. G. MURGULESCU, E. SEGAL, **Introducere în chimia fizică, Vol. II. 1. Teoria molecular-cinetică a materiei**, 1979, 1056 p.

I. G. MURGULESCU, TATIANA ONCESCU, E. SEGAL, **Introducere în chimia fizică, Vol. II. 2. Cinetică chimică şi cataliză**, 1981, 1024 p.

I. G. MURGULESCU, J. PĂUN, **Introducere în chimia fizică, Vol. I. 3. Nucleul atomic, reacţii nucleare, particule elementare**, 1982, 606 p.

I. G. MURGULESCU, RODICA VÎLCU, **Introducere în chimia fizică. Vol. III. Termodinamica chimică**, 1982, 624 p.

I. G. MURGULESCU, O. M. RADOVICI, **Introducere în chimia fizică. Vol. IV. Electrochimia**, 1986, 410 p.

C. ANDREI, I. DRĂGUŢAN, A. T. BALABAN, **Fotostabilizarea polimerilor cu amine împiedicate steric**, 1990, 240 p.

M. BREZEANU, E. CRISTUREANU, D. MARINESCU, A. ANTONIU, M. ANDRUH, **Chimia metalelor**, 1990.

R. VÎLCU, M. LECA, **Polymer Thermodynamics by Gas Chromatography**, coédition avec Elsevier, 1990, 204 p.

O. IORDACHE, M. GHERGHE, S. CORBU, **Modelarea statistică şi estimarea parametrilor proceselor chimice**, 1991, 238 p.

FL. CUIBAN, A. X. LUPEA, **Studiul structurii şi sinteza peptidelor**, 1989, 286 p.

CRISTOFOR I. SIMIONESCU, VALERIA GORDUZA, **Implicaţii bioenergetice ale coloranţilor**, 1988, 208 p.

R. VÎLCU, M. LECA, **Termodinamica polimerilor prin cromatografie de gaze**, 1987, 238 p.

I. ZUGRĂVESCU, M. PETROVANU, **Cicloadiţii 3 + 2 dipolare**, 1987, 446 p.

RAUL MIHAIL, ION GROZEANU, **Estimarea secvenţială aplicată sistemelor chimice**, 1986, 406 p.

M. BREZEANU, I. PATRON, M. ANDRUH, **Combinaţii complexe polinucleare şi aplicaţiile lor**, 1986, 244 p.

A. T. BALABAN et al., **Labelled Compounds and Radiopharmaceuticals Applied in Nuclear Medicine**, coédition avec John Wiley and Sons, 1986, 742 p.

D. PURDELA, **Nomenclatura chimiei organice — IUPAC**, 1986, 451 p.

PETRU BUDRUGEAC, **Probleme de chimie**, 1986, 280 p.

T. ONCESCU, S. G. IONESCU, **Conversie fotochimică şi stocare de energie**, 1985, 272 p.

V. DRĂGUŢAN, A. T. BALABAN, M. DIMONIE, **Olefin Metathesis and Ring-Opening Polymerization of Cyclo-Olefins**, coédition avec John Wiley and Sons, 1985, 544 p.

C. LITEANU, I. RÎCĂ, **Optimizarea proceselor analitice**, 1985, 360 p.

N. PERESCU, **Chimia extracţiei cu solvenţi şi aplicaţii**, 1985, 212 p.

1992 JUN 25

S. C. UNIVERSUL S. A. c. 3176

44 426

Lei 40

F 1103

ACADÉMIE ROUMAINE

REVUE ROUMAINE DE CHIMIE

TOME 36

N°s 9—10

Septembre —Octobre 1991

Rev. Roumaine Chim.

RRCHAX, 36, *9—10*, p. 989—1222 (1991), Bucarest

EDITURA ACADEMIEI ROMÂNE

ACADÉMIE ROUMAINE

COMITÉ DE RÉDACTION

Rédacteur en chef :

I. G. MURGULESCU, membre de l'Académie Roumaine

Rédacteurs en chef adjoints :

A. T. BALABAN et V. EM. SAHINI, membres de l'Académie Roumaine

Collège de rédaction :

ECATERINA CIORĂNESCU-NENITZESCU, CR. SIMIONESCU, P. SPACU, membres de l'Académie Roumaine ; M. BANCIU, membre correspondant de l'Académie Roumaine ; M. ANDRUH, M. D. GHEORGHIU, I. HAIDUC, D. I. MARCHIDAN, G. NIAC et D. SĂNDULESCU

La Revue Roumaine de Chimie paraît 10 fois par an. Toute commande de l'étranger sera adressée à ROMPRESFILATELIA – sectorul Export-Import Presă, P.O. Box 12–201, télex 10376 prsfi r, 78104 Bucarest, Calea Griviței nr. 64–66, Roumanie

Les manuscrits, les livres et les revues proposés en échange, ainsi que toute correspondance seront envoyés à la rédaction :

REVUE ROUMAINE DE CHIMIE

125, Calea Victoriei, 79717 Bucarest, Roumanie, téléphone 50 76 80

EDITURA ACADEMIEI ROMÂNE

125, Calea Victoriei 79717, Bucarest, Roumanie, téléphone 507680

REVUE ROUMAINE DE CHIMIE

Tome 36, Nos 9–10 **Septembre–Octobre, 1991**

EMILIAN A. BRATU (1904–1991) — Member of the Roumanian Academy . . . 991–993

N. DRAGOE and E. SEGAL, On the validity of the Coats-Redfern method in nonisothermal kinetics 995–998

VICTOR DAVID and GEORGE-EMIL BAIULESCU, A new spectrometric method for determining carbon monoxide in air, using the Pd(II)-p-nitrosodiphenylamine complex 999–1004

I. LINGVAY, RODICA GALASIU and I. GALASIU, The electrochemical behaviour of SnO_2 based semiconductor ceramic in NaCl solutions 1005–1010

I. T. FISHTIK, Thermodynamics of polynuclear complex formation reactions . . 1011–1020

N. PETRESCU, CHOI SANG GON and LUCIA GANOVICI, The synergic effect in the uranium extraction with the mixed solvent LIX 63 (5,8-diethyl-7-hydroxy-6-dodecanone oxime) and di-2-ethyl-hexyl phosphoric acid. . . 1021–1031

REMESH KUMARI, A. D. TANEJA and V. P. KUDESIA, Effect of solvents on the electronic spectra of 2, 3-dioximes derivatives of aromatic acetoacetamides 1033–1043

SERGIU P. PALII, DIMITRII V. ZAGOREVSKII, KONSTANTIN M. INDRICHAN, NIKOLAI V. GERBELEU, YURII S. NEKRASOV and VLADIMIR B. ARION, Mass spectrometry of coordination compounds of transition metals with tetradentate ligands. VIII. The redistribution of hydrogen atoms at the loss of the methyl-group from the molecular ions of nickel(II) complexes with hexaazamacrocyclic ligands on the basis of S-substituted isothiosemicarbazides and β-diketones 1045–1054

ANIȘOARA BOLD, AURELIA VASILE, ANGELICA POPA and M. CRUCEANU, Ion exchange in siliceous zeolite ZSM-8 1055–1059

R. BACALOGLU, ILSE BACALOGLU and Z. SIMON, Molecular orbital calculations with specific parametrization (MOSP). 1. Description of the method. Dipole moment calculations 1061–1074

ȘERBAN-DAN CARTIANU, Method for calculating the local electronic energy levels in semiconductors and their occupation numbers from slope variations of the Arrhenius diagram of the electric conductivity 1075–1092

LUDOVIC KURUNCZI, RADU VÂLCEANU and ZENO SIMON, Del Re calculations for phosphorus compounds. Bond and atomic properties 1093–1100

MIRCEA D. BANCIU, IOANA SIMION, ANCA BANCIU, AURICA PETRIDE and CONSTANTIN DRĂGHICI, Flow-vacuum pyrolysis of tribenzo[*a*, *e*, *i*][12]annulene 1101–1106

Rev. Roumaine de Chim. **36**, *9–10*, 989–1222 (1991), Bucarest

CORINA ILIE, AURELIA GHENCIULESCU, LUCIAN ENESCU and ILIE G. DINULESCU, The reaction of the angular dimer of 1-methyl-benzocyclobutadiene with electrophilic reagents 1107–1112

HORIA PETRIDE, Mesoionic oxazolones. VI. Hydrolysis of acylated derivatives 1113–1122

TINCA BURUIANĂ and ADRIAN CARACULACU, Synthesis and characterization of some 2, 4′-dibenzyldiisocyanate ionic polymers. VI. Biological activity at low concentrations of ionic groups 1123–1127

M. Z. A. BADR, M. M. ALY, A. A. ATTALA and S. A. MAHGOUB, Molecular rearrangements. Part XXXII. Thermolysis and photolysis of some hydroxylamine derivatives 1129–1134

IOAN AGHERGHINEI, CRISTINA PRISACARIU and ADRIAN A. CARACULACU, A new method for a kinetic study of reactions between diisocyanates and alcohols. Part II. Asymmetrical diisocyanates : 2, 4-toluylene diisocyanate 1135–1145

JEAN HERDAN, ALEXANDRU T. BALABAN, GERALD STOICA, ZENO SIMON, MIRCEA MRACEC and ION NICULESCU-DUVĂZ, Compounds with potential cancer preventing activity. I. Synthesis, physicochemical properties and quantum chemical indices of some phenolic and aminophenolic antioxidants 1147–1160

S. MISRA, B. L. DUBEY and S. C. BAHEL, Preparation, characterization and fungitoxicity of the Fe(III) complexes with mercapto azoles 1161–1168

CONSTANTIN LUCA, MIHAI BĂRBOIU and CLAUDIU T. SUPURAN, Carbonic anhydrase inhibitors. 7. Stability constants of complex inhibitors and their mechanism of action 1169–1173

CLAUDIU T. SUPURAN, RALUCA ŞTEFAN, GHEORGHE MANOLE, IOAN PUŞCAŞ and MARIUS ANDRUH, Carbonic anhydrase inhibitors. 8. Complexes of ethoxzolamide with lanthanides are powerful inhibitors of izozymes I and II 1175–1179

E. DZIWINSKI, P. KUSZ, H. SZEWCZYK, K. PYZALSKI and D. GASZTYCH, Low-boiling products of the propoxylation reaction of acetic acid 1181–1184

EMIL DUMITRIU, VASILE HULEA, KAYED YOUSEF, NICOLAE BALBA and SPIRIDON OPREA, Transalkylation of toluene with trimethylbenzene. II. Transalkylation of toluene with mesitylene over synthetic zeolites 1185–1193

GHEORGHE M. PANAITESCU, Maximum likelihood principle extended to generate selection criteria for equations of state and/ or data 1195–1201

IRINA BUCURESCU, CRISTIAN TSAKIRIS, CRISTINA MARIA, GHEORGHE MARIA and ALEXANDRU ISOPESCU, A note concerning the direct interchange area error evaluation for the radiative transfer in a radiant furnace 1203–1210

V. S. BABKIN and V. I. BABUSHOK, Bank of kinetic data and simulation of complex chemical reactions (in Russian) 1211–1217

BOOK REVIEWS 1219–1221

MŰSZAKI INFORMÁCIÓS ÉS KÖNYVTÁR 1883 ORSZÁGOS KÖZPONT

Revue Roumaine de Chimie, 36, *9–10*, 991–993 (1991)

EMILIAN A. BRATU

Member of the Roumanian
Academy
(1904–1991)

Professor Emilian A. Bratu, founder of the Roumanian chemical engineering school, a remarkable personality of our teaching, science and chemical industry community, died on 30 March 1991.

Death suddenly took him away from his familiy, friends, coworkers and students whose guide he permanently was.

Professor Emilian A. Bratu was born in Bucharest on 8 August 1904. He attended Sf. Sava High School and then the scientific section in the Gh. Lazăr High School.

Between 1923–1927 he was student at the Industrial Section of the Bucharest Polytechnic School, which later on became the Industrial Chemistry Faculty, which he graduated with "very good". He gratefully remembered his professors, among others, Traian Lalescu, David Emanuel, Vasile Bianu and Paul Staehelin, saying that "each one, by his specific way of teaching, learnt us many beautiful things in our craft but more than that, by the radiation of their personality they transferred to us something of their exemplary way of life".

In June 1928, he was appointed Assistant Professor at the Bucharest Polytechnic School, Chemical Technology and Electrochemistry Department, headed by Professor Paul Staehelin. In 1940, he became Reader of Industrial Physics, an especially designed course for the industrial chemistry students, which at his proposal, was transformed into the Unit Operations and Plants of the Chemical Industry course. It is his merit to realize the necessity and importance of such a discipline for the chemical engineers in a time when few universities in the world had it in their curriculum. As an acknowledgement of his scientific and teaching activities he was appointed Professor and Head of the Apparatus and Plants Chair, at present Chemical Engineering, till his retirement.

During his 63-year-old activity at the Industrial Chemistry Faculty, Professor Emeritus Emilian A. Bratu was a remarkable personality, marking the entire evolution of the chemical engineering teaching in Romania. Conscious of the necessity, for a scientist and a teacher, of a broad fundamental scientific and technical formation, Professor Em. Bratu started his research activity at the same time with his teaching, working abroad, for many summer holidays, in several essential domains for his future activity : methane pyrolysis for direct oxidation of nitrogen from air, at the Karlsruhe Technische Hochschule ; autoclaves and compressors for high temperature synthesis, at the famous manufacturer Andreas Hofer ; electrochemical research at the Berlin—Charlottenburg Technische Hochschule ; very high precision measurements of electromotive forces of electrochemical chains at the Vienna Physical Chemistry Institute ; applied research during stage periods in industry concerning materials quality, especially defining and verifying the achieved standards. His Ph. D. Thesis "Preparation of heavy hydrogen isotope and determination of heavy water dissociation constant" elaborated under the supervision of Professor Emil Abel, a new subject for that time, preserves its topical interest even today, the obtained results being presented in "Landolt-Börnstein Tabelles".

This broad scientific and technical formation permitted him to derive the fundamental principles of that new discipline — chemical engineering — that he developed with great success in his entire activity. His remarkable contributions to this field brought him national and international recognition.

The text books written by Professor Em. Bratu, especially Unit Operations and Plants in Chemical Industry, renewed in several editions, represent a classical chemical engineering work which has trained many generations of students and it is currently used in the Roumanian design institutes.

Being for more than 30 years the Head of the Chemical Engineering Department and for many years the Dean of the Industrial Chemistry Faculty he formed and guided a community that developed further on the chemical engineering research and teaching in the spirit of professional and civic probity.

Professor Emilian Bratu had a prodigious scientific activity ; he published many papers in scientific journals in Roumania and abroad. The domains of the research activity carried out by Prof. Em. Bratu include various aspects of chemical engineering. Many theoretical problems of this discipline have been advanced and many practical solutions were often proposed for the design of chemical plants.

All who knew Professor Emilian Bratu felt and appreciated his love for people, his trust for the youth completed with a discreet but very substantial support, the favourable influence that this strong personality exerted on all those around him.

Shining without shadowing by his perseverance, competence, modesty and delicacy, by his capacity of judging and understanding people, Professor Em. A. Bratu gained the acknowledgement of a distinguished man, professor and school chief.

An excellent organizer, possessing an extraordinary capacity for ordering and planing his activities, recognized by all who worked with him, Professor Em. A. Bratu tried and succeeded to excel in many other fields.

Academician Em. A. Bratu was a man of a vast culture. A discussion with him, no matter the subject, was a moment of high intelectual satisfaction; from a funny story to a disertation about the endeavours in the present world, depending on the subject and the environment, Professor Em. Bratu relaxed others and created intimacy using his caracteristic style and erudition, lightening discreetly but entirely the hearts and minds of those who listened.

Professor Em. A. Bratu was a nature lover and admirer. Mountains, forests, the smell of fir-trees and freshly cut grass, the purling of the spring fascinated him. He was in love with the mountain paths, knew to discover in each corner, in each lawn, each hill, beauties that alone you wouldn't have thought about.

The death of Academician Emilian A. Bratu is a great loss. He will remain in the hearts of his students, of thousands of chemical engineers that he educated, of tens of Ph. Doctors whom he, with abnegation formed, of all who knew him directly or by his illustrious work. The chemical engineering high school and science, the chemical industry lost a guide and an ingenious researcher. Let peace be with him.

Revue Roumaine de Chimie, 36, *9–10*, 995–998 (1991)

ON THE VALIDITY OF THE COATS-REDFERN METHOD IN NONISOTHERMAL KINETICS

N. DRAGOE and E. SEGAL

Department of Physical Chemistry, Faculty of Chemistry
Polytechnic Institute of Bucharest, Bulevardul Republicii 13, Bucharest, Romania

Received May 11, 1990

The authors present a test for the validity of the Coats-Redfern method used in nonisothermal kinetic analysis.

The integral method worked up by Coast and Redfern [1] is widely used to evaluate the nonisothermal kinetic parameters. The integral formula on which the method is based can be obtained from the general nonisothermal differential kinetic equation :

$$\frac{\mathrm{d}\alpha}{\mathrm{d}t} = \frac{A}{\beta}\,\mathrm{e}^{-\frac{Ea}{RT}} f(\alpha) \tag{1}$$

where all the notations have their usual meanings.[2] Through variables separation and integration equation (1) turns into :

$$\int_0^{\alpha} \frac{\mathrm{d}\alpha}{f(\alpha)} = \frac{A}{\beta}\int_{T_0}^{T} \mathrm{e}^{-\frac{Ea}{RT}}\mathrm{d}T \tag{2}$$

where T_0 is the temperature at which the reaction begins. Using the approximation :

$$\int_{T_0}^{T} \mathrm{e}^{-\frac{Ea}{RT}}\mathrm{d}T \simeq \int_0^{T} \mathrm{e}^{-\frac{Ea}{RT}}\mathrm{d}T \tag{3}$$

considering one of the usual forms of the differential function of conversion $f(\alpha)$ corresponding to the "reaction order" model :

$$f(\alpha) = (1 - \alpha)^n \tag{4}$$

where n stands for the reaction order, and introducing the integral function of conversion $F(\alpha)$ defined by the relationship :

$$F(\alpha) = \int_0^{\alpha} \frac{\mathrm{d}\alpha}{(1-\alpha)^n} \tag{5}$$

equation (2) takes the form :

$$F(\alpha) = \frac{A}{\beta} \int_0^T \mathrm{e}^{-\frac{E_a}{RT}} \mathrm{d}T \tag{6}$$

By performing the integration of the right member in (5) we get :

$$F(\alpha) = \begin{cases} \dfrac{1-(1-\alpha)^{1-n}}{1-n} & \text{for } n \neq 1 \\ -\ln(1-\alpha) & \text{for } n = 1 \end{cases} \tag{7}$$

The integral from the right member of (3),

$$I(T) = \int_0^T \mathrm{e}^{-\frac{E_a}{RT}} \mathrm{d}T \tag{8}$$

is known as the temperature integral. Introducing the notation :

$$x = -\frac{E_a}{RT} \tag{9}$$

and integrating by parts, relationship (6) turns into :

$$F(\alpha) = \frac{AE}{\beta R}\left(-\frac{\mathrm{e}^x}{x} + \int_{-\infty}^{x} \frac{\mathrm{e}^x}{x}\mathrm{d}x\right) \tag{10}$$

Using the approximation :

$$\int_{-\infty}^{x} \frac{\mathrm{e}^x}{x}\mathrm{d}x = \frac{\mathrm{e}^x}{x} \sum_{i=0}^{N} \frac{i!}{x^i} \tag{11}$$

with $N < |x|$ and $x \leqslant -10$, from (10) one obtains :

$$F(\alpha) = \frac{AE_a}{\beta R} \frac{\mathrm{e}^x}{x^2} \sum_{i=0}^{N} \frac{(i+1)!}{x^i} \tag{12}$$

Taking only two terms from the development (12) and applying the logarithms, from (12) we get :

$$\ln\frac{F(\alpha)}{T^2} = \ln\frac{AR}{\beta E_a}\left(1 - \frac{2RT}{E_a}\right) - \frac{E_a}{RT} \tag{13}$$

This is the equation used by Coats and Redfern to evaluate the nonisothermal kinetic parameters. For the correct value of the reaction order, n, the plot $\ln - \frac{E(\alpha)}{T^2}, \frac{1}{T}$ leads to a straight line whose intercept and slope allow to obtain respectively the preexponential factor A and the activation energy, E_a.

Due to some criticisms concerning the approximation of the temperature integral on which the Coats-Redfern is based, there are in the literature some attempt to check and to improve it. Among these we mention an attempt to obtain high precision values of the nonisothermal kinetic parameters using a Coats-Redfern type method. [3] For irreversible first order reactions the maximum errors of the activation energy and preexponential factor were 0.15% and 1%, respectively. Anderson and coworkers [4] worked up a corrected variant of the Coats-Redfern method. Actually the slope of the straight line $\ln\frac{F(\alpha)}{T^2}, \frac{1}{T}$ was corrected by taking into account the rest of the terms in the development (12). The corrections of the activation energy and preexponential factor values lie in the limit of experimental errors. Flynn and Wall [5] criticised also the Coats-Redfern method mainly when applied to changing order systems.

This note suggests a test for the validity of the Coats-Redfern approximation for the temperature integral.

In order to work up such a test firstly we have determined the nonisothermal kinetic parameters of the dehydration of calcium oxalate, which is a standard reaction, by using the Coats-Redfern method. The samples were heated in a derivatograph MOM Budapest in a static air atmosphere at a heating rate $\beta = 10$ K/min. The experimental data have been automatically worked up using a program written in BASIC language [6] on a TIM S computer.

The following results have been obtained $A^{CR} = 4.97 \cdot 10^7\ \mathrm{s}^{-1}$; $E^{CR} = 23.086$ cal/mole $n^{CR} = 0.8$ $r = -0.999$, r being the correlation coefficient of the linear regression. These values are in quite good agreement with the values obtained by Coats and Redfern.[1] Then we have integrated numerically the temperature integral, I, using an approximation of the Romberg type.[7] The value of the integral $I(T)$ approximated at the step k is :

$$I_k = \frac{1}{2}\left[\, I_{k-1} + \frac{b-a}{2^{(k-1)}} \sum_{i=1}^{2(k-1)} g\left(a + \frac{b-a}{2^k}\right)\right] \tag{14}$$

where a and b are the limits of the integration interval, and

$$g(x) = \mathrm{e}^{-\frac{E}{Rx}} \tag{15}$$

An extrapolation of the Richardson type

$$I = I_k + \frac{I_k - I_{k-1}}{2^n - 1} \tag{16}$$

with $n = k$ and $n \geqslant 2$ was equally used.

Using 12 steps and 256 iterations the integral

$$\int_{T}^{T_\alpha} e^{-\frac{E^{CR}}{RT}} \mathrm{d}T$$

where T_α is the temperature corresponding to the degree of conversion α, was calculated. Then using equation (6) the value of the preexponential factor A was calculated. Obviously the difference between A one A^{CR} indicates the precision of the Coats-Redfern method. The corresponding values are:

$$A = 5.41 \cdot 10^7\ \mathrm{s}^{-1}$$

and

$$A^{\mathrm{CR}} = 4.97 \cdot 10^7\ \mathrm{s}^{-1}$$

The results show that the Coats-Redfern approximations of the temperature integral is good enough to obtained correct values of the nonisothermal kinetic parameters.

REFERENCES

[1] A. W. Coats and J. P. Redfern, *Nature*, **201**, 68 (1964).

[2] E. Segal and D. Fătu, "Introduction to Nonisothermal Kinetics" (in Romanian), Ed. Academiei, Bucharest, 1983.

[3] P. Ernesto Fisher, Chon Shin Jou and Shyam S. Gokalgandhi, *I&EC RESEARCH*, **26**, 1031 (1987).

[4] H. Anderson, W. Besch and D. Haberland, "Proceedings of the fourth ICTA", Budapest 1974, vol. 1, p. 215.

[5] S. H. Flynn and L. A. Wall, *J. Res. Nat. Bur. Stand, Sect.* A, **70A** 487 (1966).

[6] N. Dragoe and E. Segal, *Thermochim. Acta*, **188**, 305 (1991).

[7] P. Davis and P. Rabinowitz, "Methods of Numerical Integration", Academic Press, New York, 1975.

Revue Roumaine de Chimie, **36**, *9–10*, 999–1004 (1991)

A NEW SPECTROMETRIC METHOD FOR DETERMINING CARBON MONOXIDE IN AIR, USING THE Pd(II)-p-NITROSODIPHENYLAMINE COMPLEX

VICTOR DAVID[a] and GEORGE-EMIL BAIULESCU[b]

[a] Institute of Chemical and Biochemical Energetics,
Splaiul Independenţei 202, 77207, Bucharest, Romania

[b] Department of Analytical Chemistry
Faculty of Chemistry, University of Bucharest
Spl. Independenţei 202, 77207, Bucharest, Romania

Received September 13, 1989

The method is based on the reaction between carbon monoxide and the Pd(II)-p-nitrosodiphenylamine complex, in a medium containing hexamethylphosphotriamide. Two reduction processes take place in this reaction: Pd(II) is reduced to Pd(O), followed by reduction of nitroso group to amino, catalyzed by Pd(O). The reaction product is spectrally characterized by an intense absorption band in the ultraviolet range, with a maximum at 285 nm. This method can be applied for determining carbon monoxide from static gas mixtures, the lower sensitivity limit being 50 ppm, for a volume of air sample of 1L.

INTRODUCTION

Carbon monoxide is a chemical compound with a very week chemical reactivity. Four classes of compounds are known today to have been used to determine CO by visible spectrometric methods: a) salts and complexes of divalent palladium;[1-4] b) salts or complex salts of silver;[5-7] c) haemoglobin and its derivatives;[8,9] and d) complexes of monovalent copper.[10]

Most of the methods for determining CO in air are based on the reduction of metallic ions, e.g. Pd(II), Ag(I), Hg(II). Only a few methods are known to determine CO by reduction of organic compounds. Thus, a method of determining CO uses the reduction of azobenzene to hydrazobenzene by carbon monoxide, in the presence of $PdCl_2$.[11] An interesting method has been achieved by Lambert and Chiang,[4] which is based on the reduction of the keto group of the yellow cacotheline compound to the hydroxy group, resulting violet cacotheline.

The authors have achieved a new method of determining carbon monoxide in air, based on the reduction of the nitroso group from the p-nitrosodiphenylamine compound. In a previous paper,[12] it was shown that the reaction between CO and Pd(II)-p-nitrosodiphenylamine complex occurs in two redox processes :

$$Pd^{2+} + CO + H_2O \rightarrow Pd^0 + CO_2 + 2H^+$$

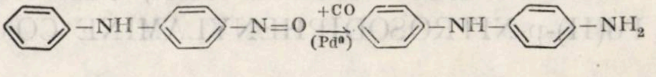

The IR spectrum has not confirmed the possibility of obtaining a carbonyl as a final product of reaction, although this may appear as an intermediate compound.[2]

EXPERIMENTAL

The authors used p-nitrosodiphenylamine and the complex having the formula $[Pd(ONC_6H_4NHC_6H_5)_2]Cl_2$, synthesized and verified by us.[13] The following stock solutions were used :

- 0.01% p-nitrosodiphenylamine in C_2H_5OH 50% ;
- 538.8 μg $[Pd(ONC_6H_4NHC_6H_5)_2]Cl_2$/mL in HMPA, corresponding to 100 μg Pd(II)/mL.

As an adequate solvent for the reaction between CO and the Pd(II)-p-nitrosodiphenylamine complex, hexamethylphosphotriamide (hexametapol or HMPA) of Merck quality was used. The solutions were prepared with deionised water.

Two sources of carbon monoxide were used : a continuous source, consisting of a Matheson cylinder with CO of Merck quality (99.5%), and a discontinuous one, made by us, and upon the decomposition of calcium formiate by conc. H_2SO_4, heated at 70°C. We obtained two based types of gas mixtures containing CO : static and dynamic. In order to obtain static gas mixtures, three calibrated bottles were used, the principle of use being given schematically in Fig. 1. The CO concentration in the last bottle is given by the following relations :[14]

$$C(n = 1) = C_0$$

$$C(n = 2) = C_0$$

$$C(n \geqslant 3) = C_0 \left(1 - \frac{v}{V}\right)^{n-2} \left[1 + (n-2)\frac{v}{V} + \left(\frac{v}{V}\right)^2 \sum_{j=1}^{n-2} j\right]$$

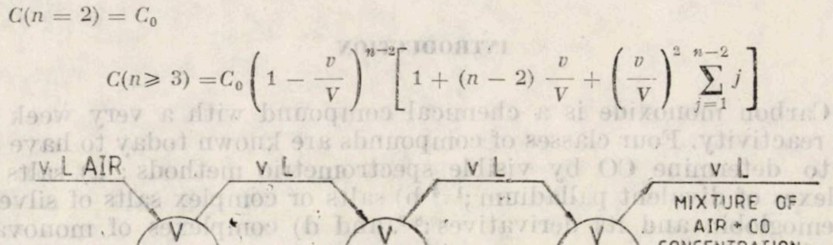

Fig. 1. — The principle of obtaining static gas mixtures.

The dynamic gas mixtures were prepared using a type OH-602 Radelkis air pump, with a small flow (0.5—1.0 L/minute). The spectra were recorded using 1-cm cells, with a Pye Unicam Spectrometer.

RESULTS AND DISCUSSIONS

Theoretical Interpretations

The UV/VIS spectra of the three solutions containing p-nitrosodiphenylamine, the Pd(II)-p-nitrosodiphenylamine complex, and with

CO bubbled into the complex solution, are given in Fig. 2. The three mentioned solutions contained the same amount of p-nitrosodiphenylamine. The effect of the reaction between Pd(II)-p-nitrosodiphenylamine complex and CO on the spectrum of the solution is an increase in intensity of the spectral band at 285 nm, and the disappearance of the spectral band at 450 nm, which is characteristic to the $-N=O$ group conjugated with the aromatic nucleus chromophore. The strengthening of the spectral band at 285 nm, specific to an n—π transition, 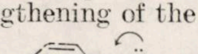, is due to the removal of p—π conjugation from the nitroso group, i.e. $-\overset{\curvearrowright}{\ddot{N}=O}$. On the other hand, the disappearance of the spectral band at 525 nm, assigned to the $d_{xy} - d_{x^2-y^2}$ transition of divalent palladium, is due to the reduction of Pd(II) to Pd(O).

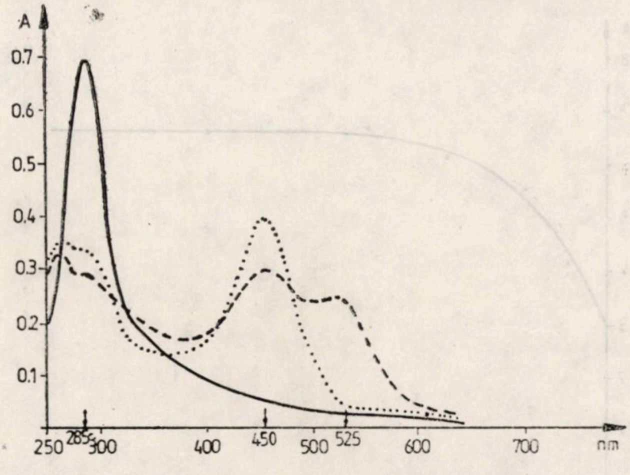

Fig. 2.— Spectra of p-nitrosodiphenylamine (. . .), Pd(II)-p-nitrosodiphenylamine (— — —), and Pd(II)-p-nitrosodiphenylamine with CO bubbled (———) solutions in HMPA.

Since p-nitrosodiphenylamine is not reduced by carbon monoxide only, we came to the conclusion that Pd(O) plays a leading part in this reaction, namely, as a catalyst of reduction of nitroso to amino group, before precipitation and, thus, decreasing its reactivity.

Stability

The reaction of CO with the $[Pd(ONC_6H_4NHC_6H_5)_2]Cl_2$ complex, in a medium containing HMPA, was found to be time-consuming. Pd(II) is reduced to Pd(O) within 5 minutes since CO has been bubbled, but the reduction of the nitroso group occurs during up to 2 hours. In Fig 3 the diagram of absorbance variation, measured at λ = 285 nm, is given for a solution containing the Pd(II)-p-nitrosodiphenylamine complex, through which CO was bubbled. The conclusion is that the absorbance maintains a constant value after about two hours, during at least 24 hours after CO bubbling.

Another novelty of this method is the use of HMPA as solvent. It was found that a 10–30% concentration of HMPA in water produced a good dispersion of Pd(O) into the reaction medium, a better absorption of CO and a good stability of the reagent medium.[15]

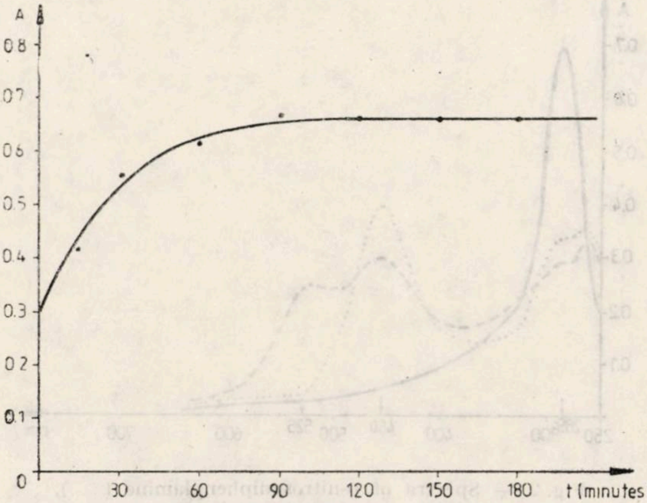

Fig. 3.— Time stability of the absorbance of a solution with 30% HMPA, containing the Pd(II)-p-nitroso-diphenylamine complex and CO bubbled.

Calibration Curve

For plotting the calibration curve of the method, two series of six calibrated flasks were used, provided with rubber stopper. We introduced 1 mL of stock solution of the complex, 1 mL of HCl 1%, 7.5 mL of HMPA and added water up to 25 mL. Then, with the aid of a Hamilton syringe, the quantities of CO given in Table 1 were introduced. The flasks were

Table 1

Dependence of the absorbance on CO quantities. The optimal calibration curve computed by the least square method: $A = 0.435\ C + 0.0095$ (C — cm^3). Correlation coeficient : $r^2 = 0.998$.

CO quantities (C_i)		Absorbances (A_i)		
cm^3	μg	I	II	Average
0.2	250	0.100	0.090	0.0950
0.4	500	0.180	0.195	0.1875
0.6	750	0.265	0.270	0.2675
0.8	1,000	0.355	0.360	0.3575
1.0	1,250	0.440	0.450	0.4450

vigorously stirred. The absorbances were measured two hours after bubbling CO, at 285 nm, against the solution without CO bubbled.

We have also noticed that the decrease of the absorbances of the same solutions, measured at 450 nm, was dependent on the taken quantities of carbon monoxide, in accordance with the Lambert-Beer law.

The reaction sensitivity limit is 5 μg/mL.

Applications and Interferences

This method can be applied for determining CO from static gas mixtures, the sensitivity limit being 50 ppm. For instance, the quantities of reagents used for plotting the calibration curve were introduced into a calibrated bottle with $V = 1$ L, containing the CO quantities given in table 1. This time, the reaction time was of 24 hours. However, this sensitivity is larger than those offered by other spectrometric methods because of the first reduction step of the reaction, i.e. Pd(II) → Pd(O). For example, the minimum reported sensitivity limit for spectrometric methods to determine CO is **0**.5 ppm,[5-7] and is based on the reduction of Ag(I) to Ag(O), although it has a major inconvenience of low time stability. But the sensitivity limit of our method allows the determination of dangerous carbon monoxide concentrations,[16] as given in table 2.

Table 2

Dependence of carbon monoxide toxicity on the concentration values [16]

ppm CO	Effects
100	Allowable for an exposure of several hours.
400–500	Can be inhaled for 1 hour without appreciable effect.
600–700	Causing a barely appreciable effect after 1 hour exposure.
1,000–1,200	Causing unpleasant but not dangerous symptoms after 1 hour.
1,500–2,000	Dangerous after exposure for 1 hour.
>4,000	Fatal in exposure of less than 1 hour.

The CO absorption-desorption equilibrium in the reaction medium enables the application of the method to determine CO from dynamic gas mixtures, the concentrations of which are less than 0.1%.

At ordinary temperature, hydrogen and saturated hydrocarbons do not interfere. In our determinations, the interferences of H_2S were eliminated by prior adsorption on silica gel, impregnated with $(CH_3COO)_2Pb$.

REFERENCES

[1] C. Winkler, *Fresenius'Z. Anal. Chem.*, **20**, 269 (1889).
[2] L. Burianec and J. Burianova, *Coll. Czech. Chem. Commun.*, **28**, 2895 (1963).
[3] J. L. Lambert and R. E. Wiens, *Anal. Chem.*, **46**, 929 (1974).

[4] J. L. Lambert and Y. C. Chiang, *Anal. Chem.*, **55**, 1829 (1983).

[5] G. Ciuhandu, *Fresenius'Z. Anal. Chem.*, **155**, 321 (1957).

[6] G. Ciuhandu, *Fresenius'Z. Anal. Chem.*, **158**, 345 (1958).

[7] G. Ciuhandu and G. Kroll, *Fresenius'Z. Anal. Chem.*, **172**, 81 (1960).

[8] M. Micloux, *Bull. Soc. Chim. France*, **3**, 818 (1923).

[9] S. E. Mehdi and A. Corsini, *Talanta*, **24**, 291 (1977).

[10] W. P. Yant and L. B. Berger, U. S. Bur. Mines, Miners' Circ., p. 34 (1963).

[11] T. V. Ramakrishna and M. Balasubramanian, *Fresenius'Z. Anal. Chem.*, **187**, 313 (1977).

[12] V. David and G. E. Baiulescu, *Rev. Roumaine Chim.*, **33**, 603 (1988).

[13] D. Todor, A. Tănase, V. David and G. E. Baiulescu, *Rev. Roumaine Chim.*, **34**, 877 (1989).

[14] V. David, P. Mărcuţă and G. E. Baiulescu, *Rev. Chim. (Bucharest)*, **40**, 512 (1989).

[15] V. David, *Anal. Lett.*, **19**, 1199 (1986).

[16] M. B. Jacobs, "The Analytical Toxicity of Industrial Inorganic Poisons", Interscience Publishers, 1967, p. 678.

Revue Roumaine de Chimie, 36, *9–10*, 1005–1010 (1991)

THE ELECTROCHEMICAL BEHAVIOUR OF SnO_2 BASED SEMICONDUCTOR CERAMIC IN NaCl SOLUTIONS

I. LINGVAY [a], RODICA GALASIU [b] and I. GALASIU [c]

[a] ICPE Bucharest
[b] Institute of Physical Chemistry, Spl. Independenţei 202, Bucharest
[c] Institute of Physical Chemistry, Spl. Independenţei 202, Bucharest, Romania

Received July 24, 1989

The results of a study on electrical and electrochemical behaviour of SnO_2-based semiconducting ceramic in NaCl solutions of various concentrations and pH are presented. It was noted that the electrical resistivity of this semiconductor material decreases with increasing current density. In the anodic range up to + 4 V against saturated calomel electrode the deposition occurs with the oxygen evolution while at more positive potentials chlorine is evolved. Likewise, the deposition of oxygen is favoured by the increase of pH i.e. of HO^- ion concentration.

INTRODUCTION

The study of electrochemical behaviour of SnO_2-based semiconductor ceramic materials presents, besides its basic interest, applications in each fields as the electrowinning of aluminium, the conversion of solar energy, the technology of sensors, etc.

The semiconductor ceramics based on SnO_2 have been consistently studied in view of their utilization in electrowinning of aluminium.[1] The electrical and electrochemical behaviour in aqueous solutions of SnO_2 based semiconductor ceramics with addition of CuO and Sb_2O_3 was also studied.[2]

This contribution presents the results of electrochemical experiments in solutions of NaCl of various concentrations and pH.

EXPERIMENTAL

As mentioned elsewhere [2], pellets of SnO_2-based ceramics were formed as follows:

Blends of 96 % SnO_2 + 2 % CuO + 2 % Sb_2O_3 were prepared, homogenized for 15–20 hours in ethylic ether or chloroform, dried and mixed with 3–5 % solution of polyvinyl alcohol in water as binder.

Pellets of 10 mm diameter and 3–5 mm height were then pressed at 150 atm. The density of these pellets was about 3.3 g/cm^3. They were sintered for 4–5 hours at 1200–1300°C in atmosphere reaching a density of 6.5–6.7 g/cm^3. The pellets were chemically plated with nickel-phosphorus alloy on one side,[3] the NiP layer obtained was annealed at 790°C. During this treatment, phosphorus diffused into the ceramic surface layer ensuring a good ohmic contact. A conducting silver paste was painted over the nickel layer and sintered at 750°C. The pellets so prepared were mounted in a glass tube to form working electrodes of the shape shown in

Fig. 1, similar to those previously described.[4] The electrical resistance of these electrodes was measured and they were employed in drawing the potentiostatic polarization curves in neutral aqueous solutions of 5–300 g/l NaCl solutions.

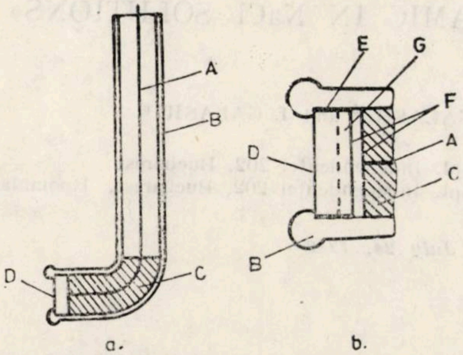

Fig. 1. — Assembling of the SnO_2 semiconductor electrode : 1 a. — general view ; 1 b. — detail ; A — copper connection wire ; B — glass tube ; C — Sn—Pb soldering alloy ; D — SnO_2 based semiconductor pellet ; E — glass — ceramic soldering ; F — metallic layer (Ni and Ag) ; G — diffused phosphorous layer.

The polarization curves were also recorded in 20 g/l NaCl solutions at various values of pH ensured by HCl or NaOH additions. The measurements were carried out at 20 ± 2°C with potentials measured against a saturated calomel electrode (SCE).

RESULTS AND DISCUSSION

To measure the electrical resistivity of the ceramic material of pellet not plated with metal the method of four tips probe was employed.[5] The semiconducting character of the ceramic resulted is proved by the strong influence of temperature upon electric conductivity. Conduction measurements were also performed by hot probe method [6] to identify the majority carrier. These measurements proved that from the stand-point of charge carriers the material is compensated i.e. the holes are numerically by electrons.

The results of measurements of current through the pellet versus voltage are shown in Fig. 2. The dependence is not linear suggesting that the electrical resistance of these ceramic masses in given working conditions (thermosetting in water) is a function of the injected current. This dependence $R = f(I)$ is plotted in Fig. 3. The curve obtained shows that below 2 mA (3.98 A/m^2) the resistance depends strongly on current which is accounted for by the increase of the number of charge carriers in the conduction band and the increase of their mobility with the increasing of injected current. This dependence varies with the composition of ceramic mass, the methods of preparation and especially of sintering this mass (time, temperature, sintering curve). Details on this phenomenon will be given in a future paper.

The results of potentiostatic determinations in the cathodic range in NaCl solutions are presented in Fig. 4 ; they show that across sintered SnO_2 — 5 — 300 g/l NaCl solution interface there is a stationary potential of 80 — 130 mV (SCE) which is more positive at low concentrations and more negative at high concentrations of NaCl. Between — 0.2 V and — 0.7 V there is a domain of Taffel linearity whose slope is $b = 0.5$ V/

decade practically independent of NaCl concentration; this domain is determined by an early process, probably the discharge of hydrogen for which exchange currents were determined graphically ranging between 0.2 A/m^2 at 5 g NaCl/1 and 1.26 A/m^2 at 300 g NaCl/1.

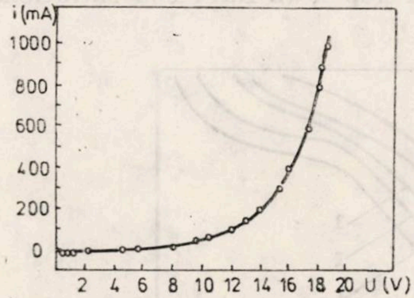

Fig. 2. — The current density through the pellet versus voltage.

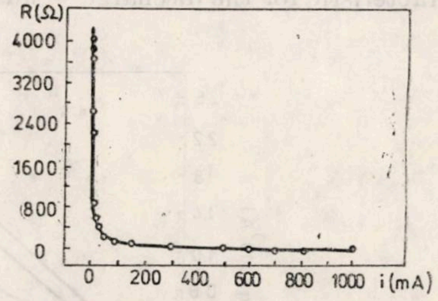

Fig. 3. — The electrical resistance of SnO_2-based semiconductor versus the current.

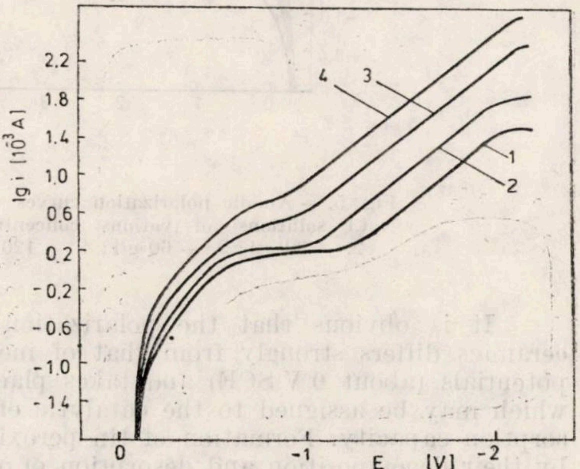

Fig. 4. — Cathodic polarization curves on SnO_2 electrode in NaCl solutions of various concentrations. 1. — 5 g/l; 2. — 20 g/l; 3. — 60 g/l; 4. — 300 g/l.

At potentials more negative than — 1 V a second process appears; it shows a Tafel characteristic whose slope is about b = 0.62 V/decade, approximately independent of NaCl concentration, and exchange currents which lie between 0.126 A/m^2 at 5 g NaCl/l and 2 A/m^2 at 300 g NaCl/l; this process is thought to consist of extraction of Sn^{4+} ions from the lattice, reduction to Sn^{2+} and transfer into solution which was confirmed by the fact that at the potentials mentioned there is a white suspension nearly the cathode which is $Sn(OH)_2$.

In the anodic domain (curves in Fig. 5) one can note that below + 4 V the process is unique i.e. discharge and evolution of oxygen which occurs in two main steps i.e. discharge — adsorption at potentials less than 2 V and desorption at potentials higher than 2 V. These two steps are distinct at lower NaCl concentrations (below 60 g/l) while at higher concentrations they appear as an overall process which unfolds according to a Tafel characteristics with b = 1.33 V/decade, a value which is characteristic for the discharge — adsorption step at all NaCl concentrations.

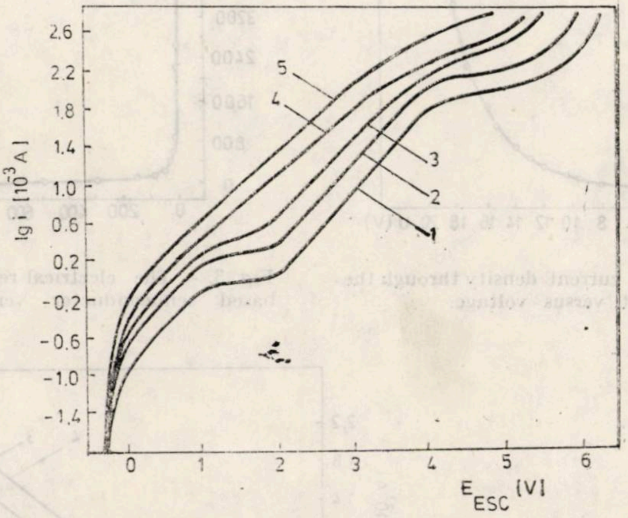

Fig. 5. — Anodic polarization curves on SnO_2 electrode in NaCl solutions of various concentrations. 1. — 5 g/l; 2. — 30 g/l; 3. — 60 g/l; 4. — 120 g/l; 5. — 300 g/l.

It is obvious that the polarization behaviour of SnO_2 — based ceramics differs strongly from that of metals: it starts at low anodic potentials (about 0 V SCE) and takes place at relatively low voltages, which may be assigned to the catalytic effect of the oxide of high adsorption capacity. Formation of tin peroxides as intermediates followed by their decomposition and desorption of oxygen is not ruled out. These findings agree to Hoare's observations regarding the anodic behaviour of platinum oxides.[7]

The exchange currents of the anodic process were also determined graphically, the values obtained being between 0.6 A/m^2 at 0.5 gNaCl/l and 5 A/m^2 at 300 g NaCl/l. At sufficiently positive potentials, i.e. over + 4 V, the desorption of oxygen is strong, it frees regions of electrode surface which may neutralize chlorine. The similar effect of hindering the discharge of chlorine on metallic oxides by blocking the active surface with adsorbed oxygen accompanied by the lowering of exchange current was previously reported.[8] Likewise, the kinetics of chlorine discharge on surface oxides was studied.[9]

The electrochemical behaviour of SnO_2-based ceramic electrodes in 20 g/l NaCl solutions of various pH's (obtained by additions of HCl and NaOH) are shown in Figs 6 (cathodic behaviour) and 7 (anodic behaviour). Examination of Fig. 6 shows that the pH strongly influences the reduction of SnO_2 and its removal from the lattice, the process being faster the more acid the medium. This fact was evidenced by the increase of exchange current whose values (obtained graphically) are : 0.085 A/m^2 at $pH = 13.5$; 0.2 A/m^2 at $pH = 9$; 0.9 A/m^2 at $pH = 6.5$; 1.6 A/m^2 at $pH = 0.5$

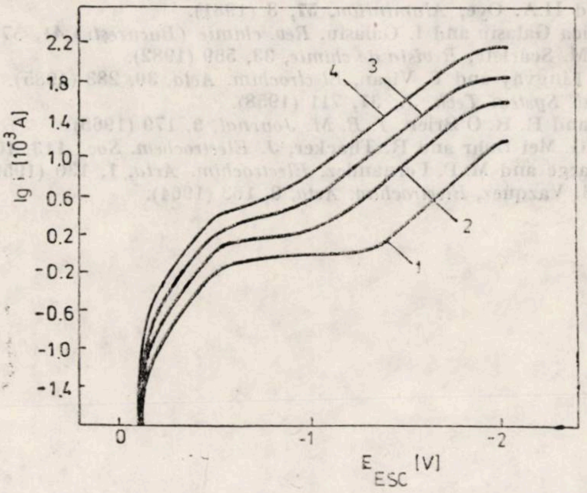

Fig. 6. — Cathodic polarization curves for SnO_2 electrode in 20 g/l NaCl solutions of various pH's. 1. $pH = 13.5$; 2. 2. $pH = 9$; 3. $pH = 6.5$; 4. $pH = 0.5$.

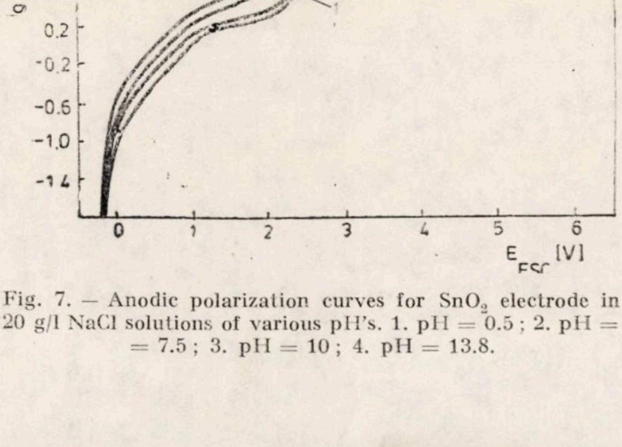

Fig. 7. — Anodic polarization curves for SnO_2 electrode in 20 g/l NaCl solutions of various pH's. 1. $pH = 0.5$; 2. $pH =$ $= 7.5$; 3. $pH = 10$; 4. $pH = 13.8$.

In the anodic range the discharge and desorption of oxygen is accelerated by the increase of pH i.e. the increase of HO^- concentration. In this domain the values of the exchange current for desorption are 0.3 A/m^2 in acid and neutral media, 0.8 A/m^2 at $pH = 10$ and 1.3 A/m^2 at $pH = 13.5$.

REFERENCES

[1] K. Billehaug and H.A. Oye, *Aluminium*, **57**, 3 (1981).
[2] I. Lingvay, Rodica Galasiu and I. Galasiu, *Rev. chimie (Bucureşti)* **41**, 577 (1990).
[3] I. Lingvay and M. Scârlete, *Revista de chimie*, **33**, 569 (1982).
[4] S. Sternberg, I. Lingvay and T. Vişan, *Electrochim. Acta*, **30**, 283 (1985).
[5] F. M. Smits, *Bell System Tech. J.*, **37**, 711 (1958).
[6] D. P. Kennedy and R. R. O'Brien, *I. B. M. Journal*, **9**, 179 (1965).
[7] J. P. Hoare, S. G. Mei Buhr and R. Thacker, *J. Electrochem. Soc.*, **113**, 1078 (1966).
[8] J. Llopis, J. Biarge and M. P. Fernandez, *Electrochim. Acta*, **1**, 130 (1959).
[9] J. Llopis and M. Vazquez, *Electrochim. Acta*, **8**, 163 (1964).

Revue Roumaine de Chimie, **36**, *9–10*, 1011–1020 (1991)

THERMODYNAMICS OF POLYNUCLEAR COMPLEX FORMATION REACTIONS

I. T. FISHTIK

Institute of Chemistry, Moldavian Academy of Sciences, 277028, Kishinev, ul. Grosula, Moldavian Republic

Received October 17, 1990

Fundamental thermodynamic relations were integrated to calculate the total Gibbs energy and enthalpy changes of polynuclear complex formation reactions. By temperature differentiation the equations for the total entropy change as well as for the heat capacity of a mixture of complexes in equilibrum are derived.

INTRODUCTION

As a result of the metal ion M and ligand L interaction usually some complexes are obtained simultaneously. Consequently the total thermodynamic function changes calculation of the complex formation reactions presents a certain interest. In other words the question is to express the total thermodynamic function changes through standard thermodynamic function changes of single reactions. For the stepwise complex formation reactions

$$M + iL = ML_i, \; i = 1, 2, \ldots, n \tag{1}$$

$$\beta_i = \frac{[ML_i]}{[M][L]^i} \tag{2}$$

the following results are known[1-5]:

$$\Delta G = -RT\ln\left(1 + \sum_{i=1}^{n} \beta_i[L]^i\right) \tag{3}$$

$$\Delta H = \sum_{i=1}^{n} f_i \Delta H_i^0 \tag{4}$$

Here f_i is the partial mole fraction of the complex ML_i; ΔH_i^0 is the standard enthalpy change of the reaction (1). By temperature differentiation,[6] the equations for the entropy and heat capacity changes can be derived

It should be noted, that equations (3) and (4) are selfconsistent. It means, that temperature differentiation of equation (3) gives equation (4) and viceversa, the integration of equation (4) gives (3). However, it is to be assumed that the ligand equilibrium concentration [L] is temperature independent. Meanwhile from general considerations it is clear that [L] is temperature dependent. Indeed, from the mass balance conditions

$$C_M = \sum_{i=0}^{n} [ML_i] = [M]\left(1 + \sum_{i=1}^{n} \beta_i [L]^i\right)$$

$$C_L = [L] + \sum_{i=1}^{n} i[ML_i] = [L] + [M]\sum_{i=1}^{n} i\beta_i [L]^i$$

it follows, that when $C_M = \text{const}$ and $C_L = \text{const}$ due to the fact that $\beta_i = \beta_i(T)$ one has $[M] = [M](T)$ and $[L] = [L](T)$. Hence, equations (3) and (4) are selfconsistent only when the temperature dependence of [L] can be neglected. This case is realized only when $C_L \gg C_M$.

The purpose of the present paper is to derive a set of selfconsistent equations for the total thermodynamic function changes of the complex formation reactions at arbitrary values of C_M and C_L as well as to consider both the formation of polynuclear complexes M_iL_j and mixed protonated complexes $M_pH_qL_r$ or hydroxocomplexes $M_p(OH)_qL_r$.

TWO-COMPONENT SYSTEM

In order to simplify the mathematical treatment, in accordance with [7] the metal ion (M) — ligand (L) system will be considered as two-component. Let the interaction between components M and L lead to polynuclear complexes of arbitrary composition M_iL_j. The reactions which take place in this system are described by the equations:

$$iM + jL = M_iL_j,\ \beta_{ij},\ \Delta H^0_{ij} \tag{5}$$

where ΔH^0_{ij} is the standard enthalpy change of the reaction (5) and β_{ij} is the stability constant:

$$\beta_{ij} = \frac{[M_iL_j]}{[M]^i\ [L]^j} \tag{6}$$

The system equilibrium composition to be calculated with equations (6) needs to be supplemented with the mass balance conditions:

$$C_M = \sum_{i=1}\sum_{j=0} i\,[M_iL_j] = \sum_{i=1}\sum_{j=0} i\beta_{ij}[M]^i\ [L]^j \tag{7}$$

$$C_L = \sum_{i=0}\sum_{j=1} j[M_iL_j] = \sum_{i=0}\sum_{j=1} j\beta_{ij}\ [M]^i\ [L]^j \tag{8}$$

First, the total Gibbs energy change calculation will be considered. To do this, let us introduce the extents of the reactions (5). As it follows from the reaction stoichiometry one has :

$$[M] = C_M - \sum_{i=1} \sum_{j=1} i\, \lambda_{ij}$$

$$[L] = C_L - \sum_{i=1} \sum_{j=1} j\, \lambda_{ij} \tag{9}$$

$$[M_iL_j] = \lambda_{ij}$$

It is known, [8] that the Gibbs energy change is equall to :

$$dG = \sum_{i=1} \sum_{j=1} \Delta G_{ij} d\lambda_{ij} = \tag{10}$$

$$= \sum_{i=1} \sum_{j=1} [\mathscr{M}(M_iL_j) - i\mathscr{M}(M) - i\mathscr{M}(L)] d\lambda_{ij}$$

where $\mathscr{M}(M)$, $\mathscr{M}(L)$ and $\mathscr{M}(M_iL_j)$ are the chemical potentials of the corresponding species and as it follows from (9) are given by :

$$\mathscr{M}(M) = \mathscr{M}^0(M) + RT \ln (C_M - \sum_{i=1} \sum_{j=1} i\lambda_{ij})$$

$$\mathscr{M}(L) = \mathscr{M}^0(L) + RT \ln (C_L - \sum_{i=1} \sum_{j=1} j\lambda_{ij}) \tag{11}$$

$$\mathscr{M}(M_iL_j) = \mathscr{M}^0(M_iL_j) + RT \ln \lambda_{ij}$$

The substitution of (11) into (10) after integration gives :

$$G = \int \sum_{i=1} \sum_{j=1} [\mathscr{M}(M_iL_j) - i\, \mathscr{M}(M) - j\, \mathscr{M}(L)]\, d\lambda_{ij} =$$

$$= - RT \ln \prod_{i=1} \prod_{j=1} \beta_{ij}^{\lambda_{ij}} + RT \ln \prod_{i=1} \prod_{j=1} \lambda_{ij}^{\lambda_{ij}} +$$

$$+ RT \ln (C_M - \sum_{i=1} \sum_{j=1} i\lambda_{ij})^{C_M - \sum_{i=1} \sum_{j=1} i\lambda_{ij}} + \tag{12}$$

$$+ RT \ln (C_L - \sum_{i=1} \sum_{j=1} i\lambda_{ij})^{C_L - \sum_{i=1} \sum_{j=1} j\lambda_{ij}} -$$

$$- RT [C_M + C_L - \sum_{i=1} \sum_{j=1} (i + j - 1)\, \lambda_{ij}] + \text{const}$$

Here it was taken into account that

$$\mathscr{M}^0(M_iL_j) - i\, \mathscr{M}^0(M) - j\, \mathscr{M}^0(L) = - RT \ln \beta_{ij}$$

By definition, the total Gibbs energy change is equal to :

$$\Delta G = G(\lambda_{ij} = \lambda^*_{ij}) - G(\lambda_{ij} = 0)$$

where λ^*_{ij} is the equilibrium value of λ_{ij}. After some transformations, one has :

$$\Delta G = -RTC_M \ln\frac{C_M}{[M]} - RT\,C_L \ln\frac{C_L}{[L]} + \\ + RT\sum_{i=1}\sum_{j=1}(i + j - 1)[M_iL_j] \tag{13}$$

Here [M], [L] and $[M_iL_j]$ are the equilibrium number of moles of the corresponding species and are determined from (6) – (8). By analogy, the enhalpy change of the reactions (5) is given by the equation[8] :

$$dH = \sum_{i=1}\sum_{j=1}\Delta H^0_{ij}\,d\lambda_{ij}$$

or, after integration

$$H = \int\sum_{i=1}\sum_{j=1}\Delta H^0_{ij} d\lambda_{ij} = \sum_{i=1}\sum_{j=1}\Delta H^0_{ij}\lambda_{ij} + \text{const}$$

The total enthalpy change by definition is equal to :

$$\Delta H = H(\lambda_{ij} = \lambda^*_{ij}) - H(\lambda = 0) = \\ = \sum_{i=1}\sum_{j=1}[M_iL_j]\,\Delta H^0_{ij} \tag{14}$$

The entropy change may be determined both by temperature differentiation of ΔG

$$\Delta S = -\frac{d\Delta G}{dT}$$

and by difference of ΔH and ΔG :

$$\Delta S = \frac{1}{T}(\Delta H - \Delta G)$$

For the heat capacity from (14) one has :

$$\Delta C_p = \frac{d\Delta H}{dT} = \sum_{i=1}\sum_{j=1}[M_iL_j]\,\Delta C^0_{p(ij)} + \sum_{i=1}\sum_{j=1}[M_iL_j]\,\Delta H^0_{ij}\frac{d\ln[M_iL_j]}{dT} \tag{15}$$

where

$$\Delta C^0_{p(ij)} = \frac{d\Delta H^0_{ij}}{dT}$$

The derivatives dln $[M_iL_j]/dT$ in accordance with (6) are equal to :

$$\frac{d\ln [M_iL_j]}{dT} = \frac{d\ln \beta_{ij}}{dT} + i\,\frac{d\ln [M]}{dT} + j\,\frac{d\ln [L]}{dT} \tag{16}$$

Further, the derivatives dln $[M]/dT$ and dln$[L]/dT$ to be determined equations (7) and (8) are to be differentiated by temperature. One has :

$$\begin{aligned} p_{11}\frac{d\ln [M]}{dT} + p_{12}\frac{d\ln [L]}{dT} &= -\sum_{i=1}\sum_{j=1} i[M_iL_j]\frac{d\ln \beta_{ij}}{dT} \\ p_{21}\frac{d\ln [M]}{dT} + p_{22}\frac{d\ln [L]}{dT} &= -\sum_{i=1}\sum_{j=1} j\,[M_iL_j]\frac{d\ln \beta_{ij}}{dT} \end{aligned} \tag{17}$$

where

$$p_{11} = \sum_{i=1}\sum_{j=0} i^2\,[M_iL_j]$$

$$p_{12} = p_{21} = \sum_{i=1}\sum_{j=1} ij\,[M_iL_j]$$

$$p_{22} = \sum_{i=0}\sum_{j=1} j^2\,[M_iL_j]$$

The solution of system (17) is :

$$\frac{d\ln [M]}{dT} = -\frac{p_{22}}{\Delta}\sum_{i=1}\sum_{j=1} i\,[M_iL_j]\frac{d\ln \beta_{ij}}{dT} + \frac{p_{12}}{\Delta}\sum_{i=1}\sum_{i=1} j\,[M_iL_j]\frac{d\ln \beta_{ij}}{dT} \tag{18}$$

$$\frac{d\ln [L]}{dT} = \frac{p_{21}}{\Delta}\sum_{i=1}\sum_{j=1} i[M_iL_j]\frac{d\ln \beta_{ij}}{dT} - \frac{p_{11}}{\Delta}\sum_{i=1}\sum_{j=1} j\,[M_iL_j]\frac{d\ln \beta_{ij}}{dT}$$

Here

$$\Delta = \begin{vmatrix} p_{11} & p_{21} \\ p_{12} & p_{22} \end{vmatrix} = p_{11}p_{22} - p_{12}p_{21}$$

On the other hand the following thermodynamic identity is valid :

$$\frac{d\ln \beta_{ij}}{dT} = \frac{\Delta H^0_{ij}}{RT^2} \tag{19}$$

The substitution of (19) into (18) and further in (16) and (15) the equation for the total heat capacity change may be obtained. However, it is more interesting the heat capacity of M, L and M_iL_j mixture in chemical equilibrium (5). The latter may be calculated from the following considerations. When $C_L = 0$ the system heat capacity C_p evidently is $C_p = C_M C_p^0(M)$, where $C_p^0(M)$ is the metal ion mole heat capacity. By analogy when $C_M = 0$ one has $C_p = C_L C_p^0(L)$ where $C_p^0(L)$ is the ligand mole heat capacity. Consequently, in the general case the system heat capacity is :

$$C_p = \Delta C_p + C_M C_p^0(M) + C_L C_p^0(L)$$

where ΔC_p is given by (15). Taking into account (16), (18) and (19) as well as :

$$\Delta C_{p(ij)}^0 = C_p^0(M_iL_j) - iC_p^0(M) - jC_p^0(L)$$

C_p may be represented as :

$$C_p = \sum_{i=0}\sum_{j=0} [M_iL_j] C_p(M_iL_j) + (RT^2)^{-1}[\sum_{i=1}\sum_{j=1} [M_iL_j] (\Delta H_{ij}^0)^2 -$$

$$- \frac{p_{22}}{\Delta} (\sum_{i=1}\sum_{j=1} i[M_iL_j]\Delta H_{ij}^0)^2 - \frac{p_{11}}{\Delta} (\sum_{i=1}\sum_{j=1} j[M_iL_j]\Delta H_{ij}^0)^2 + \qquad (20)$$

$$+ \frac{2p_{12}}{\Delta} (\sum_{i=1}\sum_{j=1} i[M_iL_j]\Delta H_{ij}^0) (\sum_{i=1}\sum_{j=1} j [M_iL_j]\Delta H_{ij}^0)]$$

The first term in this equation represents the heat capacity of a "frozen" mixture of species and the second term is due to chemical reactions.

THREE-COMPONENT SYSTEM

As a rule, the interaction between M and L is accompanied by side processes. Thus, the metal ion in aqueous solutions is subjected to hydrolysis :

$$iM + iH_2O = M_i(OH)_j + jH$$

The ligand usually is a Brönsted base and therefore is subjected to protonation :

$$L + nH = H_nL$$

In such systems quite frequently mixed protonated polynuclear complexes $M_pH_qL_r$ and hydroxocomplexes $M_p(OH)_qL_r$ are obtained. In accordance with [7] these systems may be considered as three-components. In the most general case the reactions in such a system may be described by the equations :

$$pM + qH + rL = M_pH_qL_r, \ \beta_{pqr}, \ \Delta H^0_{pqr} \tag{21}$$

where ΔH^0_{pqr} is the standard enthalpy change of reaction (21) and β_{pqr} is the stability constant :

$$\beta_{pqr} = \frac{[M_pH_qL_r]}{[M]^p[H]^q[L]^r} \tag{22}$$

Respectively, the number of the mass balance relations is increased to three :

$$\begin{aligned} C_M &= \sum_{p=1}\sum_{q=0}\sum_{r=0} p[M_pH_qL_r] = \sum_{p=1}\sum_{q=0}\sum_{r=0} p\beta_{pqr}[M]^p[H]^q[L]^r \\ C_H &= \sum_{p=0}\sum_{q=1}\sum_{r=0} q[M_pH_qL_r] = \sum_{p=0}\sum_{q=1}\sum_{r=0} q\beta_{pqr}[M]^p[H]^q[L]^r \\ C_L &= \sum_{p=0}\sum_{q=1}\sum_{r=1} r[M_pH_qL_r] = \sum_{p=0}\sum_{q=0}\sum_{r=1} r\beta_{pqr}[M]^p[H]^q[L]^r \end{aligned} \tag{23}$$

It is to be noted, that in the above equations the index q may also take negative values and consequently the formation of mixed hydroxo-complexes is taken into account. The calculation procedure of the total thermodynamic function changes in no way differs from the calculation procedure in two-component system so, here only the main results will be listed :

$$\begin{aligned} \Delta G = &- RTC_M \ln\frac{C_M}{[M]} - RTC_H \ln\frac{C_H}{[H]} - RTC_L \ln\frac{C_L}{[L]} + \\ &+ RT\sum_{p=1}\sum_{q=1}\sum_{r=1}(p + q + r - 1)[M_pH_qL_r] \end{aligned} \tag{24}$$

$$\Delta H = \sum_{p=1}\sum_{q=1}\sum_{r=1}[M_pH_qL_r]\,\Delta H^0_{pqr} \tag{25}$$

$$\begin{aligned} C_p = &\sum_{p=0}\sum_{q=0}\sum_{r=0}[M_pH_qL_r]\,C^0_p(M_pH_qL_r) + \\ &+ \sum_{p=1}\sum_{q=1}\sum_{r=1}[M_pH_qL_r]\Delta H^0_{pqr}\,\frac{d\ln[M_pH_qL_r]}{dT} \end{aligned} \tag{26}$$

Here [M], [H], [L] and $[M_pH_qL_r]$ are the equilibrium number moles of the corresponding species ; $C^0_p(M_pH_qL_r)$ is the mole heat capacity of $M_pH_qL_r$ including M, H and L. The derivatives $d\ln[M_pH_qL_r]/dT$ are obtained by temperature differentiation of equations (22) and (23) :

$$\frac{d\ln[M_pH_qL_r]}{dT}=\frac{d\ln\beta_{pqr}}{dT}+p\frac{d\ln[M]}{dT}+q\frac{d\ln[H]}{dT}+r\frac{d\ln[L]}{dT} \quad (27)$$

The last three derivatives in this equation are given by the matrix equation :

$$A = BC$$

$$A=\left|\begin{matrix}\dfrac{d\ln[M]}{dT}\\[2ex] \dfrac{d\ln[H]}{dT}\\[2ex] \dfrac{d\ln[L]}{dT}\end{matrix}\right| \qquad C=-\left|\begin{matrix}\sum\limits_{p=1}\sum\limits_{q=1}\sum\limits_{r=1}p[M_pH_qL_r]\dfrac{d\ln\beta_{pqr}}{dT}\\[2ex] \sum\limits_{p=1}\sum\limits_{q=1}\sum\limits_{r=1}q[M_pH_qL_r]\dfrac{d\ln\beta_{pqr}}{dT}\\[2ex] \sum\limits_{p=1}\sum\limits_{q=1}\sum\limits_{r=1}r[M_pH_qL_r]\dfrac{d\ln\beta_{pqr}}{dT}\end{matrix}\right|$$

$$B=\frac{1}{\Delta}\left|\begin{matrix}p_{22}p_{33}-p_{23}p_{32} & p_{13}p_{32}-p_{12}p_{33} & p_{12}p_{23}-p_{13}p_{22}\\ p_{23}p_{31}-p_{21}p_{33} & p_{11}p_{33}-p_{13}p_{31} & p_{13}p_{21}-p_{11}p_{23}\\ p_{21}p_{32}-p_{22}p_{31} & p_{12}p_{31}-p_{11}p_{32} & p_{11}p_{22}-p_{12}p_{21}\end{matrix}\right|$$

$$\Delta=\left|\begin{matrix}p_{11} & p_{12} & p_{13}\\ p_{21} & p_{22} & p_{23}\\ p_{31} & p_{32} & p_{33}\end{matrix}\right|=p_{11}p_{22}p_{33}+p_{12}p_{23}p_{31}+p_{13}p_{21}p_{32}-$$

$$-p_{11}p_{23}p_{32}-p_{12}p_{21}p_{33}-p_{13}p_{22}p_{31}$$

$$p_{11}=\sum_{p=1}\sum_{q=0}\sum_{r=0}p^2[M_pH_qL_r] \quad p_{12}=p_{21}=\sum_{p=1}\sum_{q=1}\sum_{r=1}pq[M_pH_qL_r]$$

$$p_{22}=\sum_{p=0}\sum_{q=1}\sum_{r=0}q^2[M_pH_qL_r] \quad p_{13}=p_{31}=\sum_{p=1}\sum_{q=1}\sum_{r=1}pr[M_pH_qL_r]$$

$$p_{33}=\sum_{p=0}\sum_{q=0}\sum_{r=1}r^2[M_pH_qL_r] \quad p_{23}=p_{32}=\sum_{p=1}\sum_{q=1}\sum_{r=1}qr[M_pH_qL_r]$$

It is also to be taken into account, that

$$\frac{d\ln\beta_{pqr}}{dT}=\frac{\Delta H^0_{pqr}}{RT^2}$$

The final equation for the heat capacity of M, H, L and $M_pH_qL_r$ mixture in equilibrium is not given here as it is rather cumbersome. It is to be noted only that the generalization of the obtained results to four-component systems such as M + H + 2 ligands or 2 metal ions + H + L and others is quite evident.

DISCUSSION

As it was stated above the set of equations for the total thermodynamic function changes must be selfconsistent. In this respect one can be easily convinced that the equations for ΔG and ΔH are selfconsistent. Indeed, the differentiation of (13) in accordance with

$$\Delta H = -T^2 \frac{d}{dT}\left(\frac{\Delta G}{T}\right)$$

gives

$$\Delta H = -RT^2 C_M \frac{d \ln [M]}{dT} - RT^2 C_L \frac{d \ln [L]}{dT} -$$

$$- RT^2 \sum_{i=1} \sum_{j=1} (i + j - 1)[M_i L_j] \frac{d \ln [M_i L_j]}{dT}$$

The substitution of (16) and (18) into this equation after some transformations leads to equation (14).

Under the conditions $C_L \gg C_M$ one has $C_L \cong L$ and the second term in equation (13) is equal to

$$\lim_{[L] \to C_L} C_L \ln \frac{C_L}{[L]} = \lim_{C_L \to \infty} C_L \ln \frac{C_L}{C_L - \sum\limits_{i=1} \sum\limits_{j=1} j[M_i L_j]} =$$

$$= \sum_{i=1} \sum_{j=1} j[M_i L_j]$$

Thus, equation (13) takes the form:

$$\Delta G = - RTC_M \ln \frac{C_M}{[M]} + RT \sum_{i=1} \sum_{j=1} (i - 1)\,[M_i L_j] \tag{28}$$

As can be seen when i = 1 equation (28) after normalization to 1 mole of metal ion takes the form (3).

As it follows from (20) and (26) the heat capacity of the mixture of complexes in equilibrium is a sum of two terms. One of them represents the heat capacity of a "frozen" mixture of species and the other is due to chemical reaction. Here a direct analogy with the thermal conductivity of gas mixtures in chemical equilibrium exists. It is well known[9] that in mixtures of gases in chemical equilibrium the thermal conductivity may be considerably higher than in "frozen" (nonreacting) mixtures.

Let us evaluate the term due to chemical reaction for the most simple complex formation reaction :

$$M + L + = ML, \ \Delta H^0_{11}$$

The heat capacity of M, L and ML mixture as it follows from equation (20) is equal to :

$$C_p = [M]\, C^0_p(M) + [L]\, C^0_p(L) + [ML]\, C^0_p(ML) +$$

$$+ \frac{(\Delta H^0_{11})^2}{RT^2} \frac{(C_M - [ML])\,(C_L - [ML])}{C_M C_L - [ML]^2} [ML]$$

where C_M and C_L are the total ion metal and ligand mole numbers and [M], [L] and [ML] are the equilibrium mole numbers. The last term in the above equation C_p (reaction) as a function of C_M and C_L passes through a maximum. In particular, when $C_M = C_L = C$, the maximum, as one can be easily convinced, is reached when $[ML] = C(\sqrt{2} - 1)$ and, consequently,

$$C_p(\text{reaction}) = \frac{(\Delta H^0_{11})^2}{RT^2} \frac{3\sqrt{2} - 4}{\sqrt{2}} C$$

or,

$$C_p(\text{reaction})/\text{per 1 mole of M or L} = \frac{(\Delta H^0_{11})^2}{RT^2} \frac{3\sqrt{2} - 4}{\sqrt{2}} =$$

$$= 0.1715 \frac{(\Delta H^0_{11})^2}{RT^2}$$

For T=298.15 K, $\Delta H^0_{11} = 50$ kJ/mole one has C_p(reaction)/per mole of M or L = 580 J/mole K. Thus, the heat capacity due to chemical reaction may take significant values.

REFERENCES

[1] Wyman, *J. Biophys. Chem.*, **14**, 135 (1981).

[2] D. Poland, "Cooperative Equilibria in Physical Biochemistry", Clarendon : Oxford, U. K., 1978.

[3] J. A. Schellman, *Biopolymers*, **14**, 999, (1975).

[4] J. Gill, "Biochemical Thermodynamics", Jones, M. N., Ed., Elsevier : Amsterdam, 1979, 224.

[5] A. Braibanti F. Dallavalle, E. Fisicaro and M. Pascualli, *Inorg. Chim. Acta*, 122, 135 (1986).

[6] I. F. Fishtik, *J. Phys. Chem.*, **93**, 4928 (1989).

[7] M. Beck and I. Nagypal, "Chemistry of Complex Equilibria". Akádemiai Kiado, Budapest, 1989.

[8] C. J. P. Lupis, "Chemical Thermodynamics of Materials", North-Holland : New York — Amsterdam — Oxford, 1983.

[9] J. N. Butler and R. S. Brocaw, *J. Chem. Phys.*, **65**, 1636 (1957).

Revue Roumaine de Chimie, **36**, *9–10*, 1021–1031 (1991)

THE SYNERGIC EFFECT IN THE URANIUM EXTRACTION WITH THE MIXED SOLVENT LIX 63 (5,8-DIETHYL-7-HYDROXY-6-DODECANONE OXIME) AND DI-2-ETHYL-HEXYL PHOSPHORIC ACID

N. PETRESCU [a], CHOI SANG GON [b] and LUCIA GANOVICI [c]

[a] Department of Metallurgy, Polytechnic Inst. of Bucharest, Spl. Independenţei 313, Bucharest, Romania

[b] Department of Physical Technology, Polytechnic Inst. "Kim Chek", Pyongyang, R.P.D.Korea

[c] Centre of Physical Chemistry, ICECHIM, Spl. Independenţei 202, Bucharest, Romania

Received June 17, 1989

Uranium extraction from sulphuric solutions using the organic solvent 5, 8-diethyl-7-hydroxy-6-dodecanone-oxime (LIX 63) alone or in mixture with di-2-ethyl-hexyl phosphoric acid (D2EHPA) has been studied. The aim was to reach high uranium extraction coefficients by a synergic effect of the two extractants. The experimental runs have been carried out at different concentrations of the two solvents in the extractant mixture, using initial aqueous solutions of different pH and variable uranium content. Large synergic effects have been obtained with a maximum for the molar ratio LIX 63 : D2EHPA = 10.

The synergic effect in the uranium extraction from sulphuric solutions resulting from ore leaching has been in attention since the beginning of the process development of uranium extraction with organic solvents.

Numerous synergistic systems have been studied. These may be classified as follows : (1) systems formed from a cation extractant and a neutral one : (2) two cation extractant systems ; (3) systems formed from two neutral solvents and (4) systems formed from two anion changeable extractants or an anion changeable solvent and another type of extractant.

The first systems studied for uranium synergistic extraction from sulphuric solutions were the mixtures of alkyl phosphoric acids with neutral organophosphoric compounds. For industrial purposes the most useful synergic extractant is the mixture of di-2-ethyl-hexyl phosphoric acid with tri-n-butyl phosphate (the DAPEX process).[1]

Later on, the researches have been extended to synergistic systems in the same group of extractants for uranium extraction from phosphatic ores ; on this basis industrial processes [2–4] have been developopped using a mixture of D2EHPA and TOPO (tri-n-octyl phosphine oxide).

Different other researches have been performed on synergistic systems comprising the mixture of neutral organophosphoric compounds (TBP, TOPO) or sulphoxides with chelating extractants (β-diketones [5,6] or aroylpyrazolones[7,8]), the mixtures of two chelating extractants (oximes + β-diketones[9,10]) or amines with organophosphoric acids mixtures.[11]

The researches in the present work were initially concerned with the study of the uranium extraction with a chelating extractant in the hydroxyoxime class, namely 5,8-diethyl-7-hydroxy-6-dodecanone oxime, known under the commercial designation LIX 63. The results of the uranium extraction from sulphuric solutions using LIX 63 as extractant, proved to be quite modest. So, we tried to improve the uranium extraction coefficient by combining two extractants and we obtained important synergic effects with a mixture of LIX 63 and D2EHPA. These effects were manifest in sulphuric solutions of different concentrations, including the usual compositions resulted from the ore leaching ($\sim 4.10^{-3}$ M uranium and 0.05 M H_2SO_4).

Previous researches on the uranium extraction with LIX 63 have been carried out by Akiba and Kanno[11] [12] but they worked with aqueous solutions of perchloric acid and sodium perchlorate. We have no knowledge of uranium extraction with LIX 63 from sulphuric solutions.

EXPERIMENTAL METHOD

The organic and the aqueous phases were equilibrated in a discontinuous extraction device comprising a glass extraction vessel and a magnetic stirrer. The extraction runs were carried out at constant temperature (25°C) using equal aliquots of aqueous and organic phases. The shaking time, 80 min., was experimentally established from a time extraction curve; this value is more than enough for reaching equilibrium. The aqueous phase separated from organic phase by permitting to settle, was analyzed by photocolorimetry to determine the uranium content. The aqueous solutions were prepared for colorimetric analysis by reduction of uranium hexavalent ions to tetravalent ions which form with Arsenazo III reagent a series of complexes with characteristic colour suitable for colorimetric measurements. The method allowed very low uranium contents of the order of 1 p.p.m. to be determined.

URANIUM EXTRACTION BY LIX 63

In the first series of experimental runs we have used a single solvent, LIX 63 (produced by General Mills, at p.a. level of purity) diluted in high purity kerosene (of indigenous production), and aqueous solutions of $4 \cdot 10^{-8}$ M uranium and 0.05 M H_2SO_4. In these series of runs the uranium distribution coefficient has been determined at different concentrations of the extractant and at different pH of the aqueous solution. Four values for the concentration of the organic solutions have been used, namely 0.05; 0.1; 0.2 and 0.4 M LIX 63 in kerosene. For each organic solution four values for the pH of the aqueous solutions have been used, namely pH = 2.5; 3.0; 4.0 and 5.0. To maintain the pH at a constant value, slight amounts of H_2SO_4 or NaOH were added.

The experimental results presented in double logarithmic coordinates in Fig. 1 and Fig. 2, point to a linear increase of the distribution coefficient versus the solvent concentration (Fig. 1) and versus pH (Fig. 2). The largest value for the distribution coefficient D = 7.6 was obtained for uranium extraction from an aqueous solution of pH = 5.0 with 0.4 M M LIX 63 extractant solution.

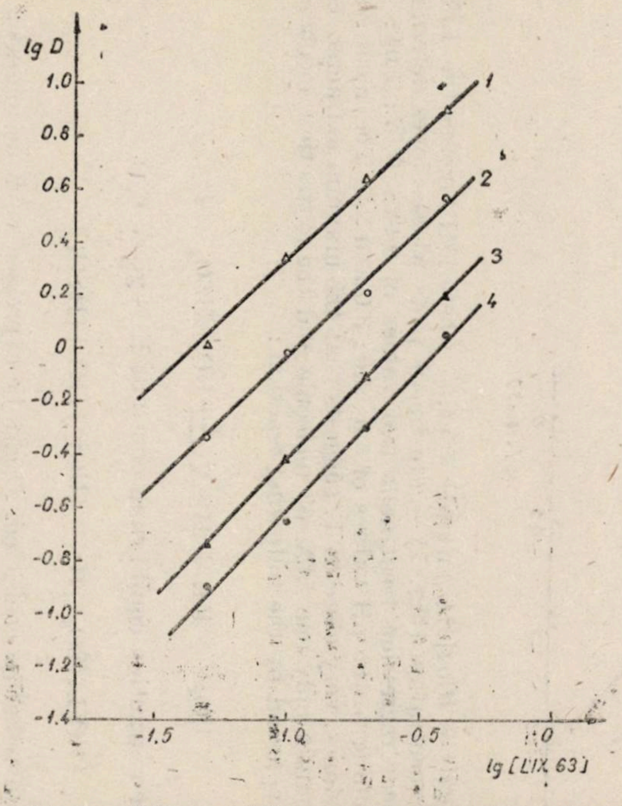

Fig. 1. — Influence of the reagent concentration on the uranium distribution coefficient;
pH = 5.0 (1); 4.0 (2); 3.0 (3); 2.5 (4).

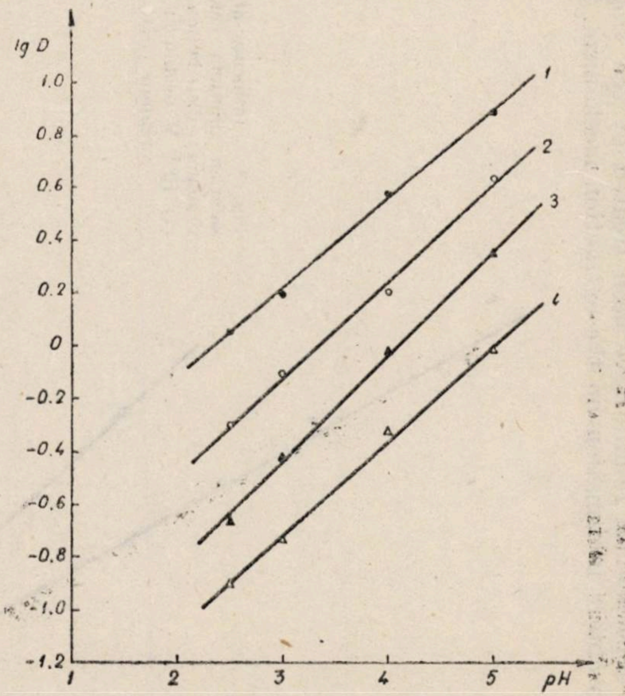

Fig. 2. — Influence of the aqueous solution pH on the uranium distribution coefficient;
[LIX 63] : 0.4 M (1); 0.2 M (2); 0.1 M (3); 0.05 M (4).

An increase of the distribution coefficient was obtained by using more dilute aqueous solution (Fig. 3).

The experimental results have been treated by the slope analysis method to obtain information on the extraction mechanism. The dependencies logD = f(log[HL]) at pH = ct, — where [HL] means the LIX 63 molar concentration (Fig. 1) — are linear plots whose slopes determined by a linear regression treatment had values of 0.94 ; 0.97 ; 1.04 ; 1.08 corresponding to the pH values of 5.0 ; 4.0 ; 3.0 and 2.5. The mean value of these slopes, very close to 1, suggests that the uranium extracted complexes contain only one LIX 63 molecule and the extraction mechanism can be expressed by the following reaction :

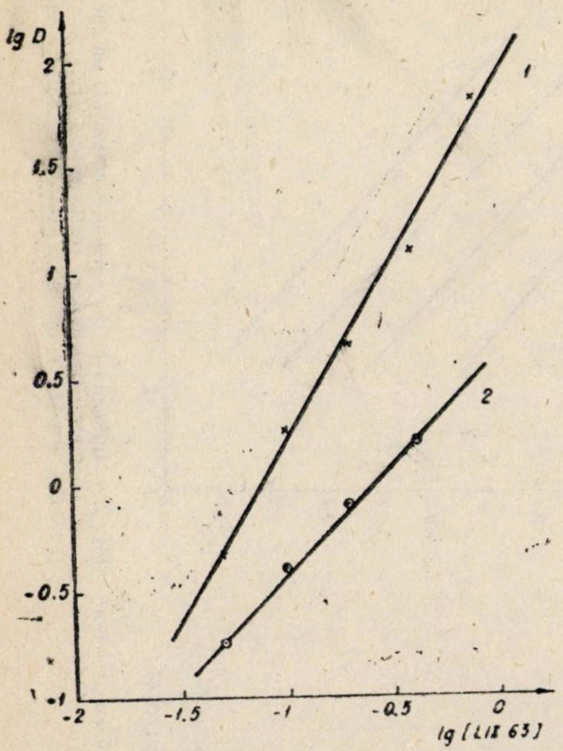

Fig. 3. — Influence of the aqueous solution uranium content on the uranium distribution coefficient ; (1) 10^{-5} M uranium ; (2) 4.10^{-3} M uranium ; pH = 3.0.

$$UO_2^{2+} + HL + HSO_4^- \overset{K}{\rightleftharpoons} UO_2LHSO_4 + H^+ \qquad (1)$$

where the extraction equilibrium constant K is given by :

$$K = [UO_2LHSO_4]\,[H^+] / [UO_2^{2+}]\,[HL]\,[HSO_4^-] \qquad (2)$$

and the distribution coefficient D can be expressed vs K as follows :

$$D = [UO_2LHSO_4] / [UO_2^{2+}] = K\,[HL]\,[HSO_4^-] / [H^+] \qquad (3)$$

or

$$\log D = \log K + \log [HSO_4^-] - \log [H^+] + \log [HL] \qquad (4)$$

The mean slope value 1.01 ± 0.03 obtained from the experimental data, confirms the extraction mechanism described by reaction (1).

By representing the distribution coefficients versus pH, according to eq. (4), a relationship of the type $\log D = a - b \log [H^+]$ is obtained, where the intercept *a* includes all the constant terms. The experimental data confirm this linear dependence, as can be seen from Fig. 2, and the slopes of the straight line calculated by the least square analysis method are : 0.33 ; 0.36 ; 0.40 and 0.36, with a mean value 0.36 + 0.01. This mean experimental slope value is much smaller than the value 1 predicted by equation (4). This fact suggests that the extraction mchanism is more complicated than that described by reaction (1).

A possible explanation is the consumption of the HSO_4^- and UO_2^{2+} ions resulting from reaction (5), to form uranium complexes (reaction 1) so that the equilibrium of reaction (5) is displaced rightwards :

$$UO_2^{2+}(SO_4)_2^{2-} + H^+ \rightleftharpoons HSO_4^- + UO_2^{2+} + SO_4^{2-} \qquad (5)$$

For low uranium containing solutions ($10 \cdot {}^{-5}M$), the slope of the straight line log D versus log [HL] calculated by the least square analysis method is 1.7 (Fig. 3), larger than the value predicted by the reaction mechanism (1). This suggests that in dilute uranium solutions (in the presence of an organic solvent excess), a second reaction mechanism takes part to the extraction process, forming another uranium complex, according to the reaction :

$$UO_2^{2+} + 2\,HL = UO_2L_2 + 2\,H^+ \qquad (6)$$

The simultaneous participation of the described reaction mechanisms account for the fractional value of 1.7 obtained from the experimental data.

URANIUM EXTRACTION BY LIX 63 – D2EHPA

The uranium extraction runs with a mixture of two solvents LIX 63 and D2EHPA, have been carried out in the same experimental conditions as the preceding runs.

The organic phase comprising a mixture of LIX 63 and D2EHPA with variable contents of the two extractants, using kerosene as a diluent.

The variation of the distribution coefficients vs the concentration of the two extractants, vs the pH of the aqueous solution and vs the uranium concentration in the initial aqueous solution has been studied. The maximum uranium loading capacity of the mixed LIX 63 – D2EHPA solvent has also been studied.

The influence of D2EHPA concentration has been studied in a set of extraction runs using mixtures in which the LIX 63 concentration was kept constant (0.2 M) and the D2EHPA concentration was changed (0.002 ; 0.005 ; 0.01 ; 0.02 ; 0.05 and 0.1 M). For each set of conditions, 5 series of extraction runs have been performed using aqueous solutions with different values for the pH (0.7 ; 1.0 ; 2.0 ; 3.0). The experimental data are presented in Fig. 4 as log D vs log [D2EHPA] plots.

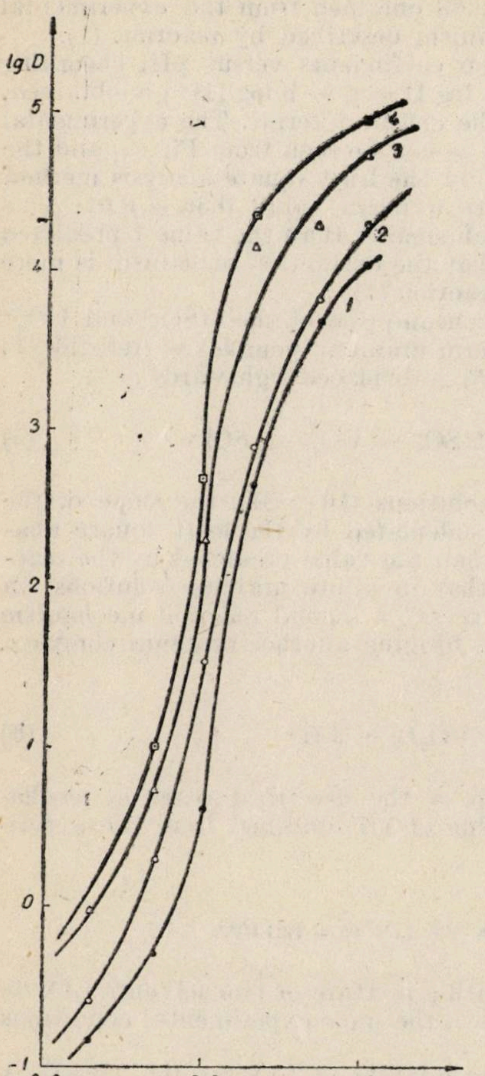

Fig. 4. — Influence of the D2EHPA concentration and of the aqueous solution pH on the uranium distribution in the extraction with 0.2 M LIX 63 + D2EHPA ; pH = 0.7 (1) ; 1.0 (2) ; 1.5 (3) ; 2.0 (4).

The results in Fig. 4 point out an important synergic effect, the distribution coefficients attaining in the best experimental conditions values up tp $10.^4$ The distribution coefficient increases in step with the D2EHPA concentration and the aqueous solution pH.

The extent of the synergic effect was appreciated by the synergic coefficient $\eta = D_{12}/(D_1 + D_2)$, where D_{12} is the uranium distribution coefficient for the mixed solvent LIX 63 – D2EHPA extraction, while D_1 and D_2 are the distribution coefficients for the extraction with the individual solvents LIX 63 and respectively D2EHPA.

The distribution coefficients D_2 were experimentally determined for a set of six extraction runs with 0.002 ; 0.005 ; 0.01 ; 0.02 ; 0.05 and 0.1 M D2EHPA solutions, the aqueous phases being sulphuric solutions with 4.10^{-3} M uranium and pH = 0.7 ; 1.0 ; 1.5 and 2.0. The experimental conditions were the same as in the previous runs. The variation of the synergic coefficient η, vs log [D2EHPA] for different values of the pH of the aqueous solutions is plotted in Fig. 5

All curves in Fig. 5 show a maximum at a molar ratio [LIX 63]/[D2EHPA] = 10. The maximum synergic coefficient $\eta = 89.2$ was obtained in the uranium extraction from an aqueous solution with pH = = 2.0 by using the mixture 0.2 M LIX 63 + 0.02 M D2EHPA.

The influence of LIX 63 concentration was studied in extraction runs where sulphuric solutions with $4 \cdot 10^{-3}$ M uranium and pH = 1.0 have been used. The extractant mixture comprised a constant concentration of D2EHPA (0.02 M) and different concentrations of LIX 63 (0.01 ; 0.02 ; 0.05 ; 0.1 and 0.2 M).

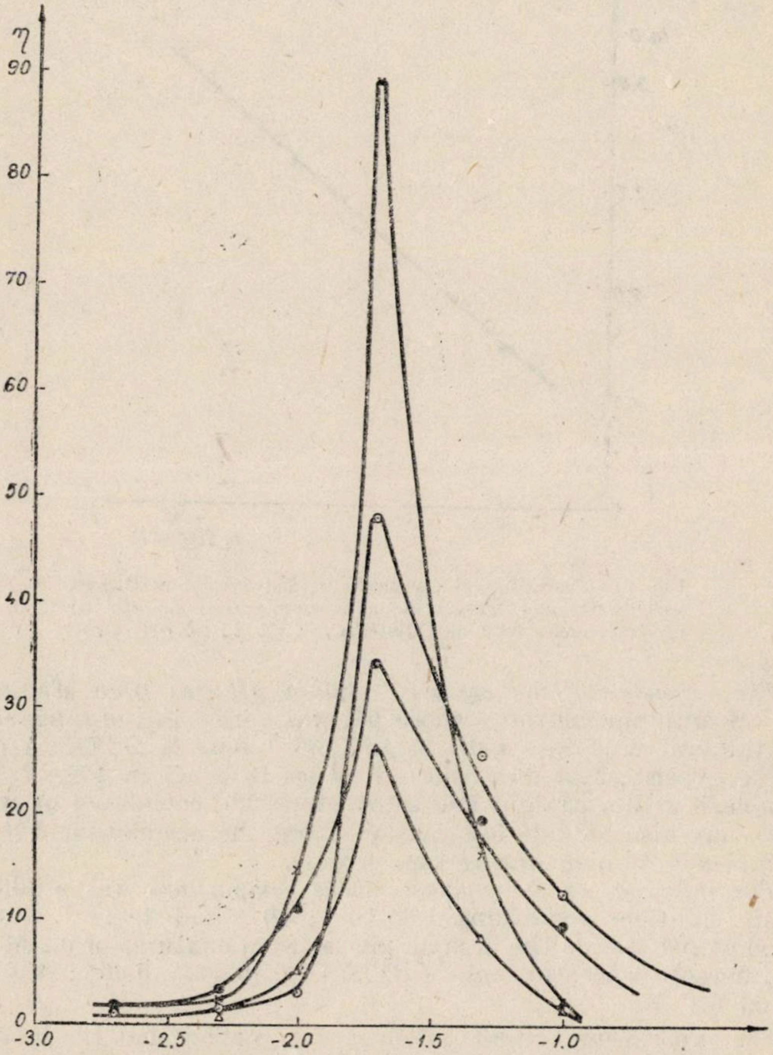

Fig. 5. — Dependence of the synergic coefficient vs the D2EHPA concentratiom, in the uranium extraction with the mixed solvent 0.2 M LIX 63 + D2EHPA ;
pH = 0.7 (⊙) ; 1.0 (●) ; 1.5 (Δ) ; 2.0 (X).

The results of this series of runs are given in Fig. 6 as a log D vs log [LIX 63] plot. The results fit satisfactorily a straight line whose slope, determined by the least square analysis method, is 0.85. The meaning of this slope is connected with the specific extraction mechanism and with the nature of the uranium complexes formed during extraction process.

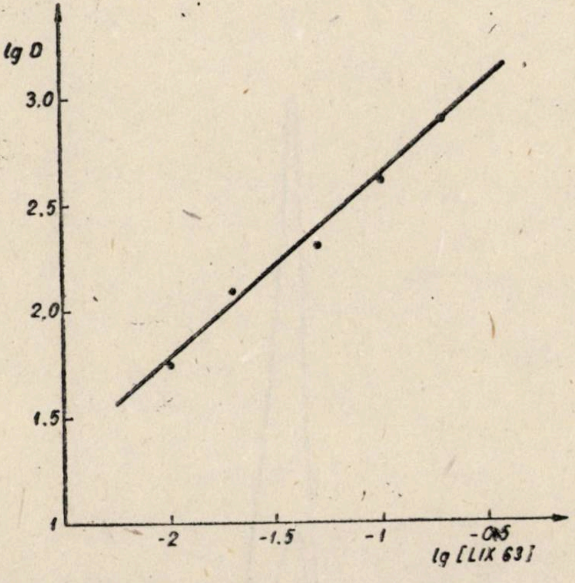

Fig. 6. — Variation of the uranium distribution coefficient vs LIX 63 concentration, in the uranium extraction with the mixed solvent 0.02 M D2EHPA + LIX 63 at pH = 1.0.

The influence of the aqueous solution pH has been studied using $4 \cdot 10^{-3}$ M uranium solutions whose pH was varied in the range 0.7—3.0. The extractant used was a 0.1 M LIX 63 + 0.01 M D2EHPA mixture.

The experimental data plotted as log D vs pH in Fig. 7 show a reasonable fit with a straight line whose slope 2.05 calculated by statistical analysis may also provide information about the mechanism of the uranium complexes forming during the process.

The influence of the aqueous phase composition was studied with sulphuric solutions containing $1.3 \cdot 10^{-2}$; 10^{-2} and $4 \cdot 10^{-3}$ M uranium adjusted at pH = 2.0. The organic phases were mixtures of 0.2 M LIX 63 with different concentrations of D2EHPA (0.002; 0.005; 0.01; 0.02; 0.05 and 0.1 M).

The experimental results given in Fig. 8 show that the best extractions have been obtained with lowest uranium containing solutions.

The maximum loading capacity of the LIX 63 — D2EHPA mixture has been determined in order to establish the practical possibilities to apply the studied synergic mixture. The experiments were carried out with LIX 63 — D2EHPA mixtures at a molar ratio 10 : 1. The mixtures

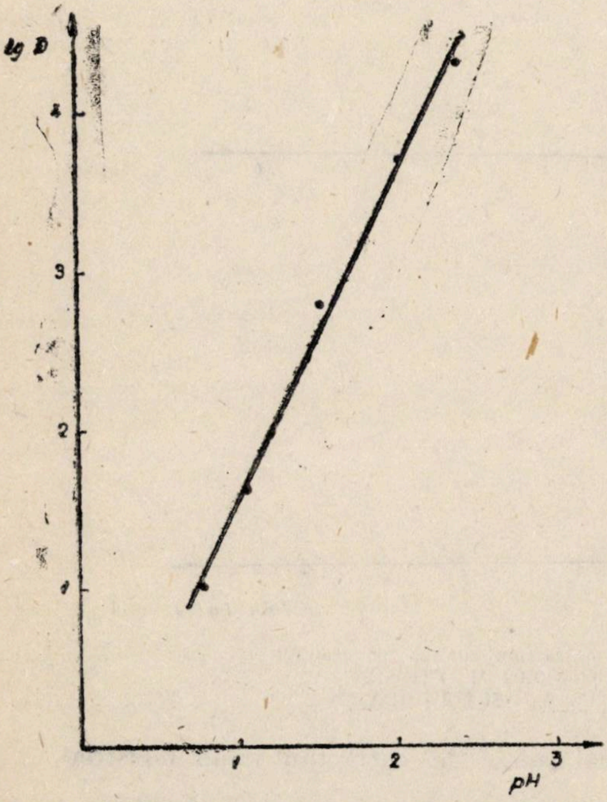

Fig. 7. — Variation of the uranium distribution coefficient vs the pH of the aqueous solution.

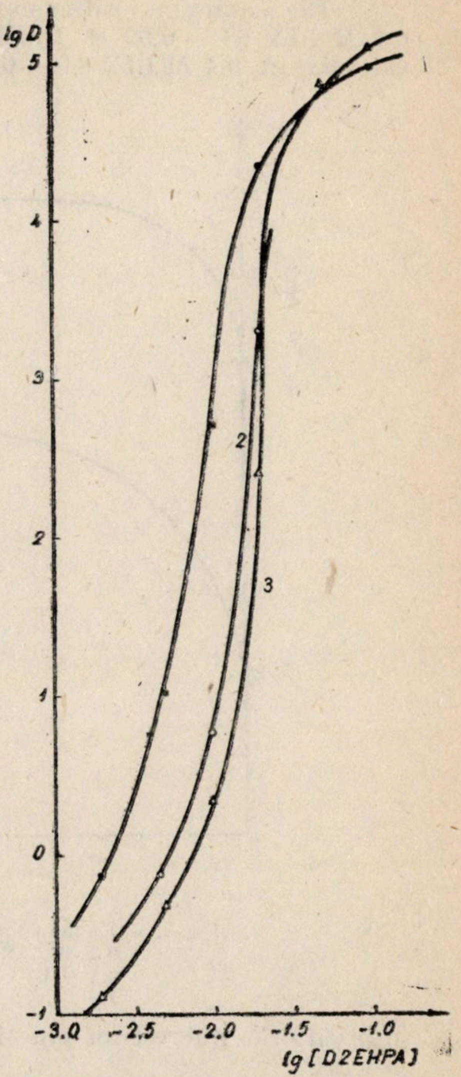

Fig. 8. — Influence of the uranium concentration in the initial solution on the extraction in solvent mixture 0.2 M LIX 63 + D2EHPA.
$4 \cdot 10^{-3}$ M uranium (1); 10^{-2} M uranium (2); $1.3 \cdot 10^{-3}$ M uranium (3).

used were 0.2 M LIX 63 + 0.02 M D2EHPA and 0.4 M LIX 63 + + 0.04 D2EHPA.

The organic phase has been equilibrated successively with sulphuric solutions of variable uranium content and pH = 3.0, up to the maximum loading capacity. The equilibrium extraction curves resulting from experiments are given in Fig. 9.

The maximum loading capacity was 5.3 g uranium/l for the mixture 0.2 M LIX 63 + 0.02 M D2EHPA and respectively 8.5 g uranium/l for the mixture 0.4 M LIX 63 + 0.04 M D2EHPA. The last value is such as to justify the interest for practical uses of this extractant in an industrial process.

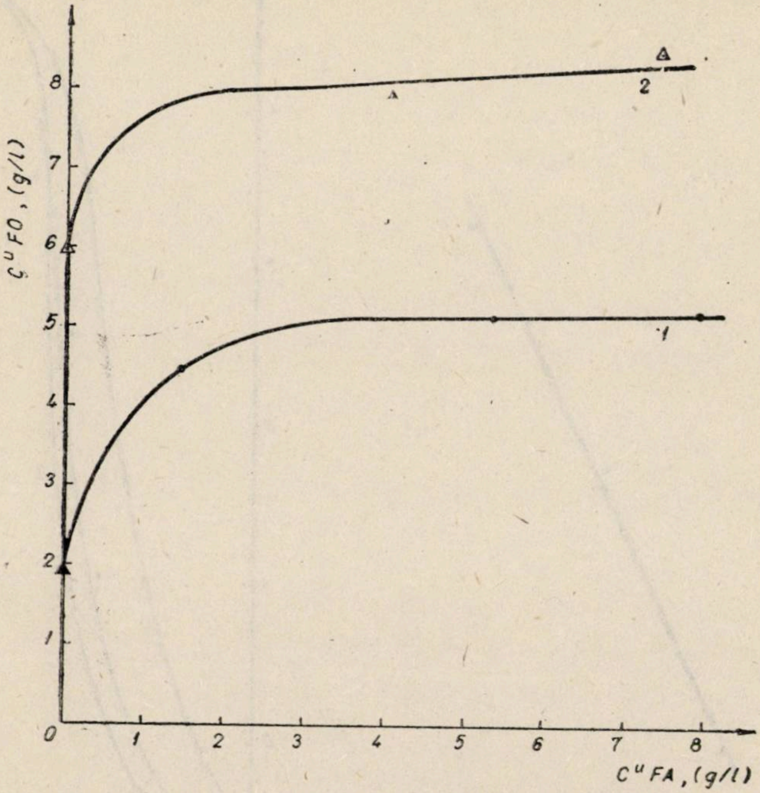

Fig. 9. — Equilibrium extraction curves for uranium; 0.2 M LIX 63 + 0.02 M D2EHPA (1); 0.4 M LIX 63 + 0.04 M D2EHPA (2).

The uranium reextraction from the mixed solvent 0.4 M LIX 63 + + 0.04 M D2EHPA was performed with 10 M HCl solution. The optimum contacting time determined experimentally, was 10 min. As an illustrative example we present the results for a reextraction experiment whose effect was a decreasing of the organic phase uranium content from 0.91 g/l to 0.08 g/l. The corresponding reextraction distribution coefficient was D = 0.09.

Concluding remarks. The experiments performed in the present study show that the mixed solvent LIX 63 — D2EHPA possesses interesting characteristics for uranium extraction: very high distribution coefficients, large loading capacity, a rapid separation of the organic and aqueous phases and favourable properties for the uranium reextraction.

REFERENCES

[1] W. D. Wilkinson, "Uranium Metallurgy", vol. I, Intersci. Publ. New York, 1962, p. 125.

[2] C. Ginisty, "Improved Dialkyl Phosphoric/Phosphine Oxide Synergistic Systems", Int. Solvent Extr. Conf., ISEC. Denver, Colorado U.S.A., 1983.

[3] H. Goreki, "Advances in Uranium Ore Processing and Recovery from Non-Conventional Resources", Proc. Techn. Comitee Meet. Adv. Uranium Ore Processing and Recovery from Non Conv. Res., I.A.E.A., Vienna, 26—29 sept. 1983, Ed. IAEA, Vienna, 1985, p. 197.

[4] D. S. Flett, *Chem. Eng.*, **1981**, 321.

[5] K. Batzar, D. E. Goldberg and L. Newman, *J. Inorg. Nuclear. Chem.*, **29**, 1511 (1967).

[6] M. S. Subramanian and S. A. Pai, *J. Inorg. Nuclear Chem.*, **32**, 3677 (1970).

[7] S. A. Pai and M. S. Subramanian, *J. Radioanal. Nuclear Chem.*, **89**, 423 (1985).

[8] W. Bacher and C. Keller, *J. Inorg. Nuclear Chem.*, **35**, 2945 (1973).

[9] Mao Jia-Jun, Chen Yu-De, Zhang Gui-Roug and Zhou Zu-Ming, *J. Radioanal. Nuclear Chem.*, **100**, 103 (1986).

[10] R. K. Malhotra, M. Sudersanan and A. K. Sundaram, *Proc. Ind. Acad. Sci. (Chem. Sci.)*, **94**, 515 (1985).

[11] C. Deptula and S. Minc, *J. Inorg. Nuclear Chem.*, **29**, 159 (1967).

[12] K. Akiba, T. Kanno, *Solvent Extr. Ion. Exch.*, **1**, 729 (1983).

[13] K. Akiba, T. Kanno, *Kakuriken Kenkyn Hokoku, (Tohoku Daigaku)*, **15**, 103 (1982).

Revue Roumaine de Chimie, 36, *9—10*, 1033—1043 (1991)

EFFECT OF SOLVENTS ON THE ELECTRONIC SPECTRA OF 2, 3-DIOXIMES DERIVATIVES OF AROMATIC ACETOACETAMIDES

REMESH KUMARI[a], A. D. TANEJA[a] and V. P. KUDESIA[b]

[a] Dept. of Plant Breeding, HAU, Hisar-125004, India
[b] D. N. College, Meerut (U.P.), India

Received September 18, 1988

Electronic absorption spectra of *para*-acetoacetanilide (PAAAH), *para*-chloroacetoacetanilide (PCAAAH), acetoacetanilide-2, 3-dioxime (AAADioxH), *ortho*-acetoaceto-toluidide-2, 3-dioxime (AATDioxH), 2, 4-acetoacetoxylidide-2, 3-dioxime (AAXDioxH), *ortho*-acetoacetanisidide-2, 2-dioxime (PAAADioxH), and *para*-chloroacetoacetanilide-2, 3-dioxime (PAAADioxH) have been examined in ultraviolet region in a series of solvents covering a broad polarity range i.e. from benzene (Z, 54.0) to ethylene glycol (Z, 85.1). Transition energies (*E*) and oscillator strengths have been calculated and *E* has been plotted against Z-values, a new empirical measurement of solvent polarity. A linear relationship was observed between the transition energy and Z-value for high energy $\Pi-\Pi^{**}$ transition due to α, β unsaturated ketones, $\Pi - \Pi^{**}$ transition and $n - \Pi^{*}$ transition due to carbonyl group. The effect of substituents present in phenyl group on λ_{max} of a compound in the same solvent has been studied. Stabilization energy of the excited state of these ligands and hence dipole moments of the excited states have been calculated in comparison with pyridinium iodide. Solvent sensitivities of these ligands have also been calculated.

During the last few years, studies on the complexes of acetoacetanilide and its derivatives with bivalent and trivalent metal have received major attention.[1-4] Harries *et al.*[5-6] have reported the determination of ionisation constant of some aromatic acetoacetamides. The purpose of the present paper is to study the electronic spectra of some acetoacetarylamides and their dioximes in different solvents of varying polarities in order to calculate their stabilization energy and solvent sensitivities. An attempt would be made to analyse the result of these investigations in terms of the solvent polarity parameter.

EXPERIMENTAL

Substituted acetoacetarylamides selected for the present studies are *para*-acetoacetanilide (PAAAH), *para-chloroacetoacetanilide* (PCAAAH), acetoacetanilide-2, 3- dioxime (AAADioxH), *ortho*-acetoaceto-toluidine-2, 3-dioxime (OAADioxH), 2, 4-acetoacetoxylidide-2, 3-dioxime (AAAXDioxH), *ortho*-acetoacetanisidide-2, 3-dioxime (OAAADioxH), *para*-acetoacetanisidide- 2, 3-dioxime (PAAADioxH), and *para*-chloroacetoacetanilide-2, 3- dioxime (PCAAADioxH). All the solvents used were either BDH, AnalaR, or E. Merck, GR quality. Freshly distilled solvents were used in all the experiments.[7-8] All the absorbance measurements were made with UV—VIS Spectrophotometer model PMO-3 using 1 cm matched quartz cells.

All the solutions were made just before use. The spectra of the above given compounds were obtained in a series of solvents varying in polarity from benzene (Z, 54.00) to ethylene glycol (Z, 85.1) at 30.0 ± 0.1°C and the results are reported in Tables 1 to 3. Transition energy (E_T) was calculated by using the standard equation.[2]

RESULTS AND DISCUSSION

It is evident from the results (cf Tables 1, 2) that accetoacetarylamides and their dioximes exhibit three intense absorption maxima in the range 199–210 nm, 246–265 nm and aromatic acetoacetamide--2,3-dioximes show three intense bands in the regions 200 to 212 nm, 248 to 267 nm, and 280 to 310 nm. These three bands have been assigned to (i) Π – Π* high energy transitions (ii) Π – Π* transitions due to carbonyl group (iii) n – Π* transitions due to carbonyl group. These assignments are in agreement with the observation of Taneja *et al.*[9] These bands exhibit a small shift in different solvents, of varying polarities being consistent with the expected spectrum of a molecule having an excited state which is more polar than the ground state.

$\pi-\pi^*$ Transitions

From the data (cf Tables 1 and 2) it can be seen that these compounds show a blue shift on going from BZ (Z, 54.0) to EG (Z, 85.1). It is also observed that, in general, absorption maxima of PCAAAH, PAAAH and PCAAADioxH occur at longer wavelength than other substituted acetoacetarylamides. Transitions observed in each case are very similar in character and occur approximately at the same wavelength range except for formamide (FA), dimethylformamide (DMF) and dimethylsulphoxide (DMSO) where there is considerable variation in intensities of these bands. Intensities of acetoacetarylamide-2,3-dioximes are more in the same solvent as compared to the PAAAH and PCAAAH. The transition energies of the above compounds in various solvents are plotted against Z-value. The correlation between Z and E gives scatter diagram for which the best straight lines were obtained by a least square fit.

The marked difference between the calculated and actual values of transitions in FA, DMF and DMSO points to a specific solute-solvent interaction. The transitions in these solvents require lesser energy than predicted by the plot of E vs Z-value. A high value of transition energy in acetonitrile (Z. 71.3) may be due to the presence of polarized Π – bonds, which enable easy acceptance of electron from the oxygen of the enolate ion by forming a complex.[10] The small shifts in other solvents are consistent with those expected from the solvent effect on the spectrum of the single species having an excited state which is more polar than the ground state.[11] It is also observed that ionisation process has a little effect on the spectra of these ketones. Since the molecules are bulky it is difficult to achieve a fruitful relationship between 'Z' and 'E' because as the solute molecules increase in size the correlation becomes less precise due to specific solute-solvent interactions, self-association and distortion of cybotactic region.[12]

If we assume that (i) the excited state dipole with the cybotactic region is directly proportional to the interaction of another somewhat

Table 1

UV Spectral data

Sr. No.	Solvent	PAAAH			PCAAAH			PAAADioxH			OAATDioxH		
		λ_{max} (nm)	E_{max} $(1\ mol)^{-1}$ cm^{-1}	E_T (kcal/ mole)	λ_{max} (nm)	E_{max} $(1\ mol)^{-1}$ $cm^{-1})$	E_T (kcal/ mole)	λ_{max} (nm)	E_{max} $(mol)^{-1}$ $cm^{-1})$	E_T (kcal/ mol)	λ_{max} (nm)	E_{max} $(mol)^{-1}$ cm^{-1}	E_T (kcal/ mole)
1	Diox	203	1865	140.83	202	1880	141.63	204	2210	140.14	205	11990	139.46
		253	12430	118.00	255	12187	112.11	256	14480	111.68	255	3280	112.11
		281	6860	101.74	280	6480	102.10	289	7665	98.92	289	7518	92.98
2	BZ	203	1803	140.83	203	1780	140.83	206	2160	138.78	208	1905	137.45
		253	12120	113.00	254	11893	112.56	256	14170	111.68	255	13270	112.11
		280	6690	102.10	279	6290	102.40	288	7602	99.27	287	7410	99.61
3	CT	202	1780	141.53	202	1710	141.53	205	2005	139.46	206	1810	138.78
		254	11910	232.56	255	11208	112.11	255	13860	112.11	256	12910	111.68
		280	6410	102.10	281	6150	101.74	287	7485	99.61	288	7312	99.27
4	CF	200	1704	136.79	200	1650	137.45	204	1970	140.14	205	1680	139.46
		252	11760	113.45	253	11095	113.00	254	13570	112.56	255	12610	112.56
		278	6210	202.84	279	6080	102.47	286	7320	99.96	289	7210	98.92
5	ACOH	199	1410	143.66	200	1520	142.95	205	1690	139.46	202	1580	141.63
		251	10157	113.90	252	10583	113.45	250	11520	114.36	252	11020	113.45
		280	6010	102.10	280	5960	102.10	283	6840	101.02	285	6850	100.31
6	DM	199	1713	143.66	201	1607	142.23	204	1904	140.00	203	1780	140.88
		250	11301	114.36	250	11238	114.36	233	12820	113.00	256	11930	111.68
		281	6340	101.74	282	6150	101.38	283	7460	101.02	284	7110	100.67
7	DE	200	1677	142.95	200	1621	142.95	202	1860	141.53	201	1660	142.53
		249	11007	114.82	251	11101	113.90	252	13710	113.45	253	11805	113.00
		279	6340	102.47	281	6240	101.74	285	7820	100.31	286	7210	99.96
8	n-BuOH	203	1813	140.83	204	1758	140.14	205	1980	139.46	204	1710	140.14
		251	11895	113.90	250	11700	237.36	286	13900	111.68	254	12802	112.56
		280	6610	102.10	277	6401	103.21	287	7980	99.61	285	7310	100.31

9	n-PrOH	202	1710	141.53	203	1661	140.83	204	1880	140.14	203	1685	140.83
		250	14407	114.36	250	11402	114.82	255	13610	112.11	253	12160	113.00
		279	6420	102.47	276	6310	103.58	286	7620	99.96	284	7220	100.67
10	EtOH	203	1650	140.83	204	1540	140.14	203	1810	140.83	202	1690	141.63
		249	11105	114.82	248	11270	115.28	254	13138	112.56	252	11880	113.45
		278	6301	102.84	274	6201	104.34	285	7440	100.15	283	7010	101.02
11	MeOH	201	1580	142.23	200	1480	142.95	202	1780	141.53	202	1561	141.53
		248	10810	115.28	247	11040	115.74	253	12830	113.00	251	11660	113.90
		277	6210	103.21	273	6090	104.72	284	7204	100.67	282	6910	101.38
12	AN	207	1910	138.11	207	1880	133.11	207	2230	138.11	208	2140	137.43
		257	12470	111.24	255	12275	112.11	249	14670	114.82	248	13710	115.28
		283	6940	101.02	284	6610	100.67	286	7512	99.96	288	7218	99.27
13	EG	200	1580	142.95	199	1620	143.66	201	1950	142.23	202	1890	141.63
		245	10240	116.69	244	10164	117.17	252	12708	113.45	251	10480	113.90
		277	6140	103.21	272	6010	105.11	282	7240	101.38	280	6770	102.10
14	Py	210	1070	136.14	210	1130	136.14	210	1304	136.14	209	1080	136.79
		—	—	—	—	—	—	—	—	—	—	—	—
		303	5067	94.35	303	5025	94.35	308	5962	92.82	309	5710	92.52
15	DMF	203	1503	140.83	203	1545	140.83	203	2040	140.83	203	1810	140.83
		265	9021	107.88	266	8957	107.48	266	12640	107.48	265	10560	107.88
		286	7010	99.96	287	6080	99.61	285	5940	100.31	287	5652	99.61
16	DMSO	202	1545	141.53	204	1519	140.44	204	1860	140.14	203	1670	140.83
		259	10735	110.38	260	9552	109.96	262	12878	109.12	261	12160	109.54
		286	6210	99.96	287	6130	99.61	286	6049	99.96	288	5880	99.27
17	FA	204	1480	140.14	203	1420	140.83	202	1580	141.53	204	1570	140.14
		269	10870	106.28	261	8760	109.54	258	10640	100.81	259	9660	110.38
		286	5870	99.96	287	5940	99.61	287	5849	99.61	289	5672	98.82

Table 2

Spectral data

Sr. No.	Solvent	PAAAH			PCAAAH			PAAADioxH			OAATDioxH		
		λ_{max} (nm)	E_{max} (1 mol)$^{-1}$ cm^{-1}	E_T (kcal/mole)	λ_{max} (nm)	E_{max} (1 mol^{-1}) cm^{-1}	E_T (kcal/mole)	λ_{max} (nm)	E_{max} (mol)$^{-1}$ cm^{-1}	E_T (kcal/mol)	λ_{max} (nm)	E_{max} (mol)$^{-1}$ cm^{-1}	E_T (kcal/mole)
1	Diox	206	2060	138.78	205	2440	139.46	207	2065	139.11	207	2080	138.11
		255	13280	112.11	257	15020	111.24	257	14930	111.24	258	14887	110.81
		288	7316	99.27	290	8420	98.58	290	8060	98.92	289	8080	98.92
2	BZ	207	1980	138.11	206	2380	138.78	208	1983	137.45	206	1960	138.78
		254	13110	112.56	256	14826	111.68	255	14620	112.11	256	14480	111.68
		286	7180	99.96	289	8218	98.92	288	7890	99.27	287	7790	99.61
3	CT	206	1880	139.78	206	2240	138.78	206	1920	138.78	206	1890	138.78
		254	12010	112.56	258	14410	110.81	256	14210	111.67	255	14108	112.11
		287	7010	99.61	288	8090	99.27	286	7810	99.96	288	7550	99.27
4	CF	205	1890	139.45	205	2202	139.45	205	1864	139.46	205	1810	139.46
		255	12680	112.11	257	13910	111.24	255	14060	112.11	256	13695	111.68
		286	7001	99.96	288	7910	99.27	287	7710	99.61	288	7480	99.27
5	AcOH	206	1662	138.78	206	2102	138.78	205	1640	139.46	207	1740	138.11
		249	11210	114.82	254	12540	112.56	251	12690	113.90	250	12280	114.36
		282	6640	101.38	286	7470	99.96	283	7640	100.31	283	7680	101.02
6	DM	206	1730	138.78	205	2330	139.46	207	1980	125.07	208	1860	137.45
		252	12410	113.45	252	14410	113.45	251	13858	113.90	253	13923	113.00
		282	6905	101.38	282	7978	101.38	285	7640	101.38	284	7450	100.87
7	DE	205	1680	139.46	206	2380	138.78	206	2083	138.78	206	1920	138.78
		251	12506	113.90	250	13900	114.36	255	14576	112.11	256	14610	111.18
		283	6902	101.02	283	7920	101.02	286	7880	99.96	286	7701	99.96
8	n.BuOH	200	1915	142.95	207	2390	138.11	204	1913	140.14	207	1907	138.11
		254	13112	112.56	256	14850	111.68	253	14001	113.00	251	13838	113.90
		286	7280	99.96	288	8106	99.27	282	7560	101.38	284	7450	100.67

9	**n-PrOH**	204	1810	140 .14	206	2340	138 .78	205	1980	138 .46	206	1861	138 .78
		253	12850	113 .00	256	14480	111 .68	254	14176	112 .56	255	14210	112 .11
		285	7140	100 .31	287	7919	99 .61	285	7705	100 .31	285	7580	100 .31
10	EtOH	203	1720	140 .83	205	2302	139 .46	205	1902	139 .46	205	1740	139 .46
		252	12460	113 .45	255	14070	112 .11	253	13780	113 .00	254	13823	122 .56
		284	7070	100 .67	287	7740	99 .61	285	7540	100 .31	284	7410	100 .67
11	MeOH	202	1620	141 .53	204	3210	140 .14	204	1808	140 .13	204	1680	140 .14
		251	11480	113 .90	254	13870	112 .56	252	13291	113 .45	252	13570	113 .45
		283	6950	101 .02	286	7601	99 .96	284	7410	100 .67	283	7240	101 .02
12	AN	207	2170	138 .11	207	2480	138 .11	207	2110	138 .11	208	2180	137 .45
		249	13240	114 .82	250	14880	114 .36	248	14870	115 .28	246	14875	116 .22
		290	7210	98 .58	287	8106	99 .61	288	8080	99 .27	289	8005	98 .92
13	EG	201	1810	142 .23	202	2106	141 .53	203	1880	140 .83	203	2020	140 .83
		250	11510	114 .36	253	12540	130 .00	251	12740	113 .90	252	13664	113 .45
		281	6970	101 .74	285	7780	100 .31	283	7740	101 .02	282	7810	101 .38
14	Py	210	1110	142 .23	202	2106	101 .53	209	1270	136 .79	211	1330	135 .49
		—	—	—	—	—	—	—	—	—	—	—	—
		305	5260	93 .72	308	5768	92 .82	307	5267	93 .12	304	6025	94 .04
15	DMF	202	1880	141 .53	204	2310	140 .14	202	1903	141 .63	204	7945	140 .14
		265	10840	107 .88	265	12110	107 .88	265	12460	107 .88	265	12820	107 .88
		288	5950	99 .27	286	7361	99 .96	289	7610	98 .92	288	7580	99 .27
16	DMSO	204	1780	140 .14	205	2240	139 .40	206	1945	138 .78	206	1819	138 .78
		262	12647	109 .12	263	13010	108 .70	259	1235	110 .38	260	12280	109 .96
		290	5870	98 .98	289	7406	98 .92	291	7510	98 .24	290	7630	98 .98
17	FA	203	1580	140 .83	204	2110	140 .14	207	1780	138 .11	205	1920	139 .46
		260	10420	109 .96	261	11810	109 .54	262	11770	109 .12	261	12420	109 .54
		291	1580	98 .24	290	7665	98 .58	292	7770	97 .91	289	7740	98 .92

large dipole with the same solvent, then we can estimate the difference in excited state stabilisation for a transition with that found for the ground state of pyridinium iodide complex dipole.[13]

Diagram 1 is a diagramatic representation of the relationship of the ground and the excited state energy levels in benzene and ethylene glycol for transitions of one of these ligands viz. AAADioxH.

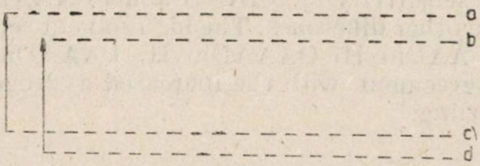

For *AAADioxH*

$$(a - c) - (b - d) = 111.68 - 113.45 = 1.77$$

$$(a - b) = (c - d) + 1.77 \qquad \text{(Eq. 3)}$$

The value of $(c - d)$ is determined by noting the shift of a particular band of PAAAH and AAADioxH from IR-spectra in benzene and ethylene glycol. The stabilization of excited state dipole of PAAAH and AAADioxH on transfer from benzene to ethylene glycol is 3.85 and 4.45 respectively. It has been observed by Kosower [1] that for the pyridinium iodide complex dipole moment of 13.90, the stabilisation was 17.3 kcal/mole- By assumption (i) the dipole moment of the excited state of AAADioxH produced by the $\Pi - \Pi^*$ transition is 5.00 D for AAADioxH in ethylene glycol. Using the method outlined above the minimum dipole moments for the excited states of other ligands have been calculated and are found to be 6.05 D for PAAAH, 6.79 D for PCAAAH, 5.01 D for DAATDioxH, 5.02 D for AAXDioxH, 4.63 D for DAAADioxH, 5.01 D for PAAADioxH and 4.99 D for PCAAADioxH. The dipole moment of an excited state is of considerable interest since it should be related to the charge distributed within the excited molecule and might permit a more precise evaluation of certain theoretical calculations for the energies of such a state.[14] The solvent sensitivities of these transitions which are a measure of transitions response to changing the polarity of the solvent, can be obtained as an experimental measure as the difference between the transition energy of this transition in ethylene glycol (Z, 85.1 highest polarity) and that in benzene (Z, 54.0 lowest polarity). This quantity is related to the degree to which the position of $\Pi - \Pi^*$ transitions responds to the polarity of the solvent. The slope averages out the changes over a range of the solvent polarities. The solvent sensitivities derived directly by the difference $E_T(\mathrm{EG}) - E_T(\mathrm{BZ})$ are listed in Table 3. The solvent sensitivity can also be evaluated from the plot of Z versus E_T as the product of slope (m) with respect of Z. i.e. the slopes and the solvent sensitivities corresponding to these slopes (obtained by multiplying the slopes by the Z-value difference ΔZ (Eq. 4) which is the difference in the Z-values of ethylene glycol and benzene (cf Table 3).

$$m = \frac{dE_T}{dZ} \qquad \text{(Eq. 4)}$$

Therefore, by changing the solvent polarity the Π — Π* transitions show a trend towards blue shift. This suggests that the Π — Π* transitions have charge-transfer character. The values obtained vary between 3.69 to 4.61 in acetoacetarylamides and 1.32 to 1.80 in case of acetoacetamide-2,3-dioximes. Marked deviation from slope or from linearity of E_T against Z plot may be regarded as an anomaly which requires rationalisation. The solvent sensitivity of PAAAH and PCAAAH is appreciably higher than that of the other diketones. The high solvent sensitivity of AAA DioxH,OAATDioxM, AADioxH, OAAADioxH, PAAADioxH and PCAA DioxH although in agreement with the increased hydrogen bonding ability is somewhat puzzling.

$n-\pi^*$ Transitions

These transitions fall in the region of 276 to 310 nm in case of PAAH, PCAAAH and 280 to 310 nm in case of acetoacetarylamide-2,3-dioximes. In this case also blue shifts are found as one goes from dioxane to acetonitrile. The plots of 'Z' vs E_T are drawn and it gives a scatter diagram from which the best straight line was obtained by a least square fit. Deviation from the regression line in case of DMF, DMSO and FA can be explained by considering the charge-transfer interactions between the carbonyl group and solvent. The deviation in case of acetonitrile may be due to the presence of polarized Π-bond in the solvent molecules which enables the easy acceptance of electrone from oxygen of carbonyl group resulting in the formation of a complex.[10] These ultraviolet spectral data permit estimation of the hydrogen bonding energy as suggested by Kosower.[10] If we consider the excited state of the transition as represented by the structure 1 and make the simple assumption that the polarisation already present in the ground state structure II, is unaffected by the excitation, the resultant dipole moment for the excited state will be very close to zero. The situation is then analogous to that for the 1-alkylpyridinium iodide complex in which the destabilisation of the excited state upon the transfer of the complex dipole from one solvent to another was equal to the stabilisation of the ground state.[10]

$$\underset{\text{I}}{>C\overset{\overset{-}{\cdot}}{=}O^{+}} \qquad \underset{\text{II}}{>\overset{\delta+}{C}=\overset{\delta-}{O}}$$

The hydrogen bonding energy is thus half of the change in the transition energy [10] from the gas phase or more simply a non-polar solvent (BZ solution in our case) to the polar solvent. This following hydrogen bonding energy or more simply, the interaction energy has been estimated for etylene glycol; PAAAH, 1 kcal/mole; PCAAAH, 1 kcal/ /mole, AAADioxH, 1.05 kal/mole, OAATDioxH, 1.42 kcal/mole, AAXDioxH, 0.89 kcal/mole, OAAADioxH, 0.68 kcal/mole, PAAADioxH, 0.87 k cal/mole and PCAAADioxH 0.88 kcal/mole.

The solvent sensitivities evaluated from the least square plot show a marked difference from the previous values. This is attributed to $Z-E$ correlation being only approximate in nature in case of bulky molecules. The solvent sensitivities of these transitions in case of PAAAH, PCAAAH, AAADioxH, AAXDioxH, OAAADioxH, PAAADioxH and PCAAADioxH are higher and low in case of OAATDioxH. The differencein solvent sensitivity values is due to increasing and decreasing electron density of ground state and the excited state of the carbonyl group.

It reveals a moderately good linear relationship between the n — Π* transitions and the Z-values which support the view thats n — Π* transitions in more polar solvents through the enol contents would be relatively less than in the non-polar solvents but due to resonance stabilization of the enolate ion the ground state would be more stabilized than the excited state.

The dipole moment of the excited state of these compounds produced by the carbonyl n — Π* transitions was calculated by using the equation (2 and 3) and the values 3.99 D for PAAAH, 5.21 D for PCAAAH. 5.27 D for AAADioxH, 5.85 for OAATDioxH, 5.00 D for AAXDioxH, 4.69 D for OAAADioxH, 4.98 D, for PAAADioxH and 4.99 D for PCAAADioxH.

High Energy Π — Π* Transitions

High energy Π — Π* transitions due to α, β-unsaturated ketone are observed in these compounds in the region at 199 to 210 nm in PAAAH and PCAAAH and 200 to 212 nm in case of acetoacetarylamide 2,3-dioximes. This band appears to be merged with the other transitions probably transitions of oxime group overlapping with it. [15]

The plots of Z vs *E* are amenable to a reasonable least square fit, though the deviation from the regression line is a rule rather than an exception. The deviation from regression line cannot be explained in all cases due to lack of knowledge of exact nature of solute-solvent interactions and due to the presence of large and bulky substituted group in the molecule. The deviation in certain cases such as DMF, DMSO, FA and An, etc. can be explained by considering the charge-transfer interactions between the ethylenic double bond and the solvent sensitivities obtained as difference of the transition energies in EG and BZ (cf. Table 3).

Table 3

Solvent sensitivity of substituted aromatic acetoacetamides and 2, 3-dioximes of aromatic acetoacetamide

Sr. No.	Compound	High energy Π — Π* transitions			Π — Π* transitions			n — Π* transitions		
		ΔE_F^* (kcal mol^{-1})	ΔE_T — mz + b		ΔE_F^* (kcal mol^{-1})	ΔE_T=mz+b		ΔE_T^* (kcal mol^{-1})	ΔE_T=mz+b	
			m (kcal)	mx ΔZ** mol^{-1}		m	mx ΔZ** (kcal mol^{-1})		m	mx ΔZ** (kcal mol)
1	PAAAH	2.12	0.620	1.93	3.69	0.0940	2.92	1.11	0.0530	1.65
2	PCAAAH	2.83	0.0933	2.91	4.61	0.1220	3.79	2.64	0.0935	2.91
3	AAADioxH	3.45	0.1214	3.78	1.77	0.0710	2.21	2.11	0.0750	2.33
4	OAATDioxH	4.08	0.1180	3.67	1.79	0.0820	2.55	2.83	0.0822	2.56
5	AAXDioxH	4.12	0.1322	4.11	1.80	0.0852	2.65	1.78	0.0740	2.30
6	OAAADioxH	2.75	0.0857	2.66	1.32	0.074	2.30	1.39	0.0600	1.56
7	PAAADioxH	3.38	0.1230	3.83	1.79	0.0730	2.27	1.75	0.0530	1.65
8	PCAAADioxH	2.05	0.0714	2.22	1.77	0.0890	2.77	1.77	0.0642	2.00

The solvent sensitivities of these transitions in case of PAAADioxH are higher and low in case of PAAAH and OAATDioxH. The dipole of the excited state of these compounds produced by this high energy $\Pi - \Pi^*$ transition has been calculated by using the equations (2 and 3) and the values are found 4.79 D for PAAAH, 5.370 D for PCAAAH, 6.34 D for AAADioxH, 6.850 D for OAATDioxH, 6.88 D for AAXDioxH 5.78 D for OAAADioxH, 6.29 D for PAAADioxH and 5.22 D for PCAAADioxH.

It is evident from the data (cf Tables 1, 2) that the substitution on the phenyl group of the nitrogen atom does not influence much the position of maxima in the same solvent. For example, the introduction of 2,4-dimetyl, 2-chloro, 2-methoxy, 2-methyl, 4-chloro or 4-dimethyl-2-chloro, 2-methoxy, 2-methyl, 4-chloro or 4-methoxy group in the benzene ring of acetoacetarylamides gives a bathochromic shift of only 2 to 5 nm in these compounds.

It can therefore be inferred that there is no resonance interaction between these substituents and the enolic group thereby, implying that there is a greater interaction within the group. Introduction of these groups does not impart much asymmetry in the chelated enol and so this may be taken as a support for the mobility of the hydrogen atom from $-CH_2-$ between the two carbonyl groups during enolisation and not the hydrogen from —NH-group.

On the basis of the present observation, it may be proposed that the difference in the λ_{max} of the bands of carbonyl group in these compounds is due to the greater electron withdrawing ability of two nitroso groups at 2 and 3 carbon of such acetoacetarylamides and thereby decreasing the electron density at carbon of carbonyl group and hence decreasing the electron density in the ground level and so more energy is required for the excitation and hence the position of λ_{max} is shifted to lower wavelength. The intensity of transition band which is related to the probability of transition is also decreased for the same region.

The $n - \Pi^*$ transitions are shifted to longer wavelength in case of acetoacetarylamide-2,3-dioximes than in the other acetoacetarylamides whereas the high energy $\Pi - \Pi^*$ transitions also shift to longer wavelength in cases of 2,3-dioximes of acetoacetarylamides. The difference in λ_{max} of the bands of 2-3-dioximes of acetoacetarylamides is due to the greater electron withdrawing ability of two-nitroso groups at 2 and 3 position.

ACKNOWLEDGEMENT. Authors are thankful to Dr. S. K. Arora, Senior Biochemist Sorghum for providing the necessaey facilities.

REFERENCES

[1] R. L. Dutta and A. Syamal, *J. Indian Chem. Soc.*, **44**, 381 (1967).
[2] D. N. Sen and P. Umapathy, *J. Indian Chem. Soc.*, **45**, 810 (1968).
[3] A. D. Taneja and K. P. Srivastava, *J. Inorg. Nucl. Chem*, **35**, 1397 (1973).
[4] A. D. Taneja and K. P. Srivastava, *J. Indian Chem. Soc.*, **49**, 889 (1972).
[5] H. J. Harries. G. Wright, *J. Inorg. Nucl. Chem*, **31**, 3149 (1969).
[6] H. J. Harries, S. Savage and G. Wright, *J. Inorg. Nucl., Chem.*, **33**, 2694 (1971).
[7] A. I. Vogel, "Practical Organic Chemistry", 3rd Ed., Longmans, London, 1962.
[8] A. Waissberger, E. S. Proskaut, J. A. Riddick, E. E. (Jr) Toops. "Technique of Organic Chemistry" vol. VII, Interscience, New York, 1955.

[9] A. D. Taneja, K. P. Srivastava and M. C. Gupta, *J. Chinese Chem. Soc.*, **20**, 95–106 (1973).
[10] E. M. Kosower, *J. Amer. Chem. Soc.*, **80**, 3261 (1958).
[11] E. M. Kosower and G. S. Wu, *J. Amer. Chem. Soc.*, **83**, 3142 (1961).
[12] G. S. Hammond, W. G. Bordjin and G. A. Guter. *J. Amer. Chem. Soc.* **81**, 4682 (1959).
[13] E. M. Kosower, *J. Amer. Chem. Soc.*, **80**, 3253 (1958).
[14] J. W. Sidman, *J. Chem. Phys*, **27**, 429 (1957).
[15] C. N. R. Rao, "Ultraviolet and Visible Spectroscopy", Butterworths, London, 1964.

Revue Roumaine de Chimie, 36, *9—10*, 1045—1054 (1991)

MASS SPECTROMETRY OF COORDINATION COMPOUNDS OF TRANSITION METALS WITH TETRADENTATE LIGANDS. VIII *

THE REDISTRIBUTION OF HYDROGEN ATOMS AT THE LOSS OF THE METHYL-GROUP FROM THE MOLECULAR IONS OF NICKEL(II) COMPLEXES WITH HEXAAZAMACROCYCLIC LIGANDS ON THE BASIS OF S-SUBSTITUTED ISOTHIOSEMICARBAZIDES AND β-DIKETONES

SERGIU P. PALII[a] **, DIMITRII V. ZAGOREVSKII[b], KONSTANTIN M. INDRICHAN[a], NIKOLAI V. GERBELEU,[a] YURII S. NEKRASOV[b] and VLADIMIR B. ARION[a]

[a] Institute of Chemistry of the Moldavian Academy of Sciences, Kishinev 277028, Moldavian Republic

[b] Institute of Organoelement Compounds of the USSR Academy of Sciences, Moscow 117334, Russia

Received June 24, 1989

The electron impact mass spectra of coordination compounds of nickel(II) with 14-members hexaazamacrocycle ligands on the basis of S-substituted isothiosemicarbazides and β-diketones with *trans*- and *cis*-arrangements of SR-group have been studied using deuterium and chemical labelling and metastable data. Molecular ions gave the most intense peaks in all cases. The common feature of molecular ions decomposition is the loss of peripheral groups. The migration capabilities of the substituents at the thiosemicarbazide sulphur atom were established. The characteristic feature of mass spectra of compounds with *trans*-arrangement of SCH_3-groups is hydrogen atom exchange between the alkylthio group and γ-positioned hydrogen of acetylacetonate residue.

INTRODUCTION

The present paper deals with the mass spectral fragmentation under electron impact of 14-members of hexaazamacrocyclic coordination compounds of Ni(II) with *trans-* (**1a-f**) and *cis-* (**2a-e**) arrangement of SR-groups.

---

* For Part I—VII, see Refs 1—7.

** Author to whom correspondence should be addressed.

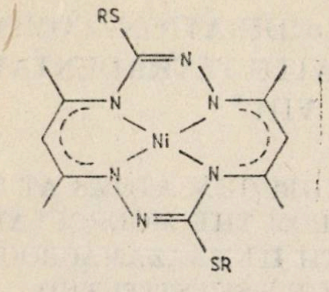

(1a - f

1a : R$=$CH$_3$;
1b : R$=$CD$_3$;
1c : R$=$C$_2$H$_5$;
1d : R$=$C$_3$H$_7$;
1e : R$=$C$_4$H$_9$;
1f : R$=$CH$_2$C$_6$H$_5$;

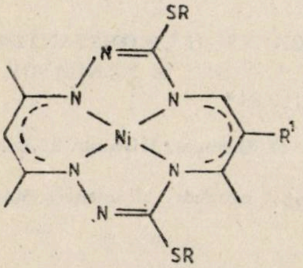

(2a - e)

2a : R$=$CH$_3$, R^1$=$H ;
2b : R$=$CD$_3$, R^1$=$H ;
2c : R$=$CH$_3$, R^1$=$COCH$_3$;
2d : R$=$CD$_3$, R^1$=$COCH$_3$;
2e : R$=$C$_2$H$_5$, R^1$=$COCH$_3$.

RESULTS AND DISCUSSION

For all the substances studied the most intense peaks are due to molecular ions. Mass spectra also contain peaks of doubly charged molecular $[M]^{2+}$, and fragment ions, $[M-R]^{2+}$, $[M-2R]^{2+}$, $[M-R-SR]^{2+}$ and so on (see Tables 1 and 2). The high stability of molecules of these compounds to the electron impact is due to their structure containing a highly conjugated system with four metallocycles.

In the region of high mass numbers in the mass spectra of **1a-f**, peaks of $[M-CH_3]^+$ ions were observed, the presence of which in spectra **1f** shows that one of the possible ways of formation of these ions is the split out of one methyl group of the acetylacetone residue.

Despite that **2b** contains three CH$_3$-groups, $[M-CH_3]^+$ ion is not registered. This indicates that, in the case of **2a**, $[M-CH_3]^+$ is formed as a result of the sulphur-carbon bond breaking. The replacement of S by Se leads to the increase in the relative intensity of the $[M-CH_3]^+$ peak (see mass spectra **2c** and **2f**).

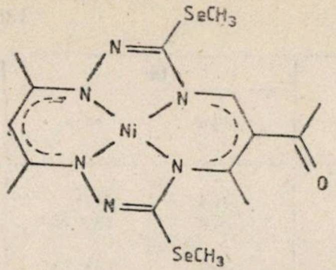

(2f)

This can be explained by the less selenium-carbon bond stability as compared to the sulphur-carbon one. The increase of the relative peak intensity of the other ions, which formed in chalcogen-carbon bond cleavage, are explained in the same manner.

For **2c**, **2d**, **2e**, and **2f** the possibility of α to CO group cleavage appears affording the $[M-CH_3]^+$ ions. This way of formation of $[M-CH_3]^+$ ions was found for coordination bivalent metal compounds with tetradentate chelating ligands containing acetyl substituent, **3**.[6,7]

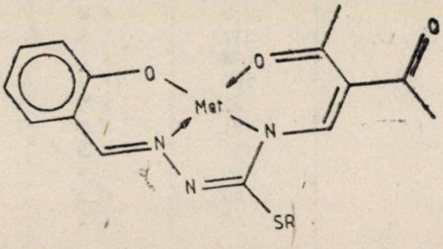

The presence of peripheral $COCH_3$-group in this compound leads also to $[M-COCH_3]^+$ and $[COCH_3]^+$ ions.[6,7] According to the Stevenson-—Audier rule the positive charge is localised presumably on the fragment which has minimal ionization energy (IE).[8] When IE of fragments are comparable the charge localization can take place on one as well as on the other fragment formed. This situation possibly occurs in the case of **3**. For **2c**, **2d**, **2**,**e** and **2**² only $[COCH_3]^+$ ions were observed. This could result from the striking difference in the IE of the fragments sited on scheme 1 (for the $CH_3CO \cdot$ IE is equal to $8.08 + 0.09$ eV).[9]

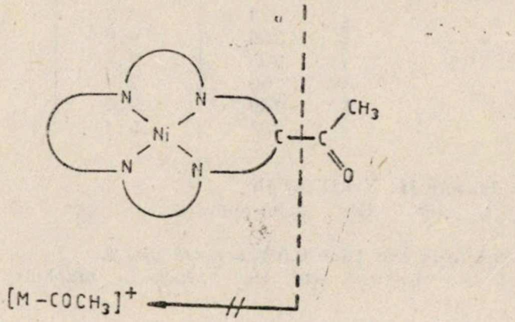

Scheme 1

Table

Electron impact mass spectra

Ions	**1a**[a]		**1b**[e]	
	m/z[b]	I[c], %	m/z	I, %
$[M]^{+\cdot}$	394	100	400	100
$[M-CH_3]^+$	379	(38.5)[d]	385	18.8
$[M-(R-H)]^+$	—	—	—	—
$[M-R]^+$	379	(38.5)	382	2.0
$[M-SY]^{+a}$	361	5.4	366	3.4
$[M-CH_3-(R-H)]^+$	—	—	—	—
$[M-(SR-Y)]^+$	348	3.5	352	1.4
$[M-SR]^+$	347	2.1	350	0.5
$[M-2(R-H)]^+$	—	—	—	—
$[M-R-(R-H)]^+$	—	—	—	—
$[M-2R]^+$	364	1.5	364	0.5
$[M-(R-H)-(SR-Y)]^+$	—	—	—	—
$[M-R-(SR-Y)]^+$	333	5.4	334	1.0
$[M-R-SR]^+$	332	9.0	332	2.5
$[M-2SR]^+$	300	2.5	300	0.5
$[NiC_6H_7YN_3S)^+$	212	4.2	213	1.6
$[NiC_6H_7N_3S]^+$	211	3.3	211	1.9
$[NiC_6H_8N_2S]^*$	198	4.2	198	5.0
$[NiC_5H_7N_2S]^+$	197	11.2	197	8.4
$[NiC_5H_3YN_2S)]^+$	182	8.0	183	2.5
$[NiC_5H_3N_2S]^+$	181	6.2	181	3.4
$[NiNCSR]^+$	131	6.2	134	3.5
$[NiNCCH_3]^+$	99	26.9	99	15.8
$[NiNCH]^+$	85	6.2	85	4.0
$[Ni]^+$	58	21.2	58	17.4
$[C_7H_7]^+$	—	—	—	—
$[M]^{2+}$	197	8.0	200	11.0
$[M-CH_3-(R-H)]^{2+}$	—	—	—	—
$[M-R]^{2+}$	189.5	0.6	191	1.0
$[M-2R]^{2+}$	182	10.5	182	8.4
$[M-R-SR]^{2+}$	166	6.8	166	3.8
Other metal-containing ions	353	1.5	199	3.7
	315	1.2	150	4.2
	306	1.7	139	4.2
	301	2.0		
	291	2.5		
	236	2.3		
	224	2.3		
	223	1.9		
	206	6.0		
	205	2.1		
	150	7.3		
	139	7.0		
	138	5.4		

[a] Y=H for **1a**, **1c**, **1d**, **1e**, and **1f**; Y=D for **1b**.

[b] Significance of m/z, for the most-popular isotopes of the corresponding elements.

[c] Peaks with relative intensity less than 0.5% are not given.

[d] The significance of the intensity (of the values in brackets) are for the related peaks.

1

(Ei = 70 eV) of compounds **1a-f**

1 e		**1 d**		**1e**		**1f**	
m/z	I, %	m/z	I, %	m/z	I, %	m/z	I, %
422	100	450	100	478	100	546	100
407	30.0	435	20.8	463	16.7	531	27.0
394	7.6	408	14.0	422	15.0	—	—
393	18.0	407	15.1	621	17.6	455	78.7
389	5.4	417	3.4	445	2.9	513	12.1
379	3.6	393	7.0	407	5.2	—	—
362	2.0	376	1.5	390	1.5	—	—
361	1.0	375	1.7	389	1.0	423	4.3
366	1.0	366	15.0	366	14.0	—	—
365	3.0	365	9.8	365	9.5	—	—
364	1.6	364	2.5	364	3.6	364	9.0
334	1.2	334	3.0	334	7.4	—	—
333	2.4	333	3.0	333	3.7	333	11.0
332	3.6	332	3.4	332	4.1	332	7.5
300	2.4	300	1.7	300	1.8	—	—
212	4.4	212	3.3	212	6.0	212	8.8
—	—	211	3.4	211	6.2	211	7.6
198	9.0	198	19.0	198	27.3	198	38.0
197	12.0	197	20.7	197	29.0	197	38.8
182	3.6	182	7.3	182	25.0	182	18.0
181	9.9	181	8.9	181	17.0	181	14.9
—	—	—	—	—	—	—	—
99	13.0	99	17.9	99	39.2	99	27.0
85	5.4	85	3.6	85	8.2	85	10.4
58	6.4	58	7.5	58	17.6	58	14.9
—	—	—	—	—	—	91	54.2
211	9.2	225	4.7	239	10.6	—	—
189.5	1.0	—	—	—	—	—	—
—	—	—	—	—	—	—	—
182	6.0	182	1.8	182	1.8	—	—
166	3.0	—	—	—	—	—	—
392	2.0	206	7.5	395	8.6	409	4.7
347	4.2			367	54.9	401	6.1
206	8.6			352	4.3	391	7.8
150	4.2			339	6.1	363	21.4
139	6.4			311	22.5	310	3.1
				310	8.0	292	7.2
				278	6.3	224	10.5
				222	5.5	223	11.0
						214	8.4

[e] Apart from values in table 1, mass spectra **1b** contains other peaks of the following ions : ion m/z (rel. int.) ; $[M-CDH_2]^+$ 384 (4.8 %) ; $[M-CD_2H]^+$ 383 (10.1 %) ; $[M-C_2H_3D_3S]^+$ 335 (4.0 %) ; $[M-C_2H_2D_4S]^+$ 334 (1.0 %) ; $[M-C_2HD_5S]^+$ 333 (1.8 %) ; $[M-C_2H_3D_3S_2]^+$ 303 (0.6 %) ; $[M-C_2H_2D_4S_2]^+$ 302 (1.5 %) ; $[M-C_2HD_5S_2]^+$ 301 (1.8 %) ; $[M-C_2H_3D_3]^{2+}$ 183.5 (3.0 %) ; $[M-C_2H_2D_4]^{2+}$ 183 (2.2 %) ; $[M-C_2HD_5]^{2+}$ 182.5 (6.2 %) ; $[M-C_2H_3D_3S]^{2+}$ 167.5 (0.7 %) ; $[M-C_2H_2D_4S]^{2+}$ 167 (4.7 %) ; which relate to H—D exchange processes.

Table

Electron impact mass spectra (Ei= 70 eV)

Ions	$2a^a$		2 b	
	m/z^b	I^c, %	m/z	I, %
$[M]^{+\cdot}$	380	100	386	100
$[M-CH_3]^+$	—	—	—	^{2}—
$[M-(R-H)]^+$	—	2—	—	—
$[M-R]^+$	365	2.2	368	16.6
$[M-2R]^+$	—	—	—	—
$[M-XY]^{+a}$	347	20.0	352	9.8
$[M-CH_3-(R-H)]^+$	—	—	—	—
$[M-(XR-Y)]^+$	334	1.8	338	0.8
$[M-XR]^+$	333	1.1	336	0.5
$[M-R-COCH_3]^+$	—	—	—	—
$[M-(R-H)-(XR-H)]^+$	—	—	—	—
$[M-R-(XR-H)]^+$	—	—	—	—
$[M-R-XR]^+$	318	12.2	318	6.2
$[NiNCXR]^+$	131	8.4	134	3.1
$[NiNCCH_3]^+$	99	22.2	99	10.7
$[NiNCH]^+$	85	12.9	85	3.8
$[Ni]^+$	58	33.3	58	11.5
$[COCH_3]^+$	—	—	—	—
$[M]^{2+}$	190	15.3	193	11.5
$[M-R]^{2+}$	182.5	7.8	184	5.7
$[M-R-(R-H)]^{2+}$	—	—	—	—
$[M-2R]^{2+}$	—	—	—	—
$[M-XR]^{2+}$	166.5	2.4	168	2.2
Other metal-containing ions	337 224 209 183 166 350 303	5.2 6.6 7.1 16.0 13.3 10.0 3.1	340 224 209 183 167	3.8 3.8 4.1 13.0 7.7

[a] X=S for **2a-e** ; X=Se for **2f** ; Y=H for **2a**, **2c**, **2e**, and **2f** ; Y=D for **2b** and **2d**.
[b] Significance of m/z, for the most—popular isotopes of the corresponding elements.

Apart from the ions, which arise as a result of simple bond cleavages, the fragments formed due to different rearrangements were also observed. Thus, the rearrangements lead to $[M-SH]^+$, $[M-(M-H)]^{+\cdot}$, $[M-(SR-H)]^{+\cdot}$ and other ions. In particular, $[M-SH]^+$ is formed as a result of a double rearrangement consisting of the migration of R-group from S atoms to the framework of molecular ion at the first stage, and hydrogen atom (or deuterium in the case of deuterium analogue **1b**, **2b**, and **2d**) to S atom at the second, with the result of SH— (or SD)group loss.

Ions $[M-(M-H)]^+$ were obtained only in the case of compounds **1c**, **1d**, **1e**, and **2e** which have hydrogen atoms at β-carbon atoms relative to the sulphur atom. The possible mechanism of this process is given in

2
of compounds 2a-f

2 c		2d		2e		2f	
m/z	I, %	m/z	I, %	m/z	I, %	m/z	I, %
422	100	428	100	450	100	518	100
407	(17.8)[d]	413	2.5	345	7.0	503	(35.3)
—	—	—	—	422	2.2	—	—
407	(17.8)	410	14.0	421	23.8	503	(35.3)
392	3.0	392	2.0	392	5.1	488	16.6
389	3.6	394	3.3	417	5.4	437	2.0
—	—	—	—	407	1.3	—	—
376	1.1	380	1.1	390	0.8	424	5.7
375	1.2	378	1.3	389	1.8	423	3.6
364	3.4	367	3.7	378	2.8	460	9.1
—	—	—	—	362	2.5	—	—
—	—	—	—	361	1.5	—	—
360	5.1	360	6.0	360	7.0	408	13.9
131	2.9	134	4.7	—	—	179	14.7
99	10.0	99	15.0	99	10.9	99	15.5
85	3.2	85	4.7	85	3.5	85	6.6
58	5.7	58	13.3	58	5.8	58	13.0
43	8.5	43	11.5	43	9.0	43	16.2
211	1.8	214	1.7	225	2.0	—	—
203.5	16.1	205	19.3	210.5	19.9	251.5	26.5
—	—	—	—	196.5	4.5	—	—
196	5.1	196	7.0	196	3.2	244	20.6
—	—	—	—	—	—	—	—
225	2.2	225	3.3	393	3.5	366	5.0
181	2.1	356	12.6	388	1.8	301	5.5
153	2.0			367	8.0	287	6.6
				357	2.3	273	6.6
				349	3.2	259	5.5
				334	5.0	234	10.9
				225	4.0	219	10.5
				167	4.0	207	23.0
				154	4.4	181	5.0
				150	4.1	153	5.5

[e] Peaks with relative intensity less than 0.5% are not given.

[d] The significance of the intensity (of the values in brackets) are for the related peaks.

Scheme 2 and includes the six-membered transition state.

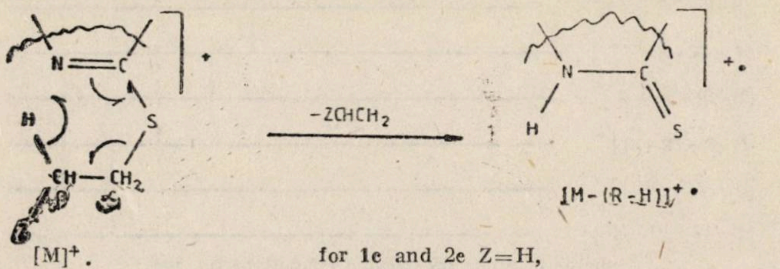

$[M]^{+}.$

for **1c** and **2e** Z=H,
1d $Z=CH_3$,
1e $Z=C_2H$.

Scheme 2

A single-act transition $[M]^{+\bullet} \rightarrow [M-(M-H)]^{+\bullet}$ is confirmed by the presence of the corresponding metastable peaks (see schemes 3 and 4). This reaction always takes place for alkylated on chalcogen atoms complexes with chalcogensemicarbazones [3,4,6,7,10,11] and chalcogencarbohydrazones, [5] starting with $R=C_2H_5$.

Both ions discussed above and many others apart from $[M-2R]^+$, $[M-R-SR]^+$, $[M-M-COCH_3]^+$ and $[M-2SR]^+$ are formed according to "even-electron" rule well known in mass spectrometry of organic compounds. It says that radicals or even-electronic ions can lose neutral even-electronic particles only.

$$AB^{+} \xrightarrow{\quad // \quad} A^{+\bullet} + B^{\bullet}$$

Meanwhile $[M-2R]^+$, $[M-M-SR]^+$, $[M-M-COCH_3]^+$ and $[M-2SR]^+$ are formed by the consequent loss of two radicals (supported by corresponding metastable transitions (see schemes 3 and 4). This reaquires at the second step the decomposition of even-electronic ions, e.g. $[M-R]^+$ with elimination of a radical which opposes the above-mentioned rule. This anomaly probably arises due to the ability of central metal atom to change its valency during fragmentation. As a result the ligand in even-electronic ion formally remains odd-electronic. Tables 1 and 2 display that the main contribution to the spectra brings peaks of ions formed by elimination of peripheral groups.

Apart from **1b-f** one extra possibility of $[M-CH_3]^+$ formation exists for **1a** due to the ability of the latter to split sulphur-carbon bond. Indeed it is realized as shown by the presence of $[M-CD_3]^+$ ions in the deuterium labelled **1b**. Besides $[M-CD_3]^+$ and $[\times-CH_3]^+$ ions which probably formed by the simple cleavage of $S-CD_3$ and $C-CH_3$ bonds the corresponding peaks of $[M-CD_1H]^+$ and $[M-CDH_1]^+$ ions appeared owing to H—D-exchange are also observed in mass spectrum of **1b**.

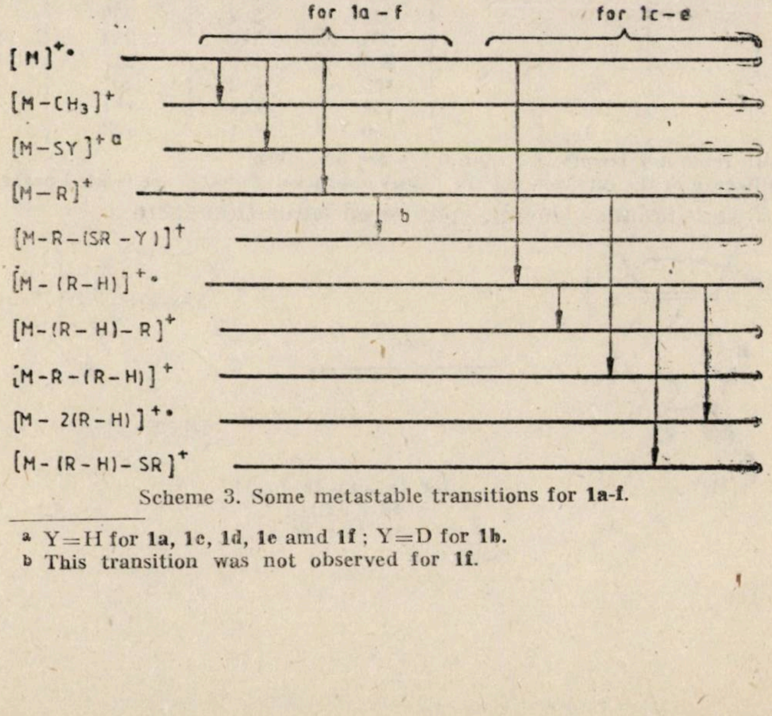

Scheme 3. Some metastable transitions for **1a-f**.

---

[a] Y=H for **1a**, **1c**, **1d**, **1e** amd **1f** ; Y=D for **1b**.

[b] This transition was not observed for **1f**.

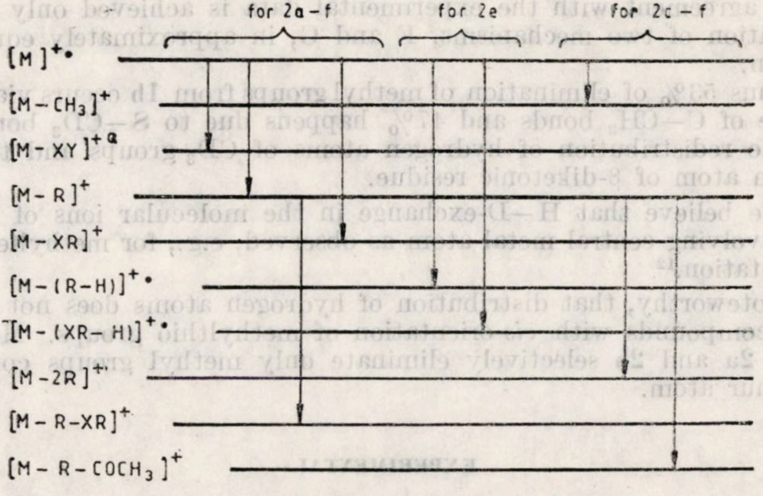

Scheme 4. Some metastable transitions for **2a-b**.

[a] X=S for **2a-e** ; X=Se for **2f** ; Y=H for **2a**, **2c**, **2e**, and **2f** ; Y=D for **2b** and **2d**.

The redistribution of hydrogen and deuterium atoms may proceed via the following mechanisms involving H—D-exchange of :

A) all 20 hydrogen atoms of the molecule (14H + 6D for **1b**);

B) hydrogen atoms of methyl groups only (12H + 6D);

C) hydrogen atoms of adjacent methyl groups and hydrogen atoms at γ-carbon atom of β-diketonic fragment (8H + 6D);

D) hydrogen atoms of adjacent methyl groups only (6H + 6D);

E) two hydrogen atoms at γ-carbon atom of β-diketonic fragment and six ones of methylthio groups (2H + 6D).

The discrepancy of observed $[M-CD_nH_{3-n}]^+$ ($n = 0-3$) abundances with the ones calculated for each mechanisms was revealed (Table 3).

Table 3

Ions	$[M-CD_3]^+$	$[M-CD_2H]^+$	$[M-CDH_2]^+$	$[M-CH_3]^+$
Mechanism	m/z 382	m/z 383	m/z 384	m/z 385
A (14H + 6D)	1.8	18.4	47.9	31.9
B (12H + 6D)	2.5	22.1	48.5	26.6
C (8H + 6D)	5.5	33.0	46.1	15.4
D (6H + 6D)	9.1	40.9	40.9	9.1
E (2H + 6D)	35.7	53.6	10.7	0
F (simple cleavage of S—C bond)	100	0	0	0
G (simple cleavage of $C-CH_3$ bond)	0	0	0	100
Experimental data	13.4 ± 2.8	28.4 ± 2.1	5.5 ± 1.7	52.7 ± 3.5

A good agreement with the experimental data is achieved only for the combination of two mechanisms, E and G, in approximately equal contribution.

Thus 53% of elimination of methyl groups from **1b** occurs via simple cleavage of $C-CH_3$ bonds and 47% happens due to $S-CD_3$ bond with complete redistribution of hydrogen atoms of CD_3-groups and those at γ-carbon atom of β-diketonic residue.

We believe that H—D-exchange in the molecular ions of **1b** proceeds involving central metal atom as observed, e.g., for methylferrocene fragmentation.[12]

Noteworthy, that distribution of hydrogen atoms does not happen in the compounds with *cis*-orientation of methylthio groups. Molecular ions of **2a** and **2b** selectively eliminate only methyl groups connected to sulphur atom.

EXPERIMENTAL

The method of synthesis of the compounds is shown in[13–15]. The electron impact mass spectra were obtained by a double focusing mass spectrometer MX-1320 using the direct inlet of samples straight to the ionisation chamber. The temperature of the inlet system was 150—180°C, and the temperature of the ionisation chamber 20—70° higher than the evaporation temperature, emission current 10 mkA, ionisation energy 70 eV. Reducing the mass spectra to mono-isotopic form was made by using "AELITA" and "ISOMETA" programs [16–17] realised on the "Nova-2/10" and "CM-3" computers respectively.

REFERENCES

[1] N. V. Gerbeleu, K. M. Indrichan and M. V. Stratulat, *Koordinatsionnaya Khimia*, **7**, 269 (1981).

[2] K. M. Indrichan and N. V. Gerbeleu, *Zh. Neorgan. Khimii*, **29**, 1178 (1984).

[3] N. V. Gerbeleu, K. M. Indrichan, S. G. Shova and M. A. Yampol'skaya, *Zh. Neorgan. Khimii*, **29**, 2293 (1984).

[4] N. V. Gerbeleu, K. M. Indrichan, M. D. Revenko and A. V. Volkova, *Koordinatsionnaya Khimia*, **10**, 1508 (1984).

[5] K. M. Indrichan, S. P. Palii, N. V. Gerbeleu and A. A. Dobrov, *Teoret. Experim. Khimia* in press.

[6] N. V. Gerbeleu, K. M. Indrichan, S. P. Palii, V. B. Arion, M. M. Timoshenko and Yu. V. Chizhov, *Zh. Structurnoy Khimii*, in press.

[7] K. M. Indrichan, S. P. Palii, D. V. Zagorevskiii, N. V. Gerbeleu, Yu. S. Nekrasov and V. B. Arion, *Izv. Akad. Nauk SSSR. Ser. khim.*, in press.

[8] H. E. Audier, *Org. Mass Spectrom.*, **2**, 283 (1969).

[9] "Chemical bonds dissociation energies. Ionization potentials and electron affinity" (Ed. V. N. Kondrat'ev), Moscow, Nauka, 1974, 351 p.

[10] N. V. Gerbeleu and K. M. Indrichan, "Mass Spectrometry of Coordination Compounds". Kishinev, Shtiintza, 1984, 340 p.

[11] N. V. Gerbeleu and K. M. Indrichan, *Zh. Neorgan. Khimii*, **26**, 291 (1981).

[12] D. V. Zagorevskii, Yu. S. Nekrasov and D. A. Lemenovskii, *J. Organometal. Chem.*, **146**, 279 (1978).

[13] N. V. Gerbeleu, Yu. A. Simonov, V. B. Arion, S. G. Shova and T. I. Malinovsky, *Dokl. Akad. Nauk SSSR*, **283**, 633 (1985).

[14] Yu. V. Simonov, N. V. Gerbeleu, P. N. Bourosh, V. B. Arion, A. A. Dvorkin and T. I. Malinovskig, *Dokl. Akad. Nauk SSSR*, **288**, 1107 (1986).

[15] Yu. A. Simonov, P. N. Bourosh, V. B. Arion, M. D. Mazus and N. V. Gerbeleu, *Kristallographiya*, **33**, 1535 (1988).

[16] Yu. N. Sukharev and Yu. S. Nekrasov, *Org. Mass Spectrom.*, **11**, 1232 (1976).

[17] Yu. N. Sukharev and Yu. S. Nekrasov, *Org. Mass Spectrom.*, **11**, 1239 (1976).

Revue Roumaine de Chimie, **36**, *9–10*, 1055–1059 (1991)

ION EXCHANGE IN SILICEOUS ZEOLITE ZSM-8

ANIȘOARA BOLD, AURELIA VASILE, ANGELICA POPA and M. CRUCEANU
Department of Chemical Technology, Polytechnic Institute, Splai Bahlui 71,
Iași, Romania

Received April 29, 1989

This paper deals with the results on kinetic and thermodynamic study of the ion exchange in siliceous zeolite ZSM-8, using Ag^+, Cu^{2+} and Zn^{2+}. The kinetic and thermodynamic quantities of the ion exchange, calculated from the experimental data, show that in the case of ZSM-8, zeolite, the ion exchange does not depend mainly on cation charge, but it depends on its size. In the presence of the Na^+ ions, zeolite ZSM-8 is not selective against the investigated cations.

INTRODUCTION

The ZSM-8 zeolite, mentioned for the first time in literature [1] in 1971, exhibits a great thermal and chemical stability due to the high silicon content. Due to its structure as well as to the possibility of replacing by ion exchange the own cations with catalytical active metal cations, the zeolite ZSM-8 can be employed as catalyst for many reactions.

The ion exchange behaviour of ZSM-8 zeolite against the Ag(I), Cu(II) and Zn(II) ions has been investigated in this paper in terms of kinetic and thermodynamic quantities of the process.

EXPERIMENTAL

The siliceous zeolite ZSM-8 was obtained by hydrothermal synthesis, using ethylenediamine as template.[2] Its crystalline structure was identified by x-ray diffraction, and chemical composition was determined by conventional chemical analysis.

Preparation of the samples for ion exchange investigation had in view the fact that the template is incorporated in the pores of zeolite network during its crystallization, troubling the ion exchange. Removal of the organic compound from the pores was performed thermally. For this reason, on the basis of TG analysis, the synthetized zeolite was calcinated at 550°C in air for 4 h.

In order to prevent the superimposion of any supplementary influences, the zeolite product was classed granulometrically by settling and passed entirely in the Na form by ion exchange with a solution of 0.1 N NaCl. The characteristics of the employed zeolite product ZSM-8 are summarized in table 1.

The ion exchange was carried out under batch conditions at 25, 35 and 50°C, with solutions of metals azotites of $4 \cdot 10^{-2}$ N.

Table 1

Characteristics of the zeolite ZSM-8

	Characteristic	
1	Crystalline network	ZSM-8
2	Crystallinity degree, %	97
3	Chemical composition, molar ratio	
	$SiO_2 : Al_2O_3$	47.7
	$Na_2O : Al_2O_3$	0.85
4	Medium radius of particles, μ	2.075

RESULTS AND DISCUSSION

The experimental results referring to the ion exchange kinetic of the three investigated cations are set out in figures 1 and 2. As it comes out from figures 1 and 2, all curves have the shape proper to high siliceous zeolites and their arrangement in decreasing order is $Ag^+ > Cu^{2+} > Zn^{2+}$, the same as for zeolite ZSM-5,[3] the equilibrium being reached after 2–4 hours.

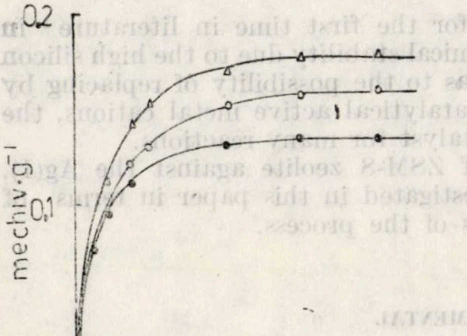

Fig. 1. — Ion exchange kinetics in zeolite ZSM-8 at 25°C ; Δ—Ag^+ ; O—Cu^{2+} ; ●—Zn^{2+}.

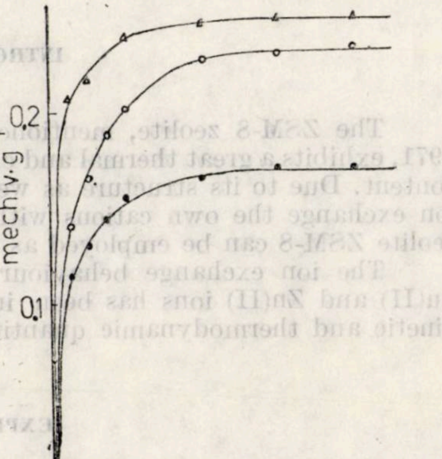

Fig. 2. — Ion exchange kinetics in zeolite ZSM-8 at 50°C ; Δ—Ag^+ ; O—Cu^{2+} ; ●—Zn^{2+}.

From the experimental data, using Boyd-Adamson's equation[4] and Reichenberg tables,[5] the apparent difussion coefficients have been calculated and from their dependence on temperature, according to Arrhenius's equation, the activation energy of exchange E_a, has been calculated. Their values are presented in table 2. The data of table 2 point out the existence of some differences on both diffusion coefficient values and activation energy values. The relatively small differences between activation energies found for monovalent and divalent ions suggest that in the case of the zeolite structure ZSM-8, the ion exchange does not depend mainly on cation charge, but only on its size.

Table 2

Apparent diffusion coefficient and activation energy of exchange

Exchangeable ion	Radius of hydrated ion, Å	Apparent diffusion coefficient, $cm^2 \cdot s^{-1}$			Activation energy, kcal · ion g^{-1}
		$t = 25°C$	$t = 35°C$	$t = 50°C$	
Ag^+	3.41	$1.971\ 10^{-12}$	$2.239\ 10^{-12}$	$2.658\ 10^{-12}$	2·279
Cu^{2+}	4.20	$1.415\ 10^{-12}$	$1.603\ 10^{-12}$	$1.878\ 10^{-12}$	2.158
Zn^{2+}	4.30	$2.037\ 10^{-12}$	$2.345\ 10^{-12}$	$2.585\ 10^{-12}$	1.815

Comparison of the values of apparent diffusion coefficient with those found for high siliceous zeolite ZSM-5,[3] shows that a relatively small difference does exist, the order of magnitude being the same (Table 3). In the case of zeolite ZSM-5 diffusion of cations takes place more easily and practically is not dependent on their charge. This fact can be attributed also to the ZSM-8 structure, specifying that the differences between diffusion coefficients of monovalent and divalent ions are a little greater but insignificant. The values of activation energy show that both siliceous structures are accessible to ion exchange.

Table 3

Comparative values of apparent diffusion coefficient and activation energy

Quantity	Exchangeable ion	NaZSM-8	NaZSM-5[3]
Apparent diffusion coefficient, $cm^2 \cdot s^{-1}$ $t = 25°C$	Ag^+	$1.971\ 10^{-12}$	$2.65\ 10^{-12}$
	Cu^{2+}	$1.415\ 10^{-12}$	$2.54\ 10^{-12}$
Activation energy, kcal · ion g^{-1}	Ag^+	2.279	1.487
	Cu^{2+}	2.158	1.353

The experimental data referring to ion exchange equilibria are given as exchange isotherms in figures 3, 4 and 5.

In the case of divalent ions at which exchange was not complete, the thermodynamic quantities have been calculated after normalization of the isotherms.[4]

For the exchange $Ag^+ \rightleftharpoons Na^+$, the selectivity coefficient determined from experimental isotherms was considered equal to the corrected selectivity coefficient, $\alpha_{Na}^{Ag} = K_c$, because the activity coefficients ratio of $AgNo_3$ and $NaNO_3$ is $\simeq 1$ in dilute solutions.[4]

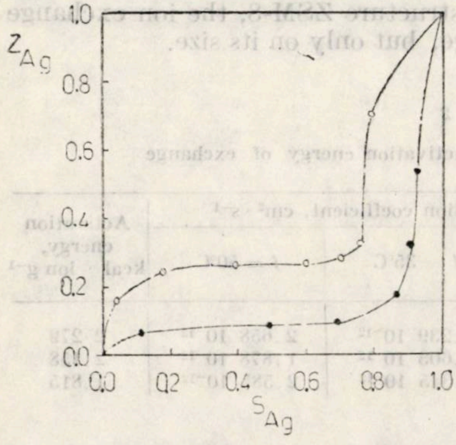

Fig. 3. — Experimental ion exchange isotherm for the reaction $Ag^+ \rightleftharpoons Na^+$ in zeolite ZSM-8 ; ● 25°C ; ○ 50°C.

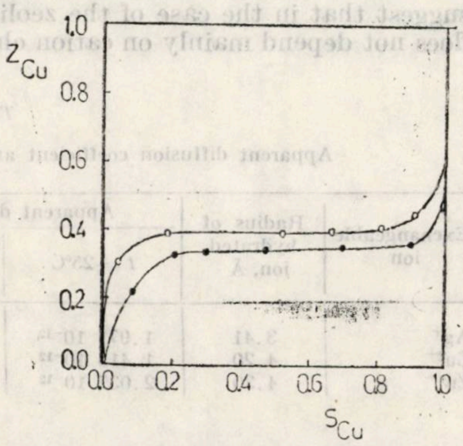

Fig. 4. — Experimental ion exchange isotherm for the reaction $Cu^{2+} \rightleftharpoons 2Na^+$ in zeolite ZSM-8 ; ● 25°C ; ○ 50°C.

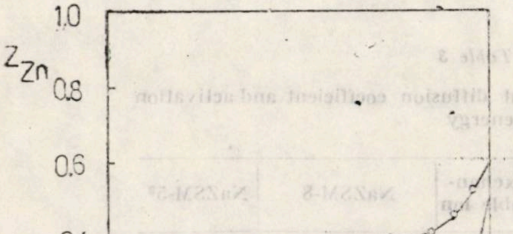

Fig. 5. — Experimental ion exchange isotherm for the reaction $Zn^{2+} \rightleftharpoons 2Na^+$ in zeolite ZSM-8 ; ● 25°C ; ○ 50°C.

In the case of divalent ions exchange $Cu^{2+} \rightleftharpoons 2Na^+$ and $Zn^{2+} \rightleftharpoons 2Na^+$, the activity coefficients of the salts in equilibrium solution was calculated using :

$$\lg \gamma_{\pm} = -0.505\, z_+ z_- \sqrt{\mu} \qquad (1)$$

where : μ — ionic strength of salt ;

z_+, z_- — charges of salt ions.

The corrected selectivity coefficient, K_c, was calculated with relation

$$K_c = \frac{A_z B_s^2}{B_z A_s} \cdot \frac{\gamma_{\pm}^4 \mathrm{BY}}{\gamma_{\pm}^3 \mathrm{AY}_2} \tag{2}$$

where :

AY_2 — $Cu(NO_3)_2$ or $Zn(NO_3)_2$;
BY — $NaNO_3$.

From the values of the corrected selectivity coefficient, K_c, the equilibrium constant Ka, and then, free enthalpy of exchange, ΔG°, have been evaluated graphically.

The standard enthalpy, ΔH°, was determined from the dependence on temperature of the equilibrium constant. Based on the found values for free enthalpy and standard enthalpy the standard entropy, ΔS° was determined. Its values are given in table 4. The positive values of free enthalpy of exchange, ΔG°, show that the zeolite ZSM-8 is not selective in the presence of Na^+ ions against the investigated cations.

Table 4

Calculated thermodynamics quantities

Exchangeable ion	ΔG°, cal · ion g^{-1} · grd^{-1}		ΔH° cal · ion g^{-1} · · grd^{-1}	ΔS° cal · ion g^{-1}
	298 K	323 K		
Ag^+	+1312	+190	+14.667	+44.8
Cu^{2+}	+ 60	−511	+ 6.854	+22.8
Zn^{2+}	+ 816	+ 90	+ 9.466	+29.0

CONCLUSIONS

Kinetic study of the ion exchange of Ag^+, Cu^{2+} and Zn^{2+} in zeolite ZSM-8 shows how easily are they exchanged and the positive influence of temperature increase. The electric field of zeolite ZSM-8 network being weak, the main factor controlling the exchange is the size of the ions diffusing through pores and not their electrical charge.

The equilibrium data of the exchange have shown that the zeolite ZSM-8 is not selective against investigated cations in the presence of Na^+ ions.

REFERENCES

1. P. Chu and N. J. Woodbury, USA Patent 3.766.093 (1973).
2. A. Vasile, V. Ababi, N. Bilba and M. Cruceanu, Romanian Patent 91.777.
3. A. Bold, A. Vasile, A. Popa, M. Cruceanu, Ev. Popovici and M. Alexandroaei, *Rev. Roumaine Chim.* in print.
4. M. Cruceanu, Ev. Popovici, L. Vlădescu, N. Bilba, R. Rusu, N. Naum and A. Vasile, "Site moleculare zeolitice". Ed. Ştiinţifică şi Enciclopedică, Bucharest, 1986, p. 341.
5. D. Reichenberg, *J. Am. Chem. Soc.*, **75**, 589 (1953).

* * * "Manualul inginerului chimist,", vol. II, Ed. Tehnică, Bucharest, 1951, p. 1765.

Revue Roumaine de Chimie, **36**, *9–10*, 1061–1074 (1991)

MOLECULAR ORBITAL CALCULATIONS WITH SPECIFIC PARAMETRIZATION (MOSP). 1

DESCRIPTION OF THE METHOD. DIPOLE MOMENT CALCULATIONS*

R. BACALOGLU [a], ILSE BACALOGLU [a] and Z. SIMON [b]

[a] Department of Chemistry, State Univ. of New Jersey, Ruthgers, Discata Way, N.J. 08855–0939 USA
[b] Department of Biophysics, Medicinal Institute of Timişoara and QSAR Group at the University of Timişoara, Pţa. 23 August, 2, 1900 Timişoara, Romania

Received July 1, 1990

A specific parametrization for the HMO,-method is proposed and used to calculate total $(\sigma + \pi)$ atomic charges. For each atom the Coulomb integral is considered to increase linearly with the p orbital electronegativity. For each bond the resonance integral is considered proportional to the overlap integral and the mean value of orbital electronegativities. The atomic σ-charges are calculated by the partial equalization of orbital electronegativities method. In turn, the orbital electronegativities are considered to decrease with the total $(\sigma + \pi)$ charge of the atom. This method is checked by a computation of molecular dipole moments for a number of 134 compounds, alkenes, arenes, heterocycles and vanious substitution derivatives. With the exception of five conjugated cyclic hydrocarbons, the differences between experimental and calculated dipole moments fall within 0.25 ± 0.25 D, comparable to the results obtained with the MINDO/3 method.

1. INTRODUCTION

Despite recent progress in quantum chemistry, semiempiric methods, especially those based upon orbital electronegativities [2–4] are used, when net atomic charges are required for calculations of interaction energies between organic molecules (the molecular mechanics method of Allinger et al. [5] as example). The Hückel Molecular Orbital method, [6]was developed into a consistent theory for π-electronic systems of unsaturated and aromatic molecules; the values for the Hamiltonian matrix elements are selected empirically in such a manner as to reproduce (for some model compounds) a given property — as well as possible. [7–19] The efective atomic charges for the σ-electronic systems are usually estimated by using the method of partial equalization of orbital electronegativities.[20–22]

The ideea of the MOSP-method is the following. The major drawback of the simple HMO method is the difficulty to account for the interactions between electrons. One major effect of electronic interactions is the decrease of atomic orbital electronegativities with an increase of net electronic charges upon the corresponding atoms. These atomic orbital electronegativities are expressed here as functions of total ($\sigma + \pi$)-atomic charges and, within an iterative procedure, one may hope to obtain a realistic molecular charge distribution. These charge distributions are tested here by dipole moment calculations. With realistic charge distributions and orbital electronegativities one may hope to obtain good results also for other molecular properties, such as ionization potentials, pK-values etc.

---

* For the first version of the MOSP-method, see Note [1].

2. ORBITAL ELECTRONEGATIVITIES AND CHARGE DISTRIBUTIONS

Sigma electrons. Effective σ-electronic charges are computed by using the method of partial equalization of orbital electronegativity.[20-22] The charge shifted from a less electronegative A-atom, to a more electronegative B-atom is estimated by the equation :

$$\Delta q = \frac{X_B - X_A}{X_A} \cdot 0.5 \tag{1}$$

with X_A and X_B the orbital electronegativities. X_A and X_B depend upon the net charges Q_A and Q_B of the two atoms. The atomic charge is equal to the initial charge (or the one obtained after the previous iteration) to which the shifts, Δq, for all bonds to the corresponding atom are added, as the corresponding π-electronic charge.

The end of computations, within this iterative procedure, is attained when, for all net atomic charges, Q_i, the differences between two iterations are less than 0.001 atomic charge units. This procedure has the advantage of a very short computation time and is quoted [20] to yield a good correlation between calculated charges and various physical and chemical properties.

Pi-electrons. It seems reasonable to relate the Coulomb integral $\alpha_i = \alpha + h_i\beta$, to the electronegativity, X_i, of the p-atomic orbital which depends, in turn, upon the net atomic charge Q_i. The proportionality of α_i and X_i was suggested, [23] as well as of h_i and the difference between X_i and the electronegativity of the C-atom. [24-27]

We attemped to correlate the most frequently used Coulombian integrals with the orbital electronegativities of Hinze and Jaffe [28]. For the figures listed in Table 1, the best correlational equation obtained by us was :

$$h_i = -3{,}2576 + 1.8117 \ln X_i, \quad r = 0.989 \tag{2}$$

We did not use this equation ; accepting charge zero for the C-atom, the dependence of Coulomb integrals (h_i) upon electronegativities (X_i) is taken as the tangent to the above curve, at the point $h_i = 0$, $X_i = 5.60$ Thus :

$$h_i = -1.8117 + 0.3238\, X_i \tag{3}$$

The orbital electronegativities X_i are considered as functions of the effective atomic charges, Q_i, of the previous subparagraph, and are given by the equation :

$$X_i = a_i + B_i Q_i + c_i Q_i^2 \tag{4}$$

The coefficients a_i, b_i, c_i for different types of atomic orbitals are listed in table 2 according to Jaffe et al.[2,28]

Table 1

Usual Coulomb integrals for p orbitals and their electronegativities

No.	Atom.	Electronic structure[a)]	Electro negativity X_i	Coulomb integrals h_i	Bonding in compounds
1	B	tr tr p	4.88 [2]	−0.45 [17]	$-\mathrm{B}=$
2	Si	tr tr tr p	5.59 [2]	−0.50 [16]	$-\mathrm{Si}=$
3	C	tr tr tr p	5.60 [2]	0.00 [17]	$-\mathrm{C}=$
4		di di p p	5.65 [2]	0.10 [14,15]	$-\mathrm{C}=$ $=\mathrm{C}=$
5	N	tr^2 tr tr p	7.95 [2]	0.50 [7]	$-\mathrm{N}=$
6		di^2 di p p	7.92 [2]	0.30 [14]	$\mathrm{N}\equiv$
7		tr tr tr p^2	12.32 [2]	1.50 [7]	$-\mathrm{N}<$
8		tr tr tr p	20.33 [28]	2.00 [7]	$-\mathrm{N}\overset{+}{=}$
9	O	tr^2 tr^2 tr p	10.08 [2]	1.00 [7]	$=\mathrm{O}$
10		tr^2 tr tr p^2	16.73 [2]	2.00 [7]	$-\mathrm{O}-$
11		tr^2 tr tr p	24.69 [28]	2.50 [7]	$-\mathrm{O}\overset{+}{=}$
12	S	tr^2 tr^2 tr p	7.73 [2]	0.46 [17]	$=\mathrm{S}$
13		tr^2 tr tr p^2	10.88 [2]	1.11 [17]	$-\mathrm{S}-$
14	P	tr^2 tr tr p	6.72 [2]	0.20 [17]	$=\mathrm{P}-$
15		tr tr tr p^2	9.47 [2]	0.75 [17]	$-\mathrm{P}-$
16	F	s p^2 p^2 p^2	31.30 [2]	3.00 [7]	$-\mathrm{F}$
17	Cl	s p^2 p^2 p^2	19.23 [2]	2.00 [7]	$-\mathrm{Cl}$
18	Br	s p^2 p^2 p^2	18.28 [28]	1.50 [7]	$-\mathrm{Br}$
19	I	s p^2 p^2 p^2	10.74 [28]	1.20 [13]	$-\mathrm{I}$

[ ] — literature quotation ; a) tr — sp^3 orbital
di — sp^2 orbital

The resonance integrals $\beta_{ij} = k_{ij}\beta$ were considered by Mulliken[29] proportional to the overlap integrals, for a given type of bond and proportional to the ratio of the S_{ij}-overlap integral and the standard S_{CC}-overlap integral for the CC-bond in benzene, by Wheland.[30] In an attempt to correlate k_{ij} with the S_{ij}-overlap integral and the X_i-electronegativities, for the values listed in table 3, the following linear correlation was obtained :

$$k_{ij} = 0.483\, S_{ij}(X_i + X_j) - 1.614,\ r = 0.939 \tag{5}$$

Overlap integrals are estimated according to tables of Mulliken et al.[31-33] which can be calculated by equation :

$$\ln S = a - bp \tag{6}$$

Table 2

The dependence of the orbital electronegativities on the charge of the atoms

No.	Atom	Electronic structure	Type of bond	a_i	b_i	c_i	Type of compounds
1	H1	1 s	σ	7.170	6.240	−0.560	−H
2	B2	tr tr p	σ	6.335	7.168	1.523	=B−
3			π	4.880	6.258	2.093	
4	C4	te te te te	σ	7.975	9.185	1.888	>C<
5	C3	tr tr tr p	σ	8.785	9.330	1.520	=C−
6			π	5.595	8.525	2.945	
7	C2	di di p p	σ	10.380	9.445	0.735	=C= −C≡
8			π	5.645	8.573	2.978	
9	N3	te^2 te te te	σ	11.540	10.82	1.355	−N<
10	N2	tr^2 tr tr p	σ	12.870	11.143	0.843	=N−
11			π	7.950	9.723	2.663	
12	N1	di^2 di p p	σ	15.680	11.698	−0.258	≡N
13			π	7.920	9.775	2.685	
14	N3	tr tr tr p^2	n	12.320	11.198	1.338	−N<
15	02	te^2 te^2 te te	σ	14.180	12.92	1.390	−O−
16	01	tr^2 tr^2 tr p	σ	17.070	13.788	0.463	=O
17			π	10.075	11.728	2.878	
18	02	tr^2 tr tr p^2	n	16.730	13.428	0.358	−O−
19	Si4	te te te te	σ	7.300	6.568	0.658	>Si<
20	Si3	tr tr tr p	σ	7.905	6.748	0.443	=Si<
21			π	5.585	6.018	1.443	
22	S2	te^2 te^2 te te	σ	10.135	9.130	1.380	−S−
23	S1	tr^2 tr^2 tr p	σ	10.880	9.485	1.320	=S
24			π	7.730	8.158	1.808	
25	S2	tr^2 tr tr p^2	n	10.88	9.338	1.203	−S−
26	P3	tr^2 te te te	σ	8.905	8.238	0.953	−P<
27	P2	tr^2 tr tr p	σ	9.665	8.530	0.735	=P−
28			π	6.720	7.410	1.590	
29	P3	tr tr tr p	n	9.470	8.525	0.935	−P<
30	F1	s^2 p^2 p^2 p	σ, n	14.660	13.850	2.310	−F
31	C11	s^2 p^2 p^2 p	σ, n	11.000	9.690	1.350	−Cl
32	Br1	s^2 p^2 p^2 p	σ, n	10.080	8.470	1.160	−Br
33	O11	s^2 p^2 p^2 p	σ, n	9.800	7.960	0.960	−I

where

$$a = 0.98976 - 0.47649\ t - 1.08213\ t^2 - 6.00277\ t^3 + 2.97511\ t^4$$

$$b = 0.56794 - 0.03172\ t - 0.63135\ t^2 - 0.22154\ t^3 - 0.38212\ t^4$$

$$p = \frac{(\mu_i + \mu_j)R}{1.058}, \quad t = \frac{\mu_i - \mu_j}{\mu_i + \mu_j}$$

Table 3

Resonance integral parameters k, bond length, overlaping integrals, and mean electronegativities of chemical bonds [2,20,28]

No.	Atom 1[a)]	Atom 2[a)]	$R_{12}^{b)}$ Å	$S_{12}^{c)}$	$(X_1 + X_2) : 2$ [2,28]	k_{12}
1	C3	C3	1 .34	0 .2597	5 .60	1 .00 [3]
2	C2	C2	1 .20	0 .3316	5 .65	1 .40 [15]
3	C3	02	1 .36	0 .1535	11 .16	1 .30 [14]
4	C3	01	1 .22	0 .2032	7 .84	1 .06 [13]
5	C3	N3	1 .40	0 .1800	8 .96	1 .30 [14]
6	C3	N2	1 .32	0 .2095	6 .78	1 .00 [9]
7	C2	N1	1 .16	0 .2835	6 .79	1 .50 [15]
8	C3	S2	1 .78	0 .0994	8 .24	0 .60 [13]
9	C3	S1	1 .56	0 .1489	6 .67	0 .81 [13]
10	C3	B3	1 .54	0 .2338	5 .24	0 .73 [13]
11	C3	Si3	1 .86	0 .1318	5 .60	0 .50 [12]
12	C3	F1	1 .33	0 .1309	10 .13	1 .25 [9]
13	C3	C11	1 .69	0 .0968	8 .30	0 .62 [13]
14	C3	Br1	1 .86	0 .0685	7 .84	0 .38 [14]
15	N2	N2	1 .25	0 .1965	7 .95	1 .00 [15]

[a)] The atoms of the bond and their coordination number

[b)] Mean values of bond length [33]

[c)] Estimated overlaping integrals [31, 32]

R is the distance between atoms i and j ; μ_i and μ_j are given by

$$\mu_i = \mu_i^0 + 0.175\ Q_i$$

Q_i is the net change of atom i. For the most important atoms the μ_i^0-values, are, according to Mulliken et al. [31.32] :

C, 1.625 ; 0.2.275 ; N, 1.950 ; F, 2.600 ; Cl, 2.033 ; Br, 2.054 ; I, 1.900 ; S, 1.817 ; P, 1.600 ; Si, 1.383 ; B, 1300

RESULTS

Comparative results of MOSP and HMO with usual parametrization for naphthalene and pyridine are listed in table 4 and table 5. Numerotation of atoms is as usual (naphthalene : α — 1, β — 2, interanular

Table 4

Orbital energies, charge densities and bond orders for naphthelane calculated with HMO and MOSP

	Orbital energies		atom charges			bond orders		
	xHMO	xMOSP	Atom	HMO	MOSP	Bond	HMO	MOSP
1	2 .303	1 .781	1	1 .000	0 .995	1—2	0 .725	0 .723
2	1 .618	1 .111	2	1 .000	0 .989	2—3	0 .603	0 .604
3	1 .303	0 .927	9	1 .000	1 .031	1—9	0 .555	0 .555
4	1 .000	0 .627				9—10	0 .518	0 .519
5	0 .618	0 .337						
6	—0 .618	—0 .641						
7	—1 .000	—0 .934						
8	—1 .303	—1 .178						
9	—1 .618	—1 .432						
10	—2 .303	—1 .993						

Table 5

Orbital energies, charge densities and bond orders for pyridine calculated with HMO and MOSP ($k_{CN} = 1$, $h_N = 0.5$)

Orbital energies			atom charges			bond orders		
	xHMO	xMOSP	Atom	HMO	MOSP	Bond	HMO	MOSP
1	2.107	1.559	1	1.195	0.969	1−2	0.654	0.654
2	1.167	0.853	2	0.923	1.069	2−3	0.669	0.684
3	1.000	0.665	3	1.005	0.953	3−4	0.665	0.655
4	−0.841	−0.772	4	0.949	0.984			
5	−1.000	−0.897						
6	−1.933	−1.661						

C-9; pyridine: N-1, C ortho-2 and 6, etc.). Molecular orbital energies, $\varepsilon = \alpha - x\beta$ and especially π-bond orders are in good correlation for these two molecules:

$$\varepsilon_{MOSP} = -0.1280 + 0.8024\,\varepsilon_{HMO}\,;\ r = 0.9997$$

The atomic charges present rather large differences, due to the influence of σ-bonds which is not included in HMO-calculations.

3. DIPOLE MOMENTS

The major part of the molecular dipole moment is the vectorial sum of dipole moments due to the net ($\sigma + \pi$) atomic charges, but there are also other contributions which must be also considered in several cases. These contributions are the homopolar dipole and the atomic dipole.[34] The first appears when the overlapping atomic orbitals are of different size and the bond charge is shifted towards the smaller atomic orbital; its contribution is between 0.1 and 1 D. The atomic dipole is due to the charge asymmetry of the hybrid orbitals at one atom. Such dipoles are quite large, 2.2 D for a sp-hybrid, 2.0 D for a sp^2-hybrid of the C-atom. These atomic dipoles are vectorially compensated, except for lone-pair electrons.

The contribution of net atomic charges to the molecular dipole is computed with standard bond lengths (Table 6) and bond angles: 109.47° for an atom with sp^3-hybridisation, 120° for sp^2-hybridisation (C, N, O), 90° for dicoordinated sulphur. All molecules are considered as planar, here. In the case of the $X-CH_3$ group, the three H-atoms are considered bonded with a 0.363 Å bond making a 180° angle with the X−C-bond. For the $XYCH_2$-group, the two H-atoms are considered in the plane of the X−C−Y bonds, with a bond length of 0.629 Å. This system simplifies the introduction of data for each atom, avoiding the second angle, usually used for defining a molecule in space.

The contributions of homopolar plus atomic dipoles are calculated as corrections for the differences between experimental dipoles and those calculated by vectorial sums via net atomic charges for some model molecules listed in table 7. The corresponding corrections for a number of 21 atoms, groups and atoms within heterocycles are also listed in table 7. Generally, these corrections are small, but sometimes they reach 1 D.

Table 6

Standard bond length Å [33, 41]

Simple bonds

X−H	C^4-H	1.09	C^3-H	1.08	C^2-H	1.06
	N^3-H	1.01	N^2-H	0.99	O^2-H	0.96
C−C	C^4-C^4	1.53	C^4-C^3	1.52	C^4-C^2	1.46
	C^3-C^3	1.46	C^3-C^2	1.45	C^2-C^2	1.38
C−N	C^4-N^3	1.47	C^3-N^3	1.40	C^2-N^3	1.33
	C^4-N^2	1.46	C^3-N^2	1.40	C^2-N^2	1.33
C−O	C^4-O^2	1.42	C^3-O^2	1.36	C^2-O^2	1.36
C−F	C^4-F	1.36	C^3-F	1.33	C^2-F	1.27
C−Cl	C^4-Cl	1.77	C^3-Cl	1.72	C^2-Cl	1.63
C−Br	C^4-Br	1.94	C^3-Br	1.88	C^2-Br	1.83
C−I	C^4-I	2.15	C^3-I	2.08	C^2-I	1.99
S−X	C^4-S^2	1.81	C^3-S^2	1.77	S^2-C^2	1.68
	S^2-S^2	1.94	S^2-Cl	1.99	S^2-H	1.35
B−X	C^4-B^3	1.56	B^3-C^3	1.54	B^3-H	1.24
	B^3-Cl	1.71				
P−X	C^4-P^3	1.85	C^3-P^3	1.80	C^2-P^3	1.79
	P^3-N^3	1.70	P^3-N^2	1.68	P^3-O^2	1.60
	P^3-S^2	2.12	P^3-Cl	2.06	P^3-F	1.58
Si−X	C^4-Si^4	1.87	C^3-Si^4	1.85	C^2-Si^4	1.82
	Si^4-Cl	2.02				
N−Y	N^3-N^3	1.45	N^3-N^2	1.45	N^2-N^2	1.45
	N^3-O^2	1.47	N^2-O^2	1.41	N^3-Cl	1.73

Double bonds

C−C	C^3-C^3	1.34	C^3-C^2	1.31	C^2-C^2	1.28
C−N	C^3-N^2	1.32	C^2-N^2	1.32		
C−O	C^3-O^1	1.22	C^2-O^1	1.16		
N−X	N^3-O^1	1.24	N^2-O^1	1.22	N^2-N^2	1.25
S−C	C^3-S^1	1.62	C^2-S^2	1.56		
Si−C	C^3-Si^3	1.83				
P−X	C^3-P^2	1.67				

Aromatic bonds

	C^3-C^3	1.40	C^3-N^2	1.40	N^2-N^2	1.40
	C^3-S^2	1.70	C^3-P^2	1.40		

Triple bonds

	C^2-C^2	1.20	C^2-N^1	1.16	N^1-N^1	1.10
	C^2-P^1	1.54				

Table 7

Experimental [35] and calculated dipole moments of model molecules; substituted benzenes (D)

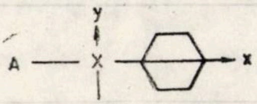

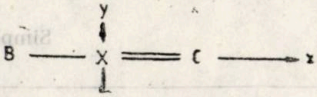

Substituents X		Experimental			Calculated			Corrections	
		x	y	t	x	y	t	x	y
F—	A	−1.57	0	1.57	−2.04	0	2.04	0.47	0
Cl—	A	−1.55	0	1.59	−1.30	0	1.30	−0.25	0
Br—	A	−1.57	0	1.57	−1.07	0	1.07	−0.50	0
I—	A	−1.40	0	1.40	−1.09	0	1.09	−0.31	0
H_3C—	A	0.37	0	0.37	0.06	0	0.06	0.31	0
Cl_3C—	A	−2.04	0	2.04	−1.56	0	1.56	−0.48	0
F_3C—	A	−2.54	0	0	−2.69	0	2.69	0.15	0
H_2N—	A	1.53	0	1.53	1.72	0	1.72	−0.19	0
O_2N—	A	−4.01	0	4.01	−5.21	0	5.21	1.20	0
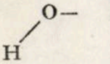	A	0	1.55	1.55	−0.49	1.11	1.22	0.49	0.44
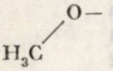	A	+0.39	1.22	1.28	−0.28	1.85	1.87	−0.67	0.65
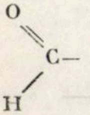	A	−2.45	1.65	2.96	−2.71	2.13	3.44	0.26	0.48
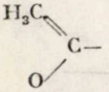	A	−1.98	2.20	2.96	−2.66	2.31	3.52	0.68	0.11
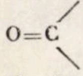		−2.27	0	2.27	−2.41	0	2.41	+0.14	0
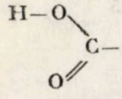	A	−1.42	−0.82	1.64	−2.24	−1.30	2.60	0.82	0.48
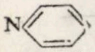		−2.22	0	2.22	−1.99	0	1.99	−0.23	0
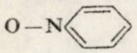		−4.24	0	4.24	−3.25	0	3.25	−0.99	0
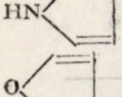		1.98	0	1.98	1.74	0	1.74	0.24	0
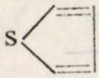		−0.66	0	0.66	−1.23	0	1.23	0.57	0
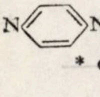		−0.55	0	0.55	−0.25	0	0.25	−0.30	0
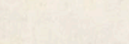		−3.56	−1.00	3.70	−3.28	−1.14	3.47	−0.47*	0

* corrected for N and NH

These corrections are used, together with the vectorial sum of dipole moments due to net atomic charges, to compute molecular dipole moments for different classes of organic compounds. As can be seen from the experimental and calculated values for different classes of compounds listed in table 8, the agreement is satisfactory.

Results for a number of 22 alkenes and aromatic hydrocarbons are listed in Fig. 1. For 17 compounds, the difference between experimental and calculated dipole moments is 0.12 ± 0.13 D. This difference is large for other five compounds, for which the names are listed below, followed by the experimental dipole moment (Debye-units), the one calculated by the MOSP-method and, respectively by the HMO method.[36] They are fulvene, 1.1 D, 3.05 D, 4.7 D ; dimethylenecyclobutene, 0.62 D, 1.13 D, — ; heptafulvene, 0.5 D, 1.86 D, ; azulene 1 D, 4.25 D, 6.9 D ; acenaphthylene, 0.93 D, 1.92 D, 2.8 D.

Table 8

Calculated and experimental dipolmoments (D) *

Substituents	$\mu_{calc.}$	$\mu_{exp.}$	$\Delta\mu$
a) substituted benzenic derivatives			
1-Nitro-4-chloro	2.54	2.57	−0.03
1-Nitro-4-bromo	2.46	2.66	−0.20
1-Nitro-4-fluoro	2.47	2.63	−0.15
1-Nitro-4-hydroxy	4.22	5.02	−0.80
1-Nitro-4-amino	6.35	6.33	0.02
1-Nitro-4-carboxy	3.43	3.50	−0.07
1-Nitro-4-formyl	2.47	2.40	0.07
1-Nitro-4-cyanato	1.98	2.27	−0.29
1-Nitro-4-thiocyanato	3.42	3.10	0.32
1-Nitro-3-chloro	3.46	3.44	0.02
1-Nitro-3-nitro	3.73	3.79	−0.06
1-Nitro-3-amino	5.01	4.85	0.16
1-Nitro-2-nitro	6.44	6.00	0.44
1-Nitro-2-chloro	4.82	4.35	0.47
1-Cyan-4-bromo	2.44	2.64	−0.20
1-Cyan-4-hydroxy	4.50	4.95	−0.45
1-Chloro-4-amino	3.04	2.99	0.05
1-Chloro-2-bromo	2.64	2.20	0.44
1-Chlor-3-bromo	1.53	1.50	0.03
1-Chlor-4-cyanato	2.68	2.71	−0.03
1-Amino-3-amino	1.49	1.79	−0.30
1-Brom-4-hydroxy	2.21	2.12	0.09
1-Hydroxy-2, 4, 6-trichloro	2.37	1.62	0.75
1-Hydroxy-2, 4, 6-tribromo	1.56	1.56	0.00

---

* Not all compounds for which dipolmoment calculations were performed is are listed in Table 8 or Figs. 1 and 2.

Table 8 (continued)

Substituents	$\mu_{\text{calc.}}$	$\mu_{\text{exp.}}$	$\Delta\mu$
b) substituted naphthalin derivatives			
1-Nitro	4.58	3.98	0.60
1-Chloro	1.55	1.56	−0.01
1-Amino	1.98	1.49	0.49
2-Chloro	1.58	1.72	−0.14
c) substituted aromatic heterocycles			
1, 2-Oxazol	2.89	2.90	−0.01
1, 3-Oxazol	1.89	1.50	0.39
1, 2-Thiazol	2.70	2.40	0.30
1, 3-Thiazol	1.42	1.61	−0.19
1, 2-Diazol	2.62	2.21	0.41
1, 3-Diazol	3.69	3.70	−0.01
1, 2, 3-Triazol	4.81	5.15	−0.34
1, 2, 4-Triazol	3.13	3.27	−0.14
1, 2, 3, 4-Tetrazol	5.15	5.15	0.00
Indol	1.96	2.13	−0.17
Benz[b]thiophen	0.66	0.62	0.04
Benzimidazol	3.33	4.02	−0.70
4-Nitropyridine	1.52	1.58	−0.06
4-Cyanpyridine	1.64	1.65	−0.01
4-Aminopyridine	3.89	3.95	−0.06
4-Chlorpyridine	0.83	0.74	0.09
1, 2-Diazine	4.02	4.22	−0.20
1, 3-Diazine	2.29	2.33	−0.04
Quinoline	2.24	2.19	0.05

The direction of the calculated dipole moments for these 5 compounds is in agreement with the experimental ones, but their value is too high. The values calculated by the simple HMO method are even higher.

The calculated and experimental values for 47 halogene derivatives are listed in Fig. 2. The correlational equation between the calculated, μ_c, and experimental, μ_e, dipole moments as well as the difference, $\Delta\mu_m$, between these values, is :

$$\mu_c = -0.02 + 1.01\,\mu_e\,; \quad r = 0.933\,; \quad \Delta\mu_m = 0.21 \pm 0.21\ \mathrm{D} \tag{7}$$

The corresponding data for 31 amino and nitroderivatives are listed in Fig. 3. The correlational results are :

$$\mu_c = -0.24 + 1.08\,\mu_e\,; \ r = 0.976\,; \ \Delta\mu_m = 0.28 \pm 0.18\ \mathrm{D} \tag{8}$$

For a series of 17 oxygenated compounds the results are :

$$\mu_c = 0.03 + 0.99\,\mu_e\,; \ r = 0.947\,; \ \Delta\mu_m = 0.22 \pm 0.19\ \mathrm{D} \tag{9}$$

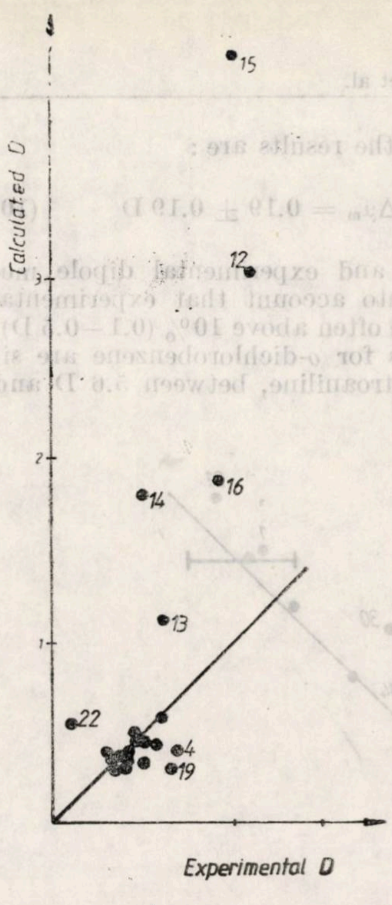

Fig. 1. – Experimental[35] and calculated dipole moments. The underlined figures (**1**, **2**, ...) correspond to the number of the point in the figure. Alkenes and arenes : **1** : propene ; **2** : butene ; **3** : 2-methylpropene ; **4** : 1, 3-pentadiene ; **5** : 2-methyl-1, 3-butadiene ; **6** : styrene ; **7** : toluene ; **8** : 1,2-xylene ; **9** : 1, 3-xylene ; **10** : 1-methylnaphthalene ; **11** : 2-methyl-naphthalene ; **12** : fulvene ; **13** : dimethylene-cyclobutene ; **14** : heptafulvene ; **15** : azulene ; **16** : acenaphthylene ; **17** : anthracene ; **18** : cyclopentadiene ; **19** : benzocyclopentene ; **20** : indene ; **21** : cyclopropene ; **22** : cyclobutene.

Fig. 2. – Experimental[35] and calculated dipole moments. Halogene derivatives : Substituted benzenes : **1** : F ; **2** : Cl ; **3** : Br ; **4** : I ; **5** : 1, 2 F_2 ; **6** : 1, 3 F_2 ; **7** : 1,2 Cl_2 ; **8** : 1, 3Cl_2 ; **9** : 1, 2Br_2 ; **10** : 1, 3 Br_2 ; **11** : 1Br, 2Cl ; **12** : 1Br, 3Cl ; **13** : 1 Br, 4 Cl ; **14** : 1 Cl, 4 I ; **15** : 1 Br, 4 F ; **16** : 1 Br, 4 CH_3 ; **17** : 1 F, 4 CH_3 ; **18** : 1 Br, 3 CH_3 ; **19** : 1 F, 3 CH_3 ; **20** : 1 Cl, 4 CH_3 ; **21** : 1 Cl, 4 CF_3 ; **22** : 1, 3I_2 ; **23** : 1 Br, 4I ; **24** : 1 F, 4 I ; **25** : 1, 2, 4 Cl_3 ; **26** : 1, 2, 3 Cl_3 ; **27** : 1, 2, 3, 4, 5 Cl_5 ; **28** : 1, 2, 3, 4, 5 Cl_5, 6 CH_3 ; Substituted naphthalenes : **29** : 1 Cl ; **30** : 2 Cl ; **31** : 1 Br ; **32** : 2 Br ; **33** : 1I ; **34** : 2I ; Substituted anthracene : **35** : 1, 8 Cl_2 ; Substituted biphenyls : **36** : 4 Br ; **37** : 4 I ; Substituted ethenes : **38** : 1 Cl ; **39** : 1 Br ; **40** : 1 I ; **41** : 1 F ; **42** : 1, 2 Cl_2 ; **43** : 1, 2 F_2 ; **44** : 1, Br_2 ; **45** : 1, 1, 2 Cl_3 ; **46** : 1, 1, 2 F_3 ; Substituted butadiene : **47** : 2 Cl.

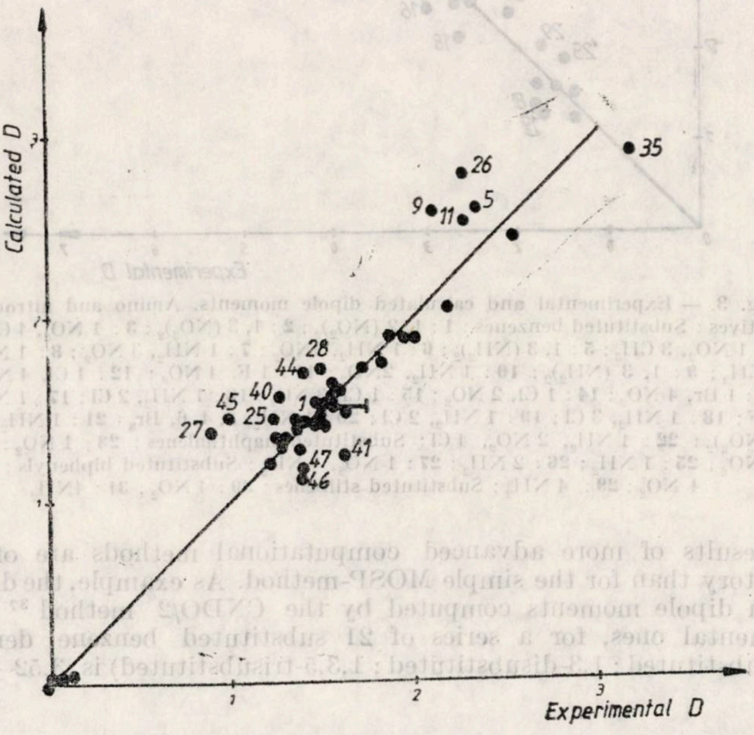

For a series of 18 aromatic heterocycles, the results are :

$$\mu_c = 0.19 + 0.94\ \mu_e\ ;\ r = 0.987\ ;\ \Delta\mu_m = 0.19 \pm 0.19\ \text{D} \qquad (10)$$

The agreement between calculated and experimental dipole moments is good, especially if one takes into account that experimental errors in dipole moment determinations are often above 10% (0.1 – 0.5 D). As example, results from different groups for *o*-dichlorobenzene are situated between 2.0 D and 2.5 D, for *p*-nitroaniline, between 5.6 D and 6.8 D[35].

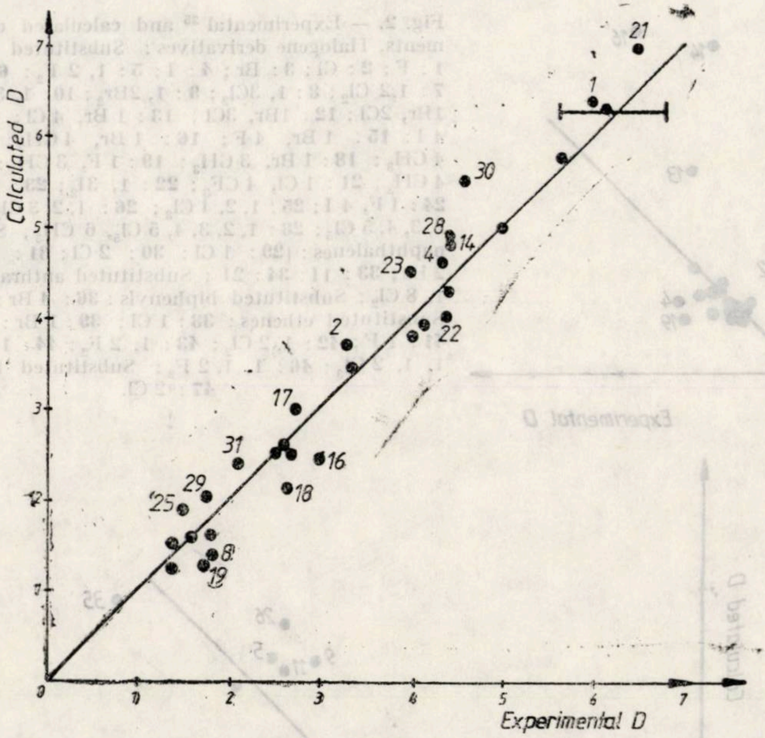

Fig. 3. – Experimental and calculated dipole moments. Amino and nitroderivatives : Substituted benzenes : **1** : 1, 2 $(NO_2)_2$; **2** : 1, 3 $(NO_2)_2$; **3** : 1 NO_2, 4 CH_3 ; **4** : 1 NO_2, 3 CH_3 ; **5** : 1, 3 $(NH_2)_2$; **6** : 1 NH_2, 4NO_2 ; **7** : 1 NH_2, 3 NO_2 ; **8** : 1 NH_2, 3 CH_3 ; **9** : 1, 3 $(NH_2)_2$; **10** : 1 NH_2, 2NO_2 ; **11** : 1 F, 4 NO_2 ; **12** : 1 Cl, 4 NO_2 ; **13** : 1 Br, 4 NO_2 ; **14** : 1 Cl, 2 NO_2 ; **15** : 1 Cl, 3 NO_2 ; **16** : 1 NH_2, 2 Cl ; **17** : 1 NH_2, 4 F ; **18** : 1 NH_2, 3 Cl ; **19** : 1 NH_2, 2 Cl ; **20** : 1 NH_2. 2, 4, 6, Br_3 ; **21** : 1 NH_2, 2, 4$(NO_2)_2$; **22** : 1 NH_2, 2 NO_2, 4 Cl ; Substituted naphthalenes : **23** : 1 NO_2 ; **24** : 2 NO_2 ; **25** : 1 NH_2 ; **26** : 2 NH_2 ; **27** : 1 NO_2, 3 NH_2 ; Substituted biphenyls : **28** : 4 NO_2 ; **29** : 4 NH_2 ; Substituted stilbenes : **30** : 4 NO_2 ; **31** : 4NH_2.

Results of more advanced computational methods are often less satisfactory than for the simple MOSP-method. As example, the difference between dipole moments computed by the CNDO/2 method [37] and the experimental ones, for a series of 21 substituted benzene derivatives (monosubstituted ; 1,3-disubstituted ; 1,3,5-trisubstituted) is 3.52 ±2.75D.

The same differences, for the MINDO/3 method, is 0.21 ±0.13 D for a series of 15 hydrocarbons, [38] 0.26 ±0.24 D for a series of 24 chlorine and fluorine derivatives [39] and 0.36 ± 0.36 D for a series of 30 oxygen and nitrogen derivatives of benzene.[40]

4. COMPUTATIONS

The calculations were performed upon a Sinclair ZX 81 computer (56 K RAM) with a program written in BASIC. The program calculates first the atomic coordinates and the σ-charges, using electronegativities considered for the initial atomic charges. The electronegativities and interatomic distances are used for calculation of Coulomb and resonance integral, with which the first HMO calculation is performed. The so obtained π-atomic charges are considered as intial charges and the calculus repeated till selfconsistency is reached. For each atom, the following values are to be given : data for rectangular coordinate calculations — two preceding atoms, the bond length of the atom with the last one and the angle of this bond with the bond between the two preceding atoms; the atoms to which the given atom is bonded; its initial charge and the charge of the atomic core for π-electronic calculations. The computer time required by our iterative method is incomparably shorter than the one required by the advanced SCF methods.

5. CONCLUSIONS

Taking into account the generally good agreement between the calculated and experimental dipole moments, one may expect an acceptable agreement of atomic charge distributions calculated by the MOSP-method and the real charge distribution.

REFERENCES

[1] R. Bacaloglu, Buletin Ştiinţif. şi Tehnic al Inst. Politehnic "Traian Vuia", Timişoara, **28**, 77 (1983).

[2] J. Hinze and H. H. Jaffe, *J. Am. Chem. Soc.*, **84**, 540 (1962).

[3] J. Hinze, M. A. Whitehead and H. H. Jaffe, *J. Am. Chem. Soc.*, **85**, 148 (1963).

[4] J. K. Labanowski, R. A. Dammkoehler and J. Moţoc, *J. Comput. Chem.*, **10**, 1016 (1989).

[5] V. Burkert and N. L. Allinger, Molecular Mechanics, American Chemical Society Washington, DC, 1982.

[6] E. Hückel, *Z. Physik*, **70**, 204 (1931) ; **72**, 310 (1932) ; **76**, 628 (1932).

[7] A. Streitwieser Jr., "Molecular Orbital Theory for Organic Chemists" J. Wiley, New York, 1961.

[8] J. D. Roberts, "Molecular Orbital Calculations", W. A. Benjamin, New York, 1962.

[9] B. Pullman and A. Pullman, "Quantum Biochemistry" J. Wiley, New York, 1963.

[10] L. Salem, "The Molecular Orbital Theory of Conjugated Systems", W. A. Benjamin, New York, 1966.

[11] H. Suzuki, "Electronic Absorption Spectra and Geometry of Organic Molecules. An Application of Molecular Orbital Theory", Academic Press, New York, 1967.

[12] E. Heilbronner and H. Bock, "Das HMO-Modell und seine Anwendung", Verlag Chemie, Weinheim, 1968.

[13] T. Yonezawa, C. Nagata, H. Kato, A. Iamamura and K. Morokuma, "An Introduction to Quantum Chemistry", Kadakudojin, Kyoto, 1983.

[14] O. E. Polansky and M.A. Grassberger, *Mh. Chem.*, **94**, 42 (1963).

[15] A. Iwohl, *Tetrahedron*, **24**, 6889 (1968).

[16] J. Eicher and J. Meziva, *Angew. Macromol. Chem.*, **19**, 31 (1971).

[17] F. A. van Catledge, *J. Org. Chem.*, **45**, 4801 (1980).

[18] G. Derflinger and H. Lischka, *Monatsh. Chem.*, **100**, 1003 (1969).

[19] A. J. Wohl. *Tetrahedron*, **24**, 6889 (1968).

[20] M. Marsili, "Ladungsverteilungen und Chemische Reaktivität in der Computergesteuerten Reaktionssimulation", Ph. D. Thésis, Organisch Chemisches Institut, Technische Universitat München, 1980.

[21] J. Gasteiger and M. Marsili, *Tetrahedron Letters*, **1978**, 3181.

[22] J. Gasteiger and M. Marsili, *Tetrahedron*, **36**, 3219 (1980).

[23] C. Sandorfy, *Bull. Soc. Chem. France*, **1949**, 615.

[24] R. S. Mulliken, *J. Chim. Phys.*, **46**, 497, 675 (1949).

[25] E. Gyverffy, *Compt. rend.*, **232**, 515 (1951).

[26] C. A. Coulson and J. de Heer, *J. Chem. Soc.*, **1952**, 483.

[27] A. Laforgue, *J. Chim. phys.*, **46**, 568 (1949).

[28] J. Hinze and H. H. Jaffe, *J. Phys. Chem.*, **67**, 1501 (1963).

[29] R. S. Mulliken, *J. Phys. Chem.*, **56**, 295 (1952).

[30] G. W. Wheland, *J. Am. Chem. Soc.*, **64**, 900 (1942).

[31] R. S. Mulliken, G. A. Roeke, D. Orloff and H. Orloff, *J. Chem. Phys.*, **17**, 1248 (1949).

[32] K. B. Wiberg, "Physical Organic Chemistry", J. Wiley, New York, 1964, p. 469.

[33] J. A. Pople, D. L. Beveridge, "Aproximate Molecular Orbital Theory", Mc. Graw Hill Book Comp., New York, 1970.

[34] C. A. Coulson, "Valence", Oxford University Press, Oxford, 1972.

[35] Landolt-Börnstein, "Zahlwerte und Funktionen aus Physik, Chemie, Astronomie, Geophysik und Technik", Vol. I/3, Molekülen, Springer, Berlin, 1951, p. 388.

[36] A. Pullman, B. Pullman, E. D. Bergmann, G. Berthier, E. Fischer, Y. Hirschberg and J. Pontis, *J. Chim. phys.*, **48**, 359 (1951); **49**, 20 (1952).

[37] J. Koudelka and O. Exner, *Coll. Czech. Chem. Commun.*, **50**, 188 (1985).

[38] R. C. Bingham, M. J. S. Dewar and D. H. Lo, *J. Am. Chem. Soc.*, **97**, 1294 (1975).

[39] R. C. Bingham, M. J. S. Dewar and D. H. Lo, *J. Am. Chem. Soc.*, **97**, 1307 (1975).

[40] R. C. Bingham, M. J. S. Dewar and D. H. Lo, *J. Am. Chem. Soc.*, **97**, 1302 (1975).

Revue Roumaine de Chimie, 36, *9–10*, 1075–1092 (1991)

METHOD FOR CALCULATING THE LOCAL ELECTRONIC ENERGY LEVELS IN SEMICONDUCTORS AND THEIR OCCUPATION NUMBERS FROM SLOPE VARIATIONS OF THE ARRHENIUS DIAGRAM OF THE ELECTRIC CONDUCTIVITY

ŞERBAN - DAN CARTIANU
Institute of Physical Chemistry of the Romanian Academy,
Splaiul Independenţei 202, Bucureşti, Romania

Received December 19, 1990

A new look at the phenomenon of electric conductivity in monocrystalline semiconductors is presented. The author conceives the usual interpretation of the temperature dependence of the electric conductivity in terms of Arrhenius diagrams merely as a parametrization. In the light of modern quantum mechanics which explains mathematically the tunneling phenomenon of quantum particles across energy barriers, there is no need to use the pre-quantum mechanics theory of Svante Arrhenius. The representation of the Arrhenius diagram can be used for deducing the place of the local energy levels and bands edges and their occupation numbers, by solving the electroneutrality equation. For a more precise determination of the energy bands, and the exact distribution of electrons on the energy levels, other phenomena must be evaluated also.

1. INTRODUCTION

The present paper gives a comprehensive account of a very interesting method of determining the parameters of the quantum states of electrons in semiconducting monocrystals, from electrical conductivity measurements interpreted according to the Svante Arrenius parametrization.

The Arrhenius formula, in the present author's conception should be regarded merely as a convenient parametrization. It was conceived before the quantum theory became available. Quantum particles do not climb potential barriers by means of activation energies for various phenomena, but by the real quantum-mechanical tunnel phenomenon.

Electrons in semiconductors are distributed on energy states E, according to the Fermi distribution function :

$$\mathrm{f}(E) = (1 + \exp((E_f - E_f)/RT))^{-1} \tag{1}$$

where the parameter E_f is called Fermi energy. If there exists an allowed level with energy $E = E_f$ the Fermi function is $f(E) = 1/2$, thus an electron would have with equal probabilities this energy. If $E \gg E_f$ the Fermi distribution tends to the classical Maxwell-Boltzmann distribution :

$$f(E) \approx \exp((E_f - E)/kT) \tag{2}$$

The positive empty energy states called holes represent a fraction equal to $(1 - f(E))$ of the quantum energy states, their distribution being :

$$1 - f(E) = (1 + \exp((E_f - E)/kT))^{-1} \tag{3}$$

The Fermi level depends on the distribution of quantum states, the total number of electrons (Avogadro) and the absolute temperature T, and the Boltzmann constant k. The distribution of electrons vs. energy results from $N(E)$, the number of quantum states on the unit of the energy scale, and from $f(E)$, the distribution function which expresses the fraction of occupied states.

By using an effective mass m_e, defined in terms of the monocrystal parameters, for each energy band, permits to express the dynamics of the electrons in the monocrystal as a dynamics of free electrons in periodic fields. The effective mass is the largest, when the energy band of allowed electron energies is the narrowest.

An energy band with a single energy minimum in the Brillouin zone and spherical constant energy surfaces, the number of quantum states on unit volume is :

$$\rho(E) = A(E - E_c)^{1/2}, \text{ where } A = (4\pi/h^3)(2m_e)^{1/2} \tag{4}$$

E_c is the minimum energy of the conduction band, h is Planck's constant. Within the range of the Maxwell-Boltzmann approximation to the Fermi distribution, the density of electrons in the energy interval $(E, E + \mathrm{d}E)$ is

$$n(E) = \rho(E) \exp((E_f - E_c)/kT) \tag{5}$$

The total number n of electrons in the conduction band on unit volume is equal to the integral of $n(E)$ between E_c and infinity :

$$n = 2(2\,\pi m_e kT/h^2)^{3/2} \exp((E_f - E_c)/kT) \tag{6}$$

The conduction band can be regarded as a single level at the conduction band edge with an effective density of states : $N_c = 2(2\pi m_e kT/h^2)^{3/2}$. The total density of holes in the valence band is :

$$p = 2(2\pi m_h kT/h^2)^{3/2} \exp((E_v - E_f)/kT) \tag{7}$$

where E_v is the energy of the edge of the valence band and m_h is the effective hole mass. The valence band is equivalent to a single level at the edge of the valence band and the effective density of states :

$$N_v = 2(2\pi m_h kT/h^2)^{3/2}.$$

If the Fermi level of the semiconducting monocrystal is near or within one of the highest two occupied bands, the integrals over the Fermi distribution must be evaluated. The number of electrons in the conduction band is then :

$$n = \int_{E_c}^{\infty} \frac{\rho(E)(E - E_c)^{1/2}\,\mathrm{d}E}{1 + \exp\left((E_c - E_f)/kT\right)} \tag{8}$$

In nondimensional variables these integrals have been tabelated, being computed by asymptotic expansions.

Near an imperfection of the crystal, its periodicity is perturbed, and the energy levels become localized. Single electronic energy levels appear in the energy gap. These impurity levels have an angular momentum degeneration, their number being respectively, for neutral donors and ionised acceptors :

$$n_d = N_d / \left(1 + \frac{1}{2} \exp((E_d - E_f)/kT)\right), \quad n_a^- = N_a/(1 + 2\exp((E_a - E_f)/kT)) \tag{10}$$

The difference from the Fermi distribution consists in the factors 1/2 and 2. The electrons can have two angular momentum states. The neutral impurity state has a double statistical weight with respect to the ionized state. For polyvalent impurities or if the wavefunction of the fundamental state of the impurity is not spherically symmetric, the degeneracy factor can differ.

The drift velocity of an electron or hole, v depends linearly on the applied electric field. For small drift velocities w.r.t. the thermal mean velocity : $v = \mu F$, F being the electric field, μ is the drift mobility of the electrons of holes. The mobility results directly from the study of the impulse photoconductivity. It is expressed in terms of an efective relaxation time $\langle \tau \rangle$, an average of the mean free path between collisions of electrons with ions and effective mass : $\mu = q\langle \tau \rangle / m^*$.

By processing the Boltzmann integrodifferential nonlinear equation, for the distribution function of the electron gas, in the nondegenerate case, the relaxation time can be expressed in terms of the collision time $\tau(E)$ by

$$\langle \tau \rangle = \int_0^{\infty} \tau(E) E^{3/2} f(E)\,\mathrm{d}E \Big/ \int_0^{\infty} E^{3/2} f(E)\,\mathrm{d}E \tag{11}$$

the weight of the various groups of electrons of energy E in $\langle \tau \rangle$ is $EN(E)$. For various types of collisions, τ depends on energy and temperature by : $\tau \sim m^*/TE^{1/2}$, for electrons colliding with phonons at usual temperatures isotropically, or $\tau \sim m^{*1/2} E^{3/2}$, when the deflection of the electron before the collision has a small probability.[1]

Within a large energy range, the relation holds: $\tau(E) = BE^{-i}$ where for collisions on the crystal i $=1/2$, and $B \sim T^{-1}$ and for collisions on impurities i $= -3/2$, B being independent of temperature.

Introducing these functions in the formula of the effective relaxation time $\langle\tau\rangle$ and using the Maxwell-Bolztmann distribution $f(E) \approx \approx \exp(-E/kT)$:

$$\langle\tau\rangle = B(kT)^{-i}\Gamma\left(\frac{3}{2} - s\right)/\Gamma(3/2) \tag{12}$$

The temperature dependence of the mobility for crystal collisions is $T^{-3/2}$ and for collisions on impurities it varies with $T^{3/2}$, just as from the above formulas.

In the majority of monocrystalline semiconductors, the temperature dependence of the mobility, deduced from Hall effect and transit time, is T^m with $-3 \leqslant m \leqslant 3/2$.

When two types of collisions predominante in a temperature range, the total collision cross section is the sum of the cross sections, and $\tau^{-1} = = \tau^{-1}_1 + \tau^{-1}_2$. In Fig. 1 such a case is illustrated: log μ vs. T. The upper line corresponds to the pure probe and depends as $T^{-3/2}$ through the collisions on phonons and for the probe with impurities, the lower line, the dependence is $T^{3/2}$ at low temperatures, through collisions on single impurities.[2]

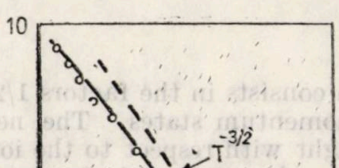

Fig. 1. — The variation of the mobility of electrons with the temperature.

In a typical semiconductor with mobility $\mu = 10^3$ cm^{2}V^{-1}s^{-1} and effective mass near the electron mass, the energy uncertainty ($\mathrm{d}E \cdot \tau \sim \hbar$) is 10^{-3} eV thus the energy levels of the electron can be precisely specified. For materials with small mobility, $\mu \sim 1$ cm^{2}V^{-1}s^{-1} and $\mathrm{d}E \sim 1$ eV. In this case energy levels in a band cannot be allocated, as for disorded materials with conduction in localized states, or molecular crystals.

The mean energy of the electrons and holes, and also their effective T is larger than that of the lattice due to the balance between the electric field applied and the losses by collisions. For large T, Ohm's rule is no longer valid, hot electrons being usual for the most important semiconductors (especially III—V, which have a differential negative conductivity).

In the present paper we make abstraction on these facts and assume that electrons are at the crystal temperature, and that their energy does not depend on T.

At the junction metal-semiconductor of type n, with ionisation potentials φ_m and φ_s, in the absence of an electric field, the metal influences the quantum state fo the semiconductor. If $\varphi_m - \varphi_s$ is positive, a limit layer appears with big resistance, and with charge depletion. If the Fermi level of the semiconductor is below that of the metal, before joining the two materials, there is an Ohmic contact.The charge at the semiconductor surface curbs the energy bands upwards. In the presence of an electric field the profiles of Fig. 2 are modified. The current flow is limited by the space charge.

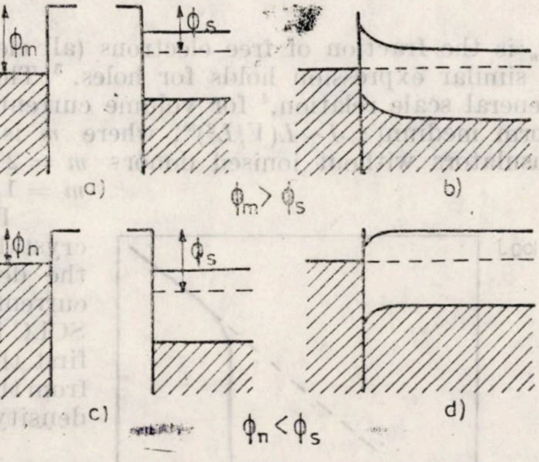

Fig. 2. — The surface potential barrier at the metal-semiconductor interface.

For Ohmic conduction :

$$J_n = nq\mu_e F \text{ and } J_p = pq\mu_h F \tag{13}$$

where q is the electronic charge, n, p and the conduction electrons and holes concentrations, J_n and J_p and μ_e, μ_h are the densities of the drift current and the mobilities of the electrons and holes.

The Arrhenius temperature dependence of the electronic conductivity $\sigma_e = nq\mu_e$ results from

$$\ln(\sigma_e) = \ln(N_c q\mu_e) - (E_c - E_f)/kT \tag{14}$$

The effective density of states in the conduction band is $\sim T^{3/2}$ and for crystal collisions $\mu_e \sim T^{-3/2}$. Thus $\ln \sigma_e$ vs. $1/T$ is an Arrhenius straight line. If the mobility is dominated by impurity collisions $\mu_e \sim T^{3/2}$, then $\ln(\sigma_e/T^3)$vs. $1/T$ is a straight line. In both cases, from the slope results the Arrhenius "energy" $\Delta E = (E_c - E_f)$ of the electronic conduction. The preexponential factor $\sigma_0 = N_c q\mu_e$ results from the intersection of the straight line with the ordinate. In this paper I will give formulas for ΔE in terms of the densities and positions of the allowed energy levels in the monocrystalline semiconductor.

The space charge limited conduction in the semiconductor is similar to the thermionic diode. The difference consists in that in the semiconductor the electrons interact with the crystal. Denoting by ε the permittivity, V the tension, L the width of the SCLC,

$$J = \frac{9}{8}\,\theta_n\,\varepsilon\,\mu_e(V^2/L^3) \tag{15}$$

θ_n is the fraction of free electrons (all electrons above the Fermi level) a similar expression holds for holes. [3] This relation is an instance of a general scale relation,[4] for volume currents with space charge in a uniform medium : $J \sim L(V/L^2)^m$, where m is a rational constant. E.g. in insulators without ionised donors $m = 2$ and for charge recombination $m = 1/2$.

Deep impurity levels in the crystal can lead to greater powers in the dependence $J(V)$. In Fig. 3 the current-voltage characteristic for SCLC is drawn, SCLC appears at the first threshold. The voltage $V_{\Omega c}$ results from the equality of the Ohmic current density with that for SCLC :

$$V_{\Omega c} = \frac{8}{9}\,(qnL^2/\varepsilon\theta_n)$$

The second threshold corresponds to a Fermi level near the single level V_{TFL} (trap filled voltage). At V_{TFL} all space charge enters the conduction or valence band, producing an abrupt increase of the characteristic $J(V)$. The threshold voltage depends on the density of impurities by : $V_{TFL} = N_m qL^2/\varepsilon$. For voltages $V > V_{TFL}$, SCLC appears. In the following the Arrhenius energies for Ohmic and SCLC conduction will be compared.

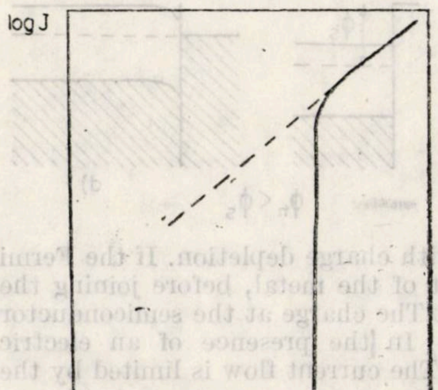

Fig. 3. — The double logarithmic diagram of the current vs. potential.

2. THE FERMI LEVEL IN MONOCRYSTALLINE SEMICONDUCTORS

In intrinsic, nondegenerate semiconductors, at high T (at which the energy gap is a small multiple of kT), in which the intrinsic excitation predominantes, by denoting m_e and m_h the effective masses, that do not differ much, the Fermi integrals reduce to the nondegenerate Maxwell-Boltzmann form. From the equality of equations (6) and (7) above, the Fermi level is :

$$E_f = \frac{1}{2}\,(E_v + E_c) + \frac{3}{4}\,kT\ln\,(m_h/m_e) \tag{16}$$

At the increase of T, E_f differs from the middle of the gap with a quantity that depends on the ratio of the effective masses of the electrons and holes. Their intrinsic concentration results from the electroneutrality equation :

$$n_0 = n = p = (N_v N_c)^{1/2} \exp (E_g/2kT) \tag{17}$$

$E_g = E_c - E_v$ is the gap width. Over the room temperature, in the majority of the materials, E_g depends linearly on $T : E_g = E_g^0 - \gamma T$. ($E_g^0 =$ = the gap at o K.) This relations is valid up to 100 K if E_g^0 is the intersection with the axis $T = 0$ of the extrapolated linear region.

In small gap semiconductors (HgTe) and degenerated, the Fermi level differs from the conduction band and the valence band only by a few kT. Also degenerated are the semiconductors with big difference between m_e and m_h. In this case the Fermi level is near the lightest charges band (InSb) where $m_h \sim 10 \cdot m_e$). The valence band is nondegenerate but the conduction band has the Fermi distribution. Thus :

$$n = N_c \cdot (\text{Fermi integral}) = N_v \exp ((E_v - E_f)/kT) \tag{18}$$

The Fermi integral is approximated by :[5]

$$\frac{\exp ((E_f - E_c)/kT)}{1 + 0.27 \exp ((E_f - E_c)/kT)} \tag{19}$$

A quadratic equation for E_f results, which in InSb is under $5kT$ from the conduction band, even at 200 K and enters the conduction band at 440 K.

In Fig. 4 the dependence of $n_0 T^{-3/2}$ on T^{-1} for InSb is represented, ($E_g^0 = 0.26$ eV, $\gamma = 2.7 \times 10^{-4}$ eV K^{-1}, $m_e = 0.1\ m$, $m_h = 0.2\ m$). The line (a) for nondegenerate statistics and the line (b) for degenerate conduction band [6].

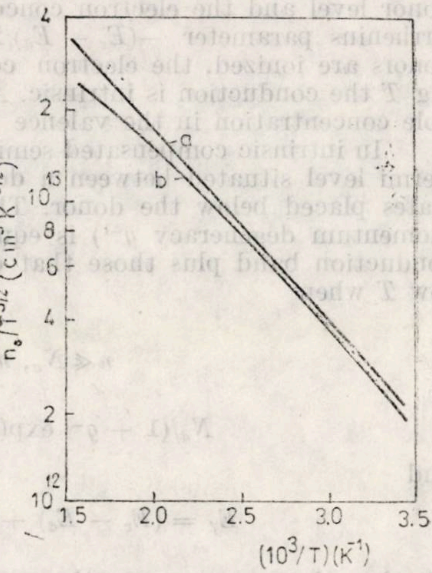

Fig. 4. — The intrinsic electron concentration dependence on temperature in a conveniently renormalized drawing.

In a solid containing both donors and acceptors,

$$p + n_d^+ = n + n_a^+ \tag{20}$$

where n_a^- and n_d^+ are the densities of acceptors and donors. Instead of solving this equations for E_f, the Fermi level E_f is determined in a few particular cases : Unique species of noncompensated impurities. We consider $N_a = 0$, and that there are enough donors for the intrinsic hole concentration to vanish. Let be N_d donors on the unit volume at the energy E_d (the degeneracy factor is considered 1). The equation reduces to $n_d^+ = n$, that is by neglecting the angular momentum degeneracy, to :

$$N_d/(1 + \exp((E_f - E_d)/kT)) = N_c \exp(E_f - E_c)/kT \tag{21}$$

By solving this equation in E_f and introducing the solution in the right term, the density of electrons results :

$$n = \frac{N_c}{2} \exp((E_d - E_c) / kT)) \left\{ -1 \pm \left(1 + \frac{4N_d}{N_c} \exp((E_c - E_d)/kT)\right)^{1/2} \right\} \tag{22}$$

(i) For low donor concentration or at high temperatures,

$(4N_d/N_a) \exp((E_c - E_d)/kT) \ll 1$. expanding the binomial we get $n = N_d$ (23)

All donor atoms are ionized and the electrons are in the conduction band.
(ii) In the limit $(4N_d/N_c)\exp((E_c - E_d)/kT) \gg 1$.

$$n = (N_c N_d)^{1/2} \exp((E_d - E_c) / 2kT) \tag{24}$$

A semilogarithmic graphic of the conductivity vs. $1/T$ for noncompensated donor species exhibits three different regions. At low T the Fermi level is near the half of the distance between the conduction band and the donor level and the electron concentration grows exponentially with an Arrhenius parameter $-(E_c - E_d)/2$. In the saturation region where all donors are ionized, the electron concentration is constant, $n = N_d$. For big T the conduction is intrinsic. An equivalent equation is valid for the hole concentration in the valence band of the semiconductor.

In intrinsic compensated semiconductors ($N_a \approx N_d$) we consider the Fermi level situated between a donor level and a set of deep acceptor states placed below the donor. The number of ionized donors (angular momentum degeneracy g^{-1}) is equal to the number of electrons in the conduction band plus those that occupy the N_a compensated states. At low T when

$$n \ll N_a,\ n_d^+ = N_a, \tag{25}$$

or

$$N_d/(1 + g^{-1} \exp((E_f - E_d)/kT)) = N_a \tag{26}$$

and

$$E_f = (E_c - E_d) + kT \ln(g(N_d - N_a)/N_a) \tag{27}$$

The free electron concentration results :

$$n = gN_c(N_d(N_a - 1) \exp((E_d - E_c)/kT) \tag{28}$$

The Arrhenius parameter for the conduction neglecting the dependence on temperature of the mobility is $(E_d - E_c)$, double the noncompensated value. In the quasiintrinsic or nonextrinsic conduction for semiconductors with large gap,[7] Fig. 5 represents the fact that at every T there exists a single predominant energy level, for each type of particle : a deep donor E_q and a deep acceptor E_m. The Fermi level is between the two predominant levels such that the electron concentration in E_m is equal to the hole concentration in E_q. The electroneutrality equation is written : $n_m = p_q$, or

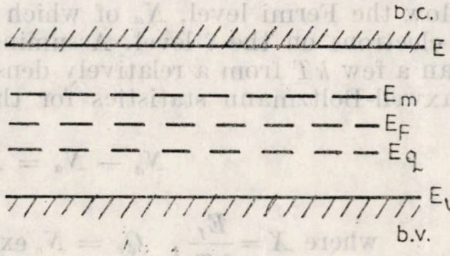

Fig. 5. — The qualitative diagram of energy states in the semiconductor gap.

$$N_m \exp((E_f - E_m)/kT) = N_q \exp((E_q - E_f)/kT) \tag{29}$$

which leads to ;

$$E_f = \frac{1}{2}(E_m + E_q) + \frac{1}{2}\, kT \ln (N_q/N_m) \tag{30}$$

To obtain the Arrhenius parameter of Ohmic conduction in n-type semiconductors, the number of electrons in the conduction band is necessary :

$$n = N_c(N_q/N_m)^{1/2} \exp((E_c - E_m)/2kT + (E_c - E_q)/2kT) \tag{31}$$

This equation leads to the Arrhenius parameter

$$\Delta E = (E_c - E_m) + (E_m - E_q)/2 \tag{32}$$

Just as in the intrinsic case, the fraction of the electron concentration which is excited out of the hole predominant level is called nonextrinsic.

3. SEMICONDUCTOR STATISTICS

The semiconductor statistics problem leads to two Arrhenius parameters the extrinsic and the nonextrinsic cases, which are distinguished by comparing the Ohmic and SCLC Arrhenius parameters.

The Fermi level is determined by the equation :

$$N = \sum_i n_i = \sum_i N_i(1 + \exp((E_i - E_f)/kT))^{-1}, \text{ where} \tag{33}$$

$N = N_v + N_d + \sum_{j=1}^{k} N_j - N_a$ is the total electron number in the system and the degeneracy factors are ignored. N_v is the effective number of valence states which contribute each with one electron, N_d is the number of donors, N_j is the number of localized states at one, the j-th, of the levels below the Fermi level, N_a of which are acceptors, and n_i is the number of electrons on the i level. Assuming that the Fermi level is no farther than a few kT from a relatively dense local level filled with electrons, the Maxwell-Boltzmann statistics for the particle distribution leads to

$$N_d - N_a = XQ_e - Q_h X^{-1} \tag{34}$$

$$\text{where } X = \frac{E_f}{kT}, \quad Q_e = N_c \exp\left(\frac{-E_c}{kT}\right) + \sum_i N_i \exp\left(\frac{-E_i}{kT}\right),$$

$$Q_h = N_v \exp\left(\frac{E_v}{kT}\right) + \sum_j N_j \exp\left(\frac{E_j}{kT}\right)$$

The largest terms of each partition function Q_e and Q_h define two dominant levels, m for electrons and q, for holes, E_m can be E_c or an E_i and E_q can be E_v or an E_j.

In n-type materials $(N_d > N_a)$ the solution of the above equation is

$$X = (N_d - N_a)/2Q_e + ((N_d - N_a)/2Q_e)^2 + Q_h/Q_e)^{1/2} \tag{35}$$

For p-type materials $(N_a > N_d)$ the negative square root must be chosen which leads to the equivalent result for holes. The formula for X leads to Arrhenius parameters which vary continuously with T. A constant value of the Arrhenius parameter, i.e. a straight Arrhenius diagram ($\ln J$ vs. $1/T$) two conditions are necessary : (i) The dominant levels in Q_e and Q_h dominate the statistics, i.e.

$$Q_e \approx N_m \exp(-E_m/kT) \text{ and } Q_h = N_q \exp(E_q/kT) \tag{36}$$

and (ii) $(N_d - N_a)$ must be $\gg 2(Q_eQ_h)^{1/2}$ or $\ll 2(Q_eQ_h)^{1/2}$. The Fermi level results :

$$E_f = E_m + kT \ln((N_d - N_a)/N_m) \text{ for } (N_d - N_a) \gg 2(Q_eQ_h)^{1/2} \tag{37}$$

$$\text{and } E_f = \frac{1}{2}(E_m + E_q) + \frac{1}{2} kT \ln(N_q/N_m) \text{ for } (N_d - N_a) \ll 2(Q_eQ_h)^{1/2}.$$

The first formula for E_f is the same, up to the degeneracy factor which was here neglected, with the case of extrinsic semiconductors, containing both donors and acceptors. The second formula is the same with formula deduced above in the non-extrinsic case (intrinsic, semiintrinsic with a conduction or valence band predominant, or when no band is predominant).

The Arrhenius parameters are contained in the variables n and θ_n of

$$J_n = nq_c\mu(V/L), \quad J_{\mathrm{SCL}} = \frac{9}{8}\,\theta_n\varepsilon\mu_s(V^2/L^3)] \tag{38}$$

where n is the free particle or hole density and θ_n is the fraction of total particles or holes $\theta_n = N_c \exp((-E_c/kT))/Q_c$. When a level dominates the electron statistics, the trapping factor simplifies to :

$Q_n = n/n_m = (N_c/N_m) \exp(-(E_c - E_m)/kT)$. To get SCLC the concentration of electrons or holes introduced must exceed the concentration of the majority particles at thermal equilibrium in the Ohmic case. Thus SCLC is always extrinsic. In the Ohmic nonextrinsic case, the Arrhenius parameters for Ohmic and SCLC conduction differ and in the extrinsic case of Ohmic conduction the Arrhenius parameters for Ohmic and SCLC conduction are equal.

The relevance of this result consists in the fact that the Arrhenius parameter for Ohmic conduction cannot be interpreted nonambiguously. Only combined with the Arrhenius parameter for SCLC it can determine the value of all relevant energy levels. Otherwise it can determine the depth of a level (extrinsically) or the mean depth of two levels (nonextrinsic). By using only the Arrhenius parameter one can determine the concentration of the dominant levels and their place in the semiconductor gap. If V_{TFL} is accessible experimentally, then one can determine also the mobility or the effective mass of the free electrons ot holes, by (14).

4. THE TEMPERATURE DEPENDENCE OF THE ARRHENIUS PARAMETERS

One of the necessary conditions for a simple Arrhenius parameter, or straight line Arrhenius diagram, is that certain energy levels should predominate in the partition functions of the electrons and holes. At each T there must be only one predominant level, for each type of charge. The diagram $\ln J$ vs. $1/T$ can be divided in a number of distinct segments, characterized by different Arrhenius parameters. The value of T for which the Arrhenius diagram has an inflexion (at the intersection of extrapolated segments) determines additional relations between the densities of states. Some rules will be examined in the following for interpreting the changes in Ohmic Arrhenius parameters. The semiconductors are assumed nondegenerate (Maxwell-Boltzmann) and with degeneracy factors equal to 1.

The difference between the electron and hole concentrations in electrically neutral materials is determined by the ionization of the impurities. By using the notation $N_1 = (n - p)$, the difference between the densities of the impurity states that lose and that gain an electron, $(np)^{1/2} = n_0$, the intrinsic charge density, and $n_0^2 = n(n - N_1)$ which leads to :

$$n = \frac{1}{2}\,N_1((1 + 4n_0^2/N_1^2)^{1/2} + 1), \; p = \frac{1}{2}\,N_1(-1 + (1 + 4n_0^2/N_1^2)^{1/2}) \tag{39}$$

These two relations become for $n_0 \ll N_1$ or $n_0 \gg N_1$, in the first case, e.g. for small $T : n \approx N_1 + (n_0^2/N_1)$, $p \approx (n_0^2/N_1)$, and in second case, e.g for large T, $n \approx n_0 + \frac{1}{2} N_1$, $p \approx n_0 - \frac{1}{2} N_1$.

The temperature change of n for a set of N_1, is represented in Fig. 6. where $E_g^0 = 0.32$ eV, $\gamma = 3 \times 10^{-4}$ eV K^{-1}, $m_e = 0.1\ m$, $m_h = 0.2\ m$, n is equal to the density of free electrons or holes, (a) $N_1 = 2 \times 10^{16}$ cm^{-3}, (b) $N_1 = 10^{15}$ cm^{-3} (c) $N_1 = 0$, intrinsic. [6]

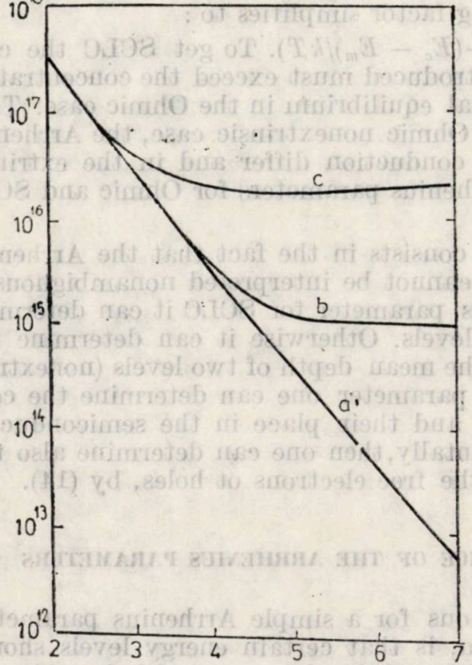

Fig. 6. — The density of electrons depending on the inverse absolute temperature.

The transition temperature between the intrinsic region (vc) and the extrinsic region depends on the difference between the intrinsic charge concentration and the impurity concentrations ($N_1 = N_d - N_a$).

The main cause of the variations in the Arrhenius parameter consists in a repopulation of the electronic states (excitation of donors, etc.) and a displacement of the Fermi level. Thus the interpretation of the variations of the Arrhenius parameter with T, resumes to the interpretation of the variations of the Fermi level.

If such a transition is due to the crossing of the Fermi level of a predominant level (of density N^*, and energy E^*) the charge balance equation is written :

$$N^* + N_d - N_a = XQ_c + N^*/(1 + X^{-1}) - Q_h/X, \quad X = \exp((E_f - E^*)/kT) \tag{40}$$

When the Fermi level crosses a localized energy level, the donor concentration or that of the acceptors varies according to the same level concentration. If the Fermi level decreases vs. T below a certain energy level, $N_d - N_a$ increases and if the Fermi level increases over a certain energy level, $N_d - N_a$ decreases. $N_d - N_a$ depends also on the concentration of the energy level crossed.

The principal causes of a transition between simple Arrhenius parameters (i) They are exhibited when the two predominant energy levels in the partition function become equal. By their equality at T_{12} (the intersection of the extrapolated straight segments of the Arrhenius diagram) for holes :

$$N_{q2} = N_{q1} ((E_{q1} - E_{q2})/kT_{12}) \tag{41}$$

where E_{q1} and N_{q2} describe the hole level most distant from the valence band. (ii) They are exhibited when the majority particles or holes change types. The majority charges are those for which the product charge x mobility is maximum. The equation :

$$N_q = N_m(\mu_c N_v/\mu_h N_v) \exp(((E_c - E_m) - (E_q - E_v))/kT_{12}) \tag{42}$$

is valid for nonextrinsic semiconductors both before and after the transition. This is the most usual case.
(iii) They are exhibited when the inequality between the extrinsic and nonextrinsic electrons or holes is reversed. The equation :

$$(N_q N_m)^{1/2} = (N_d - N_a) \exp((E_c - E_q)/2kT - (E_c - E_m)/2kT) \tag{43}$$

is valid for the extrinsic n-type case (more donors than acceptors). A similar equation holds in the p-type extrinsiv case. In the particular case of a transition nonextrinsic-extrinsic the additional relation holds

$$(N_d - N_a) \approx N_q.$$

5. THE EVALUATION OF THE ARRHENIUS DIAGRAMS

The following rules result from the above three equations :

(1) The increase of the slope with $(E_m - E_q)/2$, half the energy difference of the dominating levels, for majority and minority charges, in the extrinsic case, initially.

(2) The increase of the slope with $(E_{q1} - E_{q2})$, half of the difference of two successive energy levels dominating, of minority particles or holes, in the nonextrinsic case and if the majority charges do not change their sign.

(3) The increase of the slope is $(E_q - E_v) - (E_c - E_m)$ or the difference between the depths of the dominant levels of electrons or holes, if the initial condition is nonextrinsic and the majority charges change sign.

(4) The decrease if the slope is $(E_m - E_q)$ or half the difference between the dominant energy levels, if the final condition is extrinsic, E_q is

farther from the valence band than E_q of rule (1). Also it cannot be in the valence band.

(5) The decrease of the slope is $(E_{m2} - E_{m1})/2$ or half the difference of the successive dominant levels of majority particles or holes, if the final condition is nonextrinsic. This can happen if the initial condition is also nonextrinsic.

(6) The decrease of the slope usually implies that the initial condition is nonextrinsic. This rule is very useful for all types of semiconductors. The case of multivalent centers is described below.

The approximation of dominant levels is useful for the analysis of the Arrhenius diagrams of large gap materials. The number of electrons in a state of density N_i at the energy E_i can be written using the Maxwell-Boltzmann distribution :

$$n_i = N_i \exp((E_f - E_i)/kT), \tag{44}$$

and thus $\lg n_i = \ln N_i - 0.434\,(E_i - E_f)/kT$. Similarly for holes :

$$\lg p_j = \lg N_j - 0.434\,(E_f - E_j)/kT \tag{45}$$

Fig. 7 represents the quantity $\lg N_i$ vs. $0.434\,\varepsilon_i/kT$. A set of single localized energy levels are represented[7] with band densities N_c and N_v, $(E_i - E_f) = \varepsilon_i$ and $(E_f - E_j) = \varepsilon_j$. The continuous distribution of localized levels reduces to single equivalent densities. N_d and N_a are donor and aceptor levels which are not very deep, and the other levels are deep. The straight lines drawn have the slopes $0.434/kT$. When the peak of this V coincides with the Fermi level, the segment of the densities of states on the vertical exceeding the left side of this V, is the number of elec-

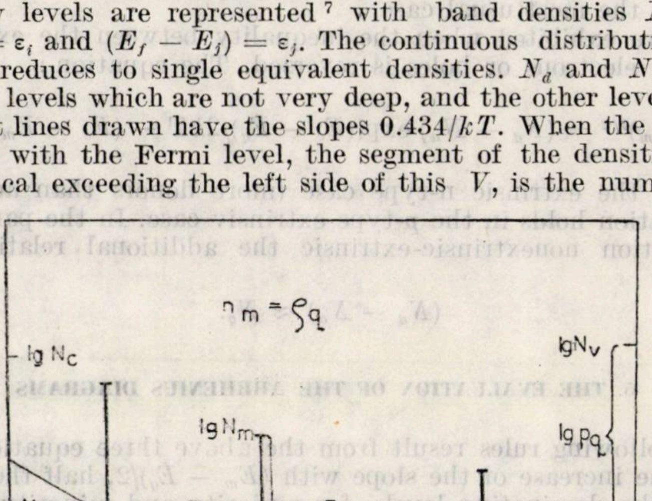

Fig. 7. — Diagram illustrating the method of evaluation of the Arrhenius graphs in the nonextrinsic case ($n_m = p_q$).

trons of those states and the segment on the vertical, of the densities of states exceeding the right side of this drawn V, is the occupation of the states with holes. The peak of this drawn V coincides with the Fermi level when one of the following two cases is valid: (1) the total number of electrons is equal with the number of holes, (nonextrinsic case), (ii) the total number of electrons or holes is equal to $(N_d - N_a)$ or $(N_a - N_d)$ which is the extrinsic condition. The drawn V is moved until the respective segments become equal. The dominant energy levels are those which exceed most above the drawn V. The total sum of the other states in the gap is often much smaller than the population of the dominant level. This is a criterion for a simple Arrhenius parameter to result. Thus one has a method to determine the Fermi level, when the Arrhenius diagram is straight, or simple. On Fig. 7 one remarks that $\lg (N_d - N_a) \sim \sim \lg N_d \ll \lg n_m$. When n_m or p_q found by this method become smaller than $N_d - N_a$ (or $N_a - N_d$) or for extrinsic materials, in order to find the Fermi level in the extrinsic case the drawn V should be moved until the maximum segment of a state density on the left (right) side of the V, becomes equal to $N_d - N_a$ (or $N_a - N_d$). This case is described in Fig. 8. [7,12]

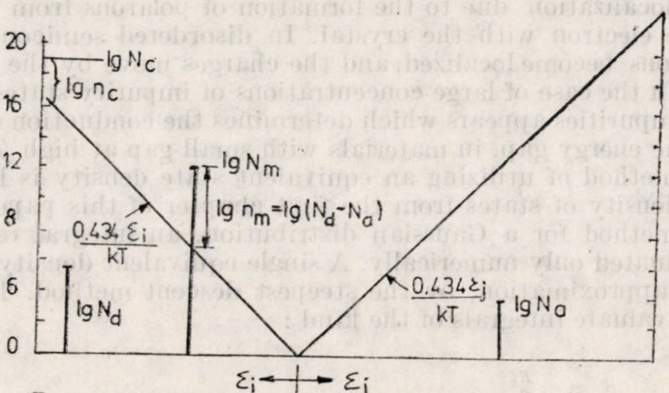

Fig. 8. — Diagram illustrating the method of evaluation of the Arrhenius graphs in the extrinsic case ($n_m = N_d - N_a$).

The result is unique for $N_d - N_a$ known. In order to place the Fermi level nonambiguously it is very important to know $N_d - N_a$ or if the extrinsic or nonextrinsic condition happens. Also it is important to know the Arrhenius parameters both in the Ohmic domain and in the SCLC. Otherwise it is sufficient to know the Arrhenius parameter for Ohmic conduction, if it is available on a large T interval and the variations of the Arrhenius parameter vs. T are followed.

Generally the Ohmic conduction measurements vs. T are not sufficient to interpret unambiguously the places of the dominant energy levels in the energy gap. There are cases in the literature when authors have interpreted incorrectly the slope of the Arrhenius diagram as an ionisation energy. Details on the characteristic energies and the concentration of localized states can be deduced from the variation both of Ohmic and SCLC conduction with T, over a large T interval.[8]

For all types of materials examined in this paper, there exists a correlation between the Arrhenius parameters and the preexponential factors for electric conduction σ_0 of the form[9]

$$\ln \sigma_0 = \alpha\, \Delta E + \beta, \quad \alpha, \beta \text{ constants} \tag{46}$$

The preexponential factor results from the ordinate at the origin of the Arrhenius diagram for the conductivity. Thus the diagram $\ln \sigma_0$ vs.ΔE is a straight line.

The following elements make difficult an evaluation by use of Arrhenius diagrams, of the energies, the densities of impurity states from the electric conductivity, even if the energy band structure is known. 1. Spatial fluctuations of the intrinsic gap and of the impurity densities. These fluctuations are considered that they move the Fermi level less than kT. The production of states in the energy gap as excited states of the donors or acceptors. The energies and angular momentum degeneration of the excited states differ from those calculated on a hydrogenoid with an effective mass and dielectric constant equal to those of the semiconductor.

The localization due to the formation of polarons from the interaction of the electron with the crystal. In disordered semiconductors the wavefunctions become localized, and the charges move by the tunnel phenomenon. In the case of large concentrations of impurity states or defects, a band of impurities appears which determines the conduction on localized states in the energy gap, in materials with small gap at high T.

The method of utilizing an equivalent state density is known for a parabolic density of states from the first chapter of this paper. By using the same method for a Gaussian distribution, an integral results which can be evaluated only numerically. A single equivalent density is obtained with good approximation, by the steepest descent method. This method is used to evaluate integrals of the kind :

$$\int_{E_1}^{E_2} N(E) \exp((-E/kT))\, \mathrm{d}E \tag{47}$$

Let $N(E)$ be the distribution defined by the function $h(E) = \ln N(E)$. It determines the partition function $Q = \int_{E_1}^{E_2} \exp(g(E))\ \mathrm{d}E$, where $g(E) = h(E) - \dfrac{E}{kT}$. The maximum value of this function lies in the interval (E_1, E_2) at E_0. By the Laplace method[17] the following value results for the integral :

$Q = (-2\pi/h''(E_0)) \exp(h(E_0))$. The function is compared with a single level placed somewhere within the distribution range, by using a Taylor expansion.

For the Gaussian distribution $N(E) = N_M \exp(-(E - E_M)/d^2)$ where N_M is the peak of the state density at the energy E_M and d is a constant. If the distribution ranges between E_A and E_B the partition function results from the equation :

$$Q_e = \int_{E_A}^{E_B} N_M \exp\left(-(E - E_M)/d^2 - E/kT\right) \mathrm{d}E. \tag{48}$$

An approximative evaluation of this integral is obtained as above : $Q_e = (2\pi kT(E_M - E_0))^{1/2} N_M \exp(-(E_M + E_0)/2kT)$, where E_0 is the energy at which the integrand is maximum. The relation takes place : $E_0 - E_M = -d^2/2kT$. The partition function is $Q_e = \mathrm{d}\pi^{1/2} \exp{(d/2kT)^2} N_M \exp{(-E_M/kT)}$. The effective density of states for a gaussian distribution around E_M is thus : $N_G = d\pi^{1/2} N_M \exp{(d/2kT)^2}$. The range of validity of this approximative formula can be studied by integrating numerically the formula for the Q_e partition function. The expressions coincide up to $5kT$.

The linear distribution is represented by equations of the form :

$$N(E) = N_y((E - E_x)/(E_y - E_x)) \tag{49}$$

where E_x and E_y are the extremes of the state distribution that varies between o and N_y. The integral in this case is exactly evaluated and results in an effective state density at E_x for a linear distribution :

$$N_L = N_y(kT)^2/(E_y - E_x) \tag{50}$$

The exponential distribution is described by $N(E) = N_E \exp((E - E_c)/kT)$ where T_c describes the way in which the concentration decreases with energy and E_x is an extremity of the distribution. The integral is exactly evaluated and results in different formulas according to $T_c > T$ or $T_c < T$.

For multivalent donors or acceptors, or amphoters (donors or acceptors according to the place of the Fermi level), the energy states are complex. For divalent donors [10,11] the energy level diagram is in Fig. 9 : (a) is the neutral state. (b) the monoionized state, (c) the double ionized state. When the Fermi level is near the conduction band edge, as in Fig. 9,

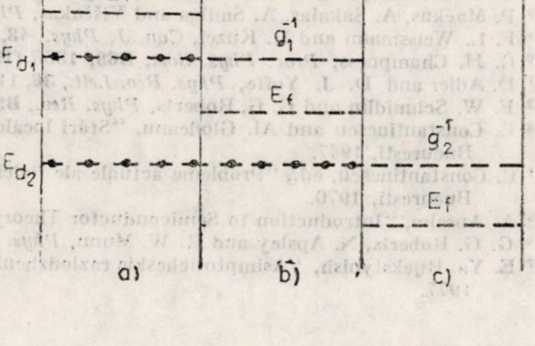

Fig. 9. — Energy levels of bivalent donors, and Fermi levels of semiconductors.

(a), each donor atom is electrically neutral and has two weakly bound electrons with binding energies $(E_c - E_{d1})$ and $(E_c - E_{d2})$. These energies can be close. In Fig. 9 (b) the Fermi level is between the energies E_{d1} and E_{d2} such that the donor is monoionized. The vacant states are at the energy E_{d1} and with statistical weight g_1^{-1}. In Fig. 9 (c) the Fermi level is below both donor levels. In this doubly ionized state the vacancy is at energies E_{d2} with statistical weight g_2^{-1}. The less deep level should be considered therefore only when an electron is trapped by a donor atom. Just as in the monovalent case, the compensation determines if the Fermi level is fixed at E_{d1} or E_{d2}. If the number of acceptor atoms is small, $N_a < N_d$ then the Fermi level is near E_{d1} at low T and :

$$n = g_1 N_c(N_d/N_a - 1)\exp((E_{d1} - E_c)/kT \tag{51}$$

where N_d is the total number of bivalent donors. If $N_d < N_a < 2N_d$, the electron density outside the saturation region is $2N_d - N_a$ and the low T region of the Arrhenius parameter equals $(E_c - E_{d2})$. Similarly for acceptors

In references [13–16] several case studies are presented and results from solving the electroneutrality equation.

Table 1

The Arrhenius parameters deduced from the electroneutrality equation (33)

Semiconductor	Electroneutrality equation	Arrhenius parameter
Intrinsic	$n = p$	$(E_c - E_v)/2$
Monoionized impurity	$n = n_d^+$	$(E_c - E_d)/2$
Extrinsic compensated	$n_d^+ = N_a$	$(E_c - E_d)$
Nonextrinsic	$n_m = p_q$	$(E_c - E_m) +$ $+ (E_m - E_q)/2$

REFERENCES

[1] E. M. Conwell and V. F. Weisskopf, *Phys. Rev.*, **77**, 388 (1950).

[2] L. V. Azaroff and J. J. Brophy, "Electronic Processes in Materials", McGraw Hill, New York, 1963, p. 217.

[3] R. H. Tedgold, "Space Charge Conduction in Solids", Elsevier, New York, 1966.

[4] P. N. Murgatroy, *Thin Solid Films*, **17**, 335 (1973).

[5] L. Austin and R. D. McClymont, *Physica*, **20**, 1077 (1954).

[6] J. S. Blakemore, "Semiconductor Statistics", Pergamon, London, 1962.

[7] G. G. Roberts, and F. W. Schmidlin, *Phys. Rev.*, **180**, 785 (1969).

[8] P. Mačkus, A. Sakalas, A. Smilga and Viščakas, *Phys. Stat. Solidi*, **A2**, 171 (1970).

[9] F. L. Weissmann and R. Kuzel, *Can. J. Phys.*, **48**, 63 (1970).

[10] C. H. Champness, *Proc. Phys. Soc.*, **B69**, 1335 (1956).

[11] D. Adler and D. J. Yoffe, *Phys. Rev. Lett.*, **36**, 1197 (1976).

[12] F. W. Schmidlin and G. G. Roberts, *Phys. Rev.*, **B9**, 1578 (1974).

[13] C. Constantinescu and Al. Glodeanu, "Stări locale în semiconductori", Editura Academiei, București, 1967.

[14] C. Constantinescu, ed., "Probleme actuale ale fizicii semiconductorilor," Editura Academiei, București, 1970.

[15] A. Anselm, "Introduction to Semiconductor Theory", Mir Publishers, Moscow, 1981.

[16] G. G. Roberts, N. Apsley and R. W. Munn, *Phys. Rep.*, **60**, 59 (1980).

[17] E. Ya. Rijckstynish, "Asimptoticheskie razlodzhenija integralov" Vol. 2. Izd. Zinatne, Riga, 1977.

Revue Roumaine de Chimie, **36**, *9–10*, 1093–1100 (1991)

DEL RE CALCULATIONS FOR PHOSPHORUS COMPOUNDS. BOND AND ATOMIC PROPERTIES

LUDOVIC KURUNCZI, RADU VÂLCEANU and ZENO SIMON[a]

Institute of Chemistry, B-dul Mihai Viteazu, 24, 1900 – Timişoara, Romania
[a] Departament of Biophysics, Institute of Medicine, P-ţa 23 August, 2, 1900 – Timişoara, Romania

Received May 9, 1990

Semiempirical Del Re molecular orbital calculations were performed for trivalent phosphorus compounds containing the PH, PC, PF, PP and PCl bonds. The obtained bond polarities (bond charges) present a satisfactory correlation with infrared bond stretching frequencies. The attempt to correlate calculated net atomic charges with nuclear magnetic resonance shifts was less successful. This because of the diversity of the NMR data (measured in varied conditions for atoms with very different molecular environment) and of the calibration of the Del Re parameters, which was performed on the basis of molecular dipole moments that are related more directly to bond polarities than to atomic charges.

INTRODUCTION

In two previous notes [1,2] we developed a Del Re method for calculation of charge distributions in trivalent phosphorus compounds which allowed a satisfactory prediction of dipole moment values. Here we try to correlate our results with other experimental parameters which also depend on electronic distribution. We chose infrared bond stretching frequencies and nuclear magnetic resonance chemical shifts: the first generally depend [3] on bond property, such as bond order (mesomeric effect) or bond polarity (inductive effect); the second is generally considered to depend on an atomic property (net atomic charge).[4]

CORRELATION OF BOND CHARGE (POLARTY) WITH IR DATA

Infrared bond stretching frequencies are, roughly speaking, dependent on bond polarity [5] and also upon *pi* contributions to the bond; the last are negligible for our compounds. [6] Experimental data concerning stretching frequencies for phosphorus atom bonds are listed in table 1 together with the corresponding bond charges (polarities) calculated with our Del Re method with the parameters as described in our second note.[2]

Bond stretching vibrations in polyatomic molecules almost always imply the coupling of vibrations of bonds. Fermi resonances may also intervene. The larger the functional groups adjacent to the studied bond

Table 1

Polarities and stretching frequencies (cm^{-1}) for bonds with P atoms

Comound	Bond^{a}										Reference
	PH^{b}		PF		PCL		PC		PC^{c}		
1	2	3	4	5	6	7	8	9	10	11	12
$HP(CF_3)_2$	−0.1941	2360							+0.1312	443	9
H_2PCF_3	−0.1281	2343.5^{d}							+0.1923	419	10
$HPCH_3(CF_3)$	−0.1036	2329					−0.1929	691	+0.2149	421	11
$(CH_3)HPP(CF_3)_2$	−0.1009	2335					−0.1862	707	+0.1786	445	12
H_2PPF_2	−0.0706	2314	+0.1021	828							13
H_2PCH_2Cl	−0.0645	2303^{e}									14
H_2PPH_2	−0.0620	2312									15
H_2PCH_3	−0.0534	2309					−0.0674	685.25^{f}			16,17
$HP(CH_3)_2$	−0.0503	2288					−0.0597	681.5^{g}			18,8
PF_3			+0.0937	892^{s}							19
$ClPF_2$			+0.0974	864.5^{s}	+0.0308	543.7					20
HPF_2			+0.0989	848^{s}							21
$FPCl_2$			+0.1015	838^{s}	+0.0441	521					22
$(CF_3)PF_2$			+0.0460	870							23
$F_2PP(CF_3)_2$			+0.0474	844					+0.1807	454	13
$FP(CF_3)_2$			+0.0523	855							23
F_2PCCl_3			+0.0651	852^{h}							23
F_2PPF_2			+0.0959	837^{i}							20
$(CH_3)PF_2$			+0.1090	806^{j}			−0.1179	701			24
$(CF_3)PCl_2$					−0.1212	523^{k}			+0.2222	429	25

$(CH_3)(CF_3)PCl$					−0.1020	516	−0.1678	700	+0.2242	425.3	11
Cl_2PPCl_2					+0.0629	507.5					26
$(CH_3)PCl_2$					+0.1057	495	−0.1070	699			27
$ClP(CH_3)_2$					+0.1744	481	−0.0868	695[l]			28,29
PCl_3					+0.0587	507					26
$(CH_3)P(CF_3)_2$							−0.3142	725			30
$(CH_3)(CF_3)PP(CF_3)(CH_3)$							−0.2025	695	+0.2114	422.3	11
$(CF_3)P(CH_3)_2$							−0.1582	696.5[m]			30
$P(CH_3)_3$							−0.0548	682[n]			31
$(CF_3)_2PP(CF_3)_2$									+0.1221	442	32
$P(CF_3)_3$									+0.0729	460[o]	33

[a] The two columns for each bond represent the bond polarity as calculated by our method, and the bond stretching frequency.

[b] The data pairs for PH_3 (−0.0589; 2325.5 cm^{-1}) [34], HPF_2 (−0.0774; 2240 cm^{-1}) [21] and $(CH_3CH_2)_2PH$(−0.0586; 2280 cm^{-1}) [35] do not correlate with the other PH containing compounds — the first two cases belonging to separate, monoatomic, series (see text), the last one probably because of sterical influences.

[c] P—C bond within the P—CF_3 fragment.

Mean values of the symmetric and antisymmetric stretching frequencies:

[d] 2339 and 2348 cm^{-1};

[e] Mean value of 2328, 2314, 2300, 2290, and 2288 cm^{-1};

[f] 676.5 and 694 cm^{-1};

[g] 660 and 703 cm^{-1};

[h] 844 and 860 cm^{-1};

[i] 831 and 843 cm^{-1};

[j] 800 and 812 cm^{-1};

[k] 520 and 526 cm^{-1};

[l] 680 and 710 cm^{-1};

[m] 680 and 713 cm^{-1};

[n] 652 and 712 cm^{-1};

[o] 455 and 464 cm^{-1};

[s] The symmetric stretching frequency.

the higher the perturbation of the "pure" stretching vibration. In condensed phase intermolecular interactions will contribute with further perturbations. Therefore only gaseous phase spectra were considered in Table 1. Spectral data from different time periods, with different accuracy had to be used. The data from table 1 are tributary also to the interpretation of the infrared spectrum; only relatively recently such interpretations are really reliable for phosphorus derivatives (improvement of the methods of purification for the utilised samples, employment of various isotopic species in the vibrational assignment, and so on).[7,8] In several cases we considered the frequencies corresponding to the absorption peaks as stretching frequencies. Where both symmetric and antisymmetric vibrations exist we used the mean value of the corresponding frequencies, if not mentioned otherwise. One cannot expect therefore a really good correlation between stretching frequencies and polarities, but the general trend may be relevant.

The results of the correlations are listed in table 2. As expected and mentioned also by other authors [5] rather small and special groups of molecules are to be considered. For PX stretching frequencies, with X monoatomic, distinct series must be worked out if the adjacent R radicals are also monoatomic or if they are functional groups (polyatomic), probably due to different vibrational couplings. Where X is also a functional group, no such distinctions are possible.

Table 2[a]

Correlational results between bond charges (polarities) and stretching frequencies in R_2PX molecules.

PX-Bond	X-type	R-type	n	r
1	2	3	4	5
PH	m	f.g.	9	−0.937
PF	m	m	4	−0.988
PF	m	f.g.	7	−0.870
PCl	m	m	3	−0.987
PCl	m	f.g.	5	−0.954
PC	f.g.	f.g.	12	−0.836
PC[b]	f.g.	f.g.	10	−0.778

[a] m — monoatomic substituent;
f.g. — functional group (polyatomic substituent);
n — number of data pairs;
r — correlation coefficient;
[b] — P—C bond within the $P-CF_3$ fragment.

The correlational results of table 2 are rather modst, as obtained also by other authors, which performed polarity *vs.* stretching frequency correlations. As expected, the more simple the molecule (both X and R monoatomic) the better the correlation; the lowest correlation coefficients are obtained when both X and R are polyatomic. The general trend nevertheless exists: the more the *sigma* bond electrons are attracted toward the P atom, the higher the stretching frequency.

CORRELATIONS WITH NUCLEAR MAGNETIC RESONANCE DATA

According to Julg [36] ^{1}H nuclear magnetic resonance signals should be a good measure for atomic carge distributions, if perturbing factors are absent. Such factors are neighbour diamagnetic anisotropic and permanent dipole moment contributions to — as well as influences of the surroundings of the molecule on — the shielding. [37]

Table 3 lists ^{1}H NMR shifts and the atomic charges at the corresponding H-atoms calculated by our Del Re method. The NMR measurements were performed in rather different and nonstandardized conditions. For the first 19 compounds, the H atom is part of a CH bond adjacent to a PC bond and there is a good correlation between the shift and the ato-

Table 3

^{1}H NMR shifts and corresponding H atom charges

No	Molecule	(ppm)[a]	Atomic charge	References
1	2	3	4	5
1	$P(C\mathbf{H}_3)_3$	0.92	0.0707	46
2	$HP(C\mathbf{H}_3)_2$	1.06	0.0729	47
3	$H_2PC\mathbf{H}_3$	0.98	0.0763	47
4	$\mathbf{H}_3CP(CH_2CH_2)_2CH(OH)$	0.88	0.0779	48
5	$ClP(C\mathbf{H}_3)_2$	1.62	0.0849	46
6	$\mathbf{H}_3CP(CH_2Cl)_2$	1.19	0.0863	49
7	$FP(C\mathbf{H}_3)_2$	1.45	0.0886	46
8	$P(C\mathbf{H}_2CH_3)_3$	1.2	0.0891	50
9	$HP(C\mathbf{H}_2CH_2)_2O$	1.75	0.0905	51
10	$Cl_2PC\mathbf{H}_3$	2.18	0.0939	52
11	$F_2PC\mathbf{H}_3$	1.41	0.0987	46
12	$H_3CP(C\mathbf{H}_2Cl)_2$	3.72	0.1031	49
13	$H_2PC\mathbf{H}_2Cl$	3.78	0.1056	53
14	$Cl_2PC\mathbf{H}_2CH_2Cl$	2.78	0.1066	54
15	$ClP(C\mathbf{H}_2Cl)_2$	3.93	0.1155	49
16	$Cl_2PC\mathbf{H}_2Cl$	4.03	0.1170	52
17	$F_2PC\mathbf{H}_2Cl$	3.36	0.1218	52
18	$Cl_2PC\mathbf{H}ClCH_3$	4.31	0.1325	54
19	$H_2PC\mathbf{H}FCHF_2$	5.27	0.1491	55
20	$P(C\mathbf{H}_2O)_3CCH_3$	4.40	0.0903	56
21	$P(C\mathbf{H}_2OH)_3$	4.07	0.0931	57
22	$\mathbf{H}_3CPCl(C(CH_3)_3)$	1.52	0.0961	58
23	$H_3C\mathbf{H}_2CPCl(C(GCH_3)_3)$	1.88	0.1088	58
24	$(F_3C)_2PP(C\mathbf{H}_3)_2$	1.52	0.1175	59
25	$\mathbf{H}_3CP(CF_3)_2$	1.20	0.1859	60
26	$\mathbf{H}P(CH_3)_2$	3.12	0.0503	47
27	$\mathbf{H}_2PCH_3$	2.64	0.0534	47
28	$\mathbf{H}P(CH_2CH_2)_2O$	3.15	0.0588	51
29	$P\mathbf{H}_3$	1.8	0.0589	61
30	$\mathbf{H}_2PCH_2Cl$	3.40	0.0645	53
31	$H_2PB\mathbf{H}_2$	2.71	0.0706	13
32	$\mathbf{H}_2PCHFCHF_2$	2.73	0.0810	55
33	$(CF_2)_3C(OH)P\mathbf{H}_2$	2.96; 3.20	0.0831	62
34	$\mathbf{H}P(CF_3)_2$	4.57	0.1941	63

[a] ^{1}H NMR shifts with respect to tetramethylsilane

mic charge ($r = 0.932$). If the next 6 compounds (**20**—**25**) are added, the correlation fails. The reasons for this failure are: — compounds **24** and **25** contain two CF_3 groups, which are known to give anomalous behaviour in several repects (stability, bond lenghts, etc).[38-41] Compounds **22**, **23** have *tertio*-butyl groups at the P atom: strong steric repulsion may produce modifications in bond angles, hybridization and hereby, atomic electronegativities. For compounds **20** and **21** atomic charges were estimated utilising [2] modified Del Re parameters for CH and CO bonds [42,43], which are proposed to improve the agreement between the calculated and experimental properties (dipole moments, correlations with chemical shifts). These modified parameters are criticized by other authors.[44] Indeed, we obtain in compounds like $P(CH_2\mathbf{O})_3CH$ $P(CH_2\mathbf{O})_3CCH_3$ and $P(\mathbf{C}H_2\mathbf{O}H)_3\mathbf{CO}$ bond charges (polarities) with the negative end at the **C** atom adjacent to the phosphorus, and hence a total dipole moment of the molecules oriented towards the P atom. But, because of the dipole moments of the nonbonded electron pairs on the oxygens from compound **20** the molecular moment must be oriented in the opposite sense.[45] And, although for $H_3CC(\mathbf{C}H_2\mathbf{O})_3\mathbf{C}CH_3$ the **CO** bond moments calculated by us (with the above-mentioned parameters) are oriented naturally, towards the oxygens, the calculated molecular moment (1.65 D) differs considerably from the experimental one (2.71 D[45]). These inadvertences may explain the lack of correlation for compounds **20** and **21**.

No NMR shift-atomic charge correlation was attempted for the ^1H—NMR shift of PH bonds, because only few data could be found and because of our parametrization method. Namely, in the optimization process, one aims at the fit of molecular dipole moment data, without taking into account the contribution of the nonbonded electron pair at the P atom. [2] Therefore, one cannot expect a really good calculated atomic charge distribution around the P atom, but only realistic overall bond polarity values. The data for compounds **26**—**34** of Table 3 illustrate this assertion.

For the methyl substituted phosphine series (H_2PCH_3, $HP(CH_3)_2$, $P(CH_3)_3$) the calculated atomic charges on the carbon (-0.1615; -0.1589; -0.1573) parallel the ^{13}C—NMR chemical shifts (-4.6 ppm; 6.9 ppm; 17.1 ppm, positive values downfield from tetramethylsilane).[64] But a disagreement between the evaluated atomic charges and shifts (as for the above-mentioned compounds **20**—**34**) was observed also for ^{13}C—NMR shifts for other alkyl phosphines. For example for $C_7P(C_3H_7)_2$, the ^{13}C chemical shifts for Cα, Cβ and Cγ were 39.35, 18.03 and respectively 15.24 ppm (with respect to tetramethylsilane)[65] while the atomic charges calculated by us are -0.2523, $+0.0472$, -0.0424. The last two charges, although small as absolute values, are unnaturally inverted.

The above disagreements suggest that a systematic search for better entrance parameters, also for other bonds than those with P atoms, is worthwhile and we intend to do this in future.

CONCLUSIONS

Our attempt to correlate bond stretching frequencies with bond polarities can be considered satisfactory, if one takes into account the perturbations of bond frequencies in polyatomic molecules. The attempts to correlate NMR shifts with atomic charges were successful in more limited series. The type of calibration of our Del Re method suggests that calculated bond polarities are more reliable than atomic charges, and this may explain some of the failures in correlation with NMR shifts. Nevertheless bond polarities can be used instead of atomic charges in calculations of electrostatic intermolecular interaction energies or molecular electrostatic potentials as used in chemical structure — biological activity studies.

REFERENCES

[1] R. Vâlceanu, Z. Simon and L. Kurunczi, *Rev. Roumaine Chim.*, **34**, 377 (1989).

[2] L. Kurunczi R. Vâlceanu and Z. Simon, *Rev. Roumaine Chim.*, submitted.

[3] M. Davies (editor), "Infra-Red Spectroscopy and Molecular Structure", Elsevier Publishing Company, Amsterdam, 1963, chap. VII.

[4] Y. Yukawa, "Handbook of Organic Structural Analysis", W. A. Benjamin Inc., New York, 1965, p. 469.

[5] R. Gupta and B. Majee, *J. Organometall. Chem.*, **36**, 71 (1972).

[6] R. Vâlceanu, L. Kurunczi and Z. Simon, *Rev. Chim. (București)*, submitted.

[7] J. R. Durig, J. A. Meadows, Y. S. Li and A. E. Stanley, *Inorg. Chem.*, **22**, 4134 (1983).

[8] J. R. Durig, S. D. Hudson, M. R. Jalilian and Y. S. Li, *J. Chem. Phys.*, **74**, 772 (1981).

[9] H. Bürger, J. Cichon, J. Grobe and R. Demuth, *Spectrochim. Acta*, **29A**, 47 (1973).

[10] H. Bürger, J. Cichon, R. Demuth and J. Grobe, *Spectrochim Acta*, **29 A** 943 (1973).

[11] A. B. Burg, K. K. Joshi and J. F. Nixon, *J. Am. Chem. Soc.*, **88**, 31 (1966).

[12] A. B. Burg and K. K. Joshi, *J. Am. Chem. Soc.*, **86**, 353 (1964).

[13] H. W. Schiller and R. W. Rudolph, *Inorg. Chem.*, **10**, 2500 (1971).

[14] B. Fontal, H. Goldwhite and D. G. Rowsell, *J. Org. Chem.*, **31**, 2424 (1966).

[15] J. D. Odom, C. J. Wurrey, L. A. Carreira and J. R. Durig, *Inorg. Chem.*, **14**, 2849 (1975).

[16] A. G. Moritz, *Spectrochim. Acta*, **22**, 1015 (1966).

[17] H. R. Linton and E. R. Nixon, *Spectrochim Acta*, **15**, 146 (1959).

[18] J. R. During, M. G. Griffin and W. J. Natter, *J. Phys. Chem.*, **81**, 1588 (1977).

[19] I. W. Levin and S. Abramovitz, *J. Chem. Phys.*, **44**, 2562)(1966).

[20] R. W. Rudolph, R. C. Taylor and R. W. Parry, *J. Am. Chem. Soc.*, **88**, 3729 (1966).

[21] J. R. Durig, A. J. Zozulin, J. D. Odom and J. B. Streusand, *J. Raman Spectrosc.*, **8**, 259 (1979).

[22] A. Müller, E. Niecke and O. Glemser, *Z. anorg. allg. Chem.*, **350**, 256 (1967).

[23] J. F. Nixon, *J. Chem. Soc.*, **1964**, 2469.

[24] J.R. Durig, A. E. Stanley and M. R. Jalilian, *J. Raman Spectrosc.*, **10**, 44 (1981).

[25] J. E. Griffiths, *Spectrochim. Acta*, **21A** 1135 (1965).

[26] S. G. Frankiss and F. A. Miller, *Spectrochim. Acta*, **21A**, 1235 (1965).

[27] J. R. Durig, F. Block and W. Levin, *Spectrochim. Acta*, **21A**, 1105 (1965).

[28] J. R. Durig and J. E. Saunders, *J. Mol. Structure*, **27**, 403 (1975).

[29] J. Goubeau, R. Baumgärtner, W. Koch und U. Müller, *Z. anorg. allg. Chem.*, **337** 174 (1965).

[30] M. A. A. Beg and H. C. Clark, *Canad. J. Chem.*, **40**, 393 (1962).

[31] M. Halmann, *Spectrochim. Acta*, **16**, 407 (1960).

[32] A. B. Burg and J. F. Nixon, *J. Am. Chem. Soc.*, **86**, 356 (1964).

[33] H. Bürger, J. Cichon, J. Grobe and F. Häfter, *Spectrochim Acta*, **28 A**, 1275 (1972).

[34] T. Shimanouchi, "Tables of Molecular Vibrational Frequencies", consolidated volume I. National Bureau of Standards, Washington, 1972.

[35] A. B. Burg and P. J. Slota, jr., *J. Am. Chem Soc.*, **82**, 2148 (1960).

[36] A. Julg in "Topics in Current Chemistry" (F. L. Boschke, Editor), vol. 58, Springer Verlag, Berlin, 1975, p. 1.

[37] J. W. Emsley, J. Feeney and L. H. Sutcliffe, "High Resolution Nuclear Magnetic Resonance Spectroscopy", Pergamon Press, Oxford, 1965, vol. 1, p. 130—133, 136—138.

[38] J. E. Griffiths and A. B. Burg : *J. Am. Chem. Soc.*, **82**, 1507 (1960).

[39] C. J. Marsden and L. S. Bartell, *Inorg. Chem.*, **15**, 2713 (1976).

[40] M. H. Whangbo and K. R. Stewart, *Inorg. Chem.*, **21**, 1720 (1982).

[41] C. J. Marsden, *Inorg. Chem.*, **23**, 1703 (1984).
[42] J. Nagy and J. Réffi, *J. Organometall. Chem.*, **22**, 565 (1970).
[43] J. Nagy and L. Párkányi, *Acta Chim. Acad. Sci. Hung.*, **71**, 159 (1972).
[44] R. Gupta and B. Majee, *J. Organometall. Chem.*, **29**, 419 (1971).
[45] R. D. Bertrand, R. D. Compton and J. G. Verkade, *J. Am. Chem. Soc.*, **92**, 2702)(1970).
[46] H. Vahrenkamp and H. Nöth : *J. Organometall. Chem.*, **12**, 281 (1968).
[47] S. L. Manatt, G. L. Juvinall, R. I. Wagner and D. D. Elleman, *J. Am. Chem. Soc.*, **88**, 2689 (1966).
[48] H. E. Shook, Jr. and L. D. Quin, *J. Am. Chem. Soc.*, **89**, 1841 (1967).
[49] L. Maier, *Helv. Chim. Acta*, **54**, 1651 (1971).
[50] J. B. Hendrickson, M. L. Maddox, J. J. Sims and H. D. Kaesz, *Tetrahedron*, **20**, 449 (1964).
[51] P. Tavs, *Angew. Chem.*, **81**, 742 (1969).
[52] J. F. Nixon and R. Schmutzler, *Spectrochim. Acta*, **22**, 565 (1966).
[53] B. Fontal, H. Goldwhite and D. G. Rowsell, *J. Org, Chem.*, **31**, 2424 (1966).
[54] L. Maier, *Helv. Chim. Acta*, **52**, 1337 (1969).
[55] R. Fields, H. Goldwhite, R. N. Haszeldine and J. Kirman, *J. Chem. Soc.*, **C**, **1966**, 2075.
[56] R. D. Bertrand, J. W. Rathke and J. G. Verkade, *Phosphorus*, **3**, 1 (1973).
[57] J. W. Rathke, J. W. Guyer and J. G. Verkade, *J. Org. Chem.*, **35** 2310 (1970).
[58] W. Wolfsberger, *Chem. Ztg.*, **110**, 449 (1986).
[59] R. G. Cavell and R. C. Dobbie, *J. Chem. Soc.*, **A**, **1968**, 1406.
[60] A. B. Burg and I. B. Mishra, *Inorg. Chem.*, **8**, 1199 (1969).
[61] E. A. V. Ebsworth and G. M. Sheldrick, *Trans. Faraday Soc.* **63**, 1071 (1967).
[62] G. W. Parshall, *Inorg. Chem.*, **4**, 52 (1965).
[63] R. Fields, M. Green and A. Jones, *J. Chem. Soc.*, **A**, **1969**, 2740.
[64] F. J. Weigert and J. D. Roberts, *Inorg. Chem.*, **12**, 313 (1975).
[65] W. Wolfsberger, *J. Organometall. Chem.*, **317**, 167 (1986).

Revue Roumaine de Chimie, **36**, *9–10*, 1101–1106 (1991)

FLOW-VACUUM PYROLYSIS OF TRIBENZO[*a*, *e*, *i*]-[12]ANNULENE

MIRCEA D. BANCIU, [a] IOANA SIMION, [b] ANCA BANCIU, [b] AURICA PETRIDE, [b] and CONSTANTIN DRĂGHICI [b]

[a] Organic Chemistry Department, Polytechnic Institute, TCH, Spl. Independenţei 313, 76206 Bucharest, Roumania
[b] Center of Organic Chemistry, Roumanian Academy, 78100 Bucharest, Roumania

Received March 15, 1991

Flow-vacuum pyrolysis of tribenzo[*a*, *e*, *i* [12] annulene (1) at 500–550°/1 Torr affords as main product tribenzo[*b*, *f*, *j*]tetracyclo][$6.4.0.0.^{4,12}0^{5,9}$]dodeca-2, 6, 10-triene (2). The reaction mechanism is discussed.

INTRODUCTION

The E, E, E-tribenzo [*a*, *e*, *i*] [12] annulene (**1**) was obtained first by Staab and co-workers [1] [2] from the Wittig reaction between the ylide of 2, 2, bis(bromomethyl)-*trans*-stylbene and *o*-phthaldialdehyde; the polycyclic hydrocarbon **2** resulted as a by-product.

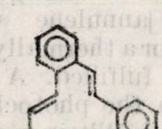

1

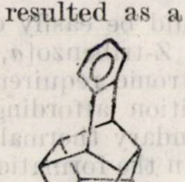

2

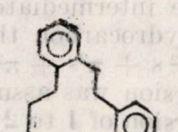

3

Later [3] the tribenzoannulene **1** was obtained by bromination-dehydrobromination of **3** (resulted on treatment of *o*-bis(bromomethyl)-benzene with sodium metal).

On the other hand, UV-irradiation of **1** affords the above-mentioned polycyclic hydrocarbon **2**.[3]

In view of these facts it seemed interesting to investigate also the thermal behaviour of tribenzo[12]annulene (**1**). The results of pyrolyses of **1** are described in the present short note.

RESULTS AND DISCUSSION

The tribenzoannulene **1**, prepared after literature data, was subjected to flow-vacuum pyrolysis in argon atmosphere. The relatively high thermal stability of **1** could be inferred from the result of pyrolysis at 500°/0.1 Torr when ⩾ 90% of the reaction product was the starting material.

Performing the same pyrolysis at 500 – 550°/1 Torr, a conversion of about 70 – 75% of **1** was achieved. The reaction mixture contains a single major component (v.p.c.-analysis) of about 40 – 45% along with unreacted **1**. Separation of this component by column chromatography permitted its identification (by ^{1}H-NMR-, IR- and UV-spectra) as tribenzo[*b*, *f*, *j*]tetracyclo$[6.4.0.0^{4.12}\,0^{5,9}]$dodeca-2,6,10-triene (**2**). The ^{1}H-NMR – (at 300 MHz) and ^{13}C-NMR spectra of **2** are presented in Fig. 1 and the attribution of the ^{13}C-signals in the following formula (δ ppm)-

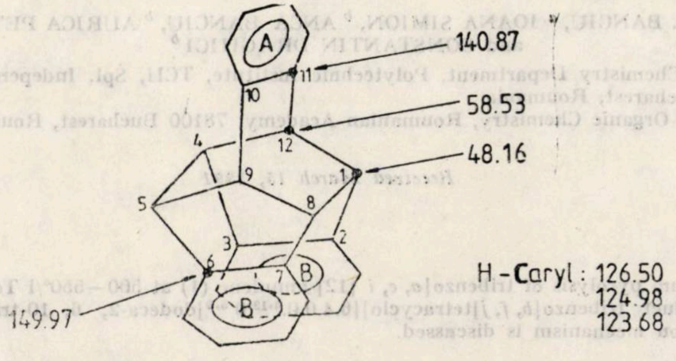

2

Pyrolyses of **1** at temperatures of ⩾ 600°/1 Torr conducted to the disappearance of the starting material accompanied by formation of **2** (24%) along with numerous minor components of about 1 – 8% each, which were not further investigated.

Formation of **2** from **1** could be easily explained assuming as unisolable intermediate the E, E, Z-tribenzo[*a*, *e*, *i*][12]annulene (**4**). In this hydrocarbon the stereoelectronic requirements for a thermally allowed $[\pi^2 s + \pi^2 s + \pi^2 s]$ cycloaddition affording **2** are fulfilled. A similar conversion was assumed as secondary thermal step in the photochemical conversion of **1** to **2** [3] as well as in the formation of **2** by Wittig reaction :[2]

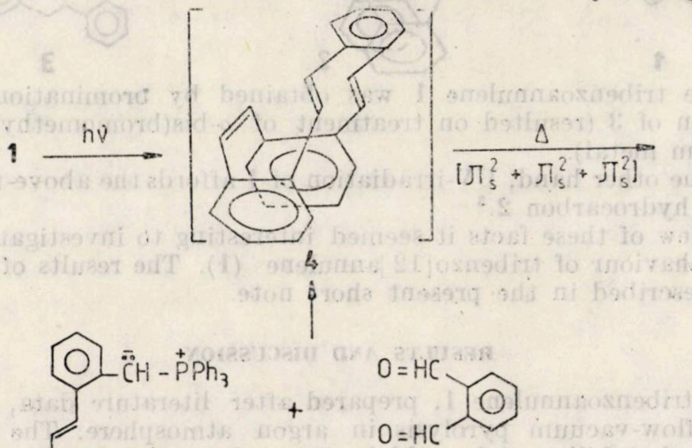

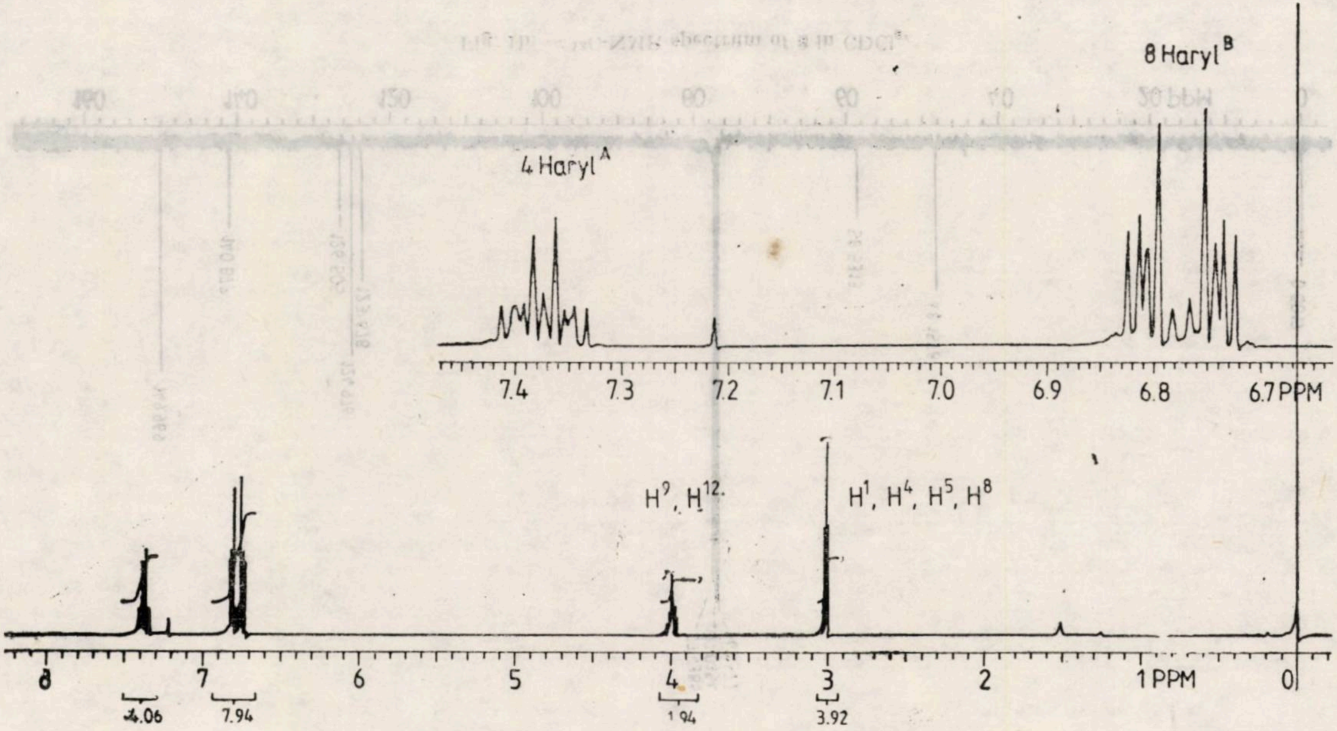

Fig. 1a.—^{1}H-NMR spectrum of **2** in $CDCl_3$.

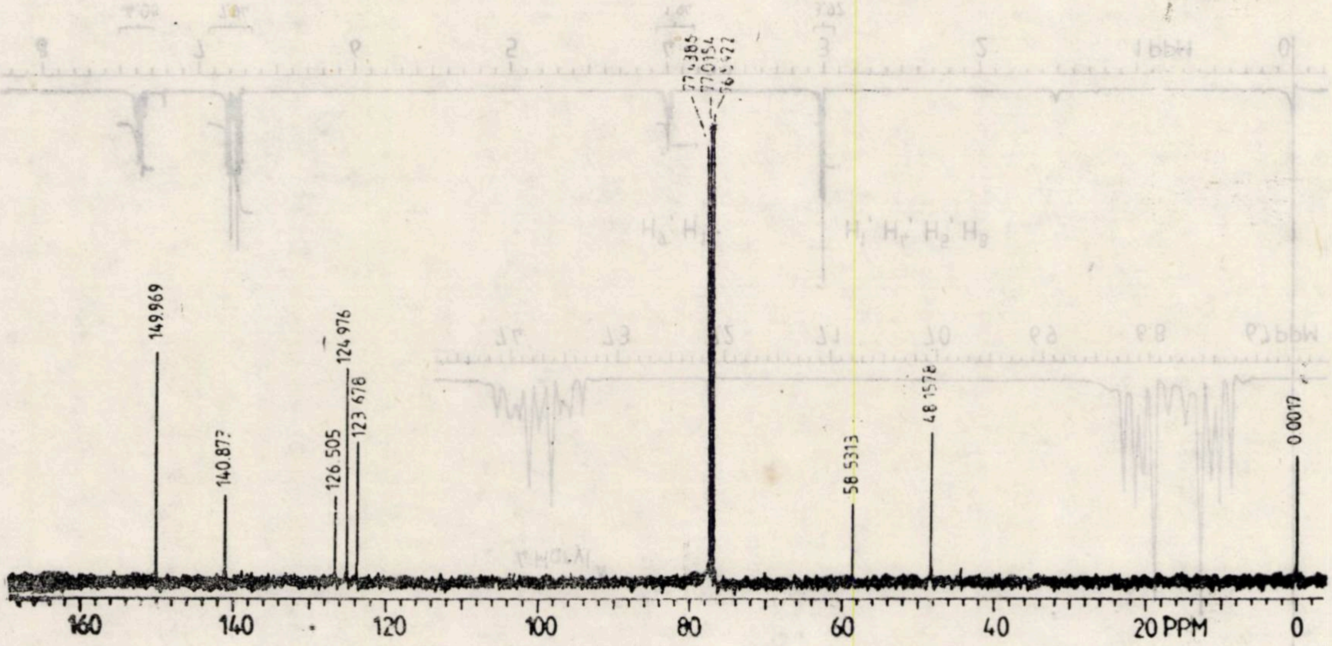

Fig. 1b. — ^{13}C-NMR spectrum of **2** in $CDCl_3$.

Concerning the thermal E → Z isomerisation of **1** to **4** a radicalic mechanism could be suggested including the diradical **5** as intermediate :

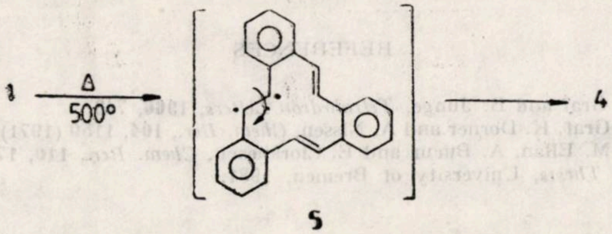

This relatively stable double benzylic diradical **5** which could occur thermally at 500–550° from **1** in gas-phase, permits the rotation around the diradicalic C–C single bond, which, followed by colligation, affords **4**.

Thus, pyrolysis of **1** seems to proceed analogously to its photolysis (**1** → **4** → **2**) the unique difference being the conditions by which the E → Z isomerisation of **1** to **4** is achieved : heating at 500–550°/1 Torr or respectively UV-illumination at room temperature.

EXPERIMENTAL

Melting points are uncorrected. NMR-Spectra were recorded on a GEMINI 300 MHz apparatus using TMS as internal standard. V.p.c-analyses were performed on a Carlo Erba model 2450 Fractovap in the following conditions : capillary glass column (25 m length ; 0 .25 mm internal diameter) with SE-methyl silicone polymer as stationary phase ; flame ionisation detector : temperature program — from 160° to 280° with 15°/min. ; carrier gas-hydrogen (2 mL/min).

E, E, E-Tribenzo[*a*, *e*, *i*][12]**annulene** (**1**) was obtained starting with *o*-bis(bromomethyl) benzene using the described procedure. The melting point (220° — after recrystallisation from acetone), IR-, UV- and ^{1}H-NMR-spectra were identical to the described ones.[1,2]

Tribenzo[*b*, *f*, *j*]**tetracyclo** [6 .4 .0 .$0^{4,12}$ $0^{5,9}$]**dodeca**-2, 6, 10-**triene** (**2**), was prepared by UV-illumination of **1**, using the described procedure.[3] The m.p. 252° (after recrystallisation from acetone), IR- UV- and ^{1}H–NMR-spectra were in agreement with the reported data.[1–4] The 300 MHz–^{1}H–NMR- and the ^{13}C–NMR spectra of **2** are presented in Fig. 1.

Flow-vacuum pyrolysis of E,E,E-tribenzo [*a*, *e*, *i*] [12] annulene (1)

The pyrolyses of **1** were performed in a pyrolysis apparatus comprising a pyrolysis quartz tube, inert gas inlet, vacuum source and a thermocouple. The sample of annulene **1** (usually 50 mg) was introduced in small portions under argon flow (4–5 mL/min) in the vertical pyrolysis tube (60 cm height, 20 mm diameter) filled with quartz chips on a portion of 30 cm ; this zone was electrically heated and the temperature was continuously measured. The vacuum of a vacuum pump was measured by a Mc-Leod manometer. The reaction product solidifies on the cold lower end of the pyrolysis tube. The obtained solid was taken in CH_2Cl_2, the solvent evaporated and the residual solid was subsequently v.p.c — analysed. For a pyrolysis at 510°/1 Torr the product contained 46 % **2**, 32 % **1** along with numerous minor components which were not further investigated. Performing the pyrolysis at 600°/1 Torr the v.p.c-analysis indicated : 24 % **2**, 2 .5 % **1** along with 20 minor components (of 1–8 % each) which were not further investigated.

From the crude pyrolysate of a reaction performed at 510°/1 Torr and using 200 mg starting material **1** a pure sample of polycyclic hydrocarbon **2** could be obtained by column chromatography on neutral alumina (Merck, activity I). Hydrocarbon **2** was eluted with petroleum ether whereas on elution with petroleum ether : diethyl ether (9 : 1) the unreacted starting material could be isolated. The hydrocarbon **2** thus obtained proved to be identical (m.p. ; IR-, ^{1}H–NMR- and UV-spectra) with the authentic sample prepared by illumination of **1** (see above).

ACKNOWLEDGEMENTS: Some technical help and useful discussions with Dr. Doina Constantinescu, Eng. Cătălina Hada and Dr. Michaela Stănescu are gratefully acknowledged.

REFERENCES

[1] H. A. Staab, F. Graf and B. Junge, *Tetrahedron Letters*, **1966**, 743.

[2] H. A. Staab, F. Graf. K. Dorner and A. Nissen, *Chem. Ber.*, **104**, 1159 (1971).

[3] M. W. Tausch, M. Elian, A. Bucur and E. Ciorănescu, *Chem. Ber.*, **110**, 1744 (1977).

[4] M. W. Tausch, *Thesis*, University of Bremen, 1981.

Revue Roumaine de Chimie, **36**, *9–10*, 1107–1112 (1991)

THE REACTION OF THE ANGULAR DIMER OF 1-METHYLBENZOCYCLOBUTADIENE WITH ELECTROPHILIC REAGENTS[1]

CORINA ILIE,[a] AURELIA GHENCIULESCU,[b] LUCIAN ENESCU[b] and
ILIE G. DINULESCU[c]

[a] Institute of Chemical and Pharmaceutical Research, Calea Vitan 112, 74373 Bucharest, Romania
[b] Organic Chemistry Department, Polytechnic Institute TCH, Spaliul Independenţei 313, 76206 Bucharest, Romania.
[c] Center of Organic Chemistry, Splaiul Independenţei 202 B, 77208 Bucharest, Romania.

Received August 31, 1990

The alkene **3** was attacked by electrophiles on the *exo* side exclusively. The structure and configuration of the obtained compounds are established by IR and ^1H–NMR spectra.

The previous papers in this series reported on the addition [2–5] and the rearrangement [6,7] reactions of the benzocyclobutadiene dimer, [8] with dibenzo [*b*, *g*] bicyclo [4.2.0] octa-2,4,7-triene (**1**) skeleton.

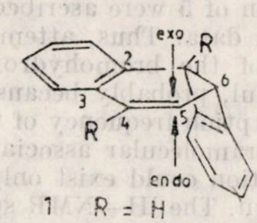

1 R = H

2 R = $C(CH_3)_3$

3 R = CH_3

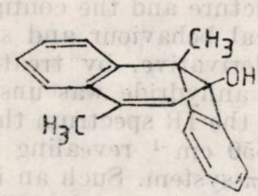

4

It has been shown that in the addition reactions, the double bond of the dimer **1** is sterically more accessible to electrophilic attack from the *exo* side of the molecule.[6]

Furthermore, the addition [11–14] and the rearrangement [13–16] reactions of the t-butyl derivative **2** were studied. In this case, the electrophilic attack occurs on the *endo* side of the molecule, because of the steric hindrance due to the t-butyl group. [10]

As a continuation of this work, we investigated the behaviour of the dimethyl derivative **3** [10] in the electrophilic additions in polar media. As regards the dimer **3**, only the oxidation in alkaline media yielding the alcohol **4** [16] has been studied.

Thus, treatment of the alkene **3** [10] with N-bromosuccinimide in glyme-water solution, produced the bromohydroxy derivative **5**, as the main compound; bromomethoxy derivative **6** was obtained when the reaction occurred in methanolic solution.

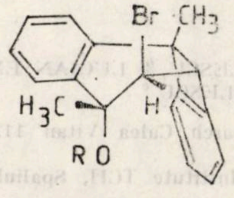

5 R = H
6 R = CH3

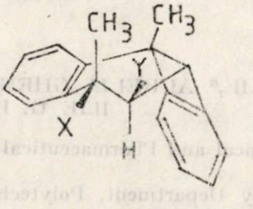

7 X = Y = OH
8 X = Y = Br

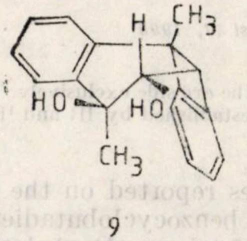

9

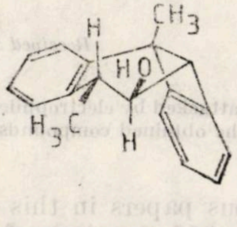

10

The structure and the configuration of **5** were ascribed on the basis of the chemical behaviour and spectral data. Thus, attempts to obtain an acetoxy derivative, by treatment of the bromohydroxy derivative **5** with acetic anhydride was unsuccessful, probably because the alcohol is tertiary. In the IR spectrum the absorption frequency of the OH group appears at 3550 cm^{-1} revealing an intramolecular association with the neighbouring π-system. Such an interaction could exist only if the 4-hydroxy group is in *endo-axial* configuration. The ^1H-NMR spectrum exhibits two doublet signals which were attributed to the protons H-5 and H-6. The value of the coupling constant $J_{5.6} = 10$ Hz, was used as an argument for an *endo-equatorial* orientation of the proton H-5 and *exo-axial* orientation of the bromine.[2,4]

In the methoxy derivative **6**, the *endo-axial* orientation of the methoxy group and *exo-axial* orientation of the bromine were also established on the basis of the coupling constant $J_{5.6} = 10.5$ Hz.[4] Furthermore, the signal of the methoxy group appears at higher field (δ 3.07 ppm), because of the shielding produced by the *endo*-oriented benzocyclobutene ring.[2]

The treatment of the bromohydroxy derivative **5** with sodium hydroxide gave the dihydroxy derivative **7**. The structure of the compound **7** was assigned by the ^1H-NMR using the results of the previous spectral studies in this series.[4] Thus, the small coupling ($J = 4.5$ Hz) between the protons H-5 and H-6 was considered an evidence for the *enodo-equatorial* orientation of the 4-hydroxy group and the *exo-equatorial* orientation of the 5-hydroxy group.[4]

The same configuration has been ascribed to the dibromo derivative **8**, obtained from alkene **3** and bromine in the methylene chloride solution. In the ^1H-NMR spectrum of this compound the protons H-5 and H-6 resonate at lower field than in the case of the dihydroxy derivative **7**, because of the bromine atom. Thus, these protons appear as two doublets at δ 4.31 ppm (H-5) and δ 4.24 ppm (H-6) with the coupling constant $J_{5,6} = 3$ Hz.[2,4]

A mixture of dihydroxy derivatives **7** and **9**, in ratio 1 : 1, was obtained from the reaction of alkene **3** with hydrogen peroxide and formic acid, followed by base-catalysed hydrolysis. Attempts to separate the hydroxy derivatives **7** and **9** were unsuccessful. The ratio and structures of the dihydroxy derivatives were assigned by ^1H-NMR spectrum of the mixture. This was compared with those of the authentic sample of **7** and other previously described compounds with similar structure.[3] Thus, the coupling constant between the protons H-5 and H-6 of dihydroxy derivative **9** ($J = 9.2$ Hz) was considered an evidence for the *exo-equatorial* configuration of the 4-hydroxy group and *endo-equatorial* configuration of the 5-hydroxy group. Moreover, the *endo-axial* oriented methyl group at C-4 exhibits an upfield signal (δ 1.71 ppm) because of the shielding produced by the benzocyclobutene ring.

The hydroboration of the alkene **3** gave the 5-hydroxy derivative **10**. The IR and ^1H-NMR spectra confirm the proposed structure of this compound. The *trans-axial* configuration for the protons H-4 and H-5 was ascribed on the basis of their coupling constant of $J_{5,4} = 8$ Hz. Moreover, the coupling constant $J_{5,6} = 6.5$ Hz, combined with the lack of the "long range" coupling between the protons H-4 and H-6 are evidences for the *exo-equatorial* orientation of the 5-hydroxy group and the *endo-equatorial* configuration of the 4-methyl group.

The observed results indicate that the electrophilic additions of the alkene **3** occur without rearrangement, likewise with the compounds **1** and **2**. The electrophile attack was produced on the *exo* side of the molecule, similarly to the unsubstituted alkene **1**, according to the usual rule.

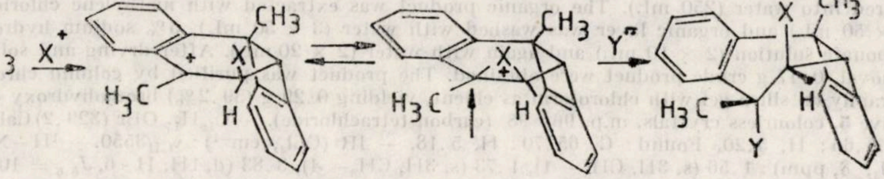

11 12 13

We assume that the intermediate ion **11** is in equilibrium with the nonclassical ion **12**. Therefore the stabilisation of this ion occurs on the *endo* side, namely at C-4 position. The position *endo*-5 is more hindered because benzocyclobutene ring.

In the reaction of the bromohydroxy derivative **5** in the presence of sodium hydroxide we have taken into account the possibility that an *endo*-epoxidic intermediate **14** was formed. This epoxide could not be isolated because of its instability.
It undergoes a ring opening by the reaction with the nucleophile at C-5 rather than at C-4 position.

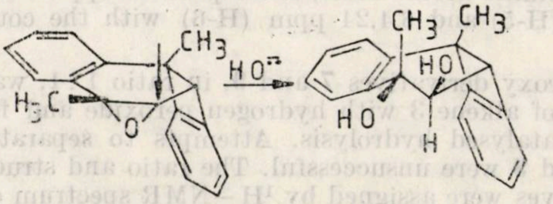

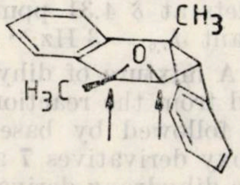

14 . 7 · 15

It is doubtless that in reaction of the alkene **3** with hydrogen peroxide and formic acid, an isomeric *exo*-epoxide **15** was formed, as unstable intermediate. The epoxidic ring opening occurred on the *endo* side, at both the C-4 and C-5 positions. In order to verify these assumptions we attempted to prepare the epoxides **14** and **15** by the usual methods, but until now unsuccessfully.

Further studies concerning the ionic reactions of the alkene **3** and of other derivatives with the same skeleton are in progress.

EXPERIMENTAL

IR spectra were recorded with a double beam Jena UR-20 spectrophotometer. ^1H-NMR spectra were performed with a Varian A-60A spectrometer. T.l.c. was carried out on plates coated with Kieselgel GF-254 (Merck) and column chromatography was performed using Aluminiumoxide 90-activity II–III (Merck) and Kieselgel 60 reinst (Merck). Petroleum ether refers to light petroleum (b.p. 35–50°).

exo-*5-Bromo-1, 4-dimethyl*-endo-*4-hydroxy-dibenzo* [b, g] *bicyclo [4.2.0] octa-2, 7-diene* (**5**). N-Bromosuccinimide (0.27 g, 1.5 mmoles) was added in small portions to a solution of the dimer **3** (0.35 g, 1.5 mmoles) in 7.8 mL glyme and 1.2 mL water; 0.1 mL conc. sulfuric acid was then added, the reaction mixture was left for 24 hrs at room temperature and then was poured into water (250 mL). The organic product was extracted with methylene chloride (3 × 50 mL) and organic layer was washed with water (3 × 50 mL), 5% sodium hydrogen carbonate solution (2 × 10 mL) and again with water (2 × 20 mL). After drying and solvent removal, 0.47 g crude product were obtained. The product was purified by column chromatography on silica gel with chloroform as eluent, yielding 0.29 g (59.2%) bromohydroxy derivative **5**, colourless crystals, m.p. 96–98° (carbon tetrachloride). – $C_{18}H_{17}OBr$ (329.2) Calcd.: C, 65.66; H, 5.20. Found: C, 65.70; H, 5.18. – IR (CCl_4, cm^{-1}): ν_{CH}3550. – ^1H-NMR (CCl_4, δ, ppm): 1.56 (s, 3H, CH_3– 1), 1.73 (s, 3H, CH_3– 4), 3.83 (d, 1H, H - 6, $J_{5.6} = 10Hz$), 4.26 (d, 1H, H – 5, $J_{5.6} = 10$ Hz), 6.90 – 7.90 (m, 8 H, aromatics).

exo-5-Bromo-1,4-dimethyl-endo-*4-methoxy-dibenzo* [*b*, g] *bicyclo* [*4.2.0*] *octa-2,7-diene* (**6**). A solution of the alkene **3** (0.56 g, 2.4 mmoles) in 23 mL methanol containing 0.1 mL conc. sulfuric acid was treated with 0.44 g (2.41 mmoles) N-bromosuccinimide in small portions (with stirring) at room temperature. The mixture was left for 24 hrs at 20°. After this time, the crystals which appeared on scratching, after cooling, were filtered and dried *in vacuo*. The product, methoxy derivative **6** (0.6 g, 72%) was a colourless compound, m.p. 143–145°. – $C_{19}H_{19}OBr$ (343.2) Calcd.: C, 66.48; H, 5.57. Found: C, 66.40; H, 5.60. – ^1H-NMR $CDCl_3$, δ, ppm): 1.58 (s, 3H, CH_3 – 1), 1.73 (s, 3H, CH_3 – 4), 3.07 (s, 3H, methoxy), 3.93

(d, 1H, H – 6, $J_{5.6}$= 10 .5 Hz), 4.36 (d, 1H, H – 5, $J_{5.6}$= 10 .5 Hz), 7 .20 – 7 .60 (m, 8H, aromatics).

endo-*4*-exo-*5-Dihydroxy-1,4-dimethyl-dibenzo* [b, g] *bicyclo* [*4.2.0*] *octa-2,7-diene* (**7**). A solution of 8 mL 0 .1 N aqueous sodium hydroxide (0 .8 mmoles) was added dropwise to a solution of 0.27 g (0.8 mmoles) bromohydroxy derivative **5** in 14 .5 mL DMFA at room temperature, and the mixture was stirred for 4.5 hrs. The mixture was extracted with methylene chloride (3 × 40 mL) and the organic layer was washed with water (3 × 50 mL) to neutral. After drying and solvent removal, 0 .18 g (85 .7 %) **7**, colourless crystals, m.p. 108 – 110°, were obtained. – $C_{18}H_{18}O_2$ (266 .3) Calcd. : C, 81 .17 ; H, 6 .81. Found : C, 81 .50 ; H, 7 .00. – IR (CCl_4, cm^{-1}) : ν_{OH}3575 large. – ^1H-NMR (CCl_4, δ, ppm) : 1 .30 (s, 3H, CH_3 – 1), 1 .86 (s, 3H, CH_3 – 4), 3 .11 (bs, 2H, OH), 3 .71 (d, 1H, H–6, $J_{5.6}$ = 4 .5 Hz), 3 .96 (d, 1H, H–5, $J_{5.6}$= 4 .5 Hz), 6 .90 –7 .80 (m, 8H, aromatics).

endo-*4*-exo-*5-Dibromo-1,4-dimethyl-dibenzo* [b, g] *bicyclo* [*4.2.0*]*octa-2,7-diene* (**8**). Bromine (0.18 g, 1.13 mmoles) in methylene chloride (10 mL) was added dropwise during 30 min to a solution of the dimer **3** (0.23 g, 1 mmole) in 20 mL methylene chloride, at room temperature. The mixture was kept at this temperature with stirring for 45 min. After solvent removal, 0.4 g crude product were obtained, containing dibromo derivative **8** and unreacted alkene **3**, in 1.5 : 1 ratio (by ^1H-NMR). This material was purified by preparative t.l.c. using petroleum ether as solvent. Attempts to separate the mixture by column chromatography were unsuccessful. Finally, 0.23 g (58.9 %) dibromo derivative **8**, colourless crystals, m.p. 127 – 130° (methylene chloride) were obtained. – $C_{18}H_{16}Br_2$ (392.1) Calcd. : C, 54.71 ; H, 4.11. Found : C, 54.84 ; H, 4.32. – ^1H-NMR ($CDCl_3$, δ, ppm) : 1.83 (s, 3H, CH_3–1), 2.23 (s, 3H, CH_3–4), 4.24 (d, 1H, H–6, $J_{5.6}$ = 3 Hz), 4.31 (d, 1H, H–5, $J_{5.6}$ = 3 Hz), 6.90–7.60 (m, 8H, aromatics).

4,5-Dihydroxy-1,4-dimethyl-dibenzo[b, g]*bicyclo* [*4.2.0*] *octa-2,7-dienes* (**7** and **9**). Alkene **3** (0.28 g, 1.2 mmoles) dissolved in 30 mL diethyl ether was treated with 3 mL (77.9 mmoles) 98 % formic acid and 1 mL (11.6 mmoles) 30 % hydrogen peroxide. The solution was refluxed for 4 hrs. The clear solution was allowed to cool to room temperature and afterwards the mixture was stirred twice for 5 min with 30 mL portions of 50 % sodium hydroxide solution. The organic phase was separated, washed with water (3 × 20 mL) until neutral and dried. Evaporation of the solvent yielded 0.27 g (85 %) crude product, m.p. 158 – 160°. T.l.c. of this mixture indicated the presence of two components. Attempts to separate the components were unsuccessful by column chromatography and preparative t.l.c. The ^1H-NMR spectrum showed a mixture of two alcohols in 1 : 1 ratio, identified as compound **7** (by comparison with an authentic sample obtained in the above experiment) and compound **9**.

exo-*4*-endo-*5-Dihydroxy-1,4-dimethyl-dibenzo* [b, g] *bicyclo* [*4.2.0*] *octa-2,7-diene* (**9**).– – IR (CCl_4, cm^{-1}) : ν_{OH} 3560 – 3590. – ^1H-NMR ($CDCl_3$, δ, ppm) : 1.26 (s, 3H, CH_3–1), 1.71 (s, 3H, CH_3–4), 3.10 (bs, 2H, OH) 3.33 (d, 1H, H–6, $J_{5,6}$ = 9.2 Hz), 3.65 (d, 1H, H–5, $J_{5,6}$ = 9 .2 Hz). 6.90–7.80 (m, 8H, aromatics).

exo-*5-Hydroxy-1,4-dimethyl-dibenzo*[b, g] *bicyclo*[*4.2.0*] *octa-2,7-diene* (**10**). Hydroboration of the alkene **3** was carried out by the classic procedure.[17] In the reaction flask 1 g (4.3 mmoles) alkene **3** in 5.3 mL tetrahydrofuran was dissolved. In the dropping funnel of the diborane generator a solution of 0.4 g (10.7 momles) sodium borohydride in 14 mL diglyme was placed and in the flask of the generator a solution of 1.8 g (12.7 mmoles) boron trifluoride etherate in 1.3 mL diglyme was placed. The installation was flushed with nitrogen and then the solution of the sodium borohydride was added dropwise for 2 hrs to the solution of boron trifluoride etherate. The diborane formed was passed through a sintered glass dispersion tube into the cooled solution contained in the reaction flask. When the addition was complete, the generator flask was warmed to 60° for 45 min. to drive residual diborane into the reaction flask. The reaction mixture was then allowed to stand at room temperature for 24 hrs. Water (0.4 mL) was added slowly, with cooling, followed by treatment with 0.5 mL of 12 % sodium hydroxide and 1 5 mL of 30 % hydrogen peroxide. The mixture was heated for 5 min on the water-bath, cooled and poured in 20 mL water. The organic phase was extracted with diethyl ether (5 × 15 mL) and the combined extracts were washed with water (3 × 20 mL). Drying and evaporation of the solvent gave 1.0 g crude product. The product was purified by column chromatography on alumina with petroleum ether as eluent, yielding 0.97 g (90.6 %) alcohol **10**, colourless crystals, m.p.

116–118°. – $C_{18}H_{18}O$ (250.3) Calcd. : C, 86.36 ; H, 7.24. Found : C, 86.20 ; H, 7.00. – IR (CCl_4, cm^{-1}) : ν_{OH} 3620. – ^1H–NMR ($CDCl_3$, δ, ppm) : 1.26 (d, 3H, CH_3–4), 1.76(s, 3H, CH_3–1), 2.15 (bs, 1H, OH), 2.97 (qv, 1H, H–4, $J_{4.Me}=7$ Hz, $J_{4.5} = 8$ Hz) 3.46 (dd, 1H, H–6, $J_{5.6} = 6.5$ Hz), 3.66 (dd, 1H H – 5, $J_{5.6} = 6.5$ Hz, $J_{4.5} = 8$ Hz), 7.10 – 7.80 (m, 8H, aromatics).

REFERENCES

[1] Part LXV in the series "Investigations in the Cyclobutane Series". For part LXIV see : L. Enescu, A. Ghenciulescu, F. Chiraleu and I. G. Dinulescu, *Rev. Roumaine Chim.*, **34**, 989 (1989).

[2] N. Ştefan, I. G. Dinulescu, F. Chiraleu and M. Avram, *Rev. Roumaine Chim.*, **20**, 1473 (1975).

[3] N. Ştefan, P. Filip, I. G. Dinulescu, F. Chiraleu and M. Avram, *Rev. Roumaine Chim.*, **29**, 631 (1984).

[4] N. Ştefan, P. Filip, F. Chiraleu and M. Elian, *Rev. Roumaine Chim.*, **29**, 861 (1984).

[5] N. Ştefan. P. Filip, I. G. Dinulescu and M. Avram, *Rev. Roumaine Chim.*, **30**, 589 (1985).

[6] N. Ştefan, I. G. Dinulescu and M. Avram, *Rev. Roumaine Chim.*, **21**, 107 (1976).

[7] N. Ştefan, P. Filip, I. G. Dinulescu and M. Avram, *Rev. Roumaine Chim.*, **30**, 791 (1985).

[8] M. P. Cava and D. R. Napier, *J. Amer. Chem. Soc.*, **79**, 1701 (1957).

[9] D. Constantinescu, I. G. Dinulescu, F. Chiraleu and M. Avram, *Tetrahedron Lett.*, 1969, 5215.

[10] P. Filip, N. Ştefan, F. Chiraleu, I. G. Dinulescu and M. Avram, *Rev. Roumaine Chim.*, **29**, 549 (1984).

[11] O. Constantinescu-Simon, I. G. Dinulescu and M. Avram. *Chem. Ber.*, **109**, 1294 (1976).

[12] O. Constantinescu-Simon, I. G. Dinulescu, D. Constantinescu, P. Filip, F. Chiraleu and M. Avram, *Chem. Ber.*, **109**- 1287 (1976).

[13] O. Constantinescu-Simon, I. G. Dinulescu and M. Avram, *Chem. Ber.*, **109**, 1301 (1976).

[14] O. Constantinescu-Simon, F. Chiraleu and M. Avram, *Chem. Ber.*, **110**, 1335 (1977).

[15] O. Constantinescu-Simon, F. Chiraleu and M. Avram, *Chem. Ber.*, **113**, 623 (1980).

[16] P. Filip, N. Ştefan, F. Chiraleu, I. G. Dinulescu and M. Avram, *Rev. Roumaine Chim.*, **29**, 557 (1984).

[17] H. C. Brown and B. C. Subha Rao, *J. Amer. Chem. Soc.*, **81**, 6428, (1959).

Revue Roumaine de Chimie, **36**, *9–10*, 1113–1122 (1991)

MESOIONIC OXAZOLONES. VI[1]

HYDROLYSIS OF ACYLATED DERIVATIVES

HORIA PETRIDE

Romanian Academy, Centre of Organic Chemistry,
Spl. Independenţei 202 B, 71141 Bucharest, Romania

Received May 26, 1989

Nonplanar acylated mesoionic oxazolones **10–16** underwent hydrolysis at ambient temperature, while their planar analogs **8–9** did it only at 100°C. The same trend in reactivity was observed in the case of the monocyclic compounds **34a** (planar) and **34b** (nonplanar). The attack takes place at the oxazolic ring of the mesoionic substrates, except in the case of **12b**. The ease of hydrolysis of **10–16** comes in between the 7-mono- and 7-dichloroacetyloxy functions in **12a** and **12b**, respectively.

The behaviour of the mesoionic oxazolones ("münchnones") towards electrophiles [2–6] as well as in (3 + 2)-cycloaddition reactions [2,7–9] is well documented but relatively few data are available concerning their reactions with nucleophiles,[2] excepting the Dakin-West ketone synthesis.[10,11] Limiting our investigation to the hydrolysis of mesoionic oxazolones it is known [12] that the monocyclic non-acylated compound **1** yields the acid **2**. The bicyclic acylated derivatives **3** gave depending on their substituent R either the ketone **4** when R = Ph (in boiling water) [13] or the 2-pyridinone **5** when R = Me (in dilute acid).[14]

In a previous paper of this series [4] the hydrolysis, ethanolysis and aminolysis of some 3-unsubstituted münchnones of type **6** (R^1 = H), Me; R^2 = H, Me, OAc) were described, their behaviour towards water (i.e. **6** → **7**) paralleling that of the monocyclic analog **1**. The ethanolysis and aminolysis of several 3-acylated derivatives of **6** were also reported.[1] A higher reactivity towards ethanol and aniline was observed for the nonplanar 3-acylated derivatives of **6** ($R^1 \neq$ H) relatively to their planar analogs (R^1 = H). Carrying on this research, the hydrolysis of the acylated bicyclic münchnones **8–16** has been investigated and the corresponding results are presented in this paper. Kinetic data along with their mechanistic implications will be published separately.[15]

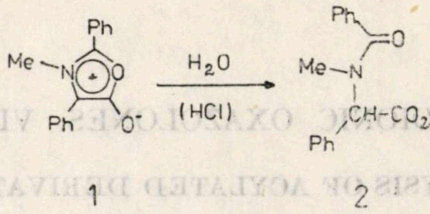

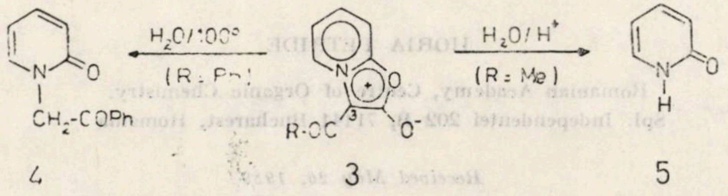

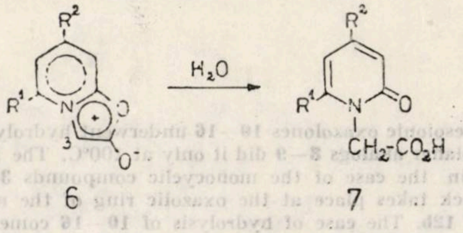

RESULTS AND DISCUSSION

Destruction of the mesoionic structure ensued from the hydrolysis of the acylated bicyclic compounds **8**–**16**. Thus, from **8**–**12a** and **13**–**16** the ketones **17**–**25** were obtained, while the acid **31** was isolated starting from **12b**. Formation of **17**–**25** implies the transient existence of the β-ketoacids KA, resulted from a nucleophilic attack at the oxazolic ring of the mesoionic substrates. When R^3 was an acetyloxy or monochloroacetyloxy group (i.e. **11a-b** and **12a**, resp.) the reaction went on further and a hydroxy-ketone was formed by the hydrolysis of the esteric function. Thus, at a short reaction time the ketones **20a-b** were obtained from **11a-b**, while the hydroxy-ketone **26a** resulted from **11a** at a longer reaction time. In the latter conditions the same compound **26a** was isolated from **20a** or directly from **2a**. In this last case also the intermediate **21a** could be separated but not in a reproducible manner due to its fast hydrolysis; it could be characterized by its ^1H—NMR spectrum. The hydrolysis of **12b** leading to the acid **31** implies a different reaction path, as discussed below.

All reactions on a preparative scale were performed with distilled water (X=H). The obtained compounds **17**–**26a** (X=H) are listed in Table 1 and their spectral features in Table 2.

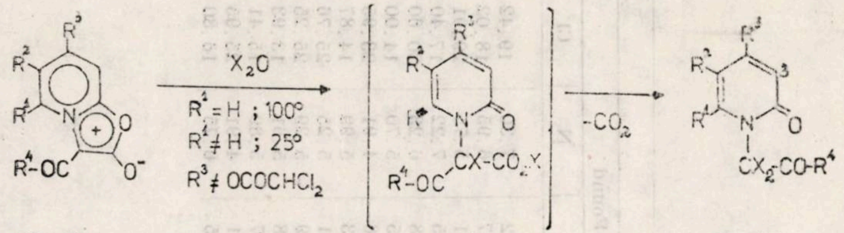

8 -16 KA 17 - 25

	R^1	R^2	R^3	
8a	H	H	H	17a
9a-b	H	H	Me	18a-b
10a-b	Me	H	H	19a-b
11a-b	Me	H	OAc	20a-b; 26a
12a-b	Me	H	$OCOR^4$	21a, 26a; 31
13a-b	Me	H	CO_2X	22a-b
14b	Me	CO_2X	H	23b
15a	Me	H	CO_2Me	24a
16a-b	benzo		H	25a-b

8-29	R^4
a	CH_2Cl
b	$CHCl_2$

17 - 31

X = H, D

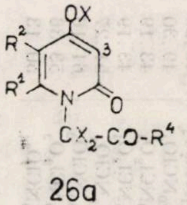

26a

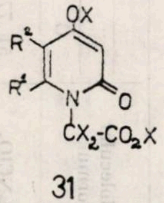

31

The hydrolysis of the nonplanar [5] mesoionic oxazolones **10**—**16** can be easily monitored by ^1H-NMR using CD_3CN/D_2O solutions. Complete deuteration occurs for the $N-CH_2$ group, but no attempts were made to isolate the corresponding reaction products **19**—**26a** (X=D) and **31** (X=D). However, this may be a very attractive route to prepare such selectively deuterium-labelled compounds. The observed spectral transformations, are in agreement with the sequence depicted in the chart. For example, **12a** is hydrolyzed at first to **21a** (X=D) which in its turn yields, more slowly, the hydroxy-ketone **26a** (X=D). Therefore, the monochloroacetyloxy function is attacked only after the oxazolic pseudo-lactonic carbonyl group.

In the particular case of **12b**, the addition of D_2O to its solution in CD_3CN (Figure 1) is followed in the first place by the replacement of the singlet corresponding to the 7-dichloroacetyloxy group by that of

Table 1

Preparation and elemental analysis of the ketones **17**–**20** and **22**–**26a** (X = H)

Compd.	Method (yield)[a] %	M.p. °C	Recrystn. solvent	Molecular formula	Elemental analysis, %							
					Calculated				Found			
					C	H	N	Cl	C	H	N	Cl
17a	A (40)	128–130[c]	CCl_4	$C_8H_8NClO_2$	51.77	4.34	7.55	19.10	51.46	4.22	7.30	19.42
18a	A (56)	130–132	CCl_4	$C_9H_{10}NClO_2$	54.15	5.05	7.02	17.76	54.31	5.27	6.95	18.02
18b	A (45)	118–120	CCl_4	$C_9H_9NCl_2O_2$	46.18	3.88	5.98	30.29	46.37	4.01	5.75	29.91
19a	B (94)	113–114	CCl_4	$C_9H_{10}NClO_2$	54.15	5.05	7.02	17.76	54.03	5.35	7.22	17.40
19b	B (87)	93–95	CCl_4	$C_9H_9NCl_2O_2$	46.18	3.88	5.98	30.29	46.27	3.78	6.23	30.60
20a	C (65)	110–112	C_6H_6	$C_{11}H_{12}NClO_4$	51.27	4.69	5.44	13.76	50.95	4.75	5.70	14.00
20b	C (78)	100–102	CCl_4	$C_{11}H_{11}NCl_2O_4$	45.23	3.80	4.79	24.28	44.98	3.96	4.91	23.95
22a	B (80)	167–169	H_2O	$C_{10}H_{10}NClO_4$	49.30	4.14	5.75	14.55	49.52	4.33	5.99	14.87
22b	B (78)	183–185	H_2O	$C_{10}H_9NCl_2O_4$	43.19	3.26	5.04	25.50	43.36	3.51	5.25	25.76
23b	B (55)	219–221	H_2O	$C_{10}H_9NCl_2O_4$	43.19	3.26	5.04	25.50	43.02	3.19	5.29	25.25
24a	B (94)	140–142	CCl_4	$C_{11}H_{12}NClO_4$	51.27	4.69	5.44	13.76	51.44	4.88	5.61	13.93
25a	B (91)	173–175	C_2H_5OH	$C_{12}H_{10}NClO_2$	61.16	4.28	5.94	15.04	60.94	4.67	5.89	15.41
25b	B (90)	133–134	C_2H_5OH	$C_{12}H_9NCl_2O_2$	53.36	3.36	5.19	26.25	53.39	3.61	4.91	25.95
26a	B[b]	196–198	AcOH	$C_9H_{10}NClO_3$	50.13	4.67	6.50	16.44	49.79	4.85	6.75	16.80

[a] see exp. part ; yields on crude products are given ;

[b] the yields are 60, 79 and 63% starting from **11a**, **12a**, and **20a**, resp.

[c] reported[16] 131–132°C (from ethanol).

Table 2

Spectral data of the ketones **17**−**26a** (X=H)

Compd.	IR data [a] ν_{CO} (cm^{-1})	^{1}H−NMR data (δ, ppm) [b,d]						UV data [c] λ_{max} (log ε)
		R^1	R^2	R^3	H$_3$	N−CH$_2$	R^4	
17a		7.2−7.6m	6.27t	as R^1	6.58d	4.88s	4.30s	
18a	1667(P) ; 1739(K)	7.22d	6.20d	2.22s	6.48s	4.86s	4.28s	296 (3.67)
18b	1665(P) ; 1752(K)	7.23d	6.21d	2.22s	6.48s	5.05s	6.34s	309 (3.65)
19a	1662(P) ; 1738(K)	2.28s	6.11d	7.30dd	6.45d	5.00s	4.30s	311.5 (3.88)
19b	1665(P) ; 1753(K)	2.28s	6.12d	7.30dd	6.45d	5.15s	6.35s	309 (3.81)
20a	1668(P) ; 1737(K) ; 1761(C)	2.30s	6.05m	2.30s	6.28m	4.97s	4.33s	
20b	1669(P) ; 1765(K) ; 1772(C)	2.28s	6.05m	2.28s	6.28m	5.16s	6.40s	
21a		2.25s	6.07m	4.43s	6.25m	4.99s	4.37s	
22a	1656(P) ; 1734(K) ; 1721(C)	2.87s	7.90m	—	7.98m	5.06s	4.15s	
22b	1647(P) ; 1749(K) ; 1712(C)	2.92s	7.92m	—	8.02m	5.19s	6.27s	327.5 (3.70)
23b	1632(P) ; 1757(K) ; 1703(C)	3.20s	—	9.09d	7.44d	5.22s	6.28s	312.5 (3.57)
24a	1664(P) ; 1727(K+C)	2.34s	6.63m	3.92s	7.08m	5.05s	4.31s	
25a	1660(Q) ; 1739(K)	7.1−7.9m		7.92d	6.72d	5.35s	4.57s	
25b	1659(Q) ; 1748(K)	7.1−7.7m		7.87d	6.80d	5.67s	6.28s	
26a	1620 ; 1650(P) ; 1753(K)	2.15s	5.53m	—	5.77m	4.85s	4.57s	

[a] spectra in CH_2Cl_2, except **22a**−**24a** and **26a** (KBr) ; carbonyl bands : pyridone (P), quinolone (Q), ketone (K), other carbonyls (C) ;

[b] spectra in $CDCl_3$, except **22a**−**23b** (TFA), **25a** (CD_3CN) and **26a** (DMSO-d_6) ; vicinal coupling constants : $J_{3,4} = 9$ for **17**−**25**, and $J_{4,5} = J_{5,6} = 7$ Hz for **17**−**24a** ;

[c] spectra in CH_3CN/H_2O (1 : 1, v/v), λ_{max} in nm.

[d] the assignments for R^2 and H$_3$ may be inverted in the case of **20**−**22**, **24a** and **26a**.

free dichloroacetic acid, as verified by pick overlapping with added acid; at the same time an upfield shift of the H_6 and H_8 signals could be observed (Figure 1b). Tentatively, this spectrum can be ascribed to the unstable münchnone **27b** (X=D). The subsequent spectral transformations are more difficult to rationalize but the finally recorded spectrum corresponds to the mixture of **31** (X=D) and Cl_2CHCO_2D in a 1 : 2 molar

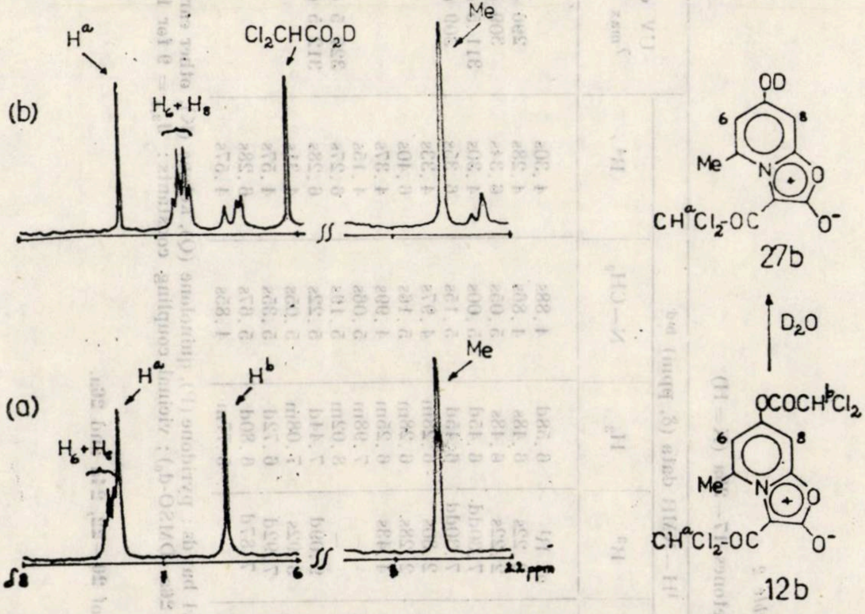

Fig. 1. — Hydrolysis of **12b** to **31** (X=D). ^1H–NMR spectra in CD_3CN (a) and CD_3CN/D_2O (b) after *ca.* 4 min.

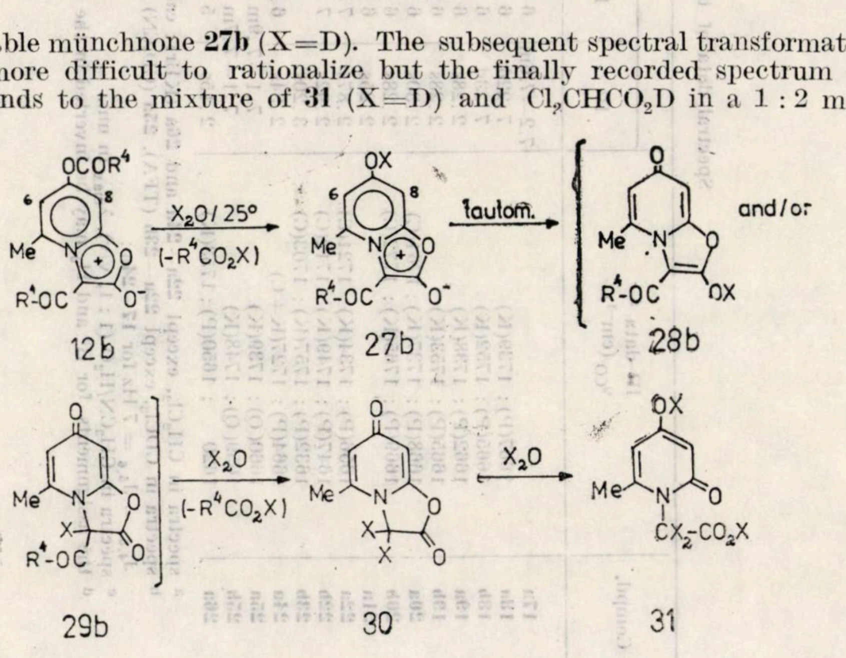
OCOR⁴
6
8
Me
N
O
R⁴-OC
O⁻
12b
X2O/25°
(-R⁴CO2X)
OX
27b
tautom.
and/or
28b
29b
X2O
(-R⁴CO2X)
30
X2O
CX2-CO2X
31

ratio. Accordingly, the reaction sequence depicted in the chart can be envisaged, namely the transient formation of **28b** (and/or **29b**; X=D) and of **30** (X=D). A similar transformation was described for a tricyclic münchnone.[3]

From these ^1H-NMR spectral transformations it results that the water molecule attacks in the first place the 7-dichloroacetyloxy function of **12b** and subsequently the new-formed lactonic ring. This is just the reverse succession to that showed by the monochloro-analog **12a**. Consequently, the reactivity towards water of the oxazolic ring of **10**—**16** is intermediate between that of the mono- and dichloroacetyloxy groups.

On the other hand, there is a sharp difference between the reactivity towards water of the planar substrates **8a** and **9a-b** relatively to that of their nonplanar analogs **10**—**16**. The latter compounds undergo hydrolysis even at room temperature. The same trend has been observed for the ethanolysis and aminolysis of these two kinds of münchnones.[1]

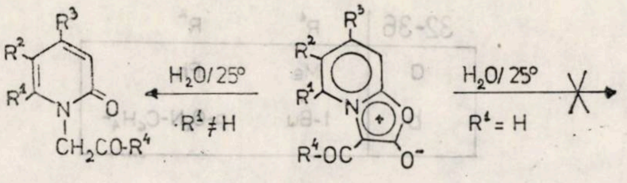

19d;20d   10d;11d//8c-d;9c

	R¹	R²	R³	
8c-d	H	H	H	-
9c	H	H	Me	-
10d	Me	H	H	19d
11d	Me	H	OAc	20d

	R⁴
c	Me
d	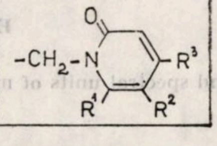

Experimental observations made in the preceding papers[4,5] find now their explanation. Thus, the nonsharp melting points (Boetius) of compounds **10**—**16** is due to partial hydrolysis, the melting points of the corresponding hydrolysis products being registered on remelting.[5] This did not occur for the planar derivatives **8**—**9**, which are more difficultly hydrolyzed. Secondly, the formation[4] of the dimeric ketones **19d** and **20d** is a result of the enhanced reactivity towards water of their precursors, the self-acylated nonplanar derivatives **10d** and **11d**, respectively.

Validity of the above conclusions was tried also in the case of monocyclic mesoionic oxazolones. Attempts to obtain the sterically hindered münchnone **34b**, using the same conditions as for the known[17] and readily isolable **34a**, led to the formation of the dimeric ketone **35b**, the hydrolysis product of the non-isolated **34b**. Similar reaction products were obtained before,[18] but no interpretation of the results was given. Obviously, the different behaviour towards water of **34a-b** may be ascribed to the non-

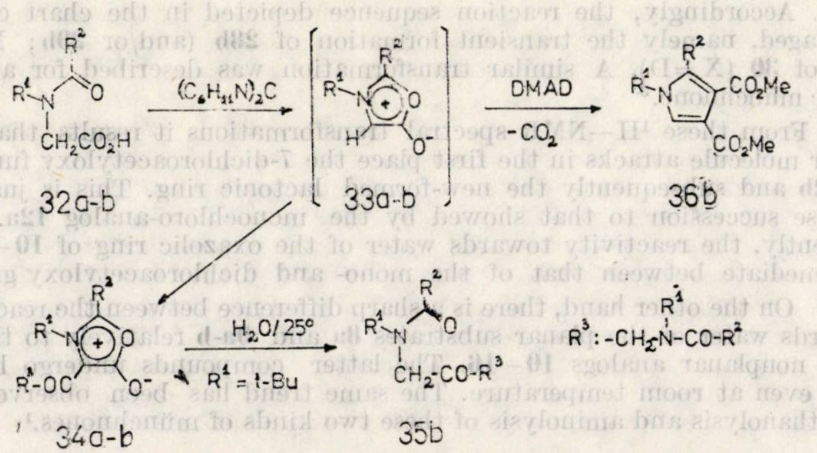

32-36	R^1	R^2
a	Me	Ph
b	t-Bu	$p\text{-}O_2N\text{-}C_6H_4\text{-}$

coplanarity between the acyl group and the mesoionic nucleus in the latter compound. The non-acylated precursor **33b** was trapped as pyrrole **36b** resulted by a (3 + 2)-cycloaddition reaction[19] with dimethyl acetylene-dicarboxylate (DMAD).

EXPERIMENTAL PART

Instruments and spectral units of measure as in the previous works.[1,4–6]

Synthesis of the ketones 17–26a (X=H)

Method A (for **17a** and **18a-b** only). A suspension of **8a** or **9a-b** (1 mmole) in 10 mL of water containing 1–2 drops of 70% aq. perchloric acid * was heated at reflux for 2–4hrs. The cooled mixture was extracted with 3 × 10 mL of dichloromethane and the collected organic layers were dried and evaporated *in vacuo* to give white solids.

Method B. To a solution of substrate (1–2 mmoles) in 10–15 mL of acetonitrile (or acetone) 2–5 mL of water were added and the homogeneous solution was left undisturbed for 3 days at room temperature. After dilution with 40 mL of water, the solution was extracted with 3 × 15 mL of chloroform and the collected organic layers were dried and evaporated *in vacuo* to give white crystalline solids.

Method C. The same as for *B* except that a short reaction time was necessary : 1–2 hrs for **20a-b** and 0.5 hr for **21a**. Attempted purification of **21a** failed.

4-Hydroxy-6-methyl-2-oxo-1(2H)pyridineacetic acid (**31** ; X = H). A suspension of 1 mmole of **12b** in 5 mL of water was left at room temperature for 3 days. The solid was filtered off and recrystallized from ethanol to afford **31** (67% yield), identical with an authentic sample.[20]

---

* The use of water or water/acetonitrile mixture required a too long reaction time, so that an acid-catalyzed [15] hydrolysis was carried out in this case.

^{1}H–NMR (DMSO-d_6) : 2.23 (3H, s, Me), 4.67 (2H, s, CH_2), 5.62 (1H, d, J = 2 Hz, H_3), 5.90 (1H, d, J = 2 Hz, H_5), 4.3–5.5 (2H, large, OH + COOH).

N-(1, 1-Dimethylethyl)-N-(4-nitrobenzoyl)-aminoacetic acid (**32b**). This compound was synthesized in two steps, *via* its ethyl ester. To a solution of 9.5 g of ethyl N-(1, 1-dimethylethyl)-aminoacetate [21] in anhydrous pyridine (20 mL) 12 g of 4-nitrobenzoyl chloride were added in small portions (max. temp. 10°C). After one hour at room temperature the reaction mixture was diluted with water (80 mL) and the deposited ethyl ester of **32b** was recovered by filtration in 82% yield. M.p. 98–99°C (from ethanol). $C_{15}H_{20}N_2O_5$ requires C, 58.43 ; N, 9.09 ; H, 6.54%. Found C, 58.65 ; N, 8.98 ; H, 6.63%.

IR (CH_2Cl_2) : 1603 (ring), 1648 (amide I), 1744 (ester).

^{1}H–NMR ($CDCl_3$) : 1.27 (3H, t, J = 7 Hz, CH_3–CH_2), 1.58 (9H, s, *t*-Bu),4.05 (2H, s, N–CH_2), 4.27 (2H, q, J = 7 Hz, O–CH_2), 7.73 (2H, d, J = 9 Hz, aromatics *meta* to nitro), 8.37 (2H, d, J = 9 Hz, aromatics *ortho* to nitro).

The ethyl ester of **32b** was hydrolyzed by refluxing for 2 hours with 10% aq. sodium hydroxide and subsequent acidification with concd. hydrogen chloride. Yield : 87%. M.p. 214–217°C (from aq. ethanol or ethanol/benzene mixture). $C_{13}H_{16}N_2O_5$ requires C, 55.71 ; H, 5.75 ; N, 10.00%. Found C, 55.67 ; H, 5.96 ; N, 10.05%.

IR (KBr) : 1593 (amide I), 1738 (CO_2H), 2200–3000 (broad, OH).

^{1}H–NMR (acetone-d_6) : 1.58 (9H, s, *t*-Bu), 4.10 (2H, s, CH_2), 7.74 (2H, d, J = 9 Hz, aromatics *meta* to nitro), 8.38 (2H, d, J = 9 Hz, aromatics *ortho* to nitro).

N, N′-(2-Oxo-1, 3-propanediyl)bis[N-(1, 1-dimethylethyl)-4-nitro-benzenecarboxamide] (**35b**). To a suspension of **32b** (0.5 g) in 30 mL of dichloromethane about 0.4 g of dicyclohexylcarbodiimide was added and the homogeneous orange solution was left at room temperature for 5 hours. After filtration of the deposited dicyclohexylurea, the solution was evaporated *in vacuo* and the residue solidified by trituration with water. Yield : 30%. M.p. 247–249°C (decomp., from ethanol). $C_{25}H_{30}N_4O_7$ requires C, 60.23 ; H, 6.06 ; N, 11.24%. Found C, 60.31 ; H, 6.25 ; N, 11.34%.

IR (KBr) : 1602, 1647 (amide I), 1740 (ketone).

^{1}H–NMR ($CDCl_3$) : 1.36 (9H, s, *t*-Bu), 3.97 (2H, s, CH_2), 7.48 (2H, d, J = 9 Hz, aromatics *meta* to nitro), 8.18 (2H, d, J = 9 Hz, aromatics *ortho* to nitro).

Dimethyl 1-(1,1-dimethylethyl)-2-(4-nitrophenyl)-1H-pyrrole-3,4-dicarboxylate (**36b**).

To a solution prepared from dicyclohexylcarbodiimide (0.4 g) and dimethyl acetylenedicarboxylate (275 mg) in 30 mL of dichloromethane an amount of 0.5 g of **32b** was added. The whole mixture was refluxed for 3 hours and the resulted dicyclohexylurea filtered off. The residue obtained after evaporation of the solvent was recrystallized from ethanol to afford pure **36b** (48% yield) with m.p. 186–188°C. $C_{18}H_{20}N_2O_6$ requires C, 59.99 ; H, 5.59 ; N, 7.77%. Found C, 60.12 ; H, 5.82 ; N, 7.88%.

IR (CH_2Cl_2) : 1603 (ring), 1711 and 1720 (CO_2Me).

^{1}H–NMR ($CDCl_3$) : 1.46 (9H, s, *t*-Bu), 3.60 (3H, s, OMe), 3.86 (3H, s, OMe), 7.58 (1H, s, H_5), 7.63 (2H, d, J = 9 Hz, aromatics *meta* to nitro), 8.31 (2H, d, J = 9 Hz, aromatics *ortho* to nitro).

REFERENCES

[1] Part V : H. Petride, *Rev. Roum. Chim.*, **35**, 747 (1990).

[2] W. D. Ollis and C. A. Ramsden, "Meso-ionic Compounds", in *Adv. Heterocyclic Chem.*, A. R. Katritzky and A. J. Boulton eds., Academic Press, New York, 1976, vol. 19, p. 1 ff. and references cited therein.

[3] Part I : E. Tighineanu, F. Chiraleu and D. Răileanu, *Tetrahedron*, **36**, 1385 (1980).

[4] Part II : H. Petride and D. Răileanu, *Rev. Roum. Chim.*, **33**, 729 (1988).

[5] Part III : H. Petride and D. Răileanu, *ibid.*, **34**, 1251 (1989).

[6] Part IV : D. Răileanu and H. Petride, *ibid.*, **35**, 459 (1990).

[7] A. Myers, W. W. Wilkerson and S. L. Council, *J. Org. Chem.*, **40**, 2875 (1975).

[8] K. T. Potts, S. J. Chen and J. Szmuskovicz, *ibid.*, **42**, 2525 (1977).

[9] T. Uchida, S. Tsubokawa, H. Harikara and K. Matsumoto, *J. Heterocycl. Chem.*, **15**, 1303 (1978).

[10] R. Knorr and R. Huisgen, *Chem. Ber.*, **103**, 2598 (1970).

[11] S. Zavyalov, N. Aronova and N. Makhova, *Reakts. Metody Issled. Org. Soedin.*, **22**, 9 (1971).

[12] R. Knorr, *Chem. Ber.*, **104**, 3633 (1971).
[13] G. V. Boyd and P. H. Wright, *J. Chem. Soc.(C)*, **1970**, 1485.
[14] A. Lawson and D. H. Miles, *J. Chem. Soc.*, **1959**, 2865.
[15] Part VII : H. Petride and D. Răileanu, *Rev. Roum. Chim*,. **36**, (1991).
[16] K. Winterfeld and H. Michael, *Chem. Ber.*, **93**, 61 (1960).
[17] C. V. Greco, R. P. Gray and V. G. Grosso, *J. Org. Chem.*, **32**, 4101 (1967).
[18] G. V. Boyd and P. H. Wright, *J. Chem. Soc. Perkin Trans.* **1**, **1972**, 914.
[19] I. Zugrăvescu and M. Petrovanu, "Cicloadiţii 3 + 2", Editura Academiei R.S. România, **1988.**
[20] S. Garratt and D. Shemin, *J. Org. Chem.*, **28**, 1372 (1963).
[21] A. J. Speziale and E. G. Jaworsky, *ibid.*, **25**, 738 (1960).

Revue Roumaine de Chimie, 36, 9–10, 1123–1127 (1991)

SYNTHESIS AND CHARACTERIZATION OF SOME 2, 4'-DIBENZYLDIISOCYANATE IONIC POLYMERS. VI

BIOLOGICAL ACTIVITY AT LOW CONCENTRATIONS OF IONIC GROUPS*

TINCA BURUIANĂ and ADRIAN CARACULACU

Institute of Macromolecular Chemistry "P. Poni" Aleea Gr. Ghica Vodă No. 41-A
6600 – Jassy, Romania

Received March 29, 1989

Antimicrobial activity of some 2, 4'-dibenzyldiisocyanate ionic polymers obtained by Menschutkin reaction was studied at low concentrations of ionic groups. It was found that polymers inhibited the growth of a bacterial culture.

In a previous paper [1] the biological activity of some "ionene" type carionic polyurethanes was presented comparatively with that of model compounds with low and high molecular weight. The above polyurethanes were synthesized by Menschutkin step reaction and exhibit an antimicrobial behaviour.

Because it was found that biological activity of some polycations depends on both the chemical structure of principal backbone, molecular weight, concentration of ammonium quaternary groups and on the contraion structure,[1,2] we have proposed to continue the study of antimicrobial behaviour of the cationic polyurethanes with lower concentration of ionic groups.[3]

RESULTS AND DISCUSSION

Cationic polyurethanes were synthesized by Menschutkin reaction of a prepolymer having dimethylamino end groups with an aliphatic or aromatic dihalide.

Prepolymer with dimethylamino end groups was prepared from poly(tetramethylene oxide) (PTHF), (MW = 2 000), or ricin oil and 2,4'-dibenzyldiisocyanate, subsequently reacted with dimethylamino ethanol.

1,4-Xilylene dichloride and 1,4-dibromobutane were used as dihalides.

---

* Presented at the 3rd National Congress of Chemistry, Bucharest, 1988.

The structure of synthesized polymers was as follows :

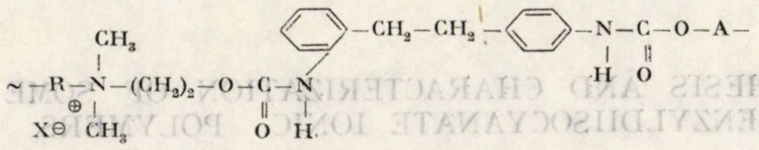

where : $A = -[(CH_2)_4O]_n-$; ricin oil rest ;

$R = -CH_2-CH_2-CH_2-CH_2-$;

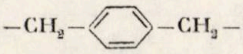

$X = Cl ; Br$;

Depending on the polyol structure (PTHF, ricin oil), linear (PU-1, PU-2) or crosslinked (PU-3, PU-4) cationic polyurethanes were obtained. They have a low concentration of quaternary ionic groups, characteristic of polyurethane ionomers.

When a dihalogenide prepolymer containing soft PTHF segments and chlorobenzyl end groups reacted with a prepolymer based on ricin oil having dimethylamino end groups, a cationic polyurethane was obtained (PU-5), with better mechanical properties than polyurethanes resulted by one step Menschutkin reaction.

Elemental analysis, IR absorption spectroscopy, mechanical measurements were used in order to characterize these polymers.

In table 1, some of structural characteristics of the above polymers are presented.

Table 1

Structural characteristics of cationic polyurethanes

Polycations	PTHF (MW = 2000)	Ricin oil	Ionic halogen content (meq/100 g)	Total halogen content (meq/100 g)
PU−1	+	−	79.49*	82.10
PU−2	+	−	67.50**	68.01
PU−3	−	+	126.31*	128.50
PU−4	−	+	127.50**	129.10
PU−5	+	+	−	107.70*

* — chloroionene ; ** — bromoionene

With the view to follow antimicrobial behaviour of synthesized polycations, their ethanol — water solutions (80 : 20 v/v) for PU-1—4, or dimethylformamide (DMF) solutions for PU-5, with different concentrations of polymer were used. Gram-negative and Gram-positive bacteria *E. Coli*, *S. Aureus*, *Proteus* and *Proteus* with *E. Coli* mixture were tried.

The tests of bacteria sensitivity against studied polycations were performed in vitro, in standardized conditions of cultivation (cultivation medium, inoculation, incubation time) with known concentrations of polymers.

Table 2 shows the results of antimicrobial behaviour of cationic polyurethanes versus utilised bacteria, ascertaining an inhibitory process of their growth at a concentration about 1 000 ppm.

Table 2

Antimicrobial activity of cationic polyurethanes at a concentration of 1000 ppm

Polycations	*E. Coli*	*S. Aureus*	*Proteus*	*E. Coli* + *Proteus*
	R_i^* (mm)			
PU−1	7	6	6	6
PU−2	5−6	5	6−7	10
PU−3	6	3−4	5	7
PU−4	6−7	6	6−7	8−9
Sulphofurazole	6	6	6	7

R_i — radius of inhibition zone ;

From the above data it can be seen a moderate sensitivity of tested bacteria for the studied cationic polyurethanes. This sensitivity is comparable with that find when an identical concentration of Sulphofurazole was used.

No evident changes regarding the sensitivity of bacteria were observed when concentration of polycation solutions decreased to 500 ppm and 250 ppm (Figs 1−4).

The results from Table 3 and Figures 1−4 show that the growth of tested bacteria is inhibited even for lower concentrations of polycations.

Table 3

Antimicrobial activity of cationic polyurethanes at low concentrations

Polycations	*E. coli*	*S. Aureus*	*Proteus*	*E. Coli* + *Proteus*
	R_i^*(mm)			
PU−1 (500 ppm)	7	5	6	7
PU−1 (250 ppm)	7	5	6	7
PU−2 (500 ppm)	6	5	7	7−8
PU−2 (250 ppm)	6	5	7	7
PU−3 (500 ppm)	7	4−5	5−6	7−8
PU−3 (250 ppm)	4−5	4−5	5−6	6
PU−4 (500 ppm)	7	5	7	5−6
PU−4 (250 ppm)	7	5	7	5−6
PU−5 (250 ppm)	6	8−9	7	6
Negram (300 ppm)	8	9	8	—
Nitrophurantoine (300 ppm)	8	7	7	—

R_i — radius of inhibition zone ;

The activity of polymers PU-1—4, versus *E. Coli* bacteria is given at two concentrations (500 and 250 ppm) in Fig. 1 and Fig. 2.

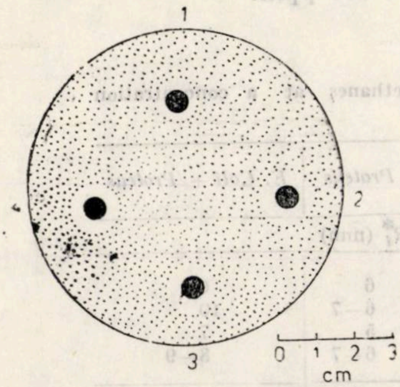

Fig. 1. — Antimicrobial activity of polymers PU—1—4 versus *E. Coli,* at 500 ppm.

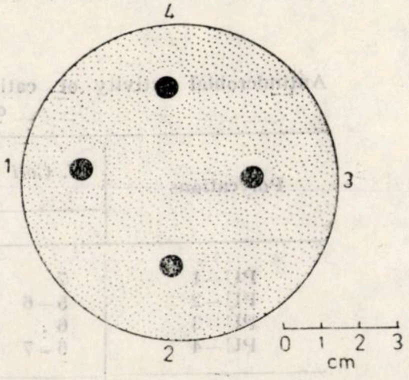

Fig. 2. — Antimicrobial activity of polymers PU—1—4 versus *E. Coli,* at 250 ppm.

Sensitivity of mixture *E. Coli* and *Proteus* versus the same polymers is presented in Fig. 3 and Fig. 4.

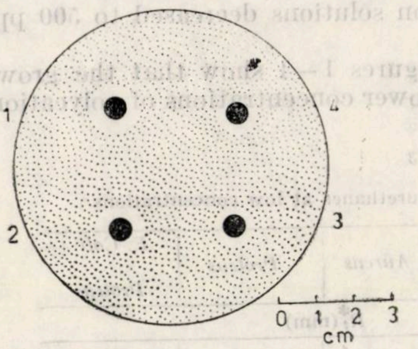

Fig. 3. — Antimicrobial activity of polymers PU—1—4 versus *E. Coli* + + *Proteus*, at 500 ppm.

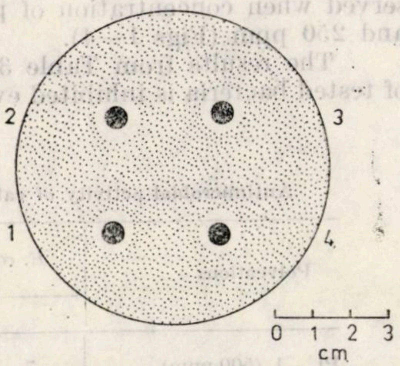

Fig. 4. — Antimicrobial activity of polymers PU—1—4 versus *E. Coli* + + *Proteus*, at 250 ppm.

Based on information from the previous paper[1] regarding the behaviour of model compound with low and high molecular weight, another model compound was synthesized with high concentration of quaternary ammonium groups.

As macromolecular model compound, a polycation of the polyurethane polyelectrolyte type was used, based on 2,4'-dibenzyldiisocyanate modified with dimethylaminoethanol and 1,4-xilylenedichloride, having the structure :

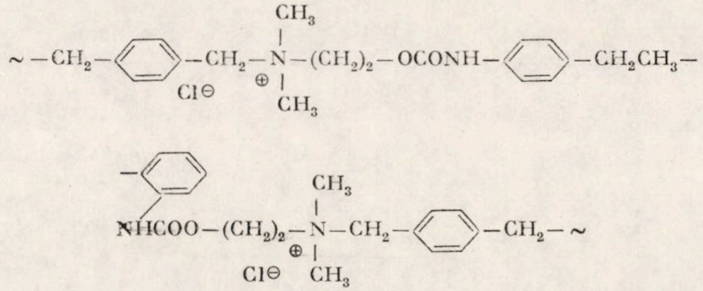

Although this model compound contains a great concentration of quaternary amonium groups, the study of its antimicrobial behaviour has indicated the insensitivity of tested bacteria at a concentration of solution of 250 ppm ($R_i = 0$).

As a conclusion, the above results confirm the previous hypothesis on the dependence of antimicrobial behaviour both on presence of ammonium quaternary groups and on their distribution along polymer backbone.

EXPERIMENTAL PART

Gram-positive and Gram-negative bacteria (obtained from a hospital) were used to study the antimicrobial activity of cationic polyurethanes.

Pellets with different polymer concentrations were placed on the surface of a nutrient agar (Mueller — Hinton type) uniformly seeded with testing germs.

A porous inert support obtained from filter paper with d = 6 mm was utilized as pellet. 0.01 ml from each solution was put on this inert support.

The zones of inhibition were measured after 18—24 hours of incubation at 37°C . It was considered that the surface of inhibition zones was directy proportional to the sensitivity of bacterium against the solution of polymer from the pellet.

REFERENCES

[1] T. Buruiană and A. Caraculacu, *Rev. Roum. Chim.*, **33**, 809, (1988).

[2] A. Rembaum, *Applied Polymer Symposium*, **22**, 299 (1973).

[3] T. Buruiană and A. Caraculacu, The IIIrd National Congress of Chimistry, Bucharest, 21—24 Sept. 1988.

Revue Roumaine de Chimie, 36, 9–10, 1129–1134 (1991)

MOLECULAR REARRANGEMENTS. PART XXXII.

THERMOLYSIS AND PHOTOLYSIS OF SOME HYDROXYLAMINE DERIVATIVES

M. Z. A. BADR, M. M. ALY, A. A. ATTALA and S. A. MAHGOUB
Chemistry Department, Faculty of Science, Assiut University, Assiut, Egypt, A.R.E.

Received September 12, 1988

Thermolysis of O-benzylhydroxylamine, N-methyl-N-phenyl-O-benzylhydroxylamine, N-phenyl-N-benzylhydroxylamine and N-benzhydryl-N-phenylhydroxylamine on heating under reflux and the formation of the identified products was explained in terms of a free-radical mechanism involving mainly the homolysis of N—O bonds in such molecules followed by the normal reaction of free radicals as dimerization, coupling, disproportionation, cyclization, oxidation or fragmentation. Similar results were also obtained on photolysis in isopropanol solution which implies that both processes are of comparable nature.

Hydroxylamine was first reported by Janny [1] to undergo pyrolysis on heating to give nitrogen, ammonia and water. Although aryl hydroxylamines are subjected to extensive studies through acid catalyzed rearrangements to give aminophenols, studies on pyrolysis or photolysis of alkyl hydroxylamines are meagre. In continuation of our previous work on hydroxylamines and related molecules,[2] the present work describes the behaviour of some hydroxylamine derivatives when heated at their reflux temperatures (ca. 180° C) or irradiated by UV light ar room temperature.

Thermolysis of O-benzylhydroxylamine was found to give rise to ammonia, water, dibenzyl, toluene, benzylalcohol, benzaldehyde, benzylamine, and benzoxazole. Such results can be accounted for in terms of a free radical mechanism involving benzyl oxygen bond homolysis (Scheme 1, route a) forming iminoxy and benzyl radicals. The iminoxy radicals may abstract hydrogen to give hydroxylamine which subsequently decomposes into ammonia and water whereas the benzyl radicals may abstract hydrogen to form toluene or dimerize to dibenzyl. Furthermore, the iminoxy radicals may undergo radical oxidative cyclization to form benzoxazole. The formation of benzylamine, benzylalcohol and benzaldehyde can be assumed to proceed through the homolysis of N—O bond (route b) to iminyl and benzyloxy radicals. Coupling of iminyl radicals with benzyl radicals affords benzylamine, whereas disproportionation of benzyloxy radicals produces benzaldehyde and benzyl alcohol.

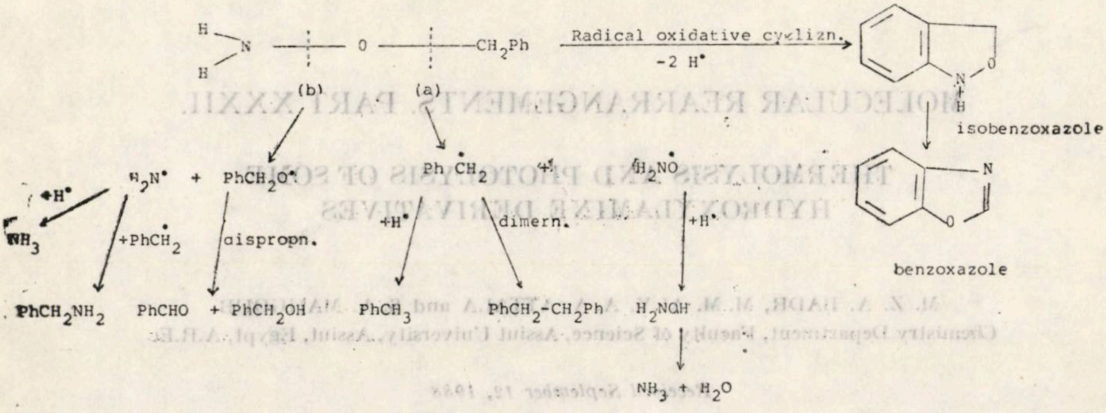
Radical oxidative cyclizn.
-2 H•
(b)
(a)
isobenzoxazole
benzoxazole
+H•
+PhCH₂
dispropn.
dimern.
PhCH₂NH₂
PhCHO + PhCH₂OH
PhCH₃
PhCH₂-CH₂Ph
H₂NOH
NH₃ + H₂O

Scheme 1

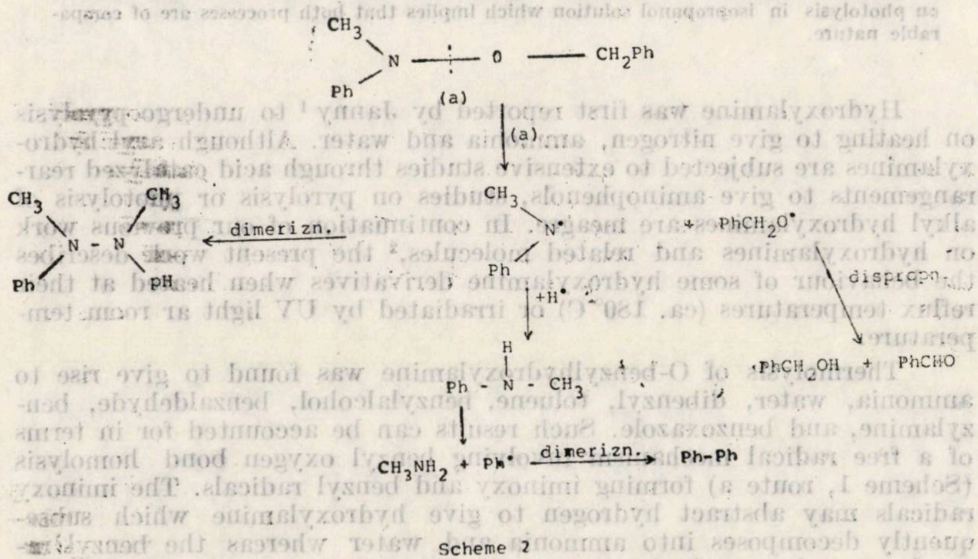
(a)
dimerizn.
+H•
disprop.
PhCH₂OH + PhCHO
dimerizn.
CH₃NH₂ + Ph•
Ph-Ph

Scheme 2

Similarly, thermolysis of N-methyl-N-phenyl-O-benzylhydroxyl amine gives : methylamine, N-methylaniline, dibenzyl, benzylacohol, and benzaldehyde through the homolysis of the N—O bond to N-methylanilino and benzyloxy radicals (c.f. Scheme 2, route a). The benzyloxy radicals disproportionate to benzyl alcohol and benzaldehyde, whereas the N-methylanilino radicals abstract hydrogen forming N-methylaniline which undergoes N-phenyl homolysis forming finally methylamine and phenyl radicals that subsequently dimerizes into diphenyl. Dimerization of N-methylanilino radicals to give 1, 2-diphenyl-1, 2-dimethyl hydrazine was not observed most probably due to the instability of the suggested N—N dimer. Moreover, C—C— dimers of mesomeric N-methylanilino radicals were not formed, a result which indicates that N-methylanilino radicals do not survive long enough to undergo such reactions due to the presence of other fast competing pathway as described previously.

Thermolysis of N-phenyl-N-benzylhydroxylamine gives benzaldehyde, dibenzyl, stilbene, azobenzene, aniline, *o*-, *p*- aminophenols and 2, 2′-azobiphenyl.

The formation of these products can be assumed to follow the same series of reactions shown in Scheme 3 which implies the preliminary homolysis of N—O bond, forming N-benzylanilino and hydrooxyl free radicals. N-Benzylanilino radicals abstract H, forming N-benzylaniline which subsequently undergoes homolysis[3] of the N-benzyl bond forming benzyl and anilino radicals. Recombination of the hydroxyl free radicals with the mesomeric anilino radicals in the *ortho*- and/or *para*-position gives rise to *o*- and *p*-amino phenols respectively. Moreover, the hydroxyl free radicals may abstract hydrogen forming water. Dimerization of anilino radicals leads to formation of hydrazobenzene which undergoes radical oxidative dehydrogenation to give finally azobenzene, whereas benzyl radicals undergo atmospheric oxidation to benzyldehyde or dimerization forming dibenzyl followed by dehydrogenation into stilbene.

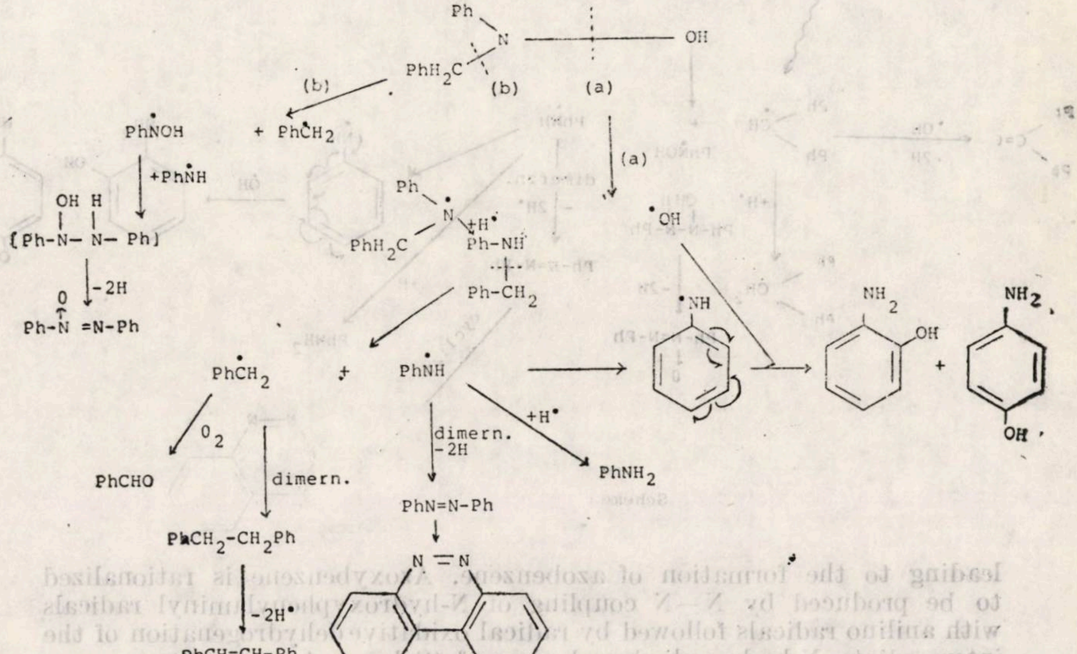

Scheme 3

Radical oxidative cyclization of azobenzene reasonably leads to formation of 2, 2′-azodiphenyl. Thermolysis of N-benzhydryl-N-phenylhydroxylamine gives benzophenone, diphenylmethane, azobenzene, azoxybenzene, aniline together with *o*- and *p*-amino phenols (cf. Scheme 4). The anilino radicals may undergo N—N radical oxidative dimerization

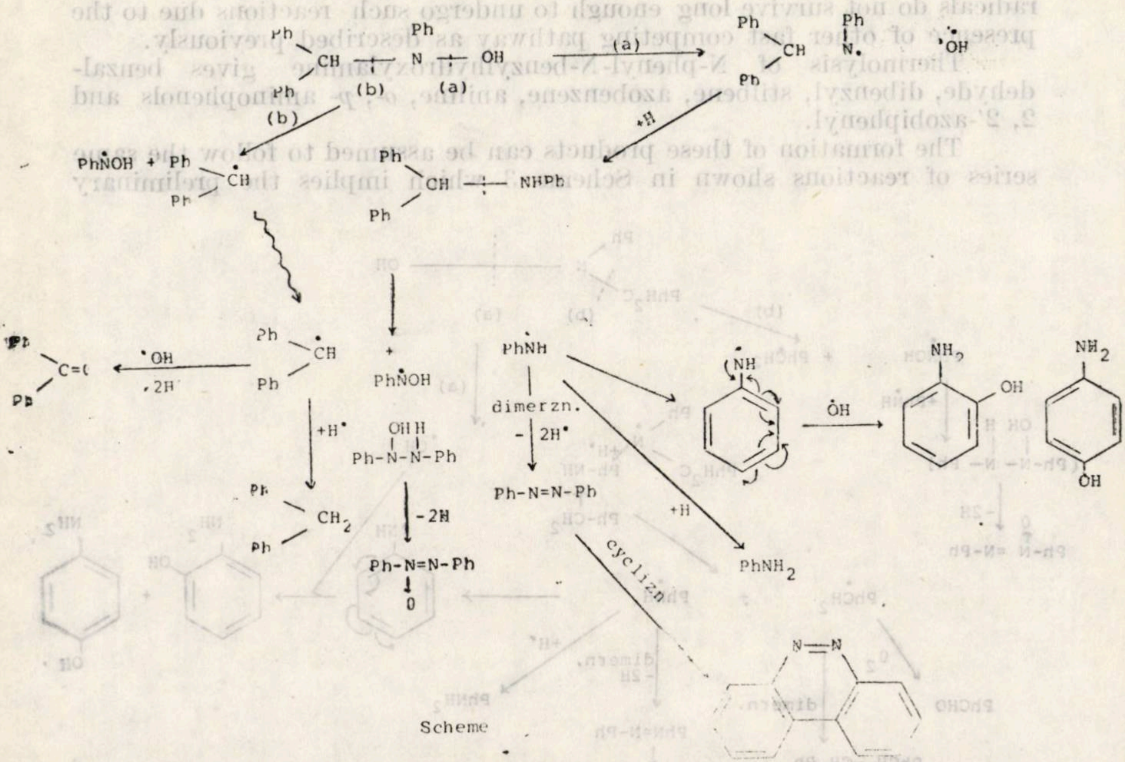

Scheme

leading to the formation of azobenzene. Azoxybenzene is rationalized to be produced by N—N coupling of N-hydroxyphenylaminyl radicals with anilino radicals followed by radical oxidative dehydrogenation of the intermediate N-hydroxyhydrazobenzene [2] (Scheme 4, route b).

Irradiation of O-benzylhydroxylamine in isopropanol solution for 10 hrs at room temperature leads to analogous products to that produced on thermolysis as shown by results of t.l.c. and g.l.c. with the exception of benzoxazole whereas irradiation of N-methyl-N-phenyl-O-benzylhydroxylamine under the same conditions gives only benzaldehyde, benzyl alcohol and diphenyl. Similarly, irradiation of N-phenyl N-benzylhydroxylamine and N-benzhydryl-N-phenyl hydroxylamine affords analogous products except 2, 2′-azodiphenyl.

The results of photolysis compared with that of thermolysis, although give only the primary photoproducts, indicate that both fragmentation processes are of comparable nature and consequently can be explained on similar grounds.

EXPERIMENTAL

All melting points are uncorrected. The IR spectroscopic analyses were carried out on a Pye-Unicam IR spectrophotometer Model SP 3—100. The gas-liquid chromatography (g.l.c.) was carried out on a Perkin-Elmer Sigma-3B chromotograph. The columns used were 4 ft × × 4 mm, packed with 30% SE 30 on Chromosorb W (35—80 mesh) or 10% SE 30 on celite

(60 : 80 mesh) at 180°C, using nitrogen as a carrier gas. Thin-layer chromatography (t.l.c) was carried out on glass plates covered with silicagel (35—40 mesh) and elutd with benzene-petroleum ether (b.p.60—80°C) (2 : 8 v/v) or acetone petroleum ether (b.p.60—80°C) (1 : 9 v/v).

General procedure

The appropriate hydroxylamine derivative (20 g) was pyrolyzed by reflux in air for 20 hrs at 180—200°C except for N-phenyl-N-benzyl-hydroxylamine which was heated in a sealed tube for 50 hrs at 150°C. The products were separated as indicated in a previous work [3] by chemical means into neutral and basic fractions followed either by fractional distillation under reduced pressure or column chromatography and identified by t.l.c., g.l.c, IR—, or mixed melting points with authentic samples whenever possible. The results are shown in Tables 1 and 2.

Table 1

Pyrolysis products of O-benzylhydroxylamine and N-methyl-N-phenyl-O-benzylhydroxylamine in g (%)

Products in g(%) / Starting materials	O-benzylhydroxylamine	N-methyl-N-phenyl-O-benzylhydroxylamine
NH_3	evolved	—
Water	0.7 (3.6)	—
Toluene [a]	few drops	—
Dibenzyl [b]	0.5 (2.5)	—
Diphenyl [c]	—	0.25 (1.25)
Benzaldehyde [d]	6.4 (32)	3.40 (17)
Benzylamine [e]	3.5 (17.5)	—
Benzylalcohol [f]	5.1 (25.5)	3.40 (17)
Benzoxazole [g]	2.23 (11.15)	—
Methylamine [h]	—	evolved
N-Methylaniline [i]	—	7.1 (35.4)
Residue	1.00 (5)	0·9 (4.5)

[a] 2,4-dinitroderivative m.p. 72—73°C

[b] b.p. 90—100°C/13 mm Hg ; m.p. and m.m.p. 50—42°C ; 4, 4′-dinitroderivative m.p. and m.m.p. 176°C.

[c] b.p. 125°C/13 mm Hg, m.p. and m.m.p. 69—72°C ; IR spectrum identic with that of an authentic sample.

[d] b.p. 120—125°C/13 mmHg ; D.N.P. derivative m.p. and m.m.p. 232—235°C.

[e] b.p. 127—135°C/13 mmHg ; benzoylderivative m.p. and m.m.p. 105°C.

[f] b.p. 85°C/13 mmHg ; *p*-nitrobenzoate derivative m.p. and m.m.p. 86°C.

[g] b.p. 65—68°C/13 mmHg ; n_D^{20} 1.5497 ; IR spectrum identic with that of an authentic sample.

[h] Trapped as its HCl salt m.p., 227°C from which the base is libertated by alkalinisation picrate from ethanol, m.p, and m.m.p. 215°C.

[i] b.p. 80—82°C/13 mm Hg n_D^{20} 1.5702 ; oxalate derivative m.p. and m.m.p. 111—113°C ; acetyl derivative m.p. and m.m.p. 102°C.

Preparation of reference compounds :

O — Benzyl hydroxylamine [1] : colourless oil b.p. 118 : 119°C/30 mmHg.,

N — Phenyl-N-benzylhydroxylamine [4] : colourless leaflets from ethanol m.p. 86°C.

N — Phenyl-N-benthydrylhydroxylamine [5] ; colourless crystals from ethanol m.p. 125°C.

N — Methyl-N-phenyl-O-benzylhydroxylamine [7] : pale yellow oil b.p. 125°C/2 mmHg ; picrate from benzene m.p. 131°C. Benzoxazole [2] : pale yellow oil b.p. 182°C ; m.p. 28—30°C ; methiodide m.p. 202°C.

2, 2′-Azodiphenyl [8] : colourless crystals from ethanol m.p. 156°C.

Table 2

Pyrolysis products of N-phenyl-N-benzylhydroxyl amine and N-phenyl-N-benzylhydroxylamie

Products in g(%) / Starting materials	N-phenyl-N-benzyl-hydroxylamine	N-phenyl-N-benzhydryl-hydroxylamine
Water	0.5 (2.5)	—
Aniline [a]	6.2 (31)	4.8 (24)
Diphenylmethane [b]	—	1.5 (7.4)
o-Aminophenol [c]	0.35 (1.75)	0.9 (4.5)
p-Aminophenol [d]	0.25 (1.25)	1.22 (6.1)
Dibenzyl [e]	0.40 (2)	—
Benzaldehyde [f]	4.00 (20)	—
Azobenzene [g]	5.00 (25)	3.10 (15.5)
Azoxybenzene	trace	0.58 (2.9)
Benzophenone	—	2.80 (14)
Stilbene [i]	0.23 (1.15)	—
Residue	3.50 (17.5)	2.30 (11.5) [j]

[a] b.p. 80—85°C/13 mmHg ; h_D^{20} 1.5836 ; acetyl deriv. m.p. and m.m.p. 113—114°C.

[b] b.p. 130°C/13 mmHg n_D^{20} 1.5770 ; 2, 2′, 4, 4′-tetranitroderivative m.p. and m.m.p. 172°C.

[c] b.p. 160—175°C/14 mmHg separated by column chromatography using acetone/petroleum ether (60—80*l*C) as eluent to *p*-aminophenol m.p. and m.m.p. 188—190°C ; diacetyl derivative m.p. 150°C and *o*-aminophenol m.p. and m.m.p. 174—176°C, diacetyl derivative m.p. 124°C.

[d] b.p. 90—100°C/14 mmHg ; m.p. and m.m.p. 50—52°C ; 4, 4′-dinitroderivative m.p. and m.m.p. 176°C.

[e] b.p. 120—125°C/13 mmHg ; D.N.P. derivative m.p. and m.m.p. 232—235°C.

[f] b.p. 185—195°C/13 mmHg ; crystals from ethanol ; m.p. and m.m.p. 66—68°C ; IR spectrum identic with that of an authentic sample.

[g] b.p. 200—210°C/13 mmHg, crystals from ethanol m.p. and m.m.p. 36°C ; IR spectrum identic with that of an authentic sample.

[h] b.p. 160°C/13 mmHg ; m.p. 48—50°C ; D.N.P. derivative m.p. and m.m.p. 238°C.

[i] b.p. 165—170°C/13 mmHg ; m.p. and m.m.p. 122—124°C.

[j] On trituration with ethanol gives 0.2 g of 2, 2′-azodiphenyl m.p. and m.m.p. with an authentic sample 154—156°C.

REFERENCES

[1] R. Janny, *Chem. Ber.*, **16**, 175 (1883).

[2] A. M. Fahmy, M. M. Aly, ; M. Z. A. Badr, and A. M. Abdel-Gawad, *Bull. Pol. Acad. Sc.* (in press) (1988).

[3] M. Z. A. Badr, and M. M. Aly; *Canad. J. Chem.*, **52**, 293 (1974).

[4] P. G. Gassman, and R. L. Cryberg, *J. Amer. Chem. Soc.*, **91**, 5176 (1969)

[5] H. Rupe, and R. Witner, *Helv. Chim. Acta*, **5**, 219 (1922).

[6] J. Meisenheimer, H. Greeske, and A. Willmersdorf, *Chem. Ber.*, **55**, 521 (1922) ; M. Mitrab., *Liebigs Ann. Chem.*, **449**, 204 (1926).

[7] R. Walter, and T. von Pulawaki *J. Prakt. Chem.*, **59**, 299 (1899).

[8] E. Tauber, *Chem. Ber.*, **24** ; 3085 (1891).

Revue Roumaine de Chimie, 36, *9–10*, 1135–1145 (1991)

A NEW METHOD FOR A KINETIC STUDY OF REACTIONS BETWEEN DIISOCYANATES AND ALCOHOLS. PART II[1].

ASYMMETRICAL DIISOCYANATES: 2,4-TOLUYLENE DIISOCYANATE

OAN AGHERGHINEI, CRISTINA PRISACARIU and ADRIAN A. CARACULACU
nstitute of Macromolecular Chemistry "P. Poni" Aleea Gr. Ghica Vodă No. 41 6600 Jassy, Romania

Received July 1, 1990

A procedure of following the kinetics of the uncatalysed reaction between 2, 4-toluylene diisocyanate (2,4-TDI) and alcohols by determining concentration variations of all molecular species by means of HPLC is described. This method allowed the determination of the rate-constants ratios valid on the whole pattern of the reaction and also calculation of the four rate-constants corresponding to the four reaction steps: $k_2/k_1 = 4.08$, $k_1/k'_1 = 4.45$, $k_2/k_2' = 4.33$

In a previous work,[1] we studied the kinetic of the uncatalysed reaction between symmetrical diisocyanates and alcohols, by determining all molecular species which coexist during reaction, using the HPLC method.

We have shown that the relation

$$F_M = \frac{1}{1 - 1/(2R)} \left(F_N^{1/(2R)} - F_N\right) \qquad (1)$$

where

F_N — the molar fraction of unreacted diisocyanate

F_M — the molar fraction of the monoreacted diisocyanate

R — the rate constants ratio k_1/k_2 corresponding to the reaction of the first and the second NCO group established by eliminating τ variable[1] from equations of bimolecular 'idealised' kinetics of the second order, where there are no catalytical effects, is experimentally verified also in the 'real' cases. The consequences had also been discussed there.

In the case of asymmetrical diisocyanates the kinetic equations of bimolecular 'idealised' system should give two functions similar to function (1) corresponding to each of the two monoreacted species m_1 and m_2 (scheme (2)).

---

[1] Part I, A. A. Caraculacu, I. Agherghinei, M. Gaspar, and C. Prisacariu, *J. Chem. Soc. Perkin Trans.*, **2**, 1343 (1990).

As in the case of symmetrical aromatic diisocyanates,[1] we distinguished two categories of asymmetrical diisocyanates : in the first the NCO groups belong to different aromatic rings (type Ac) while in the second, they belong to the same ring (type Av).

2, 4-Dibenzylediisocyanate (2,4′-DBDI) [2] can be considered a representant of the first category and 2,4-toluylenediisocyanate (2, 4-TDI) of the second. The situation of Av is the most complex case, because there exist four "very" different rate constants. The reactivities of NCO groups are different due to the substitution position and also to the alteration of their initial reactivity, as a result of the reaction of the first NCO group, which leads to consequent changes in their activating effect.

This is the reason why we considered it interesting to approach the most complex case, i.e. 2, 4-TDI.

Benzene was used as solvent, since the catalytical effects of alcohol and urethane are not overlapped by the catalytic effect of the solvent. An initial excess of isocyanate — similar to the situation in which prepolymers with NCO final groups are obtained for polyurethane synthesis — was used, i.e. $[NCO]_0/[OH]_0 = 2$.

The reaction of 2, 4-TDI with an alcohol is shown in scheme (2).

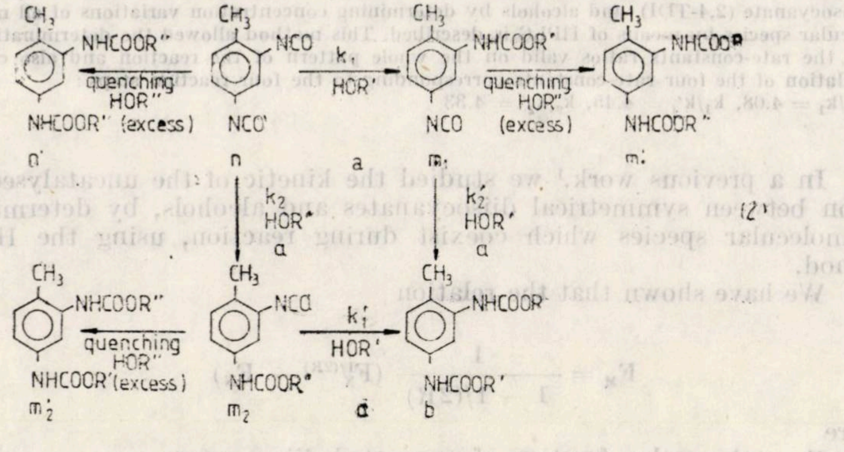
CH₃
NHCOOR"
quenching
HOR"
NHCOOR" (excess)
n'
CH₃
NCO
NCO'
n
k₁
HOR'
a
CH₃
NHCOOR'
NCO
m₁
quenching
HOR"
(excess)
CH₃
NHCOOR"
NHCOOR"
m₁'
k₂
HOR'
a
k₂'
HOR'
a
(2)
CH₃
NHCOOR"
quenching
HOR"
NHCOOR'(excess)
m₂'
CH₃
NCO
NHCOOR'
m₂
k₁'
HOR'
a
CH₃
NHCOOR'
NHCOOR'
b

The 'idealised' kinetic equations are :

$$dN/dt = -(k_1 + k_2)\,NA$$

$$dM_1/dt = (k_1\,N - k_2'\,M_1)\,A$$

$$dM_2/dt = (k_2\,N - k_1'\,M_2)\,A \qquad (3)$$

$$dB/dt = (k_2'\,M_1 + k_1'\,M_2)\,A$$

$$dA/dt = -\,[(k_1 + k_2)\,N + k_2'\,M_1 + k_1'M_2]\,A$$

where :

$N' = N$ molar concentration of unreacted diisocyanate n
$M_1' = M_2$ molar concentration of ortho monoreacted diisocyanate m_1
$M_2' = M_2$ molar concentration of *para* monoreacted diisocyanate m_2
$B =$ molar concentration of bireacted diisocyanate b
$A =$ molar concentration of alcohol
and k_1, k_2, k_1', k_2' are rate constants.

For our situation, starting from an initial condition when $[NCO]_0/[OH]_0 = 2$ and introducing the variable τ by using the relation

$$d\tau = A dt \text{ so } \tau = \int_0^t A dt \tag{4}$$

we have :

$$\begin{aligned}
F_N &= e^{-(k_1+k_2)\tau} \\
F_{M_1} &= A_2 \left(e^{-k_2'\tau} - e^{-(k_1+k_2)\tau}\right) \\
F_{M_2} &= A_1 \left(e^{-k_1'\tau} - e^{-(k_1+k_2)\tau}\right) \\
F_B &= 1 - F_N - F_{M_1} - F_{M_2} \\
A_1 &= k_2/(k_1 + k_2 - k_1') \\
A_2 &= k_1/(k_1 + k_2 - k_2')
\end{aligned} \tag{5}$$

where F_N, F_{M_1}, F_{M_2}, F_B are the fractions corresponding to the four species ($F_N + F_{M_1} + F_{M_2} + F_B = 1$).

By removing the variable τ from the system (5), the following relations are obtained :

$$\begin{aligned}
{}_{M_1} &= [R_0/(1 - R_2)] \left(F_N^{R_2} - F_N\right) \\
F_{M_2} &= [(1 - R_0)/(1 - R_1)] \left(F_N^{R_1} - F_N\right)
\end{aligned} \tag{6}$$

where

$$R_0 = k_1/(k_1 + k_2), \ R_1 = k_1'/(k_1 + k_2) \text{ and}$$

$$R_2 = k_2'/(k_1 + k_2)$$

Using the condition $dM_1/dt = dM_2/dt = 0$ and relations (3) one obtains the maximum of F_{M_1} and F_{M_2} fractions and their F_N corresponding values :

$$\begin{aligned}
(F_{M_1})_{max} &= R_0 R_2^{R_2/(1-R_2)} \dashrightarrow F_N = R_2^{1/(1-R_2)} \\
(F_{M_2})_{max} &= (1 - R_0) R_1^{R_1/(1-R_1)} \dashrightarrow F_N = R_1^{1/(1-R_1)}
\end{aligned} \tag{7}$$

We worked at lower temperatures than in the previous work [1], i.e. at 30° C, since over 50° C the process is complicated by the sensible occurrence of the secondary reaction of alophanate formation.[3]

From the same reasons, only the data obtained in the initial and average phases of the process were taken into account, i.e. up to cca. 70% of 2,4-TDI conversion.

For a more precise mathematical analysis of experimental data we propose a new search method with good performances.

EXPERIMENTAL

Materials. — 2, 4-TDI p.a. (Merck) was purified by distillation. Purity was chemically determined[4] and the isomeric purity was verified by HPLC. Benzene and petroleum ether were dried on metallic sodium and distilled before using. Butylic alcohol (p.a.) was dried on calcium hydride and distilled. Melting points were determined in a capillary tube. IR spectra were measured with a PERKIN ELMER 577 spectrophotometer (KBr pellets). ^1H-NMR measurements were made with a JEOL 60 MHz spectrometer. HPLC measurements were made with a HEWLETT PACKARD 1084 A chromatograph provided with a UV detector of variable wavelength 1030 B.

Models synthesis. — Four model substances of following structures were synthesized as standard for HPLC :

(1) $R^1 = R^2 = Me$
(2) $R^1 = R^2 = Bu^{\frown}$
(3) $R^2 = Me,\ R^2 = Bu^{\frown}$
(4) $R^1 = Bu\ ,\ R^2 = Me$

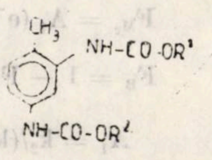

Disubstituted symmetrical models were synthesized after the general procedure used in the previous work[1]. The recrystallization solvents, the melting points and the results of elemental analysis are presented in Table 1a.

Disubstituted asymmetrical models were synthesized by a two steps reaction as follows :

Toluene (2-methyl-4-butyl) dicarbamate (3). To 10 g of 2, 4-TDI freshly distilled, solved in 15 ml anhydrous petroleum ether, a mixture of 4.2 g anhydrous butylic alcohol and a drop of pyridine were added under stirring for 40 min. The bottom liquid layer, representing the monoisocyanate, was separated in a funnel. It was solved in 50 ml anhydrous benzene and 10 ml anhydrous methylic alcohol and 0.5 ml anhydrous pyridine were added. The mixture was boiled gently. Then it was left overnight in a drying oven at 60°C. After removing the solvent by evaporation a viscous liquid was obtained which crystallized by rubbing for an hour. The crude model derivative 14.8 g recrystallized three times from a methylic alcohol-water (1 : 2 vol/vol) solution and from a water-methylic alcohol (3 : 1 vol/vol) solution to obtain 1 g model derivative of wished purity with characteristics presented in Table 1. The structure was verified by ^1H-NMR.

Toluene (2-butyl-4-methyl)dicarbamate (4). To 10 g 2,4-TDI freshly distilled, solved in 15 ml anhydrous petroleum ether, were added in drops under stirring a mixture of 1.34 g (2.31ml) methanol and a drop of anhydrous pyridine, so that mixture could gently boil. Two liquid layers were formed after about an hour. It was stirred four hours more, and thereafter, reaction mixture was cooled on ice ; the resulting solid product was separated by filtration and washed with anhydrous petroleum ether. There were obtained 10.47 g crystals, which were purified by recrystallization from 250 ml anhydrous hexane-cyclohexane (1 :1 vol/vol) mixture. The recrystalization yielded 6.46 g monoisocyanate. To 6 g monoisocyanate solved in 60 ml hot anhydrous benzene, a mixture of 10 ml anhydrous alcohol and 0.5 ml anhydrous pyridine was added. The mixture was heated overnight, at 60°C in a drying oven. The removing of the solvent left 8.05 g of crude model derivative (4), which was purified thrice by recrystallization from water-methanol (1 : 2 vol/vol) ; the recrystallization yielded 4.37 g of model compound with the melting point and the elemental analysis given in Table 1.

Table 1

HPLC models

No.	Model compound	Recrystallizations		m.p. °C	Formula	Molecular weight	Elemental analysis		
		Solvent	No.				C calc found	H calc found	N calc found
a. Models with the same substituents at the urethanic groups									
1a	Toluene-2, 4-di(methylcarbamate)	MeOH	4	171–172[a]	$C_{11}H_{14}N_2O_4$	238.24	55.46 (56.00)	5.92 (6.11)	11.76 (11.62)
1b	Toluene-2, 4-di(butylcarbamate)	MeOH MeOH–H_2O 5 : 1	1 3	80– 82[b]	$C_{17}H_{26}N_2O_4$	322.41	63.33 (63.46)	8.13 (8.03)	8.69 (8.50)
b. Models with different substituents at the urethanic groups									
1c	Toluene (2-methyl-4-butyl) dicarbamate			111–113	$C_{14}H_{20}N_2O_4$	280.33	59.98 (60.25)	7.19 (7.02)	9.99 (10.04)
1d	Toluene (2-butyl-4-methyl) dicarbamate			115–117	$C_{14}H_{20}N_2O_4$	280.33	59.98 (60.28)	7.19 (7.04)	9.99 (10.38)

[a] lit[5)] 170–171 °C

[b] lit[5)] 80– 81 °C

Kinetics. — The kinetic measurements were carried out by using the HPLC method described in the previous work[1].

Initial concentrations were the same, i.e. $C_0^{2,4-TDI} = C_0^{3-BuOH} = 0.175$ mole/l.

Benzene was used as solvent. To avoid side reactions, noted by other authors,[3] we worked at temperatures of 30°C and to conversions of 2,4-TDI up to 70%.

HPLC analysis. — The apparatus and the manner of working were the same as in the previous work.[1] The analysis was carried out in two steps : firstly only two maxima were isolated. The first corresponded to n′ species of blocked unreacted isocyanate and the second to the mixture of m_1' together with the m_2' species, representing the blocked *ortho* and respectively *para* monoreacted diisocyanates (Table 2a).

Table 2

HPLC conditions for separation

Time min	Mobile phase		Flow ml/min	Wave length (nm)	Retention time		
	Water % 80°C	Methanol % 40°C			Species	Model	min.

a. Crude separation, column Lichrosorb RP18 10μm 250 mm long, 4.6 mm Ø gradient

Time min	Water % 80°C	Methanol % 40°C	Flow ml/min	Wave length (nm)	Species	Model	min.
	40	60	1	240	n′	1	3.51
5	30	70			$m_1' + m_2'$	3 or 4	6.85
10	30	70			b	2	12.97

b. High separation, column Lichrosorb RP_{18} 5 μm 250 mm long, 4.6 mm Ø

Time min	Water % 80°C	Methanol % 40°C	Flow ml/min	Wave length (nm)	Species	Model	min.
	63	37	1	240	n′	1	7.91
					m_2'	3	57.18
					m_1'	4	60.16

In the second step we determined the ratio between the concentration of m_1 and m_2 species as shown in Table 2b.

In the latter case to shorten the analysis time after 65 min the b species was removed by washing the column with a water methanol mixture (25 : 75 vol/vol). An esential condition to have a good separation of the peaks is to use a new chromatographic column in the condition of the warranty stipulated by producer.

Concentrations from n, the sum $(m_1 + m_2)$ and b species were calculated from the first separation. The individual determination of m_1 and m_2 concentration was achieved by second separation. In Figure 1 the evolution of molar concentration of species during the reaction is plotted.

RESULTS AND DISCUSION

To test the relation group (5) the calculation of τ given by relation (4) was necessary. The determination of molar concentration of alcohol was realized indirectly, taking into account that $A = N - B$ since $A_0 = N_0$. Numerical integration was achieved through a double square

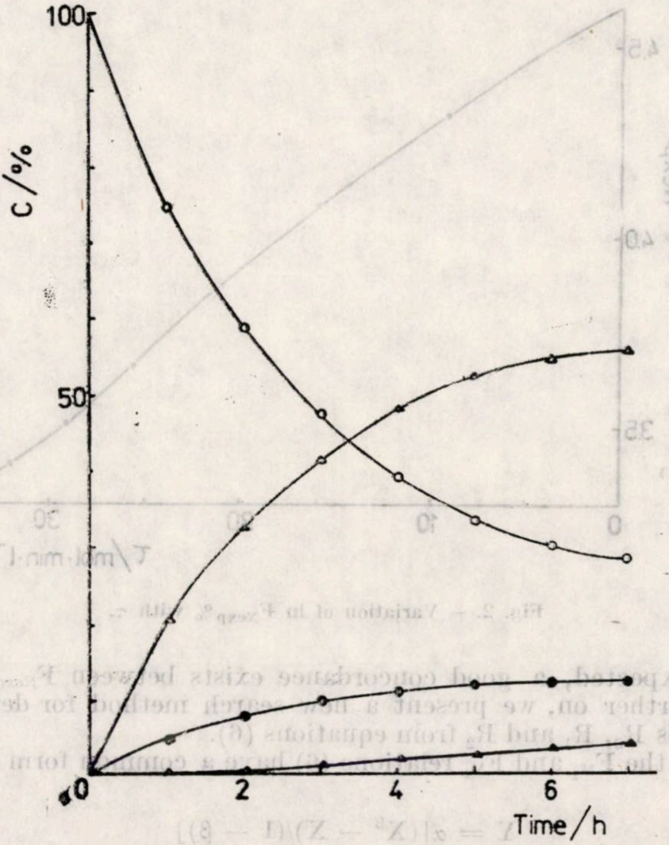

Fig. 1. — Evolution in time of molar concentration corresponding to the four molar species

O — n Δ — m_1 ● — m_2 ▲ — b

interpolation method [6]. The dependence of experimental value, F_{Nexp} versus τ is plotted in Figure 2. It is noticed that this dependence may be approximated well enough by a straight line. This fact is reflected through a relatively stable value of $k_1 + k_2$ constants sum.

Table 3 presents the experimental values F_{Nexp}, corresponding of τ values, and the $k_1 + k_2$ sum calculated with relation :

$$k_1 + k_2 = -\ln (F_{Nexp})/\tau \qquad (8)$$

As in the previous work,[1] the checking of $k_1 + k_2$ values was realized by comparing F_{Nexp} value with F_{Ncalc} one obtained through equation (9).

$$F_{Ncalc}\% = 100\ e^{-\overline{(k_1+k_2)}\tau} \qquad (9)$$

where $\overline{k_1 + k_2}$ is the arithmetical mean of the obtained values (Table 3).

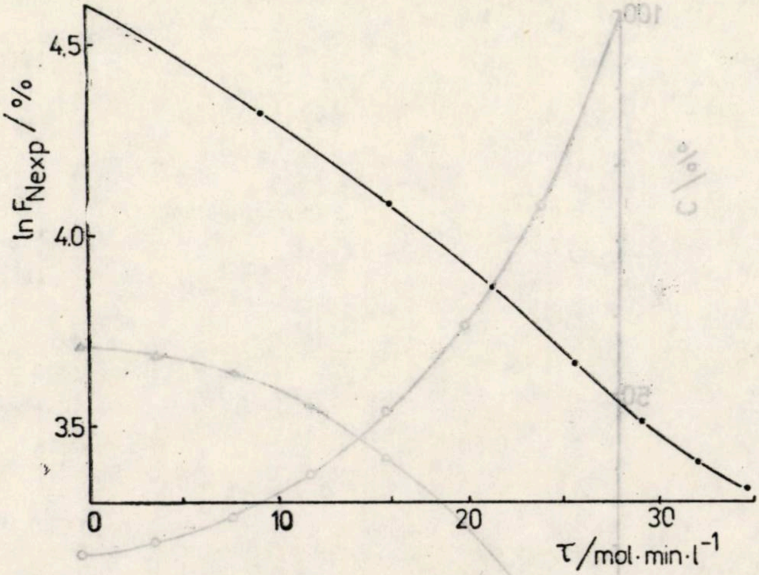

Fig. 2. — Variation of ln F_{Nexp}% with τ.

As expected, a good concordance exists between F_{Nexp} and F_{Ncalc} values. Further on, we present a new search method for determination of constants R_0, R_1 and R_2 from equations (6).

Both the F_{M_1} and F_{M_2} relations (6) have a common form as follows:

$$Y = \alpha[(X^{\beta} - X)/(1 - \beta)] \tag{10}$$

where $X = F_{Nexp}$, $Y = F_{M_1exp}$, $\alpha = R_0$ and $\beta = R_2$
or $X = F_{Nexp}$, $Y = F_{M_2exp}$, $\alpha = 1 - R_0$ and $\beta = R_1$

Table 3

Values of τ function, $(k_1 + k_2)$ sum and F_{Ncalc} %

No.	T min	F_{Nexp} %	τ mol.min.l^{-1}	$k_1 + k_2$ mol^{-1} · min^{-1} · l	F_{Ncalc} %
1	0	100.00	0.00		100.00
2	60.1	74.58	9.11	0.0322	72.31
3	120.1	58.46	15.96	0.0336	56.65
4	180.1	47.41	21.33	0.0350	46.79
5	239.9	38.86	25.62	0.0369	40.17
6	300	33.31	29.12	0.0378	35.46
7	359.9	30.02	32.10	0.0375	31.89
8	420	28.35	34.76	0.0363	29.01
			$\overline{k_1 + k_2} = 0.0356$		

We notice that :

$$Y_1 = (X^{\beta} - X)/(1 - \beta) \tag{11}$$

The procedure is as it follows : we adopt for β different equidistant values in a given interval (in our case $\beta \in [0, 1]$), considering initially an increment $\Delta\beta = 0.01$.

For a particular value of β we calculate the average value of α, corresponding to that of the n experimental data :

$$\bar{\alpha}(\beta) = \sum_{i=1}^{n} [Y(i)/Y_1(i, \beta)]/n \tag{12}$$

where Y(i) represents $F_{M_1 exp}$ or $F_{M_2 exp}$ value, and $Y(i, \beta)$ is the corresponding value calculated with equation (11). The average value is adopted with a view to calculate the sum of square mean errors.

$$S(\beta) = \sum_{i=1}^{n} [Y(i) - \bar{\alpha}(\beta)\, Y_1(i, \beta)]^2 \tag{13}$$

It was observed that, for every series of experimental data corresponding to each of the two monoreacted species the respective $S(\beta)$ values present a unique minimum. As a first β_{opt} value corresponding to minimum of S was established, the procedure is repeated in order to obtain a more precise value of β_{optim}. This time the interval $[\beta_{optim} - 0.01), \beta_{optim} + 0.01]$ was considered, taking $\Delta\beta = 0.001$ as increment. The procedure is repeated until the desired precision is obtained. This search method could be applied to all functions of the type $Y = \alpha f(X, \beta)$ The obtained data are presented in Table 4.

Table 4

Optimal values of α and β parameters for the two species obtained by search method

Type of monoreacted species	α_{opt}	β_{opt}
M_1	$\alpha_1 = R_0 = 0.107$	$\beta_1 = R_2 = 0.186$
M_2	$\alpha_2 = 1 - R_0 = 0.803$	$\beta_2 = R_1 = 0.044$

Adopting for the $(\overline{k_1 + k_2})$ sum the average value of 0.0356 $mole^{-1} \cdot min^{-1} \cdot l$ the following rate constants were calculated, by means of equation (6) :

$$k_1 = 7.013\ 10^{-3}$$

$$k_2 = 28.59\ 10^{-3}$$

$$k_1' = 1.577\ 10^{-3}$$

$$k_2' = 6.604\ 10^{-3}$$

all in $\text{mole}^{-1} \cdot \text{min}^{-1} \cdot \text{l}$.

Table 4 points out to a remarkable thing: the R_0 and $(1 - R_0)$ values, independently determined for each of the two F_{M1} and respectively F_{M1} data series, are in good agreement. This situation proves both the good precision of the experimental measurements and the efficiency of the above presented method. In Table 5 the experimental data are compared with those obtained theoretically by the substitution in equations (6) of values given in Table 4.

A very good agreement can be noticed between experimental and calculated values. The parameters R_0, R_1, and R_2 obtained before give us the possibility to calculate the final composition of the reaction mixture using also a search method, keeping in view that at the end of the reaction $F_{Nf} = F_{Bf}$. For this it starts from the last $F_{N\text{exp}}$ value and we calculate the composition of the system using equations (6) for different equidistant values of F_N and an initial increment $\Delta F_N = 0.01$. The calculation ends when $F_{Bf} > F_{Nf}$. At this point the calculation can be continued to give a more precise result by using a smaller increment for F_N. i.e. $\Delta F_N = 0.001$. The variation interval of F_N is now $[F_{Nf} - 0.01, F_{Nf}]$. Evidently the new cycle of calculations should give more precise values for the final composition. To determine a much more precise final composition the calculation should be continued with a smaller F_N increment.

Table 5

Comparison of $F_{M_1\text{exp}}$ values with $F_{M_1\text{calc}}$ values (all in %)

No.	$F_{M1\text{exp}}$	$F_{M1\text{calc}}$	$F_{M2\text{exp}}$	$F_{M2\text{calc}}$
1	4.85	4.86	20.57	20.27
2	7.63	7.74	32.54	32.93
3	9.64	9.57	41.36	41.45
4	10.94	10.87	47.88	47.92
5	11.76	11.64	52.14	52.04
6	12.11	12.06	54.47	54.43
7	12.10	12.26	55.49	55.63

The following values were thus obtained (all in %):

$$F_{Nf} = 9.47$$

$$F_{M_1f} = 13.33$$

$$F_{M_2f} = 67.77$$

$$F_{Bf} = 9.47$$

CONCLUSIONS

From the contained data we conclude that following this method of kinetic study of uncatalysed reactions between 2,4-TDI and alcohols, one could determine directly the four rate-constants of the process. The ratios of these rate-constants $k_2/k_1 = 4.08$, $k_1/k_1' = 4.45$, $k_2/k_2' = 4.33$ present constant values on the whole pattern of reaction. The found ratios allow the calculation of composition of the reaction mixture at any moment when F_N is known. Our practical determinations demonstrate that the final composition is obtained after a certain period of time, but the system has a reduced stability and the composition changes gradually due to side reactions. We must take into account that in the final stages of the reaction the incidence of side reactions increases. These side reactions occur especially between urethanic groups, which are found now in high concentrations, and the small amount of the intermediate reactive specie m_1 resulted in the reaction. Comparing our data obtained directly with some theoretical approximations [7,8] made previously, we conclude that, for a first orientation, the assumption of equality of ratio k_1/k_1' and k_2/k_2' in the case of reaction between 2,4-TDI and alcohols with small molecules is valid. The value of these ratios, averaging 4.4 is approximately the same even for other alcohols and other experimental conditions although the absolute values of rate,-constants are more different than those founded earlier [7,8]. In the case of reaction of isocyanates with alcohols having large molecules, such as the oligoesters, or the oligoethers with OH end groups [3,9], the values of this ratios can change due to the increase of steric influences of macromolecular radical bounded in the first step of the reaction. In these cases it is necessary to apply the complete procedure presented in this work.

REFERENCES

[1] A. Caraculacu, I. Agherghinei, M. Gaspar and C. Prisăcariu, *J. Chem. Soc. Perkin II*, 1343 (1990).

[2] A. Caraculacu, I. Agherghinei and C. Prisacariu, Submitted for publication to *J. Macromolecular Sci. Chem.*, **A 27**, 1547 (1990).

[3] V. P. Lodygina, Ye. V. Stovbun and S. M. Baturin, *Vysokomol. Soedineniya Ser. A.*, **27**, 921–926 (1985).

[4] S. Siggia, and J. S. Hanna, *Analyt. Chem.* **20**, 1084 (1948).

[5] D. J. David and H. B. Staley, "Analytical Chemistry of the Polyurethanes", vol. XVI, part. III Wiley-Interscience, New York, 1969, p. 581.

[6] I. Todoran, "Tratarea matematică a datelor experimentale", Ed. Academiei, Bucharest 1976, p. 193.

[7] L. C. Case, *J. Polymer Sci.*, **48**, 27 (1960).

[8] F. H. Brock. *J. Phys. Chem.*, **65**, 1638 (1961).

[9] Ye. V. Stovbun, V. P. Lodygina, Z. S. Andrianova and S. M. Baturin, *Vysokomol. Soedineniya Ser. A*, **29**, 12, 2500 (1987).

Revue Roumaine de Chimie, **36**, *9–10*, 1147–1160 (1991)

COMPOUNDS WITH POTENTIAL CANCER PREVENTING ACTIVITY. I.

SYNTHESIS, PHYSICO-CHEMICAL PROPERTIES AND QUANTUM CHEMICAL INDICES OF SOME PHENOLIC AND AMINOPHENOLIC ANTIOXIDANTS

JEAN HERDAN,[a] ALEXANDRU T. BALABAN,[b] GERALD STOICA,[c] ZENO SIMON,[d] MIRCEA MRACEC[d] and ION NICULESCU-DUVĂZ[c]

[a] Petroleum Institute of Technology, Ploiești, Roumania
[b] Polytechnic Institute, Faculty of Industrial Chemistry, Chair of Organic Chemistry, Splaiul Independenței 313, 77206 Bucharest, Roumania
[c] Oncological Institute, Dept of Carcinogenesis and Anticarcinogenesis, Sos. Fundeni 252, 72425 Bucharest, Roumania.
[d] Faculty of Medicine, Chair of Biophysics, Timișoara, Roumania

Received March 30, 1991

In an attempt to develop a QSAR analysis for a series of chemicals acting as carcinogenesis inhibitors, the physico-chemical properties as well as some quantum chemical indices of 34 compounds (substituted phenols, diphenols and aminophenols) were investigated. The synthesis of two new compounds belonging to these series (2, 6-dimethyl-4-hydroxy-thiophenol and 3, 5-di-*t*-butyl-4-hydroxybenzyl-bromoacetate) was also described. As physical properties the lipophilicities (log P) and Hammett constants (σ) were computed; ε_{HOMO}, ε_{LUMO}, and q were also calculated using HMO and ω-HMO procedures. These computations were also extended to the corresponding *p*-benzoquinones. The obtained data were used to discuss the possible mechanisms of action (scavenger effect, enzymatic inhibition etc.) by which such compounds may exert their carcinogenesis inhibitory properties.

INTRODUCTION

Cancer chemoprevention is considered to be one of the "hot spots" of the contemporary cancer research.[1–5] Many observations were reported concerning the decrease of the incidence and the reduction of severity of chemically induced malignant tumors by the intake of various chemicals, i.e. phenolic antioxidants,[6–8] selenium compounds,[9] retinoic acid[10] and other natural compounds existing in fruit, vegetables etc.[11,12].

Chemically induced carcinogenesis in experimental animals is a multistage process involving inhibition and promotion.[5,13] Therefore the carcinogenesis inhibitions were classified taking into account their mechanisms of action, as antiinitiators and antipromoters (or blocking and suppressive agents, respectively) according to Wattenberg's classification[4] (see table 1).

Table

Physico-chemical properties of the

No.	Compound	mp. (°C)
1	2	3
1	2-*t*-butyl-4-hydroxy-anisole (BHA)	62 – 62.5
2	2,6 -di-*t*-butyl-4-methylphenol (BHT)	69.5 – 70.5
3	*o*-cresol	30.4
4	*m*-cresol	11.9
5	*p*-cresol	34.7
6	2, 4-di-*t*-butylphenol	54 – 56.5
7	2, 4-di-*t*-butyl-6-mercaptophenol	64 – 65
8	2, 6-di-*t*-butylphenol	38 – 39
9	2, 6-di-*t*-butyl-4-bromphenol	83 – 83.5
10	2, 6-di-*t*-butyl-4-nitrosophenol	219
11	2, 6-di-*t*-butyl-4-mercaptophenol	84 – 85
12	3, 5-di-*t*-butyl-4-hydroxy-benzaldehyde	188 – 189
13	3, 5-di-*t*-butyl-4-hydroxy-benzaldoxime	131 – 132
14	(3, 5-di-*t*-butyl-4-hydroxy-benzyl)bromoacetate	64
15	3, 5-dimethyl-4-hydroxy-thiophenol	90 – 91
16	3, 5-di-*t*-butyl-4-hydroxy-benzyl alcohol	139 – 140
17	3, 5-di-*t*-butyl-4-hydroxy-benzyl bromide	54 – 55
18	3, 5-di-*t*-butyl-4-hydroxy-benzoic acid	210 – 211
19	resorcinol	α = 108 β = 109 – 110
20	hydroquinol	173.8 – 174.8
21	4-hydroxyanisole	53 – 56
22	2-hydroxyanisole	28.5
23	2, 5-di-*t*-butylhydroquinol	213
24	2, 6-di-*t*-butylhydroquinol	114 – 116
25	4-*t*-butylpyrocatechol	55
26	3, 5-di-*t*-butylpyrocatechol	98 – 100
27	4-aminophenol	191 – 192
28	4-(methylamino)phenol	259*
29	4-(dimethylamino)anisole	79
30	4-(dimethylamino)anisole	48 – 49
31	2-aminophenol	179
32	2-aminoanisole	liq.
33	4-aminoanisole	57 – 58
34	3-(dimethylamino)phenol	82 – 84
35	*p*-benzoquinone	115.5 – 116.5
36	2, 5-di-*t*-butyl-*p*-benzoquinone	150 – 152
37	2, 6-di-*t*-butyl-*p*-benzoquinone	68
38	3, 5-di-*t*-butyl-*o*-benzoquinone	113 – 114

a) where no otherwise noted the constants are from Beilstein ; b) synthetized by us (see

e) σ_p values only.

1

investigated phenolic antioxidants

log P 4	(log P)^2 5	σ_I 6	pK$_a$ 7	Ref. 8
1.90^d	3.61	−0.37	10.56	21.22
2.75	7.56			
5.45	29.70	p-CH$_3$ −0.17^e	14	—
1.95^d	3.80	−0.22	10.29	—
1.96^d	3.84	−0.17	10.09	—
1.93^d	3.72	−0.07	10.26	—
5.09	25.91	−0.94	11.57	—
5.28	27.88	—		23
5.09	25.91	−1.24	11.70	—
5.75	33.06	p-Br −0.23^e	10.83	24
4.77	22.75	p-NO −0.12^e	6.18	25
5.28	27.88	p-SH −0.15^e		26
4.28	27.88	p-SH −0.15^e	8.05	26
4.51	0.34	p-CH=NOH −0.10^e		28
3.77	14.21	—		(b
2.50	6.25	−0.29		(b
3.88	14.90	p-CH$_2$OH 0.00^e		29
5.68	32.26	p-CH$_2$−Br 0.14^e		30
4.57	20.88	p-CO$_2$H −0.45		31
0.53	0.28			
0.80^d	0.64	0.12	9.62	—
0.59^d	0.35	−0.37	10.12	—
1.34^d	1.80	−0.27	10.43	—
1.31^d	1.72	0.60^c	9.20	—
3.88	15.05	−1.21	11.65	—
3.88	15.05	p-OH −0.37^e		—
2.66	7.07	—		—
4.44	1.97	−0.82	>11.4	—
0.04^d	0.00	−0.66	11.15	—
0.8	0.64	−0.84	10.40K$_a$(OH) K$_a$(NH$_2$)	—
1.45	2.40	−0.83	10.25	—
1.56	2.43	—	10.22	—
0.57^d	0.32	—	5.14	—
0.95^d	0.90	—	9.7	—
0.95^d	0.90	—	4.52	—
1.56^d	2.43	—	5.29	—
0.20^d	0.04	—	9.85	—
3.76	14.14	—		—
3.76	14.14	—		—
3.76	14.14	—		—

experimental section) ; $^{c)}$ calculated with eq. 2 σ_{o,OCH_3} apparent ; $^{d)}$ experimental values ;

The phenolic antioxidants constitute an importat class of blocking agents. Currently available data demonstrate that 2-*t*-butyl-4-hydroxyanisole (BHA) **1**, 2,6-di-*t*-butyl-4-methylphenol (BHT) **2**, and some other phenolic antioxidants [14,15] are able to reduce the incidence of malignant tumors induced in experimental animals by several types of chemical carcinogens such as benzo[*a*]pyrene (BaP), 7,12-dimethyl-benzo[*a*] anthracene,[16] N-nitroso-amines [16] etc.

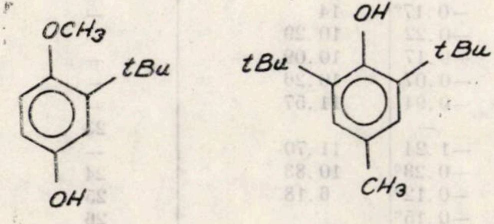

1 2

Fig. 1. — Structure of BHA (**1**) and BHT (**2**).

Reviews [3,5,6] on the mechanisms of action for antioxidants are available.

In a previous approach [17] correlational analysis between the reduction of the incidence of the forestomach tumors induced by BaP intake in mice in the presence of di- and polysubstituted phenols was undertaken in order to establish the structural features responsible for their carcinogenesis inhibitory properties. Using the Hansch procedure the following equation was obtained :

$$\log\frac{100}{100 - \mathrm{T/C}} = 0.660 + 0.669(\pm 0.092)\mathrm{MTD} - 0.087(\pm 0.079)\pi + 0.050\ (\pm 0.107)\sigma \qquad \text{(eq. 1)}$$

$$n = 12 \qquad r = 0.925 \qquad F = 15.88$$

The computed equation suggests that substituted aminophenols might be also of potential value in cancer chemoprevention (an assumption which seems to be true [18]). Moreover their oxidation products are significantly more powerful inhibitors of *in vitro* ultimate carcinogens—DNA adduct formation [18,19] as well as of the cytochrome P-450 monooxygenases [19] than the parent compunds. The obtained data suggest that probably quinoneiminic stuctures are involved in this effect. However, because these compounds are rather unstable and therefore difficult to handle as potential chemopreventive agents, we extended our investigation to the corresponding unhindered and hindered *p*-benzoquinones. The following types of compounds were investigated :

(i) cresols (n = 3) ;
(ii) substituted 2,4-di-*t*-butylphenols (n = 2) ;
(iii) substituted 2,6-di-*t*-butylphenols (n = 14) ;
(iv) unsubstituted and substituted diphenols (especially hydroquinol derivatives) (n = 7) ;

(v) substituted aminophenols (n = 7);
(vi) hindered and unhindered *p*-benzoquinones (n = 4).

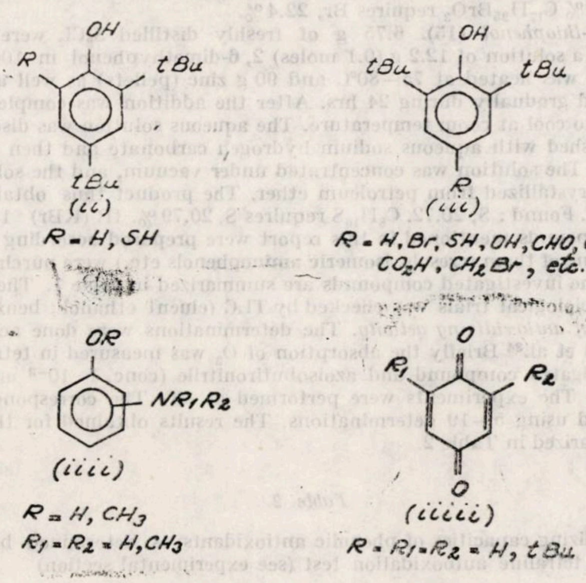

Scheme 1 — Types of investigated compounds.

We were able to demonstrate that 2,6-di-*t*-butyl-*p*-benzoquinone is very effective in protecting DNA against carcinogen interaction and is also a powerful inhibitor of cytochrome P-450 dependent monooxygenase.[19] It does not interefere with GST and may be considered to have a very low acute toxicity (DL_{50} = 3085 mg/kg b.w.).[19,20] In order to find valuable criteria for the design of better carcinogenesis inhibitory compounds, a QSAR analysis of these compounds was undertaken and will be published elsewhere. This report is concerned with:

(i) some synthetic aspects concerning the preparation of two new derivatives;
(ii) the calculation of their lipophilicity;
(iii) the determination of their antioxidant capabilities using the test of initiated O_2 absorption in tetraline;
(iv) the computation of some quantum chemical indices;
(v) the discussion of their possible mechanisms of action.

EXPERIMENTAL SECTION

Melting points were determined on a Boetius melting point apparatus and are uncorrected. IR spectra were obtained with an IR 75 Carl Zeiss Jena spectrophotometer. ^1H—NMR spectra were determined on a Varian ELM-60 spectrometer. C; H; N analyses were within ± 0.3% of theoretical values.

3,5-*Di-t-butyl-4-hydroxy-benzyl bromoacetate* (**14**). To a solution containing 2.36 g (10 mmoles) of 3,5-di-*t*-butyl-4-hydroxybenzyl alcohol in 50 mL dry pyridine (cooled at 0°C) 10 mmoles of bromoacetyl bromide were added under ice cooling and vigorous stirring. When the addition was complete (0.5 hrs at 0—5°C), the mixture was stirred for one hour at room temperature and then another hour at 50—60°C. The reaction mixture was then poured into cold water and the white precipitate thus formed was filtered and dried *in vacuo*. Recrystallization from ethanol afforded a compound with m.p. 64° (37.2% yied). IR (KBr); 1735, 3620 cm^{-1}; Anal. found Br, 22.17% $C_{17}H_{25}BrO_3$ requires Br, 22.4%.

3, 5-*Dimethyl-4-thiophenol* (**15**). 6.75 g of freshly distilled S_2Cl_2 were added during 1 hr under stirring to a solution of 12.2 g (0.1 moles) 2, 6-dimethyphenol in 100 mL benzene. The reaction mixture was heated at 75—80°C and 90 g zinc (pellets) as well as 90 mL HCl (d = 1.19) were added gradually during 24 hrs. After the addition was complete the reaction mixture was allowed to cool at room temperature. The aqueous solution was discarded and the organic layer was washed with aqueous sodium hydrogen carbonate and then dried on anhydrous sodium sulfate. The solution was concentrated under vacuum, and the solid thus formed was collected and recrystallized from petroleum ether. The product thus obtained had m.p. 90—91° (57.7%). Anal. Found : S, 20.72. $C_8H_{10}S$ requires S, 20.79%. IR (KBr) : 1590, 3450 cm^{-1}.

The other compounds mentioned in this report were prepared according to known synthetic procedures. Some of them (cresols, isomeric aminophenols etc.) were purchased from commercial sources. All the investigated compounds are summarized in table 1. The purity of the compounds used for biological trials was checked by TLC (eluent ethanol : benzene, 1 : 5 v/v).

Determination of antioxidizing activity. The determinations were done according to the procedure by Pospisil et al.[34] Briefly the absorption of O_2 was measured in tetraline solutions containing the investigated compound and azoisobutironitrile (conc. $1 \cdot 10^{-3}$ and $2 \cdot 10^{-3}$ respectively moles/liter). The experiments were performed at 80°. The corresponding regression curves were calculated using 5—19 determinations. The results obtained for the investigated compounds are summarized in Table 2.

Table 2

Antioxidizing capacities of phenolic antioxidants as determined by the tetraline autooxidation test (see experimental section)

No.	$k \cdot 10^5$ M.min^{-1}	x_0^a min	n	r^2 ^{b}	$s \cdot 10^4$ ^{c}
1	2	3	4	5	6
1	0.91	30.8	10	0.968	4.20
	1.14	50.8	8	0.984	4.24
2	1.21	11.7	11	0.993	3.73
3	1.32	− 0.9	7	0.988	3.96
4	1.00	−14.6	8	0.959	3.41
5	1.90	3.1	8	0.982	4.36
6	0.35	18.0	19	0.987	3.72
7	1.03	7.1	9	0.993	4.42
8	1.07	−10.3	10	0.975	3.54
9	1.42	3.1	9	0.989	3.82
10	0.36	21.0	12	0.981	3.77
11	3.45	1.9	6	0.998	4.00
12	1.13	0.2	8	0.975	4.00
13	0.74	14.6	10	0.984	4.26
14	0.51	1.0	10	0.997	4.00
15	2.43	3.8	9	0.996	3.33
16	3.36	7.3	7	0.995	3.64
17	0.92	− 1.3	11	0.994	3.62
18	1.94	7.2	5	0.998	4.31
19	1.72	6.7	7	0.991	4.06
20	1.18	− 3.0	7	0.999	3.70
21	0.60	9.8	9	0.997	4.31
22	0.44	− 5.5	11	0.994	3.96
23	1.44	20.0	7	0.985	4.61

[a]) latentiaton period; [b] coefficient of determination; [c] standard deviation of the estimate.

Lipophilicity parameters. For phenol, 4-hydroxyanisole, 2-*t*-butylphenol, 2-*t*-butyl-hydroquinol, 2-*t*-butyl-4-hydroxyanisole, 3- and 4-aminophenol and isomeric cresols, the experimental partition coefficients in octanol-water system were taken from the literature.[35,36] The lipophilicities (log P) for the other investigated compounds were calculated based on the additivity of the substituent constants (Π).[36,37] For the carboxylic function in some cases both Π values of unionized and ionized groups were used namely $\Pi_{CO_2H} = -0.32$ and $\Pi_{CO_2^-} = -4.36$ respectively, because we assumed that at pH = 7.0 the ionized form of the carboxylic moiety is predominant in some cases. The data thus obtained are summarized in table 1.

Hammett parameters. The Hammett substituent constants were taken from the literature.[37] For some of the derivatives for which suitable data were not found, this parameter was calculated on the basis of their basicity.[25] Accordingly the correlational equation (2) was established from literature pKa [38] data determined spectrophotometrically for a number of 13 structurally related phenols :

$$pKa = -1.298\,\Sigma\,\sigma_i + 10.084 \qquad \text{(eq.2)}$$

$$n = 13 \qquad s = 0.73 \qquad n = 0.965$$

The equation was employed to estimate some less usual values appearing in this series especially some σ *ortho* apparent values (i.e. $\sigma_{o-t-\text{butyl}}$, $-$ 0.74 ; $\sigma_{o-\text{methyl}} = -0.22$ etc.). The σ thus obtained for compounds were summarized in table 1; σ of 2, 6-di-*t*-butylphenol was re-

Table 3

Quantum chemical parameters computed by ω — HMO procedures for the investigated carcinogenesis inhibitors

No.	q_0[a]	ε_{HOMO}	ε_{LUMO}	$\Delta E = \varepsilon_{HOMO} - \varepsilon_{LUMO}$
1	2	3	4	5
1	1.941	0.729	−1.051	1.780
2	1.945	0.733	−1.156	1.889
3	1.940	0.807	−1.042	1.849
4	1.938	0.823	−1.037	1.865
5	1.940	0.779	−1.080	1.859
6	1.942	0.790	−1.059	1.849
7	1.941	0.768	−1.027	1.795
8	1.943	0.812	−1.069	1.882
9	1.942	0.789	−1.052	1.841
10	1.914	0.877	−0.012	0.889
11	1.942	0.754	−1.037	1.791
12	1.940	0.826	−0.931	1.757
13	1.939	0.597	−0.627	1.224
14	1.945	0.733	−1.156	1.889
15	1.943	0.732	−1.049	1.781
16	1.944	0.730	−1.114	1.844
17	1.944	0.732	−1.114	1.847
18	1.940	0.821	−0.939	1.760
19	1.939	0.808	−1.029	1.837
20	1.940	0.755	−1.022	1.777
21	1.940	0.750	−1.022	1.772
22	1.940	0.780	−1.030	1.810
23	1.943	0.709	−1.066	1.775
24	1.943	0.714	−1.094	1.818
25	1.941	0.751	−1.044	1.795
26	1.945	0.760	−1.019	1.779
27	1.941	0.666	−1.034	1.702
28	1.941	0.454	−1.034	1.488
29	1.942	0.273	−1.039	1.312
30	1.942	0.272	−1.040	1.312
31	1.942	0.692	−1.047	1.739
32	1.941	0.690	−1.048	1.738
33	1.941	0.290	−1.051	1.341

[a] q_0 = charge density at atom O_1.

jected because we considered that the error introduced by this kind of computation in this particular case is unacceptably large. There is also the case of some other 2, 6-di-*t*-butyl substituted phenol derivatives, in which the *o, o′*-bulky substituents induced a large inhibition of both the resonance and the hydration of the reaction center.

Quantum-chemical calculations. The computations of quantum chemical indices were performed using the ω-HMO procedure and in some cases also the HMO ones. The computations were achieved using a CORAL 4021 computer, an operating system RSX 11M and FORTRAN 77 as program language.

The energies of the highest occupied (ε_{HOMO}) and lowest empty (ε_{LUMO}) molecular orbital respectively as well as $\Delta E = \varepsilon_{HOMO} - \varepsilon_{LUMO}$, were calculated for the investigated compounds. The results thus obtained were summarized in table 3.

Atomic charge densities (q) were calculated for 2, 6-di-*t*-butylhydroquinone (see Fig. 2) taking into account also the steric hindrance introduced by the *o,o′* bulky substituents ($\beta_{OH,\text{hindered}} = 3/4\ \beta_{OH} = 0.63$).

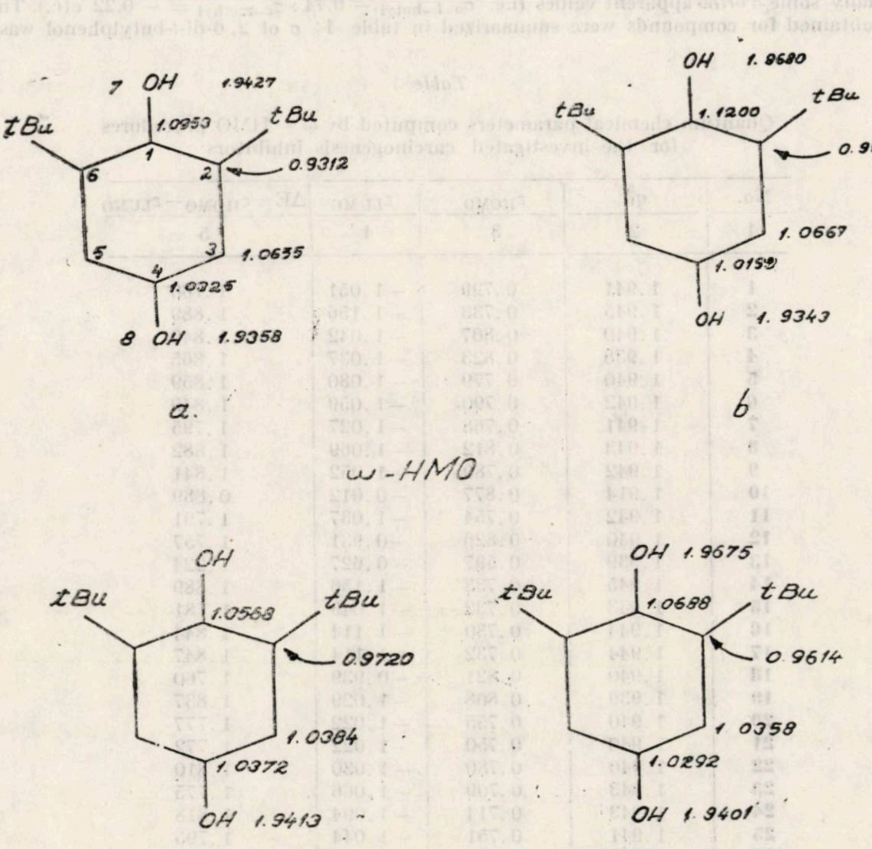
HMO
7 OH
1.9427
tBu
tBu
1.0953
1
2
6
0.9312
5
3
1.0635
4
1.0325
8 OH
1.9358
a.
OH
1.9680
tBu
tBu
1.1200
0.9126
1.0667
1.0159
OH
1.9343
b
ω-HMO
OH
tBu
tBu
1.0568
0.9720
1.0384
1.0372
OH
1.9413
a.
OH
1.9675
tBu
tBu
1.0688
0.9614
1.0358
1.0292
OH
1.9401
b.

Fig. 2. — Atomic change densities calculated for 2, 6-di-*t*-butylhydroquinone by :
A) HMO procedure
B) ω-HMO procedure
a) without steric hindrance
b) with steric hindrance.

The computation of these parameters was done using for coulombian and for the resonance integrals the values calculated by an optimization procedure developed by Mracec et al.[39] These values are given in table 4.

Table 4

Parameters used for the computation of coulombian and resonance integrals[a]

No.	Chemical function	$\alpha_x = \alpha + h_x\beta$ where h_x	Bond	$\beta_{xy} = k_{xy}\beta$[(a] where $k_{xy}^{b)}$	Ref.
1	$-OH$	2	—	—	39
2	$-C(OH)$	0.2	$C-OH$	0.84	39
3	$-C-C(CH_3)_3$	−0.2	—	—	40
4	$-CH_3$	3	$C-CH_3$	0.7	40
5	$-C(CH_3)_3$	−0.1		—	40
6	$=O$	0.2	$C=C-$	2.4	41
7	$-C=O$	0.2	—	—	41
8	$=N-$	0.5	$C=N-$	1	42, 43
9	$-NO_2$	−0.4	—	—	43
10	$-N(\text{in } NO_2)$	1.8	$N-O(\text{in } NO_2)$	0.7	42, 43
11	$-O(\text{in } NO_2)$	1.5	—	—	42, 43
12	$-C(-NO_2)$	0.25	$C-NO_2$	0.7	42, 43
13	$-NH-$	1.5	$C-NH-$	0.7	42, 43

[a] $\beta \cong 20$ kcal ; [b)] for the computation of steric hindrance : $k'_{xy} = 0.75k_{xy}$.

The same quantum chemical indices were calculated also for 2, 5-di-*t*-butyl-benzoquinones assuming both sterically hindered and non-hindered parameters. The results are summarized in table 5.

Table 5

Quantum-chemical parameters computed for tert-butyl substituted *o*- and *p*-benzoquinones

No.	Computation procedure	q_0	ε_{HOMO}	ε_{LUMO}	$\Delta E = \varepsilon_{HOMO} - \varepsilon_{LUMO}$
35	ω−HMO	1.225	0.809	−0.152	0.960
36	HMO	0.9996	0.7168	−0.7268	1.4436
	ω−HMO	1.0082	0.7184	−0.7214	1.4398
37	HMO	1.0176	0.7172	−0.7275	1.4447
	ω−HMO	1.0138	0.7186	−0.7216	1.4402
38	ω−HMO	1.0092	0.7160	−0.7230	1.4390

RESULTS AND DISCUSSION

The compounds studied in this report are candidates for cancer chemoprevention being especially investigated for their ability to prevent the initiation stage of this process. Two types of mechanisms of action may be generally involved in this effect, namely :

a) the scavenging of free radicals, especially hydroperoxy and peroxy radicals ;

b) the inhibition of the activation (phase I) enzymes with a special emphasis on cythochrome P-450 dependent monooxygenases.

Relationship between the antioxidant properties of the investigated compounds and their potential carcinogenesis inhibitory capabilities

Recent evidence substantiates the fact that *in vivo* high concentration of peroxy radicals (ROO·) could be an increased risk factor for carcinogenesis favouring both initiation and promotion stages.[44, 45]

Several types of reactions might be responsible for the *in vivo* generation of peroxy radicals namely :

- (i) lipid cooxidation reactions controlled by prostaglandin synthetase (PHS)[46] ;
- (ii) lipid peroxidation [47] ;
- (iii) reactions in which superoxide radical anions ($\mathrm{O}_2^{\overline{\cdot}}$) are formed (i.e. the so-called redox cycling).[48,49]

The peroxy radicals thus resulted may be directly involved in carcinogen cooxidation (i.e. conversion of polycyclic aromatic hydrocarbon (PAH) diols into PAH-epoxy-diols known as ultimate carcinogens) or may interact with DNA.

This was the rationale for choosing compounds with antioxidant properties able to scavenge such peroxy radicals, as candidates for cancer chemoprevention.

The phenols containing more or less bulky substituent in the 2,6-positions are fairly good inhibitors of hydrocarbon autooxidation. The formation of more persistent aroxyl radicals (unable to initiate new autooxidation chains) during their reaction with a peroxy radical is given by the following equation :

$$\mathrm{ArOH} + \mathrm{R{-}OO\cdot} \rightarrow \mathrm{ArO\cdot} + \mathrm{R{-}OOH}$$

Therefore the antioxidant ability of phenols is expected to be enhanced by an increase of the stability of the aroxyl radical. This property directly depends on the volume of the substituents located in 2 and 6 positions as well as on the effect exerted by the substituent located in 4-position. However, the data regarding the influence exerted by the *o*- and *p*-substituents are rather confusing, because the various procedures used for determining the antioxidant activities are not always comparable.[50–52] Mention should be made of the systematic studies by Pospisil et al.[34] who reported the influence exerted by the phenolic antioxidants on tetraline autooxidation. The structure of the intermediates which appeared during the interaction between phenolic antioxidants and peroxy radicals was partially elucidated and peroxycyclohexadienone, *p*-benzoquinones, stilbenequinones and dimeric products were identified (see scheme 2).[53]

It results that one molecule of an antioxidant could react with several peroxy radicals, thus preventing the initiation of several autooxidation chains. It is also obvious that the chemical nature of the substituent in position 4 is important for determining the reaction pathway. The

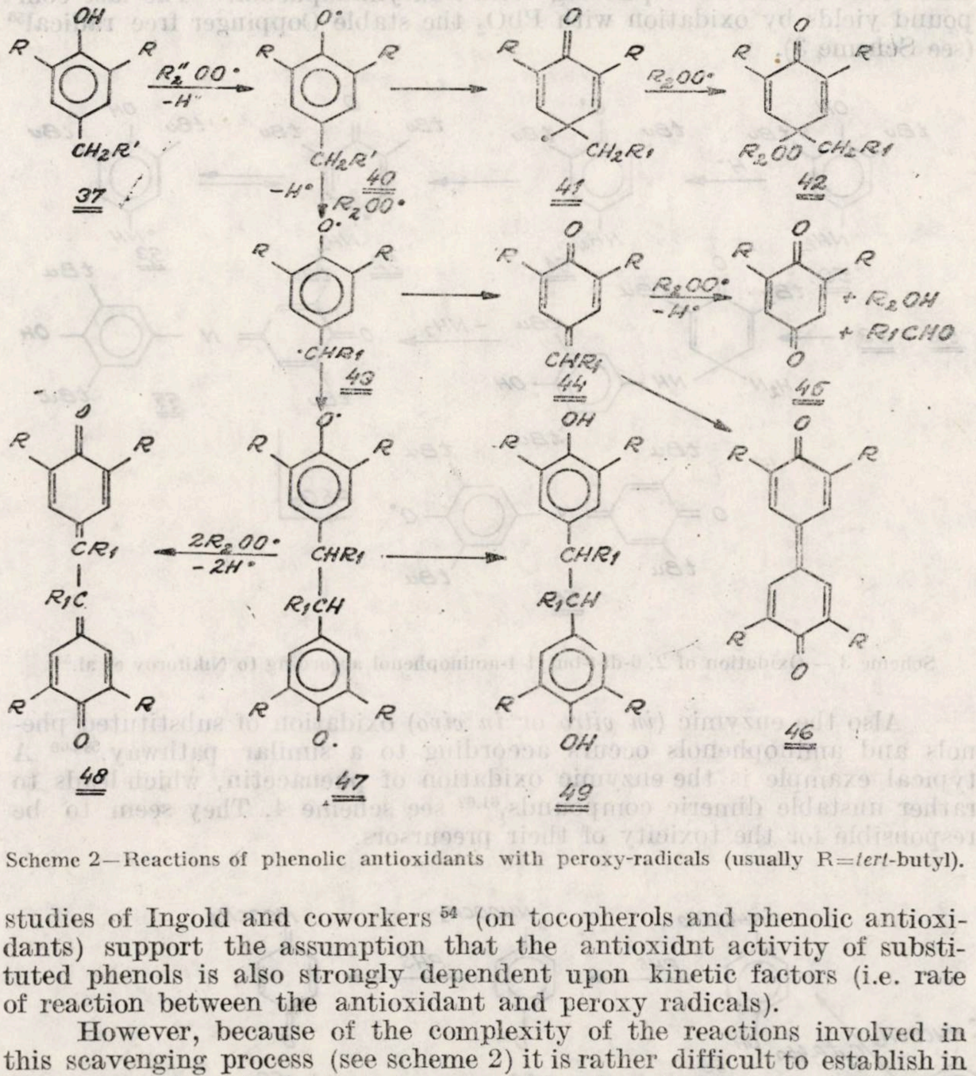
OH
R
R
R₂''OO•
-H•
CH₂R'
37
O•
CH₂R'
40
-H•
R₂OO•
O
CH₂R₁
41
R₂OO•
R₂OO
CH₂R₁
42
O•
•CHR₁
43
O
CHR₁
44
R₂OO•
-H•
+ R₂OH
+ R₁CHO
45
O
CR₁
R₁C
O
48
2R₂OO•
-2H•
CHR₁
R₁CH
O.
47
OH
CHR₁
R₁CH
OH
49
46

Scheme 2—Reactions of phenolic antioxidants with peroxy-radicals (usually R=*tert*-butyl).

studies of Ingold and coworkers [54] (on tocopherols and phenolic antioxidants) support the assumption that the antioxidnt activity of substituted phenols is also strongly dependent upon kinetic factors (i.e. rate of reaction between the antioxidant and peroxy radicals).

However, because of the complexity of the reactions involved in this scavenging process (see scheme 2) it is rather difficult to establish in most cases the rate-determining step. Therefore it would be difficult to expect to find a significant correlation between the physico-chemical or quantum mechanical parameters of the phenols and their antioxidant potencies (expressed as rates of latentiation periods, see table 2).

In fact we were not able to demonstrate such correlations in our series of compounds. However, all the determined and calculated data were used for a QSAR analysis of these series which will be reported elsewhere.

Hindered and nonhindered aminophenols also exhibit a similar behaviour. In the case of the hindered aminophenols more stable dimeric compounds with indophenolic structures could be obtained. This is the case of 2,6-di-*t*-butyl-4-aminophenol, [50] which led spontaneously, by air oxidatione to the corresponding tetra-*t*-butylindophenol.[55] The last compound yields by oxidation with PbO_2 the stable Coppinger free radical[56] (see Scheme 3).

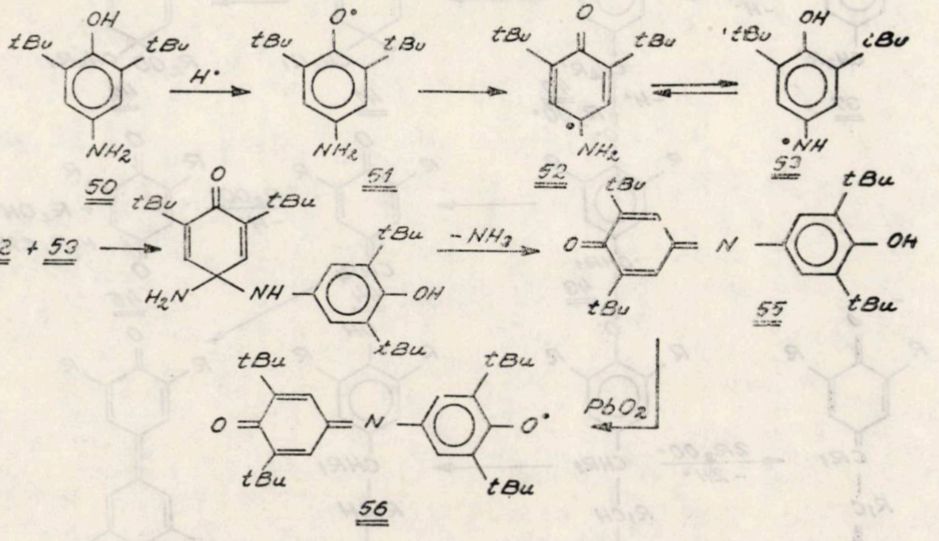
OH
tBu
tBu
H•
NH2
50
O•
51
O
52
•NH
53
52 + 53
H2N
NH
OH
−NH3
O=
N
55
PbO2
O•
56

Scheme 3 — Oxidation of 2, 6-di-*t*-butyl-4-aminophenol according to Nikiforov et al.[55]

Also the enzymic (*in vitro* or *in vivo*) oxidation of substituted phenols and aminophenols occurs according to a similar pathway.[58–60] A typical example is the enzymic oxidation of phenacetin, which leads to rather unstable dimeric compounds,[61,62] see scheme 4. They seem to be responsible for the toxicity of their precursors.

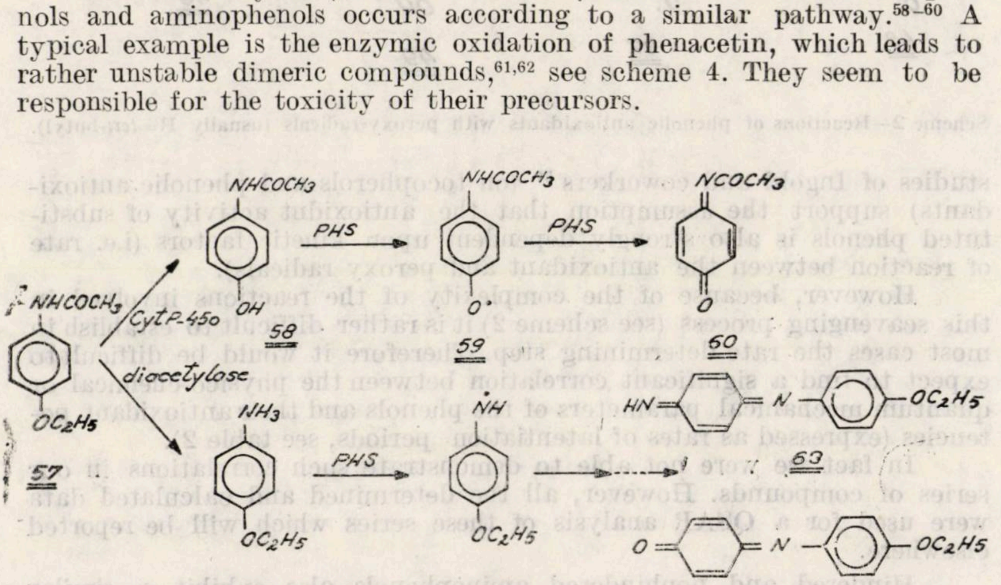
NHCOCH3
CytP-450
diacetylase
OC2H5
57
NHCOCH3
OH
58
PHS
NHCOCH3
O•
59
PHS
NCOCH3
O
60
NH3
61
PHS
•NH
OC2H5
62
63
HN=
N
OC2H5
O=
N
OC2H5
64

Scheme 4 — *In vivo* activation of phenacetin according to Ross.[62]

No experimental evidence supports the assumption that the scavenging activities of these compounds are responsible for their behaviour as antiinitiators and their ability to prevent the formation of carcinogen-DNA adducts.[63] However, this possibility could not be totally ruled out, especially since the implication of prostaglandin synthetase (PHS) in the activation of carcinogens was demonstrated. Recently some data claimed the capacity of such antioxidants to act in the promotion stage, as scavengers of radicals resulted from carcinogen activation,[64] or more likely of the superoxide anion or other oxygen radicals involved in xenobiotic cooxidation [65] or lipid peroxidation. [36]

Relationships between the physico-chemical and quantum-mechanical indices of phenolic and aminophenolic antioxidants and their inhibitory properties against monooxygenases

Other lines of evidence [66,67] suggest that the inhibition of cytochrome P-450 dependent monooxygenases may be a crucial event in preventing the initiation steps by the phenolic and aminophenolic antioxidants.[18] Our data suggest that in fact the quinones or iminoquinones resulting from the *in vivo* oxidation of these compounds are the true species responsible for the anticarcinogenesis effects.[18,19] In order to check this hypothesis a QSAR analysis using the parameters determined or computed in this report was undertaken in our laboratory. The result of this analysis will be published elsewhere.

REFERENCES

[1] L. W. Wattenberg and L. K. T. Lam, In : "Inhibition of Tumors Induction and Development", Eds. M. S. Zedeck and M. Lipton, New York, Pergamon Press, 1981, 1.

[2] J. S. Bertram, L. N. Kolonel and F. L. Meyskens, *Cancer Res.*, **47**, 3012 (1987).

[3] G. J. Keloff, F. W. Malone, C. W. Boone, C. C. Sigman and R. J. Fay, *Seminar in Oncology*, **507**, 438 (1990).

[4] L. W. Wattenberg, *Cancer Res.*, **45**, 1 (1985).

[5] N. Voiculeț and I. Niculescu-Duvăz, In : "Mecanismele moleculare ale cancerogenezei chimice", Ed. Științifică, Bucharest, 1991.

[6] a) G. Stoica, I. Niculescu-Duvăz and N. Voiculetz, *Oncologia*, **26**, 81, (1987) ; b) G. Stoica, I. Niculescu-Duvăz and N. Voiculetz, *Oncologia*, **28**, 257 (1989).

[7] P. Talalay, R. P. Batzinger, A. M. Benson, E. Bueding and Y. N. Cha, *Advan. Enzyme Regul.*, **17**, 23 (1979).

[8] A. D. Rahimtula, B. Jernstrom, L. Dock and P. Moldeus, *Biol. J. Cancer*, **45**, 935 (1982).

[9] C. Ip, *Fed. Proc.*, **44**, 2573 (1985).

[10] R. C. Moon, D. L. Mc Cormick and R. G. Mehta, *Cancer Res.*, **42**, 2469 (1983).

[11] A. W. Wood, M. T. Huang, R. L. Chang, H. L. Newmark, R. E. Lehr. H. Yagi, K.J. M. Sayer, D. M. Jerina and A. H. Conney, *Proc. Natl. Acad. Sci. USA*, **79**, 5513 (1982).

[12] J. M. Sayer, H. Yagi, A. W. Wood, A. H. Conney and D. M. Jerina, *J. Amer. Chem Soc.*, **104**, 5562 (1982).

[13] B. Weinstein, *Cancer Res.*, **48**, 4135 (1988).

[14] Y. M. Toannou, A. G. E. Wilson and M. W. Anderson, *Cancer Res.*, **42**, 1199 (1982).

[15] P. I. Adraenssens, C. M. White and M. W. Anderson, *Cancer Res.*, **43**, 3712 (1983).

[16] L. W. Wattenberg, In : "Carcinogens : Identification and Mechanisms of Action", Eds. C. Griffin and O. R. Shaw, New York, Raven Press, 299 p. 1979.

[17] I. Niculescu-Duvăz, Z. Simon, S. Tiriac, A. Ionescu, M. Mracec and N. Voiculetz, *Neoplasma*, **32**, 695 (1985).

[18] I. Niculescu-Duvăz, G. Stoica, F. Lupu, M. Arnăutu and N. Voiculetz, *Neoplasma*, **35**, 539 (1988).

[19] I. Niculescu-Duvăz, J. Herdan, Z. Simon, G. Stoica, F. Lupu, M. Arnăutu and N. Voiculetz, *Neoplasma*, **38**, 545 (1991).

[20] S. Cincă, I. Niculescu-Duvăz, N. Stafidov and N. Voiculetz, *Oncologia*, **27**, 193 (1988).

[21] A. A. Akhrem, A. V. Kamernitskii and A. M. Prohoda, *Zh. Org. Khim.*, **3**, 41 (1967).
[22] L. K. T. Lam, R. P. Pai and L. W. Wattenberg, *J. Med. Chem.*, **22**, 569 (1979).
[23] A. M. Kuliev, V. M. Farzaliev, M. A. Allakhberdiev and C. I. Mamedov, *Zn. Obsch. Khim.* **52**, 2122 (1982).
[24] A. A. Volod'kin and V. V. Ershov, *Izv. Acad. Nauk. SSSR, Ser. Khim*, **1962** (2022.
[25] M. Dexter, M. Knell and E. A. Roskih (Geigy Chemical Corp.), Patent USA, 3334046, (1967), cf. *Chem. Abstr.*, **67**, 100158 (1967).
[26] E. Müller, H. B. Stegmann and K. Scheffer, *Liebigs Annal. Chem.*, **645**, 79 (1961).
[27] T. H. Coffield, A. H. Filbey, G. C. Ecke ad A. J. Kolko, *J. Amer. Chem. Soc.*,, **79**, 5019 (1957).
[28] G. A. Nikiforov, and M. V. Dyumaev, *Izv. Akad. Nauk SSSR, Otd. Khim. Nauk*, **171** (1961).
[29] F. M. Egidis, A. A. Volod'kin and V. V. Ershov. *Izv. Akad. Nauk. SSSR, Ser. Khim.*, **1971**, 13311.
[30] G. M. Coppinger and T. W. Campbell, *J. Amer. Chem. Soc.*, **75**, 734 (1953).
[31] A. Hus-Weiler, R. Seydel and R. Stroh (Farbenfabriken Bayer ,A. G.) Patent FRG 1082278, (1960) ; cf. *Chem. Abstr.*, **55**, 27217 (1961).
[32] V. I. Isogulyants, V. N. Tishkova, G. I. Bolotova and L. N. Kirichenka, *Zh. Prikl. Khim.*, **37**, 2729 (1969).
[33] C. J. Worrel and R. L. McLean (Ethyl Corp), Patent USA 3415850, (1968) ; cf. *Chem. Abstr.*, **70**, 37476 (1969).
[34] a) J. Holicik, M. Karvas, Z. Manasek and J. Pospisil, *Collect Clzech. Chem. Commun.*, **42**, 275 (1977) ; b) L. Jirakova and J. Pospisil, *Collect. Czech. Chem. Commun.*, **40**, 2800 (1975).
[35] A. Leo, C. Hansch and D. Elkins, *Chem. Rev.*, **71**, 529 (1971).
[36] W. J. Kozumbo, J. L. Seed and T. W. Kensler, *Cancer Res.*, **43**, 2555 (1983).
[37] C. Hansch, A. Leo, S. H. Unger, K. H. Kim, D. Nakaitani and E. J. Lein, *J. Med. Chem.*, **16**, 107 (1973).
[38] T. Pliev, *Dokl. Ann. SSSR*, **69**, 1113 (1969).
[39] M. Mracec, M. Mracec and Z. Simon, *Rev. Roumaine Chem.*, **30**, 531 (1985).
[40] K. Morokuma, H. Kato and K. Fukui, *Bull. Chem. Soc. Japan*, **36**, 541 (1963).
[41] M. Mracec, personal Communication.
[42] R. Bacaloglu, C. Csundelik, L. Cotarca, H. H. Glatt, In : "Structura și proprietăţile compuşilor organici", Ed. Tehnică Bucharest, vol. 1, 1985, 137.
[43] W. P. Purcell and J. B. Sunger, *J. Chem. Eng. Data*, **12**, 235 (1967).
[44] W. Marnett, *Carcinogenesis*, **8**, 1365 (1987).
[45] T. J. Dix. R. Fontana, A. Panthani and L. W. Marnett, *J. Biol. Chem.*, **260**, 5358, (1985).
[46] T. J. Dix and L. J. Marnett, *J. Biol. Chem.*, **260**, 5351 (1985).
[47] T. A. Dix and L. J. Marnett, *Science*, **221**, 77 (1983).
[48] N. R. Bachur, M. V. Gee and R. D. Friedman, *Cancer Res.*, **42**, 1078 (1988).
[49] H. Kappus, In : "Oxidation Stress", Ed. E. Sies, Academic Press, London, 273 (1985).
[50] K. U. Ingold, *J. Phys. Chem.*, **64**, 1636 (1980).
[51] G. Scott, *Chem. Ind.*, **1963**, 27.
[52] N. A. Zakharova, K. E. Kruglyakova, G. N. Bogdanov, L. A. Keifits and N. M. Emanuel, *Zh. Obscei. Khim.*, **37**, 801 (1074).
[53] I. Buben and J. Pospisil, *Collect. Czech. Chem. Commun.*, **40**, 987 (1975).
[54] G. W. Burton and K. U. Ingold, *Acc. Chem. Res.*, **19**, 194 (1986).
[55] G. A. Nikiforov and V. V. Ershakov, *Isv. Akad. Nauk. SSSR, Ser. Kim.*, **1965**, 1097.
[56] G. Copp nger, *Tetrahedron*, **18**, 61 (1962).
[57] A. C. Crowe, A. C. Young, I. C. Calder, K. N. Ham and J. D. Tange. *Chem. Biol. Interact.*, **27**, 235 (1979).
[58] K. J. Hoffman D. B. Axworthy and T. A. Baillie, *Chem. Res. Toxicol.*, **3**, 204 (1990).
[59] S. S. Lau, T. J. Monks and J. R. Gillette, *J. Pharmacol. Exp. Ther.*, **230**, 360 (1984).
[60] R. G. Schnellman, F. P. Q. Ewell, M. Sgambati and I. J. Mandel, *Toxicol. Appl. Pharmacol.*, **90**, 420 (1987).
[61] R. Larsson, D. Ross, T. Berlin, L. I. Olson and P. Moldeus, *J. Pharmacol. Exp. Ther.*, **235**, 475 (1985).
[62] D. Ross, R. Larsson, N. Norbeck, R. Ryhage and P. Moldeus, *Mol. Pharmacol.*, **27**, 277 (1985).
[63] G. Stoica, C. Safirman, M. Arnăutu, N. Voiculetz and I. Niculescu-Duvăz, *Rev. Roum. Biochim.*, **24**, 245 (1987).
[64] A. Tkac and I. Bahna, *Neoplasma*, **30**, 197 (1983).
[65] J. N. M. Commandeur and N. P. E. Vermeulen, *Chem. Res. Toxicol.*, **3**, 171 (1990).
[66] M. W. Anderson, M. Boroujerdi and A. G. E. Wilson, *Cancer Res.*, **41** 4309 (1981).
[67] L. K. T. Lam, V. L. Sparnins, J. B. Hochalter and L. W. Wattenberg, *Cancer Res.*, **41**, 3940 (1981).

Revue Roumaine de Chimie, **36**, *9—10*, 1161—1168 (1991)

PREPARATION, CHARACTERIZATION AND FUNGITOXICITY OF THE Fe(III) COMPLEXES WITH MERCAPTO AZOLES

S. MISRA *, B. L. DUBEY and S. C. BAHEL
Department of Chemistry, University of Gorakhpur, Gorakhpur 273009 India

Received June 25, 1988

Complexes of the type Fe(Ttmmt)$_3$, Fe(Tcmmt)$_3$, Fe(Dpmo)$_3$, Fe(Tcmo)$_3$, Fe(Dpmth)$_3$ and Fe(Pmth)$_3$ (where TtmmtH = 3-(*o*-tolyloxymethyl)-5-mercapto-4-*p*-tolyl-1, 2, 4-triazole, TcmmtH = 3-(*o*-chlorophenoxymethyl)-5-mercapto-4-*p*-tolyl-1, 2, 4-triazole, DpmoH = 5-(2, 4-dimethylphenoxymethyl)-2-mercapto-1, 3, 4-oxadiazole, TomoH = = 5-(thymoloxymethyl)-2-mercapto-1, 3, 4-oxadiazole, DpmthH = 5-(2, 4-Dimethylphenoxymethyl)-2-mercapto-1, 3, 4-thiadiazole, PmthH = 5-phenyl-2-mercapto-1, 3, 4-thiadiazole) have been isolated. They have bean characterized on the basis of elemental analysis, electrical conductance, magnetic susceptibility, T.G.A., and spectral (electronic, infrared and ^{1}H$-$NMR) data. Fungitoxicity of these complexes and free ligands has been evaluated against *A. flavus* and *A. niger*.

INTRODUCTION

One of the important aspects of the use of coordination compounds of transition metals is their application as biologically active substance.[1-4] Many biocoordination compounds can be used as biologically active preparations in medicine and agriculture.[5-8] Coordination compounds containing nitrogen, sulphur, oxygen and heterocycles as ligands have attracted attention due to their important role in biological processes, pharmacological preparations and as effective plant protecting agents.[9,10] Ligands capable of undergoing thione-thiol ($HN-C=S \rightleftharpoons N=C-SH$) tautomerism can coordinate to a metal atom through nitrogen, sulphur or simultaneously through both nitrogen and sulphur. Thus the biocoordination chemistry with heterocyclic thiones continues to be of interest because of the stricking structural features and also due to their biological importance.[11–15] Structures of the ligands used in this study are given below.

---

* Author to whom correspondence should be directed.

TRIAZOLE THIONE

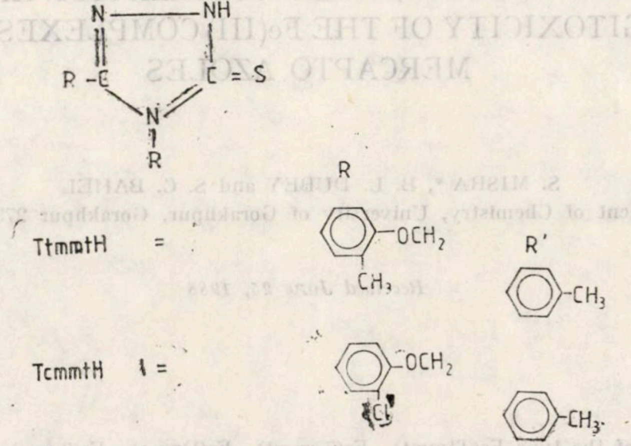
N
NH
R -C
C = S
N
R
R
TtmmtH =
OCH$_2$
CH$_3$
R'
CH$_3$
TcmmtH =
OCH$_2$
Cl
CH$_3$

OXADIAZOLE THIONE

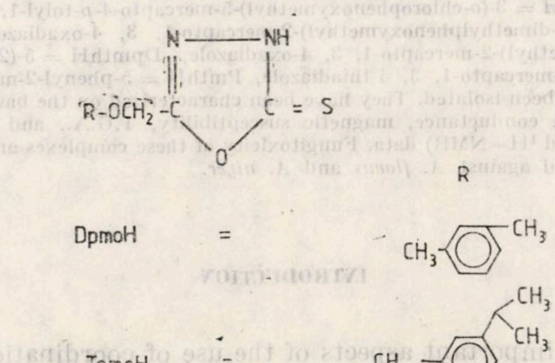
N
NH
R-OCH$_2$ -C
C = S
O
R
DpmoH =
CH$_3$
CH$_3$
TomoH =
CH$_3$
CH$_3$
CH$_3$

THIADIAZOLE THIONE

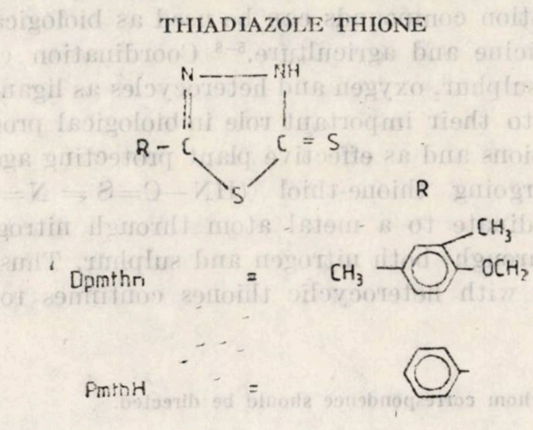
N
NH
R – C
C = S
S
R
Dpmthn =
CH$_3$
CH$_3$
OCH$_2$
PmthH =

RESULTS AND DISCUSSION

The analytical data of these complexes are given in Tables 1. All these complexes are brown coloured solids and are stable in air. The conductance measurements reveal that they are essentially nonelectrolytes.

Table 1

Analytical data of iron (III) complexes with mercapto triazoles, mercapto oxadiazoles and mercapto thiadiazoles

Complex	Found (%)						Calcd (%)					
	Metal	C	H	N	S	Cl	Metal	C	H	N	S	Cl
$Fe(Ttmmt)_3$	5.5	61.8	4.7	12.6	9.5	—	5.6	62.0	4.8	12.7	9.7	—
$Fe(Tcmmt)_3$	5.1	54.7	3.4	11.7	9.0	9.8	5.3	54.9	3.7	12.0	9.1	10.1
$Fe(Mcmo)_3$	6.6	43.5	2.7	10.1	11.5	12.6	6.7	43.7	2.9	10.2	11.6	12.9
$Fe(Dpmo)_3$	7.0	51.8	4.1	10.9	12.4	—	7.3	52.0	4.3	11.0	12.6	—
$Fe(Dpmth)_3$	6.4	48.7	3.9	10.1	23.5	—	6.8	48.9	4.0	10.3	23.7	—
$Fe(Pmth)_3$	8.5	45.0	2.2	12.9	30.0	—	8.8	45.3	2.3	13.2	30.2	—

Magnetic moment and electronic spectra

Iron (III) complexes exhibit temperature independent paramagnetic values. These values are in the range 5.70 – 5.90 B.M., a range expected for five unpaired electrons with ($^6A_{1g}/t_{2g}^3\ eg^2$) ground state of octahedral iron (III).[16–18] Moments are found to be close to the spin only value (5.92 B.M.).

The complexes with mercapto triazoles, mercapto oxadiazoles and mercapto thiadiazoles show three weak transitions[19,20] in the region 9760 – 10180, 21275 – 22180 and 24420 – 25000 cm^{-1}. They may be assigned to $^6A_{1g} \rightarrow {}^4T_{1g}(G)$, $^6A_{1g} \rightarrow {}^4T_{2g}(G)$ and $^6A_{1g} \rightarrow {}^4A_{1g}, {}^4E_g(G)$ transitions, respectively and indicate [21,22] that these complexes are octahedral in nature. An additional charge transfer band at 30500 cm^{-1} is also observed for $Fe_{e_g}\ l \rightarrow \pi^*$ (ligand) transition. Various ligand field parameters and electronic repulsion parameters have been calculated by using the equation [21–23] given below :

$$^6A_{1g} \rightarrow {}^4A_{1g}, {}^4E_g = 10B + 50 \qquad \text{(i)}$$

$$C/B = 4.73 \qquad \text{(ii)}$$

$$Dq/B = 1.1 \qquad \text{(iii)}$$

It is shown that in all the above complexes each iron atom is surrounded by an octahedral ligand field. [24]

Infrared spectra

Mercapto triazole derivatives

The ligands show four thioamide [25] bands at ca. 1550 – 1540 (I) 1250(II), 1080 – 1070(III) and IV at 780 – 770 cm^{-1}. In complexes, all thioamide bands disappear. The absence of νSH bands in the complexes is attributed to the deprotontion of thiol sulphur.[26–28] The νC=S band appears at 660–680 cm^{-1} in the complexes and the νFe–S vibration bands appear at ca. 340–370 cm^{-1}. The νC=N band splits into two in the complexes; one band at 1570–1580 cm^{-1} (as observed in spectra of the ligands) and other at ca. 1550–1565 cm^{-1}, indicating that one of the azomethine groups is coordinated to metal and the other is free and uncoordinated.[29,30] The νFe–N vibration band appears at 420–430 cm^{-1}.

Thus the IR spectra indicate that mercapto triazoles coordinate to iron atom through azomethine nitrogen and deprotonated thiol sulphur.

Mercapto oxadiazole derivatives

The νN–H at 3340 and δN–H at 1610 cm^{-1} in ligands, disappear in the complexes indicating the deprotonation of amino nitrogen. The νFe–N vibration appears at ca. 410–450 cm^{-1}. The frequencies of thioamide –III and –IV bands decrease (~20–30 cm^{-1}) upon complexation indicating[31] the coordination through thioketonic sulphur atom. The ν(Fe–S) vibration band appears at ca. 370–390 cm^{-1}. The positions of infrared bands due to oxadiazole group (C–O–C) do not change in the complexes indicating[32] that oxygen atom does not take part in coordination.

Mercapto thiadiazole derivatives

These ligands also show four thioamide bands but thioamide III and IV bands appearing at 1070–1080 and 760–780 respectively shift to lower frequencies which show that thione sulphur is coordinating.[33] The νFe–S band appears at 325–340 cm^{-1}.

The νNH and δN–H vibration bands, appearing at 3200 cm^{-1} and 1630 cm^{-1} in the ligands, disappear in the complexes indicating that ligands are coordinating to iron atom through deprotonated amino nitrogen.[31] The νFe–N is recorded [25] at 400–450 cm^{-1} in the complexes.

Bands due to C–S–C group appear at the same positions in the complexes as observed in the spectra of the ligands. This is suggestive of the fact that coordination does not occur through ring sulphur.

^{1}H–NMR spectra

The proton NHR spectra of the ligands and complexes have been recorded in deuterated chloroform and dimethylformamide. A comparison of the spectra of ligands with those of the complexes could lead to the following conclusions:

(i) The signal due to N–H proton, appearing at ca. δ 5.2–5.5 in mercapto oxadiazole and mercapto thiadiazole, disappears in the complexes suggesting the deprotonation of amino nitrogen.

(ii) A signal in the mercapto triazole ligands appears at δ 4.5 due to S–H proton which disappears in the complexes indicating the deprotonation of thiol sulphur.

Thermogravimetric studies

The thermal stability and decomposition ranges of the complexes are given in table 2. Iron (III) complexes with mercapto triazoles show two step weight loss whereas mercapto oxadiazole and mercapto thia-

Table 2

Decomposition temperature ranges (°C) of iron (III) complexes with mercapto triazoles, mercapto oxadiazoles and mercapto thiadiazoles

Complex	Decomposition	Temperature (°C)	Weight loss (%)	
			Observed	Calcd.
$Fe(Ttmmt)_3$	$Fe(Ttmmt)_3 \rightarrow Fe(SCN)_3$	220–275	76.35	76.71
	$Fe(SCN)_3 \rightarrow Fe_2O_3$	510–556	30.15	30.73
$Fe(Tcmmt)_3$	$Fe(Tcmmt)_3 \rightarrow Fe(SCN)_3$	215–260	78.00	78.08
	$Fe(SCN)_3 \rightarrow Fe_2O_3$	500–535	30.25	30.73
$Fe(Mcmo)_3$	$Fe(Mcmo)_3 \rightarrow Fe_2O_3$	260–480	80.36	80.66
$Fe(Dpmo)_3$	$Fe(Dpmo)_3 \rightarrow Fe_2O_3$	275–465	78.24	78.89
$Fe(Dpmth)_3$	$Fe(Dpmth)_3 \rightarrow Fe_2O_3$	250–435	80.10	80.34
$Fe(Pmth)_3$	$Fe(Pmth)_3 \rightarrow Fe_2O_3$	290–480	74.45	74.94

diazole complexes show single step weight loss. The end products were found to be iron trioxide as confirmed [32] by analysis and by infrared spectra. The $\nu Fe-O$ appears at about 480 cm^{-1}.

Biological activity

Compounds containing $N-C=S$ linkage show versatile biological activity.[34] The fungicidal activity of ligands and complexes was tested against *A. flavus* and *A. niger*. The fungicidal activity of each compound was screened at concentrations 1 : 1000, 1 : 10, 000 and 1 : 100,000 and the data are given in table 3. They indicate that both ligands and complexes are moderately active against both species. The fungicidal activity increases upon complexation and decreases with dilution. Iron complexes with mercapto thiadiazoles were found to be more active against both species of fungi in comparison to mercapto triazole complexes which in turn are found to be more active than mercapto oxadiazole complexes.

Table 3

Fungicidal screening data of the ligands and complexes

Compuond	Average percentage inhibition					
	Organism *A. niger*			Organism *A. flavus*		
	1 : 1000	1 : 10, 000	1 : 100,000	1 : 1000	1 : 10,000	1 : 100,000
TtmmtH	65.2	54.0	35.0	60.0	48.2	32.0
TcmmtH	62.1	48.4	30.2	58.3	44.0	28.0
DpmoH	56.5	40.2	31.0	52.0	36.2	25.2
TomoH	54.0	28.8	30.2	51.2	34.0	27.0
DpmthH	64.2	58.2	34.2	62.4	50.2	30.0
PmthH	62.2	56.0	30.6	62.2	51.2	26.2
$Fe(Ttmmt)_3$	70.2	60.0	40.4	67.8	57.2	38.0
$Fe(Tcmmt)_3$	67.8	55.8	38.4	65.6	51.0	36.4
$Fe(Dpmo)_3$	60.2	48.0	40.0	62.4	44.2	32.2
$Fe(Tomo)_3$	61.4	44.4	38.0	62.0	40.0	35.2
$Fe(Dpmth)_3$	70.2	65.8	42.4	68.8	56.2	38.5
$Fe(Pmth)_3$	72.8	64.8	44.0	68.2	51.4	34.6

The fungicidal activity against *A. niger* is greater than *A. flavus* for a given metal complex.

EXPERIMENTAL

The ligands mercapto triazoles, mercapto oxadiazoles and mercapto thiadiazoles were prepared as reported in literature.[35–37]

Preparation of complexes

All these complexes were prepared by refluxing an ethanolic solution of the appropriate ligand and sodium acetate with an aqueous solution of metal salts in desired molar ratio for different durations ranging between 1–4 hrs. The precipitate so obtained was filtered, washed with a large excess of water, hot ethanol and ether and finally dried in vacuum. Details of the amounts of reactants taken for the preparation of complexes, refluxing time, yield and colour of the products are given in table 4.

Table 4

Reactions of iron (III) chloride with mercapto triazoles, mercapto oxadiazoles and mercapto thiadiazoles

Amount of reactants taken (gm)		Molar ratio	Refluxing time (hrs)	Product, colour	Yield (%)
Metal	Ligand				
$FeCl_3 \cdot 6H_2O$ 0.9	TtmmtH 3:11	1:3	4	$Fe(Ttmmt)_3$, brown	67
$FeCl_3 \cdot 6H_2O$ 0.67	TcmmtH 2.48	1:3	4	$Fe(Tcmmt)_3$, brown	65
$FeCl_3 \cdot 6H_2O$ 0.67	McmoH 1.92	1:3	4	$Fe(Mcmo)_3$, brown	64
$FeCl_3 \cdot 6H_2O$	DpmoH	1:3	3	$Fe(Dpmo)_3$, brown	61
$FeCl_3 \cdot 6H_2O$ 0.90	DpmthH 2.52	1:3	4	$Fe(Dpmth)_3$, brown	60
$FeCl_3 \cdot 6H_2O$ 0.90	PmthH 1.94	1:3	3	$Fe(Pmth)_3$, brown	64

Physical measurements

Metal content in the complexes was estimated by the method mentioned in the literature. Sulphur was estimated as barium sulphate and chlorine as silver chloride. Carbon and hydrogen analyses were carried out at the central Drug Research Institute, Lucknow.

Magnetic susceptibilities of the complexes were determined by the Faraday method using ferrous ammonium sulphate as calibrant.

Infrared spectra of the complexes and the parent ligands were recorded on Perkin-Elmer spectrophotometer, model 621 in nujol in the 4000–2000 cm^{-1} range. Electronic spectra of the complexes were obtained on Russian CΦ/C spectrophotometer in the 750–400 nm region in chloroform, acetone, tetrahydrofuran, dimethylformamide and nujol.

Electrical conductance measurements were made on a Toshniwall conductivity bridge, type C101/01A, in nitrobenzene or dimethylformamide.

Water content of the complexes was determined by recording the weight loss on heating them at a temperature between 150–300°C. The thermogravimetry of the complexes was carried out with the help of TG-750 Stanton Red Craft (U.K.) thermogravimetry analyser, at heating rate of 10°C min^{-1} in air with chart speed 300 mm/h.

Fungitoxicity was evaluated against *A. flavus* and *A. niger* by agar plate method at three different concentrations. The average percentage inhibition caused by various compounds is recorded.

$$\text{Percentage inhibition} = \frac{(C - T) \times 100}{C}$$

where,

C = diameter of fungus colony in the control plate after 96 hours

T = diameter of the fungus colony in treated plates after 96 hours.

CONCLUSION

Iron (III) complexes were prepared with triazoles, oxadiazoles and thiadiazoles. The IR and ^{1}H-NMR studies show that triazoles coordinate to iron through azomethine nitrogen and deprotonated thiol sulphur, whereas oxadiazoles and thiadiazoles coordinate through deprotonated amino nitrogen and thioketonic sulphur.

TG studies reveal that iron(III) complexes with mercapto triazoles show two step weight loss whereas mercapto oxadiazole and mercapto thiadiazole complexes show single step weight loss.

The fungicidal data reveal that both ligands and complexes are active against *A. flavus* and *A. niger*. These data also show that for the given metal ion, the fungicidal activity of the complexes follows the sequence of ligands as follows mercapto thiadiazole > mercapt otriazole > mercapto oxadiazole. The fungicidal activity against *A. niger* was found to be greater than *A. flavus* for a particular metal complex.

ACKNOWLEDGEMENTS. The authors are thankful to University Grants Commission, New Delhi for financial assistance, and Dr. S. K. Sengupta, Chemistry Department, University of Surrey Guildferd, Surrey (U.K.) for valuable discussions.

REFERENCES

[1] M. N. Hughus, "The Inorganic Chemistry of Biological Processes", (Translated into Russian), Izd. Mir. Moscow, p. 74, 1983.

[2] K. B. Yatsimirsku, "Vuednie V Bioneorganicheskuyu Khimiyu" (Introduction to Bioinorganic Chemistry), Izd. Naukova Dumka, Kiev, p. 85, 1976.

[3] D. R. Williams, "The Metals of Life : the Solution Chemistry of Metal Ions in Biological Systems" (Translated into Russian). Izd. Mir, Mosocow, p. 21, 1975.

[4] K. B. Yatsimirsku (Editor), "Biologichesev Aspectly Koordinatsionnol Khimii" (Biological Aspects of Coordination Chemistry), Izd. Naukov Dumka, Kiev p. 3, 1977.

[5] B. A. Bovykin, *Farmatriya*, **1979**, (6) 62.

[6] M. G. Bezrukov, A. M. Belousova and V. A. Sergeev, *Uspekhi Khim.*, **51**, 696, 1982 ; *Russ. Chem. Rev.*, **4**, 1982.

[7] V. V. Lukachina, *Koord. Khim.*, **8**, 419 (1982).

[8] A. I. Stetsenko, M. A. Presnov and A. L. Konovalova Uspekhi Khim., **1981**, 50, 688 *(Russ. Chem. Rev.* (4) 1981).

[9] D. R. Williams, *Chem. Rev.*, **203**, 72 (1972).

[10] D. A. Phipps, "Metals and Metabolism", Oxford Chem. Series, Oxford, Univ., Press, 1976.

[11] C. Preti and G. Tosi, *Austral. J. Chem.*, **29**, 543 (1976) : *Canad. J. Chem.*, **54**, 1558 (1976).

[12] J. Reedijk, *J. Inorg. Nucl. Chem.*, **35**, 239 (1973).

[13] M. R. Gajendragad and U. Agarwala, *Austral. J. Chem.*, **28**, 763 (1975).

[14] B. K. Gupta, D. S. Gupta and U. Agarwala, *Bull. Chem. Soc. Japan*, **51**, 2724 (1978).

[15] S. K. Sengupta, S. K. Sahini and R. N. Kapcor, *Synth. React. Inorg. Met.-Org. Chem.*, **10**, 269 (1980).

[16] B. N. Figgis and J. Lewis, *Prog. Inorg. Chem.* **6**, 102 (1962).
[17] L. Yaramus, M. Kukia and B. R. J. Sundheim, *J. Chem. Phys.*, **40**, 33 (1964).
[18] A. Famshaw, "Introduction to Magnetochemistry", Academic Press, New York, 1968.
[19] K. B. Yatsimirskii, V. G. Golovatyi, A. S Grigoreva, E. N. Korol and E. E. Kriss, *Dokl. Akad. Nauk. SSSR.*, **226**, 144 (1976).
[20] Y. K. Bhoon, *Polyhedron*, **2**, 365 (1983).
[21] A. B. P. Lever, "Inorganic Electronic Spectroscopy", Elsevier, Amsterdam, 1968.
[22] J. J. Foster and N. S. Gill, *J. Chem. Soc.*, A **2525** (1968).
[23] G. C. Allen and K. D. Warren, *Struct. Bond.*, **9**, 104 (1971).
[24] A. H. White and R. L. Martin, *Inorg. Chem.*, **6**, 712 (1963).
[25] C. N. R. Rao, "Chemical Applications of Infrared Spectroscopy", Academic Press, London, 1963.
[26] S. K. Sengupta, *Acta Chim. Acad. Sci. Hung.*, **114**, 323 (1983).
[27] J. Singh, N. K. Singh, *Proc. Indian Acad. Sci., Chem. Sci.*, **93**, 125 (1984).
[28] B. K. Sinha, Rajeshwar Singh, J. P. Srivastava and L. K. Mishra, *J. Inorg. Nucl. Chem.*, **39**, 1797 (1977).
[29] O. P. Pandey, S. K. Sengupta and S. C. Tripathi, *Synth. React. Inorg. Met.—Org. Chem.*, **13**, 867 (1983).
[30] P. O. Pandey, S. K. Sengupta ad S. C. Tripathi, *Transition Met. Chem.*, **8**, 362 (1983).
[31] O. P. Pandey, S. K. Sengupta and S. C. Tripathi, *Inorg. Chim. Acta*, **90**, 91 (1984).
[32] D. M. Adams, "Metal-Ligand and Related Vibrations", E. Arnold, London, 1967.
[33] K. Nakamoto, "Infrared Spectra of Inorganic and Coordination Compounds", Wiley Interscience, New York, 1970.
[34] Y. L. Nene, "Fungicides in Plant Disease Control", Oxford and IBH Publishing Company, New Delhi (1971).
[35] E. Hoggarth, *J. Chem. Soc.*, 4811 (1952).
[36] R. W. Young and K. H. Wood, *J. Am. Chem. Soc.*, **77**, 4C0 (1955).
[37] A. Lowson and C. E. Searle, *J. Chem. Soc.*, 1556 (1957).

Revue Roumaine de Chimie, **36**, *9–10*, 1169–1173 (1991)

CARBONIC ANHYDRASE INHIBITORS. 7[1]

STABILITY CONSTANTS OF COMPLEX INHIBITORS AND THEIR MECHANISM OF ACTION **

CONSTANTIN LUCA [a], MIHAI BĂRBOIU [a] and CLAUDIU T. SUPURAN [b], *
[a] Polytechnic Institute, Department of Physical and Analytical Chemistry, Splaiul Independenţei 313, Bucharest, Roumania
[b] University of Bucharest, Department of Chemistry, Bd. Republicii 13, Bucharest, 1, Roumania

Received April 12, 1991

Stability constants for the coordination compounds of 6-ethoxy-benzothiazole-2-sulfonamide with Cu(II), Zn(II) and Pd(II) were determined using a spectrophotometric method. Small values for these constants indicate that the powerful inhibition observed with these complexes for the major carbonic anhydrase isozymes is due to both sulfonamido moieties as well as metal ions present in these molecules.

INTRODUCTION

In previous reports[1,2] we showed that in addition to the classical carbonic anhydrase (CA, EC 4.2.1.1) inhibitors, the aromatic/heterocyclic sulfonamides[3] and the metal-complexing anions[4] (like CN^-, N_3^-, SH^-, etc.), coordination compounds of heterocyclic sulfonamides like acetazolamide **1** (5-acetylamino-1, 3,4-thiadiazole-2-sulfonamide) and ethoxzolamide **2** (6-ethoxy-benzothiazole-2-sulfonamide) with a range of di- and trivalent cations (Zn(II),[2] Cu(II),[2] Ni(II)[1,2] Pd(II),[1] Pt(II),[1] Al(III),[5] and trivalent lanthanides[6]) act as strong inhibitors of this enzyme, their potency greatly exceeding those of the parent sulfonamides.

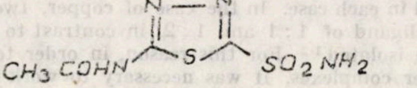

1

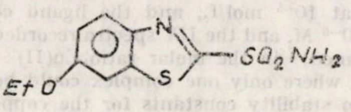

2

Although the reported compounds present a diversity of geometries (from distorted tetrahedral to square planar and (pseudo)octahedral) and stoichiometries (both mono- and bi-nuclear complexes were prepared)[1,2,5,6] all of then have two features in common : the strong inhibition of isozymes CA I and CA II, and the lack of data to explain this.

---

* Correspondence author for the biochemical data.

** Dedicated to the memory of Academician EMILIAN A. BRATU.

In a previous paper[2b] we hypothesized that due to the weak complexing ability of sulfonamides,[4b] the complex inhibitors described by us, might easily dissociate, with formation of sulfonamido anions (RSO_2NH^-, represented as L in the following equations) and metal ions, as described in a simplified manner by equation (1):

$$[ML_n] \rightleftarrows [ML_{n-1}] + L \rightleftarrows \ldots \rightleftarrows M^{n+} + nL \qquad (1)$$

The observed powerful enzyme inhibition could then be accounted for to both the anions and metal ions formed, as we hypothesized previously[2b] and as suggested by Lindskog.[7]

This fact could be of interest, especially after the finding of Silverman's group[8] that some metal ions (such as Cu(II) and Hg(II)) are selective inhibitors of the proton-shuttle in isozyme CA II, due to their binding to His-64, a residue playing a critical role for catalysis. In consequence, some of our inhibitors could display a dual role, inhibiting the enzyme both by binding to the Zn(II) ion within the active site of CA (by the sulfonamido anions) and by binding to His-64 and inhibiting the proton-shuttle (the metal ions). If this special type of interaction occurs, must be verified in future work.

In this paper we report the determination of stability constants for some of the previously reported complex inhibitors, and more precisely the complexes of Zn(II), Cu(II) and Pd(II) with ethoxzolamide, using a spectrophotometric method.[9]

EXPERIMENTAL

UV spectra were recorded with a C. Zeiss Jena UV–VIS spectrophotometer in DMSO. The source of reagents was as follows: DMSO and $Cu(NO_3)_2 \cdot 3H_2O$ from Merck; $ZnSO_4 \cdot 7H_2O$ from BDH; ethoxzolamide was prepared by literature procedures;[10] $PdCl_2$ was prepared from high purity palladium in our laboratory.

Ethoxzolamide was dissolved in hot DMSO and the stoichiometric amount of NaOH was added, in order to obtain the sodium salt $RSO_2NH^- Na^+$; solutions of the metal salts were prepared in the same solvent. UV spectra were recorded in the region 250–350 nm, where both the ligand and some of the metal ions (copper and palladium), as well as the complex have absorption bands. In a series of experiments, the metal ion concentration was maintained constant, at 10^{-5} mol/L, and the ligand concentration was varied continuously, from $1 \cdot 10^{-5}$ to $8 \cdot 10^{-5}$ M, and the UV spectra recorded in each case. In the case of copper, two complexes are formed,[2] in the molar ratio Cu(II) : ligand of 1 : 1 and 1 : 2, in contrast to Zn(II) and Pd(II), where only one complex could be isolated.[1,2] For this reason, in order to determine the two stability constants for the copper complexes, it was necessary to work (in another series of experiments) at constant concentration of ligand (10^{-5} mol/L) and variable concentrations ($1 \cdot 10^{-5}$ – $8 \cdot 10^{-5}$ mol/L) of Cu(II).

RESULTS AND DISCUSSION

The UV spectra in the region 250–350 nm for the metal complexes of ethoxzolamide with Cu(II), Zn(II) and Pd(II), at different ligand concentrations, are presented in Figs. 1–3. The molar extinction coefficient of the complex (ε_{ML_n}) was determined at high ligand concentration, taking into account the additivity rule for composed spectra[9] for each complex, at a fixed wavenumber. The relation used in these calculations was:

$$E_{\bar{\nu}} = \varepsilon_{ML_L}\cdot 10^{-5} + \varepsilon_L\cdot(C_L - n\cdot 10^{-5}) \qquad (2)$$

where: $E_{\bar{\nu}}$ = extinction value at the considered wave number $\bar{\nu}$

ε_i = molar extinction coefficient for species "i";

C_i = molar concentration of species "i"

ε_L was determined previously, recording the UV absorption spectra of ethoxzolamide, at different concentrations. The values used in our calculations were: $\varepsilon_L = 1.18\cdot 10^4$ at 36 000 cm^{-1}, and $7.54\cdot 10^3$ at 34 000 cm^{-1}. ε_M was determined in the same manner, for the ions absorbing in this region; the values obtained and used in calculations were: $\varepsilon_{Cu} = 5.25\cdot 10^3$, at 36 000 cm^{-1}, and $\varepsilon_{Pd} = 9.75\cdot 10^3$ at 36 000 cm^{-1}.

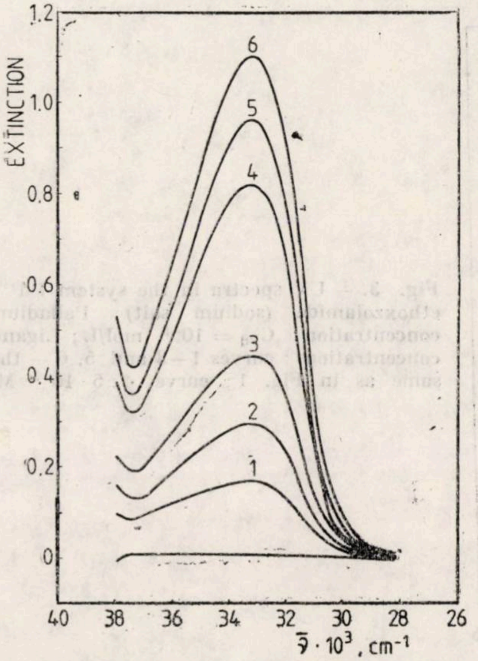

Fig. 1. — UV spectra in the system Cu^{2+}: ethoxzolamide (sodium salt); Copper concentration: $C_{Cu} = 10^{-5}$ mol/L; Ligand concentrations:
$1: 1\cdot 10^{-5}$ M; $2: 2\cdot 10^{-5}$ M; $3: 4\cdot 10^{-5}$ M; $4: 6\cdot 10^{-5}$ M; $5: 7\cdot 10^{-5}$ M; $6: 8\cdot 10^{-5}$ M.

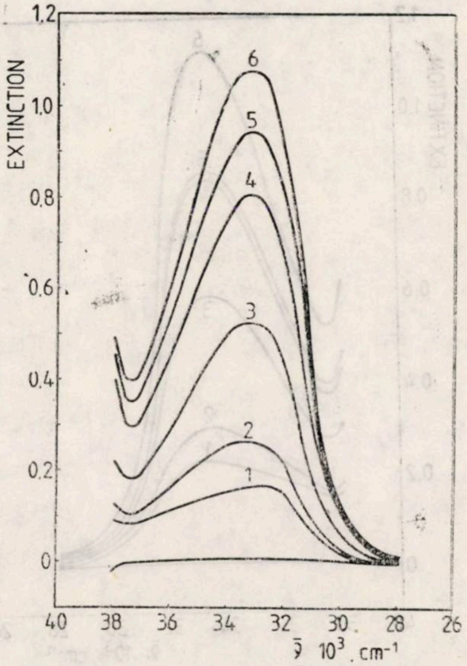

Fig. 2. — UV spectra in the system Zn^{2+}: ethoxzolamide (sodium salt); Zinc concentration: $C_{Zn} = 10^{-5}$ mol/L; Ligand concentrations are the same as in Fig. 1, for curves 1–6.

From eq. 2, the value for ε_{ML_n} was determined, and used subsequently for the calculation of complex concentration (C_{ML_n}), at low ligand concentrations (curves 1–4 in Figs. 1–3), using the same rule applied with eq. 2. The relation used in these calculations was:

$$E_{\bar{\nu}} = \varepsilon_{ML_n}\cdot C_{ML_n} + \varepsilon_M\cdot(C_M - C_{ML_n}) + \varepsilon_L\cdot(C_L - n\cdot C_{ML_n}) \qquad (3)$$

The stability constants were then calculated using relation (4):

$$K_{ML_n} = \frac{C_{ML_n}}{(C_M - C_{ML_n}) \cdot (C_L - n \cdot C_{ML_n})^n} \qquad (4)$$

The values calculated in this way are presented in Table 1. Mention must be made that only the overall stability constant could be determined for the zinc complex.

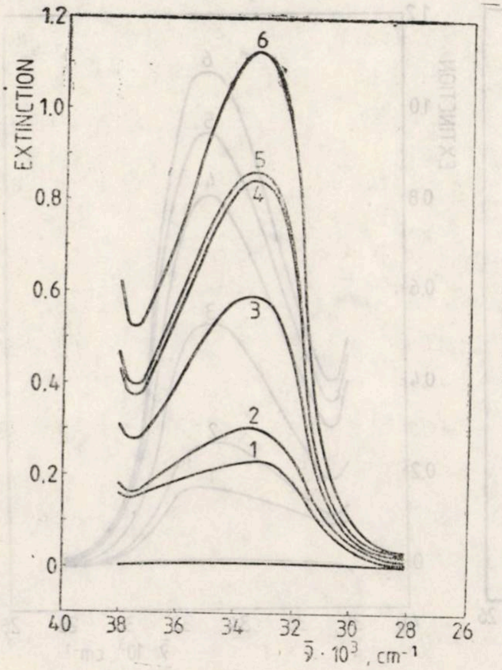

Fig. 3. — UV spectra in the system Pd^{2+} : ethoxzolamide (sodium salt); Palladium concentration: $C_{Pd} = 10^{-5}$ mol/L; Ligand concentrations: curves 1—3 and 5, 6 — the same as in Fig. 1; curve 4: $5 \cdot 10^{-5}$ M.

Table 1

Stability constants for complexes of ethoxzolamide with Cu(II), Zn(II) and Pd(II)

Complex	$\bar{\nu}^a$(cm^{-1})	$\varepsilon^b_{ML_n}$	$K^c_{ML_n}$
[CuL]	36 000	$1.17 \cdot 10^4$	$1.2 \cdot 10^6 \pm 0.8 \cdot 10^6$
[CuL$_2$]	36 000	$1.84 \cdot 10^4$	$3.4 \cdot 10^9 \pm 1.2 \cdot 10^9$
[ZnL$_2$]	34 000	$2.75 \cdot 10^4$	$4.5 \cdot 10^8 \pm 0.4 \cdot 10^8$
[PdL]	36 000	$1.99 \cdot 10^4$	$9.82 \cdot 10^2 \pm 0.2 \cdot 10^2$

[a] Wavenumber at which the calculations were done

[b] See text for details.

[c] Calculated as mean ± standard error, from six determinations.

The low stability constants for these complexes suggest that the strong enzyme inhibition observed with these compounds is indeed the result of a dual effect of both ligand (sulfonamido moieties) and cation, and that our earlier hypothesis was correct. This fact might be important for the design of novel CA inhibitors, and explains at the same time the differences in inhibitory power observed with the complex inhibitors. Thus, the palladium complex, which is very unstable, was the most effective in inhibiting CA.[1,11] Evenso, the possibility that other types of interactions occur between the enzyme and the complex inhibitors, cannot be ruled out yet.

Note added in proof: Recently, Ferrer et al. (S. Ferrer, J. Borràs and E. Garcia-España, *J. Inorg. Biochem.*, **39**, 297 (1990)) reported stability constants for complexes of acetazolamide (**1**) with Cu(II), Ni(II), Zn(II) and Co(II), determined potentiometrically in water or water : EtOH (1 : 1, v/v). The orders of magnitude for these constants are comparable with those reported by us here, for the Zn(II) and some Cu(II) complexes, and higher (10^{18}) for the Ni(II) complex. Mention must be made that the acetazolamide complexes previously reported by these authors (S. Ferrer et al., *Inorg. Chem.*, **28**, 160 (1989); S. Ferrer et al., *Inorg. Chem.* **29**, 206 (1990); S. Ferrer et al., *J. Inorg. Biochem.* **37**, 163 (1989)) have different compositions (generally containing acetazolamide anions and ammonia as ligands) of similar compounds reported by us (ref. 1, 2), which contained only sulfonamido anions and eventually inorganic anions such as Cl^-, HO^-. The complexes reported in these important works by Ferrer et al. were, unfortunately, never tested for CA inhibition.

REFERENCES

[1] Part 6 : M. Andruh, E. Cristurean, R. Stefan and C. T. Supuran, *Rev. Roumaine Chim.*, **36**, 727 (1991).

[2] a) C. Supuran, M. Andruh and I. Pușcaș, *Rev. Roumaine Chim.* **35**, 393 (1990) ; b) C. Supuran, G. Manole, A. T. Balaban, I. C. Pușcaș, M. D. Gheorghiu, A. Schiketanz, M. Andruh and I. Pușcaș, "New Types of Carbonic Anhydrase Inhibitors" in "Carbonic Anhydrase — From Biochemistry and Genetics to Pharmacology and Clinical Medicine", CA Int. Workshop Spoleto, Italia, Abstract Book pp. 128.

[3] a) T. Mann and D. Keilin, *Nature*, **146**, 164 (1940) ; b) T. H. Maren, *Physiol. Rev.* **47**, 595 (1967) ; c) T. H. Maren, *Annu. Rev. Pharmacol. Toxicol.*, **16**, 309 (1976).

[4] a) T. H. Maren, C. S. Rayburn and N. E. Liddell, *Science*, **191**, 469 (1976) ; b) J. E. Coleman, *Annu, Rev. Pharmacol.*, **15**, 221 (1975) ; c) I. Bertini and C. Luchinat, *Ann. N. Y. Acad. Sci.*, **429**, 89 (1984) ; d) I. Bertini, C. Luchinat and L. Banci, Carbonic Anhydrase International Workshop, Spoleto, Italy, 1990, Abstract Book, pp. 24.

[5] C. T. Supuran, R. Ștefan and M. Andruh, manuscript in preparation.

[6] C. T. Supuran, R. Ștefan, G. Manole, I. Pușcaș, and M. Andruh, *Rev. Roumaine Chim.*, the next paper.

[7] S. Lindskog, personal communication to C.T.S.

[8] a) C. K. Tu, G. C. Wynns and D. N. Silverman, *J. Biol. Chem.*, **256**, 9466 (1981) ; b) C. K. Tu and D. N. Silverman, *Biochemistry*, **19**, 4984 (1985).

[9] L. Sommer, "Analytical Absorption Spectrophotometry in the Visible and Ultraviolet", Akademiai Kiado, Budapest, 1989.

[10] J. Korman, *J. Org. Chem.*, **23**, 1768 (1958).

[11] The IC_{50} value for ethoxzolamide is 10 nM. while for the palladium complex 8 nM (for details see refs. 1 and 2).

Revue Roumaine de Chimie, **36**, *9–10*, 1175–1179 (1991)

CARBONIC ANHYDRASE INHIBITORS. 8[1]

COMPLEXES OF ETHOXZOLAMIDE WITH LANTHANIDES ARE POWERFUL INHIBITORS OF ISOZYMES I AND II**

CLAUDIU T. SUPURAN[a,*], RALUCA ŞTEFAN[a], GHEORGHE MANOLE[b],
IOAN PUŞCAŞ[c] and MARIUS ANDRUH[a,*]

[a] University of Bucharest, Department of Chemistry, Bd. Republicii 13, Bucharest, 1, Roumania
[b] Builders Clinical Hospital, Mandinesti Street. 3–5, Bucharest, Roumania
[c] Center for Research and Medical Assistance, Roumanian Academy, Simleu Silvaniei, Roumania

Received April 12, 1991

Coordination compounds of the type $[Ln(EZA)_3] \cdot x\ H_2O$ (where Ln = La, Ce, Pr and Er ; EZA is the anion of 6-ethoxy-benzothiazole-2-sulfonamide and x = 8 or 12) were prepared and characterized by means of TG and elemental chemical analysis, electronic and IR spectroscopy. These complexes are potent inhibitors for isozymes I and II of carbonic anhydrase.

INTRODUCTION

In addition to the thoroughly studied carbonic anhydrase (CA, EC 4.2.1.1) inhibitors, i.e., aromatic/heterocyclic sulfonamides[2] and monovalent anions,[3] we recently reported that coordination compounds of heterocyclic sulfonamides with bivalent cations such as Zn(II), Cu(II), Ni(II), Pd(II) and Pt(II) act as potent inhibitors of this enzyme.[4]

Taking into account the fact that lanthanides possess interesting properties which can be used for undercovering biologically important features of other elements, and especially of Ca^{2+} (due to the similar ionic size of these ions)[5] and because the use of lanthanides as drugs started to be considered quite recently,[6] we extended our research in the design of novel types of CA inhibitors to complexes of lanthanides with a potent sulfonamide–CA inhibitor, ethoxzolamide (6-ethoxy-benzothiazole-2-sulffonamide, **1**).

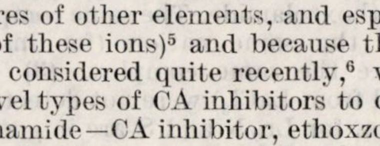
1

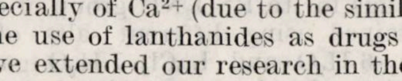
2

---

* To whom correspondence should be addressed

** Dedicated to the memory of Academician EMILIAN A. BRATU.

The interrelations between CA activity and both intra- and extracellular calcium concentrations are responsible for important physiological mechanisms such as hormone secretion, as was shown by Dietsch[7] and Drewe et al.[8] This is not at all surprising, taking into account the fact that CA, and more precisely its isozymes I and II, were identified in osteoclasts,[9] which are the cellular agents implicated in bone resorption. The role of this enzyme in such processes is to furnish H^+ ions, by catalyzing the hydration of CO_2, which in turn, are used for the mobilization of the unsoluble bone mineral, apatite, into primary/secondary soluble calcium phosphates. It was also reported that CA inhibitors such as acetazolamide (**2**) have important physiological effects, like inhibition of hypercalcemic response to parathyroid hormone or dibutyryl-3′, 5′-cAMP, or blocking the development of disuse atrophy of bone (in a rat model).[10] Endly, the culmination of research connecting CA with calcium, was the report of Sly et al.[11] of a genetic disorder of CA II deficiency, associated with osteoporosis, renal tubular acidosis and cerebral calcification. As stated by Maren[12], all these pioneering observations raised more questions than answers, so that the emergence of inhibitors that would interact both with CA and calcium, is indeed of interest.

In this paper we report the preparation and characterization of complexes of some lanthanides (La(III), Ce(III), Pr(III) and Er(III) with sulfonamide **1** and the *in vitro* inhibition studies on isozymes CA I and CA II. Due to the presence of sulfonamide moieties as well as Ln^{3+} ions in the molecules of these compounds, we presume that they would interact both with CA and with calcium (*in vivo*), so that they could be used in order to obtain new insights in this fascinating field.

RESULTS AND DISCUSSION

Reaction of lanthanide (III) chlorides or nitrates with an aqueous solution of ionized sulfonamide ($RSO_2NH^-Na^+$) in molar ratio 1 : 3 afforded the following compounds : $[La(EZA)_3] \cdot 12\,H_2O$ (**3**); $[Ce(EZA)_3] \cdot 8\,H_2O$ (**4**); $[Pr(EZA)_3] \cdot 12\,H_2O$ (**5**) and $[Er(EZA)_3] \cdot 8\,H_2O$ (**6**), where EZA stands for te RSO_2NH group of ethoxzolamide. The same compound was obtained using different salts of the same cation (for instance $La(NO_3)_3 \cdot 6\,H_2O$ and $LaCl_3 \cdot 7\,H_2O$ gave the same complex, (**3**) while chloride ions (for the compund prepared from $LaCl_3$) were not detected by elemental chemical analysis). These data, for Ln, N and S are in good agreement with the theoretical values calculated for the proposed formulas ($\pm 0.5\%$; see experimental). By thermogravimetric (TG) analysis it was proved that all the water present in the molecule of the new complexes was lost in a single step, till 175°C, with the following weight losses : for **3**, 19.01% (calcd. 19.18%); for **4**, 13.33% (calcd. 13.64%); for **5**, 18.78% (calcd. 19.15%); for **6**, 13.17% (calcd. 13.30%). This fact proves that the water molecules are equivalent and that lattice water is present in these compounds. Electronic spectra for some of the new complexes (see experimental) did not offer much information regarding the stereochemistry of these compounds, because the lanthanide complexes are of very weak field.

Taking into account the fact that we proved by TG analysis that water is not a ligand in these complexes, and the bidentate nature of the ethoxzolamide anion, as we showed in previous reports,[2] probably the donor atoms are the sulfonamidic nitrogen and the N-3 atom of the benzothiazole ring. An argument in favor of this assumption is the fact that the sulfonamido bands in the IR spectrum of complexes **3**—**6** are slightly shifted towards lower wavenumbers, as compared to the uncomplexed ligand **1** (Table 1).

Table 1

Wavenumbers (cm^{-1}) for the vibrations of SO_2 groups in ethoxzolamide (**1**) and the complex compounds **3**—**6**

Compound	$\nu_{sym}SO_2$ (cm^{-1})	ν_{as-SO_2} (cm^{-1})
1	1180	1370
3	1174	1360
4	1170	1360
5	1170	1360
6	1172	1360

The compounds were tested for inhibitory action on purified bovine isozymes CA I and CA II, using the micromethod of Maren.[13] All of them possess great efficiencies in inhibiting the enzyme, the IC_{50} values being presented in Table 2 (see experimental part for details). As expected, some differences emerged between the two isozymes. Thus, CA II is more prone to be inhibited by the complex inhibitors than the isozyme CA I, a fact that parallels the behavior of these isozymes towards aromatic/heterocyclic sulfonamides.[2] Evenso, the inhibition observed with this type of compounds is very strong and some questions remain concerning the mechanism of action for these powerful inhibitors (see ref. 1).

Table 2

IC_{50} values (mol/L) for the complex inhibitors and standard CA inhibitors (acetazolamide **2** and ethoxzolamide **1**) against isozymes CA I and CA II

Compound	1[a]	2[a]	3[b]	4[b]	5[b]	6[b]
CA I	—	—	$3 \cdot 10^{-7}$	$3.8 \cdot 10^{-7}$	$5 \cdot 10^{-7}$	$7 \cdot 10^{-10}$
CA II	10^{-9}	$8 \cdot 10^{-9}$	10^{-10}	$6 \cdot 10^{-9}$	$\leqslant 10^{-10}$	$\leqslant 10^{-11}$

[a] Human isozyme used (ref. 15).

[b] Bovine isozymes used (see experimental for details).

EXPERIMENTAL

TG analysis were done using a MOM Budapest Q-1500 D apparatus, at a heating rate $\beta = 10°/min$. Electronic spectra were recorded by diffuse reflectance technique using MgO as reference material. IR spectra were recorded in KBr pellets on a C. Zeiss-Jena double beam spectrophotometer. Inhibitors were assayed at 4°C, using Maren's micromethod[13] and the SEI (substrate — enzyme — inhibitor) technique, as described previously.[4] Stock solutions of inhibitors (10^{-2} M) were obtained in DMSO (Merck) — water and dillutions obtained thereafter with distilled deionized water. IC_{50} values represent the molar concentration of inhibitor that produces 50% inhibition of the CA catalyzed hydration of CO_2. These values were obtained from semilog plots of specific activity of enzyme vs. inhibitor molar concentration.

CA I and II (of bovine origin) were from Serva Feinbiochemica Heidelberg. With the exception of $CeCl_3 \cdot 7\,H_2O$ which was from Merck-Schuchard, the other lanthanide salts were from Merck. Ethoxzolamide was prepared by literature procedures.[14]

$[La(EZA)_3] \cdot 12\,H_2O$ (**3**) (white): IR (KBr), cm^{-1}: 440, 454, 500, 540, 565, 625, 710, 820, 910, 945, 1040, 1085, 1174, 1225, 1270, 1360, 1495, 1600, 2900, 2945, 2990, 3080 (br), 3160 (br), 3320 (br); elemental analysis: found; N, 7.68%; S, 17.60%; La, 12.80%. calcd. N, 7.46 %; S, 17.05% La, 12.34%.

$[Ce(EZA)_3] \cdot 8\,H_2O$ (**4**) (tan): IR (KBr), cm^{-1}: 440, 455, 500, 540, 560, 625, 720, 825, 910, 1040, 1080, 1170, 1225, 1275, 1360, 1495, 1600, 2990, 3060 (br), 3160 (br), 3320 (br); elemental analysis: found; N, 7.46%; S, 18.36%, Calcd. N, 7.96%; S, 18.79%.

$[Pr(EZA)_3] \cdot 12\,H_2O$ (**5**) (greenish-white): IR (KBr), cm^{-1}: 440, 455, 500, 540, 565, 625, 710, 825, 905, 1040, 1080, 1170, 1225, 1270, 1360, 1495, 1600, 2990, 3060 (br), 3170 (br), 3320 (br); electronic spectrum (MgO); λ_{max}, nm: 380, 450, 470, 490, 510 (sh), 590, 760, 825, 870, 910 (sh); elemental analysis: found; N, 7.76%, S, 16.85%; Pr, 13.00%. Calcd. N, 7.44%; S, 17.02%; Pr. 12.50%.

$[Er(EZA)_3] \cdot 8\,H_2O$ (**6**) (pinkish-white): IR (KBr), cm^{-1}: 440, 455, 500, 540, 565, 625, 715, 825, 905, 1040, 1085, 1172, 1225, 1275, 1360, 1490, 1520, 1600, 2995, 3060 (br), 3150 (br), 3320 (br); electronic spectrum (MgO); λ_{max}, nm: 380, 450, 490, 525, 575, 660, 700 (sh), 820, 860 (sh), 970, 1050 (sh); elemental analysis: found; N, 7.32%, S, 17.38%; Er, 15.00%. Calcd. N, 7.76%, S, 17.74%, Er, 15.43%.

ACKNOWLEDGMENTS. Special thanks are addressed to Professor Maria Brezeanu for helpful discussions and to Serva Feinbiochemica Heidelberg for the gift of CA isozymes.

Note added in proof: Due to the excellent inhibitory properties of the lanthanide complexes described in this paper, the study was extended; the whole series of ethoxzolamide complexes, of the type $[Ln(EZA)_3] \cdot xH_2O$, where Ln represents the other lanthanide ions, were prepared, characterized and tested on isozymes CA I and CA II. The corresponding acetazolamide complexes ($[Ln(AAZ)_3] \cdot xH_2O$) were also obtained. These results are presented in a future paper (C. T. Supuran, G. Manole & M. Andruh, *J. Inorg. Biochem.*, submitted).

REFERENCES

[1] Part 7: C. Luca, M. Bărboiu and C. T. Supuran, *Rev. Roumaine Chim.*, preceding paper.

[2] a) T. H. Maren, *Physiol. Rev.* **47**, 595 (1967); b) S. Lindskog and P. J. Wistrand, "Carbonic Anhydrase Inhibitors" in "Design of Enzyme Inhibitors as Drugs", M. Sandler Ed., Oxford Univ. Press, Oxford 1988.

[3] a) T. H. Maren, C. S. Rayburn and N. E. Liddell, *Science*, **191**, 469 (1976); b) I. Bertini, C. Luchinat and L. Banci, Carbonic Anhydrase International Workshop, Spoleto, Italy 1990, Abstract Book pp. 24.

[4] a) C. Supuran, M. Andruh and I. Puşcaş, *Rev. Roumaine Chim.* **35**, 393 (1990); b) C. Supuran, G. Manole, A. T. Balaban, I. C. Puşcaş, A. Schiketanz, M. D. Gheorghiu, M. Andruh and I. Puşcaş, Carbonic Anhydrase International Workshop, Spoleto, Italy, 1990, Abstract Book ,pp. 128; c) M. Andruh, E. Cristurean, R. Ştefan and C. T. Supuran, *Rev. Roumaine Chim.*, **36**, 727 (1991).

[5] R. J. P. Williams, *Nature*, **344**, 595 (1990).

[6] C. H. Evans, "Biochemistry of Lanthanides", Plenum Peess, 1990.

[7] P. Dietsch, "Parathyroid Hormone, Carbonic Anhydrase and Calcium Homeostasis" in "Generalized Bone Diseases", F. Kuhlencordt, P. Dietsch, E. Keck and H. P. Kruse Eds., Springer, Heidelberg 187, pp. 279–289.

[8] J. Drewe, P. Dietsch and E. Keck, *Calcif. Tissue Int.*, **43**, 26 (1988).

[9] a) C. V. Gay and W. J. Mueller, *Science*, **183**, 432 (1974). b) H. K. Väänänen and E. K. Parvinen, *Histochemistry*, **78**, 481 (1983) ; c) H. K. Väänänen, *Histochemistry*, **81**, 485 (1984) ; d) C. V. Gay, Carbonic Anhydrase International Workshop, Spoleto, Italy 1990, Abstract Book pp. 124.

[10] a) A. D. Kenny, *Pharmacology*, **31**, 97 (1974) ; b) H. H. Conaway, L. C. Waite and A. D. Kenny, *Calcif. Tissue Res.*, **11**, 323 (1973).

[11] a) W. S. Sly, D. Hewett-Emett, M. P. Whyte, Y.U. Ysl and R. E. Tashian, *Proc. Natl. Acad. Sci. USA* **80**, 2752 (1983) ; b) W. S. Sly, M. P. Whyte, V. Sundaram, R. E. Tashian, D. Hewett-Emett. P. Guibaud, M. Vainsel, H. J. Baluarte, A. Gruskin, M. Al-Misawu, H. Sakati and A. Ohlsson, *New Engl. J. Med.* **313**, 139 (1985) ; c) V. Sundaram, P. Rumbolo, J. Grubb, P. Strisciuglo and W. S. Sly, *Am. J. Hum. Genet.* **38**, 125 (1986).

[12] T. H. Maren, *New Engl. J. Med.* **313**, 179 (1985).

[13] T. H. Maren, *J. Pharmacol. Exptl. Ther.* **130**, 26 (1960).

[14] J. Korman, *J. Org. Chem.* **23**, 1768 (1958).

[15] T. H. Maren, *Drug Dev. Res.* **10**, 255 (1987).

Revue Roumaine de Chimie, **36**, *9–10*, 1181–1184 (1991)

LOW-BOILING PRODUCTS OF THE PROPOXYLATION REACTION OF ACETIC ACID

E. DZIWINSKI, P. KUSZ, H. SZEWCZYK, K. PYZALSKI and D. GASZTYCH
Institute of Heavy Organic Synthesis "Blachownia" 47–225 Kedzierzyn-Kozle
Institute of Organic Chemistry and Technology, Silesian Polytechnical University, 44–101, Gliwice, Poland

Received October 24, 1988

The low-boiling products of the catalytic acetic acid propoxylation reaction have been identified using gas chromatography– mass spectrometry method. It was found that in this process mainly 2, 3-epoxypropane-1-ol and dialkyl derivatives of 1, 3-dioxolane and 1, 4-dioxane are formed. The mechanism of the formation of these compounds has been proposed and discussed.

The main products of the catalytic acetic acid propoxylation reaction are mono- and diacetates of propylene and polyoxypropylene glycols. In an earlier paper, the gas chromatographic (GC) separation as well as qualitative and quantitative analyses of these products have been presented.

From our investigations it results that in the mentioned process many low-boiling products are also formed. In this paper, we present the results of the identification of these compounds by use of the gas chromatography – mass spectrometry (GC–MS) method.

EXPERIMENTAL

Sample for identification

The fraction boiling at 91–97°C was distilled off from the acetic acid propoxylation reaction final product.

Apparatus and GC-MS conditions

The electron impact (EI) mass spectra of the individual components of the mixture investigated were recorded on an LKB 2091 instrument equipped with the Pye 104 gas chromatograph coupled to the mass spectrometer via a Becker-Ryhage type separator.

For gas chromatography a stainless steel column (3.6m × 2.7 mm I.D.) packed with 12% Carbowax 20M–TPA on Chromosorb W–AW–DMCS, 80–100 mesh (Appl. Sci. Labs., State College, PA, USA) was used. The initial column temperature was 100°C for 1 min and then programmed to a final temperature of 220°C at the rate of 6°C/min. The injector temperature was 200°C. The helium carrier gas flow was 30 mL/min.

The EI mass spectra were obtained under the following conditions: electron beam energy, 70 eV, accelerating voltage, 3.5 kV, trap current, 50 μA, temperature, of the ion source 250°C and temperature of separator, 250°C.

RESULTS AND DISCUSSION

The GC separation of the components of the fraction investigated is shown in Figure 1.

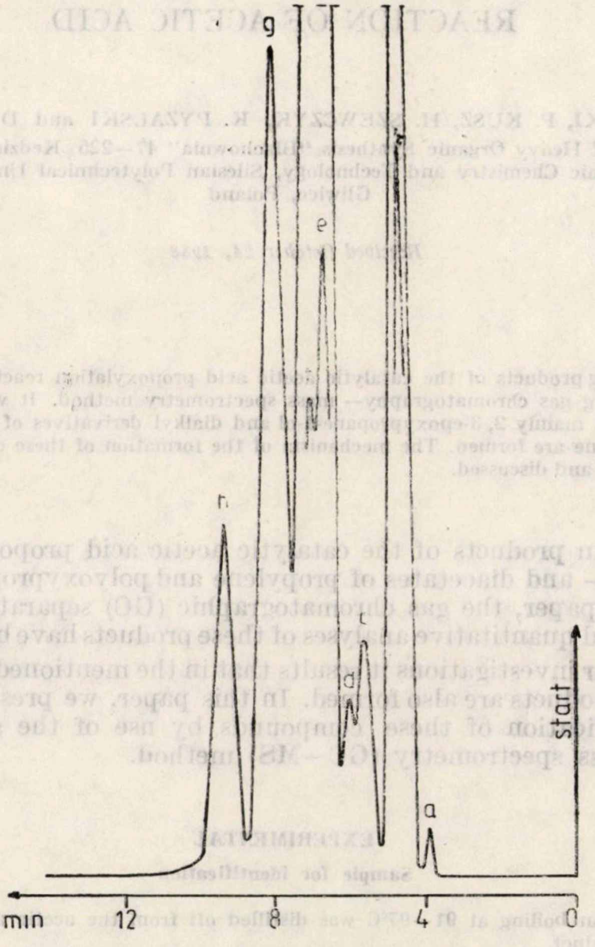

Fig. 1. — Chromatogram of the fraction (91—97°C) distilled off from the acetic acid propoxylation reaction final product. Peaks identified by GC—MS method: a and b = 1, 2-epoxypropane + 2, 3-epoxypropane-1-ol, c and d = isomers of dimethyl-1, 3-dioxolane, e and f = isomers of methylethyl-1,3-dioxolane, g = 2, 6-dimethyl-1, 4-dioxane, h = 2, 5-dimethyl-1,4-dioxane.

Their identification was based on the interpretation of the mass spectra. This was possible by using the general rules of the mass fragmentation processes of such compounds which proceed in the electron-impact type ion source of the mass spectrometer as well as by comparison of the mass spectra obtained with standard ones included in catalogues.[2,3] During the GC—MS analysis, we did not succeed to separate the peaks of the *a* and *b* components (see Fig. 1). However, from the mass spectrum obtained for the *b* peak, it is evident that it contains two compounds: propylene oxide (raw material) and a compound having a molecular weight 74. The latter was found to be 2,3-epoxypropane-1-ol:

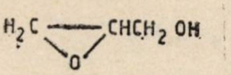

The common feature of the *c*, *d*, *e*, *f* compounds is that the $M^{+\cdot}$ molecular ions are absent in their mass spectra and therefore it is impossible to determine their molecular weights, directly. The similarity of the mass spectra of *c* and *d* compounds to those of the *e* and *f* ones proves that some isomers are present in the fraction examined. To identify these compounds, the spectra obtained were compared with the standards.[2,3] In this way, we have found the *c* and *d* components to be dimethyl-1,3-dioxolane isomers with molecular weight 102 while the main components *e* and *f* of the fraction examined, are, as it was found in a similar way, the methylethyl-1,3-dioxolane isomers having the following structure:

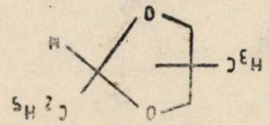

The presence of the 1,3-dioxolane alkylated derivatives in the mentioned fraction is evidenced by the $[M-1]^+$, $[M-CH_3]^+$ and $[M-C_2H_5]^+$ ions which are typical for these compounds and which are present in the mass spectra of the *e* and *f* components.

The mass spectra of the *g* and *h* components are also very similar to each other. This seems to prove that both compounds are isomeric ones as well. In this case occurrence of the molecular ions $M^{+\cdot}$ at $m/z = 116$ enabled us to determine explicitely the molecular weights. The structures of these two isomers were fully determined when the mass spectra of the *g* and *h* components were compared with the literature spectra patterns.[2,3] Here, the differences existing between the intensities of the ions having $m/z = 42$ and $m/z = 45$ were observed. In this way, the components *g* and *h* were identified as being 2,6-dimethyl-1,4-dioxane and 2,5-dimethyl-1,4-dioxane respectively.

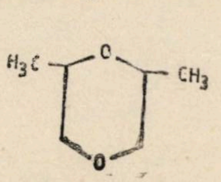

g

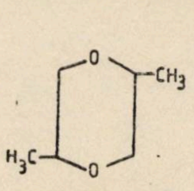

h

The main components of the fraction examined i.e. methylethyl-1,3-dioxolane isomers are formed during the propylene oxide isomerization reaction, while the dimethyl-1,4-dioxane derivatives are formed, most probably, as a result of an intramolecular cyclization of polyoxypropylene mono-ethers under the influence of an acidic catalyst, similarly to the polyoxyethylene glycols.[4] The proposed mechanism of formation of the dimethyl-1,4-dioxane in acetic acid propoxylation reaction is given in Figure 2.

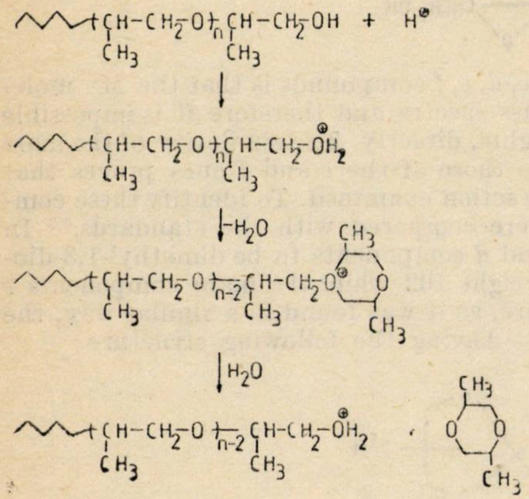

Fig. 2. — The proposed mechanism of an intramolecular cyclization reaction of the polyoxypropylene monoethers.

In conclusion it can be stated that on the basis of the mass spectra of the components investigated it was possible to identify all of them. The results obtained permit to know better the by-products of the acetic acid propoxylation reaction.

REFERENCES

[1] P. Kusk, H. Szewczyk, E. Dziwinsk , K. Pyzalski and D. Gasztych, *J. High Resolution Chromatography and Chromatography Communications*, **9**, 310 (1986).

[2] S. Stenhagen et al. "Atlas of Mass Spectral Data", Interscience Publishers, New York, 1969.

[3] "Eight Peak Index of Mass Spectra", AWRE, Aldermaston, 1974.

[4] D. J. Worsford, A. M. Easthan, *J. Amer. Chem. Soc.*, **79**, 897 (1957).

Revue Roumaine de Chimie, **36**, *9–10*, 1185–1193 (1991)

TRANSALKYLATION OF TOLUENE WITH TRIMETHYLBENZENE. II.

TRANSALKYLATION OF TOLUENE WITH MESITYLENE OVER SYNTHETIC ZEOLITES

EMIL DUMITRIU, VASILE HULEA, KAYED YOUSEF, NICOLAE BALBA and SPIRIDON OPREA

Department of Organic Chemical Technology, Faculty of Chemical Technology, Bahlui Stînga 71, Jassy 6600, Romania

Received July 29, 1989

The transalkylation of toluene with mesitylene over mordenite and Y faujasites was investigated. The influence of certain factors as : nature of catalyst, nature and mole ratio of reagents, temperature and contact time on the compositions, distribution of reaction products, conversion, activity and selectivity was studied. The experimental data have been compared with the results obtained by thermodynamic calculations.

INTRODUCTION

As it was observed from the thermodynamic study, the mesitylene can be considered as the most reactive trimethylbenzene in the transalkylation of toluene. Therefore, the aim of this paper is to study the transalkylation of toluene with mesitylene over synthetic zeolites and to follow the composition of reaction products and conversion in relation to the thermodynamic calculations and the activity and selectivity of catalysts, respectively.

EXPERIMENTAL

Reagents. Benzene, toluene. xylene and trimethylbenzenes were distilled before use.

Catalysts. The following catalysts were used :

— mordenite, H^+ form (HM), having the ratio $SiO_2/Al_2O_3 = 10.81$; this catalyst was prepared and characterized as previously reported.[1]

— SK–500 (Ventron) having the composition : 65.0 % SiO_2 ; 22.7 % Al_2O_3 ; 1.6 % Na_2O and 10.7 % RE_2O_3. Surface area was about 550 m^2g^{-1}.

The catalysts, without binder (except SK–500), were pressed, grounded and then sieved, the fraction of 0.25–0.43 mm being collected. All catalysts have been activated before use.

Apparatus and procedure. The most experiments were carried out on a microreactor connected at a GL chromatograph equipped with FID and a column with bentone 34 and dinonilphthalate on Chromosorb W. Nitrogen, free from oxygen and moisture, was used as carried gas. The amount of catalyst was about 15 mg. In order to investigate the influence of contact time, a series of experiments have been carried out on an integral fixed-bed isothermal reactor operated at atmospheric pressure. The reagents were fed at constant rate by means of a calibrated syringe pump. Nitrogen was also used as carrier gas. The reaction products were collected into a cooled trap (–30°C) and then chromatographically analysed.

RESULTS AND DISCUSSION

The aim of this paper was to study the catalytic transformation of methylbenzene in relation to the nature of reagents, the nature of catalyst, temperature and contact time. The experimental data have been interpreted by means of the thermodynamic study previously reported.

First, we must mention that the coke formation was neglected in the reaction model of transalkylation and therefore the experiments were carried out only over freshly activated catalysts, this being the reason of the microreactor use. The experiments carried out on an integral reactor show that a certain deactivation of catalyst by coke deposit occurs and this leads to a diminution of conversion and, to some extent, the distribution of reaction products is also affected.

The validity of the reaction model has been checked following the behaviour both of each aromatic compound implied in this model and of the reaction mixture for transalkylation, in the same reaction conditions, on a pulse type microreactor. The experimental data are shown in Table 1 and the following aspects can be underlined :

Table 1

The testing of reaction model validity, reaction temperature 648 K, HM catalyst

Reagent	Composition of product, % mole							
	B	T	p-X	m-X	o-X	1,3,5-TMB	1,2,4-TMB	1,2,3-TMB
Toluene (T)	16.52	71.32	2.77	6.02	2.59	0.15	0.55	0.03
p-Xylene (p-X)	3.25	21.86	12.83	21.84	10.11	7.85	19.45	2.76
m-Xylene (m-X)	3.12	23.03	12.67	27.89	9.17	5.76	16.60	1.73
o-Xylene (o-X)	4.07	26.88	14.06	28.80	21.85	6.48	16.24	3.07
1, 3, 5-Trimethylbenzene (TMB)	0.13	3.22	5.38	10.65	5.17	25.07	44.21	6.20
T + 1, 3, 5-TMB	4.04	29.53	9.25	18.35	8.92	10.31	15.85	3.72
B + 1, 3, 5-TMB	36.05	21.28	5.78	11.01	4.95	9.83	10.00	1.06

a) — the toluene is disproportionated to benzene and xylenes, the *meta* isomer being prevalent, and these are disproportionated to some extent to trimethylbenzenes ;

b) — the xylenes are firstly isomerised and then they are disproportionated in toluene and trimethylbenzenes ;

c) — 1, 3, 5-trimethylbenzene is strongly isomerised, especially to 1, 2, 4-isomer, and, to some extent, is disproportioned to xylenes and tetramethylbenzenes ;

d) — the mixture used for transalkylation (T + TMB and B + + TMB) behaves according to the thermodynamic data.

The last aspect is significantly illustred by the data shown in Figure 1, where the composition at equilibrium (calculated from the thermodynamic data) and that experimentally obtained in the transalkylation of toluene with mesitylene on mordenite HM at 648 K is presented. One observes that there is a good agreement between the experimental and calculated data. Therefore, these data demonstrate that the morphology of catalyst does not disturb the distribution of reaction products which respects the foresights of thermodynamic calculus.

Of course, the major problem of this study has been to investigate the behaviour of the three trimethylbenzene isomers in the process of transalkylation. The results for each isomer, in the same reaction conditions, are shown in Figure 2. Analysing these data, the following aspects can be mentioned ;

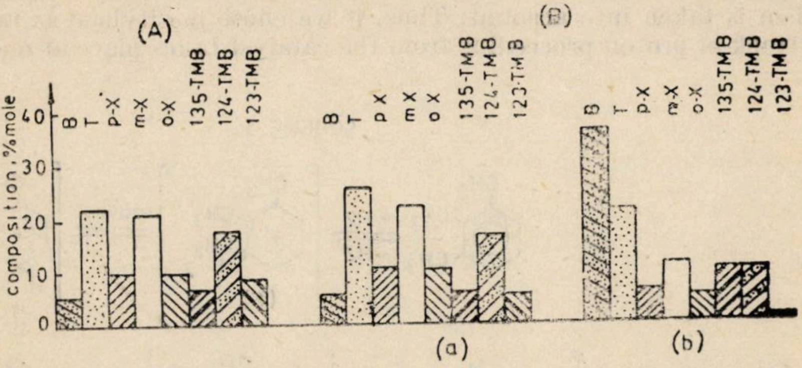

Fig. 1. — Product distribution of mesitylene transalkylation.
(A) — from thermodynamic data ;
(B) — from experimental data ; HM catalyst, T = 648 K ;
(a) — transalkylation with toluene ;
(b) — transalkylation with benzene.

a) — the conversion of toluene is greater for transalkylation with 1, 3, 5-TMB and with 1, 2, 4- than 1, 2, 3-TMB ;

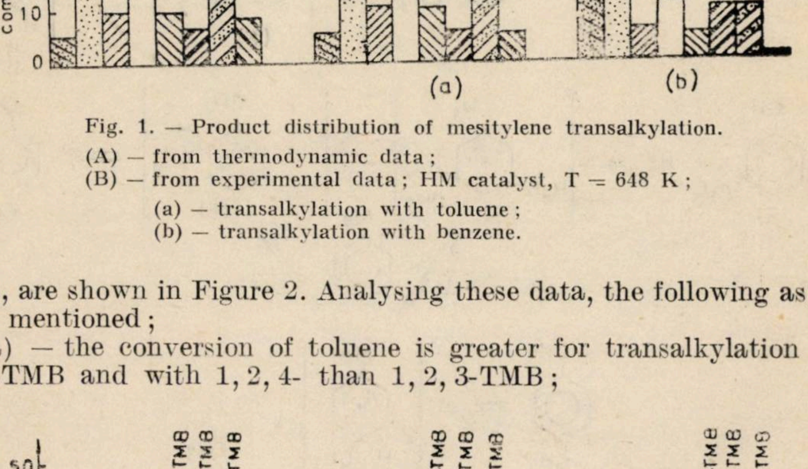

Fig. 2. — Product distribution of toluene transalkylation with :
(a) — 1, 3, 5-trimethylbenzene ; (b) — 1, 2, 4-trimethylbenzene ;
(c) — 1, 2, 3-trimethylbenzene ; HM catalyst ; T = 648 K.

b) — the distribution of xylene isomers is in agreement with the thermodynamic data, the meta isomer being in the greatest proportion, whereas the other isomers are in approximately equal proportions ;

c) — the distribution of trimethylbenzene isomers indicates that the isomerization plays an important role because, as can be observed from

Figure 2, the conversion of toluene can be correlated with the proportion of 1, 2, 4-TMB. Thus, in the case of transalkylation with 1, 2, 3-TMB, when the smallest conversion of toluene has been obtained, it is found that in this case the greatest amount of 1, 2, 4-TMB is formed. Regarding the last observation, an explanation can be offered if the reaction mechanism is taken into account. Thus, if we chose mesitylene as reactant, the attack of proton proceeding from the catalyst takes place at one of the

SCHEME I

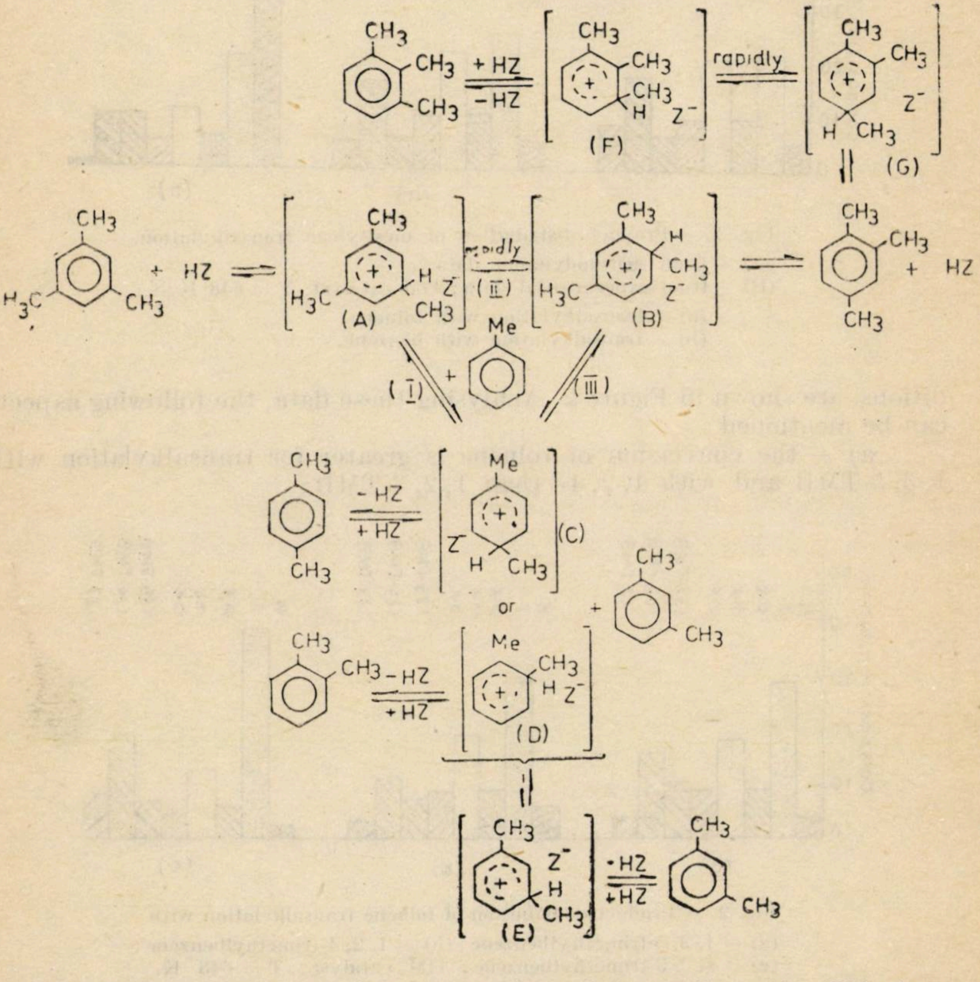

substituted carbon atoms leading to the σ intermediate (A). This intermediate can liberate the $\overset{+}{C}H_3$ carbocation with the formation of *m*-xylene isomer. The new formed carbocation ($\overset{+}{C}H_3$) will attack the molecule of substrate (toluene), the *para* and *ortho* positions being favoured due to the inductive effect of methyl group. The σ intermediates (C) or (D) are formed and they are stabilized by the proton expulsion when the *para* or *ortho*-xylene is obtained. These intermediates, (C) and (D), can generate the intermediate (E) by migration of CH_3 radical around the benzene ring, the last intermediate (E) leading to the formation of *m*-xylene. Therefore, the probability of the formation of xylene isomers can be expressed by the ratio $m : o : p = 2 : 1 : 1$, this being found by the analysis of the reaction mixture, too.

Likewise, it was experimentally observed that the mixtures of TMB obtained by transalkylation contain mainly the 1, 2, 4-TMB isomer (see Figure 2). This fact can be explained if the scheme I is taken again into consideration. Thus, the intermediate (A), by the reaction route II, gives rapidly the intermediate (B) which forms 1, 2, 4-TMB by expulsion of the proton. The same isomer is obtained taking into account the 1,2, 3-trimethylbenzene (by G intermediate). Therefore, the probability of the formation of 1, 2, 4-TMB is greater, like in the case of isomerization of *p*- or *o*-xylene to *m*-xylene.

1, 2, 4-Trimethylbenzene seems to be less reactive in transalkylation than 1, 2, 3- and 1, 3, 5-TMB as it was obtained from the thermodynamic calculus. If the reactivities of 1, 3, 5-TMB and 1, 2, 3-TMB are compared, from the experimental data results that 1, 2, 3-TMB isomerizes more easily to 1, 2, 4-TMB than mesitylene and this should explain why the conversion of toluene is smaller in this case (see Figure 2).

The above mentioned results regarding the behaviour of trimethylbenzene isomers in the transalkylation process are also confirmed by the results obtained in the isomerization and disproportionation of each isomer of TMB (see Figure 3).

It can be observed from Figure 3 that 1, 2, 3-TMB is easily isomerised and disproportioned in the presence of SK-500 catalyst whereas 1, 2. 4-TMB is more stable. Also, a certain modification of the distribution of trimethylbenzene isomers is observed. Thus, when 1, 2, 3-TMB is isomerised and diproportioned the amount of formed mesitylene is smaller than for the isomerisation and disproportionation of 1, 2, 4-TMB. This behaviour is similar for both catalysts. About the catalysts, we must quote that both the mordenite and SK-500 modified faujasite have

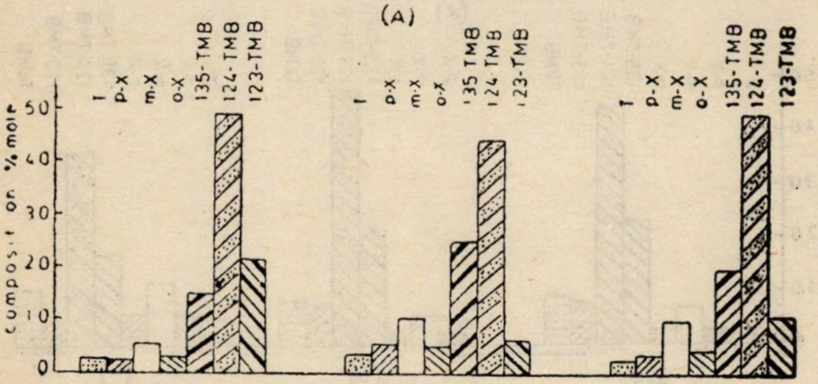

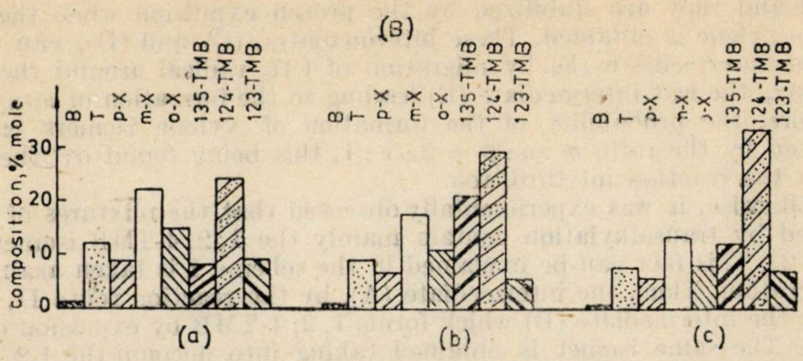

Fig. 3. — Product distribution of isomerization and disproportionation of trimethylbenzene at 648 K ; (A) — HM catalyst, (B) — SK—500 catalyst ; (a) — 1, 2, 3-trimethylbenzene ; (b) — 1, 3, 5-trimethylbenzene ; (c) — 1,2,4 -trimethylbenzene.

approximately the same activity for the isomerization reaction, but SK-500 zeolite is more active for the trimethylbenzenes disproportionation. This behaviour should be explained by the acidity difference between these catalysts rather than by the difference of porosity or size of pores.

From the above-presented data another important aspect can be quoted, namely, the thermodynamic stability of 1, 2, 4-TMB. Thus, various mixtures of trimethylbenzenes, both the equimolar mixture and the mixture corresponding to the thermodynamic equilibrium, have been subjected to the isomerization. As can be observed from Figure 4 the composition of the reaction products is very close to that obtained in the isomerization and disproportionation of 1, 2, 4-trimethylbenzene (see e.g. Fig. 4.a.). Therefore, 1, 2, 3- and 1, 3, 5-TMB isomerized and disproportionated more easily. Regarding the disproportionation process, it is interesting to note the presence of toluene which can only be explained if we admit the disproportionation of xylenes. Moreover, if a mixture of aromatic hydrocarbons, into a proportion, as resulted in the isomerization and

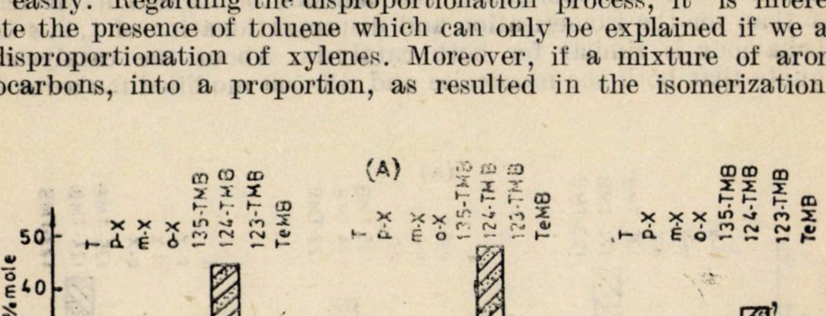

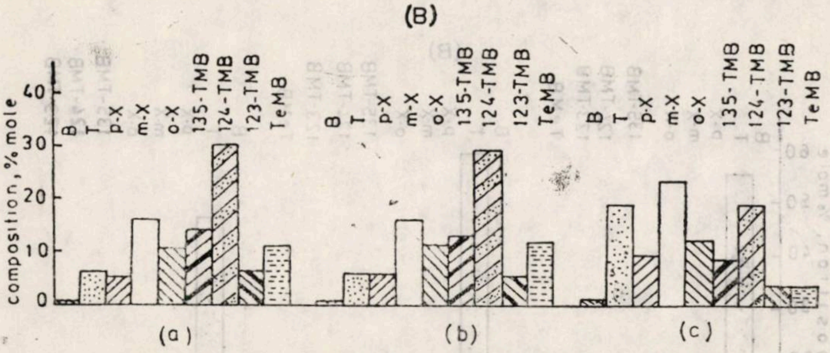

Fig. 4. — Product distribution of isomerization and disproportionation of the trimethylbenzene mixtures at 648 K ; (A) — HM catalyst, (B) — SK—500 catalyst ;
(a) — equimolar mixture ; (b) — thermodynamic mixture ; (c) — mixture of composition as those resulted from the catalytic conversion of the equimolar mixture. (TeMB = tetramethylbenzene).

disproportionation of TMB, is passed over catalyst an increase of the amount of toluene in the reaction product can be observed.

In continuation of our study, the transalkylation of toluene with these mixtures of trimethylbenzenes has been performed, and the distribution of the reaction products (Figure 5) was found also to be closer to that obtained at the transalkylation of toluene with 1, 2, 4-TMB. The differences between the activity and selectivity of the two types of catalysts are observed, too. Regarding the last observation it is interesting to quote that SK-500 catalyst favours the *o*-xylene isomer formation whereas in the presence of mordenite *o*-xylene and *p*-xylene are obtained in the same proportion.

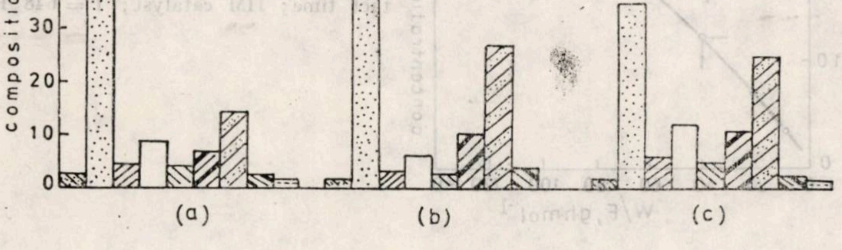

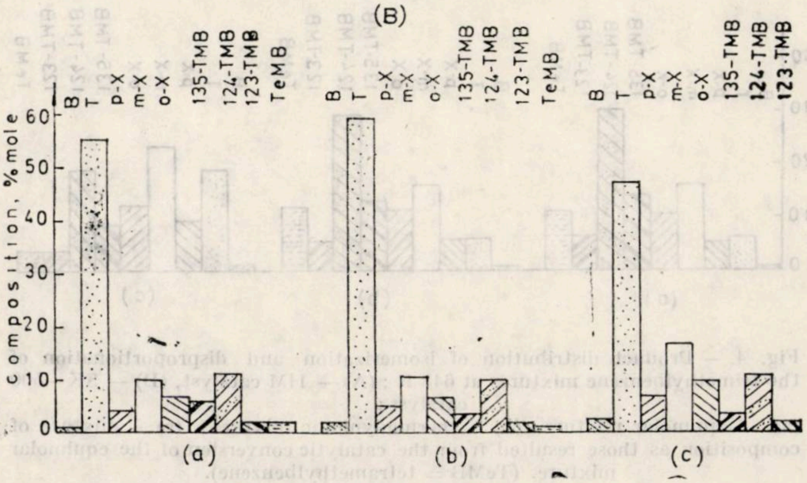

Fig. 5. — Product distribution of toluene transalkylation with trimethylbenzene mixtures at 648 K; (A) — HM catalyst, (B) — SK—500 catalyst; (a) — transalkylation with equimolar mixture of trimethylbenzene; (b) — transalkylation with thermodynamic mixture of trimethylbenzene; (c) — transalkylation with a mixture of composition similar to those obtained at the isomerization and disproportionation of an equimolar mixtures of trimethylbenzenes.

The influence of contact time has been the last factor which was investigated. In this case the proportion of 1, 2, 4-TMB and the distribution of xylenes in the reaction product has been followed. It was stated

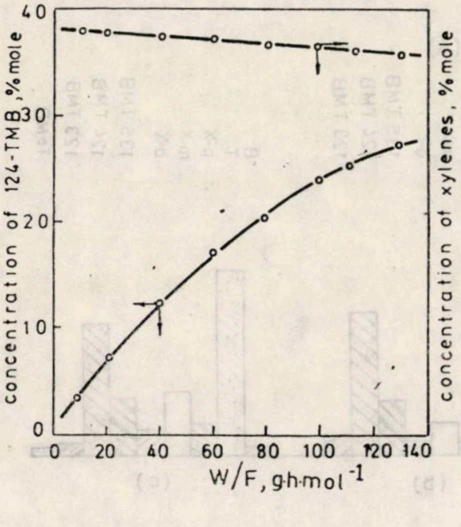

Fig. 6. — The xylenes and 1, 2, 4-trimethylbenzene concentration vs. contact time; HM catalyst; T = 648 K.

that the amount of xylenes decreases as contact time is increased due to the secondary reactions. Also, a slow accumulation of 1, 2, 4-TMB amount is observed with contact time increasing.

We can conclude that in the most cases the values of thermodynamic equilibrium have been reached, in the selected reaction conditions, and the concordances observed prove the validity of reaction model.

REFERENCES

[1] S. Oprea, E. Dumitriu, V. Hulea, P. Onu, D. Gînju and K. Yousef, *Rev. Chim.* (*Bucharest*) **36**, 807 (1985).

Revue Roumaine de Chimie, **36**, *9–10*, **1195–1201 (1991)**

MAXIMUM LIKELIHOOD PRINCIPLE EXTENDED TO GENERATE SELECTION CRITERIA FOR EQUATIONS OF STATE AND / OR DATA

GHEORGHE M. PANAITESCU

Romanian Research and Design Institute for Oil Refining and Petrochemistry,
bd. Republicii 291, Ploiești 2000, Romania

Received September 4, 1989

The use of equations of state (EOS) to model vapor-liquid equilibria has become a common practice. Difficulties appear when one must choose an EOS to be adequate to a given separation problem. There is a large variety of EOS and a lot of possible treatments of multicomponent mixtures. A comparison between experimental data and EOS predicted data is always recommended. The maximum likelihood principle applied to estimate parameters produces simultaneously criteria to select data and/or EOS. The theory on which the procedure is based and some applications are presented. The resulted criteria seem to be sound enough to be taken into account as a means for bringing more order into the area of EOS equilibrium modeling.

To choose an equation of state (EOS) adequate to a given vapor-liquid separation problem might be a difficult task. The number of EOS and their sometimes slightly different versions is really impressive. When a mixture has to be modeled, EOS coefficients must be calculated from those of the pure components and a mixing rule is needed. The mixing rules are themselves more than a few and a selection has to be made. The criteria of evaluation of the qualities of an EOS are also very diverse. It is difficult to say if some order is possible in this area. Perhaps the maximum likelihood principle offers a chance. During the maximum likelihood procedure, aimed to estimate parameters, sound criteria to eliminate erroneous experimental points and to discriminate between EOS are generated almost as a by-product of main calculation.

The maximum likelihood principle is commonly used to estimate parameters.[1] Whenever a model must be fitted to a set of data there are some parameters to be estimated.

Let X be a set of vectors of data in a one-to-one relation with a set of experimental points. Any $x \in X$ has a zero-mean random part δ, which adds to its mean value $\bar{x}$ and is assumed normally distributed.

Let y be a vector of functions which model the data and contain a vector a of parameters to be estmated.

Ideally, if both x is experimentally determined without errors and the model fits the data perfectly then

$$y(x, a) = 0 \tag{1}$$

for every experimental point. But none of the two conditions can be commonly fulfiled, thus equation (1) becomes

$$y(x, a) = \varepsilon \tag{2}$$

where ε is a non-zero component vector.

When the model describes the data in a quasiperfect manner, ε is fully justified by errors in x and a Taylor linear formula gives

$$\varepsilon = J_x\delta \tag{3}$$

where J_x is the jacobian matrix of y with respect to x and depends on experimental point. The vector ε is normally distributed and zero-mean because δ is normal and has zero-mean components. The covariance matrix of ε can be calculated from that of δ

$$W_\varepsilon = J_x W_\delta J_x' \tag{4}$$

The density of probability function [2] for ε in a given experimental point is

$$f(\varepsilon) = \sqrt{\det A}/(2\pi)^{\frac{m}{2}} \exp\left(-\frac{1}{2}\,\varepsilon' A \varepsilon\right) \tag{5}$$

where A is the inverse of W_ε and m is the dimension of ε.

The maximum likelihood values of parameters are those making probability

$$\prod_{k=1}^{n} f(\varepsilon_k) = \prod_{k=1}^{n} \left(\sqrt{\det A_k}/(2\pi)^{\frac{2}{m}}\right) \exp\left(-\frac{1}{2}\,\varepsilon_k' A\, \varepsilon_k\right) \tag{6}$$

maximum or, almost equivalently, bringing the sum

$$S = \sum_{k=1}^{n} \varepsilon_k' A_k \varepsilon_k \tag{7}$$

to a minimum. In equations (6) and (7) k counts the experimental points supposed to be mutually independent.

The estimated values of parameters have certainly some random parts. An analysis of magnitude of those parts is needed. The possible statistical equivalence of other values must be examined. To do that, let equation (2) be rewritten, the randomness of *a* compensating for the differences ε. Equation (2) has now the form (1) but equation (3) becomes

$$J_x\delta + J_a\alpha = 0 \tag{8}$$

with α the zero-mean random part of *a*. Assuming perfect data and perfect model the deviations ε are due to α only

$$J_a\alpha = v - \varepsilon \tag{9}$$

Equation (9) written for all experimental points leads to a matrix equation

$$B\alpha = -e \tag{10}$$

where B and e accumulate orderly lines of J_a and ε corresponding to the n experimental points. The vector α can be calculated from e by left multiplication of equation (10) with the generalized inverse of B

$$\alpha = -(B'B)^{-1}B'e \tag{11}$$

Averaging the product $\alpha\alpha'$ one obtains the covariance matrix of a

$$W_\alpha = (B'B)^{-1}B'W_eB(B'B)^{-1} \tag{12}$$

and the α density of probability function can be written

$$f(\alpha) = \left(\sqrt{\det Q}/(2\pi)^{\frac{l}{2}}\right)\exp\left(-\frac{1}{2}\alpha'Q\alpha\right) \tag{13}$$

where l is the number of parameters and Q is the inverse of matrix W_α.

In ε- or α-spaces there are some hypersurfaces on which the functions (5) or (13) are constant. Because both functions have as arguments in exponentials positive definite quadratic forms, the constant-f loci are hyperellipsoids. Inside every hyperellipsoid a hypervolume can be calculated. For function (13), and analogously for function (5), the measure of that hypervolume is

$$V = \left(\sqrt{\det Q}/(2\pi)^{\frac{l}{2}}\right)\iint\limits_D\cdots\int\exp\left(-\frac{1}{2}\alpha'Q\alpha\right)d\alpha \tag{14}$$

and it equals the probability that the vector α falls inside the hyperellipsoid, the domain D on which the integral is calculated. The complementary probability

$$q = 1 - V \tag{15}$$

is associated with cases when α falls outside that hypersurface. If q becomes level of significance, usually 0.05, then the hyperellipsoid contains a confidence hypervolume which in particular, for $l = 1, 2$, is known as confidence interval or confidence ellipse.[3] This is the way one can obtain the set of vectors α, and implicitly a, statistically equivalent. The integral (14) can be calculated by a double change of variable. The first change brings the quadratic form to its standard form with matrix Q diagonal. The second change transforms the hyperellipsoid in a hypersphere. One notes the radius of that hypersphere by ρ. For a given level of significance q the expression (14) becomes an equation in ρ

$$V(\rho) = 1 - q \tag{16}$$

which can be easily solved when l is even and slightly less easily, using tables for one-dimensional f, when l is odd. For a given l there is a one-to-one correspondence between values of ρ and those of q. A useful example : $l = 2$ and $q = 0.05$ give a $\rho = 2.45$.

When a model has been built and a set of parameters have been estimated through the maximum likelihood method, the individual density of probability functions of the experimental points tells a lot about the quality of both the model and the experimental data. A confidence hypervolume can be attached to each experimental point and a particular ρ value can be calculated from quadratic form appearing in (5). The radius ρ is a good criterion to discriminate between points significantly away from the model and those close to it. The discriminating value of ρ is given by an equation similar to (16). When S in equation (7) is brought to its minimum an average or global ρ can be calculated.

$$\bar{\rho} = \sqrt{(\sum \rho_k^2)/n} \tag{17}$$

which must be associated with the overall capacity of the model to fit the data. A global ρ over the critical value is a sufficient condition to reject the model.

In particular, the vectors of data could be quadruples (P, T, x, y) of pressure, temperature and concentrations in liquid and vapor phases at equilibrium. The equations modeling vapor-liquid equilibrium

$$f_i^L - f_i^V = 0 \quad (i = 1, 2, \ldots, n) \tag{18}$$

express the equality of the component fugacities in the two phases. The fugacities can be calculated, in particular, via an EOS made suitable to describe mixtures. There are parameters to be estimated from experimental data, the interaction parameters appearing in the so-called mixing rules. Following step by step the theory, it becomes possible to attach to each experimental point a confidence domain and to appreciate how well the model fits the data and/ or how good the data are. A confidence domain for the estimated parameters may also be established.

One of the most used equations, Peng-Robinson EOS[4], has been mainly used to illustrate the theory. The conventional one-binary-parameter form has been selected as a mixing rule. Data referring to three binary systems (propane-*n*-pentane, benzene-toluene, and carbon dioxide-*n*-decane) have been analysed. Because the analysis is not intended to be exhaustive, only parts of more comprehensive experiments have been processed to exemplify the theory. All over this work, except otherwise specified, the dispersions of pressure (P), temperature (T), mole fractions in liquid (x) and vapor (y) phases are supposed to be $\sigma_P^2 = 0.01$ atm ^{2}, $\sigma_T^2 = 0.01$ K^2, $\sigma_x^2 = \sigma_y^2 = 0.0001$ (mole fr.) ^{2}.

For propane-*n*-pentane [5] nine (P, T, x, y) experimental points have been retained. The maximum likelihood procedure gave $k_{12} = k_{21} = 0.01760$ and a dispersion $\sigma_k^2 = 0.00002331$. The dispersion σ_k^2 is what becomes the covariance matrix W_α when the dimension of the vector a is one. Table 1 contains the data and the values of the individual ρ for each experimental point. All ρ's are under 2.45 the critical value associa-

Table 1

Data and results for propane-*n*-pentane mixtures

	P (atm)	T (K)	x (mole %)	y (mole %)	ρ^a	ρ^b	ρ^c
1	4.08	344.25	5.80	29.50	0.638	0.871	6.574
2	5.45	344.25	12.40	48.20	1.012	1.858	6.029
3	6.80	344.25	18.90	60.00	0.777	2.000	5.353
4	8.50	344.25	27.00	70.10	0.211	4.855	4.795
5	10.20	344.25	35.00	77.00	0.574	8.283	4.362
6	13.60	344.25	50.40	86.30	1.716	17.021	3.865
7	17.00	344.25	65.70	92.00	1.945	17.997	2.487
8	20.40	344.25	79.90	95.80	1.623	14.520	1.576
9	23.80	344.25	92.50	98.60	0.939	8.009	2.786
				Global ρ	1.188	10.483	4.502

[a] Current dispersions

[b] Modified dispersions

[c] Current dispersions, Soave-Redlich-Kwong EOS

ted with a significance level of 0.05. The average ρ is also under 2.45. Peng-Robinson EOS models well the binary system in discussion.

For examining mixtures of the second pair of molecular species, benzene-toluene,[6] a set of seven (P, T, x, y) experimental points has been used. The estimation procedure led to $k_{12} = k_{21} = 0.01343$ and $\sigma_k^2 = 0.000015113$. Table 2 gives the data and the ρ's. There are ρ's over 2.45. Points # 3 and # 1 could be suspected of gross errors or the EOS could be qualified as inadequate for the subset of points with $\rho > 2.45$. The doubtful points are rather isolated cases and it seems more reasonable to eliminate them, simultaneously or one at a time, and to repeat the estimation procedure. The fact that mean ρ is under critical value is one more reason to reevaluate k_{12} after discarding the uncertain data. The two rightmost columns in Table 2 give the ρ's after the elimination

Table 2

Data and results for benzene-toluene mixtures

	P (atm)	T (K)	x (mole %)	y (mole %)	ρ	ρ^a	ρ^b
1	7.342	453.15	47.00	62.00	2.981	2.744	—
2	7.829	453.15	54.00	67.90	1.591	1.385	1.802
3	8.908	473.15	15.40	22.20	3.594	—	—
4	9.526	473.15	27.00	34.40	1.094	1.268	0.938
5	10.408	473.15	38.50	51.80	1.545	1.809	1.281
6	11.434	473.15	56.60	68.20	0.200	0.353	0.336
7	12.790	473.15	77.70	84.60	0.265	0.404	0.257
				Global ρ	2.001	1.569	1.091

[a] One point eliminated

[b] Two points eliminated

of the suspected points. A better relation between model and data is gradually attained.

A more complex case is that of the binary mixtures of carbon dioxide and *n*-decane.[7] The estimating procedure carried out on eight points gives $k_{12} = k_{21} = 0.13447$ and a dispersion $\sigma_k^2 = 0.0002491$. The data and the calculation results presented in Table 3 show an acceptable global ρ and a good agreement at lower temperatures but an unsatisfactory modeling at higher temperatures. Perhaps a temperature-dependent interaction parameter must be used with the Peng-Robinson EOS. This observation is supported by results published in the literature.[8] The problem extends to estimating two or more parameters.

Table 3

Data and results for carbon dioxide-*n*-decane mixtures

	P (atm)	T (K)	x (mole %)	y (mole %)	ρ
1	30.38	462.55	14.72	93.06	1.065
2	40.10	462.55	18.83	94.10	0.892
3	27.11	476.55	12.39	89.66	0.715
4	40.80	476.95	18.72	92.40	1.192
5	29.63	542.95	11.47	68.18	2.644
6	39.15	542.95	16.28	73.57	2.607
7	30.00	583.65	9.74	41.15	2.945
8	40.50	583.65	15.58	50.15	3.622
				Global ρ	2.220

Examining the dispersions accepted for P, T, x, y one can object about them : a $\sigma_x^2 = 0.0001$, for example, means a mean square deviation of 0.01 for x mole fraction and a particular experimental error two times larger is then possible. But careful experiments can be considerably more accurate. A σ_x^2 two orders of magnitude under the value accepted above is fully plausible. To see the effect of lower σ's for P, T, x and y a special calculation has been made for the binary system propane-*n*-pentane. The dispersions for liquid and vapor mole fractions have been modified to $\sigma_x^2 = \sigma_y^2 = 0.00001$. As expected, the ρ values increased and a variation in k_{12} was observed. The estimation procedure produces $k_{12} = k_{21} = 0.00946$ and $\sigma_k^2 = 0.0000019636$. The dispersion of k_{12} was expected to decrease but the modification of the interaction parameter itself could be considered at a first glance too important. However, the former estimation $k_{12} = k_{21} = 0.01760$ and its mean square deviation $\sigma_k = 0.0048302$ give, when considered normally distributed, a confidence interval for k_{12} between 0.00813 and 0.2706 at 0.05 level of significance because in a bilateral test[9] $z_q = 1.96$. The new value is within the confidence interval and is statistically equivalent with the previous one or, in other terms, the difference between the two values is not significant.

The values calculated with the new dispersions are given in Table 1. It seems that Peng-Robinson EOS is no longer representative for the data. In milder terms, the predictive capacity of Peng-Robinson EOS cannot be as highly accurate as the data are in the considered case. A deliberate modification of P, T, x, y dispersions can be thought of as a possible method to evaluate the risks due to EOS inadequacy, introduced in solving a separation problem.

The set of data concerning mixtures of propane and *n*-pentane has been processed to estimate the parameter appearing in the same mixing rule adopted above but with Soave-Redlich-Kwong EOS.[10] The value of the parameter k_{12} does not really matter because the global ρ almost doubles the critical value, a sound reason to reject this second EOS as a model for the data in the examined case. A global ρ beyond the critical value does not give usually too much hope for a good modeling on a subset of data. The last column of Table 1 shows values of ρ almost all over the critical value 2.45. This was a case when an EOS has been rejected by its own lack of fittness. It is possible that two or more EOS model the same set of data with global ρ's under the critical limit. The EOS with a lower ρ is preferred to the other(s). Sometimes, when the two ρ's of two EOS are close to each other, an examination of experimental points individual ρ's might be more convincing. This way one can discriminate between any EOS or any versions of the same EOS. The things change a little when more than one parameter must be estimated.

As a conclusion of this work it is very important to observe that the maximum likelihood principle gives estimates of the parameters and a confidence domain for them. Simultaneously, a criterion to eliminate gross errors in data is generated as well as a quantitative means to appreciate the adequacy of an EOS to a given mixture. The premises to develop further study on the effect of experimental errors on designing of a separation unit are also forseen.

REFERENCES

[1] J. H. Seinfeld and L. Lapidus, "Process Modeling, Estimation, and Identification", Prentice Hall Inc., Englewood Cliffs N.J., 1974, p. 201.

[2] M. Iosifescu, G. Mihoc and R. Theodorescu, "Teoria probabilităţilor şi statistică matematică", Ed. tehnică, Bucharest, 1976, p. 644.

[3] G. Panaitescu, *Int. Chem. Engng.*, **25**, 68 (1985).

[4] D. Y. Peng ad D. B. Robinson, *Ind. Eng. Chem. Fundam.*, **15**, 59 (1976).

[5] B. H. Sage and W. H. Lacey, *Ind. Eng. Chem.*, **32**, 902 (1940).

[6] J. Griswold, D. Andres and V. A. Klein, *Trans. Am. Inst. Chem. Engrs.*, **37**, 223 (1943).

[7] H. M. Sebastian, J. J. Simnik, Ho-Mu Lin and Kwang-Chu Chao, *J. Chem. Eng. Data*, **25**, 140 (1980).

[8] J. O. Valderrama and S. Obaid-ur-Rehman, *Fluid Phase Equilibria*, **40**, 217 (1988).

[9] W. H. Beyer, "Handbook of Tables for Probability and Statistics", The Chemical Rubber Co., Cleveland, Ohio, 1968, p. 125.

[10] G. Soave, *Chem. Eng. Sci.*, **27**, 1197 (1972).

Revue Roumaine de Chimie, **36**, *9–10*, 1203–1210 (1991)

A NOTE CONCERNING THE DIRECT INTERCHANGE AREA ERROR EVALUATION FOR THE RADIATIVE TRANSFER IN A RADIANT FURNACE

IRINA BUCURESCU,[a] CRISTIAN TSAKIRIS,[b] CRISTINA MARIA,[c]
GHEORGHE MARIA[b] and ALEXANDRU ISOPESCU[d]

[a] Polytechnic Institute, Polizu 1, Bucharest 78126
[b] Chemical & Biochemical Energetics Institute, Spl. Independenţei 202, Bucharest 77208.
[c] Brazi Petrochemical Works
[d] Computer Center of Chemical Industry

Received February 12, 1990

In order to obtain accurate Direct Interchange Areas (DIA) in radiant firebox, two numerical integration methods, Monte Carlo and Simpson are compared, leading to a good compromise for the required calculus precision and the computational time.

INTRODUCTION

Up to date many studies have been performed on furnace enclosure accurate simulation. It was proved that the increasing precision in every algorithm step is very important to allow satisfactory results and to base economically both the design and the operating decisions.[1,2] At present there are very accurate mathematical models concerning the coupled simulation of the radiative firebox and the thermal cracking coil (see the reviews of Rao et al., 1988, [2] Mihail et al., 1981, 1982, [3,4] Maria et. al., 1988, [5]). One of the important simulation steps concerning the complex radiative transfer in the firebox is the accurate determination of the DIA.

A coupled method based on Hottel's zone method [6,7] to simulate an industrial furnace for propane cracking was presented in previous papers. [5,8] As revealed there, a flexible division of the furnace is used in order to save computational time, by keeping a satisfactory calculus precision and refinement. The mathematical model from which the firebox tridimensional temperature field is derived, consists of thermal balance equations for each isothermal zone resulted from the box division (surface or gas volume). The model requires an adequate evaluation of the geometrical DIA, the medium properties and some parameters. For details the reader is referred to some recent papers devoted to such subjects.[9–13] The number of DIA quickly increases with the number of box divisions, but this number must be larger than some limit in order to keep a satisfactory calculus accuracy. At the same time, for this reason, this calculus step requires an important computational effort.

The aim of this note is to compare two numerical methods for computing DIA in order to find the best compromise computational time-required evaluation precision.

THEORETICAL CONSIDERATIONS

The DIA represent the fraction of the radiation leaving a radiant zone that is emitting in the direction of a receptor, multiplied by A for an emitting surface and by 4kV for an emitting gas volume (see the notations and relationships of Table 1).

Table 1

Particular expressions for DIA (see Table 3)*

---

parallel surfaces :

$$\overline{s_1 s_3} = \bar{\tau}(r)\,\frac{\Delta x^2}{\pi} \iint\limits_{A_1 A_3} \frac{\mathrm{d}A_1 \mathrm{d}A_3}{r^4}$$

rectangular surfaces :

$$\overline{s_2 s_3} = \tau(r)\,\frac{1}{\pi} \iint\limits_{A_2 A_3} \frac{\Delta x \Delta y}{r^4}\,\mathrm{d}A_2 \mathrm{d}A_3$$

volume-surface :

$$\overline{g_1 s_3} = \overline{s_3 g_1} = \bar{\tau}(r)\,\frac{1}{\pi} \iint\limits_{V_1 A_3} \frac{\Delta x}{r^3}\,\mathrm{d}V_1 \mathrm{d}A_3$$

volume-volume :

$$\overline{g_1 g_2} = \bar{\tau}(r)\,\frac{1}{\pi} \iint\limits_{V_1 V_2} \frac{\mathrm{d}V_1 \mathrm{d}V_2}{r^2}$$

---

* Used notations :
A — surface zone area
V — volume of a gas zone
r — linear distance between two elements
Δx, Δy, Δz — values of the three projections of r vector on the coordinate axis
$\bar{\tau}(r)$ — mean gas transmissivity
s — surface zone
g — gas zone

The DIA can be computed for each two gas or surface zones by multiple integration using different rules : a numerical integration method, the "shape-factor algebra", or by using combined numerical method and "shape-factor algebra". We test only two of the more usual and simple numerical methods : Monte Carlo and Simpson. These methods use different strategies to compute the multiple integrals : a deterministic quadrature, and a stochastic one. The relevant points concerning each of these methods are briefly presented below.

The Monte Carlo rule

Let us calculate an integral over the multi-dimensional volume V, namely $I = \int_V f(x)\, \mathrm{d}V$, and suppose that we pick N points, uniformly randomly in the volume V. Then the basic theorem of Monte Carlo integration[14] estimates the integral I (see relationships of Table 2).

Table 2

Relations for numerical integration quadratures *

Monte Carlo method

$$I \cong V \langle f \rangle \pm V \sqrt{\frac{\langle f^2 \rangle - \langle f \rangle^2}{N}}$$

$$\langle f \rangle \equiv \frac{1}{N} \sum_{i=1}^{N} f(x_i), \ \langle f^2 \rangle \equiv \frac{1}{N} \sum_{i=1}^{N} f^2(x_i)$$

Simpson method

$$I = \iint_{x_1 x_2} \dots \int_{x_n} f(X)\, \mathrm{d}x_1 \mathrm{d}x_2 \dots \mathrm{d}x_n = (\sum_{x_1} (\sum_{x_2} \dots (\sum_{x_n} (F(X-h) + 4F(X) +$$

$$F(X+h)) \frac{h}{3}) \dots) \frac{h}{3}) \frac{h}{3})$$

* Used notations :
The brackets $\langle \ \rangle$ denote the arithmetic mean over the N sample points
$f(X)$ — the integrand function
H — the step for numerical integration
$f(x_i)$ — value of f in the x_i point

The "plus-or-minus" term in the estimation formula is a one standard deviation error estimate for the integral, i.e. a rough indication of the expected error. As seen, the fundamental disadvantage of the Monte Carlo integration is that its accuracy increases only as the square root of N, the number of sampled points. Otherwise, the method has the advantage of a great generality.

We have adapted for our purposes the subroutine of Lautrup.[15] The integration procedure is slightly more complicated than described above, such that to optimize the increased accuracy. The unit hypercube (any finite interval to be integrated must be first scalled in a unit interval) is divided into a number of smaller subvolumes (usually, as indicated by an input parameter). Inside each subvolume, the integral and its error is estimated, and finally all contributions are added up to produce the full integral and its variance. By means of the "projections" of the errors on each axis, one determines where it is necessary to increase or diminish the density of intervals, such as to minimize the total error ; thus, if the desired accuracy has not been reached, the algorithm performs a new iteration, by using the last determined distribution and size of all the intervals.

Simpson's rule

The integral $I = \int_a^b f(x)\,\mathrm{d}x$ is evaluated by computing the values of $f(x_i)$, for $i = 1, \ldots, n$ (no. of points in which the integration interval [a, b] was divided), $f : [a, b] \to R$. By analogy with Riemann integration definition we form an approximation of $I : \hat{I} = \sum_{k=1}^{n} A_k f(x_k)$. By approximating $f(x)$ using the Lagrange polynomial the following integration formula is obtained :

$$\hat{I} = \sum_{k=1}^{n} (b - a)\, I_k^{(n)} f(x_k), \text{ where :}$$

$$I_k^{(n)} = \frac{(-1)^{n-k}}{(k-1)!)(n-k)!\,(n+2l-1)} \int_{l-1}^{n+l} \frac{(t-1)(t-2)\ldots(t-n)\,\mathrm{d}t}{t-k}\,.$$

are the Newton-Cotes coefficients, independent of x ; l indicates that the integration interval is open ($l = 1$) or closed ($l = 0$). For $n = 3$ and $l = 0$ Simpson's rule is thus derived :

$$I = \frac{b-a}{6}\left[f(a) + 4f\left(\frac{a+b}{2}\right) + f(b)\right].$$

By dividing the interval $[a, b]$ in $2m$ equal paints we obtain Simpson's formula :

$$I = \sum_{i=1}^{m} \frac{x_{2i+1} - x_{2i-1}}{6} \left(f(x_{2i-1}) + 4f(x_{2i}) + f(x_{2i+1})\right) =$$

$$= \frac{h}{3} \sum_{i=1}^{m} \left[f(x_{2i-1}) + 4f(x_{2i}) + f(x_{2i+1})\right],$$

where $h = (b - a)/m$. For the multiple integral evaluations, an analogous quadrature formula is listed in Table 2.

The estimated integration error is given by the relationship [16] :

$$R = \frac{(b-a)h^4}{2880} f^{(4)}(x) \leqslant \frac{(b-a)\,h^4\,M}{2880},$$

where $x \in [a, b]$ and $f^{(4)}(x) \leqslant$ M. The accuracy of Simpson's method increases with m, comparatively to $\sqrt{m}$ in the Monte Carlo method.

EXAMPLES AND RESULTS

In order to test and to compare the two numerical methods, many DIA are computed. The studied DIA cases are : two parallel surfaces ($\overline{s\,s}_{\|}$), two rectangular surfaces ($\overline{ss}_{\perp}$), a gas volume and a surface ($\overline{gs}$), two gas volumes ($\overline{gg}$). These examples were selected from a previous application [5] i.e. an industrial furnace simulation (Fig. 1). The zone sizes and distances are indicated in Table 3.

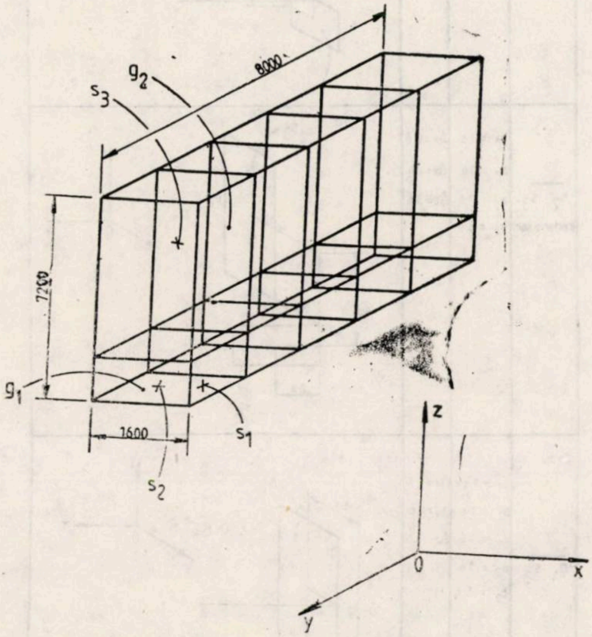

Fig. 1. — The furnace space division and the zone choice for the present example.

Now, by defining the DIA multiple integral evaluation relative accuracy as :

$$\varepsilon = \frac{|I^* - I|}{I^*},$$

where I^* is the exact value of the DIA, while I is the numerically computed one, we can represent ε vs. required CPU time for every considered case (Fig. 2a-d). The exact value of the DIA was determined by extrapolating the integral values (obtained with Simpson's rule) using an increasing number of integration steps. The relative accuracy, ε, provides from truncation error given by the numerical integration instead of analytical integration, and roundoff error given by the limitations of representing a number in a computer. Calculating the number of operations done for multiple integration (Monte Carlo or Simpson's method) the roundoff error is evaluated to 10^{-6}, two orders less than total error ε.

Table 3
Zone size and distances for the considered cases

DIA	Zone size	Distances	
$\overline{s_1 \; s_3}$ (parallel)	$a_1 = 1.6$ $b_1 = 1.6$ $a_2 = 1.6$ $b_2 = 5.6$	$\Delta x = 1.6$ $\Delta y = 1.6$ $\Delta z = 3.6$	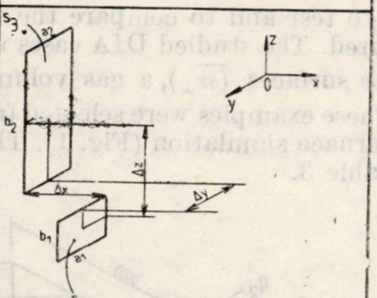 s_3 a_2 b_2 z y 0 Δz Δx Δy b_1 a_1 s_1
$\overline{s_2 \; s_3}$ (rectangular)	$a_1 = 1.6$ $b_1 = 1.6$ $a_2 = 1.6$ $b_2 = 5.6$	$\Delta x = 0.8$ $\Delta y = 2.4$ $\Delta z = 3.6$	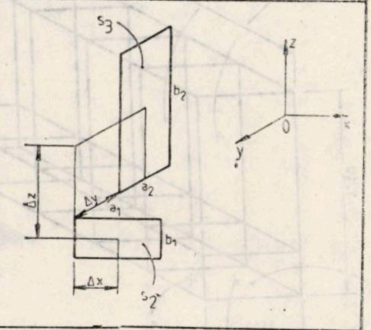 s_3 z b_2 0 x y a_2 Δy a_1 Δz b_1 Δx s_2
$\overline{g_1 \; s_3}$	$a_1 = 1.6$ $b_1 = 1.6$ $c_1 = 1.6$ $a_2 = 1.6$ $b_2 = 5.6$	$\Delta x = .8$ $\Delta y = 1.6$ $\Delta z = 3.6$	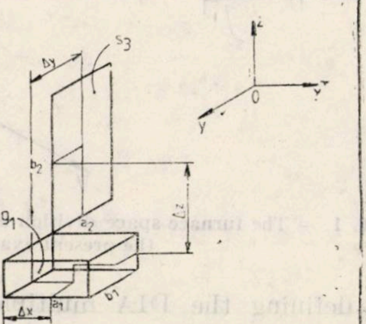 Δy s_3 z y 0 x b_2 Δz g_1 a_2 c_1 b_1 Δx
$\overline{g_1 \; g_2}$	$a_1 = 1.6$ $b_1 = 1.6$ $c_1 = 1.6$ $a_2 = 1.6$ $b_2 = 1.6$ $c_2 = 5.6$	$\Delta x = 0$ $\Delta y = 1.6$ $\Delta z = 3.6$	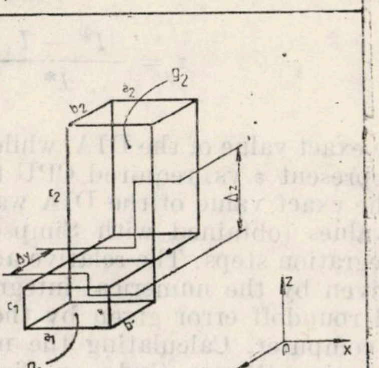 a_2 g_2 b_2 c_2 Δz Δy c_1 b_1 a_1 g_1 z x

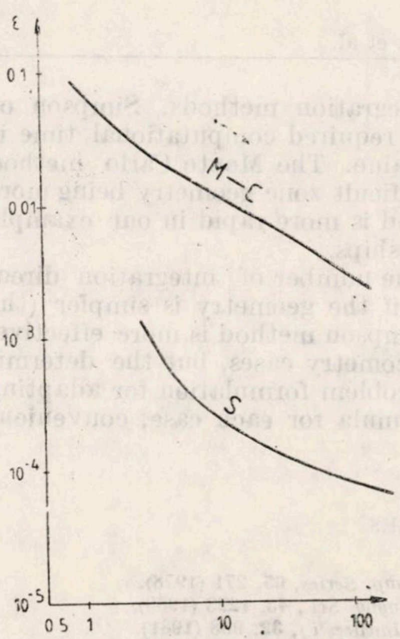

Fig. 2a. — The relative error of integration for *ss* case vs. CPU required time (MC — the Monte Carlo method; S — Simposion's method)

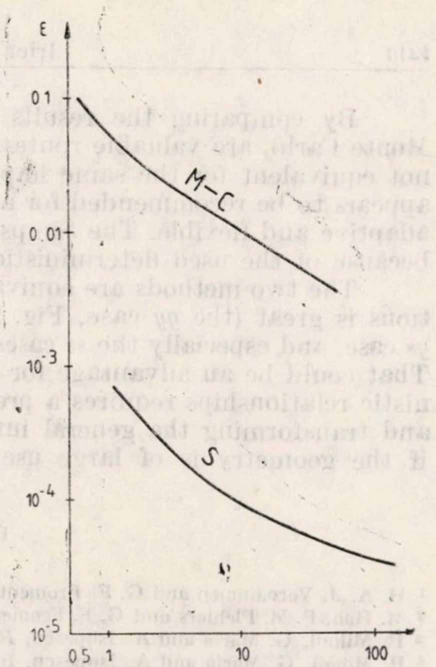

Fig. 2b. — The relative error of integration for *ss* case vs. CPU required time (MC — the Monte Carlo method, S — Simpson's method).

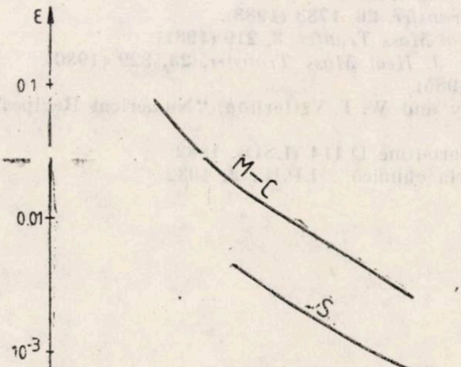

Fig. 2c. — The relative error of integration for *gs* case vs. CPU required time (MC — the Monte Carlo method, S — Simpson's method)

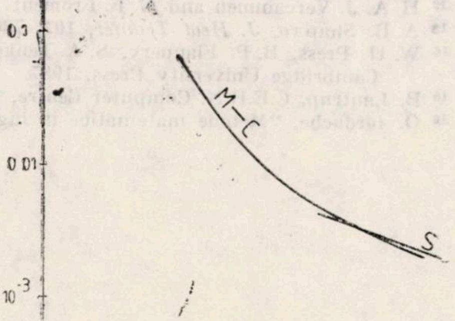

Fig. 2d. — The relative error of integration for *gg* case vs. CPU required time (MC — the Monte Carlo method, S — Simpson's method)

By comparing the results both integration methods, Simpson or Monte Carlo, are valuable routes, but the required computational time is not equivalent for the same imposed ε value. The Monte Carlo method appears to be recommended for a more difficult zone geometry being more adaptive and flexible. The Simpson method is more rapid in our example because of the used deterministic relationships.

The two methods are equivalent if the number of integration directions is great (the *gg* case, Fig. 2d), but if the geometry is simpler (the *gs* case, and especially the *ss* cases), the Simpson method is more effective. That could be an advantage for simple geometry cases, but the deterministic relationships requires a previous problem formulation for adapting and transforming the general integral formula for each case, convenient if the geometry is of large use.

REFERENCES

[1] H. A. J. Vercammen and G. F. Froment, *A.C.S. Symp. Series*, **65**, 271 (1978).
[2] M. Rao, P. M. Plehiers and G. F. Froment, *Chem. Engng. Sci.*, **43**, 1223 (1988).
[3] R. Mihail, G. Maria and A. Isopescu, *Rev. Chim. (București)*, **32**, 988 (1981).
[4] R. Mihail, G. Maria and A. Isopescu, *Rev. Chim. (București)*, **33**, 157 (1982).
[5] G. Maria, C. Tsakiris, C. Maria, A. Isopescu and G. Bozga, *Rev. Roumaine Chim*, **34**, 1377 (1989).
[6] H. C. Hottel and A. F. Sarofim, "Radiative transfer", McGraw-Hill, New York (1967).
[7] H. C. Hottel ad E. S. Cohen, *A.I.Ch.E.J.*, **4**, 3 (1958).
[8] G. Maria, C. Tsakiris, G. Bozga and A. Isopescu, *Rev. Roumaine Chim.*, **32**, 821 (1987).
[9] H. C. Hottel, *Ind. Engng. Chem. Fundls*, **22**, 153 (1983).
[10] R. Mihail and G. Maria, *Int. J. Heat Mass Transfer*, **26**, 1783 (1983).
[11] U. Gross, K. Spindler and E. Hahne, *Lett. Heat Mass Tranfer*, **8**, 219 (1981).
[12] H. A. J. Vercammen and G. F. Froment. *Int. J. Heat Mass Transfer*, **23**, 329 (1980).
[13] A. B. Shap ro, *J. Heat Tranfer*, **107**, 730 (1985).
[14] W. H. Press, B. P. Flannery, S. A. Teukolsky and W. T. Vetterling, "Numerical Recipes", Cambridge University Press, 1987.
[15] B. Lautrup, C.E.R.N. Computer Centre, Suboroutine D 114 (LSD), 1982.
[16] O. Iordache, "Metode matematice in ingineria chimică". I.P.B., 2, 1982.

Revue Roumaine de Chimie, **36**, *9–10*, 1211–1217 (1991)

БАНК КИНЕТИЧЕСКОЙ ИНФОРМАЦИИ И МОДЕЛИРОВАНИЕ СЛОЖНЫХ ХИМИЧЕСКИХ РЕАКЦИЙ

В. С. БАБКИН и В. И. БАБУШОК

Институт химической кинетики и горения
Новосибирск 90, Россия

Получено: 11 февраля 1989 г.

В работе дано общее описание разрабатываемого банка кинетической информации, его функции, структура, виды запросов и описание форматов входных данных. Показаны возможности использования баз кинетических даных для моделирования сложных химических реакций. Кратко обсуждаются результаты численного исследования колебательного режима окисления окиси углерода вблизи пределов самовоспламенения.

A general presentation of kinetic data bank under development, its functions, structure, types of requests and a description of input data formats are given in the paper. Potentialities of using the kinetic data bases for simulation of complex chemical reactions are shown. Results of numerical study of oscillatory reaction proceeding of carbon monoxide oxidation near explosion limits are briefly discussed.

На современном этапе развития науки и техники резко возросли потребности в использовании кинетической информации по химическим реакциям при решении разнообразных задач энергетики, химической технологии и экологии. Данные по газофазной химической кинетике используются, например, при моделировании процессов, протекающих в тепловых двигателях различного назнаначения, в химических и газодинамических лазерах, в атмосфере Земли, в химических реакторах и т.д. Однако, сведения об элементарных химических реакциях разбросаны по различным литературным источникам, непрерывно пополняются и уточняются. Численные значения констант скоростей отдельных стадий постоянно уточняются, причем часто весьма существенно. Для выбора достоверных значений нередко требуется проведение специального поиска и анализа большого объема литературных данных. Можно константировать, что недостаточная эффективнсость иcпользования кинетической информации для решения конкретных задач определяется отсутствием совокупности данных, которая может оперативно использоваться в необходимой форме и с достаточной надежностью. Поэтому задача систематизации кинетических данных в виде автоматизированного банка кинетической информации является актуальной.

Следует отметить, что вопрос о сборе, анализе и выработке рекомендованных кинетических данных в СССР был поставлен в конце 60-х годов по инициативе академика В. Н. Кондратьева.[1,2] Результатом явился хорошо известный справочник[3]. Появились и другие справочные издания.[4–6] Организуется периодическое издание аналогичных справочников, например.[7,8] Однако, публикация справочников не решает польностью проблему эффективного использования кинетической информации и её адаптации к решению различных задач. Кроме того, в настоящее время не эффективно ведутся работы по сбору кинетических данных, их обработке, систематизации и проверке на достоверность.

Институт химической кинетики и горения СО АН СССР начал разработку банка кинетической информации. [9] Банк кинетической информации — БАНКИН — можно определить как систему информационных, математических, программных, организационных и технических средств, предназначенную для централизованного накопления и коллективного использования кинетических данных. На первом этапе предполагается создать банк для решения задач по газофазному горению и химии атмосферы.

В банк поступает входная информация из справочников, статей, отчетов и др., которая в обработанном виде накапливается и хранится в базах данных на магнитных носителях ЭВМ. По требованию пользователя кинетическая информация поступает или прямо в виде констант скоростей элементарных стадий, или, после обработки, в виде кинетических схем сложных химических реакций, интегральной скорости реакции и т.д. Основными функциями банка являются: комплектование кинетической информацией (поиск, получение, отбор), ведение справочно-информационного фонда, первичная обработка входной информации и введение её в ЭВМ, переработка информации на ЭВМ, общение с пользователем. Наряду с обычными процедурами, присущими автоматизированным информационным системам, таким как обработка входных сообщений, накопление данных, ведение классификатора, обновление состава данных, отбор и извлечение информации из баз, управление базами данных, планируется разработка специальных процедур анализа и переработки кинетической информации (составление моделей химического процесса, решение систем кинетических уравнений, выделение важных стадий и др.). Необходимость этих процедур обусловлена их общностью для большинства кинетических задач.

Основными элементами банка кинетической информации являются базы кинетических данных, система управления базами данных (СУБД), комплекс прикладных програм (КПП). Базы кинетических данных содержат информацию о константах скоростей газофазных элементарных стадий, данные о суммарной кинетике и о кинетических моделях химических реакций. Комплекс прикладных программ совместно с базами данных позволяет автоматически формировать кинетические блоки систем уравнений моделей конкретных процессов и проводить численное решение наиболее часто встречающихся кинетических задач. Таким образом, банк осуществляет как справочную, так и расчетную функции. В обоих случаях извлечение данных из банка производится по специальному запросу, сформулированному на языке общения. Выдаваемые в справочном режиме данные могут быть либо использованы непосредственно, либо составить основу для получения вторичной информации путем их обработки. Использование банка в расчетном режиме предполагает обращение к базам данных из проблемной программы на языке высокого уровня непосредственно или через КПП, поиск необходимых данных под управлением СУБД и передача требуемых данных обратно в программу для дальнейшей обработки.

Кинетическая информацим организуется как объединение отдельных баз по различным классам данных:

— элементарные стадии (моно-, би- и тримолекулярные),

— фотохимические реакции (первичные фотохимические процессы),

— параметры суммарной кинетики,

— данные о кинетических моделях химических реакций.

Кинетические данные разделяются на рекомендованные и первичные. Рекомендованными являются такие данные, которые выбраны на основе анализа работ многих авторов, представляют наиболее точные значения в настоящее время, более предпочтительны для использования и имеют более или менее достоверную оценку абсолютной погрешности. Рекомендованные данные не носят неизменного характера. Наряду с рекомендованными значениями констант скоростей существует большой массив текущих экспериментальных данных, называемых первичными, которые важны для справочных целей, при анализе результатов моделирования и коррекции существующих данных о константах.

В базы вносятся два вида данных: рекомендованные и первичные. Порядок подготовки и выбор рекомендованных значений подлежит дополнительному определению. Работа по подготовке рекомендованных кинетических данных должна способствовать созданию единой базисной системы согласованных данных, необходимой для получения на её основе данных об иных элементарных стадиях, сопоставления результатов моделирования разными авторами, выполнения разнообразных прогнозов и. т.д.

Каждой стадии в своей базе соответстбует запись, состоящая из совокупности полей (информационных элементов записи). Конкретное представление информации в полях определяется форматом описания данных. Возможна различная степень детализации информации. Более подробное описание данных влечёт за собой увеличение объема работ при подготовке вторичных информационных документов и их вводе, к увеличению необходимой памяти, усложнению манипулирования информацией. Используемые в настоящее время форматы созданы на основе анализа различных форм представления кинетических данных в справочных изданиях и списка предполагаемых вопросов к базам. В качестве примера приведем основные элементы формата представления данных о бимолекулярной стадии в базе исходной информации:

— формула стадии,

— тип стадии (отрыв, рекомбинация, ...),

— общая характеристика способа получения данных (прямые измерения, теоретическая оценка и т.д.),

— сведения о константе скорости (предэкспоненциальной множитель, энергия активации, значение константы),

— погрешности определения константы скорости,

— интервал температур,

— интервал давлений,

— экспериментальные условия определения константы (способ воздействия на систему, тип установки, определяемые величины),

— теоретический метод,
— библиографические сведения (авторы, источники, год),
— примечания.

Каждому элементарному процессу становится в соответствие определенная термохимическая информация. Она включает изменение энтальпии ΔH, изменение энтропии ΔS и константу равновесия K_p. Для получения необходимых термохимических данных будет использоваться банк данных ИВТАНТЕРМО ИВТ АН СССР[10].

Возможны два режима функционирования банка: справочный и расчетный. В справочном режиме функционирования к базам предусматриваются следующие запросы:

— выдать все поля записи для заданной стадии, либо отдельные поля, связанные логическими условиями,

— указать по заданной левой (правой) части записи стадии все возможные правые (левые) части стадий, имеющееся в базах,

— указать по заданной частице (молекула, атом, радикал) стадии, в которых частица находится в левой (правой) части записи стадии, например, стадии её образования или расхода,

— указать по заданному списку частиц стадии, в которых участвуют эти и только эти частицы.

В расчетном режиме выполняются следующие виды работ: формирование кинетических моделей из баз кинетических данных, генерация по заданной схеме реакции программ для решения ряда кинетических задач. Предоставляемый пользователям диалоговый режим позволяет в полуавтоматическом режиме проводить формирование моделей, проводить различного рода исследовательскую работу, связанную с анализом скоростей стадий и др.

Моделирование кинетики многостадийных химических реакций включает несколько технологических стадий: создание кинетической модели, генерация программ вычисления правых частей и матрицы Якоби дифференциальных уравнений (ДУ) химической кинетики, численное решение ДУ, машинный кинетический анализ решения, упрощение больших кинетических схем и др. Система ДУ, описывающая кинетику химического превращения, имеет относительно простую структуру, фиксируемую схемой реакции. Это предопределяет целесообразность создания генератора программ правых частей и матрицы Якоби, входом для которого кроме начальных условий является кинетическая схема, задаваемая в виде близком к естественному. Созданный генератор[11] позволяет формировать программы моделирования кинетики химических реакций в изотермических и неизотермических условиях, в реакторе постоянного объема с учетом протока вещества. Предусмотрена также генерация задач для случая программированного изменения температуры. Тестовые испытания проводились на примерах хлорирования этилена, реакции цезия в верхней атмосфере, пиролиза пропана, окисления водорода и окиси углерода. Для численного решения используются неявный метод Эйлера, методы типа Розенброка[12], (m, k)-методы[13].

Опыт численного моделирования сложных кинетических систем выявил следующее обстоятельство. Численное решение уравнений модели дает огромный объем информации, который непосредственно не отвечает на интересующие конкретные вопросы (механизм реакции, роль отдельных стадий и частиц, звено цепи и др.). Необходимо создание специальных приемов машинного анализа получаемой информации, способов упрощения больших кинетических схем и техники машинного эксперимента. Для машинного анализа были предложены и исследованы различные способы: кинетическая доля стадии, тепловая доля стадии, время жизни реагирующей частицы и некоторые другие[14]. Способ кинетической доли стадии эффективен для оценки важности стадии в образовании или исчезновения реагентов в каждый момент времени, для установления механизма реакции. Способ времени жизни позволяет устанавливать текушую реакционную способность частиц, выделять звено цепи и количественно оценивать вероятность разветвления на звене цепи.

При изучении динамики тепловыделения и кинетических особенностей теплового взрыва информативными являются способ тепловой доли стадии и следующие характеристики: общая скорость тепловыделения, суммарная скорость тепловыделения экзотермических, реакций, суммарная скорость тепловыделения в эндотермических реакциях и их производные по температуре. Одновременное использование нескольких способов позволяет полно и разносторнне охарактеризовать изучаемые системы.

В качестве примера приведем результаты изучения особенностей окисления окиси углерода в околопредельной области. Для различных добавок водорода в эквимолярную смесь $CO+O_2$ проведено моделирование второго и третьего пределов самовоспламенения. Использование кинетических и тепловых характеристик машинного анализа показало, что третий предел имеет тепловую природу. Второй предел самовоспламенения является цепно-тепловым. Самовоспламенение на втором пределе обусловлено нарушением теплового баланса в результате тепловыделения по ходу цепной вспышки примеси водорода. В изотермических условиях происходит цеппое воспламенение с небольшим превращением исходных веществ и дальнейшим торможением процесса. В реальной системе, если по ходу цепной вспышки развивается скорость реакции достаточная для теплового самоускорения, то система перейдет в обычное воспламенение с полным выгоранием. Поскольку концентрация водорода мала, при низких давлениях к области обычного самовоспламенения может примыкать достаточно широкая область в которой выполняются условия цепного взрыва. Это приводит к различным кинетическим особенностям протекания реакции в околопредельной области, в том числе, колебательным режимам.

Колебательные режимы реакции окисления окиси углерода впервые наблюдались в работе P· G. Ashmore и P. C. W. Norrish в 1951г. Впоследствии колебательные режимы изучались в работах В. В. Азатяна, P. Gray с сотрудниками и др. вблизи первого и второго предела. В нашей работе колебательные режимы окисления реализованы численно[15]. В узкой температурной области, прилегающей ко второму пределу, были получены колебательные режимы различных типов в зависимости от начальных условий: колебания концентраций и температуры с относительно постоянной амплитудой, быстро затухающие колебания, колебания с раскачкой до взрыва, колебания с задержной. На рис. 1.

приведен пример колебательного режима с переходом во взрыв. При взрыве температура превышает 2000 К.

Анализ с численных результатов позволил сделать вывод о том, что колебательный режим реакции окиси углерода является последовательностью цепных вспышек. Выражение для фактора разветвления можно представить в виде

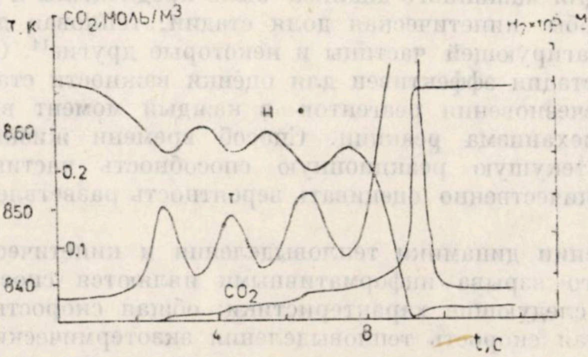

Рис. 1. — Колебательный режим с переходом во взрыв. Эквимолярная смесь $CO + O_2$, $[H_2] = 10^2$ ppm, $P = 33$ тор, $T = 838{,}3$ K, сферический сосуд, диаметр 8,8 см.

$$\varphi = [H_2] \cdot f_1 + f_2 - f_3,$$

где f_1, f_2, f_3 — положительные функции концентраций реагентов (кроме водорода) и констант скоростей. При упрощении кинетической схемы выражение приводится к виду

$$\varphi = K_5 \cdot [H_2] \cdot \left(\frac{2K_3}{K_7 [M]} - 1 \right) - K_{47} \cdot [CO] \cdot [M].$$

Здесь (3) $H + O_2 = OH + O$, (5) $O + H_2 = OH + H$;

(7) $H + O_2 + M = HO_2 + M$, (47) $CO + O + M = CO_2 + M$.

Особенность приведенных соотношений состоит в отсутствии члена с концентрацией водорода в отрицательной части. Численный анализ показал, что φ — знакопеременная величина, коррелирующая с колебательным изменением концентраций активных центров. Таким образом, колебания есть серия последовательных слабых вспышек разветвлений, каждая из которых затухает вследствие расхода водорода. Подготовка новой вспышки осуществляется путем перевода образовавшейся воды в водород по молекулярной стадии $H_2O + CO = CO_2 + H_2$. Колебательный режим окисления возможен, если характерное время перевода меньше периода задержки воспламенения. Цепная природа режима подтверждается реализацией колебаний в изотермических условиях.

Сопоставление результатов расчета с экспериментальными данными[16] показывает, что колебательный режим окисления окиси углерода наблюдается в области начальных условий близких к экспериментальным. Расчетные периоды колебаний составляют 1—5 с и соответствуют наблюдаемым экспериментально. Режим колебаний с задержкой также наблюдался экспериментально. Неплохое соответствие экспериментальных данных результатам моделирования можно рассматривать как подтверждение данного механизма колебательного окисления окиси углерода.

ЛИТЕРАТУРА

[1] В. Н. Кондратьев, *Успехи химии.*, **34,** 2081 (1965).

[2] В. Н. Кондратьев, *Кинетика и катализ*, **18**, 1093 (1977).

[3] В. Н. Кондратьев, ,,Константы скоростей газофазных реакций'', Наука, Москва, 1970.

[4] Е. Т. Денисов, ,,Константы скорости гомолитических жидкофазных реакций'', Наука, Москва, 1971.

[5] В.И. Веденеев, А. А. Кибалко, ,,Константы скорости газофазных мономолекулярных реакций'', Наука, Москва, 1972.

[6] Л. И. Вирин, Р. В. Джагацапанян, Г. В. Карачевцев, В. К. Потапов, В. Л. Тальрозе, ,,Ионно-молекулярные реакции в газах'', Наука, Москва, 1979.

[7] D. L. Baulch, J. Dixbury, S. J. Graut, D. C. Montague, ,,Evaluated Kinetic Data for High Temperature Reactions'', vol. 4, Supplement 1 to I. Phys Chem. Ref. Data, vol. 10, 1981.

[8] J. A. Kerr, M. J. Parsonage, ,,Evaluated Kinetic Data on Gas Phase Addition Reactions'', Batterworths, 1972

[9] В. С. Бабкин, В. И. Бабушок, Ю. П. Дробышев, Ю. Н. Молин, Е. А. Новиков, Г. И. Скубневская, ,,Автоматизированный банк кинетической информации. Общее описание'', препр. № 704, ВЦ СО АН СССР, Новосибирск, 1987.

[10] Л. В. Гурвич, Вестник АН СССР, № 3, 54 (1983).

[11] V. I. Babushok, E. A. Novikov, React. Kinet. Catal. Lett. *21,* N 1—2, 121 (1982)

[12] С. С. Артемьев, Г. В. Демидов, Е. А. Новиков, Л. А. Юматова, *Числ. методы механики сплошной среды*, **15**, 5 (1984).

[13] Е. А. Новиков, Ю. А. Шитов, в ,,Математические модели и методы решения задач механики сплошной среды'', Красноярск, 1986.

[14] В. И. Бабушок, В. С. Бабкин, В. И. Быков, Г. С. Яблонский в ,,Применение математических методов исследования в вопросах пожарной охраны'', Москва, 1982, с. 29.

[15] В. И. Бабушок, Е. А. Новиков. В. С. Бабкин, *Докл. АН СССР*, **271**, 878 (1983).

[16] J. R. Bond, P. Gray, J. F. Griffiths, *Proc. R. Soc. Lond.*, **A375** 43 (1981).

Revue Roumaine de Chimie, **36**, *9–10*, 1219–1221 (1991)

COMPTES RENDUS

ADVANCES IN EPITAXY AND ENDOTAXY, J. D. Hunt, University of Oxford, GB, H. D Langer, U. Broehl and J. Fruehauf, Technische Hochschule Karl Marx Stadt, GDR, V. Ruth, University of Oldenburg, FRG, L. Ikert, Department of Physics, Humboldt University, Berlin, GDR and H. G. Schneider, VEB Galvanotechnik, Leipzig, GDR. Editors : H. G. Schneider, VEB Galvanotechnik, Leipzig GDR. V. Ruth, University of Oldenburg, FRG and T. Kormany, Technical University of Budapest, Hungary. Join edition published by Académiai Kiádo, Budapest, Hungary and Elsevier Scientific Publishers Amsterdam, The Netherlands, 1990 hard cover 460 pp., ISBN 963–05–4743-0

The aim of this book is to bring together the two main aspects of the process technology for solid state devices, employing coordinated co-authorship by leading experts in the respective fields. The first aspect involves the basic principles of operation of the various electronic devices in order to achieve their best performance. The second aspect reflects the important contribution made by different materials due to specific physical properties in the functioning of a device.

The basic theory of eutectics and eutectoids is summarized in Part A. The purpose of the chapters included in is to expound the kinetics of eutectic growth, the physical and chemical properties of eutectic structures, and the influence of free energy and structure of solid phase interfaces involved in the unidirectional eutectoid decomposition processes in binary and ternary systems. The binary eutectics of germanium and siliconi with metallic phases and their electrical properties as metal semiconductor systems are dealt with in detail. The basic structure of some solid state devices are eutectic or eutectoid binary or multiple heterocrystals, especially metal systems obtained by oriented solidification or transformation. The high degree of structural perfection of the crystal volumes of the individual phases and of the phase bound aries are particularly important for such applications. One can obtain not only high qualitlayer structures but also new structures with possible new functions. Moreover, the substancey considered unstable under other conditions can be prepared easily in eutectic and eutectoids structures which is of a great importance in the development of new alloys with suitable physical properties.

In Part B the thermodynamic fundamentals of monocrystalline layer growth and the transition kinetics on the surface of different substrates are treated in a generalized form. Most of the theories and the results exposed in this section are related to semiconductor epitaxy but avoid excessive details in specific cases as well. The term epitaxy was selected, although homoepitaxy has been and still is the supporting part. In the authors' view the term epitaxy stands for a very heterogeneous complex ; in a narrower and more appropriate sense it designates the intergrowth process in all its physicochemical variety. The requirements of semiconductor epitaxy, however, could not be fully met until an efficient ultra high vacuum technique was devised.

Nucleation and layer growth in homo-epitaxy and hetero-epitaxy and the role of interfaces are also treated in extenso. In the last chapter of this part the influence of different process technologies on epitaxial layer growth is thoroughly investigated : the physical vapour deposition (PVD), the molecular beam epitaxy (MBE), the chemical vapour deposition (CVD), which raised the epitaxy planar technique or the chemical vapour-phase epitaxy and finally the liquid phase epitaxy (LPE).

In authors'opinion if now and then temporary uncertainties in evoluation have occurred, i.e. overestimation or underestimation of limits and possibilities, biased assignments and evaluations, etc., then this owed little to the subject itself which, on a realistic assessment of knowledge, disclosed well what is possible or impossible now and what will be possible or impossible in the future.

In conclusion the book gives a very comprehensive account of epitaxial and eutectic growth and eutectoid decomposition reactions. Though it is not intended to provide uniform treatment of all eutectiets and eutectoids but concentraring on the most substantial problems of this field, there is a rich and comprehensive bibliography at the end of each chapter completing and covering specific problems and application aspects.

The book produced in excellent graphic conditions and hard cover is undoubtedly a work of reference in the field and highly recommended for all those interested in interfaces between physical chemistry, mathematics and manufacturing of solid state devices.

Radu Mutihac
Faculty of Physics, University of Bucharest,
PO Box MG-11, Bucharest, 76900

"ION-SELECTIVE ELECTRODES, 5", Fifth Scientific Session on Ion-Selective Electrodes, 9—13 October, 1988 Matrafures, Hungary, Edited by E. Pungor, Pergamon Press, Akademiai Kiado.

The book "Ion Selective Electrodes" edited by Prof. E. Pungor in Pergamon Press— Akademiai Kiado includes the communications presented at the 5th Symposium on Ion Selective Electrodes held in October 9—13, 1988, Matrafures, Hungary. The book also includes the discussions occasioned by the communications.

The topics are diverse, ranging from basic aspects of membrane mechanisms involved in the design of ion selective electrodes to various analytical applications of these electrodes in science and technology.

A series of remarkable contributions on the membrane with natural and synthetic macrocyclic compounds is worth mentioning; these membranes exhibit a high selectivity which is very important in the design of ion selective electrodes.

Chemically modified electrodes is another modern field approached in communications presended by specialists.

Another series of contributions focused on biosensors.

Numerous contributions specialized in the applications of ion selective membranes in flow injection analysis systems.

The authors of the contribution presented at the Fifth Scientific Session on Ion Selective Electrodes have dedicated their works to Prof. Erno Pungor, the organizer of the meeting, with the occasion of his 65th birthday.

The event was commented in Prof. Malissa's speech.

C. Luca
Department of Analytical Chemistry
Bucharest Polytechnic, Splaiul Independenţei
313, Bucharest

M. T. BECH şi I. NAGYPAL "CHEMISTRY OF COMPLEX EQUILIBRIA", Akademiai Kiado, Budapest 1990, ISBN 963 05. 5234 5.

This book is the enlarged and completely revised version of "Chemistry of Complex Equilibria" (M. T. Beck), published by Akademiai Kiado, Budapest and Van Nostrand Reinhold Company, Ltd., London (1969).

The book relies on the authors' comprehensive experience and excellent competence and their fruitful scientific cooperation with famous schools in chemistry of complex equilibria.

In this new edition, in the pattern of the book the authors took into account the recent progress made in the fundamental complex equilibria and the large possibilities of mathematical treatment and the computerized estimation of equilibria data.

The firt two chapters of the book deal with a brief definition of the domain and types of complex equilibria in solutions.

The definition of the basic equations and the formation functions as well as the rules of the distribution of the concentration in the complex equilibrium systems are the object of Chapter 3. This chapter deals with the bases of the systematic tackling of the study of the equilibria systems and also the estimation of the stability constants.

Chapter 4 deals with the methods (optical, NMR, EPR, colorimetry kinetics, extraction, solubility, ion exchange, polarography, etc.) for determining the experimental data necessary in the study of the formation of complexes in solution. This chapter of a prime importance from the experimental standpoint is based on a vast documentation (629 refs.).

Chapter 5, "Evolution of experimental data", deals with the methods of accounting the stability constants in the function formations.

Chapter 6, "Factors determining the compositions and stabilities of metal complexes", ranks preeminently in terms of the authors' originality. This is evidenced by the interdependent character of the domain of the chemistry of complexes in solution and the usefulness of being acquainted with the significance of the equilibrium constants both fundamentally and in terms of applications.

Finally, Chapter 7, "Prospects" traces the directions and development trends in the study of the domain of the equilibrium of complex formation solutions.

On the whole, the book "Chemistry of Complex Equilibria" is a reference book of high scientific standard, dealing with one of the richest and prospective domains of modern chemistry. This book is at the same time an excelent guide in the domain of the chemistry of complexes in solutions, both fundamentally and in terms of practical experiment in the study of these equilibria.

This book is very useful to specialists in this domain as well as to chemical students and engineers.

Prof. Dr. *Constantin Luca*
Department of Analytical Chemistry
Polytechnical Institute Bucharest

"Proceedings of the Fourth European Symposium on Thermal Analysis and Calorimetry", 1987. John Wiley and Sons, Ltd., Chichester ; Akadémiai Kiadò, Budapest, 1988.

The 33th volume of the Journal of Thermal Analysis, issued in two parts, is dedicated to the contributions presented at the Fourth European Symposium on Thermal Analysis and Calorimetry, held in Jena. The modern trends as well as the recent achievements of the above scientific fields are well reflected in the scientific program of the symposium, including 17 plenary lectures, 250 poster contributions and two award lectures. The material is organised in the following sections : Plenary Lectures ; Award Lectures ; Theory ; Instrumentation of Thermal Analysis and Calorimetry ; Earth Sciences, Raw Materials ; Solid State Reactions ; Inorganic Chemistry, Glass, Ceramics ; Pharmacy, Biology, Medicine ; Organic Chemistry, Polymers ; Concluding Remarks. The most consistent section is devoted to the inorganic compounds but the field of the organic chemistry is also well represented. Many contributions are centered around the high technology materials as liquid crystals. semiconductors (both inorganic and organic), superconductors, catalysts, new polymers. Among the modern trends in instrumentation and technology it is interesting to note the combination of the thermal procedures with the spectrometric, mass-spectrometric or nuclear methods of analysis. The recent advances in the theory of the thermal analysis are also evidenced. Once again, the papers included in this volume demonstrate the involvement of the thermal and calorimetric methods in various scientific areas, as well as the contribution of these methods to the progress of the modern technology.

F. G. Bănică
Polytechnic Institute of Bucharest,
Faculty of Industrial Chemistry

Chapter 6, "Factors determining the compositions and stabilities of metal complexes", ranks preeminently in terms of the authors' originality. This is evidenced by the interdependent character of the domain of the chemistry of complexes in solution and the usefulness of being acquainted with the significance of the equilibrium constants both fundamentally and in terms of applications.

Finally, Chapter 7, "Prospects" traces the directions and development trends in the study of the domain of the equilibria of complex formation solutions.

On the whole, the book "Chemistry of Complex Equilibria" is a reference book of high scientific standard, dealing with one of the richest and prospective domains of modern chemistry. The book is at the same time an excellent guide in the domain of the chemistry of complexes in solutions, both fundamentally and in terms of practical experiment in the study of these equilibria.

This book is very useful to specialists in this domain as well as to chemical students and engineers.

Prof. Dr. Constantin Luca
Department of Analytical Chemistry
Polytechnical Institute Bucharest

Proceedings of the Fourth European Symposium on Thermal Analysis and Calorimetry 1987, John Wiley and Sons, Ltd., Chichester; Akadémiai Kiadó, Budapest, 1988.

The 33rd volume of the Journal of Thermal Analysis, issued in two parts is dedicated to the contributions presented at the Fourth European Symposium on Thermal Analysis and Calorimetry held in Jena. The modern trends as well as the recent achievements of the above scientific fields are well reflected in the scientific program of the symposium, including 17 plenary lectures, 218 poster contributions and two award lectures. The material is organised in the following sections: Plenary Lectures; Award Lectures; Theory; Instrumentation of Thermal Analysis and Calorimetry; Earth Sciences; Raw Materials; Solid State Reactions; Inorganic Chemistry; Glass; Ceramics; Pharmacy; Biology; Medicine; Organic Chemistry; Polymers; Concluding Remarks. The most consistent section is devoted to the inorganic compounds but the field of the organic chemistry is also well represented. Many contributions are centered around the high technology materials as liquid crystals, semiconductors (both inorganic and organic), superconductors, catalysts, new polymers. Among the modern trends in instrumentation and techniques it is interesting to note the combination of the thermal procedures with the spectrometric, mass-spectrometric or optical methods of analysis. The recent advances in the theory of the thermal analysis are also evidenced. Once again, the papers included in this volume demonstrate the involvement of the thermal and calorimetric methods in various scientific areas as well as the contribution of these methods to the progress of the modern technology.

[illegible] G. [illegible]
Polytechnic Institute of Bucharest,
Faculty of Industrial Chemistry

Rev. Roumanie Chim., **36**, *1–3*, 109 (1991)

MIXED LIGANDS COORDINATION COMPOUNDS OF COBALT(II) AND NICKEL(II) WITH 9,10-DIHYDRO-9,10-ETHANO-12-HYDROXYMETHYLENE ANTHRACEN-11-ONE AND 2,2-DIPYRIDYL OR 1,10-PHENANTHROLINE

MARIUS ANDRUH, MICHAELA DINA STĂNESCU, NICOLAE
STANICĂ and MARILENA FERBINŢEANU

Erratum: Instead of the published figure see:

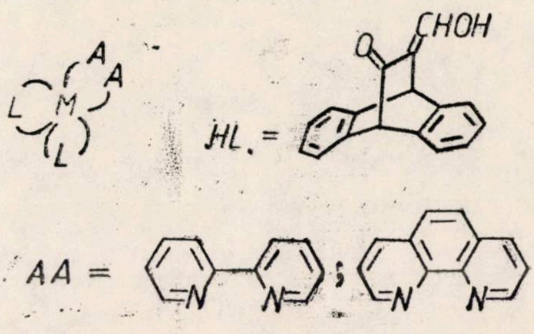

NOTE POUR LES AUTEURS

La Revue Roumaine de Chimie publie des articles en anglais, français, russe, allemand ou espagnol. Les auteurs sont priés d'envoyer des articles et des comptes rendus inédits.

Les manuscrits seront dactylographiés à double interligne. La bibliographie, les tableaux et la légende des figures seront placés après le texte.

Si l'article fait partie d'une série numérotée, la partie précédente sera donne comme première référence.

Chaque article sera précédé d'un résumé comprenant quinze lignes au maximum.

Les références bibliographiques dans le texte seront faites par des exposants sans parenthèses et paraitront à la fin de l'ouvrage.

Les publications périodiques mentionnées dans la bibliographie seront présentées suivant les prescriptions internationales : le nom de l'auteur précédé de l'initiale du prénom, le titre du périodique abrégé conformément à « Chemical Abstracts » et souligné par une ligne, le numéro du tome indiqué par des chiffres arabes et souligné par deux lignes, suivi de la première page de l'article : à la fin, l'année de la parution sera placée entre parenthèses. Le numéro de la revue ne sera pas indiqué si les pages du volume sont numérotées consécutivement.

Les textes des livres ou traités inclueront : le nom des auteurs, précédé de l'initiale du prénom, le titre du livre entre guillemets et sans être souligné, le numéro du tome précédé par l'abréviation « vol. » (ou « Bd. »), le numéro de l'édition, les éditions (the publisher), la localité de la parution du livre, l'année de la parution et la page de la référence précédée(s) par l'abréviation « p » (ou « S »).

Les brevets seront indiqués comme suit : l'auteur ou la firme, le pays et le numéro du brevet, la date de la revue (*Chem. Abstr.*). Par ex. : M. Jones (to Union Carbide Co.) Brit. Pat. 610 238, 2 Sept. 1959 : cf. *Chem. Abstr.*, 54, 12808 (1960).

Si la référence n'a pas été lue en original, on indiquera aussi la revue de références consultée.

Les diagrammes seront tracés à l'encre de Chine sur papier calque. Les tableaux et les figures (en nombre strictement nécessaire), ainsi que les courbes dans les figures seront numérotés par des chiffres arabes. Leur explication sera donnée dans la légende des figures. Prière de ne pas inscrire les mêmes données dans les tableaux et les figures. Chaque tableau aura un titre. On indiquera dans le texte la place approximative des tableaux et des figures. Les formules chimiques seront incluses dans le texte ; en outre, elles seront transcrites sur papier calque, à l'encre de Chine.

Les auteurs sont priés d'indiquer les caractères italiques (en soulignant les lettres au crayon), ainsi que tout autre caractère spécial : les préfixes *ortho*, *méta*, *para*, *cis*, *trans*, etc. seront soulignés pour indiquer leurs caractères italiques, et ne seront jamais écrits avec des majuscules.

Aucune correction à la main ne sera admise sur le manuscrit. Les corrections seront frappées à la machine. Les lettres grecques ou d'autres symboles spéciaux seront insérés à la main à l'encre clairement.

Le manuscrit sera signé par l'auteur.

Le titre courant aura 50 lettres au maximum.

L'entière responsabilité du contenu des articles appartient aux auteurs.

Sur demande on peut obtenir une note plus complète.

PRINTED IN ROMANIA

TRAVAUX PARUS AUX ÉDITIONS DE L'ACADÉMIE ROUMAINE

I. G. MURGULESCU, **Introducere în chimia fizică, Vol. I. 1 Atomi, molecule, legătură, chimică,** 1976, 560 p.

I. G. MURGULESCU, V. EM. SAHINI, **Introducere în chimia fizică, Vol. I. 2. Structura şi proprietăţile moleculelor,** 1979, 604 p.

I. G. MURGULESCU, E. SEGAL, **Introducere în chimia fizică, Vol. II. 1. Teoria molecular-cinetică a materiei,** 1979, 1036 p.

I. G. MURGULESCU, TATIANA ONCESCU, E. SEGAL, **Introducere în chimia fizică, Vol. II. 2. Cinetică chimică şi cataliză,** 1981, 1024 p.

I. G. MURGULESCU, J. PĂUN, **Introducere în chimia fizică, Vol. I. 3. Nucleul atomic, reacţii nucleare, particule elementare,** 1982, 606 p.

I. G. MURGULESCU, RODICA VÎLCU, **Introducere în chimia fizică, Vol. III. Termodinamica chimică,** 1982, 624 p.

I. G. MURGULESCU, O. M. RADOVICI, **Introducere în chimia fizică, Vol. IV. Electrochimica,** 1986, 410 p.

C. ANDREI, I. DRAGUTAN, A. T. BALABAN, **Fotostabilizarea polimerilor cu amine împiedicate steric,** 1990, 240 p.

M. BREZEANU, E. CRISTUREANU, D. MARINESCU, A. ANTONIU, M. ANDRUH, **Chimia metalelor,** 1990.

R. VÎLCU M. LECA, **Polymer Thermodynamics by Gas Chromatography,** coédition avec Elsevier, 1990, 204 p.

FL. CUIBAN, A. X. LUPEA, **Studiul structurii şi sinteza peptidelor,** 1989, 286 p.

C. SIMIONESCU, V. GORDUZA, **Implicaţiile bioenergetice ale coloranţilor,** 1988, 207 p.

R. VÎLCU M. LECA, **Termodinamica polimerilor prin cromatografie de gaze,** 1987, 238 p.

I. ZUGRĂVESCU, M. PETROVANU, **Cicloadiţii 3 + 2 dipolare,** 1987, 446 p.

RAUL MIHAIL, ION GROZEANU, **Estimarea secvenţială aplicată sistemelor chimice,** 1986, 406 p.

M. BREZEANU, I. PATRON, M. ANDRUH, **Combinaţii complexe polinucleare şi aplicaţiile lor,** 1986, 244 p.

A. T. BALABAN et. al., **Labelled Compounds and Radiopharmaceuticals Applied in Nuclear Medicine,** coédition avec John Wiley and Sons, 1986, 742 p.

D. PURDELA, **Nomenclatura chimiei organice — IUPAC,** 1986, 451 p.

PETRU BUDRUGEAC, **Probleme de chimie,** 1986, 280 p.

T. ONCESCU, S. G. IONESCU, **Conversie fotochimică şi stocare de energie,** 1985, 272 p.

V. DRAGUTAN, A. T. BALABAN, M. DIMONIE, **Olefin Metathesis and Ring-Opening Polymerization of Cyclo-Olefins,** coédition avec John Wiley and Sons, 1985, 544 p.

C. LITEANU, I. RICA, **Optimizarea proceselor analitice,** 1985, 360 p.

N. PERESCU, **Chimia extracţiei cu solvenţi şi aplicaţii,** 1985, 212 p.

1992 JUN 25

ISSN 0035-3930

S.C. UNIVERSUL S.A. c. 3185

Lei 80

F 1103

ACADÉMIE ROUMAINE

REVUE ROUMAINE DE CHIMIE

TOME 36
Nos 11–12
Novembre–Décembre 1991

Rev. Roumaine Chim.

RRCHAX, 36, *11–12*, p. 1223–1462 (1991), Bucarest

EDITURA ACADEMIEI ROMÂNE

ACADÉMIE ROUMAINE

COMITÉ DE RÉDACTION

Rédacteur en chef :

I. G. MURGULESCU, membre de l'Académie Roumaine

Rédacteurs en chef adjoints :

A. T. BALABAN et V. EM. SAHINI, membres de l'Académie Roumaine

Collège de rédaction :

ECATERINA CIORĂNESCU-NENITZESCU, CR. SIMIONESCU, P. SPACU, membres de l'Académie Roumaine; M. BANCIU, membre correspondant de l'Académie Roumaine; M. ANDRUH, M. D. GHEORGHIU, I. HAIDUC, D. I. MARCHIDAN, G. NIAC et D. SANDULESCU

La Revue Roumaine de Chimie paraît 10 fois par an. Toute commande de l'étranger sera adressée à ROMPRESFILATELIA — sectorul Export-Import Presă, P. O. Box 12—201, telex 10376 prsfi r 78104 Bucarest, Calea Griviței nr. 64—66, Roumanie

Les manuscrits, les livres et les revues proposés en échange, ainsi que toute correspondance seront envoyés à la rédaction :

REVUE ROUMAINE DE CHIMIE

125, Calea Victoriei, 79717 Bucarest, Roumanie, téléphone 50 76 80

EDITURA ACADEMIEI ROMÂNE
125, Calea Victoriei 79717, Bucarest, Roumanie, téléphone 50 76 80

REVUE ROUMAINE DE CHIMIE

Tome 36, N°s 11–12 Novembre–Décembre, 1991

ALEXANDRA SCHIOPESCU and ANCA ALBU, Thermal analysis of the ferrate (VI) ion salts with complex tetralutidinic combinations of nickel(II) and cobalt (II) 1225–1228
V. BRÂNZOI, S. STERNBERG and LILIANA APĂTEANU, Study of the electrode processes reversibility in the $PbO_2/PbSO_4$ system 1229–1237
NICOLAE ENE and ŞTEFANIA ZUCA, Electrorefining of titanium in molten alkali halide mixtures 1239–1251
ESAM A. GOMAA, Hydrogen bonding of *o*-nitroaniline in water-DMSO mixtures 1253–1258
R. R. YADAVA and S. S. YADAVA, Study of molecular interaction between acetonitrile and benzene 1259–1262
M. CONTINEANU and O. CONSTANTINESCU, Study of radical species formed at polycrystalline Ag_2SeO_3 radiolysis 1263–1268
JANOS ZSAKÓ, CSABA VÁRHELYI and ION GĂNESCU, On the dioximine complexes of transition metals. LXXXII. Study on some isoselenocyanato mixed chelates of cobalt(III) with dimethylglyoxime 1269–1273
ALEXANDRU CECAL, VIOREL CREŢU and DAN VRABIE, Inclusion of low- and intermediate-level radioactive wastes in low fusible glasses (in German) 1275–1278
FLORICA ZĂLARU, CORNELIA CERCASOV, AURELIA MEGHEA, CHRISTINA ZĂLARU and CHRISTINA JALEA, Cu(II) coordination compounds with thioamides 1279–1285
KRISTIANA GOŞA, DAN DONESCU, SORIN STRAJA, DOINA ISBĂŞESCU and ION LANGURI, Rheological modelling of emulsion copolymerization of vinyl acetate 1287–1297
HORIA PETRIDE, Mesoionic oxazolones. VII. About the mechanism of the hydrolysis of acylated derivatives 1299–1306
A. C. RĂZUŞ, E. BARTHA, Zs. ARVAY, S. A. OSADCHII, V. I. MAMATYUK and V. G. SHUBIN, Rearrangements of 1, 1a, 6,6a-tetrahydrocycloprop[a]-inden-6-ols in superacids 1307–1313
OVIDIU MAIOR, ANTONIE DINCULESCU, ION BACIU, GEORGETA BOTEZ and CLAUDIU T. SUPURAN, Synthesis of intensely coloured 2,4,6-trisubstituted pyrylium salts possessing bulky groups 1315–1320
CORNELIA MAJDIK, ALEXANDRU KOVENDI, SIMION MATEI and DORIN BREAZU, O-arylketoximes. III. Obtaining 3-(4′-methyl)-phenyl-5-nitro-benzisoxazole from O-[2-(4′-methyl)-benzoyl-4-nitro]-phenyl-ketoximes 1321–1324

KERIMAN GÜNAYDIN and OLCAY ANAÇ, Investigation of the reaction of dimethyl diazomalonate with 1-phenylcyclododecene in the presence of copper(II) acetylacetonate . . . . 1325—1329

CONSTANTIN N. CAŞCAVAL and DAN ROŞU, Phenolic and epoxy resins. I. Thermal characterization by pyrolysis — gas chromatography . . . . 1331—1336

R. M. SALEH, A. Y. SOLIMAN and F. M. A. SOLIMAN, Some reactions of chalcone epoxides. . . . . 1337—1343

CLAUDIU T. SUPURAN and MIRCEA D. BANCIU, Carbonic anhydrase inhibitors. 9. Inhibitors with modified sulfonamido groups and their interaction with the zinc enzyme . . . . 1345—1353

K. M. GHONEIM, S. EL-BASIL, A. N. OSMAN, M. M. SAID and S. A. MEGAHED, Synthesis and structure elucidation of benzothiazole-containing compounds for antimicrobial investigation . . . . 1355—1361

G. L. RADU, A. TĂNASE, MARIA CALOIANU-IORDACHEL and I. TODOR, Structural differences of some biomaterials based on collagen . . . . . 1363—1369

ADRIAN O. FULEA, The causality law in physical chemistry and chemical physics and Bohr's principle of complementarity . . . . 1371—1386

EMIL DUMITRIU, KAYED YOUSEF, VASILE HULEA and SPIRIDON OPREA, Transalkylation of toluene with trimethylbenzene. I. Thermodynamic study. . . . . 1387—1395

MARK S. CHARSON, NICULAE I. IONESCU and MIHAI S. CHIRCA, Mechanism of phenol methylation on Al_2O_3 and on MgO . . . . 1397—1401

DOINA HRITCU, GH. IONESCU and I. M. POPA, Study of the intrinsic properties of viscous flow in the ethyleneglycol (EG)-methanol (MeOH) system 1403—1408

O. RADU, As(III) — HCl — H_2O system. IV. The liquid — vapour state . . 1409—1424

TH. DELEANU, Progress of statistics applied to synthetic polymers latexes 1425—1437

AUTHORS' INDEX . . . . 1439—1454

SUBJECT INDEX . . . . 1455—1462

Revue Roumaine de Chimie, 36, *11–12*, 1225–1228 (1991)

THERMAL ANALYSIS OF THE FERRATE (VI) ION SALTS WITH COMPLEX TETRALUTIDINIC COMBINATIONS OF NICKEL(II) AND COBALT(II)

ALEXANDRA SCHIOPESCU and ANCA ALBU
Department of Chemistry, Institute of Petroleum and Gas, Bd. București 39, Ploiești, Romania

Received May 15, 1990

Salts of ferrate (VI) with nickel (II) and cobalt (II) tetralutidinic complex combinations were synthesised. Use has been made of thermal analysis to study the thermal stability of these complexes.

INTRODUCTION

Thermal behaviour of ferrate (VI) has been studied by Scholder and coworkers.[1]

This contribution deals with preparation of two types of Ni(II) and Co(II) complexes; they are salts containing tetralutidinic complex combinations of Ni(II) and Co(II) with ferrate (VI) ion. These complexes were studied by thermal analysis.

EXPERIMENTAL

Two series of Ni(II) and Co(II) complexes with lutidines containing ferrate (VI) ion were prepared. The salts are the following:

$[Ni(\alpha, \alpha'\text{-Lut})_4](FeO_4)$; $[Ni(\alpha, \gamma\text{-Lut})_4](FeO_4)$.

$[Co(\alpha, \alpha'\text{-Lut})_4](FeO_4)$; $[Co(\alpha, \gamma\text{-Lut})_4](FeO_4)$.

These complexes were analysed and studied by thermal gravimetric analysis (TGA) making use of a M.O.M. Budapest Paulik Paulik Erdey apparatus. The samples were heated in the atmosphere of the furnace to 800°C at a rate of 8°/min.

RESULTS AND DISCUSSION

The results of thermal analysis applied to salts prepared by us containing $(FeO_4)^{2-}$ ion with lutidines are presented. This study aims at explaining the thermal stability of these complex combinations as a function of some parameters of the central ion and the ligand.

The temperatures at which endothermal phenomena occur were recorded during the heating of samples in the atmosphere of the furnace.

A comparison of the thermal behaviour of ferrate(VI) ion salts with complex combinations of Ni(II) and Co(II) containing lutidine with that of thiocyanate, of some complex amines of Ni(II) and Co(II) has revealed that the complexes containing $(FeO_4)^{2-}$ ion eliminate the ligand molecules during heating in one step. This is evidenced by the presence of one endothermal process. In thiocyanates of complex amines of Ni(II) and Co(II) this elimination of the ligand takes place in two steps emphasized by two minima on curves TDA and a decrease of weight recorded by TGA curves (See Table 1).

Table 1

The temperatures corresponding to endothermal and exothermal phenomena for complex combinations of Ni(II) and Co(II) containing lutidine

Compound	Temperature of endothermal process, °C		Temperature of exothermal process, °C	
$[Ni(\alpha, \alpha'\text{-Lut})_4](SCN)_2$	188	275	428	515
$[Ni(\alpha, \gamma\text{-Lut})_4](SCN)_2$	195	300	435	520
$[Co(\alpha, \alpha'\text{-Lut})_4](SCN)_2$	190	280	430	522
$[Co(\alpha, \gamma\text{-Lut})_4](SCN)_2$	192	310	440	525

Table 2

The temperatures corresponding to endothermal and exothermal phenomena

Compound	Characteristic temperature t_m, °C	Temperature of exothermal process, °C	Temperature of endothermal process, °C
K_2FeO_4	140		620
$[Ni(\alpha, \alpha'\text{-Lut})_4](FeO_4)$	120	240	620
$[Ni(\alpha, \gamma\text{-Lut})_4](FeO_4)$	135	245	620
$[Co(\alpha, \alpha'\text{-Lut})_4](FeO_4)$	130	255	620
$[Co(\alpha, \gamma\text{-Lut})_4](FeO_4)$	140	270	620

After these two endothermal phenomena reported in Table 1, the following region corresponds to compounds $Ni(SCN)_2$, $Co(SCN)_2$; being followed by an oxidation process of $Ni(SCN)_2$ or $Co(SCN)_2$; after this a decomposition of NiO, CoO and a crystallization of these take place.

In Table 2 are reported the temperatures corresponding to endothermal and exothermal phenomena for the ferrate(VI) ion salts with complex combinations of Ni(II) and Co(II) containing lutidine. It is also shown the thermal decomposition of potassium ferrate (VI).[4]

A comparative examination of characteristic temperatures for endothermal and exothermal phenomena shows that in compounds containing $(FeO_4)^{2-}$ ion the characteristic temperature t_m of thermal decomposition and, consequently, the stability of compounds decreases on introduction of $(FeO_4)^{2-}$ ion in their molecule.

Formation of some combinations which are thermally less stable on introduction of $(FeO_4)^{2-}$ ion may be explained by a π strong bond metal-oxygen that appears in the presence of $(FeO_4)^{2-}$ ion. [2-3]

This entails a relatively high polarization of the central metallic ion which to some extent neutralizes the positive charge of the central metallic ion (Ni(II), Co(II)). Thus a decrease of the sphere of action of the central metallic ion occurs; because of its lower effective charge the attraction force exerted on the ligand polar molecules is lower. All these add up in a lower stability of the compounds containing $(FeO_4)^{2-}$ ion which is evidenced by elimination of the ligand in one step corresponding to one endothermal process.

Chemical analysis of the compounds containing $(FeO_4)^{2-}$ was carried out after heating to various temperatures: 200, 400 and 600°C. The results obtained are shown in Table 3.

Table 3

Chemical analysis of the compounds containing $(FeO_4)^{2-}$

Compound	200°C (Ni, Co) %	Fe %	400°C (Ni, Co) %	Fe %	600°C (Ni, Co) %	Fe %
$[Ni(\alpha, \alpha'\text{-Lut})_4](FeO_4)$	16.02	27.05	25.02	47.00	25.00	47.02
$[Co(\alpha, \alpha'\text{-Lut})_4](FeO_4)$	16.62	33.81	25.01	47.58	24.91	47.60
$[Ni(\alpha, \gamma'\text{-Lut})_4](FeO_4)$	16.81	33.31	24.30	46.31	24.21	46.41
$[Co(\alpha, \gamma\text{-Lut})_4](FeO_4)$	16.72	33.90	24.80	47.50	25.00	47.02

These data suggest that no unitary intermediate complexes are formed during these steps but only mixtures of metallic oxides.

From among the salts of ferrate(VI) with lutidines, the lutidinic compounds exhibit a higher stability.

The endothermal process occurring in all compounds containing $(FeO_4)^{2-}$ ion at temperatures about 620°C evidences the existence of a phenomenon which is common to all compounds. This behaviour may be accounted for by formation of ferrites of general formula $Fe_2O_3 . MO$ (where M stands for Ni(II) or Co(II) which belong to the spinel group).

Examination of thermal behaviour of potassium ferrate(VI) shows that the TDA curve starts at 620°C with a minimum assigned to the endothermal process.

Reiteration of this phenomenon in potassium ferrate(VI) favours the idea that there is a transformation in the structure of Fe_2O_3 resulted from decomposition rather than formation of spinelic compounds. This explanation is valid in all the compounds studied that contain $(FeO_4)^{2-}$.

The equilibrium of the two forms of Fe_2O_3 is

$$\gamma\, Fe_2O_3 \rightarrow \alpha\, Fe_2O_3$$

This phase transformation taking place at about 600°C[5] and corresponding to an exothermal process may not account for the thermal process recorded at 620°C in the compounds in question.

One can correlate the endothermal process occurring at 620°C with the existence of modifications of magnetic properties of Fe_2O_3. This statement is supported by the fact that the alteration of magnetic properties [6] of Fe_2O_3 is associated with an endothermal process (also evidenced in the cases considered above).

CONCLUSIONS

The behaviour of a series of salts containing ferrate(VI) ion with tetralutidinic compounds of Ni(II) and Co(II) was studied. The influence of $(FeO_4)^{2-}$ ion upon the formation of some compounds of relatively low thermal stability was evidenced.

An elimination of the ligand through a single step process was noted in all the compounds studied, which was assigned to the low stability of these compounds.

The reproductibility of the process at 620°C (which is also associated with decomposition of K_2FeO_4) is also worth noting; this suggests the existence of some changes in the magnetic properties of Fe_2O_3 (resulted from thermal decomposition) which is present in all instances in question.

REFERENCES

[1] R. Scholder, H. V. Bunsen and F. Kindervater, *Z. anorg. Chem.*, **282**, 268 (1955).
[2] I. G. Murgulescu, E. Segal and D. Fatu, *J. Inorg. Nuclear Chem.*, **27** (1965).
[3] C. J. Ballhausen and A. D. Liehr, *J. Mol. Spectroscopy*, **2**, 342 (1965).
[4] D. Fatu and A. Schiopescu, *Rev. Roumaine Chem.*, **19**, 1297 (1974).
[5] A. F. Wells, "Structural Inorganic Chemistry", ed. II, Oxford, 1962, p. 545.
[6] R. C. Mackuezie, "Differential Thermal Analysis", vol. I, Academic Press, 1970, p. 274.

Revue Roumaine de Chimie, **36**, *11–12*, 1229–1237 (1991)

STUDY OF THE ELECTRODE PROCESSES REVERSIBILITY IN THE $PbO_2/PbSO_4$ SYSTEM

V. BRÂNZOI,[a] S. STERNBERG[a]* and LILIANA APĂTEANU[b]

[a] Polytechnic Institute of Bucharest, Dept of Physical Chemistry 132, Calea Griviţei St., Bucharest, Romania

[b] Biochemical and Chemical Energetics Institute, 206 Spl. Independenţei St., Bucharest, Romania

Received October 20, 1989

Using the cyclic voltammetry method, the influence of the potential sweep rate on the processes taking place at the electrochemical oxidation of the Pb electrode to PbO_2 and on those taking place at the reduction of PbO_2 to $PbSO_4$, was studied in concentrated sulphuric acid solution. Experiments were carried out within a relatively wide range of potential sweep rates, that is from 6 to 306 mV/s. On the basis of the electrochemical parameters calculated from the polarization curves, supplementary information concerning the nature and the kinetics of the anodic oxidation and cathodic reduction in the system under study, was obtained. Conclusions on the degree of reversibility of the anodic and cathodic processes, respectively, were drawn out.

INTRODUCTION

In a previous sequence of papers [1–5] the electrode processes taking place at the Pb/H_2SO_4 interface were studied in detail, within the $(+900 \div +1850)$ mV potential range. The studies were carried out under different conditions of electrolyte concentration, temperature and composition, using for this purpose the cyclic voltammetry method.

In the present paper, the influence of the potential sweep rate on the electrode processes in the system mentioned above, was studied in order to obtain new insight and information on the nature and the kinetics of the oxidation and reduction processes, which take place in the system and within the potential range under study.

EXPERIMENTAL PART

The experimental current-potential curves, in the Pb/H_2SO_4 system, were obtained by the cyclic voltammetry method. The potential of the working electrode was swept within the $(+900 \div +1850)$ mV potential range by means of a PS-3 type potentiostat coupled with an Orion type EMG-1117 pulses generator. The voltammograms were registered by means of an X–Y recorder. A cylinder of 6 mm diameter was used as counterelectrode and $Hg/Hg_2SO_4/H_2SO_4$ 5M was used as reference electrode.

Experiments were carried out in a sulphuric acid solution of $\rho = 1.28$ g/cm³ (4,876 M) density, at potential sweep rates changing from 6 mV/s to 306 mV/s.

---

* Deceased on January 19, 1990

Before each determination, the working electrode surface was mechanically polished with glass paper of different granulations and then it was electropolished in H_2SO_4 of $\rho = 1.28$ g/cm^3 density, for 10 minutes, at a potential of -1800 mV; after that, the working electrode was cycled, with a potential sweep rate of 6 mV/s, within the $(+900 \div +1850)$ mV potential range, in the working solution, until 20 cycles were performed. Only after that, the working electrode was cycled with the different potential sweep rates mentioned above. A number of 10 cycles was carried out for each potential sweep rate. The cycling of the working electrode (20 cycles) at a small sweep rate, of 6 mV/s, before each determination, had as purpose the obtainment of an active, porous and reproducible surface. After this, preceding processing reproducible results were obtained, independently of the order in which the cycling at different potential sweep rates was performed.

The working temperature, of 25°C, was maintained constant by means of an UM-210 thermostat, with a ± 0.01°C precision.

RESULTS AND DISCUSSION

Figure 1 shows the voltammogram obtained on the lead electrode, in a H_2SO_4 solution of $\rho = 1.28$ g/cm^3 density, at the sweep of the potential within the $(+900 \div +1850)$ mV potential range, with a rate of 10 mV/s. Analysis of the figure shows that the sweep of the working electrode potential within this potential range leads to the appearance of some current maxima, that is: at the increasing anodic scan of the poten-

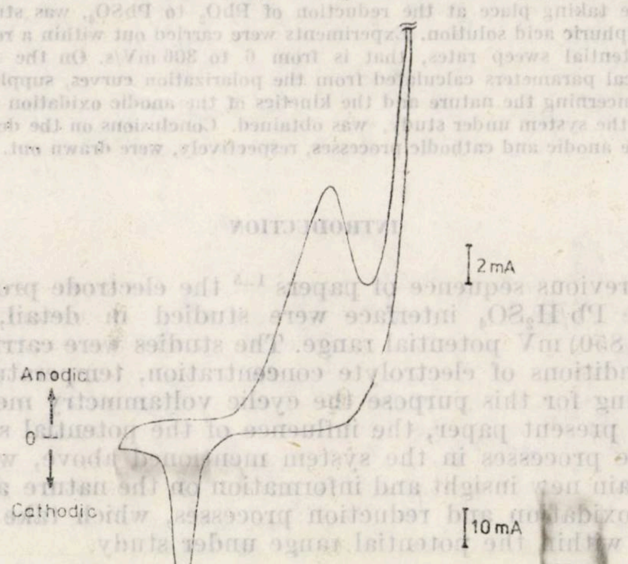

Fig. 1. — The voltammogram of lead electrode in a sulphuric acid solution, of $\rho = 1.28$ g/cm^3, obtained at the potential sweep within the $(+900 \div +1850)$ mV range, with a sweep rate of 10 mV/s.

tial, a current maximum representing the lead dioxide (α- and β-modifications) formation is obtained, after which a sudden increase of the current occurs, corresponding to the oxygen evolution. At the potential reverse sweep, a maximum current appears representing the PbO_2 to $PbSO_4$ reduction, the Pb^{4+} to Pb^{2+} ions reduction, respectively. The shape of the two peaks is much different. While the cathodic peak, of the PbO_2 to $PbSO_4$ reduction, is very sharp, pointing out that the cathodic process is under kinetic control, the anodic peak of the oxidation of lead sulphate layer and of the lead nonstoichiometric oxides and basic sulphates is not too high and lies down within a relatively wide range, pointing out that the anodic process of PbO_2 formation is under diffusive control. The processes taking place to the electrode, their characteristics, the kinetic parameters, as well as the other details have been described in detail in a previous sequence of papers.[1-5]

In the present paper the influence of the potential sweep rate of the electrode on these processes was studied, in order to establish the degree of reversibility of the system under study.

Further on, the voltammograms obtained at some potential sweep rates are presented; for the other sweep rates, only the electrochemical parameters determined from the voltammograms, will be presented.

Figures 2, 3, 4 and 5 present the voltammograms obtained at four different potential sweeps, that is: 6, 30, 180 and 300 mV/s. Analysis of the four figures shows that the shape of the voltammograms changes with the increase of the sweep rate. If at small sweep rates the two current maxima (anodic and cathodic, respectively) are very clearly outlined, the anodic peak becomes lesser outlined as the sweep rate increases; at the last sweep rates, this oxidation maximum practically appears as a shoulder, and the corresponding anodic current is much higher. This behaviour can be explained according to the Laitinen, Pohl and Pavlov [6-7] model as follows: within the potential range corresponding to the PbO_2 formation, after the formation of a thin film of PbO_2, the total anodic current at constant potential is considered as compounded from two parts, a constant part due to the gaseous oxygen evolution at the PbO_2/solution interface and a part depending on time, due to the increase of the oxide layer thickness. According to the Laitinen and Pohl mode, [6] the oxide layer is formed mainly from PbO_2 which is considered to be dense and compact.

In the recent papers [6-8] of Laitinen, Pohl, Pavlov and Rüetschi it is supposed the existence of a thin PbO layer, too. The O^{2-} oxygen ions generated at the interface diffuse through the oxide layer on the oxygen vacancies, in the crystal lattice and oxidize the underlying lead. For this reason the oxygen ions diffusion is supposed to be rate determining step. Simultaneously with the increase of the sweep rate, the same potential range is swept during a shorter and shorter time and for this reason the PbO_2 amount formed will be smaller and smaller, in such a way that, at a certain sweep rate, the PbO_2 layer formed is not enough to ensure a relative passivation of the electrode surface and to determine the decrease of the anodic current; for this reason, the anodic oxidation peak, immediatly followed by a pronounced increase of current, is no longer observ-

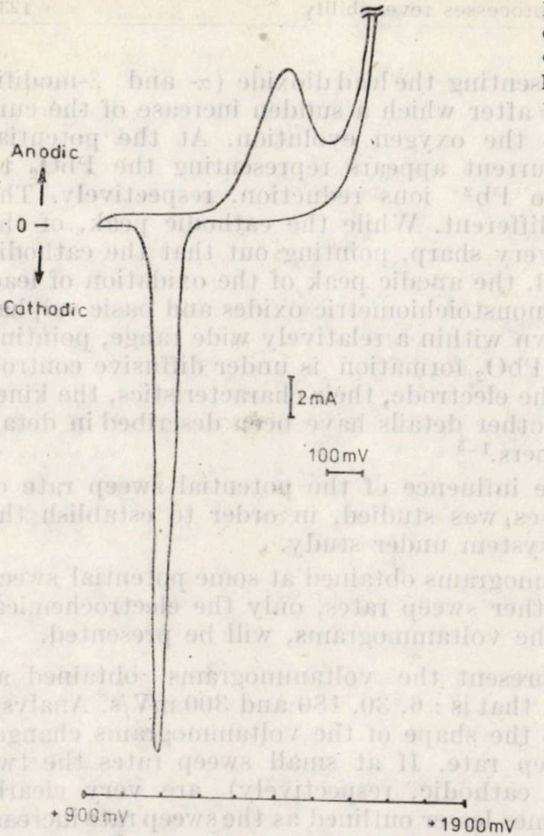

Fig. 2. — The voltammogram of lead electrode in a sulphuric acid solution, of $\rho = 1.28\ g/cm^3$, obtained at the potential sweep within the $(+\ 900 \div +\ 1850)$ mV range, with a sweep rate of 6 mV/s.

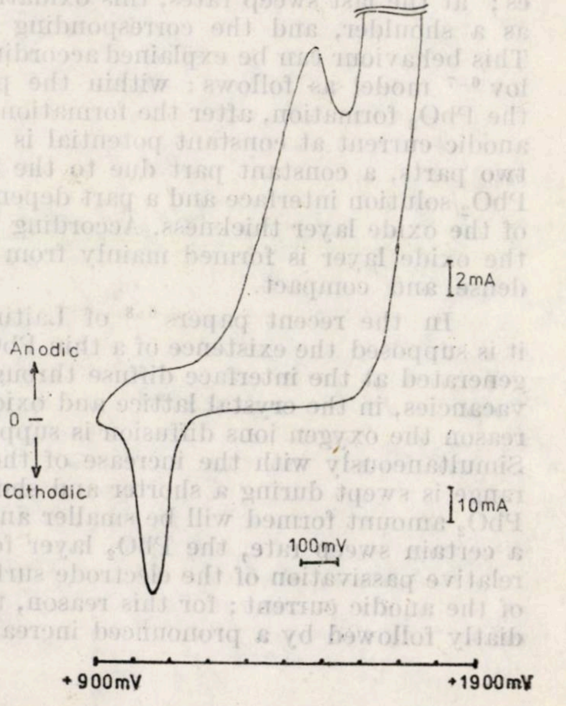

Fig. 3. — The voltammogram of lead electrode in a sulphuric acid solution, of $\rho = 1.28\ g/cm^3$, obtained at the potential sweep within the $(+\ 900 \div +\ 1850)$ mV range, with a sweep rate of 30 mV/s.

Fig. 4. — The voltammogram of lead electrode in a sulphuric acid solution, of $\rho = 1.28\ g/cm^3$, obtained at the potential sweep within the (+ 900 ÷ + 1850) mV range, with a sweep rate of 180 mV/s.

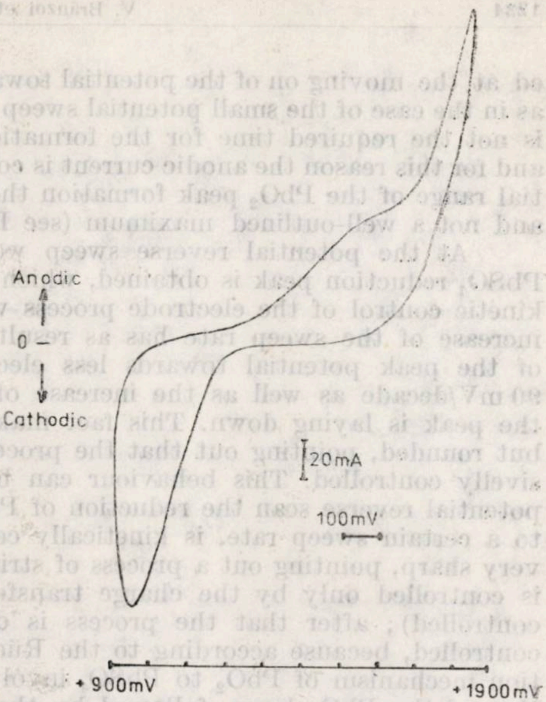

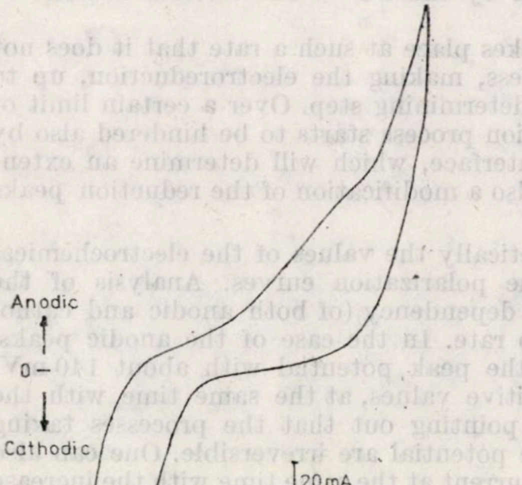

Fig. 5. — The voltammogram of lead electrode in a sulphuric acid solution, of $\rho = 1.28\ g/cm^3$, obtained at the pontential sweep within the (+ 900 ÷ + 1850) mV range, with a sweep rate of 300 mV/s.

ed at the moving on of the potential towards more electropositive values, as in the case of the small potential sweep rates. At high sweep rates there is not the required time for the formation of a passivating PbO_2 layer and for this reason the anodic current is continuous, and within the potential range of the PbO_2 peak formation there is a shoulder which appears and not a well-outlined maximum (see Figs. 4 and 5).

At the potential reverse sweep we have shown that a PbO_2 to $PbSO_4$ reduction peak is obtained, which is very sharp, pointing out the kinetic control of the electrode process within this potential range. The increase of the sweep rate has as result in this case the displacement of the peak potential towards less electropositive values, with about 90 mV/decade as well as the increase of the potential range on which the peak is laying down. This fact makes the peak be no more sharp but rounded, pointing out that the process is kinetically and also diffusivelly controlled. This behaviour can be explained as follows : at the potential reverse scan the reduction of PbO_2 to $PbSO_4$ occurs which, up to a certain sweep rate, is kinetically controlled (the reduction peak is very sharp, pointing out a process of stripping — that is a process which is controlled only by the charge transfer and which is not diffusively controlled) ; after that the process is diffusively as well as kinetically controlled, because according to the Rüetsch theory, the electroreduction mechanism of PbO_2 to $PbSO_4$ involves a stage of chemical dissolution of the PbO_2 layer, followed by the Pb^{4+} ions electroreduction to Pb^{2+} ions.

The chemical dissolution takes place at such a rate that it does not hinder the electroreduction process, making the electroreduction, up to a certain sweep rate, to be rate determining step. Over a certain limit of the sweep rate, the electroreduction process starts to be hindered also by the Pb^{4+} ions diffusion at the interface, which will determine an extension of the reduction range and also a modification of the reduction peaks shape (see Figs. 4 and 5).

Tables 1 and 2 give synthetically the values of the electrochemical parameters determined from the polarization curves. Analysis of the tables shows the peak potentials dependency (of both anodic and cathodic ones) on the potential sweep rate. In the case of the anodic peaks, one can observe a removal of the peak potential with about 140 mV/decade towards more electropositive values, at the same time with the increase of sweep rate. This is pointing out that the processes taking place at the anodic sweep of the potential are irreversible. One can also observe the increase of the peak current at the same time with the increase of the sweep rate (see table 1). For the cathodic branch, for the cathodic reduction process, respectively, one can also observe the change of the peak potential as the potential sweep rate changes. In this case, it is found a removal of the peak potential with about 90 mV/decade, towards less electropositive values, simultaneously with the increase of the potential sweep rate (see table 2).

These experimental data lead to the conclusion that the processes taking place at the cathodic sweep of the potential (corresponding to the cathodic peak) are irreversible. Also in this case, as it was otherwise expected, one can observe the increase of the peak current simultaneously with the increase of the potential sweep rate (see table 2). This behaviour can be explained by the fact that, simultaneously with the increase of the potential sweep rate, the increase of the rate of the electroreduction process occurs, too.

Table 1

The change of the electrochemical parameters of the anodic process as a function of the potential sweep rate, v

v (mV/s)	$V_{p.a}$ (mV)	$I_{p.a}$ (mA)	Q_a* (mC/cm^2)	$Q_a^{PbO_2}$ ** (mC/cm^2)
6.13	1400	8.5	2116	1150.0
12.34	1430	14.2	1507	937.7
18.63	1455	16.5	1178	771.4
25.00	1480	17.5	892	644.0
30.60	1500	19.4	807	601.6
43.20	1520	27.4	768	569.7
63.30	1550	37.0	672	488.3
95.00	1570	49.0	584	417.6
123.40	1580	51.4	435	371.5
155.74	1590	57.5	410	308.9
186.00	1600	65.0	393	283.0
215.90	1610	73.0	346	268.9
250.00	1620	84.0	319	247.7
279.40	1630	92.0	315	247.7
306.50	1640	102.0	313	247.7

* Q_a represents the electricity amount involved in the anodic process corresponding to the (+ 900 ÷ + 1650) mV potential range.

** $Q_a^{PbO_2}$ represents the electricity amount involved in the process of the PbO_2 formation (corresponding to the anodic maximum).

Tabel 2

The change of the electrochemical parameters of the cathodic process, as a function of the potential sweep rate, v

v (mV/s)	$V_{p,c}$ (mV)	$I_{p,c}$ (mA)	Q_c (mC/cm^2)	$V_p = V_{p_a} - V_{p_c}$ (mV)
6.13	1080	28.0	839	320
12.34	1070	35.9	602	360
18.63	1050	37.4	556	405
25.00	1040	41.6	531	440
30.60	1030	48.7	517	470
43.20	1020	63.0	502	500
63.30	1005	73.4	474	545
95.00	990	100.5	449	580
123.40	980	105.4	425	600
155.74	960	110.7	410	630
186.00	950	136.3	393	650
215.90	940	138.4	372	670
250.00	935	157.0	364	685
279.40	930	165.0	361	700
306.50	925	171.3	354	715

The extension of the potential range of the cathodic peak, at the increase of the sweep rate, can be explained on the basis of the fact that, as the potential sweep rate increases, the same potential range is swept during a shorter and shorter time; for this reason the electroreduction of the PbO_2 layer formed at the anodic sweep can no longer be entirely realized within the same potential range in which it was realized at a smaller sweep rate, the electroreduction being prolonged within a higher potential range, in such a way that as much as possible from the PbO_2 layer formed at the anodic oxidation can be reduced.

At the beginning of the paper we have shown that, as the sweep rate increases, the cathodic peaks are no more sharp but they become more rounded (see Figs. 4 and 5) pointing out the fact that the cathodic proces starts to be diffusively controlled. This behaviour can be explainned by the fact that at high sweep rates, the rate of the Pb^{4+} to Pb^{2+} ions electroreduction reaction is very much increasing, the Pb^{4+} ions concentration at the electrode / solution interface is rapidly decreasing and the Pb^{4+} ions diffusion from the solution at the interface becomes rate determining step; for this reason the cathodic peaks shape is changing and from very sharp peaks which are obtained at small sweep rates, corresponding to a kinetic control of the process, they become wider and more rounded, indicating a process kinetically controlled in the initial stage and further on diffusively controlled.

The further on analysis of the tables 1 and 2 shows a rapid decrease of the electricity amounts involved in the anodic (Q_a) and cathodic (Q_c) processes, respectively, simultaneously with the increase of the potential sweep rate. This behaviour can be explained by the fact that, at the increase of the potential sweep rate, the same potential range is swept during a shorter and shorter time, hence the thickness of the active layer from the elctrode surface, which takes part in the reactions at the interface, becomes smaller and smaller, contributing to the diminishing of the cathodic and anodic processes and consequently, to the diminishing of Q_a and Q_c.

One can also consider that the sweep being performed with higher and higher rates, the electrolyte has not the necessary time to penetrate into the depth of the active layer from the electrode surface; as a consequence a smaller and smaller amount of the active layer from the electrode surface takes part, in the reactions at the interface resulting in the diminishing of the anodic and cathodic processes, of the electricity amounts involved in these processes, respectively. One can consider, hence, that the thickness of the passivating film (of PbO_2 in this case) changes as a function of the sweep rate as it also result from the tables 1 and 2.

This behaviour is different from that usually indicated in literature,[9–12] in which a constant thickness of the passivating layer is considered, independently of the potential sweep rate. The various mathematical models from literature [9–12], which are suggesting $I_p = f(Q)$ relations, refer to constant electricity amounts Q. In our case, such an equation must take into account the existence of a variable Q and will be discussed in a future paper.

A mathematical modelling of the electrode processes with insoluble films formation, based on the assumption of the existence of a variable Q, was performed and discussed for the Pb/Pb^{2+} electrode processes.[13,14]

CONCLUSIONS

The study of the influence of the potential sweep rate on the electrode processes at the Pb/H_2SO_4 interface, within the $(+900 \div +1850)$ mV potential range, leads to the following conclusions:

— the increase of the sweep rate over a certain limit leads to the change of the voltammograms shape;

— the potential corresponding to the anodic maximum changes with the potential sweep rate, moving with about 140 mV/decade towards more electropositive values simultaneously with the increase of the sweep rate;

— the potential corresponding to the cathodic maximum also changes with the sweep rate, that is it moves with about 90 mV/decade towards less electropositive values simultaneously with the increase of the sweep rate;

— the change of the peak potentials with the sweep rate points out the irreversibility of the anodic and cathodic processes, corresponding to the two maxima;

— the electricity amounts involved in the anodic and cathodic processes are very much changing, that is they are decreasing with the increase of the potential sweep rate. For this reason, the thickness of the passivating layer on the electrode surface is also changing simultaneously with the sweep rate;

— a mathematical model for the computation of the E—I curves has to take into account the existence of a variable and not constant Q, as appearing in literature.

REFERENCES

[1] S. Sternberg, A. Mateescu, V. Brânzoi and Liliana Apăteanu, *Rev. Roumaine Chim.*, **29**, 727 (1984).

[2] S. Sternberg, V. Brânzoi, A. Mateescu and Liliana Apăteanu, *Rev. Roumaine Chim.*, **30**, 955 (1985).

[3] S. Sternberg, A. Mateescu, V. Brânzoi and L. Apăteanu, *Electrochim. Acta*, **32**, 349(1987).

[4] V. Brânzoi, S. Sternberg and Liliana Apăteanu, *Rev. Roumaine Chim.*, **34**, 937 (1989).

[5] V. Brânzoi, S. Sternberg and Liliana Apăteanu, *Rev. Roumaine Chim.*, **34**, 1457 (1989).

[6] T. Laitinen and J. Pohl, *Electrochim. Acta*, **34**, 377 (1989).

[7] D. Pavlov, *Electrochim. Acta*, **23**, 845 (1978).

[8] P. Rüetschi, *J. Power Sources* **2**, 3 (1977/78).

[9] S. Srinivasan and E. Gileadi, *Electrochim. Acta*, **11**, 321 (1966).

[10] N. R. de Tacconi, A. J. Calandra and A. J. Arvia, *Electrochim. Acta*, **18**, 571 (1973).

[11] A. J. Calandra, N. R. de Tacconi, R. Pereiro and A. J. Arvia, *Electrochim. Acta*, **19**, 901 (1974).

[12] D. Devilliers, F. Lantelme and M. Chemla, *Electrochim. Acta*, **31**, 1235 (1986).

[13] S. Sternberg, V. Brânzoi and Liliana Apăteanu, *Rev. Roumaine Chim.*, **34**, 1281 (1989).

[14] S. Sternberg, Liliana Apăteanu, V. Brânzoi and M. Gaust, *Rev. Roumaine Chim.*, **34**, 1581 (1989).

Revue Roumaine de Chimie, **36**, *11–12*, 1239–1251 (1991)

ELECTROREFINING OF TITANIUM IN MOLTEN ALKALI HALIDE MIXTURES

NICOLAE ENE and ȘTEFANIA ZUCA
Institute of Physical Chemistry, Spl. Independenței 202, Bucharest, Romania

Received July 1, 1990

The electrorefining of titanium metal in alkali halide melts has been investigated. The characteristics of electrodeposited metal, as a function of electrolyte composition at constant current density and temperature, were studied. The influence of atomic ratio F/Cl and/or Ti/F on the mechanism of generation and growth of crystals was established. This dependence was qualitatively explained in terms of the influence exerted upon the thermodynamic stability of the complex hexafluorocoordinated anion of titanium in the melt.

Although titanium metal is produced exclusively by the well-known Kroll process, numerous researches on the alternative of direct electroreduction of $TiCl_4$ to metallic titanium in molten salt baths have been developed over the last 50 years in different laboratories. However only in 1988 the Ginatta SpA (Italy) and RMI (USA) announced in a press release,[1] that they were installing an electrolytic plant to produce 100–150 tons of titanium sponge per year in advantageous conditions of both quality and cost price comparatively to the existing sponge technology.

In our opinion, another aspect related to the electrowinning of titanium which is becoming more important to industry is the processing of the titanium scrap metal by electrorefining. Compared to the recovery by chemical methods, that transform scrap metal into chloride, hydride or iodide to process them farther by specific methods of obtaining pure metal, electrorefining affords the direct metal-metal transformation in a unique operation. Besides, during electrorefining, complicating factors as the depletion of titanium from the electrolyte and the anodic gases evolution with the related technical problems of separating the anode from the cathode compartments are absent. Moreover the main feature of electrolysis in fused salts, i.e. operation in a wide range of current densities, ensures by means of an adequate control of this parameter, the cathodic deposition of metallic powders of variable granulometric distribution suitable for the direct processing by the metallurgy of powder. Due to the above discussed features and taking into account that the cathodic process, which plays a determining role in the deposition of the metal, is expected to be the same during electrorefining and electrolysis, we chose to study the characteristics of electrodeposited metallic Ti as a function of electrolyte composition in a electrorefining cell. During the experiments the operating parameters (temperature and current density), were kept constant. The structural characteristics of the deposits were determined by optical methods and scanning electron microscopy.

EXPERIMENTAL

The alkali halides employed in this study were p.a. grade lithium, sodium and potassium fluorides and chlorides. Special precautions were taken in preparing and melting them. Before melting they were dried by heating for at least 48 h at 150—200°. LiCl, NaCl and KCl were melted while either argon gas saturated with CCl_4 or gaseous HCl was bubbled through the melt in order to remove traces of water and hydrolysis products; after freezing they were stored under CCl_4 and were checked for neutrality before utilization. Stoichiometric K_2TiF_6 was prepared in this laboratory by a method described elsewhere [2] and was dried over P_2O_5 in desiccator for many days.

All studied molten salt mixtures were obtained by remelting the necessary amounts of the components, directly in the electrolysis cell under vacuum by gradually rising the temperature to 400°C during 48 hours followed by rapid heating to working temperature while purified argon (oxygen and nitrogen content lower than 15—20 ppm) was allowed into the cell.

The cell assembly used in these experiments is shown in Fig. 1 and consisted of a stainless steel (V4A extra) tube closed at the bottom and the upper cathode cover assembly.

This cell could accomodate a metallic (V4A extra) crucible of 10 cm diameter, having a capacity of about 500 cm^3 of electrolyte. It contained also the titanium scrap metal placed between the crucible wall and the concentric separator made of stainless steel net whose openings were of 1—6 mm. The crucible was the anode (connected to the positive terminal of the power supply through the metallic tube), and the scrap metal the anodically dissolved material during electrorefining. It consisted of chipping scraps, powder or any other scraps cropped at desired size, washed in $HNO_3-H_2O_2-HF$ solution, water and acetone and dried in air at 60°C before use. A brass fitting provided with an O-ring for vacuum-tight closing of the lid, was attached to the top of the metallic tube. Water-cooled castings were provided at the upper part of the cell. The cathode, a stainless steel tube of 0.7 cm diameter, was introduced into the cell through special electrically insulating O-ring seal located in the center of the lid. This seal allowed the vertical displacement of cathode in conditions of adequate tightness. A Pt—Pt 10% Rh thermocuple was inserted into the cathodic tube to measure the working temperature when the cathode was immersed into the melt. The cell was also provided with side connections to vacuum and argon supply. It was checked for leaks prior to its use, and its ability to hold vacuum for extended periods of time was tested. The experimental procedure involved loading the crucible with the appropiate amounts of salts and scrap metal and then lowering it into the electrolysis cell which was covered and evacuated. With the cathode kept in the cold part of the cell, the salts were melted as described above. Then the cathode was lowered to the desired depth and electrolysis was started. All experiments were conducted in galvanostatic conditions at a c.d. of $0.5\ A \cdot cm^{-2}$. The temperature was kept constant at 750 ± 5°C.

At the end of the experiment, the cathode was lifted over the melt level and left there to drain the entrapped melt. Then, it was withdrawn to the cold part of the cell and the assembly was cooled down to room temperature.

A vertical kanthal furnace was used; by zone heating a temperature gradient of less than 5°C was ensured along a 20 cm height where the crucible was placed.

The cathodic deposits were recovered in water, washed in $HNO_3-H_2O_2-HF$ solution and acetone, air dried and stored in stoppered tubes. Samples of titanium powder were analyzed for chemical purity and their structural characteristics were determined by optical methods and scanning electron microscopy.

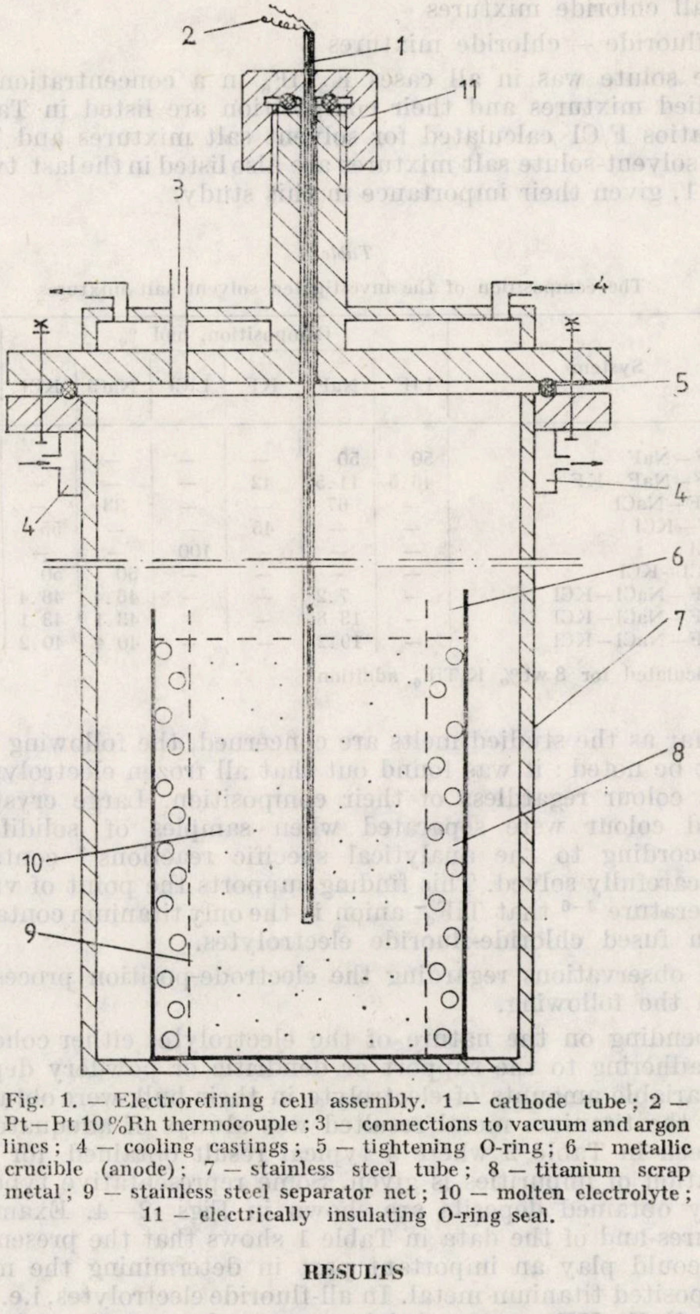

Fig. 1. — Electrorefining cell assembly. 1 — cathode tube ; 2 — Pt—Pt 10%Rh thermocouple ; 3 — connections to vacuum and argon lines ; 4 — cooling castings ; 5 — tightening O-ring ; 6 — metallic crucible (anode) ; 7 — stainless steel tube ; 8 — titanium scrap metal ; 9 — stainless steel separator net ; 10 — molten electrolyte ; 11 — electrically insulating O-ring seal.

RESULTS

To establish the influence of electrolyte composition upon the characteristics of cathodic deposit various types of solvent salt mixtures containing common or different cations were tested :

— all fluoride mixtures

— all chloride mixtures

— fluoride — chloride mixtures

The solute was in all cases K_2TiF_6 in a concentration of 8wt%. The studied mixtures and their composition are listed in Table 1. The atomic ratios F/Cl calculated for solvent salt mixtures and Ti/F calculated for solvent-solute salt mixtures are also listed in the last two columns of Table 1, given their importance in this study.

Table 1

The composition of the investigated solvent salt mixtures

No.	System	Composition, mol %						atomic ratio	
		LiF	NaF	KF	LiCl	NaCl	KCl	F/Cl	Ti/F*
1	LiF—NaF	50	50	—	—	—	—	∞	0.039
2	LiF—NaF—KF	46.5	11.5	42	—	—	—	∞	0.040
3	NaF—NaCl	—	67	—	—	33	—	1.087	0.041
4	KF—KCl	—	—	45	—	—	55	0.438	0.060
5	LiCl	—	—	—	100	—	—	0	0.420
6	NaCl—KCl	—	—	—	—	50	50	0	0.420
7	NaF—NaCl—KCl	—	7.2	—	—	46.4	46.4	0.04	0.284
8	NaF—NaCl—KCl	—	13.8	—	—	43.1	43.1	0.085	0.215
9	NaF—NaCl—KCl	—	19.2	—	—	40.4	40.2	0.126	0.172

*Calculated for 8 wt% K_2TiF_6 addition

As far as the studied melts are concerned, the following interesting fact must be noted : it was found out that all frozen electrolytes were of pink-lilac colour regardless of their composition. Large crystals of the mentioned colour were separated when samples of solidified melts, which according to the analytical specific reactions [3] contained Ti^{3+} ion were carefully solved. This finding supports the point of view advanced in literature [4-6] that TiF_6^{3-} anion is the only titanium containing ionic species in fused chloride-fluoride electrolytes.

The observations regarding the electrode-position process are discussed in the following.

Depending on the nature of the electrolyte, either coherent dense deposits adhering to the support or dendritic or powdery deposits that include variable amounts of electrolyte in their bulk were obtained. After recovery, the titanium metal resulted was always of adequate purity as can be seen in Table 2 where a typical result obtained for maximum concentration of impurities is given. Some representative types of experimentally obtained deposits are shown in Figs 2—4. Examination of these figures and of the data in Table 1 shows that the presence of fluorine ion could play an important part in determining the morphology of the deposited titanium metal. In all-fluoride electrolytes, i.e. LiF—NaF and LiF—NaF—KF systems, bright compact layers adherent to cathode surface were obtained. Unlike the first electrolyte, in the second, containing KF, metallic K condensed on the cold zones of the electrolysis cell. The phenomenon was mentioned also by other authors [7,8] and was assign-

Table 2

Maximum content of impurities in deposited metallic titanium

Element	Conc. 10^{-3} %	Element	Conc. 10^{-3} %
O_2	82	Mg	⩽1
N_2	5.6	Mn	⩽1
Fe	1	Cu	⩽1
Cr	2	Pb	⩽1
Sn	⩽1	Ni	1−3
Si	1−3	B	⩽1
Al	1−5	P	⩽1
Na	⩽1	K	⩽1

ed to the exchange reaction :

$$Ti + nKF = TiF_n + nK$$

with the value of n close to 4. This is evidently confirmed in the electrorefining process. Thus, in the presently employed cell assembly the applied voltage was of 0.1 V, while the decomposition voltage of any alkali halide, as it is well known, exceeds 3 V.

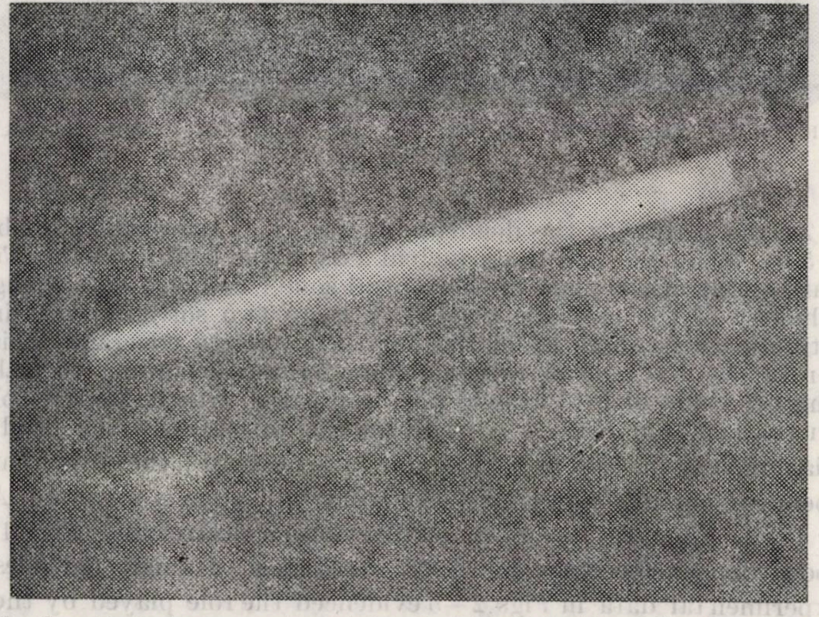

Fig. 2. — Typical compact adherent deposit of Ti obtained in all fluoride solvent melts (1).

Unlike all-fluoride electrolytes, in chloride-fluoride ones the deposits resulted were bulky (Fig. 3), with variable amounts of electrolyte entrapped. Examination of metallic deposits obtained in NaCl−NaF and KCl—KF electrolytes by optical and scanning electron microscopy has revealed that plates were formed in both cases whose discontinuous structure was generated by interpenetration of thready crystals in an ordered lattice (Fig. 5 a).

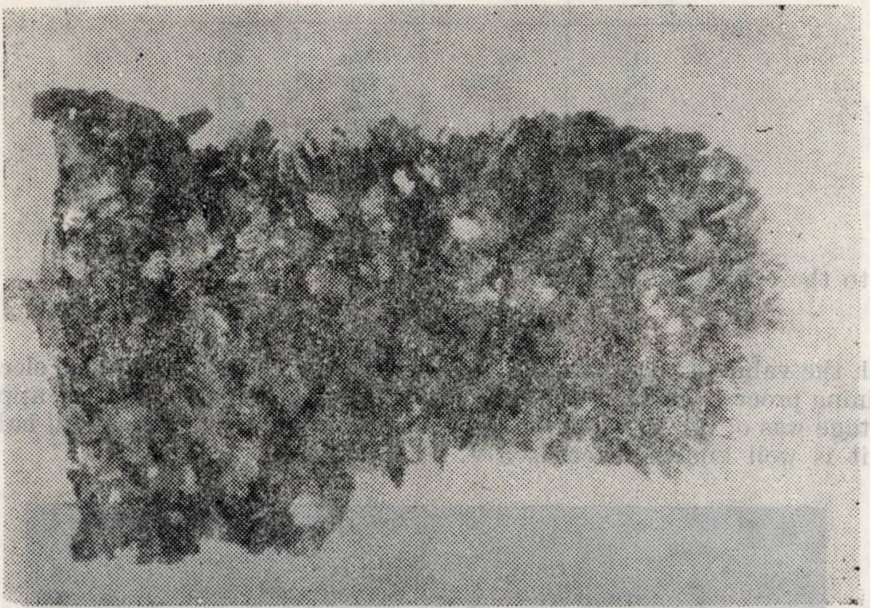

Fig. 3. — Typical dendritic deposit of Ti obtained in fluoride — chloride solvent melts ($\times 0.6$).

At the periphery the dendritic character of the deposit is obvious (Fig. 5 b), the angle with the principal axis of the dendrite being 55—60° similar to that of the plate in the central zone (see Fig. 5 a). Although the morphology of the cathodic deposit in these two solvents was similar, a distinction was observed in the degree of surface coverage. This was higher in the NaCl—NaF solvent characterised, according to Table 1, by a higher value of F/Cl atomic ratio compared with KCl—KF solvent. Given the fact that $F/Cl = \infty$ in all-fluoride mixtures, which yield compact layers, it seems that as F/Cl atomic ratio decreases, the growth through independent crystals formed by electrocrystallisation is favoured. At the other limit, when $F/Cl = 0$, as in all chloride electrolytes (Fig. 4), the cathodic deposit becomes powdery, consisting of small particles. All he experimental data in Figs 2—5 evidenced the role played by the concentration of F^- ion in determining the morphology of the cathodic deposit. In order to define more accurately the influence of F/Cl atomic ratio on the mechanism of generation and growth of crystals a series of experiments with NaCl—KCl electrolyte was carried out in which variable amounts of NaF were added (solvents 7—9 in Table 1).

Examination of Figs 6–8 shows indeed that the morphology of titanium deposit changes as the NaF content and implicitely the F/Cl atomic ratio increase. At the first 5% NaF addition (F/Cl = 0.04) the

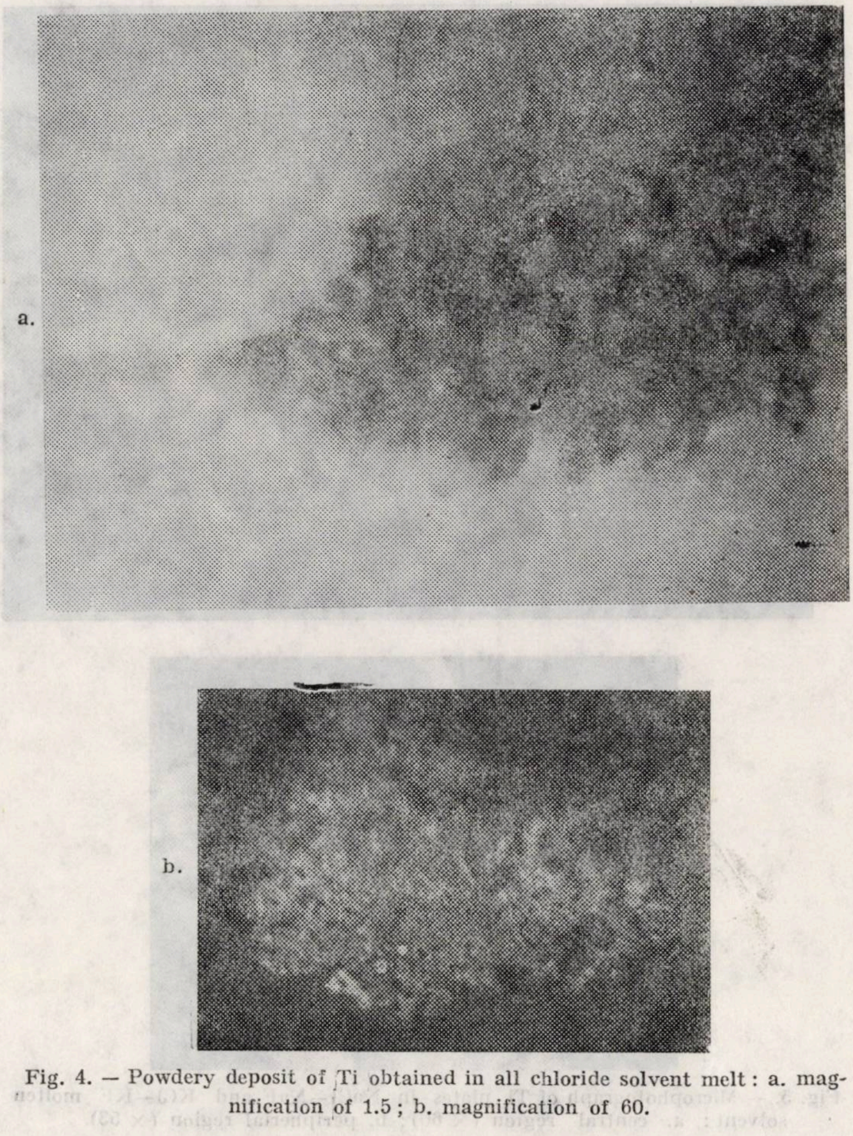

Fig. 4. — Powdery deposit of Ti obtained in all chloride solvent melt: a. magnification of 1.5; b. magnification of 60.

titanium crystal begins to structure with intersecting edges (Fig. 6) but a bright uniform surface on which no well crystallized zones, with basic hexagonal structure characteristic to the unit cell of titanium crystal, may be distinguished.

At 10% NaF addition ($F/Cl = 0.085$) the crystal becomes dendritic with obvious principal direction of growth and secondary direction of triggering of the growth of new dendritic structures (Fig. 7 a).

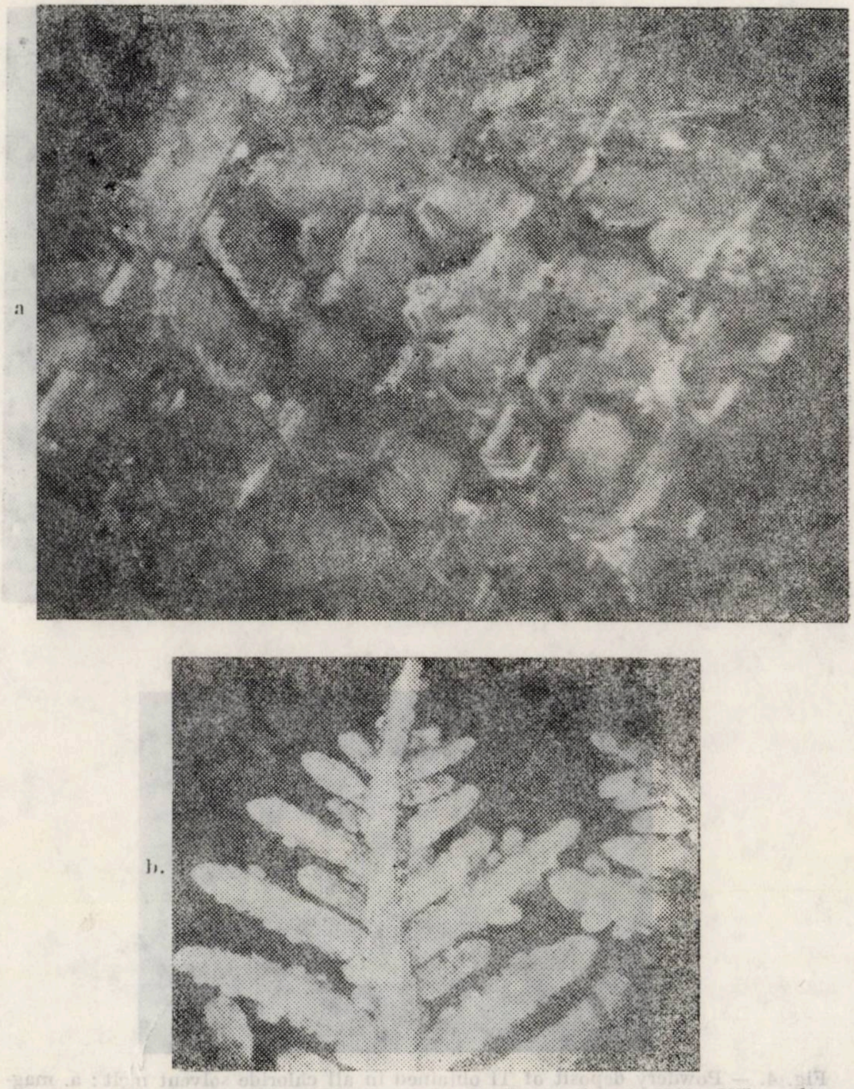

Fig. 5. -- Microphotograph of Ti plates in NaCl—NaF and KCl—KF molten solvent: a. central region (× 60); b. peripherial region (× 53).

At higher magnification (Fig. 7b) one can note the mechanism of layer growth of basic hexagonal structures.

Further increase of NaF content to 15% ($F/Cl = 0.126$) alters again the morphology of titanium deposit which shows a non-uniform

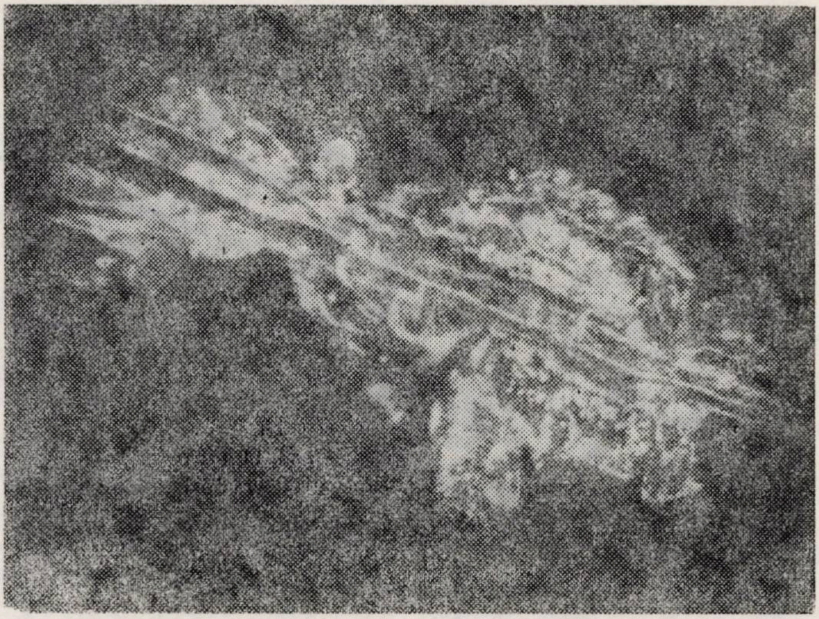

Fig. 6. — Typical Ti crystal obtained in NaCl$-$KCl + 5 % NaF solvent (× 70).

structure formed by the growth of primary pyramidal structures. Because the rate of growth is probably large the apex of the pyramid disappears. Due also to the fact that the rate of growth of the initial pyramids is different, the crystal surface is finally non-uniform-zig-zag shaped (Fig. 8). The growth scheme of such a crystal is shown in Fig. 9.

We consider that this series of experiments evidences beyond doubt the influence of F/Cl atomic ratio upon the coherence of the cathodic deposit; the coherence increases as F/Cl increases.

From among these experiments the $LiCl-K_2TiF_6$ electrolyte exhibited an unusual behaviour. With LiCl as solvent the atomic ratio F/Cl$=$0 as in the case of NaCl$-$KCl solvent discussed above. However the morphologic aspect of the cathodic deposit is completely different; it is characterised by needle-like crystals of size ranging within 0.3$-$1.5 cm and almost constant thickness of 0.1 cm. As seen in Fig. 10 their cross-section is either rectangular or V-shaped with an angle of intersection of the planes of $\sim 110°$. It is also obvious from Fig. 10 that the crystal grows by completion of successive layers and the face that grows at higher rate disappears.

It is very likely that this special behaviour observed in $LiCl-K_2TiF_6$ electrolyte may be correlated with some specific steric effect exorted by Li^+ ion which may influence the orientation of preferential growth direction. In fact it was found out[9] that in fused alkali nitrates Li^+ ion hinders effectively the rotation of NO^-_3 anion.

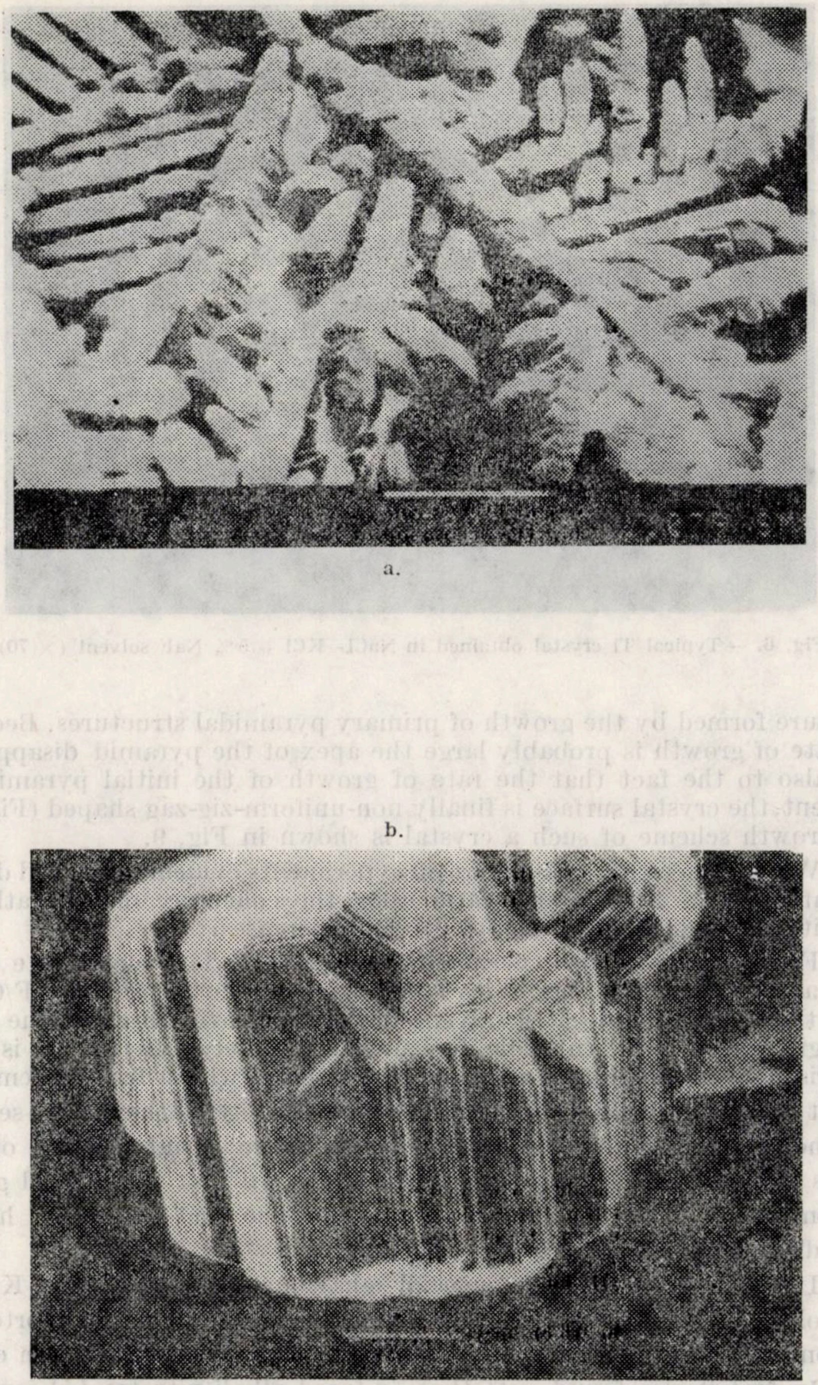

Fig. 7. — Microphotograph of Ti crystal in NaCl—KCl + 10 %NaF solvent ;
a. magnification of 24 ; b. magnification of 229.

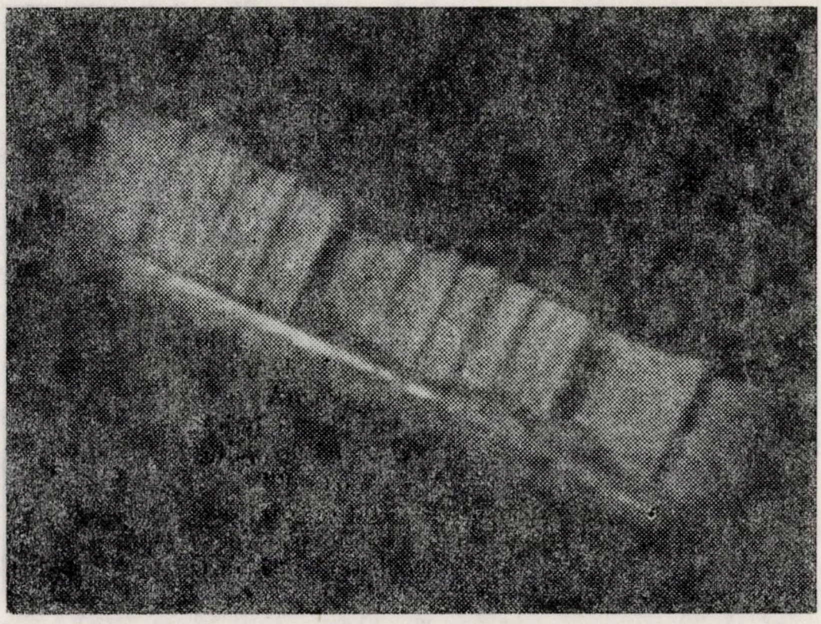

Fig. 8. — Microphotograph of Ti crystal in NaCl—KCl + 15 %NaF solvent (×40).

Fig. 9. — Growth mechanism of Ti crystal in NaCl—KCl + 15 %NaF solvent.

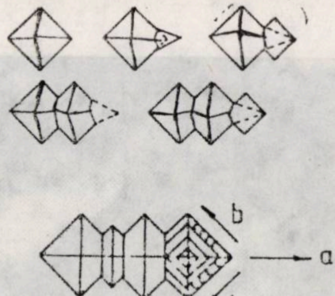

DISCUSSION

The specific effect of F⁻ ion and implicitly of F/Cl atomic ratio upon the morphology of titanium cathodic deposit may be understood, at least qualitatively, if one admits the influence they may exert upon the stability of electroactive species in the electrolyte. One may postulate that if the thermodynamic stability of the hexacoordinated anionic complex of titanium is not sufficiently high then the dissociation constant is large enough and the concentration of metallic cations available in the electrolyte is sufficient to favour deposition by electroreduction of dendrites and powders. On the contrary coherent deposition from molten

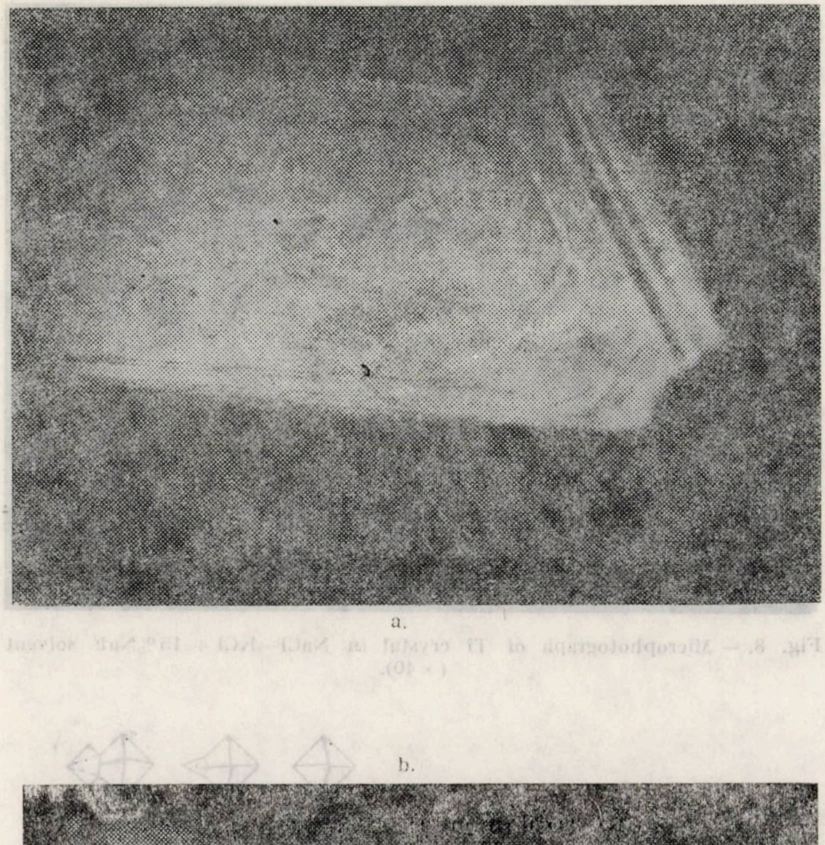

Fig. 10. — Different types of Ti crystals obtained in LiCl—K_2TiF_6 solvent ; a. rectangular crystal (× 70) ; b. V-shaped crystal (× 70).

salts implies a much higher thermodynamic stability of the complex anion in order that the electrocrystallisation centres be relatively reduced.

Potassium hexafluorotitanate is a stable compound. However its thermodynamic stability may be influenced by the anions of the solvent. There is no doubt that the hexafluorinated anion is much more stable than the hexachlorinated one. Consequently, the presence of alkali fluorides may be regarded as an additional stabilising element. On the contrary the alkali chlorides may increase the activity of titanium ions in the electrolyte, perhaps because of an exchange reaction of the type[10,11] :

$$2K_2TiF_6 + Ti + 2xKCl = 2K_{x+1}TiF_4Cl_2 + K_2TiF_4$$

which favours powdery deposits as noted in all-chloride electrolyte NaCl—KCl (see Fig. 5). By adding NaF in this electrolyte the Ti—Cl bond is replaced with a much stronger one Ti—F and thus the activity of Ti ions in the electrolyte is lowered which alters the process of electroreduction of the electroactive species, as emphasized by Figs 6—8. According to Table 1 the modification of F/Cl atomic ratio is naturally accompanied by a corresponding modification of Ti/F atomic ratio : the increase of the former entails the decrease of the latter accompanied by the consequent decrease of the electrochemical activity of titanium ion in the electrolyte. Obviously the transition from amorphous deposits through dendritic ones to coherent continuous and adherent deposits is promoted by the increase of F/Cl atomic ratio or/and decrease of Ti/F atomic ratio.

Thus, keeping constant the operating parameters of electrorefining (temperature, current density and voltage) one may vary the character of titanium deposition (compact layer, dendritic or powdery) by modifying the composition of the electrolyte and so altering the F/Cl or/and Ti/F atomic ratio.

REFERENCES

[1] *Molten Salts Bulletin*, M. Gaune-Escard ed., **41**, 24 (1990).

[2] "Handbook of Preparative Inorganic Chemistry", G. Brauer ed. vol. 2., 2nd edition., Academic Press, New York, 1965, p. 1163.

[3] J. G. Wurm, L. Gravel and R. J. A. Potvin, *J. Electrochem. Soc.*, **104**, 301 (1957).

[4] D. Inman and S. H. White, *J. Appl. Electrochem.*, **11**, 291 (1981).

[5] M. V. Smirnov and N. A. Loginov, "Electrochemistry of Molten and Solid Electrolytes", vol. 1, 2nd edition., Academic Press, 1964, p. 22.

[6] F. H. N. Bright, *Can. J. Chem.*, **36**, 615 (1957).

[7] G. W. Mellors and S. Senderoff, *J. Electrochem.*, **112**, 266 (1965).

[8] G. W. Mellors, Proc. Inst. Austral. Conf. on Electrochem., N. Friend and E. Gutman ed., Pergamon Press, New York, 1964, p. 521.

[9] B. J. Fortin and J. G. Wurm, *J. Electrochem. Soc.*, **106**, 428 (1959).

[10] Chen Guang-Sen, Masuzumi Okido and Takeo Oki., *J. Appl. Electrochem.*, **17**, 849 (1987).

[11] L. P. Polyakova and P. T. Stangrit, *Electrochimica Acta*, **31**, 159 (1986).

salts implies a much higher thermodynamic stability of the complex anion in order that the electrocrystallisation centres be relatively reduced.

Potassium hexafluoropotitanate is a stable compound. However its thermodynamic stability may be influenced by the anions of the solvent. There is no doubt that the hexafluorinated anion is much more stable than the hexachlorinated one. Consequently, the presence of alkali fluorides may be regarded as an additional stabilising element. On the contrary the alkali chlorides may increase the activity of titanium ions in the electrolyte, perhaps because of an exchange reaction of the type[10,11]:

$$2K_2TiF_6 + Ti + 2xKCl = 2K_{x+1}TiF_4Cl_x + K_2TiF_4$$

which favours powdery deposits as noted in all-chloride electrolyte NaCl–KCl (see Fig. 5). By adding NaF in this electrolyte the Ti–Cl bond is replaced with a much stronger one Ti–F and thus the activity of Ti ions in the electrolyte is lowered which alters the process of electroreduction of the electroactive species, as emphasized by Figs 6–8. According to Table I the modification of F/Cl atomic ratio is naturally accompanied by a corresponding modification of Ti/F atomic ratio: the increase of the former entails the decrease of the latter accompanied by the consequent decrease of the electrochemical activity of titanium ion in the electrolyte. Obviously the transition from amorphous deposits through dendritic ones to coherent continuous and adherent deposits is promoted by the increase of F/Cl atomic ratio or and decrease of Ti/F atomic ratio.

Thus, keeping constant the operating parameters of electrorefining (temperature, current density and voltage) one may vary the character of titanium deposition (compact layer, dendritic or powdery) by modifying the composition of the electrolyte and so altering the F/Cl or and Ti/F atomic ratio.

REFERENCES

[1] *Molten Salts Bulletin*, M. Grune Record ed. 4, 21 (1980).
[2] "Handbook of Preparative Inorganic Chemistry", G. Brauer ed. vol. 2., 2nd edition, Academic Press, New York, 1965, p. 1168.
[3] J. G. Wurm, L. Gravel and R. J. A. Potvin, *J. Electrochem. Soc.*, 104, 301 (1957).
[4] D. Inman and S. H. White, *J. Appl. Electrochem.*, 11, 201 (1981).
[5] M. V. Smirnov and N. A. Loginov, "Electrochemistry of Molten and Solid Electrolytes", vol. 1, 2nd edition, Academic Press, 1961, p. 22.
[6] E. H. N. Bright, *Can. J. Chem.*, 36, 615 (1957).
[7] G. W. Mellors and S. Senderoff, *J. Electrochem.*, 112, 266 (1965).
[8] G. W. Mellors, Proc. Inst. Austral. Conf. on Electrochem., N. Friend and F. Gutman ed., Pergamon Press, New York, 1964, p. 321.
[9] B. L. Toffin and J. G. Wurm, *J. Electrochem. Soc.*, 106, 428 (1959).
[10] Chen-Guang-Sen, Masazumi Okido and Takeo Oki, *J. Appl. Electrochem.*, 17, 849 (1987).
[11] L. P. Polyakova and P. T. Stangrit, *Electrochimica Acta*, 31, 159 (1986).

Revue Roumaine de Chimie, **36**, *11–12*, 1253–1258 (1991)

HYDROGEN BONDING OF *o*-NITROANILINE IN WATER-DMSO MIXTURES

ESAM A. GOMAA*

Chemistry Department, Faculty of Science, Mansoura University, Mansoura, Egypt

Received June 25, 1988

From the solubility of *o*-nitroaniline and *p*-nitroaniline at 25°C in $H_2O-DMSO$ mixtures, the values of H-bonding of *o*-nitroaniline have been estimated. Also, the solute-solute interaction and the single ion thermodynamics for both *ortho*- and *para*-nitroanilinium ions have been discussed.

INTRODUCTION

Valuable information [1–4] on the nature of solute-solvent interaction in mixed systems can be obtained from a study of the dissociation equilibria. The effect of solvent on pK's of nitroanilines in various amphiprotic-water mixtures [2–4] and in protic-dipolar aprotic solvent mixtures [5–7] has been reported. This paper reports the result of hydrogen bonding of *o*-nitroaniline on the variation of pK's of *o*-nitroaniline and *p*-nitroaniline in water-DMSO mixtures at 25°C over a complete range of solvent compositions.

EXPERIMENTAL

o-Nitroaniline (2-nitroaniline) and *p*-nitroaniline (4-nitroaniline), analytical grade from Merck Co. were used. The saturated solutions of *o*-nitroaniline and *p*-nitroaniline in the aqueous dimethyl sulphoxide mixtures were prepared by dissolving them in the mixed solvents and passing N_2 gas in closed test tubes. The tubes were shaken in a water thermostat for three days, then left for another one day without shaking to reach the necessary equilibrium. The solubilities of *o*- and *p*-nitroanilines were determined gravimetrically by taking 1 mL of the saturated solution on a small aluminium disk and evaporated using infrared lamp.

RESULTS AND DISCUSSION

The solubilities of *o*-and *p*-nitroanilines in mixed $H_2O/DMSO$ solvents in molal scale are determined experimentally and tabulated in Table 1. The solubility was estimated in seven mole fractions of dimethylsulphoxide (X_s) ranging from 0–1 as listed in Table 1. The solute-solute interaction of both organic anilines was calculated using Debye-Hückel equation.[8] The activity coefficients which expressed the solute-solute interaction were calculated using the following equation:

---

* All communications should be sent to : Teachers Training College, Salalah-P.O. 19905, Sultanate of OMAN

$$\log \gamma_{\pm} = -\frac{A(Z_1 Z_2)\sqrt{C}}{1 + Ba\sqrt{C}}$$

where $A = 1.8246 \times 10^6/(T \cdot \varepsilon)^{3/2}$, $B = 50 \cdot 29 \times 10^8/(T \cdot \varepsilon)^{1/2}$, Z_1Z_2 are the charges of both ions, C the molal solubility and a is the solvated radius. The solvated radius was calculated as the closest approach which equals the Van der Waals radius of the solute plus the scaled particle theory radius of the mixed solvent under consideration.[9] The intermolecular Van der Waals radii of both *o*- and *p*-nitroanilines was calculated by applying the Bondi[10] model and found to be 3.811 Å for both anilines. It is clear from Table 1 that the solute–solute interaction (activity coefficient) between the *o*-nitroaniline ions was greater than that between *p*-nitroaniline ions. The solubility products pK of both nitroanilines were calculated by using equation 1.

$$\mathrm{pK} = -\log C^2 + 2 \log \gamma_{\pm} \tag{1}$$

where C is the molal solubility. The solubility products of both *o*- and *p*-nitroaniline are shown in Table 1, showing greater solubility product values of nitroaniline than *p*-nitroaniline. The free energies were calculated using the relation $\Delta G^\circ = -2.303\ RT \log C$. The transfer free energies of *o*-nitroaniline (ONA) and *p*-nitroaniline (PNA) from water (w) to the mixed solvent (s) were calculated using equations 2 and 3 or 4 and 5.

$$\Delta G_t^\circ(\mathrm{ONA}) = 2.303\ RT \log \frac{C_{\mathrm{ONA(w)}}}{C_{\mathrm{ONA(s)}}} \tag{2}$$

$$\Delta G_t^\circ(\mathrm{PNA}) = 2.303\ RT \log \frac{C_{\mathrm{PNA(w)}}}{C_{\mathrm{PNA(s)}}} \tag{3}$$

or

$$\Delta G_t^\circ(\mathrm{ONA}) = 2.303\ RT \cdot \Delta\mathrm{pK(ONA)} \tag{4}$$

$$\Delta G_t^\circ(\mathrm{PNA}) = 2.303\ RT\ \Delta\mathrm{PK\ (PNA)} \tag{5}$$

where C is the molal solubility and ΔpK is the difference in solubility products of the solute between the mixed solvent under consideration and the reference solvent (water). The free energies and the free energies of transfer data of *o*- and *p*-nitroanilines are explained in Table 2. The free energies of both salts decrease with the addition of DMSO, whereas the free energies of transfer increase. The increase of the latter (free energy of transfer) is an indication of the increasing of the solute-solvent interaction; *o*-and *p*-nitroanilines may be solvated through the positively charged amino group by the more negative oxygen atoms of DMSO, while the small solvation in water proceeds through the negatively charged

Table 1

Molal solubilities, activity coefficients and pK's of *o*-nitroaniline and *p*-nitroaniline in mixed DMSO/H_2O mixtures at 25°C

Vol. % of DMSO	X_s DMSO	a in A°	*o*-nitroaniline			*p*-nitroaniline		
			Solubility	$\log \gamma_\pm$	pK	Solubility	$\log \gamma_\pm$	pK
0	0	6.541	4.864×10^{-5}	-3.51×10^{-3}	8.633	6.414×10^{-3}	-3.483×10^{-3}	4.393
50	0.237	7.191	0.1499	−0.111	1.870	0.1049	−0.101	2.159
60	0.327	7.391	0.3949	−0.143	1.094	0.3749	−0.114	1.080
70	0.433	7.631	0.9042	−0.171	0.429	0.5758	−0.162	0.804
80	0.504	7.771	1.4299	−0.197	0.084	0.7883	−0.176	0.559
90	0.696	8.131	2.5583	−0.220	−0.375	1.917	−0.215	0.159
100	1.0	8.481	3.6575	−0.218	−0.689	2.9223	−0.215	−0.502

Solubilities are in molal scale (g. mole/1000 g solvent)

Table 2

Free energies of hydrogen bonding of *o*-nitroaniline in mixed DMSO/H_2O solvents at 25°C (kcal/mole)

X_s DMSO	ΔG° (ONA)	ΔG_t° (ONA)	ΔG° (PNA)	ΔG_t° (PNA)	$\Delta\Delta G^\circ$ (ONA)	$\Delta\Delta G^\circ_{\text{H-bonding}} = \Delta\Delta G_t^\circ$ (ONA)
0	11.775	0	5.992	0	5.784	0
0.237	2.551	−9.225	2.946	−3.046	−0.396	−6.179
0.327	1.493	−10.283	1.474	−4.518	0.0191	−5.765
0.433	0.586	−11.189	1.096	−4.895	−0.424	−6.295
0.504	0.114	−11.661	0.762	−5.229	−0.649	−6.431
0.696	−0.512	−12.287	0.217	−5.775	−0.729	−6.413
1	−0.941	−12.716	−0.684	−6.676	−0.256	−6.040

All ΔG values are in kcal/mole.

oxygen atoms ($-NO_2$). Therefore, the affinity of *o*- and *p*-nitroanilines for H_2O-DMSO mixtures seems to be greater than that for water. In addition to the dipole-dipole interactions mentioned above, the increase of solubility for *o*- and *p*-nitroanilines may also be caused by dispersion effects. The $\Delta\Delta\overset{\circ}{G}$(ONA) was calculated by using equation 6 and the values are reported in Table 2.

$$\Delta\Delta G^\circ(\text{ONA}) = \Delta G^\circ(\text{ONA}) - \Delta G^\circ(\text{PNA}) \tag{6}$$

p-Nitroaniline has no hydrogen bonding (intermolecular hydrogen bonding) and the hydrogen bond formation of *o*-nitroaniline can be estimated by substracting its free energy of solute-solvent interaction from the free energy of the same compound having the same structure, the same volume and the same radius without forming intermolecular hydrogen bonding. *p*-Nitroaniline fullfils the character of the neutral compound that did not form hydrogen bonds. Therefore, the hydrogen bonding of *o*-nitroaniline can be calculated using equation 7.

$$\Delta\Delta G^\circ_{\text{H-bonding}} = \Delta\Delta G_t^\circ(\text{ONA}) = \Delta G_t^\circ(\text{ONA}) - \Delta G_t^\circ(\text{PNA}) \tag{7}$$

The calculated values of hydrogen bonding for *o*-nitroaniline are shown in both Table 2 and Fig. 1, with nearly a constant value in $H_2O-DMSO$ mixtures. The mean value of this hydrogen bonding is −6.187 kcal/mole (−25.87 KJ/mole), which lies in the order of bond energy of H-bonding.[11]

The values of ΔG°_t (hydrogen ion) are taken from ref. [9] and used for further calculation (Table 3). The free energies of transfer for *o*- and *p*-nitroanilinium ions in mixed H_2O/DMSO solvents at 25°C are calculated using equations 8 and 9. The ΔG_t° values are listed in Table 3.

$$\Delta G_t^\circ(\text{ONA}^-) = \Delta G_t^\circ(\text{ONA}) - \Delta G_t^\circ(\text{H}^+) \tag{8}$$

$$\Delta G_t^\circ(\text{PNA}^-) = \Delta G_t^\circ(\text{PNA}) - \Delta G_t^\circ(\text{H}^+) \tag{9}$$

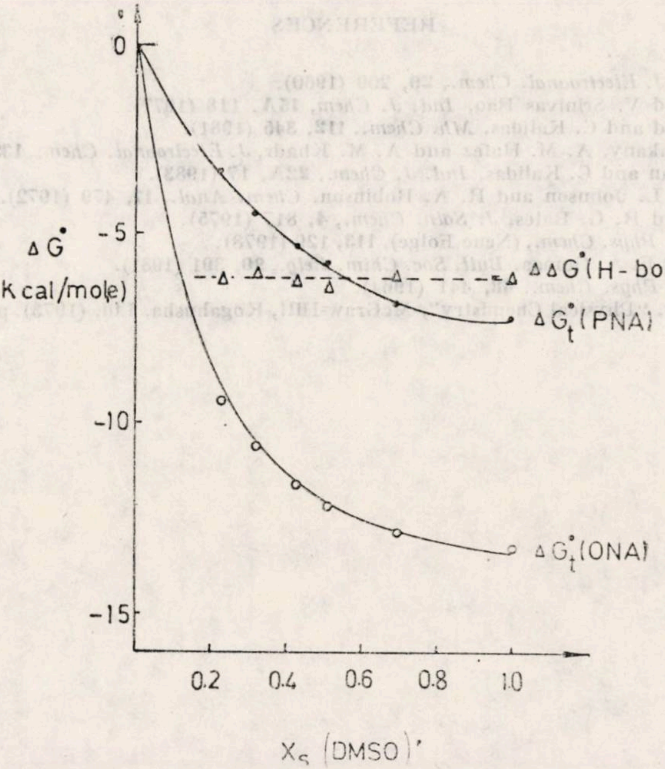

Fig. 1. — Free energies of transfer of *o*- and *p*-nitroaniline and $\Delta\Delta G$ (H-bonding) of *o*-nitroaniline in mixed DMSO/H_2O solvents.

Also, the ΔG_t° values for the ions (Table 3) indicate the increase of both the free energies of transfer of *o*- and *p*-nitroanilinium ions on adding more DMSO due to the increase in the solute-solvent interaction as mentioned before.

Table 3

Free energies of transfer for *o*- and *p*-nitroanilinium ions in mixed DMSO/H_2O solvents at 25°C (kcal/mole)

X_s DMSO	ΔG_t° H^+	ΔG_t° ONĀ	ΔG_t° PNĀ
0	0	0	0
0.237	−2.751	−6.474	−0.294
0.327	−4.210	−6.073	−0.308
0.433	−5.024	−6.166	+0.129
0.504	−5.119	−6.542	−0.111
0.696	−4.952	−7.335	−0.823
1.0	−4.325	−8.391	−2.351

REFERENCES

[1] R. G. Bates, *J. Electroanal. Chem.*, **29**, 209 (1960).
[2] C. Kalidas and V. Srinivas Rao, *Ind. J. Chem*, **15A**, 118 (1977).
[3] P. Siva Prasad and C. Kalidas, *Mh. Chem.*, **112**, 345 (1981).
[4] A. A. El-Harakany, A. M. Hafez and A. M. Khadr, *J. Electroanal. Chem.*, **132**, 345 (1982).
[5] S. Janardhanan and C. Kalidas, *Ind. J. Chem.*, **22A**, 17 (1983).
[6] R. G. Bates, L. Johnson and R. A. Robinson, *Chem. Anal.*, **17**, 479 (1972).
[7] Z. Pawlak and R. G. Bates, *J. Soln. Chem.*, **4**, 817 (1975).
[8] J. I. Kim ; *Z. Phys. Chem.*, (Neue Folge), **113**, 129 (1978).
[9] J. I. Kim and E. A. Gomaa, *Bull. Soc. Chim. Belg.*, **90**, 391 (1981).
[10] A. Bondi, *J. Phys. Chem.*, **68**, 441 (1964).
[11] G. M. Barrow, "Physical Chemistry", McGraw-Hill, Kogahusha, Ltd, (1973) pp. 493 518.

Revue Roumaine de Chimie, 36, *11–12*, 1259–1262 (1991)

STUDY OF MOLECULAR INTERACTION BETWEEN ACETONITRILE AND BENZENE

R. R. YADAVA [a] and S. S. YADAVA [b]

[a] Chemistry Department, Gorakhpur University, Gorakhpur-273 009, India

[b] Chemistry Department, Garhwal University Campus, Pauri (Garhwal)—246001, India

Received September 5, 1988

The dielectric constants (ε) and refractive indices (*n*) of binary mixtures of polar solute, acetonitrile in an inert solvent, cyclohexane and non-polar aromatic solvent, benzene, have been measured at 307.4 K. The values of dipole moments of acetonitrile in cyclohexane (μ_{inert}) and in benzene (μ_{sol}) have been calculated by Guggenheim's method. It is concluded that the dipole-induced dipole interaction operates between acetonitrile and benzene.

INTRODUCTION

Many studies [1] have been made on molecular interactions governed by the reaction

$$A + B \rightleftharpoons A\ldots B \qquad (1)$$

in solution. The product A...B in the reversible equilibrium with the component molecules A and B has attracted much attention [2,3] due to the unusual behaviour of liquid mixture caused by its presence in such mixture.

The existence of the complexes in solution can be confirmed[4] by large heats of mixing. The knowledge of heats of mixing together with the optical studies gives a better understanding of the interactions. In most of the molecular interaction studies, the purpose of investigation has been to find information about nature and strength of the interaction and position of the equilibrium. A number of works[5,6] have used spectroscopic methods for gaining information about either one or more of the above points. Schneider,[7] on the basis of an NMR study, has proposed that the interaction between polar molecule and a non-polar reactive molecule is dipole-induced dipole in nature.

However, it is shown [8] that the dielectric studies can also be used as a potential means to obtain significant information regarding the molecular interactions. Earp and Glasstone[9] have studied the interactions between two substances A and B which yield a molecular complex of 1 : 1 stoichiometry by dielectric polarisation calculations. Hamick [10] and Few and Smith [11] have also used the polarisation study to determine the position of the equilibrium. Yadava et al.,[12] by measuring dielectric constants of polar aliphatic molecules in various symmetrical aromatic hydrocarbons, have established the nature of the molecular interaction.

The present study suggests the determination of the induced dipole moment, μ_{ind} from the difference of the dipole moment of polar solute in an interacting solvent, μ_{sol} and that in an inert solvent, μ_{inert}. The value of the μ_{ind} gives information regarding the nature of the interaction.

EXPERIMENTAL

The binary systems studied were acetonitrile + cyclohexane and acetonitrile + benzene. Polar solute acetonitrile (Sisco Chem.) was used after purification followed by distillation over one meter long fractionating column. The inert solvent cyclohexane and the reactive aromatic solvent benzene were of spectroscopic grade.

A series of solutions of polar solute acetonitrile in cyclohexane and benzene were prepared in sealed vials keeping the weight fractions of the acetonitrile in solution within the range of 0.00 to 0.03. The liquids were inserted by means of a syringe. The dielectric constant of each solution was measured with an accuracy of ±0.0001 by Dekameter (Type Dk 03, W T W, Germany) using M F L – 1/s (No. 2078) type of cell at a frequency of 1.8 MHz/s. The temperature of the solution kept in the cell was maintained constant by circulating water around the cell from a water thermostat regulated at 307.4 ± 0.1 K. The refractive indices of each solution were measured at 307.4 K by circulating water around the prism boxes employing an Abbe refractometer with an accuracy of ± 0.0002 using white light.

Various methods[13] have been suggested for the calculation of the dipole moment of polar molecule in solution. However, one way or the other each of them involves the evaluation of orientation polarisation, P_0, which is related with the dipole moment of the molecule. The orientation polarisation is obtained by deducing distortion polarisation, P_D, from the solute polarisation at infinite dilution, P_∞, in solution where solute is supposed to behave in solution like a gas. P_∞ can be obtained either graphically by extrapolating the curve between solute polarisation and the mole fraction of the solute at infinite dilution or mathematically by an equation suggested by Halverstadt and Kumler.[14] The above procedures depend on the accurate measurement of the solution densities which is found to be difficult normally. The Guggenheim[15] procedure, which requires the density of pure solvent with an accuracy of 0.1 % in the calculation avoids the measurements of the solution densities, was used in the present work.

The procedure is based on the Debye equation and employs the relation given in equation (2) ;

$$P_0 = \frac{4}{9}\pi N \frac{\mu^2}{kT} = \frac{3\,M_2}{\rho_1(\varepsilon_1 + 2)^2} \lim_{w_2 \to 0} \left(\frac{\partial \varepsilon_{12}}{\partial w_2} - \frac{\partial n_{12}^2}{\partial w_2} \right) \tag{2}$$

where P_0, μ, M_2 and w_2 are the orientation polarisation, dipole moment, molecular weight and weight fraction of the solute. ρ_1 and ε_1 are the density and the dielectric constant of the pure solvent and ε_{12}, n_{12} are the dielectric constant and refractive index of the solution respectively. N, k and T are Avogadro's number, Boltzmann constant and the temperature of the measurement on absolute scale. $\lim\limits_{w_2 \to 0} \frac{\partial \varepsilon_{12}}{\partial w_2}$ and $\lim\limits_{w_2 \to 0} \frac{\partial n_{12}^2}{\partial w_2}$ are the limiting slope of the curve by plotting ε_{12} versus w_2 and n_{12}^2 versus w_2 when $w_2 = 0$. These curves can be expressed by equation (3) ;

$$\left.\begin{aligned} \varepsilon_{12} &= \varepsilon_1 + a w_2 + a' w_2^2 \\ n_{12}^2 &= n_1^2 + b w_2 + b' w_2^2 \end{aligned}\right\} \tag{3}$$

where n_1 is the refractive index of the pure solvent. On substitution of the limiting slopes of the curves at $w_2 = 0$ given by equation (4);

$$\left.\begin{aligned} \frac{\partial \varepsilon_{12}}{\partial w_2} &= a \\ \frac{\partial n_{12}^2}{\partial w_2} &= b \end{aligned}\right\} \tag{4}$$

into equation (2), we have

$$\mu^2 = \frac{10^{36}}{N} \cdot \frac{27\, k\, T\, M_2}{4\pi \rho_1 (\varepsilon_1 + 2)^2} (a - b) \tag{5}$$

where the term 10^{36} has been introduced in the above expression to obtain the value of dipole moment of the polar solute in Debye unit directly.

RESULTS AND DISCUSSION

The values of weight fractions of the solute, dielectric constant and square of the refractive index of each solution at 307.4 K for acetonitrile + cyclohexane and acetonitrile + benzene systems are recorded in tables 1

Table 1

Weight fractions of the solute (w_2) dielectric constants (ε_{12}) and squares of refractive indices (n_{12}^2) for acetonitrile + cyclohexane system at 307.4 K

S.N.	w_2	ε_{12}	n_{12}^2
1	0.0000	2.0003	2.0062
2	0.0034	2.0659	2.0051
3	0.0071	2.1392	2.0045
4	0.0112	2.2098	2.0039
5	0.0136	2.2577	2.0028
6	0.0168	2.3155	2.0022
7	0.0204	2.3861	2.0011
8	0.0236	2.4467	2.0005
9	0.0245	2.4594	2.0000

Table 2

Weight fractions of the solute (w_2), dielectric constants (ε_{12}) and squares of refractive indices (n_{12}^2) for acetonitrile + benzene system at 307.4 K

S.N.	w_2	ε_{12}	n_{12}^2
1	0.0000	2.2556	2.2201
2	0.0035	2.3522	2.2177
3	0.0060	2.4192	2.2165
4	0.0102	—	2.2141
5	0.0118	2.5821	2.2130
6	0.0149	2.6654	2.2112
7	0.0190	2.7789	2.2088
8	0.0208	2.8325	2.2082
9	0.0243	2.9214	2.2058
10	0.0273	3.0010	2.2040

Table 3

Values of dipole moment (μ) of acetonitrile in gas phase and in cyclohexane and benzene

	μ (in debye unit)
Gas phase*	3.90
Cyclohexane	3.12
Benzene	3.34

* A. A. Maryott and F. Buckley, "Table of Dielectric Constants and Electric Dipole Moments of Substances in the Gaseous State", N B S Circular 537, Washington D.C. (1953).

and 2 respectively. The dipole moment of the solute, acetonitrile in gas phase and that in cyclohexane and benzene obtained experimentally are listed in table 3.

A perusal of table 3 shows that the value of the dipole moment of acetonitrile in gas phase, where there is no molecular interaction and the molecules are oriented independently of one another in the externally applied field, is higher than that in cyclohexane and benzene. This is in accordance with the earlier view[16] that the dipole moment values of polar molecules in solution should be consistently different from those measured in the vapour state and varied from one solvent to another.

The solution dipole moment of acetonitrile in benzene, μ_{sol} is higher than that in an inert solvent cyclohexane, μ_{inert}. The induced dipole moment μ_{ind}, which is the difference of μ_{sol} and μ_{inert} is found to be 0.22 D. Although benzene itself is non-polar, it possesses π-electrons which enable it to be easily polarised by neighbouring solute with dipole moment μ_{inert}. If the interaction is such that the solute polarises the aromatic, this results in a dipole moment being induced in the latter. The process is then followed by electrostatic attraction between the interacting molecules. At the same time the solute experiences the resultant dipole moment of its own and that induced in the aromatic leading to an increase in the dipole moment. In general it might be considered that the more polar is the solute, the larger is the induced moment, μ_{ind}. Hence it is possible to conclude that the interactions in such systems are governed by dipole-induced dipole mechanism.

ACKNOWLEDGEMENTS. The authors are thankful to the Head, Chemistry Department, Gorakhpur University for providing necessary facilities.

REFERENCES

[1] R. Foster, "Organic Charge – Transfer Complexes", Academic Press, New York, 1969,

[2] I. D. (Jr) Kuntz and F. P. Gasparro, *J. Am. Chem. Soc.*, **90**, 4778 (1968).

[3] R. Foster, "Progress in NMR Spectroscopy", Vol. 4, Pergamon Press, Oxford, 1969.

[4] M. Tamers, S. Searles, E. M. Leighly and D. W. Mohrman, *J. Am. Chem. Soc.*, **76** 3983 (1954).

[5] M. W. Hanna and A. L. Ashbaugh, *J. Phys. Chem.*, **68**, 811 (1964).

[6] J. Homer, M. H. Everdell, C. J. Jackson and P. M. Whitney, *J. Chem. Soc. Faraday Trans. II*, **68**, 874 (1972).

[7] W. G. Schneider, *J. Phys. Chem.*, **66**, *2653* (1962).

[8] P. J. Huke, "Study on Molecular Interactions in Solution", Ph. D. Thesis, University of Aston in Birmingham, 1968.

[9] D. P. Earp and S. Glasstone, *J. Chem. Soc.*, **1935**, 1709.

[10] D. L. Hamick, A. Norris and L. E. Sutton, *J. Chem. Soc.*, **1938**, 1755.

[11] A. V. Few and J. W. Smith, *J. Chem. Soc.*, **1949**, 2781.

[12] R. R. Yadava and S. S. Yadava, *Indian J. Chem.*, **16 A**, 826. (1978).

[13] C. P. Smyth, "Dielectric Behaviour and Structure", Mc Graw – Hill Book Company, Inc., N.Y., 1955.

[14] I. F. Halverstadt and W. D. Kumler, *J. Am. Chem. Soc.*, **64**, 2988 (1942).

[15] E. A. Guggenheim, *Trans. Faraday Soc.*, **47**, 573 (1951).

[16] F. H. Müller, *Trans. Faraday Soc.*, **30**, 731 (1934).

Revue Roumaine de Chimie, **36**, *11–12*, 1263–1268 (1991)

STUDY OF RADICAL SPECIES FORMED AT POLYCRYSTALLINE Ag_2SeO_3 RADIOLYSIS

M. CONTINEANU [a] and O. CONSTANTINESCU [b]

[a] Faculty of Chemical Technology, Polytechnic Institute of Bucharest, Romania
[b] Institute of Physics and Nuclear Engineering, Bucharest, Romania

Received October 14, 1989

The paramagnetic centres formed at irradiation of polycrystalline Ag_2SeO_3 have been identified. The recombination kinetics of SeO_2^- radicals during thermal annealing have been studied. An adequate radiolysis mechanism has been established.

EPR measurements of irradiated metal selenites allow us to obtain information on the nature of paramagnetic centres and on the changes occurring in the properties of these compounds. Atkins [1] et al. have for the first time evidenced SeO_2^- and SeO_3^- radicals formation in the alkali selenites and selenates radiolysis. Cook[2] et al. have studied, using the same technique, the spectrum of SeO_2^- radicals formed during X irradiation of a $NaHSeO_3$ monocrystal. Results of γ radiolysis of Ca and Ba selenates studied by means of EPR technique were reported by Spitzyn[3].

The present note presents the results of γ radiolysis of polycrystalline Ag_2SeO_3 in order to characterize the spectral properties and the thermal behaviour of the formed radicals.

EXPERIMENTAL

It was used Ag_2SeO_3 prepared from $AgNO_3$ and H_2SeO_3 according to the literature. [4] Polycrystalline Ag_2SeO_3 samples were irradiated with Co^{60} γ rays 5.6×10^{12} Bq activity and doses of 10^4 Gy/h. Irradiations using an electron beam of 0.5 MeV produced by a Van der Graaff accelerator were also used. EPR spectra of irradiated sample were recorded using an ART 5 spectrograph operating in X-band having high-frequency modulation (100 KHz). For g-Landé factor determination, Mn^{2+} ion in $CaCO_3$ matrices was used. Reflectance spectra were recorded using a Pye-Unicam SP 1800 spectrograph provided with a reflectance device.

RESULTS AND DISCUSSION

Ag_2SeO_3 samples γ-irradiated at the room temperature are grey-coloured and present complex EPR spectra containing less intense signals. Figure 1 illustrates EPR spectrum of an Ag_2SeO_3 sample γ irradiated with $5 \cdot 10^4$ Gy compared with those of an irradiated $NaHSeO_3$ and H_2SeO_3 samples.

In order to establish the Ag_2SeO_3 radiosensitivity compared with that of other selenites, the same amounts of Ag_2SeO_3, $Na_2SeO_3 \cdot 5\,H_2O$, $NaHSeO_3$, $(NH_4)_2SeO_3$ and H_2SeO_3 were irradiated and their EPR spectra recorded under the same conditions. Signal intensities are given in table 1, where it may be seen that Ag_2SeO_3 is the least radiosensitive.

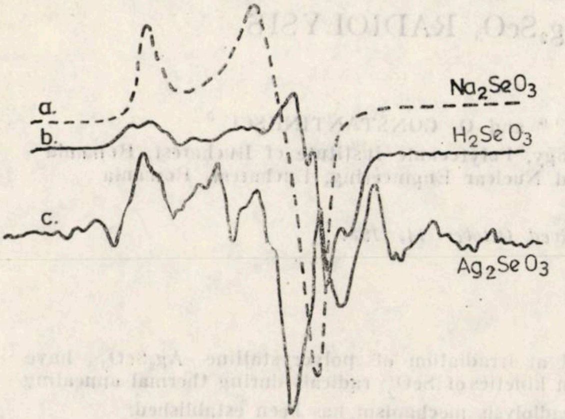

Fig. 1. — EPR spectrum of some selenites γ-irradiated at room temperature and recorded at the same temperature a) Na_2SeO_3 ; b) H_2SeO_3 ; c) Ag_2SeO_3.

Table 1

The relative radiosensitivity of some selenites estimated from EPR spectra

Compound	Ag_2SeO_3	H_2SeO_3	$NaHSeO_3$	$(NH_4)_2SeO_3$	$Na_2SeO_3 \cdot 5H_2O$
EPR signal intensity	1	79	106	166	298

As shown in fig. 1, γ irradiated Ag_2SeO_3 EPR spectrum is more complex if compared with those of other selenites, which suggest an overlapping of signals originated from two radicals. To check this assumption a sample was stepwise heated to higher temperatures and EPR spectra were accordingly recorded. A lowering of signal intensity with the temperature increase was observed, accompanied by a change of signal shape, especially in the central part of the spectrum. Beginning with 110°, the signal shape remains practically unchanged, its structure being presented in figure 2.

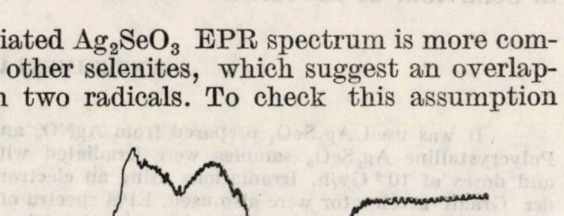

Fig. 2. — EPR spectrum of some Ag_2SeO_3 samples γ-irradiated at room temperature and then heated at 160°C.

A detailed analysis of EPR spectrum leads to the following g tensor values : $g_x = 2.0007$, $g_y = 2.0295$; $g_z = 2.0087$ $\langle g \rangle = 2.0129$. In contrast with other selenites[5] the hyperfine structure due to ^{77}Se isotope (nuclear spin $I = 1/2$) cannot be observed owing to the relativelly small intensity of the signal. The peak shape and g tensor values are similar to those recorded for other selenites.[6] This strongly suggests the assignements of the spectrum to radical species of the SeO_2^- type. This assignement agrees with its high thermal resistance compared with other Se oxianions as SeO_3^- and SeO_4^-. The analysis of this spectrum revealed the existence of a small splitting of ~6 G recorded in each component of g-tensor, probably caused by the interaction with nuclear spin $I = 1/2$ of ^{107}Ag (51.35%) and ^{109}Ag (48,65%).

EPR spectrum of γ-irradiated $AgSeO_3$ sample presented in figure 1c can be interpreted as follows : in central part of the spectrum over the signal corresponding to SeO_2^- radical a further one is present, characterised by the parameters ; $g_\perp = 2.0159$ and $g_\parallel = 2.0048$. These values, the spectrum shape and low thermal resistance suggest the assignement to the SeO_3^- radical.[7] It is worth mentioning that SeO_3^- radical formed at the Ag_2SeO_3 irradiation has a relatively higher thermal resistance compared with that of the same species occurred in the irradiation of other selenites, such as : $Na_2SeO_3 \cdot 5H_2O$, H_2SeO_3, $(NH_4)_2SeO_3$, where the SeO_3^- radicals were detected only to lower temperatures.[7] Grey colour of γ irradiated Ag_2SeO_3 sample is probably due to metal silver formation.

The radical accumulation with γ ray dose at the room temperature is illustrated in figure 3, which presents the signal intensity variation for the SeO_2^-, SeO_3^- radicals as well as the whole spectrum.

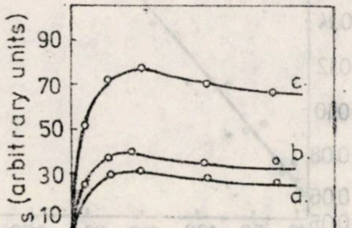

Fig. 3. — Dependence of EPR signal intensities of integral dose for an Ag_2SeO_3 sample γ irradiated at room temperature ($D = 6 \cdot 4 \times 10^3$ Gy/h) : a) SeO_2^- radical accumulation ; b) SeO_3^- radical accumulation ; c) accumulation of both radicals.

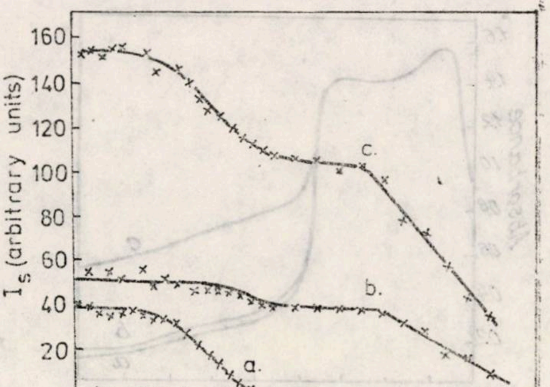

Fig. 4. — Variation of EPR signal intensity function of heating temperature for an Ag_2SeO_3 γ-irradiated using 5×10^5 Gy dose for : a) SeO_3^- radical ; b) SeO_2^- radical ; c) both radicals.

As may be seen, the signal intensity increases at the beginning with the irradiation time, until a maximum is reached and then remains almost constant. This behaviour suggests the fact that during irradiation besides the radical formation, a radical recombination process takes place also. If the radical accumulation is studied as a function of time for electrons produced by accelerator, a similar variation with of γ-irradiation is obtained.

To study the thermal stability of the formed radicals, the isochronous variation of signal intensity with heating of irradiated Ag_2SeO_3 samples has been studied from the room temperature up to 210°C. The results are given in fig. 4.

Curve 4a shows that the signal of SeO_3^- radical decreases beginning with 50°C and disappears completly at about 100°C. This behaviour agrees with that expected for a SeO_3^- radical which, in the case of all other selenites and selenates, has a lower thermal resistance than that of the SeO_2^- radicals. On curve 4c, which shows the variation of the sum signal, two processes can be noticed : a process of about 30% taking place up to 100°C and caused by the SeO_3^- disappearance and another one between 150—210° attributed to the SeO_2^- radical disappearance.

Reflectance spectra of unirradiated and irradiated samples of Ag_2SeO_3 were recorded and presented in fig. 5. In contrast with the previously studied selenites,[8] the absorption maximum characteristic to the radical species cannot be obtained due to the low concentration of the radicals formed by radiolysis.

It is seen that the spectrum of irradiated and heated sample moves vertically upwards in the long wave region, which can be due to the appearance of the red Se modification.

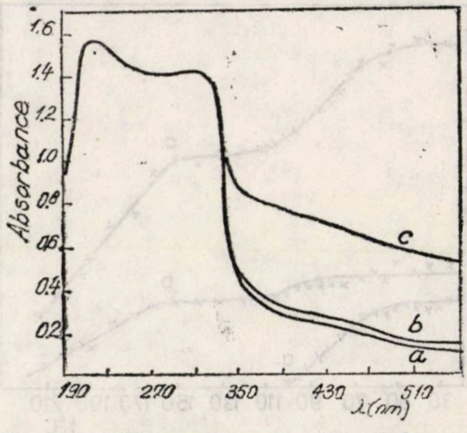

Fig. 5. — Reflectance spectra of Ag_2SeO_3 samples : a) unirradiated b) irradiated ; c) irradiated and then heated 10′ at 230°C.

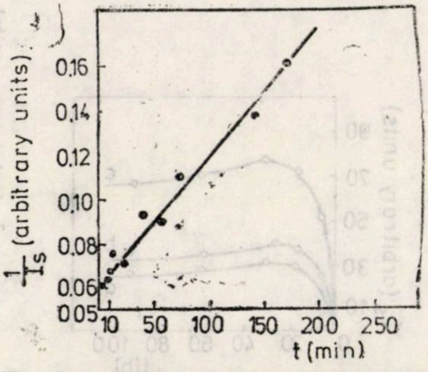

Fig. 6. — The plot of $1/I$ as a function of time for an Ag_2SeO_3 sample γ-irradiated and then heated at 196.5°C.

Reaction isothermal curves of γ-irradiated samples were made for temperatures comprised between 170—210°C where only SeO_2^- radical is present. If the reciprocal of EPR signal intensity is plotted against time, straight lines were obtained for all working temperatures. Fig. 6 illustrated such a dependence for the temperature of 196.5°C.

The slope of the straight lines thus obtained yielded the rate constants at the temperatures under investigation (table 2).

Table 2

Rate constants for the SeO_2^- radical disappearance at different temperatures

T°C	214	205	196.5	181.5	179.5
$k \cdot 10^8$	2.24	1.75	0.58	0.214	0.208

An Arrhenius plot of these data (Fig. 7) enabled the evaluation of the activation energy for the process of SeO_2^- decay : $E_a = 127.2$ kcal/mol.

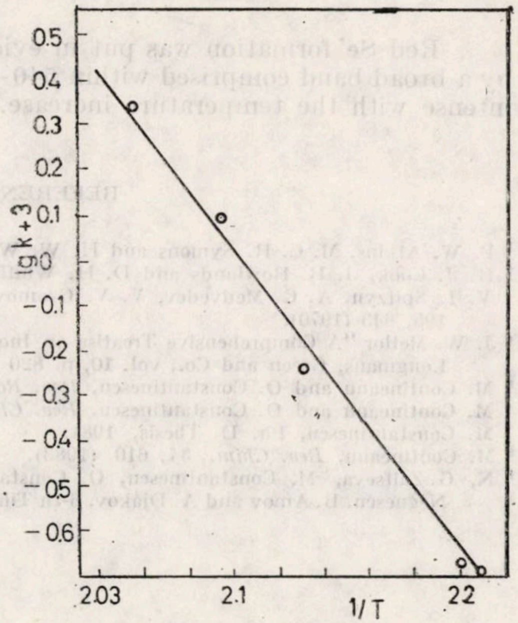

Fig. 7. — Plotting lg *k* versus 1/*T*.

The results herein reported allowed us to outline the following mechanism for Ag_2SeO_3 radiolysis.[9]

$$SeO_3^{2-} \rightsquigarrow SeO_3^- + e^-$$

$$SeO_3^{2-} \rightsquigarrow (SeO_3^{2-})^* \rightarrow SeO_2^- + O^-$$

$$SeO_3^{2-} + e^- \rightarrow (SeO_3^{3-})^* \rightarrow SeO_2^- + O^{2-}$$

According to this scheme the primary radiochemical processes lead to SeO_3^- and SeO_2^- radicals formation evidenced by EPR spectra. In contrast with other selenites [6,7] of the first group metals, in the case of Ag_2SeO_3, SeO_3^- radical is stable at room temperature.

The kinetic data previously reported have shown that SeO_2^- radicals disappear by heating, following a second order kinetics :

$$SeO_2^- + SeO_2^- \longrightarrow \left| \begin{array}{l} \rightarrow SeO_3^- + Se^{\bullet} + O^- \\ \rightarrow SeO_4^{2-} + Se^{\bullet} \end{array} \right.$$

For the disappearance of SeO_3-radicals the following reactions are possible :

$$SeO_3^- + e^- \rightarrow SeO_3^{2-}$$

$$SeO_3^- + SeO_3^{2-} \rightarrow SeO_4^{2-} + Se^{\bullet} + O_2^-$$

Red $Se^{\bullet}$ formation was put in evidence in the reflectance spectrum[8] by a broad band comprised within 540–570 nm and which becomes more intense with the temperature increase.

REFERENCES

[1] P. W. Atkins, M. C. R. Symons and H. W. Wardale, *J. Chem. Soc.*, 5215, (1964).

[2] R. J. Cook, J. R. Rowlands and D. H. Whiffen, *Mol. Phys.*, **8**, 195 (1964).

[3] V. I. Spitzyn, A. C. Medvedev, V. V. Gromov and V. F. Stanko, *Dokl. Akad. Nauk*, **3**, 195, 643 (1970).

[4] J. W. Mellor "A Comprehensive Treatise on Inorganic and Theoretical Chemistry" London, Longmans, Green and Co., vol. 10, p. 820 (1952).

[5] M. Contineanu and O. Constantinescu, *Rev. Roum. Phys.* In press.

[6] M. Contineanu and O. Constantinescu, *Rev. Chim.*, **28**, 845 (1977).

[7] M. Constantinescu, Ph. D. Thesis, 1981.

[8] M. Contineanu, *Rev. Chim.*, **34**, 610 (1983).

[9] N. G. Zaitseva, M. Constantinescu, O. Constantinescu, R. Georgescu, M. Contineanu, I. Neguescu, B. Amov and A. Djakov, 6-th Tihany Symp. on Radiation Chemistry,

Revue Roumaine de Chimie, **36**, *11–12*, 1269–1273 (1991)

ON THE DIOXIMINE COMPLEXES OF TRANSITION METALS. LXXXII.*

STUDY ON SOME ISOSELENOCYANATO MIXED CHELATES OF COBALT(III) WITH DIMETHYLGLYOXIME

JÁNOS ZSAKÓ [a], CSABA VÁRHELYI [a] and ION GĂNESCU [b]
[a] Faculty of Chemical Technology, "Babeş-Bolyai" University,
Cluj-Napoca, Arany János str. 11, Romania
[b] Departament of Chemistry, University of Craiova, Craiova,
Alexandru Ion Cuza str. 13,Romania

Received December 4, 1989

A number of 15 new isoselenocyanato mixed chelates of cobalt(III) of the type $[Co(DH)_2(NCSe)(Am)]$ (DH_2-dimethylglyoxime, Am – primary aromatic and tertiary heterocyclic amine) were obtained by substitution reactions from $K[Co(DH)_2(NCSe)_2]$ and the corresponding amine ligand in aqueous alcoholic ammonium acetate buffer solutions. The new products were characterized by chemical methods, electrical conductivity measurements and IR spectra. Force constants for the ν_{CN} and ν_{CSe} vibrations of the coordinated NCSe were calculated and discussed in terms of metal-ligand π-bond formation.

INTRODUCTION

The NCX^- ($X = O, S, Se, Te$) ions are ambidentate ligands and are coordinated to the transition metal ions through the N – or X – donor atoms as a function of the nature, valence state of the central ion and of sterical factors. This linkage isomerism problem was studied by X-ray and IR-spectral measurements.

The number of the selenocyanato-coordination compounds, as compared to the thiocyanato-derivatives is much smaller owing to the light decomposition of the $NCSe^-$, especially in acidic media. Various homogeneous ($[Co(NCSe)_4]^{2-}$, $[Cr(NCSe)_6]^{3-}$, $[Hg(SeCN)_4]^{2-}$, $[Pt(SeCN)_6]^{2-}$ [1–4] and mixed ligand complexes : $[Cu(en)_2(NCSe)_2]$[5], $[Pd(tetraen)(SeCN)]$[6], $[M(pyridine)_4(NCSe)_2]$ (M = Co, Ni, Cu, Zn, Cd)[7], etc. were obtained and characterized.

In our previous papers [8–10] the formation of some $H[Co(Diox.H)_2(NCSe)_2]$ (Diox. H_2 – dimethylglyoxime, nyoxime, pentoxime) monobasic complex acids has been reported. From the $NCSe^-$-groups one can be substituted easily in aquation processes in acidic media.

---

* Part LXXXI. Cs. Várhelyi, B. Burus and F. Makkay, *Stud. Univ. Babeş-Bolyai, Chem.*, **1989** (2), in press.

$$[Co(Diox.\,H)_2(NCSe)_2]^- + H_2O = [Co(Diox.\,H)_2(NCSe)(H_2O)] + NCSe^-.$$

In basic solution also the second $NCSe^-$ can be replaced in a complicated olation reaction[11], e.g.

$$[Co(Diox.\,H)(Diox)(OH)(NCSe)]^- + OH^- = [Co(Diox.\,H)(Diox)(OH)_2]^- + NCSe^-$$

($Diox.\,H^-$, $Diox^{2-}$) — mono — and double deprotonated dioxime molecule)

RESULTS AND DISCUSSION

We observed that one $NCSe^-$ group can be substituted also with amines and phosphines in ammonium acetate buffer solution:

$$[Co(Diox.\,H)_2(NCSe)_2]^- + Am = [Co(Diox.\,H)_2(NCSe)(Am)] + NCSe^-$$

(Am — primary aromatic amine, NH_3, tertiary heterocyclic amine or tertiary alkyl-aryl-phosphine ($pK_b = 6-13$). The very weak bases ($pK_b = 14-16$) are not suitable for this purpose, also as in the case of the analogous thiocyanato-derivatives.

15 new compounds of this type with Diox. H_2-dimethylglyoxime are characterized in Table 1.

Table 1

New nonelectrolytes of the type $[Co(DH)_2(NCSe)(amine)]$

Formula	Yield (%)	Aspect		Analysis	
				calcd.	found
$[Co(DH)_2(NCSe)(pyridine)]$	60	brown short prisms	Co	12.45	12.41
			N	17.75	17.72
$[Co(DH)_2(NCSe)(\gamma\text{-picoline})]$	60	yellow-brown thin plates	Co	12.09	11.96
			N	17.24	17.18
$[Co(DH)_2(NCSe)(\beta\text{picoline})]$	60	yellow-brown plates	Co	12.09	11.94
			N	17.24	17.16
$[Co(DH)_2(NCSe)(imidazole)]$	50	rhomb. yellow-brown prisms	Co	12.75	12.69
			N	21.20	21.09
$[Co(DH)_2(NCSe)(2\text{-methyl-imidazole})]$	50	yellow-brown square prisms	Co	12.37	12.30
			N	20.58	20.49
$[Co(DH)_2(NCSe)(benzimidazole)]$	70	yellow-brown cryst. crops	Co	11.50	11.41
			N	19.13	19.06
$[Co(DH)_2(NCSe)(aniline)]$	40	irregular yellow-brown thin plates	Co	12.09	11.96
			N	1724	17.10
$[Co(DH)_2(NCSe)(o\text{-toluidine})]$	40	brown irregular crops	Co	11.75	11.65
			N	16.75	16.66
$[Co(DH)_2(NCSe)(m\text{-toluidine})]$	40	yellow-brown dendrites	Co	11.75	11.65
			N	16.75	16.70
$[Co(DH)_2(NCSe)(p\text{-toluidine})]$	45	yellow-brown square prisms	Co	11.75	11.60
			N	16.75	16.68
$[Co(DH)_2(NCSe)(p\text{-anisidine})]$	40	yellow-brown hexagonal plates	Co	11.39	11.24
			N	18.21	18.15
$[Co(DH)_2(NCSe)(p\text{-phenetidine})]$	45	yellow-brown rhomb. prisms	Co	11.09	10.93
			N	15.81	15.77
$[Co(DH)_2(NCSe)(benzylamine)]$	50	yellow-brown thin needles	Co	11.75	11.69
			N	16.75	16.68
$[Co(DH)_2(NCSe)(\beta\text{-naphthylamine})]$	70	brown, hexagonal plates	Co	10.97	10.88
			N	15.63	15.57

Majority of these derivatives are very sparingly soluble in water and dil. HCl. The diluted mineral acids do not separate elementary selenium from these compounds (unlike the ionic metallic selenocyanates : M NCSe (M = Na, K, Rb, NH_4, etc). This phenomenon proves a strong covalent Co- selenocyanate bonding. They dissolve easily in DMF, THF, DMSO and acetone.

The molar electrical conductivity of some more soluble derivatives is 2—15 ohm cm² mole^{-1}, V = 1000—2000 mole/l, i.e. the above mentioned mixed chelates have a nonelectrolytic character.

In the IR spectra of the $[Co(DH)_2(NCSe)(Am)]$ type compounds the weak bands characteristic for the short O—H..O hydrogen bridges, observed also in the case of the $[Co(DH)_2(Am)_2]X$ and $H(Co(DH)_2X_2]$ type complexes[12] appear at 2300—2350 cm^{-1} (w) and 1700—1740 cm^{-1} (w) (ν_{O-H} and $\delta_{O-H..O}$). These bands suggest a *trans* geometric configuration.

The ν_{N-H} stretching frequencies of the coordinated primary amines appear at 3250—3200 and 3080—3030 cm^{-1} (s) shifted towards lower frequency values as compared to the free, non-coordinated amines (3500, 3300 cm^{-1}), showing a strong covalent character of the Co—N (amine) bonds.

Concerning the vibrations of the coordinated NCSe group, the ν_{CN}, ν_{CSe} and δ_{NCSe} bands could be identified. The corresponding wave numbers are given in Table 2.

Table 2

Vibration wave numbers (in cm^{-1}) and force constants (dyne/cm) for the coordinated NCSe group in $[Cc(DH)_2(NCSe)(amine)]$ type complexes

group	amine	ν_{CN}	ν_{CSe}	δ_{NCSe}	$k_{CN} \times 10^6$	$k_{CSe} \times 10^6$
a	aniline	2116	615	420	19.97	1.476
	m-toluidine	2120	612	426	20.18	1.470
	p-toluidine	2120	625	423	20.18	1.533
	p-anisidine	2106	623	426	20.05	1.532
	β-naphthylamine	2125	616	415	20.58	1.508
	benzylamine	2113	610	423	20.04	1.460
	mean value			422	20.17	1.496
b	pyridine	2112	643	417	19.76	1.604
	β-picoline	2113	660	433	19.91	1.700
	γ-picoline	2116	663	435	19.97	1.716
	2-methyl-imidazole	2118	620	432	19.90	1.494
	benzimidazole	2130	632	433	20.69	1.589
	NH_3	2113	665	426	19.05	1.663
	mean value			429	19.88	1.628

As well known the ambidentate ligand NCSe may form a linear M — NCSe or an angular M—SeCN structure. For the linear isoselenocyanato structure $\nu_{CN} < 2100$ cm^{-1}, $620 < \nu_{CSe} < 640$ cm^{-1} and $\delta_{NCSe} >$

400 cm^{-1} and for the angular selenocyanato structure $\nu_{CN} > 2100$ cm^{-1}, $520 < \nu_{CSe} < 550$ cm^{-1} and $\delta_{NCSe} < 400$ cm^{-1} are indicated.[13,14] Inspection of Table 2 shows that the ν_{CSe} and δ_{NCSe} values are in good agreement with those indicated above for the isoselenocyamato complexes. Although the ν_{CN} stretching wave numbers slightly exceed 2100 cm^{-1}, we consider the studied complexes to be isoselenocyanato ones.

We made an attempt to calculate the k_{CN} and k_{CSe} force constants in a very rough approximation, by considering the whole complex to be a diatomic molecule A–B, viz. with A = $Co(DH)_2$(amine)N and B = CSe, when k_{CN} is calculated and with A = $Co(DH)_2$(amine)NC and B = Se, for calculating k_{CSe}. Reduced masses μ were calculated in both the above assumptions and force constants could be derived as

$$k = 4\,\pi^2\nu^2\mu.$$

Results are also presented in Table 2.

Amine ligands are disposed in two groups. In group *a* the ligand has no π type orbitals available for the Co atom. In group *b* the coordinated N – atom participates in a delocalized π – bond system, the only exception being NH_3, but on the basis of the k_{CN} and k_{CSe} values it resembles more the *b* group amines than the *a* group ones.

The force constants k_{CN} in group *a* are larger as compared to group *b*, reversely, k_{CSe} values are less with group *a* amines than with group *b* ones.

The NCSe ligand may form retrodative π bonds with the Co atom. Thus t_{2g} electrons of the Co arrive in the antibonding π orbitals of the ligand, which leads to the diminution of the N–C π bond order and may entail the increase of the C–Se π bond order. If the amine ligand in the *trans* position is also able to form retrodative π bonds, the appearance of a larger π-bond system has a stabilizing effect, consequently k_{CN} diminishes and k_{CSe} increases, as observed in Table 2. The behaviour of NH_3 seems to be anomalous, but this could also be explained by presuming a hyperconjugation,[15] allowing a π bond formation.

A small difference between *a* and *b* group amines is observed also with respect to the δ_{NCSe} deformation vibration. Wave numbers are a little higher with *b* type amines as compared to *a* group ones. This effect is also consistent with the above given explanation, since the enhanced π-bond formation diminishes the difference between the π-bond orders of the two neighbouring N–C and C–Se bonds, making the ligand less deformable.

EXPERIMENTAL

$K[Co(DH)_2(NCSe)_2]$ – solution. 25 g cobalt acetate (0.1 mol) in 200 ml water and 23.2 g dimethylglyoxime (0.2 mol) in 800 ml methanol were oxidized by air bubbling for 4–5 hours. Then 0.22 moles KCNSe (29 g) in 150 ml water were added drop by drop and the oxidation continued further 2–3 hours. The brown solution formed was filtered off from the oxidation byproducts and some red elementary selenium and used for substitution reactions.

$[Co(DH)_2(NCSe)(amine)]$ nonelectrolytes 10 mmoles $K[Co(DH)_2(NCSe)_2]$ in 100 ml dil. methanol (1 :1) were treated on a water bath with 3—4 g ammonium acetate and 15 mmoles amine in 10—15 ml methanol. After 30—45 minutes warming the crystalline product precipitated was filtered off, washed with dil. metahnol (1 : 3) and dried on air.

The *IR spectra* of the complexes were recorded in KBr pellets with a Specord UR spectrophotometer (Carl Zeiss Jena).

Analysis. Cobalt was determined complexometrically and nitrogen gasvolumetrically by the usual microanalytical method.

REFERENCES

[1] F. A. Cotton, *Inorg. Chem.*, **1**, 565 (1962).
[2] K. Michelson, *Acta Chem. Scand.*, 17, 1811 (1963).
[3] A. Rosenheim and M. Pritze, *Z. anorg. Chem.*, **63**, 275 (1909).
[4] G. B. Bickton, *Liebigs Ann. Chem.*, **92**, 280 (1854).
[5] G. Morgan and F. H. Burstall, *J. Chem. Soc.*, **1927**, 1259.
[6] J. L. Burmeister and H. Gysling, J. *Chem. Soc. Chem. Commun.*, **11**, 543 (1967).
[7] G. Spacu and R. Ripan, *Bul. Soc. St. Cluj*, **4**, 3 (1928).
[8] Cs. Várhelyi, J. Zsakó and Z. Finta, *Monatsh.*, **101**, 1013 (1970).
[9] Cs. Várhelyi, Z. Finta and J. Zsakó, *Z. anorg. Chem.*, **374**, 326 (1970).
[10] Cs. Várhelyi, J. Zsakó and Z. Finta, *Stud. Univ. Babeș-Bolyai, Chem.*, **15** (1), 81 (1970).
[11] J. Zsakó, Z. Finta and Cs. Várhelyi, *J. inorg. nuclear Chem.*, **35**, 2839 (1973).
[12] A. Nakahara, *Bul. Chem. Soc. Japan.*, **28**, 473 (1955).
[13] A. Sabatini and J. Bertini, *Inorg. Chem.*, **4**, 959, 1665 (1965); **5**, 1025 (1966).
[14] J. L. Burmeister and M. Y. Al. Yanabi, *Inorg. Chem.*, **4**, 962 (1965).
[15] A. Streitwieser, Jr., "Molecular Orbital Theory for Organic Chemists", John Wiley and Sons, New York-London, 1961, Chapter 5.7.

Re vue Roumaine de Chimie, **36**, *11–12*, 1275–1278 (1991)

DAS EINSCHLIESSEN RADIOAKTIVER ABFÄLLE KLEINER UND MITTLERER AKTIVITÄT IN LEICHTSCHMELZBARE GLÄSER

ALEXANDRU CECAL[a], VIOREL CREŢU[b] und DAN VRABIE[a]
[a] Fakultät für Chemische Technologie des Polytechnischen Instituts aus Iaşi, Rumänien
[b] Glasfabrik Dorohoi, Rumänien

Eingegangen am 5 December, 1989

This work studies the possibility of treatment and storage of low- and intermediate-level radioactive wastes using low fusible glasses. Several types of these glasses including ^{60}CoO, as simulated radioactive waste, were carried out. Then, by means of the radioactive tracer ^{60}Co, the solubility in time of these solid glasses in different chemicals, was followed.

Diese Arbeit umfasst eine Untersuchung über die Möglichkeit einer Einschmelzung radioaktiver Abfälle von kleiner und mittlerer Aktivität in leichtschmelzbarem Glas als eine Variante der Aufbereitungs- und Deponierungsmethoden für diese, für das ökologische System so gefährlichen Rückstände. Zu diesem Zweck wurden mehrer leichtschmelzbare Glasarten synthetisiert, die dieselbe Menge von Kobaltoxyd mit dem Radioisotop ^{60}Co beeinhalten, ; danach wurde der Löslichkeitsgrad dieser festen Proben in Wasser und in Gegenwart einiger chemischer Lösungsmittel in Abhängigkeit von der Zeit verfolgt.

EINFÜHRUNG

Radioaktive Abfälle mittlerer und kleiner Aktivität in flüssigem oder festen Zustand werden im allgemeinen in Zement oder Bitumenmassen [1–3] eingeschlossen, nachdem ihr Volumen durch Eindampfung, Einäscherung oder Verfestigung reduziert worden ist.

Um die in Labors anfallenden Mengen, wo mit offenen Strahlungsquellen gearbeitet wird, von radioaktiven Ionen zu reinigen, appeliert man auch an andere Methoden, wie z.B. an ihre Abscheidung in Ionenaustauschern oder durch Molekularsiebe.[4–5]

In dieser Arbeit wird eine Methode für die Behandlung und Lagerung radioaktiver Abfälle mittlerer und kleiner Aktivität aus nuklearen Anlagen oder aus Labor, wo mit offenen Strahlungsquellen gearbeitet wird, vorgeschlagen. Die Methode basiert auf der Einschliessung dieser Abfälle als radioaktive Oxyde (der Art^{60}CoO) in leichtschmelzbare Gläser. Bei Temperaturen von ca. 300°C gehen die radioaktiven Ionen in schwerlösliche Verbindungen, wie Borate und Phosphate, über, während die Hinzufügung anderer Metalloxyde bewirkt, dass jenes leichtschmelzbare Glas widerstandsfähiger gegenüber der Wirkung chemischer Lösungsmittel wird.

EXPERIMENTELLER TEIL

Es wurden leichtschmelzbare Gläser unterschiedlicher Zusammensetzung mit Erweichungspunkten von ca. 300°C hergestellt. In diesen Gemischen, war die ^{60}CoO-Menge konstant (30 %), während die Mengen der anderen Oxyde (Glasformer und Modifikatoren) variierten. Die Zusammensetzung dieser leichtschmelzbaren Gläser ist in Tabelle 1 dargestellt.

Tabelle 1 (*und Abb. 1—8*)

Die Zusammensetzung (%) einiger leichtschmelzbarer Gläser

Abb. Nr.	Oxydtyp (%)	PbO	B_2O_3	P_2O_5	Tl_2O	Bi_2O_3	^{60}CoO
1		20	50	—	—	—	30
2		20	—	50	—	—	30
3		40	30	—	—	—	30
4		40	—	30	—	—	30
5		30	30	10	—	—	30
6		30	30	—	10	—	30
7		30	30	—	—	10	30
8		65	5	—	—	—	30

Die Oxydgemische wurden in Schmelztiegeln mit einem Bunsenbrenner geschmolzen, wobei darauf zu achten ist, dass die Erweichungstemperatur langsam erreicht wird. Danach wurden die entsprechenden Gemische bei Zimmertemperatur abgekühlt und in Berzeliusgläser gefüllt, die bereits je 300 ml Lösungsmittel für die radioaktiven Ionen jener festen Proben enthielten, und zwar: Wasser, Salzsäure (1 :1) oder Ammoniak (25 %).

Getrennt wurden auch schwerlosliche Grundverbindungen aus leichtschmelzbaren Gläsern nachder Literaturhinweisen,[7] $^{60}Co_3(BO)_2$ bzw. $^{60}Co_3(PO_4)_2$, hergestellt, deren Lösungsgrad in Wasser dann verfolgt wurde. Auf diese Weise wurde die Rolle der zusätzlich in den schwerschmelzbaren Gläsern enthaltenen Oxyde herausgestellt und zwar die der Vergrösserung der Stabilität gegenüber chemischer Mittel.

Zur Verfolgung des Losungsgrades in der Zeit wurden Proben zu je 0,5 ml aus den Lösungen über den Niederschlägen entnommen. Diese Lösungsproben wurden in Porzellantiegel umgefüllt. Nach Verdampfung der Lösungen durch eine Infrarotlampe wurde die Radioaktivität der Rückstände in den Tiegeln mit Hilfe eines γ-Zähler, der an einen Apparat Vakutronik VA—M—14 angeschlossen war, gemessen.

Zum Zwecke einer erhöhten Sicherheit bei der Einlagerung radioaktiver Abfälle in leichtschmelzbare Gläser wird die Verwendung eines "Gehauses" aus Polymethylmethakrylat (Plexiglas) vorgeschlagen. Deshalb wurden Abfälle dieses Polymers genommen, die wenn sie auf ca. 100°C erwärmt werden, erweichen und somit über die festen Proben aus den leichtschmelzbaren Gläsern, in die vorher die radioaktiven Abfälle eingelagert wurden, gegossen werden können.

ERGEBNISSE UND DISKUSSION

Die erhaltenen praktischen Ergebnisse sind in den Abbn. 1—8 dargestellt.

Es ist bekannt, dass durch totalen oder teilweisen Ersatz des Siliziumdioxyd (und des Aluminiumoxyds) als Basis schwerschmelzbarer Gläser durch Bor- oder Phosphoroxyde man Glaszusammensetzungen erhielt, die bei weit niedrigen Temperaturen schmelzen, jedoch weniger stabil sind als gewöhnliche Gläser.

Zur Vergrösserung der Stabilität leichtschmeltzbarer Gläser bei Einwirkung chemischer Mittel, wie Wasser, Säuren, Hydroxyde u.s.w., werden ihren Zusammensetzungen verschiedene Oxyde, wie Bleioxyd,

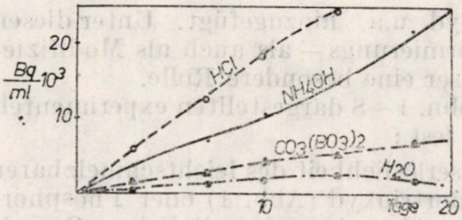

Fig. 1

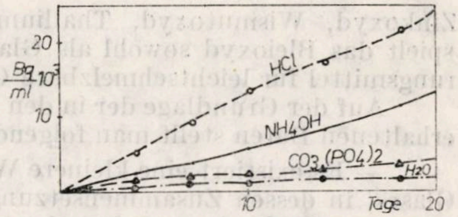

Fig. 2

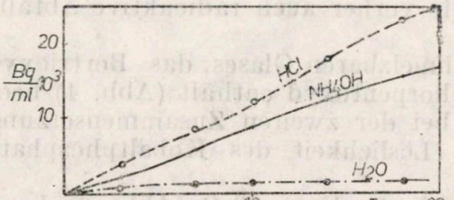

Fig. 3

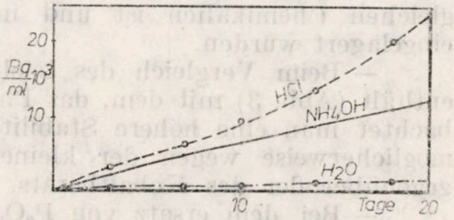

Fig. 4

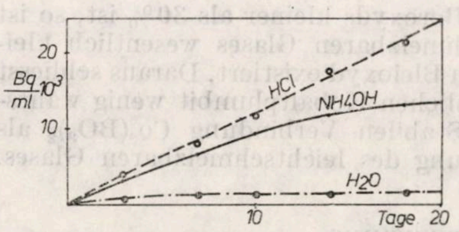

Fig. 5

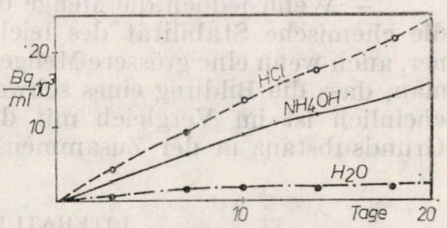

Fig. 6

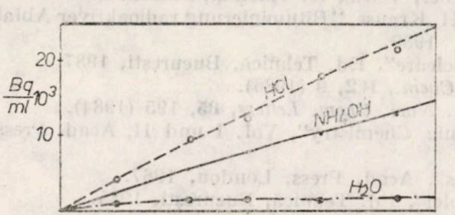

Fig. 7

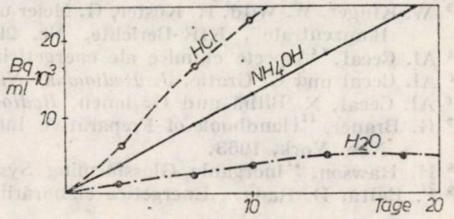

Fig. 8

Abbildungen 1—8. Die Abhängigkeit zwischen dem Löslichkeitsgrad der Versuchsproben aus leichtschmelzbarem Glas unterschiedlicher Zusammensetzung und der Kontaktzeit im gegebenen aggresieven Medium:

Zinkoxyd, Wismutoxyd, Thalliumoxyd u.a. hinzugefügt. Unter diesen spielt das Bleioxyd sowohl als Glasformierungs — als auch als Modifizierungsmittel für leichtschmelzbare Gläser eine besondere Rolle.

Auf der Grundlage der in den Abbn. 1—8 dargestellten experimentell erhaltenen Daten stellt man folgendes fest :

— Es existiert eine kleinere Wasserlöslichkeit des leichtschmelzbaren Glases, in dessen Zusammensetzung Bortrioxyd (Abb. 1) oder Phosphorpentoxyd (Abb. 2) enthalten ist, gegenüber der schwerlöslichen Grundverbindungen : $^{60}Co_3(BO_3)_3$ bzw. $^{60}Co_3(PO_4)_2$.

— In Anwesenheit einiger aggressiever Substanzen wie HCl oder NH_4OH stellt man eine wesentlich prägnantere Löslichkeit der leichtschmelzbaren Gläser gegenüber ihrer Löslichkeit in Wasser fest, eine Tatsache, die gleichbedeutend mit der Löslichkeit einiger Kalzinate in den gleichen Chemikalien ist und in die vorher auch radioaktive Abfälle eingelagert wurden.

— Beim Vergleich des leichtschmelzbaren Glases, das Bortrioxyd enthält (Abb. 3) mit dem, das Phosphorpentoxyd enthält (Abb. 4) beobachtet man eine höhere Stabilität bei der zweiten Zusammensetzung möglicherweise wegen der kleineren Löslichkeit des Kobaltphosphats gegenüber der des Kobaltborats.

— Bei dem ersatz von P_2O_5 (Abb. 5) durch Tl_2O (Abb. 6) bzw. Bi_2O_3 (Abb. 7) stellt man eine relative Verkleinerung des Stabilität des leichtschmelzbaren Glases fest, ein Beweis dafür, dass das Phosphorpentoxyd die Rolle eines Formierungsmittels für das entsprechende Glas hat.

— Wenn jedoch die Menge des Boroxyds kleiner als 30% ist, so ist die chemische Stabilität des leichtschmelzbaren Glases wesentlich kleiner, auch wenn eine grössere Menge von Bleioxyd existiert. Daraus schliesst man, dass die Bildung eines schwerlöslichen Kobaltplumbit wenig wahrscheinlich ist im Vergleich mit der Stabilen Verbindung $Co_3(BO_3)_2$ als Grundsubstanz in der Zusammensetzung des leichtschmelzbaren Glases.

LITERATURVERZEICHNIS

[1] C. A. Mawson, "Processing of Radioactive Wastes", I.A.E.A., Vienna, 1961.

[2] G. Höhlein, "Behandlung schwach- und mittelaktiver Abfälle", in „Chemie der Nuklearen Entsorgung", Teil II, Hrsg. F. Baumgärtner, Verlag K. Thiemig, München, 1978.

[3] W. Kluger, W. Wild, R. Köster, G. Meier und H. Krause, "Bituminierung radioaktiver Abfallkonzentrate", KfK-Berichte, Nr. 2975, 1980.

[4] Al. Cecal, "Aspecte chimice ale energeticii nucleare", Ed. Tehnică, Bucureşti, 1987.

[5] Al. Cecal und C. Gratie, *J. Radioanal. Nucl. Chem.*, **102**, 9 (1986).

[6] Al. Cecal, N. Bilbă und G. Iancu, *Radioanal. Nucl. Chem. Letters*, **85**, 195 (1984).

[7] G. Brauer, "Handbook of Preparative Inorganic Chemistry", Vol. I und II, Acad. Press, New York, 1963.

[8] H. Rawson, "Inorganic Glassforming Systems", Acad. Press, London, 1967.

[9] P. Baltă, D. Radu, „Energetica elaborării sticlei", Ed. Tehnică, Bucureşti, 1985.

Revue Roumaine de Chimie, **36**, *11–12*, 1279–1285 (1991)

Cu(II) COORDINATION COMPOUNDS WITH THIOAMIDES

FLORICA ZĂLARU, CORNELIA CERCASOV, AURELIA MEGHEA, CHRISTINA ZĂLARU and CHRISTINA JALEA
Faculty of Chemical Technology, Polytechnic Institute, Bucharest, Romania

Received May 36, 1989

The present paper reports on several new coordination compounds of the CuL_4Cl_2 and CuL_2Br_2 types, where L = cinnamthioamide (*o*, *m*, *p*-substituted) and N, N′-disubstituted phenylthioacetamide. The compounds were characterized by elemental chemical analysis, electronic, IR and ESR spectra. The ligands coordinated monodentately by the N or S atoms as a function of the thioamide structure.

INTRODUCTION

Thioamides may coordinate by both N and S donor atoms or only by the N atom and the S atom, respectively, as a function of the nature of the metallic ion.[1] For a given metallic ion, the donor properties of thioamides might be determined by the particular structure of the thioamide.

The paper presents the coordination behaviour, under the same experimental conditions, of several aromatic thioamides belonging to the following types: I, II, III.

I. Cinnamthioamides

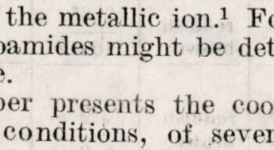

x = Cl; CH₃O– y, z = H
y = Cl x, z = H
z = Cl x, y = H

II. α-phenylcinnamthioamides

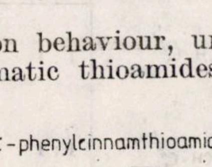

x = NO₂, Cl, N(CH₃)₂, CH₃O

III. Tertiary thioamides

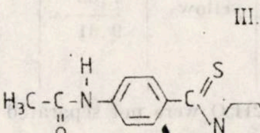

IIIa.

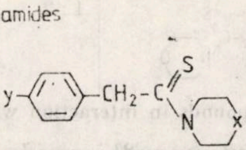

x = C, O y = H
x = O y = CH₃, Br

IIIb.

Cu(II) ion was used as metallic ion, and ethanol as a reaction medium. The reactions were performed with $CuCl_2 \cdot 2H_2O$ and $CuBr_2$ halides at room temperature.

RESULTS AND DISCUSSION

Cinnamthioamides (*I*). During the interaction of the Cu(II) halides with *o*, *m*, *p*-substituted cinnamthioamides in ethanol, at a Cu : L = 1 : 1 and 1 : 4 molar ratio, brick-red and brown compounds were obtained (noted **1**–**4**, Table 1). The influence of the anion nature in CuX_2 on the type of the separated compound was evidenced. From the Cl-substituted *m* and *p* cinnamthioamides, the compounds were obtained only after the interaction with $CuBr_2$.

Table 1

Type of the compound. Analytical data

No.	Ligand	Molar ratio Cu : L	Compound	Colour	Cu % found / calcd	Cl % found / calcd	Br % found / calcd
1	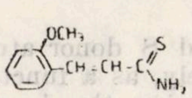	1 : 1	CuL_4Cl_2	brick-red	6.72 7.00	6.35 7.83	
2		1 : 4	CuL_2Br_2	reddish brown	9.85 10.42		25.90 26.22
3	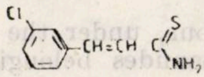	1 : 1	CuL_2Br_2	reddish brown	7.2 8.9		22.06 22.05
4	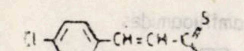	1 : 1	CuL_2Br_2	reddish brown	7.10 8.90		22.63 22.50
5	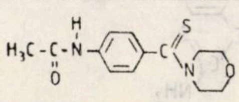	1 : 1 1 : 4	CuL_2B_2	yellow	8.94 8.51		23.27 21.70
6	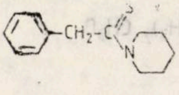	1 : 2	CuL_2Br_2	yellow	7.58 9.61		26.35 27.20
7	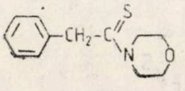	1 : 2	CuL_2Br_2	yellow	7.08 9.61		26.87 27.02

The compounds in interaction with $CuCl_2 \cdot 2H_2O$ were not separated

α-Phenylcinnamthioamides. Unlike cinnamthioamides, α-phenylcinnamthioamides (type II) do not react with Cu(II) halides under the same experimental conditions (molar ratio Cu : L, reaction medium, temperature). The presence of the benzenic nucleus in the α position seems to reduce the coordination ability of these thioamides.

Tertiary thioamides. Thioamides of the type IIIb are different from the thioamides of the types I, II and IIIa by the functional group and phenyl, interrupted by the $>CH_2$ group; p-π conjugation between the unshared pair of electrons of the N atom and the π electrons of the S atom in the functional group (NCS) will be determined by steric reasons, at the N atom.

Sändström[2] showed, on the basis of several theoretical observations, that the steric hindrances do not favour the plane configuration of the molecule, the thioamide group and the rest of the molecule revolving one against the other. The molecule nonplanarity might influence the coordination behaviour of this type of thioamides.

p-Acetylaminothiobenzmorpholide (IIIa) and the N,N-disubstituted phenylthioamides interact only with $CuBr_2$. In each case a complex yellow compound, formulated on the basis of the elemental chemical analysis CuL_2Br_2 was obtained. Interaction of the ligand ethanolic solutions, with the $CuCl_2$ ethanolic solution led to a syrup-like state that could not be characterized.

Electronic spectra. The reflectance electronic spectra have a common feature: a strong and broad band or a shoulder around 400 nm (380 nm for the compounds **6** and **7**), 460 nm for the compounds **1** and **2** and 500 nm for the compounds **3**, **4** and **5**. The band stretches to about 600 nm (Table 2).

Table 2

Diffuse reflectance spectra (400—1000 nm)

No.	Complex	λ_{max}	
1	CuL_4Cl_2	460	
2	CuL_2Br_2	450 sh	
3	CuL_2Br_2 2s	500	940
4	CuL_2Br_2 2s	500	740
5	CuL_2Br_2	450 sh	950
6	CuL_2Br_2	380 sh	
7	CuL_2Br_2	360 sh	

sh = shoulder
L = the same ligand as in table 1.

Unlike the compounds **1**, **2**, **6** and **7** which show no other absorption in the visible, the spectra of the compounds **3**, **4** and **5** show a weak band with $\lambda_{max} \sim 800-900$ nm.

The analysis of the electronic spectra on the number of the absorption bands and the position of their maxima suggests that the Cu(II) ion adopts probably a geometry of flattened tetrahedron in the compounds **1**, **2**, **6** and **7** and plane-square in the compounds **3**, **4** and **5**. According to Campbel,[3] the presence in the spectrum of chromofore CuN_2S_2 in the compounds of the CuL_2X_2 type of two absorptions with $\lambda = 500$ nm and ~ 700 nm would be typical of the plane-square geometry. Weill and

Khann[4] show the difference between the electronic spectra of the $CuCl_4^{2-}$ chromophore in solid Cs_2CuCl_4 with known geometry of distorted tetrahedron and plane-square solid $[N(C_2H_5)_4]_2[CuCl_4]$. The electronic spectrum of the compound Cs_2CuCl_4 shows only an absorption around 400 nm whereas the spectrum of the plane-square compound shows two absorptions with $\lambda_{max} = 500$ and $\lambda_{max} = 800-900$ nm. The broad and strong band, close to 400 nm might be the result of a TCL→M band overlapping the d−d band expected for the tetracoordinated Cu(II) ion. This charge transfer might explain the less usual red, red-brown colour of the compounds. The literature associates this colour to a dimeric structure accompanied by an intense absorption at $\lambda_{max} = 375$ nm,[5] but it has been shown that the adsorption also appears in compounds with monomeric structures. Likewise, the red-brown colour was attributed to a geometry of distorted tetrahedron of the tetracoordinated Cu(II) ion or to an L→M charge transfer.[6,7] Moreover, Blumberg et al.[8] assigned the red colour of some Cu(II) compounds with N and S donor atom ligands to a delocalization of the odd electron of the Cu(II) ion favoured by the nonsaturated character of the ligand molecule.

ESR spectra. The ESR spectra determined at room temperature on crystalline powders do not show any signal. The possible existence, in the compounds of the Cu(I) ion with d^{10} configuration, as a consequence of the reducing action of the ligands is excluded, as the compounds absorb in the visible.

IR spectra. The IR spectra of the ligands and compounds were recorded by the disc technique in KBr and the main bands were assigned (Tables 3 and 4).

The typical spectra of the thioamides are found in the range of the "finger print" and very often they cannot be clearly recorded; the vibrations of the (CSN) group are shadowed by a strong coupling with other vibrations of the molecule.[9] The changes undergone by the bands characteristic of the functional group containing N and S donor atoms may indicate the donor atom.

The thioamide group presents only two mesomeric forms :

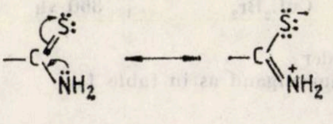

If coordination is achieved by the N atoms, the (a) form will be favoured and then the bands corresponding to the vibration frequencies for the NH_2 group (ν_{NH} decreases and δ_{NH_2} increases) will be modified; also a slight increase of the I and II thioamide bands is noticed.[1] If coordination is achieved by the S atom, the (b) form will be favoured and the bands corresponding to the vibration frequencies, ν_{C-S} and $\nu_{C=N}$, will be modified.

It was found,[10,11] for the Cu(II) complex compounds with thiosemicarbazone, that the band due to ν_{CS} is usually a proof for forming the

Table 3

The main bands in the IR spectrum (cm⁻¹)

No.	Ligand and compound	$\nu_{NH\ asym}$ $\nu_{NH\ sym}$ (3500–3100)	δ_{NH_2} 1600–1500	B_I $\delta_{NH}+\delta_{CH}+$ $+\nu_{CN}$ 1520–1460	B_{II} $\delta_{NH}+\delta_{CH}$ $\nu_{C=N}+\nu_{C=S}$ 1460–1200	B_{III} $\nu_{C=N}+\nu_{C=S}$ 1000–900	B_{IV} $\nu_{C=S}$ 900–700	ν_{C-S} 700–600
1	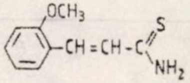	3540 w 3400–3290 3190 s	1610 vs 1580 vs	1480 m 1455 m	1420 s 1315 s	1005 m	787 m 762 vs	660–685 w
	CuL_4Cl_2	3260–3290 vs 3180–3130 vs	1580 1605 vs	1485 m 1460 w	1430 w 1312 vs	990 m	783 w 753 sv	
2	CuL_2Br_2	3290 vw 3190 vw	1580 1600 s	1485 w 1460 m	1310	985 w	754 s	
3	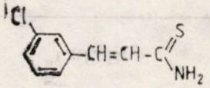	3370 m 3260 w 3160 m	1630 s	1495 m	1395 s 1318 s	1010 m 970 m	825 s 740 m	
	$CuL_2Br_2\cdot 2S$		1620 m	1490 w	—	1010 w 960 w	800 m	
4	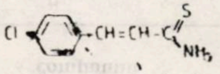	3390 m 3270 w 3165 m	1640 s	1565 w	1480 w 1400 vs 1325 s	1015 w 970 s	855 w 885 w 795 m 750 m	690
	$CuL_2Br_2\cdot 2L$		1620 s	1558 w	1400–1475 1300–1335	840–890 w 770 m		670

vs = very strong; s = strong; m = medium; w = weak; vw = very weak

Table 4

The main bands in the IR spectrum (cm^{-1})

No.	Ligand and compound	$\nu_{NH\,asym}$ $\nu_{NH\,sym}$ (3500−3100)	δ_{NH_2} 1600−1500	B_I $\delta_{NH}+\delta_{CH}+\nu_{CN}$ 1520−1460	B_{II} $\delta_{NH}+\delta_{CH}$ $\nu_{CN}+\nu_{CS}$ 1460−1200	B_{III} $\nu_{CN}+\nu_{CS}$ 1000−900	B_{IV} ν_{CS} 800−600
5	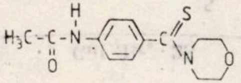	3340 s 3110 w	1675 vs 1580 vs 1520−1475 vs		1320 m 1305 m	1045 s 1010 m	695−785 m 650 w 600 w
	CuL_2Br_2	3250−3330 w	1670 m 1580 m		1320 m 1320 m	1045 m 1000 m	
6	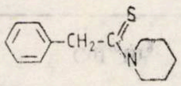			1500 vs 1465−1440 s	1300 s 1260−1250 s 1200 m 1120 s	1010 s 950 m 900 m	850 m 820 w 750 s 710 s
	CuL_2Br_2			1500 vs−1450 1440 s	1280−1240 m 1180 vw 1100 s	1000 m 940 w 900 w	830 w 820 vw 770−750 m 680 m
7	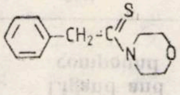			1510 vs 1460−1440 s (doublet)	1390 m 1310−1290− −1270 s (triplet) 1200−1190 m	1120 vs 1070 m 1040 s 965 s	865 m 840 m 740 s 715 s
	CuL_2Br_2			1550 vs 1465−1470 m	1340 m 1270 m 1180 vw	1120 s 1070 m 1040 s 975 vw	865 vw 840 w 760 m 710 m

M—S bond; the band is shifted towards less frequencies or even disappears. The band in the 1100 cm^{-1} range, that may include ν_{C-S}, has a similar behaviour in complexation.

The changes noticed in the spectrum of the compounds **1**—**4** (Table 3), compared to that of the ligands, mainly the changes undergone by the corresponding ν_{NH} and ν_{NH} bands might indicate the coordination by the N atom. The ligand would act monodentately. The other two coordinating points would be the halide atoms. The ligands being tertiary thioamides, the thioamide bands I—IV are interesting for the compounds **5**, **6** and **7**. Such changes as slight shifts of the bands positions towards less frequencies and weakening of their intensity, are noticed. These changes suggest the coordination by the S atom and not by the N atom disubstituted with voluminous substituents.

In conclusion, the correlation of the data given by the electronic and IR spectra shows that, in all the compounds studied, the Cu(II) atom is tetracoordinated. In terms of the ligand nature, the donor atom is either the N or the S atom. The other two coordinating points might be the halide atoms. The geometry of the Cu^{2+} ion in the CuL_2X_2 compounds might be either a distorted tetrahedron or a square planar.

EXPERIMENTAL

$CuCl_2 \cdot 2H_2O$ and $CuBr_2$ p.a were used and the ligands were prepared according to the indications in the literature.[12] Molar ratio Cu : L = 1 : 1; 1 : 2 or 1 : 4 in ethanol medium. The compounds were prepared by the following general procedure: the solutions containing ligands and metal halide were mixed and the products separated from solution as microcrystalline poweders. The compounds obtained were separated by filtration under vacuum, washed with small quatities of ethanol and dried at room temperature. Composition of the complexes and their colour are given in table 1.

Copper was determined gravimetrically after breakdown of the complex with H_2O_2 and concentrated H_2SO_4. Chlorine and bromine were determined gravimetrically.

Electronic spectra. Diffuse-reflectance spectra were recorded on a VSU_2 Zeiss-Jena spectrophotometer within the 300—1100 nm range in dilution with MgO at a compound/MgO ratio : 1 : 3.

Infrared spectra were recorded in the region of 4000—700 cm^{-1}, using a Specord 71 spectrophotometer. The samples were mounted in potassium bromide disks.

Electron spin resonance spectra were made on ART-5-IFA spectrograph. The klystron frequency was 9060 MHz and the modulation of the magnetic field was 100 kc/s.

REFERENCES

[1] B. Singh, R. Singh and R. V. Chaudhary, *Indian J. Chem.*, **11** (2), 174 (1973).

[2] J. Sändström and B. Pearsson, *Acta Chem. Scand.*, **18**, 1059 (1964).

[3] M. J. M. Campbell, *Coord. Chem. Rev.*, **15**, 279 (1975).

[4] M. A. Khan and M.J. Schwing-Weill, *Inorg. Chem.*, **15** (9), 202 (1976).

[5] M. Kato, H. B. Jonassen and J. C. Fanning., *Chem. Rev.*, **64**, 99 (1964).

[6] J. M. Klotz, G. H. Gzerlinski and H. A. Fiess, *J. Am. Chem. Soc.*, **80**, 2920 (1958).

[7] A. Cotton and G. Wilkinson, "Advanced Inorganic Chemistry", Interscience, N.Y., 2nd Ed., 1966, pp. 901, 903.

[8] W. E. Blumberg and J. Peisach, *J. Chem. Phys.*, **49**, 1793 (1968).

[9] K. Jansen and P. H. Nielsen, *Acta Chim. Scand.*, **20**, 597 (1966).

[10] M. Akbar Ali and S. E. Livingstone, *Coord. Chem. Rev.*, **13**, 101 (1974).

[11] A. T. Pilipenko and H. V. Melnikova, *Dokld. Acad. Nauk.*, **50**, 312 (1979).

[12] C. Fulea-Cereasov, Doctoral Thesis, 1975.

Revue Roumaine de Chimie, 36, *11–12*, 1287–1297 (1991)

RHEOLOGICAL MODELLING OF EMULSION COPOLYMERIZATION OF VINYL ACETATE

KRISTIANA GOŞA [a], DAN DONESCU [a], SORIN STRAJA [b], DOINA ISBĂŞESCU [c] and ION LANGURI [d]

[a] Center of Plastic Materials Research

[b] Institute of Chemical and Biochemical Energetics

[c] Institute of Chemical Research, Splaiul Independenţei no. 202, 77208 Bucharest, Romania

[d] ICSITPSC, Soseaua Olteniţei no. 105, Bucharest, Romania

Received December 5, 1989

This paper endeavours to explain the pseudoplastic behaviour of the emulsion of vinyl acetate (VAc) copolymers and the interpretation of the viscosity modifications during the copolymerization process on the basis of the Ree-Eyring model. By means of the Ree-Eyring model parameters values, the pseudonetwork structure of these emulsions was established. In the case of the copolymer emulsions with the same average particle diameter but having different polydispersion degrees, the parameters of the model differ only for the non-Newtonian unit which determines the flowing at very low shearing rates. The formation of two distinct structures is rendered evident during copolymerization of VAc in the presence of hydroxyethylcellulose in semicontinuous system of monomer adding.

The rheological properties of the polymers emulsions were intensively studied as a function of volume fraction, average size of particles, size distribution, nature and concentration of the emulsifier used.[1-8]

The paper[9] shows that in the case of vinyl acetate (VAc), copolymerization with di-2 ethylhexyl maleate (EHM) in the presence of hydroxyethylcellulose (HEC) as emulsifier and sulphosuccinate of nonyl pehnol ethoxylated with 6 moles of ethylene oxide (NFSSEO) as coemulsifier, the viscosity decreases towards the end of polymerization and finally it increases again, probably due to the agglomeration and to the nucleation of new particles.

The emulsions of polyvinyl acetate (PVAc) and of VAc copolymers have a pseudoplastic behaviour. Eagland and Kay [2] consider that the larger particles which occur in such emulsions are, in fact, aggregates, and one of the main reasons of pseudoplasticity consists in the breaking of the aggregates.

In the case of PVAc emulsions obtained in the presence of polyvinyl alcohol (PVA),[1] the pseudoplastic behaviour was explained by the tendency of association of the PVA chains, the links being broken under the action of the shear forces.

This paper attempts to explain the pseudoplastic behaviour of the emulsions of VAc—EHM copolymers and the interpretation of the viscosity modifications during the copolymerization process on the basis of the Ree-Eyring model. The Ree-Eyring model [2,10–13] based on the theory of the activated complex allows the calculation of some kinetic and thermodynamic parameters of the flowing of the polymer emulsions.

The model considers the fluid to be made up of molecular groups named "flow units". At rest, these groups make a pseudonetwork, each flow unit oscillating around a point of minimum free energy.

Assuming the existence of n types of flow units, the relation between the apparent viscosity η_a of the polymers dispersion and the applied shear $\dot{\gamma}$ can be written in the form :

$$\eta_a = \sum_{i=1}^{n} \frac{x_i \beta_i}{\alpha_i} \frac{\sin h^{-1} \beta_i \dot{\gamma}}{\beta_i \dot{\gamma}} \tag{1}$$

where α_i is the volume fraction occupied by the flow unit i. The relaxation time β_i of the flow unit i is defined by the equation :

$$\beta_i = \left(\frac{\lambda}{\lambda_1} \cdot 2k' \right)_i^{-1} \tag{2}$$

λ is the distance between two equilibrium positions in the direction of movement and λ_1 is the distance between two parallel planes of flow units of the same type. The values λ and λ_1 are not identical but, being of the same order of magnitude, they can be considered equal at a first approximation.[13]

The rate constant k'_i for the movement of a flow unit over the potential barrier is calculated on the basis of the theory of activated complex by means of the equation :

$$k'_i = \frac{kT}{h} \mathrm{e}^{-\Delta G_i/RT} \tag{3}$$

in which ΔG is the free energy of flow activation (in the absence of any force), R is the universal constant of gases and h is the Planck constant.

The rheological behaviour of some PVAc emulsions, obtained in the presence of a sodium salt of an ionic emulsifier was analysed by Eagland and Kay [2] based on the Ree-Eyring model with three units : a Newtonian one which predominates at high applied shearing rates and two non-Newtonian flow units which predominate at low and intermediate range of applied shearing.

Equation (1) can be written in the form :

$$\eta_a = \eta_\infty + (\eta_0 - \eta_\infty) \frac{\sin h^{-1} \beta_2 \dot{\gamma}}{\beta_2 \dot{\gamma}} + (\eta'_0 - \eta_0) \frac{\sin h^{-1} \beta_3 \dot{\gamma}}{\beta_3 \dot{\gamma}} \tag{4}$$

where η_0' represents the total zero shearing viscosity and η_0 is the contribution of the first two flow units at the η_0' viscosity, η_∞ is the viscosity at infinite shearing. Eagland and Kay observed the dependence of the rheological parameters of the model on the size and volume fraction of the particles. The relaxation time β_2 of the unit that causes the flow at intermediate range of applied shearing increases together with the increase of the particles diameter, but it does go beyond 1 s, while the relaxation time β_3 of the unit that predominates the flow at low applied shearing has high values (between 1—100 s) which increase with the lowering of the particles diameter. The paper mentioned does not estimate the free energy of activation or the k_i' rate constants.

EXPERIMENTAL

The emulsions of VAc—EHM (EC 1—5) copolymer were obtained by copolymerization in the presence of 2% HEC and 0.5% NFSSEO as emulsifier and coemulsifier, respectively, and 1.5% n-butyl alcohol as transfer agent at various stirring rates in the reactor. No transfer agent was used to prepare REC-6 emulsion. The emulsion of EH-7 homopolymer was prepared under the same conditions like the EC 1—5 emulsions. The VAc homopolymerization process in the presence of 10% PVA completely saponificated was also investigated, for comparison.

The polymerizations in the semicontinuous system of adding the monomers carried out in the way previously described[14] were stopped at different degrees of conversion (or solid content) and the viscosity was presently measured at 30°C.

The apparent viscosity was measured with a Rheotest 2 type viscometer. Emulsion films were obtained by drying at room temperature and were subjected to successive extractions in water and in benzene.

The particles diameter was determined by means of an electronic microscope JEOL 200 CX, the samples being prepared by the freezing method.

The NMR spectra were recorded with an IFA spectrometer, type T 71, with stable working frequency of 10 MHz.

The rheological parameters of the Ree-Eyring model were calculated on the basis of a computing programme in Fortran II run on an IBM 11.30 computer, using Marquard-Fletcher method.

RESULTS AND DISCUSSION

1. The "pseudonetwork" structure of the finite emulsions of AVAc-EHM copolymer

As mentioned in the previous papers,[15-17] during the VAc polymerization and copolymerization in the presence of HEC or PVA between the growing radical and the macromolecular emulsifier, there appear transfer reactions leading to the formation of block or grafted copolymers, soluble in water and in benzene, or insoluble. Even when a transfer agent is used, the grafting reactions are not completely removed because the weight of the water soluble fraction is bigger than the concentration of the emulsifier used. Figure 1 shows the curves of the apparent viscosity variation as a function of the gradient of shearing rates.

In the case of copolymer emulsions obtained with transfer agent (EC 1—5) which have the same average diameter of the particles, but different size distributions (Table 1), the curves differ only in the field of low shearing rates. At low shear rates, the apparent viscosity is higher when the polydispersion interval is wider. Although the EC—6 copolymer emulsion (obtained without transfer agent) has the average particles diameter much bigger, the apparent viscosity is higher in the whole range of shearing rates.

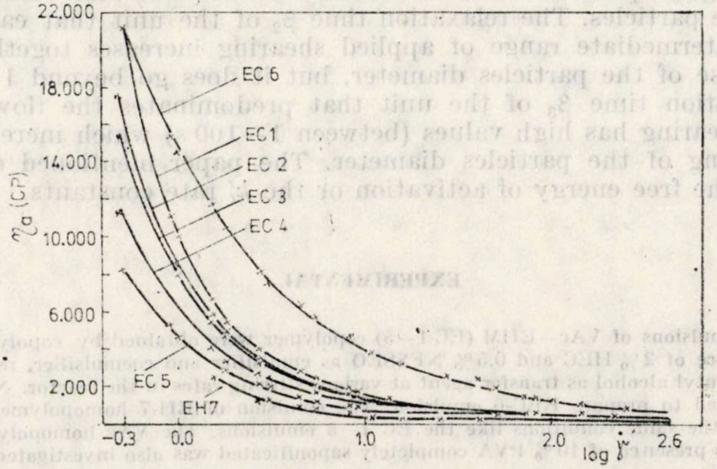

Fig. 1. — Rheological curves of the PVAc based finite emulsions.

The apparent viscosity of the homopolymer (EH—7) is smaller than the one of the copolymer emulsions in the whole range of shearing rates.

The rheological parameters of the Ree-Eyring model are given in Table 1.

For all the emulsions investigated, the two relaxation times β_2 and β_3 of the non-Newtonian flow units differ between each other with several magnitude orders. According to the rheological model adopted, the bigger the size of the flow units is, the longer their relaxation time is and the interval of shearing rates in which they predominantly occur at ever lower shearing rates.

The very high values of η_0' and β_3 show that both at zero shearing rate and at small shearing rates inside the emulsions, multiple interactions are established so that the emulsions can be considered in their totality as three-dimensional networks. But most of the junctions of there networks have low energy because viscosity dramatically decreases with the increase of the shearing rate.

In the case of EC—6 copolymer emulsion, obtained in the absence of the transfer agent, the apparent viscosity lowers more slowly with the increase of the velocity gradient. Thus, the interactions between the components of the emulsion are stronger, due to the structure of grafted and crosslinked copolymer.

In Table 1, η_0' and β_3 decrease with some orders of magnitude with the narrowing of the polydispersion interval. One can also observe a decrease of the free energy of activation ΔG_3 and an increase of the rate constant k_3' for the non-Newtonian unit which predominates the flow at low shearing rates (Table 2).

Table 1

Characteristics of PVAc based emulsions

Emulsion	Polymers structure			Particle size		Rheological parameters of the Ree-Eyring model					
	Water soluble fraction (%)	Benzene soluble fraction (%)	Insoluble fraction (%)	$D_{av}10^6$ (mm)	$(D_{min} - D_{max})10^6$ (mm)	η'_0 (cP)	η_0 (cP)	η_∞ (cP)	β_3 (s)	β_2 (s)	Standard error
EC−1	5.1	94.9	0	788	300...1400	$2.7.10^{11}$	4200	0.1	$5.6.10^8$	0.042	406
EC−2	5.2	94.9	0	—	—	$7.3.10^{10}$	558	124	$1.8.10^8$	0.011	170
EC−3	6.0	94.0	0	729	277...1250	$7.0.10^{11}$	610	187	$2.1.10^9$	0.032	100
EC−4	6.4	93.6	0	671	417...1111	$5.1.10^9$	583	202	$1.6.10^7$	0.046	97
EC−5	5.5	94.5	0	797	552...1111	$2.6.10^6$	405	176	$5.6.10^3$	0.041	44
EC−6	6.74	51.63	41.63	2068	740...3320	$3.6.10^7$	7947	726	$5.7.10^4$	0.896	55
EH−7	5.3	94.7	0	543	180...300	$1.0.10^{10}$	203	84	$8.0.10^7$	0.017	41

D_{av} — average diameter
D_{min} — minimum diameter
D_{max} — maximum diameter

Table 2

Kinetic parameters of the Ree-Eyring model

Emulsion	1st non-Newtonian unit		2nd non-Newtonian unit	
	ΔG_3 (KJ/mol)	$K'_3(s^{-1})$	ΔG_2 (KJ/mol)	$K'_2(s^{-1})$
EC−1	−122	$8.9.10^{-10}$	−66	11 .9
EC−2	−120	$2.8.10^{-9}$	−62	45 .4
EC−3	−126	$2.4.10^{-9}$	−65	15 .6
EC−4	−114	$3.1.10^{-8}$	−66	10 .9
EC−5	−94	$8.9.10^{-5}$	−66	12 .2
EC−6	−100	$8.7.10^{-6}$	−73	0 .56
EH−7	−118	$6.1.10^{-9}$	−63	29 .4

Thus, the more uniform the particles size of the emulsion is, the easier the flow is at small shearing rates and the smaller the apparent viscosity is.

As suggested by the experimental data (because the curves in Figure 1 overlap at medium shearing rates) the relaxation time β_2 does not depend on the degree of polydispersion. The relaxation time β_2 of the emulsion EC 6 (without transfer agent) is higher by an order of magnitude than that of the other copolymer emulsions. Thus, the dimensions of the non-Newtonian unit which dominate the flow at intermediate shearing rates are higher when an insoluble fraction exists in the copolymer. The existence of an insoluble fraction determines the persistence of the network at intermediate shearing rates.

For the non-Newtonian unit corresponding to the intermediate shearing rates, one can observe no dependence on the degree of polydispersion for the free energy of activation ΔG_2 and the rate constant k'_2. For the EC-6 emulsion, ΔG_2 has a higher value and the k'_2 constant a much smaller one due to the structure of "pseudonetwork" which hinders the flow.

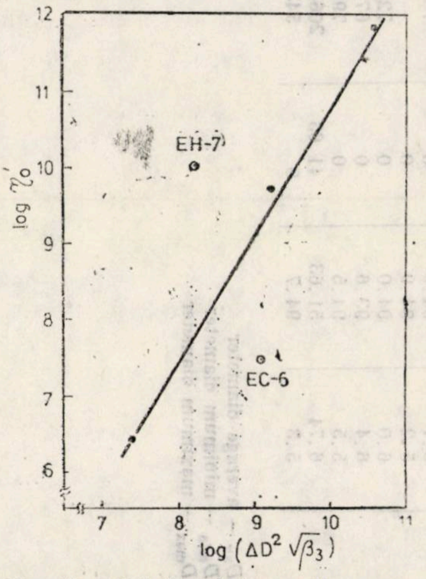

Fig. 2. — Relation between the parameters of the Ree-Eyring model and the width of the polydispersion interval.

The values of the standard errors from Table 1 show that the rheological behaviour of the emulsions is well approximated by the model chosen in the field of low and intermediate range of applied shearing, but it does not allow the exact calculation of the Newtonian component η_∞ of the viscosity.

The data presented in Table 1 point to the existence of a correlation between η'_0 and β_3, allowing us to write the equation :

$$\eta'_0 = a \cdot c_S \cdot \Delta D^2 \sqrt{\beta_3} \qquad (5)$$

where C_S is the solid content (%) of the emulsion, ΔD is the width of the polydispersion interval and the constant $a = 1 \cdot 10^{-6}$.

Thus, the points corresponding to the EH-7 homopolymer and to the EC-6 copolymer (obtained without a transfer agent) are located outside the line plotted in Figure 2.

Equation (5) is similar to equation (6):

$$\eta_0' = k \cdot c^2 \cdot M \sqrt{\beta_p} \tag{6}$$

for polymer solutions, where c is the concentration of the solution in (%), M is the molecular weight of the polymer while β_p is the relaxation time of the main unit. The k constant has the value $2 \cdot 10^{-5}$ for the solution of polyacrylonitrile in dimethylformamide [2] and $3.2 \cdot 10^{-4}$ for the solution of cellulose nitrate in butyl acetate. [2]

2. Restructuring phenomena during the copolymerization of vinyl acetate with di-ethylhexyl maleate

In the process of VAc homo- and copolymerization in the presence of macromolecular emulsifiers, in semi-continuous system of monomer adding, the apparent viscosity of the reaction mixture varies non-monotonously, having a maximum at a certain moment, followed by a minimum, after which the viscosity increases again.

For instance, in the case of VAc polymerization in the presence of PVA, the viscosity increases up to the value of 40% solid content, decreases suddenly down to 45% solid content and then increases again to the end of the polymerization (56% solid content) (Fig. 3). When the maximum viscosity is reached, the emulsion is polydispersed and agglomerated, the average diameter of the particles being of $2 \cdot 10^{-3}$ mm. As the polymerization process goes on, the particles regain their individuality, still remaining very crowded, the average diameter is of $3 \cdot 10^{-3}$

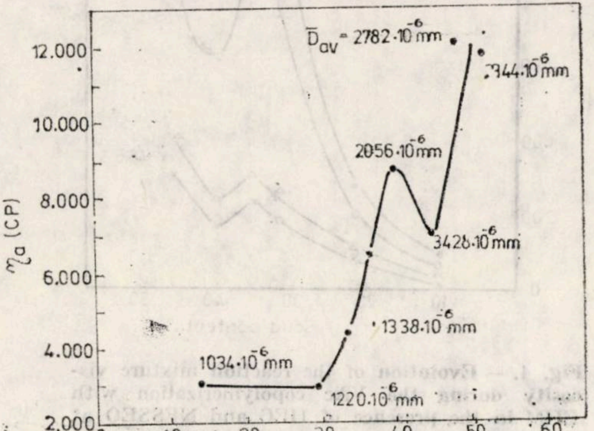

Fig. 3. — Evolution of the viscosity of the reaction mixture during VAc polymerization in the presence of 10% completely saponificated PVA (at shearing rate = 5.4 s^{-1}).

mm, although very large particles of $5.5 \cdot 10^{-3}$ mm appear and the viscosity is minimum. The fact should be mentioned that during the whole process of polymerization, the reaction mixture also contains small particles of about $1.2 \cdot 10^{-3}$ mm, but the viscosity of solution is due to the largest sizes.

This evolution of the particles size was mentioned in other papers, too, and it was explained on the basis of continuous nucleation and agglomeration of the newly formed particles.

In the case of VAc copolymerization with EHM in the presence of HEC and NFSSEO, the maximum viscosity occurs at 35% solid content and the minimum at 40% solid content (Fig. 4).

These experimental data indicate that during the VAc polymerization and copolymerization process in semicontinuous process, a phenomenon of emulsion restructuration appears.

The availabilities of the Ree-Eyring model of following the process of VAc copolymerization with EHM are illustrated in the present paper by establishing the rheological parameters.

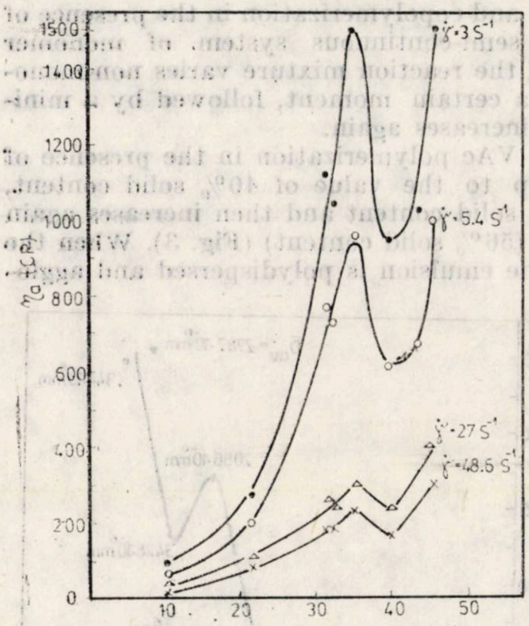

Fig. 4. — Evolution of the reaction mixture viscosity during the VAc copolymerization with EHM in the presence of HEC and NFSSEO at different values of the shearing rate.

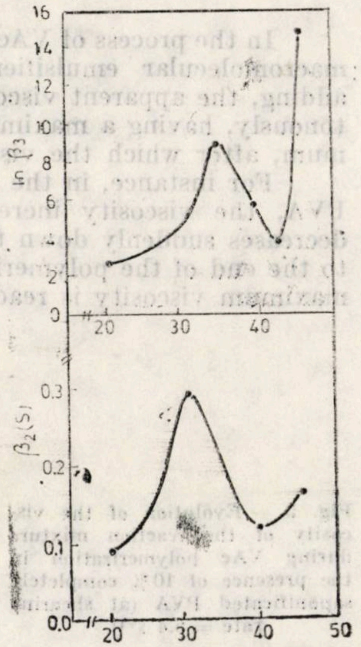

Fig. 5. — Relaxation times of the two non-Newtonian flow units during the copolymerization process.

For all the moments of the copolymerization process, the two relaxation times β_2 and β_3 of the two non-Newtonian units differ from one another from the point of view of the magnitude order (Fig. 5).

The maximum values of η'_0 and β_3 correspond to the maximum value of the apparent viscosity η_a from 35% solid content, and to the maximum apparent viscosity of the final emulsion. Consequently, in the maximum point and in the final emulsion, in the absence of any force and at low shearing forces there are multiple interactions, so that the emulsions can be considered three-dimensional networks. In contrast with the paper [2], nonmonotonous variation of β_3 with emulsion concentration is noticed. The minimum values of η'_0 and β_3 correspond to the minimum apparent viscosity and indicate the fact that at that moment there is no more a three-dimensional network, because it is destroyed by the occurrence of big particles in the system.

The phenomenon is similar with the one observed in the case of mixtures of two emulsions — one emulsion with high apparent viscosity of above 10,000 cP and particles with a very small diameter and another emulsion with viscosity of 300 cP and big particles. The mixture 50/50 has the apparent viscosity of 500 cP.

The free energy of flow activation in the absence of any force is maximum in the point with maximum apparent viscosity because the jump over the potential barrier is made difficult under the conditions of a network structure and a lower energy of activation when there are no multiple interactions, that is at the point of minimum (Fig. 6).

The formation of two distinct structure during copolymerization is rendered evident by the evolution of the rate constant (Fig. 7). The points corresponding to the rate constant as a function of the solid content of the polymerization mixture are situated on two distinct lines.

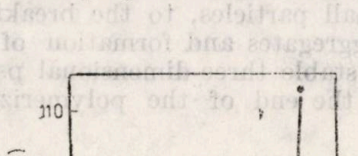

Fig. 6. — Modification of the free energy of activation of the non-Newtonian flow unit which dominates the flow at low shearing rates during the copolymerization process.

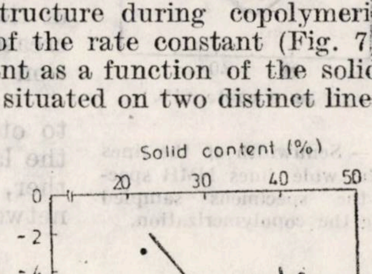

Fig. 7.—Evolution of the rate constant of the non-Newtonian flow unit from the low shearing rates zone during the copolymerization.

In the wide lines of the NMR spectra of the specimens sampled during the polymerization, there appear two distinct components having the semiwidth δH_1 and δH_2 (Fig. 8). The transition points determined by the intersection of the tangent to the curve correspond to that value of solid content for which restructuration is indicated by the viscometry.

The fact should be mentioned that at concentrations of up to 40% solids for which there is the first three-dimensional structure, the NMR line also has a dispersion component besides the absorption one, each one with different intensity. The spectra of the samples with concentrations of more than 40% solids do not exhibit the dispersion component, which proves that the species with high mobility disappeared.

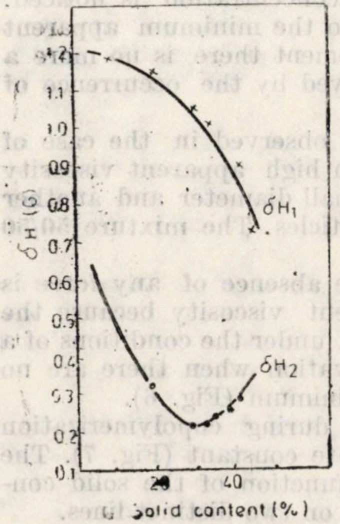

Fig. 8. — Semiwidth of the lines from the wide lines NMR spectra of the specimens sampled during the copolymerization.

The conclusion can be drawn that during VAc polymerization and copolymerization in the presence of HEC, in semicontinuous system of monomer adding, the diameter of the particles varies ununiformly due to the continuous nucleation.

The existence of very small particles allows the formation of a three-dimensional pseudonetwork. In a certain stage of the reaction, very big particles, well individualized, appear which lead to the destruction of the network and induce the abrupt decrease of the viscosity of the polymerization mixture.

The progressing of the reaction leads to other small particles, to the breaking of the large aggregates and formation of another, more stable three-dimensional pseudonetwork in the end of the polymerization.

CONCLUSIONS

The Ree-Eyring model, based on the theory of the activated complex proved to fit well the interpretation of the rheological behaviour of the VAc-EHM copolymers emulsions.

By means of the Ree-Eyring model parameters values, the pseudonetwork structure of these emulsions was established, explaining their pseudoplastic behaviour in this way.

In the case of the copolymer emulsions with the same average particles diameter but having different polydispersion degrees, the parametrs of the mofel differ only for the non-Newtonian unit which determines the flowing at very low shearing rates.

The copolymer emulsions which also contain a fraction of crosslinked copolymer (insoluble) behave like a more resistant network, while the three-dimensional structure is maintained at intermediate shearing rates, too.

The Ree-Eyring model also proved efficient in the study of the copolymerization process, rendering evident the formation of two distinct network structures and allowing us to notice the restructuring moment.

REFERENCES

[1] R. A. Ghani and A. S. Dunn, *Polymer Communications*, **24**, 285 (1983).

[2] D. Eagland and M. Kay, *Colloid Interf. Sci.*, **34**, 249 (1970).

[3] O. Quadrat and J. Jr. Snuparek, *J. Colloid Interf. Sci.*, **119**, 597 (1987).

[4] V. L. Kuznetzov, E. A. Dorohova, V. Iu. Erofeev and B. K. Basov *Koloidnyi J.*, **4**, **806 (1985)**.

[5] S. Hecht, H. Herold, W. Poge, A. Wichmann and R. Zenker, *Plaste und Kuntschuk*, **30**, 551 (1983).

[6] W.-D. Hergeth and K. Schmutzler, *Acta Polymerica*, **36**, 565 (1985).

[7] H. Zecha, *Acta Polymerica*, **36**, 57 (1985).

[8] B. R. Vijayendran, *Makromol. Chem. Suppl.*, 1**0** **11**, 271 (1985).

[9] D. Donescu, K. Goşa and I. Languri, *Acta Polymerica*, in press.

[10] T. Ree and H. Eyrig, *J. Appl Phys.*, **26**, 793 (1955).

[11] A. F. Gabrish, H. Eyring, M. Shimzer and J. Assay, *J. Appl. Phys.*, **34**, 261 (1963).

[12] W. K.-Kim, N. Hirai, T. Ree, *J. Appl. Phys.*, **31**, 358 (1960).

[13] I. G. Murgulescu and E. Segal "Introducere în chimia fizică" vol. 2 part 1, Ed. Academiei, Bucharest 1979, p. 808.

[14] D. Donescu, K. Goşa, S. Bogdănescu, G. Symide, C. Manolache, L. Paşcanu and A. Poşa, Romanian Patent no. 90166 (1986).

[15] D. Donescu, I. Deaconescu, K. Goşa, M. Mazăre and I. Gavăt, *Rev. Roum. Chim.*, **25**, 975 (1980).

[6] D. Donescu, K. Goşa and I. Languri, *Acta Polymerica*, **40**, 49 (1989).

[7] D. Donescu, K. Goşa and Â. Ciupiţoiu, *J. Macromol. Sci.-Chem.*, **A22**, 931 (1985).

Revue Roumaine de Chimie, **36**, *11–12*, 1299–1306(1991)

MESOIONIC OXAZOLONES. VII[1]

ABOUT THE MECHANISM OF THE HYDROLYSIS OF ACYLATED DERIVATIVES

HORIA PETRIDE

Centre of Organic Chemistry- Romanian Academy, Spl. Independenţei 202 B, 78141 Bucharest
12, Romania

Received November 29, 1989

The kinetics of the hydrolysis of bicyclic 3-acylated mesoionic oxazolones **5–8** was investigated. For the nonplanar compounds **6–8** an izokinetic relationship $\Delta H^*/\Delta S^*$ was found. Different mechanisms of the hydrolysis were proposed for the planar (**5**) and nonplanar derivatives. The first step might be the protonation of the substrate.

In the preceding papers of this series [1–3] we presented the behaviour towards nucleophiles (water, ethanol, aniline) of several mesoionic oxazolones ("münchnones") with an oxazolo [3,2-a] pyridinium - or quinolinium-2-olate structure, especially from the point of view of reaction products. Thus, the hydrolysis of the 3-unsubstituted derivatives **1** and **2**, generated *in situ*, afforded easily the acids **3** and **4**, respectively.[2] Analogously reacted the 3-acylated compounds **5–8** giving the ketones **9–12**, as decarboxylation products of the transient keto-acids KA.[1] The mesoionic oxazolones **5a-b** ($R^1 = H$) having the acyl group coplanar[4] with the mesoionic nucleus displayed a smaller reactivity towards water[1] than their analogs **6–8** in which the acyl group and the rest of the molecule are no longer coplanar (the increase of the steric demand of the $R^1 = Me$ substituent).[4]

Rate constants have been determined for the ethanolysis of **2** and **6a-b** but not for **5a-b**, because the reaction products were unstable in this last case.[2,3] However, a complete set of kinetic measurements was obtained for the hydrolysis of planar (**5a-b**) as well for the nonplanar acylated compunds (**6–8**). These results, along with their mechanistic implications, are presented in this paper. To our knowledge these are the first examples concerning a quantitative assessment for the reactivity towards water of acylated münchnones.

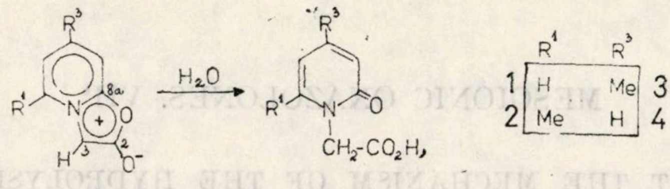

1-2 3-4

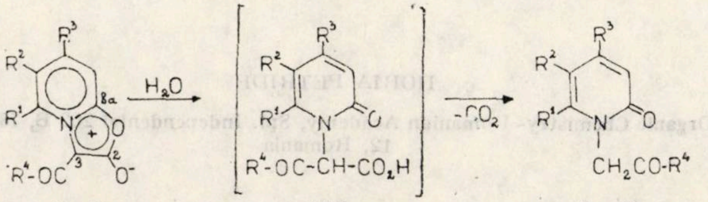

5-8 KA 9-12

	R¹	R²	R³	
5a-b	H	H	Me	9a-b
6a-b	Me	H	H	10a-b
7b	Me	H	CO_2H	11b
8b	Me	CO_2H	H	12b

5-12	R⁴
a	CH_2Cl
b	$CHCl_2$

RESULTS AND DISCUSSION

Similarly to the hydrolysis of the 3-unsubstited compounds **1** and **2**,[2] the analogous reaction of their acylated derivatives **5**–**8** was performed in aqueous acetonitrile (pseudo-first order reaction conditions) and followed spectrophotometrically.

Preliminary trials showed that the observed rate constants are dependent on the relative water concentration and also on the presence of strong acids. The room temperature hydrolysis of **6a** in aqueous acetonitrile had measurable reaction rates if : (i) the water concentration is over 1 M, or (ii), keeping the water content at a lower value (*ca.* 0.1 M), a strong acid is added. Analogously reacted the planar derivative **5a**, but a higher temperature was needed, as expected.

The acid catalysis of the hydrolysis of the studied compounds implies that either a protonation reaction is the slowest step or that protonation occurs before the rate-determining step. Table 1 presents the observed rate constants for the perchloric acid-catalyzed hydrolysis of **6a**. These data suggest that the rate-determining step is the nucleophilic attack of the water molecule at the previously protonated substrate.

The hydrolysis of **5**–**8** was performed also in neutral acetonitrile-water solutions (1 : 1, v/v), that is under comparable conditions with those employed for compounds **1** and **2**.[2] The corresponding rate constants and activation parameters are given in Table 2 and 3, respectively.

Table 1

Acid-catalyzed hydrolysis of **6a** in aqueous acetonitrile. (Temperature : 25°C ; [**6a**] = 2×10^{-4} mole.L^{-1} ; Acid : $HClO_4$)

Nr.	$10^3 \times [H_3O^+]$ (mole.L^{-1})	$10^2 \times [H_2O]$ (mole.L^{-1})	$10^3 \times k_{obs}$ (s^{-1})	$\frac{k_{obs}}{[H_3O^+][H_2O]}$
1	2.47	7.46	0.52	2.82
2	2.84	7.76	0.66	2.99
3	2.84	14.43	0.99	2.41
4	3.56	14.27	1.31	2.58
5	4.89	13.24	1.53	2.36
				mean = 2.63

Table 2

Rate constants for the hydrolysis of bicyclic münchnones **5**–**8**

Compd.	Temp. (°C)	$10^4 \times k_{obs}$ (s^{-1})	Compd.	Temp. (°C)	$10^4 \times k_{obs}$ (s^{-1})
		Planar acylated compounds			
5a	92.2	1.8	**5b**	105.3	1.6
	105.4	5.2		117.7	4.2
	118.0	13.5		130.6	10.75
		Nonplanar acylated compounds			
6a	10.5	1.9	**6b**	24.5	1.8
	24.5	8.0		36.5	6.3
	36.5	21.4		46.5	19.0
7b	24.5	1.8	**8b**	21.7	3.1
	46.5	19.1		31.0	7.7
				40.0	19.0

Table 3

Activation parameters[a] in the hydrolysis of bycyclic münchnones.

Compd.	ΔH^* (kcal.mole^{-1})	ΔS^* (e.u.)	k_{rel} [b]
	Non-acylated compunds		
1[c]	17.4	−18.9	(1)
2[c]	17.4	−18.9	(1)
	Nonplanar acylated compounds		
6a	15.6	−20.3	7.2
6b	19.4	−10.5	3.5
7b	19.6	− 9.8	3.7
8b	17.5	−15.2	5.5
	Planar acylated compounds		
5a	21.4	−17.6	0.0050
5b	2.22	−17.2	0.0019

[a] estimated errors : $\Delta H^* \pm 0.2$; $\Delta S^* \pm 0.7$. [b] extrapolated at an intermediate temperature (65°C). [c] from ref.[2].

As it can be seen from the last column of Table 2, the parent münchnones **1** and **2** possess towards water a reactivity intermediate between those of their planar and nonplanar acylated derivatives. They are 3—7 times less reactive than the nonplanar **6**—**8**, but 200—500 times more reactive than their planar analogs **5a-b**. It emerges that, in comparison with **1** and **2**, the nonplanar acylated münchnones have a smaller perturbation of the electronic distribution than their planar acylated derivatives, as advanced in a preceding paper.[4]

Interesting aspects are revealed by plotting ΔH* *vs.* ΔS* (Fig. 1). Through the points corresponding to the nonplanar acylated compounds an isokinetic line[5] may be drawn (slope β ~ 109°C), indicating that one and the same mechanism is in action. At the same time, the points related to the planar acylated derivatives lie far from this line. This dichotomy suggests different hydrolysis mechanisms for the two types of the studied acylated münchnones, i.e. the nonplanar and planar ones. The point corresponding to the non-acylated precursors **1** and **2** is not on the

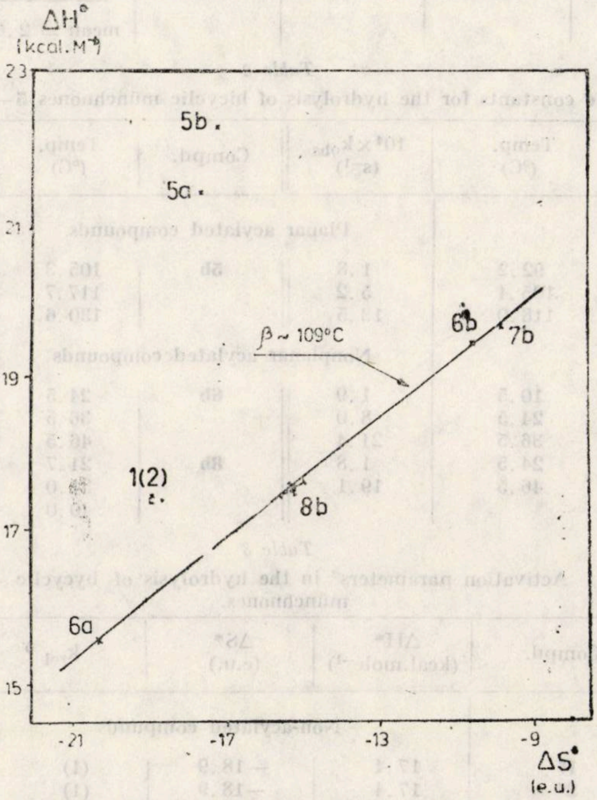

Fig. 1. — Correlation of the activation parameters in the hydrolysis of bicyclic münchnones. (the axes of the errors ellipsoid are shown for one point only ; the numbers correspond to the substrates).

isokinetic line, but very near of it. Therefore, these last two compounds might undergo hydrolysis by a similar, though not identical, mechanism with that of their nonplanar acylated analogs. However, more data are needed to test this last hypothesis.

Only few data are available for the hydrolysis mechanism of mesoionic oxazolones. Thus, it was shown by Knorr[6] that water attacks the selectively ^{18}O-labelled monocyclic münchnone **13** at both 2 and 5* positions, the first pathway prevailing (70%). Although the reaction occurred in acidic medium (1 N HCl in aq. THF), the transient formation of a cation like **14**[7] was not considered. On the other hand, Huisgen *et. al.* supposed[7] that the behaviour of **13** towards nucleophiles could be better understood if the valence tautomer **15** is postulated as intermediate. However, from **15** a sole hydrolysis product can result, namely that derived from the nucleophilic attack at its *sp*-carbon atom, in contradiction with Knorr's work. By consequence, the implication of the ketene **15** in the hydrolysis of **13** can be rejected, and this might be also the case for our bicyclic münchnones.

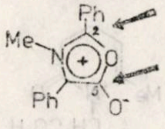

13

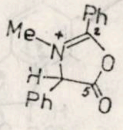

14

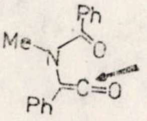

15

As presented before, the acid-catalyzed hydrolysis of **5**—**8** indicated a protonation reaction as a first step. To the extent of this being true also for a neutral hydrolysis, one may write two types of protonated forms. As previously reported,[8] the nonplanar acylated compounds **6**—**8** undergo protonation at the C_3 carbon atom, while their planar analogs **5a-b** at the oxygen atom of the acyl group. Accordingly, the cations **16**** and **17** are formed from **6**—**8** and **5a-b**, respectively. Obviously, these protonated species are more powerful electrophiles than the parent münchnones.

The behaviour towards water of **16** and **17** is also known.[8] At room temperature, the cation **16** (derived from **6a**) easily undergoes hydrolysis to the ketone **10a**, while **17** (derived from **5a**) affords the parent substrate **5a**. This resembles the behaviour of compounds **18** and **19**, respectively, as previously discussed. Thus, in the same conditions in which **18** gives the acid **4**, the perchlorate **19** does not react at all (see exp. part). The hydrolytic cleavage of the oxazolic ring in **19** to yield the acid **20** occurs only with warm sodium hydroxide solution.[9] All these data suggest that the cations **16**, **17** and their parent münchnones present similar tendencies in their reactivity towards water (with destruction of the oxazole nucleus).

---

* Positions 2 and 5 of the monocyclic compounds **13**, **14**, and **26**—**28** are equivalent to the positions 8a and 2, resp., of the bicyclic derivatives **1**, **2**, **5**—**8** and **16**—**23**.

** For simplicity, only the substituents positions are indicated in the chart for **16**, **17** and **21**—**24**.

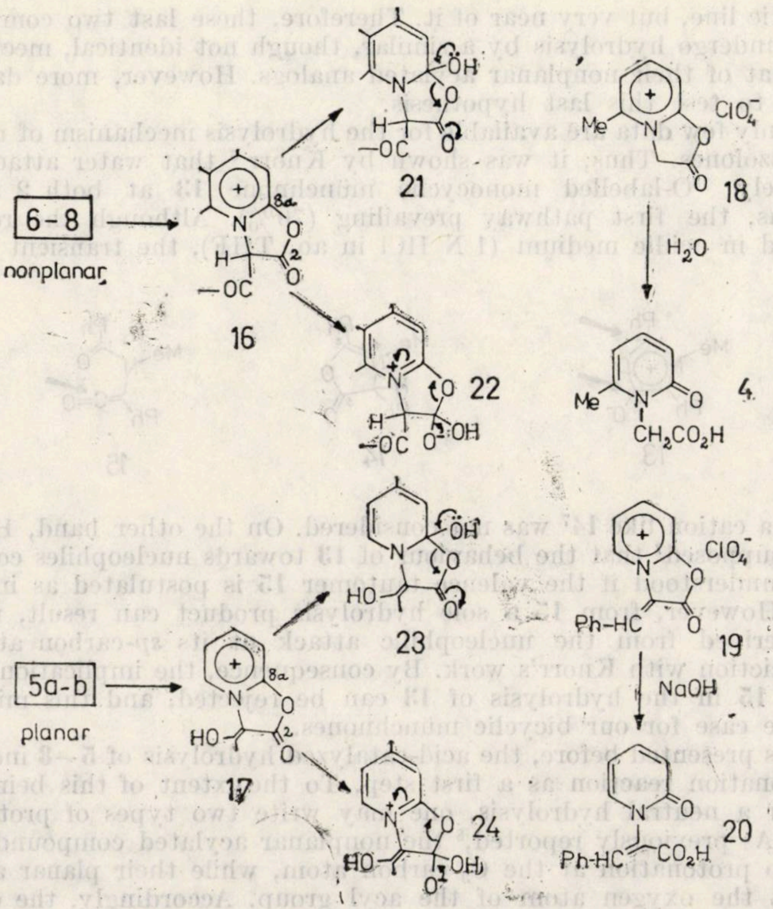

Additional interesting deductions can be made by considering the two virtual electrophilic sites of **16** and **17**, as suggested by the described behaviour of **13**. Thus, depending on the position of the nucleophilic attack (C_{8a} and/or C_2), two types of tetrahedral intermediates may result from **16** and **17**, namely **21**—**22** and **23**—**24**, respectively. The energies required for the formation of these intermediates are expected to be different. Thus, the transformation **16**→**22** might be favoured relatively to **16**→**21**, because in this case the pyridinium ring aromaticity is preserved. Obviously, this does not occur during the hydrolysis of the monocyclic münchnone **13**. Moreover, it is known [10] that the pyridine **25** is hydrolyzed *only* by attack at its carbonyl carbon atom. For the concurrent transformations **17**→**23** and **17**→**24**, the energetic requirements might be not so different. Indeed, the first pathway destroys the pyridinium ring aromaticity, but preserves the conjugation between carbonyl and the *exo*-ethylenic bonds; the opposite is true for the second alternative route. It results that the ratio "attack at C_{8a}/attack at C_2" may be smaller for **16** as compared to **17**.

To the same conclusion one may arrive if azlactones **26**–**28** are taken into consideration. Cation **27** and a nitrogen-protonated form of **28** are model compounds for **16** and **17**, respectively. Hydrolysis of the azlactone **26** occurs exclussively *via* attack at C_5 in neutral, basic or acidic medium.[11] At the same time, the cation **27** (R=Me, Ph) undergoes

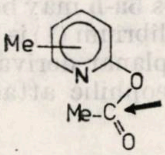

25

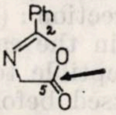

26

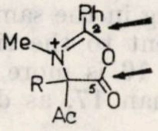

27

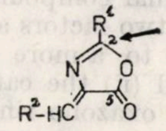

28

acidolysis at both 2 and 5 positions,[6,12] indicating a higher electrophilicity at position 2 relatively to that of the corresponding position in **26**. On the other hand, the methylene-azlactones **28** are attacked only at C_2 for R^1 = alkyl.[13] It emerges that the nucleophilic attack at C_2 will occur to higher extent for a nitrogen-protonated form of **28**. The behaviour of **13** (probably through its protonated form **14**) is in agreement with these data.

All these considerations lead to the following general scheme for the hydrolysis of the studied münchnones **5**–**8**:

$$(1) \qquad M + HA \underset{k_{-1}}{\overset{k_1}{\rightleftarrows}} MH^+ + A^- \qquad (HA : H_3O^+, H_2O)$$

$$(2) \qquad MH^+ + Nu \xrightarrow{k_2} T \qquad (Nu : H_2O, OH^-)$$

$$(3) \qquad T \longrightarrow \text{product}$$

The first step is a reversible protonation of the münchnone M yielding the cation MH^+ by either hydronium ion (in acid-catalyzed reactions) or by water molecule (in neutral conditions). The protonated species is attacked subsequently by a nucleophile (Nu) leading to a tetrahedral intermediate (T). As nucleophile may act water or even the hydroxyl anion (generated in step (1) in neutral medium), if living sufficiently closely to the substrate as lyate ion. The third step is a composite one, including the formation and decarboxylation of the acids KA. By analogy with esters and azlactones hydrolyses, this last step may be not rate-determining. Therefore, as suggested also by the data of Table 1, the observed rate constants are given by

$$k_{obs} = (k_1/k_{-1})k_2 \qquad (k_{-1} \gg k_2[Nu]),$$

implicating the second step as the slowest one.

Accordingly, the nonplanar acylated münchnones **6**—**8** undergo hydrolysis by a different mechanism than their planar analogs **5a**-**b**. In the first case, the substrate is protonated to **16** which in turn yields mainly the tetrahedral intermediate **22**. In the second case, different structures are expected for both protonated species (**17**) and tetrahedral intermediate (more probably **23**). The enhanced reactivity towards water of the nonplanar compounds **6**—**8** relatively to their planar analogs **5a**-**b** may be due to two factors acting in the same direction : (i) the equilibrium (1) is shifted to a more extent to the right in the case of nonplanar derivatives and (ii) the cation **16** is more susceptible to the nucleophilic attack at its oxazolic ring than **17**, as discussed before.

EXPERIMENTAL PART

Kinetic data were obtained by spectrophotometric measurements, as described.[2,3] The reactions were monitored by the decay of the electronic absorption at 333 nm (357 nm for **7b**) for 3—4 half-life times. For the more reactive compounds **6**—**8**, the progress of the reaction was observed in the thermostated cell of the UV apparatus ; for **5a**—**b**, previously heated glass ampoules were analyzed. The evolved carbon dioxide did not disturb the measurements.

The pseudo-first order rate constants k_{obs} were obtained with the least-squares method from the equation :

$$\ln(\log(T_\infty/T)) = -k_{obs} \cdot t + \text{const.}, \qquad (1)$$

where T_∞ and T are the transmission at time "infinite" and at the considered time t, respectively.

If the origin of time is accurately known, the constant of equation (1) is given by :

$$\text{const.} = \ln((\varepsilon_M - \varepsilon_P) \cdot c_0 \cdot d), \qquad (2)$$

where ε_M, ε_P are the molar extinction coefficients of the mesoionic substrate and the reaction product, respectively (at the considered wavelength), c_0 is the initial concentration of the münchnone, and d the cell length. Because ε_P is known from separate determinations or from the transmission at "infinite" time the ε_M value of the more reactive compounds **6**—**8** may be calculated from equations (1) and (2). Because of the uncertaintes upon the exact "zero" time an approximate value of $\log \varepsilon_M$ is 4.1 at the longest λ_{max}.[4]

The isokinetic line (Figure 1) had a correlation coefficient of 0.99. The criteria of Exner[14] are satisfied for this relationship.

At 25°C, the solution of **18** in acetonitrile containing 0.1 M of water and 0.001 M of perchloric acid displayed $\lambda_{max} = 281$ nm ($\log \varepsilon = 3.90$) within two minutes, a spectrum identical to that of the acid **4** in the same conditions. Analogous treatment of the perchlorate **19** presented $\lambda_{max} = 369$ nm ($\log \varepsilon = 4.05$) ; the spectrum remained unchanged after one day. Its hydrolysis product **20** displayed a very different spectrum ($\lambda_{max} = 286.5$ nm ; $\log \varepsilon = 3.90$) in the same conditions.

REFERENCES

[1] Part VI : H. Petride, *Rev. Roumaine Chim.*, **35**, 1107 (1991).
[2] Part II : H. Petride and D. Răileanu, *Rev. Roumaine Chim*, **33**, 729 (1988).
[3] Part V : H. Petride, *Rev. Roumaine Chim*, **35**, 747 (1990).
[4] Part III : H. Petride and D. Răileanu, *Rev. Roumaine Chim.*, **34**, 1251 (1989).
[5] J. E. Leffler and E. Grundwald, "Rates and Equiliria of Organic Reactions", J. Wiley &Sons, New York, 1963.
[6] R. Knorr, *Chem. Ber.*, **104**, 3633 (1971).
[7] H. O. Bayer, R. Huisgen, R. Knorr and F. C. Schaefer, *Chem. Ber.*, **103**, 2581 (1970).
[8] Part IV : D. Răileanu and H. Petride, *Rev. Roumaine Chim.*, **35**, 459 (1990).
[9] G. V. Boyd and P. H. Wright, *J. Chem. Soc. (C)*, **1970**, 1485.
[10] S. Oae and S. Kozuka, *Tetrahedron*, **20**, 2691 (1964).
[11] T. C. Curran, C. R. Farrar, O. Niazy and A. Williams, *J. Amer. Chem. Soc.*, **102** 6828 (1980).
[12] G. Höfle, A. Prox and W. Steglich, *Chem. Ber.*, **105**, 1718 (1972).
[13] W. Steglich, V. Amstel and A. Prox, *Angew. Chem.*, **80**, 701 (1968).
[14] O. Exner, *Coll. Czech. Chem. Commun.*, **29**, 1094 (1964).

Revue Roumaine de Chimie, **36**, *11–12*, 1307–1313 (1991)

REARRANGEMENTS OF 1,1a,6,6a-TETRAHYDROCYCLOPROP-[a]INDEN-6-OLS IN SUPERACIDS

A. C. RĂZUŞ,[a] E. BARTHA,[a] Zs. ARVAY,[a] S. A. OSADCHII,[b] V. I. MAMATYUK[b] and V. G. SHUBIN[b]

[a] Center of Organic Chemistry, Spl. Independenţei 202B, 78141, Bucharest, Romania
[b] Institute of Organic Chemistry, Siberian Division of the Academy of Sciences, Prosp. Acad. Lavrentyev, 9, 630090, Novosibirsk, USSR

Received May 10, 1990

Rearrangements of the methyl substituted 1, 1a, 6, 6a-tetrahydrocycloprop[a]inden-6-ols (**1b-d**) in superacids (HSO_3F-SO_2FCl (A) or $HSO_3F-SbF_5-SO_2FCl$ (B)) are described Carbinols **1c**, **d** rearrange into 4- and 2-methyl-1H-napthalenonium ions, respectively, even at −95°C, while carbinol **1b** gives 6-methyl-1, 1a, 6, 6a-tetrahydrocycloprop[a]inden-6-yl cation (**2b**) which transforms into 1-methyl-3-fluorosulphonyloxymethyleneindan-1-yl cation (**5**) at −25°C.

Sterically hindered cyclopropylcarbinyl ions, 1,1a, 6, 6a-tetrahydrocycloprop[a] inden-6-yl cations (**2a-d**), were suggested to be intermediates in the acid-catalyzed rearrangements of 1, 1a, 6, 6a-tetrahydrocycloprop[a]inden-6-ols (**1a-d**) : [1]

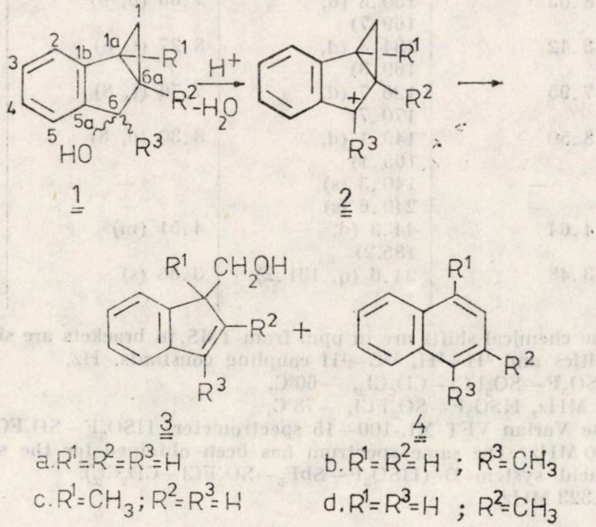

a. $R^1=R^2=R^3=H$ b. $R^1=R^2=H$; $R^3=CH_3$
c. $R^1=CH_3$; $R^2=R^3=H$ d. $R^1=R^3=H$; $R^2=CH_3$

SCHEME 1

The mechanism of this rearrangement may be supported by the data reported by Olah and coworkers[2] who have found that the 1, 1a, 6, 6a-tetrahydrocycloprop[a]inden-6-yl cation (**2a**) generated under stable ion conditions (HSO_3F-SO_2FCl or $HSO_3F-SbF_5-SO_2FCl$, −78°C) rearranges at increased temperature to the 1H-naphthalenonium ion, while the 6-methyl-1, 1a, 6, 6a-tetrahydrocycloprop[a]inden-6-yl cation (**2b**) is more stable.

We report here an attempt to generate the methyl-substituted cations (**2b-d**) under stable ion conditions and to study their transformations in order to obtain some additional information on the mechanism of the above rearrangement.

The cation **2b** has been generated from 6-methyl-1, 1a, 6, 6a-tetrahydrocycloprop[a]inden-6-endo-ol (**1b**) in acid system A, $HSO_3F-SO_2FCl-CD_2Cl_2$ and in acid system B, $HSO_3F-SbF_5-SO_2FCl-CD_2Cl_2$ (the ratio HSO_3F/SbF_5 is 2/1 in moles) at −95°C. The ^1H NMR data for this ion are consistent with the data reported in the literature, [2] while the ^{13}C NMR data somewhat differ (Table 1). The assignement of the ^{13}C resonances were made on the basis of signal multiplicities and the values of residual splitting of the signals in the "off-resonance" spectrum, which are known[3] to be proportional to the values of differences between irradiation frequency and signal frequencies of the correspoding hydrogen atoms in the ^1H NMR spectrum.

Table 1

^1H and ^{13}C NMR spectra of ion 2b[a)]

Position	Literature data [2]		Data of this work[b)]	
	$\delta\ ^1H$[c)]	$\delta\ ^{13}C$[d)]	$\delta\ ^1H$[e)]	$\delta\ ^{13}C$[f)]
1	3.22, exo- 3.60, endo-	89.1 (dd, 171.7, 174.7)	3.12 (m), exo-; 3.50 (m), endo-	89.2 (dd, 170.0, 174.4)
1a	4.85	49.0 (d, 186.5)	4.73 (m)	44.2 (d, 185.0)
1b	—	169.6 (s)	—	169.5 (s)
2	8.05	130.8 (d, 169.7)	7.88 (d, 8)	126.8 (d, 170.8)
3	8.42	134.4 (d, 169.3)	8.27 (t, 8)	149.2 (d, 165.2)
4	7.95	126.7 (d, 170.7)	7.76 (t, 8)	130.9 (d, 170.4)
5	8.50	149.1 (d, 165.1)	8.30 (d, 8)	134.4 (d, 169.6)
5a	—	140.3 (s)	—	140.2 (s)
6	—	249.6 (s)	—	249.1 (s)
6a	4.64	44.3 (d, 185.2)	4.51 (m)	49.0 (d, 186.0)
CH_3	3.48	24.6 (q, 131.2)	3.38 (s)	24.8 (q, 131.0)

[a)] The chemical shifts are in ppm from TMS, in brackets are signal multiplicities and $^1H-^1H$, $^{13}C-^1H$ coupling constants, Hz.

[b)] $HSO_3F-SO_2FCl-CD_2Cl_2$, −60°C.

[c)] 60 MHz, HSO_3F-SO_2FCl, −78°C.

[d)] The Varian VFT XL-100—15 spectrometer, HSO_3F-SO_2FCl, −78°C.

[e)] 200 MHz. The same spectrum has been obtained for the solution in the acid system B ($HSO_3F-SbF_5-SO_2FCl-CD_2Cl_2$).

[f)] 50.323 MHz.

As shown by the ^1H, ^{13}C (Table 2) and ^{19}F NMR data (singlet at -204.4 ppm from C_6F_6) as the temperature raised up to −25°C, the ion

Table 2

^{1}H and ^{13}C NMR spectra of ion 5a), b)

Position	δ ^{1}Hc)	δ ^{13}Cd)
1	—	252.7 (s)
2	3.63 (d, J_{gem} 26.5[6]) and 4.2 (m)e)	51.0 (t, 132.0)
3	4.2 (m)e)	45.0 (d, 135.2)
3a	—	174.4 (s)
4	8.18 (d, 8)	128.7 (d, 170.0)
5	8.7f)	155.4 (d, 166.0)
6	8.05 (t, 7)	133.5 (d, 170.0)
7	8.7f)	136.4 (d, 170.0)
7a	—	144.9 (s)
CH_3	3.52 (s)	25.7 (q, 130.4)
CH_2O	5.04g)	74.3 (t, 156.0[8,9])

a) The chemical shifts are in ppm from TMS, in brackets are signal multiplicities and $^1H-^1H$, $^{13}C-^1H$ coupling constants, Hz. b) Acid system A, −50°C. c) 200 MHz. d) 50.323 MHz. e) The signals of one of C^2H_2 protons and the 3-H proton are overlapping. f) The signals of the 5-H and 7-H protons are overlapping. g) A symmetric multiplet of 8 peaks, part AB of the ABX system.[10]

2b generated in the acid system A is transformed to the cation containing the OSO_2F group. (cf. ^{19}F NMR resonance for such a group [4,5]). For this cation there are four possible isomeric structures, **5**—**8**:

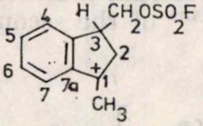

5

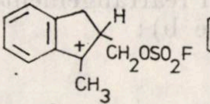

6

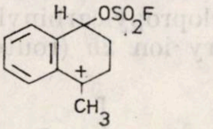

7

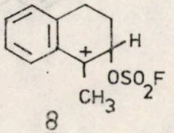

8

The structures **7** and **8** are rejected, because the chemical shift for the $\underline{C}HOSO_2F$ carbon (d, 45.0 ppm) is much smaller than that expected for these structures (~70 ppm[4,12]). The choice between the structures **5** and **6** in favour of **5** has been made from the data obtained by the LRJMD method.[11] Thus, on irradiation of CH_2OSO_2F protons (5.04 ppm, the signals of carbons 45.0 d, C^3), 51,0 (t, C^2) and 174.4 (s, C^{3a}) are observed in the ^{13}C NMR spectrum, the geminal and vicinal J_{CH} couplings being developed. The assignment of the ^{1}H and ^{13}C resonances for the cation **5** (Table 2) have been made by analogy with the data for ions **2a**, **2b**, indanyl cations,[6,7] and neutral compounds $C_2H_5OSO_2F$ and $CH_3O\ SO_2F$.[4]

It is possible that the cation **5** results from the C^1-C^{6a} bond cleavage of the cyclopropane ring of ion **2b**. Such cleavages have earlier been observed either in the solvolytic conditions[1] or under stable ion conditions.[13]

The attempts to generate the 1a-methyl-1,1a,6,6a-tetrahydrocycloprop[a]inden-6-yl cation (**2c**) in the acid systems A and B from a mixture of epimeric 1a-methyl-1,1a,6,6a-tetrahydrocycloprop[a]inden-6-ols (**1c**-endo/exo ~ 3/2) failed. As shown by the ^{1}H NMR spectrum, even at −95°C, the 4-methyl-1H-naphthalenonium ion **9**[14] was formed instead of the expected ion **2c**. An attempt to generate the 6a-methyl-1,1a 6,6a-tetrahydrocycloprop[a]inden-6-yl cation (**2d**) by dissolution of the 6a-methyl-1,1a,6,6a-tetrahydrocycloprop[a]inden-6-endo-ol (**1d**) in the acid system B was also unsuccessful, the ^{1}H NMR spectrum at −95°C indicated the formation of the 2-methyl-1H-naphthalenonium ion (**10**).[14] The cations **2c** and **2d** are probably formed as a result of ionisation of the alcohols **1c** and **1d** but they are readily isomerized to the corresponding naphthalenonium ions **9** and **10** even at −95°C.

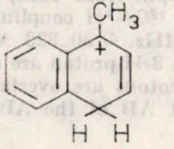

9

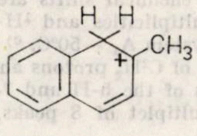

10

As the cation **9** seems to be generated according to scheme 2 and the isomeric cation **2b** is quite stable in these conditions, the absence of the signals of the latter in the ^{1}H NMR spectrum indicates the low rate of the cyclopropylcarbinyl rearrangement[15,16] of the secondary ion **2c** to the tertiary ion **2b** (route b):

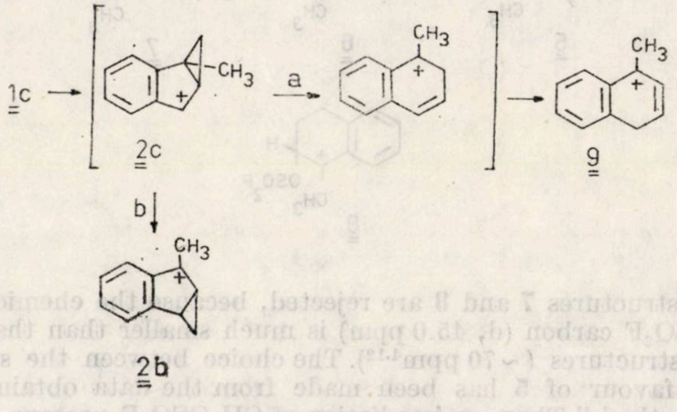

SCHEME 2

The increase in the isomerization rate of the ions **2c** and **2d** as compared to ion **2b** is probably due to cleavage of the cyclopropane ring which proceeds in the former two ions with transformation of the secondary carbocations to the more stable tertiary ones, whereas in the latter case the situation is just reverse. These results are consistent with the transformation of the alcohols **1c** and **1d** into 1- and 2-methylnaphthalene, respectively, in acid-catalyzed conditions.[1,15]

EXPERIMENTAL

The ^{1}H NMR spectra of neutral compounds and carbocationic salts were recorded on Bruker AC 200, Bruker WP 200 SY and Varian A56/60A instruments. For the solutions of neutral compounds, hexamethyldisiloxane was used as an internal standard (δ_H 0.04 ppm), for the solutions of carbocationic salt, CH_2Cl_2 (δ_H 5.33 ppm). The ^{13}C NMR spectra were recorded on Bruker AC 200 and Bruker WP 200 SY (50.323 MHz) instruments in different conditions : a) complete decoupling ; b) off-resonance irradiation of protons ; c) monoresonance. For the solutions of carbocationic salts, CD_2Cl_2 was used as internal standard (δ_C 53.3 ppm). For recording the LRJMD spectra, the program by Salnikov[17] was used.

The ^{19}F NMR spectra of the cation **5** were recorded on a Bruker WP 200 SY instrument (188.28 MHz), with SO_2FCl as internal standard (δ_F 269.1 ppm from C_6F_6[18]). For generation of carbocations, the doubly distilled HSO_3F (b.p. 158—161°C) was used, as well as SO_2FCl obtained according Woyski.[19] The latter was purified by boiling with SbF_5,[20,21] by keeping over anhydrous KF,[21] SbF_3, and by passing the vapour through conc. H_2SO_4. Sampling of on salts solutions for the NMR spectroscopic study was carried out as described earlier.[22]

I. Synthesis of starting compounds

In the literature[15,23,24] there are described the synthesis and the ^{1}H NMR spectra of alcohols **1b**, **1c** and **1d** using spectrometers with an operating frequency 60 MHz.[2] This paper gives some additional ^{1}H NMR data for these alcohols obtained using spectrometer with an operating frequency 200 MHz, as well as the ^{13}C NMR data for these compounds (Table 3).

II. Generation of carbocations

1. 6-Methyl-1, 1a, 6, 6a-tetrahydrocycloprop[a]inden-6-yl cation (**2b**).

a) In the acid system A. To a stirred solution of 0.13 g of 6-methyl-1, 1a, 6, 6a-tetrahydrocycloprop[a]inden-6-endo-ol (**1b**[15]) in 0.6 mL CD_2Cl_2 cooled to −100°C, was added dropwise, by means of a pipette cooled in liquid nitrgen, 1.5 mL of HSO_3F-SO_2FCl (1 : 4 v/v) mixture cooled to −100°C. The light red solution was stirred at −100°C for 5 min.

b) In the acid system B. The solution of 0.13 g of alcohol **1b**, 0.6 mL CD_2Cl_2 and 1.5 mL of SO_2FCl prepared as described above, was added dropwise with stirring to a solution of 1.11 g of HSO_3F-SbF_5 (2 : 1 in moles) mixture in 1.5 mL of SO_2FCl cooled to −100°C. The mixture was stirred at −100°C for 5 min.

2. 1-Methyl-3-fluorosulphonyloxymethyleneindan-1-yl cation (**5**). A solution of the salt of ion **2b**, prepared in the acid A system as described in section II-1a, was heated to −25°C and kept at this temperature for 20 min.

3. 4-Methyl-1H-naphthalenonium ion (**9**) is formed from a mixture of epimeric 1a-methyl-1, 1a, 6, 6a-tetrahydrocycloprop[a]inden-6-ols[15] (**1c**-endo/exo ~ 3 :2) under the section II-1b conditions. The ^{1}H NMR spectra recorded at −95°C and −60°C coincide with those for the solution prepared under the same conditions from 0.11 g 1-methylnaphthalene. The ^{1}H NMR spectrum (60 MHz, −60°C) : 3.43 t (3H, J 2.5 Hz, CH_3), 4.96 broad signal (2H, CH_2), 7.8—8.6 m (4H, 3-H, 6-8-H), 8.83 d (1H, J 8 Hz, 5-H), 9.17 d (1H, J 8 Hz, 2-H).

4. 2-Methyl-1H-naphthalenonium ion (**10**) is formed from 6a-methyl-1, 1a, 6, 6a-tetrahydrocycloprop[a]inden-6-endo-ol (**1d**)[15] and also from 2-methylnaphthalene (0.11 g) under the section II-1b conditions. The ^{1}H NMR spectrum (200 MHz, −60°C) : 3.06 s (3H, CH_3), 5.02 s (2H, CH_2) ; ABCD system : 7.96 t (1H, J 8 Hz, 6-H), 8.09 d (1H, J 8 Hz, 8-H), 8.26 t (1H, J 8 Hz, 7-H), 8.37 d (1H, J 8 Hz, 5-H) ; 8.00 d (1H, J 8 Hz, 3-H), 9.38d (1 H, J 8 Hz, 4-H).

Table 3

^{1}H and ^{13}C NMR spectra of alcohols[a] **1b**, **1c**[b] and **1d**

Position	**1b**-endo[c]		**1c**-endo		**1c**-exo		**1d**-endo[d]	
	δ^1H	δ^{13}C	δ^1H	δ^{13}C	δ^1H	δ^{13}C	δ^1H	δ^{13}C
1	endo : 0.62 (m) exo : 1.02 (ddd, 8.0, 7.5 7.5 and 4.8)	17.5 (t, 162)	endo : 0.70 (t, 4.0) exo : 0.82 (dd, 8.0 and 4.0)	21.9 (t)	endo : 0.22 (t, 4.0) exo : 1.04 (dd, 8.0 and 4.0)	26.1 (t)	endo : 0.57 (dd, 4.0 and 3.5) exo : 0.85 dd, 8.0 and 4.0)	23.2 (t)
1a	2.45 (ddd, 7.5, 5.8 and 3.3)	21.8 (d, 172)	—	29.0 (s)	—	28.7 (s)	2.20 (dd, 8.0 and 3.5)	29.4 (d)
1b, 5a	—	144.8 (s), 146.0 (s)	—	142.0 (s), 148.6 (s)	—	143.3 (s), 149.2 (s)	—	143.2 (s), 146.8 (s)
2–5	7.2–7.3 (m)	123.1[e] 123.7[e] 126.0[e] 127.5[e]	7.2–7.3 (m)	121.5 (d), 125.3 (d), 126.0 (d), 127.6 (d)	7.2–7.3 (m)	121.7 (d), 125.6 (d), 125.7 (d), 128.1 (d)	7.1–7.3 (m)	122.9 (d), 124.4 (d), 125.7 (d), 127.6 (d)
6	—	81.2 (s)	exo : 5.52 (d, 6.5)	75.5 (d)	endo : 4.80 (s)	75.5 (d)	5.24 (s)	81.5 (d)
6a	1.85 (ddd, 8.0, 5.8 and 4.3)	26.0 (d, of multiplets, 170)	1.79 (ddd, 8.0, 6.5 and and 4.0)	27.4 (d)	1.84 (dd, 8.0 and 5.0)	33.4 (d)	—	26.6 (s)
CH_3	1.66 (s)	30.0 (q, 127)	1.55 (s)	16.6 (q)	1.60 (s)	17.1 (q)	1.46 (s)	19.1 (q)
OH		—	2.70 (broad signal)	—	2.70 (broad signal)	—	2.70 (broad signal)	—

[a] The chemical shifts are in ppm from TMS, in brackets are signal multiplicities and $^1H-^1H$, $^{13}C-^1H$ coupling constants, Hz. ^{1}H NMR spectra were recorded using 200 MHz instrument, the ^{13}C spectra—50.323 MHz. [b] A mixture of epimers, **1c**, endo/exo 3 : 2, 10% solution in $CDCl_3$, cf. lit. data[15,24,25] [c] 10% solution in $CDCl_3/CD_3OD$:4/1, cf. lit. data [2,15,23] [d] 10 % solution in CD_2Cl_2, cf. lit. data [15] [e] doublet, J_{CH} 160 Hz.

REFERENCES

[1] A. C. Răzuş, V. Wertheimer, A. M. Glatz, Zs. Arvay and F. Badea, *Rev. Roumaine Chim.*, **26**, 457 (1981).

[2] G. A. Olah, G. Liang and S. P. Jindal, *J. Org. Chem.*, **40**, 3259 (1975).

[3] H. Gunther, "NMR Spectroscopy. An Introduction", Mir, Moscow, 1984, p. 394.

[4] A. Diaz, I. L. Reich and S. Winstein, *J. Amer. Chem. Soc.*, **91**, 5637 (1969); R. C. Kumar, S. A. Kinkead and J. M. Shreeve, *Inorg. Chem.*, **23**, 3112 (1984).

[5] G. A. Olah, G. K. S. Prakash and J. Sommer, "Superacids", J. Wiley and Sons, New York, 1985, p. 35; O. A. Gavrilyuk, D. V. Korchagina, Yu. V. Gatilov, V. Manatyuk, S. A. Osadchii, E. A. Fisher, Zh. V. Dubovenko and V. A. Barkhash, *Zhur. Org. Khim.*, **23**, 457 (1987).

[6] C. U. Pittman and W. G. Miller, J. *Amer. Chem. Soc.*, **95**, 2947 (1973).

[7] N. C. Deno, C. U. Pittman and J. O. Turner, *J. Amer. Chem. Soc.*, **87**, 2153 (1965); G. A. Olah, G. Asencio and H. Mayr, *J. Org. Chem.*, **43**, 1518 (1978); G. A. Olah, G. K. S. Prakash, A. L. Berrier and G. Liang, *Nouv. J. Chim.*, **4**, 691 (1980).

[8] H.-O. Kalinowski, S. Berger and S. Braun, "Carbon-13 NMR Spectroscopy", J. Wiley and Sons, New York, 1988, p. 497.

[9] B. E. Hansen, in "Progress in Nuclear Magnetic Resonance Spectroscopy", Ed. by J. W. Emsley, Pergamon Press, Oxford, 1981, vol. 14, part 4, p. 191; Pal Sohar, "Nuclear Magnetic Resonance Spectroscopy", CRC Press, Boca Raton, Florida, 1983, vol. 2, p. 214.

[10] J. W. Emsley, J. Feeney and L. H. Sutcliffe, "High Resolution Nuclear Magnetic Resonance Spectroscopy", Mir, Moscow, 1968, vol. 1, p. 349.

[11] H. Seto and K. Furihata, *JEOL News*, **21**A, 2 (1985).

[12] See ref.,[8] p. 174.

[13] T. S. Sorensen and K. Rajeswari, *J. Amer. Chem. Soc.*, **93**, 4222 (1971).

[14] G. A. Olah, G. D. Mateescu and Y. K. Mo, *J. Amer. Chem. Soc.*, **95**, 1865 (1973); G. A. Olah, J. S. Staral, G. Asencio, G. Liang, D. A. Forsyth and G. D Mateescu, *J. Amer. Chem. Soc.*, **100**, 6299 (1978); N. V. Bodoev, V. I. Mamatyuk, A. P. Krysin and V. A. Koptyug, *Zhur. Org. Khim.*, **14**, 1929 (1978).

[15] V. Wertheimer, A. M. Glatz and A. C. Răzuş, *Rev. Roumaine Chim.*, **22**, 1505 (1977).

[16] R. F. Childs and S. Winstein, *J. Amer. Chem. Soc.*, **90**, 7146, (1968); V. A. Koptyug, V. I. Mamatyuk, L. I. Kuzubova and I. S. Isaev, *Izv. Akad. Nauk SSSR, ser. khim.*, **1969** (7), 1635; P. Vogel, M. Saunders, N. M. Hasty and J. A. Berson, *J. Amer. Chem. Soc.*, **93**, 1551 (1971); G. A. Olah, G. K. S. Prakash and T. N. Rawdah, *J. Org. Chem.*, **45**, 965 (1980); D. P. Kelly, D. R. Leslie and B. D. Smith, *J. Amer. Chem. Soc.*, **106**, 687 and 6119 (1984).

[17] G. E. Salnikov, "ABACUS Program Library Catalog", Spectrospin AG, Fallanden, Switzerland, March 1988.

[18] G. A. Nisnevich, V. I. Mamatyuk and V. A. Barkhash, *Zhur. Org. Khim.*, **18**, 1660 (1982); * * * Pure Appl. Chem., *45*, 217 (1976).

[19] M. M. Woyski, *J. Amer. Chem. Soc.*, **72**, 919 (1950).

[20] J.-Y. Calves and R. J. Gillespie, *J. Amer. Chem. Soc.*, **99**, 1788 (1977).

[21] G. A. Olah, M. R. Bruce and J. Welch, *Inorg. Chem.*, **16**, 2637 (1977).

[22] S. A. Osadchii, M. P. Polovinka, D. V. Korchagina, N. A. Pankrushina, Zh. V. Dubovenko, V. A. Barkhash and V. A. Koptyug, *Zhur. Org. Khim.*, **17**, 1211 (1981).

[23] H. O. House, W. C. McDaniel, R. F. Sieloff and D. Vanderveer, *J. Org. Chem.*, **43**, 4316 (1978).

[24] E. C. Friedrich, D. B. Taggart and M. A. Saleh, *J. Org. Chem.*, **42**, 1437 (1977).

[25] V. S. Watts and J. H. Goldstein, *J. Chem. Phys.*, **46**, 4165 (1967).

Revue Roumaine de Chimie, **36**, *11–12*, 1315–1320 (1991)

SYNTHESIS OF INTENSELY COLOURED 2,4,6-TRISUBSTITUTED PYRYLIUM SALTS POSSESSING BULKY GROUPS[1]

OVIDIU MAIOR[a], ANTONIE DINCULESCU[b], ION BACIU[a], GEORGETA BOTEZ[c], and CLAUDIU T. SUPURAN[a]*

[a] University of Bucharest, Department of Organic Chemistry, Bd. Republicii 13, Bucharest 1 Roumania
[b] Chemical-Pharmaceutical Research Institute Bucharest, Vitan Street 112, Bucharest, Roumania
[c] Oncological Institute Bucharest, Roumania.

Received March 5, 1991

Novel pyrylium salts possessing bulky groups in positions 2 or 4 were prepared by reaction of 2,4,6-trimethyl-, 2-methyl-4,6-diphenyl- or 4-methyl-2,6-diphenyl-pyrylium perchlorates with aromatic/heterocyclic aldehydes. The newly prepared compounds, which possess intense colours, were characterized by means of UV–VIS, IR and ^{1}H–NMR spectra.

INTRODUCTION

Pyrylium salts versatility in organic syntheses as well as their importance for theoretical organic chemistry (representing an extreme case of aromaticity with a strong perturbation due to the presence of the positively charged heteroatom) explains the well-deserved attention this topic received in the last years, major contribution in this field being done by Balaban's group.[2]

In addition to the thoroughly studied reactions with nucleophiles, alkyl-substituted pyrylium salts undergo condensation reactions with aldehydes, leading to styryl-pyrylium derivatives. This reaction was discovered by Dilthey and Fischer[3] who prepared in this way 2,6-diphenyl-4-styryl- and 2,4-diphenyl-6-styryl-pyrylium salts. It was later extended to other compounds by Dorofeenko's[4] and Balaban's[5] groups. It was also shown that benzaldehydes substituted with electron-donating groups react more easily and in higher yields, probably due to the enhanced electrophilicity of their carbonyl group.[4b,6]

In the case of 2,4,6-trimethyl pyrylium perchlorate, the 4-methyl group is the first which undergoes this condensation reaction,[5–7] a common feature with the deuteration reaction of the same methyl groups in this and related alkyl-substituted pyrylium salts.[8] This is the reason why the reaction of 2,4,6-trimethyl-pyrylium perchlorate with substituted benzaldehydes affords the corresponding 2,6-dimethyl-4-substitued styryl-pyrylium salt.

---

* To whom correspondence should be addressed.

In previous reports,[9,10] we showed that tri-, tetra- or penta-substituted pyrylium salts are versatile synthons for obtaining a large variety of biologically active compounds such as enzyme inhibitors (for carbonic anhydrase[10] and cholinesterase[11] among others), coccidiostatics,[9b,12] ganglionic blocking agents,[9] all these substances possessing interesting properties like membrane impermeability, due to the presence of positive charge(s). These facts prompted us to extend our research to novel pyrylium salts, possessing other types of groups in positions 2 or 4, which, eventually would confer them and to the compounds prepared from them, desired properties, such as intense colour. Taking into account the intense colour of compounds like **1a**[5,6] (deep blue) and **1b**[3] (green), and our intention to design coloured carbonic anhydrase inhibitors,[10,13] which would allow us to study the interaction enzyme – inhibitor by means of UV–VIS spectroscopy, we focused our interest in obtaining novel pyrylium salts by reaction of 2,4,6-trimethyl-, 2-methyl-4,6-diphenyl- and 4-methyl-2,6-diphenyl-pyrylium perchlorates with aromatic/heterocyclic aldehydes; reaction of the substituted pyrylium salt pepared in this way with certain nucleophiles, would yield subsequently coloured enzyme inhibitors of type **2**[10] or **3**[9,10b] as was previously reported.

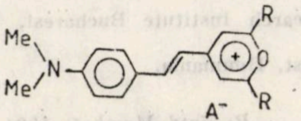

1 a: R = Me
b: R = Ph

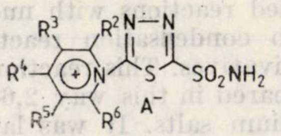

2

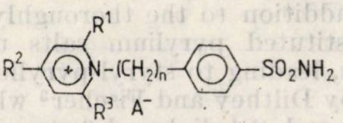

3 a: n = 0
b: n = 1

RESULTS AND DISCUSSION

In this paper we report the synthesis of 2,4,6-trisubstituted pyrylium salts possessing a bulky group (**7, 8, 10**), obtained by reaction of pyrylium perchlorates **4, 5, 9,** with bi- or tricyclic aromatic/heterocyclic aldehydes (**6**) (Schemes 1 and 2). The following aldehydes were used in these syntheses: 2-hydroxy-naphthalene-1-carboxaldehyde,[14] anthracene-9-carboxaldehyde,[15] phenoxathiine-2-carboxaldehyde,[16] and 10-methyl-phenothiazine-3-carboxaldehyde.[17]

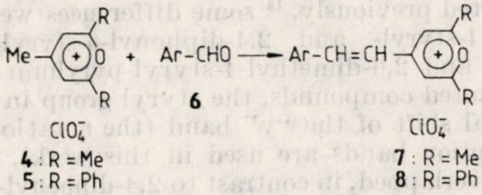

Me
R
R
O
+
Ar-CHO
6
Ar-CH=CH
ClO4⁻
4 : R = Me
5 : R = Ph
7 : R = Me
8 R = Ph

Compound	Ar	Yield (%)	Colour
7a	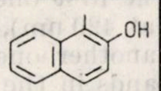	59	deep red
8a		73	purple
7 b	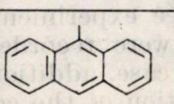	63	violet
8b	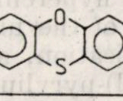	81	red-brown
8c	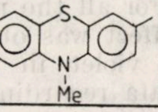	65	blue

Scheme 1

The syntheses of enzyme inhibitors and the studies of enzyme – inhibitor interaction will be reported elsewhere.[13]

The structure of the newly prepared compounds was assigned using UV–VIS, IR and ^1H–NMR spectroscopy, while their purity was determined by thin-layer chromatography (tlc).

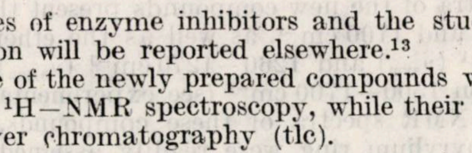

Ar-CHO +
Ph
Me
O
Ph
ClO4⁻
Ar-CH=CH
Ph
6
9
10

Compound	Ar	Yield (%)	Colour
10 a	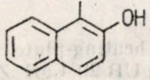	27	red-violet
10 b	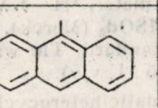	61	violet

Scheme 2

In the electronic absorption spectra of compounds **7**, **8** and **10**, the specific absorption bands of the aromatic and vinylic systems were detected. As reported previously,[18] some differences were observed between 2,6-diphenyl-4-styryl- and 2,4-diphenyl-6-styryl-pyrylium salts, and between these and 2,6-dimethyl-4-styryl-pyrylium derivatives. For the diphenyl-substituted compounds, the styryl group in position 4 induces a bathochromical shift of the "y" band (the notations of Balaban et al.[19] for the absorption bands are used in this work), so that the "x" and "y" bands are overlapped, in contrast to 2,4-diphenyl-6-styrylpyrylium salts which possess two distinct bands, x and y, respectively. This is also the case of our compounds **8a**-**c** and **10a**, **b**, this fact being very obvious for the two isomers **8a** and **10a**. The first one has only one absorption band in the interval 360–500 nm (at 420 nm), while the second one has a band at 364 nm (probably y) and another one at 471 nm (probably x). All these compounds have broad bands in the visible region, due to the conjugated chromophore system (see experimental part). No differences were detected when the spectra were recorded in acidified methanol, excepting for compoud **8c**. In this case, addition of concentrated hydrochloric acid to the methanolic solution of the compound led to a modified spectrum; the hypsochromic and hyperchromic shifts observed may be accounted for by the protonation of the nitrogen within the phenothiazinic ring, with formation of a dication, as reported previously for 2,6-dimethyl-4(*p*-dimethylamino-styryl)-pyrylium perchlorate **1a**, which undergoes a similar protonation.[5] For all the newly prepared compounds a strong positive solvatochromic effect was observed; for instance **8a** is red in dichloromethane solution, violet in acetone and deep blue in dimethyl-sulfoxide (quantitative data regarding this effect will be presented elsewhere).

The IR spectra of the new compounds present the intense perchlorate bands at 625 and 1100 cm^{-1}, as well as the ether stretching vibrations at 1020 cm^{-1} ($\bar{\nu}_{sym}$) and 1260–1270 cm^{-1} ($\bar{\nu}_{asym}$) and the aromatic bands in the region 1500–1700 cm^{-1} (see experimental part).

In the ^{1}H–NMR spectra of these compounds, the two protons attached to the pyrylium ring were readily assigned as singlet signals at δ 7.9–8.5 ppm. In some cases the two vinylic protons had signals which did not overlap the aromatic protons,but this was not always the case. In some cases the spectra could be interpreted by comparing the 2,6-dimethyl and 2,6-diphenyl-pyrylium salts possessing the same group in position 4.

EXPERIMENTAL

Melting points were determined on a heating-plate microscope and are not corrected. IR spectra were recorded in KBr pellets with a UR 20 Carl Zeiss Jena spectrometer, UV–VIS spectra on a Specord UV–VIS Zeiss spectrometer. ^{1}H–NMR spectra were taken at 60 MHz with a Varian EM 360 L spectrometer in DMSOd$_6$ (Merck). Chemical shifts are reported as δ values (ppm) relative to Me_4Si as internal standard. Tlc was done on silica (Kieselgel Fertigplatten from Merck) in benzene-acetone (5 : 1, v/v).

Pyrylium salts **4**[20], **5**[2] and **9**[2] and aromatic/heterocyclic aldehydes[14–17] were prepared by literature procedures.

General procedure for preparation of pyrylium salts 7, 8 10

20 mMoles of trisubstituted pyrylium perchlorate (4, 5 or 9) were suspended in 50 mL absolute methanol and heated to reflux temperature. 20 mMoles of aromatic/heterocyclic aldehyde dissolved in a small amount of MeOH were added dropwisely, over a period of two hours in the reaction mixture. Reflux was continued for other three hours, then the mixture was cooled in a refrigerator and left overnight. The crystallized condensation product was filtered off and recrystallized from acetic acid containing 5—10% $HClO_4$.

2,6-Dimethyl-4-(2-hydroxy-naphth-1-yl-etheno)-pyrylium perchlorate (7a)

Deep red crystals, m.p. 192—4°C. UV—VIS (MeOH)λ_{max} : 234, 272 (sh), 340, 425, 584 (sh), 640 nm ; IR (KBr) : 625, 1100, 1260, 1560 cm^{-1} ; ^{1}H-NMR (DMSO-d_6) (δ) : 2.80 (s, 6H, 2,6-Me_2), 6.60—6.90 (m, 2H, CH = CH), 7.15—8.10 (m, 6H, ArH from naphthyl), 8.22 (s, 2H, ArH from pyrylium) ppm. Tlc (benzene : acetone 5/1, v/v)R_f = 0.48.

2,6-Diphenyl-4-(2-hydroxy-naphth-1-yl-etheno)-pyrylium perchlorate (8a)

Purple crystals, m.p. 275—7°C. UV—VIS (MeOH) λ_{max} : 240, 352, 580, 640 (sh) nm ; IR(KBr) : 625, 710, 1100, 1510, 1620 cm^{-1} ; ^{1}H—NMR (DMSO-d_6) : 6.6—6.9 (m, 2H, CH=CH), 7.30—7.90 (m, 16H, ArH), 8.21 (s, 2H, ArH from pyrylium) ppn ; tlc (benzene : acetone 5/1, v/v), R_f = 0.53.

2,6-Dimethyl-4-(9-anthryl-etheno)-pyrylium perchlorate (7b)

Violet crystals, m.p. 234—6°C. UV—VIS (MeOH) : 225, 257, 370, 388, 510 (sh) nm ; IR(KBr) : 625, 740, 1020, 1100, 1260, 1560 cm^{-1} ; ^{1}H—NMR (DMSO—d_6) : 2 9 (s, 6H, 2,6—Me_2), 6.8—7.0 (m, 2H, CH = CH), 7.10—8.15 (m, 9H, ArH from anthryl), 8.00 (s, 2H, ArH from pyrylium) ppm ; tlc (benzene : acetone 5/1, v/v), R_f = 0.46.

2,6-Diphenyl-4-(phenoxathiin-2-yl-etheno)-pyrylium perchlorate (8b)

Red-brown crystals, m.p. 267°C. UV—VIS (MeOH) λ_{max} : 217, 244, 289, 420, 515 697 nm ; IR(KBr) : 625, 1020, 1100, 1190,1270, 1455, 1600 cm^{-1} ; ^{1}H—NMR (DMSO-d_6) : 6.8—6.95 (m, 2H, CH = CH), 7.05—8.50) (m, 17H, ArH), 8.80 (s, 2H, ArH from pyrylium) ppm ; tlc (acetone : benzene 1/5, v/v), R_f = 0.51.

2,6-Diphenyl-4-(10-methyl-phenothiazin-2-yl-etheno)-pyrylium perchlorate (8c)

Deep blue crystals, m.p. 260°C. UV—VIS (MeOH) λ_{max} : 218, 244, 260, 300, 420, 580 (sh), 650 nm ; in MeOH acidified with HCl : 215, 240, 260, 280, 415, 575 (sh), 650 (strong hyperchromic shift for the last three bands) ; IR(KBr) : 625, 680, 950, 1100, 1140, 1200, 1260, 1290, 1470, 1555 cm^{-1} ; ^{1}H—NMR (DMSO-d_6) : 3.32 (s, 3H, N—Me), 6.52 (m, 2H, CH = CH), 6.65—8.00 (m, 17H, ArH), 8.15 (s, 2H, ArH from pyrylium) ppm ; tlc (benzene : acetone 5/1, v/v), R_f = 0.39. An isomer of this compound, possessing the N-methyl-phenothiazinyl-etheno group in position 6 was reported previously by Wizinger and Rembold [21] and was characterized by elemental analysis and UV—VIS spectrum.

2,4-Diphenyl-6-(2-hydroxy-naphth-1-yl-etheno)-pyrylium perchlorate (10a)

Red-violet crystals, m.p. 268°C. UV—VIS (MeOH) λ_{max} : 252, 310, 364, 471, 665 nm ; IR(KBr) : 625, 670, 1050, 1100, 1270, 1480, 1550 cm^{-1} ; ^{1}H—NMR (DMSO-d_6) : 6.80—6.95 (m, 2H, CH = CH), 7.1—8.15 (m, 16H, ArH), 8.35 (s, 2H, ArH from pyrylium) ppm ; tlc (benzene : acetone 5/1, v/v), R_f = 0.49.

2,4-Diphenyl-6-(9-anthryl-etheno)-pyrylium perchlorate (10b)

Deep violet crystals, m.p. 189°C. UV—VIS (MeOH) λ_{max} : 220, 250, 308 (sh), 326, 338, 362, 380, 510 (sh) nm ; IR(KBr) : 625, 660, 770, 1050, 1100, 1270, 1480, 1550 cm^{-1} ; ^{1}H-NMR (DMSO-d_6) : 7.0—7.2 (m, 2H, CH = CH), 7.30—8.30 (m, 19H, ArH) ; 8.60 (s, 2H, ArH from pyrylium) ppm ; tlc (benzene acetone 5/1, v/v), R_f = 0.47.

ACKNOWLEDGMENT. Thanks are addressed to Professor Mircea D. Banciu for helpful discussions.

REFERENCES

[1] This paper is dedicated to Professor Alexandru T. Balaban on the occasion of his 60th anniversary and to Professor Petre Spacu on the occasion of his 85th anniversary.

[2] a. A. T. Balaban, W. Schroth and G. Fischer, *Adv. Heterocycl. Chem.*, **10**, 241 (1969); b. A. T. Balaban, A. Dinculescu, G. N. Dorofeenko, G. W. Fischer, A. V. Koblik, V. M. Mezheritskii and W. Schroth, "Pyrylium Salts: Syntheses, Reactions and Physical Properties" in *Adv. Heterocycl Chem.*, Suppl. 3, A. R. Katritzky Ed; Academic Press, New York 1982, and references cited therein.

[3] a. W. Dilthey and J. Fischer, *Ber. Dtsch. Chem. Ges.*, **56**, 1012 (1923); b. W. Dilthey and J. Fischer, *ibid.*, **57**, 1653 (1924).

[4] a. Y. A. Zhdanov, G. N. Dorofeenko, V. A. Palchkov and G. P. Safaryan, *Dokl. Akad. Nauk SSSR*, **155**, 1115 (1964) (*Chem. Abstr.* **61**, 3070 (1974)); b. G. N. Dorofeenko, O. E. Shelepin, Z. N. Nazarova, V. N. Novikov and G. P. Tikhonova, *Zh. Obsch. Khim.*, **35**, 570 (1965) (*Chem. Abstr.*, **63**, 1766 (1965)), c. Y. A. Zhdanov, G. N. Dorofeenko and V. A. Palchkov, *Khim. Geterotsikl. Soedin.*, 812 (1965) (*Chem. Abstr.*, **65**, 2205 (1965)); d. G. N. Dorofeenko, Y. A. Zhdanov, A. D. Semenov; V. A. Palchkov and S. V. Krivun, *Zh. Obsch. Khim.* **36**, 1728 (1966) (*Chem. Abstr.*, **66**, 55327 (1967)).

[5] D. C. Oniciu, A. Marton, T. S. Balaban, S. Vlad and A. T. Balaban, *Rev. Roumaine Chim.*, **35**, 561 (1990).

[6] M. Simalty, H. Strzelecka and H. Khejida, *Tetrahedron*, **27**, 3503 (1971).

[7] J. Kelemen and R. Wizinger, *Helv. Chim. Acta*, **45**, 1918 (1962).

[8] a. A. T. Balaban, E. Romas and C. Rentia, *Tetrahedron*, **22**, 1 (1966); b. E. Gârd, A. Vasilescu, G. D. Mateescu and A. T. Balaban, *J. Labelled Compd.*, **3**, 196 (1967).

[9] a. A. Dinculescu, Ph. D. Thesis, Polytechnic Institute, Bucharest 1979; b. A. Dinculescu and A. T. Balaban, *Rev. Roumaine Chim.*, **25**, 1505 (1980).

[10] a. C. T. Supuran, A. T. Balaban, M. D. Gheorghiu, A. Schiketanz, A. Dinculescu and I. Puscas, *Rev. Roumaine Chim.*, **35**, 399 (1990); b. C. T. Supuran, A. Dinculescu, G. Manole, A. Schiketanz, M. D. Gheorghiu, I. Puscas and A. T. Balaban, ***J. Pharm.** Sci. in press.*

[11] E. Stepan and A. T. Balaban, *Rev. Roumaine Chim.*, **28**, 707 (1983).

[12] A. Dinculescu and A. T. Balaban, *Roumanian Pat.* 71870 (1978).

[13] C. T. Supuran, A. Dinculescu and A. T. Balaban, manuscript in preparation.

[14] A. Russel and L. B. Lockhart, *Org. Synth. Coll. Vol.*, **3**, 463 (1955).

[15] E. Campaigne and W. L. Archer, *J. Amer. Chem. Soc.*, **75**, 989 (1953).

[16] a. O. Maior and A. Gioabă, *Ann. Univ. Bucharest*, XXII, 47 (1973); b. G. Vasiliu, A. Gioabă and O. Maior, *ibid.*, **11**, 175 (1962).

[17] V. Fărcăşan, I. Oprean and C. Bodea, *Rev. Roumaine Chim.*, **19**, 1841 (1954).

[18] H Khejida, H. Strzelecka and M. Simalty, *Bull. Soc. Chim. Fr.*, 3173 (1972).

[19] A. T. Balaban, V. E. Sahini and E. Keplinger, *Tetrahedron*, **9**, 163 (1960).

[20] A. T. Balaban and C. D. Nenitzescu, *Org. Synth. Coll. Vol.*, **5**, 1106 (1973).

[21] R. Wizinger and H. Rembold, *Chimia*, 156 (1959).

Revue Roumaine de Chimie, **36**, *11–12*, 1321–1324 (1991)

O-ARYLKETOXIMES. III[1]

OBTAINING 3-(4′-METHYL)-PHENYL-5-NITRO-BENZISOXAZOLE FROM O-[2-(4′-METHYL)-BENZOYL-4-NITRO]-PHENYL-KETOXIMES

CORNELIA MAJDIK, ALEXANDRU KOVENDI, SIMION MATEI and DORIN BREAZU
Chemical-Pharmaceutical Research Institute, str. Fabricii no. 126, 3400 Cluj-Napoca, Romania

Received June 10, 1989

Refluxing O-[2-(4′-methyl)-benzoyl-4-nitro]-phenyl-ketoximes (**3**) in ethanol saturated with hydrocloric acid, besides ketones **5**, 3-(4′-methyl)-phenyl-5-nitro-benzisoxazole **4** was obtained instead of the corresponding benzofurans **6**. The formation of **4** is possible by spliting the oximic bond of **3** into 0-[2-(4′-methyl)-benzoyl-4-nitro]-phenylhydroxylamine **8** and ketones **5**, under acid catalysis. Further on, the arylhydroxylamine **8** turns into **4** by cyclization, a new intramolecular oximic bound being formed.

Following our works on the ketoximes O-arylation[2] and the conversion of O-arylated derivatives into benzofurans,[1] we aimed at replacing the nitro activating group in chlorobenzenes (used as O-arylating agents) by the aroyl ones. If a benzoyl group stands in a *para* position to the halogen (4-chlorobenzophenones), arylation occurs under our conditions (THF-DMSO in the presence of KOH) at 70 to 80°C. By placing the benzoyl group in the *ortho* position to the chlorine atom (2-chlorobenzophenons), arylation did not occur even at high temperatures. The reaction was possible only after a nitro group has been placed in the *para* position to the halogen. The reaction develops under mild conditions (40°C, within 1.5 to 2 hours), using 2-chloro-5-nitro-4′-methyl-benzophenone (**1**) as arylating agent for the ketoximes **2**; the O-arylketoximes **3** were isolated with 80–90% yields.

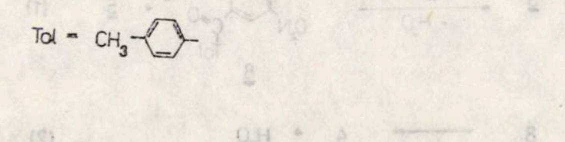

	a	b	c	d
R_1	CH_3	C_6H_5	p-$CH_3OC_6H_4$	C_6H_5
R_2	CH_3	CH_3	CH_3	C_2H_5

Subjecting the ketoximes **3 a-c** to transposition-cyclization to get benzofurans, [1,4] in ethanol saturated with gaseous hydrochloric acid under reflux, instead of the expected 5-nitrobenzofurans **6**, besides the ketones **5**, the same product **4** was isolated, heaving a m.p. 146°C and characteristics (determined by elemental analysis) corresponding to the molecular formula $C_{14}H_{10}N_2O_3$. We assume that another reaction took place affording 3-(4′-methyl)-phenyl-5-nitro-benzisoxazole (**4**) which can be identified with the help of its classic synthesis[5] namely the cyclization of 2-chloro-5-nitro-4′-methyl-benzophenonoxime (**8**) in the presence of potassium hydroxide. The products obtained by both these methods have the same m.p., which is not decreased in their mixture and their I.R. spectra are identical.

In the case of propiophenonoxime **3d**, besides **4d**, 2-phenyl-3-methyl-5-nitro-7-(4′-methyl)-benzoyl-benzofuran **6 d** was isolated, with a ratio of 60 : 40%. The formation of **6 d** in a concurrent reaction may be explained by the higher reactivity of the O-(4-nitrophenyl)propiophenonoximes an the corresponding acetophenonoximes in the transposition reaction.[1]

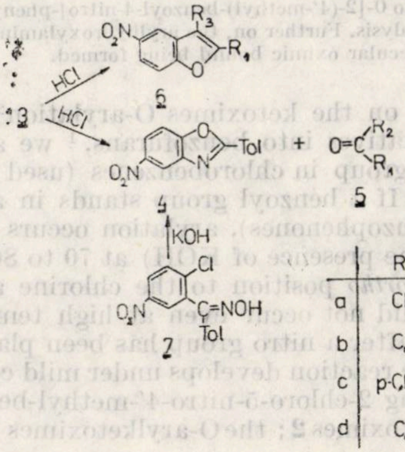

	R_1	R_2	R_3
a	CH_3	CH_3	H
b	C_6H_5	CH_3	H
c	p-$CH_3OC_6H_4$	CH_3	H
d	C_6H_5	C_2H_5	CH_3

The formation of the heterocycle **4** presumably involves the following two-step mechanism :

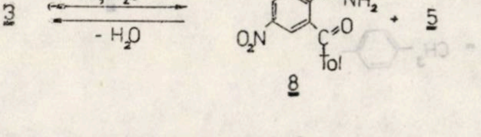

(1)

$$\mathbf{8} \longrightarrow \mathbf{4} + H_2O \qquad (2)$$

a) During the first step (1), under acid catalysis in equilibrium reaction, oximic bound (C=N—) in the **3** is splitted into O-/2-(4′-methyl)-benzoyl-4- nitro/-phenylhydroxylamine (**8**) and the ketones **5**.

b) In the second step (2), **8** is subjected to an intramolecular cyclization and a new oximic bond is formed to the benzisoxazole **4**. This mechanism is in agreement with the facts observed and with certain characteristics of O-aryl-and O-alkylketoximes : a) the ketonic component of **3** is formed in the reaction medium as ketones **5** ; b) literature provides information[6,7] on breaking the oximic bond of O-alkylketoximes by acid hydrolysis, with the formation of O-alkylhydroxylamines and the respective ketones ; c) the intramolecular cyclization of the proposed intermediated **8** is in fact a reaction yielding O-arylketoximes from O-arylhydroxylamines and ketones, already know in the literature.[4,8,9]

EXPERIMENTAL PART

Melting points are uncorrected. IR spectra were recorded on a C. Zeiss Jena Specord 75 IR with KBr discs.

Ketoximes **2**, were prepared as decribed in the literature.[10–13]

2-Chloro-5-nitro-4 -methylbenzophenone (**1**), was obtained by the Comubert and Mamel[14] method ; m.p. 92–93° C ; lit.[14] m.p. 93°C.

2-Chloro-5-nitro-4′-methylbenzophenonoxime, (**7**), was obtained from **1** and hydroxylamine hydrochloride in an analogous manner as previously described by Pagliarini *et al.*,[5] with 68 % yield and m.p. 160–161°C (benzene). Found : C, 57.80 ; H,3.92 ; Cl. 12.25 ; N, 9.70 %. Calcd. for $C_{14}H_{11}Cl\,N_2O_3$: C, 57.84 ; H, 3.81 ; Cl, 12.20 ; N, 9.66 %.

O-/2-(4′-methyl)-benzoyl-5nitro/-ketoximes, (**3**). Over a stirred solution of 0.1 mole (**1**) and 0.1 mole **2** in 50 mL DMSO and 50 mL THF add 6.5g KOH in small portions, during 15 to 20 minutes, so that the temperature gets not higher than 40°C. Keep the mixture with stirring at the same temperature for other 1.5 to 2 hours, until a sample shows chromatographically (thin layer) no ketones (**2**). Cool at room temperature and pour into water under continuos stirring. Filter the precipitate thus formed, wash it with water and dry it. The ketoximes **3** are then recrystallized from toluene.

O-/2-(4′-methyl)-benzoyl-4-nitro -acetoxime, (**3a**). Yield 85% ; m.p. 169–170°C. Found : C, 65.61 ; H, 4.93 ; N, 9.03 %. Calcd. for $C_{17}H_{15}N_2O_4$: C, 65.58 ; H, 8.45 ; N, 9.00 %. IR *spectrum* (KBr ; cm^{-1}) : 1667 (C = O), 1617 (C=N), 1595 (C=C), 1527, 1330 (NO_2), 1253, 1085 (=C–O), 930 (N–O).

O-2-(4′-methyl)-benzoyl-4-nitro/-acetofenonoxime, (**3b**). Yield 85 % ; m.p. 118°C. Found : C, 64.56 ; H, 4.21 ; N, 6.79 %. Calcd. for $C_{22}H_{17}N_2O_4$: C, 64.62 ; H, 4.19 ; N, 6.85 %. IR *spectrum* (KBr ; cm^{-1}) : 1667 (C=O), 1605 (C=N), 1580 (C=C) 1513, 1315 (NO_2), 1250, 1080 (=C–O), 967(N–O)

O- 2′-(4″-methyl)-4′-nitro-4-methoxy-acetophenonoxime, (**3c**) Yield 90 % ; m.p. 150–151°C. Found : C, 68.50 ; H, 4.65 ; N, 6.90 %. Calcd for $C_{23}H_{19}N_2O_5$: C, 68.48 ; H, 4.70 ; N, 6,95 %.

IR *spectrum* (KBr ; cm^{-1}) : 1660 (C=O), 1610 (C=N), 1585 (C=C) 1513, 1320 (NO_2), 1250, 1080 (=C–O), 968 (N–O).

O-/-(4′-methyl)benzoyl-4-nitro/-propiophenonoxime (**3d**). Yield : 85 % ; m.p. 110–111°C. Found C, 72.18 ; H, 5.22 ; N, 7.38 %. Calcd. for $C_{23}H_{20}N_2O_4$: C, 75.11 ; H. 19 ; N, 7.21 %. IR *spectrum* (KBr : cm^{-1}) : 1660 (C=O), 1605 (C=N), 1585 (C=C), 1527, 1350 (NO_2), 1228, 1073 (=C–O), 953 (NO).

3-(4′-Methyl)-phenyl-5-nitro-benzisoxasole, (**4**). To 3 g of oxime **7** in 200 mL of ethanol add 1 g of potassium hydroxide and reflux for one hour. Wash the organic layer with water and dry it over anhydrous natrium sulphate. Distille the solvent under vacuum and recrystallize the residue from alcohol : benzene. The resulting 1.5 g of **4**, m.p. 145–146°C. Found : C, 66.20 ; H, 4.10 ; N, 11.10 % Calcd for $C_{14}H_{10}N_2O_3$: C, 66.14 ; H, 3.94 ; N, 11.03 %. IR *spectrum* (KBr ; cm^{-1}) : 1616 (C=N), 1600 (C=C), 1527, 1305 (NO_2), 1267, 1085 (=C–O), 980 (N–O).

Benzisoxazole **4** *from* **3a-c**. A mixture of 10 g **3a** and 100 mL etnanol saturated with 17% gasous hydrochloric acid and 30 mL toluene was refluxed with stirring for 6 hours. Unlike the case of benzofurans no deposit of ammonium chloride is formed. Cool at room temperature and pour it into water. Add 100 mL toluene, stirr and decant the toluene layer. Extract the aqueous fraction with toluene. Wash the combined organic fraction with water, dry it over anhydrous natrium sulphate and evaporate the solvent under reduced pressure. To the remained residue add alcohol-benzene when **4** crystallizes. The resulting 6g of substance have a melting point of 144–146°C and no depression is observed on addition of a sample of **4** obtained from **7**. The IR spectrum is identical to that of **4** obtained from **7**. Found : C, 66.25 ; H. 4.10 ;

N, 11.12%. Calcd. for $C_{14}H_{10}N_2O_3$: C, 66.14 ; H, 3.94 ; N, 11.02 %. Under similar conditions the same product (**4**) may be obtained out of **3b** and **3c**, having the same characteristics. In this case, after removing toluene, acetophenone **5b** and 4-methoxyacetophenone **5c** are also removed from the remaining residue by steam distillation.

Transposition of propiophenonoxime **3d**. Start with 10 g of **3d** and proceed as shown above. After the reaction mixture is poured into water, the precipitate thus formed is filtered *and washed with cold toluene on the filter; 3.8 g of 2-phenyl-3-methyl-5-nitro-7-(4′-methyl)*-benzoyl-benzofuran (**6d**) with m.p. 170–171°C (toluene) is formed. Found : C, 74.35 ; H, 4.50 ; N, 3.82%. Calcd. for $C_{23}H_{17}NO_4$: C, 74.70 ; H, 4.50 ; N, 3.77 %.

IR *spectrum* (KBr ; cm^{-1}) : 3100, 2945 (C–H), 1667 (C=O), 1610, 1580 (C=C), 1540, 1325 (NO_2), 1285, 1080 (=C–O). From the filtrate the toluene layer is separated and the aqueous one is again extracted with toluene. Remove the toluene under vacuum and propiofenone **5d** by steam distillation. Cool and filter the solid fraction : 3.3 g of **4** are obtained. After recrystallization from alcohol : benzene, the product thus obtained has a m.p. of 143–145°C and does not show depression when mixed with an authentic specimen.

REFERENCES

[1] Part. II. C. Majdik, Al. Kovendi, S. Matei and D. Breazu, *Rev. Chim. (București)*, in press.

[2] C. Majdik, Al. Kovendi, S. Matei and D. Breazu *Rev. Chim. (București)*, in press.

[3] C. Majdik, Al. Kovendi, S. Matei and D. Breazu, manuscript in preparation.

[4] T. Sheradsky, *J. Heterocycl. Chem.*, **1967**, 413.

[5] G. Pagliarini, G. Cignarella and E. Testa, *Farmaco (Pavia) Ediz. Sci.*, **20**, 686 (1965).

[6] L. Semper and L. Lichenstadt, *Ber. dtsch. chem. Ges.*, **51**, 930 (1918).

[7] L. Bardy and R. P. Mehta, *J. Chem. Soc.*, **125**, 2298 (1924).

[8] T. Sheradsky, *Tetrahedron Letters*, **1966**, 5225.

[9] C. L. Bumgardner and R. L. Lilly, *Chem. and Ind.*, **1962**, 539.

[11] *Houben-Weyl, "Methoden der Organischen Chemie", Stuttgart 1953, Bd II/5, p. 458.*

[10] S. Nenoki and B. Stoeber, *Ber. dtsch. chem. Ges.*, **30**, 1769 (1897).

[12] Pauly and Likemann, *Ber. dtsch. chem. Ges.*, **48**, 1812 (1915)

[13] K. Anwers, *Ber. dtsch. chem. Ges.*, **45**, *996 (1912)*

[14] R. Comubert and A. Mamel, *Ber. dtsch. chem. Ges.*, **64**, 2384 (1931).

Revue Roumaine de Chimie, **36**, *11–12*, 1325–1329 (**1991**)

INVESTIGATION OF THE REACTION OF DIMETHYL DIAZOMALONATE WITH 1-PHENYLCYCLODODECENE IN THE PRESENCE OF COPPER(II) ACETYLACETONATE

KERIMAN GÜNAYDIN and OLCAY ANAÇ
Department of Chemistry, Faculty of Science Technical University of Istanbul, Turkey

Received April 1, 1989

$Cu(AcAc)_2$ catalyzed reaction of dimethyl diazomalonate (dmdm) with 1-phenylcyclododecene was realized under different molar ratios and new compounds were obtained. The best procedures for synthesis of the addition products were noticed and the presence of a triploid-type carbenoid was claimed.

The reactions of α-diazocarbonyl compounds with various olefins have been studied under photochemical, thermal and catalytic conditions yielding addition, insertion and carbene dimerization products.[1–5] It is generally recognized that singlet and triplet carbene is formed in direct and sensitized irradiation but there are still no distinct mechanistic and synthetic explanations on metal salt-catalyzed reactions.[6–10] Some of the present mechanistic approaches suggest a carbenoid intermediate, a carbene-catalyst complex.

In our previous papers,[11–13] we have reported the synthesis of some new N,N-dimethoxycarbonylbicyclo [n.1.0] dimethoxycarbonylcyclopropane and cyclopropene derivatives using catalytic and photolytic reactions.

In the present work, a crowded olefin, 1-phenylcyclododecene[14,15] (92.3% *cis*, 7.7% *trans*), which was synthesized in our laboratory, was used to determine its reactivity towards dimethyl diazomalonate (dmdm). For this purpose the catalyzed reaction of this olefin with dmdm was carried out at different molar ratios of dmdm to olefin and the optimum condition for the formatios of the addition product was found. Excess benzene was used as solvent. Other details of the reactions are described in the experimental section.

RESULTS AND DISCUSSION

Typical reactions postulated for the formation of compounds obtained in this study are illustrated in Scheme I and the relative % weight ratios of products to the amount of total products are given Table 1. As shown above, it is stereochemically possible to obtain *cis-* and *trans-*

Table 1

Products, percentages (based on glc) and yields of cycloadducts from reactions of dmdm with 1-phenylcyclododecene

Experiment	Molar ratio of dmdm to olefin	Relative % weight ratios of compounds						Yields of total cycloadducts (g) (1+2)
		1	2	3	4	Unidentified	Unreacted olefin *cis*+*trans*	
1	3/1	53.3	5.5	32.1	9.1	—	—	7
2	1/1	73.9	13.9	3.3	1.3	8.6	—	6.1
3	1/3.9	22.9	1.1	1.7	1.8	18.6	48.6+5.2	4.8

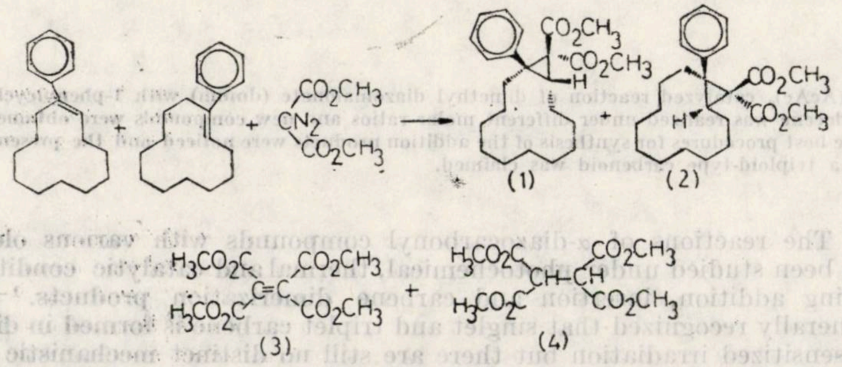

Scheme 1

addition products in the reaction of dimethoxycarbonylcarbenoid with 1-phenylcyclododecene both of which being rather sterically crowded. An interesting point is that when stoichiometric molar ratios (experiment 2) and 3 : 1 molar ratios (experiment 1) are used, cycloaddition products are found to be in higher yields than 1 : 3.9 molar ratios (experiment 3). Moreover, the experiment 2 would be considered as the most convenient procedure since the synthesis of the two starting compounds (dmdm and olefin) required multi step reactions and the procedure using excess dmdm in experiment 1 resulted only in a relatively weak increase in yields. These results are in complete contrast with the findings of other workers[10,9,6]. It has been claimed that excess olefin should be used in order to obtain cyclo-addition products in high yields. At a molar ratio of dmdm/olefin 3 : 1, carbene-dimers **3** and **4** were formed in higher percentages as expected. Experiment 2 also affords these dimers but in lower percentage.

In experiments 1 and 2, the reaction was continued until all the reactants were consumed. In experiment 3, the conditions were such that only dmdm is consumed totally. As described in the experimental section, the olefin used was 92.3% *cis* and 7.7% ***trans***. At the end of the reactions, the percentage ratios of *cis*- and *trans*- addition products to the % of total addition products are 90.6 %, 9.4 % and 84.0%, 16.0% in experiments 1 and 2 respectively. Experiment 3 was not deliberately taken into consideration in this respect as excess olefin was used. Consequently the percentage ratios of *trans* addition at the end of the reaction in experiments 1 and 2, are greater than they should have been if the reaction had been totally stereospecific. The reason of this increase may be due to :

i) Under present conditions the olefin undergoes a *cis-trans* isomerization before the reaction with the carbene takes place, or

ii) The presence of a triploid-type carbenoid intermediate may possibly result in a non-stereospecific addition reaction.

In order to clarify the first problem pure *cis*-olefin was heated only with catalyst for long times and the results showed that there was not a *cis-trans* isomerization under our thermal catalysis conditions. Then the experiments were repeated using pure *cis*-olefin, dmdm and catalyst. The results are summarized in Table 2.

Table 2

Products and percentages (based on glc) from the reactions of dmdm with *cis*-1-phenylcyclododecene

Experiment	Molar ratio of dmdm to olefin	Relative % weight ratios of compounds					Unreacted olefin *cis*+*trans*
		1	**2**	**3**	**4**	Uni-dent.	
1	3/1	57.3	1.5	31.7	9.1	—	—
2	1/1	83.1	5.2	3.2	0.9	7.1	—
3	1/3.9	23.2	1.1	1.7	1.7	5.4	53.4+0.0

As shown in Table 2, *trans*-adduct formation was observed in some extent even though the starting olefin was the *cis*-isomer in all cases. Furthermore, the absence of the *trans*-alkene in the unreacted olefin is an additional evidence for insignificance of *cis-trans* alkene isomerization when dmdm, alkene and catalyst are all present in the reaction conditions.

EXPERIMENTAL

Spectroscopic and Gas Chromatographic Studies

Infrared spectra were measured on a Schimadzu IR-400 Model Spectrophotometer and ^{1}H-NMR on a Varian T-60 model instrument using TMS as an internal standard. Some of the IR and ^{1}H-NMR spectra were also measured in the Sadtler Research Laboratories, Inc., Philadelphia. Gas chromatographic studies were performed on a Schimadzu instrument, model 5A, equipped with F.I.D. detector. An OV-17 % on Chromosorb W 100/120 mesh, 3 mm I.D. × 3 m column was used. The following conditions were imposed : Injector and detector temperature : 250°C, carrier gas (N_2), 100 mL/min, temperature programme : 5'isothermal at 100°C ;→ 160°C at 10°C/min ; 160° → 190°C at 2°C/min ; 190°C → 295°C at 10°C/min, heating rate; Integrator : ITG-4A. Reproducibility of results on Table was ±0.6 under the same conditions. Internal standard was used for calculation. Elemental analyses were performed by Hereaeus Microstandard equipment.

Preparative Thin-Layer Chromatographyc Studies

PTLC studies were carried out using Silicagel HF_{25} layers (1 mm) and $CH_2Cl_2 : CCl_4 :$ *n-Hexane : Ethylacetate* (75 : 10 : 10 : 5) solvent. As detection spray (for only pattern plate) : 3.5% ethanolic solution of phosphomolybdic acid is used. The plate is heated to 160°C and kept at 160°C for 30 mins. The sample is applied to the plate by DESEGA Microdoser equipment.

Preparation of Starting Materials

p-Toluene sulphonylazide was prepared by the method of Baumgarten.[16] Yield was 91% (higher than the value quoted in the literature [10]). Dimethyldiazomalonate (from *p*-toluene sulphonylazide), tetramethoxycarbonylethylene (**3**) and tetramethoxycarbonylethane (**4**) were prepared by the method of Wulfman and co-workers.[10] 1-Phenylcyclododecene was synthesized by dehydration of 1-phenylcyclododecanol which was prepared from cyclododecanone and phenylmagnesium bromide by Grignard reaction.[14,15]

General Procedure for Catalyzed Reactions

The amount of used $Cu(AcAc)_2$ and benzene are 0.14 mmol and 0.5 mol in all three experiments. 0.06 mol dmdm and 0.2 mol olefin were used in experiment 1, 0.02 mol dmdm and 0.02 mol olefin were used in experiment 2 and 0.02 mol dmdm and 0.078 mol olefin were used in experiment 3.

A solution of the catalyst in the olefin and half of the total amount of benzene (0.25 mol) was refluxed while a solution of dmdm in the remaining part of benzene (0.25 mol) was added dropwise at the rate of 6 drops per minute. After addition samples taken from the continuing reaction at several times, were analyzed by VPC and IR in order to ensure the end of reaction. Reactions were stopped when both of reactants were consumed in experiment 1 and 2 and when dmdm disappeared in experiment 3. After filtration of the catalyst and evaporation of benzene the three residues were analysed by VPC and PTLC. After extraction of zones corresponding to **1** and **2** from PTLC, the compounds obtained were again controlled by VPC o ensure their purities. Results were summarized in Table 1. The data for compounds **1** and **2** re shown below : (**1**) *cis*-1-phenyl-13, 13-dimethoxycarbonylbicyclo[10.1.0]tridecane : IR (cm^{-1}): 060, 3030, 2930, 2860 (vs C—H), 1740 (vs C=O), 1605 (vs C=C), 1495, 1475, 1450, 1440 vs C—H). ^1H—NMR (δ) ($CDCl_3$) :0.10—2.20 (m-20H, ring), 2.36 (d-1H, J = 10 c/s, bridgehead), 3.32 (s-3H, ester), 3.79 (s-3H, ester), 7.21 (d-5H, J = 2 c/s, aromatic)-Anal : Calcd. for $C_{23}H_{32}O_4$: C, 74.16 ; H, 8.66 ; found : C, 74.24, H, 8.58%. (**2**) *trans*-1-phenyl, 13, 13-dimethoxycarbonylbicyclo[10.1.10]tridecane : IR (cm^{-1}) : 3025, 2935, 2850 (vs C—H), 1740 (vs C=O), 1610 (vs C=C), 1490, .1445 (vs C—H). ^1H—NMR (δ) ($CDCl_3$) : 0.15—2.20 (m-20H, ring), 2.35 (d-1H, *J* = 5 *c/s*, bridgehead), 3.33 (s-3H, ester), 3.80 (s-3H, ester), 7.20 (d-5H, J = 4.5 c/s, aromatic). Anal : Calcd. for $C_{23}H_{32}O_4$:C, 74.16 ; H, 8.66 ; found : C, 74.21 ; H, 8.71%.

Preliminary test for cis-olefin

A solution of catalyst (0.014 mmol) in *cis*-olefin (0.002 mol) was heated at 80°C for 48 hours. After filtration of the catalyst, olefin was analysed by glc and the data obtained showed that there was no *cis-trans* isomerization under these conditions. Experiments were repeated using *cis*-olefin in small amounts. Results were summarized in Table 2.

REFERENCES

[1] M. Jones, Jr. and R. A. Moss, "Carbenes", Wiley-Interscience, 1973.

[2] N. S. Isaacs, "Reactive Intermediates in Organic Chemistry", Wiley Interscience, 1974, 375.

[3] M. Jones and R. A. Moss, "Reactive Intermediates, A Serial Publication", Wiley-Interscience, 1978, 1, 69.

[4] W. Kirmse, "Carbene Chemistry", Organic Chemistry, A Series of Monographs, Academic Press, 1971.

[5] E. Müller, Houben-Weyl, "Methoden der Organischen Chemie", Photochemie II, 4/5b, George Thieme Verlag, 1975, 1158.

[6] D. S. Wulfman, N. V. Thinh, R. S. Mc. Daniel and B. W. Peace, *J. Chem. Soc. Dalton. Trans.* **1975** 522.

[7] D. S. Wulfman, *Tetrahedron* **32**, 1231 (1979).

[8] D. S. Wulfman, R. S. Mc. Daniel and B. W. Peace, *Tetrahedron*, **32**, 1241 (1976).

[9] D. S. Wulfman, B. W. Peace and Mc. Daniel, *Tetrahedron*, **32**, 1251, 1976.

[10] D. S. Wulfman, B. G. Mc. Gibboney, E. K. Steffen, N. V. Thinn, R. S. Mc. Daniel and B. W. Peace, *Tetrahedron*, **32**, 1257 (1976).

[11] O. Anaç and C. Aydoğan, *Chim. Acta Turc.*, **10** (2), 113 (1982).

[12] O. Anaç, C. Aydoğan and Y. Yağci, *Chim. Acta. Turc.*, **11** (2), 221 (1983).

[13] O. Anaç, *Rev. Roumaine Chim.*, **31** (8), 787 (1986).

[14] K. Günaydin and Ü. Oyman, *Chim. Acta. Turc.*, **13**, 539 (1985).

[15] K. Günaydin and Ü. Oyman, *Rev. Roumaine Chim*, **31** (5), 497 (1986).

[16] H. E. Baumgarten, *Organic Synthesis*, **5**, 179 (1973).

Revue Roumaine de Chimie, 36, *11–12*, 1331–1336 (1991)

PHENOLIC AND EPOXY RESINS. I

THERMAL CHARACTERIZATION BY PYROLYSIS – GAS CHROMATOGRAPHY

CONSTANTIN N. CAŞCAVAL and DAN ROŞU
"Petru Poni" Institute of Macromolecular Chemistry,
Aleea Gr. Ghica Vodă, no. 41A, Iaşi–6600, Romania

Received March 10, 1989

Pyrolysis in combination with gas chromatography was used in the study of the thermal behaviour of some phenolic resins (phenol-formaldehyde and nonylphenol-formaldehyde) as well as the epoxy resins, commercialized under the name of Novox and Dinox, respectively. Pyrolysis of phenolic and epoxy resins at temperatures higher than 600° leads to products with low boiling points (hydrocarbons C_1-C_5), phenol and substituted phenols. Together with these products, an aromatic fraction is also formed, which consists in benzene and benzene alkylic derivatives. The identification of the thermal degradation products and their semi-quatitative estimation show the presence of a complex degradation mechanism of the phenolic and epoxy resins.

INTRODUCTION

Phenolic resins are the reaction products of phenol with formaldehyde. A large variety of resins are possible, depending on the choice of phenol, the phenol/formaldehyde molar ratio, the type and amount of catalyst and the time and temperature of the reaction.

Epoxy resins can be defined as condensation products of bisphenol A with epichlorhydrin.

There are few papers which deal with the study of the phenolic resins by pyrolysis in combination with gas chromatography (P–GC). This thing is due to the complexity of the thermal decomposition process, which takes place by formation of a great number of organic and anorganic compounds.

Jackson and Conley [1] have reported the presence of phenol and some methylalkylphenols among the pyrolysis products of the phenolic resins, but an important attention was given to the products with low boiling points, particularly to carbon monoxide, carbon dioxide and methane.

Martinez and Guiochon [2] studied the thermal behaviour of the phenolformaldehyde resins with reticulated structure. They found a quantitative relationship between the content in phenol, 3-methylphenol and

3,5-xylenol, evolved as the main pyrolysis products, and the initial composition of the mixture used on synthesis.

Jamao and Iida[3] analyzed and identified by P–GC the thermal degradation products of the phenolic resins as follows: phenol, *o*-cresol, *p*-cresol, 2,4-xylenol and 2,6-xylenol, respectively.

Phenol and its derivatives, evolved on pyrolysis of some phenolformaldehyde resins, were analyzed by P–GC as acetate esters.[4,5]

Up to now, the epoxy resins were less studied by P – GC[6]; they were more characterized by pyrolysis-mass spectrometry.[7–9]

This paper reports the results obtained by P–GC in the analysis of some phenolic and epoxy resins. The experimental conditions used in analysis allowed us to separate the aromatic hydrocarbons, which were already notified as the thermal degradation products of the phenolic resins,[10] but not completely identified till now.

EXPERIMENTAL PART

The study by P-GC was carried out both on two resins synthesised in laboratory (phenol-formaldehyde resin and *p*-nonylphenol-formaldehyde resin) and two epoxy resins, which are commercially known under the name of Dinox and Novox, respectively.

The phenolic resins were prepared in acidic condition (H_2SO_4) with the molar ratio phenol/formaldehyde of 1 :0.8 for the phenol-formaldehyde resin and the molar ratio *p*-nonylphenol/formaldehyde of 1 :0.75 for the *p*-nonylphenol-formaldehyde resin.

The Dinox epoxy resin is a commercial resin prepared by the condensation reaction between bisphenol A and epichlorhydrin with the general formula as follows:

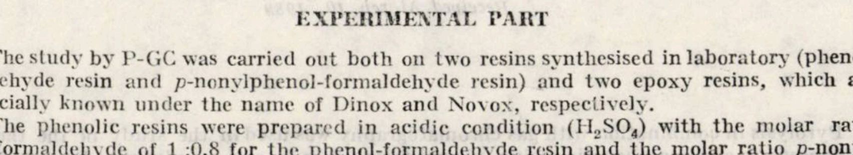

The Novox epoxy resin is another commercial resin obtained by the reaction between the phenol-formaldehyde resin of Novolac type and epichlorhydrin with the general formula:

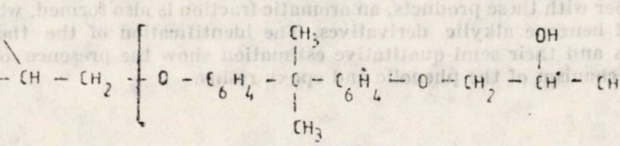

The resin samples were pyrolyzed in argon as carrier gas (flow rate 30 ml/min), using a filament type pyrolysis unit described elsewhere.[11] Separation and analysis of the pyrolysis products were carried out with a Siemens gas chromatograph type L-400, provided with a flame ionization detector. The following operational conditions have been used: the cromatographic column of stainless-steel (2m × 3mm, i.d.) was packed with Chromosorb W (60—80 mesh) acid washed and coated with 5 % free fatty acid polymer (FFAP); the column temperature was first programmed from 60 to 180°C at 7°/min and then operated isothermally at 180°C. The polymer samples weighed in small platinum boats were pyrolysed at temperatures higher than 600°.

Identification of the pyrolysis products was carried out by using the relative retention times of various reference substances. In this way we also recorded the IR spectra of the resin subjected to analyse to have additional information upon the products which could form on degradation. The IR spectra were recorded with the aid of a Perkin-Elmar spectrophotometer, type 577.

RESULTS AND DISCUSSION

Thermal degradation of the phenolic resins starts above 300°, when water, carbon monoxide, carbon dioxide, methane, phenol, cresols and xylenols are expelled. At temperatures higher than 400° aromatic hydrocarbons are also fermed.

Using the P—GC technique we identified the aromatic hydrocarbons evolved by pyrolysis of some phenolic resins as well as the epoxy resins, respectively.

With a view to identify the thermal degradation products first we have recorded the IR spectra of the resins and the characteristic absorption bands are shown in Table 1.

Table 1

The IR absorption bands of the phenolic and epoxy resins

Wave number, cm^{-1}	Assigning
700—900	ν(CH), substituted aromatic compounds
950—1150	ν(CH), ν(C=C), aromatic compounds, olephines
1100—1230	ν(C—OH), alcohols, phenols
1400—1500	ν(C=C), ν(CH), aliphatic compounds, alkenes
1510—1600	ν(C—OH), phenols
1600—1650	ν(CH), condensed aromatic hydrocarbons
1700—2700	Weak bands
2750—3300	ν(C—OH), ν(CH), aliphatic compounds, alkenes, aromatic compounds, phenols.

The IR spectra of the phenolic and epoxy resins show the presence of some vibrations which belong to a great number of the organic compounds (alkenes, aromatic hydrocarbons, hydroxylic compounds and so on).

The IR spectra recorded for the four types of resins do not evidence the important difference in the nature of the characteristic bands, the resins being differentiated only by the intensities of the bands (especially in the region 700—1600 cm^{-1}).

The P—GC study showed that the thermal degradation of the phenolic and epoxy resins takes place by a complex mechanism. Thus, the pyrograms recorded for the four types of resins evidence a great number of the degradation products, with important variations in the height of the peaks. As an example, Figs. 1–4 show the pyrograms obtained at 720° for phenol-formaldehyde resin (Fig. 1), nonylphenol-formaldehyde resin (Fig. 2), Novox resin (Fig. 3) and Dinox resin (Fig. 4), respectively.

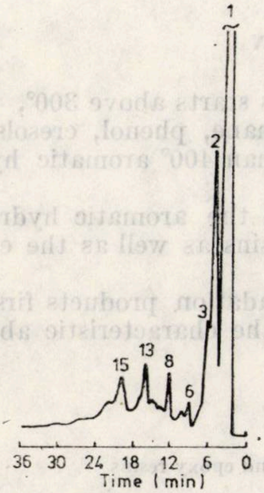

Fig. 1 — Pyrogram of phenol-formaldehyde resin.

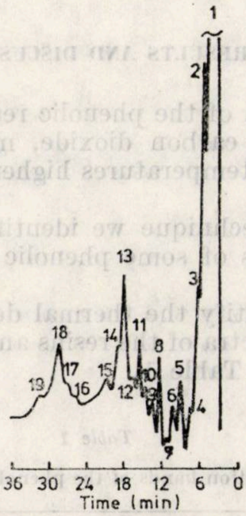

Fig. 2 — Pyrogram of nonylphenol-formaldehyde resin.

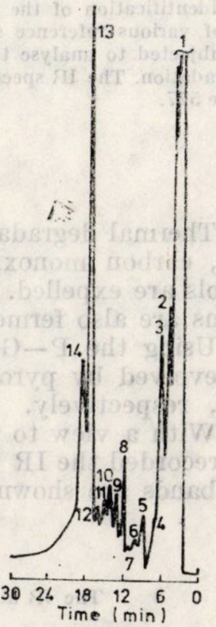

Fig. 3 — Pyrogram of Novox resin.

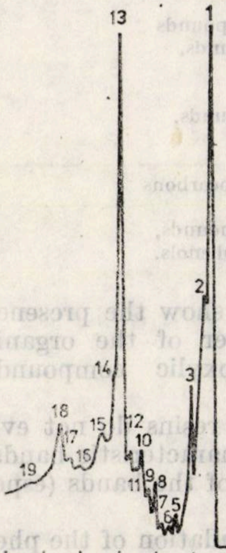

Fig. 4 — Pyrogram of Dinox resin.

The thermal degradation products of the analyzed resins are listed in Table 2. Their identification was carried out taking into consideration the retention times of some standard substances. Considering that the response of the flame ionization detector is the same for all analyzed substances, the relative weight sensitivity of each product was approximately regraded as a unit. In this way a semi-quantitative determination of the pyrolysis products of the resins was accomplished and the result are also listed in Table 2.

The data in Table 2 show that the main degradation products of the phenolic and epoxy resins, analyzed in the same experimental conditions, are as follows: gases with high volatility (hydrocarbons C_1—C_5), phenol, benzene, toluene, isopropylbenzene, m-crezol and alkyl-phenols.

Table 2

Composition of the pyrolysis products of the phenolic and epoxy resins, pyrolysed at temperature of 720°

Peak	Compound	Resin			
		Phenol-formaldehyde	Nonylphenol-formaldehyde	Novox	Dinox
		Semiquantitative content (%)			
1	Gases with high volatility (C_1-C_5)	63.68	58.42	41.82	37.28
2	Benzene	15.12	7.68	9.08	10.16
3	Toluene	7.34	2.84	8.24	4.14
4	Ethylbenzeme	—	1.12	1.16	—
5	*m*, *p*-Xylenes	1.64	2.96	3.18	0.82
6	*o*-Xylene	1.52	1.18	0.64	0.74
7	Unknown	—	0.12	—	0.56
8	Isopropylbenzene	3.24	3.86	4.68	1.82
9	Unknown	0.82	1.06	2.16	0.86
10	Ethyltoluene	—	0.96	2.22	1.12
11	1,2,4-Trimethylbenzene	0.56	2.14	1.32	0.28
12	1,3,5-Trimethylbenzene	0.44	0.78	0.96	0.88
13	Phenol	3.18	6.84	18.26	33.04
14	*m*-Cresol	0.98	1.92	6.16	2.12
15–19	Substituted phenols	1.12	7.78	—	6.06

The phenolic and epoxy resins can be differentiated after the content in gases with high volatility and the content in phenol, respectively. Thus, on the thermal degradation, the phenolic resins lead to gases with high volatility in a greater quantity than that found on pyrolysis of the epoxy resins. This thing is more or less connected with the structure of the resin. It is due to the complexity of the thermal degradation mechanism, which takes place by the random rupture of the polymeric chain, with recombinations of the radicals and the products at high temperatures.

CONCLUSIONS

The pyrolysis of the phenolic and the epoxy resins takes place by a complex degradation mechanism.

Besides the phenol and substituted phenols, the thermal degradation of phenolic and epoxy resins leads and to aromatic hydrocarbons, which consist in benzene, toluene, xylenes, ethylbenzene, isopropylbenzene, ethyltoluene and trisubstituted benzenes.

The pyrolysis of the phenolic and epoxy resins at high temperatures akes place, also with formation of a great amount of gases with high volatility (hydrocarbons C_1-C_5).

REFERENCES

[1] W. M. Jackson and R. T. Conley, *J. Appl. Polym. Sci.*, **8**, 2163 (1964).

[2] J. Martinez and G. Guiochon, *J. Gas Chromatog.*, **5**, 146 (1967).

[3] M. Yamao and Y. Iida, *Bunseki Kagaku*, **21**, 1602 (1973) ; C. A. 6036u (1973). vol. 79.

[4] H. P. Higginbottom, H. M. Culbertson and J. C. Woothey, *Analyt. Chem.*, **37**, 1021 (1965).

[5] R. Gnauck and D. Habisch, *Plaste u. Kautschuk*, **9**, 485 (1980).

[6] L.-H. Lee, *J. Polym. Sci.*, **A-3**, 859 (1965).

[7] P. J. Gale, B. L. Bentz and W. Harrington, *RCA Rev.*, **47**, 380 (1986).

[8] L. M. Lukashenko, R. A. Khmel'nitskii, E. S. Brodskii, G. A. Kalinkovich, N. M. Kovaleva and U. P. Batizot, *Visokomol, Soedin.*, **18**, 1133 (1976).

[9] G. A. Kalinkevich, L. M. Lukashenko, R. A. Khmel'nitskii, E. S. Brodskii, N. M. Kovaleva and U. P. Batizat, *Plast, masî*, **8**, 16 (1977).

[10] M. Ladacki, J. V. Hamilton and S. Cohz, *A.I.A.A⁻. Journal*, 4, 1798 (1966).

[11] C. N. Caşcaval, H. Oleinek, I. Zugrăvescu and I. A. Schneider, *Makromol. Chem.*, **109**, 129 (1973).

Revue Roumaine de Chimie, **36**, *11–12*, 1337–1343 (1991)

SOME REACTIONS OF CHALCONE EPOXIDES

R. M. SALEH[a], A. Y. SOLIMAN[b] and F. M. A. SOLIMAN[c]

[a] Faculty of Engineering, Suez Canal University, Port Said, Egypt
[b] Faculty of Education at Al Fayoum, Cairo University, Egypt
[c] Faculty of Science (For Girls), Al Azhar University, Cairo, Egypt

Received May 13, 1989

Epoxidation of chalcones **1 a**,**b** gives the epoxyketones **2 a**, **b**. Compound **2a** reacts with hydrazine hydrate, phenylhydrazines, hydroxylamine hydrochloride and semicarbazide hydrochloride to give hydroxypyrazolines **3**, **4 a**, **b**, isoxazoline derivative **5**, and carbamidopyrazoline **6** respectively. Compound **2** reacts with various aromatic hydrocarbons and amines to yield the triarylpropiophenones **7 a-e** and α-hydroxy-β-alkylamine-β-arylpropiophenones **8 a-d** respectively. The reaction of **2** with primary amines affords the Schiff bases **9 a**, **b**. Compound **2 a** reacts with sodium hydroxide to give the propane-1,2-dione **10** and its rearranged product **11** which is the nitrobenzylglycolic acid derivative.

It is known that hydrogen peroxide reacts with α, β-unsaturated carbonyl compounds to give α, β-epoxy ketones.[1–3] This reaction has now been applied to the chalcones **1a**, **b** with the aim of synthesizing some new oxirane derivatives **2a**, **b**. Thus, treatment of an alkaline solution of the chalcones **1a**, **b** in methanol – acetone mixture with hydrogen peroxide yielded the corresponding oxirane derivatives **2a**, **b** respectively. The proposed structures for **2a** and **2b** are supported by the following evidences :

i) The infrared spectra indicated strong bands characteristic of carbonyl (1700–1685 cm^{-1}) and epoxylinkage at 1290 cm^{-1}.

ii) The ^{1}H-NMR spectrum of **2a** reveals the presence of $-CH_3$ group as a singlet at δ 2.51, the system of the oxirane ring as a doublet at δ 4.25 – 4.45, the $-OCH_3$ as a singlet at δ 3.96 and a doublet at δ 6.9 and 6.99 for the the hydrogen protons of the aromatic ring (A) while the multiplet at δ 7.6–8.49 is due to the aromatic hydrogen protons of ring (B).

In analogy with the recently reported reactions of 1,2-epoxy ketones, [2,3,6,7,8] the treatment of the epoxide **2a** with different nucleophilic reagents results in the opening of the oxirane ring of the epoxide. Thus, reaction of **2a** with hydrazine hydrate in boiling ethanol yields the aryl 4-hydroxypyrazoline derivative **3**. The structure of **3** is supported by the following :

i) It gives the colour test of pyrazolines.[9,10]

ii) Its infrared spectrum shows well defined absorbed bands at 1530, 3225, and 3420 cm^{-1} attributable to νC = N, νNH and νOH respectively.

iii) Compound **3** yields the diacetyl derivative by treatment with acetyl chloride, which shows νC = N at 1635 cm^{-1} and νC = O at 1670 cm^{-1} with the lack of any νOH stretching or νNH stretching in its infrared spectrum.

iv) Treatment of compound **3** with methanolic HCl affected its dehydration with the formation of the corresponding pyrazole derivative which was characterised by its infrared spectrum, showing absorption bands at 1635 and 1620 cm^{-1} due to νC = N and νC = C and revealing the absence of νOH group.

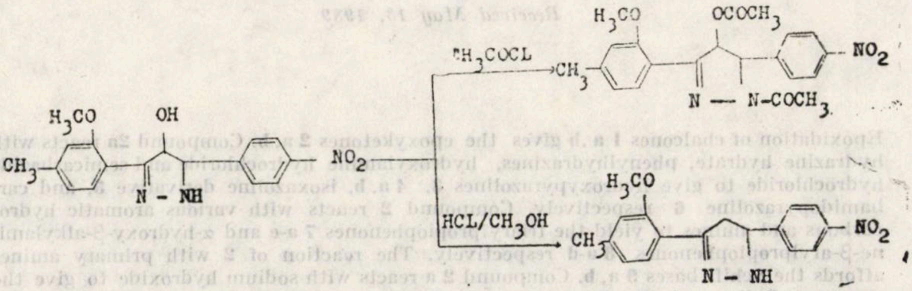

The reaction of chalcone epoxide **2a** with nitrogen nucleophiles has extended to include its reaction with phenylhydrazine and 2,4-dinitrophenylhydrazine to yield new pyrazoline derivatives **4a** and **4b** respectively.

Structures of **4a** and **4b** were proved by:

i) The infrared spectra which reveal the presence of νC = N and νOH at 1605 and 3495 cm^{-1} in case of **4a**, and the presence of νC = N and νOH at 1605 and 3395 cm^{-1} in case of **4b**.

ii) The ^{1}H-NMR spectrum of **4a** shows the — CH_3 group as a singlet at δ 1.32, the methine proton at δ 2.6—2.8, the — OCH_3 group as a singlet at δ 3.4, the olefinic hydrogen at δ 6.7, while the multiplet at δ 7.4—8.5 belongs to the aromatic hydrogen protons.

Treatment of **2a** with hydroxylamine in boiling pyridine and/or semicarbazide hydrochloride in ethanol yielded the isoxazoline **5** and the carbamidopyrazoline **6** derivatives respectively.

The infrared spectrum of **5** shows bands at 1585 cm^{-1} due to ν C = N while νOH and νNH are absent. Similarly, the infrared spectrum of **6** exhibits strong absorption bands at 1585, 1625, 3305, 3405, and 2940 cm^{-1} attributable to νC = N, νC = O, νNH, νOH, and νCH_2 respectively.

Treatment of **2a** with various aromatic derivatives, namely, toluene, m—xylene and chlorobenzene in the presence of anhydrous aluminium chloride under Friedel — Crafts conditions yielded the corresponding triarylpropiophenone derivatives **7a-c** respectively.

The structure of **7a-c** is confirmed by their infrared spectra which show intense absorption bands at 1690—1670 cm^{-1} due to νC = O stretching frequency of the aryl ketone.[4]

The reaction of chalcone epoxides with amines has been previously studied by several authors,[11–13] which reported that the oxirane ring in the chalcone epoxide was readily cleaved with amines at the β-carbon atom. In our present work, the reaction of **2a** with different amines, namely aniline, 4-anisidine, 2-aminopyridine, and 2-aminothiazole was studied and the results were in accordance with the previously reported ones. The resulting α-hydroxy-β-arylamino-β aryl propiophenones **8a-d** were characterized by their infrared spectra which show strong absorption bands at about 3370—3450 cm^{-1} due to νOH or νNH and at a range 1640—1635 cm^{-1} due to νC = O.

The ^{1}H-NMR spectra of **8b** revealed the presence of a —CH_3 group at δ 3.4 (*s*, 3H, 4 — tolyl); a — OCH_3 at 3.8 (*s*, 3H); 2 CH_2 groups at δ 4.3 (*s*, 2H, methylene group), a methine group at δ 6.2 (*s*, 1H, olefinic proton) and the aromatic protons as a multiplet at δ 6.6—7.7 (*m*, 11H, Ar—H).

In the reaction of **2a** with methylamine and/or benzylamine as primary amines, two molecules of the amine are incorporated with the formation of the corresponding Schiff bases **9a** and **9b** respectively.

Compounds **9a** and **9b** showed the presence of νC = N at 1610, 1620 cm^{-1} and absence of the hydroxyl and carbonyl groups stretching frequency in their infrared spectra.

The reaction of **2a** with aqueous sodium hydroxide solution proceeds also with opening of the oxirane ring of the epoxide and yields a mixture of two products. The first is 1 — (2′-methoxy-4′-methylphenyl)-3-4-nitrophenyl)-propane 1,2-dione **10** and the other one is its rearranged product (2′-methoxy-4′-methylphenyl)-4-nitrobenzylglycolic acid **11**. The structure of **10** was proved by:

i) Its infrared spectrum showing strong absorption bands at 1700 and 1620 cm^{-1} characteristic for the carbonyl group.

ii) The acid **11** could also be prepared by boiling the diketone **10** with aqueous sodium hydroxide, a fact which explained that the glycolic acid was obtained from the oxirane derivative via the stable isolated intermediate diketone **10**.

EXPERIMENTAL

Melting points are uncorrected. The IR spectra were carried on a Pye Unicam Sp—200 G spectrophotometer using KBr wafer technique. The ^{1}H—NMR spectra were run on a Varian 60 instrument. Yields and physical properties are shown in table.

Expoxidation of chalcones. Formation of **2a** *and* **2b**. A solution of the chalcone **1a** or **1b** (0.01 mole) in acetone (40 mL) and methanol (15 mL) was treated with 8% aqueous sodium hydroxide (12 mL) followed by the addition of hydrogen peroxide (30%; 15 mL). The solution was shaken occasionaly and left aside while cooling for 2 hours. The solid that separated was crystallized from a suitable solvent to yield **2a** and **2b**.

Reaction of the epoxides with hydrazines. Formation of **3**, **4a** *and* **4b**. The epoxide (0.01 mole) in 30 mL ethanol was refluxed with hydrazine hydrate, phenylhydrazine, and/or 2,4-dinitrophenylhydrazine (0.01 mole) for 6 hours. The reaction mixture was poured onto ice water in case of **3** and into ice-cold dilute hydrochloric acid in cases of **4a** and **4b**. The product was crystallized from a suitable solvent to yield **3**, **4a** and **4b** respectively.

Acetylation of the pyrazoline derivative **3**. A mixture of **3** (0.01 mole) and acetyl chloride (8 mL) was refluxed for 2 hours. The excess of the acetyl chloride was removed. The diacetyl derivative was crystallized from ethanol as white crystals. m.p. 248°.

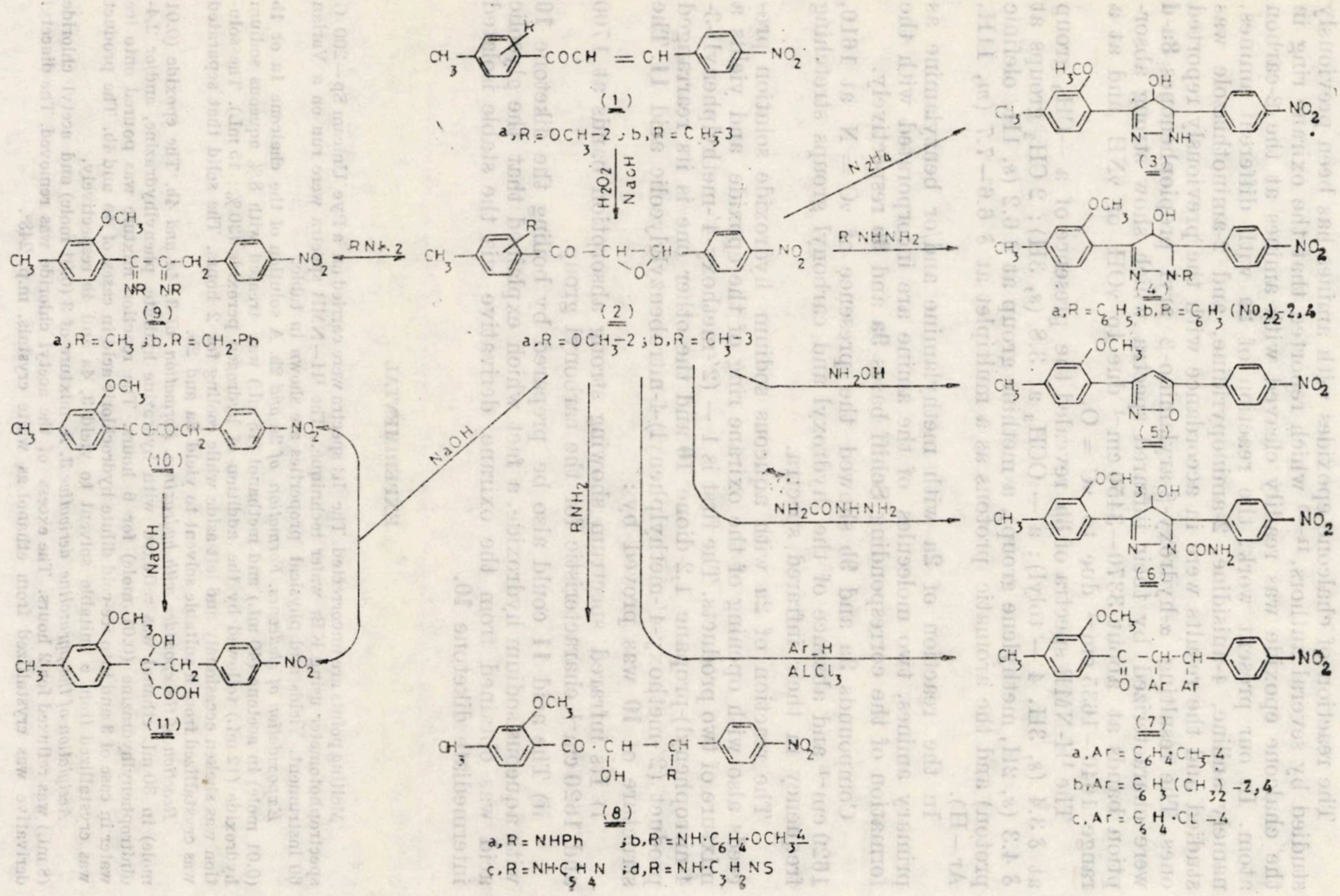
(1)
a, R = OCH3-2 ; b, R = CH3-3
H2O2
NaOH
(2)
a, R = OCH3-2 ; b, R = CH3-3
N2H4
(3)
R NHNH2
(4)
a, R = C6H5 ; b, R = C6H3 (NO2)2-2,4
NH2OH
(5)
NH2CONHNH2
(6)
Ar_H
AlCl3
(7)
a, Ar = C6H4·CH3-4
b, Ar = C6H3 (CH3)2-2,4
c, Ar = C6H4·Cl-4
RNH2
(8)
a, R = NHPh ; b, R = NH·C6H4·OCH3-4
c, R = NH·C5H4N ; d, R = NH·C3H2NS
RNH2
(9)
a, R = CH3 ; b, R = CH2·Ph
NaOH
(10)
NaOH
(11)

aquous sodium hydroxide (0.2 g/mL) for 3 hours. The ethanol was removed and 40 mL of water were added to the residue. The alkaline solution was extracted with ether, and evaporation of the ethereal layer gave the diketone **10**. Acidification of the alkaline solution gave the glycolic acid derivative **11**. The product was crystallized from the proper solvent.

Conversion of the diketone **10** *to glycolic acid derivative* **11**. A mixture of **10** (0.01 mole) in 10 mL of ethanol and 30 mL of aqueous sodium hydroxide (20%) was heated under reflux for 3 hours. The alkaline solution was acidified to give a crystalline product which was found to be the glycolic acid **11** via the m.p. and m.m.p determinations.

REFERENCES

[1] Harry H. Wasserman and Norman E. Aubery, *J. Amer. Chem. Soc.*, **77**, 590 (1955).

[2] A. Sammour and M. El Kassaby, *U.A.R. J. Chem.*, **13**, no. 2, 151, (1970).

[3] M. A. Al Hashash and M. El Kady, *Rev. Roumaine Chim.*, **23**, 1581 (1978).

[4] L. J. Bellamy, "The Infrared Spectra of Complex Molecules", Methuen and Co., Ltd., London (1962).

[5] S. C. Bhrara, A. C. Jain and T. R. Seshadri, *Tetrahydron*, **20**, 1141 (1964).

[6] F. Piozzi and C. Fuganti, *Ann. Chim. (Rome)*, **56**, 1248 (1966); *Chem. Abstr.*, **67**, 73473 (1967).

[7] N. H. Cromwell and J. L. Martin, *J. Org. Chem.*, **33**, 1890 (1968).

[8] G. Kobayashi, S. Furukawa and Y. Matsuda, *Yakugaku Zasshi*, **86** (1966); *Chem. Abstr.*, **67**, 108594 (1967).

[9] Benh. Micolet, *J. Amer. Chem. Soc.*, **57**, 1098 (1935).

[10] M. M. Mohamed, M. A. El Hashash, M. A. El Naggar, F. Said and W. M. Ali, *Pakistan J. Sci. Ind. Res.*, **23**, 4 (1980).

[11] J. Tischenko, K. Vesti and P. M. Molasko, *Ser. Khim, Nauk*, **6**, 103 (1969); *Chem. Abstr.*, **72**, 110717 (1970).

[12] N. H. Cromwell, F. H. Schunachere, and J. L. Adelfang, *J. Amer. Chem. Soc.*, **83**, **974** (1961).

[13] A. Sammour, M. Selim and A. A. Hamed, *Egypt J. Chem.*, **16** 2, 101–113 (1973).

Revue Roumaine de Chimie, **36**, *11–12*, 1345–1353 (1991)

CARBONIC ANHYDRASE INHIBITORS. 9[1]

INHIBITORS WITH MODIFIED SULFONAMIDO GROUPS AND THEIR INTERACTION WITH THE ZINC ENZYME

CLAUDIU T. SUPURAN[a] and MIRCEA D. BANCIU[b]

[a] Department of Chemistry, University of Bucharest, Bd. Republicii 13, Bucharest 1, Roumania
[b] Organic Chemistry Department, The Polytechnic – TCH, Spl. Independentei 313, 76206 Bucharest, Roumania

Received March 15, 1991

A number of 20 compounds, containing modified sulfonamido groups were prepared and tested as carbonic anhydrase inhibitors on the bovine enzyme. Novel classes of inhibitors were evidenced, and a new mode of binding for bidentate inhibitors was proposed, both for the native and Co(II) substituted enzyme.

INTRODUCTION

Sulfonamide inhibitors of the zinc metallo-enzyme carbonic anhydrase (CA, EC 4.2.1.1) were extensively studied since the discovery of Mann and Keilin[2] that sulfanilamide strongly inhibits this enzyme. Such studies are motivated by the fact that the eight isozymes of CA[3] are present in a variety of tissues[4] where they play important physiological roles connected with secretory processes, transport of ions, regulation of pH,[5] etc. Inhibition of CA with sulfonamides may be clinically exploited, in the treatment of glaucoma,[5b] edema,[4] minor seizure,[6] and mountain sickness[7] among others.

The discovery of Krebs[8] that CA inhibitory effect is drastically reduced by N-substitution of sulfonamides (in compounds of the type $ArSO_2NHR$, where R = acetyl, guanidyl, acetamido, heterocyclyl, etc. which generally act as antimicrobial sulfonamides[9]) had as result a thorough investigation of unsubstituted sulfonamides as CA inhibitors,[10] and a lack of data concerning other types of inhibitors. Only recently Blackburn et al.[11] and Duffel et al.[12] showed that compounds of the type **1** (Fig. 1) may act as powerful inhibitors, with potencies comparable in some cases with those of the unsubstituted sulfonamides. Moreover, it was shown that compounds of type **1c, d** may act as topically active CA inhibitors in lowering elevated intraocular pressure in glaucoma.[12] On the other hand, using ^{15}N-labelled **1a** (X = F), and ^{15}N- and ^{111}Cd-NMR spectroscopy, Blackburn et al.[11] showed that the inhibitor is directly bound to the metal ion through the nitrogen atom, similarly with the binding of unsubstituted sulfonamides, previously demonstrated using different spectroscopic techniques,[10-13] as well as X-ray diffraction studies of enzyme — inhibitor complexes.[14]

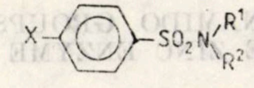

1

Fig. 1. — Chemical structure of reported CA inhibitors, possessing modified sulfonamido groups;
a : $R^1 = H$, $R^2 = OH$
b : $R^1 = H$, $R^2 = OMe$
c : $R^1 = OH$, $R^2 = Me$
d : $R^1 = H$, $R^2 = Me$.
$X = H$, NO_2, halogeno, Me;

In this paper we report novel classes of CA inhibitors, showing that other types of substitutions may be achieved at the sulfonamido moiety, without loss of inhibitory action. The compounds reported by us are not strong CA inhibitors and our goal was not to develop potential candidates for clinical studies, but to bring new insights into the catalytic and inhibition mechanism of this enzyme.

RESULTS AND DISCUSSION

The compounds included in our study (**2**—**4**) were selected upon the following criteria:

i) imidazole, as wel as related azoles (for instance 1,2,4-triazole, tetrazole, thiadiazole, etc)[15] interact with CA; Khalifah[16a] discovered

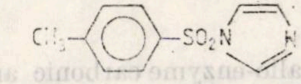

2

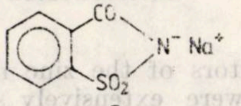

3

$Ar-SO_2NH-R$

4

that imidazole is the unique CO_2 competitive inhibitor of CA I. Recently, Khalifah et al.[16b] studied the interaction of such inhibitors with Co(II)-substituted as well as carboxymethylated CA I and II. Luchinat et al.[17] studied the interaction of imidazole with the native and Co(II)-substituted CA I, by means of ^{13}C- and ^{1}H-NMR spectroscopy, showing its mode of binding within the active site. On the other hand, Parkes and Coleman[18] and Silverman's group[19] showed that imidazole is an activator of CA II and CA III respectively. We[20] have also shown that histamine and histidine (imidazole derivatives) may act as potent CA activators. It appeared of interest to see if a molecule containing both a sulfonamido moiety ($SO_2N\langle$) and an imidazole ring, like in **2**, would interact with the enzyme;

ii) saccharine (**3**) contains an acylated sulfonamido group, and although it was reported that 2-substituted benzenesulfonamides are less potent CA inhibitors, due to steric constraints,[21] it was of interest to see whether such a widely used chemical does not possess an unexpected effect, i.e; to inhibit CA;

iii) although Blackburn et al.[11] prepared and tested N-hydroxy- and N-methoxy-sulfonamides (**1a**, **b**), it is quite strange that they did not extend the study to the amino analogues of type **4e, f**. We extended then the series of substituents to even larger groups (R in formula **4**) also because we tried to evidence novel types of interactions between inhibitor and the active site.

Table 1

CA Inhibition by compounds **1–4**

$$Ar-SO_2NH-R$$

4

Compound	Ar	R	IC_{50}(μM)	enzyme assay
1a	$4-F-C_6H_4$	OH	0.249	a); ref. 11
1d	$4-Cl-C_6H_4$	Me	584	b); ref. 12
2	for formula *vide supra*		34	a)
3			97	a)
4a	$4-Me-C_6H_4$	H	11	a)
4b	Ph	OH	13	a)
4c	$4-Me-C_6H_4$	OH	9	a)
4d	$4-Me-C_6H_4$	OMe	173	a)
4e	Ph	NH_2	64	a)
4f	$4-Me-C_6H_4$	NH_2	53	a)
4g	$4-Me-C_6H_4$	Me	217	a)
4h	$4-Me-C_6H_4$	NMe_2	328	a)
4i	$4-Me-C_6H_4$	NHPh	119	a)
4j	Ph	$CONH_2$	325	a)
4k	$4-Me-C_6H_4$	$CONH_2$	379	a)
4m	Ph	$C(NH)NH_2$	431	a)
4n	$4-Me-C_6H_4$	$C(NH)NH_2$	>500	a)
4o	$4-Me-C_6H_4$	$NHCONH_2$	462	a)
4p	$4-Me-C_6H_4$	$NHCSNH_2$	411	a)
4q	$4-Me-C_6H_4$	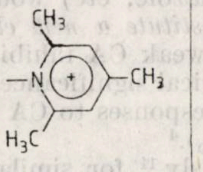	337	a)
4r	$4-Me-C_6H_4$	Ts	>500	a)
4s	$4-Me-C_6H_4$	CH_2NHTs	>500	a)

a) Bovine CA II from Sigma was used.
b) The source of enzyme and its type are not specified.

Two facts prompted us to increase the volume of these groups although we expected to obtain somehow weaker inhibitors, as showed by the classical study of Krebs. The first one was the recent report of Gerig's group[22] that fluorobenzenesulfonamides bind to the zinc enzyme in a strange stoichiometry: two moles of inhibitor per mole of enzyme; using NMR techniques, these authors showed that the two inhibitor molecules are near the Zn(II) ion of the active site. This means that there is sufficient place there, even for compounds with bulkier SO_2NHR groups. The second fact was that although for the native enzyme it seems to be clear that the sulfonamide binds in a monodentate fashion, with the nitrogen atom occupying the fourth position in a tetrahedral geometry,[10,13,14] in the case of the Co(II)-substituted CAs things are rather complicated, because both tetra- and pentaco-ordinated states were evidenced when inhibitor binds to the metal ion within the active site.[13,23] These two facts, together with the recent report of hexa- or heptaco-ordinated Zn(II) ions in other metallo-enzymes,[24] prompted us to design bidentate inhibitors like **4j-p.** A putative binding for such a compound is shown in Fig. 2.

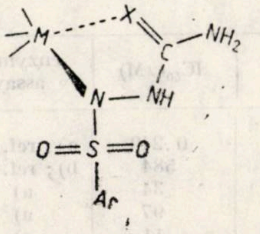

Fig. 2. — Putative mode of binding for a bidentate CA inhibitor; M = Zn(II) (native enzyme) or Co(II) (Cobalt-substituted enzyme); X = O, S, NH.

The inhibition data of our compounds are presented in Table 1, together with literature data for a strong (**1a**) and a very weak (**1d**) structurally-related inhibitor, as well as 4-toluene-sulfonamide (**4a**), a moderate inhibitor, for comparison.

N-Tosyl-imidazole (**2**) proved to be an inhibitor of CA II (bovine isozyme, see experimental), although its mode of binding to enzyme cannot be stated yet precisely. Probably the coordination centre is the N-3 atom, although binding with the oxygen atom(s) of the $-SO_2-$ group cannot be ruled out (participation of the π electrons system of the heterocyclic ring to binding with the Zn(II) ion seems to be highly improbable). We also predict that N-arylsulfonyl-azoles (derivatives of triazoles, tetrazole, thiadiazole, etc) would act as CA inhibitors. *Thus, arylsulfonylated azoles constitute a new class of CA inhibitors.*

Saccharine (**3**) is a weak CA inhibitor too, but this fact seems to be without great physiological significance at the doses used in humans (in order to obtain relevant responses to CA inhibition, the enzyme must be inhibited more than 99%).[4]

As reported previously[11] for similar compounds, N-hydroxy derivatives **4b, c** are among the strongest inhibitors in this series. To our greatest surprise, the hydrazino derivatives **4e ,f** are also moderate CA inhibitors, *this constituting another novel class of compounds which possess such an activity*. Probably that by changing the Ar group with a heterocyclyl one, some potent inhibitors of this type can be expected. It is again very strange that the derivative of N,N-dimenthyl-hydrazine (**4h**) is a much weaker inhibitor than the N-phenyl-derivative **4i**, although the last one is much bulkier. In contrast to the data reported by Blackburn et al.[11] which claimed that the N-methoxy compounds prepared by them had high IC_{50} values (which could not be determined), we found that the N-methoxy-derivative **4d** is a weak CA inhibitor, anyhow more effective than the N-methyl-sulfonamide **4g**. It seems that the electronegative oxygen atom of the methoxy group favours the interaction between inhibitor and the enzyme. Detailed data for such an interaction, studied on the Co(II)-substituted enzyme will be presented elsewhere.[25]

Although the compounds with bulkier groups (4j-s) still present a weak inhibitory action, this is quite unsignificant and might be accounted for by the affinity of the apoenzyme to such compounds. [26] So, it seems that at least for the native enzyme, bidentate binding of the inhibitors to the active site does not occur.

In conclusion, in this paper we reported two novel classes of CA inhibitors, the arylsulfonylated azoles and the arylsulfonylhydrazides and derivatives. As far as we know, this is the first comparative study on such a structurally diverse series of sulfonamides with substituted groups. It is also noteworthy that we discovered an unexpected effect of a common, widely used chemical, i.e., saccharine, which is a weak CA inhibitor.

EXPERIMENTAL

Compounds **2**, **3** and **4a** were from Merck. The other compounds were prepared by literature procedures, from tosyl chloride or benzene-sulfonyl-chloride and the appropriate nucleophile, as it will be specified in each case. With the exception of O-methylhydroxylamine which was prepared by literature procedures, [27] the other nucleophiles used were commercial samples, used without further purification. The prepared compounds were characterized by IR spectroscopy, in KBr pellets (using a C. Zeiss Jena double beam spectrophotometer) and ^{1}H-NMR spectroscopy (in solvents specified in each case) using a Varian EM-360 L spectrometer, working at 60 MHz. Chemical shifts are reported as δ values (ppm) relative to TMS as internal standard. Melting points were recorded on a heating-plate microscope and are not corrected. Bovine CA II was from Sigma Chemical Company.

The inhibitors were tested using the micromethod of Maren [28] and the substrate — enzyme — inhibitor (SEI) technique, as described elsewhere.[20] Stock solutions of inhibitor ($10^{-2}-10^{-3}$ M) were prepared in distilled deionized water — DMSO (max. 10%, v/v) and dilutions obtained thereafter with distilled deionized water, till $10^{-7}-10^{-8}$ M. In this concentration range, DMSO is not inhibitor of CA.[11,20] IC_{50} values, obtained from semilog plots of specific activity of enzyme *vs.* inhibitor concentration represent the molar concentration of inhibitor which produced the 50% decrease of enzyme specific activity. The enzyme concentration in the assay cell was approx. 10^{-8} M.

All inhibitors were at least doubly recrystallized (solvents specified in each case, *vide infra*) prior to assaying.

N-Hydroxy-sulfonamides 4b and 4c

These compounds were prepared by reaction of the corresponding sulfonyl chloride with hydroxylamine, using literature procedures. [11 29]

N-Hydroxy-benzenesulfonamide 4b

M.p. 104—106°C (lit. [29] m.p. 107°C from benzene). This compound was doubly recrystallized from MeOH. IR (KBr), cm^{-1}: 578, 655, 730, 780, 830, 910, 1160, 1320, 1395, 1590, 3210, 3370 (br); ^{1}H-NMR (TFA), δ, ppm : 6.90—7.90 (m, 5H, ArH); 9.10 (s, 1H, NH), 10.10 (s, 1H, OH).

N-Hydroxy-4-toluenesulfonamide 4c

M.p. 149°C, from MeOH (Lit. [29] m.p. 148°C, from benzene); IR (KBr), cm^{-1}: 550, 570, 735, 825, 905, 1000, 1085, 1170, 1315, 1390, 1595, 3210, 3375 (br); ^{1}H-NMR (TFA), δ, ppm : 2.50 (s, 3H, Me); 7.10—7.90 (m, AB, 4H, ArH); 9.20 (s, 1H, NH), 10.10 (s, 1H, OH).

N-Methoxy-4-toluenesulfonamide 4d

The compound was prepared by the reaction of tosylchloride with o-methyl-hydroxylamine, [27] as described in the literature. [29,30] M.p. 111°C, from MeOH (lit. [30] m.p. 113°C, from CCl_4); IR (KBr), cm^{-1}: 550, 565, 738, 830, 910, 1050, 1095, 1180, 1325, 1400, 1597, 2940, 3220;

^{1}H-NMR ($CDCl_3$), δ, ppm : 2.40 (s, 3H, 4-Me) ; 3.75 (s, 3H, OMe) ; 7.20–7.90 (m, AB, 4H, ArH) ; 7.10 (br s, 1H, NH). The last signal was attributed after addition of D_2O in the NMR tube, when it disappeared, due to the isotopic exchange reaction.

Arylsulfonylhydrazides 4e and 4f

The two compounds were prepared by reaction of the corresponding sulfonyl chloride with hydrazine hydrate in THF, using reported procedures.[31]

Benzenesulfonylhydrazide 4e

M.p. 93–95°C, from MeOH (lit.[31] m.p. 98°C, from benzene) ; IR (KBr), cm^{-1} : 520, 970, 1080, 1110, 1330, 1410, 1500, 1570, 3000(br), 3250(br) ; ^{1}H-NMR (AcOH-d_4), δ, ppm : 7.00–7.90 (m, 5H, ArH) ; 11.95 (s, 3H, $NHNH_2$).

4-Toluenesulfonylhydrazide 4f

M.p. 109°C, from MeOH : water (9 : 1, v/v) (lit.[31] m.p. 109–110°C) IR (KBr), cm^{-1} : 510, 705, 980, 1090, 1115, 1350, 1490, 1570, 1610, 3000 (br), 3260 (br) ; ^{1}H-NMR (AcOH-d_4), δ, ppm ; 3.50 (s, 3H, Me) ; 7.30–8.10 (m, AB, 4H, ArH), 12.00 (s, 3H, $NHNH_2$).

N-Methyl-4-toluenesulfonamide 4g

The compound was prepared by reaction of tosylchloride with aqueous methylamine (33%), in the presence of NaOH, as reported in the literature.[32] M.p. 78°C, from MeOH (lit.[32] m.p. 78°C) : IR (KBr), cm^{-1} : 570, 745, 820, 1030, 1070, 1170, 1330, 1400, 1600, 2955, 3230 ^{1}H--NMR (TFA), δ, ppm : 2.50 (s, 3H, Me from tolyl) ; 3.90 (s, 3H, N–Me) ; 7.10–7.80 (m, AB, 4H, ArH) ; 9.25 (s, 1H, NH).

N-Substituted-arylsulfonylhydrazides 4h and 4i

The title compounds were prepared by reaction of tosylchloride with N,N-dimethylhydrazine and phenylhydrazine, respectively, by literature procedures.[33]

N,N-Dimethyl-4-toluenesulfonylhydrazide 4h

M.p. 80°C, from MeOH : water 7 : 3 (v/v) (lit.[33] m.p. 79–81°C, from MeOH — water). IR (KBr), cm^{-1} : 520, 710, 930, 1075, 1120, 1340, 1495, 1590, 1600, 3230 ; ^{1}H-NMR (TFA), δ, ppm : 2.50 (s, 3H, 4-Me) 3.85 (s, 6H, NMe_2), 7.10 – 7.80 (m, AB, 4H, ArH), 9.10 (s, 1H, NH).

N'-Phenyl-4-toluenesulfonylhydrazide 4i

M.p. 160–162°C, from MeOH (lit.[33] m.p. 163°C, from benzene) ; IR (KBr), cm^{-1} : 500, 605, 660, 770, 820, 1090, 1160, 1315, 1490, 1595, 3240, 3330 ; ^{1}H-NMR (TFA), δ, ppm : 2.50 (s, 3H, Me) ; 7.10–8.80 (m, 9H, ArH) ; 10.05 (s, 2H, NHNH).

N-Arylsulfonylderivatives of urea, guanidine, semicarbazide and thiosemicarbazide 4j–4p

These compounds were pepared by acylation of urea, guanidine carbonate, semicarbazide and thiosemicarbazide respectively, with arylsulfonylchlorides, in the presence of potassium carbonate (to neutralize the HCl formed in the reaction), in THF–MeOH. Mention should be made that such acylation reactions were reported to be unsuccessful for urea and guanidine until now,[34] the corresponding compounds being prepared from N-cyano-toluenesulfonamide by other methods.[34] In contrast to Kurzer and Powell[34] which tried to acylate these nucleophiles in pyridine and did not succeed, we performed the reactions with good results in THF–MeOH. The only compound that could not be acylated in these conditions was thiourea.

N-Phenylsulfonylurea 4j

M.p. 197°C, from THF — benzene (4 : 1, v/v) (lit. [34] m.p. 198—200°C, from dioxane); IR (KBr), cm^{-1} : 560, 690, 720, 760, 870, 1015, 1025, 1140, 1370, 1445, 1560, 1675, 1730, 3180 (br), 3370(br); ^1H-NMR (DMSO-d_6), δ, ppm ; 4.90 (br s, 2H, NH_2); 7.30—7.95 (m, 5H, ArH); 8.00 (s, 1H, NH).

N-(4-Toluenesulfonyl)urea 4k

M.p. 190°C, from water (lit. [34] m.p. 191—192°C) ; IR (KBr), cm^{-1} : 560, 690, 815, 1010, 1035, 1150, 1375, 1450, 1570, 1670, 1700, 3190(br), 3360(br) ; ^1H-NMR (DMSO-d_6), δ, ppm : : 2.25 (s, 3H, Me) ; 5.20 (br s, 2H, NH_2) ;6.90—7.60 (m, AB, 4H, ArH) ; 8.05 (s, 1H, NH).

N-Phenylsulfonylguanidine 4m

M.p. 212—214°C, from water (lit.[34] m.p. 214°C) ; IR (KBr), cm^{-1} : 540, 690, 730, 750, 1120, 1315, 1430, 1580, 1690, 3190(br), 3350(br) ^1H-NMR (TFA), δ, ppm : 6.40 (br s, 3H, NH_2 + NH) ; 7.10—7.90 (m, 5H, ArH).

N-(4-Toluenesulfonyl)guanidine 4n

M.p. 233—235°C, from EtOH (lit.[34] m.p. 235°C) ; IR (KBr), cm^{-1} : 540, 575, 650, 690, 700, 820, 1010, 1035, 1130, 1315, 1590, 1680, 3200 (br), 3350 (br) ; ^1H-NMR (TFA), δ, ppm : 2.50 (s, 3H, Me) ; 6.25 (br s, 3H, NH_2 + NH) ; 6.20—8.05 (m, AB, 4H, ArH) ; 8.85 (br s, 1H,NH).

N^4-(4-Toluenesulfonyl)semicarbazide, 4o

M.p. 237—238°C, from EtOH (lit.[34] m.p. 337°C) ; IR (KBr), cm^{-1} : 550, 620, 730, 1050 1100, 1180, 1330, 1440, 1590, 1670, 3080(br), 3200, 3380 ; ^1H-NMR (DMSO-d_6), δ, ppm : 2.40 (s, 3H, Me) ; 6.00 (br s, 3H, NH + NH_2), this signal disappears in time after addition of D_2O in the NMR tube ; 7.20—7.80 (m, AB, 4H, ArH).

N^4-(4-Toluenesulfonyl)thiosemicarbazide 4p

M.p. 186—187°C, from MeOH (lit.[34] m.p. 187°C, from EtOH) ; IR (KBr), cm^{-1} : 550 720, 840, 1010, 1170, 1330, 5120, 1630, 2800, 3000 (br), 3180(br), 3320, 3450 ; ^1H-NMR (TFA) δ, ppm : 2.50 (s, 3H, Me) ; 7.20—8.00 (m, AB, 4H, ArH) ; in this acidic solvent, the amidic protons are not seen.

N-(2,4,6-trimethyl-pyridinium)-4-toluenesulfonamide perchlorate 4q

This compound was prepared by the reaction of tosylhydrazide 4f with 2,4,6-trimethylpyrylium perchorate,[35] by literature procedures.[36] M.p. 234°C, from MeOH (lit.[35] m.p. 235°C). IR (KBr), cm^{-1} ; 625, 835, 1100, 1315, 1440, 1600, 3070, 3240 ; ^1H-NMR (TFA), δ, ppm : 2.50 (s, 3H, Me from tolyl) ; 2.70 (s, 6H, 2,6-Me_2 from pyridinium) ; 2.95 (s. 3H, 4-Me from pyridinium), 7.20—7.90(m, 6H, ArH).

Bis(4-toluenesulfonyl)amine 4r

This compound was prepared from toluenesulfonamide and tosylchloride, using reported procedures. [37] M.p. 155°C, from water (lit.[37] m. p. 155°C, from water) ; IR (KBr), cm^{-1} : 550, 660, 810, 900, 1100, 1180, 1300, 1520, 1590, 3255, 3360 ; ^1H-NMR (TFA), δ, ppm : 2.50 (s, 6H, 2 Me) ; 7.40—8.20 (m, AB, 8H, ArH) ; 9.1 (s, 1H, NH).

Bis (4-toluenesulfonamido)methane 4s

The compound was prepared by condensation of 4-toluenesulfonamide with formaldehyde in aqueous solution as reported in literature.[38] M.p. 137°C, from MeOH (lit.[38] m.p. 136°C). IR (KBr), cm^{-1} : 550, 675, 1120, 1330, 1590, 3260 ; ^1H-NMR (TFA), δ, ppm : 2.50 (s, 6H 2Me) ; 3.90 (s, 2H, CH_2), 7.40—8.20 (m, AB, 8H, ArH).

ACKNOWLEDGMENTS. Special tanks are addressed to Professor Ivano Bertini (University of Florence, Italy) for his invaluable help and advices, and to Mrs. Engineer Ana Schiketanz for recording some of the NMR spectra.

REFERENCES

[1] Part 8: C. T. Supuran, R. Stefan, G. Manole, I. Puscas and M. Andruh, *Rev. Roumaine Chim.*, **36**, 1073 (1991).

[2] T. Mann and D. Keilin, *Nature*, **146**, 164 (1940).

[3] P. J. Venta, J. C. Montgomery and R. E. Tashian, "Molecular Genetics of Carbonic Anhydrase Isozymes" in "Isozymes: Current Topics in Biological and Medical Research", M. C. Rattazzi, J. G. Scandalios and G. S. Whitt Eds., Alan R. Liss, New York, 1987, pp. 59–72.

[4] T. H. Maren, *Physiol. Rev.* **47**, 595 (1967).

[5] T. H. Maren, *Ann. N.Y. Acad. Sci.* **429**, 568 (1984); b) T. H. Maren, *Drug. Dev. Res.* **10** 255 (1987).

[6] D. M. Woodbury, "Carbonic Anhydrase Inhibitors" in "Antiepileptic Drugs: Mechanism of Action", G. H. Glaser, J. K. Penry and D. M. Woodbury Eds., Raven Press, New York, 1980, pp. 617–633.

[7] E. B. Larsson, R. C. Roach, R. B. Schoene and T. T. Hornbein, *J. Am. Med. Ass.* **248**, 328 (1982).

[8] H. A. Krebs, *Biochem. J.* **43**, 525 (1948).

[9] G. L. Mandell and M. A. Sande, "Antimicrobial Agents" in "The Pharmacological Basis

[10] I. E. Coleman, *Ann. Rev. Pharmacol.*, **15**, 221 (1975).

of Therapeutics", A. Goodman Gilman et al. Eds., Macmillan, New York 1987, seventh edition, pp. 1095–1114.

[11] G. M. Blackburn, B. E. Mann, B. F. Taylor and A. F. Worrall, *Eur. J. Biochem.*, **153**, 553 (1985).

[12] M. W. Duffel, I. S. Ing., T. M. Segarra, J. A. Dixson, C. F. Barfknecht and R. D. Schoenwald, *J. Med. Chem.*, **29**, 1488 (1986).

[13] I. Bertini, C. Luchinat and A. Scozzafava, *Struct. Bonding* **48**, 45 (1982).

[14] a) K. K. Kannan, I. Vaara, B. Notstrand, S. Lövgren, A. Borell, K. Fridborg and M. Petef, "Structure and Function of Carbonic Anhydrase: Comparative Studies of Sulfonamide Binding to Human Erythrocyte CA B and CA C" in "Drug Action at Molecular Level", G. C. K. Roberts Ed., University Park Press, Baltimore 1977, pp. 73–91; b) E. A. Eriksson, T. A. Jones and A. Liljas, "Crystallographic Studies of Human Carbonic Anhydrase II" in "Zinc Enzymes", I. Bertini, C. Luchinat, W. Maret and M. Zeppezauer Eds., Birkhäuser, Basel, 1986, pp. 317–328.

[15] I. Bertini, C. Luchinat, *Acc. Chem. Res.* **16**, 272 (1983).

[16] a) R. G. Khalifah, *J. Biol. Chem.* **246**, 2561 (1971); b) R. G. Khalifah, J. I. Rogers and J. Mukherjee, *Biochemistry*, **26**, 7057 (1987).

[17] C. Luchinat, R. Monnanni and M. Sola, *Inorg. Chim. Acta*, **177**, 133 (1990).

[18] J. L. Parkes and P. S. Coleman, *Arch. Biochem. Biophys.* **275**, 459 (1989).

[19] a) C. Tu and D. N. Silverman, *Biochemistry*, **28**, 7913 (1989); b) C. Tu, S. R. Paranawithana, D. A. Jewell, S. M. Tanhauser, P. V. LoGrasso, G. C. Wynns, P. J. Laipis and D. N. Silverman, *Biochemistry* **29**, 6400 (1990).

[20] a) I. Pușcaș, C. Supuran and G. Manole, *Rev. Roumaine Chim.* **35**, 683 (1990); b) C. T. Supuran, A. Dinculescu, G. Manole, F. Săvan, I. Pușcaș and A. T. Balaban, *Rev. Roumaine Chim.*, **36**, 936 (1991).

[21] N. Kakeya, N. Yata, A. Kamata and M. Aoki, *Chem. Pharm. Bull. (Tokyo)* **17**, 2558 (1969).

[22] a) L. B. Dugad and J. T. Gerig, *Biochemistry* **27**, 4310 (1988); b) L. B. Dugad, C. R. Cooley and J. T. Gerig, *Biochemistry* **28**, 3955 (1989).

[23] a) I. Bertini, G. Canti, C. Luchinat and A. Scozzafava, *J. Amer. Chem. Soc.* **100**, 4873 (1978); b) I. Bertini, G. Canti, C. Luchinat and F. Mani, *J. Amer. Chem. Soc.* **103**, 7784 (1981); c) I. Bertini, A. Dei, C. Luchinat and R. Monnanni, *Inorg. Chem.* **24**, 301 (1985); d) L. Banci, I. Bertini, C. Luchinat, R. Monnanni and J. Moratal Mascarell, *Gazz. Chim. Italiana* **119**, 23 (1989).

[24] a) L. Garcia-Iniguez, L. Powers, B. Chance, S. Sellin, B. Mannervik and A. S. Mildvan, *Biochemistry* **23**, 685 (1984); b) K. T. Douglas, "Glutathione-dependent Enzymes — Chemistry" in "Enzyme Mechanisms", M. I. Page and A. Williams Eds., Royal Soc. Chemistry, London 1989, pp. 442—467.
[25] I. Bertini et al., in preparation.
[26] R. W. King and A. S. W. Burgen, *Proc. R. Soc.* **B193**, 107 (1976).
[27] A. Chimiak and T. Kolasa, *Bull. Acad. Pol. Sci. Ser. Chim.* **22**, 195 (1974).
[28] T. H. Maren, *J. Pharmacol. Exp. Ther.* **130**, 26 (1960).
[29] M. Fujimoto and M. Sakai, *Chem. Pharm. Bull. (Tokyo)* **13**, 248 (1965).
[30] S. Murakami and S. Nashima, *Mem. Inst. Scient. Ind. Res. Osaka Univ.* **10**, 175 (1953).
[31] a) L. Friedman, R. L. Litle and W. R. Reichle, *Org. Synth.* **40**, 93 (1960); b) L. Friedman, R. L. Litle and W. R. Reichle, *Org. Synth. Coll. Vol.* V, 1055 (1973).
[32] T. J. de Boer and H. J. Backer, *Org. Synth. Coll. Vol.* IV, 943 (1972).
[33] J. Wawzonek and V. Meyer, *J. Amer. Chem. Soc.* **76**, 2918 (1954).
[34] a) F. Kurzer and J. R. Powell, *J. Chem. Soc.* **1955**, 1497; b) F. Kurzer and J. R. Powell, *J. Chem. Soc.* **1955**, 1503.
[35] A. T. Balaban and C. D. Nenitzescu, *Org. Synth. Coll. Vol.* V, 1106 (1973).
[36] R. Neidlein and P. Witerzens, *Arch. Pharm. (Weinheim)*, **309**, 649 (1976).
[37] M. Dychanow, *J. Obshch. Chim.* **29**, 3602 (1959).
[38] C. D. Egginton and A. J. Lambie, *J. Chem. Soc.* **1969**, 1623.

Revue Roumaine de Chimie, **36**, *11–12*, 1355–1361 (1991)

SYNTHESIS AND STRUCTURE ELUCIDATION OF BENZOTHIAZOLE-CONTAINING COMPOUNDS FOR ANTIMICROBIAL INVESTIGATION

K. M. GHONEIM, S. EL-BASIL, A. N. OSMAN, M.M. SAID and S. A. MEGAHED *
Organic and Microbiology * Departments, Faculty of Pharmacy, Cairo University, Cairo, Egypt

Received November 12, 1988

Attempted cycloaddition of benzimidazole-2-thiol with arylidenemalononitriles 1 was unsuccessful. 2-Cyanomethyl-1,3-benzothiazole 6 condensed with certain aromatic aldehydes to produce 7, cycloaddition of which with cyanoacethydrazide 3 yielded 8. Structure of the newly synthesized compounds was substantiated by spectroscopic data and/or unambiguous synthesis. Representative compounds were screened for antimicrobial activity.

INTRODUCTION

In 1981, a group of Japanese investigators [1] — in an extension of their studies on pesticidal heterocyclic compounds — prepared the pyridine derivatives (**2**, $R = C_6H_5$ or $2\text{-}H_2N{\cdot}C_6H_4$) through the reaction of benzenethiol and/or 2-aminobenzenethiol with arylidenemalononitriles **1** in ethanol containing triethylamine (TEA), or by initial reaction of the thiol with malononitrile followed by addition of **1**. Based on these data, it was thought to prepare an analogous pyridine series by replacing the aforementioned benzenethiol with benzimidazole-2-thiol.

On the other hand, some Egyptian authors [2,3] reported that the reaction of cyanoacethydrazide **3** with **1** afforded pyridine-containing products **4** and **5**. However no mechanism was laid down.

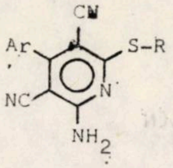

(2)

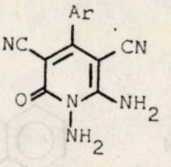

(4)

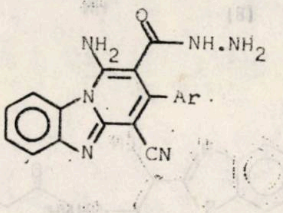

(5)

Consequently, it was decided to carry out the reaction of **3** with arylidenemalononitriles containing the benzothiazole ring, aiming at the synthesis of heterocyclic compounds of microbiological interest, since some benzothiazole derivatives have been reported to exhibit antimicrobial activity.[4–9]

RESULTS AND DISCUSSION

Six arylidenemalononitriles **1** became accessible [10-12] through Knoevenagel condensation of aromatic aldehydes with malononitrile and were allowed to react with benzimidazole-2-thiol adopting the two routes reported earlier. [1] However, the starting materials were recovered. Refluxing the reactants for 24 hours in ethanol alone, ethanol containing base (TEA, piperidine, K_2CO_3) and/or dioxane containing TEA brought about the same result. Moreover, carrying out the reaction in alc. NaOH or fusion of the reactants for 10 hours did not improve matters, and the target compounds (**2**, R = 2-benzimidazolyl) were not obtained.

Failure of benzimidazole-2-thiol to condense with **1** in a Michael type reaction may be ascribed to entering the lone electron pair of the mercapto group sulphur into conjugation with benzimidazole ring system and hence its lower nucleophilicity. Steric factors may have played a role too. Such an interpretation may be supported by what has been reported by Kada et al. [13] who reacted 4,5-dibromo-2-furfurylidenemalononitrile with the sodium salt of benzimidazole-2-thiol. The reaction was found to be S-arylation rather than a Michael type addition.

On the other hand, certain arylidenemalonitriles containing the benzothiazole ring **7** were prepared, starting with 2-aminobenzenethiol. These were then allowed to interact with **3** in boiling enthanol and in presence of piperidine. Mass spectral data of the products revealed that

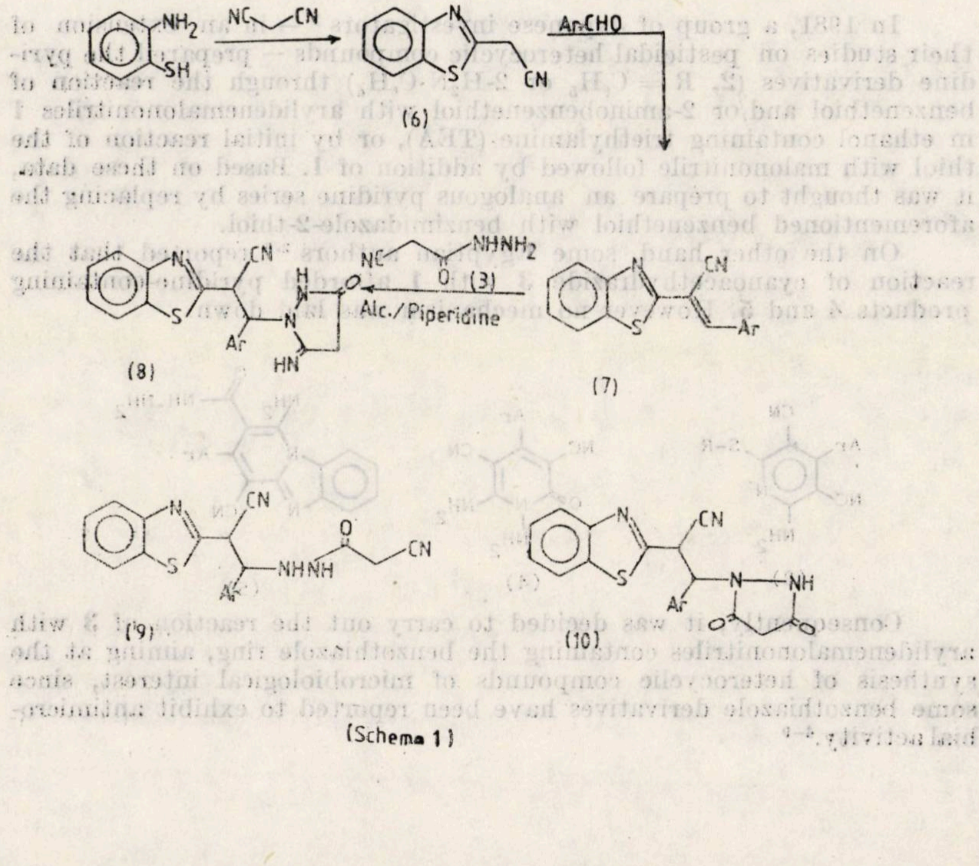

(Schema 1)

they represent 1 :1 adducts. Based on IR, ^1H-NMR and mass spectral data, three possible structures **8**—**10** may be assigned for these reaction products.

This indicated that attack by the amino function in **3** on the olefinic double bond in **7** *via* Michael addition is the most probable pathway. For clarification of this conjecture, cyanoacethydrazide **3** was condensed with benzaldehyde to obtain the corresponding azomethine **11**, [14,15] which was then allowed to react with **6**, (Route A). The product was identical with that obtained from the reaction of **3** with **7a**. Literature survey showed that **3** undergoes cyclization to 5-aminopyrazolin-3-one **12**, under reaction conditions [16] similar to those applied in the present work. Based on this experimental finding, the proposed structure **9** might be expected to undergo cyclization to provide either **8** or **10**. Therefore **12** was prepared [16] and introduced to react with **7a**, (Route B). The product was the same as that obtained by (Route A), which in turn was the same as that produced from the reaction of **3** with **7a**. This synthesis (Route B) has been taken as an evidence that **3** has reacted with **7** to afford the iminopyrazolidinone derivatives **8**. Hence the other two alternative structures **9** and **10** were rejected.

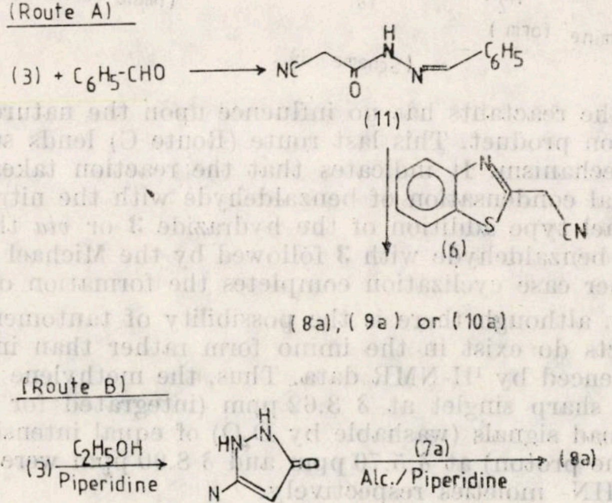

(Scheme 2)

Consequently, the most compatible mechanism that can account for the reaction of **3** with **7** in presence of piperidine may be portrayed by the following scheme (Scheme 3).

Alternatively **3** may undergo cyclization into **12** which may then attack the arylidenes **7** to afford the final products **8** as evidenced by (Route B).

Furthermore **8a** has also been obtained by a one-step procedure (Route C) involving the reaction of a mixture of benzaldehyde, **3** and 2-cyanomethylbenzothiazole **6** in ethanol containing TEA. The order of addition of the reactants has no influence upon the nature or the yield of the reaction product. This last route (Route C) lends support to the suggested mechanism. It indicates that the reaction takes place either through initial condensation of benzaldehyde with the nitrile **6** followed by the Michael type addition of the hydrazide **3** or *via* the initial condensation of benzaldehyde with **3** followed by the Michael type addition of **6**. In either case cyclization completes the formation of **8a**.

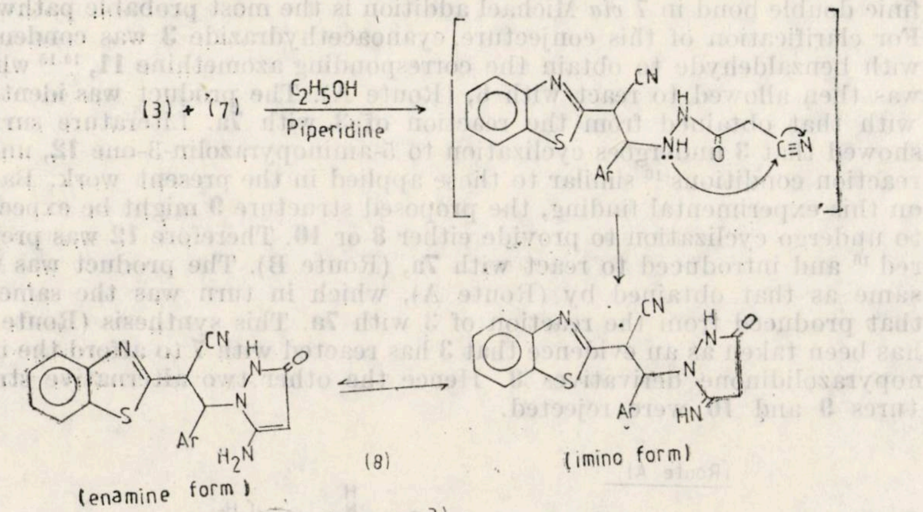

(Scheme 3)

Finally, although there is the possibility of tautomerism in **8**, yet these products do exist in the imino form rather than in the enamine form as evidenced by ^{1}H-NMR data. Thus, the methylene group protons appeared as sharp singlet at δ 3.62 ppm (integrated for two protons), while the broad signals (washable by D_2O) of equal intensity (each integrated for one proton) at δ 5.70 ppm and δ 8.90 ppm were assignable to $=$NH and HN- moieties respectively.

EXPERIMENTAL

Melting points are determined by open capillary method and are uncorrected. Microanalysis was carried out at the Microanalytical Center, Cairo University. IR-spectra were performed in KBr discs on a Perkin Elmer 457 or Pye Unicam sp 1100 IR-spectrophotometers. ^{1}H-NMR spectra were carried out on Variant T-60 ^{1}H-NMR spectrometer, using TMS as internal standard. Mass spectra were performed by the Mass Spectrometry Laboratory, Department of Chemistry, University of Alberta, Edmonton, Alberta, Canada.

Arylidenemalononitriles (**1**) [10–12]; *2-benzothiazolylacetonitrile* (**6**) [17]; *cyanoacetic acid hydrazide* (**3**) [18]; *cyanoacetic benzylidene hydrazide* (**11**) [14,15] and *5-aminopyrazolin-3-one* (**12**) [16] were prepared using reported methods.

Table 1

1-Aryl-2-cyano-2-(2-benzothiazolyl)ethylenes **7**

7	Ar	Yield %	M.p. °C	Molecular Formula	Analysis Calcd/Found		
					C	H	N
a*	C_6H_5	80	121–3	$C_{16}H_{10}N_2S$	—	—	—
b	2-$C_6H_4OCH_3$	74	160	$C_{17}H_{12}N_2OS$	69.86 69.5	4.10 4.3	9.58 9.2
c*	4-$C_6H_4OCH_3$	68	143–4	$C_{17}H_{12}N_2OS$	—	—	—
d	3,4,5-$C_6H_2(OCH_3)_3$	72	140	$C_{19}H_{16}N_2O_3S$	64.77 64.9	4.54 4.4	7.95 7.6
e	2-C_6H_4Cl	80	162	$C_{16}H_9ClN_2S$	64.75 64.5	3.03 3.4	9.44 9.6
f	3-C_6H_4Cl	78	135	$C_{16}H_9ClN_2S$	64.75 65.0	3.03 3.4	9.44 9.6
g*	4-C_6H_4Cl	67	148–50	$C_{16}H_9ClN_2S$	—	—	—
h	3-$C_6H_4NO_2$	83	197	$C_{16}H_9N_3O_2S$	62.54 62.8	2.90 3.0	13.68 14.0
i	4-$C_6H_4NO_2$	84	160	$C_{16}H_9N_3O_2S$	62.54 62.8	2.90 3.2	13.68 13.5
j	2-Furyl	73	135	$C_{14}H_8N_2OS$	66.66 67.0	3.17 3.6	11.11 11.1
k	2-Thienyl	72	148	$C_{14}H_8N_2S_2$	62.68 63.0	2.98 3.2	10.44 10.8

* As reported [17].

Table 2

1-Aryl-1-(5-iminopyrazolidin-3-one-1-yl)-2-cyano-2-(2-benzothiazolyl)ethanes **8**

8	Ar	Yield %	M.p. °C	Molecular Formula	Analysis Calcd/Found		
					C	H	N
a	C_6H_5	68	222	$C_{19}H_{15}N_5O_5$	63.15 63.3	4.15 4.0	19.39 19.8
b	2-$C_6H_4OCH_3$	69	288	$C_{20}H_{17}N_5O_2S$	61.38 61.9	4.34 3.6	17.94 17.5
c	4-$C_6H_4OHC_3$	69	230	$C_{20}H_{17}N_5O_2S$	61.38 61.4	4.34 4.0	17.94 17.5
d	3,4,5-$C_6H_4(OCH_3)_3$	75	190	$C_{22}H_{21}N_5O_4S$	58.53 58.1	4.65 5.0	15.52 15.1
e	2-C_6H_4Cl	73	210	$C_{19}H_{14}ClN_5OS$	57.64 57.7	3.53 3.4	17.69 18.1
f	3-C_6H_4Cl	71	260	$C_{19}H_{14}ClN_5OS$	57.64 58.3	3.53 3.4	17.69 18.0
g	4-C_6H_4Cl	73	314	$C_{19}H_{14}ClN_5OS$	57.64 57.5	3.53 3.3	17.69 17.1
h	2-$C_6H_4NO_2$	74	312	$C_{19}H_{14}N_6O_3S$	56.15 56.5	3.44 3.7	20.68 20.2
i	4-$C_6H_4NO_2$	75	330	$C_{19}H_{14}N_6O_3S$	56.15 56.4	3.44 3.6	20.68 20.3
j	2-Furyl	67	230	$C_{17}H_{13}N_5O_2S$	58.11 58.0	3.70 3.5	19.94 20.0
k	2-Thienyl	65	250	$C_{17}H_{13}N_5OS_2$	55.58 55.5	3.54 3.6	19.07 18.7

1-*Aryl-2-cyao-2-(-2-benzothiazolyl) ethylenes*, (**7a-k**).

General Procedure.

To a solution of **6** (1.7 g, 0.01 mole) in absolute ethanol, a few drops of TEA and the appropriate aldehyde (0.01 mole) were added. The mixture was stirred at room temperature for 4 hours and then allowed to stand overnight. The separated solid was filtered and crystallized from ethanol (Table 1).

IR-spectra : 3220 cm^{-1} ($\nu C{\equiv}N$).

^1H-NMR-spectrum (**7c** in $CDCl_3$) : δ 7.0—7.6 ppm (m., 4H, benzothiazole aromatic protons), δ 7.90—8.25 ppm (m., 4H, 2-chlorophenyl group protons), δ 8.6 ppm (s., 1H, $-CH=$)-

1-Aryl-1-(5-iminopyrazolidin-3-one-1-yl)-2-cyano-2-(2-benzothiazolyl)ethanes (**8a-k**).

General Procedure.

A solution of the appropriate **7** (0.01 mole) and **3** (1 g, 0.01 mole) in absolute ethanol (20 mL) was heated under reflux for 3—4 hours in presence of a few drops of piperidine. The reaction mixture was cooled and the precipitate was filtered and crystallized from ethanol (Table 2).

IR-spectra : 3480, 3340, 3240 cm^{-1} (ν_{NH}), 2220 cm^{-1} ($\nu C{\equiv}N$), 1690—1645 cm^{-1} ($\nu C{=}O$),

^1H-NMR-spectrum (**8a** *in DMSO-D_6*) : δ 3.62 ppm (s., 2H, $-CH_2-$) ; δ 4.55 ppm (m., 1H, $-\overset{|}{C}H-Ar$) ; δ 5.65 ppm (m., 1H, $-CH-CN$) ; δ 5.70 ppm (broad, 1H, $=NH$) ; δ 7.55 ppm (s., 5H, C_6H_5) ; δ 7.4—8.0 ppm (m., 4H, benzothiazole protons) ; and δ 8.90 ppm (broad, 1H, $HN-\overset{|}{C}=O$). Signals at δ 5.70 and δ 8.9 ppm disappeared upon deuteration.

Mass spectrum of **8a** : m/z 361 ($C_{19}H_{15}N_5OS$, 76 %, M) ; m/z 262 ($C_{19}H_{10}N_2S$, 100 %, M--pyrazolidinone ring $C_3H_5N_3O$) ; m/z 187 ($C_{10}H_9N_3O$, 28.6 %, M-$C_9H_6N_2S$) ; m/z 174 (benzothiazoleacetonitrile $C_9H_6N_2S$, 81 %, M—$C_{10}H_9N_3O$).

Mass spectrum of **8g** : m/z 395($C_{19}H_{12}ClN_5OS$, 18 %, 60 %, M-H_2) ; m/z 364, 362 ($C_{18}H_9ClN_5S$, 14 %, 30 %, M—H_2, —OH, —CH_2) ; m/z 43 (CHNO, 100 %, base, M—$C_{18}H_{13}ClN_4S$).

Separate synthesis of (**8a**).

This compound was further prepared by three other routes.

Route A.

Equimolecular amounts of **6** and **11** (0.01 mole each) were refluxed in absolute ethanol in presence of a few drops of piperidine for 3 hours. The solid which separated at cooling was filtered and crystallized from ethanol. M.p. 222°C, yield 2.1 g (60 %).

Route B.

A mixture of **12** (1 g, 0.01 mole), **7a** (2.6 g, 0.01 mole), a few drops of piperidine and absolute ethanol (10 mL) was refluxed for 2 hours. The separated solid after cooling was filtered and crystallized from ethanol. M.p. 222°C, yield 1.8 g (50 %).

Route C.

A mixture of **6** (1.74 g, 0.01 mole), **3** (1 g, 0.01 mole), benzaldehyde (1 g, 0.01 mole) and a few drops of piperidine was refluxed in absolute ethanol (10 mL) for 4 hours. After cooling, the separated solid was filtered and crystallized from ethanol. M.p. 222°C, yield 2.1 g (60 %).

Samples of **8a** prepared by the general procedure and through the routes (A—C) showed identical m.p. and IR spectra. Mixed m.p. showed no depression.

Screening for Antimicrobial Activity.

Suspensions of several microorganisms were prepared by inoculating fresh stock cultures into separate broth tubes, each containing 7 mL of nutrient broth (peptone 0.3 %, beed extract 0.3 %). The inoculated tubes were incubated at 37°C for 24 hours. The microbial suspensions were plated in triplicates as follows :

Talls of sterile culture media (test tubes, each containing 15 mL of nutrient agar for bacteria, or of Sabouraud dextrose agar for fungi) were melted and poured each in an empty sterile petri-dish (100 and 5 mm) and were left to solidify. The overnight broth cultures of each organism were spread with a dry sterile swab on the surface of the previously prepared plates.

Sterile discs of Whatmann No. 3 (6 mm diameter) were impregnated with each of the compounds (**8a, b, e, f-h, j, k**) solutions in dimethylformamide (DMF), left to dry and then placed on the surface of the inoculated plates. These plates were incubated at 37°C for 24 hours for bacteria and at 25°C for 7 days for fungi then visually examined, and zones of inhibition, if any, were measured (Table 3).

Table 3

Results of the antimicrobial testing*

(8)	Staph. aureus	Bacillus subtilis	Esch. coli	Candida albicans	Myco. phlei	Asper. niger	Trichophyton mentagrophites	Phycomyces blackesleeanus
a	—	—	—	—	—	—	—	—
b	—	—	+++	—	—	—	—	—
e	—	—	++	—	—	—	—	—
f	—	—	—	—	—	—	—	—
g	—	—	++	—	—	—	—	—
h	—	—	—	—	—	—	—	—
j	—	—	+	+	—	—	—	—
k	—	—	—	—	—	—	—	—

* Inhibition zones are measured in mm. The concentration used is 20 mg/disc. Control discs were performed with DMF.

(—) Resistant, (+) moderately sensitive giving a zone of inhibition 11 mm, (++) sensitive giving a zone of inhibition 12 mm, (+++) very sensitive giving a zone of inhibition 13 mm.

CONCLUSION

Compounds **8b, e, g, j** showed activity against Escherichia coli. In addition, compound **8j** was found to be effective against the yeast *Candida albicans*. However compounds **8a, f, h, k** were shown to be inactive.

REFERENCES

[1] S. Kambe and F. Saito, *Synthesis*, **7**, 531 (1981).

[2] E. M. Zayed, E.A. A. Hafez, S. A. S. Ghozlan and A. A. H. Ibrahim, *Heterocycles*, **22** 2553 (1984).

[3] M. A. Hammad, M. M. Kamel, M. M. Abbasi, M. T. El-Wassimi and H. N. A. Hassan, *Pharmazie*, **41**, 141 (1986).

[4] E. L. Everitt, and M. X. Sullivan, *J. Wash. Acad. Sci.*, **30**, 125 (1940); *Chem. Abstr.* **34**, 4104 (1960).

[5] J. Hata, M. Tsuruoka, I. Utsumi and T. Ida, *J. Pharm. Soc. Japan*, **74**, 245 (1954); *Chem. Abstr.*, **48**, 7780^e (1954).

[6] S. Nakajima, I. Tanaka, T. Seki and T. Anmo, *Yakugaku Zasshi*, **78**, 1378 (1958); *Chem. Abstr.*, **53**, 8124^h (1959).

[7] V. Sutoris, P. Foltinova and G. Blockinger, *Chem. Zvest.*, **27**, 698 (1973); *Chem. Abstr.*, **80**, 95814^g (1974).

[8] S. Eva and O. Zelmira, Czech., CS, 189, 212 (Cl. CO7D 277/68), 25 Sept. 1981; *Chem. Abstr.* **96**, 162686n (1982).

[9] P. Ram and V. S. Rajendra, *Indian Drugs* **23**, 21 (1985); *Chem. Abstr.*, **104**, 2837s (1986).

[10] B. B. Corson and R. W. Stoughton, *J. Amer. Chem. Soc.*, **50**, 2825 (1928).

[11] H. G. Sturz, and C. R. Noller, *J. Amer. Chem. Soc.*, **71**, 2949 (1949).

[12] F. Freeman, *Chem. Rev.*, **69**, 609 (1969).

[13] R. Kada, V. Knoppova, J. Kovac, and P. Cepec, *Collection Czechoslovak. Chem. Commun.*, **49**, 984 (1984).

[14] D. Chakravarty, A. Bose and S. Bose, *J. Pharm. Sci. 53*, 1036 (1964). *Chem. Abstr.*, **61**, 14632c (1964).

[15] G. Geissler, M. Hippius and G. Tomaschewski, *J. Prakt. Chem.*, **324**, 910 (1982).

[16] B. Hepner and S. Fajersztejn, *Bull. Soc. Chim.* **5**, 854 (1937); *Chem. Abstr.*, **31**, 8511 (1937).

K. Saito, S. Kambe, Y. Nakano, A. Sakurai and H. Midorikawa, *Synthesis*, 3, 210 (1983).

R. V. Fotherburg, *Chem. Ber.*, **27**, 687 (1894).

Revue Roumaine de Chimie, **36**, *11–12*, 1363–1369 (1991)

STRUCTURAL DIFFERENCES OF SOME BIOMATERIALS BASED ON COLLAGEN

G. L. RADU [a], **A. TĂNASE** [b], **MARIA CALOIANU-IORDACHEL** [a] **and I. TODOR** [b]

[a] **Institute of Biological Sciences, Spl. Independenţei no. 296 Bucharest, Romania**

[b] **Research and Production Entreprise for Electronic Materials, Bucharest, Romania**

Received October 20, 1989

Collagen became the basic material to obtain biomaterials used in various medical fields. The physico-chemical and biological properties of biomaterials are dependent, among other factors, on the structure. The paper characterises certain spongy biomaterials, by thermal analysis. The thermograms obtained on the temperature range 20 – 500° are specific for each biomaterial and may become their "fingerprint". "Structural water" was detected in an approximate amount of 1 %, its elimination being done within the temperature range of 180–210°. The denaturation of the collagen contained in samples, revealed by DTA curves, is preceded and accompanied by mass loss evidenced by TG and DTG curves. It is considered that this mass loss (probably water) is determining the denaturation.

INTRODUCTION

The animal protein, generically called "collagen" is in the last years the object of intense structural investigations [1–4] because of its biological importance and the fact that it is used as natural material in various fields such as: medicine, chemico-pharmaceutical industry and cosmetics.

The further use of collagen-based biomaterials in practice requires certain biological, physical and chemical properties.

Collagen can be extracted from those animal tissues that contain it in large quantities, both accessible and available. [5]

The biological variety of sources and the diversity of the extraction procedures did not permit a standardisation during the stage of isolation. Each variety of extracted collagen and biomaterial should be independently characterised by applying analvtical methods and techniques. The methods of thermal analysis, widely applied in the study of natural and synthetical polymers[6] were used in the case of collagen where a correlation of some elements of the native structure of the protein was possible with the thermal effects[7,8] detected as such.

Therefore, the paper presents a characterisation by thermal analysis of some collagen-based biomaterials, correlating the structural differences with the parameters of the incipient stage of extracting collagens.

EXPERIMENTAL

The biomaterials analysed by us contain collagen (a mixture of type I and type III) extacted from bovine derm and conditioned as dry and spongy matter by lyophilisation.

The collagen from biomaterials as : $C\ 0.8_{Ac}$, $C\ 1_{Ac}$, $C\ 0.8_{Ta}$, $C\ 1_{Ta}$ $C\ 0.8_{Ox}$, $C\ 1_{Ox}$ was obtained after a controlled treatment of derm with a solution of 2 M NaOH, followed by a solubilisation in solutions of 0.5 M acetic acid, 0.5 M tartric acid, 0.5 M oxalic acid.

The collagen solutions were obtained in two variants differentiated by the concentration of collagen of 0.8 g/dL and 1 g/dL respectively. The quantity of collagen was estimated according to the method described in literature.[9]

The biomaterials C_1, C_2, C_3 partly insoluble were obtained from the solution of collagen of concentration 1 g/dL in 0.5 M acetic acid.

The various solubilities were determined by reticulation of collagen with formaldehyde (art. 400 Merk). The gravimetrical relationships collagen/formaldehyde were : $C_1 - 1/0.036$; $C_2 - 1/0.108$; $C_3 - 1/0.182$.

The thermal analyses were carried out by using the derivatographer MOM type Q — -1500 D which recorded simultaneously the temperature increase (T) of the thermogravimetric curves (TG), the differential thermogravimetric curves (DTG) and differential thermal analysis curves (DTA). Samples of 200 mg were heated in air to 500° with a rate of 2.5°/min and 5°/min ; sensitivities for DTG and DTA were of 500 uV and 250 uV respectively ; alumine was taken as standard.

RESULTS AND DISCUSSION

Collagen was extracted with a nondenaturated or partly denaturated molecular structure comparing to the native one. In the analysed biomaterials collagen is organised as molecular superstructure (supranetworks) whose structural peculiarities depend on a series of factors.[10,11]

For all analysed samples the temperature scale was considered between the environmental temperature and 500°; beyond this, the occurring pyrolysis process is of no interest.

The thermal curves of samples $C\ 0.8_{Ac}$, $C\ 1_{Ac}$(Fig. 1) starting from the environmental temperature to 130°, present a good effect induced

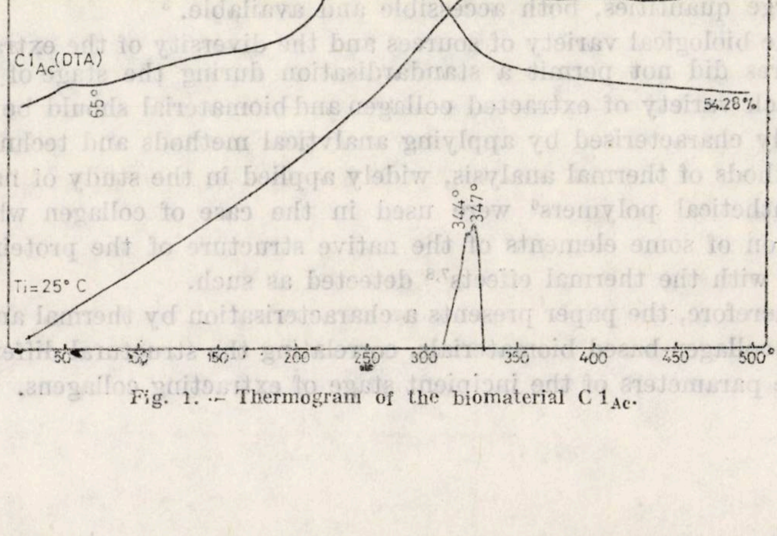

Fig. 1. — Thermogram of the biomaterial $C\ 1_{Ac}$.

by the release of water from the structure of the biomaterial; the mass loss in this range of temperature is of about 7% (Table 1). For C 0.8_{AC} the value of 69° and for C 1_{Ac} the value of 65° are characteristic as denaturation points for collagen. Between 135° and 180°, in both cases, the curves of mass variation (DTG and TG) show a good thermal stability of samples. When temperature increases over 200°, two exothermal effects appear on the curve DTA, with the maximum values at 229° and 330° and 237° respectively 347°. These effects are accompanied by a mass loss representing 37.18% and 41.19%. We ascribe these effects to the break and elimination of the functional groups from collagen structure, this process being also followed by the break of the peptidic chains and the pyrolysis of the organic matter not entirely oxidated to 500° with a carbonic waste.

In the involved temperature range, the thermal curves of the samples C 0.8_{Ta}; C 1_{Ta} (Fig. 2) are similar, some differences appear as regards he maximum points and expansion of thermal effects. The denaturation points of collagen extracted in tartric acid are at 67° for the biomaterial C 0.8_{Ta} and at 75° for C 1_{Ta}. The mass loss at the temperature of 130° is higher (Table 1) than in case of biomaterials based on collagen

Table 1

The per cent mass loss (m.l.)* of biomaterials C 0.8_{Ac}, C 1_{Ac}, C 0.8_{Ta}, C 1_{Ta}, C 0.8_{Ox}, C 1_{Ox} on the temperature range (t°) characteristic of the thermograms

	$C0.8_{Ac}$ $C1_{Ac}$		$C0.8_{Ta}$ $C1_{Ta}$		$C0.8_{Ox}$ $C1_{Ox}$	
	t°	m.l.	t°	m.l.	t°	m.l.
A–B	24–125 25–120	7.12 6.33	20–140 25–127	11.19 13.13	15–140 20–150	11.7 14.05
B–C	125–185 120–190	1.5 1.3	140–193 127–200	0.91 1.09	140–220 150–200	1.8 1.17
C–D	185–355 190–350	37.18 41.19	193–365 200–366	33.54 35.02	220–363 200–376	31.03 26.34
D–E	355–510 350–510	4.07 5.4	365–500 366–500	6.58 4.9	363–500 376–500	24.27 26.04
E	510	49.87 54.28	500	52.22 55.27	500	68.8 67.6

* The per cent mass loss were determined from the curves of thermogravimetry (TG) without the correction for water release.

extracted in acetic acid; the exothermal effects between 200—350° have the maximum points around the same temperature values ($C\ 0.8_{Ta}$—232° and 337°; $C\ 1_{Ta}$—223° and 327°) but with reduced amplitudes.

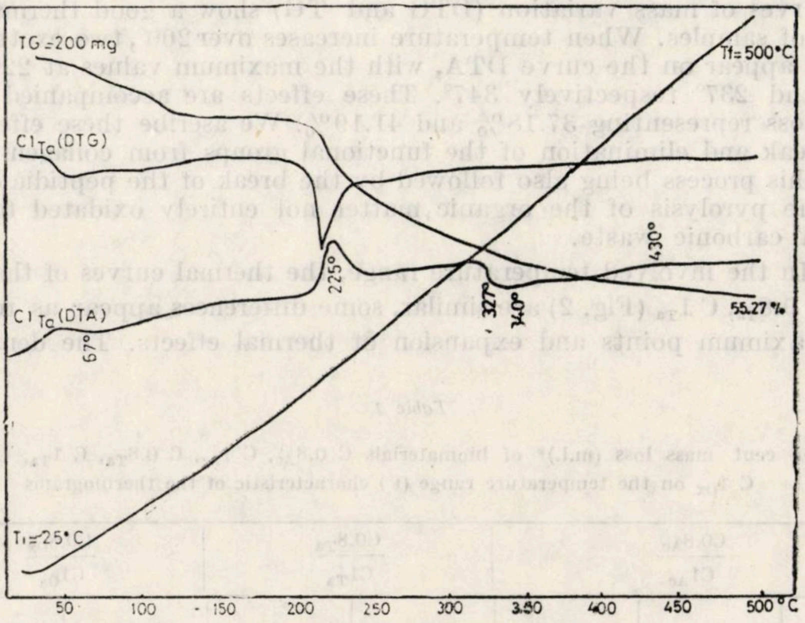

Fig. 2. — Thermogram of the biomaterial $C1_{Ta}$.

In case of biomaterials $C\ 0.8_{ox}$ (Fig. 3) and $C\ 1_{ox}$ in the temperature range 20—150°, the endothermal effects are more intense the denaturation points of collagen being higher (95° and 85°) than for the smaples analysed so far. The thermal stability is noticed in the range 150—200°. Starting from 200°, a thermal phenomenom with an explosive character occurs, the mass loss is produced at a high speed (an evident effect on the curve DTG at 240°, Fig. 3); at the same time caloric energy is released (exothermal effect on the curve DTA). In fact the thermal effect should be considered as unitary in the temperature range 200—350°. Over 350° the thermal degradation of the proteic substance occurs, starting with autooxidation; the mass loss at 500° of the biomaterials $C\ 0.8_{ox}$ and $C\ 1_{ox}$ is important (Table 1).

The thermograms of biomaterials C_1, C_2, C_3 (Fig. 4) present in the range of water release (20—130°) two effects. The former, placed the maximum value at 65° and coincides with the denaturation point of collagen in the biomaterial $C\ 1_{Ac}$, the latter endothermic effect has the maximum value at about the temperature of 100°. The mass loss (Table 2) increases with the increase of insolubilisation with increasing also the quantity of reticulant (formaldehyde). The biomaterials present between 120° and approximately 200° a good thermal stability, with a little mass loss on this interval. Over 200° a thermal degradation of samples takes place,

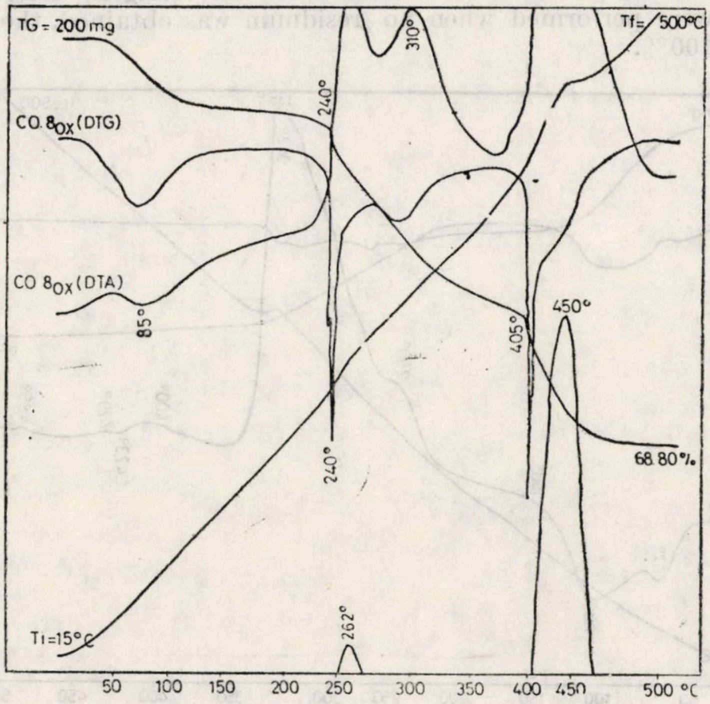

Fig. 3. — Thermogram of the biomaterial $CO.8_{OX}$.

revealed by the curves DTA by an evident exothermal effect accompanied by the release of the volatile compounds from the system, at 500° a residuum being left, calculated and presented in table 2. The exothermal effect with the maximum value at 350° for the biomaterial C_3, which contains the highest quantity of formaldehyde has a unitary aspect in comparison with the thermal effects of other biomaterials : C_1 and C_2.

Table 2

The per cent mass loss (m.l.)* of biomaterials C_1, C_2, C_3 on the temperature range (t°) characteristic of the thermograms

	C_1 (Residuum$_{500°}$ = 39.67 %)		C_2(Residuum$_{500°}$ = 38.67 %)		C_3(Residuum$_{500°}$ = 35.84 %)	
	t°	m.l.	t°	m.l.	t°	m.l.
A–B	22–120	27.33	25–138	28.54	23–141	31.05
B–C	120–200	1.2	138–207	1.19	141–210	1.38
C–D	200–357	29.5	207–343	29.15	210–345	27.29
D–E	357–500	2.3	343–500	2.45	345–500	4.14
E	500	60.33	500	61.33	500	64.16

* The per cent mass losses were determined from the curves of thermogravimetry (TG) without the correction for water release.

For all samples of biomaterials based on collagen, determinations to 1000° were performed when no residuum was obtained, the mass loss being of 100%.

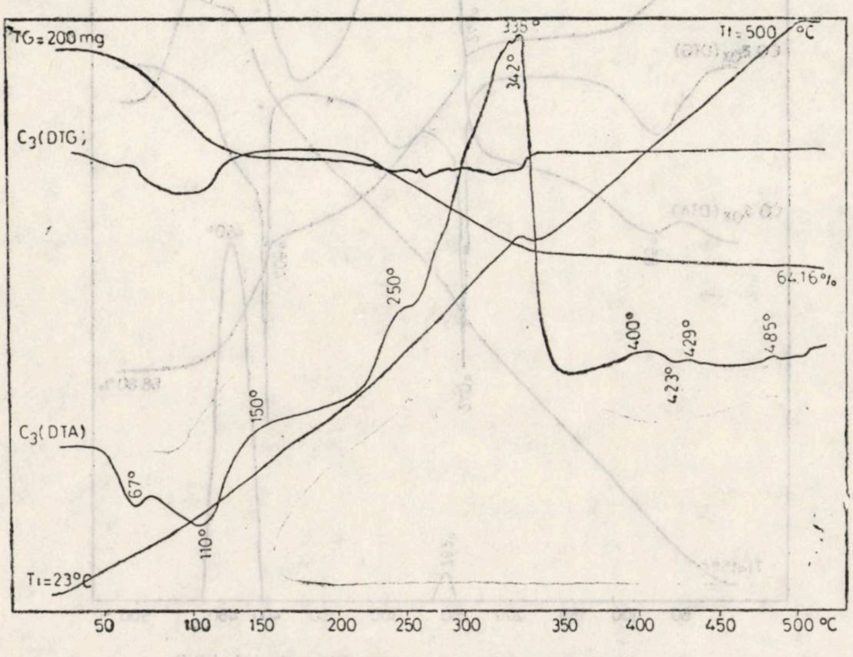

Fig. 4. — Thermogram of the biomaterial C_3.

CONCLUSIONS

The various biomaterials analysed in the paper presented differences as regards the extent and importance of processes, the characteristic temperatures and the mass loss accompanying the thermal effects. These differences were mentioned in other papers as well.[7,8]

The thermograms on the temperature range under investigation can be divided into four stages. The first stage between 20–130° includes the process of releasing water (in variable quantities depending on the method to extract collagen and obtain the biomaterial) and denaturing collagen. We consider that the denaturation is preceded and determined by a mass loss of the samples presented by the curves DTG of thermograms. The second stage, of thermal stability is ranged between 130–200°. However, there is a small variation in this stage (about 1%) ascribed to the loss of the "structural water". Its presence and quantitative estimation was performed by other analytical methods.[12] The decomposition stage, the third, ranges in the temperature interval of 200–350° (excepting the biomaterials $C\ 0.8_{ox}$ and $C\ 1_{ox}$ where the upper limit is of 500°). The mass loss in this interval is considerable. During the last stage, a slow oxidative degradation of the proteic substance is recorded at 500° with a residuum of variable quantities according to each material.

The thermograms can be used as "fingerprint" to characterise specifically each biomaterial based on collagen.

REFERENCES

[1] A. P. Mould, D. F. Holmes, K. E. Kadler and J. A. Chapman, *J. Ultrastruct. Res.*, **91**, 66 (1985).

[2] K. Kuhn, *Rheumatology*, **10**, 26 (1986).

[3] M. I. Millionova, *Biofizika*, **30**, 578 (1985).

[4] K. A. Piez, "Encyclopedia of Polymer Science and Engineering", vol. 3, J. Willey & Sons, New York, 1985, p. 669.

[5] G. L. Radu and M. Caloianu Iordăchel, *St. cerc. biochim.*, **30**, 198 (1987).

[6] J. Mitchel jr. and J. Chiu, *Anal. Chem. Rew.*, **47**, 289 (1975).

[7] I. V. Yannas, *J. Macromol. Sci. Rev. Macromol. Chem.*, **7**, 49 (1972).

[8] G. Angel, M. Caloianu Iordăchel and M. Costea, *Rev. Roum. Biochim.*, **17**, 3 (1980).

[9] I. Jamall, V. Finelli and S. S. QueHee, *Anal. Biochem.*, **112**, 70 (1981).

[10] W. Traub and B. Steinmann, *FEBS Lett.*, **198**, 213 (1986).

[11] J. L. Brokaw, C. J. Doillon, R. A. Hahn, D. E. Birk, R. A. Berg and F. H. Silver, *Int. J. Biol. Macromol.*, **7**, 135 (1985).

[12] D. Bourgoin, *J. Fr. Biophys. Med. Nucl.*, **1**, 53 (1977).

Revue Roumaine de Chimie, 36, *11—12*, 1371—1386 (1991)

THE CAUSALITY LAW IN PHYSICAL CHEMISTRY AND CHEMICAL PHYSICS AND BOHR'S PRINCIPLE OF COMPLEMENTARITY*

ADRIAN O. FULEA **

Home address : Calea Plevnei No. 127, Bucharest R-77103, Romania

Received June 8, 1987
Revised April 27, 1990

A new law of causality is derived starting from Curie's law of symmetry (1894)[2] : (I) For occurring a phenomenon, in a system, there should hold three necessary (but not sufficient) conditions : (a) The existence of an ordering or a regularity pattern. (b) Provided that condition (a) is met, Curie's dissymmetry condition (1894) should be met too. (c) Between the system and environment, a proper matching should exist between their geometrical or/and energetical characteristics. (II) Curie's law of symmetry (1894).[2] More generally, sometimes a phenomenon is having some similar or even identical characteristics with the one occurring in a system with a much higher symmetry (Fulea – 1986). It is further shown that this law of causality, suggested to be called Curie-Fulea law, is an expression of Bohr's principle of complementarity (1961) in Physical Chemistry and Chemical Physics. Our causality law proves wrong Born's opinion on the so-called "multiple causes" (1949) ; in the causality quest, sometimes a causality aspect of the Galelian cause could indeed come in the forefront, but we should seek all of them. Phenomena known as "violation of Curie's principle" and "the breaking of symmetry" are explained as consequences of corpuscular character of matter whose consequence is the present causality law too, as well as Curie's law of symmetry.[1a]

INTRODUCTION

Prior to Curie's principle of symmetry in Physics, Neumann was the first who introduced a principle of symmetry in the Physics of Crystals. Its reformulation, due to Voigt, is : "The elements of the symmetry of any physical property of a crystal have to include the elements of symmetry of the punctual group of the crystal". [3,***]

Curie had been preoccupied by the problem of using the symmetry in Physics, Chemistry and Crystallography just from the beginning of his scientific life,[4,5] and the symmetry in Physics was in fact a preoccupation of his whole scientific life.[5] After finishing the joint work on Radioactivity with M. Curie, during her doctoral thesis work (for which they shared with Becquerel the Nobel Prize in Physics, in 1903), Curie returned to his preoccupation of the symmetry problem. His first lecture, as a Sorbonne Professor (at the Chair created for him, in 1904) was devoted to the symmetry in Physics. Unfortunately, the science lost Curie, who died at 47, in an accident, on April 19, 1906.

---

* See firstly ref. 1a ; a short abstract of ref. la appeared in print earlier.[1b] I dedicate this paper to the memory of my father, Dumitru Fulea (1907–1977).

** I was retired by the Romanian competent authorities on April 16, 1987, by claiming me a schizophrenic since 1973.

*** The fundamental importance of this statement was repeatedly asserted by Voigt, who called it the Neumann-Voigt principle. Neumann's initial formulation of it was : "The symmetry of the macroscopic properties of the crystals is determined by the point group of symmetry of the crystal and *not by the space group*'' [3]. (Italics ours).

In the first part of this century, the French philosopher, Louis Rougier tried to apply Curie's ideas on symmetry in the causality quest in Physics, Chemistry and Biology in a nice and logical way[6], as far as we could say *.

In the present paper we will mainly try:

— To complete and to rewrite Curie's law of symmetry on the basis of the new knowledge and understanding in science, since Curie stated it in 1894[2];

— To link Curie's law of spatial symmetry as completed by us: (C—F)l, to Bohr's principle of complementarity;

The areas of the applications of (C—F)l, deduced partly by Curie in 1894 and by us in 1987, are those, which nowadays, in the American universities are taught and reasearched mainly (or are increasingly studied) in the Chemistry Departments and in the Physical Chemistry Departments, if existing separately; decades ago some of these topics were studied mainly in the Physics Departments **, i.e. the areas of Physical Chemistry and Chemical Physics ***.

---

* We had reached most of the conclusions of this paper till early 1987, while we found, rather by chance, ref. 6 in Summer 1988. Although we do not know French at all, we have managed to understand some of Rougier's logical deductions, using a French-Romanian dictionary, helped also by their convergence, in some respects, with ours. However, in other cases, Rougier's assertions are at variance with the ideas presented here, but we could catch quite easily his errors.

** It is a privilege for us to have the opinion of the Canadian Professor G. Herzberg, expressed in his letter on March 1, 1977, addressed to us, kindly responding to our letter of February 15, 1977: "...at the present time the great majority of courses in molecular spectroscopy are done in chemistry departments or physical chemistry departments if there is a separate department in the field. I only need to refer to the situation at Harvard University, where the Physics Department is concerned with nuclear physics, while almost all the research and teaching in molecular spectroscopy is done in the Chemistry Department. The fact that my Nobel Prize was awarded in chemistry even though I am a physicist is indicative of the change that has taken place in the last few decades. The reason for the shift from physics to chemistry, it seems to me easy to understand since molecules after all are the basis of chemistry and whatever we can find out from the spectrum about structure of molecules is of great interest to chemists". We may add that even in 1903, the Nobel Prize Committee firstly thought to award to Arrhenius a half of Nobel Prize in Physics, and a half of it in Chemistry.[7]

*** We also further add that the Soviet Professor A. M. Prokhorov, Nobel Laureate in Physics (1964) for his work in laser area, was the Chairman of the Scientific Committee of the 3rd National Congress of Chemistry held in Bucharest, Romania, September 21—24, 1988. The shift from physics to chemistry of molecular spectroscopy, pointed out by Herzberg in 1977, has already taken place, in our opinion for the entire area of Chemical Physics, the rend continuing for Solid State Physics (see for example the high temperature superconductivity) because there the chemical structure is essential too.

A. CURIE'S LAW OF SPATIAL SYMMETRY AS COMPLETED BY FULEA — (C—F)I*

Part I. *In order to occur a phenomenon in a system, three necessary (but not sufficient) conditions should be met :*

(a) *There should exist a sort of regularity or ordering of the particles (parts) of the system, at the time scale of the experiment.* Otherwise there will be a stochastic cancellation of the effects of the particles of the system. We reached this conclusion before being aware of Hacken's Synergetics just by thinking at the explanation of Farina and Bresan[8] of the lack of optical activity of the high molecular weight polyethylene solution, and, especially, by trying to reconciliate the concept of Mislow and Bickart of stochastic achirality[9] with Curie's law of symmetry,[2] realizing that it is a heuristic problem : the observations of Mislow and Bickart seemed very keen to us ; on the other hand, Curie's law of symmetry (1894) implies that we cannot define operationally the chirality **. We discussed already in ref. (1a) the cases (d_2) and (d_3) of Section B,[1a] which are in fact, clear-cut examples of (C—F)I (Ia).

Let us follow this (Gedanken)experiment : Suppose that we take a quartz crystal, melt it and, afterwards, we quench the melted SiO_2 to a glass state. We further cut a piece from this glass having exactly the same form as the initial crystal of quartz, i.e. this macroscopic piece of glass is transformed into itself, at the *macroscopic* scale, by any symmetry operation of the point group of quartz. Though this has, according to Neumann-Curie ideas, the same Curie's necessary dissymmetry, it certainly will not be expected to exhibit the birefringence, for example, which quartz does, according to the previous experience.

Furthermore, in Physical Chemistry of Macromolecules, it has been already established that in the case of the polymeric materials, the birefringence is due to the orientation rather than crystallization. Thus if a visco-elastic polymer is extended, cooled below T_g and then it is viewed between crossed polars, the *glass* *** will appear birefringent. This is because by such a deformation of the polymeric material the chains became oriented.[10] As a matter of fact, the morphology of a polymer controls all the optical properties ; thus the presence of spherulites greatly reduces the transparence of a polymer.[10]

The uncovering of condition (Ia) was, in fact, long overdue in the causality explanation. Thus, in 1883, Bücking envisaged an experiment in which by applying pressure on a piece of glass choped in a form of a cube it became birefringent. The phenomenon is reversible[11] ; after ceasing the pressure, the piece of glass becomes isotropic again. Curie himself was preoccupied by the problem, but, unfortunately, his way of sol-

---

* In the new law we write in French that part which Curie envisaged in 1894[2] and which, to date, is known as Curie's principle (law) of symmetry[1,2,3,5].

** Because the effects can be more symmetrical than the causes[2] it is principially erroneous to seek "operational criteria" either to define or to detect chirality or achirality. Mislow and Bickart remarked that : "the term cryptochiral takes explicit cognizance of both the chirality of the model, and the inactivity of the sample"[9]. However, the "stochastic achirality" implied an operational definition for chirality.[9] In Physics and Chemistry, the best definition *of a phenomenon* is the operational one, as considered in gnoseology already.

*** Italic ours.

ving was erroneous: "Nous avons supposé que la matière non cristallisée et non douée de pouvoir rotatoire n'apportait par elle-même aucune dissymétrie dans un système: nous avons fait implicitement la même supposition pour le milieu qui remplit les espaces vides de matière. Cette supposition bien naturelle, *mais toute gratuite**, est indispensable, elle montre bien que nous ne pouvons avoir raison de la symètrie absolue; nons devons choisir arbitrairement une symétrie pour un certain milieu et en déduire la symétrie des autres milieux".[2] Much more recently, Holden also erroneously solved a similar problem (in ref. 12, p. 66), which, correctly explained, could have led to the discovery of Part (Ia) of (C–F)1.

Finally, in the Physical Chemistry of polymers there has been used for quite a long time the degree of crystallinity of polymers, when obtained from X-ray diffraction data, the weight expressed in percents from the whole probe of polymer which is sufficiently ordered as to exhibit an XRD characteristic to crystalline material. Therefore, in our (Ia) necessary condition we may also introduce the attribute of "*sufficient ordering*" or "*sufficient*" *regularity pattern*; it is well known for example that even the liquid state has a short range ordering.

Part (Ib). *Provided that the necessary condition (Ia) holds, it is further necessary to be met "Curie's dissymmetry condition", i.e. the absence of certain symmetry elements, at the time scale of the experiment.* Otherwise there will be a cancellation of the effects of the particles (parts) of the system by symmetry reasoning, as in the case (e) in Section B of ref. 1a. Other examples are the selection rules in vibrational spectroscopy.

Part (Ic). *In case of the interaction between the system and environment, or between systems* (as in the case of the (bio)-chemical reactions) *there should necessarily be a sort of matching in their geometrical pattern*** *or/and energetically* ***.

Note: During the whole paper we speak of a phenomenon as required of Bohr[13]: i.e. having defined very precisely the conditions of observation, including the experimental arrangement.

The *specifics* of the above three necessary conditions are a function of the *specifical phenomenon* we look on, and they are observed experimentally, usually, by the so-called "crucial experiments".

Even if the above three necessary conditions: Part (Ia), Part (Ib) and Part (Ic) of (C–F)1 are met there is no guarantee that the respective system will undergo or exhibit the respective phenomenon, because of other characteristics of the system structure which make it either too weak to be detected with the sensibility of our (macroscopic) apparatus****, i.e. "in practice" it does not exist (as Curie penetratingly observed, in 1894), or it is just forbidden, as also observed by Curie in regard to his "dissymmetry" condition[2].

---

* Italics ours.

** In many areas such as Biochemistry, Psychiatry and Psychology, the so-called condition of "key and lock" is well known; sometimes symmetry can play a central role, as in infrared dichroism or in the Woodwards-Hoffmann rule.

*** As the resonance in the spectroscopy.

**** In Physical Chemistry and Chemical Physics we usually are working with a number of particles of the magnitude of Avogadro's number.

Note. The above discussion of Part I of (C—F)l shows that Curie's well-known assertion "C'est la dissymétrie qui crée le phénomène" [*,2] is erroneous. Unfortunately, this error is still in force to date in science being accepted even by Wigner and, as far as we could see, it is the core of Mislow's school errors in the area of spectroscopy, we have already discussed in our paper [1a] and our communication [1b]; Mislow cites affirmatively this error of Curie in at least two papers, as far as we know, [9,14] while himself correctly observed previously "molecular dissymmetry is a necessary but not a sufficient condition for optical activity" [15], i.e. contrasting Curie's error. However, Mislow's more recent statement is: "a phenomenon is expected and can in principle be observed *only* ** because certain elements of symmetry are absent from the system". [9]

The correct statement would have been simply that the symmetry does not forbid the phenomenon, as we pointed out previously, [1a] just before being aware of Curie's work.[2] Rougier observed also that symmetry considerations (can) enter the law of causality. Another equivalent corrected statement is simply that 'dissymmetry' does not permit to have nullified the phenomenon by symmetry reasons.

We note that, when speaking of "cause" in Physics and Chemistry, we are referring to the Galelian causality which considers the cause as the necessary and sufficient conditions for the phenomenon (vide infra).

Part (IIa). *Lorsque certaines causes produisent certains effets, les éléments de symétrie des causes doivent se retrouver dans les effets produits. Lorsque certains effets révèlent une dissymétrie, cette dissymétrie doit se retrouver dans les causes qui lui ont donné naissance.*

Part (IIb). *La réciproque de ces deux propositions n'est pas vraie, au moins pratiquement, c'est-à-dire que les effets produits peuvent être plus symétriques que les causes* (Curie 1894) [2]. *More generally, sometimes a certain phenomenon is having some characteristics similarly with another one occurring in a system with the same kind or alike particles, but with a* (*much*) *higher symmetry* ***.

Note. While Part I of (C—F) l is, in reality, the part dealing mainly with the ontological aspects of the cause, Part II of (C—F)l is, in fact, dealing mainly with ontological relationships between the cause and the effect only from the viewpoint of spatial symmetry ****, the latter being attached by Curie (1894)[2] to any phenomenon. As far as Part (IIb) is concerned see also however our conclusion (2) in ref. [1a]

B. (C—F)l and Bohr's principle of complementarity

The symmetry is an advanced form of ordering, being sometimes considered (especially in the art work) the most advanced form of orde-

---

[*] "It is the dissymmetry which creates the phenomenon" (our translation). See also I. Hargittai, *Symmetry*, 1 (1), 1 (1990)" phenomena are created by dissymmetry".

[**] Italics ours.

[***] We drew this conclusion from the theory we developed for vibrational spectra of polymers, in 1986. [16]

[****] For the definition of spatial symmetry, see ref. [17]

ring or regularity. Therefore, by linking * (Ia) with (Ib) in C—F)l, we already reached, independently, Bohr's principle of complementarity, in the most general form, which Bohr put down in 1961, while visiting Lomonosov University in Moskow ** : "Contraria non contradictoria sed complementa sunt". This formulation of Bohr's complementarity principle in the most concise but at the same time it does not contain any reference to the concrete physical phenomena,[18] and also has the greatest degree of generality.***,[18]

As far as we know, previously to our work[16] there was no attempt to link Curie's law of symmetry with Bohr's principle of complementarity, though both are referring to causality. In our work[16] we reached the conclusion that Curie's law of symmetry is expressing in fact Bohr's principle of complementarity in Physical Chemistry and Chemical Physics reasoning in that way : following Descartes' view that a problen should be firstly searched by its different aspects and because of the importance of symmetry in a many bodies problem, we think that it is very useful to view the molecular structure*** by two kinds of rather opposits classes of characteristics : the first, the symmetry, and the second, the kind and the interaction between the forming atoms. We may view them as 'contrary' characteristics as when we refer to spatial symmetry we need a molecular model, which, by its idealization, neglects some characteristics of the other class of molecular properties ; molecular models are indeed only idealizations and not realities (see ref.[15]), however very helpful in reaching the understanding of reality, in the realm of our way of thinking and doing research. Therefore we reached in 1986, Bohr's : "*Contra ia non contradictoria sed complementa sunt*" in Physical Chemistry and Chemical Physics (even in a more general way[16]) i.e. in an area where Bohr did not discuss it at all, though, towards the end of his life, he perceived it as acting in any area of human knowledge.[21]

In his principle of complementarity Bohr underlined the relationship of mutual exclusion between those aspects of the reality he viewed as complementary, based on his own experience in Atomic Physics **** (the Heivsenberg uncertainty principle) and his knowledge in Biology, Psychology and Psychiatry. However, at variance with the Atomic Physics, in Chemical Physics and Physical Chemistry we are dealing with assemblies of around $10^{20}-10^{23}$ atoms (or molecules); the uncertainty relations do not have, therefore, at least in practice, usually, the impact of mutual exclusionship in determining the complementary aspects by the experimental device(s), the apparatus having usually, the dimensions which are comparable from the viewpoint of atom numbers (i.e. by considering the order of the number of the atoms) with those of the studied system, though we can still find cases where the uncertainty relations are relevant (even in practice) as in the case of the natural bandwidth, in spectroscopy. For instance, in the case of the geminal chemical shift of syn NCH_2 protons in *ortho*(thio)benzamides, the complementary aspects of the Galelian cause : the necessary diastereotopic condition and the conformer populations preference [1a,24], do not require *in practice* mutually *exclusive* experiments. We therefore reached the complementarity principle in Physical Chemistry and Chemical Physics as a "logical relationship, referring to our way of describing and communicating our experience", "the complementarity enables us, so far as we can judge, to account for all aspects of phenomena", [21*] as it is already admitted nowadays.[21]

---

* Laplace defined as a scientific discovery the linking, in a logical way, of two things in science which previously seemed not related in that way. This definition can still be used even today, inside the present theory of creativity in science.

** Bohr wrote it in the office of the fellow scientist Dimitri Ivanenco and signed below Niels Bohr. It remained unerased to date there.

*** The Romanian philosopher Lucian Blaga introduced in 1940 "the method of the transfigurated antinomy" very close to Bohr's complementarity principle, according to Toro.[18] The Romanian genius, Mihai Eminescu (1850—1889), for whom, in 1989, UNESCO commemorated one hundred years from his death, observed also very penetratingly the complementarity principle in the poetry (see for example his comments on the hexameter rhythm in.[19]) See also Prigogine's view of complementarity[20].

**** For the definition of molecular structure see ref.[15]

***** Although it is generally claimed that, in achieving the complementarity principle, Bohr started from the Heisenberg uncertainty relations, Jammer[22] considers that Bohr started from Psychology, after reading the monumental book of James[23] and that the Heisenberg relations were only a proof of his already rather formed idea, which seems to us a real possibility, based on our own experience, too, in Psychiatry's studying.

In many cases one of the complementary aspects of the Galelian cause may appear in the forefront to a researcher, or even to an entire scientific community[**], for a while, at least. At the beginning of our scientific career we pointed out [27] that not only the energy of the molecular orbitals should be taken into account in defining the frontier orbitals defined by Fukui and his coworkers[***], but also their probability of localization in the molecule. Sometimes, by considering only one complementary aspect of the causality explanation one still can get valid results. Thus, we fall into such an error in [29] in the NMR spectroscopy. Longinescu's final view on the association of liquids was considering only the crowding aspect of liquids, while denying the real association [30] (such as in the case of hydrogen bonding) following the idea of one of his pupils Dr. G. Chaborski. However, as pointed out by Balaban and Simionescu, [31] Longinescu's formula is his main achievement, leading to results in agreement with the reality[****] in respect of boiling temperatures. [31]

However, in general, by considering only one of the complementary aspects of causality, as Born advocates his view of "multiple causes",[32]

---

[*] Referring to piezoelectricity, the phenomenon discovered by Curie and his brother Jacques Curie and which Curie studied in his paper on symmetry in Physics [2], we found thus in a book of Physical Chemistry [25] : "piezoelectricity is met at crystals without a center of symmetry"; "when a real pyroelectricity appears the crystal has a polar axis" [25], whereas in another book [26] : "the condition of the occurrence of pyroelectricity and piezoelectricity in crystals is that the latter should be dielectrics and exhibit an ionic structure" [26] (Translation from the Romanian by us). In reality there is a complementarity relation, each handbook [25,26] presenting only one of the complementarity aspects of the cause.

[**] This situation was firstly realized by this author after reading Psychiatry, where the secondary symptoms of Bleuler for schizophrenia appear in the forefront of the primary symptoms of Bleuler for this disease.

[***] For a review see ref. [28].

[****] Such cases may raise problems in the area of Philosophy of Science, especially for the logical neo-positivism, whose main representative is probably Carnap. We heard firstly of Carnap during a discussion with the psychiatrist Marin Stancu, on May 25, 1987, at the Cula madhouse, being under strong psychotropic medication and complete exhaustion, and guarded by police 24 hours a day; on May 23, 1987, seven policemen rushed into our house yelling out to us to go to their chief and, by a waggon, police took us to that madhouse, in the Popeşti-Leordeni village (till May 28, 1987).

is at least an oversimplification, if not a starting point for further errors and futile polemics. It is also in disagreement with Bohr's idea of complementarity as the ideal causality quest,[33] as well as with the present view on causality in Romanian literature, [34] illustrated also in this work, for the Physical Chemistry and Chemical Physics.

C. ON THE CONFUSION OF THE SPATIAL SYMMETRY WITH ORDER IN THE LITERATURE, ON THE APPARENT VIOLATION OF THE (C—F)I AND ON BREAKING OF THE SYMMETRY OF THE CAUSE

C_1. In many cases there is a tendency in the literature to erroneously consider some ordering pattern of the particles of the system as its spatial symmetry. A clear-cut example of this error is found in the case of the liquid crystals for which it is considered that "the most important property of the liquid is the anisotropy *due to the lower symmetry of them in regard to liquids. Qualitatively this means* that*** the liquid crystals are more ordered than the liquids".[35]

The correct explanation for the properties of liquid crystals which are not exhibited by the normal liquids is comprised in our proposed Part Ia of (C—F)l: the crystal liquids do meet the necessary condition (Ia), while the normal liquids do not. The above misconception can be very well contrasted just with Ursu's reported NMR results, [36] obtained from the studies on nuclear spin-spin and spin-lattice relaxation in the vicinity of the order-disorder transition, in 1-X adamantanes, underlying in the causality relationship the complementarity of molecular symmetry and the decrease of order in the plastic phase of the crystal for T_2^{36} (see especially the conclusion 2 in ref.[36])***.

A similar confusion of ordering with symmetry**** is observed in the literature of (bio)polymers.[39]

Thus, Monod considers order as the symmetry[39]; with extremely few exceptions (one of them found by chance by us [1a,43], in 1972) most of the polymers have, strictly speaking, the symmetry C_1, i.e. no symmetry: as we have already pointed out, the translation is not a symmetry operation [1a]; at this we have to add the fact that many polymers are coiled and also have to take into account the effects of the side and end groups. However in many cases we can approximate a *point group symmetry*, as we did in [43]; but we cannot approximate a line group (or in the case of the crystals a spatial group of the 230 Feudorov groups!)*****

---

* Profesor I. Ursu, who wrote the foreword for Mushcutariu's work [35] observed [36]: "Knowing why is an irreductible prerequisite of knowing how". We are indebted to Professor D. Fiat, International Society of Magnetic Resonance Founding Chairman, for sending, at our request, finally, a xerox copy of [36].

** Translation from the Romanian as well as italics ours: the latter points out the inconsistency, as well as the overlooking of the definition of spatial symmetry.[17]

*** See also Sălceanu's results, [37] Kerr effect. [38]

****Reciprocal is true: the symmetry is a very advanced kind of ordering. Unfortunately, we could see only ref. [40], but not ref.[41] or ref.[42]. We thank Professor Balaban for a xerox of ref. 40.

***** This assertion should be elaborated and further discussed, especially because of its implications in the Solid State Physics. If time, health and money for a living permit us, we will certainly do it.

In the light of (C—F)l presented in this paper, the confusing of order with plain spatial symmetry may lead to contradictions or a false belief in understanding. Thus Monod is claiming that "there is more symmetry in the sense of structural order* of biopolymers".**,[39]

Pasteur's view was that the life. as it appears to us now, is a function of the universe's dissymmetry.[5] Monod's and Pasteur's views can be simply reconciliated while observing that Monod is speaking in fact of structural order and that the two views are complementary and in agreement with Part I of (C—F)l.

The concepts of stochastic achirality and cryptochirality of Mislow and Bickart[9] can be also very nicely integrated in our Part I of (C—F)l; thus for the cryptochirality the order or regularity is enough for *some* phenomena, while for the others they are not. It makes sense for cryptochirality to seek the Curie dissymmetry condition (Ib). In the case of the stochastic achirality the disorder is so high that there is no sense of further seeking Curie's dissymmetry necessary condition; we already have a firm (negative) answer from Part (Ia). It is interesting, however, that, when a phenomenon does not take place, either in case of cryptochirality or in case of stochastic achirality, the formal explanation is the same: the condition (Ia) of (C—F)l does not hold — there is a stochastic cancellation of the actions of the particles at the sensibility of our apparatus (in practice, at least)***. This implies that: 'too much' order (at the time scale of the experiment) i.e. a special symmetry operation, has the same effect sometimes as an insufficient specifical order at the same time scale (including the complete *chaos*) for the existence of a property in Physical Chemistry and Chemical Physics, at least, i.e. the nullifying of the specific property.

The above more specific assertion is included in fact in our general conclusion (2).[1a] Whereas we drew conclusion (2)[1a] from the NMR spectra and the symmetry principle of Curie (1894),[2] which, as we have pointed out, deals mainly with the ontological relations of the cause-effect, the last conclusion is a direct result of Part (Ia) and Part (Ib) of (C—F)l, dealing mainly with the ontological relationships in the cause. It seems to us that the effect-cause are the contrary and complementary parts of the dialectical unitary process of causality explanation (thinking) and the contrary character of these two entities is expressed by the continuous changing of our world; therefore the cause-effect explanation**** is a beautiful example of Bohr's complementarity principle, in the area of epistemology, reflected in (C—F)l.

---

* Whereas structural order includes the symmetry, the reciprocal is not always true; it would have been much more correct to speak just of structural order, at which we may refer in (Ia) of (C—F)l.

** The same could be said for stereopolymers.

*** Mislow and Bickart observed: "A more sensitive method... capable of distinguishing between samples would remove the condition of cryptochirality". However, according to the definifion of phenomena of Bohr, it will be in fact *another* phenomenon!

**** The causality is the most advanced explanation in Physics and Chemistry; we can have also other different explanations such a particular law or a particular equation relating two or more different quantities, such as Maxwell eqs.

C_2. Because the spatial symmetry is imperfect*, sometimes Curie's dissymmetry necessary condition could appear on the surface as being broken: well-known examples are: the Herzberg-Teller stealing intensity,[46,47] anomalous optical properties in *anomalous* crystals.[11] Also the nonobedience ** of Cauchy relations seems to violate Part II of (C—F)l. However, in high resolution NMR no such phenomena of violation of (C—F)l were ever detected experimentally; this can be easily explained because of the long time scale of the experiment; thus by averaging the thermal motion, the spatial symmetry is becoming less unperfect at this time scale.

C_3. The examples of breaking the symmetry of the causes without an apparent cause from ref.[48] could be explained in our view by taking into account the corpuscular character of the matter of which (C—F)l is itself a consequence[1a]; the fact that in these cases it is taken into account only the "macroscopic" spatial symmetry (see our Gedankenexperiment with a quartz crystal mold — Section A), it is not correct**. In the example of falling of the pencil in ref.[48] we can explain this: a) by putting it in the vertical position it is very probably that a (small) force will still act on it from our hand, with a component perpendicular to the pencil, while raising our hand from it, (b) even if its force is not from our hand, the pencil seems only macroscopically balanced; at the structural scale it is certainly more "heavy" in some parts than on the others and because of this component of gravity it will tilt a little. Afterwards the following takes place: increasing of that component of gravity force and the further tilting of the pencil (destroying the axial symmetry) go on synergetically.

D. ON THE NECESSITY OF INTRODUCING (C—F)l IN THE HANDBOOKS OF PHYSICS AND CHEMISTRY, AS THE CAUSALITY LAW

(α) Causality is the most important part of any scientific explanation. As Born put down: cause is the supreme law of the physical world,[32] whereas causality research means discovery of how a physical situation (the effect) depends on another one**** (the cause.)[32] Science insists on a

---

* See for example refs.[9,15]: for the problem of dynamic symmetry, to which Emmy Noether's theorem refers, see refs.[44,45]

** Nowadays this aspect is the most attractive and important aspect of Cauchy's relations.

*** Therefore in applying (C—F)l we should always consider the spatial symmetry at the corpuscular level for the object (i.e. of its structure). Macroscopic symmetry arguments, while using (C—F)l, are in general unwarranted. They may very well fail. On the other hand, if an argument of macroscopic symmetry works this could be always explained also at the corpuscular level of the matter (i.e. at structural level).

**** Born states (Appendix II, p. 8)[32]: "any event may have several causes... actually the 'number' of causes seems to me a rather meaningless notion". In the light of this paper this opinion is erroneous. Taking into account the great authority of Born in Physics and the Philosophy of Science, of which he was a Professor at the Edinburgh University, it is also dangerous. We note that we call a casuality aspect of the Galileian cause, what Born calls simply "cause" in his statement.

For the cause of a phenomenon see the definition in ref.[49] under the "causation". In our discussion we consider that an event's cause is the set of those things which are separacriterion for dependence, namely repetitive observation or experiment which are systematically thought. [32] (C—F)l is a great help in this direction, as observed by Langevin in 1906, for Curie's principle, [2] and also by Curie himself, in the conclusions of his paper[2]. "There are rules to be observed : isolation of the sytem considered, restriction on the variable factors, varying the conditions until the dependence of a single factor becomes evident". [32] However, in the search of the complementarity aspects of the Galilean cause in the causality quest does not stop here. After finding this "factor"[32] or one of the complementary aspects of the cause, other experiments should be sought in order to identify another causality aspect, until we reach not only a necessary condition, but also the sufficiency for the existence of the phenomenon (the effect).

Here it seems, at least on the surface, that we are confronted with an inconsistency between the opinions of Bohr and Born, on the phenomenon and its causality, unobserved to date to our knowledge. Bohr requests a full description of the conditions in which the phenomenon takes place; changing them, according to him, we get another phenomenon. Born's [32] above recommendations for causality relationship research are certainly contrary to Bohr's ideas of the phenomenon used by us, too. However, Born's description of the way we do the reasearch [32] is just according to the experimental way the real scientific creative work is done *. One may however firstly observe that Born's description of the experimental creative research [32] is referring mainly to the finding of the cause, while Bohr's definition is that for *a* phenomenon (the effect). Secondly, in doing science, we are transferring not only the previous knowledge already got, by other scientists, but also *our* knowledge obtained in experiments as those described by Born, [32] to the one different, but forming a class with those which we previously experimented. We propose the name of an '*epistemologic class*' of experiments (phenomena) for this class. Forming such classes it may require a real scientific art and it reflects the unitary differentiation-integration process **, at a superior level. While Bohr's definition of a phenomenon is primarily concerned with the differentiation, Born's view of scientific research [32] shows

---

tely necessary and together sufficient for the event's occurrence,[49] as we did in fact in our other works such as [1a,27] without being aware of this precise definition, or of the causality problem in general.

* Repeating some experiments or calculations, after one did them firstly — just on different systems, without any real novelty in science and without bringing anything new in science, besides a new paper for the author — is not considered by this author as a real, creative scientific research. See also a recent view on a scientist in ref. [50] as well ref. [51] It should be noted that, on the other hand, introducing a new law in science is the expression of an "emergent creativity", which is the highest level of creativity and the rarest form of manifestation of creativity,[51b] while the profound and essential modification of a law is an "innovative creativity".[51b]

** As it is well known in Psychology and Psychiatry, this differentiation-integration process is impaired in psychoses and neuroses, the worst aspect being usually found in schizophrenia, whose formal explanation, as Bleuler observed, in the loosening power of association. The schizophrenic autism (dereistic and pervasive) may be a consequence of the inability to cope with the true (real) world, in this dreadful disease.

the importance of integration. As von Bertalanffy [52] very penetratingly observed "the fantastic world constructions from the science surpass any schizophrenic's ... *the integration makes for the difference* ... the scientific notions happen to be 'true' that is, *they fit into an integrated scheme*". [52]

We had shown in this paper how necessary it is Bohr's definition of a phenomenon in the search of causality. Now we see Born's approach to the research for causality. So, the two are rather opposite entities entering the causality, they are complementary, i.e. in agreement with Bohr's complementarity principle *. In respect to this, (C—F)l is giving us some segments of regularity in Physical Chemistry and Chemical Physics, from which we afterwards can much more easily and more logically find the (other) complementary aspects of a cause of a phenomenon, as defined by Bohr, following, however, Born. [32] We deduced the (C—F)l mainly deductively. To discover the Galilean cause fully, we need also the checking of observing the reality, a point emphasized by Born. However, in regard to his emphatic statement "I do not hesitate to call a man foolish if he rejects the teaching of experience because no logical proof is forthcoming", [32]** we should add at Born's remark : at least in that stage of research, because the causality search is done for improving our understanding. (C—F)l provides the starting points for the causality understanding ***.

(β) Without being aware of Curie's principle of symmetry, we had to teach (and supervise) several generations of undergraduate students (1980—1984)**** of the Polytechnic Institute of Bucharest, our employer at that time, a lab work[55] which :

(i) was flagrantly against Curie's principle of symmetry; in 1988, we found out that Rougier (ref. 6. p. 32) was giving it as an example which, because of lack of the necessary Curie dissymmetry, did not work, showing also how its necessary condition may be introduced and, thus, how could the experiment be, however, performed.

---

* We believe that this is related just with the process of thinking, which we believe that, in psychoanalytic terms was envisaged by Arieti [53] as the tertiary process (in fact being closed to Jung's "Self"). However Arieti considered it to be valid only for creativity.

It is interesting to see how close Eminescu's genius intuited the creativity process of Arieti (described in psychoanalytical terms by the latter). In a manuscript letter : Vienna, in 17/6/870, Eminescu wrote : "...fantasy *implies* reflection. However, speaking rightly, the mother of the images, the fantasy, seems to me an essential condition of poetry — whereas reflection is only the skeleton which in the works of art is not at least seen ... In some one is predominant, in others the other predominates, the *unification of both of them is perfection, its carrier is a genius*. Dimitrescu is not a genius, though he is a poet". "(...(he) has a lot of talent although the fantasy is overpowering the reflection)". (Translation from the Romanian and italics ours).

** We are more prone to fully accept Descartes' "Dubito ergo cogito, cogito ergo sum" in epistemology too (as well as in any areas of human knowledge).

*** Once more, it seems that we are dealing in fact with Bohr's complementarity principle between the inductive and deductive thinking. Furthermore, deduction presumes induction.[54]

**** At that time this author had a Licentiate degree in Chemistry (1964), a Licentiate degree in Physics (1970) and a Ph.D. (1976), but also a diagnosis of paranoid schizophrenia put in 1977—1978 by the Romanian psychiatrists, being under strong psychotropic medication and repeated hospitalizations, by force, too.

(ii) was also against the doctoral work of our Professor G. Atanasiu *, done at Sorbonne, under Cotton (see ref.[56]).

(iii) we did not understand it at all, and we were in the awful position of "explaining" it to the asking students, in their really commendable search for the scientific truth (creating conflicts between us and students).

To our knowledge this spurious lab work[55] was done by several thousands of ungraduate (freshmen) students at the Polytechnic Institute of Bucharest.

(γ) Curie's principle of symmetry, it is stated, when not completely omitted in handbooks of Physical Chemistry, such as: "Macroscopic causes cannot have more elements of symmetry than the effects they produce"[57].

(δ) The discussion of the birefringence **, in the famous handbook of Physics[58] containing the two year course taught at the California Institute of Technology, by Nobel Laureate (1965) R. Feynman, seems to us to lack some logical connections necessary for a good understanding of the exposed subject just because it did not take fully into account the ideas contained in our causality law — i.e. it rather overlooks the formal explanation of Curie's dissymmetry conditions in terms of the corpuscular character of the matter. Feynman states, *without explaining why*, that "A cubic crystal, which has the symmetry of a cube certainly could not birefringent".[58] A better insight into the problem was at hand after taking into account also his previous observation (p. 495)[58] that "an atom is emitting for 10^{-8}s and if an atom emits light of a certain polarization, and then another atom emits light of a different polarization, the polarization will change at every 10^{-8}s. If the polarization changes faster than we can detect it, we say that the light is not polarized, because, by the process of averaging, the effects of polarization are nil".[58] Feynman states also that "in a birefringent substance, an alignment of the asymmetrical molecules should exist in a certain degree.[58] One therefore could reasonably inquire the instructor *** why NaCl, for instance, which is crystallising in a cubic lattice and which has therefore an alignment of asymmetrical molecules, does not exhibit birefringence, being one of the so-called "optically isotropic substances".[11] It would have also been nice to point out in this course, here, that in the case of an optical isotropic crystal, the symmetry of the optic phenomenon (i.e. the effect) is much higher than the symmetry of the crystal, the former having an infinite number of axes of rotation and of symmetry planes [11] — a beautiful illustration of Curie's principle of symmetry. In our view the intrinsic value of Feynman's handbook of Physics[58] resides mainly in containing a lot of euristic reasoning, while most of the handbooks are using mainly the algorithmic one. If the above reasonings of Feynman had followed our ideas from (C—F)I, especially bringing into the forefront also the dissymmetry condition, the logic discourse would have been improved, even in the Physics course of one of the brightest minds of our times, because the euristic thinking is requiring a lengthier elaboration than the algoritmic one *.

---

* Prof. G. Atanasiu taught us the last of the three courses of Experimental Physics, at the Faculty of Chemistry of University of Bucharest (1960—1961).

** The reader should also take some care there because of seemingly confusing by Feynman et al.[58] of an operational definition with a *structural* property, probably due to the same verbalization: the operational definition is referring to "a quater wave lamella" which is "a lamella whose thickness in exactly as to introduce a phase difference of 90^0 between the polarizations x and y respectively" (p. 496),[58] while the property statement is: "the cellophane foils used in commercial wrapping have a thickness very close to that of a half wave" (p. 498)[58] — in the context, correctly it should have been: the cellophane foils used in comercial wrapping have a thickness of two quaters wave lamellas. (All translations from the Romanian version of Feynman's handbook[58] are made by us).

*** This way of communication between the student and instructor, is very common in the American universities, not only during the tutorials, but just during the time of the course and, in our view, it is beneficial for both the students and the instructor, and it was one of the facts we liked most during our Ph. D. studies at the University of Calgary, Canada (1972—1975).

(ε) We suggest as an abbreviation for the name of the law put down in this paper: "Curie-Fulea causality law". Firstly it is not containing only symmetry propositions. It is also easy to be distinguished by Curie's law of symmetry, which contains only symmetry properties, lacking however Curie's dissymmetry condition. Secondly, it parallels the way Voigt introduced Neumann-Voight principle of symmetry in the Physics of Crystals, after modifying somehow Neumann's principle of symmetry. Last, but not least, it avoids confusion in the subject indexes with Curie's law of symmetry, Curie's law and Curie-Weissmann's law from magnetism.

As Rougier thought at the beginning of this century, that Curie's principle of symmetry could be also of use beyond the boundaries of Physics, we think that Curie-Fulea's law of causality might be, in a way or another, introduced in the General System Theory of von Bertallanfy.[59] Curie-Fulea's law is also a very good example of conception developmental i.e. of increasing differentiation and hierarchic integration[60] (in the causality quest) and in the formation of concept and especially in the scientific creativity area.[61]

REFERENCES

[1] (a) A. O. Fulea, *Rev. Roum. Chim.*, **33**, 39 (1988); (b) A. O. Fulea "Abstracts Book" 9th Meeting of the International Society of Magnetic Resonance", Rio de Janeiro, June 29 — July 5, 1986, A24, p. 38.

[2] P. Curie, *J. Phys. (Paris)*, 3^e serie, **III**, 393 (1894), reprinted in "Oeuvres de Pierre Curie", Gauthier-Villars, Paris, 1905, p. 118.

[3] I. I. Sirotin and M. P. Shaskolsksia, "Fizica cristalelor", Ed. Ştiinţifică şi Enciclopedică, Bucharest, 1981, p. 210 (the translation into Romanian from the Russian original "Osnovi Cristallofiziki", Nauka, Moskow, 1975).

[4] P. Curie, *Bull. Soc. miner. France*, **VII**, 89 (1884).

[5] E. Cotton, "Cei patru Curie şi radioactivitatea", Ed. Ştiinţifică, Bucharest, 1965 (translation into Romanian from the French original "Les Curies").

[6] L. Rougier, "En marge de Curie, de Carnot et d'Einstein", Paris, 2nd Ed. 1929.

[7] Asimov's Biographical Encyclopedia of Science and Technology, Doubleday and Company, Inc., Garden City, New York, 1966.

[8] M. Farina and G. Bresan, in "The Stereochemistry of Macromolecules", A. D. Ketley Edit., vol. 11, New York, 1968, p. 183.

[9] K. Mislow and P. Bickart, *Isr. J. Chem.*, **15**, 1, *1976, 1977*.

---

* As any new real scientific discovery, our causality law is in fact replacing a lot of euristic thinking with an algorithmic thinking (in the causality quest in the case of this law).

[10] C. T. Greenwood and W. Banks, "Synthetic High Polymers", Oliver and Boyd, Edinburgh, 1968, p. 80, 148.

[11] V. N. Latiu, "Cristalografia fizică", Ed. Tehnică, Bucharest, 1958, p. 104, 231.

[12] A. Holden, "The Nature of Solids", Columbia University, New York, 1965, p. 11, 63–64, 66.

[13] N. Bohr, "Unity of the Knowledge" (1954) in N. Bohr, "Fizica atomică și cunoașterea umană", Ed. Științifică, Bucharest, 1969, p. 90 (the translation into Romanian of N. Bohr "Atomic Physics and Human Knowledge" (1955)).

[14] K. Mislow and J. Siegel, *J. Am. Chem. Soc.*, **106**, 3319 (1984).

[15] K. Mislow, "Introduction to Stereochemistry", W. A. Benjamin, New York, 1965, pp. 1 22, 51 – Second paragraph is very important; I. D. Iroff and K. Mislow, *J. Am' Chem. Soc.*, **100** 2121 (1978).

[16] A. O. Fulea, unpublished work – ref. 52 in re .[1a].

[17] J. P. Mathieu, A. Kastler and J. Flory, "Dictionnaire de Physique", Massen, Paris, 1983.

[18] I. Toro, "Fizica modernă și filozofia", Ed. Facla, Timișoara, 1973, p. 25.

[19] M. Eminescu, "Opere" vol. XIV, Ed. Academiei, 1983, p. 319.

[20] I. Prigogine and I. Stengers, "Noua alianță, Metafizica științei", Ed. politică, Bucharest, 1984 (the translation of the French original into Romanian).

[21] "Dictionary of Scientific Biography", Charles Schreibner's Sons Publishers, 1970, vol. 11, pp. 249.

[22] M. Jammer, "The Conceptual Development of Quantum Mechanics", McGraw-Hill, New York, 1966.

[23] W. James "The Principles of Psychology", McMillan, London, 1891.

[24] A. O. Fulea, Communication presented at the 4th Conference of Chemistry and of Chemical Engineering of the Polytechnic Institute of Bucharest, Oct. 18, 1985.

[25] I. G. Murgulescu and V. E. Sahini, "Introducere in Chimia Fizică", vol. 2, "Structura și proprietățile moleculelor" Ed. Academiei, 1978, p. 1209.

[26] R. Apostolescu, "Cristalografie, mineralogie", Ed. Didactică și Pedagogică, 1982, p. 201.

[27] a) A. O. Fulea, *Anal. Univ. București, Chimie*, **XIX** (1), 109 (1970); b) D. A. Isăcescu and A. O. Fulea, Communication presented at the 3rd Republican Conference of Chemistry, Timișoara, June 28, 1966; c) A. O. Fulea, A. Botea, D. A. Isăcescu, *Anal Univ. Bucharest, Chimia*, **16**, 65 (1967).

[28] K. Fukui, *Int. J. Quant. Chem.*, **XII**, Supl. 1. 277 (1977).

[29] a) A. O. Fulea and P. J. Krueger, *Tetrehedren Lett.*, **1975**, 3135; b) P. J. Krueger, A. O. Fulea, C. Fulea and F. F. Cernea, *Spectroscopy Letters*, **8**, 141 (1975); c) A. O. Fulea, *Rev. Roum. Chim.*, **24**, 1107 (1979).

[30] G. G. Longinescu, *Chem. Rev.*, **VI** (3), 381 (1929).

[31] "Istoria generală a științei", R. Taton, Ed., vol. IV, Știință contemporană, Ed. Științifică și Enciclopedică, Bucharest, p. 17, 308, 444 (translation of the French original "Histoire générale des Sciences" R. Taton (Ed.) Presse Universitaire de France).

[32] M. Born, "Natural Philosophy of Cause and Chance", Clerendon, Oxford, 1949, pp. 5 129.

[33] N. Bohr, "Asupra noțiunii de cauzalitate și complementaritate", in "Materialismul dialectic și științele contemporane" (translation into Romanian of N. Bohr's "Kausalität und Komplementaritat", *Naturwiss.* **21**, 13, (1933)).

[34] Ș. Calmare, "Determinism și cauzalitate", Ed. Științifică și Enciclopedică, Bucharest, 1979, p. 52.

[35] I. Mushcutariu, "Cristale lichide și aplicații", Seria Fizica modernă aplicată, Ed. Tehnică, Bucharest, 1981, p. 88.

[36] I. Ursu, *Bull. Mag. Reson.*,**7**, 105 (1985).

[37] C. Sălceanu, *Compt. rend.*, **190**, 757 (1930).

[38] S. P. Davis in "The Encyclopedia of Physics", R. M. Besançon (Ed.) Reinhold, Co. New York, 1966.

[39] J. Monod, "Symmetry and Function of Biological Systems at Molecular Level", in Proceedings of the 11th Nobel Symposion held August 26–29, 1968, Sodergarn, Lidingo in the county of Stockholm, A. Engstrom and B. Strandberg Eds., Almquist and Wieksel, Stockholm, 1969.

[40] A. T. Balaban, *Comp. and Math. with Appl.*, vol. **12B** (3/4), 999–1020 (1986), reprinted in Ref.[41]

[41] "Symmetry Unifying Human Understanding", I. Hargittai (Ed.), Pergamon Press, Oxford, 1987.

[42] F. M. Jaeger, cited in References of Ref.[40] : "Le principe de la symétrie et ses applications", Gauthier-Villars, Paris, (1945).

[43] A. O. Fulea, *Rev. Roum. Chim.*, **30**, 357, (1985).

[44] A. Zee, "Fearful Symmetry, The Search for Beauty in Modern Physics", Mac Millan Publishing Company, 1988, New York.

[45] Z. Folescu, "Quarkurile, supersimetria și superstringurile", Ed. Științifică și Enciclopedică, Bucharest, 1989.

[46] A. R. Bacon, J. M. Hollas and T. Ridley, *Can. J. Phys.*, **62**, 1254 (1984) and the references cited therein.

[47] M. Orchin and H. H. Jaffé, "Symmetry, Orbitals and Spectra" (S.O.S), Wiley-Interscience, New York, 1971, p. 222.

[48] "Encyclopedia Universalis", Paris, 1973, vol. **15**, p. 630, 631, 634.

[49] A. R. Lacey, "Dictionary of Philosophy", Routlenge and Ken Paul, London, p. 19.

[50] D. K. Simonton, *The Scientist*, February 6, 1989.

[51] a. I. G. Murgulescu, "În știință trebuie creați mai întîi specialiștii" (In science, firstly to be created the professionals) in A. Matei Săvulescu (Cine a rostit întîiul "Evrika"? (Who said firstly 'Evrika?') Ed. Politică, Bucharest, 1987, pp. 161–164.

[51] b. C. Rusu, O. Mihăilescu and E. Pelinescu, "Creația științifico-tehnică și inovarea industrială" Ed., Politică, Bucharest, 1989 pp. 29–30.,

[52] L. Von Bertallanfy, "General System Theory and Psychiatry", in "American Handbook of Psychiatry", S. Arieti (Ed.), vol. III, Basic Books, Inc. Publishers, New York, 1966, p. 705.

[53] S. Arieti, "Creativity and its Cultivation", in "American Handbook of Psychiatry", S. Arieti (Ed.) vol. III, Basic Books, Inc. Publishers, New York, 1966, p. 722.

[54] "Dicționar de Filosofie", O. Chezatu and R. Sommer (Eds in-Chief), Ed. Politică, Bucharest, 1978, p. 180.

[55] N. Demian, E. Butuceanu, Ioana Demetrescu, E. Jurconi and B. Popescu, "Aplicații și probleme de chimie generală", Ed. Didactică și Pedagogică, 1980, Bucharest, pp. 95–99 (see especially Fig. 39). (Applications and Problems of General Chemistry)

[56] L. Müller, in Irina G. Atanasiu, "George Atanasiu", Ed. Științifică și Enciclopedică, Bucharest (see especially Fig. 10, p. 190).

[57] W. J. Moore, "Physical Chemistry", 4th Ed. Prentice-Hall Inc. Englewood Cliffs, New Jersey, 1972, p. 360.

[58] R. P. Feynman, "Fizica modernă — Mecanica, Radiația și Căldura". Ed. Tehnică, Bucharest, 1969, pp. 495–498 ; the translation into Romanian and scientific revision by Prof. M. Gavrilă of the English original "The Feynman Lectures on Physics" Mainly Mechanics, Radiation and Heat, by R. P. Feynman, R. B. Leighton and M. Sands, Addison-Wesley, Reading, Massachussetts.

[59] L. von Bertalanfy, "General System Theory", Penguin Books, Middlesex, 1973.

[60] B. Kaplan, "The Comparative Developmental Approach" in American Handbook of Psychiatry", S. Arieti (Ed.), vol. III, Basic Books Inc. Publishers, New York, 1967, p. 659.

[61] A. O. Fulea, unpublished works.

Note added in proof. We acknowledge the presentation of the Curie-Fulea causality law at Eötvős Lorant University in Budapest, on October 31, 1990 and thank Professor Pal Sohár for offering this possibility to us, while we were living in Bicske Refugees Camp, Hungary (October 8 — December 13, 1990).

Revue Roumaine de Chimie, **36**, *11–12*, 1387–1395 (1991)

TRANSALKYLATION OF TOLUENE WITH TRIMETHYLBENZENE. I

THERMODYNAMIC STUDY

EMIL DUMITRIU, KAYED YOUSEF, VASILE HULEA and SPIRIDON OPREA
Department of Organic Chemical Technology, Faculty of Chemical Technology, Bahlui Stînga 71, Jassy 6600, Romania

Received July 29, 1989

On the basis of thermodynamic properties of the reagents and products implied in the transalkylation process of toluene, the Gibbs enthalpy, the equilibrium constants and the conversions at equilibrium vs. temperature and molar ratio were calculated. We have taken into account a large scheme of secondary reactions.

INTRODUCTION

At the beginning, the transalkylation reaction of alkylaromatics was considered as a secondary reaction accompanying the alkylation, disproportionation or isomerization of these hydrocarbons. Now, the transalkylation has become a valuable route for some aromatic hydrocarbons, e.g. the xylene manufacture by transalkylation of toluene with trimethylbenzene (see XYLENE-PLUS method).[1,2]

Various studies of the transalkylation process have been done and the influence of reaction conditions and nature of catalysts upon the product distribution was especially investigated. [3–5] Also, some reaction scheme and mechanisms were proposed.[6–9] All these studies revealed that the transalkylation process is very complex because a great number of secondary reactions are implied. The restriction of the rection product distribution represents the most important problem, which together with the increase of reaction rate, must be solved on the basis of finding of a proper catalyst. Here we present the results of a thermodynamic study, which can be a theoretical support for the above-mentioned aim.

THE CHEMICAL MODEL OF PROCESS

To establish a chemical model able to describe as exactly as possible the actual process of aromatic transalkylation it is necessary to take into account a great number of reactions which are responsible for the presence in the final reaction mixture of a large scale of products such as : lower alkanes, benzene, toluene, xylenes, tri- and tetramethyl-benzene etc. All these products have been identified in the toluene transalkylation with trimethylbenzenes using synthetic zeolites as catalysts. [10,11]

Therefore, on the basis of the above-mentioned observation, as well as of some theoretical considerations previously reported,[12] a chemical model was elaborated and it is shown in Table 1.

Table 1

The chemical model of the process

I. The transalkylation reaction of toluene

$$1,3,5\text{-}C_6H_3(CH_3)_3 + C_6H_5CH_3 \left\{ \begin{array}{ll} \xrightleftharpoons{K_1} 2m-C_6H_4(CH_3)_2 & (1) \\ \xrightleftharpoons{K_2} o\text{-}C_6H_4(CH_3)_2 + m\text{-}C_6H_4(CH_3)_2 & (2) \\ \xrightleftharpoons{K_3} p\text{-}C_6H_4(CH_3)_2 + m\text{-}C_6H_4(CH_3)_2 & (3) \end{array} \right.$$

$$1,2,4\text{-}C_6H_3(CH_3)_3 + C_6H_5CH_3 \left\{ \begin{array}{ll} \xrightleftharpoons{K_4} 2\ o\text{-}C_6H_4(CH_3)_2 & (4) \\ \xrightleftharpoons{K_5} 2\ p\text{-}C_6H_4(CH_3)_2 & (5) \\ \xrightleftharpoons{K_6} 2\ m\text{-}C_6H_4(CH_3)_2 & (6) \\ \xrightleftharpoons{K_7} p\text{-}C_6H_4(CH_3)_2 + o\text{-}C_6H_4(CH_3)_2 & (7) \\ \xrightleftharpoons{K_8} p\text{-}C_6H_4(CH_3)_2 + m\text{-}C_6H_4(CH_3)_2 & (8) \\ \xrightleftharpoons{K_9} o\text{-}C_6H_4(CH_3)_2 + m\text{-}C_6H_4(CH_3)_2 & (9) \end{array} \right.$$

$$1,2,3\text{-}C_6H_3)CH_3 + C_6H_5CH_3 \left\{ \begin{array}{ll} \xrightleftharpoons{K_{10}} 2\ o\text{-}C_6H_4(CH_3)_2 & (10) \\ \xrightleftharpoons{K_{11}} 2\ m\text{-}C_6H_4(CH_3)_2 & (11) \\ \xrightleftharpoons{K_{12}} o\text{-}C_6H_4(CH_3)_2 + m\text{-}C_6H_4(CH_3)_2 & (12) \\ \xrightleftharpoons{K_{13}} o\text{-}C_6H_4(CH_3)_2 + p\text{-}C_6H_4(CH_3)_2 & (13) \\ \xrightleftharpoons{K_{14}} m\text{-}C_6H_4(CH_3)_2 + p\text{-}C_6H_4(CH_3)_2 & (14) \end{array} \right.$$

II. The transalkylation reactions of benzene

$$1,3,5\text{-}C_6H_3(CH_3)_3 + C_6H_6 \xrightleftharpoons{K_{15}} C_6H_5CH_3 + m\text{-}C_6H_4(CH_3)_2 \qquad (15)$$

$$1,2,4\text{-}C_6H_3(CH_3)_3 + C_6H_6 \left\{ \begin{array}{ll} \xrightleftharpoons{K_{16}} C_6H_5CH_3 + p\text{-}C_6H_4(CH_3)_2 & (16) \\ \xrightleftharpoons{K_{17}} C_6H_5CH_3 + m\text{-}C_6H_4(CH_3)_2 & (17) \\ \xrightleftharpoons{K_{18}} C_6H_5CH_3 + o\text{-}C_6H_4(CH_3)_2 & (18) \end{array} \right.$$

$$1,2,3\text{-}C_6H_3(CH_3)_3 + C_6H_6 \left\{ \begin{array}{ll} \xrightleftharpoons{K_{19}} C_6H_5CH_3 + m\text{-}C_6H_4(CH_3)_2 & (19) \\ \xrightleftharpoons{K_{20}} C_6H_5CH_3 + o\text{-}C_6H_4(CH_3)_2 & (20) \end{array} \right.$$

III. The disproportionation reactions of toluene

$$2\,C_6H_5CH_3 \begin{cases} \xrightleftharpoons{K_{21}} C_6H_6 + o\text{-}C_6H_4(CH_3)_2 & (21) \\ \xrightleftharpoons{K_{22}} C_6H_6 + p\text{-}C_6H_4(CH_3)_2 & (22) \\ \xrightleftharpoons{K_{23}} C_6H_6 + m\text{-}C_6H_4(CH_3)_2 & (23) \end{cases}$$

IV. The isomerization reactions of trimethylbenzenes

$$1,3,5\text{-}C_6H_3(CH_3)_3 \xrightleftharpoons{K_{24}} 1,2,4\text{-}C_6H_3(CH_3)_3 \tag{24}$$

$$1,3,5\text{-}C_6H_3(CH_3)_3 \xrightleftharpoons{K_{25}} 1,2,3\text{-}C_6H_3(CH_3)_3 \tag{25}$$

$$1,2,4\text{-}C_6H_3(CH_3)_3 \xrightleftharpoons{K_{26}} 1,2,3\text{-}C_6H_3(CH_3)_3 \tag{26}$$

V. The isomerization reactons of xylenes

$$p\text{-}C_6H_4(CH_3)_3 \xrightleftharpoons{K_{27}} m\text{-}C_6H_4(CH_3)_3 \tag{27}$$

$$p\text{-}C_6H_4(CH_3)_3 \xrightleftharpoons{K_{28}} o\text{-}C_6H_4(CH_3)_3 \tag{28}$$

$$m\text{-}C_6H_4(CH_3)_3 \xrightleftharpoons{K_{29}} o\text{-}C_6H_4(CH_3)_3 \tag{29}$$

As can be observed, the most important reactions such as : transalkylation of toluene, isomerization of xylenes and trimethylbenzenes, disproportionation of toluene and transalkylation of benzene have been taken into account. Also, it can be mentioned that some of these reactions are linear combinations of the independent reactions.

The reactions having a small contribution such as : hydrodealkylation, condensation, coke formation etc. have been neglected.

THE THERMODYNAMIC CALCULATIONS

Using the well-known thermodynamic relations (eqs. 1—3) and based on the thermodynamic properties of organic compounds implied in the above model, the following parameters were calculated : Gibbs free energy, equilibrium constant and composition at equilibrium. A large range of temperatures (473—823 K) was investigated.

The following relationships were used :

$$\Delta C_p = \Delta a + \Delta b \cdot T + \Delta c \cdot T^2 + \Delta d \cdot T^3 \tag{1}$$

$$\Delta G_T = \Delta H_{298} + \int_{298}^{T} \Delta C_p \cdot \mathrm{d}T - T \left[\Delta S_{298} + \int_{298}^{T} (\Delta C_p / T \mathrm{d}T) \right] \tag{2}$$

$$K_T = \exp\left(-\Delta G_T / RT\right) \tag{3}$$

where $R = 8310\ \mathrm{J \cdot kmol^{-1} \cdot K^{-1}}$

The thermodynamic properties of the implied substances are shown in Table 2.

Table 2

Thermodynamic properties of substances [13–16]

Substances	ΔH_{298} KJ · mol⁻¹	ΔS_{298} J · mol⁻¹K⁻¹	a J · mol⁻¹K⁻¹	b × 10² J · mol⁻¹K⁻²	c × 10⁶ J · mol⁻¹K⁻³	d × 10⁹ J · mol⁻¹K⁻⁴
Benzene	82.84	268.94	−36.16	48.39	−315.17	77.49
Toluene	49.95	319.43	−34.33	56.75	−344.01	80.25
p-Xylene	17.93	352.08	−22.29	59.44	−333.73	71.18
m-Xylene	17.22	357.34	−27.31	62.30	−369.13	83.81
o-Xylene	18.97	352.41	−15.84	59.73	−349.19	78.58
1,3,5-TMB*	−16.05	385.18	−15.68	66.91	−377.07	83.79
1,2,4-TMB	−13.92	396.01	−8.19	65.05	−360.77	78.53
1,2,3-TMB	−9.57	395.97	−6.39	65.08	−360.52	78.56

* TMB = Trimethylbenzene

The calculations were performed on a FELIX-256 computer.

RESULTS AND DISCUSSION

Using equations (1—2) and the thermodynamic properties of substances which are shown in Table 2, the Gibbs free energy was calculated. The values of Gibbs free energy, presented in Table 3, for a large range of temperatures (473—823 K), point out some interesting aspects regarding the studied reactions.

Table 3

Gibbs free energy values

Reaction	ΔG, kJ · mol⁻¹							
	473K	523K	573K	623K	673K	723K	773K	823K
1	−4.366	−4.829	−5.285	−5.716	−6.118	−6.486	−6.817	−7.117
2	−0.312	−0.690	−1.091	−1.512	−1.953	−2.413	−2.892	−3.389
3	−0.809	−1.061	−1.335	−1.641	−1.987	−2.382	−2.834	−3.355
4	6.717	7.076	7.399	7.696	7.959	8.194	8.399	8.579
5	5.725	6.332	6.909	7.437	7.893	8.257	8.516	8.646
6	−0.966	−0.769	−0.558	−0.251	−0.070	0.211	0.512	0.835
7	6.219	6.704	7.156	7.566	7.926	8.227	8.457	8.613
8	2.173	2.563	2.960	3.359	3.757	4.151	4.536	4.905
9	2.670	2.933	3.205	3.488	3.792	4.119	4.477	4.871
10	2.426	2.833	3.216	3.496	3.918	4.239	4.536	4.812
11	−5.666	−5.448	−5.172	−4.833	−4.415	−3.913	−3.311	−2.598
12	−1.619	−1.308	−0.979	−0.628	−0.249	0.161	0.612	1.111
13	1.930	2.462	2.970	3.448	3.884	4.268	4.595	4.846
14	−2.116	−1.679	−1.224	−0.757	−0.283	0.193	0.669	1.141
15	−10.41	−11.45	−12.47	−13.45	−14.39	−15.30	−16.15	−16.95
16	−3.877	−4.058	−4.222	−4.373	−4.518	−4.662	−4.804	−4.955
17	−7.259	−7.868	−8.420	−9.019	−9.683	−10.46	−10.97	−11.67
18	−3.381	−3.688	−3.977	−4.243	−4.486	−4.691	−4.863	−4.988
19	−11.72	−12.07	−12.36	−12.57	−12.69	−11.73	−12.65	−12.46
20	−7.692	−7.930	−8.160	−8.361	−8.524	−8.650	−8.729	−8.755
21	10.23	11.16	12.13	13.14	14.19	15.29	16.45	17.65
22	9.617	10.74	11.94	13.23	14.61	16.41	17.70	19.31
23	6.118	6.775	7.452	8.153	8.881	9.636	10.42	11.24
24	−2.982	−3.624	−4.293	−5.001	−5.746	−6.532	−7.369	−8.261
25	1.307	0.618	−0.111	−0.884	−1.704	−2.575	−3.504	−4.494
26	4.289	4.243	4.176	4.117	4.041	3.957	3.865	3.765
27	−3.549	−3.770	−3.950	−4.076	−4.133	−4.106	−3.980	−3.738
28	0.496	0.370	0.244	0.129	0.034	−0.031	−0.056	−0.033
29	4.046	4.141	4.193	4.206	4.167	4.075	3.923	3.705

Firstly, concerning the transalkylation of toluene, one observes that only for transalkylation with 1, 3, 5-trimethylbenzene and 1,2,3-trimethylbenzene $\Delta G < 0$. In the case of 1,2,4-trimethylbenzene $\Delta G > 0$, but due to the small value of Gibbs free energy, the probability of occurring of this transalkylation is not excluded because the range of the thermodynamic probability of chemical reactions is extended up to $G \leqslant 40$ kJ·mol^{-1}.

Another interesting aspect consists in the fact that all reactions of benzene transalkylation with trimethylbenzene (irrespective of isomer) have $\Delta G < 0$ and these Gibbs free energy values are greater than that corresponding to the toluene transalkylation (as absolute value), in spite of the increased reactivity of alkyl substituted aromatics as toluene. For both case ΔG increases with the temperature rising.

Concerning the isomerization reactions, it can be remarked that the greatest probability shows *p*-xylene to *m*-xylene isomerization and then *o*-xylene to *m*-xylene, but for the trimethylbenzenes isomerization the order is 1,3,5-TMB$\rightleftharpoons$1,2,4-TMB$>$1,2,4-TMB$\rightleftharpoons$1,2,3-TMB.

The thermodynamic study of toluene disproportionation was previously reported in detail.[12]

More exact information about the priority of chemical transformation of the aromatic hydrocarbons from this system is obtained determining the value of equilibrium constants for the reactions making up the above model. These values are shown in Table 4 and they are calculated for the same range of temperatures.

Table 4

Equilibrium constants for the chemical model of transalkylation process

Reaction	Equilibrium constants at:							
	473K	523K	573K	623K	673K	723K	773K	823K
1	3.027	3.036	3.031	3.014	2.984	2.941	2.886	2.819
2	1.083	1.172	1.257	1.339	1.417	1.494	1.568	1.641
3	1.228	1.276	1.323	1.373	1.426	1.486	1.554	1.633
4	0.181	0.196	0.212	0.226	0.241	0.256	0.271	0.286
4	0.234	0.233	0.235	0.238	0.244	0.253	0.266	0.283
6	1.278	1.194	1.124	1.049	1.013	0.965	0.923	0.885
7	0.206	0.214	0.233	0.237	0.243	0.253	0.268	0 284
8	0.576	0.555	0.537	0.523	0.511	0.502	0.494	0.488
9	0.507	0.510	0.511	0.510	0.508	0.504	0.498	0.491
10	0.540	0.522	0.509	0.501	0.497	0.495	0.494	0.495
11	4.221	3.499	2.961	2.541	2.201	1.917	1.674	1.462
12	1.509	1.351	1.228	1.128	1.046	0.973	0.908	0.851
13	0.612	0.568	0.536	0.514	0.500	0.492	0.490	0.493
14	1.712	1.471	1.293	1.157	1.052	0.968	0.901	0.847
15	14.091	13.912	13.680	13.401	13.093	12.734	12.340	11.902
16	2.679	2.542	2.425	2.326	2.242	2.171	2.111	2.062
17	6.295	6.071	5.822	5.672	5.612	5.567	5.484	5.471
18	2.361	2.334	2.304	2.269	2.228	2.182	2.130	2.072
19	19.651	16.033	13.363	11.300	9.656	8.298	7.154	6.171
20	7.026	6.189	5.542	5.021	4.587	4.214	3.886	3.592
21	0.074	0.076	0.078	0.089	0.079	0.078	0.077	0.076
22	0.086	0.084	0.081	0.077	0.073	0.065	0.063	0.059
23	0.211	0.210	0.209	0.207	0.204	0.201	0.197	0.193
24	2.134	2.300	2.463	2.625	2.790	2.963	3.146	3.334
25	0.717	0.867	1.024	1.186	1.356	1.535	1.725	1 929
26	0.336	0.377	0.415	0.452	0.486	0.518	0.548	0.577
27	2.465	2.379	2.291	2.196	2.092	1.980	1.857	1.727
28	0.881	0.918	0.950	0.975	0.994	1.005	1.009	1.013
29	0.357	0.386	0.415	0.444	0.475	0.508	0.543	0.582

An important aspect is pointed out from this table, namely that for the most rections, excepting the benzene transalkylation, the equilibrium constant is ranging between the following limits $0.2 < K_T < 5$.

In order to facilitate a comparison between the reactions describing this process, the most representative reactions from each type have been chosen and the variation of equilibrium constant *vs*. temperature was shown in Figure 1.

As can be observed from this figure, the equilibrium constants are disposed in the following order:

$$K_{\text{tsansB}} > K_{\text{isoTMB}} > K_{\text{isoX}} > K_{\text{transT}} > K_{\text{dispT}}$$

Therefore, one can conclude that the transalkylation of toluene with mesitylene is preceded by the isomerization, which leads to the trimethylbenzenes more less reactive than the mesitylene (see Figs. 2 and 3); the equilibrium constants for the isomerization of trimethylbenzenes are greater than that for the toluene transalkylation and only mesitylene, from the three isomers, has the greatest equilibrium constant for transalkylation and also this constant is favoured by temperature.

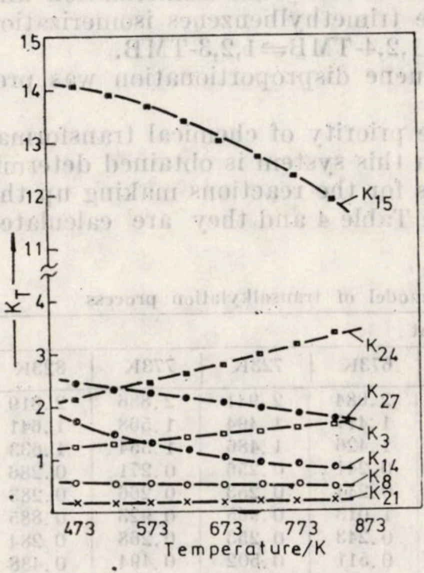

Fig. 1. — The variation of equilibrium constants *vs*. temperature.

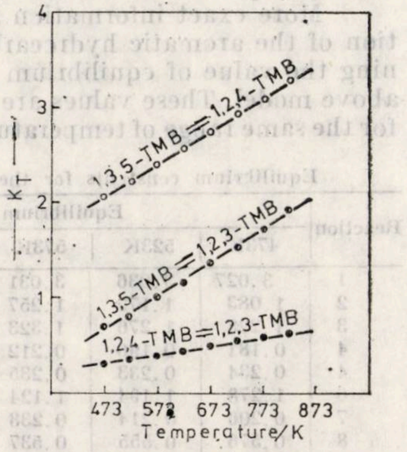

Fig. 2. — The variation of equilibrium constants for isomerization of trimethylbenzenes *vs*. temperature.

Both Table 3 and Fig. 2 show that for the isomerization of trimethylbenzenes the order of magnitude of the equilibrium constants is: $K_{24} > K_{25} > K_{26}$, while from Figure 3 one remarks the small values of equlibrium constants for the transalkylation reaction of toluene with 1,2,4-trimethylbenzene. Also, in relation to the influence of temperature, we can observe that only in the transalkylation of toluene with 1,3,5-trimethylbenzene the formation of *p*- and *m*-xylene or *o*- and *m*-xylene is favoured by the temperature increase (see Fig. 3a, curves K_2 and K_3).

Another interesting aspect can be observed in relation to the transalkylation of benzene. Both the thermodynamic and experimental data demonstrate that a certain amount of toluene is disproportioned to benzene and xylene. As is observed from Table 3, the equilibrium constants

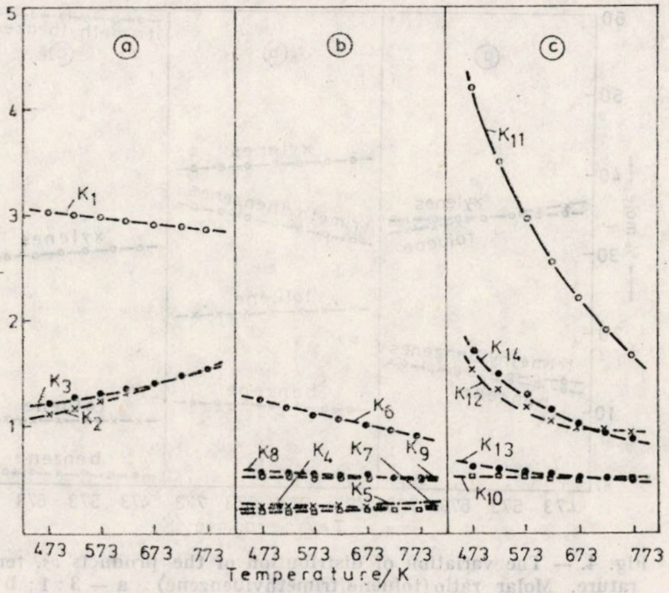

Fig. 3. — The variation of equilibrium constants for the toluene transalkylation with trimethylbenzene *vs.* temperature.
a — 1, 3, 5-TMB ;b — 1,2,4-TMB ; c — 1,2,3-TMB

for the benzene transalkylation have the greatest values of all, and this represents a favourable situation for the efficiency of the process because the amount of benzene will be reduced, whereas the amount of xylene will be increased.

As is known, the composition at thermodynamic equilibrium depends on the contribution of each reaction at the overall equilibrium. Generally, the composition at equilibrium is influenced by temperature and molar ratio between reagents. On the basis of thermodynamic calculations the composition of the reaction products was evaluated for the same temperature range (473—823 K) and for the following toluene/mesitylene molar ratios : 1/1 ; 2/1 ; 3/1 ; 1/2 and 1/3.

Analysing the data shown in Figure 4 the following conclusions are releaved :

(i) — the xylene percent decreases as far as the temperature is increased, irrespective of mole ratio between reagents;

(ii) — the percent of xylenes is maintained at a satisfactory level, 32—41.5% (mole), on overall range of temperatures;

(iii — the percent of benzene increases as temperature is increased and it is favoured by an excess of toluene.

It is interesting to study the influence of temperature and molar ratio upon the distribution of xylenes and trimethylbenzenes, respectively. The following aspects can be observed from Figure 5 :

(i) — the distribution of xylene and trimethylbenzene isomers is unaffected by the molar ratio of reagents ;

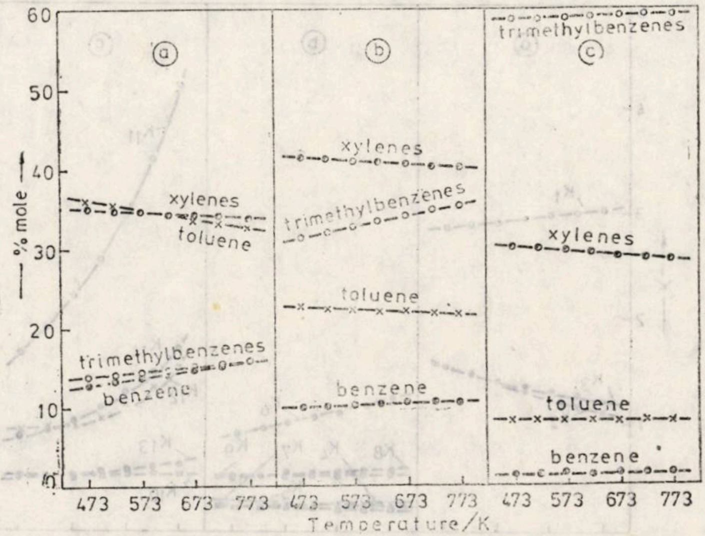

Fig. 4. — The variation of distribution of the products *vs*. temperature. Molar ratio (toluene/trimethylbenzene) : a — 3 : 1 ; b — 1 : 1 : 1 ; c — 1 : 3.

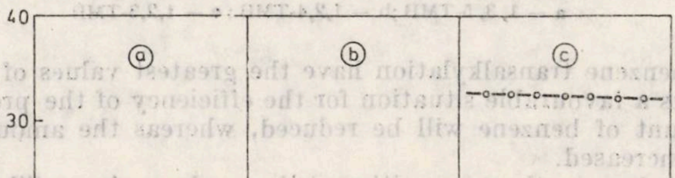

Fig. 5. — The variation of distribution of the xylene and trimethylbenzene isomers *vs*. temperature.
(●) — *o*-xylene ; (◐) — *m*-xylene ; (×) — *p*-xylene ; (▭) — 1, 2, 3-TMB ; ( ) — 1, 2, 4-TMB ; (○) — 1, 3, 5-TMB. Molar ratio (toluene/TMB) : a — 3 : 1 ; b — 1 : 1 ; c — 1 : 3

(ii) — the distribution of the above-mentioned isomers is influenced by temperature, namely : both the amount of *m*-xylene and the amount of mesitylene decrease in favour of the corresponding isomers as far as the temperature is increased.

The maximum conversions, which are thermodynamically possible, can be determined if the composition at equilibrium is known. The influence of molar ratio of reagents upon the conversion is shown in Figure 6.

As can be observed from this figure, the results are referred to the limiting reagent. When the toluene is the limiting reagent, the conversion increase is more stronger than when the mesitylene is limiting reagent. This behaviour can be explained by the fact that, in the first case, there is a higher concentration of mesitylene, in spite of a certain decrease of the concentation of this due to the isomerization, whereas, in the second case, there is a lower concentration of mesitylene, from the same reason. In the last case, the small increase observed is due to the high concentration of toluene.

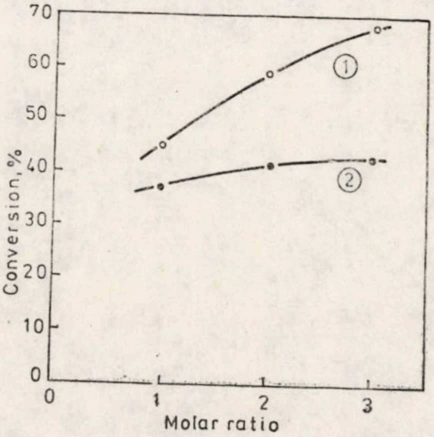

Fig. 6. — The variation of conversion *vs.* mole ratio of reagents. (1) — TMB/toluene ; (2) — toluene/TMB.

This information, obtained by thermodynamic calculations, is useful in order to explain the experimental data, as can be seen in the following paper.

REFERENCES

[1] J. P. Gignier, *Revue de l'Assoc. Fr. Techn. Pétrole*, **17**, 201 (1970).

[2] S. Otani, S. Matsnoka and M. Seto, *Jap. Chem. Quart.*, **4**, 16 (1968).

[3] E. L. Pollitzer (Universal Oil Products Co.), U.S. 3, 527, 825, 08. Sept. 1970, *Chem. Abstr.*, **73**, 98576 (1970).

[4] E. L. Pollitzer (Universal Oil Products Co.), U.S. 3, 527, 824, 08.Sept.1970, *Chem. Abstr.*, **73**, 98577 (1970).

[5] R. M. Aliev, *Neftepereryv. Neftekhim.* (Moscow), **3**, 30 (1977).

[6] V. G. Lipovich, A. V. Vysotskii and V. V. Chenets, *Neftekhimiya*, **11**, 656 (1971).

[7] V. G. Lipovich, *Neftekhimiya*, **11**, 838 (1971).

[8] T. Yashima and Y. Matsuoko, *Sekiyn Gakkai Shi*, **15**, 487 (1972).

[9] R. Chojnacki, *Przem. Chem.*, **53**, 338 (1974).

[10] S. Oprea, E. Dumitriu, V. Hulea, P. Onu, D. Gînju and K. Yousef, *Rev. Chim.* (Bucharest), **36**, 807 (1985).

[11] V. Hulea, E. Dumitriu and S. Oprea, "Lucrările sesiunii jubiliare de comunicări ştiinţifice", Jassy 10—12 nov 1988, vol. X, p. 104.

[12] S. Oprea, A. Azzouz, E. Dumitriu and M. Constantinescu, *Bull. Soc. Chim. Belg.*, **92**, 289 (1983).

[13] Manualul Inginerului Chimist, Edit. Tehnică. Bucharest, vol. II, 1972, p. 1458 and 1562.

[14] P. Whnitier, "Raffinage et Génie Chimique", Technip Paris, tome I, p. 147, 1972.

[15] K. L. Hanson and A. J. Enger, *A. J. Chem. Eng. I.*, **13**, 260 (1967).

[16] C. R. C. Handbook of Chemistry and Physics", Ed. 52 (R. C. Weast), Cleveland (1971—1972), p. D76, D130, D132.

Revue Roumaine de Chimie, **36**, *11–12*, 1397–1401 (1991)

MECHANISM OF PHENOL METHYLATION ON Al_2O_3 AND ON MgO

MARK S. CHARSON[a], NICULAE I. IONESCU[b] and MIHAI S. CHIRCA[b]

[a] Institute of Organic Chemistry of the Academy of Science of U.S.S.R., Leninski prospekt 47, Moscow, U.S.S.R.

[b] Institute of Physical Chemistry of the Romanian Academy, Spl. Independenţei 202, Bucharest, Romania

Received July 23, 1990

Based on kinetic and IR data, the mechanism for phenol methylation on Al_2O_3 and on MgO is discussed. For both catalysts a Langmuir-Hinshelwood mechanism seems the most probable. An Eley-Rideal mechanism for anisole formation can also be partially supported by the experimental data.

In our previous papers some aspects concerning the kinetics of phenol methylation on Al_2O_3 [1–5] and on MgO[6], as well as the IR investigation of the adsorbed species of phenol and methanol on MgO surface were presented. Based on these data in this paper an attempt is made to ascertain the mechanism of phenol methylation on Al_2O_3 and on MgO.

EXPERIMENTAL

The kinetics of phenol methylation was studied in a flow system, using either an integral or a differential one-pass reactor. In the experimental area covered by our measurements, the reaction rate was not influenced by the intra- or extragranular transfer, as shown by preliminary tests.

The reaction was carried out at atmospheric pressure in a glass reactor kept a constant temperature in a molten salts bath. The condensed products were analysed by gas chromatography in order to determine the phenol conversion. More details are presented in our previous papers.[1,2,5,6]

RESULTS AND DISCUSSION

The phenol methylation on Al_2O_3 and respectively on MgO shows some similarities, but important differences can be found between the catalytic activities and the selectivities of these two catalysts.

One of the first experimental observations was that in order to obtain comparable conversion for phenol, the process must be conducted at different temperatures: about 300°C for Al_2O_3 and 500°C for MgO. The experimentally determined values for the apparent activation energy vary in the same manner: 77.0 kJ · mol^{-1} for Al_2O_3, respectively 158.7 kJ · mol^{-1} for MgO.[6]

Another distinction between the phenol methylation on these two catalysts is that for low conversion of phenol only *o*-cresol is obtained on MgO, while on Al_2O_3 three main products are always obtained : *o*-cresol, anisole and 2,6-xylenol. These data show that in phenol methylation on Al_2O_3 at least four parallel and consecutive reactions must be taken into account, as presented in scheme 1.

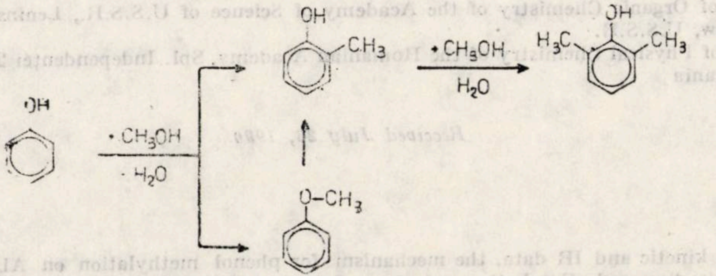

Scheme 1. — Parallel and consecutive reactions in phenol methylation.

From the above scheme is absent the anisole formation by *o*-cresol isomerization, since our experimental data showed that this reaction is improbable. Thus, a methanol-*o*-cresol mixture gives, in conditions similar with those used for phenol methylation on Al_2O_3, only 2,6-xylenol, *o*-methylanisole and 2.4,6-trimethylphenol, but no anisole. Yet a methanol-anisole mixture gives, in the same conditions, 2,6-xylenol, phenol, *o*-cresol, *o*-methylanisole and 2,4,6-trimethylphenol, in this order of selectivities. It is to note that the isomerization of anisole in *o*-cresol and the absence of the reverse reaction was also observed on alumina-silica catalyst.

The kinetic studies of phenol methylation were realized using the method of initial reaction rates, which seemed adequate for such a complex reaction system. These studies revealed the resemblance between the phenol methylation on Al_2O_3 and on MgO, because on both catalysts the initial reaction rates are better described by rate equations which presume that the rate determining step is the surface reaction between adjacent chemisorbed species.

The kinetic data can be correlated with the information obtained from IR spectra in order to suggest a plausible mechanism for phenol methylation on the surface of Al_2O_3 and on MgO catalysts. The IR studies published by Taylor[9], Shabalin [10] and Kagel [11] show that on Al_2O_3 phenol is chemisorbed as phenolate species and methanol as methoxide species. The same chemisorbed species were identified by IR investigation of MgO.[7]

The IR studies prove also the competition of phenol and methanol for the same type of active centers of Al_2O_3, respectively of MgO surface. But neither by IR investigations, nor by kinetic studies a clear distinction between the chemisroption with or without dissociation of phenol and methanol on the catalyst surface can be made.

Based on these data, a possible mechanism for phenol methylation on Al_2O_3 was presented in scheme 2.

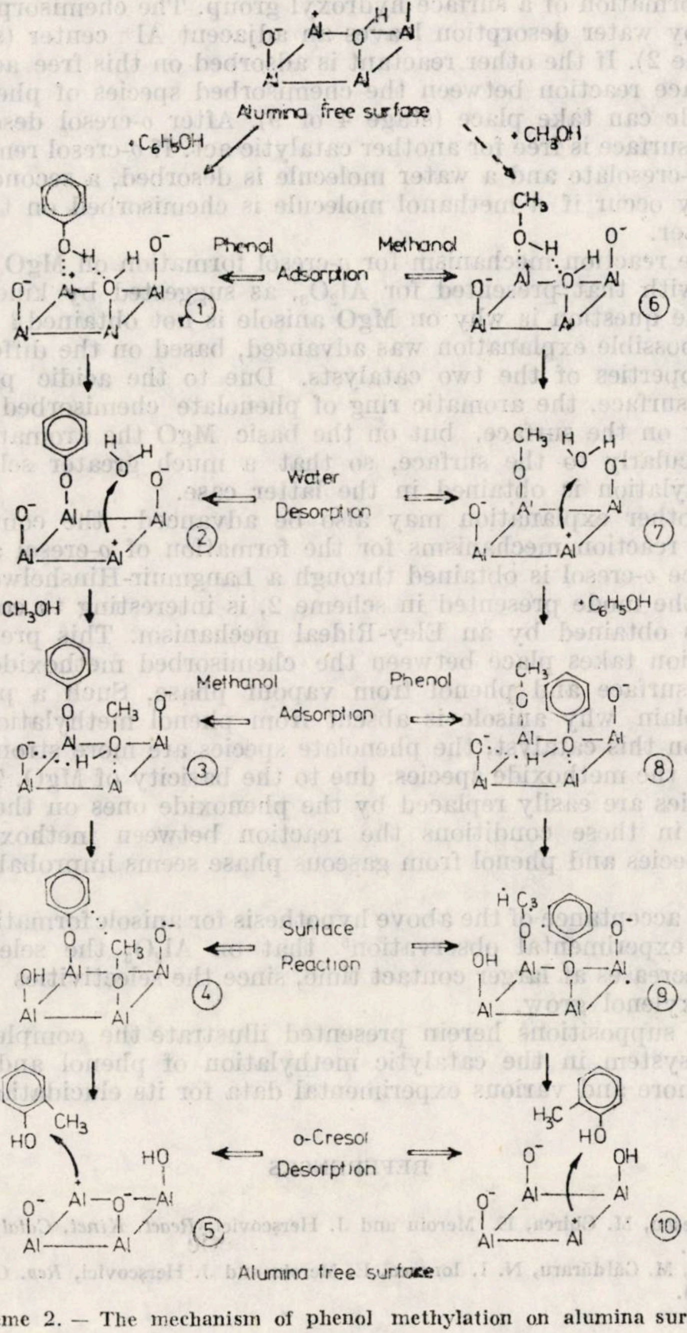
Alumina free surface
+C6H5OH
+CH3OH
Phenol
Adsorption
Methanol
1
6
Water
Desorption
2
7
+CH3OH
+C6H5OH
Methanol
Adsorption
Phenol
3
8
Surface
Reaction
4
9
o-Cresol
Desorption
5
10
Alumina free surface

Scheme 2. — The mechanism of phenol methylation on alumina surface.

In this scheme, two alternative routes for phenol methylation are presented, which differ by the order in which the two reactants are chemisorbed on adjacent active centers of the alumina surface. Both phenol and methanol adsorption may be accompanied by water desorption or by the formation of a surface hydroxyl group. The chemisorption accompanied by water desorption leaves an adjacent Al^+ center (stage 2 or 7 in scheme 2). If the other reactant is adsorbed on this free active center, the surface reaction between the chemisorbed species of phenoxide and methoxide can take place (stage 4 or 9). After *o*-cresol desorption, the catalyst surface is free for another catalytic act. If *o*-cresol remains adsorbed as *o*-cresolate and a water molecule is desorbed, a second alkylation step may occur if a methanol molecule is chemisorbed on the new free Al^+ center.

The reaction mechanism for *o*-cresol formation on MgO is probably similar with that presented for Al_2O_3, as suggested by kinetic and IR data. The question is why on MgO anisole is not obtained?

A possible explanation was advanced, based on the different acido-basic properties of the two catalysts. Due to the acidic properties of alumina surface, the aromatic ring of phenolate chemisorbed species lies obliquely on the surface, but on the basic MgO the aromatic ring lays perpendicularly to the surface, so that a much greater selectivity for ortho-alkylation is obtained in the latter case.

Another explanation may also be advanced: the competition of different reaction mechanisms for the formation of *o*-cresol and of anisole. Since *o*-cresol is obtained through a Langmuir-Hinshelwood mechanism in the mode presented in scheme 2, is interesting to consider that anisole is obtained by an Eley-Rideal mechanism. This presumes that the reaction takes place between the chemisorbed methoxide species on alumina surface and phenol from vapour phase. Such a presumption may explain why anisole is absent from phenol methylation on MgO, because on this catalyst, the phenolate species are more strongly chemisorbed as the methoxide species, due to the basicity of MgO. The methoxide species are easily replaced by the phenoxide ones on the MgO surface and in these conditions the reaction between methoxide chemisorbed species and phenol from gaseous phase seems improbable on MgO catalyst.

The acceptance of the above hypothesis for anisole formation explains also the experimental observation[5] that on Al_2O_3 the selectivity for anisole decreases at larger contact time, since the selectivities for *o*-cresol and 2,6-xylenol grow.

The suppositions herein presented illustrate the complexity of the reaction system in the catalytic methylation of phenol and point the need of more and various experimental data for its elucidations.

REFERENCES

[1] **N. I. Ionescu, M. Chirca, E. Meroiu and J. Herşcovici,** *React. Kinet. Catal. Lett.*, **15,** 42 (1980).

[2] **M. Chirca, M. Căldăraru, N. I. Ionescu, E. Meroiu and J. Herşcovici,** *Rev. Chim.*, **32,** 117 (1981).

[3] N. I. Ionescu and M. Chirca, "The Kinetics of the Heterogeneous Catalytic Reactions. Methodical Problems of Kinetics. Thematic collection" (in Russian), Tchernogolovka, 1983, p. 34.
[4] M. Chirca, I. Suciu, B. Albu, R. Boeru, E. Meroiu and N. I. Ionescu, *Rev. Chim.*, **37**, 218 (1986).
[5] N. I. Ionescu, M. Chirca, E. Meroiu, B. Albu, A. Nicolau, M. Enăchescu, T. Bota and M. S. Charson, *Z. phys. Chem., Leipzig*, **268**, 1201 (1987).
[6] M. Chirca, M. S. Charson, N. I. Ionescu and M. M. Kostiukovski, *Kin. Kat.*, **26**, 1254 (1985).
[7] N. I. Ionescu, M. S. Charson and M. S. Chirca, *React. Kinet. Catal. Lett.*, **33**, 447 (1987)
[8] K. Tanabe and F. Nishizaki, *Proc. 6-th Int. Congr. Catal., London*, **2**, 863 (1976).
[9] D. R. Taylor and K. H. Lundum, *J. Phys. Chem.*, **76**, 2882 (1972).
[10] I. I. Shabalin, E. A. Kiva, M. V. Ciurkin, L. A. Rusanova and M. F. Macitov, *Kin. Kat.*, **15**, 1540 (1974).
[11] R. O. Kagel, *J. Phys. Chem.*, **71**, 844 (1967).

Revue Roumaine de Chimie, 36, *11–12*, 1403–1408 (1991)

STUDY OF THE INTRINSIC PROPERTIES OF VISCOUS FLOW IN THE ETHYLENEGLYCOL (EG)-METHANOL (MeOH) SYSTEM

DOINA HRITCU, GH. IONESCU and I. M. POPA
Polytechnic Institute of Jassy, Faculty of Chemical Technology,
Department of Physical Chemistry, Splai Bahlui 71, Jassy 6600, Romania

Received June 10, 1989

The paper discusses the determination, for ethyleneglycol-methanol solutions, of the intrinsic properties of viscous flow: dynamic viscosity, parameters of the Guzmán-Andrade equation, Eyring parameters of flow activation, as well as the potential compound of the internal energy. Such parameters are necessary in the explanation of the solutions behaviour in prcesses of flow, stirring, distillation, and so on. The concentration of the solutions investigated are those usually employed in industrial processes.

1. INTRODUCTION

The parameters of viscous flow represent essential characteristics of solutions, in various physical and chemical processes in which they are involved. The EG—MeOH solution has a special practical importance especially in polyester fibers industry, in transesterification and dimethylterephthalate (DMT) recovery.

Establishment of the conditions of flow, stirring, distillation, implies knowledge of the viscous flow parameters.

The present paper aims at determining the solution's viscosity, in the case of some industrial concentrations and different temperatures. Starting from such experimental data, there have been tested: the applicability of the Guzmán-Andrade equation, the value of E_{vis} and B parameters, belonging to this equation, the value of the activation parameters of the viscous flow, expressed by $\Delta H^{\ddagger}_{\text{vis}}$, $\Delta S^{\ddagger}_{\text{vis}}$ and $\Delta G^{\ddagger}_{\text{vis}}$, as well as the potential compound of the internal energy $(\partial U/\partial V)_T$.

2. REAGENTS AND EQUIPMENT

Ethyleneglycol and methanol were of p.a. purity, anhydrous versus the Karl-Fischer reagent.

An Ostwald type viscosimeter was used, equipped with a capillary tube, ensuring leakage times over 200 s, thus eliminating the necessity of the correction required by the perturbation of laminar flow when entering the capillary tube and thermostated with an accuracy of 0.2°.

The densimeter, provided with an inner thermometer, was thermostated at the same accuracy degree. Preparation of the solutions was performed through weighing. This operation employed for solutions synthesizing and for density determining was performed with accuracy of 0.0001 g.

Viscosity was determined as relative, on using a standard liquid (EG = the solvent). As, according to literature data [1], EG viscosity is given accurately only for two temperatures on the range taken into study, the necessity of determining its viscosity at other temperatures, too, was felt. For such determinations, the standard liquid employed was isobutylic alcohol, as literature offers precise viscosity data, on a larger temperature range, for this substance.

Experimental data referring to the solutions' viscosity, at various temperatures and concentrations, are given in Table 1.

Table 1

Viscosities (Pa.s) for EG-MeOH solutions

x_{EG}	t, °C	15	22	29	36
1	—	26.3	19.72	14.29	11.28
0.8901	—	19.53	14.92	11.22	8.542
0.8085	—	14.43	11.00	8.266	6.704
0.7227	—	11.04	8.983	6.864	5.670
0.7008	—	7.980	6.550	5.420	4.519

3. CHECKING THE APPLICABILITY OF THE GUZMÁN-ANDRADE EQUATION AND THE DETERMINATION OF E_{vis} AND B PARAMETERS

In the case of liquids, the dependence of viscosity on temperature is expressed, with the great majority of nondissociating compounds, through the semi-experimental equation proposed by Guzmán and Andrade[2,3]:

$$\eta = B \cdot \exp \cdot (E_{vis}/RT) \qquad (1)$$

B = viscosity value for $T \to \infty$;
E_{vis} = energy barrier with the flow, known as activation energy of the viscous flow.

Equation (1), having an experimental character, has to be checked with respect to its applicability for the system considered. Thus, experimental data from Table 1 have been processed in co-ordinates $\ln \eta$ and $1/T$, a case in which, after logarithmation, the equation should be linear, if applied in the case under study, i.e.:

$$\ln \eta = \ln B + \frac{E_{vis}}{RT} \qquad (2)$$

Table 2

Processing of experimental data in co-ordinates $\ln\eta$ and $10^3/T$

$\frac{10^3}{T}$, K^{-1}	x_{EG}				
	1	0.8901	0.8085	0.7227	0.7008
3.472	−3.638	−3.936	−4.238	−4.506	−4.831
3.390	−3.926	−4.205	−4.510	−4.712	−5.028
3.311	−4.248	4.490	−4.796	−4.982	−5.218
3.236	−4.485	−4.763	−5.005	−5.173	−5.400

The diagram plotted in Fig. 1 evidences that, within the (15 . . .36)°C range, equation (1) is being satisfied, for all concentrations of the solutions employed.

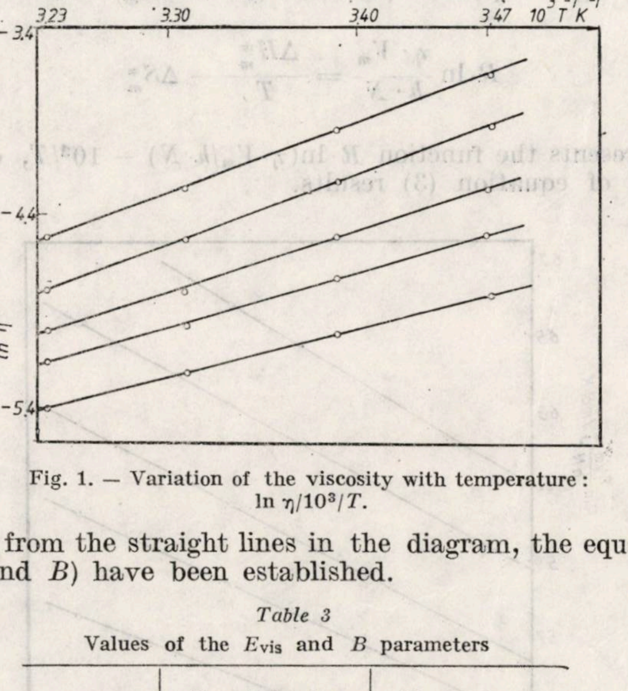

Fig. 1. — Variation of the viscosity with temperature: ln $\eta/10^3/T$.

Starting from the straight lines in the diagram, the equation parameters (E_{vis} and B) have been established.

Table 3

Values of the E_{vis} and B parameters

x_{EG}	E_{vis}, kJ/mole	$10 \cdot B$, Pa · s
1	30.25	8.57
0.8901	29.22	9.88
0.8085	27.34	15.79
0.7227	23.98	49.92
0.7008	20.03	186.0

4. CALCULATION OF THE PARAMETERS OF VISCOUS FLOW ACCORDING TO EYRING

Eyring, on applying the "theory of the absolute reaction rates" to the process of viscous flow, which is similar to the shifting of molecules from an equilibrium position towards another, over a potential barrier, proposes the equations :[4,5]

$$\eta = \frac{h \cdot N}{V_m} \cdot \exp \cdot (\Delta G^{\neq}_m / RT) \tag{3}$$

$\Delta G^{\neq}_m$ = free Gibbs' energy of activation of flow corresponding to 1 mole ; N = Avogadro's number ; V_m = molar volume ; k = Planck's constant. As,

$$\Delta G^{\neq}_{\text{vis}} = \Delta H^{\neq}_{\text{vis}} - T \cdot \Delta S^{\neq}_{\text{vis}}, \tag{4}$$

on substituting in equation (3) and logarithming, there results :

$$R \cdot \ln \frac{\eta \cdot V_m}{h \cdot N} = \frac{\Delta H^{\neq}_m}{T} - \Delta S^{\neq}_m \tag{5}$$

Figure 2 presents the function $R \cdot \ln(\eta \cdot V_m / h \cdot N) - 10^3/T$, out of which verification of equation (3) results.

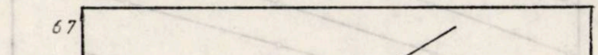

Fig. 2. — Checking the applicability of the Eyring equation (3).

In equations (3) and (5), respectively, calculate V_m from the density values, on applying for solutions the equation :

$$V_m = \rho^{-1} [M_{\text{EG}} + x_{\text{MeOH}}(M_{\text{MeOH}} - M_{\text{EG}})] \tag{6}$$

From the parameters of the straight lines and from equation (4), Table (4), including the values of the activation parameters from the Eyring's equation, has been drawn.

Table 4

Eyring parameters of activation of viscous flow

x_{EG}	$\Delta H^{\neq}_m$, kJ/mole	$\Delta S^{\neq}_m$, J/mole·K	$\Delta G^{\neq}_m$, kJ/mole
1	29.79	35.19	19.16
0.8901	28.03	31.91	18.39
0.8085	26.81	30.39	17.63
0.7227	32.45	21.09	17.08
0.7008	19.51	10.11	16.46

5. DETERMINATION OF THE POTENTIAL COMPOUND OF INTERNAL ENERGY

A liquid may be treated according to the following physical model: the molecules having their own volume, v_0, move in a free volume, v_f, in the field of potential energy created by the intermolecular forces. The potential energy is therefore an intrinsic value of the liquid, belonging to its internal energy and being expressed through its potential compound $(\partial U/\partial V)_T$.

Glastone, Hirschfelder and other have established, for this compound, the following equation[6,7,8]:

$$(\partial U/\partial V)_T = (\alpha \cdot R \cdot T/(V_m^{2/3} \cdot V_{mf}^{1/3}) \tag{7}$$

$$\alpha = \frac{\sigma^3}{v}\,[(3v_f/4 \cdot \pi \cdot \sigma^3)^{1/3} + 1]^3 \tag{8}$$

$$v_f = v - v_0 = M/(\rho \cdot N) - \pi \cdot \sigma^3/6 \tag{9}$$

$$v_{mf} = V_m - v_0 \cdot N \tag{10}$$

In these equations, α represents the packing degree of molecules, while σ = molecular diameter. In the case of MeOH, $\sigma = 3.76$ A°, while for EG, $\sigma = 4.41$ A⁰. [9,10]

On applying the data of solution densities $V_m = M/\rho$ and the set of equations 7—10, the value of the potential compound of the internal energy has been calculated (see Table 5):

Table 5

Values of $10^6 \cdot (\partial U_m/\partial V_m)_T$, J·mole/m³; $t = 29$°C

x_{EG}	1	0.8901	0.8085	0.7227	0.7008
$(\partial U_m/\partial V_m)_T$	—	262	234	210	199

6. CONCLUSIONS

The values η and E_{vis}, as well as Eyring's activation parameters of viscous flow are numerically determined by the intensity of the intermolecular forces. In the EG-MeOH system, there also appear additional hydrogen bonds, whose number depends upon the concentration of the HO$^-$ groups; this explains the decrease of viscosity and of E_{vis} with increasing the concentration of MeOH, and also the positive and relatively high values of $\Delta H_m^{\ddagger}$ and $\Delta S_m^{\ddagger}$, as compared with solutions among whose compounds such links do not appear. As to $\Delta G_m^{\ddagger}$, it varies much slower with decreasing the concentration of the HO$^-$ groups, showing values comparable to those of the solutions having molecules that cannot be associated through hydrogen links. This is explained by the fact (that the entropy variation being positive, the influence of the hydrogen bonds upon the entropy and enthalpy variation is reciprocally compensated, in the Gibbs equation of free activation energy. To the same effect that is, formation of hydrogen bonds) there pleads the high value of the potential compound of the internal energy, met with the solutions considered, as well as its decrease with decreasing the concentration of the HO$^-$ groups. With the values of concentration and temperature employed, the Guzmán-Andrade and Eyring equations are being satisfied.

REFERENCES

[1] Landolt-Börnstein, "Eigenschaften der Materie in ihren Aggregatzuständen",5.Teil, Bandteil a, Transportphänomenen I (Viscosität und Diffusion), Springer-Verlag, Berlin-Heidelberg-New York, 1969.

[2] J. De Guzmán, *Anales Soc. Esp. Fiz. Quim.*, **11**, 353 (1913).

[3] E. N. De C. Andrade, *Phil. Mag.*, **17**, 497, 1934.

[4] H. Eyring, *J. Chem. Phys.*, **4**, 283 (1936).

[5] H. Eyring and R. H. Ewell, *J. Chem. Phys.*, **5**, 726 (1937).

[6] S. Glastone, "Theoretical Chemistry", Van Nostrand, Princeton 1966.

[7] J. O. Hirschfelder, C. F. Curtis, and R. B. Bird, "Molecular Theory of Gases and Liquids", John Wiley, New York 1954.

[8] M. Diaz and A. Roig, "Quimica Fisica", Ed. Alhambra, Madrid 1975.

[9] K. P. Michenko, Kratkij spravocinik fiziko-himiceskih velicin", Izd. Himia, Leningrad 1967.

[10] O. Bastiansen, *Acta Chimica Scandinavica*, **2**, 415 (1949).

Revue Roumaine de Chimie, **36**, *11–12*, 1409–1424 (1991)

As(III) – HCl – H_2O SYSTEM. IV*

THE LIQUID–VAPOUR STATE

O. RADU

Institute for Research and Production of Semiconductors, Sos. Gării Cățelu No. 5, Sector 3, Bucharest, Romania

Received March 14, 1989

The liquid – vapour state of As(III) – HCl – H_2O system formed by dissolution of As_2O_3 in HCl solutions is studied. The experiments consisted of drawing distillation curves which represent the plots of elemental concentrations in the distillate versus its volume. Some important regularities in the behaviour of the system are thus evidenced. Extrapolation of some of these curves to zero volume supplies information regarding the values of elemental concentrations in vapour at equilibrium. Adequate interpretation of these values has been facilitated by introducing the notions of conventional vapour system, the condition of azeotrope and the deviation from it. Thus it has become possible to calculate molecular composition of phases and evidence the azeotropic and quasi-azeotropic behaviour. Then the inter-phase equilibrium equations and diagrams and the coefficient of activity were defined with respect to the initial standard state. The independence of vapour composition of the liquid phase composition over a wide concentration range has suggested the hypothesis of an interaction between $AsCl_3$ and HCl in vapour phase which was confirmed by modelling a direct relation between phase compositions.

The procedure employed in this study was exposed in three previous notes [1,2,3]; it consists of establishing relations between the initial state (the known values of two parameters which define the interaction of sytem forming) and the final state (the parameters of the equilibrium state of the system formed); these relations assume that inter-phase equilibria are determined only chemically. The inter-phase liquid-vapour state at boiling temperature (110°C) has not been studied so far except in some contributions of technological interest.[4,5]

1. THE METHOD OF STUDY

1.1. Distillation curves

In the following one understands by distillation curves the variation of distillate composition versus its volume : they are obtained from a discontinuous fractional distillation in which several fractions of small and very small volume are collected and their elemental concentrations (chlorine, arsenic) are determined. The variations of concentrations in the distillate with its volume are found after adding up each fraction to the sum of the previous fractions. Summing up of non-additive volumes of distillate fractions is achieved by substituting them with the volumes of the initial corresponding states according to the relations between the states. [1] The volumes of fractions are non-additive because they originate in different phasic states and are of different concentrations; each fraction is characterized separately. The characterization of a certain distillate fraction d_i, is ensured by additive composition parameters $n_{Cl(d_i)}$ and $n_{As(d_i)}$ and non-additive volumes $V_{(d_i)}$. Fractional distillation of a final homogeneous state, characterized by n_{Cl}, n_{As}, V_s, yields, after complete transfer of liquid phase into the distillate, i fractions and a residuum. The final volume of the distillate (V_d) being approximately equal to that of initial solution, the material balance is:

---

* Part III is ref. 3.

$$V_d \simeq V_s$$

$$\sum_{1}^{i} n_{As(d_i)} + \sum_{1}^{i} n_{As(rez)} = n_{As}$$

$$\sum_{1}^{i} n_{Cl(d_i)} + \sum_{1}^{i} n_{Cl(rez)} = n_{Cl}$$

The coordinate system takes account of the balance relations. Thus the increasing volumes of distillate are expressed as dimensionless fractions of solution volume.

$$Y_{V(d)} = V_{d_i}/V_s$$

The distillate composition is expressed in two ways: 1) non-dimensionally, as fractions of total chlorine and arsenic transferred into the distillate after collecting i of its fractions:

$$Y_{Cl(d)} = \frac{\sum_{1}^{i} n_{Cl(d_i)}}{n_{Cl}} \qquad Y_{As(d)} = \frac{\sum_{1}^{i} n_{As(d_i)}}{n_{As}}$$

2) dimensionally, in terms of elemental concentration in distillate, $C_{Cl(d)}$ and $C_{As(d)}$, after collecting i fractions of distillate.

1.2. Determination of elemental composition of vapour phase

Extrapolation of semi-dimensional distillation curves $C_{Cl,As(d)} = f[Y_{V(d)}]$ to the point $Y_{V(d)} = 0$ (the method of zero point) yields the values $C_{Cl(v)}$ and $C_{As(v)}$ which express the elemental concentrations of vapour at equilibrium with liquid phase. To adequately exploit these values they are regarded as elemental composition of a conventional system which is assumed isolated from the real one, condensed, without loss and at equilibrium in standard conditions. Thus, the conventional homogeneous or two-phase systems of vapours may be characterized by the equations previously presented.[1,2,3] The conventional liquid-liquid system are assumed ideally homogenized i.e. similar to homogeneous state. The conventional system of vapour may not be compared to liquid phase in any conditions because its volume is not measurable; however the molecular concentrations of the two phases may be correctly expressed as mole fractions by assigning the conventional system an arbitrary volume.

1.3. The condition of azeotropy and the deviation from it

It is admitted that a standard initial state behaves azeotropically when the equations of distillation curves are linear, as follows:

$$\frac{Y_{As(d)}}{Y_{V(d)}} = \frac{C_{As(d)}}{C_{As}} = 1$$

$$\frac{Y_{Cl(d)}}{Y_{V(d)}} = \frac{C_{Cl(d)}}{C_{Cl}} = 1 \qquad \text{IV}-1$$

The deviation from unity of the ratio of these values over any value of $Y_{V(d)}$ determines the quasi-azeotropic behaviour of the initial state in question. The deviation from azeotropy at equilibrium is defined as the deviation from unity of the value of these ratios at $Y_{V(d)} = 0$:

$$A_{As} = \frac{C_{As(v)}}{C_{As}} \qquad A_{Cl} = \frac{C_{Cl(v)}}{C_{Cl}} \qquad \text{IV}-2$$

2. EXPERIMENTAL

Sets of determinations were carried out by discontinuous fractional distillations with collection and characterization of many small volume fractions. A still made of silica, glass and teflon of 1 TT efficiency allows the maintaining under total reflux to reach the stationary regime and fractional distillation with collecting of small and very small volume samples accurately determined in burette-type graduated test tubes.

Controlled transition methods in homogeneous phase [2,3] were employed in elemental characterization of two-phase fractions. The validity of distillation curve is confirmed by the material balance.

Sets of distillation curves were drawn in the range $C_{HCl} \geqslant 6$ and $2 \leqslant R \leqslant 12$ and mostly in the range $C_{HCl} \geqslant 7.5$ over which quasi-azeotropic behaviour was noted. Figs. IV—1. . . IV—4 show some of the determinations at $C_{HCl} = 8.9$. Chlorine semi-dimensional distillation curves are not shown because their correct extrapolation to zero was not possible. However correct values of $C_{Cl(v)}$ were obtained by extrapolation of $R_d = f[Y_{i(d)}]$ curves (Figs. IV—5 and IV—6).

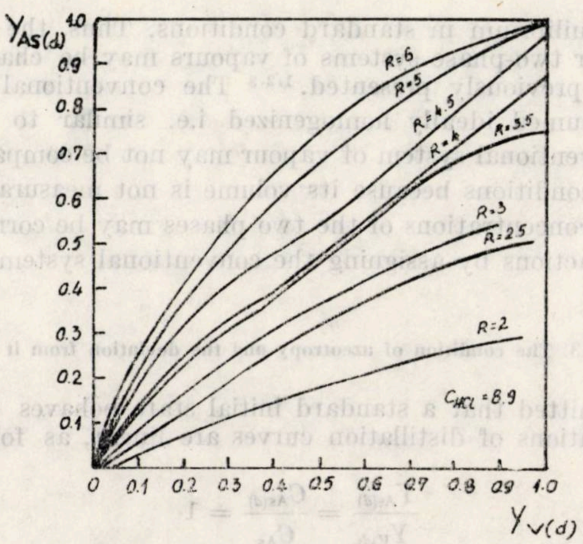

Fig. IV — 1. — Distillation curves of arsenic in dimensionless coordinates valid over the whole range $C_{HCl} > 7.5$.

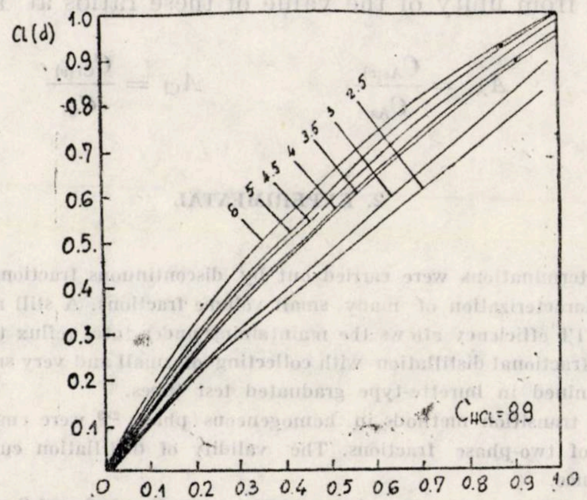

Fig. IV—2. — Distillation curves of chlorine in dimensional coordinates valid over the whole range $C_{HCl} > 7.5$.

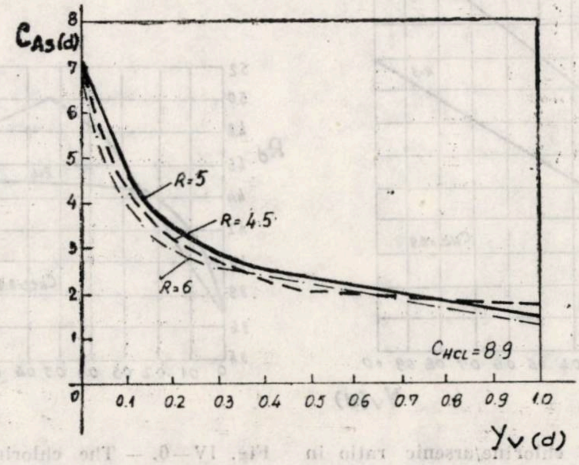

Fig. IV—3. — Distillation curves of arsenic in semi-dimensional coordinates extrapolated (in $C_{As(v)} = f(C_{HCl})$ domain).

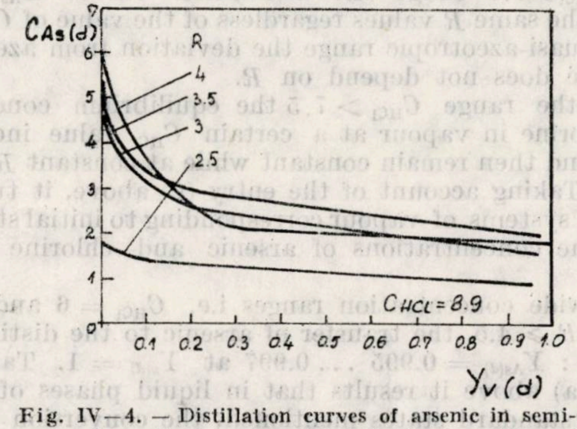

Fig. IV—4. — Distillation curves of arsenic in semi-dimensional coordinates extrapolated (in $C_{As(v)} = f(C_{HCl}, R)$ domain).

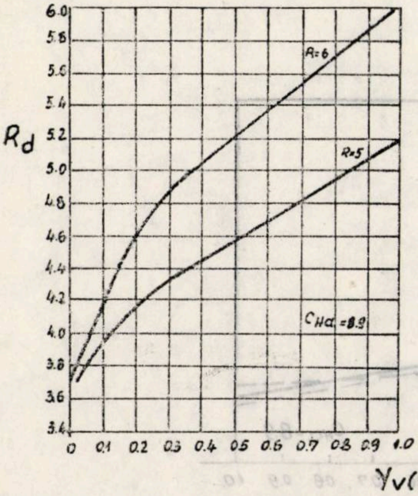

Fig. IV – 5. – The chlorine/arsenic ratio in distillate (R_d) versus the distilled volume fraction.

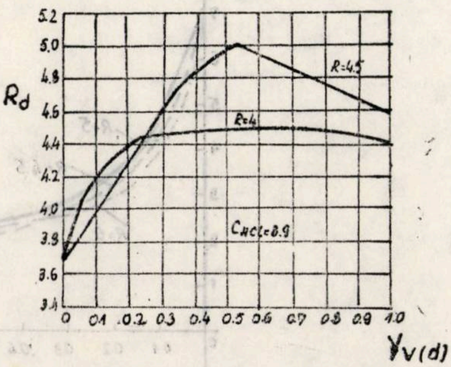

Fig. IV – 6. – The chlorine/arsenic ratio in distillate versus the distilled volume fraction.

3. RESULTS AND INTERPRETATION

The comprehensive examination of extrapolated sets of dimensionless and semi-dimensional distillation curves reveals some significant regularities :

(a) The R_d ratio is always larger than three even if in initial state R <3. It results that arsenic passes into vapour state only as $AsCl_3$ accompanied by free HCl and water.

(b) The initial state $C_{HCl} = 6.1$ and $R = 6.05$ exhibits an azeotropic behaviour and the states in $C_{HCl} > 7.5$ range are quasi-azeotropic.

(c) In $C_{HCl} > 7.5$ range the distillation curves $Y_{As,Cl(d)} = f[Y_{v(d)}]$ are identical at the same R values regardless of the value of C_{HCl}. It results that over the quasi-azeotropic range the deviation from azeotropic behaviour of arsenic does not depend on R.

(d) Over the range $C_{HCl} > 7.5$ the equilibrium concentrations of arsenic and chlorine in vapour at a certain C_{HCl} value increase with R up to $R \simeq 4.5$ and then remain constant while at constant R they increase with C_{HCl}. Taking account of the entry (c) above, it turns out that in conventional systems of vapour corresponding to initial states $C_{HCl} \geqslant 7.5$ and R $\geqslant 4.5$ the concentrations of arsenic and chlorine depend only on C_{HCl}.

(e) Over wide concentration ranges i.e. $C_{HCl} = 6$ and $R \geqslant 6$ and $C_{HCl} \geqslant 7.5$ and $R \geqslant 4.5$, the transfer of arsenic to the distillate is practically complete : $Y_{As(d)} = 0.995 \ldots 0.997$ at $Y_{v(d)} = 1$. Taking account of the finding (a) above it results that in liquid phases of the systems with the initial standard states mentioned, the conversion of arsenic to $AsCl_3$ is total at boiling temperature : $X^{x}_{AsCl_3(f)} = 0.997$. Thus the minimum values of atomic ratio Cl/As needed in total specific conversion of arsenic at boiling temperature R_{xf} for a wide range of initial states are obtained :

C_{HCl}	R_{xf}
6	6
$\geqslant 7.5$	4.5

Hence it also results the extent of concentration range where standard initial multicomponent states (5 to 9 molecular species) become ternary at boiling temperature ($AsCl_3 + HCl + H_2O$) :

C_{HCl}	R
6 . . . . . .7.5	6 . . . .4.5
$\geqslant 7.5$	$\geqslant 4.5$

(f) The initial states generate, at the total conversion above, conventional liquid — liquid systems in which C'_{HCl} takes the maximum standard value, the solubility of $AsCl_3$ is minimum and the hydrochloric phase has constant composition [3] such that the increase of C_{HCl} is sensed only through the increase of $AsCl_3$ phase volume.

(g) The initial states at non-total conversion generate homogeneous conventional systems whose composition is constant and related to the standard solubility of $AsCl_3$.

(h) The increase of R in initial states entails the progressive concentration of $AsCl_3$ in vapour which causes the homogeneous → liquid-liquid transition to occur in their conventional systems. A relationship was established between the value of $R'_{lim}{}^3$ of this conventional transition and the value of $R_{lim}{}^2$ for liquid →solid-liquid transition in the corresponding real system.

4. THE COMPOSITION OF PHASES

4.1. Molar concentrations in conventional systems of initial state vapour $C_{HCl} \geqslant 7.5$

The previous findings for conventional vapour systems suggest the following equation :

$$C^*_{As(v)} = f(C_{HCl}) \qquad R \geqslant R_{xf} \qquad \text{IV}-3$$

Because $C_{As} = RC_{Cl}$ and $C_{Cl} = C^*_{Cl}$ provided that $R \leqslant 8^1$ and making use of eqs. IV—2 and IV—3 one may write :

$$A_{As} = \frac{C^*_{As(v)}}{C^*_{Cl}} R \qquad \text{IV}-4$$

The constant value of concentration ratio is calculated from the data obtained for the states $C_{HCl} = 8.9$. Thus one obtains the equation of linear variation of the deviation from azeotropy of arsenic :

$$A_{As} = 0.8426\, R \qquad R \geqslant 4.5 \qquad \text{IV}-5$$

The relations between the states [1] and eqs. IV–4 and IV–5 yield the equation of constant arsenic concentration in terms of the initial state :

$$C^*_{\mathrm{As}} = 0.8426 \quad C^*_{\mathrm{Cl}} = 0.8426\,(a_1 C_{\mathrm{HCl}} + b_1) \qquad \mathrm{IV{-}6}$$

$$R \geqslant 4.5$$

The R-dependent arsenic concentration in the range of non-total conversion, over which the deviation from azeotropy is a non-linear function of R, results from the equation :

$$C_{\mathrm{As}(v)} = A_{\mathrm{As}} \frac{C^*_{\mathrm{Cl}(v)}}{R} = A_{\mathrm{As}} \frac{a_1 C_{\mathrm{HCl}} + b_1}{R} \qquad \mathrm{IV{-}7}$$

$$R < 4.5$$

In conventional liquid-liquid systems eqn. III–13[3] holds true ; assuming that $V_e = 1$ litre and $C_{\mathrm{Cl}} = C_{\mathrm{As}} R$, the following equation is obtained :

$$C'_{\mathrm{HCl}(v)} = \frac{C_{\mathrm{As}(v)}(R_v - 3)}{1 - 0.0843\, C_{\mathrm{As}(v)}} \qquad \mathrm{IV{-}8}$$

which is a ratio of the conventional number of chlorine atoms over the conventional volume of the acid at dissolution. The equation is employed in calculation of R^*_v in the range of constant concentration in which $C'_{\mathrm{HCl}} = \text{maximum} = 12.7$:

$$R^*_v = \frac{12.7(1 - 0.0843\, C^*_{\mathrm{As}(v)})}{C^*_{\mathrm{As}(v)}} + 3 \qquad \mathrm{IV{-}9}$$

$$R \geqslant 4.5$$

Utilization of eqn. IV–9 allows the obtention of a simple expression for R^*_v in terms of the initial state :

$$R^*_v = \frac{15.07}{C^*_{\mathrm{Cl}}} + 1.93 = \frac{15.07}{a_1 C_{\mathrm{HCl}} + b_1} + 1.93 \qquad \mathrm{IV{-}10}$$

$$R \geqslant 4.5$$

Hence it results that for constant chlorine concentration in the conventional system :

$$C^*_{\mathrm{Cl}(v)} = 1.93\, C^*_{\mathrm{As}(v)} + 12.7 \qquad \mathrm{IV{-}11}$$

$$R \geqslant 4.5$$

in which the terms of real states, the initial ones included, take the form :

$$C^*_{\mathrm{Cl}(v)} = 1.626\, C^*_{\mathrm{Cl}} + 12.7 = 1.626\,(a_1 C_{\mathrm{HCl}} + b_1) + 12.7 \qquad \mathrm{IV{-}12}$$

$$R \geqslant 4.5$$

The R-dependent chlorine concentration two-phase solid-liquid systems of final states at non-total conversion and constant R_v is :

$$C_{\mathrm{Cl}(v)} = A_{\mathrm{As}} \frac{1.93 C^*_{\mathrm{Cl}} + 15.07}{R} = A_{\mathrm{As}} \frac{1.93\,(a_1 C_{\mathrm{HCl}} + b_1) + 15.07}{R} \qquad \text{IV}-13$$

Because the only molecular species of As(III) in vapour is $\mathrm{AsCl_3}$, eqs. IV—6 or IV—7 and IV—12 or IV—13 allow calculation of molecular concentrations in the vapour of initial states with $C_{\mathrm{HCl}} \geqslant 7.5$ by making use of the equations :

$$C_{\mathrm{AsCl_3}(v)} = C_{\mathrm{As}(v)} \qquad \text{IV}-14$$

$$C_{\mathrm{HCl}(1,v)} = C_{\mathrm{Cl}(v)} - 3\,C_{\mathrm{As}(v)} \qquad \text{IV}-15$$

4.2. Molar concentrations in liquid phase

On the basis of the foregoing one may write the equation of nonspecific conversion of As(III) to $\mathrm{AsCl_3}$ similarly with the conversion in standard conditions ^{1} :

$$X'_{\mathrm{AsCl_3}(f)} = \frac{X^x_{\mathrm{AsCl_3}(f)}}{R_{xf}}\,R$$

where $X^x_{\mathrm{AsCl_3}(f)}$ is the total specific conversion = 0.997, $R_{xf} = 4.5$ in the $C_{\mathrm{HCl}} > 7.5$ range and $R_{xf} = 6.05$ for $C_{\mathrm{HCl}} \leqslant 6.1$.

Hence the equations for linear variation of the degree of nonspecific conversion in quasi-azeotropic and azeotropic state results :

$$X'_{\mathrm{AsCl_3}(f)} = 0.2216\,R \text{ quasi-azeotropic } C_{\mathrm{HCl}} > 7.5 \;\; R < 4.5 \qquad \text{IV}-16$$

$$X'_{\mathrm{AsCl_3}(f)} = 0.1648\,R \text{ azeotropic } C_{\mathrm{HCl}} = 6.1 \;\; R < 6.05 \qquad \text{IV}-17$$

The data obtained afford the deduction of the relations for elemental and molecular concentrations listed in the following table :

Concentration	The relation over $R \leqslant R_{xf}$ range	The relation over $R \geqslant R_{xf}$ range
$C_{\mathrm{Cl}(f)}$	$\dfrac{R_{xf} C_{\mathrm{HCl}}}{R_{xf} + 0.0488\, C_{\mathrm{HCl}}}$	$\dfrac{R C_{\mathrm{HCl}}}{R + 0.0488\, C_{\mathrm{HCl}}}$
$C_{\mathrm{As}(f)}$	$\dfrac{1}{R}\,\dfrac{R_{xf} C_{\mathrm{HCl}}}{R_{xf} + 0.0488\, C_{\mathrm{HCl}}}$	$\dfrac{C_{\mathrm{HCl}}}{R + 0.0488\, C_{\mathrm{HCl}}}$
$C_{\mathrm{AsCl_3}(f)}$	$\dfrac{0.997\, C_{\mathrm{HCl}}}{R_{xf} + 0.0488\, C_{\mathrm{HCl}}}$	$\dfrac{0.997\, C_{\mathrm{HCl}}}{R + 0.0488\, C_{\mathrm{HCl}}}$
$C_{\mathrm{HCl}(1,f)}$		$\dfrac{C_{\mathrm{HCl}}}{R + 0.0488\, C_{\mathrm{HCl}}}(R - 2.991)$

IV—18

4.3. Molar fractions in vapour at equilibrium

The molar fractions in vapour at equilibrium with liquid phase as a function of mole concentration in mole/litre in the conventional system may be deduced by assigning the conventional system an arbitrary volume equal to unity.:

(a) homogeneous conventional system

$$y_{AsCl_3} = \frac{C_{As(v)}}{49.60 - 0.5\,C_{As(v)}} \qquad \text{IV}-19$$

$$y_{HCl(1)} = \frac{11.78 - 3\,C_{As(v)}}{49.60 - 0.5\,C_{As(v)}} \qquad \text{IV}-20$$

b) Liquid-liquid conventional system in $R < 4.5$ range

$$y_{AsCl_3} = \frac{C_{As(v)}}{C_{As(v)}(R_v^* - 2) + n_{H_2O}} \qquad \text{IV}-21$$

$$y_{HCl(1)} = y_{AsCl_3}(R_v^* - 3) \qquad \text{IV}-22$$

(c) Liquid-liquid conventional system in $R \geqslant 4.5$ range

$$y_{AsCl_3} = \frac{C^*_{As(v)}}{C^x_{As(v)}(R_v^* - 2) + n_{H_2O}} \qquad \text{IV}-23$$

$$y_{HCl(1)} = y_{AsCl_3}(R_v^* - 3) \qquad \text{IV}-24$$

4.4. Molar fractions in liquid phase at equilibrium

Converting the concentrations expressed as mole/liter into mole fractions involves the density of hydrochloric acid (d_{HCl}) corresponding to C_{HCl}.

(1) In the $R < 4.5$ range:

$$x_{AsCl_3} = \frac{C_{HCl}/4.5}{55.49 d_{HCl} - 1.13 C_{HCl}} \qquad \text{IV}-25$$

Over this range of non-total conversion the liquid phase is multicomponent containing besides HCl (1), $As(OH)_3$, $As(OH)_2Cl$ and also $As(OH)Cl_2$ whose concentrations may not be determined[1].

(2) In the $R \geqslant 4.5$ range:

$$x_{AsCl_3} = \frac{C_{HCl}/R}{55.49 d_{HCl} - C_{HCl}\left(\dfrac{0.5}{R} + 1.02\right)} \qquad \text{IV}-26$$

$$x_{HCl(1)} = x_{AsCl_3}(R - 3) \qquad \text{IV}-27$$

5. LIQUID – VAPOUR EQUILIBRIUM

The relations for phase composition at equilibrium in terms of mole fraction have allowed calculation of the equations of inter-phase equilibrium as a function of the initial state for various degrees of conversion in liquid phase and different inter-phase nature of vapour conventional state. A set of six equations has thus resulted for the inter-phase equilibrium of arsenic trichloride and a set of three equations for free hydrochloric acid. The liquid-vapour inter-phase equilibrium diagrams at 110°C as a function of the initial state (R and C_{HCl}) obtained by graphical transposition of the two sets of nine equations are plotted in Figs. IV—7 and IV—8.

The expressions for calculation of phase composition at equilibrium in terms of mole fraction were used in calculation of the activity

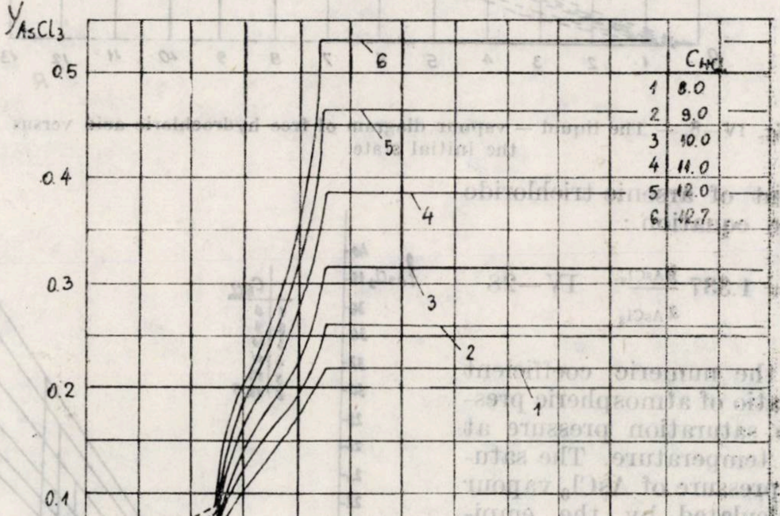

Fig. IV—7. — The liquid — vapour equilibrium diagram of arsenic trichloride versus the initial state.

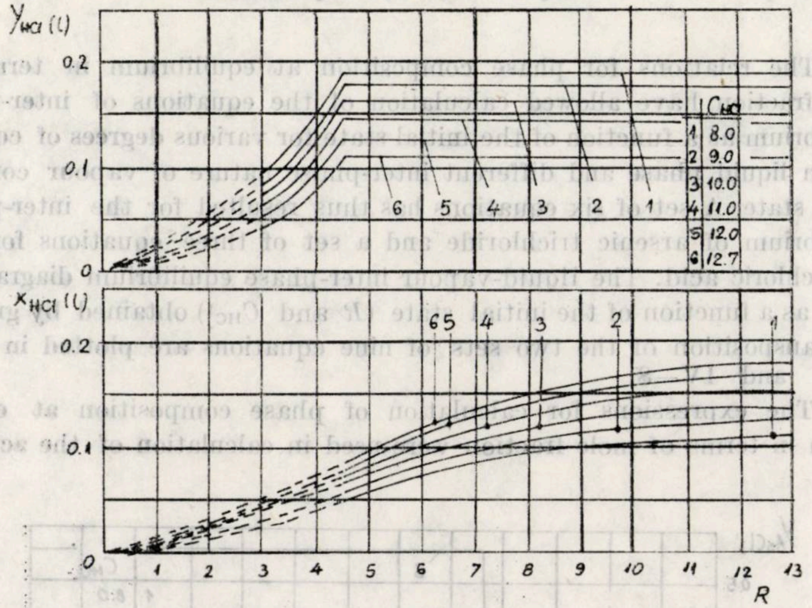

Fig. IV—8. — The liquid — vapour diagram of free hydrochloric acid versus the initial state.

coefficient of arsenic trichloride by the equation :

$$f_{\mathrm{AsCl_3}} = 1.337 \frac{y_{\mathrm{AsCl_3}}}{x_{\mathrm{AsCl_3}}} \qquad \text{IV}-28$$

where the numeric coefficient is the ratio of atmospheric pressure to saturation pressure at boiling temperature. The saturation pressure of AsCl$_3$ vapour was calculated by the empirical equation [6] :

$$\log p^0_{\mathrm{AsCl_3}} = -\frac{2,660}{T} + 24.76 - 5.83\,T$$

Fig. IV—9 shows the variation of the activity coefficient of AsCl$_3$ versus the initial state. Large positive deviations from the Raoult law are evidenced which increase with C_{HCl} and increase linearly with R.

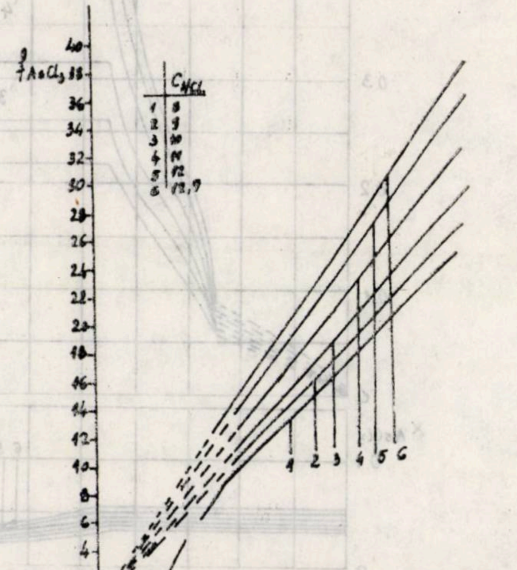

Fig. IV—9. — The activity coefficient of arsenic trichloride versus the initial state.

6. DISCUSSION

It is unusual and significant about liquid-vapour inter-phase equilibrium that the composition of vapour is apparently independent of the composition of liquid phase in ternary states in which arsenic exists only as trichloride. Such a behaviour may be accounted for in terms of an interaction between components. One may assume that chemical interactions are not restricted to total conversion of arsenic to trichloride; most probable they would consist of $AsCl_3 + HCl$ with formation of an $xAsCl_3 \cdot yHCl$-type compound or else $(AsCl_x)H_{x-3}$ ($x \geqslant 4$). Thus, at constant temperature the mole fraction of newly formed compound would depend on mole fraction of components attending the interaction.

The practically linear variation of the activity coefficient with R might be a measure of the interaction. The general equation of straight lines passing through the origin is:

$$f_{AsCl_3} = k_{HCl}R \quad C_{HCl} \geqslant 7.5 \quad R \geqslant 4.5 \qquad \text{IV}-29$$

k_{HCl} being a C_{HCl}-dependent constant.

It is very likely that the $HCl + AsCl_3$ interaction advances together with the increasing of the ratio of molar fractions of reactants:

$$R' = x_{HCl(1)}/x_{AsCl_3}$$

Because R' increases linearly with R it results that the molar ratio of components would be responsible for the linear increase of the activity coefficient. Expressing f_{AsCl_3} by eqn. IV—28 and R in terms of R' and multiplying both sides with x_{AsCl_3} yields a first direct relation between phases composition:

$$y_{AsCl_3} = k_x(x_{HCl(1)} - 3x_{AsCl_3}) \qquad \text{IV}-30$$

where $k_x = k_{HCl}/1.337$

The linear relation between f_{AsCl_3} and R' is confirmed as it gives constant values of y_{AsCl_3}; indeed provided that C_{HCl} is constant one gets:

$$x_{CHl(1)} + 3x_{AsCl_3} = x_{HCl} = \text{const.}$$

Since $x_{HCl} = 0.137$ at $C_{HCl} = 7.5$ one may state the condition of ternary system i.e. the condition of validity of eqn. IV—30:

$$x_{HCl(1)} + 3x_{AsCl_3} \geqslant 0.137$$
$$x_{HCl(1)}/x_{AsCl_3} \geqslant 1.5$$

The constant k_x depends on the sum in parentheses; eqn. IV—30 may be used without resorting to the parameters of initial state.

A similar reasoning might be employed to develop the interphase equilibrium equation for free hydrochloric acid:

$$y_{HCl(1)} = k'_x(X_{HCl(1)} + 3x_{AsCl_3}) \qquad \text{IV}-31$$

Fig. IV—10 shows the liquid-vapour inter-phase equilibrium diagram of ternary systems as a direct relation between phase composition.

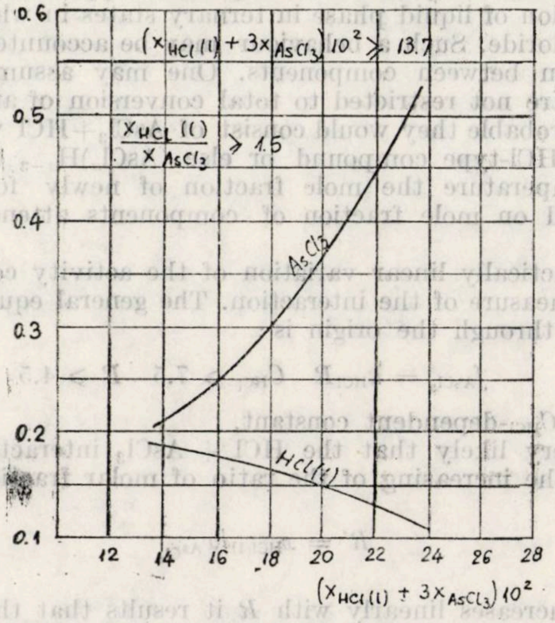

Fig. IV—10. — The liquid — vapour equilibrium diagram expressed through the direct relation between phase compositions for ternary molecular system at 110°C.

6. CONCLUSIONS

This note and the previous three [1,2,3] were devoted to As(III)—HCl—H_2O system which has been scarcely studied and in fact not defined as such; it is ionic, slightly dissociated, multicomponent, of unknown molecular composition, in multi-pole phase and possessing azeotropic and quasi-azeotropic properties.

Taking account of the exclusive chemical determination of the system its characterization has consisted of developing relations between the initial state (the parameters of system forming) and the final state (equilibrium parameters). Relations between states were also necessary in the homogeneous phase because of volume variations which were then the decisive element in establishing these relations. Asserting that arsenic trichloride is the only responsible for these variations has led to elucidation of molecular compositions. Detecting some physical factors that perturb standard inter-phase equilibria has imposed the introduction of the notion of stability limit of homogeneous phase. In the study of liquid-vapour phase use has been made of distillation curves representing the variation of distillate composition versus its volume and of their extrapolation. The full checking of these curves has required introduction of the notions of conventional vapour system, the conditions of azeotropy and deviations from them. Thus, it was possible to establish :

(1) the molecular composition of phases, the equations (diagrams) of inter-phase equilibria and the transitions between them ;

(2) the domain of stability, the concentration and stability of $AsCl_3$;

(3) the solubility of $AsCl_3$;

(4) the unique azeotropic composition, the domain of quasi-azeotropic concentrations and the variation of activity coefficient of arsenic trichloride in this domain.

The hypothesis was advanced of a HCl + $AsCl_3$ interaction which accounts for the large linear deviations from the Raoult law and consequently for quasi-azeotropic behaviour ; the satisfactory behaviour of the hypothesis has led to a direct relationship between the liquid and vapour phase. Thus some basic theoretical aspects of the system formed on dissolution of As_2O_3 or $AsCl_3$ in hydrochloric acid solutions (a system with wide technological applications) were elucidated.

LIST OF SYMBOLS

$n_{As(d)}$, $n_{Cl(d)}$ = number of gram atoms of arsenic and chlorine respectively in the distillate
V_s = the volume of initial solution (litres)
V_d = the volume of the distillate (litres)
$Y_{v(d)}$ = the fraction of total volume transferred to the distillate
$Y_{As(d)}$, $Y_{Cl(d)}$ = the fraction of the total number of gram atoms of arsenic and chlorine, respectively, transferred to the distillate
$C_{As(v)}$, $C_{Cl(v)}$ = the concentration of arsenic and chlorine, respectively, in the conventional vapour system (gram atoms per litre)
$C_{As(d)}$, $C_{Cl(d)}$, R_d = concentrations and molar ratios in the distillate
A_{As}, A_{Cl} = the deviation from the azeotropy of arsenic and chlorine, respectively
$C^*_{As(v)}$, $C^*_{Cl(v)}$, $R^*_{(v)}$ = concentrations and molar ratios independent of R in the conventional vapour system
R_{xf} = minimum R value needed for total conversion of $AsCl_3$ in liquid phase at boiling temperature
$C^{A}{}_{sCl_3(v)}$ = molar concentration of $AsCl_3$ in vapour
$C_{HCl(1)}$, $C_{HCl(1,v)}$ = molar concentration of free hydrochloric acid in aqueous phase and vapour, respectively
x_{AsCl_3}, y_{AsCl_3} = molar fractions of $AsCl_3$ in liquid and vapour, respectively
$x_{HCl(1)}$, $y_{HCl(1)}$ = same for free HCl
f_{AsCl_3} = activity coefficient of $AsCl_3$
k_{HCl}, k_x, k'_x = C_{HCl} — dependent constants

See also parts I—III of this paper [1,2,3]

REFERENCES

[1] O. Radu, *Rev. Roumaine Chim.*, **33**, 585 (1988).
[2] O. Radu and C. Gheorghiu, *Rev. Roumaine Chim.*, **33**, 677 (1988).
[3] O. Radu and C. Gheorghiu, *Rev. Roumaine Chim.*, **36**, 43 (1991).
[4] V. V. Krapuhin and I. A. Sokolov, *Isv. Vissh. Uceb. Zaved. Tsved. Met.*, **13**, 140 (1970).
[5] V. V. Krapuhin and I. A. Sokolov, *Isv. Vissh. Uceb. Zaved. Tsved. Met.*, **14**, 84 (1971).
[6] C. J. Smithels, "Metals Reference Book", p. 616, 1962.

Revue Roumaine de Chimie, **36**, *11–12*, 1425–1437 (1991)

PROGRESS OF STATISTICS APPLIED TO SYNTHETIC POLYMERS LATEXES

TH. DELEANU

Central Institute of Chemistry, Department of Research of Plastics, Splaiul Independentei 202, Bucharest, Romania

Received October 2, 1989

The suggestion of using two statitical indices to synthetic polymers latexes is fundamented. One of them refers to the Wilcoxon test. It helps to check the previously calculated distribution and the experimentally found hystogram adequacy. The analysed hystogram refers to the statistic distribution of the studied latex particles diameters. The comparison efficiency of the statistic indices is qualitatively discussed as well as the necessary orientation for the successful application of the Wilcoxon test. By using normal statistic distributions, the second statistic index, which refers to the informational energy of Onicescu, is examined. The importance of this informational energy was reported in a previous paper. These tests can be used to nonliniar regression, for which few experiments are available.

The preocupation to evaluate the copolymerization constants with an acceptable exactness aroused many controversies. The analysis of the physico-chemical properties or of the corresponding equations did not allow the obtention of the desired results. In a previous paper [1], this topic was approached from a general point of view, i.e., the mathematical analysis of regression. For the same purpose, different equations can be used, which obviously lead to different regression, even if the same adjusting parameters are used, particularly the same copolymerization constants. For the adequate choice of the regression, the use of two statistical indices was suggested. The former index envisages the evaluation of media displacements and the latter one tries to evaluate the exactness with which one can calculate some sums. The informational energy of Onicescu proves [2-4] to be the best value for this purpose. For instance, it is essential to know whether a certain sum contains one significant term or three of the six ones.

One can talk about the existence of a preliminary step in the adequate choice of the equations in order to effectively apply the statistical (ST) evaluations. Besides an analysis of errors, the regression analysis also implies a testing on the computer of the deviations behaviour at the simulation of different ST distributions of errors, similar to the experimental ones. The comparison of these simulations must be done by means of the same indices.

The Wilcoxon test (TW)[5] is the only one independent of the nature of probable distribution of errors and it can be applied to the small volume selections, too. Still, after more than three decades since this test has been known, there are no eloquent classes of examples regarding the successful use of TW in chemistry. Thus, an important class of such processes must be found (i), the reasons for which TW was generally avoided must be explained (ii) and one also has to show the way in which the normal objections against TW application can be overcome (iii).

Surprisingly, there are some differences not enough explained, regarding the use of TW tables from[6] and[7]. This fact represents a supplementary difficulty in applying TW. A means of avoiding this impediment had to be found, at least in this initial phase, referring to TW use in chemistry.

It is known that subsequent measurements of the same physicochemical characteristic, generally, have a normal distribution. But, generally, the extension of the supposition of the existing of a normal distribution to the deviations from a law, too, that is from a dependence between measured values is not justified. The current literature about experimental investigations evidences that, generally, the deviations are neither distributed independently of the value from the abscissa nor make up a bidimensional gaussian distribution. Therefore, in such cases the application of the Fisher and Student tests is hazardous. In two previous papers,[8,9] a way of avoiding this difficulty was suggested. The statistical straggling was supposed to originate from several causes which act independently. Each cause leads to a gaussian scattering of the deviations and one has to render evident the dominant cause. This way, the Fisher and Student tests are reconsidered for distributions that are not gaussian, too. The main element for the likelihood direction discussed in[9] in comparison with the classical one[5] takes into account the possibility that the increase of the deviations distributions function be no more necessary. In fact, this approach corresponds to the reality, because the deviations causes are not entirely objective. They also depend on the characteristics of the instrumentation used and on the way it is installed as well as on the possible human contribution if automatization is not complete. The easy access to high performance computers in the last few years suggests the resuming of some investigations, of TW type, neglected without justification. In the first part of the paper, TW application to the analysis of the hystograms of the synthetic polymers latex particles diameters is examined. This preocupation is a preliminary phase of TW application to regression. The second part of the paper analyzes the fundamenting of the importance of the use of informational energy. The element that unites the two endeavours envisages the common objective of using them to regression.

THE WILCOXON TEST

The distribution function is noted by $F(u)$

$$F(u) = \text{Prob}\ (v : v < u) = \int_{-\infty}^{u} P(w)\,\mathrm{d}w \tag{1}$$

$P(w)$ is the probability density. This value is positive or null. TW compares two distributions. In this case, a real finite distribution is compared with a fictitious distribution containig an infinity of events with the $F(u)$ distribution. The statistical hypothesis consists exactly in the adequate selection of the distribution function. This assumption represents a completion of the physico-chemical hypothesis regarding the wording of the law which could govern the phenomena observed. Here, u is the deviation from the physico-chemical law taken into consideration.

If no physico-chemical law is taken into consideration, u represents the measured value, whose scattering is to be studied. The use of infinite assemblies is avoided, considering a set of M_1 particles with $F(u)$ distribution where M_1 is supposedly very high. Equation (1) can be interpreted this way : $M_1F(u)$ stands for the number of deviations from the second set, which are smaler than the u deviations from the first set.

The values are defined

$$\bar{F} = (F(u_1) + F(u_2) + \ldots + F(u_N))/N \tag{2}$$

$$\Delta = \sqrt{12N}(\bar{F} - 1/2) \tag{3}$$

where N is the number of experiments and u_i represents the deviations from the accepted physico-chemical law. The TW test can be expressed in this case :

$$|\Delta| \leqslant D = u_{1-q} \tag{4}$$

where u_{1-q} is the inverse function of the $\Phi(D) = 1 - q$ normal integral distribution. This function can be found in the tables from the most usual ST books. If $1 - q = .5$, then $D = 0$. If $1 - q = .999$, then $D = 3$ represents a value that can be considered as infinite. Even $D = 2.4$ is a very high value.

Since the literature does not explicitely mention this form of the TW test, it was checked by an example.[10] One could observe the existence of a minimum degree of reliability $1 - q = .86$ for accepting a $F(u)$ distribution corresponding to a normal distribution. The Liliefors test is used in [10], which gives a minimum degree of reliability much below .8. Thus, the relative exigency of the TW test was proved once more.

With a view to apply TW to hystograms, a sample of polybutadiene emulsion was analysed, as an example, with particles of 580–2960 Å. The average diameter of the latex particles is of 2245 Å. The usual average was considered, which can be compared with the evaluations carried out by means of the surface tension.

Column 1 from table 1 gives the i index of the d_i diameter of the investigated latex particles from $d_i - d/2$ to $d_i + d/2$ ($d_i = id + e$). Column 2 indicates the N_i number of particles with the nominal diameter d_i. Here e represents the possible instrumental correction which must be carried out. Generally, this correction should be small. For estimating

Table 1

Size distribution of polybutadiene latex particles with sizes between 580 and 4960 Å

No. of diameter	No. of particle	No. of calc. particles	Sum of the no. of part.	Sum of the no. of calc. particle	Sum of column 2 × column 3	TW test $i-1$ line i line
1	2	3	4	5	6	7
2	12	8.3791	12	8.3791	50.2746	0
3	8	13.9950	20	22.3741	173.2874	−1.7467157
4	41	31.0879	61	53.462	1727.9275	1.7842546
5	30	35.204	91	88.666	3859.8475	−1.5836522
6	96	117.745	187	206.411	18023.544	−0.15411772
7	282	247.635	469	454.046	111147.98	2.2994999
8	177	185.104	646	639.15	207895.83	−1.5633142
9	63	71.0799	709	710.2299	250401.3	−0.40132179
10	28	27.305	737	737.5349	270670.01	0.9834348
11	22	19.9811	759	757.516	287115.57	0.21365502
12	16	17.4341	775	774.9501	299375.3	−0.47949732
13	20	17.9665	795	792.9166	315053.97	0.49926833
14	11	12.3809	806	805.2975	323844.15	−0.51229173
15	9	7.9187	815	813.2162	331127.46	0.46408021
16	3	4.4417	818	817.6579	333573.77	−0.65632833
17	7	5.7092	825	823.3671	339317.36	0.75363172
18	4	4.8365	829	828.2036	342620.5	−0.54554742
19	5	4.2882	834	832.4918	346772.24	0.44480516
20	2	2.7089	836	835.2007	348439.93	−0.4650099
21	3	2.1115	839	837.3122	350948.7	0.62669626
22	0	1.2965	839	838.6087	350948.7	−1.1409155
23	5	3.6551	844	842.2638	355150.88	1.0136898
24	2	2.9882	846	845.252	356838.4	−0.7513899
25	4	3.2469	850	848.4989	360225.9	0.61962647
26	2	2.7288	852	851.2277	361925.63	−0.5228167
27	4	3.3503	856	854.578	365337.24	0.49069771
28	2	2.3705	858	856.9485	367048.77	−0.34327961
29	2	2.0083	860	858.9568	368764.68	0.14651307
30	2	1.7043	862	860.6611	370484.3	−0.1449982

Column 2 represents the number of particles with the diameters from $d_i - d/2$ to $d_i + d/2$ of the latex particles ; $d = id + e$, when d is the space between two diameters donsidered ; the value at i is mentioned in the first column the same line.
Column 3 — number of particles calculated with diameters between $d_i - d/2$ and $d_i + d/2$.
Column 4 sums up column 2 in accordance with eq. (5).
Column 5 sums up column 3 in accordance with eq. (6).
Column 6 is calculated in accordance with eq. (15).
Column 7 applies the Wilcoxon test [4] to the censorized results, taking into consideration only the $i-1$ and i lines.
From column 7 the final conclusion can be drawn that there appears an exceeder of the acceptable statistical deviations between the measured values and the calculated ones. The computing was performed on a Felix 130 computer with 14 memories.

the $F(u)$ function, it is assumed that $u = d_i$, the diameter of the measured latex particle.

The question can be asked whether a certain calculation method of the probable scattering leads or not to an agreement with the experimentally found hystogram, i.e. with the values from columns 1 and 2. Column 3 comprises right these values, resulted from a certain computing method. For instance, for simplification, one can note by "3_i" the value from column 3, where the line is noted by i in column 1. Thus, $2_i = N_i$, that is this is the number of particles having the diameters in the interval mentioned above. There is going to be a scale-up factor, M, also obtained by computing, so that by definition

$$3_i = M(F(d_i) - F(d_{i-1}))$$

A first criterion of accepting the computing method has in view the relative closeness between the total number N of measured particles and the value of M scale-up factor, that is the computed number of particles resulted from the analysis of the hystogram. The following columns from table 1 result from the computing:

$$4_i = 4_{i-1} + 2_i = 2_1 + 2_2 + \ldots + 2_i \tag{5}$$

$$5_i = 5_{i-1} + 3_i = 3_1 + 3_2 + \ldots + 3_i \tag{6}$$

where m is the value of i from column 1 for the last line for which 2_i or 3_i are different from zero. In accordance with (5), the total number of measured particles will be equal to 4_m. Thus, the distribution function used is

$$F(d_i) = 5_i/5_m\ ;\ M = 5_m \tag{7}$$

At the first approximation, the equivalent of the sum from (2) multiplied by M is:

$$\sum_1^i M2_jF(d_j) = 6_i = 6_{i-1} + 2_i5_i = 2_15_1 + \ldots + 2_i5_i \tag{8}$$

If the corresponding experimental results for lines $j > i$ are censored, one can obtain from (2):

$$\bar{F} = 6_i/(4_i5_i) \tag{9}$$

If only the lines from i to j, inclusively, are used, $j > i$ and the other lines from table 1 are censorized, then the presumed equivalent of column 6 has contained in the last line the values:

$$X = 6_j - 6_{j-1} - (4 - 4_{i-1})5_{i-1} = \tag{10}$$

$$X = 3_i2_i + (3_i + 3_{i+1})2_{i+1} + \cdots + (3_i + 3_{i+1} + \cdots + 3_j)2_j \tag{11}$$

From the similarity of eq. (11) with eq. (8), one can conclude that this would have been the value to be noted in column 6 if the mentioned censorisation were used. In (10), the same value can be computed in a simpler way, using table 1 for uncensorised data. So that the value corresponding to eq. (9) for censorized data will be

$$\bar{F} = X/((4_j - 4_{i-1})(5_j - 5_{i-1})) \tag{12}$$

Eq. (8) is true only if 2_i is very small. This means that, generally, $2_i = 0$ and only from time to time $2_i = 1$. In the real cases, $F(d)$ is supposed to be a continuous function, that is :

$$MF(d_k) = 5_{i-1} + \int_0^{\lambda} (5_i - 5_{i-1})\mathrm{d}x\,;\ k = i - 1 + \lambda\,;\ 0 \leqslant \lambda \leqslant 1 \qquad (13)$$

It is also assumed that the 2_i particles are evenly distributed on the $(i - 1,\ i)$ interval and even "continuously". In this case :

$$6_k \quad 6_{i-1} + \int_0^{\lambda} MF(\mathrm{d}_{i-1+x})2_i\,\mathrm{d}x \qquad (14)$$

for $\lambda = 1$, one obtains :

$$6_i = 6_{i-1} + 5_{i-1}2_i + 3_i 2_i/2 \qquad (15)$$

If eq. (15) is used instead of eq. (8), then only (11) changes its shape. But eq. (11) is not going to be used to numerical calculation. Column 7 from table 1 presents the Δ values computed from (3), using only the $i-1$ and i lines ; the other lines are considered censorized. One can evaluate exactly the fields in which the computing method used is wrong. The systematic charater of these values from column 7, obtained at many hystograms, points to the existing error of method for the computing of the $F(u)$ distribution function. The values from column 7 should have a gaussian distribution and it should not be dependent on the value of i. Thus, for a correctly computed $F(u)$ distribution, the results from column 7 should be statistically analysed and they should give values within acceptable limits. If only the Δ values, without censorship were mentioned, the results would be excellent, even if the hi-square test indicates obviously unacceptable values. The hi-square test is concludent only if the events distribution is approximately even on all the degrees of freedom and their number^5 is higher than 15–20. The difficulty to satisfy these conditions was one of the reasons for which TW was used.

The example from Table 1 explains the very general meaning of the following sentence, mentioned in every statistics book : the positive answer to statistic test means, *ad literam*, that the statistic hypothesis is not contradicted by the respective set of events. This does not imply that the respective statistical hypothesis *should be accepted as plausible.* Only one fact in favour of thesis is generally far from representing a proof. Hence, the requirement of using a relatively high number of statistical tests results. The importance of TW lies exactly in its very high flexibility. Each value from column 7 (Table 1) represents a TW test. The mentioned relations allow a natural increase of the number of these tests. The overall statistical tests, like the hi-square test, can only give one value — these tests cannot be used at censorized results. Just like in the case of arguments in favour of a thesis, their "power" has importance. The numerical values of the power of the statistic tests are not listed in the way the acceptabe values are, on the basis of certain level of confidence. It is known that the positive answer to the TW test has a relatively low power. But the negative answer to the mentioned test has a very high power. So that will be less negative answers required by this test in order to accept the opposite hypothesis as plausible, i.e., in these cases, that $F(u)$ computed by the method used for column 3 from Table 1 is not acceptable.

It is known that the TW power can be compared with the power of Student test.[5] If these tests are used only when one or two values are acceptable, their power is obviously higher. That is why TW was used at censorized results.

It is known that the main element in statistics is the sampling (picking-up of samples), the so-called selection.

There should be somebody else, not the microscope expert, to specify which field is to be photographed by the electronic microscope. For instance, the choice of field could be made by a computer by using a system of generating random numbers. In this manner, the subjective preferences of the operator are excluded. If this aim cannot be achieved (for example when there are very few regions which have enough particles and these are not overlapped), then everything will never depend not only on the examined polymer but also on the emulsifier used at polymerization. In some emulsions, the photographed and then measured particles could possibly not represent an eloquent selection of the emulsion which is going to be investigated. Random oral statements indicate that, for some photographs, an excessively good coincidence was found between two sets of particles. From a statistical point of view, a too good coincidence is suspect, itself.

THE INFORMATIONAL ENERGY OF ONICESCU

— There is a habitude of evaluating the importance of some events, according to their closeness to a value previously considered as preferentially estimated.

— The exactly opposite alternative is also accepted : it is recommended that the statistics should not use preconceived ideas : all the events must be similarly treated, given the same share, that is given the same importance.

This discussion started from an average[10] mainly subsequently denoted by $n\bar{p}$ by means[1] of which the informational energy of Onicescu[2–4] can be compared with the informational entropy. For the mentioned example[2,8], the value of the difference between the two $n\bar{p}$ averages does not exceed 0.4%. For this example $n\bar{p}=1.12$ in the case of the informational energy and $n\bar{p} = 1.064$ for the informational entropy ; in the respective case, $n\bar{p}$ can have values between 1 and 16. Thus, the relative difference between the two averages could be calculated — only 0.4%. Thus, the fact is proved that no domain for which the informational energy of Onicescu is useful for the practicians has been found yet. It was checked once more that the correct intuition sincerely expressed has a higher value than the mathematical formalism which resulted in the elaboration of the name of "informational energy".

Examination of different expressions that could be used to exact estimations of the copolymerization constants [1], shows that some sums must be estimated with a relatively high statistical exactness. The terms of these sums contain few values of the random values used. So that the exactness with which one can know these sums depends on the number of important terms comprised. The sum of these terms only should represent a relatively high fraction, for example at least 70%, from the total value of the discussed sum. The reverse of the informational energy represents exactly the number of "important" terms. Then, only these terms must be summed up, in the order of their magnitude. It was checked that the sum computed in this way represents at least 74% of the total sum. From the point of view of the mathematical analysis, such a value does not have and it cannot have a theoretical basis. It is enough to consider a bimodal distribution with widely different variances in order to justify this negative statement. But, in fact, some distributions — like the normal distribution — have a very great share, so that an even more general statement considers that the sum of "important" terms is higher than 70—80% from the total sum. Everything depends on whether the probability density in the case of continuous distributions does not exhibit "too great variations" in the neighbourhood of its maximum. Appendix A fully illustrates those mentioned above. One of the difficulties encountered 40 years ago and unsufficienetly explained consists in the shift from the discontinuous case to the continous one in the case of entropy, or more recently in the case of informational energy. It was indirectly seen that these classical considerations were lacking exactly what it was understood by "importance". [1] There could be possibily used a Greek originating term, analogous with "cybernetics". In this case, the "simasia" term is suggested [11] (σιμασία). The touchstone of these considerations seems to be the Weibull distribution [12,13]:

$$F(u) = 1 - \exp - u^{\gamma}$$

If γ is sub-unitary, the density of probability tends to infinite when $u \to 0$. If $\gamma \leqslant 0.5$, the informational energy is infinite, too. In the examples quoted in [13], the minimum value of γ is 0.73, which corresponds to a sum of the "important" terms of 74% from the total sum. In the case [12], the minimum value of the γ coefficient was 0.85, for the examples quoted. The theoretical basis of the importance of the Weibull distribution is mentioned in [5,14]. But only in[5] the name Weibull is quoted. These distributions are mentioned on the occasion of the order statistics.[5]

Finally, one should rewind the contrast existing between the relative simplicity of the approach of copolymerization in most works from the science of polymers and the obvious analysed complexity of [1].

If there were not any controversies in literature, the mathematical analysis developed in [1] would have no object.

The main element which is well-known but, still, as if ignored, is the fact that copolymerization is an *unstable* process. So that the determinations carried out at small conversions cannot satisfactorily characterize the copolymerization process at high conversions. The instability of the copolymerization process is essential in the neighbourhood of azeotropy, i.e. exactly where one is interested to get most exact values. However, an answer must be cleared-up : at what conversions it is desirable to perform the determinations of concentrations. And once these determinations performed, what can be hoped to obtain by their means. Thus, a general method of approaching this subject is discussed.

The main steps of this method of computing are the following :

— A) The usual equations of copolymerization at low conversions are used for orientative determinations of the copolymerization constants. The best known such equation is the equation of Mayo.

— B) The adequate confidence domains are developed, by means of known methods.

—C) The sensitivity curve of the analysis method is plotted as a function of conversion, with respect to the determination of the concentrations from the system.

—D) The extreme values are considered acceptable from the confidence domain developed at point B.

—E) By using the extreme values of the acceptable copolymerization constant computed at point D, one estimates the conversion at which relatively high differences of concentration will be able to appear in comparison with the curve of deviations estimations from C. At these values of the conversion, the concentrations values will be determined both by computing and experimentally so that the copolymerization constants could be corrected if necessary.

—F) Finally, the last corrections of the copolymerization constants are computed.

At first sight the copolymerization process is not influenced by the amount of synthesized polymer until the respective moment. Even the exactness of the determinations of monomers concentrations is much higher at low conversions. But it is usually forgotten that during the polymerization process, the "like-low-conversions" systems are correlated, in fact.

Let M_{10} represent the initial "1" type comonomer concentration In a similar way, M_{11} denotes the relative "1" type monomer concentration from a given conversion. Supposing that the copolymerization constants were determined at a negligible conversion, M_{11} must also result from computing. From the possible difference between the calculated value and the measured one at known conversions, the copolymerization constants can be corrected. If M_{11} is considered like at negligible conversion, one more supplementary determination is available. Thus, the respective contribution to the exactness of knowing the copolymerization constants is insignificant. The unusual element appeared in these considerations is the point C. The curve of experimental errors plays a decision making part here : by means of this curve one can learn the conversion at which the experimental determination of the conversions from the system is going to be carried out.

APPENDIX A

First, the probability densities $P(x)$ are considered [1], which are monotonous decreasing functions, without singularities. One assumes

$$\int_{\varepsilon}^{a} P(x)\,\mathrm{d}x = 1\,;\quad a > \varepsilon\,;\quad P(x) \geqslant 0 \tag{1A}$$

This equation has the finite equivalent

$$\sum P(x_i)\delta x = 1\,;\; p_i = P(x_i)\delta x\,;\; \delta x = x_i - x_{i-1}\,;\; i = 1, 2, \ldots, N \tag{2A}$$

$$x_0 = \varepsilon\,;\; x_n = a\,;\; n\delta x = a - \varepsilon\; n = N$$

Generally, N is different from n; n represents the number of p_i probabilities values. In the example from Table 1, $N = 862$ and $n = 29 = m - 1$. The informational energy [2-4] for the finite case will be:

$$\bar{p} = \sum p_i^2 = \delta x \sum (P(x_i))^2\, \delta x \tag{3A}$$

Thus $\bar{p}$ also represents the average probability. For finite "ε, a" the $n\bar{p}$ product will have a finite value. In the case of continuous distributions

$$n\bar{p} = (a - \varepsilon)\int_{\varepsilon}^{a} (P(x))^2\,\mathrm{d}x \tag{4A}$$

Always

$$n\bar{p} \geqslant 1 \tag{5A}$$

It is enough to express the value of the mean square deviation of the p_i probabilities:

$$\sum(p_i - \bar{p})^2 = (n\bar{p} - 1)\bar{p} \geqslant 0 \tag{6A}$$

In the case of averaging resulted from the use of the informational entropy, another $\bar{p}$ value is obtained

$$\ln(n\bar{p}) = \sum p_i \ln(np_i) = \sum \delta x P(x_i) \ln(n\delta x P(x_i)) \tag{7A}$$

Taking into account (2A) for the continuous case

$$n\bar{p} = (a - \varepsilon)\exp\int_{\varepsilon}^{a} P(x)\ln P(x)\,\mathrm{d}x \tag{8A}$$

If at least one of the integration limits tends to infinite, then the $n\bar{p} =$ = "importance" cannot be used any more. At continuous distribution, one can notice first an important (ε, x_0) domain :

$$I = \int_{\varepsilon}^{x_0} P(x)\,\mathrm{d}x\,; \quad I \leqslant 1\,; \; a \geqslant x_0 \geqslant 1 \qquad (9\mathrm{A})$$

The term of n_0 number of "important events" was justified[1]:

$$n_0 = n/(n\bar{p}) = n/\left((a-\varepsilon)\int_{\varepsilon}^{a} (P(x))^2\,\mathrm{d}x\right) \qquad (10\mathrm{A})$$

One can put

$$x_0 - \varepsilon = n_0 \delta x = 1/\int_{\varepsilon}^{a} (P(x))^2\,\mathrm{d}x \qquad (11\mathrm{A})$$

In this case, a can tend to infinite. The same considerations can be extended to the informational entropy :

$$x_0 - \varepsilon = \exp - \int_{\varepsilon}^{a} P(x) \ln P(x)\,\mathrm{d}x \qquad (12\mathrm{A})$$

The $x_0 - \varepsilon$ value calculated from (12A) is higher than the one form (11A). Similar relations are extended to the other generalized informational energies

$$n\bar{p} = (a-\varepsilon)\left(\int_{\varepsilon}^{a} (P(x))^{\nu}\,\mathrm{d}x\right)^{1/(1-\nu)} \qquad (13\mathrm{A})$$

The informational energy of Onicescu corresponds to the value $\nu = 2$. If gamma distribution is considered :

$$p(x) = x^{\nu-1} \mathrm{e}^{-x} / \Gamma(\nu) \qquad (14\mathrm{A})$$

with $\varepsilon = 0$ and $a = \infty$ then the respective function has only one maximum for $x = \nu - 1$. Such a function does not consider the monotony condition. In this case, the conditions from [1] will require that the important domain be from x_1 to x_0, where :

$$P(x_1) = P(x_0)\,; \; x_0 - x_1 = 1/\int_{\varepsilon}^{a} (P(x))^2\,\mathrm{d}x\,; \quad I = \int_{x_1}^{x_0} P(x)\,\mathrm{d}x \qquad (15\,\mathrm{A})$$

Formally, x_1 is substituted for "ε" from (9A). So, this is the main difference between the monotonous distributions and those which accept only one maximum. Thus both types of distribution from Table 2 can be treated in this manner.

Table 2

Characteristics of different distributions connected with the "importance"

Type of distribution	Informational energy			Informational entropy		
	x_0	x_1	I	x_0	x	I
normal $P(x) = (2n)^{-0.5}\exp-\frac{x^2}{2}$	1.73	−1.73	0.916	2.0664	−2.0664	0.963
exponential $P(x) = e^{-x}$	2	0	0.8647	2.7183	0	0.934
gamma $\nu = 2$ $P(x) = x^{\nu-1}\exp-x/\Gamma(\nu)$	4.06926	0.06926	0.9111	9.8616	$5.14 10^{-5}$	0.9994
uniform $P(x) = 1 \quad 0 \leqslant x \leqslant 1$	0	0	1	1	0	1

x_0 represents the higher integration limit (15A)
x_1 represents the lower integration limit (15A)
I is the value of the respective "importance" domain (15A)

NOTES

Δ — measure of (integral or censorized) real distribution deviation as against the accepted statistical hypothesis. This value is defined by eq. (3).
$\delta x_i = x_i - x_{i-1}$, represents the constant finite increase.
$\bar{F}$ — average of $F(u)$ distribution values for the u_i deviations experimentally observed.
$F(u)$ — function of distribution, defined by (1). This function is chosen as statistical hypothesis.
m — maximum value from column 1, Table 1 ;4_m represents the number of measured particles.
M — number of particles calculated in the process of $F(u)$ function estimation ; M must be close to N
M_1 — positive values, supposed to be very high, measuring number of fictitious evaluations with the $F(u)$ distribution.
M_{10}, M_{11} — relative concentrations of the "1" comonomer at null conversion and at given, finite conversion.
N — number of actually performed evaluations, In Table 1 $N = 862$
n — number of frequencies or of considered probabilities. In Table 1, $n = m = 29$
$P(w)$ — the usual density of probability which satisfies eq. (1A)
ST — short for statistics
u_i, u — deviation from the considered laws. If no laws are considered, u_i represents the experimentally found result
TW — short for Wilcoxon test.
$2_i, 3_i, \ldots 7_i$ — represent the values from Table 1, columns 2, 3, ... 7. The index i designates the line noted in column 1 by the definition $i = 1$.

REFERENCES

[1] Th. Deleanu, *Rev. Chim. (Bucharest)* **40**, 581 (1989).

[2] O. Onicescu and V. Ştefănescu "Elemente de statistică informaţională cu aplicaţii", Ed. Tehnică Bucharest, 1979.

[3] I. Petrică and V. Ştefănescu, "Aspecte noi ale teoriei informaţionale", Ed. Academiei, Bucharest, 1982.

[4] I. Parcaru, "Informaţie şi corelaţie", Ed. Enciclopedică, Bucharest, 1988.

[5] B. Mihoc and V. Craiu, "Tratat de statistică matematică", Vol. 1—4, Ed. Academiei, 1976—1981.

[6] S. Aïvasian, "Etude statistique des dependences", Mir. Moscow, 1970.

[7] B. E. Cooper "Statistics for Experimentalists" Pergamon Press, London, 1969.

[8] Th. Deleanu, *Rev. Chim. (Bucharest)*, **39**, 322 (1988).

[9] Th. Deleanu, *Rev. Chim. (Bucharest)*, **39**, 582 (1988).

[10] D. V. Iliescu and V. Vodă "Statistică şi toleranţe", Ed. ştiinţifică Bucharest, p. 73, 1977.

[11] D. Scorţescu, personal communication.

[12] Al. Isaic-Maniu, "Metoda Weibull, aplicaţii" Ed. Academiei, 1983.

[13] U. Wiener, Al. Isaic Maniu and V. Vodă, "Aplicaţii ale reţelelor probabiliste în tehnică", Ed. Tehnică, Bucharest, 1983.

[14] L. Tovissi and V. Vodă, "Metode statistice", Ed. Ştiinţifică şi Enciclopedică, Bucharest, 1982.

Revue Roumaine de Chimie, **36**, *11–12*, 1439–1454 (1991)

INDEX DES AUTEURS

ABBASI S. A., Atomic absorption spectrometric determination of manganese in natural waters and industrial effluents after extractive separation of its ternary complex with n-phenyl-2-furohydroxamic acid and trioethylmethyl-ammonium cation in MIBK 901

ABDEL LATIF TAHA M., v. KANDILE G. NADIA 245

ACERETE CARMEN and MARIA LUISA BANON, PILAR CABILDO, ROSA MARIA CLARMUNT, JOSÉ ELGUERO, JOSE LUIS LAVANDERA, Basicity-structure relationships in bisazolyl-methanes and -ethanes 629

AGHERGHINEI IOAN and PRISACARIU CRISTINA, CARACULACU A. ADRIAN, A new method for a kinetic study of reactions between diisocyanates and alcohols. Part II. Asymmetrical diisocyanates : 2,4-toluylene diisocyanate 1135

ALBU ANCA, v. SCHIOPESCU ALEXANDRA 65

ALBU ANCA, v. SCHIOPESCU ALEXANDRA 859

ALBU ANCA, v. SCHIOPESCU ALEXANDRA 1225

ALEXANDRU TATIANA, v. CONTINEANU IULIA 435

ALKOURASHY A. and A. S. EL-SHAHAWY, Electronic spectral analysis of benzo [b]pyrido [3,2-F] thiepin, 8-chlorobenzo [b]pyrido [3,2-F] thiepin and 8-chlorobenzo [b]pyrido [3,2-F] thiepin-6(5H)-one 235

ALY M. M., v. BADR M. Z. A. 1129

ANAÇ OLCAY, v. GÜNAYDIN KERIMAN 1325

ANDREESCU REMUS, v. POPESCU MONICA 741

ANDRUH MARIUS, Thermal behaviour of the complex cation-complex anion-type coordination compounds. III. Thermochromism in tris(phenanthroline)nickel (II)-tetrachloro-palladate complexes 101

ANDRUH MARIUS and MICHAELA STĂNESCU, NICOLAE STANICA, MARILENA FERBINTEANU, Mixed-ligands coordination compounds of cobalt(II) and nickel(II) with 9, 10-dihydro-9, 10-ethano-12-hydroxy-methylene-anthracen-11-one and 2,2′-dipyridyl or 1, 10-phenanthroline 109

ANDRUH MARIUS and STĂNESCU MICHAELA, FLORIANA MUSUROI, MARIA BREZEANU, Coordination compounds of cobalt(II), nickel(II) and copper(II) with 9, 10-dihydro-9, 10-ethano-12-hydroxymethylene anthracen-11-one 113

ANDRUH MARIUS, v. BREZEANU MARIA 545

ANDRUH MARIUS and ELENA CRISTUREAN, RALUCA ŞTEFAN, CLAUDIU T. SUPURAN, Carbonic anhydrase inhibitors. 6. Novel coordination compounds of Pd(II), Pt(II) and Ni(II) with 6-ethoxy-benzothiazole-2-sulfonamide 727

ANDRUH MARIUS, v. SUPURAN T. CLAUDIU 1175

ANITESCU GH., v. VILCU R. 421

APATEANU LILIANA, v. BRANZOI V. 1229

ARBELOT MICHEL, v. BARONE RÉNÉ 581

ARION B. VLADIMIR, v. PALII P. SERGIU 1045

ARRVAY ZS., v. RAZUS A. C. 1307

ATTA A. A., v. YASSIN S. 197

ATTALA A. A., v. BADR M. Z. A. 1129

BABKIN V. S. and V. I. BABUSHOK, Bank of kinetic data and simulation of complex chemical reactions (in Russian) 1211

BABUSHOK V. I., v. BABKIN V. S. 1211

BACALOGLU ILSE, v. BACALOGLU RADU 1061

BACALOGLU RADU and ILSE BACALOGLU, Z. SIMON, Molecular orbital calculations with specific parametrization (MOSP). 1. Description of the method. Dipole moment calculations 1061

BACIU ION, v. MAIOR OVIDIU 1315

BADEA FLORIN and A. T. BALABAN, ION COSTEA, FLORIN IORDACHE, AURELIA MEGHEA, DANIELA CARMEN ONICIU, Reaction of 3,5-di-t-butyl-nitrosobenzene with alkoxides and carbanions 157

BADR M. Z. A. and M. M. ALY, A. A. ATTALA, S. A. MAHGOUB, Molecular rearrangements. Part XXXII. Thermolysis and photolysis of some hydroxylamine derivatives 1129

BAHEL S. C., v. MISRA S. 1161

BAIULESCU GEORGE EMIL, v. DAVID VICTOR 995

BALABAN A. T. and J. BRUNVOLL, S. J. CYVIN, Chemical graphs. Part 54. Enumeration of unbranched catacondensed polyhexes with equidistant linearly condensed segments 145

BALABAN A. T., v. BADEA FLORIN 157

BALABAN T. ALEXANDRU, v. SUPURAN T. CLAUDIU 937

BALABAN T. ALEXANDRU, v. HERDAN JEAN 1147

BALABAN TEODOR-SILVIU and MARIANA BOGATIAN, MARIANA PLAVETI, VIRGIL M. BADESCU, GH. MIHAI, Diacylation of olefins. XXV. New pyrylium and pyridinium salts derived from hexahydropseudoionone 229

BALDY ANDRÉ, v. BARONE RÉNÉ 581

BALINT ION, v. VASS I. MIHAI 829

BANCIU ANCA, v. BANCIU D. MIRCEA 1101

BANCIU D. MIRCEA, v. STĂNESCU MICHAELA DINA 119

BANCIU D. MIRCEA, v. SARAMET IOANA 127

BANCIU D. MIRCEA, v. SARAMET IOANA 135

BANCIU D. MIRCEA and CATALINA HADA, MICHAELA DINA STĂNESCU, FILIP CHIRALEU, ECATERINA CIORĂNESCU, Heterocycles with annelated dibenzocycloalkane skeletons. VI. Six membered heterocycles with annelated 7H-dibenzo [a, c] cycloheptene skeletons 671

BANCIU D. MIRCEA and MIRCEA POP, AURICA PETRIDE, MICHAELA DINA STĂNESCU, Flow-vacuum pyrolysis of dibenzo[c, g]tricyclo $[4.2.2.0^{2,5}]$-deca-3, 7, 9-triene (*syn*-diabenzo[c, g] Nenitzescu's hydrocarbon) and of tribenzo [c, g, j]tricyclo $[4.2.2.0^{2,5}]$ deca-3, 7, 9-triene (tribenzo-Nenitzescu's hydrocarbon). . 907

BANCIU D. MIRCEA and IOANA SIMION, ANCA BANCIU, AURICA PETRIDE, CONSTANTIN DRAGHICI, Flow-vacuum pyrolysis of tribenzo[a, e, i] [12] annulene 1101

BANCIU D. MIRCEA, v. SUPURAN T. CLAUDIU 1345

BANON MARIA LUISA, v. ACERETE CARMEN 629

BARAS-DIUDEA ANGELA, v. KACSÓ E. IREN 455

BARONE RÉNÉ and MICHEL ARBÊLOT, ANDRÉ BALDY, MICHEL CHANON, ROGER GALLO, RENE (REaction geNErator): a program to propose new reactions by construction of isomers and related reactive sets of simple functionalized compounds. Application to acids and esters 581

BARTHA E., v. RAZUS C. AL. 215

BARTHA E., v. RAZUS A. C. 1307

BAYOUMY B. E., v. YASSIN F. A. 201

BAYOUMY B. E., v. EL-BAHAIE S. 209

BĂDESCU M. VIRGIL, v. BALABAN TEODOR-SILVIU 229

BĂRBOIU V., v. SCUTARU D. 721

BĂRBOIU MIHAI, v. LUCA CONSTANTIN 1169

BÂLBĂ NICOLAE, v. DUMITRIU EMIL 1185

BEJAN DOINA, v. DUCA ALEXANDRU 439

BEJAN DOINA, v. DUCA ALEXANDRU 863

BERCEA MARIA, v. IOAN SILVIA 749

BICHER MARIANA, v. JITARU I. 983

BIRYUKOV V. YU, v. KLETSKY M. E. 341

BITAR M. B., v. SELIGER H. 171

BOESE ROLAND, v. NEIDLEIN RICHARD 601

BODOR NICHOLAS, v. NISHITANI SHINJI 635

BODOR NICHOLAS, v. BREWSTER E. MARCUS 647

BOGATIAN MARIANA, v. BALABAN TEODOR-SILVIU 229

BOLD ANISOARA and AURELIA VASILE, ANGELICA POPA, M. CRUCEANU, Ion exchange in siliceous zeolite ZSM-8 1055

BOLOCAN ION and FLAVIAN CUIBAN, Thermal decomposition of propylene . . . 819

BONCHEV D., v. MEKENYAN O. 363

BOTEZ GEORGETA, v. MAIOR OVIDIU 1315

BRAUN T. and S. ZSINDELY, Trends and tendencies in instrumental analytical techniques with special emphasis on environmental analysis 481

BRĂGĂREA ŞTEFAN, v. POPOESCU MONICA 741

BRÂNZOI V. and STERNBERG S., LILIANA APATEANU, Study of the electrode processes reversibility in the $PbO_2/PbSO_4$ system 1229

BREAZU DORIN, v. MAJDIK CORNELIA 1321

BREWSTER MARCUS E. and MING-JU HUANG, JAMES J. KAMINSKI, EMIL POP, NICHOLAS BODOR, Use of semiempirical molecular orbital parameters to probe dihydropyridine stability-implications to brain-targeting chemical delivery systems 647

BREZEANU MARIA, v. ANDRUH MARIUS 113

BREZEANU MARIA and L. PATRON, OANA CARP, MARIUS ANDRUH, N. STANICA, Coordination compounds as raw materials for spinelic oxides 545

BREZINSKI Z. JACEK, v. KATRITZKY ALAN 573

BRUNVOLL J., v. A. T. BALABAN 145

BRUNVOLL J., v. CYVIN S. J. 313

BUCURESCU IRINA and CRISTIAN TSAKIRIS, CRISTINA MARIA, GHEORGHE MARIA, ALEXANDRU ISOPESCU, A note concerning the direct interchange area error evaluation for the radiative transfer in a radiant furnace 1203

BUDRUGEAC P. and E. SEGAL, Derivatographic investigatin of the compound *eva* submitted to thermal accelerated ageing thermooxidative oxidation of the compound *eva*. 429

BULACOVSCHI V., v. MIHAILESCU CAMELIA 783

BURUIANA TINCA and CARACULACU ADRIAN, Synthesis and characterization of some 2,4-dibenzyldiisocyanate ionic polymers. VI. Biological activity at low concentrations of ionic groups 1123

BUTUCELEA AL., v. SPACU P. 519

CABILDO PILAR, v. ACERETE CARMEN 629

CALOIANU-IORDĂCHEL MARIA, v. RADU G. L. 1363

CAPITAN-VALLVEY L. F., v. MOLINA-DIAZ A. 77

CAPROSU MARIA and EUGENIA STEFANESCU, MARGARETA UNGUREANU, MAGDA PETROVANU, New physiologically active pyridazines and phthalazines (in French) 657

CARACULACU ADRIAN, v. BURUIANA TINCA 1123

CARACULACU A. ADRIAN, v. AGHERGHINEI IOAN 1135

CARAGHEORGHEOPOL AGNETA, v. STANCIUC G. 733

CARP OANA, v. BREZEANU M. 545

CARTIANU ŞERBAN-DAN, Method for calculating the local electronic energy levels in semiconductors and their occupation numbers from slope variations of the Arrhenius diagram of the electric conductivity 1075

CASCAVAL N. CONSTANTIN and DAN ROSU, Phenolic and epoxy resines. I. Thermal characterization by pyrolysis-gas chromatography 1331

CĂLDĂRARU H., v. STANCIUC GABRIELA 733

CĂPROIU M. T., v. STANCIUC GABRIELA 733

CECAL ALEXANDRU and VIOREL CRETU, DAN VRABIE, Inclusion of low- and intermediate-level radioactive wastes in low fusible glasses (in German) 1275

CERBELEU V. NIKOLAI, v. PALII P. SERGIU 1045

CERCASOV CORNELIA, v. ZALARU FLORICA 1279

CHANON MICHEL, v. BARONE RÉNÉ 581

CHARSON S. MAREK and NICOLAE I. IONESCU, MIHAI S. CHIRCA, Mechanism of phenol methylation on Al_2O_3 and on MgO 1397

CHIRALEU FILIP, v. STANESCU MICHAELA DINA 119

CHIRALEU FILIP, v. BANCIU D. MIRCEA 671

CHIRALEU FILIP, v. ROSCA SINZIANA 693

CHIRCA M. S., v. N. I. IONESCU 809

CHIRCA S. MIHAI, v. CHARSON S. MAREK 1397

CHOI SANG GON, v. PETRESCU N. 1021

CIORANESCU ECATERINA, v. BANCIU D. MIRCEA 671

CIUBOTARIU D., v. GOGNEA V. 465

CLARAMUNT ROSA MARIA, v. ACERETE CARMEN 629

COCIRLA I. and LUCIA TATARU, M. VAŢĂ, D. SCUTARU, I. MAZILU, LUMINIŢA WAGNER, CAMELIA PETRESCU, Absorption electronic spectra and reactivity of some As-naphthols 877

COJOCARU M., v. WEINBERG J. 417

CONSTANTINESCU O., v. CONTINEANU M. 1263

CONSTANTINESCU TITUS, v. MUTIHAC LUCIA 91

CONTINEANU IULIA and LUMINIŢA WAGNER, TATIANA ALEXANDRU, D. I. MARCHIDAN, The enthalpies of combustion and formation of 5-nitro-benzimidazol-2-one; 5-amino-benzimidazol-2-one and 5-acetoacetyl-amino-benzimidazol-2-one 435

CONTINEANU MIHAI, On intermediates involved in thermal decomposition of anzibenzyl. Part I 931

CONTINEANU M. and O. CONSTANTINESCU, Study of radical species formed at polycrystalline Ag_2SeO_3 radiolysis 1263

CONTESCU ADRIANA, v. SPACU P. 5

COSEAC TEODOR and EUGEN SEGAL, Basic program to generate the TG and DTG curves corresponding to thermal decompositions in solid-gas systems 257

COSTEA ION, v. BADEA FLORIN 157
COTÂRȚĂ ADINA, v. STERNBERG S. 13
CRĂCIUN LILIANA, v. MAGER SORIN 665
CRETU VIOREL, v. CECAL ALEXANDRU 1275
CRISTEA I., v. MAGER SORIN 665
CRISTUREAN ELENA, v. ANDRUH MARIUS 727
CRIȘAN D., v. SPACU P. 5
CRUCEANU M., v. BOLD ANIȘOARA 1055
CUIBAN FLAVIAN, v. BOLOCAN ION 819
CYVIN S. J., v. A. T. BALABAN 145
CYVIN B. N., v. CYVIN S. J. 313
CYVIN S. J. and J. BRUNVOLL, B. N. CYVIN, Enumeration and classification of coronoid hydrocarbons. Part 12. Triple coronoids 313

DAVID VICTOR and GEORGE-EMIL BAIULESCU, A new spectrometric method for determining carbon monoxide in air, using the Pd(II)-p-nitrosodiphenyl-amine complex 999
DELEANU TH., Progress of statistics applied to synthetic polymers latexes 1425
DERETEY E., v. GOGONEA V. 465
DIMITROV D. N., v. MEKENYAN O. 363
DIMONIE M. V. and N. N. MARINESCU, D. S. VASILESCU, Radical polymerization of acrylamide in homogeneous and heterogeneous systems. II. Emulsifier aggregates in organic media 757
DINCULESCU ANTONIE, v. SUPURAN T. CLAUDIU 937
DINCULESCU ANTONIE, v. MAIOR OVIDIU 1315
DINULESCU G. ILIE, v. ILIE CORINA 1107
DIUDEA V. MIRCEA and IOAN SILAGHI-DUMITRESCU, Molecular topology. 2. A computer program for multiple bond, cycle and radical approximations of DS index 263
DIUDEA V. MIRCEA, v. KACSÓ E. IRÉN 455
DIUDEA M., v. MAGER SORIN 665
DONESCU ALEXANDRINA, v. WEINBERG JOSETTE 417
DONESCU DAN, v. GOSA KRISTIANA 1287
DRAGOE N. and E. SEGAL, On the validity of the coats-redfern method in nonisothermal kinetics 995
DRAGHICI CONSTANTIN, v. SARAMET IOANA 127
DRAGHICI CONSTANTIN, v. SARAMET IOANA 135
DRAGHICI CONSTANTIN, v. BANCIU D. MIRCEA 1101
DUBEY S. L., v. MISRA S. 1161
DUCA ALEXANDRU and DOINA BEJAN, Cyclic voltammetry of *p*-phenylendiamine 439
DUCA ALEXANDRU and MARIA GABURICI, DOINA BEJAN, Polarography of cysteine, cystine and thiourea with various electrodes (DME, ME, MFE) 863
DUMITRASCU FLOREA and MARIETA PLAVETI, DAN RAILEANU, New convenient methods for the synthesis of 1, 2-dihydro-3H-indazol-3-one and its 1-acyl derivatives 917
DUMITRIU EMIL and KAYED YOUSEF, VASILE HULEA, SPIRIDON OPREA, Transalkylation of toluene with trimethyl benzene. I. Thermodynamic study . 1387
DUMITRIU EMIL and VASILE HULEA, KAYED YOUSEF, NICOLAE BALBA, SPIRIDON OPREA, Transalkylation of toluene with trimethylbenzene. II. Transalkylation of toluene with mesitylene over synthetic zeolites 1185

DUMITRIU MARIA, v. DUMITRIU SEVERIAN 947

DUMITRIU SEVERIAN and MARIA DUMITRIU, Bioactive polymers. 69. Cross-linked xanthan as drug-carrier matrices 947

DZIWINSKI E. and P. KUSZ, H. SZEWCZYK, K. PYZALSKI, D. GASZTYCH, Low-boiling products of the propoxylation reaction of acetic acid 1181

EL-ALEEM ABD A. H., v. YASSIN S. 197

EL-BADAWI M., v. EL-BARBARY A. A., 619

EL-BAHAEI S., v. EL-SAFTY M. A. 187

EL-BAHAIE S. and B. E. BAYOUMY, Synthesis of some new 1, 2, 3-selena- and 1, 2, 3-thiadiazolopyrimidines 209

EL-BARBARY A. A. and M. FAHMY, M. EL-BADAWI, K. EL-BREMBALY, N. R. EL-BROLLOSI, Studies on 4-amine-5-aryl-1,2, 4-triazole-3-thiones 619

EL-BASIL S., v. GHONEIM K. M. 1355

EL-BREMBALY K., v. EL-BARBARY A. A. 619

EL-BROLLOSI N. R., v. EL-BARBARY A. A. 619

EL-FARARGY A., v. EL-SAFTY M. A. 187

EL-FARARGY A. F., v. YASSIN F. A. 201

EL-HASHASH M. A., v. EL-SAFTY M. A. 187

EL MARAGHY SALAH, v. LINERT WOLFGANG 507

EL-SAFTY M. A. and S. EL-BAHAEI, M. A. EL-HASHASH, A. EL-FARARGY, F. YASIN, Studies in the field of heterocyclic compounds synthesis and behaviour of 4-(4-chloro-3-methyl)phenyl-1-(2H)-phthalazinone towards some electrophiles and nucleophiles 187

EL-SAFTY M. A., v. YASSIN F. A. 201

EL SAYED WAFAA A., v. KANDILE G. NADIA 245

EL-SHAHAWY A. S., v. ALKOURASHY A. 235

ELGUERO JOSÉ, v. ACERETE CARMEN 629

ENE NICOLAE and STEFANIA ZUCA, Electrorefining of titanium in molten alkali halide mixtures 1239

ENESCU LUCIAN, v. ILIE CORINA 1107

FAHMY M., v. EL-BARBARY A. A. 619

FAZAKAS JÁNOS, v. ZUGRĂVESCU GH. PAUL 39

FERBINTEANU MARILENA, v. ANDRUH MARIUS 109

FISHTIK I. T., Thermodynamics of polynuclear complex formation reactions 1011

FULEA O. ADRIAN, The causality law in physical chemistry and chemical physics and Bohr's principle of complementarity 1371

GALASIU I., v. LINGVAY I. 1005

GALASIU RODICA, v. LINGVAY I. 1005

GALLO ROGER, v. BARONE RÉNÉ 581

GANOVICI LUCIA, v. PETRESCU N. 1021

GASZTYCH D., v. DZIWINSKI E. 1181

GĂBURICI MARIA, v. DUCA ALEX. 863

GĂINAR I., v. VILCU RODICA 421

GĂNESCU I., v. ZSAKÓ J. 1269

GHENCIULESCU AURELIA, v. ILIE CORINA 1107

GHEORGHE CONSTANŢA, v. RADU O. 43

GHEORGHIU D. MIRCEA, v. RAZUS C. AL. 215

GHEORGHIU D. MIRCEA, v. SUPURAN CLAUDIU 251
GHEORGHIU D. MIRCEA, v. POPESCU ANGELA 683
GHEORGHIU D. MIRCEA, v. POPESCU ANGELA 707

GHONEIM K. M. and S. EL-BASIL, A. N. OSMAN, M. M. SAID, S. A. MEGAHED, Synthesis and structure elucidation on benzothiazole-containing compounds for antimicrobial investigation 1355
GLUZ E. B. and M. E. KLETSKY, R. M. MINYAEV, Electronic and geometrical structure of 10π -electron systems : cyclooctatetraene dianion and its heteroatomic analogs 333
GLUZ E. B., v. M. E. KLETSKY 341
GOGONEA V. and D. CIUBOTARIU, E. DERETEY, M. POPESCU, I. IORGA, M. MEDELEANU, Surface area of organic molecules : a new method of computation 465
GOMAA A. ESAM, Hydrogen bonding of *o*-nitroaniline in water-DMSO mixtures . . . 1235
GONZALEZ VALIENTE P. v. SALINAS F. 71
GOSA KRISTIANA and DAN DONESCU, SORIN STRAJA, DOINA ISBASESCU, ION LANGURI, Rheological modelling of emulsion copolymerization of vinyl acetate. 1287
GOLDNER E., v. SELIGER H., ... 171
GURAN CORNELIA, v. I. JITARU 983
GUTMAN IVAN, Topological properties of benzenoid systems Merrifield-Simmons indices and independence polynomials of unbranched catafusenes 379
GUTMANN VIKTOR, v. LINERT WOLFGANG 507
GÜNAYDIN KERIMAN, The synthesis of some 1-naphthylcycloalkanols and 1-naphthylcycloalkenes. 925
GÜNAYDIN KERIMAN and OLCAY ANAC, Investigation of the reaction of dimethyl diazomalonate with 1-phenylcyclododecene in the presence of copper(II) acetylacetonate. 1325

HADA CATALINA, v. BANCIU D. MIRCEA 671
HAIDUC IONEL and IOAN SILAGHI-DUMITRESCU, The richness of structures available to P_2N_2 inorganic heterocycles. A topological and molecular orbital (EHMO) analysis. 527
HERDAN JEAN and ALEXANDRU T. BALABAN, GERALD STOICA, ZENO SIMON, MIRCEA MRACEC, ION NICULESCU-DUVAZ, Compounds with potential preventing activity. I. Synthesis, physico-chemical properties and quantum chemical indicies of some phenolic and aminophenolic antioxidants 1147
HRITCU DOINA and GH. IONESCU, I. M. POPA, Study of the intrinsic properties of viscous flow in the ethyleneglycol (EG)-methanol (MeOH) system 1403
HAUNG MING-JU, v. BREWSTER E. MARCUS 647
HULEA VASILE, v. DUMITRIU EMIL 1185
HULEA VASILE, v. DUMITRIU EMIL 1387

ILIE CORINA and AURELIA GHENCIULESCU, LUCIAN ENESCU, ILIE G. DINULESCU, The reaction of the angular dimer of 1-methyl-benzocyclobutadiene with electrophilic reagents 1107
INDRICHAN M. KONSTANTIN, v. PALII P. SERGIU 1045
IOAN SILVIA and MARIA BERCEA, BOGDAN C. SIMIONESCU, Flexibility parameter of high molecular weight polymers. 2. Polystyrene in solvent-nonsolvent mixtures 749

IONESCU GH., v. HRITCU DOINA . . . 1403

IONESCU N. I. and M. S. CHIRCA, D. I. MARCHIDAN, The catalytic oxidation of methanol in oscillatory regime . . . 809

IONESCU I. NICOLAE, v. CHARSON S. MAREK . . . 1397

IORDACHE FLORIN, v, BADEA FLORIN . . . 157

IORGA I., v. GOGONEA V. . . . 465

IRIMIE F., v. MAGER SORIN . . . 665

ISBASESCU DOINA, v. GOSA KRISTIANA . . . 1287

ISMAIL I. I., v. YASSIN S. . . . 197

ISOPESCU ALEXANDRU; v. BUCURESCU IRINA . . . 1203

IVANUSEVIĆ MILAN and SONJA NIKOLIĆ, NENAD TRINAJSTIC, A QSAR study of antidotal activity of H-oximes . . . 389

JALEA CHRISTINA, v. ZALARU FLORICA . . . 1279

JECU LUIZA, v. POPESCU MONICA . . . 741

JINESCU GHEORGHITA and VASILE LAVRIC, The multistage immobilised living yeast cells bioreactor . . . 789

JINESCU V. VALENTIN, The degradation of matter . . . 797

JITARU IOANA and CORNELIA GURAN, MARIANA BICHER, Zinc chromite obtained from a residual chromium acetate solution . . . 983

KACSÓ E. IRÉN and ANGELA BARAS-DIUDEA, MIRCEA V. DIUDEA, Molecular topology. 10. Fragmentation of molecular graphs within (Randic (75 Ran)) and Y(90DIU) topological indices . . . 455

KAMINSKI J. JAMES, v. BREWSTER E. MARCUS . . . 647

KANDILE G. NADIA and TAHIA M. ABDEL LATIF, WAFAA A. EL SAYED, Synthesis and some reactions of 4-(N-acetyloxindolylidene)-2-aryl-5 (4H) oxazolones . . . 245

KATRITZKY ALAN and JACEK Z. BREZINSKI, JAMSHED N. LAM, 1-Cyanobenzotriazole : a safe and convenient source of CN^+ . . . 573

KILIAN G. G., v. SELIGER H. . . . 171

KING R. B., Metal cluster topology. 12. Nickel carbonyl clusters . . . 353

KITTEL I., v. SELIGER H. . . . 171

KLETSKY M. E., v GLUZ E. B. . . . 333

KLETSKY M. E. and E. B. GLUZ, V. YU. BIRYUKOV, R. M. MINYAEV, V. I. MINKIN, Electronic and geometrical structure of six-membered π-electron redundant systems . . . 341

KOVENDI ALEX., v. MAJDIK CORNELIA . . . 1321

KOZAKIEWICZ GISELA, v. SCHMITZ ERNST . . . 599

KRAMER WALTER, v. NEIDLEIN RICHARD . . . 601

KRASS NORBERT, v. OLAH A. GEORGE . . . 567

KUDESIA V. P., v. KUMARI REMESH . . . 1033

KUMARI REMESH and A. D. TANEJA, V. P. KUDESIA, Effect of solvent on the electronic spectra of 2, 3-dioximes derivatives of aromatic acetoacetamides . . . 1033

KURUNCZI LUDOVIC and RADU VALCEANU, ZENO SIMON, Del Re calculations for dipole moments of phosphorus compounds. Parametrization and results . . . 473

KURUNCZI LUDOVIC and RADU VALCEANU, ZENO SIMON, Del Re calculations for phosphorus compounds. Bond and atomic properties . . . 1093

KUSZ P., v. DZIWINSKI E. . . . 1181

LAM N. JAMSHED, v. KATRITZKY ALAN . . . 573

LANGURI ION, v. GOSA KRISTIANA 1287
LAVANDERA JOSÉ LUIS, v. ACERETE CARMEN 629
LAVRIC VASILE, v. JINESCU GHEORGHITA 789
LAZARESCU VALENTINA and M. VASS, Oxygen interaction with silver-gold alloy films 851
LINERT WOLFGANG and VIKTOR GUTMANN, ALI TAHA, EL MARAGHY SALAH, Studies on chromotropic nickel (II)-complexes 507
LINGVAY I., v. STERNBERG SOLOMON 13
LINGVAY I. and RODICA GALASIU, I. GALASIU, The electrochemical behaviour of SoO_2 based semiconductor ceramic in NaCl solutions 1005
LIXANDRU TATIANA, v. SCUTARU D. 721
LUCA CONSTANTIN, v. MUTIHAC LUCIA 85
LUCA CONSTANTIN, v. MUTIHAC LUCIA 91
LUCA CONSTANTIN, v. MUTIHAC LUCIA 551
LUCA CONSTANTIN and MIHAI BARBOIU, CLAUDIU T. SUPURAN, Carbonic anhydrase inhibitors. 7. Stability constants of complex inhibitors and their mechanism of action 1169

MAGER SORIN and I. CRISTEA, LILIANA CRACIUN, F. IRIMIE, M. DIUDEA, New aminopyrimidinonic derivatives with potential biological activity 665
MAHGOUB S. A., b. BADR M. Z. A. 1129
MAIOR OVIDIU, v. STOICESCU DAN 715
MAIOR OVIDIU and ANTONIE DINCULESCU, ION BACIU, GEORGETA BOTEZ, CLAUDIU SUPURAN, Synthesis of intensely coloured 2, 4, 6-trisubstituted pyrylium salts possessing bulky groups 1315
MAJDIK CORNELIA and ALEXANDRU KOVENDI, SIMION MATEI, DORIN BREAZU, O-arylketoximes. III. Obtaining 3-(4′-methyl)-phenyl-5-nitro-benzisoxazole from O-(2-(4′-methyl)-benzoyl-4-nitro)-phenyl-ketoximes 1321
MAKOSZA MIECZYSLAW and ZBIGNIEW WROBEL, Vilsmeyer-Haack reaction of nitrobenzylic sulfones and nitriles 563
MAMATYUK V. I., v. RAZUS A. C. 1307
MANOLE GHEORGHE, v. SUPURAN T. CLAUDIU 251
MANOLE GHEORGHE, v. SUPURAN T. CLAUDIU 937
MANOLIU LIGIA, v. STERNBERG S. 13
MARCHIDAN D. I., v. CONTINEANU IULIA 435
MARCHIDAN D. I., v. N. I. IONESCU 809
MARIA CRISTINA, v. BUCURESCU IRINA 1203
MARIA GHEORGHE, v. BUCURESCU IRINA 1203
MARINESCU N. N., v. DIMONIE M. V. 757
MATEESCU A. and C. D. MATEESCU, V. S. TEODORESCU, I. C. NISTOR, The influence of ClO_4^- ions upon the electrochemical system $Pb/H_2SO_4/PbO_2$ 883
MATEESCU C. D., v. MATEESCU A. 883
MATEI IRINA, v. POPESCU ANGELEA 707
MATEI SIMION, v. MAJDIK CORNELIA 1321
MAZILU I., v. SCUTARU D. 721
MAZILU I., v. COCIRLA I. 877
MĂMĂLIGĂ ION, v. TUDOSE Z. RADU 771
MEDELEANU M., v. GOGONEA V. 465
MEGAHED S. A., v. GHONEIM K. M. 1355
MEGHEA AURELIA, v. BADEA FLORIN 157

MEGHEA AURELIA, v. BADEA FLORIN 157
MEGHEA AURELIA, v. ZALARU FLORICA 1279
MEHEDINŢEANU LAURENŢIU, v. POPESCU ANGELA 683
MEKENYAN O. and D. BONCHEV, D. N. DIMITROV, Information-theoretic approach to the aromaticity of chemical compounds based on superdelocalizability indices 363
MERICĂ ECATERINA, v. TUDOSE Z. RADU 771
METZGER JACQUES, v. ROUSSEL CHRISTIAN 613
MIHAI GHEORGHE, v. BALABAN TEODOR-SILVIU 229
MIHAILESCU CAMELIA and V. BULACOVSCHI, C. I. SIMIONESCU, Phase transfer free radical reactions. V. Copolymerization of methyl methacrylate with styrene under phase transfer conditions 783
MINKIN V. I., v. KLETSKY M. E. 341
MINYAEV R. M., v. GLUZ E. B. 333
MINYAEV R. M., v. KLETSKY M. E. 341
MISRA S. and S. L DUBEY, S. C. BAHEL, Preparation, characterization and fungitoxicity of the Fe(III) complexes with mercapto azoles 1161
MOLINA-DIAZ A. and M. I. PASCUAL-REGUERA, L. F. CAPITÁN-VALVEY, Study of the system iron(III)-3-nitrobenzohydroxamic acid-adogen 464 in toluene 77
MOMIRLAN MAGDALENA and EUGEN PINCOVSCHI, Oxidation of the titanium alloy Ti6Al4V in air and oxygen 845
MOTOC IOAN and OSKAR E. POLANSKY, The effect of molecular topology on π-molecular orbital energies of pyridazine, pyrimidine and pyrazine topomer triple . . 399
MRACEC MIRCEA, v. HERDAN JEAN 1147
MURGULESCU G. ILIE and EUGENIA SALAGEANU, The estimation of thermodynamic properties of fused silver halides 411
MUTIHAC LUCIA and CONSTANTIN LUCA, Separation by extraction of aminoacids with macrocyclic ligands 85
MUTIHAC LUCIA and CONSTANTIN LUCA, TITUS CONSTANTINESCU, MARIETA OPREA, MIHAI RADU, The influence of operational parameters upon the extraction of amino acids with macrocyclic ligands 91
MUTIHAC LUCIA and RADU MUTIHAC, TITUS CONSTANTINESCU, CONSTANTIN LUCA, Mathematical modelling of ion pair carrier mediated transport through liquid membranes 551
MUTIHAC RADU and ALEXANDRU OPREA, Thin films of Al_2O_3 and Ta_2O_5 obtained by magnetion reactive sputtering 49
MUTIHAC RADU, v. MUTIHAC LUCIA 551
MUSUROI FLORIANA, v. ANDRUH MARIUS 113

NECRASOV S. YURII, v. PALII P. SERGIU 1045
NEIDLEIN RICHARD and ZHIHUA SUI, WALTER KRAMER, ROLAND BOESE, Synthesis and structure analysys of 4-quinazolone derivatives from alkyl dicyanoacetates 601
NEVADO BERZAS J. J., v. SALINAS F. 71
NICOLIĆ SONJA, v. IVANUŠEVIĆ IVAN 389
NICULESCU-DUVAZ ION, v. HERDAN JEZN 1147
NISHITANI SHINJI and NICHOLAS BODOR, Polymer supported 1-benzyl-1,2-dihydroisonicotinamides as reducing agents 635
NISTOR L. C., v. MATEESCU A. 883

OLAH A. GEORGE and QI WANG, NORBERT KRASS, K. G. SURYA PRAKASH, Oxyfunctionalization of hydrocarbons 16. Electrophilic hydroxylation and oxygenation of hydrocarbons with sodium percarbonate trifluoromethanosulfonic acid. 567

ONICIU DANIELA CARMEN, v. BADEA FLORIN 157

OPREA ALEXANDRU, v. MUTIHAC RADU 49

OPREA MARIETA, v. MUTIHAC LUCIA 91

OPREA SPIRIDON, v. DUMITRIU EMIL 1185

OPREA SPIRIDON, v. DUMITRIU EMIL 1387

OSADCHII S. A., v. RAZUS A. C. 1307

OSMAN A. N., GHONEIM K. M. 1355

PALII P. SERGIU and DIMITRII V. ZAGOREVSKII, KONSTANTIN M. INDRICHAN, NIKOLAI V. CERBELEU, YURII S. NEKRASOV, VLADIMIR B. ARION, Mass spectrometry of coordination compounds of transition metals with tetradentate ligands. VIII. The redistribution of hydrogen atoms at the loss of the methyl-group from the molecular ions of nickel (II) complexes with hexaazamacrocyclic-ligands on the basis of S-substituted isothiosemicarbazides and β-diketones 1045

PANAITESCU M. GHEORGHE, Maximum likelihood principle extended to generate selection criteria for equations of state and/or data 1195

PASCUAL-REGUERA M. I., v. MOLINA-DIAZ A. 77

PATRON LUMINITA, v. SPACU P. 5

PATRON LUMINITA, v. SPACU P. 519

PATRON LUMINITA, v. BREZEANU MARIA 545

PARVULESCU LUMINITZA, v. POPESCU ANGELA 683

PERISANU STEFAN, v. VILCU R. 421

PETRESCU CAMELIA, v. COCIRLA I. 877

PETRESCU N. and CHOI SANG GON, LUCIA GANOVICI, The synergic effect in the uranium extraction with the mixed solvent LIX 63 (5,8-diethyl-7-hydroxy-6-dodecanone oxime 1021

PETRIDE AURICA, v. BANCIU D. MIRCEA 907

PETRIDE AURICA, v. BANCIU D. M. 1101

PETRIDE HORIA, Mesoionic oxazolones. VI. Hydrolysis of acylated derivatives . . . 1113

PETRIDE HORIA, Mesoionic oxazolones. VII. About the mechanism of the hydrolysis of acylated derivatives 1299

PETROVANU MAGDA, v. CAPROSU MARIA 657

PETRUS O., v. TUDOSE Z. RADU 771

PINCOVSCHI EUGEN, v. MOMIRLAN MAGDALENA 845

PLĂVETI MARIETA, v. BALABAN T.-S. 229

PLĂVETI MARIA, v. POPESCU ANGELA 683

PLĂVEŢI MARIETA, v. DUMITRASCU FLOREA 917

PLOSTINARU SILVIA, v. SPACU PETRE 5

PLOSTINARU SILVIA, v. SPACU PETRE 519

POLANSKY OSKAT E., v. MOTOC IOAN 399

POP EMIL, v. BREWSTER E. MARCUS 647

POP MIRCEA, v. BANCIU D. MIRCEA 907

POPA ANGELICA, v. BOLD ANISOARA 1055

POPA I. M., v. HRITCU DOINA 1403

POPA MARCEL and CLEOPATRA VASILIU OPREA, Mechanochemical reactions at the spinning from solution of the acrylonitrile-vinyl acetate-α-methyl styrene based ternary copolymer . . . 761

POPESCU ANGELA and LUMINITZA PÂRVULESCU, LAURENŢIU MEHENDINTEANU, MARIA PLĂVEŢI, MIRCEA D. GHEORGHIU, Synthesis of 1α, 2α-5,9-methano-5H-benzo[3, 4]cyclobuta[1, 2]cycloheptene derivatives. Molecular and crystal structure of 7-chloro-8-keto-1α, 2α-5, 9-methano-5H-benzo[3, 4] cyclobuta[1 ,2]cycloheptene . . . 683

POPESCU ANGELA and MATEI IRINA, MIRCEA D. GHEORGHIU, K. M. TURDIBEKOV, Yu. T. STRUCHKOV, The synthesis of 8-substituted compounds of 7-H and 7-chloro-1β, 2β-5, 9-methano-5H-benzo[3, 4]cyclobuta[1, 2]cycloheptenes. Molecular and crystal structure of 7, 8α-dibrome-1β, 2β-5, 9-methano-5H-benzo [3, 4]cyclobuta[1, 2]cycloheptene . . . 707

POPESCU M., v. GOGONEA V. . . . 465

POPESCU MONICA and REMUS ANDREESCU, SILVIA STANESCU, ŞTEFAN BRAGAREA, LUIZA JECU, An estimation of the possibilities for obtaining carotenoid- and chlorophyl-derived pigments from vegetal raw materials . . . 741

PRAKASH SURYA K. G., v. OLAH A. GEORGE . . . 567

PRISACARU CRISTINA, v. AGHERGHINEI IOAN . . . 1135

PUSCAS IOAN, v. SUPURAN CLAUDIU . . . 251

PUSCAS IOAN, v. SUPURAN T. CLAUDIU . . . 937

PUSCAS IOAN, v. SUPURAN T. CLAUDIU . . . 1175

PYZALSKI K., v. DZIWINSKI E. . . . 1181

RADU G. L. and A. TANASE, MARIA CALOIANU-IORDACHEL, I. TODOR, Structural differences of some biomaterials based on collagen . . . 1363

RADU MIHAI, v. MUTIHAC LUCIA . . . 91

RADU O. and CONSTANTA GHEORGHIU, As(III) -HCl—H_2O system. III. The liquid-liquid state . . . 43

RADU O., As(III)—HCl—H_2O system. IV. The liquid — vapor state . . . 1409

RAJOHARISON G. HARIVELLO, v. ROUSSEL CHRISTIAN . . . 613

RĂILEANU DAN, v. DUMITRASCU FLOREA . . . 917

RAZUS C. ALEXANDRU and M. D. GHEORGHIU, EMERIC BARTHA, Dihydropyrans obtained in the reaction between 2-(acenaphthylen-1-yl)-ethanol and carbonylic derivatives . . . 215

RĂZUS A. A. and BARTHA E., Zs. ARVAY, S. A. OSADACHII, V. I. MAMATYUK, V. G. SHUBIN, Rearrangements of 1, 1a 6, 6a-tetrahydrocycloprop [a]inden-6-ols in superacids . . . 1307

ROSCA SINZIANA and FILIP CHIRALEU, SORIN I. ROSCA, Electrophilic aromatic substitution in arene-tricarbonyl-chromium complexes . . . 693

ROSCA SORIN, v. STERNBERG S. . . . 25

ROSCA I. SORIN, v. ROSCA SINZIANA . . . 693

ROSU DAN, v. CASCAVAL CONSTANTIN . . . 1331

ROUSSEL CHRISTIAN and HARIVELA G. RAJOHARISON, JACQUES METZGER, Acylation of alkenes using trifluoromethanesulphonic acid/acid halogenide acylation system (in French) . . . 613

SAHINI N. EM., v. WEINBERG J. . . . 417

SAID M. M., v. GHONEIM K. M. . . . 1355

SALEH R. M., and SOLIMAN A. Y., SOLIMAN F. M. A., Some reactions of chalcone epoxide . . . 1337

SALINAS F. and J. J. BERZAS NEVADO, P. VALIENTE GONZÁLEZ, Iron determination by solvent extraction with salycylaldehyde guanylhydrazone and atomic absorption spectrophotometry . . . 71

SAVAN FLORINA, v. SUPURAN T. CLAUDIU 937
SĂLĂGEAN EUGENIA, v. MURGULESCU ILIE G. 411
SĂNDULESCU D., v. SCHIOPESCU ALEXANDRA 65
SCHIKETANZ ANA, v. SUPURAN CLAUDIU 251
SCHIOPESCU ALEXANDRA and ANCA ALBU, D. SĂNDULESCU, The ferrate(VI) $(FeO_4)^{2-}$ as oxidizing agent. 65
SCHIOPESCU ALEXANDRA and ANCA ALBU, Ferrate(VI) ion employed in preparation of some salts of the tetralutidinic complex combinations of nickel(II) and cobalt(II) 859
SCHIOPESCU ALEXANDRA and ALBU ANCA, Thermal analysis of the ferrate(VI) ion salts with complex tetralutidinic combinations of nickel(II) and cobalt(II) 1225
SCHMITZ ERNST and GISELA KOZAKIEWICZ, Formation of an α-lactone 599
SCUTARU D. and I. MAZILU, M. VÂTA, LUCIA TATARU, TATIANA LIXANDRU, V. BARBOIU, Functional derivatives of ferrocen-S-modified thioglycol acids (in German) 721
SCUTARU D., v. COCIRLA I. 877
SEGAL EUGEN, v. COSEAC TEODOR 257
SEGAL E., v. BUDRUGEAC P. 429
SEGAL E., v. DRAGOE N. 995
SELIGER H. and M. B. BITAR, E. GÖLDNER, I. KITTEL, H. G. KILIAN, Preparation and properties of oligomers of defined chain length and structure as models for technical copolymers 171
SHUBIN V. G., v. RAZUS A. C. 1307
SILAGHI-DUMITRESCU IOAN, v. DIUDEA V. MIRCEA 263
SILAGHI-DUMITRESCU IOAN, v. HAIDUC IONEL 527
SILAGHI-DUMITRESCU IOAN, v. DIUDEA V. MIRCEA 975
SIMION IOANA, v. BANCIU D. MIRCEA 1101
SIMIONESCU C. BOGDAN, v. IOAN SILVIA 749
SIMIONESCU C. I., v. MIHAILESCU CAMELIA 783
SIMON ZENO, v. KURUNCZI LUDOVIC 473
SIMON Z., v. BACALOGLU RADU 1061
SIMON ZENO, v. KURUNCZI LUDOVIC 1093
SIMON ZENO, v. HERDAN JEAN 1147
SLANINA ZDENEK and FILIP UHLIK, MICHAEL C. ZERNER, $C_5H_5^+$ isomeric structures : relative stabilities at high temperatures 965
SOLIMAN A. Y., v. SALEH R. M. 1337
SOLIMAN F. M. A., v. SALEH R. M. 1337
SPACU P. and SILVIA PLOSTINARU, LUMINIŢA PATRON, ADRIANA CONTESCU, D. CRISAN, N. STANICA, Coordination compounds as raw materials for mixed oxides. VII. Mixed coordination compounds of lanthanides and Mn(II) as procursors of manganites 5
SPACU P. and LUMINIŢA PATRON, SILVIA PLOSTINARU, Al. BUTUCELEA, Complex compounds of lanthanoids with Ba(II) and Cu(II) with malic acid . . 519
STANCIUC GABRIELA and M. T. CAPROIU, AGNETA CARAGHEORGHEOPOL, H. CALDARARU, Preparation and EPR spectra of capto-dative N.alkoxy-2,6-dinitre-α,α,α -trifluoro-p-tolyl-aminyls 733
STANESCU MICHAELA, v. ANDRUH MARIUS 109
STANESCU MICHAELA, v. ANDRUH MARIUS 113
STANESCU MICHAELA DINA and MIRCEA D. BANCIU, FILIP CHIRALEU, Heterocycles with annelated dibenzobarrelene and dibenzohomobarrelene skeletens. 119

STANESCU MICHAELA DINA, v. BANCIU D. MIRCEA 671

STANESCU MICHAELA DINA, v. BANCIU D. MIRCEA 907

STANESCU SILVIA, v. POPESCU MONICA 741

STANICA N., v. SPACU P. 5

STANCA NICOLAE, v. ANDRUH MARIUS 109

STANICA NICOLAE, v. M. BREZEANU 545

STERNBERG S. and T. VISAN, LIGIA MANOLIU, ADINA COTÂRȚĂ and I. LINGVAY, Polarization behaviour of the n-type and p-type silicon in hydroxide solutions 13

STERNBERG S. and MIHAELA UNGUREANU, SORIN ROSCA, Electrochemical oxidation of carboxylic acids. II. Electrode processes in electrochemical oxidation of natrium monomethyl adipate on platinum 25

STERNBERG S., v. BRANZEI V. 1229

STOICA GERALD, v. HERDAN JEAN 1147

STOICESCU DAN and OVIDIU MAIOR, Phenoxatiin chemistry. Synthesis of pyrido(2,3-b) phenoxatiin 715

STRAJA SORIN, v. GOSA KRISTIANA 1287

STRUCHKOV YU. T., v. POPESCU ANGELA 683

STRUCHKOV YU. T., v. POPESCU ANGELA 707

SUI ZDIHUA, v. NEIDLEIN RICHARD 601

SUPURAN CLAUDIU and GHEORGHE MANOLE, ANA SCHIKETANZ, MIRCEA D. GHEORGHIU, IOAN PUSCAS, Carbonic anhydrase inhibitors. IV. Bifunctional derivatives of 5-amino-1, 3, 4-thiadiazole-2-sulfonamide 251

SUPURAN T. CLAUDIU, v. ANDRUH MARIUS 727

SUPURAN T. CLAUDIU and ANTONIE DINCULESCU, GHEORGHE MANOLE, FLORIANA SAVAN, IOAN PUSCAS, ALEXANDRU T. BALABAN, Carbonic anhydrase activators. Part 2. Amino acids and some of their derivatives may act as potent enzyme activators. 937

SUPURAN T. CLAUDIU, v. LUCA CONSTANTIN 1169

SUPURAN T. CLAUDIU and RALUCA ȘTEFAN, GHEORGHE MANOLE, IOAN PUSCAS, MARIUS ANDRUH, Carbonic andhydrase inhibitors. 8. Complexes of ethoxzolamide with lanthanides are powerful inhibitors of isozymes I and II 1175

SUPURAN T. CLAUDIU, v. MAIOR OVIDIU 1315

SUPURAN T. CLAUDIU and MIRCEA D. BANCIU, Carbonic anhydrase inhibitors. 9 Inhibitors with modified sulfonamide groups and their interaction with the zinc enzyme 1345

SZEWCZYK H., v. DZIWINSKI E. 1181

ȘARAMET IOANA and MIRCEA D. BANCIU, CONSTANTIN DRAGHICI, Synthesis and characterization of some 4,5-disubstituted-3-mercapto-1,2,4-triazoles . . . 127

ȘARAMET IOANA and BANCIU D. MIRCEA, CONSTANTIN DRAGHICI, Synthesis and characterization of some 5-substituted-3-mercapto-1, 2, 4-triazoles 135

ȘTEFAN RALUCA, v. ANDRUH MARIUS 727

ȘTEFAN RALUCA, v. SUPURAN T. CLAUDIU 1175

ȘTEFĂNESCU EUGENIA, v. CAPROSU MARIA 657

TAHA ALI, v. LINERT WOLFGANG 507

TANEJA A. D., v. KUMARI RAMESH 1033

TANASE A., v. RADU G. L. 1363

TĂTARU LUCIA, V. SCUTARU D. 721

TĂTARU LUCIA, v. COCIRLA I. 877

TEODORESCU V. S., v. MATEESCU A. 883

TODOR I., v. RADU G. L. 1363
TRINAJSTIĆ NENAD, v. IVANUSIVIĆ IVAN 389
TSAKIRIS CRISTINA, v. BUCURESCU IRINA 1203
TUDOSE Z. RADU and ECATERINA MERICA, ION MAMALIGA, O. PETRUS, Study on mass transfer in thin film flow of suspensions 771
TURDIBEKOV M. K., v. POPESCU ANGELA 683
TURDIBEKOV M. K., v. POPESCU ANGELA 707

UHLIK FILIP, v. SLANINA ZDENEK 965
UNGUREANU MARGARETA, v. CAPROSU MARIA 657
UNGUREANU MIHAELA, v. STERNBERG S. 25

VÁRHEYI C., v. ZSAKÓ J. 1269
VASILE AURELIA, v. BOLD ANISOARA 1055
VASILESCU D. S., v. DIMONIE M. V. 757
VASILIU OPREA CLEOPATRA, v. POPA MARCEL 761
VASS I. MIHAI and ION BALINT, Oxidative coupling of methane. The influence of reactant diffusion on the reaction 829
VASS M., v. LAZARESCU VALENTINA 851
VÂLCEANU RADU, v. KURUNCZI LUDOVIC 473
VÂLCEANU RADU, v. KURUNCZI LUDOVIC 1093
VÂŢĂ M., v. SCUTARU D. 721
VÂŢĂ M., v. COCÎRLĂ I. 877
VISAN T., v. STERNBERG S. 31
VÎLCU R. and GAINAR I., GH. ANITESCU, ST. PERISANU, A physical method for determining the solubility of gases in liquids at high pressures 421
VLADUTESCU RADU, Anionic layer optimization in a demineralization scheme using ion exchangers (in French) 55
VRABIE DAN, v. CECAL ALEXANDRU 1275

WAGNER LUMINITA, v. CONTINEANU IULIA 435
WAGNER LUMINIŢA, v. COCIRLA I. 877
WANG QI, v. OLAH A. GEORGHE 567
WEINBERG JOSETTE and ALEXANDRINA DONESCU, V. EM. SAHINI, M. COJOCARU, β-Lactam antibiotics. III. Electronic structure and physico-chemical properties of some antibiotic molecules and their intermediates 417
WROBEL ZBIGNIEW, v. MAKOSZA MIECZYSLAW 563

ZAGOREVSKII V. DIMITRII, v. PALII P. SERGIU 1045
ZALARU CHRISTIANA, v. ZALARU FLORICA 1279
ZALARU FLORICA and CORNELIA CERCASOV, AURELIA MEGHEA, CHRISTIANA ZALARU, CHRISTINA JAIEA, Cu(II) coordination compounds with thioamides. 1279
ZERNER C. MICHAEL, v. SLANINA ZDENEK 965
ZSAKÓ J., VÁRHELYI, I. GĂNESCU, On the dioximine complexes of transition metals. LXXXII. Study of some isoelenocyanato mixed chelates of cobalt(III) with dimethylglyoxime 1269
ZSINDELA S., v. BRAUN T. 481
ZUCA STEFANIA, v. ENE NICOLAE 1239
ZUGRAVESCU GH. PAUL and JÁNOS FAZAKAS, The hollow cathode current as a factor affecting the influence of pressure on spectral line overlaps in electrothermal atomic absorption spectrometry 39

YADAVA R. R. and S. S. YADAVA, Study of molecular interaction between aceto-

nitrile and benzene 1259
YADAVA S. S., v. YADAVA R. R. 1259
YASIN F., v. EL-SAFTY M. A. 187
YASSIN S. and I. I. ISMAIL, A. H. ABD EL-ALLEM, A. A. ATTA, Some reactions of sultones 197
YASSIN F. A. and M. A. EL-SAFTY, B. E. BAYOUMY, A. F. EL FARARGY, Synthesis of 4, 5, 6, 7-tetraphenyl-8(substituted)-3(2H)-phthalazinone derivatives with potential antihypertensive activity 201
YOUSEF KAYED, v. DUMITRIU EMIL 1185
YOUSEF KAYED, v. DUMITRIU EMIL 1387

Revue Roumaine de Chimie, **36**, *11–12*, 1455–1462 (1991)

INDEX DES SUJETS

Absorption electronic spectra and reactivity of some As-naphthols. I. COCIRLA, L. TATARU, M. VÂŢĂ, D. SCUTARU, I. MAZILU, L. WAGNER and C. PETRESCU 877

Acylation of alkenes using trifluoromethanesulphonic acid/acid halogenide acylation system (in French). C. ROUSSEL, H. G. RAJOHARISON and J. METZGER 613

Al_2O_3 and Ta_2O_5 films obtained by magnetron reactive sputtering. R. MUTIHAC and A. OPREA 49

4-Amino-5-aryl-1,2,4-triazole-3-thiones. A. A. EL-BARBARY, M. FAHMY, M. EL-BADAWI, K. EL-BREMBALY and N. R. EL-BROLLOSI 619

Anionic layer optimization in a demineralization scheme using ion exchangers. R. VLADUTESCU 55

As(III)-HCl–H_2O system. III. The liquid-liquid state. O. RADU and C. GHEORGHIU 43

As(III)-HCl–H_2O system. IV. The liquid-vapor state. O. RADU 1409

Atomic absorption spectrometric determination of manganese in natural waters and industrial effluents after extractive separation. S. A. ABBASI 901

Bank of kinetic data and simulation of complex chemical reactions V. S. BABKIN and V. I. BABUSHOK 1211

Basic program to generate the TG and DTG curves corresponding to thermal decompositions in solid-gas systems. T. COSEAC and E. SEGAL 257

Basicity-structure relationship in bisazolyl-methanes and -ethanes. C. ACERETE, M. L. BANON, P. CABILDO, R. M. CLARMUNT, J. ELGUERO and J. L. LAVANDERA 629

Bioactive polymers. 69 Cross-linked xanthan as drug-carrier matrices. S. DUMITRIU and M. DUMITRIU 947

Carbonic anhydrase activators:
  — amino acids and some of their derivatives may act as potent enzyme activators. C. SUPURAN, A. DINCULESCU, GH. MANOLE, F. SAVAN, I. PUSCAS and A. T. BALABAN 937

Carbonic anhydrase inhibitors:
  — novel coordination compounds of Pb(II), Pt(II) and Ni(II) with 6-ethoxy-benzothiazole-2-sulfonamide. M. ANDRUH, E. CRISTUREAN, R. STEFAN and C. T. SUPURAN 727
  — complexes of ethoxzolamide with lanthanides are powerful inhibitors of isozymes I and II. CLAUDIU T. SUPURAN. R. STEFAN. GH. MANOLE, I. PUSCAS and M. ANDRUH 1175
  — stability constants of complex inhibitors and their mechanism of action. C. LUCA, M. BARBOIU and CLAUDIU T. SUPURAN 1169
  — inhibitors with modified sulfonamide groups and their interaction with the zinc enzyme. CLAUDIU T. SUPURAN and M. D. BANCIU 1345
  — bifunctional derivatives of 5-amino-1,3,4-thiadiazole-2-sulfonamide. CLAUDIU C. SUPURAN, GH. MANOLE, A. SCHIKETANZ, M. D. GHEORGHIU and I. PUSCAS 251

Causality law in physical chemistry and chemical physics and Bohr's principle of complementarity. A. O. FULEA 1371

$C_5H_3^+$ isomeric structures : relative stabilities at high temperatures. Z. SLANINA, F. UHLIK and M. C. ZERNER 965

Chemical graphy. Part 54. Enumeration of unbranched catacondensed polyhexas with equidistant linearly condensed segments. A. T. BALABAN, J. BRUNVOLL and S. J. CYVIN 145

Complex compounds as raw materials for mixed oxides. VIII. Complex compounds of lanthanides with Ba(II) and Cu(II) with malic acid. P. SPACU, L. PATRON, S. PLOSTINARU and AL. BUTUCELEA 519

Compounds with potential preventing activity. I. Synthesis, physico-chemical properties and quantum chemical indices of some phenolic and aminophenolic antioxidants. J. HERDAN, A. T. BALABAN, G. STOICA, Z. SIMON, M. MRACEK and I. NICULESCU-DUVAZ 1147

Computer program for multiple bond, cycle and radical approximations of DS index. M. V. DIUDEA and I. SILAGHI-DUMITRESCU 263

Coordination compounds of cobalt(II), nickel(II) and copper(II) with 9, 10-ethane-12-hydroxy-methylene anthracen-11-one. M. ANDRUH, M. STANESCU, F. MUSUROI and M. BREZEANU 113

Coordination compounds of cobalt(II) and nickel(II) with 9,10-dihydro-9,10-ethano-12-hydroxy-methylene-anthracen-11-one and 2,2′-dipyridyl of 1,10-phenanthroline. M. ANDRUH, M. STANESCU, M. STANICA, N. STANICA and M. FERBINTEANU 109

Coordination compounds as raw materials for mixed oxides. VII. Mixed coordination compounds of lanthanides and Mn(II) as precursors of manganites. P. SPACU, S. PLOSTINARU, L. PATRON, A. CONTESCU, D. CRISAN and N. STANICA

Coordination compounds as raw materials for spinelic oxides. M. BREZEANU, L. PATRON, O. CARP, M. ANDRUH and N. STANICA 545

Cu(II) coordination compounds with thioamides. F. ZALARU, C. CERCASOV, A. MEGHEA, C. ZALARU and C. JAIEA 1279

1-Cyanobenzotriazole : a safe and convenient source of CN^+. A. KATRITZKY, J. Z. BREZINSKI and J. N. LAM 573

Cyclic voltametry of *p*-phenylendiamine. A. DUCA and D. BEJAN 439

Degradation of matter. V. V. JINESCU 797

Del Re calculations for dipole moments of phosphorus compounds. Parametrization and results. L. KURUNCZI, R. VALCEANU and Z. SIMON 473

Del Re calculations for phosphorus compounds. Bond and atomic properties. L. KURUNCZI, R. VALCEANU and Z. SIMON 1093

Direct interchange area error evaluation for the radiative transfer in a radiant furnace. I. BUCURESCU, C. TSAKIRIS, C. MARIA, GH. MARIA and A. ISOPESCU 1203

Derivatographic investigation of the compound *eva* submitted to thermal accelerated ageing. Thermooxidative oxidation of the compound *eva*. P. BUDRUGEAC and E. SEGAL 429

Diacylation of olefins. XXV. New pyrylium and pyridinium salts derived from hexahydropseudoioneue. T. S. BALABAN, M. BOGATIAN, M. PLAVETI, V. M. BADESCU and GH. MIHUI 229

Dihydropyrans obtained in the reaction between 2-(acenaphthylen-1-yl)-ethanol and carbonylic derivatives. A. C. RAZUS, M. GHEORGHIU and E. BARTHA . . 215

Dioximine complexes of transition metals. LXXXII. Study on some isoelenocyanato mixed chelates of cobalt(III) with dimethylglyoxime 1269

Effect of solvents on the electronic spectra of 2,3-dioximes derivatives of aromatic acetoacetamides. R. KUMARI, A. D. TANEJA and V. P. KUDESIA 1033
Electrochemical behaviour of SeO_2 based semiconductor ceramic in NaCl solutions. I. LINGVAY, R. GALASIU and I. GALASIU 1005
Electrochemical oxidation of carboxylic acids. S. STERNBERG, M. UNGUREANU and S. ROSCA 25
Electronic and geometrical structure levi-electron systems : cyclooctatetraene dianion and its heteroatomic analogs. E. B. GLUZ, M. E. KLETSKY and R. M. MINYAEV 333
Electronic spectral analysis of benzo(b)pyrido(3,2-F) thienpin, 8-chlorobenzo(b)pyrido(3,2-F)thienpin and 8-chlorobenzo(b)pyrido(3,2-F)thiepin-6(5H)-one. A. ALKOURASHY and A. S. EL-SHAHAWY 235
Electrophilic aromatic substitution in arene-tricarbonyl-chromium complexes. S. ROSCA, F. CHIRALEU and S. I. ROSCA 693
Electrorefining of titanium in molten alkali halide mixtures. N. ENE and S. ZUCA 1239
Electrothermal atomic absorption spectrometry — the hollow cathode current. P. ZUGRAVESCU and J. FAZAKAS 39
Enthalpies of combustion and formation of 5-nitro-bezimidazol-2-one ; 5-amino-benzimidazol-2-one and 5-acetoacetyl-amino-benzimidazol-2-one. I. CONTINEANU, L. WAGNER, T. ALEXANDRU and D. I. MARCHIDAN 435
Enumeration and classification of coronoid hydrocarbons. Part 12. Triple coronoids. S. J. CYVIN, J. BRUNVOLL and S. J. CYVIN 313
EPR spectra of capto-dative N-alkoxy-2-6-dinitro-trifluoro-p-tolylaminyls. G. STANCIUC, M. T. CAPROIU, A. CARAGHEORGHEOPOL and H. CALDARARU 733
Estimation of the possibilities for obtaining caretenoid- and chlorophyl-derived pigments from vegetal raw materials. M. POPESCU, R. ANDREESCU, S. STANESCU, ST. BRAGAREA and L. JECU 741

F$eO)^{2-}$ as oxidizing agent. A. SCHIOPESCU, A. ALBU and D. SANDULESCU . . 65
Ferrate (VI) ion employed in preparation of some salts of the tetralutidinic complex combinations of nickel(II) and cobalt(II). A. SCHIOPESCU and A. ALBU . . 1225
Flexibility parameter of high molecular weight polymers. S. IOAN, M. BERCEA and B. C. SIMIONESCU 749
Flow-vacuum pyrolysis of dibenzo[c, g] tricyclo[$4.2.2.0^{2,5}$]-deca-3, 7, 9-triene (*syn*-dibenzo[c, g]Nenitzescu's hydrocarbon) and of tribenzo[c, g, j]tricyclo[$4.2.2.0^{2,5}$]deca-3, 7, 9-triene (tribenzo-Nenitzescu's hydrocarbon). M. D. BANCIU, M. POP, A. PETRIDE and M. D. STANESCU 907
Flow-vacuum pyrolysis of tribenzo[*a*, *e*, *i*] [12] annulene. M. D. BANCIU, I. SIMION, A. BANCIU, A. PETRIDE and C. DRAGHICI 1101
Formation of an α -lactone. E. SCHMITZ and G. KOZAKIEWICZ 599
Functional derivatives of ferrocen-S-modified thioglycol acids (in German). D. SCUTARU, I. MAZILU, M. VÂȚĂ, L. TATARU, T. LIXANDRU and V. BARBOIU 721

Heterocycles with annelated dibenzocycloalkane skeletons. V. Pyrimidines with annelated dibenzobarrelene. M. D. STANESCU, M. D. BANCIU and F. CHIRALEU . . 119
Heterocycles with annelated dibenzocycloalkane skeletons. VI. Six membered heterocycles with annelated 7H-dibenzo [a, c] cycloheptene skeletons. M. D. BANCIU, C. HADA, M. D. STANESCU, F. CHIRALEU and E. CIORANESCU 671
Hydrogen bonding of *o*-nitroaniline in water-DMSO mixtures. E. A. GOMAA . . . 1253

Ion exchange siliceous zeolite ZSM-8. A. BOLD, A. VASILE, A. POPA and M. CRUCEANU 1055

Inclusion of low- and intermediate-level radioactive wastes in low fusible glasses (in German). A. CECAL, V. CRETU and D. VRABIE 1275

Influence of ClO_4^- ions upon the electrochemical system $Pb/H_2SO_4/PbO_2$. A. MATEESCU, C. D. MATEESCU, V. S. TEODORESCU and L. C. NISTOR 883

Influence of operational parameters upon the extraction of aminoacids. L. MUTIHAC, C. LUCA, T. CONSTANTINESCU, M. OPREA and M. RADU 91

Information-theoretic approach to the aromaticity of chemical compounds based on superdelocalizability indices. O. MEKENYAN, D. BONCHEV and D. N. DIMITROV 363

Intermediates involved in thermal decomposition of azibenzyl. Part. I. M. CONTINEANU 931

Investigation of the reaction of dimethyl diazomalonate with 1-phenylcyclododecene in the presence of copper(II) acetylacetonate. K. GÜNAYDIN and O. ANAÇ 1325

Iron determination by solvent extraction with salicylaldehyde guanylhydrazone. F. SALINAS, J. J. BERZAS NEVADO and P. V. GONZALES 71

Iron (III)-3-nitrobenzohydroxamic acid-adogen 464 in toluene. A. M. DIAZ, M. I. P. REGUERA and L. F. CAPITAN-VALLVEY 77

β-Lactam antibiotics. III. Electronic structure and physico-chemical properties of some antibiotic molecules and their intermediates. J. WEINBERG, A. DONESCU, V. EM. SAHINI and N. COJOCARU 417

Low-boiling products of the propoxylation reaction of acetic acid. E. DZIWINSKI, P. KUSZ, H. SZEWCZYK, E. PYZALSKI and D. GASZSYCH 1181

Mass spectrometry of coordination compounds of transition metals with tetradentate ligands. VIII. The redistribution of hydrogen atoms at the loss of the methylgroup from the molecular ions of nickel (II) complexes with hexaazamacrocyclic ligands on the basis of S-substituted isothiosemicarbazides and β-diketone. SP. PALII, D. V. ZAGOREVSCKII, K. M. INDRICHAN, N. V. CERBELEU, Y. S. NEKRASOV and V. B. ARION 1045

Mathematical modelling of ion pair carrier mediated transport through liquid membranes. L. MUTIHAC, R. MUTIHAC, T. CONSTANTINESCU and C. LUCA . . 551

Maximum likelihood principle extended to generate selection criteria for equations of state and/or data. GH. M. PANAITESCU 1095

Mechanism of phenolmethylation on Al_2O_3 and on MgO. M. S. CHARSON, N. I. IONESCU and M. S. CHIRCA 1397

Mechanichemical reactions at the spining from solution of the acrylonitrile-vinyl acetate-α-methyl styrene based ternary copolymer. M. POPA and CL. VASILIU-OPREA 761

Mesoionic oxazolones. VI. Hydrolysis of acylated derivatives. H. PETRIDE . . . 1113

Mesoionic oxazolones. VII. About the mechanism of the hydrolysis of acylated derivatives. H. PETRIDE 1299

Metal cluster topology. 12. Nickel carbonyl clusters. R. B. KING 353

Method for calculating the local electronic energy levels in semiconductors and their occupation numbers from slope variations of the Arrhenius diagram of the electronic conductivity. Ş.-D. CARTIANU 1075

Molecular orbital calculations with specific parametrization (MOSP). 1. Description of the method. Dipole moment calculations. R. BACALOGLU, I. BACALOGLU and Z. SIMON 1061

Molecular rearrangements. Part XXXII. Thermolysis and photolysis of some hydroxylamine derivatives. M. Z. A. BADR, M. A. ALY, A. A. ATTALA and S. A. MAHGOUB. 1129

Molecular topology. 2. A computer program for multiple bond, cycle and radical approximations of DS index. M. V. DIUDEA and I. SILAGHI-DUMITRESCU . . 263

Molecular topology. 10. Fragmentation of molecular graphs within (Randic (75 Ran)) and Y (90 Diu_1) topology indices. I. E. KACSO, A. BARAS-DIUDEA and M. V. DIUDEA 455

Molecular topology on π-molecular orbital energies of pyridazine, pyrimidine and pyrazine topomer triple. I. MOTOC and O. E. POLANSKY 399

Multistage immobilised living yeast cells bioreactor. GHEORGHITA JINESCU and V. LAVRIC. 789

New aminopyrimidionic derivatives with potential biological activity. S. MAGER, I. CRISTEA, L. CRACIUN, F. IRIMIE and M. DIUDEA 665

New convenient methods for the synthesis of 1,2-dihydro-3H-indazol-3-one and its 1-acyl derivatives. F. DUMITRASCU, M. PLAVETI and D. RAILEANU 917

New method for a kinetic study of reactions between diisocyanates and alcohols. Part II. Asymmetrical diisocyanates. I. AGHERGHINEI, C. PRISACARIU and A. A. CARACULACU 1135

New physiologically active pyridazines and phthalazines (in French). M. CAPROSU, E. STEFANESCU, M. UNGUREANU et M. PETROVANU 657

O-arylketoximes. III. Obtaining 3-(4 -methyl)-phenyl-5-nitro-benzisoxazole from O-(2-(4′-methyl)-benzoyl-4-nitro)-phenyl-ketoximes. C. MAJDIK, A. KOVENDI, S. MATEI and D. BREAZU . . . .

Oxidation of the titanium alloy Ti 6Al 4V in air and oxygen. M. MOMIRLAN and E. PINCOVSCHI 845

Oxidative coupling of methane M. I. VASS and I. BALINT 829

Oxidation (catalytic) of methanol in oscillatory regime. N. I. IONESCU, M. S. CHIRCA and D. I. MARCHIDAN 809

Oxygen interaction with silver-gold alloy-films. V. LAZARESCU and M. VASS . . . 851

Oxyfunctionalization of hydrocarbons. 16. Electrophilic hydroxylation and oxygenation of hydrocarbons with sodium percarbonate/trifluoromethane sulphonic acid. G. A. OLAH, QI WANG, N. KRASS and G. K. S. PRAKASH 567

Phase transfer free radical reactions. C. MIHAILESCU, V. BULACOVSCHI and C. I. SIMIONESCU 783

Phenolic and epoxy resines. I. Thermal characterization by pyrolysis — gas chromatography. C. N. CASCAVAL and D. ROSU 1331

Phenoxatiin chemistry. Synthesis of pyrido(2,3-b) phenoxatiin. D. STOICESCU and O. MAIOR 715

Physical method for determining the solubility of gases in liquids at high pressures. R. VILCU, I. GAINAR, GH. ANITESCU and ST. PERISANU 421

Polarization behaviour of the n-type and p-type silicon in hydroxide solutions. STERNBERG S., T. VISAN, L. MANOLIU, A. COTÂRȚĂ and I. LINGWAY 13

Polarography of cysteine, cystine and thiourea with various electrodes (IME, ME, MFE). A. DUCA, M. GABURICI and D. BEJAN 863

Polymer supported 1-benzyl-1,2-dihydroisonicotinamides as reducing agents. S. NISHITANI and N. BODOR 635

Preparation, characterization and fungitoxicity of the Fe(III) complexes with mercapto azoles. S. MISRA, S. L. DUBEY and S. C. BAHEL 1161

Preparation and properties of oligomers of defined chain length and structure as models for technical copolymers. H. SELIGER, M. B. BITAR, E. GOLDNER, I. KITTEL and H. G. KILIAN 171

Program to propose new reactions by construction of isomers and related reactive sets of simple functionalized compounds. Application to acids and esters. R. BARONE, M. ARBELOT, A. BALDY, M. CHANON and R. GALLO 581

Progress of statistics applied to synthetic polymers latexes. Th. DELEANU 1425

Radical polymerization of acrylamide in homogeneous and heterogeneous systems. M. V. DIMONIE, N. N. MARINESCU and D. S. VASILESCU 757

Reaction of the angular dimer of 1-methyl-benzocyclobutadiene with electrophilic reagents. C. ILIE, A. GHENCIULESCU, L. ENESCU and I. G. DINULESCU 1107

Reaction of 3,5-di-t-butylnitrosobenzene with alkoxides and carbanions. F. BADEA, A. T. BALABAN, I. COSTEA, F. IORDACHE, A. MEGHEA and D. C. ONICIU 157

Rearrangements of 1, la 6, 6a-tetrahydrocycloprop [a]-inden-6-ols in superacids. A. C. RAZUS, E. BARTHA, Z. ARVAY, S. A. OSADACHII, V. I. MAMATYUK and V. G. SHUBIN 1307

Rheological modelling of emulsion copolymerization of vinyl acetate. K. GOSA, D. DONESCU, S. STRAJA, D. ISBASESCU and I. LANGURI 1287

Richness of structures available to P_2N_2 inorganic heterocycles. A topological and molecular orbital (EHMO) analysis. I. HAIDUC and SILAGHI-DUMITRESCU 527

Separation by extraction of amino acids with macrocyclic ligands. L. MUTIHAC and C. LUCA 85

Some reactions of chalcone epoxide. R. M. SALEH, A. Y. SOLIMAN and F. M. A. SOLIMAN . . . . . .

Some reactions of sulfones. S. YASSIN, I. I. ISMAIL, A. H. ABD EL-ALEEM and A. A. ATTA 197

Spectrometric method for determining carbon monoxide in air, using the Pd(II)-p-nitrosodiphenylamine complex. V. DAVID and G. E. BAIULESCU 999

Structural differences of some biomaterials based on collagen. G. L. RADU, A. TANASE, M. C. IORDACHEL and I. TODOR 1363

Studies on chromotropic nickel (II)-complexes. W. LINERT, V. GUTMANN, A. TAHA and EL-M. SALAH 507

Studies in the field of heterocyclic compounds. Synthesis and behaviour of 4-(4-chloro-3 methyl)phenyl-1-(2H)-phthalazinone towards some electrophiles and nucleophiles. M. A. EL-SAFTY, S. EL-BAHAEI, M. A. EL-HASHASH, A. EL-FARARGY and F. YASIN 187

Study of the electrode processes reversibility in the $PbO_2/PbSO_4$ system. V. BRÂNZOI, S. STERNBERG and L. APĂTEANU 1229

Study of the intrinsic properties of viscous flow in the ethyleneglycol (EG)-methanol (MeOH) system. D. HRITCU, GH. IONESCU and I. M. POPA 1403

Study on mass transfer in thin film flow of suspensions. R. Z. TUDOSE, E. MERICA, I. MAMALIGA and O. PETRUS 771

Study of molecular interaction between acetonitrile and benzene. R. R. YADAVA and S. S. YADAVA 1259

Study (QSAR) of antidotal activity or H-oximes. I. IVANUSEVIĆ, S. NIKOLIĆ and N. TRINAJSTIĆ 389

Study of radical species formed at polycrystalline Ag_2SoO_3 radiolysis. M. CONTINEANU and O. CONSTANTINESCU 1263

Synergic effect in the uranium extraction with the mixed solvent LIX 63. N. PETRESCU, CHOI S. GON and L. GANOVICI 1021

Synthesis and characterization of some 2,4'-dibenzyldiisocyanate ionic polymers. VI. Biological activity at low concentrations of ionic groups. T. BURUIANA and A. CARACULACU 1123

Synthesis and characterization of some 4,5-disubstituted-3-mercapto-1, 2, 4-triazoles. I. SARAMET, M. D. BANCIU and C. DRAGHICI 127

— 5-substituted-3-mercapto-1, 2, 4-triazoles. I. SARAMET, M. D. BANCIU and C. DRAGHICI 135

Synthesis of intensely coloured 2, 4, 6-trisubstituted pyrylium salts possessig bulky groups. O. MAIOR, A. DINCULESCU, I. BACIU, G. BOTEZ and CLAUDIU T. SUPURAN 1315

Synthesis of 1,2-5, 9-methano-5H-benzo[3,4]cyclobuta[1, 2]cycloheptene derivatives. Molecular and crystal structure of 7-chloro-8-keto-1α, 2α-5, 9-methano-5H-benzo [3,4]cyclobuta[1,2]cycloheptane. A. POPESCU, L. PARVULESCU, L. MEHEDINTEANU, M. PLAVETI and M. D. GHEORGHIU 683

Synthesis of some 1-naphthylcycloalkanols and 1-naphthylcycloalkanes. K. GÜNAYDIN 925

Synthesis of some new 1, 2, 3-thiadiazolo-pyrimidines. S. EL-BAHAIE and B. E. BAYOUMY 209

Synthesis and some reactions of 4-(N-acetyloxindolylidene)-2-aryl-5-(4H) oxazelones. N. G. KANDILE, T. M. A. LATIF and W. A. EL SAYED 245

Synthesis and structure analysis of 4-quinazolone derivatives from alkyl dicyanoacetates. R. NEIDLEIN, Z. SUI, W. KRAMER and R. BOESE 601

Synthesis and structure elucidation of benzothiazole containing compounds for antimicrobial investigation. K. M. GHONEIM, S. EL-BASIL, A. N. OSMAN, M. M. SAID and S. A. MEGAHED 1355

Synthesis of S-substituted compounds of 7-H and 7-chloro-1β, 2β-5, 9-methano-5H-benzo [3, 4]cyclobuta[1, 2]cycloheptene. Molecular and crystal structure of 7, 8 α-dibromo-1β, 2β-5, 9-methano-5H-benzo[3, 4]cyclobuta[1, 2]cycloheptene. A. POPESCU, I. MATEI, M. D. GHEORGHIU, K. M. TURDIBEKOV and Yu. T. STRUCHOV 707

Synthesis of 4, 5, 6, 7-tetraphenyl-8(substituted)-3(2H)-phthalazinone derivatives with potential antihypertensive activity. F. A. YASSIN, M. A. EL-SAFTY, B. E. BAYOUMI and A. F. EL FARARGY 201

Surface area of organic molecules : a new method of computation. V. GOGONEA, D. CIUBOTARIU, E. DERETEY, M. POPESCU, I. IORGA and M. MEDELEANU. 465

Thermal analysis of the ferrate (VI) ion salts with complex tetralutidinic combinations of nickel (II) and cobalt (II). A. SCHIOPESCU and A. ALBU 1225

Thermal behaviour of the complex cation — complex anion-type coordination comdounds. M. ANDRUH 101

Thermal decomposition of propylene. I. BOLOCAN and F. CUIBAN 819

Thermodynamic properties of fused silver halides. I. G. MURGULESCU and E. SALAGEANU. . . . .

Thermodynamics of polynuclear complex formation reactions. I. T. FISHTIK 1005

Topological properties of benzenoid systems. Merrifield-Simmons indices and independence polynomials of unbranched catafusenes. I. GUTMAN 379

Transalkylation of toluene with trimethylbenzene. I. Thermodynamic study. E. DUMITRIU, K. YOUSEF, V. HULEA and S. OPREA 1387

Transalkylation of toluene with trimethylbenzene II. Transalkylation of toluene with mesitylene over synthetic zeolites. E. DUMITRIU, V. HULEA, KYYOUSEF, N. BALBA and S. OPREA 1185

Trends and tendencies in instrumental analytical techniques with special emphasis on environmental analysis. T. BRAUN and S. ZSINDELY 481

Use of semiempirical molecular orbital parameters to probe dihydropyridine stability-implications to brain-targeting chemical delivery system. M. E. BREWSTER, M.-JU. HUANG, J. J. KAMINSKI, E. POP and N. BODOR 647

Validity of the coats-redfern method in nonisothermal kinetics. N. DRAGOE and E. SEGAL 995

NOTE POUR LES AUTEURS

La Revue Roumaine de Chimie publie des articles en anglais, français, russe, allemand ou espagnol. Les auteurs sont priés d'envoyer des articles et des comptes rendus inédits.

Les manuscrits seront dactylographiés à double interligne. La bibliographie, les tableaux et la légende des figures seront placés après le texte.

Si l'article fait partie d'une série numérotée, la partie précédente sera donnée comme première référence.

Chaque article sera précédé d'un résumé comprenant quinze lignes au maximum.

Les références bibliographiques dans le texte seront faites par des exposants sans parenthèses et paraîtront à la fin de l'ouvrage.

Les publications périodiques mentionnées dans la bibliographie seront présentées suivant les prescriptions internationales : le nom de l'auteur précédé de l'initiale du prénom, le titre du périodique abrégé conformément à « Chemical Abstracts » et souligné par une ligne, le numéro du tome indiqué par des chiffres arabes et souligné par deux lignes, suivi de la première page de l'article ; à la fin, l'année de la parution sera placée entre parenthèses. Le numéro de la revue ne sera pas indiqué si les pages du volume sont numérotées consécutivement.

Les textes des livres ou traités incluеront : le nom des auteurs, précédé de l'initiale du prénom, le titre du livre entre guillemets et sans être souligné, le numéro du tome précédé par l'abréviation « vol. » (ou « Bd. »), le numéro de l'édition (the publisher), la localité de la parution du livre, l'année de la parution et la page de la référence précédée par l'abréviation « p. » (ou « S. »).

Les brevets seront indiqués comme suit : l'auteur ou la firme, le pays et le numéro du brevet, la date et la revue (*Chem. Abstr.*) Par ex. : M. Jones (to Union Carbide Co), Brit. Pat. 601 238, 2 Sept. 1959 ; cf. *Chem. Abstr.*, **24**, 12808 (1960).

Si la référence n'a pas été lue en original, on indiquera aussi la revue de référencs consultée.

Les diagrammes seront tracés à l'encre de Chine sur papier calque. Les tableaux et les figures (en nombre strictement nécessaire) ainsi que les courbes dans les figures seront numérotés par des chiffres arabes. Leur explication sera donnée dans la légende des figures. Prière de ne pas inscrire les mêmes données dans les tableaux et les figures. Chaque tableau aura un titre. On indiquera dans le texte la place approximative des tableaux et des figures. Les formules chimiques seront incluses dans le texte ; en outre, elle seront transcrites sur papier calque, à l'encre de Chine.

Les auteurs sont priés d'indiquer les caractères italiques (en soulignant les lettres au crayon), ainsi que tout autre caractère spécial ; les préfixes *ortho*, *meta*, *parc*, *cis*, *trans*, etc. seront soulignés pour indiquer leurs caractéres italiques et ne seront jamais écrits avec des majuscules.

Aucune correction à la main ne sera admise sur le manuscrit. Les corrections seront frappeés à la machine. Les lettres grecques ou d'autres symboles spéciaux seront insérés à la main à l'encre clairement.

Le manuscrit sera signé par l'auteur.

Le titre-courant aura 50 lettres au maximum.

L'entière responsabilité du contenu des articles appartient aux auteurs.

Sur demande ou peut obtenir une note plus complète.

PRINTED IN ROMANIA

TRAVAUX PARUS AUX ÉDITIONS DE L'ACADÉMIE ROUMAINE

I. G. MURGULESCU, **Introducere în chimia fizică, Vol. I. 1. Atomi, molecule, legătură chimică,** 1976, 560 p.
I. G. MURGULESCU, V. EM. SAHINI, **Introducere în chimia fizică, Vol. I. 2. Structura şi proprietăţile moleculelor,** 1979, 604 p.
I. G. MURGULESCU, E. SEGAL, **Introducere în chimie fizică, Vol. II. 1. Teoria molecular-cinetică a materiei,** 1979, 1036 p.
I. G. MURGULESCU, TATIANA ONCESCU, E. SEGAL, **Introducere în chimia fizică, Vol. II. 2. Cinetică chimică şi cataliză,** 1981, 1024 p.
I. G. MURGULESCU, J. PAUN, **Introducere în chimia fizică, Vol. I. 3. Nucleul atomic, reacţii nucleare, particule elementare,** 1982, 606 p.
I. G. MURGULESCU, RODICA VÎLCU, **Introducere în chimia fizică, Vol. III. Termodinamica chimică,** 1982, 624 p.
I. G. MURGULESCU, O. M. RADOVICI, **Introducere în chimia fizică, Vol. IV. Electrochimia.** 1986, 410 p.
C. ANDREI, I. DRAGUTAN, A. T. BALABAN, **Fotostabilizarea polimerilor cu amine împiedicate steric,** 1990, 240 p.
M. BREZEANU, E. CRISTUREANU, D. MARINESCU, A. ANTONIU, M. ANDRUH, **Chimia metalelor,** 1990.
R. VÎLCU, M. LECA, **Polymer Thermodynamics by Gas Chromatography,** coédition avec Elsevier, 1990, 204 p.
FL. CUIBAN, A. X. LUPEA, **Studiul structurii şi sinteza peptidelor,** 1989, 286 p.
C. SIMIONESCU, V. GORDUZA, **Implicaţiile bioenergetice ale coloranţilor,** 1988, 207 p.
R. VÎLCU, M. LECA, **Termodinamica polimerilor prin croomatografie de gaze,** 1987, 238 p.
I. ZUGRAVESCU, M. PETROVANU, **Cicloadiţii 3 + 2 dipolare,** 1987, 446 p.
RAUL MIHAIL, ION GROZEANU, **Estimarea secvenţială aplicată sistemelor chimice,** 1986, 406 p.
M. BREZEANU, I. PATRON, M. ANDRUH, **Combinaţii complexe polinucleare şi aplicaţiile lor,** 1986, 244 p.
A. T. BALABAN et al., **Labelled Compounds and Radiopharmaceuticals Applied in Nuclear Medicine,** coédition avec John Wiley and Sons, 1986, 742 p.
D. PURDELA, **Nomenclatura chimiei organice — IUPAC,** 1986, 451 p.
PETRU BUDRUGEAC, **Probleme de chimie,** 1986, 280 p.
T. ONCESCU, S. G. IONESCU, **Conversie fotochimică şi stocare de energie,** 1985, 272 p.
V. DRAGUTAN, A. T. BALABAN, M. DIMONIE, **Olefin Metathesis and Ring-Opening Polymerization of Cyclo-Olefins,** coédition avec John Wiley and Sons, 1985, 544 p.
C. LITEANU, I. RICA, **Optimizarea proceselor analitice,** 1985, 360 p.
N. PERESCU, **Chimia extracţiei cu solvenţi şi aplicaţii,** 1985, 212 p.

1992 JUN 2

ISSN 0035—3930

S.C. UNIVERSUL S.A.—c. 3186

Lei 80